F 1103

Fa

ACADÉMIE DE LA RÉPUBLIQUE SOCIALISTE DE ROUMANIE

REFERÁLVA

R

REVUE ROUMAINE DE CHIMIE

TOME 22
N° 1
Janvier 1977

EDITURA ACADEMIEI REPUBLICII SOCIALISTE ROMÂNIA

Rev. Roumaine Chim.

RECHAX, 22, *1*, p. 1–160 (1977), Bucarest

ACADÉMIE DE LA RÉPUBLIQUE SOCIALISTE DE ROUMANIE

COMITÉ DE RÉDACTION

Rédacteur en chef:

I. G. MURGULESCU, membre de l'Académie de la République Socialiste de Roumanie

Rédacteurs en chef adjoints:

A. T. BALABAN et V. EM. SAHINI, membres correspondants de l'Académie de la République Socialiste de Roumanie

Collège de rédaction:

EM. BRATU, ELENA CEAUŞESCU, ECATERINA CIORĂNESCU-NENITZESCU, C. DRĂGULESCU, CR. SIMIONESCU, membres de l'Académie de la République Socialiste de Roumanie; P. SPACU, membre correspondant de l'Académie de la République Socialiste de Roumanie; MARGARETA AVRAM, I. HAIDUC, D. I. MARCHIDAN, I. MOLDOVAN, G. NIAC et D. SĂNDULESCU

La Revue Roumaine de Chimie paraît 10 fois par an. Toute commande de l'étranger (fascicules ou abonnements) sera adressée à ILEXIM — Departamentul Export-Import Carte (Livres)/Departamentul Export-Import Presă (Revues), P.O.B. 136—137, télex 11226, Bucarest, 3, str. 13 Decembrie, Roumanie

Les manuscrits, les livres et les revues proposés en échange, ainsi que toute correspondance seront envoyés à la rédaction :

REVUE ROUMAINE DE CHIMIE

23, str. Dumbrava Roşie, Bucarest, Roumanie, téléphone 12 41 60

EDITURA ACADEMIEI REPUBLICII SOCIALISTE ROMÂNIA
125, Calea Victoriei, 71021, Bucarest, Roumanie, téléphone 507680

ORSZÁGOS MŰSZAKI KÖNYVTÁR ÉS DOKUMENTÁCIÓS KÖZPONT 1883

REVUE ROUMAINE DE CHIMIE

Tome 22, N° 1 Janvier 1977

The 75th Anniversary of Academician I. G. Murgulescu 3–6

D. I. MARCHIDAN and LIANA PANDELE, Thermal properties of the mixture $BaCl_2-KCl$ 7–11

B. F. MARKOV, Thermodynamic information on the structure of molten salt systems with chemical interaction between the components 13–20

S. STERNBERG and LUCIA BEJAN, Thermodynamic properties of fused salt ternary system AgI + NaI + CsI by formation cell method 21–25

L. DENIELOU, J. P. PETITET, C. TEQUI, Étude dilatométrique et volumétrique de sels fondus — application au sulfate d'argent, aux sulfates, chromates, molybdates et tungstates alcalins 27–33

MARILENA ŞERBAN, On the viscosity of molten metals. IV. A comparison between gas and liquid viscosities 35–37

V. E. SAHINI and A. SAVIN, On the stability of aromatic hydrocarbons. IV. On the linearity of the delocalization energy relationships 39–44

A. T. BALABAN, Chemical graphs. XXVIII. A new topological index for catafusenes : L-transform of their three-digit codes 45–47

Q CR. I. SIMIONESCU and ADELAIDA LIGA, Researches in the terpolymerization field. VIII. Theoretical structural study of the high conversion acrylonitrile — methacrylic acid — methyl methacrylate terpolymer 49–54

C. DRĂGULESCU, SEPTIMIA POLICEC and T. SIMONESCU, Complexes of anthranil-N,N-diacetic acid with trivalent metals. IV. Stability interpretation 55–59

P. SPACU and LUCIA ANTONESCU, Contribution to the coordination chemistry of molybdenum. IV. Biguanidonium aquo-tetrachloro-oxomolybdates (V) 61–67

TATIANA ONCESCU and ECATERINA JURCONI, Thermal decomposition of Bis(oxalato)diaquomanganese(III). Complex in acidic aqueous solution 69–75

M. VLAD and E. SEGAL, A kinetic analysis of addition polymerization reaction 77–86

Z. SIMON and E. DRASKOVITS-SCHUCH, Partition coefficients and intermolecular force parameters 87–95

Q I. V. NICOLESCU, OLGA ŞERBAN, I. SĂNDULESCU and LILIANA STOICESCU, The origin and the type of active centers in solid acid catalysts. II. Transalkylation of toluene on $Al_2O_3-SiO_2$ catalyst 97–102

R. H. SCHUSTER und I. A. SCHNEIDER, Mediumeinflüsse bei der Solvolyse von Alkylhalogeniden. II. Solvolyse von *t*-Butylchlorid in Aceton-Wasser-Gemischen mittlerer Konzentration 103–116

Rev. Roumaine Chim., 22, *1*, p. 1–160 (1977), Bucarest

ILEANA I. STĂNOIU, F. CHIRALEU, EUGENIA GÂRD and A. T. BALABAN, Isotopic exchange of active methyl hydrogens. VIII. Deuterium kinetic isotope effects for α-and γ-isopropyl-substituted pyrylium salts 117–126

R – SOFIA MARCHIDAN, Polarographic reduction of some s-triazine herbicides 127–132

D. FĂTU, VIORICA CIMPU et D. CAMBOLI, La décomposition thermique des combinaisons complexes thiocyaniques du Pd(II) avec la thio-urée 133–136

R – N. TOTIR, SOFIA MARCHIDAN, C. VOLANSCHI, N. CIMPOERU, RODICA ANDREI and ILEANA FUNDUC, Quantitative determination of trace amounts of s-triazine herbicides in waste waters by physico-chemical methods 137–143

O. RADOVICI, MARIA MAVRODIN-TĂRĂBÎC, IOANA ONACA and I. SOLACOLU, Oxygen reduction on silver gas electrodes. V. The effect of compression and sintering conditions on electrode performances 145–152

COMPTES RENDUS 153–159

PROFESSOR I. G. MURGULESCU

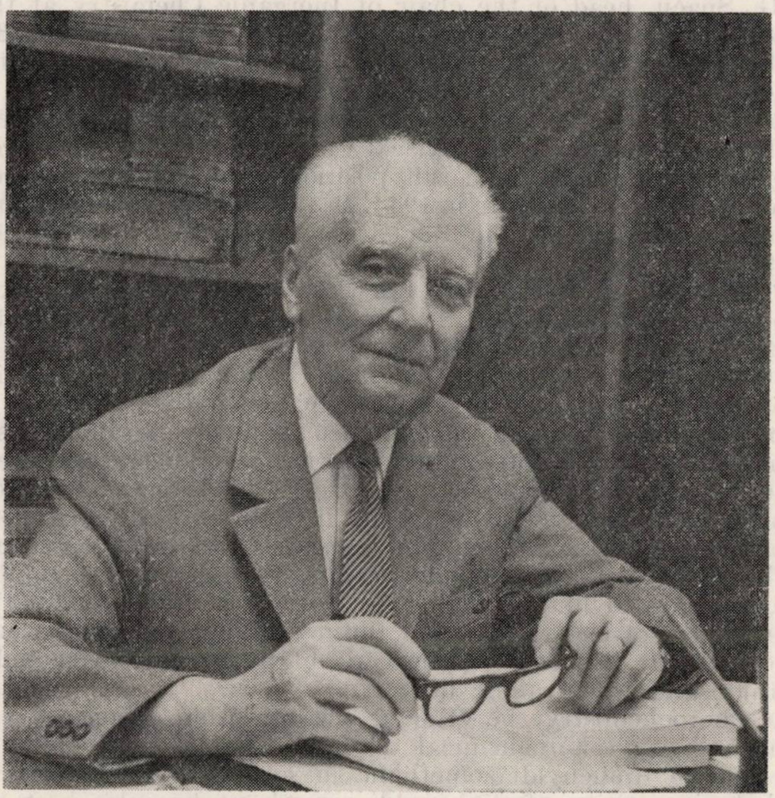

Professor Dr. I. G. Murgulescu, member of the Academy of the Socialist Republic of Romania, Professor Emeritus of Physical Chemistry at the Bucharest University, and Director of the Centre of Physical Chemistry, is seventy five years old on January 27, 1977.

His scientific personality, his important contribution in creating a modern school of physical chemistry in Romania, and his multiple activities in teaching and scientific research have been unanimously recognized and appreciated.

Professor Dr. I. G. Murgulescu was born at Cornu, Oltenia. He studied at the elementary school in his native village and he followed the high school in Craiova. As a student at the Science Faculty of the Cluj University he has proven his ingenuity in numerous occasions.

He started his didactic activity at the Science Faculty of the Cluj University where, he was appointed assistant in 1928, after having graduated from the same Faculty with the highest honours. In 1930 he obtained his Ph. D degree, with a thesis on Copper Thiosulphate Complexes, which was approved with „Magna Cum Laude" by the Cluj University.

His scientific personality has been appreciated by the late Professor G. Spacu, head of the chair of Inorganic Chemistry at the Cluj University. Professor I. G. Murgulescu spent the years 1932—1933 at the Institute of Physical Chemistry of the Leipzig University working with Professor F. Weigert on photochemical problems.

Returning home in 1934, Professor I. G. Murgulescu became reader in Analytical Chemistry and Physical Chemistry at the Timișoara Polytechnic Institute, and he held this position until he was appointed full professor at the same Institute in 1944. In 1949 he was appointed professor of physical chemistry at the Bucharest University where he lectured until 1972.

Professor Murgulescu's research work covers a wide field : kinetics, thermodynamics, electrochemistry, spectroscopy, inorganic and analytical chemistry, molten salt chemistry.

Starting from the studies of complex combinations he identified new types of complex silver and copper thiosulphates in the presence of ammonium, potassium and sodium, and extended these investigations by spectrophotometric, cryoscopic, and conductometric measurements ; he determined thus the composition of Durrand's salt. He also investigated spectrophotometrically the copper and cobalt salts in solution and the type of the chemical bond of complex chromium, manganese, iron and cobalt oxalates.

The study of the refractometric properties of aqueous solutions of electrolytes allowed him to elaborate new methods for calculating the refractive index of electrolytes and the individual ionic refractions. One of these methods has been applied to obtain the refractive indices of ferricyanide and ferrocyanide ions.

In photochemistry, he studied the quantum efficiency and the mechanism of the photochemical decomposition of potassium cobaltic oxalate and of diphenyldiazomethane in solution. The kinetics of the thermal decomposition of diphenyldiazomethane has also been studied by Professor Murgulescu and his coworkers.

Professor I. G. Murgulescu studied the kinetics of the alcoholysis of some benzyl halides and decomposition of the cobaltic oxalates in aqueous solution.

Another problem in which Professor I. G. Murgulescu became interested was the anodic passivation of metals and alloys. His studies on the electrochemical behaviour of thin films and on the determination of electrode potentials are well known.

His contribution to chemical thermodynamics dealt mainly with thermal decomposition of calcium carbonate, thermodynamic activity of solutions and alloys and free energy of chemical substances. By ebullioscopy he obtained the dissociation constant of α-nitroso-β-naphthol in solution. By calorimetry he obtained the heat of dissolution of sodium iodate, both anhydrous and hydrated.

In analytical chemistry Professor I. G. Murgulescu has elaborated new analytical methods for mercury and he was the first to use o-chlorobenzoic acid in alkalimetry and acidimetry. He developed a new conductometric method for titrating molybdates and wolframates using silver nitrate, and also for complex iron cyanides enriching the theory of precipitation processes in the physico-chemical analysis. He has published studies on the theory of the equivalence point in titrimetry, and the determination of normal electrode potentials.

In 1957 Professor I. G. Murgulescu concentrated on the area of research for which he became best known, the physical chemistry of molten salts. His contributions to this field are both theoretical and experimental. Professor Murgulescu's researches in molten salts cover a wide field : thermodynamic properties of binary mixtures of molten salts by the methods of electromotive forces ; cryometry and vapour pressure measurements ; transport properties of molten salts, namely viscosity, electric conductivity ; optical properties of molten salts (refractive indices) ; heat of mixing, heat of melting, heat capacity of molten salts, etc.

The results of his scientific research have been published in over 200 articles issued in Romanian and foreign journals.

In 1948 Professor I. G. Murgulescu was elected Member of the Academy of the Socialist Republic of Romania. As a recognition of his merits he was elected Vicepresident between 1959—1963 and President of the Academy of the Socialist Republic of Romania between 1963—1966.

The Centre of Physical Chemistry was formed in 1963 under Professor Murgulescu's leadership and he has been the Director of this institute ever since.

The stimulating atmosphere which prevails in Professor Murgulescu's activity at the Centre of Physical Chemistry and the Bucharest University, has provided an excellent starting point for many young scientists who are now engaged in research and teaching in different fields of physical chemistry. The same atmosphere has been beneficial for a few young scientists from abroad during their affiliation with the Centre of Physical Chemistry.

Under his scientific guidance, over 20 young researchers have completed their graduate studies (Ph. D.).

As a recognition of his remarkable organizing aptitudes, Professor I. G. Murgulescu was nominated Rector of the Timișoara Polytechnic Institute (1947—1949), Rector of the Bucharest University (1949—1950), Deputy Minister of Education (1950—1956) and then Minister of Education (1960—1963).

In carrying out his duties, Professor Murgulescu has given an example of perseverance and tenacity to all his co-workers and pupils. His devotion to teaching and research, which he succeeded in combining throughout his career, was the most characteristic feature of his multilateral activity. Among the public offices he detained in Romania, we would quote : member of the Grand National Assembly (1948—1965), Vice President of the State Council (1965—1967) and Vice President of the Grand National Assembly (1967—1975).

As an international recognition of his scientific merits, he was elected member of the USSR Academy of Sciences, of the Czechoslovak Academy of Sciences, of the Hungarian Academy of Sciences and of the Bulgarian Academy of Sciences. He is a member of the editorial board of scientific journals : *Electrochimica Acta* and *Corrosion Science*. He is editor-in-chief of the chemical scientific journal *Revue Roumaine de Chimie* and was also editor-in-chief of *Studii și Cercetări de Chimie — Academia R. S. România*.

For his scientific and public activity, Professor I. G. Murgulescu was awarded several distinctions, medals and prizes such as : Romanian State Prize (1963), Professor Emeritus (1964), Emeritus Scientist (1969), the Gold Medal of the 39th International Congress of Industrial Chemistry (1970), Hero of Socialist Labour (1971).

Professor Murgulescu's personality is an example for the Romanian scientists who hold him in high esteem. We wish him a long and fruitful life serving high scientific and patriotic ideals.

D. I. MARCHIDAN

Revue Roumaine de Chimie, **22**, *1*, 7–11 (1977)

THERMAL PROPERTIES OF THE MIXTURE $BaCl_2$–KCl

D. I. MARCHIDAN and LIANA PANDELE
Centre of Physical Chemistry, Str. Galaţi 31, Bucharest 13, România

Received May 12, 1976

The thermal properties of the binary mixture $BaCl_2$–KCl were determined by means of drop-calorimetry. Measurements were carried out for both solid and for liquid states. The experimental data were processed to evaluate heat capacities, heats of fusion and heat capacities of mixing.

It is extremely important to study the thermal properties of molten salts and of their mixture due to their theoretical and practical applications.

Fused-salts systems provide an important testing ground for theories of liquids and of solutions and for the study of oxidation states.

Also, the study of the thermochemical properties of fused salts has a practical importance due to their utilization in diverse fields such as metallurgy, electrochemistry and nuclear technology.

The study of the binary mixture $BaCl_2$ – KCl constitutes a part of a wider programme developed in our laboratory in view of determining the thermal properties of alkaline and alkaline-earth halides.

The thermal properties of pure salts, namely $BaCl_2$ and KCl were previously investigated [1,2].

EXPERIMENTAL SECTION

The experimental technique and the installation has been described in detail in a previous paper.[3] The accuracy of the measurements is considered to be within reproducibility, i.e. ± 0.4 percent. The essential features of the installation are the furnace with an inoxiterm steel core and the copper-block calorimeter proper. The temperature of the furnace was kept constant by means of a proportional thermoregulating device and was verified using a thermocouple, Pt–PtRh (10%). The temperature variations of the calorimeter proper were measured by means of a thermistor characterized by a high sensitivity and reproducibility, which permitted the measurement of a small temperature variations of 0.001 K.

In order to account for the heat content of the container and the heat lost during the drop, similar experiments were made with the empty container at the same temperatures.

Potassium chloride and barium chloride (purity 99.9%, British Drug House) were dried and purified, according to previously described method [1,2] they were then melted together and sealed into the platinum containers under vacuum.

---

[1] D. I. Marchidan and L. Pandele, *Rev. Roumaine Chim.*, **20**, 299 (1975).

[2] D. I. Marchidan and L. Pandele, *Rev. Roumaine Chim.* **20**, 1227 (1975).

[3] D. I. Marchidan and M. Ciopec, *Studii şi Cercetări Chim., Acad. R. S. România*, **17**, 737 (1969).

RESULTS AND DISCUSSION

Heat content measurements for 2 compositions, namely those corresponding to eutectic mixtures,[4] were carried out.

The first studied mixture has the composition 25.9 mol % $BaCl_2$ and 74.1 mol % KCl and the melting point 931.1 K.

Table 1

Experimental and calculated enthalpy increments for solid and liquid mixture of 25.9 mole % $BaCl_2$ and 74.1 mole % KCL composition. Deviation of experimental data from the calculated curve

T(K)	$H_T - H_{298.15}$ (cal mole^{-1})		Deviation	
	exp.	calc.	cal mole^{-1}	%
		Solid		
762.9	7631.7	7575	56.7	0.74
780.1	7801.9	7842	−40.1	−0.51
797.8	7956.7	8121	−164.3	−2.02
820.3	8470.1	8474.5	−4.4	−0.05
841.2	8859.6	8802	57.6	0.65
849.7	9103.2	8936	167.3	1.87
875.2	9248.6	9336.4	−87.2	−0.93
904.2	9744.9	9801.1	56.2	0.57
925.4	9977.9	10124	146.1	1.44
931.3	10758.4	—	—	—
		Liquid		
936	16050	16009	41	0.26
983.6	17031	17035	−4	−0.02
1011.4	17550	17634	−84	−0.47
1031.1	18118	18057	61	0.33
1060	18700	18682	18	0.09

The heat content was determined within the temperature range 762−1060 K. The experimental results are listed in table 1 and plotted in figure 1.

The experimental results were processed by the least squares method to obtain for the mixture in the solid state the following equation :

$$H_T - H_{298.15} = (15.70\ \mathrm{T} - 4404.2)\ \mathrm{cal\ mol^{-1}}$$

By deriving equation in terms of absolute temperature we obtained :

$$C_p = 15.70\ \mathrm{cal \cdot K^{-1} mol^{-1}}$$

The experimental data for the liquid state were processed to obtain an equation of the form :

$$H_T - H_{298.15} = (21.55\ \mathrm{T} - 4161.65)\ \mathrm{cal\ mol^{-1}}$$

---

[4] C. Krolin, *Acta Chem. Scand.*, **20**, 1 (1966).

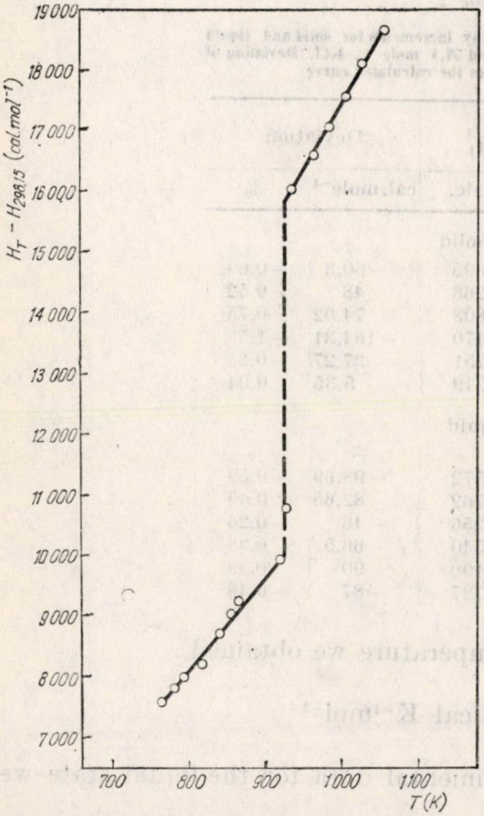

Fig. 1. — Enthalpy variation of the mixture of 25.9 mol % $BaCl_2$ and 74.1 mol % KCl composition in terms of temperature

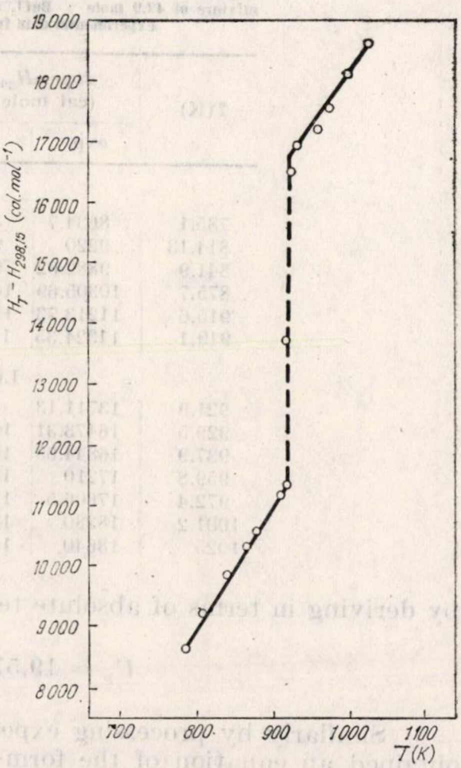

Fig. 2. — Enthalpy variation of the mixture of 42.9 mol % $BaCl_2$ and 57.1 mol % KCl composition in terms of temperature

The equation derived in terms of absolute temperature leads to the value:

$$C_p = 21.55 \text{ cal K}^{-1}\text{mol}^{-1}$$

For the enthalpy of fusion we obtained the value 5.40 kcal mol⁻¹.

The second studied mixture had the composition 42.9 mol % $BaCl_2$ and 57.1 mol % KCl and the melting point 921 K.

The heat content was determined within the temperature range 785—1025 K. The experimental results are listed in table 2 and plotted in figure 2.

The experimental data for the mixture in the solid state were processed to obtain the equation:

$$H_T - H_{298.15} = (19.57\ T - 6667.6)\text{cal mol}^{-1}$$

Table 2

Experimental and calculated enthalpy increments for solid and liquid mixture of 42.9 mole % $BaCl_2$ and 57.1 mole % KCl. Deviation of experimental data from the calculated curve

T(K)	$H_T - H_{298.15}$ (cal mole^{-1}) exp.	$H_T - H_{298.15}$ (cal mole^{-1}) calc.	Deviation cal. mole^{-1}	Deviation %
		Solid		
785.1	8634.7	8695	−60.3	−0.69
814.13	9220	9268	−48	−0.52
841.9	9882.02	9808	74.02	0.75
875.7	10305.69	10470	−164.31	−1.56
915.6	11213.73	11251	−37.27	−0.33
919.1	11324.35	11319	5.35	0.04
		Liquid		
921.9	13711.13	—	—	—
929.5	16473.31	16572	−98.69	−0.59
937.9	16844.65	16762	82.65	0.49
959.8	17210	17256	−46	−0.26
972.4	17606.5	17540	66.5	0.38
1001.2	18280	18190	90	0.49
1025	18640	18727	−87	−0.46

by deriving in terms of absolute temperature we obtained :

$$C_p = 19.57 \text{ cal } K^{-1} mol^{-1}$$

Similarly by processing experimental data for the liquid state we obtained an equation of the form :

$$H_T - H_{289.15} = (22.56\ T - 4397.55) \text{ cal mol}^{-1}$$

The equation derived in terms of absolute temperature leads to the value :

$$C_p = 22.56 \text{ cal } K^{-1} mol^{-1}$$

The value $\Delta H_f = 5.55$ kcal mol^{-1} is obtained for the enthalpy of fusion.

The values previously reported [1,2] for the heat capacities of the pure salts were used to calculate the heat capacities of mixing. The results are listed in table 3.

ΔC_p^M is found to have the same sign in both systems. A similar behaviour from the viewpoint of heat capacity change on mixing has been found by Markov [5] in $KCl-CaCl_2$ system (in compositions corresponding to euthectics) ; this system is similar to the one under study both as nature of salts involved and charge asymmetry and as phase diagrams.

---

[5] B. F. Markov and T. A. Tishura, *Ukrain. Khim. Zhur.*, **39**, 757 (1973).

Table 3

Heat capacities of mixing

System	C_p(comp.) cal K^{-1} $mole^{-1}$	C_p(mixture) cal K^{-1} $mole^{-1}$	ΔC_p^M cal K^{-1} $mole^{-1}$
25.9 mol % $BaCl_2$+ 74.1 mol % KCl	19.55	21.55	2.00
42.9 mol % $BaCl_2$+ 57.1 mol % KCl	21.10	22.56	1.46

In conclusion one can say that the two studied compositions of the $BaCl_2$—KCl system exhibit in molten state a similar thermochemical behaviour namely the heat content and heat capacity values are similar over the whole temperature range covered; the heat capacity change on mixing has the same sign for the two compositions.

Revue Roumaine de Chimie, **22**, *1*, 13 – 20 (1977)

THERMODYNAMIC INFORMATION ON THE STRUCTURE OF MOLTEN SALT SYSTEMS WITH CHEMICAL INTERACTION BETWEEN THE COMPONENTS

B. F. MARKOV

Institute of General and Inorganic Chemistry, Ukrainian SSR Academy of Sciences, Kiev, USSR

Received January 21, 1976

A method of calculating the structural elements of a melt has been developed, which relies on the combination of experimental thermodynamic data and structural models, for molten binary salt systems with chemical interaction between the components. The results of the calculation for the systems $CoCl_2-NaCl$, $CoCl_2-KCl$, $MgCl_2-NaCl$, and $MgCl_2-KCl$ are given as plots : molar fraction of the structural element vs. initial composition of the mixture. The free energy of formation of the complex compounds $NaCoCl_3$, $NaMgCl_3$, $KCoCl_3$, $KMgCl_3$, Na_2CoCl_4, Na_2MgCl_4, K_2CoCl_4 and K_2MgCl_4 has been determined. The thermodynamic activity of $CoCl_2$ or $MgCl_2$ is equal to the concentration of the free, not complexed part of the component expressed in molar fraction relative to all equilibrium forms of the species in the melt.

1. INTRODUCTION

The large negative values of the integral excess thermodynamic properties of molten binary salt systems, such as enthalpy of mixing and free excess Gibbs energy, indicate that a chemical interaction between the components takes place in the melt, which manifests itself in the formation of complex compounds (complex ions). The existence of complexes in such molten salt systems is first of all proved by the results of the study of the structure of the melts by spectral methods.

The excess thermodynamic functions describing the energy characteristics of the formation of the solution have in this case a formal thermodynamic meaning and do not characterize the structural elements of the melt, in particular complex compounds.

As will be shown below, it is possible to obtain information on the structure of the solution, that is, on its model involving the dependence of the content of each structural element on the composition and their thermodynamic characteristics, from the partial thermodynamic properties of the solution components determined experimentally.

2. METHOD OF CALCULATION

Since in systems with chemical interaction of the components there is a thermodynamic equilibrium between all structural elements of the melt — between the complexes and the components in free state — we can assume that the chemical potential of any structural component of the solution is given by the equation

$$\mu_i = \mu^0_{i\ x_i=1} + RT \ln x_i \tag{1}$$

where x_i is the molar fraction of the i-th structural component which has been determined relative to all coexisting structural forms.

As to the first component, which is regarded as complexing agent, its thermodynamic activity, determined experimentally, must be equal to the concentration of the free, not complexed part expressed in molar fraction relative to all existing structural forms.

This condition is to be regarded as validity criterion of the assumed model of the solution. We have taken as example binary salt systems with assymmetrically charged ions of the type MeX_2 (*A* component) — MX (*B* component), i.e. melts formed by halides of univalent and bivalent metals.

Components *A* and *B* form complex compounds $M\,MeX_3$ and M_2MeX_4, which are, naturally, dissociated in the melt into ions. The existence of the coordinatively saturated compound $M_2\,MeX_4$ in the melt is confirmed by spectral studies: when the content of the *A* component in the mixture is small, the tetrahedral complex $[MeX_4]^{2-}$ [1-3] prevails in the melt.

Thus, we consider the model of the melt consisting of the following structural elements : *A*, *AB*, AB_2, *B*.

In the calculations we deal with one mole of the mixture.

At any initial composition there are n_1 moles of *A*, n_2 moles of *B*, n_3 of *AB* and n_4 moles of AB_2 in equilibrium in the mixture.

The material balance condition

$$n_1 + n_2 + 2n_3 + 3n_4 = 1 \tag{2}$$

and the equation of relation to the initial composition

$$n_1 + n_3 + n_4 = N_A \tag{3}$$

are apparently satisfied.

The mole fractions of *A*, *B*, *AB* and AB_2 at equilibrium are found from the equations

$$x_1 = \frac{n_1}{n_1 + n_2 + n_3 + n_4} \tag{4}$$

etc.

---

[1] K. Balasubrahmanyan and L. Nanis, *J. Chem. Phys.*, **40**, 2657 (1964).

[2] R. B. Ellis, *J. Electrochem. Soc.*, **113**, 485 (1966).

[3] V. A. Marani, E. J. Hathaway and E. J. Cairns, *J. Phys. Chem.*, **75**, 155 (1971).

The standard free energy of formation of the compound AB from components may be expressed in terms of equilibrium constant (or a reciprocal of it).

$$\Delta G^0_{AB} = RT \ln K_1$$

In its turn

$$K_1 = \frac{x_1 \cdot x_2}{x_3} = \frac{n_1 \cdot n_2}{n_3(n_1 + n_2 + n_3 + n_4)} \tag{5}$$

Similarly for the AB_2 compound

$$K_2 = \frac{x_1 \cdot x_2^2}{x_4} = \frac{n_1 \cdot n_2^2}{n_4(n_1 + n_2 + n_3 + n_4)^2} \tag{6}$$

If K_1 and K_2 have been determined independently, then one can find n_1, n_2, n_3 and n_4 and hence also x_1, x_2, x_3, x_4 at various initial compositions (N_A) by combined solution of equations (2), (5) and (6) as one can specify one of unknown quantities.

Determination of K_2

To find K_2 it is enough to estimate $\Delta G^0_{AB_2}$. At low concentrations of the A component in the mixture, i.e. at very large excess of the B component, the whole of the A component is practically in the form of AB_2 compound according to equation (6). The dependence of the partial free energy of A ($\Delta\bar{G}_A$) on the composition (N_A) in the region of low values of N_A is known from practice.

We now make up a thermodynamic cycle, assuming that the whole of the component A added to the melt is complexed.

The equation of the cycle reads as follows:

$$\Delta\bar{G}_{A_{N_A \to 0}} = RT \ln \frac{N_A}{1-2N_A} + \Delta G^0_{AB_2} - 2RT \ln \frac{1-3N_A}{1-2N_A}$$

The change in free energy on the return of the released B component can be neglected as a small value.

Then the above equation reduces to

$$\Delta G^0_{AB_2} \cong \Delta G_A - RT \ln \frac{N_A}{1-2N_A} \tag{7}$$

We will demonstrate the calculation of $\Delta G^0_{AB_2}$ from the experimental data $\Delta\bar{G}_A$ on the system $CoCl_2-KCl$, which has been studied before by the e.m.f. method[4] (see table 1).

---

[4] D. C. Hamby and A. B. Scott, *J. Electrochem. Soc.*, **117**, 319 (1970).

Table 1

Standard free energy of formation of K_2CoCl_4 ($\Delta G^{0}_{K_2CoCl_4}$) at varions composition of the molten mixture(N_{CoCl_2}) in the system $CoCl_2$ – KCl at 1073 K

N_{CoCl2}	$-\ \Delta G_{CoCl2}$ cal.mole^{-1}	$RT \ln \frac{N_{CoCl2}}{1\text{-}2N_{CoCl2}}$ cal.mole^{-1}	$-\Delta G^{o}_{KCoCl_4}$ cal.mole^{-1}	$-G^{E}_{CoCl_2}$ cal.mole^{-1}
0.001	29700	−14730	14970	14970
0.003	27400	−12375	15025	15010
0.007	25600	−10550	15050	15020
0.020	23300	−8255	15045	14960
0.050	21200	−6163	15037	—
		average	15030	15000

As the mole fraction of $CoCl_2$ almost coincides with the mole fraction of K_2CoCl_4 at high dilution, the average value of $\Delta G^0_{K_2CoCl_4}$ (−15.05 kcal) agrees with the partial free excess energy of $CoCl_2$, $\bar{G}^E_{CoCl_2}$ (−15 kcal).

In the case of less stable compounds, some variation of $\Delta G^0_{AB_2}$ is observed: the variation decreases gradually with decreasing N_A.

One should, naturally, use the limiting value of $\Delta G^0_{AB_2}$ at $N_A \to 0$.

Determination of K_1

We make up a thermodynamic cycle consisting of the following steps: formation of solution from 0.5 mole of A and 0.5 mole of B, separation of the solution into equilibrium components A, B, AB and AB_2, splitting of AB and AB_2 into original components. Summation of changes of free energies in the cycle yields the equation

$$0.5\,\Delta\bar{G}_A + 0.5\,\Delta\bar{G}_B = n_1RT\ln\frac{n_1}{\sum n} + n_2RT\ln\frac{n_2}{\sum n} + \\ + n_3RT\ln\frac{n_3}{\sum n} + n_4RT\ln\frac{n_4}{\sum n} + n_3RT\ln K_1 + n_4RT\ln K_2 \tag{8}$$

When K_2 is known, the combined solution of equations (2), (5), (6) and (8) for the condition $n_1 + n_3 + n_4 = 0.5$ makes it possible to determine K_1. It will be noted that the mathematical problems were solved using "MIR−2" computer.

3. RESULT AND CONCLUSION

The above method was used for treating the literature thermodynamic data, which had been obtained from e.m.f. measurements on reversible chemical cells with molten binary electrolytes $CoCl_2-NaCl$, $CoCl_2-KCl$[4] and $MgCl_2-NaCl$, $MgCl_2-KCl$.[5]

The calculated standard free energies of formation of the complex

Table 2

Standard free energy of formation of AB and AB$_2$ compounds from components

System	TK	$-\Delta G^0_{AB}$ cal. mole^{-1}	K_{AB}	$-\Delta G^0_{AB_2}$ cal. mole^{-1}	K_{AB_2}
$MgCl_2-NaCl$	1098	5350	0.086336	7200	0.0369
$CoCl_2-NaCl$	1073	7200	0.034114	9100	0.01402
$MgCl_2-KCl$	1073	10350	0.0078125	11800	0.003952
$CoCl_2-KCl$	1073	11000	0.00574	15030	0.00088

compounds AB and AB_2 and K_{AB_2} and K_{AB} values corresponding to them are summarized in table 2.

The calculated values of x_1, x_2, x_3 and x_4 at different initial compositions were used for plotting the mole fraction of structural element (x_i) versus composition (N_A) (Figures 1—4). The plots show the variation of the ratio between the equilibrium forms during the variation of the stability of complexes.

Mole fractions of the A component (x_A) in free, not complexed state versus initial composition (N_A) are shown in figures 5—8 (solid lines). The same figures contain the experimental activity values of the first component (circles). As is seen from the figures, there is a good agreement between the experimental values a_A and calculated values x_A. This con-

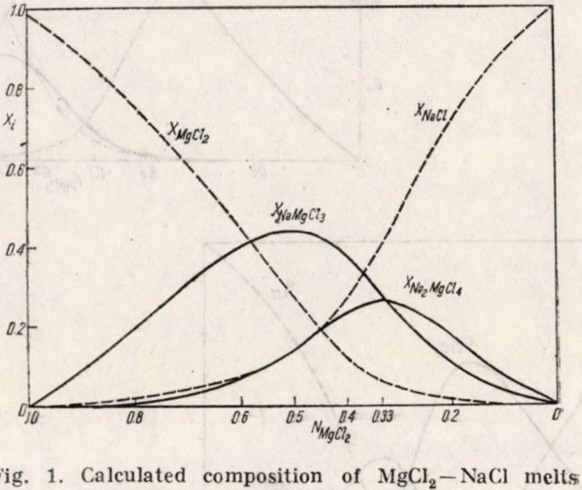

Fig. 1. Calculated composition of $MgCl_2-NaCl$ melts at 1098 K

---

[5] D. E. Neil, H. M. Clark and R. H. Wiswall, *J. Chem. and Eng. Data*, **10**, 21 (1965).

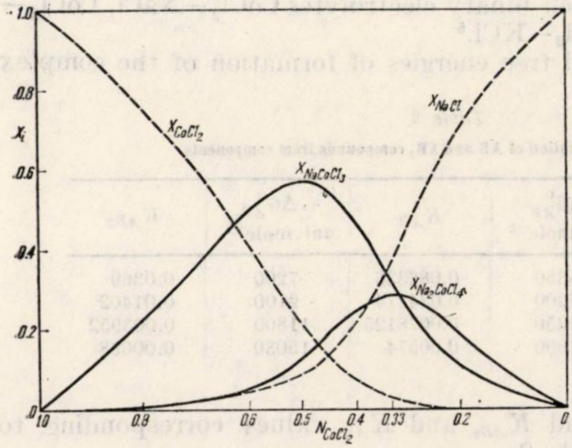

Fig. 2. Calculated composition of $CoCl_2-NaCl$ melts at 1073 K

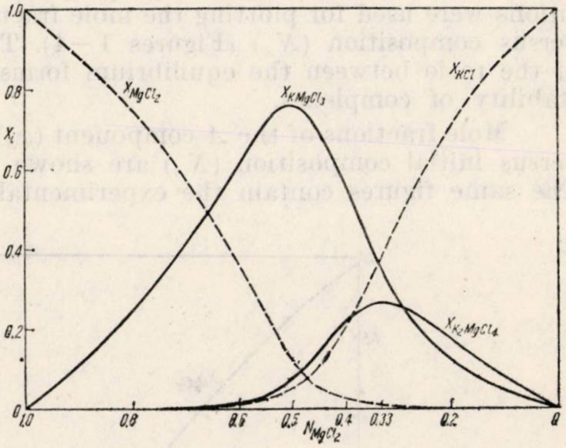

Fig. 3. Calculated composition of $MgCl_2-KCl$ melts at 1073 K

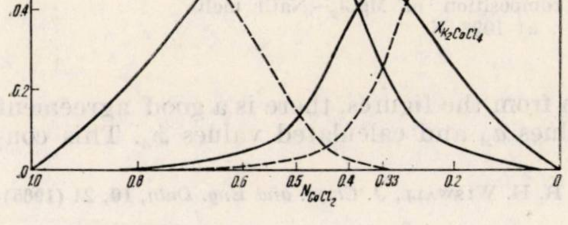

Fig. 4. Calculated composition of $CoCl_2-KCl$ melts at 1073 K

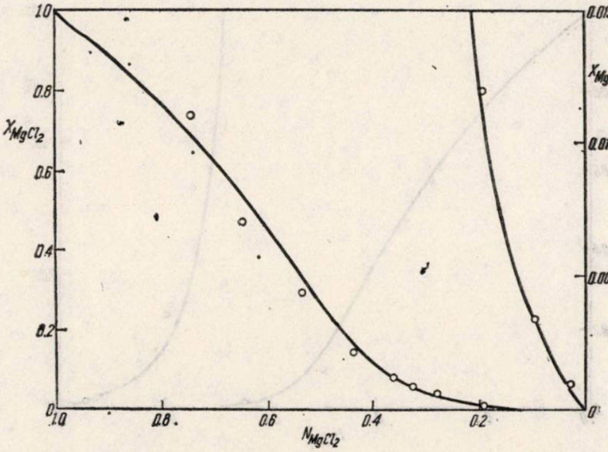

Fig. 5. Comparison between the calculated molar fraction of $MgCl_2(X_{MgCl_2})$ and the experimental activity of $MgCl_2$ (circles) of $MgCl_2-NaCl$ melts at 1098 K

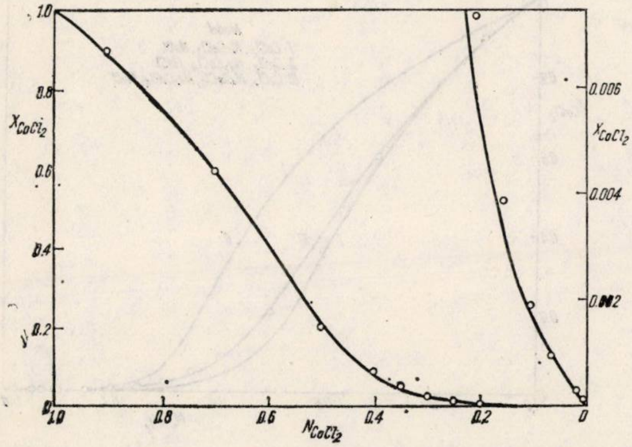

Fig. 6. Comparison between the calculated molar fraction of $CoCl_2(X_{CoCl_2})$ and the experimental activity of $CoCl_2$ (circles) of $CoCl_2-NaCl$ melts at 1073 K

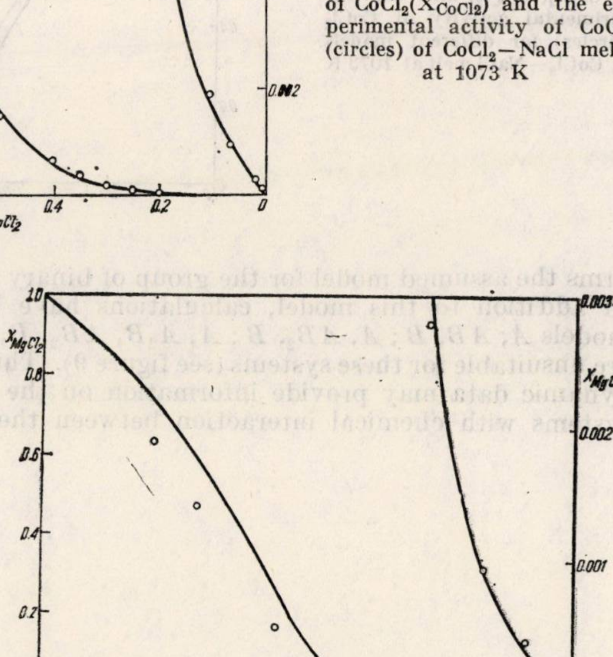

Fig. 7. Comparison between the calculated molar fraction of $MgCl_2(X_{MgCl_2})$ and the experimental activity of $MgCl_2$ (circles) of $MgCl_2-KCl$ melts at 1073 K

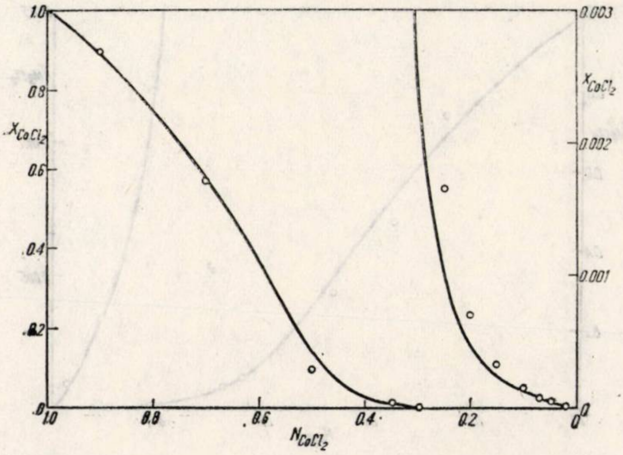

Fig. 8. Comparison between the calculated molar fraction of $CoCl_2(X_{CoCl_2})$ and the experimental activity of $CoCl_2$ (circles) of $CoCl_2-KCl$ melts at 1073 K

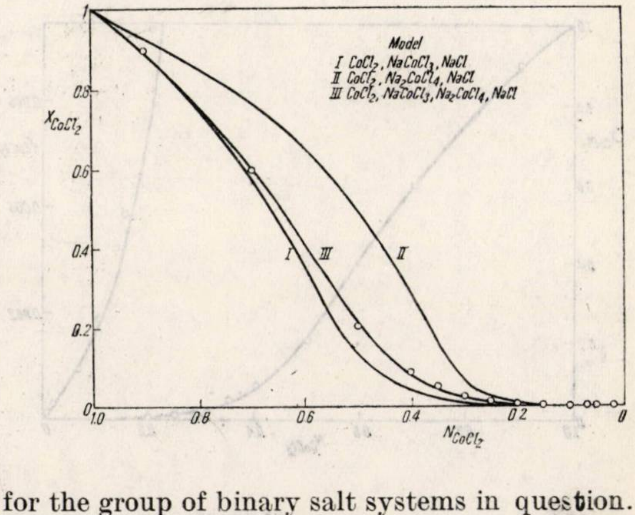

Fig. 9. Comparison between the calculated molar fraction of $CoCl_2(X_{CoCl_2})$ and the experimental activity of $CoCl_2$ (circles) for different models of $CoCl_2-NaCl$ melt at 1073 K

firms the assumed model for the group of binary salt systems in question. In addition to this model, calculations have been carried out for the models A, AB, B; A, AB_2, B; A, A_2B, AB_2, B, which showed that they are unsuitable for these systems (see figure 9). Thus, experimental thermodynamic data may provide information on the structure of molten salt systems with chemical interaction between the components.

Revue Roumaine de Chimie, 22, 1, 21–25 (1977)

THERMODYNAMIC PROPERTIES OF FUSED SALT TERNARY SYSTEM AgI + NaI + CsI BY FORMATION CELL METHOD

S. STERNBERG and LUCIA BEJAN
Centre of Physical Chemistry, Str. Galaţi 31, Bucharest, Romania

Received August 4, 1975

Measurements of e.m.f. on formation cells with fused AgI + NaI + CsI ternary system have been carried out in the 870–1020 K temperature range. The thermodynamic activity, activity coefficient and excess partial molar chemical potential of AgI in the given system have been calculated.

INTRODUCTION

Several works [1–5] have dealt with thermodynamic properties of ternary fused salt mixtures. Likewise, we have reported in a previous work [6] a thermodynamic study of the ternary fused AgI + NaI + KI system.

In the present work we expose a similar thermodynamic study of the AgI + NaI + CsI ternary system based upon e.m.f. of the formation cell.

$$\mathrm{Ag(s)} \,\|\, \mathrm{AgI}(l,\, x_1) + \mathrm{NaI}(l,\, x_2) + \mathrm{CsI}(l,\, x_3) \,\|\, \mathrm{I_2}\ (\mathrm{g},\ 1\ \mathrm{atm.})\ \mathrm{graphite}$$

Details on the cell and on the reversible iodine electrode have been given elsewhere.[7–8] The electromotive forces of the cells were measured to within ± 1–2 mV with a L.M. 1440.2 type Solartron digital voltmeter. Experiments were carried out in different compositions and in the 820–1020 K temperature range. Temperatures were chosen so that only homogeneous liquids were present for all compositions.

---

[1] J. Guion, M. Blander, D. Hengstenberg and H. Hagemark, *J. Phys. Chem.*, **72**, 2086 (1968).

[2] A. D. Pelton and S. N. Flengas, *J. Electrochem. Soc.*, **118**, 1307 (1971).

[3] B. F. Markov, *Rev. Roumaine Chim.*, **17**, 203 (1972).

[4] B. F. Markov and V. Holbekk, *Ukrain. Khim. Zhur.* **40**, 82 (1974).

[5] M. F. Lantratov, *Zhur. priklad. Khim.*, **46**, 2205 (1973).

[6] S. Sternberg and L. Bejan, *Rev. Roumaine Chim.* (in press).

[7] S. Sternberg, I. Adorian and I. Galasiu, *J. Chim. phys.*, **62**, 63 (1965).

[8] S. Sternberg and L. Bejan, *Rev. Roumaine Chim.*, **14**, 303 (1969).

RESULTS AND DISCUSSIONS

The experimental e.m.f.'s for the AgI + NaI + CsI ternary system are given in Table 1. $E = f(T)$ equations have been found by least squares method from 20—25 points.

Table 1

Experimental e.m.f.'s versus temperature in AgI + NaI + CsI

x_{AgI}	$x' = \frac{x_2}{x_2 + x_3}$	$\frac{E}{V}$	Average standard deviation
1		$0.5510 - 0.272 \times 10^{-3} (T - 873)$	±0.0021
0.7	0.7	$0.5789 - 0.240 \times 10^{-3} (T - 873)$	±0.0014
0.5		$0.6064 - 0.199 \times 10^{-3} (T - 873)$	±0.0015
0.3		$0.6487 - 0.193 \times 10^{-3} (T - 873)$	±0.0010
0.7	0.5	$0.5810 - 0.234 \times 10^{-3} (T - 873)$	±0.0029
0.5		$0.6149 - 0.205 \times 10^{-3} (T - 873)$	±0.0010
0.3		$0.6594 - 0.176 \times 10^{-3} (T - 873)$	±0.0028

From the values of e.m.f. it was possible calculate the thermodynamic activity, the activity coefficient, the partial molar and excess potentials of AgI by equations:

$$\ln a_1 = -\frac{n\mathcal{F}}{RT} [E(x_1) - E^\circ] \tag{1}$$

$$\gamma_1 = \frac{a_1}{x_1} \tag{2}$$

$$\Delta\mu_1 = \mu_1 - \mu_1^0 = \mathcal{F}[E(x_1) - E^\circ] \tag{3}$$

$$\mu_1^E = \Delta\mu_1 - \Delta\mu_1^{id} = -\mathcal{F}[E(x_1) - E^\circ] - RT \ln x_1 \tag{4}$$

respectively, where E° refers to the cell with single AgI while $E(x_1)$ to that with ternary mixture, x_1 is the mole fraction of AgI and a_1 its activity.

x_1 and x' were chosen as composition variables, x_1 being x_{AgI} and

$$x' = \frac{n_{NaI}}{n_{NaI} + n_{CsI}} = \frac{x_2}{x_2 + x_3} \tag{5}$$

For constant x', the ternary system may be treated as a quasi — binary one.

Table 2 lists the experimental values of activity, activity coefficient and excess partial molar chemical potentials of AgI in the AgI + NaI + + CsI system at 873 K and 973 K.

Figure 1 displays on two quasi — binary curves, $x' = 0.7$ and $x' = 0.5$, the experimental excess partial molar chemical potentials of AgI in AgI + NaI + CsI ternary system versus $(1 - x_1)$ at 973 K. On the same figure are also plotted the experimental partial molar chemical

Table 2

Experimental thermodynamic functions of AgI in AgI + NaI + CsI ternary system at 873 K and 973 K; x_1 is the mole fraction of AgI

x_1	$x' = \frac{x_2}{x_2 + x_3}$	a_1		γ_1		$\Delta\mu_1$ cal. mole^{-1}		μ_1^E cal. mole^{-1}	
		873 K	973 K	873 K	973 K	873 K	973 K	873 K	973 K
0.7	0.7	0.6902	0.6901	0.9860	0.9859	− 643	− 717	− 25	− 28
0.5		0.4789	0.4734	0.9578	0.9468	−1278	−1446	− 75	−105
0.3		0.2729	0.2838	0.9097	0.9460	−2253	−2435	−164	−107
0.7	0.5	0.6712	0.6682	0.9589	0.9546	− 692	− 780	− 73	− 90
0.5		0.4277	0.4309	0.8554	0.8618	−1474	−1628	−271	−288
0.3		0.2367	0.2448	0.7890	0.8160	−2500	−2721	−411	−393

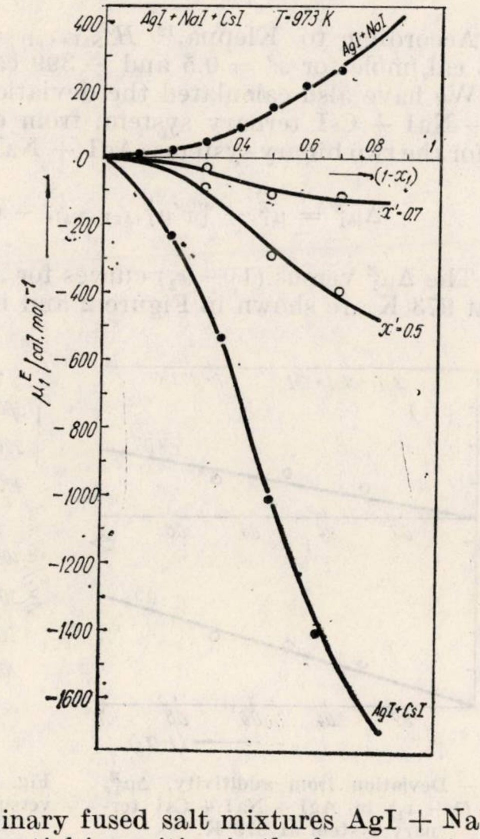

Fig. 1 — Experimental values of excess partial molar chemical potentials of AgI versus $(1 - x_1)$ in AgI + NaI + CsI ternary system at 973 K.

potentials of AgI in the two binary fused salt mixtures AgI + NaI and AgI + CsI [9]; the chemical potential is positive in the former system and negative in the latter.

---

[9] S. Sternberg and I. Adorian, *Electrochim. Acta*, **13**, 1647 (1968).

Like in AgI + NaI + KI system previously studied, in AgI + + NaI + CsI the curves of excess partial molar chemical potentials lie betwen the corresponding curves of binary systems.

According to the quasi – chemical theory extended by Hagemark [1,10] to ternary systems, the excess partial molar chemical potential of AgI is given by equation :

$$\mu_1^E = x'\,\mu^E_{1\,(\mathrm{AgI+NaI})} + (1 - x')\,\mu^E_{1\,(\mathrm{AgI+CsI})} - (1 - x_1)^2\,H^E_{(\mathrm{NaI+CsI})} + (1 - x_1)^2 f(x') \tag{6}$$

where $f(x')$ is a term specific to ternary systems (calculated from the quasi-chemical approximation).

If $f(x')$ were negligible and when $x_1 \to 0$, equation (6) gives the Alcock and Richardson's [11] relation :

$$\mu_1^E = x'\mu^E_{1\,(\mathrm{AgI+NaI})} + (1 - x')\,\mu^E_{1\,(\mathrm{AgI+CsI})} - H^E_{(\mathrm{NaI+CsI})} \tag{7}$$

According to Kleppa,[12] $H^E_{(\mathrm{NaI+CsI})} = -\,x'(1 - x')\,1900$; -475 cal./mole for $x' = 0.5$ and $-\,399$ cal./mole for $x' = 0.7$.

We have also calculated the deviation from additivity ($\Delta\mu_1^E$) in the AgI + NaI + CsI ternary system, from our experimental data and the data for the two binary systems (AgI + NaI and AgI + CsI), by equation :

$$\Delta\mu_1^E = \mu_1^E - [x'\mu^E_{1\,(\mathrm{AgI+NaI})} + (1 - x')\mu^E_{1\,(\mathrm{AgI+CsI})}] \tag{8}$$

The $\Delta\mu_1^E$ versus $(1 - x_1)$ curves for $x' = 0.7$ and $x' = 0.5$ at 873 K and at 973 K are shown in Figure 2 and in Figure 3, respectively.

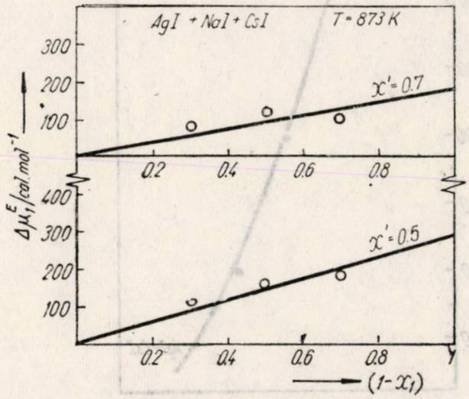

Fig. 2 – Deviation from additivity, $\Delta\mu_1^E$, versus $(1 - x_1)$ in AgI + NaI + CsI ternary system at 873 K.

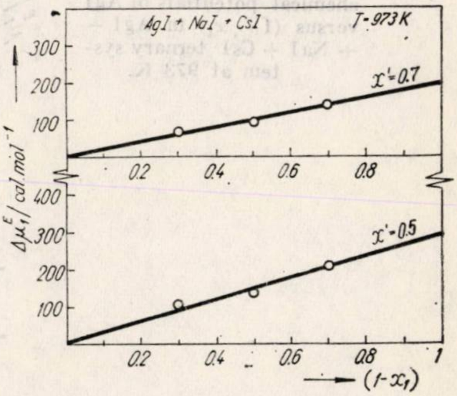

Fig. 3 – Deviation from additivity, $\Delta\mu_1^E$, versus $(1 - x_1)$ in AgI + NaI + CsI ternary system at 973 K.

---

[10] K. Hagemark, *J. Phys. Chem.*, **72**, 2316 (1968).

[11] C. B. Alcock and F. D. Richardson, *Acta. Met.*, **6**, 385 (1958).

[12] L. S. Hersh and O. J. Kleppa, *J. Chem. Phys.*, **42**, 1309 (1965)-

Equation (6) deduced on the basis of Hagemark's theory would yield $\Delta\mu_1^E$ equal to $-(1 - x_1)^2 H^E_{(\mathrm{NaI+CsI})}$ if $f(x')$ were negligible. However, the analysis of these curves both for AgI + NaI + CsI and in AgI + + NaI + KI systems has led to a linear and not quadratic dependence of $\Delta\mu_1^E$ on $(1 - x_1)$. An equation of the following type holds roughly

$$\Delta\mu_1^E = -2\alpha(1 - x_1)H^E_{(\mathrm{NaI+CsI})}$$

where $\alpha \simeq 0.3$ in AgI + NaI + CsI system.

For $x' = 0.5$ and $x_1 = 0$ at both temperatures (873 K and 973 K) $\Delta\mu_1^E \simeq 290$ cal/mole instead of 475 cal/mole. For $x' = 0.7$ and $x_1 = 0$, $\Delta\mu_1^E \simeq 180$ cal/mole at 873 K and $\simeq 200$ cal/mole at 973 K instead of 399 cal/mole.

One may say that besides the endothermal effect brought about by the heat of mixing $H^E_{(\mathrm{NaI+CsI})}$ an exothermal term is present which lowers $\Delta\mu_1^E$. In the AgX + (K, Rb, Cs)X binary systems the interaction potential $b_{\mathrm{Ag-Me}}$ takes negative values imposed by the polarization energy which increases from K to Cs. In the case of the AgI + NaI + CsI ternary system, on mixing three differently sized cations ($r_{\mathrm{Ag^+}} = 1.24$ °A, $r_{\mathrm{Na^+}} = 0.95$ °A and $r_{\mathrm{Cs^+}} = 1.69$ °A, $r_{\mathrm{I^-}} = 2.16$ °A), the contribution of nonchemical interaction energies (polarization energy) may possibly be more pronounced and may cause the deviation found by us.

Revue Roumaine de Chimie, **22**, *1*, 27–33 (1977)

ÉTUDE DILATOMÉTRIQUE ET VOLUMÉTRIQUE DE SELS FONDUS – APPLICATION AU SULFATE D'ARGENT, AUX SULFATES, CHROMATES, MOLYBDATES ET TUNGSTATES ALCALINS

LUCIEN DENIELOU, JEAN-PIERRE PETITET, CHRISTOPHE TEQUI
Laboratoire de Thermodynamique du Liquide Salin, Université Pierre et Marie Curie,
4, Place Jussieu, 75005 Paris, FRANCE

Reçu le 5 mars 1975

Une méthode de mesure directe de volume spécifique par repérage de la hauteur d'un sel fondu dans un creuset parfaitement étalonné en volume est décrite. Le repérage est fait à l'aide d'une aiguille vibrante assurant un contact électrique intermittent. Ce procédé de repérage électrique permet une reproductibilité de l'ordre de 1/100 mm. Outre le volume molaire et la densité, le coefficient de dilatation peut être obtenu sans report intégral des erreurs de volume. On donne les résultats pour un ensemble de sels alcalins à anion polyatomique tétraédrique (sulfate, chromate, tungstate, molybdate).

La méthode de détermination des volumes molaires, densités et coefficients de dilatation que nous présentons dans cet article est basée sur la mesure de la hauteur d'une masse connue de sel fondu dans un creuset parfaitement étalonné en volume.

La bonne conductibilité électrique des sels fondus est exploitée en vue de repérer le niveau à l'aide d'une aiguille conductrice en platine. Pour éliminer certaines erreurs et rendre la mesure dynamique, nous avons utilisé une aiguille vibrant verticalement.

La méthode a été exploitée à la mesure du volume molaire, du coefficient de dilatation et de la densité des sulfates, chromates, molybdates et tungstates alcalins, ainsi que le sulfate d'argent.

PRINCIPE ET MÉTHODE

Soit $x = -A \cos \omega t$ la représentation du mouvement de la pointe autour de sa position moyenne x_m prise pour origine ($x_m = 0$) et soit x_0 le niveau du liquide ($A > x_0 > -A$). Le dispositif, alimenté par une d.d.p. E, possède en série une résistance R grande devant la résistance de contact de l'aiguille de platine et du sel fondu (fig. 1). On peut écrire :

condition (a) $\quad x > x_0 \qquad i = 0$

condition (b) $\quad x < x_0 \qquad i = E/R = I$

Le circuit est ainsi parcouru par un courant « rectangulaire ». Un galvanomètre indique le courant moyen i_m, soit :

$$i_m = 1/T \int_0^\tau i \, dt = I\tau/T$$

où τ représente la durée d'immersion de la pointe. Tout calcul fait :

$$\begin{aligned} i_m &= E/R\ (1/2 + 1/\pi \arcsin (x_0/A)) \\ &= E/R\,(1/2 + x_0/A\pi + x_0^3/6A^3\pi + \cdots) \end{aligned}$$

Pour x_0 suffisamment proche de x_m, le courant moyen varie linéairement avec x_0, avec une pente $E/\pi RA$ autour de $E/2R$.

La nécessité de rendre négligeable la variation des f.e.m. parasites impose le choix d'une forte valeur pour E (45 V) et par suite une forte valeur pour R afin de ne pas trop augmenter l'intensité circulant dans le sel fondu. Ainsi pratiquée, la méthode a donné d'assez bons résultats et présente l'avantage de permettre l'enregistrement.[1] La nécessité de faire des mesures autour d'un courant moyen égal à I/2, et pour de faibles variations de celui-ci (cette condition est nécessaire non seulement à la linéarité mais aussi à la stabilité de réponse du système) nous a suggéré la réalisation d'un montage en pont. Dans ce montage on superpose au courant du circuit un contre-courant de valeur $-$ I/2 qui permet au galvanomètre de travailler avec des courants de valeur moyenne voisine de zéro et d'amplifier autant qu'on le désire sans entraîner de fortes élongations galvanométriques (fig. 2).

D'autre part la vapeur de certains sels (notamment ceux de K, Rb, Cs) montre une conductibilité électrique telle que la condition (a) n'est plus réalisée. On se trouve alors contraint de diminuer la valeur de la résistance R du circuit afin de rendre négligeable le courant de fuite par l'atmosphère saline. Il a toujours été possible de rendre la résistance de cette atmosphère grande devant celle du circuit, tout en maintenant cette

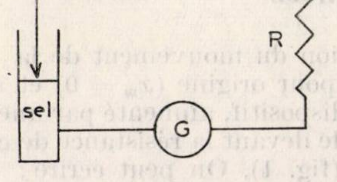

Fig. 1. — Schéma de principe.

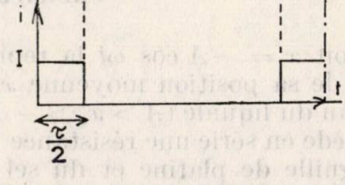

Fig. 2. — Signal délivré par l'aiguille vibrante.

---

[1] G. Petit et L. Denielou, *Rev. Int. Hautes Tempér. et Réfract.*, **5,** 13 (1968).

dernière grande devant la résistance de contact du sel. Malgré tout, cette condition entraîne une augmentation du courant traversant le sel, qui n'est pas souhaitable et nous a incité à développer une technique pratiquement mieux adaptée.

Il s'agit d'une méthode de zéro qui permet de régler la position moyenne de l'aiguille à une distance constante du niveau du liquide. Soit :

$$E = E_0 \cos \omega t$$

la tension d'alimentation du vibreur. Le mouvement de l'aiguille est :

$$x = A \cos(\omega t - \varphi)$$

où φ est un retard de phase assez voisin de $\pi/2$, provoqué par la self du vibreur et la masse de son équipage. Le circuit est alimenté maintenant par la tension E et donne aux bornes de la résistance R une tension alternative tronçonnée comme le montre la figure (fig. 4). Un générateur d'impulsions G.I. (fig. 3) est déclenché par la crête γ et fournit une impulsion en phase avec l'entrée de l'aiguille dans le sel (dans la pratique il existe un déphasage entre l'impulsion et la crête γ, mais ce déphasage étant constant n'introduit aucune erreur). Ce signal, mélangé à une impulsion déclenchée avec une phase constante par la tension E, est envoyé sur un oscillographe. Par déplacement de la hauteur de l'aiguille, on peut régler la position de l'impulsion que celle-ci déclenche ; amener cette impulsion à coïncider avec l'impulsion de référence permet de régler l'aiguille à une distance constante et précise du niveau liquide. On peut d'ailleurs ajuster cette distance en jouant sur le déphasage de l'impulsion de référence, ce qui permet de choisir une faible distance pour obtenir une réponse plus stable et diminuer l'erreur due aux fluctuations de la tension d'alimentation.

Cette méthode permet d'utiliser un courant de valeur moyenne presque nulle, que l'on peut encore diminuer en utilisant une forte résistance du circuit et en amplifiant fortement le signal. Elle n'est absolument pas perturbée par la variation de la conductibilité du liquide ou de la vapeur saline. Mais elle n'offre pas de possibilité simple d'enregistrement.

PARTIE MÉCANIQUE

Toutes les pièces du montage sont fixées sur une colonne d'acier, verticale, de 60 mm de diamètre qui assure la grande stabilité exigée par la sensibilité du dispositif de repérage électrique. De même la plate-forme (P) (fig. 5) qui supporte le tube dilatométrique est fixée rigidement et définitivement à la colonne (C). Ainsi le dégagement du tube dilatométrique (T) doit se faire par déplacement du four (F) mobile le long de la colonne. Le support du vibreur (V) peut être animé d'un mouvement rapide par crémaillère (dégagement de l'aiguille et recherche du niveau du sel) et d'un mouvement lent par vis micrométrique (Vm), utilisé en cours de manipulation. Toujours aux fins de stabilité et de précision, l'ensemble est guidé sur une grande longueur (180 mm). Le repérage de la position de l'aiguille se fait par mesure directe de la hauteur séparant le support du vibreur de la plate-forme (P), à l'aide d'un comparateur au micron et d'un jeu de cales (Co et Ca). Cette technique nécessite la mesure de la hauteur de l'aiguille

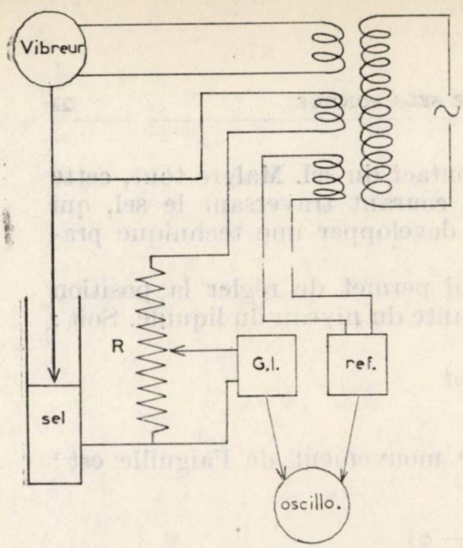
Vibreur
R
sel
G.I.
ref.
oscillo.

Fig. 3. — Montage électrique.

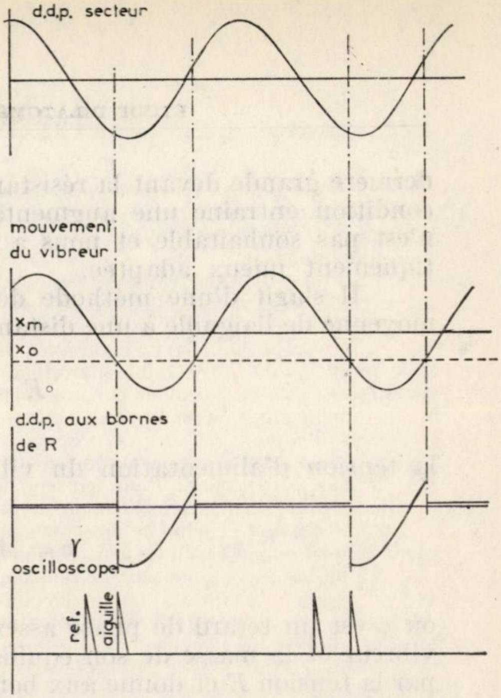
d.d.p. secteur
mouvement du vibreur
x_m
x_o
o
d.d.p. aux bornes de R
oscilloscope
ref.
aiguille

Fig. 4. — Schéma de fonctionnement.

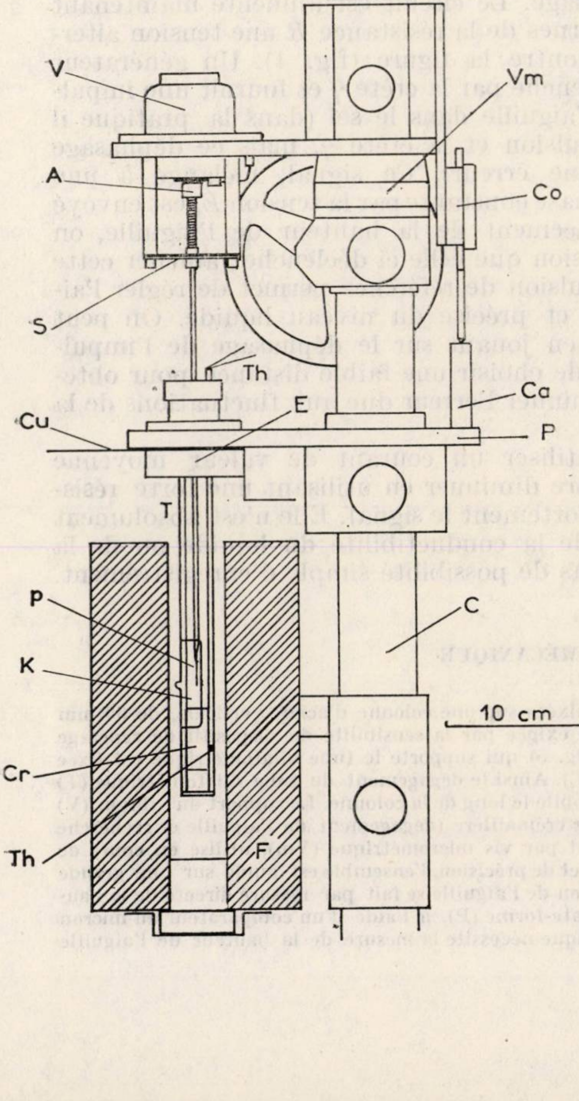
V
Vm
A
Co
S
Th
Cu
E
Ca
P
T
P
K
Cr
Th
F
C
10 cm

Fig. 5. — Appareil de mesure.

pour un emplacement repéré du vibreur, au cathétomètre et avant manipulation. Cette mesure est refaite après manipulation pour vérification. La colonne (C) repose sur un socle réglant sa verticalité. Une circulation d'eau et une plaque de cuivre, (E) et (Cu), protègent la partie haute du montage.

Le tube dilatométrique (T) supportant le creuset est en silice. Il est fixé à la plateforme (P) à l'aide d'une collerette en invar. Sa verticalité est assurée lors du collage du tube de silice sur la collerette à l'araldite. Une ouverture latérale permet de placer le creuset ; elle est fermée par un couvercle de silice (K) durant les manipulations. L'aiguille est un mince tube de silice dont la très faible dilatation ($\alpha = 0{,}5.10^{-6}$) est compensée pai celle du tube dilatométrique. Elle est terminée par une fine pointe (Ø = 0,1 mm) de platine rhodié 30 % scellée sur le tube de silice (à chaud et sous vide) ; ce fil se prolonge à l'intérieur du tube pour être raccordé au circuit.

Le creuset (Cr) est en platine rhodié 15 % de 1,5 mm d'épaisseur, suffisamment résistant pour ne pas se déformer ; d'une hauteur de 53 mm et d'un diamètre intérieur de 17 mm, il a été tourné puis rectifié. Avant chaque mesure, son diamètre intérieur est mesuré tous les 2 mm en partant du haut et selon 20 directions pour chaque hauteur à l'aide d'un comparateur d'alésage au micron ; ces résultats sont exploités sur ordinateur et fournissent un relevé « topographique » du creuset permettant de tenir compte des petites irrégularités de diamètre (fluctuations n'excédant pas 0,2 %). Afin d'exploiter cet étalonnage la position du haut du creuset est repérée au cathétomètre avant manipulation.

L'aiguille est fixée en A à un vibreur (V) de 5 W et 10 kHz de bande passante, dont la rigidité latérale a été renforcée par adjonction d'une membrane de salleron (S) quatre centimètres plus bas. La fréquence de 50 Hz étant satisfaisante, on utilise le secteur comme alimentation.

Le chauffage est assuré par un four de type Chevenard-Joumier à trois enroulements pour diminuer les gradients de température et équipé d'un cycle thermique et d'un régulateur de température. La température est relevée près du creuset à l'aide d'un thermocouple Pt—Pt Rh 10 % (Th). Une série de mesures nous a montré une différence inférieure à 1/10e de degré entre cette température et celle du sel dans le creuset.

DISCUSSION ET RÉSULTATS

Un grand nombre d'erreurs systématiques (mauvaise définition du fond du creuset, ménisque dû à la tension superficielle, déformation de ce dernier par la vibration de la pointe etc ...) est facilement éliminé par une double mesure parce qu'elles ne dépendent que de la température. En effet :

$$h_c^2 - h_c^1 = (h_m^2 + \delta h(t)) - (h_m^1 + \delta h(t)) = h_m^2 - h_m^1$$

h_m^1 et h_c^1 sont les hauteurs mesurées et corrigées pour une masse de sel m_1 et $\delta h(t)$ représente la correction, fonction de la température seule. L'évaporation crée une erreur qui dépend aussi du temps ; une solution a été proposée[1] à cette difficulté que nous n'exposerons pas ici, les sels étudiés étant suffisamment peu volatils.

Dans la pratique une première série de mesures est faite sur une faible quantité de sel m_1, qui sert, par interpolation polynomiale, de correction aux mesures faites sur une grande quantité de sel. L'ensemble des calculs est fait automatiquement sur ordinateur CII 10070 par la méthode des moindres carrés. Le coefficient α s'étant avéré très peu variable dans les gammes de température étudiées, la forme mathématique retenue est :

$$V_T = V_F \exp(\alpha(T - T_F))$$

et

$$\rho_T = \rho_F \exp(-\alpha(T - T_F))$$

V_T, V_F sont les volumes molaires à la température T et à la fusion ; ρ est la densité.

Les erreurs sur les pesées et sur la température sont à peu près négligeables ; l'erreur d'étalonnage du creuset est faible mais il convient d'y ajouter l'erreur sur la correction de dilatation, le coefficient de dilatation du platine rhodié 15% étant mal connu.

Les plus grosses erreurs viennent des mesures de hauteur au cathétomètre avant manipulation, auxquelles il convient d'ajouter celles sur le déplacement du vibreur mesuré au comparateur (celles-ci sont en général assez faibles). L'erreur sur ρ est de l'ordre de 0,5%. D'autre part les erreurs de visée cathétométrique, provoquant des translations des courbes $h(T)$, n'affectent pas leur pente et ne doivent pas être prises en considération pour l'erreur sur α. Ainsi l'erreur sur α est en général de l'ordre de 2 à 3%.

Le sulfate d'argent, les sulfates, chromates, molybdates et tungstates alcalins ont été étudiés par cette technique. La pureté des produits utilisés est garantie par les fournisseurs. Le tableau 1 fournit quelques détails expérimentaux : la provenance du produit, la gamme de température étudiée, le nombre de déterminations expérimentales pour une petite quantité, NP et pour une grande quantité, NG. Dans le tableau 2 figurent les

Tableau 1

Détails expérimentaux

Sel	Provenance	Gamme de température (°C)	NP	NG
Li_2SO_4	Mallinckrodt	869–1143	10	12
Na_2SO_4	Merck	895–1150	13	14
K_2SO_4	Merck	1080–1219	11	15
Rb_2SO_4	Koch-Light	1077–1176	13	10
Cs_2SO_4	Koch-Light	1010–1134	10	8
Li_2CrO_4	K. and K.	508–1005	15	14
Na_2CrO_4	Merck	797–1095	14	17
K_2CrO_4	Merck	979–1162	14	13
Rb_2CrO_4	ROC.RIC	983–1167	15	16
Cs_2CrO_4	Merck	968–1149	11	12
Li_2MoO_4	K. and K.	702–1105	15	15
Na_2MoO_4	K. and K.	695–1173	18	13
K_2MoO_4	K. and K.	934–1140	14	14
Rb_2MoO_4	ROC.RIC	900–1098	16	17
Cs_2MoO_4	ROC.RIC	949–1136	11	13
Li_2WO_4	K. and K.	740–1139	20	20
Na_2WO_4	Hopkins-W.	705–1165	14	14
K_2WO_4	B.D.H.	932–1147	14	16
Rb_2WO_4	ROC.RIC	960–1100	11	12
Cs_2WO_4	ROC.RIC	950–1156	13	15
Ag_2SO_4	Prolabo	662– 819	10	13

résultats sous la forme exponentielle indiquée précédemment, ainsi qu'un estimateur statistique de la variance des valeurs lissées défini par :

$$\sigma = \sqrt{\frac{(\delta V)^2}{NG(NG-m)}}$$

Tableau 2

Densité et volume molaire à la température de fusion et coefficient de dilatation

Sel	T_F (°C)	Densité à la fusion (g cm^{-3})	Vol. molaire à la fusion (cm^3 mol^{-1})	σ (cm^3 mol^{-1})	Coefficient de dilatation × 10^3
Li_2SO_4	857	2,02	54,36	0,004	0,192
Na_2SO_4	882	2,08	68,19	0,011	0,215
K_2SO_4	1068	1,90	91,59	0,004	0,237
Rb_2SO_4	1066	2,60	102,86	0,006	0,255
Cs_2SO_4	1001	3,11	116,52	0,029	0,267
Li_2CrO_4	488	2,24	58,11	0,085	0,164
Na_2CrO_4	797	2,25	72,11	0,007	0,221
K_2CrO_4	980	2,03	95,68	0,006	0,257
Rb_2CrO_4	980	2,69	106,79	0,007	0,250
Cs_2CrO_4	960	3,15	121,30	0,009	0,258
Li_2MoO_4	701	2,85	60,93	0,009	0,181
Na_2MoO_4	689	2,93	70,22	0,027	0,224
K_2MoO_4	926	2,35	101,31	0,011	0,247
Rb_2MoO_4	960	2,88	114,85	0,009	0,273
Cs_2MoO_4	936	3,32	128,40	0,033	0,258
Li_2WO_4	740	4,30	60,91	0,002	0,188
Na_2WO_4	694	3,91	75,17	0,017	0,228
K_2WO_4	930	3,19	102,08	0,027	0,271
Rb_2WO_4	958	3,65	114,65	0,018	0,284
Cs_2WO_4	950	3,98	129,22	0,011	0,262
Ag_2SO_4	652	4,81	64,85	0,004	0,156

où m est le nombre de paramètres calculés par lissage, δV est la différence entre les volumes expérimentaux et théoriques.

Les valeurs des densités antérieurement publiées, lorsqu'elles existent, sont en bon accord avec celles présentées ici [2 à 7]. Cependant la comparaison est moins satisfaisante pour les coefficients de dilatation dont les valeurs publiées jusqu'ici semblaient très dispersées. Remarquons que ces mesures ont été faites par la méthode d'Archimède et souvent très au-dessus de la température de fusion.

[2] F. M. Jaeger, *Z. anorg. Chem.*, **101**, 16 (1917).

[3] F. M. Jaeger et B. Kapma, *Z. anorg. Chem.*, **113**, 27 (1920).

[4] R. G. Gossink et J. M. Stevels, *J. of Non Cryst. Sol.*, **5**, 217 (1971).

[5] J. C. Th. G. M. van der Wielen, H. N. Stein et J. M. Stevels, J. *of Non Cryst-Sol.*, **1**, 18 (1968).

[6] K. B. Morris et P. L. Robinson, *J. Chem. Eng. Data*, **9**, 444 (1964).

[7] K. B. Morris, M. I. Cook, C. Z. Sykes et M. B. Templeman, *J. Amer. Chem. Soc.* **77**, 851 (1955).

Revue Roumaine de Chimie, **22**, *1*, 35–37 (1977)

ON THE VISCOSITY OF MOLTEN METALS. IV [1]

A COMPARISON BETWEEN GAS AND LIQUID VISCOSITIES

MARILENA ŞERBAN
Chemistry Institute, Department of Physical Chemistry, Bd. Republicii 13, Bucharest, Romania

Received February 6, 1975

The paper demonstrates that under boiling point conditions the equation deduced in two previous notes for the viscosity of simple liquids leads to the same expression as for the gas state.

In parts II [2] and III [1] a general equation was derived,

$$\eta = A\rho T\, e^{E/RT}, \tag{1}$$

which can be used to calculate the viscosity of simple liquids, near their melting points only from experimental data and molecular constants.

To deduce this equation, the liquid was supposed to have a cellular structure with the most compact packing. Each particle performs harmonic oscillations around its lattice position, considered the equilibrium position, with a constant frequency, a slightly smaller than its frequency in the solid state. [3] In the abnormal metallic elements, some particles are dimers, which gradually dissociate when the temperature increases.

The viscous flow consists of successive jumps of particles from one equilibrium position to another; the potential barrier which these particles have to jump over is the same as the vibration energy of particles at the melting point.

In order to obtain equation (1), we have started from the relationship

$$\eta = h\,\frac{\lambda_1}{\lambda_2\lambda_3\lambda^2}\,\frac{F}{\overset{*}{F}}\,e^{E/RT}, \tag{2}$$

where the different symbols have been defined in part II. According to the supposed structural model, it was considered that: $\lambda_1/\lambda_2\lambda_3\lambda^2 = 1/a^3$, $F/\overset{*}{F} = kT/h\nu$, and E is the vibration energy for $3N$ harmonic oscillators.

---

[1] Part III. I. G. Murgulescu and M. Şerban, *Rev. Roumaine Chim.*, **20**, 591 (1975).

[2] I. G. Murgulescu and M. Şerban, *Rev. Roumaine Chim.*, **19**, 1417 (1974).

[3] N. F. Mott, *Proc. Roy. Soc.*, **146**, 465 (1934).

As soon as the boiling point is reached, the vibration amplitude tends toward extreme values and the vibration changes into translation motion. As can be observed from equation (5), part III, the activation energy vanishes.

The momentum transfer is now provided by the colliding particles. If we assume that each oscillation which changes into translation results in a collision, the vibration frequency may be substituted for the actual collision number, Z, per time unit.

In these conditions, if we suppose that $\lambda_1 = \lambda_2 = \lambda_3 = \lambda = a$, where a is the mean separation in the gas state, equation (2) becomes :

$$\eta = \frac{1}{a^3}\,\frac{kT}{Z} = \frac{R}{a^3N}\,\frac{T}{\sqrt{2}\,\pi\sigma^2 n\bar{c}} = \frac{R}{a^3N}\,\frac{T}{\sqrt{2}\,\pi\sigma^2 n}\left(\frac{\pi M}{8RT}\right)^{1/2} =$$

$$= \frac{R^{1/2}}{4\pi^{1/2}N}\,\frac{M^{1/2}}{a^3 n\sigma^2}\,T^{1/2},$$

provided that the collision number is given by Maxwell equation.

As the number of particles per volume unit, n, is $1/a^3$, one finally obtains :

$$\eta = 2.135 \times 10^{-21}\,\frac{M^{1/2}}{\sigma^2}\,T^{1/2} \tag{3}$$

or

$$\eta = 2.135 \times 10^{-21}\,\frac{M^{1/2}}{\sigma^2\left(1+\frac{C}{T}\right)}\,T^{1/2} \tag{4}$$

if we consider the Sutherland correction, which takes into account the existence of weak attraction forces, besides repulsive forces.

Except for the numerical coefficient, equation (4) is similar to the equation derived for the gas viscosity,

$$\eta = A\,n\,m\,\bar{c}\,l,$$

where the following substitutions have to be made : $m = M/N$, $\bar{c} = (8RT/\pi M)^{1/2}$, $l = 1/\sqrt{2}\pi\sigma^2 n(1 + C/T)$; A is a numerical coefficient.

In the obtained equation :

$$\eta = A' \times 10^{-21}\,\frac{M^{1/2}}{\sigma^2\left(1+\frac{C}{T}\right)}\,T^{1/2} \tag{5}$$

A' is a numerical coefficient equal to [4]: 1.813 for the approximate Maxwell relation, 1.905 or 1.687 for the corrected relations and 2.716 for the Chapman equation which is considered the best.

The numerical coefficient from equation (4) is within these values. If we take into account that actually the vibration frequency is not equal to the collision number Z, this coefficient takes other values, different from 2.135. In order to find the correct relationship between these two quantities, it is necessary to know the true collision number which accounts for the momentum transfer. In this way, both the numerical coefficient evaluation and the real temperature dependence of the gas viscosity could be solved.

---

[4] E. H. KENNARD, "Kinetic Theory of Gases", Mc. Graw Hill, New York, 1938, p. 136—160.

Revue Roumaine de Chimie, **22**, *1*, 39–44 (1977)

ON THE STABILITY OF AROMATIC HYDROCARBONS. IV[1]

ON THE LINEARITY OF THE DELOCALIZATION ENERGY RELATIONSHIPS

V. E. SAHINI* and A. SAVIN**

* Laboratory of Physical Chemistry, Polytechnic Institute, Bucharest.
** Computation Center of the Ministry of Mines, Oil and Geology, Bucharest

Received February 17, 1976

Some formulas for the calculation of the delocalization energy of aromatic hydrocarbons are obtained using the perfect aromatic limit structure.

In a previous paper [2] a linear relationship has been established between the Hückel Molecular Orbital delocalization energy (HDE) of the *ortho*-condensed aromatic hydrocarbons and two parameters: the number of hexagonal rings and the number of non-Kekulé rings in the mesomeric limit structure with the maximum number of Kekulé rings. The aim of the present paper is to develop the mentioned procedure by obtaining the coefficients with a higher degree of accuracy and by the modification of the parameters.

METHOD OF CALCULATION

We will consider a linear form for the delocalization energy (DE):

$$DE = a\,M + b\,N + c$$

where:

M, N are molecular parameters and

a, b, c are the coefficients which were obtained using the least-squares method to fit the HDE values of some hydrocarbons. *

In order to estimate the precision of the results the following criteria were used:

a) the variance

$$d = \sum_{i=1}^{n} (DE_i - HDE_i)^2/(n-3)$$

where

n is the number of compounds used in parametrization, shows the magnitude of the scattering of the *DE*, but is unit-dependent *. b) the determination coefficient (= 100 k, where

---

* The *HDE* values were found in reference.[3]

[1] Part III, V. E. Sahini, *Rev. Chim.* (Bucureşti), **1964**, 551.

[2] V. E. Sahini, *J. Chim. phys.*, **59**, 177 (1962).

[3] E. Heilbronner and P. Straub, "Hückel Molecular Orbitals", Springer Verlag, Berlin, 1966.

$$k = 1 - \sum_{i=1}^{n} (DE_i - HDE_i)^2 / \sum_{i=1}^{n} \left(DE_i - \sum_{j=1}^{n} HDE_j/n \right)^2 \Big) ;$$

a value close to 1 expresses a good relationship between the *HDE* and the parameters ; the determination coefficient is not unit-dependent **.

SELECTION OF THE PARAMETERS

The parameters are found by using the mesomeric limit formula. [2]

We obtained M by using the number of single bonds M' ($M = M'/3$; in *ortho*-condensed hydrocarbons M is the number of cycles). The second parameter, N was determined from the formula with maximum number of benzenoid rings (the formula which minimizes N)***. N reflects the existence of subsystems in arenes. When $c \neq 0$ they are not additive :

$$DE = \mathbf{a}M + \mathbf{b}N + \mathbf{c} = \mathbf{a}(M - N) + (\mathbf{a} + \mathbf{b})N + c$$

(the energy is not a sum of terms corresponding to the energies of N subsystems with delocalization energy $a + b$ and $M - N$ subsystems with delocalization energy a). Three cases were studied :

1) The original [2] choice of N, which is discussed on the basis of localized molecular orbitals in reference[6] ; N is the number of rings that have not a perfect aromatic character. For *ortho*-condensed arenes **** N can be easily determined from the topology of the molecule, as shown by Balaban.[7]

---

* In this paper we use β units.

** The variance and the determination coefficient are simmilar to those used in statistics.

*** The formula with maximum number of perfect aromatic benzenoid rings is defined in reference.[2] It is known that it is the best picture of the molecule with localized bonds (from experiment : Fries'rule [4] ; from theory : localized molecular orbitals [5,6]).

**** Exceptions are molecules such as pentaphene, where a ring with imperfect aromatic character is used by more than one group of three linearly condensed rings.

[4] L. F. Fieser and M. Fieser, "Textbook of Organic Chemistry", D. C. Heath, Boston, 1950.

[5] W. England, S. Salmon and K. Ruedenberg, *Fortschr. Chem. Forsch.*, **23**, 31 (1967).

[6] V. E. Sahini and A. Savin, to be published.

[7] A. T. Balaban, *Match*, **1**, 33 (1975) and references cited therein.

2) The value of N represents the number of rings that are not isolable benzenoid subsystems in arenes (e.g. in naphthalene there is only one such subsystem). It is related to Clar's ideas [8] and finds a theoretical basis in reference.[9] *

3) The value of N represents the number of double bonds not included in rings with perfect aromatic character. This rests on the fact that localized molecular orbitals that belong to rings with perfect aromatic character have an energy that differs from that of the localized molecular orbitals which do not belong to these rings.[6]

The value of N as the number of double bonds not included in isolable benzenoid subsystems will not be discussed here independently, as it is connected with that determined in the second case.

The differences between the three choices of N are confirmed by the following example : for 000^{00}, 000^{0}_{0}, ${}^{0}000^{0}$, ${}_{0}00^{0}_{0}$ N is $(1, 3, 1), (1, 2, 0), (1, 2, 1)$, viz. $(0, 2, 0)$ (the numbers show the values of N in the first, second, and third choice, respectively).

RESULTS

Table 1 presents the formulas for the delocalization energies, the three choices corresponding to formulas 1—4, 5, 6 respectively. Benzene was not always used in interpolation, providing an exception in many cases. The analysis of the variance shows good results in all cases, the determination coefficients have very high values. If we consider as normal the distribution of the *HDE* we can define the probability of finding a *HDE* value in a domain bounded by $M-\mathbf{a}/2$ and $M+\mathbf{a}/2$ or $N-\mathbf{b}/2$ and $N+\mathbf{b}/2$. The high value of $\mathbf{a}$ determines a probability of 1.0 in the former case ; in the latter, it is of over 0.9 (formulas 1, 3, 4, 5), 0.8 (formula 2 with rounded coefficients), 0.6 (formula 8, because the coefficient b used in this formula is approximately one half of the one used in formulas 1—5 ; if we define the domain by the bounds $N-b$ and $N+b$, the probability is of over 0.9).

Formula 4 shows that the use of a new type of molecules (*peri*-condensed hydrocarbons) does not modify essentially the values of the $\mathbf{a}$, $\mathbf{b}$, $\mathbf{c}$, the variance or the determination coefficient.

---

* A graphical method could be used here, based on the fact that two isolable benzenoid subsystems cannot be joined together. N is then obtained by subtracting from M the number of possible eliminations of cycles which are not connected with more than one cycle and the cycles linearly connected with the former.

[8] E. CLAR, "Polycyclic Hydrocarbons", Academic Press, London, 1964.

[9] O. E. POLANSKY and G. DERFLINGER, *Internat. J. Quantum Chem.*, **1**, 379 (1967).

The results obtained with formula 2 show that the rounding of the coefficients does not alter essentially the values of the variance and the determination coefficient. Formula 2 differs from the one obtained in the first paper of this series [2] only by the value of the last coefficient.

Table 1

The linear equations : DE = a.M − b.N + c

	a	b	c	variance	determination coefficient
1 *	1.754	−.131	.201	.0016	99.97
2 **	1.75	−. 15	. 20	.0035	99.94
3 ***	1.761	−.132	.167	.0015	99.96
4 ****	1.757	−.129	.185	.0015	99.98
5 ***	1.813	−.165	.205	.0019	99.95
6 ***	1.737	−.070	.241	.0015	99.97

* The 24 *cata*-annelated hydrocarbons of reference[3] were used in parametrization.

** The coefficients of formula 1 were rounded to halves of tenths.

*** Benzene was not used in parametrization.

**** The 24 *cata*-annelated and the 6 *peri*-condensed hydrocarbons of reference [3] were included in parametrization.

As the formal analysis shows good results, it can be expected that the *HDE* could be calculated by using the linear relationship.

As N has the same meaning in formulas 1, 3 and 4 the differences between the coefficients **a, b, c** are small (also **a** and **c** are of opposite sign) only one value of the *DE* is presented in tables 2, 3 and 4 (that calculated with formula 4).

The values for the *DE* are listed in tables 2 and 3. Knowing the values of the variance, it is not surprising to find that there are only remarkably small errors for the energy values.

Table 4 presents the relative errors (100 $(DE_i - HDE_i) HDE_i$) for the first ten n-acenes. In this limit case the formula $DE = 1.75\ M - 0.13\ N + 0.19$ (obtained by interpolation from the values of the *HDE* of the acenes) is remarkably close to formula 2.

The values presented in the tables prove that the linear equations can be used in order to determine the delocalization energies, having the same degree of confidence as the *HMO* values.

We would like to express our indebtedness to Professor A. T. Balaban for providing many results prior to publication and for critically reading and commenting on the manuscript.

We have benefited from the kind assistence of the Computation Center of the University of Bucharest.

Table 2

Delocalization energies of the cata-annelated molecules used in parametrization

Molecule	*HDE*	*DE* formula			
		1.34	2	5	6
O	2.00	1.94	1.95	2.02	1.98
OO	3.68	3.70	3.70	3.67	3.71
OOO	5.31	5.33	5.30	5.31	5.31
$\mathrm{OO^{O}}$	5.45	5.46	5.45	5.48	5.45
OOOO	6.93	6.95	6.90	6.96	6.91
$\mathrm{OOO^{O}}$	7.10	7.08	7.05	7.12	7.12
$\mathrm{{}^{O}OO^{O}}$	7.19	7.21	7.20	7.12	7.19
$\mathrm{OO^{OO}}$	7.19	7.21	7.20	7.12	7.19
$\mathrm{{}^{O}_{O}OO}$	7.27	7.21	7.20	7.29	7.19
OOOOO	8.54	8.58	8.50	8.61	8.59
$\mathrm{OOOO_{O}}$	8.73	8.71	8.65	8.78	8.71
$\mathrm{OOO^{O^{O}}}$	8.76	8.84	8.80	8.78	8.85
O $\mathrm{OOO^{O}}$	8.83	8.84	8.80	8.78	8.85
$\mathrm{OOO^{OO}}$	8.84	8.84	8.80	8.78	8.85
$\mathrm{{}^{O}OOO^{O}}$	8.88	8.84	8.80	8.94	8.85
$\mathrm{O^{OOO^{O}}}$	8.88	8.84	8.80	8.94	8.85
$\mathrm{OOO^{O}_{O}}$	8.94	8.84	8.80	8.94	8.92
OO $\mathrm{OO^{O}}$	8.94	8.97	8.95	8.94	8.92
$\mathrm{O^{OO}OO}$	8.94	8.97	8.95	8.94	8.92
$\mathrm{OO^{OO^{O}}}$	8.94	8.97	8.95	8.94	8.92
$\mathrm{{}^{O}_{O}OO^{O}}$	9.00	8.97	8.95	8.94	8.92
$\mathrm{OOOO^{OO}}$	10.46	10.47	10.45	10.42	10.45
$\mathrm{OOO^{OO^{O}}}$	10.59	10.60	10.55	10.59	10.59
OOO $\mathrm{OOO^{O}}$	12.24	12.23	12.15	12.24	12.26

Table 3

Delocalization energy for not cata-condensed benzenoid hydrocarbons

Molecule	*HDE*	*DE* calculated using formula			
		1, 3, 4	2	6	5
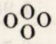	6.50	6.50	6.47	6.54	6.52
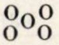	8.25	8.26	8.22	8.35	8.17
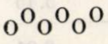	9.25	9.30	9.23	9.36	9.22
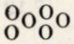	9.43	9.43	9.38	9.50	9.38
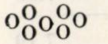	10.55	10.60	10.55	10.66	10.42
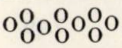	14.50	14.46	14.33	14.57	14.32
O_O	4.38	4.28	4.28	4.29	4.44
O_O‾O	6.77	6.63	6.62	6.61	6.85
O_O_O	6.77	6.63	6.62	6.61	6.85

Table 4

Relative errors obtained for the delocalization energy of n-acenes

N° of rings	Relative errors, formula			
	1, 3, 4,	2	5	6
2 *	.4	.4	−.2	.4
3 *	.4	−.2	.0	.0
4 *	.3	−.4	.4	−.3
5 *	.5	−.5	.8	−.4
6	.4	−.6	1.0	−.6
7	.5	−.6	1.1	−.6
8	.5	−.6	1.3	−.6
9	.6	−.6	1.4	−.6
10	.6	−.6	1.5	−.6

* Used in parametrization.

Revue Roumaine de Chimie, **22**, *1*, 45–47 (1977)

CHEMICAL GRAPHS. XXVIII [1]

A NEW TOPOLOGICAL INDEX FOR CATAFUSENES: L-TRANSFORM OF THEIR THREE-DIGIT CODES

ALEXANDRU T. BALABAN
Institute of Chemistry, The Polytechnic, Bucharest, Romania
Correspondence address: Institute of Atomic Physics, POB 5206, Bucharest

Received March 22, 1976

The three-digit code, proposed earlier and consisting of digits 0, 1, and 2, for catafusenes, may be reduced to a two-digit code, consisting of symbols 0 and I, which may be read as a binary number and conveys information analogously to Hosoya and Yamaguchi's sextet polynomial.

It was shown earlier [2] that condensed benzenoid polycyclic hydrocarbons (polyhexes) can be conveniently classified on the basis of their characteristic graphs * having as vertices the centres of hexagons; an edge connects two vertices whenever the respective hexagons are condensed (*ortho*-fused): the polyhex is a catafusene (*cata*-condensed) when this graph is a tree, and is a perifusene when this graph has circuits.

Catafusenes can be enumerated by algebraic formulas (which are simple for non-branched systems,[2] but complicated for the branched ones[4]), and coded [2] by a string of digits 0, 1, and 2, expressing the topology of annelation (0 stands for angle 180° between two successive edges of the dualist graph, 1 and 2 for angles 120° and 240°, starting from a free end). Branched systems have codes [5] with brackets following the digit symbolizing the branching point. The uniqueness of the code is assured by the convention that the string of digits affords the smallest number when alternative endpoints or 1 *versus* 2 assignments are possible. The topology of the catafusene is completely expressed by this code, therefore it was not surprising that correlations between the code and the resonance energies or other properties of catafusenes were found.[6] However, for some of these correlations, the whole topology is not necessary; the purpose of the present paper is to indicate how catafusenes can be further subdivided, or grouped together, according to a reduced (incomplete) molecular topology.

---

* We now prefer to name them dualist graphs, in order to emphasize both the similarity with, and the difference from, dual graphs.[3]

[1] A. T. Balaban, *Rev. Roumaine Chim.* part XXVII, **21**. 1049 (1976).
[2] A. T. Balaban and F. Harary, *Tetrahedron*, **24**, 2505 (1968).
[3] F. Harary, "Graph Theory", p. 113, Addison-Wesley, Reading, Mass., 1969.
[4] F. Harary and R. C. Read, *Proc. Edinburgh Math. Soc.* Ser. II, **17**, 1 (1970).
[5] A. T. Balaban, *Tetrahedron*, **25**, 2949 (1969).
[6] A. T. Balaban, *Rev. Roumaine Chim.*, **15**, 1243 (1970).

As a digression, it is interesting [1,7] that the numbers of conformers of n-alkanes with minimal energies when only the carbon skeletons are taken into account (named for brevity staggered n-alkane C-rotamers) are identical to those of non-branched catafusenes; branched catafusenes also are in a one-to-one correspondence with C-rotamers of branched alkanes without quaternary carbons. Such branched or non-branched alkane C-rotamers can be coded either in terms of four digits symbolizing the four orientations of edges on a diamond lattice, [8,9] or by the above 1—1 correspondence in terms of three digits, 0, 1, and 2, each of which is equivalent to a triplet of the four digits in a degenerate (overlapping) code: thus 0 corresponds to the *trans* conformation of the carbon skeleton of n-butane, while 1 and 2 correspond to the two enantiomeric *gauche* conformations of the same skeleton. Staggered C-rotamers of alkanes are dualist graphs of diamondoid hydrocarbons; thus, a new enumeration, codification, and nomenclature of diamondoid hydrocarbons is possible.[10]

A less detailed topological description of catafusenes than that given by their complete codes is possible by what we call the **l**-*transform* of their three-digit codes.

To convert the three-digit code of a catafusene into the **l**-transform, the following operations must be effected:

(i) In the three-digit codes, digits 1 and 2 are replaced by the letter **l**.

(ii) One **l** is added at the beginning of the resulted code.

(iii) For non-branched catafusenes, the resulted string, denoted by **B**, of **0**'s and **l**'s is read as a binary number, where **l** stands for 1, and, if wanted, converted into a decimal number, denoted by **D**.

Either in binary form, **B**, or in decimal form, **D**,* this **l**-transform is a *reduced topological index* which contains in compact form both the numerical information about the number of benzenoid rings (because of the added initial **l**) and the topological information about the mode of condensation of benzenoid rings, namely whether this condensation is in linear (**0**'s) or angular (**l**'s) fashion. However, the passage from the full three-igit code to the reduced topological index which is a two-digit code, is irreversible, i.e. the lost information can no longer be restored.

(iv) For branched catafusenes, the **l**-transform as an index **B** also results by operations (i) — (iii) above ignoring brackets, but the information about branching is indicated as follows: each pair of brackets is conventionally symbolized in both indices **B** and **D** by one initial zero; thus, the number of branching points corresponds to the number of initial **0**'s; secondly, one zero is introduced into the **l**-transform in the place of each opening bracket; thus, "(" is coded by "**0**" in the place where it appears in the string of digits.

Therefore, a branch of one vertex on the dualist graph of a catafusene, symbolized [5] in the three-digit code by (.), is read in the **l**-transform as **0** in the place of the code where the branch was indicated, in addition

---

[7] A. T. Balaban, *MatCh*, Nr. 2, 51 (1976).

[8] M. Saunders, *Tetrahedron*, **23**, 2105 (1967).

[9] A. T. Balaban, in "Chemical Applications of Graph Theory" (edited by A. T. Balaban), Academic Press, London, 1976, p. 73.

[10] Manuscript in preparation, in collaboration with P. von R. Schleyer.

* The conversion of index **B** into **D** is easily reverted.

to one initial **0** added to the **1**-transform ; similarly, a branch of two linearly condensed rings, symbolized in the three-digit code by (**0**) is read in the **1**-transform as **00** ; a branch of two angularly condensed benzenoid rings symbolized by (1) or (2) is read in the **1**-transform as **01** (again, in addition to this, an initial **0** indicates one branch).

It results that a branched or a non-branched catafusene with k condensed benzenoid rings has an index B of k − 1 symbols **1** and/or **0**, counting from the first **1**, i.e. ignoring the initial **0**'s indicating the number of branching points.

A one-to-one correspondence exists between either of these indices **B** or **D**, and the sextet polynomial introduced by Hosoya and Yamaguchi.[11] Therefore these indices have the same information content as the sextet polynomial for correlations with molecular properties or with other indices proposed in the literature,[11] and in addition have the advantage of compactness and of easy reconstitution (less the distinction between 1- and 2-type annelation, and sometimes the position of the branches) of the catafusene topology. Their only limitation is the fact that they do not apply to perifusenes, and, of course, that they cannot be applied for nomenclature purposes : in this case, the full three-digit code is necessary for retrieval of molecular topology.

The published extensive tables of non-branched [2] and branched [5] catafusenes included their three-digit codes ; by the above operations (i)−(iv), these codes can be easily converted into indices **B** and **D**. The following table presents these indices only for those catafusenes which were included in ref. 11.

Table 1

k	Catafusene [12]	3−D.C.[2,5]	**B**	**D**	Sextet polynomial [11]
2	Naphthalene	.	**1**	**1**	$1 + 2X$
3	Anthracene	0	**10**	**2**	$1 + 3X$
,,	Phenanthrene	1	**11**	**3**	$1 + 3X + X^2$
4	Tetracene	00	**110**	**4**	$1 + 4X$
,,	Tetraphene	01	**101**	**5**	$1 + 4X + 2X^2$
,,	3.4-Benzophenanthrene	11	**111**	**7**	$1 + 4X + 3X^2$
,,	Chrysene	12	,,	,,	,,
,,	Triphenylene	1(.)	**0110**	**06**	$1 + 4X + 3X^2 + X^3$
5	Pentacene	000	**1000**	**8**	$1 + 5X$
,,	1.2-Benzotetracene	001	**1001**	**9**	$1 + 5X + 3X^2$
,,	Pentaphene	010	**1010**	**10**	$1 + 5X + 4X^2$
,,	1.2-Benzotetraphene	011	**1011**	**11**	$1 + 5X + 5X^2$
,,	3.4-Benzotetraphene	012	,,	,,	,,
,,	1.2,7.8-Dibenzoanthracene	101	**1101**	**13**	$1 + 5X + 5X^2 + X^3$
,,	1.2,5.6-Dibenzoanthracene	102	,,	,,	,,
,,	3.4,5.6-Dibenzophenanthrene	111	**1111**	**15**	$1 + 5X + 6X^2 + X^3$
,,	5.6-Benzochrysene	112	,,	,,	,,
,,	Picene	121	,,	,,	,,
,,	1.2,3.4-Dibenzoanthracene	01(.)	**01010**	**010**	$1 + 5X + 5X^2 + 2X^3$
,,	1.2-Benzochrysene	11(.)	**01110**	**014**	$1 + 5X + 6X^2 + 2X^3$

Note ; 3−D.C. is the abbreviation of three-digit code.

---

[11] H. Hosoya and T. Yamaguchi, *Tetrahedron Letters*, 4659 (1975).

[12] E. Clar, "Polycyclic Hydrocarbons", vol. 1, Academic Press, London, 1964.

Revue Roumaine de Chimie, **22**, *1*, 49–54 (1977)

RESEARCHES IN THE TERPOLYMERIZATION FIELD. VIII*)

THEORETICAL STRUCTURAL STUDY OF THE HIGH CONVERSION ACRYLONITRILE – METHACRYLIC ACID – METHYL METHACRYLATE TERPOLYMER

CR. I. SIMIONESCU and ADELAIDA LIGA
Institute of Macromolecular Chemistry "Petru Poni"
Aleea Gr. Ghica Vodă 41 A, Jassy, Romania

Received August 6, 1975

The variations of the main structural parameters characteristic of acrylonitrile-methacrylic acid-methyl methacrylate terpolymer have been calculated as a function of conversion. The used relationships are valid for any ternary system of monomers.

The acrylonitrile (A)-methacrylic acid(B)-methyl methacrylate(C) terpolymer, synthetised as in the previously reported paper[1] can become technically important, its applicability depending on its composition and its obtainment conditions.[2,3] For this reason it seems very useful to examine its sequences distribution up to high conversions, i.e. the intramolecular mean inhomogeneity of composition as a function of conversion.

The investigated parameters (terpolymer composition, molar fractions of the central monomer units in compositional triads, mean sequences length) have been calculated up to different values of conversion, by eqn.[4] :

$$\overline{P_n(\ )} = 1/\mathrm{m}\int_0^m P_n(\ )\,\mathrm{d}m \tag{1}$$

where $\overline{P_n(\ )}$ represents the average value of the examined parameter over the observed conversion, $P_n(\ )$ is its instantaneous value and m is the mole-fractional conversion.

According to the usual copolymerization theory, these calculations were carried out by the following procedure [4] :

1. The instantaneous monomer compositions A, B and C were calculated as a function of mole-fractional conversion, using the integrated form of the simplified terpolymerization equations.[5]

---

*) Part VII : see ref. 11.

[1] Cr. I. Simionescu and A. Liga, *Makromol. Chem.*, **110**, 278 (1967).

[2] Cr. I. Simionescu and A. Liga, Rom. Pat. 60033, Oct. 1974.

[3] Cr. I. Simionescu and A. Liga, Rom. Pat. 59707, Ian. 1975.

[4] Y. Yamashita, K. Ito, H. Ishii, S. Hoshino and M. Kai, *Macromolecules*, **1**, 529 (1968).

[5] A. Valvassori and G. Sartori, *Adv. Polymer Sci.*, **5**, 28 (1967).

2. The instantaneous copolymer composition, $P_1(\ )$, molar fractions of the central monomer units, $P_3(\ )$ and mean sequences length, $\bar{n}_M$, were calculated by eqns. (2)−(4)[6–8]:

$$P_1(A) = \frac{P_{BA}\,P_{CA}}{P_{BA}\,P_{CA} + P_{AB}\,P_{CA} + P_{AC}\,P_{BA}} \tag{2a}$$

$$P_1(B) = \frac{P_{AB}P_{CB}}{P_{BA}P_{CB} + P_{AB}\,P_{CB} + P_{BC}\,P_{AB}} \tag{2b}$$

$$P_1(C) = 1 - \{P_1(A) + P_1(B)\} \tag{2c}$$

$$P_3(AAA) = P^2_{AA}\,;\ P_3(AAB) = 2\ P_{AA}P_{AB}\,;\ P_3(AAC) = 2\ P_{AA}P_{AC}\ \text{etc.} \tag{3}$$

$$\bar{n}^A_M = \sum_{n=1}^{\infty} n\ P\,(A)_n / \sum_{n=1}^{\infty} P\,(A)_n \quad \text{etc.} \tag{4}$$

where

$$P(A)_n = \left(\frac{A}{A + B/r_{AB} + C/r_{AC}}\right)^{n-1} \cdot \left(1 - \frac{A}{A + B/r_{AB} + C/r_{AC}}\right) \text{etc.} \tag{5}$$

$$P_{AB} = \frac{B}{A r_{AB} + B + C\,r_{AB}/r_{AC}} \tag{6a}$$

$$P_{BA} = \frac{A}{A + B\,r_{BA} + C\,r_{BA}/r_{BC}} \tag{6b}$$

etc.

In these relations, P_{AB} for example is the conditional probability of an A unit being followed by a B unit in the copolymerization propagation sequence of a ternary system[8]; $P(A)_n$ represents the numerical fraction of A sequences composed by n monomer units.[9] The quantities r_{AB}, $r_{BA}\ldots$, etc. are the respective comonomer reactivity ratios that were obtained from the data on low-conversion copolymers in the usual manner[1] as:

$r_{AB} = 0.093$ $\qquad r_{AC} = 0.15$ $\qquad r_{BC} = 0.92$

$r_{BA} = 2.5$ $\qquad r_{CA} = 1.09$ $\qquad r_{CB} = 0.6$

3. Finally, the mean values of the three examined parameters during the mole-fractional conversion, m, were obtained by numerically integrating the corresponding instantaneous relations (2)−(4) by eq. 1.

---

[6] G. E. Ham, *J. Polymer Sci.*, **A. 2**, 2735 (1964).

[7] C. Tosi, *European Polymer J.*, **6**, 161 (1970).

[8] G. Goldfinger and T. Kane, *J. Polymer Sci.*, **3**, 462 (1948).

[9] T. Alfrey and G. Goldfinger, *J. Chem. Phys.*, **12**, 205 (1944).

Figures 1—6 show typical results of these calculations for the terpolymers of different monomer compositions in the feed.

The changes depending on conversion of the monomer and terpolymer compositions lead to the following conclusion : over the whole theoretical range of conversion, the content of the less reactive monomer (acrylonitrile) increases continuously both in the monomer mixtures and in the terpolymer (Fig. 1). These graphs, based on the integrated data, give a general picture of some homogeneous reaction products from the point of view of the components. The smooth variations of the three comonomer concentrations show the existence of the terpolymer only, and not of a physical mixture of homopolymers. In the case of the first terpolymer (with prevalent content of acrylonitrile in the initial mixture), Fig. 1a shows that by the end of the polymerization reaction the other two como-

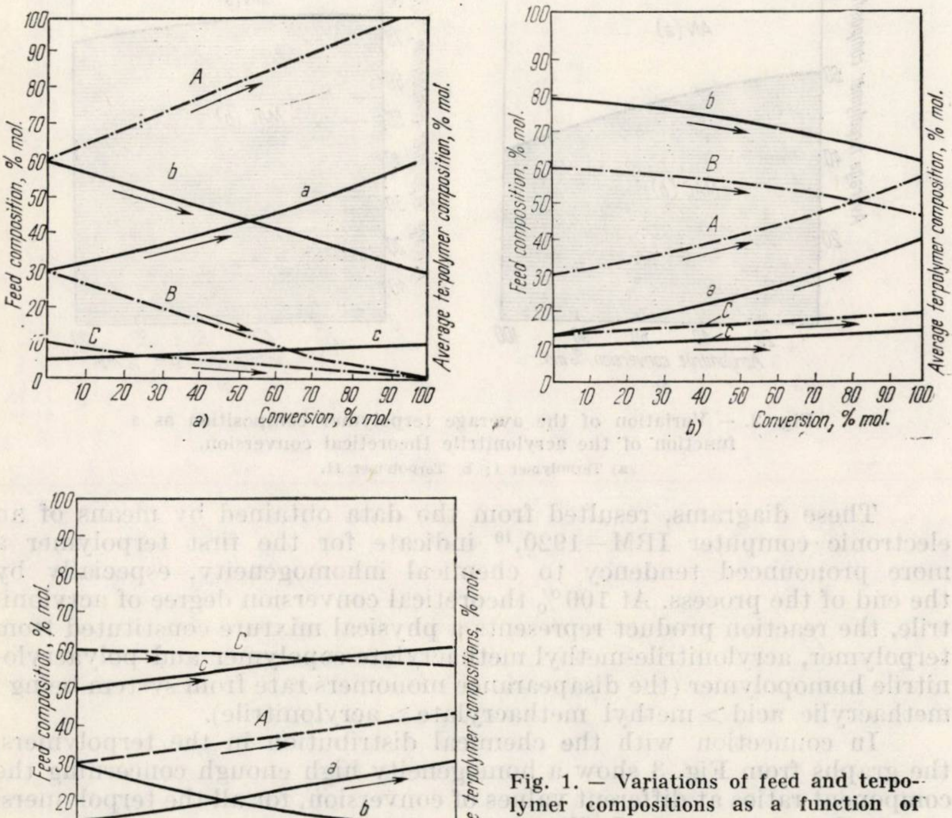

Fig. 1. — Variations of feed and terpolymer compositions as a function of conversion.

a) Terpolymer I: [AN]/[MAc]/[MMA] = 0.6/0.3/0.1 (moles) ; b) Terpolymer II: [AN]/[MAc]/[MMA] = 0.3/0.6/0.1; c) Terpolymer III: [AN]/[MAc]/[MMA] = 0.3/0.1/0.6.

nomers (methacrylic acid and methyl methacrylate) tend to vanish from the mixture and the homopolymer of acrylonitrile can appear.

The examination of the three comonomers behaviour as a function of theoretical conversion of the less reactive monomer leads to the conclusion presented in Fig. 2.

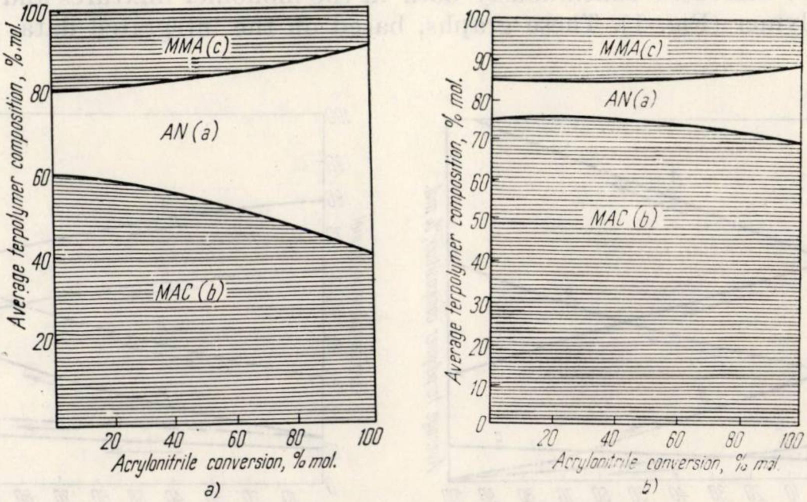

Fig. 2. — Variation of the average terpolymer composition as a function of the acrylonitrile theoretical conversion.
a) Terpolymer I; b) Terpolymer II.

These diagrams, resulted from thə data obtained by means of an electronic computer IBM—1920,[10] indicate for the first terpolymer a more pronounced tendency to chemical inhomogeneity, especially by the end of the process. At 100% theoretical conversion degree of acrylonitrile, the reaction product represents a physical mixture constituted from terpolymer, acrylonitrile-methyl methacrylate copolymer and polyacrylonitrile homopolymer (the disapearance monomers rate from system being : methacrylic acid > methyl methacrylate > acrylonitrile).

In connection with the chemical distribution in the terpolymers, the graphs from Fig. 3 show a homogeneity high enough concerning the component ratios at different values of conversion, for all the terpolymers, except the same system I (Fig. 3a).

A detailed study of the conversional chemical inhomogeneity is possible by using the curves of compositional distribution in the integrated and differential forms. This problem is not the aim of the present paper.

Theoretical variation of the instantaneous sequences is shown in Fig. 4, as a function of conversion. One can see the decrease of BAB, BBB type sequences, corresponding to the reduction of the content of the more reactive monomer B (methacrylic acid) in the monomer mixture, on the one hand and the increases of A and C monomers (acrylonitrile and

---

[10] N. Asandei, A. Liga and A. Biro, *European Polymer J.*, **7**, 317 (1971).

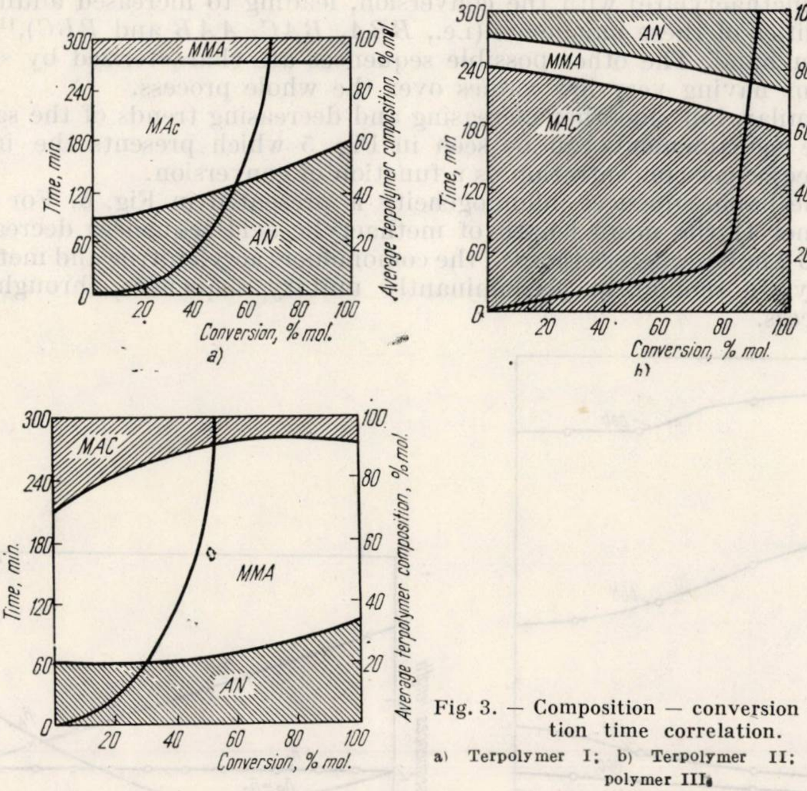

Fig. 3. — Composition — conversion — reaction time correlation.

a) Terpolymer I; b) Terpolymer II; c) Terpolymer III.

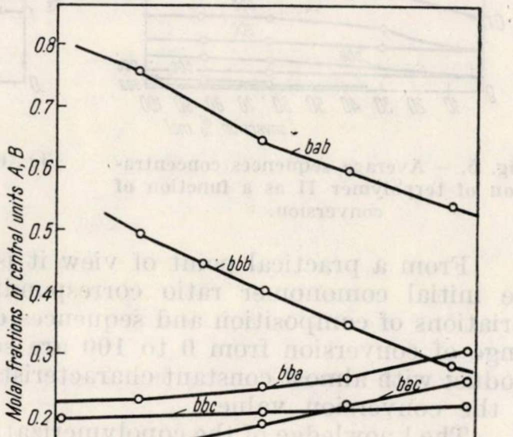

Fig. 4. — Instantaneous sequences concentration of terpolymer II as a function of conversion.

methyl methacrylate) with the conversion, leading to increased addition probabilities of these monomers (i.e., *BBA*, *BAC*, *AAB* and *BBC*),[11] on the other hand. The other possible sequences are characterized by slow variations having very low values over the whole process.

Similar, but smoother increasing and decreasing trends of the same probable enchainements can be seen in Fig. 5 which presents the integrated sequences concentration as a function of conversion.

The homosequences inhomogeneity is presented in Fig. 6. For the terpolymer II the mean length of methacrylic acid sequences decreases from 4 to 2 units, whereas those of the comonomers acrylonitrile and methyl methacrylate remain in predominantly unitary sequences, throughout the process.

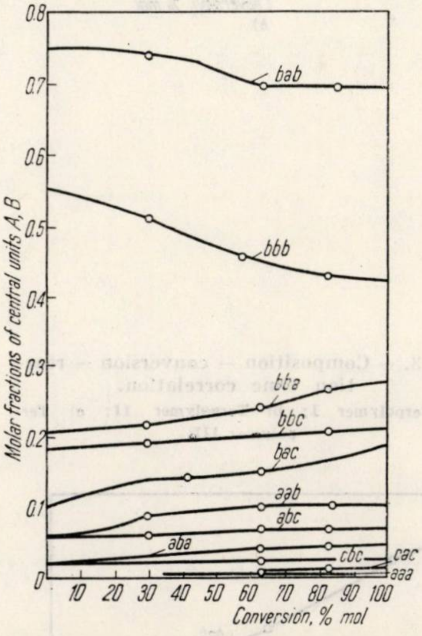

Fig. 5. — Average sequences concentration of terpolymer II as a function of conversion.

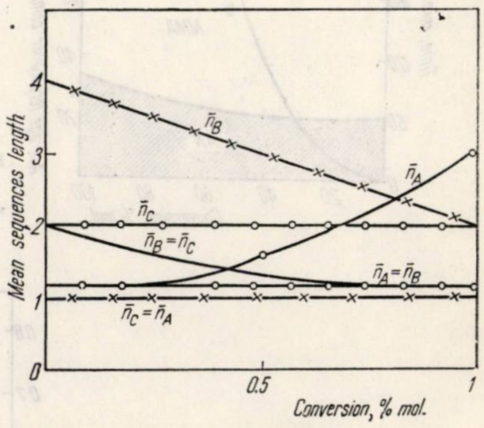

Fig. 6. — Mean sequences length as a function of conversion.
— × — × Terpolymer II.

From a practical point of view it is important to remark that for the initial comonomer ratio corresponding to the terpolymer II, the variations of composition and sequences distribution over the theoretical range of conversion from 0 to 100 are somewhat slow, meaning that a product with almost constant characteristics can be obtained, irrespective of the conversion value.

The knowledge of the copolymerization behaviour of a certain monomers mixture on the basis of such theoretical diagrams is useful for practical purposes, as it provides some valuable data related to the best initial comonomer ratio leading to a chemically homogeneous product.

---

[11] Cr. I. Simionescu and A. Liga, *Rev. Roumaine Chim.*, **21**, 1555 (1976).

Revue Roumaine de Chimie, 22, 1, 55–59 (1977)

COMPLEXES OF ANTHRANIL-N,N-DIACETIC ACID WITH TRIVALENT METALS. IV[1]

STABILITY INTERPRETATION

C. DRĂGULESCU, SEPTIMIA POLICEC and T. SIMONESCU
Centre of Chemistry, Bv. Mihai Viteazul, 24, Timişoara, Romania

Received June 23, 1975

The stability of the M—ANDA complex compounds, where M(III) = Ga, In, Sc, Y, La and ANDA = anthranil-N,N-diacetic acid, is interpreted as a function of the reaction enthalpy. By means of some criteria as the e/r ratio, polarizing action, ionization potential, distortion capacity of the metal ions and the electronegativity and size of both central ions and donor atoms, the following stability sequences have been established: Ga < In and Sc > Y > La, with no possibility to clearly attribute a ionic or covalent character to the M-Ligand bond.

INTRODUCTION

In a previous study concerning the chelating reaction of the anthranil-N,N-diacetic acid (ANDA) with the trivalent metal ions Ga^{3+}, In^{3+}, Sc^{3+}, Y^{3+}, La^{3+}, the liquid phase equilibrium of the corresponding systems has been investigated. Stability constants, computed by means of spectrophotometric data have proved the formation of mononuclear, equimolar compounds with medium stability [2] (table 1, column 2). The reaction enthalpies, determined thermometrically.[3] have shown that the complexation reactions between ANDA and the Ga^{3+}, In^{3+}, Sc^{3+}, Y^{3+} and La^{3+} ions are endothermic (table 1, column 3) being energetically improbable. The entropy change calculation of these systems [1] showed an entropy increase during the reaction, big enough to compensate the unfavourable energetic balance (table 1, column 4). It has been concluded hereafter that the stability of the investigated chelate compounds is dependent on entropy factors only.

These results obtained in our previous work may be correlated in order to interpret the enthalpy contribution to the stability of the investigated complexes; the entropy change contribution to the same stability has already been considered in a previous paper.[1]

---

[1] Part III: C. Drăgulescu, S. Policec and T. Simonescu, *Rev. Roumaine Chim.*, **19**, 801 (1974).

[2] C. Drăgulescu, S. Policec et T. Simonescu, *Talanta*, **13**, 1451 (1966); **13**, 1543 (1966).

[3] S. Policec, T. Simonescu and C. Drăgulescu, "Third National Conference on Analytical Chemistry", Braşov, Romania, vol. IV, 1971, p. 354.

In order to have an overall account of the investigated reactions, the principal characteristics of the reaction partners will be presented below.

THE LIGAND

The anthranil-N,N-diacetic acid can act as a tri- or quadridentate ligand by means of a nitrogen donor atom and two or three oxigen donor atoms. Both types of donor atoms are hard bases, after Pearson's [6] classification. It is thus expected that ANDA should form the most stable chelates with metal ions of class **a**.[7]

Table 1

Thermodynamic functions of the chelating reaction : M^{3+} + ANDA → M – ANDA and some characteristics of the metal ions

Metal ion	K [2]	ΔH [3] joule/mol	ΔS [1] joule/mol °K	Electronic configuration of the ion	Ionic radius [4] A°	Electro-negati-vity [5]	Third ionization potential [4] eV
1	2	3	4	5	6	7	8
Ga^{3+}	$1.4.10^6$	35,700	237.8	[Ar] $3d^{10}$	0.62	1.6	30.60
In^{3+}	$1.8.10^6$	28,600	215.3	[Kr] $4d^{10}$	0.81	1.7	27.90
Sc^{3+}	$6.6.10^5$	32,200	222.7	[Ar]	0.81	1.3	24.75
Y^{3+}	$3.0.10^5$	28,000	198.7	[Kr]	0.93	1.2	20.52
La^{3+}	$3.4.10^5$	20,600	174.7	[Xe]	1.15	1.1	19.17

As the nitrogen donor atom of the ligand is part of a tertiary aminic group, it will have a medium complexation capacity due to its high degree of substitution ; the benzene ring being one of its substituents, there is a decrease of the nitrogen atom basicity. Due to the higher electronegativity of the oxigen atom compared to that of the nitrogen atom, the last one has generally a higher tendency to form donor-acceptor bonds. Due to the basicity decrease of the nitrogen atom in ANDA, there is a uniformization of the electron donor capacity of the two types of ligand donor atoms.

By means of the dissociation constants of the anthranil-N,N-diacetic acid, determined by Schwarzenbach [8] ($pK_1 = 2.3$; $pK_2 = 2.9$; $pK_3 = 7.7$), which show a conjugate base of medium strength, a strong base, respectively, it is considered that ANDA can exhibit a medium, respectively a strong tendency to form complex compounds with metal ions.

Thermodynamic investigations have shown [9] that the stability of a complex depends on entropy factors especially when the atom is oxygen, and the bonds are predominantly ionic, and on enthalpy factors when the donor atom is nitrogen and the bonds have a more covalent character.

---

[4] F. A. Cotton and G. Wilkinson, "Advanced Inorganic Chemistry", Wiley, New York, 1966.

[5] M. J. Sienko and R. A. Plane, "Chemistry", Mc Graw-Hill, New York, 1961.

[6] R. G. Pearson, *J. Amer. Chem. Soc.*, **85**, 3533 (1963) ; *J. Chem. Educ.*, **9**, 581 (1968) ; **10**, 643 (1968).

[7] S. Ahrland, J. Chatt and N. R. Davies, *Quart. Rev.*, **12**, 265 (1958).

[8] G. Schwarzenbach, A. Willi and R. O. Bach, *Helv. Chim. Acta*, **30**, 1303 (1947).

[9] E. Uusitalo, *Ann. Acad. Sci. Fennicae*, *Ser. A*, **2**, 87 (1957).

The Metal Ions which were investigated in the present study Ga^{3+}, In^{3+}, Sc^{3+}, Y^{3+} and La^{3+}, belong to class **a** [7] elements, and are hard acids.[6] For systems in which **a** class metals interact with ligands having hard base character the electrostatic model is meaningful, the ionic radius and charge being important characteristics.

After Schwarzenbach's classification,[10] Sc^{3+}, Y^{3+} and La^{3+} are group A ions (noble gas core). The same group may also include Ga^{3+} and In^{3+} ions, due to their big positive charge. The electrostatic character is prevailing when interpreting the metal-ligand bond formed with elements of this group.

The electronegativity difference between the metal ion and the ligand donor atoms is another useful criterion for considering the polar character of the M—L bond : the bigger the difference, the more important are the electrostatic model criteria; the smaller this difference, the more important is the covalent contribution.

CHELATE STABILITY INTERPRETATION BY MEANS OF THE REACTION ENTHALPY

Enthalpy values which result during the investigated M—ANDA chelate formation reactions (table 1) show an energetically unfavourable change. The currently used criteria to interpret the complex stability by means of the partially ionic or covalent nature of the metal-ligand bond have in this case a minor importance. This does not mean that their effect is small, but that the effect of the interactions which are shifting the equilibrium in the sense opposite to chelate formation is greater. However, regardless of the driving force leading to the metal-ligand bond formation, its nature is still dependent on several characteristics of the metal ions and of the ligand. These will be considered below.

Among the investigated metal ions, those having a noble gas configuration, namely Sc^{3+}, Y^{3+} and La^{3+}, with a typical **a** class character, will supposedly form with the donor atoms of the anthranil-N,N-diacetic acid predominantly ionic bonds. The Ga^{3+} and In^{3+} ions, with a high positive charge, also belong to class **a**, and the same considerations are valid concerning the metal-ligand bond character.

In order to prove the electrovalent nature of the bond, different authors [11-13] have correlated the stability constant with a function of the metal ion radius, positive deviations being attributed to covalent contributions. Table 2 gives logK values for the investigated M^{III}—ANDA chelates, together with the corresponding charge/radius ratio. The stability sequence $Ga > In$ is not followed, possibly indicating a covalent contribution to the In—ANDA bonds. The $Sc > Y > La$ sequence is followed with a small deviation for lanthanum, which also supposes a covalent contribution. Concerning these disagreements, it is pointed out that e/r is a suitable criterion, especially for small anionic ligands. Jazimirski[14] has shown that in the case of bulky anionic ligands, small cations form less stable complexes than the large ones.

---

[10] G. Schwarzenbach, *Experientia* Suppl., **5**, 162 (1956).

[11] C. W. Davies, *J. Chem. Soc.*, **1951**, 1256.

[12] H. Irving and R. J. P. Williams, *Nature*, **162**, 746 (1948).

[13] G. Mattock, *Acta Chem. Scand.*, **8**, 777 (1954).

The different behaviour of ions having the same charge and approximately the same radius, but different electronic structures, may be qualitatively explained by means of the electrostatic model, completed with polarization reprezentations. The In^{3+} ion, resulting from an atom with an 18 electrons outer shell, i.e. with strong polarizability, is a typical complex forming agent. Sc^{3+} and Y^{3+} ions, with noble gas outer shell configuration, thus with reduced polarizability, will have a smaller tendency to form complex compounds.

Table 2

M^{III} – ANDA complex stability constants related to the corresponding charge per radius values

Metal ion	Ga^{3+}	In^{3+}	Sc^{3+}	Y^{3+}	La^{3+}
log K	6.14	6.25	5.82	5.48	5.53
e/r	4.8	3.7	3.7	3.5	2.6

The electronic configuration has also influence on the distortion capacity of the metal ion. Sc^{3+}, Y^{3+} and La^{3+} ions, with noble gas configuration, are very difficult to be distorted. Those with an 18 electrons outer shell configuration, Ga^{3+}, In^{3+}, are much easier distorted. As the complexation capacity is paralleling the degree of distortion, Ga^{3+} and In^{3+} ions really do form easier complexes than Sc^{3+}, Y^{3+} and La^{3+} ions, as expected.

The difference concerning the distortion capacity between group III A and B cations is small. Likewise the difference in their complex formation capacity is also small and thus the resultant chelates exhibit comparable stability (table 2).

The unfavourable enthalpy of the investigated complexation reactions may also be interpreted by means of the polarizability difference of metal ions, due to their electronic configuration. For metal ions with small polarizability (noble gas electronic configuration) the main factor in the metal-ligand interaction is attributed to the permanent momentum of the ligand. The noble gas configuration metal ions, Sc^{3+}, Y^{3+}, La^{3+}, will thus prefer the ligand with higher dipole-moment, i.e. water instead of ANDA, the corresponding aquo-complexes being enthalpically favoured compared to the respective ANDA ones. Metal ions with higher polarizability exhibit stronger external fields inducing an additional momentum to the ligand molecule. Such metal ions, as Ga^{3+}, In^{3+}, will have a greater affinity for ANDA than the metal ions with noble gas configuration. But the positive enthalpy values of the Ga–, In–ANDA complex formation reactions show that in these cases too, the corresponding aquo-complexes are favoured enthalpically. It follows hereafter that in the stability sequence of the complexes formed by the five discussed metal ions in presence of ANDA in aqueous solutions, the enhanced stability of the Ga–, In–ANDA complexes compared to that of the Sc–, Y–, La–ANDA ones may be also attributed to polarizability factors.

Due to relatively small electronegativity differences between the investigated metal ions and the ligand donor atoms, and due also to the large size of the central metal ions, it is assumed that the metal-ligand bonding has a partially covalent character. This allows to interpret the stability sequence in the case of the Ga—ANDA and In—ANDA complexes. Indium which, compared to gallium, has a larger size and electronegativity, will have a greater covalent contribution to the metal-ligand bond than gallium. Therefore the In-ANDA complex is supposed to have and actually exhibits a greater stability than the Ga—ANDA complex.

---

[14] K. B. Jazimirski and W. P. Wassiljew, "Instabilitätskonstanten von Komplexverbindungen", V.E.B. Deutscher Verlag der Wissenschaften, Berlin, 1963.

The stability constants have also been correlated to other characteristics of the metal ions. Thus the ionization potential has been first correlated to stability constants by Mellor and Maley [15] and then by others.[16,17] It was assumed [18], [12] that a linear function means bond formation with covalent character. Comparing the third ionization potential of the investigated metal ions (table 1, column 8) with the stability constants of the corresponding complexes (same table, column 2) the conclusion was analogous to that reached for the e/r criterion, the sequences $In > Ga$, $Sc > Y < La$ being valid in this case, too. If for the same metal ions, correlations are possible between K both with a radius function and/ with the ionization potential, leading to analogous results, it follows that it is not possible to attribute a ionic or covalent character to the metal-ligand bond, by means of those correlations only. [19]

---

[15] D. P. Mellor and L. Maley, *Nature*, **159**, 370 (1947).

[16] J. C. Bailar, "The Chemistry of the Coordination Compounds", Reinhold, New York, 1956.

[17] A. E. Martell und M. Calvin, "Die Chemie der Metallchelat-Verbindungen", Verlag Chemie, Berlin, 1958.

[18] M. Calvin and N. C. Melchior, *J. Amer. Chem. Soc.*, **70**, 3270 (1948).

[19] F. J. C. Rossotti, "The Thermodynamics of Metal Ion Complex Formation in Solution", in "Modern Coordination Chemistry", (J. Lewis and R. G. Wilkins, ed.), Interscience, New York, 1964.

Revue Roumaine de Chimie, 22, 1, 61–67 (1977)

CONTRIBUTION TO THE COORDINATION CHEMISTRY OF MOLYBDENUM. IV[1]

BIGUANIDONIUM AQUO-TETRACHLORO-OXOMOLYBDATES (V)

P. SPACU and LUCIA ANTONESCU

Department of Inorganic Chemistry of the Faculty of Chemistry of Bucharest
University, Splaiul Independenţei, n⁰ 89

Received April 11, 1975

Pure (RBigH) $[MoOCl_4(H_2O)]$ compounds were isolated and characterized from a chemical point of view [where RBig = N^1-*p*-chloro-phenyl-N^5-isopropyl-biguanide (Pald); N^1-*p*-chloro-phenyl-biguanide (Cl-PhBig); N^1-phenyl-biguanide(PhBig); N^1-morpholine-biguanide(Morph. Big) and N^1-dimethyl-biguanide (Me_2Big)]. The obtained biguanidonium salts have a green colour and present a good stability in perfectly dry air. The oxidation state of molybdenum was cerimetrically verified. The structure was elucidated by visible, UV and IR spectra, by EPR spectra and also by magnetic and electric conductivity measurements.

INTRODUCTION

Molybdenum(V) is known to form a series of monomer compounds with general formulas $R_2[MoOX_5]$, (X = Cl, Br, F) and $R[MoOX_4]$, (X = Cl, Br), where R may be ammonium, an alkaline metal or an organic base.[2–9]

Under similar reaction conditions, Allen et al.[10] obtained in the case of cations with large volume (such as the $RBigH^+$ biguanidonium ion), complexes having the form $R[MoOX_4]$.

More recent studies made by Rillema and Brubaker both by chemical approach and by EPR and IR spectroscopy revealed the formation of compounds $(C_4H_9)_4N[MoOCl_4]$ and $(C_3H_7)_4N[MoOCl_4]$.[11,12] Polish research workers specify that oxo-tetrachloro- and oxo-tetrabromo-aquo-molibdate(V) anions appear in compounds of type R[$MoOX_4$], in agreement with the hexacoordination of molybdenum atom.[13–15]

---

[1] Part III, L. Antonescu, *Anal. Şti. Univ. Bucureşti*, **21**, 135 (1972).

[2] J. F. Allen and H. M. Neumann, *Inorg. Chem.*, **3**, 1612 (1964).

[3] M. C. Haldar and H. K. Saha, *J. Indian Chem. Soc.*, **44**, 231 (1967).

[4] H. K. Saha and M. C. Haldar, *J. Indian Chem. Soc.*, **44**, 741 (1967).

[5] D. Grandjean and R. Weiss, *Bull. Soc. chim. France*, **1967**, 3054.

[6] H. K. Saha and A. K. Banerjee, *J. Indian Chem. Soc.*, **45**, 660 (1968).

[7] H. K. Saha and M. C. Haldar, *Z. anorg. Chem.*, **377**, 221 (1970).

[8] H. K. Saha and M. C. Haldar, *Z. anorg. Chem.*, **380**, 97 (1971).

[9] H. K. Saha, S. Roy and S. Chakravertý, *J. Indian Chem. Soc.*, **49**, 299 (1972).

[10] E. A. Allen, B. J. Brisdon, D. A. Edwards, G. W. A. Fowles and R. G. Williams, *J. Chem. Soc.*, **1963**, 4649.

[11] D. P. Rillema and C. H. Brubaker, Jr., *Inorg. Chem.*, **8**, 1645 (1969).

[12] D. P. Rillema and C. H. Brubaker, Jr., *Inorg. Chem.*, **9**, 397 (1970).

The crystalline and molecular structure of complex anions [$MoOX_4(H_2O)]^-$ was studied by X ray diffraction and IR studies [16] and exhibits similarities with [$ReOBr_4(H_2O)]^-$ anion investigated by Cotton and Lippard.[17]

The present paper describes the preparation and the properties of some biguanidonium salts of the form (RBigH) [$MoOCl_4(H_2O)$].

EXPERIMENTAL

Mo(V) solutions have been obtained by $Na_2MoO_4 . 2H_2O$ reduction with $N_2H_4 . HCl$. Substituted biguanide derivatives, such as chlorohydrates *R*Big.HCl were prepared according to literature.[18] Molybdenum was gravimetrically determined with 8-hydroxyquinoline, subsequent to the decomposition of compounds with hydrogen peroxide in ammonia medium. Nitrogen was determined by microcombustion using Pregl's method, while chlorine was determined by precipitation with 5% $AgNO_3$ in the presence of HNO_3. The oxidation state of molybdenum was determined by titration in acid medium with cerium sulphate(IV) in the presence of ferroin as indicator.

Visible and UV electronic spectra were recorded in HCl 10 M and DMF, for solutions with concentrations of 10^{-2}M and 10^{-4}M, respectively, using a UNICAM SP 800 D spectrophotometer. IR spectra were recorded with a UR Zeiss-Jena spectrophotometer using the technique of KBr pelletted powders.

The magnetic susceptibilities were measured on solid samples using the Gouy method. Molar conductivity determinations were performed on a type OK 102/1 Radelkis conductometer with platinum electrodes. Measurements were made on 10^{-3}M solutions in DMF at a temperature of 25°.

EPR spectra were recorded in DMF and HCl solutions using a spectrograph operating in X band, having a high-frequency modulated magnetic field. Disulphonated peroxylamine and Mn(II) were used as standards.

PREPARATION

a) 15 ml concentrated HCl and 1.5 g N_2H_4HCl were added to 1 g $Na_2MoO_4 . 2H_2O$. The solution was heated to obtain a clear green solution. Biguanide derivatives under the form of hydrochlorides are added while stirring, in a 1 :1 molybdenum : biguanide molar ratio (1 g Pald.HCl, 0.9 g Cl—PhBig.HCl, 0.8 g PhBig.HCl, 0.8 g Morph.Big.HCl, respectively 0.7 g Me_2Big.HCl). The mixture is heated for another 5—10 minutes. If the solution turns brown, gaseous hydrochloric acid will be bubbled until it turns green again when it is allowed to stand on ice, to crystallize. Deep green precipitates obtained were filtered in vacuo in a closed device in a HCl atmosphere. They are washed with some concentrated HCl and dried on calcium chloride until they reach the constant weight. Working with a 1 :2 molybdenum : biguanide molar ratio, one obtains again compounds shown in table 1.

b) A lower yield of the same compounds (RBig.H)[$MoOCl_4(H_2O)$] could be obtained by treating some molybdenum(V) oxo-complexes and oxo-chloro-complexes : Mo_2O_3(*R*Big)$_4$, Mo_2O_4(*R*Big)$_2(H_2O)_2$ and (*R*Big.H)$_2$[$Mo_2O_4Cl_4(H_2O)_2$] with concentrated HCl.

---

[13] B. Jezowska-Trzebiatowska and M. Rudolf, *Roczniki Chem.*, **42**, 1221 (1968).

[14] B. Jezowska-Trzebiatowska and M. Rudolf, *Roczniki Chem.*, **44**, 1031 (1970).

[15] B. Jezowska-Trzebiatowska and M. Rudolf, *Roczniki Chem.*, **44**, 745 (1970).

[16] J. G. Scane, *Acta Cryst.*, **23**, 85 (1967).

[17] F. A. Cotton and B. J. Lippard, *Inorg. Chem.*, **4**, 1621 (1965).

[18] H. King and J. M. Tonkin, *J. Chem. Soc.*, **1946**, 1063.

Table 1

Elemental analysis data

Compounds	Mo %		N %		Cl %	
	calcd.	found	calcd.	found	calcd.	found
(Pald.H) [$MoOCl_4(H_2O)$]	18.21	18.27	13.28	13.34	26.94	27.03
(Cl−PhBig.H) [$MoOCl_4(H_2O)$]	19.80	19.62	14.44	14.56	29.30	29.14
(PhBig.H) [$MoOCl_4(H_2O)$]	20.62	20.57	15.55	15.65	31.84	31.93
(Me_2Big.H) [$MoOCl_4(H_2O)$]	23.82	23.96	17.36	17.23	35.23	35.42
(Morph.Big.H) [$MoOCl_4(H_2O)$]	21.62	21.60	15.76	15.98	31.98	32.04

RESULTS AND DISCUSSION

Experimental data show that compounds of type (RBig.H) [$MoOCl_4(H_2O)$] are formed by reducing sodium molybdate in a concentrated HCl solution with hydrazine hydrochloride and adding biguanide substituted derivatives (RBig.HCl). It must be emphasized that due to a strong hydrochloric reaction medium, salts containing the aquo-tetrachloro-oxo-molybdate(V) ion could be prepared not only from aryl-substituted biguanide but also from biguanide alkyl derivatives, such as dimethyl biguanide and morpholin biguanide.

The synthetized compounds are green, a specific colour of such monomer chloro-derivatives of pentavalent molybdenum, and they are extremely hygroscopic. In wet air, they release hydrochloric acid, and the colour gradually turns blue as a result of oxidation. In dry air, they are stable and may keep the same aspect and properties for a longer period.

We observe the higher stability in the air of biguanidonium salts (RBig.H)[$MoOCl_4(H_2O)$] with aryl-substituted derivatives which display the interaction between electrons π of benzene cycles and electrons π of biguanide. Among these, phenylbiguanide exhibits the higher stability and also the minimum solubility in hydrochloric acid, hence the highest reaction yield, probably due to the chlorine absence in the biguanide derivative.

In aqueous, alcoholic solutions, in DMF and DMSO, green solutions are obtained which shortly turn brown with a simultaneous hydrochloric acid release. We assume that complexes of the form $MoOCl_3 \cdot$RBig have formed in these solutions, similar to those with dipyridyl phenanthroline, phosphine, arsine, etc.[19-22] However we have failed to isolate them in a pure state. A reverse reaction takes place when bubbling gaseous HCl through the brown solutions, with the formation of [$MoOCl_4(H_2O)]^-$ ion.

Modifications occurring in a 10^{-3}M solution in DMF were revealed by molar conductivity measurements. The calculated values (table 2)

---

[19] S. M. Horner and S. Y. Tyree, Jr., *Inorg. Chem.*, **1**, 122 (1962).

[20] P. C. H. Mitchell, *J. Inorg. Nuclear Chem.*, **25**, 963 (1963).

[21] W. M. Carmichael and D. A. Edwards, *J. Inorg. Nuclear Chem.*, **30**, 2641 (1968).

[22] H. K. Saha and A. K. Banerjee, *J. Indian Chem. Soc.*, **46**, 180 (1969).

are included in the 195−214 $ohm^{-1}\cdot cm^2\cdot mol^{-1}$ interval and correspond to a type 3 : 1 electrolyte, according to data reported in the literature.[23,24] This confirms the formation of $MoOCl_3\cdot RBig$ complexes in solution, which dissociate into MoO^{3+} and $3Cl^-$ ions.

Table 2

Electrical conductivity and magnetic moment

Compounds	$\lambda(\Omega^{-1}cm^2\ mol^{-1})$	μ_{ef} B.M. 300 K
(Pald.H) $[MoOCl_4(H_2O)]$	202.8	1.84
(Cl−PhBig.H) $[MoOCl_4(H_2O)]$	213.2	1.76
(PhBig.H) $[MoOCl_4(H_2O)]$	195	1.78
(Me_2Big.H) $[MoOCl_4(H_2O)]$	214	1.71
(Morph.Big.H) $[MoOCl_4(H_2O)]$	208	1.80

Attempts were made to obtain these complexes by thermal decomposition in a nitrogen atmosphere, according to reaction :

$$(RBig\cdot H)[MoOCl_4(H_2O)] \xrightarrow{t^0} MoOCl_3\cdot RBig + HCl + H_2O$$

By raising the temperature to 150°, the decomposition reaction is observed to begin with the formation of a brown compound and with hydrochloric acid release. Calcination continued at 160−170°, to complete the reaction, led to the organic compound decomposition so that complex compounds of type $MoOCl_3\cdot RBig$ could not be synthesized through this approach, either.

— The +5 oxidation state of molybdenum in the aquo-tetra-chloro-oxomolybdate ion was verified both chemically by titration with cerium sulphate (IV) and by magnetic and EPR measurements. The magnetic moments calculated for all the compounds (table 2) show values between 1.71 B.M. and 1.84 B.M. which may be considered very close to the 1.73 B. M. value, within the limits of experimental errors. This latter value is characteristic of monomer species containing pentavalent molybdenum with d^1 configuration and unpaired spins.

The IR vibration spectroscopy should that the water molecule attached to the anion is very weakly bound and for this reason the molybdenum-oxygen bond stretching is altered. Thus compounds $R[MoOX_4(H_2O)]$ reveal in the IR spectrum a sharp band at about 980 cm^{-1} assigned to the stretching frequency Mo = 0.[25,26]

Complex ions $[MoOX_5]^{2-}$ belonging to the C_{4V} symmetry group, present this stretching frequency ν (Mo = 0) at shorter wavenumbers,[27] in the 950−960 cm^{-1} domain.

---

[23] D. J. Phillips and S. Y. Tyree, Jr., *J. Amer. Chem. Soc.*, **83**, 1806 (1961).

[24] W. J. Geary, *Coord. Chem. Rev.*, **7**, 81 (1971).

[25] C. G. Barraclough, J. Lewis and R. S. Nyholm, *J. Chem. Soc.*, **1959**, 3552.

[26] F. A. Cotton and R. M. Wing, *Inorg. Chem.*, **4**, 867 (1965).

[27] A. Sabatini and I. Bertini, *Inorg. Chem.*, **5**, 204 (1966).

All complexes prepared by us, (*R*Big·H) [$MoOCl_4(H_2O)$] present a stretching vibration Mo = 0 at 970—975 cm^{-1} (table 3), which confirms that the structure suggested as a result of the chemical analysis and of the study of properties is the real one.

Since we deal with biguanidonium salts, their IR spectrum also reflects the main vibrations characteristic of biguanide, respectively the vibrations of groups CN, NCN and NH_2 around 1,540 cm^{-1}, 1,500 cm^{-1} respectively 1,100 and 1,630 cm^{-1}.[28]

Broad bands also appear at higher frequencies than 3,000 cm^{-1}, specific both of biguanide and of O—H vibrations of the coordinated water.

Table 3

Stretching frequencies ν(Mo = O)

Compounds	ν(Mo = O) cm^{-1}
(Pald.H) [$MoOCl_4(H_2O)$]	970
(Cl—PhBig.H) [$MoOCl_4(H_2O)$]	975
(PhBig.H) [$MoOCl_4(H_2O)$]	970
(Me_2Big.H) [$MoOCl_4(H_2O)$]	970
(Morph.Big.H) [$MoOCl_4(H_2O)$]	975

The formulation of the aquo-tetrachloro-oxo molybdate(V) complex anion as biguanidonium salt is also in agreement with visible and UV spectral measurements made in a 10 M hydrochloric acid solution. Gray and Hare [29] consider that both $[MoOCl_5]^{2-}$ and $[MoOCl_4(H_2O)]^-$ species may exist in a 10 M HCl solution. Absorption maxima were assigned by taking the discussed orbital molecular scheme for $(NH_4)_2$ [$MoOCl_5$], as reference. Allen et al. [10] also underline that M^I [$MoOX_4$] salts dissolved in halogenated acid have the same electronic spectrum as the M^I_2 [$MoOX_5$] salts, assuming that $[MoOX_4]^-$ anion accepts a halogen ion from the solution.

Thus, the electronic spectrum of synthesized biguanidonium salts (RBig·H) [$MoOCl_4(H_2O)$] presents absorption maxima at wavelengths and with intensities which are very close to those reported for $(NH_4)_2$ [$MoOCl_5$].

Two weak bands appear in the visible domain for all synthesized monomer compounds, as a result of transitions involving d' orbitals of the

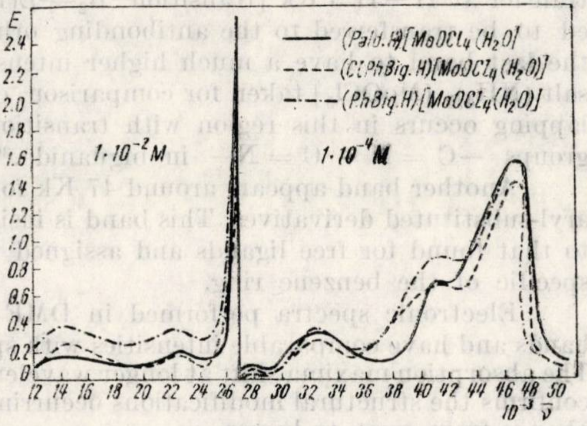

Fig. 1. —Electronic spectra in 10 M HCl of compounds with biguanide aryl-derivatives.

---

[28] M. Tahimoto, *Nippon Kagaku Lasshi*, **85**, 168 (1964).

[29] H. B. Gray and C. R. Hare, *Inorg. Chem.*, **1**, 363 (1962).

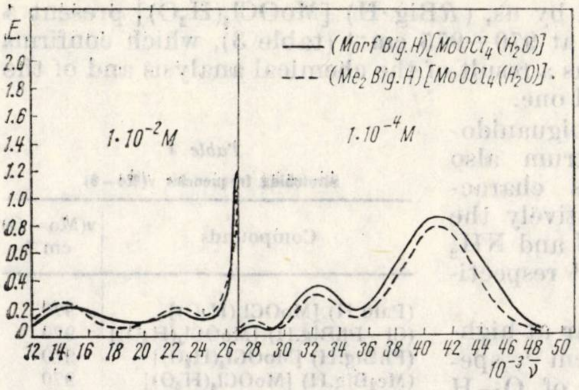

Fig. 2. — Electronic spectra in 10 M HCl of compounds with biguanide alkyl derivatives.

metal. The band found around 14 Kk is a d—d band and is due to transition $^2B_2 \to {}^2E(\mathrm{I})$ by the transfer of electron $b_2(\mathrm{d}_{xy})$ from the ground state into the $\mathrm{e}^*\pi(d_{xz}, d_{yz})$ excited state. The second band of the ligand field, observed at 22.5—22.7 Kk corresponds to transition $^2B_2 \to {}^2B_1$ as a result of the electron b_2 passing into the $b_1[(d_{xy})^1 \to (d_{x^2-y^2})^1]$ excited state.

According to the orbital-molecular scheme anticipated by Gray and Hare,[29] the three high intensity bands in the UV domain were assigned to transitions involving an electron transfer from a bonding orbital $\mathrm{e}\pi$ associated with the oxygen atom, to antibonding orbitals with an essentially d character.

The band at 28—28.3 Kk with a relatively low extinction coefficient is produced by a $\mathrm{e}\pi$ electron transfer to the antibonding orbital $b_2(d_{xy})$ and is described to result from the $^2B_2 \to {}^2E(\mathrm{II})$ transition. The band at 32.5 Kk $[{}^2B_2 \to {}^2B_2(\mathrm{I})]$ transition appears when a $\mathrm{e}\pi$ electron is transferred to an antibonding orbital $e^*\pi\ (d_{xz}, d_{yz})$. For the third band with charge transfer at 41—41.5 Kk [transition $^2B_2 \to {}^2E(\mathrm{III})$], electron $e\pi$ is considered to be transferred to the antibonding orbital $b_1^*(d_{x^2-y^2})$. We consider the last band to have a much higher intensity than in the ammonium salt $(NH_4)_2$ [MoOCl$_5$] taken for comparison, due to the fact that an overlapping occurs in this region with transitions due to the chromophore groups $-\mathrm{C}=\mathrm{N}-\mathrm{C}=\mathrm{N}-$ in biguanide.[30]

Another band appears around 47 Kk for compounds with biguanide aryl-substituted derivatives. This band is insignificantly shifted compared to that found for free ligands and assigned to some $\pi - \pi^*$ transitions, specific of the benzene ring.

Electronic spectra performed in DMF basically exhibit the same bands and have comparable intensities with spectra recorded in 10 M HCl. The absorption maxima shift at longer wavelengths for the DMF spectrum, confirms the structural modifications occurring in solution with the colour change from green to brown.

---

[30] D. Sen and A. Maitra, *J. Indian Chem. Soc.*, **49**, 153 (1972).

EPR spectra [31] in DMF and concentrated HCl solutions have confirmed the monomer structure assigned to those compounds formulated (RBig.H) $[MoOCl_4(H_2O)]$, the resonance absorption being recorded for all of them with intense assymmetrical signals.

It has also been found that solutions in DMF kept in the air for several hours present a decrease in the EPR signals intensity, simultaneously with the change of colour towards brown. After a longer period the complete dissappearance of the signal is observed. By adding concentrated HCl, the colour turns again green and EPR signals appear again with initial characteristics. This behaviour qualitatively observed and used by us in the synthesis of various types of Mo(V) compounds suggests the occurrence in time of a dimerization process in DMF solutions and the addition of concentrated HCl causes the dimers conversion into paramagnetic monomer species.

---

[31] P. Spacu, C. Gheorghiu, M. Constantinescu and L. Antonescu, *J. Less-Common Metals*, **44**, 161 (1975).

Revue Roumaine de Chimie, 22, *1*, 69–75 (1977)

THERMAL DECOMPOSITION OF BIS(OXALATO) DIAQUOMANGANESE(III). COMPLEX IN ACIDIC AQUEOUS SOLUTION

TATIANA ONCESCU and ECATERINA JURCONI

Physical Chemistry Department, Bucharest Institute of Chemistry, Bd. Republicii 13, Romania.

Received June 26, 1975

The pH influence on the kinetics and mechanism of the thermal decomposition of $[Mn(C_2O_4)_2(H_2O)_2]^-$ in aqueous solutions has been investigated at various temperatures and the activation parameters have been reported. The rate constant values show a specific acid catalysis over a pH ranging from 1.8 to about 4 and a region practically uncatalyzed at pH values greater than 4. The inert salt effect on the reaction exhibits a decelerating effect with increasing of the salt concentration.

1. INTRODUCTION

The problem of decomposition reaction of oxalato Mn(III) complexes has formed the subject of some papers, most of them dealing with studies on the tris (oxalato) complex. The bis (oxalato) complexes were supposed to form in the reduction of the permanganate by oxalate in acidic media [1] and in the decomposition of the trisoxalato complex. [2] The purpose of the present paper is to investigate the behaviour of bisoxalato Mn(III) complexes in solutions of various pH and the medium effect on its thermal decomposition.

2. EXPERIMENTAL

The crystalline yellow isomer$[Mn(C_2O_4)_2(H_2O)_2]K.3H_2O$ was prepared according to published procedure,[3] using reagent grade chemicals. In order to investigate the role of hydrogen ion, the aqueous solutions were acidified using HNO_3 Merck p.a. The acidity was established thereby to within ± 0.02 pH unit at the beginning of each kinetic experiment. An attempt to buffer the solutions failed, since the basic components of the buffer mixtures react with the complex in an anation reaction. The inert salt effect on the reaction was measured at different potassium nitrate concentrations. The use of nitrates was justified by the definite advantage over the perchlorates in respect to solubilities and the equally negligible tendency of the anion to undergo an anation reaction with the complex. Kinetic runs were made in a SP 800 Pye Unicam spectrophotometer, using a thermostated cell compartment capable of temperature control ± 0.3°. The changes in optical density of the reaction solutions were recorded at $\lambda = 450$ nm in the absorption band of the complex (fig. 1).

---

[1] H. Taube, *J. Amer. Chem. Soc.*, **70**, 1216 (1948).

[2] M. Wronska and T. Ernst, *Roczniki. Chem.*, **46**, 643 (1972).

[3] G. H. Cartledge and W. P. Eriks, *J. Amer. Chem. Soc.*, **58**, 2061 (1936).

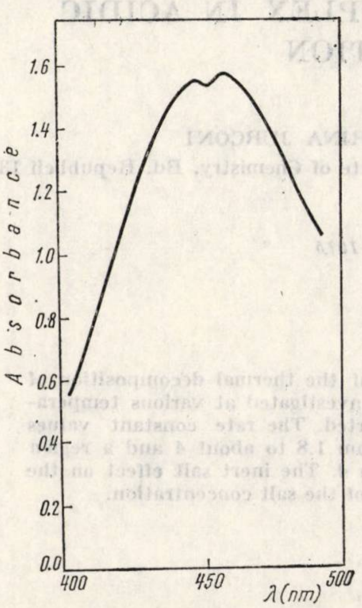

Fig. 1. — Absorption spectrum of bis(oxalato) diaquomanganese (III) in acidic solution of pH=2.7

3. RESULTS

A principal aim of our experiments was to determine the order of reaction with respect to Mn(III) complex concentration. For individual run, plot of $\log\frac{A_0}{A_t}$ (where A is absorbance) against time gives a good straight line, as seen in Figure 2. This seeming by first order dependence on Mn(III) complex concentration was confirmed by all series of runs; therefore we calculated the rate constant values by applying the least square method. These values at $T = 20°$ are summarized in Table 1 for all working pH values. The error of these determinations was about 3%.

The temperature dependence of the rate is shown in Figure 3, which presents the results of experiments at pH = 2.3 at three various temperatures : 15.7°, 20° and 25°. The resulting activation energy is 17.6 ± ± 0.5 kcal mole^{-1}. The corresponding values for the enthalpy and entropy of activation are respectively $\Delta H^{\neq} = 17.0$ kcal/mole and $\Delta S^{\neq} = -5.96$ u.e.

Series of experiments were carried out to determine the effects of the ionic strength on the reaction rate, yielding the data presented in Figure 4. It includes the runs made in presence of KNO_3 over the concentration range 0.1—3.0 M, at two pH values : 2.9 corresponding to the catalyzed region and 5.35 to uncatalyzed part.

4. DISCUSSION

It is known [3] that by dissolving the complex in water the following equilibrium is established :

$$[Mn(C_2O_4)_2(H_2O)_2]^- + H_2O \overset{K}{\rightleftharpoons} [Mn(C_2O_4)_2OH\ H_2O]^{--} + H_3O^+ \quad (E)$$

This behaviour is confirmed by changing suddenly the pH of the complex solution to about 4, even at its dissolution.[4] In our experimental con-

---

[4] I. G. Murgulescu and T. Oncescu, *Rev. Roumaine Chim.*, **10**, 3 (1965).

Table 1

Rate constants in aqueous solutions of different pH

$a = 2 \times 10^{-3}$ M $T = 20°$

pH	k_{obs} (sec^{-1})
1.87	0.00532
2.05	0.00374
2.3	0.00219
2.45	0.00165
2.6	0.00120
2.7	0.000939
2.9	0.000325
3.1	0.000504
3.5	0.000450
4.0	0.000479
4.5	0.000456
4.73	0.000410
5.0	0.000400
5.5	0.000383
5.83	0.000385
5.9	0.000364
6.35	0.000384
6.5	0.000359
6.65	0.000344
6.9	0.000381
7.42	0.000356

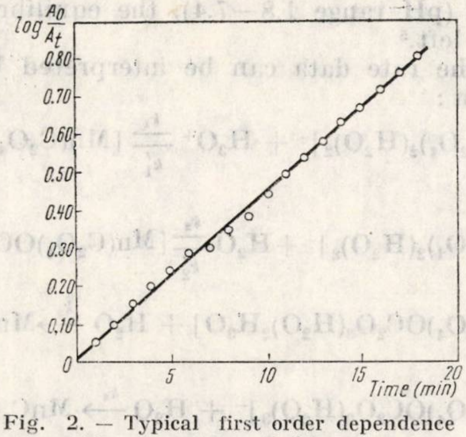

Fig. 2. — Typical first order dependence at conditions : $a = 2 \times 10^{-3}$ M, pH = 2.6, $T = 20°$

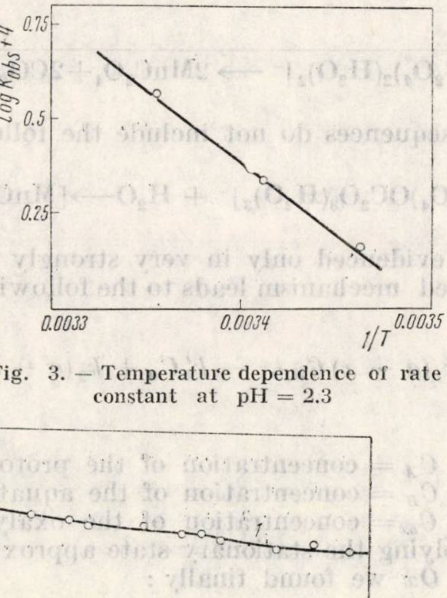

Fig. 3. — Temperature dependence of rate constant at pH = 2.3

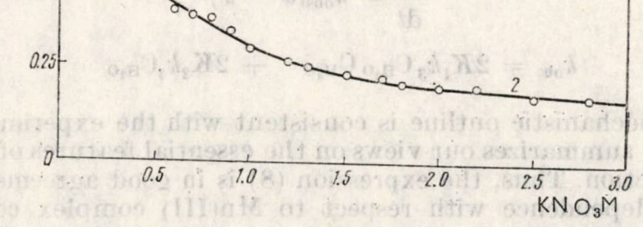

Fig. 4. — Variation of rate constant with ionic strength at pH = 2.9 (curve 1) and pH = 5.35 (curve 2); $T = 20°$

ditions (pH range 1.8—7.4), the equilibrium (E) is practically shifted to the left.[5]

The rate data can be interpreted by the following reaction mechanism :

$$[Mn(C_2O_4)_2(H_2O)_2]^- + H_3O^+ \underset{k_1'}{\overset{k_1}{\rightleftharpoons}} [Mn(C_2O_4)OC_2O_3(H_2O)_2)H_3O]\ K_1(1)\ \text{rapid}$$

$$[Mn(C_2O_4)_2(H_2O)_2]^- + H_2O \underset{k_2'}{\overset{k_2}{\rightleftharpoons}} [Mn(C_2O_4)OC_2O_3(H_2O)_3]^- \qquad K_2(2)\ \text{rapid}$$

$$[Mn(C_2O_4)OC_2O_3(H_2O)_2H_3O] + H_2O \xrightarrow{k_3} MnC_2O_4 + C_2O_4^{\cdot -} + 3H_2O + H_3O^+ \qquad (3)\ \text{slow}$$

$$[Mn(C_2O_4)OC_2O_3(H_2O)_3]^- + H_2O \xrightarrow{k_4} MnC_2O_4 + C_2O_4^{\cdot -} + 4H_2O \qquad (4)\ \text{slow}$$

$$2[Mn(C_2O_4)_2(H_2O)_2]^- + 2C_2O_4^{\cdot --} \xrightarrow{k_5} 2MnC_2O_4 + 4CO_2 + 2C_2O_4^{--} + 4H_2O \qquad (5)\ \text{rapid}$$

$$2[Mn(C_2O_4)_2(H_2O)_2]^- \longrightarrow 2MnC_2O_4 + 2CO_2 + C_2O_4^{--} + 4H_2O \qquad (6)\ \text{overall}$$

These sequences do not include the following step :

$[Mn(C_2O_4)OC_2O_3(H_2O)_3]^- + H_2O \longrightarrow [MnC_2O_4(H_2O)_4]^+ + C_2O_4^{--}$, because

it was evidenced only in very strongly acidic media[1] at $pH < 1$. The suggested mechanism leads to the following differential kinetic equation :

$$\frac{dx}{dt} = k_1(a - x)\,C_{H_3O^+} - k_1' C_A + k_2(a - x)\,C_{H_2O} - k_2' C_B + k_5(a - x)^2 C_{ox}^2 \tag{7}$$

where C_A = concentration of the protonated complex
C_B = concentration of the aquated complex
C_{ox} = concentration of the oxalyl radical ion

By applying the stationary state approximation to the intermediates A, B and Ox we found finally :

$$\frac{dx}{dt} = k_{obs}(a - x) \tag{8}$$

where

$$k_{obs} = 2K_1 k_3\, C_{H_2O}\, C_{H_3O^+} + 2K_2 k_4 C_{H_2O}^2 \tag{9}$$

This mechanistic outline is consistent with the experimental observations and summarizes our views on the essential features of the decomposition reaction. Thus, the expression (8) is in good agreement with the first order dependence with respect to Mn(III) complex concentration

---

[5] T. ONCESCU and E. JURCONI unpublished data.

(Fig. 2) revealed from our experimental data. On the other hand, the expression (9) shows that at higher hydrogen ion concentration (in our case pH < 4), $K_1 > K_2$, and consequently:

$$k_{obs} = k_H C_{H_3O^+} \tag{10}$$

$$\log k_{obs} = \log k_H - \text{pH} \tag{11}$$

where $k_H = 2K_1k_3C_{H_2O}$, K_1 is the protonation preequilibrium constant and k_3 is the first order constant of the rate determining step in acidic media. Equation (11) is typical of the specific acid catalysed reactions, and its plot gives a straight line with a slope of about unity, verified satisfactorily in our case, as seen in Figure 5.1.

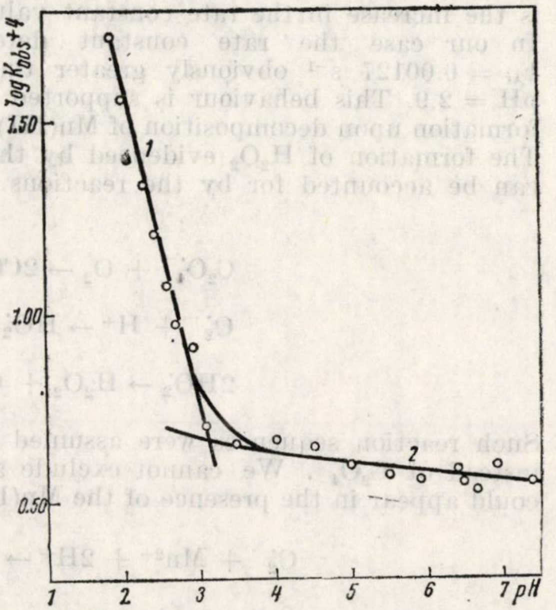

Fig. 5. — Variation of rate constant with pH, at $T = 20°$: curve 1 at pH < 4; curve 2 at pH > 4.

At lower hydrogen ion concentration (pH $= 4-7.4$), $K_1 < K_2$, the second term in expression (9) becomes preponderant and therefore:

$$k_{obs} = k \tag{12}$$

where
$$k = 2K_2k_4C^2_{H_2O} \tag{13}$$

These k values correspond to Figure 5.2. The mechanism of the thermal decomposition of the investigated system in basic solution forms the subject of another paper.[5] It is certain that in such solutions the acidified water ligands undergo proton abstraction changing into (hydroxo) ligands at corresponding basicities.

Another interesting observation resulting from the proposed mechanism is the presence of the protonated and aquated intermediates A and B, which we suggest by analogy to the decomposition of Co(III) and Rh(III) tris(oxalato) complexes.[6-8]

---

[6] D. Barton and G. M. Harris, *Inorg. Chem.*, **1**, 251 (1962).

[7] A. L. Porte, H. S. Gritowsky and G. M. Harris, *J. Chem. Phys.*, **34**, 66 (1961).

[8] C. A. Burton, J. H. Carter, D. R. Llewellyn, Ch. O'Connor, S. Y. Yih and A. L. Odell, *J. Chem. Soc.*, **43**, 4615 (1964).

The reaction mechanism involves also the production of the free radical $C_2O_4^{\cdot -}$ which reattacks the substrate to form additional Mn(II). The theoretical basis for the appearance with a greater probability of $C_2O_4^{\cdot -}$ in opposition to $CO_2^{\cdot -}$ is offered by Simon.[9] Some additional evidence has been provided by the observation that this thermal decomposition leads to the acrylonitrile[10,11] or vinyl polymerization.[12] The E.S.R. spectra obtained in the photolysis of $[Mn(C_2O_4)_2(H_2O)_2]K$ in DMF[13] and of $[Mn(C_2O_4)_3]K_3$ in aqueous solution[14] on irradiation at nitrogen temperature present a signal corresponding to $C_2O_4^{\cdot -}$. Also, the formation of $HC_2O_4^{\cdot}$ radical in very acidic solution is probable.[15] Another proof of the free radical mechanism in the acid catalyzed redox decomposition is the increase in the rate constant values in deoxygenated solutions.[16] In our case the rate constant determined in presence of argon is $k_{Ar} = 0.00127\ s^{-1}$ obviously greater than $k_{air} = 0.000825\ s^{-1}$ both at $pH = 2.9$. This behaviour is supported also by the hydrogen peroxide formation upon decomposition of Mn(III) complex in presence of oxygen. The formation of H_2O_2 evidenced by the colour reaction with $Ti(SO_4)_2$ can be accounted for by the reactions :

$$C_2O_4^{\cdot -} + O_2 \rightarrow 2CO_2 + O_2^{\cdot -} \qquad (a)$$

$$O_2^{\cdot -} + H^+ \rightarrow HO_2^{\cdot} \qquad (b)$$

$$2HO_2^{\cdot} \rightarrow H_2O_2 + O_2 \qquad (c)$$

Such reaction sequences were assumed by Kolthoff[17] involving $CO_2^{\cdot -}$ instead of $C_2O_4^{\cdot -}$. We cannot exclude also redox path by which H_2O_2 could appear in the presence of the Mn(II) formed in the reaction :

$$O_2^{\cdot -} + Mn^{2+} + 2H^+ \rightarrow Mn^{3+} + H_2O_2 \qquad (d)$$

This reaction which competes with the process (b) takes place in strongly acidic media. By adding $Mn(NO_3)_2$ in the reaction samples one observes the increasing of H_2O_2 amount, and at the same time an accelerating effect on the decomposition rate presented in Figure 6 and Table 2.
This last behaviour is supported by the following reactions :

$$Mn^{3+} + H_2O \rightarrow Mn^{2+} + H^+ + OH^{\cdot} \qquad (e)$$

$$OH^{\cdot} + C_2O_4^{--} \rightarrow C_2O_4^{\cdot -} + OH^- \qquad (f)$$

---

[9] Z. Simon, *Rev. Roumaine Chim.*, **14**, 705 (1969).

[10] T. Oncescu, *Rev. Roumaine Chim.*, **15**, 209 (1970).

[11] I. G. Murgulescu, T. Oncescu and I. Vlagiu, *J. Chem. Phys.*, **10**, 1487 (1971).

[12] T. B. Copstake and N. Uri, Proc. Roy. Soc. Ser. A., **228**, 252 (1955).

[13] I. G. Murgulescu, T. Oncescu and S. G. Ionescu, *Rev. Roumaine Chim.*, **17**, 3 (1972).

[14] A. L. Pozniac, G. A. Shagisultanova and L. N. Neokladnova, *Teoreticheskaya i eksperimentalnaya Khimia*, **4**, 567 (1968).

[15] N. S. Rowan, M. Z. Hoffman and R. M. Milburn, *J. Amer. Chem. Soc.*, **96**, 6060 (1974).

[16] N. S. Rowan, K. M. Mulburn and M. Z. Hoffman, *Inorg. Chem.*, **11**, 2272 (1972).

One can observe that process (f) yields again $C_2O_4^{\cdot -}$ which reacts with the substrate and contributes therefore to the decomposition of the initial complex. Such processes are supposed to be intermediate steps in the reduction of permanganate by oxalate according to Gupta and Gosh.[18]

Table 2

Rate constants at different concentrations of added $Mn(NO_3)_2$
pH = 2.7 T = 20°

$Mn(NO_3)_2$ M	0	0.87×10^{-3}	1.74×10^{-3}	3.43×10^{-3}
k_{obs}	0.00939	0.0146	0.0170	0.0990

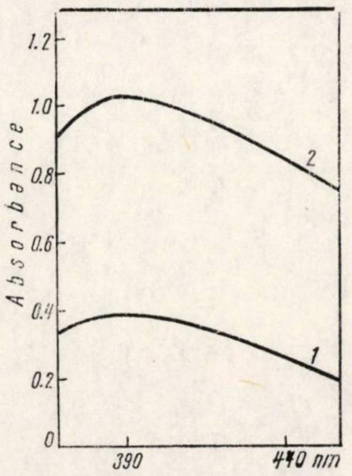

Fig. 6.—The increasing of final absorption of the solution by adding $Ti(SO_4)_2$, in absence (1) and in presence (2) of 1.74×10^{-3} M $Mn(NO_3)_2$.

The inert salt effects observed in this study show that the rate constants are slightly affected by ionic strength. Because there is no quantitative theory for the salt effects in the concentration range between 0.1—3M, we can give only a qualitative explanation. Thus, as can be seen in Figure 4, the change of the rate constant as a function of ionic strength is larger for pH = 5.35 than for 2.9. This seems understandable in terms of the charge of the complex involved in the rate determining step : in the first case the rate determining step (4) involves a negative ion and in the second case an uncharged complex.

In conclusion, this study has the advantage that, starting directly from $[Mn(C_2O_4)_2(H_2O)_2]K$, not from the reaction between MnO_4^- and $C_2O_4^{--}$ (in which it is involved only as an intermediate), it provides more precise information regarding the decomposition mechanism of this complex. In favour of the aquation mechanism are also the results obtained from the decomposition of this complex in DMF—H_2O [19] and DMSO—H_2O [20] mixtures. At the same time, these investigations help to elucidate the decomposition of $[Mn(C_2O_4)_3]K_3$.

---

[17] I. M. Kolthoff, E. J. Meehan and M. Kimura, *J. Phys. Chem.*, **75**, 3343 (1971).

[18] Y. K. Gupta and S. Ghosh, *Z. phys. Chem.* (Leipzig) **208**, 368 (1957).

[19] T. Oncescu and E. Jurconi, *Rev. Roumaine Chim.*, **21**, 6, 805 (1976).

[20] T. Oncescu and E. Jurconi, *Rev. Roumaine Chim.*, **21**, 7, 985 (1976).

Revue Roumaine de Chimie, 22, *1*, 77–86 (1977)

A KINETIC ANALYSIS OF ADDITION POLYMERIZATION REACTION

M. VLAD and E. SEGAL
Polytechnic Institute of Bucharest, Institute of Chemistry, Department of Physical Chemistry and Electrochemical Technology, Bd. Republicii 13

Received January 21, 1976

A detailed kinetic analysis of the reaction system $M_1 + M_1 \xrightarrow{k_1} M_2$; $M_2 + M_1 \xrightarrow{k_2} M_3$; … ; $M_n + M_1 \xrightarrow{k_n} M_{n+1}$; … is presented. Supposing that $k_1 \neq k_2 \neq \ldots \neq k_n$, $k_n = k_{n+1} = \ldots$ the authors suggest a method for determination of the rate constants $k_1, \ldots, k_n$ from the experimental data. A computational method of the functions $M_i = M_i(z)$ $i = 1, 2, \ldots$, $\left(z = \int_0^t M_1 \mathrm{d}t\right)$ is elaborated. This method is applied to the case $n = 2$ ($k_1 \neq k_2$, $k_2 = k_3 = \ldots$). For certain values of $\eta = k_2/k_1$ ($\eta \ll 1$, $\eta \cong 1$ and $\eta \gg 1$) it is possible to determine the analytic dependence $z = z(t)$.

The most simple mechanisms for addition polymerization are :

$$\begin{array}{ll}
\mathrm{I} & \mathrm{II} \\
\mathrm{I} + M_1 \xrightarrow{k_1} \mathrm{I}M_1 & M_1 + M_1 \xrightarrow{k_1} M_2 \\
\mathrm{I}M_1 + M_1 \rightarrow \mathrm{I}M_2 & M_2 + M_1 \xrightarrow{k_2} M_3 \\
\ldots\ldots\ldots\ldots & \ldots\ldots\ldots\ldots \\
\mathrm{I}M_n + M_1 \xrightarrow{k_{n+1}} \mathrm{I}M_{n+1} & M_n + M_1 \xrightarrow{k_n} M_{n+1} \\
\ldots\ldots\ldots\ldots & \ldots\ldots\ldots\ldots \\
(M_1 \neq \mathrm{I}) & (M_1 = \mathrm{I})
\end{array}$$

Flory[1] and Leighton[2] Natta and Mantica[3] and Gold,[4] dealt with the first scheme. A kinetic analysis of the second mechanism was made by Benson[5]. He determined the analytic dependence of monomer concentration M_1 versus $z = \int_0^t M_1 \mathrm{d}t$. The present report contains a more detailed kinetic analysis of the second scheme.

---

[1] P. J. Flory, *J. Amer. Chem. Soc.*, **62**, 1561 (1940).

[2] B. Leighton and H. Peebles Jr., "Molecular Weight Distribution in Polymers", Wiley — Interscience, New York, 1971.

[3] G. Natta and E. Mantica, *J. Amer. Chem. Soc.*, **74**, 3152 (1952).

[4] L. Gold, *J. Chem. Phys.*, **28**, 91 (1958).

[5] S. W. Benson, "The Foundations of Chemical Kinetics", McGraw-Hill, New York, 1960.

The rate equations corresponding to the mechanism II are

$$\frac{dM_1}{dz} = -\,2k_1M_1 - \sum_{i=2}^{\infty} k_iM_i\,; \tag{1}$$

$$\frac{dM_i}{dz} = k_{i-1}M_{i-1} - k_iM_i\,, \qquad i = 2, 3, \ldots \tag{2}$$

where $\quad z = \int_0^t M_1 \mathrm{d}t$

(Our k_1 is Benson's $k_1/2$)

Supposing that $M_1(t = 0) = M_0$ and $M_i(t = 0) = 0$, $i = 2, 3, \ldots$, (1) and (2) become:

$$s\bar{M}_1 - M_0 = -\,2\,k_1\bar{M}_1 - \sum_{i=2}^{\infty} k_i\bar{M}_i\,; \tag{3}$$

$$s\bar{M}_i = k_{i-1}\bar{M}_{i-1} - k_iM_i, \qquad i = 2,\ 3, \ldots \tag{4}$$

where $\bar{M}_i(s) = \int_0^\infty \mathrm{e}^{-sz} M_i(z)\mathrm{d}z = \mathfrak{L}\, M_i(z)$ are the Laplace transforms [6] of variables $M_i(z)$.

The solutions of algebraic equations (3) and (4) are:

$$\bar{M}_1(s) = \frac{M_0}{s + 2k_1 + k_1 \sum\limits_{i=2}^{\infty} \prod\limits_{u=2}^{i} \left(\frac{k_u}{s + k_u}\right)}\,; \tag{5}$$

$$\bar{M}_i(s) = \frac{M_0}{s + 2k_1 + k_1 \sum\limits_{i=2}^{\infty} \prod\limits_{u=2}^{i} \left(\frac{k_x}{s + k_u}\right)} \prod_{u=2}^{i} \left(\frac{k_{u-1}}{s + k_u}\right), \quad i = 2,\ 3,\ \ldots \tag{6}$$

If $k_n = k_{n+1} = \ldots$ the sumatiom of series $\sum\limits_{i=2}^{\infty} \prod\limits_{2}^{i} (k_u/(s + k_u))$ yields:

$$\sum_{i=2}^{\infty} \prod_{u=2}^{i} \left(\frac{k_u}{s + k_u}\right) = \frac{k_2}{s}, \qquad n \leqslant 2\,;$$

$$\sum_{i=2}^{\infty} \prod_{u=2}^{i} \left(\frac{k_u}{s + k_u}\right) = \sum_{i=2}^{n-1} \prod_{u=2}^{i} \left(\frac{k_u}{s + k_u}\right) + \prod_{u=2}^{n-1} \left(\frac{k_u}{s + k_u}\right) \frac{k_n}{s}, \qquad n > 2$$

Then:

$$\bar{M}_i(s) = \frac{M_0 s}{s^2 + 2k_1 s + k_1 k_2}\left(\frac{k_1}{k_2}\right)^{1-\delta_{1i}}\left(\frac{k_2}{s + k_2}\right)^{i-1}, \qquad n \leqslant 2 \tag{7}$$

and

$$\bar{M}_1(s) = \frac{M_0 s}{P_n(s)}\prod_{u=2}^{n-1}(s + k_u), \qquad n > 2; \tag{8}$$

$$\bar{M}_i(s) = \frac{M_0 s}{P_n(s)}\prod_{u=i+1}^{n-1}(s + k_u)\prod_{v=1}^{i-1}k_v, \qquad 1 < i < n - 1,\ n > 2; \tag{8'}$$

$$\bar{M}_i(s) = \frac{M_0 s}{P_n(s)}\prod_{v=1}^{n-2}k_v\left(\frac{k_{n-1}}{k_n}\right)^{1-\delta_{n-1i}}\left(\frac{k_n}{s + k_n}\right)^{i-n+1}, i \geqslant n - 1,\ n > 2; \tag{8''}$$

where

$$P_n(s) = s^2 + 2k_1 s + k_1 k_2,\ n = 1,\ 2;$$

$$P_3(s) = s(s + 2k_1)(s + k_2) + sk_1k_2 + k_1k_2k_3;$$

$$P_n(s) = s(s + 2k_1)\prod_{u=2}^{n-1}(s + k_u) + s\sum_{i=2}^{n-2}\prod_{u=i+1}^{n-1}(s + k_u)\prod_{v=1}^{i-1}k_v + (s + k_n)\prod_{v=1}^{n-1}k_v, \qquad n > 3$$

and δ_{ij} is Kronecker delta.

From (7) and (8)—(8″) it follows that:

$$S_1(s) = \frac{1}{M_0}\sum_{i=1}^{\infty}\bar{M}_i = \frac{s + k_1}{s^2 + 2k_1 s + k_1 k_2}, \qquad n \leqslant 2; \tag{9}$$

$$S_1(s) = \frac{1}{P_n(s)}\left[s\prod_{u=2}^{n-1}(s + k_u) + s\sum_{i=2}^{n-2}\prod_{u=i+1}^{n-1}(s + k_u)\prod_{v=1}^{i-1}k_v + (s + k_{n-1})\prod_{v=1}^{n-2}k_v\right], \qquad n > 2; \tag{9'}$$

$$S_2(s) = \frac{1}{M_0}\sum_{i=1}^{\infty}i^2\bar{M}_i = \frac{s^3 + 4s^2k_1 + 5sk_1k_2 + 2k_1k_2^2}{s^2(s^2 + 2k_1 s + k_1 k_2)}, \qquad n \leqslant 2; \tag{10}$$

$$S_2(s) = \frac{1}{s^2 P_n(s)}\left\{s^3\prod_{u=2}^{n-1}(s + k_u) + s^3\sum_{i=2}^{n-2}i^2\prod_{u=i+1}^{n-1}(s + k_u)\prod_{v=1}^{i-1}k_v + \right.$$

$$\left. + [(n - 1)^2 s^3 + n^2 s^2 k_{n-1} + (2n + 1)sk_{n-1}k_n + 2k_{n-1}k_n^2]\prod_{v=1}^{n-2}k_v\right\}, \quad n > 2 \tag{10'}$$

As $\overline{M}_i(s)$ are ratios of polynomials, the originals $M_i(z)$ can be obtained with Heaviside's theorem [6]:

$$M_i(z) = \mathfrak{L}^{-1}\overline{M}_i(s) = \mathfrak{L}^{-1} \frac{Q_i(s)}{\prod\limits_{1}^{r} (s - s_u^{(i)})^{m_u^{(i)}}} = \tag{11}$$
$$= \sum_{u=1}^{r} \sum_{k=0}^{m_u^{(i)}-1} \frac{z^{m_u^{(i)}-k-1}\, \mathrm{e}^{s_u^{(i)} z}}{(m_u^{(i)}-k-1)\,!\,k\,!} \cdot \frac{d^k}{ds^k} \left[(s - s_u^{(i)})^{m_u^{(i)}} \overline{M}_i(s)\right]_{s=s_u^{(i)}}$$

Similarly, we obtain the following expressions for number average and weight average polymerization degrees:

$$\bar{n}_n = \frac{\sum i M_i(z)}{\sum M_i(z)} = [\mathfrak{L}^{-1} S_1(s)]^{-1} \tag{12}$$

$$\bar{n}_w = \frac{\sum i^2 M_i(z)}{\sum i M_i(z)} = \mathfrak{L}^{-1} S_2(s) \tag{13}$$

In the case $n = 2(k_2 = k_3 = \ldots)$, Benson suggests a method of determination for rate constants k_1 and k_2 from the curve $M_1 = M_1(t)$. Using Eqs. (7), (8) and (11) we can easily generalize Benson's method. We get:

$$M_1(z) = \frac{M_0}{s_1 - s_2} (s_1\ \mathrm{e}^{s_1 z} - s_2 \mathrm{e}^{s_2 z}), \qquad n = 2 \tag{14}$$

$$M_1(z) = M_0 \sum_{j \neq i} \frac{s_j \prod\limits_{u=2}^{n-1} (k_u + s_j)}{\prod\limits_{j \neq i} (s_j - s_i)}\, \mathrm{e}^{s_j z}, \qquad n > 2 \tag{14'}$$

where, for the sake of simplicity we supposed that the equation $P_n(s) = 0$ has n distinct solutions $s_j\ j = 1, \ldots, n$ and $s_j \neq k_\lambda j = 1, \ldots, n;\ \lambda = 2, \ldots, \ldots, n - 1$.

The variable z can be obtained from the curve $M_1 = M_1(t)$ through numerical (or graphical) integration. Then it is easy to determine the solutions s_i from Eqs. (14) or (14′) by fitting the experimental data to the standard methods.[7] Further, by using the identity

---

[6] M. Lavrentiev and B. Chabat, "Méthodes de la théorie des fonctions d'une variable complexe", Publish. H. Mir., Moscow, 1972, p. 496.

[7] C. Penescu, G. Ionescu, M. Tertișco and E. Creangă, "Identificarea experimentală a proceselor automatizate", Ed. tehnică, Bucharest, 1971, p. 64, 95.

$$\prod_{i=1}^{n}(s-s_i)=P_n(s) \tag{15}$$

we get a system of n algebraic equations :

$$f_i(s_1,\ldots,s_n,k_1,\ldots,k_n)=0,\ i=1,\ldots,n \tag{16}$$

The system (16) renders possible the determination of the rate constants $k_1,\ldots,k_n$.

If the rate constants $k_1,\ldots,k_n$ are known, the dependence $t=f(z)$ can be obtained from the relationship :

$$M_1(z)=\frac{\mathrm{d}}{\mathrm{d}t}\int_0^t M_1\mathrm{d}t=\frac{\mathrm{d}z}{\mathrm{d}t} \tag{17}$$

or

$$t=\int_0^z\frac{\mathrm{d}z}{M_1(z)}=f(z) \tag{17'}$$

Then

$$M_i(t)=M_i(z=g(t)) \tag{18}$$

where $f(g(t))=t$
At equilibrium ($t=\infty$) Eq. (18) becomes :

$$M_i(\infty)=M_i(z(t=\infty)) \tag{18'}$$

Taking into account that

$$M_1(t=\infty)=0$$

$z_\infty=z(t=\infty)$is given by the equation

$$M_1(z_\infty)=0 \tag{19}$$

Further on, we shall apply the equations derived above to the case $n=2$. We get :

1. $\eta=k_2/k_1<1$ $(k_1>k_2)$

$$M_1(z)=M_0\mathrm{e}^{-k_1z}\left(\cosh\beta k_1z-\frac{\sinh\beta k_1z}{\beta}\right); \tag{20}$$

$$\begin{aligned} M_i(z) &= \frac{M_0\gamma \mathrm{e}^{-\eta k_1 z}}{2(1-\eta)} \sum_{q=0}^{i-2} \frac{(\eta k_1 z)^{i-q-2}}{(i-q-2)!}\left[\left(1+\frac{1}{\beta}\right)^q + \left(1-\frac{1}{\beta}\right)^q\right] - \\ &- \frac{M_0\eta \mathrm{e}^{-k_1 z}}{2(1-\eta)}\left[\left(1+\frac{1}{\beta}\right)^{i-2} \cdot \mathrm{e}^{\beta k_1 z} + \left(1-\frac{1}{\beta}\right)^{i-2} \mathrm{e}^{-\beta k_1 z}\right] = \\ &= \frac{M_0\eta \mathrm{e}^{-\eta k_1 z}}{1-\eta} \sum_{q=0}^{i-2} \frac{(\eta k_1 z)^{i-q-2}}{(i-q-2)!} \frac{\cosh \varphi q}{\cosh^q \varphi} - \\ &- \frac{M_0\eta \mathrm{e}^{-k_1 z}}{1-\eta} \frac{\cosh[\beta k_1 z + \varphi(i-2)]}{\cosh^{i-2}\varphi}, \qquad i = 2, 3, \ldots ; \end{aligned} \tag{21}$$

$$\bar{n}_n(z) = \frac{\mathrm{e}^{k_1 z}}{\cosh \beta k_1 z} ; \tag{22}$$

$$\bar{n}_w(z) = 1 + 2\eta k_1 z + 2\beta e^{-k_1 z} \sinh \beta k_1 z ; \tag{23}$$

$$U_n(z) = \frac{\bar{n}_w(z)}{\bar{n}_n(z)} - 1 = (1 + 2\eta k_1 z) e^{-k_1 z} \cosh \beta k_1 z + e^{-2k_1 z} \sinh 2\beta k_1 z - 1 ; \tag{24}$$

$$t(z) = \frac{1}{M_0 k_1} \int_0^{k_1 z} \frac{eydy}{\cosh \beta y - \dfrac{\sin h \beta y}{\beta}} \tag{25}$$

where $\beta = \sqrt{1-\eta}$, tanh $\varphi = \beta^{-1}$ and U_n is the polymer polydispersity.[8]

2. $\eta = 1$ $(k_1 = k_2)$

$$M_i(z) = \frac{M_0 (k_1 z)^{i-1}}{(i-1)!} e^{-k_1 z} \left(1 - \frac{k_1 z}{i}\right); \qquad i = 1, 2, \ldots ; \tag{21'}$$

$$\bar{n}_n(z) = e^{k_1 z} ; \tag{22'}$$

$$\bar{n}_w(z) = 1 + 2k_1 z ; \tag{23'}$$

$$U_n(z) = (1 + 2k_1 z) e^{-k_1 z} - 1 ; \tag{24'}$$

$$t = \frac{1}{M_0 k_1} \int_0^{k_1 z} \frac{e^y}{1-y} \mathrm{d}y = \frac{e}{M_0 k_1} [E_i(-1) - E_i(k_1 z - 1)] \tag{25'}$$

---

[8] C. V. Schultz, *Z. phys. Chem.*, **B43**, 25, 49 (1939).

or

$$z = \frac{1}{k_1}\{1 + \arg E_i[E_i(-1) - e^{-1}M_0k_1t]\} \tag{26}$$

with [9]

$$E_i(x) = \int_{-\infty}^{x} \frac{e^y}{y}\,\mathrm{d}y \quad \text{and} \quad \arg E_i(E_i(x)) = x$$

3. $\eta > 1$ $(k_1 < k_2)$

$$M_1(z) = M_0e^{-k_1z}\left(\cos\beta k_1z - \frac{\sin\beta k_1z}{\beta}\right); \tag{20'}$$

$$M_i(z) = \frac{M_0\eta e^{-k_1z}}{\eta - 1}\cdot\frac{\cos[\beta k_1z - \varphi(i-2)]}{\cos^{i-2}\varphi} -$$

$$- \frac{M_0\eta e^{-\eta k_1z}}{\eta - 1}\sum_{q=0}^{i-2}\frac{(\eta k_1z)^{i-q-2}}{(i-q-2)!}\,\frac{\cos\varphi q}{\cos^q\varphi} \qquad i = 2, 3, \ldots ; \tag{21''}$$

$$\bar{n}_n(z) = \frac{e^{k_1z}}{\cos\beta k_1z}; \tag{22''}$$

$$\bar{n}_w(z) = 1 + 2\eta k_1z - 2\beta e^{-k_1z}\sin\beta k_1z; \tag{23''}$$

$$U_n(z) = (1 + 2\eta k_1z)e^{-k_1z}\cos\beta k_1z - \beta e^{-2k_1z}\sin 2\beta k_1z - 1; \tag{24''}$$

$$t = \frac{1}{M_0k_1}\int_0^{k_1z}\frac{e^y\mathrm{d}y}{\cos\beta y - \dfrac{\sin\beta y}{\beta}}; \tag{25''}$$

with $\beta = \sqrt{\eta - 1}$ and $\sin\varphi = 1/\sqrt{\eta}$.

At equilibrium $(t = \infty)$ we have:

1. $\eta < 1$

$$M_1(z_\infty) = e^{-k_1z_\infty}\left(\cosh\,\beta k_1z_\infty - \frac{\sin h\beta h_1z_\infty}{\beta}\right) = 0$$

---

[9] N. N. Lebedev, "Funcţii speciale şi aplicaţiile lor", Ed. tehnică, Bucharest, 1957, p. 55 (translated from Russian).

and then

$$k_1 z_\infty = \frac{\operatorname{argtanh} \beta}{\beta} = \frac{1}{2\beta} \ln \left(\frac{1+\beta}{1-\beta} \right), \tag{27}$$

$$M_i(\infty) = \frac{M_0 \eta}{2(1-\eta)} \left(\frac{1+\beta}{1-\beta} \right)^{-\eta/2\beta} \sum_{q=0}^{i-2} \frac{1}{(i-q-2)!} \left[\frac{\eta}{2\beta} \ln \left(\frac{1+\beta}{1-\beta} \right) \right]^{i-q-2} \cdot$$

$$\cdot \left[\left(1 + \frac{1}{\beta} \right)^{q} + \left(1 - \frac{1}{\beta} \right)^{-q} \right] - \frac{M_0 \eta}{2(1-\eta)} \left(\frac{1+\beta}{1-\beta} \right)^{-1/2\eta} \left[\left(1 + \frac{1}{\beta} \right)^{i-2} \cdot \right.$$

$$\left. \cdot \sqrt{\frac{1+\beta}{1-\beta}} + \left(1 - \frac{1}{\beta} \right)^{i-2} \sqrt{\frac{1-\beta}{1+\beta}} \right]; \tag{28}$$

$$\bar{n}_n(\infty) = \sqrt{\eta} \left(\frac{1+\beta}{1-\beta} \right)^{1/2\beta}; \tag{29}$$

$$\bar{n}_w(\infty) = 1 + \frac{\eta}{\beta} \ln \left(\frac{1+\beta}{1-\beta} \right) + 2\sqrt{\eta} \left(\frac{1+\beta}{1-\beta} \right)^{-1/2\beta}; \tag{30}$$

$$U_n(\infty) = \left(\frac{1+\beta}{1-\beta} \right)^{-1/2\beta} \left[\frac{1}{\sqrt{\eta}} + \frac{\sqrt{\eta}}{\beta} \ln \left(\frac{1+\beta}{1-\beta} \right) + 2 \left(\frac{1+\beta}{1-\beta} \right)^{-1/2\beta} \right] - 1; \tag{31}$$

2. $\eta = 1$

$$k_1 z_\infty = 1; \tag{27'}$$

$$M_i(\infty) = \frac{M_0 e^{-1}}{i!} (i-1); \tag{28'}$$

$$\bar{n}_n(\infty) = e = 2.73; \tag{29'}$$

$$\bar{n}_w(\infty) = 3; \tag{30'}$$

$$U_n(\infty) = 3/e - 1 = 0.103 \tag{31'}$$

3. $\eta > 1$

$$k_1 z_\infty = \frac{\arctan \beta}{\beta} = \frac{\arccos(1/\sqrt{\eta})}{\beta} = \frac{\pi - 2\varphi}{2\beta}; \tag{27''}$$

$$M_i(\infty) = \frac{M_0 \eta}{\eta - 1} \exp \left(\frac{2\varphi - \pi}{2\beta} \right) \frac{\sin[(i-1)\varphi]}{\cos^{i-2} \varphi} - \frac{M_0 \eta}{\eta - 1} \exp \cdot$$

$$\cdot\left[\frac{\eta(2\varphi-\pi)}{2\beta}\right]\sum_{q=0}^{i-2}\frac{1}{(i-q-2)!}\left[\frac{\eta(\pi-2\varphi)}{2\beta}\right]^{i-q-2}\frac{\cos\varphi q}{\cos^q\varphi}; \tag{28''}$$

$$\bar{n}_n(\infty)=\sqrt{\eta}\exp\left(\frac{\pi-2\varphi}{2\beta}\right); \tag{29''}$$

$$\bar{n}_w(\infty)=1+\frac{\eta}{\beta}(\pi-2\varphi)-2\left(1-\frac{1}{\eta}\right)\exp\left(\frac{2\varphi-\pi}{2\beta}\right); \tag{30''}$$

$$U_n(\infty)=\left[\frac{1}{\sqrt{\eta}}+\frac{2\sqrt{\eta}}{\beta}-\frac{2}{\sqrt{\eta}}\left(1-\frac{1}{\eta}\right)\exp\left(\frac{2\varphi-\pi}{2\beta}\right)\right]\exp\left(\frac{2\varphi-\pi}{2\beta}\right)-1 \tag{31''}$$

These equations turn into a simple form for certain special values of η. We distinguish the following cases :

a. $1 \gg \eta \cong 0$

$$t \cong \frac{1}{M_0k_1}\lim_{\beta\to 1}\int_0^{k_1z}\frac{e^y\mathrm{d}y}{\cosh\beta y-\frac{\sin h\beta y}{\beta}}=\frac{1}{2M_0k_1}(e^{2k_1z}-1); \tag{32}$$

$$k_1z \cong \frac{1}{2}\ln(2M_0k_1t-1); \tag{32'}$$

b. $0 \cong \eta > 1$ or $1 > \eta \cong 0$

Starting from Eqs. (25) and (25'') we can show that

$$k_1z \cong 1+\arg E_i[E_i(-1)-e^{-1}M_0k_1t] \tag{26'}$$

c. $\eta \gg 1$

As $z \leqslant z_\infty$, $z_\infty(\eta=\infty)=0$ and $(\beta k_1z_\infty)_{\eta=\infty}=\pi/2$ it turns out that

$$\cos\beta y-\frac{\sin\beta y}{\beta}\cong\sin(\pi/2-\beta y)\cong\pi/2-\beta y$$

and

$$t \cong \frac{1}{M_0\beta k_1}\int_0^{k_1z}\frac{e^y\mathrm{d}y}{\pi/2\beta-y}=\frac{e^{\pi/2\beta}}{M_0\beta k_1}[E_i(-\pi/2\beta)-E_i(k_1z-\pi/2\beta)]; \tag{33}$$

$$k_1z \cong \pi/2\beta+\arg E_i[E_i(-\pi/2\beta)-e^{-\pi/2\beta}M_0\beta k_1t] \tag{33'}$$

But [9]

$$\lim_{x\to 0} E_i(-x) = \gamma + \ln x + 0(x)$$

Then

$$t \cong -\frac{e^{\pi/2\beta}}{M_0\beta k_1}\ln\left(1-\frac{2\beta k_1 z}{\pi}\right) \cong \frac{1}{M_0\beta k_1}\ln\left(1-\frac{2\beta k_1 z}{\pi}\right); \tag{34}$$

$$k_1 z \cong \frac{\pi}{2\beta}\left[1-\exp\left(-M_0\beta k_1 t\right)\right]; \tag{34'}$$

$$\bar{n}_n(t) \cong \frac{\exp\left\{\frac{\pi}{2\beta}\left[1-\exp\left(-M_0\beta k_1 t\right)\right]\right\}}{\sin\left[\frac{\pi}{2}\exp\left(-M_0\beta k_1 t\right)\right]}; \qquad t < \infty\,!; \tag{35}$$

$$\bar{n}_n(\infty) \cong \sqrt{\eta}\,; \tag{35'}$$

$$\bar{n}_w(t) \cong 1 + \pi\sqrt{\eta}\left[1-\exp\left(-M_0\beta k_1 t\right)\right] - 2\beta\exp\cdot$$

$$\cdot\left\{-\frac{\pi}{2\beta}\left[1-\exp\left(-M_0\beta k_1 t\right)\right]\right\}\cdot\cos\left[\frac{\pi}{2}\exp\left(-M_0\beta k_1 t\right)\right]; \tag{36}$$

$$\bar{n}_w(\infty) \cong \pi\sqrt{\eta}\,; \tag{36'}$$

$$U_n(t) \cong \left\{1+\pi\sqrt{\eta}\left[1-\exp\left(-M_0\beta k_1 t\right)\right]\right\}\sin\left[\frac{\pi}{2}\exp\left(-M_0\beta k_1 t\right)\right] -$$

$$-\beta\exp\left\{-\frac{\pi}{\beta}\left[1-\exp\left(-M_0\beta k_1 t\right)\right]\right\}\sin\left[\pi\exp\left(-M_0\beta k_1 t\right)\right], \quad t < \infty\,!; \tag{37}$$

$$U_n(\infty) \cong \pi - 1 = 2.14 \tag{37'}$$

Revue Roumaine de Chimie, 22, 1, 87–95 (1977)

PARTITION COEFFICIENTS AND INTERMOLECULAR FORCE PARAMETERS

Z. SIMON and E. DRASKOVITS-SCHUCH
Department of Chemistry, University of Timişoara, Bd. V. Pârvan, No. 4
Timişoara, Romania

Received February 27, 1975

Partition coefficients for benzene-water, chloroform-water, ethyl ether-water and oil-water are correlated with 7 intermolecular force parameters for the partitioned molecules (Hansch hydrophobicity-π, character in hydrogen bonding, proton donating or accepting, strong or weak—HDS, HDW, HAS, HAW, aromaticity—AR, and separate atoms with sp^2 hybridization—PI). The correlational coefficients obtained are respectively r : 0.944, 0.876, 0.783 and 0.986, i.e. rather low for solvents with a pronounced double hydrophilic-hydrophobic character (chloroform and ethyl ether). The highest partial correlation coefficients were obtained for the π, HDS and AR—parameters. No correlation is obtained with minimal steric differences with respect to the solvents.

Partition coefficients depend on the free energies of interaction between the molecular species of the two solvents and thus it is possible to obtain correlations between these partition coefficients and intermolecular force parameters. In previous papers [1,2,3] we used a set of intermolecular force parameters in structure — biologic activity correlations. The correlation coefficients thus obtained were rather low, $r = 0.7-0.75$, probably because the steric fit of the effector molecules with the rather rigid sites for biologic activity were not taken into account.

Here, we shall try to correlate organic solvent : water partition coefficients, P_{solv}, for series $i = 1, 2 \ldots$, n of molecular species. Such partition coefficients give good linear correlations with Hansch-hydrophobicities, $\pi = \log P_{oct}$, if one considers separately molecules which are good proton donors and respectively acceptors in hydrogen bonds.[4] The whole series of molecular species will be considered here, irrespective of their hydrogen bonding character. Steric fit should not intervene in partition between liquid phases, allowing a good correlation with intermolecular force parameters. On the other hand, the same solvent molecules may interact by different atomic groups with solute molecules differing in hydrophilic/hydrophobic character or proton donor/acceptor character,

---

[1] Z. Simon *Rev. Roumaine Biochim.*, **5**, 319 (1968).

[2] Z. Szabadai and Z. Simon *Rev. Roumaine Biochim.*, **9**, 337 (1972).

[3] R. Vîlceanu, A. Chiriac, Z. Szabadai and Z. Simon *Stud. Biophys.* (*Berlin*), **34**, 1 (1972), *Rev. Roumaine Biochim.*, **10**, 239 (1973).

[4] A. Leo, C. Hansch and D. Elkins *Chem. Rev.*, **71**, 525 (1971).

Table 1

Intermolecular force parameters and partition coefficients

N°	Substance	HDS	HDW	HAS	HAW	AR	PI	lg P_{OCT}	lg P_{BZ}	lg P_{OLF}	lg P_{ET}	lg P_{OIL}
1	$HCOOH$	1	0	2	0	0	3	−0.54	−2.95	−2.20	−0.45	−1.84
2	CH_3COOH	1	0	2	0	0	3	−0.17	−1.97	−1.50	−0.35	−1.60
3	$CH_2BrCOOH$	1	0	2	0	0	3	0.41	−1.41	−1.41	—	−0.72
4	$CH_3CHBrCOOH$	1	0	2	0	0	3	0.92	−0.62	−0.61	—	−0.18
5	C_2H_5COOH	1	0	2	0	0	3	0.33	−1.20	−0.78	—	−0.80
6	$CH_3CH:CHCOOH$	1	0	2	0	0	5	0.72	−0.91	−0.50	0.72	—
7	$C_2H_5CHBrCOOH$	1	0	2	0	0	3	1.42	−0.08	0.08	—	0.14
8	$n-C_3H_7COOH$	1	0	2	0	0	3	0.79	−0.65	−0.27	0.66	−0.21
9	$n-C_5H_{11}COOH$	1	0	2	0	0	3	1.88	0.67	1.05	1.88	0.83
10	C_2H_5OH	0	1	0	2	0	0	−0.32	−1.58	−0.85	−0.58	−1.52
11	$n-C_3H_7OH$	0	1	0	2	0	0	0.34	−0.87	−0.21	0.28	−0.85
12	$n-C_4H_9OH$	0	1	0	2	0	0	0.88	−0.19	0.45	0.89	−0.28
13	$n-C_5H_{11}OH$	0	1	0	2	0	0	1.40	0.19	—	—	0.36
14	$CH_3COOOCH_3$	0	0	2	0	0	3	0.18	0.47	—	0.43	−0.37
15	$CH_3COOC_2H_5$	0	0	2	0	0	3	0.73	1.01	—	0.93	0.40
16	CH_3COCH_3	0	0	2	0	0	2	−0.24	−0.04	0.72	−0.21	−0.70
17	CH_3NH_2	0	0	1	0	0	0	−0.57	−1.34	−0.56	−1.64	—
18	$(CH_3)_3N$	0	0	1	0	0	0	0.27	−0.33	0.54	−0.34	—
19	$n-C_4H_9NH_2$	0	0	1	0	0	0	0.88	0.14	0.99	0.11	—
20	$(C_2H_5)_2NH_2$	0	0	1	0	0	0	0.57	−0.02	0.81	−0.28	—
21	$n-(C_3H_7)_2NH_2$	0	0	1	0	0	0	1.73	1.05	—	0.95	—
22	$(C_2H_5)_3N$	0	0	1	0	0	0	1.44	1.13	—	—	—
23	Cyclo $C_5H_{10}NH$	0	0	1	0	0	0	0.85	−0.06	0.92	−0.24	—
24	C_6H_6(benzene)	0	0	0	0	1	0	2.13	2.97	—	—	2.22
25	C_5H_5N (pyridine)	0	0	1	0	1	0	0.64	0.42	1.43	0.08	−0.02
26	C_6H_5COOH	1	0	2	0	1	3	1.87	0.21	0.71	1.89	0.66
27	C_6H_5OH	1	0	0	0	1	1	1.46	0.36	0.00	1.64	0.81
28	C_6H_5CHO	0	0	2	0	1	2	1.48	2.10	—	1.74	—
29	$C_6H_5NH_2$	0	2	0	0	1	1	0.90	1.00	1.42	0.85	—
30	$C_6H_5CONH_2$	0	2	2	0	1	3	1.75	−0.71	0.11	−0.22	−0.51
31	$C_6H_5CH_2NH_2$	0	0	1	0	1	0	1.09	0.61	1.18	0.28	—

32	$C_6H_5B(OH)_2$	2	0	0	0	1	3	1.58	−0.80	—	—	—
33	*o*−HOC_6H_4COOH	2	0	2	0	1	4	2.26	0.45	0.48	2.37	1.00
34	*m*−$O_2NC_6H_4COOH$	1	0	6	0	1	6	1.83	0.21	0.48	0.64	—
35	*p*−$O_2NC_6H_4COOH$	1	0	6	0	1	6	1.89	0.31	0.86	—	—
36	*o*−$H_2NC_6H_4COOH$	1	1	1	0	1	4	1.21	−0.27	0.57	1.43	—
37	*m*−$CH_3C_6H_4OH$	1	0	0	0	1	1	1.96	0.88	—	1.80	1.29
38	*m*−$CH_3C_6H_4NH_2$	0	2	0	0	1	1	1.40	1.51	—	—	—
39	*o*−$CH_3C_6H_4NH_2$	0	2	0	0	1	1	1.29	1.53	—	—	—
40	*p*−$CH_3C_6H_4NH_2$	0	2	0	0	1	1	1.39	1.43	1.99	—	—
41	*o*−$C_6H_4(NH_2)_2$	0	4	0	0	1	2	0.15	−0.28	—	−0.06	—
42	*m*−$HOC_6H_4NH_2$	1	2	0	0	1	2	0.17	−1.36	—	2.20	—
43	*o*−$HOC_6H_4NH_2$	1	2	0	0	1	2	0.62	−0.84	—	—	—
44	*p*−$HOC_6H_4NH_2$	1	2	0	0	1	2	0.04	−1.65	—	—	—
45	*m*−$BrC_6H_4NH_2$	0	2	0	0	1	2	2.10	2.20	—	—	—
46	*p*−$BrC_6H_4NH_2$	0	2	0	0	1	2	2.26	2.06	—	—	—
47	*m*−$ClC_6H_4NH_2$	0	2	0	0	1	2	1.88	1.93	—	—	—
48	*o*−$ClC_6H_4NH_2$	0	2	0	0	1	2	1.90	2.13	—	—	—
49	*p*−$ClC_6H_4NH_2$	0	2	0	0	1	2	1.83	1.82	—	—	—
50	*m*−$HOC_6H_4NO_2$	0	0	4	0	1	4	2.00	0.38	—	—	—
51	*o*−$HOC_6H_4NO_2$	0	0	3	0	1	4	1.79	2.33	2.54	2.18	—
52	*p*−$HOC_6H_4NO_2$	1	0	4	0	1	4	1.91	0.15	0.08	2.04	—
53	*2,4,6*−$HOC_6H_2(NO_2)_3$	0	0	11	0	1	10	2.03	1.69	—	—	—
54	*m*−$H_2NC_6H_4NO_2$	0	2	4	0	1	4	1.37	1.31	1.61	1.71	—
55	*o*−$H_2NC_6H_4NO_2$	0	1	3	0	1	4	1.44	1.78	2.13	1.95	—
56	*p*−$H_2NC_6H_4NO_2$	0	2	4	0	0	6	1.39	0.92	1.23	1.48	—
57	*p*−$H_2NC_6H_4SO_2NH_2$	0	4	0	4	1	1	−0.83	−2.05	−1.40	−0.72	—
58	$(CH_3O)_2P(O)OCH:CCl_2$	0	0	2	4	0	6	1.40	1.46	1.43	1.36	—
59	$(CH_3O)_2P(O)OCH_2CCl_3$	0	0	2	6	0	2	0.51	−0.82	−0.10	−0.29	—
60	$C_6H_5COCH_3$	0	0	2	0	1	2	1.39	2.20	—	1.75	—
61	$C_6H_5CH_2COOH$	1	0	2	0	1	3	1.41	−0.03	0.45	1.57	0.35
62	$C_{10}H_{14}N_2$(nicotine)	0	0	2	0	1	0	1.17	0.98	1.89	—	—
63	$C_8H_{10}N_4O_2$(caffeine)	0	0	5	0	1,5	2	−0.07	−0.16	1.33	−1.30	−0.40

while the rather rigid sites for biologic activity will always present the same atomic groups for interaction. Also, the experimental values for partition coefficients have a higher precision than those for biological activities, where good correlations between partition and intermolecular force parameters are obtained, and the results may be used for gauging of regressional coefficients in correlational equations.

METHOD AND COMPUTATIONS

The structural parameters used here are essentially those defined in a paper published in 1968.[1] For a characterisation of the ability to give Van der Waals interactions the molecular weight, M, of the molecular species may be used. A better alternative is the Hansch hydrophobicity, $\pi = \log P_{\mathrm{oct}}$, related to the octanol : water partition. This parameter implicitely contains the effect of different interactions with water of different molecules.

The difference in proton donating or accepting character is taken into account by the number, HD, of proton donating X—H groups and the number, HA, of proton accepting lone electron pairs, Y : These groups are classified into strong (S) and weak (W) according to the following criteria. Generally we shall consider only X—H groups or lone electron pairs Y : which yield a high water solubility and a sensible increase of boiling temperatures for the respective pure liquids. Groups will be considered to be „strong" if partial electric charges favour hydrogen bonds, due to conjugation. The alcoholic OH—group and the NH groups of aromatic ammines and amides will be considered weak hydrogen donor groups, HDW. The NH group of aliphatic ammines will not be considered as hydrogen donor group, because NH_3 and aliphatic ammines have normal boiling temperatures — their NH groups do not form hydrogen bonds with the lone electron pairs of the N atoms. The OH groups of carboxylic acid and phenols will be considered strong hydrogen donor groups, HDS.

The two lone electron pairs of alcoholic—OH, and of etheric —O— will be considered weak hydrogen acceptor groups, HAW. The two lone electron pairs for O atoms in nitro groups, carboxyl groups (double bonded) and the one lone electron pair on the N atoms of aliphatic ammines and pyridine (basic character) will be considered strong hydrogen acceptor groups, HAS. The O atoms of OH groups in phenols and carboxylic groups will not be considered proton accepting, because these atoms have partial positive charges due to conjugation. The number of proton donating and accepting groups involved in intramolecular hydrogen bonds is substracted from the HD and HA values.

Another parameter is the number AR of aromatic cycles, as aromatic molecules have a higher affinity for aromatic solvents than for aliphatic ones.[5] For condensed cycles, AR will be given by the number of atoms of these cycles divided by 6; for benzene and pyridine AR=1. As double bonds and sp^2 hybridized atoms conjugated with phenyl cycles such as nitro groups etc., enlarge the planar conjugated system, another parameter will be introduced, PI— the number of sp^2 hybridized atoms not included into an aromatic cycle.

Table 1 lists the 63 molecular species for which the logarithms of partition coefficients for the systems n-octanol : water (P_{OCT}); benzene : water (P_{BZ}); chloroform : water (P_{CLF}); ethyl-ether : water (P_{ET}) and oil (glycerine palmitate, oleate, stearate) (P_{OIL}), have been extracted from the review of Leo, Hansch and Elkins.[4] The values for the HDS, HDW, HAS, HAW, AR and PI are also listed.

The computations were performed on an IRIS—computer of the Territorial-Computing Center of Timişoara, using the COLIN program written by S. Holban, D. Ciubotariu, I. Moţoc and M. Mracec.

Intercorrelation coefficients between the structural parameters, M, π, HDW, HDS, HAW, HAS, AR and PI are given in table 2 and between the reduced set of parameters : π, AR, PI, HD=HDS+HDW and HA=HAS+HAW in table 3. The intercorrelation coefficients are rather low, only those for the PI—M, PI—HAS and PI—HA intercorrelation exceed 0.5. The interdependence between our structural parameters is thus rather low.

---

[5] H. A. SCHERAGA *Ber. Bunsengesellschaft Phys. Chem.*, **68**, 838 (1964).

Table 2

Intercorrelation coefficients between intermolecular force parameters (complete set)

	M	π	HDS	HDW	HAS	HAW	AR	PI
M	1.000	0.416	0.050	0.060	0.489	0.343	0.426	0.566
π	0.416	1.000	0.107	−0.093	0.191	−0.253	0.427	0.293
HDS	0.050	0.107	1.000	−0.293	0.099	−0.229	0.042	0.360
HDW	0.060	−0.093	−0.293	1.000	−0.381	0.121	0.403	−0.131
HAS	0.489	0.191	0.099	−0.381	1.000	−0.118	0.119	0.778
HAW	0.343	−0.253	−0.229	0.121	−0.118	1.000	−0.273	−0.069
AR	0.426	0.427	0.042	0.403	0.119	−0.273	1.000	0.179
PI	0.566	0.293	0.360	−0.131	0.778	−0.069	0.179	1.000

Table 3

Intercorrelation coefficients between intermolecular force parameters (reduced set)

	π	HD	HA	AR	PI
π	1.000	−0.036	0.041	0.427	0.293
HD	−0.036	1.000	−0.305	0.431	0.062
HA	0.041	−0.305	1.000	−0.035	0.674
AR	0.427	0.431	−0.035	1.000	0.179
PI	0.293	0.062	0.674	0.179	1.000

Partial correlation coefficients of structural parameters with partition coefficients for various solvents are given in table 4. Correlations with minimal steric differences, MSD, refer to the partner solvent of water in the pair; the molecule is superposed over the molecule of the organic solvent and the unsuperposable second raw atoms are counted.[6] The values in brackets for the MSD$-\log P_{\mathrm{OCT}}$ correlation refer exclusively to the aliphatic molecules from table 1, those for the MSD$-\log P_{\mathrm{BZ}}$ correlation, only to aromatic molecules.

Table 5 lists the correlational equations for different sets of parameters, linear correlation coefficients, r, the number N of molecules to which the equation refers, and the mean standard deviation, s. Correlational equations are also given for sets of parameters reduced by eliminating the parameters for which the partial correlation coefficients have a significance below 95 % (i.e. for partial correlation coefficients below 0.20−0.25) for the series of substances used in the respective correlation.

RESULTS AND DISCUSSION

As it results from tables 2 and 3 the intercorrelation coefficients are rather low and the structural parameters, independent. The rather high values, over 0.5, for the PI−M, PI−HAS and PI−HA intercorrelations are rather difficult to explain; for the PI−HAS pair the high intercorrelation can be explained by the fact that sp^2 hybridized atoms favour conjugations which produce partial negative charges on atoms and thus favour stronger proton acceptance. The MSD values with respect to n-octanol are approximatively antiparallel to the π-hydrophobicities; additions of CH_2 groups will increase π, and generally decrease MSD with respect to n-octanol, a rather large molecule ($C_8H_{17}OH$).

---

[6] Z. Simon and Z. Szabadai *Stud. Biophys.* (*Berlin*), **39**, 123 (1973).

Table

Partial correlation coefficients logarithms of partition constants

	M	π	HDS	HDW	HD	HAS
$\lg P_{OCT}$	0.416	1.000	0.106	−0.116	—	0.194
$\lg P_{BZ}$	0.278	0.743	−0.437	0.050	−0.195	0.076
$\lg P_{CLF}$	—	0.517	−0.429	0.003	—	−0.091
$\lg P_{ET}$	—	0.685	0.433	0.078	—	0.148
$\lg P_{OIL}$	—	0.870	0.145	−0.242	—	−0.240

Table 5

Correlational equations

$$\lg P_{OCT} = 0.049 + 0.014\,\mathrm{M} - 0.363\,\mathrm{HDS} - 0.266\mathrm{HDW} - 0.244\ \mathrm{HAS} - 0.441\mathrm{HAW} - 0.095\mathrm{AR} + 0.130\ \mathrm{PI}; \; r = 0.697,\; s = 0.566,\; N = 63 \tag{1}$$

$$\lg P_{OCT} = 0.047 + 0.012\mathrm{M} - 0.358\mathrm{HAW} - 0.042\mathrm{PI}; \qquad r = 0.614 \tag{1a}$$

$$\lg P_{BZ} = -0.068 + 0.011\mathrm{M} - 2.123\mathrm{HDS} - 0.725\mathrm{HDW} - 0.579\mathrm{HAS} - 0.498\mathrm{HAW} + 0.903\mathrm{AR} + 0.462\mathrm{PI}; \quad r = 0.838, \quad s = 0.687, \quad N = 63 \tag{2}$$

$$\lg P_{BZ} = -0.326 + 0.004\mathrm{M} - 1.043\mathrm{HDS} + 0.922\mathrm{AR}; \qquad r = 0.626 \tag{2a}$$

$$\lg P_{BZ} = -0.256 + 0.989\,\pi - 1.664\mathrm{HDS} - 0.378\mathrm{HDW} - 0.285\mathrm{HAS} - 0.167\mathrm{HAW} + 0.612\mathrm{AR} + 0.249\mathrm{PI}; \quad r = 0.944, \quad s = 0.414, \quad N = 63 \tag{2b}$$

$$\lg P_{BZ} = -0.692 + 1.198\,\pi - 1.183\mathrm{HDS} + 0.278\mathrm{AR}; \qquad r = 0.912 \tag{2c}$$

$$\lg P_{BZ} = -0.565 + 1.022\,\pi - 0.389\mathrm{HD} - 0.054\mathrm{HA} + 0.721\mathrm{AR} - 0.065\mathrm{PI}; \quad r = 0.809, \quad s = 0.739, \quad N = 63 \tag{2d}$$

$$\lg P_{BZ} = -1.068 + 1.107\,\pi + 0.285\mathrm{AR}; \qquad r = 0.750 \tag{2e}$$

$$\lg P_{CLF} = 0.601 + 0.840\,\pi - 1.830\mathrm{HDS} - 0.421\mathrm{HDW} - 0.263\mathrm{HAS} - 0.166\mathrm{HAW} + 0.462\mathrm{AR} + 0.207\mathrm{PI}; \quad r = 0.876, \quad s = 0.539, \quad N = 40 \tag{3}$$

$$\lg P_{CLF} = 0.132 + 1.042\,\pi - 1.356\mathrm{HDS} + 0.022\mathrm{AR}; \qquad r = 0.818 \tag{3a}$$

$$\lg P_{ET} = 0.111 + 0.511\,\pi + 0.046\mathrm{HDS} - 0.153\mathrm{HDW} - 0.344\mathrm{HAS} - 0.094\mathrm{HAW} + 0.423\mathrm{AR} + 0.306\mathrm{PI}; \quad r = 0.783, \quad s = 0.653, \quad N = 41 \tag{4}$$

$$\lg P_{ET} = -0.162 + 0.589\,\pi + 0.391\mathrm{HDS} + 0.184\mathrm{AR} + 0.077\mathrm{PI}; \; r = 0.736 \tag{4a}$$

$$\lg P_{OIL} = -0.479 + 1.111\,\pi - 0.677\mathrm{HDS} - 1.035\mathrm{HDW} - 0.056\mathrm{HAS} + 0.151\mathrm{HAW} + 0.165\mathrm{AR} + 0.013\mathrm{PI}; \quad r = 0.986, \quad s = 0.157, \quad N = 24 \tag{5}$$

$$\lg P_{OIL} = -0.984 + 0.907\,\pi + 0.235\mathrm{AR}; \qquad r = 0.877 \tag{5a}$$

As for the partial correlation coefficients of table 4 and the respective coefficients in equations (1—5) of table 5 the following conclusions are resulting. There is no statistically significant correlation with MSD values when the organic solvent molecule is used as standard. The rather high values of r (MSD) for octanol especially for aliphatic molecules is due to antiparallelism of MSD with π-values, as discussed above. The effect of the molecular configuration upon partition coefficients is negligible, as expected, if the corresponding solvents are practically randomised as compared to the crystalline state.

The solvents, among which partition are used here, with the exception of oils, triesthers of fatty acids, have only one type of proton donating or accepting groups for hydrogen bonds (the "weak" type). One can expect therefore a constant quotient of the regressional coefficients for the structural parameters HDS and HDW and respectively for HAS and HAW in the correlational equations. This is not observed

4

ve, intermolecular force and MSD parameters

HAW	HA	AR	PI	$\frac{\text{MSD}}{\text{(SOLV)}}$
−0.274	—	0.181	0.302	−0.367(−0.527)
−0.216	−0.045	0.411	0.061	−0.037(−0.081)
−0.158	—	0.393	−0.015	—
−0.219	—	0.395	0.466	+0.039
−0.235	—	0.511	−0.123	—

for the OCT/H_2O, BZ/H_2O, ET/H_2O and OIL/H_2O solvent pairs, the quotients of the HDS :HDW coefficients in the equations of table 5 being respectively +1.35 ; +4.4 ; +4.35 ; −0.3 and +0.65 while for the quotients of the HAS :HAW coefficients they are +0.55 ; +1.7 ; +1.6 ; +3.65 and −0.35. Strong proton donating groups, HDS, decrease significantly the BZ/H_2O, CLF/H_2O partition coefficients but increase the coefficient for the ET/H_2O partition (ethyl-ether presents 2 proton accepting lone electron pairs). The reduced set of parameters which does not distinguish between "strong" and "weak" proton donor and acceptor groups gives a sensibly reduced correlation coefficient for the BZ/H_2O partitions (compare eqs. 2b and 2d).

Aromatic species, AR, have an increased BZ/H_2O partition coefficient, but the CLF/H_2O, ET/H_2O and OIL/H_2O partition coefficients are also increased. The influence of sp^2 hybridized atoms (PI) not included in aromatic cycles is more difficult to ascertain. According to the correlational equation this structural feature increases the solubility in non-aqueous solvents, while partial correlation coefficients (with respect to PI, tab. 4) are often low.

As for the correlation coefficients obtained (tab. 5), they are lower than those obtained with the pair of correlational equations (for proton donor, *D*, and acceptor, *A*, species respectively) ; [4]

$$\lg P_S = a_s^{D,A}\,\pi + b_s^{D,A} \tag{6}$$

The use of π instead of M (compare eqs. 2 and 2b, tab. 5) increases sensibly the correlation for the BZ/H_2O partition ; the effect of a different solvent environment for different molecules is accounted for by π, at least for one of the solvents (H_2O) in the pair. The correlation is best for BZ/H_2O and OIL/H_2O partition, i.e. for organic solvents with rather unpolar molecules (benzene, oil) than for organic solvents with a marked dipolar character (octanol, ethyl-ether). The correlation will be sensibly decreased if the number of structural parameters is reduced, by substituting HDS and HDW with HD and respectively HAS and HAW by HA, or if the parameters with a significance below 95% are eliminated.

The concentrations X_s^k of the "sites" for different types k of intermolecular forces in different solvents S were calculated according to:

$$X_s^k = \frac{1.000\cdot\bar{\rho}_s}{\bar{M}_s}(X_s^s\, x_s^k + X_{\mathrm{H_2O}}^S\cdot x_{\mathrm{H_2O}}^k) \therefore \bar{M}_s = X_S^S M_S + X_{\mathrm{H_2O}}^S\cdot M_{\mathrm{H_2O}} \quad (7)$$

X_S^S and $X_{\mathrm{H_2O}}^S$ are the molar fractions of pure solvent and water in the solvent saturated with water; they are taken from the review of Leo, Hansch and Elkins,[4] as well as the corresponding mean densities $\bar{\rho}_s$. The results are listed in table 6. An equilibrium constant a_k for the interaction of each intermolecular force type of the molecule with the complementary type on the solvent was computed according to:

$$a_k = \frac{C_s^k}{X_s^k - X_{\mathrm{H_2O}}^k} \quad (8)$$

with C_s^k the regressional coefficient for the structural parameter k in the correlational equation for S/H_2O partition of table 5. The calculated a_k constants are listed in table 7.

Table 6

Intermolecular force characteristics for solvents saturated with water
($X_S^K \equiv$ concentrations of sites for intermolecular forces)

Solvent S,	K : X_S^K K = π	HDS	HDW	HAS	HAW	AR	PI
H_2O	−65.5	0	55.5	0	1.11	0	0
OCT $C_8H_{17}OH$	17.8	0	6.27	0	12.55	0	0
CLF $CHCl_3$	4.9	0	0.68	0	1.36	0	0
BZ C_6H_6	23.9	0	0.025	0	0.05	11.1	0
ET $(C_2H_5)_2O$	9.0	0	0.70	0	20.32	0	0

Table 7

"Normalized" correlation coefficients (a_k, for eqs 1–5)

Solvent S	$a_k : K=\pi$	HDS	HDW	HAS	HAW	AR	PI
OCT/H_2O	—	0.0037	0.0026	0.0050	0.0090	—	—
BZ/H_2O	0.010	0.0191	0.0065	0.0051	0.0030	0.54	—
CLF/H_2O	0.012	0.0038	0.0024	0.0047	0.0030	—	—
ET/H_2O	0.007	−0.0005	0.0017	0.0062	0.0017	—	—

The pairs $\pi-\pi$, HDS and HDW—HAS and HAW, and AR—AR were considered as complementary intermolecular force types according to our previous papers.[1,2] They differ much from one solvent pair to another, indicating that intermolecular interactions cannot be classified into complementary pairs and interactions between types of forces as π—PI, HDS—AR, etc. cannot be neglected. Also the way the X_s^k concentrations of intermolecular types are computed (eq. 7) neglects the possibility of differential interactions of a solvent with different molecular species.

CONCLUSIONS

The use of a set of 7 intermolecular force parameters characteristic for different molecules increases sensibly the correlation with solvent : water partition coefficients, as compared with the results obtained by the use of Hansch hydrophobicities only, without separating the solvents in proton donors and proton acceptors. Good correlation, with $r > 0.90$, are obtained only for solvents with molecules having a uniform spatial distribution of groups able to form different types of intermolecular forces (i.e. not polar and apolar molecular ends). Configurational similarity of molecules with the solvent does not seem to have any influence.

It is not easy to explain the values of regressional coefficients in the correlational equations. An attempt to obtain interaction constants for pairs of complementary intermolecular force types, has failed.

The set of intermolecular force parameters used here (π, AR, HDS, HDW, HAS, HAW) may be used for orientative predictions of solubility or partitions between pairs of nonmiscible solvents.

Revue Roumaine de Chimie, **22**, *1*, 97 – 102 (1977)

THE ORIGIN AND THE TYPE OF ACTIVE CENTERS IN SOLID ACID CATALYSTS. II[1]

TRANSALKYLATION OF TOLUENE ON $Al_2O_3-SiO_2$ CATALYST

I. V. NICOLESCU, OLGA ŞERBAN, I. SĂNDULESCU and
LILIANA STOICESCU
Institute of Chemistry, Department of Chemical Technology & Catalysis, Splaiul
Independenţei Nr. 89, Bucharest 6, Romania

Received February 11, 1975

The transalkylation of toluene has been studied as depending on the thermal treatment of alumina-silica catalyst (25% Al_2O_3), which influences the formation and concentration of acid centers. A lower temperature thermal treatment was proved to ensure a maximum selectivity of the catalyst towards transalkylation reaction. The authors consider that, very likely, the presence of B+L (Brönsted + Lewis) center couple in given concentration favours the dealkylation, which accompanies the transalkylation reaction.

1. INTRODUCTION

In the process of alkylbenzene transalkylation amorphous acid catalysts have been used such as $Al_2O_3-SiO_2$,[2,3] $Al_2O_3-B_2O_3$,[4] $Cr_2O_3-B_2O_3-Al_2O_3$,[5] and synthetic zeolites.[6,7]

The catalysts are characterized by their acidic function, which achieves the main transalkylation reaction as well as secondary isomerization and dealkylation reactions.

The studies of transalkylation reaction have suggested that the active centers are protonic centers of Brönsted type.

In the present work a study of the activity of alumina-silica catalyst in the transalkylation of toluene has been undertaken aiming at specifying the distinct species of acid centers which participate in the formation of reaction intermediaries.

---

[1] Part I: I. V. Nicolescu, O. Şerban, A. Ionescu and O. Popescu-Vlădoianu, *Anal. Univ. Bucureşti Chimie*, **2**, 51 (1971).

[2] E. Boldcker, U. S. Pat. 2 795 629 July 2 1952; *Chem. Abstr.*, **52**, 12247 (1958).

[3] A. Mamoru, E. Etsuro and A. Ozaki, *Bull. Jap. Petr. Inst.*, **7**, 46 (1965).

[4] V. Izumi and T. Shiba, *Bull. Chem. Soc. Japan*, **37**, 1797 (1964).

[5] S. Kovach and G. O. Michaels, U. S. Pat. 3 260 764, July 11 1966; *Chem. Abstr.* **64**, 11125 (1966).

[6] J. Isakov and K. Minachev, *Neftekhimia*, **7**, 561 (1967).

[7] H. Matsumoto and Y. Morita, *Bull. Jap. Petr. Inst.*, **10**, 8 (1968); **11**, 40 (1969).

Use has been made of industrial alumina-silica (25% Al_2O_3) which is employed in the catalytic cracking of fuel oil. The alumina-silica was subjected to various thermal treatments which influence the concentration of acid centers as well as their formation and transformation.

a. The transalkylation reaction:

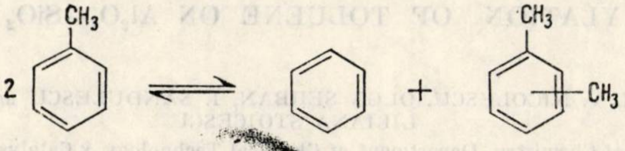

b. The dealkylation reaction:

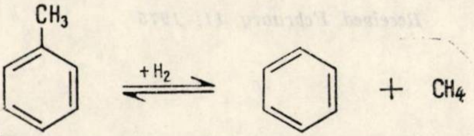

c. The isomerization reaction:

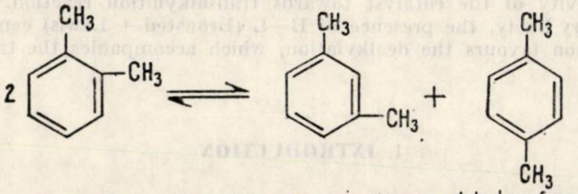

d. The cracking reaction with carbon deposition on catalyst surface.

2. RESULTS AND DISCUSSION

The study of toluene transalkylation has been conducted as a function of the thermal treatment of the catalyst, of the volume rate and of the reaction temperature.

The alumina-silica has been calcined for three hours at 500, 600, 600 and 800°.

In this paper the catalysts are labelled by subscripts according to the temperature of the thermal treatment, like $Al-Si_{500}$, $Al-Si_{600}$, $Al-Si_{700}$, $Al-Si_{800}$. The catalysts were granulated to 1.6 :1.25 mm. A fresh catalyst sample was employed in every reaction; reactions were carried out in microreactors with dynamic flow which eliminate the diffusion effects.

The reaction products were analyzed chromatographically on a column of 3.5 m length and 4 mm diameter; the stationary phase was Silicone Oil MS 555 + Bentone 34 on W-Chromosorb of 80—100 mesh.

The catalyst activity has been expressed as apparent reaction rate according to the simplified equation:

$$r_c = F_A/W \cdot X_c \ (\mathrm{mol \cdot g^{-1} \cdot h^{-1}})$$

where F_A stands for the number of moles of raw material fed in, W for the amount of catalyst (in grams) and X_c for the conversion of toluene as resulted from chromatographic data.

In order to elucidate how the reaction proceeds, the transalkylation of toluene was studied first as a function of the volume rate on one catalyst, that is $Al-Si_{600}$, and at various temperatures.

The experimental results for a variable volume rate, but constant temperature (500°) and for variable temperature are shown in Figures 1 and 2, respectively.

Examination of these figures shows that the reactions which express the conversion of toluene are favoured by the maximal time of contact and by the higher temperatures.

The B/X ratio, that is the ratio moles of benzene over xylene sum, shown in Figure 3 is larger than unit for the lowest reaction temperature i.e. 440°. At the maximum reaction temperature, 500°, this ratio increases to 1.85 due to the pronounced reaction of toluene dealkylation; for this condition of reaction the toluene conversion is highest (Fig. 3).

The variation of the reaction rate with temperature follows Arrhenius' law, which is shown in Figure 4; the slope of the line has given an apparent activation energy of reaction of $E_a = 8.9$ kcal/mole, which is similar to values given elsewhere.[8]

Further on, the influence of the thermal treatment upon the behaviour of the catalyst has been investigated.

The reaction was carried out at 500°, which corresponds to minimum selectivity of the transalkylation reaction and to maximum dealkylation, so that B/X ratio was maximum. Thus one can give qualitative indications on the specificity of active centers which are involved in dealkylation and transalkylation reactions.

The experimental data have indicated that the amount of benzene originating both in transalkylation reactions of toluene is largest in case of $Al-Si_{600}$ catalyst.

A plot of the variation of the apparent reaction rate versus the thermal treatment of the catalyst (Fig. 5) shows that the former is maximum for the $Al-Si_{600}$ catalyst.

It is worth studying the change of B/X ratio in case of the same catalyst with various thermal effects (Fig. 6). Regardless of the thermal effect of $Al_2O_3-SiO_2$ catalyst, B/X is larger than unit. Special references should be made of $Al-Si_{500}$ and $Al-Si_{600}$; the former favours the optimal selectivity towards the main transalkylation reaction, the B/X ratio being close to unit while in the latter the maximum of dealkylation reaction appears, besides the transalkylation reaction and B/X is maximum.

---

[8] K. TANABE, "Solid Acids and Bases, their Catalytic Properties", Academic Press, New York, 1970.

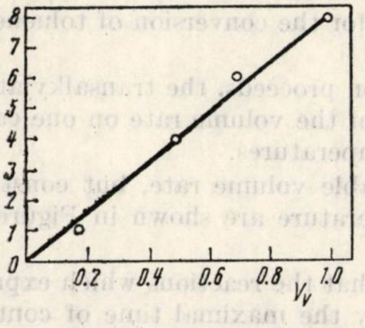

Fig. 1. — The apparent reaction rate versus volume rate.

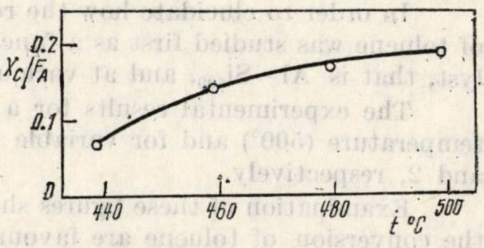

Fig. 2. — Variation of X_c/F_A ratio with the reaction temperature.

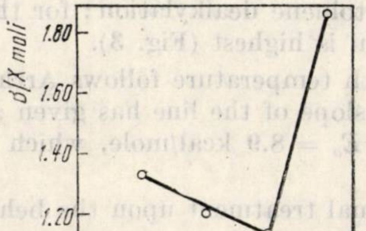

Fig. 3. — Variation of B/X ratio with the reaction temperature.

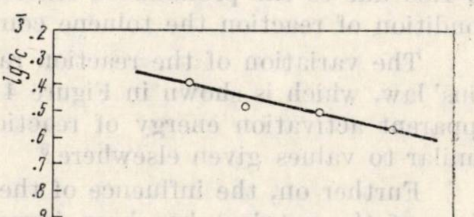

Fig. 4. — The plot of log r_c vs. $1/T$.

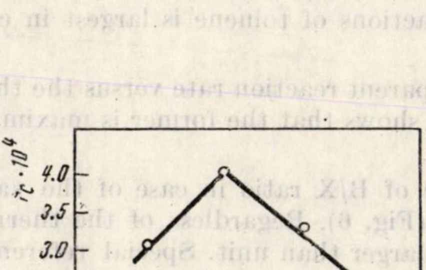

Fig. 5. — The apparent reaction rate versus the thermal treatment of the catalyst.

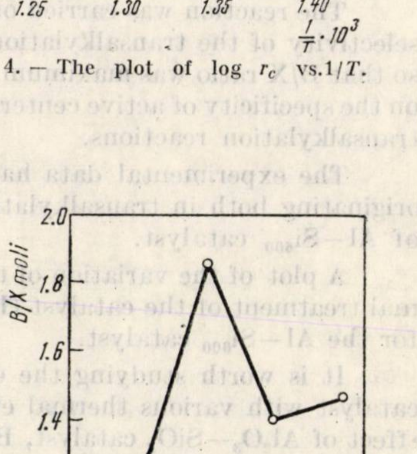

Fig. 6. — B/X ratio versus the thermal treatment of catalyst.

For higher thermal treatments, i.e. $Al-Si_{700}$ and $Al-Si_{800}$, B/X is nearly constant.

These results have determined us to affirm that this complex reaction is also controlled by species of various active centre concentrations which characterize one or another of the possible reactions. These findings have previously been pointed out elsewhere.[9,10]

In our case the formation of different active centers originates in alterations of original alumina-silica due to temperature, which have been confirmed by IR spectra in the solid as well as by IR spectra of pyridine adsorbed on $Al-Si_{600}$ and $Al-Si_{800}$ catalysts (Figs. 7 and 8).

The thermal treatment does not break the lattice of alumina-silica. The TDA diagram (Fig. 9) of the initial catalyst exhibits only the elimination of moleculary adsorbed water at 170° and an elimination of structural water at 430°.

The IR spectra within the range 1450—1800 and 3000—3800 cm^{-1} of differently treated catalysts (Fig. 7) indicate the gradual disapearance of bands characteristic of twisting vibrations of molecular water and free hydroxyls or those bonded by hydrogen bonds, respectively.

The condensed lattice of alumina-silica is formed as an effect of the thermal treatment and may result in a decrease of Brönsted acidity and the formation of acid centers of Lewis type.

The IR spectra of pyridine (Py) adsorbed upon $Al-Si_{600}$ and $Al-Si_{800}$ after processing of samples at 10^{-6} mm Hg, adsorption and desorption of pyridine at 10^{-2} mm Hg, indicate diferent concentrations of LPy and BPy centers in $Al-Si_{800}$ sample as compared to $Al-Si_{600}$ (Fig. 8).

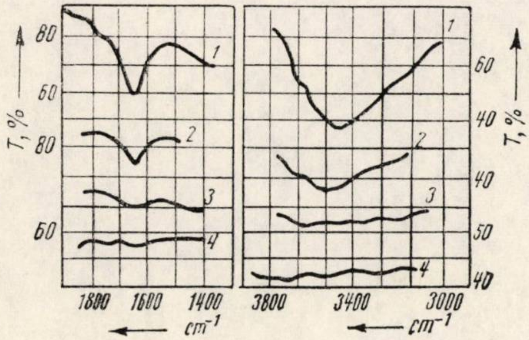

Fig. 7. — IR spectra of $Al_2O_3-SiO_2$ with various thermal treatments: *1* — 500°; *2* — 600°; *3* — 700°; *4* — 800°.

Fig. 8. — IR spectra. Pyridine adsorbed on $Al_2O_3-SiO_2$ catalyst thermally treated: *1* — 600°; *2* — 800°. →

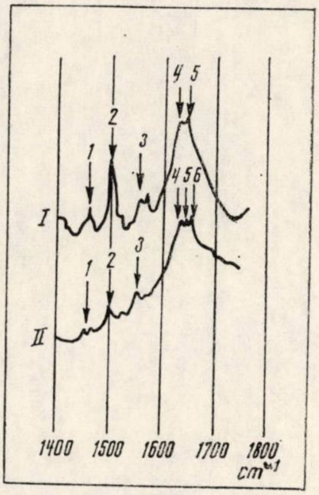

---

[9] I. V. Nicolescu and O. Şerban, *Rev. Chim.* (*Bucureşti*), **20**, 585 (1969).

[10] I. V. Nicolescu and O. Şerban, *Rev. Chim.* (*Bucureşti*), **23**, 589 (1972).

From our results one can conclude that the thermal treatment of amorphous alumina-silica catalyst with 25% Al_2O_3 influences the formation and concentration of acid centers and determines the selectivity of the catalyst towards the transalkylation reaction of toluene. The lower temperature thermal treatment ensures the maximal selectivity of the catalyst towards the transalkylation reaction.

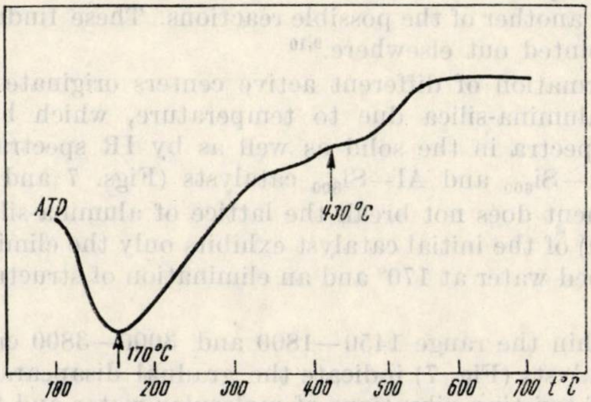

Fig. 9. — The TDA diagram of $Al_2O_3-SiO_2$ catalyst.

Very likely the presence of B+L (Brönsted + Lewis) center couples in given concentrations favours the dealkylation reaction which accompanies the transalkylation reaction. In a next work we will clear up this problem.

Revue Roumaine de Chimie, **22**, *1*, 103–116 (1977)

MEDIUMEINFLÜSSE BEI DER SOLVOLYSE VON ALKYLHALOGENIDEN. II*

SOLVOLYSE VON *t*-BUTYLCHLORID IN ACETON-WASSER-GEMISCHEN MITTLERER KONZENTRATION

R. H. SCHUSTER ** und I. A. SCHNEIDER ***
** Zentrum für physikalische Chemie, Str. Galaţi 31, Bukarest.
*** Lehrstuhl für physikalische Chemie, Institut für Chemie Iassy

Eingegangen am 27. September 1975

In Aceton-Wasser-Gemischen wurde die Reaktionsgeschwindigkeit der Solvolyse von *t*-Butylchlorid bei den Wassermolbrüchen von 0,311; 0,505; 0,636; 0,731 und 0,803 konduktometrisch im Temperaturbereich 283,1–323,1 K bestimmt. Anschließend wird die Anwendbarkeit von klassischen, auf elektrostatischer Kontinuumstheorie beruhenden Gleichungen, insbesondere die der Amis-Gleichung, zur Erklärung des Lösungsmitteleffektes diskutiert. Die Ergebnisse, sowie die „Reaktionsordnung" in bezug auf Wasser lassen auf ein polymolekulares Reaktionschema schließen. Der bestimmende Lösungsmitteleinfluß auf das gesamte Reaktionsgeschehen, (vor allem in der Aktivierungsenergie widerspiegelt) kann ausschließlich auf die Lösungsmittelstruktur zurückgeführt werden.

Zum Unterschied zu den Reaktionen in der Gasphase die einer theoretischen Besprechung einigermaßen zugänglich sind, weisen die Reaktionen in flüssiger Phase infolge der Komplexität der intermolekularen Wechselwirkungskräfte zwischen den Molekülen des Lösungsmittels und der Reaktanten erhebliche Schwierigkeiten auf. Aus diesem Grunde scheint, trotz des erstaunlichen Arbeitsaufwandes auf diesem Gebiet, eine genauere Korrelation der Reaktionsgeschwindigkeit und der Aktivierungsparameter einer Reaktion mit der Lösungsmittelzusammensetzung binärer und umsomehr ternärer Systeme noch immer ungelöst zu sein.

Die zwischenmolekularen Kräfte, die eine Assotiation der gelösten Reaktanten mit den Lösungsmittelmolekülen bewirken, sind nicht nur unspezifische und nichtabsättigbare Richt-, Induktions- und Dispersionskräfte, die eventuelle quantitative Berechnungen zulassen würden, sondern sie umfassen auch Wechselwirkungskräfte, wie z.B. Wasserstoffbrükken-Bindungskräfte, die eine spezifische Solvatation bewirken und deren Berücksichtigung bei den Ausgangsverbindungen, wie auch beim Übergangszustand eine Reihe von Aspekten prägt, denen eine quantitative Berechnung und auch die Korrelationen mit makroskopischen Größen des Lösungsmittels kaum gerecht werden kann.

---

* R. H. Schuster und I. A. Schneider, *Rev. Roumaine Chim.*, **18**, 1841 (1973).

Wie bekannt, kommt bei nucleophilen Substitutionen der Solvatation des austretenden Anions einige Bedeutung zu. Da diese durch protonische Lösungsmittel besonders begünstigt wird, scheint es von Interesse die Substitution in binären Gemischen von protonischen und aprotonischen Lösungsmitteln zu untersuchen.

Unsere Bemühungen gingen dann dahin, das Verhalten von Alkylhalogeniden, und speziell von *t*-Butylchlorid, in binären Lösungsmitteln zu untersuchen, von denen der eine Partner Wasser ist. Die Wahl von wässerigen Systemen kann kaum originell gewertet werden da eine Reihe grundlegender Arbeiten vorliegen,[1-6] doch scheint sie gerechtfertigt, da Wasser tatsächlich eine einzigartige Flüssigkeit darstellt [7-9] und immer neue Gesichtspunkte zu Tage fördert.

Die Solvolyse des *t*-Butylchlorids (*t*-BuCl) in Aceton-Wasser-Gemischen wurde schon von Fainberg und Winstein [1] und Kohnstam [10] bei verschiedenen Temperaturen und Molbrüchen Wasser untersucht. Der vorliegende Beitrag versucht daher, Lücken bei der Solvolyse des *t*-BuCl im Bereich mittlerer Wasserkonzentration zu schließen und gleichzeitig einige Gesichtspunkte im Zusammenhang mit einer anschaulichen Lösungsmittelstruktur und einem Solvolyseschema zu beleuchten.

EXPERIMENTELLER TEIL

t-Butylchlorid „Merck" (von der Firma freundlicherweise zur Verfügung gestellt), frisch destilliert ($K_p = 51{,}0°$) und dann in trockenem Aceton gelöst. Diese Standardlösung, die im Exikator bei tieferer Temperatur aufbewahrt wird, konnte etliche Wochen verwendet werden, ohne daß Konzentrationsänderungen festgestellt wurden.

Wasser für Leitfähigkeitsmessungen.

Aceton „Reactivul", wurde destilliert, anschließend getrocknet und dann fraktioniert.

Die binären Lösungsmittelgemische wurden in genügender Menge hergestellt, so daß alle Versuche in demselben Lösungsmittelgemisch ausgeführt wurden.

Kinetische Messungen. Die Versuche wurden in einer auf ± 0,05° thermostatierten Zelle eigener Konstruktion ohne freies Gasvolumen über der Lösung durchgeführt, wobei bei jedem Versuch mindestens 30 Minuten vorthermostatiert wurde. In die mit Lösungsmittel angefüllte Zelle wurde ein verhältnismäßig kleines Volumen (0,2 ml) von der Standardlösung *t*-BuCl in Aceton, bekannter Konzentration, mittels einer Hamiltonspritze eingeführt, wobei immer darauf geachtet wurde, daß die Mischzeit von geringem Wert blieb. Testversuche ergaben eine Mischzeit von cca 1 Sekunde. Die Konzentration der entstandenen Salzsäure wurde konduktometrisch, mit Hilfe eines Radelkis- Konduktometers Typ OK 102/1 bestimmt. Die Elektroden der Meßzelle waren so angebracht, daß sie eine zusätzliche Turbulenz in der magnetisch gerührten Flüssigkeit hervorriefen. Vorversuche ergaben, daß mit konzentrierter *t*-BuCl Standardlösungen kleinere Reaktionsgeschwindigkeiten erzielt werden und erst durch entsprechende Verdünnung ein Anwachsen der Reaktionsgeschwindigkeit auf konstante und gut reproduzierbare Werte erfolgte.

---

[1] S. Winstein und A. H. Fainberg, *J. Amer. Chem. Soc.*, **79**, 1602, 1608, 4146, 5937 (1957).

[2] R. E. Robertson, *Progr. Phys. Org. Chem.*, **4**, 213 (1967).

[3] J. B. Hyne, *J. Amer. Chem. Soc.*, **85**, 304 (1963).

[4] J. B. Hyne, *J. Amer. Chem. Soc.*, **85**, 3650 (1963).

[5] E. M. Arnett und D. R. Mc Kelvey, *Rec. Chem. Progr.*, **26**, 185 (1965).

[6] E. M. Arnett, W. G. Bentrude, J. J. Burke und P. McC Dugglebby, *J. Amer. Chem. Soc.*, **87**, 1965 (1965).

[7] F. Frank und D. Ives, *Quart. Rev.*, **20**, 1 (1966).

[8] H. S. Frank und W. Y. Wen, *Disscuss. Faraday Soc.*, **24**, 133 (1967).

[9] G. Nemethy und H. Scheraga, *J. Chem. Phys.*, **36**, 3401 (1967).

[10] G. Kohnstam, *J. Chem. Soc.*, **1961**, 2045.

Um den Beitrag einer Reaktion in heterogener Phase möglichst auszuschließen, kamen deshalb in Folge nur verdünnte Standardlösungen zur Anwendung.

Für eine größere Sicherheit der Meßergebnisse, sorgte ein fünfmaliges Wiederholen der Messungen, wonach der kleinste und der größte Wert von der mittleren Reaktionsgeschwindigkeitskonstante ausgeschlossen wurden. Dieses führte zu ziemlich kleinen Standardfehlern. Die größten Fehler werden im Bereich kleiner Reaktionsgeschwindigkeiten durch zeitlich sehr kleine Konzentrationsänderungen hervorgerufen, die durch die angewandte Methode schwer zu erfassen sind.

VERSUCHSERGEBNISSE UND DISKUSSION

Die Meßergebnisse der Solvolyse von *t*-BuCl in Aceton-Wasser-Gemischen für Wassermolbrüche (X_w) von 0,311; 0,505; 0,636; 0,731; 0,803 im Temperaturbereich 283,1—323,1 K sind in Tabelle 1 angeführt.

Tabelle 1

Reaktionsgeschwindigkeitskonstanten der Solvolyse von *t*-BuCl im binären System Aceton-Wasser bei verschiedenen Temperaturen (k × 10^7/sec^{-1})

Temp. K	Wassermolbruch (X_w)				
	0,311	0,505	0,636	0,731	0,803
283,1	0,116±0,003	2,46±0,03	17,0± 0,2	77,1± 0,9	320± 3
288,1	0,245±0,006	5,06±0,07	34,6± 0,5	155 ± 2	634± 6
293,1	0,505±0,001	10,15±0,2	68,3± 0,9	302 ± 4	1220± 13
298,1	0,983±0,002	19,9 ±0,3	130 ± 1,5	581 ± 7	2280± 30
303,1	1,88 ±0,03	37,2 ±0,6	245 ± 3	1050 ±10	4110± 40
308,1	3,50 ±0,07	69,3 ±1,9	445 ± 5	1890 ±20	7300± 60
313,1	6,38 ±0,02	126 ±2	787 ± 9	3310 ±40	12320±100
318,1	11,8 ±0,3	222 ±5	1360 ±20	5660 ±60	20700±180
323,1	20,9 ±0,3	381 ±5	2300 ±30	9550 ±90	34000±300

Im allgemeinen steigt die Reaktionsgeschwindigkeitskonstante (RGK) bei konstanter Temperatur mit etwas mehr als drei Größenordnungen an, wenn der Wassermolbruch von 0,311 auf 0,803 vergrößert wird. Im untersuchten Temperaturintervall von 40°, verzeichnet die RGK ebenfalls einen Anstieg um etwa drei Größenordnungen. Der beschleunigende Einfluß des protonischen Lösungsmittel Wasser auf das Reaktionsgeschehen ist wie bekannt charakteristisch für S_N1 Prozesse.

a) ABHÄNGIGKEIT DER RGK VON DER LÖSUNGSMITTELZUSAMMENSETZUNG

Wird, in erster Annäherung, ein empirischer Zusammenhang zwischen RGK und Lösungsmittelzusammensetzung angestrebt, so ergibt sich- daß log *k* von der molaren Wasserkonzentration in diesem Konzentra, tionsbereich entsprechend einer quadratischen Gleichung der Form:

$$\log k = A + Bx + Cx^2$$

abhängt, wobei den Konstanten A, B, C kaum eine Bedeutung zugeschrieben werden kann.

Sinnvoller scheint eine Korrelation von $\log k$ mit dem Wassermolbruch, die im Bereich mittlerer Wasserkonzentration ($X_w = 0{,}311 - 0{,}731$) fast linear verläuft (Abb. 1).

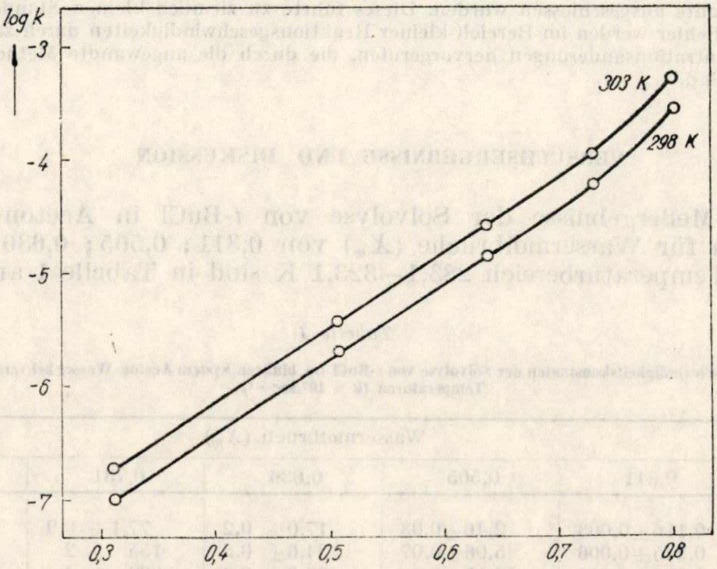

Abb. 1 – Korrelation von $\log k$ mit dem Molbruch Wasser (X_w) für zwei Temperaturen.

Der Wert für $X_w = 0{,}805$ liegt deutlich außerhalb dieser Geraden. Dieses Verhalten, das auch in der Aktivierungsenergie widerspiegelt wird, kann durch ein anschauliches Modell der Lösungsmittelstruktur erklärt werden.

Wie eingangs erwähnt, ist Wasser eine „extreme“ Flüssigkeit die aufgrund ihrer Wasserstoffbrückenbindungen quasi-kristalline Raumgitter „flickering clusters“[8] bilden kann. Bei Zugabe von apolaren oder dipolaren Nichtelektrolyten erfolgt zunächst eine Festigung der reinem Wasser entsprechenden Struktur.[9] Diese Struktur, die u.a. eine hydrofobe Hydratation bewirken kann, kann je nach Größe und Polarität des zugegebenen Nichtelektrolyten bis zu $X_w = 0{,}9 - 0{,}8$ beibehalten werden. Wird dieser Bereich überschritten, dann wird die stabile Wasserstruktur stetig abgebaut, und eine umso ungeordnetere Struktur angestrebt, je mehr Nichtelektrolyt hinzugegeben wird.

Da unsere Messungen im Bereich $X_w = 0{,}311 - 0{,}803$ erfolgten, wo also auch die obere Grenze noch an den geordneten Lösungsmittelbereich herankommt, kann angenommen werden, daß im Bereich $0{,}3 - 0{,}7$ eine lineare Korrelation zwischen $\log k$ und X_w möglich ist, da eine ungeordnete Struktur vorliegt und das Anwachsen der Konzentration des protonischen Lösungsmittels die Reaktion ungehemmt durch spezifische Solvatation der Reaktanten und (oder) des Übergangszustandes beschleunigen kann. Das Abweichen von dieser linearen Korrelation im Bereich

$X_w = 0{,}7-0{,}8$ kann nur dadurch hervorgerufen werden, daß der hinzukommende Wasseranteil in eine statistisch bestimmte, kompakte Raumstruktur eingeklemmt wird, wodurch die Solvatation des Reaktanten oder des Übergangszustandes beeinträchtigt wird. Strukturmodifikationen des Lösungsmittelgemisches scheinen somit die bedeutendsten Faktoren für die nichtlinearen Lösungsmitteleffekte zu sein.

b) ABHÄNGIGKEIT DER RGK VON DER DIELEKTRIZITÄTSKONSTANTEN DES MEDIUMS

Wie bekannt überwiegen bei einer Reaktion zwischen neutralen aber dipolaren Molekülen, die keine Wasserstoffbrückenbindung eingehen, die elektrostatischen Richtkräfte.

Ist das Reaktionsmedium im Idealfalle ein Kontinuum mit der Dielektrizitätskonstante D, so beschränkt sich der Mediumseinfluß auf eine Änderung der freien Enthalpie der Reaktanten und des Übergangszustandes. Nach Kirkwood[11] beträgt die Änderung:

$$\Delta G = -\frac{\mu}{r^3} \cdot \frac{D-1}{2D+1} \tag{1}$$

wenn als Bezugsmedium Vakuum angenommen wird ($D = 1$); wo μ das molekulare Dipolmoment und r den Molekülradius bedeuten. In die Grundgleichung der Theorie des Übergangszustandes eingesetzt, erhält man die Laidler-Eyringsche Beziehung:[12]

$$\ln k = \ln k_0 - A\,\frac{D-1}{2\,D+1} \tag{2}$$

wo A eine vom Lösungsmittel unabhängige Konstante und k_0 eine hypothetische RGK im Vakuum darstellen.

Quantitativ ist somit ein linearer Zusammenhang zwischen $\ln k$ und $(D-1)/(2D+1)$ zu erwarten. Für typische SN_2 Reaktionen wie z.B. Menschutkin-Reaktion ist das auch der Fall,[13] obwohl A stark von dem Lösungsmittel abhängt.

Unsere Meßergebnisse für die Solvolyse von t-BuCl in Aceton-Wasser-Gemischen erlauben es jedoch nicht von einer linearen Korrelation zu sprechen wie aus Abb. 2 hervorgeht, da die Abweichungen weitaus größer, als der Vertrauensbereich der Meßergebnisse sind.

Tabelle 2

Vertrauensbereiche der gemessenen log k Werte bei 298,1 K

log k	Molbruch Wasser (X_w)				
	0,311	0,505	0,636	0,731	0,803
log k (min)	−7,00838	−5,70730	−4,88739	−4,24162	−3,64666
log k (max)	−7,00656	−5,69508	−4,87517	−4,23084	−3,63658

---

[11] J. G. Kirkwood, *J. Chem. Phys.*, **2**, 51 (1934).

[12] S. Glasstone, K. J. Laidler und H. Eyring, „The Theory of Rate Processes", Mc Grow Hill, New York, 1941, 400−476.

[13] E. Tommila, *Acta Chem. Scand.*, **13**, 622 (1959).

Somit ist aber die Anwendbarkeit des obenerwähnten Modells mit Kontinuum-Dielektrizitätskonstanten zur Erklärung des Lösungsmitteleinflusses im Falle dieser Reaktion in Frage gestellt.

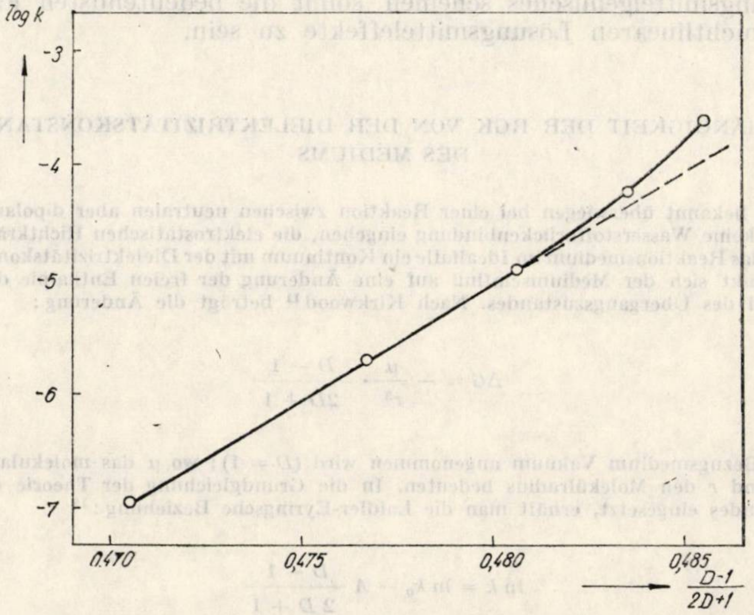

Abb. 2 – Korrelation von log k mit dem Proportionalitätsfaktor $(D-1)/(2D+1)$ der Laidler-Eyring-Gleichung.

Dieses geht noch deutlicher hervor, wenn statt der Laidler-Eyring-Gleichung, die für größere Dielektrizitätskonstanten gänzlich analoge, Amis-Gleichung[14] herangezogen wird. In dieser Gleichung wird die Coulombische Wechselwirkungsenergie zweier dipolarer Moleküle mit den Dipolmomenten μ_1 und μ_2 und einem Molekülkomplexradius $r_{\neq}$:

$$E_c = \frac{2\mu_1\,\mu_2 \cos\theta_1 \cos\theta_2}{Dr^3_{\neq}} + \frac{\mu_1\mu_2 \sin\theta_1 \sin\theta_2}{Dr^3_{\neq}} \tag{3}$$

der Aktivierungsenergie gleichgesetzt. Für eine lineare Anordnung des Komplexes ergibt sich :

$$E_c = \frac{2\,\mu_1\mu_2}{Dr^3_{\neq}}, \tag{4}$$

so daß sich für ein hypothetisches Bezugsmedium mit unendlicher Dielektrizitätskonstante $(D = \infty)$ die bekannte Gleichung ergibt[14] :

$$\ln k_D = \ln k_\infty - \frac{2\mu_1\,\mu_2}{k_B\,Tr^3_{\neq}} \cdot \frac{1}{D} = \ln k - B\,\frac{1}{D} \tag{5}$$

---

[14] E. S. Amis, *J. Chem. Educ.*, **30**, 351 (1953).

wobei k_D und k_∞ die RGK im Medium mit der Dielektrizitätskonstanten D bzw. ∞ bedeuten.

Ohne auf eine mögliche Nichtlinearität der Korrelation in k_D gegen $1/D$ näher einzugehen, läßt sich die Gleichung (5) zur Abschätzung von $r_{\neq}$ verwenden. Somit erhielt Amis[15] mit den Meßdaten von Hughes[16] für die Solvolyse von t-BuCl in Äthanol-Wasser-Gemischen für $r_{\neq}$ den Wert 0,75 Å.

Unsere Meßergebnisse bei 298,1 führen mit B(Neigung) gleich 170, und $\mu_{H_2O} = 1{,}87{,}10^{-18}$ ues. cm bzw. $\mu_{t-\mathrm{BuCl}} = 2{,}10.10^{-18}$ ues. cm zu:

$$r_{\neq} = \sqrt[3]{\frac{2.1{,}87.2{,}10.10^{-36}}{2{,}303.1{,}38.298.170.10^{-16}}} = 0{,}78.10^{-8}\mathrm{cm}$$

also einen fast gleichen Wert für $r_{\neq}$ in Aceton-Wasser-Gemischen, wie im System Äthanol-Wasser. Aus einem einfachen geometrischen Modell läßt sich aber unter Berücksichtigung der Van der Waalsschen Radien ein plausibler Wert für $r_{\neq}$ bestimmen, der für den Molekülkomplex t-BuCl $-$ H_2O bei ungefähr 3,5 Å liegen sollte und demnach 4$-$5 mal größer als der aus der Amis-Gleichung errechnete ist.

Außerdem ergeben die Berechnungen der Dipol-Dipol Wechselwirkungen für verschiedene $r_{\neq}$ und D Werte, unter Berücksichtigung, daß die makroskopische Dielektrizitätskonstante mit der in der unmittelbaren Reaktionsumgebung nicht identisch ist sondern um ungefähr eine Größenordnung kleiner ist, für den Molekülkomplex t-BuCl$-H_2O$, mit $r_{\neq} = 3{,}5$ Å Werte die um ungefähr zwei Größenordnungen unter der experimentellen Aktivierungsenergie liegen und somit der Grundhypothese der Amis-Gleichung nicht entsprechen (Tab. 3).

Tabelle 3

Dipol-Dipol Wechselwirkungsenergien (kcal/Mol) des Molekülpaares t-BuCl $-$ H_2O für verschiedene mikroskopische Dielektrizitätskonstanten und Komplexradien

D	Radien (Å)			
	0,78	2,0	3,5	4,0
1	23,842	1,413	0,236	0,175
2,5	9,536	0,562	0,102	0,070
3,5	8,137	0,480	0,089	0,060
4,0	4,767	0,282	0,052	0,035

Bei protonischen Reaktionsmedien sollte man daher auf keinen Fall den Beitrag von starken Wasserstoffbrückenbindungen (5 kcal/Mol) und von van der Waals Kräften ($\simeq$ 2 kcal/Mol) übersehen, was aber von der Amis Gleichung prinzipiell getan wird. Das wäre somit schon ein Grund diese oder ähnliche Gleichungen nicht zu der Erklärung des Lösungsmitteleffektes bei der Solvolyse von tertiären Alkylhalogeniden in protonischen Lösungsmitteln heranzuziehen.

Amis[15] schlug auch einen bimolekularen Reaktionsmechanismus als ersten Reaktionsschritt vor:

$$t\text{-BuCl} + H_2O \rightleftarrows t\text{-Bu}^+ + Cl^- \ldots H_2O$$

$$t\text{-Bu}^+ + 2H_2O \rightarrow t\text{-BuOH} + H_3O^+$$

---

[15] E. S. AMIS, „Solvent Effects on Reaction Rate and Mechanism", Acad. Press, New York, 1966, S. 66.

[16] E. D. HUGHES, *J. Chem. Soc.*, **1935**, 255.

Nun folgt aber aus dem oben Erwähnten, daß der erste Schritt der Reaktion, d.h. die Ionisation oder gar Dissoziation der C—Cl Bindung, energetisch nicht von einer einzigen Dipol-Dipol Wechselwirkung gesichert werden kann, schon eher von einem komplexen Beitrag sämtlicher Moleküle der Solvatationssphäre (sowohl der protonischen als auch der aprotonischen dipolaren Moleküle), die ein ,,Solvatationsfeld" bilden.

Man kann daher auch streng genommen nicht von einer bimolekularen Reaktion im eigentlichen Sinne im geschwindigkeitsbestimmenden Schritt sprechen, sondern viel wahrscheinlicher liegt eine polymolekulare Reaktion vor, bei der aber nur ein Lösungsmittelmolekül im Endprodukt auftritt, während die restlichen Moleküle durch ihr Feld die Ionisation der C—Cl Bindung ermöglichen.

Der Lösungsmitteleinfluß beruht demnach hauptsächlich auf Wasserstoffbrückenbildung zwischen Reaktanten und protonischen Lösungsmittelmolekülen und damit einbegriffen auf einer Ionisation des Reaktanten im Sinne des Winstein'schen Reaktionsschemas.[17] Das Vorhandensein dieser Wasserstoffbrücken ermöglicht aber auch aufgrund einer besseren Solvatation das Austreten des Anions mit einer geringeren freien Enthalpie. Das Cosolvens Aceton kann höchstens den positiven Ladungsschwerpunkt des Ionenpaares $t\text{-Bu}^+ \ldots \text{Cl}^-$ effizient solvatieren und trägt infolge spezifischer Solvatationseffekte weniger zu der RG-Beschleunigung bei.

Es darf also nicht verwundern wenn die auf elektrostatischer Grundlage abgeleiteten Gleichungen auch in äußerst großzügigen Grenzen bei der Solvolyse von t-BuCl nicht entsprechen, da sie erstens keinen wahrscheinlichen Reaktionsmechanismus vorsehen und zweitens bedeutende Wechselwirkungen vernachlässigen.

Man kann somit allgemein behaupten, daß bei Lösungsmittelgemischen von denen ein Partner protonisch ist, alle vom klassischen elektrostatischen Modell mit Kontinuums-Dielektrizitätskonstanten abgeleitete Beziehungen zwischen RGK und Lösungsmittelzusammensetzung, nur einen Teil der vorhandenen Wechselwirkungen erfassen, was in allen Fällen ein recht grobes Bild für den Lösungsmitteleffekt vermittelt.

Daher verwundert es einigermaßen, daß diese Reaktion des öfteren als Beispiel für eine lineare Korrelation $\log k$ gegen $(D-1)/(2D+1)$ oder $1/D$ herangezogen wurde.

c) KORRELATION VON $\log k$ MIT DER WASSERKONZENTRATION

Wird aufgrund des Vorhergesagten nun angenommen, daß am geschwindigkeitsbestimmenden Schritt der Reaktion die Wassermoleküle der Solvatationssphäre mit einem viel bedeutenderen Anteil als die Acetonmoleküle beteiligt sind, kann man für die Reaktionsgeschwindigkeit schreiben:

$$-\frac{\mathrm{d}\,(t\text{-BuCl})}{\mathrm{d}t} = k'\,[\mathrm{H_2O}]^{\alpha}\,[t\text{-BuCl}] \tag{6}$$

wobei die gemessene RGK sich als:

$$k = k'\,[\mathrm{H_2O}]^{\alpha} \tag{7}$$

ergibt. Der Ausdruck (7) ermöglicht dabei eine einfache, aber formelle Beschreibung des Lösungsmitteleffektes. Durch Logarithmieren erhält man:

$$\log k = \log k' + \alpha\,\log[\mathrm{H_2O}] \tag{8}$$

wo die Wasserkonzentration in Mol/l angegeben ist.

---

[17] E. S. GOULD, ,,Mechanismus und Struktur in der organischen Chemie" 2. Aufl. Verlag Chemie Weinheim, 1964, S. 297—361.

Nach der Meinung einiger Autoren[18,19] bedeutet α die Reaktionsordnung in bezug auf Wasser. Die aus unseren Daten ermittelten Werte deuten eine Temperaturabhängigkeit an und betrugen im Mittel 5,3 bei 283,1°K und 4,6 bei 323,1°K. Daraus könnte man schließen, daß sich ungefähr fünf Wassermoleküle in der Solvatationssphäre des Übergangszustandes befinden, was die Annahme eines polymolekularen Reaktionsmechanismus bestärken würde.

Nach Moelwyn-Hughes[19] kann α für Methanol-Wasser-Gemische aus dem Ausdruck:

$$\alpha = -\frac{V_w}{V_m}\left(\frac{\mathrm{d}\ln k}{\mathrm{d}\,x_m}\right)_{x_m \to 0} \tag{9}$$

bestimmt werden, wo V_w und V_m die partiell molaren Volumina für Wasser bzw. Methanol bedeuten. Im Mittel liegt der für den Grenzpunkt $x_m \to 0$ bestimmte Wert für *t*-BuCl, *t*-BuBr und *t*-BuJ bei $\alpha = 5{,}06 \pm 0{,}17$, d.h. nahe zu den von uns erhaltenen Werten. Tommila[18] dagegen mediiert den α-Wert graphisch über zwei willkürlich angenommene Lösungsmittelbereiche von 0—50% Gew. (I) und 50—100% Gew. Wasser(II). Für Aceton- oder Dioxan-Wasser-Gemische der Gruppe I erhält der Autor für die Solvolyse von Benzolsulfonsäure-isopropyl-ester einen viel geringeren α-Wert ($\simeq 2$) als für die der Gruppe II (6—7) und nimmt an, daß der α-Wert ein Kriterium zur Bestimmung des Mechanismus sei, wobei der Übergang von niederen zu höheren α-Werten eine Verschiebung von SN_2 nach SN_1 andeute.

Mit unseren Meßdaten (Tabelle 1) erhielten wir beim Auftragen von $\log k$ gegen $\log[H_2O]$ Kurven deren Neigung zu den in Tabelle 4 angegebenen α-Werten führten.

Tabelle 4

α-Werte der Solvolyse von *t*-BuCl in Aceton-Wasser bei einigen Temperaturen

Molbruch Wasser (X_w)	Temperatur (K)				
	283,1	293,1	303,1	313,1	323,1
0,311	4,3	4,1	3,8	3,6	3,5
0,505	4,5	4,4	4,3	4,0	3,9
0,636	5,0	4,9	4,8	4,6	4,5
0,731	5,7	5,5	5,3	5,2	5,1
0,803	6,9	6,6	6,4	6,2	6,1

Es wäre zu bemerken, daß die α-Werte stetig, aber nicht linear mit steigender Wasserkonzentration (Abb. 3) ansteigen und ebenfalls nicht linear mit der Temperatur abfallen (Abb. 4), Eigenheiten, auf die in den erwähnten Arbeiten nicht eingegangen wurde.

Wir sind aber nicht der Ansicht, daß in unserem Falle eine Mechanismusänderung von $SN_2 \to SN_1$ vorliegt, obwohl am Bereichsanfang die

---

[18] E. Tommila, *Acta chem. Scand.*, **9**, 975 (1955).

[19] E. A. Moelwyn-Hughes, *J. Chem. Soc.* **1962**, 5301.

α-Werte wie auch bei Tommila stets kleiner sind um dann stetig anzusteigen, da wir keinerlei Beschleunigung durch OH^- Ionen feststellen konnten. Eine solche Beschleunigung die auf einen SN_2 Beitrag hingewiesen

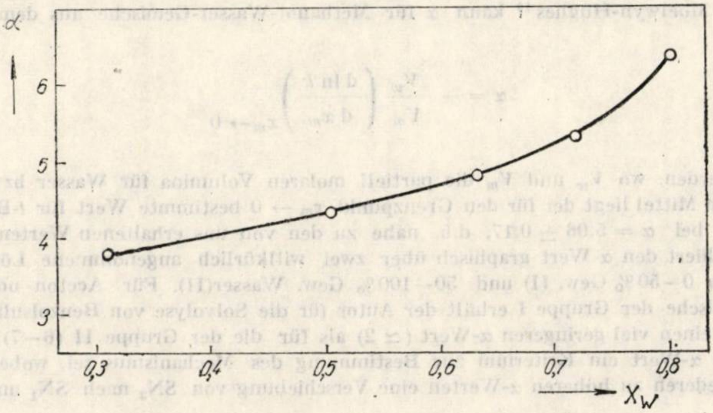

Abb. 3 – Verlauf der α-Werte mit dem Molbruch Wasser (X_w).

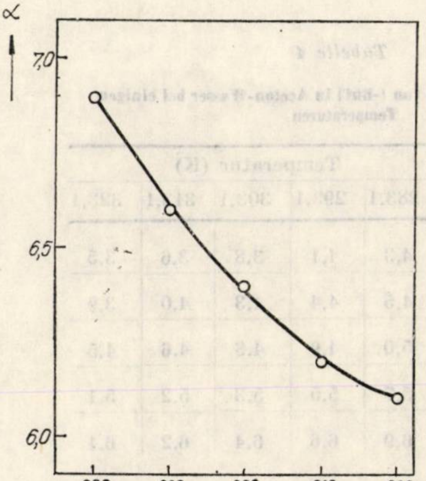

Abb. 4 – Temperaturabhängigkeit der α-Werte.

hätte wurde auch in 80% Dioxan-Wasser und Äthanol-Wasser[20] nicht gefunden. Es handelt sich eher um eine spezifische Solvatation der Reaktanten und des Übergangszustandes gemäß eines polymolekularen Solvolyseschemas wie auch aus der guten linearen Korrelation der $\Delta H^{\neq}$ mit den α-Werten geschlossen werden kann.

---

[20] O. T. Benfey, E. D. Hughes und C. K. Ingold, *J. Chem. Soc.*, **1952**, 2494.

Die Temperaturabhängigkeit der α-Werte deutet darauf hin, daß bei höheren Temperaturen eine geringere Anzahl von protonischen Molekülen die nötige Aktivierungsenergie aufzubringen vermögen, wobei in dem von uns untersuchten Konzentrationsbereich eine Temperaturerhöhung von 40° den Verlust an Wechselwirkungsenergie von ungefähr einem Wassermolekül aufwiegt.

d) AKTIVIERUNGSPARAMETER

Um die Änderung der Aktivierungsenergie mit der Lösungsmittelzusammensetzung zu erklären wurden eine Reihe von Ansätzen gemacht, wobei sich aber noch keine Ansicht allgemein durchgesetzt hat. In einer grundlegenden Arbeit versuchte Winstein[1] das Verhalten mit der Ionisationsstärke Y, ein empirischer Parameter, in Verbindung zu bringen, wogegen Hyne[21,22] die Aktivierungsenergieänderungen durch Änderungen in der spezifischen Solvatation des Ausgangszustandes und vor allem des Übergangszustandes erklärte. Arnett[23] dagegen ist der Ansicht, daß die Änderung der Solvatation des Grundzustandes ausschlaggebend sei, was auch durch mikrokalorimetrische Messungen erklärt wird.

In dem von uns untersuchten Lösungsmittelbereich sind im Großen zwei Gebiete zu unterscheiden und zwar von $X_w = 0{,}3-0{,}7$ und zwischen $X_w = 0{,}7$ gegen $X_w = 0{,}8$ wo die Lösungsmittelfestigkeit einem Maximum zustrebt, was durch ein Maximum der freien Mischungsenthalpie angezeigt ist.[24] Es ist daher anzunehmen, daß auch die Aktivierungsparameter diesen Übergang anzeigen werden.

Die aus den kinetischen Meßdaten (Tabelle 1) erhaltenen mittleren Arrhenius-Aktivierungsenergien sind in Tabelle 5 angegeben. Da, wie auch anderweitig in der Literatur[2,10,19] eine Temperaturabhängigkeit der Aktivierungsenergie aufgefunden wurde, sind die E_A Werte für 303,1 K angegeben. Auf die Temperaturabhängigkeit der Aktivierungsparameter möchten wir in einer folgenden Arbeit näher eingehen.

Tabelle 5

Mittlere Arrhenius Aktivierungsenergie für 303,1 K (kcal/Mol)

Molbruch Wasser (X_w)	0,311	0,505	0,636	0,731	0,803
E_A (kcal/Mol)	23,670	22,830	22,270	21,840	21,160

Es ist ein allgemeiner Abfall der E_A Werte zu bemerken der aber in dem Bereich $X_w = 0{,}731-0{,}803$ betonter ist. Der Verlauf der Aktivierungsenthalpie die nach :

$$\Delta H^{\neq} = E_A - RT$$

---

[21] J. B. Hyne, R. Wills und R. E. Wonka, *J. Amer. Chem. Soc.*, **84**, 2914 (1962).

[22] J. B. Hyne, *J. Amer. Chem. Soc.*, **82**, 5129 (1960).

[23] E. M. Arnett, P. Mc.C Duggleby und J. J. Burke, *J. Amer. Chem. Soc.*, **85**, 1350 (1963).

[24] A. G. Mitchell und W. K. F. Wynne Jones, *Disscuss. Faraday Soc.*, **15**, 161 (1953).

berechnet wurde, zeigt wie aus Abb. 5 hervorgeht denselben Verlauf an. Zur Erklärung dieses Verhaltens könnten nun die Auffassungen von Hyne[22] und Arnett[23] herangezogen werden. Mit steigender Wasserkonzentration im Bereich von $X_w = 0{,}3 - 0{,}7$, dem eine lockere Mischstruktur Aceton-Wasser entspricht, kann infolge der etwas besseren Solvatation des Ionenpaars, ähnlichen Übergangszustandes, als des Grundzustandes die Aktivierungsenthalpie linear abfallen. Von ungefähr $X_w = 0{,}7$ aufwärts beginnt sich eine kompaktere Mischstruktur herauszubilden, wobei zunächst die Wassermoleküle in festere tridimensionale Raumgebilde eingebaut werden und daher vor allem die Solvatation des Grundzustandes beeinträchtigt wird. Die Wechselwirkungskräfte eines dipolaren Moleküls reichen weniger aus die Wassermoleküle zur Bildung einer festen Solvatationshülle aus einer kompakten Struktur herauszulösen, als die des vorionisierten Übergangszustandes $t\text{-Bu}^+ \cdots \text{Cl}^-$. Die Folge davon ist eine viel schwächere Solvatation des Grundzustandes als des Übergangszustandes, und daher ein deutlicher Abfall des $\Delta H^{\neq}$ Wertes in diesem Konzentrationsbereich.

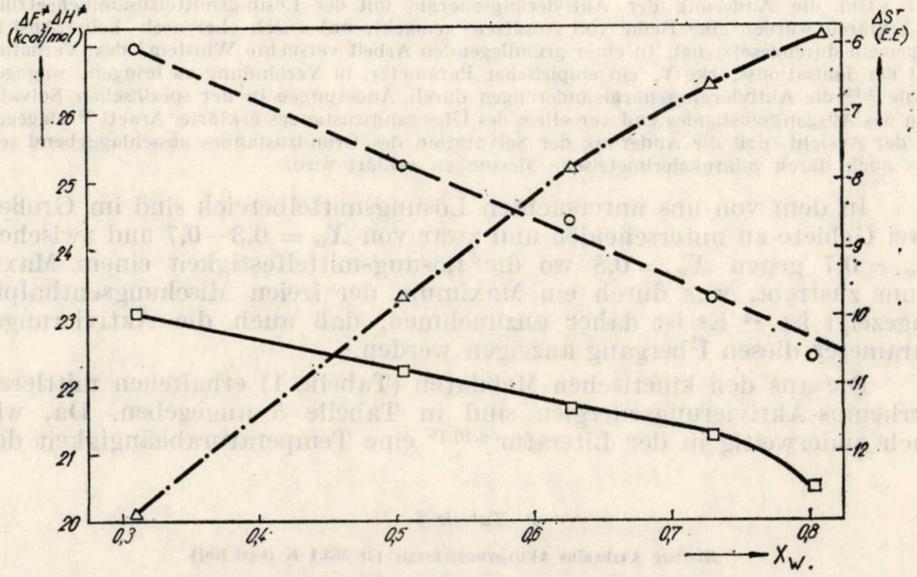

Abb. 5 – Abhängigkeit der Aktivierungsparameter von dem Molbruch Wasser (X_w) ——— $\Delta H^{\neq}$; – – – $\Delta F^{\neq}$; –.–.–.–.– $\Delta S^{\neq}$.

Wird nun der Verlauf der Aktivierungsentropie betrachtet, so ergeben sich, dem Kompensationseffekt entgegengesetzt, ansteigende $\Delta S^{\neq}$ Werte. Dieser Befund ist aber keinesfalls befremdend, da bei kleineren X_w Werten von einem viel ungeordneteren Ausgangszustand ausgehend als bei höheren X_w Werten, der geordnetere Übergangszustand erreicht wird. Diese Differenz in der Ordnung des Ausgangszustandes ist demnach für das Anwachsen der $\Delta S^{\neq}$ Werte maßgebend.

Im Rahmen der Fehlergrenze zeigen dagegen die $\Delta F^{\neq}$ Werte einen Lösungsmittel-unabhängigen Abfall.

Eine interessante Korrelation ergibt sich noch zwischen den $\Delta H^{\neq}$ und den α-Werten (Abb. 6).

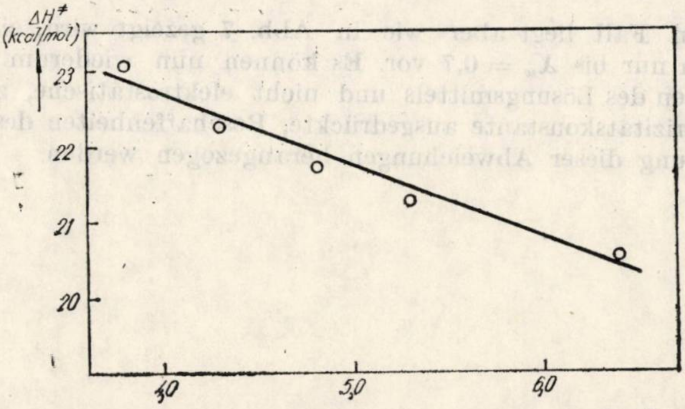

Abb. 6 — Korrelation von $\Delta H^{\neq}$ mit den α-Werten.

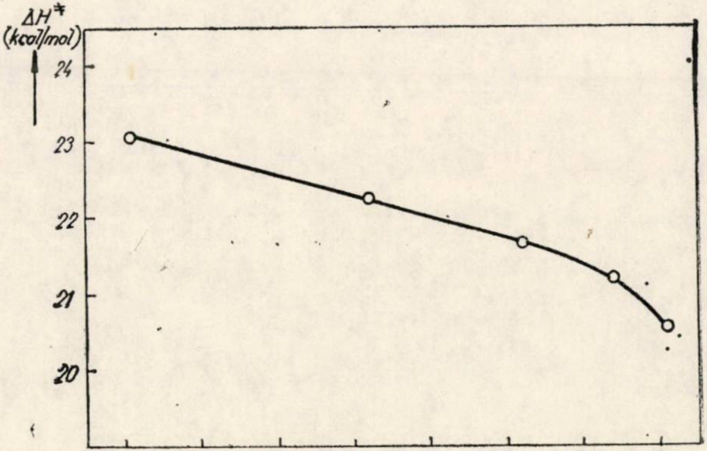

Abb. 7 — Korrelation von $\Delta H^{\neq}$ mit $\Delta S^{\neq}$ im Aceton-Wasser-Gemisch.

Wenn α die „Reaktionsordnung" in bezug auf Wasser darstellt, sind demnach an der Ionisationsarbeit des Reaktanten bei höheren X_w Werten mehr Wassermoleküle beteiligt. Das hat zur Folge, daß die Temperaturabhängigkeit der RGK etwas abfällt. Außerdem stärkt diese

Korrelation wiederum die Vorstellung eines polymolekularen Ionisationsmechanismus.

Die lineare Korrelation zwischen $\Delta H^{\neq}$ und $\Delta S^{\neq}$ wurde oft diskutiert[25] und kann aufgrund von linearen Beziehungen für Entropie und Enthalpie im Ausgangs- und Übergangszustand sowie auch durch elektrostatische Annahmen belegt werden.

In unserem Fall liegt aber wie in Abb. 7 gezeigt wird, eine lineare Korrelation nur bis $X_w = 0,7$ vor. Es können nun wiederum Struktureigenschaften des Lösungsmittels und nicht elektrostatische, z.B. durch die Dielektrizitätskonstante ausgedrückte, Beschaffenheiten des Mediums zur Erklärung dieser Abweichungen herangezogen werden.

---

[25] E. Grunwald und J. E. Leffler, „Rates and Equilibria of Organic Reactions", Wiles, New York, 1963, S. 315–402.

Revue Roumaine de Chimie, 22, 1, 117–126 (1977)

ISOTOPIC EXCHANGE OF ACTIVE METHYL HYDROGENS. VIII[1]

DEUTERIUM KINETIC ISOTOPE EFFECTS FOR α- AND γ-ISOPROPYL-SUBSTITUTED PYRYLIUM SALTS

ILEANA I. STĂNOIU,[a] FILIP CHIRALEU,[b] EUGENIA GÂRD[a]
and ALEXANDRU T. BALABAN[a,c,d]

[a] Institute of Atomic Physics, P.O.B. 5206, Bucharest, Romania
[b] Centre of Organic Chemistry, Bucharest
[c] Chair of Organic Chemistry, Polytechnic Institute, Bucharest
[d] To whom correspondence should be addressed

Received May 24, 1976

Rate constants were determined by NMR for the deuteration and de-deuteration of 2,6-dimethyl-4-isopropyl-pyrylium and 2,6-diisopropyl-4-methylpyrylium perchlorates in buffered media. An apparent kinetic isotope effect of (2.1 – 2.4 ± 0.3) was obtained in H_2O or D_2O, respectively; when acetonitrile-d_3 was employed as solvent, to eliminate solvent effects due to the isotopic composition of water, a value k_H/k_D of 1.6 ± 0.3 was found. This is interpreted as involving the formation of an intermediate α- or γ-methylene-pyran (anhydrobase). γ-Standing isopropyl groups exchange faster than α-standing ones.

In previous papers of this series, it was noted that benzylic hydrogens bonded to α- or γ-standing alkyl groups in pyrylium salts undergo isotopic exchange with D_2O or CH_3COOD. The kinetic parameters for 2,4,6-trimethylpyrylium salts were determined[1] in various buffered solutions of deuterium oxide in the pH range 1 – 4; the higher rate at higher pH values (not so high pH that pseudobase formation can lead to ring opening), as well as theoretical calculations,[2,3] indicate that this isotopic exchange involves anhydrobases (methylenepyrans). It was observed earlier[4] that the deuteration proceeds faster than the de-deuteration at the same temperature; however, these experiments were effected in non-buffered media and rested on the assumption that CH_3, CH_2D and CHD_2 groups are deuterated with the same rate, which is valid only approximately. For 2,4,6-trimethylpyrylium perchlorate, both the α and the γ methyl protons gave an isotopic effect of 2.08 (in H_2O/D_2O at 100°C)[4].

In the present paper we report the investigation of this isotopic effect in buffered solutions. In order to make the exchange simpler, we used isopropyl-substituted pyrylium salts I and V which have only one exchangeable hydrogen.

---

[1] Preceding part, E. Gârd, I. Stănoiu, F. Chiraleu and A. T. Balaban, *Rev. Roumaine Chim.*, **18**, 257 (1973).

[2] G. V. Boyd, *Rev. Roumaine Chim.*, **12**, 1133 (1967).

[3] A. T. Balaban and C. C. Renţia, *Rev. Roumaine Chim.*, **11**, 1193 (1966).

[4] E. Gârd, A. Vasilescu, G. D. Mateescu and A. T. Balaban, *J. Labelled Comp.*, **3**, 196 (1967).

The exchange of isopropyl groups was followed by integrating the ^1H-NMR signals at various times. The spectra of I and V at different degrees of deuteration are presented in figures 1 and 2, respectively (since only external TMS was employed, the absolute τ values are only approximative, but the relative peak positions are accurate).

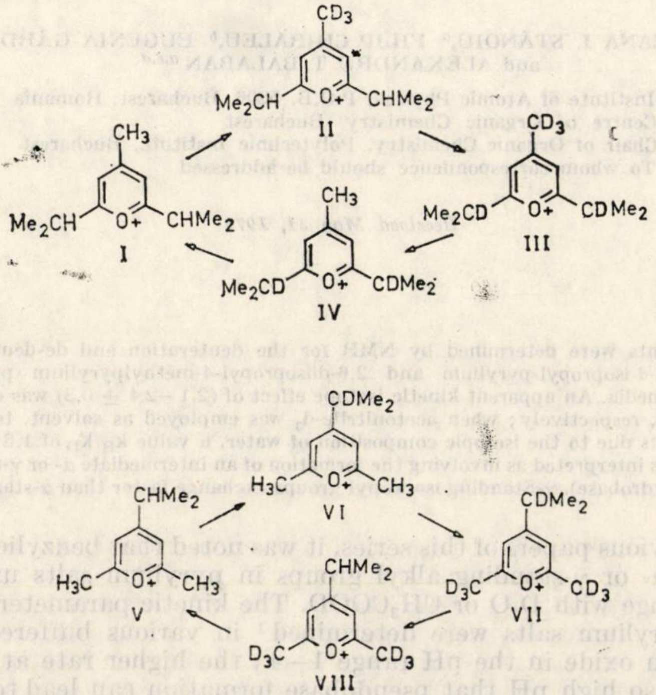

It may be observed that the deuteration has the following effects on the ^1H-NMR spectra of I and V in H_2O [or D_2O : the gradual disappearance of methyl peaks and of CH septets, and the coalescence of the methyl doublets from the isopropyl groups into a central poorly resolved closely-spaced triplet : whereas the proton (with spin 1/2) splits the methyl peak into a doublet with $J = 6.9$ Hz, the deuteron (with spin 1) produces a triplet with $J = 0.7$ Hz.

Since direct measurement of the intensity of the isopropyl CH septet is very imprecise, owing to the wide extension of this signal, to its low intensity (0–1 protons) and to overlap with the methyl peak (for V), we have chosen an indirect method for following the course of isotopic exchange : the distribution of peak intensities for methyl hydrogens belonging to the isopropyl group. The total intensity remains constant because there is no isotopic exchange of these hydrogens, but the partition between the two marginal peaks h_1 and h_2 (due to CH) and the central unresolved triplet d (due to CD) allows the kinetic measurements (h_1, h_2 and d are integral intensities measured in mm).

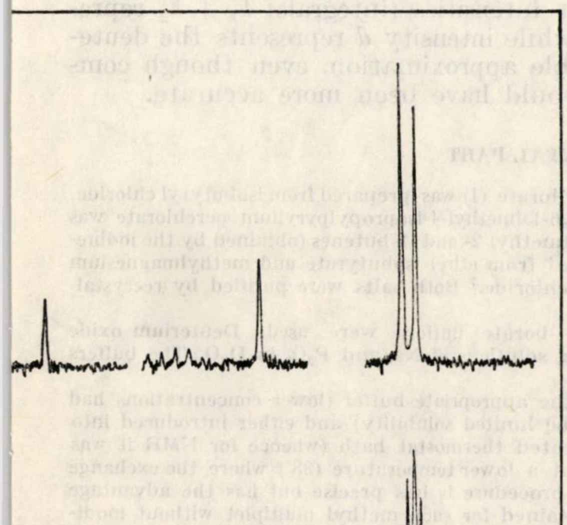

.1 .— ^{1}H–NMR spectra of 2,6-diisopropyl-4-methyl-
rylium perchlorate at various deuteration degrees :
per spectrum, non-deuterated I in H_2O ; middle spectrum,
tly deuterated II in D_2O ; lower spectrum, completely
deuterated III in D_2O (external TMS).

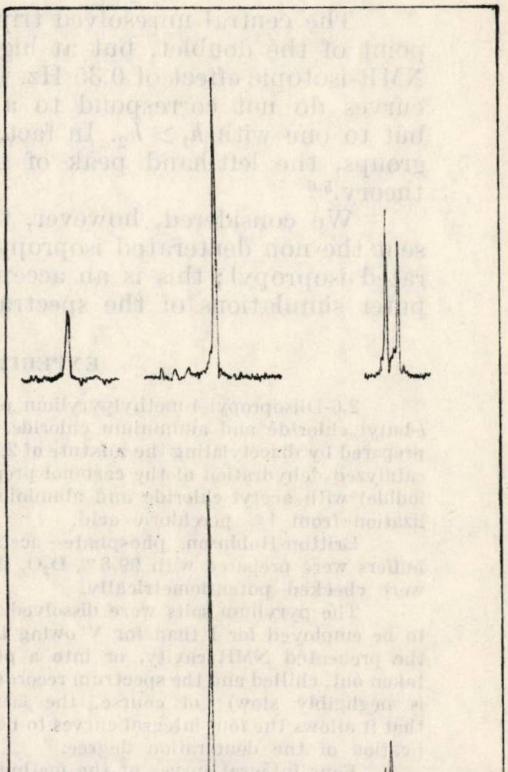

Fig. 2. — ^{1}H–NMR spectra of 2,6-dimethyl-4-isopropylpyrylium perchlorate at various deuteration degrees : upper spectrum, non-deuterated V in H_2O ; middle spectrum, partly deuterated VI in D_2O ; lower spectrum, completely deuterated VII in trifluoroacetic acid (external TMS).

The central unresolved triplet does not appear exactly at the midpoint of the doublet, but at higher field than this midpoint : this is an NMR-isotopic effect of 0.35 Hz. Because of this dissymmetry, the integral curves do not correspond to a distribution $h_1 + d + h_2$ with $h_1 = h_2$, but to one with $h_1 > h_2$. In fact, even for the non-deuterated isopropyl groups, the left-hand peak of the doublet is higher, in agreement with theory.[5,6]

We considered, however, that intensities (integrals) $h_1 + h_2$ represent the non deuterated isopropyl while intensity d represents the deuterated isopropyl; this is an acceptable approximation, even though computer simulations of the spectra would have been more accurate.

EXPERIMENTAL PART

2,6-Diisopropyl-4-methylpyrylium perchlorate (I) was prepared from isobutyryl chloride, *t*-butyl chloride and aluminium chloride. [7] 2,6-Dimethyl-4-isopropylpyrylium perchlorate was prepared by diacetylating the mixture of 2,3-dimethyl-2- and -1-butenes (obtained by the iodine-catalyzed dehydration of the carbinol prepared from ethyl isobutyrate and methylmagnesium iodide) with acetyl chloride and aluminium chloride.[7] Both salts were purified by recrystallization from 1% perchloric acid.

Britton-Robinson phosphate—acetate—borate buffers were used. Deuterium oxide buffers were prepared with 99.8% D_2O, using solutions of Na and P_2O_5 in D_2O. The buffers were checked potentiometrically.

The pyrylium salts were dissolved in the appropriate buffer (lower concentrations had to be employed for I than for V owing to the limited solubility) and either introduced into the preheated NMR cavity, or into a preheated thermostat bath (whence for NMR it was taken out, chilled and the spectrum recorded at a lower temperature (38°) where the exchange is negligibly slow); of course, the latter procedure is less precise but has the advantage that it allows the four integral curves to be obtained for each methyl multiplet without modification of the deuteration degree.

Four integral curves of the methyl region were recorded for each exchange time, and the intensities h_1, h_2 and d were averaged statistically. Small changes in the spectrometer sensitivity at time t relatively to the initial time t_1 were corrected by multiplying with a factor f which represents the ratio of total intensities $\Sigma = h_1 + h_2 + d$ at times t_1 and t.

Examples are presented in tables 1—4 where the coefficients for the linear variation of lg k *versus* time were determined by the method of least squares. Since points for longer exchange times than ca. one hour tended to be affected by larger errors, these points were omitted so that all slopes correspond to the initial part of the curves. Regressions $\lg (fd/\Sigma)$ *vs.t* for de-deuterations and $\lg (1 - fd/\Sigma)$ *vs.t* should pass through the origin; the fact that they do not (as seen in tables 1—4 there is an apparent negative t_0 of a few minutes) is due to incomplete deuteration of the sample (in de-deuterations) and to the time necessary to set up the instrument. Since, however, reactions are pseudounimolecular, this does not affect the results.

Measurements were effected with a Varian A 60 A NMR spectrometer.

RESULTS AND DISCUSSION

As in the case of deuterium exchange with methyl groups,[1-4] it was found that also with isopropyl groups, the exchange in γ proceeds faster than in α. This is due to the higher stability hence higher stationary state concentration, of γ- (IX, XI) than of α-isopropylidene-pyran

---

[5] J. W. Emsley, J. Feeney and L. H. Sutcliffe, "High Resolution Nuclear Magnetic Resonance Spectroscopy", Pergamon Press, Oxford, 1966, vol. 1, p. 341.

[6] H. Günther, "NMR-Spektroskopie", Georg Thieme Verlag, Stuttgart, 1973, pp. 45, 152.

[7] A. T. Balaban and C. D. Nenitzescu, *Liebigs Ann Chem.*, **625**, 74 (1959).

Table 1

Deuteration of 2,6-dimethyl-4-isopropylpyrylium perchlorate in D_2O buffer at pH 2.25 and 67°

Time (hrs)	Integral averaged intensities (mm)					$-\lg[(h_1+h_2)f/\Sigma]$	
	Measured				Corrected		
	h_1	h_2	d	Σ	$(h_1+h_2)\,f/\Sigma$	Experim.	Calc.
0.033	78.5	60.0	37.2	175.7	0.788	0.103	0.125
0.066	68.5	51.8	53.2	173.5	0.701	0.154	0.165
0.116	56.5	40.0	71.0	167.5	0.604	0.219	0.225
0.166	51.0	30.5	94.0	175.5	0.464	0.333	0.285
0.250	43.0	25.0	109.2	177.2	0.381	0.419	0.386
0.333	38.0	19.5	122.0	179.5	0.313	0.504	0.486
0.417	32.7	17.2	128.5	178.5	0.276	0.560	0.587

$-\lg[(h_1+h_2)\ f/\Sigma] = 0.086 + 1.202\ t.$

The correlation coefficient is 0.98.

The apparent t_0 is $-0.086/1.202 = -0.071$ hrs.

Table 2

De-deuteration of 2,6-dimethyl-4-isopropylpyrylium perchlorate in H_2O at pH 4.1 and 65°

Time t (hrs)	Integral averaged intensities (mm)					$-\lg(fd/\Sigma)$	
	Measured				Corrected		
	h_1	h_2	d	Σ	fd/Σ	Exper.	Calc.
0.050	26	14	116	156	0.744	0.130	0.133
0.100	31.5	19.5	112.5	163	0.661	0.166	0.170
0.167	37.5	22	106	165.5	0.605	0.216	0.220
0.233	42	29.5	91	162.5	0.537	0.274	0.270
0.300	49	31	79.5	159.5	0.479	0.317	0.320
0.433	57	44	59	160	0.360	0.441	0.419
0.500	61	45	58	164	0.336	0.474	0.469
0.583	65.5	49.5	49	164	0.284	0.526	0.531
0.667	68	49	44	161	0.254	0.582	0.593

$-\lg(fd/\Sigma) = 0.0966 + 0.745\ t.$

The correlation coefficient is 0.99.

The apparent t_0 is $-0.0966/0.745 = -0.13$ hrs.

Table 3

Deuteration of 2,6-diisopropyl-4-methylpyrylium perchlorate in D_2O buffer at pH 2.25 and 85°

Time t hrs	Integral averaged intensities (mm)					$-\lg[(h_1+h_2)f/\Sigma]$	
	Measured				Corrected		
	h_1	h_2	d	Σ	$(h_1+h_2)f/\Sigma$	Exper.	Calc.
0	55.7	49.7	33.2	138.7	0.761	0.118	0.090
0.083	44.2	38.2	45.7	128.2	0.694	0.158	0.151
0.166	38.7	36.2	55.2	130.2	0.609	0.215	0.213
0.250	33.5	31.0	64.5	129.0	0.536	0.271	0.275
0.350	28.0	27.5	75.0	130.5	0.451	0.346	0.346
0.416	24.5	24.2	78.5	137.2	0.357	0.447	0.398

$-\lg[(h_1+h_2)\,f/\Sigma] = 0.09 + 0.742\ t.$

The correlation coefficient is 0.97.

The apparent t_0 is $-0.09/0.742 = -0.12$ hrs.

Table 4

De-deuteration of 2,6-diisopropyl-4-methylpyrylium perchlorate in H_2O buffer at pH 4.1 and 85°

Time t hrs	Integral averaged intensities (mm)					$-\lg(fd/\Sigma)$	
	Measured				Corrected		
	h_1	h_2	d	Σ	fd/Σ	Exper.	Calc.
0.083	16	9	108	133	0.811	0.091	0.083
0.167	22	14.5	90	126.5	0.749	0.125	0.122
0.333	30	21	74.5	125.5	0.629	0.201	0.198
0.500	35.5	25.5	64	125	0.545	0.263	0.275
0.667	40	29	52.5	121.5	0.474	0.324	0.352
0.916	49.5	40	39	128.5	0.315	0.502	0.467
1.267	52	47	29.5	128.5	0.238	0.623	0.629

$-\lg(fd/\Sigma) = 0.045 + 0.461\ t$.

The correlation coefficient is 0.99.

The apparent t_0 is $-0.045/0.461 = -0.098$ hrs.

(X, XII) intermediates. Thus VI is formed much faster than VIII, and II much faster than IV. Therefore in order to obtain convenient times, reactions I→II→III and III→IV→I were effected at 80–85° while reactions V→VI and VII→VIII were performed at 65–67° (in the latter case, the α-methyl groups are only slightly affected, whereas in the former case the γ-methyl reacts completely, much faster than the more sluggish α-isopropyl groups). Therefore, methyl and isopropyl groups undergo deuteration and de-deuteration with comparable rates when this comparison is made for the same position (α or γ) of the pyrylium ring; the stability of the methylene-pyran intermediate is therefore not much influenced by its end-group $=CH_2$ (from methylpyrylium) or $=CMe_2$ (from isopropylpyrylium).

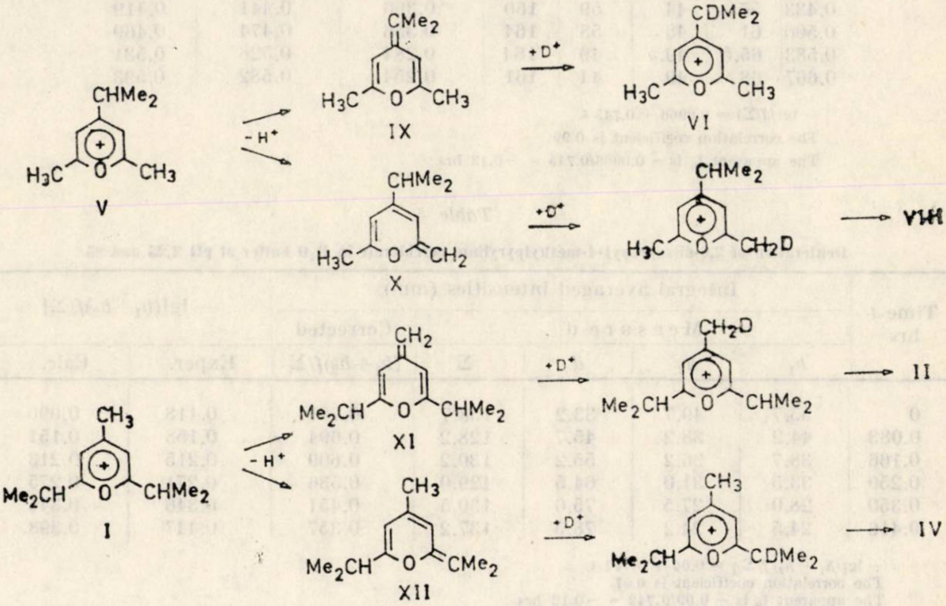
CHMe2
H3C
O
CH3
V
- H+
CMe2
H3C
O
CH3
IX
+D+
CDMe2
H3C
O
CH3
VI
CHMe2
H3C
O
CH2
X
+D+
CHMe2
H3C
O
CH2D
VIII
CH3
Me2CH
O
CHMe2
I
- H+
CH2
Me2CH
O
CHMe2
XI
+D+
CH2D
Me2CH
O
CHMe2
II
CH3
Me2CH
O
CMe2
XII
+D+
CH3
Me2CH
O
CDMe2
IV

Figures 3 and 4 illustrate the course of the deuteration of I and de-deuteration of VII, respectively (only the methyl signals of the isopropyl groups are shown).

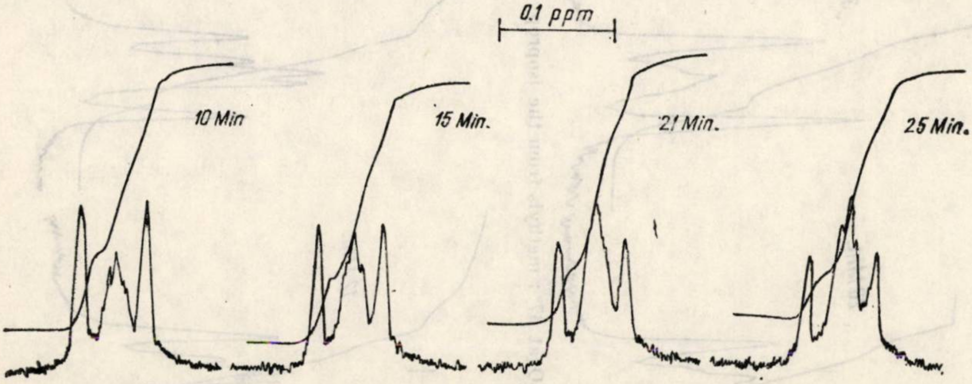

Fig. 3. — Deuteration of 2,6-diisopropyl-4-methylpyrylium perchlorate (I) in buffered D_2O at 85° : methyls of the isopropyl group.

Table 5 presents the final results with the rate constants k_H and k_D and the resulting isotope effects k_H/k_D. It may be noted that for reactions performed in H_2O or D_2O as solvent, a kinetic isotope effect of $(2.1-2.4) \pm 0.3$ is obtained.

This kinetic isotope effect k_H/k_D found for the exchange of the benzylic hydrogen in H_2O/D_2O of α- or γ-standing isopropyl groups in pyrylium salts requires first a critical examination, in order to see whether it is a real phenomenon, or on the contrary, is an artifact due to change in solvent, temperature, or reaction conditions. The last factors were excluded by employing exactly the same instrument, NMR vials, and calculation procedure for obtaining the reaction rate. The change in solvent and temperature were unavoidable, and were imposed by the reactions to be studied : deuterations had to be performed in D_2O, and de-deuterations in H_2O.

However, a check was made on the influence of the solvent on the reaction rate by performing both the deuteration of V and the de-deuteration of VII in an inert main solvent (acetonitrile-d_3) with an addition of D_2O or H_2O buffers (pH 4.2) as reaction partners (pyrylium salt concentration ca. 10 times lower than H_2O or D_2O concentration). It is noteworthy that in these conditions (fig. 5) the deuterium hyperfine splitting of the $CDMe_2$ methyl peaks is much better resolved than in D_2O or H_2O (figures 3 and 4). The results are also included in table 5.

As seen from table 5, the effect of raising the temperature from 65 to 85° is to lower somewhat the isotopic effect, in agreement with theory. However, when the temperature differences (between deuterations and de-deuterations used for calculating kinetic isotope effects) are smaller than 3°, these differences do not affect the results more than other experimental error-introducing factors.

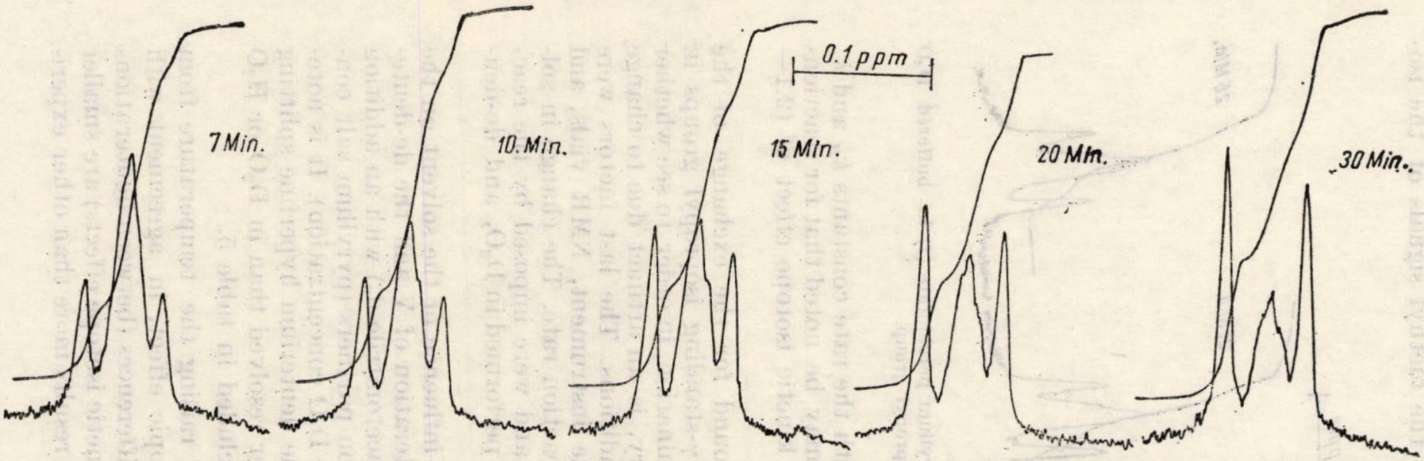

Fig. 4.—De-deuteration of 2,6-dimethyl-4-isopropylpyrylium perchlorate (VII) in buffered H_2O at 67° : methyls from the isopropyl group

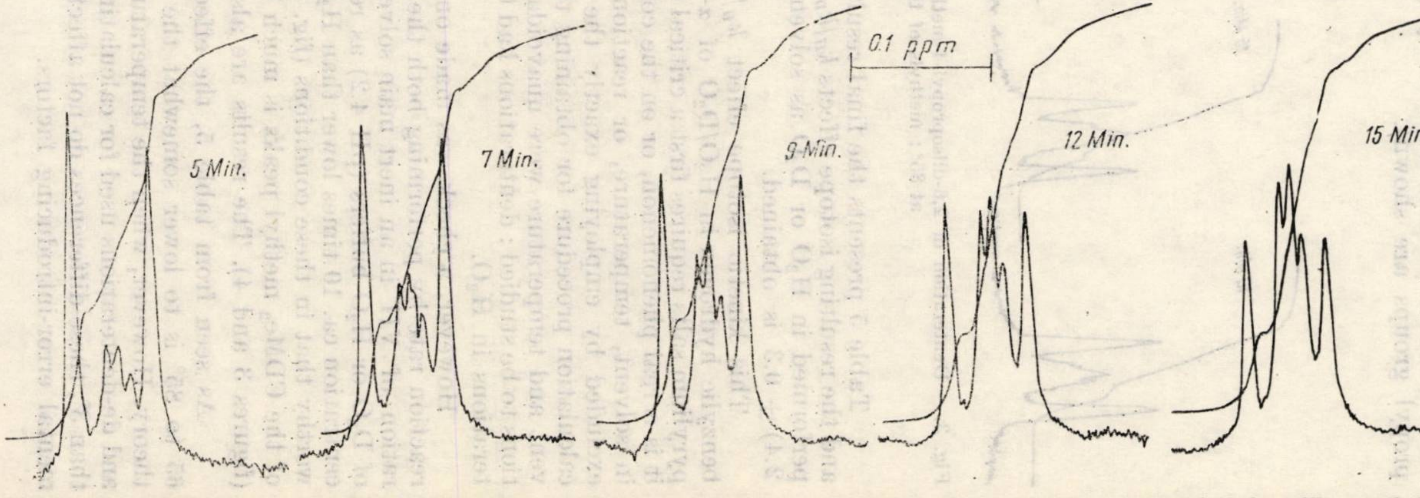

Fig. 5. — Deuteration of 2,6-dimethyl-4-isopropylpyrylium perchlorate in D_3C-CN with an excess of buffered D_2O at 67° : methyls of the isopropyl group.

The effect of the pH, apparent from table 5, is in agreement with previous data[1] and with the proposed mechanism: the higher the pH, the more readily is the reaction intermediate (methylenepyran) formed, and the higher the reaction rate. The enhancement factor in raising the pH from 1 to 4 is 1.2—1.4. It is known that the autoprotolysis factor of D_2O is different from that of water so that pD = pH reading + 0.40[8,9] However, these differences lead to errors smaller than the generous margin of ± 0.3 in the k_H/k_D values.

Table 5

Rate constants of deuterations and de-deuterations of α- or γ-standing isopropyl groups $-CHMe_2 \rightleftharpoons -CDMe_2$ in pyrylium salts and kinetic isotope effects

Temp. °C	pH	Initial		Process	k_H hrs^{-1}	k_D hrs^{-1}	k_H/k_D
		Comp.	Solvent				
2,6-Dimetyl-4-isopropylpyrylium perchlorate							
67	4.2	V	D_2O	Deuteration	2.00 2.43		2.4±0.3
65	4.1	VII	H_2O	De-deuteration		0.745 0.895	
67	2.25	V	D_2O	Deuteration	1.202		2.1±0.3
67	1.87	VII	H_2O	De-deuteration		0.603 0.760	
67	4.2	V	D_3CCN+D_2O	Deuteration	1.09		1.6±0.3
67	4.2	VII	D_3CCN+H_2O	De-deuteration		0.685	
2,6-Diisopropyl-4-methylpyrylium perchlorate							
80	4.2	I	D_2O	Deuteration	0.977		2.1±0.3
85	4.1	III	H_2O	De-deuteration		0.461	
85	2.25	I	D_2O	Deuteration	0.742		2.1±0.3
85	1.87	III	H_2O	De-deuteration		0.301 0.366	
80	4.2	I	D_3CCN+H_2O	Deuteration	0.418		1.6±0.3
80	4.2	III	D_3CCN+H_2O	De-deuteration		0.255	

Table 5 evidences that, if D_2O/H_2O as solvent is replaced by D_3CCN as solvent with a small addition of D_2O/H_2O as reagents, the observed isotope effects become smaller, namely 1.6 ± 0.3. Therefore we consider that the larger values, $(2.1-2.4) \pm 0.3$ contain both a solvent isotope effect and a kinetic isotope effect. At the same time, we have to consider

---

[8] A. F. Thomas, "Deuterium Labeling in Organic Chemistry", Appleton-Century-Crofts, New York, 1971, p. 401.

[9] P. K. Glasoe and F. A. Long, *J. Phys. Chem.*, **64**, 188 (1960).

that the kinetic isotope effect of ca. 1.6 is real, and to interpret it in terms of the reaction mechanism. It is generally agreed[10-16] that, in reactions involving only one hydrogen atom, a kinetic isotope effect $k_H/k_D > 3$ has to be interpreted as primary, and that smaller isotope effects are due to various other causes. In our case we interpret it as involving the formation of reactive intermediates (anhydrobases).

We may assume steady-state concentration of the intermediate anhydrobase (methylenepyran):

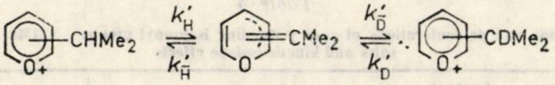

$$K_H = \frac{k'_{\bar{H}}}{k'_H}\,; \quad K_D = \frac{k'_{\bar{D}}}{k'_D}$$

Considering constant pH and overwhelming excess of H_2O or D_2O, the ratio of initial rates gives the isotope effect as

$$\frac{k_H}{k_D} = \frac{k'_{\bar{D}}\,k'_H}{k'_D\,k'_{\bar{H}}} = \frac{K_D}{K_H}$$

The experimental finding, that the isotope effect k_H/k_D is ca. 2, indicates therefore that the protoloytic equilibria involving the anhydrobase have different constants, $K_D \cong 2\,K_H$. A crude rationalization of this phenomenon considers that the ratio $k'_{\bar{D}}/k'_{\bar{H}}$ of deuteronation and protonation rates of the anhydrobase should be close to 1, while the ratio k'_H/k'_D of C—H and C—D bond breaking rates must be higher than 1 owing to the different zero-point energies; since the product of these two ratios is the isotope effect, the value of ca. 2 found experimentally is in agreement with the reaction mechanism involving the anhydrobase.

---

[10] K. B. Wiberg, *Chem. Rev.*, **55**, 713 (1955).

[11] F. H. Westheimer, *Chem. Rev.*, **61**, 265 (1961).

[12] E. R. Thornton and E. R. Thornton, in "Isotope Effects in Chemical Reactions" (ed. C. J. Collins and N. P. Bowman), Van Nostrand, New York, 1970, pp. 213, and especially p. 221.

[13] L. Melander, "Isotope Effects on Reaction Rates", Ronald Press, New York, 1960.

[14] E. A. Halevi, *Progr. Phys. Org. Chem.*, **1**, 109 (1963).

[15] W. H. Saunders Jr., *Survey Prog. Chem.*, **3**, 109 (1966).

[16] C. J. Collins, *Adv. Phys. Org. Chem.*, **2**, 3 (1964).

Revue Roumaine de Chimie, 22, 1, 127–132 (1977)

POLAROGRAPHIC REDUCTION OF SOME s-TRIAZINE HERBICIDES

SOFIA MARCHIDAN

Centre of Physical Chemistry, 31 Galaţi Street, Bucharest, Romania

Received February 4, 1976

The polarographic behaviour of Atrazine, Prometryne, and Igran has been studied as a function of pH. The experimental conditions for the analytical application of the procedure to s-triazines determination between 10^{-4} and 10^{-6} M concentration range have been established.

Some substituted s-triazines at 2,4,6 position are herbicide chemicals widely used in agriculture.

There are few reported data dealing with the polarography of s-triazines [1] and with reduction mechanism of some chlorotriazine derivatives.[2,3]

In the present paper the polarographic behaviour of Atrazine (2-chloro-4-ethylamino-6-isopropylamino-s-triazine), Prometryne (2-methylthio-4,6-bis-isopropylamino-s-triazine), and Igran (2-methylthio-4-ethylamino-6-t-buthylamino-s-triazine) was studied in order to establish a procedure for the quantitative analysis within a low concentration range of these s-triazines. Special attention was given to methylthio-s-triazine compounds scarcely investigated till now.

EXPERIMENTAL

APPARATUS

A classical equipment was used namely LP 60 polarograph with EZ 2 recorder. All experiments were carried out in Novak type cells, immersed in a thermostated bath. The working electrode was a DME. The reference electrode used was an external low-resistance SCE connected to the electrolysis cell through a salt bridge. Dissolved oxygen was removed by means of a purified argon steam. The capillary characteristics were : $m = 3.9$ mg sec^{-1}, $t = 3.02$ sec at $h_{Hg} = 35$ cm in distilled water and open circuit. An U 10 ultrathermostat and a Radiometer 22 pH-meter with G 200 B glass and K 130 calomel electrodes were used.

REAGENTS AND SOLUTIONS

All reagents were p.a. grade and s-triazines were of Geigy provenance. The following solutions were used :

– standard solutions of Atrazine, Prometryne, and Igran in 2% NaCl ;

---

[1] M. H. B. Hayes, M. Stacey and J. M. Thompson, *Chem. and Ind.*, **28**, 1222 (1967).

[2] G. S. Supin, I. A. Melnikova, T. N. Bykhovskaya and N. N. Melnikov, *Zhur. obshcheĭ Khim.*, **44**, 1208 (1974).

[3] E. Yu. Khmelnitskaya, *Elektrokhimya*, **10**, 173 (1974).

— buffer solutions of pH ranging from 1 to 11 ;

— 2% NaCl solution.

The standard solutions were prepared by dissolving a weighted amount of s-triazine (50 mg) in 5—10 ml CH_3OH and bringing it to 1000 ml volumetric flask with 2% NaCl solution.

PROCEDURE

The polarographic sample solutions were prepared in a 10 ml volumetric flask taking with the pipette different volumes of the standard solution, and adding NaCl solution up to 5 ml ; after that the buffer solution was added up to the mark and the pH value was measured. The polarograms were recorded in the potential range between —0.4 and —1.2 V (*vs.* SCE) after thermostating at 25±0.1°C and deaeration for 30 minutes.

RESULTS AND DISCUSSION

Atrazine, Prometryne, and Igran are polarographically active and yield well-defined and reproducible reduction waves (figure 1).

As can be seen in figure 1 the reduction of Prometryne and Igran occurs in a single step. For Atrazine the process proceeds in two very close, nearly overlapped steps, which could be resolved only in very strong acid solutions.

The pH of the medium has a great influence upon the reduction process. In order to establish optimum conditions for analytical purposes

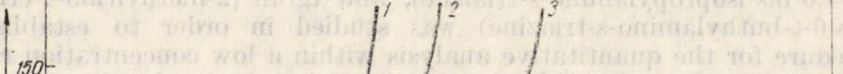

Fig. 1. — Polarograms of (1) Atrazine 10 mg/l, (2) Prometryne 20 mg/l, (3) Igran 20 mg/l, (4) residual-current curve ; pH 1.2 ; $t = 25 \pm 0.1°$.

all the pH range was investigated by using buffered solutions at pH 1 to 11 and unbuffered solutions at a pH smaller than 1 and higher than 11. Thus figure 2 shows the pH influence upon the wave height. For Atrazine the wave height decreases sensibly at a pH greater than 1.2 ; at a pH of 3 the wave becomes rather poorly defined and completely disappears at pH values greater than 4. In strong alkaline media ($pH > 12$) only a small wave occurs.

For Prometryne and Igran well-developed waves are obtained over a wide pH range but they become distorted and poorly defined as the pH values increase. In strong alkaline solutions much smaller waves than in acid medium were obtained. Thus, the pH range suitable for determinations lies between pH 1 and 2 and most of the subsequent experiments were carried out at $pH = 1.2$ in HCl—KCl buffered solutions.

The half-wave potential shifts towards more negative values as the pH increases. A linear shift of about 60 mV/pH unit is obtained between pH 0.4 and pH 6 (figure 3). This behaviour indicates the participation of one hydrogen ion in the reaction for Prometryne and Igran.

In order to define the electrode process the influence of mercury column height on the limiting current was studied. As can be seen in figure 4 at a pH 1.2 a linear dependence was obtained for Atrazine (curve 1), Prometryne, and Igran (curve 2—3) which suggests that the process is mainly diffusion-controlled. The logarithmic analysis of the polarograms, $\log i/(i_d - i)$ *vs.* E (figure 5) gives a straight line for Prometryne (curve 2) or Igran (curve 3) confirming the same diffusion character. The half-wave potentials are very close $E_{1/2} = -0.924$ V (*vs.* SCE) and -0.943 V (*vs.* SCE) respectively. The slopes of the log-plot analysis are 0.037 V and 0.036 V respectively, very near to the case of a two-electron reversible reduction process. In table 1 are listed the slopes obtained within the whole pH range. With pH decreasing, the slopes become closer to the theoretical value for a two-electron reversible reduction. At higher pH values the slopes increase, showing a modification of the electrode process.

Table 1

The slopes from log-plot analysis at various pH values

pH	Slope (volts)			
	Atrazine		Prometryne	Igran
	Ist wave	2nd wave		
0.4	0.070 *	0.036 *	0.032 *	0.029 *
1.2	0.072	0.052	0.037	0.036
2.3	0.074	0.064	0.045	0.047
3.1			0.043	
4.05			0.044	0.058
5.1	0.130 *		0.048	0.076
6.2			0.073	
10.3			0.156	
12.6			0.182 *	

* Values obtained in unbuffered media

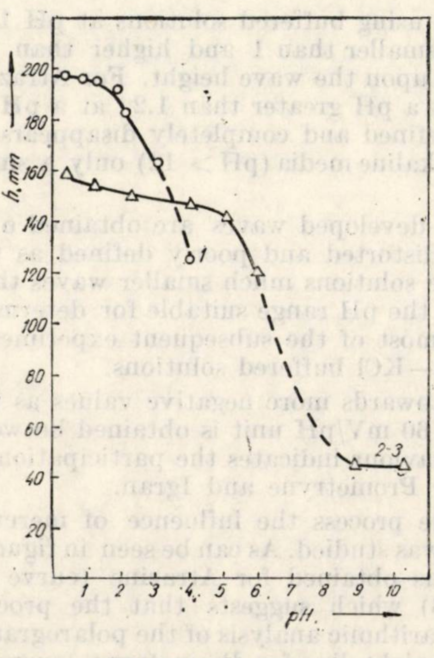

Fig. 2. — Effect of pH upon the wave height of (1) Atrazine, (2—3) Prometryne—Igran.

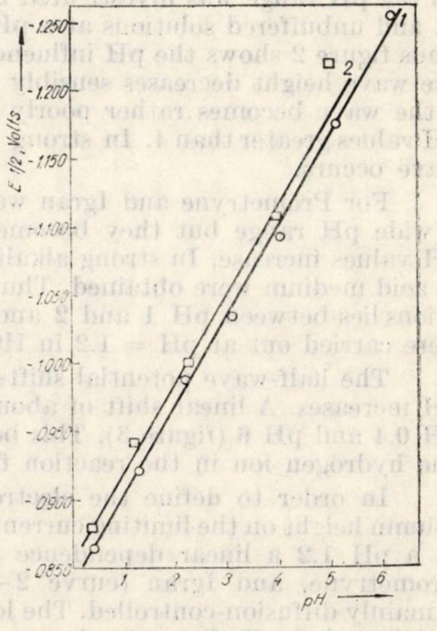

Fig. 3. — Effect of pH upon the half-wave potential of (1) Prometryne, (2) Igran.

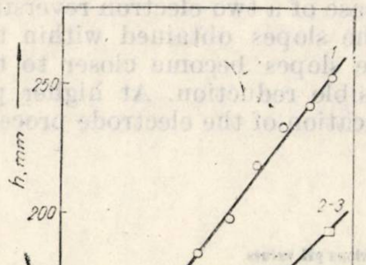

Fig. 4. — Influence of mercury column height on the wave height of (1) Atrazine, (2—3) Prometryne—Igran; pH 1.2.

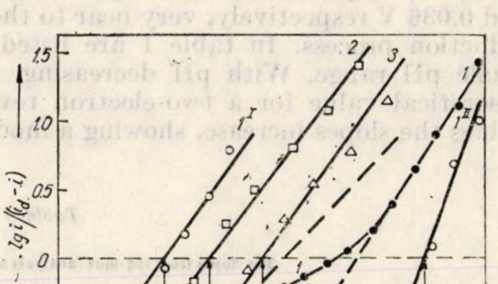

Fig. 5. — Log-plots of (1) Atrazine (total wave) pH 1.2, (1^{I}) Atrazine lst wave and (1^{II}) Atrazine 2nd wave pH 0.4, (2) Prometryne pH 1.2, (3) Igran pH 1.2.

The reduction process for Atrazine occurs in two steps which almost merge at a pH greater than 1 (figure 1, curve 1) and lead to the logarithmic plot 1, figure 5. This curve is a total diagram and presents two linear portions corresponding to the asymptotic functions of the two individual steps.[4] At a pH lower than 1, when the waves are better separated, each wave yields a straight line (figure 5, curves 1^{I} and 1^{II}) of different slopes (0.070 V and 0.036 V respectively) and different half-wave potentials ($E^{I}_{1/2} \simeq -0.58$ and $E^{II}_{1/2} \simeq -0.77$ V *vs.* SCE). In such processes both $E_{1/2}$ values and the slopes obtained directly from the usual logarithmic diagram are approximate. The complete and accurate characterization of stepwise electrode procesess depends on the degree of reversibility of each step and on the stability of the intermediate.[4] However in table 1 one can notice that the slope of the first wave of Atrazine does not depend on the pH, its value is closer to a one-electron reduction and shows an irreversible character. The second wave in strong acid media exhibits a behaviour close to that for a two-electron reversible reduction but its character rapidly changes with the increasing of pH.

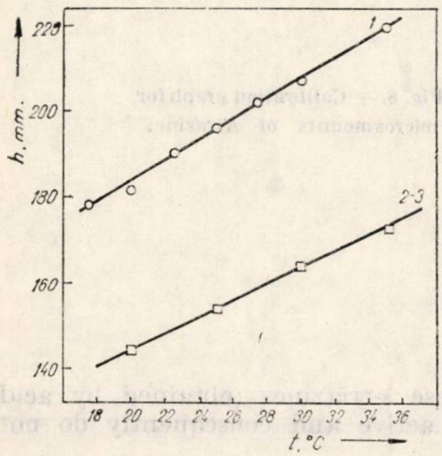

Fig. 6. — Influence of temperature upon the wave height of (1) Atrazine, (2—3) Prometryne—Igran.

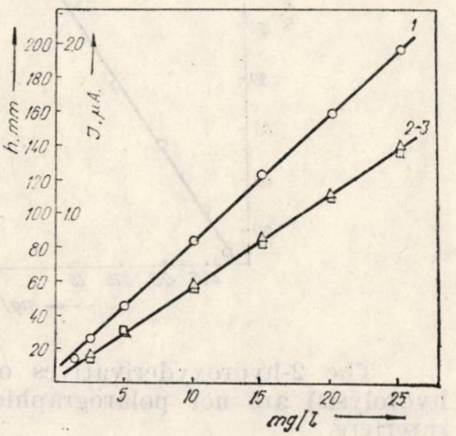

Fig. 7. — Calibration graphs of (1) Atrazine (2) Prometryne, (3) Igran.

In figure 6 the variation of the wave height with temperature is given. The temperature coefficients : 1.33% $\deg^{-1}$ for Atrazine and 1.21% $\deg^{-1}$ for Prometryne and Igran represent usual values in polarographic reduction when the process is diffusion-controlled. The shift of the half-wave potential, about + 2 mV $\deg^{-1}$, lies within the normal limits too.

A direct proportionality between concentration of s-triazines and the wave height was established for analytical application. Thus, the calibration graphs in figure 7 show a perfectly linear dependence for Atrazine,

---

[4] I. Ruzić, *Electroanalyt. Chem.*, **52**, 331 (1974).

Prometryne, and Igran between 1.25 and 25 mg/l ($10^{-4}-10^{-5}$ M). The same linear dependence is found (figure 8) at lower concentrations, between 0.125 and 1.5 mg/l. Thus, the lowest concentration of s-triazine which could be polarographically determined with a classical equipment is about 0.1 ppm (1.10^{-6} M). The very close values of the half-wave potentials of s-triazines do not allow their separate determination when they are simultaneously in solution.

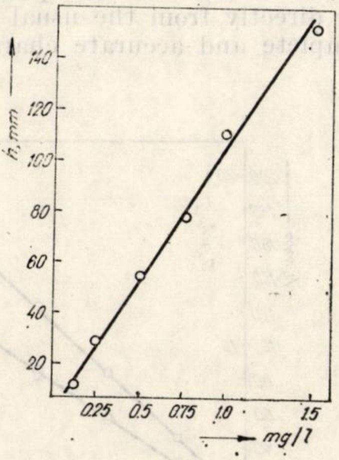

Fig. 8. — Calibration graph for microamounts of Atrazine.

The 2-hydroxyderivatives of these s-triazines (obtained by acid hydrolysis) are not polarographically active and consequently do not interfere.

To evaluate the precision of the polarographic method, samples with known amounts of s-triazines were analyzed. The statistical processing of experimental data *e.g.* for atrazine are given in table 2.

For a probability P of 95% ($\alpha = 0.05$) the variation coefficient for six runs was of 0.5%.

Table 2

Statistical processing of data at polarographic determination of Atrazine

N° of runs	Average	Standard deviation of the average	Significance level	Student parameter	$\bar{x} \pm t_\alpha S_{\bar{x}}$	$CV = \frac{S_{\bar{x}}}{\bar{x}} 100$
n	$\bar{x}$	$S_{\bar{x}}$	α	t_α		
6	196	0.974	0.05	2.571	196±2.50	0.5

Revue Roumaine de Chimie, **22**, *1*, 133–136 (1977)

LA DÉCOMPOSITION THERMIQUE DES COMBINAISONS COMPLEXES THIOCYANIQUES DU Pd(II) AVEC LA THIO-URÉE

D. FĂTU, VIORICA CIMPU et D. CAMBOLI
Institut Polytechnique, Faculté de Chimie Industrielle, 1, str. Polizu
Bucarest, Roumanie

Reçu le 18 janvier 1975

L'étude de la décomposition thermique des combinaisons complexes thiocyaniques de Pd(II) avec la thio-urée prouve que le processus de l'élimination du ligand est précédé par la fusion. Les combinaisons étudiées ne présentent pas des différences importantes en ce qui concerne la stabilité thermique.

La présente note a comme objet certains résultats sur le comportement thermique des combinaisons complexes :

$[\mathrm{Pd.\ thio_2(SCN)_2}]$; (a) $[\mathrm{Pd.\ thio_4}][\mathrm{Pd(SCN)_4}]$ (b) et $[\mathrm{Pd.\ thio_4}](\mathrm{SCN})_2$ (c)

On continue donc les études thermiques des combinaisons complexes du Pd(II).[1] La synthèse des combinaisons a été effectuée selon le procédé décrit dans une note antérieure.[2]

En utilisant un « Dérivatographe MOM Paulik-Paulik-Erdey », on a tracé simultanément les courbes thermogravimétrique (ATG), thermogravimétrique dérivée (ATGD), celle d'analyse thermique différentielle (ATD) et celle de la variation de la température (T), qui indiquent, dans des unités arbitraires, la variation de la masse de l'échantillon Δm durant la décomposition, la vitesse de la variation de la masse $\mathrm{d}m/\mathrm{d}t$, ainsi que la différence des températures de l'échantillon et du matériel inerte de référence (α—Al_2O_3 calciné à 1000° pendant quelques heures) (fig. 1).

RÉSULTATS ET DISCUSSIONS

L'examen des courbes démontre que toutes les combinaisons complexes étudiées présentent un processus endothermique qui ne conduit pas à une variation de la masse de l'échantillon. Les observations directes prouvent que ce processus est dû à la fusion, qui est ensuite suivie par la décomposition thermique de la substance, avec l'élimination dans une première étape de toutes les molécules d'amine, selon les équations :

---

[1] D. Camboli, D. Fătu et V. Cimpu, *Rev. Roumaine Chim.*, **21**, 000 (1976).
[2] P. Spacu et D. Camboli, *Anal. Univ. Sti. Bucureşti*, **14**, 101 (1965).

$$[\mathrm{Pd.\,thio_2(SCN)_2}]_{(l)} \rightarrow \mathrm{Pd(SCN)_2}_{(s)} + 2\ \mathrm{thio}_{(g)} \uparrow \qquad (I)$$

$$[\mathrm{Pd.\,thio_4}][\mathrm{Pd(SCN)_4}]_{(l)} \rightarrow 2\mathrm{Pd(SCN)_2}_{(s)} + 4\ \mathrm{thio}_{(g)} \uparrow \qquad (II)$$

$$[\mathrm{Pd.\,thio_4}](\mathrm{SCN})_{2\,(l)} \rightarrow \mathrm{Pd(SCN)_2}_{(s)} + 4\ \mathrm{thio}_{(g)} \uparrow \qquad (III)$$

Ce processus, lequel est aussi endothermique et qui, pour les complexes *a* et *b* se superpose en partie à la fusion, est favorisé par cette dernière, qui le précède, car en état liquide la réactivité de la substance s'accroît. Ceci est illustré par le fait que pour le complexe *c*, ayant une température de fusion plus basse, on constate que la décomposition commence à 182°, tandis que les complexes *a* et *b* sont stables jusqu'à 210° (fig. 1, courbes ATG et ATGD).

On remarque une grande ressemblance dans le comportement thermique des complexes *a* et *b*. Ainsi, par exemple, leurs températures de fusion sont très proches, situées à environ 200°, pour une vitesse de chauffage de 10°/min.

Ces valeurs résultant de l'examen des courbes ATD sont environ dix degrés plus élevées que celles déterminées pour les échantillons chauffés en tube capillaire à une vitesse beaucoup plus lente. La forme des courbes d'analyse thermique des combinaisons *a* et *b* est à peu près la même. Cette ressemblance accusée est due au fait que le second complexe de type Vauquelin est le dimère du premier. Le complexe **c**, plus riche en composant volatil, présente une température de fusion beaucoup plus basse, située sur la courbe ATD à 120°.

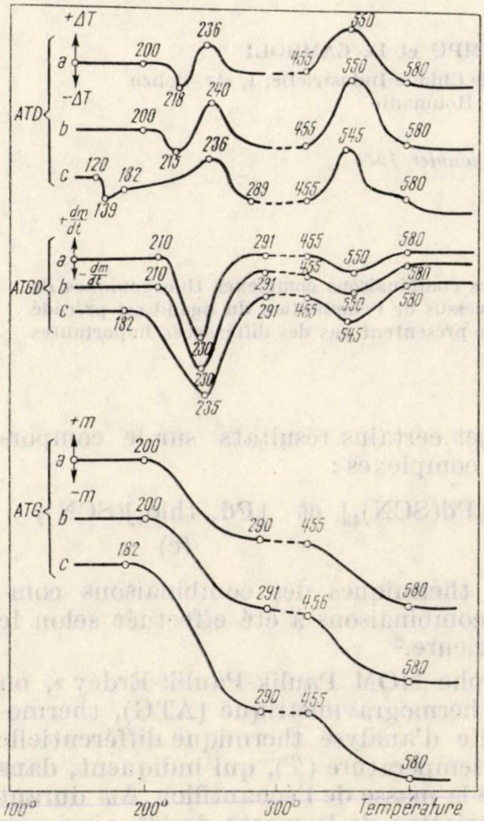

Fig. 1. — Courbes ATG, ATGD et ATD de combinaisons complexes thiocyanique du Pd(II) avec la thio-urée.

a — $[\mathrm{Pd.\,thio_2(SCN)_2}]$; *b* — $[\mathrm{Pd.\,thio_4}][\mathrm{Pd(SCN)_4}]$; *c* — $[\mathrm{Pd.\,thio_4}](\mathrm{SCN})$.

La différence par rapport au comportement thermique des combinaisons complexes thiocyaniques du Pd(II) avec la pyridine et les pyridines méthylées [1] consiste dans le fait que celles-ci présentent plusieurs étapes d'élimination des molécules d'amine et que la fusion intervient après l'élimination partielle de l'amine. Pour les complexes avec la thio-urée, les liaisons dans le réseau cristallin sont moins énergiques que celles entre l'ion métallique et les ligands, donc la destruction du réseau — la fusion — précède la décomposition avec l'élimination du ligand.

La courbe thermogravimétrique obtenue pour le complexe **c** peut être utilisée pour l'étude de la cinétique du processus de l'élimination de l'amine, car l'étape initiale de ce processus n'est pas perturbée par l'effet thermique dû à la fusion.

Pour évaluer les paramètres cinétiques à partir des données thermogravimétriques on utilise deux méthodes de calcul. La première est basée sur une programmation de chauffage hyperbolique [3] et utilise les équations :

$$\left.\begin{array}{l} -\lg\left[\dfrac{1-(1-\alpha)^{1-n}}{1-n}\right]_{n\neq 1} \\[2ex] -\lg[-\ln(1-\alpha)]_{n=1} \end{array}\right\} = \frac{E}{2{,}303R}\cdot\frac{1}{T} - \lg\frac{ZR}{bE} \qquad (1)$$

Le second procédé élaboré par Coats et Redfern [4] s'applique pour une vitesse de chauffage constante et permet de calculer les paramètres cinétiques en employant les équations :

$$\left.\begin{array}{l} \lg\left[\dfrac{1-(1-\alpha)^{1-n}}{T^2(1-n)}\right]_{n\neq 1} \\[2ex] \lg\left[\dfrac{\ln(1-\alpha)}{T^2}\right]_{n=1} \end{array}\right\} = \lg\frac{ZR}{E}\left(1-\frac{2RT}{\beta E}\right) - \frac{E}{2{,}303\,R}\cdot\frac{1}{T} \qquad (2)$$

Dans les expressions (1) et (2) n, E et Z représentent respectivement l'ordre de la réaction, l'énergie d'activation et le facteur préexponentiel, α est le degré de la décomposition, R — la constante des gaz, T — la température en degrés Kelvin, tandis que β et b sont des constantes qui caractérisent la programmation du chauffage utilisée.

Ci-dessous on présente, par comparaison, les données obtenues par les deux méthodes, ainsi que la masse **m** des échantillons et les valeurs des constantes β et b :

Méthode du chauffage hyperbolique	*Méthode Coats et Redfern*
$m = 0{,}0908$ g	$m = 0{,}0920$ g
$b = 5{,}6 \cdot 10^{-6}(°\mathrm{K})^{-1}$	$\beta = 8{,}7$ °C/min
$n = 1$	$n = 1$
$E = 22{,}7$ kcal/mole	$E = 21{,}3$ kcal/mole
$Z = 8{,}7 \cdot 10^{6}\ \mathrm{s}^{-1}$	$Z = 2{,}8 \cdot 10^{6}\ \mathrm{s}^{-1}$

La valeur de l'énergie d'activation a été calculée à partir de la pente des droites représentées sur les figures 2 et 3. On remarque une bonne concordance entre les valeurs des paramètres cinetiques obtenues par les deux procédés de calcul.

---

[3] D. FĂTU et E. SEGAL, *Rev. Roumaine Chim.*, **16**, 343 (1971).

[4] A. W. COATS et P. J. REDFERN, *Nature*, **21**, 68 (1964).

L'élimination de la thio-urée de la combinaison complexe **c** est un processus cinétique du premier ordre, ce qui s'explique par le fait que la décomposition a lieu en état de fusion, donc sur le processus de la décomposition monomoléculaire ne se superpose pas celui de la diffusion. La diffusion du composant volatil joue un rôle déterminant, quand la décomposition a lieu en phase solide.[5]

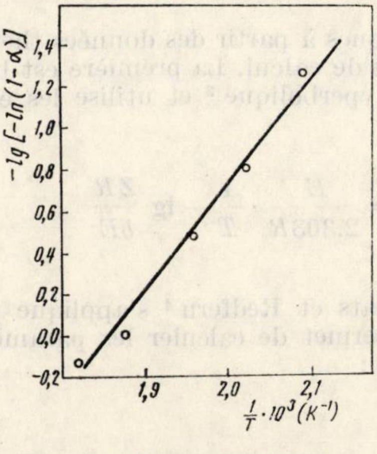

Fig. 2. — Vérification graphique de l'équation (1).

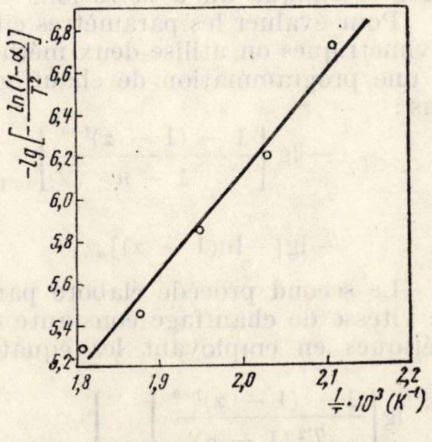

Fig. 3. — Vérification graphique de l'équation (2).

Quand on effectue l'analyse thermique dans l'air atmosphérique, la thio-urée, qui est éliminée dans la dernière étape de la décomposition, est oxydée. Ce processus exothermique se superpose au processus endothermique de la décomposition de la combinaison complexe, qui est complètement masqué ; en conséquence, sur la courbe ATD on constate un maximum exothermique. L'élimination de l'amine s'achève à des températures inférieures à 300°.

La dégradation thermique du $Pd(SCN)_2$ constitue la dernière étape de la décomposition. Ce processus est aussi exothermique, car les groupes SCN sont oxydés dans l'air.

CONCLUSIONS

1. Les complexes **a**, **b** et **c** présentent des stabilités thermiques comparables.

2. La stabilité thermique varie dans le même sens que la température de fusion.

3. La dernière étape de la décomposition est identique pour toutes les combinaisons ; elle consiste dans la dégradation thermique du $Pd(SCN)_2$. Le seul produit final solide est le palladium métallique.

4. L'élimination de la thio-urée de la combinaison complexe **c** fondue a lieu — comme on peut conclure des données thermogravimétriques — selon une cinétique du premier ordre.

---

[5] I. G. Murgulescu, D. Fătu et E. Segal, *J. Thermal Anal.*, **1**, 17 (1969).

Revue Roumaine de Chimie, 22, 1, 137–143 (1977)

QUANTITATIVE DETERMINATION OF TRACE AMOUNTS OF s-TRIAZINE HERBICIDES IN WASTE WATERS BY PHYSICO-CHEMICAL METHODS

N. TOTIR, SOFIA MARCHIDAN, C. VOLANSCHI, N. CIMPOERU,
RODICA ANDREI and ILEANA FUNDUC
Centre of Physical Chemistry, 31 Galaţi St., Bucharest, Romania

Received February 4, 1976

A comparative study of physico-chemical determination of s-triazine herbicides in waste waters is given. Among the procedures applied for carrying out the extraction, the method with methylene chloride as solvent gave the best results. A complex mixture of s-triazine herbicides in very diluted aqueous solutions can be properly analysed only by applying the gas-chromatographic method.

During the last two decades many attempts have been made to elaborate a specific method for the quantitative determination of s-triazine herbicides.[1–10]

Mattson, Kahrs and Murphy [11] have reviewed the literature in regard to the determination of s-triazine residues in soils by chemical analysis. Delley *et al.* [12] have discussed, in an early paper, the known methods for the determination of s-triazine herbicides in biological materials.

A review, placing particular emphasis on the versatility of chromatographic procedures has been published by Fishbein.[13]

None of these paper is dealing specifically with the quantitative determination of s-triazine herbicides from the waste waters.

[1] H. Gysin and E. Knüsli, "Advances in Pesticides Control Research", Vol. III, Editor R. L. Metcalf, Intersience, New York, 1960, p. 289.

[2] J.-Y. T. Chen, *J. Assoc. Offic. Anal. Chemists*, **50**, 595 (1967).

[3] H. P. Burchfield and P. H. Schuldt, *J. Agric. Food Chem.*, **6**, 106 (1958).

[4] M. H. B. Hayes, M. Stacey and J. M. Thompson, *Chem. Ind.*, **28**, 1222 (1967).

[5] E. D. Chilwell and D. Hughes, *J. Sci. Food Agr.*, **13**, 425 (1962).

[6] A. M. Mattson, R. A. Kahrs and J. Schneller, *J. Agric. Food Chem.*, **13**, 120 (1965).

[7] S. S. Brody and J. E. Chaney, *J. Gas Chromatogr.*, **4**, 42 (1966).

[8] W. P. Cochrane and B. P. Wilson, *J. Chromatogr.*, **63**, 364 (1971).

[9] R. C. Tindle, C. W. Gehrke and W. Aue, *J. Assoc. Offic. Anal. Chemists*, **51**, 682 (1968).

[10] H. G. Henkel and W. Ebing, *J. Chromatogr.*, **14**, 283 (1964).

[11] A. M. Mattson, R. A. Kahrs and R. T. Murphy, "Residue Reviews", Vol. 32, Editor F. A. Gunther, Springer-Verlag, New York, 1970, p. 371.

[12] R. Delley, K. Friedrich, B. Karlhuber, G. Székely and K. Stammbach, *Z. analyt. Chem.*, **228**, 23 (1967).

[13] L. Fishbein, *Chromatog. Rev.*, **12**, 167 (1970).

The aim of this paper was a comparative study of the possibilities of s-triazine herbicides analysis from waste waters by using polarographic, UV spectrophotometric, and gas-chromatographic methods.

EXPERIMENTAL

A LP 60 polarograph with EZ 2 recorder for polarographic analysis, a Beckman DK 2 for spectrophotometric measurements and a Carlo Erba model 2300 gas-chromatograph, equipped with a specific detector were used.

Polarographic measurements were performed in a Novak type cell thermostated at 25±0.1°. A dropping mercury electrode was used as the working electrode. The oxygen was removed from the solution by bubbling through it purified argon for 30 minutes.[14]

All the substances were of P.A. purity except the s-triazine herbicides which were of Geigy provenance. The following solutions were used : standard solutions of s-triazine herbicides containing 20 mg/l in 2% NaCl and buffered solution pH 1.2 (0.2 N KCl + 0.2 N HCl) as supporting electrolyte. The s-triazine herbicides were dissolved first in a small amount of methyl alcohol (5—10 ml) and then in 2% NaCl solution, which was then mixed with buffer solution, in a 1 to 1 ratio.

Polarographic waves were recorded in the potential range between —0.3 and —1.1 volts, *vs.* mercury pool anode. The characteristics of the capillary were : $m = 3.9$ mg $\sec^{-1}$ and $t = 3.02$ sec in distilled water at $E = 0.0$ V and $h_{Hg} = 35$ cm.

Spectrophotometric measurements were performed following a known method.[15] Initially it was necessary to determine by experiments the conditions for a total hydrolysis to the respective 2-hydroxyderivatives. The hydrolysis was obtained by heating the sample for a predetermined temperature and time with sulphuric acid.

Thus, the atrazine, propazine and terbutazine were determined after heating 1 ml of the sample to be analysed with 5 ml of sulphuric acid 50% and 4 ml distilled water. After keeping the solution at 50° for 15 minutes and cooling, the UV spectrum was recorded in a 3 cm optic pathway cell using sulphuric acid 25% as reference. The concentration was calculated by using the extinction value at 240 mμ.

The hydrolysis of prometryne and igran was performed in a mixture containing 1 ml solution to be analysed, 5 ml sulphuric acid 2 N and 4 ml distilled water. After heating the sample for 90 minutes in a water bath at 100° and cooling, the sample was analysed spectrophotometrically in the same way as for atrazine.

Gas chromatographic measurements were performed by using a Gas Chromatograph FRACTOVAP Mod. 2300 (Carlo Erba) with an alkali-flame thermionic detector having a high selectivity towards nitrogen and phosphorous compounds.

Three different chromatographic columns were used :

a) a 2 meters glass column with 3 mm inner diameter filled with 5% OV_1/GAS CHROM Q, 100/120 mesh, conditioned for 48 hours at 300°. The working temperature was 200°,

b) a 1 meter glass column with 3 mm inner diameter filled with 5% DC 200/GAS CHROM Q, 80/100 mesh + 7.5% QF_1/CHROM WHP 80/100 mesh conditioned for 48 hours at 210°. The column was used at 180°,

c) a 1 meter glass column with 3 mm inner diameter filled with 8% REOPLEX 400/CHROM W HMDS 80/100 mesh and conditioned for 48 hours at 195°. The working temperature for this column was 190°.

The temperature of the injector for all three columns was 225°. Nitrogen as used as a carrier gas.

The ranges of the flow rates were the following :

40— 60 ml/min for nitrogen
28— 31 ml/min for hydrogen
250—300 ml/min for air.

The solvent used, n-hexane, produced a zero blank signal.

A large variety of methods are described in the literature for the extraction of s-triazine herbicides from different media. In our experiments we have used three of these methods namely : extraction of s-triazine herbicide from water with ethyl ether,[12] extraction with methylene chloride [11] and extraction with hexane-ether 2+1 mixture.[16]

---

[14] I. G. Murgulescu, O. Radovici and N. Totir, *Rev. Roumaine Chim.*, **12**, 231 (1967).

[15] G. Zweig (Editor), "Analytical Methods for Pesticides, Plant Growth Regulators and Food Additives", vol. 4, Academic Press, New York, 1964.

Only the extraction with ethyl ether was applied exactly as it is described in the literature.

The extraction with methylene chloride was modified as follows : to a 300 ml separatory funnel, transfer 180 ml waste water and add 10 ml saturated solution of sodium sulphate. Extract the aqueous solution with 12.5 ml freshly distilled methylene chloride by mechanically shaking the funnel for three minutes. After ten minutes the phases separate and the methylene chloride is filtered through a 3 cm pad of anhydrous sodium sulphate (35 g) into a 100 ml Erlenmeyer flask. Repeat the extraction two more times following the same procedure and wash the sodium sulphate with 15 ml of methylene chloride. Using a water bath heated at 40° the solvent is slowly evaporated to dryness.

For hexane-ether extraction the procedure is the following: to a 300 ml separatory funnel transfer 150 ml waste water. Extract three times the aqueous solution with 10 ml hexane-ether (2+1) mixture and filter through a 3 cm pad of anhydrous sodium sulphate into a 100 m Erlenmeyer flask. The extraction follows then the same procedure as for methylene chloride.

RESULTS

All five s-triazines studied can be polarographically reduced in the potential range $-0.3 \div -1.1$ V *vs.* mercury pool anode. The supporting electrolyte used (2% NaCl in buffered solution) gave no interference.

The pH of the solution has a great influence on the reduction process. It has been established, by studying the polarographic behaviour of s-triazine herbicides in all the pH range, that it is possible to obtain well-defined, well-developed and reproducible waves for analytical purposes only in acid media. For prometryne and igran the reduction process occurs in one step. Atrazine gives two very closed waves. The limiting current and the half-wave potential depend on the pH value. For this reason buffered solution with pH 1.2—1.3 were used in all experiments. The half-wave potentials have been found to shift towards more negative values with increasing pH. There is a linear dependence of about 60 mV/pH unit (between pH 1 and 5 for prometryne and igran) showing the participation of one hydrogen ion into reaction.

The reduction process is diffusion-controlled as proved by the linear dependence between the height of the reduction wave and the square root of the height of the mercury column ; there is also a linear dependence between $\log i/(i_d - i)$ *vs.* E for prometryne and igran with a slope of about 36 mV comparable with the theoretical value. This indicates a reduction reaction slightly irreversible with participation of two electrons. The slopes obtained for different pH show that the irreversible character diminishes for lower pH values and is very strong at pH greater than 2.

For atrazine, prometryne and igran there is a linear dependence between the amount of the substance and the intensity of the diffusion current in the concentration range 0.125—25 mg/l. Therefore the lowest concentration which can be detected by polarographic method is 0.125 mg/l or 0.1 ppm. Unfortunately because the half-wave potentials for all s-triazines studied are very close it is not possible to analyze separately the triazines from a mixture of these substances. We were not able to prove the linear dependence for propazine and terbutazine owing the low solubility of these substances in water. All solutions containing the 2-hydroxyderivatives obtained by acid hydrolysis are not polarographically active and consequently do not interfere.

---

[16] W. D. Hörmann, G. Formica, K. Ramsteiner and D. O. Eberle, *J. Assoc. Offic. Anal. Chemists*, **55**, 1031 (1972).

The analysis by spectrophotometry was performed by using a described method. In our experimental conditions we found a direct proportionality between extinction coefficient and the s-triazine concentration in 0.5—5 mg/l range.

In fact by using this method the respective hydroxyderivatives resulting after acid hydrolysis are determined as has been shown previously.

For the analysis of s-triazines mixtures (atrazine, propazine, terbutazine, prometryne and igran) by gas chromatography, three different columns were tested (Fig. 1—3). No one of the columns was able to separate all five components of the mixture. The first column (Fig. 1) seems to be the best one because it has a good selectivity. The only substances which could not be determined separately were atrazine and propazine.

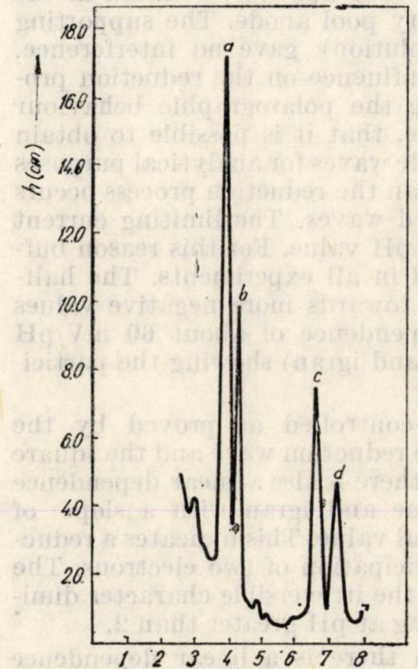

Fig. 1. — Gas-chromatographic separation of herbicidal triazines.

GLC conditions; 2.0 m × 3 mm I.D. Pyrex column packed with 5% OV_1/GAS CHROM Q, 100—120 mesh; column temperature 200°; flow rates N_2 = 60 ml/min; H_2 = 30 ml/min; air = 300 ml/min; *a* = 1.2 ng/µl atrazine + propazine; *b* = 0.4 ng/µl terbutazine; *c* = 0.8 ng/µl prometryne; *d* = 0.8 ng/µl igran.

The second column (Fig. 2) permits also the separation of the same four components but the delimitation of the obtained peaks are not as good as for the previous one. The same is true for the third column (Fig. 3).

For the first column which gave the best results we found a good proportionality between the surface of the chromatographic peaks in the 0.1—5.0 ng/l concentration range of the s-triazine herbicides.

In order to find out the proper way to analyse trace amounts of s-triazine herbicides from waste waters, the efficiency of extraction with ethyl ether, methylene chloride and hexane-ether (2+1) was investigated.

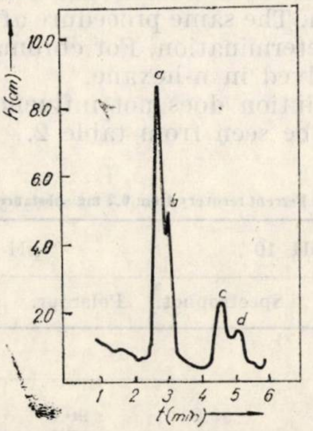

Fig. 2. — Gas-chromatographic separation of herbicidal triazines.

GLC conditions; 1.0 m × 3 mm I.D. Pyrex column packed with 5% DC 200/GAS CHROM Q, 80–100 mesh + 7.5% QF_1/CHROM WHP 80–100 mesh; column temperature 180°; flow rates N_2 = 60 ml/min; H_2 = 30 ml/min; air = 300 ml/min; *a* = 1.2 ng/µl atrazine + propazine; *b* = 0.4 ng/µl terbutazine; *c* = 0.8 ng/µl prometryne; *d* = 0.8 ng/µl igran.

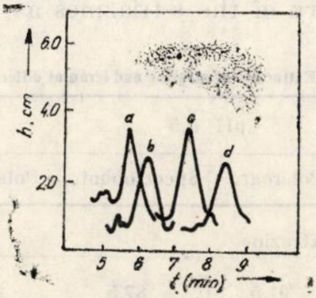

Fig. 3. — Gas-chromatographic separation of herbicidal triazines.

GLC conditions; 1.0 m × 3 mm I.D. Pyrex column packed with 8% REOPLEX 400/CHROM WHMDS 80–100 mesh; column temperature 190°; flow rates N_2 = 60 ml/min; H_2 = 30 ml/min; air = 300 ml/min; *a* = 2 ng/µl propazine; *b* = 2 ng/µl terbutazine; *c* = 4 ng/µl atrazine; *d* = 4 ng/µl igran.

Table 1

Recovery of s-triazine herbicides (added to water) after extraction with (I) ethyl ether, (II) methylene chloride, (III) hexane-ether 2+1

s-Triazine added to water	Amount of s-triazine added	Amount of s-triazine found					
		I		II		III	
	mg	mg	%	mg	%	mg	%
Atrazine	0.100 0.100 0.100	0.033 0.038 0.052	33 38 52	0.092 0.080 0.079	92 80 79	0.072 0.064 0.052	72 64 52
			41±7		84±6		63±7
Prometryne	0.100 0.100 0.100	0.067 0.081 0.068	67 81 68	0.091 0.090 0.081	91 90 81		
			72±6		87±4		
Igran	0.100 0.100 0.100	0.050 0.061 0.056	50 61 56	0.087 0.089 0.088	87 89 88	0.086 0.086 0.086	86 86 86
			56±4		88±1		86±0

As it can be seen from table 1 the best extraction results were obtained by using methylene chloride as solvent. The analysis of the extract was performed by the polarographic method after evaporation to dryness of the solvent, solving the residue in 0.5 ml methanol and bringing it to a volume of 10 ml with aqueous solution. The same procedure after extraction was used for spectrophotometric determination. For chromatographic analysis the residue was directly dissolved in n-hexane.

The pH value of the aqueous solution does not influence sensibly the recovery of the s-triazines as can be seen from table 2.

Table 2

Extraction of atrazine and igran at different pH. Percent recovery from 0.2 mg substance

Run Nr.	pH 6.5		pH 10		pH 12	
	Polarogr.	Spectrophot.	Polarogr.	Spectrophot.	Polarogr.	Spectrophot.
	Atrazine					
1	91.5	87.5	93.0	95.0	90.0	94.5
2	82.5	86.5	97.5	97.5	87.5	74.5
3	91.0	92.0	96.0	97.0	89.5	91.5
4	96.0	92.5	99.0	87.0	96.5	87.0
5		90.0			92.5	88.5
Average	90.5±3.8	89.5±2.2	96.5±1.9	94±3.6	91±2.6	87±5.2
	Igran					
1	68.5	66.0	73.5	73.5	85.0 *	78.5 *
2	82.5		93.5	91.5	88.0 *	84.5 *
3	96.5	94.5	92.0	93.0	87.5 *	78.5 *
4	97.0	91.5	67.0	63.0	77.0 *	67.0 *
5	92.0	88.0	85.0	78.0	78.0 *	68.0 *
6	91.5 *	83.5	95.0	94.5		
Average	88.0±8.3	84.5±8.0	84.5±9.3	82.5±10.7	83.0±4.5	75.5±6.2

* The amount recovered after five consecutive extractions.

The results for extraction of prometryne, propazine and terbutazine obtained at a pH = 10 are given in table 3.

Tabel 3

Extraction of some s-triazine herbicides at pH 10. Percent recovery from 0.2 mg prometryne, respectively 0.05 mg propazine and 0.05 mg terbutazine

Run N°	Prometryne		Propazine		Terbutazine
	Polarogr.	Spectrophot.	Chromatogr.	Spectrophot.	Chromatogr.
1	82.0	88.5	88.0	68.0	92.0
2	92.0	80.5	94.0	98.0	100.0
3	75.5	94.0	88.0	92.0	
4	93.0	95.5	86.0	96.0	96.0
5	75.5	81.0	88.0	82.0	94.0
Average	83.5±6.7	88.0±5.7	89.0±2.2	87.2±9.8	95.6±2.5

The s-triazine concentrations in the solutions to be extracted were about 1 ppm for atrazine, igran and prometryne and about 0.25 ppm for propazine and terbutazine.

For atrazine, propazine and terbutazine the recovery was reproducible around 90% and for igran and prometryne around 85% with a good concordance between the polarographic, spectrophotometric or chromatographic results.

The analysis of waste waters with very low amounts of atrazine and prometryne are given in table 4.

Table 4

Gas-chromatographic analysis of waters with trace amounts of s-triazines

Sample N°	Atrazine			Prometryne		
	Added mg	Found		Added mg	Found	
		mg	%		mg	%
1	0.01	0.0094	94.0	0.01	0.	90.0
2	0.01	0.0088	88.2	0.01	0.	80.0
			91.1 ± 2.9			85.0 ± 5.0

As can be seen from table 4 we found the same good results in the concentration range of 0.05 ppm. In this case, as for s-triazines mixture, after extraction only the chromatographic method can be used.

In conclusion our experiments show the possibility of analysing waste waters with very low concentration of s-triazines using an extraction procedure with methylene chloride and by applying the gas chromatographic method as described above.

Revue Roumaine de Chimie, 22, 1, 145–152 (1977)

OXYGEN REDUCTION ON SILVER GAS ELECTRODES. V[1]

THE EFFECT OF COMPRESSION AND SINTERING CONDITIONS ON ELECTRODE PERFORMANCES

O. RADOVICI, MARIA MAVRODIN-TĂRĂBÎC, IOANA ONACA and
I. SOLACOLU
Centre of Physical Chemistry, str. Galaţi 31, Bucharest, Romania

Received: *Apr 2, 1975*

MSK and DSK type silver gas electrodes have been prepared. The DSK type electrodes presented lower overpotentials in oxygen reduction in KOH medium. The effect of compression pressure ($1.5-2.5\cdot10^{8}$ N.m^{-2}), temperature (350–370°) and time of sintering (10–15 minutes) on electrode structure and on electrode polarization has been studied. Polarization measurements were carried out by potentiostatic method. The lowest overpotentials were performed by the electrodes compressed at $2.5\cdot10^{8}$ N·m^{-2} and sintered at 350–360° for 15 minutes (230–250 mA·cm^{-2} at 350 mV) and by the electrodes compressed at 2.10^{8} N.m^{-2} and sintered at 370° for 15 minutes (230 mA·cm^{-2} at 350 mV).

As it is known, the improved performances of porous electrodes over nonporous electrodes are the result of active area magnification.[2,3] The high apparent current densities (referred to the external electrode surface) are due to this very large internal surface (m^2/cm^3) of the gas electrodes. This internal surface cannot be greatly extended by reducing the pore diameter (i.e. by the increase in the number of the active pores), due to the obvious increase of the diffusion polarization. Obviously, for every fuel or oxidant-electrolyte set there is an optimum porous system in which the cappilary forces ensure a large active surface and a good diffusion of the products and reactants. The achievement of a suitable porous system [4] depends on the structure type, on the composition and granulometric repartition of the powder mixture, on the preparation conditions (compression pressure, sintering conditions), etc. This is a very difficult problem, due to the correlation of all the technological parameters involved in the gas electrode preparation. The literature does not offer detailed information concerning the effect of these parameters on the electrode performances. Data concerning the preparation of silver gas electrodes are reported in some patents.[5-7]

---

[1] Part IV: I. SOLACOLU, M. MAVRODIN-TĂRĂBÎC and I. ONACA, *Rev. Roumaine Chim.* in press.

[2] J. O'M. BOCKRIS and S. SRINIVASAN, "Fuel Cells", McGraw-Hill, New York, 1969, p. 233.

[3] E. JUSTI and A. WINSEL, "Kalte Verbrennung", Steiner Verlag, Wiesbaden, 1962, p. 59.

[4] E. JUSTI and A. WINSEL, *Naturwiss.*, **47**, 289 (1960).

In this work, in order to improve the silver gas electrode performances, their preparation conditions have been studied.

1. EXPERIMENTAL

1.1. ELECTRODE PREPARATION

Silver gas electrodes with different structures and porosities have been achieved :

— *MSK type electrodes with small pores* (*MSK 1*). Silver carbonate powder (grain size below 5 μm) has been pressed at 2.10^8 N.m^{-2}, in steel matrix. The pellets (10 mm diameter, 0.6 mm thickness) have been sintered at 360° for 15 minutes, in hydrogen atmosphere.

— *MSK type electrodes with large pores* (*MSK 2*). A mixture of 80% silver oxide (grain size below 5 μm) and 20% ammonium dicarbonate (grain size of about 40—60 μm) has been pressed at 2·10 N.m^{-2}. The pellets have been sintered in the same conditions.

— *DSK type electrodes.* A series of mixtures of silver carbonate (grain size below 5 μm) — ammonium dicarbonate (grain size of about 40—60 μm) have been pressed at 2.10^8 N.m^{-2}. The percentage composition was : 95—5 (DSK 1), 90—10 (DSK 2), 85—15 (DSK 3), 80—20 (DSK 4), 75—25 (DSK 5). The pellets have been sintered in the same conditions.

In order to determine the effect of the preparation conditions (compression pressure, temperature, sintering time) upon the electrode polarization, these have been varied in the range $1.5-2.5\cdot10^8$ N·m^{-2}, 350—370° and for 10—15 minutes, respectively. The electrodes were noted from 1.1.1. to 3.3.2. and indexed as follows :

— the 1st number indicates the compression pressure ($1 = 2.5\cdot10^8$ N·m^{-2}; $2 = 2\cdot10^8$ N·m^{-2}; $3 = 2.5\cdot10^8$ N·m^{-2}),

— the 2nd, the sintering temperature (1 = 370°; 2 = 360°; 3 = 350°),

— the 3rd, the sintering time (1 = 15 minutes, 2 = 10 minutes).

In order to obtain a porous structure, the electrodes were heated with 2.5°/minute. A constant level was maintained, for an hour, at 100° and 140° (for H_2O and CO_2 removal) and for 10 or 15 minutes at sintering temperature. The cooling was carried out with 3°/minute decrease of temperature. The hydrogen flow was of 1.5 dm^3/minute.

1.2. STRUCTURE AND POROSITY DETERMINATION

The sintering degree and the electrode structure have been studied by using an IOR MC—1 type metallographic microscope (500X).

The total porosity was determined by weighing the electrodes before and after impregnation with toluene (at 80°, for 4 hours).

1.3. ELECTROCHEMICAL MEASUREMENTS

The polarization curves were obtained for each type of silver gas electrodes in oxygen reduction in KOH medium, at different oxygen overpressures comprised between 300 and 660 mm Hg by potentiostatic method, by applying potential steps of 10 mV at 1 minute intervals. The wiring scheme, gas supply system at constant overpressure and working cell have been previously described.[8]

---

[5] A. M. Moos, US Patent 3 276 909, October 4, 1966 ; *Chem. Abstr.*, **69**, 112887 (1968)

[6] W. V. Childs, Ger. Patent 1 806 408, October 2, 1969 ; *Chem. Abstr.*, **69**, 117232 (1970).

[7] H. C. Lies, Ger. Patent 1 273 642, July 25, 1968 ; *Chem. Abstr.*, **69**, 64125 (1968).

[8] O. Radovici, M. Mavrodin-Tărăbîc, I. Onaca and I. Solacolu, *Rev. Roumaine Chim.*, **17**, 1153 (1972).

A Radelkis type OH 404/A potentiostat (± 1 mV precision), a DU 20 type milliampermeter (1% precision) and a Radiometer 22 type electronic millivoltmeter (± 1 mV precision) have been used. The auxiliary electrode was a 99.9% nickel tape. Potentials are referred to the SCE. The electrolyte concentration was 6N. The working temperature was 20°.

2. RESULTS AND DISCUSSIONS

2.1 DETERMINATION OF THE MOST EFFICIENT STRUCTURE AND POROSITY

In order to establish the most suitable structure, MSK type silver gas electrodes with homoporous structure (MSK 1, which small pores and MSK 2, with large pores) and DSK type silver gas electrodes with various porosities (DSK 1 — DSK 5) have been prepared. Different electrode porosities were obtained by using different silver carbonate/ammonium dicarbonate ratio (between 19 :1 and 3 :1).

Microscopic examination of the electrodes has evidenced an advanced degree of sintering and an uniform repartition of the pores. The total porosities were : 11.5% (MSK 1), 58.3% (MSK 2),18.4% (DSK 1), 32.5% (DSK 2), 50.1% (DSK 3), 63.2% (DSK 4), 75.2% (DSK 5). The DSK 5 type electrodes had not a suitable mechanical strength for their electrochemical study.

The conclusions concerning the efficiency of the different electrodes were obtained by comparing their polarization curves in oxygen reduction in KOH medium. The polarization curves were determined at different oxygen overpressures (300, 400, 500, 600, 660 mm Hg). The lowest overpotentials were performed at 400 mm Hg overpressure (for the MSK 2 electrodes) and at 660 mm Hg overpressure (for the other electrodes). The optimum overpressure of 400 mm Hg for the MSK 2 electrodes, lower than the optimum overpressure for the DSK 4 electrodes, with about the same porosity, is due to their structure characterized only by large pores. In this case the reaction conditions at overpressures higher than 400 mm Hg are not favorable. For the electrodes which have not presented an optimum overpressure in the range under study (MSK 1, DSK 1 — DSK 4), the differential variation of the apparent current density, at constant overvoltage, decreases greatly with increasing overpressure. For instance, in the case of the DSK 4 electrode, the apparent current densities at 350 mV are : 51 mA $\cdot$cm^{-2} (300 mm Hg), 83 mA $\cdot$cm^{-2} (400 mm Hg), 100 mA $\cdot$cm^{-2} (500 mm Hg), 113 mA $\cdot$cm^{-2} (600 mm Hg), 116 mA $\cdot$cm^{-2} (660 mm Hg).

The polarization curves, characteristic for the silver gas electrodes with different structures and porosities, for the optimum overpressure conditions are shown in Fig. 1.

2.1.1. The effect of electrode structure

As seen in Fig. 1 (curves 1 and 3) the overpotentials characteristic for the MSK 2 electrodes are lower than those corresponding to the MSK 1 electrodes. The apparent current densities are of 7 and 9 mA $\cdot$cm^{-2}, respectively (100 mV), 37 and 29 mV $\cdot$cm^{-2}, respectively (200 mV), 75 and 52 mA $\cdot$cm^{-2}, respectively (350 mA). The MSK 2 electrodes have a structure characterized by large pores (of about 5—15 μ m diameter), where the active surface is localized. In these pores the diffusion of reactants and products is faster than in the MSK 1 electrodes characterized by small pores.

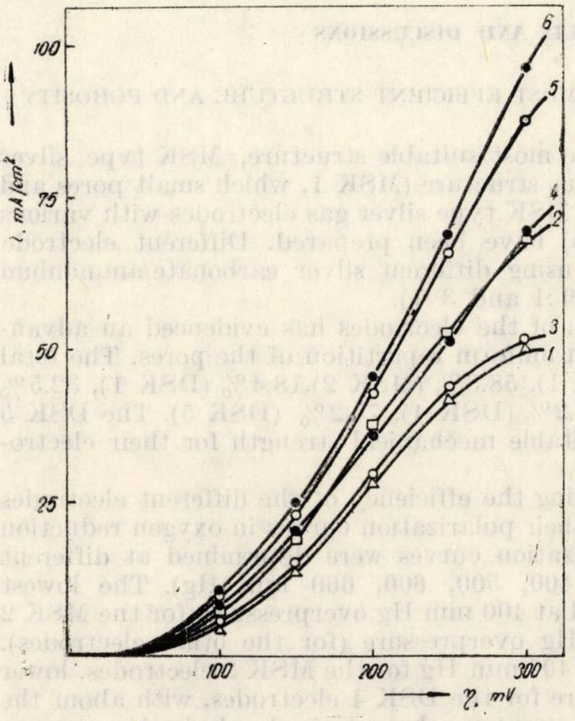

Fig. 1. — Polarization curves for oxygen reduction reaction in KOH medium on silver gas electrodes.

1 – MSK 1 electrode; 2 – MSK 2 electrode; 3 – DSK 1 electrode; 4 – DSK 2 electrode; 5 – DSK 3 electrode; 6 – DSK 4 electrode.

In order to establish the effect of DSK structure upon the electrode polarization, overpotential data of DSK 4 electrodes are compared with overpotential data of MSK 2 electrodes with about the same porosity. The curves 2 and 6 of Fig. 1 show that the DSK 4 electrodes presented much lower overpotentials than the MSK 2 electrodes. The apparent current densities for different overpotentials are: 9.5 mA $\cdot$cm^{-2} (DSK 4) in comparison with 7 mA $\cdot$cm^{-2} (MSK 2) at 100 mV, 42 and 37 mA $\cdot$cm^{-2}, respectively (200 mV), 117 and 75 mA $\cdot$cm^{-2}, respectively (350 mV). The higher the overpotential is the larger are these differences due to diffusion polarization effect. The DSK structure favours the electrode process since the fine pores have a role in eliminating the products and reactants created in the meniscus (which is localized in the large pores). Thus, a high ratio OH^-/O_2H^- is maintained by removal of O_2H^- from the active surface.[9] H_2O_2 decomposition takes place in the fine pores of the DSK structure.

From these data it results that the most suitable electrode structure is the two-disperse structure of DSK type.

---

[9] W. Latimer, "The Oxidation Potentials", Prentice Hall, New York, 1964, p. 98.

2.1.2. The effect of porosity

The polarization curves 3, 4, 5 and 6 in Fig. 1, characteristic for the DSK type electrodes with 18.4%, 32.5%, 50.1% and 63.2% porosities, show that the DSK 4 electrodes presented the lower overpotentials. The apparent current densities at different overpotentials for the DSK 1, DSK 2, DSK 3 and DSK 4 electrodes are:

— 100 mV — 5, 7, and 9.5 mA·cm^{-2}, respectively;
— 200 mV — 31, 35.5, 40, and 41.5 mA·cm^{-2}, respectively;
— 350 mV — 54, 81.5, 100, and 117 mA·cm^{-2}, respectively.

The higher apparent current density values of the DSK 4 electrodes are due to a more extended active reaction zone. These electrodes were performed by compressing and sintering of a powder mixture with 20% poroforming (grain size of about 40—60 μm). By the poroforming decomposition, pores with large diameters are formed, where the active reaction zone is localized. The number of active pores, refering to the external surface, is much greater by comparing with the DSK electrodes prepared from a powder mixture containing a smaller poroforming amount. It is to note that the DSK electrodes performed from a powder mixture with 25% poroforming had not presented a suitable mechanical strength.

Thus, the gas electrodes with the lowest overpotentials in oxygen reduction in KOH medium are the electrodes of DSK 4 type (63.2% porosity). These have been performed from a powder mixture containing 80% silver carbonate and 20% ammonium dicarbonate, by compressing at $2 \cdot 10^8$ N·m^{-2} and sintering at 360° for 15 minutes, in hydrogen atmosphere.

2.2. THE EFFECT OF PREPARATION PARAMETERS

The improvement of the gas electrodes performances depends on the correct determination of the preparation conditions (compression pressure, sintering temperature, sintering time, etc). These conditions, correctly correlated, lead to a favorable porous system.

In order to establish the preparation parameters of the gas electrodes, powder mixtures of 80% silver carbonate and 20% ammonium dicarbonate have been compressed at various pressures (1.5, 2 and $2.5 \cdot 10^8$ N·m^{-2}); the pellets have been sintered, in hydrogen atmosphere, at different temperatures (350, 360 and 370°), for 10 or 15 minutes.

Microscopic determinations have evidenced various degrees of sintering which depend on compression and sintering conditions. The average total porosities of electrodes are: 60.9% (1.1.1.), 61.5% (1.1.2.), 61.7% (1.2.1.), 62.1% (1.2.2.), 63.1% (1.3.1.), 63.8% (1.3.2.), 62.8% (2.1.1.), 63.5% (2.1.2.), 63.2% (2.2.1.), 64.1% (2.2.2.), 64.3% (2.3.1.), 64.9% (2.3.2.), 76.2% (3.1.1.), 77.7% (3.1.2.), 76.9% (3.2.1.), 78.1% (3.2.2.), 78.8% (3.3.1.), 80.2% (3.3.2.).

The polarization curves of these electrodes, in potentiostatic conditions, at oxygen overpressure of 300, 400, 500, 600 and 660 mm Hg, have been determined. In all cases the best results were obtained at 660 mm Hg overpressure.

In order to illustrate the effect of the preparation parameters upon the electrode polarization, Fig. 2 shows some characteristic polarization curves.

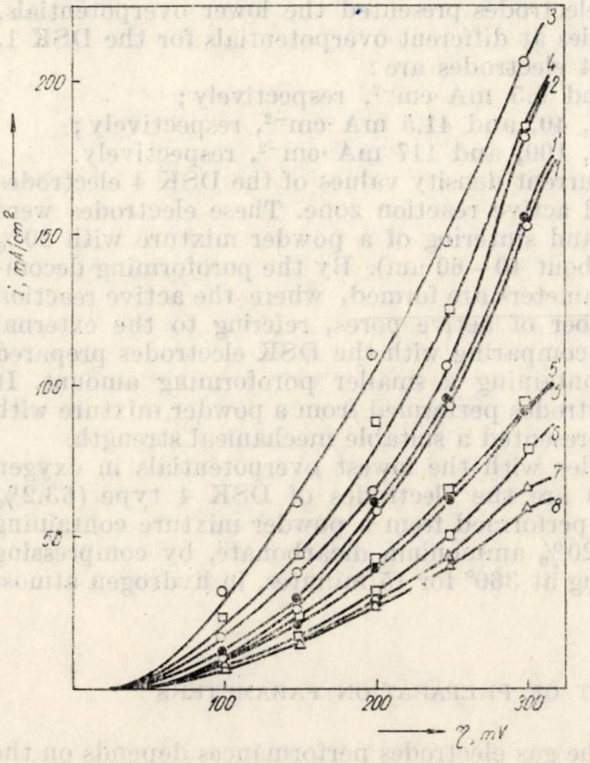

Fig. 2. — Polarization curves for oxygen reduction reaction in KOH medium on DSK type silver gas electrodes.

1 – 1.1.1. electrode ($2.5.10^8$ N/m², 370°, 15 min); 1′ – 1.1.2. electrode ($2.5.10^8$N/m², 370°, 10 min); 2 – 1.2.1, electrode ($2.5.10^8$ N/m², 360°, 15 min); 3 – 1.3.1. electrode ($2.5.10^8$ N/m², 350°, 15 min); 4 – 2.1.1, electrode (2.10^8N/m² 370°, 15 min); 5 –2.2.1, electrode (2.10^8 N/m², 360°, 15 min); 5′ – 2.2.2. electrode (2.10^8 N/m², 360°, 10 min); 6 – 2.3.1. electrode (2.10^8N/m², 350°, 15 min), 7 – 3.1.1. electrode ($1.5.10^8$ N/m². 370°, 15 min); 8 – 3.2.1. electrode ($1.5.10^8$ N/m², (360°, 15 min).

2.2.1. The effect of compression pressure

Comparative examination of the polarization curves 1, 4 and 7 (Fig. 2), for the electrodes sintered at 370° for 15 minutes, and compressed at different pressures (2.5, 2 and $1.5 \cdot 10^8$ N $\cdot$m^{-2}, respectively), shows that the increase of compression pressure from $1.5 \cdot 10^8$ N$\cdot$m^{-2} (curve 7) to $2 \cdot 10^8$ N $\cdot$m^{-2} (curve 4) leads to an important decrease of the electrode overpotentials, while the increase of the compression pressure to $2.5 \cdot 10^8$ N $\cdot$m^{-2} (curve 1) leads to an important increase of the electrode overpotentials. The apparent current densities, at different overpotentials, characteristic for the 3.1.1., 2.1.1. and 1.1.1. electrodes are:

— 100 mV — 8, 7.5 and 10 mA $\cdot$cm^{-2}, respectively;
— 200 mV — 31.5, 88 and 62.5 mA $\cdot$cm^{-2}, respectively;
— 350 mV — 75, 228 and 195 mA $\cdot$cm^{-2}, respectively.

Thus, the increase of the compression pressure up to $2 \cdot 10^8$ N $\cdot$m^{-2} leads to a suitable electrode structure with a large active surface. The increase of the compression pressure over this value leads to a very advanced degree of sintering, i.e. to a smaller active surface and as result the overpotential increases.

Comparative examination of the polarization curves 2, 5 and 8 in Fig. 2, for the electrodes sintered at 360° for 15 minutes, and compressed at different pressures (2.5. 2 and $1.5 \cdot 10^8$ N $\cdot$m^{-2}, respectively), shows that the increase of the compression pressure causes a decrease of the electrode overpotential, in the range under study. This effect is more evident in the range of $2-2.5 \cdot 10^8$ N $\cdot$m^{-2}.

The apparent current densities, at different overpotentials, for the 3.2.1., 2.2.1., and 1.2.1. electrodes are :

— 100 mV — 7.5, 9 and 19.5 mA $\cdot$cm^{-2}, respectively;
— 200 mV — 27.5, 41.5 and 64 mA $\cdot$cm^{-2}, respectively;
— 350 mV — 64.5, 117 and 227 mA $\cdot$cm^{-2}, respectively.

Thus, these sintering conditions require a higher compression pressure, in order to obtain a suitable porous system.

2.2.2. The effect of sintering temperature

Comparative examination of the polarization curves 3, 2 and 1 in Fig. 2, characteristic for the electrodes compressed at $2.5 \cdot 10^8$ N $\cdot$m^{-2}, and sintered at 350, 360, and 370°, respectively, for 15 minutes, in hydrogen atmosphere, shows that the increase of the sintering temperature leads to an increase of the electrode overpotential. This effect is illustrated by the apparent current densities, at different overpotentials, for the 1.3.1., 1.2.1., and 1.1.1. electrodes :

— at 100 mV — 32, 19.5 and 10 mA $\cdot$cm^{-2}, respectively;
— at 200 mV — 106, 64 and 62.5 mA $\cdot$cm^{-2}, respectively;
— at 350 mV — 255, 227 and 195 mA $\cdot$cm^{-2}, respectively.

At high compression pressures, the increase of the temperature leads to a very advanced sintering degree, i.e. to the corresponding decrease of pore diameters. Thus, one obtains porous structures unfavorable for reactant and product diffusion. As a result, the electrode polarization increases as seen in Fig. 2.

The polarization curves 6, 5 and 4 in Fig. 2, for the electrodes compressed at $2 \cdot 10^8$ N $\cdot$m^{-2}, and sintered at 350, 360 and 370°, for 15 minutes, show a favorable effect of the sintering temperature increase in the range under study. This effect is more evident in the range of 360—370°. The apparent current densities, at different overpotentials, for the 2.3.1., 2.2.1., and 2.1.1. electrodes are :

— at 100 mV — 8.5, 9 and 22.5 mA $\cdot$cm^{-2}, respectively;
— at 200 mV — 34, 41.5 and 88 mA $\cdot$cm^{-2}, respectively;
— at 350 mV — 103, 117 and 228 mA $\cdot$cm^{-2}, respectively.

Comparative examination of the polarization curves shows an evident decrease of the overpotential, due to the suitable electrode structure.

2.2.3. The effect of sintering time

Comparative examination of 1 and 1′ and 5 and 5′ polarization curves in Fig. 2, for the 1.1.1., 1.1.2. and 2.2.1., 2.2.2. electrodes shows that the variation of the sintering time between 10 and 15 minutes has not an important effect upon the silver gas electrode overpotentials.

2.3. THE DETERMINATION OF THE ELECTRODE PREPARATION CONDITIONS

The study of the effect of the preparation parameters upon the DSK type electrode polarization shows that the compression pressure and the sintering temperature are the parameters with significant influence. These two effects are correlated ; the correct determination of the compression pressure-sintering temperature leads to suitable porous systems and to lower overpotentials oxygen reduction in KOH medium.

As a final result of our work the most efficient porous systems are obtained from powder mixtures of 80% silver carbonate — 20% ammonium dicarbonate, either by pressing at $2.5 \cdot 10^8$ N $\cdot$m^{-2} and sintering at 350°, or by pressing at $2 \cdot 10^8$ N $\cdot$m^{-2} and sintering at 370°. Obviously, for the exact determination of the preparation optimum parameters, it is necessary to carry out an optimization study.

3. CONCLUSIONS

1. The silver gas electrodes with DSK type two-disperse structure are characterized by lower overpotentials than those having a MSK type homoporous structure.

2. The lowest overpotentials correspond to the electrodes prepared from a powder mixture of 80% silver carbonate and 20% ammonium dicarbonate (total porosity 63.2%).

3. The variation of the compression pressure in the range of 1.5—$2.5 \cdot 10^8$ N $\cdot$m^{-2}, and of the sintering temperature, in the range 350—370°, has an important effect upon the electrode structure.

4. The variation of the sintering time between 10 and 15 minutes has not an evident effect upon electrode structure.

5. The lowest overpotentials correspond to the electrodes prepared either by compressing at $2.5 \cdot 10^8$ N $\cdot$m^{-2} and sintering at 350° (22 mA $\cdot$cm^{-2} at 100 mV, 106 mA $\cdot$cm^{-2} at 200 mV, 255 mA $\cdot$cm^{-2} at 350 mV), or by compressing at $2 \cdot 10^8$ N $\cdot$m^{-2} and sintering at 370° (22.5 mA $\cdot$cm^{-2} at 100 mV, 88 mA $\cdot$cm^{-2} at 200 mV, 228 mA $\cdot$cm^{-2} at 350 mV).

Revue Roumaine de Chimie, 22, 1, 153–159 (1977)

COMPTES RENDUS

I. G. MURGULESCU, ,,Introducere în chimia fizică'' (Introduction to physical chemistry), vol. I, 1. Atomi, molecule, legătura chimică (Atoms, molecules, chemical bond). The printing House of the Academy of Science of Socialist Republic of Romania, Bucharest, 1976, 560 p.

Designed as an extensive work to be issued in several volumes, ,,Introduction to Physical Chemistry'' by Acad. Prof. I. G. Murgulescu, is much more than just a treatise of physical chemistry; it is a window opened to physical chemistry, to basic knowledge required for smoothing out the way to handbooks, to articles in journals, to improving the qualification of those involved in any kind of chemistry.

The work is to be issued in three volumes subdivided in six parts whose topics are:

I. 1. Atoms, molecules, chemical bond; I. 2. Structure and properties of molecules; I.3. Atomic nucleus, nuclear reactions, elementary particles; II.1. Molecular theory of the states of matter: gas, solid, liquid and solutions; II.2. Chemical kinetics. Catalysis; III. Chemical thermodynamic.

These volumes represents an extension and systematization of the lectures on physical chemistry given by the author, who has brilliantly lead the physical chemistry chair of Department of Chemistry, University of Bucharest, close to a quarter of a century of teaching and scientific activity; these lectures has permanently been updated with the newest achievements in the field.

The first part of volume I covers atoms, molecules and chemical bond. It consists of five parts, 25 chapters, 17 appendixes and numerous references. The author has chosen for presentation the criterion of historical evolution since, according to his oppinion, it mirrors most faithfully the logical evolution of knowledge in science.

The first part treats the beginnings of atomic theory, its development in 18-th century as well as the classical atomic theory.

The second part deals with discovery and characterization of the electron, anodic (canal) rays and separation of isotops.

In Part III are presented the experimental and theoretical foundations of atomic models (Bohr-Sommerfeld), the vectorial model, the theory of the periodic table of elements (Mendeleef), the theory of X ray spectra, the first theories of chemical bond.

In part IV are exposed the quantum atomic theory, the theoretical and experimental foundations of quantum mechanics. quantum treatment of some simple systems, the theory of hydrogenous atoms, approximations in quantum mechanics, the applications of the methods of stationary perturbations and of variations, the electronic spin in quantum mechanics (consequences), the emission and absorption of light and rules of selection.

The last part encompasses the quantum theory of chemical bond with extension to the method of valence bond, the method of molecular orbitals, the coordination and metallic bond.

This topic is exposed systematically to make the work accessible though of higher level.

The book is intended for chemists and chemical engineers, physicists and metallurgical engineers, geo- and biochemists, research staff and graduate students in various fields, highly qualified specialists in various fields as well as undergraduate students.

D.I. Marchidan

RODICA VÎLCU, "Termodinamica chimică" (Chemical Thermodynamics), Bucharest, Ed. tehnică, 1975, 650 p.

The present book on Chemical Thermodynamics provides a rigorous and unitar, handling of the field and covers the most representative aspects of this general discipline:

— "traditional" thermodynamics of physico-chemical equilibrium processes presented in a modernized form,

— chemical thermodynamics of irreversible processes, a largely developing field initiated hree decades ago, which includes the fundamentals on the treatment of phenomena in evolution and

— the statistical thermodynamics which steadily substantiates the results of phenomenological thermodynamics.

Statistical thermodynamics calculations are supported by elements of statistical mechanics systematized in a readily accessible form in appendix I of the book.

A well-balanced plan is followed in presenting this rich material : the basic notions which are permanently referred to, such as partial molar values, state parameters, etc., are exposed in the introductory part of the work, followed by general principles of equilibrium thermodynamics and of irreversible thermodynamics, classically and statistically substantiated. The material is completed by the most representative applications of thermodynamics principles and also by complex applications of the basic laws in the field which imply the previous definition of thermodynamics values and functions both in a phenomenological and in a statistical manner. This part of the treatise places a special emphasis on the characterization of the chemical equilibrium, of the reaction yield and of the equilibrium conversion, while also revealing the role of the chemical affinity and its thermodynamics substrate.

The term "chemical affinity" is not regarded strictly statically but in correlation with the elements of the systems in evolution : (affinity and the extent of reaction ; affinity and the reaction rate, a.o.). In fact, chapter XI points out to the intervention of the time parameter in the systems dynamics characterization also revealing the particularities of the methods studying the processes in evolution over the methods of equilibrium thermodynamics.

After establishing the general laws and the correlations between thermodynamic functions specific of pure bodies or of systems, the book deals with the particularities of homogeneous ideal and real systems in gas-phase and in condensed media (non-electrolyte solutions and aqueous electrolyte solutions). The material has been completed by statistical handlings of liquids and of solutions, with preponderance on treatments according to models.

The handling of heterogeneous systems has been based on the laws of the field, extensively presented and followed by thermodynamic phase-stability criteria. The presentation of physical equilibria points to the laws of ideal systems and to methods of obtaining some functions of deviation from ideality in the treatment of non ideal phases in equilibrium. The book also reveals the correspondence between the phase-diagram form and the specific equations of equilibrium curves between phases, with the thermodynamic justification of the thermodynamic equations obtained.

Each of the 17 chapters of the book underlines the physical meaning of phenomena and also their implications in laboratory and in industrial operations substantiated in terms of quantity by a rigorous mathematization of the presentation. Each symbol referred to has a precise correspondent in the real world, each equation includes determined relations between the physical values being defined.

The presented material is supported by a rich bibliography including the most representative works of the world literature, some of which open new avenues in various fields. The contributions of the Romanian school of Physical Chemistry in the last two decades have not been omitted, either.

In the present exposition even same subtleties of the field are readily accessible to those interested in it, due to a gradual assimilation of notions and in particular of their physical meaning.

D. Marchidan

L. MÁZOR, "Analytical Chemistry of Organic Halogen Compounds", Akademiay Kiado Publishing House, Budapest 1975, 290 p.

The organic halogen compounds were known today for their important applications in the chemical and pharmaceutical industry as plastics, solvents, lacquers, dyes, medical drugs, and in agriculture as herbicides, insecticides, represent a class of substances growing in time numerically, quantitatively and in different uses. The industrial synthesis, storage and utilisation of the above compounds are connected with their chemical analysis revealing in fact, their halogenic nature and content quicklier, more precisely, having lower and lower detection limits.

The diversity of analytical gravimetrical, volumetrical or instrumental methods used for the great number of various halogen compounds, led in time, to a vast accumulation of bibliographical materials in this field.

In only 290 pages including 8 chapters, the author selects, organizes and presents, in a detailed and accesible form a series of procedures and analytical methods for the determinations and dosing of the halogens from the organohalogenated compounds.

Following a laboratory experience of 20 years in this field, these methods are considered by the author, the best from the applicative point of view.

The book is addressed to the analytical chemists working in organic laboratories or to the professorial staff and students from the chemical institutes.

The analytical methods and procedures are classified according to the halogen quantity to be dosed in : macro, semimicro and micro, ultramicro. The description is started with the classical methods : gravimetrical and volumetrical continuing with the instrumental ones : spectrophotometrical, colorimetrical and finishing with more pretentious ones as : N.M.R., E.P.R., and Mass Spectrometry.

We can draw the conclusion that the author wanted to put at the specialists' disposal those methods needing cheap apparata, easy to be handeled and maintained in the good order in time, although the book does not ignore the modern instrumental methods, presenting their importance and possibilities.

When dealing with micro, ultramicro methods, the author presents in detail by drawings and explicative texts, the special equipment made from glass and metals, necessary for carrying out the analyses. There are disscused in parallel with the conditions that must be fullfilled and the measures that have to be taken for carrying out the most precisely analysis. The book insists upon sampled quantity of compound, the interference between elements that can appear during the analysis, leading to anomalies in obtaining the best results.

Chapter I contains generalities regarding the halogens and organohalogenated compounds from the physicochemical point of view, presented according to the latest theories.

Chapter II describes the methods for halogen detection in organic compounds : by thermal decomposition, non-selective detection reactions, specific detection reactions and halogenated compound analysis based on the apparition of some known organic derivatives in the reactions.

Chapter III refers in details to the determination and dosing of chlorine, bromine and iodine in organohalogenated compounds.

Chapter IV presents only the analyses for fluorine.

Chapter V describes the ultramicro methods used for dosing the halogen traces in organic compounds. An important chapter is the VI-th where there are taken into consideration the qualitative and quantitative investigations of the organohalogenated compounds based on the different reactivity of the halogens.

Very interesting and at the same time usefull for the analyst is chapter VII, where there are described the interfference effects of the halogens and the methods used for their elimination, to perform the analyses of other elements : carbon, nitrogen, sulphur, phosphorus and oxigen.

Finally, chapter VIII contains a list of physico-chemical contants for 1000 of the most important organohalogenated compounds currently used in the chemical and pharmaceutical industry.

Dan Ciomartan

"Atlas of Thermoanalytical Curves", Edited by G. Liptay, Akadémiai Kiadó, Budapest coedition with Heyden & Son Ltd., London Volume 1, 1971, 50 diagrams ; Volume 2, 1973, 75 diagrams ; Volume 3, 1974, 75 diagrams ; Volume 4, 1975, 75 diagrams.

Methods of thermal analysis have rapidly developed during the last two decades, and have found widespread practical application. Today, thermoanalytical methods are important tools in research and routine analysis.

Owing to the very rapid developement of thermal analysis, it seemed desirable to start the continuous publication of a collection of diagrams to assist the work of researchers and chemists in industrial laboratories engaged in thermal analysis.

This collection of diagrams is to be broadened in scope, so as to develop it by international collaboration (using instruments other than the Derivatograph developed by Paulik — Z. anal. Chem. 160 (1958) 241 and Talanta 13(1966) 1405) into a handbook which can be used all over the world, and will be of good service to the steadily increasing number of thermal analysts. The present collection of diagrams (275) is part of a larger, comprehensive work in preparation. This volume is dealing with the measuring techniques and practical problems of thermoanalysis. In order to ilustrate the differences caused by the conditions of recording, this Atlas contains several curves for each substance taken under different experimental conditions. These diagrams have been especially prepared for this purpose and for this Atlas. The users of the Atlas of Thermoanalytical Curves will certainly find useful the much more complete information provided for the same material, in many cases, by combining the simultaneous technique with parallel recordings on instruments of other type (Mettler Recording Thermoanalyser, Sartorius Thermogravimat, Du Pont 990 Thermal Analysis System).

The experimental conditions may seem rather arbitrary. However, the selection was made in consideration of having due regard to the practical uses and possibilities, to the ICTA recommendations. The authors use this opportunity to call the attention of scientists and researchers active in the field of thermal analysis to the possibility of joint work. They welcome inquiries for cooperation.

The Atlas containing the collection of diagrams is very useful and will furnish guidance and assistance to those engaged in thermal analysis.

D. I. Marchidan

Structure and bonding, 22 (Structură și legătură). Springer Verlag, Berlin, Heidelberg, New York, 1975, 180 p.

Under the coverage "Rare earths", the 22-nd volume is devoted to the lanthanide elements. The interest of the subject is evidenced by the veritable explosion of papers and reports in the last decade. Also a large part of the 13th volume in the series refers to structural aspects of the lanthanide chemistry.

The present volume includes four large chapters. The object of the first is "The lanthanide ions as structural probes in biological and model systems". The substitution of metal ions in biochemical macromolecules by others of similar chemical reactivity, but possessing improved physical properties has proved to be a versatile research tool. The simple ionic chemistry of the lanthanide ions plays a dominant role in the chemistry of living systems and their application as structural probes is the result of their favourable physico-chemical properties. With this background the article written by E. Niebeer is a review of the methods employed and their success in providing information about the immediate and distant environment of the trivalent lanthanide ions when incorporated in model systems, or when complexed with low molecular weight molecules and macromolecules of biological interest. The most firmly established application of rare earths ions as structural probes is in NMR spectroscopy.

The following three chapters of the volume are dealing with theoretical developments in the matter. Under the heading "Partly filled shells constituting anti-bonding orbitals with higher ionization energy than their bonding counterparts", C. K. Jørgensen discusses in detail: one electron substitution in the lowest configuration, the Copenhagen principle of final states and the partly covalent bonding in respect to the lanthanides.

A topic largely developed in the volume is also "The intensities of lanthanide $f \leftrightarrow f$ transitions" reviewed by R.D. Peacock. The interest in the subject had begun with Van Vleck's paper published in 1937. At that time it had not been established whether the sharp lines in the spectra of trivalent lanthanide ions were in fact due to transitions within the $4f^N$ configuration or to transitions between that configuration and one of the higher energy (for example $4f^{N-1}5d$). Van Vleck concluded that, while the intensity produced by the allowed electric dipole mechanism was too large (ruling out $f \rightarrow d$ transitions), any of the other mechanisms could account for the observed intensities. He interpreted the many "extra" lines found in the spectra of most solid lanthanide compounds as being due to vibronic transitions and this gave weight to his point of view that much of the intensity was the result of the vibronically induced absorption of the electric dipole radiation. He also noted that since the $f \leftrightarrow f$ transitions of Eu(III), Gd(III) and Tb(III) are spin forbidden in zero order, magnetic dipole transitions should be relatively of more importance in the spectra of these ions.

The next step forward took place in 1942 when the group of spectroscopists at the University of Amsterdam began a systematic study of the solution spectra of the lanthanide aquo-ions. An important paper was published on the origin of intensities which reached somewhat different conclusions from those of Van Vleck. Further they calculated the oscillator strengths of the Pr^{3+}, Tm^{3+} and Yb^{3+} aquo ions considering only a static forced electric dipole mechanism and remarked that except for two transitions one in the spectrum of Pr^{3+} and one in that of Tm^{3+} this mechanism could account for all the intensity. Although based on semiquantitative calculations, the ideas included in this paper are broadly in agreement with the present-day opinion.

Except a compilation of the oscillator strengths of all the aquo ions issued in 1948 and an unpublished report in 1952, no other intensity data appear in the literature until after the publication of the theory of lanthanide intensities by B.R. Judd and G. S. Ofelt. This last theory has obviously been a great help in understanding lanthanide intensities and have prompted all recent studies in the topic. Although not really subjected to sufficient test, it appears to be a good working model at least for the non-hypersensitive transitions, provided the perturbation is not considered to be due to the electrostatic field of the ligands.

Most of the $f \leftrightarrow f$ transitions of the trivalent lanthanides have intensities which are little affected by the environment of the ion. A few however, called hypersensitives by Judd and Jørgensen, are very sensitive to the environment and are usually more intense when the ion is complexed than they are in the corresponding aquo ions. Spectra of aqueous solutions of Nd^{3+}, Eu^{3+}, Ho^{3+} and Er^{3+} nitrates of varying concentration obtained by Selwood in 1930 show clear hypersensitivity associated with certain absorption bands although the phenomenon was not commented upon at the time. Judd and Jørgensen treated few hypersensitive transitions of the trivalent lanthanides and concluded that they follow certain selection rules. On the whole it may be noted that Judd, the inhomogeneous dielectric and the dynamic coupling theories may all be considered to some extent to account for hypersensitivities. It may be also noticed that the interest generated in lanthanide spectral intensities has perhaps to some extent been responsible for the recent renewal of interest in the intensities of the transition metal spectra.

The last review of the volume is "Radiative and non-radiative transitions of rare earth ions in glasses". The author Renata Reisfeld discusses her experimental data in the domain in view of the theoretical approach of radiative transitions using the Judd-Ofelt theory. One of the important features of this theory is that once a set of three parameters for a specific rare earth ion in a given host has been obtained, they can be used to calculate absorption and emission probabilities between any f^N levels of the system. From the data presented it can be seen that the Judd-Ofelt model is able to predict with satisfactory accuracy (within 5 — 10%) the observed electric dipole absorption intensities in a large number of rare earths in different glasses. It is also possible to calculate correctly the radiative transitions probabilities and branching ratios of the rare earths in glasses using this model. Concluding, it is also believed that the radiative transition probabilities in many new glasses can be obtained and their validity as lasers predicted. The highest energy phonons in agreement with the theories concerning the multiphonon processes relaxation, are responsible for the nonradiative relaxation in glasses.

The compendium is written with the cooperation of outstanding specialists. The material included is presented in a clear and concise manner with tables and diagrams wherever necessary. Each article ends with an up-to-date bibliography including treaties, monographs, thesis, comprehensive articles, private communications, a large number of original papers, and even future literature, so that the volume provides the specialists with an useful guide to selected topics in the current research work.

Florica Popea

"*Topics in Current Chemistry*, Fortschritte der chemischen Forschung, 56, Theoretical Inorganic Chemistry" Springer Verlag, Berlin, Heidelberg, New York, 1975, 159 p.

The series presents critical reviews of the present position and future trends in modern chemical research. The volume comprises four large chapters. In the first "Continuum effects indicated by hard and soft anti-bases (Lewis acids) and bases" C. K. Jørgensen begins with a comprehensive historical introduction discussing the chemical affinity, the determination of complex formations constants (A) and (B) trends in complex chemistry, hard and soft anti-bases and bases, inorganic symbiosis and preparative chemistry. With this background spontaneous deviations from the highest symmetry available, electric dipolar polarizabilities and the approximately additive molar refractivities, quantum-chemical comments, softness parameters, hydration and ionization energies are further presented.

The following review is "Stereochemistry of the reactions of optically active organometallic transition metal compounds". Optically active organometallic compounds in which the transition metal is the center of chirality have been known since 1969, when the first manganese compounds were reported. In the meantime cyclopentadienyl and carbonyl transition metal complexes with 4, 5 and 6 ligands have been obtained in optically active form. H. Brunner describes in this article of the volume the stereochemical results obtained with the new optically active organometallic compounds, subdivided according to the stereochemical outcome into : retention, inversion, racemization and epimerization reactions.

In the third report of the book, I. H. Pignolet reviews "the dynamics of intramolecular metal-centered rearrangement reactions of tris-chelate complexes". Since the time of A. Werner, inorganic chemists have been intrigued by the observation of widely varying rates for isomerization reactions of metal complexes. Many studies have been carried out on reactions such as geometric isomerization and racemization especially with complexes which isomerize slowly, i. e. with half-lives of several hours or longer. In this category there are complexes of the traditionally non-labile metal ions such as Co(III), Cr(III), Rh(III), Ru(III) and Pt(II, IV). The extent of these kinetically "slow" reactions was usually pursued by spectrophotometric or polarimetric means, although chromatographic techniques have been employed. Since these techniques require isomer separation and ion resolution, it was very tedious to carry out experiments. Recently nuclear magnetic resonance (NMR) spectroscopy has been used to measure rates of isomerization reactions. This technique greatly simplifies isomer detection and with faster reactions often permits kinetic measurements without isomer separation. NMR line broadening techniques (DNMR) have now been extensively used to measure rates of reactions in which magnetically nonequivalent environments are averaged or interchanged on the NMR timescale. Reactions with rates between cca. 10^{-2} to 10^{6} sec^{-1} are best suited for DNMR studies and usually involve the kinetically "fast" metal ions such as Fe (III), Mn(III), V(III), Co(II), Ti(IV), Sc(III), Al(III) and Ga (III). Classical rate measurements seldom lead to unambiguous mechanistic predictions. Only with DNMR can detailed environmental site interchanges be directly observed and with this information the most probable mechanism can sometimes be deduced. In the present article the kinetics and probable mechanism for metal centered rearrangement reactions of this chelate complexes are presented, with respect to the β-diketonates, α-β-tiopolonates and dithiocarbamates separately. These three classes have been the most extensively studied and have yielded the most firm mechanistic conclusions. It is obvious that rates and mechanisms depend markedly on metal ion and ligand type. The problem of explaining these results is also approached by considering the effect of ground state geometry as determined from X-ray data on the kinetic parameters and mechanism for rearrangement.

The purpose of the last chapter is to develop and verify a reasonably simplified "theoretical approach to heterogeneous reactions in a nonisothermal low pressure plasma". With this purpose in mind, S. Vepřeck first considers a simple statistical model of the plasma which has brought about a better understanding of the dependence of the chemical composition of the plasma on energy. The comparison of this model with several real systems which had been experimentally investigated illustrates the applicability of the theoretical ideas to such systems as well as their limitations. The energy level diagrams, which can be compiled and used by any experimental chemists, represent a qualitative assessment of the dependence of chemical equilibrium composition of heterogeneous systems on the plasma parameters. The theoretical approach described in this review makes it possible to predict the direction of chemical transport as well as the relative amount of plasma energy which is necessary for the transport to take place. Such considerations also allow a choice of the most suitable heterogeneous system for chemical evaporation and/or deposition of a particular solid. The main subject was the theoretical aspects of plasma chemical vapour deposition processes. The results obtained so far show that the plasma of intense low pressure discharges offers new techniques of crystal growth. But the contribution of this theoretical approach presented is more in the nature of a challenge to perform more experimental work and to develop new ideas on the subject.

On the whole, the book succeeds in highlighting some very interesting and complex problems. All chapters are written by specialists currently doing research on the specific topics being covered. Provided with tables and diagrams whenever necessary, summing a large and updated information, the volume is addressed to all research and industrial chemists who wish to keep abreast of advances in their subject.

Florica Popea

NOTE POUR LES AUTEURS

La Revue Roumaine de Chimie publie des articles en anglais, français, russe, allemand ou espagnol. Les auteurs sont priés d'envoyer des articles et comptes rendus inédits.

Les manuscrits seront dactylographiés à deux intervalles. La bibliographie, les tableaux et la légende des figures seront placés après le texte.

Si l'article fait partie d'une série numérotée, le titre de la partie précédente sera indiqué dans une note au bas de la première page.

Chaque article sera précédé d'un résumé comprenant quinze lignes au maximum.

Les références bibliographiques dans le texte seront faites par des exposants sans parenthèse, et paraîtront comme des notes au bas de chaque page.

Les publications périodiques mentionnées dans la bibliographie seront présentées suivant les prescriptions internationales : le nom de l'auteur précédé de l'initiale du prénom, le titre du périodique abbrégé conformément à « Chemical Abstracts », et souligné par une ligne, le numéro du tome indiqué par des chiffres arabes et souligné par deux lignes, suivi de la première page de l'article ; à la fin, l'année de la parution sera placée entre parenthèses. Le numéro de la revue ne sera pas indiqué si les pages du volume sont numérotées consécutivement.

Les textes des livres ou traités incluеront : les noms des auteurs, les initiales du prénom, le titre du livre entre guillemets et sans être souligné, le numéro du tome précédé par l'abbréviation « vol. » (ou « Bd. »), le numéro de l'édition, les éditions (the publisher), la localité de la parution du livre, l'année de la parution et la page de la référence précédée(s) par l'abbréviation « p » (ou « S »).

Les brevets seront indiqués comme suit : l'auteur ou la firme, le pays et le numéro du brevet, la date et la revue (Chem. Abstr.). Par ex. : M. Jones (to Union Carbide Co.), Brit. Pat. 601 238, 2 Sept. 1959, *Chem. Abstr.*, **54**, 12808 (1960).

Les diagrammes seront tracés à l'encre de Chine sur papier calque. Les tableaux et les figures (en nombre strictement nécessaire) seront numérotés par des chiffres arabes. Les courbes dans les figures seront numérotées par des chiffres arabes et leur explication sera donnée dans la légende des figures. Prière de ne pas inscrire les mêmes données dans les tableaux et les figures. Chaque tableau aura un titre. On indiquera dans le texte la place approximative des tableaux et des figures. Les formules chimiques seront incluses dans le texte ; en outre, elles seront transcrites sur papier calque, à l'encre de Chine.

Les auteurs sont priés d'indiquer les caractères italiques (en soulignant les lettres au crayon), ainsi que tout autre caractère spécial ; les préfixes *ortho*, *meta*, *para*, *cis*, *trans*, etc. seront soulignés pour indiquer leurs caractères italiques et ne seront jamais écrites avec des majuscules.

Aucune correction à main ne sera admise sur le manuscrit. Les corrections seront frappées à la machine. Les lettres grecques ou autres symboles spéciaux seront insérés à la main à l'encre clairement.

Le manuscrit sera signé par l'auteur.

Le colonne-titre aura 50 lettres au maximum.

L'entière responsabilité du contenu des articles appartient aux auteurs.

TRAVAUX PARUS AUX ÉDITIONS DE L'ACADÉMIE DE LA RÉPUBLIQUE SOCIALISTE DE ROUMANIE

I. G. MURGULESCU, **Introducere în Chimia fizică. Vol. I. Atomi, molecule, legătură chimică** (Introduction à la Chimie Physique. Ier vol. Atomes, molécules, liaison chimique), 1976, 559 p., 36 lei.

P. BALTĂ, E. BALTĂ, **Introduction to the physical chemistry of the vitreous state**, co-édition avec Abacus Press, 1976, 400 p., 39 lei.

I. GĂLĂŢEANU, **Radiochimia aplicată. Metode şi probleme** (La radiochimie appliquée. Méthodes et problèmes), 1976, 305 p., 19 lei.

FR. A. GOTHARD, **Echilibre lichid-vapori. I. Baze teoretice şi metode de calcul** (Equilibres liquide-vapeurs. I. Bases théoriques et méthodes de calcul), 1975, 262 p., 28 lei.

CONST. GH. MACAROVICI, DAN MACAROVICI, **Chimia oxizilor dubli şi utilizările lor** (La Chimie des oxydes doubles et leurs utilisations), 1975, 194 p., 13 lei.

ELENA CEAUŞESCU, **Research work on synthesis and caracterization of macromolecular compounds. Contributions**, 1974, 251 p., 20 lei.

I. ZUGRĂVESCU et MAGDA PETROVANU, **Chimia N-Ilidelor** (La chimie des N-Ylures), 1974, 347 p., 19 lei.

MARGARETA AVRAM, **Antidăunători** (Pesticides), 1974, 494 p., 41 lei.

CR. SIMIONESCU, VIORICA RUSAN et N. POPA, **Chimia algelor marine** (La Chimie des algues marines), 1974, 211 p., 18 lei.

TIBERIU NĂŞCUŢIU, **Metode radiochimice de analiză** (Méthodes radiochimiques d'analyse), 1973, 384, p., 23 lei.

MARIA FITI, **Dozimetria chimică a radiaţiilor ionizate** (La dosimétrie chimique des radiations ionisantes), 1973, 240 p., 13,50 lei.

MIHAI FLORESCU, **Eficienţa economică a cercetării ştiinţifice** (L'efficience économique de la recherche scientifique), 1972, 115 p., 15 lei.

GEORGETA LĂZĂRESCU, **Sistematizarea informaţiilor în Chimia organică** (La systématisation des informations dans la Chimie organique), 1972, 252 p., 10,50 lei.

LYDIA-MARIA VAICUM, **Biodegrabilitatea detergenţilor** (La biodégrabilité des détergents), 1971, 254 p., 16 lei.

TIBERIU NĂŞCUŢIU, **Metode radiometrice de analiză** (Méthodes radiométriques d'analyse), 1971, 346 p., 19,50 lei.

I. ZUGRĂVESCU et L. STOICESCU-CRIVETZ, **Polimeri heterociclici** (Polymères hétérocycliques), 1971, 190 p., 9,50 lei.

1977 JUN 09

I. P. INFORMAŢIA c. 1566

43426

Lei 25.—

F 1103

ACADÉMIE DE LA RÉPUBLIQUE SOCIALISTE DE ROUMANIE

REFERÁLVA

REVUE ROUMAINE DE CHIMIE

TOME 22
N° 2
Février 1977

2 50 !

EDITURA ACADEMIEI REPUBLICII SOCIALISTE ROMÂNIA

Rev. Roumaine Chim.

RECHAX, 22, 2, p. 161 – 318 (1977), Bucarest

ACADÉMIE DE LA RÉPUBLIQUE SOCIALISTE DE ROUMANIE

COMITÉ DE RÉDACTION

Rédacteur en chef:

I. G. MURGULESCU, membre de l'Académie de la République Socialiste de Roumanie

Rédacteurs en chef adjoints:

A. T. BALABAN et V. EM. SAHINI, membres correspondants de l'Académie de la République Socialiste de Roumanie

Collège de rédaction:

EM. BRATU, ELENA CEAUŞESCU, ECATERINA CIORĂNESCU-NENITZESCU, C. DRĂGULESCU, CR. SIMIONESCU, membres de l'Académie de la République Socialiste de Roumanie; P. SPACU, membre correspondant de l'Académie de la République Socialiste de Roumanie; MARGARETA AVRAM, I. HAIDUC, D. I. MARCHIDAN, I. MOLDOVAN, G. NIAC et D. SĂNDULESCU

La Revue Roumaine de Chimie paraît 10 fois par an. Toute commande de l'étranger (fascicules ou abonnements) sera adressée à ILEXIM – Departamentul Export-Import Presă (Revues), P.O.B. 136–137, télex 11226, Bucarest, 3, str. 13 Decembrie, Roumanie

Les manuscrits, les livres et les revues proposés en échange, ainsi que toute correspondance seront envoyés à la rédaction :

REVUE ROUMAINE DE CHIMIE

23, str. Dumbrava Roşie, Bucarest, Roumanie, téléphone 12 41 60

EDITURA ACADEMIEI REPUBLICII SOCIALISTE ROMÂNIA

125, Calea Victoriei, 71021, Bucarest, Roumanie, téléphone 50 76 80

ORSZÁGOS MŰSZAKI KÖNYVTÁR ÉS DOKUMENTÁCIÓS KÖZPONT 1883

REVUE ROUMAINE DE CHIMIE

Tome 22, N° 2 Février 1977

LUCIA CIOHODARU, The electronic structure of some stilbene derivatives. III. The infrared spectra of some nitro-containing *trans*-stilbene derivatives . 163–170

LUCIA CIOHODARU, V. EM. SAHINI and ELENA VOLANSCHI, The electronic structure of some stilbene derivatives. IV. ESR spectra of some nitro-containing stilbene anion-radicals 171–179

K. POLINSZKY, E. VASANITS and J. FÜLÖP, Approximate analytic determination of the average values of potential functions occurring in chemical transport phenomena. 181–190

A A. BIELAŃSKI and J. M. ŁAGAN, An EPR study of oxygen and nitrous oxide chemisorption on manganese substituted X-type zeolites 191–199

CAMELIA BELDIE and OLIMPIA MIHĂILESCU, Dielectric constants and refractive indices in polyelectrolyte solutions 201–211

J. M. CACHAZA, J. CASADO y A. VARELA, Estudio de reacciones de Arbuzov. I. Mecanismo de reacciones de trialquil (-aril) fosfitos con yoduros de alquilo 213–220

MARGARETA TEODORESCU and MARIA BREZEANU, Steric effects in a series of tetracoordinated complexes of Co(II) containing phenanthroline derivatives 221–225

GH. MARCU and MARIANA RUSU, Heteropolytungstates with U(IV) as central atom. Synthesis and physico-chemical study of the $K_{10}[U(PW_{11}O_{39})_2]\cdot 22H_2O$ complex 227–235

N. VOICULESCU, Reactions of coordinated ligands. IX. Chloroaluminum-organic derivatives of coordinated dimethyl- and diphenylglyoxime 237–241

A. T. BALABAN, Chemical graphs. XXX. Reaction graphs for degenerate rearrangements of homovalenium cations 243–255

A D. C. SUSTER, G. BOTEZ, L. V. FEYNS, V. DOBRE and I. NICULESCU-DUVĂZ, Potential anticancer agents. XI. Derivatives prepared from diazotized pyrimidines 257–261

P. BUCHWALD and F. DOMNARIU, Cyanoethylation of ketoximes. III. Preparation of *para*-substituted-(benzylidene-aminoxy)-propionic acids . . . 263–269

EM. A. BRATU, CORNELIA BALABAN and GHEORGHIȚA I. JINESCU, Mass transfer from dispersed particles to continuous fluid media. II. Oscillating fluid media, particularly due to ultrasonic energy 271–282

CR. I. SIMIONESCU, ADELAIDA LIGA and N. ASANDEI, Researches in the terpolymerization field. IX. Chemical structure — properties correlation 283–291

Rev. Roumaine Chim. **22**, *2*, p. 161–318 (1977), Bucarest

C. LITEANU, GH. RĂDULESCU, GY. STEINBRECHER, A. MASCAŞ and M. PREDA, Study of the rectification properties of heterogeneous membranes. V. Behaviour of the celluloid membrane systems : Cationite-Ag+ +Anionite-S, Cationite-Ag+Anionite-Cl, Cationite-Hg+Anionite-Br . 293–300

GR. POPA and S. MOLDOVEANU, Theoretical study of the acidity of some organic reagents 301–304

S. FIŞEL et CATINCA SIMION, Concentration et séparation d'éléments à l'aide de chélateurs par la méthode de la zone fondue. I. Systèmes Cu(II)-Co(II) ou Cu(II)-Ni(II) et mercaptoacétanilide 305–311

COMPTES RENDUS 313–317

Revue Roumaine de Chimie, 22, 2, 163 – 170 (1977)

THE ELECTRONIC STRUCTURE OF SOME STILBENE DERIVATIVES. III[1]

THE INFRARED SPECTRA OF SOME NITRO-CONTAINING *TRANS*-STILBENE DERIVATIVES

LUCIA CIOHODARU

Department of Physical Chemistry, Polytechnic Institute,
Str. Polizu 1, Bucharest, Romania

Received September 5, 1975

The infrared spectra of 28 nitro-containing *trans*-stilbene derivatives are reported and discussed. New Hammett-type relations are obtained.

In two previous papers [1,2] we have reported and discussed the electronic absorption spectra of some nitro-containing *trans*-stilbene derivatives, in order to correlate them with molecular structure and to point out the electronic interactions in these extensive conjugated molecules depending on the substituent effects.

The present paper continues the discussion with reference to the infrared spectra of some stilbene derivatives.

The syntheses (according to the literature data) were reported in a previous paper. [2] The infrared spectra were recorded by means of a UR-10 Carl Zeiss Jena spectrophotometer with KBr pellets.

RESULTS AND DISCUSSION

The studied stilbene derivatives possess the following general formula, where A – G are the substituents listed in Table 1.

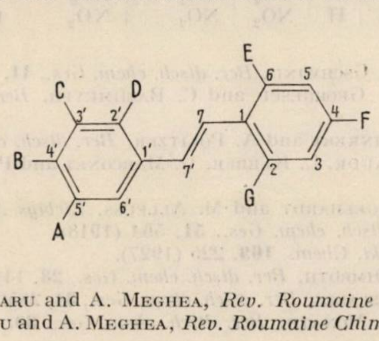

---

[1] Part II : L. Ciohodaru and A. Meghea, *Rev. Roumaine Chim.*, **21**,1127 (1976).
[2] Part I :L. Ciohodaru and A. Meghea, *Rev. Roumaine Chim.*, **21**,1473 (1976).

There are in the literature no data referring to the infrared spectra of these stilbene derivatives by now.

From the infrared spectra there were identified and specified the bands corresponding to $\gamma_{=C-H}$, $\nu_{C\equiv H}$, $\nu^{sym}_{NO_2}$, $\nu^{asym}_{NO_2}$, γ_{C-H}, as well as the bands corresponding to the frequencies of the characteristic group vibrations due to CO, NMe_2, OCH_3, $CONH_2$, OH.

Table 1

The nitro-containing trans-stilbene derivatives

No.	A	B	C	D	E	F	G	M.p.(°)	Ref.	Comments
1	H	H	H	H	H	NO_2	CN	141	[3]	
2	H	H	H	H	H	NO_2	$CONH_2$	262	[4]	2-cyano-
3	H	H	H	H	H	NO_2	COOH	206	[4]	4-nitro-
4	H	OH	H	H	H	NO_2	CN	219	[5]	*trans*-
5	H	OCH_3	H	H	H	NO_2	CN	197	[6]	stilbene
6	H	NMe_2	H	H	H	NO_2	CN	209	[6]	derivatives
7	H	NMe_2	H	H	H	NO_2	COOH	206	[7]	
8	H	H	H	H	H	CN	NO_2	168	[3]	
9	H	H	H	H	H	$CONH_2$	NO_2	180	[3]	
10	H	H	H	H	H	COOH	NO_2	233	[3]	
11	H	OH	H	H	H	CN	NO_2	230	[8]	2-nitro-
12	H	OCH_3	H	H	H	CN	NO_2	153	[6]	4-cyano-
13	H	NMe_2	H	H	H	CN	NO_2	180	[6]	*trans*-
14	H	NMe_2	H	H	H	$CONH_2$	NO_2	228	[5]	stilbene
15	H	NMe_2	H	H	H	COOH	NO_2	265	[5]	derivatives
16	H	$NHCOCH_3$	H	H	H	CN	NO_2	244	[9]	
17	$O-CH_2-O$		H	H	H	CN	NO_2	191	[6]	
18	OCH_3	OH	H	H	H	CN	NO_2	210	[8]	
19	OCH_3	$OCOCH_3$	H	H	H	CN	NO_2	168.5	[8]	
20	H	H	H	H	H	NO_2	NO_2	140	[10]	
21	H	H	H	NO_2	H	NO_2	NO_2	190	[11]	2,4-dinitro-
22	H	H	NO_2	H	H	NO_2	NO_2	179	[11]	*trans*-
23	H	NO_2	H	H	H	NO_2	NO_2	238	[11]	stilbene
24	H	NMe_2	H	H	H	NO_2	NO_2	174	[11]	derivatives
25	H	H	H	H	NO_2	NO_2	NO_2	155	[12]	2,4,6-trinitro-
26	H	OCH_3	H	H	NO_2	NO_2	NO_2	165	[6]	*trans*-
27	H	Cl	H	H	NO_2	NO_2	NO_2	154	[6]	stilbene
28	H	NO_2	H	H	NO_2	NO_2	NO_2	190	[3]	derivatives

---

[3] F. Ullmann and M. Gschwind, *Ber. dtsch. chem. Ges.*, **41**, 2291 (1908).

[4] E. Macovschi, I. I. Georgescu and C. Bachmeyer, *Ber. dtsch. chem. Ges.*, **74**, 1279 (1941).

[5] P. Pfeiffer, L. Klinkert and A. Politzer, *Ber. dtsch. chem. Ges.*, **49**, 2426 (1916).

[6] P. Pfeiffer, S. Braude, L. Kléber, G. Marconet and P. Wittkop, *Ber. dtsch. chem. Ges.*, **48**, 1797 (1915).

[7] P. Pfeiffer, J. Engelhardt and M. Allfuss, *Liebigs Ann. Chem.*, **467**, 158 (1928).

[8] P. Pfeiffer, *Ber. dtsch. chem. Ges.*, **51**, 564 (1918).

[9] P. Pfeiffer, *J. prakt. Chem.*, **109**, 225 (1927).

[10] J. Thiele and O. Dimroth, *Ber. dtsch. chem. Ges.*, **28**, 1412 (1895).

[11] J. Thiele and R. Escales, *Ber. dtsch. chem. Ges.*, **34**, 2850 (1901).

[12] P. Pfeiffer and P. Monath, *Ber. dtsch. chem. Ges.*, **39**, 1306 (1906).

The bands could be attributed to individual vibrations by an empirical procedure, using results of some studies on similar compounds.[13-19]

The infrared spectra point out a difference between the positional isomers, even between the closely related compounds, and this is of use for an analytical study.

Examining the obtained IR spectra of the 28 investigated nitro-containing *trans*-stilbene derivatives, the following can be noticed:

1. The $\gamma_{=C-H}$ deformation vibration frequency appears at 968 cm^{-1} for the unsubstituted *trans*-stilbene, while for the studied derivatives it appears between 946 and 982 cm^{-1} (Table 2). In most cases, this band has two maxima, according to the literature data with reference to other stilbene derivatives.

Table 2

The out-of-plane in-phase vibration of the two trans-ethylenic hydrogen atoms ($\gamma = C-H$)

N°	$\gamma = C-H$	N°	$\gamma = C-H$
1	958 shm, 972 m	15	956 s
2	968 s, 981 m	16	955 shw, 970 m
3	967 m	17	968 m, 986 w
4	958 w, 970 m, 982 w	18	958 m
5	970 m, 982 m	19	960 shw, 969 m
6	953 m, 970 m	20	963 m, 978 m
7	952 s, 960 s, 971 m	21	978 m
8	975 s	22	968 m
9	967 m	23	963 m, 974 m
10	958 m	24	950 m, 974 s
11	970 w	25	946 w, 980 m
12	970 m	26	946 w, 987 m
13	950 m, 967 m	27	961 w, 981 m
14	950 m, 963 m	28	967 m, 978 m

s – strong; m – medium; w – weak; sh – shoulder.

---

[13] A. W. Thompson, E. E. Vago, M. C. Corfield and S. F. D. Orr, *J. Chem. Soc.*, **1950**, 214.

[14] K. Lunde and L. Zechmeister, *Acta Chem. Scand.*, **8**, 1421 (1954).

[15] De Los F. De Tar and L. A. Carpino, *J. Amer. Chem. Soc.*, **78**, 475 (1956).

[16] O. H. Wheeler and H. N. Battle de Pabon, *J. Org. Chem.*, **30**, 1473 (1965).

[17] S. F. D. Orr, *Spectrochim. Acta*, **8**, 218 (1956).

[18] A. R. Katritzky, A. J. Boulton and D. J. Short, *J. Chem. Soc.*, **1960**, 1519.

[19] H. Veschambre and A. Kergomard, *Bull. Soc. chim. France*, **1**, 336 (1966).

The displacements of the $\gamma_{=C-H}$ characteristic vibrations of every stilbene derivative are due to :

— the electron-withdrawing or electron-donating nature of the substituents in molecules ;

— the position of the substituents in molecules ;

— the size of the substituents in *ortho*-position to the ethylenic bridge, that is the extent of steric hindrance to planarity.

Of course, "the weight" and the relative extent of each of the above effects cannot be estimated. Therefore, the given appreciatons refer to the overall substituent effects on the mentioned vibrations.

Furthermore, the $\gamma_{=C-H}$ values are depending on the substituent constants σ ; that is why we attempt to obtain new Hammett-type relations. The substituent constants σ are according to the literature data.[20-22] The values of the correlation coefficients were verified [23] with reference to the possibility to decline the assumption of the correlation of the above variables.

Accordingly :

— for 2-cyano-4-nitro-stilbene derivatives ;

$\gamma_{=C-H} = 975.6 + 30.6\ \Sigma\sigma,\ r = 0.680$;

— for 2-nitro-4-cyano-stilbene derivatives :

$\gamma_{=C-H} = 972.8 + 30.4\ \Sigma\sigma,\ r = 0.710$;

— for 2,4-dinitro-stilbene derivatives :

$\gamma_{=C-H} = 960.2 + 13.5\ \Sigma\sigma,\ r = 0.965$;

— for 2,4,6-trinitro-stilbene derivatives :

$\gamma_{=C-H} = 951.0 + 21.8\ \sigma\Sigma,\ r = 0.948$.

Table 3

The stretching vibration frequency corresponding to the cyano group ($\nu_{C\equiv N}$)

N°	$\nu_{C\equiv N}$	N°	$\nu_{C\equiv N}$
1	2 230 s	12	2 237 m
4	2 246 m	13	2 230 m
5	2 232 m	16	2 242 m
6	2 230 m	17	2 235 m
8	2 234 s	18	2 246 s
11	2 235 w	19	2 237 m

s – strong ; m – medium ; w – weak

2. The frequencies of the $\nu_{C\equiv N}$ stretching vibration band of cyano-stilbene derivatives are between 2230 and 2246 cm^{-1} (Table 3), according to the literature data[24] with reference to the cyano-benzene derivatives, being, however, a little higher. The presence of two electron-withdrawing substituents in one benzene ring and of one or two electron-donating substituents in another one increases the conjugation over the whole molecule and produces a displacement of $\gamma_{C\equiv N}$ towards higher values. It is the same conclusion as resulted from the electronic absorption spectra,[2] as well as by comparison of the molecular diagrams,[25] namely that in the first

---

[20] L. P. Hammett, "Physical Organic Chemistry", McGraw-Hill Book Company, Inc., New-York, 1940, p. 188.

[21] H. Bekkum, P. E. Verkade and B. M. Wepster, *Rec. Trav. chim.*, **78**, 815 (1959).

[22] D. Fărcașiu, *Studii și cercetări chim. Acad. R.S.R.*, **14**, 37(1966).

[23] D. Ceaușescu, "Tratarea statistică a datelor chimico-analitice", Editura tehnică, București, 1973, p. 225.

[24] M. Avram and Gh. D. Mateescu, "Spectroscopia în infraroșu. Aplicații în chimia organică", Editura tehnică, București, 1966, p. 511 – 513.

[25] L. Ciohodaru (to be published).

electronically excited state the π-bond order of C—CN bond increases. In consequence, the force constant of this bond and, also, the corresponding frequency, increase.

The $\gamma_{C\equiv N}$ values are well defined for the couple of positional isomers : no. 1 and 8 ; 4 and 11 ; 5 and 12 ; 6 and 13.

Also, a Hammett-type relation between the $\gamma_{C\equiv N}$ values and the substituent constants σ is reported, but only for 2-nitro-4-cyano-stilbene derivatives :

$$\nu_{C\equiv N} = 2238.5 + 12.3\ \Sigma\sigma,\ r = 0.763.$$

3. The frequency of the symmetric stretching vibration band of the nitro group, $\gamma_{NO_2}^{sym}$, appears between 1330 and 1368 cm^{-1} (Table 4). This band is of essentially constant position for the positional isomers no.21, 22 and 23 as well as for the 2,4,6-trinitro-stilbene derivatives. It does follow that the position of the nitro group in the second benzene ring does not influence $\nu_{NO_2}^{sym}$; neither does the presence, even in 4′-position, of some different electron-donating or electron-withdrawing substituents (Cl, OCH_3, NO_2). Therefore, in these extensive conjugated systems, the introduction of a new substituent in a second benzene ring does not influence $\nu_{NO_2}^{sym}$ for the nitro group in the first ring in contrast with the nitro-benzene derivatives where a displacement of the corresponding band of about 40 — — 50 cm^{-1} is recorded. These data suggest a much weaker transmission of substituent effects in the investigated stilbene derivatives as compared to the benzene derivatives, according to the literature data referring to similar compounds.[19]

Table 4

The symmetric stretching vibration frequency corresponding to the nitro group ($\gamma_{NO_2}^{sym}$)

N⁰	$\nu_{NO_2}^{sym}$	N⁰	$\nu_{NO_2}^{sym}$
1	1348 vs, 1360 vs	15	1350 vs, 1373 vs
2	1330 shvs, 1346 vs	16	1356 m
3	1352 shm, 1372 m	17	1352 s
4	1350 vs	18	1368 s
5	1350 s	19	1358 s
6	1340 m, 1380 m	20	1343 m, 1358 m
7	1330 vs	21	1354 s
8	1362 vs	22	1355 vs
9	1355 m, 1366 m	23	1353 vs
10	1350 m	24	1342 vs
11	1350 m	25	1351 m, 1366 m
12	1362 m	26	1354 vs
13	1347 m, 1368 m	27	1355 vs
14	1359 s	28	1355 vs

vs – very strong ; s – strong ; m – medium ; w – weak ; sh – shoulder.

For the studied stilbene derivatives, the frequency of the antisymmetric stretching vibration band of the nitro group, $\nu_{NO_2}^{asym}$, occurs between 1493 and 1560 cm^{-1} (Table 5). Generally, a number of one to three bands appear in the infrared spectra of the nitro-containing stilbene derivatives, this number being greater in the presence of more nitro groups. The assignment of these frequencies (Table 5) is only tentative and is based on the following: [26]

Table 5

The antisymmetric stretching vibration frequency corresponding to the nitro group ($\nu^{asym}_{NO_2}$) and the assignment of the vibration

N°	$\nu^{asym}_{NO_2}$	N°	$\nu^{asym}_{NO_2}$
1	1525 vs(1)	17	1515 s(3), 1535 m(4), 1556 m(5)
2	1493 m (2), 1508 m, 1532 s, 1560 shm	18	1502 m, 1516 shm(3), 1530 s (4), 1545 s
4	1523 vs(1)	19	1522 s(3), 1538 s(4), 1506m(5)
5	1515 shs, 1525 s(1)	20^a	1516 shm(3), 1530 m-broad(6)
6	1490 shm, 1520 m(1), 1538 m	21^b	1493 m(2), 1516 shm(3), 1530 s(4)
7	1490 s(2), 1515 shvs, 1523 vs(1), 1541 vs	22^b	1498 shm(2), 1516 shs(3), 1537 vs(4) or (6)
8	1512 m(3), 1540 vs(4), 1560 s(5)	23^b	1480 shm(7), 1516 shs(2), 1532 vs(4)
9	1492 m, 1516 shm(3), 1532 s(4)	24^b	1515 shs(3), 1525 shvs (1), 1539 vs(4) or (6)
10	1528 m, 1560 m(5)		
11	1520 m(3, 1532 shm(4), 1542 shm	25^b	1505 m(2), 1528 shs(1), 1548 s(8)
12	1526 m(3), 1560 w(5)	26^b	1512 shs(3), 1524 vs(1), 1548 vs(8)
13	1516 shm(3), 1530 m(4), 1560 m(5)	27^b	1523 shm(1), 1544 s(4) or (6) or (8), 1560 s(5) 1560 s(5)
14	1538 s(4), 1560 shm(5)		
15	1492 s, 1530 vs (4), 1560 s(5)	28^c	1500 shm(2), 1526 vs(1), 1553 vs(8), 1560 shm(5)
16	1498 shm, 1535 s(4), 1555 s		

(1) the nitro group in 4-position, other W substituent in 2-position; (2) conjugated nitro group in 4-position; (3) conjugated nitro group in 2-position; (4) out-of-plane nitro group in 2-position; (5) the nitro group in 2-position, other W substituent in 4-position; (6) two nitro groups in *meta* position with each other, unconjugated due to steric reasons; (7) two nitro groups in 4,4′-positions; (8) three nitro groups in *meta* positions with each other; W-withdrawing substituent; ^{a}-stilbene derivative having two nitro groups and two bands; ^{b} – stilbene derivative having three nitro groups and three bands; ^{c} – stilbene derivative having four nitro groups and four bands; vs – very strong; s – strong; m – medium; w – weak; sh – shoulder.

— when the nitro group is found in the benzene ring plane, $\nu^{asym}_{NO_2}$ appears at 1498 cm^{-1};

— when there are two nitro groups in *meta* positions with each other, $\nu^{asym}_{NO_2}$ appears between 1520 and 1540 cm^{-1};

— in case of steric hindrance to planarity, the $\nu^{asym}_{NO_2}$ becomes greater; the π-bond order, as well as the ν_{N-O} frequency, increases, due to the decreasing conjugation with the benzene ring. Again, it is the same conclusion we have already reported as resulted from the molecular diagrams.

Accordingly, we can mention that there is a tendency of the neutral molecules of some nitro-containing stilbene derivatives to adopt a non-planar conformation, although the out-of-plane deviations are small. This effect is stronger especially for the nitro group in *ortho* position to the ethylenic bridge or for two nitro groups in *meta* positions with each other.

---

[26] B. Franck, H. Hörmann and S. Scheibe, *Chem. Ber.*, **90**, 330 (1957).

4. In comparison with the corresponding benzene derivatives, for the studied stilbene derivatives, the frequency of the deformation vibration for the ring hydrogens depending on the benzene ring substitution, γ_{C-H}, appears in about the same regions, without significant displacements (Table 6).

Table 6

The deformation vibration frequency of the ring hydrogens depending on the benzene ring substitution (γ_{C-H})

N^o	Mono-subst.	Disubstitution			Trisubstitution (1, 2, 4,)	Tetrasubst. (1, 2, 3, 5)
		o	*m*	*p*		
1	750 s	758 m	780 m	823 m	823 m, 871 m	
2	738shm	750m	780m	810m, 823m	810m, 823m, 862m, 872m	
3	753m	770shm	790w	830w	830w, 874shw	
4	748m	768m	785m	805m, 815m	805m, 828m, 848m, 866w	
5	748m	755m	790m	825m	825m, 870m	
6	745m		785m	800m	820m, 860m	
7	747s	765m	782m	808s	825s, 885m	
8	748s	768m	778m	823m	823m, 879m	
9	750w	763m	780shw	823w	823w, 862w, 875w, 892w	
10	736m	767s	770s, 785w	830w	830w, 860w, 880w	
11		760w		800w, 825w	825w, 865w	
12	750w	770w	782w	822w	822w, 837w	
13		760m	780m	800m, 820m	820m, 880m	
14	752m		782m	813s	813s, 836m, 881m	
15		760m	780m	810s, 823m	823m, 885m	
16		762w	778w	812w, 823m	823m, 835m, 848m, 870w, 885w	
17		762w		796m, 822m	802m, 836m, 870m	
18	745m	769m	787m	830m	805m	
19	748w	767w	780w	828w	828w, 878m	
20		758m			835m, 875w	
21		758m	770w	818m	834m, 862m	
22		748m		818m	839m, 868w	
23		752m		820m	836m, 878m	
24	735m, 743m		768w	813s	830s, 863m, 879m	
25	738m	752m	766w, 780w	823w	823w	850w
26	752w	763m	782w	830s	830s, 878w	862w, 878w
27	740m	753w	777w	826m	831m, 882w	882w
28	740m	754m	780w	829m	829m, 870m, 890m	853w, 870m 890m

s – strong; m – medium; w – weak; sh – shoulder.

5. The assignments of the characteristic vibration group frequencies of the other substituents (CO, NMe_2, OCH_3, $CONH_2$, OH) are in agreement with the literature data, without great displacements.

The following conclusions can be drawn from the infrared spectra of the stilbene derivatives dealt with in this paper :

— the transmission of the substituent effects through the ethylenic bridge is much weaker in the investigated stilbene derivatives as compared to the corresponding benzene derivatives ;

— the neutral molecules of the *ortho*-nitro-stilbene derivatives tend to adopt nonplanar conformations ;

— linear dependences between the characteristic frequencies of some vibrations ($\gamma_{=C-H}$, $\nu_{C\equiv N}$) and substituent constants σ are reported ;

— the assignment of the bands corresponding to the $\nu_{NO_2}^{asym}$ stretching vibration frequency was made, based on the consideration of the molecular structure of every stilbene derivative.

Revue Roumaine de Chimie, **22**, *2*, 171 – 179 (1977)

THE ELECTRONIC STRUCTURE OF SOME STILBENE DERIVATIVES. IV[1]

ESR SPECTRA OF SOME NITRO-CONTAINING STILBENE ANION-RADICALS

LUCIA CIOHODARU, V. EM. SAHINI and ELENA VOLANSCHI

Department of Physical Chemistry, Polytechnic Institute, Bd.Republicii 13,
Bucharest, Romania

Received September 15, 1975

ESR spectra of some polysubstituted nitro-stilbene anion-radicals are reported. The effect of the substituents on the spin-distribution is evidenced by comparison with the corresponding toluene anion-radicals. The modifications in the electronic structure are well accounted by MO calculations in the framework of Hückel and McLachlan approximations.

The electronic distribution in the stilbene anion-radical as reflected by its ESR spectra was already investigated by several authors. [2-4] However substituted derivatives from this molecule are little investigated, the existing studies involving only 4-nitro-, 4,4′-dinitro- and 4-nitro-4′-amino-stilbene.[5-7] Therefore, we consider interesting to study the effect of several substituents on the spin-distribution, and especially in the presence of the strongly perturbing nitro group. In order to better evidence the effect of the substituents on the stilbene molecule, their influence was compared to that on a single benzene ring, and, therefore, the corresponding polysubstituted toluenes were also investigated.

EXPERIMENTAL

2-cyano-4-nitro-4′-methoxy-stilbene (m.p. = 196°), (1), 2-nitro-4-cyano-4′-methoxy-stilbene (m.p. = 153°), (2), 2,4,4′-trinitro-stilbene (m.p. = 238°) (3), 2-cyano-4-nitro-toluene (m.p. = 106°), (4), 2-nitro-4-cyano-toluene (m.p. = 107°) (5), 2,4-dinitro-toluene (m.p. = 70°),

---

[1] Part III : L. Ciohodaru, *Rev. Roumaine Chim.*, **22**,163 (1977).

[2] V.V. Voevodski, S. P. Solodovnikov and V. M. Cibrikin, *Doklady Akad. Nauk S.S.S.R.*, **129**, 1082 (1959).

[3] R. Chang and C. S. Johnson, *J. Chem. Phys.*, **41**, 3273(1964) ; *ibid.*, **43**, 3183 (1965).

[4] N. M. Atherton, F. Gerson and J. N. Ockwell, *J. Chem. Soc., Inorg., Phys. Theor.*, **A2**, 109(1966).

[5] L. S. Degtiarev and Iu. A. Krugliak, *Teor. i. eksper. Khimiya*, **2**, 184 (1966).

[6] A. I. Brodski, B. I. Gordienko and L. S. Degtiarev, *Electrochim. Acta*, **13**, 1095(1968).

[7] B. I. Sapiro, V. M. Kozakova and Ia. K. Sirkin, *Zhur. strukt. Khim.*, **4**, 540 (1965).

(6) were synthetised as indicated in the literature.[8,9] The anion-radicals were prepared using an electrochemical *"in situ"* technique previously described,[10] with dimethyl-formamide (DMF) as solvent and tetra-n-butyl ammonium iodide in concentration of 0.1M as supporting electrolyte. The chemical reduction with sodium or potassium in DMF was also used, leading, in general, to better resolved spectra. The ESR spectra were recorded on a JES-3B Spectrometer in the X-band frequency, using peroxylammine disulphonate as standard ($a_N = 13$ *Gs*).

MO CALCULATIONS

The MO calculations were carried out in the frame of Hückel and McLachlan approximations on Felix C-256 and IBM 370/135 computers.

The parameters and the equations used in the spin-density calculations, together with the corresponding references are contained in *Table 1*. For the splitting constant of the nitro group nitrogen two sets of values were used for the $\sigma - \pi$ parameters : the set (a) was suggested by Rieger and Fraenkel [11] in their study of several nitrobenzenes ; the set (b) was suggested by Degtiarev and Krugliak [5] for the nitrostilbene derivatives.

Table 1

Parameters and equations used in the MO calculations

	h_X	k_{CX}	*Reference*
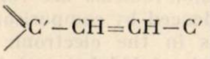	$h_C = 0$ $h_{C'} = 0$	$k_{CC'} = 0.9$ $k_{CC} = 1.1$	3
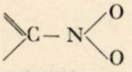	$h_N = 2.2$ $h_0 = 1.4$	$k_{CN} = 1.2 \div 0.8$ $k_{NO} = 1.67$	11
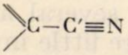	$h_{C'} = 0$ $h_N = 1.0$	$k_{C'N} = 2.0$ $k_{CC'} = 0.9$	11
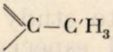 (conjugative model)	$h_{H_3} = -0.5$ $h_{C'} = -0.1$	$k_{C' \equiv H_3} = 2.5$ $k_{CC'} = 0.9$	11
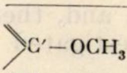 (heteroatom model)	$h_{OCH_3} = 1.9$	$k_{C'OCH_3} = 0.8$	13

$$a_N^{CN} = (23.1 \pm 1.4)\, \rho_N^{\pi} - (6.8 \pm 2.2) \rho_{c'}^{\pi} \quad {}^{11}$$

$$\text{(a) } a_N^{NO_2} = \pm\, (99.0 \pm 10.2)\, \rho_N^{\pi} \mp 2(35.8 \pm 5.9))\rho_0^{\pi} \quad {}^{11}$$

$$\text{(b) } a_N^{NO_2} = 185\, \rho_N^{\pi} - 2 \times 63\, \rho_0^{\pi 5}$$

$$\text{(c) } a_H^{CH_3} = 27.2\, \rho_c^{\pi 12}$$

$$\text{(d) } a_H^{CH_3} = 220\, \rho_{H_3}^{\pi 12}$$

$$a_H^H = Q_{CH}^H\, \rho_c^{\pi} ; Q_{CH}^H = /24/\text{Gs.}$$

---

[8] J. Thiele and R. Escales, *Ber. dtsch. chem., Ges.*, **34**, 2850 (1901).

[9] P. Pfeiffer, S. Braude, J. Kléber, G. Marconet and P. Wittkop, *Ber. dtsch. chem. Ges.*, **48**, 1797 (1915).

[10] E. Volanschi, C. Vlădescu and C. Volanschi, *Rev. Roumaine Chim.*, **19**, 755 (1974).

[11] P. H. Rieger and G. K. Fraenkel, *J. Chem. Phys.*, **39**, 609 (1963).

For the methyl group splitting two models were used: in model (c) a McConnell type formula with $Q^{\mathrm{H}}_{\mathrm{CH_3}} = 27.2$ Gs was employed, in model (d) the spin-density in the π-orbital of the pseudo-atom H_3, $\rho^{\pi}_{\mathrm{H_3}}$, was used with $Q^{\mathrm{H}}_{\mathrm{CH_3}}=220$ Gs, according to Fraenkel.[12] The calculated hyperfine splitting (hfs) constants, together with the experimental ones are collected in *Table 2*.

RESULTS AND DISCUSSION

The ESR spectra of the anion-radicals obtained from the polysubstituted stilbenes (1), (2) and (3) are presented in Figures 1 – 3 and were analysed with the splitting constants in *Table 2*. The analysis of the spec-

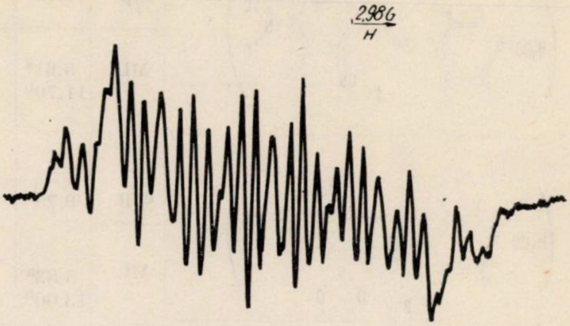

Fig. 1. – ESR spectrum of the 2-cyano-4-nitro-4′-methoxy-stilbene anion-radical (Na, DMF).

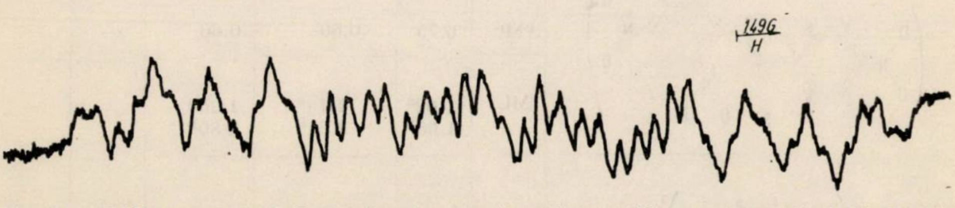

Fig. 2. – ESR spectrum of the 2-nitro-4-cyano-4′-methoxy-stilbene anion-radical (K, DMF).

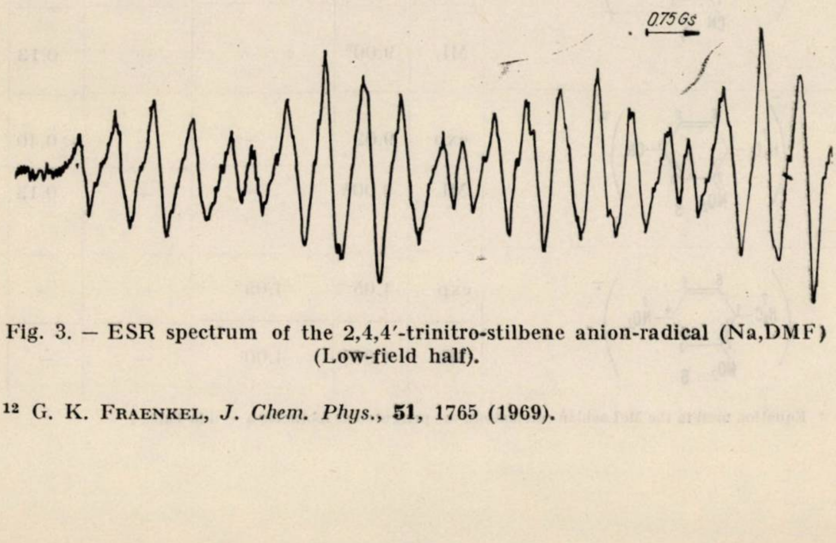

Fig. 3. – ESR spectrum of the 2,4,4′-trinitro-stilbene anion-radical (Na,DMF) (Low-field half).

---

[12] G. K. Fraenkel, *J. Chem. Phys.*, **51**, 1765 (1969).

Table

Experimental and calculated*

Anion-radical		$a_{N_8}^{NO_2}$	$a_{N_9}^{NO_2}$	$a_{N_{10}}^{NO_2}$	a_N^{CN}	a_H^2
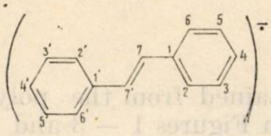	exp	—	—	—	—	2.96
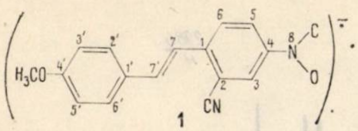 1	exp	7.50	—	—	<0.40	—
	ML	5.61[a] 11.70[b]	—	—	0.02	—
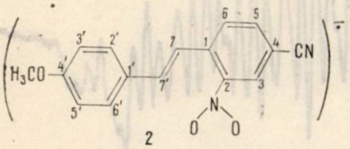 2	exp	9.75	—	—	<0.30	—
	ML	5.83[a] 13.00[b]	—	—	0.03	—
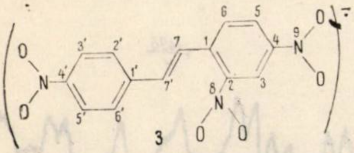 3	exp	6.75	0.60	0.60	—	—
	ML	1.02[a] 1.65[b]	1.14[a] 2.34[b]	1.25[a] 2.80[b]	—	—
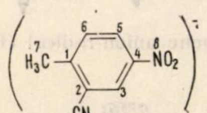 4	exp	9.10	—	—	<0.40	—
	ML	9.00[a]	—	—	0.13	—
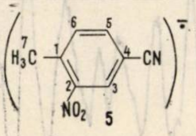 5	exp	9.02	—	—	<0.40	—
	ML	9.00[a]	—	—	0.13	—
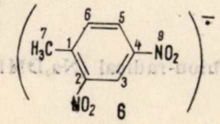 6	exp	4.05	4.05	—	—	—
	ML	4.00[a]	4.00	—	—	—

* Equation used in the McLachlan calculations are presented as footnotes a — d in Table 1.

2

hfs constants (Gauss)

a_H^3	a_H^4	a_H^5	a_H^6	a_H^7	$a_H^{7'}$	$a_H^{02'}$	$a_H^{3'}$	$a_H^{4'}$	$a_H^{5'}$	$a_H^{6'}$	Line width (*Gs*)
0.81	3.89	0.30	1.90	4.37	4.37	2.96	0.81	3.89	0.30	1.90	
3.39	—	3.39	0.90	<0.40	4.95	0.90	<0.40	—	<0.40	0.90	0.40
2.09	—	3.15	0.96	0.40	3.96	0.96	0.32	—	0.32	0.96	
2.10	—	3.48	2.10	<0.30	4.05	0.60	<0.30	—	<0.30	0.60	0.30
1.66	—	3.79	1.29	0.37	3.81	0.93	0.31	—	0.31	0.93	
<0.20	—	2.63	<0.20	<0.20	3.15	<0.20	<0.20	—	<0.20	<0.20	0.20
0.40	—	2.77	0.45	1.03	2.99	0.57	0.67	—	0.67	0.57	
3.34	—	3.65	1.22	4.56	—	—	—	—	—	—	0.40
2.86	—	3.52	1.13	4.66[c] 4.17[d]	—	—	—	—	—	—	
2.70	—	3.60	0.97	4.50	—	—	—	—	—	—	0.40
3.18	—	4.17	1.12	3.92[c] 4.04[d]	—	—	—	—	—	—	
1.05	—	2.85	1.95	4.80	—	—	—	—	—	—	0.40
0.39	—	6.30	1.70	7.22[c] 7.04[d]	—	—	—	—	—	—	

trum in Fig. 2 is more difficult, as its aspect is complicated by alternating line-width effects. The hfs constants reported in *Table 2* give a good fit with the unbroadened central component and are reasonable as compared with the other studied derivatives.

The assignment of the hfs constants to different positions is only tentative and is based on the best fit with the calculated splitting constants.

The hfs constants of the corresponding substituted toluenes are also contained in *Table 2*. The assignment for these molecules is facilitated and verified by comparison with many substituted benzenes.[11,14] Therefore, the influence of every substituent will be first evidenced in the polysubstituted toluenes and then used in interpreting the data for the substituted stilbenes. The effect of the extended conjugation and the perturbing role of the ethylenic bond on the electronic distribution will be further evidenced by comparison with the unsubstituted stilbene radical, which is, therefore, also contained in *Table 2*.

Examining the experimental hfs constants reported for compounds (4), (5) and (6), the following may be stated :

— when a single nitro group is present, it has the greatest splitting constant, pointing out a high spin-density on the nitrogen atom. The introduction of a second nitro group reduces the nitrogen splitting constant to about one half and brings about small modifications in the proton splittings of the *ortho* and *para* positions (3 and 5) ;

— the splitting of the methyl group is that expected for a methyl in *ortho* or *para* to a nitro group in a benzene ring[11] and its presence does not perturb the spin-distribution.

Therefore, it may be concluded that the dominant perturbing role in the polysubstituted toluene anion-radicals is exerted by the nitro group.

Examining the data reported for the unsubstituted stilbene anion-radical, it may be noticed that the odd electron is mainly delocalized on the ethylenic bond and symmetrically in the two benzene rings, the a_H being in the order *para* (4,4′) > *ortho* (2,2′, 6,6′) > *meta* (3,3′, 5,5′).

If a single nitro group is introduced (radicals (2) and (3)), the greatest hfs constant is that of this nitrogen atom and its presence in one ring determines an asymmetry in the spin-distribution. This asymmetry is apparent from the similitude of the experimental splittings of the nitro-containing ring in radicals (1) and (2) to the corresponding positions in the "halves" of the molecules, that is in radicals (4) and (5), respectively. From the second ring only two protons appear in the experimental spectrum with smaller hfs constants, and these are presumably those from the 2′ and 6′ sites, as it is pointed out by the comparison with the stilbene radical and with spin-density calculations. The same asymmetry is evidenced by the appearance in the experimental spectrum of a single proton with a hfs constant in the range 4 - 5 Gs ; the similitude of this splitting to the methyl hfs constant in the corresponding substituted toluenes and to the ethylenic protons in the unsubstituted stilbene anion-radical, on one

[13] H. Güsten and L. Klasinč, *Tetrahedron Letters*, **30**, 2923 (1967).

[14] A. H. Maki and D. H. Geske, *J. Amer. Chem. Soc.*, **83**, 1852 (1961).

side, and the good agreement with the calculated hfs constants, on the other side, made us assign it to position 7′.

The perturbation effect due to the nitro group is also reflected in the line-width alternation observed in the spectrum of radical (2).(fig. 2). The greater nitrogen splitting observed for this compound could be assigned to a steric hindrance which may force it to get out of the plane of benzene ring. [11] It was pointed out by Freed and Fraenkel [15] that steric hindrance may also enhance line-width alternation, that is fluctuations of the same order of magnitude in the splitting constant of hindered and unhindered anion-radicals may bring about greater changes in the former ones. This may also be an explanation for the appearance of such phenomena in our case for radical (2) and not for (1), although both were produced by chemical reduction *.

The presence of three nitro groups in the molecule (anion-radical (3)) determines a decrease of the nitrogen hfs constants, two nitrogens appearing as equivalent with 0.60 Gs and one with 6.75 Gs. A possible assignment is that suggested in *Table 2*, justified by comparison with the 4,4-dinitro-stilbene anion-radical. [7] A discussion of the proton splittings in this compound is not conclusive, as in the experimental spectrum only two protons are resolved.

The cyano and methoxy substituents in the stilbene molecule have practically no influence on the spin-distribution, their splittings being under the resolution of the experimental spectrum in both cases, a fact which is in good agreement with the calculated spin-densities.

A comparison of the calculated hfs constants contained in *Table 2* points out a better overall agreement for the substituted toluenes than for the stilbene anion-radicals; this fact is explainable if we take into account the size of the molecule and the presence of several substituents, which introduce additional approximations. As concern the nitrogen splittings, a very good agreement is obtained for compounds (4), (5) and (6) using Rieger-Fraenkel's formula. For the anion-radicals (1), (2) the experimental nitrogen splittings are between those calculated by Rieger-Fraenkel's formula (a) and Degtiarev-Krugliak's formula (b). For the anion-radical (3) all the formulae fail, but the presence of three nitro groups in the stilbene molecule makes this failure explainable.

In order to better evidence the effect of the substituents in the stilbene anion-radical as compared to that on the neutral molecule, π-bond orders for compounds (1), (2) and (3) were calculated. The results are contained in *Table 3*. Their examination points out a lowering of the bond-order of the ethylenic bond in the anion-radicals, which is greatest for

---

* Line-width alternation in a molecule which contains a single nitro group was observed in the case of the nitrobenzene reduced with potassium in acetonitrile solutions.[16] For a single nitrogen atom the line-width is given by: $T_2^{-1}(m) = j(0)m^2 + T_{2,0}^{-1}$, where $j(0)$ and $T_{2,0}^{-1}$ have the usual significance in the relaxation-matrix theory. Therefore, the $m = 1$ components of the nitrogen atom ($I = 1$) will be broadened, while the central component ($m = 0$) will be not broadned by this mechanism.

[15] J. H. Freed and G. K. Fraenkel, *J. Chem. Phys.*, **41**, 699 (1964).

[16] G. K. Fraenkel, *J. Chem. Phys.*, **71**, 139 (1967).

Table 3

π – bond orders in the studied stilbene derivatives

Compound	Bond	π-bond order Neutral mol.	 Anion-radical
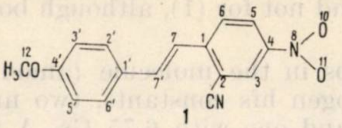 1	1′—2′	0.6116	0.6028
	2′—3′	0.6845	0.6855
	3′—4′	0.6343	0.6254
	1′—7′	0.3849	0.4033
	7 —7′	0.8497	0.8024
	1 —7	0.3958	0.4454
	1 —6	0.6067	0.5676
	5 —6	0.6948	0.7294
	4 —5	0.5910	0.5261
	4 —8	0.3820	0.4683
	2 —9	0.2838	0.2898
	4′—12	0.2624	0.2537
	8 —10	0.6688	0.5445
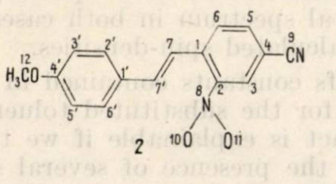 2	1′—2′	0.6114	0.6026
	2′—3′	0.6845	0.6853
	3′—4′	0.6342	0.6334
	1′—7′	0.3855	0.4037
	7 —7′	0.8482	0.8019
	1 —7	0.3994	0.4478
	1 —6	0.6188	0.6086
	5 —6	0.6807	0.6996
	4 —5	0.6178	0.5773
	4 —9	0.2806	0.2872
	2 —8	0.3869	0.4751
	8 —10	0.6524	0.5078
	4′—12	0.2625	0.2541
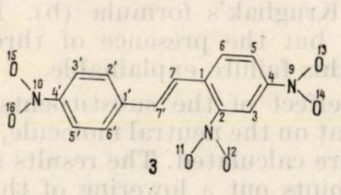 3	1′—2′	0.6043	0.5727
	2′—3′	0.6945	0.7204
	3′—4′	0.5967	0.5644
	1′—7′	0.3894	0.4491
	7 —7′	0.8433	0.7761
	1 —7	0.4038	0.4714
	1 —6	0.6123	0.5800
	5 —6	0.6898	0.7194
	4 —5	0.5853	0.5397
	4—9	0.3786	0.4147
	9—13	0.6684	0.6349
	2 —8	0.3834	0.4179
	4′—10	0.3788	0.4252

compound (3), and, simultaneously, an increase of the bond-order of the adjacent bonds 1 — 7 and 1′ — 7′. In the benzene rings the bond-orders of the bonds parallel to the long axes increase and, simultaneously, the others are reduced. The bond order of the carbon-nitro bond is increased and that of the N-O bonds decreased in the anion-radicals in comparison to the neutral molecule. All these data suggest a greater "weight" of quinoid type structure :

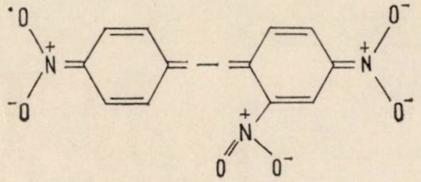

in the anion-radical in comparison to the neutral molecule. They also suggest a stronger transmission of the substituent effect in the anion-radical as compared to the neutral molecule and a tendency for the former to adopt a planar conformation.

In conclusion, it may be stated that in the polysubstituted stilbenes studied, the presence of nitro groups brings about a strong modification of the spin-distribution, while the cyano or methoxy groups do practically not influence it ; this effect is stronger for a single nitro group in *ortho* to the ethylenic bond and is, in general, comparable, although smaller, to that exerted in a single benzene ring, that is in the corresponding polysubstituted toluenes.

Revue Roumaine de Chimie, 22, 2, 181 – 190 (1977)

APPROXIMATE ANALYTIC DETERMINATION OF THE AVERAGE VALUES OF POTENTIAL FUNCTIONS OCCURRING IN CHEMICAL TRANSPORT PHENOMENA

K. POLINSZKY, E. VASANITS and J. FÜLÖP
Research Institute for Technical Chemistry of the Hungarian Academy of Sciences,
Budapest, Hungary

Received February 11, 1975

A relatively simple method has been worked out, which enables, with certain restrictions, to determine by an approaching analytic way the average values of the potential functions occurring in heat and mass transfer processes. The method is based on the introduction of an auxiliary function, the approaching form of which can be directly determined by Laplace transformation from the system of differential equations. By numerical calculations it can be shown that the approaching method is of satisfying reliability in the interval of the independent variable in which we are interested from the practical point of view.

NOMENCLATURE

a : specific thermal conductivity, m;
c : specific heat, kcal/kg °K;
L : thickness of reactor, m;
R : radius of spheres, m;
r : radial coordinate of the spheres, m;
T : temperature of the charge, °K;
$\bar{T}$: average temperature of the charge, °K;
v : velocity of spheres, m/s;
x : rectangular coordinate, m;
y : rectangular coordinate, m;
α : thermal diffusivity, kcal/m^2.hr.°K;
γ : density, kg/m^3;
λ : thermal conductivity, kcal/m.hr.°K;
ε : fractional void space;
ν : the number of the spheres in specific volume, m^{-3}.

SUBSCRIPTS

O : entering value
K : average volume

SUPERSCRIPTS:

' : gas phase.

1. INTRODUCTION

Some transport phenomena occurring in chemical unit operations may be described by partial differential equation systems. The approximate method we have worked out can be applied under the following conditions:

1) The process is stationary and the differential equation system describing it contains two independent variables.

2) The partial differential equation figuring in the equation system is a Fourier function the boundary condition of which is the general Newton's linear boundary conditions.

3) The differential equation system is linear.

4) Both potential functions converge to the saturation value.

5) The parameters figuring in the differential equations are constants.

The above conditions are fulfilled in a lot of transport phenomena occurring in chemical unit operations.

In problems of *heat transfer* our method may be applied to flowing stationary systems. The heat transfer problems taking place between flowing, dispergating or continuous solid phases and flowing gas (if the source of heat in the dispergating or continuous phase is a linear function of heat) belong to this category. As an example we want to refer to the heat transfer problems taking place between flowing, dispergating heaps and flowing gas as well as the description of tunnel furnaces.

The method may also be applied to *diffusion* problems. In case the diffusion is not followed by some other process (e.g. adsorption), the method can be applied, similarly to the heat transfer problems, to stationary systems.

The method can also be applied to processes where *diffusion and adsorption* (resp. desorption) are taking place at the same time and if the isotherm of the adsorption is assumed to be linear. Otherwise condition 3, is not fulfilled, that means that the differential equation system is not linear.

The method is also applicable to *absorption* processes between a liquid and a gas phase, between two liquids, respectively, i.e. in this case the relation between the two phases — considering the Henry constant — — can be given similarly to Newton's boundary condition. If a chemical reaction is taking place in the liquid phase, the method can be applied only if the chemical reaction is of first degree.

In the case of processes where *heat- and mass transfer* are taking place *at the same time* the method is only applicable if the functions representing the source (heat or mass source) do not effect the linearity of the differential equation system. Algorithms qualified as practically "treatable" serving for the mathematical solution of system of the type mentioned above — partly consist of partial, partly of general differential equations — are at disposal only for some systems of special structure.

These algorithms require a big mathematical apparatus. The results obtained with their help are of a complicated structure, uneasy to survey and can be applied to numerical calculations only be employing a digital computer.

Therefore, it was necessary to find an approximate analytic solution which, on the one hand, does not need a too complicated mathematical apparatus, is simply derivable and where, on the other hand, the results received are easy to survey and suitable for numerical calculations, too.

This idea of the approximate analytic solution and its construction for some cases have been already proposed by Kondratiew [1] and Heiligenstädt. [2] Heiligenstädt has derived his approximate coherences from the exact solution of the differential equation he examined; thus, he could only achieve the aim to get a simple form for the solutions easy to survey. Kondratiew elaborated a method rendering possible the approximate solution in a direct way, too, but only in cases when the potential function of the surroundings was constant. In these cases we have got no differential equation system but the Fourier partial differential equation. For this function the exact solution can also be looked upon as worked out. Kondratiew's method cannot be generalized according to a previously given algorithm in cases when the potential value of the surroundings (e.g. the temperature of gas) is not constant (that is when we are confronted with a differential equation system).

2. GENERAL DESCRIPTION OF THE APPROXIMATE METHOD

Let the two potential functions figuring in condition (1) be u and u' : and the two independent variables x and y. Let satisfy the function with two variables $u(x, y)$ e.g. the Fourier partial differential equation plotted in Descartes coordinates : in the region

$$v_x \frac{\partial u}{\partial x} = a \left(\frac{\partial^2 u}{\partial x^2} + \frac{\partial^2 u}{\partial y^2} \right) \tag{1}$$

and

$$-L \leqq y \leqq +L$$

$$0 \leqq x \leqq \infty$$

This function describes a stationary process where the medium, determined by the potential function u is moving forward in direction x with velocity v_x.

---

[1] G. M. KONDRATIEW, "Regularni teplovi regim", Moscow, 1954.

[2] W. HEILIGENSTÄDT, "Wärmetechnische Rechnungen für Industrieöfen", Düsseldorf, 1951.

The other equation of the differential equation system with two unknowns is of the following form :

$$L\,(u, u') = 0 \tag{2}$$

where we have only to assume that it is a linear differential equation.

The Newton boundary condition of equation (1) generally is of the form :

$$\left(\frac{\partial\, u}{\partial\, y}\right)_{y=L} = h\,[u' - u\,(x, L)] \tag{3}$$

$\left(\text{where } h = \dfrac{\alpha}{\lambda}\right)$

and

$$\left(\frac{\partial u}{\partial y}\right)_{y=-L} = -\,h\,[u' - u\,(x, L)] \tag{4}$$

Let the potential function $u(x, y)$ denote the average value in direction y :

$$\bar{u}\,(x) = \frac{1}{2\,L}\int_{-L}^{+L} u\,(x, y)\,d\,y \tag{5}$$

Let us integrate both sides of equation (1) with respect to y from $-L$ to $+L$. Then we obtain the following general differential equation :

$$v_x\,\frac{d\,\bar{u}}{d\,x} = a\,\frac{d^2\,\bar{u}}{d\,x^2} + \frac{a\,h}{2L}\left[\left(\frac{\partial\,u}{\partial\,y}\right)_{y=L} - \left(\frac{\partial\,u}{\partial\,y}\right)_{y=-L}\right] \tag{6}$$

Substituting the boundary conditions (3) and (4) into equation (6):

$$v_x\,\frac{d\,\bar{u}}{d\,x} = a\,\frac{d^2\,\bar{u}}{d\,x^2} + \frac{ah}{L}\,[u' - u\,(x,\,L)] \tag{7}$$

We should like to stress that x is the only independent variable in differential equation (7). If u' is only a function of x, the above mentioned statement is trivially true, if, however, $u' = u'(x, y)$ the boundary value $u'(x, L)$ is figuring in equation (7). We can assume in the following $u' = u'(x)$ — without diminishing the generalization — that means it is a function with one variable only. From the view-point of physical considerations this assumption is reasonable because u' generally represents the potential function of the gas or liquid flowing round the solid phase and in this direction, perpendicular to the flowing direction x, the value of the potential function is not changing.

The differential equation (2) being linear after integrating with respect to y we get a linear differential equation of the form :

$$L'(\bar{u}, u') = 0 \tag{8}$$

In equation (8), too, x is the only independent variable. The solution of the system consisting of the general differential equations (7) and (8), too, is ambiguous including three unkown functions :

$$\bar{u}(x), u'(x) \text{ and } u(x, L)$$

Let us introduce the following function with one variable :

$$z(x) = \frac{u'(x) - u(x, L)}{u'(x) - \bar{u}(x)} \tag{9}$$

In every stationary transport phenomena where there exist lim $u(x, y)$ and lim $u'(x)$, function $z(x)$ will obviously show the following qualities :

a) $z(0) = 1$

b) $\lim\limits_{x=\infty} z(x) = z_\infty$ where $0 < z_\infty < 1$

c) $z(x)$ is decreasing monotonously in the interval $x > 0$

The main point of our approximation is :

$$z(x) \cong z_\infty \tag{10}$$

in the case of every $x > 0$. With application of the equations (9) and (10) the differential equation system (7) and (8) can be solved with respect to $u(x)$ and $u'(x)$ as a function of z_∞ , as the number of the unknown functions has been reduced by one.

Our aim now is to determine the boundary value z_∞. In the course of the determination we shall not use the exact mathematical solution of the partial differential equation system we started from.

3. DETERMINATION OF THE LIMIT z_∞

It can be proved that there exists a solution of the starting partial differential equation system in the following form :

$$u(x, y) = \sum_{k=1}^{\infty} A_k(y)\, e^{-\lambda_k^2 x} \tag{11}$$

and

$$u'(x) = \sum_{k=1}^{\infty} B_k\, e^{-\lambda_k^2 x} \tag{12}$$

The eigenvalue equation of the partial differential equation system generates the values λ_k. Between the eigenvalues λ_k there exists the following well-known relation[3]

$$\lambda_1 < \lambda_2 < \lambda_3 \ldots < \lambda_k < \lambda_{k+1} < \ldots$$

The form of $\bar{u}\,(x)$ got by integrating $u\,(x, y)$ is the following:

$$\bar{u}\,(x) = \sum_{k=1}^{\infty} \bar{A}_k \, e^{-\lambda_k^2 x} \tag{13}$$

By comparison of the equations (9), (11), and (12) and (13), passing to the limit and considering the relation:

$$\lambda_k < \lambda_{k+1}:$$

$$z_\infty = \frac{B_1 - A_{1f}}{B_1 - \bar{A}_1} \tag{14}$$

where A_{1f} denotes the value of the function $A_{1(y)}$ on the surface $y = L$. The values of B_1, A_{1f} and $\bar{A}_1$ can be determined with the application of the Laplace transform without knowledge of the solutions of the partial differential equation system $u(x, y)$ and $u'(x)$.

Let us form the Laplace transforms[4] with respect to x of the equations (11), (12) and (13):

$$\int_0^\infty u\,(x, y)\, e^{-px} \, dx = V\,(p, y) = \sum_{k=1}^{\infty} \frac{A_k\,(y)}{\lambda_k^2 + p} \tag{15}$$

$$\int_0^\infty u'\,(x)\, e^{-px} \, dx = V'\,(p) = \sum_{k=1}^{\infty} \frac{B_k}{\lambda_k^2 + p} \tag{16}$$

$$\int_0^\infty \bar{u}\,(x)\, e^{-px} \, dx = V^*\,(p) = \sum_{k=1}^{\infty} \frac{\bar{A}_k}{\lambda_k^2 + p} = \frac{1}{2\,L} \int_{-L}^{+L} V\,(p, y)\, dy \tag{17}$$

In equations (15) and (16) $V(p, y)$ and $V'(p)$ are the solving functions of the Laplace transformed equation system of the starting differential equation system. In a given case these functions can be determined after forming the Laplace transform of the starting differential equation system.

---

[3] H. S. Carslaw and J. C. Jaeger, "Conduction of heat in solids", 2nd ed., Oxford, Univ. Press, 1959.

[4] M. R. Spiegel, "Theory and problems of Laplace transforms", Mc Graw-Hill, London, 1965.

Multiplying both sides of equations (15), (16) and (17) with $(\lambda_1^2 + p)$ and passing to the $p \to -\lambda_1^2$, we get:

$$A_{1f} = A_1(L) = \lim_{p=-\lambda_1^2} V(p, L)(\lambda_1^2 + p) \tag{18}$$

$$B_1 = \lim_{p=-\lambda_1^2} V'(p) \quad (\lambda_1^2 + p) \tag{19}$$

$$\bar{A}_1 = \lim_{p=-\lambda_1^2} V^*(p)(\lambda_1^2 + p) \tag{20}$$

By substitution of the expressions (18), (19) and (20) into function (14) and after reduction, we get:

$$z = \lim_{p=-\lambda_1^2} \frac{V'(p) - V(p, L)}{V'(p) - V^*(p)} \tag{21}$$

Summing up we can note the following:

1) Applying the approximation according to expression (10) for the determination of the functions $\bar{u}(x)$ and $u'(x)$ we get the system consisting of the general differential equations (7) and (8). In differential equation (7) after applying the approximation of (10) the limit value z_∞ appears.

2) The limit value z_∞ can be solved *without exact solution* of the starting differential equation system on the basis of equation (21) only by knowledge of the Laplace transforms $V(p, y)$ and $V'(p)$.

3) With knowledge of the necessary initial conditions the differential equation system consisting of (7) and (8) can be solved for the functions $\bar{u}(x)$ and $u'(x)$ with the application of the equations (9) and (10) as well as using the value z_∞ got from function (21). In the following it will be shown that the functions $\bar{u}(x)$ and $u'(x)$ we got from equations (7) and (8) give a very good approximation of the functions $\bar{u}(x)$ and $u'(x)$ received by the exact solution of the starting differential equation system in the whole interval of $x > 0$.

4. THE APPLICATION OF THE APPROACHING METHOD

4.1. PHYSICAL MODEL OF AN ADIABATIC HEATING

It can be shown the application of the approaching method to a given heat transfer model. In the adiabatic reactor a charge consisting of spheres with the same radius R is moving — with constant velocity v — into x coordinate and gas is flowing in direct flow.

The temperature of the heating gas $T'(x)$ is only a function of the height coordinate x. The temperature of the spheres $T(x, r)$, however, is a function with two variables, one of the independent variables being also the height coordinate x, the other being the radial coordinate r of the charge.

The differential equation being valid for the temperature distribution of flowing gas :

$$\frac{d\,T'}{d\,x} = -\frac{4\,R^2 \pi \nu \alpha}{v' \varepsilon c' \gamma'} \left[T'(x) - T(x, R) \right] \tag{22}$$

The temperature distribution of the spheres can be determined from the Fourier equation :

$$v \frac{\partial\,T}{\partial\,x} = a \left(\frac{\partial^2 T}{\partial\,r^2} + \frac{2}{r} \frac{\partial\,T}{\partial\,r} \right) \tag{23}$$

The Newton boundary condition (3) is also valid and in the center of the spheres the limit of the heat flux is zero :

$$\lim_{r=0} \left[r^2 \frac{\partial\,T}{\partial\,r} \right] = 0 \tag{24}$$

The initial conditions are : the temperature of the spheres and of the gas entering the apparatus at $x = 0$:

$$T/0, r/ = T_0 \tag{25}$$

$$T'/0/ = T_0' \tag{26}$$

4.2. THE DETERMINATION OF z_∞

According to equation (21) the value of z_∞ can be determined from the Laplace transforms — with respect to x — of the differential equations (22) and (23) and of the Newton boundary condition, and boundary condition (24) :

$$z_\infty = \frac{\beta_1^2}{3\,Nu\,(1+q)} \tag{27}$$

where β_1 is the smallest positive root of the eigenvalue equation,

$$Nu = \frac{\alpha\,R}{\lambda} \text{ is the Nusselt number} \tag{28}$$

and

$$q = \frac{4 \cdot v\,c\,\gamma\,\nu\,R^3\,\pi}{3 \cdot v' c' \gamma' \varepsilon} \tag{29}$$

is the quotient of the heat capacity of the charge and the flowing gas.

By application of function (27) the solution of the system of differential equations is as follows:

$$\frac{T_0' - \bar{T}_k(w)}{T_0' - T_0} = \frac{1}{1+q}\left(q + e^{-\beta_1^2 w}\right) \tag{30}$$

$$\frac{T_0' - T_k'(w)}{T_0' - T_0} = \frac{q}{1+q}\left(1 - e^{-\beta_1^2 w}\right) \tag{31}$$

where $w = \dfrac{a\,x}{R^2\,v}$ is an independent variable without dimension.

It can be stated that the functions (30), (31) are of quite a simple structure and well suitable for numerical calculations, too. From these equations can be expressed the approximate solution for the average temperature of the spheres: $\bar{T}_k(w)$ and for the temperature of the gas: $T_k'(w)$.

4.3. ERROR ESTIMATE OF THE APPROXIMATE SOLUTIONS

Let the relative error — between the deviations of the exact and the approximate solutions compared with the maximum temperature difference in the apparatus — be:

$$\eta(w) = \left| \frac{\bar{T}(w) - \bar{T}_k(w)}{T_0' - T_0} \right| \tag{32}$$

$$\eta'(w) = \left| \frac{T'(w) - T_k'(w)}{T_0' - T_0} \right| \tag{33}$$

The form of the relative error function on the basis of the exact solutions and the approximate solutions of the system of differential equations is the following:

$$\bar{\eta}(w) = \left| \frac{1}{1+q}\left(q + e^{-\beta_1^2 w}\right) - \sum_{k=1}^{\infty} \varphi_k \left(q + e^{-\beta_k^2 w}\right) \right| \tag{34}$$

and

$$\eta'(w) = \left| \frac{q}{1+q}\left(1 - e^{-\beta_1^2 w}\right) - q \sum_{k=1}^{\infty} \varphi_k \left(1 - e^{-\beta_k^2 w}\right) \right| \tag{35}$$

Equations (34) and (35) have been evaluated by a digital computer for some values of Nu (0.1 — 10) and q/0.5 — 1.5/ to be met with in practice, too. The results for $Nu = 10$ and $q = 0.8$ are shown in figure 1.

The equations $\bar{\eta}(w)$ and $\eta'(w)$ are all starting from the origin and in case of $w \to \infty$ converge to zero.

Thus, all these functions have a local maximum. It can be stated that these maximum values of the functions with increasing Nusselt number show a growing tendency. The maximum relative error — when $Nu = 0.1$ — is smaller than $0.1\,^0/_{00}$ for the whole interval $w > 0$. The error curves are very interesting in case of $Nu = 10$ (see Fig. 1.) In this case the maximum error reaches 10 — 12 %; however, the approximate functions can be applied all the same very well as the relative error curves show a very sharp relative maximum. In other words, this means that the approximate equations yield only in the interval of $0 \leqq w \leqq 0.2$ less precise values than the exact solution. In case of $w > 0.2$ the relative error is already less than 2 %.

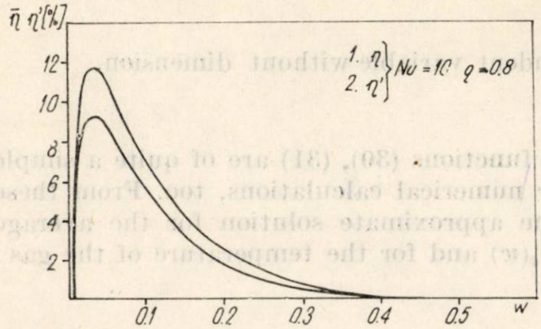

Fig. 1. — The error curves.

Our numerical calculations also show that at a given Nu the relative error in the interval of $0.5 < q < 1.5$ does not differ considerably.

Revue Roumaine de Chimie, 22, 2, 191 – 199 (1977)

AN EPR STUDY OF OXYGEN AND NITROUS OXIDE CHEMISORPTION ON MANGANESE SUBSTITUTED X-TYPE ZEOLITES

A. BIELAŃSKI, and J.M. ŁAGAN
Jagellonian University, Department of Chemistry, 30—060 Kraków, Krupnicza 41, Poland

Received January, 10, 1975

The effect of the cation exchange degree and the dehydration conditions on the chemisorption of O_2 and NO in MnNaX zeolites was studied using the EPR method. No chemisorption of oxygen took place after the dehydration had been carried out in vacuo at temperatures of 70 – 500°. This has been explained by the assumption that dehydrated Mn^{2+} cations migrated to the positions inaccessible to the oxygen molecules. The interaction of O_2 molecules with Mn^{2+} cations was however observed if oxygen was present in the system already in the course of dehydration. Mn^{2+} cations reacted then with O_2 molecules immediately after loosing totally or partially their hydration shells still before migration could be effectuated. Similar results were obtained with NO.

It is considered that charge-transfer processes resulting in the formation of organic radicals may strongly influence the course of some reactions catalyzed by zeolites containing transition metal cations [1-4]. It has been shown that the transition metal cations introduced into the zeolite may, in some cases at least, encourage the formation of centres for generating radicals. The transfer of electrons between transition metal cations and the adsorbed molecules has recently been observed in the case of chemisorption of inorganic molecules on zeolites.

Vansant and Lunsford [5] have shown that chemisorption of oxygen on CoY zeolite results in the oxidation of Co^{2+} to Co^{3+} with the simultaneous formation of the superoxide radical O_2^-. Similar effects were discovered by Neikam [6] who investigated $Ce^{III}Y$ zeolites. The formation of O_2^- radical occurred in both cases spontaneously without any previous irradiation with ultraviolet light or γ-rays as reported in [7-10].

[1] J. T. Richardson, *J. catalysis*, **9**, 172 (1967).
[2] *ibid.*, p. 182.
[3] C. M. Naccache, and Y. Ben Taarit, *ibid.*, **22**, 171 (1971).
[4] W. C. Neikam, *ibid.*, **21**, 102 (1971).
[5] E. F. Vansant, and J. H. Lunsford, *Adv. Chem. Series*, **121**, 441 (1973).
[6] W. C. Neikam, and M. A. Vannice, *J. Catalysis*, **27**, 207 (1972).
[7] P. H. Kasai, *J. Chem. Phys*, **43**, 3322 (1965).
[8] K. M. Wang, and J. H Lunsford, *J. Phys. Chem*, **74**, 1512 (1970).
[9] *ibid.*, **75**, 1165 (1971).
[10] *ibid.*, **73**, 2069 (1969).

Kasai and Bishop [11] observed charge transfer processes also in the case of $Ni^{II}Y$ zeolite on which nitrous oxide was adsorbed. In this case, however, the electron has been transferred from the ad-molecule to the nickel cation which was reduced to the oxidation state +1.

All these processes that are closely connected with the catalytic properties of transition metal substituted zeolites deserve more thorough investigation. The questions which should be asked also include the problem of how the charge-transfer processes are influenced by the position and coordination of the cations in the zeolite. In order to get some insight into this problem the effect of dehydration and cation exchange degree of oxygen and nitrous oxide chemisorption on Mn substituted X-type zeolites was studied in the present research using EPR technique. Manganese zeolite has been chosen because in this case cation migration processes occurring in the course of dehydration have already been studied[12-15]. Dyrek [16] also investigated in this laboratory oxygen chemisorption on MnO-MgO solid solutions in which the behaviour of easily accessible Mn^{2+} cations isolated in diamagnetic matrix could be studied. Therefore this paper enables more ample discussion of the results obtained with manganese substituted zeolites.

EXPERIMENTAL

MnNaX zeolites were obtained from a preparation of a 13 X sodium zeolite (composition of the anhydrous unit cell was $Na_{83}(AlO_2)_{83}$ $(SiO_2)_{109}$) by treating it with a solution of $MnCl_2$ of appropriate concentration. The degree of cation exchange had been calculated from the analytical determination of manganese; in the preparations MnNaX zeolites with the exchange degrees 59, 8 and 0.01% (symbols MnX-59, MnX-8 and MnX-001 resp.) were obtained.

Oxygen was obtained by thermal decomposition of $KMnO_4$ and nitrous oxide by the action of H_2SO_4 on a solution containing K.J and $NaNO_2$ in a special device connected to a vacuum apparatus. Both gases were freed from contamination by passing them through a solid CO_2 trap.

The preparations (about 0.05 g) were dehydrated in glass tubes joined to the vacuum apparatus. Two different procedures were applied:

(i) dehydration under dynamic vacuum (10^{-5} Torr) was carried out for 5 hours at one of the following temperatures: 70, 190 or 500°. After cooling the samples at room temperature oxygen was introduced and adsorbed at the pressure of 70 Torr, (ii) the dehydration in an atmosphere of oxygen (70 Torr) in a static system in which water vapour was condensed in a trap cooled with a solid CO_2 — acetone mixture.

The tubes with the samples prepared according to (i) or (ii) were sealed off and inserted into the cavity of an EPR spectrometer.

The EPR measurements were carried out using a spectrometer ZPT-IV constructed in the Laboratory of Telecommunication, Technical University, Wrocław, working in X band (ν =9.3GHz) and also with an EPR spectrometer Varian E-3. The changes in the number of spins were estimated by comparing the integrated signal intensity of a given sample with that of a standard sample of MnNaX zeolite dehydrated in vacuo at 500° and sealed in a glass tube. The determinations of the absolute number of spins were not undertaken. The integrated signal intensities (ISI) were calculated from the usual differential plots by double integration using the ODRA-1204 computer and the program designed by one of the present authors [17].

---

[11] P. H. Kasai, and R. J. Bishop, *J. Amer Chem. Soc*, **94**, 5560 (1972).

[12] T. J. Barry, and L. A. Lay, *J. Phys. Chem. Solids*, **27**, 1821 (1966).

[13] *ibid.*, **29**, 1395 (1968).

[14] N. N. Tihomirova I. V. Nikolaeva, V. V. Demkin, E. N. Rosolovskaya, and K. V. Topchieva, *J. Catalysis*, **29**, 105 (1973).

[15] *ibid.*, **29**, 500 (1973).

[16] K. Dyrek, *Bull. Acad. Polon. Sci., Ser. Sci. chim.*, **22**, 213 (1974).

RESULTS

1. ADSORPTION OF OXYGEN

In the first series of experiments the samples were dehydrated in vacuo (procedure i) at various temperatures. The parameters of the signals observed in MnX-59 and MnX-8 preparations before and after adsorption of oxygen are collected together in Table 1. All these signals were relatively broad. The former did not exhibit hyperfine structure and in the latter it was poorely resolved (Fig. 1). Table 1 also contains the data con-

Table I

Results of the investigations of O_2 adsorption on Mn NaX samples dehydrated in vacuo

Zeolite	% of charge	Dehydration conditions	Parameters of EPR signal (after dehydration)		
			ΔH_{max} (G)	g-factor	S (arbitrary units)
MnX-59	59	$t = 500°$ vacuum time = 5 hrs	400	2.02	3.90×10^4
MnX-59	59	$t = 190°$ vacuum time = 4 hrs	420	2.02	6.64×10^4
MnX-8	8	$t = 70°$ vacuum time = 2 hrs	530	2.02	4.03×10^4
		Adsorption conditions	Parameters of EPR signal (after adsorption)		
MnX-59	59	oxygen(p = 68 Torr) room temp. time = 15 min	400	2.02	3.95×10^4
MnX-59	59	oxygen (p = = 71 Torr room temp. time = 15 min	420	2.02	6.60×10^4
MnX-8	8	oxygen (p = = 72 Torr) temp. = 70° time = 1.5 hr	530	2.02	4.08×10^4

---

[17] J. M. Lagan, *Roczniki Chem.*, **47**, 199 (1973).

cerning the conditions of the experiments. It is seen that the adsorption of oxygen carried out at room temperature on the samples MnX-59 which had been dehydrated at 500 or 900° did not change the integrated intensities of the signals. Also other parameters : g — factor and line width were not influenced by the presence of oxygen. The sample dehydrated at 500° was subsequently heated in oxygen at 500°, and the sample originally dehydrated at 190° for 3 hours at 300°, again without any change of the signals being found.

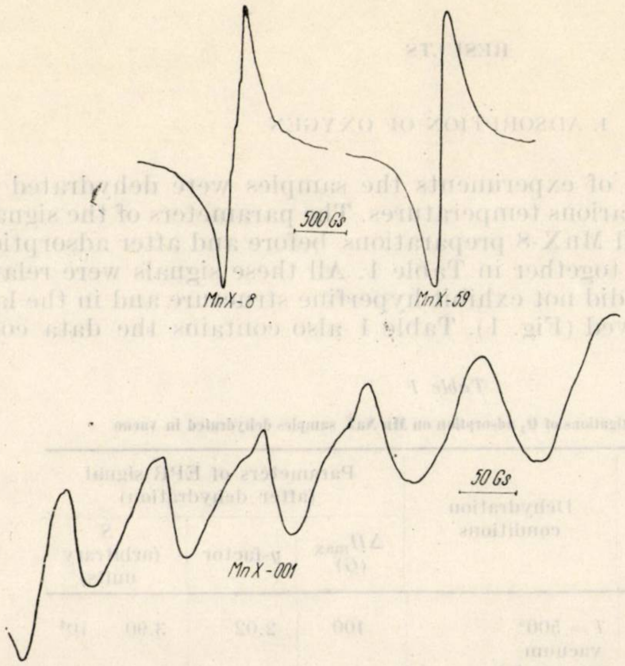

Fig. 1. — EPR signals of manganese substituted X-type zeolites with various degrees of exchange.

Table 1 shows also the data obtained for the sample MnX-8 dehydrated in vacuo at 70° for 2 hours. Also in this case no changes of signal could be registered after admitting oxygen into the system.

All these results strongly suggested that in the dehydrated zeolite Mn^{2+} cations occupied positions at which they were not accessible to O_2 molecules. The migration of cations, located in supercages when hydrated, would therefore take place in the course of, or after, the process of their dehydration. Similar migration of cations to the sites in which they can reach high coordination number was postulated by Barry and Lay [12,13] and also by Tihomirova and coll. [14,15] who studied EPR spectra of X and Y zeolites containing various diamagnetic cations and also very small amounts of Mn^{2+}. From the changes of the well resolved hyperfine structure of Mn^{2+} signal they concluded that this ion shows a distinct tendency to migrate to the sites of nearly octahedral symmetry i.e. to the sites *SI* in the hexagonal prism. Our results however suggest that the migration of cations is a much faster process than it could be assumed on the basis of the results given in [12,13].

Assuming the migration of Mn^{2+} cations to the sites inaccessible to O_2 molecules as the working hypothesis we carried out a second series of experiments in which dehydration occurred in the presence of oxygen.

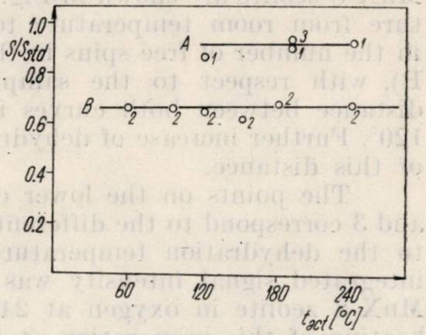

Fig. 2. — Dependence of EPR signal intensity on dehydration temperature for MnX-59 preparation in vacuum (*A*) and oxygen (*B*).

"1" samples dehydrated in vacuo for 2 hours;
"2" samples dehydrated in oxygen for 2 hours;
"3" dehydration in vacuo followed by the adsorption of oxygen at room temp.

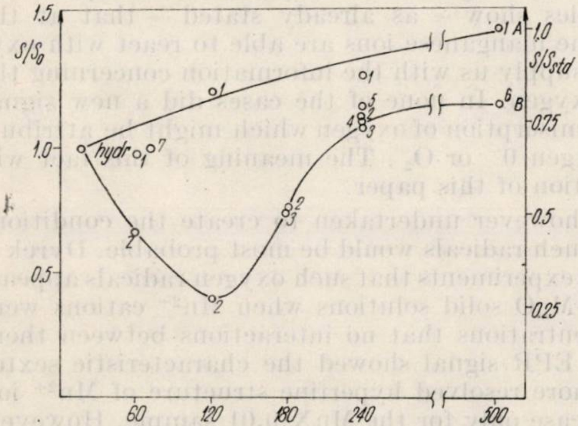

Fig. 3. — Dependence of EPR signal intensity on dehydration temperature for MnX-8 preparation in vacuum (*A*) and oxygen (*B*)

"1" samples dehydrated in vacuum; "2" dehydration in oxygen (slow heating to the final temperature) for 2 hours; "3" samples dehydrated in oxygen (fast heating to the final temperature) for 2 hours; "4" samples dehydrated in oxygen for 5 hrs at 240°; "5" samples dehydrated in oxygen for 22 hrs at 240°; "6" samples dehydrated in oxygen for 2 hrs at 240°; and subsequently for 4.5 hrs at 500°; "7" dehydration in vacuo followed by the adsorption of O_2 at temp. 70°.

In particular it was hoped that there existed a certain time between the act of total or partial dehydration and the reaching by the migrating cation of the site inaccessible to oxygen. During this period it was possible that the reaction between the Mn^{2+} cation and O_2 molecule might occur, similar to the reaction between Mn^{2+} cation and oxygen on the easily accessible surface of the MnO — MgO solid solutions.[16]

In this series of experiments dehydration procedure (ii) was applied. The relative signal intensities S/S_{std} (S and S_{std} are integrated signal intensities of the investigated sample and the standard preparation resp.) for the MnX 59 samples dehydrated in vacuo (line A) and in oxygen (line B) are given in Fig. 2 as a function of the temperature of dehydration. It is clearly seen that the samples dehydrated in vacuo show higher signal intensity and therefore a higher number of free spins. The presence of oxygen contributes to the decrease of the signal intensity and to the number of free spins as similarly observed by Dyrek[16] in the case of

MnO-MgO solid solution. Such an effect is evidently due to the oxidation of Mn^{2+} to Mn^{3+} (d^4) which is a non Kramers ion and exhibits no EPR signal. Simultaneously a negatively charged oxygen species must be formed.

The results of a similar series of experiments carried out with MnX MnX-8 zeolite are shown in Fig. 3. It is seen that the raising of temperature from room temperature to 120° contributes to a strong decrease in the number of free spins in the samples dehydrated in oxygen (curve B), with respect to the samples dehydrated in vacuo (curve A). The distance between both curves is largest at the point corresponding to 120°. Further increase of dehydration temperature results in the decrease of this distance.

The points on the lower curve in Fig. 3 marked with numbers 2 and 3 correspond to the different rates of heating from room temperature to the dehydration temperature. No effect is observed. Similarly the integrated signal intensity was not changed by prolonged heating of MnX-8 zeolite in oxygen at 240° (points 4 and 5). Also the second heating of this preparation at 500° did not change the signal.

The above-described investigations of oxygen chemisorption on MnX-59 and MnX-8 samples show — as already stated — that at the moment of dehydration some manganese ions are able to react with oxygen. However, they do not supply us with the information concerning the form of the chemisorbed oxygen. In none of the cases did a new signal appear in the course of chemisorption of oxygen which might be attributed to radical forms of oxygen 0^- or O_2^-. The meaning of this fact will be discussed in the last section of this paper.

Some attempts were however undertaken to create the conditions in which the occurrence of such radicals would be most probable. Dyrek [16] observed in the course of her experiments that such oxygen radicals appeared on the surface of MnO-MgO solid solutions when Mn^{2+} cations were present in such small concentrations that no interactions between them occurred and the observed EPR signal showed the characteristic sextet of hyperfine structure. A more resolved hyperfine structure of Mn^{2+} ion signal was observed in our case only for the MnX-0.01 sample. However, the presence of paramagnetic oxygen species could not be detected with the samples dehydrated in the presence of oxygen at 120 and 240° (EPR spectrum, recorded at 77°K with Varian spectrometer).

2. ADSORPTION OF NITROUS OXIDE NO

Experiments with the adsorption of nitrous oxide were carried out using MnX-8 preparation. The results are similar to the results obtained with oxygen. Adsorption of NO on the zeolite sample previously dehydrated in vacuo at 500° practically did not change the integrated signal intensity despite the fact that the shape of the signal was somewhat different. On the other hand the dehydration in the atmosphere of nitrous oxide contributed to a decrease of the intensity of the signal produced by Mn^{2+} ions. The results of the latter experiments are shown in Fig. 4. The upper line shows the integrated signal intensities of the samples dehydrated in vacuo and not treated with NO atmosphere, the lower line those of the samples dehydrated at the same temperature but in an atmosphere of NO. The graph shows that if NO is present in the course of the dehydration the molecules of the gas react with Mn^{2+} ions, thus decreasing the number of unpaired electrons observed by EPR method. The diagram is very similar to that in Fig. 3, the difference being that the minimum of the lower curve is shifted towards lower temperatures.

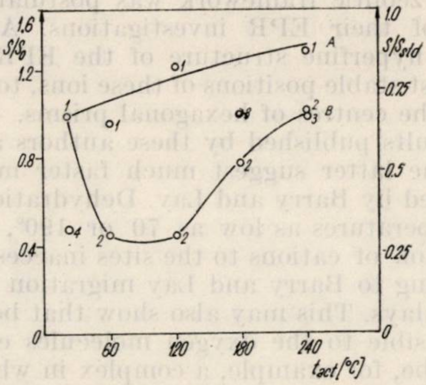

Fig. 4. — Dependence of EPR signal intensity on dehydration temperature for MnX-8 preparation. Dehydration in vacuo (*A*) and in NO(B)
"1" samples dehydrated in vacuo for 2 hours; "2" samples dehydrated in NO atmosphere (slow heating); "3" samples dehydration in NO atmosphere (fast heating); "4" dehydration in vacuum for 3 hrs followed by NO adsorption at room temp.

Point 4 in Fig. 4 corresponds to the experiment in which the sample had been in contact with NO at room temperature. The sample was previously outgassed for 3 hours. Under these conditions the hydration shells of Mn^{2+} cations are not destroyed. The decrease in the integrated signal intensity was then very distinct which indicated that the substitution of some water molecules in the coordination sphere of Mn^{2+} cations by NO molecules took place.

DISCUSSION

Direct contact between adsorbed reagent molecules and the cations present in the zeolite seems to be necessary if the zeolite is to be active catalyst.[1,2] For this reason the investigation of chemisorption of gases, which may form charge-transfer complexes with the cations in zeolites, is important. In the course of the present investigation two gases were used : oxygen, which is known as an acceptor of electrons, and nitrous oxide, behaving as an electron donating ligand.

The results of the investigation of oxygen chemisorption on manganese zeolite may be summarized as follows : oxygen may be chemisorbed not only on the semiconducting transition metal oxides but also on the zeolites modified with transition metal cations, at least on the Mn form of X zeolite, if these cations are accessible to the O_2 molecules.

Adsorption of oxygen on the zeolite hydrated or outgassed at temperatures within the range 70 — 500° is not accompanied by any charge-transfer processes decreasing the number of unpaired spins on Mn^{2+}

cations. In the former case the cations are obviously shielded by their hydration envelopes, in the latter the only explanation is the migration of cations, in the course of heating in vacuo, to the sites inaccessible to the oxygen molecules. As already stated, such migration of Mn^{2+} cations in the zeolitic framework was postulated by Barry and Lay [12] on the basis of their EPR investigations. According to their interpretation of the hyperfine structure of the EPR signals exhibited by Mn^{2+} ions the most stable positions of these ions, to which they migrate, are positions *SI* in the centres of hexagonal prisms. The essential difference between the results published by these authors and the results obtained by us is that the latter suggest much faster migration of the cation than was supposed by Barry and Lay. Dehydration for 2 – 5 hours in vacuo, even at temperatures as low as 70 or 190°, is already accompanied by the migration of cations to the sites inaccessible to oxygen molecules, while according to Barry and Lay migration in such conditions may last even 2 – 3 days. This may also show that besides the *SI* sites other positions inaccessible to the oxygen molecules exist in the X-type zeolites. This might be, for example, a complex in which a partially dehydrated cation coordinates some oxygen atoms of the alumino-silicate framework such as $[Mn(H_2O)_5O]$, $[Mn(H_2O)_24O]$, etc.

The situation is quite different if the dehydration of zeolite is carried out in an atmosphere of oxygen. The presence of O_2 molecules in the zeolitic channels, in the near vicinity of cations, enables the reaction of oxygen with Mn^{2+}, cations, fully or partly dehydrated, before the latter can migrate to inaccessible sites. The decrease in the number of unpaired spins is, in this case, very distinct. In the MnX-8 preparations the number of Mn^{2+} cations which become oxidized does initially increase with increasing temperature of the treatment (Fig. 3). Above 120° however, the effect becomes weaker and one might think that many cations reach the sites inaccessible to oxygen before they enter into the reaction. However if such an explanation should be correct, one would expect the effect to be dependent on the rate of heating to the final temperature. Points 2 (slow heating) and 3 (fast heating) corresponding to the temperatures 180° and 240° show however that the final signal intensity reached at a given temperature is independent of heating rate. The alternative explanation seems therefore to be more probable and viz. that with increasing temperature desorption of oxygen takes place and is accompanied by the transfer of an electron from the negatively charged oxygen species to Mn^{3+} ions. The increased number of free spins is manifested by an increase of the integrated signal intensity.

The behaviour of the zeolite MnX-59 is different. The decrease of the integrated signal intensity of manganese cations resulting from the adsorption of oxygen is independent of the temperature at which dehydration in the atmosphere of oxygen takes place (Fig. 2) and equal to about 30% of the value reached by the preparations treated only in vacuo. It should be stated here that the number of manganese cations in this sample is equal to 26 per unit cell. This number is larger than the number of SI sites equal to 16. The result of the experiment suggests that, already in the hydrated zeolite, all these positions are occupied by Mn^{2+} cations, and that only the remaining cations may, in the appropriate conditions, become the centres of adsorption.

The problem of which form is the oxygen adsorbed in the manganese substituted X zeolites cannot be answered univocally on the basis of our results. The fact that no signals of paramagnetic oxygen radicals O^- and O_2^- could be observed, might be taken as the indication that oxygen is bonded in the form of diamagnetic O^{2-} ions. However the second possibility also exists viz. the signals of such forms under the influence of O_2 molecules present in the zeolitic cavities become so broad that they cannot be distinguished on the backgroud of the signals generated by Mn^{2+} ions. Such broadening of the signal of the oxygen radical species under the influence of oxygen from the gas phase was observed by Dyrek [16] in the case of diluted MnO — MgO solid solutions.

The formation of O^{2-} — ion might occur only in the zeolites in which the concentration of Mn^{2+} ions is high enough to supply an O_2 molecule with 4 electrons. Evidently they cannot be given by one Mn^{2+} ion. On the other hand, if Mn^{2+} ions are situated far apart from each other, electron transfer becomes difficult, and the formation of O_2^- ion may be expected. Entering of the species as a ligand to the complexes of the type $[Mn^+(H_2O)_5O_2]$ also seems probable.

Many complexes of transition metals containing NO ligand are known in which oxidation number of the central atom is reduced by the electron transfer from the antibonding orbital of NO molecule. The so produced nitrosonium cation NO^+ is doubly bonded to the central atom, the low degree of oxidation of which is considered to be stabilized by the π-back donation of an electron pair. Among aquo-nitrosylo complexes of such kind the brown complex $[Fe^+/H_2O/_5NO/^+]^{2+}$ is most widely known.

A complex of manganese of similar type is very likely to be formed in the course of dehydration of MnNaX zeolite carried out in nitrous oxide atmosphere at temperatures of 25 — 240°. The observed decrease in the integrated EPR signal intensity of manganese is well explained by the formation of Mn^+ (d^6) cations which as non Kramers ions, do not yield EPR signal at room temperature.

The formation of manganese nitrosyl complexes is fast even at room temperature when most probably hydration shell of Mn^{2+} cations is not yet destroyed, and the observed process might be treated as the exchange of ligands. The complexes are stable at temperatures up to 120°. Heating above this temperature results in the increase of the integrated EPR signal intensity which is interpreted as the decomposition of the nitrosyl complexes and the migration of Mn^{2+} cations that has been already discussed.

Revue Roumaine de Chimie, 22, 2, 201 – 211 (1977)

DIELECTRIC CONSTANTS AND REFRACTIVE INDICES IN POLYELECTROLYTE SOLUTIONS

CAMELIA BELDIE and OLIMPIA MIHĂILESCU
Department of Physical Chemistry, Polytechnic Institute of Jassy, str. Splai Bahlui nr. 71, Jassy

Received February 3, 1975

The refractive index and the dielectric constant of some samples of polyacrylic acid (PAA) and polymethacrylic acid (PMA) of different molecular weights, in aqueous, alcoholic, ethanol-water mixture and hydrogen chloride solutions, within 25 – 35° temperature range, were measured. These data enable us to make some remarks on the behaviour and the conformation of the above polyelectrolytes in solutions of different compositions.

Although many studies have been developed on the polyelectrolyte solutions, especially in the last decades, the interpretation of the experimental results is complicated by different phenomena occurring in such a solution. [1]

The dissociation degree of the carboxylic groups is dependent on the solvent and polyelectrolytic chemical nature and, at the same time, on the polyelectrolyte concentration. Due to the structure of the monomer unit, it can readily form inter- and intramolecular hydrogen bondings, which will be influenced by concentration, solvent nature and temperature.

The refractive index is determined by the numbers of various kinds of atoms (molecules) and ions in a unit volume (density) and their polarizabilities. Since the polarizability of atoms or ions is not much affected by the state of interaction between them, the density in the solution can be related simply to the refractive index.

The dielectric constant of such a solution can be calculated with the following equation : [2]

$$E = E + 4\pi P ; \quad P = \sum_i N_i \alpha_i \quad {}_i \qquad (1)$$

where the summation is carried out for all macroions and the other molecules in the solution, and E is the static electric field, E' – internal electric field, α-the polarizability given by the equation ;

---

[1] R. Fowler and E. Guggenheim, "Statistical thermodynamics", Cambridge Univ. Press, London, 1948.

[2] Fumio Oosawa, "Polyelectrolytes", Marcel Dekker, Inc., New York 1971, p. 54, 61.

$$\alpha = (3/4\ \pi)\ v\ \varepsilon_0$$

where v is the volume in which all counter ions are retained.

The polarizability is determined by the volume of the macroion, independent of the charge or the charge density of the macroion. [2] More exactly, it is determined by the volume in which bound counter ions are moving, but not by the charge density of the macroion.

The dielectric constant has high values for large volumes and an extended conformation for the range within which bound counter ions are moving.

The relative dielectric increment ($\Delta\varepsilon = \varepsilon - \varepsilon_0$), in which ε_0 is the dielectric constant of the solvent, is proportional to the apparent volume concentration of the macroions.

Experimental results suggested that the dielectric increment depends on the shape of the macroions ; rodlike macroions give a much larger increment than spherical macroions. Moreover, the dielectric increment due to rodlike macroions was found to increase rapidly with the increasing length of the macroions.[3]

The present paper deals with the behaviour of the poly(acrylic) acid (PAA) and poly(methacrylic) acid (PMA), in aqueous, alcoholic and hydrochloric acid solutions, depending on the solvent nature, the temperature and the solution concentration. Refractive index and dielectric constant measurements were used for this purpose.

EXPERIMENTAL RESULTS AND DISCUSSION

The dielectric constant was measured with a Multidecameter 06WTW model. The frequency range was 0.1 — 12 MHz ± 0.5%, with a precision of $\frac{\Delta\varepsilon}{\varepsilon} = 2\times10^{-3} \sim 2\times10^{-4}$.

The dielectric increments of the two polyelectrolytes in solutions were calculated.

Three poly(acrylic) acid samples of different average molecular weights PAA(1), $\overline{M}_w = 150{,}000$; PAA(2), $\overline{M}_w = 300{,}000$; PAA(3) $\overline{M}_w = 450{,}000$, and one poly(methacrylic) acid sample (PMA), $\overline{M}_w = 150{,}000$ were prepared in laboratory, through monomer polymerization in solution.[4] The average molecular weight was measured by viscosimetry.

As solvent were used : Water, ethanol, ethanol-water mixture and dilute chloride solution within 25 — 35° temperature range. Thus we were able to follow the influence of the molecular weight of the polyelectrolyte, of the solvent nature, of the polyelectrolyte concentration, of the temperature and of the frequency on the dielectric constants of the solutions.

In the same solutions we have also measured the refractive index, by using an immersion refractometer with a precision of 10^{-6} order. All measurements (refractive index) were carried out at 20 and 25°. The refractive index increments and the molar refraction referred to the monomer were calculated with these data.

All measurements (dielectric constant and refractive index) were carried out in 24 hours and the used concentration range was $3.3186 \times 10^{-3} - 0.13005 \times 10^{-3}$ equix./liter.

---

[3] S. Takashima, *J. Phys. Chem.*, **70**, 1372 (1966) ; *Biopolymers*, **5**, 899 (1967).

[4] A. Packter, *J. Polymer Sci.*, A, **1**, 3021 (1963).

a. DIELECTRIC CONSTANTS

All studied solutions present negative dielectric increments, since the dielectric constants of the solutions were lower than those of the solvent. This fact can be seen in tables 1 and 2.

Table 1

Dielectric constants in aqueous solutions

Sample	Conc. (moles monomer per liter)	ε					
		12,000 KHz		500 KHz		120 KHz	
		25°	35°	25°	35°	25°	35°
PAA(1)	0.003144	77.25	74.75	—	—	53.75	49.75
	0.002111	77.00	74.25	—	—	59.00	59.75
	0.001188	76.75	73.75	—	—	67.75	66.00
	0.000247	76.50	73.00	—	—	77.25	72.75
	0.000113	76.25	73.25	—	—	77.50	73.75
PAA(2)	0.003240	77.50	74.25	—	—	56.50	51.50
	0.001825	77.25	74.00	—	—	69.00	66.25
	0.000688	77.00	73.50	—	—	74.50	71.75
	0.000152	76.75	73.25	—	—	75.75	72.75
	0.000088	76.50	73.00	—	—	77.25	73.50
PAA(3)	0.003472	80.25	—	—	—	55.25	—
	0.001897	79.50	—	90.00	—	67.50	—
	0.000500	79.00	—	87.75	—	80.50	—
	0.000166	78.25	—	84.25	—	82.00	—
PMA	0.002920	78.50	75.25	—	—	37.25	—
	0.001441	77.75	74.50	—	—	46.50	—
	0.000725	77.25	74.25	90.00	—	58.75	23.25
	0.000144	76.75	73.75	90.00	—	66.00	55.00

Table 2

Dielectric constants in ethanol-water mixture

Sample	Conc. (moles monomer per liter)	ε					
		12,000 KHz		500 KHz		120 KHz	
		25°	35°	25°	35°	25°	35°
a. Ethanol 25%							
PAA(1)	0.003019	65.25	61.25	77.00	73.25	61.50	58.50
	0.002858	65.50	62.25	76.00	73.75	60.25	59.50
PAA(2)	0.002890	67.75	65.50	81.50	79.25	60.25	58.00
	0.002660	68.00	65.25	80.75	79.00	60.50	57.25
PAA(3)	0.002944	69.25	—	78.50	—	66.75	—
PMA	0.002369	65.50	62.25	73.50	74.00	61.00	53.25
	0.002123	66.00	62.50	75.50	75.50	60.00	52.75
b. Ethanol 50%							
PAA(1)	0.002902	51.50	48.25	55.50	53.75	51.25	48.75
	0.002741	51.75	48.50	55.75	54.00	51.50	49.00
PAA(2)	0.003008	57.25	54.75	62.50	60.75	56.00	52.25
	0.002708	57.50	55.25	64.25	63.00	56.25	52.75
PAA(3)	0.002944	59.75	—	66.25	—	58.00	—
PMA	0.002434	51.00	48.75	55.00	55.00	51.25	47.25
	0.002393	51.25	49.00	55.25	55.00	51.50	47.50

Table 2 (continued)

Sample	Conc. (moles monomer per liter)	ε					
		12,000 KHz		500 KHz		120 KHz	
		25°	35°	25°	35°	25°	35°
		c. Ethanol 75%					
PAA(1)	0.003030	36.50	34.25	38.75	37.25	37.75	35.75
	0.002700	37.00	34.75	38.25	37.00	37.50	35.50
PAA(2)	0.003050	37.00	35.25	38.25	37.00	37.00	35.25
	0.002722	36.50	34.50	38.75	37.50	36.50	35.75
PAA(3)	0.002972	41.75	—	43.50	—	43.75	—
PMA	0.002372	37.00	35.00	39.25	39.00	37.50	34.75
	0.002162	37.50	35.25	39.75	38.75	37.75	35.00
		d. Ethanol 99%					
PAA(1)	0.002958	23.50	22.00	23.75	22.50	23.75	22.50
	0.002788	23.50	22.00	23.75	22.50	23.75	22.75
PAA(2)	0.002763	23.50	22.00	23.75	22.50	23.75	22.75
	0.002686	23.75	22.00	23.75	22.50	23.75	22.75
PAA(3)	0.002933	28.00	—	28.50	—	28.75	—
PMA	0.0024186	23.75	22.75	25.50	23.75	24.00	22.25
	0.002356	23.75	22.50	25.50	24.00	24.00	22.50

The effect of the polyelectrolyte concentration occurs especially at lower frequencies (Fig. 1), at which the dielectric constants change much more significantly with the change of the polyelectrolyte concentration, in the studied range, and much less at higher frequencies (Fig. 2).

Fig. 1 presents the change of the dielectric constants depending on the solution concentration at lower frequencies (120 KHz). Fig. 2 presents the same change at higher frequencies (12,000 KHz).

In ethanol and ethanol-water mixture, the dielectric constants change less, in terms of concentration, than in water (Fig. 3).

In all cases the dielectric constants have lower values at lower frequencies and higher ones at higher frequencies, as it can be seen in Tables 1 and 2.

This behaviour is not the same as in salt added polyelectrolyte solutions, when the dielectric constant decreases with the increasing frequency.[5]

The dielectric constants decrease, in all cases, with the increasing temperature as for other polyelectrolytes.

The dielectric constants for the first two samples ($\overline{M}_w$=150,000 and 300,000), are not actually influenced by the increasing molecular weight. For the third sample ($\overline{M}_w$ = 450,00), higher values than in the first two samples were obtained.

The viewpoints of some authors on the change of the dielectric constants with the change of the molecular weight of the polyelectrolyte are not concordant. Some authors found that the molecular weight influences the dielectric constant, others claimed the contrary.[5,6] Mandel and Jenard found that ε_∞ (dielectric constant extrapolated at infinite frequency) is independent of the degree of polymerization[5] as for uncharged macromolecules whose dielectric increment is also molecular weight independent.

---

[5] M. Mandel and A. Jenard, *Trans. Faraday Soc.*, **59**, 2158 (1963).

[6] L. G. Augen and S. Roswall, *J. Polymer Sci.*, **23**, 635 (1957).

We are tempted to believe that the average molecular weight of a polyelectrolyte influences the dielectric constant, while a lower limit

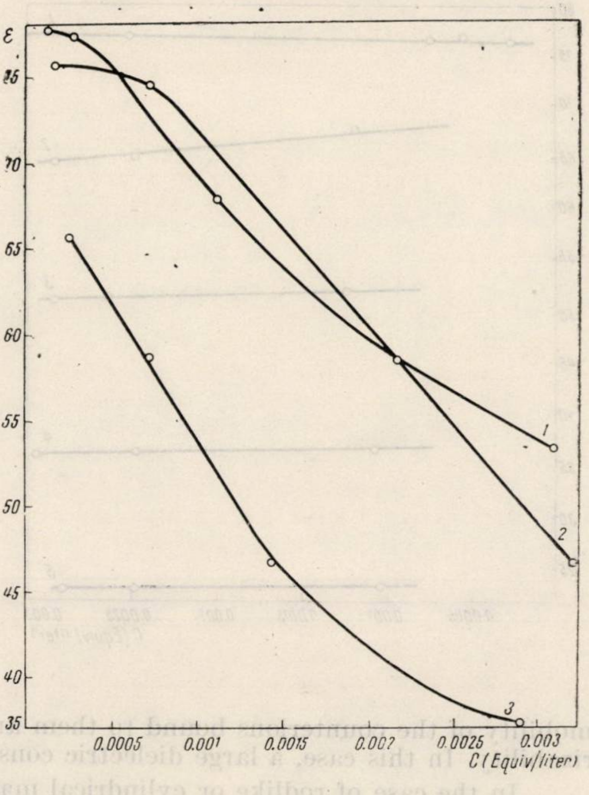

Fig. 1. — Change of dielectric constant in terms of concentration, at lower frequencies (120 KHz) 1-PAA (1); 2-PAA (2); 3-PMA

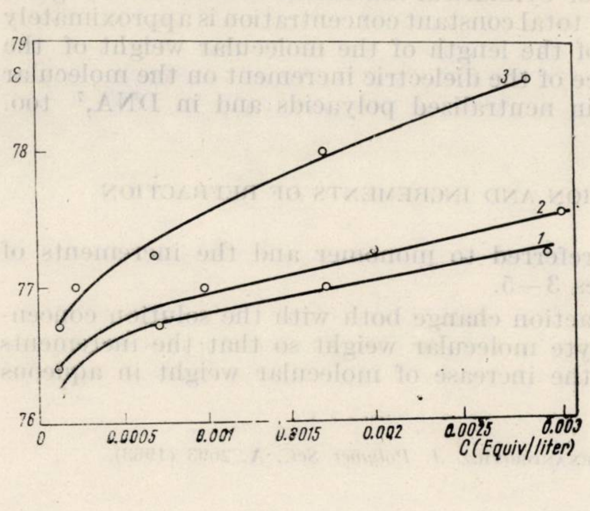

Fig. 2. — Change of dielectric constant in terms of concentration, at higher frequencies (12,000 KHz) 1-PAA (1); 2-PAA (2); 3-PMA.

exists, at the same time, from which the effect is discernible. Roughly speaking, the same behaviour was found by Augen and Roswall[6] in aqueous solutions of sodium alginate.

A uniform and continuous distribution of charged groups and the mobility of the counterions bound to them are essential for a large polarizability. In this case, a large dielectric constant is observed.[2]

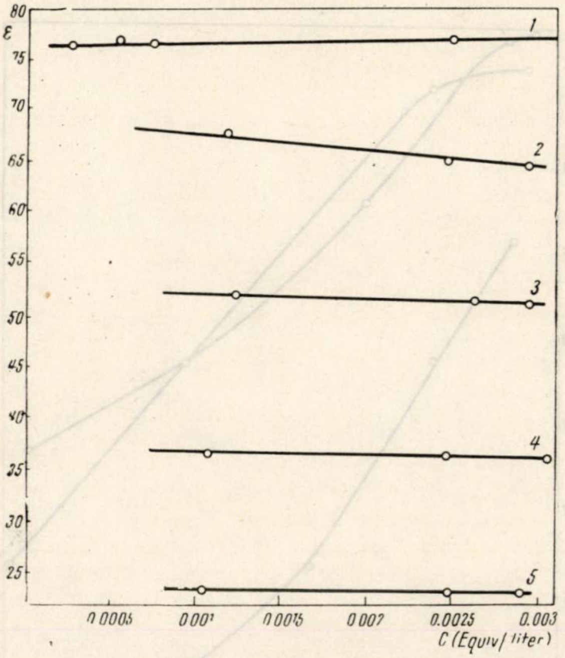

Fig. 3. — Dependence of the dielectric constant in PAA(1) solutions, upon concentration. 1-*Water*; 2-Ethanol 125%; 3-Ethanol 50%; 4-Ethanol 75%; 5. Ethanol 99% (in volumes).

In the case of rodlike or cylindrical macroions of different lengths, the dielectric increment at a total constant concentration is approximately proportional to the square of the length of the molecular weight of the macroion.[2] Such a dependence of the dielectric increment on the molecular weight was actually found in neutralized polyacids and in DNA,[7] too.

b. INDICES OF REFRACTION AND INCREMENTS OF REFRACTION

The molar refraction referred to monomer and the increments of refraction are listed in tables 3—5.

The increments of refraction change both with the solution concentration and the polyelectrolyte molecular weight so that the increments of refraction increase with the increase of molecular weight in aqueous

---

[7] A. Katchalsky and Z. Alexandrovicz, *J. Polymer Sci.*, **A**, 2093 (1963).

Table 3

Aqueous solution

Sample	Conc. (moles monomer per liter)	Δn_D	r	R
PAA(1)	0.003925	0.000185	0.206650	14.87916
25°C	0.002027	0.000117	0.206640	14.87829
	0.000277	0.000068	0.206700	14.88254
PAA(2)	0.004141	0.000078	0.206828	14.89161
20°C	0.001516	0.000029	0.206834	14.89204
	0.000233	0.000004	0.206807	14.89010
PAA(3)	0.004352	0.000110	0.206804	14.88990
20°C	0.001569	0.000058	0.206827	14.89161
	0.000194	0.000019	0.206829	14.89178
PMA	0.003534	0.000210	0.206625	17.76981
20°C	0.001386	0.000150	0.206640	17.77106
	0.000186	0.000100	0.206637	17.77079

Table 4

Alcoholic solutions 20°C

Sample	Conc. (moles monomer per liter)	Δn_D	r	R
		a. Ethanol 25%		
PAA(1)	0.0028690	0.000872	0.220905	15.905182
PAA(2)	0.0028444	0.000539	0.220245	15.873910
PAA(3)	0.0027916	0.000465	0.220599	15.883150
PMA	0.0024558	0.000354	0.220561	18.973120
		b. Ethanol 50%		
PAA(1)	0.0029080	0.000417	0.235073	16.925282
PAA(2)	0.0028770	0.000921	0.236245	17.009683
PAA(3)	0.0029444	0.001083	0.236189	17.005650
PMA	0.0023906	0.000705	0.236189	20.312310
		c. Ethanol 75%		
PAA(1)	0.0028720	0.000623	0.254329	18.311691
PAA(2)	0.0029305	0.000530	0·254410	18.317581
PAA(3)	0.0029361	0.000483	0·254310	18.310320
PMA	0.0024116	0.000448	0.254927	21.923730
		d. Ethanol 99%		
PAA(1)	0.0029080	0.000972	0.279883	20.151599
PAA(2)	0.0028694	0.000727	0.280914	20.225875
PAA(3)	0.0028694	0.000937	0.279787	20.144730
PMA	0.00242558	0.001077	0.279802	24.062970

Table 5

0.02 MHCl Solutions at 20° C

Sample	Conc. (moles monomer per liter	Δn_D	r	R
PAA(1)	0.0037970	0.000156	0.206974	14.902167
	0.0014833	0.000117	0.206980	14.902608
	0.0001305	0.000077	0.206980	14.902595
PAA(2)	0.0039277	0.000175	0.206938	14.899559
	0.0014944	0.000132	0.206950	14.900446
	0.0001861	0.000083	0.206948	14.900285
PAA(3)	0.0038380	0.000193	0.207000	14.904037
	0.0015000	0.000149	0.207035	14.096557
	0.0001440	0.000088	0.207071	14.909145
PMA	0.0033180	0.000195	0.206931	17.796084
	0.0012060	0.000117	0.206900	17.793414
	0.0001460	0.000039	0.206870	17.790820

and HCl solutions, as can be seen in Fig. 4, which shows the change of the refractive index increments depending on solution concentration (aqueous solutions), for different molecular weights of PAA.

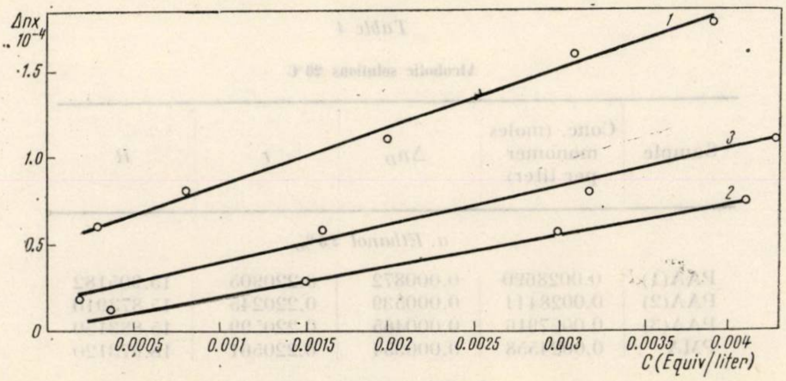

Fig. 4. — Dependence of the refractive increment upon solution concentration (aqueous solutions) 1-PAA(1); 2-PAA(2); 3-PAA(3),

Such a behaviour was also found by Margerison and co-workers [8] in solutions of polystyrene in toluene.

The molar refraction changes very little with the molecular weight of the polyelectrolyte in such a way that we could use the average values of these refractions, which are in aqueous solutions : 14.88745 for PAA and 17.77099 for PMA, respectively.

In a water-ethanol mixture, the molar refractions increase by increasing alcohol content in the mixture from 14.894037 in pure water up to 20.218754 in alcohol 99%, for PAA samples.

---

[8] D. Margerison, D. R. Bain and B. Kiely, *Polymer*, **14**, 133 (1973).

The same behaviour was also found for PMA as can be seen in Tables 3–5.

The index of refraction and the molar refraction are commonly correlated by Lorentz-Lorenz equation, but it gives questionable results when it is applied to polymers. For this reason, Albert and Malone [9] have proposed a new relation which correlates the index of refraction to the total parachor and the number of the bonds of a given molecule, and, after the authors' opinion, it can be applied successfully both to polymers and monomers. This is :

$$n = A\left[\frac{3\bar{n}-1}{(\bar{n}-2)P}\right] - B \tag{2}$$

in which : n is the index of refraction,

$\bar{n}$ is the polymerization degree,

P is the parachor,

A and B are two constants for the same homologous polymer series.

By using this equation, knowing the index of refraction and the parachor, the mean polymerization degree and then the mean molecular weight could be determined.

In the present work, the parachor was not determined, therefore we were not able to verify the above relation.

Looyenga [10] has shown that the molar refraction can be expressed more satisfactorily by the relation ;

$$n^{2/3} - 1 = \rho[R_L]/M, \tag{3}$$

where : n is the index of refraction,

R_L is the molar refraction,

M is the molecular weight,

ρ is the solution density.

This equation has a much more reduced temperature coefficient than the Lorentz-Lorenz's equation.

In order to avoid knowledge of the molecular weight of a polymer, the Lorentz-Lorenz equation applied to polymers [11,12] in the form

$$\frac{(n^2-1)}{(n^2+2)} = \rho[R_{LL}]/M \tag{4}$$

---

[9] R. Albert and W. M. Malone, *J. Macromol. Sci., Chem.*, **A6**, 347 (1972).

[10] H. Looyenga, *Mol. Phys.*, **9**, 501 (1965).

[11] R. B. Beevers, *Lab. Pract.*, **22**, 272 (1973).

[12] R. H. Wiley, *Ind. Eng. Chem.*, **38**, 959 (1946).

was replaced by Beevers[13] by relation (5)

$$\frac{(n^2-1)}{(n^2+2)} = \rho[{}_uR_{LL}]/M_r \qquad (5)$$

where M_r is the residue molecular weight and $[{}_uR_{LL}]$ is defined as the unit molar refractivity.

The same authors propose to use in the future the analogous expression

$$n^{2/3} - 1 = \rho\,[{}_uR_L]/M_r \qquad (6$$

derived from equation (4) for the above reason.

We use for our data equation (6) and, at the same time, equation (5), in the form ;

$$R_m = \frac{(n^2-1)}{(n^2+2)}\frac{M_m}{\rho} \qquad (7)$$

where-R_m is the molar refraction referred to monomer, the unit molar refraction, M_m, is the monomer molecular weight, and we found the results listed in Table 6 where we can see that the unit molar refractions obtained by using equation (6) are closer to those obtained by using the additivity law than the values calculated with equation (7), for all solutions.

Table 6

Unit molar refractions

Sample	Solvent	Additivity law	Equation (7)	Equation (6)
PAA	Water	17.809	14.8875	15.2966
	Alcohol 25%	”	15.8874	16.3583
	Alcohol 50%	”	16.9802	17.5200
	Alcohol 75%	”	18.3132	18.9067
	Alcohol 99%	”	20.1741	20.8113
	HCl 0.02M	”	14.9031	15.3171
PMA	Water	22.427	17.7710	18.2656
	Alcohol 25%	”	18.9731	19.5340
	Alcohol 50%	”	20.3123	20.9620
	Alcohol 75%	”	21.9237	22.6385
	Alcohol 99%	”	24.0630	24.8433
	HCl 0.02M	”	17.7936	18.2594

Beevers' equation has the advantage that it needs no data on the parachor or on the molecular weight of the polymer.

With the same data, the additivity law in presence of common electrolytes was verified. The index of refraction of such a solution is thus described as a superposition of the individual properties of the pure components by an additivity law, as can be seen in Tables 3—6. Although this law is very disputed in reference material, [7,14–16] it has kept its validity in these cases.

---

[13] R. B. Beevers, *J. Polymer Sci.*, **12**, 1407 (1974).

CONCLUSION

From our experimental data of dielectric constant and refractive index measurements in PAA and PMA solutions in different solvents, we can conclude as follows:.

The two polyelectrolytes in aqueous, water-ethanol mixture and alcoholic solutions can be approximated by a cylindrical shape of the macroion.

In aqueous solutions, the macroion is less extended than in the alcoholic one.

Equation (6) proposed by Beevers was verified to correlate the refractive index and the unit molar refractivity.

Between the particles in solution, different kinds of interaction are also exerted, which depend on the polyelectrolyte chemical nature and solution concentration and, on the other hand, on the solvent nature and temperature.

---

[14] Z. Alexandrowicz, *J. Polymer Sci.*, **56**, 115 (1962).

[15] G. Manning, *J. Chem. Phys.*, **43**, 4260 (1965).

[16] B. H. Zimm and G. Manning, *J. Chem. Phys.*, **43**, 4250 (1965).

Revue Roumaine de Chimie 22, 2, 213 – 220 (1977)

ESTUDIO DE REACCIONES DE ARBUZOV. I

MECANISMO DE REACCIONES DE TRIALQUIL(-ARIL)FOSFITOS CON YODUROS DE ALQUILO

J. M. CACHAZA, J. CASADO y A. VARELA
Departamento de Química física. Universidad de Santiago. Laboratorio de Investigaciones Químicas, C.S.I.C., España

Recibido el 26 Abril 1975

A kinetic study of some Arbuzov's reactions has been carried out, finding two clearly differentiated groups of processes. Conductimetric and spectrographic (I.R.) techniques have been used. Kinetic and thermodynamic parametres have been calculated proposing a reaction-mechanism that explains the experimental facts observed and that includes the genesis of an intermediate ionic compound.

I. INTRODUCCIÓN

Un grupo de reacciones de interés creciente, tanto por su papel en procesos de síntesis, como por sus relaciones con importantes procesos industriales y con especies implicadas en el polémico campo de los insecticidas, es el que genéricamente se denomina "reacciones de Arbuzov":

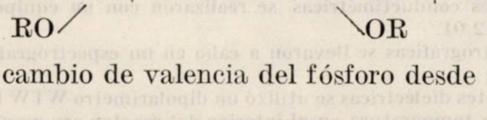

$$(RO)_3P + R'X \rightarrow R'-P(O)(OR)_2 + RX$$

que implican un cambio de valencia del fósforo desde su estado trivalente a pentavalente.

Aunque este tipo de reacciones aparece con frecuencia en la bibliografía, suele hacerlo a través de trabajos de orientación preparativa, abordando muy superficialmente (cuando lo hacen) aspectos cinéticos y mecanicistas de los procesos estudiados. [1-9]

---

[1] A. MICHAELIS y R. KAEHNE, *Ber. dtsch. chem. Ges.*, **31**, 1048 (1898).

[2] A. E. ARBUZOV, *J. Russ. Phys. Chem. Soc.*, **38**, 161, 293, 687 (1906).

[3] A. H. FORD-MOORE y W. HOWARTH, *J. Chem. Soc.*, **1947**, 1465.

[4] A. E. ARBUZOV, *Diss. Kazan*, **1914**, 148.

[5] B. A. ARBUZOV, A. V. FUZHENKOVA. V. S. VINOGRADOVA y T. E. TOLKACHEVA, Khim. i Primeneneie Fosfororgan. Soedinenií, Akad. Nauk S.S.S.R., Trudy 1-oí Konferents, 1955, 62, *Chem. Abstr.*, **52**, 239 (1958).

[6] B. A. ARBUZOV y A. V. FUZHENKOVA, *Izvest. Akad. Nauk. S.S.S.R., Otdel khim. Nauk*, 1928 (1959).

[7] B. A. ARBUZOV, *Pure Appl. Chem.*, **9**, 307 (1964).

[8] V. MARK y J. VAN WAZER, *J. Org. Chem.*, **1964**, 1006.

[9] a) A. N. PUDOVIC y V. K. KRUPNOV, *Zhur. obshchei Khim.*, **38**, 1287 (1968).
b) N. I. RIZPOLOZHENSKI y F. S. MUKHAMETOV, *Izvest. Akad. Nauk. S.S.S.R., Otdel. khim. Nauk.*, **1968**, 2163.

Staronka [10] da cuenta en 1927 de resultados de interés cinético sobre este tipo de reacciones, pero no es hasta 1944 cuando se aborda sistemáticamente [11] el estudio de reacciones de trialquil fosfitos con haluros de alquilo, aunque con una metodología de alcance limitado. Rumpf [12] sugiere más tarde la conveniencia de un estudio físicoquímico de esos sistemas. Buck y Yoke [13] se sirven de la conductimetría para estudiar la reacción entre yoduro de etilo y tributil fosfitos. Un año después, Aksnes y Aksnes [14] utilizan la espectrografía de I.R. para estudiar la reacción entre trietil fosfito y yoduro de etilo, encontrando resultados en contradicción con los de Buck y Yoke (loc. cit.). Posteriormente, Aksnes y Aksnes [15,16] reafirman la formación de compuestos intermedios de fosfonio, interpretando diversos resultados observados experimentalmente.

II. PARTE EXPERIMENTAL

Analizadas algunas de las discrepancias observadas por autores que utilizan diferentes técnicas (loc. cit.), y con el fin de realizar un estudio sistemático, se seleccionó como magnitud observable la conductividad del sistema reaccionante, sin excluir el manejo complementario de la espectrografía de I.R. Esa selección se hizo atendiendo, entre otros factores, a:

1. La posible aparición de un compuesto iónico intermedio.
2. El medio de reacción elegido, acetonitrilo ($\varepsilon = 36$).

La bibliografía, (Aksnes y Aksnes, loc. cit.) apunta como posible fuente de error la presencia de humedad en el medio de reación. Por ello, en este trabajo se ha llevado un riguroso control del acetonitrilo, procediendo a sucesivas destilaciones cuando la conductividad presentaba valor superior a uno umbral que se fijó en 10^{-6} mhos cm^{-1} (Buck y Yoke fijaron este límite en 10^{-5}).

Por la misma razón se ha utilizado como reactor una cápsula de cuello esmerilado cuyo cierre estaba constituido por la propria célula de conductividad, también de cuello esmerilado. El grado de garantía del método fue verificado introduciendo en la cápsula muestras de acetonitrilo que se mantuvieron allí durante periodos superiores a cuarenta y ocho horas, sin que se apreciara variación en el valor de la conductividad. La preparación de disoluciones se llevó a cabo en caja seca.

Las determinaciones conductimétricas se realizaron con un equipo Radiometer CDM3, con célula Philips PR9512/01.

Las medidas espectrográficas se llevaron a cabo en un espectrógrafo Perkin-Elmer I.R. 20A.

Para medir constantes dieléctricas se utilizó un dipolarímetro WTW DMO1.

La constancia de la temperatura en el interior del reactor era mantenida sumergiéndolo en un ultratermostato convencional que garantizaba un error no superior a ± 0,02°.

Se utilizaron reactivos Fluka

Dada la toxicidad de las especies manejadas, hubo necesidad de tomar las precauciones habituales en este tipo de trabajo.

III. RESULTADOS

En este trabajo se han estudiado cinéticamente las reacciones de trietil, tributil y trifenil fosfitos (TEtP, TBuP y TPhP), respectivamente con yoduros de metilo, etilo y propilo (IMe, IEt e IPr) utilizando acetonitrilo como medio de reacción.

---

[10] W. Staronka, *Roczniki. Chem.*, **7**, 42 (1927).

[11] G. M. Kosolapoff, *J. Amer. Chem. Soc.*, **66**, 109 (1944).

[12] P. Rumpf, *Bull. Soc. chim. France*, **1951**, 128.

[13] F. C. Buck y J. T. Yoke, *J. Org. Chem.*, **27**, 3675 (1962).

[14] G. Aksnes y D. Aksnes, *Acta Chem. Scand.*, **17**, 2121 (1963).

[15] G. Aksnes y D. Aksnes, *Ibid.*, **18**, 38 (1964).

[16] G. Aksnes y D. Aksnes, *Ibid.*, **19**, 898 (1965).

Antes de pasar a detallar los resultados obtenidos en cada caso, debe indicarse que se han observado dos situaciones claramente diferenciables : Mientras que en las reacciones entre IEt e IPr con TEtP, TBuP y TPhP,

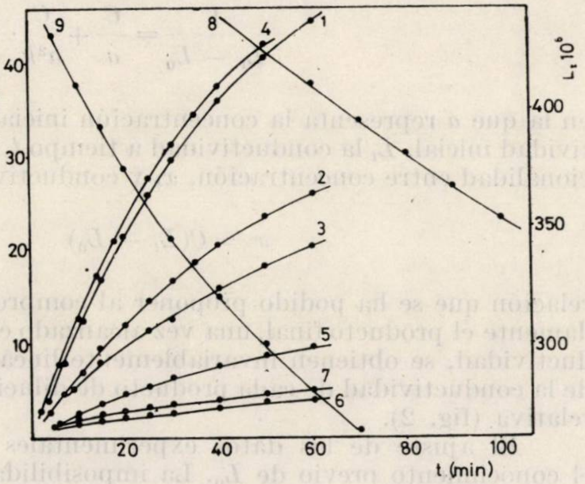

Fig. 1. — Variación de la conductividad con el tiempo para las reacciones :

1) TEtP + IMe, c_i = 0.0336 M, 25°;
2) TEtP + IEt, c_i = 0,1332 M, 30°;
3) TEtP + IPr, c_i = 0,1693 M, 30°;
4) TBuP + IMe, c_i = 0,0328 M, 25°;
5) TBuP + IEt, c_i = 0,1820 M, 30°;
6) TBuP + IPr, c_i = 0,1075 M, 30°;
7) TPhP + IMe, c_i = 0,1990 M, 30°;
8) TEtP + IMe, c_i = 0,3059 M, 40°;
9) TBuP + IMe, c_i = 0,7615 M, 40°.

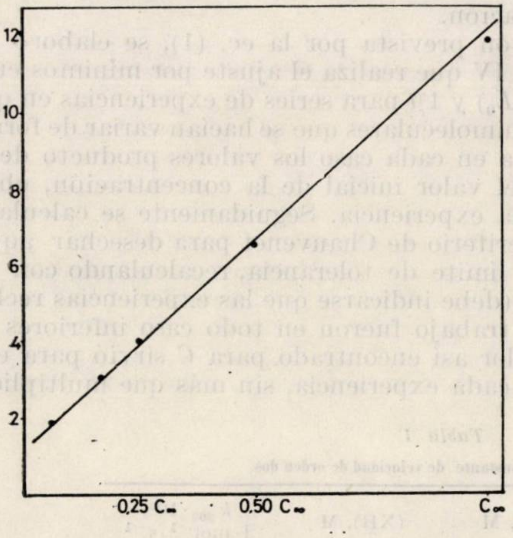

Fig. 2. — Reacción TBuP + IEt.

se manifestó invariablemente un crecimiento progresivo de la conductividad con el tiempo, hasta alcanzar un valor estacionario, en las de IMe con TEtP y TBuP, tras ese aumento inicial, se observó un lento descenso en los valores de la conductividad, descenso que concluía cuando se alcanzaba un valor ligeramente superior al inicial para cada experiencia. La fig.1 ilustra ese comportamiento.

Como veremos más adelante, se ha identificado el tramo ascendente de la conductividad con la génesis de una especie iónica, intermedia, propia de esas reacciones de Arbuzov.

Resulta fácil mostrar que, si los resultados observados se ajustasen a un proceso de orden dos, debería satisfacerse la expresión :

$$\frac{1}{L_t - L_0} = \frac{C}{a} + \frac{C}{a^2 k} \cdot \frac{1}{t} \qquad (1)$$

en la que a representa la concentración inicial de reactivos, L_0 la conductividad inicial, L_t la conductividad a tiempo t, y C el coeficiente de proporcionalidad entre concentración, x, y conductividad :

$$x = C(L_t - L_0) \qquad (2)$$

relación que se ha podido proponer al comprobar que, al diluir reiteradamente el producto final, una vez alcanzado el valor estacionario de la conductividad, se obtienen invariablemente líneas rectas como representación de la conductividad de cada producto de dilución frente a su concentración relativa (fig. 2).

El ajuste de los datos experimentales de la ecuación (1) supone el conocimiento previo de L_0. La imposibilidad de conocer experimentalmente este valor de manera directa, ha obligado, en cada caso, a efectuar su determinación por extrapolación.

Para verificar la correlación prevista por la ec. (1), se elaboró un programa de cálculo en Fortran IV que realiza el ajuste por mínimos cuadrados de los valores de $1/(L_t - L_0)$ y $1/t$ para series de experiencias en que se utilizaron concentraciones equimoleculares que se hacían variar de forma sistemática. El programa calcula en cada caso los valores producto de la ordenada en el origen por el del valor inicial de la concentración, obteniendo así el valor de C en cada experiencia. Seguidamente se calcula el valor medio de C, aplicando el criterio de Chauvenet para desechar aquellos valores que sobrepasan su límite de tolerancia, recalculando con los restantes un nuevo valor medio (debe indicarse que las experiencias rechazadas con esta metodología de trabajo fueron en todo caso inferiores en número al 3% del total). El valor así encontrado para C sirvió para calcular la velocidad específica en cada experiencia, sin más que multiplicar

Tabla 1

Cálculo de la constante de velocidad de orden dos

Reacción	$(P(OR)_3)$, M	(XR), M	$k_{303} \cdot 10^3$, $l \cdot mol^{-1} \cdot s^{-1}$
TEtP + IMe	0,0734 – 0,0337	0,0740 – 0,0336	7,17 ± 0,49
TEtP + IEt	0,5055 – 0,3040	0,5013 – 0,3001	1,51 ± 0,18
TEtP + IPr	0,4908 – 0,1693	0,4950 – 0,1693	1,61 ± 0,09
TBuP + IMe	0,0720 – 0,0336	0,0702 – 0,0328	7,51 ± 0,21
TBuP + IEt	0,1880 – 0,0450	0,1820 – 0,0450	2,05 ± 0,43
TBuP + IPr	0,1408 – 0,0537	0,1080 – 0,0540	6,55 ± 0,42
TPhP + IMe	0,1990	0,2022	3,11

el valor recíproco de la pendiente de la recta (1) por C/a^2. La fig. 3 ilustra genéricamente los resultados obtenidos a lo largo de 67 experiencias. Debe indicarse que el coeficiente de correlación lineal presentó siempre valores no inferiores a 0,9950. En la Tabla 1 se da cuenta de los valores obtenidos

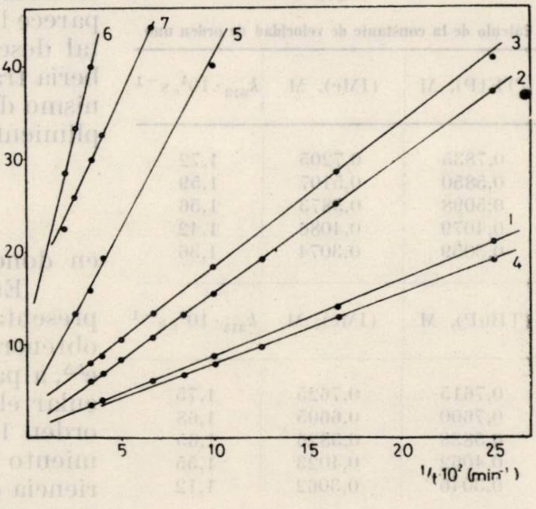

Fig. 3. — Comprobación de la ecuación (1).

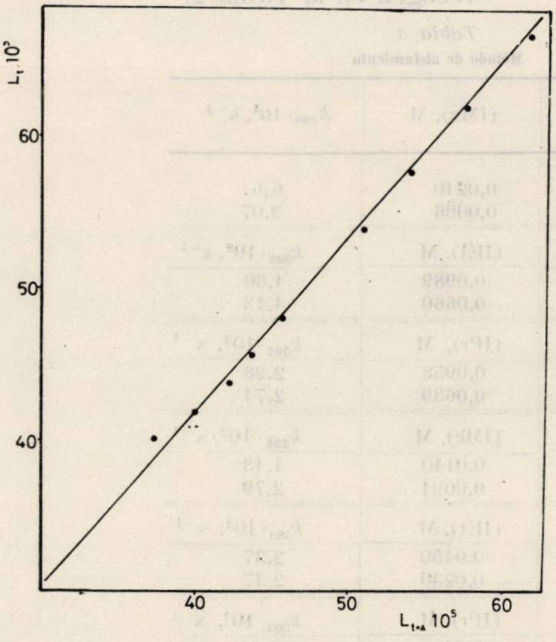

Fig. 4. — Reacción TEtP + IMe, $c_i = 0{,}7845$ M, 40°.

para k en cada caso. Debe advertirse que, dado que no se ha observado variación significativa de la constante de velocidad con la concentración en los intervalos de trabajo, los valores que en ella figuran son valores medios.

Al estudiar la reacción entre yoduro de metilo y trietil y tributil fosfitos, las respectivas curvas conductividad/tiempo permitieron observar, como ya queda dicho, un tramo decreciente, probable reflejo de la descomposición de la especie iónica intermedia (véase fig. 1). En principio, parece lógico pensar que, de producirse tal descomposición monomolecular, debería transcurrir a través de un mecanismo de orden 1, lo que supondría cumplimiento de la ecuación (3) :

$$L_{t1} = e^{k\Delta} L_{t1+\Delta} \qquad (3)$$

en donde $\Delta = t_2 - t_1$.

Esta expresión supone que, al representar L_{t1} frente a $L_{t1+\Delta}$, debería obtenerse una línea recta de pendiente $e^{k\Delta}$, a partir de cuyo valor se puede calcular el de la constante de velocidad de orden 1. La fig. 4 muestra el cumplimiento de tal linealidad para una experiencia estándar. Los valores de *k* se recogen en la Tabla 2.

Tabla 2

Cálculo de la constante de velocidad de orden uno

(TEtP), M	(IMe), M	$k_{313} \cdot 10^4$, s^{-1}
0,7835	0,7205	1,72
0,5850	0,5107	1,59
0,5098	0,5873	1,56
0,4079	0,4086	1,42
0,3059	0,3074	1,36
(TBuP), M	(IMe), M	$k_{313} \cdot 10^4$, s^{-1}
0,7615	0,7625	1,75
0,7600	0,6605	1,68
0,5838	0,5826	1,65
0,4062	0,4023	1,55
0,3046	0,3062	1,12

Tabla 3

Método de aislamiento

(TEtP), M	(IMe), M	$k_{298} \cdot 10^4$, s^{-1}
0,1257	0,0240	6,64
0,1257	0,0096	3,07
(TEtP), M	(IEt), M	$k_{303} \cdot 10^3$, s^{-1}
0,8198	0,0989	4,80
0,8198	0,0660	4,13
(TEtP), M	(IPr), M	$k_{303} \cdot 10^3$, s^{-1}
0,7785	0,0958	2,98
0,7785	0,0639	2,74
(TBuP), M	(IMe), M	$k_{298} \cdot 10^3$, s^{-1}
0,0720	0,0140	4,43
0,0720	0,0091	2,79
(TBuP), M	(IEt), M	$k_{303} \cdot 10^3$, s^{-1}
0,2480	0,0450	2,37
0,2480	0,0230	2,47
(TBuP), M	(IPr), M	$k_{303} \cdot 10^3$, s^{-1}
0,1803	0,0540	2,34
0,1803	0,0270	1,62
(TPhP), M	(IMe), M	$k_{313} \cdot 10^4$ s^{-1}
0,1990	0,0272	3,73
0,1990	0,0204	4,19

Para confirmar el orden global 2 en las reacciones estudiadas, se llevaron a cabo experiencias encaminadas a la determinación de los órdenes parciales respecto a cada reactivo, utilizando el método de aislamiento. Así se encontraron pseudoórdenes unitarios en ambos casos. Para el cálculo de las constantes de velocidad se siguió el método de Guggenheim. Algunos de los resultados obtenidos en esta serie se recogen en la Tabla 3.

Tabla 4

Parámetros de activación

Reacción	$\Delta E_a^{\neq}$, $k\mathrm{Jmol}^{-1}$	$\Delta H^{\neq}$, $k\mathrm{Jmol}^{-1}$	$-\Delta S^{\neq}$, $\mathrm{Jmol}^{-1}\mathrm{K}^{-1}$
TEtP + IMe	58,6	56,0	100,4
TEtP + IEt	68,5	65,9	80,4
TEtP + IPr	57,7	55,1	115,8
TBuP + IMe	64,1	61,6	80,2
TBuP + IEt	72,6	70,0	63,4
TBuP + IPr	53,6	51,0	121,5
TPhP + IMe	45,6	43,0	149,1
TEtP + IMe	53,3	50,8	150,6
TBuP + IMe	44,4	41,9	181,7

(Las dos últimas filas corresponden al proceso de descomposición).

Con objeto de calcular los valores de las energías, entalpias y entropías de activación, se realizaron experiencias a diferentes temperaturas, pudiendo observar satisfactorio cumplimiento de la ecuación de Arrhenius y de las previsiones derivadas de la teoría del complejo activado, tanto para el proceso de supuesta formación de la especie iónica intermedia como, en su caso, para el de su descomposición. En la Tabla 4 se recogen tales resultados.

IV. DISCUSIÓN DE RESULTADOS: MECANISMO DE REACCIÓN

Factor clave en el estudio mecanicista de reacciones de Arbuzov es la génesis de enlace P = O en los fosfonatos que resultan como productos de reacción. Tal enlace es uno de los más fuertes que se conocen (500/600 kJmol^{-1}), de modo que su aparición ha de ser muy favorable termodinámicamente, permitiendo inferir que la formación de enlaces P = O sea una de las fuerzas directrices en éstas y otras reacciones comparables. Por ello se llevó a cabo un estudio espectrográfico en la región I. R. sobre el sistema TEtP/IMe. Pudo así observarse que, a medida que transcurre el tiempo de reacción, se produce una intensificación de las bandas centradas en 1250, 1310 y 1200 cm^{-1}. La primera de ellas se asigna a la vibración de tensión del enlace P=O y la segunda a la vibración de tensión $P-CH_3$. La última frecuencia iría asociada al IEt formado en el curso de la reacción. Esta banda desaparece cuando, después de un tiempo suficientemente largo, se somete a destilación la mezcla de reacción debido, sin duda, a la mayor volatilidad de esa especie.

Resulta de interés observar que, invariablemente, en aquellas reacciones en que no se observaba descenso de la conductividad, tampoco pudo detectarse espectrográficamente la presencia del grupo P = O en los productos de reacción.

A la vista de los resultados y consideraciones precedentes, se propone el siguiente mecanismo de reacción para los procesos de Arbuzov estudiados en esta investigación:

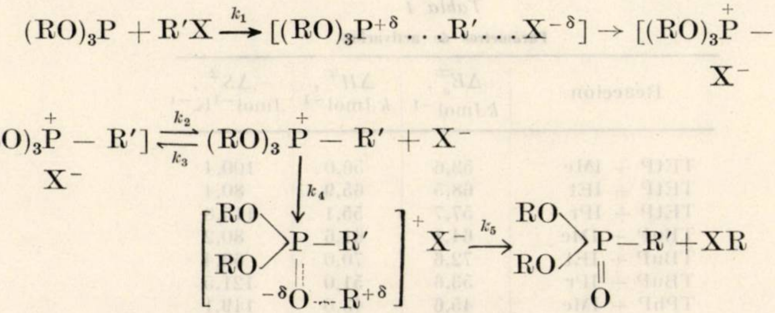

$$(RO)_3P + R'X \xrightarrow{k_1} [(RO)_3P^{+\delta}\ldots R'\ldots X^{-\delta}] \rightarrow \underset{X^-}{[(RO)_3\overset{+}{P} - R']}$$

$$\underset{X^-}{[(RO)_3\overset{+}{P} - R']} \underset{k_3}{\overset{k_2}{\rightleftharpoons}} (RO)_3\overset{+}{P} - R' + X^-$$

$$\xrightarrow{k_4} \left[\begin{array}{l} RO \\ \quad \rangle P-R' \\ RO \quad \vdots \\ \quad {}^{-\delta}O \cdots R^{+\delta} \end{array}\right]^+ X^- \xrightarrow{k_5} \begin{array}{l} RO \\ \quad \rangle P-R' + XR \\ RO \quad \| \\ \quad\; O \end{array}$$

El continuado incremento de la conductividad observado invariablemente ha permitido postular la formación de una especie en equilibrio con sus iones. El valor negativo de la entropía de activación para el proceso de formación de tal especie, confirma que transcurre a través de una reordenación, sin olvidar la participación de procesos de solvatación.

Los resultados han puesto también en evidencia que, en aquellos procesos de Arbuzov en los que sólo se aprecia el tramo creciente de la curva de conductividades, el intervalo de variabilidad de esta magnitud es muy reducido mientras que, cuando se observa tramo descendente, ese intervalo es mucho mayor (la variación puede ser de 10^{-6} a 10^{-3} Siemens). Eso induce a pensar que el equilibrio entre las formas indisociada y disociada de la especie propuesta, debe de estar mucho más desplazado hacia la derecha en el segundo caso, hipótesis coherente con el valor negativo de la entropía de activación encontrado asimismo para el segundo proceso.

Si se tiene en cuenta que las especies ionizadas han sido las utilizadas para el seguimiento cinético de la reacción, y supuesto cumplimiento de la condición de estado estacionario, puede deducirse con facilidad que:

$$V_r = k_1((RO)_3P)\,(XR') - k_5((RO)_3PR')^+ \qquad (4)$$

La ecuación de velocidad (4) resulta acorde con los hechos experimentales, es decir orden global dos para el proceso de formación de la especie intermedia y orden uno cuando tiene lugar el proceso de transformación de la misma en los productos finales.

Finalmente debe apuntarse que, al estudiar la reacción entre TBuP y IEt, no se observó merma de la conductividad una vez formado el compuesto intermedio, lo cual se encuentra acorde con los resultados espectrográficos de Aksnes y Aksnes (loc. cit.).

Revue Roumaine de Chimie, 22, 2, 221 – 225 (1977)

STERIC EFFECTS IN A SERIES OF TETRACOORDINATED COMPLEXES OF Co(II) CONTAINING PHENANTHROLINE DERIVATIVES

MARGARETA TEODORESCU and MARIA BREZEANU
Laboratory of Inorganic Chemistry of the Chemical Faculty, Bucharest,
Str. Splaiul Independenţei, 89

Received February 24, 1975

A correlation has been made between the steric effects of the aromatic ligands such as 2-methyl-1,10-phenanthroline (mephen) and 2,9-dimethyl-1, 10-phenanthroline (dmphen) and the orbital parameter Δ estimated from the electronic spectra of the tetracoordinated compounds of Co(II) of the type : $[Co(II)_2L_2Cl_2]Cl_2.4HCl$ and $[Co(II)\,LCl_2]$ (L-organic ligand as mephen and dmphen), in order to see the steric hindrance influence on the σ metal-ligand bonding strength. The proposed structural formulas, as derived from the spectral behaviour, agree with magnetic and chemical properties.

INTRODUCTION

From the direct reaction between ligand (mono- and dimethyl-phenanthroline derivatives) and Co(II) chloride (see the experimental part), two types of tetracoordinated Co(II) complexes were obtained : (a) binuclear complexes of the type $[Co(II)_2L_2Cl_2]Cl_2.4HCl$, and (b) tetrahedral diammine of the type $[Co(II)LCl_2]$

The syntheses, chemical analyses and physico-chemical properties of the mentioned compounds with 2,9-dimethyl-1,10-phenanthroline were reported in an earlier paper. [1] In a similar manner, complexes of Co(II) with 2-methyl-1,10-phenanthroline were also obtained. The aim of the present note is to characterize the above mentioned compounds, and to compare their optical and magnetic properties in order to obtain information concerning the steric hindrance influence on the metal-ligand chemical bonds.

EXPERIMENTAL

The synthesis and the chemical analysis of Co(II) complexes with dimethyl-phenanthroline were reported in an earlier paper.[1]

$[Co(II)_2mephen_2Cl_2]Cl_2.4HCl$-green. Solid organic ligand is added to a concentrated aqueous solution of cobalt chloride at the molar ratio 1 :2, and then concentrated hydrochloric acid and cold hydrogen peroxide. The solution is heated and dried on water bath and then the precipitate is washed in acetone, a green compound being separated thereby. working at ratio 1 :1 or 1 :3($CoCl_2.6H_2O$-base) the same compound is obtained. The green compound was separated wor-

---

[1] M. Teodorescu, M. Brezeanu and P. Spacu, *Rev. Roumaine Chim.*, **17**, 1191 (1972).

king in the same way but without peroxide. The chemical analysis calc. for $[Co(II)_2 mephen_2 Cl_2]Cl_2.4HCl$ gives : C%39.30 ; N%7.06 ; Cl% 35.73 ; Co% 14.85. Found : C% 39.90 ; N% 7.28 ; Cl%35.80 ; Co%14.42.

[Co(II)mephenCl$_2$]-violet. The same preparation method as for the green form is used, solving the green residue in methanol, ethanol or DMF. A violet compound is thus obtained. The same violet form may be obtained by heating the green compound. The chemical analysis calc. for $[Co(II) mephenCl_2]$ gives : C%48.19 ; N% 8.64 ; Cl% 21.89 ; Co% 18.19. Found : C% 48.56 ; N% 8.79 ; Cl% 21.82 ; Co% 17.94.

The magnetic moment was determined by means of Faraday method[2] using the formula $\mu = 2.84(\chi'_m.T)^{1/2}$ where $\chi'_m = \chi_m - \chi_{dia}\, \chi_{dia\ mephen} = -131.6{,}10^{-6}$ and $\chi_{dia\ Cl^-} = -40.2{,}10^{-6}$ u.c.g.s.

The electronic spectra were recorded for the solid state using a spectrophotometer Zeiss VSU$_1$ equipped with a reflectance device, and MgO as standards.

RESULTS AND DISCUSSIONS

The electronic spectra of compounds containing 2-methyl-1,10-phenanthroline recorded for the solid state are plotted in fig. 1. The reflectance spectra of the similar compounds containing 2,9-dimethyl-1,10-phenanthroline were presented and briefly discussed in an earlier paper.[1] The absorption maxima and their assignment in Co(II) compound with phenanthroline derivatives are listed in table 1.

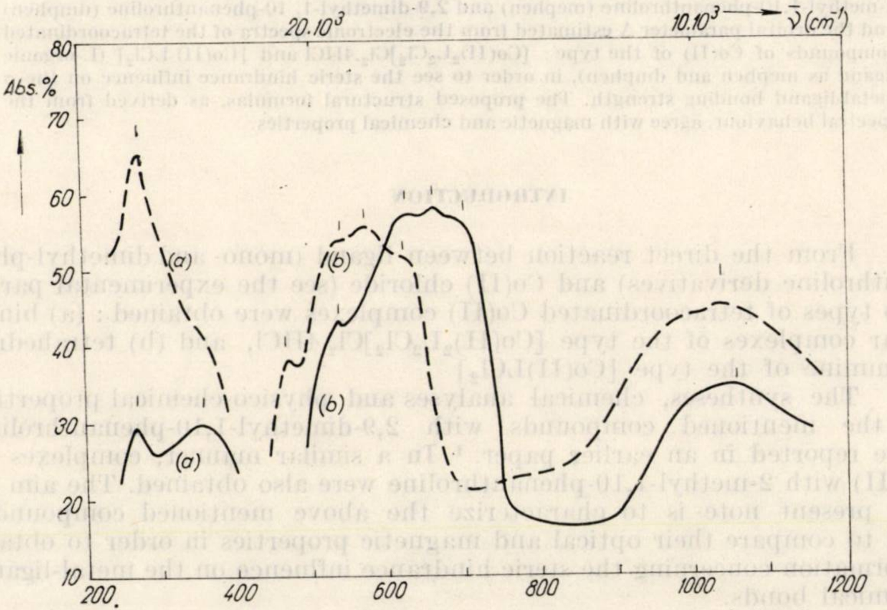

Fig. 1. — Electronic spectra of compounds : $[Co(II)_2 mephen_2Cl_2]Cl_2.4HCl$ green form (full line)and $[Co(II) mephenCl_2]$ violet form (dashed line) recorded for the solid state.

a) ratio 1 : 3(complex : MgO)
b) ratio 1 : 1(complex : MgO)

---

[2] B. N. Figgis and J. Lewis in "Modern Coordination Chemistry" K. Lewis and R. G. Wilkins, Ed. Interscience Publ., Inc. New York, 1960.

Table 1

The absorption maxima and their assignment in Co(II) compounds with phenanthroline derivatives

Compound	Absorption maxima mμ(cm^{-1})				
[Co(II)$_2$mephen$_2$Cl$_2$]Cl$_2$.4HCl green	1060(9400)	700(14 300) 660(15 150) 630(15 870)	535(18 700)	365(27 400)	275(36 360)
[Co(II)mephen Cl$_2$] violet	1040(9600)	620(16 130) 570(17 540) 540(18 510)	475(21 000)	365(27 400)	275(36 360)
[Co(II)$_2$dmphen$_2$Cl$_2$]Cl$_2$.4HCl green	—	690(14 490) 650(15 380) 625(16 000)	535(18 700) 500(20 000)	350(28 570)	275(36 360)
[Co(II)dmphenCl$_2$] blue	—	650(15 380) 600(16 670) 570(17 540)	475(21 000)	350(28 570)	280(35 700)
Assignment	$^4A_2 \rightarrow {}^4T_1(F)$ ν_2	$^4A_2 \rightarrow {}^4T_1(P)$ ν_3	$^4A_2 \rightarrow {}^2E$	MO(d^7)→π*	π→π**

In the electronic spectra of the Co(II) compounds containing methylphenanthroline occurs in the i.r. range a broad band ascribed to a spin allowed transition (ν_2), which is out of the instrumental accessibility for the compounds containing dimethylphenanthroline. In the visible range of the spectra[3], like $[Co(II)X_4]^{-2}$ (where X-halide ions) an absorption band at 15 – 12 000 cm^{-1} occurs, split by the spin-orbit coupling. This band (ν_3) is attributed to a spin allowed d-d transition, up to the spectral term $^4T_1(P)$. Absorption maxima comparatively of lower intensity at ~20 – 21 000 cm^{-1} were ascribed to spin forbidden transitions up to the doublet ^2E ($^4A_2 \rightarrow {}^2E$). In the u.v. range, the absorption bands could be assigned to a charge transfer $M \rightarrow L$ mechanism.

Characteristic for the tetrahedral d^7 configuration is the spin allowed transition ν_3,[4] which will be comparatively studied for all the four Co(II) compounds.
The energy of this transition is :[5]

$$\nu_3 = 1.5\ \Delta + 7.5\ B + Q$$

where

$$Q = 1/2[(0.6\Delta - 15B)^2 + 0.64\ \Delta^2]^{1/2}$$

Taking the mean value $B \approx 700$ cm^{-1}, the following values for the orbital parameter Δ are obtained : (Tab. 2)

---

[3] F. A. Cotton, D.M.L. Goodgame and M. J. Goodgame, *J. Amer. Chem. Soc.*, **83**, 469^{0} (1961).

[4] Y. Tanabe and S. Sugano, *J. Phys. Soc. Japan*, **9**, 753(1954).

[5] A. B. Lever "Inorganic Electronic Spectroscopy" Els. Publ. Comp. Amsterdam, 1968

Table 2

Calculated values for the parameter Δ

Compound	Δ (cm^{1-})
$[Co(II)_2mephen_2Cl_2]Cl_2.4HCl$	3 700
$[Co(II)mephenCl_2]$	5 300
$[Co(II)_2dmphen_2Cl_2]Cl_2.4HCl$	3 800
$[Co(II)dmphenCl_2]$	4 600

For $[Co(II)Cl_4]^{2-}$ $\Delta = 4\,780\ cm^{-1}$ (Cotton)[3].

As may be seen from the spectral value of Δ, one may conclude :

(i) $$\Delta_{T[Co(II)mephenCl_2]} > \Delta_{T[Co(II)dmphenCl_2]}$$

which agrees with the suggestion that the methyl groups attached to the aromatic ring close to the nitrogens, involved in coordinative bonds with the central metal ion, produce a lowering of the σ chemical bond strength, in direct proportion with their increase.

(ii) it may be stated that the 2,9-dimethylphenanthroline is close to chloride ion in the spectrochemical series, since

$$\Delta_{[Co(II)dmphenCl_2]} \approx \Delta_{[Co(II)Cl_4]^{2-}}$$

(iii) the ligand field strength in the green compounds (type a) is lower than in the blue compounds (type b), in agreement with the bridge formulation (Fig. 2), the bridge chemical bonds Co---Cl being weaker than the terminal Co – Cl bonds in $[Co(II)Cl_4]^{2-}$.

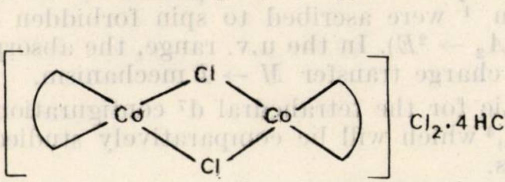

The chemical behaviour of the compounds (see the experimental part) is thus supported by their spectral properties and by the magnetic measurements made at room temperature.

The magnetic results for the new Co(II) compounds with methylphenanthroline (see tabl. 3) are characteristic of high spin tetrahedral d^7 complexes.[6] They are in agreement with those calculated by means of the formula :

$$\mu_{obs} = \mu_s - \frac{15.59\,\lambda}{\Delta}, \quad \text{where}$$

---

[6] B N. Figgis "Introduction to Ligand Fields" Interscience Publ., New York, 1967.

μ_s is the spin only magnetic moments (3.88 M.B. for three uncoupled electrons), Δ—the orbital splitting parameter and λ—spin-orbit coupling constant, equal for Co(II) to -178 cm^{-1}.

Table 3

Magnetic moments of Co (II) complexes

Compound	μ_{eff} (BM)	
	obs.	calc.
	4.72	4.63
$[Co(II)_2mephen_2Cl_2]Cl_2.4HCl$	4.66	4.40
$[Co(II)mephenCl_2]$	4.84*	4.61
$[Co(II)_2dmphen_2Cl_2]Cl_2.4HCl$	4.74*	4.48
$[Co(II)dmphenCl_2]$		

* results reported in an earlier paper [1]

As may be seen from table 3, the magnetic measurements are in agreement with the high-spin tetrahedral arrangement of the complexes of Co(II), in agreement with spectral behaviour of the complexes.

Revue Roumaine de Chimie, 22, 2, 227 – 235 (1977)

HETEROPOLYTUNGSTATES WITH U(IV) AS CENTRAL ATOM. SYNTHESIS AND PHYSICO-CHEMICAL STUDY OF THE $K_{10}[U(PW_{11}O_{39})_2].22H_2O$ COMPLEX

GH. MARCU and MARIANA RUSU

Laboratory of Radioactive Element. Chemistry "Babeş-Bolyai" University of Cluj-Napoca, Romania, str. Arany Janos, nr. 11

Received February 14, 1975

The ion U(IV) reacts rapidly with unsaturated heteropolyanions, forming complexes of the UL_2 type where $L = PW_{11}O_{39}^{7-}$ and $P_2W_{17}O_{61}^{10-}$. The potassium salt of the heteropolyanion $[U(PW_{11}O_{39})_2]^{10-}$ and the corresponding acid were isolated. The combination ratio and oxidation state of uranium in the heteropolycompound are discussed.

INTRODUCTION

It is well known that unsaturated heteropolyanions $L = PW_{11}O_{39}^{7-}$, $SiW_{11}O_{39}^{8-}$ and $P_2W_{17}O_{61}^{10-}$, react with M^{2+}, M^{3+} and M^{4+} cations of the transition metals to form heteropolycompounds represented as ML, which are members of a large class of heteropolyanions.[1-7]

Peacock and Weakley [8] have observed that the cations of lanthanides form anionic complexes of ML and ML_2 type and have isolated their salts. Botar and Weakley [9] have isolated salts of ThL_2 complexes (where $L = SiW_{11}O_{39}^{8-}$, $PW_{11}O_{39}^{7-}$ and $P_2W_{17}O_{61}^{10-}$).

We found that ion U(IV) forms a heteropolycompound of UL_2 type (where $L = PW_{11}O_{39}^{7-}$, $SiW_{11}O_{39}^{8-}$ and $P_2W_{17}O_{61}^{10-}$).[10]

In this paper we report the investigation of the compound $K_{10}[U(PW_{11}O_{39})_2].22H_2O$. The heteropolycompounds of ML and ML_2 type, where $L = PW_{11}O_{39}^{7-}$, are derived from the anion $PW_{12}O_{40}^{3-}$ by replacing one tungsten atom with a metal atom M. [11] These heteropoly-

---

[1] S. A. Malik and T J. R. Weakley, *J. Chem. Soc.(A)*., **1968**, 2647.

[2] C. M. Tourné and G. F. Tourné, *Compt. rend.*, **266**, 1363 (1968).

[3] C M Tourné and G. F. Tourné, *Bull. Soc. chim. France.*, **4**, 1124 (1969).

[4] C. M. Tourné, *Compt. rend.*, **266**, 702 (1968).

[5] C. M. Tourne, G, F. Tourné, S. A. Malik and T. J. R. Weakley, *J. Inorg. Nuclear Chem.*, **32**, 3875 (1970).

[6] T. J. R. Weakley and S. A. Malik, *J. Inorg. Nuclear Chem.*, **29**, 2935 (1967).

[7] L. C. W. Baker and J. S. Figgis, *J. Amer. Chem. Soc.*, **92**, 3794 (1970).

[8] R. D. Peacock and T. J. R. Weakley, *J. Chem. Soc (A)*., **1971**, 1836.

[9] A. V. Botar and T. J. R. Weakley, *Rev. Roumaine Chim.*, **18**, 1155 (1973).

[10] Gh. Marcu, M. Rusu and A. V. Botar, *Rev. Roumaine Chim.*, **19**, 827 (1974).

[11] P. Souchay, *Ann. Chim. (France)*, **20**, 73 (1967).

anions are formed by incomplete degradation of $PW_{12}O_{40}^{3-}$ type anions with potassium acetate or potassium bicarbonate, up to pH = 6 – 7 in presence of the metal atom M, introduced in various oxidation states.[12] In each 12-tungstate heteropolyanion the atom M replaces only one octaedrally coordinated M.

EXPERIMENTAL PART

The salt $K_{10}[U(PW_{11}O_{39})_2].22H_2O$, was prepared by a similar method to that used previously for related complexes.[1-8] The optimal conditions for the formation of the complex were first establised photocolorimetrically.[13] A solution of $K_7PW_{11}O_{39}.15H_2O$,[14] was warmed to 70° after adjustment of the pH to 4.5 with 2N H_2SO_4. A solution containing the theoretical amount of $U(SO_4)_2$ (prepared by the reduction of UO_2SO_4 with zinc amalgam [15]) was added slowly with continuous stirring. The mixture was cooled to 5° and filtered. Deep brown microcrystals separated after 48 h at 5° and were recrystallized three times from distilled water (70°, pH = 4.5).

The chemical analysis of the heteropolycompound obtained involved the analysis method generally applied to heteropolycompounds of this type.[16] Uranium was measured photocolorimetrically with Arsenazo III, at 665 nm using cuvettes of 1 cm.[17] Tungsten was determined by precipitation with chinchonine and ignition to WO_3.[18] Phosphorus was determined by precipitation as magnesium ammonium phosphate and ignition to $Mg_2P_2O_7$.[19] Potassium was determined with tetraphenylborate.[20] The water content of the complex was determined by heating at 500 – 550° during 1h.

The results of chemical analysis are indicated in table 1.

Table 1

Chemical analysis data of K_{10} $(U(PW_{11}$ $O_{39})_2).22H_2O$

%	K	U	P	W	water
calc.	6.12	3.72	0.97	63.29	6.15
found	6.18	3.70	0.99	63.40	6.42

---

[12] S. A. Malik and T.J.R. Weakley. *Chem. Comm.*, **1967**, 1094.

[13] Gh. Marcu and M. Rusu, *Rev. Roumaine Chim.* (under press).

[14] P. Souchay, "Ions Mineraux Condensés", Masson et Cie, Paris, 1969, p. 93.

[15] J. H. Kenedy, *Analyt. Chem.*, **32**, 150 (1960).

[16] V. E. Simmons, Ph. D. Thesis, Boston University, 1963.

[17] B. S. Savvin, *Talanta*, **8**, 673 (1961).

[18] A. I. Vogel "A Text Book of Quantitative Inorganic Analysis", 2nd. ed. London, **1951**, pp. 418.

[19] A. I. Vogel, "Quantitative Inorganic Analysis", 3 nd. edn., London, 1961, p. 575.

[20] G. H. Glass, *Chemist Analyst.*, **42**, 50(1953).

OTHER MEASUREMENTS

The basicity was measured by conductometric titration of 50 ml solution of the salt $K_{10}[U(PW_{11}O_{39})_2].22H_2O(T_w = 0.0335)$ with a solution of thalium acetate $(T_{Tl} = 0.0405)$ as indicated in figure 1.

The measurement was made on a Radelkis conductometer type OK-102.

The basicity of the acid corresponding to our heteropolycompound was determined by conductometric and potentiometric titration with 0.1 N NaOH. The results are plotted in figure 2.

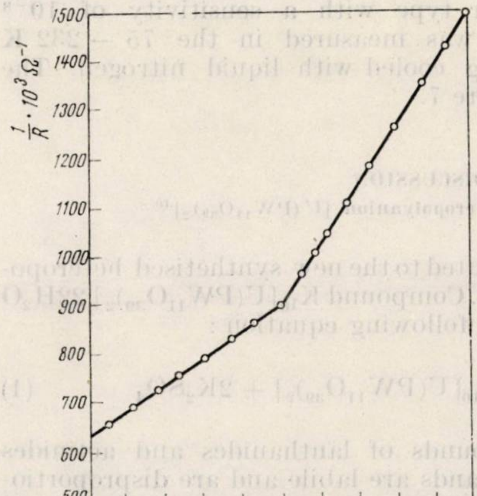

Fig. 1. – Conductometric titration curve of 50 ml solution $K_{10}[U(PW_{11}O_{39})_2].22H_2O$ with $T_W = 0.0335$ with CH_3COOTl with $T_{Tl} = 0.0409$.

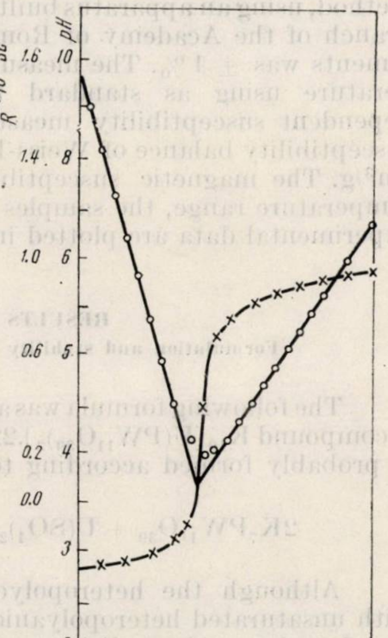

Fig. 2. – Conductometric and potentiometric titration curve of 50 ml $H_{10}[U(PW_{11}O_{39})_2]$ with $T_W = 0.0080$, with 0.1 N NaOH with $T_{NaOH} = 0.0039$.

The measurements were made on a Radelkis conductometric type Ok-102, respectively a pH-meter MV-11 equipped with a glass electrode.

The spectrophotometric determination of uranium was made on a Zeiss "Spekol" spectrophotometer.

The purity of the substance was also demonstrated by electrophoresis (by obtaining a single spot). The electrochromatograms were recorded using a paper electrophoresis device according to Consden, Gordon and Martin [21] in 1 M NaCl, on chromatographic paper Schleicher-Schüll 2043b during 30 minutes at 900 V and 15 mA.

---

[21] R. Consden, A. H. Gordon and A. P. Martin, *Biochem. J.*, **40**, 33 (1946).

The chemical individuality of K_{10} $[U(PW_{11}O_{39})_2].22H_2O$ in solution was controlled by recording the UV electronic spectrum on a "Specord UV-VIS" spectrophotometer with automatical recording (figure 3) and with the aid of polarograms recorded on a Radelkis polarograph, the indicator electrode being a normal dropping mercury electrode, and the reference electrode being a saturated calomel electrode (figure 4). The measurements were conducted at room temperature.

The electronic diffuse reflectance spectrum (figure 6) of pellets (1 :1) dilution with MgO was recorded on a Zeiss-1-WSH spectrophotometer.

Magnetic susceptibility measurements were made by the Gouy method, using an apparatus built at the Institute of Chemistry, Cluj-Napoca branch of the Academy of Romanian sciences. The precision of measurements was ± 1 %. The measurements were carried out at room temperature using as standard twice distilled water. The temperature-dependent susceptibility measurements were done by using a magnetic susceptibility balance of Weiss-Forrer type with a sensitivity of 10^{-8} cm^3/g. The magnetic susceptibility was measured in the 75 – 232 K temperature range, the samples being cooled with liquid nitrogen. The experimental data are plotted in figure 7.

RESULTS AND DISCUSSION

Formulation and stability of heteropolyanion $[U(PW_{11}O_{39})_2]^{10-}$

The following formula was attributed to the new synthetised heteropolycompound $K_{10}[U(PW_{11}O_{39})_2].22H_2O$. Compound $K_{10}[U(PW_{11}O_{39})_2].22H_2O$ is probably formed according to the following equation :

$$2K_7PW_{11}O_{39} + U(SO_4)_2 = K_{10}[U(PW_{11}O_{39})_2] + 2K_2SO_4 \tag{1}$$

Although the heteropolycompounds of lanthanides and actinides with unsaturated heteropolyanion ligands are labile and are disproportionated under acid conditions, we were able to prepare the free acid $H_{10}[U(PW_{11}O_{39})_2]$ by cation exchange (Zerolit 225 H^+ form). The conductometric and potentiometric titration confirm the expected basicity. The total basicity of 10, prescribed theoretically without difficulty, as the oxidation state of the central atom is known precisely, is in good agreement with that determined by conductometric titration of potassium salt of heteropolyanion $[U(PW_{11}O_{39})_2]^{10-}$ as well as by conductometric and pH-metric titration of the corresponding acid.

The UV absorption spectra of the potassium salt of heteropolyanion $[U(PW_{11}O_{39})_2]^{10-}$ with $c_W = 2.5.10^{-4}$, is similar to the absorption spectrum of the ligand $K_7PW_{11}O_{39}$ (figure 3). The characteristic bands at 38,910 cm^{-1} (257 nm) and at 39,476 cm^{-1} (253 nm) indicate the formation of two different polywolframic species and are attributed to the electron transition in the 3 central W-O-W bonds.[22] The spectrum of the compound $K_{10}[U(PW_{11}O_{39})_2].22H_2O$ presented a more attenuated peak and shifted to more reduced frequencies than the peak corresponding to the compound $K_7PW_{11}O_{39}$. This intensity reduction (ε) and the observed shift are due to the replacement of W by U.

---

[22] V. I. Spitsyn, E. A. Topcenkova, L. P. Kazanski and P. Baidala, *Z. Chem.*, **1**, 1 (1974).

The absorption bands at 49,825 cm^{-1} (200.5 nm) in the heteropolycompound, and at 49,295 cm^{-1} (203.5 mm) in the free ligand, could be assigned to a $p_\pi - d_\pi$ transition in the W = O bond.[23] This former band

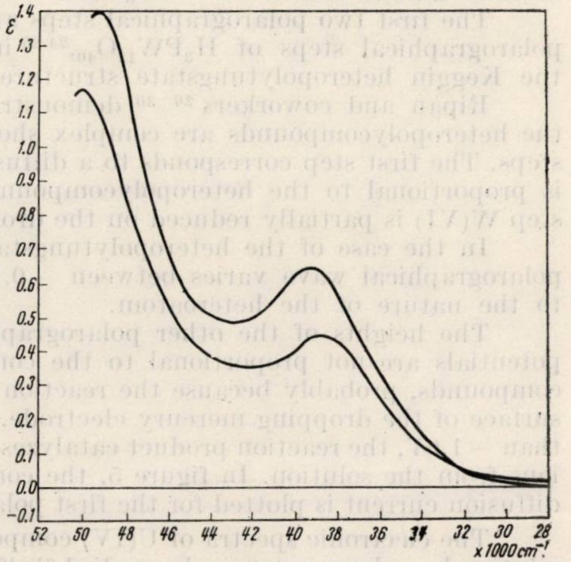

Fig. 3. — UV electronic absorption spectrum recorded on a $K_{10}[U(PW_{11}O_{39})_2].22H_2O$ solution with $c_W = 2.5.10^{-4}$ M at room temperature.

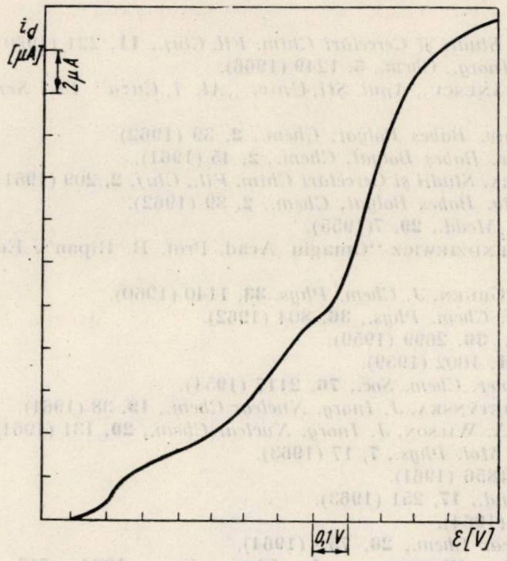

Fig. 4. — Polarogram of $K_{10}[U(PW_{11}O_{39})_2].22H_2O$ solution with $c_W = 10^{-3}$ M in (base electrolyt) 1M $NaClO_4$ at room temperature.

---

[23] Hynsoo So and M. T. Pope, *Inorg. Chem.*, **11**, 1441 (1972).

is shifted according to the strength of the $p_\pi - d_\pi$ transition which is much stronger in the complex than in the free ligand, and therefore this determines the shift of this band toward higher energies.

The polarographic reduction on dropping mercury electrode of $K_{10}[U(PW_{11}O_{39})_2]\cdot22H_2O$ (at a concentration of 10^{-3} M_W in a base solution of 1 M in $NaClO_4$ in the 0 — 1 V potential range) (figure 4) shows three well defined steps at —0.23V ; —0.67V ; —0.93V, of the polarogram, which are also maintained at $5.10^{-4}M_W$ and $10^{-4}M_W$ concentrations (figure 4).

The first two polarographical steps are almost identical to the first polarographical steps of $H_3PW_{12}O_{40}$,[24,25] indicating the preservation of the Keggin heteropolytungstate structure in our heteropolycompound.

Ripan and coworkers [26-30] demonstrated that the polarograms of the heteropolycompounds are complex showing at least three reduction steps. The first step corresponds to a diffusion current and in all cases it is proportional to the heteropolycompound concentration. In this first step W(VI) is partially reduced on the dropping mercury electrode.

In the case of the heteropolytungstates, the potential of the first polarographical wave varies between —0.12 V and —0.03 V according to the nature of the heteroatom.

The heights of the other polarographical waves at more negative potentials are not proportional to the concentration of the heteropolycompounds, probably because the reaction products are absorbed on the surface of the dropping mercury electrode. At more negative potentials than —1.0V, the reaction product catalyzes the reduction of the hydrogen ions from the solution. In figure 5, the concentration dependence of the diffusion current is plotted for the first polarographical step.

The electronic spectra of U(IV) compounds in the solid state and in solution have been extensively studied.[31-46]

---

[24] R. Ripan, A. Duca and N. Calu, *Studii și Cercetări Chim. Fil. Cluj.*, **11**, 221 (1960).

[25] M. T. Pope and G. M. Varga Jr., *Inorg., Chem.*, **5**, 1249 (1966).

[26] R. Ripan, M. Pușcașiu and D. Stănescu., *Anal. Şti. Univ. ,,Al. I. Cuza'' Iași Ser. Mat-Fiz-Chem.*, **4**, 869 (1960).

[27] R. Ripan and N. Calu, *Stud. Univ. Babes Bolyai, Chem.*, **2**, 39 (1962).

[28] R. Ripan and N. Calu, *Stud. Univ. Babeș Bolyai, Chem.*, **2**, 45 (1961).

[29] R. Ripan, M. Puscasiu and A. Duca, *Studii și Cercetări Chim. Fil., Cluj*, **2**, 209 (1961).

[30] R. Ripan and N. Calu, *Stud. Univ. Babes Bolyai, Chem.*, **2**, 39 (1962).

[31] C. K. Jorgensen, *Dan. Mat. Fys. Medd.*, **29**, 7(1955).

[32] B. J. Trzebiatowska and J. Legendziewicz "Omagiu Acad. Prof. R. Ripan", Ed. Acad. R.S.R., 1966, pp. 613.

[33] R. A. Saten, D. Yung and D. M. Gruen, *J. Chem. Phys.* **33**, 1140 (1960).

[34] S. A. Pollak and R. A. Saten, *J. Chem. Phys.*, **36**, 804 (1962).

[35] R. Mc. Laughlin, *J. Chem. Phys.*, **36**, 2699 (1959).

[36] J. G. Conway, *J. Chem. Phys.*, **31**, 1002 (1959).

[37] D. M. Gruen and M. Fred, *J. Amer. Chem. Soc.*, **76**, 2117 (1954).

[38] B. J. Trzebiatowska and K. Bukietynska, *J. Inorg. Nuclear Chem.*, **19**, 38 (1961).

[39] W. E. Keder, J. L. Ryan and S. A. Wilson, *J. Inorg. Nuclear Chem.*, **20**, 131 (1961).

[40] J. L. Ryan and C. K. Jorgensen, *Mol. Phys.*, **7**, 17 (1963).

[41] J. L. Ryan, *J. Phys. Chem.*, **65**, 1856 (1961).

[42] C. K. Jorgensen, *Acta Chem. Scand.*, **17**, 251 (1963).

[43] J. L. Ryan, *Inorg. Chem.*, **3**, 211 (1964).

[44] D. G. Karraker, *I. Inorg. Nuclear Chem.*, **26**, 751 (1964).

[45] H. A. C. McKay and J. L. Woodhead, *J. Chem. Soc.*, **1964**, 717.

[46] K. W. Bagnall, D. Brown, P. J. Jones and P. S. Robinson, *J. Chem. Soc.* (A)., **1964**, 2527.

Jorgensen [31] made an attempt to identify the electronic transitions in the U(IV) spectrum. He assumed that the ground state of U(IV) of $5f^2$ structure is $3H_4$. U(IV) has the typical properties of an ion with 5f structure. The bands appearing in the U(IV) spectrum are caused by the internal transition between the *f* orbitals, which are forbidden by the selection rules. The ligand field always affects the absorption spectrum of U(IV) in the visible region. If comparing the absorption spectra of some U(IV) compounds with the absorptions spectrum of the U(IV) heteropolycompound described here, important information about this last compound can be obtained. The electronic absorption spectrum is shown in Figure 6.

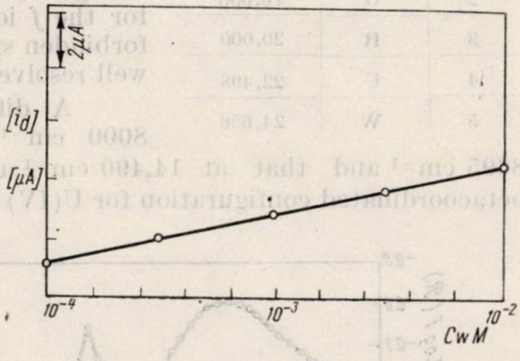

Fig. 5. — Variation of diffusion current with concentration.

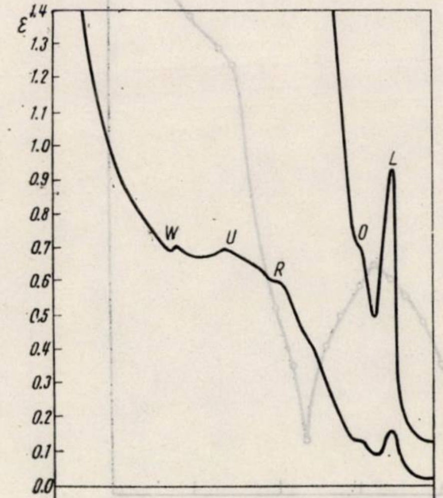

Fig. 6. — Absorption spectrum in visible region, recorded on a $K_{10}[U(PW_{11}O_{39})]_2.22H_2O$ solution with $c_W = 10^{-2}$ M and 5.10^{-2} M at room temperature.

In the range of lower energies we can expect the occurrence of the transition bands which characterize the f^2 configuration. In the literature [23] resolved transition bands for the UCl_6^{2-} group in Cs_2UCl_6 [47] are discussed. From these, in the spectrum recorded by us, the L band (14,490 cm^{-1})

---

[47] R. Pappalardo and C. K. Jorgensen, *Helv. Phys. Acta.*, **37**, 79 (1964).

at $c_W = 5.10^{-2}$M is well resolved and at greater dilution ($c_W = 10^{-2}$M) a tendency to resolve also the bands O, R, U and W is observed. These bands occur in $K_{10}[U(PW_{11}O_{39})_2].22H_2O$ at greater energy values, which indicates a stronger crystalline field in the studied compound than that determined by the 6 chlorine atoms in Cs_2UCl_6. The intensive absorption begins at a value lower than 26,000 cm^{-1}. The broad absorption at 20 — — 25,000 cm^{-1} (figure 6) with superimposed f — f peaks, results from the U(IV) to W(VI) charge transfer. It is worth mentioning that for the *f* ions, in contrast to the *d* ions, the forbidden spin transitions are also relatively well resolved (bands 0 and U, table 2).

Table 2

Electronic transition bands in the absorption spectrum recorded in visible region of $K_{10}[U(PW_{11}O_{39})_2]$. $22H_2O$

No.	Band	ν cm^{-2}
1	L	14,490
2	O	16,000
3	R	20,000
4	U	22,498
5	W	24,656

A diffuse reflectance spectrum to 8000 cm^{-1} was recorded. The bands at 8695 cm^{-1} and that at 14,490 cm^{-1} according to Bagnall [46] suggest an octacoordinated configuration for U(IV) (figure 7).

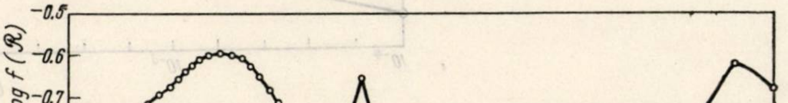

Fig. 7. — Reflectance spectrum recorded $K_{10}[U(PW_{11}O_{39})_2].22H_2O$, for pellets diluted with MgO (1 :1).

As a proof of this statement, the relatively high intensity of the reflection bands, specific of the U(IV) compounds with coordination number higher than 6, can be mentioned. The two transition bands are due to the electronic transitions between U(IV) and W(VI) using the oxygen atom or directly the metal-metal orbitals.

According to Gans,[48] U(IV) compounds having a high intensity reflection spectrum are octacoordinates, and therefore U(IV) heteropolytungstates which were studied here belong to the same class of U (IV) compounds.

These results were completed with magnetochemical measurements. In the literature the effective magnetic moments measured for the different U(IV) compounds are comprised between 2.3 and 3.8 B.M.

Trzebiatowska [49] classifies the U(IV) compounds according to the symmetry of the crystalline field, in two groups :

1. Compounds with cubic symmetry slightly distorted with $\mu_{ef} = 2.8$ B.M., or with a little temperature-independent paramagnetism.

2. Compounds with rhombic symmetry with $\mu_{ef} = 3.3-3.8$ B.M.

U(IV) being an $(n-2)f^2$ element screened against the ligand field, orbital angular momentum is quenched, so the magnetic moment has its spin-only value which for d^2 elements has a value of 2.83 B.M.[50]

To obtain other structural data about the heteropolytungstates a magnetochemical study was performed. The effective magnetic moment was computed according to the following formula :

$$\mu_{ef} = 2.839\sqrt{(\chi_{Mcor}) \cdot T} \tag{1}$$

The value of μ_{ef} is 2.73 B.M. The temperature-dependence of the susceptibility fitted the equation :

$$\chi = C/(T - \theta)_p \tag{2}$$

where C is Curie constant, and θ is Weiss constant.

The effective magnetic moment over the temperature range 75 – 232 K is 2.78 B.M. ; it was calculated from :

$$\mu_{ef} = 2.839 \quad C^{1/2} \tag{3}$$

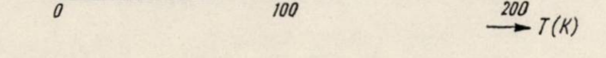

Fig. 8. — Variation of $1/\chi$ depending on temperature T(75 – 232K) for $K_{10}[U(PW_{11}O_{39})_2.22H_2O$.

If the value of C is that given in figure 8, the diamagnetic contribution to the total magnetic susceptibility being $1.658.10^{-3}$ e.m.u./mol, then a value of 2.78 BM is found for the μ_{ef}.

The values of the effective magnetic moment obtained by the two methods suggest that $K_{10}[U(PW_{11}O_{39})_2].22H_2O$ belongs to the class of octacoordinated U(IV) compounds, and the ion U(IV) is in a site of high cubic symmetry, having the state of oxidation equal to +4.

---

[48] P. GANS, B. L. HATHAWAY and B. C. SMITH, *Spectrochim. Acta.* **21**, 1589 (1965).

[49] B. J. TREZEBIATOWSKA, *J. Chem. Phys.*, **60**, 843 (1963).

[50] C. A. CANDELA *J. Chem. Phys.*, **27**, 707 (1957).

Revue Roumaine de Chimie, 22, 2, 237 – 241 (1977)

REACTIONS OF COORDINATED LIGANDS. IX[1]

CHLOROALUMINUM-ORGANIC DERIVATIVES OF COORDINATED DIMETHYL- AND DIPHENYLGLYOXIME

N. VOICULESCU
Institute of Macromolecular Chemistry "P. Poni"
Aleea Grigore Ghica Vodă, nr. 41 A, Jassy

Received February 22, 1975

A series of aluminumorganic compounds of dimethyl- and diphenylglyoxime were obtained from the reaction of diethylaluminum chloride with Ni(II) $(DMGH)_2$, Pd(II)$(DMGH)_2$ and Ni(II)$(DPGH)_2$ (DMG and DPG are divalent radicals of dimethylglyoxime and diphenylglyoxime). The resulted compounds were isolated under the form of solid powders and characterized by chemical analyses, IR absorption spectra, X-ray diffraction spectra, ^{1}H nmr magnetic measurements. The synthesized compounds form adducts with nitrogen Lewis bases. Only pyridine-containing adducts were isolated and characterized. The substitution of O – H. . . .O bonds existing in chelates, by O – Al – O bridges determines, as in the case of other aluminumorganic derivatives of coordinated oximes, the closure of some hexaatomic metallocycles, M – N – O – Al – O – N, without carbon.

We have reported in earlier works[1–6] aluminumorganic compounds of some coordinated oximes resulted from the reaction of oximates with trialkyl- and triarylaluminum derivatives. Based on results obtained, we assumed that the most likely formula of aluminumorganic compounds of dimethyl- and diphenylglyoxime coordinated with Ni(II), Pd(II) and Cu (II) ions is formula I.

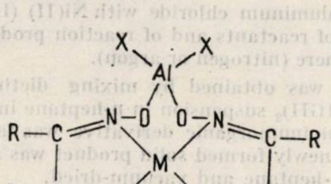

$$R = CH_3—,\ C_6H_5— ;\ X = C_2H_5—,\ iC_4H_9—,\ C_6H_5— ;$$
$$M = Ni(II),\ Pd(II),\ Cu(II)$$

---

[1] N. Voiculescu, *Rev. Roumaine Chim.*, (to be published).
[2] N. Voiculescu and I. Popescu, *Rev. Roumaine Chim.*, **17**, 719 (1972).
[3] N. Voiculescu, I. Popescu and L. Roman, *Rev. Roumaine Chim.*, **18**, 1595 (1973).
[4] N. Voiculescu and I. Popescu, *Rev. Roumaine Chim.*, **18**, 1911 (1973).
[5] N. Voiculescu, *Rev. Roumaine Chim.*, **18**, 1919 (1973).
[6] N. Voiculescu, A. Airinei and I. Popescu, *Rev. Roumaine Chim.*, **19**, 399 (1974).

In all the cases, aluminumorganic derivatives of coordinated oximes result by substitution of intramolecular hydrogen bridges existing in such compounds, by O—Al—O aluminum bridges. This substitution is also accompanied by a modification in the physico-chemical properties of oximates. We suggest that modifications occurring in the behaviour of reaction products are mainly due to radicals left at the aluminum atom. However, the introduction of AlX_2 groups into Ni(II), Pd(II) and Cu(II) bisdimethylglyoximates has a practically negligible influence upon the intimate structure of complex compounds. Thus, the existing square planar structure in Ni(II) and Pd(II) bisdimethylglyoximates is also maintained in their aluminumorganic compounds in which the aluminum atom achieves a sp^3 bond.

In this paper we report aluminumorganic compounds resulted from the reaction of dimethylaluminum chloride with Ni(II) and Pd(II) bisdimethylglyoximates and with Ni(II) bisdiphenylglyoximate. Likewise, we report amine-containing adducts of such aluminumorganic compounds. Chloroaluminumorganic compounds of oximates and their pyridine-containing adducts were isolated under the form of amorphous powders and characterized by chemical analyses, IR absorption spectra, X-ray diffraction spectra and magnetic measurements. The presence of C_2H_5 radicals in the final products was verified by ^{1}H nmr.

EXPERIMENTAL

Ni(II) and Pd(II) bisdimethylglyoximate and Ni(II) bisdiphenylglyoximate were synthesized according to methods reported in the literature [7,8] by other authors, and were recrystallized from nitrobenzene.

Solvents used as reaction medium or as washing agents were anhydrized by distillation on metallic sodium .

The reaction of diethylaluminum chloride with Ni(II) $(DMGH)_2$, Pd(II) $(DMGH)_2$, and Ni(II)$(DPGH)_2$, the handling of reactants and of reaction products took place in Schlenk vessels in a dry and inert atmosphere (nitrogen or argon).

$Ni(DMG)_2Al_2(C_2H_5)_2Cl_2$ was obtained by mixing diethylaluminum chloride dissolved in n-heptane with a Ni(II)$(DMGH)_2$ suspension in n-heptane in the proportion required by the reaction stoichiometry. The aluminumorganic derivative was taken in excess. It was stirred for 2h at room temperature. The newly-formed solid product was allowed to settle. It was decanted, repeatedly washed with n-heptane and vacuum-dried.

$Pd(DMG)_2Al_2(C_2H_5)_2Cl_2$. The same procedure as in the case of the nickel derivative was applied to obtain this product.

$Ni(DPG)_2Al_2(C_2H_5)_2Cl_2$. This product was obtained similarly to ethylaluminum chloride of nickel bisdimethyl-glyoximate, except for the stirring time which was much longer.

These reactions were repeated at different temperatures, varying the stirring time, and the reaction products obtained in all cases had the same chemical formula. The colour and the results of chemical analyses of the reaction products are presented in table 1.

Adducts preparation. Adducts with pyridine or with any other tertiary amine, of aluminumorganic derivatives reported in this work were prepared by adding amine (dried on potassium hydroxide and distilled) in excess to the aluminumorganic derivative. In all the cases, the aluminum-organic derivative of the coordinated oxime is converted to solution after a few

---

[7] G. Basu, G. M. Cook and R. L. Belford, *Inorg. Chem.*, **3**, 1361 (1964).

[8] F. W. Atack, *J. Chem. Soc.*, **1913**, 1317.

minutes of stirring at room temperature. An exception is palladium derivative which is first converted to a gelatinous product and after a few days of stirring it is converted to solution. Adducts were separated from solution either by vacuum-evaporation of the amine in excess or by precipitation with liquid aliphatic or aromatic hydrocarbon. Among amine-containing adducts, only those with pyridine were isolated and characterized (table 1).

Table 1

Analyses and characteristics of the synthetized products

Compound	Colour	Magnetic characteristics	Analyses					
			C Calc. Found %	H Calc. Found %	Al Calc. Found %	N Calc. Found %	Cl Calc. Found %	M Calc. Found %
$Ni(DMG)_2Al_2(C_2H_5)_2Cl_2$	yellow	diamagnetic	30.63	4.68	11.48	11.91	15.10	12.55
			29.95	4.60	11.60	11.80	15.05	12.43
$Pd(DMG)_2Al_2(C_2H_5)_2Cl_2$	yellowish	diamagnetic	27.85	4.25	10.44	10.83	13.73	20.50
			27.10	4.15	10.50	10.65	13.60	20.35
$Ni(DPG)_2Al_2(C_2H_5)_2Cl_2$	orange	diamagnetic	53.48	4.17	7.52	7.79	9.88	8.21
			53.10	4.15	7.60	7.70	9.80	8.05
$Ni(DMG)_2Al_2(C_2H_5)_2Cl_2.2Py$	yellow	diamagnetic	42.03	5.09	8.12	13.37	11.30	9.39
	reddish		41.50	5.05	8.25	13.20	11.15	9.20
$Pd(DMG)_2Al_2(C_2H_5)_2Cl_2.2Py$	yellow	diamagnetic	39.05	4.73	7.98	12.42	10.50	15.82
			38.50	4.60	7.80	12.05	10.25	15.80
$Ni(DPG)_2Al_2(C_2H_5)_2Cl_2.2Py$	orange	diamagnetic	57.53	4.56	6.16	9.58	8.10	6.73
			57.10	4.40	6.25	9.40	8.00	6.50

IR absorption spectra for the 3600—650 cm^{-1} range were recorded on a Unicam SP-200 apparatus. Samples were pelleted in KBr.

X-ray diffraction spectra were obtained by the powder method on a TUR M 60 apparatus using CuK_α radiation and nickel filter. Samples were exposed in Lindemann glass capillaries at 40 kV and 12 mA, for 8 hours.

Magnetic properties were verified on a Gouy balance in nonhomogeneous magnetic field.

The presence of C_2H_5 — radicals in the reaction products was verified on a JEOL-60 HL spectrometer working on 60 MHZ, at room temperature.

DISCUSSION

The reaction between diethylaluminum chloride and nickel and palladium oximates occurs according to the following chemical equation :

$$M(II)\ (LH)_2 + 2Al(C_2H_5)_2Cl \text{ —— } ML_2Al_2(C_2H_5)_2Cl_2 + 2C_2H_6$$

$$M = Ni, Pd\ ;\ L = DMG, DPG$$

We think that the probable mechanism determined by reactants particularities is a two-step reaction similar to that proposed by us in the case of other aluminumorganic derivatives [3].

Due to the diethylaluminum chloride heterogeneity, its reaction with coordinated oximes may occur in two manners. In the first case the Al—Cl bond would split with hydrochloric acid release and in the second case an Al—C bond would split with ethane release. The reaction products result from the second reaction and correspond to formula II.

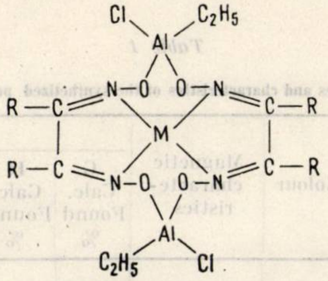

As can be seen from formulas I and II, the reaction of aluminumorganic derivatives with bisdimethylglyoximates and bisdiphenylglyoximates of some transitional metals occurs with the substitution of hydrogen bridges, O—H . . . O by aluminum bridges, O—Al—O. The introduction of aluminum bridges into the molecule of coordinated oximes determines the closure of some hexaatomic metallocycles, M—N—O—Al—O—N, without carbon atoms. The closure of hexaatomic metallocycles without carbon presents an increased interest for the chemistry of inorganic cyclic compounds in general and specifically for macrocyclic compounds.

The reaction between oximates under study and diethylaluminum chloride presents some particularities probably determined by the chlorine atom bound to aluminum. Thus, the formation of the new compounds is weakly exothermal and the reaction products are immediately separated under the form of coloured powders insoluble in hydrocarbons and highly sensitive to moisture. However, the formation reaction of pyridine-containing adducts is not basically different from adduct formation in the case of other aluminumorganic derivatives or with regard to the number of bound amine molecules or to the bonding manner (formula III).

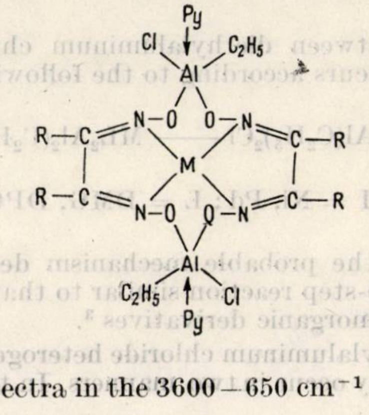

IR absorption spectra in the 3600—650 cm⁻¹ range (table 2).

Table 2

IR absorption spectra of the synthetized products (Values given in cm^{-1})

$M(DMG)_2Al_2(C_2H_5)_2Cl_2$		$M(DPG)_2Al_2(C_2H_5)_2Cl_2$	Assignment
Ni	Pd	Ni	
1635 s	1630 s	1625 vs	CN
1590 s	1580 s	1580 s	
1440 s	1440 s	1550 s, 1490 s	
1380 s	1380 s	1440 vs, 1360 s	
1235 vs	1245 vs	1295 vs	
1100 vs	1100 vs	1145 vs	NO
980 s	990 s	1045 vs, 940 s,	
875 s	875 w	915 s, 880 s,	
790 s	795 s	815 s, 745 vs, 700 vs	

show that the substitution of O—H ... O bridges by O—Al—O bridges determines the disappearance of absorption maxima characteristic of OH groups in oximates and a shift towards higher frequencies of absorption maxima characteristic of C=N and NO groups compared to their position in oximates[2] or in other aluminumorganic derivatives [1-4] of coordinated oximes. We suggest that the more marked shift in the case of compounds with Al $(C_2H_5)Cl$ groups is due to the polarizing action of chlorine atoms in the aluminum atom. In this spectral domain, absorption spectra of adducts present no observable modifications compared to those of aluminumorganic derivatives.

X-ray diffraction spectra of both aluminumorganic derivatives and of pyridine containing adducts are characteristic of amorphous substances. Chelates having a crystalline structure are again obtained by hydrolysis or alcholysis reactions.

In a nonhomogeneous field, all compounds reported in this paper have the typical behaviour of diamagnetic substances. This fact indicates, particularly in the case of adducts, that the square-planar chelate structure has not undergone essential modifications during chemical conversions and amine molecules bonding occurs at the aluminum atom rather than at the central metallic atom.

The amorphous structure of compounds and the loss of the coordination capacity of central metallic atoms prompt us to think that the introduction of aluminumorganic groups into oximates affects the behaviour of the ligand and also that of the central metallic ion.

Revue Roumaine de Chimie, **22**, *2*, 243–255 (1977)

CHEMICAL GRAPHS. XXX[1]

REACTION GRAPHS FOR DEGENERATE REARRANGEMENTS OF HOMOVALENIUM CATIONS

ALEXANDRU T. BALABAN
Department of Organic Chemistry, The Polytechnic, Bucharest

Received August 12, 1976

Degenerate rearrangements *via* 1,2-shifts of carbenium ions derived from homovalenes $(CH)_{2n+1}^{+}$ are analyzed. Two examples of reaction graphs are discussed in detail, one with 30 vertices for the completely degenerate rearrangement (topomerization) of homotetrahedryl II, and a second one with 120 vertices for the partly degenerate rearrangement (automerization) of bicyclo[2.1.0]pentenyl V, also involving cyclopentadienyl cations VI. Homoprismyl (VII, VIII), homocubyl (III), and other cations afford reaction graphs which are too complicated to be analyzed in detail.

1. INTRODUCTION

The present paper analyzes from the standpoint of graph theory the 1,2-rearrangements of carbon – carbon bonds in carbenium ions derived from homovalenes.[2] Such rearrangements proceed with low activation energies and lead to a fluctuating structure and to the scrambling of isotopic labels. This analysis may be relevant also to the still prevailing controversy over non-classical carbocations.[3–5]

2. DEFINITIONS

Reaction graph is a graph whose vertices represent molecular species : in the present case, a vertex symbolizes one carbenium ion with a certain permutation of its carbon atoms or, more exactly, CH groups. Two vertices are *adjacent*, i.e. are connected by an edge in such a reaction graph, if they represent molecular species which can be formed from one another by an elementary reaction step symbolized by that edge : in the present case, two vertices are adjacent if they symbolize cations which differ by one 1,2-rearrangement of one C — C bond. Reaction graphs may be *directed* (*digraphs*) if the reactions they symbolize are irreversible, or may be *non-directed* when, as in the present case, the reactions are reversible, so that there is no reason to have oriented edges.

---

[1] Preceding part, A. T. BALABAN, E. M. PALMER and F. HARARY, *Rev. Roumaine Chim.* **22**, No. 4, to appear (1977).

[2] A. T. BALABAN, *Rev. Roumaine Chim.*, **19**, 1611 (1974).

[3] H. C. BROWN, *Acc. Chem. Res.*, **6**, 377 (1973) ; *Tetrahedron*, **32**, 179 (1976).

[4] G. A. OLAH, *Acc. Chem. Res.*, **9**, 41 (1976) ; "Carbocations and Electrophilic Reactions", Verlag Chemie, Weinheim, and Wiley, New York, 1974.

[5] P. D. BARTLETT "Nonclassical Ions", W. A. Benjamin, New York, 1965 ; G. D. SARGENT, in "Carbonium Ions" (G. A. OLAH and P. von R. SCHLEYER, editors), vol. 3, p. 1099, Wiley-Interscience, New York, 1972 ; R. E. LEONE, J. C. BARBORAK and P. von R. SCHLEYER, *ibid.*, vol. 4, chapter 33, 1973.

In a *constitutional graph*, [6] vertices symbolize atoms or groups of atoms, and edges represent covalent bonds ; organic structural formulas are examples of constitutional graphs.

Homovalene[2] is a hydrocarbon $(CH)_{2n}CH_2$, where n is a natural number, while *homovalenium cation* is a carbenium ion $(CH)^+_{2n+1}$ derived from a homovalene by loss of one hydride anion, or from a valence isomer of an annulene (i.e. a valene[2]) by formal addition of CH^+.

A *degenerate rearrangement* is a reaction where product and reactant are structurally identical, though chemical bonds have been modified, e.g. the fluctuation of bullvalene (unimolecular reaction), or isotopic exchange with isotopically unlabelled materials (bimolecular reaction). Rearrangements may be *totally degenerate* if all vertices of the reaction graph represent one and the same molecular species, differing only in the permutation of its atoms (CH groups in the case of bullvalene or in the present case) ; for brevity, we will use the terms *topomerization**,[7] for a totally degenerate rearrangement, and *automerization**,[8] when the rearrangement is *partly degenerate*, for its degenerate portion, i.e. when the vertices of the reaction graph symbolize two or more molecular species, which are structurally different, but a vertex of one type is linked to a vertex of the same type.

In a graph, the number of edges meeting at a vertex is called the *degree* of that vertex. Graphs whose vertices all have the same degree are called *regular graphs* ; some graphs examined in the present paper will be regular of degree four, or *tetravalent* ; regular graphs of degree three are called *trivalent* or *cubic graphs*. Valence isomers of annulenes or valenes $(CH)_{2n}$ have structural graphs (with vertices representing CH groups) which are cubic graphs.[9]

A graph is called *planar* if it can be represented in a plane without crossing edges ; all constitutional graphs corresponding to known molecules are always planar, and this is likely to remain so (unless the restriction that one edge corresponds to a covalent bond in constitutional graphs is removed ; in this case, with an edge representing a chain of covalent bonds, it may be possible to prepare molecules corresponding to non-planar graphs). Most reaction graphs, however, are non-planar. In the present paper, we will restrict ourselves to discussing planar constitutional graphs, and most of the resulted reaction graphs will be non-planar.

---

* This is a new connotation of these terms, not originally included in the initial references.[7,8]

[6] A. T. Balaban, editor, "Chemical Applications of Graph Theory", Foreword, Academic Press, London, 1976.

[7] G. Binsch, E. L. Eliel and H. Kessler, *Angew. Chem.*, **83**, 618 (1971) ; *Angew. Chem. Internat. Edit.*, **10**, 570 (1971).

[8] A. T. Balaban and D. Fărcaşiu, *J. Amer. Chem. Soc.*, **89**, 1958 (1967) ; A. T. Balaban, D. Fărcaşiu, V. A. Koptyug, I. S. Isaev, M. I. Gorfinkel and A. I. Rezvukhin, *Tetrahedron Letters*, **1968**, 4757.

[9] A. T. Balaban, *Rev. Roumaine Chim.*, **11**, 1097 (1966) ; Erratum, *ibid.*, **12**, No. 1, 103 (1967).

A graph is *vertex-transitive* if for any two vertices there exists an automorphism interconverting these vertices. A similar definition, replacing in the preceding phrase vertex by edge, applies to ***edge-transitive graphs.***

3. DEGENERATE REARRANGEMENTS OF HOMOVALENIUM CATIONS

There exists exactly one planar general cubic graph with one loop and four vertices[2] (one of these vertices is the loop-point which is to be cancelled to afford the constitutional graph of the homovalene, with the vertex of degree two representing the CH_2 group symbolized by the point where the loop had been attached). Therefore there exists exactly one homovalene C_3H_4, namely cyclopropene, hence one homovalenium cation $(CH)_3^+$, namely the cyclopropenyl cation. It was shown[2] that the numbers v of homovalenium cations $(CH)^+_{2n+1}$ are those presented in table 1. All graphs with $n \leqslant 4$, giving rise to homovalenes with 3, 5, 7, and 9 carbon atoms, were depicted.[2] Restricting ourselves only to these graphs, and inspecting their structures for spotting which of these graphs can afford degenerate rearrangements, it appears that only the following homovalenium cations can give completely degenerate rearrangements : cyclopropenyl I, homotetrahedryl II, and homocubyl III (since graph theory only considers topological factors, the formulas I – III and subsequent ones disregard geometrical factors) as well as vinylic cations (see section 3.1).

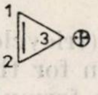

I

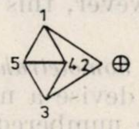

II

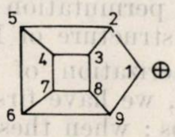

III

Table 1

Numbers v of homovalenium cations
$(CH)^+_{2n+1}$

n	1	2	3	4	5
v	1	4	18	96	502

In a 1,2-shift involving three vertices i, j, and k of a constitutional graph, a vertex (i) once removed from the vertex (k) bearing the positive charge becomes adjacent to it, leaving the positive charge on the vertex (j) which had been adjacent to it :

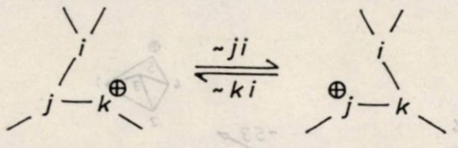

Therefore an edge changes one of its endpoints, using the other endpoint (i) as a pivot. In all 1,2-shifts, the endpoint which is changed is adjacent to the vertex bearing the positive charge ; as a result of the 1,2-shift, this endpoint and the positive charge change places. The pivot may also be adjacent to the vertex bearing the positive charge, if this charge is on a cyclopropyl or cyclopropenyl ring, but more often the pivot is more remote from the positive charge.

3.1. COMPLETELY DEGENERATE REARRANGEMENTS (TOPOMERIZATIONS)

The reaction graphs of topomerizations have vertices which represent isomorphic constitutional graphs, therefore these reaction graphs will be regular.

We will analyze the above three topomerizations of I — III in order to obtain their reaction graphs.

The case of *cyclopropenyl* I is trivial : the reaction graph is regular of degree two (because there is only one edge once removed from the vertex bearing the positive charge, and this edge is a double bond), and its number of vertices is three (fig. 1). Moreover, since the vertices of the reaction graph only represent the delocalization of π-electrons in the aromatic cyclopropenyl cation, they do not symbolize different permutations of atoms, but one and the same permutation ; however, this is an exception due to the particular simple structure of I.

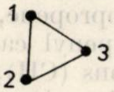

Fig. 1. — Reaction graph for the topomerization of the cyclopropenyl cation I.

To analyze the topomerization of the *homotetrahedryl* (tricyclo-[2.1.0.0^{3,5}]pentyl-2) cation II, we have first to devise a notation for the permutations of its CH groups : when these are numbered as in formula II, we can symbolize this particular permutation by (2,45), i.e. by two groups of unordered digits separated by a comma, and indicating first the CH group bearing the positive charge, and after the comma the two CH groups bonded by the edge twice removed from the CH group bearing the positive charge.

Since there exist four edges once removed from the positive charge, and since each of these four edges can be shifted 1,2 to yield a different permutation, it results that the reaction graph representing the topomerization of homotetrahedryl will be regular of degree four.

On the lines of the portion of the reaction graph presented in fig. 2, the C—C bond which undergoes the 1,2-shift is noted by its two vertices : the first one is the vertex adjacent to the positive charge, and the second one is the pivot vertex ; in the reverse shift, the pivot is the same but the

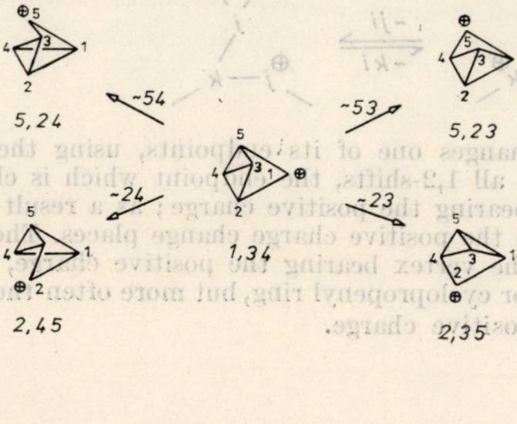

Fig. 2. — Adjacent vertices in the reaction graph for the topomerization of homotetrahedryl II.

first vertex is not ; this convention is adopted throughout the present paper, and always the symbol of the 1,2-shift (~) will precede this type of notation. In fig. 2, edges of the reaction graph bear arrows in order to evidence which vertex is pivot, but arrows will no longer be used in subsequent figures.

As shown in fig. 2, one can devise a set of adjacency rules for vertices in this reaction graph : if *abcde* represents one permutation of the five digits 1 — 5, a vertex (*a*, *bc*) representing one homotetrahedryl cation is adjacent to vertices : (*d*, *be*) ; (*d*, *ce*) ; (*e*, *bd*) ; (*e*, *cd*). Expressed in words, a vertex (*a*, *bc*) is adjacent to vertices which have the positive charge at a CH group denoted by digit *d* or *e* which does not appear in the notation of the initial vertex (*a*, *bc*), while the two unordered digits after the comma in the notations of these adjacent vertices are : (i) the other digit, *e* or *d*, which does not appear in the notation (*a*, *bc*), and (ii) one of the two digits *b* or *c* following the comma in the notation (*a*, *bc*).

With these adjacency rules it is easy to construct the reaction graph of the topomerization of homotetrahedryl (II). Since the digit before the comma is one out of five, and since the digits after the comma are two out of the remaining four, the reaction graph has $C_5^1 \times C_4^2 = 30$ vertices. It is represented in fig. 3 with a fourfold symmetry. The Hamiltonian circuits found so far do not have a symmetrical representation. Through one vertex there pass two 4-circuits, two 5-circuits, sixteen 6-circuits, and many circuits with ⩾ 7 vertices. The graph has diameter 4, each point (*a*, *bc*) having one "antipode" at distance four denoted by (*a*, *de*). The graph is vertex- and edge-transitive.

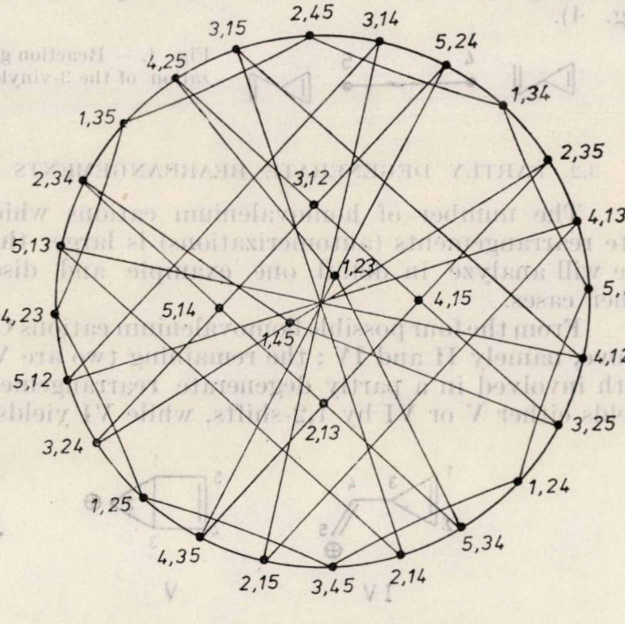

Fig. 3. — Reaction graph for the topomerization of homotetrahedryl II.

For the *homocubyl* cation,[10] one may also devise a notation on a similar basis : if vertices are numbered as shown in III, this particular permutation is denoted by (1, 29, 3856, 47), (1, 29, 5638, 47), (1, 92, 8365, 74), or (1, 92, 6583, 74), indicating in turn : the vertex bearing the positive charge, its two adjacent vertices (in any order), a partly ordered group of four digits indicating the endpoints of the edges completing (with the vertices already indicated) a bicyclo[2.2.1]heptane skeleton and starting for both edges with the vertices adjacent to the first vertex indicated in the group of two digits, and finally an ordered group of two digits indicating the endpoints of the edge antipodal to the positive charge. It may be deduced that the reaction graph for the topomerization of the homocubyl cation will be regular of degree four, vertex- and edge-transitive, and that it will have $\frac{1}{2} C_9^1 C_8^2 A_6^2 A_4^2 = 45630$ vertices. Since this large number precludes a detailed investigation of the reaction graph, and since for topomerizations of homovalenium cations $(CH)_v^+$ with $v = 2n + 1 > 9$ the number of vertices in the reaction graph will be even larger, we conclude here this discussion.

In addition to the three topomerizations discussed above for I – III, there exist 20 homovalenium cations $(CH)^+_{2n+1}$ with $n \leqslant 4$ which have a vinylic cation structure, e.g. IV, and which yield a trivial topomerization whose reaction graph is the complete graph K_2 with two points of degree one (fig. 4).

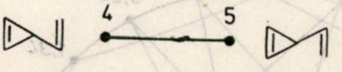

Fig. 4. — Reaction graph for the topomerization of the 3-vinylcyclopropene cation IV.

3.2. PARTLY DEGENERATE REARRANGEMENTS (AUTOMERIZATIONS)

The number of homovalenium cations which give partly degenerate rearrangements (automerizations) is larger than for topomerizations. We will analyze in detail one example and discuss summarily a few other cases.

From the four possible homovalenium cations $C_5H_6^+$, two were discussed above, namely II and IV ; the remaining two are V and VI, and these are both involved in a partly degenerate rearrangement (of V only, since V. yields either V or VI by 1,2-shifts, while VI yields only V by 1,2-shifts)

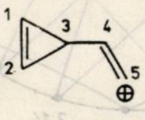

IV

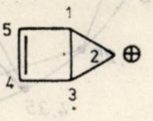

V

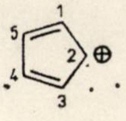

VI

To analyze the automerization of V, we start again by devising notations for V and VI. With the numbering indicated on the formulas, we will denote the particular permutation of V by (2, 451) or (2, 543) and

---

[10] R. E. Leone and P. von R. Schleyer, *Angew. Chem.*, **82**, 889 (1970) ; *Angew. Chem. Internat. Edit.*, **9**, 860 (1970).

VI by [2, 451] or [2, 543], i.e. for both V and VI, before the comma, the digit indicating where the positive charge is located, and after the comma, a group of three ordered digits indicating a chain of three CH groups which are in turn non-adjacent, non-adjacent, and adjacent to the first vertex of the constitutional graph.

As indicated in fig. 5, it is possible to devise a set of adjacency rules for the vertices in the reaction graph. If *abcde* is a permutation of

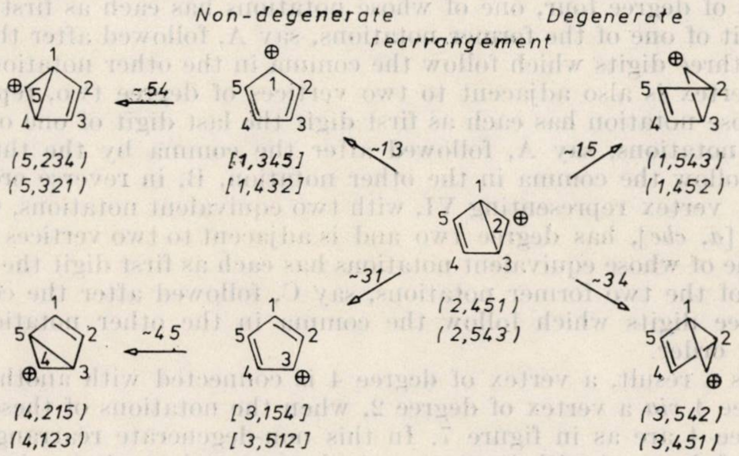
Non-degenerate
Degenerate
rearrangement
-54
-13
-15
-31
-34
-45
(5,234)
(5,321)
[1,345]
[1,432]
(1,543)
(1,452)
(2,451)
(2,543)
(4,215)
(4,123)
[3,154]
[3,512]
(3,542)
(3,451)

Fig. 5. — Interconversions of bicyclo [2.1.0] pentenyl (V) and cyclopentadienyl (VI) cations.

digits 1 — 5, using as model fig. 5, figure 6 presents these generalized adjacency rules, employing both possible notations for each vertex of the reaction graph.

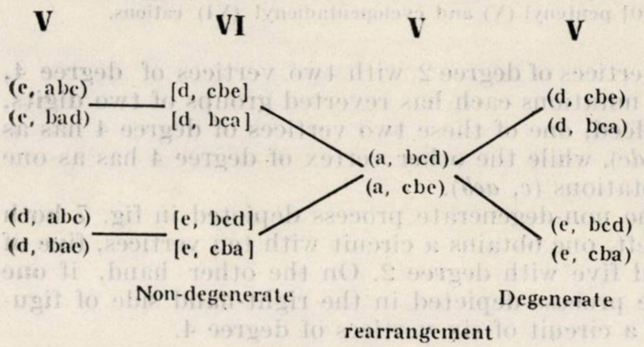
V
VI
V
V
(e, abc)
(e, bad)
[d, cbe]
[d, bca]
(d, cbe)
(d, bca)
(a, bcd)
(a, cbe)
(d, abc)
(d, bae)
[e, bcd]
[e, cba]
(e, bcd)
(e, cba)
Non-degenerate
Degenerate
rearrangement

Fig. 6. — Adjacent vertices in the reaction graph for the partly degenerate rearrangement of bicyclo[2.1.0]pentenyl V.

The two equivalent notations for each vertex always have the same first digit and differ in the other digits after the comma : the first two digits after the comma are permuted, and the last digit is one or the other of the two digits which are not identical to the three digits so far used. Thus, knowing one notation, it is simple to obtain the second, equivalent, notation both for V and for VI. Though it seems tedious to have for each vertex two equivalent notations which can be deduced quite simply from one another as it was just shown, it was found convenient[*] to keep both notations since they are complementary and lead to simple adjacency rules. Later we will find a simpler form of expressing this dual notation of each vertex.

The adjacency rules (fig. 6) may be expressed as follows : let a vertex of the reaction graph represent V with two equivalent notations: A (*a*, *bcd*), and B (*a*, *cbe*) ; this vertex has degree four and is adjacent to two vertices of degree four, one of whose notations has each as first digit the last digit of one of the former notations, say A, followed after the comma by the three digits which follow the comma in the other notation, B. The same vertex is also adjacent to two vertices of degree two, representing VI, whose notation has each as first digit the last digit of one of the two former notations, say A, followed after the comma by the three digits which follow the comma in the other notation, B, in reverse order.

A vertex representing VI, with two equivalent notations, C [*a*, *bcd*] and D [*a*, *cbe*], has degree two and is adjacent to two vertices of degree four, one of whose equivalent notations has each as first digit the last digit of one of the two former notations, say C, followed after the comma by the three digits which follow the comma in the other notation, D, in reverse order.

As a result, a vertex of degree 4 is connected with another vertex of degree 4 *via* a vertex of degree 2, when the notations of these vertices of degree 4 are as in figure 7. In this non-degenerate rearrangement, a vertex of degree 4 with its two equivalent notations A (*a*, *bcd*) and B (*a*, *cbe*) is linked *via* two vertices of degree 2 with two vertices of degree 4, one of whose equivalent notations each has reverted groups of two digits, ignoring the comma : indeed, one of these two vertices of degree 4 has as one of its notations (*b*, *adc*), while the other vertex of degree 4 has as one of its two equivalent notations (*c*, *aeb*).

	(b, adc)		[e, dcb]		(a, bcd)		[d, ebc]		(c, aeb)	
··· —	(b, dae)	—	[e, cda]	—	(a, cbe)	—	[d, bea]	—	(c, ead)	— ···
	V		**VI**		**V**		**VI**		**V**	

Fig. 7. — Notations for adjacent vertices in the non-degenerate rearrangement of bicyclo [2.1.0] pentenyl (V) and cyclopentadienyl (VI) cations.

If one continues the non-degenerate process depicted in fig. 7 both to the right and to the left, one obtains a circuit with ten vertices, five of which have degree 4 and five with degree 2. On the other hand, if one continues the degenerate process depicted in the right-hand side of figures 5 and 6, one obtains a circuit of six vertices of degree 4.

---

[*] It would, however, be possible to adopt one notation for each vertex of the reaction graph, by specifying only two ordered digits after the comma (thus the permutation numbered as in V would be (2,54) and VI would be [2,54]), namely those not adjacent to the positively charged CH group, as in II; the order of these digits would, however, depend on those adjacent to them (which are at the same time adjacent to the CH^+ group and do not appear in the notation) : the first digit after the comma is that one which is adjacent to the CH group denoted by the smaller digit. Though apparently simpler, this notation does not lead to simple adjacency rules, needs more practice, and will therefore not be used in the present paper.

In order to further simplify the notation of vertices, so as to be able to depict the whole reaction graph without writing for each vertex two notations, we will observe that in the right-hand side of figures 5 and 6, two adjacent vertices of degree 4, with their two equivalent notations each, have one of these notations with the same digits following the comma, as required by the adjacency rules. Therefore it will be simpler to symbolize such a degenerate rearrangement by two vertices with just their first digit (the digit before the comma in the full notations), and to write the common three digits (following the comma in the full notations) on the edge joining these two vertices, as shown in figure 8. For the non-degenerate rearrangement, figure 8 shows a similar convention, to write for all vertices only their first digit (black points for degree 4, white points for degree 2), and to note on the edges the common digits which, in the full notation, appear after the comma (in direct order for vertices of degree 4, in reverse order for those of degree 2). No confusion with other symbols on the edges can occur, such as edges undergoing 1,2-shifts. A comparison between the full and simplified notations, for the degenerate six-membered and non-degenerate ten-membered circuits is presented in figures 9 and 10, respectively.

It can be observed that the 6-circuit depicted in figure 9 has as first digits a triplet of digits repeated twice, namely 245. Since this "hexagon triplet" can be read in both rotation senses, starting from any digit, it is an unordered triplet. The first two digits which label the six edges of this hexagon are complementary to this triplet. Since the triplet nota-

Fig. 8. — Simplified notation for degenerate and non-degenerate processes involving cations V and VI.

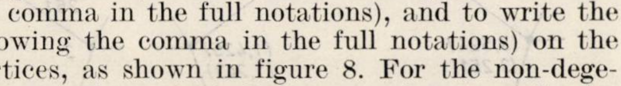

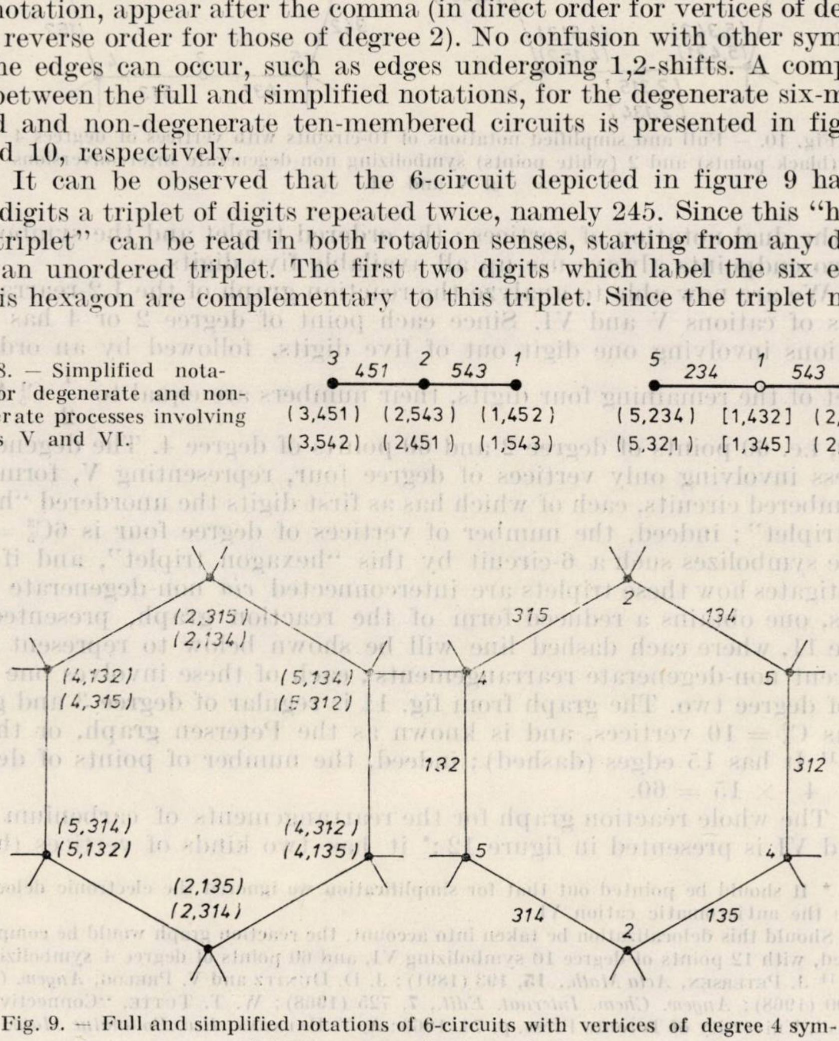

Fig. 9. — Full and simplified notations of 6-circuits with vertices of degree 4 symbolizing automerizations of V.

tions for these edges result easily from the first digits of endpoints (fig. 9), these triplets may be omitted. It must be borne in mind that this labelling of edges with ordered triplets is only another convention for symbolizing the dual notation of vertices : the ordered triplet and the symbols of its two endpoints always use up all available five digits.

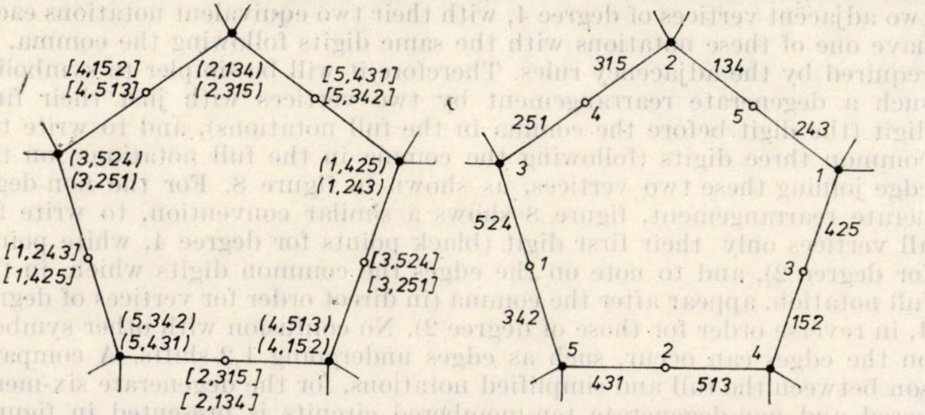

Fig. 10. — Full and simplified notations of 10-circuits with vertices of degrees 4 (black points) and 2 (white points) symbolizing non-degenerate interconversions of V and VI.

We are now able to analyze the reaction graph of the 1,2-rearrangements of cations V and VI. Since each point of degree 2 or 4 has two notations involving one digit out of five digits, followed by an ordered triplet of the remaining four digits, their numbers are equal to $\frac{1}{2} C_5^1 A_4^3 = 60$, i.e. 60 points of degree 2 and 60 points of degree 4. The degenerate process involving only vertices of degree four, representing V, form ten 6-membered circuits, each of which has as first digits the unordered "hexagon triplet"; indeed, the number of vertices of degree four is $6C_5^3 = 60$. If one symbolizes such a 6-circuit by this "hexagon triplet", and if one investigates how these triplets are interconnected *via* non-degenerate processes, one obtains a reduced form of the reaction graph, presented in figure 11, where each dashed line will be shown below to represent four different non-degenerate rearrangements; each of these involves one vertex of degree two. The graph from fig. 11 is regular of degree 3 and girth 5, has $C_5^3 = 10$ vertices, and is known as the Petersen graph, or the 5-cage.[11] It has 15 edges (dashed); indeed, the number of points of degree 2 is $4 \times 15 = 60$.

The whole reaction graph for the rearrangements of carbenium ions V and VI is presented in figure 12;* it has two kinds of vertices (black

---

* It should be pointed out that for simplification we ignored the electronic delocalization in the antiaromatic cation VI.

Should this delocalization be taken into account, the reaction graph would be completely changed, with 12 points of degree 10 symbolizing VI, and 60 points of degree 4 symbolizing V.

[11] J. Petersen, *Acta Math.*, **15**, 193 (1891); J. D. Dunitz and V. Prelog, *Angew. Chem.*, **80**, 700 (1968); *Angew. Chem. Internat. Edit.*, **7**, 725 (1968); W. T. Tutte, "Connectivity in Graphs", University of Toronto Press, p. 74, 1966; A. T. Balaban, *Rev. Roumaine Math. Pures Appl.*, **17**, 3 (1972).

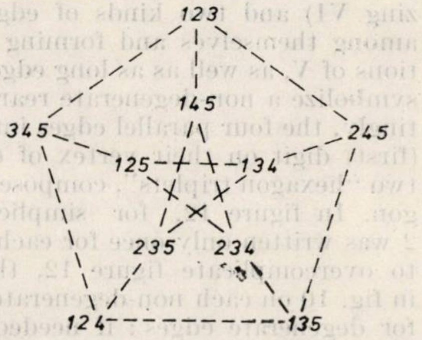

Fig. 11. — Reduced form of the reaction graph representing interconversions between cations V and VI. Each triplet of unordered digits is adjacent to triplets having one common digit, and symbolizes a 6-circuit as in fig. 9.

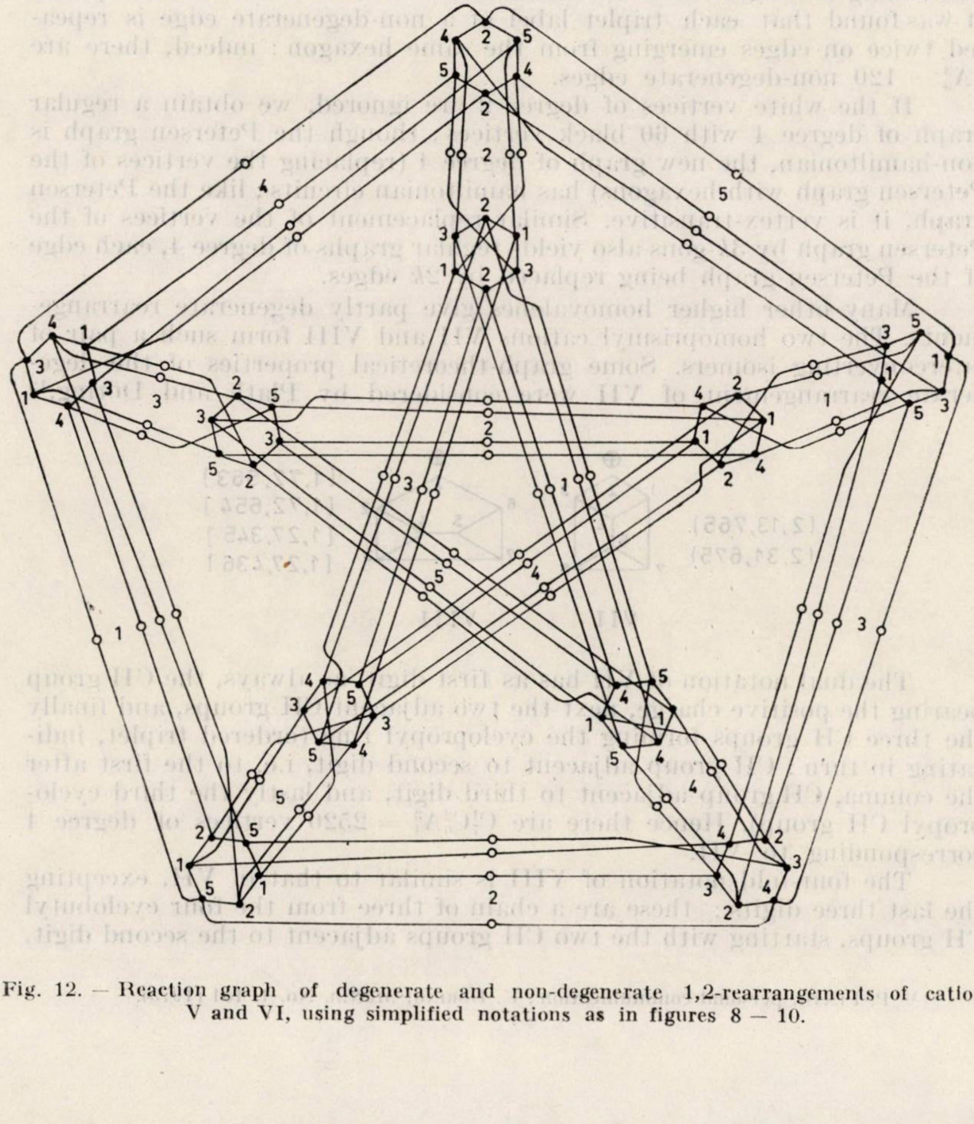

Fig. 12. — Reaction graph of degenerate and non-degenerate 1,2-rearrangements of cations V and VI, using simplified notations as in figures 8 — 10.

points of degree 4 symbolizing V, and white points of degree 2 symbolizing VI) and two kinds of edges (short edges connecting black points among themselves and forming hexagons, which symbolize automerizations of V, as well as as long edges linking a black to a white point, which symbolize a non-degenerate rearrangement involving V and VI). Interestingly, the four parallel edges interlinking two hexagons all have the same (first) digit on their vertex of degree two : this digit is common to the two "hexagon triplets", composed of the first digits of vertices in the hexagon. In figure 12, for simplicity, this first digit of vertices of degree 2 was written only once for each group of four vertices. Also, in order not to overcomplicate figure 12, the triplets of the simplified notation as in fig. 10 on each non-degenerate edge were omitted like the other triplets for degenerate edges : if needed, they can be found quite easily as the triplet of a hexagon edge having the same black point as one endpoint, and ending in a digit which is different from the label of the white endpoint. It was found that each triplet label of a non-degenerate edge is repeated twice on edges emerging from the same hexagon : indeed, there are $2A_5^3 = 120$ non-degenerate edges.

If the white vertices of degree 2 are ignored, we obtain a regular graph of degree 4 with 60 black vertices ; though the Petersen graph is non-hamiltonian, the new graph of degree 4 (replacing the vertices of the Petersen graph with hexagons) has hamiltonian circuits ; like the Petersen graph, it is vertex-transitive. Similar replacement of the vertices of the Petersen graph by $3k$-gons also yields regular graphs of degree 4, each edge of the Petersen graph being replaced by $2k$ edges.

Many other higher homovalenes give partly degenerate rearrangements. The two homoprismyl cations VII and VIII form such a pair of interconverting isomers. Some graph-theoretical properties of the degenerate rearrangement of VII were considered by Plath and Döring.[12]

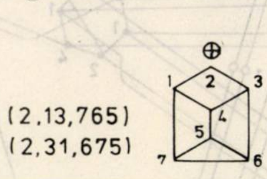

VII

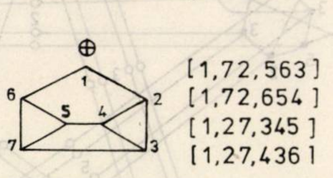

VIII

The dual notation of VII has as first digit, as always, the CH group bearing the positive charge, next the two adjacent CH groups, and finally the three CH groups forming the cyclopropyl ring (ordered triplet, indicating in turn : CH group adjacent to second digit, i.e. to the first after the comma, CH group adjacent to third digit, and lastly the third cyclopropyl CH group). Hence there are $C_7^1C_6^2A_4^3 = 2520$ vertices of degree 4 corresponding to VII.

The four-fold notation of VIII is similar to that of VII, excepting the last three digits : these are a chain of three from the four cyclobutyl CH groups, starting with the two CH groups adjacent to the second digit, i.e. the first after the comma. Hence there are 1760 vertices of degree 4 corresponding to VIII.

---

[12] P. Plath, personal communication ; U. Döring, *MatCh*, No. 1, 151 (1975).

A vertex VII is adjacent to two VII-type (automerization) and to two VIII-type vertices, while a vertex VIII is adjacent to four VII-type vertices (non-degenerate rearrangement). The resulting reaction graph of degree four with a total of 4280 vertices is too complicated to be analyzed in detail, but it can be shown that it has 12-membered circuits representing degenerate rearrangements (fig. 13) similar to the hexagons in the case of V.

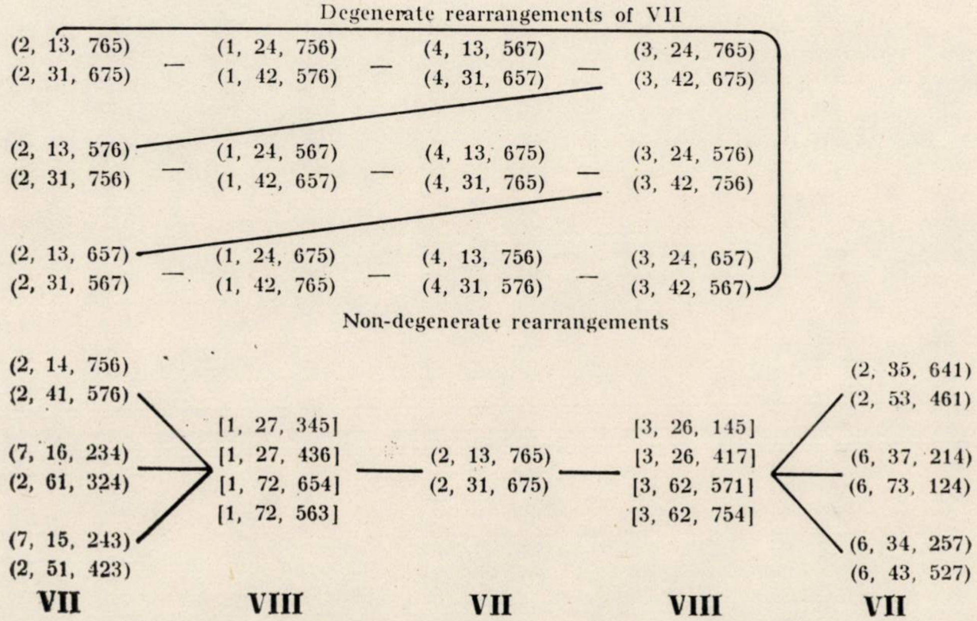
Degenerate rearrangements of VII

Non-degenerate rearrangements

(2, 13, 765)
(2, 31, 675)
(1, 24, 756)
(1, 42, 576)
(4, 13, 567)
(4, 31, 657)
(3, 24, 765)
(3, 42, 675)
(2, 13, 576)
(2, 31, 756)
(1, 24, 567)
(1, 42, 657)
(4, 13, 675)
(4, 31, 765)
(3, 24, 576)
(3, 42, 756)
(2, 13, 657)
(2, 31, 567)
(1, 24, 675)
(1, 42, 765)
(4, 13, 756)
(4, 31, 576)
(3, 24, 657)
(3, 42, 567)
(2, 14, 756)
(2, 41, 576)
(7, 16, 234)
(2, 61, 324)
(7, 15, 243)
(2, 51, 423)
[1, 27, 345]
[1, 27, 436]
[1, 72, 654]
[1, 72, 563]
(2, 13, 765)
(2, 31, 675)
[3, 26, 145]
[3, 26, 417]
[3, 62, 571]
[3, 62, 754]
(2, 35, 641)
(2, 53, 461)
(6, 37, 214)
(6, 73, 124)
(6, 34, 257)
(6, 43, 527)
VII
VIII
VII
VIII
VII

Fig. 13. — Degenerate rearrangements (automerizations) of VII forming a 12-circuit, and interconversions of VII—VIII (non-degenerate).

Most other homovalenium cations which give automerizations also lead to reaction graphs with too many vertices to be analyzed in detail, but similar in principle to those discussed above. Many automerizations of homovalenium cations involve more than two species, e.g. six different classical $(CH)_7^+$ valence isomers are involved in the 1,2-rearrangements presented in figure 14.

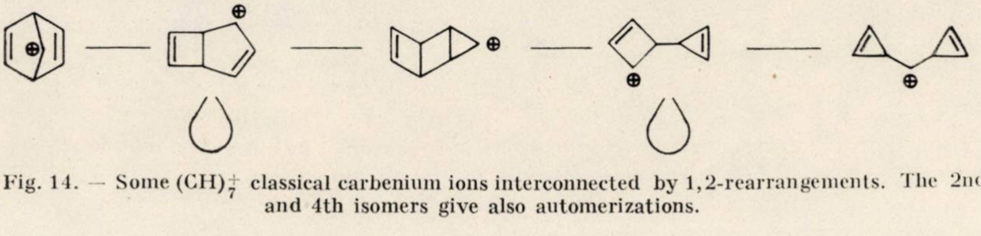

Fig. 14. — Some $(CH)_7^+$ classical carbenium ions interconnected by 1,2-rearrangements. The 2nd and 4th isomers give also automerizations.

Revue Roumaine de Chimie, **22**, 2, 257 – 261 (1977).

POTENTIAL ANTICANCER AGENTS. XI[1]

DERIVATIVES PREPARED FROM DIAZOTIZED PYRIMIDINES

D. C. SUSTER, G. BOTEZ, L. V. FEYNS, V. DOBRE and I. NICULESCU-DUVĂZ
Oncological Institute Bucharest Bul. 1 Mai 11, Romania

Received, September 16, 1975

In search for biologically active pyrimidine derivatives a series of new compounds (5-fluoro and 5-azo-pyrimidines) were prepared from diazotized pyrimidines and tested for antitumor activity. Only 2,4-diamino-6-hydroxy derivatives displayed moderate activity against L-1210 leukemia.

The intensive studies performed on pyrimidine antimetabolites led to derivatives with outstanding activity against L-1210 mouse leukemia (e.g. 2,4,5-triamino-pyrimidine,[2] 2,4,6-triamino-5-aryl-azo-pyrimidines,[3,4] etc.) some of them (e.g. 5-fluorouracyl [5,6]) being under clinical use.

The synthesis and biological properties of a series of 5-aryl-azo-pyrimidines are already reported in the literature.[4]

Roy-Burman and Sen[7] reported that these compounds act as antagonists of folic acid. On the other hand the biological results obtained with aryl-azo-pyrimidines having an alkylating side chain suggested that they function as "site-directed irreversible inhibitors" of nucleic acid biosynthesis.[8]

In search of pyrimidine derivatives with improved anticancer activity, we prepared some new 5-fluoro- and 5-azo-pyrimidines.

1. SYNTHESIS

Similarly to the aromatic amines, the diazotized 5-amino-pyrimidines may react by :

— displacing the diazo group ;

— maintaining it, in a coupling reaction.

---

[1] Part X. D. C. Suster, L. V. Feyns, G. Ciuştea, G. Botez, V. Dobre, R. Bick and I. Niculescu-Duvăz, *J. Med. Chem.*, **17**, 758 (1974).

[2] J.A.R. Mead, H. B. Wood and A. Goldin, *Cancer Chemother. Rep.* (*Part. 2*) **1**, 273 (1968).

[3] K. Tanaka, E. Omura, T. Sugawa, Y. Sanno, Y. Ando, K. Imai and K. Kavashina, *Chem. Pharm. Bull.* (*Tokio*), **7**, 1 (1959).

[4] J. Hampshire, P. Hebborn, A. M. Triggle, D. J. Triggle and S. Vickens, *J. Med. Chem.*, **8**, 745 (1965).

[5] A. R. Curreni, E. J. Ansfield, F. A. McIver, H. A. Waisman and C. Heidelberger, *Cancer Res.*, **18**, 478, 484 (1958).

[6] L. F. Larionov "Chimioterapia Tumorilor Maligne", Ed. Med. Bucureşti, 1963.

[7] P. Roy-Burman and D. Sen, *Biochem. Pharmacol.*, **13**, 1437 (1964).

[8] B. R. Baker "Design of Active-Site-Directed Irreversible Enzyme Inhibitors", Wiley, New York, 1967.

A. *5-Fluoropyrimidines.* Surprisingly, few examples are known in which the displacement of the diazo group was used as a preparative route to 5-substituted pyrimidines (e.g. the synthesis of 5-halo (Cl, Br, I)-pyrimidines),[9,10] 5-mercapto-uracyl,[11] 5-hydroxy-2-carboxy-pyrimidine[10] and 5-cyano-uracyl [12]).

As an alternate method of synthesis for 5-fluoropyrimidines, we extended the Schiemann reaction [13,14] to pyrimidines.

The 5-diazonium salts of 2,4,5-triamino-6-hydroxy and 2,4,5,6-tetra-amino-pyrimidine were obtained from the corresponding amines by diazotization in aqueous solution of tetrafluoroboric acid. The 5-pyrimidyl diazonium fluoroborates were separated as white solid stable products and after drying they were subjected (in paraffin oil) to thermal decomposition in order to afford the corresponding 5-fluoro-pyrimidines.

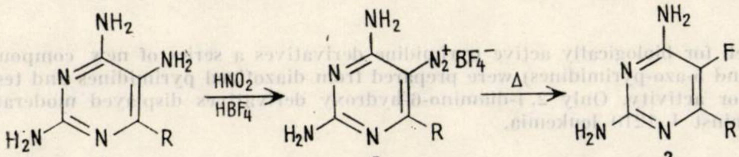

1 2 3

a) $R = NH_2$
b) $R = OH$

The conditions of this reaction are similar to those described for Schiemann procedure.[13,14]

B. *5-Azo-pyrimidines.* They may be obtained [15] by coupling : a) the 5-diazo-pyrimidines with an aromatic amine or a phenol (including pyrimidine derivatives) ; [9,16,17] b) an aromatic diazonium salt with a 5-unsubstituted pyrimidine [18-24] (followed by a reduction of the azo group, this reaction was used for the insertion of an amino group at the 5-position of the pyrimidine ring).

The substituted 5-azo-pyrimidines were synthetized in good yields by coupling a 5-pyrimidyl diazonium salt with an appropriate pyrimidine (with free 5-position) in an acetate buffer at pH 5.5.

---

[9] F. L. Rose, *J. Chem. Soc.*, **1952**, 3448.

[10] T. Yoshikawa, *J. Pharm. Soc. Japan*, **76**, 776 (1956).

[11] T. J. Bardos, R. R. Herr and T. Enkogi, *J. Amer. Chem. Soc.*, **77**, 960 (1955).

[12] Chang Sae Hee, *Daehan Hwahak Hwoejee*, **13**, 177 (1969) ; *Chem. Abstr.*, **71**, 112880.

[13] G. Balz and G. Schiemann, *Ber. dtsch. chem. Ges.*, **60B**, 1186 (1927).

[14] A. Roe in "Organic Reactions", vol. 5, R. Adams-Editor, Wiley, New York, 1960, p.193.

[15] D. J. Brown, "The Pyrimidines", Wiley, New York, 1962.

[16] M. T. Bogert and D. Davidson, *Proc. Nat. Acad. Sci. U.S.A.*, **18**, 215 (1932).

[17] T. B. Johnson, O. Baudisch and A. Hoffmann, *Ber. dtsch. chem. Ges.*, **64B**, 2629 (1931).

[18] J. W. F. McOmie and J. H. Chesterfield, *Chem. Ind. (London)*, **1956**, 1453.

[19] H. G. Garg and R. A. Sharma, *J. Med. Chem.*, **14**, 1248 (1971).

[20] S. S. Chatergee, S. Ludwig, J. F. Moran, D. J. Triggle and A. Wayne, *J. Med. Chem.*, **14**, 1237 (1971).

[21] H. G. Garg and R. A. Sharma, *J. Med. Chem.*, **13**, 763 (1970).

[22] R. E. Harmon, F. E. Dutton and H. D. Warren, *J. Med. Chem.*, **11**, 627 (1968).

[23] M. Chadwick, J. Hampshire, P. Hebborn, A. M. Triggle and D. J. Triggle, *J. Med. Chem.*, **9**, 874 (1966).

[24] S. S. Chatergee, D. R. Garrison, R. Kaprowe, J. F. Moran, A. M. Triggle, D. J. Triggle and A. Wayne, *J. Med. Chem.*, **14**, 499 (1971).

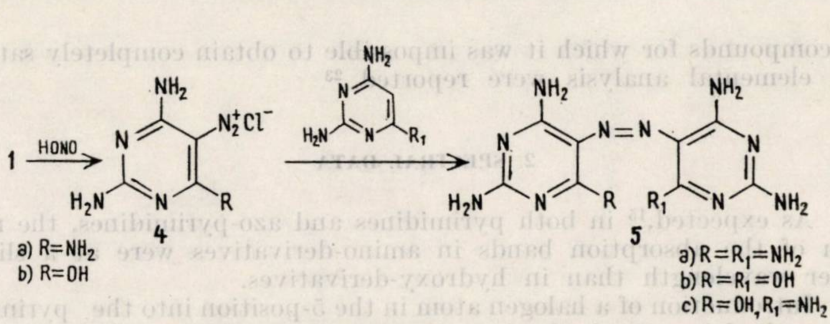
1
HONO
NH₂
N₂⁺Cl⁻
H₂N
R
4
a) R=NH₂
b) R=OH
NH₂
H₂N
R₁
NH₂
N=N
R
R₁
NH₂
H₂N
5
a) R=R₁=NH₂
b) R=R₁=OH
c) R=OH, R₁=NH₂

By this procedure, only the symmetric azo-pyrimidines ($R = R_1$, *5a, b*) were obtained satisfactorily pure (as determined by TLC) (see U.V. spectra Fig. 1).

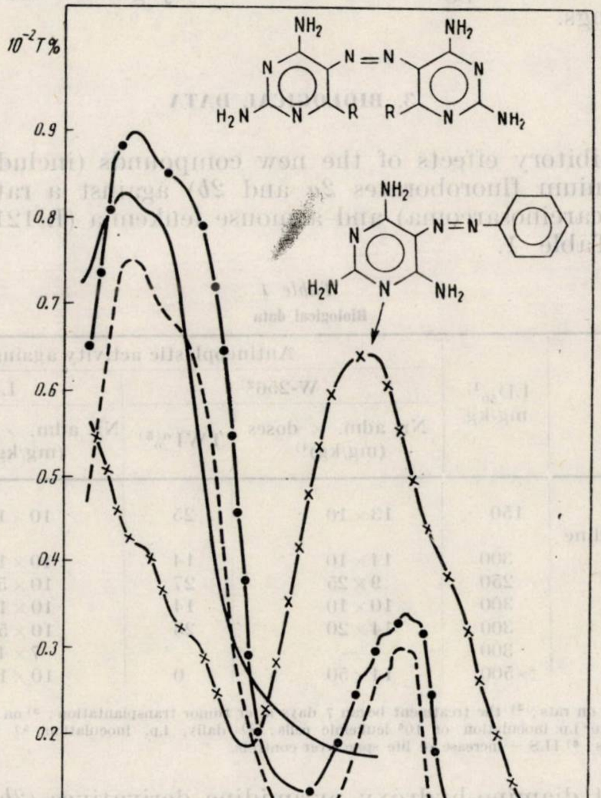

Fig. 1

No suitable methods of purification were found for compound *5c*. Its formation was ascertained by the U.V. spectrum. Other pyrimidyl-azo compounds for which it was impossible to obtain completely satisfactory elemental analysis were reported.[23]

2. SPECTRAL DATA

As expected,[15] in both pyrimidines and azo-pyrimidines, the maximum of the absorption bands in amino-derivatives were at a slightly higher wavelength than in hydroxy-derivatives.

Introduction of a halogen atom in the 5-position into the pyrimidine ring resulted in some bathochromic shifts of the U.V. absorption.[25] This rule did not apply for the fluorine atom in our derivatives (λ_{max} for 2,4-diamino-6-hydroxy-pyrimidine-266 nm and for 2,4,6-triamino-pyrimidine-272 nm, both at pH 2.3).[26]

The low position of the first two bands in azo-pyrimidines (probably $\pi - \pi^*$ transitions) suggested a lack of conjugation between the two pyrimidine rings.

3. BIOLOGICAL DATA

The inhibitory effects of the new compounds (including the pyrimidyl-5-diazonium fluoroborates *2a* and *2b*) against a rat solid tumor (Walker 256 carcinosarcoma) and a mouse leukemia (L-1210) were summarized in Table 1.

Table 1

Biological data

Compound	LD$_{50}$ 1) mg/kg	Antineoplastic activity against :			
		W-256 2)		L-1210 3)	
		Nr. adm. × doses (mg/kg) 4)	TWI % 5)	Nr. adm. × doses (mg/kg) 4)	ILS % 6)
2,4,6-triamino-5-phenylazo-pyrimidine	150	13×10	25	10×10	0
2a	300	14×10	14	10×10	0
2b	250	9×25	27	10×50	17
3a	300	10×10	14	10×10	0
3b	300	14×20	23	10×50	0
5a	300	—	—	7×40	0
5b	>500	14×50	0	10×100	27

1) determined on rats; 2) the treatment began 7 days after tumor transplantation; 3) on BDF$_1$ mice, the treatment began 24 hrs. after i.p. inoculation of 10^6 leukemic cells; 4) daily, i.p. inoculation; 5) TWI – tumor weigth inhibition over controls; 6) ILS – increase of life span over controls.

Only 2,4 diamino-hydroxy pyrimidine derivatives (*2b* and *5b*) displayed in our test a moderate activity against L-1210 leukemia. This observation agreed with those of Chattergee[20] who found that the 6-OH group increased the biological activity of such compounds.

---

[25] T. NISHIWAKI, *Tetrahedron*, **1966**, 2401.

[26] L. CAVALIERI and H. BENDICH, *J. Amer. Chem. Soc.*, **72**, 2587 (1950).

EXPERIMENTAL SECTION

U.V. spectra were run on a CF_4 spectrophotometer Optica Milano in 0.1 N HCl solution. TLC was performed on Merck plates.

1. **2,4,6-triamino-5-fluoro-pyrimidine (3a)**

To a solution of 10.5 g (0.05 moles) of 2,4,5,6-tetraamino-pyrimidine dihydrochloride (obtained by recrystallization of bisulphite salt of 2,4,5,6-tetraaminopyrimidine in HCl solution) in 100 ml H_2O, 300 ml of tetrafluoroboric acid 35% was added. A saturated aqueous solution of $NaNO_2$ was dropped under vigorous stirring after cooling to 0°. After the end of the reaction (iod-amidon paper) the solution was stirred for 1 hr.below 0°. 2,4,6-triamino-5-pyrimidyl-diazonium fluoroborate *2a* was collected by filtration, washed with 10 ml cold H_2O and dried under vacuum (P_2O_5).

The dry solid was suspended in paraffin oil and heated to 225° until the gas evolution ceased. After cooling to 100°, the suspension was filtered. The crude product was washed with petroleum ether. After recrystallization from N,N-dimethylformamide-toluene it resulted 4.7 g (65%) *3a* (Found : C, 33.80 ; H, 4.10 ; N, 49.80 ; Calc : for $C_4H_6N_5F$: C, 33.60 ; H, 4.20 ; N, 49.50%). $\lambda_{max.}^{0.1NHCl}$ 256 nm (log ε 3.89) and 277 nm (sh) (log ε 3.56).

2. **2,4-diamino-6-hydroxy-5-fluoro-pyrimidine (3b)**

By the same procedure, the 2,4,5-triamino-6-hydroxy-pyrimidine was converted to *3b* (yield 60%) (Found : C, 33.30 ; H, 3,47 ; N, 38.50 ; Calc for $C_4H_5N_4OF$: C, 33.40 ; H, 3.60 ; N, 38,90%). $\lambda_{max.}^{0.1NHCl}$ 256 nm (log ε 3.738) and 268 nm (sh)(log ε 3.681).

3. **2,4,6-triamino-5(2′,4′,6′-triamino-pyrimidyl)-azopyrimidine (5a)**

A solution of 1 g (0.004 moles) 2,4,5,6-tetraamino-pyrimidine dihydrochloride dihydrate in 10 ml 1 NHCl, cooled at 0° was diazotized with a saturated aqueous solution of $NaNO_2$.

To a suspension of 0.5 g (0.004 moles) 2,4,6-triamino-pyrimidine, in an acetate buffer (5 g CH_3CO_2Na sicc. in 20 ml H_2O), cooled at 0°, the previous prepared diazonium salt was added under stirring.

The pH (5.0) was maintained by addition of crystalline sodium acetate. After another 0.5 hrs. of stirring at 0°, the mixture was kept overnight at room temperature. The formed precipitate removed by filtration, washed with cold water, gave 0.7 g (yield 63%) of *5a* (Found : C, 35.09 ; H, 4.34 ; N, 60.88. Calc. for $C_8H_{12}N_{12}$: C, 34.80 ; H, 4.47 ; N, 61.37%) $\lambda_{max.}^{0.1NHCl}$256 (log ε 4.37), 276 nm (sh) (log ε 4.30) and 390 nm (log ε 3.44).

4. **2,4-diamino-6-hydroxy-5-(2′,4′-diamino-6′-hydroxy-pyrimidyl)-azopyrimidine (5b)**

By a similar procedure, the compound *5b* was obtained with a yield of 52% using as starting materials 2,4,5-triamino-6-hydroxy-pyrimidine and 2,4-diamino-6-hydroxypyrimidine (Found : C, 35.46 ; H, 3.40 ; N, 49.33. Calc. for $C_8H_{10}N_{10}O_2$: C, 34.53 ; H, 3.59 ; N, 50.4%) $\lambda_{max.}^{0.1NHCl}$ 251 nm (log ε 4.14) and 366 nm (sh) (log ε 4.12).

Revue Roumaine de Chimie, **22**, *2*, 263 – 269 (1977)

CYANOETHYLATION OF KETOXIMES. III[1]

PREPARATION OF *PARA*-SUBSTITUTED-(BENZYLIDENE-AMINOXY)-PROPIONIC ACIDS

P. BUCHWALD and F. DOMNARIU
Chemical-Pharmaceutical Research Institute, str. Fabricii 126, Cluj-Napoca, Romania

Received: *January 31, 1975*

The preparation of some new *para*-substituted-(benzylidene-aminoxy)-propionic acids with marked antiinflammatory and analgesic properties is described. They were obtained by the conversion of the — CN group of the corresponding cyano-ethylated acetophenone oximes into -COOH group. The intermediate iminoether hydrochlorides, free iminoether bases and ethylic esters of the above acids have been also isolated and characterized.

INTRODUCTION

In the course of previous studies we described the cyanoethylation of some *para*-substituted acetophenone oximes [2] and the failure of -CN conversion into -COOH in the resulted cyanoethyl derivatives using the classical acid and alkaline hydrolysis method.[1]

Our aim being the synthesis of some new *para*-substituted-(benzylidene-aminoxy)-propionic acids which might be expected to show antiinflammatory and analgesic properties,[3] for the conversion of the -CN group of cyanoethyl derivatives into -COOH we chose an indirect way: through iminoethers.

It is well known,[4] that absolute ethanol adds to nitriles in the presence of anhydrous hydrogen chloride to form the corresponding iminoether hydrochlorides. Using water hydrolysis, the latter can be easily converted into ethylic esters of the appropriate *para*-substituted-(benzylidene-aminoxy)-propionic acids. Further, these esters were allowed to react with dilute sodium hydroxide, reaction which gave with good yields the alkali salts of the carboxylic acids, from which the desired *para*-substituted-(benzylidene-aminoxy)-propionic acids would be liberated upon acidification.

---

[1] P. Buchwald and L. Fey, *Rev. Roumaine Chim.*, **20**, 379 (1975).

[2] P. Buchwald and A. Kövendi, *Rev. Roumaine Chim.*, **20**, 245 (1975)

[3] J. Van Dijk, I.M.A. Zwagemakers and V. Classen (N. V. Philips'-Gloeilamphen fabrieken), Ger. Offen. 1960 910; *Chem. Abstr.*, **73**, 76833 (1970).

[4] Houben-Weyl "Methoden der Organischen Chemie", Band 8., G. Thieme Verlag, Stuttgart, 1952, p. 697.

Thus, we used the following reaction scheme to obtain the desired acids from the cyanoethyl derivatives of *para*-substituted acetophenone oximes :

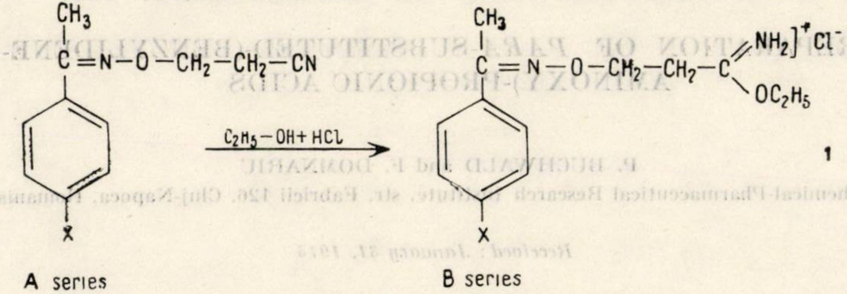

C₂H₅—OH+ HCl
A series
B series

1

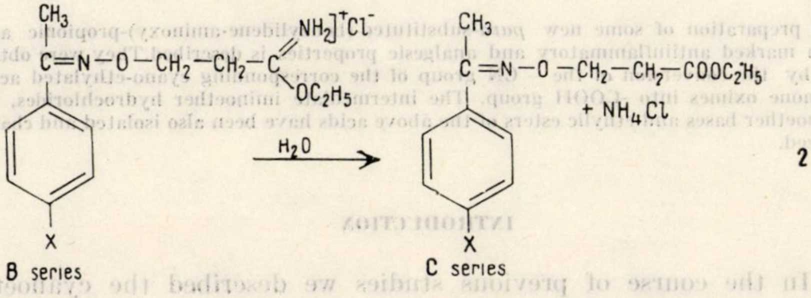

H₂O
+ NH₄Cl
B series
C series

2

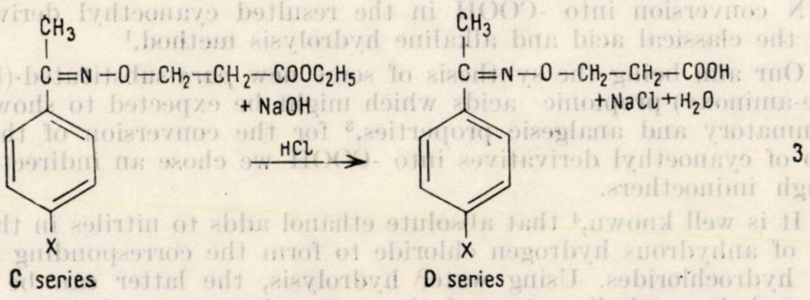

+ NaOH
HCl
+NaCl+H₂O
C series
D series

3

where : X = H (I); NO_2 (II); Cl (III); Br (IV); CH_3 (V); C_2H_5 (VI).
CH_3O (VII); C_2H_5O (VIII) and CH_3—CO—NH (IX)

RESULTS AND DISCUSSION

The iminoether hydrochlorides were prepared by the action of dry gaseous hydrogen chloride upon the cyanoethyl derivatives of *para*-substituted acetophenone oximes and absolute ethanol (reaction 1).

The reaction was carried out by bubbling anhydrous hydrogen chloride through an absolute ethereal solution of the cyanoethyl derivative and absolute ethanol, required in 1 : 1 molar proportions. The cyanoethylated *para*-acetylamino-acetophenone oxime (A IX) being insoluble in ether, the formation of B IX was carried out in chloroform. The reactions take place at 0 — 5° and are slightly exothermic, therefore cooling was necessary. The most part of resulted iminoether hydrochlorides crystallize on standing and cooling. If an oily material remains, the crystallization may be induced by scratching the vessel with a glass rod or by seeding. However, no crystallization of derivatives B I, B VI and B IX occured.

The crystallized iminoether hydrochlorides are sensitive to heat, hence their purification by recrystallization is not possible. The pure iminoether hydrochlorides may be obtained by dissolving the crude product in a small amount of acetic acid and dropping diethyl ether until no more hydrochloride precipitates. The obtained needles are well crystallized. After filtration and washing with ether, they are stable at room temperature and melt with decomposition.

The free iminoether bases may be liberated from hydrochlorides by treatment with saturated (33%) potassium carbonate solution at 0°. After the etheral extraction of the alkaline aqueous layer, the iminoether base was isolated by removing the organic solvent. Most iminoethers were oily materials (except for the *para*-nitro derivative : plates with m.p. 66°), which decomposed during vacuum distillation. They are generally soluble in organic solvents such as ether, benzene or alcohols, sparingly soluble in petroleum ether and hexane, and are insoluble in water. They are also dissolved by dilute hydrochloric acid, but decompose with ethylic ester formation of the corresponding (benzylidene-aminoxy)-propionic acids.

The infrared spectra of the obtained iminoether bases and hydrochlorides show disappearance of the band at 2260 $\mathrm{cm^{-1}}$ (nitrile absorption) which is present in the starting materials *. Further, the intensity of the absorption band at 1610 $\mathrm{cm^{-1}}$ becomes very strong and is shifted at a higher value : 1650 $\mathrm{cm^{-1}}$ ($C = N$ stretching frequency). The spectrum of hydrochlorides shows a broad absorption band in the ranges 2400 — — 3200 $\mathrm{cm^{-1}}$ which is superposed on C — H valence vibration values. This band is missing in I.R. spectra of the free bases.

The characteristics of the crystallized iminoether hydrochlorides and their characteristic vibration frequencies are presented in Tables 1 and 2 respectively.

The reaction of the iminoether hydrochlorides with water (reaction 2), or of the iminoether bases with dilute hydrochloric acid, gave with good yields the corresponding ethylic esters of the *para*-substituted-(benzylidene-aminoxy)-propionic acids. The obtained esters separated as oily layers. After extraction with an organic solvent (the most convenient was proved to be diethyl ether) and washing the organic layer with saturated sodium bicarbonate solution, the solvent was dried and removed. The resulted esters were distilled at reduced pressure. The *para*-nitro-(C II) and *para*-acetyl-amino-(C IX) derivatives crystallized on standing.

---

* The characteristic vibration frequencies of the cyanoethylated acetophenone oximes were presented in our previous paper [2].

After recrystallization from ethanol the pale yellow crystalls of C II melted at 62°. For the purification of C IX no suitable solvent could be found.

The obtained esters, their boiling or melting points, refractive indexes and elementary analysis are presented in Table 3.

The alkaline hydrolysis of esters into acids (reaction 3) was carried out with dilute sodium hydroxide in aqueous-alcoholic solution at 40 — 60°. After 2 — 3 hours, the alkaline solution was cooled at room temperature, acidified with dilute hydrochloric acid to pH = 1 — 1,5 and extracted with benzene. After separation, the organic layer was extracted repeatedly with sodium bicarbonate solution. From the combined aqueous-alkaline layer the desired acids were precipitated by acidulation with dilute hydrochloric acid. The obtained *para*-substituted-(benzylidene-aminoxy)-propionic acids are well crystallized stable plates. They are insoluble in water and are generally soluble in organic solvents such as acetic acid, acetone and alcohols. The adequate solvent for their recrystallization has been proved to be the aqueous acetic acid or aqueous ethanol and light petroleum.

The prepared *para*-substituted-(benzylidene-aminoxy)-propionic acids, the solvents of recrystallization, their melting points and analysis are presented in Table 4.

The infrared spectra of the obtained carboxylic acids and esters show very strong absorption bands at 1710 cm^{-1} (carboxylic carbonyl stretching). Further, the spectrum of the acids reveals a broad absorption band in the ranges 2500 — 3000 cm^{-1} specific of associated carboxylic groups.

The characteristic vibration frequencies of the *para*-substituted (benzylidene-aminoxy)-propionic acids and of their ethylic esters are presented in Tables 5 and 6 respectively.

The preliminary pharmacological test results were supplied by Dr. E. Neuman from the Clinica Chirurgicală Nr. 1, Cluj-Napoca. The results show, that the obtained acids posses marked antiinflammatory and analgesic activity, comparable with Hydrocortisone and Mialgin. An ample study of pharmacological activity determination of these compounds will be described in a next paper.

EXPERIMENTAL PART

The melting points are uncorrected.

The I.R. spectra of the acids, esters and iminoether bases were recorded on a Perkin-Elmer Infracord 137-B spectrophotometer in chloroform, and that of the iminoether hydrochlorides, on a Shimadzu I.R.-27 G spectrophotometer, using KBr pellets.

The cyanoethylated *para*-substituted acetophenone oximes described in our previous paper[2] were used as starting materials.

1. PREPARATION OF THE IMINOETHER HYDROCHLORIDES (B SERIES)

General procedure : In all experiments, the anhydrous hydrogen chloride was passed into an absolute ethereal solution of cyanoethylated *para*-substituted acetophenone oximes (A series) and absolute ethanol, required in 1 :1 molar proportions. The reactions were carried out at 0 — 5° under stirring and cooling. Removal of the solvent by filtration or decantation left a crystal-

Table 1

The melting points and elementary analysis of the iminoether hydrochlorides with general formula: p-X-$C_6H_4-C(CH_3)=N-O-(CH_2)_2-C(OC_2H_5)=NH_2/^+Cl^-$

Compound	X =	m.p. °C	Empirical formula	Analysis C% Calcd. Found	H% Calcd. Found	N% Calcd. Found	Cl% Calcd. Found	Br% Calcd. Found
				49.40	5.74	13.30	10.10	—
B II	NO_2	134–5	$C_{13}H_{18}ClN_3O_4$	49.60	5.89	12.90	10.25	—
				51.20	5.94	9.20	23.23	—
B III	Cl	112–3	$C_{13}H_{18}Cl_2N_2O_2$	51.27	6.02	9.50	23.50	—
				44.70	5.20	8.02	10.17	22.82
B IV	Br	126	$C_{13}H_{18}BrClN_2O_2$	44.40	5.25	8.37	10.20	22.65
				59.04	7.43	9.83	12.45	—
B V	CH_3	113	$C_{14}H_{21}ClN_2O_2$	58.80	7.60	9.91	12.70	—
				56.00	7.03	9.30	11.80	—
B VII	CH_3O	88–9	$C_{14}H_{21}ClN_2O_3$	56.35	7.32	9.27	12.00	—
				57.25	7.35	8.92	11.30	—
B VIII	C_2H_5O	102–3	$C_{15}H_{23}ClN_2O_3$	56.90	7.70	9.05	11.45	—

Table 2

The characteristic vibration frequencies of the iminoether hydrochlorides (B series)

Compound	cm^{-1}
B II	2800vs; 1640vs; 1515vs; 1440m; 1370s; 1045vs; 890s; 830s;
B III	2750vs; 1640vs; 1440m; 1375s; 1040vs; 890s; 830s;
B IV	2850vs; 1660vs; 1440m; 1370s; 1050s;
B V	2800vs; 1660vs; 1440s; 1360s; 1060s; 950m; 890m; 830s;
B VII	2800vs; 1650vs; 1440m; 1370s; 1240s; 1050s; 930m; 840vs;
B VIII	2800vs; 1660vs; 1440m; 1360vs; 1240s; 1030s; 940w; 840vs;

Table 3

The characteristics of ethylic esters with general formula p-$X-C_6H_4-C(CH_3)=N-O-CH_2-CH_2-COOC_2H_5$

Comp.	X =	m.p. b.p. °C °C/Hgmm	n_D^{21} =	Empirical formula	Analysis C% Calcd. Found	H% Calcd. Found	N% Calcd. Found	Hal.% Calcd. Found
C I					66.40	7.30	5.96	—
	H	— 118–20/3	1.5188	$C_{13}H_{17}NO_3$	66.30	7.63	6.24	—
C II					55.70	5.75	10.00	—
	NO_2	62 —	—	$C_{13}H_{16}N_2O_5$	55.75	6.10	10.18	—
C III					58.00	6.00	5.03	13.20
	Cl	— 150–2/2	1.5326	$C_{13}H_{16}ClNO_3$	58.08	6.42	5.20	13.35
C IV					49.60	5.12	4.46	25.41
	Br	— 155–6/2	1.5485	$C_{13}H_{16}BrNO_3$	49.40	5.16	4.60	25.51
C V					67.50	7.70	5.62	—
	CH_3	— 165–7/3	1.5200	$C_{14}H_{19}NO_3$	68.00	7.96	5.90	—
C VI					68.50	8.00	5.33	—
	C_2H_5	— 166–7/2	1.5176	$C_{15}H_{21}NO_3$	68.30	8.30	5.30	—
C VII					63.50	7.20	5.30	—
	CH_3O	— 140–2/3	1.5280	$C_{14}H_{19}NO_4$	63.50	7.45	5.70	—
C VIII					64.75	7.55	5.00	—
	C_2H_5O	— 160–2/3	1.5256	$C_{15}H_{21}NO_4$	64.75	7.83	5.06	—

Table 4

The characteristics of the *para*-substituted (benzylidene-aminoxy)-propionic acids with general formula:
$para-X-C_6H_4-C(CH_3)=N-O-CH_2-CH_2-COOH$

Comp.	X =	Solvent of recrystall.	m.p. °C	Empirical formula	C% Calcd. Found	H% Calcd. Found	N% Calcd. Found	Hal.% Calcd. Found
D I	H	$CH_3COOH:H_2O$	73–4	$C_{11}H_{13}NO_3$	63.80 64.05	6.35 6.78	6.76 6.89	— —
D II	NO_2	$C_2H_5-OH:H_2O$	115	$C_{11}H_{12}N_2O_5$	52.30 52.75	4.80 5.10	11.10 10.78	— —
D III	Cl	light petrol.	85–6	$C_{11}H_{12}ClNO_3$	54.40 54.73	5.02 5.37	5.80 5.95	14.70 14.80
D IV	Br	light petrol	87–8	$C_{11}H_{12}BrNO_3$	46.10 46.30	4.24 4.55	4.90 4.89	28.00 28.20
D V	CH_3	light petrol.	76	$C_{12}H_{15}NO_3$	65.00 64.90	6.85 6.95	6.45 6.30	— —
D VI	C_2H_5	petrol.ether	53	$C_{13}H_{17}NO_3$	66.40 66.25	7.28 7.40	5.97 6.05	— —
D VII	CH_3O	benzene+ light petrol.	109	$C_{12}H_{15}NO_4$	61.00 61.18	7.15 7.00	5.90 6.10	— —
D VIII	C_2H_5O	benzene + light petrol.	111	$C_{13}H_{17}NO_4$	62.20 62.41	6.83 6.90	5.58 6.00	— —
D IX	$CH_3-CO-NH$	H_2O	169–70	$C_{13}H_{16}N_2O_4$	59.00 58.75	6.10 6.47	10.60 10.71	— --

Table 5

The characteristic vibration frequencies of the *para*-substituted (benzylidene-aminoxy) – propionic acids (D series)

Compound	cm^{-1}
D I	2940vs; 2700s; 1710vs; 1600w; 1370s; 1030s; 890s; 840w;
D II	2940vs; 2700s; 1710vs; 1590s; 1505m; 1340vs; 1090m; 1040s; 890s; 850s;
D III	2940vs; 2700s; 1710vs; 1600w; 1370s; 1090s; 1040s; 890vs; 830s;
D IV	2940vs; 2700s; 1710vs; 1600w; 1360s; 1090s; 1040s; 890s; 830s;
D V	2940vs; 2700s; 1710vs; 1600w; 1045s; 890s; 835m
D VI	2940vs; 2700s; 1710vs; 1600m; 1050s; 890s; 830m
D VII	2940vs; 2700s; 1710vs; 1600s; 1360s; 1250s; 1030m; 880s; 830s;
D VIII	2940vs; 2700s; 1710vs; 1600s; 1360s; 1245s; 1040m; 880s; 830s
D IX	3360s; 2940vs; 2700s; 1710vs; 1670vs; 1600m; 1050s; 890s; 830m;

line or heavy oily product, which was dissolved in a small amount of acetic acid, from which the pure iminoether hydrochlorides were precipitated with anhydrous ether and dried at room temperature.

The yields are between 75 — 85%.

2. OBTENTION OF FREE IMINOETHER BASES

A representative experiment: the obtention of the iminoether base of *para*-nitro derivative from its hydrochloride is described.

7 g of B II suspended in 50 ml diethyl ether were treated at 0°, under stirring and cooling, with 8.5 ml saturated (33%) aqueous potassium carbonate solution. After separation of the organic layer, removal of the solvent left a crystalline product, which after recrystallization from 30 ml hexane melts at 66°.

Yielded 4 g (64%) of *para*- O_2N-C_6H_4-$C(CH_3)=N$-O-CH_2-CH_2-$C(OC_2H_5)=NH$
Found : C, 56.28 ; H, 6.30 ; N, 15.00. Calcd. for $C_{13}H_{17}N_3O_4$: C, 56.00 ; H, 5.88 ; N, 15.08%

The other obtained iminoether bases were heavy oily materials, which decomposed during vacuum distillation.

Table 6

The characteristic vibration frequencies of the ethylic esters of the *para*-substituted (benzylidene-aminoxy)-propionic acids (C series)

Compound	cm^{-1}
C I	2980vs ; 1730vs ; 1440m ; 1370vs ; 1170vs ; 1030s ; 990m ; 890m ;
C II	2940vs ; 1720vs ; 1570vs ; 1440m ; 1340vs ; 1170m ; 1030s ; 945m ; 910s ; 855s ;
C III	2950vs ; 1720vs ; 1600w ; 1490m ; 1370s ; 1310s ; 1160s ; 1090vs ; 945m ; 905s ; 890s ; 835s ;
C IV	2940vs ; 1730vs ; 1600w ; 1490w ; 1370s ; 1310w ; 1160s ; 1090s ; 1030s ; 945m ;890m ; 825s ;
C V	2940vs ; 1710vs ; 1600w ; 1370vs ; 1310m ; 1160s ; 1090m ; 1045s ; 940m ; 890m ; 820m ;
C VI	2950vs ; 1710vs ; 1600w ; 1460w ; 1370vs ; 1160s ; 1040vs ; 945m ; 890s ; 830m ;
C VII	2940vs ; 1710vs ; 1600s ; 1440m ; 1350s ; 1300m ; 1260s ; 1170s ; 1040vs ; 940m ; 890s ; 830s ;
C VIII	2940vs ; 1710vs ; 1600vs ; 1500w ; 1460s ; 1350s ; 1170vs ; 1040vs ; 890s ; 830s ;
C IX	3370s ; 2950vs ; 1730vs ; 1640m ; 1370vs ; 1165vs ; 1030s ; 990m ; 890m ;

vs = very strong s = strong m = medium w = weak

3. OBTENTION OF ETHYLIC ESTERS OF *PARA*-SUBSTITUTED (BENZYLIDENE-AMINOXY)-PROPIONIC ACIDS (C SERIES)

General procedure : In all experiments, 0.1 mole of iminoether hydrochloride (B series) was dissolved in 200 ml water and stirred for 3 hours at room temperature. It was then extracted with two portions of ether (2 × 100 ml). The combined ether extracts were washed succcessively with water and 10% sodium bicarbonate solution and dried over anhydrous sodium sulfate. Removal of the solvent left a residue which was distilled at reduced pressure.

The yields are between 90 — 93%.

4. OBTENTION OF *PARA*-SUBSTITUTED-(BENZYLIDENE-AMINOXY)-PROPIONIC ACIDS (D SERIES)

General procedure : A mixture of 0.04 moles of above ester (C), 50 ml ethanol and 20 ml 10% aqueous sodium hydroxide was stirred at 50° until homogeneous (about 3 hours). After addition of 200 ml water, the reaction mixture was cooled to room temperature and made acid with dilute hydrochloric acid solution. The precipitated carboxylic acids were taken up in 150 ml benzene by extraction in a separatory funnel. After separation, the organic layer was washed twice with 150 ml saturated bicarbonate solution. After acidulation of the combined aqueous alkaline layer with dilute hydrochloric acid, the crystalls of the obtained *para*-substituted (benzylidene-aminoxy)-propionic acids were filtered off, washed with water and recrystallized from an adequate solvent.

The yields are between 92 — 95%.

Acknowledgement : we are indebted to Livia Moraru and Iolanda Mureşan for performing the elemental analysis.

Revue Roumaine de Chimie, 22, 2, 271 – 282 (1977)

MASS TRANSFER FROM DISPERSED PARTICLES TO CONTINUOUS FLUID MEDIA. II.*

OSCILLATING FLUID MEDIA, PARTICULARLY DUE TO ULTRASONIC ENERGY

EM. A. BRATU, CORNELIA BALABAN and GHEORGHIŢA I. JINESCU
Chair of Chemical Engineering, Polytechnic Str. Polizu 1, Bucharest, Romania

Received 15 November, 1975

The mass transfer from dispersed particles to a continuous fluid phase is analysed, when in the transfer interfaces a turbulence of oscillation is created. Ultrasonic energy was used as agent of turbulence and an intensification of 150 – 200% of mass transfer was obtained in comparison with the same system in the absence of ultrasonic energy. A relation was obtained for the mass transfer coefficient in the presence of ultrasonic energy as a function of (i) the mass transfer coefficient in the absence of ultrasonic energy, (ii) the magnitude of the gas bubble and (iii) the characteristics of the ultrasonic energy.

1. INTRODUCTION

The present study of mass transfer was undertaken within the framework of the general tendency towards the intensification of the fundamental processes of mass transfer in view of increasing the productivity of installations and improving the product quality.

The intensification of mass transfer results from the application of technological methods which enhance favourable factors or which reduce the influence of un favourable factors.

In the case of the interphase mass transfer for the systems formed from dispersed particles (solid, liquid, gas) and a continuous fluid medium, the intensification of the mass transfer is achieved mainly through the following factors :

— attainment of favourable hydrodynamic conditions at the interface between the two phases ;

— the increase of the interphase mass transfer area ;

— uniformization of the contact time of the particles dispersed in the continuous phase ;

— the increase or the conservation of the mass transfer driving force.

---

[*] Part I is ref. 22.

In order to influence all these factors, various techniques were employed, ranging from simple alterations in the construction of the apparatus or in the circulations of the fluids, to very complex working techniques. Sometimes, the intensification is achieved through the combination of two or more such techniques. Several procedures for the mass transfer intensification have been known and used, such as packed columns, fluidized beds, foaming beds, systems which increase the turbulence of the phases, the introduction into the system of mobile elements. More recently, mass transfer intensification was achieved by modifying the physical properties of the transfer interface : the utilization of surface active agents, or the modifications of the flow conditions through vibrations, pulsations or the use of ultrasonic and/or sonic energy. Such procedures perturb the system through a supplementary energy which alters the flow conditions in the contact interfaces creating a "turbulence of oscillation".

Throughout this work, "oscillations" denote all perturbations which can introduce into the system a turbulence of oscillation : these are vibrations, pulsations, sonic energy, and ultrasonic energy.

2. THE INFLUENCE OF OSCILLATIONS ON THE MASS TRANSFER

The influence of oscillations on the mass and heat transfer is very disputed.[1] Several authors [2–5] assert that mechanical vibrations and pulsations increase the mass and heat transfer for systems formed from particles and a continuous phase, other authors[6,7] consider that the efect is negligible or even unfavourable. These controversies result from the different influence of the oscillations as a function of the geometry of the system, the initial hydrodynamic conditions, the nature and the characteristics of the oscillations.

The first positive results in the use of oscillations (namely of pulsations) were reported in the case of liquid-liquid extraction.[8,9] Later, pulsations as well as vibrations were also used for other operations.[10–12] Experimental and theoretical studies were made in the case of the mass transfer intensification in vibrated fluidized beds,[13,14] and in the case of rectification in mechanically vibrated columns.[15] Ultrasonic energy was applied for the evaporation of liquids in a capillary tube,[16] in the liquid-liquid extraction,[17] and in the absorption in wetted-wall columns.[18] Sonic energy was used in absorption.[19]

---

[1] R. Lemlich, *Chem. Eng.*, **68** 171 (1961).

[2] M. R. Fand and J. Kaye, *J. Heat Transfer Trans. ASME*, **83** C, 133 (1961).

[3] R. Lemlich, *Ind. Eng. Chem.*, **47**, 1175 (1955).

[4] S. Bretsznajder, M. Jaszczak and W. Pasiuk, *Internat. Chem. Eng.*, **3**, 496 (1963).

[5] C. R. Martinelli and L.M.K. Boelter, *Proc. 5th Int. Congr. Appl. Mech.*, 578 (1938).

[6] G. B. Nevil, G. E. Commerford and I. A. Raben, *J. Acoust. Soc. Amer.*, **35**, 928 (1963).

[7] G.B. Darling, *Petroleum (London)*, **22** 177 (1950).

[8] W.J.O., Van Diyck, U. S. Patent 2011186, 13 August 1935.

[9] W. D. Jamrack, "Rare Metal Extraction by Chemical Engineering Techniques", Pergamon Press, London, 1963.

[10] S. F. Zhigalov "Protessy i apparaty sveklisaharnogo proizvodstva" Pishchepomizdat, Moscow, 1958.

[11] E. M. Mitkeevich *Zhur. priklad. Khim.*, **33**, 1263 (1960).

[12] O. V. Isaev, L. A. Ruslanova, V. A. Chilenov, L. Ia. Margolis and N. V. Mihailov, *Khim. Prom.*, **41**, 471 (1965).

[13] Em. A. Bratu and Gh. I. Jinescu, *Génie chim.*, **104**, 1657 (1971).

[14] Em. A. Bratu and Gh. I. Jinescu, *Brit. Chem. Eng.*, **16**, 691 (1971).

Oscillations act on the mass transfer by influencing especially the hydrodynamic conditions in the transfer interfaces. In order to estimate the influence of the oscillations in the mass transfer intensification, it is necessary to study comparatively the hydrodynamics of the transfer interfaces and the mass transfer mechanism, both in the system with, and without oscillations. The hydrodynamics of the systems without and with oscillations was the object of two previous papers.[20,21] The mass transfer in the absence of oscillations constituted the first part of this work.[22]

A systematical survery of the literature data for the mass transfer in the presence of oscillations is difficult because of the various methods for producing oscillations and because of the different nature and form of the particles. For the systems formed from a dispersed solid, liquid or gaseous phase, and a continuous liquid phase, the following methods were used in the literature for mass transfer intensification by oscillations :

— vibration and spinning of the solid particles ;

— pulsation of the continuous phase ;

— utilisation of sonic and/or ultrasonic energy.

Table 1 presents the relationships from the literature for the mass transfer in the presence of oscillations as a function of the physical nature of the particles involved.

From experimental and theoretical investigations[4,16-19,23-33] it results that the mass transfer may be intensified by the correct utilisation of oscillations. The main factors which intensify the mass transfer in the presence of oscillations for the systems formed from dispersed particles and fluid media are :

— pulsating movement of the particles ;

— reduction of the speed of the moving particles, or inversion of their sense of circulation, leading to a longer contact time ;

---

[15] Em. A. Bratu and F. A. Cothard, *Rev. Chim. (București)*, **18**, 683 (1967).

[16] H. S. Fogler and K. D. Timmerhaus, *Amer. Inst. Chem. Eng. J.*, **12**, 90 (1966).

[17] H. A. Woodle, J. and F. C. Vilerand, *Amer. Inst. Chem. Eng. J.*, **6**, 296 (1960).

[18] V. Ju. Orlov and M. M. Zhavoronkov, *Doklady Akad. Nauk. S.S.S.R.*, **129**, 161 (1959).

[19] K. L. Harbaum and G. Haughton, *Chem.Eng. Sci.*, **13**, 90 (1960).

[20] C. Balaban and G. Jinescu, *Rev. Chim. (București)*, **25**, 970(1974).

[21] G. Jinescu and C. Balaban, *Rev. Chim. (București)*, **26**, 138 (1975).

[22] G. Jinescu and C. Balaban, *Rev. Roumaine Chim.*, **20**, 1141 (1975).

[23] S. Bretsznajder and W. Pasiuk, *Bull. Acad. polon., Sci. Ser. chim.* **7**, 591 (1959).

[24] S. Bretsznajder and W. Pasiuk, *Bull. Acad. polon. Sci. Ser. Sci. chim.* **10**, 153 (1962).

[25] Em. A. Bratu and R. Z. Tudose, *Rev. Roumaine Chim.*, **11**, 607 (1966).

[26] G. Houghton, *Canad. J. Chem. Eng.*, **46**, 79(1968).

[27] R. Saint-James and G. P. Graham, *Génie Chim.*, **86**, 1(1961).

[28] V. A. Doronin, N. M. Zhavoronkov and A. M. Nikolaev, *Khim Mashinostr.*, **5**, 21 (1962).

[29] E. Ruckenstein and O. Muntean, *Chem. Eng. Sci.*, **25**, 1159 (1970).

[30] R. Lemlich and M. R. Levy, *Amer. Inst. Chem. Eng. J.*, **7**, 240 (1961).

[31] P. Noordsiy and J. W. Rotte, *Chem. Eng. Sci.*, **22**, 1475 (1975).

[32] H. Gilbert and H. Angelino *Canad. J. Chem. Eng.* **51**, 319 (1973).

[33] T. K. Ross and M. F. Azim. *Chem. Eng. Sci.*, **26**, 1771 (1971).

Table 1

Relations for the mass transfer in the presence of oscillations

Characteristics of the system	Relation	Reference
Vertically vibrating cylinders of naphthalene in air	$\frac{k'_g}{k_g} = 0.117\ Re_v^{0.85}$;	30
	$\frac{k'_g}{k_g} = 0.038\ Re_v^{0.85}\ Sc^{1.13}$	30
Rotating sphere	$Sh = 10 + 0.43\ Re_r^{1/2} Sc^{1/2}$ at $0.8\times10^3 < Re_r < 27\times10^3$ $0.5\times10^3 < Sc < 2\times10^3$ $Re_r = \frac{\omega\, d_p^2}{\nu}$	31
Vibrating sphere	$Sh = 2 + 0.24\,(Re_v \cdot S_c)^{1/2}$ at $10^2 < (Re_v\ Sc) < 16\times10^2$ $0.5\times10^3 < Sc < 2\times10^3$ $0.03 < \frac{a}{d_p} < 0.063$	31
Solid spheres in pulsed liquid	$Sh.\ Sc^{-1/3} = 0.593\left[Re_v\left(\frac{2a}{d_p}\right)^{1/2}\right]^{0.538}$ for $\frac{2a}{d_p} \leqslant 1.5$	32
	$Sh.\ Sc^{-1/3} = 0.661\ Re_v^{0.538}$ for $\frac{2a}{d_p} \geqslant 1.5$ $Re_v = \frac{d_p\,(4a\,f)}{\nu}$	32
Solid spheres vibrated in the liquid	$Sh.\ Sc^{1/3} = 0.624\left[Re_v\left(\frac{2a}{d_p}\right)^{1/3}\right]^{0.538}$ for $\frac{2a}{d_p} \leqslant 1.5$	32
	$Sh.\ Sc^{-1/3} = 0.711\ Re_v^{0.538}$ for $\frac{2a}{d_p} \geqslant 1.5$	32

Table 1 (continued)

Characteristics of the system	Relation	Reference
Gas bubbles in oscillating liquid	$k_l = \frac{2}{\sqrt{\pi}} \frac{D}{\delta}$	29
	$Sh = \frac{2}{\sqrt{3\pi}} \left(\frac{d_p u_p}{D} \right)^{1/2}$	29
Mass transfer for the liquid-liquid interface	$\frac{k_l}{2fa} \left(\frac{\nu}{D} \right)^{0.66} = 0.4\ Re_v^{-0.21}$	33
	$Re_v = \frac{2\ d_p\ f\ a}{\nu}$	
	$Re_v = 250 - 3600$	

— variation in time of the relative speed of the dispersed phase ;

— creation of so-called "turbulence of oscillation" in the mass transfer interfaces ;

— variation of the interface area, in the case of particles with mobile interface ;

— creation of a vibrational field caracterized by a vibrational acceleration $(a\omega^2)$.

From all the systems which introduce oscillations into a system, the most advantageous seems to be, especially for industrial installations, the utilisation of sonic and ultrasonic energy. When using mechanical vibrations one acts generally on the whole installation or a substantial part of it, with a considerable expenditure of electric power, and with difficult mechanical problems (transmission and mechanical resistance). In the pulsation of the continuous phase the resulting oscillating movement acts on the whole height of the fluid column, not only in the area where the intensification is necessary. The sonic or ultrasonic energy may be introduced in several points distributed along the height of the fluid column, only in the area where the intensification is necessary. It is possible to utilize different intensities of power depending on the necessities of local mass transfer.

The utilisation of ultrasonic energy in chemical engineering is only 20 years old, and it was dependent on the posibility of constructing the generators with convenient power and high efficiency.[34] The information from the literature is insufficient and sometimes rather contradictory concerning the effect of sonic and ultrasonic energy on the mass transfer ; in order to create a theoretical and experimental basis, necessary for the utilisation of ultrasonic energy on an industrial scale for the intensification of mass transfer, technical investigations in the case of each unit operation are necessary.

---

[34] M. J. Ashlei, *Chem. Eng.*, **81**, 368 (1974).

3. EXPERIMENTAL

The mass transfer from individual gas bubbles in free ascension in a liquid column in the presence of oscillations produced by ultrasonic energy was determined.

The experimental set-up (fig. 1) is composed mainly from an absorbtion column (1) made from sections of cylindrical glass tubing of 10 and 15 cm height, with a diameter of 5cm. The height of the liquid column penetrated by the ultrasonic energy was varied by using a different number of glass sections. The gas volume utilized in absorption was measured with a calibrated syringe (2), and was introduced under a metallic cup (3). By turning the cup upside down, the gas bubble starts to rise freely and its speed was measured between two marks on the column. By a system of stopcocks of the installation, the absorption column is completely filled with liquid, and after absorption, the unabsorbed gas is eliminated from the system. In order to prevent absorption of the gas during the formation of the bubble under the cup, a mercury layer was used in the bottom of the column.

The amount of absorbed gas was measured using the method of Ledig and Weaver,[35] modified by Johnson et al.[36] The same method was used by one of us[37] for studying absorption of gas bubbles in the presence of mechanical vibrations.

For producing ultrasonic energy a magnetostrictive generator with a resonance frequency of 21 kHz was used; it dissipated in the liquid a power of 35W. The ultrasonic generator (4) was introduced directly into the absorption column. By varying the electrical intensity of the generator, different values for the dissipated power, ultrasonic intensity and amplitude of the liquid motion were obtained. The system carbon dioxide-distilled water was used. For this system, mass transfer resistance is concentrated in the liquid film, on which the oscillations produced by the ultrasonic energy are in fact acting.

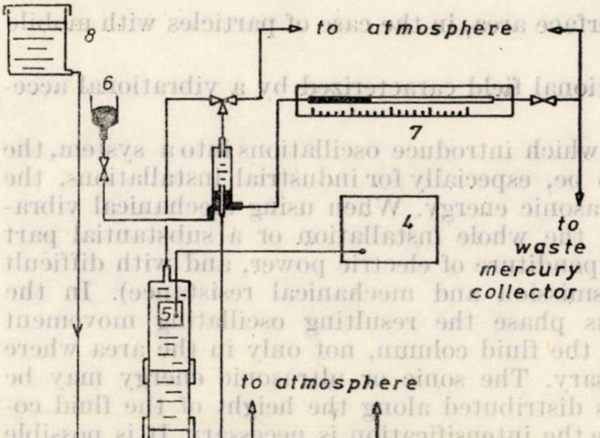

Fig. 1. — Experimental apparatus 1, glass column; 2, gas injection system; 3, metallic cup; 4. electric impulse generator; 5, ultrasonic transducer; 6, mercury level control system; 7, gas volume measuring system; 8, distilled water reservoir.

---

[35] P. G. Ledig and E. R. Weaver, *J. Amer. Chem. Soc.*, **46**, 650 (1924).

[36] A. I. Johnson, F. Besik and A. E. Hamielec, *Canad. J. Chem. Eng.*, **47**, 559 (1964).

[37] C. Balaban, Gh. Dobraniş and R. Mihail, *Rev. Roumaine Chim.*, **18**, 1829 (1973).

In the experimental work, we varied the height of the liquid column penetrated by ultrasonic energy, the magnitude of the bubble and the specific intensity (I) of the ultrasonic energy. The intensity of the mass transfer was expressed by the partial mass transfer coefficient in the liquid phase (k_l), determined from the amount of absorbed gas.

4. RESULTS AND DISCUSSIONS

The partial mass transfer coefficient in the liquid phase k_l, was calculated by means of the relation :[22]

$$k_l = \frac{\Delta V}{\Delta \tau \bar{S}_b} \tag{1}$$

where : $\frac{\Delta V}{\Delta \tau}\left[\frac{\text{cm}^3}{\text{s}}\right]$ is the ratio between the volume of absorbed carbon dioxide and the absorption time.

$\bar{S}_b[\text{cm}^2]$ is the average between the initial and final area of the bubble, considered as a sphere. All bubbles were small enough for this approximation to be valid.

The variation of the mass transfer coefficient k_l, as a function of the equivalent diameter of the gas bubble, for heights of the liquid column equal to 30, 40 and 50 cm are given in figures 2, 3 and 4.

The highest vales of the mass transfer coefficient obtained in this work were for a height of liquid column of 30 cm. This fact may be explained through the attenuation of the oscillation intensity and of the turbulence of oscillation along the height of the liquid column. It is necessary to determine in each case the optimal height of the liquid column as a function of the characteristics of the oscillations produced by ultrasonic energy, the properties of the liquid, the geometry of the system and the hydrodynamic conditions.

For the height of 30 cm, for which the absorption was maximal in our case, the intensity of the mass transfer expressed by Sherwood's number, was plotted as a function of the initial volume V_1 of the bubble gas (fig. 5).

From the experimental data it results that for the ultrasonic power used in this work the values of the mass transfer coefficient and of Sherwood's number, present a maximum for the bubbles with an initial volume $V_1 \in (0.7-1.0)\,\text{cm}^3$. For the bubbles with V_1 smaller than 0.3 cm the effect of the ultrasonic energy on the mass transfer was negligible.

The variation of Sherwood's number as a function of the intensity of the ultrasonic energy dissipated in the system shows a dependence with maxima and minima. Similar variations with peaks of the mass transfer coefficient k_l or of the product $k_l A$ were obtained also by other authors in the case of absorption in pulsed column and in the case of using sonic energy.[19] The maxima of the absorption coefficient are attributed to the existence of enhanced oscillations of the bubble when resonance occurs between the proper frequency of the bubble oscillations and the frequency of the external oscillations.

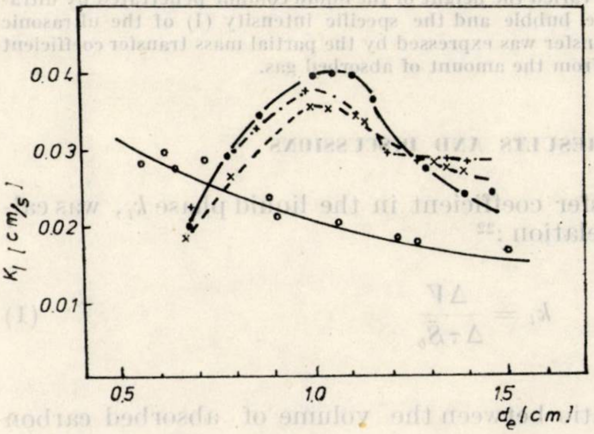

Fig. 2. — Variation of partial mass transfer coefficient, k_l, *versus* gas bubbles for $H_c = 30$ cm. Specific intensity of ultrasonic energy, I: ○, $I = 0$; ×, $I = 1.07$; +, $I = 1.34$; ●, $I = 1.16$.

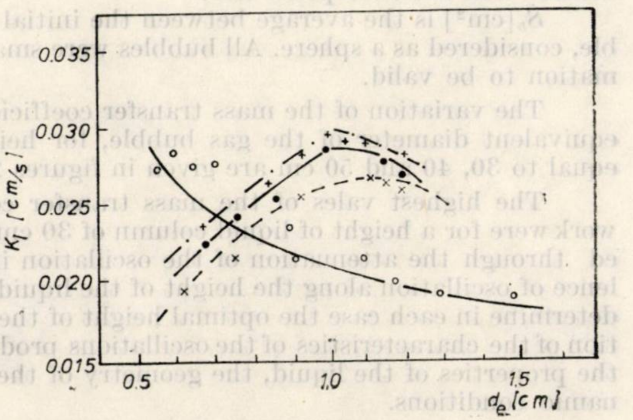

Fig. 3. — Variation of partial mass transfer coefficient, k_l, *versus* the equivalent diameter of the gas bubbles, for $H_c = 40$ cm : ○, $I = 0$; ×, $I = 1.07$; ●, $I = 1.16$; +, $I = 1.25$.

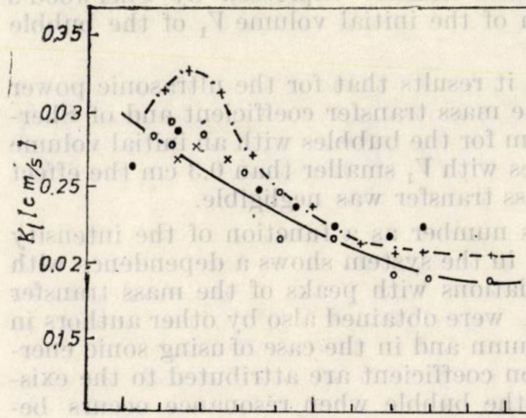

Fig. 4. — Variation of partial mass transfer coefficient, k_c, *versus* the equivalent diameter of the gas bubbles for $H_c = 50$ cm : ○, $I = 0$; □, $I = 0.98$; +, $I = 1.25$; ●, $I = 1.07$.

The intensification of the mass transfer through ultrasonic energy was expressed by the ratio k_l'/k_l, between the mass transfer coefficient in the presence of ultrasonic energy (k_l'), and the same coefficient in the absence of this energy (k_l). The ratio k_l'/k was considered as the intensification coefficient of the mass transfer. For the utilised ultrasonic power, we calculated the ratio $a\omega^2/g$, which represents a measure of the intensity of the vibrational field in comparison with the gravitational field. The variation of the intensification coefficient k_l'/k_l as a function of the ratio $a\omega^2/g$ and of the volume of the gas bubble is given in figure 6.

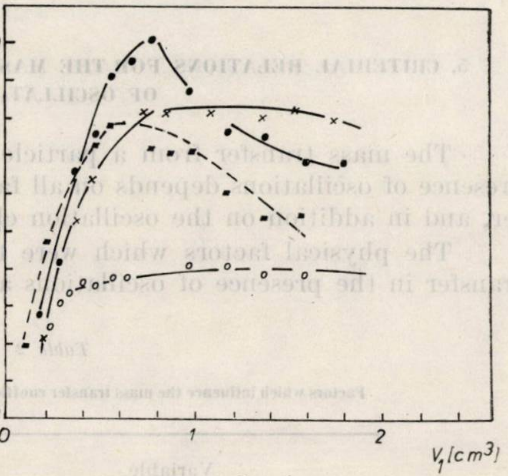

Fig. 5. — Variation of Sherwood number *versus* the initial volume of gas bubles for H_c=30 cm : ○, $I = 0$; ■, $I = 1.34$; × $I = 1.07$; ●, $I = 1.16$.

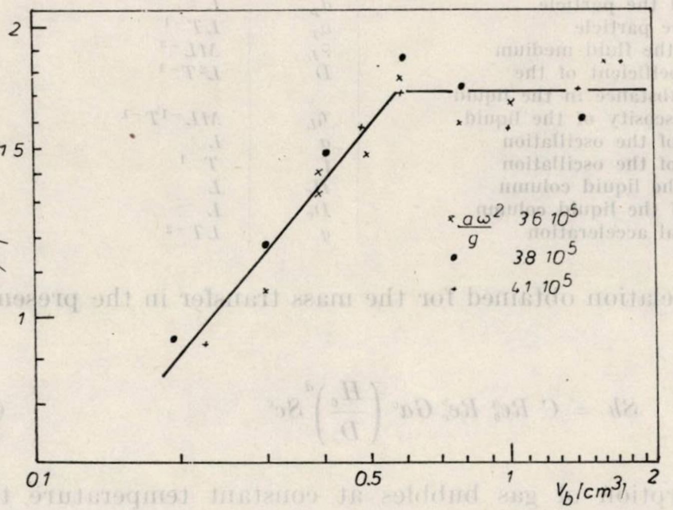

Fig. 6. — Variation of the intensification coefficient k_l'/k_l *versus* the volume of *de* gas bubbles.

The above experimental data lead to relations (2) and (3) which allow the appreciation of the partial mass transfer coefficient in the presence of ultrasonic energy, if the value k_l in the absence of ultrasonic energy is known:

$$\frac{k'}{k_l} = 2.45\, V_b^{0.7} \qquad \text{for } 0.2 < V_b < 0.6 \text{ cm}^3 \tag{2}$$

$$\frac{k'_l}{k_l} = 1.7 = \text{const.} \qquad \text{for } 0.6 < V_b < 2 \text{ cm}^3 \tag{3}$$

5. CRITERIAL RELATIONS FOR THE MASS TRANSFER IN THE PRESENCE OF OSCILLATIONS

The mass transfer from a particle to a continuous medium in the presence of oscillations depends on all factors influencing the mass transfer, and in addition on the oscillation characteristics.

The physical factors which were taken into account in the mass transfer in the presence of oscillations are given in table 2.

Table 2

Factors which influence the mass transfer coefficient k'_l in the presence of oscillations

Variable	Symbol	Dimensional formula
Diamater of the particle	d_p	L
Speed of the particle	u_r	LT^{-1}
Density of the fluid medium	ρ_L	ML^{-3}
Diffusion coefficient of the soluble substance in the liquid	D	L^2T^{-1}
Dynamic viscosity of the liquid	η_L	$ML^{-1}T^{-1}$
Amplitude of the oscillation	a	L
Frequency of the oscillation	f	T^{-1}
Height of the liquid column	H_c	L
Diameter of the liquid column	D_c	L
Gravitational acceleration	g	LT^{-2}

The criterial relation obtained for the mass transfer in the presence of oscillations is:

$$Sh = C\, Re_b^a\, Re_v^b\, Ga^c \left(\frac{H_c}{D_c}\right)^d Sc^e \tag{4}$$

For the absorption of gas bubbles at constant temperature the Schmidt number Sc is a constant and may be introduced into the constant. The values of this constant and of the exponents were determined from the experimental data obtained for the absorption of carbon dioxide in distilled water in the presence of ultrasonic energy. We used the least square fitting of relation (4) on a computer.

$$Sh = 2.24\ Re_b^{0.85}\ Re_v^{0.66}\ Ga^{-0.1} \left(\frac{H_c}{D_c}\right)^{1{,}12} \tag{5}$$

$$\text{for } Re_b < 2200$$

6. CONCLUSIONS

The correct utilisation of oscillations produced by mechanical vibrations, pulsations, sonic or ultrasonic energy, intensifies the mass transfer in the case of the systems formed by dispersed particles and a continuous fluid phase.

The intensification of the mass transfer in the presence of ultrasonic energy was determined experimentally in the absorption of carbon dioxide in distilled water. An intensification of the mass transfer was obtained ranging from 100 to 200% as a function of the magnitude of the bubble, the intensity of the dissipated ultrasonic energy in the system, and the height of the liquid column penetrated by this energy.

A criterial relation (5) was obtained for the mass transfer in the presence of ultrasonic energy.

NOTATION

a — amplitude of oscillation, cm.
d_e — equivalent diameter of spherical particle, cm.
d_p — diameter of particle, cm.
D — diffusion coefficient of gas in liquid, cm²/s.
D_c — diameter of liquid column, cm.
f — frequency of oscillation, Hz.
H_c — height of the liquid column, cm.
I — specific intensity of ultrasonic energy, W/cm².
k_g — mass transfer coefficient in the gas film, cm/s.
k'_g — mass transfer coefficient in the gas film in the presence of oscillation, cm/s.
k_l — mass transfer coefficient in the liquid film, cm/s.
k'_l — mass transfer coefficient in the presence of oscilations, cm/s.
V_b — volume of gas bubble, cm³.
V_1 — initial volume of gas bubble, cm³.
u_p — speed of the particle, cm/s.
δ — thickness of diffusion boundary layer, cm.
ρ — density of liquid, g/cm³.
τ — time, s.

η — viscosity, g/cm.s.

ν — kinematic viscosity, cm^2/s.

ω — angular velocity, rad/s.

Ga — Galileo number, $\frac{g\, d_p^3}{\nu^2}$

Re — Reynolds number, $\frac{w\, d_p\, \rho}{\eta}$

Re_v — Reynolds number for vibration, $\frac{f\, d_p\, a}{\nu}$

Re_r — Reynolds number for rotation, $\frac{\omega d_p^2}{\nu}$

Sc — Schmidt number, $\frac{\nu}{D}$

Sh — Sherwood number, $\frac{k_l d_p}{D}$

Revue Roumaine de Chimie, 22, 2, 283 – 291 (1977)

RESEARCHES IN THE TERPOLYMERIZATION FIELD. IX*)

CHEMICAL STRUCTURE – PROPERTIES CORRELATION

CR. I. SIMIONESCU, ADELAIDA LIGA and N. ASANDEI
Institute of Macromolecular Chemistry "Petru Poni" Aleea Gr. Ghica Vodă, N° 41 A,
Jassy, Romania

Received August 6, 1975

The present paper correlates the thermal behaviour of some terpolymers based on acrylonitrile, methacrylic acid and methyl methacrylate with their main structural parameters (composition and sequences distribution).

The dependence of physico-mechanical or chemical properties of a copolymer on its chemical structure is insufficiently treated because of the numerous experimental and computing difficulties. At present only the dependence of the properties on the comonomer ratios in the copolymers is studied.

The present paper tries to establish for acrylonitrile-methacrylic acid-methyl methacrylate terpolymer a correlation between structural factors (represented by composition and sequences distribution) and properties, particularly thermal behaviour. The results of this study will complete and clarify some previous conclusions.[1]

For this purpose, the behaviours of terpolymers, of physical mixtures (with the same composition as the terpolymers) and of homopolymers were compared in thermal-oxidative degradation conditions. The results of the study made on homopolymers and terpolymers, neglecting the influence of molecular weight on degradation rate, are presented in Table 1.

The comparison of the terpolymers and physical mixtures is represented in Table 2 together with the data referring to the theoretical mixtures. It is observed that in every case $\Delta W_{T,\,\mathrm{theor}} > \Delta W_{T,\,\mathrm{real}}$ meaning that the degradation of real physical mixtures is retarded due to interactions between homopolymers.

By means of functional groups, the real mixtures form more resistant structures from the thermal point of view. From the same table the following general order is established :

$$\Delta\ W_{T,\,\mathrm{theor.}} > \Delta W_{T,\,\mathrm{real}} > \Delta\ W_{T,\,\mathrm{terpolymers}}$$

---

*) Part VIII: see ref. 2.

[1] N. ASANDEI, A. LIGA and A. BIRO, *European Polymer J.*, 7, 317 (1971).

Table 1

Weight losses and activation energies for homo *) – and terpolymers **) at the temperature corresponding to maximum degradation rate

Sample	Degrad. step	Temper. range, °	Temper. mx. degr., °	ΔW %	n	*E* kcal/mol
PAN	I	130–268	170	8	1.6	18.5
	II	268–400	330	11	2	52
	III	400–720	595	81	2	33
PMAc	I	90–327	205	57	0.4	14.9
	II	327–463	463	38	0.5	44.7
	III	463–570	—	5	—	—
PMMA	I	100–220	178	18	2.8	26.4
	II	220–332	288	54	1.8	20.7
	III	332–570	388	28	0.75	27.4
Terpolymer I	I	130–278	211	18	2.4	23.6
	II	278–465	369	57	2.2	37.3
	III	465–600	548	25	1.1	42.5
Terpolymer II	I	80–322	305	14	0	2.9
	II	322–458	393	63	1.3	40
	III	458–552	535	23	0.3	25.4
Terpolymer III	I	100–260	178	5.8	1.6	22.6
	II	260–430	393	64	0.75	26.2
	III	430–563	520	13	0.7	27.4

* PAN – polyacrylonitrile; PMAc – poly(methacrylic acid); PMMA – poly(methyl methacrylate).

**) Terpolymers I, II and III represent the products with predominant content of acrylonitrile (M_1), methacrylic acid (M_2) and methyl methacrylate (M_3), respectively.

Table 2

Weight losses at various temperatures for the theoretical and real physical mixtures of homopolymers and for the terpolymers

Predominant homopolymer	Temp. °C	$\Delta W^{a)}_{T,\,\mathrm{theor.}}$ %	$\Delta W_{T,\,\mathrm{real}}$ %	$\Delta W_{T,\mathrm{terpolym.}}$ %
PAN	200	16.6	13.4	6.5
	300	33.6	21.0	20.0
	400	51.0	40.0	58.0
PMAc	200	23.7	14.7	3
	300	46.7	28.2	13
	400	86.4	45.6	55
PMMA	200	14.7	9.1	5
	300	50.8	41.7	16
	400	83	79.2	71

a) Calculated with additivity relation; [1]

$$\Delta W_{T,\,\mathrm{theor}} = \Delta W_{T,\mathrm{PAN}} \cdot P_{\mathrm{PAN}} + \Delta W_{T,\mathrm{PMAc}} \cdot P_{\mathrm{PMAc}} + \Delta W_{T,\mathrm{PMMA}} \cdot P_{\mathrm{PMMA}}$$

where

$\Delta W_{T,\,\mathrm{theor}}$ – weight loss of the theoretical physical mixture up to T temperature;

P – % homopolymer in mixture;

$\Delta W_{T,\,\mathrm{PAN}}$; $\Delta W_{T,\mathrm{PMAc}}$; $\Delta W_{T,\mathrm{PMMA}}$ – weight losses up to the degradation T temperature of homopolymers.

This order is maintained up to approximatively 320°, after which the degradation of terpolymers occurs at higher rate. The results from Tables 1 and 2 suggest that the discussion on the thermostability of homo- and terpolymers, respectively, could be centered on three criteria: a) the initial temperature of degradation; b) the value of weight losses during a common interval of temperature; c) the temperature at which the maximum degradation is found.

Regarding the homopolymers, all three ways of tackling the problem lead to the same order of stability, i.e.:

Polyacrylonitrile > Poly(methyl methacrylate) > Poly(methacrylic acid)

The terpolymer study, based on these three points of view and as a function of the predominant homopolymer, presents a reverse order regarding the weight losses within the same temperature range (criterion b) and the temperature at which the maximum degradation is found (criterion c). Thus, while for the temperature at which degradation begins (criterion a), the order of thermostability is that imposed by the predominant homopolymer, namely

Terpolymer I > Terpolymer III > Terpolymer II,

Table 2 shows that, according to the values of weight losses, the order changes unexpectedly in favour of terpolymer II (predominant content of methacrylic acid). The temperature of maximum degradation also pleads for this order (Table 1, Fig. 1):

Terpolymer II > Terpolymer III > Terpolymer I.

This surprising behaviour, not corresponding to the predominant homopolymer, must be correlated with other structural factors, the most important being the distribution of comonomer units in the macromolecular chain, which favours interactions of certain types of adjacent functional groups.

In this paper we shall try to interpret the behaviour of the three terpolymers as a function of the chemical structure of each of them.

Terpolymer I. Table 1 and Fig. 1 show that this terpolymer has a similar behaviour as polyacrylonitrile concerning the initial degradation temperature (~130°). This process takes place much more rapidly in the terpolymer, so that in all the three steps of degradation, within limited intervals of temperature, the terpolymer shows greater losses than the homopolymer.

In the terpolymer, as result of the preferential addition of the monomers methacrylic acid and methyl methacrylate to the acrylonitrile radical during copolymerization, long sequences of acrylonitrile are missing; in consequence the interaction of adjacent CN groups is inhibited and the cyclizations which lead to the known thermal stability of PAN do not occur. According to structural calculations[2], the acrylonitrile units are present in this terpolymer as predominantly isolated units (the maximum value of mean sequence length is $\bar{n}_{mx} = 2$), meaning that most acrylonitrile units (M_1) are isolated among units of methacrylic acid (M_2) or methyl methacrylate (M_3). Most acrylonitrile units (about 60%) are to be found

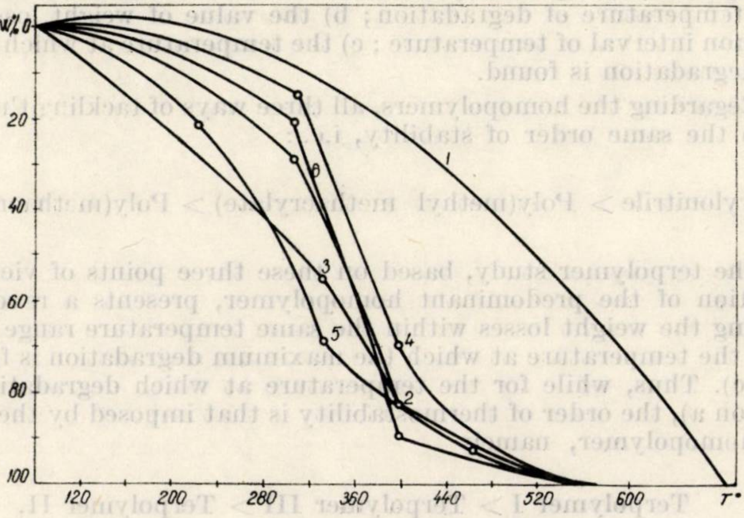

Fig. 1. — The diagram of weight losses against temperature for homopolymers and terpolymers.
1 — Polyacrylonitrile; 2 — Terpolymer I; 3 — Poly(methacrylic acid); 4 — Terpolymer II; 5 — Poly(methyl methacrylate); 6 — Terpolymer III.

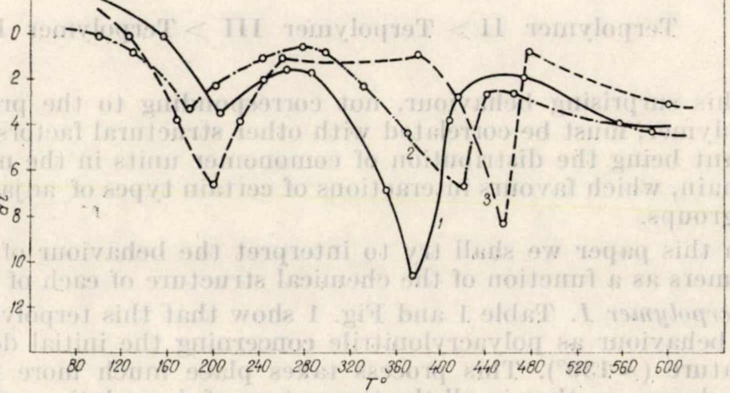

Fig. 2. — Variation of the decomposition rate of the terpolymer I depending on temperature.
1 — Terpolymer I; 2 — Physical mixture; 3 — Polyacrylonitrile.

---

[2] Cr. I. Simionescu and A. Liga, *Rev. Roumaine Chim.*, **22**, 000 (1977).

in sequences $M_2M_1M_2$ or $M_2M_1M_3$ (Tab. 3). These structures, together with $M_1M_1M_2$ (about 24%), are responsible for the different behaviour of this terpolymer compared with the PAN homopolymer.

The highest weight loss of this copolymer is recorded at 363°, i.e. about 100° lower than for the homopolymer (Fig. 2).

The behaviour of the physical mixtures is intermediate between that of the homopolymer and that of the terpolymer ; this fact underlines both the role of the chemical links and of the average length of the acrylonitrile sequences in assigning thermal properties to the three products.

Terpolymer II. Though the degradation begins at a lower temperature than in the corresponding homopolymer, the first stage is characterized by much smaller losses (14.3% at 305°, in comparison with 57% at 205°, see Table 1). This fact is due to the shortening of consecutive sequences of methacrylic acid, corresponding to the reduction of the probability of the existence of long sequences of acid (in comparison with the homopolymer), because of addition of acrylonitrile and methyl methacrylate units. The mean length of methacrylic acid sequences is given by $\bar{n}_2 = 2.5$; from the total units of this monomer, only about 30% are linked in the triad $M_2M_2M_2$ (Table 3), while 27% are found in the triad $M_2M_2M_1$ and about 22% in $M_2M_2M_3$. The rest (about 20%) of methacrylic acid units form the centre of three other types of triads which, being fewer, have a less significant role. The units of methacrylic acid belonging to various sequences are separated by methyl methacrylate units and especially by acrylonitrile units. As shown in Table 3, the frequency of acrylonitrile on the macromolecular chain is about twice or three times greater than that of methyl methacrylate.

In inner sequences $M_2M_2M_1$ or $M_2M_1M_2$, some interactions of functional groups may occur

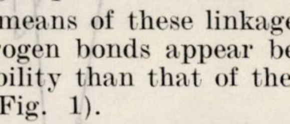

leading to the formation of cycles and increase of thermostability in the first stage, in comparison with the homopolymer. Intramolecular links C—O—C can also appear after water elimination between two neighbouring carboxylic groups in the same chain.

The cyclization by means of these linkages is intensified at higher temperatures, when hydrogen bonds appear between chains, the result being higher thermal stability than that of the other terpolymers in all the degradation steps (Fig. 1).

The activation energy in the principal stage of the degradation is $E_a = 40$ Kcal/mol, near the value corresponding to reticulated structures of poly(methacrylic acid). The maximum degradation rate is realised at 393° i.e. about 30° higher than in the terpolymer with acrylonitrile (Fig. 3).

Terpolymer III. The presence of acrylonitrile affects the depolymerization of poly(methyl methacrylate) in many ways. At first it inhibits almost completely monomer production at 220° by blocking of the chain ends.

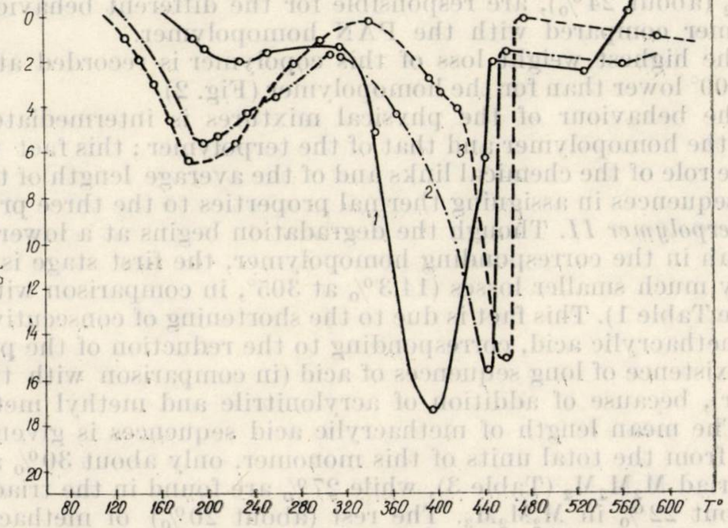

Fig. 3. — Variation of the decomposition rate of the terpolymer II depending on temperature.

1 — Terpolymer II; 2 — Physical mixture; 3 — Poly(methacrylic acid).

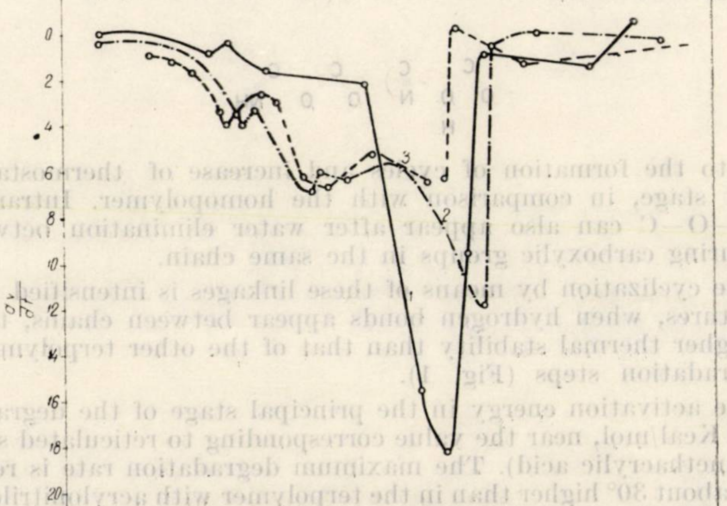

Fig. 4. — Variation of the decomposition rate of the terpolymer III depending on temperature.

1. Terpolymer III; 2 — Physical mixture; 3 — Poly(methyl methacrylate).

The degradation occurs in the first stage by a process initiated at random, consequently with a much smaller speed than in homopolymer. Indeed, at 300° the weight losses reach 16.5% in terpolymer as compared to 54% in poly(methyl methacrylate). The maximum loss of 64% is found at 393° as compared with 288° in homopolymer (Fig. 4).

The behaviour of terpolymer III with predominant methyl methacrylate content is affected especially by the presence of acrylonitrile and less by that of methacrylic acid. The structural calculations[2] show that besides the triads $M_3M_3M_3$ (37%), those which contain acrylonitrile ($M_3M_3M_1$) are similar in number (37.5%), while the $M_3M_3M_2$ sequences which contain methacrylic acid represent only 10%. The probability that the continuous sequences of methyl methacrylate should be interrupted by an acrylonitrile unit is about two times greater than the same probability regarding methacrylic acid (Table 3, see N_i). At high temperatures, terpolymer degradation becomes efficient by the acrylonitrile units.

To conclude, the data from Tables 1 — 3 and Figures 1 — 4 show that, by including comonomers, increasing thermostability is obtained, comparing the terpolymers with predominant content of methacrylic acid and methyl methacrylate to corresponding homopolymers; on the other hand, decreasing thermal stability in comparison with the homopolymer is found when acrylonitrile is predominant in terpolymer. In both situations the reason is the disturbance of the chemical structure peculiar to homopolymers, i.e. the interruption of homosequences formed from the predominant monomer, by the addition the two comonomers.

The comparative study of the three terpolymers supplies us with information about the way in which their behaviour may be affected by the proportion in which comonomers are present and, implicitly, by their chain distribution, both being dependent on the feed composition of monomers and on their reactivities. As under identical conditions of reaction the values of the reactivities remain unchanged, for the same system every feature represents theoretically a variable dependent only on the initial reactant ratios.

Practically, the problem of obtaining copolymers with controlled properties may be realised by choosing both the corresponding feed composition and the synthesis method, which will lead to the optimum microstructure of the chains. For example, in the present case of acrylonitrile-methacrylic acid-methyl methacrylate terpolymer, the thermal stability of the PAN and its fibre-forming characteristics may be obtained under the conditions in which acrylonitrile is present in maximum proportion and as long sequences; this means the use of an initial comonomer ratio which is rich in acrylonitrile, or, possibly, the application of a prepolymerization method of acrylonitrile which should provide long sequences in competition with the more reactive monomers, methacrylic acid and methyl methacrylate.

Table

Correlations between chemical structure and thermal stability

Polymer	Initial chemical structure of polymers								
	Average composition % mol.			Predominant sequence	Sequence concentration mole %	$\bar{n}_i$			
	M_1	M_2	M_3			$\bar{n}_1$	$\bar{n}_2$	$\bar{n}_3$	N_1
PAN	100	0	0	$(M_1)_{n1}$	100	$\bar{n}_1$	—	—	—
Terpolymer I	60	35.6	4.4	$\left.\begin{matrix}-M_2-M_1-M_2-\\-M_2-M_1-M_3-\end{matrix}\right\}$ $-M_1-M_1-M_2-$	60 24	1.5	1	1	1
PMAc	0	100	0	$(M_2)_{n_2}$	100	—	$\bar{n}_2$	—	—
Terpolymer II	27	67	6	$-M_2-M_2-M_2-$ $-M_2-M_2-M_1-$ $-M_2-M_2-M_3-$	30 27 22	1	2.5	1	3.5
PMMA	0	0	100	$(M_3)_{n_3}$	100	—	—	$\bar{n}_3$	—
Terpolymer III	20	13	67	$-M_3-M_3-M_3-$ $-M_3-M_3-M_1-$ $-M_3-M_3-M_2-$	37 37.5 10	1	1	3	3.7

M_1 = acrylonitrile ; M_2 = methacrylic acid ; M_3 = methyl methacrylate

$\bar{n}_i$ = mean sequence length ; N_i = average number of m_j and m_k units comprised between two successive units of m_is

---

[3] C. Tosi, *European Polymer J.*, **6**, 161 (1970).

3

of AN – MAc – MMA terpolymer of different composition

N_i		Degradation step and the corresponding temperature °C	Weight losses Δw% —	Chemical structure realised by heating	Observations
N_2	N_3				
—	—	I 100–268 II 268–400 III 400–720	8 11 81	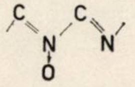	The cyclization determines the stabilization up to 600°
2	18	I 130–278 II 278–465 III 465–600	18.2 57.9 24	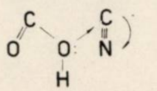	Initially, inhibits the degradation process; over 130° the thermostability decreases, since the cyclization is hindered. The $\bar{n}_M$ of AN decreases
—	—	I 90–327 II 327–463 III 463–570	57 38 5	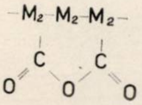	Rapid depolymerization in the first stage; certain stabilisation over 200°
1	8	I 80–322 II 322–458 III 458–552	14,3 63 22,4	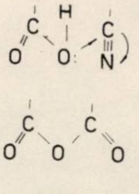 bonds	The sequences of methacrylic acid are shortened, the depolymerization probability decreases. Provides stability up to 300°
—	—	I 100–220 II 220–332 III 332–570	18 54 28	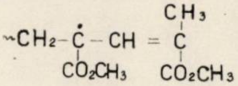 $\sim CH_2-\dot{C}(CO_2CH_3)-CH=C(CH_3)(CO_2CH_3)$ unstable at 220°	Determines a rapid depolymerization up to 270° (50%)
6	1.5	I 100–260 II 260–430 III 430–563	5,8 64 13	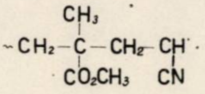 $\sim CH_2-C(CH_3)(CO_2CH_3)-CH_2-\dot{C}H(CN)\cdot$	Inhibits monomer production by unsaturated structures. At high temperatures depropagation passes efficiently through the AN units

Revue Roumaine de Chimie, **22**, 2, 293 – 300 (1977)

STUDY OF THE RECTIFICATION PROPERTIES OF HETEROGENEOUS MEMBRANES. V*

BEHAVIOUR OF THE CELLULOID MEMBRANE SYSTEMS: CATIONITE-Ag + ANIONITE-S, CATIONITE-Ag + ANIONITE-Cl, CATIONITE-Hg + ANIONITE-Br

C. LITEANU*, GH. RĂDULESCU**, GY. STEINBRECHER***, A. MASCAŞ**
and M. PREDA***

* University "Babeş-Bolyai" Cluj-Napoca, str. Arany J. N° 11
** Pedagogical Institute Oradea, str. Armata Roşie N° 5
***University of Craiova, Calea Bucureşti N° 165

Received February 22, 1975

Based on the analogy between semiconductors with $p - n$ junction and the contact of opposite charge ionitic membranes, the paper elaborates on the rectification properties of some ion-exchanger membranes. The characteristic curve, the rectification coefficient φ, the rectification output R_r and the frequency influence have been studied to characterize the rectification effect in systems formed of R-Ag/R-S, R-Ag/R-Cl and R-Hg/R-Br Based on I – V direct current characteristic curves the rectification capacity is shown to increase considerably with the increase in the stability of the compound that may form by the contact of the two membranes.

The rectification phenomenon of the current through membranes has been reported in a number of publications having an experimental as well as a theoretical character.[1-33]

---

* Part IV. Gh. Rădulescu, C. Liteanu, and G. Steinbrecher, *J. Chim. phys.*, **68**, 1412 (1971).

[1] Gh. Rădulescu, C. Liteanu and E. Marinescu *Studia Univ. Babeş-Bolyai*, **14** (2), 33(1969).

[2] H. Reiss, *J. Chem. Phys.*, **21**, 1209 (1953).

[3] C. S. Fuller *Rec. Chem. Progr.*, **17**, 75 (1956).

[4] B. Lovrecek, A. Despic and J. O'M. Bockris, *J. Phys. Chem.*, **63**, 750 (1959).

[5] S. Schreiber, *Compt. rend.*, **264** (C), 652 (1967).

[6] V. N. Maslov and A. V. Ovodova, *Zhur. fiz. Khim.*, **34**, 413 (1960).

[7] B. Lovrecek and B. Kunst, *Nature*, **189**, 804 (1961).

[8] B. Lovrecek and B. Kunst, *Croat. Chem. Acta*, **34**, 137, 219 (1962); **35**, 7 (1963).

[9] J. Oshida and Y. Sugunuma, *Bull. Kobayashi Inst. physic. Res.*, **13**, 96(1963); *Chem. Abstr.*, **62**, 7408 (1965).

[10] M. Seno and T. Yamabe, *Bull. Chem. Soc. Japan*, **37**, 668 (1964).

[11] H. I. Friedlander, *J. Polymer Sci. Ser. C*, **4**, 1447 (1969).

[12] P. Läuger, *Ber. Bunsengesellschaft Phys. Chem.*, **68**, 534 (1964).

[13] S. Oshki, *J. Phys. Soc. Japan*, **20**, 1674 (1965).

Using the analogy made by Reiss[2] and Fuller[3] between the electron excess and deficit in Si and Ge containing impurities which correspond to semiconductors of type *n* and *p* on the one hand, and between the proton excess and deficit corresponding to acidic or basic solutions on the other hand, Lovrececk, Despic and Bockris [4] have experimentally shown the possible rectification of the alternating electric current by means of type *p* and *n* electrolyte junctions.

A *p* — *n* type electrolyte junction may consist of a two-compartment device. One of them contains an electrolyte with a slightly mobile anion and mobile protons (a polyacidic or a cationic R—H type membrane) whereas the other compartment of the system contains an electrolyte with a slightly mobile cation and mobile hydroxyl ions (a polybase or an anionitic R—OH type membrane).

In general, such a junction may be obtained of whatever phase possessing a slightly mobile anion and a mobile cation, associated with an alternate phase possessing a slightly mobile cation and a mobile anion.

If the two compartments contain liquid phases, the construction of the contact separating them will play an important role with regard to rectification properties, as was shown by Schreiber.[5]

A series of papers have been published latelay on the rectification properties of bipolar double membranes, systems formed by joining an anionitic membrane with a cationitic one. Such a problem is of interest due to the analogy between both artificial membranes and biological ones and bipolar membranes and semiconductor diodes.[16]

The experimental works concerned with the rectification effect by membranes have used H^+ and OH^- ions as mobile ions, water molecules being formed at the membrane interface hence a sparingly dissociable product.

---

[14] A. I. Tchernova, I. A. Melnik, V. I. Maslov and Iu. A. Zotov, *Doklady Akad. Nauk S.S.S.R.*, **174**, 895 (1967).

[15] K. Shimizu, M. Seno and H. Nozaki, *Bull. Chem. Soc. Japan*, **41**, 803 (1968).

[16] A. Mauro, *Biophys. J.*, **2**, 179 (1962).

[17] A. Katchalski and O. Kedem, *Biophys. J.*, **2**, 553 (1962).

[18] C. Liteanu and Gh. Rădulescu *Rev. Roumaine Chim.*, **14**, 1257 (1969).

[19] C. Forgács and G. Stein, *Israel J. Chem.*, **2**, 209 (1964).

[20] C. Liteanu, Gh. Rădulescu and Cs. Jámbor, *Anal. Sti. Univ. Craiova*, **1**, 175 (1970).

[21] Gh. Rădulescu and C. Liteanu. *Anal. Sti. Univ. Craiova*. **1**, 181 (1970),

[22] V. M. Maslov, Iu. A. Zotov, A. I. Tchernova, I. A. Melciuk, and M. I. Nuralova, *Doklady Akad. Nauk S.S.S.R.*, **183**, 1371 (1968).

[23] T. Teorell, *Proc. Soc. exp. Biol. Med.*, **33**, 282 (1953).

[24] K. H. Meyer and F. F. Sievers *Helv. Chim. Acta*, **19**, 649 (1936).

[25] Gh. Rădulescu, C. Liteanu and G. Steimbrecher, *J. Chim. phys.*, **68**, 1412 (1971).

[26] Gh. Rădulescu, C. Liteanu and G. Steimbrecher, *J. Chim. phys.*, **68**, 1405 (1971).

[27] N. S. Lidorenko, V. Ya. Bartenev and G. A. Dameshek, *Doklady Akad. Nauk. S.S.S.R.*, **205**, 1 (1972).

[28] N. S. Lidorenko and A. L. Muler, *Doklady Akad. Nauk S.S.S.R* ..**187**, 1 (1969).

[29] L.L. Odinets, *Zhur. fiz. Khim.*, **35**, 6(1961).

[30] G. Bahr, *Ber. Bunsengesellschaft Phys. Chem.*, **71**, 8 (1967).

[31] D. Woermann, *Ber Bunsengesellschaft Phys. Chem.*, **71**, 1 (1967).

[32] U. F. Franck, *Ber. Bunsengesellschaft Phys. Chem.*, **71**, 8 (1967).

[33] G. Kolf, *Ber. Bunsengesellschaft Phys. Chem.*, **71**, 8 (1967).

It is known that in the case of semiconductors, the equation below holds both for the direct and for the inverse region :

$$I = I_0 \left(\exp \frac{eV}{kT} - 1 \right) \tag{1}$$

where I stands for the total junction current and I_0 represents the sum of the two field currents, k being Boltzman's constant ($k = 1.38 \times 10^{-23}$ J. grd.$^{-1}$) and e — the elementary charge ($e = 1.602 \times 10^{-19}$ C).

For $\frac{kT}{e} > 0.026$ V (at room temperature), the parenthesized unit of equation (1) may be neglected, the equation becoming :

$$I = I_0 \exp \left(\frac{eV}{kT} \right) \tag{2}$$

Considering that equation (2) describes the theoretical characteristic under the above conditions and comparing it to the experimental characteristic which may be usually expressed in the form :[20]

$$I = I_0 \exp \left(\frac{eV}{\eta kT} \right) \tag{3}$$

it is possible to estimate the deviation from the theoretical predictions since the deviation of the η coefficient from the unity indicates the deviation of the experimental characteristic from the ideal rectification characteristic.

A plot of $\ln I = f(V)$, respectively

$$\ln I = \ln I_0 + \frac{e}{\eta kT} V \tag{4}$$

for the considered membrane system enables the determination of the η value.

Similarly, by applying equation [26] to such a system with "ionic" junction :

$$I = A V e^{-Vq/kT} \tag{5}$$

and plotting $\log I/V = f(V)$, this relation may be found to describe with a good approximation the rectification phenomenon by bipolar double membrane, a fact which confirms the correctness of the assumption underlying the theoretical background of this relation [26] and its aplicability in $p - n$ "ionic" junction systems.

The present paper studies the rectification effect obtained with heterogeneous double membranes at whose interface sparingly dissociable products are formed such as silver or mercury halides and silver sulphide, respectively.

The membranes were prepared using Allassion CSNA cationite of a R—Ag and R—Hg type, and Dowex-1 anionite of a R—Cl, R—Br and R—S type. The membrane support was formed of celluloid. The ion-exchange resin was brought to a fine granulation passing through a 0.10 mm sieve and was then mixed with a solution of celluloid dissolved in acetone. When the mixture was considered to be homogeneous it was poured onto a glass plate and dried, readily detaching the membrane of the glass plate thereafter. The membrane used was 0.20 mm thick.

Membranes prepared in the medium described above are soaked in water and then placed between two platinum electrodes [10] with 1 cm^2 surface. The system is closed by paraffining in order to provide a constant humidity which is important for obtaining good rectification effects.[1, 18, 20]

1. THE CATIONITE-AG + ANIONITE+S SYSTEM

Fig. 1 plots the I — V direct current characteristic curve showing that a 14 × 10^3 μA value was obtained for I_d at a 10 volts maximum applied tension, which could obviously not be represented in the diagram, and that a 56 μA value was obtained for the I_i reverse current. Considering these magnitudes, it is possible to infer from the current-tension curve the values for R_d, R_i, $\varphi = I_d/I_i$ and for the R_r rectification efficiency [20] calculated by relation :

$$R_r = \frac{I_d - I_i}{I_d} 100 \tag{6}$$

The values obtained are listed in Table 1 and prove that the system has good rectification properties.

Table 1

The values of rectification parameters of some heterogeneous membrane systems

Parameters	Membrane system		
	R—Ag/R—S	R—Ag/R—Cl	R—Hg/R—Br
R_d	7×10^2	4×10^4	3×10^4
R_i	1.7×10^5	14×10^5	1×10^5
φ	250	40	5.5
R_r (%)	99.6	97	81.9
η	40(V < 10) 193(V > 10)	39(V < 4) 88(V > 4)	48(V < 5) 124(V > 5)

The diagram in fig. 10 a illustrates the shape of the rectified curve on the oscillograph and the 10 volts sinusoidal tension applied to the system at 50 Hz frequency.

Fig. 1. — I — V direct-current characteristic curve system for the R—Ag/R—S system.

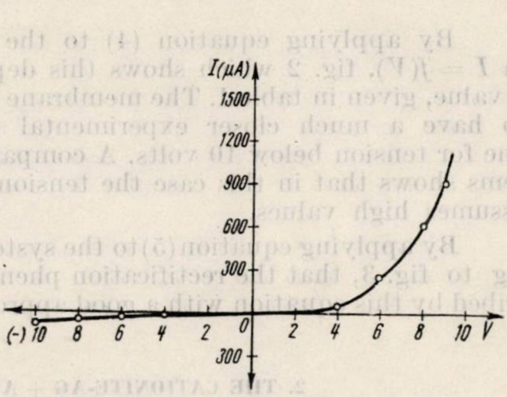

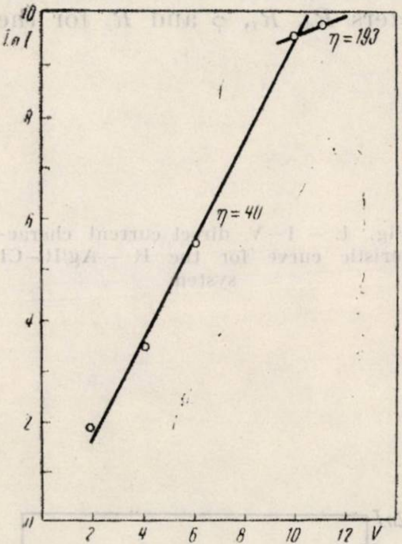

Fig. 2. — ln I = $f(V)$ dependence for the R—Ag/R—S system.

Fig. 3. — log I/V = $f(V)$ dependence for the R—Ag/R—S system.

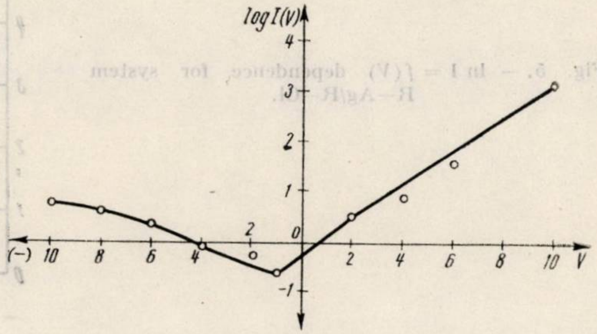

By applying equation (4) to the membrane system and plotting $\ln I = f(V)$, fig. 2 which shows this dependence, helps to determine the η value, given in table I. The membrane system under study is thus found to have a much closer experimental characteristic to the theoretical one for tension below 10 volts. A comparison with other investigated systems shows that in this case the tension for which the deviation is small assumes high values.

By applying equation (5) to the system and plotting, it results, according to fig. 3, that the rectification phenomenon for such a system is described by this equation with a good approximation.

2. THE CATIONITE-AG + ANIONITE-CL SYSTEM

The procedure applied was analogous to the preceding systems. Fig. 4 exhibits the I —V direct current characteristic curve which was used for calculating the values of parameters R_d, R_i, φ and R_r for the

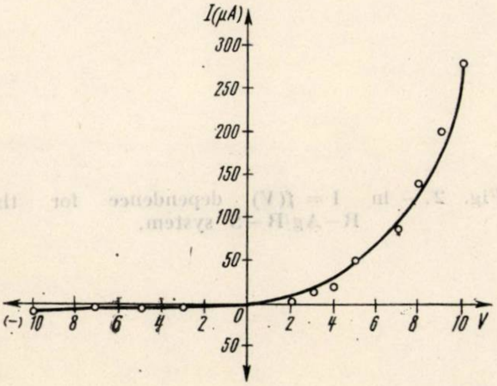

Fig. 4. — I—V direct current characteristic curve for the R — Ag/R—Cl system

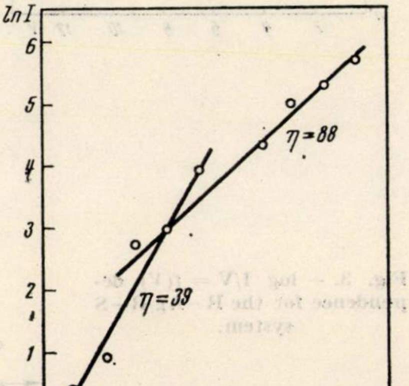

Fig. 5. — ln I = $f(V)$ dependence for system R—Ag/R—Cl.

10 volts maximum tension applied to the system. The values obtained are listed in table 1.

The diagram of fig. 10 b illustrates the shape of the rectified curve on the oscillograph and the 10 volts sinusoidal tension applied to the system at 50 Hz frequency.

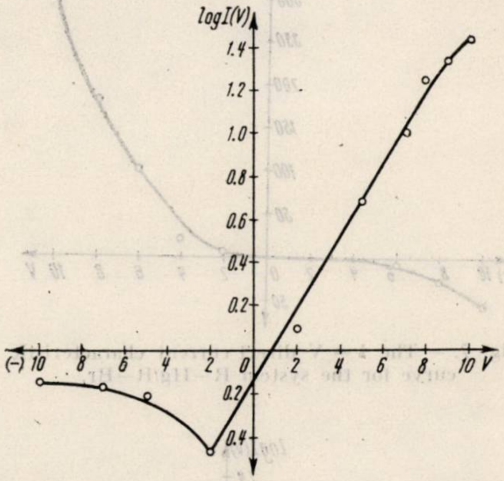

Fig. 6. — log I/V = $f(V)$ dependence for the system R—Ag/R—Cl.

Applying equation (4) to the system, the η values may be determined from fig. 5 and are listed in table 1.

Considering equation (5), it results from fig. 6 that the rectification phenomenon by this system is described by the mentioned equation with a good approximation.

3. THE CATIONITE-Hg + ANIONITE-Br SYSTEM

The study of this system shows a similar behaviour to that of the other systems analyzed above.

Fig. 7 plots the current-tension curve used for calculating the values of parameters R_d, R_i, φ and R_r listed in table 1 for the 10 volts maximum applied tension.

The diagram of fig. 10 c illustrates the shape of the rectified curve on the oscillograph and the 10 volts sinusoidal tension applied to the system at 50 Hz frequency.

By applying equation (4) to the system, one obtaines from fig. 8 the η values which are listed in table 1.

Considering equation (5), fig. 9 shows that in this case too, the phenomenon is described by this equation with a good approximation.

CONCLUSIONS

An examination of data included in table 1 shows that the rectification process occurs with the formation of a sparingly dissociated compound. For this reasons, the rectification parameters should by correlated to the stability of the compound which may form.

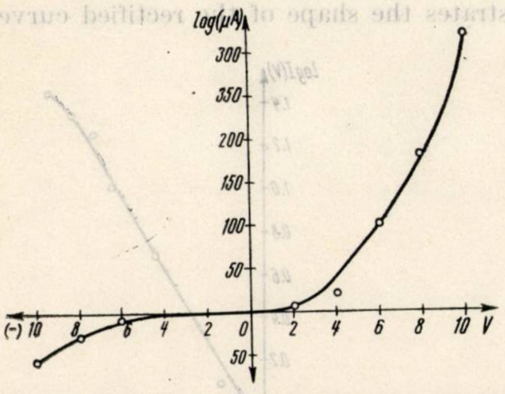

Fig. 7. — The I — V direct current characteristic curve for the system R—Hg/R—Br.

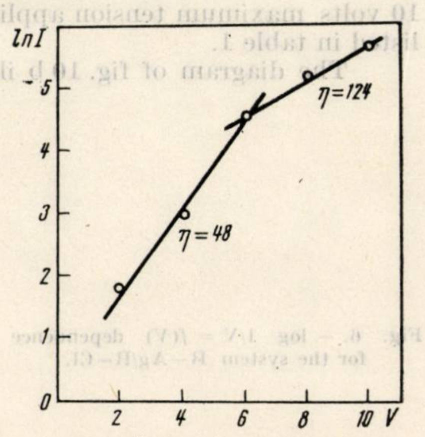

Fig. 8. — ln I = $f(V)$ dependence for the R—Hg/R—Br system.

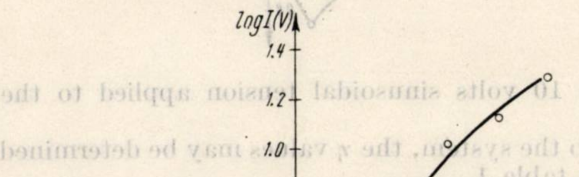

Fig. 9. — log I/V = $f(V)$ dependence for the R — Hg/R — Br system.

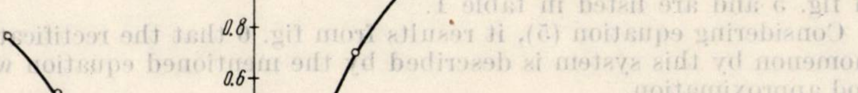

a b c

Fig. 10. — Rectified curve (1) obtained on the oscillograph and the sinusoidal 10 volts tension (2) applied at 50 Hz frequency for systems : *a*) R — Ag/R—S, *b*) R—Ag/R—Cl, *c*) R—Hg/R—Br.

Revue Roumaine de Chimie, 22, 2, 301 – 304 (1977)

THEORETICAL STUDY OF THE ACIDITY OF SOME ORGANIC REAGENTS

GR. POPA and S. MOLDOVEANU
I.P.B., Institute of Chemistry, Faculty of Chemistry, Str. Splaiul Independenţei 89, Bucureşti

Received February 3, 1975

This paper deals with the relation between pK_a of some weak organic acids and the charge density in the molecule. A linear dependence has been theoretically found and then proved on four phenols. For the computation of charge density, an ω technique method has been used.

The acidity of organic reagents which are used in analytical chemistry is an important factor which governs the equilibrium of the chemical reactions.

Taking for example a reagent for a metal M^+, which is a weak acid LH, whose acidity constant is K_a, we can write the equilibrium :

$$LH + M^+ \overset{K}{\rightleftarrows} LM + H^+$$

and the expression for K :

$$K = \frac{[LM][H^+]}{[LH][M^+]} = K_s K_a \tag{1}$$

where

$$K_s = \frac{[LM]}{[M^+][L^-]} \tag{2}$$

and

$$K_a = \frac{[H^+][L^-]}{[LH]} \tag{3}$$

A theoretical study of K_s is rather difficult, but a study of K_a is a feasible problem, using some approximations and limiting ourselves only to some organic reagents. So, in this paper we deal with the problem of the relation between the charge density in an organic reagent which contains delocalised π and n electrons, and its acidity, namely its K_a.[1]

---

[1] A. Albert, R. Goldacre and J. Phillip, *J. Chem. Soc.*, **1948**, 2240.

Considering the equilibrium :

$$LH \overset{K}{\rightleftarrows} H^+ + L^-$$

we have :

$$RT \ln K_a = -\Delta G \tag{4}$$

or using the approximation

$$\Delta G \simeq \mathcal{N} \Delta E + \Delta G_{\mathrm{solv}} - T \Delta S \tag{5}$$

where $\mathcal{N}$ is Avogadro's number, ΔE is the variation of the energy of the system due to the reaction, apart from solvation, ΔS is the variation of the entropy of the system due to the reaction, apart from the solvation and ΔG_{solv} is the variation of the free enthalpy of the system due to the solvation, following the reaction, we have :

$$RT \ln K_a \simeq (\mathcal{N} \Delta E + \Delta G_{\mathrm{solv}} - T \Delta S)$$

Taking now $\Delta S \simeq 0$ and $\Delta E \simeq \Delta E^{\pi}$ for those molecules with delocalised electrons, we have :

$$\Delta G \simeq \mathcal{N} \Delta E^{\pi} + \Delta G_{\mathrm{solv}} \tag{5'}$$

or

$$\ln K_a \simeq -\frac{\Delta E^{\pi}}{kT} - \frac{\Delta G_{\mathrm{solv}}}{RT}$$

and

$$pK_a = \frac{1}{2.302} \cdot \left(\frac{\Delta E^{\pi}}{kT} + \frac{\Delta G_{\mathrm{solv}}}{RT} \right) \tag{6}$$

where k is Boltzmann's constant.

For ΔE^{π} we can now use a formula [2] which is obtained by using the ω technique for the computation of energy in organic molecules with delocalised electrons, namely :

$$\Delta E^{\pi} \simeq \sum_j n_j c_{1j}^2 \Delta \alpha_1 + \sum_j n_j c_{2j}^2 \Delta \alpha_2 + \ldots + 2 \sum_j n_j c_{1j} c_{2j} \Delta \beta_{12} + \ldots \tag{7}$$

where

$$\alpha_{\mu} = -11.54 + (1 - Q_A) \cdot \omega_A \cdot (-2.8)\ eV$$

$$Q_A = \sum_{\mu} q_{\mu}$$

---

[2] A. Streitwieser Jr. "Molecular Orbital Theory for Organic Chemists", J. Wiley pub. Co., New York, 1962.

which is the charge on A centre in the molecule,

$$q_{\mu} = \sum_{j} n_j c_{\mu j}^2$$

which is the charge on μ orbital,

$$\omega_A = \omega \cdot h_A$$

$$\omega \simeq 1.4$$

which is a parameter in ω technique

$$\beta_{\mu\nu} = k_{\mu\nu}\beta$$

$$\beta \simeq -2.8\,eV$$

and where h_A and $k_{\mu\nu}$ are parameters[3] used for heteroatoms in the mentioned method for energy computation.

Using formula (7) we can obtain for ΔE^{π} in the case in which the hydrogen atom is bound by the A atom in the organic molecule and supposing that only the energy of delocalised electrons are modified :

$$\Delta E^{\pi} \simeq q_1 \Delta\alpha_1 + q_2 \Delta\alpha_2 + \dots \tag{8}$$

$$\Delta\alpha_i \simeq 2.8\,(\omega h_A \cdot \Delta Q_A)$$

$$\Delta E^{\pi} \simeq 2.8 \sum_{i \in A} q_i\,(\omega h_A \Delta Q_A)$$

$$\Delta E^{\pi} \simeq 4\,Q_A h_A \tag{9}$$

Therefore :

$$pK_a \simeq \frac{4\,h_A}{2.302\,kT}\,Q_A + \frac{G_{\text{solv}}}{2.302\,RT} \tag{10}$$

In order to prove formula (10), the computations have been achieved by the method of LCAO-MO type, ω technique, for some phenols. These computations have been carried out using a FORTRAN program for ω technique obtained by QCPE. The program has been run using a IBM 360/30 computer*.

---

* The program was run in the Computing Centre of the University of Bucharest.

[3] G. W. Wheland and D. E. Mann, *J. Chem. Phys.*, **17**, 24 (1949).

In these computations we choose the value $h_o = 0.15$ and $k_{C-o} = 0.8$, formula (11) being in this case :

$$pK_a = 10.1460\, Q_A + 0.734\, \Delta\, G_{\mathrm{solv}} \tag{11}$$

The results of computation of Q_A and the experimental value of pK_a[4,5] are given in table 1.

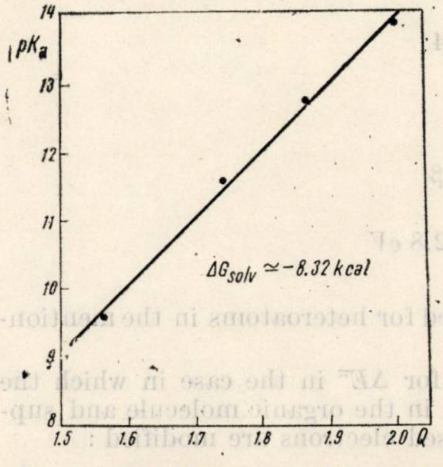

Fig. 1. — The dependence between the charge density and the pK_a of four phenols.

Table 1

Charge densities and pK_a values for four phenols

Phenols	Q_A	pK_a (25°)
Phenol	1.5645	9.62
Pyrocatechol	1.8620	12.8
Resorcinol	1.7438	11.6
Pyrogallol	1.9803	14.0

Plotting Q_A against pK_a we obtain a straight line which is given in fig. 1, proving the dependence given by formula (11).

The value of ΔG_{solv} obtained graphically is $\Delta G_{\mathrm{solv}} \simeq -8.32 \dfrac{\mathrm{kcal}}{\mathrm{mol}}$ for 25°.

These results show the possibility to make a theoretical study of the acidity of some weak acids which are organic molecules with delocalised electrons. Rough approximations which have been introduced still lead to good results but restrain the application of this theory to a reduced range of molecules.

---

[4] "Stability Constants", Special Publication, N° 17, The Chemical Society, London, 1964.

[5] "Stability Constants, Supplement N° 1", Special Publication, N° 25, The Chemical Society, London, 1971.

Revue Roumaine de Chimie, **22**, *2*, 305 - 311 (1977)

CONCENTRATION ET SÉPARATION D'ÉLÉMENTS À L'AIDE DE CHÉLATEURS PAR LA MÉTHODE DE LA ZONE FONDUE. I

SYSTÈMES Cu(II) – Co(II) OU Cu(II)-Ni(II) ET MERCAPTOACÉTANILIDE

SIMON FIŞEL et CATINCA SIMION
Chaire de Chimie inorganique et analytique, Institut Polytechnique Iaşi, 71, str. Splai Bahlui,

Reçu le 5 février 1975

La technique de la zone fondue a été appliquée à la concentration et à la séparation des chélates de Cu(II), Co(II) et Ni(II) avec le mercaptoacétanilide (HA). On décrit et on étudie les systèmes CuA_2-HA, CoA_2—HA, NiA_2—HA, CuA_2—HA—diphényle, CoA_2—HA—diphényle et NiA_2—HA—diphényle. Lorsque la vitesse est fixée à 15 mm/h, après 57 passages, le cuivre est séparé à la partie inférieure de la colonne, du cobalt et du nickel. On obtient la même séparation, après 35 passages, en utilisant les systèmes MA_2—HA—diphényle.

1. INTRODUCTION

La méthode de la zone fondue [1] est adoptée comme méthode de purification des substances organiques[2-4] de concentration et séparation des composés minéraux[5,6] et de concentration des traces d'éléments après leur extraction avec un excès de ligand.[7-10]

Dans le présent travail on décrit les recherches concernant la concentration et la séparation du Cu(II), du Co(II) et du Ni(II) par la méthode de la zone fondue des chélates de ces éléments (MA_2) avec le mercaptoacétanilide (HA). Les systèmes étudiés sont du type MA_2—HA et MA_2—HA-diphényle.

---

[1] W. G. Pfann, "Zone Melting", John Wiley, New York, 1958.
[2] R. Kieffer, *Bull. Soc. chim. France*, **1965**, 633.
[3] T. Chaudron et P. Rumpf, *Chim. analyt.*, **47**, 583 (1965).
[4] J. C. Maire et J. Moritz, *Bull. Soc. chim. France*, **1963**, 210.
[5] P. Süe, J. Pauly et A. Novaille, *Bull. Soc. chim. France*, **1958**, 593.
[6] D. Ecklin, *Helv. Chim. Acta*, **50**, 1107 (1967).
[7] H. Kaneko, H. Kobayashi, H. Kanagawa et K. Ueno, *Talanta*, **14**, 1411 (1967).
[8] H. Kaneko, H. Kobayashi, K. Ueno et H. Kanagawa, *Talanta*, **14**, 1403 (1967).
[9] K. Ueno et H. Kaneko, *Microchem. J.*, **10**, 244 (1966).
[10] M. Mashima et K. Marayama, *Bull. Chem. Soc. Japan*, **44**, 2693 (1971).

2. PARTIE EXPÉRIMENTALE

Les expériences ont été effectuées à l'aide d'un appareil [11] qui comprend un dispositif de chauffage et de refroidissement avec huit zones à chauffage électrique, chacune ayant une longueur de 6 mm et huit zones de refroidissement, chacune d'une longueur de 45 mm, un système mécanique qui assure le déplacement des colonnes de purification à une vitesse comprise entre 5 mm/h et 60 mm/h ; huit colonnes de purification en verre, avec une longueur (L) de 500 mm et un diamètre de 10 mm.

Le remplissage des colonnes de purification a été réalisé à l'aide d'un dispositif[11] qui a assuré l'homogénéité de l'échantillon essayé (remplissage uniforme). Après solidification et refroidissement du mélange, le tube a été rempli d'azote.

Le mercaptoacétanilide et ses chélates de Cu(II), de Co(II) et de Ni(II) ont été préparés et purifiés selon les indications trouvées dans la littérature.[12,13] On a obtenu ainsi les chélates CuA_2, CoA_2 et NiA_2. Après un certain nombre de passages la colonne est divisée en zones de 10 mm de longueur. Chaque zone a été calcinée, le résidu a été dissous en acide chlorhydrique et nitrique et on a ensuite déterminé par spectrophotométrie la concentration en ions métalliques : le Cu(II) par le diéthyldithiocarbamate de sodium, le Co(II) avec le nitrozo-R et le Ni(II) à l'aide de la diméthylglioxime.[14] Le degré de pureté du mercaptoacétanilide des zones supérieures des colonnes a été évalué par analyse thermique en régime dynamique de température à l'aide de la méthode du film mince.[15]

3. RÉSULTATS ET DISCUSSION

Pour l'étude quantitative du processus, on a construit les diagrammes de phase des systèmes binaires CuA_2-HA, CoA_2-HA et NiA_2-HA (fig. 1A, B, C).

Les coefficients de distribution (K) ont été calculés [15] en utilisant la relation :

$$t_y = t_0 - \frac{C_s \cdot C_1 \cdot p}{C_1 + y(C_s - C_1)}$$

où C_1 est la concentration des impuretés dans la fondue, C_s la concentration des impuretés dans la phase solide, y la fraction molaire de la zone fondue, p le pourcentage molaire d'impureté, t_0 le point de fusion de la substance pure et t_y le point de fusion de la substance contenant des impuretés.

On a calculé les valeurs C_s, C_1 pour plusieurs paires de valeurs y et t_y, en traçant les graphiques température-composition (fig. 2A, B, C).

A partir de ces graphiques on a calculé la pente de la courbe solidus (C_s) et la pente de la courbe liquidus (C_1), K étant défini par le rapport C_s/C_1. Pour le système CuA_2-HA, K = 0,34, CoA_2-HA, K = 0,13 et NiA_2 — HA, K = 0,12. Les coefficients de distribution calculés ayant des valeurs plus faibles que l'unité, pour la concentration et la séparation des chélates on a dû réaliser un grand nombre de passages zonaux (n) (la concentration s'effectuant dans la direction de déplacement de la zone fondue).

---

[11] C. SIMION et GH. BENDESCU, *Rev. Chim.*, (*Bucureşti*), **24**, 998 (1973).

[12] L. HARTWIG, *J. prakt. Chem.*, **74**, 25 (1906).

[13] P. W. WEST et A. MEGGER, *Analyt. Chim. Acta*, **15**, 271 (1956).

[14] N. H. FURMAN, "Standard Methods of Chemical Analysis", Ier vol. Van Nostrand Company, New York, 1962, p. 388, 407, 704.

[15] W. M. SMIT, *Rec. Trav. chim.*, **75**, 1309 (1956).

Les résultats obtenus par les diagrammes de phase des systèmes binaires ont été interprétés par la méthode des moindres carrés en obtenant les équations des courbes liquidus des diagrammes étudiés. La fonction inconnue a été représentée sous la forme d'un polynôme du second degré ;

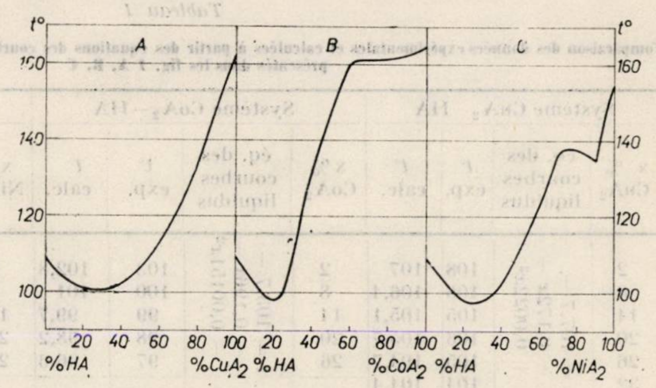

Fig. 1. A. — Diagramme de phase, température-composition du système binaire HA—CuA_2 ; B. — Diagramme de phase, température-composition du système binaire HA—CoA_2 ; C. — Diagramme de phase, température-composition du système binaire HA—NiA_2.

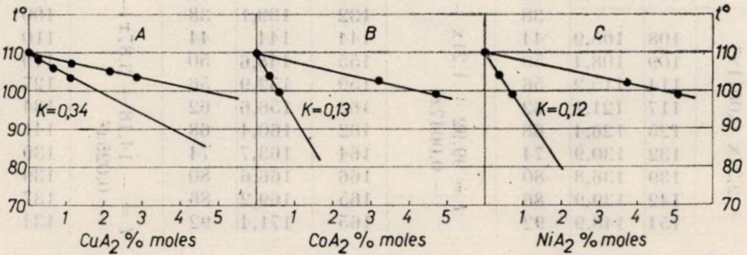

Fig. 2. — A. — Détermination du coefficient de distribution pour CuA_2 ; B. — Détermination du coefficient de distribution pour CoA_2 ; C. Détermination du coefficient de distribution pour NiA_2.

$$t = b_0 + b_1 x + b_2 x^2$$

où b_0, b_1, b_2 sont les coefficients de régression, x la concentration (en pourcentage) des composants du système, t les températures de fusion des mélanges de compositions x.

Les coefficients de régression du polynôme ont été calculés à l'aide de la méthode des moindres carrés, en utilisant le système :

$$mb_0 + \sum_{i=1}^{m} x_i b_1 + \sum_{i=1}^{m} x_i^2 b_2 = \sum_{i=1}^{m} t_i$$

$$\sum_{i=1}^{m} x_i b_0 + \sum_{i=1}^{m} x_i^2 b_1 + \sum_{i=1}^{m} x_i^3 b_2 = \sum_{i=1}^{m} x_i t_i$$

$$\sum_{i=1}^{m} x_i^2 b_0 + \sum_{i=1}^{m} x_i^3 b_1 + \sum_{i=1}^{m} x_i^4 b_2 = \sum_{i=1}^{m} x_i^2 t_i$$

dans lequel m est le nombre de déterminations.

Les résultats présentés dans le tableau 1 montrent une concordance satisfaisante entre les données expérimentales et celles calculées.

Tableau 1

Comparaison des données expérimentales et calculées à partir des équations des courbes liquidus des diagrammes de phase présentés dans les fig. 1 A, B, C

Système CuA_2—HA				Système CoA_2—HA				Système NiA_2—HA			
x % CuA_2	éq. des courbes liquidus	$t°$ exp.	$t°$ calc.	x % CoA_2	éq. des courbes liquidus	t° exp.	$t°$ calc.	x % NiA_2	éq. des courbes liquidus	$t°$ exp.	$t°$ calc.
2	$t = 107,7 - 0,172x + 0,0022x^2$	108	107	2	$t = 103.7 - 0,196x - 0,00151x^2$	103	102,8	2	$t = 102,87 - 0,3x - 0,00177x^2$	103	102,2
8		106	106,4	8		100	101	8		99	100,3
14		105	105,1	14		99	99,7	14		97	98,3
20		106	105,7	20		98	98,2	20		96	96,1
26		105	104,7	26		97	96,6	26		95	93,8
32		104	104,4	32	$t = 99,92 + 1,21x - 0,0047x^2$	105	133	32	$t = -14,18 + 3,87x - 0,025x^2$	98	88
38		105	104,3	38		132	139,1	38		100	100,7
44	$t = 22,64 + 2,27x + 0,0011x^2$	108	105,9	44		144	144	44		110	111,7
50		109	108,4	50		155	148,6	50		119	120,8
56		114	115,2	56		159	152,9	56		127	128,1
62		117	121,1	62		162	156,6	62		134	133,6
68		125	126,4	68		162	160,4	68		141	147,2
74		132	130,9	74		164	163,7	74		139	139,3
80		139	136,8	80		166	166,6	80		139	139,5
86		142	139,9	86		165	169,2	86		137	137,7
92		154	148,9	92		165	171,4	92		134	135

Les résultats de l'analyse de la distribution des chélates métalliques après le processus de fusion de zone sont donnés dans les figures 3, 4. Les courbes de distribution montrent une bonne concentration des chélates et une bonne séparation des chélates CuA_2 de CoA_2 et CuA_2 de NiA_2. En partant de 514 μg de Cu(II), 482 μg de Co(II) et 480 μg de Ni(II) dans le système initial, on a réussi, après 57 passages zonaux, à la vitesse (V) de 15 mm/h, sur une portion de 10%, respectivement 7,5% et 5% de la longueur de la colonne, à concentrer et à séparer en moyenne 416 μg de Cu(II), 400 μg de Co(II) et 395 μg de Ni(II).

Puisque la séparation exige dans le cas précédent une longue période de temps, on a utilisé un « solvant solide », le diphényle, dans le but de réduire le temps de séparation. La forme des diagrammes de phase des systèmes binaires HA-diphényle, CuA_2-diphényle, CoA_2-diphényle et NiA_2-diphényle (fig. 5A, B, C, D), montre que pour réduire le temps de concentration et de séparation on doit utiliser une concentration d'environ 25% dans le solvant.

On a obtenu ainsi une meilleure séparation effectuant seulement un nombre de 35 passages zonaux (fig. 6).

Pour montrer la variation du coefficient de distribution en fonction de la concentration on a déterminé la distribution du chélate CuA_2 dans le système HA-CuA_2, après un nombre de 10 passages zonaux à la vitesse de 15 mm/h.

En utilisant l'équation d'état du système :

$$\frac{C}{C_0} = K(1-g)^{(K-1)}$$

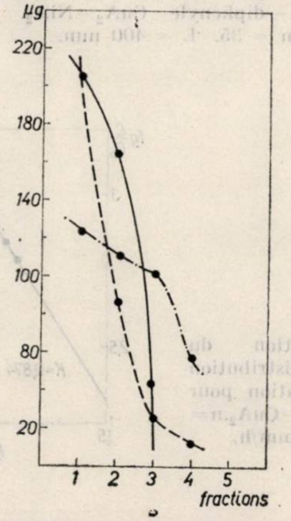

Fig. 3. — Courbes de distribution des chélates métalliques après la zone fondue : ---- CuA_2, -·-·-·$CoA_2 - N_iA_2$.

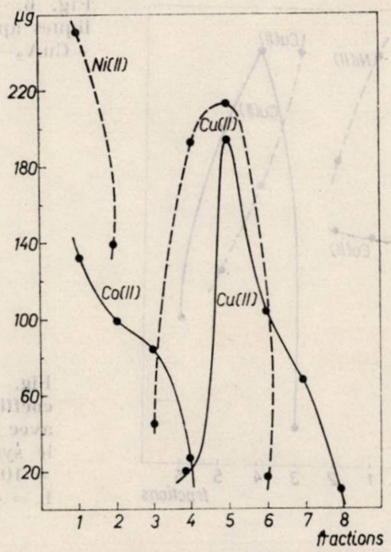

Fig. 4. — Courbes de distribution de chélates métalliques après la zone fondue, pour le système : $CuA_2 - CoA_2 - HA$, $CuA_2 - NiA_2 - HA$. n = 57, V = 15 mm/h, L = 400 mm.

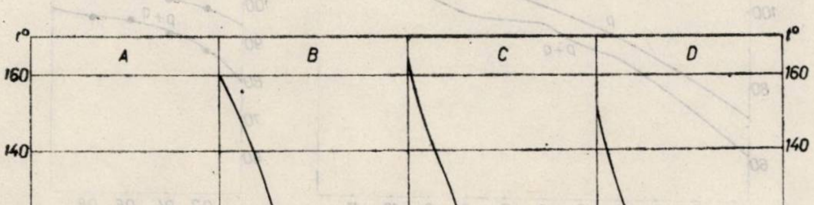

Fig. 5.A. — Diagramme de phase du système diphényle-HA ; B. Diagramme de phase du système diphényle-CuA_2 ; C. Diagramme de phase du système diphényle-CoA_2 ; D. Diagramme de phase du système diphényle-NiA_2.

(où C est la concentration des impuretés dans la phase solide quand le volume (v) a cristallisé, C_0 la concentration initiale, g le nombre des portions cristallisées) ; à partir du graphique donnant log C/C_0 en fonction de log $(1 - g)$, on a déterminé la valeur log K(fig. 7).

Les valeurs de K croissent avec l'augmentation de la concentration.

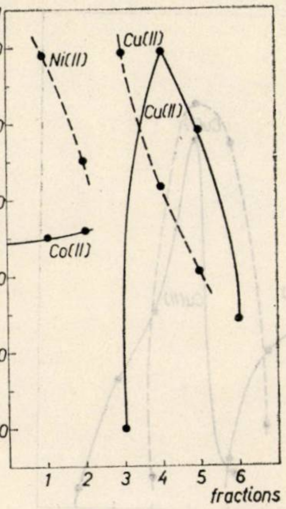

Fig. 6. — Courbes de distribution des chélates métalliques après la zone pour le système : HA-diphényle —CuA$_2$—CoA$_2$, HA—diphényle—CuA$_2$—NiA$_2$. V = 15 mm/h, n = 35, L = 400 mm.

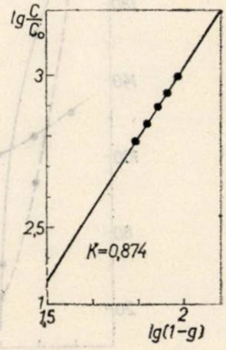

Fig. 7. — Variation du coefficient de distribution avec la concentration pour le système HA—CuA$_2$.n = = 10, V = 15 mm/h, L = 400 mm.

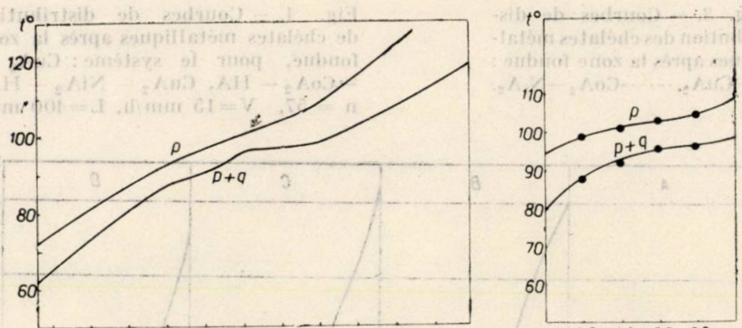

Fig. 8. — Détermination de la pureté de mercaptoacétanilide, les courbes de fusion pour p moles % d'impuretés et $(p + q)$ moles % d'impuretés,

Pour déterminer le degré de pureté de la mercaptoacétanilide contenue dans les zones supérieures de la colonne de purification à partir des courbes de fusion du HA et de la mercaptoacétanilide, à laquelle on a ajouté 0,2 moles de diphényle (fig. 8), on a sélectionné les températures nécessaires au calcul de la pureté d'après l'équation :

$$p = \frac{(t_2 - t_1) \cdot q}{(t_2' - t_1') - (t_2 - t_1)}$$

où t_1 et t'_1 sont les températures prises sur les courbes de fusion des échantillons d'essais qui contiennent p moles % et $(p + q)$ moles % d'impuretés correspondant à la fraction molaire de la fondue y_1 ; t_2 et t'_2 sont les températures prises sur les courbes de fusion des échantillons d'essais qui contiennent p moles % et $(p + q)$ moles % d'impuretés, correspondant à la fraction molaire de fondue y_2 ; q moles % de contaminant. On a déterminé $p = 0{,}20$ ce qui correspond à une pureté de 99,80 %.

4. CONCLUSIONS

Les résultats de ces recherches indiquent qu'il est possible de concentrer et de séparer le Cu(II) du Co(II) et le Cu(II) du Ni(II) par la méthode de la zone fondue après leur extraction par un excès de mercaptoacétanilide. Pour réduire le temps de séparation on a utilisé comme «solvant solide» le diphényle, en diminuant ainsi le nombre des passages zonaux.

Revue Roumaine de Chimie, 22, 2, 313–317 (1977)

COMPTES RENDUS

"Topics in Flavonoid Chemistry and Biochemistry" – Proceedings of the Fourth Hungarian Bioflavonoid Symposium, Keszthely, 1973, Edited by L. Farkas, M. Gabor and F. Kállay, Akadémiai Kiadó, Budapest, 1975

The book contains 27 communications which were presented at the IVth Hungarian Bioflavonoid Symposium. From 46 contributors 26 are Hungarian (among which the known research-workers: L. Farkas, F. Kállay, R. Bognar and M. Gabor) and 20 foreigner (some of them also known investigators in this field as: H. Wagner, L. A. Griffiths, G. B. Marini-Bettolo, K. Weinges, O. Seligmann, D.M.X. Donnelly and J. Chopin). As the communications clearly show, the field of flavonoid compounds, which has great traditions in Hungary beginning with the well-known works of Géza Zemplen, is actively investigated nowadays.

Most communications describe topics from chemistry of flavonoids including synthesis and reactions. New applications of some classical or modern reactions from this field are presented, e.g.: oxidative rearrangements of chalchones in presence of $Tl(NO_3)_3$; Neber rearrangement for the synthesis of amino-thiaflavanonesulfones; $TiCl_4$ – catalysed reaction of flavonoid carbonyl group with amines; Elbs persulfate oxidation; selective demethylation of flavone derivatives with $AlCl_3/CH_3CN$; Baker-Venkataraman rearrangement of acetophenonebenzoates to hydroxy-dibenzoylmethanes, etc. Other interesting problems described in the book should also be mentioned: synthesis of optically active flavan derivatives; ring enlargement of flavanones to benzoxazepinones: reactions of azaflavonoid derivatives (compounds which make a transition from flavonoids to alkaloids); interconversions of neoflavonoids and of isoflavonoids; synthesis of pyridinium isoflavans, etc.

The physical methods utilized in this field for structure determination are largely expounded in special papers (^{13}C–NMR spectroscopy and mass spectrometry) or in connection with the chemistry of flavonoids (UV spectra; ^{1}H–NMR spectra; NMR spectra with LIS reagents, etc.).

Other topics appearing in the book concern the biochemistry of flavonoids. The metabolism of flavonoids is discussed underlining the important position of modern physical methods, e.g.: ^{14}C– and ^{3}H–studies or thin-layer chromatography connected with fluorescence spectrometry. Some interesting biologic activities of flavonoids are also discussed e.g.: antiviral activity on herpesviruses, antioxidant effect on ascorbic acid, oestrogenic action and cardiovascular effect.

In this connection the communication of Z. Dinya and E. Hetényi concerning the relationship between the electronic structure and biological action of some flavonoids deserves special mention due to the effort to explain the relation structure – action using quantum chemical methods.

The book is completed with an author index and a sufficiently detailed subject index.

Except a few minor mistakes (e.g. the absence of an NMR signal of cordoin at page 13 and *n*-butylimine instead of n-butylamine at page 62) the entire text is correct and very well printed.

In conclusion, the book is very interesting and useful for organic chemists and biochemists with interest in this field as well as for all chemists which may develop their knowledge.

M. Banciu

MELVIN D. JOESTEN and L. J. SCHAAD, "Hydrogen Bonding", Marcel Dekker, Inc., New York, 1974, 622 p.

Since the publication of Pimentel and McClellan's book on hydrogen bonding in 1959, a large number of papers dealing with various aspects of hydrogen bonding have appeared. The recent book by M. D. Joesten and L. J. Schaad (both authors from Vanderbilt University, Nashville, Tennessee, U.S.A.) provides a comprehensive coverage of those topics which account for a large percentage of the hydrogen bonding papers published from 1960 through 1973.

The topics of the book are presented in five chapters, namely spectroscopical studies and correlations, theory of hydrogen bond, thermodynamics and kinetics, and intramolecular hydrogen bonding. Each chapter includes a brief general introduction with a comprehensive review of developments during the past fourteen years.

The first chapter deals with the detection methods of homo- and hetero-intermolecular hydrogen bonds by means of spectroscopic methods (infrared, far i.r., near i.r., electronic, n.m.r., etc.) and X-ray diffraction.

Chapter 2 (theory of the hydrogen bond — written by Professor Schaad) has an introduction to quantum mechanics followed by a critical analysis of the present theoretical position of hydrogen bonding (energy and geometry, vibrational, electronic and n.m.r. spectra, and the origin and the nature of the hydrogen bond). The thermodynamics and kinetics of hydrogen bonding for 1 : 1 adducts are treated in Chapter 3.

The vast amount of literature data concerning theoretical studies on hydrogen — bonded systems (from 1960 through 1973) was condensed in a table at the end of the second chapter, while thermodynamic data are given in a suitable manner, as an Appendix.

Frequency shifts (i.r. and n.m.r.) and other correlations involving hydrogen bonding are reviewed in chapter 4, while the last chapter deals with intramolecular hydrogen bonds and self-association of hydrogen bonding compounds.

The bibliography of the book is very rich : over three thousand references, and the format of the bibliography is similar to that used by Pimentel and McClellan (i.e. author(s), journal, volume, page and the year of publication, followed by a key title of the paper) and both text and bibliography were indexed. The subject and author indices of the book, together with those of Pimentel and McClellan's book, assure the updating of the bibliography in this field and provide ready access to the literature on this rapidly expanding field of chemistry. However, in spite of the great volume of bibliographical material (which uses 25 per cent of the graphical space of the book) there are many papers which were not referenced by the authors. Consequently, the reader interested in an exhaustive coverage of the bibliography on hydrogen bonding must examine carefully the pertinent reference sources.

We appreciate that this monograph will be a valuable tool for all people which are interested in this field of chemistry, therefore the book should be present on the shelf of all scientific libraries.

I. I. Bădilescu

KINETIK DER ELEKTRODENPROZESSE, Tibor Erdéy — Gruz, 581 Seiten, 111 Abbildungen.

Das Buch wie schon vom Titel aus ersichtlich, behandelt Fragen der Kinetik der heterogenen Reaktionen, die and der Trennungsfläche Elektrode-Elektrolyt stattfinden. Seine Ersscheinung ist besonders willkommen, da auf diesem Gebiet der Elektrochemie in den letzten Jahren äusserst wichtige Fortschritte zu verzeichnen waren und der Verfasser eine Autorität auf piesem Gebiet darstellt, indem er zu den Pionieren der experimentellen und theoretischen Forschung auf dem Gebiet der elektrochemischen Kinetik zählt.

Das Buch umfasst sieben Kapiteln und einen Anhang. Die Kapiteln sind, wie folgt, benennt : 1) Grundprinzipien der Kinetik und die durch den Ladungsübertritt bestimmte Geschwindigkeit der Elektrodenprozesse ; 2) Elektrodenprozesse, mit durch chemische Reaktionen bestimmter Geschwindigkeit ; 3) Elektrodenprozesse, deren Geschwindigkeit die Diffusion bestimmt. 4) Einzelheiten der Kinetik einiger Elektrodenprozesse 5) Elektrodenprozesse in Salzschmelzen 6) Elektrodenprozesse an der Grenze von Halbleitern. 7) Kinetik der anodischen Filmbildung.

Im ersten Kapitel werden die Grundprinzipien der Kinetik der Elektrodenprozesse dargestellt. Die Begriffe der Polarisation und der Überspannung, so wie die Überspannungstypen werden erläutert. Es werden die Grundlagen der Theorie der Übertrittsüberspannung, sowie der Einfluss der Temperatur, der Struktur der elektrolytischen Doppelschicht und der Konzentra-

tion der Reaktanten auf die Geschwindigkeit der Durchschnittsüberspannung dargestellt. Die wichtigsten Methoden zwecks Bestimmung der Mechanismen der Elektrodenreaktionen werden vorgeführt. Das Kapitel schliesst mit einem kurzen Überblick der an der Elektrodenoberfläche auftretenden Adsorptionserscheinungen.

Das zweite Kapitel ist der Reaktionsüberspannung gewidmet. Es werden Elektrodenprozesse, deren langsame Etappe eine homogene chemische Reaktion ist, sowie solche deren Geschwindigkeit von einer heterogenen chemischen Reaktion bestimmt wird, ausführlich diskutiert.

Im dritten Kapitel wird die Problematik der Transportüberspannung behandelt. Die Rolle des Stofftransportes im Rahmen der Elektrodenprozesse, sowie der Diffusionsstrom und die Faktoren, die ihn beeinflussen, werden besprochen. Der Einfluss der Bewegung der Flüssigkeit aud die Diffusionsschichtdicke, wird erläutert und die rotierende Scheibenelektrode vorgestellt. Die Bedingungen der nichtstationären Diffusion werden behandelt und die zeitliche Abänderung der Diffusionsgrenzstromdichte und der Transportüberspannung werden gezeigt. Der Einfluss des Wechselstromes auf die Transportüberspannung wird diskutiert.

Im vierten Kapitel werden die wichtigsten experimentellen Ergebnisse, sowie die theoretischen Schlussfolgerungen hinsichtlich einiger konkreter Elektrodenprozesse dargestellt.

Ausführlich wird die Kinetik einiger Gaselektroden, besonders die der Wasserstoff- und Sauerstoffelektrode, die Kinetik einiger Oxydo-Reduktions Reaktionen, sowie die Kinetik der Abscheidung und der Auflösung einiger Metalle behandelt.

Dementsprechend werden die Theorien hinsichtlich des Mechanismuses, sowie der Einfluss der verschiedenen Faktoren auf den Wert der Entladungs- und des Ionisationsüberspannung dargestellt. Die zeitlichen Änderungen der Wasserstoffüberspannung unter nichtstationären Bedingungen werden diskutiert.

Ähnliche werden auch die Besonderheiten der Sauerstoffelektrode diskutiert, wobei ungefähr die selben Probleme behandelt werden.

Etwas kürzer, wobei aber die Hauptprobleme noch immer behandelt werden, wird dann die Kinetik der Chlorelektrode und einiger Oxydo-Reduktionsreaktionen, sowie Fe^{2+}/Fe^{3+}, Ce^{3+}/Ce^{4+}, Tl^{+}/Tl^{3+}, Sn^{2+}/Sn^{4+}, Ti^{3+}/Ti^{4+}, Mn^{2+}/Mn^{3+}, Ag^{+}/Ag^{2+}, Cr^{2+}/Cr^{3+}, Br_2/Br^{-}, I_2/I^{-}, HNO_2/HNO_3 und Chinone/Hydrochinone behandelt.

Eine besondere Aufmerksamkeit wird den Problemen der Kinetik der elektrolytischen Abscheidung und Auflösung der Metalle gewidmet. Die Abscheidungsprozesse eines Metalls an einer flüssigen Elektrode oder an einer fremden festen Elektrode, sowie die daran gebundenen Überspannungen werden diskutiert. Es werden sowohl allgemeine Probleme, wie z.B. die theoretischen Grundlagen der Elektrokristallisation, sowie gewisse spezielle Probleme, wie das Kristallwachstum in Spiralform, die Bildung dendritischer Niederschläge oder die Textur metallischer Niederschläge behandelt. Die Kinetik der elektrolytischen Abscheidung der Metalle wird diskutiert. Das Kapitel schliesst mit der Darstellung der kinetischen Besonderheiten einiger Metallelektroden, wie Cu/Cu^{2+}, Ag/Ag^{+}, Cd/Cd^{2+}, Zn/Zn^{2+}, Fe/Fe^{2+}, Ni/Ni^{2+}, In/In^{3+}, Bi/Bi^{3+} etc.

Im 5ten Kapitel werden die Hauptprobleme der Elektroden-prozesse in Salzschmelzen dargestellt. Die Struktur der geschmolzenen Salze, sowie einige wichtigere kathodische und anodische Prozesse werden diskutiert. Dementsprechend wird die Entladung des Wasserstoffes aus Schmelzen, die Besonderheiten der Abscheidung der Metalle unter flüssiger oder kristalliner Form, die Elektrodenprozesse bei der Abscheidung der Alkalimetalle und des Aluminiums, bei der Reduktion einiger sauerstoffhaltiger Anionen, sowie bei der Entladung des Sauerstoffes und des Chlors behandelt.

Im 6ten Kapitel werden die Besonderheiten der an Halbleiterelektroden stattfindenden Elektrodenprozesse behandelt. Die Grundlagen der Theorie und die allgemeinen Eigenschaften der Halbleiter werden dargestellt und die Elektrodenprozesse, die am Halbleiterelktroden sowohl durch Elektronen-als auch durch Ionenübertragung stattfinden, werden besprochen.

Das letzte Kapitel ist der Kinetik der Bildung von anodischen Filmen gewidmet. Das Auftreten der Kristallisationskeime, sowie deren Weiterwachsen im Falle der Bildung einer schwerlöslichen Verbindung, wird diskutiert.

Der Anhang behandelt kurz einige Probleme aus benachbarten Gebieten, ohne denen das Verstehen der Fragen der elektrochemischen Kinetik nicht möglich wäre. Dementsprechend werden die Grundprinzipien der elektrochemischen Thermodynamik, der Theorie der elektrochemischen Doppelschicht, der Theorie der absoluten Reaktionsgeschwindigkeit und der experimentellen Methoden der Kinetik der Elektrodenprozesse behandelt.

Im Vorwort kennzeichnet der Verfasser das Buch als eine untermediäres Werk das eine Mittelstellung einnimmt, zwischen einer Monographie, die ein beschränktes Gebiet erschöpfend behandelt und einem Lehrbuch, das einen allgemeinen Überblick über ein ausgedehntes Gebiet

der Elektrochemie ermöglicht. Meiner Meinung nach widerspiegelt diese Charakterisierung sehr gut die Hauptmerkmale des Buches. Durch sein hohes Niveau spricht das Buch vor allem Spezialisten an, die darin Antwort auf die meisten Fragen der Kinetik der Elektrodenprozesse finden. Ein äusserst reiches Literaturverzeichnis, das einschliesslich 1974 erschienenen Arbeiten anführt, ermöglicht Interessierten die nötigen Informationen in besonderen Problemen zu erhalten. Durch ihre Klarheit und durch fliessenden Stil wendet sich das Buch aber auch an einen weiten, aus Metallurgie-Physik- und Chemie-Ingenieuren und Studenten gebildeten Lesekreis, die sich auf diesem Gebiet der Elektrochemie, das sich z.Z. so explosionsartgi entwickelt, Grundbegriffe aneignen wollen.

Gh. Facskò

CONSTANTIN V. UGLEA « La chromatographie sur gel perméable. Nouveaux domaines d'application ». Ed. Academiei, Bucarest, 1976, 122 pages, 55 fig.

Le but de ce travail est de présenter aux spécialistes la chromatographie sur gel perméable, une nouvelle méthode d'analyse, qui trouve des domaines d'application de plus en plus importants et de plus en plus variés.

Le matériel est divisé en quatre chapitres.

Dans le premier chapitre, on présente les principes de base de la chromatographie sur gel perméable, ainsi que certaines indications sur les principaux gels commerciaux utilisés dans les colonnes de séparation. On démontre que la chromatographie sur gel perméable n'est pas une méthode absolue et pour interpréter les résultats expérimentaux, il est nécessaire, au préalable, de tracer la courbe de calibrage, qui donne un sens qualitatif à la séparation.

Le deuxième chapitre « La séparation des substances organiques micromoléculaires, par chromatographie sur gel perméable » examine le comportement des principales catégories de substances organiques, au passage par les colonnes remplies de gel (hydrocarbures saturées, alcools, acides carboxyliques, dérivés halogénés, amines, aldéhydes, cétones, composés aromatiques, phénols, etc.). Cela permet de mettre en évidence l'influence de certaines particularités structurales du solvat, comme — par exemple — le groupe fonctionnel de ce dernier.

A base du matériel expérimental analysé, l'auteur détache une série de règles qui permettent de faire la différence entre le comportement des composés organiques.

Le troisième chapitre a comme titre « L'application de la chromatographie sur gel perméable pour la caractérisation des mélanges à poids moléculaire réduit ».

La chromatographie sur gel perméable est utilisée pour caractériser des substances ou des mélanges de substances qui contiennent seulement des produits à poids moléculaire réduit, des restes de monomères ou des fractions à poids moléculaire réduit (oligomères).

En même temps, cette nouvelle technique a permis de définir la cinétique de certains processus de polymérisation et de clarifier certains aspects importants en ce qui concerne la nature de l'interaction entre le solvat et le solvant, dans les systèmes qui utilisent des substances polaires comme milieu de dissolution.

L'auteur montre que la chromatographie sur gel perméable est une méthode ayant un large domaine d'application, soit comme méthode d'analyse quantitative soit pour diriger certains processus technologiques de grande finesse. On indique de nombreux domaines d'utilisation dans l'étude des verres époxy, des différents polymères, des résines, etc.

Particulièrement, il faut signaler l'application de la chromatographie sur gel perméable à l'analyse du pétrole, des fractions de distillation de ce dernier, ainsi que des résines qu'on sépare après la distillation.

De cette façon, la chromatographie sur gel perméable a été utilisée avec succès pour l'analyse des asphaltes, ou on a effectué une séparation dans des fractions ayant des poids moléculaires différents, suivie d'une étude par d'autres méthodes pour déterminer la structure chimique. L'ordre des techniques appliquées, ainsi que le choix des méthodes de séparation, dépendent d'un cas à l'autre.

Le dernier chapitre du livre s'occupe des « Installations et procédés utilisés en chromatographie sur gel perméable ».

On indique les schémas de principe des installations de laboratoire pour chromatographie sur gel perméable, le mode et les conditions classiques d'utilisation, ainsi qu'une série de modifications qu'on peut appliquer. On mentionne aussi les gelchromatographes commerciaux.

Une partie de ce chapitre est réservée à l'analyse des effets et des conditions expérimentales sur la séparation et sur les résultats qu'on obtient par la chromatographie sur gel perméable.

Le travail est complété par 141 indications de bibliographie.

Le matériel présente un intérêt informatif et pratique pour ceux qui travaillent dans différents domaines de la chimie, car il expose les principes, le mécanisme et les applications de cette nouvelle méthode de séparation, la chromatographie sur gel perméable, qui s'est rapidement développée ces dernières années.

Maria Gruia

P. DAY, editor "Electronic States of Inorganic Compounds : New Experimental Techniques", D. Reidel Publishing Company, Dordrecht-Holland, NATO Advanced Study Institutes Series C, vol. 20, 1975, 541 p.

The present volume, published in the NATO Advanced Study Institute Series, includes a series of lectures given at the Inorganic Chemistry Laboratory and St. John's College, Oxford (8 — 18 September 1974) by a group of experts in the field of electronic structures of inorganic compounds.

These lectures provide a general survey of the basic theories and experimental procedures relevant to the different techniques developed in the last years for investigating the electronic structures of inorganic compounds.

After a general introduction in the basic theory of the molecular electronic states by C. J. Ballhausen and in the band theory of solids by J. M. Thomas, the following lectures in the book are dedicated to various experimental techniques, which are extremely disparate in background and involve, among others, linearly and circularly polarised electromagnetic radiation, electron kinetic energy analysis and neutron scattering.

Among the methods based on polarised radiation dealt with in this volume, the magnetic circular dichroism (MCD) is today the most extensively used and is accordingly given a wide space. The MCD has found interesting applications as an analytical or spectroscopic tool, providing information which is complementary to absorption spectroscopy and other physical techniques, especially with regard to the magnetic properties of the ground state of inorganic compounds. All aspects — theoretical, experimental and applicative — of the MCD spectroscopy are covered in 5 lectures by various authors.

Of equal weight in this volume is the group of lectures in photoelectron spectroscopy (PES), namely the ultraviolet PES of molecules in the gas phase and of transition metal compounds, and the X-ray PES of solids, interfaces and openshell ions. These PES techniques are now widely used in studying valence and core-electron ionisations of various compounds. Some related techniques like electron impact energy loss spectroscopy (ELS), Penning ionization (PI), Auger electron spectroscopy (AES) and ion neutralization spectroscopy (INS) are briefly presented, particularly emphasizing their relationship to photoelectron spectroscopy and demonstrating the use of the results in understanding the chemical bond in inorganic molecules.

The inelastic neutron scattering, for studying the excited electronic states of inorganic materials, constitutes the subject of only one lecture in the book.

The volume is much more than a set of "Proceedings" ; by its completeness it is rather a textbook of the new methods, and is recommended as such to all inorganic chemists interested in the electronic structures, both of isolated molecules and continuous lattice solids.

Rodica Beldie

NOTE POUR LES AUTEURS

La Revue Roumaine de Chimie publie des articles en anglais, français, russe, allemand ou espagnol. Les auteurs sont priés d'envoyer des articles et des comptes rendus inédits.

Les manuscrits seront dactylographiés à deux intervalles. La bibliographie, les tableaux et la légende des figures seront placés après le texte.

Si l'article fait partie d'une série numérotée, le titre de la partie précédente sera indiqué dans une note au bas de la première page.

Chaque article sera précédé d'un résumé comprenant quinze lignes au maximum.

Les références bibliographiques dans le texte seront faites par des exposants sans parenthèse et paraîtront comme des notes au bas de chaque page.

Les publications périodiques mentionnées dans la bibliographie seront présentées suivant les prescriptions internationales : le nom de l'auteur précédé de l'initiale du prénom, le titre du périodique abbrégé conformément à «Chemical Abstracts», et souligné par une ligne, le numéro du tome, indiqué par des chiffres arabes et souligné par deux lignes, suivi de la première page de l'article ; à la fin, l'année de la parution sera placée entre parenthèses. Le numéro de la revue ne sera pas indiqué si les pages du volume sont numérotées consécutivement. Pour les revues dont les tomes ne sont pas numérotés (par ex. Bull. Soc. Chim. France, etc.), l'année de la parution soulignée par deux lignes précèdera l'indication de la page.

Les textes des livres ou traités inclueront : les noms des auteurs, les initiales du prénom, le titre du livre entre guillemets et sans être souligné, le numéro du tome précédé par l'abbréviation ,,vol.'' (ou ,,Bd.''), le numéro de l'édition, les éditeurs (the publisher), la localité de la parution du livre, l'année de la parution et la page de la référence précédée par l'abbréviation ,,p'' (ou ,,S'').

Les brevets seront indiqués comme suit : l'auteur ou la firme, le pays et le numéro du brevet, la date et la revue (Chem. Abstr.). Par ex. : M. Jones (to Union Carbide Co.), Brit. Pat. 601 238, 2 septembre 1959, *Chem. Abstr.*, 54, 12808 (1960).

Si la référence n'a pas été lue en original, on indiquera aussi la revue de référence consultée.

Les diagrammes seront tracés à l'encre de Chine sur papier calque. Les tableaux et les figures (en nombre strictement nécessaire) seront numérotés par des chiffres arabes et leur explication sera donnée dans la légende des figures. Prière de ne pas inscrire les mêmes données dans les tableaux et les figures. Chaque tableau aura un titre. On indiquera dans le texte la place approximative des tableaux et des figures. Les formules chimiques seront incluses dans le texte ; en outre, elles seront transcrites sur papier calque, à l'encre de Chine.

Les auteurs sont priés d'indiquer les caractères italiques (en soulignant les lettres au crayon), ainsi que tout autre caractère spécial ; les préfixes *ortho*, *meta*, *para*, *cis*, *trans*, etc. seront soulignés pour indiquer leurs caractères italiques et ne seront jamais écrits avec des majuscules.

Aucune correction à la main ne sera admise sur le manuscrit. Les corrections seront frappées à la machine. Les lettres grecques ou d'autres symboles spéciaux seront insérés à la main à l'encre clairement.

Le manuscrit sera signé par l'auteur.

La colonne-titre aura 50 lettres au maximum.

L'entière responsabilité du contenu des articles appartient aux auteurs.

1977 JUL 26

TRAVAUX PARUS AUX ÉDITIONS DE L'ACADÉMIE DE LA RÉPUBLIQUE SOCIALISTE DE ROUMANIE

I. G. MURGULESCU, **Introducere în Chimia fizică. Vol. I. Atomi, molecule, legătură fizică** (Introduction à la Chimie Physique, Ier vol. Atomes, molécules, liaison chimique), 1976, 559 p., 36 lei.

E. P. BALTĂ, E. BALTĂ, **Introduction to the physical chemistry of the vitreous state**, co-édition avec Abacus Press, 1976, 400 p., 39 lei.

I. GĂLĂŢEANU, **Radiochimia aplicată. Metode şi probleme** (La radiochimie appliquée. Méthodes et problèmes), 1976, 305 p., 19 lei.

FRANCISC A. GOTHARD, **Echilibre lichid-vapori. I. Baze teoretice şi metode de calcul** (Equilibres liquide-vapeurs. I. Bases théoriques et méthodes de calcul), 1975, 263 p., 2 pl., 28 lei.

CONST. GH. MACAROVICI, D. MACAROVICI, **Chimia oxizilor dubli şi utilizările lor** (La chimie des oxydes doubles et leur utilisation), 1975, 195 p., 41 lei.

ELENA CEAUŞESCU, **Research work on synthesis and characterization of macromolecular compounds. Contributions**, 1974, 251 p., 20 lei.

M. AVRAM, **Antidăunători** (Pesticides), 1974, 496 p., 41 lei.

DUMITRU COSTACHE, **Analiza chimică prin metoda cinetică** (L'Analyse chimique par la méthode cinétique), 1974, 276 p., 15,50 lei.

G. A. RĂDULESCU, **Proprietăţile ţiţeiurilor româneşti** (Les propriétés des pétroles roumains), 1974, 267 p., 2 pl., 18 lei.

CR. SIMIONESCU, VIORICA RUSAN, V. POPA, **Chimia algelor marine** (La chimie des algues marines), 1974, 212 p., 1 pl., 18 lei.

I. ZUGRĂVESCU, MAGDA PETROVANU, **Chimia n-ilidelor** (La chimie des n-Ilures, 1974, 348 p., 19 lei.

MARIA FITI, **Dozimetria chimică a radiaţiilor ionizante** (La dosimétrie chimique des radiations ionisantes), 1973, 240 p., 13,50 lei.

TIBERIU NĂŞCUŢIU, **Metode radiochimice de analiză** (Méthodes radiochimiques d'analyse), 1973, 384 p., 23 lei.

CRISTOFOR SIMIONESCU, MARGARETA GRIGORAŞ, AGATA CERNĂTESCU-ASANDEI, ROZMARIN GHEORGHE, **Chimia lemnului în România. Plopul şi salcia** (La Chimie du bois en Roumanie. Le peuplier et le saule), 1973, 299 p., 13 pl., 26 lei.

MIHAI FLORESCU, **Eficienţa economică a cercetării ştiinţifice** (L'efficience économique de la recherche scientifique), 1972, 115 p., 14 lei.

I.P.I. – o. 1627

43426

Lei 25.–

F1103

ACADÉMIE DE LA RÉPUBLIQUE SOCIALISTE DE ROUMANIE

REFERÁLVA

REVUE ROUMAINE DE CHIMIE

TOME 22
N° 3
Mars 1977

427 l.

EDITURA ACADEMIEI REPUBLICII SOCIALISTE ROMÂNIA
Rev. Roumaine Chim. RECHAX, **22**, *3*, p. 319–480 (1977), Bucarest

ACADÉMIE DE LA RÉPUBLIQUE SOCIALISTE DE ROUMANIE

COMITÉ DE RÉDACTION

Rédacteur en chef:

I. G. MURGULESCU, membre de l'Académie de la République Socialiste de Roumanie

Rédacteurs en chef adjoints:

A. T. BALABAN et V. EM. SAHINI, membres correspondants de l'Académie de la République Socialiste de Roumanie

Collège de rédaction:

EM. BRATU, ELENA CEAUŞESCU, ECATERINA CIORĂNESCU-NENITZESCU, C. DRĂGULESCU, CR. SIMIONESCU, membres de l'Académie de la République Socialiste de Roumanie; P. SPACU, membre correspondant de l'Académie de la République Socialiste de Roumanie; MARGARETA AVRAM, I. HAIDUC, D. I. MARCHIDAN, I. MOLDOVAN, G. NIAC et D. SĂNDULESCU

La Revue Roumaine de Chimie paraît 10 fois par an. Toute commande de l'étranger (fascicules ou abonnements) sera adressée à ILEXIM Departamentul Export-Import Presă (Revues), P.O.B. 136 — 137, télex 11226, Bucarest, 3, str. 13 Decembrie, Roumanie

Les manuscrits, les livres et les revues proposés en échange, ainsi que toute correspondance seront envoyés à la rédaction :

REVUE ROUMAINE DE CHIMIE

23, str. Dumbrava Roşie, Bucarest, Roumanie, téléphone 12 41 60

EDITURA ACADEMIEI REPUBLICII SOCIALISTE ROMÂNIA

125, Calea Victoriei, 71021, Bucarest, Roumanie, téléphone 50 76 80

ORSZÁGOS MŰSZAKI KÖNYVTÁR ÉS DOKUMENTÁCIÓS KÖZPONT 1883

REVUE ROUMAINE DE CHIMIE

Tome 22, N° 3 Mars 1977

S. STERNBERG and T. VIŞAN, A chronopotentiometric study of the strontium(II) ion in molten potassium nitrate 321–325

EMILIA CONSTANTIN et J. CH. ABBE, Étude des réactions entre D_2^+ et CH_nD_{4-n} à l'aide d'un spectromètre de masse à deux étages 327–333

F. ARCE, J. CASADO, M. A. RÍOS y V. TATO, Estudio teorico de la naturaleza de constantes de fuerza. I. Moleculas diatomicas 335–343

F. ARCE, J. CASADO, M. A. RÍOS y V. TATO, Estudio teorico de la naturaleza de constantes de fuerza. II. Moleculas triatomicas 345–352

N. I. IONESCU et B. AURIAN-BLĂJENI, Considérations sur le modèle de Landsberg relatif à l'équation logarithmique 353–359

RALUCA RIPAN, GH. POP, ILEANA POP et CRISTINA NAŞCU, Acide ascorbique comme agent réducteur. V. Cinétique de la réduction des ions Au(III) par acide ascorbique 361–370

MARIA BREZEANU and IOANA JITARU, Cr(III) coordination compounds with 3-amino-1-propanol. 371–378

ILEANA BALÁZS, VALER FĂRCĂŞAN and IONEL HAIDUC, Synthesis of di- and triphenyllead polychloroacetates 379–383

CONSTANŢA GHEORGHIU, CRISTINETA MĂRCULESCU, MARIA CONSTANTINESCU and O. CONSTANTINESCU, Contributions to the coordination chemistry of *s*-triazines. III. The condensation reaction of phenylbiguanide with phenylisothiocyanate in the presence of Cu ions 385–394

L. RAMAKRISHNAN and S. SOUNDARARAJAN, Quinoline-1-oxide complexes of lanthanide iodides 395–399

M. MRACEC, S. RADULY, Z. SIMON, AURELIA BOLDEA and C. DRUGĂRIN, New urea and thiourea derivatives. II. HMO and Del Ré molecular orbital calculations. 401–409

I. M. ISSA, A. A. EL-SAMAHY, R. M. ISSA, H. S. EL-KASHEF and S. H. ETAIW, The electronic and vibrational spectra of some N-substituted carbazoloquinones 411–419

Z. SZEKELY, TEODORA PANEA and C. BODEA, Hydroxyphenothiazine-5,5-dioxides (Hydroxyphenothiazine-sulphones). II. Determination of dissociation constants of some 3-hydroxyphenothiazine-sulphones 421–426

R IOVANCA HAIDUC, STELUŢA BEICU and C. LITEANU, Determination of xanthates from flotation pulps with an Ag_2S membrane electrode . . . 427–433

Revue Roumaine Chim. **22**, *3*, p. 319–480(1977), Bucarest

T. SIMONESCU and V. RUSU, New analytical applications of some sulphonamide compounds. V. Arsenic traces determined with silver sulphanilamide . 435–441

I. C. POPESCU and MARIANA HĂLĂLĂU, Studies on the electroanalytical behaviour of membrane-electrodes under current. VI. Potentiometry at continuous and constant current using a Hg/AgI–Ag_2S membrane-electrode 443–449

N. VOICULESCU, Reactions of coordinated ligands. X. Aluminumorganic compounds of salicylaldoxime with Ni(II), Pd(II) and Cu(II) ions and their adducts with nitrogen Lewis bases 451–457

G. BOURCEANU, V. ABABI, GH. POPA and M. SANDULOVICIU, Phenol obtainment from benzene in oxygen plasma generated by a high frequency discharge. II. The phenol formation mechanism 459–469

J. P. FAYET, M. C. VERTUT, P. MAURET, R. M. CLARAMUNT et J. ELGUERO, Azolides. IX. Étude de la conformation des azolides par dipôlemétrie 471–474

COMPTES RENDUS 475–479

Revue Roumaine de Chimie, **22**, *3*, 321–325 (1977)

A CHRONOPOTENTIOMETRIC STUDY OF THE STRONTIUM(II) ION IN MOLTEN POTASSIUM NITRATE

S. STERNBERG and T. VIŞAN
Dept. of Physical Chemistry and Electrochemical Technology
Polytechnic Institute, Bucharest

Received January 30, 1976

Strontium discharge on platinum electrode is studied in the mixtures $KNO_3-Sr(NO_3)_2$ and KNO_3-SrCl_2 at various temperatures (350 – 420°). The values of interdiffusion coefficients of strontium (II) ion, the activation energy for diffusion and the pre-exponential factor have been evaluated by chronopotentiometric method.

1. INTRODUCTION

The alkaline-earth metal ions are electrochemically considered to have a very negative reducing potential.

There may be changes in the potential series of different ions of various molten halide systems,[1-3] but in all the cases the electrode potentials of the alkaline-earth cations (with the exception of magnesium ion) are very close to the alkali metals (sodium and potassium), the difference being within the range 0.01 – 0.25 V.

This close-range of the discharging potentials has discouraged the chronopotentiometric and polarographic studies of the cations from the second main group (II-A) dissolved in a salt of the alkali metals.

There is a larger difference within the molten nitrates between the alkali metal ion and the divalent ion, because of the secondary reactions appearing at the cathode.[4]

In the present paper we present the chronopotentiometric study of the strontium (II) ion in molten potassium nitrate.

2. EXPERIMENTAL

The working galvanostatic device for the chronopotentiometric determinations was described in the previous publications.[5,6]

---

[1] Iu. K. Delimarskii and B. F. Markov, "Elektrokhimyia Rasplavlenikh Solei", Metallurghizdat, Moscow, 1960.

[2] A. F. Alabyshev, M. F. Lantratov and A. G. Morachevskii, "Electrody Sravnenyia dlia Rasplavlenikh Solei", Metallurghizdat, Moscow, 1965.

[3] R. W. Laity, *J. Chem. Educ.*, **39**, 67 (1962).

[4] H. E. Bartllet and K. E. Johnson, *J. Electrochem. Soc.*, **114**, 64 (1967).

[5] S. Sternberg and C. Herdlicka, *Rev. Roumaine Chim.*, **14**, 991 (1969).

[6] T. Vişan, D. P. Geană and S. Sternberg, *Rev. Roumaine Chim.*, **21**, 1153 (1976).

The cathode (s = 0.4 — 0.7 cm^2) and the anode (s = 3 — 4 cm^2) are made from platinum foils. The reference electrode consists of a platinum wire dipped into the working molten electrolyte and placed into a special small compartment.

The chronopotentiograms were recorded on a Philips X — Y recorder (either in conjunction with a low frecquency waveform generator or with a Philips time base).

Some chronopotentiometric transients were photographed on the screen of a C—1—19 oscilloscope.

Strontium ions were introduced into the melt as $Sr(NO_3)_2$ or $SrCl_2$. Strontium salts were heated at 200° for several hours. KNO_3 solvent was recrystallised with bidistilled water, twice melted and dried at 200°.

The current was reversed after each chronopotentiogram for redissolution of the deposited cathodic product.

Before each determination 10 — 15 minutes were allowed in order to establish the stationary electrode potential.

3. RESULTS AND DISCUSSION

Strontium chronopotentiograms were obtained in $KNO_3-Sr(NO_3)_2$ and KNO_3-SrCl_2 molten systems at different temperatures (350 — 420°) and Sr^{2+} concentrations ($0.8 - 8.4 \times 10^{-2}$ mol/l). The current densities were 1 — 30 mA/cm^2. Under these conditions the transition time measured by drawing tangents [7] was 0.5 — 2.0 s.

Typical chronopotentiograms obtained in $KNO_3-Sr(NO_3)_2$ and KNO_3-SrCl_2 solutions are shown in Fig. 1 — 2. They have a similar behaviour. For a given concentration in Sr^{2+} ion, the product $i\,\tau^{1/2}$ (i is the current density and τ the transition time) is constant at different current densities. We have also found the constancy of $i\,\tau^{1/2}/c^{\circ}$ ratio (c° is the concentration of Sr^{2+} ion) at any concentration.

The interdiffusion coefficients of strontium (II) ion in molten KNO_3 were calculated from the Sand equation. The results are listed in Table 1.

The temperature dependence of interdiffusion coefficient (D) is represented by an Arrhenius-type equation. Figure 3 shows the $\log D - 1/T$ dependence, which corresponds to the following equation:

$$D = 6.63 \times 10^{-3} \exp\left(-\frac{8150}{RT}\right), \quad (350 - 420^{\circ}) \qquad (1)$$

The numerical values of the activation energy for diffusion and the pre-exponential factor were determined by the least squares method.

To calculate the interdiffusion coefficient of strontium (II) ion, the assumption has been made that the number (n) of electrons which participate in the cathodic reaction is n = 2.

In the molten nitrates, the electrode potential for the reduction of strontium ion to metal:

$$Sr^{2+} + 2e \rightarrow Sr \qquad (2)$$

is not known, but one could consider that strontium metal should be produced at very negative potentials.

---

[7] S. Sternberg and T. Vişan, *Rev. Roumaine Chim.*, **18**, 221 (1973).

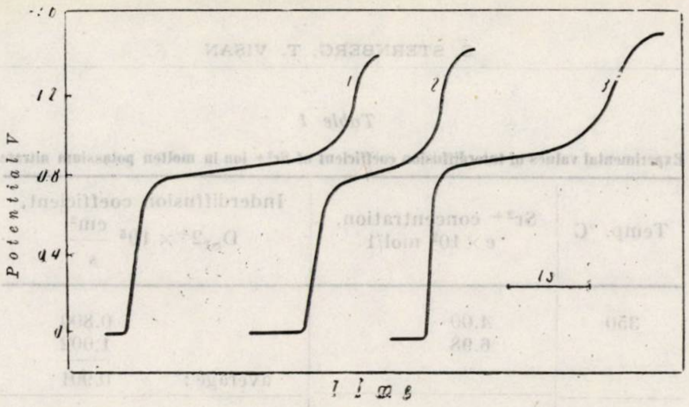

Fig. 1. — Chronopotentiograms for the cathodic reduction on Pt of strontium ion from $KNO_3-Sr(NO_3)_2$ systems.

Temperature ; 380° ; $1 - c = 3.08 \times 10^{-2}$ mol/l ; $i = 13.5 \times 10^{-3}$ A/cm² ; $2 - c = 3.08 \times 10^{-2}$ mol/l ; $i = 16 \times 10^{-3}$ A/cm² ; $3 - c = 7.0 \times 10^{-2}$ mol/l ; $i = 30 \times 10^{-3}$ A/cm².

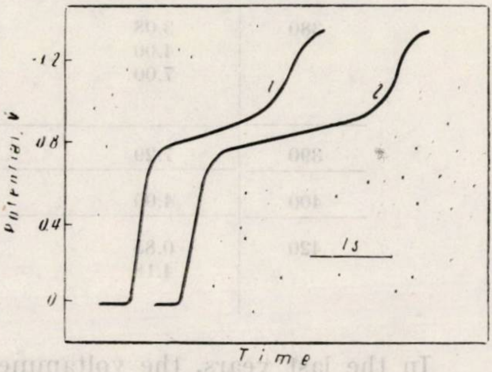

Fig. 2. — Chronopotentiograms for the cathodic reduction on Pt of strontium ion from KNO_3-SrCl_2 system.

Temperature ; 400° ; concentration = 4×10^{-2}mol/l ; $1 - i = 24 \times 10^{-3}$ A/cm² ; $2 - i = 14 \times 10^{-3}$ A/cm²

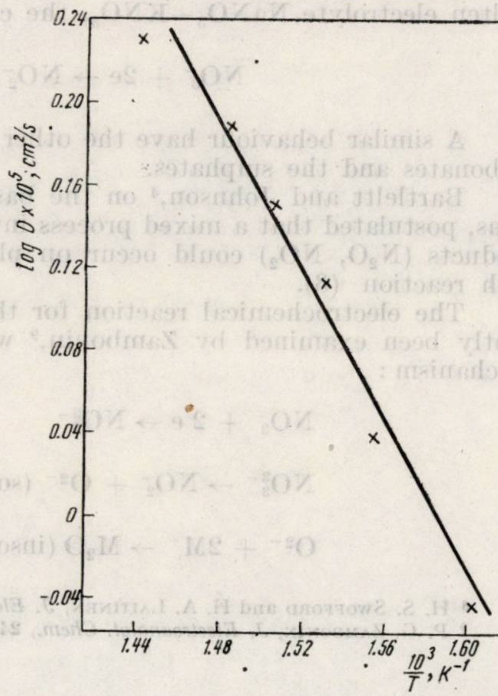

Fig. 3. — Arrhenius dependence of the strontium ion interdiffusion coefficient in molten KNO_3.

Table 1

Experimental values of interdiffusion coefficient of Sr^{2+} ion in molten potassium nitrate

Temp. °C	Sr^{2+} concentration, $c \times 10^2$ mol/1	Inderdiffusion coefficient, $D_{Sr^{2+}} \times 10^5 \frac{cm^2}{s}$
350	4.00	0.800
	6.98	1.002
		average : 0.901
370	6.06	1.150
	6.20	1.230
	8.40	0.900
		average : 1.093
380	3.08	1.300
	4.00	1.388
	7.00	1.200
		average : 1.296
390	7.29	1.410
400	4.00	1.539
420	0.85	1.710
	4.18	1.710
		average : 1.710

In the last years, the voltammetric studies[8] indicate that, in the molten electrolyte $NaNO_3-KNO_3$, the cathodic reaction is :

$$NO_3^- + 2e \rightarrow NO_2^- + O^{2-} \tag{3}$$

A similar behaviour have the other oxianionic molten salts e.g., the carbonates and the sulphates.

Bartlelt and Johnson,[4] on the basis of thermodynamic considerations, postulated that a mixed process involving the formation of gaseous products (N_2O, NO_2) could occur on platinum electrode concomitantly with reaction (3).

The electrochemical reaction for the reduction of NO_3^- ion has recently been examined by Zambonin,[9] who has suggested the following mechanism :

$$NO_3^- + 2\,e \rightarrow NO_3^{3-} \tag{4}$$

$$NO_3^{3-} \rightarrow NO_2^- + O^{2-} \text{ (soluble} \tag{5}$$

$$O^{2-} + 2M^+ \rightarrow M_2O \text{ (insoluble)} \tag{6}$$

---

[8] H. S. SWOFFORD and H. A. LAITINEN, *J. Electrochem. Soc.*, **110**, 814 (1963).

[9] P. G. ZAMBONIN, *J. Electroanalyt. Chem.*, **24**, 365 (1970).

The mechanism illustrated by the reactions (4 — 6) develops at a potential of ~ 1.5 V more electropositive than the reaction similar to (2), and we can consider, on the whole, that the cathodic process is depolarized by the presence of alkali metal ion in oxidant nitrate medium.

The strontium ion in molten KNO_3 shifts the potential of reaction (3) towards more positive values. We have found for $E_{\tau/4}$ (the potential at the point where $t = \tau/4$) in $KNO_3-Sr(NO_3)_2$ and KNO_3-SrCl_2 systems having strontium concentrations of $\sim 10^{-2}$ mol/l values with 0.4 — 0.8 V more positive than the cathodic reduction potential of the solvent.

In conclusion, we suggest for cathodic deposition of the strontium ion a mechanism which can be described by the equations:

$$NO_3^- + 2e \rightarrow NO_2^- + O^{2-} \qquad (7)$$

$$O^{2-} + Sr^{2+} \rightarrow SrO \quad \text{(insoluble)} \qquad (8)$$

This mechanism justifies the n = 2 value introduced into the Sand equation to calculate the interdiffusion coefficient of strontium ion in molten potassium nitrate.

These chronopotentiometric results have been confirmed by the cyclic voltammetric study of the same molten systems.[10]

---

[10] S. STERNBERG and T. VIŞAN, *Rev. Roumaine Chim.*, to be published.

Revue Roumaine de Chimie, **22**, *3*, 327–333 (1977)

ÉTUDE DES RÉACTIONS ENTRE D_2^+ ET CH_nD_{4-n} À L'AIDE D'UN SPECTROMÈTRE DE MASSE À DEUX ÉTAGES

EMILIA CONSTANTIN* et J. CH. ABBE**

* Faculté de Physique, Cluj, 1, str. Kogălniceanu, Roumanie

** Centre de Recherches Nucléaires, Laboratoire de Chimie Nucléaire, 67037 Strasbourg CEDEX, FRANCE

Reçu le 25 avril 1975

Les résultats expérimentaux obtenus avec un spectromètre de masse à deux étages, de type longitudinal montrent que les collisions entre D_2^+ et CH_nD_{4-n} conduisent aux ions CX_4^+, CX_3^+, CX_2^+, CX_5^+ (X = H, D). On présente la dépendance des sections efficaces relatives de l'énergie du projectile D_2^+ (2 — 100 eV) et les effets isotopiques reliés au transfert de charge.

INTRODUCTION

Dans le présent travail on donne les résultats détaillés concernant une note précédente.[1]

On a étudié les réactions entre D_2^+ et CH_nD_{4-n} avec un spectromètre de masse à deux étages de type longitudinal[2] ayant D_2^+ comme projectile (2 — 100 eV) et CH_nD_{4-n} dans la chambre de collisions. Le but du travail consiste à établir la dépendance de l'énergie pour les sections efficaces relatives des ions secondaires et les effets isotopiques H — D concernant la formation de ces ions.

On va noter :

1) σ_r, la section efficace relative définie comme $\sigma_r = I_s/I_t$ où I_s désigne le courant ionique qui correspond à l'espèce secondaire et I_t représente le courant ionique total : $I_t = \Sigma I_s$;

2) $CX_n^+ (X = H, D)$ — les ions ayant le nombre total d'atomes $H + D$ égale à « n » ;

3) « A » — les processus de transfert de charge sans dissociation ;
« B » — les processus de transfert de charge avec dissociation ;
« C » — réactions ion — molécule.

On a marqué par un point (ex. $\dot{D}_2^+$) les atomes qui peuvent être transférés de l'ion primaire pendant une interaction de type C(ex. $\dot{D}_2^+ + CH_4 \rightarrow CH_2\dot{D}^+$).

---

[1] J. Ch. Abbe et E. Constantin, *Int. J. Mass Spectrom. Ion Phys.*, **12**, 91 (1973).

[2] J. P. L'Hote, J. Ch. Abbe, J. M. Paulus et R. Igerseim, *Int. J. Mass Spectrcm. Ion Phys.*, **7**, 309 (1971).

RÉSULTATS EXPÉRIMENTAUX

Ions secondaires. Les résultats expérimentaux montrent la formation des ions secondaires par les processus A, B, C : A — ions CX_4^+, B — ions CX_3^+, CX_2^+, C3 — ions CX_3^+, C4 — ions CX_4^+, C5-ions CX_5^+. La section efficace fonction de l'énergie présente un comportement caractéristique pour chaque processus.[1] Ce comportement est évident quand il n'y a pas de juxtapositions des ions de nature différente à la même valeur de m/e. Si une telle juxtaposition existe, la forme de la courbe $(I_1 + I_2)/I_t$ est plus compliquée, mais on peut la prévoir en connaissant la dépendance de l'énergie de ses composants.

Sur la figure 1 (courbes I — IV) on peut poursuivre la variation de I_s/I_t pour les ions ayant m/e égale à celui de l'ion moléculaire CX_4^+ : m/e = = 16, 17, 18, 19, 20. Dans le cas des courbes I — III on remarque la portion initiale descendante déterminée par les ions de type CX_3^+, qui ont m/e égale à celui de l'ion moléculaire. Ainsi, à m/e = 16 a sont présents en même temps les ions CH_4^+ et $CH_2\dot{D}^+$ (courbe I) :

$$\text{m/e} = 16 \qquad \dot{D}_2^+ + CH_4 \rightarrow CH_4^+ \ \text{(processus A)}$$
$$\rightarrow CH_2\dot{D}^+ \ \text{(processus C3)}$$

Des juxtapositions du même type interviennent à m/e = 17 (courbe

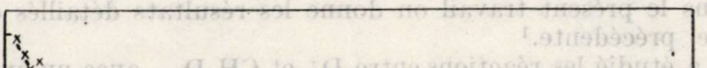

Fig. 1. — Dépendance de l'énergie des sections efficaces relatives pour les ions ayant m/e de l'ion moléculaire (courbes I — V) et ceux formés par la perte de D (courbes VI — IX).

II) et m/e = 18 (courbe III), dans les réactions de D_2^+ avec CH_3D et CH_2D_2 :

$$m/e = 17 \quad \dot{D}_2^+ + CH_3D \rightarrow CH_3D^+ \quad (A)$$
$$\rightarrow CHD\dot{D}^+ \quad (C3)$$

$$m/e = 18 \quad \dot{D}_2^+ + CH_2D_2 \rightarrow CH_2D_2^+ \quad (A)$$
$$\rightarrow CD_2\dot{D}^+ \quad (C3)$$

Dans le cas du système $\dot{D}_2^+$ et CD_3H, aussi bien que D_2^+ et CD_4, les processus C3 donnent des ions CD_3^+ ayant la masse différente de celle des ions moléculaires CD_3H^+ et CD_4. Par conséquent il n'y a pas de juxtapositions et on a seulement les ions moléculaires à m/e = 19 (courbe IV), respectivement 20 (courbe V) — processus A.

Les sections efficaces relatives des ions CX_3^+ qui peuvent provenir de l'ion moléculaire par la perte de D sont représentées sur la fig. 1, courbes VI — IX. On remarque que les courbes pour CD_4, CD_3H, CH_2D_2 (VI — VIII) présentent des portions caractéristiques pour les ions formés par le processus C3. Ainsi :

$$\dot{D}_2^+ + CD_4 \rightarrow CD_3^+ \quad (B)$$
$$\rightarrow CD_2\dot{D}^+ \quad (C3)$$

$$\dot{D}_2^+ + CD_3H \rightarrow CD_2H^+ \quad (B)$$
$$\rightarrow CD\dot{D}H^+ \quad (C3)$$

$$\dot{D}_2^+ + CH_2D_2 \rightarrow CH_2D^+ \quad (B)$$
$$\rightarrow CH_2\dot{D}^+ \quad (C3)$$

Il y a un seul système pour lequel les ions CX_3^+ proviennent seulement du transfert de charge (courbe IX) :

$$D_2^+ + CH_3D \rightarrow CH_3^+ \quad (B)$$

Dans ce cas, la section efficace des ions CX_3^+ présente un maximum. Les autres ions CX_3^+ ont une section décroissante suivie d'un palier.

Les sections efficaces relatives des ions formés à partir de l'ion moléculaire par la perte de H se trouvent sur la figure 2. Il y a de nouveau des juxtapositions des ions formés soit par des processus C3, soit par B, excepté les ions CX_3^+ de la réaction (courbe I) suivante :

$$D_2^+ + CH_4 \rightarrow CH_3^+ \quad (B)$$

dont la valeur de m/e est différente de celle de CD_2H^+ formé par R.I.M. Par conséquent, la courbe de CH_3^+ correspond au transfert de charge.

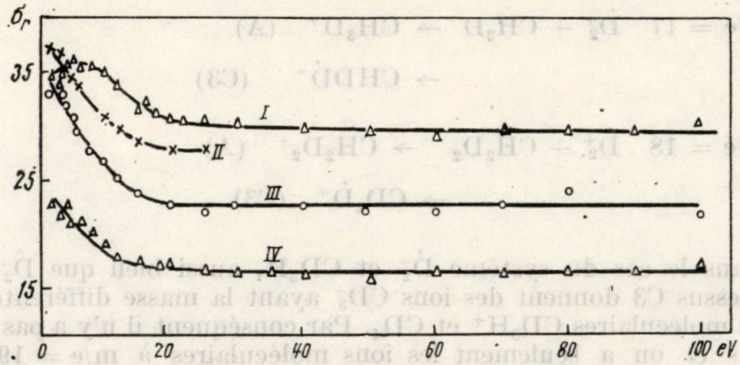

Fig. 2. — Dépendance de l'énergie des sections efficaces relatives des ions $CX_3^+ (X = H, D)$ formés dans les réactions : I. $D_2^+ + CH_4 \rightarrow CH_3^+$; II. $\dot{D}_2^+ + CH_3D \rightarrow CH_2D^+ + CH_2\dot{D}^+$; III. $\dot{D}_2^+ + CH_2D_2 \rightarrow CD_2H^+ + CD\dot{D}H^+$; IV. $\dot{D}_2^+ + CD_3H \rightarrow CD_3^+ + CD_2\dot{D}^+$.

Le comportement des ions CDH^+ et CH_2^+ formés par la perte de $D_2(2D)$ est donné par les courbes I et II de la fig. 3, pendant que les courbes I et II de la figure 4 correspondent aux ions formés par la perte de $DH(D + H)$ à partir des mêmes molécules : CD_3H et CH_2D_2. La courbe III (fig. 4) se réfère aux ions $CH_2^+ + CD^+$ provenant de CH_3D.

Sur la figure 5 on peut voir l'évolution des sections efficaces relatives pour les ions CX_4^+ (courbe III — VI) et CX_5^+ (courbes I, II) provenant des réactions ion — molécule. On remarque que la section des ions CX_4^+ décroît lorsque l'énergie augmente, pendant que celle des ions CX_5^+ augmente à de faibles énergies et décroît légèrement à de hautes énergies.

$\dot{D}_2^+ + CH_3D \rightarrow CH_3D\dot{D}^+$ (C5) courbe I

$\dot{D}_2^+ + CH_3 \rightarrow CH_4\dot{D}^+$ (C5) courbe II

$\dot{D}_2^+ + CH_3D \rightarrow CH_2D\dot{D}^+$ (C4) courbe III

$\dot{D}_2^+ + CH_4 \rightarrow CH_3\dot{D}^+$ (C4) " IV

$\dot{D}_2^+ + CH_2D_2^+ \rightarrow CHD_2\dot{D}^+$ (C4) " V

$\dot{D}_2^+ + CHD_3 \rightarrow CD_3\dot{D}^+$ (C4) " VI

Effets isotopiques. Les effets isotopiques concernant la formation des ions CX_3^+ et CX_2^+ sont présentés sur les figures 6 et 7. Les effets sont appréciés en considérant les rapports suivants :

1. y_e pour les ions CX_3^+ :

$$y_e = \frac{I(CX_3^+)}{I(CH_3^+)CH_4}$$

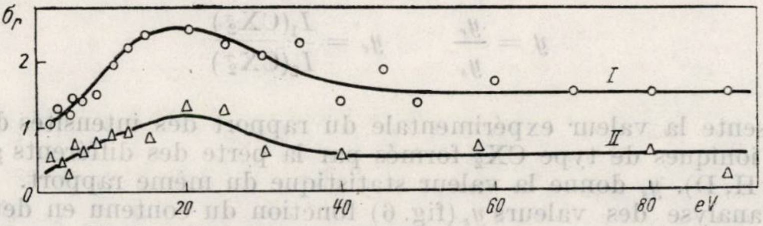

Fig. 3. — Variation de σ_r avec l'énergie pour les ions CX_2^+ :
I. $D_2^+ + CD_3H \rightarrow CDH^+$; II. $D_2^+ + CH_2D_2 \rightarrow CH_2^+$.

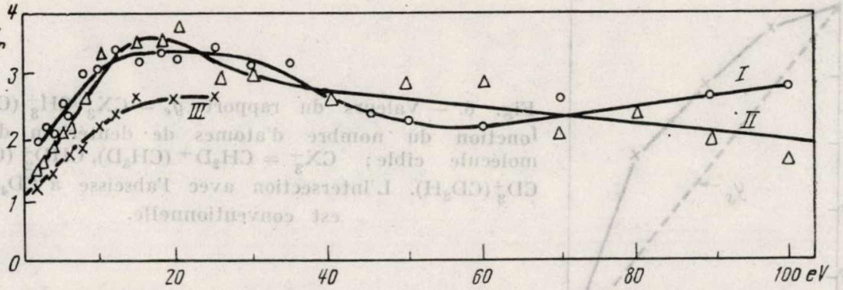

Fig. 4. — Variation de σ_r avec l'énergie pour les ions CX_2^+ :
I. $D_2^+ + CD_3H \rightarrow CD_2^+$; II. $D_2^+ + CH_2D_2 \rightarrow CDH^+$; III. $D_2^+ + CH_3D \rightarrow CH_2^+$.

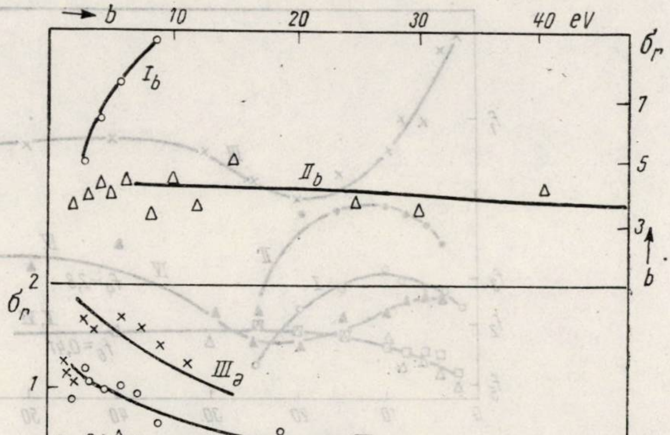

Fig. 5. — Dépendance de l'énergie des sections efficaces relatives pour les ions formés par processus C5 — courbes I, II et C_4 — courbes III — VI.

$I(CX_3^+)$ représente l'intensité d'une espèce ionique qui se forme par la perte de H :

$$CX_3^+ = CH_2D^+\ (CH_3D),\ \ CHD_2^+(CH_2D_2),\ \ CD_3^+(CD_3H)$$

2. y pour les ions CX_2^+ :

$$y = \frac{y_e}{y_s} \qquad y_e = \frac{I_1(CX_2^+)}{I_2(CX_2^+)}$$

y_e représente la valeur expérimentale du rapport des intensités de deux espèces ioniques de type CX_2^+ formés par la perte des différents groupes X_2(X = H, D). y_s donne la valeur statistique du même rapport.

L'analyse des valeurs y_e (fig. 6) fonction du contenu en deutérium de l'ion primaire montre que les effets sont du même type qu'en fragmen-

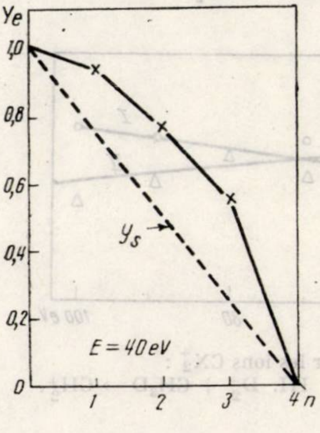

Fig. 6. — Valeurs du rapport $y_e = CX_3^+/CH_3^+\ (CH_4)$ en fonction du nombre d'atomes de deutérium dans la molécule cible ; $CX_3^+ = CH_2D^+\ (CH_3D)$, $CHD_2^+\ (CH_2D_2)$, $CD_3^+(CD_3H)$. L'intersection avec l'abscisse à CD_4(n = 4) est conventionnelle.

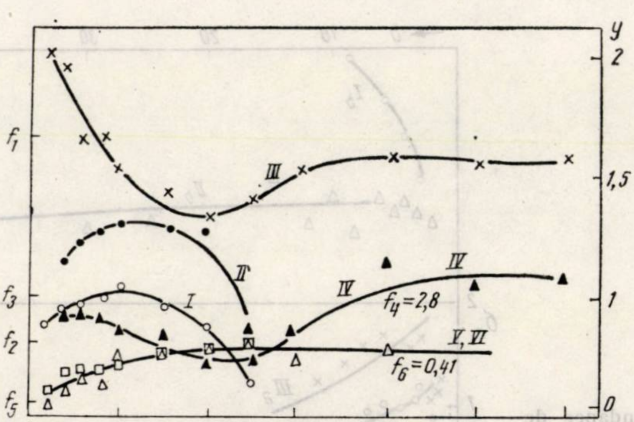

Fig. 7. — I. $CDH^+(CD_3H)/CD_2^+(CD_4)$; II. $CH_2^+(CH_2D_2)/CD_2^+\ (CD_4)$; III. $CD_2^+(CD_3H)/CDH^+(CD_3H)$; IV. $CDH^+(CH_2D_2)/CH_2^+(CH_2D_2)$; V. $CDH^+(CH_2D_2)/CD_2^+(CD_3H)$; VI. $CH_2^+(CH_3D)/CD_2^+(CD_3H)$.

tation. La perte de H est donc plus probable pour les composés deutérés que pour le CH_4. L'effet croît avec le nombre d'atomes de D de la molécule-cible : l'écart par rapport aux valeurs statistiques, marquées par la droite descendante, augmente de CH_3D vers CD_3H. L'effet reste constant en commençant de 35 à 40 eV.

En même temps, les valeurs[2] du rapport $CD_3^+(CD_3H)/CD_2H^+(CD_3H)$ montrent que la perte de H pour CD_3H est plus probable que celui de D. A 40 eV, la valeur expérimentale est égale à 0,87 et celle statistique à 0,33, ainsi que l'effet est $y = 2{,}62$.

La figure 7 donne y pour les ions CX_2^+. On a noté par f_i les valeurs correspondant à la fragmentation. Il résulte de cette figure :

— les courbes I et II ont des allures croissantes suivies des maximums. Le $CDH^+(CD_3H)$ se forme moins aisément que le $CD_2^+(CD)$ pendant que pour le $CH_2^+(CH_2D_2)$ la situation est inverse. Il résulte donc que les probabilités P de perte de 2D s'arrangent dans l'ordre suivant : $P(CH_2D_2) > > P(CD_4) > P(CD_3H)$. Les valeurs de f_2 et f_1 marquées sur la figure 7 indiquent des effets inverses par rapport à la fragmentation (électrons ayant 70 eV) ;

— on compare la formation de $CD_2^+(CD_3H)$ et $CHD^+(CD_3H)$ d'une part et celle de $CDH^+(CD_2H_2)$ et $CH_2^+(CH_2D_2)$ à l'aide des courbes III respectivement IV. Les courbes descendent, passent par un minimum, puis elles restent constantes. Les valeurs pour CD_3H sont supérieures à l'unité ou bien la formation de CD_2^+ est favorisée par rapport à CDH^+. La nature de l'effet correspond à celui de la fragmentation. Pour CH_2D_2 cette correspondance existe dès le moment où $y > 1$, aux énergies plus élevées que 35 eV. Il paraît donc que la formation de $CDH^+(CH_2D_2)$ devient favorisée à partir de cette énergie ;

— les courbes V, VI montrent que les probabilités de formation de $CDH^+(CH_2D_2)$ et $CH_2^+(CH_3D)$ sont inférieures à la probabilité de formation de $CD_2^+(CD_3H)$. D'autre part, y_5 et y_6 sont qualitativement en concordance avec f_5 et f_6.

CONCLUSION

Les résultats présentés ci-dessus montrent que l'interaction entre D_2^+ et les méthanes deutérés conduit au transfert de charge et R.I.M. A faibles énergies, la plus importante des RIM est celle qui détermine la formation des ions CX_3^+.

Les sections efficaces relatives dépendent de l'énergie.

Dans le transfert de charge avec dissociation on a mis en évidence des différences entre la probabilité de perte de H et D.

Les résultats concernant les systèmes $D_2^+ + CH_nD_{4-n}$ sont en accord avec ceux obtenus pour $H_2^+ + CH_nD_{4-n}$.[3]

Remarques et remerciements. Le présent travail a été réalisé à l'Institut de Chimie Nucléaire, Strasbourg, France. Les auteurs remercient M. R. Keller pour la partie technique du travail.

---

[3] E. Constantin et J. Ch. Abbe, *Int. J. Mass Spectrom. Ion Phys.*, envoyé pour publication.

Revue Roumaine de Chimie, 22, 3, 335–343 (1977)

ESTUDIO TEORICO DE LA NATURALEZA DE CONSTANTES DE FUERZA. I

MOLECULAS DIATOMICAS

F. ARCE, J. CASADO, M. A. RÍOS y V. TATO
Departamento de Química Física, Facultad de Ciencias, Universidad de Santiago, Centro Coordinado del C.S.I.C., España

28 apr. 1975

The energetic interpretation of the force constants of diatomic molecules is analyzed by the CNDO/2 and CNDOBW approximations. Both methods give the same vision of the phenomenon in terms of energetic contributions. The dissimilarity of the force constant results by these methods is also discussed.

1. INTRODUCCION

En esta investigación se intenta dar una interpretación del campo de fuerzas molecular y, en última instancia, de las correspondientes constantes de fuerza, a través de los efectos que los movimientos intramoleculares ejercen sobre ciertos términos energéticos mecanocuánticos, como energía total y energías de canje, repulsión y penetración. Estos términos se evalúan dentro del ámbito de la aproximación Born-Oppenheimer, utilizando métodos CNDO.

2. PLANTEAMIENTO DEL METODO

Dentro de la aproximación CNDO, la energía total molecular puede expresarse como suma de términos energéticos físicamente significativos,[1] que, a partir de ahora, serán denominados en este trabajo "energías de partición":

$$E_U^A = \sum_{\mu \in A} P_{\mu\mu} U_{\mu\mu}$$

---

[1] H. Fischer y H. Kollmar, *Theor. Chim. Acta*, **16**, 163 (1970).

que representa la suma de las energías cinética y potencial de los electrones situados sobre el átomo A.

$$E_J^A = \frac{1}{2} P_A^2 \gamma_{AA}$$

es la energía de repulsión de los electrones situados sobre el centro A;

$$E_K^A = -\frac{1}{4} \gamma_{AA} \sum_{\mu \in A} \sum_{\nu} P_{\mu\nu}^2$$

corresponde a interaciones de canje monocétricas;

$$E_V^{AB} = -P_A V_{AB} - P_B V_{BA}$$

representa la energía potencial de interacción de la densidad electrónica del átomo A con el núcleo B más la de los electrones de B con el campo del núcleo A;

$$E_R^{AB} = 2 \sum_{\mu \in A} \sum_{\nu \in B} P_{\mu\nu} \beta_{AB}^0 S_{\mu\nu}$$

es la contribución de las integrales de resonancia a la energía del enlace $A - B$, siendo la principal característica del enlace covalente;

$$E_J^{AB} = P_A P_B \gamma_{AB}$$

es la energía de repulsión entre los electrones de los átomos A y B;

$$E_K^{AB} = -\frac{1}{2} \gamma_{AB} \sum_{\mu \in A} \sum_{\nu \in B} P_{\mu\nu}^2$$

representa la estabilización debida a interacciones de canje; por último E_N^{AB} es la energía de repulsión entre cores, que se calcula según un modelo electróstático sencillo.

Para desplazamientos atómicos suficientemente pequeños, la energía total molecular puede expresarse[2]

$$2E_T = \sum_{i,j} K_{ij} S_i S_j$$

---

[2] T. SHIMANOUCHI, "Physical Chemistry. An Advanced Treatise", vol. IV, Academic Press, Nueva York, 1970, p. 233.

donde

$$K_{ij} = \left(\frac{\partial^2 E_T}{\partial S_i \partial S_j} \right)$$

son las constantes de fuerza y

$$S_i = q_i - q_{io}$$

en la que q_{io} indica la coordenada interna q_i en el equilibrio y q_i la misma coordenada desplazada.

Expresiones equivalentes pueden ser establecidas para los valores de las energías correspondientes a los términos energéticos de partición. Puesto que la suma de estas energías es la energía total molecular, la constante de fuerza de la molécula será también la suma de las constantes de fuerza originadas por estos terminos energéticos; estas constantes se denominarán en el presente trabajo "constantes de partición".

3. APLICACION A MOLECULAS DIATOMICAS

Para la realización de este estudio se han elegido las aproximaciones CNDO/2, propuesta por Pople y Segal,[3] y CNDO BW III, propuesta por Boyd y Whitehead.[4]

Las moleculas estudiadas con la aproximación CNDO/2 han sido: H_2, Li_2, C_2, N_2, O_2, F_2, LiH, BH, NH, FH, FLi y CO, y con la CNDOBW III: H_2, B_2, C_2, N_2, O_2, F_2, BH, NH, FB, y CO.

En el caso de moleculas diatómicas la elección de los parámetros internos q_i, y el establecimiento de los desplazamientos S_i resultan sencillos, pues la única coordenada interna que expresa la posición relativa de los núcleos es la distancia internuclear, R, de modo que la función, potencial puede expresarse:

$$2E_T = K(\Delta R)^2$$

El cálculo de la energía total molecular se llevó a cabo para diez distancias interatómicas diferentes tomadas con intervalos de 0,01 Å en torno a la de equilibrio y los valores de la energía total y las distancias se ajustaron a un polinomio de segundo grado mediante el criterio de mínimos cuadrados.

---

[3] J. A. Pople y G. A. Segal, *J. Chem. Phys.*, **44**, 32 89 (1966).

[4] R. J. Boyd y M. A. Whitehead, *J. C. S. Dalton*, **1972**, 73.

4. RESULTADOS Y DISCUSION

En la tabla 1 se comparan las constantes de fuerza obtenidas en este trabajo con los correspondientes valores experimentales.[5]

La aproximación CNDO/2 conduce a unos valores excesivamente elevados para las constantes de fuerza, como consecuencia de lo inadecuado de su parametrización para este tipo de cálculos, aspecto en el que se insistirá más adelante. Por ello se repitió el proceso empleando la aproximación CNDOBW III que permitió obtener unos resultados más acordes con la experiencia, si bien se ha de tener en cuenta que el objeto del trabajo no es tanto la obtención de valores numéricos de constantes de fuerza, como la interpretación teórica de las mismas.

Tabla

Constantes de fuerza

	H_2	C_2	N_2	O_2	F_2	BH
K(CNDO/2)	10,12	35,57	50,96	56,80	56,70	8,71
K(CNDOBW)	6,23	14,95	22,84	21,54	13,88	3,77
K(exp.)	5,69	12,20	23,00	11,80	4,73	3,04

Los valores obtenidos para las constantes de fuerza y constantes de partición aplicando las aproximaciones CNDO/2 y CNDOBW III aparecen en las tablas 2 y 3 respectivamente.

La discusión de las constantes de fuerza en términos de las constantes de partición que figuran en las Tablas 2 y 3 se hace difícil debido a la gran cantidad de términos que aparecen y a la diversidad de magnitud de los diferentes términos al pasar de unas moléculas a otras. En orden a una mayor sistematización, es mejor hacer la discusión basándose en "porcentajes de constante de fuerza", es decir, en la relación entre las constantes de partición y las constantes de fuerza total de la molécula; de ese modo se observa mejor el peso con que contribuye cada constante de partición a la constante total al pasar de una molécula a otra.

En las Tablas 4 y 5 se muestran las contribuciones de las distintas constantes de partición en las aproximaciones CNDO/2 y CNDOBW, respectivamente, expresadas en tantos por uno.

Como puede observarse, las formas energéticas que más contribuyen a la magnitud de la constante de fuerza son E_N^{AB}, E_J^{AB}, y E_V^{AB} es decir, los términos electrostáticos bicéntricos. Sólo resultan altas las contribuciones monocéntricas E_U y E_J en el caso de las moléculas heteronucleares en las que aparece un átomo de flúor. Ni el signo ni la magnitud de las contribuciones guardan relación alguna con la naturaleza de los átomos presentes en la molécula; es por esto conveniente agrupar de otra forma las contribuciones energéticas, teniendo en cuenta la naturaleza de las mismas; estas nuevas agrupaciones son: suma de términos monocéntricos o bicéntricos, suma de términos repulsivos (E_J, E_N) y términos electrostáticos (E_J, E_V, E_N). En la Tabla 6 aparecen estos términos para las dos aproximaciones empleadas.

---

[5] D. R. Herschbach y V. W. Laurie, University of California, Radiation Laboratory Report, UCRL 9694 (Berkeley, California 1961).

1

en mdin/Å

NH	FH	BF	CO	Li_2	B_2	FLi	LiH
15,06	20,40	18,04	42,05	0,84	—	2,09	1,95
6,48	11,80	9,15	20,52	—	3,94	—	—
6,03	9,66	8,07	19,00	0,26	3,58	2,48	1,03

El que la constante de fuerza sea una propiedad del enlace se deduce de que el porcentaje de contribución de la suma de términos bicéntricos es cercano a la unidad en casí todos los casos; hay que notar el hecho de que, aunque las contribuciones E_U y E_J monocéntricas sean apreciables, siempre son de signo contrario y de magnitud muy parecida.

En las columnas 5, 6, 10, y 11 de la Tabla 6 aparece la relación del porcentaje de repulsiones y de términos electrostáticos al restante. El hecho de que la relación entre los términos repulsivos y los que no lo son sea siempre superior a la unidad indica que la constante de fuerza es de naturaleza repulsiva. Análoga conclusión se puede deducir en el caso de los términos electrostáticos, si bien aquí se presentan como excepciones el BF y FLi en las aproximaciones CNDOBW y CNDO/2, respectivamente.

El carácter dinámico de la constante de fuerza se pone de manifiesto por el hecho de que no guarda relación alguna la magnitud de la contribución energética de un término a la energía total con la magnitud de su constante de fuerza de partición.

La visión de la constante de fuerza que se obtiene con las dos aproximaciones empleadas en el cálculo es cualitativamente la misma. Sin embargo no se obtienen valores parecidos para las constantes de fuerza en las dos metodologías. La causa de este comportamiento radica en que las contribuciones más importantes (E_V^{AB}, E_N^{AB}, E_J^{AB}) son muy superiores en el CNDO/2 a las mismas contribuciones en el CNDOBW y, por lo tanto, su suma también lo es. De estos tres términos sobre los que recae el peso de la constante de fuerza, dos son dependientes de la integral de repulsión γ_{AB} y de la carga electrónica de los átomos, P_A y P_B. Dado que las cargas obtenidas por ambos métodos son parecidas, y en el caso de moléculas homonucleares son, por supuesto, iguales, puede decirse que esta diferencia de contribuciones es debida al distinto comportamiento de γ_{AB} con la

Tabla 2

Contribuciones a las constantes de fuerza en mdin/Å (CNDO/2)

AB	E_T	E_U^A	E_U^B	E_K^A	E_K^B	E_J^A	E_J^B	E_K^{AB}	E_J^{AB}	E_R^{AB}	E_V^{AB}	E_N^{AB}
H_2	10,12	0,00	0,00	0,00	0,00	0,00	0,00	−0,21	0,42	−0,18	−0,82	10,92
Li_2	0,84	− 0,02	− 0,02	0,00	0,00	0,00	0,00	0,02	0,00	0,38	0,02	0,45
C_2	35,57	0,03	0,03	−1,53	−1,53	0,00	0,00	−0,16	4,60	−6,52	−9,20	48,42
N_2	50,96	1,29	1,29	0,00	0,00	0,00	0,00	−1,23	20,46	−6,79	−40,93	76,81
O_2	56,80	1,60	1,60	0,00	0,00	0,00	0,00	−1,43	51,59	−7,70	−103,3	114,4
F_2	56,7	2,35	2,35	0,00	0,00	0,00	0,00	−1,00	99,7	−8,30	−199,4	161,1
LiH	1,95	− 0,01	− 0,14	0,01	−0,10	− 0,03	0,20	0,03	− 0,06	0,77	0,08	1,18
BH	8,71	− 1,28	0,90	−0,32	0,56	1,95	−1,10	−0,16	− 0,50	0,60	−0,18	8,24
NH	15,06	− 0,50	0,19	−0,13	0,08	1,09	−0,18	−0,36	2,27	−0,40	−6,63	19,60
FH	20,40	− 3,30	0,40	−0,40	0,20	4,80	−0,40	−0,50	4,30	−3,40	−14,60	33,40
FB	18,04	26,59	− 5,11	2,86	−0,45	−25,46	6,11	−2,04	20,24	−8,27	−31,80	35,37
FLi	2,09	5,90	− 0,16	0,77	−0,02	− 6,33	0,10	−0,26	2,10	−1,03	−2,29	3,22
CO	42,05	− 4,00	10,67	−0,70	−0,53	5,25	−9,47	−0,30	21,25	−8,10	−40,06	65,75

Tabla 3

Contribuciones a las constantes de fuerza en mdin/Å (CNDOBW)

AB	E_T	E_U^A	E_U^B	E_K^A	E_K^B	E_J^A	E_J^B	E_K^{AB}	E_J^{AB}	E_R^{AB}	E_V^{AB}	E_N^{AB}
H_2	6,23	0,00	0,00	0,00	0,00	0,00	0,00	0,05	0,08	0,21	0,18	5,88
B_2	3,94	0,16	0,16	0,07	0,07	0,00	0,00	−0,19	0,50	−0,92	−0,98	5,36
C_2	14,95	0,45	0,45	0,00	0,00	0,00	0,00	−0,49	1,67	−3,67	−3,34	19,98
N_2	22,84	0,86	0,86	0,00	0,00	0,00	0,00	−0,20	3,26	−1,08	−6,54	25,67
O_2	21,54	1,28	1,28	0,00	0,00	0,00	0,00	−0,42	15,00	−5,26	−29,98	39,66
F_2	13,88	1,16	1,16	0,00	0,00	0,00	0,00	−0,27	26,60	−5,02	−53,19	43,45
BH	3,77	0,23	−0,05	0,01	−0,04	−0,05	0,05	−0,06	0,20	0,53	−0,55	3,47
NH	6,48	−2,26	0,62	−0,31	0,22	2,64	−0,44	0,06	−1,97	0,35	0,91	6,66
FH	11,80	−6,02	0,84	−0,67	0,24	6,93	−0,46	0,19	−3,92	−0,33	1,23	13,76
FB	9,15	11,11	−2,32	1,10	−0,20	−9,99	2,52	−1,06	10,04	−2,94	−14,60	15,49
CO	20,52	−0,48	2,17	−0,56	−0,61	0,90	−0,62	0,28	6,22	−1,77	−11,78	26,84

Tabla 4

Porcentajes de constantes de partición (CNDO/2)

$A-B$	E_U^A	E_U^B	E_K^A	E_K^B	E_J^A	E_J^B	E_K^{AB}	E_J^{AB}	E_R^{AB}	E_V^{AB}	E_N^{AB}
H_2	—	—	—	—	—	—	−0,02	0,04	−0,02	−0,08	1,08
Li_2	−0,02	−0,02	—	—	—	—	0,02	−0,01	0,46	0,02	0,53
C_2	0,00	0,00	−0,04	−0,04	—	—	0,00	0,13	0,18	−0,26	1,36
N_2	0,02	0,02	—	—	—	—	−0,02	0,40	−0,13	0,80	1,53
O_2	0,03	0,03	—	—	—	—	−0,02	0,84	−0,12	−1,69	1,93
F_2	0,04	0,04	—	—	—	—	−0,01	1,59	−0,11	−3,18	2,65
LiH	−0,01	−0,07	0,01	−0,05	−0,02	0,10	0,02	−0,03	0,39	0,04	0,61
BH	−0,14	0,10	−0,04	0,06	0,22	−0,12	−0,02	−0,06	0,07	−0,02	0,94
NH	−0,03	0,01	−0,01	0,00	0,07	−0,01	−0,02	0,15	−0,03	−0,44	1,30
FH	−0,16	0,02	−0,02	0,01	0,23	−0,02	−0,03	0,21	−0,17	−0,71	1,33
BF	−0,28	1,47	−0,02	0,16	0,34	−1,41	−0,11	1,12	−0,46	1,76	1,96
FLi	2,82	−0,07	0,37	−0,01	−3,03	0,05	−0,13	1,00	−0,49	−1,10	1,54
CO	−0,09	0,25	−0,02	−0,01	0,12	−0,22	0,00	0,50	−0,19	−0,95	1,56

distancia. Esto se pone de manifiesto en la representación de las dos expresiones de las integrales de repulsión utilizadas.[6] Las expresiones teóricas que usan base de Slater (CNDO/2), presentan mayor pendiente que las semiempíricas de Ohno (CNDOBW). Hay que añadir además que en la parametrización de Boyd y Whitehead, E_N depende de la integral de repulsión, con lo que la relación entre los términos E_J, E_V y E_N está más equilibrada.

Tabla 5

Porcentajes de constantes de partición (CNDOBW)

$A-B$	E_U^A	E_U^B	E_K^A	E_K^B	E_J^A	E_J^B	E_K^{AB}	E_J^{AB}	E_R^{AB}	E_V^{AB}	E_N^{AB}
H_2	—	—	—	—	—	—	0,00	0,01	0,03	0,03	0,93
B_2	0,04	0,04	−0,01	−0,01	—	—	−0,05	0,13	−0,23	−0,26	1,35
C_2	0,03	0,03	0,00	0,00	—	—	−0,03	0,11	−0,24	−0,23	1,33
N_2	0,04	0,04	—	—	—	—	0,00	0,14	−0,05	−0,29	1,12
O_2	0,06	0,06	—	—	—	—	−0,02	0,70	−0,24	−1,39	1,83
F_2	0,08	0,08	—	—	—	—	−0,02	1,92	−0,36	−3,83	3,13
BH	0,06	−0,01	0,00	−0,01	−0,01	0,01	−0,02	0,05	0,14	−0,15	0,92
NH	−0,35	0,09	−0,05	0,03	0,41	−0,07	0,00	−0,30	0,05	0,14	1,03
FH	−0,51	0,07	−0,06	0,02	0,59	−0,04	0,02	−0,33	−0,03	0,10	1,16
BF	−0,25	1,21	−0,02	0,12	0,28	−1,09	−0,12	1,10	−0,32	−1,59	1,69
CO	−0,02	0,11	−0,03	−0,03	0,04	−0,03	0,01	0,30	−0,09	−0,57	1,31

[6] J. N. MURREL y A. J. HARGET, "Semiempirical SCF Molecular Orbital Theory of Molecules", Wiley-Interscience, Nueva York., 1972.

Tabla 6

Estudio comparativo de las distintas contribuciones energéticas

Molecula	CNDO/2					CNDOBW				
	Electrost.	Repuls.	Bicentr.	Electr. / otros	Repuls. / otros	Electrost.	Repuls.	Bicentr.	Electr. / otros	Repuls. / otros
H_2	1,04	1,12	1,00	26,0	9,3	0,97	0,94	1,00	32,3	23,5
C_2	1,29	1,49	1,08	4,5	3,0	1,21	1,44	0,94	5,8	3,3
N_2	1,13	1,93	0,96	8,7	2,1	0,97	1,26	0,92	32,3	4,8
O_2	1,08	2,77	0,94	13,5	1,6	1,14	1,53	0,88	8,1	2,9
F_2	1,06	4,24	0,92	17,7	4,0	1,22	5,05	0,84	5,5	1,2
BH	0,96	0,98	0,91	24,0	49,0	0,82	0,97	0,96	4,6	32,3
NH	0,97	1,51	0,96	32,3	3,0	1,21	1,07	0,92	5,8	15,3
FH	1,34	2,05	0,93	3,9	2,0	1,48	1,38	0,92	3,1	3,6
BF	3,73	1,83	1,73	1,4	2,2	0,39	1,98	0,76	0,6	2,0
CO	1,11	1,96	0,92	10,1	2,0	1,05	1,62	0,96	21,0	2,6
B_2	—	—	—	—	—	1,22	1,48	0,94	5,5	3,1
LiH	0,70	0,66	0,93	2,3	1,5	—	—	—	—	—
FLi	−1,54	3,52	0,82	−0,6	1,4	—	—	—	—	—
Li_2	0,54	0,52	1,04	1,2	1,1	—	—	—	—	—

Revue Roumaine de Chimie, **22**, *3*, 345–352 (1977)

ESTUDIO TEORICO DE LA NATURALEZA DE CONSTANTES DE FUERZA. II[1]

MOLECULAS TRIATOMICAS

F. ARCE, J. CASADO, M. A. RÍOS y V. TATO
Departamento de Química Física. Facultad de Ciencias. Universidad de Santiago. Centro Coordinado del C.S.I.C. España

28 apr. 1975

The stretching, bending and interaction force constants of triatomic molecules are discussed in terms of energy partitioning using the CNDOBW approximation. The force constants, equilibrium geometries and vibrational frequencies are evaluated for some triatomic molecules.

1. INTRODUCCION

Empleando la metodología indicada en un trabajo anterior,[1] se pretende ahora dar una interpretación teórica a los distintos tipos de constantes de fuerza que aparecen en el campo de fuerzas cuadrático de algunas moléculas triatómicas, analizando la contribución a las mismas de términos energéticos mecanocuánticos con significado físico.

Los sistemas objeto de estudio son : CH_2, H_2O, O_3 y HCN. El cálculo de las energías moleculares se realiza mediante la aproximación CNDOBW[2].

2. APLICACION A MOLECULAS TRIATOMICAS

Para el estudio de moléculas triatómicas hemos considerado conveniente especificar las configuraciones moleculares en función de las coordenadas internas de simetría las cuales, junto con la notación de su correspondiente constante de fuerza, se indican en la Tabla 1.

Para el cálculo de las energías, se varía una coordenada de simetría cada vez, de forma que, una vez optimizada una coordenada, se mantiene fija y se optimiza la siguiente hasta obtener una configuración molecular de energía mínima. Las variaciones de longitud se toman en intervalos de 0,01 Å y las de ángulo, de 1°.

---

[1] Part I: F. ARCE, J. CASADO, M. A. RIOS y V. TATO, *Rev. Roumaine Chim.*, **22**, 335 (1977).

[2] R. J. BOYD y M. A. WHITEHEAD *J. C. S. Dalton*, **1972**, 73.

Tabla 1

Coordenadas internas de simetria

Molécula	Coord. interna	Constante de fuerza
CH_2	$S_1 = (\Delta r_{CH_1} + \Delta r_{CH_2})/\sqrt{2}$	σ_{11}
	$S_2 = r_{CH} \cdot \Delta\Phi$	σ_{22}
	$S_3 = (\Delta r_{CH_1} - \Delta r_{CH_2})/\sqrt{2}$	σ_{33}
OH_2	$S_1 = (\Delta r_{OH_1} + \Delta r_{OH_2})/\sqrt{2}$	σ_{11}
	$S_2 = r_{OH} \cdot \Delta\Phi$	σ_{22}
	$S_3 = (\Delta r_{OH_1} - \Delta r_{OH_2})/\sqrt{2}$	σ_{33}
O_3	$S_1 = (\Delta r_{OO_1} + \Delta r_{OO_2})/\sqrt{2}$	σ_{11}
	$S_2 = r_{OO} \cdot \Delta\Phi$	σ_{22}
	$S_3 = (\Delta r_{OO_1} - \Delta r_{OO_2})/\sqrt{2}$	σ_{33}
CO_2	$S_1 = (\Delta r_{CO_1} + \Delta r_{CO_2})/\sqrt{2}$	σ_{11}
	$S_2 = (\Delta r_{CO_1} - \Delta r_{CO_2})/\sqrt{2}$	σ_{22}
	$S_3 = r_{CO} \cdot \Delta\Phi$	σ_{33}
CNH	Δr_{CH}	k_{11}
	Δr_{CN}	k_{22}
	$\Delta\Phi$	k_{33}

Tabla

Constantes de fuerza de

		E_T	E_U^A	E_U^X	E_K^A	E_K^X	E_J^A	E_J^X	E_K^{AX}
	k_{11}	5,56	– 0,58	0,13	– 0,15	0,05	0,84	– 0,11	–0,01
	k_{12}	0,02	– 0,49	0,07	– 0,09	0,03	0,46	– 0,07	0,03
CH_2	k_{13}	– 0,04	– 0,04	0,00	– 0,02	0,00	– 0,03	0,01	0,01
	k_{33}	0,66	– 3,53	0,60	– 0,62	0,29	3,56	– 0,58	0,14
	k_{11}	8,91	– 4,62	0,42	– 0,55	0,13	5,54	– 0,27	0,08
H_2O	k_{12}	0,17	0,02	– 0,01	– 0,12	0,00	0,02	0,02	0,08
	k_{13}	0,26	– 0,13	0,00	0,12	0,00	0,06	0,00	– 0,06
	k_{33}	0,59	– 7,64	0,62	– 1,83	0,21	8,27	– 0,44	0,87
	k_{11}	12,11	–16,60	9,04	– 5,22	– 6,44	15,86	– 6,82	1,46
	k_{12}	4,13	30,92	–15,35	5,40	4,64	–27,47	13,87	– 1,13
O_3	k_{13}	0,48	44,94	–18,87	4,50	– 0,49	–37,60	20,79	– 2,46
	k_{33}	1,47	– 1,22	– 0,78	2,43	0,49	– 2,25	1,27	– 1,44
	k_{11}	13,15	– 8,08	7,74	– 1,77	– 1,15	5,72	– 7,28	0,38
CO_2	k_{12}	2,65	13,98	–12,79	1,09	– 0,33	–1,78	13,07	0,34
	k_{33}	0,48	– 2,31	1,94	–0,36	0,10	1,56	– 2,03	0,13

El par de constantes de fuerza que interaccionan y su correspondiente constante de fuerza de interacción se calculan ajustando los valores de la energía obtenidos al variar esas dos a un polinomio del tipo

$$2V = aS_1^2 + 2bS_1S_2 + cS_2{}^2$$

según el criterio de mínimos cuadrados.

3. RESULTADOS Y DISCUSION

Con objeto de facilitar la discusión de los resultados, es conveniente considerar constantes de fuerza de las coordenadas internas de valencia (distancias de enlace y ángulos) en lugar de las coordenadas de simetría, visualizándose así mejor el problema, de acuerdo con los modelos más sencillos de la química estructural.

Las transformaciones elevadas a cabo son,[3] para las moléculas no ineales, AX_2,

$$k_{11} = (\sigma_{11} + \sigma_{33})/2$$

$$k_{12} = (\sigma_{11} - \sigma_{33})/2$$

$$k_{13} = \sigma_{12}/\sqrt{2}$$

$$k_{33} = \sigma_{22}$$

2

valencia (Moléculas AX_2) mdin /Å

E_K^{XX}	E_J^{AX}	E_J^{XX}	E_R^{AX}	E_R^{XX}	E_V^{AX}	E_V^{XX}	E_N^{AX}	E_N^{XX}
– 0,01	– 0,19	– 0,23	0,29	– 0,06	– 0,08	0,21	2,65	0,06
– 0,01	– 0,11	0,16	0,11	– 0,12	0,16	– 0,45	– 0,12	0,37
– 0,01	0,00	– 0,06	0,09	– 0,10	– 0,02	0,06	0,02	– 0,05
– 0,15	– 0,72	– 0,08	0,47	– 0,60	0,76	– 0,53	0,00	0,69
0,02	– 1,85	– 0,60	0,06	0,09	0,71	0,94	4,79	– 0,02
– 0,08	0,02	0,18	0,12	– 0,25	– 0,20	– 0,51	0,07	0,68
0,04	0,00	– 0,11	0,06	0,00	0,00	0,21	0,00	0,10
– 0,84	– 2,21	– 0,13	0,94	– 1,59	1,68	– 0,42	0,00	1,43
4,54	8,99	– 2,31	0,12	– 0,41	–16,10	– 3,90	17,30	5,06
– 4,02	– 8,95	25,47	– 2,21	0,88	7,14	–31,50	– 0,05	8,52
– 0,87	69,03	106,65	–20,48	1,27	–157,80	–188,20	103,50	83,42
– 1,46	– 0,96	446,21	– 2,33	3,76	0,91	–863,35	0,004	23,03
0,60	8,64	2,71	– 0,34	0,22	–10,50	–10,38	11,04	7,59
– 0,61	–12,37	19,65	– 0,12	– 0,50	10,30	–26,22	0,00	0,82
– 0,04	1,11	7,20	0,56	0,09	0,12	–17,61	0,00	8,09

---

[3] T. Shimanouchi, "Physical Chemistry. An Advanced Treatise", vol. IV, Academic Press, New York, 1970, p. 233.

siendo k_{11} la constante de fuerza del enlace AX, k_{33} la constante de fuerza de flexión y k_{12} y k_{13} las constantes de fuerza de interacción entre enlaces y entre enlace y ángulo, respectivamente.

Para una molécula AX_2 lineal,

$$k_{11} = (\sigma_{11} + \sigma_{22})/2$$

$$k_{12} = (\sigma_{11} - \sigma_{22})/2$$

$$k_{33} = \sigma_{33}$$

donde las constantes k_{ij} tienen el mismo significado que anteriormente.

Tabla 3

Constantes de fuerza de valencia (molécula HCN) mdin/Å

	k_{22}	k_{11}	k_{12}	k_{33}
E_T	17,76	5,86	0,05	0,25
E_U^H	− 2,74	0,38	0,16	0,25
E_U^C	9,60	− 0,96	0,42	− 1,60
E_U^N	− 1,34	− 0,14	− 1,38	1,05
E_K^H	− 1,16	0,14	0,07	0,00
E_K^{CH}	− 0,04	− 0,02	− 0,03	0,10
E_K^C	0,24	− 0,16	− 0,09	− 0,35
E_K^{NH}	− 0,08	0,00	0,02	0,00
E_K^{CN}	1,12	− 0,02	0,20	0,10
E_K^N	− 1,22	0,04	− 0,32	0,00
E_J^H	2,32	− 0,30	− 0,15	− 0,15
E_J^{CH}	4,96	− 0,46	− 0,21	− 0,54
E_J^C	− 9,40	0,96	− 0,50	1,15
E_J^{NH}	7,44	− 0,16	0,73	0,00
E_J^{CN}	− 7,18	1,16	0,38	0,95
E_J^N	2,18	0,18	1,42	− 0,95
E_R^{CH}	0,52	0,46	0,00	0,25
E_R^{NH}	0,06	− 0,04	0,00	0,00
E_R^{CN}	− 0,32	0,02	0,26	0,19
E_V^{CH}	− 4,96	− 0,14	0,24	0,70
E_V^{NH}	− 8,10	− 0,82	− 1,69	− 0,70
E_V^{CN}	4,20	− 1,10	− 0,44	− 0,84
E_N^{CH}	0,00	5,98	0,00	0,00
E_N^{NH}	0,96	0,96	0,96	0,65
E_N^{CN}	20,72	0,00	0,00	0,00

En las Tablas 2 y 3 aparecen las constantes de fuerza y constantes de partición de las moléculas estudiadas, en mdin /Å.

La dificultad en la interpretación de los datos disponibles es mayor que en el caso de las moléculas diatómicas, ya que se hace muy alto el número de constantes de partición. Es conveniente, por eso, agrupar estos datos de otro modo; para ello se han utilizado tres criterios:

a) Criterio geométrico mediante el cual se agrupan las distintas aportaciones en contribuciones monocéntricas del átomo central (E^A), monocéntricas de los átomos terminales (E^X), bicéntricas entre átomos enlazados (E^{AX}) y bicéntricas entre átomos no enlazados (E^{XX}) (Tabla 4).

Tabla 4

Contribuciones a las constantes de fuerza (tanto por uno)

Molécula		E^A	E^X	E^{AX}	E^{XX}
CH_2	k_{11}	0,02	0,03	0,96	−0,01
	k_{12}	−6,00	3,00	7,00	−3,00
	k_{13}	2,25	−0,50	−5,00	4,25
	k_{33}	−0,90	0,94	1,97	−1,01
H_2O	k_{11}	0,04	0,06	0,85	0,05
	k_{12}	−0,47	0,12	1,06	0,12
	k_{13}	0,19	0,00	0,46	0,38
	k_{33}	−2,03	1,32	4,34	−2,63
O_3	k_{11}	−0,49	−0,70	1,94	0,25
	k_{12}	2,14	1,53	−2,52	−0,16
	k_{13}	24,67	5,96	−34,21	4,73
	k_{33}	−0,71	1,20	−5,20	5,58
CO_2	k_{11}	−0,31	−0,10	1,40	0,06
	k_{12}	5,01	−0,03	−1,39	−2,58
	k_{33}	−2,31	0,04	8,00	−4,73
HCN	k_{11}	−0,03	0,02	0,99(1)	0,00(2)
	k_{22}	0,02	−0,11	1,04(5)	0,04(6)
	k_{12}	−3,40	−4,00	8,00(3)	0,40(4)
	k_{33}	−3,20	0,80	3,64	−0,20(4)

(1) Referido al enlace CH; (2) Referido a enlaces CH y NH;
(3) Referido a enlaces CN y CH; (4) Referido al enlace NH;
(5) Referido al enlace CN; (6) Referido a enlaces NH y CH.

b) Criterio energético, en el que se agrupan las contribuciones correspondientes a los términos energéticos de penetración, canje, resonancia, repulsión electrónica, repulsión nuclear, términos electrostáticos y repulsivos, expresadas como suma de las contribuciones individuales (Tabla 5).

c) Criterio mixto geométrico-energético, que agrupa las contribuciones de enlace y de no-enlace (tipo geométrico) y las electrostáticas y repulsivas (tipo energético) también como suma de contribuciones individuales (Tabla 6).

Dichas contribuciones se expresan en todos los casos en tantos por uno.

Tabla 5

Contribuciones a las constantes de fuerza (tanto por uno)

Molécula		Penetración	Canje	Repulsión electrónica	Resonancia	Repulsión nuclear	Electrost.	Repulsivos
CH_2	k_{11}	— 0,04	—0,01	0,01	0,09	0,98	1,00	0,99
	k_{12}	— 24,00	1,00	13,00	5,00	6,50	13,00	19,50
	k_{13}	0,50	0,25	1,75	— 2,00	0,25	1,50	2,00
	k_{33}	— 2,03	0,13	1,33	0,51	1,05	3,88	2,38
H_2O	k_{11}	— 0,15	—0,02	0,07	0,03	1,08	1,42	1,15
	k_{12}	— 5,36	—0,24	1,66	— 0,05	4,82	4,12	6,48
	k_{13}	0,31	0,15	—0,19	0,46	0,38	1,00	0,19
	k_{33}	— 5,86	—0,86	4,80	0,49	2,42	12,21	7,22
O_3	k_{11}	— 2,85	—0,88	1,48	— 0,01	3,28	1,78	4,76
	k_{12}	— 4,12	2,04	1,90	— 0,87	2,90	— 0,23	3,94
	k_{13}	~ —1 000	—4,73	~500	~ —83	~600	73,60	~1 100
	k_{33}	~ — 500	—0,64	~300	— 0,62	~300	4,14	~ 600
CO_2	k_{11}	— 1,82	—0,20	0,86	— 0,04	2,26	0,73	3,12
	k_{12}	— 6,49	0,20	7,27	0,09	2,86	8,02	10,13
	k_{33}	— 32,92	0,13	14,41	2,53	16,85	— 4,93	31,30
HCN	k_{11}	— 0,47	0,00	0,23	0,07	1,18	1,06	1,41
	k_{22}	— 0,19	—0,07	0,02	0,01	1,22	0,73	1,23
	k_{12}	— 53,80	—2,80	33,40	5,20	19,20	10,00	52,60
	k_{33}	— 4,56	—0,60	1,84	1,76	2,60	1,08	4,44

Tabla 6

Contribuciones a las constantes de fuerza (tanto por uno)

Molécula		Bicéntricos electrost. de enlace	Bicéntricos elecrost. de no enlace	Bicéntricos repulsivos de enlace	Bicéntricos repulsivos de no enlace
CH_2	k_{11}	0,88	0,01	0,90	— 0,03
	k_{12}	— 3,00	4,00	—23,00	26,50
	k_{13}	0,00	1,25	— 1,00	2,75
	k_{33}	0,12	0,13	—2,18	0,93
H_2O	k_{11}	0,82	0,04	0,66	0,07
	k_{12}	— 1,30	2,06	1,06	5,06
	k_{13}	0,00	—0,04	0,00	— 0,04
	k_{33}	— 1,80	1,49	— 7,50	2,20
O_3	k_{11}	1,68	—0,09	4,34	0,23
	k_{12}	— 0,90	0,60	— 4,36	8,23
	k_{13}	61,38	3,88	~719	~396
	k_{33}	— 0,06	4,01	— 1,30	~591
CO_2	k_{11}	1,40	0,00	3,00	0,79
	k_{12}	— 1,56	0,39	— 9,34	10,28
	k_{33}	5,12	—4,84	4,62	31,85
HCN	k_{11}	0,91	0,00	0,94	0,33
	k_{22}	0,99	0,00	0,76	0,75
	k_{12}	— 0,60	0,00	3,40	33,80
	k_{33}	1,08	—0,20	1,64	2,60

i) *Constantes de fuerza de tensión.* De las tablas 4 y 5 se desprende que este tipo de constante está dominanda por las energías bicéntricas de enlace, mostrando su naturaleza repulsiva y electrostática, debida al factor geométrico del enlace AX en todos los casos, tal como se deduce de la Tabla 6. Para moléculas con átomos terminales distintos del hidrógeno se observan además contribuciones de términos repulsivos de no enlace muy acentuadas.

ii) *Constantes de fuerza de flexión.* No se definen por ningún factor geométrico determinado; lo único comun a todas las moléculas es que no depende de la energía monocéntrica del átomo central, lo que está causado por el hecho de que, aunque las contribuciones E_J^A, E_K^A y E_U^A son apreciables, se compensan entre sí, según los datos de las Tablas 2 y 3. El que las anteriores formas de energía tengan contribuciones importantes indica que el movimiento de flexión hace variar apreciablemente la carga electrónica del átomo central (alta E_J^A), así como su distribución entre orbitales atómicos (alta E_U^A), alterándose también los elementos no diagonales de la matriz densidad de carga correspondientes (alta E_K^A), lo que demuestra que el movimiento de flexión repercute grandemente en el carácter híbrido de los orbitales del átomo central; esta última afirmación es admisible si se tiene en cuenta la definición de "Hibridación natural" dada por McWeeny.[4]

Los terminos energéticos más determinantes son las repulsiones nucleares y electrónicas, siendo el de penetración siempre negativo; esta oposición de signos era de esperar, ya que el efecto de las repulsiones es centrífugo y el de las penetraciones centrípeto. De la Tabla 6 se desprende que las contribuciones de más peso son las correspondientes a las repulsiones entre átomos no enlazados.

iii) *Constantes de interacción enlace-enlace.* No parecen estar dominadas por ningún factor geométrico particular, aunque muestran naturaleza repulsiva.

Los términos electrostáticos y repulsivos de no enlace dan siempre contribuciones positivas en este caso; esto quiere decir que esta constante es tanto más alta cuanto mayor sea la contribución electrostática y repulsiva entre átomos no enlazados, lo que parece estar de acuerdo con el fundamento del campo de fuerzas de Urey-Bradley.[5] Sin embargo, este hecho no se manifiesta siempre en la energía total de interacción E^{XX} debido a que las contribuciones de canje y resonancia entre átomos no enlazados son siempre negativas y apreciables, lo que provoca que la energía total de interación entre átomos no enlazados no sea determinante de la magnitud de esta constante de fuertza a causa de efectos puramente mecanocuánticos, como son el canje y la resonancia.

iv) *Constantes de interacción enlace-ángulo.* No puede deducirse ninguna conclusión de caráter general para esta constante, que parece ser una propiedad de la molécula como conjunto, no attribuible a ningún factor en particular.

---

[4] R. McWeeny, *Rev. Mod. Phys.*, **32**, 335 (1960).

[5] H. C. Urey y C. A. Bradley, *Phys. Rev.*, **38**, 1969 (1931).

Se han obtenido las frecuencias normales de vibración de las moléculas estudiadas, conocida la geométria molecular evaluada teóricamente que aparece en la Tabla 1 y las constantes de fuerza calculadas, haciendo uso del método de Wilson.[6] Estas frecuencias se comparan con las experimentales para CO_2,[7] H_2O,[8] HCN [9] y O_3 [10] en la tabla 8.

Tabla 7

Distancias (Å) y angulos de enlace (°)

CH_2	$P_{CH} = 1{,}109$	—	$H\hat{C}H = 93{,}4$
OH_2	$R_{CH} = 0{,}958$	—	$H\hat{O}H = 82{,}8$
HCN	$R_{CH} = 1{,}089$	$R_{CN} = 1{,}155$	$H\hat{C}N = 180$
CO_2	$R_{CO} = 1{,}182$	—	$O\hat{C}O = 180$
O_3	$R_{OO} = 1{,}257$	—	$O\hat{O}O = 116{,}7$

Tabla 8

Frecuencias vibracionales (cm^{-1})

	CO_2		H_2O		O_3		HCN	
	Calc.	Exp.	Calc.	Exp.	Calc.	Exp.	Calc.	Exp.
ν_1	1295	1353,96	4040	3832,2	1630	1124	2085	2128,67
ν_2	611	673,17	1430	1648,5	772	719	749	727,10
ν_3	2021	2396,29	3941	3942,5	1441	1102	3317	3441,16

La concordancia de los valores teóricos con los experimentales es consistente con los valores de las constantes de fuerza obtenidos. La diferencia de números de onda entre las vibraciones simétrica y antisimétrica se predice bien, en general, excepto para el H_2O, debido al alto valor obtenido para la constante de interacción enlace-enlace.

---

[6] E. B. Wilson, *J. Chem. Phys.*, **7**, 1047 (1939); **15**, 736 (1947).

[7] I. Suzuki, *J. Mol. Spectroscopy*, **25**, 479 (1968).

[8] W. S. Benedict, N. Gailar y E. K. Plyler, *J. Chem. Phys.*, **24**, 1138 (1956).

[9] T. Nakagawa y Y. Morino, *Bull. Chem. Soc. Japan.*, **42**, 2212 (1969).

[10] T. Tanaka y Y. Morino, *J. Mol Spectroscopy*, **33**, 538 (1970).

Revue Roumaine de Chimie, 22, 3, 353–359 (1977)

CONSIDÉRATIONS SUR LE MODÈLE DE LANDSBERG RELATIF À L'ÉQUATION LOGARITHMIQUE

N. I. IONESCU et B. AURIAN-BLĂJENI
Centre de Chimie Physique, str. Galaţi 31, Bucarest, Roumanie

Reçu le 22 mars 1975

Le modèle de Landsberg, appliqué aux processus d'adsorption gaz-solide, peut aussi représenter, par une modification convenable, l'équation logarithmique de la désorption. De même, ce modèle pourrait être généralisé.

Dans un travail antérieur nous avons montré[1] les raisons pour lesquelles l'équation logarithmique dans sa forme intégrale

$$Q = \frac{1}{b}[\ln(t + t_0) - \ln t_0] \tag{1}$$

et dans sa forme différentielle

$$\frac{dQ}{dt} = a \exp(-bQ) \tag{2}$$

où Q représente une quantité variable dans le temps t, a et b sont des constantes, et $t_0 = \frac{1}{ab}$, si pour $t = 0, Q = 0$ [2,3] pourrait représenter non seulement des processus de chimisorption, mais aussi d'autres phénomènes physiques ou chimiques.

Dans la présente note nous nous sommes proposé d'étudier d'autres aspects concernant le modèle de Landsberg,[4,5] qui conduit à la forme intégrale de l'équation logarithmique, utilisée pour la description formelle de l'évolution cinétique de quelques processus gaz-solide.

---

[1] N. I. Ionescu et B. Aurian-Blăjeni, *Rev. Roumaine Chim.*, **18**, 203 (1973).

[2] J. Zeldovich, *Acta Physicochim. U.R.S.S.*, **1**, 449 (1934).

[3] S. Z. Roginsky, J. Zeldovich, *Acta Physicochim. U.R.S.S.*, **1**, 554 (1934).

[4] P. T. Landsberg, *J. Chem. Phys.*, **23**, 1079 (1955).

[5] P. T. Landsberg, *J. Appl. Phys.* **33**, 2251 (1962).

RÉSULTATS ET DISCUSSIONS

Le modèle de Landsberg est représenté par le système

$$\frac{\mathrm{d}Q}{\mathrm{d}t} = Np$$

$$-\frac{\mathrm{d}p}{\mathrm{d}t} = kNp^2 \tag{3}$$

où Q représente un processus probabilistique discontinu, qui progresse par des étapes discrètes sur un fond de fluctuations, alors que N est le nombre des événements par unité de temps ; ces deux grandeurs sont en principe capables de faire avancer le processus mais seulement pour une probabilité $p = p(t)$; k est une constante. La signification physique des grandeurs N et p des équations (3) est celle du nombre de collisions des molécules du gaz avec la surface par unité de temps et respectivement le nombre des centres libres.

Par l'intégration des équations (3) on obtient une relation analogue à la formule (1) bien connue sous le nom de l'équation R.Z.E. (Roginsky, Zeldovich, Elovich).

Revenons aux équations (3) et soit maintenant un processus Q dans lequel le nombre d'événements N capables de le faire progresser a, en principe, une probabilité p^m de la faire, m étant une constante positive quelconque. Aussi, dans le cas de ce processus, soit que chaque étape fasse baisser la probabilité de formation de l'étape suivante avec une quantité proportionnelle à la puissance r de la probabilité p, qui existe à ce moment, r étant une autre constante positive. Dans ce cas, les équations (3) deviennent :

$$\frac{\mathrm{d}Q}{\mathrm{d}t} = Np^m$$

$$-\frac{\mathrm{d}p}{\mathrm{d}t} = kNp^{r+1} \tag{4}$$

En effectuant les calculs on arrive à la relation :

$$\mathrm{d}Q = \frac{Np_0^m}{(1 + kNrp_0^r\, t)^{m/r}}\,\mathrm{d}t \tag{5}$$

où $p_0 = p(0)$.

De la relation (5) il résulte que, pour que, par son intégration, la grandeur Q acquiert une forme logarithmique, il est nécessaire et suffisant que

$$\frac{m}{r} = 1 \tag{6}$$

Si

$$\frac{m}{r} = a > 1 \tag{7}$$

il résultera alors pour la grandeur Q l'expression

$$Q = \frac{-p_0^a}{(a-1)\,kr(1 + kNrp_0^r\,t)^{a-1}} \tag{8}$$

qui n'est plus logarithmique.

Pour le cas

$$\frac{m}{r} = a < 1 \tag{9}$$

les calculs conduisent à la relation

$$Q = \frac{p_0^a(1 + k\,Nrp_0^r\,t)^{1-a}}{(1-a)\,kr} \tag{10}$$

qui aussi n'a plus une forme logarithmique.

Le cas où des grandeurs m et r sont fonctions de t conduit aux équations difficilement utilisables. Le cas dans lequel $N = N(t)$ a été traité par Landsberg.[5]

Ainsi, on peut tirer la conclusion que le modèle de Landsberg déduit dans une forme générale montre qu'il existe une infinité de systèmes d'équations, selon la valeur donnée à la grandeur r, qui toutes conduisent à l'équation logarithmique (1). Le modèle donné par Landsberg se réfère au cas particulier $r = 1$.

La conclusion antérieure soutient l'idée qu'il existe beaucoup de possibilités pour justifier formellement une équation logarithmique du type (1).

L'impossibilité de proposer un mécanisme de chimisorption basé seulement sur la concordance des données expérimentales avec l'équation (Λ) peut être attribuée, à la suite des recherches entreprises jusqu'à présent, à trois causes, notamment :

— la non-équivalence physique des modèles qui conduisent aux formes (1) et (2) de l'équation logarithmique[1] ;

— le modèle basé sur le processus d'association des centres actifs ;

— l'existence d'un modèle généralisé de Landsberg.

Toutes ces causes pourraient expliquer pourquoi des mécanismes physiques et chimiques complètement différents entre eux[6] peuvent être décrits dans leur évolution cinétique par le même formalisme.

Un autre problème posé par le modèle de Landsberg est la signification des signes plus et minus dont sont affectées les équations (3) sur le résultat de l'intégration de ce système.

Dans le cas des systèmes d'équations (3), les constantes k et N sont positives et ont une signification physique précise. Admettons que ces constantes soient positives.

Soit maintenant le système d'équations :

$$\begin{aligned} = \frac{\mathrm{d}Q_1}{\mathrm{d}t} &= N_1 p_1 \\ = \frac{\mathrm{d}p_1}{\mathrm{d}t} &= k_1 N_1 p_1^2 \end{aligned} \qquad (11)$$

Par l'intégration de la dernière équation du système (4) on obtient :

$$\frac{p_{0_1}}{p_1} = 1 + k_1 N_1 \, p_{0_1} t \qquad (12)$$

où $p_{0_1} = p_1(0)$.

Compte tenu de la relation (12) la première équation du système (11) devient

$$Q_1 = \frac{1}{k_1} [\ln t_0' - \ln(t + t_0')] \qquad (13)$$

où $t_0' = \dfrac{1}{k_1 N_1 p_{0_1}}$.

La formule (13) représente une forme intégrale de l'équation logarithmique de la désorption.

Dans ce cas, du point de vue physique, Q représente une quantité de gaz qui reste adsorbée au temps t par la surface sur laquelle a lieu le processus de désorption et p_1 — une grandeur proportionnelle au nombre des centres de la surface couverts par le gaz. D'ailleurs, cette définition de la grandeur Q peut être retrouvée aussi dans le cas de la désorption.[7,8] La constante N_1 a la signification d'un nombre des fréquences de vibration des molécules adsorbées, perpendiculaires à l'unité de surface.

Avec ces notations, les équations (11) décrivent un processus de désorption. C'est-à-dire, la vitesse du processus de désorption est proportionnelle au nombre de centres occupés. Par contre, tandis que le gaz se désorbe, la probabilité de trouver des centres occupés sur la surface est plus petite, fait décrit justement par la deuxième relation des équations (11). Cette relation se réfère à un processus dans lequel chaque étape décroît la probabilité de production de la suivante avec une quantité proportionnelle à la probabilité qui existe à un moment donné $p_1(t)$.[5]

---

[6] I. S. McLintock, *J. Catalysis*, **16**, 126 (1970).

[7] D. O. Hayward, B. M. W. Trapnell, «Chemisorption», 2e Ed., Butterworths, Londres, 1964, p. 143.

[8] G. C. Bond, «Catalysis by Metals», Academic Press, Londres 1962, p. 106.

Malheureusement, le résultat exprimé par l'équation (13) n'a pas une signification physique précise pour deux raisons.

En premier lieu, Q_1 reçoit seulement des valeurs négatives, ce que contrevient à la signification des symboles (la quantité de gaz ne peut avoir que des valeurs positives). En deuxième lieu, quand $t = 0$, $Q = 0$, ce qui est absurde, parce que, au moment où commence un processus de désorption, la surface est couverte par une quantité quelconque de gaz, c'est-à-dire conformément à la définition, $Q > 0$ et fini même à partir de $t = 0$.

Pour éliminer cette difficulté, on a eu recours à l'hypothèse de l'existence d'une quantité maximale Q_m, adsorbée sur la surface. Une fois cette hypothèse admise, il résulte immédiatement :

$$Q_m = Q_{\mathrm{ad}} + Q_{\mathrm{des}} \tag{14}$$

où Q_{ad} et Q_{des} représentent les quantités de gaz adsorbées et respectivement désorbées par la surface.

On a $Q_1 = Q_{\mathrm{ad}}$. La relation (14) mène à

$$\mathrm{d}Q_{\mathrm{des}} = \mathrm{d}(Q_m - Q_{\mathrm{ad}}) = -\,\mathrm{d}Q_{\mathrm{ad}} \tag{15}$$

et

$$\mathrm{d}(Q_m - Q_{\mathrm{ad}}) = N_1 p_1 \tag{16}$$

$$-\frac{\mathrm{d}p_1}{\mathrm{d}t} = k_1 N_1 p_1^2$$

qui, par intégration conduit à la formule :

$$Q_m - Q_{\mathrm{ad}} = \frac{1}{k_1}[\ln(t + t_0') - \ln t_0'] \tag{17}$$

La relation (17) montre qu'à $t = 0$, $Q_m = Q_{\mathrm{ads}}$ et donc $Q_{\mathrm{des}} = 0$; aussi Q_{des} a seulement des valeurs positives étant une fonction qui croît avec le temps.

Avec ces adnotations, le modèle modifié de Landsberg peut décrire une équation logarithmique de désorption. Ce modèle peut aussi être généralisé, comme nous l'avons montré plus haut.

Considérons maintenant les deux autres systèmes d'équations qui dérivent du modèle de Landsberg. Soient donc les équations :

$$= \frac{\mathrm{d}Q_2}{\mathrm{d}t} = N_2 p_2$$

$$\frac{\mathrm{d}p_2}{\mathrm{d}t} = k_2 N_2 p_2^2 \tag{18}$$

Par leur intégration on obtient :

$$Q_2 = \frac{1}{k_2} \left[\ln/t - t_0''/ - \ln t_0''\right] \tag{19}$$

Aussi par l'intégration des équations

$$\frac{\mathrm{d}Q_3}{\mathrm{d}t} = N_3 p_3$$

$$\frac{\mathrm{d}p_3}{\mathrm{d}t} = k_3 N_3 p_3^2 \tag{20}$$

il résulte :

$$Q_3 = \frac{1}{k_3} \left[\ln t_0''' - \ln/t - t_0'''/\right] \tag{21}$$

Les équations (19) et (20) sont aussi des équations logarithmiques, mais pour leur justification on n'a pu encore trouver aucun modèle physique approprié dans le cas des processus d'adsorption gaz-solide. Mais cela ne signifie pas que, dans d'autres cas de phénomènes physiques et chimiques, on ne puisse pas trouver une interprétation logique des grandeurs qui interviennent dans les équations (19) et (21).

Ainsi comme nous l'avons montré dans une autre circonstance[1] et d'après ce qui résulte de la note présente, l'élément essentiel pour obtenir la relation logarithmique (1) est la deuxième équation des systèmes (3) et (11) que décrit le processus de décroissement de la probabilité de production du phénomène.

Les résultats peuvent être synthétisés dans le tableau 1.

En conclusion, d'après nos recherches, il résulte que le modèle de Landsberg avec une modification appropriée peut représenter aussi l'équation logarithmique de la désorption. Le modèle peut être généralisé ce qui constitue une nouvelle explication du fait que l'équation logarithmique (1) décrit une telle variété de phénomènes physiques et chimiques.

Tableau 1

Des équations qui dérivent du modèle de Landsberg

Signe de la première équation du système (3)	Signe de la deuxième équation du système (3)	Equation finale obtenue
+	–	Equation logarithmique de l'adsorption (R.Z.E.).
–	–	Equation logarithmique de la désorption
–	+	Equation logarithmique
+	+	Equation logarithmique

Revue Roumaine de Chimie, **22**, *3*, 361–370 (1977)

ACIDE ASCORBIQUE COMME AGENT RÉDUCTEUR. V[1]

CINÉTIQUE DE LA RÉDUCTION DES IONS Au(III) PAR ACIDE ASCORBIQUE

RALUCA RIPAN, GHEORGHE POP, ILEANA POP et CRISTINA NAŞCU
Institut de Chimie de Cluj-Napoca str. Donath 65 — 103, Roumanie

Reçu le 1 août 1975

Dans ce travail on a étudié la cinétique de la réduction des ions Au(III) à l'or métallique par acide ascorbique en présence des ions de chlore et d'hydrogène. On a étudié aussi l'influence de la température, en établissant une relation, caractérisant quantitativement la valeur de la vitesse de réaction :

$$v_{1/2} = -\frac{d[AuCl_4^-]}{dt} = K_{Au}\frac{[Au^{3+}][Asc]}{[H^+][Cl^-]^2}\,e^{-E_{Au}/RT} \qquad (I)$$

Asc — acide ascorbique
K_{Au} — coefficient préexponentiel

Pour la première fois Stathis[2,3] a utilisé la réaction de réduction des ions Au(III) à l'or métallique par acide ascorbique pour l'identification des petites quantités d'or en solutions (10^{-6} g/ml) et pour le dosage gravimétrique.

D'autres auteurs [4,5] ont établi les conditions optimales de titrage potentiométrique de l'or par acide ascorbique.

Nous avons établi[6,7] une méthode de séparation de l'or du mélange sélénium-tellure par réduction sélective avec de l'acide ascorbique, en indiquant les conditions optimales pour la réduction quantitative de l'or au métal en présence des deux éléments.

La réduction à l'état métallique des ions d'or (III) par acide ascorbique a lieu conformément à la réaction :

$$2Au^{3+} + 3C_6H_8O_6 \xrightarrow{HCl} 2Au + 3C_6H_6O_6 + 6H^+ \qquad (II)$$

---

[1] R. Ripan, Gh. Pop et I. Pop, *Rev. Roumaine Chim.*, **19**, 1593 (1974).
[2] E. C. Stathis, *Praktika Akademy Athens*, **17**, 74 (1942).
[3] E. C. Stathis et H. C. Gatos, *Ind. Eng. Chem. Analyt. Edit.*, **18**, 810 (1946).
[4] N. K. Pchenitzin et S. I. Ginzburg, *Izvest. Sekt. Platiny*, **30**, 171 (1955).
[5] L. Erdey et G. Rady, *Talanta*, **1**, 159 (1958).
[6] R. Ripan et Gh. Pop, *Rev. Chim. (Buc.)*, **14**, 411 (1963).
[7] R. Ripan et Gh. Pop, *Rev. Chim. (Buc.)*, **14**, 413 (1963).

Des données expérimentales obtenues on a établi l'ordre de réaction, l'énergie d'activation et le facteur préexponentiel. Aussi on a observé que l'or (III) catalyse la réaction de réduction des ions Pd(II) et Ag(I) par acide ascorbique.

PARTIE EXPÉRIMENTALE

Réactifs nécessaires

1. Solution de chlorure d'or (III) *p.a.* 0,33N
2. Solution d'acide ascorbique *p.a.* 0,68 N
3. Acide chlorhydrique concentré *p.a.*
4. Acide bromhydrique *p.a.* 63%
5. Acide bromhydrique *p.a.* 37,8%
6. Solution de bromure de potassium *p.a.* 3M
7. Solution d'iodure de potassium *p.a.* 3M
8. Solution de chlorure de sodium 4M

Pour déterminer la vitesse de réduction de l'or (III) par acide ascorbique en présence des halogènes on a suivi la diminution de la concentration des ions d'or (III) en fonction du temps, l'analyse d'or étant effectuée par la spectrométrie de fluorescence à rayons X. On a utilisé un spectromètre Philips PW 1410, avec une tube à anticathode de chrome à 80kV, 30 mA. On a mesuré la ligne AuLα en utilisant en tandem le comptoir de scintillation, avec flux gazeux (gaz P 10) et un analyseur automate de hauteur des impulsions. Pour poursuivre les grandes vitesses de réaction, les mesures ont été effectuées potentiométriquement, en utilisant un potentiomètre de type MV 11, couplé à un enregistreur électronique de type EZ 2.

La vitesse de réaction, exprimée en M/s est mesurée par la méthode des tangentes au point où la concentration d'or est arrivée à la moitié de la concentration initiale.

La température de travail a été maintenue à l'aide de l'ultrathermostat de type U 10. L'agitation a été effectuée avec un agitateur électromécanique type LR 40.

La réduction de l'or (III) est arrêtée dans le HBr 4,7 M.

RÉSULTATS ET DISCUSSIONS

La réduction de l'or (III) par acide ascorbique a lieu en deux étapes conformément au mécanisme suivant :[5]

$$[AuCl_4]^- + 2\,e \rightleftharpoons [AuCl_2]^- + 2Cl^- \quad (E_0 = 0{,}95\ V)$$

$$[AuCl_2]^- + e \rightleftharpoons Au + 2Cl^- \quad (E_0 = 1{,}13\ V) .$$

Les données expérimentales attestent l'existence d'une période d'induction comme pour la réduction des ions Pt(II)[1] et Pd(II)[8] à l'état métallique par acide ascorbique. La période d'induction qui caractérise les réactions redox entre les ions des métaux précieux et l'acide ascorbique est une période nécessaire pour la formation des noyaux qui catalysent plus loin le processus de réaction. [9]

L'aspect général d'une courbe représentant la variation de la concentration d'or (III) dans le mélange de réaction en fonction du temps est indiqué par la figure 1.

---

[8] R. Ripan et Gh. Pop, *Rev. Roumaine Chim.*, **12**, 7 (1967).

[9] L. N. Berdichevskaya et N. I. Dankov, *Compt. Rend. Acad. Sci. U.R.S.S.*, **24**, 545 (1939).

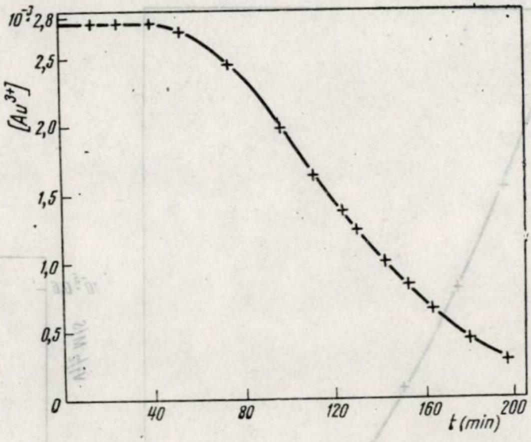

Fig. 1. — Réduction des ions d'or (III) par acide ascorbique en milieu de HCl 7,22 M ($t = 25°$, Au^{3+} = $= 2{,}76.10^{-3}$ M, Asc = $= 8{,}5.10^{-3}$M).

DÉTERMINATION DE L'ORDRE DE RÉACTION

On a suivi l'influence de la concentration des ions d'or (III) et d'acide ascorbique dans un milieu de HCl 7,22 N, à 25°.

En utilisant différentes concentrations d'or avec une concentration constante d'acide ascorbique on constate une relation proportionnelle entre les valeurs des vitesses de réaction et la concentration de l'or (III) conformément aux données expérimentales présentées (figures 2 et 3).

Il ressort que la réaction est du premier ordre par rapport au premier réactant Au(III).

Dans des conditions identiques, mais à une concentration constante d'or (III) $8{,}3.10^{-3}$N, on a étudié l'influence de la concentration d'acide ascorbique sur la vitesse de réaction, à 25°.

Les données expérimentales illustrées par les figures 4 et 5 prouvent une dépendance directement proportionnelle entre la vitesse de réaction et la concentration d'acide ascorbique, donc la réaction est du premier ordre par rapport au deuxième réactant.

Les figures 2 et 4 indiquent aussi évidemment que la période d'induction est d'autant plus petite que la concentration des ions d'or (III) et d'acide ascorbique est plus grande, comme dans le cas de la réduction du Pd(II) avec l'acide ascorbique[8] quand a été établi que la période d'induction est inversement proportionnelle au produit des concentrations des réactants.

L'ordre total de réaction est II, fait vérifié par l'introduction des données expérimentales dans l'équation cinétique du second ordre :

$$k_{\text{II}} = \frac{2{,}303}{t(a-b)} \log \frac{b(a-x)}{a(b-x)} \qquad \text{(III)}$$

obtenant à différents intervalles de temps la même constante de la vitesse de réaction, conformément aux données du tableau 1.

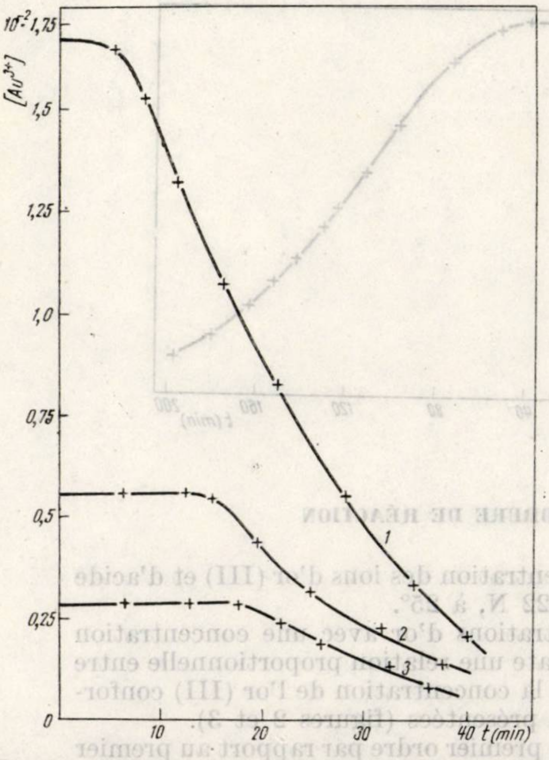

Fig. 2. — Influence de la concentration des ions d'or (III) sur la vitesse de réaction en milieu de HCl 7,22M, Asc = 5.10^{-2} M, t = 25°, 1 — $1{,}66.10^{-2}$ M Au(III), 2 — $0{,}54.10^{-2}$ M Au(III), 3 — $0{,}27.10^{-2}$ M Au(III).

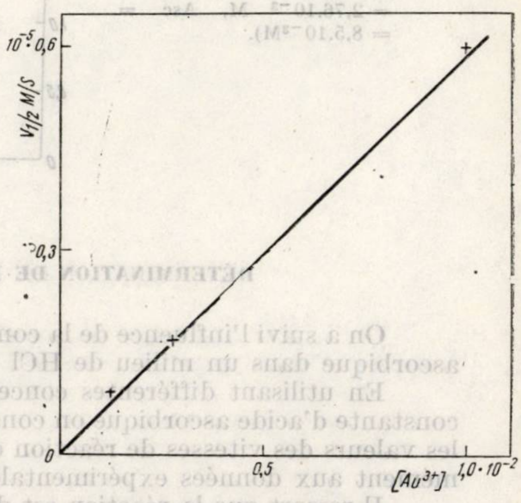

Fig. 3. — Dépendance de la vitesse de réaction de la concentration d'or (III).

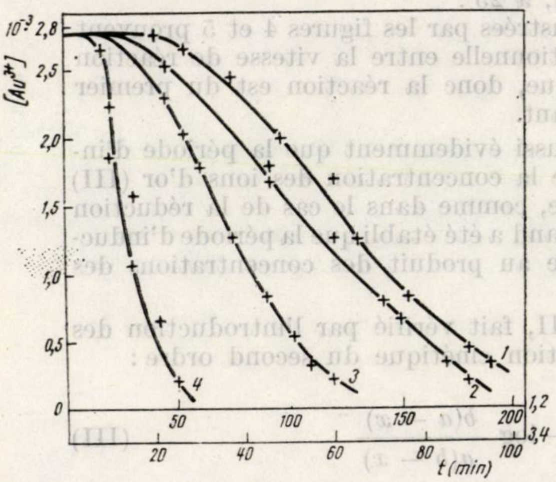

Fig. 4. — Influence de la concentration de l'acide ascorbique sur la vitesse de réaction en milieu de HCl 7,22 M, $t = 25°$, Au^{3+} = $2{,}76.10^{-3}$M; 1 — $0{,}85.10^{-2}$ M Asc, 2 — $1{,}5.10^{-2}$ M Asc, 3 — 5.10^{-2} M Asc, 4 — $8{,}5.10^{-2}$ M Asc.

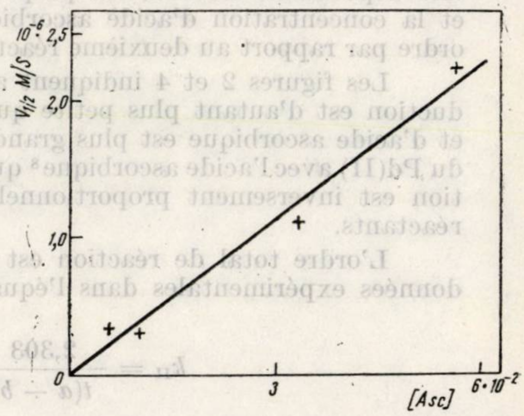

Fig. 5. — Dépendance de la vitesse de réaction de la concentration d'acide ascorbique.

(k_{II} — la constante de la vitesse de réaction du second ordre
t — le temps
a — la concentration d'acide ascorbique correspondante *après avoir réagi* 33% de l'or (III) initial
b — la concentration de l'or (III) *après avoir réagi* 33% de l'or (III) initial. À cause de la période d'induction de réaction l'équation cinétique d'ordre II se vérifie seulement après *avoir réagi approximativement* 33% de quantité initiale d'or
x — la diminution de la concentration initiale d'or (III) jusqu'au moment t)

Tableau 1

Constantes de vitesse de réaction à la réduction des ions d'or (III) par acide ascorbique, aux différents intervalles du temps (température = 25°, HCl = 7,22 M, Au^{+3} = $2{,}76 \cdot 10^{-3}$ M, Asc = $8{,}5 \cdot 10^{-3}$ M)

t min.	k_1 $M^{-1}.\ s^{-1}$
115	$3{,}7.\ 10^{-2}$
123	$4{,}10^{-2}$
130	$3{,}85.10^{-2}$
141	$3{,}8.10^{-2}$
150	$3{,}97.10^{-2}$

L'erreur de détermination est ± 5%.

INFLUENCE DE LA CONCENTRATION DES IONS D'HYDROGÈNE (H_2SO_4) SUR LA VITESSE DE RÉACTION

En modifiant la concentration des ions d'hydrogène entre 0,44 — 3,52 M (H_2SO_4) en présence de NaCl 1,6 M, à 25°, aux concentrations constantes des réactants, on constate que la vitesse de réaction diminue à la croissance de l'acidité. En représentant graphiquement la vitesse de réduction en fonction de $1/H^+$ on obtient une ligne droite (figure 6), qui prouve que la vitesse est directement proportionnelle à l'inverse de la concentration des ions d'hydrogène.

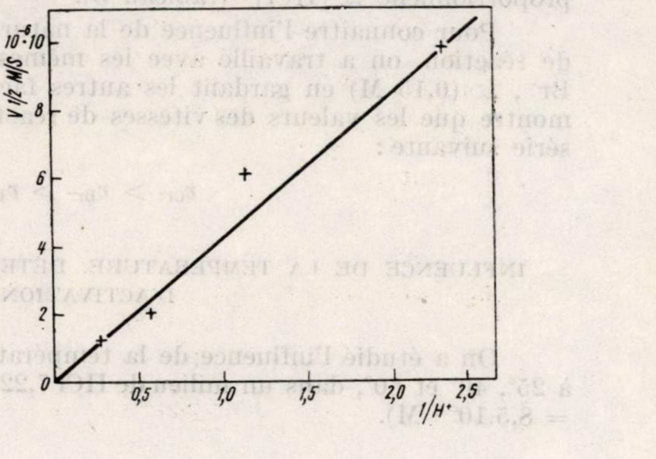

Fig. 6 — Dépendance de la vitesse de réaction en fonction de l'inverse de la concentration des ions d'hydrogène (H_2SO_4), Au^{3+} = $1{,}2.10^{-3}$, M, Asc = $3{,}4.10^{-3}$ M, $t = 25°$, H^+ = 0,44 — 3,52M.

INFLUENCE DE LA NATURE ET DE LA CONCENTRATION DES HALOGÈNES SUR LA VITESSE DE RÉACTION

On a effectué une étude en détail concernant l'influence des ions Cl^- sur la vitesse de réaction, vu que le HCl est le milieu le plus souvent utilisé pour la réduction de l'or (III).

En maintenant constantes les concentrations des réactants ($Au^{3+} = 1{,}2.10^{-3}$ M, Asc $= 3{,}4 \cdot 10^{-3}$M) et des ions d'hydrogène ($H^+(H_2SO_4) = 2{,}64$ M), à 25°, on a modifié la quantité des ions Cl^-(NaCl) entre les limites de concentration de 0,2 à 3,2 M. On observe une baisse de la vitesse de réaction avec l'augmentation de la concentration des ions de chlore. La vitesse de réaction déterminée est inversement proportionnelle au carré de la concentration des ions Cl^-. Cette dépendance est illustrée dans la figure 7.

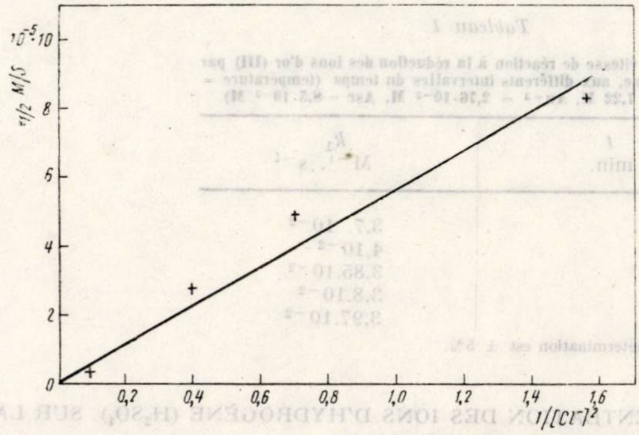

Fig. 7. — Dépendance de la vitesse de réaction en fonction de $1/[Cl^-]^2$, $Au^{3+} = 1{,}2.10^{-3}$, M, Asc $= 3{,}4.10^{-3}$M, $H^+(H_2SO_4) = 2{,}64$ M, $Cl^- = 0{,}8 - 3{,}2$ M.

On a suivi aussi l'influence de la concentration de l'acide chlorhydrique sur la vitesse de réaction, en observant qu'elle est inversement proportionnelle à $[HCl]^3$ (tableau 3).

Pour connaître l'influence de la nature des halogènes sur la vitesse de réaction, on a travaillé avec les mêmes concentrations des ions Cl^-, Br^-, I^- (0,15 M) en gardant les autres facteurs constants. La figure 8 montre que les valeurs des vitesses de réaction dans ce cas respectent la série suivante :

$$v_{Cl^-} > v_{Br^-} > v_{I^-}$$

INFLUENCE DE LA TEMPÉRATURE. DÉTERMINATION DE L'ÉNERGIE D'ACTIVATION

On a étudié l'influence de la température sur la vitesse de réaction à 25°, 40° et 60°, dans un milieu de HCl 7,22 M ($Au^{3+} = 2{,}76.10^{-3}$M, Asc $= 8{,}5.10^{-3}$ M).

Fig. 8. – Influence de la nature des halogènes sur la vitesse de réduction des ions d'or (III) par acide ascorbique, $Au^{3+} = 1{,}2.10^{-3}$ M, Asc = $= 3{,}4.10^{-3}$M, $H^+(H_2SO_4) = 3{,}52$ M, t = 25°, 1 – 0,15 M (Cl^-), 2 – 0,15M (Br^-), 3 – 0,15 M (I^-).

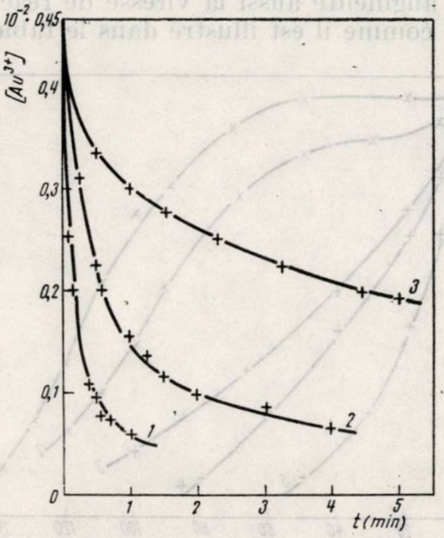

La dépendance entre les constantes des vitesses de réaction et l'inverse de la température absolue est représentée dans la figure 9.

L'énergie d'activation (9,32 kcal/mole) est calculée graphiquement de la pente de la ligne droite. On a calculé aussi le facteur préexponentiel A, en obtenant pour log A la valeur 5,26.

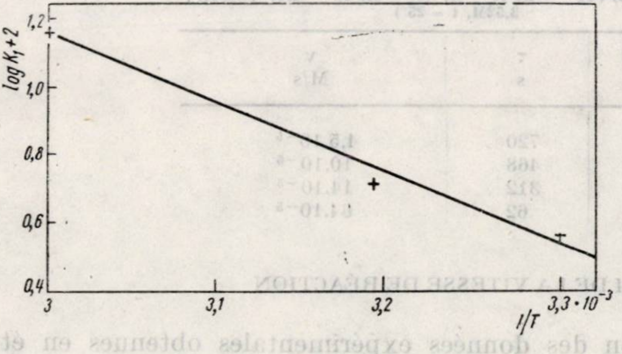

Fig. 9. – Variation de log k_1 en fonction de 1/T, $Au^{3+} = 2{,}76.10^{-3}$ M, Asc = $8{,}5.10^{-3}$ M, HCl = = 7,22 M, $t = 25 - 60°$.

INFLUENCE DE L'OR(III) SUR LA RÉDUCTION DES IONS PD(II) ET AG(I) PAR ACIDE ASCORBIQUE

En étudiant la réduction des ions Pd(II) par acide ascorbique en présence des ions d'or (III) dans un milieu de HCl 0,25 M, à 25°, on constate que l'or (III) augmente la vitesse de réaction et en même temps diminue la période d'induction, phénomène illustré par la figure 10.

Dans le cas de la réduction des ions Ag(I) par acide ascorbique en présence de l'or (III), dans un milieu de H_2SO_4 3,52 M, à 25°, on constate que l'or augmente aussi la vitesse de réaction et diminue la pérode d'induction, comme il est illustré dans le tableau 2.

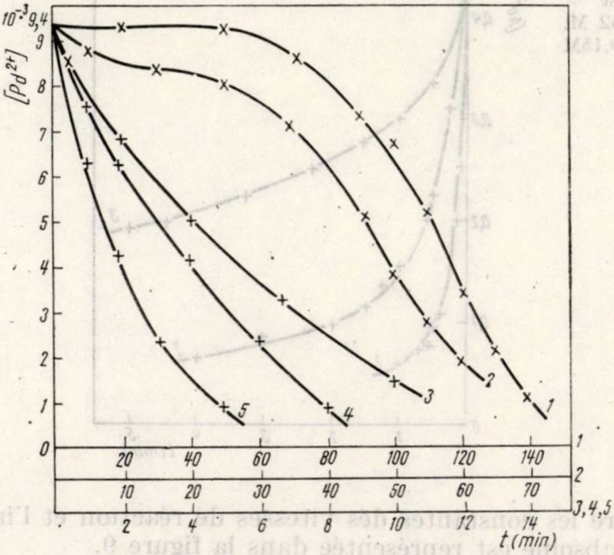

Fig. 10. — Influence des ions d'or (III) sur la réduction du Pd(II) par acide ascorbique à $t = 25°$, $HCl = 0,25$ M, $Pd^{2+} = 9,4.10^{-3}$M, Asc $= 5,7.10^{-2}$ M, 1 — 0 g Au(III) %, 2 — $0,5.10^{-2}$ Au(III) %, 3 — $1,25.10^{-2}$ Au(III) %, 4 — $2,5.10^{-2}$ Au(III) %, 5 — 5.10^{-2} Au(III) %.

Tableau 2

Valeurs de la période d'induction et de la vitesse de réaction à la réduction d'Ag(I) par acide ascorbique pour différentes concentrations d'Au (III) ($Ag^{+} = 4,5 \cdot 10^{-2}$ M, Asc $= 5,6 \cdot 10^{-2}$ M, $H^{+}(H_2SO_4) = 3,52$M, $t = 25°$)

Au(III) g	τ s	v M/s
0	720	$4,5.10^{-5}$
4.10^{-5}	468	10.10^{-5}
10.10^{-5}	312	14.10^{-5}
20.10^{-5}	62	64.10^{-5}

LOI DE LA VITESSE DE RÉACTION

Par l'interprétation des données expérimentales obtenues en étudiant l'influence de la concentration des réactants, du milieu de réaction et de la température sur la vitesse de réduction des ions Au (III) avec l'acide ascorbique, on est arrivé à l'expression suivante, caractérisant quantitativement la valeur de la vitesse de réaction :

$$v_{1/2} = -\frac{dc}{dt} = K_{Au}\frac{[Au^{3+}][Asc]}{[H^{+}][Cl^{-}]^{2}}\,e^{-E_{Au}/RT} \qquad (I)$$

K_{Au} — le coefficient préexponentiel
$\log K_{Au} = 7,82$ (calculé des données expérimentales)

En connaissant la valeur K_{Au} et les conditions de réaction on peut calculer la vitesse de réaction, en utilisant l'expression I.

La loi établie se vérifie dans les conditions expérimentales suivantes : $Au^{3+} = 1{,}2.10^{-3} - 16{,}66.10^{-3}$ M, Asc $= 0{,}85.10^{-2} - 8{,}5.10^{-2}$ M, $H^+(H_2SO_4$ ou HCl$) = 0{,}44 - 9$ M, Cl^- (NaCl ou HCl) $= 0{,}8 - 9$M, T $= 298{,}16 - 333{,}16$°K.

Le tableau 3 montre une bonne concordance entre les valeurs des vitesses de réaction déterminées expérimentalement et celles calculées à l'aide de l'expression établie.

T ableau 3

Valeurs comparatives des vitesses de réaction à la réduction des ions d'or (III) par acide ascorbique, déterminées expérimentalement et calculées à l'aide de l'expression établie (I)

N° crt.	$V_{1/2}$ M/s lculée	$V_{1/2}$ M/s déterm. exp.	Au(III)M	Asc M	H^+M	Cl^- M	T° K
1	2	3	4	5	6	7	8
1	$2{,}21.10^{-7}$	$3{,}20.10^{-7}$	$1{,}38.10^{-3}$	$6{,}43.10^{-3}$	7,22	7,22	298,16
2	$4{,}54.10^{-7}$	$3{,}5.10^{-7}$	$1{,}38.10^{-3}$	$12{,}93.10^{-3}$	7,22	7,22	298,16
3	$16{,}8.10^{-7}$	$11{,}9.10^{-7}$	$1{,}38.10^{-3}$	$47{,}93.10^{-3}$	7,22	7,22	298,16
4	$29{,}1.10^{-7}$	$29{,}0.10^{-7}$	$1{,}38.10^{-3}$	$82{,}93.10^{-3}$	7,22	7,22	298,16
5	$8{,}55.10^{-7}$	$5{,}6.10^{-7}$	$0{,}685.10^{-3}$	$48{,}97.10^{-3}$	7,22	7,22	298,16
6	$3{,}23.10^{-6}$	$2{,}03.10^{-6}$	$2{,}765.10^{-3}$	$45{,}86.10^{-3}$	7,22	7,22	298,16
7	$7{,}96.10^{-6}$	$6{,}66.10^{-6}$	$8{,}33.10^{-3}$	$37{,}5.10^{-3}$	7,22	7,22	298,16
8	$1{,}82.10^{-6}$	$1{,}50.10^{-6}$	$1{,}38.10^{-3}$	$6{,}43.10^{-3}$	3,60	3,60	298,16
9	$3{,}95.10^{-7}$	$5{,}6.10^{-7}$	$1{,}38.10^{-3}$	$6{,}43.10^{-3}$	6,00	6,00	298,16
10	$1{,}44.10^{-7}$	$1{,}66.10^{-7}$	$1{,}38.10^{-3}$	$6{,}43.10^{-3}$	9,00	9,00	298,16
11	$6{,}17.10^{-7}$	$5{,}00.10^{-6}$	$1{,}38.10^{-3}$	$6{,}43.10^{-3}$	2,40	2,40	298,16
12	$8{,}53.10^{-6}$	$8{,}30.10^{-6}$	$0{,}60.10^{-3}$	$2{,}50.10^{-3}$	2,64	0,80	298,16
13	$3{,}79.10^{-6}$	$5{,}50.10^{-6}$	$0{,}60.10^{-3}$	$2{,}50.10^{-3}$	2,64	1,20	298,16
14	$2{,}12.10^{-6}$	$2{,}86.10^{-6}$	$0{,}60.10^{-3}$	$2{,}50.10^{-3}$	2,64	1,60	298,16
15	$5{,}33.10^{-7}$	$0{,}46.10^{-6}$	$0{,}60.10^{-3}$	$2{,}50.10^{-3}$	2,64	3,20	298,16
16	$1{,}28.10^{-5}$	$1{,}73.10^{-5}$	$0{,}6.10^{-3}$	$2{,}50.10^{-3}$	0,44	1,60	298,16
17	$6{,}39.10^{-6}$	$7{,}50.10^{-6}$	$0{,}6.10^{-3}$	$2{,}50{,}10^{-3}$	0,88	1,60	298,16
18	$3{,}19.10^{-6}$	$2{,}54.10^{-6}$	$0{,}6.10^{-3}$	$2{,}50.10^{-3}$	1,76	1,60	298,17
19	$1{,}50.10^{-6}$	$1{,}22.10^{-6}$	$0{,}6.10^{-3}$	$2{,}50.10^{-3}$	3,52	1,60	298,16
20	$4{,}78.10^{-7}$	$5{,}00.10^{-7}$	$1{,}38.10^{-3}$	$6{,}43.10^{-3}$	7,22	7,22	313,16
21	$1{,}17.10^{-6}$	$1{,}00.10^{-7}$	$1{,}38.10^{-3}$	$6{,}43.10^{-3}$	7,22	7,22	333,16

En utilisant les données du tableau 3, la vitesse de réduction, la concentration des réactants et du milieu de réaction on calcule les constantes de vitesse pour les températures de 25°, 40° et 60° :

$$v_{1/2} = -\frac{dc}{dt} = k_1[Au^{3+}][Asc] \qquad \text{(IV)}$$

$$v_{1/2} = -\frac{dc}{dt} = k_2\frac{[Au^{3+}][Asc]}{[H^+][Cl^-]^2} \qquad \text{(V)}$$

$k_{1(25°)} = 2{,}36.10^{-2}$ M^{-1} s^{-1}, $k_{1(40°)} = 5{,}63.10^{-2}$ M^{-1} s^{-1}, $k_{1(60°)} =$
$= 11{,}2.10^{-2}$ M^{-1} s^{-1} pour $H^+ = 7{,}22$ M, $Cl^- = 7{,}22$ M.
$k_{2(25°)} = 9{,}02$ M^2 s^{-1}, $k_{2(40°)} = 21{,}2$ M^2 s^{-1}, $k_{2(60°)} = 42{,}41$ M^2 s^{-1}.

Les valeurs des constantes de vitesse k_1 et k_2 sont calculées pour chaque température entre 25° — 60° et à l'aide des expressions suivantes :

$$k_1 = \frac{K_{\mathrm{Au}}\,\mathrm{e}^{-E_{\mathrm{Au}}/RT}}{[\mathrm{H}^+][\mathrm{Cl}^-]^2} \tag{VI}$$

$$k_2 = K_{\mathrm{Au}}\,\mathrm{e}^{-E_{\mathrm{Au}}/RT} \tag{VII}$$

En effectuant le rapport des relations (VI) et (VII) et en considérant que

$$k_1 = A\,\mathrm{e}^{-E_{\mathrm{Au}}/RT} \qquad \text{(VIII) on obtient}$$

$$k_2 = A[\mathrm{H}^+][\mathrm{Cl}^-]^2\,\mathrm{e}^{-E_{\mathrm{Au}}/RT} \qquad \text{(IX), d'où}$$

$$K_{\mathrm{Au}} = A[H^+][\mathrm{Cl}^-]^2 \tag{X}$$

La valeur K_{Au} diffère du facteur préexponentiel A de la relation (VIII) par le produit $[\mathrm{H}^+][\mathrm{Cl}^-]^2$.

La relation I est similaire à celle établie à la réduction du Pt(II)[1] et du Pd(II)[8] par acide ascorbique :

$$v_{1/2} = K_{\mathrm{Me}}\,\frac{[\mathrm{Me}^{n+}][\mathrm{Asc}]}{[\mathrm{H}^+][\mathrm{Cl}^-]^2}\,\mathrm{e}^{-E_{\mathrm{Me}}/RT} \tag{XI}$$

$\mathrm{Me}^{n+} = \mathrm{Pt}^{2+}, \mathrm{Pd}^{2+}$

$E_{\mathrm{Pd}} = 18500$ cal/mole, $E_{\mathrm{Pt}} = 27036$ cal/mole.

En considérant les valeurs $\log K_{\mathrm{Au}} = 7{,}82$, $\log K_{\mathrm{Pd}} = 10{,}40$ $\log K_{\mathrm{Pt}} = 13{,}32$, on peut déduire la possibilité de séparation des trois éléments, avec des applications dans la chimie inorganique et analytique, ce qui a constitué le but du cycle de travaux cités.

Le mécanisme de cette réaction redox est dans notre attention.

Nous remercions le Dr Gheorghe Morar pour l'aide accordée à l'exécution des analyses d'or par spectrométrie de fluorescence à rayons X.

Revue Roumaine de Chimie, **22**, *3*, 371–378 (1977)

Cr (III) COORDINATION COMPOUNDS WITH 3-AMINO-1-PROPANOL

MARIA BREZEANU and IOANA JITARU

Institute of Chemistry, Bucharest, Laboratory of Inorganic Chemistry, Splaiul Independenței, 87, Bucharest, Romania.

Received January 21, 1976

A series of chromium (III) coordination compounds with 3-amino-1-propanol were obtained; they belong to the following general types: $[Cr(AOH)(AO)_2(H_2O)]\ X.nH_2O$ ($X = Cl, Br, n = 0; X = I, n = 1; X = CNS, n = 2$) and $[Cr_2(AOH)_3(AO)_3]X_3.nH_2O$ ($X = 1/2SO_4$, $n = 12$) where $AOH = H_2N-C_3H_6-OH$ and $AO = H_2N-C_3H_6-O^-$. The compounds obtained were characterized by elemental chemical analysis, molecular weight determinations, conductivity measurements, electronic and vibrational spectra, thermodifferential analysis. Attempts were made to establish the most probable stereochemistry of the compounds studied, based on data obtained.

The paper is a part of a more extended study on the coordination capacity of some higher aminoalcohols, namely of propanolamines.

In a previous note[1] we have reported the results obtained in the synthesis and characterization of some coordination compounds of copper (II) with 3-amino-1-propanol (monopropanolamine).

This paper reports the results of the study performed in view of characterizing some new chromium (III) coordination compounds with monopropanolamine.

In order to obtain the largest possible variety of complex compounds containing monopropanolamine under the form of neutral or anionic ligand, we have performed the synthesis under different experimental conditions with regard to: the molar ratio of the components (chromium (III) salt and monopropanolamine), the nature of anion X, the solvent nature and the pH of the reaction medium.

Conducting the synthesis under different conditions with regard to the above mentioned parameters we have been able to characterize a series of chromium (III) coordination compounds which belong to the following general types: $[Cr(AOH)(AO)_2(H_2O)]\ X.n\ H_2O$ ($X = Cl, Br, n = 0; X = I, n = 1; X = CNS, n = 2$), $[Cr_2(AOH)_3(AO)_3]X_3.n\ H_2O$($X = 1/2SO_4$, $n = 12$) where $AOH = HO-C_3H_6-NH_2$ and $AO = H_2N-C_3H_6-O^-$.

---

[1] N. Brezeanu and I. Jitaru, *Rev. Roumaine Chim.*, **18**, 2039 (1973).

The compounds obtained were characterized by elemental chemical analysis, molecular weight determinations, conductivity measurements, electronic spectra, vibrational spectra, thermal analysis.

RESULTS AND DISCUSSIONS

Each of the different parameters in this study has a special contribution in the stabilization of a certain type of compound and in particular in the manner in which the monopropanolamine ligand acts.

The compounds belonging to the first mentioned type $[Cr(AOH)(AO)_2(H_2O)]$ X.n H_2O were obtained in a medium of slightly basic methyl alcohol (pH = 8) at a 1 :5 molar ratio of components.

With regard to the nature of anion X, it could be mentioned that by using chromium nitrate or acetate we have failed to isolate well defined compounds.

As it also results from the suggested general formula, not all the three monopropanolamine (AOH) ligands are present as anionic species, although this should be the form of existence of aminoalcohols in an alkaline medium.

To obtain a compound containing three AOH ligands of an anionic type, the synthesis was conducted in a strongly basic medium obtained with an excess of monopropanolamine.

In such conditions, however, the complex compound obtained was similar to that obtained at pH 8, i.e. $[Cr(AOH)(AO)_2(H_2O)]X.nH_2O$.

Attempts to obtain such a complex compound from a strongly basic aqueous solution have also failed to yield results. No well defined compounds have been obtained in these conditions. Likewise, due to the basic character of monopropanolamine, it was difficult, in fact virtually impossible to obtain by direct synthesis complex compounds of chromium (III) containing only the neutral ligand species.

The anionic coordinated ligands could however be partially or totally protonated by the action of acids on the respective compounds. Thus, depending on the strength and the concentration of the acid, compounds of the form $[Cr(AOH)(AO)_2(H_2O)]X$ would be expected to lead either to the formulation of some compounds of the $[Cr(AOH)_2(AO)]X_2$ type or the $[Cr(AOH)_3]X_3$ type, or to polynuclear complex compounds in which the oxygen of the deprotonated aminoalcohol would act as a bridge.

The attempts performed in this sense yielded no results. The isolation of such compounds in solid state, under the action of diluted or concentrated acids, from any of the $[Cr(AOH)(AO)_2(H_2O)]X.nH_2O$ compounds was not possible. Nevertheless, the change in the colour of the reaction mixture (from blue to red) indicates a chemical interaction which is most likely of the above mentioned type.

The second reported compound, i.e. $[Cr_2(AOH)_3(AO)_3]_2(SO_4)_3.12H_2O$ was obtained in a direct reaction between chromium sulphate and monopropanolamine (see the experimental section).

Molecular weight measurements. The molecular weight determinations have confirmed the data of the chemical analysis, showing that the first compounds $[Cr(AOH)(AO)_2(H_2O)]X.nH_2O$ are mononuclear whereas the complex sulphate $[Cr_2(AOH)_3(AO_3]_2(SO_4)_3.12\ H_2O$ is binuclear (see Table 1).

Table 1

Molecular weights and melting points of the studied compounds

Compound	Melting point	Molecular weight	
		found	calculated
$[Cr(AOH)(AO)_2(H_2O)]Cl$	155	328.44	321.50
$[Cr(AOH)(AO)_2(H_2O)]Br$	170	372.89	369.20
$[Cr(AOH)(AO)_2(H_2O)]I.H_2O$	165	437.89	432.35
$[Cr(AOH)(AO)_2(H_2O)]CNS.2\ H_2O$	150	386.99	383.55
$[Cr_2(AOH)_3(AO)_3]_2(SO_4)_3.12\ H_2O$	250	1710.80	1706.52

$AOH = H_2N-C_3H_6-OH$ and $AO = (H_2N-C_3H_6-O)^-$

Table 1 lists the values of molecular weights obtained for the complexes under study.

Conductivity measurements. The formulation assigned to the complexes obtained, in the sense of establishing the electrolyte type, was supported by the determination of their molecular electrical conductivities. The data obtained are presented in table 2.

Table 2

Molar electrical conductivities of the compounds under study

Compound	Molar electrical conductivity ($\Omega^{-1}\ cm^2\ mol^{-1}$)	Electrolyte type
$[Cr(AOH)(AO)_2(H_2O)]Cl$	85.30	1 : 1
$[Cr(AOH)(AO)_2(H_2O)]Br$	80.45	1 : 1
$[Cr(AOH)(AO)_2(H_2O)]I.H_2O$	75.20	1 : 1
$[Cr(AOH)(AO)_2(H_2O)]CNS.2H_2O$	83.70	1 : 1
$[Cr_2(AOH)_3(AO)_3]_2(SO_4)_3.12\ H_2O$	390.25	2 : 3

Sol. 10^{-3} M, in DMF, $t = 25°$.

Electronic spectra. Some data on the structure of the studied complexes were obtained by recording their reflexion electronic spectra.

The electronic spectra of $[Cr(AOH)(AO)_2(H_2O)]\ X.nH_2O$ ($X = Cl, Br, n = 0$; $X = I, n = 1$; $X = CNS, n = 2$) compounds can be interpreted satisfactorily in terms of an octahedral structure, tetragonally distorted (fig. 1).

According to the Tanabe Sugano diagram, the band appearing at 420 nm (23.800 cm^{-1}) is attributed to the $^4T_{1g}(F) \leftarrow {}^4A_{2g}$ transition, while that appearing at 570 nm (17.500 cm^{-1}) to a $^4T_{2g} \leftarrow {}^4A_{2g}$ transition. The asymmetry of this band could be interpreted based on a tetragonal distorsion from the octahedral symmetry, which may sometimes result in a marked splitting of the band corresponding to the $^4T_{2g} \leftarrow {}^4A_{2g}$ transition. The third band, of a high energy (about 30,000 cm^{-1}) and a small intensity, corresponding to the $^4T_{1g}(P) \leftarrow {}^4A_{2g}$ transition, assumed for a d^3 configuration in an octahedral symmetry field, is in general overlapped by the charge transfer bands or by those belonging to the ligand.[2,3]

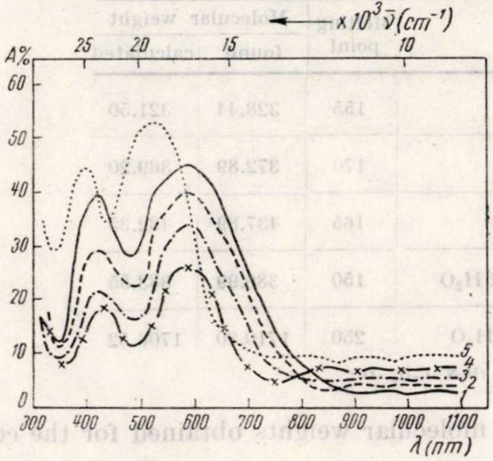

Fig. 1. — Electronic reflexion spectra of compounds :
1. $[Cr(AOH)(AO)_2(H_2O)]Cl$;
2. $[Cr(AOH)(AO)_2(H_2O)]Br$;
3. $Cr(AOH)(AO)_2(H_2O)]\,I.H_2O$;
4. $[Cr(AOH)(AO)_2(H_2O)]CNS.2H_2O$;
5. $[Cr_2(AOH)_3(AO)_3]_2(SO_4)_3.12H_2O$

The electronic spectrum recorded for the $[Cr_2(AOH)_3AO)_3]_2(SO_4)_3$ $.12H_2O$ compound is very similar to those of compounds $[Cr(AOH)(AO)_2(H_2O)]X.n\,H_2O$. This permits the assignment of a similar configuration, i.e. octahedral configuration tetragonally distorted.

However, considered comparatively, the spectra of these compounds indicate a slight difference with regard to the position of bands in the sense of a shift towards higher frequencies for the binuclear compound (Fig. 1). This difference may be attributed to the intensity growth of the crystalline field by the transition from the binuclear compound to mononuclear ones.

Infrared spectra. The IR spectra recorded for the compounds under study were interpreted by establishing the coordination manner of the monopropanolamine ligand (neutral molecule, mono or bidentated anion).

From this point of view, two most appropriate spectral ranges are those for which the absorption is attributed to O—H (ν_{OH}), C—O (ν_{CO})

---

[2] L. S. Forster and K. D. Armond, *J, Chem. Phys.*, **34**, 2193 (1961).
[3] R. M. Mac Farlane, *J. Chem. Phys.*, **39**, 3118 (1963).

and N—H (ν_{asNH} and ν_{sNH}) stretching vibrations of the monopropanolamine ligand.

In order to assign the IR spectra of the studied compounds as correctly as possible, the spectrum of the free ligand was also recorded. In the ligand spectrum, the OH (ν_{OH}) stretching vibration appears at 3450 cm^{-1}. Compared to the ν_{OH} stretching vibration in primary alcohols (3650 — — 3590 cm^{-1}) this value indicates the presence of the inter and intramolecular hydrogen bonds in monopropanolamine.

Table 3 shows the IR characteristic frequencies of some chromium (III) complexes studied and the probable assignments.

A study of the data included in table 3 suggests the following : -a shift of the frequencies attributed to the vibration modes of the amino groups (ν_{asNH}, ν_{sNH} and δ_{NH_2}) towards lower values, in all the studied complexes, relative to the free aminoalcohol, may be interpreted as an evidence of its coordination by means of nitrogen.[4]

— in the spectra of all the mononuclear compounds under study, both anhidrous $[Cr(AOH)(AO)_2(H_2O)]X$ (X = Cl, Br) and crystallohydrates $[Cr(AOH)(AO)_2(H_2O)]\ X.n\ H_2O$ (X = I, n = 1 ; X = CNS, n = = 2) (table 3 presents one compound for each type) and also of binuclear compounds $[Cr_2(AOH)_3(AO)_3]_2(SO_4)_3.12\ H_2O$, the absorption band assigned to the OH stretching vibration appears (3450 cm^{-1}) within the same range as for the free ligand. This indicates the presence of at least one monopropanolamine molecule as a neutral monodentated ligand, coordinated only by nitrogen of the amino group ;

— the absorption bands appearing in the spectra of compounds $[Cr(AOH)\ (AO)_2(H_2O)]X$ (X = Cl, Br, CNS) at about 970 cm^{-1} and about 1010 cm^{-1} were attributed to the stretching vibrations of coordinated water molecule. The absence of such bands in the spectrum of the binuclear compound $[Cr_2(AOH)_3(AO)_3]_2(SO_4)_3.12\ H_2O$ supports this assignement[5];

— in the spectrum of $[Cr_2(AOH)_3(AO)_3]_2(SO_4)_3.12\ H_2O$ compound in which monopropanolamine acts in a different manner (neutral molecule and anionic ligand) the absorption band attributed to the C—O stretching vibration appears split into two components (in the spectra of the other compounds $[Cr(AOH)(AO)_2(H_2O)]$ X this thing is more difficult to emphasize since the range of the C—O stretching vibration is overlapped by the bands assigned to the stretching vibration of the coordinated water molecule) ;

— the position of the bands attributed to the vibration modes of the CNS^- and SO_4^{2-} anions in the spectra of compounds $[Cr(AOH)(AO)_2(H_2O)]$ CNS.2 H_2O and $[Cr_2(AOH)_3(AO)_3]_2(SO_4)_3.12\ H_2O$ indicates their presence in the respective compounds.[6,7]

---

[4] L. J. Bellamy, "Infrared Spectra of Complex Molecules", Academic Press, New York, 1958, p. 108.

[5] K. Nakamoto, "Infrared Spectra of Inorganic Coordination Compounds", Aacdemic Press, New York, 1963, p. 159.

[6] K. Nakamoto, "Infrared Spectra of Inorganic Coordination Compounds", Academic Press, New York, 1963, p. 165.

[7] B. M. Gatehouse, S. E. Livingstone and R. S. Nyholm., *J. Chem. Soc.*, **1957**, 422.

Table

Characteristic IR frequencies

Compound	ν_{OH}	ν_{asNH}	ν_{sNH}
AOH	3450(s, b)	3290(s, b)	3170(sh)
$[Cr(AOH)(AO)_2(H_2O)]Cl$	3450(m)	3220(m)	3115(m)
$[Cr(AOH)(AO)_2(H_2O)]$ (CNS)$.2H_2O$	3450(m, b) 3320(m, b)	3250(m, b)	3090(w)
$[Cr_2(AOH)_3(AO)_3]_2(SO_4)_3.12H_2O$	3450(m, b) 3310(m, b)	3260(m,b)	3080(w)

s-strong, w-weak, b-broad, sh-shoulder.

Thermal analysis. The thermodifferential analysis of some complex compounds studied was performed, to obtain data on their thermal stability. The data thus obtained were used to elucidate the proposed structures and particularly to establish the nature of water involved in the composition of these complexes, i.e. water of crystallization or water of coordination.

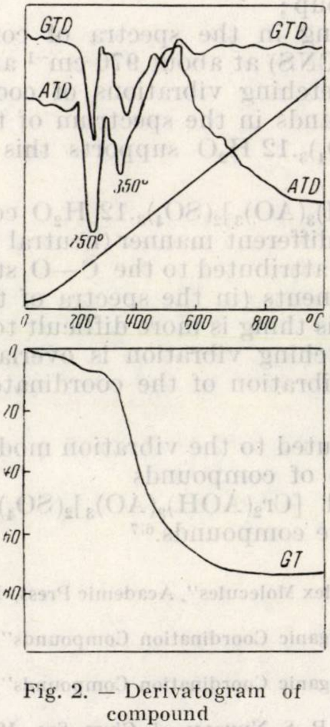

Fig. 2. — Derivatogram of compound $[Cr(AOH)(AO)_2(H_2O)]Cl$.

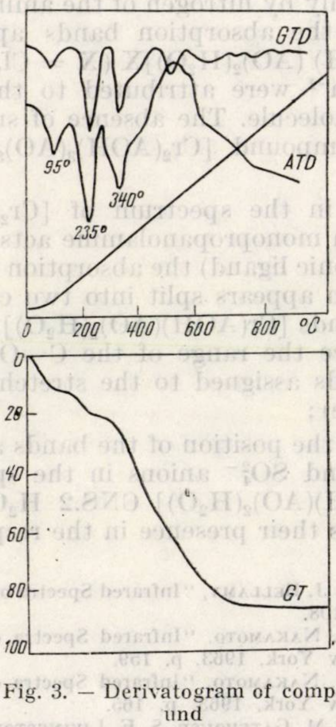

Fig. 3. — Derivatogram of compound $[Cr(AOH)(AO)_2(H_2O)]CNS.2H_2O$.

3

of the obtained compounds

δ_{NH_2}	ν_{CO}	ν coordinated (H_2O)	$\nu_{CN(CNS)}$ $\nu_{CS(CNS)}$	$\nu_{SO(SO_4)}$
1615(m, b)	1055(s)	—	—	—
1570(m)	coordin H_2O band	975(s) 1010(m)	—	—
H_2O bands	coordin H_2O band	970(s) 1015(m)	1960(s)(ν_{CN})	—
H_2O bands	1040(s) 1030(sh)	—	—	1140(s) (ν_3) 625(s)(ν_4)

From this point of view it is worth studying the behaviour on heating of the complexes of type $[Cr(AOH)(AO)_2(H_2O)]X$ (X = Cl, Br) respectively $[Cr(AOH)(AO)_2(H_2O)]$ X.n H_2O (X = I, n = 1 and X = = CNS, n = 2). The derivatogram of compound $[Cr(AOH)(AO)_2(H_2O)]Cl$ illustrated in figure 2 presents two distinct endoeffects at 250° and 350°, respectively. The first endoeffect corresponds to a 5.55% weight loss (theoretically 5.48%) and may be attributed to the loss of the water molecule from the coordination sphere. The endoeffect at 350° corresponds to the total thermal decomposition of the complex compound. The absence of an endoeffect at temperatures around 100° which would be accompanied by an obvious weight loss is an evidence in support of the formulation of the respective compound with water of coordination rather than with water of crystallization.

Another evidence in support of this formulation is provided by the derivatogram recorded for compound $[Cr(AOH)(AO)_2(H_2O)]CNS.2\,H_2O$ (Fig. 3) which presents an additional endoeffect at a temperature of 95° attributed to the elimination of water of crystallization (actual weight loss 9.35%, theoretical, 9.29%).

EXPERIMENTAL DATA

I. SYNTHESIS OF COMPOUNDS

1. $[Cr(AOH)(AO)_2(H_2O)]X.nH_2O$ (X = Cl, Br, n = 0; X = I, n = 1; X = CNS, n = 2)

An amount of methanolic solution of 3 amino 1 propanol (1 : 5) corresponding to a chromium (III) : AOH = 1 : 5 molar ratio was added to a methanolic solution of chromium salt. The solution containing in suspension the green grey gelations precipitate initially formed is refluxed for 8 — 10 hours on a water bath at 50 — 60° (in the case of chromium chloride) or it is kept for 7 — 10 days in the cold with addition of new amounts of methanol (in the case of chromium bromide, iodide and thiocyanide). During this time, the gelatinous precipitate is macerated forming a dark blue solution. The solution obtained in this way is filtered to remove the possible unreacted chromium hydroxide traces and is then evaporated on a water bath (at 50 — 60°) until the first crystals are formeed. The solution is then left in the desiccator on calcim chloride until dark blue crystals have been formed. The substance obtained in this way is filtered and washed with small amounts of methyl alcohol.

The reaction between the chromium nitrate or acetate and 3-amino-1-propanol in methyl alcohol leads to the formation of some bluedark violet solutions from which we have failed to isolate well defined compounds.

Calcd.: Cr, 15.82; N, 12.79; Cl, 10.79%
Found: 15.90; 12.75; 10.92 %
Calcd.: Cr, 13.94; N, 11.26; Br, 21.42 %
Found: 14.10; 11.35; 21.60%
Calcd.: Cr, 11.86; N, 9.58; I, 28.95 H_2O,4.11 %
Found: 11.65; 9.65; 28.80 3.95 %
Calcd.: Cr, 13.42; N, 10.84; CNS,14.99; H_2O,9,29 %
Found.: 13.55; 10.90; 15.10; 9.00

2. $[Cr_2(AOH)_3(AO)_3]_2(SO_4)_3.12\ H_2O$. An amount of a methanolic solution of 3 amino 1 propanol (1 :5) corresponding to a chromium(III) : AOH = 1 : 7 molar ratio is added to a solution of chromium sulphate, $Cr_2(SO_4)_3.6H_2O$ in water + methyl alcohol (1 + 1). The mixture obtained is refluxed for 1 — 2 hours on a sand bath at 90 — 100°. During this period the sulphate is totally dissolved and a blue solution is formed. The solution thus obtained is filtered, concentrated on a water bath at 50 — 60° and evaporated to dryness in the desiccator on calcium chloride. By working out the viscous mixture obtained with methyl alcohol pink red crystals will separate. These are filtered and washed with methyl alcohol.

Calcd: Cr, 12.18; N, 9.84; SO_4 16.88; H_2O, 18.52%
Found: 12.10; 9.75; 16.70; 18.20

II. MOLECULAR WEIGHT MEASUREMENTS

The molecular weight of the compounds under study were determined by means of the Rast method. The solvent used for this purpose was camphor.

III. CONDUCTIVITY MEASUREMENTS

The molecular electric conductivity measurements were peformed on a type II K. Zeiss Yena conductometer (Czechoslovakia) with the cell constant k = 0.52. We used 10^{-3} M solutions in dimethylformamide at a temperature of 25°.

The assignement of the electrolyte type was made based on the indications reported in the literature with regard to the methods for the determination of the electrolyte type in a dimethylformamide solution.

IV ELECTRONIC SPECTRA

The reflexion electronic spectra were recorded at room temperature using a VSU 1 K. Zeiss Yena spectrophotometer and the reference material was magnesium oxide. The electronic spectra in solution were recorded at room temperature using a VSU 2 G spectrophotometer.

V. INFRARED SPECTRA

IR spectra were recorded by means of a Perkin Elmers spectrophotometer in Nujol solutions or in KBr pellet.

VI. THERMAL ANALYSIS

The thermodifferential analysis was conducted on a Paulik Paulik Erdey derivatograph (Hungary) with the concomitent recording of T. TG, DTG, DTA. The temperature range used was 20 — 1000°. The curves were recorded in the air, the heating rate was 5°/minute, the sensitivity of the heating system was 100 mg and the standard sample used was calcined Al_2O_3.

Revue Roumaine de Chimie, **22**, *3*, 379–383 (1977)

SYNTHESIS OF DI- AND TRIPHENYLLEAD POLYCHLOROACETATES[a]

ILEANA BALÁZS, VALER FĂRCĂŞAN and IONEL HAIDUC[b]
Chemistry Department, Babeş-Bolyai University, Str. Arany Janos 11, 3400 Cluj-Napoca

Received October 11, 1975

The synthesis of di- and triphenyllead mono-, di- and trichloroacetates is described. The compounds were prepared by the reaction of triphenyllead hydroxide or diphenyllead oxide with the appropriate polychloroacetic acid, in good yield. A satisfactory alternative preparation was the cleavage of phenyl groups from tetraphenyllead with an appropriate polychloroacetic acid, in 1 :1 molar ratio to give $Ph_3PbOCOR$, and 1 : 2 molar ratio to give $Ph_2Pb(OCOR)_2$ ($R = CH_2Cl$, $CHCl_2$ and CCl_3). Some decarboxylation experiments were also performed. Infrared spectra of the compounds prepared are discussed briefly.

INTRODUCTION

Organolead compounds, in particular organolead carboxylates, have been found to exhibit biological activity, and some of them are of potential interest as fungicides, insecticides or bactericides.[1] Thus, triphenyllead acetate hinders the growth of *Escherichia Coli*,[2] increases the resistance of cotton to spillage[3] and is a good preservative for high quality marine antifouling paints[4] or hydroxyethylmetacrylate polymers.[5] Triphenyllead propionate exhibits antiseptic properties[6] whereas other triphenyllead carboxylates show biocidal activity against *Candida albicans* and *Aspergillus niger*.[7]

---

[a] The general term "polychloroacetates" is designated to include all members of the $Cl_n\ CH_{3-n}\ COOH$ series with $n = 1 - 3$.

[b] Author to whom all the correspondence concerning this paper should be addressed.

[1] H. Shapiro and F. W. Frey, "The Organic Compounds of Lead", Interscience, New York, 1968, p. 399.

[2] H. Kourai, K. Takeichi, M. Okaraki, T. Enatsu and I. Shibasaki, *Hakko Kagaku Zasshi*, **50**, 34 (1972) ; *Chem. Abstr.*, **76**, 136251 (1972).

[3] D. J. Donaldson, W. A. Guice, G. L. Drake and W. R. Reeves, *U.S. Patent* 3,420, 701 (1969) ; *Chem, Abstr.*, **70**, 58871 (1969).

[4] R. J. Dick and L. J. Nowacki, *J. Paint Technol.*, **42**, 535 (1970) : *Chem. Abstr.*, **73**, 132028 (1970).

[5] T. H. Shepherd and F. E. Gould, *Ger. Offen.*, 2, 161, 630 (1972) ; *Chem Abstr.*, **77**, 128200 (1972).

[6] M. Buschkoff, *Ger. Offen.*, 2,032,299 (1971) ; *Chem. Abstr.*, **76**, 59754 (1972).

[7] H. Kourai and K. Takeichi, *Hakko Kagaku Zasshi*, **47**, 603 (1969) ; *Chem. Abstr.*, **72**, 63923 (1970).

These results suggested that other organolead carboxylates might be of interest as potential biocide compounds and our attention turned towards phenyllead polychloroacetates. This investigation was a part of a larger research program, in which several types of organometallic compounds, including phenyllead phosphorodithioates,[8] phenylmercury phosphorodithioates[9] and other compounds, were prepared with the purpose of evaluating their biological activity.

Organometallic derivatives of mono- di-, and trichloroacetic acids are of particular interest, since these acids themselves exhibit biological activity and are used as herbicides.[10,11] The literature on phenyllead polychloroacetates is very scarce and incomplete.[12–14] Diphenyllead bis(monochloroacetate)[12] and diphenyllead bis(trichloroacetate)[13,14] have been reported, but to the best of our knowledge no triphenyl polychloroacetate has been described. Therefore, a complete investigation of this type of compound seemed appropriate.

RESULTS AND DISCUSSION

Triphenyllead polychloroacetates were prepared by two different methods:

a. The reaction of triphenyllead hydroxide with the free acid, in anhydrous ethanol:

$$Ph_3Pb-OH + RCOOH \rightarrow Ph_3Pb-OCOR + H_2O \qquad (A)$$

$$R = CH_2Cl,\ CHCl_2 \text{ and } CCl_3$$

b. The reaction of tetraphenyllead with the appropriate acid, in toluene, under heating, in 1 :1 molar ratio :

$$PbPh_4 + RCOOH \rightarrow Ph_3Pb-OCOR + C_6H_6 \qquad (B)$$

Since triphenyllead hydroxide itself is prepared from tetraphenyllead[15] and the yields in method B are at least as good as in method A, the preparation of triphenyllead polychloroacetates from tetraphenyllead seems to be the method of choice for the synthesis of these compounds. The yields, melting points, analytical data and infrared data (ν_{CO_2} stretchings) for the compounds prepared are listed in Table 1.

---

[8] I. Haiduc, F. Martinaş, D. Ruse and M. Curtui, *Syn. React. Inorg. Metal-Org. Chem.* **5**, 103 (1975).

[9] I. Haiduc and E. Veres, *Syn. React. Inorg. Metal-Org. Chem.*, **5**, 115 (1975).

[10] C. Popa and R. Drimuş, "Chimia produselor fitofarmaceutice", Editura Tehnică, Bucureşti, 1965, p. 311.

[11] M. Avram, "Antidăunătorii", Editura Academiei, Bucureşti, 1974, p. 416.

[12] E. M. Panov and K. A. Kocheshkov, *Zhur. obshchei khim.*, **25**, 489 (1955) ; *Doklady Akad. Nauk S.S.S.R.*, **85**, 1037 (1952).

[13] A. E. Goddard, J. S. Ashley and R. B. Evans, *J. Chem. Soc.*, **121**, 978 (1922).

[14] F. Huber, H. Horn and H. J. Haupt, *Z. Naturforsch.*, **22b**, 918 (1967) ; *Chem. Abstr.*, **68**, 49695 (1968).

[15] E. Lieber and F. M. Keane, *Inorg. Synth.*, **8**, 57 (1966).

Table 1

Phenyllead polychloroacetates

Compound	Method of preparation	Yield %	M.p.[a] °C	Analytical data found (calc)		I.R. data	
				Pb %	Cl %	$\nu_{as}CO_2$ cm^{-1}	$\nu_{sym}CO_2$ cm^{-1}
$Ph_3Pb-OCOCH_2Cl$	A	90	205−6	39.08	6.80	1583	1410
	B	92		(38.95)	(6.66)		
$Ph_3Pb-OCOCHCl_2$	A	93	216−17	36.54	12.60	1603	1392
	B	96		(36.58)	(12.52)		
$Ph_3Pb-OCOCCl_3$	A	73	183(dec)	34.47	17.60	1610	1390
	B	88		(34.49)	(17.70)		
$Ph_2Pb(OCOCH_2Cl)_2$	C	91	223	37.81	13.08	1590	1410
			(dec.)[b]	(37.79)	(12.93)		
	D	88					
$Ph_2Pb(OCOCHCl_2)_2$	C	98	240	34.29	23.00	1610	1405
	D	88	(dec.)	(33.57)	(22.95)		
$Ph_2Pb(OCOCCl_3)_2$	C	94	303−4	30.55	31.00	1620	1415
	D	80	(dec.)[c]	(30.20)	(30.80)		

[a] Melting points are not corrected ; [b] Lit. m.p. 185 − 205° (dec.)[12] [c] Lit. m.p. 210°for $Ph_2Pb(OCOCCl_3)_2 . CCl_3COOH$[13]

If the reaction of tetraphenyllead with a polychloroacetic acid is carried out in 1 : 2 molar ratio, two phenyl groups are cleaved, to give diphenyllead bis(polychloroacetates) (method C) :

$$PbPh_4 + 2\ RCOOH \rightarrow Ph_2Pb(OCOR)_2 + 2C_6H_6 \qquad (C)$$

$$R = CH_2Cl,\ CHCl_2,\ CCl_3$$

Therefore, the stoichiometric ratio must be rigorously observed in these reactions.

An alternative procedure for the synthesis of diphenyllead bis(polychloroacetates) is the reaction of diphenyllead oxide with the appropriate acid (method D) :

$$Ph_2PbO + 2\ RCOOH \rightarrow Ph_2Pb(OCOR)_2 + H_2O \qquad (D)$$

The results are given in Table 1. The yields in method D are slightly lower than in method C. It follows that for diphenyllead derivatives the preparation using tetraphenyllead as starting material is again the method of choice.

Each compound was prepared by two different methods and the identity of products was demonstrated by melting point (mixed melting point), elemental analysis and infrared spectra.

The absorption bands due to ν_{sym} CO_2 and ν_{as} CO_2 are listed in Table 1. The $\nu_{C=}O$ at 1760−1730 cm^{-1} in the free acids is missing from the spectra of the organolead derivatives. The bands at ca. 1620−1580cm^{-1}

and 1415—1390 cm^{-1} are assigned to ν_{as} CO_2 and ν_{sym} CO_2, respectively, based on the fact that these bands are not present in the starting materials. The shift of the bands due to carboxylic groups seems to suggest that in the compounds investigated the carboxylato groups act as bidentate ligands, increasing the coordination number of lead from four to five (in $Ph_3Pb-OCOR$) and six (in $Ph_2Pb(OCOR)_2$), as illustrated by the following structures:

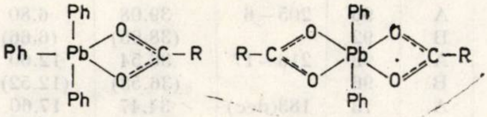

The infrared spectra of the compounds investigated exhibit some other absorption bands of interest. Thus, the bands at ca 795—790 cm^{-1} are due to C—Cl stretchings. A band at ca 1025 cm^{-1}, present in the spectra of all phenyllead derivatives investigated, may be assigned to $Pb-C_6H_5$ groups, this band being diagnostic for aryllead derivatives.[16]

It was observed during repeated recrystalizations of triphenyllead dichloro-and trichloroacetate, that some chemical transformation occurs. Two different possible reactions could be taken into consideration, namely a disproportionation (reaction E) or a decarboxylation (reaction F):

$$2\ Ph_3Pb-OCOR \xrightarrow{t} Ph_2Pb(OCOR)_2 + PbPh_4 \qquad (E)$$

$$Ph_3Pb-OCOR \xrightarrow{t} Ph_3Pb-R + CO_2 \qquad (F)$$

In order to clarify this matter, a decarboxylation of the two compounds mentioned was attempted, by refluxing in pyridine, according to a decarboxylation procedure decribed in the literature[17] for other derivatives. No individual product could be isolated, but the absorption bands of carboxylic groups were absent in the infrared spectra of the product, thus indicating a decarboxylation process to occur. A comparison of the products formed during recrystallization, with those formed in refluxing pyridine with the aid of thin layer chromatography, showed that during recrystallization only some disproportionation occurs. Thin layer chromatography data showed that some tetraphenyllead and diphenyllead dicarboxylate was formed during the process.

EXPERIMENTAL PART

The organolead reagents used in this work were prepared according to the literature.[16] A sample of triphenyllead chloride was received from the Organic Chemistry Institute TNO, Utrecht (Holland). The polychloroacetic acids were commercial products (reagent grade) and were used as received, without further purification. Infrared spectra were recorded on a UR-20 Carl Zeiss, Jena (DDR) instrument, in KBr pellets.

---

[16] J. G. Noltes, M. G. Henry and M. J. Janssen, *Chem. & Ind.* (*London*), **1959**, 298.
[17] G. B. Deacon and P. W. Felder, *Austral. J. Chem.*, **23**. 1359 (1970).

PREPARATION OF TRIPHENYLLEAD POLYCHLOROACETATES

Method A. A saturated hot solution of triphenyllead hydroxide (3 mmoles) in 15 ml ethanol was treated with 3 mmoles of acid and the mixture was refluxed for 5 minutes, then cooled. The crystals separated were filtered, washed with some ethanol and dried. A small additional crop of compound was obtained by adding 10 — 15 ml water to the filtrate.

Method B. A concentrated solution containing 2.5 mmoles of tetraphenyllead in 10 ml. hot toluene was treated with 2.5 mmoles of polychloroacetic acid. The mixture was heated for another few minutes at reflux, then allowed to cool and to stand overnight. The crystals deposited were filtered, dried in vacuo under 80° and, if necessary, recrystallized from ethanol.

The triphenyllead polychloroacetates are insoluble in water and ligroin, but dissolve in chloroform, dimethylformamide, hot ethanol, benzene, xylene or toluene.

PREPARATION OF DIPHENYLLEAD BIS(POLYCHLOROACETATES)

Method C. This method is similar to method B, except that a double amount of the acid is used.

Method D. A hot suspension of 3 mmoles of Ph_2PbO in 35 ml acetone was treated with 6 mmoles of polychloroacetic acid, then heated under gentle reflux for 1 hr on a water bath. The acetone was removed by distillation and the solid product deposited was separated and dried. Instead of acetone 20 ml. of toluene can be used.

Diphenyllead bis (polychloroacetates) are insoluble in water and ligroin, but are readily soluble in ethanol, acetone, sparingly soluble in benzene, toluene and xylene. In chloroform only $Ph_2Pb(OCOCCl_3)_2$ is soluble.

DECARBOXYLATION OF TRIPHENYLLEAD DI- AND TRICHLOROACETATES

A solution of 2.5 mmoles of triphenyllead derivative in 4 ml. pyridine was refluxed for 1 hr. The solvent was removed by vacuum distillation or the compound dissolved was precipitated by addition of water.

The products were chromatographed on silica gel plates, bonded with carboxymethylcellulose. The thin layer plates were activated by heating at 110° for 30 min and cooled in an exsiccator. Acetone-chloroform solutions were placed at the start and the plates were developed with a chloroform : benzene : ethanol (3 : 2 : 1) mixture, at room temperature. The plates were then dried at 100° for 10 min., then sprayed with an aqueous solution of 2N mercury (II) chloride. A white spot was observed for the compounds, while the plate was still wet.

Revue Roumaine de Chimie, **22**, *3*, 385–394 (1977)

CONTRIBUTIONS TO THE COORDINATION CHEMISTRY OF *s*-TRIAZINES. III[1]

THE CONDENSATION REACTION OF PHENYLBIGUANIDE WITH PHENYLISOTHIOCYANATE IN THE PRESENCE OF Cu IONS

CONSTANŢA GHEORGHIU*, CRISTINETA MĂRCULESCU **, MARIA CONSTANTINESCU *** and O. CONSTANTINESCU ***

* Department of Inorganic Chemistry, University of Bucharest, Splaiul Independenţei 89, Bucharest
** Center of Physical Chemistry, str. Dumbrava Roşie 23, Bucharest
*** Institute of Atomic Physics, P.O. Box 35

Received March 18, 1975

We discussed a hypothesis concerning the existence of a thiourea derivative, as an intermediate in the reaction of phenylbiguanide condensing with phenylisothiocyanate, which is supported by the separation of a Cu(II) complex with the formula $CuLCl_2$, where this derivative has the role of the ligand (L). The formulation of the ligand L (thiocarbamoylbiguanide) as a thiourea derivative in the $CuLCl_2$ complex is confirmed by the I.R. spectra and EPR spectra. The possibilities of coordination are also discussed.

In previous papers [1-3] we showed that by condensing phenylbiguanide with phenylisothiocyanate, there result *s*-triazines derivatives, respectively thioammeline, melamine and isomelamine. The formation of these cyclic derivatives according to the scheme below, implies the existence of an intermediate acyclic compound, thiocarbamoylbiguanide (L), form III, which may be considered as a thiourea derivative.

It was also shown that diphenyl-2-thioammeline (TA) and diphenyl melamine (ME) form coordination compounds of the $CuTAX_2$ and $CuMEX_2$ type, in which X = Cl, Br, I, SCN, SeCN.

In this work, we have attempted to elucidate the mechanism of the cyclisation reaction in the process of phenylbiguanide condensing with phenylisothiocyanate as well as to establish the conditions for the intermediate compound isolation, using chemical and physico-chemical methods (conductometric determinations, I.R., reflectance and EPR spectra).

---

[1] Part II, C. Gheorghiu and C. Mărculescu, *Rev. Roumaine Chim.*, **20**, 345 (1975).
[2] P. Spacu and C. Mărculescu, *Rev. Roumaine Chim.*, **16**, 513 (1971).
[3] C. Gheorghiu and C. Mărculescu, *Rev. Roumaine Chim.*, **21**, 707 (1975).

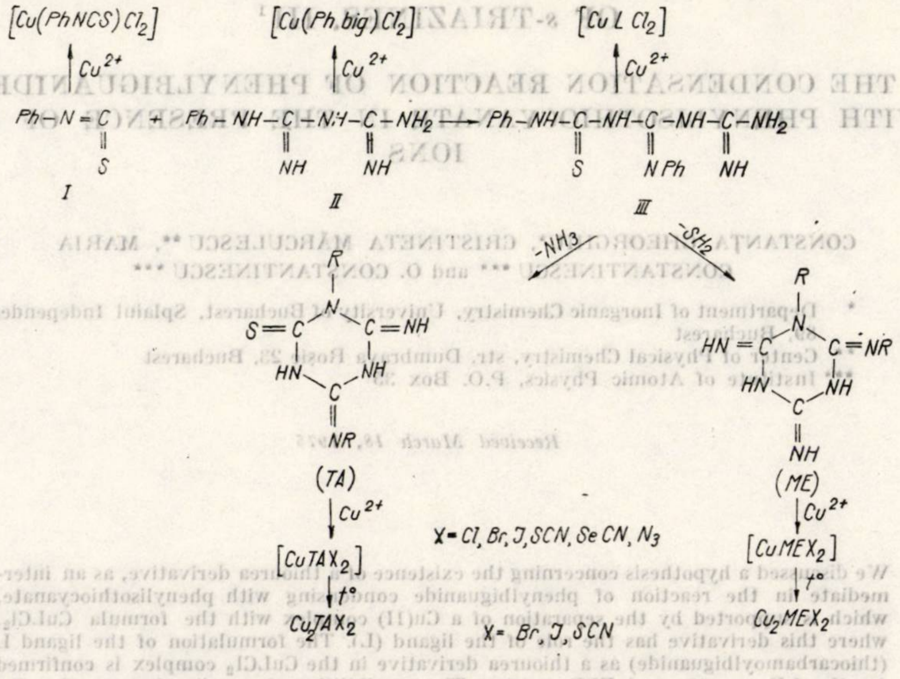

EXPERIMENTAL

The phenylbiguanide base (Ph.Big.) and the phenylisothiocyanate (PhNCS) were synthetized according to the literature.[2]

Reflectance spectra were effected with a spectrophotometer VSU-1 Zeiss-Jena in the 260 — 1100 nm range. I.R. spectra were recorded on solid state, using a UR−10−Zeiss−Jena spectrophotometer and KBr pellets.

The molar electric conductivity was determined in DMF solution at 25°, by using an OK 102/1 Radelkis conductometer within the range of 0,1 μs — 0,5 s. For the determinations of magnetic susceptibility the Gouy method was used with Hg(II) tetracyanocobaltate(II) as standard.

The E.P.R. spectra of the powder samples and of the solutions in DMF were recorded at room temperature as well as at 77 K using a spectrograph operating in X band. For the g-values determinations, DPPH and Mn_2^+ were used as standards.

PREPARATION OF $CuLX_2$. DMF TYPE COMPOUNDS (X = CL, Br)

Phenylisothiocyanate was added to a concentrated solution in anhydrous DMF of phenylbiguanide base (molar ratio 1 : 1) and the yellow-reddish solution was kept for two hours at room temperature, stirring from time to time. Then $CuCl_2.2H_2O$ or $CuBr_2$ concentrated solutions in DMF, also in 1 : 1 molar ratio, was added, when the solution gradually become red-brown. The mixture was allowed to stand for 10 minutes and then we added anhydrous diethyl ether, maintaining it on ice. This operation is repeated by settling until the viscous pro-

duct, initially formed, changes into another brick-red microcrystalline product, which is filtered and washed with anhydrous ethyl ether. By vacuum drying, the product colour becomes greenish in case one uses the copper chloride and brown in case the copper bromide is used.
$CuC_{15}H_{16}N_6SCl_2.DMF$; *Found* : C, 42.04 ; Cu, 11.52 N, 19.06 % ; Requires : C, 42.08 ; Cu, 11.42 ; N, 18.88 %. electr. cond. 85.28 ohm^{-1} cm^2mol^{-1} ; magnetic moment : 1.79 M.B.

$CuC_{15}H_{16}N_3SBr_2$: *Found* : C, 36.25 ; Cu, 10.15 ; N, 16.25 % Requires : C, 36.25 ; Cu, 9.89 ; N, 16.26 %.
electr. cond. 77.48 ohm^{-1} cm^2 mol^{-1} ; m.p. 112 — 113°.

PREPARATION OF $Cu(Ph.Big.)Cl_2.DMF$

The phenylbiguanide base and $CuCl_2.2H_2O$ in 1 : 1 molar ratio, in DMF solution were maintained for two hours at room temperature. The mixture was then treated with diethyl ether, on ice, and then it was dried in the air.
$CuC_8H_{11}N_5Cl_2$: *Found* : C, 33.05 ; Cu, 18.35 ; N, 22.30 %
Requires : C, 32.77 ; Cu, 18.25 ; N, 22.12 %.
electr. cond. 65.82 $ohm^{-1}cm^2mol^{-1}$.

The preparation of $Cu(PhNCS)Cl_2$ was accomplished by the reaction between PhNCS and $CuCl_2.2H_2O$ in DMF concentrated solution 7 1 : 1 molar ratio, maintained at room temperature for two hours. Then anhydrous diethyl ether was added on ice obtaining after repeated washing a pale green product which was filtered and washed with a small amount of diethylether
$CuC_7H_5NSCl_2$: *Found* : C, 30.83 ; Cu, 23.76 ; N, 5.34 %.
Requires : C, 31.14 ; Cu, 23.54 ; N, 5.19 %

RESULTS AND DISCUSSIONS

The reaction between phenylbiguanide and phenylisothiocyanate in equimolecular ratio in DMF solution at room temperature at $p_H = 0.5 - 1$, in time occurs with H_2S or NH_3 elimination, leading to the formation of some s-triazine derivatives. The same reaction conducted under the above mentioned conditions, but at $p_H = 5$ and in the presence of $CuCl_2.2H_2O$ occurs without release of H_2S or NH_3 leading in a short time to a khaki product which was separated from DMF medium by repeated treatments with ethyl ether. This compound is air-stable at room temperature, soluble in DMF and DMSO but insoluble in ethanol, acetone and diethyl ether. It presents a melting point at 120 — 122° and an electric conductivity determined in DMF solution at 85 ohm^{-1} cm^2mol^{-1}. The determined value of 1.79 M.B. for magnetic moments indicates that copper is divalent in this compound.

The reflectance spectra revealed two bands in UV : one at 270 nm (37.040 cm^{-1}) and the other at 330 nm (30.300 cm^{-1}), $\pi \rightarrow \pi^*$ and $n \rightarrow \pi^*$ transitions. In the visible range, two bands of low intensity were observed : the one at 440 nm (22.717 cm^{-1}) corresponding to the ${}^2B_{1g} \rightarrow {}^2E_g$ transition and the other at 780 nm (12.814 cm^{-1}) corresponding to the ${}^2B_{1g} \rightarrow {}^2B_{2g}$ transition. On the basis of the obtained results we attributed to this compound the formula $CuLCl_2$(where L = thiocarbamoylbiguanide, a thiourea derivative).

To elucidate the above mentioned mechanism of condensing reaction in presence of Cu (II) ions or generally speaking in presence of transition metals, we studied this process by modifying the addition order of the reactants, in the same molar ratio. In both possible cases, the compound obtained was Cu(Ph.Big)Cl_2. This proves the remarkable stability of the product Cu(Ph.Big.)Cl_2 which once formed cannot condense with PhNCS so as to lead either to a cyclic derivative (a *s*-triazine derivative) or to an acyclic derivative (a thiourea derivative).

For the same reason the chemical and physico-chemical properties of the $CuMEX_2$ and $CuTAX_2$ compounds have been studied earlier.[1,3]

Thus in contrast to $CuTACl_2$ and respectively $CuMECl_2$ which are able to form substitution products of the form $CuTAX_2$ and respectively $CuMEX_2$ (X = Br, I, NCS, NCSe) the compound $CuLCl_2$ does not form substitution products with the halides or pseudohalides of the other metals.

Similarly in contrast to $CuTABr_2$ and $CuMEBr_2$ which in DMF solution as well as in ethanol solution undergo a reducing process by refluxing, changing into a microcrystalline, pale yellow compound with the form of Cu_2TABr_2 respectively Cu_2MEBr_2 under the same conditions, the compound $CuLBr_2$ settles into a brown-grey product containing copper (I) sulphide.

By treating $CuLCl_2$ in DMF solution with concentrated HCl and then with cold water (conditions under which TA and ME synthesis takes place), a gelatinous precipitate results with an inhomogeneous composition, behaving totally different from $CuTACl_2$ or $CuMECl_2$. This proves that after the formation of the compound $CuLCl_2$ supposed to have the ligand (L) with linear-chain a thiourea derivative the cyclisation is hindered and does not result in Cu(II) compounds with *s*-triazine derivatives.

I.R. spectra also evidenced (table 1) the lack of triazine cycle in $CuLCl_2$, because a series of bands from the spectra of $CuTACl_2$, TA and respectively $CuMECl_2$, and ME, bands which are characteristic of the triazine cycle (770 cm^{-1}, 815 – 865 cm^{-1}) and for $C-NH_2$ exocycle groups (620 – 635 cm^{-1}) do not appear.

The I.R. spectrum of $CuLCl_2$ compound reflected five characteristic bands (670, 695 – 705, 920 cm^{-1} and 1160 – 1185 and 1460 cm^{-1}) which can be attributed to the vibration frequencies of C = S groups from simple or N,N′-disubstituted thiourea. The first band from 670 cm^{-1} is shifted (676 cm^{-1}) in Cu(ASETU)[4]-spectrum and the following (695 – – 705 cm^{-1}) as well as the band from 700 cm^{-1} in N,N′-diphenylthiourea were attributed to a vibration which has 50% C = S character.[5] The band from 920 cm^{-1} as well as that from 1160 – 1183 cm^{-1} were attributed to the C = S group analogous with the bands from 959 and 1183 cm^{-1} which are characteristic of N,N′-disubstituted thiourea.[6] In thiourea Stewart[7] attributed the vibration frequencies of C = S group, to a band from 1413 cm^{-1}, which in our compounds appears shifted towards higher frequencies (1460 cm^{-1}) probably due to the coordination. These bands characteristic in most cases of C = S group do not appear in $CuTACl_2$ and TA spectra, but they are some times also evidenced in these compounds, which have an exocycle C = S group in the molecule.

---

[4] A. Paingankar and B. C. Haldar, *J. Inorg. Nuclear Chem.*, **31**, 2409, (1969).

[5] R. K. Ritchie, H. Spedding and D. Steele, *Spectrochim. Acta*, **27A**, 234 (1971).

[6] R. Mercke and F. Langenbucher, "Infrared Spectra of Selected Chemical Compounds" Ed. Heyden, New York, 1962.

[7] J. Stewart, *J. Chem. Phys.*, **26**, 248 (1957).

Table 1

Infrared Spectra

$CuLCl_2$ cm^{-1}	$CuTACl_2$ cm^{-1}	$CuMECl_2$ cm^{-1}	$Cu(ASETU)_2^*$ cm^{-1}	ATU** cm^{-1}	Assignments
—	620— 35	—	—	—	$C-NH_2$ exocycle
670	668	—	676	—	$\nu_{C=S}$
695—705	697— 705	—	—	701	C = S 50%
745— 760	—	—	—	744—763	C = S/N—C—N
—	770	775	—	—	triazine cycle
—	815— 865	835	—	—	δ-triazine cycle N-subst.
920	920— 960	—	—	945	C = S
1085	1080	1090	—	1069	ρ_{NH_2} and N—C—N
1160—1185	1180	—	—	1190	C = S
—	1235	1240	—	—	$C-NH-C_6H_5$
1260	1260	—	1250	—	$>C-S-$
1340	1360	—	1380	1326	ν_{C-N}
1400	1410	1410	—	1426	ν_{C-N} and C—C
1460	1460	—	—	—	C = S
1500	1500	—	—	1499	$\nu_{C=N-}$
1580	1580	—	1560	—	ν_{C-N}
1640—60	1630—66	1640	1615	1663	$\nu_{C=N}$and δ_{NH_2} and Thioamm

ASETU = S — ethylamidinothiourea ; ATU = 1—amidino-2-thourea ;
* Literature (4) ; **Literature (8).

The band from 745 — 760 cm^{-1} is split and it appears in the same form also in 1-amido-2-thiourea and diphenylthiourea (744 — 763 and 758 — 763 cm^{-1}) being attributed to a mixture of C = S/N—C—N vibrations, following Yamaguki[8] indications for the band from 730 cm^{-1} in thiourea. It was not observed in $CuTACl_2$ spectrum.

Another series of bands which appear in $CuLCl_2$, I.R. spectrum at 1340 cm^{-1}, 1500 — 1580 cm^{-1} and 1640—1660 cm^{-1} were attributed to the ν_{C-N} vibration frequencies. The band from 1340 cm^{-1} is located between the values mentioned in the literature (1310—1343 cm^{-1}) for the band which dominates aryl-thiourea spectrum[5] and the bands from 1500

---

[8] Ch. Yamaguki, *J. Amer. Chem. Soc.*, **80**, 527 (1958).

Table 2

EPR Spectra Parameters

Nr.	Complex	Powders				DMF sol.		DMF sol. 77 K				$E\Delta_{xy}$ cm^{-1}	ΔE_{xz} cm^{-1}
		$g_\parallel$	$g_\perp$	$<g>$	ΔH [G]	g_0	A_0 [G]	$g_\parallel$	$A_\parallel$ [G]	$g_\perp$	$A_\perp$ [G]		
1	$CuTACl_2$			2.1234	328	2.1267	60.3	2.2274	136.1	2.0624	~ 22.4	12 900	24 100
2	$CuTABr_2$			2.1058	252	2.1793	56.9	2.3753	129.2	2.0813	~ 20.7	13 070	23 810
3	$CuTAI_2$					2.1687	55.2	2.3482	132.0	2.0789	~ 16.8	12 890	—
4	$CuTA(SeCN)_2$	2.2041	2.0741	2.1174		2.1730	~62	2.3577	145.7	2.0806	~ 20.1	12 820	—
5	$CuMECl_2$	2.1865	2.0528	2.0974		2.1650	50.6	2.3281	117.8	2.0834	~ 17.1	11 630	23 260
6	$CuMEBr_2$			2.1509	277	2.1823	55.4	2.3776	124.0	2.0846	~ 21.2	11760	24 690
7	$Cu(PnBig)Cl_2$	2.1892	2.0519	2.0977		2.1213	77.7	2.2195	177.5	2.0582	~ 18.5	15 380	—
8	$CuLCl_2$			2.1056	164	2.1768	59.1	2.3721	149.0	2.0792	− 14.3	12 814	22 717

— 1580 cm^{-1} and 1640—1660 cm^{-1} are broad bands which were also found in $Cu(ASETU)_2$ spectrum at 1560 and 1615 cm^{-1} being attributed to ν_{C-N}

Although accentuated bands also appear in $CuTACl_2$ and TA spectra, about in the same range (1340 — 1650 cm^{-1}) these have a quite different shape being sharp, in contrast with those from $CuLCl_2$, which are broader, like in the spectra of 1-amido-2-thiourea and diphenylthiourea. Consequently, the above mentioned facts, constitute additional arguments to consider the ligand L from $CuLCl_2$ compounds as a thiourea derivative (thiocarbamoylbiguanide) and not a cyclic derivative of *s*-triazine.

EPR studies were effected to obtain more detailed information concerning the chemical bond in the considered complexes. The considered compounds in undiluted magnetically polycrystalline powders present EPR spectra without hyperfine structure in X band.

In the case of compounds marked 1, 2, 6 and 8, the EPR spectrum is a large singlet on which $<g>$ values were determined, while the other complexes present typical spectra for the polycristalline powders with axial symmetry for which $g_{||}$ and $g_{||}$ values were determined (table 2).

In DMF solutions at room temperature isotropic spectra were recorded which present a poor resolved hyperfine structure with four components, corresponding to the interaction of the impaired electron with the nuclear spins of ^{63}Cu, ^{65}Cu, both equal to $I = \frac{3}{2}$. An exception is the complex $CuATCl_2$ for which a well resolved hyperfine structure was observed and to a certain extent, the complex $CuLCl_2$.

It should be noted that neither splitting from ^{65}Cu and ^{63}Cu nor superhyperfine structure from the ligand were observed to be solved most likely due to lines broadening. These spectra helped to determine the isotropic values of the spectroscopical splitting factors g_0 and of hyperfine structure constants A_0.

EPR spectra of the frozen DMF solutions of the considered complexes show two sets of hyperfine lines (fig. 1) corresponding to $g_{||}$ and $g_{\perp}$. From these spectra the $g_{||}$, $A_{||}$ and $g_{\perp}$ were accurately determined.

As for the $A_{\perp}$ values, these were generally obtained using the formula of Kivelson[9] and Mc. Connell[10] : $3A_0 = A_{||} + 2A_{\perp}$

The obtained results are summarised in table 2. The consideration of the EPR parameters from table 2 enables us to make a series of remarks and comparisons. Thus comparing the parameters of $CuTACl_2$ and $CuMECl_2$ complexes in which the triazine derivative is changed marked differences were obtained in the powder spectra as well as in the DMF solution, recorded at room temperature and at 77 K. Thus, for example in the DMF solutions at room temperature the g_0 value obtained for the complex with TA is smaller than that corresponding to the complex with ME, while the A_0 value in the first case is larger than in the second one. As concerns the DMF frozen solution at 77°K, the $g_{||}$ and $g_{\perp}$ values of the complex with TA are much smaller than that obtained in the complex with ME, while the $A_{||}$ and $A_{\perp}$ values are smaller in the complex with ME. Thus, it results that the substitution of the TA ligand by the ME ligand leads to some important modifications in the EPR spectra, suggesting in the first case the presence of a Cu ion bonding in which the atom of sulphur is implied. In fact, this is in good agreement with the results obtained from IR spectra.

---

[9] D. Kivelson, *J. Chem. Phys.*, **33**, 1094 (1960).

[10] H. M. Connell, *J. Chem. Phys.*, **25**, 709 (1956).

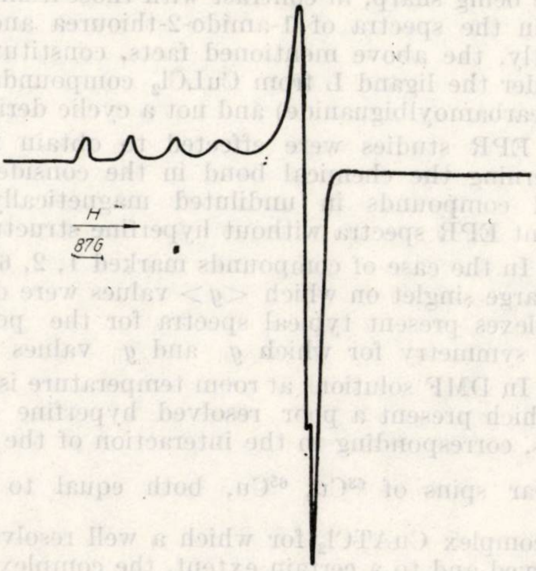

Fig. 1. – EPR Spectra of the frozen DMF solutions.

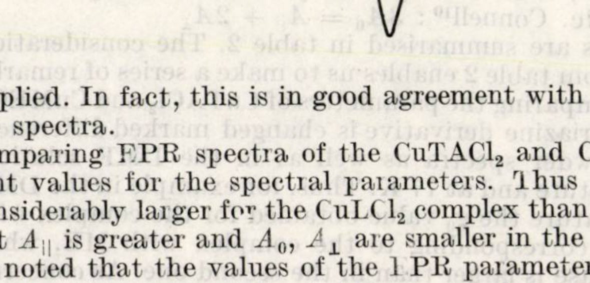

Fig. 2. – EPR spectra of the DMF solutions at room temperature.

Comparing EPR spectra of the $CuTACl_2$ and $CuLCl_2$ one observes different values for the spectral parameters. Thus g_0, $g_{\|}$ and $g_{\perp}$ values are considerably larger for the $CuLCl_2$ complex than that of $CuTACl_2$ complex but $A_{\|}$ is greater and A_0, $A_{\perp}$ are smaller in the TA complexes. It should be noted that the values of the EPR parameters in the $CuLCl_2$ complex are closer to that of the $CuMECl_2$ complex, suggesting the existence of a metal-ligand bond in which the same type of atoms (nitrogen atoms) are implied. Certainly, a superhyperfine structure observed in the EPR spectra of all considered complexes, would provide us direct information on the way the Cu atom is bound to ligands. But unfortunately, such a solved structure was not observed, till now, in the experimental conditions used.

On the basis of the EPR and electronic spectra, parameters of the considered complexes, Kivelson's and Neiman's[11] and Gersman's and Swallen's[12] approximate MO-theory was used to calculate the molecular orbital parameters with notations employed in our previous papers.[13,14] Thus, using the wave functions and the approximation from our work[14] and taking for the overlap integral S a value of 0.0803, for $T(\mathrm{n}) = -0.036$ the respective media for the coordination by the Cl, S, and N atoms and ΔE_{xy} from the electronic spectra (table 2), the α^2 values for the considered complexes were calculated with the relationship :

$$\alpha^2 = -\frac{A_{\|}}{P} + (g_{\|} - 2.0023) + \frac{3}{7}(g_{\perp} - 2.0023) + 0.4 \qquad (1)$$

where $P = -0.036 \text{ cm}^{-1}$.

The α^2 values obtained (table 3) were used for the α'^2 values calculations from the normalization condition.

The values of α_z^2 were also calculated using the formula given by Zamaraev :[15]

$$\alpha_z^2 = \frac{1}{K}\left(\frac{A_0}{P} + g_0 - 2\right) + 0.02 \qquad (2)$$

in which only the isotropic values of the g tensors and hyperfine structure were used. The obtained values are fairly close to those calculated by relationship (1).

Table 3

LCAO-MO parameters

Nr.	Complex	α^2	α'^2	α^2_z	β^2
1	$CuTACl_2$	0.68	0.398	0.69	0.69
2	$CuTABr_2$	0.84	0.225	0.81	0.91
3	$CuTAI_2$	0.82	0.502	0.77	0.86
4	$CuTA(SeCN)_2$	0.87	0.193	0.82	0.82
5	$CuMECl_2$	0.76	0.328	0.73	0.80
6	$CuMEBr_2$	0.83	0.243	0.80	0.84
7	$Cu(PhBig)Cl_2$	0.79	0.288	0.79	0.67
8	$CuLCl_2$	0.90	0.163	—	0.84

---

[11] D. Kivelson and R. Neiman, *J. Chem. Phys.*, **35**, 149 (1961).

[12] H. R. Gersman and J. D. Swalen, *J. Chem. Phys.*, **36**, 3221 (1962).

[13] P. Spacu, G. Gheorghiu, O. Constantinescu, and I. Pascaru, *Rev. Roumaine Chim.*, **16**, 667 (1971).

[14] P. Spacu, G. Gheorghiu, M. Constantinescu, O. Pascaru and O. Constantinescu, *Z. anorg. Chem.*, **384**, 184 (1971).

[15] K. I. Zamaraev, *Zhur strukt. Khim.*, **1**, 33 (1969).

But it must be mentioned that in the case of the considered complexes, the $g_{||}$ and $A_{||}$ were obtained more accurately. A consideration of the α^2 values shows that the $CuTACl_2$ complex presents a marked covalent character of the σ bonding. This character decreases in the complexes $CuMECl_2$ and respectively in $CuLCl_2$. The β^2 values (table 3) which describe the covalent character of the in-plane π bonding were calculated using the α^2 and α'^2 values. From the table one observes a marked covalent character of the in-plane π bonding in the case of the $CuTACl_2$ complex. We must also notice in this case that the substitution of the TA ligand by ME ligand respectively by thiocarbamoylbiguanide (L) leads to the diminishing of the in-plane π bonding covalent character.

From the above results one can conclude that our hypothesis concerning the existence of a thiourea derivative as an intermediate (III — Scheme) in the reaction of PhNCS condensing with Ph.Big. is supported by the separation of a Cu(II) complex with the formula $CuLCl_2$ where the derivative has the role of the ligand (L).

Although the thiourea derivative obviously lead to Cu(I) complexes guanilthiourea and S-amidinothiourea which have a structure very close to that of the ligand (L) give rise to similar Cu(II) type complexes. The formulation of the ligand (L) —thiocarbamoylbiguanide-as a thiourea derivative in the $CuLCl_2$ complex is supported by the I.R. spectra, in which the specific bands of the triazine cycle are absent by the EPR spectra and by the diminishing of the reductible character which would exclude the possibility of sulphur atom implication in the coordination.

Thus, the coordination of this ligand to Cu(II) by two nitrogen atoms (N^1, N^4 or N^2, N^4) would account for the low reductible influence of the $C = S$ group and for impossibility of triazine cycle formation.

Revue Roumaine de Chimie, **22**, *3*, 395–399 (1977)

QUINOLINE-1-OXIDE COMPLEXES OF LANTHANIDE IODIDES

L. RAMAKRISHNAN and S. SOUNDARARAJAN
Department of Inorganic and Physical Chemistry Indian Institute of Science, Bangalore-560012
India

Received April 12, 1975

Complexes of lanthanide iodides of the formulae $La(QNO)_5I_3.4H_2O$, $Ln(QNO)_5I_3.3H_2O$ where Ln = Pr or Nd and $Ln(QNO)_6I_3$ where Ln = Tb, Dy, or Er and QNO = Quinoline-1-Oxide have been prepared and characterized by analyses, conductance, molecular weight and IR spectral data. IR spectral data are interpreted in terms of the coordination of the ligand through the oxygen atom of the N→O group. The conductance data show a coordination number seven for the lighter lanthanides and eight for the heavier lanthanides.

INTRODUCTION

Only a few complexes of aromatic amine oxides with lanthanides are known.[1] Even though complexes of lanthanide perchlorates, chlorides, and nitrates have been well studied, only a few complexes of lanthanide iodides are known.[2,3] The lanthanide iodide complexes show a similarity in stoichiometry to the corresponding perchlorate complexes.[4,5] In the presence of iodide as the anion, we can expect the coordination of the anion to the metal, thus making the coordination number of the metal higher than that in the corresponding perchlorate complex. So a study of lanthanide iodide complexes was undertaken. Quinoline-1-oxide (QNO) was chosen as the ligand because it behaves as a 2,3-disubstituted pyridine-1-oxide in its complexes with transition metal ions.[1] QNO complexes of lanthanide chlorides[6] and complexes of the formula $[Ln(QNO)_7]$ $[Cr(SCN)_6]$[7] have already been prepared and characterized in different laboratories. In the present communication we describe the preparation and characterization of six lanthanide iodide complexes with QNO.

---

[1] N. M. Karayannis, L. L. Pytlewski and C. M. Mikulski, *Coord. Chem. Rev.*, **11**, 93(1973).

[2] T. Moeller and V. Galasyn, *J. Inorg. Nuclear Chem.*, **12**, 259 (1960)

[3] J. K. Marsh, *J. Chem. Soc.*, **1951**, 1337.

[4] S. S. Krishnamurthy and S. Soundararajan, *Canad. J. Chem.*, **47**, 995(1969).

[5] V. N. Krishnamurthy and S. Soundararajan, *J. Inorg. Nuclear Chem.*, **29**, 517 (1967)

[6] J. V. Kingston, E. M. Krankovits and R. Magee, *J. Inorg. Nuclear Chem.*, **31**, 3181 (1969).

[7] V. V. Serebrennikov, E. S. Pavelenko, V. N. Kumok and N. T. Belousova, *Zuhr. obshchei Khim.*, **39**, 306 (1969).

EXPERIMENTAL

Lanthanide iodides were prepared by dissolving the corresponding lanthanide oxide (99.9% pure. Obtained from the Lindsey Chemical division of the American Potash and Chemicals Corporation) in hydriodic acid and evaporating the product on a water-bath. Excess of hydriodic acid was removed by washing the salt several times with benzene till the washings were colourless.

QNO was prepared by oxidizing quinoline with peracetic acid according to the method given in reference.[8] The compound obtained was purified by vacuum distillation (170°C/4 mm) and was dried over phosphorus (V) oxide in a vacuum desiccator.

All the solvents used were purified before use as given in the literature.[9]

Preparation of the complex : About 0.5 g of the hydrated lanthanide iodide was dissolved in 10 ml of acetone and about 1 g of QNO was also dissolved in 10 ml of the same solvent. The two solutions were mixed with constant stirring. Stirring was continued for about 10 minutes, after which 10 ml of chloroform was added to this mixture with constant stirring. The complex started separating out slowly. During the precipitation of the complex, the colour of the solution changed rapidly showing a play of colours. Generally the colour changed in the order : yellow→greenish yellow→green→blue. In a few cases the colour changed again to the original colour. The final colours of all the complexes are given in table 1. The complexes were separated by filtration under suction, washed well with chloroform and dried over phosphorus (V) oxide in a vacuum desiccator.

Analyses : The metal content of the complexes was determined by EDTA titrations using xylenol orange as indicator.[10] Iodide content of the complexes was estimated by Volhard's method. QNO content was estimated for a few complexes by spectrophotometry (at 313 nm) using the calibration curve method.[11] The analytical data are given in table 1.

Physical measurements : The molar conductances of the complexes were determined in nitrobenzene with a Siemen's Conductivity bridge using an immersion cell (type LTA). The complexes dissolved with difficulty in nitrobenzene. The concentrations of the solutions used were of the order of 0.001M. The conductance data are given in table 2.

The IR spectra of the ligand in CCl_4 solutions and KBr pellet and of the complexes in Nujol mulls and KBr pellets were recorded in a Carl-Zeiss UR-10 spectrophotometer. The important IR bands and their assignments are given in table 3.

Molecular weights of two of the complexes were determined in water using the Beckman's freezing point method. The results are given in table 2.

Table 1

Analytical data

Complex	Colour	% Metal		% Iodide		% QNO	
		Found	*Calc.*	*Found*	*Calc.*	*Found*	*Calc.*
$La(QNO)_5I_3.4H_2O$	yellow	10.37	10.54	28.51	28.84	55.56	55.09
$Pr(QNO)_5I_3.3H_2O$	pale green	10.97	10.82	29.34	29.27	..	..
$Nd(QNO)_5I_3.3H_2O$	yellowish pink	11.06	11.04	29.02	29.18	54.68	55.67
$Tb(QNO)_6I_3$	yellow	11.39	11.27	26.83	26.99	..	..
$Dy(QNO)_6I_3$	yellow	11.42	11.49	26.95	26.93	60.55	61.86
$Er(QNO)_6I_3$	blue	11.93	11.80	27.06	26.83	..	..

---

[8] E. Ochiai, "Aromatic Amine Oxides", Elsevier Publishing Co,. Amsterdam, 1967, p. 24.

[9] A. Weissberger and E. S. Proskauer, "Organic Solvents", Techniques of Organic Chemistry, Vol. 7, Interscience, New York, 1961.

[10] I. M. Kolthoff and P. J. Elwing, "Treatise on Analytical Chemistry", Part, II, Vol.8, Interscience, New York, 1963.

[11] H. H. Willard, L. L. Merrit and J. A. Dean "Instrumental Methods of Analysis" 4th ed., Affiliated East-West Press Pvt., Ltd., New Delhi, 1965, p. 89.

Table 2

Conductance and Molecular weight data

Complex	Molar conductance ohm^{-1}cm^{2}mole^{-1}	Molecular weight in water	Number of species
$La(QNO)_5I_3.4H_2O$	30.68	. .	. .
$Pr(QNO)_5I_3.3H_2O$	28.93	144.3	9
$Nd(QNO)_5I_3.3H_2O$	28.89	. .	. .
$Tb(QNO)_6I_3$	30.35	. .	. .
$Dy(QNO)_6I_3$	26.77	140.6	10
$Er(QNO)_6I_3$	24.52	. .	. .

Table 3

Some important IR bands (in cm^{-1}) and their assignment

QNO	La	Pr	Nd	Tb	Dy	Er	Assignment
	3500 b	3500 b	3500 b	3500 b	3500 b	3500 b	Sym. and antisym. O−H stretch
	1633 w	1633 w	1632 w	1632 w	1632 w	1635 w	H−O−H bending
1587 m	1589 m	1589 m	1589 m	1590 m	1590 m	1590 m	C=N stretch
1530 m	1527 m	1528 w	1528 w	1526 w	1526 m	1526 m	Ring stretching
1459 m*	1472 vs	1473 vs	1472 vs	1470 vs	1470 vs	1470 vs	
1407 vs	1404 s	1404 s	1403 s	1402 s	1405 s	1402 s	Ring stretching
1317 vs	1323 w	1323 w	1322 w	1325 w	1324 w	1323 w	
1280 s	1271 s	1272 s	1277 s	1276 s	1275 m	1275 m	C−H in-plane deformation
1245 vs	1240 s	1241 s	1242 s	1242 s	1242 s	1241 s	N−O stretching
1216 w	1220 m	1220 w	1219 m	1217 m	1217 m	1216 s	
1144 m	1150 m	1148 m	1152 m	1154 m	1152 m	1158 m	C−H in-plane deformation
1099 m	1107 m	1101 w	1101 m	1101 m	1101 m	1101 m	
892 m	890 m	891 m	890 s	890 m	891 m	893 m	N−O bending
800 vs**	804 vs	801 s	802 s	802 s	804 vs	804 vs	
770 s**	767 s	768 m	769 s	767 s	770 vs	770 vs	C−H out of plane vibrations
731 s**	735 s	732 m	732 s	733 m	733 m	733 s	

* This band merges with the mull band in the spectra of the complexes and appears in the spectra of the complexes taken in KBr pellets. Spectra of the complexes in nujol mulls are reported.

** QNO spectrum in KBr pellet. All the other bands (QNO) are from the spectrum in CCl_4 solution. Abbreviations; vs = very strong; s = strong; m = medium; w = weak; b = broad.

RESULTS AND DISCUSSION

The complexes analyse for the formulae $La(QNO)_5I_3.4H_2O$, $Ln(QNO)_5I_3.3H_2O$, where Ln = Pr or Nd and $Ln(QNO)_6I_3$, where Ln = = Tb, Dy or Er. The colours of all the complexes are different from the corresponding metal salts. All the complexes are sensitive to atmospheric moisture and turn colour on standing in atmosphere. All the complexes decompose completely in water as shown by the molecular weight data.

Conductance data in nitrobenzene show that the complexes behave as 1 : 1 electrolytes in this solvent.[12] This means that two of the iodide ions are coordinated to the metal ion while the third is non-coordinated. Taking into account the non-coordinating nature of water in these complexes as shown by IR data, a coordination number of seven for the lighter lanthanides and eight for the heavier lanthanides can be postulated. It is generally believed that the coordination number will decrease or remain the same on going from lanthanum to lutetium.[13] The coordination number inferred from the conductance data clearly shows that this is not the case in the present complexes. An increase in the coordination number on going from La to Lu has also been observed in the QNO complexes of the lanthanide chlorides.[6] These observations can be explained as follows : On going from La to Lu, the size of the trivalent lanthanide ion decreases and hence the steric effect will influence the coordination number of the lanthanides leading to a lower coordination number for the heavier lanthanides. At the same time the ionic potential of the trivalent lanthanide ions increases on going from La to Lu. As bonding in the lanthanide complexes is mainly electrostatic,[14] the heavier lanthanides tend to attract more ligands than the lighter lanthanides. In the present complexes, the electrostatic effect may be prominent leading to a higher coordination number for the heavier lanthanides than for the lighter lanthanides.

The IR spectra of the complexes show no significant dependence on the central metal ion. N — O stretching vibration of the pure ligand occurring at 1245 cm^{-1} (in CCl_4) does not undergo any appreciable shift upon complexation. IR studies of QNO complexes of transition metal ions show either a positive shift or no shift at all for the N — O stretching frequency of the ligand. The absence of any shift in the N — O stretching frequency has been attributed to two opposing effects: [1](a) Complexation through oxygen leading to a decrease in the N — O bond order and hence a shift of the N — O stretching frequency to lower wave-numbers, and (b) kinematic coupling of the N — O stretching frequency with the vibrations of the quinoline ring leading to the shift in the frequency to higher wave-numbers. The other possible effect which affects the N — O stretching frequency is the $d\pi - p\pi$ backbonding which is not observed in the lanthanide complexes. A shift of ca. 5 cm^{-1} in the N — O stretching frequency upon complexation may indicate that the effects (a) and (b) are almost equal in magnitude. Other bands occurring in the region 1340 cm^{-1} to 1280 cm^{-1} which have been assigned to N — O stretching vibrations[15] undergo small shifts towards lower frequency region. The intensiy of the band at 1317 cm^{-1} in the free ligand is much affected upon complexation (s to w). The C—H in-plane vibrations show very small shifts in the complexes. As in the other aromatic amine oxide complexes, the N — O bending vibration occurring at 892 cm^{-1} in the free ligand does not undergo any appreciable shift. The γ—C—H vibrations of the ligand could not be identified in the spectrum of QNO in CCl_4 because of the interference of the ν_3 band of the solvent in this region. A spectrum of the ligand taken in KBr pellet shows that $\gamma-C-H$ vibrations occur in the region 700 — — 800 cm^{-1}. These vibrations do not undergo any appreciable shift upon complexation.

---

[12] W. J. GEARY, *Coord. Chem. Rev.*, **7**, 81 (1971).

[13] K. K. BHANDARY, PH. D. thesis, Indian Institute of Science, 1973.

[14] L. J. CHARPENTIER and T. MOELLER *J. Inorg. Nuclear Chem.*, **32**, 3575 (1970).

[15] H. SHINDO *Chem. Pharm. Bull.* (*Tokyo*), **8**, 1603 (1958).

All the complexes show absorption at about 3400 cm^{-1} (broad) due to the presence of water. The $H-O-H$ bending vibration occurs at about 1620 cm^{-1}. The absence of any new absorption band in the region 650—880 cm^{-1} indicates[16] that the water molecules are not coordinated, leading to the conclusion that in the La, Pr and Nd complexes water is present as lattice water. Other complexes show bands due to absorbed water as all these complexes are hygroscopic.

Achnowledgements. The author thank Mr. P. Mukund, Department of Organic Chemistry, Indian Institute of Science, for the help in the preparation of the ligand. One of the authors (L.R) thanks the authorities of the Indian Institute of Science for financial assistance.

---

[16] N. NAKAMOTO, "Infrared Spectra of Inorganic and Coordination Compounds", Wiley Interscience, New York, 1970, p. 167.

Revue Roumaine de Chimie, **22**, *3*, 401–409 (1977)

NEW UREA AND THIOUREA DERIVATIVES. II

HMO AND Del Ré MOLECULAR ORBITAL CALCULATIONS

M. MRACEC, S. RADULY, Z. SIMON, AURELIA BOLDEA and C. DRUGĂRIN
Department of Technologic Chemistry and Department of Chemistry University of Timişoara
1900—Timişoara, Bd. V. Pârvan 4

Received January 15, 1975

Molecular orbital calculations are performed by the HMO, ω-HMO and Del Ré methods for urea and thiourea derivatives, including some new compounds described in note I. Molecular diagrams calculated by the ω-HMO and Del Ré methods are given, as well as the energies for the frontier orbitals. The first transition calculated by the HMO method is in acceptable agreement with the position of the first absorption band in the electronic spectra of these compounds.

In the first note[1] of this series the synthesis and the UV and IR spectra of some phenylurea, *p*-chlorophenylurea and phenylthiourea derivatives was described. Here we give the results of molecular orbital calculations by the HMO, ω-HMO and Del Ré[2] methods for some of these molecules and for other seven simple derivatives of urea and thiourea. Work in this field, especially that of the Pullman's group [3] and of the group of Cammarata [4], demonstrated the importance of this type of calculations for understanding of mechanisms determining biological activity in various classes of compounds.

The results of the ω-HMO calculations will be used for calculating bond orders and total atomic charges in which charges determined by σ bonds are calculated by the Del Ré method ; this procedure yields good agreement with experimental dipole moments and with atomic charges calculated by advanced methods.[5]

The notations of the new molecules described in the previous note [1] are as follows :

I : N-phenyl-carbamoyl-*p*-aminobenzoyl-diethylaminoethanol
II : N-phenyl-thiocarbamoyl-*p*-aminobenzoyl-diethylaminoethanol
III : N-phenyl-carbamoyl-*p*-aminobenzoyl-glycine
IV : N-phenyl-thiocarbamoyl-*p*-aminobenzoyl-glycine
V : N-phenyl-carbamoyl-sulphanilyl-5-amino, 1-phenyl-pyrazole
VI : N-phenyl-carbamoyl-sulphanilyl-6-amino, 2,4-dimethyl-pyrimidine

---

[1] Part I. : A. Boldea, C. Drugărin, M. Mracec and Z. Simon, *Rev. Roumaine Chim.*, **21**, 1345 (1976).

[2] G. Del Ré., *J. Chem. Soc.*, **1958**, 403.

[3] B. Pullman and A. Pullman, "Quantum Biochemistry", Wiley Interscience, New York, 1963.

[4] A. Cammarata, in "Molecular Orbital Studies Chemical Pharmacology", Symposium, E. B. Kier and B. Lemot editors, Springer, New York, 1970, p. 156.

[5] A. Pullman, *Modern Quantum Chemistry*, **3**, 283 (1965).

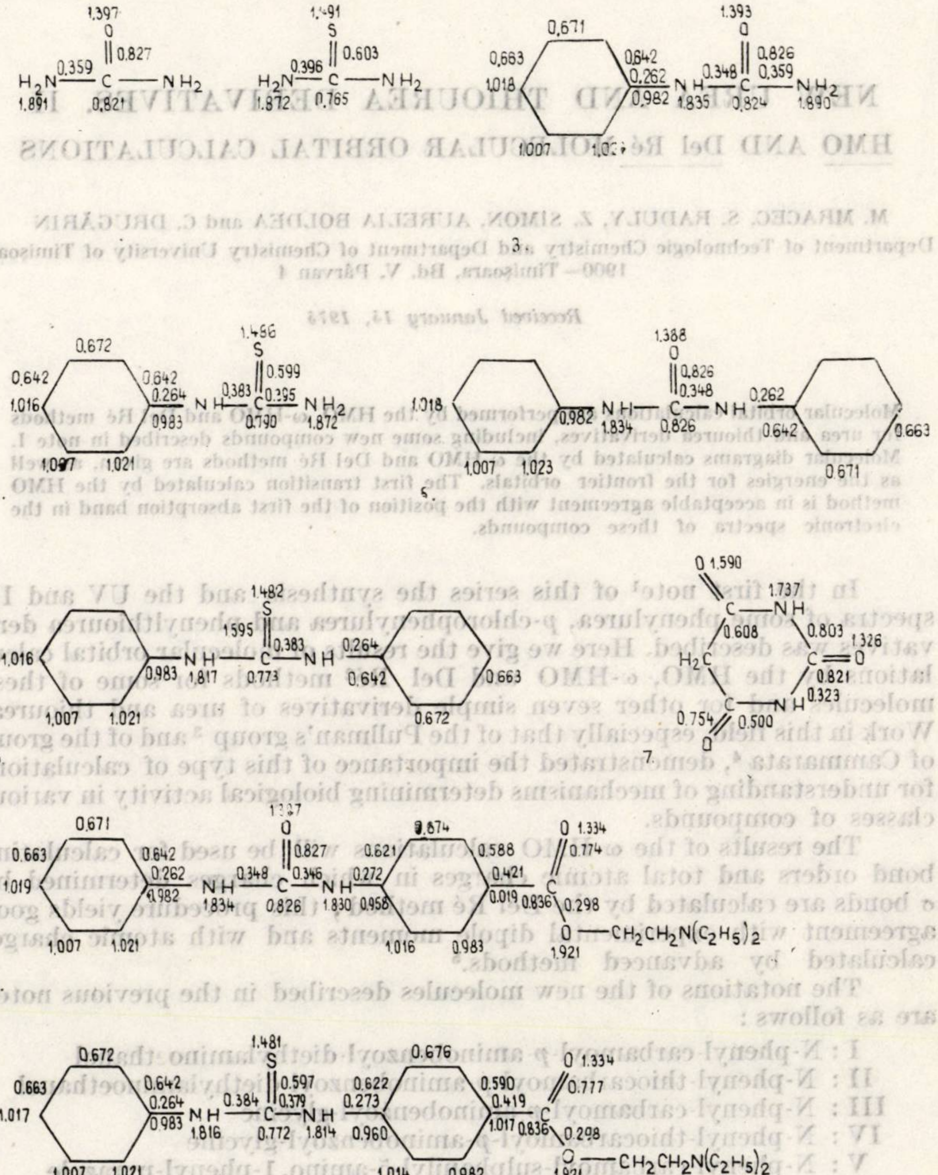
1.397
O
0.827
H_2N
0.359
C
NH_2
1.891
0.821
1
1.491
S
0.603
0.396
0.765
1.872
0,671
0,663
1,018
0,642
0,262
0,982
1.007
1.393
0.826
0.348
0.359
NH
1.835
0.824
1.890
3
1.486
0.672
0.642
1.016
0.264
0.983
0.599
0.383
0.395
0.790
1.872
1,021
4.
1.388
1.018
0.982
1.834
0.826
0.348
0.262
0.642
0.663
0.671
1.023
5.
1.482
1.595
0.383
0.773
1.817
0.264
0.642
0.663
0.672
1.007
1.021
6.
O 1.590
1.737
0.608
0.803
1.326
H_2C
0.821
0.323
0.754
0.500
7.
0.671
0.663
1.019
0.642
0.262
0.982
0.348
0.827
0.346
0.826
1.834
1.830
0.874
0.621
0.272
0.958
0.588
0.421
0.019
O 1.334
0.774
0.836
0.298
$O—CH_2CH_2N(C_2H_5)_2$
1.921
1.016
0.983
1.007
1.021
8.
1.481
0.672
0.663
1.017
0.642
0.264
0.983
1.816
0.384
0.597
0.379
0.772
1.814
0.676
0.622
0.273
0.960
0.590
0.419
1.017
O 1.334
0.777
0.836
0.298
1.921
1.014
0.982
1.007
1.021
9

Fig. 1

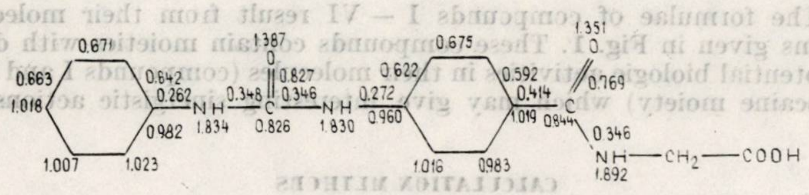
0.671
0.663
1.018
1.007
1.023
0.642
0.262
0.982
N H
1.834
0.348
1.387
O
0.827
0.346
C
0.826
N H
1.830
0.622
0.272
0.960
0.675
0.592
0.414
1.019
1.016
0.983
1.351
O
0.769
C
0.844
0.346
N H
1.892
CH2
COOH

10

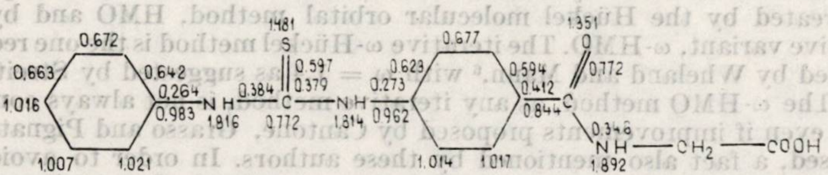
0.672
0.663
1.016
1.007
1.021
0.642
0.264
0.983
N H
1.816
0.384
1.481
S
0.597
0.379
C
0.772
N H
1.814
0.623
0.273
0.962
0.677
0.594
0.412
0.844
1.014
1.017
1.351
O
0.772
C
0.346
N H
1.892
CH2
COOH

11.

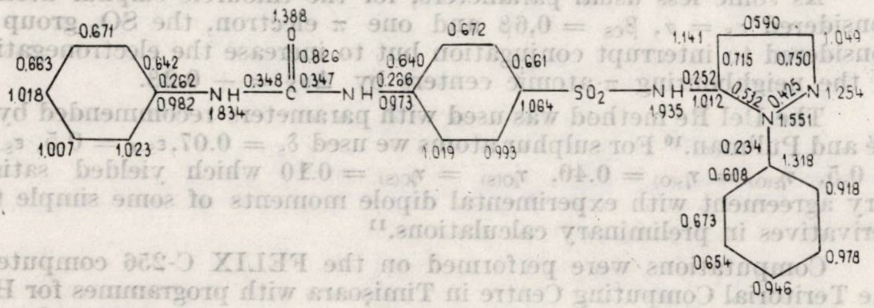
0.671
0.663
1.018
1.007
1.023
0.642
0.262
0.982
N H
1.834
0.348
1.388
O
0.826
0.347
C
N H
0.640
0.286
0.973
0.672
0.661
1.064
1.019
0.993
SO2
N H
1.935
0.252
1.012
1.141
0.590
1.049
0.715
0.750
0.532
0.425
N 1.254
N 1.551
0.234
1.318
0.608
0.918
0.673
0.654
0.978
0.946

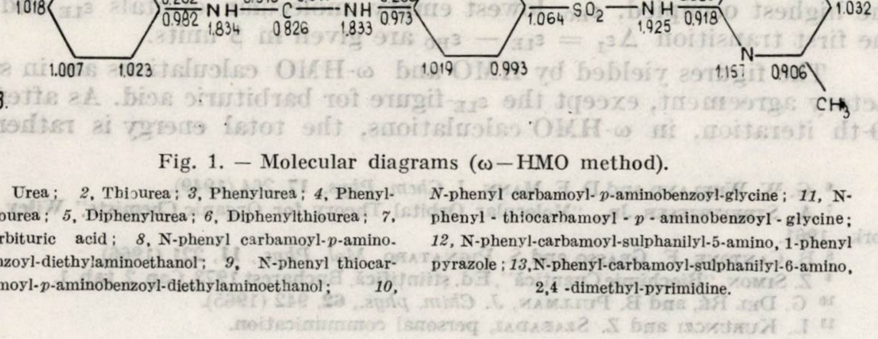
0.671
0.663
1.018
1.007
1.023
0.642
0.262
0.982
N H
1.834
0.348
1.388
O
0.826
0.347
C
0.826
N H
1.833
0.640
0.266
0.973
0.672
0.661
1.064
1.019
0.993
SO2
N H
1.925
0.283
0.918
CH3
0.651
N
0.627
0.653
1.032
N
1.157
0.906
CH3

13.

Fig. 1. — Molecular diagrams (ω—HMO method).

1, Urea; *2*, Thiourea; *3*, Phenylurea; *4*, Phenylthiourea; *5*, Diphenylurea; *6*, Diphenylthiourea; *7*, Barbituric acid; *8*, N-phenyl carbamoyl-*p*-aminobenzoyl-diethylaminoethanol; *9*, N-phenyl thiocarbamoyl-*p*-aminobenzoyl-diethylaminoethanol; *10*, *N*-phenyl carbamoyl-*p*-aminobenzoyl-glycine; *11*, N-phenyl-thiocarbamoyl-*p*-aminobenzoyl-glycine; *12*, N-phenyl-carbamoyl-sulphanilyl-5-amino, 1-phenyl pyrazole; *13*, N-phenyl-carbamoyl-sulphanilyl-6-amino, 2,4-dimethyl-pyrimidine.

The formulae of compounds I — VI result from their molecular diagrams given in Fig. 1. These compounds contain moieties with different potential biologic activities in their molecules (compounds I and II — a novocaine moiety) which may give interesting sinergistic actions.

CALCULATION METHODS

The π-electronic systems of the molecules discussed in this paper are treated by the Hückel molecular orbital method, HMO and by its iterative variant, ω-HMO. The iterative ω-Hückel method is the one recommended by Wheland and Mann,[6] with $\omega = 1{,}4$ as suggested by Streitwieser.[7] The ω-HMO method, as any iterative method, is not always convergent, even if improvements proposed by Cantone, Grasso and Pignatoro[8] are used, a fact also mentioned by these authors. In order to avoid an excessive length of computation times we considered that 10 iterations are sufficient to attest the degree of convergence for each system studied. The α and β parameters are those recommended by Streitwieser[7] and currently used by our group.[9]

As some less usual parameters, for the thioureic sulphur atom we considered $\alpha_S = \alpha$, $\beta_{CS} = 0{,}6\beta$ and one π electron, the SO_2 group was considered to interrupt conjugation but to increase the electronegativity of the neighbouring π-atomic centers by $\Delta\alpha_X = +\ 0.2\beta$.

The Del Ré method was used with parameters recommended by Del Ré and Pullman.[10] For sulphur atoms we used $\delta_S = 0.07, \varepsilon_{S-C} = 0.5$, $\varepsilon_{S-O} = 0.5$, $\eta_{S(O)} = \eta_{S(O)} = 0.40$, $\eta_{O(S)} = \eta_{C(S)} = 0.10$ which yielded satisfactory agreement with experimental dipole moments of some simple thioderivatives in preliminary calculations.[11]

Computations were performed on the FELIX C-256 computer of the Teritorial Computing Centre in Timişoara with programmes for HMO and ω-HMO calculations adapted for this type of computer and a programme for Del Ré calculations written by one of us (S. Raduly).

RESULTS

The results of HMO and ω-HMO calculations describing the π-electronic system are given in Tab. 1. For both methods, the energies of the highest occupied, ε_{HO}, lowest empty molecular orbitals ε_{LE} and for the first transition $\Delta\varepsilon_1 = \varepsilon_{LE} - \varepsilon_{HO}$ are given in β units.

The figures yielded by HMO and ω-HMO calculations are in satisfactory agreement, except the ε_{LE}-figure for barbituric acid. As after the 10-th iteration, in ω-HMO calculations, the total energy is rather far from constant, the energetic parameters as calculated by the simple HMO-method are to be considered more reliable.

---

[6] G. W. WHELAND and D. E. MANN, *J. Chem. Phys.*, **17**, 264 (1949).

[7] A. STREITWIESER JR., "Molecular Orbital Theory for Organic Chemists" Wiley, New York, 1961.

[8] B. CANTONE, F. GRASSO and S. PIGNATARO, *Mol. Phys.*, **11**, 221 (1966).

[9] Z. SIMON, "Biochimie Cuantică", Ed. ştiinţifică, Bucharest 1973, Cap. 2, tab. 1.

[10] G. DEL RÉ, and B. PULLMAN, *J. Chim. phys.*, **62**, 942 (1965).

[11] L. KURUNCZI and Z. SZABADAI, personal communication.

For all molecules listed in Tab. 1, the first transition in the electronic spectra has an extinction coefficient ε_{max} of about $10^4 - 10^5$ (see data listed in note I¹) and the position of the first band increases rather monotonously with the molecular size, indicating the $\varepsilon_{HO} - \varepsilon_{LE}$ transition in the π-electronic systems as probably responsible for these first bands. Spectral data for the first seven compounds refer to ethanolic solutions and are those listed by the tables of Organic Electronic Spectral Data.[12] Tab. 2 lists the corresponding experimental wave lengths, λ_{exp}, the

Table 1

Results of HMO and ω-HMO calculations

Molecule	HMO method (β-units)			ω−HMO method (β-units)		
	ε_{LE}	ε_{HO}	$\Delta\varepsilon_1$	ε_{LE}	ε_{HO}	$\Delta\varepsilon_1$
urea	−1.008	+1.189	−2.197	−0.959	+0.895	1.854
thiourea	−0.768	+1.068	1.836	−0.711	+0.799	1.510
phenylurea	−0.917	+0.707	1.624	−0.896	+ .732	1.628
phenylthiourea	−0.719	+0.872	1.591	−0.671	+0.733	1.404
diphenylurea	−0.865	+0.744	1.609	−0.854	+0.711	1.565
diphenylthiourea	−0.679	+0.744	1.432	−0.636	+0.724	1.360
barbituric acid	−0.618	+0.151	0.769	−0.197	+0.085	0.282
I	−0.507	+0.757	1.264	−0.506	+0.705	1.211
II	−0.484	+0.760	1.244	−0.478	+0.757	1.235
III	−0.527	+0.757	1.284	−0.526	+0.701	1.227
IV	−0.502	+0.760	1.262	−0.498	+0.713	1.211
V	−0.592	+0.386	1.607	−0.629	+0.455	1.607
VI	−0.849	+0.758	1.607	−0.849	+0.758	1.607

Table 2

Wavelengths of experimental and calculation maxima of absorption bands (nm units)

Urea derivatives	λ_{exp} (nm)	λ_{calc} (nm)	$\Delta\lambda$¹⁾ (nm)	Thiourea derivatives	λ_{exp} (nm)	λ_{calc} (nm)	$\Delta\lambda$¹⁾ (nm)	$\Delta\lambda_{exp.}$²⁾$_{S,O}$	$\Delta\lambda_{calc.}$³⁾$_{S,O}$
Urea	229	202	−27	Thiourea	235	241	+ 6	+ 6	+39
Phenyl urea	273	273	0	Phenyl thiourea	276	279	+ 3	+ 3	+ 6
Diphenyl urea	256	275	+19	Diphenyl thiourea	272	309	+37	+30	+34
I	288	351	+63	II	299	356	+57	+11	+4
III	275	345	+70	IV	289	352	+63	+14	+7
Barbituric acid	264	251	−13	—	—	—	—	—	—
V	280	275	− 5	—	—	—	—	—	—
VI	263	275	+12	—	—	—	—	—	—

¹ $\Delta\lambda = \lambda_{calc} - \lambda_{exp}$; ² $\Delta\lambda_{exp.S,O} = \lambda_{exp}$ (thiourea derivatives) $- \lambda_{exp}$ (urea derivatives) ; ³ $\Delta\lambda_{calc.S,O} = \lambda_{calc}$ (thiourea derivatives) $- \lambda_{calc}$ (urea derivatives).

---

[12] "Organic Electronic Spectral Data", Vol. II, Interscience Publishers, New York, 1953−1955.

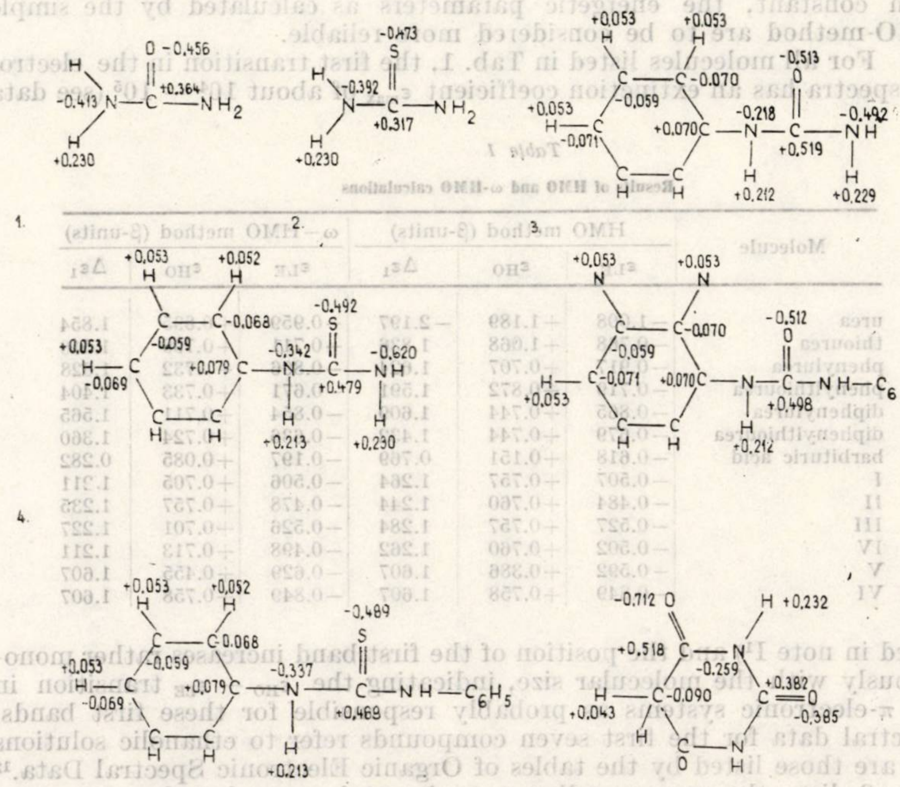
O -0.456
H
+0.364
-0.413 N — C — NH2
H
+0.230
1.
-0.473 S
H
-0.392
N — C — NH2
+0.317
H
+0.230
2.
+0.053 H
+0.053 H
-0.513 O
C — C -0.070
-0.059
+0.053
H — C
-0.071
+0.070C — N — C — NH
-0.218
-0.492
+0.519
H +0.212
H +0.229
3.
+0.053 H
+0.052 H
C — C -0.068
-0.492 S
+0.053
-0.059
-0.342
-0.620
H — C +0.079 C — N — C — NH
-0.069
+0.479
H +0.213
H +0.230
4.
+0.053 N
+0.053 N
-0.512 O
C -0.070
-0.059
H — C -0.071 +0.070C — N — C — NH — C6H5
+0.053
+0.498
H +0.212
+0.053 H
+0.052 H
C — C -0.068
-0.489 S
+0.053
-0.059
-0.337
H — C +0.079C — N — C — NH — C6H5
-0.069
+0.469
H +0.213
6.
-0.712 O
H +0.232
+0.518 C — N
-0.259
H — C -0.090
+0.382
C = O
+0.043
-0.385
H
C — N
O H
7.
+0.053 H
+0.054 H
-0.064
-0.501 O
-0.059
-0.351
-0.327
H — C -0.072 +0.134C — N — C — N — C
+0.053
+0.604
+0.158
H +0.195
H +0.195
+0.054 H
+0.053 H
-0.059
-0.398 O
C — C -0.035
-0.037C — C
+0.330
-0.178 O — C — C — N -0.410
+0.053 +0.048
-0.023 +0.033
+0.048 +0.040
C +0.033 CH -0.109
C2H5
8
+0.053 H
+0.054 H
-0.064
-0.507 S
-0.059
-0.308
-0.304
H — C -0.074 +0.144C — N — C — N — C
+0.053
+0.606
+0.165
H +0.196
H +0.196
+0.054 H
+0.053 H
-0.059
-0.398 O
C — C -0.035
-0.035C — C
+0.327
-0.178 O — C — C — N -0.410
+0.053 +0.048
-0.023 +0.033
+0.048 +0.040
C +0.033 CH -0.109
C2H5
9.

Fig. 2

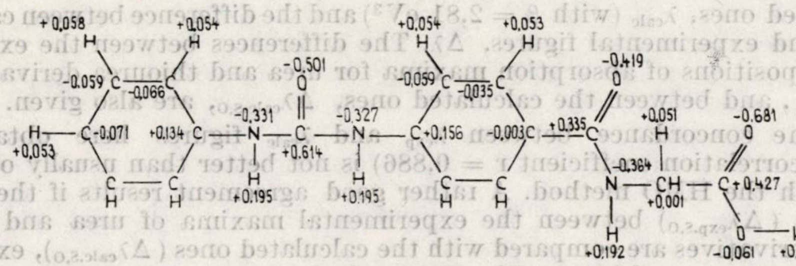
+0.058 H
+0.054 H
-0.059 C
-0.066 C
H—C-0.071
+0.053
+0.134 C
C
H
C
H
-0.501 O
-0.331 N
C +0.614
H +0.195
-0.327 N
H +0.195
+0.054 H
+0.053 H
-0.059 C
-0.035 C
C+0.156
-0.003 C
C H
C H
-0.419 O
+0.335 C
+0.051 H
-0.364 N
CH +0.001
H +0.192
-0.681 O
C+0.427
O—H
-0.061 +0.319

10.

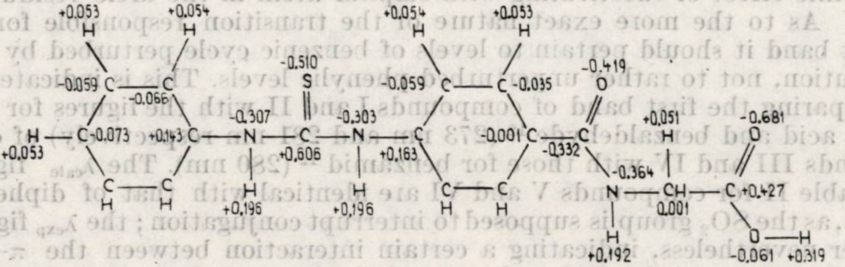
+0.053 H
+0.054 H
-0.059 C
C
-0.066
H—C-0.073
+0.053
+0.143 C
C H
C H
-0.510 S
-0.307 N
C +0.606
H +0.196
-0.303 N
+0.163
H +0.196
+0.054 H
+0.053 H
-0.059 C
C -0.035
-0.001 C
-0.332 C
C H
C H
-0.419 O
+0.051 H
-0.364 N
CH 0.001
H +0.192
-0.681 O
C +0.427
O—H
-0.061 +0.319

11.

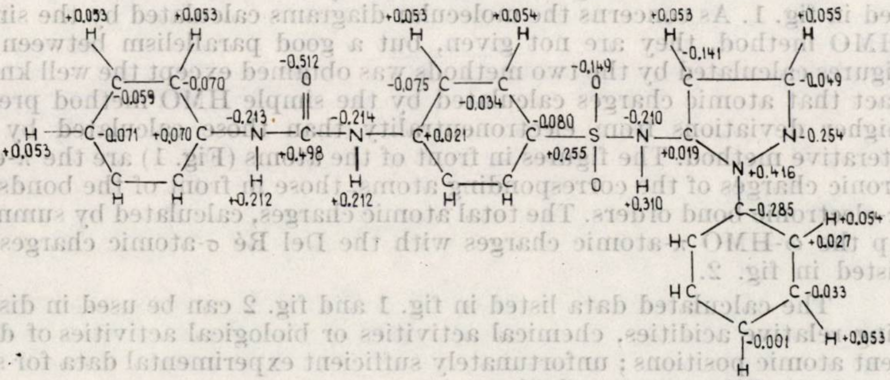
+0.053 H
+0.053 H
C -0.070
-0.059
H—C-0.071
+0.053
+0.070 C
C H
C H
-0.512 O
-0.213 N
C +0.498
H +0.212
-0.214 N
H +0.212
+0.053 H
+0.054 H
-0.075 C
-0.034 C
C+0.021
-0.080 C
C H
C H
-0.149 O
S
+0.255
O
-0.210 N
H +0.310
+0.053 H
-0.141 C
+0.019
+0.055 H
C -0.049
N -0.254
N +0.416
C -0.285
H +0.054
HC
C +0.027
HC
C -0.033
C -0.001
H +0.053
H +0.053

12.

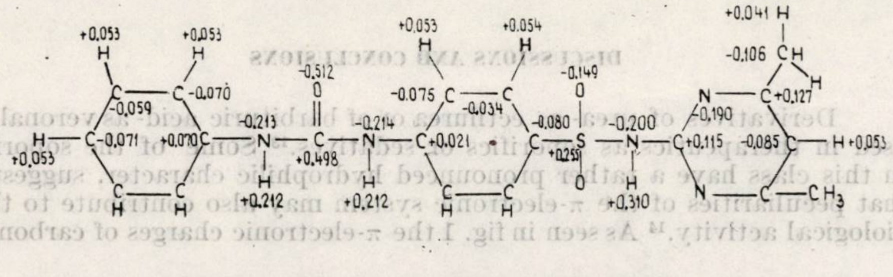
+0.053 H
+0.053 H
C -0.070
-0.059
H—C-0.071
+0.053
+0.070 C
C H
C H
-0.512 O
-0.213 N
C +0.498
H +0.212
-0.214 N
H +0.212
+0.053 H
+0.054 H
-0.075 C
-0.034 C
C+0.021
-0.080 C
C H
C H
-0.149 O
S
+0.255
O
-0.200 N
H +0.310
+0.041 H
-0.106 CH
H
N
C+0.127
-0.190
C+0.115
-0.085 C
H +0.053
N
C—CH3

13.

Fig. 2. — Molecular diagrams (Del Ré method).

1, Urea; *2*, Thiourea; *3*, Phenylurea; *4*, Phenylthiourea; *5*, Diphenylurea; *6*, Diphenylthiourea; *7*, Barbituric acid; *8*, N-phenyl carbamoyl-*p*-aminobenzoyl-diethylaminoethanol; *9*, N-phenyl thiocarbamoyl-*p*-aminobenzoyl-diethylaminoethanol; *10*, N-phenyl carbamoyl-*p*-aminobenzoyl-glycine; *11*, *N*-phenyl thiocarbamoyl-*p*-aminobenzoyl-glycine; *12*, *N*-phenyl carbamoyl-sulphanilyl-5-amino, 1-phenyl pyrazole; *13*, N-phenyl carbamoyl-sulphanilyl-6-amino, 2,4-dimethyl-pyrimidine.

calculated ones, λ_{calc} (with $\beta = 2{,}81$ eV[3]) and the difference between calculated and experimental figures, $\Delta\lambda$. The differences between the experimental positions of absorption maxima for urea and thiourea derivatives $\Delta\lambda_{exp.S,O}$, and between the calculated ones, $\Delta\lambda_{calc.S,O}$, are also given.

The concordance between λ_{exp} and λ_{calc} figures here obtained (linear correlation coefficient $r = 0{,}886$) is not better than usually obtained with the HMO method. A rather good agreement results if the differences ($\Delta\lambda_{exp.S,O}$) between the experimental maxima of urea and thiourea derivatives are compared with the calculated ones ($\Delta\lambda_{calc.S,O}$), except the first pair, urea-thiourea. The HMO calculations explain thus the batochromic effect of substituting with sulphur atom in the ureic residue.

As to the more exact nature of the transition responsible for the first band it should pertain to levels of benzenic cycle perturbed by substitution, not to rather unperturbed phenylic levels. This is indicated by comparing the first band of compounds I and II with the figures for benzoic acid and benzaldehyde[12] (273 nm and 281 nm respectively) of compounds III and IV with those for benzamid[12] (280 nm). The λ_{calc} figures of table II for compounds V and VI are identical with that of diphenylurea, as the SO_2 group is supposed to interrupt conjugation; the λ_{exp} figures differ nevertheless, indicating a certain interaction between the π-electronic systems of the diphenylurea and the heterocyclic moieties in these molecules.

The molecular diagrams calculated by the ω-HMO method are listed in fig. 1. As concerns the molecular diagrams calculated by the simple HMO method, they are not given, but a good parallelism between the figures calculated by the two methods was obtained except the well known fact that atomic charges calculated by the simple HMO method present higher deviations from electroneutrality than those calculated by the iterative method. The figures in front of the atoms (Fig. 1) are the π-electronic charges of the corresponding atoms, those in front of the bonds the π-electronic bond orders. The total atomic charges, calculated by summing up the ω-HMO π-atomic charges with the Del Ré σ-atomic charges are listed in fig. 2.

The calculated data listed in fig. 1 and fig. 2 can be used in discussing relative acidities, chemical activities or biological activities of different atomic positions; unfortunately sufficient experimental data for such correlations are not available.

DISCUSSIONS AND CONCLUSIONS

Derivatives of urea- as ectilurea or of barbituric acid- as veronal are used in therapeutics as soporifics or sedatives.[13] Some of the soporifics in this class have a rather pronounced hydrophilic character, suggesting that peculiarities of the π-electronic system may also contribute to their biological activity.[14] As seen in fig. 1 the π-electronic charges of carbonylic oxygens in positions 1 and 6 of barbituric acid (1.59 e.u) is much higher than in urea and urea derivatives (1.30 – 1.40 e.u.). Also, the energy of the lowest empty orbital, ε_{LE}, is sensibly lower for barbituric acid than for the other compounds (see Tab. 1.).

---

[13] S. Goodman and A. Gilman, "The Pharmacological Basis of Therapeutics", 2nd. edition, McMillan Company, U.S.A., 1955.

[14] C. Drugărin, J. Dick and D. Drugărin, *Ann. pharm. franç.*, **26**, 691 (1968).

Correlational equations predicting several types of biologic activities for sulphonamidic derivatives are known, for example the one given by Martin[15] for sulphamides of the type :

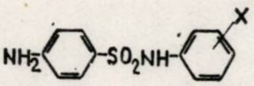

Nevertheless, the π-electronic parameters for our sulphamides V and VI could not be used directly for such predictions as they contain large groups differing sensibly from those of the sulphamide classes in the above cited correlational studies. The large steric differences which appear are not accounted by existing correlational equations, but they certainly will have great effects upon the biological activity.

---

[15] Y. C. Martin, cited by A. Cammarata (see ref. 4).

Revue Roumaine de Chimie, **22**, *3*, 411–419 (1977)

THE ELECTRONIC AND VIBRATIONAL SPECTRA OF SOME N-SUBSTITUTED CARBAZOLOQUINONES

I. M. ISSA*, A. A. EL-SAMAHY*, R. M. ISSA, H. S. EL-KASHEF* and S. H. ETAIW**
Chemistry Department, Faculty of Science, Tanta University, A. R. Egypt
* Assiut University.

Received March 28, 1975

The electronic absorption spectra of Some 6-hydroxy-2,7-dimethoxy-N-substituted phenyl carbazoloquinones are studied in organic solvents of different polarities. Band assignment, effect of substitution on band position, intensity and energy of intramolecular charge transfer are given. The spectra are also investigated in aqueous buffer solutions. The variation of absorbance with pH is utilized for the determination of pK_a. The ir-spectra are analysed to the extent that appears possible.

INTRODUCTION

Although the absortion spectra of quinones were the subject of many investigations,[1–6] few spectrophotometric studies have been carried out on quinones with a heterocyclic moeity.[7–9] In the present investigation, the electronic absorption spectra of some carbazoloquinones are investigated in organic solvents of varying polarities and in buffer solutions. The important bands in the ir-spectra are assigned and discussed in relation to molecular structure.

EXPERIMENTAL

Synthesis of carbazoloquinones was carried out according to the method of Inove et al.[10] by the condensation of 4,4— dimethoxydiquinone with primary aromatic amines, giving N—substituted carbazoloquinones of the type I.

---

* Extracted from the Ph.D. Thesis of Safaa El-Din Hassan Etaiw Mar. 1973.

[1] R. M. Issa, A. S. Hammam, I. I. Ezzat and R. Abdel-Hamid, *J. Chem. U.A.R.*, **14**, 113 (1971).

[2] A. S. Hammam, R. M. Issa and A. M. Osman, *J. Chem. U.A.R.*, **13**, 391 (1971).

[3] R. M. Issa, A. S. Hammam and S. H. Etaiw, *Z. phys. Chem. (Leipzig)*, **251**, 177 (1972).

[4] J. W. Sidman, *J. Amer. Chem. Soc.*, **78**, 2363 (1956).

[5] J. W. Sidman, *Chem. Rev.*, **58**, 685 (1958).

[6] R. A. Morton and W. T. Eorlam, *J. Chem. Soc.*, **1941**, 159.

[7] S. N. Singh, Indian *J. Pure Appl. Phys.* **5**, 430 (1967).

[8] T. K. Clumbalov, *Zhur. priklad. Sepcktrosk.*, **6**, 832 (1967).

[9] M. S. El-Ezaby, T. M. Salem, A. H. Zewail and R. Issa, *J. Chem. Soc.* B, **2**, 1293 (1958).

[10] A. Inove, Y. Nomura, N. Kuroke and R. Konishi, *Yûki Gâei Kagaki Shi.*, **16**, 536 (1958).

The products were crystallised several times from appropriate solvents. The solvents used for spectral measurements were purified by recommended procedures.[11] The universal buffer series of(pH 2 – 12), were prepared as reported by Britton. [12] The pH of the solutions were checked using a radiometer pH meter, model 28, accurate to ± 0.05 units.

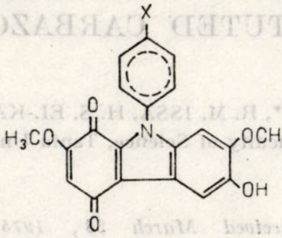

I

where X = H(a) : $NHCOCH_3$(b) : OCH_3 (c) : OH (d) : CH_3 (e) : Cl (f) : COOH (g).

The absorption spectra in the uv and visible region, were recorded on a UNICAM S.P. 8000 spectrophotometer, using I.O cm matched silica cells. The ir-spectra were obtained by a UNICAM S.P. 200 infrared spectrophotometer, using the KBr-disc technique.

RESULTS AND DISCUSSION

Band Assignment :

The spectra of these compounds in ethanol (Fig. 1 and table 1) can be considered as comprising five absorption bands each. The two absorption bands within the 230 – 265 nm region, can be assigned to ^IL_a and ^IL_b transitions of the phenyl ring. A broad band appears within the range 285 – 294 nm, which may be attributed to $\pi - \pi^*$ transition with in the carbonyl groups. The band located near 325 nm being not sensitive to substitution effects, would then correspond to a $\pi - \pi^*$ transition within

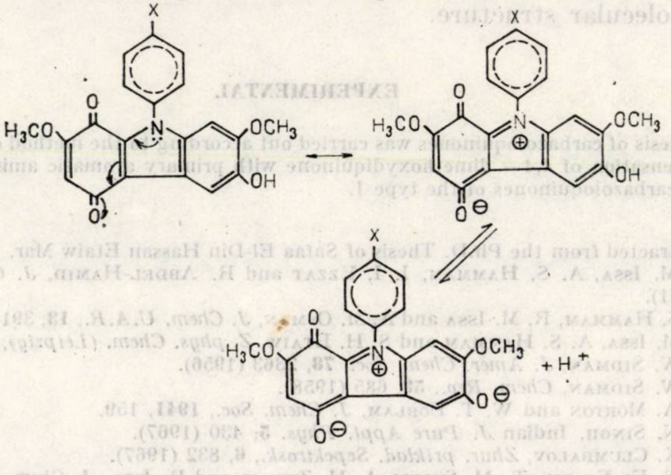

---

[11] A. I. Vogel, "Practical Organic Chemistry", Longmas, London, 1956.

[12] H. T. S. Britton, "Hydrogen Ions", Fourth Edition, Chapman and Hall, London, 1952, p. 364.

the ethylenic system of the quinone nucleus. The band in the visible side, not characteristic of locally excited transitions of carbazoloquinone nucleus, must be assigned to an intramolecular charge transfer interaction.

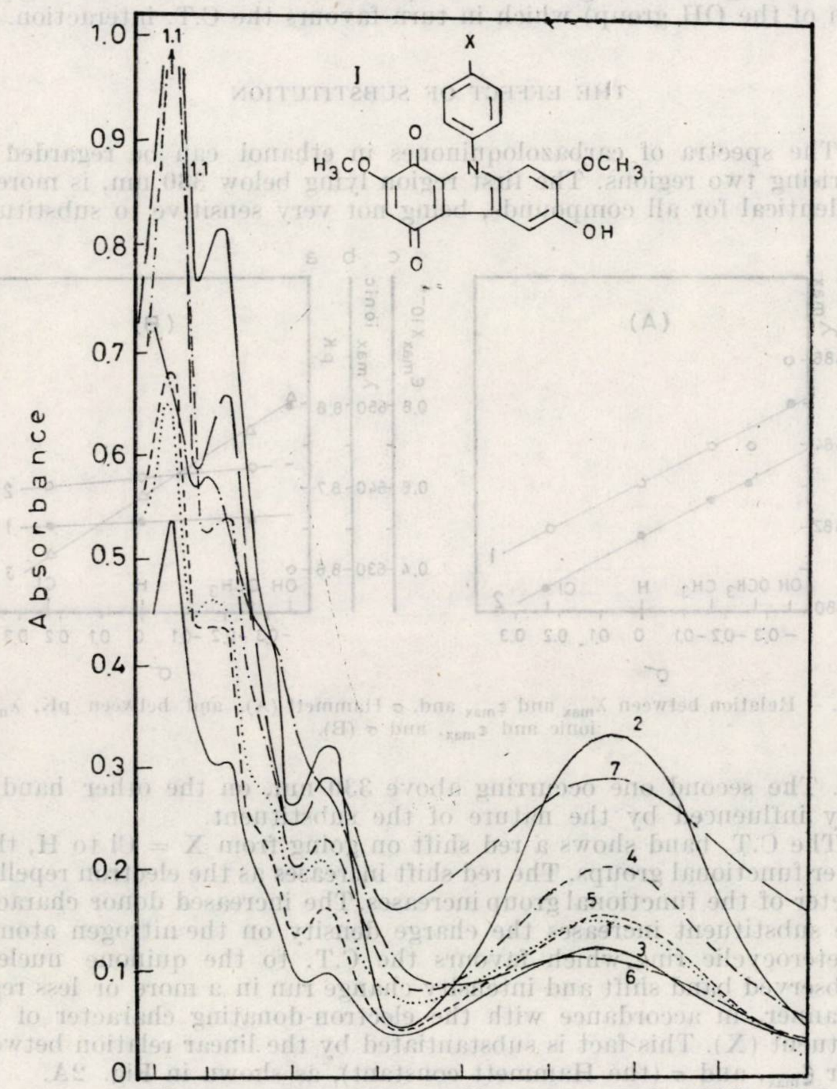

Fig. 1. — Electronic absorption spectra in ethanol (X):

(X) ; (1) H 2.0×10^{-5} gm moles/litre ; (2) $NHCOCH_3$ 4.25×10^{-5} hm moles/litre ; (3) $OCH._3$ 1.60×10^{-5} gm.moles/litre ; (4) OH 2.0×10^{-5} gm. moles/litre ; (5) CH_3 2.0×10^{-5} gm. moles/litre ; (6) Cl. $4.0 \times$ $\times 10^{-5}$ gm.moles/litre ; (7) COOH 1.60×10^{-5} gm. moles/litre.

The C.T. nature of the 480 nm band is supported by considering the spectral behaviour in alkaline solutions. The solutions in alkaline media acquire a bluish to bluish green colour, and the maximum absorption shifts to longer wavelength (tables 1 and 3). The large red shift is mainly due to the negative charge left on the phenate ion, (as a result of the ionization of the OH group) which in turn favours the C.T. interaction.

THE EFFECT OF SUBSTITUTION

The spectra of carbazoloquinones in ethanol can be regarded as comprising two regions. The first region lying below 330 nm, is more or less identical for all compounds, being not very sensitive to substituent effect. The second one occurring above 330 nm, on the other hand, is readily influenced by the nature of the substituent.

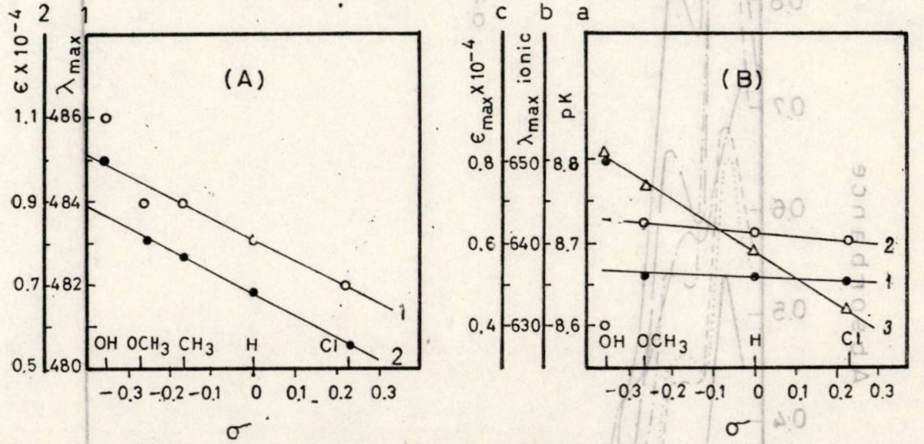

Fig. 2. — Relation between λ_{max} and ε_{max} and, σ Hammett (A), and between pK, λ_{max} ionic and ε_{max}, and σ (B).

The C.T. band shows a red shift on going from X = Cl to H, then to other functional groups. The red shift increases as the electron repelling character of the functional group increases. The increased donor character of the substituent increases the charge density on the nitrogen atom of the heterocyclic ring, which favours the C.T. to the quinone nucleus. The observed band shift and intensity change run in a more or less regular manner, in accordance with the electron-donating character of the substituent (X). This fact is substantiated by the linear relation between λ_{max} or ε_{max}, and σ (the Hammett constant), as shown in Fig. 2A.

THE EFFECT OF THE POLARITY OF THE MEDIUM

The bands display some changes in their appearance, position and relative intensity depending on the molecular structure and the polarity of the medium used (table 1). Generally, C.T. bands are solvent-sensitive,

Table 1

Effect of solvent and substituent on λ_{max} $\in$ and $_{max}$ of some carbazoloquinones

X^a	Ethanol		$CHCl_3$		Ether^s	CCl_4^s	Cyclohexane
	λ_{max}	$\in_{max} \times 10^{-4}$	λ_{max}	$\in_{max} \times 10^{-4}$	λ_{max}	λ_{max}	λ_{max}
H	230	3.25			232		
	262	2.30			255		
	285	1.30	292	1.15	293	293	291
	321	1.05	320	1.05	317	317	313
	483	0.68	469	0.80	462	456	446
	230	2.58			230		
	262	1.90			259		
$NHCOCH_3$	285	0.90			290	—	—
	324	0.75	322	2.31	317		
	490	0.76	480	2.12	465		
	230	3.37			231		
	265	1.94	265	1.95	263		260
OCH_3	293	1.00	292	1.15	293	293	290
	324	0.63	320	0.90	316	315	312
	484	0.80	470	0.85	460	452	450
	230	4.70					
	264	2.75	265		264		
OH	287	1.55	292	s	294	295	—
	321	1.15	322		316	315	
	486	1.00	472		462	458	
	231	3.42					
	263	2.17			256		
CH_3	286	1.05	291	1.20	293	295	292
	324	0.80	320	1.20	318	315	314
	484	0.77	468	1.00	461	455	450
	231	3.40					228
	259	2.85			253		252
Cl	287	2.05	291	0.81	293	290	290
	326	1.35	324	0.58	321	321	320
	482	0.55	468	0.23	462	455	450
	230	6.87			231		
	263	3.28	263	s	260		
COOH	294	1.06	285		288	—	—
	324	1.15	322		319		
	488	1.15	466		462		

a = λ_{max} in nm, $\in_{max}$ in cm^2 $mole^{-1}$. s = Saturated solution.

while L.E. bands are relatively not sensitive to such changes. The bands corresponding to ^1L_a and ^1L_b transitions, show no pronounced solvent effect. The band due to $\pi - \pi^*$ transition within the $C = O$ group, shows a slight blue shift on changing the solvent from a non-polar to a polar one. This observed, shift, would be the resultant of different factors, as was explained before.[13]

---

[13] I. M. Issa, R. M. Issa, K. A. Idris and A. M. Hammam, *Egypt. J. Chem. (Special Issue)* **1973**, 67.

The band corresponding to the $\pi - \pi^*$ transition within the ethylenic system, is red shifted on going from non-polar to polar solvents. The C.T. band on the other hand, is red shifted on going from ethanol as a polar solvent to cyclohexane as a non-polar one. The observed red shifts in both cases in presence of ethanol, chloroform and ether are the esultant of the superposition of dipole-dipole forces as well as hydrogen bonding effects. The intermolecular hydrogen bonds, formed between the polar solvents and the hydroxyl hydrogen of solute, increase the mesomeric effect of the OH-group of the solute. This leads to an increase of the charge density towards the heteroatom, which is not the case with cyclohexane and carbontetrachloride. As a result of the charge transfer from the heteroatom to the quinone nucleus, the dipole moment of the solute is expected to increase in the C.T. state but remains in the same direction as that of the ground state. Also, solvents capable of forming hydrogen bonds with the methoxyl group at position 2 lower its mesomeric effect towards the quinone nucleus, thus decreasing the antagonism for C.T. from the heterocyclic ring to the quinone.

Table 2

Results obtained for the solvation energy values

Solvent	I_a			I_c			I_e			I_f		
	C.T. Band	E	ΔE	C.T. Band	E	ΔE	C.T. Band	E	ΔE	C.T. Band	E	ΔE
Cyclohexane	446	64.2	—	450	63.6	—	450	63.6	—	450	63.6	—
CCl_4	456	62.7	1.41	452	63.3	0.28	455	62.9	0.69	455	62.9	0.69
Ether	462	61.9	2.23	460	62.3	1.38	461	62.1	1.52	462	61.9	1.65
$CHCl_3$	469	61.1	3.15	470	60.9	2.71	468	61.2	2.45	468	61.2	2.44
Ethanol	483	59.3	3.92	484	59.2	4.47	484	58.8	4.80	482	59.1	4.47

E and ΔE in k cal/mole

The maximum wavelengths of the charge transfer band, the corresponding energy of each band and the values of the difference between C.T. energy in cyclohexane and ethanol are depicted in table 2. This C.T. energy difference is taken as the difference in solvation energies between cyclohexane and other solvents

$$\Delta E = E_s - E \text{ cyclohexane}$$

The values indicate that ΔE for CCl_4 is very low and does not exceed in most cases 0.70 kcal/mole, which lies within the lower range of the solvation energy values. For ether, $CHCl_3$ and ethanol the values vary between 1.38 – 4.9 K cal./mole. These values indicate that such solvents can form intermolecular hydrogen bonding with the solute molecules. The strength of hydrogen bonding runs in the order.

$$\text{Ether} < CHCl_3 < \text{Ethanol}$$

SPECTRA IN BUFFER SOLUTIONS

The absorption spectra for the carbazoquinone compounds in universal buffer solutions (Fig. 3) show mainly two bands. The first band appearing within the lower wavelength side is mainly due to absorption by the neutral species of the dye. On gradually increasing the $_{p}$H of the solution the ionisation of the proton from the OH group takes place, a process which increases the π—electron density on the phenyl ring. Accordingly, the effect of rise in $_{p}$H, (that leads to the ionisation of the OH group and thus increases the proportion of the ionic from in solution) is to enhance the interamolecular charge tranfer from the heterocyclic ring to the quinone system. In consequence to this, the absorption band due to the ionic from will be located at longer wavelengths. A clear isosbestic point is observed bear 535 nm indicating the existence of an acid-base equilibrium between the nonionised and ionised forms. The dissociation constant of some compounds are determined applying the methods discussed previously [14,15] namely :

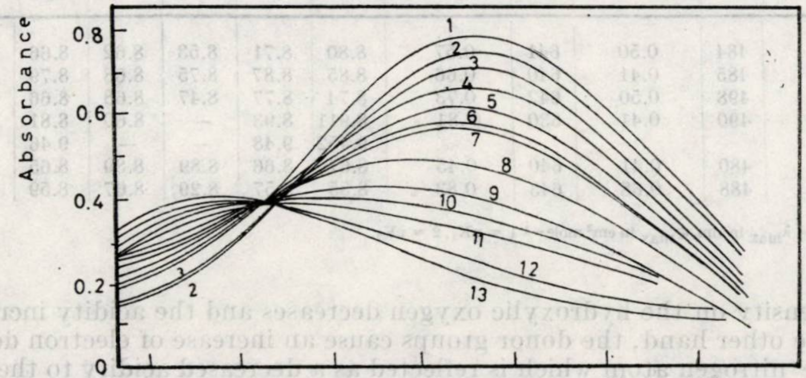

Fig. 3. — The spectra of 1 × 10^{-4} M (Id) in universal buffer solutions.
pH ; *1*, 11.90 ; *2*, 11.02 ; *3*, 10.04 ; *4*, 9.46 ; *5*, 9.43 ; *6*, 9.40 ; *7*, 9,24 ; *8*, 8.97 ; *9*, 8.94 ; *10*, 8.77 ; *11*, 8.72 ; *12*, 8.70 ; *13*, 8.48.

1 — Half-height method.[14]
2 — The modified limiting absorbance.
3 — The isosbestic point method.[15]
4 — The modified Colleter method.[15]

The results obtained are depicted in table 3. The values indicate that the acceptor groups cause a decrease of the electron density on the nitrogen atom. The mesomeric interaction between the OH group and the phenyl ring increases towards the heterocyclic ring. As a result the elect-

---

[14] R. M. Issa, A. S. Hammam, I. Ezzat and R. Abd-El-Hamid, *Z. physik Chem. (Frankfurt)*, **74**, 17 (1971) *Egypt J. Chem.* **14**, 113 (1971).

[15] J. C. Colleter, *Ann. Chim. (France)* **5**, 415 (1960).

Table 3

Dissociation constant of some carbazloquinone compounds

Compound^a	Nonionic form		Ionic form		Methods for calculation pK					ΔG^* kcal/mole
	λ_{max}	$\varepsilon_{max} \times 10^{-4}$	λ_{max}	$\varepsilon_{max} \times 10^{-4}$	1	2	3	4	Average	
I_a	484	0.50	641	0.57	8.80	8.71	8.53	8.62	8.66	11.67
I_b	485	0.41	640	0.66	8.85	8.87	8.75	8.68	8.79	11.85
I_c	498	0.50	642	0.73	8.74	8.77	8.47	8.68	8.66	11.67
I_d	490	0.41	630	0.81	8.911	8.93	—	8.60	8.81	11.87
					9.452	9.48	—	—	9.46	
I_f	480	0.41	640	0.45	8.67	8.66	8.89	8.89	8.65	11.66
I_g	488	0.68	643	0.83	8.55	8.57	8.29	8.67	8.59	11.58

a = λ_{max} in nm, $\in_{max}$ in cm^2 mole^{-1} 1 = pK_1, 2 = pK_2.

ron density on the hydroxylic oxygen decreases and the acidity increases. On the other hand, the donor groups cause an increase of electron density on the nitrogen atom which is reflected as a decreased acidity to the compound. 6-Hydroxy-2,7-dimethexy-N-(*p*-hydroxyphenyl) carbazole-1,4-quinone has two pK values amounting to 8.81 and 9.46. The former belongs to ionisation of the OH-group at position 6 and the other belongs to ionisation of the OH-group at the para-position of the phenyl ring attached to the nitrogen atom. The apparent influence of the substituent on the band intensity, the band position and pK is substantiated by the linear relation between f_{max}, $\in_{max}$ and pK and σ-(Hammett constant) as shown in Fig. 2B.

IR-SPECTRA

The ir-spectra of some carbazoloquionoes are reported in table 4 and the important bands are interpreted to the extent that appears possible. The broad band appearing within the 3200 —3490 cm^{-1} region corresponds to the stretching vibrations of the OH-groups. The broadening and the low frequency of the band indicate the presence of an intermolecular hydrogen bond probably formed between the hydroxyl hydrogen of one carbazoloquinone molecule and the carbonyl oxygen of other molecule.

In the spectra of all compounds, there are three bands in the 1600—1690 cm^{-1} region which are characteristic of the quinone system. The first two bands, appearing near 1670 cm^{-1} and 1650 cm^{-1}, correspond to stretching vibrations of the nonpolarised (position 1) and polarised carbonyl group (position 4) respectively. The carbonyl group in position four is polarised under the influence of charge transfer from the heteroatom.

Also, the methoxyl group at position 2 increases the delocalisation of the π-orbitals of the ethylenic bond together with those of the 4-carbonyl group, the case which antagonises the C.T. from the heteroatom. The third band which appears near 1620 cm^{-1}, corresponds to stretching

Table 4

Solid state(a), common feature, infrared data for I

a	b	c	d	e	f	g	Vibrational assignment
3200^{s}	3320^{m}	3220^{b}	3400vb	4300^{b}	3400^{b}	3490^{m}	ν_{OH}
1670^{m}	1690^{sh}	1668^{s}	—	1665^{w}	1660^{sh}	1680^{sh}	$\nu_{C=O}$
1652^{sh}	1662^{m}	1660^{sh}	1660^{sh}	1655^{sh}	1645^{sh}	$165\ ^{m}$	$\nu_{\text{polarised } C=O}$
1620^{s}	1620^{s}	1615^{s}	1625^{s}	1632^{m}	1630^{s}	1630^{sh}	$\nu_{\text{ethylenic } C=C}$
1600^{s}	1600^{s}	1595^{w}	1600^{s}	1610^{s}	1605^{s}	1600^{s}	$\nu_{asym.}$ C = C
1585^{sh}	1583^{sh}	1576^{w}	1580^{sh}	1582^{sh}	1580^{sh}	1580^{sh}	$\nu_{sym.}$ C = C
1500^{s}	1510^{s}	1505^{s}	1510^{s}	1505^{s}	1498^{s}	1505^{m}	In plane sheletal vib. aliphatic
1450^{w}	1450^{w}	1450^{w}	1455^{w}	1450^{m}	1450^{w}	1450^{m}	$\delta_{asym.\,C-H}$
1340^{w}	1338^{w}	1335^{m}	1339^{m}	1338^{s}	1338^{w}	1340^{m}	δ_{sym} aliphatic C–H
1320^{sh}	1315^{w}	1310^{m}	1315^{w}	1308^{s}	1310^{b}	1305^{sh}	δ_{OH}
1250^{s}	1250^{s}	1250^{s}	1250^{s}	1245^{s}	1250^{m}	1250^{m}	$\nu_{asym.}$= C–O–C
1095^{s}	1090^{s}	1090^{s}	1095^{s}	1093^{s}	1095^{s}	1090^{s}	ν C–OH
1048^{s}	1044^{s}	1045^{w}	1745^{s}	1045^{s}	1045^{w}	1045^{s}	$\nu_{sym.}$=C–O–C
870^{s}	870^{s}	875^{s}	875^{sh}	870^{s}	875^{w}	868^{s}	γ isolated H-ring atom

(a) As KBr disk, (b) Band intensities are given by s = strong, b = broad, m = medium, w = weak, sh = shoulder.
(c) Absorption band frequencies are expressed in cm^{-1}.

vibrations of the ethylenic bond in the quinone ring. The existance of these three bands reveals that the ethylenic and the carbonyl systems are not strongly interacting i.e. are at least partly isolated.

The plot of $\nu_{C=O}$ with σ gives a straight line indicating that the polarised carbonyl is directly affected by the nature of the substituent (Fig. 4).

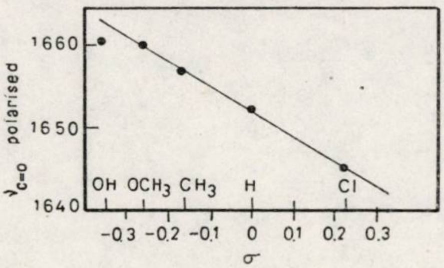

Fig. 4. — Relation between $\nu_{C=0}$ and σ (Hammett constant).

Bands due to stretching of C = C, C—OH and = C—O—C bonds and of deformation of the OH—group are expected to appear within the region 1600 — 100 cm^{-1}. On the other hand, bands due to the C—H out-of-plane deformation appear below 1000 cm^{-1}.

Revue Roumaine de Chimie, 22, 3, 421–426 (1977)

HYDROXYPHENOTHIAZINE-5,5-DIOXIDES (HYDROXYPHENOTHIAZINE-SULPHONES)[*]. II[**]

DETERMINATION OF DISSOCIATION CONSTANTS OF SOME 3-HYDROXYPHENOTHIAZINE-SULPHONES

Z. SZEKELY, TEODORA PANEA and C. BODEA
Institute of Chemistry, Cluj-Napoca str. Donath 65 — 103

Received April 8, 1975

In the present investigations we have determined, by spectrophotometric method, the dissociation constants of some 3-hydroxyphenothiazine-sulphones. The acid character of these compounds is situated between that of acetic acid and phenol. In addition these data demonstrate the contribution of the halogen atoms in increasing the acidity.

Hitherto no determinations have been made of dissociation constants in the hydroxyphenothiazine series. A reason for this may be the high sensitivity of 3-hydroxy-phenothiazines to oxidants (even atmospheric oxygen), which turn them into phenothiazones.

In previous papers[1–3] we have described the preparation of a new type of hydroxy-phenothiazines, namely 3-hydroxyphenothiazine-sulphones, presenting an increased stability of the hydroxy-group. Due to the higher electron attracting effect of the sulphone group as compared to the unsubstituted sulphur atom, an increase in the acidic character of hydroxy sulphones may also be expected.

As it was shown previously by recording the UV-spectra of some 3-hydroxyphenothiazine-sulphones, the electronic state of these compounds undergoes no significant change in acidic medium, whereas in basic medium a bathochromic shift of all four bands is observed. [4]

Taking into account these observations we considered useful to determine the dissociation constants of several 3-hydroxyhalophenothiazine-sulphones.

---

[*] The term hydroxyphenothiazine-sulphones will be used here because it is much more suggestive for the purposes of this paper.

[**] Part. I. : T. Panea, V. Fărcăşan and C. Bodea, *Rev. Roumaine Chim.*, **18**, 7, 1259 (1973).

[1] T. Panea, Dissertation, Cluj, 1971.

[2] T. Panea and C. Bodea, Rom. pat. 60238, 14 iunie 1969.

[3] T. Panea and C. Bodea, Rom. pat. 64734, 20 oct. 1970.

[4] C. Bodea, T. Panea and V. Fărcăşan, *Rev. Roumaine Chim.*, **15**, 1923 (1970).

EXPERIMENTAL

In order to estimate the dissociation constants, conductometric, potentiometric and spectrophotometric methods are usually applied.

In the present investigations we have chosen the spectrophotometric method [5,6] as it is not only precise but provides also the advantage that very low concentrations ($C.10^{-4}M$) can be used.

Since the 3-hydroxy- sulphones are not soluble enough in water, but the solubility can be increased using a mixture of water and a miscible organic solvent (e.g. dioxane, alcohol, acetone, etc.), the recordings were performed by means of dioxane-water solutions. In this way the so-called apparent dissociation constants were obtained.

The dissociation constant can be calculated by means of absorption values at different pH-values. The difference between the optical density of the dissociated and undissociated form being rather large at the used wavelength, the precision of the calculated dissociation constants is satisfactory.

The most simple case for calculating dissociation constants (K) is that in which the optical densities of both ionized and unionized forms (A^-, resp. HA) are available. Since, in our case, some difficulties have arisen in obtaining these values (due to low solubilities in acidic medium, secondary phenomena in more basic solutions) this simple method was not applicable. Therefore a procedure developed by Rosenblatt was used.[7] This method requires only three solutions with different pH's and optical densities. By resolving simultaneously three equations of the type:

$$a_n D_n \frac{1}{K} - a_n D_{\mathrm{HA}} \frac{1}{K} - D_{\mathrm{A}} = D_n, \tag{1}$$

K is available where D_n is the optical density of a mixture at H^+ activity a_n, supposing that the cell length and total acid concentration (C) are constants $C = C_{\mathrm{HA}} + C_{\mathrm{A}^-}$, D_{A^-} and D_{HA}, respectively, are the optical density of the solution containing only A^-, respectively HA;

Equation (1) may be resolved by means of determinants, and the value of K is obtained as follows [8]:

$$K = \frac{D_1(a_1a_2 - a_1a_3) + D_2(a_2a_3 - a_2a_1) + D_3(a_3a_1 - a_3a_2)}{D_1(a_3 - a_2) + D_2(a_1 - a_3) + D_3(a_2 - a_1)} \tag{2}$$

Fig. 1 — 4 represent the absorption spectra of hydroxyphenothiazine-sulphones at different pH-values. The appearance of isosbestic points in the studied pH-intervals indicates the existence of an equilibrium between only two species in solution, the dissociated and the undissociated form of the hydroxy-sulphone, according to the general equilibrium : $AH \rightleftarrows A^- + H^+$, and that no interaction with solvents and buffer substances appears.

To permit a comparison, Fig. 5 and Fig. 6 show the absorption spectra at different pH-values of phenothiazine-sulphone (5) and of 3-methoxyphenothiazine-sulphone (6). As these compounds have no acidic character, pH modifications do not influence the spectra.

Hydroxyphenothiazine-sulphones were prepared in our laboratory [2] and their purity was checked by thin-layer chromatography; in addition m.p. control was made. Freshly distilled dioxan and twice distilled CO_2 free water with phosphate and borate buffer were used for preparing solutions with exact pH-values.

Spectra were recorded between 210 — 400 nm. at different pH-values, using a Beckmann DK-2A Spektrophotometer thermostated at 20 ± 0.2.

---

[5] J. Fruwert, G. Geisler, H. Hübner, W. Knathe, E. Müller, H. D. Nagel, H. Otto E. Pilz, K. Schmiedel, W. Schimmrich, F. Stache und H. Steffens, "Ausgewählte physikalische Methoden der organischen Chemie", vol. II, editor G. Geiseler, Akademie Verlag Berlin, 1963, S. 60.

[6] R. A. Robinson and R. H. Stokes, "Electrolyte Solutions", Ed. II, Butterworths, London, 1959, p. 344.

[7] D. H. Rosenblatt, *J. Phys. Chem.*, **58**, 40 (1954).

[8] P. Cecchi, *Res. Sci.*, **28**, 2526 (1958).

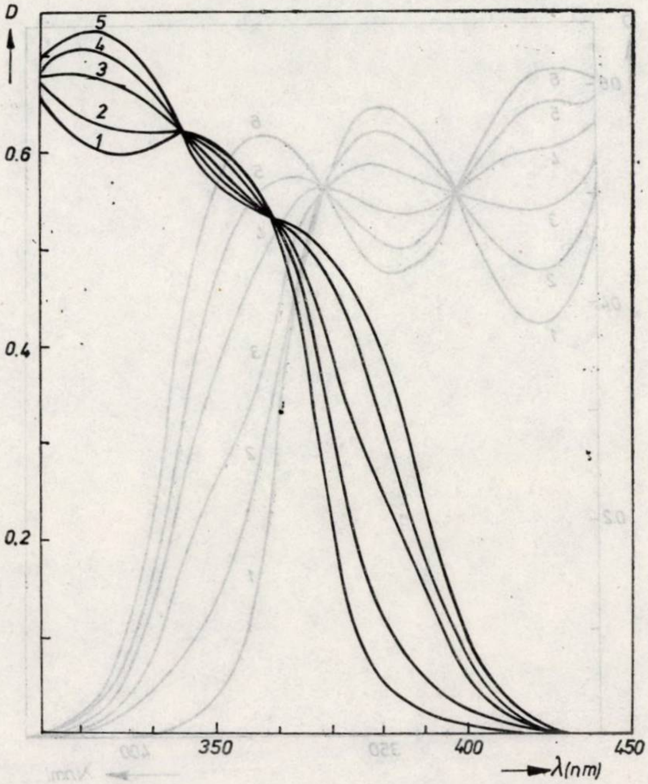

Fig. 1. — Absorption spectra of compound **(1)** at different pH-values. C = $1.050.10^{-4}$M; 22°, pH: 1) 7.00; 2) 8.20 3) 8.60 4) 8.80 5) 9.22.

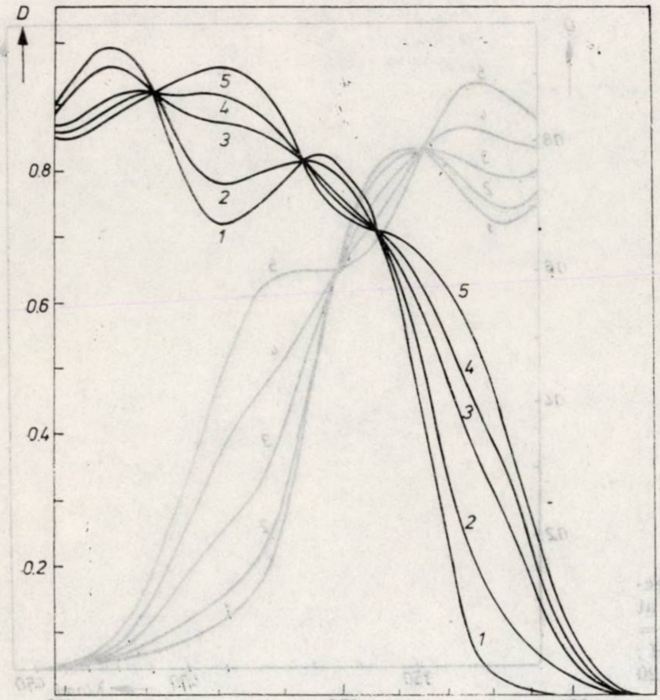

Fig. 2. — Absorption spectra of compound **(2)** at different pH-values C = = $0.72.10^{-4}$M; 22°, pH: 1) 7.00 2) 7.20 3) 8.60 4) 8.80 5) 9.22.

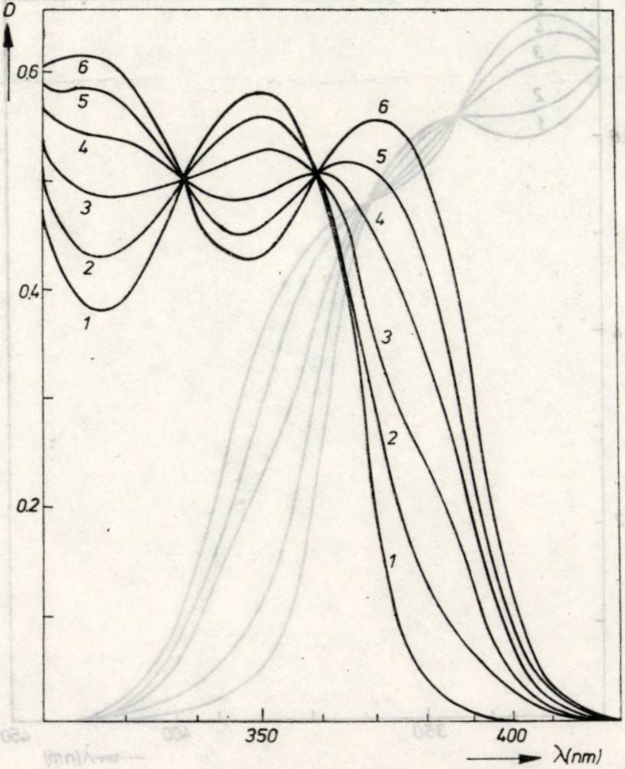

Fig. 3. — Absorption spectra of compound **(3)** at different pH-values $C = 0.715.10^{-4}$M; 22°. pH: 1) 6.40 2) 7.20 3) 7.60 4) 8.00 5) 8.40 6) 9.22.

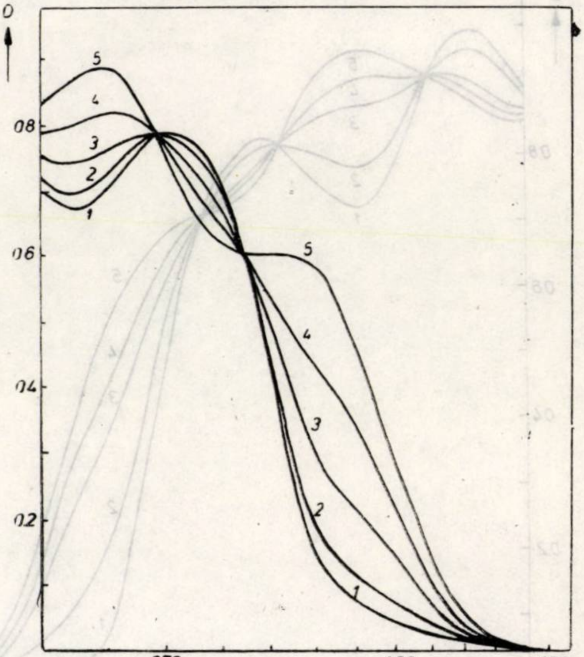

Fig. 4. — Absorption spectra of compound **(4)** at different pH-values $C = 0.725.10^{-4}$M; 22°. pH: 1) 6.20 2) 6.80 3) 7.20 4) 7.80 5) 8.60.

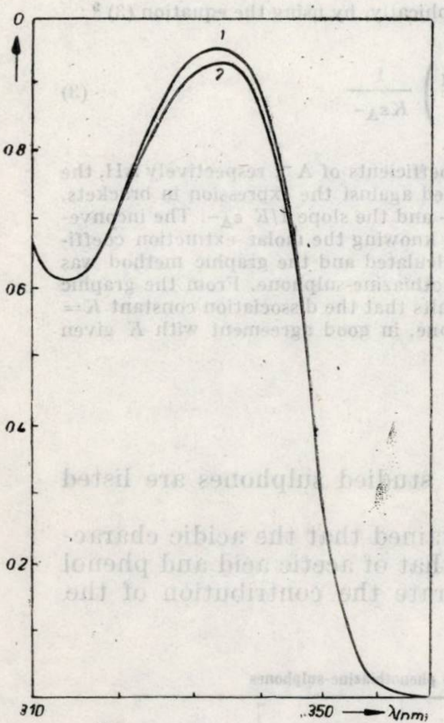

Fig. 5. — Absorption spectra of compound **(5)** at different pH-values C = 0.84.10⁻⁴M; 22°. pH : 1) 4.75 2) 9.22.

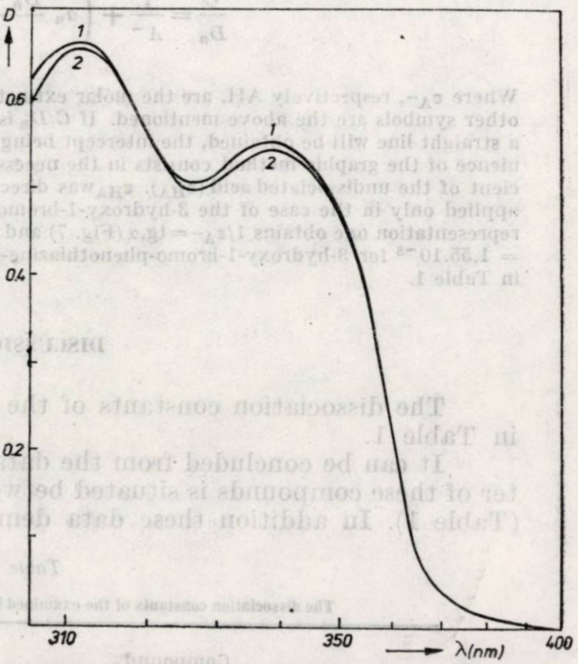

Fig. 6. — Absorption spectra of compound **(6)** at different pH-values C = 0.82.10⁻⁴M; 22°. pH : 1) 4.75 2) 9.22.

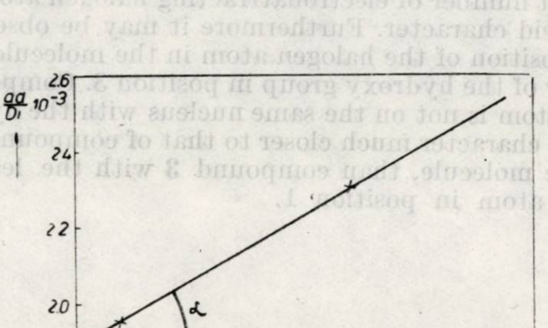

Fig. 7.—The diagram for evaluation of dissociation constant of compound **(3)** by graphic method.

The dissociation constant can also be obtained graphically, by using the equation (3) [9]:

$$\frac{C}{D_n} = \frac{1}{A^-} + \left(a_n \frac{D_n - \varepsilon_{AH}}{D_n} \right) \frac{1}{K \varepsilon_{A^-}} \tag{3}$$

Where ε_{A^-}, respectively AH, are the molar extinction coefficients of A^-, respectively AH, the other symbols are the above mentioned. If C/D_n is plotted against the expression in brackets, a straight line will be obtained, the intercept being $1/\varepsilon_{A^-}$ and the slope $1/K\ \varepsilon_{A^-}$. The inconvenience of the graphic method consists in the necessity of knowing the molar extinction coefficient of the undissociated acid (ε_{HA}). ε_{HA} was directly calculated and the graphic method was applied only in the case of the 3-hydroxy-1-bromo-phenothiazine-sulphone. From the graphic representation one obtains $1/\varepsilon_{A^-} = \text{tg}.\alpha$ (Fig. 7) and it results that the dissociation constant $K = 1.55.10^{-8}$ for 3-hydroxy-1-bromo-phenothiazine-sulphone, in good agreement with K given in Table 1.

DISCUSSION

The dissociation constants of the four studied sulphones are listed in Table 1.

It can be concluded from the data obtained that the acidic character of these compounds is situated between that of acetic acid and phenol (Table 1). In addition these data demonstrate the contribution of the halogen atoms to increasing the acidity. Compound **4**, containing the largest number of electronattracting halogen atoms has the most pronounced acid character. Furthermore it may be observed how the nature and the position of the halogen atom in the molecule influence the acidic character of the hydroxy group in position 3. Compound **2**, in which the chlorine atom is not on the same nucleus with the hydroxy group, displays an acidic character much closer to that of compound **1**, with no halogen atom in the molecule, than compound **3** with the less electronattracting bromine atom in position 1.

Table 1

The dissociation constants of the examined hydroxy phenothiazine-sulphones

Compound	K_a	pK_a
3-Hydroxyphenothiazine-sulphone(1)	$2.30.10^{-9}$	8.64
3-Hydroxy-7-chloro-phenothiazine-sulphone (2)	$2.44.10^{-9}$	8.61
3-Hydroxy-1-bromo-phenothiazine-sulphone (3)	$1.8.10^{-8}$	7.75
3-Hydroxy-1, 7, 9-trichloro-phenothiazine-sulphone(4)	$4.33.10^{-8}$	7.35

---

[9] A. Agren, *Acta Chem. Scand.*, **9**, 49 (1955).

Revue Roumaine de Chimie, **22**, *3*, 427–433 (1977)

DETERMINATION OF XANTHATES FROM FLOTATION PULPS WITH AN Ag_2S MEMBRANE ELECTRODE

IOVANCA HAIDUC, STELUȚA BEICU and CANDIN LITEANU

Chair of Analytical Chemistry, Babeș-Bolyai University, Cluj-Napoca, str. Arany János nr. 11

Received March 21, 1975

The determination of xanthate ions in pure solutions of $10^{-3} - 10^{-4}$ M concentrations can be performed by potentiometric titration with $AgNO_3$ with the aid of an Ag_2S membrane electrode. In flotation pulps (of non-ferrous ores) the uncomplexed xanthate can be determined by the method of known addition of a standard reagent which either increases or decreases the level of xanthate concentration, by using the Ag_2S electrode. Interfering ions S^{2-} and CN^- are masked with $Zn(OH)_2$. The CO_3^{2-}, NO_3^- and CrO_4^{2-} anions are not interfering. This method affords the determination of 8 mg xanthate with an error of ± 6%.

INTRODUCTION

Xanthates may constitute an analytical problem due to their use as flotation agents for nonferrous ores and in the manufacture of artificial silk and rayon.[1] In order to monitor the flotation process and for the recirculation of waste water from industrial processes [2] it is necessary to know very small concentrations of xanthate (in the range of $10^{-5} - 10^{-6}$ M) in these waters. To date, the determination of xanthates was performed by titrimetric,[3-18] polarographic,[19,20] spectrophotometric methods,[21-29]

---

[1] K. Otmer, "Encyclopedia of Chemical Technology", sec. ed., vol. 22, Intersci. Publ. John Wiley, New York, 1964, p. 419.

[2] B. Philipp and C. Fichte, *Faserforsch.u Textiltech.*, **11**, 118, 172 (1960) ; *Chem. Abstr.*, **54**, 16139 (1960).

[3] I. Iwasaki and S. R. B. Cooke, *J. Amer. Chem. Soc.*, **80**, 285 (1958).

[4] W. S. Calcott, F. L. English and F. B. Downing, *Eng. Mining J. Press.*, **1974**, 118, 980.

[5] K. S. Panwar, S. P. Rao and J. N. Gaur, *Analyt. Chim. Acta*, **25**, 218 (1961).

[6] E. Rolia, *Trans. Instr. Min. Metall.*, C 207 – C209 (1970) ; *Analyt. Abstr.*, **21**, 2735 (1971).

[7] V. Hejl and V. Fejfar, *Chem. průmysl.*, **14**, 87 (1964).

[8] S. Veibel and M. Wronski, *Acta Chem. Scand.*, **20**, 849 (1966).

[9] L. Kekedy and F. Makkay, *Stud. Univ. Babeș-Bolyai, Chem.*, **9** (2), 55 (1964).

[10] S. Karaivanov, D. Dimitrov and S. Magaeva, *Z. analyt. Chem.* **244**, 319 (1969).

[11] P. N. Krishnan Nabbisan and C. G. Ramachandran Nair, *Analyt. Chim. Acta*, **52**, 475 (1970).

[12] A. L. J. Rao and S. Singh, *Z. analyt. Chem.*, **260**, 367 (1972).

[13] L. Kekedy and F. Makkay, *Stud. Univ. Babeș-Bolyai, Chem.*, **7**(1), 139 (1962).

[14] A. L. J. Rao and S. Singh, *Prepr. Semin. Electrochem.*, **13 II**, 133 (1972) ; *Chem. Abstr.*, **80**, 11581 (1974).

ESR [30] (the xanthate is precipitated with copper ions and the Cu(II) excess is then determined by ESR), atomic absorption spectroscopy [31] (the xanthate is precipitated with Ag(I) and the excess of Ag(I) is determined by atomic absorption spectroscopy). There are few papers dealing with the determination of xanthates in industrial waters.

Rolia et al.[16] have used an Orion Ag_2S electrode in the determination of xanthates, but they do not give quantitative data in their paper.

In this work we report a method for determining the uncomplexed xanthate in the flotation pulps, by using an Ag_2S electrode prepared by Liteanu and Popescu [32] and the technique of known addition. [33]

EXPERIMENTAL

Reagents. A stock solution of potassium ethylxanthate (KEX) 10^{-1}M, was prepared from reagent grade salt, in buffer solution with pH = 9.5.

Potassium ethylxanthate solutions $10^{-2} - 10^{-4}$ M were prepared by diluting the stock solution with a buffer solution of pH = 9.5.

The buffer solution was prepared from $NaHCO_3$ 0.025 M ; Na_2CO_3 0.025 M (1 : 1).

Industrial pulps were obtained from Baia Mare factory.

The silver nitrate stock solution 10^{-2} M was obtained from reagent grade salt and bidistilled water, the constant ionic strength being adjusted with KNO_3 10^{-1}M. $AgNO_3$ solutions $10^{-2} - 10^{-4}$M were prepared by diluting the stock solution with bidistilled water and adjusting the constant ionic strength with 10^{-1}M KNO_3.

Apparatus. A Clamann Grahnert pH-meter, type MV 85, magnetic stirrer, microburette, Ag_2S membrane-electrode (type LCCA-Cluj-Napoca), saturated calomel electrode (SCE) and agar-agar in KNO_3 10^{-1} M syphone were used.

The electrochemical chain involved in the measurements was :

(−) Hg, metallic contact	Ag_2S membrane	Xanthate (solution)	Agar-agar bridge	SCE(+)

---

[15] L. Kekedy and F. Makkay, *Stud. Univ. Babes-Bolyai, Chem.*, **7**(2), 105 (1962).

[16] E. Rolia and J. G. Ingles, *Canadian Mining J.*, **1971**, 94.

[17] I. M. Plaskin, *Zavodskaya Lab.*, **56**, 28 (1956).

[18] Z. Kurzawa, W. Wojciak and R. Solecki, *Chem. Analit.*, **12**, 1007 (1967)

[19] R. V. Dronina, Yu. S. Gorodetskii and A. A. Mamakov, *Izvest. Akad. Nauk Mold. S.S.S.R., Ser. fiz. tekn. matem. Nauk*, **1971**, 56.

[20] B. Philipp, *Faserforsch. u Textiltech.*, **10**, 493 (1959) ; *Analyt. Abstr.*, **7**, 2846 (1960).

[21] P. J. C. Fierens, J. Adams and E. Royers, "Comptes Rendus du Congres International de Chimie Industrielle, 31e Liège", vol. 2, 1958, p. 770.

[22] J. Dyer and L. H. Phifer, *Macromolecules*, **1969**, 111.

[23] R. Joedodibroto, Ph. D. Thesis, Syracuse Univ., Syracuse, N. Y., 1963.

[24] M. Wronski and S. Plaza, *Chem. Analit.*, **14**, 1129 (1969).

[25] C. Pohlandt, E. B. T. Cook and T. W. Steele, *Talanta*, **16**, 1129 (1969).

[26] H. Dautzenberg, J. Schumann and B. Philipp, *Faserforsch. u Textiltech.*, **23**, 256 (1972) ; *Analyt. Abstr.*, **24**, 224 (1973).

[27] V. Masin, *Chem. průmysl.*, **20**, 383 (1970).

[28] V. A. Kremer and L. A. Zatuchnaya, *Izvest. V.U.Z., Khim. i khim. tekhnol.*, **9**, 375 (1966).

[29] K. Bicovski and P. Bicovska, *Coll. Czech. Chem. Comm.*, **24**, 3099 (1959).

[30] P. M. Solozhenkin, N. I. Kopitskaya and L. F. Vasilenko, *Doklady Akad. Nauk Tadzhik. S.S.R.*, **12**, 27 (1969).

[31] H. K. Gupta and D. F. Boltz, *Microchem.*, J., **16**, 571 (1971).

[32] C. Liteanu, I. C. Popescu and V. Ciovîrnache, *Talanta*, **19**, 985 (1972).

[33] *Orion Newsletter*, **2** (11), 50 (1970).

For Gran plots semi-antilogarithmic graph papers, developed by Orion, was used : the electrode potential (mV) is plotted on the vertical, antilogarithmic axis, against titrant added (ml) on the horizontal linear axis.

RESULTS AND DISCUSSION

THE RESPONSE OF Ag_2S MEMBRANE ELECTRODE TO XANTHATE

The Ag_2S membrane electrode has a nernstian response towards potassium ethylxanthate, with a slope of 60 mV/pc (Fig. 1) in the concentration range from 10^{-2} to 10^{-6} M. The ionic strength during the electrode function was $J = 0.1$M, achieved by KNO_3 and the pH of the solution was in the range 10.5 — 11.

THE DETERMINATION OF POTASSIUM ETHYLXANTHATE BY POTENTIOMETRIC TITRATION WITH $AgNO_3$ AND Ag_2S MEMBRANE ELECTRODE

The solutions of potassium ethylxanthate in the range $10^{-1}-10^{-4}$ M were titrated potentiometrically with $AgNO_3$ $10^{-1}-10^{-4}$ M solutions, by using the Ag_2S membrane electrode as indicating electrode. In fig. 2 the titration curves of ethylxanthate $10^{-2}, 10^{-3}$ and 10^{-4} M solution, are given as an illustration.

The determinations are precise only for the concentration range from $10^{-1}-10^{-3}$ M. For 10^{-3}M solution, $\Delta E_{\pm 1\%} = 120$ mV and the relative error for 75 mg is $\pm$ 2%. For the titration of 10^{-4} M (7.5 mg in the sample), $\Delta E_{\pm 1\%} = 35$ mV and the relative error is $e = \pm 7\%$.

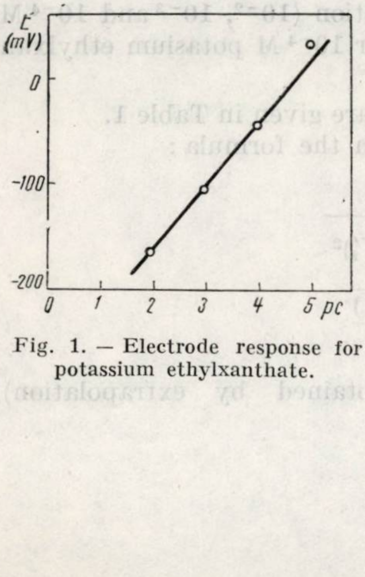

Fig. 1. — Electrode response for potassium ethylxanthate.

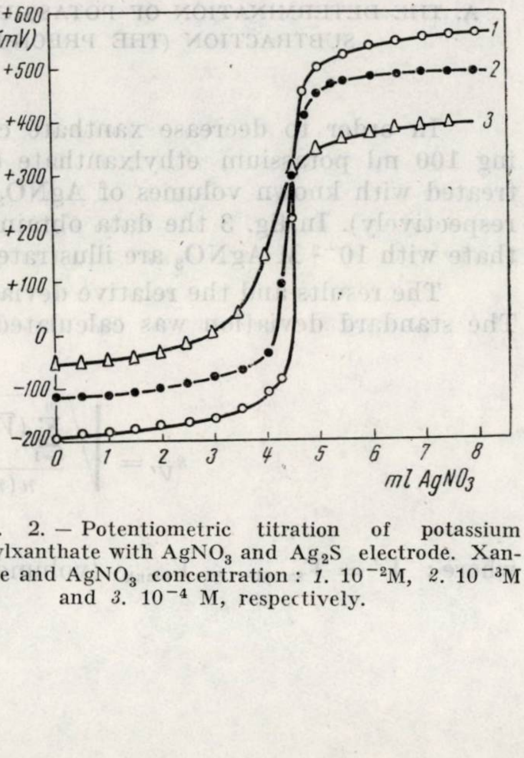

Fig. 2. — Potentiometric titration of potassium ethylxanthate with $AgNO_3$ and Ag_2S electrode. Xanthate and $AgNO_3$ concentration : *1.* 10^{-2}M, *2.* 10^{-3}M and *3.* 10^{-4} M, respectively.

THE DETERMINATION OF POTASSIUM ETHYLXANTHATE BY THE TECHNIQUE OF KNOWN ADDITION AND SUBTRACTION

Within this technique,[33] both alternatives were used, including the increase of the xanthate concentration in the sample, and the decrease of the xanthate concentration by precipitation with $AgNO_3$.

In both alternatives the e.m.f. of the cell is measured when the Ag_2S membrane electrode is in the xanthate solution of unknown concentration (c_x) and the e.m.f. of the cell after each addition of standard solution (which can increase or decrease the xanthate concentration in the sample). A Gran plot on semiantilogarithmic paper (as mentioned in the experimental part : e.m.f. values *vs.* the volume of standard solution added) gives a straight line, which extrapolated back to the horizontal axis gives the concentration of the xanthate in the unknown solution, according to the relation :

$$c_x = c_s \, (V_{\text{extrapolated}} / V_0)$$

where c_s = the concentration of standard solution
$V_{\text{extrapolated}}$ = the volume obtained by extrapolation to the horizontal axis
V_0 = the initial volume of the sample, in which the xanthate concentration is c_x.

A. THE DETERMINATION OF POTASSIUM ETHYLXANTHATE BY KNOWN SUBTRACTION (THE PRECIPITATION AGENT $AgNO_3$)

In order to decrease xanthate concentration, the sample containing 100 ml potassium ethylxanthate ($10^{-4} - 10^{-6}$ M) at J = 0.1 was treated with known volumes of $AgNO_3$ solution (10^{-2}, 10^{-3} and 10^{-4} M, respectively). In fig. 3 the data obtained for 10^{-4} M potasium ethylxanthate with 10^{-2} M $AgNO_3$ are illustrated :

The results and the relative deviation are given in Table 1. The standard deviation was calculated with the formula :

$$s_{\overline{V}'} = \sqrt{\frac{\sum_{i=1}^{n} (\overline{V}' - V'_i)^2}{n(n-1)}}$$

where : $V' = V_{\text{sample}} - V_{\text{blank}}$ (volumes obtained by extrapolation).

The blank sample was treated with the same volumes of $AgNO_3$ solution and after plotting on Gran diagrams V_{blank} was determined by extrapolation back to the horizontal axis.

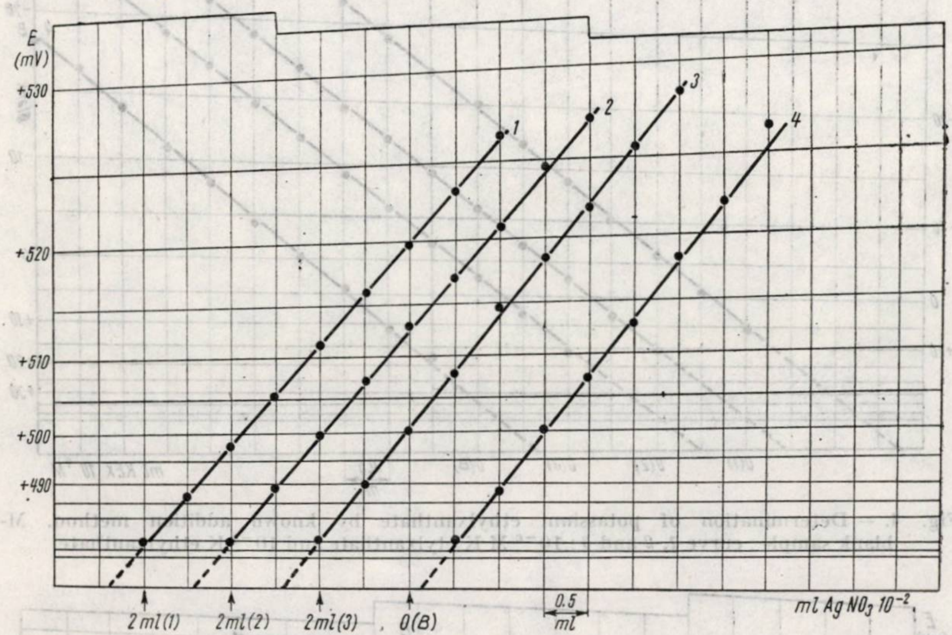

Fig. 3. — Determination of potassium ethylxanthate by known subtraction method. M — blank sample; curve *1*, *2*, and *3* : 10^{-4} M K ethylxanthate and 10^{-2} M $AgNO_3$.

Table 1

Determination of xanthate by known subtraction

Experiment	[xanthate] sample	$[AgNO_3]$	V_{extr} ml	V' ml	$\overline{V}'$ ml	$\lvert V'_i - \overline{V}'_i \rvert$ ml	$\frac{s}{\overline{V}'}$
Blank	0	10^{-2}	0.1	—	—	—	—
1	10^{-4}	10^{-2}	1.6	—		0	0
2	10^{-4}	10^{-2}	1.6	1.5	1.5	0	
3	10^{-4}	10^{-2}	1.6			0	
Blank	0	10^{-3}	0.34	—	—	—	—
1	10^{-5}	10^{-3}	1.35	1.01		0.08	0.0607
2	10^{-5}	10^{-3}	1.30	0.96	0.93	0.03	(6.07 %)
3	10^{-5}	10^{-3}	1.16	0.82		0.11	
Blank	0	10^{-4}	0.5	—	—	—	—
1	10^{-6}	10^{-4}	1.15	0.65		0.033	0.0206
2	10^{-6}	10^{-4}	1.20	0.70	0.68	0.016	(2.06 %)
3	10^{-6}	10^{-4}	1.20	0.70		0.016	

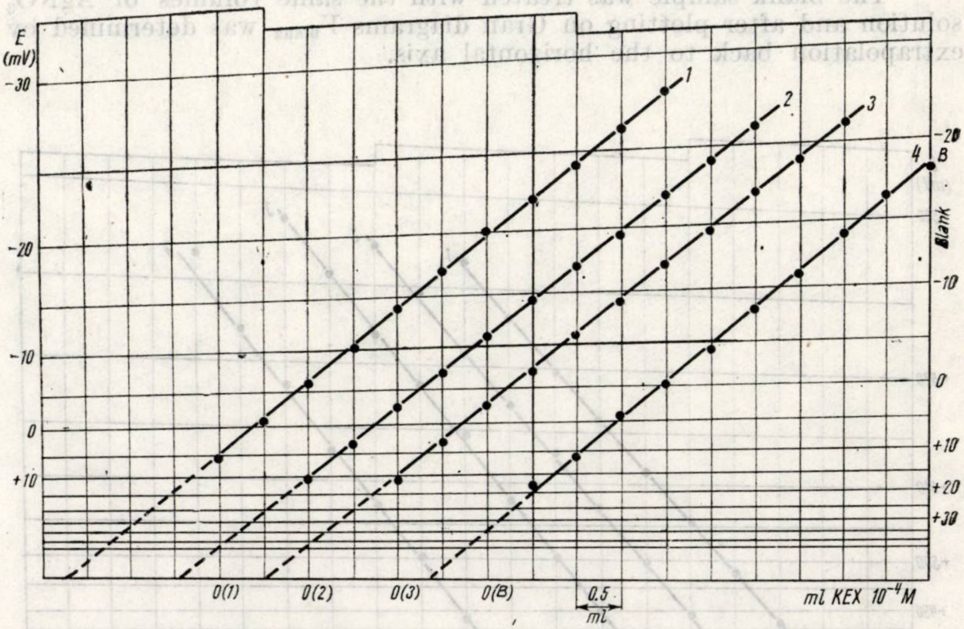

Fig. 4. — Determination of potassium ethylxanthate by known addition method. M-blank sample : curve *1*, *2* and *3* : 10^{-6} M K etylxanthate and 10^{-4} K ethylxanthate.

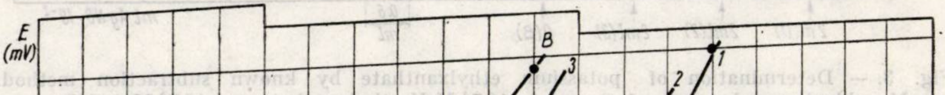

Fig. 5. — Determination of xanthate by the known addition method in flotation pulps : M-blank sample, 1. $[CN^-] = 10^{-5}$ (sequestered with Zn^{2+}) *2*. $[S^{2-}] = 10^{-5}$ (sequestered with Zn^{2+}). *3*. $[S^{2-}]10^{-4}$ M (sequestered with Zn^{2+}).

B. THE DETERMINATION OF POTASSIUM XANTHATE BY THE KNOWN ADDITION METHOD

The sample containing 100 ml $10^{-4} - 10^{-6}$ M potassium ethylxanthate at $J = 0.1$ was treated with known volumes of potassium ethylxanthate(10^{-2},10^{-3} and 10^{-4} M). The data obtained in the determination of 10^{-6} M potassium ethylxanthate by known addition of 10^{-4} M ethylxanthate are plotted in Fig. 4 and the results of determination are given in Table 2.

Table 2

Determination of xanthate by known addition

Experiment	[Xanthate]	[xanthate] added	$V_{\text{extr.}}$ ml	V ml	$\bar{V}'$ ml	$\lvert V' - \bar{V}'_i \rvert$ ml	$\frac{s}{\bar{V}'}$
Blank	0	10^{-2}	0	—	—	—	—
1	10^{-4}	10^{-2}	1.0	1.0		0.033	
2	10^{-4}	10^{-2}	1.1	1.1	1.033	0.067	0.03
3	10^{-4}	10^{-2}	1.0	1.0		0.033	(3%)
Blank	0	10^{-3}	0.13	—	—	—	
1	10^{-5}	10^{-3}	0.90	0.77		0.01	
2	10^{-5}	10^{-3}	0.90	0.77	0.76	0.01	0.013
3	10^{-5}	10^{-3}	0.87	0.74		0.02	(1.31%)
Blank	0	10^{-4}	0.5	—	—	—	
1	10^{-6}	10^{-4}	1.6	1.1		0.133	
2	10^{-6}	10^{-4}	1.4	0.9	0.96	0.066	0.068
3	10^{-6}	10^{-4}	1.4	0.9		0.066	(6.85%)

In order to eliminate the influence of interfering ions, able to consume Ag(I) in the determination of xanthate from flotation pulps, the method of known addition was used. The constant ionic force and the optimal pH were achieved by adding to each 50 ml sample a volume of 50 ml buffer solution (pH $= 9 - 9.5$ from $Na_2CO_3 + NaHCO_3$). The S^{2-} and CN^- interfering ions for xanthate, were sequestered with $ZnCO_3$ (to each sample was added $1 - 2$ ml Zn(II) 10^{-1} M solution). Fig. 5 and Table 3 give the results obtained in the analysis of flotation pulps.

Table 3

Determination of xanthate in a cuprous concentrate (industrial sample)

Experiment	CN^-	[xanthate] sample mg/l	[xanthate] added	xanthate found (mg/l)	Observations
1	10^{-5}	2.0	10^{-3}	2.05	
2	10^{-6}	—	10^{-3}	1.05	after 48 h
3	10^{-6}	—	10^{-3}	0.75	after 96 h

Revue Roumaine de Chimie, 22, 3, 435–441 (1977)

NEW ANALYTICAL APPLICATIONS OF SOME SULPHONAMIDE COMPOUNDS. V*

ARSENIC TRACES DETERMINED WITH SILVER SULPHANILAMIDE

TULIU SIMONESCU and VASILE RUSU
University of Timişoara, The Laboratory for Analytical Chemistry, Strada Pestalozzi 16

Received March 26, 1975

The silver compound of sulphanilamide in alkaline solution is proposed as a reagent for the determination of arsenic microamounts. The method has multiple applications and its errors do not exceed 2%.

It has been well known for a long time that the silver salts in diluted solutions are reduced by arsenic hydride to metallic silver. Although this reaction was studied systematically by different authors in order to apply it for colorimetrical purposes, it has not been achieved yet.

Vašák and Šedivec [1] proposed a solution of silver diethyldithiocarbamate in pyridine as a colour reagent for arsenic, after its previous reduction to arsenic hydride. Bode and Hackmann [2] showed that as a result of this reaction a silver colloidal solution is obtained.

Ciuhandu et al. [3,4] propose for the determination of arsenic the same reduction to arsenic hydride followed by the reaction with the silver compound of *p*-sulphamoylbenzoic acid in strong alkaline solution. From this reaction a silver colloidal solution is obtained whose absorption of light is measured at about 420 nm wavelength. This last method is more sensitive than that of Vašák and Šedivec. As the reagent is sensitive towards hydrogen [5] too, the blank tests have a remarkable absorption of light disturbing thus the precision of the determination, especially when this is achieved on the initial part of the standard curve.

Assuming that the formation of coloured colloidal solutions with arsenic hydride might be also characteristic of other silver compounds of sulphonamides in alkaline medium, we directed our research to obtain a reagent with a great sensitivity towards arsenic hydride but inefficient towards hydrogen.

---

[*] Part IV. T. Simonescu, V. Rusu and L. Kiss., *Rev. Chim. (Bucureşti).*, **26**, 75 (1975).

[1] V. Vašák and V. Šedivec, *Chem. listy.*, **46**, 341 (1952).

[2] H. Bode and K. Hackmann, *Z. analyt. Chem.*, **241**, 18 (1968).

[3] G. Ciuhandu and M. Rocsin, *Z. analyt. Chem.*, **172**, 268 (1960).

[4] G. Ciuhandu, A. Roşcovanu and M. Cuţui, *Chem. analyt.*, **50**, 489 (1968).

[5] G. Ciuhandu and A. Chicu, *Z. phys. Chem. (Leipzig)*, **249**, 133 (1972).

EXPERIMENTAL PART

APPARATUS

The absorption of light of the silver sol was carried out by means of a spectrophotolmeter type "Spekol" made at Carl Zeiss Jena.

Conductometric determinations were performed with a Radelkis Type OK—102 conductometer.

Potentiometric determinations were made with a MV-11 milivoltmeter "Clamann-Grahnert".

The electric charge of the silver sol was determined with an electrophoresis device made at "Electrotehnica" Bucharest.

REAGENTS

2×10^{-2} M silver nitrate (*p. a.* Merck) solution.
2×10^{-2} M sulphanilamide (*p.a.* Austranal-Wien) solution.
10^{-1} M sodium hydroxide (*p.a.* Chemapol) solution.
Hydrocloric acid containing stannous chloride. Dissolve 1 gram $SnCl_2.2H_2O$ in 100 ml of hydrochloric acid not less than 32 — 34 % (p.a. U.C.B.).
Potassium iodide (*p.a.* "Reactivul" Bucharest) 12% solution.
Lead acetate (*p.a.*Merck) 10% solution.
Zinc filings (*p.a.* Carlo Erba).
Standard arsenic (As_2O_3 *p.a.* Merck) solution containing 100 μg As/ml.
The reagent is prepared on need by mixing equal volumes of 2×10^{-2} M silver nitrate with 2×10^{-2}M sulphanilamide. After homogenization a volume of 10^{-1} M sodium hydroxide is added. The reagent has to be colourless and perfectly clear.

RESULTS AND DISCUSSION

THE REACTION OF SILVER NITRATE WITH SULPHANILAMIDE

Potentiometric and conductometric studies of the reaction of silver nitrate with sulphanilamide were carried out. By titrating a 2×10^{-2} M silver nitrate solution, conductometrically or potentiometrically with a 2×10^{-2}M sulphanilamide solution, the titration curves indicate a slight interaction of these two compounds. The reaction might be formulated as follows:

$$AgNO_3 + H_2N-SO_2-C_6H_4-NH_2 \rightleftharpoons AgHN-SO_2-C_6H_4-NH_2 + HNO_3 \quad (1)$$

The shifting of the equilibrium to the left is due to the fact that under these conditions sulphanilamide undergoes a very slight dissociation. By adding an equimolecular mixture of silver nitrate and sulphanilamide with sodium hydroxide, the equilibrium is shifted to the right due to the deprotonation reactions of the sulphanilamide. In figures 1 and 2 the potentiometric (silver indicating electrode) and conductometric titrations curves are plotted, for an equimolecular mixture of silver nitrate and sulphanilamide with sodium hydroxide.

The potentiometric curve shows a well-marked jump coresponding to the addition of an equivalent of sodium hydroxide, and a less marked jump corresponding to the interaction with two equivalents of sodium hydroxide. The conductometric curve plotted in figure 2 explains doubtlessly the existence of two stages when sodium hydroxide is added.

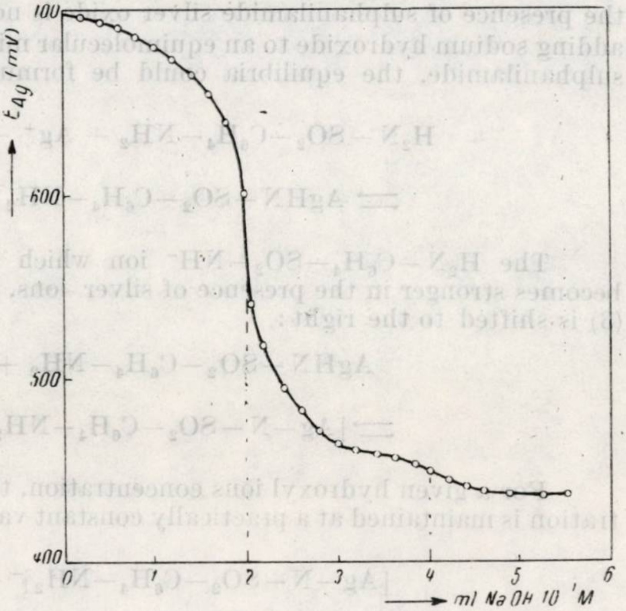

Fig. 1. — Silver electrode potential (E_{Ag}) in milivolts, at the titration of 20 ml 1 : 1 mixture of 2×10^{-2} M silver nitrate and 2×10^{-2}M sulphanilamide with 10^{-1} M sodium hydroxide.

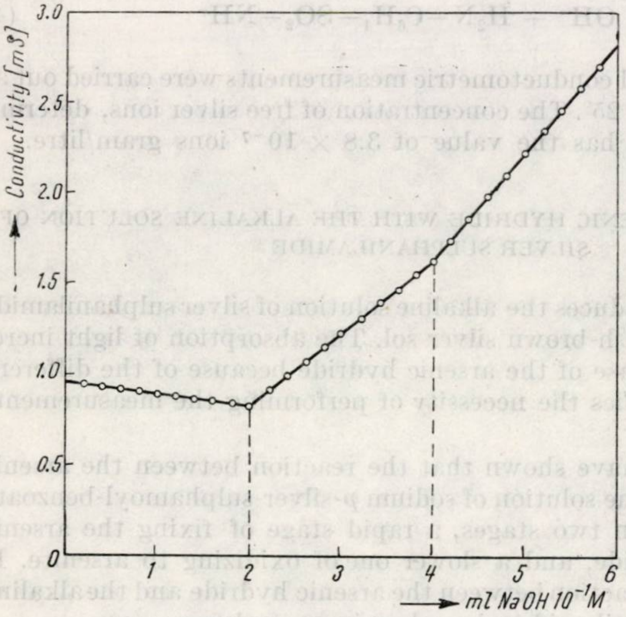

Fig. 2. — Conductivity (mS) at the titration of 20 ml 1 : 1 mixture of 2×10^{-2} M silver nitrate and 2×10^{-2} M sulphanilamide with 10^{-1} M sodium hydroxide.

As it results from the potentiometric curve when the equimolecular mixture of silver nitrate and sulphanilamide is alkalized, the concentration of the free silver ions in solution lowers very much. We mention that in the presence of sulphanilamide silver oxide is not formed. In the case of adding sodium hydroxide to an equimolecular mixture of silver nitrate and sulphanilamide, the equilibria could be formulated as follows:

$$H_2N-SO_2-C_6H_4-NH_2 + Ag^+ + OH^- \rightleftharpoons$$

$$\rightleftharpoons AgHN-SO_2-C_6H_4-NH_2 + H_2O \qquad (2)$$

The $H_2N-C_6H_4-SO_2-NH^-$ ion which is a weak anionic acid becomes stronger in the presence of silver ions, and thus the equilibrium (3) is shifted to the right:

$$AgHN-SO_2-C_6H_4-NH_2 + OH^- \rightleftharpoons$$

$$\rightleftharpoons [Ag-N-SO_2-C_6H_4-NH_2]^- + H_2O \qquad (3)$$

For a given hydroxyl ions concentration, the free silver ions concentration is maintained at a practically constant value by the equilibrium(4):

$$[Ag-N-SO_2-C_6H_4-NH_2]^- + H_2O \rightleftharpoons$$

$$Ag^+ + OH^- + H_2N-C_6H_4-SO_2-NH^- \qquad (4)$$

Potentiometric and conductometric measurements were carried out at constant temperature of 25°. The concentration of free silver ions, determined potentiometrically, has the value of 3.8×10^{-7} ions gram/litre.

THE REACTION OF ARSENIC HYDRIDE WITH THE ALKALINE SOLUTION OF SILVER SULPHANILAMIDE

Arsenic hydride reduces the alkaline solution of silver sulphanilamide giving a yellow to reddish-brown silver sol. The absorption of light increases even after the release of the arsenic hydride because of the different reaction rate. This implies the necessity of performing the measurements at a standard time.

Ciuhandu et al.[4] have shown that the reaction between the arsenic hydride and the alkaline solution of sodium *p*-silver-sulphamoyl-benzoate takes place up to 30° in two stages, a rapid stage of fixing the arsenic hydride as silver arsenide, and a slower one of oxidizing to arsenite. It is very likely that the reaction between the arsenic hydride and the alkaline solution of silver sulphanilamide takes place in an analogous way.

The negative charge of the silver sol was established by electrophoresis.

DETERMINATION OF ARSENIC MICROAMOUNTS

TECHNIQUE

A 10 ml sample containing 0.05 to 8 μg As/ml is introduced into a reagent tube, then 1 ml of potassium iodide solution and 2 ml of hydrochloric acid are added. After 15 minutes, 1 g of zinc fillings is added and the tube is closed with a rubber stopper through which a glass tube ending with a capillary reaches the bottom of a narrow tube containing 4 ml of alkaline silver sulphanilamide solution.

Hydrogen sulphide eventually present is retained by a filter paper pad impregnated with lead acetate. The experimental device used [4] allows the thermostatic control of the reagent.

For a fluid height of at least 100 mm a quantitative absorption of arsenic hydride takes place. Reaction duration is of an hour from the moment the zinc was added.

RESULTS

Under the experimental conditions proposed, a complete absorption of arsenic hydride by the silver sulphanilamide reagent can be achieved. The absorption of light was measured at 400 nm wavelength, the absorption peak for the sol as it results from figure 3.

As the oxidizing reactions take place in various stages and with different speeds, it implies that the measurements should be performed at a well-determined moment. The standard curves obtained in the given conditions are plotted in figure 4. Within an hour arsenic is completely reduced to arsenic hydride.

As blank test the reagent solution is used after its previous bubbling with hydrogen resulted from zinc and hydrochloric acid under the same conditions with the other tests. Thus, errors caused by arsenic eventually present in the reagents, as well as those caused by hydrogen reduction of the reagent could not appear.

The five standard curves yielded the following molar extinction coefficients; $\varepsilon_1 = 1.64 \times 10^4$ l/mole × cm., $\varepsilon_2 = 1.94 \times 10^4$ l/mole × cm., $\varepsilon_3 = 2.54 \times 10^4$ l/mole × cm., $\varepsilon_4 = 3.12 \times 10^4$ l/mole × cm., $\varepsilon_5 = 4.16 \times 10^4$ l/mole × cm.

The method proposed has a good reproducibility as it results from the data in table 1.

If the solution to be analysed contains reducible anions or other compounds which can interfere, like phosphides, sulphides or thiosulphates, it is recommended to remove them by a previous vaporization with sulphuric acid. Antimony must not be present because with the reagent it behaves just like arsenic.

The alkaline solution of silver sulphanilamide is very well fitted for the determination of arsenic. It allows an enlargement of the application range of silver sulphonamide compounds in micro-analysis. Arsenic concentrations in 0.05 to 8 μg/ml range can be determined with errors not exceeding 2%.

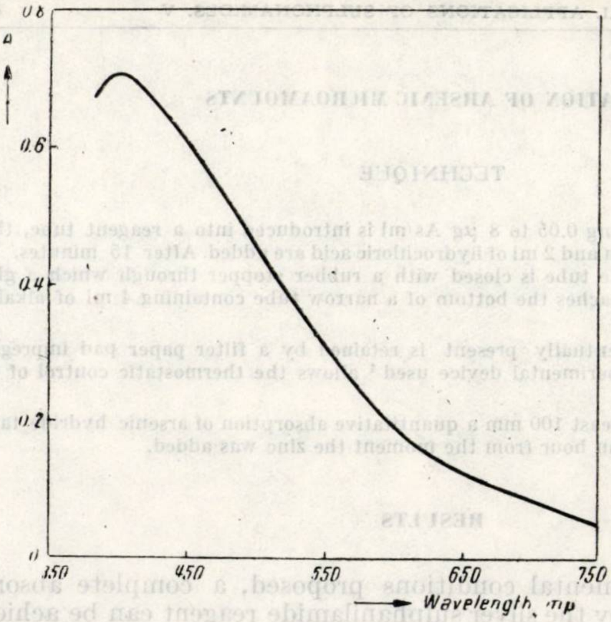

Fig. 3. — Absorption of light (*A* — absorbance modulus) of the silver sol plotted versus wavelength.

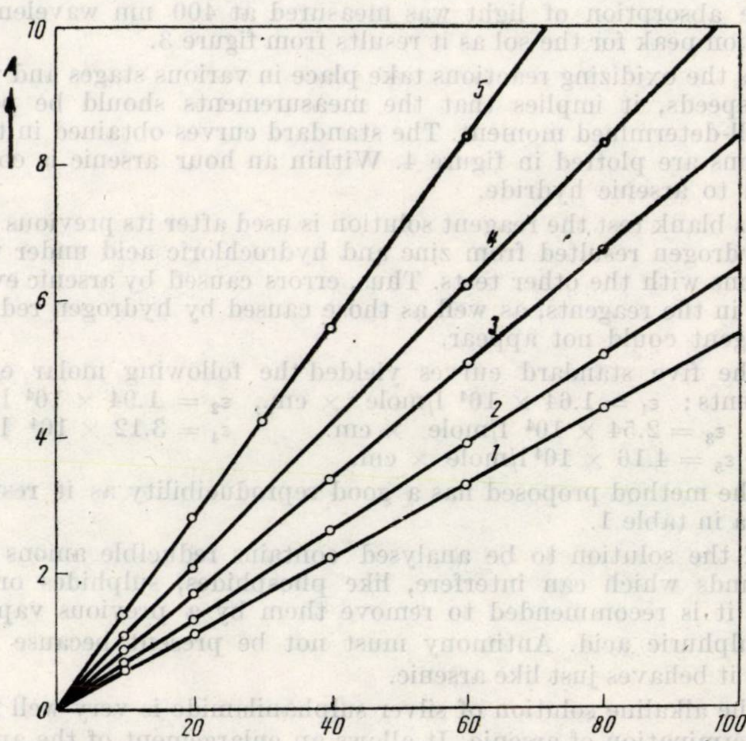

Fig. 4. — Standard curves for the determination of arsenic (A-absorbance modulus).

1, Reducing duration 60 minutes. Reagent temperature 15°. Instant photometry. *2*, Reducing duration 30 minutes. Reagent temperature 25°. Instant photometry. *3*, Reducing duration 60 minutes. Reagent temperature 25°. Instant photometry. *4*, Reducing duration 60 minutes. Reagent temperature 25°. Photometry after 60 minutes from the end of reduction. *5*, Reducing duration 60 minutes. Reagent temperature 35°. Instant photometry.

The method proposed might find application in the determination of microamounts of arsenic in biological material, petrol products, food, toxic gases, chemical products, sewage as well as for other purposes.

Table 1

Results of checking determinations on samples known contents of 20 μg As
($\overline{X}$ = 19.97 μg As., s = 2.1×10^{-1}, $s_{\overline{X}} = 8.5 \times 10^{-2}$)

μg As found in sample	Deviation in μg	Error %
20.24	+0.24	+1.2
20.24	+0.24	+1.2
19.6	−0.4	−2
19.6	−0.4	−2
19.76	−0.24	−1.2
19.80	−0.2	−1
19.95	−0.05	−0.25
19.95	−0.05	−0.25
20.3	+0.3	+1.5
20.3	+0.3	+1.5

Revue Roumaine de Chimie, 22, 3, 443–449 (1977)

STUDIES ON THE ELECTRO-ANALYTICAL BEHAVIOUR OF MEMBRANE-ELECTRODES UNDER CURRENT. VI*

POTENTIOMETRY AT CONTINUOUS AND CONSTANT CURRENT USING A Hg/AgI-Ag$_2$S MEMBRANE-ELECTRODE

I. C. POPESCU and MARIANA HĂLĂLĂU
Chair of Analytical Chemistry, "Babeş-Bolyai" University, Str. Arany J. Nr. 11, Cluj-Napoca, Romania

Received April 1, 1975

The paper includes a preliminary study devoted to the effect of a continuous and constant electric current upon electrodic functions $E - pAg$ and $E - pI$ and also upon the end point of Ag$^+$ ion with I$^-$ ion titration, achieved with a I$^-$ selective membrane-electrode (Hg/AgI $-$ Ag$_2$S). It has been found that, in the investigated field of intensities of external polarization (0.3 $-$ 3 μA) the utilized indicator system metal-membrane-solution behaves quasi-reversibly and the improvement effect of the end point indication fails to appear. An explicative hypothesis has been formulated based on the interpretation of cyclic voltamograms recorded in solutions of various compositions.

Investigations carried out with regard to the behaviour of membrane-electrodes under current[1–6] have shown that under the influence of an appropriately selected external electric polarization the electrodic functions and, implicitly, the titration curves corresponding to the studied membrane-electrodes (membrane-electrode of parchment impregnated with BaSO$_4$[1–3,6] membrane-electrode of Ag$_2$S[4,6] and membrane-electrode of plastifier PVC [5]) are profoundly modified. As a result, an effect appears of a clear improvement of the indication of the end point of titrations conducted, effect proved to be generated by the appearance of a concentration polarization in the liquid layer adhering to membrane.[4]

In this context, extending the field of investigated membrane-electrodes, the present paper has studied a I$^-$ — selective membrane-electrode achieved in the constructive variant metal-membrane-solution. The electrode in question was used in zero and non-zero current potentio-

---

[*] Part. V : E. HOPÎRTEAN and C. LITEANU, *Rev. Roumaine Chim.*, **19**, 145 (1974).

[1] C. LITEANU and I. C. POPESCU, *Rev. Roumaine Chim.*, **18**, 319 (1973).
[2] C. LITEANU, I. C. POPESCU and M. PREDA, *Rev. Roumaine Chim.*, **18**, 1811 (1973)
[3] I. C. POPESCU, C. LITEANU and M. PREDA, *Rev. Roumaine Chim.*, **18**, 1819 (1973)
[4] I. C. POPESCU, C. LITEANU and L. SAVICI, *Rev. Roumaine Chim.*, **18**, 1983 (1973)
[5] E. HOPÎRTEAN and C. LITEANU, *Rev. Roumaine Chim.*, **19**, 145 (1974).
[6] C. LITEANU, I. C. POPESCU and E. HOPÎRTEAN, "Ion Selective Electrodes, Symposium", 1972, ed. by E. Pungor, Akad. Kiadó, Budapest, 1973, p. 51.

metric measurements and the behaviour found was explained and proved by means of cyclic voltamograms recorded in solutions of various compositions.

EXPERIMENTAL

PROCEDURE FOR OBTAINING I^- — SELECTIVE MEMBRANE-ELECTRODE

I^-— selective membrane-electrodes used, whose construction was previously described,[7] were achieved by pressing an $AgI - Ag_2S$ mixture.[8] Electrodes thus obtained, having membranes of various AgI/Ag_2S compositions were tested as I^- — selective electrodes, by measuring the emf of the cell:

$$\text{ESC} \left\| \begin{array}{l} \text{Salt bridge} \\ \text{KNO}_3\ 10^{-1}\text{M agar-agar} \end{array} \right\| \text{Test solution} \left| \begin{array}{l} \text{Membrane} \\ \text{AgI}-\text{Ag}_2\text{S} \end{array} \right| \text{Hg, Cu} \qquad (1)$$

As test solutions we used KI solutions obtained by dilution from a KI 10^{-1} M stock solution prepared by weighing. Results obtained at variable or constant ionic strength ($J = 10^{-1}$ M KNO_3) ranging within a field of concentrations 10^{-1}— 10^{-6} M (room temperature, magnetic stirring) are presented in table 1.

Table 1

The influence of membrane composition upon the $E-p$I electrode function

Molar percent AgI	Linearity domain		Slope		$\dfrac{\Delta E/\Delta pI}{2{,}3\ RT/F} - 1$ (%)	
	J = var.	J = 1 M	J = var.	J = 1 M	J = var.	J = 1 M
100	$10^{-1} - 10^{-5}$	$10^{-2} - 10^{-6}$	48.7	58.2	−17.6	−1.5
90.5	$10^{-1} - 10^{-6}$	$10^{-2} - 10^{-6}$	44.8	60.1	−24.2	+1.7
80.8	$10^{-1} - 10^{-6}$	$10^{-2} - 10^{-6}$	41.4	—	−29.9	—
71.1	$10^{-1} - 10^{-5}$	$10^{-1} - 10^{-6}$	53.3	53.0	−9.8	−10.3
65.3	$10^{-1} - 10^{-5}$	$10^{-2} - 10^{-6}$	73.8	63.2	+24.9	+6.9
56.3	$10^{-2} - 10^{-6}$	$10^{-2} - 10^{-5}$	60.6	62.8	+2.5	+6.3
41.3	$10^{-1} - 10^{-5}$	$10^{-2} - 10^{-6}$	53.8	59.3	− 8.9	+0.3
31.1	$10^{-3} - 10^{-6}$	$10^{-2} - 10^{-6}$	87.4	61.6	+47.9	+4.2

Since membrane-electrodes of AgI/Ag_2S composition approximately corresponding to the 1 : 1 ratio present minimal deviations from the nernstian value of the slope of the electrodic function $E - p$I (table 1, column 7), further use was made of a membrane-electrode achieved of an equimolar mixture of $AgI - Ag_2S$. The electrode functions $E - p$I and $E - p$Ag corresponding to it are presented in figure 1.

BEHAVIOUR OF THE I^- — SELECTIVE MEMBRANE-ELECTRODE UNDER CURRENT

Using the assembly of fig. 2, it was possible to establish the electrodic functions $E - p$Ag and $E - p$I at various intensities of cathodic polarization. Results obtained are plotted in figure 3.

---

[7] I. C. Popescu and C. Liteanu, *Rev. Roumaine Chim.*, **17**, 1629 (1972).

[8] Orion Research Inc., Brit. Patent 1,150, 698 (1969).

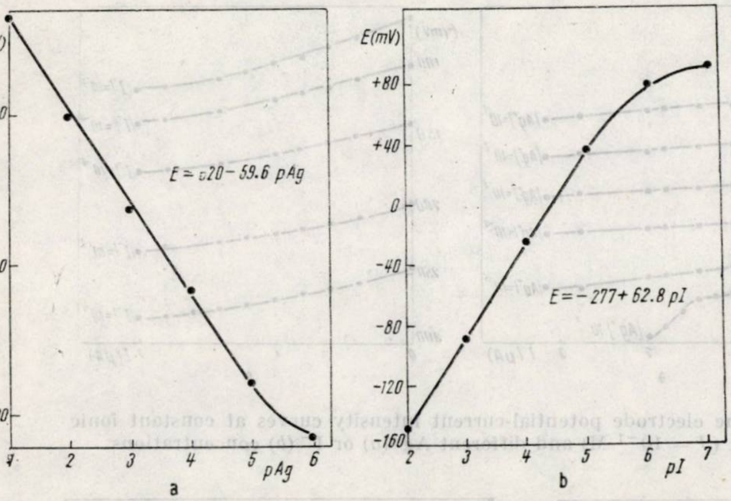

Fig. 1. — The $E - p\text{Ag}$ (a) and $E - p\text{I}$ (b) electrode functions ($J = 10^{-1}$ M).

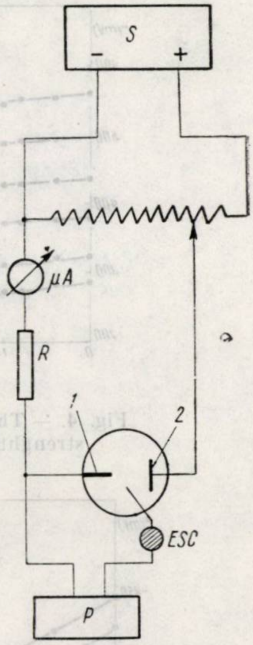

Fig. 2. — The used assembly for potentiometric measurements at non-zero current. *1*, membrane-electrode; *2*, counter-electrode; S = d.c. source; *P*-electronic potentiometer; *R*-660 KΩ rezistance.

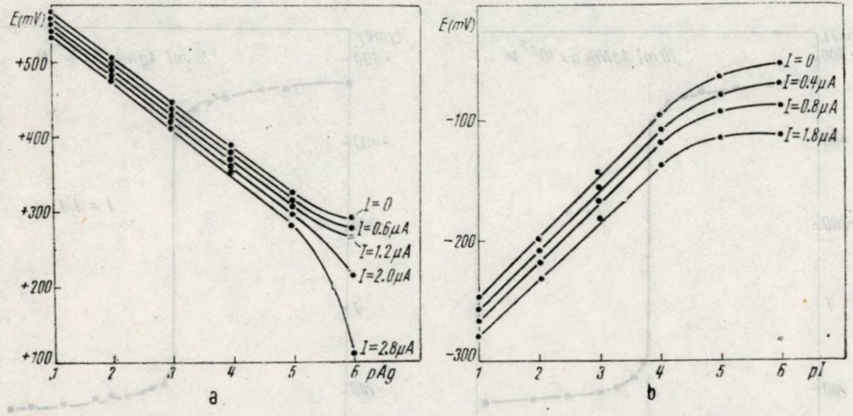

Fig. 3. — The $E - p\text{Ag}(a)$ and $E - p\text{I}$ (b) electrode functions at different intensities of cathodic polarization ($J = 10^{-1}$ M).

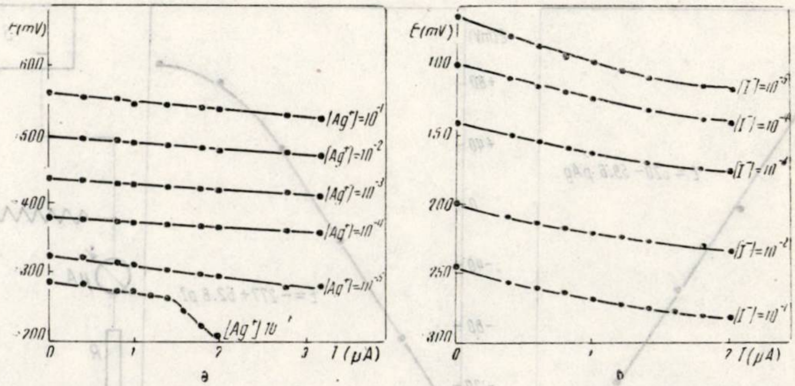

Fig. 4. — The electrode potential-current intensity curves at constant ionic strenght ($J = 10^{-1}$ M) and different Ag^+(*a*) or I^- (*b*) concentrations.

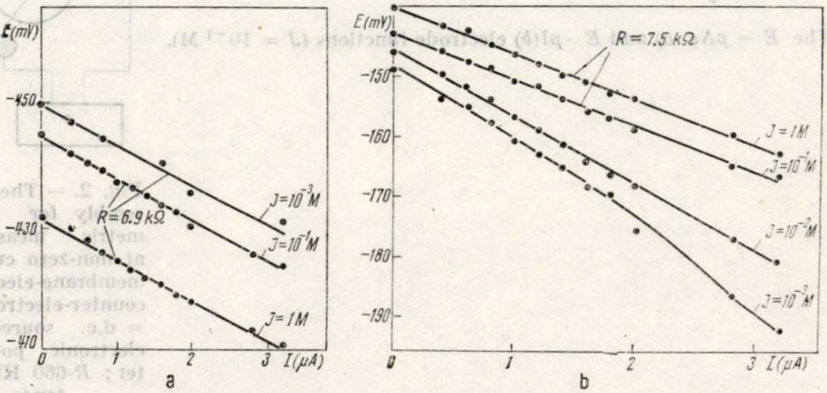

Fig. 5. — The electrode potential-current intensity curves at different ionic strenghts and fixed concentration (10^{-3} M) of Ag^+ (*a*), or I^- (*b*).

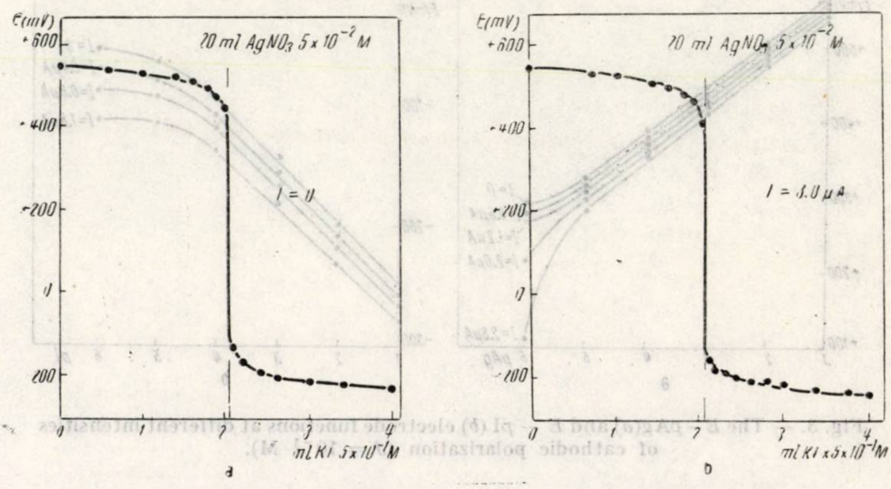

Fig. 6. — The 5×10^{-2} M $AgNO_3$ with 5×10^{-1} M KI titration at zero (*a*) and nonzero current (*b*) (cathodic polarization).

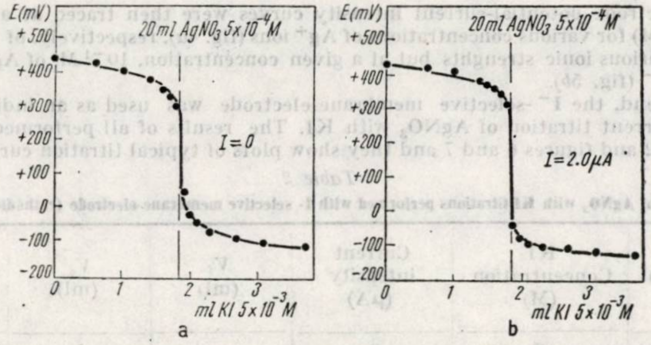

Fig. 7. — The 5×10^{-4}M $AgNO_3$ with 5×10^{-3}M KI titration at zero (*a*) and nonzero current (*b*) (cathodic polarization).

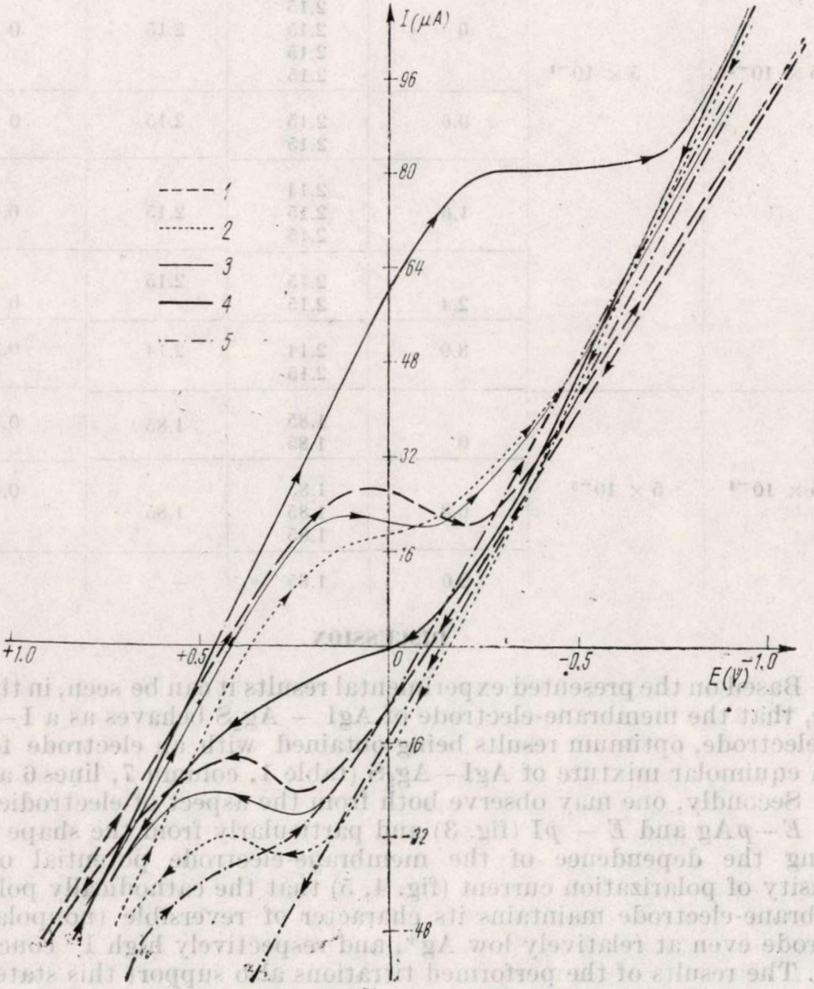

Fig. 8. — The cyclic voltammogrames for I^--selective membrane electrodes. *1*, 10^{-1} M KNO_3; *2*, 10^{-1} M KNO_3 after O_2 remove; *3*, 10^{-1} M KNO_3, 10^{-1}M HNO_3; *4*, 10^{-1} M KNO_3, 10^{-3} M $AgNO_3$; *5*, 10^{-1} M KNO_3, 10^{-3} M KI.

The electrode potential-current intensity curves were then traced at a constant ionic strength (10^{-1}M) for various concentrations of Ag^+ ions (fig. 4*a*), respectively, of I^- ions (fig. 4*b*) as well as at various ionic strenghts but at a given concentration, 10^{-1} M, of Ag^+ (fig. 5*a*), respectively of I^- (fig. 5*b*).

At the end, the I^--selective membrane-electrode was used as an indicator electrode in non-zero current titration of $AgNO_3$ with KI. The results of all performed titrations are listed in table 2 and figures 6 and 7 and they show plots of typical titration curves.

Table 2

The results of $AgNO_3$ with KI titrations performed with I- selective membrane-electrode (cathodic polarization)

$AgNO_3$ Concentration (M)	KI Concentration (M)	Current intensity (μA)	V_i (ml)	$\overline{V_i}$ (ml)	$^s\overline{V_i}/\overline{V_i}$ (%)
1	2	3	4	5	6
5×10^{-2}	5×10^{-1}	0	2.15 2.15 2.15 2.15 2.15	2.15	0
		0.6	2.15 2.15	2.15	0
		1.6	2.14 2.15 2.15	2.15	0.1
		2.4	2.15 2.15	2.15	0
		3.0	2.14 2.15	2.14	0.2
5×10^{-4}	5×10^{-3}	0	1.85 1.85	1.85	0.1
		0.8	1.85 1.85 1.85	1.85	0.1
		2.0	1.85	—	—

DISCUSSION

Based on the presented experimental results it can be seen, in the first place, that the membrane-electrode of AgI — Ag_2S behaves as a I—selective electrode, optimum results being obtained with an electrode formed of an equimolar mixture of AgI—Ag_2S (table 1, column 7, lines 6 and 7).

Secondly, one may observe both from the aspect of electrodic functions $E-p$Ag and $E-p$I (fig. 3) and particularly from the shape representing the dependence of the membrane-electrode potential on the intensity of polarization current (fig. 4, 5) that the cathodically polarized membrane-electrode maintains its character of reversible (nonpolarized) electrode even at relatively low Ag^+, and respectively high I^- concentrations. The results of the performed titrations also support this statement. Thus, one may observe (fig. 6,7) that in the investigated field of cathodic polarization intensities, the shape and even the position of titration curves are independent of the intensity value of the polarization current.

Based on the above, we may conclude that, apparently, the behaviour under current of the membrane-electrode of $AgI-Ag_2S$ negates our previous investigations [4] with regard to the membrane-electrode formed of Ag_2S. Thus, although the investigated field of cathodic polarization intensities was approximately the same in both situations, yet, in the case of the membrane-electrode of $AgI-Ag_2S$ the concentration polarization was not found to appear and consequently the improvement effect of the end-point indication was not revealed either, not even in the case of titration of some $AgNO_3$ solutions having a much lower concentration (fig. 7 and fig. 4 of note [4]).

In order to be able to explain this (apparent) contradiction it is necessary to examine the manner in which the existing difference in the structure of the two compared electrochimical systems are reflected in their operation under current. First, it is obvious that the different nature of electrodic materials cannot be the cause of the difference found in their behaviour. Indeed it is known that silver sulphide [9] as well as silver iodide[10] present a marked ionic conductibility at room temperature, accompanied by the possibility of an electronic conduction, particularly in the case of silver sulphide. Second, the fact is known that the weight with which each of the two types of conduction mechanism participates in the achievement of the global charge transfer through the membrane is strongly influenced by the type of conduction through the phases adjacent to the membrane.[11,12] Therefore, in the case of the electrochemical system $Hg/AgI-Ag_2S$ solution, used in achieving the I^--selective membrane-electrode, the electronic conduction mechanism is expected to be favoured by the presence of an electronic conductor (Hg) in direct contact with the membrane.

This assumption was checked by recording the cyclic voltamograms (0.5 V/min, unstirred solution) of the I^--selective membrane-electrode located in the electrochemical cell (*1*). An examination of curves obtained (fig. 8) shows that, under the influence of a cathodic external polarization Ag^+ ions present in solution are the first involved in the transport process of electric charges through the membrane-solution interface. But in the absence of Ag^+ ions (fig. 8, curve *5*) or, in general, as a result of some external polarizations exceeding the value of the limit current corresponding to the reduction of Ag^+ ions (ascending branches of curves *1*—*5* of fig. 5) other chemical species (H^+ ions, impurities) are immediately involved in the electrode reaction so that in practice the membrane-electrode will not polarize.

In conclusion, based on experimental data reported in this paper, one may state that, due to depolarization possibilities by redox-type reactions, possibilities generated by the presence of an electronic conductor in direct contact with the membrane, the electrochemical system metal-ion selective membrane-solution fails to permit the occurrence of the improvement effect of the end of titration indication, effect found in the case of the system solution-ion selective membrane-solution.

[9] M. H. Hebb, *J. Chem. Phys.*, **20**, 185 (1962).

[10] C. Tubandt, *Handbuch Exp. Phys.*, **12**, 383 (1932).

[11] K. S. Fletcher, III and R. T. Mannion, *Analyt. Chem.*, **42**, 287 (1970).

[12] J. W. Ross, Jr., *Orion Research Inc. Newsletter*, **1**, 12 (1969).

Revue Roumaine de Chimie, **22**, 3, 451–457 (1977)

REACTIONS OF COORDINATED LIGANDS. X[1]

ALUMINUMORGANIC COMPOUNDS OF SALICYLALDOXIME WITH Ni(II), Pd(II) AND Cu(II) IONS AND THEIR ADDUCTS WITH NITROGEN LEWIS BASES

N. VOICULESCU

Institute of Macromolecular Chemistry "P. Poni", Aleea Grigore Ghica Vodă, N⁰ 41 A, Jassy

Received February 22, 1975

Chloroaluminum organic compounds of coordinated salicylaldoxime resulted from the reaction of Ni(II), Pd(II) and Cu(II) bissalicylaldoximates with diethylaluminum chloride were isolated under the form of coloured powders and characterized by chemical analyses, IR absorption spectra, X ray diffraction spectra and magnetic measurements. Substitution of O–H ...O bonds in chelates by O–Al–O aluminum bridges determines the closure of pentaatomic metallocycle M–O–Al–O–N without carbon atoms. Among amine-containing adducts of aluminum organic derivatives of coordinated salicylaldoxime only those with pyridine were isolated and characterized. Since the adducts of nickel derivative with four pyridine molecules and of copper derivative with three molecules are crystalline and paramagnetic, they depart from the general chemical behaviour of aluminumorganic derivatives of coordinated salicylaldoxime.

Free [2] and coordinated [3–5] salicylaldoxime with Ni(II), Pd(II) and Cu(II) ions proved capable of giving substitution reactions with a series of aluminumorganic [2–4] and zincorganic [5] compounds. Studies made on the reaction products have revealed that both in the case of salicylaldoxime and of dimethyl[6–8] and diphenylglyoxime [1,9] reaction products result from the substitution of O–H. . . O hydrogen bridges existing in such compounds, by O–Al–O aluminum bridges or O–Zn–O zinc bridges.

Aluminumorganic compounds of salicylaldoxime [3,4] resulted from the reaction of Ni(II), Pd(II) and Cu(II) bissalicylaldoximates with triphenylaluminum and triisobutylaluminum correspond to formula I. Introducing AlX_2 groups into the molecule of Ni(II), Pd(II) and Cu(II) bissalicylaldoximates the behaviour of the ligand as well as that of the central metallic ion was found to change.[2] Among others, the coordination capacity of bissalicylaldoximates, particularly of nickel [10–12] is modified in that Lewis bases are bound to aluminumorganic derivatives of coordinated salicylaldoxime at the aluminum atom [8] rather than at the central metallic ion.

---

[1] N. Voiculescu, *Rev. Roumaine Chim.*, **22**, 2, 237 (1977).

[2] N. Voiculescu, *Rev. Roumaine Chim.*, **18**, 1919 (1973).

[3] N. Voiculescu, I. Popescu and N. Luchian, *Rev. Roumaine Chim.*, **18**, 1601 (1973).

[4] N. Voiculescu and I. Popescu, *Rev. Roumaine Chim.*, **18**, 1911 (1973).

[5] N. Voiculescu, L. Roman and I. Popescu, *Rev. Roumaine Chim.*, **20**, 7, 945 (1975).

[6] N. Voiculescu and I. Popescu, *Rev. Roumaine Chim.*, **17**, 719 (1972).

[7] N. Voiculescu, I. Popescu and L. Roman, *Rev. Roumaine Chim.*, **18**, 1595 (1973).

[8] N. Voiculescu, A. Airinei and I. Popescu, *Rev. Roumaine Chim.*, **19**, 399 (1974).

[9] N. Voiculescu, *Rev. Roumaine Chim.*, **20**, 8, 1071 (1975).

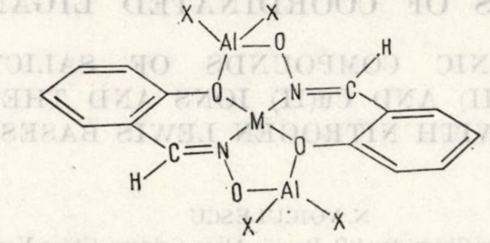

$X = iC_4H_9,\ C_6H_5;\ M = Ni,\ Pd\ Cu$

In this paper we report chloroaluminum organic compounds resulted from the reaction of Ni(II), Pd(II) and Cu(II) bissalicylaldoximates with diethylaluminum chloride and their amine-containing adducts. All compounds reported in this paper were isolated under the form of solid coloured powders and were characterized by chemical analyses, IR absorption spectra, X ray diffraction spectra and magnetic properties. The presence of C_2H_5 radicals in the synthesized products was verified by ^1H nmr.

EXPERIMENTAL

Ni(II), Pd(II) and Cu(II) bissalicylaldoximates were prepared according to the methods reported in the literature[13–15] and purified by recrystallization from chloroform.

Solvents used as reaction medium and as washing agents were distilled on metallic sodium in presence of benzophenone as anhydrization identification agent.

$Ni(C_7H_5O_2N)_2Al_2(C_2H_5)_2Cl_2$ was obtained by adding diethylaluminum chloride to Ni(II) bissalicylaldoximate suspension in petroleum ether in a 2 : 1 molar ratio. The reaction vessel was cooled with solid carbon dioxide. It was stirred for a few hours. The solid compound was allowed to settle. The liquid fraction was removed by decanting. It was repeatedly washed with petroleum ether and vacuum-dried.

$Pd(C_7H_5O_2N)_2Al_2(C_2H_5)_2Cl_2$ was prepared as in the case of the nickel derivative.

$Cu(C_7H_5O_2N)_2Al_2(C_2H_5)_2Cl_2$. Diethylaluminum chloride was added to copper bissalicylaldoximate suspended in petroleum ether in a 1 : 2 molar ratio. The reaction vessel was cooled with solid carbon dioxide. After approx. 12 hr of constant stirring, a solid grey product and a green liquid were formed. After removal of the liquid fraction, it was repeatedly washed with petroleum ether and vacuum-dried.

$Ni(C_7H_5O_2N)_2Al_2(C_2H_5)_2Cl_2.4Py$. Dry pyridine in excess was added to the aluminumorganic derivative with nickel obtained by the above described method. The reaction occurred immediately with a weak heat release. A blue powder deposited after a few hours of stirring at room temperature. The solid product was separated, repeatedly washed with petroleum ether end vacuum-dried.

$Pd(C_7H_5O_2N)_2Al_2(C_2H_5)_2Cl_2.2Py$ was obtained by adding pyridine in excess to the aluminumorganic derivative. The solid product was converted to solution a few minutes after mixing the reactants. The amine excess was removed in vacuum. A solid powder was obtained whose colour slightly differed from that of the aluminumorganic derivative.

---

[10] I. Csaszar and I. Szeghalmi, *Acta Univ. Szeged., Acta Phys. Chem.*, **12**, 117 (1966).

[11] M. Robtelsky and E. Iungreis, *J. Inorg. Nuclear Chem.*, **3**, 38 (1956).

[12] F. Maggio, V. Romano, T. Pizzino and L. Pellerito, *Ann. Chim.(Ital.).*, **58**, 725 (1968).

Table 1

Analyses and characteristics of the synthetized products

Compound	Colour	Magnetic characteristics	Analyses					
			C Calcd. Found %	H Calcd. Found %	Al. Calcd. Found %	N Calcd. Found %	Cl Calcd. Found	M Calcd. Found %
$Ni(C_7H_5O_2N)_2Al_2(C_2H_5)_2Cl_2$	yellow	diamagnetic	42.18	3.90	10.54	5.46	13.86	11.52
			41.80	3.85	10.60	5.45	13.75	11.40
$Pd(C_7H_5O_2N)_2Al_2(C_2H_5)_2Cl_2$	brown	diamagnetic	38.57	3.57	9.64	4.96	12.67	19.10
			38.05	3.57	9.80	4.85	12.45	18.70
$Cu(C_7H_5O_2N)_2Al_2(C_2H_5)_2Cl_2$	green	paramagnetic	41.77	3.86	10.44	5.41	13.73	12.37
			41.10	3.85	10.55	5.30	13.65	12.20
$Ni(C_7H_5O_2N)_2Al_2(C_2H_5)_2Cl_2.4Py$	blue	paramagnetic	55.07	4.83	6.52	10.14	8.57	7.12
			54.50	4.80	6.75	10.10	8.45	7.03
$Pd(C_7H_5O_2N)_2Al_2(C_2H_5)_2Cl_2.2Py$	brown	diamagnetic	46.79	4.17	7.52	7.79	9.88	14.90
			46.02	4.15	7.63	7.60	9.83	14.87
$Cu(C_7H_5O_2N)_2Al_2(C_2H_5)_2Cl_2.3Py$	blue-greenish	paramagnetic	52.51	4.64	7.59	9.28	9.41	8.48
			52.03	4.52	7.58	9.26	9.33	8.43

$Cu(C_7H_5O_2N)_2Al_2(C_2H_5)_2Cl_2.3Py$. Pyridine in excess was added to the aluminumorganic derivative prepared as above, stirring until the solid product was totally converted to solution. After a few days, nicely coloured blue-azure crystalline agglomerates deposited on the walls of the vessel. Crystals were isolated and vacuum-dried.

Chemical analyses of the synthesized products are presented in table 1.

Reactants and reaction products were worked up in an inert and dry atmosphere.

IR absorption spectra for the 3600 – 650 cm^{-1} range were recorded on a Unicam SP 200 apparatus. Samples were pelletted in KBr.

X ray diffraction spectra were obtained by the powder method on a TUR M 60 apparatus using CuK_α radiation and nickel filter. Samples were exposed in glass capillaries at 40 kV and 12 mA.

The magnetic properties of compounds reported in this paper were verified on a Gouy balance in nonhomogeneous magnetic field.

The presence of C_2H_5 radicals in the synthesized compounds was revealed on a JEOL JNM 60 HL spectrometer working with 60 MHZ at room temperature.

DISCUSSION

The formation of aluminumorganic compounds resulted from the reaction of diethylaluminum chloride with Ni(II), Pd(II) and Cu(II) bissalicylaldoximates may be described by the following equation:

$$M(II)\ (C_7H_6O_2N)_2 + 2Al(C_2H_5)_2Cl\ -$$

$$M(C_7H_5O_2N)_2Al_2(C_2H_5)_2Cl_2 + 2C_2H_6$$

M = Ni, Pd, Cu

The mechanism producing chloroaluminumorganic compounds of Ni(II), Pd(II) and Cu(II) bissalicylaldoximates is probably a two-step reaction. The first step involves the formation of an addition compound between chelate and two diethylaluminum chloride molecules with hydrogen release from O–H · · ·O bridges. The second step involves the elimination of two ethane molecules and the closure of the M–O–Al–O–N pentaatomic metallocycles (form II).

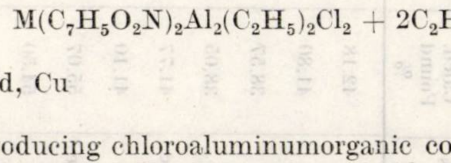

M = Ni, Pd, Cu

Aluminumorganic compounds and pyridine-containing adducts exhibited in table 1 were isolated under the form of coloured powders insoluble in liquid hydrocarbons and unstable to water, acids and bases. The reaction course and the physico-chemical behaviour of reaction products is somehow similar to that found in the case of other aluminumorganic derivatives of coordinated salicylaldoxime.[3,5] However there are a few exceptions in their behaviour which will be further discussed. The common property of aluminumorganic derivatives of coordinated oximes to form adducts with a series of amines presents some particularities with regard to the bonding manner and to the number of bound molecules. Nickel and copper derivatives display the most different behaviour. The aluminumorganic derivative with nickel binds four pyridine molecules, and the derivative with copper three (see table 1). The bonding of three pyridine molecules in the case of the aluminumorganic derivative with copper seems surprising only compared to other aluminumorganic derivatives. However, taking into account the divalent state of copper in the derivative with $Al(C_2H_5)$ Cl groups, the bonding of the three pyridine molecules seems no more surprising since two molecules are bound to the aluminum atoms and the third one to the central metallic ion. This situation does not contradict the data from the literature and also proves that copper has maintained its valence two and the ability to form pentacoordinated derivatives [16,17] (formula III).

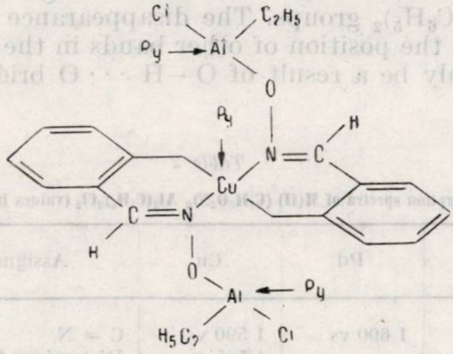

The bonding of the third amine molecule results from the pairing of the dz_2 orbital of copper (II) with the p orbital of the donor atom.

The most likely formula of $Ni(C_7H_5O_2N)_2Al_2(C_2H_5)_2Cl_2.4\,Py$ is in our opinion formula IV in which two pyridine molecules are bound to the aluminum atoms and two to nickel (II). This modification in the coordination capacity of central metallic ions in the case of aluminumorganic derivatives with nickel and copper is certainly the result of the influence of groups $Al(C_2H_5)Cl$ upon the central metallic ion, as they induce a more marked positive charge in contrast to other aluminum-organic groups.

[13] F. Epharim, *Ber. dtsch. Chem. Ges.*, **63 B**, 1928 (1930).
[14] F. Epharim, *Ber. dtsch. Chem. Ges.*, **64**, 1210, 1215 (1931).
[15] E. Crause and P. Dittmar, *Ber. dtsch. Chem. Ges.*, **63**, 2401 (1930).
[16] D. Dyrssen and M. Hennichs, *Acta Chem. Scand.*, **15**, 47 (1961).
[17] D. Dyrssen and D. Petrovic, *Acta Chem. Scand.*, **19**, 653 (1965).
[18] K. K. Ramaswamy, C. I. Jose and D. N. Sen, *Indian J. Chem.*, **5**, 156 (1967).

The formation of amine-containing adducts in the case of aluminumorganic derivatives of coordinated oximes regardless whether amine bonding occurs at the aluminum atom or at the central metallic ion, was interpreted by us based on the Lewis acidic-basic concept.[4]

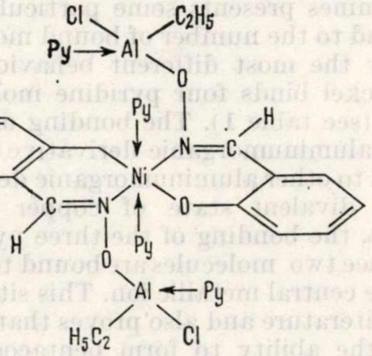

IR absorption bands exhibited in table 2 may be attributed and interpreted [3,4] as in the case of aluminumorganic derivatives with $Al(iC_4H_9)_2$ and $Al(C_6H_5)_2$ groups. The disappearance of some bands and the modification in the position of other bands in the chelates absorption spectrum[18] can only be a result of O—H ··· O bridges substitution by $Al(C_2H_5)Cl$ groups.

Table 2

IR absorption spectra of $M(II)\ (C_7H_5O_2N)_2\ Al_2(C_2H_5)_2Cl_2$ (values in cm^{-1})

Ni	Pd	Cu	Assignment
1 600 vs	1 600 vs	1 590 vs	C = N
1 550 s	—	1 565 w	Distortion C = N
1 480 s	1 480 s	1 485 s	
1 445 s	1 445 vs	1 440 vs	*Ortho*
1 370 w	1 365 w	1 395 w	
1 320 w	—	1 360 s	C—H in the plane
1 285 vs	1 235 s	1 230 s	
1 200 s	1 205 s	1 210 vs	NO
1 150 s	1 140 s	1 145 s	Vibration to the benzen ring
1 120 s	1 115 w	—	
1 060 vs	1 065 vs	1 070 vs	
1 030 s	1 045 s	1 040 s	CO
920 vs	860 s	950 s	NO
830 w	780 vs	875 s	
760 vs	760s	755 vs	C—H outside the plane
680 s	700 vs	685 vs	

The most important observation obtained from X ray diffraction spectra of the studied compounds is the crystalline structure of pyridine-containing adducts of aluminumorganic derivatives with nickel and copper. The other compounds have an amorphous structure.

The paramagnetism of derivative $Ni(C_7H_5O_2N)_2Al_2(C_2H_5)_2Cl_2.4Py$ indicates the octahedral (sp^3d^2) structure of nickel. In the case of copper derivatives, the paramagnetism is an evidence of the copper divalent state in such compounds.

Studies carried out until now on compounds resulted from the reaction of bissalicylaldoximates [2–5] of bisdimethyl-glyoximates [6–8] and of bisdiphenylglyoximates [1,9] of some transitional metals with aluminumorganic derivatives lead to the following conclusions :

— Aluminumorganic compounds of coordinated oximes result from the substitution of O—H. . . O hydrogen bonds, existing in chelates, by O—Al—O aluminum bridges.

— The substitution of hydrogen bridges by aluminum bridges determines the closure of hexaatomic metallocycles without carbon atoms, M—N—O—Al—O—N in the case of coordinated dimethyl- and diphenylglyoxime and of pentaatomic metallocycles, M—O—Al—O—N in the case of coordinated salicylaldoxime.

Revue Roumaine de Chimie, **22**, *3*, 459–469 (1977)

PHENOL OBTAINMENT FROM BENZENE IN OXYGEN PLASMA GENERATED BY A HIGH FREQUENCY DISCHARGE. II[1]

THE PHENOL FORMATION MECHANISM

G. BOURCEANU*, V. ABABI,* GH. POPA** and M. SANDULOVICIU**
*Faculty of Chemistry and Chemical Engineering, Polytechnic Institute of Jassy, Splai Bahlui 71 ;
**Faculty of Physics, "Al. I. CUZA" University, Jassy, Calea 23 August 11, Romania

Received April 2, 1975

This paper provides an explanation of the reason why phenol is formed under conditions in which the oxygen to benzene ratio is larger than 25, but it does not occur at a value of this ratio ranged from 1.0 to 10.0. Taking into account these observations we consider that the species which lead to the development of a series of secondary reactions are the atomic oxygen in the states $O(^3P)$, $O(^1D)$ and $O(^1S)$, atomic hydrogen and phenyl radical. It is assumed that at a value of the oxygen to benzene ratio larger than 25, the reactions responsible for phenol formation are $\dot{C}_6H_5 + O_2 \rightarrow C_6H_5-O-\dot{O}$ and $C_6H_5-O-\dot{O} + H_2O \rightarrow C_6H_5OH + \dot{H}O_2$.

The excited electronic states of benzene have been the subject of many theoretical and experimental investigations. Benzene has been investigated by means of absorption spectroscopy[2–7] and more recently by means of the electron impact method. Doering [8,9] and Hubin-Franskin,[10] using this method, evidenced six excited electronic states from which three are singlet that correspond to 5.0, 6.2 and 6.9 eV respectively, which are of the type $^1B_{2u}$, $^1B_{1u}$ and $^1E_{1u}$, respectively.

The other three triplet states correspond to 3.9, 4.7 and 5.6 eV, respectively and are of the type $^3B_{1u}$, $^3E_{1u}$ and $^3B_{2u}$, respectively.

---

[1] Part. I: G. Bourceanu, V. Ababi, Gh. Popa and M. Sanduloviciu, *Rev. Roumaine Chim.*, **20**, (1975).

[2] G. Herzberg, "Electronic Spectra of Polyatomic Molecules", Van Nostrand, New-York, 1967, p. 555.

[3] S. D. Colson and E. R. Bernstein, *J. Chem. Phys.*, **43**, 2661 (1965).

[4] S. D. Colson and E. R. Bernstein, *J. Chem. Phys.*, **45**, 3873 (1966).

[5] P. G. Wilkinson, *Canad. J. Phys.*, **34**, 596 (1956).

[6] D. F. Ewans, *Nature*, **178**, 534 (1956).

[7] A. Skerbele and E. N. Lassettre, *J. Chem. Phys.*, **42**, 395 (1965).

[8] J. P. Doering, *J. Chem. Phys.*, **51**, 2866, (1969).

[9] J. P. Doering and A. J. Williams, III, *J. Chem. Phys.*, **47**, 4180 (1967).

[10] M. J. Hubin-Franskin and J. E. Collin, *Int. J. Mass. Spectrom. Ion Phys.*, **5**, 163 (1970).

Both the phenomenon of dissociative capture of oxygen and its excitation by means of the electron impact have been widely studied by Schulz,[11] Rapp [12] and more recently by Sabadil.[13]

1. ESTABLISHING THE NATURE OF REACTIVE SPECIES

Taking into account the electrons energy in plasma in comparison with the data in the cited literature, one of the possible mechanisms of the electrons energy transfer to the molecules of oxygen is the dissociative capture.

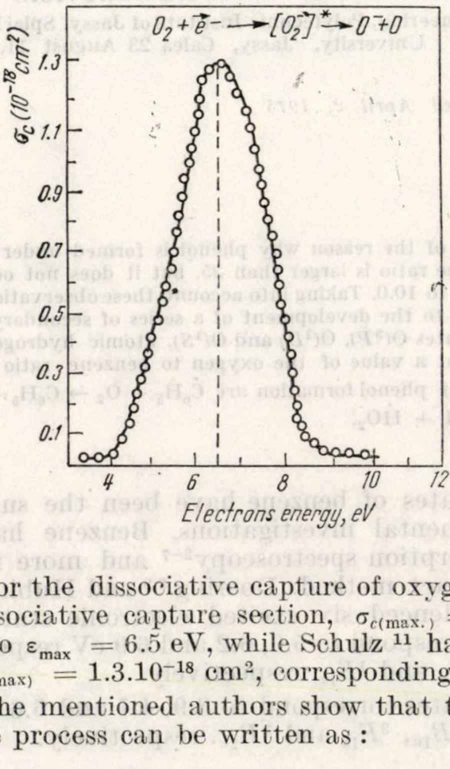

Fig. 1. — Dependence of the dissociative capture of oxygen molecule on electrons energy.

For the dissociative capture of oxygen molecule, Rapp [12] has found the dissociative capture section, $\sigma_{c(\max.)} = 1.8.10^{-18}$ cm², which corresponds to $\varepsilon_{\max} = 6.5$ eV, while Schulz [11] has obtained for oxygen molecule too, $\sigma_{c(\max)} = 1.3.10^{-18}$ cm², corresponding to $\varepsilon_{\max.} = 6.7$ eV (Fig. 1).

The mentioned authors show that the reaction of this dissociative capture process can be written as:

$$O_2 + \vec{e}^- \rightarrow [(O_2^-)^*] \rightarrow O^- + O. \qquad (1)$$

The intermediate molecular ion $(O_2^-)^*$ has its half life by order of 10^{-13} s, because within Franck-Condon's range it corresponds to a repulsive energetic curve, [12,14] so that $(O_2^-)^*$ dissociates spontaneously according to the reaction (1), Fig. 1.

[11] G. J. Schulz, *Phys. Rev.*, **128**, 178 (1962).
[12] R. S. Rapp and D. Briglia, *J. Chem. Phys.*, **43**, 1480 (1965).
[13] H. Sabadil, *Plasma Physik*, **13**, 235 (1973).
[14] L. G. Christophorou and J. A. D. Stokdale, *J. Chem. Phys.*, **48**, 1965 (1968).

The formation of the stable molecular ion was seen only in the case of triple collisions necessary for taking the energy excess. Schulz,[15] operating with oxygen at high pressure, by means of the electron impact method, has evidenced the stable O_2^-. Curran [16] shows that the value of molecular oxygen affinity is of -0.58 eV, while Phelps [17] has found it of -0.46 eV. More recent data as regards the dissociative capture of molecular oxygen according to reaction (1) are given by Sabadil [13] who shows that in an electric discharge at low pressure, in oxygen atmosphere, the ion O^- appears and the molecular ion O_2^- does not occur.

Since the mean energy of electrons in plasma, measured by means of a triple probe,[18] under operating conditions, was found to be about 6.0 eV (Table 1), we consider that the reaction (1) took place with a high probability.

Table 1

Mean energy of the electrons in plasma at various power and molecular oxygen flow rates for benzene flow rate of 0.05 mol/h

O_2 flow rate mol/h	Mean energy of the electrons for the power of 305 W, eV	Power of generator, *W*	Mean energy of the electrons for oxygen flow rate of 6,69 mol/h, eV
4.01	6.0 − 6.3	220.5	2.0 − 2.8
4.95	5.6	265.5	3.8 − 4.2
5.80	5.0	305.5	5.0
6.69	4.2 − 5.0		
7.58	3.1	364.5	6.0 − 6.2

It can be seen that, under the same power, the mean energy of electrons decreases as molecular oxygen flow rate increases, leading to a pressure increase and, therefore, to a diminishing of the mean free path of the electrons.

In Tab. 2 the values of the rate constant for the dissociative capture of the oxygen molecules are given. Calculation was carried out using relation [19]

$$k = \left[\frac{8}{\mu\pi(KT)^3}\right]^{1/2} \varepsilon_0 \exp\left(-\frac{\varepsilon_0}{KT}\right)\int_0^\infty \sigma(\varepsilon)\,d\varepsilon \qquad (2)$$

where μ is the reduced mass of the e^- and O_2 system. Because the mass of electron is much less than that of O_2, for the first approximation, we can take : $\mu = m_e = 9.1.10^{-28}$ g ; $K = 8.9.10^{-5}$ eV/K ; $\varepsilon_0 = \varepsilon_{c(\max)} = 6.7$ eV (for the dissociative capture to O_2) ; $\int_0^\infty \sigma(\varepsilon)d\varepsilon = 8.24.10^{-19}$ cm^2.eV[11].

---

[15] G. J. Schulz, *Bull. Amer. Phys., Soc.*, 6, *387* (1961).

[16] R. K. Curran, *J. Chem. Phys.*, **35**, 1849 (1961).

[17] S. V. Phelps and J. L. Pack, *Bull. Amer. Phys. Soc.*, **7**, 131 (1962).

[18] Sin-Li Chen and T. Sekiguri, *J. Appl. Phys.*, **36**, 2363 (1965).

[19] * * * "Reactions under Plasma Conditions", vol. II, Edited by M. Venugopolan, Wiley-Interscience, New York, 1972, p. 35.

Since $T_e \gg T_{O_2}$, only the kinetic temperature of electrons can be considered. Its calculation is made using the equation :

$$\frac{m_e \cdot v_e^2}{2} = \frac{3}{2} KT \tag{3}$$

If $m_e \cdot v_e^2/2 = 1$ eV, then $T = 7700$ K.

Table 2

Rate constants for the dissociative capture of O_2 at various powers and molecular oxygen flow rates for benzene flow rate of 0.05 mol/h

O_2 flow rate, mol/h	Rate constant, k, for power of 305.5 W, $cm^3 \cdot s^{-1}$	Power of generator, W	Rate constant k, for oxygen flow rate of 6.69 mol/h, $cm^3 \cdot s^{-1}$
4.01	$1.48.10^{-7}$	220.5	$0.037.10^{-7}$
4.95	$1.19.10^{-7}$	265.5	$0.35.10^{-7}$
5.80	$0.81.10^{-7}$	305.5	$0.81.10^{-7}$
6.69	$0.45.10^{-7}$		
7.58	$0.10.10^{-7}$	364.5	$1.48.10^{-7}$

The O^- ion, generated by the reaction (1) can be destroyed by the most important reaction :[13,20]

$$O^- + O \rightarrow O_2 + e^- + 3.6 \text{ eV} \tag{4}$$

This type of reaction is usually called the electron detaching reaction. The rate constant of this reaction is $k = 3.1.\ 10^{-10}\ cm^3.s^{-1}$ and $\sigma \cong \cong 10^{-11}\ cm^2$. Another possible path of the O^- ion disapearance is through action of radiations in plasma, according to reaction [21]

$$O^- + h\nu \rightarrow O + e^- \tag{5}$$

with the efficacious section of electron photodetaching $\sigma_{4000} < \lambda < 6000 = = 6.3.10^{-18}\ cm^2$.

Sabadil [13] shows that the concentration of O^- becomes extremely low, only due to reaction (4) without taking into account the O^- destruction by reaction (5).

It must be mentioned that the destruction process of the negative ions O^- does not take place to the wall, it takes place only in the discharge zone, because the diffusion coefficient of O^- to the wall is a negative one.[13]

If we take into consideration that the affinity of benzene is -1.35 eV according to Hubin-Franskin [10] and -1.6 eV established by Parr,[22] and

---

[20] F. C. FEHSENFELD, E. E. FERGUSON and A. L. SCHMELTEKOPF, *J. Chem Phys.*, **45**, 1844, (1966).

[21] G. C. TISONE, and L. M. BRANSKOMB, *Phys. Rev.*, **170**, 169 (1968).

[22] R. S. PARR, "The Quantum Theory of Molecular Electronic Structure", W. A. Benjamin Inc., New York, 1964, p. 74.

that the mean energy of electrons is much higher (Tab. 1) and the process of dissociative capture is seen as a resonance phenomenon, it results that

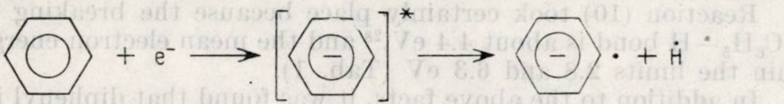

(6)

cannot take place under the utilized conditions.

Taking into account the electronic excited states of benzene and oxygen, the mean energy of electrons in plasma as well as the breaking energy of the $O = O$ and C_6H_5-H bonds, another possible mechanism of the electron energy transfer to the molecule of O_2 and C_6H_6 could be the excitation of these molecules, followed by their dissociation according to the reactions :

$$O_2^3\Sigma\bar{g} + \vec{e}^- \longrightarrow O(^3P) + O(^3P) + e^- \qquad (7)$$

$$O_2^3\Sigma\bar{g} + \vec{e}^- \longrightarrow O(^3P) + O(^1D) + e^- \qquad (8)$$

$$O_0^3\Sigma\bar{g} + \vec{e}^- \longrightarrow O(^3P) + O(^1S) + e^- \qquad (9)$$

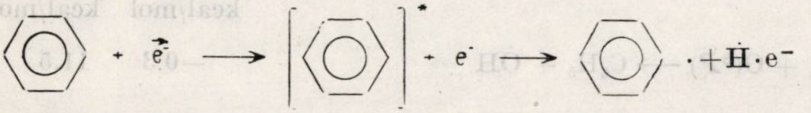

(10)

The energetical states of the occurred oxygen atoms depend on the energy of the incident electrons. Schulz [23] has evidenced the fact that through electron impact the dissociation of oxygen starts in the state $^3\Sigma_u^+$, namely the energetical state which corresponds just to the dissociation energy of oxygen molecule that is of 5.1 eV, [23] resulting in two atoms of oxygen in the ground state $O(^3P) + O(^3P)$, according to reaction (7). At 7.05 eV, the molecules of oxygen can dissociate in atomic oxygen only in the states $O(^3P) + O(^1D)$ in accordance with Wigner and Witmer [24] due to reaction (8).

Over 8.6 eV, the molecular oxygen can dissociate in the states $O(^1D)+O(^1D)$ and $O(^3P)+O(^1S)$. The excited states $O(^1D)$ and $O(^1S)$ are metastable states which correspond to energies of 2.0 eV and 4.2 eV, respectively. [25]

Herron,[26] performing discharges in microwaves in an oxygen atmosphere, has observed in any point of the discharge zone the metastable states :$O_2(^1\Delta g)$ and $O_2(^1\Sigma_g^+)$ which correspond to 0.98 eV and 1.6 eV respectively. Since these species are not reactive enough, they cannot generate any type of reaction at the normal temperature, i.e. 298 K,[27] but probably neither at 320 K as it was in our operating conditions.

---

[23] G. J. Schulz and J. T. Dowell, *Phys. Rev.*, **128**, 174 (1962).

[24] G. Herzberg, "Spectra of Diatomic Molecules", d. Van Nostrand Company Inc., New York, 1969, p. 447, 448.

[25] E. Bădărău and I. Popescu, "Gaze ionizate, procese fundamentale", Editura tehnică București, 1963, p. 63.

[26] J. T. Herron and R. E. Huic, *J. Phys. Chem.*, **73**, 1326 (1969).

Reaction (10) took certainly place because the breaking energy of the C_6H_5-H bond is about 4.4 eV,[28] and the mean electron energy ranged within the limits 2.8 and 6.3 eV (Tab. 1).

In addition to the above facts, it was found that diphenyl is obtained by carrying out electrical discharge only in a benzene atmosphere.

From the data presented above, it results that the reacting species responsible for both the nature of the formed products and their proportion are atomic oxygen either in ground state or in excited state, atomic hydrogen and phenyl radical, which can lead to a series of secondary reactions.

2. REACTIONS POSSIBLY OCCURRING IN PLASMA

Both the nature of these reactions and their preponderence depend widely on the oxygen to benzene molar ratio.

a. THE OXIGEN TO BENZENE MOLAR RATIO RANGED FROM 1.0 TO 10.0

	ΔH kcal/mol	ΔE_a kcal/mol	
$C_6H_6 + O(^3P) \longrightarrow \dot{C}_6H_5 + \dot{O}H$	−0.3	11.5	(11)
$C_6H_6 + O(^1D) \longrightarrow \dot{C}_6H_5 + \dot{O}H$	−46.0	0.0	(12)
$C_6H_6 + O(^1S) \longrightarrow \dot{C}_6H_5 + \dot{O}H$	−96.6	0.0	(13)
$C_6H_6 + \dot{O}H \longrightarrow \dot{C}_6H_5 + H_2O$	−13.1	8.9	(14)
$C_6H_6 + H \longrightarrow \dot{C}_6H_5 + H_2$	−2.0	11.2	(15)
$\dot{O}H + O(^3P) \rightarrow O_2 + \dot{H}$	−15.5	7.7	(16)
$\dot{O}H + O(^1D) \rightarrow O_2 + H$	−61.5	0.0	(17)
$\dot{O}H + O(^1S) \rightarrow O_2 + \dot{H}$	−107.5	0.0	(18)
$\dot{C}_6H_5 + \dot{C}_6H_5 \longrightarrow C_6H_5 - C_6H_5$	−100.7	0.0	(19)
$\dot{C}_6H_5 + C_6H_6 \longrightarrow C_6H_5 - C_6H_5 + \dot{H}$	2.6	13.1	(20)

---

[27] G. W. **Mayer** and L. **Schiler**, *J. Phys. Chem.*, **72**, 2628 (1968).

[28] M. **Szwarc**, *Chem. Rev.*, **47**, 75 (1950).

$$\dot{O} + \dot{H} \longrightarrow \dot{O}H \qquad -103.2 \qquad 0.0 \qquad (21)$$

$$\dot{O}H + \dot{H} \longrightarrow H_2O + h\nu \qquad -117.7 \qquad 0.0 \qquad (22)$$

$$\dot{O}H + H_2 \longrightarrow H_2O + \dot{H} \qquad -12.0 \qquad 8.5 \qquad (23)$$

$$O(^1D) + H_2 \longrightarrow \dot{O}H + \dot{H} \qquad -44.0 \qquad 0.5 \qquad (24)$$

$$O(^1D) + H{-}OH \rightarrow \dot{O}H + \dot{O}H \qquad -29.0 \qquad 4.4 \qquad (25)$$

$$O(^3P) + H{-}OH \rightarrow \dot{O}H + \dot{O}H \qquad -16.0 \qquad 15.5 \qquad (26)$$

$$\dot{O}H + \dot{O}H \longrightarrow H_2O + \dot{O} \qquad -17.0 \qquad 7.3 \qquad (27)$$

Knowing the formation enthalpies of both radicals [29, 30] and molecules, the reaction enthalpies for each reaction presented above have been computed. The reaction activation energies have been computed using the empirical relation given by Semenov [29] which for the exothermal reactions has the form

$$E_a = 11.5 - 0.25\,\Delta H \qquad (28)$$

and for endothermal

$$E_a = 11.5 + 0.25\,\Delta H \qquad (29)$$

ΔH, being the reaction enthalpy. For the reactions between radicals, the activation energies are equal to zero through their definition.

When the experiments are operated with oxygen to benzene molar ratios ranged from 1.0 to 10.0 phenol does not occur, but only diphenyl occurs dissolved in unreacted benzene, and the gaseous mixture made up of acetylene, ethylene and propylene as well as polymer deposited on the discharging tube. Acetylene, ethylene and propylene occur only due to the breaking of the C=C bonds in benzene nucleus, caused by the electron impacts.

At low oxygen flow rates which are ranged between the above ratios, the concentration of atomic oxygen in the molecular oxygen is larger, because, as can be seen in Tab. 3, the electron energy and atomic oxygen concentration in the molecular oxygen decreases as the molecular oxygen flow rate increases, and therefore, as pressure increases.

In Tab. 3, values of both electron energies and atomic oxygen concentration are given for the oxygen to benzene molar ratios ranged from 80 to 150. But, at oxygen to benzene molar ratios, ranged from

---

[29] N. N. SEMENOV, "O nekatorykh problemakh khimicheskoi kinetiki i reactsioni sposnosti" Izd. Akad. Nauk S.S.S.R., Moskva, 1958, p. 31, 42.

[30] G. KLOPMAN and B. O'LEARY "All Valence — Electrons S. C. F. Calculation of Large Organic Molecules", Springer Verlag, Berlin, 1970, p. 499.

Table 3

Atomic oxygen concentration* against the electrons energy and molecular oxygen flow rate to the power of 305 W and benzene flow rate of 0.05 mol/h

O_2 flow rate, mol/h	Mean energy of electrons, eV	Molar ratio oxygen to benzene	Concentration of O_2, %
4.01	6.0 – 6.3	80	26.43
4.95	5.6	99	22.41
5.80	5.0	116	17.60
6.69	4.0 – 5.0	134	11.78
7.58	3.1	151	6.25

* The atomic oxygen concentration was calculated from pressure variation in the discharge tube before and after plasma realization.

1.0 to 10.0, both the electron energy and atomic oxygen concentration in the molecular oxygen increases more and more.

The atomic oxygen generated by reactions (1) and (7 — 9) reacts with benzene according to reactions (11 — 13). For the reaction $CH_3{-}H + \dot{O} \rightarrow CH_3 + \dot{O}H$[31] the rate constant has the value $1.6.10^9\ cm^3\ mol^{-1}s^{-1}$. Since the enthalpy of this reaction, $\Delta H = +\ 0.5$ kcal/mol, is very close to enthalpy of the reaction (11), $\Delta H = -0.3$ kcal/mol, it results that they have the same activation energy. If we consider that the value of $\left(\frac{\sigma_A + \sigma_B}{2}\right)^2$ in the impacts relation[32]

$$k = \left(\frac{\sigma_A + \sigma_B}{2}\right)^2 \left(\frac{8\pi KT}{\mu}\right)^{1/2} \exp\left(-E/RT\right) \tag{30}$$

is the same, it results that the rate constant of reaction (11) will be less than that for reaction $CH_3{-}H + \dot{O}$ with ratio of reduced masses, i.e. with 1.65, wherefrom it results that $k_{(11)} = 10^9\ cm^3 mol^{-1}s^{-1}$. For the reaction (12) and (13) the rate constants are larger if the reaction enthalpies are taken into consideration.

The OH radical occurred according to (11 — 13) reacts with benzene yielding the phenyl radical and water. The rate constant of $CH_3{-}H + \dot{O}H \rightarrow CH_3 + H_2O$[26] is $k = 10^{12} cm^3\ mol^{-1}s^{-1}$. Making the same reasoning as above it can be said, in the first approximation, that $k_{14} = 10^{12}\ cm^3\ mol^{-1}s^{-1}$. On the other hand, it is observed that the OH radical is used up also in the reaction (16) which has its rate constant $k_{16} = 10^{13} cm^3\ mol^{-1}s^{-1}$. For the reactions (17) and (18) the rate constants increase in comparison with $k(16)$ with the same value as increase the rate constants of the reactions (12) and (13). If we take into account only reactions (11), (14) and (16) whose rate constants are known and which are among the initial reactions, it can be said that the OH radical that occurs in the highest proportion according to reaction (11) is used up 1000 times faster in reaction (14) and 10.000 times faster in reaction (16) than it occurs from reaction (11). It is seen that OH radical occurs also from reaction (21) which takes place among the first reactions in the discharge zone, but, on the other hand, it is used up in reactions (22) and (23). Therefore, it results that, in the first approximation, the above reasoning is correct, namely the steady concentration of the OH radical is extremely low.

---

[31] J. Barassin and J. Combourien, *Bull. Soc. chim. France*, **1**, 1 (1974).

[32] I. A. Schneider, "Cinetică chimică", Editura didactică și pedagogică, București, 1974, p. 64.

The phenyl radicals occur from reactions (11) — (15), but in higher proportion due the direct collision among the electrons and the molecules of benzene according to reaction (10).

Since the OH radicals are used up in the above reaction, the phenyl radicals react according to reactions (19) and (20) resulting in diphenyl identified by analyses, or they go into the composition of polymer deposited on the discharge tube.

Because phenol is not detected together with diphenyl, dissolved in unreacted benzene, although we made analyses on two chromatographs having different stationary phases at various flow rates of carrying gas in programmed temperature regime, we must admit that the reaction between phenyl and hydroxyl to form phenol did not take place under used operating conditions.

Undoubtedly, reactions (11) — (14) took place in the discharge zone because an aqueous layer was also separated in the obtained mixture. Reaction (22) has been evidenced by Podley [33] who thinks that the blue emission of 5000 — 6000 Å, in a discharge of microwaves in the $H_2 + O_2$ mixture is due to the radiative recombination $\dot{O}H + H \rightarrow H_2O + h\nu$. The intensity of light is proportional to concentration of $\dot{H}$ and $\dot{O}H$.[33] Under the same conditions, Ticktin [34] evidences the formation of the OH radical from O and H according to reaction (21). Reaction (23) was more recently studied by Semenov.[35] Reactions (24) — (26) have been studied by Mc Grath,[36] Basco[37] and Philips.[38]

An additional argument which justifies the fact that the atomic oxygen leads to reactions (11 — 15) is the negative influence of nitrogen in the discharge zone on the phenol yield. Indeed, starting from the observation that the phenol yield increases as oxygen flow rate increases, it was initially assumed that a resonant transfer of energy could be from the molecules of oxygen to the molecules of benzene, and the transfer is followed by the breaking of the C_6H_5-H bond.

If there were a resonant transfer of energy to the molecules of benzene followed by phenol occurrence, then the use of a mixture of oxygen and nitrogen would be more indicated because the energy transfer takes place with a higher probability when the molecules are found in a metastable state. Or, the molecular nitrogen has a metastable state which corresponds to a transition of 6.2 eV[25] equal exactly with the electronic excited state $^1\mathrm{Bi}_{1u}$ of benzene.[8,39] The energy of the metastable states in both cases of molecular oxygen and atomic oxygen, which correspond to 1.64 eV,[25,26] and 4.2 eV, respectively, is less than the breaking energy of the C_6H_5-H bond that is of 4.4 eV.[28] Starting from this consideration, the discharge was realized in the mixture of benzene and air. Air was admitted in with a flow rate of 6.69 mol/h so that the mean energy of the electrons should not be too much modified as against the case when we worked with pure oxygen having the same flow rate. At the air flow rate of 6.69 mol/h, the molar ratio oxygen to benzene is 30. According to the analyses carried out on the reaction products, contrary to expectation, diphenil was also obtained together with phenol. Or, in case of using only pure oxygen, with the molar ratio oxygen to benzene larger than 25, only phenol is obtained.

---

[33] P. J. Padley, *Trans Faraday Soc.*, **56**, 449 (1960).

[34] S. Ticktin, G. Spindler and H. I. Schiff, *Discuss. Faraday Soc.*, **44**, 218 (1967).

[35] V. V. Azatian and N. N. Semenov, *Kinetica i kataliz*, **13**, 17 (1972).

[36] W. D. Mc Grath and R. S. W. Norrish, *Proc. Roy. Soc.*, A, 254, 317 (1960).

[37] N. Basco and R. S. W. Norrish, *Proc. Roy. Soc.*, A **260**, 293 (1961).

[38] L. F. Phillips and H. I. Schiff, *J. Chem. Phys.*, **37**, 1233 (1962).

Sabadil[40] shows that, in the presence of nitrogen in an oxygen plasma, the atomic oxygen concentration increases very much. If the atomic oxygen concentration increases and, consequently, the molar oxygen concentration decreases, it results that the preponderance of reactions (11) — (13) increases too and therefore this would be the reason due to which the phenol yield decreases and diphenyl occurs even when we operate with an airflow rate of 6.69 mol/h which corresponds to an oxygen to benzene molar ratio of about 30.

b. THE OXYGEN TO BENZENE MOLAR RATIO LARGER THAN 25

When the oxygen to benzene molar ratio ranges from 10.0 to 25.0f both diphenyl and phenol are obtained. In the case when the value oe this ratio is larger than 25, only phenol dissolved in unreacted benzen, is obtained and, in the aqueous layer, hydrogen peroxide and water occur. A gaseous mixture made up by components mentioned above and a polymer deposited on the discharge tube were also obtained, but both the gaseous mixture and the polymer in a smaller proportion.

Excluding the reaction of the diphenyl formation (which was not identified even as traces) we assume that also under these conditions all reactions written above take place and, in addition, the following reactions which are responsible for the phenol and hydrogen peroxide formation :

$$\Delta H(\mathrm{kcal/mol})$$

$$\left.\begin{array}{l} \dot{C}_6H_5 + O_2 \longrightarrow C_6H_5-O-\dot{O} \\ C_6H_5-O-\dot{O} + HOH \rightarrow C_6H_5-OH + \dot{H}O_2 \end{array}\right\} -32.0 \qquad (31)$$

$$\dot{H} + O_2 \longrightarrow \dot{H}O_2 \qquad -47.0 \qquad (32)$$

$$\dot{H}O_2 + \dot{H}O_2 \longrightarrow H_2O_2 + O_2 \qquad -43.6 \qquad (33)$$

---

[39] E. N. Lassettre, A. Skerbele, M. A. Dillon and K. J. Ross, *J. Chem. Phys.*, **48**, 5066 (1958).

[40] H. Sabadil, *Plasma Physik*, **11**, 327 (1971).

The arguments pleading in favour of this mechanism of phenol formation in such conditions are :

— Phenol does not occur at low oxygen flow rates, when the molecular oxygen concentration is low, due to its high dissociation degree in atomic oxygen, a fact that does not favour the development of the reaction (31);

The phenol yield increases as molecular oxygen flow rate increases, and hence it results that reaction (31) is favoured;

— The phenol yield increases appreciably when the discharge is realized in the ($C_6H_6 + O_2 + H_2O$) mixture and therefore, reaction (31) is favoured (Tab. 4);

— The phenol yield decreases when the discharge is realized in the air-benzene mixture, due to the atomic oxygen concentration increase and consequently, reactions (11) — (13) are promoted.

Table 4

Phenol yield at the power of 305.5 W, molar ratio benzene to water of 1.0 and various oxygen flow rates

O_2 flow rate, mol/h	Phenol yield of reaction $C_6H_6 + O_2$, %	Phenol yield of reaction $C_6H_6 + O_2 + H_2O$, %
4.01	7.92	10.31
4.95	16.54	17.43
5.80	22.72	23.15
6.69	26.28	26.50

In order to evidence the contribution of the direct reaction

$$\dot{C}_6H_5 + \dot{O}H \rightarrow C_6H_5 - OH \qquad (34)$$

discharges were carried out in the mixture benzene-water using the benzene to oxygen molar ratio of about $0.05/0.05 \cong 1.0$ and that of benzene to water of about $0.1/0.1 \simeq 1.0$, at the generator power ranging from 265.5 to 364.5 W. In all cases the phenol yield did not exceed 0.15 % as against initial benzene. Just for this reason we think that the contribution of reaction (34) is extremely small even under the conditions when the molar ratio, oxygen to benzene, is larger than 25.

From the data presented above it results that reactions (31) and (32) are responsible for the phenol formation.

Revue Roumaine de Chimie, 22. 3. 471–474 (1977)

AZOLIDES. IX[*]

ÉTUDE DE LA CONFORMATION DES AZOLIDES PAR DIPÔLEMÉTRIE

J. P. FAYET, M. C. VERTUT et P. MAURET
Université Paul Sabatier, Laboratoire de Chimie organique structurale 118, route de Narbonne, 31077 TOULOUSE CEDEX, France

R. M. CLARAMUNT et J. ELGUERO
Université des Sciences et Techniques du Languedoc, Centre de Chimie organique, Place E. Bataillon, 34060 MONTPELLIER CEDEX, France

Reçu le 28 avril 1975

La comparaison des moments dipolaires expérimentaux (dans le dioxanne à 25° et à 45°) et calculés (méthode CNDO/2) a permis de déterminer la position de l'équilibre E/Z pour un certain nombre de dérivés acétylés des azoles.

Il est surprenant de constater que la conformation des dérivés C-acylés des hétérocycles π-excédents (pyrrole, furanne, thiophène) a fait l'objet de très nombreuses études (voir parmi les plus récentes les références,[1–4] tandis que la conformation des dérivés N-acylés des azoles n'a été étudiée que par nous-mêmes.[5–9] Toutes nos études étaient basées sur l'emploi de la résonance magnétique du proton ; en vue de contrôler les résultats obtenus, nous avons fait appel à l'une des méthodes semi-empiriques de la chimie théorique (méthode PCILO) pour des calculs d'énergie ;[10] puis nous avons procédé à l'étude expérimentale de ces équilibres par la méthode dipôle-métrique couplée à des calculs CNDO/2.

Pour simplifier, nous n'avons considéré que les formes planes[**] pour lesquelles nous avons adopté la nomenclature E/Z habituellement réservée à la description de la configuration et très généralement adoptée dans le cas des amides. Nous avons choisi de comparer une propriété moyenne d'un azolide en solution (le carré du moment dipolaire électrique déterminé expérimentalement) avec cette propriété dans le cas des formes E et Z (le carré du moment dipolaire électrique calculé). Cette méthode nous a donné d'excellents résultats dans le cas d'équilibres tautomères.[12-15]

---

[*] L'acétyl-1 bromo-4 pyrazole est plan à l'état cristallin.[11]

[**] Part VIII : M. C. Pardo, J. Elguero et L. Pappalardo, *Anal. Quim.* (sous presse).

[1] B. R. Larsen, F. Nicolaisen et J. T. Nielsen, *Acta Chem. Scand.*, **26**, 1736 (1972).

[2] M. Farnier et T. Drakenberg, *Tetrahedron Letters*, **1973**, 429.

[3] B. P. Roques et S. Combrisson, *Canad. J. Chem.*, **51**, 573 (1973).

[4] C. L. Cheng, I. G. John, G. L. D. Ritchie et P. H. Gore, *J. Chem. Soc. (Perkin II)*, **1974**, 1318.

[5] L. Pappalardo, J. Elguero et C. Marzin, *C. R. Acad. Sci.* (Paris), **277C**, 1163 (1973).

[6] J. Elguero, C. Marzin et L. Pappalardo, *Bull. Soc. Chim. France*, **1974**, 1137.

[7] J. Elguero, A. Fruchier, L. Knutsson, R. Lazardo et J. Sandström, *Canad. J. Chem.*, **52**, 2744 (1974).

[8] L. Pappalardo, J. Elguero et A. Fruchier, *Anal. Quim.* (sous presse).

[9] J. Elguero, C. Marzin et M. E. Peek, *Org. Magn. Res.* (soumis pour publication).

[10] H. Sauvaitre, J. Teysseyre et J. Elguero, *Bull. Soc. Chim. France* (soumis pour publication).

[11] J. Lapasset, A. Escande et J. Falgueirettes, *Acta. Cryst.*, **B 28**, 3316 (1972).

PARTIE EXPÉRIMENTALE

L'acétyl-1-imidazole **3** est un produit commercial. La synthèse des autres azolides se trouve décrite dans d'autres publications de cette série : acétyl-1-pyrrole **1**,[6,9] acétyl-1-pyrazole **2**,[6] acétyl-1-indole **4**,[9] acétyl-1-benzimidazole **5**.[14]

Les moments électriques ont été mesurés dans le dioxanne à 25° et à 45°. La formule de Debye a été utilisée, ainsi que la méthode d'extrapolation mathématique d'Halverstadt et Kumler[12] pour le calcul de la polarisation totale du soluté. La préparation des solutions a été effectuée en boîte à gants sous atmosphère d'azote R. Les résultats figurent dans le tableau 1.

Tableau 1

Résultats expérimentaux

Composés	t°C	α	β	RM_D	P_{200}	μ_D
acétyl-1-pyrrole **1**	25	7,51	−0,10	30,29	162,54	2,54
acétyl-1-pyrazole **2**	25	2,75	−0,09	28,63	77,88	1,55
	45	2,61	−0,08	28,63	77,58	1,60
acétyl-1-imidazole **3**	25	9,04	−0,16	28,51	189,93	2,81
	45	8,65	−0,06	28,51	192,19	2,92
acétyl-1-indole **4**	25	7,12	−0,11	46,53	226,41	2,97
	45	6,63	−0,15	46,53	218,67	3,00
acétyl-1-benzimidazole **5**	25	5,26	−0,15	44,75	176,83	2,54
	45	5,02	−0,17	44,75	174,94	2,61

CALCUL DES MOMENTS DIPOLAIRES

Si, en raison de sa symétrie, l'acétyl-1-pyrrole ne peut exister que sous une seule forme, les quatre autres produits peuvent présenter une isomérie E/Z

[12] P. Mauret, J. P. Fayet, M. Fabre, J. Elguero et M. C. Pardo, *J. Chim. Phys.*, **70**, 1483 (1973).

[13] P. Mauret, J. P. Fayet, M. Fabre, J. Elguero et J. de Mendoza, *J. Chim. Phys.*, **71**, 115 (1974).

[14] J. P. Fayet, M. C. Vertut, P. Mauret, J. de Mendoza et J. Elguero, *J. Het. Chem.*, **12**, 197 (1975).

[15] J. P. Fayet, M. C. Vertut, R. M. Claramunt, K. M. Fabrega et L. Knutsson, *Bull. Soc. chim. France*, **1975**, 393.

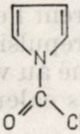

1

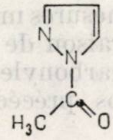

2E

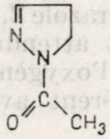

2Z

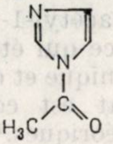

3E

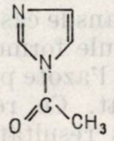

3Z

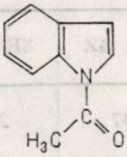

4E

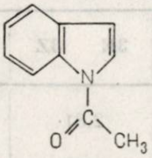

4Z

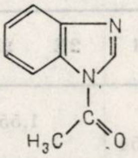

5Z

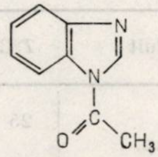

5E

Les moments dipolaires ont été calculés par la méthode CNDO/2.[16] Les résultats obtenus figurent dans le tableau 2.

Tableau 2

Moments dipolaires calculés (unités Debye)

Produit	1	2E	2Z	3E	3Z	4E	4Z	5E	5Z
moment calculé	2,80	1,87	5,46	2,01	3,94	2,58	3,26	2,12	3,49

Des études antérieures [12–15] sur d'autres hétérocycles azotés ont montré que les résultats CNDO, même avec des géométries idéales, étaient généralement en accord avec les moments expérimentaux à ± 0,3 D près.

GÉOMÉTRIES UTILISÉES DANS LES CALCULS CNDO

Cycles réguliers de 1,39Å de côté ; distance C-H aromatique ou hétérocyclique : 1,00 Å ; groupe acétyle : NC : 1,33 ; CO : 1,23 ; CC : 1,52 et CH : 1,10 Å ; angle NCO : 120°.

DISCUSSION

Nous avons conduit les calculs des pourcentages des formes E et Z à l'équilibre de deux façons :

1) avec les valeurs μCNDO ;

2) avec les valeurs $\mu_T = (\mu_{CNDO} - 0,25)$ D, afin de retrouver la valeur expérimentale dans le cas de l'acétyl-1-pyrrole **1**, qui ne présente pas de problème conformationnel.

---

[16] J. A. Pople et G. A. Segal, *J. Chem. Phys.*, **44**, 3289 (1966).

Les valeurs expérimentales, les valeurs de μ_{CNDO} et de μ_T figurent dans le tableau 3, à côté des pourcentages de E calculés de deux manières.

Dans le cas de l'acétyl-1-pyrazole **2**, nos mesures montrent l'existence de la seule forme E, ce qui était attendu en raison de la répulsion de la paire de l'azote pyridinique et de l'oxygène du carbonyle situé au voisinage immédiat. Ce résultat est cohérent avec nos précédents calculs [5,6] et avec les résultats théoriques.[10]

Tableau 3

Constantes d'équilibre E/Z

Produit	T°C	**1**	**2E**	**2Z**	**3E**	**3Z**	**4E**	**4Z**	**5E**	**5Z**
moment exp. (D)	25	2,54	1,55		2,81		2,97		2,54	
	45		*1,60*		2,92		*3,00*		2,61	
$\mu_{\text{CNDO}}(D)$		2,80	1,87	5,46	2,01	3,94	2,58	3,26	2,12	3,49
$\mu_T(D)$		*2,55*	*1,62*	5,21	1,76	3,69	2,33	*3,01*	1,87	3,24
%E(CNDO)	25	—	100 %		66 %		46 %		75 %	
	45				61 %		40 %		70 %	
%E(T)	25	—	100 %		54 %		7 %		58 %	
	45				48 %		2 %		53 %	

Dans le cas de l'acétyl-1-imidazole **3** la présence des formes E et Z en pourcentages sensiblement égaux, en solvant non polaire, est en bon accord avec le fait qu'elles ont pratiquement la même énergie[10]; l'étude RMN avait montré que leur abondance relative varie avec le solvant utilisé. [6,7]

Pour l'acétyl-1-benzimidazole **5** nos résultats corroborent les études basées sur la RMN qui donnaient de 75 à 90% de forme E.[6,8,17] Un calcul théorique PCILO [10] montre également la prédominance de la forme E.

Mais la méthode devient difficilement applicable à l'acétyl-1-indole **4** à cause du faible écart entre les moments calculés pour les formes E et Z. On remarquera que les valeurs corrigées ne seraient pas incompatibles avec l'existence de ce produit uniquement sous la forme Z.[9,10]

Le calcul CNDO/2 pour l'acétyl-1-indole **4** conduit, pour la forme **4Z** à un $\mu = 3{,}26$ D ; une rotation de 21°5, qui a été proposée pour le groupe acétyl à la suite de déterminations infrarouges, [18] ne modifie pratiquement pas cette valeur (3,23 D).

La méthode d'étude des équilibres conformationnels basée sur les moments dipolaires ne peut fournir des résultats précis que s'il existe un écart suffisant entre les polarités des deux formes.

---

[17] J. M. Gross et D. G. Rush, *Chem. Ind.*, **1968**, 1766.

[18] G. V. Garner, O. Meth-Cohn et H. Suschitzky, *J. Chem. Soc. (C)*, **1971**, 1234.

IUPAC, "The chemistry of non-benzenoid aromatic compounds — II" (Plenary lectures presented at the 2nd International Symposium on this topic, held in Lindau, Federal Republic of Germany, 23 — 27 September 1974), Butterworths, London, 1975 (J. Kreher, editor)

According to a well-established tradition, the full texts of plenary lectures presented at IUPAC symposia are printed in *Pure and Applied Chemistry*, and reprinted in bound volumes. The volume under discussion represents issue 4 of the above journal, **44**, 691—948 (1975) with the original page numbers.

The organizing committee of the second international symposium on the Chemistry of non-benzenoid aromatic compounds, held in Lindau/Bodensee, was headed by Klaus Hafner.

The volume includes ten plenary lectures, whose titles are given below in brackets after the authors'names. The length of these lectures varies from three pages (a synopsis of E. Heilbronner's lecture, with a note indicating that the material has either been published or submitted for publication) to sixty (A. G. Anastassiou's lecture), but most lectures are ca. 25 pages long. They are arranged in alphabetical order of first author's name.

A. G. Anastassiou's lecture (Synthesis and study of select heterocycles) emphasized the unique character of hetero [9] annulenes (heteronins), where the electronegativity of the heteroatom (also influenced by side-chains attached to it) determines whether the compound is aromatic or not. The next higher heteroannulenes after Hückel's 4n + 2 π-electron rule has 13 atoms , and these have also been prepared and studied, both in Karlsruhe and in Syracuse. Benzoheteroannulenes and bicyclic valence tautomers of the heteroannulenes are also described and discussed. The disagreement with Masamune's published work on certain aspects remains to be settled by experimental evidence.

V. Boekelheide's lecture (Intrusion of substituents into the cavity of aromatic π-electron clouds) describes bridged [14] annulenes, bridged [18] annulenes, tetra-bridged cyclophanes and [22] *meta-para* cyclophanes as well as heteroanalogues of the latter. Diatropic ring current effects in NMR spectra are of the same magnitude for ^1H and ^{13}C for the same position in space relative to the π-electron cloud.

M.J.S. Dewar's lecture (M.O. Studies of some nonbenzenoid aromatic systems) described the results of the MINDO/3 semiempirical SCF MO method : cyclobutadiene appears to be very antiaromatic and is predicted to have a rectangular singlet ground state ; by the same method, its valence isomer, tetrahedrane, is predicted to be a stable species. The pyramidal $(CH)_5^+$ and the analogous $(CH)_9^+$ cations are rationalized theoretically. It appears that azulene needs X-ray investigations to establish whether its bonds are equalized or not. Paradoxically, it seems that thiophene has more bond alternation than furan, and this in turn than pyrrole, therefore the lack of reactivity of thiophene is an illusion due to its lower basicity (nothing is said about the diene behaviour).

P. J. Garratt (Polycyclic systems containing small-membered rings) described systems containing four-membered rings fused to aromatic systems (benzenoid and/or heterocyclic), such as heterobenzo-cyclobutadienes.

H. Günther and H. Schmickler (Results of ^{13}C—NMR spectroscopy in the field of cyclic conjugated π-electron systems) emphasized the multiple applications of this method, starting from the fact that "most chemical laboratories have acquired pulse Fourier transform facilities by now. . .and that. . .^{13}C—NMR spectroscopy by definition must be regarded as *the* spectroscopy of organic molecules". Though ring current effects are not always detectable, as in ^1H—NMR, ^{13}C—NMR is much more sensitive to other minor structural variations in aromatic systems.

E. Heilbronner's synopsis (Photoelectron spectra of nonbenzenoid cyclic conjugates π-electron systems) ends as follows : "It is fortunate that the photoelectron spectroscopic data known to date . . . do not allow the formulation of yet another aromaticity criterion".

Y. Kitahara's (8-Oxoheptafulvene) is at the same time a ketene and a heptafulvene. It presents many interesting reactions such as cycloadditions.

S. Masamune gave in his lecture (Some aspects of strained systems. [4] Annulene and its CH^+ adduct) experimental evidence confirming several theoretical predictions contained in Dewar's talk : NMR spectra of $(CH)_5^+$ demonstrate its pyramidal structure whereas the synthesis and X-ray structural investigation of the crystalline methoxycarbonyl-tri-t-butyl-cyclobutadiene reveals a rectangular singlet ground state of a [4] annulene. The unsubstituted [4] annulene, for which a triplet ground state was advocated on the basis of its IR spectrum in an argon matrix is also supposed to have, instead, a singlet ground state, by analogy.

M. Nakagawa (Acetylene-cumulene dehydroannulenes) reported on tetradehydro [18] — and— [22] annulenes, a field first explored by F. Sondheimer. An elegant experiment showed the identity of a pentadiynic chain and a cumulenic chain in such compounds. The ring current decreases strongly in the tetra-t-butyl-didehydro $[4n + 2]$ annulenes with 14 – 30 atoms.

The last lecture is that of G. Schröder (Höhergliederige Annulenylionen und Bemerkungen zur Frage der Konfigurations- und Konformations-stabilität bei Annulenen). By variable temperature NMR spectroscopy it was possible to examine the configurational and conformational stability of annulenes and their ions : the rearrangements may be degenerate or nondegenerate.

The printing is accurate, with well-drawn formulas (except for formulas **1**, p. 752 and **8**, p. 756 where lines intersect awkwardly). Errors are few : Lindan instead of Lindau on the cover and the binding, formula **4** on p. 774 lacks a double bond, formula $(CH)_n(CH)_{2m}$ on p. 861 should probably be $(CH)_n(CH_2)_m$, while on p. 701, instead of $>$ Nb the anion $>N^-$ is meant. Though this causes little difficulty, it would have been nice to present all ^{1}H-NMR spectra with the same scale (either δ, or τ); most spectra are in the τ scale, but a few in the δ-scale; the spectrum on p. 864 does not even mention what the scale is.

Erich Hückel was honorary president of the symposium. "There are, in the history of chemistry, few rules that have withstood experimental tests as extensively as his $(4n + 2)$-postulate" (Masamune); however, „die erste Blütezeit der Annulenchemie geht zu Ende" (Schröder). Nevertheless, the symposium, as reflected in the present volume, shows that organic chemistry still presents fascinating areas.

Although some of the lectures are admittedly non-exhaustive in their literature coverage (e. g. Masamune's paper does not quote either Maier, or Avram and Nenitzescu's pertinent data), all lectures present an up-to-date report of the most prominent producers of new chemical data.

At a modest hard-cover price of 18.75 US $, the book is highly recommended to all chemical libraries and organic chemists who do not subscribe to *Pure and Applied Chemistry*.

Alexandru T. Balaban

O. WEISSBACH : "THE BEILSTEIN GUIDE", a manual for the use of Beilstein Handbuch der organischen Chemie, Ed. Springer, Berlin, 1976, 95 pages.

For those accustomed with organic compounds, "Beilsteins Handbuch der organischen Chemie" needs no introduction at all. For over 60 years, consecutive supplements to this monograph have appeared so that it reached 150 volumes in 1976, due to the care of Beilstein Institute. Prepared by one of the experts of the Beilstein Institute, this Guide is meant to provide practical and comprehensive instructions for the use of the treatise, giving exact explanations on how to find a certain compound.

As it is known, Beilstein is the only organic chemistry encyclopaedia including the most complete and consistent data on carbon compounds, known and precisely characterized from the point of view of their composition and constitution. It does not cover e.g. macromolecular compounds such as cellulose or proteins as they have not perfectly defined chemical formulas and are not included in inorganic compounds. All the concrete data are checked and critically analysed by the editors so that in many cases the reader may find the necessary information without consulting the original article for which the authors, the journal and the pages in question are cited. In general the following data are given for each compound in Beilstein : natural sources and isolating manner ; preparation and purification ; physical properties ; chemical properties and reactions, identification of the compound, its derivatives, analytical methods and possible instructions on the handling manner. Each expression has precise references in the periodicals literature based on which the completed volumes have been developed and sometimes even additional information sources from monographs, patents or doctoral theses.

In the differently coloured series of 27 volumes, simple or multiple, Beilstein covers at present the literature processed until 1960 :

	Hauptwerk	1910	green
I.	Ergänzungswerk	1910–1920	red
II.	Ergänzungswerk	1920–1930	white
III.	Ergänzungswerk	1930–1950	blue
IV.	Ergänzungswerk	1950–1960	black

to which volumes are added containing indexes of the compound name and of formulas.

An efficient use of knowledge included in these volumes is not possible without knowing the content and the basic principles of its organization, which constitutes the Beilstein system. The author of the guide amply explains in a few chapters the coverage of Beilstein, its organization, the way for retrieving data (index of formulas, of names, the Beilstein system, the ordering and classification of compounds, derivatives, tautomers, etc.) the presentation and organization of an article and he gives as an appendix some additional rules for the principal compounds and for derivatives. At the end of the guide, apart from an index of subjects there is a restricted German-English-French vocabulary containing the most frequent words and expressions. It helps those who do not master the German language but have appropriate knowledge of English or French.

The accomplished graphical presentation of the manual, highlighting the basic rules and definitions by coloured blocks renders the reading attractive and readily assimilable. It is worth mentioning the faithful and fluent translation of H.M.R. Hoffmann (University College, London) of the German version issued by the same editors under the name "*Beilstein-Leitfaden*".

For those who are frequently faced with organic compounds without being organic chemists, the consultation of the guide and the reading of Beilstein is irreplaceable. A preliminary documentation, on a certain subject involving organic compounds on the part of specialists in industry, research, designing and education as well as of undergraduate students in chemistry faculties is a prerequisite. For this reason almost all the units carrying on activities in the field of organic chemistry have Beilstein Collections at present which will be better used by means of this guide. The guide has an exceptional utility, particularly for the numerous students in developing countries who study abroad and who could not have access to the Beilstein encyclopaedia without this guide.

F. Cuiban

P. BALTĂ and E. BALTĂ, "Introduction to the physical chemistry of the vitreous state", Ed. Academiei, Bucharest, Romania and Abacus Press, Tunbridge Wells, Kent, England, 1976, 287 p.

In the field of vitreous state, the structural research is faced with difficulties because of the disordered character of this state, which determines a lowering efficiency of investigation methods of crystalline structure. Then, it is necessary to carry out the research at high temperatures for viscous fluids or for solids. For this reason, the knowledge about vitreous state has developed slowly.

The present work is remarkably valuable, because the authors have pointed out that only the consistent use of up-to-date knowledge and of methods promoted by chemistry, physical chemistry and the physics of the solid state, leads to a correct understanding of the problems connected with the vitreous state.

The work is divided into six chapters.

The first chapter deals with the methods with enable the obtaining of solid with non-crystalline structure; by thermal energy by melting, by mechanical energy, by the effect of neutron rays on crystalline materials, by reactions from solutions, electrochemical processes a.s.o. Also, using the concept of energy profile, intuitive images of the energy state corresponding to different degrees of order have been developed. The amorphous notion has been defined by considering the concept of coefficient of linear and space repetition and the configurational entropy.

The second chapter presents syntheses of vitreous state by melts supercooling, special attention being paid with good reason, to explaining the manner in which the nature of chemical bonds influences the tendency towards vitrification by supercooling. Different concepts have been treated concerning the nature of chemical bonds in glasses, showing that each of them contributes to a certain extent to demonstrating some aspects which tend to present an almost complete theory for getting an insight into the nature of the vitreous state. The authors also point out the role of the chemical bonds in obtaining the vitreous state, such as sigma bonds, the structural bridges which give rise to tridimensional, bidimensional or linear heteropolymeric formation and donor-acceptor bonds. Exemplifying different structures of melts, to obtain vitreous state substances, the authors treat in detail the kinetics of their cooling process.

Chapter 3 is concerned with some problems related to the approach to the vitreous state through the prism of polymeric structures. The structure alway consists of a mixture of polymers whose size and concentration depend on composition and on some external factors i.e. : the history of melting (the temperature and the duration of melting) and the thermal one, very important in defining the properties of glass depending on the technological obtention conditions. Chapter 3 deals with processes leading to the formation of the vitreous state i.e. : structural disordering, structure of the melts, the variation in polymer distribution with respect to various factors included, structural equilibrum established within melts, the influence of this equilibrium on the history of melting properties, the change occurring in melts cooling up to the temperature Tg, a.s.o.

Chapter 4 is concerned with the type of bonds that exist between the frequent elements in glass and some structural implication, i.e. : the chemical bonds in hydrogenide glasses, organic glasses, oxide glasses (B_2O_3 glasses, SiO_2 glasses, GeO_2 glasses and glasses with P_2O_5), chalcogenide glasses, halide glasses, salinogenide glasses. Although reflecting the great structural diversity of the substance that can be supercooled in vitreous state, the presented date point out certain regularities regarding the nature of chemical bonds, very clearly emphasized for all categories of substances.

Chapter 5 deals with the separation phenomenon of the vitreous microphases into glasses. The authors present the thermodynamical theory of the phenomenon, the causes determining the unsual variation of free energy in certain regions of temperature and compositions and the opinions of various researchers on this phenomenon. The conclusion reached is that immiscibility cannot appear if the silicates solutions will not have a polymer structure, or if the bonds of these structures will be too rigid. The mechanism and kinetics of vitreous microphase separation and the practical importance of this process in the technology of vitroceramic products is also discussed. The study of vitreous microphase separation will lead to a noticeable improvement in the quality of some products, to the establishment of better technological processes and even to the development of totally new articles and technologies.

Chapter 6 is concerned with the optical processes in the vitreous solid. It presents the interaction of electromagnetic radiations with the vitreous state, the behaviour of the ions of transition metal in coloured glasses based on the ligand field theory and on the light absorption by charge transfer. The study of redox processes in glasses is presented in connection with obtaining various colours and shades. The authors show researches in the field of photosensitive glasses and in the laser field that demonstrate that glass is an adequate medium for achieving a stimulated light emission. Some practical applications of the optical fibres are also briefly mentioned.

The work has a highly original character, by its conception, the way in which the material is organised and the original ideas presented in all chapters. The authors come up with a scientific unitary conception in the study of noncrystalline solids, contributing to the development of fundamental and applicative research.

By its content and high level, the work is useful for chemical engineers, specializing in silicate technology, for chemists and physicists interested in the problems of the vitreous state and also for students who are being trained in the field.

Maria Crişan

M. KLEITZ and J. DUPUY, "Electrode processes in solid state ionics, theory and application to energy conversion and storage", D. Reidel Publishing Company, Dordrecht-Holland/ Boston, U.S.A., 1976, 484 p.

This work is a collection of all the texts of the teaching courses, presented over the twelve days of study in a Summer School at the Proceedings of the NATO Advances Study Institute held at Ajaccio (Corsica), 28 August — 9 September 1975.

The idea of an "Advanced Study Institute" on the theme of electrode reactions on solid electrolytes was put forward by Dr. J. Dupuy at the meeting of the International Society for Electrochemistry in Eindhoven in September 1973.

Phenomena of matter and electricity transfer at the junction between an electronic and a solid ionic conductor, as well as the related elementary processes, have been the subject of research in fields as different as solid physics, electrochemistry, and adsorption phenomena physical chemistry.

A great deal of development work on aplications in solid electrolyte cells comes up against interfacial phenomena which appreciably reduce anticipated performances.

Numerous potential applications of specific electrodes or gauges appear that would benefit from a more systematic approach.

From a more fundamental viewpoint, interface phenomena on ionic crystals are the subject of independent investigations in quite distinct research fields such as solid state physics and electrochemistry.

The most eminent proponents of the different approaches brought together to take part in the meeting, have attempted to formulate a synthesis of the various models put forward.

In the first part of this book there are the courses conected with the following themes :

— Structure, energetics and defects at ionic surface and how these influence chemical activity at surface. Here one can mention :

"Structure and energetics of the ionic surface", by P. Mark, Department of Electrical Engineering, Princeton University (USA).

"Structure and defects at ionic crystal surface", by J. M. Blakely, Cornell University, Ithaca (USA).

"Adsorption and catalysis on ionic solids," by B. Claudel, Institut de Recherches sur la Catalyse, and Institut National des Sciences Appliquées de Lyon Villeurbanne (France).

— The electrochemical double layer in solid electrolytes, electrode polarization and mechanism.

This theme was illustrated in :

"The Electrochemical double layer in solid electrolytes", by D. O. Raleigh, Science Center, Rockwell International Thousand Oaks, California (USA).

"Space charge polarization", by J. Ross Macdonald, Department of Physics and Astronomy, University of North Carolina (USA).

"Polarization studies on solid state electrolytes", by J. B. Wagner, Jr., Materials Research Center and Department of Materials Science and Engineering, Northwestern University Evanston, Illinois (USA).

— Description of junctions, and ion transfer of the interface between an electronic and ionic conductor.

This theme was presented in :

"Descriptions of junctions between electronic and solid ionic conductors", by M. Kleitz, P. Fabry, E. Schouler, Laboratoire de Cinétique Electrochimique Minérale Associé au CNRS (France).

"Ion transfer at the interface between an electronic and ionic conductor", by H. Gerischer, Fritz-Haber-Institut d. Max Planck-Gesellschaft, Berlin (Federal Republic of Germany).

Particular mention can be made of cells used for storage and conversion of energy and also : (a) various types of gauges, some of which are already used in metallurgy or for monitoring exhaust fumes or gases, (b) various specific electrodes used in laboratory or industrial analysis (the miniaturization of these electrodes will answer a long felt need in the field of medical instrumentation), and (c) electronic components such as large capacitance capacitors, coulometers, timers, and data storage units.

All these themes were presented in work sessions on the following courses :

"Impedance diagrams for solid electrolyte cells", by R. D. Armstrong, Electrochemistry Research Laboratories, School of Chemistry, University of Newcastle-upon-Tyne (England).

"High temperature fuel cells and electrolysers", by B. C. H. Steele, Imperial College, London (England).

"The application of solid state ionics to batteries", by R. M. Dell, AERE Harwell, Didcot, Oxon (UK).

"Rechargeable solid electrolyte traction batteries", by R. M. Dell and L. S. Evans, AERE, Harwell, Oxfordshire (UK).

"Various utilisations of solid electrolytes", by M. Voïnov, BATTELE, Geneva Research Centre (Switzerland).

At the end of each course a summary of the discussions that followed are presented. This second part of the book has a very practical value, because it offers a complete review of these applications and particularly of electrode phenomena in the light of the different theoretical approaches discussed in the first part.

Both the qualities of contents and the graphic presentation make the book titled : "Electrode processes in solid state ionics", edited by M. Kleitz and J. Dupuy, a very valuable reference source for researchers who are working in fields where electrode processes in solid state are involved.

Iuliana Vartires

NOTE POUR LES AUTEURS

La Revue Roumaine de Chimie publie des articles en anglais, français, russe, allemand ou espagnol. Les auteurs sont priés d'envoyer des articles et des comptes rendus inédits.

Les manuscrits seront dactylographiés à deux intervalles. La bibliographie, les tableaux et la légende des figures seront placés après le texte.

Si l'article fait partie d'une série numérotée, le titre de la partie précédente sera indiqué dans une note au bas de la première page.

Chaque article sera précédé d'un résumé comprenant quinze lignes au maximum.

Les références bibliographiques dans le texte seront faites par des exposants sans parenthèse et paraîtront comme des notes au bas de chaque page.

Les publications périodiques mentionnées dans la bibliographie seront présentées suivant les prescriptions internationales : le nom de l'auteur précédé de l'initiale du prénom, le titre du périodique abbrégé conformément à « Chemical Abstracts » et souligné par une ligne, le numéro du tome, indiqué par des chiffres arabes et souligné par deux lignes, suivi de la première page de l'article ;à la fin, l'année de la parution sera placée entre parenthèses. Le numéro de la revue ne sera pas indiqué si les pages du volume sont numérotées consécutivement. Pour les revues dont les tomes ne sont pas numérotés (par ex. Bull. Soc. Chim. France, etc.), l'année de la parution soulignée par deux lignes précèdera l'indication de la page.

Les textes des livres ou traités inclueront : les noms des auteurs, les initiales du prénom, le titre du livre entre guillemets et sans être souligné, le numéro du tome précédé par l'abbréviation « p » (ou « S »).

Les brevets seront indiqués comme suit : l'auteur ou la firme, le pays et le numéro du brevet, la date et la revue (Chem. Abstr.). Par ex. : M. Jones (to Union Carbide Co.), Brit-Pat. 601 238, 2 Sept. 1959, *Chem. Abstr.*, **54**, 12808 (1960).

Si la référence n'a pas été lue en original, on indiquera aussi la revue de références consultée.

Les diagrammes seront tracés à l'encre de Chine sur papier calque. Les tableaux et les figures (en nombre strictement nécessaire) seront numérotés par des chiffres arabes et leur explication sera donnée dans la légende des figures. Prière de ne pas inscrire les mêmes données dans les tableaux et les figures. Chaque tableau aura un titre. On indiquera dans le texte la place approximative des tableaux et des figures. Les formules chimiques seront incluses dans le texte ; en outre, elles seront transcrites sur papier calque, à l'encre de Chine.

Les auteurs sont priés d'indiquer les caractères italiques (en soulignant les lettres au crayon), ainsi que tout autre caractère spécial ; les préfixes *ortho*, *meta*, *para*, *cis*, *trans*, etc. seront soulignés pour indiquer leurs caractères italiques et ne seront jamais écrites avec des majuscules.

Aucune correction à main ne sera admise sur le manuscrit. Les corrections seront frappées à la machine. Les lettres grecques ou d'autres symboles spéciaux seront insérés à la main à l'encre clairement.

Le manuscrit sera signé par l'auteur.

Le colonne-titre aura 50 lettres au maximum.

L'entière responsabilité du contenu des articles appartient aux auteurs.

1977 JUL 28

TRAVAUX PARUS AUX ÉDITIONS DE L'ACADÉMIE DE LA RÉPUBLIQUE SOCIALISTE DE ROUMANIE

GR. POPA, Ş. MOLDOVEANU, **Reactivii organici în chimia analitică** (Les réactifs organiques dans la Chimie analytique), 1976, 255 p., 18 lei.

P. BALTĂ, E. BALTĂ, **Introduction to the physical chemistry of the vitreous state**, 1976, co-édition avec Abacus Press, 287 p., 31 lei.

I. GĂLĂŢEANU, **Radiochimia aplicată** (La Radiochimie appliquée), 1976, 307 p., 19 lei.

I. G. MURGULESCU, **Introducere în Chimia fizică. Vol. I. Atomi, molecule, legătură fizică** (Introduction à la Chimie physique. Ier vol. Atomes, molécules, liaison chimique), 1976, 559 p., 36 lei.

CONST. V. UGLEA, **Cromatografia pe gel permeabil. Noi domenii de aplicare** (La chromatographie sur gel perméable. Nouveaux domaines d'application), 1976, 123 p., 6,75 lei.

FRANCISC A. GOTHARD, **Echilibre lichid—vapori. I. Baze teoretice şi metode de calcul** (Equilibres liquide—vapeurs. I. Bases théoriques méthodes de calcul), 1975, 263 p., 2 pl., 28 lei,

CONST. GH. MACAROVICI, D. MACAROVICI, **Chimia oxizilor dubli şi utilizările lor** (La chimie des oxydes doubles et leur utilisation), 1965, 195, p., 13 lei.

M. AVRAM, **Antidăunători** (Pesticides), 1974, 496 p., 41 lei.

ELENA CEAUŞESCU, **Research work on synthesis and characterization of macromolecular compounds. Contributions**, 1974, 251 p., 20 lei.

DUMITRU COSTACHE, **Analiza chimică prin metoda cinetică** (L'Analyse chimique par la méthode cinétique), 1974, 275 p., 15,50 lei.

G. A. RĂDULESCU, **Proprietăţile ţiţeiurilor româneşti** (Les propriétés des pétroles roumains), 1974, 267 p., 2 pl. 18 lei.

CR. SIMIONESCU, VIORICA RUSAN, V. POPA, **Chimia algelor marine** (La chimie des algues marines), 1974, 212 p., 1 pl., 18 lei.

I. ZUGRĂVESCU, MAGDA PETROVANU, **Chimia n-ilidelor** (La chimie des n-Illures), 1974, 348 p., 19 lei.

MARIA FITI, **Dozimetria chimică a radiaţiilor ionizante** (La dosimétrie chimique des radiations ionisantes), 1973, 240 p., 13,50 lei.

TIBERIU NAŞCUŢIU, **Metode radiochimice de analiză** (Méthodes radiochimiques d'analyse), 1973, 384 p., 23 lei.

CRISTOFOR SIMIONESCU, MARGARETA GRIGORAŞ, AGATA CERNĂTESCU-ASANDEI, ROZMARIN GHEORGHE, **Chimia lemnului în România. Plopul şi salcia** (La Chimie du bois en Roumanie. Le peuplier et le saule), 1973, 299 p. 13 pl. 26 lei.

Lei 25.—

$ 35 (pour un abonnement annuel)

I.P.I. c. 1694

43426

F 1103

ACADÉMIE DE LA RÉPUBLIQUE SOCIALISTE DE ROUMANIE

REFERÁLVA

REVUE ROUMAINE DE CHIMIE

Hommage au Professeur
CORIOLAN DRĂGULESCU
à l'occasion de son 70ᵉ anniversaire

TOME 22
N° 4
Avril 1977

EDITURA ACADEMIEI REPUBLICII SOCIALISTE ROMÂNIA

Rev. Roumaine Chim., RECHAX, 22, 4, p. 481–644 (1977), Bucarest

ACADÉMIE DE LA RÉPUBLIQUE SOCIALISTE DE ROUMANIE

COMITÉ DE RÉDACTION

Rédacteur en chef:

I. G. MURGULESCU, membre de l'Académie de la République Socialiste de Roumanie

Rédacteurs en chef adjoints:

A. T. BALABAN et V. EM. SAHINI, membres correspondants de l'Académie de la République Socialiste de Roumanie

Collège de rédaction:

EM. BRATU, ELENA CEAUȘESCU, ECATERINA CIORĂNESCU-NENITZESCU, C. DRĂGULESCU, CR. SIMIONESCU, membres de l'Académie de la République Socialiste de Roumanie; P. SPACU, membre correspondant de l'Académie de la République Socialiste de Roumanie; MARGARETA AVRAM, I. HAIDUC, D. I. MARCHIDAN, I. MOLDOVAN, G. NIAC et D. SĂNDULESCU

La Revue Roumaine de Chimie paraît 10 fois par an. Toute commande de l'étranger (fascicules ou abonnements) sera adressée à ILEXIM Departamentul Export-Import Carte (Livres)/Departamentul Export-Import Presă (Revues), P.O.B. 136–137, télex 11226, Bucarest 3, str. 13 Decembrie, Roumanie

Les manuscrits, les livres et les revues proposés en échange, ainsi que toute correspondance seront envoyés à la rédaction:

REVUE ROUMAINE DE CHIMIE

23, str. Dumbrava Roșie, Bucarest, Roumanie, téléphone 12 41 60

EDITURA ACADEMIEI REPUBLICII SOCIALISTE ROMÂNIA

125, Calea Victoriei, 71021, Bucarest, Roumanie, téléphone 50 76 80

ORSZÁGOS MŰSZAKI KÖNYVTÁR ÉS DOKUMENTÁCIÓS KÖZPONT 1883

REVUE ROUMAINE DE CHIMIE

Tome 22, N° 4 Avril, 1977

Professor CORIOLAN DRĂGULESCU 483–489

П. К. АГАСЯН, Е. Р. НИКОЛАЕВА, Р. Д. ЧАВДАРОВА, Кулонометрические методы определения рения 491–501

И. П. АЛИМАРИН, А. П. ГОЛОВИНА и В. К. РУНОВ, Ионные ассоциаты родаминовых красителей с анионными хелатами и их химико-аналитическое использование 503–509

ILSE-IRINA BACALOGLU, R. BACALOGLU, D. MARTIN und ANNA PRÜFER, Struktur-Reaktivitätsuntersuchungen mit heterosubstituiertem Nitrilen. XVII. Kinetik und Mechanismus der Trimerisation der Arylcyanate in Gegenwart von $AlCl_3$ 511–515

A. T. BALABAN, E. M. PALMER and F. HARARY, Chemical graphs. XXIX. Numbers of isomers with naphthalene and adamantane skeletons . . . 517–523

P. BALTĂ and D. RADU, Some information about the geometry of the molecules in molten and solid glasses 525–530

R. BELCHER, HELENA PUZANOWSKA-TARASIEWICZ and W. I. STEPHEN, An examination of various phenothiazine derivatives as indicators in vanadometry 531–537

MARIA BREZEANU and MAGDALENA DINCULESCU, Polynuclear complex compounds of iron, cobalt and nickel. I. Mercury-containing complex compounds 539–544

M. CAIS, P. ASHKENAZI and J. GOTTLIEB, Spin-trapping experiments with pentadienyl- and cycloheptadienyl-iron tricarbonyl cations 545–549

N. CALU, N. FOCA and M. LUCHIAN, The UV, VIS and IR spectra of the $Pd(p\text{-}NO.C_6H_4N(CH_3)_2)_2Cl_2.H_2O$ 551–555

A. CĂLUȘARU, Hydroxide precipitation and metal dendrite formation at the limiting current on DME 557–562

D. CEAUȘESCU and V. ELIU-CEAUȘESCU, The equivalence point and the confidence interval of linear titration curves in the outlook of normal bidimensional distribution of branches 563–567

M. B. ĆELAP and M. J. MALINAR, Synthesis and absolute configuration of the nitrobis(aminoacidato)amminecobalt(III) complexes 569–574

R. A. CHALMERS and A. F. J. JACKSON, Critical evaluation of fluorimetric assay methods for morphine 575–581

GH. CIUHANDU, OLGA BÉCZY und GH. OANCEA, Photometrische Bestimmung einiger aromatischer Amine durch Kupplung mit dem *p*-Nitrobenzoldiazonium-Ion 583–586

Revue Roumaine Chim. **22**, *4*, 481–644 (1977) Bucarest

J. M. DANCE, A. TRESSAUD, J. PORTIER et P. HAGENMULLER, Sur quelques nouvelles séries de fluorures ferrimagnétiques 587–600

CIRILA DJORDJEVIC, Heteroligand peroxo complexes of some d^0 transition metal ions 601–605

ILEANA DRĂGUŢAN, M. ELIAN and ECATERINA CIORĂNESCU, Rearrangements of the benzobicyclo[3.2.2] nonene to the benzobicyclo[3.3.1]nonene system 607–610

GH. FACSKÓ, C. RADOVAN und C. DAMINESCU, Eine Deutung des Einflusses der Arbeitsbedingungen auf die Stromausbeute bei der elektrolytischen Abscheidung von metallischen Pulvern 611–617

V. GUTMANN, Ladungsdichteveränderungen durch Donator-Acceptor-Wechselwirkungen 619–624

I. HAIDUC, GH. MARCU and MARIA CURTUI, Solvent extraction of uranium(VI) with dialkylphosphorodithioic acids. V. Synergistic effect of tributylphosphate 625–632

L. KÉKEDY and M. ŞERBAN, Zero-current bipotentiometric end-point indication with pretreated electrodes. IV. Use of pretreated silver electrodes . . . 633–638

W. KLEMM, Some considerations on the nomenclature of inorganic chemistry 639–643

Prof. CORIOLAN DRĂGULESCU

Professor CORIOLAN DRĂGULESCU

Professor Dr. Doc. Coriolan Drăgulescu, member of the Romanian Academy, President of the Section of chemical sciences of the Romanian Academy, Professor of inorganic chemistry at the Polytechnic Institute "Traian Vuia" in Timişoara and also Director of the Research Base of the Academy and Director of the Centre of chemistry, both located in Timişoara, is 70 years old on the 4th of April, 1977. His scientific personality, his determining role in creating a modern school of inorganic chemistry in the capital of Banat and his manysided activity in the chemical higher education and in scientific research are known and unanimously appreciated throughout the world.

This issue of our journal includes papers of numerous Romanian and foreign researchers who want to pay him thereby their respect.

Professor Coriolan Drăgulescu was born in Banat, Vărădia village, Caraş-Severin district, on April 4, 1907.

After completing his primary studies in his native village, he attended the courses of the high-school "C. Diaconovici-Loga" in Timişoara, from which he graduated in 1925.

As a student of the Cluj University, in the chemistry section of the faculty of sciences, he stands out by his enthusiastic work both in the laboratory and in the library, obtaining in 1930 B. Sc. degree in chemistry.

Working thereafter with the Laboratory of physical chemistry as an instructor, he prepares his doctoral thesis in this field under the guidance of Professor D. Rădulescu and obtains the doctoral degree in 1936.

As early as 1934 he is employed as an assistant-professor at the chair of inorganic and analytical chemistry, becoming a collaborator of Professor Gheorghe Spacu under whose guidance he was trained as a valuable researcher in inorganic and analytical chemistry.

As the faculty of science of Cluj had moved to Timişoara due to conditions imposed by World War II, he was appointed lecturer in 1944 at the same chair, headed by that time by the distinguished Professor Raluca Ripan.

In 1945 he moves to the Polytechnic Institute in Timişoara holding the position of permanent professor of general and agricultural chemistry at the new faculty of Agronomy established in the framework of the Polytechnic. His contribution to its establishment was substantial.

In 1948, owing to his enthusiastic and competent work developed together with Professor I. G. Murgulescu, Rector of the Polytechnic Institute in Timişoara, his name becomes associated with a very important achievement for the chemical engineering in our country namely the creation of the Faculty of industrial chemistry in Timişoara. On this occasion he becomes the head of the Chair of inorganic and analytical chemistry at the new faculty, being at the same time Dean of this faculty. He held this position until 1956 when he was appointed Rector of the Polytechnic Institute in Timişoara and shortly thereafter he became Deputy Minister of Education.

In 1957 he resumes his function as a dean, fulfilling it until 1963 when he is appointed Director of the Scientific Research Base of the Romanian Academy in

Timişoara. Since 1951 he was given the task to organize and directiy control the chemical research activities in this institute.

Initially as a chemistry section then a research centre, the Centre of Chemistry in Timişoara — which is at present a component unit of the Central Institute for Chemical Research of the Ministry of Chemical Industry, has been and is led by Prof. Coriolan Drăgulescu.

Between 1962—1968 he worked as a professor of Inorganic chemistry and head of department at the faculty of chemical engineering of the Polytechnic Institute of Bucharest as well as Director of the Centre of Inorganic Chemistry of the Academy, in Bucharest.

As a recognition of his special merits in his scientific activity, in higher education and in the cultural movement, professor Drăgulescu is elected corresponding member of the Academy in 1955, becoming full member in 1963 and president of the section of chemical sciences of the Academy in 1974.

During his unremitting didactic and scientific activities he has always supported the new directions appearing both in theory and in the experimental activity. The twenty-five series of chemical engineers whose teacher he has been, meet every year to celebrate their graduation and on such occasions, the "festive courses" held by Prof. C. Drăgulescu, attractive by the novelty of their content and by their subtle humour, are followed with pleasure and interest.

The scientific work of Professor Coriolan Drăgulescu reflected in over 230 publications — among which 4 books — and in his contribution to the training of more than 40 researchers who have obtained a doctoral degree, is primarily materialized along the following directions:

— separation and obtention of metal compounds from local natural resources by the most up-to-date methods;

— original contributions to the study of the chemistry of metal compounds such as: bismuth, zirconium, hafnium, thorium, uranium, niobium, tantalum and others, either in view of obtaining new coordination compounds or to establish or improve analytical methods;

— original studies in the coordination chemistry of metal complexes with complexing ligands namely new synthesis and separation approaches in nonaqueous solvents or by means of volatile compounds.

The methods which he has constantly advanced in research work include the latest scientific advances. His creative theoretical interpretations have been made in the light of the most recent scientific views.

His original results have been presented at important scientific events in Romania and abroad. His papers presented at I.U.P.A.C. congresses and at related conferences : I.C.C.C. and I.C.N.A.S. were among communications reported at 36 scientific events.

His devotion to fundamental principles, his modesty and humane attitude have characterized his entire activity and his relationships with colleagues, co-workers and students. These distinguished features have made people love and esteem him.

He has constantly worked with abnegation and perseverance — even in the hardest moments of his life — and keeps working in this way. As a member of numerous working groups in Romania and abroad, representative of our country to I.U.P.A.C. and Pugwash conferences, he has developed a fruitful activity, deserving the respect of his co-workers.

Animated by the generous ideals of socialism ever since his university studies, he has continuously developed an intense political and social activity, permanently militating for the triumph of justice and equity. Being a member of the Communist Party since the period of its underground activity (1941), he has accomplished for the last 35 years numerous and important tasks which have evidenced his wisdom and generosity.

Taking into account the highly important role played by him as a scientist, professor and organizer, and also his outstanding cultural and social merits, Professor Coriolan Drăgulescu was awarded several medals, distinctions and honorary titles such as the Order of Work (1962) the Order of Scientific Merit (1966), emeritus scientist (1970).

All his achievements, results of his untiring activity, have brought Professor Coriolan Drăgulescu the high appreciation and profound esteem on the part of Romanian and foreign chemists and the love of his colleagues, collaborators and students.

On the occasion of his 70th birthday, the Editorial Board of "Revue Roumaine de Chimie" whole-heartedly join all those who have known and loved him, wishing him a long and happy life, full of spiritual freshness, so that he may carry on his important creative activity.

THE EDITORIAL BOARD

Owing to his activity of over 45 years in the field of chemistry, **Professor Coriolan Drăgulescu**, member of the Romanian Academy, has won an outstanding place in our chemical industry, which, based on the tradition of an old shcool of Romanian chemists, is now competitive on the world market and has an important weight in the national economy.

His clear insight, a particular feature of future-oriented personalities, made Professor Coriolan Drăgulescu publish as early as 1930 works on petroleum and its economic importance, relating this raw-material, which at present governs the world, to the policy of big international concerns involved by that time in the management of petroleum all over the world.

Hardly a quarter of a century has passed since 1930, when the young graduate from the University of Cluj, Coriolan Drăgulescu started his activity, then petroleum became the basic raw material for the new field of petrochemistry, including the whole line of products, from petroleum products with high characteristics, to new organic synthesis products, monomers, polymers, elastomers, synthetic fibers, pesticides, pharmaceuticals, dyestuffs and laquers, etc.

Small refineries with their old technology have been replaced by huge plants producing millions of tons and with the most sophisticated and up-to-date technological processes for the best use of raw materials.

Born in the Banat region, Professor Coriolan Drăgulescu has remained devoted to those beautiful places. However, he developed his activities, full of abnegation and whole-heartedly, in Cluj, between 1930 and 1940, at the Polytechnic Institute of Timişoara since 1945 until now; in Bucharest he was professor at the chair of inorganic chemistry of the Faculty of Chemical Engineering of the Polytechnic Institute, and Deputy Minister of Education.

He has participated in many important scientific events both in Romania and abroad — U.S.A., Federal Republic of Germany, France, Italy, Spain, Switzerland, Austria, Czechoslovakia, Hungary, USSR, Poland, Japan, Israel and India — where, as a messenger of his country he showed the results of our research school in the large field of analytical and of inorganic chemistry.

As a result of his rich scientific activity he was elected member and national representative on the I.U.P.A.C. Council and honorary member of the Industrial Chemistry Society in Paris.

As an initiator and active participant in a number of technical-scientific events in Romania, in congresses, symposia or other meetings, he contributed with personal papers, introducing to the chemical research work young specialists who have subsequently been remarked as distinct personalities.

As an organizer and participant in such events of a high scientific level Professor Coriolan Drăgulescu delivered prestigious papers, taking an active part in discussions and proposals and standing out as a researcher with a vast scientific activity closely related to the practical applicability. He also proved to be a passionate forerunner of innovation. It is hard to review the over 250 titles, papers and books, written in more than 46 years of manysided activity. Nevertheless we must mention the studies evidencing modern methods of determination and analyses of chemical products, such as: potentiometric titration of the antimony ion; determination of the mixed silver and thallium phosphate; potentiometric titration of arsenic, tin etc; conductimetric titration of selenocyanides, of lead, of bismuth, etc; conductimetric study of the formation of bismuth phosphate; solubility of the mixed silver and thorium phosphate; new methods for determining some elements in the family of lanthanides and actinides; studies on the precipitation of ammonium uranates, precipitation of uranium salts with aromatic amines, etc.

He has particularly supported the technological processes in view of turning to good accounts some valuable subproducts from the manufacturing of phosphoric acid by acid attack of phosphatic ores. An important contribution was made in the elucidation of basic aspects in the obtention of magnesium oxide from various locally available materials, etc.

As a highly appreciated professor, he has carried on a permanent training programme, not only in chemistry but also as an educator, a good patriot and citizen, winning thereby the appreciation of whole generations of engineers and chemists.

On the political and social level, he has linked his entire activity to the interests of the working class and of the Romanian people.

From his professional activity we note only a few works, such as "Practical Manual of Physical Chemistry, Thermodynamics and Kinetics" (Timişoara, 1941); "A Course in Inorganic Chemistry, Part I and II (1954—1955) and "Modern Inorganic Chemistry" (1975).

A retrospective view on the vast activity developed by Prof. Coriolan Drăgulescu on the occasion of his 70th anniversary in the social-educational and political field, as a guide, on councils state and faculty committes or in editorial boards of various publications, in all the domains approached, reveals the scientific-objective nature of this activity.

In the political domain where he has worked ever since he was a student he published several articles from which we cite:

— "The Sino-Japanese conflict", published in 1932;
— "Managers of a fascist system" (1933);
— "The force and the organization of the red army" (1933);
— "Hitlerism failed to keep its promises to peasants" (1936);
— "The condition of middle classes in Germany" (1937);

The value of such article and studies has increased for us both due to their combativity and to the courageous attitude of a fighter who has overtly expressed his opinions even when the shadows of fascism had started to darken the horizon.

The fundamental and applicative research activity at the Chemistry Centre of the Romanian Academy, the Timişoara branch, organized by Prof. Coriolan Drăgulescu and later on, the activity developed by the Centre of Chemical Research in the same city have achieved a solid link between theory and practice, between fundamental and applicative research. It can be stated that this aspect is reflected by all the works prepared under the guidance of Prof. Coriolan Drăgulescu.

By developing applicative research, he established a close link between the chemical enterprises in Craiova, Piteşti, Făgăraş, Victoria, Ocna Mureş, Valea Călugărească and Turnu Măgurele and the preoccupations of the Centre of Chemical Research in Timişoara as well as those of the chairs of the Faculty of Chemical engineering in Timişoara.

Valuable chemists, endowed with solid training, know-how, love for their work and patriotism, have gathered around him.

The merits of Prof. Coriolan Drăgulescu strongly revealed by his brilliant results place him, after an activity of almost half a century, in the first rank of chemists in our country, confirm him as an appreciated representative of analytical and inorganic chemistry, a name that has passed the borders of our country with important works and a lively, tonic and unexhausted enthusiasm.

On the occasion of his 70 years anniversary, we express our unanimous, grateful appreciations, full of admiration for his rich activity, for his dignified behaviour, for his untiring work as a university professor and clear-sighted guide of our chemical industry, a young and promising branch of our national economy. May the eighth decade of his life be filled with fruitful activities in the field of Romanian chemistry, developed together with all of us who appreciate and esteem him — as a brilliant representative among those who have contributed to the advance of Romanian chemical science and technology.

MIHAIL FLORESCU
Minister of the Chemical Industry

Revue Roumaine de Chimie, **22**, *4*, 491–501 (1977)

Посвящается проф. Кориолану Дрэгулеску
по случаю его 70-летия

КУЛОНОМЕТРИЧЕСКИЕ МЕТОДЫ ОПРЕДЕЛЕНИЯ РЕНИЯ

П.К. АГАСЯН, Е. Р. НИКОЛАЕВА, Р.Д. ЧАВДАРОВА
Московский государственный университет им. М. В. Ломоносова
Высший химико-технологический институт, София

Получена 12 августа 1976 г.

Установлены оптимальные условия внутренней электрогенерации Sn(II), Ti(III) и Mn(III) из соответствующих солей в сильно кислых средах (HCl и H_2SO_4) на угольном электроде, пропитанном парафином под вакуумом. Указанные титранты использованы для кулонометрического титрования Re(VII), (V) и (IV). Разработанные методики определения рения применены к модельным растворам и при анализе некоторых рений содержащих производственных материалов.

Многообразие степеней окисления рения (от -1 до + 7) является теоретической предпосылкой для разработки электроаналитических методов его определения.

Электрохимическое восстановление рения (VII) на макроэлектродах из различного материала в потенциостатическом [1–5] и амперостатическом[6–9] режимах использовано для изучения механизма соответствующих процессов и получения различных форм окисления рения. Лишь в работе[3] приведены условия, при которых Re(VII) количественно восстанавливается на сетчатом Pt-электроде до Re (IV), между тем, как в потоке жидкости на электроде из пористого стекла, покрытого черной платиной, в тех же условиях — с участием только одного электрона. Этот факт автор объясняет различием в скоростях реакций электрохимического восстановления Re (VII) до Re(VI), являющегося быстрой стадией и диспропорционирования Re(VI) до Re(VII) и Re(IV) — медленной.

[1] J. C. Hindman and P. Wehner, *J. Amer. Chem. Soc.*, **75**, 2869 (1953).

[2] P. Wehner and J. C. Hindman, *J. Amer. Chem. Soc.*, **75**, 2873 (1953).

[3] J. A. Shropshire, *Electroanal. Chem.*, **9**, 80 (1965).

[4] J. A. Shropshire, *Electroanal. Chem.*, **16**, 275 (1968).

[5] С. И. Синякова, А. М. Демкин и Л. В. Борисова, *Ж. аналит. химии*. **28**, 1974(1973)

[6] Д. И. Рябчиков, В. А. Заринский и И.И. Назаренко, *Ж. неорг. химии*, **6**, 1138 (1961).

Электрохимическое окисление металлического рения в кислой и щелочной средах протекает количественно с образованием Re(VII), [10–13] что использовано для разработки прямого кулонометрического метода определения рения в сплавах и покрытиях, осажденных на более благородных металлах. Определение проводят в кислой среде при постоянной величине анодного тока растворения по резкому изменению потенциала анода в момент завершения окисления рения.[10,11]

Из известных для титриметрического определения рения окислительно-восстановительных реакций [14–22] в кулонометрии применены лишь ряд редуктометрических методов определения Re(VII). Так, в качестве промежуточного реагента использован Ti(III), внутренне генерированный при 85° из 8 М раствора H_2SO_4 0,6М по $Ti(SO_4)_2$ и 0,2 М по H_3PO_4 на сетчатом Pt-электроде; при этом Re(VII) восстанавливается до Re (IV). Индикация конечной точки титрования (к.т.т.) осуществлена потенциометрически. Определено 0,4—4 мг Re(VII) с относительным стандартным отклонением 0,9—0,1%. [23]

При электрогенерации Cu(I) и Sn(II) из активных электродов конечным продуктом титрования Re(VII) является только Re(V), [24,25,13] в то время как полученный аналогичным путем кулонометрический титрант-Cr(II) вызывает, как и Ti(III), более глубокое восстановление — до Re(IV). [26]

Оптимальной средой для генерации всех указанных титрантов является HCl [1 М — для Sn(II) и Cr(II), 6М — для Cu(I)]; Sn(II) можно получить и на 1 М фоне NaOH. В случаях несовместимости условий

---

[7] Я. Тоул, Н. Г. Игнатьева и В. М. Пешкова, *Ж. аналит. химии*, **19**, 224 (1964).

[8] Д. И. Рябчиков, В. А. Заринский и И. И. Назаренко, *Ж. неорг. химии*, **6**, 641 (1961).

[9] G. Henze und R. Geyer, *Z. Chem.*, **11**, 437 (1968).

[10] S. Tribalat et D. Mofidi, *Compt. rend.* **258**, N 13, 3477 (1964).

[11] S. Tribalat, C. Piolet et D. Mofidi, *Bull. Soc. chim. France*, N 2, 844 (1968).

[12] A. Giraudeau, P. Lemoine et M. Gross, *Corrosion Sci.*, **13**, 421 (1973).

[13] М. И. Евгеньев, «Автореферат диссертации на соискание ученой степени кандидата химических наук», Изд. МГУ, (1976).

[14] Д. И. Рябчиков, В. А. Заринский и И. И. Назаренко, *Ж. аналит. химии*, **14**, 737 (1959).

[15] Д. И. Рябчиков, В. А. Заринский и И. И. Назаренко, *Ж. аналит. химии*, **15**,. 752 (1960).

[16] В. А. Заринский и В. А. Фролкина, *Ж. аналит. химии*, **17**, 75 (1962).

[17] З. А. Галлай, Т. Я. Рубинская и А. В. Фурсова, *Ж. аналит. химии*, **21**, 584(1966).

[18] Т. Я. Рубинская, Л. Б. Хусид и З. А. Галлай, *Ж. аналит. химии*, **22**, 1519 (1967).

[19] З. А. Галлай и Т. Я. Рубинская, *Ж. аналит. химии*, **21**, 961 (1966).

[20] G. Henze und R. Geyer, *Z. analyt. Chem.*, **200**, 434 (1964).

[21] I. Drwiega, *Chem. Analit.*, **13**, 281 (1968).

[22] З. А. Галлай и Т. Я. Рубинская, *Ж. аналит. химии*, **22**, 1378 (1967).

[23] Ch. Sheytanov, R. Chavdarova and M. Konstantinova, *Compt. rend. Acad. bulg. Sci.*, **19**, 1147 (1966).

[24] А. И. Костромин и Р. М. Бадакшанов, *Заводск. лаборатория*, **37**, 1057 (1973).

[25] А. И. Костромин, М. И. Евгеньев и Л. А. Новикова, *Ж. физ. химии*, **49**, 509 (1975).

[26] А. И. Костромин и М. И. Евгеньев, *Ж. аналит. химии*, **30**, 2047(1975).

химических и электрохимических реакций авторы использовали внешнюю генерацию титрантов. Для нахождения к.т.т. применяли потенциометрию и биамперометрию. При определении 0,1—0,3 мг рения относительное стандартное отклонение составляло в среднем ~1%.

Наши исследования посвящены изучению возможности использования углеродного электрода при внутренней генерации как восстановительных, так и окислительных кулонометрических титрантов: Sn(II), Ti(III) и Mn(Ш) для определения наиболее устойчивых и аналитически важных степеней окисления рения (+7, +5 и +4).

ЭКСПЕРИМЕНТАЛЬНАЯ ЧАСТЬ

Экспериментальная работа выполнена с реагентами ч.д.а. и х.ч. Ртуть (ч.д.а.) дополнительно очищали дистилляцией. Висмут и кадмий имели чистоту 99,999%. Все эксперименты проводили в атмосфере азота (99,999%).

В работе использованы: потенциостат-гальваностат ИПГ-410 В; спектрофотометр Pye Unicam SP 8000; электролитическая ячейка, описанная в [27]; рабочий электрод из стержня спектрального углерода (видимая поверхность $S = 28{,}3$ мм^2) пропитанный парафином под вакуумом;[28] платиновые пластины размером 1×1 см как вспомогательный и индикаторные электроды, а нас. к.э. как электрод сравнения (потенциалы в тексте выражены относительно нормального водородного электрода); сернокислые и солянокислые растворы $Ti(SO_4)_2$, $TiCl_4$, NH_4ReO_4 и $MnSO_4$ соответствующей концентрации.

Растворы $ReOCl^{2-}$ получили восстановлением Re(VII) в HCl конц. двумя эквивалентами KJ, [29,30] а сернокислые растворы Re(V) и Re(IV) — амальгамами висмута и кадмия соответственно в 9 и 4,5 M растворах H_2SO_4.[31] Концентрации Re(V) и Re (IV) в исходных растворах контролировали титрованием 0,01 M растворами $K_2Cr_2O_7$ или $Ce(SO_4)_2$ с потенциометрическим обнаружением к.т.т.

Растворы Re(V) и (IV) индентифицировали по спектрам их поглощения в видимой области. Результаты наших экспериментов, хорошо согласуемые с литературными данными[30,32,33] показали, что желто-зеленый раствор $ReOCl^{2-}$ с максимумами поглощения при 414, 480 и 780 нм обладает наибольшей устойчивостью (до 20 суток в HCl конц.). Синий же раствор Re(V) в 9 M H_2SO_4(λ макс. 590 нм) устойчив ~ 2 часа. Его разбавление водой до концентрации H_2SO_4 7 M приводит к быстрому изменению окраски в желтую (λ макс.$=440$ нм), отвечающий Re (IV)[33], а равным объемом HCl конц. — к образованию $ReOCl^{2-}$ с вышеуказанным спектром поглощения.

Для нахождения оптимальных условий кулономертического титрования Re(VII), (V) и (IV) изучали кривые поляризации C-электрода на различных фонах (4—10 M HCl и H_2SO_4 в катодной и 2—8 M H_2SO_4 в анодной областях потенциалов) и в присутствии вспомогательных реагентов (0,01—1 M $SnCl_4$; 0,1—1 M $TiCl_4$ и Ti $(SO_4)_2$; 0,2—0,4 M $MnSO_4$) и титруемых компонентов [10^{-4}—10^{-3} г-ион/л Re(VII), (V) и (IV)] в отдельности.

Оптимальные условия биамперометрической индикации к.т.т. устанавливали на основании изучения катодно-анодных кривых поляризации Pt-электрода в растворах при различной степени оттитрованности определяемого компонента электрогенерированным титрантом. Составы фонов для проведения намеченных исследований были выбраны на остовании сопоставления оптимальных условий химического взаимодействия различных степеней окисления рения с соответствующими титрантами (литературные данные) и их кулонометрического генерирования (наши данные). По этим же кривым можно было судить и о механизме соответствующих процессов титрования·

---

[27] Хр. Шейтанов и Р. Чавдарова, *Изв. отдел. хим. науки БАН*, **3**, 183(1970).

[28] П. К. Агасян и Т. К. Хамракулов, *Заводск. лаборатория*, **35**, 644(1969).

[29] W. F. Jakob und B. Jezows a, *Z. anorg. Chem.*, **220**, 16 (1934).

[30] Б. Ежовска-Тшебятов ка, С. Вайда и М. Балука, *Ж. структ. химии*, **8** 519 (1967).

[31] А. И. Лазарев, *Ж. неорг. химии*, **1**, 385 (1956).

[32] M. Pavlova, *J. Inorg. Nuclear Chem.*, **36**, 1623 (1974).

[33] Н. Йорданов и М. Павлова, *Ж. аналит. химии*, **24**, 865 (1969).

РЕЗУЛЬТАТЫ И ИХ ОБСУЖДЕНИЕ

Сравнение кривых катодной поляризации C- и Pt-электродов в 4—10 M растворах HCl и H_2SO_4 показало, что перенапряжение водорода на первом электроде в среднем на $\sim$0,9 в отрицательнее и зависит в большей степени от концентрации HCl, чем — H_2SO_4 (увеличение концентрации кислоты на 2 моль/л в указанных пределах концентраций вызывает смещение потенциала разряда фона на углероде в сторону менее отрицательных потенциалов на 0,1 и 0,05 в соответственно).

Перенапряжение анодного процесса фона (2 M раствора H_2SO_4) на C -электроде на $\sim$0,4 в больше, чем на платине. С увеличением концентрации кислоты на 2 моль/л начало разряда фона на платине остается практически неизменным, в то время как на C-электроде оно смещается на 0,1 в сторону менее положительных значений потенциалов.

Введение Re(VII) в растворы фонов не вызывает изменения в положении и форме кривых катодной и анодной поляризации Pt- и анодной — C -электрода, в то время как катодные кривые последнего смещаются в область менее отрицательных потенциалов с увеличением концентрации Re(VII). При постоянстве его содержания в растворе изменение концентрации HCl или H_2SO_4 вызывает такое же смещение кривых, как и в отсутствие Re (VII).

Электролиз с C-электродом в 6 M растворе HCl, содержащем 2.10^{-5} моль/л NH_4ReO_4 при I=1 ма в течение 10 мин не вызывал практически изменения потенциала рабочего электрода, а катодно-анодные кривые поляризации C- и Pt-электродов, снятые в растворе до и после электролиза, полностью совпали. Аналогичные результаты получены и в среде 8 M H_2SO_4. Следовательно, в данных условиях Re(VII) электронеактивен, хотя вызывает понижение перенапряжения водорода на C-электроде. С этим фактором следует считаться при оценке эффективности тока электрогенерации соответствующих промежуточных реагентов.

В катодной области потенциалов Re(V) и (IV) электронеактивны, что доказано совпадением кривых поляризации C- и Pt-электродов на всех изученных нами фонах в отсутствие и присутствии этих ионов.

Анодные кривые поляризации C- и Pt-электродов в присутствии Re(IV) на фонах HCl и H_2SO_4 имеют одинаковый характер — двухступенчатая волна окисления с $E_{1/2} \approx 0,6$ и 0,9 в.

В присутствии Re(V) на фонах 5—10 M H_2SO_4, содержащих 1 моль/л HCl, 4—8 M HCl и 8—10 M H_2SO_4 на кривых анодной поляризации Pt-электрода имеется волна окисления с $E_{1/2} \approx 1,0$ в, а C-электрода — с $E_{1/2} \approx 0,85$ в (кр. 5, рис. 1, в) В отсутствие ионов Cl^- в среде $\leqslant$ 7M H_2SO_4 анодная кривая для Re(V) аналогична кривой окисления Re(IV) (кр. 6, рис. 1 в). Этот факт следует объяснить диспропорционированием Re (V) на Re(VII) и Re (IV). Мгновенное диспропорционирование Re(V) обнаружено и в 8—10 M растворах H_2SO_4, содержащих 0,5 моль/л $Ti(SO_4)_2$ в отсутствие ионов Cl^-, что отмечено также в работе.[27]

На выше рассмотренных фонах в интервале концентраций от 0,01 до 1 и 0,1 до 1 моль/л $SnCl_4$ и $TiCl_4$ соответственно катодные кривые поляризации C-электрода смещаются в сторону менее отрицательных потенциалов с увеличением концентраций вспомогательных реагентов.

При постоянной концентрации Sn(IV) форма и расположение кривых i=f(E) С-электрода не зависит от концентрации HCl и H_2SO_4 в то время как при фиксированной концентрации Ti(IV) увеличение кислотности фона вызывает смещение кривых катодной поляризации в сторону положительных потенциалов.

С увеличением концентрации ионов Mn(II) от 0,2 до 0,4 моль/л кривые анодной поляризации этого же электрода на фоне 2—8 моль/л H_2SO_4 сдвигаются в сторону менее положительных потенциалов. Изменение концентрации H_2SO_4 не влияет на форму и расположение кривых при постоянном содержании Mn(II).

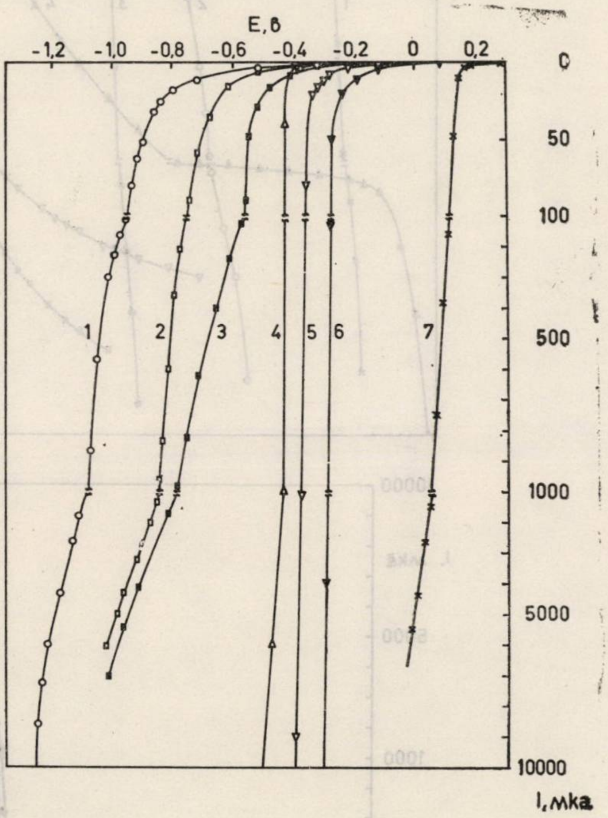

Рис. 1. — а) Кривые катодной поляризации углеродного (1-6) и платинового (7) электродов в 6 М растворе HCl (1; 7), содержащем: (2) $1{,}7 \cdot 10^{-4}$; (3) $8{,}3 \cdot 10^{-4}$ г-ион/л Re(VII); (4) 0,01; (5) 0,1; (6) 1,0 г-ион/л Sn(IV);

б) Кривые катодной поляризации углеродного электрода в 8 М растворе H_2SO_4 (1), содержащем: (2) $3{,}8.10^{-5}$; (3) $4{,}2.10^{-4}$ г-ион/л Re(VII); (4) 0,1; (5) 0,5; (6) 1,0 г-ион/л Ti(IV);

в) Кривые анодной поляризации углеродного электрода в 4 М растворе H_2SO_4 (1), содержащем: (2) 0,3 г-ион/л Cl^-; (3) 0,23; (4) 0,40 г-ион/л Mn(II); (6) $4{,}5.10^{-4}$ г-ион/л Re(V); и в 9 М растворе H_2SO_4, содержащем $4{,}5.10^{-4}$ г-ион/л Re(V) (5).

В присутствии Cl^- -ионов (0,3 г-ион/л) кривые поляризации С-электрода на фонах в отсутствие и присутствии Mn(II) практически совпадают, что делает невозможным генерацию Mn(III) в таких условиях.

В качестве примера на рис. 1 приведены кривые $i = f(E)$ С-электрода на фонах 6М HCl, 8 и 4 М H_2SO_4 в присутствии вспомогательных реагентов $SnCl_4$, $TiCl_4$ и $MnSO_4$ соответственно.

Расчеты на основание соответствующих кривых поляризации выхода по току электрогенерации кулонометрических титрантов на С-электроде показали, что 100% эффективность тока достигается в следующих усло-

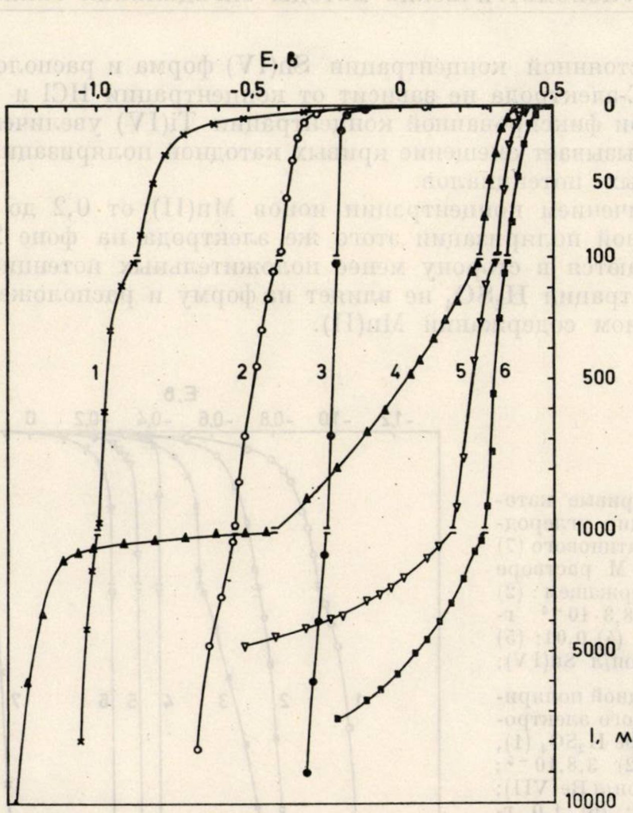
E, в
-1.0
-0.5
0
0.5
0
50
100
500
1000
5000
10000
I, мка
1
2
3
4
5
6

Рис. 1б

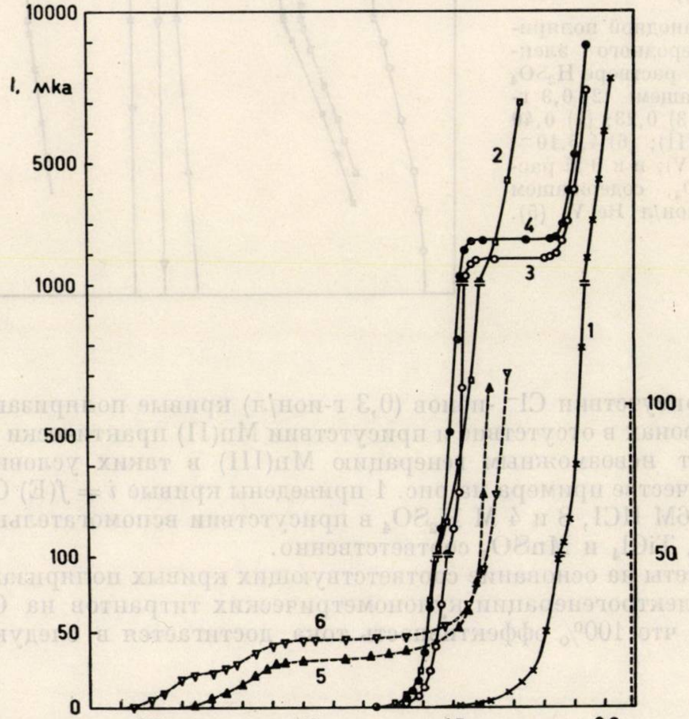
10000
I, мка
5000
1000
500
100
50
0
0.5
1.0
1.5
2.0
E, в
1
2
3
4
5
6
100
50

Рис. 1в

виях: Sn(II) —при $C_{Sn(IV)} \geqslant 0{,}1$ моль/л и $i = 0{,}3$—30 ма/см² на всех ранее указанных фонах; Ti(III) при $C_{Ti(IV)} \geqslant 0{,}5$ моль/л и $i = 0{,}3$—18 ма/см² в средах 10 М HCl и 6—8 М H_2SO_4; Mn(III) — при $C_{Mn(II)} \geqslant 0{,}4$ моль/л и $i = 0{,}3$—8 ма/см² на фоне 2 и 4 М H_2SO_4.

Эффективность тока генерации Sn(II) и Ti(III), вычисленная с учетом влияния Re(VII) на перенапряжение разряда фона, составляет 100% при несколько меньшем верхнем пределе плотности тока.

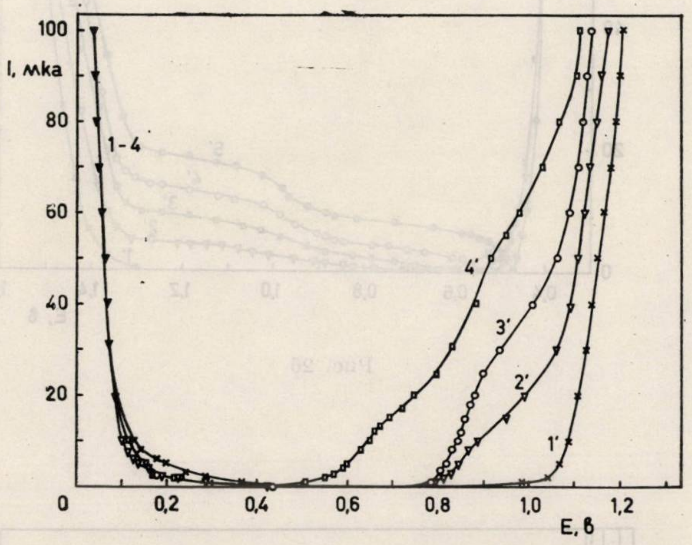

Рис. 2а. — Кривые катодно-анодной поляризации Pt-электрода: В 6 М растворе HCI, 0,143 М по $SnCI_4$, содержащем $7{,}78.10^{-5}$ г-ион/л Re(VII) (1) после электрогенерации $n.10^{-5}$ г-ион/л Sn(II), где n=3,89 (2); 7,78 (3); 11,7 (4); б) В 8 М растворе H_2SO_4, 0,5 М по $Ti(SO_4)_2$, содержащем $7{,}78.10^{-5}$ г-ион/л Re(VII) (1) после электрогенерации $n.10^{-4}$ г-ион/л Ti(III), где n=0,778 (2); 1,56 (3); 2,33(4); 3,11 (5); в) В 4 М растворе H_2SO_4 0,40 М по $MnSO_4$ (0), после внесения $4{,}28, 10^{-5}$ г-ион/л Re (V) (1) и электрогенерации $n.10^{-5}$ г-ион/л Mn(III), где n=4,28 (2); 8,56 (3); 12,8 (4).

Изучение катодно-анодных кривых Pt-электрода при различной степени оттитрованности растворов ранее перечисленными кулонометрическими титрантами показало, что восстановление Re(VII) оловом (II) на фоне 8 М H_2SO_4 и титаном (III) в средах 8М HCl или 8М H_2SO_4, содержащей 2 г-ион/л Cl^- происходит двухступенчато до Re(IV) через Re (V), что делает возможным раздельное титрование Re(VII) и (V) в их смеси. Восстановление Re(VII) оловом (II) в среде 6 М HCl (рис. 2а) протекает одностадийно до Re(V), а титаном (III) на фоне 8М H_2SO_4, не содержащей ионов Cl^- (рис. 2, б) или в присутствии лишь незначительных его концентраций ($\leqslant 0{,}03$ г-ион/л) — также одностадийно до Re(IV).

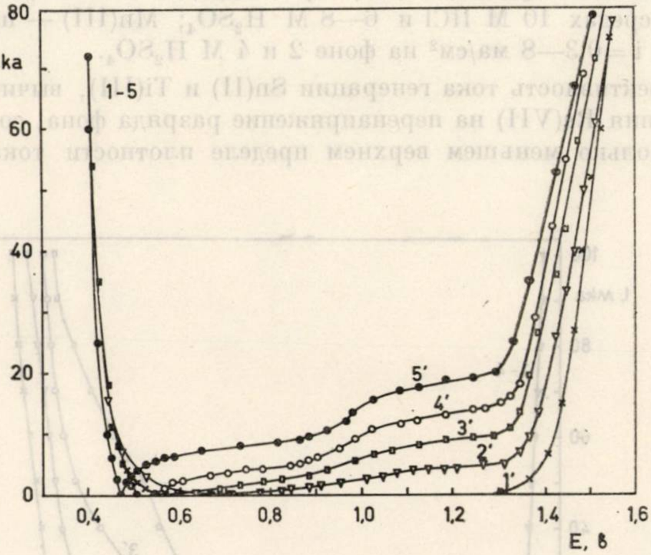
I, мка
80
60
40
20
0
1-5
5'
4'
3'
2'
1'
0,4
0,6
0,8
1,0
1,2
1,4
1,6
E, в

Рис. 2б

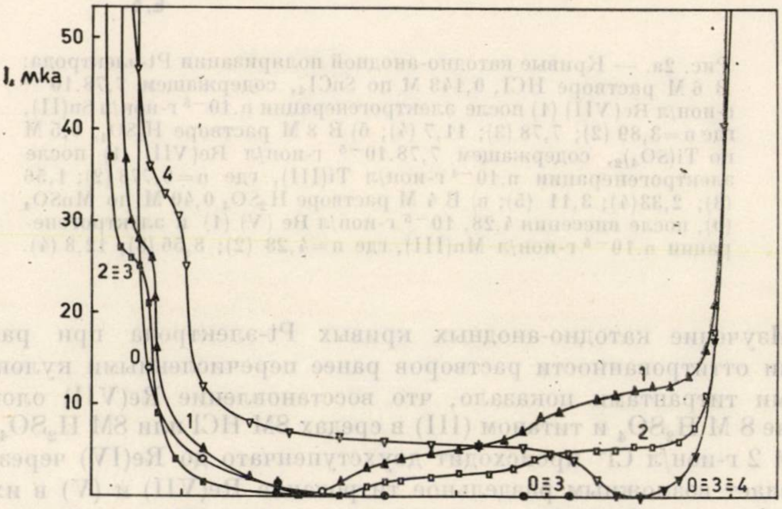
50
I, мка
40
30
20
10
0
4
2≡3
0
1
1
2
0≡3
0≡3≡4
0
0,2
0,4
0,6
0,8
1,0
1,2
1,4
E, в

Рис. 2в

Из-за диспропорционирования Re(V), кулонометрическое титрование в среде 4M H_2SO_4 растворов Re(IV) и (V) генерированным Mn(III) протекает как одностадийное окисление Re(IV) до Re(VII) (рис. 2, в).

На основании тех же катодно-анодных кривых Pt-электрода выбраны оптимальные напряжения (ΔE), налагаемые на индикаторные электроды при кулонометрическом титровании с биамперометрическим обнаружением к.т.т.

Несмотря на высокий выход по току и возможность биамперометрической индикации в широком диапазоне состава и кислотности среды, при проведении кулонометрического титрования в некоторых случаях возникли ограничения, связанные с получением плохо воспроизводимых и заниженных результатов. Это может быть обусловлено недостаточно большой скоростью протекания соответствующих электрохимических и химических реакций, а также упомянутой выше реакции диспропорционирования. В таблице приведены результаты кулонометрического титрования, проведенные в оптимальных условиях, обеспечивающих получение хороших воспроизводимости и правильности.

Методики кулонометрического титрования Re(VII)с биамперометрическим обнаружением к.т.т. электрогенерированным Sn(II) и Ti(III) опробированы при анализе, соответственно, молибденового концентрата и рениево-молибденового сплава, содержащего 48% Re (найдено $\overline{X}=$ $=47{,}7\pm0{,}5\%$). Для концентрата результат анализа ($0{,}623\pm0{,}008$) г/кг Re сравнили с данными, полученными спектрофотометрическим роданидным методом ($0{,}61_5\pm$ $0{,}02$) г/кг.

Сопоставляя результаты разработанных нами методик, можно заключить, что кулонометрические титранты Sn(II) и Ti(III) могут быть успешно применены для определения Re(VII) в зависимости от состава фонового раствора (HCl и H_2SO_4, соответственно). Духступенчатое протекание восстановления Re (VII) генерированным Ti(III) в среде 8M H_2SO_4, 0,5 M по $TiCl_4$ дает возможность раздельно титровать Re(VII) и (V) в их смеси. При определении небольших количеств Re(V) следует предпочесть оксидиметрическое титрование электрогенерированным Mn (III), так как при этом расходуется в два раза больше электронов, чем при редуктометрическом титровании, что увеличивает чувствительность метода в два раза. Диспропорционирование Re(V) в условиях титрования кулонометрически генерированным Mn(III) не делает возможным раздельное титрование этим титрантом Re(V) и (IV) в смеси. Это определение можно выполнить двумя последовательными титрованиями: Re(V) — электрогенерированным Ti(III) и смеси Re(V) и (IV) — электрогенерированным Mn(III).

Таблица

Результаты кулонометрического титрования Re (IV), (V) и (VII

Титрант, среда	Ток электролиза ма	Re(IV), мг	
		взято	найдено $\bar{X} \pm \varepsilon$
Mn(III)	1	0,248	0,249 ± 0,002
$C_{MnSO_4} = 0{,}4$ моль/л	1	0,124	$0{,}122_5$ ± 0,001
$C_{H_2SO_4} = 4$ моль/л	0,5	0,031	0,030 ± 0,001
Sn(II)	4		
$C_{SnCl_4} = 0{,}114$ моль/л	2		
$C_{HCl} = 6$ моль/л	1		
	2		
	1		
	1		
Ti(III)			
$C_{Ti(SO_4)_2} = 0{,}5$ моль/л	2		
$C_{H_2SO_4} = 8$ моль/л	0,5		
$C_{TiCl_4} = 0{,}5$ моль/л	2		
$C_{H_2SO_4} = 8$ моль/л	1		
	0,5		
	2		
	2		
	1		
	1		

1

электрогенерированными титрантами (V = 45 мл; n = 5; α = 0,95)

Re(V), мг		Re(VII), мг		Индикация к.т.т.
взято	найдено $\overline{X} \pm \varepsilon$	взято	найдено $\overline{X} \pm \varepsilon$	
0,368	0,366 ± 0,003			биампером.
0,184	0,184 ± 0,002			(ΔE = 500 мв)
0,046	0,047 ± 0,001			,,
		1,333	1,335 ± 0,006	потенциом.
		0,666	0,665 ± 0,006	($i = 0$)
		0,133	0,134 ± 0,002	,,
		0,666	0,664 ± 0,002	биампером.
		0,133	0,134 ± 0,001	(ΔE = 600 мв)
		0,066$_6$	0,067 ± 0,001	,,
0,536	0,537 ± 0,004	0,330	0,329 ± 0,004	биампером.
0,080	0,081 ± 0,002	0,033	0,034 ± 0,001	(ΔE = 200 мв)
1,340	1,338 ± 0,005	0,330	0,328 ± 0,003	биампером.
0,134	0,136 ± 0,002	0,133	0,133 ± 0,002	(ΔE = 100 мв)
0,043$_5$	0,044 ± 0,001	0,033	0,032 ± 0,001	,,
Смесь Re(V) + Re(VII)				
Re(V), мг		Re(VII) мг		
взято	найдено $\overline{X} \pm \varepsilon$	взято	найдено $\overline{X} \pm \varepsilon$	
1,340	1,343 ± 0,005$_5$	0,133	0,132 ± 0,002	,,
0,134	0,136 ± 0,003	0,665	0,665 ± 0,005	,,
0,134	0,132 ± 0,003	0,133	0,134 ± 0,002	,,
0,670	0,671 ± 0,004	0,066$_5$	0,065 ± 0,001	,,

Revue Roumaine de Chimie, **22**, *4*, 503–509 (1977)

Посвящается проф. Кориолану Дрэгулеску
по случаю его 70-летия

ИОННЫЕ АССОЦИАТЫ РОДАМИНОВЫХ КРАСИТЕЛЕЙ С АНИОННЫМИ ХЕЛАТАМИ И ИХ ХИМИКО-АНАЛИТИЧЕСКОЕ ИСПОЛЬЗОВАНИЕ

И. П. АЛИМАРИН, А. П. ГОЛОВИНА и В. К. РУНОВ
Институт геохимии и аналитической химии им. В. И. Вернадского
АН СССР, Москва

Получена 16 июля 1976 г.

В последнее время ионные ассоциаты, содержащие элементы, органические лиганды и основные красители,находят применение в аналитической химии. В данной работе систематизированы результаты исследований ионных ассоциатов ряда элементов с 8-оксихинолином, его производными и родаминовыми красителями. Обсуждается влияние природы лиганда, красителя на возможность определения элементов в виде таких ассоциатов. Особое внимание уделено спектрально-люминесцентным свойствам образующихся соединений.

В последнее время в литературе появляются работы по изучению ионных ассоциатов, содержащих элементы, органические лиганды и основные красители. В качестве лигандов использовано более 100 соединений различных классов: карбоновые кислоты, β-дикетоны, нитрозофенолы и -нафтолы, 8-оксихинолин и его производные. Катионами ассоциатов обычно служат родаминовые и трифенилметановые красители. Интерес к таким соединениям обусловлен рядом причин. Во-первых, расширяется круг элементов, образующих ионные ассоциаты с основными красителями. Это позволяет определить те элементы, для которых не характерно образование ионных ассоциатов основных красителей с металлогалогенидными комплексами (табл. 1). Во-вторых, усложнение структуры ионных ассоциатов основных красителей за счет анионного хелата может привести к повышению селективности определения элементов, входящих в этот ассоциат.

Нами исследовались ионные ассоциаты ряда элементов с 8-оксихинолином, его производными и родаминовыми красителями. Известно, что флуоресцентные свойства ионных ассоциатов этих красителей с металлогалогенидными комплексами определяются их катионной частью, то есть родамином. Мы ожидали, что его ассоциаты с анионными хелатами будут также интенсивно флуоресцировать. Но оказалось, что некоторые из них вообще не флуоресцируют. Поэтому представляло интерес выяснить причины, приводящие к тушению флуоресценции.

В спектрах поглощения исследуемых соединений имеются две полосы. Длинноволновая — характерна для родаминового красителя и коротковолновая — для хелата. Флуоресцентные свойства этих соединений зависят от природы элемента, хелатообразующего реагента и родаминового красителя.

Таблица 1

Элементы, образующие ионные ассоциаты с органическими лигандами и основными красителями

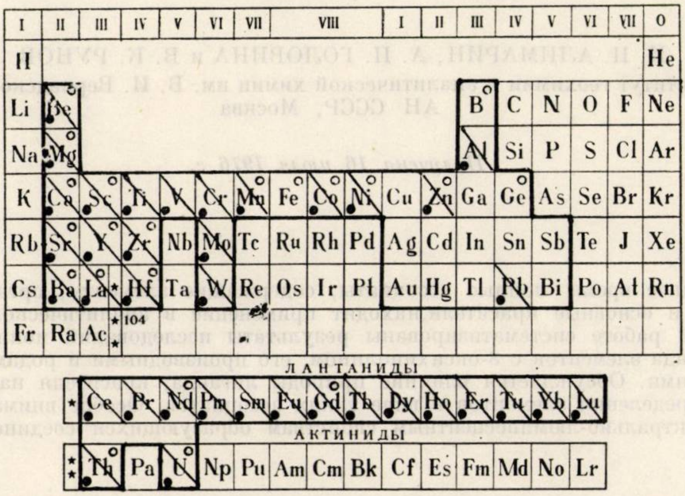
I II III IV V VI VII VIII I II III IV V VI VII 0
H He
Li Be B C N O F Ne
Na Mg Al Si P S Cl Ar
K Ca Sc Ti V Cr Mn Fe Co Ni Cu Zn Ga Ge As Se Br Kr
Rb Sr Y Zr Nb Mo Tc Ru Rh Pd Ag Cd In Sn Sb Te J Xe
Cs Ba La* Hf Ta W Re Os Ir Pt Au Hg Tl Pb Bi Po At Rn
Fr Ra Ac ** 104
ЛАНТАНИДЫ
* Ce Pr Nd Pm Sm Eu Gd Tb Dy Ho Er Tu Yb Lu
АКТИНИДЫ
** Th Pa U Np Pu Am Cm Bk Cf Es Fm Md No Lr

□° – имеются методики определения;

□ – указывается на возможность определения;

⧄ – не известны ионные ассоциаты с металлогалогенидными комплексами.

Интенсивно флуоресцируют ионные ассоциаты урана (VI), магния, кальция, цинка, кадмия, стронция, иттрия, лантана, тория с 5,7-динитро-8-оксихинолином и родамином В. На рис. 1 в качестве примера приведены спектры поглощения и флуоресценции ионного ассоциата тория с 5,7-динитро-8-оксихинолином и родамином В. Переходные металлы (железо, кобальт, никель, марганец) тушат флуоресценцию этих соединений. Флуоресценция ассоциатов лантанидов зависит от их природы. Наиболее интенсивно флуоресцируют ассоциаты лютеция (с заполненной

4f-оболочкой), гадолиния, имеющего высокую энергию возбуждения. Остальные лантаниды тушат флуоресценцию родаимна В, особенно церий и неодим.

Ионные ассоциаты, содержащие 8-оксихинолин, его 5,7-дигалоидпроизводные, 5-нитрозо-8-оксихинолин, не флуоресцируют независимо от входящего в их состав элемента.

Интересно отметить, что флуоресцентные свойства ассоциатов катионов красителей с анионами хелатообразующих реагентов (без элементов) также различаются. Эти соединения не флуоресцируют, если анионом служит диссоциированная молекула 8-оксихинолина или его 5-нитрозо и 5,7-дигалоидпроизводного, флуоресцирует в случае 5,7-динитропроизводного.

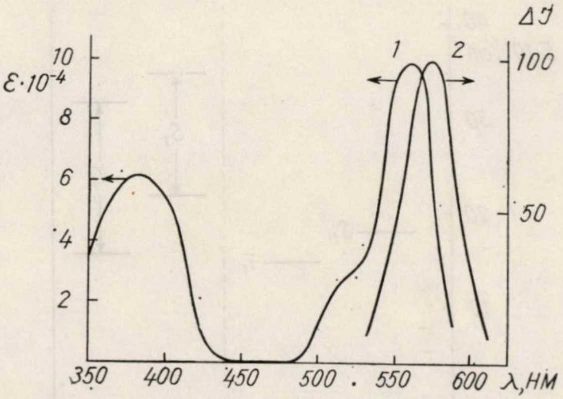

Рис. 1. — Спектры поглощения (1) и флуоресценции (2) бензольного экстракта ионного ассоциата теория с 5,7-динитро-8-оксихинолином $[HOx(HO_2)]_2$ и родамином B(RhB); pH = 1,80, $C_{HOx(NO_2)_2} = 3{,}8 \cdot 10^{-5}$ M, $C_{RhB} = 7{,}0.10^{-5}$ M.

Ранее [1] мы высказали предположение, что флуоресцентные свойства подобных соединений зависят от взаимного расположения синглетных и триплетных энергетических уровней молекул родаминовых красителей и органических лигандов. Для подтверждения этого предположения исследовались также ионные ассоциаты родаминовых красителей с фенолом, 2-нафтолом, бензойной, салициловой, 2-пиридинкарбоновой кислотами, 1-фенил-3-метил-4-бензоилпиразолоном-5. Энергии синглетных и триплетных уровней всех рассмотренных органических лигандов оценены по результатам спектрально-люминесцентных исследований, квантово-механических расчетов и по литературным данным. [2,3] Энергии нижнего синглетного уровня лигандов изменяются ~от 22 000 до 35 000 $см^{-1}$, а нижнего триплетного ~от 15 000 до 32 000 $см^{-1}$ (рис. 2). Оказалось, что интенсивно флоуресцирующие ионные ассоциаты образуют органические лиганды, энергии нижнего триплетного уровня которых ~15 000 $см^{-1}$ (5,7-динитро-8-оксихинолин) или ~25 000 — 32 000 $см^{-1}$ (фенол, бензойная, салициловая, 2-пиридинкарбоновая кислоты). Результаты проведенных исследований показывают, что тушение флуоресценции родаминовых красителей в таких ассоциатах осуществляется с участием триплетного состояния органического лиганда. Основываясь на этих данных, можно априори выбирать органические лиганды для экстракционно-фотометрического и -флуориметрического методов определения элементов.

---

[1] И. П. Алимарин, А. П. Головина, В. К. Рунов *Изв. АН СССР. Сер. хим.*, **6**, 1423 (1974).

[2] С. И. Мак-Глинн, Т. Адзуми, М. Киносита, «Молекулярная спектроскопия триплетного состояния», Москва, изд. «Мир», 1972.

[3] Р. Н. Нурмухаметов, «Поглощение и люминисценция ароматических соединений», Москва, «Химия», 1971.

Так, разработаны экстракционно-флуориметрические методы определения урана (VI) и тория в виде ионных ассоциатов с 5,7-динитро-8-оксихинолином и родамином В,[1,4,5] предел обнаружения 0,007 мкг/мл.

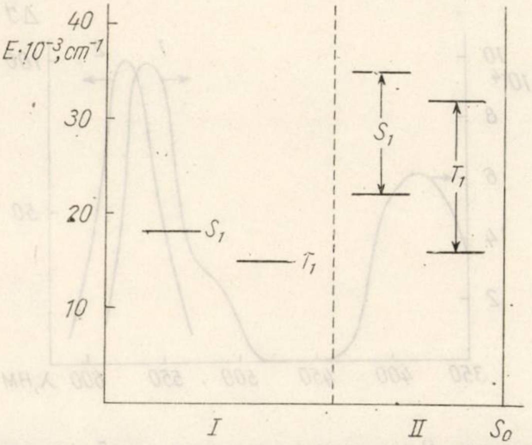

Рис. 2. — Относительное расположение нижних синглетных (S_1) и триплетных (T_1) энергетических уровней молекул родаминовых красителей (I) и органических лигандов (II).

Это выгодно отличает их от экстракционно-фотометрических методов определения урана (VI) с 8-оксихинолином и бутилродамином В[6] и тория с 5,7-дибром-8-оксихинолином и родамином В[7] с пределом обнаружения 0,04 мкг/мл. Экстракционно-фотометрический и -флуориметрический методы определения урана (VI) использованы для анализа урановых руд.[4,6]

При определении элементов в виде ионных ассоциатов с органическими лигандами в ряде случаев наблюдается значительная экстракция родаминового красителя с анионом лиганда (холостой опыт). Это приводит к увеличению предела обнаружения и ухудшает воспроизводимость анализа. Величина холостого опыта зависит от рН, концентрации и природы красителя и органического лиганда.

Причем самое существенное влияние оказывает природа красителя. Мы исследовали этерифицированные (3В, 6G, 3GO, бутилродамин В) и неэтерифицированные родаминовые красители, в частности родамин В.

---

[4] А. П. Головина, Н. Б. Зоров, В. К. Рунов, В сб. «Оптические методы контроля химического состава материалов», Москва, МДНТП им. Ф. Э. Дзержинского, 1974, 35.

[5] Ю. В. Грановский, В. К. Рунов, И.С. Тищенко и А. П. Головина, *Ж. аналит. химии*, **29**, 1959 (1974).

[6] А. П. Головина, В. К. Рунов и И. П. Алимарин, Ю. В. Грановский, Тез. докл. Всесоюзного семинара «Геохимические методы изучения вещественного состава горных пород», Душанбе, 1974, т. 2, 109.

[7] А. П. Головина, В. К. Рунов, В сб. «Успехи аналитической химии», Москва, «Наука», 1974, 184.

При pH 2—11 родамин В существует главным образом в виде биполярного иона, концентрация его катионной формы очень мала. Поэтому родамин В практически не экстрагируется в виде ионных ассоциатов с 8-оксихинолином, его 5,7-дигалоидпроизводными, давая небольшой холостой опыт. Этерифицированные родамины в указанном интервале pH находятся в основном в катионной форме, что приводит к увеличению холостого опыта. Поэтому родамин В имеет практическое преимущество перед другими исследованными родаминами. Однако в определенных условиях можно использовать и этерифицированные родамины. Например, элементы, хелаты которых с 5,7-дигалоидпроизводными 8-оксихинолина экстрагируются при $pH<4$, можно определять в виде их ионных ассоциатов с родамином 3В. В случае 8-оксихинолина с этим красителем можно определять, элементы, оксихинолинаты которых экстрагируются при $pH<7$, такие как, кадмий, цинк, никель, кобальт, марганец, уран(VI).

Для уменьшения предела обнаружения и повышения селективности может оказаться полезным предварительное концентрирование. Так, при определении урана в морской воде и монацитовом песке мы проводили предварительное концентрирование его раствором 8-оксихинолина ($5{,}0.10^{-1}$M) в бензоле или толуоле. Исследовались возможность определения урана (VI) в полученном концентрате в виде ионного ассоциата с бутилродамином В. Поиск оптимальных условий проводили методом математического планирования эксперимента в варианте Бокса-Уилсона.[8,9] В первой серии опытов в качестве факторов были выбраны концентрация красителя (x_1), изменявшаяся от $1{,}0.10^{-4}$ до $2{,}0.10^{-4}$M, и pH (x_2)—от 4,89 до 6,32. Параметром оптимизации (y) служила величина ΔA — разность между оптическими плотностями экстрактов ионного ассоциата и холостого опыта. По результатам эксперимента построена модель, адекватно ($F_{\text{эксп}} = 3{,}7$ при $F(3;\ 9;\ 0{,}05)=3{,}9$) описывающая процесс:

$$\hat{y} = 0{,}28311 - 0{,}00967x_1 - 0{,}07050x_2 - 0{,}03175x_1x_2 - 0{,}01167x_1^2 - 0{,}10017x$$

$$S^2\{\bar{y}\} = 1{,}8\ 10^{-4}, \qquad \Delta b_0 = \pm 0{,}02011, \qquad \Delta b_i = \pm\ 0{,}01243,$$

$$\Delta b_{ij} = \pm\ 0{,}01514, \qquad \Delta b_{ii} = \pm 0{,}02147$$

или в канонической форме:

$$Y - 0{,}2956 = -0{,}0089X_1^2 - 0{,}1029X_2^2, \quad \text{где}$$

$$X_1 = 0{,}985x_1 - 0{,}172x_2 - 0{,}144$$

$$X_2 = 0{,}172x_1 + 0{,}985x_2 + 0{,}345$$

Геометрической интерпретацией канонического уравнения является система контурных кривых равного выхода, представляющих собой эллипсы, сильно вытянутые вдоль оси X_1, с центром (максимумом) в точке S

---

[8] Ю. В. Грановский, «Основы планирования эксперимента для оптимизации многофакторных технологических процессов», Москва, изд. МИНХ им. Г.В. Плеханова, 1971.

[9] Л. П. Рузинов, «Статистические методы оптимизации химических процессов», Москва, «Химия», 1972.

(рис. 3). Найденные оптимальные условия — концентрация красителя $1{,}5.10^{-4}$M, pH=5,75 характеризуются небольшой воспроизводимостью анализа (1,8±0,7 мкг урана (VI) при n=3, $\alpha = 0{,}95$). Это обусловлено значительной величиной холостого опыта ($A_0 > 1{,}5$ при $l = 1$ см), которую можно снизить, уменьшая концентрацию родамина. Между тем это не приводит к существенному уменьшению величины параметра оптимизации. Число контурных кривых равного выхода, пересекаемых прямыми, параллельными оси x_1, мало (рис. 3). В следующей серии экспериментов исследовалась возможность улучшения воспроизводимости анализа. В качестве фактора была выбрана концентрация бутилродамина В (x_1). Она изменялась от $2{,}5.10^{-5}$ до $7{,}5.10^{-5}$M, значение pH=5,75. Параметром оптимизации (y) служила величина относительного стандартного отклонения $S_r = S/\overline{\Delta A}$ для n=3. По результатам эксперимента получено уравнение, адекватно ($F_{\text{эксп}} = 3{,}0$ при $F(2;\ 5;\ 0{,}05) = 5{,}8$) описывающее исследуемый процесс:

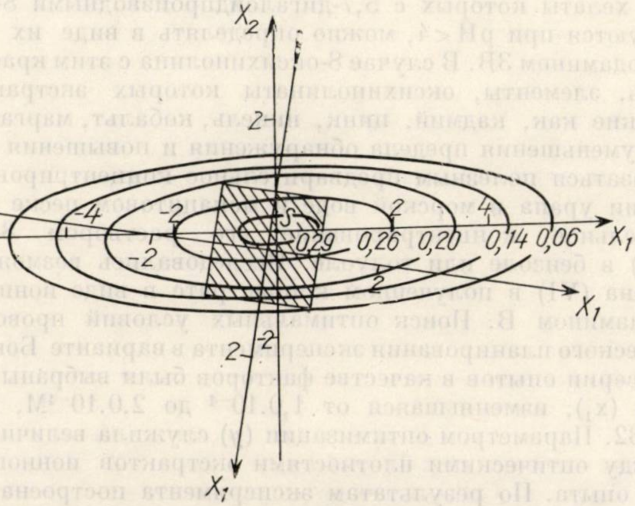

Рис. 3. — Система контурных кривых равного выхода для ионного ассоциата урана (VI) с 8-оксихинолином и бутилродамином В; Cu=1 мкг/мл, $l = 1$ см, $\lambda = 564$ нм.
▨ — область определения факторов.

$$\hat{y} = 0{,}03926 - 0{,}01220x_1 + 0{,}05514x_1^2$$

$$S^2\{y\} = 2{,}4\ 10^{-5},\quad \Delta b_0 = \pm 0{,}00949,\quad \Delta b_1 = \pm 0{,}00861,\quad \Delta b_{11} = \pm 0{,}01456$$

Найдена концентрация красителя ($5{,}0 \cdot 10^{-5}$M), при которой величина параметра оптимизации минимальна. Воспроизводимость анализа (2,0±0,1 мкг урана (VI) при n=3, $\alpha = 0{,}95$) улучшена в 7 раз по сравнению с результатами первой серии опытов. Разработанный метод использован для определения урана в морской воде (до 10^{-7}%) и монацитовом песке.[6]

Можно предположить, что предварительное разделение или концентрирование элементов экстракцией их хелатов (например, оксихинолинатов) будет способствовать увеличению селективности и снижению предела обнаружения. Поэтому важным является вопрос о возможности образования элементом ионных ассоциатов с органическими лигандами и основными красителями. Существенным является способность элемента образовывать анионный хелат. Известно, например, более 50 элементов, образующих оксихинолинаты.[10] Но лишь немногие из них экстрагируются в виде ионных ассоциатов с родаминовыми красителями (табл. 2). Необходимым условием их образования и экстракции является способность элемента давать с 8-оксихинолином координационно-ненасыщенный хелат.

Введение в молекулу 8-оксихинолина заместителей, обладающих электронно-акцепторными свойствами (Cl, Br, J, NO_2), приводит к увеличению числа элементов, образующих ионные ассоциаты такого типа (табл. 2).

Таблица 2

Элементы, образующие ионные ассоциаты с 8-оксихинолином ● его 5,7-дигалоидпроизводными ○, 5,7-динитро-8-оксихинолином[11] ☐ и родаминовыми красителями

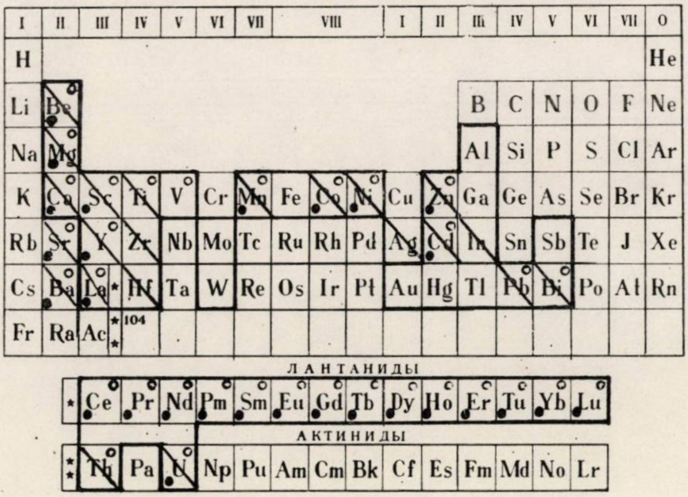
I II III IV V VI VII VIII I II III IV V VI VII 0
H He
Li Be B C N O F Ne
Na Mg Al Si P S Cl Ar
K Ca Sc Ti V Cr Mn Fe Co Ni Cu Zn Ga Ge As Se Br Kr
Rb Sr Y Zr Nb Mo Tc Ru Rh Pd Ag Cd In Sn Sb Te J Xe
Cs Ba La * Hf Ta W Re Os Ir Pt Au Hg Tl Pb Bi Po At Rn
Fr Ra Ac ** 104
ЛАНТАНИДЫ
* Ce Pr Nd Pm Sm Eu Gd Tb Dy Ho Er Tu Yb Lu
АКТИНИДЫ
** Th Pa U Np Pu Am Cm Bk Cf Es Fm Md No Lr

⧅ – образуют координационно-ненасыщенные оксихинолинаты[12,13]

---

[10] И. Стары, «Экстракция хелатов», Москва, изд. «Мир», 1966.

[11] С. В. Бельтюкова, В. Н. Двобязко, Л. И. Кононенко, Н. С. Полуэктов *Укр. хим. ж.*, **42**, 83 (1976).

[12] R. Hollingshead „Oxine and Its Derivatives", London, Butterworth, 1954, v. 1, 2.

[13] F. Z. Umland, *Analyt. Chem.*, **190**, 186 (1962).

Revue Roumaine de Chimie, 22, 4, 511–515 (1977)

Herrn Professor Dr Coriolan Drăgulescu
zum 70. Geburtstag gewidme

STRUKTUR-REAKTIVITÄTSUNTERSUCHUNGEN MIT HETEROSUBSTITUIERTEN NITRILEN. XXI[1]

KINETIK UND MECHANISMUS DER TRIMERISATION VON ARYLCYANATEN IN GEGENWART VON $AlCl_3$

ILSE-IRINA BACALOGLU*, RADU BACALOGLU **, DIETER MARTIN ***
und MONIKA BAUER ***

* Chemiezentrum, Bd. M. Viteazul 24 Timişoara
** Laboratorium für Organische Chemie, Technische Hochschule „Traian Vuia", Str. Bocşa 6 Timişoara
*** Zentralinstitut für Organische Chemie der Akademie der DDR, Berlin-Adlershof, Rudower Chaussee 5, DDR

Eingegangen am 3. September 1976

Die Geschwindigkeit der $AlCl_3$–katalysierten Trimerisation von Arylcyanaten in $CH_2Cl_2/C_6H_5NO_2$–Lösungen wurde IR–spektroskopisch verfolgt. Aus den kinetischen Daten ergibt sich als langsamster Schritt der Bruttoreaktion die intramolekulare Übertragung eines Chloridions vom $AlCl_3$ auf die OCN-Gruppe eines Arylcyanat-$AlCl_3$-Komplexes.

Arylcyanate trimerisieren sich in Gegenwart von Brönsted-oder Lewis-Säuren unter milden Reaktionsbedingungen oder in Gegenwart von Basen bei erhöhter Temperatur zu 2,4,6-Tris(aryloxy)-1,3,5-triazinen. [2-4]

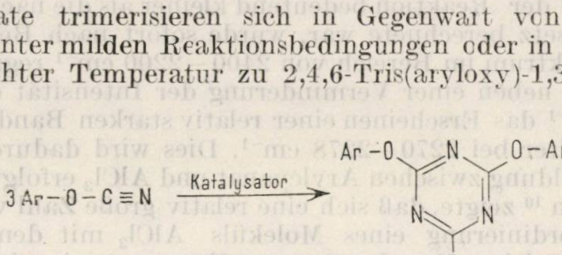

---

[1] Mitt. XXX. : S. El. Negoumi, R. Bacaloglu, D. Martin, *J. prak. Chem.*, **1977**, im Druck.

[2] D. Martin, *Z. Chem.*, **7**, 123 (1967).

[3] E. Grigat und R. Pütter, *Angew. Chem.*, **79**, 219 (1967).

[4] W. A. Pankratow, W. W. Korschak, S. W. Winogradova und A. G. Putschin, *Plaste und Kautschuk*, **20**, 481 (1973).

Aus Literaturangaben geht hervor, daß $AlCl_3$ die Trimerisationsreaktion bei höherer[5,6] oder mäßiger[7] Temperatur mit quantitativer Ausbeute katalysiert. In der vorliegenden Arbeit wurde die Kinetik und der Mechanismus der Trimerisation von Arylcyanaten in Gegenwart von $AlCl_3$ studiert. Dieser Katalysator wurde deshalb gewählt, weil er für die Polycydotrimerisation der Aryldicyanate zu makromolekularen Stoffen, mit guten technischen Verwendungsmöglichkeiten, besonders geeignet ist.[4,8]

VORVERSUCHE UND IDENTIFIZIERUNG DER PRODUKTE

Die Versuche zeigten, daß selbst in Gegenwart von kleinen Mengen $AlCl_3$ (0,1 Mol $AlCl_3$/1Mol PhOCN) die Trimerisation des Phenylcyanates mit quantitativer Ausbeute in Dekalin, Benzol, Acetonitril, und Methylenchlorid, abläuft. Von den angegebenen Lösungsmitteln ist nur CH_2Cl_2 geeignet, weil das Reaktionsgemisch homogen bleibt, was aber nur bei kleinen, schwer kontrollierbaren $AlCl_3$-Mengen der Fall ist. Um ein homogenes Reaktionssystem auch bei größern $AlCl_3$-Mengen zu erhalten, wurde Nitrobenzol zur $CH_2Cl_2 =$ Lösung hinzugefügt, wodurch sich ein Komplex bildet,[9] und somit die Löslichkeit erhöht wird. Unter diesen Bedingungen bleibt die Ausbeute an Triazin quantitativ, die Reaktionsdauer ist relativ klein und das System homogen.

REAKTIONSKINETIK UND DISKUSSIONEN

Die kinetischen Messungen wurden IR-spektroskopisch anhand des Verschwindens der$-$OCN Valenzschwingung ($2250-2280$ cm^{-1}) durchgeführt. Zum Zeitpunkt Null wurden die Lösungen des PhOCN in CH_2Cl_2 und die des $AlCl_3$ in $CH_2Cl_2-PhNO_2$ zusammengemischt und in eine thermostatierte Küvette mit Si-Fenster eingeführt.

Da im Falle aller Arylcyanate die extrapolierte Extinktion für den Zeitpunkt Null der Reaktion bedeutend kleiner als die nach dem Lambert Beer'schem Gesetz berechnete war, wurde sofort nach Beginn der Reaktion ein IR-Spektrum im Bereich von $2400-2200$ cm^{-1} registriert. Das IR Spektrum zeigt neben einer Verminderung der Intensität der Bande von $2250-2280$ cm^{-1} das Erscheinen einer relativ starken Bande bei 2320 cm^{-1} mit einer Schulter bei $2270-2278$ cm^{-1}. Dies wird dadurch erklärt, daß eine Komplexbildung zwischen Arylcyanat und $AlCl_3$ erfolgt. Das Studium der IR Spektren[10] zeigte, daß sich eine relativ große Zahl von Komplexen durch die Koordinierung eines Moleküls $AlCl_3$ mit dem freien Elektronenpaar des Stickstoff$-$oder Sauerstoffatoms, sowie mit den π Elektronen des aromatischen Kerns, bilden können. Es besteht auch die Möglich-

---

[5] M. Hedayatullah, *Bull. Soc. chim. France*, **1967**, 422.

[6] M. Hedayatullah und A. Nunes, *Compt. rend.*, **265**, 1125 (1967).

[7] E. Grigat und R. Püter, *Chem. Ber.*, **97**, 3012 (1964).

[8] R. Kubens, H. Schultheis, R. Wolf und E. Grigat, *Kunststoffe*, **1968**, 3.

[9] P. Gagneaux, D. Janjic und B. P. Susz, *Helv. Chim. Acta*, **41**, 1323 (1958).

[10] D. Martin und A. Weise, *Chem. Ber.*, **100**, 3747 (1967).

keit, daß sich zwei Moleküle $AlCl_3$ mit einem Molekül Arylcyanat, oder zwei Moleküle Arylcyanat mit einem Molekül $AlCl_3$ koordinieren. [10] Von den obengenannten Komplexen haben wir die Assoziationsgleichgewichte zwischen Arylcyanat und $AlCl_3$ im Verhältnis 1 : 1 und 1 : 2 hervor, weil sie zu aktiven Zwischenprodukten bei der Trimerisation führen können :

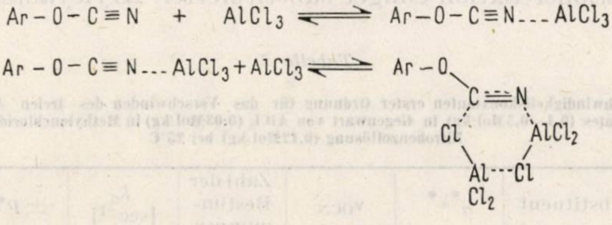

Ar-O-C≡N + AlCl3 ⇌ Ar-O-C≡N---AlCl3
Ar-O-C≡N---AlCl3 + AlCl3 ⇌ Ar-O
C≡N
Cl
AlCl2
Al---Cl
Cl2

Anhand des Verschwindens der entsprechenden Bande des freien Arylcyanates in Abhängigkeit von der Zeit konnten die Geschwindigkeitskonstanten erster Ordnung bis zu einer Konversion von cca 90% berechnet werden (Tabelle 1)

Tabelle 1

Geschwindigkeitskonstanten erster Ordnung für das Verschwinden des freien Phenylcyanates (ν_{OCN} = = 2270 cm^{-1}) in CH_2Cl_2 bei 25°C

PhOCN [Mol/kg]	$AlCl_3$ [Mol/kg]	$PhNO_2$ [Mol/kg]	k_0 [Sec^{-1}]
0,135	0,014	0,061	3,48
0,193	0,028	0,056	4,26
0,189	0,068	0,126	7,86
0,155	0,095	0,664	10,32
0,191	0,107	0,272	11,28
0,165	0,111	0,499	13,98
0,170	0,117	0,644	15,42
0,306	0,130	0,476	16,62
0,197	0,130	0,202	17,34
0,272	0,150	0,533	18,00
0,278	0,155	0,155	20,04

Wie aus Tabelle 1 ersichtlich ist, steigen die Konstanten mit der Konzentration des $AlCl_3$, so daß eine Korrelation folgender Form möglich ist :

$$k_0 = 2{,}34 + 60{,}00\,[AlCl_3] + 351{,}6\,[AlCl_3]^2 \qquad r = 0{,}986 \qquad (1)$$

Die Reaktionsgeschwindigkeit der Trimerisation kann folgendermaßen ausgedrückt werden :

$$v = k_1[ArOCN]_1 + k_2[ArOCN]_1\,[AlCl_3] + k_3[ArOCN]_1\,[AlCl_3]^2 \qquad (2)$$

wo $[ArOCN]_1$ die Konzentration des freien Arylcyanates ist.

Daraus geht hervor, daß die nichtkatalysierte Trimerisation eine relativ geringe Rolle spielt, während bei kleinen $AlCl_3$-Konzentrationen der Komplex 1 : 1 eine größere Bedeutung hat. Bei größeren $AlCl_3$ Konzentrationen tritt auch die katalytische Wirkung des Komplexes 1 : 2 hervor.

In Tabelle 2 sind die Geschwindigkeitskonstanten erster Ordnung der Trimerisationsreaktion einiger substituierter Arylcyanate aufgeführt.

Tabelle 2

Geschwindigkeitskonstanten erster Ordnung für das Verschwinden des freien Arylcyanates (0,1 – 0,5Mol/kg) in Gegenwart von $AlCl_3$ (0,03Mol/kg) in Methylenchlorid und Nitrobenzollösung (0,12Mol/kg) bei 25°C

Substituent	$\sigma^{*}{}_{*}{}^{*}$	ν_{OCN}	Zahl der Bestimmungen	k_0 $[sec^{-1}]$	$\pm p^{**}$
$p-CH_3-O-$	$-0{,}268$	2280	3	10,66	0,51
$p-CH_3-$	$-0{,}170$	2270	3	12,64	0,68
$m-CH_3-$	$-0{,}069$	2260	4	8,71	0,72
H	0	2270	—	5,30 *	—
$m-CH_3-O-$	$+0{,}115$	2280	3	3,34	0,40
$m-Cl-$	$+0{,}373$	2270	6	15,28	0,79
$m-NO_2-$	$+0{,}710$	2260	2	41,40	2,30

* ber. nach Gl. (1). ** ber. nach $p = [\Sigma(\bar{X}-X_i)^2/(p-1)n]^{0,5}$. $*_{*}*$ aus l.c. [11] entnommen.

Eine Korrelation zwischen diesen Konstanten und den σ-Werten ist nicht möglich, weil die ersten einen Gesamtwert darstellen. Es ist zu bemerken, daß sowohl die elektronenanziehenden als auch die elektronenabstoßenden Substituenten die Trimerisation begünstigen und die Reaktionsgeschwindigkeit zeigt ein Minimum bei *m*-Methoxyphenylcyanat.

Dies kann erklärt werden, wenn man annimmt, daß im langsamen Schritt die Komplexe 1 : 1 bzw. 1 : 2 eine monomolekulare Umwandlung erleiden, wo sowohl der elektrophile, als auch der nukleophile Charakter der Arylcyanate zur Geltung kommen. Eine Umwandlung solcher Art könnte die Übertragung eines Chloratoms vom $AlCl_3$ zum Kohlenstoffatom sein.

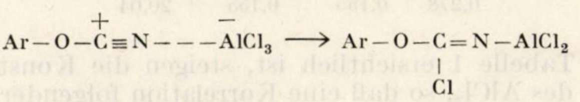

$$Ar-O-\overset{+}{C}\equiv N---\overset{-}{A}lCl_3 \longrightarrow Ar-O-\underset{\substack{|\\Cl}}{C}=N-AlCl_2$$

Die elektronenabastoßenden Substituenten begünstigen die Eliminierung des Chloridions aus dem $AlCl_3$, während die elektronenanziehenden den nukleophilen Angriff desselben am Kohlenstoffatom fördern. Das so gebildete Zwischenprodukt erleidet eine schnelle Umwandlung zum Trimeren und gleichzeitig bildet sich das $AlCl_3$ zurück.

---

[11] J. E. Leffler und E. Grunwald, „Rates and Equilibria of Organic Reactions" J. Wiley, New York, 1963, S. 173.

Da die Konzentration des Nitrobenzols keinen Einfluß auf die Reaktionsgeschwindigkeit hat (Tabelle 1, Nr. 5—7 ; 8, 9) kann man annehmen, daß die Übertragung des Chloratoms im Komplex 1 : 1 oder 1 : 2 intramolekular erfolgt, und somit nicht von der Solvatationsfähigkeit des Reaktionsmediums beinflußt wird.

EXPERIMENTELLER TEIL

SUBSTANZEN

Die Arylcyanate wurden durch thermische Zersetzung der substituierten Thiatriazole, dargestellt [12].

Das CH_2Cl_2 p.a. wurde über K_2CO_3 getrocknet, destilliert und anschließend über aktiviertem Molsieb (5Å) aufbewahrt.

Nitrobenzol p.a. wurde destilliert und anschließend über aktiviertem Molsieb (5Å) aufbewahrt.

Aluminiumchlorid war ein p.a. wasserfreies sublimiertes E. Merck-Produkt.

IDENTIFIZIERUNG DER REAKTIONSPRODUKTE

0,52 g Phenylcyanat wurden in 10 ml CH_2Cl_2, 0,39 g $AlCl_3$ in einem Gemisch von 10 ml CH_2Cl_2 und 1 ml Nitrobenzol gelöst. Das Reaktionsgemisch wurde in eine Küvette mit Si-Fenstern eingeführt und von Zeit zu Zeit das IR-Spektrum bis zum völligen Verschwinden der charakteristischen Bande des freien Phenylcyanates bei $2270 cm^{-1}$, registriert. Das auf diese Weise erhaltene Reaktionsgemisch wurde eingedampft, mit 10 ml heißem mit HCl angesäuertem Wasser versetzt und abgesaugt. Man erhielt 1,54 g Produkt, das ein identisches IR Spektrum mit dem einer authentischen Probe von 2,4,6-Tris(aryloxy)-1,3,5-triazin, aufwies. Ausbeute 99%.

REAKTIONSKINETIK

Die Lösung der eingewogenen Arylcyanate in 10 ml CH_2Cl_2 und die des $AlCl_3$ in 10 ml CH_2Cl_2 dem die bestimmte Menge $PhNO_2$ hinzugefügt wurde, wurden im Zeitpunkt Null zusamengemischt und in eine thermostatierte Küvette mit Si-Fenster (Schichtdichte 0,1 mm) eingeführt. Das Verschwinden der charakteristischen OCN Bande (Tabelle 2) wurde mit einem IR Spektrograph UR—IO (VEB Carl-Zeiss Jena) mit Zweitschreiber Gl Bl (VEB Funkwerk Erfurt) registriert.

Die Geschwindigkeitskonstanten erster Ordnung wurden nach folgender Gleichung, mit Hilfe eines Hewlett Packard-Modells. 9810, berechnet

$$k_0 t = \ln [(E_0 - E_\infty)/(E_t - E_\infty)]$$

wo E_0, E_t, E_∞ die Extinktionen im Zeitpunkt Null, t und Unendlich sind. Es wird hervorgehoben, daß die Bestimmungen unbedingt wasserfrei durchgeführt werden müssen, um eine genaue Reproduzierbarkeit zu gewährleisten.

---

[12] D. Martin, *Chem. Ber.*, **97**, 2989 (1964).

Revue Roumaine de Chimie, **22**, *4*, 517–523 (1977)

Dedicated to the 70th anniversary
of Professor Coriolan Drăgulescu

CHEMICAL GRAPHS. XXIX.[1] NUMBERS OF ISOMERS WITH NAPHTHALENE AND ADAMANTANE SKELETONS

A. T. BALABAN,[a,b] E. M. PALMER[c] and F. HARARY[d]
[a] The Polytechnic, Organic Chemistry Department, Bucharest, Romania
[b] Correspondence address : Institute of Atomic Physics, P.O.Box 5206, Bucharest, Romania
[c] Michigan State University, East Lansing 48823, U.S.A.
[d] University of Michigan, Ann Arbor 48109, U.S.A.

Received September 11, 1976

Pólya's Enumeration Theorem is used for calculating the number of isomers of naphthalene and adamantane, on replacing the carbon atoms of naphthalene, or the carbon or hydrogen atoms of adamantane, by other types of atoms.

In part IV of the present series,[2] Pólya's Enumeration Theorem was applied to monocyclic and *cata*-condensed polycyclic systems, and a general formulation of the cycle index was found for bicyclic systems. As one of the examples for bicyclic systems naphthalene was chosen. The number of isomers was computed, when the ten atoms of the skeleton can be of three types, X, Y, and Z, as proposed earlier,[3,4] so that the molecular formula of the compund becomes $X_xY_yZ_z$ with $x + y + z = 10$.

We wish to correct two numbers of isomers given earlier,[2] namely 329 for $x^6y^2z^2$ should be replaced by 330, and 807 for $x^4y^4z^2$ should be replaced by 810. The errors resulted from the inadvertent omission of one term in the expansion of $(x + y + z)^2\,(x^2 + y^2 + z^2)^4$.

A related problem was discussed by Masinter *et al.*,[5] namely the labelling of objects having symmetry. In examining the labelling of the decalin skeleton, these authors found for partition $x^6y^2z^2$ a number of 330 isomers.

---

[1] Previous part, A. T. Balaban *Rev. Roumaine Chim.*, **21** (1976).

[2] A. T. Balaban and F. Harary, *Rev. Roumaine Chim.*, **12**, 1511 (1967).

[3] A. T. Balaban, *Studii și Cercetări Acad. R. P. România*, **7**, 257 (1959).

[4] A. T. Balaban and Z. Simon, *Tetrahedron*, **18**, 315 (1962) ; *Rev. Roumaine Chim.*, **10**, 1059 (1965).

[5] L. M. Masinter, N. S. Sridharan, R. E. Carhart, and D. H. Smith, *J. Amer. Chem. Soc.*, **96**, 7714 (1974).

All numbers of isomers for naphthalene or decalin (ignoring stereoisomerism in the latter case) in which the carbon atoms are replaced by up to three types of heteroatoms are presented in Table 1. They were calculated using the cycle index

$$Z = \frac{1}{4}(y_1^{10} + y_1^2y_2^4 + 2y_2^5). \tag{1}$$

It was noted that for cyclohexane, if the conformational interconversion is averaged, a coplanar six-membered ring is a useful model[6,7] and this can be obviously generalized to decalin. However decalin is too flexible for the application of Pólya's theorem to derive chemically interesting results. Therefore, in the present paper we disregard the geometrical isomerism of decalin, treating carbon-labelled naphthalene and decalin as if they were topologically identical.

By applying Pólya's theorem to the porphyrin skeleton, the number of isomers was obtained,[8] leading to the same numerical results as those found by Masinter *et al.*,[5] and correcting an erroneous result in the literature.[9]

A molecule which was discussed at length by Masinter *et al.*[5] is adamantane. It is the opposite of decalin, having no flexibility. So far only one application of Pólya's theorem to adamantane seems to have been reported[10a]*, but Ruch *et al.* enumerated substituted adamantanones by using double cosets.[10b] We now report, therefore, an analysis of adamantane using Pólya's theorem.

A *C-labelled adamantane* is an adamantane molecule in which one or more carbon atoms are substituted by heteroatoms with valence at least two (or three for the bridgehead atoms). Adamantanes in which one or more hydrogen atoms are replaced by univalent substituents will be called *H-labelled adamantanes*.

As a geometrical configuration, adamantane (I, fig. 1) possesses four C_3 axes, three mutually coincident C_2 and S_4 axes, and six reflection planes or S_1 axes orthogonal to these planes. A C_3 axis passes through one carbon and one hydrogen atom ; a C_2 axis passes through two carbon atoms and no hydrogen atom ; an S_4 axis coincides with a C_2 axis and passes through the same atoms as that axis ; an S_1 axis passes through no atom, but is equivalent to a reflection plane which passes through eight

---

* Only cycle indices (4) and (5) below coincide with previous results, corresponding to relations numbered (2) and (1), respectively, in ref. 10a

[6] J. E. Leonard, G. S. Hammond and H. E. Simmons, *J. Amer. Chem. Soc.*, **97**, 5052 (1975).

[7] R. L. Flurry, Jr., *J. Phys. Chem.*, **80**, 777 (1976).

[8] A. T. Balaban, *Rev. Roumaine Chim.*, **20**, 239 (1975).

[9] D. Blackman, *J. Chem. Educ.*, **50**, 258 (1973) ; cf. also R.L.C. Pilgrim, *ibid.*, **51**, 316 (1974).

[10a] M. Yu. Kornilov, *Zhur. Strukt. Khim.*, **16**, 495 (1975).

[10b] E. Ruch, W. Hässelbarth and B. Richter, *Theoret. Chim. Acta, (Berlin)*, **19**, 288 (1970).

Table 1

Number of isomers

	Relation	x^{10}	x^9y	x^8y^2	x^8yz	x^7y^3	x^7y^2z	x^6y^4	x^6y^3z	$x^6y^2z^2$	x^5y^5	x^5y^4z	$x^5y^3z^2$	$x^4y^4z^2$	$x^4y^3z^3$
C-Labelled decalin ignoring stereoisomerism	(1)	1	3	15	23	32	92	60	212	330	66	318	636	810	1056
C-Labelled adamantane including stereoisomerism	(2)	1	2	5	8	14	32	22	74	110	24	108	216	270	360
C-Labelled adamantane excluding stereoisomerism	(4)	1	2	5	7	11	22	17	47	67	18	66	126	155	240

	Relation	x^{16}	$x^{15}y$	$x^{14}y^2$	$x^{14}yz$	$x^{13}y^3$	$x^{13}y^2z$	etc.
H-Labelled adamantane including stereoisomerism	(3)	1	2	12	20	50	140	
H-Labelled adamantane excluding enantiomerism but including diastereomerism	(5)	1	2	9	16	32	79	
H-Labelled adamantane excluding stereoisomerism	(15)	1	2	6	8	15	30	

atoms, as indicated in Fig. 1 : in formula I, only one axis of each type is presented for the clarity of the drawing.

If only the proper C_2 and C_3 axes are considered, there exist 12 symmetry operations : the identity, the three C_2 rotations, and the eight C_3 rotations (four axes, times two rotation angles : 120° and 240°). Thus the cycle indices for adamantane as a geometrical object, i.e. including stereoisomerism, are :

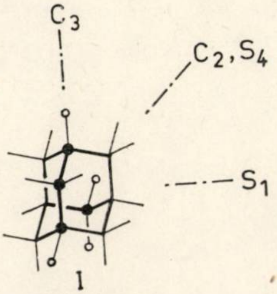

Fig. 1. — Adamantane (I) with its symmetry axes. The four black points (carbon atoms) and four white circles (hydrogen atoms) are all contained in one reflection plane orthogonal to the improper axis S_1 indicated on the figure.

$$Z = \frac{1}{12}(y_1^{10} + 3y_1^2y_2^4 + 8y_1y_3^3) \quad \text{C-labelled} \qquad (2)$$

$$Z = \frac{1}{12}(y_1^{16} + 3y_2^8 + 8y_1y_3^5) \quad \text{H-labelled} \qquad (3)$$

Note that in the C_2 rotations, the two carbon atoms lying on the C_2 axis do not permute (leading to $3y_1^2y_2^4$), and that since there are no hydrogens on the C_2 axes, all hydrogens permute pairwise in the C_2 rotations (leading to $3y_2^8$).

When the improper S_4 and S_1 axes are also considered, the cycle index will have to include the six rotations-reflections on S_4 with angles 90° and 270°, and the six reflections. Note that again there are no hydrogens, but there are two carbons on the S_4 axis. On each reflection plane there are four carbon and four hydrogen atoms which do not permute on operations S_1. Therefore the cycle indices are :

$$Z = \frac{1}{24}(y_1^{10} + 3y_1^2y_2^4 + 8y_1y_3^3 + 6y_2y_4^2 + 6y_1^4y_2^3) \qquad (4)$$

for C-labelled adamantanes excluding stereoisomerism ; and

$$Z = \frac{1}{24}(y_1^{16} + 3y_2^8 + 8y_1y_3^5 + 6y_4^4 + 6y_1^4y_2^6) \qquad (5)$$

for H-labelled adamantanes excluding enantiomerism but including diastereomerism.

A C-labelled adamantane, viewed as a graph, is a complete graph K_4, whose six edges are each subdivided by one vertex (II, Fig. 2). To find the cycle indices (2) and (4) above for C-labelled adamantane by an alternative procedure, we have to coalesce the cycle indices of the symmetric group $\mathbf{S}_4$ on four vertices, and the symmetric pair group $\mathbf{S}_4^{(2)}$ on six edges :[11a]

$$Z(\mathbf{S}_4) = \frac{1}{24}(s_1^4 + 3s_2^2 + 8s_1s_3 + 6s_1^2s_2 + 6s_4) \tag{6}$$

$$Z(\mathbf{S}_4^{(2)}) = \frac{1}{24}(t_1^6 + 3t_1^2t_2^2 + 8t_3^2 + 6t_1^2t_2^2 + 6t_2t_4). \tag{7}$$

By multiplying the corresponding terms in the above cycle indices, we find :

$$Z(\mathbf{S}_4^{(1,2)}\,;\, s_k\,;\, t_k) = \frac{1}{24}(s_1^4t_1^6 + 3\,s_2^2t_1^2t_2^2 + 8\,s_1s_3t_3^2 + 6\,s_1^2s_2t_1^2t_2^2 + 6s_4t_2t_4) \tag{8}$$

If now we replace in (8) both s_k and t_k by y_k, we obtain (4) directly.

It is well known[11b] that the cycle index of the alternating group $\mathbf{A}_4$ is

$$Z(\mathbf{A}_4) = \frac{1}{12}(s_1^4 + 3s_2^2 + 8s_1s_3). \tag{9}$$

Similarly, we have :

$$Z(\mathbf{A}_4^{(1,2)}) = \frac{1}{12}(s_1^4t_1^6 + 3s_2^2t_1^2t_2^2 + 8s_1s_3t_3^2) \tag{10}$$

and again replacing both s_k and t_k by y_k in (10), we obtain (2) directly.

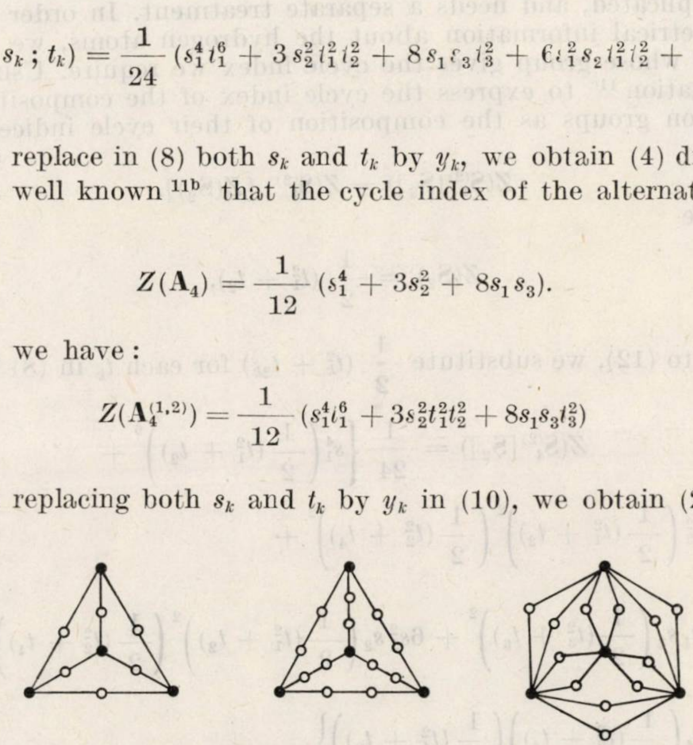
II III IV

Fig. 2. — Graphs associated with adamantane : II for C-labelled, III and IV for H-labelled adamantane. Black points symbolize tertiary carbons (in II) or hydrogens bonded to them (in III and IV); white circles symbolize secondary carbons (in II) or hydrogens bonded to them (in III and IV).

An H-labelled adamantane, viewed as a graph which preserves geometrical information on how the hydrogens are bonded, is a complete graph K_4, whose edges are subdivided by two points each ; all points of

---

[11] F. Harary and E. M. Palmer, "Graphical Enumeration", Academic Press, New York, 1974 : a, p. 84 ; b, p. 36 ; c, p. 98.

the resulting graph III represent hydrogen atoms. Coalescing the relevant cycle indices once more, we obtain

$$Z = \frac{1}{24}(s_1^4 t_1^{12} + 3s_2^2 t_2^6 + 8s_1 s_3 t_3^4 + 6s_1^2 s_2 t_1^2 t_2^5 + 6s_4 t_4^3) \tag{11}$$

whence on replacing s_k and t_k by y_k, we obtain (5). On replacing the symmetric group $\mathbf{S}_4$ by the alternating group $\mathbf{A}_4$ as before, we obtain cycle index (3).

The case of H-labelled adamantane excluding stereoisomerism is more complicated, and needs a separate treatment. In order to exclude any geometrical information about the hydrogen atoms, we start from graph IV, whose group gives the cycle index we require. Using conventional notation[11c] to express the cycle index of the composition of two permutation groups as the composition of their cycle indices, we may write:

$$Z(\mathbf{S}_4^{(2)}[\mathbf{S}_2]) = Z(\mathbf{S}_4^{(2)})\,[Z(\mathbf{S}_2)]. \tag{12}$$

Since

$$Z(\mathbf{S}_2) = \frac{1}{2}(t_1^2 + t_2), \tag{13}$$

according to (12), we substitute $\frac{1}{2}(t_k^2 + t_{2k})$ for each t_k in (8) to obtain:

$$\begin{aligned} Z(\mathbf{S}_4^{(2)}[\mathbf{S}_2]) = \frac{1}{24}\Bigg\{ & s_1^4\left(\frac{1}{2}(t_1^2 + t_2)\right)^6 + \\ & + 3s_2^2\left(\frac{1}{2}(t_1^2 + t_2)\right)^2\left(\frac{1}{2}(t_2^2 + t_4)\right)^2 + \\ & + 8s_1 s_3\left(\frac{1}{2}(t_3^2 + t_6)\right)^2 + 6s_1^2 s_2\left(\frac{1}{2}(t_1^2 + t_2)\right)^2\left(\frac{1}{2}(t_2^2 + t_4)\right)^2 + \\ & + 6s_4\left(\frac{1}{2}(t_2^2 + t_4)\right)\left(\frac{1}{2}(t_4^2 + t_8)\right)\Bigg\}. \end{aligned} \tag{14}$$

Effecting, as before, the replacement of s_k and t_k by y_k in (14), we obtain finally:

$$\begin{aligned} Z = \frac{1}{1536}(& y_1^{16} + 6y_1^{14}y_2 + 15\,y_1^{12}y_2^2 + 20\,y_1^{10}y_2^3 + 15\,y_1^8 y_2^4 + \\ & + 30y_1^6 y_2^5 + 61y_1^4 y_2^6 + 48y_1^2 y_2^7 + 12y_2^8 + 24y_2^6 y_4 + 12y_2^4 y_4^2 + \\ & + 96y_2^2 y_4^3 + 96y_4^4 + 48y_1^6 y_2^3 y_4 + 24y_1^6 y_2 y_4^2 + 120y_1^4 y_2^4 y_4 + \\ & + 60y_1^4 y_2^2 y_4^2 + 96y_1^2 y_2^5 y_4 + 48y_1^2 y_2^3 y_4 + 128\,y_1 y_3^5 + \\ & + 256y_1 y_3^3 y_6 + 128y_1 y_3 y_6^2 + 96y_2^2 y_4 y_8 + 96y_4^2 y_8). \end{aligned} \tag{15}$$

This is precisely the cycle index for H-labelled adamantane ignoring stereoisomerism !

The numbers of isomers presented in Table 1 were calculated by substituting

$$y_k = x^k + y^k + z^k$$

and finding the coefficients of each term $x^p y^q z^r$. If p atoms of C or H in adamantane are substituted by heteroatoms or substituents P, and q atoms by Q-type substituents/heteroatoms, while remaining r atoms are either unsubstituted or replaced by heteroatoms/substituents R, then the number of isomers is, according to Pólya's theorem, the coefficient of the term $x^p y^q z^r$. The smaller numbers (up to 40 isomers) from Table 1 were checked manually by constructing all possible isomers, and these provided further verification.

Revue Roumaine de Chimie, 22, 4, 525–530 (1977)

Dedicated to the 70th anniversary
of Professor Coriolan Drăgulescu

SOME INFORMATION ABOUT THE GEOMETRY OF THE MOLECULES IN MOLTEN AND SOLID GLASSES

P. BALTĂ and D. RADU
Institute of Chemistry, Polytechnic Institute of Bucharest

Received September 6, 1976

Starting from the polymer distribution in silicate melts and glasses and using the present data on the nature of the chemical bonds it becomes possible to obtain information concerning the shape and the size of the silicate molecules. Arguments supporting the obtained data may be supplied by calculating some properties of the melts and glasses by means of the rigid sphere theory. An application to sodium metasilicate is presented.

1. INTRODUCTION

A correlation between the structure and the properties of glasses is still difficult, due especially to the insufficiently concrete knowledge concerning the structure. As a result, in most published works, the authors try to obtain information about the structure starting from properties.

The data gathered so far show that the polymer distribution is a very important structural feature, which becomes now experimentally accessible. The latest works in this field are summarized in references. [1,2]

Interesting information about the dimensions of the structural units in some melts has been obtained by means of the rigid sphere theory. [3–6] The data presented in some works seem to show a satisfactory agreement with the old structural models of phosphates and silicates. However, these works have not considered the information concerning the polymer distribution in phosphate and silicate melts. Consequently, the obtained data are probably only average values.

---

[1] P. Baltă, E. Baltă and V. Ceaușescu, *J. Non-Crystalline Solids*, **20**, 323 (1976).

[2] P. Baltă and E. Baltă "Introduction to the Physical Chemistry of the Vitreous State", Editura Academiei R.S.R. and Abacus Press, București—Tunbridge Wells, 1976.

[3] H. Reiss and H. L. Frisch, *J. Chem. Phys.*, **31**, 369 (1959).

[4] A. J. G. Boyer, D. J. Fray and T. R. Meadowcraft, *Phys. Chem. Glasses*, **8**, 96 (1967).

[5] D. J. Fray, *Phys. Chem. Glasses*, **11**, 219 (1970).

[6] G. Vasu, *Rev. Roumaine Chim.*, **15**, 1011 (1970).

The authors present a first attempt to use the rigid sphere theory taking into account that the polymer distribution implies the existence of a broad spectrum of values for the rigid sphere diameters.

2. CALCULATION OF THE RIGID SPHERE DIAMETERS ON THE BASIS OF POLYMER DISTRIBUTION

This problem of essential importance was resolved using up-to-date data concerning the structure and the chemical bonding in silicate, which are reviewed in references. [1,2] For this study was selected sodium metasilicate for which sufficient data are available.

The spatial models of the molecules SiO_4Na_4, $Si_6O_{18}Na_{12}$ and $Si_{12}O_{33}Na_{18}$ were built up. For this purpose the atoms were represented by expanded polystyren balls, their radii being proportional to covalent radii of Si and O atoms and to ionic radius of Na atom (the scale was 1Å = 1,5 cm). When building up models it was considered that in the molecules with more than 5 silicon atoms there are rings with 6 tetrahedra, because of their maximum stability, although in reality there may be also rings with a different number of tetrahedra. The average value of 140° was taken for Si—O—Si angles. Except for the orthosilicate which may be considered as spherical, the other molecules shapes are close to that of an ellipsoid. Two of the models are presented in figure 1. Taking into account the possible existence of a great number of isomers it was assumed that the rigid sphere diameter may be approximated by the great axis of the ellipsoid. Direct measuring or interpolation helped to determine the diameters of the molecules with up to 17 silicon atoms. This limit was established on the basis of the calculated polymer distribution curve [7] (figure 2). At larger values of x the weight of the respective molecules in melt decreases below 1 molal percent so that they were neglected. For orthosilicate it was possible to compare the value of the anion diameter measured on the model with the calculated one:

$$d_1 = 2(D_{Si-O} + r_0) = 2(1.62 + 0.66) = 4.56\ \text{Å} \qquad (1)$$

As it is known, for simple ionic melts, the rigid sphere diameter is obtained by adding up the radii of the ions: r^+ and r^-. Fray compared the rigid sphere diameters estimated by calculus with those deduced from models in which the cations were neglected justifying this by the large size of the anions and by the fact that they are only approximately spherical.

Consequently, it was assumed as possible to use the rigid sphere diameters obtained on the basis of three hypotheses:

1) assuming that the anions are the solvent and the cations the solute, the rigid sphere diameter will be: $a_{x(1)} = \dfrac{d_x + 2r_{Na}}{2}$;

2) the same as above but assuming that the non-bonding oxygen atom is ionic, that is, the anion diameter ($a_{x(2)}$) includes the ionic radii (not the covalent ones as above) of this oxygen species;

---

[7] P. Baltă, *Rev. Roumaine Chim.*, **17**, 969 (1972).

3) neglecting the cations and assuming that the anions are in contact with other anions of the same species so that : $a_{x(3)} = \frac{2d_x}{2}$.

Figure 3 presents the variation in the diameters of the rigid spheres as a function of the number of silicon atoms in the molecule. Points (*1*)

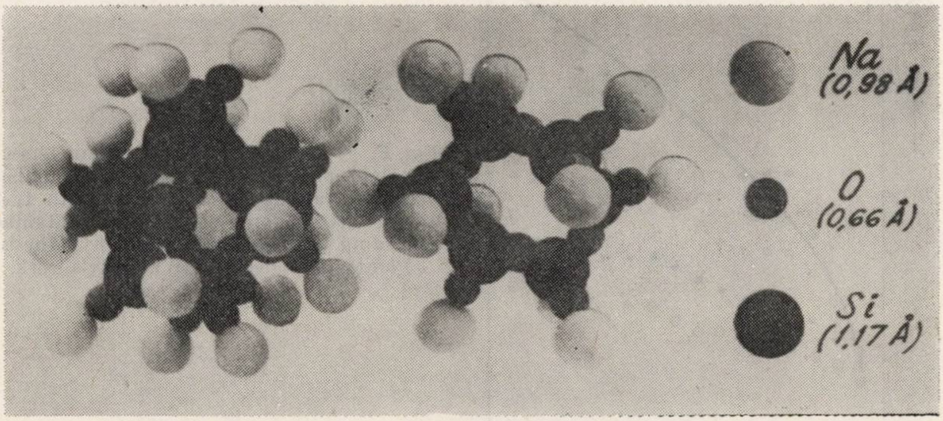

Fig. 1.—The models of two silicate molecules. From right to left: the component atoms; the molecule $Si_6O_{18}Na_{12}$; the molecule $Si_{12}O_{33}Na_{18}$.

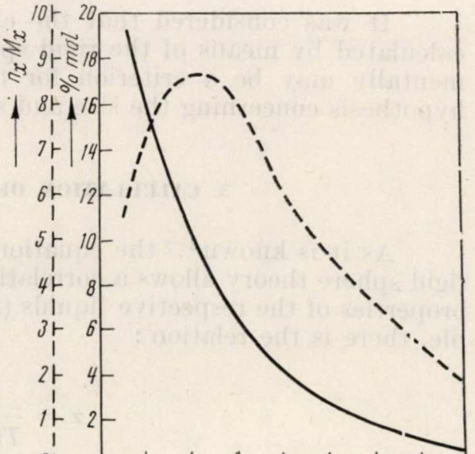

Fig. 2. — Calculated polymer distribution curves for sodium metasilicate.

and (*2*) are the values obtained by direct measuring on the models or by calculus starting from the spatial models according to hypotheses 1) and 2). On the curve (*3*) there are the values used in the calculation according to hypothesis 3). The discontinuities marked by the points which are not on the curve appear in the values of x where some ring closures are possible. Therefore, the values on curve (*3*) would roughly correspond to the situation in which the existence of rings with less than 6 silicon atoms is also admitted. Points (*4*) are the rigid sphere diameters obtained by Fray [5] for the compositions with the same ratio between oxides.

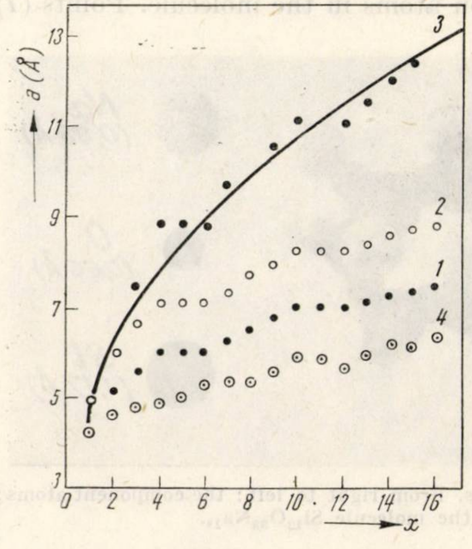

Fig. 3. — The variation of the diameters o the rigid spheres as a function of the number of sodium atoms in molecule. With 1, 2 and 3 are denoted the points obtained according to the corresponding hypothesis. Points 4 are deduced from Fray's work.

It was considered that the closeness of values of some properties calculated by means of the rigid sphere theory to those obtained experimentally may be a criterion for the selection of the most verisimilar hypothesis concerning the size and shape of molecules in silicate.

3. CALCULATION OF SOME PROPERTIES

As it is known [3–5] the equation of state deduced on the basis of the rigid sphere theory allows a correlation between their diameters and some properties of the respective liquids (melts). For the expansitity, for example, there is the relation :

$$\alpha = \frac{1 - y^3}{T(1 + 2y)^2} \tag{2}$$

where

$$y = \frac{\pi a^3 N}{6V} \tag{3}$$

a being the rigid sphere diameter, *N* Avogadro's number and *V* the molar volume. In relation (2) *T* is the absolute temperature. The molar volume was calculated using the molar weight of each of the 17 species of molecules existing in sodium metasilicate and the corresponding densities at

1400°, obtained by interpolating the Tickle's data.[8] In order to obtain the rigid sphere diameters (a) at 1400° it was assumed that the molecules are stable in the melt and therefore they expand like the solids. Consequently, the expansivities calculated for each species by a simple additive formula were used.[9]

In this manner it became possible to calculate y. Relations (2) and (3) were then used to calculate the expansivity of each molecule species at 1400°. The expansivity of the metasilicate melt must be the weighted mean of the values obtained for different component species.

In this stage of calculus, attempts were made to take into account the fact that in reality, in the case of hypothesis (3), a molecule of a given species may also border a molecule of a different species, resulting in an alteration in the value of the rigid sphere diameter. Since an accurate treatment of this question is fairly difficult, only the probability was considered that a given molecule may have as neighbour a molecule of the same species. This probability is proportional to the number of molecules of the given species. Accordingly, in the case of hypothesis (3), the weighted mean was calculated by means of the formula:

$$\alpha = \frac{\sum\limits_{x=1}^{n} \alpha_x P_x p_x}{\sum\limits_{x=1}^{n} P_x p_x} \tag{4}$$

where p_x is the concentration of the species x in weight percents and P_x the concentration in molar percents. The magnitude α_x is the expansivity of the species x at 1400°.

The compressibility and the surface tension were calculated in a similar manner, using the corresponding relations. The obtained values are compared with some experimental data listed in table 1.

Table 1

Comparison between some calculated and experimental properties of sodium metasilicate melt at 1400°

Property	Calculated	Experimental	Reference
Expansivity K^{-1}	$12.4 \cdot 10^{-5}$	$12.6 \cdot 10^{-5}$	8
Compressibility $cm^2\ dyne^{-1}$	$13.2 \cdot 10^{-12}$	$5.9 \cdot 10^{-12}$ (at 1200°)	5
Surface tension $dyne\ cm^{-1}$	170	305 (at 1350°)	10

---

[8] R. E. Tickle, *Phys. Chem. Glasses*, **8**, 116 (1967).

[9] P. Baltă "Glass Technology", Ed. didactică și pedagogică, Bucharest, 1966.

4. DISCUSSION

The obtained results may be considered totally satisfactory. For the expansivity, for example, the following values were obtained : $27.6 \times \times 10^{-5}$ K^{-1}, according to the first assumption; 18.4×10^{-5} K according to the second assumption and 12.4×10^{-5}K according to the third assumption. All these values are comparable with $(12.6 \pm 0.05) \times 10^{-5}$ K obtained experimentally [8]. The calculation manner (according to hypothesis (3) gives the closest value (practically identical) to the experimental one. On this basis this assumption may be considered to best fit the reality. As a result, the other properties were calculated according to hypothesis (3). The obtained results were also satisfactory.

The calculated compressibility is 13.2×10^{-12} cm^2 dyne^{-1}, comparable with 5.88×10^{-12} cm^2 dyne^{-1} at 1200° after Fray. [5] For surface tension the calculated value 170 dyne cm^{-1} is also comparable with the experimental data known for near temperatures[10].

These data permit to consider that within the limits of some approximations which cannot be avoided at present, the image concerning the shape and the size of the molecules in the metasilicate melt according to hypothesis (3) and also the polymer distribution are wholly confirmed.

Emphasis is also placed on the possibility to investigate theoretically, by using the rigid sphere theory, the correlation between the polymer distribution and the properties of melts which can be supercooled as glasses. It seems that at present this is the only possibility to study theoretically this correlation of essential importance for the industrial practice.

5. CONCLUSIONS

The rigid sphere theory was applied in correlation with the polymer distribution to investigate the structure of silicate melts and glasses.

Starting from the diameters of the polymer molecules estimated by means of some spatial models and from polymer distribution in sodium metasilicate, the values of some properties were calculated and they turned out to be very near to or comparable with those obtained experimentally. In this way it was possible to select the structural model of the silicate molecules which assures the best agreement and corresponds to the present ideas concerning the nature of the chemical bonds and the size and shape of the structural units in silicate.

An interesting avenue is also opened for theoretical investigation of the correlation between the structure and the properties of the non-crystalline solids obtained by melt supercooling.

---

[10] M. A. Bezborodow, H. M. Bobkowa, S. M. Brehowckih, H. H. Ermolenko, E. E. Mazo and E. A. Porai-Kositz "The Diagrams of Glassforming Systems", Beloruskyi Polytechn. Inst., Minsk, 1959, p. 84 (in Russian).

Revue Roumaine de Chimie, 22, 4, 531–537 (1977)

Dedicated to the 70th anniversary
of Professor CORIOLAN DRĂGULESCU

AN EXAMINATION OF VARIOUS PHENOTHIAZINE DERIVATIVES AS INDICATORS IN VANADOMETRY

R. BELCHER, HELENA PUZANOWSKA-TARASIEWICZ* and W. I. STEPHEN,
Department of Chemistry, University of Birmingham, Birmingham, B15 2TT, U.K.

Received September 14, 1976

The following phenothiazine derivatives, chlorpromazine and diethazine hydrochlorides, perphenazine, promazine hydrochloride, trifluorperazine, levomepromazine and methopromazine maleates have been studied as indicators in redox titrimetry. The colour change at the equivalence point is from bluish-green to dark-red with the first three compounds, to dark-violet with levomepromazine and methopromazine maleates or to green-orange with the remaining compounds. The end-points obtained are sharper than with conventional indicators. The spectra of the indicator forms have been determined. The transition potentials of the indicators have been determined. Three of the ten have been determined previously and the results, in general, are in agreement. The values obtained confirm the suitability of these indicators for this particular titration.

Phenothiazine derivatives (PD) form coloured oxidation products with a number of oxidants (e.g. Ce(IV), VO_3^-, $Cr_2O_7^{2-}$, BrO_3^-, IO_3^-, IO_4^-, NO_2^-, NO_3^-, etc.) in acid medium. These properties enable certain phenothiazine derivatives to be used as indicators in various redox titrations. In the present work, which is a continuation of previous studies,[1-4] the behaviour of ten phenothiazine indicators in vanadometric titration has been examined.

Sanke Gowda[5-7] and his colleagues were the first to study methopromazine and chlorpromazine hydrochloride as indicators in vanadometric titrations; they determined both the oxidation potentials and transition potentials. Later they examined diethazine and prochlorperazine as indicators in the titration of zinc with ferrocyanide. Three of these indicators

---

[*] Visiting Fellow, Technical University, Bialystok, Poland.

[1] H. BASINSKA, H. PUZANOWSKA-TARASIEWIEZ and M. TARASIEWICZ, *Chem. Analit.*, **14**, 889 (1969).
[2] H. PUZANOWSKA-TARASIEWIEZ, *Chem. Analit.*, **15**, 939 (1970).
[3] H. PUZANOWSKA-TARASIEWIEZ, *Chem. Analit.*, **18**, 435 (1973).
[4] H. PUZANOWSKA-TARASIEWIEZ, *Mikrochim. Acta*, **1972**, 876.
[5] H. SANKE GOWDA and R. SHAKUNTHALA, *Talanta*, **13**, 1375 (1966).
[6] H. SANKE GOWDA, R. SHAKUNTHALA and P. G. RAMAPPA, *Talanta*, **15**, 266 (1968).
[7] H. SANKE GOWDA and B. KESAVAN, *Talanta*, **16**, 1103 (1969).

have been included in the present study. The spectra of the non-oxidised and oxidised forms have also been determined.

In studies of this nature it is usual to select iron(II) as the reducing agent. In the present investigation it was decided to utilise uranium(IV), because this is also a stable reducing agent and its redox behaviour is well-authenticated.

Phenothiazine derivatives are oxidised to intensely coloured free radicals or semiquinones which are stable in acid solution.[8] This reaction is reversible, but the free radicals are further oxidised irreversibly by strong oxidising agents to a colourless sulphoxide [9,10]. This reaction e.g. for chlorpromazine may be represented as follows:

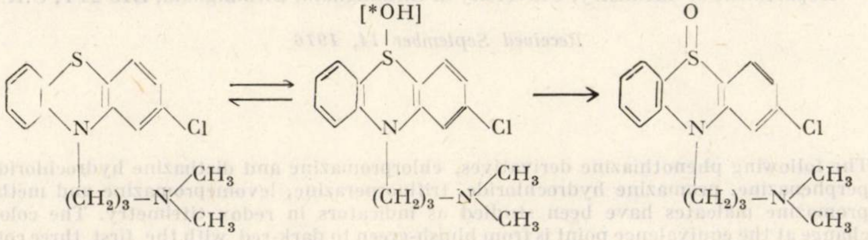

Colourless non-oxidised form

Red free radical

Colourless Sulphoxide

EXPERIMENTAL

REAGENTS USED

Uranium(IV) solution (0.05 N) in 1.0 N sulphuric acid was prepared from pure uranyl acetate. This solution was reduced in a Jones reductor (in 2.0N sulphuric acid), then a stream of air was passed through the reduced solution for about 10 min. to oxidise any uranium(III) to uranium(IV). The solution was standardised against a standard ceric sulphate solution.[11]

Ammonium vanadate solution (0.05N) was prepared by dissolving 5.35 g of the salt in 80 ml. of 1 : 1 sulphuric acid before dilution to 1 litre. The solution was standardised against iron(II).

Phenothiazine indicators were prepared as aqueous 0.1 % solutions by dissolving the PD bases or salts : I, II, IV and VI in water ; III, V, VIII, IX in 0.3N hydrochloric acid ; X in 1 : 2 ethanol-water (Table I).

PRELIMINARY TESTING

For each test, 2 drops of 0.05N solution of ammonium vanadate were added to 5 ml of 0.1 % solution of PD in 2N hydrochloric acid. The colours of the oxidised forms are given in Table 2.

[8] L. Levy, Thomas H. Tozer and D. Tuck, *Med. Chem.*, **15**, 898 (1972).

[9] J. S. Forrest, F. M. Forrest and M. Berger, *Biochim. Biophys. Acta.* **29**, 441 (1958)

[10] K. Korezak-Fabierkiewiez, *Nature*, **211**, 147 (1966).

[11] N. Birnbaum and S. M. Edmonds, *Analyt. Chem.*, **12**, 155 (1940).

Table 1

Phenothiazine derivatives examined as redox indicators

Number	Chemical name	Trivial name	Substituents mean R$_1$	Substituents mean R$_2$	Supplier
I	2-chlor-10-(3-dimethylamino-propyl)-phenothiazine hydrochloride	Chlorpromazine—HCl	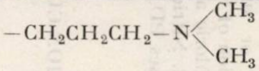 $-CH_2CH_2CH_2-N(CH_3)_2$	$-Cl$	EGYT — Budapest
II	10-(3-diethylamino-propylo)-phenothiazine hydrochloride	Diethazine—HCl	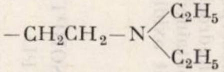 $-CH_2CH_2-N(C_2H_5)_2$	$-H$	EGYT — Budapest
III	2-chloro-10-[3-(4-β-hydroxyethyl-1-piperazinyl)-propyl]-phenothiazine	Perphenazine	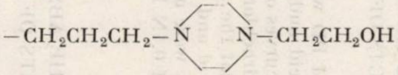	$-Cl$	SPECIA — Paris
IV	10-(3-dimethylamino-propyl)-phenothiazine hydrochloride	Promazine—HCl	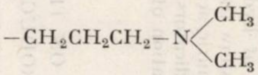 $-CH_2CH_2CH_2-N(CH_3)_2$	$-H$	EGYT — Budapest
V	10-[3-(4-methyl-1-piperazinyl-propylo]-phenothiazine	Perazine	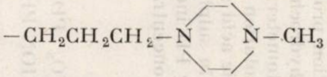	$-H$	PROMONTA — Hamburg
VI	2-trifluomethyl-10-{3-[4-(2-hydroxyetyl)1-piperazinyl]-propyl}-phenothiazine dihydrochloride	Fluphenazine—2HCl	$-CH_2CH_2CH_2-N\ N-CH_2CH_2OH$	$-CF_3$	SPECIA — Paris
VII	2-trifluomethyl-10-[3-(4-methyl-1-piperazinyl)-propyl]-phenothiazine	Trifluoperazine	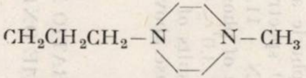	$-CF_3$	MEDIMPEX — Moscow
VIII	2-methoxy-10(3-dimethyl-amino-2-methylpropyl)-phenothiazine maleate	Levomepromazine maleate	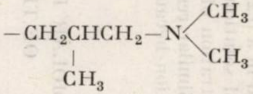 $-CH_2CH(CH_3)CH_2-N(CH_3)_2$	$-OCH_3$	EGYT — Budapest
IX	2-methoxy-10(3-dimethyl-amino-propyl)-phenothiazine maleate	Methopromazine maleate	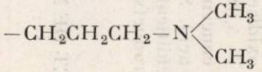 $-CH_2CH_2CH_2-N(CH_3)_2$	$-OCH_3$	SPECIA — Paris
X	2-methylthio-10-[2-(1-methyl-2-piperidyl)-ethyl]-phenothiazine hydrochloride	Thioridazine—HCl	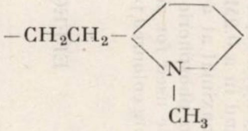	$-SCH_3$	SPOFA — Prague

Table 2

Oxidation of PD indicators by NH_4VO_3

Pink-red	*Orange*	*Violet*	*Blue*
Chlorpromazine	Promazine	Levomepromazine	Thioridazine
Diethazine	Perazine	Methopromazine	
Perphenazine	Fluphenazine Trifluoperazine		

EFFECT OF ACID CONCENTRATION ON THE ABSORPTION CURVES OF THE OXIDATION PRODUCTS OF PD

The absorption curves of the oxidation products of PD with ammonium vanadate in varying concentrations of sulphuric acid, hydrochloric acid and phosphoric acid were established using a Unicam SP1800 spectrophotometer. The curves obtained for chlorpromazine hydrochloride oxidised in a 0.2N — 11.0N solution of hydrochloric acid or sulphuric acid, and in a 0.2M — 5.0M solution of phosphoric acid show that the absorption of the solution is maximal at a concentration of 3.0 — 4.0N in sulphuric acid and hydrochloric acid and 3.5M in phosphoric acid. Similar results of other PD indicators were obtained. Nitric acid cannot be used for acidification because above a concentration of 0.1N it oxidises PD solution forming coloured products.

EFFECT OF MOLAR RATIO NH_4VO_3 : PD ON THE ABSORPTION CURVES OF THE OXIDATION PRODUCTS OF PD

The absorption curves obtained for NH_4VO_3-chlorpromazine hydrochloride, NH_4VO_3 promazine hydrochloride, NH_4VO_3-levomepromazine maleate and NH_4VO_3-thioridazine hydrochloride systems in 2N hydrochloric acid, show that the maximum absorption was obtained at the molar ratio NH_4VO_3 : PD = 1.1 independently of the type of PD tested. Similar results were obtained for the other PD indicators.

ABSORPTION CURVES OF NON-OXIDISED AND OXIDISED PD FORMS

As mentioned previously, the PD indicators are oxidised reversibly by ammonium vanadate with the formation of coloured free radicals, which are further oxidised irreversibly of colourless sulphoxides. The ultra-violet spectra of the non-oxidised and oxidised forms of chlorpromazine and promazine hydrochlorides, levomepromazine maleate and thioridazine hydrochloride were prepared. Absorption curves of the oxidation products of PD were obtained at a molar ratio NH_4VO_3 :PD=1.1, sulphoxides of PD at NH_4VO_3 :PD = 5.1 in 4.0N solution of hydrochloric acid at room temperature. Absorption spectra of the free radicals of PD usually show bathochromic shifts, sulphoxides hyperchromic shifts with respect to the non-oxidised PD forms. Table III summarises the results of these experiments.

TRANSITION POTENTIALS

25 ml of 0.05N solutions of uranium(IV) in 1.0M sulphuric acid containing 2 ml. of syrupy phosphoric acid were titrated potentiometrically against 0.05N solutions of ammonium vanadate of the same acid concentration in the presence of 1 ml. of 0.1% of phenothiazine indicator solution. Just before the theoretical end-point, the 0.05N solution of ammonium

Table 3

Values of λ_{max} and of non-oxidized forms of PD and their oxidation products

Number	Name of phenothiazine derivative	Values of PD							
		non-oxidized forms		free radicals				sulphoxides	
				ultra-violet region		visible region			
		λ_{max}	ε	λ_{max}	ε	λ_{max}	ε	λ_{max}	ε
I	Chlor-promazine-HCl	209 254	24000 33000	217 268 275	26000 45000 43600	525	9800	239 274 299 347	33700 10200 7200 5500
II	Diethazine—HCl	206 249	23000 31500	212 265 272	23500 38500 36000	515	9600	236 267 292 336	31500 10000 5500 5500
III	Perphenazine	208 255	23500 30900	215 267 276	26000 43700 42900	525	8000	235 273 300 342	33200 11900 6900 5400
IV	Promazine—HCl	206 252	21700 30000	213 266 271	26200 45000 45100	515	9000	232 274 304 345	26500 12200 7500 5500
V	Perazine	207 252	18000 24800	214 266 272	5000 26500 24000	515	5900	233 273 301 344	20000 7500 5500 4300
VI	Fluphenazine—2HCl	206 255	20200 32500	213 274	20200 48500	514	5300	234 272 301 347	25200 12700 7000 5800
VII	Trifluoperazine	206 255	17000 24700	214 273	15700 34100	501	5200	234 272 301 348	20100 7000 5500 4500
VIII	Levomepromazine-maleate	211 250	26000 23300	221 251 279	23300 33700 29500	560	5600	252 279 300 335	25300 9000 5500 4500
IX	Methopromazine-maleate	212 250	27000 25700	220 277	18600 23000	560	6500	253 279 300 338	24200 9700 5000 4000
X	Thioridazine—HCl	262 297	40500 8000	267 296	26700 33800	646	5700	225 280 350	11700 40100 4700

vanadate was replaced by a 0.01N solution which was added dropwise. The transition potential was obtained when the first trace of the appropriate colour appeared. The results obtained are given in Table IV.

Table 4

Transition potentials of PD indicators at 18°—20° referred to the normal hydrogen electrode

Indicator	Potential V(1N H_2SO_4)	Indicator	Potential V(1N H_2SO_4)
Chlorpromazine—HCl	0.73	Fluophenazine—2HCl	0.76
Diethazine—HCl	0.76	Trifluoperazine	0.76
Perphenazine	0.74	Levomepromazine maleate	0.65
Promazine—HCl	0.71	Methopromazine maleate	0.64
Perazine	0.72	Thioridazine—HCl	0.66

The values of the transition potentials of the phenothiazine indicators tested confirm that they are suitable for use in vanadometric titration. The redox potentials of three (chlorpromazine, diethazine and promazine) have already been reported by Sanke Gowda and other investigators; [3, 5, 6, 7, 12] although our value for promazine hydrochloride is somewhat lower, the other results are identical.

·DETERMINATION OF URANIUM(IV) WITH AMMONIUM VANADATE

N-phenylanthranilic acid [13,14] has been used in the titration of uranium(IV) with ammonium vanadate in 2.5—6.8M sulphuric acid. When oxalic acid is used as a catalyst the sulphuric acid concentration required is only 2M. [15] Diphenylbenzidine [15—17] has been proposed as redox indicator with oxalate catalysis, the titration being done at 50°. When both oxalic and phosphoric acids are present it can be done at room temperature. Copper-phthalocyaninetetrasulphonic acid [18] functions only in 6M sulphuric acid solution containing 3 ml of syrupy phosphoric acid.

We find that nine of the phenothiazine indicators tested can be employed satisfactory as reversible indicators in the uranium(IV)-vanadate titration at room temperature in sulphuric acid or hydrochloric acid media. Only thioridazine hydrochloride cannot be used. This indicator forms a blue oxidation product, similar in colour to vanadyl ions and it does not give a sharp end-point.

RECOMMENDED CONDITIONS FOR TITRATION

Adjust the acidity to 2.0—4.0N in sulphuric or hydrochloric acid and add a small amount of syrupy phosphoric acid (2—3 ml), to promote the reaction of the oxidised form of the phenothiazine indicator with uranium(IV).

Add 1 ml of 0.1% PD solution for a titration volume of 50—100 ml and titrate to the appropriate end-point.

---

[12] H. Puzanowska-Tarasiewiez, *Chem. Analit.* in print.

[13] V. S. Syrokomskii and Yu. V. Klimenko, *Zavodskaya Lab.*, **7**, 1093 (1938).

[14] *Idem. ibid.*, **9**, 1077 (1940).

[15] V. P. Rao, B. V. S. R. Murthy and G. G. Rao, *Z. analyt. Chem.*, **147**, 161 (1955).

[16] M. N. Sastri and G. G. Rao, *Current Sci.*, **18**, 402 (1949).

[17] U. V. Rao, *Z. analyt. Chem.*, **177**, 190 (1960).

[18] G. G. Rao and T. P. Sastri, *Z. analyt. Chem.*, **167**, 1 (1959).

The colour of the test solution changes as follows :

—	Chlorpromazine hydrochloride Diethazine hydrochloride Perphenazine	Bluish-green → blue → dark-red
—	Trifluophenazine Promazine hydrochloride Perazine Fluophenazine dihydrochloride	Bluish-green → blue → green-orange
—	Levomepromazine maleate Methopromazine maleate	Bluish-green → blue → dark-violet

At higher acidities this reduction is slow resulting in premature end-points. A sharp end-point is not obtained when the acidity is less than 1N even in the presence of phosphoric acid.

The indicator blanks were never greater than 0.05 ml of 0.05N ammonium vanadate.

Phenothiazine indicators were compared with other indicators used in the vanadometric titration of uranium(IV), e.g. diphenylbenzidine and N-phenylanthranilic acid. It was found that all the phenothiazine indicators tested (except thioridazine hydrochloride) gave sharper end-points.

INTERFERENCES

Iron(II), Sn(II), Ce(IV), Cr(VI) and HNO_3 interfere in the titration of uranium (IV) with ammonium vanadate.

Acknowledgements. One of us, Helena Puzanowska-Tarasiewicz thanks the School of Engineering, Bialystock, Poland for providing a Fellowship.

Revue Roumaine de Chimie, **22**, *4*, 539–544 (1977)

Dedicated to the 70th anniversary
of Professor Coriolan Drăgulescu

POLYNUCLEAR COMPLEX COMPOUNDS OF IRON, COBALT AND NICKEL. I

MERCURY-CONTAINING COMPLEX COMPOUNDS

MARIA BREZEANU and MAGDALENA DINCULESCU
Chemistry Institute, Laboratory of Inorganic Chemistry, Splaiul Independenţei, 89, Bucharest

Received August 31, 1976

A series of polynuclear complex compounds containing mercury and respectively iron, cobalt, nickel were synthesized; they correspond to the following general formulas: $Fe(HgCl_2)_n(NH_3)_{2n}(OH)_3$, $n = 1, 2, 4$; $M(HgCl_2)_n(NH_3)_{2n}(OH)_2$; $M = Co, Ni$; $n = 1, 2, 4$. The compounds obtained were characterized by elemental chemical analysis, electronic spectra and molecular electric conductivity measurements.

This paper is a part of a more extended study on the capability of iron, cobalt and nickel elements to form polynuclear complex compounds containing two different metals and it is concerned with the systems: $FeX_3-M'X_n-$Base; $MX_2-M'X_n-$Base($M=Co,Ni$; $M'=$ bivalent metal, trivalent metal; $X=Cl$, NO_3; Base: NH_3, en, Py).

The paper reports the results obtained in the synthesis and characterization of compounds formed in the systems:
$FeCl_3-HgCl_2-NH_3$; $MCl_2-HgCl_2-NH_3$ ($M=Co$, Ni).

The selection of such systems is mainly justified by the fact that the literature mentions only a few polynuclear compounds containing these elements and also by the fact that some of this type of compounds present catalytic properties.

Among the known complex compounds we can mention: $Fe(CO)_4\cdot\cdot(HgX)_2$,[1] $Hg[Co(CO)_4]_2$,[2–4] $Hg[Co(CO)_3L]_2$,[5–7] $(\pi-C_5H_5)Co(CO)_2\cdot nHgX_2$,[8,9] in which $X = Cl$, Br, I. For nickel no such compounds are known.

---

[1] J. Lewis and S. B. Wild, *J. Chem. Soc. A*, **1966**, 69.

[2] G. M. Sheldrick and R. N. Simpson, *J. Chem. Soc. A*, **1968**, 1005.

[3] H. Stammreich and K. Kawai, *J. Chem. Phys.*, **35**, 2175 (1961).

[4] J. M. Burlitch and S. W. Ulmer, *J. Organometal. Chem.*, **19**, 11 (1969).

[5] A. R. Manning, *J. Chem. Soc. A*, **1968**, 1018.

[6] A. R. Manning and J. R. Miller, *J. Chem. Soc. A*, **1970**, 3352.

[7] L. M. Bower and M. H. Stiddard, *J. Organometal. Chem.*, **13**, 325 (1968).

[8] D. J. Cook and J. L. Lawes, *J. Chem. Soc. A*, **1967**, 1547.

[9] B. Demersman and G. Bouquet, *J. Organometal. Chem.*, **35**, 341 (1972).

A series of polynuclear complex compounds containing the above-mentioned elements have been obtained as a result of this study. They may be represented by the following general formulas:
$Fe(HgCl_2)_n(NH_3)_{2n}(OH)_3$; $M(HgCl_2)_n(NH_3)_{2n}(OH)_2$ (M = Co, Ni; n = 1, 2, 4).

These compounds were characterized by elemental chemical analysis, electronic spectra and molecular electric conductivity determinations.

RESULTS AND DISCUSSION

The nature of species being formed in the systems under study was established by conducting the synthesis of these compounds under various conditions with regard to the following parameters: the $MCl_n : HgCl_2$ ratio; the pH of the reaction medium; the nature of base.

The contribution of the first parameter, the components ratio was established by performing two series of determinations: one, in which the amount of iron, cobalt and nickel chloride, respectively, has been kept constant while progressively varying the amount of mercury chloride from a ratio of 1 : 1 to 1 : 8 and another in which the amount of mercury chloride has been kept constant while progressively varying the same limits of the $MCl_n : HgCl_2$ ratio (from 1 : 1 to 1 : 8).

We present below the results obtained from the first series of determinations. In such conditions, three complex compounds have been obtained for each of the systems under study. They are represented by the following general formulas: $Fe(HgCl_2)_n(NH_3)_{2n}(OH)_3$; $M(HgCl_2)_n(NH_3)_{2n}(OH)_2$ (M = Co, Ni; n = 1, 2, 4).

It must be noted that for each system, the maximum amount of fixed mercury chloride corresponds to a 1 : 4 $MCl_n : HgCl_2$ ratio even if using in the synthesis a high excess of mercury chloride ($MCl_n : HgCl_2 = 1 : 8$).

This behaviour may be interpreted as an indication of the fact that the maximum number of direct or bridged metal-mercury bonds possibly formed in such compounds is four.

A characteristic property of complex compunds containing bivalent cobalt as a central metal ion is their existence in two differently coloured modifications, i.e. light blue and light pink. The blue modification represents the stable species in solution. In solid state, it will change in time to the pink modification, the conversion being irreversible.

The change from the blue modification to the pink one occurs without any variation in weight and under different conditions, as a function of the composition of the compound under consideration. Thus, for compounds $Co(HgCl_2)_2(NH_3)_4(OH)_2$ and $Co(HgCl_2)_4(NH_3)_2(OH)_2$ the conversion occurs within approximately one week whereas the compound $Co(HgCl_2)(NH_3)_2(OH)_2$ undergoes practically no change.

As will be shown below, the electronic spectra helped to attribute a tetrahedral configuration to the blue modifications and an octahedral one to the pink modifications.

The stability of the modification with an octahedral structure (pink) in solid state may be the result of some packing effects in the crystalline lattice.

The complex compounds of iron and nickel were obtained in one single modification which represents the stable species both in aqueous solution and in solid state.

Based on electronic spectra, the nickel complex compounds were assigned an octahedral configuration while iron compounds were attributed a tetrahedral configuration.

The formulation of those compounds is a relatively difficult problem due primarily to the fact that both direct and bridged mercury-metal bonds are possible and also to the fact that both chlorine and hydroxyl could act as a bridged ligand.

Since in the series of compounds obtained the number of the hydroxyl groups does not vary with their mercury content, it has been concluded that chlorine very likely acts as a bridged ligand.

Based on the spectral data correlated with the molecular electric conductivity determinations, the compounds of the form $M(HgCl_2)(NH_3)_2(OH)_2$ where M = Co, Ni, were assigned a tetrahedral structure having very likely the form

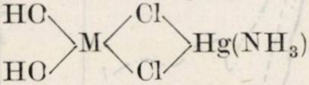
HO
HO
M
Cl
Cl
Hg(NH3)2

Based on the same data, compunds of the form $M(HgCl_2)_2(NH_3)_4(OH)_2$ where M = Co, Ni were assigned an octahedral structure having very likely the form :

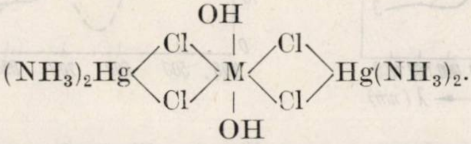
OH
(NH3)2Hg
Cl
Cl
M
Cl
Cl
Hg(NH3)2.
OH

The most probable formulation for the iron complex compounds $Fe(HgCl_2)_n(NH_3)_{2n}(OH)_3$ in which n = 1,2,4, would be

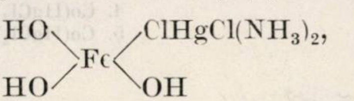
HO
HO
Fe
ClHgCl(NH3)2,
OH

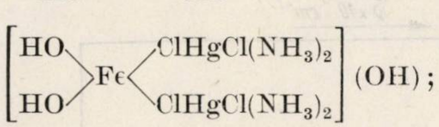
HO
HO
Fe
ClHgCl(NH3)2
ClHgCl(NH3)2
(OH) ;

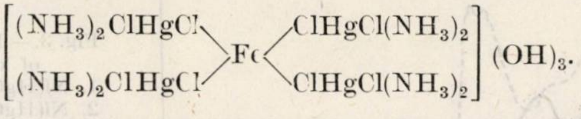
(NH3)2ClHgCl
(NH3)2ClHgCl
Fe
ClHgCl(NH3)2
ClHgCl(NH3)2
(OH)3.

Based on spectral and conductivity data, the cobalt and nickel complex compounds of type $M(HgCl_2)_4(NH_3)_8(OH)_2$ were assigned a tetrahedral structure, very probably of the form :

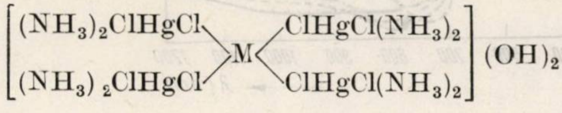
(NH3)2ClHgCl
(NH3)2ClHgCl
M
ClHgCl(NH3)2
ClHgCl(NH3)2
(OH)2

ELECTRONIC SPECTRA

Electronic reflexion spectra were recorded to obtain some information on the structure of complex compounds isolated in the systems under consideration.

A study of the electronic spectra of compounds $Fe(HgCl_2)_n(NH_3)_{2n}(OH)_3$ ($n = 1, 2, 4$) shows that their most likely structure is tetrahedral (fig. 1). The band at approx. 800 nm was attributed to the $^6A_1 \rightarrow {}^4E$ spin-forbidden transition.

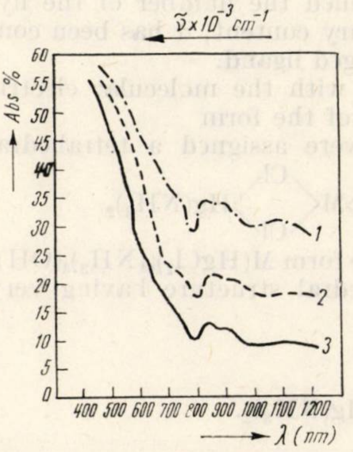

Fig. 1. — Electronic spectra of compounds : 1. $Fe(HgCl_2)(NH_3)_2(OH)_3$; 2. $Fe(HgCl_2)_2(NH_3)_4(OH)_3$; 3. $Fe(HgCl_2)_4(NH_3)_8(OH)_3$.

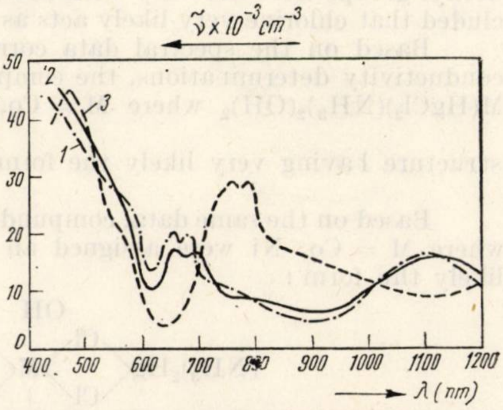

Fig. 2. — Electronic spectra of compounds :
1. $Co(HgCl_2)_2(NH_3)_4(OH)_2$-pink ;
2. $Co(HgCl_2)_4(NH_3)_8(OH)_2$-pink ;
3. $Co(HgCl_2)(NH_3)_2(OH)_2$-blue ;
4. $Co(HgCl_2)_2(NH_3)_4(OH)_2$-blue ;
5. $Co(HgCl_2)_4(NH_3)_8(OH)_2$-blue.

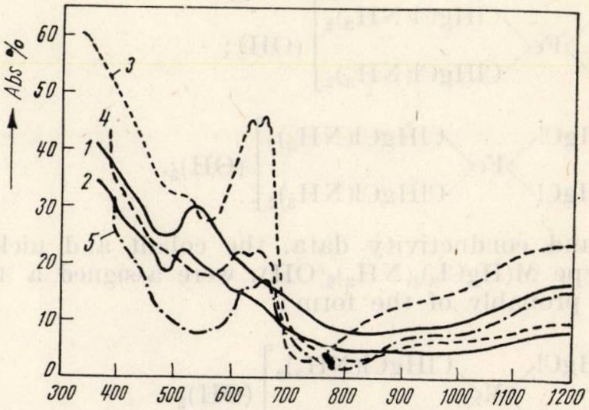

Fig. 3. — Electronic spectra of compounds :
1. $Ni(HgCl_2)_2(NH_3)_4(OH)_2$;
2. $Ni(HgCl_2)_4(NH_3)_8(OH)_2$;
3. $Ni(HgCl_2)(NH_3)_2(OH)_2$.

The electronic spectra recorded for the compounds $Co(HgCl_2)_n(NH_3)_{2n}\cdot$ $\cdot(OH)_2$ (n = 2, 4) coloured pink (fig. 2—1, 2) may be interpred on the base of an octahedral structure. Thus the band appearing in the domain of long wavelengths (aprox. 1150 nm) is attributed to the $^4T_{1g} \rightarrow {}^4T_{2g}$ transition and that at 530 nm, to the $^4T_{1g} \rightarrow {}^4T_{1g}(P)$ transition. For the corresponding blue compounds (fig. 2—3, 4, 5) the spectra indicate a tetrahedral structure.

The band found in these spectra at approx. 650 nm is attributed to the $^4A_2 \rightarrow {}^4T_1$ (P) transition. Its fine structure is due to the spin-orbit coupling which determines the splitting of the $^4T_1(P)$ term. [10]

Based on the electronic spectra (fig. 3) the compounds $Ni(HgCl_2)_n\cdot$ $\cdot(NH_3)_{2n}(OH)_2$(n = 2, 4) were assigned an octahedral structure and the existing bands were attributed as follows: the band at approx. 700 nm, to the $^3A_{2g} \rightarrow {}^3T_{1g}(F)$ transition, the splitting being due to the spin-orbit coupling which determines the mixing of the $^3T_{1g}(F)$ and ^1E_g states and the band appearing at approx. 1100 nm, to the $^3A_{2g} \rightarrow {}^2T_{2g}$ transition.

The nickel compound corresponding to n = 1 has a tetrahedral structure analogous to the cobalt compound.

MOLECULAR ELECTRIC CONDUCTIVITY DETERMINATIONS

The formulations attributed to these complex compounds were confirmed by their molecular conductivity determinations. The nature of the ionic dissociation was attributed based on the data reported in the literature relative to the limits comprising the various electrolyta types. [11] Table 1 indicates the results obtained for the compounds under study.

Table 1

Molecular electric conductivities of the obtained compounds in DMF solutions

Complex compound		Molecular conductivity $\Omega^{-1}cm^2mol^{-1}$	Type of electrolyte
$Fe(HgCl_2)(NH_3)_2(OH)_3$		26.4	non-electrolyte
$Fe(HgCl_2)(NH_3)_4(OH)_3$		68.5	1 : 1
$Fe(HgCl_2)_4(NH_3)_8(OH)_3$		194.0	1 : 3
$Co(HgCl_2)(NH_3)_2(OH)_2$	(blue)	13.7	non-electrolyte
$Co(HgCl_2)_2(NH_3)_4(OH)_2$	(blue)	163.1	1 : 2
$Co(HgCl_2)_2(NH_3)_4(OH)_2$	(pink)	18.3	non-electrolyte
$Co(HgCl_2)_4(NH_3)_8(OH)_2$	(blue)	186.2	1 : 2
$Co(HgCl_2)_4(NH_3)_8(OH)_2$	(pink)	16.4	non-electrolyte
$Ni(HgCl_2)(NH_3)_2(OH)_2$		19.5	non-electrolyte
$Ni(HgCl_2)_2(NH_3)_4(OH)_2$		18.6	non-electrolyte
$Ni(HgCl_2)_4(NH_3)_8(OH)_2$		32.4	non-electrolyte

---

[10] Y. Tanabe and S. Sugano, *J. Phys. Soc. Japan*, **6**, 457 (1954).

[11] D. J. Phillips and S. Y. Tyree, *J. Amer. Chem. Soc.*, **83**, 1806 (1961).

EXPERIMENTAL DATA

SYNTHESIS AND ANALYSIS OF COMPOUNDS

1. *$Fe(HgCl_2)_n(NH_3)_{2n}(OH)_3$ ($n = 1, 2, 4$).* To a solution obtained by dissolving 0.25 g $FeCl_3 \cdot 6H_2O$ in 3 ml water one adds 0.25 g, 0.5 g and 1 g $HgCl_2$, respectively, corresponding to 1 :1, 1 :2 and 1 :4 $FeCl_3 : HgCl_2$ ratio. About 25 ml alcohol are added to totally dissolve the salts. To the final solution one adds ammonia up to a pH = 8. After approx. 24hr the separated substance is filtered and washed with alcohol.
The compound $Fe(HgCl_2)_4(NH_3)_8(OH)_3$ is also obtained at $FeCl_3 : HgCl_2 > 1:4$ ratios, i.e. 1 :6 and 1 :8.

Calcd.:	Hg,	48.66;	Fe,	13.56;	Cl,	17.19;	N,	6.77%	n=1
Found:		48.35;		13.42;		17.51;		6.32	
Calcd.:	Hg,	55.91;	Fe,	7.78;	Cl,	19,74;	N,	7.78%	n=2
Found:		55.73;		7.82;		19.85;		7.65	
Calcd.:	Hg,	60.38;	Fe,	4,21;	Cl,	20.71;	N,	8.41%	n=4
Found:		60.15;		4.16;		20.60;		8.69	

2. *$(CO(HgCl_2)_n(NH_3)_{2n}(OH)_2$ ($n = 1, 2, 4$).* To a solution obtained by dissolving 0.2 g $CoCl_2 \cdot 6\,H_2O$ in 3 ml water and approx. 25 ml ethyl alcohol one adds 0.25 g, 0.5 g and 1 g $HgCl_2$ respectively, corresponding to a 1 :1, 1 :2 and 1 :4 $CoCl_2 : HgCl_2$ ratio. After total dissolution of salts, one adds ammonia up to a pH=8. The separated substance is filtered after 24 hr. and thoroughly washed with alcohol.

Calcd.:	Hg,	50.40;	Co,	14.80;	Cl,	17.79;	N,	7.02%	n=1
Found:		50.28;		14.52;		18.39;		7.69	
Calcd.:	Hg,	57.02;	Co,	8.37;	Cl,	20.14;	N,	7.94%	n=2
Found:		57.56;		8.48;		20.95;		7.87	(blue form)
Calcd.:	Hg,	57.32;	Co,	8.25;	Cl,	20.63;	N,	7.84%	n=2
Found:		57.26;		8.13;		20.18;		7.56	(pink form)
Calcd.:	Hg,	61.01;	Co,	4.55;	Cl,	21.58;	N,	8.51%	n=4
Found:		61.66;		4.38;		21.51;		8.23	(blue form)
Calcd.:	Hg,	61.23;	Co,	4.35;	Cl,	21.37;	N,	8.45%	n=4
Found:		61.45;		4.48;		21.63;		8.62	(pink form)

The compound $Co(HgCl_2)(NH_3)_8(OH)_2$ is also obtained for a ratio $CoCl_2 : HgCl_2 > 4$, i.e. for 1 :6 and 1 :8.

3. *$NiCl_2(HgCl_2)_n(NH_3)_{2n}(OH)_2$ ($n=1, 2, 4$).* To a solution obtained by dissolving 0.2 g $NiCl_2 \cdot 6\,H_2O$ in 3 ml water and 2 ml alcohol one adds 0.25 g, respectively 0.5 g or 1 g $HgCl_2$. To the final solution one adds ammonia up to a pH=8. After 24 hr. the separated substance is filtered and washed with alcohol. The compound $NiHgCl_2(NH_3)_2(OH)_2$ is obtained only in the presence of a high excess of $NiCl_2$($HgCl_2 : NiCl_2$ 1 :6 ratio).

Calcd.:	Hg,	57.45;	Ni,	8.45;	Cl,	20.12;	N,	8.04%	n=2
Found:		57.26;		8.70;		20.58;		8.51	
Calcd.:	Hg,	61.72;	Ni,	4.50;	Cl,	21.58;	N,	8.62 %	n=4
Found:		61.54;		4.23;		21.93;		8.75	
Calcd.:	Hg,	50.63;	Ni,	14.90;	Cl,	17.80;	N,	7.12%	n=1
Found:		50.42;		15.02;		18.11;		7.35	

All these compounds decompose when heated to 110°. The chemical analyses performed have shown that the whole amount of mercury and ammonia is lost in the compounds through decomposition. The residues left have the composition of basic salts.

The electronic spectra were recorded at room temperature using a VSU_1 spectrophotometer and magnesium oxide as a reference.

Molecular conductivity determinations were performed by means of an UK–120/1 conductometer.

Revue Roumaine de Chimie, 22, 4, 545–549 (1977)

Dedicated to the 70th anniversary
of Professor Coriolan Drăgulescu

SPIN-TRAPPING EXPERIMENTS WITH PENTADIENYL- AND CYCLOHEPTADIENYL-IRON TRICARBONYL CATIONS

MICHAEL CAIS, P. ASHKENAZI and J. GOTTLIEB
Department of Chemistry, Technion — Israel Institute of Technology, Haifa, Israel

Received September 24, 1976

The reaction between dienyliron tricarbonyl cations and nitroso-derivatives leads to the formation of nitroxide radicals which can be detected and characterized by ESR spectroscopy. The structure of these nitroxide radicals and their mode of formation are analogous to those observed in the α-ferrocenylcarbonium ions/nitrosoderivatives system.

INTRODUCTION

The distinctive stability of α-ferrocenylcarbonium ions has continued to generate a lively and diverse interest in the study of this class of compounds.[1–6]

Recently we have presented results which demonstrated the occurrence of electron transfer reactions between tertiary amines and α-ferrocenyl carbonium ions[7] and the spin-trapping of radicals in the α-ferrocenylcarbonium ions/nitrosobenzene system.[8]

---

[1] a) M. Cais, *Organometal. Chem. Rev.*, **1**, 435 (1966); b) M. Cais, in "Aromaticity, Pseudo-aromaticity, Anti-aromaticity", eds. E. D. Bergmann and B. Pullman, Academic Press, New York, 1971, pp. 97–113.

[2] R. Gleiter and R. Seeger, *Helv. Chim. Acta*, **54**, 1217, (1971).

[3] S. Lupan, M. Kapon, M. Cais and F. H. Herbstein, *Angew. Chem. Internat. Edn.*, **11**, 1025, (1972).

[4] A. Eisenstadt and M. Cais, *J. Chem. Soc., Chem. Commun.*, **1972**, 216.

[5] V. I. Sokolov, P. V. Petrovski and O. A. Reutov, *J. Organometal. Chem.*, **59**, C27, (1973).

[6] For additional pertinent references see e.g. a) T. D. Turbitt and W. E. Watts *J. Chem. Soc., Perkin Trans.*, **2**, 177, (1974); b) J. W. Larsen and P. Ashkenazi, *J. Amer. Chem. Soc.*, **97**, 2140, (1975).

[7] M. Cais, P. Ashkenazi, S. Dani and J. Gottlieb, *J. Organometal. Chem.*, (1976), in press.

[8] M. Cais, P. Ashkenazi, S. Dani and J. Gottlieb, *J. Organometal. Chem.*, (1976), in press.

In this communication we wish to report data on the extension of this work to organometallic cations incorporating the iron tricarbonyl moiety.

EXPERIMENTAL

ESR spectra were recorded on a Varian E—4 spectrometer, using a three-pronged Pyrex semi-capillary vessel which allowed for degassing (usually ten cycles) and sealing under vacuum prior to mixing of reactants. NMR spectra were measured on a Varian T—60 spectrometer. IR spectra were obtained with a Perkin-Elmer Model 237 grating spectrometer. Mass spectra were recorded with an Atlas CH—4 spectrometer. All solvents and reagents used were of analytical grade. Nitroso-derivatives were resublimed prior to use. Cycloheptadienyliron tricarbonyl fluoroborate was generously supplied by Dr. A. Eisenstadt. Pentadienyliron tricarbonyl fluoroborate salts were prepared from precursor carbinols. [8]

RESULTS AND DISCUSSION

Upon mixing a well degassed solution of 1-methylpentadienyliron tricarbonyl fluoroborate (I, R = H) in dichloromethane with nitrosobenzene, an ESR nitroxide radical spectrum (a_N 10.9 Gauss) was exhibited within about 20—30 minutes. This spectrum was not resolved so well as those obtained with α-ferrocenylcarbonium ions [8] and therefore the hyperfine splitting constants could not be determined accurately for all the hydrogen substituents. However, the general appearance of the spectrum was very similar to that of spectra obtained with the ferrocenyl systems,[8] indicating strongly the formation of nitroxide radicals of analogous structure. Due to the absence of high resolution, the ESR spectrum did not afford data for distinguishing between the two possible nitroxide radicals, II and III (Scheme 1).

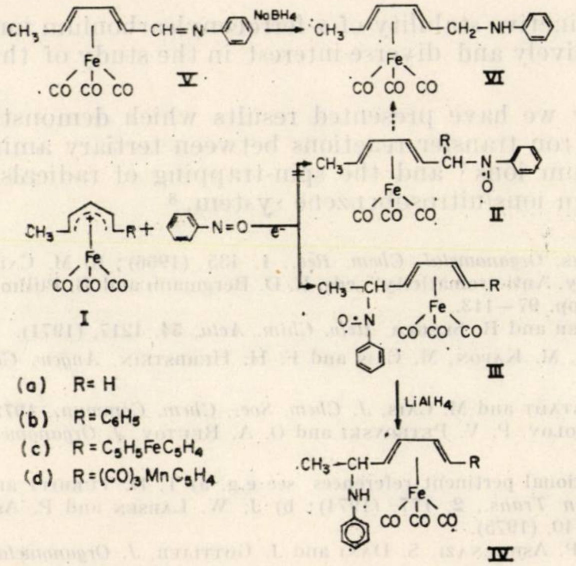

Scheme 1. — Products from reaction of pentadienyliron tricarbonyl fluoroborate with nitrosobenzene.

The answer to this question was obtained by the following experiments. The nitroxide obtained from a mixture of 1-methylpentadienyliron fluoroborate and excess nitrosobenzene was reduced [8] with $LiAlH_4$ and the spectral properties (NMR, IR) of the resulting amine were found to fit those expected for amine IV which would be derived from nitroxide III. Additionally, oxidation of this amine with *m*-chloroperbenzoic acid, *in situ*, gave a nitroxide ESR spectrum identical to that obtained from the reaction of I (R = H) with nitrosobenzene.

Furthermore, amine VI (expected to form from nitroxide III) was synthesized independently. Tricarbonyliron sorbaldehyde was reacted [8] with aniline in the presence of $TiCl_4$ to produce the imine V. Reduction of V with $NaBH_4$ yielded the amine VI, which exhibited different properties (NMR, IR) from those of IV. The proof was completed when the cation I was reacted with nitroso-*tert*-butane to obtain a simplified ESR spectrum which exhibited a triplet of doublets with hyperfine splitting constants a_N 15.5 Gauss and a_{HB} 2.95 Gauss, as expected for a nitroxide analogous to III but not to II (R = H) (which would have shown a triplet of triplets). The ESR spectrum obtained with cycloheptadienyliron tricarbonyl fluoroborate and nitrosobenzene is shown in Fig. 1. A compu-

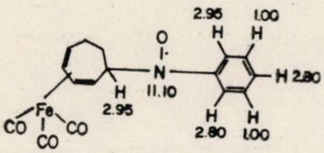

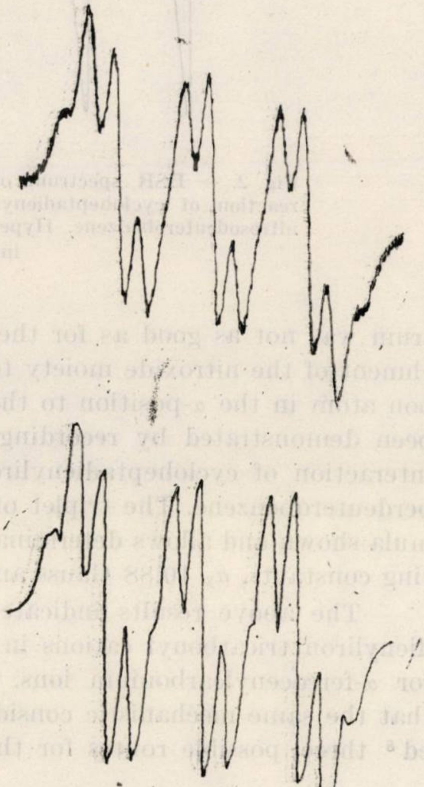

Fig. 1. — ESR spectrum of nitroxide radical obtained from reaction of cycloheptadienyliron tricarbonyl fluoroborate and nitrosobenzene (top); and (bottom) the computer simulation obtained with hyperfine splitting constants (Gauss) shown in formula.

ter simulated ESR spectrum gave a good fit with the hyperfine splitting constants shown on the formula in the figure. In this case too, as for the 1-methylpentadienyliron tricarbonyl cations, the resolution of the spectrum was not as good as for the ferrocenyl cations.[8] The point of attachment of the nitroxide moiety to the ring was as expected,[9] on the carbon atom in the α-position to the dieneiron tricarbonyl system. This has been demonstrated by recording the ESR spectrum obtained from the interaction of cycloheptadienyliron tricarbonyl fluroborate with nitrosoperdeuterobenzene. The triplet of doublets, shown in Fig. 2, fits the formula shown and allows determination by inspection of the hyperfine splitting constants, a_N 10.88 Gauss and a_{HB} 3.00 Gauss.

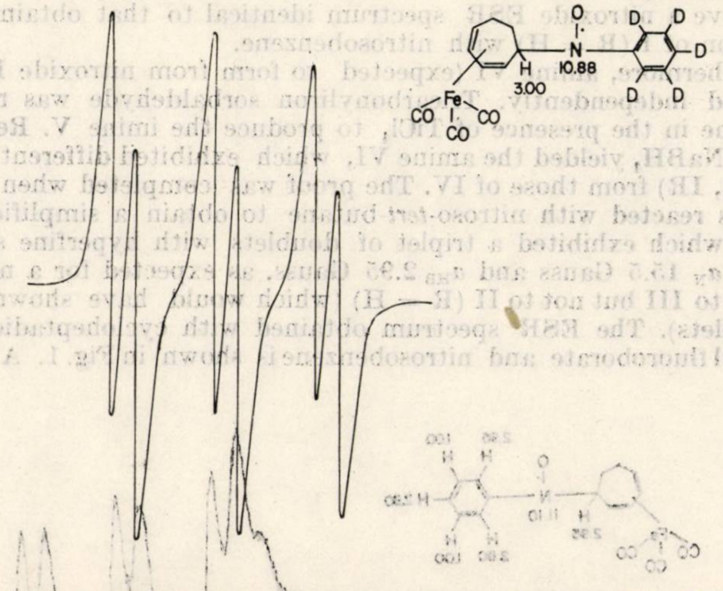

Fig. 2. — ESR spectrum of nitroxide radical obtained in the reaction of cycloheptadienyliron tricarbonyl fluoroborate with nitrosodeuterobenzene. Hyperfine splitting constants (Gauss) shown in formula.

The above results indicate that nitroso compounds interact with dienyliron tricarbonyl cations in an analogous manner to that observed for α-ferrocenylcarbonium ions. Therefore, we feel justified to suggest that the same mechanistic consideration should prevail. We have proposed[8] three possible routes for the formation of the nitroxide radicals in this system (Scheme 2):

---

[9] A. J. Birch, I. D. Jenkins and A. J. Liepa, *Tetrahedron Letters*, **21**, 1723 (1975).

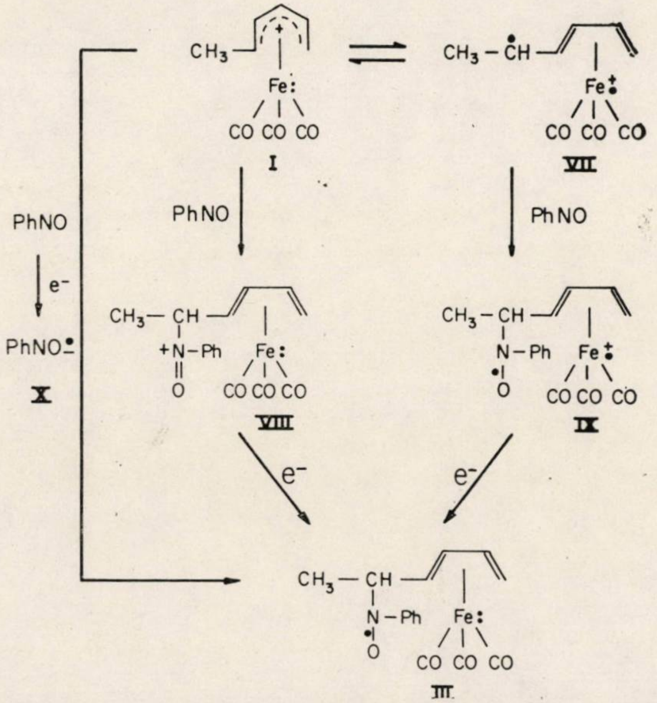
CH₃
Fe:
CO CO CO
I
CH₃ – CH
Fe
CO CO CO
VII
PhNO
PhNO
PhNO
e⁻
PhNO⁻
X
CH₃ – CH
+N – Ph
O
Fe:
CO CO CO
VIII
CH₃ – CH
N – Ph
O
Fe
CO CO CO
IX
e⁻
e⁻
CH₃ – CH
N – Ph
O
Fe:
CO CO CO
III

Scheme 2. — Mechanistic pathways for formation of nitroxide radicals in the reaction of dienyliron tricarbonyl cations with nitrosobenzene.

(i) the "electron tautomerism" representation I $\rightleftarrows$ VII for the formation of a cation-diradical species, VII, which is spin-trapped by the nitroso compound to form the cation radical IX. This is then reduced to the neutral nitroxide radical III;

(ii) a nucleophilic attack by the nitroso moiety on the carbonium ion center to form the immonium intermediate VIII is followed by a one-electron reduction to yield the nitroxide radical III, and

(iii) a one-electron reduction of the nitroso compound to form an anion radical X which then reacts with the carbonium ion to produce the observed nitroxide radicals. At the present time we cannot exclude any of the above possibilities.

Revue Roumaine de Chimie, **22**, *4*, 551–555 (1977)

Dedicated to the 70th anniversary of Professor CORIOLAN DRĂGULESCU

THE UV, VIS AND IR SPECTRA OF THE $Pd(p\text{-}NO.C_6H_4N(CH_3)_2)_2Cl_2.H_2O$

N. CALU, N. FOCA and M. LUCHIAN

Inorganic Chemistry Department, Polytechnical Institute of Iassy, Splaiul Bahlui 71,
R–6600–Iassy, Romania

Received August 28, 1976

The complex PdL_2Cl_2 exhibits an electronic spectrum that can be interpreted on the basis of molecular orbital diagram in D_{4h}. Thus, in UV and VIS, the complex exhibits three bands with metal-ligand (*p*-nitrosodimethylaniline) charge transfer and three bands by the crystalline field type, very weak, characteristic of the complexes with Pd(II) having ligands with π system in D_{4h}. In addition to this, the complex PdL_2Cl_2 exhibits in visible two bands of ligand-metal charge transfer.

The IR spectrum of the complex PdL_2Cl_2 is examined in comparison with that of the ligand (*p*-nitrosodimethylaniline). Thus, it has been found that the coordination of *p*-nitrosodimethylaniline to Pd(II) by means of the group –NO is admitted.

In the $PdCl_2$-*p*.nitrosodimethylaniline system the complexes $PdLCl_2$ and PdL_2Cl_2* are generated step by step[1]. These complexes have their UV and VIS spectra with bands of the crystalline field type and with charge transfer spectra which provide information about their structure. Similarly, their IR spectra bring information as regards their characteristic metal-ligand bond.

Further on, the UV, VIS, and IR spectra of the PdL_2Cl_2 complexes are presented.

EXPERIMENTAL

The complex PdL_2Cl_2 was obtained in solution using $PdCl_2$ and $p\text{-}NOC_6H_4(CH_3)_2$, in stoichiometric ratios, during an approximative reaction time of 25 minutes, and concentration $5-10^{-5}$ moles/l. It was obtained in the crystalline form too.

The UV and VIS spectra have been recorded for the complex obtained in both aqueous or ethyl alcohol 85–90% solution and crystallyzed and dissolved in some organic solvents.

The IR spectra have been recorded on the complex PdL_2Cl_2 pelletized with KBr.

---

* Taking into account the metal to ligand ratio, the complexes in this system are symbolized with $PdLCl_2$ (1 : 1) and PdL_2Cl_2 (1 : 2).

[1] N. CALU and N. FOCA, *Bul. Inst. Politeh. Iaşi*, In press.

RESULTS AND DISCUSSION

a. THE UV AND VIS SPECTRA OF THE PdL_2Cl_2 COMPLEX

The absorption bands of the PdL_2Cl_2 complex can be distinguished from those of reactants (occurring on the same field), watching the electronic spectrum during its formation reaction. Therefore, the bands whose intensity increases during the reaction of formation have been attributed to the complex, only, Figs. 1 and 2.

Generally, the complexes PdL_2X_2 have a square-planar shape and a microsymmetry not so good as that of D_{4h}. It can be either D_{2h} or C_{2v}, corresponding to the *trans* and *cis* forms ; in the trans form, sterical repulsions between ligands are minimized.

The electronic spectrum of the PdL_2Cl_2 complex in UV and VIS is similar to that of the Pd(II) complexes from D_{4h}. It seems that the complex deformation caused by the two different ligands is small and consequently, its electronic spectrum can be interpreted on the basis of molecular orbitals diagram from D_{4h},[2] the case of the ligands with a π electron system ; Fig. 3.

Therefore, in UV, the complex PdL_2Cl_2 is characterized by three bands with metal-ligand (*p*-nitrosodimethylaniline) charge transfer : ν_{1c}, ν_{2c} and ν_{3c}. λ_{max} of these bands are 45050, 34130 and 32470 cm^{-1} respectively and they correspond to the transitions $^1A_{1g} \rightarrow {}^1E_u$, $^1A_{1g} \rightarrow {}^1A_{2u}$ and $^1A_{1g} \rightarrow {}^1B_{1u}$ respectively, in D_{4h}. The band ν_{1c} is the most intense of all, such as theoretically predicted. [2]

The band ν_{c1} with $\lambda_{max} \sim 36230$ cm^{-1} represents an intraligand transition, at the coordinated ligand. It results from the ν_{31} ligand band which undergoes both a weak bathochromic effect and a hypsochromic effect during the formation of the complex.

The remaining bands in UV such as those corresponding to the chlorine — paladium transitions are covered by the above-mentioned bands.

In VIS, the complex PdL_2Cl_2 exhibits two ligand-metal charge transfer bands : ν_{4c} and ν_{5c}. Their λ_{max} are 19900 and 18900 cm^{-1} respectively. They correspond to some electron transitions from π molecular orbitals (eventually π and π^*) localized, especially, on the ligand (*p*-nitrosodimethylaniline), in the orbital $d_{x^2-y^2}$, particularly, localized on metallic atom, consequently some transitions $^1A_{1g} \rightarrow {}^1A_{2u}$ and others in D_{4h}.

Certain bands of the ligand and complex behave similarly when the nature of the solution of the two compounds changes. Thus, the bands ν_{5l} and ν_{5c} occur well shaped when the ligand and complex respectively are found in prevalent alcoholic solution ; others appear as a shoulder when the two compounds are found in aqueous solution with a low content of ethyl alcohol. They have been called "alcohol bands".

It is possible that the asymmetry of the π electron cloud of nitroso group in ligand (*p* nitrosodimethylaniline) may be reflected in both the $n \rightarrow \pi^*$ or eventually $\pi \rightarrow \pi^*$ transitions in ligand and ligand-metal transition in complex.

---

[2] H. B. GREY and C. J. BALLHAUSEN, *J. Amer. Chem. Soc.* **85**, **260**, (1963).

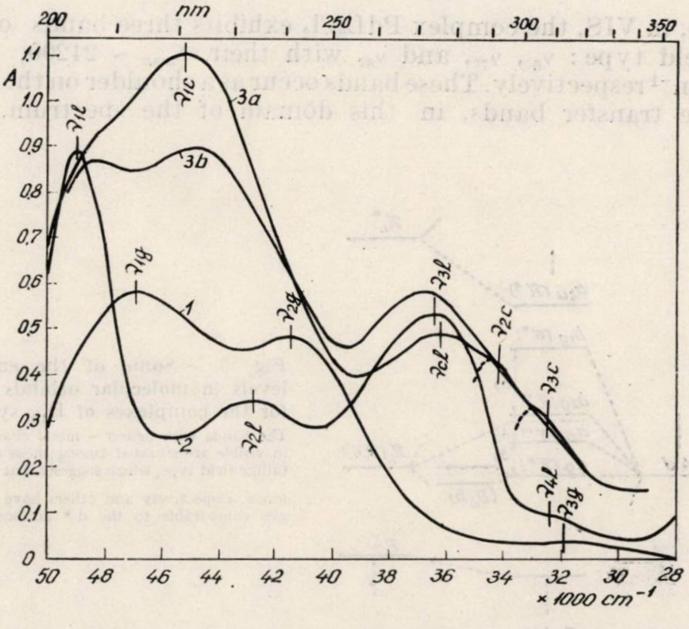

Fig. 1. — UV spectra recorded on the $PdCl_2$ — *p*-nitrosodimethylaniline system.

1. $PdCl_2(HCl)$ — 1.10^{-4} moles/1, in aqueous solution with pH = 3.6; bands ν_{ig}, i = = 1—3. 2. p $NOC_6H_4N(CH_3)_2$— 2.10^{-4} moles/1, in ethyl alcohol 90%; bands ν_{il}, i = = 1—4. 3. PdL_2Cl_2 — 1.10^{-4} moles/1, in 90% ethyl alcohol. Reaction time: 3 a—1 minute and 3b—25 minutes (considered from reactants joining); bands ν_{ic}, i = 1—3 and ν_{cl}. Thickness of sample = 0.5 cm.

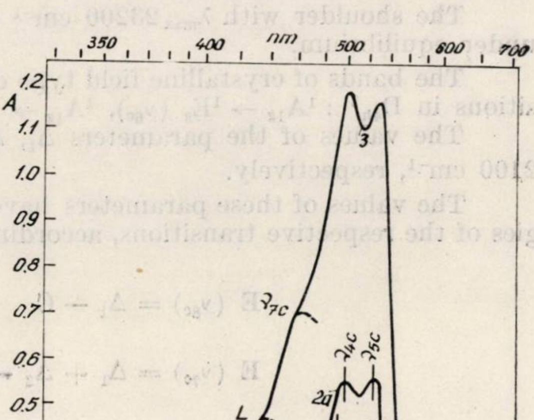

Fig. 2. — The VIS spectra recorded on the $PdCl_2$ — *p*-nitrosodimethylaniline system.

1. *p*-$NOC_6H_4N(CH_3)_2$ 5.10^{-5} moles/1; 1a — in 90% ethyl alcohol; 1b — in aqueous solution with ∼ 5% ethyl alcohol; bands ν_{il}, *i* = 5 and 6. 2. PdL_2Cl_2 — 5.10^{-5} moles/1, 2a — in ethyl alcohol ∼90%; 1b — in aqueous solution with ∼ 5% ethyl alcohol; bands ν_{ic}, i = 4 and 5. 3. PdL_2Cl_2 — 1.10^{-4} moles/1; in ethyl alcohol ∼90%; bands ν_{ic} i = 6—8. Thickness of sample = 0.2 cm.

Also, in VIS, the complex PdL_2Cl_2 exhibits three bands of the crystalline field type: ν_{6c}, ν_{7c}, and ν_{8c} with their $\lambda_{max} \sim 24200$, 21400 and $\sim 16000\ cm^{-1}$ respectively. These bands occur as a shoulder on the ligand-metal charge transfer bands, in this domain of the spectrum. The most obvious of them is the ν_{7c} band. The other ones, very weak, can be visible in more concentrated solutions.

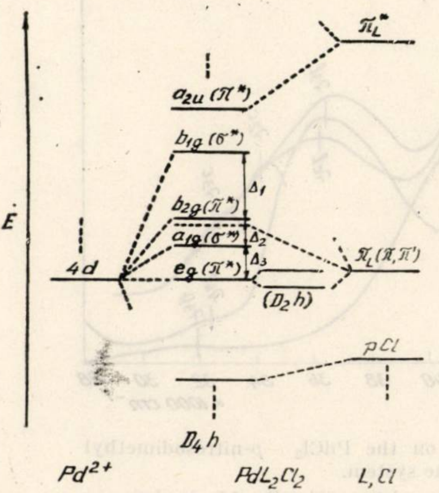

Fig. 3. — Some of the energetical levels in molecular orbitals diagram for the complexes of D_{4h} symmetry. The bands with ligand — metal charge transfer in visible are situated among those of the crystalline field type, which suggests that π_L and b_{2u} levels, respectively and others have their energies comparable to the d* antibonding ones

The shoulder with λ_{max} 23200 cm^{-1} is attributed to the free ligand, under equilibrium.

The bands of crystalline field type correspond to the following transitions in D_{4h}[3] : $^1A_{1g} \rightarrow {}^1E_g$ (ν_{6c}), $^1A_{1g} \rightarrow {}^1B_{1g}$ (ν_{7c}) and $^1A_{1g} \rightarrow {}^1A_{2g}$ (ν_{8c}).

The values of the parameters Δ_1, Δ_2 and Δ_3 are 18600, 8150 and 2100 cm^{-1}, respectively.

The values of these parameters have been computed from the energies of the respective transitions, according to the equations.

$$E\ (\nu_{8c}) = \Delta_1 - C$$

$$E\ (\nu_{7c}) = \Delta_1 + \Delta_2 - 4B - C$$

$$E\ (\nu_{6c}) = \Delta_1 + \Delta_2 - 3B - C$$

in which, for Pd^{2+}, the Racah's parameters, namely $B = 683$ and $C = 2620$ [3] have been utilized.

---

[3] A. B. P. Lever, "Inorganic Electronic Spectroscopy", Elsevier, Amsterdam, 1968, 164, 351.

b. IR SPECTRUM OF THE COMPLEX PdL_2Cl_2

The IR spectrum of the complex PdL_2Cl_2 is examined in comparison with that of ligand on the basis of characteristic group-frequencies.

The ligand, *p*-nitrosodimethylaniline, exhibits a spectrum with several absorbtion bands. Among these, especially the frequencies attributed to the substituents – NO and $-N(CH_3)_2$ on benzenic nucleus are examined.

When the ligand coordinates Pd(II) in the complex PdL_2Cl_2 important modifications occur, besides others, near the frequency ν (NO). This shows that ligand-metal bond in complex takes place by means of the –NO group of *p*-nitrosodimethylaniline.

For nitrosoderivates monomers R–NO, the frequency ν(NO) is situated between 1490 and 1621 cm^{-1} and for dimers, $(RNO)_2$, between 1180 and 1430 cm^{-1}.[4,5] It depends on the position and nature of substituents in aromatic nucleus.

In the case of *p*-nitrosodimethylaniline, the monomer form is more stable.

For –NO group, *p*-nitrosodimethylaniline monomer exhibits three vibrations, namely, δ(RNO), ν(CN) and ν(NO) with their frequencies of 830, 1122 and 1540 cm^{-1}, respectively. These frequencies are modified for the ligand coordinated in PdL_2Cl_2. The first two are displaced towards higher frequencies, at 840 and 1140 cm^{-1} respectively, and the last, ν(NO), is markedly displaced towards lower frequencies namely at 1510 cm^{-1}. Obviously, by ligand coordination at Pd(II), in which –NO group is used with its π electron cloud the order of its nitrogen-oxygen bond and the force constant diminish, which influences the frequency ν(NO).

The very weak frequencies of ν(NO) at 1400 and 1430 cm^{-1} show that the ligand contains *cis*-dimer traces too.

At the group $-N(CH_3)_2$, *p*-nitrosodimethylaniline exhibits the vibrations ν′(CN) at 1240 cm^{-1}, $\delta(CH_3)$ at 1370 and 1460 cm^{-1} and $\nu(NCH_3)$ at 2940 cm^{-1}. These frequencies are modified at the ligand coordinated in PdL_2Cl_2. Therefore, ν′(CN) is displaced at 1230 cm^{-1}; $\delta(CH_3)$ at 1380 and 1470 cm^{-1}, and $\nu(NCH_3)$ at 2940 cm^{-1}. Generally, the modifications of these frequencies are less than ν(NO).

The $Pd(p\text{-}NOC_6H_4N(CH_3)_2)_2Cl_2.H_2O$ complex investigated contains water, and its IR spectrum brings information in this respect. Thus, the IR spectrum of dehydrated complex shows modifications of frequencies as against the usual one, in the vibration range of –OH group such as π(OH), out of plane deformations, at 940–970 cm^{-1}, δ(OH) between 1300 and 1400 cm^{-1} and ν(OH) between 2500 and 2600 cm^{-1}.

---

[4] W. LUTTKE, *Z. Electrochem.*, **61**, **303** (1957). **61**, **976** (1957).

[5] D. BÎRCĂ-GĂLĂŢEANU, L. ARCAN şi C. LUPU, *Studii şi cercetări fizică*, **10**, **417** (1959).

Revue Roumaine de Chimie, **22**, *4*, 557–562 (1977)

Dedicated to the 70th anniversary
of Professor Coriolan Drăgulescu

HYDROXIDE PRECIPITATION AND METAL DENDRITE FORMATION AT THE LIMITING CURRENT ON DME

A. CĂLUȘARU
Institute of Atomic Physics, P.O.B. 5206, Bucharest, Romania

Received August 25, 1976

The process of hydroxide precipitation and dendrite formation in the limiting current region has been studied. In the presence of gelatine the hydroxide layer on the surface of the mercury drop is more uniform and compact. The growth of dendrites is favoured by the addition of gelatine in the case of Bi, Cu and Cd, but in the case of Tl and Pb the same process is hindered. The formation potential and the shape of silver dendrites are considerably influenced by the presence of the colloidal AgCl in solution. In the case of copper ions the shape of the drop is determined by the value of the voltage applied at the mercury electrode. These processes were interpreted on the basis of the quantum mechanism of the elementary act of the electrochemical reactions in the limiting current region.

The metal dendrite formation on the dropping mercury electrode (DME) has been studied, considering both the characteristic potential of this process and the threshold of the metal ion concentration at which the dendrites are formed.[1,2]

The aim of the present work is to show that in the limiting current region on the dropping mercury electrode the metal dendrites are formed together with the hydroxide precipitation. Since this process is more intensive in the relative concentrated solutions, only these last ones are studied.

EXPERIMENTAL

A polarographic cell provided with an optical window, suitable for photographing the mercury drop, has been used.

The capillary constants are : $t_1 = 180$ s, $w = 0.189$ mg s^{-1} at $h = 80$ cm, in 2 M KNO_3 and open circuit.

The installation for the photography of the mercury drop consists of an objective of small increment (2X) located at a relative large distance from the film (about 50 cm). In this way

---

[1] A. Călușaru and J. Kůta, *Nature*, **211**, 1080 (1966).
[2] A. Călușaru and J. Kůta, *J. Electroanlyt. Chem.*, **20**, 383 (1969).

the relief of the drop and dendrites does not disturb the clarity of the image at an increment of 15–20X.

High sensitivity films (27 DIN) were used. All the substances were reagent grade.

EXPERIMENTAL RESULTS

The experiments were carried out in conditions which eliminate the effect of the light irradiation, appearing to be sometimes very strong. The illumination for the photography was performed only a few tenths of seconds, before the changes produced by the irradiation with strong light sources.

1. HYDROXIDE PRECIPITATION AND EFFECT OF THE SURFACTANTS

When small concentrations of the metal ion are used,[1,2] no visible hydroxide precipitation has been observed. At concentrations larger than 0.1 M the formation of the hydroxides occurs in the case of copper, if the potential of the drop is negative enough. In fig. 1, Cu, frame 1, for 0.2 M Cu^{2+}, at -1.4 V, only the copper hydroxide is formed around the drop. At lower concentration (0.1 M) metal dendrites are formed together with hydroxide precipitation. Owing to the hydroxide film the drop cannot grow spherically, being strongly deformed (frame 2, Cu). The addition of the gelatine (frame 3) allows the continuous formation of the film and thas is why the drop has a quasi-cylindrical form.

A weaker deformation effect has been found in the case of silver ion (fig. 1, Ag). For comparison the non-deformed mercury drop is shown in the frame 1, Ag. When the circuit is open (potential of the maximum on the electrocapillary curve) a spontaneous formation of silver oxides occurs at the mercury drop, visibly deformed (frame 2); this effect is very reproducible. At 0.0 V in the presence of the colloidal AgCl, the adsorbed film is of grey-blue colour and the deformation near the capillary is obvious (frame 3).

In solutions containing Cd^{2+} ions, without gelatine, an intensive precipitation of cadmium hydroxide occurs (Fig. 1, Cd, frame 1), as in the case of copper. In the presence of gelatine very bright dendrties are formed. On the first polarised drop white hydroxide and metal dendrites are formed together, while on further drops practically only the dendrites can be observed.

The addition of gelatine favours the dendrite formation in the case of Bi, Cu and Cd, but in the case of Tl and Pb the dendrite growth is in general hindered by the surfactant.

2. EFFECT OF THE COMPOSITION OF THE ADSORBED FILM

The effect of the surfactant, already presented, shows that the nature of the adsorbed films has a visible influence on the metal dendrite growth. In the case of silver it was possible to study the case of the films having different chemical compositions.

When a small quantity of chloride ions is present, the colloidal AgCl fragments migrate to the mercury drop and cover its surface with a thin AgCl film, well visible at 0.0 V (fig. 1, Ag, frame 1). In 0.1 M $AgNO_3$ + 2 M KNO_3 (fig. 2) the dendrites grow at about −0.3 V in the form of a bunch having a punctual bond to the drop surface, as in the case shown for −0.4 and −0.5 V (fig. 2). At more negative potentials (over −0.6 V) abundant dendrite growth occurs on the drop surface. During the growth the film is broken, the dendrite contacts directly the mercury and dissolves into drop very fast. The influence of the electrode potential is strongly dependent on the precipitation conditions of AgCl.

A different picture is obtained when no traces of AgCl are present in solution. The films on the mercury surface are always formed, but in the absence of chlorides, these films are composed of silver oxide. In this case the dendrites grow at more positive potentials (fig. 3) and are amalgamated by the mercury. The influence of the potential is shown in fig. 3.

The shape of the dendrites and of the whole drop is very different at the same potential during the dendrite growth. In fig. 4 different shapes of the mercury drop at 0.2 V are shown. The frames on the lower part of fig. 4 are taken short time before the drop fall off.

3. EFFECT OF THE ELECTRODE POTENTIAL

Figs. 2 and 3 show in fact the effect of the electrode potential on silver dendrite formation in both the presence and absence of AgCl. A further study of a peculiar influence of the dendrite growth was carried out in the case of Cu.

In fig. 5 the shape of the drop as a function of the potential is shown for 0.1 M Cu^{2+} in KNO_3 and gelatine. The formation of the hydroxide film produces the deformation of the drop when the potential is increased towards the negative side. The peculiar form of the drop can be explained by a non-uniform adsorption of the hydroxide on the surface, owing to the electrical screening produced by the vicinity of the capillary : the lower part of the drop is more negative as compared with the upper one. Owing to this different electrical polarisation the adsorption of the colloids is more strong at the lower part of the drop. During the increase of the applied voltage, the polarisation becomes stronger and is extended towards the upper part; only the drop region in the immediate vicinity to the capillary remains not enough polarised to allow the adsorption of the colloids and of the gelatine. Owing to its compactness and uniformity the adsorbed film hinders the normal growth of the drop, producing a quasi-cylindrical form (fig. 5, potential −1.4 V).

DISCUSSION

The electrocrystallisation is a crystallisation process accompanied by a preceding electron transfer reaction. The rate of crystallisation itself cannot determine the value of the current, but the mechanism involved during this process changes when the oversaturation changes in wide limits. The electrocrystallisation in the limiting current region can be identified with a crystallisation process taking place in conditions of a strong oversaturation. This case corresponds to the dendritic growth. Although the mechanism of dendrite crystallisation was thoroughly studied for crystallisation of germanium dendrites from melts, [8–10] the fundamental aspects of this mechanism have a general applicability. The most peculiar aspect is represented by the existence of the twining planes in the core of the dendrites. [5–7] The twining planes are produced in conditions of a high oversaturation or by the influence of impurities. The same general mechanism is also responsible for the electrocrystallisation of dendrites. The characteristic aspect in this last case is represented by the creation of the oversaturation state.

In the special case of electrocrystallisation the electrochemical equivalent of the oversaturation is represented by the overvoltage at which the crystallisation process occurs. [11]

The overvoltage corresponding to bi-dimensional nuclei is of the order of 10 mV and for the three-dimensional ones 100 mV. [11] In the limiting current the ions are discharged at an overvoltage of 100–1 000 mV. In order to explain the mechanism of the elementary electrochemical process, a quantum mechanical theory based on tunnel effect transition has been proposed. [12–17] According to this theory the average neutralisation distance increases when the potential becomes more negative. In this way the atoms formed by the electrochemical reactions are not only the ad-atoms but also quasi-free atoms. Owing to the total insolubility of the metal atoms in water the quasi-free atoms are in a state of high oversaturation; from this state the growth of the dendrites is the preferred path of the crystallisation process.

The quantitative interpretation of this process involves the numerical calculation of the quantum formulas of the electrochemical current, i:

$$i = 2\,e\left(\frac{m}{2\pi\hbar}\right)^{3}\int_{v_m}^{v_M} v_x\, D(E_x)\, N(E_x)\, dv_x \iint_{-\infty}^{+\infty} f(E)\, dv_y dv_z \qquad (1)$$

[3] E. Billig, *Proc. Roy. Soc.*, **A229**, 346 (1955).

[4] A. J. Bennett and R. L. Longini, *Phys. Rev.*, **116**, 53 (1959).

[5] D. R. Hamilton and R. G. Seidensticker, *J. Appl. Phys.*, **31**, 1165 (1960).

[6] D. R. Hamilton and R. G. Seidensticker, *J. Appl. Phys.*, **34**, 1450 (1963).

[7] R. G. Seidensticker and D. R. Hamilton, *J. Appl. Phys.*, **34**, 3113 (1963).

[8] E. Billig and P. J. Holmes, *Acta Cryst.*, **8**, 353 (1955).

[9] E. Billig and P. J. Holmes, *Acta Met.*, **5**, 53 (1957).

[10] E. Billig, *Acta Met.*, **5**, 54 (1957).

[11] A. Căluşaru, "Depunerea electrolitică a pulberilor metalice", Ed. ştiinţifică şi enciclopedică, Bucharest, 1976.

[12] A. Căluşaru, Thesis, Inst. Politehn. Bucureşti, 1957.

[13] A. Căluşaru and I. Atanasiu, *Studii cercet. metalurg.*, **4**, 365 (1959); idem, *Rev. Metallurgie*, **5**, 291 (1960).

[14] A. Căluşaru, *Electrochim. Acta*, **12**, 1507 (1967).

[15] A. Căluşaru and A. Moldovan, *Electrochim. Acta.*, **17**, 1299 (1972).

[16] A. Căluşaru and A. G. Moldovan, *Electrochim. Acta*, **19**, 341 (1974).

[17] A. G. Moldovan, A. Căluşaru and M. Rizea, *Rev. Roum. Phys.*, **21**, 547 (1976).

$\hbar$ is the Planck constant divided with 2π, E_x is the kinetic energy in barrier direction, v_i is the velocity of the electron in i direction, $D(E_x)$ is the transparence coefficient of the potential barrier in x direction, $N(E_x)$ is the repartition function of the free electron levels in solution, $f(E)$ is the repartition function of the occupied electron levels in metal (Fermi-Dirac function). It has been shown that for the case of the limiting current $N(E_x)$ can be considered as a constant.[12] The Fermi-Dirac function can be integrated from 0 to ∞, and the equation of the limiting current is:

$$i_l = 2e(kT)^2 \frac{2\pi}{(2\pi)^3 \hbar^3} mK \int_{u_m}^{u_M} D(u_x) \ln \frac{e^{u_x}}{1 + e^{u_x}} \, du_x \tag{2}$$

u_x is a function of E_x. Equation (2) was calculated numerically for the case when $D(u_x)$ is a rectangular barrier.[16] In general it is accepted that a parabolic barrier is an improved approximation.[18,19] In this case $D(u_x)$ can be well approximated by the following equation:[20]

$$D(F_x) = \left[\exp\left(- \frac{E_x - \varphi_0 - e\varepsilon}{\alpha_0} \right) + 1 \right]^{-1} \tag{3}$$

where φ_0 is the height of the barrier, ε is the voltage applied to the electrode and α_0 is given by the formula:

$$\alpha_0 = \frac{\hbar}{\pi s} \left(\frac{2\varphi_0}{m} \right)^{1/2} \tag{4}$$

s is barrier width and m electron mass.

With eq. (3) the equation of the limiting current (2) becomes:

$$i_l = -A \int_{u_m}^{u_M} \left[\exp\left(- \frac{kTu_x + E_F - \varphi_0}{\alpha_0} \right) + 1 \right]^{-1} \ln \frac{e^{u_x}}{1 + e^{u_x}} \, du_x \tag{5}$$

We have carried out computer calculation of this formula using a computer IBM 370/135 with the method described previously.[16,17]

For the low integration limit, u_m we have used the following equation, describing the variation of the potential energy of the free electron level in solution as a function of the distance from the electrode surface:

$$\varphi(s) = a\left(1 + \frac{b}{s} + \frac{c}{s^2}\right) \tag{6}$$

where a, b, c are constants.

---

[18] I. Giavier, "Tunneling Phenomena in Solids" (Ed. E. Burstein and S. Lundquist), Plenum, New York, 1969.

[19] C. B. Ducke, "Tunneling in Solids", Academic Press, New York, 1969.

[20] D. D. Landau and E. M. Lifshitz, "Kvantovaia Mechanika", Moscow, 1963, p. 214.

The results of the computer calculations are shown in fig. 6 for two initial values of s (3 and 5 Å) and three values of the constant a, eq. (6) (1, 3 and 5 eV) and $\varepsilon = 0.2$ V. In all cases a considerable increase of the neutralisation distance occurs, when the electrode potential is increased. For instance at 1.0 V, s is equal to ~ 5 Å if the initial value for calculation was 3 Å and ~ 7 Å for 5 Å. The same values at 2 V are: 5.5 and 7.5 Å, respectively.

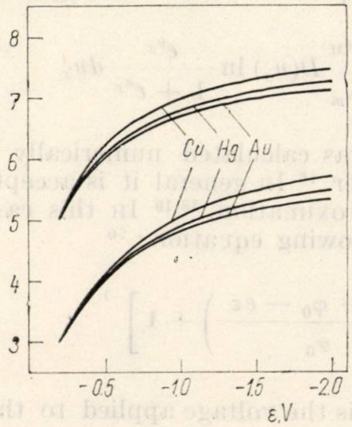

Fig. 6. — Variation of the neutralisation distance s as a function of the electrode potential ε for Cu, Hg, and Au; parabolic barrier; variable free electron level in solution. Difference between Fermi level in metal and the highest level in solution, 1 eV. Initial values for computer calculation: $s = 3$ and 5 Å, $\varepsilon = -0.2$ V.

These results confirm the formation of the quasi-free atoms and therefore the crystallisation in the conditions of a high oversaturation.

The precipitation of the hydroxides can be interpreted considering the interaction of the free atoms with water. In the same manner the precipitation of the iron hydroxides in the limiting current region was interpreted by Hilbert [21] and Hilbert and Darwisch.[22]

---

[21] F. Hilbert, *Naturwiss.*, **56**, 215 (2969).

[22] F. Hilbert and N. A. Darwisch, *Monatsh.*, **102**, 498 (1971).

Revue Roumaine de Chimie, **22**, *4*, 563–567 (1977)

Dedicated to the 70th anniversary
of Professor Coriolan Drăgulescu

THE EQUIVALENCE POINT AND THE CONFIDENCE INTERVAL OF LINEAR TITRATION CURVES IN THE OUTLOOK OF NORMAL BIDIMENSIONAL DISTRIBUTION OF BRANCHES

DUMITRU CEAUŞESCU * and VICTOR ELIU-CEAUŞESCU **

* University of Timişoara, str. Pestalozzi, 16
** Centre of Chemistry, Timişoara, Bd. Mihai Viteazul, 24, Romania

Received July 26, 1976

Because both the "titration value" measurement and that of the "followed property" are error-affected (random) variables, in the proposed model the two branches of the titration curve correspond to normal bidimensional distributions, with close correlation. The intersection results from the condition that its probability density is the product of the statistically independent densities of the two branches. The maximum of this normal distribution corresponds to the most probable (average) value, accordingly the intersection point. Putting the distribution into the canonic form, the dispersion is obtained. Based on the standard deviation the confidence interval is formulated. A numerical example is given.

The treatment of the equivalence point and its confidence interval in the case of linear titrations, considering the branches of the titration curve as regression straight-lines is given in a foregoing note.[1] In this case the volume of the reagent added during titration was taken as an independent variable, unaffected or less affected by errors. This consideration, though usual, is in fact artificial, because both the measurement of titration volume and that of the followed property (conductibility etc.) are error-affected operations. In this note a model is proposed by which a closely correlated bidimensional normal distribution corresponds to each branch of the titration curve.

Let $f_{\mathrm{I}}(x, y)$ and $f_{\mathrm{II}}(x, y)$ be the normal bidimensional frequency function (probability density) of the two branches of the titration curve I and II. Their product, also a bidimensional frequency function :

$$f_{\mathrm{I}}(x, y) \cdot f_{\mathrm{II}}(x, y) = f(x, y)$$

---

[1] D. Ceauşescu and V. Eliu-Ceauşescu, *Z. analyt. Chem.* **282**, 45–46 (1976).

represents the intersection *. The expression of the normal bidimensional function is (e.g. [2]):

$$f(x,y)=\frac{1}{2\pi\sigma_x\sigma_y\sqrt{1-\rho^2}}\, e^{-\frac{1}{2(1-\rho^2)}\left[\frac{(x-\mu_x)^2}{\sigma_x^2}-2\rho\frac{(x-\mu_x)(y-\mu_y)}{\sigma_x\,\sigma_y}+\frac{(y-\mu_y)^2}{\sigma_y^2}\right]}$$

where x and y are the random variables : the reagent volume respectively the measured property, μ_x and μ_y are their general averages, σ_x, σ_y are the standard deviations and ρ the correlation coefficient : $\rho = \frac{\mathrm{cov}(x,y)}{\sigma_x\,\sigma_y}$.

To facilitate the following summation of the exponents these are written in the explicit square form :

$$\alpha x^2 + \beta y^2 + 2\gamma xy + \delta x + \varepsilon y + z$$

where :

$$\alpha = \frac{1}{2(1-\rho^2)\sigma_x^2} \quad \beta = \frac{1}{2(1-\rho^2)\sigma_y^2} \quad \gamma = \frac{-\rho}{2(1-\rho^2)\sigma_x\,\sigma_y}$$

$$\delta = \frac{1}{1-\rho^2}\left(\frac{\rho\mu_y}{\sigma_x\sigma_y}-\frac{\mu_x}{\sigma_x^2}\right) \quad \varepsilon = \frac{1}{1-\rho^2}\left(\frac{\rho\mu_x}{\sigma_x\,\sigma_y}-\frac{\mu_y}{\sigma_y^2}\right)$$

z — further unnecessary for the calculations.

The indices I and II are used to note the statistical parameters belonging to the first respectively the second branch of the titration curve. In the composed function no index or the index i is used. The exponent of the frequency function representing the intersection has the coefficients : $\alpha = \alpha_{\mathrm{I}} + \alpha_{\mathrm{II}}$ etc., since the product $f_{\mathrm{I}}(x, y)\cdot f_{\mathrm{II}}(x, y)$ leads to the summation of the exponents.

The "intersection point" of the two branches is the most probable value of the bidimensional frequency function, accordingly the maximum of the normal bidimensional surface. This point is obtained by equating to zero the partial derivatives of the frequency function :

$$\frac{\partial f}{\partial x} = -(2\alpha x + 2\gamma y + \delta)\cdot f(x, y) = 0$$

$$\frac{\partial f}{\partial y} = (2\beta y + 2\gamma x + \varepsilon)\cdot f(x,y) = 0$$

---

[2] G. U. YULE and M. C. KENDALL "An Introduction to the Theory of Statistics", ed. 14, cap. X, C. Griffin, London, 1965.

* Instead of the "discrete value" of the intersection, we consider here the bidimensional distribution obtained by multiplying the probability density functions of the two branches. Indeed, in order to get the intersection, we carry out the logic operation "both ... and", namely the intersection belongs *both* to the first *and* to the second branch, which in the case of independent probabilities corresponds to their product.

$f(x, y)$ is different from zero, therefore only the brackets can be cancelled. By solving the linear system it results:

$$X_i = \frac{1}{2}\cdot\frac{\gamma\varepsilon - \beta\delta}{x\beta - \gamma^2} = \mu_x \quad Y_i = \frac{1}{2}\cdot\frac{\gamma\delta - \alpha\varepsilon}{\alpha\beta - \gamma^2} = \mu_y$$

where X_i is the equivalence volume, Y_i the value of the measured property at equivalence. Identifying the square terms'coefficients, the other parameters of the intersection frequency function are obtained:

$$\rho_i = \frac{\gamma}{\sqrt{\alpha\beta}} \quad \sigma^2_{x_i} = \frac{1}{2\alpha(1-\rho_i^2)} \quad \sigma^2_{y_i} = \frac{1}{2\beta(1-\rho_i^2)}$$

(We stress that $\alpha = \alpha_{I} + \alpha_{II}$, $\beta = \beta_{I} + \beta_{II}$ etc.)
The same expression of the standard deviation is obtained by cancelling the second derivative:

$$\frac{\partial^2}{\partial x^2} f(x, y)_y = \mu_y = 0$$

All the parameters defined above belong to the whole population and are expressed by means of their estimates based on the experimental data of the selection — compare tab. II.

Taking the experimentally obtained equivalence volume as x_i, the ratio:

$$\frac{x_i - X_i}{s_{x_i}} = t$$

has an approximate Student distribution, since x_i is an average, see.[3] The confidence interval is:

$$X_i = x_i \pm t \cdot s_{x_i}$$

where t has $n = n_{I} + n_{II} - 2$ degrees of freedom; n_{I}, n_{II} are the number of (x, y) value pairs on the two branches of the titration curve.

As an example we take the same experimental data treated in the foregoing note.[1] These data are given in table 1. Table 2 shows the results of data processing. The obtained result for the equivalence volume is:

$$x_i \pm \Delta x_i = 4.077 \pm 0.070$$

The true equivalence volume is $X_i = 4.073$.

---

[3] D. Ceaușescu "Tratarea statistică a datelor chimico-analitice", Ed. tehnică, Bucharest, 1973, pag. 95.

We remark the fact that the dispersion of the "intersection point" depends on ρ_i, the correlation coefficient of the intersection distribution frequency :

$$\sigma^2_{x_i} = \frac{1}{2(\alpha_{I} + \alpha_{II})(1 - \rho_i^2)}$$

Table 1

25 ml of a 0.004949 M solution of chlorine in water and 75 ml distiled water are titrated conductometrically with a 0.01013 M solution of KI.[4]

ml KI x	$\frac{100-a}{a}$ y	n^*
0.00	0.641	$n_1 = 5$
1.00	0.774	
2.00	0.890	
3.00	1.013	
4.00	1.141	
5.00	1.137	$n_2 = 5$
6.00	1.128	
7.00	1.118	
8.00	1.104	
9.00	1.092	

* The points belonging to the first respectively to the second branch of the titration curve were previously established by a graphical method.

The optimum condition corresponds to $\rho_i = 0$ which is fulfilled when $\gamma = 0$. We also stress that the maximum of the frequency function $f(x, y)$ is not necessarily identical with the intersection of the regression straight lines of the two branches of the titration curve.

---

[4] D. CEAUŞESCU, *Studii şi Cercetări Chim. Fil. Cluj*, **3–4**, 281 (1957).

Table 2

The Results of calculations

The parameters considered			branch I	branch II	intersection
of the whole population	the estimate of the selection	the formula of the estimate	n = 5	n = 5	n = 10
μ_x	$\bar{x}$	$\frac{1}{n}\Sigma x$	2.00	7.00	—
μ_y	$\bar{y}$	$\frac{1}{n}\Sigma y$	0.8918	1.1158	—
σ_x^2	s_x^2	$\frac{1}{n-1}\Sigma(x-\bar{x})^2$	2.50	2.50	—
σ_y^2	s_y^2	$\frac{1}{n-1}\Sigma(y-\bar{y})^2$	0.038392	0.0003272	—
σ_{xy}	s_{xy}	$\frac{1}{n-1}\Sigma(x-\bar{x})(y-\bar{y})$	0.30975	-0.02850	—
ρ	r	$\frac{s_{xy}}{s_x s_y}$	0.99981	-0.99648	—
$1-\rho^2$	$1-r^2$	—	0.000382	0.007029	—
α	a	$\frac{1}{2(1-r^2)\cdot s_x^2}$	$a_{\mathrm{I}} =$ 523.067	$a_{\mathrm{II}} =$ 28.452	$a = a_{\mathrm{I}} + a_{\mathrm{II}} =$ 551.519
β	b	$\frac{1}{2(1-r^2)\cdot s_y^2}$	$b_{\mathrm{I}} =$ 34060.3	$b_{\mathrm{II}} =$ 217391.3	$b = b_{\mathrm{I}} + b_{\mathrm{II}} +$ 251451.6
γ	c	$\frac{1}{2(1-r^2)s_x s_y}$	$c_{\mathrm{I}} =$ -4220.08	$c_{\mathrm{II}} =$ 2478.26	$c = c_{\mathrm{I}} + c_{\mathrm{II}} =$ -1741.82
δ	d	$\frac{1}{1-r^2}\left(\frac{r\mu_y}{s_x s_y} - \frac{\mu_x}{s_x^2}\right)$	$d_{\mathrm{I}} =$ 5434.66	$d_{\mathrm{II}} =$ -5928.82	$d = d_{\mathrm{I}} + d_{\mathrm{II}} =$ -494.16
ε	e	$\frac{1}{1-r^2}\left(\frac{r\mu_x}{s_x s_y} - \frac{\mu}{s_x^2}\right)$	$e_{\mathrm{I}} =$ -43869.7	$e_{\mathrm{II}} =$ -519810.2	$e = e_{\mathrm{I}} + e_{\mathrm{II}} =$ -563679.9
X_i^*	x_i^*	$\frac{1}{2}\cdot\frac{ec-bd}{ab-c^2}$	—	—	4.0770
Y_i^*	y_i^*	$\frac{1}{2}\cdot\frac{cd-ae}{ab-c^2}$	—	—	1.1491
ρ_i^*	r_i^*	$-\frac{c}{\sqrt{ab}}$	—	—	0.14791
σ_{xi}^{2*}	s_{xi}^{2*}	$\frac{1}{2a(1-r^2)}$	—	—	0.00092686
	t	$t(P = 95\%,\ f = 8)$	—	—	2.306
	Δx_i	$t\cdot s_{x_i}$	—	—	0.0701

the parameters taken into account beginning with the asterisk refer only to the intersection; in the table you can find the values of the dispersions, the standard deviations result by square root.

Revue Roumaine de Chimie, **22**, *4*, 569--574 (1977)

Dedicated to the 70th anniversary
of Professor Coriolan Drăgulescu

SYNTHESIS AND ABSOLUTE CONFIGURATION OF THE NITROBIS(AMINOACIDATO)AMMINECOBALT(III) COMPLEXES*

M. B. ĆELAP and M. J. MALINAR
Institute of Chemistry, Faculty of Sciences,
University of Beograd, P.O. Box 550, 11001 Beograd, Yugoslavia

Received July 14, 1976

cis(O)-*trans*(NH_2)-Nitrobis(aminoacidato)amminecobalt(III) complexes with L-α-aminobutyric acid, L-norvaline, L-valine, L-norleucine and L-isoleucine, have been prepared. The synthesis was achieved by the nucleophilic substitution of ligands of the complex ion of Erdmann salt by the corresponding aminoacidato chelate ligands. Their geometrical configuration was determined by means of electronic spectroscopy. The absolute configurations of the isolated optical isomers of *cis*(O)-*trans*(NH_2)-nitrobis(aminoacidato)-amminecobalt(III) complexes were examined by comparing their CD spectra with the CD spectra of *cis*(NO_2)-*trans*(N)-isomer of dinitrobis(aminoacidato)-cobaltate(III) ion.[1-3] All the $(-)_{589}$-isomers exhibited negative Cotton effect in the region of the first absorption band, on the side of lower energy, and on this basis they were assigned the Δ absolute configuration.

RESULTS AND DISCUSSION

In one of our earlier papers[4] the synthesis and the geometrical configuration of *cis*(O)-*trans*(NH_2)-nitrobis(aminoacidato)amminecobalt(III) complexes with glycine, L-alanine and β-alanine, are described. Continuing these investigations, in this paper we wanted to study the absolute configurations of complexes of the above mentioned type which contain optically active amino acids, and therefore, we have prepared complex compounds with L-α-aminobutyric acid, L-valine, L-norvaline,

---

* Presented at the 2nd Yugoslav Congress for Industrial Chemistry, Skopje, Yugoslavia, 1976.

[1] R. G. Denning, M. P. Ćelap and D. J. Radanović, *Inorg. Chim. Acta*, **2**, 58 (1968).

[2] M. B. Ćelap, R. G. Denning, D. J. Radanović and T. J. Janjić, *Inorg. Chim. Acta*, **5**, 9 (1971).

[3] W. H. Watson, D. R. Johnson, M. B. Ćelap, and B. Kamberi, *Inorg. Chim. Acta*, **6**, 591 (1972).

[4] M. B. Ćelap, M. J. Malinar and T. J. Janjić, *Rev. Chim. min.*, **13**, 175 (1976).

L-norleucine and L-isoleucine. In contrast with the procedure of direct synthesis which was applied in the case of previously used amino acids,[4] in this paper the synthesis was achieved by the nucleophilic substitution of one ammonia molecule and three nitro groups of the complex ion of Erdmann salt [5] with the corresponding aminoacidato chelate ligands :

$$NH_4[Co(NH_3)_2(NO_2)_4] + 2MAm = [Co\,NH_3Am_2NO_2] + NH_4NO_2 + \\ + 2MNO_2 + NH_3$$

Out of six theoretically possible geometrical isomers of this complex ion (Figure 1), we succeeded to obtain in the reaction with each amino acid studied (except with L-norleucine and L-isoleucine) two internal

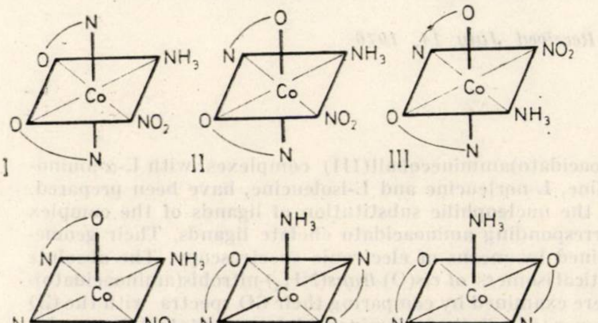

Fig. 1. — Geometrical isomers of the nitrobis (amminoacidato)-amminecobalt(III) complex.

diastereisomers of *cis*(O)-*trans*(NH_2)-geometrical isomer (I) ; in the reaction with L-norleucine and with L-isoleucine we also obtained two isomers, but only one of them was found to represent the expected$(-)_{589}$-diastereoisomer, whereas the configuration of the other isolated isomer could not be examined because of its insolubility. The yields of the complexes obtained amounted to about 10% (the above reaction gives rise also to the previously described dinitrobis(aminoacidato) [1,2] and trinitro(aminoacidato)amminecobaltate(III) complexes, [6] respectively).

All the isolated compounds exhibited electronic spectra identical with the spectra of the previously obtained [4] *cis*(O)-*trans*(NH_2)-nitrodiglycinato-, and nitrobis(L-alaninato)amminecobalt(III) complexes, respectively (Table 1) ; on this basis it was concluded that they have the same geometrical configuration.

Taking into consideration the fact that the previously described *cis*(NO_2)-*trans*(N)-isomer of dinitrobis(aminoacidato)-cobatate(III) ion[1,2], whose absolute configuration was confirmed by X-ray analysis [3], and the *cis*(O)-*trans*(NH_2)-isomer of nitrobis(aminoacidato)amminecobalt(III) complex have similar ligand field symmetry (Figure 2) we have assumed that their optical isomers, exhibiting Cotton effect of the same sign, would have the same absolute configuration. This assumption was supported by the fact that these two complexes exhibited similar CD spectra (Figure 3).

---

[5] S. M. Jörgensen, *Z. anorg. Chem.* **17**, 455 (1898).

[6] M. B. Ćelap, M. J. Malinar and T. J. Janjić, *Z. anorg. Chem.*, **383**, 341 (1971).

Table 1

Absorption maxima λ(nm) and log ε of the *cis*(O)-*trans*(NH_2)-isomers of nitrobis (aminoacidato)amminecobalt(III) complexes

	Compound	λ_1	log ε_1	λ_2	logε_2	λ_3	log ε_3
1	$[Co\ NH_3gly_2NO_2]^4$	478	2.12	335	3.56	248	4.24
2	$(-)-[Co\ NH_3(L\text{-}ala)_2NO_2]^4$	478	2.12	335	3.03	246	4.30
3	$(+)-[Co\ NH_3(L\text{-}ala)_2NO_2]^4$	478	2.10	335	3.12	246	4.30
4	$(-)-[Co\ NH_3(L\text{-}abu)_2NO_2]$	480	2.12	335	3.12	246	4.28
5	$(+)-[Co\ NH_3(L\text{-}abu)_2NO_2]$	478	2.11	333	3.40	247	4.52
6	$(-)-[Co\ NH_3(L\text{-}nva)_2NO_2]$	478	2.12	335	3.15	246	4.22
7	$(+)-[Co\ NH_3(L\text{-}nva)_2NO_2]$	478	2.13	335	3.13	246	4.29
8	$(-)-[Co\ NH_3(L\text{-}val)_2NO_2]$	478	2.15	335	3.12	247	4.12
9	$(+)-[Co\ NH_3(L\text{-}val)_2NO_2]$	480	2.12	335	3.12	246	4.25
10	$(-)-[Co\ NH_3(L\text{-}nle)_2NO_2]$	479	2.15	336	3.24	247	4.28
11	$(-)-[Co\ NH_3(L\text{-}ile)_2NO_2]$	480	2.17	335	3.23	250	4.20

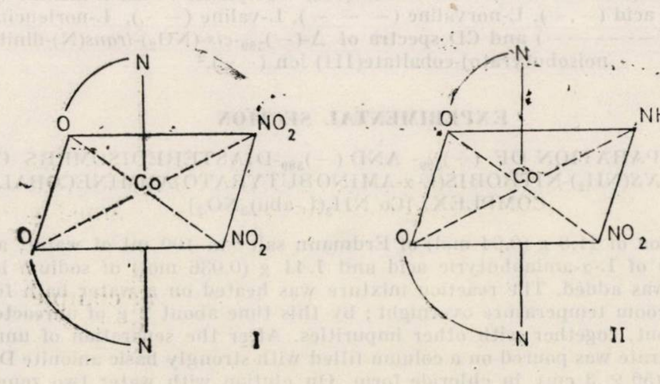

Fig. 2. — *cis*(NO_2)-*trans*(N)-Dinitrobis(aminoacidato)-cobaltate(III) (I) and *cis*(O)-*trans*(NH_2)-nitrobis(aminoacidato)amminecobalt(III) (II) complexes.

From figure 3 it may be seen that all the $(-)_{589}$-isomers of *cis*(O)-*trans*(NH_2)-nitrobis(aminoacidato)amminecobalt(III) complex exhibit negative Cotton effect in the region of the first absorption band, on the side of lower energy, similar to the $(-)_{589}$-*cis*(NO_2)-*trans*(N)-dinitrobis(aminoacidato)cobaltate(III) ion, whose M(C_2), and the Δ absolute configuration, respectively, was determined by Ćelap and coworkers.[1,2] On this basis they were also assigned the Δ absolute configuration.

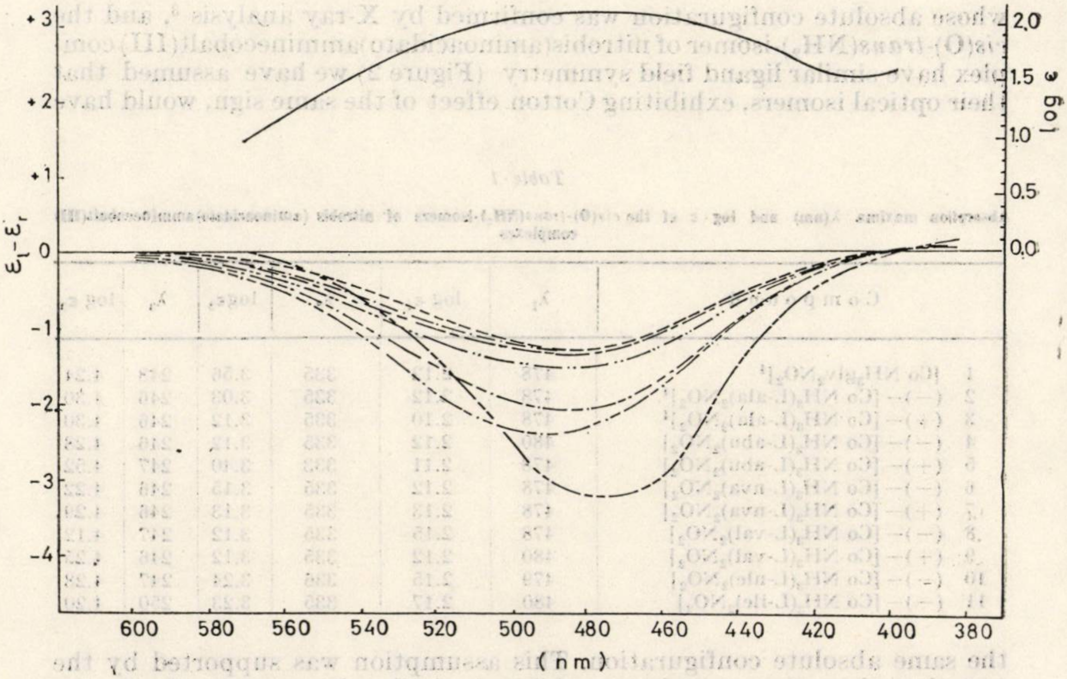

Fig. 3. — Circular dichroism spectra ($\varepsilon_1 - \varepsilon_r$) and absorption spectra (log ε) of $(-)_{589}$-*cis*(O)-*trans*(NH_2)-nitrobis-(aminoacidato)amminecobalt(III) complexes with L-alanine (— —.— —), L-α-aminobutyric acid (—.—), L-norvaline (— — —), L-valine (— -.), L-norleucine (—..—..), and L-isoleucine (————————) and CD spectra of Δ-$(-)_{589}$-*cis*-(NO_2)-*trans*(N)-dinitrobis(α-aminoisobutyrato)-cobaltate(III) icn (—--).[2]

EXPERIMENTAL SECTION

1. PREPARATION OF $(+)_{589}$- AND $(-)_{589}$-DIASTEREOISOMERS OF *CIS*(O)-*TRANS*(NH_2)-NITROBIS(L-α-AMINOBUTYRATO)AMMINECOBALT(III) COMPLEX, [Co NH_3(L-abu)$_2NO_2$]

To a solution of 11.8 g (0.04 mol) of Erdmann salt[5] in 100 ml of water, a solution of 4.12 g (0.04 mol) of L-α-aminobutyric acid and 1.44 g (0.036 mol) of sodium hydroxide in 40 ml of water, was added. The reaction mixture was heated on a water bath for one hour, and then left at room temperature overnight; by this time about 2 g of unreacted Erdmann salt crystallized out, together with other impurities. After the separation of unreacted Erdmann salt, the filtrate was poured on a column filled with strongly basic anionite Dowex 1—X4 (200—400 mesh) (50 × 3 cm), in chloride form. On elution with water two zones descended down the column and one remained fixed at the top. The eluate of the first zone (first 10 ml was discarded) was red coloured and contained $(+)_{589}$- and $(-)_{589}$-diastereoisomers of the *cis*(O)-*trans*(NH_2)-nitrobis-(L-α-aminobutyrato)amminecobalt(III) complex *. On evaporation the eluate yielded first crystals of common salts. Further evaporation gave a red-violet substance which was found to represent $(+)_{589}$-diastereoisomer of nitrobis(L-α-aminobutyrato)-amminecobalt(III) complex. The yield was 0.6 g (9%). The substance was recrystallized from hot water till constant optical rotation $[\alpha]_D^{22°} = +320°$. Concentration of the filtrate gave another red-violet substance which was identified as $(-)_{589}$-diastereoisomer of nitrobis(L-α-aminobutyrato)amminecobalt(III). The yield was 0.32 g (5%). The substance for analysis was recrystallized from hot water till constant optical rotation $[\alpha]_D^{22°} = -600°$, and then it was dried at 105° till constant weight.

---

* The eluate of the second zone, which sometimes could not be well separated from the first zone, was yellow coloured and contained a mixture of substances of nitro-ammine type and small amounts of *cis*(NO_2)-*trans*(NH_2, NH_3)- and *trans*(NO_2)-isomers of dinitro(L-α-aminobutyrato)diamminecobalt(III) complex.[4] At the top of the column there remained fixed the substances of anionic type: *cis*(NO_2)-*trans*(N)-isomer of dinitrobis(L-α-aminobutyrato)cobaltate (III) ion[7] and the meridional *trans*(NH_2, NH_3)-trinitrc(L-α-aminobutyrato)amminecobaltate (III) ion.[6]

[7] M. B. Čelap, M. B. Dimitrijević, D. J. Radanović, F. A. Čoha, T. I. Nikolić i T. J. Janjić, *Glasnik Hem. društva Beograd*, **35**, 449 (1970).

ANALYSIS

Calculated for $CoC_8H_{19}N_4O_6$ (M = 326.21)	C, 29.46 ; H, 5.87 ; N, 17.18
Found for $(+)_{589}$-diastereoisomer :	C, 29.88 ; H, 6.13 ; N, 17.21
Found for $(-)_{589}$-diastereoisomer :	C, 29.64 ; H, 6.06 ; N, 16.97

2. PREPARATION OF $(+)_{589}$-DIASTEREOISOMERS OF *CIS*(O)-*TRANS*-(NH_2)-NITROBIS(L-NORVALINATO)AMMINECOBALT(III), [Co NH_3(L-nva)$_2$$NO_2$]

These diastereoisomers were obtained by the procedure used for the preparation of the corresponding diastereoisomers with L-α-aminobutyric acid ; the yields were as follows : The diastereoisomer with optical rotation of $[\alpha]_D^{22°} = +300°$ was obtained in a yield of 5%, and the diastereoisomer having $[\alpha]_D^{22°} = -600°$ in a 7% yield.

ANALYSIS

Calculated for $CoC_{10}H_{23}N_4O_6$ (M = 354.27) :	C, 33.90 ; H, 6.54 ; N, 15.82
Found for $(+)_{589}$-diastereoisomer :	C, 33.75 ; H, 6.50 ; N, 15.65
Found for $(-)_{589}$-diastereoisomer :	C, 33.64 ; H, 6.35 ; N, 15.50

3. PREPARATION OF $(+)_{589}$- AND $(-)_{589}$-DIASTEREOISOMERS OF *CIS*(O)-*TRANS*(NH_2)-NITROBIS(L-VALINATO)AMMINECOBALT(III) COMPLEX, [Co NH_3(L-val)$_2$$NO_2$]

These diastereoisomers were obtained by a procedure analogous to that already described ; only, in this case, a part of $(+)_{589}$-diastereoisomer separated out already in the course of the reaction. The diastereoisomer $[\alpha]_D^{22°} = +300°$ was obtained in a yield of 6%, and the diastereoisomer having optical rotation $[\alpha]_D^{22°} = -1000°$ in a 17% yield.

ANALYSIS

Calculated for $CoC_{10}H_{23}N_4O_6$ (M = 354.27) :	C, 33.90 ; H, 6.54 ; N, 15.82
Found for $(+)_{589}$-diastereoisomer :	C, 33.82 ; H, 6.57 ; N, 15.95
Found for $(-)_{589}$-diastereoisomer :	C, 33.73 ; H, 6.57 ; N, 15.84

4. PREPARATION OF $(-)_{589}$-DIASTEREOISOMERS OF *CIS*(O)-*TRANS*(NH_2)-NITROBIS(L-NORLEUCINATO)- AND BIS(L-ISOLEUCINATO)-AMMINE-COBALT(III) COMPLEXES, [Co $NH_3Am_2NO_2$]

These diastereoisomers were also obtained by a procedure analogous to that already described. But in the course of these reactions, in both cases, a sparingly soluble crystalline product of pale-violet colour separated out ; the results of microanalysis showed that isomeric substances were in question, probably the corresponding $(+)_{589}$-diastereoisomers. This assumption could not be confirmed since their optical rotations could not be determined on account of their very small solubilities in water.

The yield of the L-norleucinato complex having optical rotation $[\alpha]_D^{22°} = -700°$ as well as the yield of the L-isoleucinato complex with optical rotation $[\alpha]_D^{22°} = -500°$ was 7 %, whereas the yields of the corresponding insoluble substances amounted to about 10 %.

ANALYSIS

Calculated for $CoC_{12}H_{27}N_4O_6$ (M = 382.32) : C, 37.70 ; H, 7.21 ; N, 14.66

Found for insoluble substance containing :

L-norleucine : C, 37.49 ; H, 7.08 ; N, 14.66

L-isoleucine : C, 37.40 ; H, 7.18 ; N, 14.76

Found for

$(-)_{589}$-L-norleucinato diastereoisomer : C, 37.84 ; H, 7.34 ; N, 14.99

$(-)_{589}$-L-isoleucinato diastereoisomer : C, 37.62 ; H, 7.32 ; N, 14.80

Acknowledgement. The authors are grateful to the Serbian Republic Research Fund for financial support, and to Dr. Ružica Tasovac and Mrs. Zorica Lukanić for elemental microanalyses ; thanks are also due to Dr. D. Radanović for CD spectra and Mr. P. Radivojša for help in typing of the manuscript.

Revue Roumaine de Chimie, **22**, *4*, 575–581 (1977)

Dedicated to the 70th anniversary
of Professor Coriolan Drăgulescu

CRITICAL EVALUATION OF FLUORIMETRIC ASSAY METHODS FOR MORPHINE

ROBERT A. CHALMERS and A. F. J. JACKSON *
Chemistry Department, University of Aberdeen, Old Aberdeen, Scotland

Received August 31, 1976

A comparison has been made of the native fluorescence and oxidative fluorescence methods for determination of morphine. The native fluorescence method gives the better precision, but is less sensitive and much less selective.

Irrespective of the definitions and interpretations used, the values reported for the sensitivity and limit of detection of fluorimetric methods depend on the experimenter and the apparatus and reagents used. Thus, a compound found to be non-fluorescent by one worker[1] may later be found to be weakly fluorescent by another.[2] When several methods for the same compound are described by different workers using different instruments, it may not be easy to assess their relative merits. Several fluorimetric methods have been reported for the assay of morphine,[1–15] and form three basic groups.[1,5,9] The purpose of the present investigation was to assess them in terms of simplicity, sensitivity, selectivity and precision.

[1] R. Brandt, S. Ehrlich-Rogozinsky and N. D. Cheronis, *Microchem. J.*, **5**, 215 (1961).

[2] G. A. Wadds Ph. D. Thesis, University of Aberdeen, 1969.

[3] C. Fulton, *J. Am. Pharm. Assoc.*, **26**, 726 (1937).

[4] G. Nadeau and G. Sobolewski, *Can. J. Biochem. Physiol.*, **36**, 625 (1958).

[5] J. P. Delcambre, Thèse doct., Université (Pharm.) de Lille, 1960.

[6] P. Balatre, M. Traisnel and J. P. Delcambre, *Bull. Soc. Pharm. Lille* **1960**, 143.

[7] P. Balatre, C. Claeys, J. P. Delcambre and M. Traisnel, *Bull. Soc. chim. France*, **1962**, 1654.

[8] R. Brandt, M. J. Olsen and N. D. Cheronis, *Science*, **139**, 1063 (1968).

[9] H. Kupferberg, A. Burkhalter and E. L. Way, *J. Pharmacol. Exptl. Therap.*, **145**, 247 (1964).

[10] A. E. Takemori and M. W. Stenwick, *ibid.*, **154**, 586 (1966).

[11] A. E. Takemori, *Biochem. Pharmacol.*, **17**, 1627 (1968).

[12] W. Matusiak and L. A. Dal Cortivo, *Chem. Eng. News*, **1968**, Sept, 23 42.

[13] J. R. Broich, *Fluorescence News*, **4**, 7 (1969).

[14] R. A. Chalmers and G. A. Wadds, *Analyst*, **95**, 234 (1970).

[15] S. J. Mule and P. L. Hushin, *Analyt. Chem.*, **43**, 708 (1971).

* Present address : Chemistry Department, Fourah Bay College, Freetown, Sierra Leone.

THE THREE BASIC METHODS

NATIVE FLUORESCENCE

Morphine fluoresces in 0.1N sulphuric acid fairly strongly, but only weakly in 0.1M sodium hydroxide. In the acid medium it has two excitation peaks at 245 and 285 nm, the latter being the more intense, and an emission peak at 350 nm (or 345 nm).[2] The range for linear proportionality is reported to be 0.1 – 50 μg/ml.

HALOFLUORESCENCE

When morphine (or some other of the opium alkaloids) is heated with conc. sulphuric acid, cooled, then heated with conc. ammonia solution, it yields an unidentified fluorescent product. The fluorescence is very sensitive to ultraviolet light. Delcambre [5–7] used the reaction for determination of morphine. Excitation at 365.5 nm resulted in emission peaks at 427.5 and 440 nm. With four hours of heating at 50° with conc. ammonia solution, the method gave a linear response for 0.5 – 4 μg of morphine. A modified and faster method has been described.[12]

OXIDATION[9]

Several mild oxidants [16,17] convert morphine into pseudomorphine which is potentially more strongly fluorescent. [9] The rate of formation and the stability of pseudomorphine are functions of the quantity of oxidant, pH, and the amount of morphine. Kupferberg *et al.*[9] used pyrophosphate buffer (pH 8.5) and a 16 :1 molar ratio ferricyanide/ferrocyanide oxidation buffer to oxidise morphine. The product had excitation peaks at 250, 280 and 320 nm (the intensity increasing in that order). Excitation at 250 nm gave an emission peak at 440 nm, and this combination gave the lowest blank reading for the reagents used in extraction of morphine from tissue. The limit of detection was 0.1 μg and the linear range 0.1 – 8 μg. Takemori [10] improved the sensitivity tenfold, mainly by decreasing the reaction volume.

EXPERIMENTAL

REAGENTS AND APPARATUS

Analytical-reagent grade chemicals were used throughout. The 0.1M pyrophosphate buffer (pH 8.5, adjusted with 1M hydrochloric acid) was prepared fresh each day to avoid the effect of hydrolysis.[9] The oxidant stock solution was prepared weekly by dissolving 115.4 mg

[16] L. Kieffer, *Liebigs Ann. Chem.*, **103**, 271 (1859).

[17] C. Fulton, *Am. J. Pharm.*, **105**, 103 (1933).

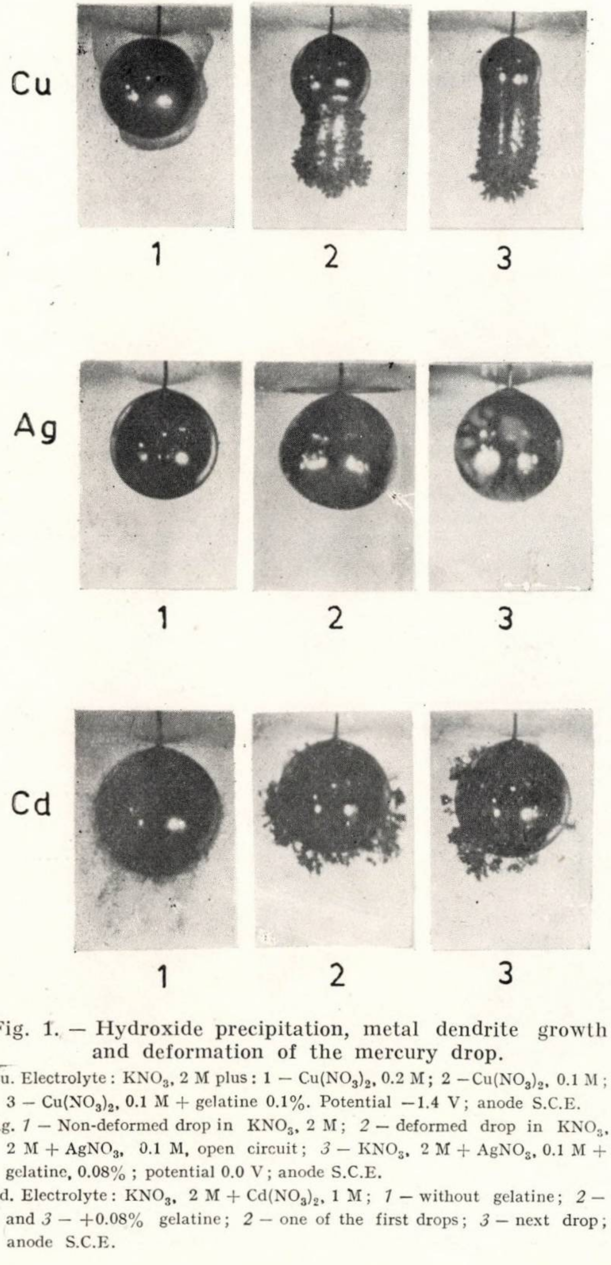

Fig. 1. — Hydroxide precipitation, metal dendrite growth and deformation of the mercury drop.

Cu. Electrolyte: KNO_3, 2 M plus: 1 — $Cu(NO_3)_2$, 0.2 M; 2 — $Cu(NO_3)_2$, 0.1 M; 3 — $Cu(NO_3)_2$, 0.1 M + gelatine 0.1%. Potential −1.4 V; anode S.C.E.

Ag. *1* — Non-deformed drop in KNO_3, 2 M; *2* — deformed drop in KNO_3, 2 M + $AgNO_3$, 0.1 M, open circuit; *3* — KNO_3, 2 M + $AgNO_3$, 0.1 M + gelatine, 0.08%; potential 0.0 V; anode S.C.E.

Cd. Electrolyte: KNO_3, 2 M + $Cd(NO_3)_2$, 1 M; *1* — without gelatine; *2* — and *3* — +0.08% gelatine; *2* — one of the first drops; *3* — next drop; anode S.C.E.

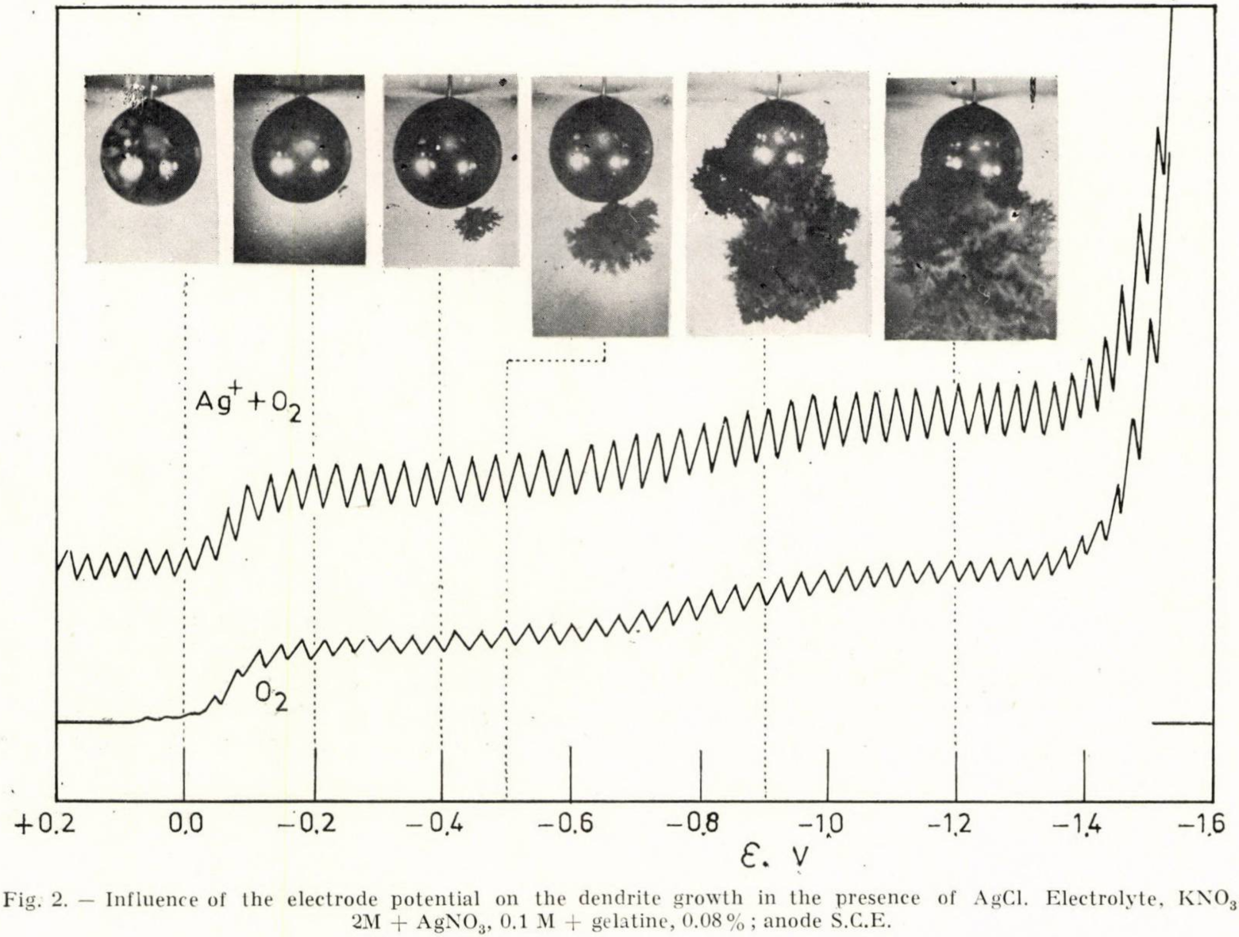

Fig. 2. — Influence of the electrode potential on the dendrite growth in the presence of AgCl. Electrolyte, KNO_3, 2M + $AgNO_3$, 0.1 M + gelatine, 0.08 % ; anode S.C.E.

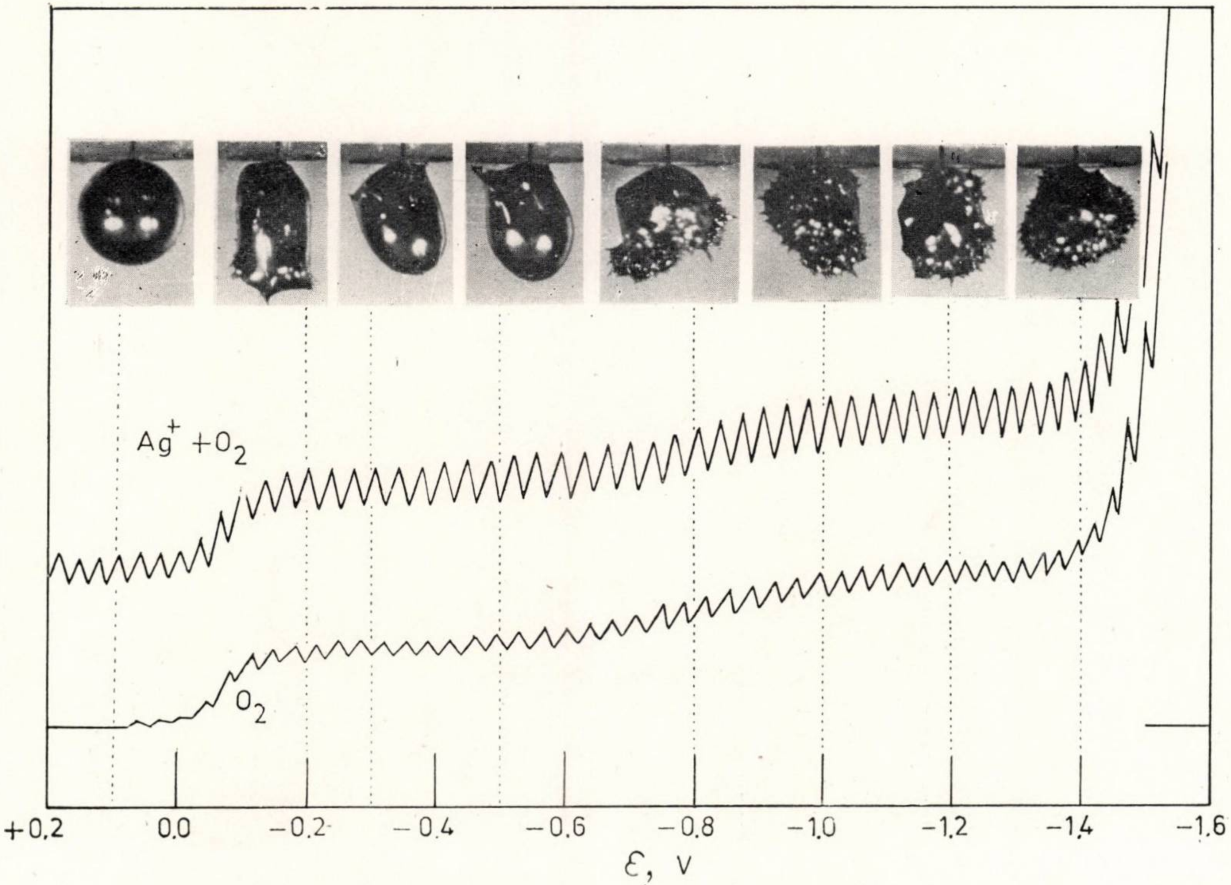

Fig. 3.—Influence of the electrode potential on the growth of silver dendrites in the absence of AgCl. Electrolyte : KNO_3, 2M + $AgNO_3$, 0.1 M. Potential scale is given against S.C.E.

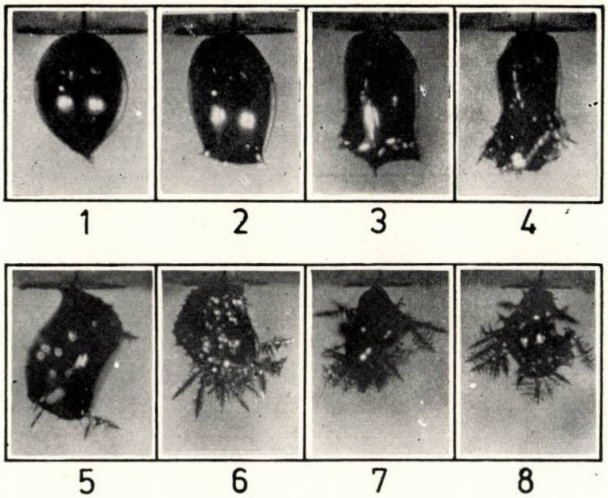

Fig. 4. — Different shapes of the mercury drop at -0.2 V (S.C.E.) from fig. 3. The photographs from the low part correspond to the moment preceding the fall down of the drop (about 1 s).

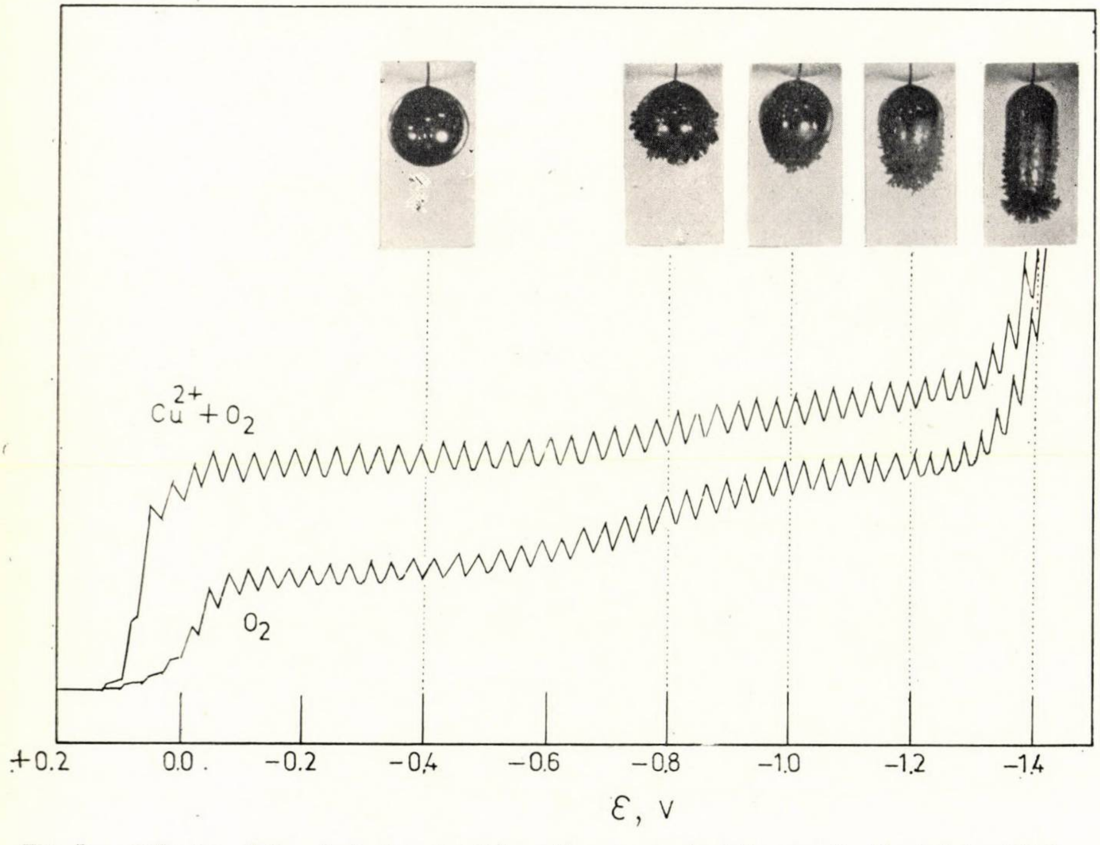

Fig. 5. — Influence of the electrode potential on the copper dendrite growth. Electrolyte : KNO_3, 2 M + $Cu(NO_3)_2$, 0.1 M + gelatine, 0.1 % ; anode S.C.E.

of $K_3Fe(CN)_6$ and 9.8 mg of $K_4Fe(CN)_6 \cdot 3H_2O$ in 200 ml of water, and stored in a refrigerator; a portion was diluted tenfold immediately before use.

A Farrand spectrofluorimeter was used, with 10 nm bandwidth slits and 10 × 10 × 48 mm quartz cells, and an IP 28 photomultiplier tube. The spectra were not corrected for instrumental response.

NATIVE FLUORESCENCE

About 40 mg of morphine hydrochloride (BP) was accurately weighed, dissolved in 0.1N sulphuric acid, and made up to volume in a 100-ml standard flask, with the same acid. Aliquots were diluted appropriately with the acid to give the concentrations required. The excitation (245, 285 nm) and emission (345 nm) peak wavelengths reported by Wadds[2] were confirmed. The 285-nm peak was used for excitation. The fluorescence intensity of very dilute morphine solutions was found to increase with time on exposure to ultraviolet light, presumably because of oxidation, so all morphine solutions were deaerated by passage of nitrogen for 10—15 minutes, before the fluorescence was measured. The acid was also deaerated before use. The fluorescence intensities were measured in order of increasing alkaloid concentration, starting with a solvent blank, and with a fluorescence standard (0.1 ppm 2-aminopyridine[18]) before and after the morphine solutions. The blank value was subtracted, and the net intensities were corrected to correspond to those for a 0.0400% stock morphine solution, and then referred to the average intensity of the standard at the same wavelength combination (285/345 nm). A calibration graph was plotted from the means of eleven sets of measurements, each set based on a fresh morphine stock solution. The standard deviation of the blank values was used as an estimate of the noise level, and the limit of detection was taken as four times this standard deviation. The selectivity was examined by consideration of the fluorescence characteristics of codeine, thebaine, papaverine, narcotine, narcotine hydrochloride, cotarnine hydrochloride, laudanosine, cryptopine, narceine and sinomenine hydrochloride.

OXIDATION

About 40 mg of morphine hydrochloride, accurately weighed, was dissolved in distilled water and diluted to volume in a 100-ml standard flask. Aliquots were diluted to give the desired concentrations. In the procedures described earlier,[9-11] the reaction volumes were relatively small, as the object was determination of small amounts of morphine in biological media. With larger volumes, it was found necessary first to establish the optimum conditions. The excitation peaks were found to have their maxima at 250, 280 and 321 nm, and the emission peak had its maximum at 435 nm. The 320/435 nm combination was used because it had the highest sensitivity.

An aliquot of morphine solution was placed in a standard flask, some pH 8.5 buffer was added, then after 5—10 minutes the oxidant was added by pipette and the solution was diluted to volume with buffer and mixed. The reaction was timed from addition of the oxidant. A portion of reaction mixture was placed in the cuvette and its fluorescence intensity was measured every 2—3 minutes, the cuvette being removed between readings (to minimise oxidation by the ultraviolet light). The intensity of a standard was read before, between, and after the readings of the pseudomorphine intensities. The blank value was measured and subtracted, and the net fluorescence intensities (corrected to correspond to 0.0400% stock solution) relative to the standard (0.1 ppm 2-aminopyridine solution) were plotted against time (figs. 1—3).

From this investigation it was concluded that 5 ml of oxidant should be used for a total volume of 50 ml, the fluorescence being measured 15—20 minutes after addition of the oxidant. Eleven sets of calibration measurements were taken on fresh morphine stock solutions, with 0.1 ppm 2-aminopyridine solution as standard, and corrected as usual.

The selectivity was tested by taking stock solutions of the other alkaloids examined in the native fluorescence work, treating them at pH 8.5 with 5 or 10 ml of oxidant, and comparing the fluorescence characteristics with those at pH 7—13 in the absence of the oxidant.

[18] R. Rusakowicz and A. C. Testa, *J. Phys. Chem.*, **72**, 2680 (1968).

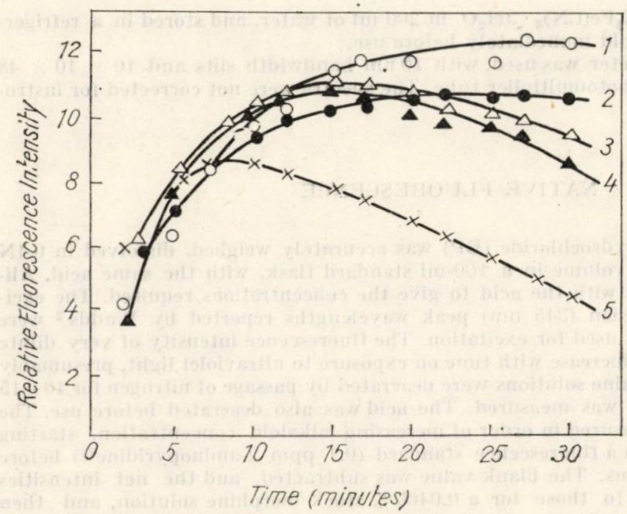

Fig. 1. — The effect of oxidant on 0.1 ppm morphine hydrochloride :

1, Oxidant 2 ml, solution 50 ml ;
2, Oxidant 2 ml, solution 100 ml ;
3, Oxidant 4 ml, solution 100 ml ;
4, Oxidant 5 ml, solution 50 ml ;
5, Oxidant 10 ml, solution 50 ml

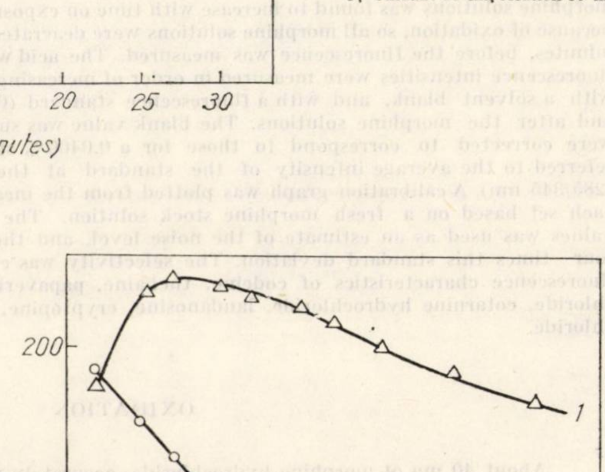

Fig. 2. — The effect of oxidant on 0.5 and 1.0 ppm morphine hydrochloride solutions (50 ml) :

1, 1 ppm, oxidant 5 ml ; *2*, 0.5 ppm, oxidant 2 ml ; *3*, 0.5 ppm, oxidant 3 ml ; *4*, 1.0 ppm, oxidant 10 ml ; *5*, 0.5 ppm, oxidant 5 ml ; *6*, 0.5 ppm, oxidant 10 ml.

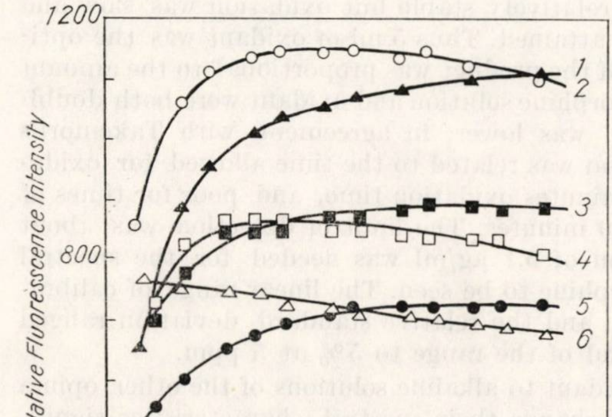

Fig. 3. —The effect of oxidant on 5 ppm morphine solution:
1, Oxidant 5 ml, solution 50 ml;
2, Oxidant 10 ml, solution 50 ml;
3, Oxidant 10 ml, solution 100 ml;
4, Oxidant 15 ml, solution 100 ml;
5, Oxidant 5 ml, solution 100 ml;
6, Oxidant 20 ml, solution 100 ml.

The fluorescence was also measured at the wavelength combination 320/435 nm to assess possible interference with the morphine determination.

COMPARATIVE EXPERIMENTS

Because of the difference in fluorescence intensity of the standard at different excitation and/or emission wavelength combinations, the calibration curves could not be used for direct comparison of the blanks and fluorescence intensities for the two methods. Therefore, two sets of 1, 2 and 5 ppm morphine hydrochloride solutions were prepared and the fluorescence intensities and blanks for both methods were measured on the same occasion.

RESULTS AND DISCUSSION

NATIVE FLUORESCENCE

The limit of detection (the concentration giving a signal, on the linear portion of the graph, four times that of the background noise) was about 0.05 μg/ml. The maximum relative standard deviation was about 10% for 0.1 ppm of morphine and the minimum was 2% for ppm concentrations. The linear range of calibration was from 0.1 to 8 ppm. The fluorescence characteristics of the other opium alkaloids were generally the same as those reported by Wadds.[2,14] The large overlap of the fluorescence spectra of morphine, codeine, laudanosine and cryptopine is a serious source of interference.

OXIDATION

When 50 ml of the morphine hydrochloride solution (0.1—5 ppm) were oxidised with more than 5 ml of the oxidant, the rate of oxidation was high but the stability of the product was low. With less than 5 m of oxidant the product was relatively stable but oxidation was slow and maximum intensity was not attained. Thus 5 ml of oxidant was the optimum volume. The stability of the product was proportional to the amount present. If the volumes of morphine solution and oxidant were both doubled the resultant intensity was lower, in agreement with Takemori's observations.[10,11] The precision was related to the time allowed for oxidation, being best for 15–20 minutes oxidation time, and poor for times of more than 30 or less than 10 minutes. The limit of detection was about 5 ng/ml, but a concentration of 0.1 μg/ml was needed for the spectral characteristics of pseudomorphine to be seen. The linear range of calibration was from 0.1 to 5 ppm, and the relative standard deviation ranged from 25% at the bottom end of the range to 5% at 5 ppm.

The addition of the oxidant to alkaline solutions of the other opium alkaloids did not appear to change their spectral characteristics significantly, but in almost every case some quenching of the fluorescence was observed. In the case of cotarnine hydrochloride a momentary increase in the intensity (measured at 365/470 nm) was observed, but started to disappear after about 10 minutes. This effect appeared to be due to a shift of the broad emission peak first towards and then away from 470 nm. The presence of cotarnine hydrochloride seems to be the only source of interference in morphine determination. The high selectivity seems to be due to the presence and position of the phenolic group on the morphine nucleus. Pseudomorphine is formed by phenolic coupling [19] of two morphine molecules at the 2,2′-positions. Only a few of the opium alkaloids, for example sinomenine and oripavine, have phenolic groups. Although disinomenine (two sinomenine molecules linked in the 1,1′-positions) can be prepared by the action of potassium ferricyanide,[20] no fluorescence was observed when the experimental conditions for formation of pseudomorphine were applied to sinomenine hydrochloride. Possibly the dimer is formed but does not fluoresce. However, besides the absence of a 4,5-oxide ring in sinomenine, the phenolic group is on C–4 whereas in morphine it is on C–3, and the lack of analytically useful fluorescence from sinomenine emphasises the role played by structure in the fluorescence behaviour of molecules.

COMPARATIVE STUDIES

The fluorescence intensity of the oxidation product of morphine hydrochloride was found to be about 17 times the native fluorescence intensity at the same concentration, but the blank value was twice that for 0.1N sulphuric acid. The excitation peak at 321 nm for pseudomorphine was about three times as intense as the peak at 250 nm and twice as intense as the one at 280 nm. The blank values were also higher, however.

---

[19] D. H. R. Barton and T. Cohen "Festschrift A. Stoll", Birkhäuser, Basle, 1957, p. 117.
[20] K. Goto and H. Sudzuki, *Bull. Chem. Soc. Japan*, **4**, 107 (1929).

At the wavelength combinations used for the calibration curves, the relative intensity for the standard at 285/345 nm (used for the native fluorescence) was 2.7 times that at 320/435 nm (used for the oxidation method).

CONCLUSIONS

The best precision can be obtained by using the native fluorescence method, but at the expense of sensitivity and selectivity, for which the oxidative method is best. The halofluorescence method is reported to give poor selectivity, and it was not investigated in the present work. It is recommended to work at about the 5 ppm concentration level if possible, and to use the oxidation method unless it is known that the alkaloids that interfere in the native fluorescence method are absent or can be corrected for.

Revue Roumaine de Chimie, 22, 4, 583–586 (1977)

Herrn Professor Dr Coriolan Drăgulescu
zum 70. Geburtstag gewidmet

PHOTOMETRISCHE BESTIMMUNG EINIGER AROMATISCHER AMINE DURCH KUPPLUNG MIT DEM *p*-NITROBENZOLDIAZONIUM-ION

GH. CIUHANDU, OLGA BÉCZY und GH. OANCEA
Labor f. organische Chemie, Universität Timişoara, Str. Pestalozzi 16

Eingegangen am 12. Juli 1976

Die Kupplung zwischen Diazoniumion und Amin erfolgt praktisch quantitativ in 5 min, in Gegenwart eines Essigsäure-Acetat-Puffers. Die erhaltenen Triazene oder Azofarbstoffe weisen charakteristische Absorptionsmaxima auf. Das Lambert-Beer-Gesetz wird bis 100 μg Amin gut verfolgt. Es wird eine Bestimmungsmethode für Methyl- und Dimethylanilin nebeneinander erarbeitet.

Die Bestimmung der aromatischen Amine ist für die Reinheitskontrolle der Atmosphäre oder der industriellen Abwässer häufig von Bedeutung. Zu diesem Zweck ist von besonderem Interesse eine Verschiebung der absorptiometrischen Messungen vom ultravioletten dem sichtbaren Bereich zu, wo sie leichter zugänglich sind. Die Kupplung der aromatischen Amine mit einem Diazoniumion ist besonders geeignet.

m-Phenylendiamin kuppelt mit Diazoderivaten in acetatgepufferten Lösungen indem es mono-, dis- und tris-Azoverbindungen bildet.[1] Die Kupplung mit Diazobenzolsulfanilamiden [2] oder mit bis-Diazobenzidin [3] ermöglicht die Bestimmung von Diamin bis zur Mikrogrammgrenze, sowie von Benzol, *m*-Nitranilin, Nitro- und Dinitrobenzol, welche durch Nitrierung und Reduktion leicht in Diamin übergeführt werden können. Unter diesen Bedingungen bilden die aromatischen Monoamine im allgemeinen Diazoaminoderivate (Triazene). Es wird allerdings nicht erwähnt unter welchen Bedingungen die Reaktion quantitativ verläuft und inwieweit sie von der Struktur des Amins beeinflußt wird.

---

[1] F. Muzik und Z. J. Allan, *Coll. Czech. Chem. Comm.*, **20**, 623 (1955); *Chem. listy*, **49**, 212 (1955); H. Zollinger, „Azo and Diazo Chemistry", Interscience Publishers, New York, 1961, S. 262,

[2] G. Ciuhandu und M. Mracec, *Z. analyt. Chem.*, **238**, 104 (1968).

[3] G. Ciuhandu und M. Mracec, *Rev. Roumaine Chim.*, **15**, 757 (1970).

In vorliegender Arbeit werden einige Angaben auf Grund der Kupplungsreaktion mit dem *p*-Nitrobenzoldiazoniumion (I) gebracht, welches infolge des stark elektronenanziehenden Substituenten in der *p*-Stellung eine bedeutende elektrophile Kraft aufweist. Auf dieser Basis wurde eine allgemeine Bestimmungsmethode für aromatische Amine bis zur Mikrogrammgrenze erarbeitet, welche sich zur Bestimmung von Methyl- und Dimethylanilin im Gemisch, an Stelle des alten thermometrischen Verfahrens mit Essigsäureanhydrid [4] als gut geeignet erwies. Dagegen kuppeln die entsprechenden Anilide, wegen der Desaktivierung des aromatischen Kerns, mit I nicht was inzwischen die Verfolgung der Reaktionskynetik bei der Hydrolyse und der Decarbonylierung einiger Formanilide in saurer Lösung ermöglichte. [5]

EXPERIMENTELLER TEIL

1. REAGENZIEN

1. Anilin, Methyl- (MA), Dimethyl- (DMA), Äthyl-, Propyl-, *o*-Chlor-, *m*-Chlor-, Benzyl- und *o*-Hydroxybenzylanilin sowie *o*- und *p*-Toluidin, Diphenylamin und α-Naphthylamin : 50 mg Amin wurden in 100 ml-Meßkolben gewogen, mit einigen Tropfen konz. Salzsäure versetzt und mit Wasser auf Marke gebracht. Zur Aufstellung der Eichkurven wurden diese Lösungen weiter mit Wasser verdünnt.

2. Eisessig *p.a.*

3. *p*-Nitranilin : 0,5 g wurden in 25 ml Eisessig gelöst. In braunen Flaschen aufbewahrt ist die Lösung maximal 1 Monat haltbar.

4. Natriumnitrit 1%, etwa 2 Wochen haltbar.

5. Natriumacetat gesättigt, etwa 5 M.

6. Ammoniumsulfamat *p.a.*

7. i-Amylalkohol, durch Schütteln mit Diazosulfanilsäure und Natriumhydroxyd gereinigt und nochmals destilliert. [2]

8. Diazoreagens : In einem graduierten Glasstöpselprobierrohr werden 0,5 ml essigsaures *p*-Nitranilin, 0,5 ml konz. Salzsäure und 1 ml Nitrit gemischt und gut geschüttelt, dann 30 min im Dunkeln stehen gelassen. Man gibt 2—3 Sulfamatkristalle hinzu, verdünnt auf 10 ml und rührt gut durch. Da das Reagens lichtempfindlich ist, soll es sofort benützt werden. Die Epruvette wird nötigenfalls in einer dunklen Flasche aufbewahrt.

o-Hydroxybenzylanilin wurde von uns durch Kondensieren von Salicylaldehyd mit Anilin und nachfolgende Hydrierung erhalten.

2. EICHUNG UND BESTIMMUNG

In einem graduierten 15 ml-Glasstöpselprobierrohr werden 0—100 µg Amin zu 6 ml verdünnt, mit 1,7 ml Acetat und 0,3 ml Essigsäure gepuffert, gut gemischt, mit 1 ml Diazoreagens versetzt, auf 10 ml weiter verdünnt, gut gerührt und 5 min im Dunkeln stehen gelassen. Dann schüttelt man gut mit 5 ml Amylalkohol und trennt mit einer ausgezogenen Pipette vollkommen die untere wässerige Schicht. Die organische Phase wird weiter mit wenig Na_2SO_4 geklärt und gegen eine Blindprobe mit demselben Diazoreagents photometriert.

---

[4] H. E. Fierz-David und L. Blangey, „Grundlegende Operationen der Farbenchemie", Springer-Verlag, Wien, 1952, S. 130.

[5] G. Ciuhandu, M. Mracec, A. Tîrnăveanu und N. Hanţu, *J. prakt. Chem.*, **317**, 98 (1975).

ERGEBNISSE

Das stark elektrophile I-Ion reagiert quantitativ mit den aromatischen Aminen in 5 min, unter Bildung von Triazenen oder Azofarbstoffen, welche charakteristische Absorptionsmaxima aufweisen (Tabelle 1, Spektralphotometer VSU-2P, Zeiss, Jena).

Tabelle 1

Kupplungsprodukte

Amin	Produkt	Farbe	Maximum nm	$\varepsilon \cdot 10^{-4}$ $1.mol^{-1} \cdot cm^{-1}$	k_λ
Anilin	Triazen	Gelb	390	2,42	19,2
Methylanilin	Triazen	Gelb	390	2,51	21,3
Dimethylanilin	Azoverbindung	Orange	480	2,58	23,5
Äthylanilin	Triazen	Gelb	390	2,42	25,5
Propylanilin	Triazen	Gelb	390	2,41	28,9
o-Chloranilin	Triazen	Gelb	385	1,93	33,8
m-Chloranilin	Triazen	Gelb	385	3,07	20,8
Benzylanilin	Triazen	Gelb	395	3,00	30,8
o-Hydroxybenzylanilin	Triazen	Gelb	390	3,27	30,4
o-Toluidin	Triazen	Gelb	395	2,25	23,3
p-Toluidin	Triazen	Gelb	390	2,82	19,0
Diphenylamin	Azoverbindung	Rot	490	2,18	38,8
α-Naphthylamin	Azoverbindung	Purpur	520	2,42	29,6

Bei Triazenen liegt das Absorptionsmaximum bei 385—395 nm, bei Azoverbindungen dagegen weit im sichtbaren Bereich. Diphenylamin liefert kein Triazen sondern einen Azofarbstoff, wegen der starken Konjugation des freien Elektronenpaares von Stickstoff mit den beiden Benzolkernen. α-Naphthylamin liefert ebenso nur einen Azofarbstoff. Benzyl- und *o*-Hydroxybenzylanilin bilden Triazene; die *o*-ständige OH-Gruppe beeinflußt nicht den elektrophilen Angriff des Diazoniumions am Stickstoffatom.

In allen Fällen erreicht der molare Extinktionskoeffizient in Amylalkohol die 10^4-Größenordnung.

Das Lambert-Beer-Gesetz wird bis zu 100 μg Amin erfüllt. In diesem Bereich wird die Aminkonzentration in linearer Abhängigkeit vom Extinktionsmodul ermittelt:

$$c = k_\lambda \cdot m_\lambda$$

Die Steilheitsfaktoren sind in Tabelle 1 wiedergegeben.

Der Abstand von etwa 90 nm zwischen den Absorptionsmaxima bei MA (Triazen) und DMA (Azofarbstoff) veranlaßte uns auch ihre Bestimmung nebeneinander zu versuchen. Für die beiden Amine sind bei 390 bzw. 480 nm folgende Gleichungen gültig:

$$c^{\mathrm{MA}} = k_{390}^{\mathrm{MA}} \cdot m_{390}^{\mathrm{MA}} = k_{480}^{\mathrm{MA}} \cdot m_{480}^{\mathrm{MA}}$$

$$c^{\mathrm{DMA}} = k_{390}^{\mathrm{DMA}} \cdot m_{390}^{\mathrm{DMA}} = k_{480}^{\mathrm{DMA}} \cdot m_{480}^{\mathrm{DMA}}$$

wobei

$$m_{390} = m_{390}^{\mathrm{MA}} + m_{390}^{\mathrm{DMA}}$$

$$m_{480} = m_{480}^{\mathrm{MA}} + m_{480}^{\mathrm{DMA}}$$

Daraus ergibt sich :

$$c^{\mathrm{MA}} = \frac{k_{390}^{\mathrm{MA}} \cdot k_{480}^{\mathrm{MA}}}{k_{390}^{\mathrm{DMA}} \cdot k_{480}^{\mathrm{MA}} - k_{480}^{\mathrm{DMA}} \cdot k_{390}^{\mathrm{MA}}} \left| k_{390}^{\mathrm{DMA}} \cdot m_{390} - \cdot k_{480}^{\mathrm{DMA}} \, m_{480} \right|$$

$$c^{\mathrm{DMA}} = \frac{k_{390}^{\mathrm{DMA}} \cdot k_{480}^{\mathrm{DMA}}}{k_{390}^{\mathrm{DMA}} \cdot k_{480}^{\mathrm{MA}} - k_{480}^{\mathrm{DMA}} \cdot k_{390}^{\mathrm{MA}}} \left| k_{480}^{\mathrm{MA}} \cdot m_{480} - k_{390}^{\mathrm{MA}} \cdot m_{390} \right|$$

Die entsprechenden Steilheitsfaktoren betragen $k_{480}^{\mathrm{MA}} = 368$ bzw. $k_{390}^{\mathrm{DMA}} = 69{,}2$.

Die Kontrollanalysen sind in Tabelle 2 wiedergegeben.

Tabelle 2

Kontrollanalysen

Einnahme : μg MA + DMA	Gefunden : μg					Mittelwert : μg
11,8+94,7	MA	11,9	10,0	10,9	12,9	11,4
	DMA	94,6	94,3	94,8	94,5	94,5
23,7+74,7	MA	23,5	23,9	23,8	24,5	23,9
	DMA	74,3	75,3	74,6	75,2	74,8
47,4+42,1	MA	47,3	46,6	46,7	46,8	46,9
	DMA	42,4	43,4	43,7	42,1	42,9
59,2+11,5	MA	59,5	59,7	57,8	60,6	59,5
	DMA	11,5	11,3	10,8	11,0	11,1

Revue Roumaine de Chimie, **22**, *4*, 587–600 (1977)

Dédié au Professeur Coriolan Drăgulescu
à l'occasion de son 70e anniversaire

SUR QUELQUES NOUVELLES SÉRIES DE FLUORURES FERRIMAGNÉTIQUES

JEAN-MICHEL DANCE, ALAIN TRESSAUD, JOSIK PORTIER
et PAUL HAGENMULLER
Laboratoire de Chimie du Solide du C.N.R.S., Université de Bordeaux I, 33405, Talence, France

Reçu le 15 octobre 1976

Several new ferrimagnetic fluorides have been synthetized in the last years at Bordeaux. Their magnetic properties have been studied using magnetization, Mössbauer resonance and neutron diffraction measurements, either on polycrystalline samples or on single crystals. The various magnetic behaviours have been correlated to the nature of the inserted transition element and the crystallographic structure.

Si les oxydes ferrimagnétiques sont connus depuis l'antiquité, ce n'est qu'en 1958 que Knox et Geller découvrirent le premier fluorure ferrimagnétique $Na_5Fe_3F_{14}$ de structure chiolite.[1] Dix ans plus tard M. W. Shafer et al. et indépendamment Smolensky et al. mirent en évidence le ferrimagnétisme de $RbNiF_3$ de type $BaTiO_3$ hexagonal.[2,3] D'autres fluorures ferrimagnétiques de ce type furent découverts à la même époque dans divers laboratoires, dont le nôtre.[4,5] La transparence des fluorures dans une partie du spectre visible justifiait la poursuite et l'extension de ces recherches en vue d'applications magnétooptiques.

Le but de cet article est l'étude cristallochimique et magnétique de nouvelles séries de fluorures ferrimagnétiques mises en évidence au cours des dernières années au laboratoire :

— les chiolites $Na_5M_3^{III}F_{14}$ (M = V, Cr, Fe, Co),

— les wébérites $Na_2M^{II}\,M^{III}\,F_7$ et $Ag_2M^{II}M^{III}F_7$ (M = élément 3d),

---

[1] K. Knox et S. Geller, *Phys. Rev.*, **110**, 771 (1958).

[2] M. W. Shafer, T. R. McGuire, B. E. Argyle et G. J. Fan, *Appl. Phys. Letters*, **10**, 202 (1967).

[3] G. A. Smolensky, N. M. Yudin, P. P. Syrnikov et A. B. Sherman, *J.E.T.P. Letters*, **8**, 2368 (1967).

[4] K. Kohn, R. Fukuda et S. Iida, *J. Phys. Soc. Japan*, **22**, 333 (1967).

[5] J. Portier, A. Tressaud, R. Pauthenet et P. Hagenmuller, *Compt. rend.*, **267**, 1329 (1968).

– les fluorures de formule $M^{II}M^{III}F_5$ (M^{II} = Cr, Mn ; M^{III} = Ti, V, Fe),
– les perovskites hexagonales 12L de formule $Cs_2MnM^{II}F_6$ (M = élément 3d).

I – TECHNIQUES EXPÉRIMENTALES

Les composés sont généralement obtenus par synthèse directe à partir des binaires, en tubes d'or ou de platine scellés. L'utilisation du fluor élémentaire permet également de préparer des fluorures dans lesquels les éléments de transition sont à des degrés d'oxydation élevés.[6,7]

Des monocristaux ont été obtenus par les méthodes de Bridgman-Stockbarger et de flux en présence de chlorures fondus.

Après étude analytique, les fluorures sont soumis à un contrôle radiocristallographique. Les études structurales sont menées à l'aide d'un diffractomètre automatique. Les mesures magnétiques sont effectuées de 4,2 à 500 K au moyen de balances de type Faraday et d'un magnétomètre à échantillon vibrant. Les études par résonance Mössbauer ont été réalisées pour ^{57}Fe en collaboration avec F. Menil à l'aide de spectromètre fonctionnant selon le mode multi-échelle, la source utilisée étant le ^{57}Co dilué dans le palladium. Les études par diffraction neutronique ont été effectuées au C.E.N. Grenoble en collaboration avec M. Wintenberger.

II – LES CHIOLITES $Na_5M_3^{III}F_{14}$(M = V, Cr, Fe, Co)

1 – ÉTUDE CRISTALLOCHIMIQUE

L'étude radiocristallographique et par analyse thermique différentielle de $Na_5Fe_3F_{14}$ [8] montre que ce composé possède trois variétés allotropiques de structures assez proches, la variété de haute température γ dérivant de la chiolite $Na_5Al_3F_{14}$. [9] Dans cette phase le fer comporte un environnement octaédrique distordu, les octaèdres $(FeF_6)^{3-}$ mettant leurs sommets en commun de manière à former des couches de formule $(Fe_3F_{14})_n^{5n-}$ (fig. 1*a*). La structure de chaque couche peut être décrite comme formée de chaînes d'octaèdres pontées. Un tiers des octaèdres partage quatre de ses sommets avec ses voisins (Fe en sites (2a)), les deux autres tiers ne comportent que deux sommets communs (Fe en sites (4d)) (fig. 1*b*). Dans les lacunes à l'intérieur de chaque couche s'insèrent un cinquième des atomes de sodium (sites (8 g)) avec la coordinence huit ; les autres atomes de sodium se placent entre les couches en coordinence six.

2 – ÉTUDE MAGNÉTIQUE

Toutes les chiolites dont les cations dérivent d'éléments de transition possèdent des propriétés ferrimagnétiques (fig. 2). Toutefois, en dessous du point de Curie, il est difficile d'atteindre la saturation de l'aimantation même pour un champ appliqué de 20 kOe ; les valeurs σ_s (fig. 2*b*)

---

[6] R. Bougon, J. Ehretsmann, J. Portier et A. Tressaud, « Preparative Methods in Solid State Chemistry », P. Hagenmuller Ed., Academic Press, New York, 1972, p. 401.

[7] J. Grannec, Thèse de Doctorat ès Sciences, Université de Bordeaux, I, 1970.

[8] M. Vlasse, F. Menil, C. Moriliere, J. M. Dance, A. Tressaud et J. Portier, *J. Sol. State Chem.*, **17**, 291 (1976).

[9] C. Brosset, *Z. anorg. Chem.*, **238**, 201 (1938).

sont obtenues en extrapolant à champ infini les droites $\sigma = f(1/H)$. Les données magnétiques sont réunies au tableau 1.

L'agencement structural des octaèdres (MF_6) au sein du réseau permet d'interpréter les résultats obtenus. Les interactions magnétiques résultent d'un couplage par superéchange à 180° par l'intermédiaire des orbitales p du fluor. Elles sont antiferromagnétiques et conduisent au ferrimagnétisme en raison de la différence d'occupation des deux sous-réseaux. Les valeurs expérimentales du moment magnétique à saturation

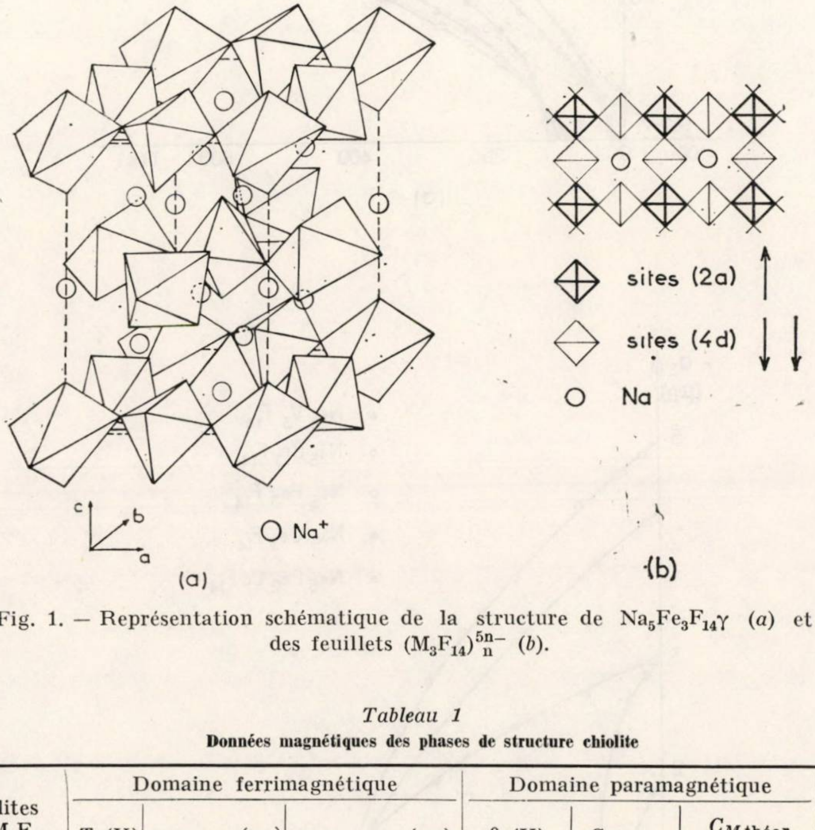

Fig. 1. — Représentation schématique de la structure de $Na_5Fe_3F_{14}\gamma$ (*a*) et des feuillets $(M_3F_{14})_n^{5n-}$ (*b*).

Tableau 1

Données magnétiques des phases de structure chiolite

Chiolites $Na_5M_3F_{14}$	Domaine ferrimagnétique			Domaine paramagnétique			Réf.
	T_C(K)	σ_s OK exp.(μ_B)	σ_s OK théor.(μ_B)	θ_p(K)	C_M exp.	C_M théor. (spin only)	
$Na_5V_3F_{14}$	21	1,94	2	− 48	2,44	3	11
$Na_5Cr_3F_{14}$	18	2,97	3	− 32	5,44	5,61	10
$Na_5Fe_3F_{14}\gamma$	90	4,98	5	− 95	11,55	13,14	11
$Na_5Fe_2CoF_{14}$	94	4,33	(4, 5 (désord.) (6 (ord.)	−100	10,53	11,76	11
$Na_5Co_3F_{14}$	108	3,10	4	−110	8,50	9	11

[10] J. P. Mirandayy, G. Ferey, C. Jacoboni, J. M. Dance, A. Tressaud et R. De Pape, *Rev. Chim. Miner.*, **12**, 187 (1975).

[11] H. Mc Kinzie, J. M. Dance, A. Tressaud, J. Portier et P. Hagenmuller, *Mat. Res. Bull.*, **7**, 673 (1972).

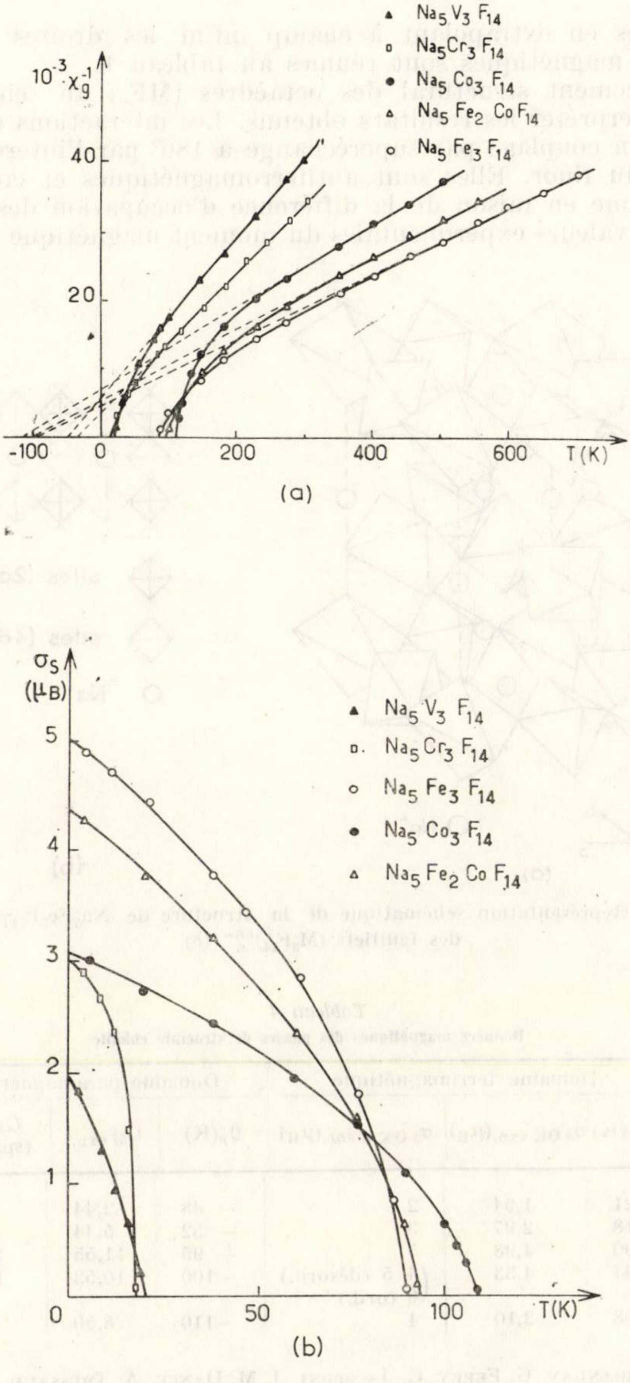

Fig. 2. — Variation avec la température de l'inverse de la susceptibilité (*a*) et de l'aimantation à saturation (*b*) des phases $Na_5M_3F_{14}$.

absolue $\sigma_{\text{sOK exp.}}$ sont en bon accord avec celles calculées à l'aide de la formule : $\sigma_{\text{sOK théor.}} = 2\,\overrightarrow{\text{M(4d)}} - \overrightarrow{\text{M(2a)}}$.

Les composés du vanadium et du chrome possèdent des températures de Curie nettement plus faibles (tableau 1). Ce résultat s'explique par le fait que dans le cas de V^{3+} et Cr^{3+} interviennent seulement des couplages $t_{2g} - p\pi - t_{2g}$, alors que pour le fer et le cobalt s'ajoutent les couplages $e_g - p\sigma - e_g$ qui sont prédominants du fait d'un plus grand recouvrement des orbitales concernées.

Des mesures d'aimantation sur monocristal ont permis de tracer les cycles d'hystérésis de $Na_5Fe_3F_{14}$ α en fonction du champ magnétique appliqué pour diverses orientations, l'aimantation étant maximale perpendiculairement aux couches du réseau (fig. 3).[12]

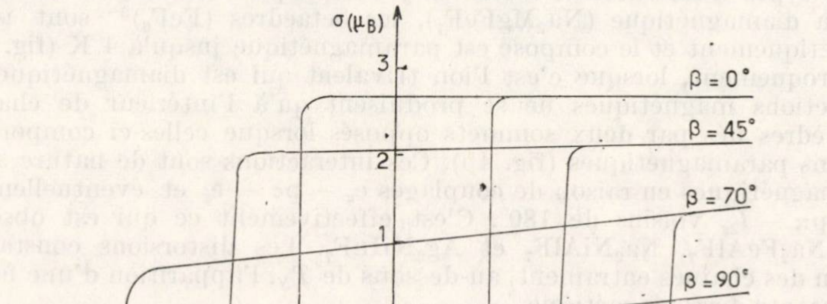

Fig. 3. — Cycles d'hystérésis de $Na_5Fe_3F_{14}$ α perpendiculairement à l'axe $\mathfrak{b}$ ($T = 4{,}2$ K ; β = angle formé par l'axe de facile aimantation et l'axe du champ magnétique appliqué).

L'étude de $Na_5Fe_3F_{14}$ γ par résonance Mössbauer a confirmé le rapport 1/2 existant entre les atomes de fer situés en sites (2a) et (4d) ainsi que la valeur de la température de Curie.

La structure magnétique de $Na_5Fe_3F_{14}$ γ a été déterminée par diffraction neutronique. La maille magnétique est identique à la maille cristallographique comme l'a montré l'identité des raies de diffraction au-dessus et en dessous de la température de Curie. La mesure de l'intensité des raies comportant une contribution magnétique a effectivement permis de conclure au parallélisme des moments avec l'axe $\boldsymbol{c}$ du réseau ; le groupe d'espace magnétique est $P4_2 2_1' 2'$.

[12] A. Tressaud, J. M. Dance, M. Vlasse et J. Portier, *Compt. rend.*, **282**, 1105 (1976).

III - LES WÉBÉRITES $Na_2M^{II}M^{III}F_7$ ET $Ag_2M^{II}M^{III}F_7$ (M = élément 3d)

De nombreux composés de formules $Na_2M^{II}M^{III}F_7$ et $Ag_2M^{II}M^{III}F_7$ ont été obtenus en substituant dans la wébérite Na_2MgAlF_7 divers éléments divalents et trivalents au magnésium et à l'aluminium. Par analogie avec Na_2MgAlF_7,[13] on peut penser que l'élément divalent se situe en sites (4c) et l'élément trivalent en sites (4d). Les octaèdres $(M^{II}F_6)^{4-}$ mettent en commun tous leurs sommets avec les octaèdres adjacents, alors que les octaèdres $(M^{III}F_6)^{3-}$ ne partagent que quatre sommets (fig. 4*c*). La structure wébérite comporte une grande analogie avec celle de la variété hexagonale des bronzes de tungstène et avec la structure pyrochlore.

La présence des ions diamagnétiques divalents (Mg^{2+}) ou trivalents (Al^{3+}, In^{3+}) illustre la diversité des propriétés magnétiques en isolant les divers types d'interactions mises en jeu. Lorsque l'élément divalent est un ion diamagnétique (Na_2MgFeF_7), les octaèdres $(FeF_6)^{3-}$ sont isolés magnétiquement et le composé est paramagnétique jusqu'à 4 K (fig. 4*a*). Réciproquement, lorsque c'est l'ion trivalent qui est diamagnétique, les interactions magnétiques ne se produisent qu'à l'intérieur de chaînes d'octaèdres liés par deux sommets opposés lorsque celles-ci comportent des ions paramagnétiques (fig. 4b). Ces interactions sont de nature antiferromagnétiques en raison de couplages $e_g - p\sigma - e_g$ et éventuellement $t_{2g} - p\pi - t_{2g}$ voisins de 180°. C'est effectivement ce qui est observé pour Na_2FeAlF_7, Na_2NiAlF_7 et Ag_2NiInF_7. Les distorsions constatées au sein des chaînes entraînent, au-dessous de T_N, l'apparition d'une faible composante ferromagnétique.

Lorsque les ions divalents et trivalents sont simultanément paramagnétiques, il existe deux types d'interactions : celles qui apparaissent entre ions divalents au sein des chaînes et celles qui se produisent entre ions divalents et ions trivalents voisins. Ces couplages s'effectuent toujours par superéchange, puisque tous les octaèdres sont liés par des sommets (fig. 4*c*, tableau 2). Heger et Viebahn-Hansler, en déterminant la

Tableau 2

Données magnétiques relatives aux phases de structure wébérite

Wébérites $A_2^IM^{II}M^{III}F_7$	Domaine ferrimagnétique			Domaine paramagnétique			Réf.
	T_C(K)	σ_s OK exp. (μ_B)	σ_s OK théor. (μ_B)	θ_p(K)	C_M exp.	$C_{M\text{théor.}}$ (spin only)	
Na_2MnFeF_7	$T_N = 97$*	0,14 **	—	−134	8,19	8,76	14
Na_2FeFeF_7	84	0,75	1	−104	7,42	7,38	14
Na_2CoFeF_7	80	1,2	2	−100	7,35	6,26	14
Na_2NiFeF_7	90	1,5	3	−50	4,60	5,38	15
Na_2NiCoF_7	126	0,9	2	−88	4,27	4	14
Ag_2NiCrF_7	10	— ***	1	−28	3,08	2,87	16
Ag_2NiFeF_7	103	2,1	3	−61	4,51	5,38	16

* Antiferromagnétique par compensation ; ** Composante ferromagnétique ; *** non déterminée (T_C trop basse

---

[13] A. Byström, *Arkiv. Kemi*, **18B**, 1 (1944).

[14] A. Tressaud, J. M. Dance, J. Portier et P. Hagenmuller, *Mat. Res. Bull.*, **9**, 1219 (1974).

[15] R. Cosier, A. Wise, A. Tressaud, J. Grannec, R. Olazcuaga et J. Portier, *Compt. rend.*, **271**, 142 (1970).

[16] J. M. Dance, J. Grannec, C. Jacobini et A. Tressaud, *Compt. rend.* ,**279**, 601, (1974).

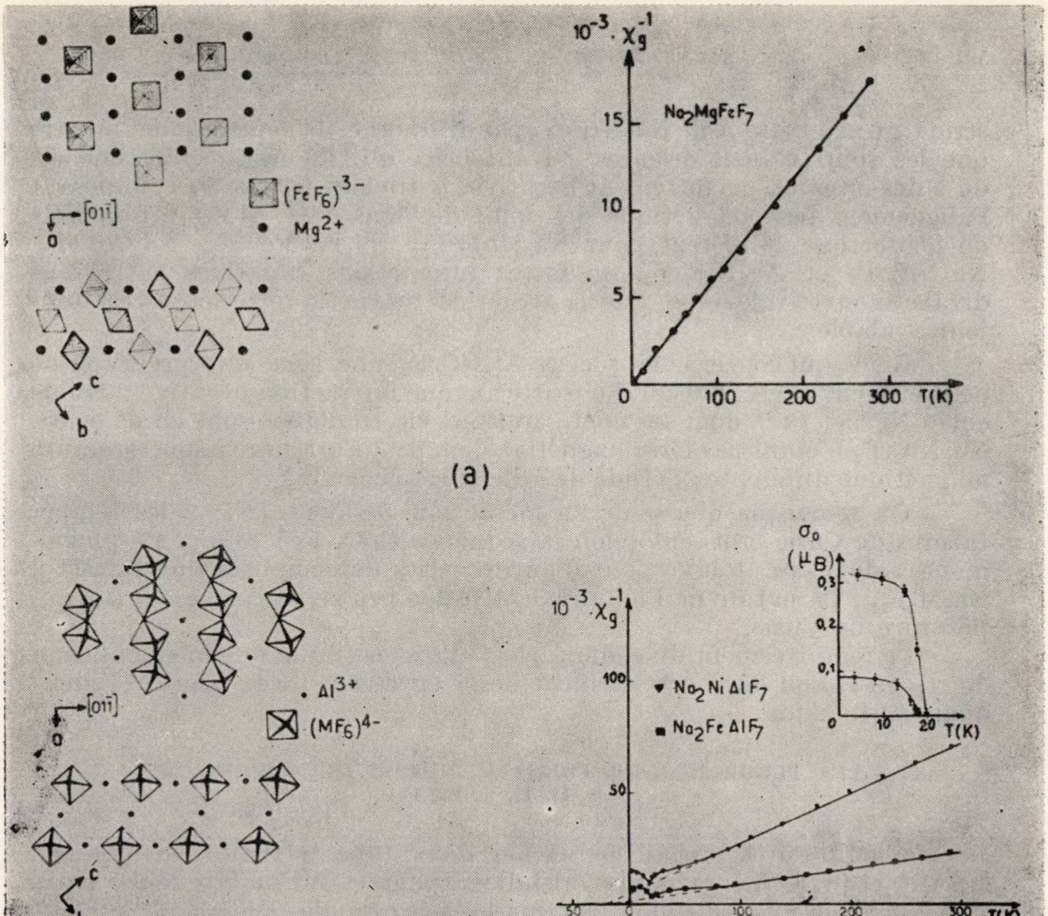

Fig. 4. — Les divers types de comportement magnétique observés dans les wébérites $A_2^{I}M^{II}M^{III}F_7$ (les octaèdres représentent les environnements des ions magnétiques).

structure magnétique de Na_2NiFeF_7 par diffraction de neutrons, ont montré que les spins étaient orientés suivant l'axe ***a***[17]. Le ferrimagnétisme est dû à des interactions fortement négatives entre ions Ni^{2+} et Fe^{3+} imposant l'alignement ferromagnétique des spins des ions Ni^{2+}. Il est raisonnable de penser que subsistent pour Na_2MnFeF_7, $Na_2Fe^{II}Fe^{III}F_7$, Na_2CoFeF_7, Na_2NiCoF_7 et Ag_2NiFeF_7, de fortes interactions négatives entre ions divalents et trivalents et que la structure magnétique proposée est toujours valable.

En ce qui concerne les phases $A_2^INiCrF_7$, une telle interprétation ne peut être envisagée, puisqu'il n'existe aucune interaction négative possible entre Ni^{2+} et Cr^{3+} dont les configurations électroniques sont en d^8 et d^3. Na_2NiCrF_7 n'étant pas ferromagnétique, on peut s'attendre à une structure magnétique différente ; l'étude de celle-ci est en cours.

On remarque que pour un même ion divalent (Ni^{2+}), les températures de Curie croissent selon la séquence Cr^{3+}, Fe^{3+}, Co^{3+}. Ce phénomène a déjà été observé pour d'autres séries de composés fluorés (MF_3, $Na_5M_3F_{14}$). La nature de l'ion divalent influe peu en revanche sur la température de Curie.

Le remplacement du sodium par l'argent entraîne une augmentation de T_C en raison de l'accroissement de la covalence de la liaison élément monovalent-fluor.

IV – LES FLUORURES DE FORMULE $M^{II}M^{III}F_5$(M^{II} = Cr, Mn ; M^{III} = = Al, Ti, V, Cr, Fe)

Ces fluorures cristallisent selon deux types structuraux voisins : $MnAlF_5$ et Cr_2F_5. Leurs mailles cristallographiques ont pu être reliées entre elles, ainsi qu'aux mailles d'autres fluorures de formule générale $M^{II}M^{III}F_5$.[18] La figure 5 montre les relations existant entre les réseaux de $MnAlF_5$ et de Cr_2F_5.

1 – LA PHASE $MnAlF_5$ ET LA SOLUTION SOLIDE $MnAl_{1-x}Fe_xF_5$

a – Propriétés magnétiques de $MnAlF_5$

Dans $MnAlF_5$ les chaînes d'octaèdres $(MnF_6)^{4-}$ liés par des arêtes sont isolées les unes des autres par des chaînes d'octaèdres $(AlF_6)^{3-}$ associés par les sommets.[19] Le composé ne présente un ordre antiferromagnétique qu'en dessous de 2,3 K. Ce résultat est dû à une compensation presque parfaite des deux interactions majeures existant entre atomes de manganèse : d'une part un couplage ferromagnétique par double échange à 90° Mn–F–Mn, d'autre part à travers les arêtes communes des octaèdres un couplage antiferromagnétique direct Mn–Mn légèrement prédominant.

Une étude par diffraction neutronique a montré que la maille magnétique de $MnAlF_5$ était doublée selon les axes ***b*** et ***c***, les moments étant dirigés parallèlement à ***b***. La faible résultante des couplages entre atomes de manganèse à l'intérieur d'une même chaîne est du même ordre de grandeur que l'interaction existant entre chaînes.

---

[17] G. Heger et R. Viebahn-Hänsler, *Solid State Commun.*, **11**, 1119 (1972).

[18] J. M. Dance et A. Tressaud, *Compt. rend.*, **277**, 379 (1973).

[19] A. Rimsky, J. Thoret et W. Freundlich, *Compt. rend.*, **270**, 407 (1970).

b — La solution solide $MnAl_{1-x}Fe_xF_5$

Etant donnée l'existence de deux sites différents pour l'aluminium et le manganèse dans $MnAlF_5$ il était tentant de remplacer l'aluminium par le fer. En fait la substitution totale n'est pas possible, mais une solution solide de formule $MnAl_{1-x}Fe_xF_5$ a été mise en évidence à 700° pour des valeurs de x comprises entre 0 et 0,58. Au-delà de $x = 0,58$, la solution solide limite coexiste avec MnF_2 et FeF_3 · $MnAlF_5$ et la solution solide sont isostructuraux.

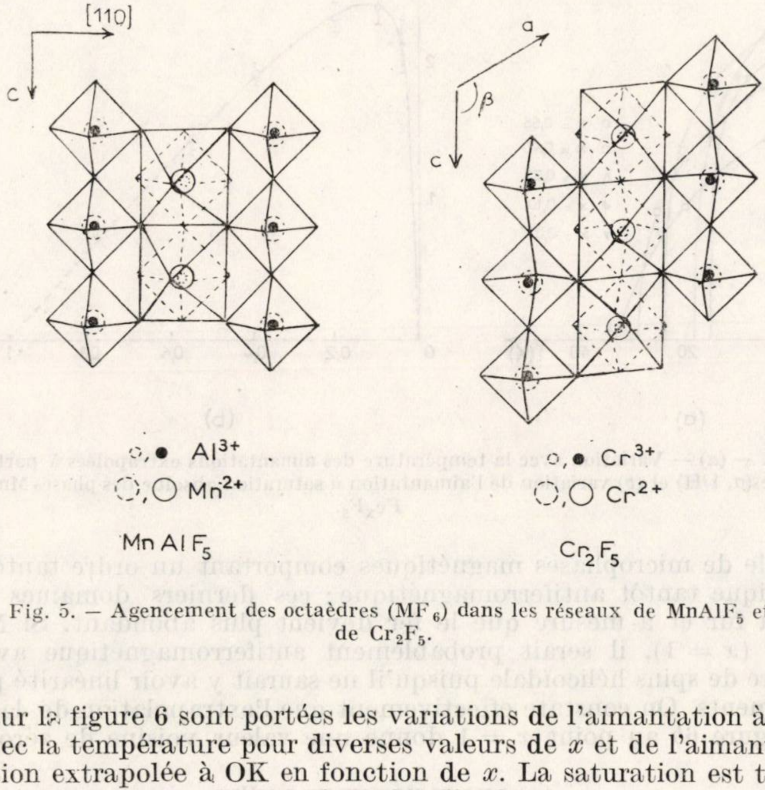

Fig. 5. — Agencement des octaèdres (MF_6) dans les réseaux de $MnAlF_5$ et de Cr_2F_5.

Sur la figure 6 sont portées les variations de l'aimantation à saturation avec la température pour diverses valeurs de x et de l'aimantation à saturation extrapolée à OK en fonction de x. La saturation est toutefois difficile à atteindre en dessous du point d'ordre.

Le ferrimagnétisme observé résulte sans nul doute de l'absence de compensation entre les sous-réseaux (4 a) et (4 b) qui contiennent respectivement les ions Mn^{2+} et les ions Al^{3+} et Fe^{3+}. La température de Curie paramagnétique augmente avec x en raison de l'accroissement du nombre d'interactions ; il en est de même pour la température de Curie.

En collaboration avec J. B. Goodenough, nous avons proposé une explication à l'évolution de l'aimantation à saturation absolue avec x

(fig. 6*b*). La substitution d'un atome d'aluminium par un atome de fer crée un microdomaine (cluster) ferrimagnétique dans lequel le moment du fer est orienté antiparallèlement à ceux des six atomes de manganèse les plus proches. Tant que x reste faible les ions Fe^{3+} tendent à former des clusters ferrimagnétiques de plus en plus étendus dans lesquels les moments des ions Fe^{3+} et Mn^{2+} sont orientés antiparallèlement. Mais à partir du moment où deux ions Fe^{3+} deviennent premiers voisins dans une même file, les interactions Fe—F—Fe antiferromagnétiques entrent en compétition avec les interactions Mn—F—Fe et l'ordre magnétique à l'intérieur du cluster est alors plus complexe. La solution solide consiste alors en un ensemble de microphases magnétiques comportant un ordre tantôt ferrimagnétique tantôt antiferromagnétique ; ces derniers domaines s'étendent au fur et à mesure que le fer devient plus abondant. Si $MnFeF_5$ existait ($x = 1$), il serait probablement antiferromagnétique avec une structure de spins hélicoïdale puisqu'il ne saurait y avoir linéarité parfaite des moments. On constate effectivement que l'extrapolation de la courbe de la figure 6*b* au point $x = 1$ donne une valeur voisine de zéro.

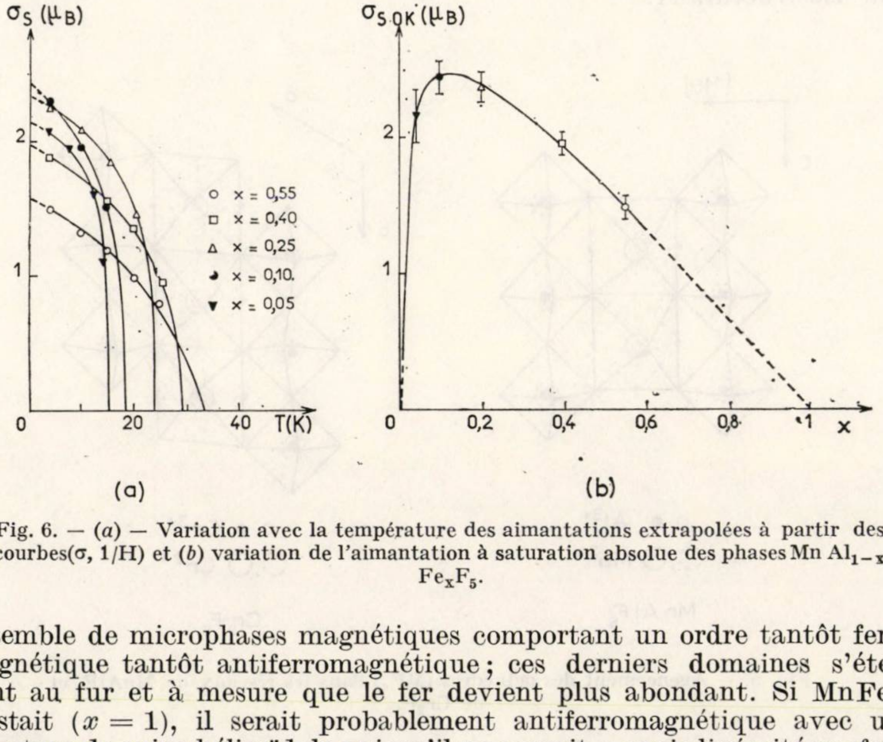

Fig. 6. — (*a*) — Variation avec la température des aimantations extrapolées à partir des courbes(σ, 1/H) et (*b*) variation de l'aimantation à saturation absolue des phases $MnAl_{1-x}Fe_xF_5$.

2 — LES FLUORURES $CrM^{II}F_5$

Trois fluorures isotypes de Cr_2F_5 ont été préparés : $CrAlF_5$, $CrTiF_5$, $CrVF_5$. Les données magnétiques relatives à ces composés sont rassemblées au tableau 3. $CrAlF_5$ est paramagnétique dans le domaine de température étudié. Le caractère antiferromagnétique de Cr_2F_5 qui avait été envisagé par Osmond [20] est confirmé par nos propres mesures magné-

---

[20] W. P. Osmond, *Proc. Phys. Soc.*, **87**, 767 (1966).

Tableau 3

Données magnétiques relatives aux fluorures ferrimagnétiques de type Cr_2F_5

Composé	T_C(K)	σ_{s0K} (μ_B)	θ_p (K)	C_M exp.	C_M théor. (mom. orb. bloqué)
$CrTiF_5$	26±3	1,78	−78	3,59	3,88
$CrVF_5$	40±3	0,86	−51	4,02	4,40

tiques. La figure 7 représente les courbes obtenues pour $CrTiF_5$ et $CrVF_5$. Goodenough explique les propriétés ferrimagnétiques de ces deux phases par une compétition entre les interactions magnétiques.

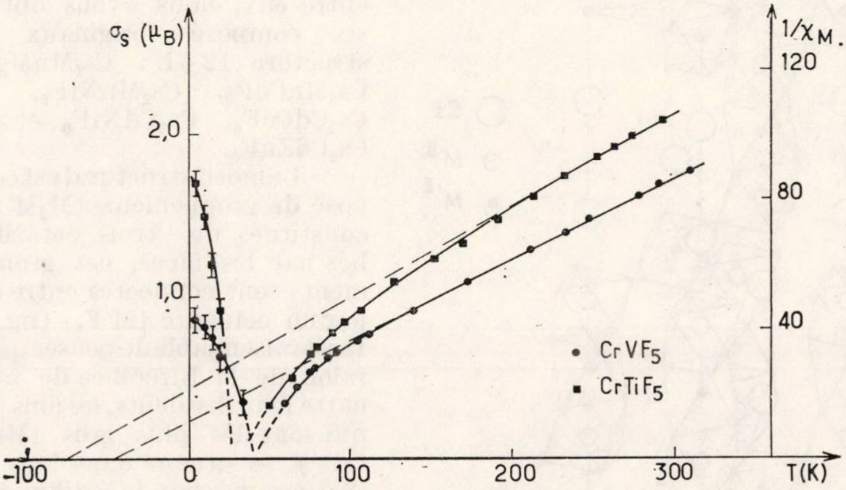

Fig. 7. — Comportement magnétique de $CrTiF_5$ et $CrVF_5$.

Dans $CrTiF_5$ les interactions $Cr^{2+}-F-Ti^{3+}$ prépondérantes s'effectuent entre les orbitales *d* à moitié pleines des ions Cr^{2+} et les orbitales *d* vides des ions Ti^{3+} ; elles sont ferromagnétiques. D'autre part les couplages entre ions Ti^{3+} sont antiferromagnétiques du fait de l'occupation préférentielle de l'orbitale d_{xy} par le seul électron *d* présent. L'anisotropie magnétique stabilisant les moments des ions Ti^{3+} le long de l'axe ***c***, on peut s'attendre à une composante ferromagnétique parallèlement à l'axe ***b*** et à une composante antiferromagnétique le long de l'axe ***c*** pour les chaînes d'ions Ti^{3+} et Cr^{2+}.

Dans $CrVF_5$ l'ion V^{3+} ($3d^2$) introduit un fort couplage spin-orbite en dessous de la température d'ordre. Les signes des interactions magnétiques sont les mêmes que pour $CrTiF_5$; cependant la forte anisotropie associée à l'ion V^{3+} écarte fortement les moments magnétiques de l'axe ***b***.

V – LES PEROVSKITES HEXAGONALES $Cs_2M^{II}M'^{II}F_6$

Le caractère ferrimagnétique de $RbNiF_3$ et $CsFeF_3$ de structure 6L, polytype de la perovskite, nous a incité à rechercher dans les familles des perovskites hexagonales des structures susceptibles de conduire au ferrimagnétisme.

1 – ÉTUDE CRISTALLOCHIMIQUE

C'est ainsi qu'en substituant dans les fluorures $Cs_2NaM^{III}F_6$ de structure 12L[21] le couple sodium-élément trivalent par deux éléments de transition divalents dont la taille diffère suffisamment pour qu'un ordre puisse s'établir entre eux, nous avons obtenu six composés originaux de structure 12 L : Cs_2MnMgF_6, Cs_2MnCoF_6, Cs_2MnNiF_6, Cs_2CdCoF_6, Cs_2CdNiF_6 et Cs_2CdZnF_6.

Le motif structural est composé de groupements $(M_2M'F_{12})$ constitués de trois octaèdres liés par les faces, ces groupements sont connectés entre eux par un octaèdre $(M'F_6)$ (fig. 8). Il est raisonnable de penser qu'en raion de la différence de taille entre ions divalents, les ions M^{2+} qui sont les plus gros (Mn^{2+}, Cd^{2+}) se situent dans les sites (6c) occupés par le sodium dans Cs_2NaMF_6, alors que les ions M'^{2+} de taille plus petite (Mg^{2+}, Co^{2+}, Ni^{2+}, Zn^{2+}) occupent les sites (3a) et (3b) de l'élément trivalent.

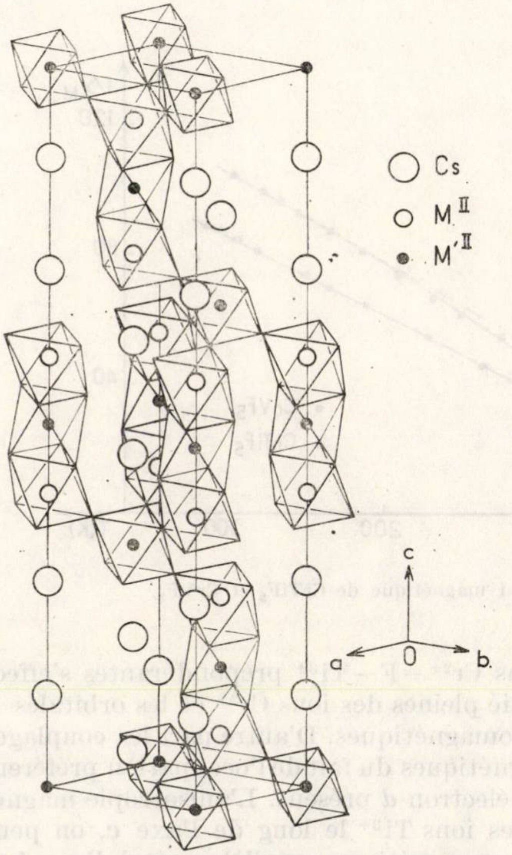

Fig. 8.—Maille hexagonale des composés $Cs_2MM'F_6$.

2 – ÉTUDE MAGNÉTIQUE

Le tableau 4 et la figure 9 reproduisent respectivement les données magnétiques et les courbes $\sigma = f(T)$ et $\chi^{-1} = f(T)$ relatives aux composés ferrimagnétiques Cs_2MnCoF_6 et Cs_2MnNiF_6.

La présence dans la structure 12L de trois sites cristallographiques distincts explique le caractère ferrimagnétique des phases obtenues lorsque ces sites sont tous occupés par des ions paramagnétiques. A l'intérieur des

---

[21] D. Babel, R. Haegele, G. Pausewang et F. Wall, *Mat. Res. Bull.*, 8, 1371 (1973)

Tableau 4

Données magnétiques relatives aux fluorures ferrimagnétiques de type $Cs_2MM'F_6$

Composé	T_C (K)	$\sigma_{s\ 0K}(\mu_B)$	θ_p (K)	C_M exp.
Cs_2MnCoF_6	53±2	1,99	−61	8,19
Cs_2MnNiF_6	61±2	2,40	−78	5,96

groupements $(Mn_2M'F_{12})(M' = Co, Ni)$ les interactions magnétiques résultent de couplages directs à travers les faces des octaèdres et par superéchange à 90° par l'intermédiaire du fluor. Il existe également des interactions entre les ions Mn^{2+} situés aux extrémités de ces groupements et les ions Ni^{2+} (ou Co^{2+}) des octaèdres qui partagent avec eux leurs sommets. Ces couplages antiferromagnétiques par superéchange à 180° de type e_g-$p\sigma$-e_g sont certainement très importants.

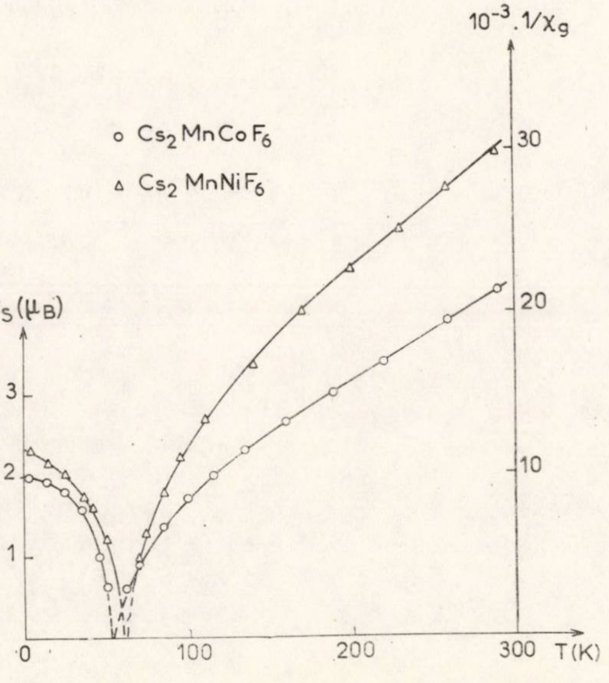

Fig. 9. — Variation avec la température de l'aimantation à saturation et de la susceptibilité réciproque des phases $Cs_2MM'F_6$.

Une étude par diffraction de neutrons actuellement en cours permettra de déterminer l'orientation exacte des moments et de préciser la nature et l'importance des divers couplages.

V – CONCLUSIONS

Du point de vue fondamental l'ensemble de ce travail a permis de vérifier les prévisions de Goodenough[22] sur la nature des interactions magnétiques mises en jeu dans les divers édifices structuraux obtenus. D'un point de vue plus appliqué et malgré les valeurs relativement basses des températures de Curie obtenues, l'étude des fluorures ferrimagnétiques s'est révélée particulièrement intéressante en raison de l'intérêt que peuvent présenter du point de vue magnétooptique des matériaux possédant de fortes aimantations spontanées, isolants électroniques et transparents dans une partie du visible

---

[22] J. B. Goodenough, «Magnetism and the Chemical Bond», Interscience Publ., Ville, 1963.

evue Roumaine de Chimie, **22**, *4*, 601–605 (1977)

Dedicated to the 70th anniversary
of Professor Coriolan Drăgulescu

HETEROLIGAND PEROXO COMPLEXES OF SOME d^0 TRANSITION METAL IONS

CIRILA DJORDJEVIC
College of William and Mary
Williamsburg, Virginia 23185, U.S.A.

Received September 6, 1976

A brief survey is given of the heteroligand peroxo complexes of the early transition metals in their highest oxidation state. Only the compounds characterized in the solid state are considered. The article is focused on more recent investigations, with a special emphasis on the heteroligand peroxo complexes of pentavalent vanadium, niobium and tantalum. Formation and properties of mono-, di-, and tri-peroxo heteroligand complexes are discussed. Two novel series of crystalline peroxo complexes of tervalent lanthanides of the formula
$KLnEDTA \times H_2O_2yH_2O$ **and** $K_3Ln(O_2)EDTA \times H_2O_2yH_2O$,
respectively, are described. Characteristic trends concerning the coordination polyhedra observed, and the types of the heteroligand field present in this group of complexes, are discussed.

Metal ions of the d^0 electron configuration are derived from the early transition metal elements in the following oxidation states : M(VI) for the chromium group metals, M(V) for the vanadium group metals, M(IV) for the titanium group metals, and M(III) for the lanthanides. Heteroligand peroxo complexes have now been reported for most of these elements, and a brief review is presented here, outlining some thought provoking trends, and summarizing some recent results obtained by studying the solid crystalline peroxo complexes. The numerous solution investigations are not included.

Most of the early transition metals have been known to form fairly stable peroxo complexes [1] in their higher oxidation states for a long time. The well known blue "peroxochromic acid", CrO_5, has been of interest since 1847, and has been studied by many chemists.[2, 3] The yellow titanium and niobium peroxo species in aqueous solutions too have been used

[1] J. A. Connor and E. A. V. Ebsworth, *Adv. Inorg. Chem. Radiochem.*, **6**, 279 (1964).
[2] J. E. Ferguson, C. J. Wilkins, and J. F. Young, *J. Chem. Soc.*, **1962**, 2136.
[3] R. Stomberg, *Arkiv Kemi.*, **24**, 283 (1965), and references therein.

in analytical chemistry for a long time. However, the proper characterization and understanding of the molecular structure and bonding in complexes of this type has really come much later.

The presence of coordinated peroxo group can be derived from the chemical evidence, [1] which, however, by itself may be misleading, in particular if the metal ion displays variable oxidation states.[4] The infrared spectra have proved to be very helpful in supplying further evidence for the presence of a coordinated peroxo group.[5,6] It has been shown that characteristic additional band appears between 800–900 cm^{-1} in the spectra of the compounds containing a peroxo ligand. Even the number of such additional bands has been related to the number of the peroxo ligands.[7] These infrared bands are originated in the peroxo group (O–O) stretching mode. In the heteroligand fields, however, for ligand spheres comprising bulky molecules and displaying a rich absorption in the infrared by itself, the location of such additional bands is more difficult. In addition, the terminal oxo group usually displays a band in this region, due to the M=O stretching. Consequently, the infrared evidence, along with the chemical characterization of the heteroligand peroxides, has to be taken "cum grano salis". The final and most reliable source of information on the molecular structure of a heteroligand metal peroxide still remains a well done X-ray structural analysis. Fortunately, there are several structural analyses available today providing invaluable insight into the chemistry of this class of compounds.

Heteroligand peroxo complexes were first characterized for chromium, and a number of structures were done by R. Stomberg.[3] The compounds investigated were mononuclear diperoxo derivatives of Cr(IV) and Cr(VI), involving therefore d^2 and d^0 metal ions, respectively. The complexes of the latter can be represented by the formula $[CrO(O_2)_2L]$, where L = pyridine, dipyridyl [8] and *o*-phenanthroline, respectively. The peroxo groups occupy the equatorial positions in a pentagonal bipyramidal arrangement. Molybdenum and tungsten complexes have been studied as well, and they were found to form similar heteroligand peroxo spheres. The complexes are, however, not prepared as easily as for chromium.[3,5]

The structural data on the complexes investigated support generally the bidentate model of the peroxo group coordination, and not the π-donor description of the peroxo ligand, which was put forward earlier, based on the presumption of the O–O bond shortening upon coordination, due to the antibonding electrons' delocalization.[3,5] Further structural studies have disclosed a fairly constant O–O bond length ranging from 1.42 to 1.47 Å, and thus not differing significantly from the oxygen distances found in the peroxo ion or hydrogen peroxide itself.[1] Peroxo group is therefore regarded here as a bidentate group.

---

[4] N. Vuletic and C. Djordjevic, *J. Chem. Soc. Dalton*, **1973**, 1137.

[5] W. P. Griffith, *J. Chem. Soc.*, **1964**, 5248.

[6] E. Wendling, *Bull. Soc. chim. France*, **1967**, 16.

[7] R. N. Shchelovok, E. N. Traggeim, M. A. Michnik, and K. I. Petrov, *Zhur. neorg. Khim.*, **17**, 1270 (1972).

[8] R. Stomberg and J. B. Ainalem, *Acta Chem. Scand.*, **22**, 1431 (1968).

The d^0 tetraperoxides of the type $K_3M(O_2)_4$, M(V) = V, Nb, Ta have been found to be isomorphous [2] with the d^1 $K_3Cr(O_2)_4$, with a dodecahedral ligand polyhedron.[3] Since then several heteroligand peroxocomplexes were prepared of these metals,[4,9,10] and some important X-ray structures are available.[11–13] Mono-, di-, and tri-peroxo heteroligand complexes are known. Indeed, there seem to be some regularity in the heteroligand field formation. Monoperoxo derivatives are generally formed in presence of electronegative monodentate ligands, giving rise to species of the formula $M(O_2)X_n^{y-}$, where M(V) = V, Nb, Ta; X = F, Cl and n ranges from 4 to 6. An interesting monoperoxopentafluorotantalate (V) was reported recently [10] of the formula $K_2/Ta(O_2)F_5/KHF_2$. Physical and chemical properties of this compound imply the presence of the coordinated peroxo group and an independent HF_2^- ion. Lately[14] a strange structure of this complex was published, describing an asymmetrical polyhedron which the authors called "an irregular octahedron with one corner located in the middle of the peroxo bond." The unexpected feature of this structure is the O—O bond length of 1.64 A, however, longer than in the ionic peroxide or hydrogen peroxide itself. The deviation of this value is not reported.

Diperoxo derivatives are the most common ones for this group of metals, with an oxo group appearing frequently in the coordination spheres, along with the additional mono or bidentate ligands of various electronegativity. The complexes of the formula $MO(O_2)_2L$ and $M(O_2)_2L_2$ are known, where M(V) = V, Nb and M(V) = Nb, Ta, respectively, and L = fluoride, oxalate, dipyridyl or *o*-phenanthroline.[4,9,10] Trisperoxo derivatives are less common, established so far only for M(V) = Nb, Ta, showing the formula $M(O_2)_3L$, where L = dipyridyl,[9] *o*-phenanthroline,[9] and oxalate.[7]

It is interesting that in these complexes vanadium resembles more molybdenum than niobium and tantalum. The heteroligand sphere for vanadium and molybdenum comprises invariably an oxo group, terminal or bridging, revealing the well known stronger tendency of these metal ions towards the metal-oxo bond formation.[4] This similarity of vanadium and molybdenum has been confirmed recently, when the structure of the $K_3[VO(O_2)_2(C_2O_4)]H_2O$ was determined,[13] revealing the presence of an isostructural complex peroxo ion with the previously reported [15] compound $K_2/MoO(O_2)_2(C_2O_4)/$. The two compounds are not isomorphous, due to the different charge and thus the number of potassiums, but the complex ions are isostructural. The coordination polyhedron is a pentagonal bipyramid with the oxo group occupying the apical position, and the two peroxo groups placed in the equatorial position, having an average (O—O) distance of 1.46 Å. The vanadium, and the molybdenum atom are displaced from the pentagonal plane towards the oxo oxygen for 0.28 and 0.35 Å, respectively. Under analogous conditions the niobium and tantalum form the eight coordinated dodecahedral complexes of the formula $K_3/M(O_2)_2(C_2O_4)_2/ \cdot H_2O$.

---

[9] C. Djordjevic and N. Vuletic, *Inorg. Chem.*, **7**, 1864 (1968); *idem, Chem. & Ind.*, **1968**, 1360.

[10] N. Vuletic and C. Djordjevic, *J. Less-Common Metals*, **45**, 85 (1976).

[11] G. Mathern, R. Weiss, and R. Rohmer, *Chem. Commun.*, **1969**, 70; idem, *Acta Cryst.*, **B 27**, 1572 (1971).

[12] G. Mathern, R. Weiss, and R. Rohmer, *Chem. Commun.*, **1970**, 153; idem, *Acta Cryst.*, **B 27**, 1971 (1971).

[13] D. Begin, F. W. B. Einstein, and J. Field, *Inorg. Chem.*, **14**, 1784 (1975).

[14] Z. Ruzic-Toros, B. Kojic-Prodic, and M. Sljukic, *Acta Cryst.*, **B 32**, 1096 (1976).

[15] R. Stomberg, *Acta Chem. Scand.*, **24**, 2024 (1970).

The formation of the heteroligand peroxo sphere of a given composition, obtained by crystallization from aqueous solutions, is also highly pH dependent. This is nicely illustrated on the peroxo fluoro niobates and tantalates,[10] and on the peroxooxalato niobates[7] systems. Monoperoxo species are generally formed at lower pH, the di- and tri-peroxo derivatives forming upon the pH increase, and ending finally with the homeo ligand sphere of the type $M(O_2)_4{}^{3-}$, the only species existing at high pH.

Lately two structures of some interesting heteroligand peroxo complexes were reported for titanium.[16,17] In both, the dipicolinatoperoxo complex of the formula $K_2[O\{Ti(O_2)(C_7H_3O_4N)\}_2]\ 5H_2O$, and the nitrilotriacetatoperoxo complex of the formula $Na_4[O\{Ti(O_2)(C_6H_6O_6N)\}_2]\ 11H_2O$ the coordination polyhedron is approximately a pentagonal bipyramid sharing an apical μ-oxygen, and the peroxo group occupies equatorial site, with a O—O distance of $1.45 + .01$ Å.

In contrast to the rest of the d^0 metal ions, the tervalent lanthanides do not form easily peroxo derivatives, and the only known compounds so far are the poorly characterized and thermally unstable oxo-hydroxo-peroxo hydrates.[1,18] Only recently, crystalline peroxo-EDTA-Ln(III) complexes have been obtained.[19] It has been observed that hydrogen peroxide will not replace water molecules coordinated to the lanthanide ions in acid solutions containing EDTA, where species of the composition $Ln(EDTA)^-_{aq}$ have been found to exist.[20] However, on raising the pH to about 6—7, it is possible to separate from the solutions compounds of the formula $KLnEDTA\ x\ H_2O_2yH_2O$, where $x = 0.5$, $y = 4$ for Y(III) : $x = 2, y = 5$ for Ln(III) = La, Nd ; $x = 0.5, y = 6$ for Ln(III) = Eu, Gd. On heating at 100° in vacuo, these complexes gradually decompose. The infrared spectra do not show the additional band expected for a terminal bidentate coordinated peroxo group, indicating the presence of perhydrates or, in some complexes, a bridging peroxo group. Indeed, for complexes of Ln(III) = La, Nd, it seems that two different kinds of peroxides are present. The first mole of hydrogen peroxide oxygen is lost in vacuo over phosphorous pentoxide at 25°, and the second one is removed only at 100°. It is also significant that isomorphism has been established for the three types of stoichiometric formulae, which vary in amount of peroxo oxygen and water molecules.

Thermally much more stable crystalline peroxo-EDTA complexes were obtained from the alkaline media. They correspond to the formula

---

[16] D. Schwarzenbach, *Inorg. Chem.*, **9**, 2391 (1970).

[17] D. Schwarzenbach and K. Girgis, *Helv. Chem. Acta*, **58**, 2391 (1975).

[18] K. B. Jacimirskii, N. A. Kostromina, Z. A. Sheka, N. K. Davidenko, E. E. Kriss, and V. I. Ermolenko, "Khimia Kompleksnih Soedinenii Redkozemelnih Elementov", Naukova Dumka, Kiev, 1966.

[19] C. Djordjevic and N. Vuletic, "Proceeding 12th Rare Earth Research Conference", Vail, Colo., 1976, p. 158.

[20] T. Moeller, in "MTP Internation Review of Science, Inorganic Chemistry, Series One", Vol. 7 (K. W. Bagnall, Ed.), Butterworths, London, 1972, p. 275—298.

$K_3Ln(O_2)EDTA$ x H_2O_2 y H_2O, where $x = 0$, $y = 3$ for Y(III); $x = 0$, $y = 6$ for Ln(III) = La, Nd; and $x = 1$, $y = 5$ for Ln(III) = Eu, Gd. Heated in vacuo over phosphorous pentoxide to about 130°, these complexes do not lose oxygen, and they can be dehydrated without decomposition. The thermal stability, as well as the infrared spectra, indicate that a bidentate peroxo group is present in the ligand sphere, comprising also the polydentate EDTA. These complexes represent the first class of stable peroxo lanthanide derivatives. Isomorphous series are found in accord with the proposed formulae, shown above. Infrared spectra, useful for detecting the presence of a coordinated peroxo group, are very complex for these compounds, due to the EDTA bands. It is however plausible to assign a characteristic additional band, appearing at 850 cm^{-1} in the spectra of all these complexes, to a coordinated peroxo group stretching.

Sterochemically, the heteroligand peroxo complexes of the d^0 transition metal ions prepared and investigated so far indicate some interesting peculiarities. First of all, in hexacoordinated complexes pentagonal pyramidal structure arrangement was found for various chromium[3] and then for a vanadium compound.[21] Further on, it is observed that the seven coordinated species are invariably assuming a pentagonal bipyramidal polyhedron, with the peroxo groups always placed in the equatorial plane. Coordination eight, however, in all the complexes studied displays a dodecahedral arrangement.

Heteroligand spheres are in general a challenge to chemists. The mutual interactions of the ligands present, ranging from the simple spacial hindrances to complex perturbations of energy levels of the bonding and nonbonding electrons, result in properties of the complexes, which differ significantly from the ones found in corresponding simple symmetrical homeoligand fields. For example, changes in vibrational and electronic spectra occur, and marked differences are frequently observed in the thermodynamic and/or kinetic stability of the heterocomplex species. Predictions of particular trends for such changes, as dependent upon the ligand architecture, are as yet very uncertain. Besides, they are empirical in nature. Consequently, in order to get insight into the formation, structure and properties of particular heteroligand fields, as many correlations as possible, derived from the existing series of heteroligand complexes, are useful. This topic is of crucial interest among various problems of current coordination chemistry, because in spite of great progress in recent decades, it still remains to be understood why only certain ligand fields, in combination with given metal ions, reversibly bind oxygen, molecular nitrogen, or a number of other important and interesting ligands.

---

[21] R. E. Drew and F. W. B. Einstein, *Inorg. Chem.*, **11**, 1079 (1972).

Revue Roumaine de Chimie, **22**, *4*, 607–610 (1977)

Dedicated to the 70th anniversary
of Professor CORIOLAN DRĂGULESCU

REARRANGEMENTS OF THE BENZOBICYCLO [3.2.2] NONENE TO THE BENZOBICYCLO[3.3.1]NONENE SYSTEM

ILEANA DRĂGUŢAN, M. ELIAN and ECATERINA CIORĂNESCU
Organic Chemistry Centre, Bucharest, Spl. Independenţei, 202 B, Romania

Received September 24, 1976

The stability of the systems **2**, **3** and **7** in acidic and buffered medium was studied. Under all the employed conditions **7** was stable. In the presence of acids **2** rearranged to **3**. A mechanism of this rearrangement is proposed.

Acetolysis of 7-(β-tosyloxyethyl)-benzo[*a*]-1,3-cycloheptadiene **(1-OTs)** gave rise to 24% benzo[*b*]bicyclo[3.2.2]nonen-4-yl acetate **(2-OAc)** and 21% benzo[*b*]bicyclo[3.3.1]nonen-4-yl acetate **(3-OAc)**.[1] Both these acetates are obviously a result of double bond participation, but the latter cannot be a direct π-route product.

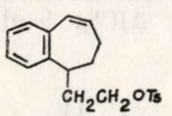

1-OTs

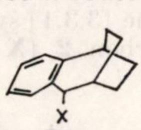

2-X

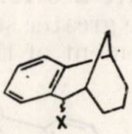

3-X

The question was to establish which were the rearrangements leading to **3-OAc**. The corresponding ion **4** could be generated starting from either of the two initial π-route intermediates, **5** and **6**.

In order to understand this mechanism we undertook the study of the relations between the benzobicyclo[3.2.2]-and-[3.3.1]nonene systems. To our knowledge similar studies have not yet been reported.

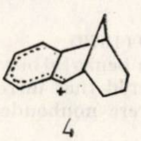

4

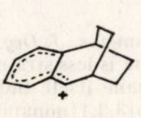

5

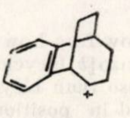

6

---

[1] I. DRĂGUŢAN, C. DRĂGHICI and E. CIORĂNESCU, *Rev. Roumaine Chim.*, **20**, 283 (1975).

The behaviour of the system **7** in acidic medium was followed by nmr spectroscopy. Both the treatment of the authentic **7-OH** [1] with trifluoroacetic acid or *p*-toluenesulphonic acid in AcOH and the buffered acetolysis of the corresponding tosylates **(7-OTs)** lead to unrearranged products (**7-OAc** or **7-OCOCF)$_3$**. The stability of the system **7-X** could be ascribed to the intervention of the aromatic ring, the ion **8**, rather than **6**, being the intermediate (phenyl migration in **8** gives the same system, **7-X**).

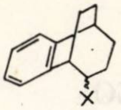

7-X

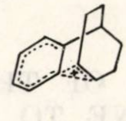

8

The other alternative, the formation of the system **3** from **2**, was then checked. As expected, the acetates **2-OAc**, [1] corresponding to the ion **5**, were recovered unchanged after refluxing in acetic acid—sodium acetate. Instead, in the presence of *p*-toluenesulphonic acid, the alcohol **2-OH** [1] rearranged to a mixture of *exo*- and *endo*-benzo[*b*]-bicyclo[3.3.1]-nonen-4-yl acetates **(3-OAc)** (*exo*/*endo* = 3 : 1). This *exo*/*endo* ratio is similar to that obtained in the buffered acetolysis of **1-OTs** and, as previously pointed out, [1] can be accounted for by the steric conditions favouring the attack of the solvent on the *exo* side of the ion **4**.

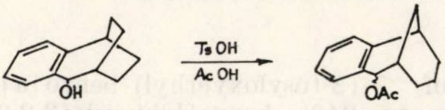

2-OH 3-OAc

Thus, the acetates **3-OAc** are thermodynamically more stable than the acetate **2-OAc**.

The greater stability of the [3.3.1] system was also inferred from the rearrangement of the hydrocarbon **2 (X = H)** by AlCl$_3$, leading practically only to **3 (X = H)**. As reported by Roberts, [2] the dibenzo analog **9** gives rise, under the same conditions, to 77% 2,3 : 6,7-dibenzobicyclo[3.3.1]nona-2,6-diene. The driving force of the [3.2.2] → [3.3.1] rearrangement is in both cases release of strain. [2,3]

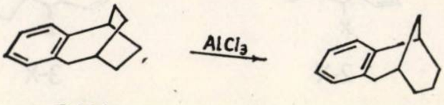

2,X=H 3,X=H

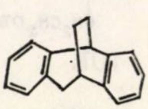

9

---

[2] Chow-Eng Low and R. M. Roberts, *J. Org. Chem.*, **38**, 1909 (1973).

[3] Benzo[*b*]bicyclo [3.3.1] nonene is less strained not only than benzo[*b*]bicyclo[3.2.2]nonene but also than bicyclo [3.3.1] nonane itself. Indeed, it is considered that introduction of a double bond in position 3 of bicyclo[3.3.1]nonane removes the severe nonbonded interaction of the hydrogen atoms at C$_3$ and C$_7$.[4]

[4] W. A. Brown, G. Eglington, J. Martin, W. Parker and G. A. Sim, *Proc. Chem. Soc.*, **1964**, 57 ; E. L. Eliel, "Stereochemistry of Carbon Compounds", 2nd ed., Mc Graw-Hill. New York, 1966, p. 295.

The rearrangement **2** → **3** may be conceived in many ways. The following mechanistic scheme may be favoured :

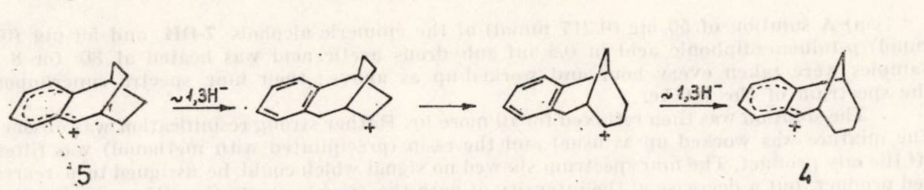

Each of the two 1,3-hydride shifts could be replaced by two successive 1,2-shifts but this would imply the intervention of two bridgehead, less stable intermediates. 1,3-Type hydrogen migrations were proved to proceed in favourable circumstances.[5] Besides, such shifts are with these systems quite probable.[6] Even the formation of the benzo[*b*]bicyclo[3.3.1]nonene **(3, X = H)** by dehydration (in acidic conditions) of 1-benzylcyclohexanol very likely proceeds *via* such migrations.[9]

The above experiments indicate that the benzylic ion **5**, and not **6**, is the intermediate responsible for the products obtained in the acetolysis of **1-OTs**. Competition of solvent capture of the ion **5** with its multistep rearrangement to the ion **4** gives rise to the acetates **2-OAc** and **3-OAc** observed in the buffered acetolysis.

EXPERIMENTAL

Behaviour of benzo[b]- or benzo[f]bicyclo[3.2.2]nonene acetates **(2-OAc** *or* **7-OAc)** *in buffered acetic solution*

A solution of 40 mg (0.174 mmol) acetate **2-OAc** (or **7-OAc**) and 21.4 mg (0.26 mmol) anhydrous sodium acetate in 5 ml glacial acetic acid was refluxed for 48 hr. The mixture was then neutralized with $NaHCO_3$ and extracted with ether. After washing, drying over $MgSO_4$ and evaporation, the extracts yielded 30 mg oil, which in each case showed the same nmr spectrum as the starting material.[1]

---

[5] J. D. Roberts, C. C. Lee and W. H. Saunders, Jr., *J. Amer. Chem. Soc.*, **76**, 4501 (1954); K. Humski, S. Borcic and D. E. Sunko, *Croat. Chem. Acta*, **37**, 3 (1965).

[6] Reutov and co-workers[7] have evidenced the occurrence of 1,3-hydride shifts in the cyclohexyl system. Furthermore, it is known[8] that if the stereochemistry of the cation is such that the migration terminus and origin are closely constrained higher-order shifts might be important.

[7] O. A. Reutov, *Pure Appl. Chem.*, **7**, 203 (1963); Yu. G. Bundel, V. A. Savin, A. A. Lubovich and O. A. Reutov, *Doklady. Akad. Nauk S.S.S.R.* **165**, 1078 (1965), *Proc. Acad. Sci. U.S.S.R. Chem. Sect.* (English Transl.), **165**, 1180 (1965).

[8] J. L. Fry and G. J. Karabatsos in "Carbonium Ions", Vol. II, Ed. G. A. Olah and P. von R. Schleyer, Interscience Publishers, New York, 1970, p. 555.

[9] J. W. Cook and C. L. Hewett, *J. Chem. Soc.*, **1936**, 62.

Behaviour of the benzo[f]bicyclo[3.2.2]nonen-2-ols **(7-OH)** *in acidic medium*

a) A solution of 50 mg (0.217 mmol) of the epimeric alcohols **7-OH** and 50 mg (0.29 mmol) *p*-toluenesulphonic acid in 0.4 ml anhydrous acetic acid was heated at 80° for 8 hr. Samples were taken every hour and worked-up as above; their nmr spectra superimposed the spectrum of the **7-OAc**.

The solution was then refluxed for 10 more hr. Rather strong resinification was observed. The mixture was worked up as usual and the resin (precipitated with methanol) was filtered off the oily product. The nmr spectrum showed no signal which could be assigned to a rearranged product, but a decrease of the intensity of both the signals due to the CH_3 groups and the proton adjacent to OAc was evident, indicating that some elimination had occurred.

b) The nmr spectrum of 30 mg **7-OH** in 0.2 ml trifluoroacetic acid was recorded, then the solution was allowed to stand at room temperature. After 4 hr the trifluoroacetate **7-OCOCF$_3$** was formed (the signal assigned to the proton adjacent to the functional group shifted from 4.0 ppm to 5.16 ppm). After 110 more hours at room temperature and heating for 35 hr at 70—75° the same nmr spectrum was obtained.

Buffered acetolysis of benzo[f]bicyclo[3.2.2]nonen-2-yl tosylates **(7-OTs)**

A solution of the crude epimeric tosylates **7-OTs** (prepared from **7-OH** and *p*-TsCl in pyridine in the usual manner) (145 mg; 0.42 mmol) and anhydrous sodium acetate (50 mg; 0.61 mmol) in 3 ml glacial acetic acid was heated under reflux for 25 hr. The usual work-up afforded 77.4 mg product whose ir and nmr spectra matched those of the authentic **7-OAc**.

Rearrangement of the system 2 in acidic medium

a) *Rearrangement of benzo[b]bicyclo[3.2.2]nonen-4-ol* **(2-OH)**

A solution of 0.15 g (0.8 mmol) **2-OH** and 0.15 g (0.87 mmol) *p*-TsOH in 3 ml acetic acid was heated at 95° for 2 hr. The work-up yielded 0.15 g of an oily product which was analysed by vpc; 64.8% *exo*-**3-OAc**, 20.1% *endo*-**3-OAc** and 5.5% unrearranged **2-OAc** were identified by means of authentic samples.

If an acetic solution of **2-OH**, containing *p*-TsOH, was refluxed for 5 hr, only resinified material was recovered.

b) *Rearrangement of benzo[b]bicyclo[3.2.2]nonene* **(2, X = H)** [10]

In the $AlCl_3$ catalyzed reaction of **2, X = H** the same conditions as reported by Roberts [2] were employed. After 2 hr at room temperature the reaction mixture was worked up showing the composition (vpc): 56.8% **3, X = H,** 0.05% **2, X = H,** 9.3% and 23.8% two unidentified components, the remainder being 12 other smaller components. The retention times and the aspect of the peaks corresponding to the 9.3% and 23.8% components indicate higher molecular weights.

---

[10] I. Drăguţan and E. Ciorănescu, *Org. Prep. Proced. Int.*, **7**, 75 (1975).

Revue Roumaine de Chimie, 22, 4, 611–617 (1977)

Herrn Professor Dr. Coriolan Drăgulescu
zum 70. Geburtstag gewidmet

EINE DEUTUNG DES EINFLUSSES DER ARBEITSBEDINGUNGEN AUF DIE STROMAUSBEUTE BEI DER ELEKTROLYTISCHEN ABSCHEIDUNG VON METALLISCHEN PULVERN

GH. FACSKÓ, C. RADOVAN und C. DAMINESCU
Polytechnisches Institut ,,T. Vuia'' Timişoara, Str. Bocşa nr. 6

Eingegangen am 11. September, 1976

In der Arbeit wird der Einfluß der Stromdichte, der Temperatur und der Metallkonzentration im Bade auf die Stromausbeute bei der Herstellung von Nickelpulver dargestellt. Zwecks Deutung der festgestellten Zusammenhänge wird ein Modell dargestellt, das die Festlegung gewisser Gesetzmäßigkeiten, die in gutem Einklang mit unseren Ergebnissen sind, erlaubt. Die festgesetzten Gesetzmäßigkeiten können für alle pulverförmigen Niederschläge von Metallen, die weniger edel als Wasserstoff sind, verallgemeinert werden.

In der gegenwärtigen Arbeit wurde der Einfluß der Arbeitsparameter auf die Stromausbeute bei der elektrolytischen Herstellung von Nickelpulver, sowie die Erklärung der erhaltenen Gesetzmäßigkeiten verfolgt. Die festgestellten Abhängigkeiten können aber für alle pulverförmigen Niederschläge der Metalle, die weniger edel als Wasserstoff sind, verallgemeinert werden.

Die Versuche wurden in einer 800 ml Elektrolysezelle durchgeführt, die mit einer Serpentine zwecks Termostatierung versehen war. Es wurden kombinierte Nickel-Graphit-Anoden, die zwecks Verhinderung der Verunreinigung des Nickel-Pulvers mit anodischem Schlamm in Säcke gelagert wurden und Kathoden aus glänzendem 0,5 mm starkem V2A Stahlblech verwendet. Es wurden von Drozdov[1] empfohlene Elektrolytlösungen, aufgrund von Nickelsulphat mit Zugaben von NH_4Cl (40 g/l) und NaCl (70 g/l) bei pH-Werten von 7-7,2, verwendet, wobei der Durchfluß einer Elektrizitätsmenge von 5 Ah gewährleistet wurde. Von den von uns untersuchten Arbeitsparametern wird in gegenwärtiger Arbeit nur der Einfluß der Nickelkonzentration im Bade, der Stromdichte und der Temperatur dargestellt. Es wurde bei Konzentrationen von 11, 20 und 40 g/l Nickel, bei Temperaturen von 24, 40 und 60° und Stromdichten von 1000–8000 A/m² gearbeitet.

---

[1] B. V. Drozdov, *Zhur. priklad. Khim.*, **38**, 45 (1955).

Unsere Feststellungen hinsichtlich der Niederschläge haben gezeigt, daß die pulverförmigen Niederschläge bei einer Konzentration von 11g/l Nickel und einer Temperatur von 24°, d.h. unter den für das Auftreten einer betonten Transportüberspannung günstigen Bedingungen, erhalten wurden. Mit dem Anstieg der Nickelkonzentration und der Temperatur ist eine Neigung zur Betonung der Agglomerierung des Pulvers, sowie zur Kompaktisierung des Niederschlages festzustellen, der hierdurch hart und von der Kathode schwer zu entfernen wird. So z.B. beginnt der Bereich der Stromdichten, die zu pulverförmigen Niederschlägen führen, bei 40 g/l Nickel und 24° erst über 5000 A/m² wobei, bei gleicher Temperatur und 11 g/l Nickel dieser Bereich schon bei 1000–1500A/m² anfängt. Unter den für die Bildung von pulverförmigen Niederschlägen besonders günstigen Bedingungen ist eine beonte Stabilität des Systems festzustellen. Mit dem Anstieg der Konzentration und der

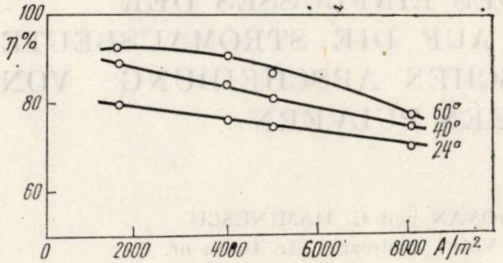

Abb. 1 – Stromausbeute als Funktion der Stromdichte bei der elektrolytischen Herstellung von Nickelpulver; Badzusammensetzung: Nickel 11 g/l; NH_4Cl 40 g/l; NaCl 70 g/l.

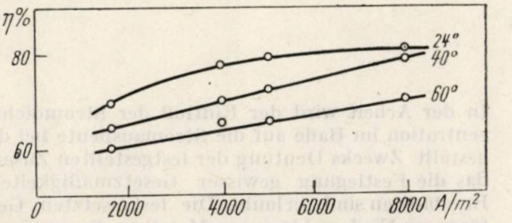

Abb. 2. – Stromausbeute als Funktion der Stromdichte bei der elektrolytischen Herstellung von Nickelpulver; Badzusammensetzung: Nickel 20 g/l; NH_4Cl 40g/l; NaCl 70 g/l.

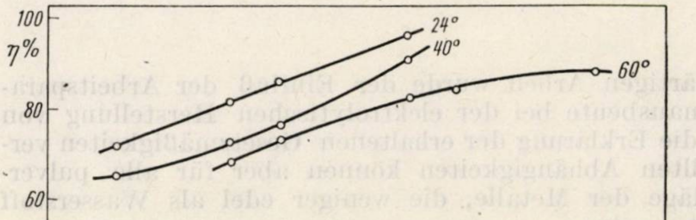

Abb. 3. – Stromausbeute als Funktion der Stromdichte bei der elektrolytischen Herstellung von Nickelpulver; Badzusammensetzung: Nickel 40 g/l; NH_4Cl 40g/l; NaCl 70 g/l.

Temperatur neigen die anfänglich pulverförmigen Niederschläge, falls sie von der Kathode nicht entfernt werden, zur Bildung von kompakten bis zu dendritischen Niederschlägen.

Ebenfalls konnte festgestellt werden, daß die kathodischen Stromausbeuten von der Stromdichte, der Nickelkonzentration und der Temperatur auf eine Art abhängen, die auf den esten Blick keiner klaren Gesetzmäßigkeit entspricht.

Die Abhängigkeit der kathodischen Stromausbeuten von der Stromdichte, bei Nickelkonzentrationen von 11, 20 und 40 g/l und Temperaturen von 24, 40 und 60° wird in folgenden Abbildungen wiedergeben.

Wie ersichtlich nehmen bei 11 g/l Nickel die Stromausbeuten mit dem Anstieg der Stromdichte ab, wobei sie beispielweise bei 24° zwischen 79%, bei 1500 A/m^2, und 68,5%, bei 8000 A/m^2, betragen. Ebenfalls konnte ein Anstieg der Stromausbeuten mit dem Anstieg der Temperatur festgestellt werden.

Im Gegensatz, konnte bei höheren Nickelkonzentrationen, z.B. bei 20 g/l oder noch augenscheinlicher bei noch höheren Konzentrationen, z.B. bei 40 g/l, ein Anstieg der Stromausbeuten mit dem Anstieg der Stromdichte und eine Abnahme mit dem Anstieg der Temperatur festgestellt werden.

DISKUSSION DER ERGEBNISSE

Nickel, ein Metall, das sich in der Reihe der Standardpotentiale nach Wasserstoff befindet, mit ε° gleich $-0{,}25$ V,[2] scheidet sich an der Kathode gleichzeitig mit der Entwicklung von Wasserstoff ab. Dies führt zu kathodischen Stromausbeuten, die kleiner als 100% sind. In den Abbildungen 4 a und b wird der allgemeine Fall, der gleichzeitigen Abscheidung eines beliebigen Metalls mit Wasserstoff wiedergeben, wobei das Gleichgewichtspotential des Metalls negativer, als das des Wasserstoffes ist und die Metallkonzentration der Lösung zwei verschiedene, hypothetische Werte aufweist. Beginnend mit dem Potential $\varepsilon_{\mathrm{Me}}$ findet die gleichzeitige Abscheidung statt, wobei Polarisationskurve 3 das Resultat der Addition von Kurve 1, für das Metall und 2, für Wasserstoff, darstellt.

In den Abbildungen werden auf den Ordonaten einige beliebige Stromdichten bezeichnet, sowie die entsprechenden Stromausbeuten, aus dem Abstand zwischen der Abszisse und den beiden Polarisationskurven berechnet. Wie ersichtlich, geht die Stromausbeute mit der Stromdichte durch ein Maximum, bei einer Stromdichte, die wir als kritisch i(kr) bezeichnen. Dieses Maximum fällt mit dem Beginn der Grenzstromdichte für das Metall zusammen, wobei sein Wert und seine Lage von der Form und der reziproken Lage der beiden Polarisationskurven 1 und 2 (Abb. 4) abhängt. So z.B bewirkt der Anstieg der Metallkonzentration im Bade einen starken Anstieg der Grenzstromdichte der Polarisationskurve des Metalls. 1, ohne die der Entladung des Wasserstoffes entsprechende Kurve 2 zu beeinflussen, wodurch ein bedeutender Anstieg der kritischen Stromstärke und der maximalen Stromausbeute bewirkt wird. Wie aus Abb. 4 a ersichtlich, beträgt z.B. bei einer Konzentration c_1 die aus den Abständen zwischen der Abszisse und den beiden Polarisationskurven berechneten Stromausbeuten, einen Maximalwert von cca. 66,6 %, bei einer konventionellen Stromdichte von 66 Einheiten, wobei bei einer doppelten Konzentration, c_2, (Abb. 4b) die maximale Stromausbeute cca. 80 % beträgt, bei einer konventionellen Stromdichte von 105 Einheiten.

---

[2] V. Latimer, ,,Okislitelinoe sostoyana elementov i ikh potentsialy v vodnykh rastvorakh'', Moskva. Inostr. Lit., 1954, S. 206.

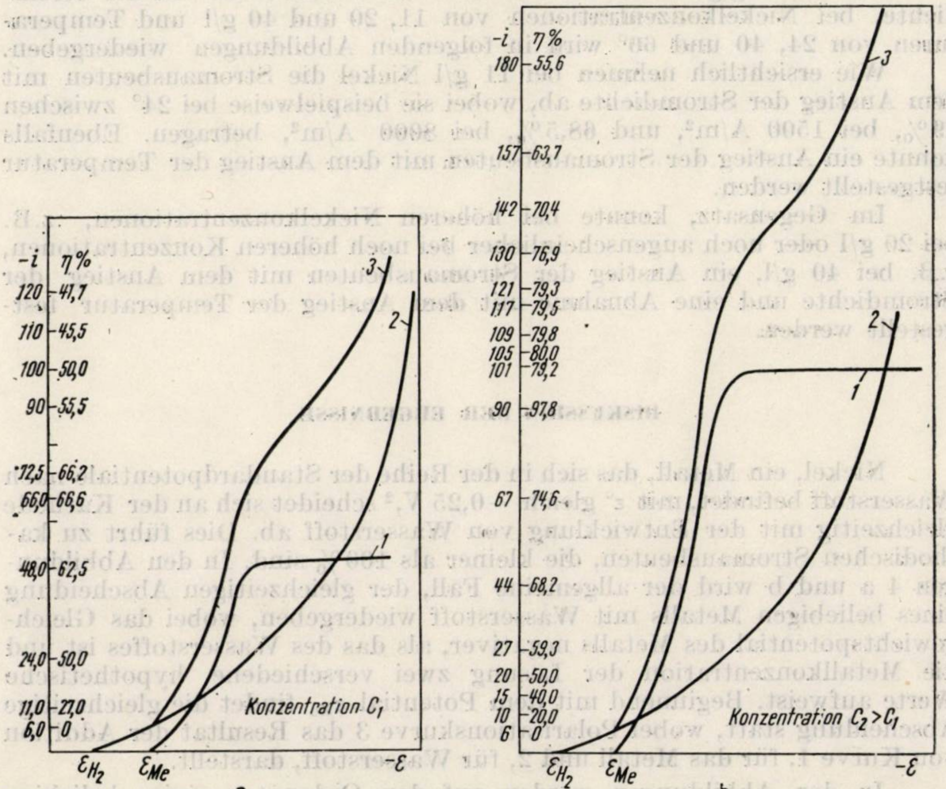

Abb. 4. — Polarisationskurven, für das Metall (1), für Wasserstoff (2) und deren Resultante (3), im Falle gleichzeitiger Abscheidung eines Metalls mit Wasserstoff, bei zwei verschiedenen Konzentrationen.

Abb. 5 wiedergibt die Abhängikeit der Stromausbeute von der Stromdichte, die an Hand angenommener, wie in den Abbildungen 4 a und b wiedergegebenen Polarisationskurven berechnet wurden.

Der Anstieg der Temperatur beeinflußt beide Polarisationskurven, wobei eine Abnahme der Überspannung beider Prozesse und ein bedeutender Anstieg der kritischen Stromstärke zu verzeichnen ist.

Abbildung 6 a und b wiedergibt die Polarisationskurven des Metalls (1), des Wasserstoffes (2) und deren Resultante (3) im Falle der gleichzeitigen Abscheidungen eines Metalls mit Wasserstoff bei zwei verschie-

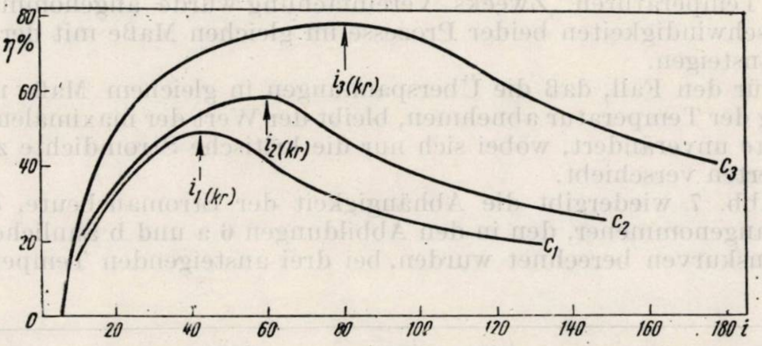

Abb. 5. — Die Abhängigkeit der Stromausbeute von der Stromdichte, bei drei verschiedenen Konzentrationen, im Falle gleichzeitiger Abscheidung eines Metalls mit Wasserstoff.

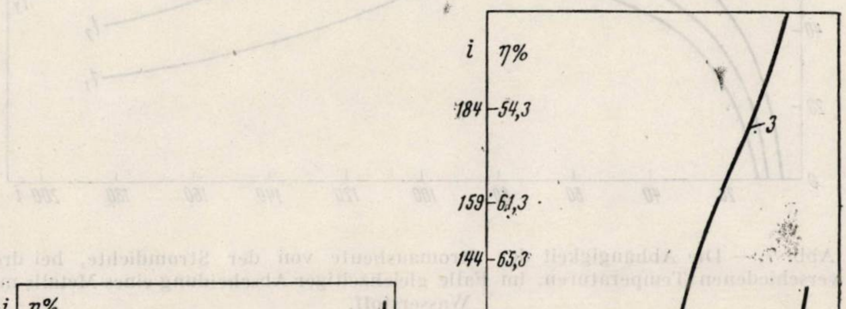

Abb. 6. — Polarisationskurven, für das Metall (1), für Wasserstoff (2) und deren Resultante (3) im Falle gleichzeitiger Abscheidung eines Metalls mit Wasserstoff, bei zwei verschiedenen Temperaturen.

denen Temperaturen. Zwecks Vereinfachung wurde angenommen, daß die Geschwindigkeiten beider Prozesse im gleichen Maße mit der Temperatur ansteigen.

Für den Fall, daß die Überspannungen in gleichem Maße mit dem Anstieg der Temperatur abnehmen, bleibt der Wert der maximalen Stromausbeute unverändert, wobei sich nur die kritische Stromdichte zu höheren Werten verschiebt.

Abb. 7 wiedergibt die Abhängigkeit der Stromausbeute, die aufgrund angenommener, den in den Abbildungen 6 a und b ähnlichen Polarisatilonskurven berechnet wurden, bei drei ansteigenden Temperaturen.

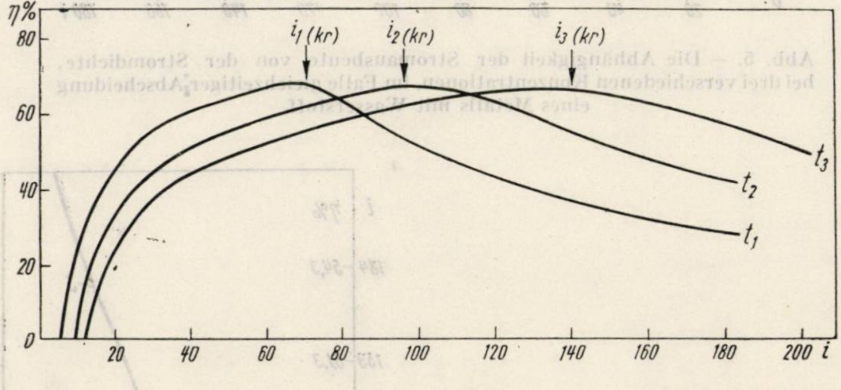

Abb. 7. — Die Abhängigkeit der Stromausbeute von der Stromdichte, bei drei verschiedenen Temperaturen, im Falle gleichzeitiger Abscheidung eines Metalls mit Wasserstoff.

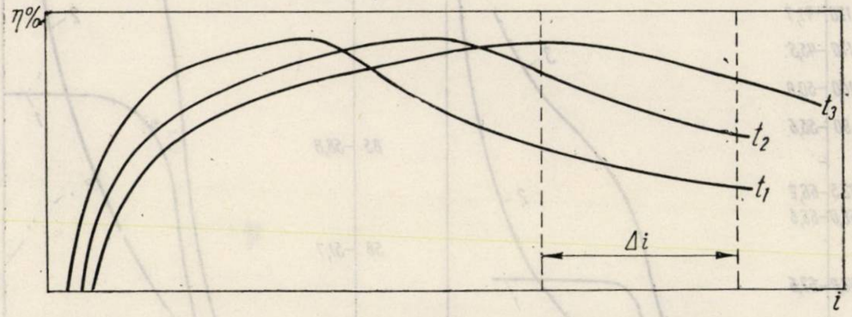

Abb. 8. — Zusammenhang zwischen dem Wert der Stromausbeute und der Stromdichte, in einem Intervall Δi, bei kleinen Metallkonzentrationen im Bad.

Falls der Einfluß der Temperatur ungleich ist, nimmt die maximale Stromausbeute zu oder ab, bedingt durch das Überwiegen der Abnahme der Nickelüberspannung oder die des Wasserstoffes. Die Form der Kurven bleibt aber unverändert.

Angesichts obiger Erwägungen können die von uns festgestellten experimentellen Abhängigkeiten erklärt werden, die auf den ersten Blick vollkommen willkürlich erschienen.

Ein klarer Unterschied muß gemacht werden, zwischen den Situationen, in denen wir uns oberhalb der kritischen Stromdichten i(kr) und denen, in welchen wir uns unterhalb dieser Werte befinden. Im ersten Fall nehmen die Stromausbeuten mit dem Anstieg der Stromdichte ab, im zweiten Fall hingegen zu. Für den Fall, daß wir uns in einem Gebiet befinden, das den Wert der kritischen Stromstärke enthält, weist die Kurve ein Maximum auf.

Abb. 8 wiedergibt den Fall kleiner Nickelkonzentrationen, wobei das Gebiet der untersuchten Stromdichten Δi weit oberhalb der kritischen Stromdichten lag. Wie aus derAbbildung ersichtlich, nimmt unter diesen Arbeitsbedingungen die Stromausbeute mit dem Anstieg der Stromdichte und der Abnahme der Temperatur erwartungsgemäß ab.

Zum Vergleich können unsere experimentellen Ergebnisse dienen, die in einem 11 g/l Nickel enthaltendem Bad erhalten wurden (Abb. 1). Wie ersichtlich, stimmt die Form der Kurven mit der erwartungsgemäßen überein.

Im Falle höherer Nickelkonzentrationen im Bad und höherer Temperaturen, wenn das System weniger stabil ist, wobei eine Neigung zur Betonung der Agglomerierung des Pulvers, sowie zur Kompaktisierung oder sogar zum Übergang zu kompakten, dendritischen Niederschlägen festzustellen ist, befinden wir uns in einem Stromdichtegebiet Δi, das sich unterhalb der kritischen Stromdichten oder eventuell in der Nähe dieses Wertes befindet.

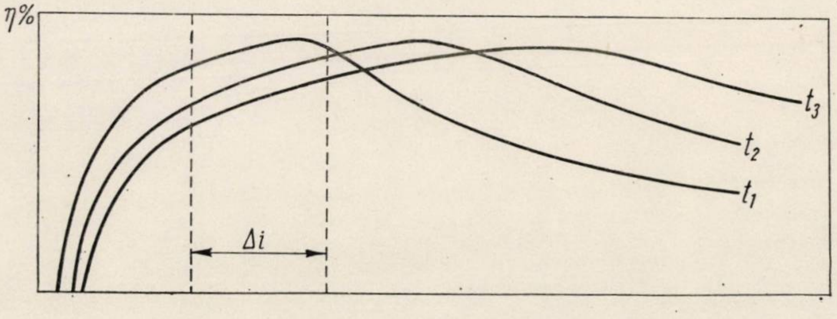

Abb. 9. — Zusammenhang zwischen, dem Wert der Stromausbeute und der Stromdichte, in einem Intervall Δi, bei hohen Metallkonzentrationen im Bad.

Abb. 9 wiedergibt diese Lage. Erwartungsgemäß bleibt die Form der Kurven dieselbe wie bei niedrigen Nickelkonzentrationen, wobei sich nur die kritischen Stromdichten zu höheren Werten verschieben, was einer Verschiebung des untersuchten Stromdichtegebietes Δi näher zum Koordonatenursprung gleichkommt.

Wie aus der Abbildung ersichtlich, ist unter diesen Arbeitsbedingungen ein Anstieg der Stromausbeute mit dem Anstieg der Stromdichte und der Abnahme der Temperatur zu erwarten.

Zwecks Vergleich können unsere experimentellen Ergebnisse, die in einem 20 g/l Nickel enthaltendem Bad erhalten wurden (Abb. 2), dienen. Wie ersichtlich, entspricht die Form der Kurven der erwartungsgemäßen.

Revue Roumaine de Chimie, 22, 4, 619–624 (1977)

Herrn Professor Dr. Coriolan Drăgulescu
zum 70. Geburtstag gewidmet.

LADUNGSDICHTEVERÄNDERUNGEN DURCH DONATOR-ACCEPTOR-WECHSELWIRKUNGEN

VIKTOR GUTMANN
Institut für Anorganische Chemie der Technischen Universität Wien, Getreidemarkt 9, A—1060 Wien

Sowohl die Überführung von Elektronenladung vom Donator zum Acceptor als auch Polarisationseffekte bedingen eine Verringerung der Elektronendichte am Acceptoratom („Ladungsmitführungseffekt") und eine Erhöhung der Elektronendichte am Donatoratom („Aufstaueffekt"). Letzterer ist besonders groß bei der Koordination an harten Metallionen, wo der Ladungsübergang wegen Nichteintreten des Ladungsmitführungseffektes im Acceptor relativ klein ist. Daher sind bei Kation-Ligand-Wechselwirkungen die elektrostatischen Wechselwirkungsanteile entsprechend hoch.

I. ALLGEMEINES

Jede Donator-Acceptor Wechselwirkung führt zu Ladungsumverteilungen als Folge gegenseitiger Polarisationswechselwirkungen einerseits und durch Ladungsübergang andererseits.[1] Diese beiden Effekte die voneinander nicht zu trennen sind, führen zu strukturellen Veränderungen[1–4]: Die der Donor-Acceptor-Wechselwirkung unmittelbar benachbarten σ-Bindungen werden in ihrer Polarität erhöht,[2,3] d.h. die internuklearen Abstände werden größer,[5] ihre Heterolysierbarkeit erleichtert und die chemischen Eigenschaften entsprechend verändert:

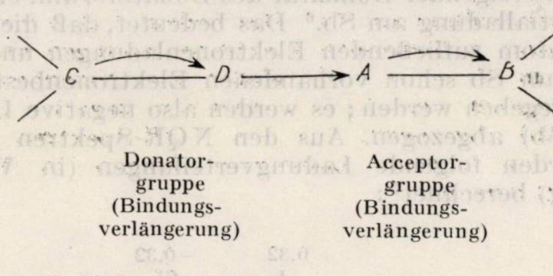
C
D
A
B
Donatorgruppe (Bindungsverlängerung)
Acceptorgruppe (Bindungsverlängerung)

---

[1] R. Paetzold, *Z. Chem.*, **15**, 377 (1975).

[2] V. Gutmann, *Coord. Chem. Revs.*, **15**, 207 (1975).

[3] V. Gutmann, *Coord. Chem. Revs.*, **18**, 225 (1976).

[4] V. Gutmann, *Structure and Bonding*, **15**, 141 (1973).

[5] I. Lindqvist, „Inorganic Adduct Molecules of Oxo Compounds", Springer Verlag, Berlin, 1963.

Die Ladungsumverteilungen erstrecken sich auf den Gesamtbereich der Moleküle, bzw. des Komplexes. [2] In der Regel werden diejenigen Bindungen verlängert, an denen der Elektronenzug von elektropositiveren zum elektronegativeren Partner erfolgt und diejenigen gekürzt, an denen dieser in entgegengesetzter Richtung erfolgt, z.B. :

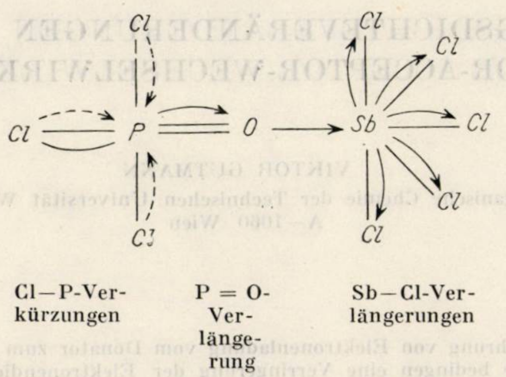

Die Pfeile geben die Richtung des Elektronenzuges an, die ausgezogenen symbolisieren Bindungsverlängerung, die strichlierten Bindungsverkürzung.

2. LADUNGSVERÄNDERUNGEN IM ACCEPTORBEREICH

Während über die Veränderung der Bindungsabstände und der damit verknüpften spektroskopischen Eigenschaften, und ihre Beziehungen zum veränderten chemischen Verhalten, reichlich Material vorliegt, [1–4] sind keine Regeln für die Veränderungen der Partialladungen der Kerne formuliert worden.

Die ESCA-Untersuchung von mit verschiedenen Donatoren komplexiertem $SbCl_5$ zeigt ein Ansteigen der Elektronenbindungsenergie der 3 $d_{5/2}$-Orbitale mit steigender Donizität des Donators, d.h. einer Erhöhung der positiven Partialladung am Sb.[6] Das bedeutet, daß die vom Donator an das Acceptoratom zufließenden Elektronenladungen unter Mitnahme eines Teiles des am Sb schon vorhandenen Elektronenbestandes an die Cl-Atome weitergegeben werden ; es werden also negative Ladungen vom Akzeptoratom (Sb) abgezogen. Aus den NQR-Spektren von JCl und C_5H_5N-JCl wurden folgende Ladungverteilungen (in Vielfachen der Elektronenladung) berechnet[7] :

$$\begin{array}{ccccc} & & +0{,}32 & & -0{,}32 \\ & & \mathrm{J} & \text{———} & \mathrm{Cl} \\ +0{,}26 & & +0{,}35 & & -0{,}61 \\ \mathrm{C_6H_5N} & \longrightarrow & \mathrm{J} & \text{———} & \mathrm{Cl} \end{array}$$

---

[6] K. Burger und E. Fluck, *Inorg. Nucl. Chem. Letter*, **10**, 171 (1974).

[7] G. A. Bowmaker und S. Hacobian, *J. Austr. Chem.*, **21**, 551 (1968).

Demnach werden 0,26 Ladungseinheiten zwischen Donator und Acceptor übertragen, wobei durch „Mitführung“ von 0,03 Ladungseinheiten vom Acceptoratom (Jodatom) das Acceptorendatom, nämlich das Chloratom einen Ladungszuwachs von 0,29 Ladungseinheiten erfährt. Ebenso zeigen die Ergebnisse von ^{129}J-Mößbauer Untersuchungen am Hexamethylentetramin-Jod-Komplex, daß durch die Komplexierung die Ladung des Brückenjodatoms verringert und diejenige des endständigen Jodatoms erhöht wird.[8]

Die experimentellen Ergebnisse finden Bestätigung in den Ergebnissen quantenchemischer Berechnungen. Bei der Bildung von Ammoniumchlorid aus Ammoniak und Chlorwasserstoff werden alle Wasserstoffatome positiver und sowohl das Stickstoffatom, als auch Chloratom negativer[9]:

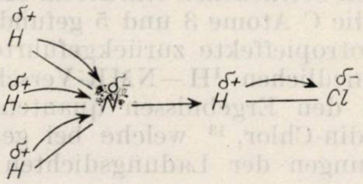

Die Verminderung der positiven Partialladung am Acceptoratom zeigt die Berechnung der Reaktion von Ammoniak mit Fluor,[10] sowie von zu Wasserstoffbrückenbindungen führenden Wechselwirkungen, z.B. die Assoziation von zwei Wassermolekülen, wofür folgende Ladungsveränderungen errechnet wurden[11]:

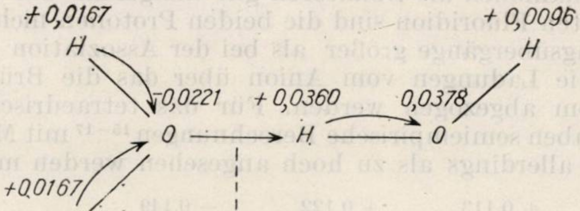

Die Erscheinung der Verringerung der Elektronendichte am Acceptoratom selbst ist für die Erhöhung der Bindungspolarität der Acceptorgruppe entscheidend und möge als ”Mitführungseffekt“ oder „Ausspüleffekt“ bezeichnet werden, da ursprünglich am Acceptoratom vorhandene negative Ladung von diesem ”ausgespült“ wird.

---

[8] S. Ichiba, H. Sakai und H. Negita, *J. Chem. Phys.* **54**, 1627 (1971).

[9] E. Clementi, *J. Chem. Phys.*, **46**, 3851 (1967).

[10] L. A. Carreira, W. B. Person, *J. Amer. Chem. Soc.*, **94**, 1485 (1972).

[11] D. Hankins J. W. Moskowitz und F. H. Stillinger, *J. Chem. Phys.*, **53**, 4544 (1970).

3. LADUNGSVERÄNDERUNGEN IM DONATORBEREICH

Die Ladungsumverteilung innerhalb des Donatormoleküls kann den schon angeführten Ergebnissen entnommen werden. Die Abgabe von Elektronenladung vom Donatoratom zum Acceptor wird dadurch kompensiert, daß die Elektronendichten in anderen Molekülbereichen (vor allem an den Endatomen der Donator Komponente verringert werden. In der Regel führt dies zur „Aufstauung“ von Elektronenladung am Donatoratom. Ein solcher „Aufstaueffekt“ am Donatoratom wurde z.B. für die Reaktion von NH_3 mit HCl[9] und die Dimerisation von Wassermolekülen[11] errechnet. Innerhalb des Donormoleküls Pyridin kann die Ladungsumverteilung aus ^{13}C NMR-Messungen im $C_5H_5N-J_2$-Komplex abgeleitet werden.[12] Dabei werden Verschiebungen zu niedrigerem Feld für die C-Atome 2 und 6 und in beträchtlich stärkerem Maße für C-Atom 4, sowie zu höherem Feld für die C-Atome 3 und 5 gefunden. Dieses ursprünglich auf magnetische Anisotropieffekte zurückgeführte Ergebnis spiegelt sich auch in den unterschiedlichen ^1H-NMR-Verschiebungen. Dies ist in Übereinstimmung mit den Ergebnissen quantenchemischer Berechnungen am System Pyridin-Chlor,[13] welche bei geringer Ladungsübertragung folgende Änderungen der Ladungsdichten durch Komplexierung ergab[13]:

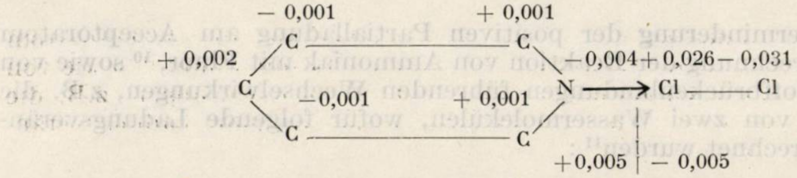

Für Atomanionen als Donatoren gilt sinngemäß das Gleiche: Im hydratisierten Fluoridion sind die beiden Protonen nicht äquivalent[14] und die Ladungsübergänge größer als bei der Assoziation von HF-Molekülen wobei die Ladungen vom Anion über das die Brücken bildende Wasserstoffatom abgezogen werden. Für das tetraedrisch koordinierte Fluoridion ergaben semiempirische Berechnungen[15–17] mit Modellcharakter Werte, welche allerdings als zu hoch angesehen werden müssen[18]:

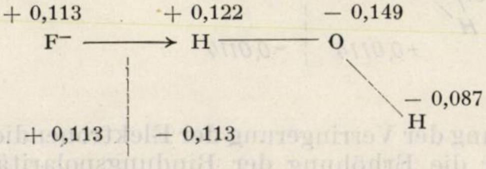

Das Eintreten des Mitführungseffekts am Acceptoratom kann sowohl diesen, als auch den in Tab. 1 angeführten Rechenergebnissen entnommen werden:

---

[12] J. P. Larkindale und D. J. Simkin, *J. Chem. Phys.*, **55**, 5048 (1971).

[13] J. La Grange, L. Leroy und G. Louterman-Leloup, Private Communication.

[14] H. G. Hertz und C. Raedle, *Ber. Bunsengellschaft Phys. Chem.*, **77**, 521 (1973).

[15] P. Schuster, *Int. J. Quantum Chem.*, **3**, 851 (1969).

[16] P. Schuster, *Theoret. Chim. Acta*, **19**, 212 (1970).

[17] P. Schuster, W. Jakubetz und W. Marius, *Topics in Current Chem.*, **60**, 1 (1975).

[18] P. Russegger, H. Lischka und P. Schuster, *Theoret. Chim. Acta*. **24**, 191 (1972).

Tabelle 1

Änderungen der Nettoladungen an Donor und Acceptoratomen durch Komplexbildung [13,19–21]

Komplex	„Aufstaueffekt" am Donor Atom	„Mitführungseffekt" am Acceptor Atom	Ladungsüberführung
$H_3N - Cl_2$	$-0{,}003$	$+0{,}30$	0,008
$HCN - Cl_2$	$-0{,}002$	$+0{,}018$	0,001
$H_2O - Cl_2$	$-0{,}369$	$+0{,}023$	0,003
$H_2S - Cl_2$	$-0{,}001$	$+0{,}007$	0,005
$H_2CO - Cl_2$	$-0{,}191$	$+0{,}014$	0,001

4. KOORDINATION AN METALLIONEN

An einem harten Metallkation kann der vom Donator erhaltene Zuwachs der Elektronendichte nicht weitergegeben werden. Daher kommt es durch Wechselwirkungen mit Donatoren zu einer Bremsung des Elektronenüberganges zwischen Donator- und Acceptor. Der Ladungsübergang bleibt gering.[22] Durch die Aufstaueffekte an den Donatoratomen werden die elektrostatischen Anteile der Donator-Acceptorwechselwirkung entsprechend erhöht.

Die Veränderung der internuklearen Abstände bei der Wechselwirkung von Li^+ und Ameisensäure im Molverhältnis 1 : 4 wurde aus ramanspektrographischen Ergebnissen abgeleitet[23]: die $C=O$ und die $O-H$-Bindung werden gedehnt und die $C-O$-Bindung gekürzt. Ab initio-Berechnungen erbrachten folgende Veränderungen der Nettoladungen[24]:

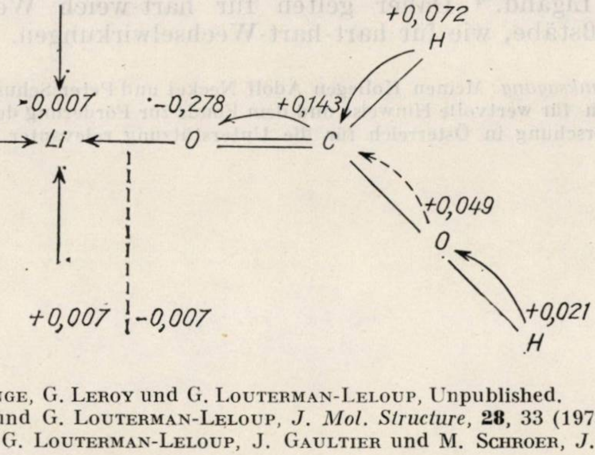

---

[19] J. La Grange, G. Leroy und G. Louterman-Leloup, Unpublished.

[20] G. Leroy und G. Louterman-Leloup, *J. Mol. Structure*, **28**, 33 (1973).

[21] G. Leroy, G. Louterman-Leloup, J. Gaultier und M. Schroer, *J. Mol. Structur*, **25**, 205 (1975).

[22] P. Schuster, W. Marius, A. Pullman und H. Berthod, *Theor. Chim. Acta*, **40**, 323 (1975).

[23] B. M. Rode, *Chem. Phys. Letters*, **32**, 38 (1975).

[24] B. M. Rode, M. Breuss und P. Schuster, *Chem. Phys. Letters*, **32**, 34 (1975).

Dem geringen Ladungsübergang zwischen Liganden und Kation steht ein relativ hoher Zuwachs der Ladungsdichte am Donatoratom gegenüber. Ähnliche Verhältnisse liegen in anderen Solvaten vor (Tab. 2).

Tabelle 2

Änderung der Ladungsdichten (Mulliken-Populationen) an C- und O-Atomen der C = O-Gruppe durch Koordination an Metallkationen[25]

Kation	Ligand	Δq_0	Δq_C
Li^+	HCHO	$-0,293$	$+0,117$
Li^+	HCOOH	$-0,239$	$+0,137$
Li^+	DMF	$-0,284$	$+0,113$
Na^+	HCHO	$-0,213$	$+0,095$
Be^{2+}	HCHO	$-0,707$	$+0,272$
Be^{2+}	DMF	$-0,700$	$+0,243$

Ist das Metallion mit teilweise besetzten d-Orbitalen ausgestattet, so kann der Ladungsübergang vom Donator zum Acceptor die Funktion des letzteren als π-Elektronendonator hervorrufen. Hiedurch wird die Erhöhung der Elektronendichte am „weichen“ Acceptor durch back-donation überkompensiert und dadurch ein „Ausspüleffekt“ induziert. Voraussetzung zu dieser Funktionsausübung ist aber neben der erwähnten Fähigkeit des Acceptors die Aufnahmebereitschaft des π-Donators für Elektronen. Dieser wirkt dem durch Koordination entstehenden Aufstaueffekt entgegen. Daher kommt es zwischen weichem Acceptor und harten Liganden ebensowenig zur Bindungsverstärkung durch back-donation, wie bei der Wechselwirkung von hartem Acceptor und weichem Liganden. Nur wenn das Ligandenmolekül eine entgegen dem Aufstaueffekt wirkende Veränderung der Ladungsverteilung durchführen kann („weich-weich-Wechselwirkung“) kommt es zum Netto-Ladungsübergang Acceptor → Ligand.[4] Daher gelten für hart-weich Wechselwirkungen ähnliche Maßstäbe, wie für hart-hart-Wechselwirkungen.

Danksagung: Meinen Kollegen Adolf Neckel und Peter Schuster danke ich herzlich für wertvolle Hinweise und dem Fonds zur Förderung der wissenschaftlichen Forschung in Österreich für die Unterstützung relevanter Forschungsprojekte.

---

[25] B. M. Rode, Private Mitteilung.

Revue Roumaine de Chimie, 22, 4, 625—632 (1977)

Dedicated to the 70th anniversary
of Professor Coriolan Drăgulescu

SOLVENT EXTRACTION OF URANIUM(VI) WITH DIALKYLPHOSPHORODITHIOIC ACIDS. V*

SYNERGISTIC EFFECT OF TRIBUTYLPHOSPHATE

IONEL HAIDUC, GH. MARCU and MARIA CURTUI
Chemistry Department, Babeş-Bolyai University, R—3400 Cluj-Napoca

Received August 31, 1976

It was found that in the solvent extraction of uranium(VI) with dialkylphosphorodithioic acids in benzene, tributhylphosphate (TBP) exhibits a synergistic effect. In order to establish the composition of the extractable species, the variation of the distribution coefficient *versus* the parameters of the extraction system was measured. It was established that the organic phase contains mixed ligand complexes (synergistic adducts) with a combination ratio U : HDTP : TBP = 1 : 2 : 1. The good solubility of these adducts in benzene explains the large values of the synergistic increase of the distribution coefficients. The extraction constants and stability constants of the synergistic adducts were also determined. The extraction data are supported by spectral measurements.

INTRODUCTION

Within our investigations upon the extraction of uranium(VI) with organic solvents as complexes of dialkylphosphorodithioic acids (HDTP),[1-4] it was found that the presence of a polar oxygen-containing compound in the system, greatly increases the distribution coefficient of the metal. In this work, we have investigated the influence of tributylphosphate (TBP) upon the extraction of uranium(VI) with diethyl-, dipropyl- and dibutylphosphorodithioic acids (HDTP) in benzene.

It is common knowledge the fact that the particular importance of TBP in the solvent extraction of uranium, has stimulated much theoretical research in this field in recent years. In addition to the application of TBP in the extraction of metals based upon the great efficiency of TBP as solvent, of remarkable importance is its use in extraction systems made up of solvent mixtures, usually in association with acidic extraction agents.

---

* Part IV: in preparation

[1] M. Curtui, Gh. Marcu and I. Haiduc, *Stud. Univ. Babeş-Bolyai. Chem.*, **21**, 74 (1976).

[2] M. Curtui, Gh. Marcu, M. Diaconeasa and I. Haiduc, *Stud. Univ. Babeş-Bolyai, Chem.*, **21**, 63 (1976).

[3] Gh. Marcu, M. Curtui and I. Haiduc, *J. Inorg. Nuclear Chem.*, in press.

[4] M. Curtui, Thesis, Univ. of Cluj-Napoca, 1976.

Tributylphosphate is known to exhibit a synergistic effect in rather various systems, involving the solvent extraction of alkali metals, alkaline earths, lanthanides, actinides and others, and is of particular importance in uranium chemistry.[5]

EXPERIMENTAL

Reagents and equipment. The dialkylphosphorodithioic acids, $HS(S)P(OR)_2$, used in this work, have been prepared by the reaction between tetraphosphorus decasulfide and the appropriate anhydrous alcohol, according to known procedures,[6] and were purified by vacuum distillation. All other reagents were used as received from commercial sources and were of analytical grade purity.

The concentration of hydrogen ions in the aqueous phase was determined potentiometrically, with an MV—11 pH-Meter (DDR). The spectral measurements in ultraviolet range were performed with a Spekord C. Zeiss, Jena (DDR) spectrophotometer, and in the infrared range with an UR—20 C. Zeiss, Jena (DDR) instrument. The extinction measurements in the quantitative determination of uranium(VI) with Arsenazo III as colour reagent,[7] were made with a Spekol C. Zeiss, Jena spectrophotometer (at 665nm).

Preparation of the aqueous and organic phases. From freshly prepared and distilled dialkylphosphoroditioic acids, 1M standard benzene solutions were prepared. From these, by successive dilutions, solutions of desired concentration were obtained. To the solution of HDTP in benzene, determined amounts of TBP (0.1M in benzene) were added.

The aqueous phases, with a variable uranium content, were prepared from a solution of uranyl perchlorate 0.1M, (standardized gravimetrically) by successive dilutions. Various pH values were attained by using perchloric acid and sodium perchlorate, in such a ratio as to give a constant 1M ionic strength. In certain cases the pH of the solution was adjusted with NaOH.

Determination of the distribution coefficients (D) of uranium. Equal volumes (10 ml) of organic and aqueous phases were mixed and shaken together. Preliminary experiments have shown that 2—3 minutes were enough for the system to attain the partition equilibrium. In order to avoid volume variations during the extraction, caused by the high acidity of the aqueous solutions, the phases were preequilibrated. The uranium concentration in the aqueous and organic phases determined spectrophotometrically was used in the calculation of the distribution coefficients (D).

It was noticed that the presence of an appreciable amount of HDTP in the aqueous phase makes difficult the quantitative determination of uranium, by acting upon the Arsenazo III reagent. Therefore, the spectrophotometric measurements were made immediately after the addition of the reagent.

RESULTS AND DISCUSSION

The distribution coefficients of uranium, defined as the ratio between the total concentration of uranium in the organic phase and the uranium concentration in the aqueous phase, were measured in solvent systems of total molar concentration of 0.1 M dialkylphosphorodithioic acid + tributylphosphate. The data presented in table 1 afford some

---

[5] Y. Marcus and A. S. Kertes, "Ion Exchange and Solvent Extraction of Metal Complexes", J. Wiley, Interscience, 1969, p. 425.

[6] K. Sasse, "Organische Phosphor Verbindungen(Houben-Weil Methoden der Organischen Chemie)" Teil 2, G. Thieme Verlag, Stuttgart, 1964, p. 684.

[7] S. B. Savin, *Talanta*, **8**, 673 (1961)

Table 1

Extraction of uranium from aqueous solution at pH = 6.5 ($NaClO_4 + HClO_4 = 1$ M) with a 0.1 TBP + HDTP mixture[a]

Concentration of TBP (%)	Distribution coefficient (D)		
	HEtDTP−TBP	HPrDTP−TBP	HBuDTP−TBP
0	0.063	0.159	0.219
10	1.41	24.0	50.1
20	3.55	50.1	107.2
30	5.62	63.1	134.9
40	6.03	60.3	129.4
50	5.41	50.1	103.4
60	5.20	41.3	89.1
70	3.55	20.0	39.8
80	2.00	15.9	24.0
90	0.89	8.9	6.03
100	0.01	0.01	0.01

[a] Abbreviation used: HEtDTP = $HS(S)P(OEt)_2$; HPrDTP = $HS(S)P(OPr)_2$; HBuDTP = $HS(S)P(OBu)_2$.

conclusions about the effect of TBP upon the partition of the metal. It was found that tributylphosphate alone in benzene in 0.1 M concentration at pH = 0.65, extracts very poorly the uranium from aqueous solutions. Under the same conditions, benzene solutions of diethyl-, dipropyl- and dibutyl-phosphorodithioic acids (without TBP) extract the uranium with distribution coefficients which are 6, 16 and 22 times, respectively, higher than those obtained with pure TBP. With 0.1 M HDTP−TBP mixtures, when 30−40% of HDTP was replaced by TBP, the magnitude of the distribution coefficients for the three acids mentioned is 6.03, 60.3 and 134.9 respectively; this represents synergistic increases of 95, 398 and 617 times for diethyl-, dipropyl- and dibutyl-phosphorodithioic acids. It follows that TBP exhibits a rather pronounced synergistic effect upon the extraction of uranium(VI) with HDTP in benzene. This effect is strongly illustrated by the extraction curves given in Fig. 1.

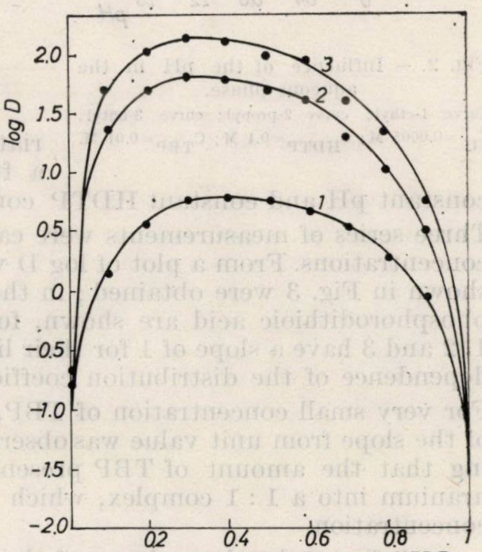

Fig. 1. — Extraction of uranium(VI) with HDTP−TBP mixture (0.1 M)

Curve 1-ethyl; curve 2-propyl; curve 3-butyl; $C_U = 0.0005$M

In order to establish the extraction mechanism of uranium with HDTP + TBP mixtures, the variation of the distribution coefficient with the pH of the aqueous phase, concentration of TBP and concentration of HDTP in the organic phase were investigated.

THE INFLUENCE OF THE AQUEOUS PHASE ACIDITY

At constant concentrations of HDTP (0.1 M) and TBP (0.01 M), the influence of the aqueous phase acidity upon the distribution coefficients of uranium is illustrated by curves shown in Fig. 2, where the plots of log D versus pH are given.

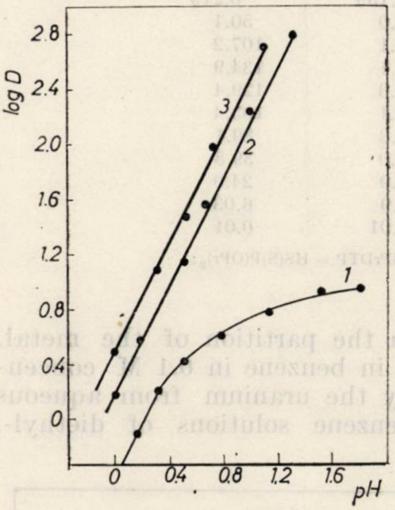

Fig. 2. — Influence of the pH in the aqueous phase.

Curve 1-ethyl; curve 2-propyl; curve 3-butyl; $C_U = 0.0005$ M; $C_{HDTP} = 0.1$ M; $C_{TBP} = 0.01$ M.

A slope of two for the linear range of curves 1, 2 and 3 (in Fig. 2) suggests a second power dependence of the distribution coefficient versus the pH of the aqueous phase. Therefore, the extraction of uranium(VI) with HDTP + TBP mixtures occurs via an ion exchange process, with participation of two HDTP molecules.

A deviation of the slope of curve 1 from the value of 2, beginning with pH = 1, can be explained by some complexation of uranium(VI) in the aqueous phase, with the diethylphosphorodithioic anion, which reduces the amount of uranium passed into organic phase.

THE INFLUENCE OF THE TBP CONCENTRATION

It was also investigated the variation of the distribution coefficient as a function of TBP concentration, at constant pH and constant HDTP concentration.

Three series of measurements were carried out, for three different HDTP concentrations. From a plot of log D versus log $[TBP]_o$, curves of the type shown in Fig. 3 were obtained; in the figure only the curves for diethylphosphorodithioic acid are shown, for other acids being similar. Curves 1, 2 and 3 have a slope of 1 for their linear range, indicating a first degree dependence of the distribution coefficient versus TBP concentration.

For very small concentration of TBP, $[TBP]_o \leqslant [UO_2^{2+}]$ some deviation of the slope from unit value was observed. This can be explained by assuming that the amount of TBP present is not enough to transform all the uranium into a 1 : 1 complex, which seems to be formed at higher TBP concentration.

A first order dependence of the distribution coefficient versus TBP concentration is observed even in the range of large TBP concentrations (0.1 — 0.97 M). Compared with other extraction systems, [8-10] where the

---

[8] T. V. Healy, D. F. Peppard and G. W. Mason, *J. Inorg. Nuclear Chem.*, **24**, 1429 (1962).

[9] T. V. Healy, *Nucl. Sci. Eng.*, **16**, 413 (1963)

[10] M. Zangen, *J. Inorg. Nuclear Chem.*, **28**, 1693 (1966).

presence of large amounts of TBP produces a decrease of synergistic effect, in our system such behaviour does not occur. This suggests that strong interactions between HDTP and TBP molecules do not occur, a supposition supported by the infrared spectra of mixtures of the two compounds, in benzene.

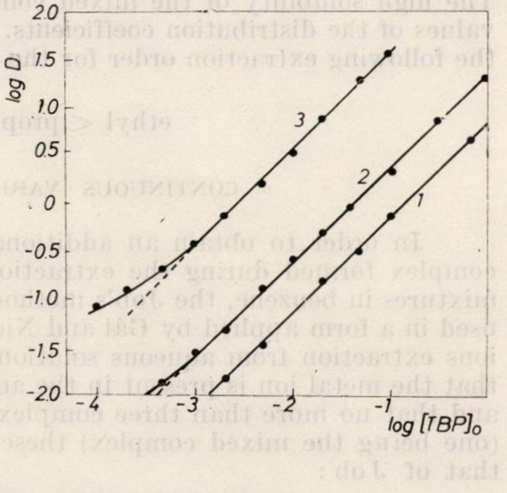

Fig. 3. — Influence of TBP concentration.

$C_U = 0.0005$ M; $C_{HEtDTP} = 0.01$ M (curve 1); 0.02 M (curve 2) and 0.1 M(curve 3).

THE INFLUENCE OF HDTP CONCENTRATION

The variation of the distribution coefficients versus HDTP concentration, at constant pH and constant TBP concentration is shown in Fig. 4. For dipropyl- and dibutyl-phosphorodithioic acids the plots are linear, with a slope of 2, which confirms the participation of two acid molecules in the formation of the complex in the organic phase. In the case of diethylphosphorodithioic acid (curve 1) the slope of the curve deviates from 2 (its value is 1.73), which is explained by some complexation of uranium with diethylphosphorodithioic anion in the aqueous phase.

The results presented above, relative to the influence of pH in the aqueous phase and TBP and HDTP concentration in the organic phase upon the distribution coefficients, suggest that the extraction of uranium (VI) with a mixture of TBP and HDTP occurs through the formation of a mixed ligand complex in benzene (synergistic adduct), with a combination ratio U : HDTP : TBP = 1 : 2 : 1. The overall reaction mechanism

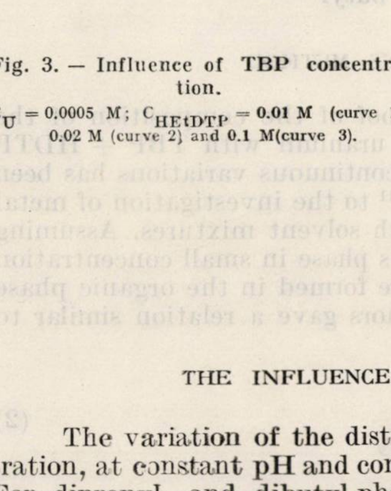

Fig. 4. — Influence of HDTP concentration.

$C_U = 0.0005$ M; $C_{TBP} = 0.01$ M; pH = 0.65;

can be written as follows:

$$UO_2^{2+} + 2[HDTP]_o + [TBP]_o \rightleftarrows [UO_2(DTP)_2TBP]_o + 2H^+ \qquad (1)$$

where the index "o" indicates the species present in the organic phase. The high solubility of the mixed complex in benzene explains the high values of the distribution coefficients. The curves given in Fig. 1 suggest the following extraction order for the synergistic adducts:

$$\text{ethyl} < \text{propyl} < \text{butyl}$$

CONTINUOUS VARIATIONS METHOD

In order to obtain an additional proof of the composition of the complex formed during the extraction of uranium with TBP + HDTP mixtures in benzene, the Job's method of continuous variations has been used in a form applied by Gál and Nicolič [11] to the investigation of metal ions extraction from aqueous solutions with solvent mixtures. Assuming that the metal ion is present in the aqueous phase in small concentration and that no more than three complexes are formed in the organic phase (one being the mixed complex) these authors gave a relation similar to that of Job:

$$m/y = \frac{x_y}{1 - x_y} \qquad (2)$$

where m/y is the molar ratio of the two ligands in the mixed complex (HDTP/TBP) and x_y is the molar fraction of one of the ligands (TBP) for which a maximal distribution coefficient is obtained.

For the system UO_2^{2+} − HDTP − TBP the Job's method was employed by using the data shown in Table 1.

Table 2

Extraction and stability constants for the compounds $UO_2[S_2P(OR)_2]_2 \cdot OP(OBu)_3$

Compound	Extraction constant log K′	Stability constant log β′
R = Et	3.40±0.15	3.71
Pr^n	4.23±0.17	4.34
Bu^n	4.50±0.06	4.48

A maximum value for the distribution coefficient is obtained for $x_y = 0.3 - 0.4$, which suggests the formation of the complex $UO_2(DTP)_2TBP$ (which requires $x_y = 0.33$).

---

[11] I. J. Gál and R. M. Nicolič, *J. Inorg. Nuclear Chem.*, **28**, 563 (1966).

INFRARED SPECTRA

The organic phases obtained during the extraction of uranium with a HDTP–TBP mixture were examined by infrared spectroscopy. The spectra obtained for the three systems investigated contain all a band at 940 cm^{-1}, which is due to the asymmetric stretching of the dioxouranium (UO_2^{2+}) group.

The bands due to PS_2 groupings, which in the free acids are found in the range 540–700 cm^{-1}, are changed only in their intensity and shape. No shift of the band position is observed.

The band due to the P = O group stretching in TBP, which in the spectrum of the free ligand occurs at 1270 cm^{-1}, is shifted towards lower wave numbers. This confirms the coordination of TBP through the P = O group, and therefore, the participation of TBP in the extraction process as a dioxouranium complex.

DETERMINATION OF THE EXTRACTION AND STABILITY CONSTANTS

The extraction constant related to equation (1) can be written as follows :

$$K = \frac{D[H^+]^2}{[HDTP]_0^2[TBP]_0} \qquad (3)$$

By using the data from Figures 2 and 3, with the aid of relation (2) extraction constants were calculated, which are given in Table 2. The extraction order indicated by the magnitude of the distribution coefficients is confirmed by the order of extraction constants.

The stability constants of the synergistic adducts in benzene (Table 2) were determined with the aid of Sillén's curve overlap method,[12,13] by using the curves shown in Fig. 5 and the relation :

$$D/D_0 = 1 + \sum_1^y \beta_y[TBP]_0^y \qquad (4)$$

where D is the distribution coefficient of uranium in the presence of TBP and D_0 is the distribution coefficient in the absence of TBP ; β_y – the stability constant of the adduct ; y = the number of TBP molecules in the complex.

It can be seen that the magnitudes of the stability constants of the synergistic adducts derived from the three dialkylphosphorodithioic acids are rather close, which reflects the structural similarity of the acidic

---

[12] L. G. Sillén, *Acta Chem. Scand.*, **10**, 186 (1956).

[13] L. G. Sillén and D. Dyrssen, *Acta Chem. Scand.*, **7**, 663 (1953).

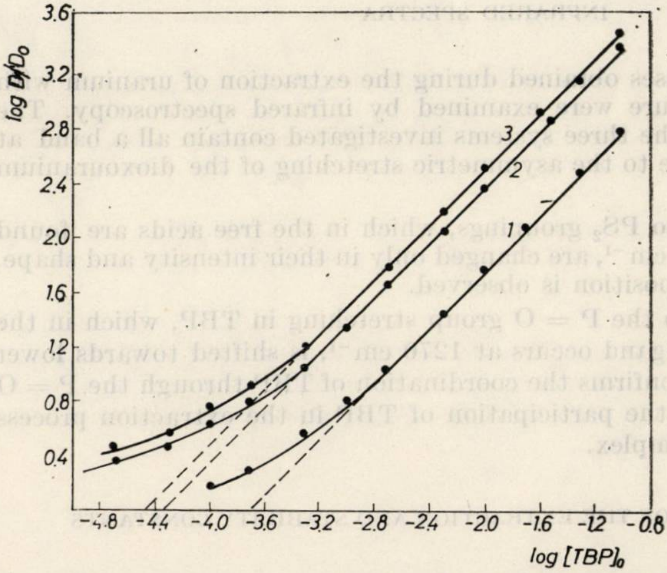

Fig. 5. — Determination of the stability constants of the synergistic adducts.

Curve 1-ethyl; curve 2-propyl; curve 3-butyl;

ligands. The differences observed in the synergistic increases of the distribution coefficients are due to solubility effects, since the synergistic adducts of long-chain dialkylphosphorodithioates exhibit higher solubility in benzene.

Revue Roumaine de Chimie, 22, 4, 633–638 (1977)

Dedicated to the 70th anniversary
of Professor Coriolan Drăgulescu

ZERO-CURRENT BIPOTENTIOMETRIC END-POINT INDICATION WITH PRETREATED ELECTRODES. IV*

USE OF PRETREATED SILVER ELECTRODES

L. KÉKEDY ** and M. ŞERBAN ***

** Department of Analytical Chemistry, "Babes-Bolyai" University, Str. Arany J. N° 11, Cluj-Napoca, Romania

*** Chair of Analytical Chemistry, Medical and Pharmaceutical Institute, Str. Pasteur N° 4, Cluj-Napoca, Romania

Received July 20, 1976

Experimental data are presented for the zero-current bipotentiometric indication of the end-point in titration of Ag^+ with I^- ions, based on the use of two differently pretreated silver indicator electrodes. The bipotentiometric end-points are compared and related with the potentiometric ones calculated by three different methods.

The principles of zero-current bipotentiometry have been outlined in our previous papers (e.g. Part II of this series [1]), pretreatment effects on platinum [2] and on gold [1] respectively being used for end-point indication in oxidimetric titrations. A mathematical simulation of the forms of titration curves obtained has been also suggested. [3] A review article concerning the present status in bipotentiometry is also available. [4] This paper reports on pretreatment effects on silver electrodes, the phenomenon being used for the zero-current bipotentiometric indication of the Ag^+-ion titration with I^-.

The literature contains few pertinent data on pretreatment of silver, most of them referring to anodization and oxide film formation in alkaline medium.[5] In sulphuric acid the formation of a Ag_2SO_4 film was reported which on further anodization transforms in oxide and peroxisulphate respectively.[6–8] On anodization in nitric acid a black film is first formed, which in the presence of water transforms slowly into Ag_2O.[9] Other electrochemical pretreatments have also been reported[10] as well as mechanical ones.[8,11] Two platinum wires plated with silver in different conditions (freshly plated, aged, with stress in deposit, without stress) have been used by Hanselman, Shade and Rogers[12] for the indication of Ag^+ titration with I^- by a technique which at present is considered as zero-current bipotentiometry. Recently the same titration was reported using a pair of differently pretreated silver electrodes, one of them being heated, the other ground with emery paper or plated with a thin AgI film respectively (adsorption-polarized electrodes as termed by the authors).[13]

---

* Previous part, L. Kékedy and P. Ney, *Talanta*, **22**, 478 (1975).

[1] L. Kékedy and A. Popescu, *Talanta*, **22**, 135 (1975).

[2] L. Kékedy and F. Makkay, *Rev. Roumaine Chim.*, **18**, 717 (1971).

[3] L. Kékedy and P. Ney, *Talanta*, **22**, 478 (1975).

[4] L. Kékedy, *Reviews in Analyt. Chem. (Tel-Aviv)*, **3**, 27 (1975).

[5] B. V. Tilak, R. S. Perkins, H. A. Kozlowska and E. B. Conway, *Electrochim. Acta*, **17**, 1447 (1972).

EXPERIMENTAL

Conventional titration assembly was used as described earlier.[1] 25.00 ml 10^{-3}M $AgNO_3$ which contained also 0.1M KNO_3 was titrated with $5 \cdot 10^{-3}$M I^-. Near the equivalence point the titration was continued with a tenfold diluted iodide solution. The titrant volumes were read with a precision of 1/100 ml, the thousands being estimated. Two, approximately identical (18 mm^2) silver wires (The British Drug Houses Ltd.) served as indicating electrodes, the potential difference between them being followed during the titration. At the same time, for comparison, the potentials of each silver electrode against a SCE (KNO_3 salt bridge) electrode were also recorded. The potentiometric equivalence volumes were calculated using three independent methods (see Table 1). The bipotentiometric ones were identified as follows: in the case of the curves similar to the first derivative of a normal S-shaped potentiometric curve with the abscissa of the peak, in the case of the second derivative-like curves with the abscissa corresponding to zero ordinate value, and in the case of intermediate forms with the abscissa corresponding to the half of the potential break between the two peaks respectively. Chemical pretreatments were used in the form of dipping the silver electrodes for 15 s in one of the following solutions: 2N HNO_3, 0.1% $KMnO_4$ in 0.1N $HClO_4$, 5% $KMnO_4$ in 0.1N $HClO_4$, 30% H_2O_2, 0.5M $FeSO_4$ in 0.1N $HClO_4$, 0.5M $SnCl_2$ in 0.1N $HClO_4$, 0.5M KCN or successive dipping in 2N HNO_3, then in 2N NH_3. Electrochemical pretreatment consisted in freshly plating with silver. After pretreatment the electrodes were thoroughly washed with doubly distilled water, then fixed in the titration cell, being connected directly to the meter (MV 84 Type pH-meter). Analytical grade chemicals and doubly distilled water were used throughout.

RESULTS AND DISCUSSION

Small pretreatment effects can be observed even on the usual potentiometric titration curves (Fig. 1) apparently consisting in differences in the potential break. The very small delay between the two curves against the X axis (degree of titration) cannot be evidenced in Fig. 1. It appears only on the bipotentiometric curves of the same titration, causing the

---

[6] G. P. Jones and H. R. Thirsk, *Trans. Faraday Soc.*, **50**, 732 (1954).

[7] G. W. D. Briggs, I. Dugdale and W. F. K. Wynne-Jones, *Electrochim. Acta*, **4**, 55 (1961).

[8] I. Dugdale, M. Fleischmann and W. F. K. Wynne-Jones, *ibidem*, **5**, 229 (1961)

[9] A. B. Neiding and I. A. Kazarnovskii, *Doklady Akad. Nauk S.S.S.R.*, **78**, 713 (1951).

[10] L. Müller, P. Ianietz and P. Landsberg, *Electrokhimiija*, **5**, 1001 (1969).

[11] P. Jones and H. R. Thirsk, *Trans. Faraday Soc.*, **50**, 732 (1954).

[12] R. B. Hanselman, G. H. Shade Jr. and L. B. Rogers, *Analyt. Chem.*, **32**, 761 (1960).

[13] E. Schumacher and F. Umland, *Z. analyt. Chem.*, **272**, 257 (1974).

formation of a first derivative-like curve with a very sharp peak at the end-point (Fig. 2).[3] The majority of the pretreatment combinations used yielded titration curves of this form, e.g. when one electrode was treated with HNO_3, the other with $SnCl_2$, or one with H_2O_2, the other with KCN, etc. The only difference was in the height of the peaks on the titration curves obtained, the highest peak (300 mV) being obtained with the last above-mentioned treatment combination. The smallest peak was exhibited by an electrode pair consisting of an electrode treated with HNO_3 and the other with $SnCl_2$. Bipotentiometric titration curves similar to the second derivative of a sigmoidal curve were obtained in the cases represented in Fig. 3. Unlike the second derivative type bipotentiometric titration curves obtained in redox titrations, in the present argentometric titrations first derivative type titration curves appeared in most cases. This same form was obtained exclusively by Schumacher and Umland.[13] Most likely this is due to a simpler structure of the surface films on silver. It is known that anodization of silver provides one of the few examples

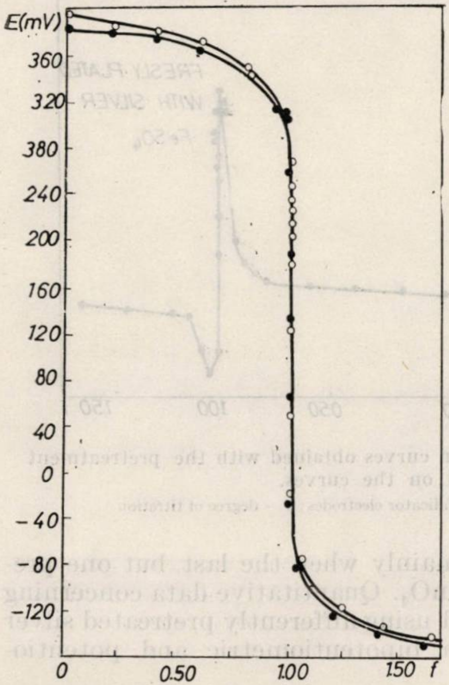

Fig. 1. — Potentiometric titration curves of 10^{-3}M Ag^+ with $5 \cdot 10^{-3}$M I^-, obtained with differentlyp retreated silver indicator electrodes.

Pretreatments: ○ — with $FeSO_4$; ● — with HNO_3; f — degree of titration

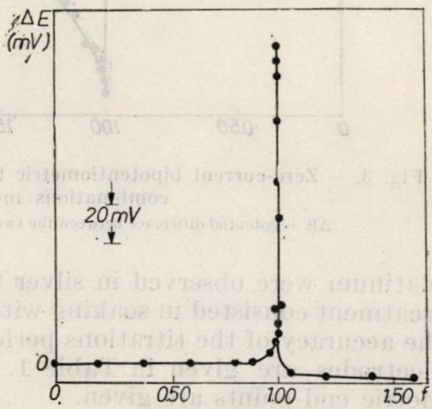

Fig. 2. — Zero-current bipotentiometric curve of the same titration as in Fig. 1. ΔE — potential difference between the two silver indicator electrodes; f — degree of titration. Pretreatments as in Fig. 1.

of clearly separated stages of surface oxidation of a metal corresponding to different valence states. [5] This determines a simpler mechanism for the establishment of the electrode potential. Memory effects observed in platinum were observed in silver too, mainly when the last but one pretreatment consisted in soaking with $KMnO_4$. Quantitative data concerning the accuracy of the titrations performed using differently pretreated silver electrodes are given in Table 1. Both bipotentiometric and potentiometric end-points are given.

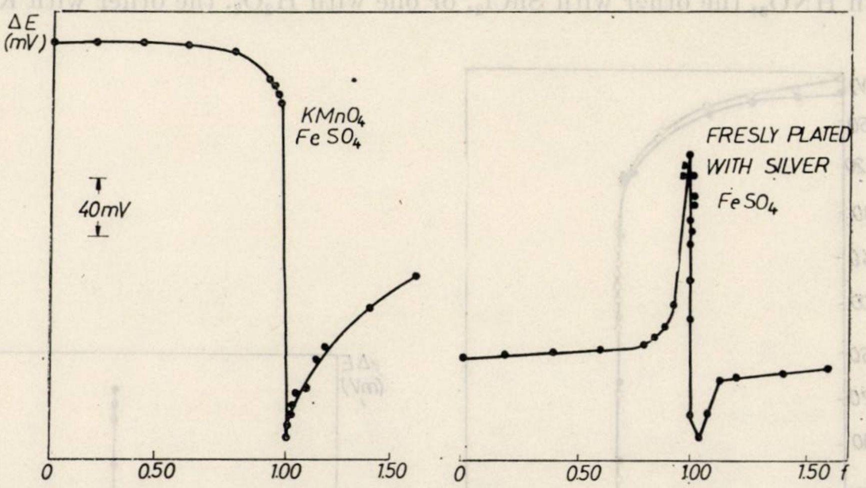

Fig. 3. — Zero-current bipotentiometric titration curves obtained with the pretreatment combinations indicated on the curves.
ΔE — potential difference between the two silver indicator electrodes; f — degree of titration

From the potentiometric data the following can be concluded: a) The most accurate results are obtained using electrodes pretreated with $FeSO_4$. b) The freshly plated (with silver) electrode exhibited a significant potential drift most likely due to the variation of the activity of the metal. c) No electrodes treated with 5% $KMnO_4$ gave good results, either in potentiometric titrations or in bipotentiometric ones. Electrodes treated with more diluted $KMnO_1$ (0.1%) showed improved qualities. d) Treatment with $SnCl_2$ or KCN ensured good results; soaking with H_2O_2 yielded electrodes with less favourable properties. e) Different calculation procedures in some cases yielded similar equivalence values. In other cases significant differences can be observed. This is due partly to different approximations made, partly to differences in the intimate structure of the potentiometric titration curves strongly affected by pretreatment.

The bipotentiometric titration data prove the following: The best couple of indicating electrodes consists of a silver wire treated with HNO_3, the other being soaked in $FeSO_4$. This indicator system yields titration curves with a very sharp peak, enabling the very exact location of the end-point (Fig. 2). The pretreatments involved are simple and reproducible. The end-point values thus obtained are the most accurate ones (see Table 1), the reproducibility being also good (Table 2).

Table 1

Comparison of the bipotentiometric equivalence volumes with the potentiometric ones calculated by three different methods. Effect of pretreatment and prehistory

Pretreatment of the electrode pair used	Equivalence volume, ml, and % absolute error				
	Potentiometric, calculated by the method			Bipotentiometric	Theoretical
	Hostetter-Roberts[14]	Liteanu-Cörmöş[15]	Gran[16,17]		
2N HNO_3	2.473(− 0.36%)	2.488(+ 0.24%)	2.451(− 1.25%)	2.482(0.00%)	2.482
0.5M $FeSO_4$	2.482(0.00%)	2.496(+ 0.56%)	2.482(0.00%)		
0.1% $KMnO_4$	2.476(− 0.24%)	2.500(+ 0.73%)	2.461(− 0.85%)	2.483(+0.04%)	2.482
0.5M $FeSO_4$	2.482(0.00%)	2.496(+ 0.56%)	2.482(0.00%)		
Plated	2.367(− 4.63%)	2.479(− 0.12%)	2.307(− 7.05%)	2.490(+0.32%)	2.482
0.5M $FeSO_4$	2.486(+ 0.16%)	2.504(+ 0.89%)	2.486(+ 0.16%)		
0.5M $FeSO_4$	2.451(− 0.85%)	2.475(+ 0.12%)	2.451(− 0.85%)	2.460(−0.49%)	2.472
0.5M $FeSO_4$	2.451(− 0.85%)	2.473(+ 0.04%)	2.472(0.00%)		
5% $KMnO_4$	2.467(− 0.84%)	2.474(− 0.56%)	2.682(+ 7.80%)	2.540(+2.09%)	2.488
0.5M $FeSO_4$	2.544(+ 2.25%)	2.497(+ 0.36%)	2.507(+ 0.76%)		
2N HNO_3 a)	2.215(−10.97%)	2.216(−10.93%)	2.102(−15.51%)	2.410(−3.14%)	2.488
0.5M $FeSO_4$	2.544(+ 2.25%)	2.497(+ 0.36%)	2.507(+ 0.76%)		
2N HNO_3 a)	2.215(−10.97%)	2.216(−10.93%)	2.102(−15.51%)	2.410(−3.14%)	2.488
0.5M $SnCl_2$	2.485(− 0.12%)	2.478(− 0.40%)	2.483(− 0.20%)		
2N HNO_3 b)	2.358(− 5.22%)	2.489(+ 0.04%)	2.463(− 1.01%)	2.470(−0.72%)	2.488
0.5M $SnCl_2$	2.492(+ 0.16%)	2.504(+ 0.64%)	2.490(+ 0.08%)		
0.5M $FeSO_4$ c)	2.433(− 2.21%)	2.398(− 3.61%)	2.355(− 5.35%)	2.474(−0.56%)	2.488
0.5M $FeSO_4$	2.503(+ 0.60%)	2.503(+ 0.60%)	2.499(+ 0.44%)		
30% H_2O_2 d)	2.478(− 0.40%)	2.482(− 0.24%)	2.231(−10.33%)	2.496(+0.32%)	2.488
2N HNO_3,					
2N NH_3	2.501(+ 0.52%)	2.507(+ 0.76%)	2.512(+ 0.97%)		
30% H_2O_2	2.468(− 0.56%)	2.470(− 0.48%)	2.395(− 3.51%)	2.472(−0.40%)	2.482
0.5M KCN	2.486(+ 0.16%)	2.495(+ 0.54%)	2.494(+ 0.48%)		
2N HNO_3,	2.461(− 0.85%)	2.467(− 0.60%)	2.427(− 2.21%)	2.470(−0.48%)	2.482
2N NH_3					
0.5M KCN	2.491(+ 0.36%)	2.491(+ 0.36%)	2.490 (+ 0.32%)		

Prehistory (before the treatment indicated):

a) previous use, as treated with 5% $KMnO_4$, followed by treatment with 2N HNO_3, 0.1N hot oxalic acid and wet grounding with fine emery.

b) previous use as a) followed by treatment with hot 2N HNO_3 and wet grounding with fine emery.

c) previous use as b) followed by treatment with 2N HNO_3 and 0.5 M$FeSO_4$.

d) previous use as c), then treated with 2N HNO_3, grounded with fine emery and dipped in 2N HNO_3.

---

[14] J. C. Hostetter and H. S. Roberts, *J. Amer. Chem. Soc.*, **41**, 1337 (1919).

[15] C. Liteanu and D. Cörmöş, *Talanta*, **7**, 25 (1960).

[16] G. Gran, *Acta Chem. Scand.*, **4**, 559 (1950).

[17] G. Gran, *Analyst*, **77**, 661 (1952).

Table 2

Reproducibility of the titrations represented in Fig. 2

Ag^+ taken mg	Ag^+ found mg	%(X)	Error $(X-\overline{X})$ %	Statistical data
2.835	2.831	99.86	−0.09	$\overline{X} = 99.95\,\%$ $n = 5$ $s_{\overline{x}} = 0.162$ $P = 95\,\%$ $t = 2.78$ $A = 99.95 \pm 0.45\,\%$ $(A = \overline{X} \pm t \cdot s_{\overline{x}})$ Mean $(\overline{X}) = 99.95\,\%$
2.835	2.835	100.00	0.00	
2.835	2.827	99.72	−0.23	
2.730	2.730	100.00	0.00	
2.730	2.734	100.15	+0.20	

CONCLUSIONS

The zero-current bipotentiometric indication of the given argentometric titration has several advantages over the conventional potentiometry: a) Rapid establishment of the analytical signal (potential difference between the electrodes), showing smaller fluctuations than the individual electrode potentials, b) Simplicity, no need for reference electrode or for salt bridge, possible further advantages in nonaqueous media, c) Rapid identification of the equivalence point without laborious calculations. The data of Table 1 show that such calculations do not ensure higher precision unless the transference function of the electrode remains invariable during the experiments, d) Great sensibility, solutions down to $C_{Ag^+} = 10^{-7}$ M could be titrated with good results. This limit, according to our experiments coincides with the validity of the Nernst equation for the Ag/Ag^+ system.

Revue Roumaine de Chimie, 22, 4, 639–643 (1977)

Dedicated to the 70th anniversary
of Professor CORIOLAN DRĂGULESCU

SOME CONSIDERATIONS ON THE NOMENCLATURE OF INORGANIC CHEMISTRY

WILHELM KLEMM
Institut für Anorganische Chemie der Universität Münster/Westfalen
D 4400 Münster, Theresiengrund 22

Received September 11, 1976

The application of the Rules for Nomenclature of Inorganic Chemistry, elaborated by the International Union of Pure and Applied Chemistry, encounters some difficulties, especially as a consequence of the introduction of alphabetic order. Examples are given and proposals made for improvement.

Some years ago, the International Union of Pure and Applied Chemistry (IUPAC) has published the Second Edition of the Rules for Nomenclature of Inorganic Chemistry. This book is the result of very careful deliberations of distinguished experts of many countries during the period of more than ten years, and we all should be grateful for the unselfish efforts of this group in the interest of the chemical community. The question arises whether these nomenclature rules solve in a satisfactory manner the needs of inorganic chemists concerning nomenclature, or whether there are problems which are still open.

In order to give an answer we must consider the general lines of the IUPAC Nomenclature Rules. Of importance for our considerations are the following items :

1). It stands to reason that the Rules should be international, or at least that they should be adaptable to other languages with as few difficulties as possible.

2). Furthermore, the Second Edition of the Rules emphasizes the alphabetical order. This means that the first letter of the chemical symbol and the initial letter of the name should be, as far as possible, the same in order to avoid that the sequence in tables, indexes *etc.* becomes different if one makes use of formulae or names.

3). Finally, the general principle of the nomenclature is the following : very many compounds consist, or can be regarded as essentially consisting, of two parts (binary type) with an electropositive and an electronegative constituent.[1]

In the following we will discuss how far the "Rules" are applicable in all cases.

I. The first question is whether principle *3*) can cover the totality of inorganic chemistry. Roughly speaking, the elements can be metals or nonmetals. As a consequence we have salts (metal and nonmetal) and compounds which consist only of metals (alloys) and only of nonmetals (*e.g.*, organic compounds, but also an increasing number of inorganic compounds). The general principle *3*) of the IUPAC Nomenclature Rules covers of course the salts (including coordination compounds) and those intermetallic compounds which are saltlike and those nonmetallic compounds which consist of atoms of different electronegativity (*e.g.*, NO_2), but there are difficulties with compounds like Na_2K or $H_2N-N=N-NH_2$. It seems to me that the nomenclature of these two groups should be rediscussed from the very beginning. The solution will not be easy because it will become necessary to introduce new principles.

II. The general principle, adopted by IUPAC, to consider all substances as being binary with an electropositive and an electronegative constituent requires a decision as to which constituent of a compound is positive and which is negative. This is easy for NaCl, but what about F_2O (or OF_2) or Na_2K? It would be logical to take the values of the electronegativity as a base. But the course of the electronegativity in the Periodic Table is complicated. Therefore the IUPAC Commission has proposed, in accordance with established practice, that in compounds of nonmetals the component should be placed first which appears earlier in the sequence : Rn,[2], Xe, Kr ; B ; Si, C ; Sb, As, P, N ; H ; Te, Se, S ; At, I, Br, Cl ; O ; F. Examples : XeF_2, CH_4, NH_3, H_2S, S_2Cl_2, OF_2. Now according to section 2.15 (p. 14) of the Rules, the electropositive constituent should always be placed first in formulae. It is a little difficult to consider H in CH_4 as electronegative[3] and the systematic name as "carbon hydride". Here it becomes clear that the principle of the "binary structures" is a rather crude one and brings difficulties for compounds in which the difference of electronegativity is very small. But at present there is no better solution. Moreover, for the volatile hydrides one can avoid the difficulty by using another principle : one cites the root of the name of the element followed by the suffix -ane (example, sulfane H_2S). We shall come back to this question later on.

III. Whereas the problems discussed up to now will need a rather long time for their solution, there are some questions which can be solved at least in part rather quickly. For the application of the alphabetic order it is desirable that the initial letter of the name be the same as the first letter of the formula. This concerns above all the elements. For the majority of the elements there is no difficulty. But there is a group of elements the names of which differ from one language to the other and which do not correspond, in general, with the symbols, e.g., antimony, lead, iron, gold, copper, silver, tin. This is intolerable for the indexes. Here, the IUPAC Commission has thought out a remedy : one makes use of the Latin names, that means : stibium, plumbum, ferrum, aurum, cuprum, argentum, stannum. This method is very simple and should be strongly recommended. Ferrum(II)chloride is as simple and generally understood as iron(II) chloride, but this name has the advantage of being the same in all languages. These Latin names shall of course be valid only for scientific purpose ; in colloquial usage names like iron and gold will naturally be retained.

---

[1] IUPAC—Nomenclature of Inorganic Chemistry 1970, Section 2.2 (p. 15).

[2] Section 2.161 (p. 14).

[3] In section 0.1 (p. 5) of the Rules the charges in CH_4 are considered as H^+ and C^{4-} which is in contradiction to the rule cited above.

The situation is more difficult in English and French with Na, K and Hg. It is difficult to understand why one uses the symbols Na and K, but the names sodium and potassium ; historically, both systems have the same foundation. In the future one should use the names natrium and kalium. With Hg the situation is still more difficult, as neither mercury nor quicksilver have H as the initial letter. A possible solution might be the use of hydrargyrum as the name for Hg. In any case for reasons of continuity, here and in other cases it seems advantageous to retain the symbol and to change the name !

The names brought into discussion by IUPAC and strongly recommended here and the names proposed in this paper are summarized in Table 1. Here and for all other elements the names have the same initial letter as the symbols. But one must admit that the second letter of the symbol does often not correspond to the alphabetic order of the names. However for most purposes it will no more be necessary to make use of two alphabetic tables of the elements, one according to the symbols and one according to the names.

Table 1

Names proposed for elements (for scientific purposes)

Symbol	Proposed Name	IUPAC-Name
Ag	Argentum (Silver)	Silver (Argentum)
Au	Aurum (Gold)	Gold (Aurum)
Cu	Cuprum (Copper)	Copper (Cuprum)
Fe	Ferrum (Iron)	Iron (Ferrum)
Hg	Hydrargyrum (Mercury)	Mercury
K	Kalium	Potassium
Na	Natrium	Sodium
Ni	Niccolum (Nickel)	Nickel
Pb	Plumbum (Lead)	Lead (Plumbum)
Sn	Stannum (Tin)	Tin (Stannum)
Sb	Stibium (Antimony)	Antimony
Zn	Zincum (Zinc)	Zinc

The harmonization of names and symbols of the elements introduces various difficultier for different languages. For German there was no difficulty with Na and K, but some othes

problems arose. A Commission composed of members of the Federal Republic of Germany, of Austria and of Switzerland recommended :

1) The proposal of IUPAC to make use of names like ferrum *etc.* instead of iron *etc.* is supported.

2) The following German names are to be changed : Wismut (Bi) into Bismut (Bi), Kobalt (Co) into Cobalt (Co), Jod (J) into Iod (I) Vanadin (V) into Vanadium (V) and Zirkon (Zr) into Zirconium (Zr).

3) To use instead of the names : Wasserstoff, Kohlenstoff, Stickstoff, Sauerstoff and Schwefel the names : Hydrogen, Carbon, Nitrogen, Oxygen and Sulfur, especially for the names of compounds.

4) The IUPAC Commission is asked to propose a new name for Hg and to recommend for Na and K the names Natrium and Kalium.

IV. Great difficulties arise because H_2O (water) and NH_3 (ammonia) have names which are by no means systematic and which are (for water) different in many languages. For complexes, Alfred Werner has therefore proposed to make use for H_2O of the name "aquo" ; IUPAC, in the Second Edition of the Rules, has decided to write instead "aqua".[1] But alphabetically both, aquo or aqua, do not fit, either to H_2O or to OH_2 ; the sequence of ligands of coordination compounds comes into disharmony.

The name for NH_3 (ammonia, in coordination compounds — ammine) does also not fit alphabetically to the formula. Here we experience difficulties not only for coordination compounds but also for ternary salts :

$Al(NH_3)_3F_6$ aluminium ammonium fluoride
$Fe(NH_3)_3F_6$ ammonium iron(III) fluoride

It is true that the IUPAC Rules admit (p. 36) that such differences exist, but apparently the IUPAC Commission is of the opinion that such differences are of no importance. We, on the contrary, think that they should be avoided ; their number is much too great. One should look for ways to remove these difficulties. There are two possibilities :

1) The names for groups like H_2O, NH_3, NH_4^+ *etc.* and the alphabetical order are retained, but special rules are introduced for the sequence.

a) In formula and in the name of ***complexes*** one places first H_2O (aqua), second OH (hydroxo), third NH_3 (ammine), fourth NH_2 (amido) and NH (imido), fifth other inorganic ligands and then the organic ligands in alphabetical order according to the special rules of IUPAC.

b) For the formula and the name of ***ternary compounds*** the sequence is determined by the ionic charge, *e.g.*, $(NH_4)_3AlF_6$ ammonium-aluminium hexafluoride, $NH_4MgPO_4 \cdot 6H_2O$ ammonium magnesium phosphate hexahydrate.

2) Another possibility exists in allocating other names to H_2O and NH_3. According to the IUPAC Rules for hydrides the names ***oxane*** for H_2O and ***nitrane*** for NH_3 correspond to sulfane (H_2S) and phosphane (PH_3). The name oxane should of course be used only in the names of complexes ; normally one says water as before. Nitrane could be used everywhere, for example for NH_3 in the free state.

The names for H_3O^+ and NH_4^+ become oxonium (no change !) and *nitronium*. Whereas the names of OH (hydroxyl) and OH^- remain unchanged, names for $-NH_2$ and $>NH$ (respectively NH_2^- and NH^{2-}) still have to be found — a task which is not easy. $N\equiv$(nitrilo) and N^{3-} (nitride) are clear again. In considering this problem one must admit that the system at present in use is far from being satisfactory, as is indicated by the following extract of the IUPAC-rules :

---

[1] The fact that aqua is more correct than aquo has been known for twenty years ; but the influence of the late Werner was so strong that the decision in favour of aqua was not possible before the generation of the immediate pupils of Werner was practically extinct.

atom or group	as uncharged atom, molecule or radical	as cation or cationic radical	as anion	as ligand	as prefix for substituent in organic compounds
N	(mono)nitrogen		nitride	nitrido	nitrilo, $N\equiv$
NH	aminylene	aminylene	imide	imido	imino
NH_2	aminyl	aminyl	amide	amido	amino
NH_3	ammonia			ammine	ammonio, H_3N^+-
NH_4		ammonium			

The harmony between the initial letter of the names and the formulae is very poor. Therefore it may be worthwhile to look for a totally new system for NH_x in its different forms.

It may be mentioned here that E. Wiberg in his well-known textbook (71.—80 edition, p. 542) discusses names like Azane NH_3, N_2H_4 Diazane and Diazene (N_2H_2). Such names should also be taken into consideration, but in this case the name of the element should be changed into the former French name Azote, in order to harmonize names and formulae.

It was the purpose of this paper to demonstrate that there are still open questions in the field of Nomenclature of Inorganic Chemistry. We hope that the IUPAC Commission on the Nomenclature of Inorganic Chemistry will find adequate solutions.

NOTE POUR LES AUTEURS

La Revue Roumaine de Chimie publie des articles en anglais, français, russe, allemand ou espagnol. Les auteurs sont priés d'envoyer des articles et comptes rendus inédits.

Les manuscrits seront dactylographiés à deux intervalles. La bibliographie, les tableaux et la légende des figures seront placés après le texte.

Si l'article fait partie d'une série numérotée, le titre de la partie précédente sera indiqué dans une note au bas de la première page.

Chaque article sera précédé d'un résumé comprenant quinze lignes au maximum.

Les références bibliographiques dans le texte seront faites par des exposants sans parenthèse et paraîtront comme des notes au bas de chaque page.

Les publications périodiques mentionnées dans la bibliographie seront présentées suivant les prescriptions internationales : le nom de l'auteur précédé de l'initiale du prénom, le titre du périodique abrégé conformément à « Chemical Abstracts » et souligné par une ligne, le numéro du tome, indiqué par des chiffres arabes et souligné par deux lignes, suivi de la première page de l'article ; à la fin, l'année de la parution sera placée entre parenthèses. Le numéro de la revue ne sera pas indiqué si les pages du volume sont numérotées consécutivement. Pour les revues dont les thèmes ne sont pas numérotés (par. ex. Bull. Soc. Chim. France, etc.), l'année de la parution soulignée par deux lignes précèdera l'indication de la page.

Les textes des livres ou traités inclueront : les noms des auteurs, les initiales du prénom, le titre du livre entre guillemets et sans être souligné, le numéro du tome précédé par l'abréviation « p » (ou « S »).

Les brevets seront indiqués comme suit : L'auteur ou la firme, le pays et le numéro du brevet, la date et la revue (Chem. Abstr.). Par ex. : M. Jones (to Union Carbide Co.), Brit. Pat. 601 238, 2 septembre 1959, *Chem. Abstr.*, **54**, 12808 (1960).

Si la référence n'a pas été lue en original, on indiquera aussi la revue de références consultée.

Les diagrammes seront tracés à l'encre de Chine sur papier calque. Les tableaux et les figures (en nombre strictement nécessaire) seront numérotés par des chiffres arabes et leur explication sera donnée dans la légende des figures. Prière de ne pas inscrire les mêmes données dans les tableaux et les figures. Chaque tableau aura un titre. On indiquera dans le texte la place approximative des tableaux et des figures. Les formules chimiques seront incluses dans le texte ; en outre, elles seront transcrites sur papier calque, à l'encre de Chine.

Les auteurs sont priés d'indiquer les caractères italiques (en soulignant les lettres au crayon), ainsi que tout autre caractère spécial ; les préfixes *ortho*, *meta*, *para*, *cis*, *trans*, etc. seront soulignés pour indiquer leurs caractères italiques et ne seront jamais écrits avec des majuscules.

Aucune correction à main ne sera admise sur le manuscrit. Les corrections seront frappées à la machine. Les lettres grecques ou autres symboles spéciaux seront insérés à la main à l'encre clairement.

Le manuscrit sera signé par l'auteur.

Le colonne-titre aura 50 lettres au maximum.

L'entière responsabilité du contenu des articles appartient aux auteurs.

TRAVAUX PARUS AUX ÉDITIONS DE L'ACADÉMIE DE LA RÉPUBLIQUE SOCIALISTE DE ROUMANIE

I. G. MURGULESCU, **Introducere în Chimia fizică. Vol. I. Atomi, molecule, legătură chimică** (Introduction à la Chimie Physique, Ier vol. Atomes, molécules, liaison chimique), 1976, 559 p,. 36 lei .

P. BALTĂ, E. BALTĂ, **Introduction to the physical chemistry of the vitreous state**, co-édition avec Abacus Press, 1976, 400 p., 39 lei.

I. GĂLĂŢEANU, **Radiochimia aplicată. Metode şi probleme** (La radiochimie appliquée. Méthodes et problèmes), 1976, 305 p., 19 lei.

FR. A GOTHARD, **Echilibre lichid-vapori. I. Baze teoretice şi metode de calcul** (Equilibres liquide-vapeurs, I. Bases théoriques et méthodes de calcul), 1975, 262 p., 28 lei.

CONST. GH. MACAROVICI, DAN MACAROVICI, **Chimia oxizilor dubli şi utilizările lor** (La Chimie des oxydes doubles et leurs utilisation), 1975, 194 p,. 13 lei.

ELENA CEAUŞESCU, **Research work on synthesis and caracterization of macromolecular compounds. Contributions**, 1974, 251 p., 20 lei.

I. ZUGRĂVESCU et MAGDA PETROVANU, **Chimia N-Ilidelor** (La chimie des N-Ylures), 1974, 347 p., 19 lei.

MARGARETA AVRAM, **Antidăunători** (Pesticides), 1974, 494 p., 41 lei.

CR. SIMIONESCU, VIORICA RUSAN et N. POPA, **Chimia algelor marine** (La Chimie des algues marines), 1974, 211 p., 18 lei.

TIBERIU NĂŞCUŢIU, **Metode radiochimice de analiză** (Méthodes radiochimiques d'analyse), 1973, 384, p. 23 lei.

MARIA FITI, **Dozimetria chimică a radiaţiilor ionizate** (La dosimétrie chimique des radiations ionisantes), 1973, 240 p., 13,50 lei.

MIHAI FLORESCU, **Eficienţa economică a cercetării ştiinţifice** (L'efficience économique de la recherche scientifique), 1972, 115 p., 15 lei.

GEORGETA LĂZĂRESCU, **Sistematizarea informaţiilor în Chimia organică** (La systématisation des informations dans la Chimie organique), 1972, 252 p., 10,50 lei.

LYDIA-MARIA VAICUM, **Biodegrabilitatea detergenţilor** (La biodégrabilité des détergents), 1971, 254 p., 16 lei.

TIBERIU NĂŞCUŢIU, **Metode radiometrice de analiză** (Méthodes radiométriques d'analyse), 1971, 346 p., p., 19,50 lei.

I. ZUGRĂVESCU et L.. STOICESCU-CRIVETZ, **Polimeri heterociclici** (Polymères hétérocycliques) 1971, 190 p., 9,50 lei.

1977 JUN 09

I. P. INFORMAŢIA c. 7053

43426

Lei 25.—

F1103

REFERÁLVA

ACADÉMIE DE LA RÉPUBLIQUE SOCIALISTE DE ROUMANIE

REVUE ROUMAINE DE CHIMIE

TOME 22
N° 5
Mai 1977

EDITURA ACADEMIEI REPUBLICII SOCIALISTE ROMÂNIA

Rev. Roumaine Chim. RECHAX, 22, *5*, p. 645–804 (1977), Bucarest

ACADÉMIE DE LA RÉPUBLIQUE SOCIALISTE DE ROUMANIE

COMITÉ DE RÉDACTION

Rédacteur en chef:

I. G. MURGULESCU, membre de l'Académie de la République Socialiste de Roumanie

Rédacteurs en chef adjoints:

A. T. BALABAN et V. EM. SAHINI, membres correspondants de l'Académie de la République Socialiste de Roumanie

Collège de rédaction:

EM. BRATU, ELENA CEAUŞESCU, ECATERINA CIORĂNESCU-NENITZESCU, C. DRĂGULESCU, CR. SIMIONESCU, membres de l'Académie de la République Socialiste de Roumanie; P. SPACU, membre correspondant de l'Académie de la République Socialiste de Roumanie; MARGARETA AVRAM, I. HAIDUC, D. I. MARCHIDAN, I. MOLDOVAN, G. NIAC et D. SĂNDULESCU

La Revue Roumaine de Chimie paraît 10 fois par an. Toute commande de l'étranger (fascicules ou abonnements) sera adressée à ILEXIM — Departamentul Export-Import Carte (Livres)/Departamentul Export-Import Presă (Revues), P.O.B. 136—137, telex 11226, Bucarest, 3, str. 13 Decembrie, Roumanie

Les manuscrits, les livres et les revues proposés en échange ainsi que toute correspondance seront envoyés à la rédaction:

REVUE ROUMAINE DE CHIMIE

23, str. Dumbrava Roşie, Bucarest, Roumanie, téléphone 12 41 60

EDITURA ACADEMIEI REPUBLICII SOCIALISTE ROMÂNIA

125, Calea Victoriei, 71021, Bucarest, Roumanie, téléphone: 50 76 80

ORSZÁGOS MŰSZAKI KÖNYVTÁR ÉS DOKUMENTÁCIÓS KÖZPONT 1883

REVUE ROUMAINE DE CHIMIE

Tome 22, N° 5 Mai 1977

R

G. LIPTAY, L. LIGETHY und E. BRANDT-PETRIK, Thermoanalytische Untersuchungen von Polyäthylen 647–651

C. LITEANU, ELENA HOPÎRTEAN and EUGENIA STEFĂNIGĂ, Liquid-membrane electrodes. XI. Tetrafluoroborate-selective liquid membrane-electrode 653–656

CONST. GH. MACAROVICI und E. CHIŞ, Ein neues Reagenz vom EDTA-Typus. II. Komplexsalze der 4,4′-Diaminodiphenylmethan-N,N′-diessigsäure mit verschiedenen Metallionen 657–664

F. MATHIS, Quelques aspects de la recherche en chimie organique du phosphore : résultats et perspectives 665–674

MARIA MRACEC, ANA MAURER, SEPTIMIA POLICEC und Z. SIMON, Bildung und Stabilität von Metallchelaten mit Liganden die Donoratome aus der 6. Gruppe enthalten. I. HMO-Berechnungen an den Liganden (*o*-Carboxyphenoxy)-essigsäure und (*o*-Carboxyphenylthio)-essigsäure 675–682

I. G. MURGULESCU and CR. TELEA, Heat capacities in molten alkaline halides 683–689

ANA NIMARĂ and I. JULEAN, Contributions to the bismuth hydrolysis study. IV. Equilibrium and rate constants of bismuth perchlorate hydrolysis studied by polarography 691–695

TATIANA ONCESCU, S. G. IONESCU and C. ANDREESCU, On the photolysis of [Mn $(C_2O_4)_2(H_2O)_2$]K in dimethyl-formamide. II. Concentration and oxygen effects 697–704

G. OSTROGOVICH, MARIA NUŢIU and R. NUŢIU, Studies in the field of biuret reaction. X. Infrared absorption spectra for some copper(II) complexes of the cyanuric acid 705–712

B. I. PETROV, V. V. STRELKOV, A. I. BUSEV und P. NENNING, Zur Komplexbildung bei der Hf-Extraktion aus chloridhaltigen Lösungen unter Verwendung von Hexyldiantipyrilmethan 713–717

E. PETROVICI et IULIANA LUPU, Hexachloroantimonates(V) métalliques complexes ayant comme ligand la pyridine 719–724

GR. POPA et LUMINIŢA VLĂDESCU, Séparation et concentration du magnésium des fontes au graphite sphéroïdal au moyen des résines échangeuses d'ions 725–732

Rev. Roumaine Chim. **22**, *5*, p. 645 – 804, (1977) Bucarest

O. A. REUTOV and K. P. BUTIN, Equilibria of redistribution reactions of organometallic compounds 733–737

K. SAITO, Circular dichroism of optically active square planar complexes containing η^2-olefins 739–743

H. SANKE GOWDA, K. N. THIMMAIAH and B. NARAYANA ACHAR, Spectrophotometric determination of palladium(II), cerium(IV). Arsenic (III) and nitrite with fluphenazine hydrochloride 745–751

R CR. SIMIONESCU and I. MAZILU, Ferrocene polymers as polymerization initiators 753–759

I. SITARU and E. SEGAL, On preferential orientation of thin magnesium films supported on glass 761–764

H. SONTHEIMER, Chemische Parameter der Gewässerverschmutzung . . . 765–771

V. I. SPITSINE et L. I. MARTYNENKO, Effets des particularités cinétiques des complexes des éléments des terres rares sur le mécanisme du processus de séparation par échange ionique 773–779

A. TAKEUCHI and S. YAMADA, Isomerism in copper(II) complexes with N-isopropyl- and N-cyclohexyl-salicylaldiminates 781–786

T. P. TĂVALĂ, N. GR. BRÎNZAN and V. FLOREA, Red-brown pigments in the $Cr_2O_3-TiO_2-WO_3$ system 787–792

P. TRIBUNESCU, ECATERINA MERCA und OTILIA FACSKÓ, Die thermische Zersetzung einiger Hexacyanokomplexen. I. Silber Ammonium oder Alkylammonium Hexacyanoferrate 793–799

R K. YAMASAKI and Y. YOSHIKAWA, Correlation between absolute configurations of cobalt(III) complexes and their chromatographic behaviour on ion-exchange cellulose 801–804

Revue Roumaine de Chimie, **22**, 5, 647–651 (1977)

Herrn Professor Dr. CORIOLAN DRĂGULESCU
zum 70. Geburtstag gewidmet

THERMOANALYTISCHE UNTERSUCHUNGEN VON POLYÄTHYLEN

G. LIPTAY *, L. LIGETHY ** und E. BRANDT-PETRIK *
* Institut für Anorganische Chemie, Technische Universität, Budapest,
** Ungarische Kabelwerke, Budapest

Eingegangen am 24. September 1976

Die thermischen Eigenschaften der — in der Mittel- und Hochspannungsisoliertechnik angewandten — verschiedenen Polyäthylenen wurden durch dynamische und isotherm thermoanalytische Methoden untersucht. Die Proben sind mit anderen, im elektrischen Feld gealterten Proben verglichen worden. Es konnte festgestellt werden, daß bei den im elektrischen Feld gealterten Proben für Wärmeeinwirkung dieselben Vorgänge ablaufen, wie bei den ungealterten, jedoch ist die Ablaufszeit kleiner.

Wegen seinen ausgezeichneten elektrischen Eigenschaften wird das Polyäthylen in wachsendem Maße in der Isoliertechnik für Mittel- und Hochspannungsgebiete verwendet. Es ist ein wertvolles Isoliermaterial für Energieverteilungskabel, und weist zahlreiche Anwendungs- und Betriebsvorteile auf, gegenüber den herkömmlichen Materialen. Die Anwendungs- und Betriebseigenschaften von Polyäthylen haben sich bei Reaktionen, die durch Wärme ablaufen bewährt, deswegen können Studien der thermischen Eigenschaften des Polyäthylens vor der Herstellung des Produktes entscheidend sein.

In unserer früheren Arbeit [1] wurde nachgewiesen, daß die thermoanalytischen Methoden zum Vergleich : Thermostabilität, thermische oder thermooxidative Eigenschaften von verschiedenen Elektroisolierstoffen anwendbar sind. Diese Ergebnisse wurden für die Untersuchungen der thermooxidativen Eigenschaften bei elektrisch beanspruchten Polyäthylenen angewandt und weiterentwickelt.

Bei einigen Untersuchungen wurden die dynamischen thermischen Methoden angewandt.

Hier soll erwähnt werden, daß die Untersuchungen nicht in Sauerstoff-Atmosphäre durchgeführt wurden (obgleich in der letzten Zeit solche Untersuchungen öfter veröffentlicht wurden) einerseits um die neuen Daten mit den früheren zu vergleichen, andererseits da die hohe Sauerstoffkonzentration nicht den Vorgängen folgt, welche unter Normalständen ablaufen.

---

[1] L. Ligethy und G. Liptay : „Thermal Analysis" ed. I. Buzás Proc. 4th ICTA, Vol. 3. Akadémiai Kiadó, Budapest, 1975, S. 389.

Neben den dynamischen Meßmethoden wurden auch die Isothermen verwendet.

Aus den Voruntersuchungen und auch aus früheren gefundenen Ergebnissen haben wir die Temperatur von 150°, als Untersuchungstemperatur für Isotherm-Untersuchungen ausgewählt.

Es wurden drei Typen von Polyäthylenen geprüft. (In weiterem PÄ.) Eine normal-Hochdruckpolyäthylen-Qualität, eine spannungsstabilisierte Qualität (besteht aus dem erwähnten normal Polymer und aus einer speziellen Aminverbindung die zugemischt wird), bzw. vernetztes Polyäthylen (mit Benzoilperoxyd vernetzt). Die Proben sind in einer Glaszelle einer elektrischen Beanspruchung unterworfen worden.

Die PÄ-Proben zeigten bis cca 180° eine Gewichtsstabilität. In diesem Temperaturbereich zeigt die DTA Kurve den Vorgang des Schmelzens mit endothermen Effekten. Der Vorgang selbst — entsprechend unseren früheren Ergebnissen — besteht aus zwei Teilen : aus einem langsamen Anstieg und aus einer späteren markanten Spitze. (Abb. 1)

Die Derivatogramme der elektrisch-beanspruchten PÄ-Folien weichen ein wenig von den nichtbeanspruchten ab. Die Abweichungen sind meist gering, sind aber viel größer als die Empfindlichkeit der Methode ; aus den Unterschieden der thermoanalytischen Kurven kann man einige Folgerungen ziehen. Die Derivatogramme der in elektrischem Feld gealterten Proben sind wegen der Übersichtlichkeit mit gestreiften Linien neben den ungealterten dargestellt.

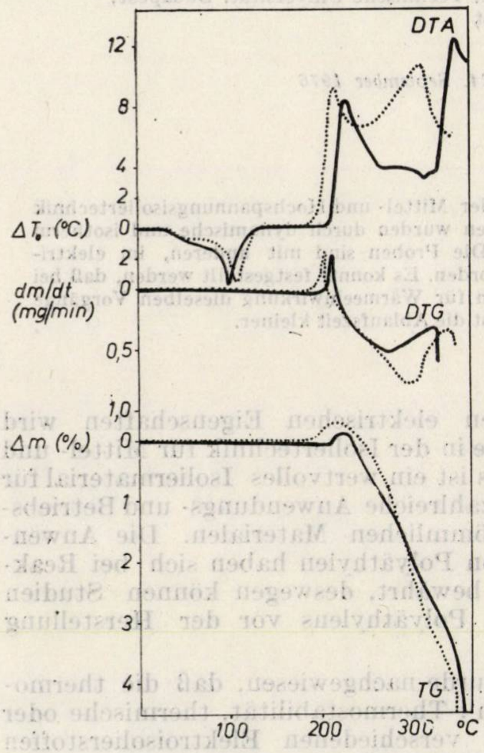

Abb. 1 — Derivatogramm von Hochdruckpolyäthylen.

———— ungealterte Probe; .... in elektrischem Feld gealterte Probe.

Die Oxydation von elektrisch-gealterten Proben beginnt und läuft mit um 20° niedrigerer Temperatur ab, als im Falle von nichtgealterten Proben. Außer diesen quantitativen Abweichungen zeigt die DTA Kurve auch qualitative Unterschiede besonders im höheren Temperaturbereich.

Es kann festgelegt werden, daß der Gewichtsverlust der gealterten Probe größer ist, als der von ungealterten.

In spannungsstabilisierten Proben sind die thermischen Umwandlungen ein wenig verschoben, aber geringer als bei dem Grundpolymer. (Abb. 2). Man kann festlegen, daß sich ein Exotherm-Effekt der elektrisch beanspruchten Proben um 300°, vor dem vollständigen Abbau, als DTA Kurve zeigt.

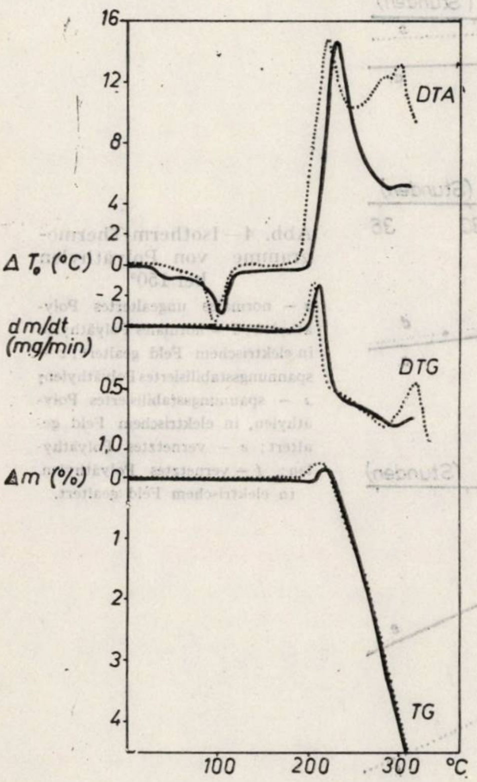

Abb. 2 — Derivatogramm von spannungsstabilisierten Hochdruckpolyäthylenen

——— ungealterte Probe; .... in elektrischem Feld gealterte Probe.

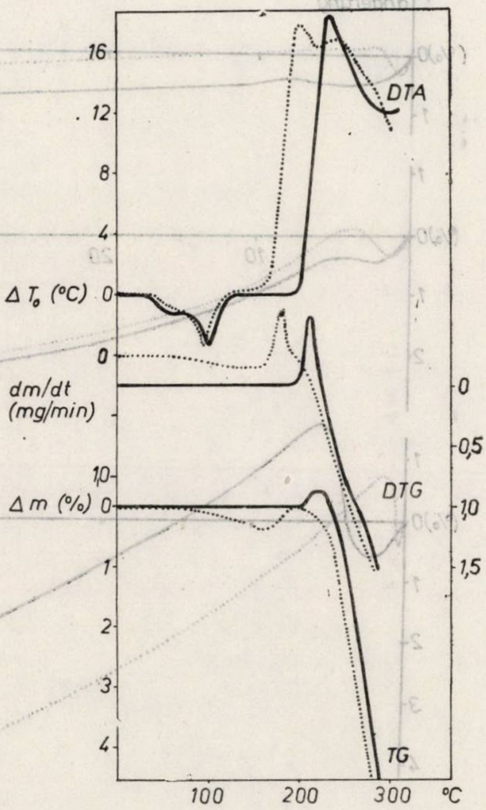

Abb. 3 — Derivatogramm von vernetztem Polyäthylen

——— ungealterte Probe; .... in elektrischem Feld gealterte Probe.

Vernetztes Polyäthylen (Abb. 3) weist keinen Gewichtsverlust nach dem Erweichen bis zum Beginn der Oxydation auf. Das Erweichen der elektrisch beanspruchten Proben folgt mit einer geringen Gewichtsabnahme von cca 0,5% (gegenüber den früheren Proben!) und nachdem bei beiden Proben sich eine Gewichtszunahme cca 0,5% zeigt. Diese Temperatur ist aber niedriger, als bei den früher erwähnten Proben. Der Charakter der DTA Kurven ändert sich auch und es ist keine waagerechte Strecke zu finden, wie in früheren Fällen. Der Abbau der auf die Oxydation folgt, ist bei ungealterten und bei gealterten Proben wesentlich höher, als bei früheren Proben.

Bei isothermen Untersuchungen aller Proben zeigten sie eine geringe Gewichtsabnahme und danach trat in allen Fällen eine Gewichtszunahme (Oxydation) auf. (Abb. 4)

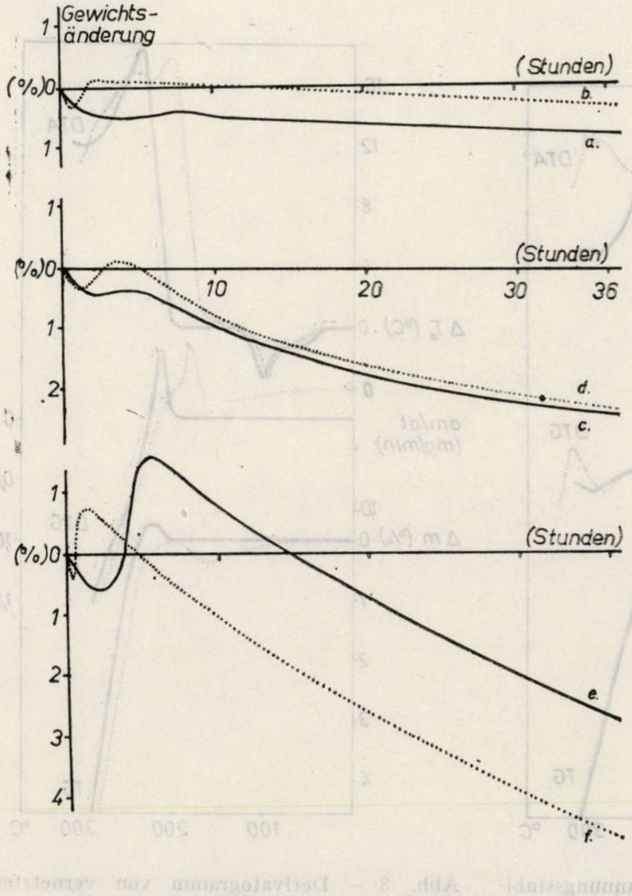

Abb. 4 — Isotherm-Thermogramme von Polyäthylen bei 150°

a — normales ungealtertes Polyäthylen; *b* — normales Polyäthylen in elektrischem Feld gealtert; *c* — spannungsstabilisiertes Polyäthylen; *d* — spannungsstabilisiertes Polyäthylen, in elektrischem Feld gealtert; *e* — vernetztes Polyäthylen; *f* — vernetztes Polyäthylen, in elektrischem Feld gealtert.

Bei der 150° isotherm-thermogravimetrischen Kurve weist das Grundpolymer (Kurve *a*) einen Anfangsgewichtsverlust (0,5%) während 5 Stunden auf, gefolgt von einer geringen Gewichtszunahme (0,1%). Danach tritt eine monoton ermäßigte Gewichtsabnahme ein. Im Falle des Grundpolymers, gealtert in elektrischem Feld (Kurve *b*) sind die früher erwähnten Vorgänge binnen kürzerer Zeit, aber markanterweise abgelaufen. Die Zeit der Anfangsgewichtsabnahme verkürzte sich auf 1 Stunde, gefolgt von einer schnellen bedeutenden Gewichtszunahme (0,4%). Die Probe zeigte nachdem — ähnlich wie die ungealterte Probe — eine ermäßigte monotone Gewichtsabnahme.

Auch die Isotherma der spannungsstabilisierten ungealterten Probe (Kurve *c*) zeigt eine Anfangsgewichtsabnahme, welche von der Oxydation des Polyäthylens gefolgt wird, bestätigt durch eine Gewichtszunahme (0,1%). Danach erleidet die Probe eine Degradation in wesentlich größerem Maß, als das Grundpolymer. Die Stelle des Maximums des Oxydationsvorgangs in der Zeitabhängigkeit gemessen war kleiner (3 Stunden anstatt 5 Stunden), jedoch von größerem Umfang (0,45% anstatt 0,1%). Der Verlauf der weiteren Degradation scheint ganz gleich, wie bei der ungealterten Probe. (Kurve *d*).

Im Falle des vernetzen Polymers waren die Oxydations- und Degradationsvorgänge die größten. Bei der ungealterten Probe (Kurve *e*) erhielten wir eine Gewichtszunahme von 2%, danach verlief aber die Degradation wesentlich schneller, als bei den früher erwähnten nichtvernetzten Proben. Bei den gealterten Proben (Kurve *f*) liefen die Effekte binnen kürzerer Zeit, aber in kleinerem Maß ab. Die Oxydationsvorgänge der vernetzten Probe zeigen sich wesentlich stärker, weil Tertiärkohlenstoffatome die während der Vulkanisation entstanden sind, eine geringere Wärmestabilität aufweisen.

Durch Vergleichen der Isothermen kann festgestellt werden, daß die Degradation bei dem Grundpolymer die kleinste ist und die höchste bei den vernetzten Proben. Insofern laufen für Wärmeeinwirkung die gleichen Vorgänge bei ungealterten Proben wie bei gealterten ab, nur die Vorgänge zeigen im zweiten Fall einen geringeren Zeitverbrauch.

Revue Roumaine de Chimie, 22, 5, 653–656 (1977)

Dedicated to the 70th anniversary
of Professor CORIOLAN DRĂGULESCU

LIQUID-MEMBRANE ELECTRODES. XI *

TETRAFLUOROBORATE-SELECTIVE LIQUID MEMBRANE-ELECTRODE

C. LITEANU, ELENA HOPÎRTEAN and EUGENIA STEFĂNIGĂ

Department of Analytical Chemistry, University of Cluj-Napoca, str. Arany J. No. 11,
Cluj-Napoca, Romania

Received June 14, 1975

The results with regard to the obtention of BF_4^- - selective liquid membrane-electrode by using tetraphenylphosphonium bromide as electrode active component in tetrachloroethane as solvent are presented. The electrode response towards $10^{-1} - 10^{-4}$M BF_4^- (J = const., achieved by Na_2SO_4 or NaH_2PO_4) is nernstian. The selectivity series of the electrode was established.

INTRODUCTION

There are few reports dealing with BF_4^--selective liquid membrane-electrodes. These refer to the practical application of the electrode in determining the boron content of water, [1] soil, [2] plant tissues, [2] $Al_2O_3-BC_4$[3] and of silicones in semiconductor devices.[4] Orion BF_4^--selective electrode was used having quaternary ammonium salt as liquid ion exchanger. In the present paper the response towards tetrafluoroborate of a liquid membrane-electrode obtained from tetraphenylphosphonium bromide in tetrachloroethane is studied.

EXPERIMENTAL

The liquid membrane-electrode has been obtained by soaking the pores of a glass frit G_4 support made hydrophobic, attached to the extremity of a glass tube, by a 0.2% tetraphenylphosphonium bromide (PPh_4Br) solution in tetrachloroethane. The organic solution was used as internal solution too. Saturated calomel electrodes have been used as inner and outer reference electrodes.

---

* Part X. E. HOPÎRTEAN, *Rev. Roumaine Chim.*, in press.

[1] R. M. CARLSON and J. L. PAUL, *Analyt. Chem.*, **40**, 1292 (1968).

[2] R. M. CARLSON and J. L. PAUL, *Soil Sci.*, **108**, 266 (1969).

[3] H. E. WILDE, *Analyt. Chem.*, **45**, 1526 (1973).

[4] P. LANZA and P. L. BULDINI, *Analyt. Chim. Acta*, **75**, 149 (1975).

Potential measurements have been performed with a MV−85 pH-meter (± 1 mV precision), by measuring the e.m.f. of the electrochemical cell:

SCE ‖ Internal organic solution | Liquid membrane in glass frit | Test solution ‖ SCE

Determinations were performed at room temperature in nonstirred solutions.

Reagents and solutions. All reagents were of analytical grade. Standard $10^{-1} - 10^{-5}$M $NaBF_4$ solutions have been prepared by successive dilutions of the 1M $NaBF_4$ stock solution, the ionic strength being adjusted with Na_2SO_4 to $J = 0.15$ M or with NaH_2PO_4 to $J = 0.1$M. Standard series of $NaBF_4$ containing 10^{-1}M HF have also been prepared. In order to check the electrode selectivity in the presence of Cl^-, Br^-, AcO^- and CO_3^{2-} anions, standard solutions of $NaBF_4$ containing the above-mentioned anions in a 10^{-1}M concentration, have been prepared.

RESULTS AND DISCUSSIONS

The liquid membrane-electrode formed by 0.2% tetraphenylphosphonium bromide in tetrachloroethane was conditioned by maintaining it in a 10^{-1}M $NaBF_4$ solution, till a constant potential has been reached (3–4 hours). Between the determinations series the electrode was maintained in a 10^{-1} M $NaBF_4$ solution.

Electrode functions obtained for $NaBF_4$ in standard solutions containing HF, Na_2SO_4 and NaH_2PO_4, respectively, are given in Fig. 1. The characteristic electrode response data are given in table 1. Na_2SO_4 and NaH_2PO_4 are good adjusting agents for the ionic strength of the standard $NaBF_4$ solutions. In the presence of these electrolytes the electrode gives a practical nernstian response for BF_4^- in $10^{-1}-10^{-4}$M concentration range. The 10^{-1}M HF present in the standard $NaBF_4$ solutions reduces the concentration range of the electrode response, without a significant affecting in its sensitivity. The electrode standard potential is shifted to more negative values.

The electrode functions for BF_4^- in the presence of 10^{-1} M chloride, bromide, acetate and carbonate, respectively, were established. The results thus obtained are given in Fig. 2 and table 2. Fig. 2 also represents the electrode function for BF_4^- obtained in standard $NaBF_4$ solutions without adjusting the ionic strength with an electrolyte. Carbonate and acetate have been proved to be indifferent while chloride interferes significantly, decreasing both the linear response range and the electrode sensitivity. Bromide produces a great interference. The following selectivity series is given for the studied electrode:

$$ClO_4^- > SCN^- > I^- > BF_4^- > NO_3^- > Br^- > Cl^- > CO_3^{2-},\ H_2PO_4^-,$$
$$AcO^-,\ SO_4^{2-}.$$

As to the electrode response time, it varies from 20–30 sec in solutions having concentrations higher than 10^{-2}M to 5–10 min for concentrations lower than 10^{-3}M.

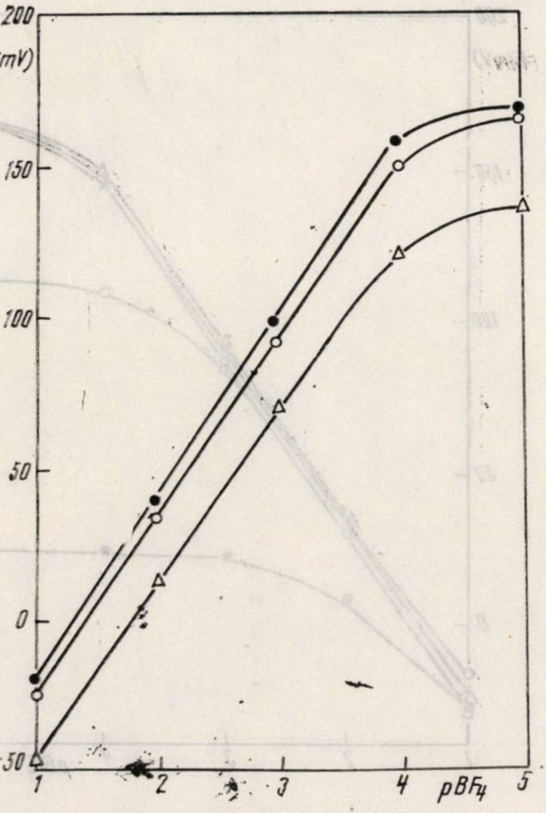

Fig. 1. — Electrode functions for BF_4^-.

— ● — J = 0.15 M (Na_2SO_4); — ⊙ — J = = 0.1 M (NaH_2PO_4); — △ — HF (c = 10^{-1} M).

Table 1

Behaviour of the liquid membrane-electrode from PPh_4Br in tetrachloroethane towards BF_4^-

Foreign electrolyte	Concentration range of BF_4^-	Slope (mV)
Na_2SO_4 (J = 0.15 M)	10^{-1} – 10^{-4} M	59.5
NaH_2PO_4 (J = 0.1 M)	10^{-1} – 10^{-4} M	58.0
HF (c = 10^{-1} M)	10^{-1} – 2×10^{-4}M	57.5

CONCLUSIONS

Liquid membrane-electrode with PPh_4Br as active component in tetrachloroethane as solvent shows a nernstian behaviour towards 10^{-1} – 10^{-4}M tetrafluoroborate ion (constant ionic strength, achieved by Na_2SO_4 or NaH_2PO_4). The 10^{-1} M HF present in standard solutions shifts the electrode potential to more negative values. Acetate and carbonate (c = 10^{-1}M) do not disturb the electrode response to BF_4^-. Bromide and chloride interferences upon the electrode response as well as the general selectivity series have been established.

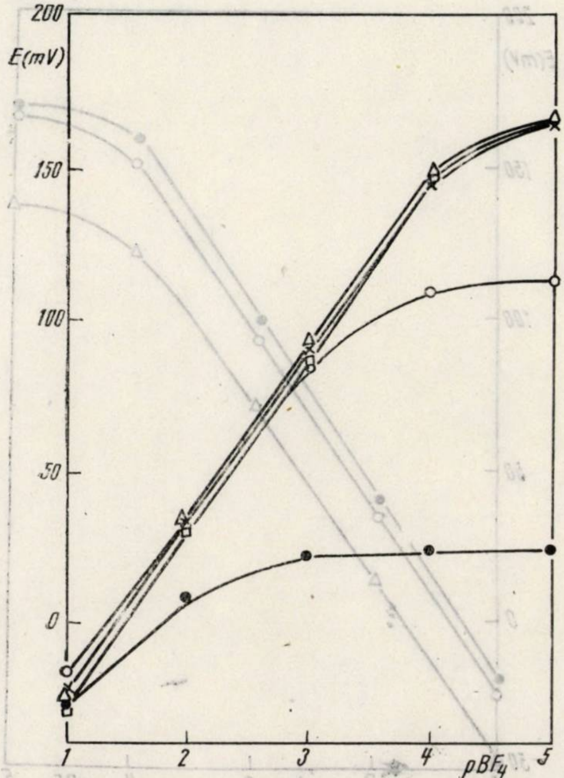

Fig. 2.— Influence of some anions ($c = 10^{-1}$M) on the electrode function for BF_4^-.

— × — without foreign anion ; — △ — CO_3^{2-} ; — □ — AcO^- — ○ — Cl^- ; — ● — Br^-.

Table 2

Behaviour of the liquid membrane-electrode from PPh_4Br in tetrachloroethane towards BF_4^- in the presence of some anions

Foreign anion ($c = 10^{-1}$M)	Concentration range of BF_4^-	Slope (mV)
—	$10^{-1}-10^{-4}$ M	57.0
CO_3^{2-}	$10^{-1}-10^{-4}$ M	56.0
AcO^-	$10^{-1}-10^{-4}$ M	57.5
Cl^-	$10^{-1}-10^{-3}$ M	52.0
Br^-	$10^{-1}-10^{-2}$ M	35.0

Revue Roumaine de Chimie 22, 5, 657–664 (1977)

Herrn Professor Dr. Coriolan Drăgulescu
zum 70. Geburtstag gewidmet

EIN NEUES REAGENZ VOM EDTA-TYPUS. II*

KOMPLEXSALZE DER 4,4′-DIAMINODIPHENYLMETHAN-N, N′-DIESSIGSÄURE MIT VERSCHIEDENEN METALLIONEN

CONST. GH. MACAROVICI ** und EUGEN CHIŞ ***
** Fakultät für Chemie der „Babeş-Bolyai“-Universität, Cluj-Napoca
*** Fakultät für Physik-Chemie der Universität, Braşov

Eingegangen am 4. August 1976

Es wird über neue Chelatverbindungen verschiedener I-, II-, III- und IV- wertiger Metallionen mit 4,4′-Diaminodiphenylmethan-N,N′-diessigsäure als Ligand berichtet. Auf Grund der chemischen und thermogravimetrischen Analysen, der IR- und Elektronenspektren und der magnetischen Bestimmungen wurden die wahrscheinlichen Strukturschemata der synthetisierten Komplexverbindungen festgelegt. Die Verwendung des Liganden als Fällungsreagenz wird vorausgesehen.

In einer vorhergehenden Veröffentlichung [1] wurde über die Darstellung von 4,4′-Diaminodiphenylmethan-N, N′-diessigsäure, RAc_2H_2, und deren Natriumsalz RAc_2Na_2 mitgeteilt ($R = -NH \cdot C_6H_5-CH_2-$ $-C_6H_5 \cdot NH-$; $Ac = -CH_2COO^-$).

In vorliegender Arbeit berichten wir über die Untersuchung von neuen Komplexverbindungen der angeführten Säure mit I-, II-, III- und IV- wertigen Metallionen bezüglich ihrer Eigenschaften und Struktur.

EXPERIMENTELLER TEIL

Die Synthesen der Komplexverbindungen wurden durch Zufügen, unter ständigem Rühren, von alkoholischen oder alkoholisch-wäßriger Lösungen der betreffenden Metallchloride, in stöchiometrischen Verhältnissen zu einer alkoholischen Lösung des Natriumsalzes oben angegebener Säure durchgeführt. Die ausgefällten Niederschläge wurden nach 1–3 Stunden filtriert, mit destilliertem Wasser bis zur gänzlichen Entfernung der Cl^--Ionen und nachher mit Methylalkohol und Äther gewaschen. Getrocknet wurde in einem Vakuumexikator bei Zimmertemperatur.

---

* Mitteilung I : *Rev. Roumaine Chim.*, **19**, 1855 (1974).

[1] Const. Gh. Macarovici und E. Chiş, *Rev. Roumaine Chim.* **19**, 1855 (1974).

Einige dieser neuen Komplexverbindungen sind gefärbt; vor allem jene mit Übergangsmetallen. Mit Ausnahme der den Alkali- und Erdalkalimetallen angehörenden Verbindungen sind alle unlöslich in Wasser und Alkohol, in dem sie sich manchmal sogar bei ziemlich niedrigem pH-Wert (unter 5) bilden. Dieses in Verbindung mit erhaltenen Resultaten mit den gravimetrischen Bestimmungsversuchen einiger der verwendeten Metallionen, eröffnet die in der vorherigen Mitteilung angegebene Möglichkeit der Anwendung des Natriumsalzes RAc_2Na_2 als Niederschlagsreagenz.

Die Ergebnisse der Elementaranalyse und einige Eigenschaften der erhaltenen Komplexverbindungen sind in Tabelle 1 enthalten.

Tabelle 1

Chemische Analyse der durch Synthese erhaltenen Substanzen

Synthetisierte Substanz	Farbe	Schmelzpunkt	Gehalt an: % C		% N		% Metall		% H_2O	
			Ber.	Gef.	Ber.	Gef.	Ber.	Gef.	Ber.	Gef.
RAc_2Li_2	gelb	—	62,59	62,21	8,59	8,48	4,25	4,11		
$[RAc_2]_2Ca_2$	”	—	57,94	57,88	7,95	7,86	11,37	11,34		
$[RAc_2]_2Ba_2$	”	—	45,42	45,44	6,23	6,18	30,54	30,43		
$[RAc_2]_2Pb_2$	weiß	> 300	39,30	39,08	5,39	5,29	39,88	39,62		
$[RAc_2]_2Mn_2 \cdot 4H_2O$	”	> 300	50,60	50,49	6,94	7,12	13,62	13,38	8,93	9,12
$[RAc_2]_2Co_2 \cdot 6H_2O$	rosa	—	48,01	47,81	6,58	6,34	13,85	13,71	12,71	12,60
$[RAc_2]_2Ni_2 \cdot 6H_2O$	hellgrün	—	48,04	48,18	6,58	6,37	13,81	13,38	12,71	12,56
$[RAc_2]_2Cu_2 \cdot 4H_2O$	dunkel-grün	< 300	49,57	49,21	6,81	7,09	15,42	15,21	8,74	8,82
$[RAc_2]_2Zn_2$	weiß	—	54,06	53,02	7,41	6,54	17,31	17,04		
$[RAc_2]_2Cd_2 \cdot 4H_2O$	,,	> 300	44,32	44,36	6,08	5,92	24,39	24,33	7,81	7,69
$[RAc_2]_3Al_2$	,,	—	61,81	62,03	8,48	8,39	5,44	5,41		
$[RAc_2]_3Cr_2 \cdot 4H_2O$	graugrün	—	55,03	54,78	7,55	6,98	9,34	9,34	6,47	6,58
$[RAc_2]_3In_2$	weiß	> 300	52,51	51,76	7,20	6,72	19,68	19,19		
$[RAc_2]_3Fe_2 \cdot 4H_2O$	braun	—	54,64	54,81	7,49	7,42	9,69	10,35	6,43	6,67
$[RAc_2]_3La_2$	weiß	—	50,42	50,38	6,92	6,78	22,87	22,78		
$[RAc_2]_3Ce_2$	”	—	50,33	50,46	6,90	7,21	23,02	22,89		
$[RAc_2]_4Th_2 \cdot 8H_2O$	”	—	43,97	43,89	6,03	5,85	24,98	24,71	7,75	7,62
$[RAc_2]_4Ti_2$	”	—	60,72	59,91	8,33	8,12	7,12	7,07		

$R = -NH-C_6H_4-CH_2-C_6H_4-NH-$; $Ac = -CH_2COO-$.

Zwecks weiterer Informationen zur Strukturbestimmung der synthetisierten Stoffe wurden folgende Analysen durchgeführt. Die thermogravimetrischen Analysen wurden mit Hilfe eines Derivatographen (F. Paulik, J. Paulik, L. Erdely) im Temperaturbereich bis 1000° ausgeführt.

Tabelle 2

Thermische Zersetzung der Verbindungen

Komplexe Substanz	Molmasse	Temperaturbereich in dem die exothermen Effekte stattfinden °C	Nach der thermischen Zersetzung zurückgebliebene Substanz: Zusammensetzung	Gehalt, %: Ber.	Gef., TG
RAc_2Li_2	326,21	180—900	Li_2CO_3	22,64	23,12
$[RAc_2]_2Cu_2 \cdot 4H_2O$	823,74	140—520	CuO	19,21	18,99
$[RAc_2]_3Al_2$	990,95	200—660	Al_2O_3	10,28	10,55
$[RAc_2]_3Cr_2 \cdot 4H_2O$	1113,07	200—540	Cr_2O_3	13,63	13,87
$[RAc_2]_3Fe_2 \cdot 4H_2O$	1120,75	150—690	Fe_2O_3	14,24	14,83
$[RAc_2]_4Th_2 \cdot 8H_2O$	1857,20	200—670	ThO_2	28,42	28,54

$R = -NH-C_6H_4-CH_2-C_6H_4-NH-$; $Ac = -CH_2COO^-$.

Die IR-Spektren wurden mir einem Perkin-Elmer Spektrophotometer ausgeführt, unter Benützung von KBr-Pastillen (Tabelle 3). Die Reflexionselektronenspektren wurden mit einem Carl-Zeiss VSU–2P Spektrophotometer im Bereich 320–1500 nm aufgenommen (Tabelle 4). Für die magnetischen Suszeptibilitätbestimmungen gelangt die Gouy Methode oder die Faraday Methode, unter Benützung der Standarde $CuSO_4 \cdot 5H_2O$ bzw. $Co[Hg(SCN)_4]$ zur Anwendung (Tabelle 5).

Tabelle 3

Zuordnung der in den IR-Spektren der synthetisierten Substanzen erschienenen Banden

Zugeordnete Banden / Substanz	ν—CH_2—	vas—NH—CH_2COO^- ν—COO—M	Ar—NH—CH_2—	ν_s—COO^-	Ar—NH—CH_2—	ν C—N $>$C—NH—CH_2—	ν—CH_2 COOH
RAc_2H_2	2920 m	1615 ss	1515 s	1430 s	—	1190 m	1715 m
RAc_2Li_2	2923 ms	1618 ss	1518 ss	1420 ss	1315 ss	1180 m	—
$[RAc_2]_2Ca_2$	2920 ms	1615 ss	1515 ss	1430 s	1320 ms	1180 msw	—
$[RAc_2]_2Ba_2$	2920 s	1615 ss	1510 s	1430 ss	1310 ms	1185 msw	—
$[RAc_2]_2Pb_2$	2920 ms	1615 ss	1518 ss	1388 ss	1305 s	1185 m	—
$[RAc_2]_2Mn_2 \cdot 4H_2O$	2928 m	1615 ss	1518 ss	1405 s	1320 ms	1185 msw	—
$[RAc_2]_2Co_2 \cdot 6H_2O$	2922 ms	1598 ss	1515 ss	1410 s	1318 m	1180 m	—
$[RAc_2]_2Ni_2 \cdot 6H_2O$	2930 ms	1615 ss	1518 ss	1410 s	1320 m	1180 m	—
$[RAc_2]_2Cu_2 \cdot 4H_2O$	2925 ms	1620 ss	1515 ss	1435 ms	1325 ms	1185 sw	—
$[RAc_2]_2Zn_2$	2925 m	1615 ss	1515 ss	1405 ss	1320 ms	1185 sw	—
$[RAc_2]_2Cd_2 \cdot 4H_2O$	2925 ms	1620 ss	1515 ss	1400 ss	1318 ms	1185 sw	—
$[RAc_2]_3Al_2$	2925 ms	1620 ss	1520 ss	1435 m	1315 s	1185 m	—
$[RAc_2]_3In_2$	2920 ms	1618 ss	1518 ss	1385 s	1315 s	1185 m	—
$[RAc_2]_3Cr_2 \cdot 4H_2O$	2925 m	1615 ss	1515 ss	1435 m	1315 ms	1180 ms	—
$[RAc_2]_3Fe_2 \cdot 4H_2O$	2925 ms	1618 ss	1518 ss	1405 s	1312 s	1185 ms	—
$[RAc_2]_3La_2$	2920 ms	1615 ss	1515 ss	1410 ss	1305 s	1185 m	—
$[RAc_2]_3Ce_2$	2920 ms	1615 ss	1520 ss	1405 ss	1320 s	1185 m	—
$[RAc_2]_4Th \cdot 8H_2O$	2925 ms	1615 ss	1520 ss	1430 s	1310 s	1182 msw	—
$[RAc_2]_4Ti_2$	2925 m	1618 ss	1518 ss	1405 m	1310 ms	1185 m	—

$R = -NH-C_6H_4-CH_2-C_6H_4-NH-$; $Ac = -CH_2COO-$; ss = sehr stark; s = stark; m = mäßig; ms = mäßig-stark; sw = schwach; msw = mäßig-schwach.

Tabelle 4

Reflexionsspektren (cm^{-1}) einiger Komplexverbindungen

Komplexverbindung	ν_1	ν_2	ν_3	Ladungsübertragung
$[RAc_2]_3Cr_2 \cdot 4H_2O$	$^4T_{2g} \leftarrow {}^4A_{2g}$ 17000	$^4T_{1g} \leftarrow {}^4A_{2g}$ 23300	$^4T_{1g}(P) \leftarrow {}^4A_{2g}$ (F) 28000	—
$[RAc_2]_2Co_2 \cdot 6H_2O$	$^4T_{2g} \leftarrow {}^4T_{1g}$ 7700	$^4T_{2g} \leftarrow {}^4T_{1g}$ 18800	$^4T_{1g}(P) \leftarrow {}^4T_{1g}(F)$ 26400	—
$[RAc_2]_2Ni_2 \cdot 6H_2O$	$^3T_{2g} \leftarrow {}^3A_{2g}$ 8700	$^3T_{1g} \leftarrow {}^3A_{2g}$ 14500	$^3T_{1g}$ (P) $\leftarrow {}^3A_{2g}(F)$ 25400	— 30300
$[RAc_2]_2Cu_2 \cdot 4H_2O$	$^2T_{2g} \leftarrow {}^2E_{2g}$ 15000	—	—	25000

$R = -NH-C_6H_4-CH_2-C_6H_4-NH-$; $Ac = -CH_2COO-$.

Tabelle 5

Magnetische Eigenschaften einiger Komplexverbindungen

Komplexverbindung	TK	$\chi_g 10^{-6}$	$\chi_{Mcor} 10^{-6}$	μBM	Methode
$[RAc_2]_3Cr_2 \cdot 4H_2O$	296	11,25	6453	3,93	Gouy
	297	11,65	6675	3,99	Faraday
$[RAc_2]_2Co_2 \cdot 6H_2O$	296	21,02	9093	4,65	Gouy
$[RAc_2]_2Ni_2 \cdot 6H_2O$	297	8,24	3657	2,95	Gouy
$[RAc_2]_2Cu_2 \cdot 4H_2O$	296	2,44	1115	1,64	Gouy
	297	2,39	1097	1,64	Faraday

$R = -NH-C_6H_4-CH_2-C_6H_4-NH-$; $Ac = -CH_2COO^-$.

ERGEBNISSE UND DISKUSSION

Die chemische Analyse (Tabelle 1) bestätigt die Zusammensetzung bzw. das Bindungsverhältnis M : L der folgenden synthetisierten Komplexverbindungen:

$RAc_2M_2^I$; (2M : 1L) ; $M^I = Li$

$[RAc_2]_2M_2^{II} \cdot xH_2O$; (2M : 2L) ; M^{II} = Ca, Ba, Pb, Mn, Co, Ni, Cu, Zn, Cd.

x = 0, 2, 6 ;

$[RAc_2]_3M_2^{III} \cdot xH_2O$; (2M : 3L) ; M^{III} = Al, In, Cr, Fe, La, Ce.

x = 0, 4 ;

$[RAc_2]_4M_2^{IV} \cdot xH_2O$; (2M : 4L) ; M^{IV} = Th, Ti ;

x = 0, 8 ;

$R = -NH-C_6H_4-CH_2-C_6H_4-NH-$; $Ac = -CH_2COO^-$.

Aus den thermogravimetrischen Diagrammen der Li-, Al-, Fe-, Cr-, Cu- und Th-Salze geht hervor, daß diese sogar unter 100° sich zu zersetzen beginnen. Die Zersetzung geht bis ungefähr 200° langsam vor sich und wird bei höherer Temperatur verstärkt, wobei bei Temperaturen über 600° gewisse Bereiche der Registrierkurven dem Li_2CO_3 oder den Oxyden, im Falle anderer Salze, entsprechen.

Die DTA-Kurven zeigen klar, daß ungefähr zwischen 140° und 700° exotherme Vorgänge stattfinden (Tabelle 2). Es werden nur exotherme Vorgänge verzeichnet, die durch Verbrennung des Liganden bewirkt sind. Was die Art der Produkte der thermischen Zersetzung anbelangt, nehmen wir an, daß diese dieselben sind wie die die während des Erhitzens dieser Stoffe im offenen Glasrohr entstehen. Es entweichen Wasserdämpfe und farblose Gase, von denen mittels bekannter Reaktionen CO_2, CO, NH_3 sowie Ruß (Kohlenstoff) identifiziert wurden.

Durch Vergleich der IR-Spektren der synthetisierten Substanzen mit dem Spektrum des freien Liganden RAc_2H_2 geht hervor, daß in den

Spektren der synthetisierten Komplexverbindungen die charakteristischen Absorbtionsbanden der freien Carboxylgruppe nicht mehr vorhanden sind ; dafür treten die der $-COO^-$, $-NH-CG_2$- und $-NH-CH_2COO^-$-Gruppen auf. Aus diesen Daten (Tabelle 3) kann geschlossen werden, daß das Metallion direkt an die Carboxylgruppen und wahrscheinlich koordinativ an den Stickstoff gebunden ist. Ebenfalls ist ersichtlich, daß die IR-Spektren der synthetisierten Substanzen sehr wenig von der Natur des Metallions beeinflußt sind. Die betreffenden Schwingungen weisen untereinander sehr kleine Verschiebungen auf, ohne daß eine bestimmte Regelmäßigkeit festgelegt werden kann.

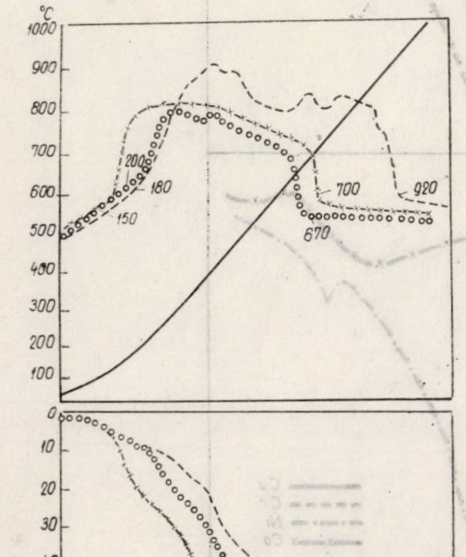

Abb. 1 — GTA- und DTA-Diagramme der Komplexverbindungen :
1. RAc_2Li_2 ; 2. $[RAc_2]_3Fe_2.4H_2O$; 3. $[RAc_2]_4Th_2.8H_2O$.

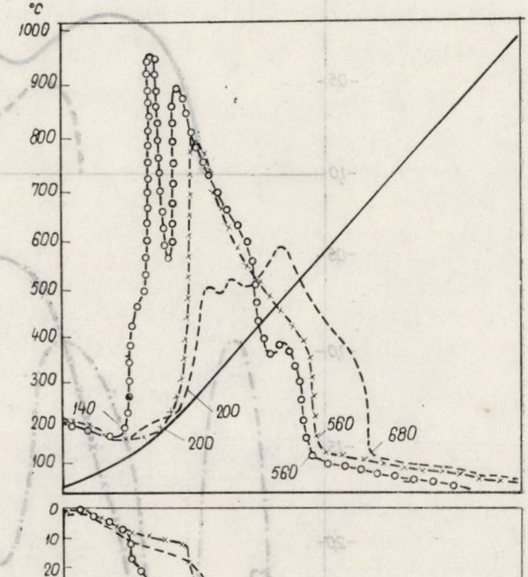

Abb. 2 — GTA- und DTA-Diagramme der Komplexverbindungen :
1. $[RAc_2]_2Cu_2.4H_2O$; 2. $[RAc_2]_3Al_2$; 3. $[RAc_2]_3Cr_2.4H_2O$.

Es wurden die diffusen Elektronenreflexionsspektren der Cr^{3+}-, CO^{2+}-, Ni^{2+}- und Cu^{2+}-Komplexverbindungen für die Übergänge d-d (Tabelle 4) aufgenommen.

Die Maxima der breiten Banden aus den diffusen Reflexionsspektren zeigen für die untersuchten Komplexverbindungen eine Hexakoordinierung mit oktaedrischer, ein wenig verzerrter Symmetrie.[2,3] Diese Tatsache wurde durch Bestimmung der magnetischen Momente bestätigt (Tabelle 5).

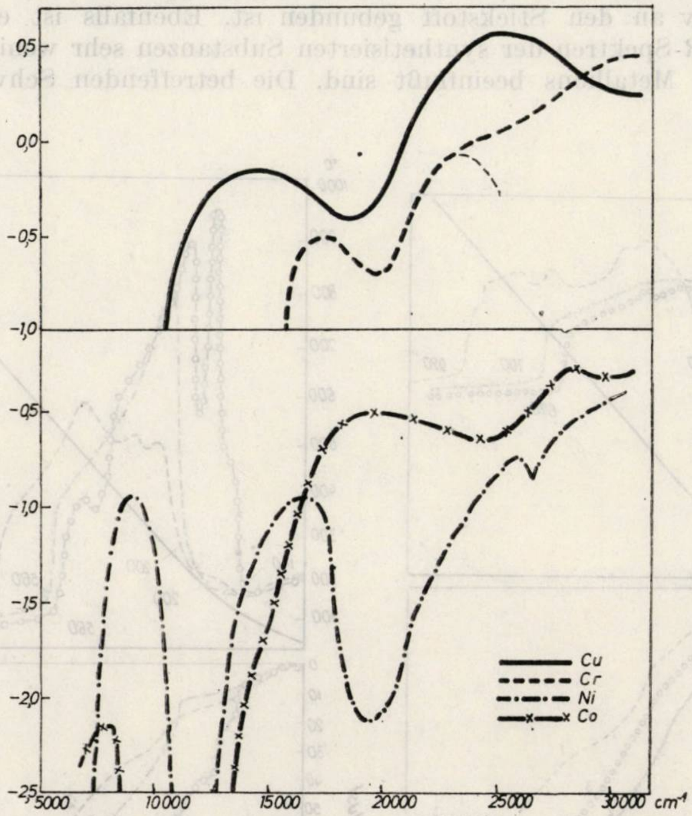

Abb. 3 — Reflexionsbeugungsspektren der Komplexverbindungen :
1. $[RAc_2]_2Cu_2.4H_2O$; 2. $[RAc_2]_3Cr_2.4H_2O$; 3. $[RAc_2]_2Co_2.6H_2O$; 4. $[RAc_2]_2Ni_2.6H_2O$.

Ähnlich verhalten sich auch die Äthylendiamin-N, N′-diessigsäure und -monoessigsäure bei der Bildung der Cr(III)- und Ni(II)-Komplexe, die von Fujii und Mitarb.[4,5] erhalten wurden.

Demnach hat das magnetische Moment der Ni^{2+}-Komplexverbindungen einen Wert, der sich dem Werte des reinen Spinmoments (2,83 MB) nähert, so wie es für ein hexakoordiniertes Ni^{2+}-Ion, mit dem $^3A_{2g}$ Grund-

---

[2] B. N. Figgis, „Introduction to Ligand Fields", Interscience, Ind. Ed. New York, 1967, S. 257.

[3] A. D. P. Lewer, „Inorganic Electronic Spectroscopy", Elsevier, Amsterdam, S. 249–261.

[4] Y. Fujii, E. Kyuno und R. Tsuchiya. *Bull. Chem. Soc. Japan*, **42**, 1569 (1969).

[5] Y. Fujii, *ibid*, **43**, 2815 (1970).

term zu erwarten ist. Andererseits hat die CO^{2+}-Komplexverbindung ein viel größeres magnetisches Moment als das nur dem Spin angehörige (3,88 BM). Dies zeigt, daß der Grundterm ein orbitales Triplett $^4T_{1g}$, das den oktaedrischen Komplexverbindungen entspricht, ist. Die größeren Werte sind durch die Spin-Bahn-Kopplungen aus dem Inneren des $^4T_{1g}$ Termes und der Kopplungen desselben Typs mit dem nächsten höherangeregten Term verursacht worden.

Der Wert von 1,64 BM, der kleiner als 1,73 BM ist, der der Cu^{2+}-Komplexverbindung angehört, konnte auf eine dimere oder polymere Struktur mit komplexen antiferromagnetischen Wechselwirkungen angesehen werden oder könnte durch eine mit Cu(I) verunreinigte Probe hervorgerufen worden sein.

Die Ergebnisse der chemischen Analyse, die spektralen und magnetischen Untersuchungen die mit Komplexverbindungen der 4,4'-Diaminodiphenylmethan-N, N'-diessigsäure durchgeführt wurden, erlauben die wahrscheinlichen Strukturen aufzustellen.

Für die Alkalimetallionen entstehen einfache Salze der Säure $RAc_2M^I_2$:

(I) $M^I-OOC-CH_2-NH-C_6H_4-CH_2-C_6H_4-NH-CH_2COO-M^I$

Für die zweiwertigen Metallionen Ca, Ba, Pb und Zn kann eine dimere oder eher polymere tetrakoordinierte (tetraedrische) Struktur folgender Form angenommen werden;

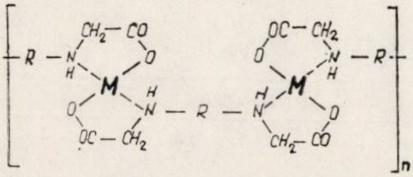

worin $R = -C_6H_4-CH_2-C_6H_4-$, und fünf-gliedrige Chelatringe gebildet werden; man könnte aber genau so gut annehemen, daß es sich nur um einfache Salze, wie im Falle der Alkalimetalle, handelt.

Die Komplexverbindungen der zweiwertigen Ionen von Mn, Co, Ni, Cu und Cd enthalten auch je 4 oder 6 Wassermoleküle. Die spektrale und magnetische Analyse deutet auf eine Hexakoordinierung in oktaedrischer Umgebung. In diesem Fall kann die mögliche Struktur als Formel II dargestellt werden, wobei um das Metallion das Oktaeder mit Wassermolekülen in den trans-Positionen ergänzt wird.

Die Komplexverbindungen der dreiwertigen Metalle Al, In, Cr, Fe, La, und Ce können auch als hexakoordiniert und polymer folgender schematischer Struktur angesehen werden:

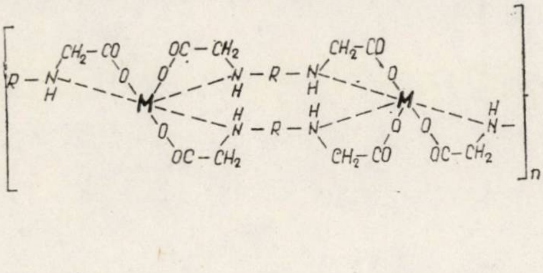

wobei das Koordinationsoktaeder folgendermaßen gebildet wird:

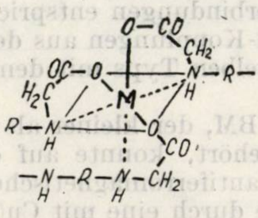

Im Falle der Metallionen Ti^{4+} und Th^{4+} in den gebildeten Komplexverbindungen $[RAc_2]_4Ti_2$ und $[RAc_2]_4Th_2 \cdot 8H_2O$ kann eine größere Koordinierung als sechs vorausgesetzt werden. Dies erweist sich vorläufig noch als eine schwierig festzustellende Annahme.

Revue Roumaine de Chimie, 22, 5, 665–674 (1977)

Dédié au Professeur CORIOLAN DRĂGULESCU
à l'occasion de son 70e anniversaire

QUELQUES ASPECTS DE LA RECHERCHE EN CHIMIE ORGANIQUE DU PHOSPHORE : RÉSULTATS ET PERSPECTIVES

F. MATHIS
Doyen honoraire de la Faculté des Sciences, Université Paul Sabatier, Toulouse, France

Reçu le 6 septembre 1976

On indique brièvement quelques résultats récents relatifs à la chimie organique du phosphore : les dérivés phosphorylés de l'hydrazine, les acides aminophosphoniques, la création de la liaison phosphore-carbone à partir de dérivés du phosphore tricoordiné, l'addition des phosphoranes à liaison P—H sur les doubles liaisons C = O et C = C, les processus de passage entre la coordinence 5 et la coordinence 4 du phosphore, la formation de dérivés du phosphore hexacoordiné et celle de dérivés du phosphore dicoordiné.

I – INTRODUCTION

Comme les autres métalloïdes de la ligne correspondante du tableau de Mendeleev et ceux des lignes suivantes, le phosphore peut présenter plusieurs indices de coordination : 2, 3, 4, 5, 6. On peut donc, dans la chimie des composés organiques du phosphore, distinguer les réactions qui conservent l'indice de coordination et celles qui font passer d'une coordinance à l'autre selon le schéma 1.

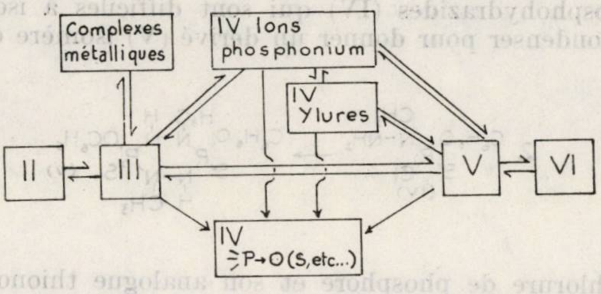

Schéma 1 — Passages mutuels entre les diverses coordinences de l'atome de phosphore.

Donner ici une vue d'ensemble de la recherche sur la chimie organique du phosphore est hors de question. Je voudrais seulement indiquer quelques sujets parmi ceux qui paraissent devoir bénéficier d'un développement croissant dans un proche avenir.

II – QUELQUES DÉRIVÉS NOUVEAUX DU PHOSPHORE TÉTRACOORDINÉ

a) HYDRAZIDES DÉRIVÉS DU PHOSPHORE

J. P. Majoral, J. Navech et al., au laboratoire, ont développé récemment une chimie des dérivés phosphorylés ou thiophosphorylés de l'hydrazine ; un composé renfermant le groupement $P(O)Cl_2$ peut réagir sur une hydrazine [1] pour donner un phosphohydrazide tel que (I) :

$$C_6H_5P(O)Cl_2 + 2H_3C-NH-NH_2 \rightarrow C_6H_5P(O)[N(CH_3)-NH_2]_2 \qquad (I)$$

Ce dihydrazide peut réagir sur un aldéhyde ou une cétone pour former un dérivé (II) de la perhydrotétrazaphosphorine-1, 2, 4, 5, 3 :

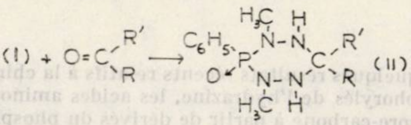
(II)

Dans certaines conditions, un dérivé analogue à (I) peut réagir sur une seconde molécule du dérivé dichloré de départ pour former [2] un dérivé (III) de la tétrazadiphosphorine-1, 2, 4, 5, 3, 6 :

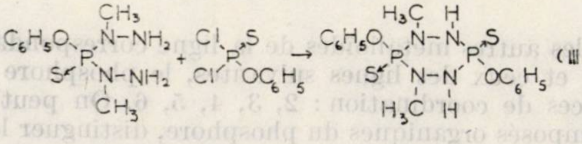
(III)

La formation de dihydrazides tels que (I) passe par l'intermédiaire de chlorophosphohydrazides (IV) qui sont difficiles à isoler, mais qui peuvent se condenser pour donner un dérivé (V) isomère de (III) :

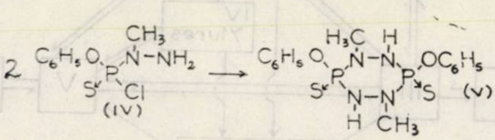
(IV) (V)

L'oxychlorure de phosphore et son analogue thiono donnent des trihydrazides ; si le trihydrazide renferme, comme (VI), trois groupements NH_2 en β de l'atome de phosphore, il se condense avec le méthanal pour former un composé (VII) de structure adamantanique :

---

[1] J.-P. Majoral, R. Kraemer, J. Navech et F. Mathis, *Tetrahedron Letters*, **1975**, 1481.

[2] J.-P. Majoral, R. Kraemer, J. Navech et F. Mathis, *Bull. Soc. chim. France*, **1975**, 2367.

$$S \leftarrow PCl_3 + H_3C-NH-NH_2 \rightarrow \quad S \leftarrow P[N(CH_3)-NH_2]_3 \qquad (VI)$$

$(VI) + O = CH_2 \rightarrow$

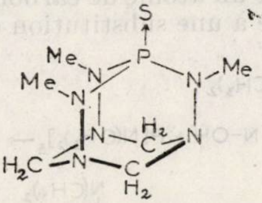

(VII)

Il se peut que de tels composés aient des applications pharmacodynamiques intéressantes : des essais sont en cours à ce sujet. En ce qui concerne la synthèse organique, nous attendons beaucoup plus des dérivés analogues du phosphore tricoordiné ; ceux-ci ne paraissent pas directement accessibles, mais il semble possible de désulfurer les thionophosphohydrazides (Majoral et Riess, communication personnelle).

b) ACIDES AMINOPHOSPHONIQUES

On sait depuis un quart de siècle (voir Neuzil [3]) que l'acide amino-2--éthylphosphonique (VIII a) est présent dans certains protozoaires et dans divers coelentérés

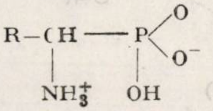

$$R-\underset{\underset{NH_3^+}{|}}{C}H - \underset{\underset{OH}{|}}{P}\begin{matrix} \diagup O \\ \diagdown O^- \end{matrix}$$

(VIII a, R = CH_3
VIII b, R = H)

La diffraction des rayonx X (Darriet et al. [4]) confirme la structure zwitterionique, a priori probable, de (VIII b).

Ces composés ressemblent aux acides α-aminocarboxyliques, et il paraît possible qu'ils interfèrent avec le métabolisme de ceux-ci. Dans cet ordre d'idées, l'école de Neuzil [5,6] a montré que (VIII a) et ses dérivés sont incorporés par le foie et le rein, et que (VIII a) et (VIII b) peuvent inhiber la croissance bactérienne.

III – FORMATION DE LIAISONS PHOSPHORE-CARBONE

Des liaisons phosphore-carbone peuvent être créées par de multiples voies qui sont décrites par exemple dans le livre de Purdela et Vîlceanu ou dans l'ouvrage collectif de Kosolapoff et Maier [8] : réaction de Friedel et Crafts, emploi d'organomagnésiens, réaction d'Arbuzov,...

---

[3] E. Neuzil et M. Labadie, « Composés organiques du phosphore », Colloque du C.N.R.S., Toulouse, 1965 (édité en 1966), p. 349.

[4] M. Darriet, J. Darriet, A. Cassaigne et E. Neuzil, *Acta Cryst.*, **31**, 469 (1975).

[5] M. Tamari, A. Cassaigne, A. M. Lacoste et E. Neuzil, *Biochimie*, **57**, 97 (1975).

[6] A. M. Lacoste, A. Cassaigne et E. Neuzil, *Compt. rend.*, *280D*, 1173 (1975).

[7] D. Purdela et R. Vîlceanu, « Chimia compuşilor organici al fosforului şi al acizilor lui », Ed. Academiei, Bucarest, 1965.

[8] « Organic Phosphorus Compounds », G. M. Kosolapoff et L. Maier éditeurs, 6 volumes, Wiley Interscience, New York, (1972).

Or Barrans et Lopez,[9,10] au laboratoire, ont observé une réaction qui ne parait pas entrer dans les rubriques classiques et dont, aujourd'hui encore, le mécanisme nous est inconnu ; la formation observée de la liaison entre le phosphore et un atome de carbone aromatique dans (IX) ne paraît pas pouvoir être due à une substitution électrophile sur le noyau.

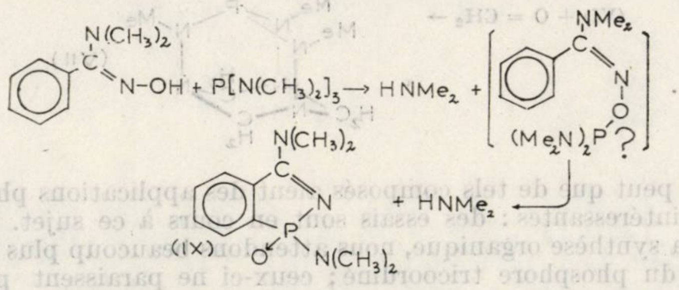
N(CH₃)₂
C
N-OH + P[N(CH₃)₂]₃ ⟶ HNMe₂ +
NMe₂
C
N
O
(Me₂N)₂P ?
N(CH₃)₂
C
N
+ HNMe₂
P
(IX)
O
N(CH₃)₂

Si cette réaction peut être généralisée, elle conduira à des synthèses intéressantes.

Morel et al.[11] ont décrit une réaction qui n'est pas sans analogie avec celle d'Arbuzov :

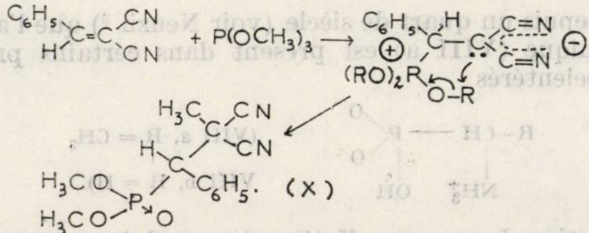
C₆H₅
H
C=C
CN
CN
+ P(OCH₃)₃ ⟶
C₆H₅
H
C–C
C≡N
C≡N
⊕
⊖
(RO)₂R
O–R
H₃C
CN
C
CN
H
C
C₆H₅
H₃CO
P
O
H₃CO
(X)

Actuellement sont en cours dans le laboratoire de R. Burgada et dans le nôtre des recherches sur la création de la liaison P—C dans des phosphoranes tels que (XI) et (XII). Elles utilisent l'addition de la liaison PH sur la double liaison C = 0[12] et sur des liaisons C = C « activées »[13].

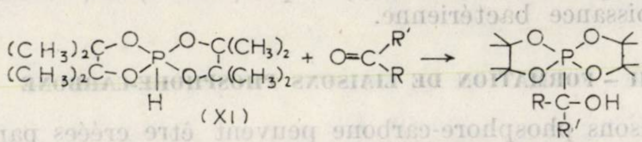
(CH₃)₂C–O
(CH₃)₂C–O
P
O–C(CH₃)₂
O–C(CH₃)₂
H
(XI)
+ O=C
R'
R
⟶
R-C-OH
R'

$(R = H, R' = C_6H_5 ; R = CF_3, R' = CH_3$ ou $CF_3)$

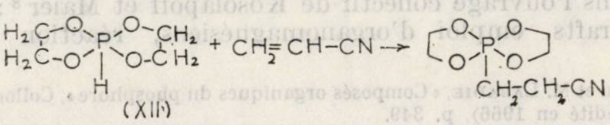
H₂C–O
H₂C–O
P
O–CH₂
O–CH₂
H
(XII)
+ CH₂=CH–CN ⟶
CH₂–CH₂–CN

---

[9] L. Lopez et J. Barrans, *Compt. rend.*, **273**, 1591 (1971).

[10] L. Lopez, Thèse d'Etat, Toulouse 1974.

[11] G. Morel, R. Seux et A. Foucaud, *Bull. Soc. chim. France*, **1976**, 177.

[12] H. Germa et R. Burgada, *Bull. Soc. chim. France*, **1975**, 2607.

[13] M. Willson, R. Burgada et F. Mathis, « Colloque National sur la chimie du phosphore », Toulouse, septembre 1976, p. 8.

L'orientation de ces additions suggère que le phosphore se comporte comme nucléophile, ce qui n'est possible que si le phosphorane réagit sous une forme tautomère à phosphore tricoordiné.

L'intérêt synthétique de ce travail nous paraît être le suivant. Comme on va le voir, les oxyphosphoranes se transforment aisément en dérivés du phosphore tétracoordiné à liaison P → 0. En choisissant bien le reste qui s'élimine, on peut espérer préparer des phosphonates à structure fixée à l'avance selon le schéma 2.

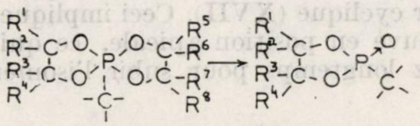

Schéma 2 — Passage d'un spirotétraoxyphosphorane à un phosphonate.

Il se peut que de telles synthèses soient plus commodes que celles auxquelles on recourt actuellement.

IV – LE PASSAGE DU PHOSPHORE DE LA COORDINENCE 5 À LA COORDINENCE 4 ET VICE-VERSA

Le passage de dérivés du phosphore tricoordiné ou pentacoordiné à des dérivés du phosphore tétracoordiné est bien connu ; il est très facile quand il entraine la formation d'une liaison phosphoryle P → 0 (voir par exemple Ramirez [14]). Nous avons observé par exemple au laboratoire (M. Willson, travail en cours) la décomposition de (XIII) :

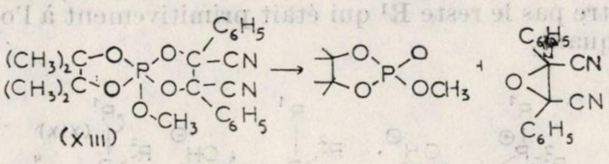

Apparemment, le passage d'un phosphorane à un dérivé phosphorylé est sans retour. Cependant, le passage inverse est postulé pour l'interprétation des réactions de substitution sur un atome de phosphore tétracoordiné. Celles-ci doivent passer par un stade rappelant l'état de transition SN2 dans la chimie du carbone. Or on est certain que dans beaucoup de cas ce stade à phosphore pentacoordiné n'est pas un état de transition, mais un intermédiaire ayant une durée de vie non nulle. Ceci résulte par exemple des travaux de Hudson et Brown. [15-17]

---

[14] F. Ramirez, *Bull. Soc. chim. France*, **1970**, 3491.

[15] R. F. Hudson et Ch. Brown, *Accounts Chem. Res.*, **5**, 204 (1972).

[16] R. F. Hudson, « Composés organiques du phosphore », Colloque du C.N.R.S., Toulouse, 1965 (édité en 1966), p. 35.

[17] R. F. Hudson, *Ind. chim. belge*, **8**, 777 (1964).

L'éthylène phosphate de méthyle (XIV), par exemple, s'hydrolyse en milieu acide pour donner deux diesters, l'un cyclique (XVII), l'autre non (XVIII). Comme dans la réaction SN2, on admet que l'attaque nucléophile (ici par l'eau, sur l'ester protoné) est apicale ; elle conduit à un édifice phosphoranique (XV). Dans cet édifice, le cycle ne peut occuper que la position apicale-équatoriale ; dans cette position, la contrainte de cycle est soulagée, ce qui explique que (XIV) soit beaucoup plus facilement hydrolysé en milieu acide que ses analogues acycliques. Le départ étant, lui aussi, apical, (XV) ne peut donner que (XVIII). Or il se fait aussi 40 % de l'ester cyclique (XVII). Ceci implique que le groupe méthoxyle partant se trouve en position apicale, ce qui n'est possible que si (XV) subsiste assez longtemps pour subir l'isomérisation conduisant à (XVI).

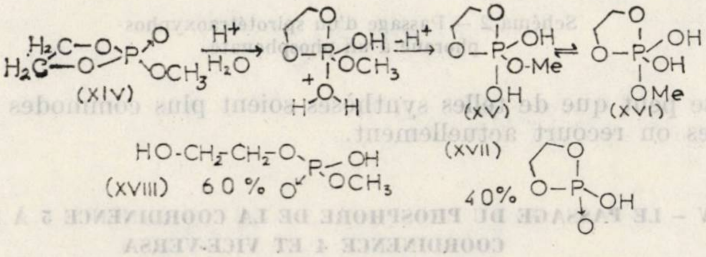

On observe quelque chose d'analogue dans l'hydrolyse alcaline des sels de phosphonium, sur laquelle Soleiman [18] a fait une mise au point récente. Cette hydrolyse passe par un intermédiaire phosphoranique (XIX) dans lequel l'oxygène de l'hydroxyle attaquant occupe une position apicale. Si le départ apical est immédiat, le groupe partant ne peut être que R 1, et il y a inversion de configuration. Si le départ est plus tardif (XIX) a le temps de s'isomeriser : il y a racémisation, et le groupe partant peut n'être pas le reste R¹ qui était primitivement à l'opposé de l'hydroxyle attaquant.

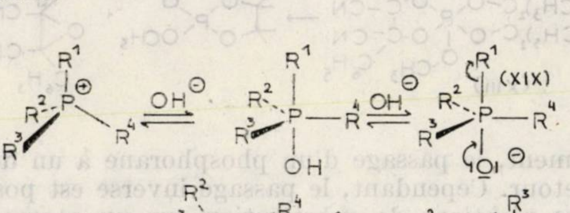

Le passage d'un ion phosphonium à un dérivé phosphorylé a été étudié par Castro et al. [19,20] Une « phosphine » (au sens large) peut réagir sur le tétrachlorure de carbone pour donner un sel du cation (XX). En présence d'un alcool ROH, ce cation se transforme en alcoxyphosphonium (XXI), qui peut être extrait en phase aqueuse en présence d'anion perchlorate. Le cation (XXI) peut réagir avec des nucléophiles (que l'anion ClO_4^- ne concurrence pas) en passant à l'état de dérivé phosphorylé (XXII) :

---

[18] M. Soleiman, Thèse d'Etat, Montpellier 1976.

[19] B. Castro et C. Selve, *Bull. Soc. chim. France*, **1971**, 2296.

[20] B. Castro et C. Selve, *Bull. Soc. chim. France*, **1971**, 4368.

$$[(CH_3)_3N]_3P + CCl_4 \rightarrow \underset{(XX)}{(Me_2N)_3P-Cl^+, CCl_3^-}$$

$$\underset{(XXI)}{(Me_2N)_3P-OR^+, \ ClO_4^-}$$

$$(Me_2N)_3P-OR^+ + C_6H_5S^- \rightarrow \underset{(XXII)}{(Me_2N)_3P \rightarrow O} + C_6H_5-S-R$$

Castro a utilisé ces réactions pour la préparation de dérivés des oses [21,22]. Il a montré que le cation (XX) peut, en réagissant sur un diol, conduire à un phosphorane : suivant que la bétaïne intermédiaire (XXIII) peut ou ne peut pas prendre la conformation appropriée, il se forme le phosphorane (XXIV), ou directement (XXII) et l'époxyde (XXV).

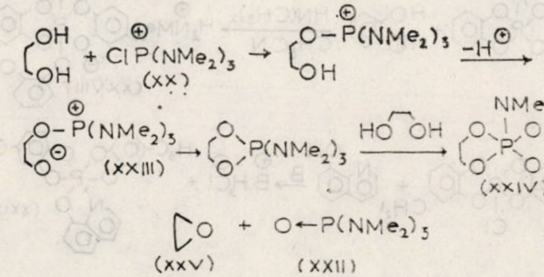

OH
OH
+ Cl P(NMe₂)₃
(XX)
O−P(NMe₂)₃
OH
−H⊕
O−P(NMe₂)₃
O⊖
(XXIII)
P(NMe₂)₃
HO OH
NMe₂
P
(XXIV)
O
+ O←P(NMe₂)₃
(XXV)
(XXII)

Il existe encore une voie de passage de la coordinence 4 à la coordinence 5, c'est celle qui mène d'un ylure à un phosphorane, comme dans la réaction observée par Turcant et Le Corre [23] qui conduit à un phosphorane cyclopropanique (XXVI).

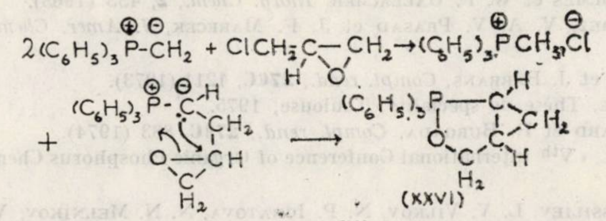

2(C₆H₅)₃P−CH₂ + ClCH₂C−CH₂→(C₆H₅)₃PCH₃Cl
H O
(C₆H₅)₃P−C H
CH₂
+
O−CH
C
H₂
(C₆H₅)₃P−C H
CH₂
O−C H
H₂
(XXVI)

---

[21] R. A. Boigegrain, B. Castro et B. Gross, *Bull. Soc. chim. France*, **1974**, 2623.

[22] B. Castro, Y. Chapleur et B. Gross, *Bull. Soc. chim. France*, **1973**, 3034.

[23] A. Turcant et M. Le Corre, *Tetrahedron Letters*, **1976**, 1277.

C'est probablement sous la forme tautomère ylure-alcool (XXVII) que le phosphorane (XXVI) réagit sur les aldéhydes :

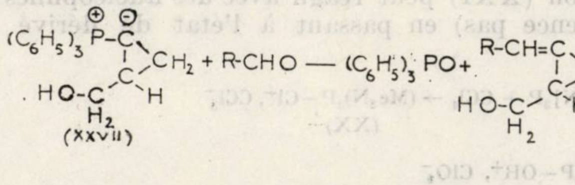

V – LES «COORDINENCES RARES» : 2 ET 6

Le phosphore pentacoordiné est électrophile (Holmes et Gallagher [24], Ramirez et al. [25]). Toutefois, le nombre de dérivés connus du phosphore hexacoordiné est actuellement assez petit. Il est vrai que, conformément à la prédiction de Hellwinkel (réf. 8, vol. 3, chap. 5B), il croît rapidement. Au laboratoire même, plusieurs ont été obtenus, soit anioniques comme (XXVIII) (Lopez et Barrans [26]), soit neutres comme (XXIX) (Gence [27]).

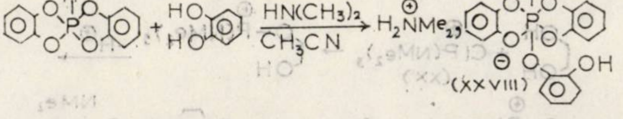

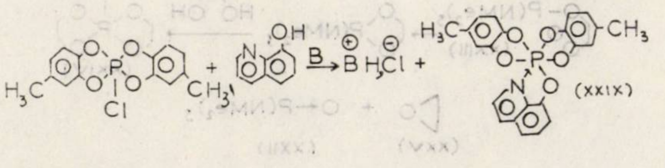

Voir aussi sur ce sujet Bernard et Burgada. [28]

En ce qui concerne le phosphore dicoordiné, on connaît les phosphorines de Märkl [29] et les diazaphospholes de Vassiliev. [30] Barrans, Charbonnel et Chaabane [31-33] ont obtenu une nouvelle famille de composés dérivant du triazaphosphole-1, 2, 4, 3, composés qui sont remarquablement stables et qui paraissent avoir un caractère aromatique. Les équations suivantes résument la synthèse des deux isomères (XXX) et (XXXI).

---

[24] R. R. Holmes et W. P. Gallacher, *Inorg. Chem.*, **2**, 433 (1963).

[25] F. Ramirez, V. A. V. Prasad et J. F. Marecek, *J. Amer. Chem. Soc.*, **96**, 7269 (1974).

[26] L. Lopez et J. Barrans, *Compt. rend.*, **276C**, 1211 (1973).

[27] G. Gence, Thèse de spécialité, Toulouse, 1975.

[28] D. Bernard et R. Burgada, *Compt. rend.*, **279C**, 883 (1974).

[29] G. Märkl, « Vth International Conference of Organic Phosphorus Chemistry », Gdańsk, septembre 1974.

[30] A. F. Vassiliev, L. V. Vilkov, N. P. Igratova, N. N. Melnikov, V. V. Negrebetskii et L. S. Khaikin, *Doklady Akad. Nauk S.S.S.R.*, **183**, 95 (1968).

[31] Y. Charbonnel et J. Barrans, *Compt. rend.*, **278C**, 355 (1974).

[32] Y. Charbonnel, Thèse d'Etat, Toulouse 1975.

[33] A. Chaabane, Thèse de Spécialité, Toulouse, 1974.

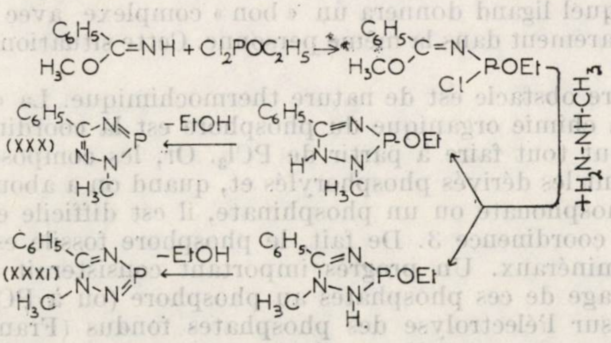

CONCLUSION

Les applications actuelles des dérivés organiques du phosphore sont déjà très nombreuses : insecticides, herbicides, fungicides (voir [7]), catalyseurs, ignifugeants, etc... Ces domaines continuent à se développer, et on peut essayer de prévoir quelques nouveautés.

Beaucoup de systèmes catalytiques, dont certains sont employés industriellement, sont des complexes de phosphines (voir Booth [34]). Il est naturel de songer à utiliser un catalyseur formé d'un haut polymère supportant les sites catalytiques. Effectivement, Tkatchenko [35] a décrit un polystyrène sur lequel sont greffés des restes de β-diphosphine, et les atomes de phosphore complexent des métaux de transition :

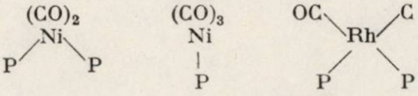

D'autre part, les systèmes capables de fixer l'azote moléculaire et d'assurer sa réduction en ammoniac sont presque tous des complexes de phosphines (voir Chatt, [36,37] Allen et al. [38]) comme (XXXII).

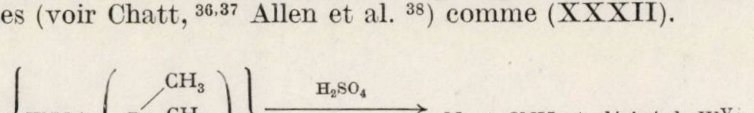

$$\text{cis}\left\{W(N_2)_2\left(P\begin{matrix}CH_3\\CH_3\\C_6H_5\end{matrix}\right)_4\right\}\xrightarrow[\text{tétrahydrofuranne}]{H_2SO_4} N_2 + 2NH_3 + \text{dérivé de } W^{VI}$$

(XXXII)

---

[34] G. Booth, réf. 8 ci-dessus, vol. I, chap. 3A.

[35] I. Tkatchenko, *Compt. rend.*, **282C**, 229 (1976).

[36] J. Chatt, *J. Organometal. Chem.*, **100**, 17 (1975).

[37] J. Chatt, A. J. Pearman et R. L. Richards, *J. Organometal. Chem.*, **101**, C45 (1975).

[38] A. D. Allen, R. O. Harris, B. R. Loescher, J. R. Stevens et R. N. Whiteley, *Chem. Rev.*, **73**, 11 (1973).

Les recherches sur ce sujet conduiront peut-être à une « technologie douce » de la synthèse de l'ammoniac.

Un obstacle au progrès dans cette voie est que l'entraînement pratique pour le synthèse de ligands phosphorés et celui qui est nécessaire pour savoir quel ligand donnera un « bon » complexe avec tel ou tel ion se trouvent rarement dans la même personne. Cette situation peut changer rapidement.

Un autre obstacle est de nature thermochimique. La « plaque tournante » de la chimie organique du phosphore est la coordinence 3. A la limite, on peut tout faire à partir de PCl_3. Or, les composés stables du phosphore sont les dérivés phosphorylés et, quand on a abouti à un phosphate, un phosphonate ou un phosphinate, il est difficile et coûteux de revenir à la coordinence 3. De fait, le phosphore fossile est à l'état de phosphates minéraux. Un progrès important consisterait à abaisser le coût du passage de ces phosphates au phosphore (ou à PCl_3). Peut-être les travaux sur l'électrolyse des phosphates fondus (Franks [39]) fourniront-ils le commencement d'une solution. Certes, je ne prétends pas que la fusion des phosphates ne nécessite pas de températures élevées ; mais on peut songer à la réaliser au moyen de l'énergie solaire, dont précisément certains pays riches en phosphates disposent en abondance.

---

[39] E. Franks et D. Inman, *Electroanalyt. Chem. Interfacial Electrochem.*, **26**, 13 (1970).

Revue Roumaine de Chimie, 22, 5, 675–682 (1977)

Herrn Professor Dr. Coriolan Drăgulescu
zum 70. Geburtstag gewidmet

BILDUNG UND STABILITÄT VON METALLCHELATEN MIT LIGANDEN DIE DONORATOME AUS DER 6. GRUPPE ENTHALTEN. I

HMO BERECHNUNGEN AN DEN LIGANDEN (*o*-CARBOXYPHENOXY)-ESSIGSÄURE UND (*o*-CARBOXYPHENYLTHIO)-ESSIGSÄURE

MARIA MRACEC *, ANA MAURER *, SEPTIMIA POLICEC * und Z. SIMON **
* Forschungszentrum für Chemie, Bv. Mihai Viteazul 24, Timişoara, Rumänien,
** Laboratorium für Chemie der Universität Timişoara, Bv. V. Pârvan 4, Rumänien.

Eingegangen am 16. Juli 1976

Mit Hinblick auf die Verwendung von (*o*-Carboxyphenoxy)-essigsäure (I) und (*o*-Carboxyphenylthio)-essigsäure (II) als Liganden zur Komplexbildung mit Metallionen, wurden durch Berechnungen die zur Koordinationsbindung nötige Elektronendisponibilität der Donoratome erörtet. Einfache Hückelberechnungen führten zu guten Übereinstimmungen zwischen den experimentellen und berechneten Elektronenspektren von Verbindung (I). Im Falle von (II) mußte die Coulomb-Integralle für das Schwefelatom durch Variationsberechnungen umgeändert werden, um zu guten Übereinstimmungen zwischen den experimentellen und berechneten $\pi \rightarrow \pi^*$ Transitionen zu gelangen. Die effektiven Ladungsverteilungen auf die Atome, deren Autopolarisabilitäten, wie auch die Werte der höchsten besetzten Molekülorbitalen (HOMO) führten zum Ergebnis, daß (I) eine relativ härtere Base als (II) ist, wie es auch das Prinzip von harten und weichen Säuren und Basen (HSAB) voraussieht.

Eine Reihe von vorherigen Arbeiten behandeln die Komplexbildung der Anthranyl-N,N-diessigsäure (ANDA), [1]

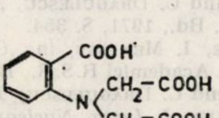

---

[1] C. Drăgulescu, T. Simonescu und R. Anton, *Studii şi Cercetări Şti., Chim., Acad. R.P.R., Timişoara*, 1, 21 (1959).

mit verschiedenen Metallionen in Lösungen, [2] in bezug auf ihre Bildungkonstanten die auf spektrophotometrischem [3] oder thermometrischem Wege [4] bestimmt wurden. Einige dieser Komplexverbindungen wurden im festen Zustand erhalten und vom strukturellen Standpunkt aus untersucht, [5] andere dienen als Grundlage für analytische Methoden zur gleichzeitigen Bestimmung von verwandten Metallpaaren, wie z.B. Zirkonium u. Hafnium.[6]

Um vergleichende Studien bezüglich der Donoreigenschaften der Elemente aus der 5. und 6. Gruppe durchführen zu können, wird im Folgenden die Fähigkeit zur Chelatbildung der Liganden

(I)

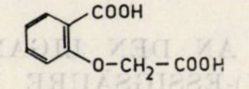

(*o*-Carboxyphenoxy)-essigsäure

(II)

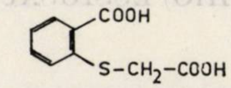

(*o*-Carboxyphenylthio)-essigsäure

untersucht. Diese können als Analogen des ANDA mit Donoratomen aus der 6. Gruppe betrachtet werden.

Untersuchungen über die Stabilität der Komplexe von (I) und (II) mit einigen zweiwertigen Metallen wurden bereits von Suzuki und Yamasaki durchgeführt. [7]

Unsere Arbeiten bezwecken das Erhalten von Komplexverbindungen mit großer Stabilität; als Richtlinie dazu diente das Prinzip von harten und weichen Säuren und Basen (HSAB). [8] In diesem Sinne erwies sich die Berechnung der Verfügbarkeit der Elektronen aus den Donoratomen von (I) und (II) zur Ausbildung von Koordinationsbindungen als notwendig. Diese Berechnungen zusammen mit den daraus hervorgehenden Schlußfolgerungen über die Elektronenstruktur der behandelten Liganden bilden den Gegenstand dieser Veröffentlichung.

EXPERIMENTELLES

Die (*o*-Carboxyphenoxy)-essigsäure (I) wurde nach Meyer u. Duczmal hergestellt,[9] während die (*o*-Carboxyphenylthio)-essigsäure (II) aus Anthranylsäure dargestellt wurde.[10] (II) wurde aus Äthylacetat, nach Behandeln mit Aktivkohle umkristallisiert. Die Verbindungen wurden potentiometrisch am Potentiographen Metrom Herisau E 336 A titriert; dabei wurde ein Reinheitsgrad von 99,98–100% erhalten. Die U.V. Spektren wurden mit dem Spektrophotometer UNICAM SP 800 an ethanolischen Lösungen von (I) und (II) ($c = 10^{-3}M$) aufgenommen. Die Maxima aus den experimentellen Spektren stimmen mit jenen aus der Fachliteratur überein. [11]

---

[2] C. Drăgulescu, T. Simonescu, I. Menessy und R. Anton, *Rev. Chim. Acad. R.P.R.*, 7, 161 (1962).

[3] C. Drăgulescu, S. Policec und T. Simonescu, *Talanta*, **13**, 1451 (1966).

[4] S. Policec, T. Simonescu und C. Drăgulescu, „III. Nationale Konferenz für Analytische Chemie", Braşov, România, 4. Bd., 1971, S. 354.

[5] C. Drăgulescu, R. Pomoje, I. Menessy, in „Omagiu Acad. Prof. Raluca Ripan", C. Drăgulescu, Herausgeber, Editura Academiei R.S.R., Bucureşti, 1966, S. 225–34.

[6] S. Policec, T. Simonescu und C. Drăgulescu, *Talanta*, **17**, 567 (1970).

[7] K. Susuki und K. Yamasaki, *J. Inorg. Nuclear Chem.*, **24**, 1093, (1962).

[8] R. G. Pearson, *J. Amer. Chem. Soc.*, **85**, 3533 (1963); *J. Chem. Educ.*, **45**, 581, 643 (1968).

[9] R. Meyer und C. Duczmal, *Ber. dtsch. chem. Ges.*, **46**, 3366 (1914).

[10] H.E. Fierz-David und L. Blangly, „Grundlegende Operationen der Farbenchemie", 8. Ausg., Springer Verlag, Wien, 1952, S. 322–324.

BERECHNUNGEN UND DISKUSSIONEN

Zur Erhaltung der Elektronenstruktur der Liganden (I) und (II), sowie der Ladungverteilung auf sämtliche Atome beider Verbindungen wurden einfache Hückel Berechnungen durchgeführt welche nach der Variante von Coulson und Longuet-Higgins erweitert wurden.

Sämtliche in den Berechnungen verwendete Parameter sind in Tabelle 1 und 2 zu finden. Die Gruppe $-CH_2-$ wurde als ein Heteroatom assimiliert, das sich mit 2 Elektronen am π-System beteiligt. Weiter wurde angenommen, daß auch das O-Atom der Äthylgruppe und das S-Atom der Thioäthergruppe sich am π-System mit je zwei Elektronen beteiligen. Da die Fachliteratur nicht über genügend Daten bezüglich der Resonanzintegralen der Bindungen $-\ddot{O}-CH_2-$ und $-\ddot{S}-CH_2-$ verfügt, wurden diese annährend durch Multiplizieren bekannter Resonanzintegralen für ähnliche Bindungen erhalten, wie aus Tabelle 2 aus den Klammern ersichtlich ist.

Tabelle 1

Werte der Coulomb-Integralen (in β-Einheiten)

Atom		Coulomb-Integralen		Literatur-nachweis
		a	b	
$C=$	(aromatisch)	α	α	12
$-C\langle$	(der Carbonylgr.)	$\alpha + 0{,}2\ \beta$	$\alpha + 0{,}2\ \beta$	13
$\rangle C-$	(aus substituiertem Benzolring)	$\alpha + 0{,}2\ \beta$	$\alpha + 0{,}2\ \beta$	13,14
$-CH_2-$	(hyperkonjugiert)	$\alpha + 2\ \beta$	$\alpha + 2\ \beta$	12
$=O$	(der Carbonylgr.)	$\alpha + 1{,}8\ \beta$	$\alpha + 1{,}18\ \beta$	14,15
$-OH$	(der Carbonylgr.)	$\alpha + 0{,}6\ \beta$	$\alpha + 2{,}06\ \beta$	13–15
$-\ddot{O}-$	(aus Äthergr.)	$\alpha + 2\ \beta$	$\alpha + 2\ \beta$	16
$-\ddot{S}-$	(aus Thioäthergr.)	α	$\alpha + 1{,}11\ \beta$	16,17

Aus Tabelle 3 resultieren die höchsten besetzten Niveaus, 2 an der Zahl (HO), die drei ersten freien niedrigsten (LE); wie auch die entsprechenden berechneten Transitionen, im Vergleich mit den Maxima der experimentellen Spektren von (I) und (II).

---

[11] L. Lang, „Absorption Spectra in the Ultraviolet and Visible Region", 1. Bd., 2. Ausg., Publishing House of the Hungarian Academy of Sciences, Budapest, 1961, S. 97–100.

[12] A. Streitwieser, Jr., „Molecular Orbital Theory of Organic Chemists", John Wiley, New York, 1961, 5. Kap.

[13] H. Yamabe, T. Yonezawa und H. Kato, *Bull. Chem. Soc. Japan*, **43**, 3029 (1970).

[14] G. Klopman und J. Nasielski, *Bull. Soc. chim. belges*, **70**, 490 (1961).

[15] G. Derflinger und H. Lischka, *Monatsh.*, **100**, 1003 (1969).

[16] W. R. Purcell und J. A. Singer, *J. Chem. and Eng. Data*, **12**, 235 (1967).

[17] M. Mracec und M. Mracec, „IV. Nationale Konferenz für allgemeine und angewandte physikalische Chemie", Bukarest, Romania, **1974**, S. 11.

Tabelle 2

Resonanzintegralen (in β-Einheiten)

Bindung	Resonanzintegralen		Literaturnachweis
	a	b	
C$\overset{\cdots}{-}$C(arom.)	β	β	12
$\overset{\cdots}{-}\mathrm{C-C}\langle$	β	β	13,14
$\overset{\cdots}{-}\mathrm{C-\ddot{O}-}$	0,9 β	0,9 β	16
$\overset{\cdots}{-}\mathrm{C-\ddot{S}-}$	0,6 β	0,6 β	16
$>\mathrm{C=O}$	1,41β	1,93β	13–15
$>\mathrm{C-OH}$	0,7 β	1,31β	13–15
$-\mathrm{CH_2-C}$	0,6 β	0,6 β	12
$-\mathrm{CH_2-\ddot{O}-}$	$0{,}5\ \beta \approx \left(\beta_{\overset{\cdots}{-}\mathrm{C-\ddot{O}-}} \cdot \beta_{-\mathrm{CH_2-C}\langle}\right)$	0,5 β	
$-\mathrm{CH_2-\ddot{S}-}$	$0{,}4\ \beta \approx \left(\beta_{-\mathrm{C-\ddot{S}-}} \cdot \beta_{-\mathrm{CH_2-C}\langle}\right)$	0,4 β	

Im Falle von (I) werden zufriedenstellende Übereinstimmungen zwischen den experimentellen und berechneten Transitionen beobachtet. Sämtliche Transitionen können als $\pi \rightarrow \pi^*$ betrachtet werden. Auch ist der Unterschied zwischen den experimentellen und berechneten Niveaus fast konstant und ungefähr gleich mit 100 nm. Diese Differenz könnte dem Polymorphismus der eingesetzten Parameter und den verhältnismäßig großen Molekülen zugeschrieben werden.

Die für (II) erhaltenen Resultate sind der Wirklichkeit relativ weit entfernt; eine Sache die hauptsächlich den angewandten Parametern zuzuschreiben ist.

Es sind verhältnismäßig wenig Daten über das Coulomb-Integral für das S-Atom der Thioäthergruppe vorhanden, deshalb wird dieses Integral nach Coulson und Longuet-Higgins modifiziert.[18] Betrachtet man die Formel:

$$\frac{\partial E_i}{\partial \alpha_i} = q_{ri} \qquad (1)$$

und nimmt die Variation des Coulomb-Integrals des S-Atoms gleich mit 1,1 β an, so werden die entsprechenden Ergebnisse aus Tabelle 3 erhalten, welche wie ersichtlich, den experimentellen Daten viel näher kommen.

Wird im Falle des Liganden (II) nicht Formel (1) verwendet sondern $\alpha_{-\ddot{S}-}$ mit α gleichgesetzt, so ist das höchste besetzte Niveau gleich mit $\alpha + 0{,}0009\ \beta$, d.h. es ist dem Nichtbindungsniveau ganz nahe. Werden die Berechnungen nach (1) durchgeführt, so deplasiert sich das höchste besetzte Niveau genügend und die berechneten Transitionen sind nicht mehr so weit von den experimentellen entfernt. Diese Transitionen sind

---

[18] C. A. Coulson und H. C. Longuet-Higgins, *Proc. Roy. Soc.*, **A 191**, 39 (1947); **A 192**, 16 (1947); **A 193**, 447, 456 (1948); **A 195**, 188 (1948).

Tabelle 3

Experimentelle und berechnete Spektren (mittels bestimmter Parameter) für Verbindungen (I) und (II)

Verbindung	ε_{HO}	ε_{LE}	Hückel-Trans. mit Param. aus Tab. 1 u. 2, Kol. a. nm	Trans. nach Goodman u. Shull nm	ε_{HO}	ε_{LE}	Hückel-Trans. mit Param. aus Tab. 1 u. 2, Kol. b. nm	Trans. aus exp. Spektren nm
(*o*-Carboxyphenoxy)-essigsäure (I)	$\alpha+0{,}7722\ \beta$ $\alpha+0{,}7244\ \beta$	$\alpha-0{,}5039\ \beta$	414	316	$\alpha+1{,}0645\ \beta$ $\alpha+0{,}8293\ \beta$	$\alpha-0{,}7612\ \beta$	327	289
		$\alpha-0{,}9507\ \beta$	310	237		$\alpha-1{,}0196\ \beta$	285	230
		$\alpha-1{,}0217\ \beta$	297	228		$\alpha-1{,}6677\ \beta$	281	208
(*o*-Carboxyphenylthio)-essigsäure (II)								
$\alpha_{-\ddot{S}-} = \alpha$	$\alpha+0{,}7530\ \beta$ $\alpha+0{,}0009\ \beta$	$\alpha-0{,}5676\ \beta$	914	696				316
		$\alpha-0{,}9507\ \beta$	546	415				258
		$\alpha-1{,}0471\ \beta$	496	377				230
$\alpha_{-\ddot{S}-} = \alpha+1{,}1\ \beta$	$\alpha+0{,}7567\ \beta$ $\alpha+0{,}7504\ \beta$	$\alpha-0{,}6807\ \beta$	363		$\alpha+0{,}0613\ \beta$ $\alpha+0{,}7186\ \beta$	$\alpha-0{,}7486\ \beta$	354	316
		$\alpha-0{,}9510\ \beta$	304			$\alpha-0{,}9939\ \beta$	304	258
		$\alpha-1{,}1520\ \beta$	262			$\alpha-1{,}6677\ \beta$	288	230

in gutem Einklang mit jenen des Liganden (I), der eine große strukturelle Ähnlichkeit aufweist.

Nach der Berechnung der Elektronenniveaus und der Koeffizienten der Molekülorbitalen gemäß der Hückel-Methode, wurden noch Berechnungen nach Goodman und Shull aufgestellt,[19] welche im allgemeinen zur Berechnung der Elektronenspektren monosubstituierter Benzolringe verwendet werden. Beim Einsetzten der degenerierten, bindenden bzw. lockernden Molekülbahnfunktionen des Benzols in die letzten drei besetzten und die ersten drei freien Niveaus der entsprechenden Verbindungen, konnten keine Aufteilung der Molekülorbitalen der beiden Verbindungen in zwei ireduktible, verschiedene Repräsentationen erhalten werden, wie es die Methode von Goodman u. Shull verlangt. Deshalb wurde nach dem Vorschlag derselben Autoren ein Mittelwert des Resonanzintegrals in Betracht gezogen, der dem Werte $\beta = 3{,}14$ eV entspricht.[19] Mit diesem Wert wurden die Energieniveaus und die entsprechenden Transitionen wieder berechnet. Die erhaltenen Ergebnisse sind ebenfalls in Tabelle 3, Kolonne 5 enthalten.

Wie aus der Tabelle ersichtlich, besteht im Falle von (I) Übereinstimmen zwischen den berechneten und experimentellen Werten; bei (II) hingegen nur wenn man $\alpha_{-\ddot{S}-} = \alpha + \beta$ annimmt.

Die schwachen Ergebnisse die für (II) erhalten wurden, sind hauptsächlich dem für das Schwefelatom verwendenten Coulomb-Integral zuzuschreiben. Verwendet man die Methode von Coulson und Longuet-Higgins so ergibt sich, daß für $\alpha_{-\ddot{S}-}$ der Wert $\alpha + 1{,}1\beta$ verwendet werden müßte.

Zu fast gleicher Schlußfolgerung gelangt man, wen man die Differenz zwischen $\alpha_{=O} = \alpha + \beta$[12] (für das O der Carbonylgruppe) und $\alpha_{-O-} = \alpha + 2\beta$ (für das O aus einem Äther) vergleicht. Die Differenz der beiden Integrale stellt gerade eine Einheit β dar. Nehmen wir an, daß dieselbe Differenz auch zwischen den entsprechenden Coulomb-Integralen des Schwefelatoms besteht, müßte für den Fall $\alpha_{=S} = \alpha$, das α_{-S-} ungefähr mit $\alpha + \beta$ gleich sein.

Für diese Behauptung plädiert auch der Vergleich des ersten Ionisationspotentials des Benzols, der dem Werte 9,2 eV entspricht, mit dem des $S(CH_3)_2$, gleich mit 8,7 eV.[20] Da diese beiden Potentiale ungefähr dieselben sind, können wir ruhig annehmen, daß in beiden Verbindungen das höchste besetzte Niveau dem Werte $\alpha + \beta$ entspricht.In der Verbindung $S(CH_3)_2$ wird das höchste besetzte Niveau größtenteils durch das Schwefelatom bestimmt, somit kann α_{-S-} als ungefähr gleich mit $\alpha + \beta$ angenommen werden.

Zu ungefähr denselben Werten gelangt man durch die graphische Methode der Parameteroptimisierung,[21] welche für Thiophen, Thiosalicylsäure u.s.w. angewandt wurde.[17]

Verwendet man die verbesserten Parameter aus Tabelle 1 und 2, Kolonne b, so werden Werte erhalten, die den experimentellen viel näher stehen. Siehe Kolonne 8 aus Tabelle 3.

---

[19] L. Goodman und H. Shull, *J. Chem. Phys.*, **27**, 1388 (1957).

[20] R. P. Blaustein und L. Cristiphoren, *Radiation Res. Rev.*, **3**, 69 (1971).

[21] M. Mracec, M. Mracec und Z. Simon, *Rev. Roumaine Chim.*, in Druck.

Aus den erhaltenen Daten, wie dem Wert der höchsten besetzten Orbitale (HOMO), der effektiven Ladungsverteilung auf die Atome, der Autopolarisabilität der Atome, können Schlußfolgerungen bezüglich der relativen Basizität der beiden Verbindungen gezogen werden.

Da die Verbindungen (I) und (II) bezüglich ihrer Zusammensetzung und chemischen Struktur sehr ähnlich sind und der einzige Unterschied im Aufbau der Moleküle in den Atomen von Position (10), Abb. 1 besteht, sind diese beiden Atome, bzw. die berechneten Werte ihrer charakteristischen Eigenschaften von größter Bedeutung; sie allein sind für das spezifische Verhalten von (I) und (II) verantwortlich.

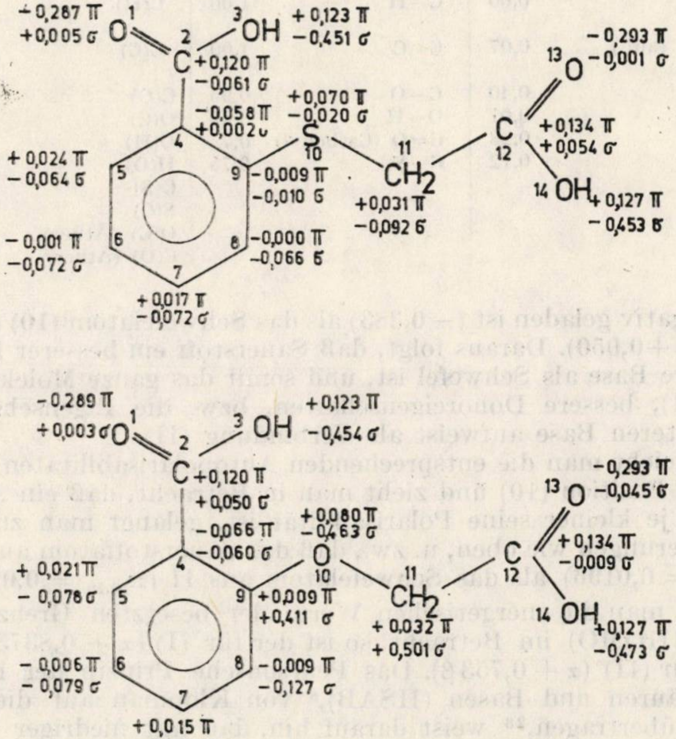

-0,287 π
+0,005 σ
1
O
2
C
3
OH
+0,123 π
-0,451 σ
+0,120 π
-0,061 σ
-0,058 π
+0,002 σ
4
+0,070 π
-0,020 σ
S
10
11
CH2
+0,031 π
-0,092 σ
12
C
+0,134 π
+0,054 σ
13
O
-0,293 π
-0,001 σ
14
OH
+0,127 π
-0,453 σ
+0,024 π
-0,064 σ
5
-0,001 π
-0,072 σ
6
7
+0,017 π
-0,072 σ
8
-0,000 π
-0,066 σ
9
-0,009 π
-0,010 σ
-0,289 π
+0,003 σ
1
O
2
C
3
OH
+0,123 π
-0,454 σ
+0,120 π
+0,050 σ
-0,066 π
-0,060 σ
4
+0,080 π
-0,463 σ
O
10
11
CH2
+0,032 π
+0,501 σ
12
C
+0,134 π
-0,009 σ
13
O
-0,293 π
-0,045 σ
14
OH
+0,127 π
-0,473 σ
+0,021 π
-0,078 σ
5
-0,006 π
-0,079 σ
6
7
+0,015 π
-0,088 σ
8
-0,009 π
-0,127 σ
9
+0,009 π
+0,411 σ

Abb. 1.— Numerierung der Atome und die effektiven Ladungsverteilungen δ und π auf die Atome, berechnet durch Verwenden der Parameter aus Kolonne b, Tab. 1 und 2, und Tab. 4.

Wie bereits erwähnt, kann die Basizität mit der effektiven Ladungsverteilung auf die Atome in Verbindung gebracht werden. Im Falle der Verbindungen (I) und (II) kann durch die Hückel-Methode allein kein korrekter Wert für die Basizität berechnet werden, da sie nicht die unbeteiligten Elektronen des Sauerstoff- und Stickstoffatoms in Betracht zieht, die diese stark beeinflussen. Deshalb führten wir noch Berechnungen nach Del Re[22] durch, die sich auf die lokalisierten σ-Bindungen beziehen. Dazu benützten wir die in Tabelle 4 verzeichneten Parameter.

Betrachtet man σ u. π, die effektiven Landungen der Atome, bemerkt man, daß das Sauerstoffatom (10) der Verbindung (I) aus Abb. 1 viel stärker negativ geladen ist ($-0{,}383$) als das Schwefelatom (10) der Verbindung (II) ($+0{,}050$). Daraus folgt, daß Sauerstoff ein besserer Donor bzw. eine härtere Base als Schwefel ist, und somit das ganze Molekül der Verbindung (I), bessere Donoreigenschaften, bzw. die Eigenschaften einer relativ härteren Base aufweist als Verbindung (II).

Tabelle 4

Parameter für die Berechnungen nach Del Re[22]

Atom	δ_i^0	Bindung	η_{ij}	γ_{ij}	
H	0,00	C−H	1,00	C(H)	0,3
−C− (alif.)	0,07	C−C	1,00	C(C)	0,1
−O−	0,40	C−O	0,95	C(O)	0,1
−S−	0,07	O−H	0,45	O(C)	0,1
O=	0,28	C=O (Carbonyl)	0,7	O(H)	0,3
>C=	0,12	C−S	0,75	H(O)	0,4
				C(S)	0,2
				S(C)	0,4
				O(C) (Äther)	0,05
				C(O) (Äther)	0,50

Vergleicht man die entsprechenden Autopolarisabilitäten der beiden Atome aus Position (10) und zieht man in Betracht, daß ein Atom umso härter ist, je kleiner seine Polarisabilität ist, gelangt man zu ähnlichen Schlußfolgerungen wie oben, u. zw., daß das Sauerstoffatom aus (I) härter ist ($\pi_{10.10} = 0{,}0196$) als das Schwefelatom aus II ($\pi_{10.10} = 0{,}0240$).

Zieht man die energetischen Werte der besetzten Grenzmolekularorbitalen (HOMO) im Betracht, so ist der für (I) ($\alpha + 0{,}8373\,\beta$) kleiner als jener für (II) ($\alpha + 0{,}753\,\beta$). Das Pearsonsche Prinzip der harten und weichen Säuren und Basen (HSAB),[8] von Klopman auf die Quantenmechanik übertragen,[23] weist darauf hin, daß mit niedriger werdenden Werten für die HOMO die Basenhärte ansteigt. Somit plädiert in unserem Falle auch die soeben behandelte Größe für eine relativ größere Durität von (I) gegenüber von (II).

Schlußfolgerung: Die Hückel-Methode kann, bei Anwendung der richtigen Parameter, zur Voraussage der Basizität von Verbindungen eingesetzt werden. Die dadurch definierte Basizität stimmt mit der nach dem HSAB-Prinzip vorausgesetzten überein.

---

[22] G. Del Re, *J. Chem. Soc.*, **1958**, 4031;
G. Del Re und B. Pullman, *J. Chim. phys.*, **62**, 942 (1965);
M. Martin und R. Carbo, *Rev. Roumaine Chim.*, **17**, 1963 (1973).

[23] G. Klopman, *J. Amer. Chem. Soc.*, **90**, 223 (1968).

Revue Roumaine de Chimie, **22**, 5, 683–689 (1977)

Dedicated to the 70th anniversary
of Professor CORIOLAN DRĂGULESCU

HEAT CAPACITIES IN MOLTEN ALKALINE HALIDES

I. G. MURGULESCU and CR. TELEA
Center of Physical Chemistry Bucharest, Str. Galați No 31, Romania

Received June 2, 1976

The heat capacities in molten alkaline halides were measured on a Calvet calorimeter near the melting point. The data reported in the literature for the dilatation coefficient and the adiabatic compressibility coefficient were used to calculate the C_v. The values obtained were compared to the values resulted from the theory of holes considering the holes concentration equal with the volume variation on melting.

Although the heat capacities of molten salts are directly related to the motion state of ions in the melt, they have been less studied due both to the experimental difficulties and to the absence of an adequate theory. In molten alkaline halides, the heat capacities were exclusively obtained by drop calorimetry. Usually the measurements precision is not better than 1% when determining the heat content and 2% for heat capacities. An inspection of table 2 shows that an agreement of 3% between the data obtained by different authors may be looked upon as satisfactory.

No systematic measurements exist with regard to the temperature dependence of heat capacities in molten alkaline halides. Mcleod[1] has performed complete measurements on pure alkaline fluorides and in mixtures and has found a c_p increase with temperature.

EXPERIMENTAL

Direct c_p measurements in conduction calorimetry rely on the existence in stationary regime of a θ temperature difference between the internal and the external chamber. Knowing θ and measuring ΔQ we may obtain c_p. The θ temperature rises can be achieved by the Joule effect, by Peltier effect or by programming the temperature of the calorimeter; they are of the order of hundredths of degree and difficult to measure directly. For this reason comparative measurements have been carried on, recording the areas (for Joule effect or for Peltier effect) or the maximal deviations (in temperature programming) for the case in which the working cell contains:

the standard substance (A_e, Δ_e, c_{pe})
the substance under study (A_x, Δ_x, c_{px}) (1a)
the cell is empty (A_0, Δ_0, c_{p0})

---

[1] A. C. MCLEOD, *J. Chem. Soc. (Faraday Trans. 1)*, **69**, 2026 (1973).

Since the temperature rises are similar, we obtain [2]

$$\frac{c_{px}}{c_{pe}} = \frac{A_x - A_0}{A_e - A_0} \quad (1a) \qquad \frac{c_{px}}{c_{pe}} = \frac{\Delta_x - \Delta_0}{\Delta_e - \Delta_0} \quad (1b)$$

The measurements were performed on a high-temperature Calvet calorimeter (SETRAM). In view of standardization Al_2O_3 (synthetic sapphire microcrystals) was used considering the c_p values given by Frederickson and Chasnov. [3]

The salts used were dissolved, filtered and recrystallized and after drying they were melted in a hydracid current; after melting rubidium and cesium salts were redissolved and the cycle was repeated once or twice. The quartz contained was filled with salt in a vacuum plant by repeated meltings in an argon current and by its subsequent sealing under vacuum. Determinations were performed over a 50—100° temperature above the melting point without recording a c_p variation with temperature.

Equation (1b) is similar to the relation used for c_p measurements in scanning calorimetry. [4] Its correctness was tested in the case of Calvet calorimeter using various heating rates and by comparison to eqn. (1a). As seen in table 1, the data agree within the limit of experimental errors of 1—2%.

Table 1

Heat capacities

Salt	c_p cal/mole			
	$v = 5°/h$	$v = 8°/h$	$v = 10°/h$	Peltier effect
RbCl	17.8	17.3	17.56	—
CsCl	18.2	18.1	18.13	18.6

The values thus obtained for molten alkaline halides are listed in Table 2. Although the measurements precision is not better than 1% the comparative differences between salts are probably more exactly given. For this reason c_p was listed in the table with two decimals. Knowing c_p, we can calculate the c_v constant volume heat capacity and the β_T isothermal compressibility according to relations:

$$\frac{c_p}{c_v} = 1 + \frac{\alpha^2 VT}{\beta_s c_p} \quad (2a) \qquad \beta_s = \frac{1}{u^2 \rho} \quad (2b)$$

$$\frac{c_p}{c_v} = \frac{\beta_T}{\beta_s} \quad (2c)$$

where the α dilatation coefficient is obtained from ρ density measurements [12] and the β_s adiabatic compressibility, from the u ultrasounds velocity in molten salts. [13,14] Table 2 also contains the volume variation on melting [12] and the melting heat [15] necessary to calculate the energy of holes formation.

As can be seen, c_v is of approximately 12 cal/mole for most molten alkaline halides. The regularities observed in the c_v variation with the ions dimensions, with the cation and anion nature will be explained by the ionic interactions and taking into account the structure of molten salts.

---

[2] E. Calvet, in "Microcalorimetrie et Thermogenese", ed. C.N.R.S., Paris, 1967, p. 95.

[3] D. R. Frederickson and M. G. Chasonov, *J. Chem. Thermodynam.*, **2**, 63 (1970).

[4] M. J. O'Neill, *Analyt. Chem.*, **38**, 1331 (1966).

[12] E. R. Schinke and F. Sauerwald, *Z. anorg. Chem.*, **287**, 313 (1956).

[13] V. Vasilescu, Ph. D. Thesis, Univ. București, 1971.

[14] J. O'M Bockris and N. E. Richards, *Proc. Roy. Soc.*, **241A**, 44 (1957).

[15] A. S. Dworkin and M. A. Bredig, *J. Phys. Soc.*, **64**, 269 (1960).

Table 2

Experimental heat capacities

Salt	T °K	V cm^3 [12]	$\alpha 10^4$ $°K^{-1}$	$\beta_S \cdot 10^4$ cm^3 [13,14]/cal	$\frac{\Delta V}{V_S}$ [12]	ΔH ·kcal/mole[15]	c_p cal/mole	
							own data	data from the literature
NaCl	1073	37.5	3.49	8.74	0.250	6.69	16.50	16.0 [5]
KCl	1043	48.8	3.84	10.63	0.173	6.34	17.49	17.6 [6]; 18.4[7] 17.8 [8]
RbCl	995	54.0	3.95	11.17	0.143	5.67	17.56	17.5 [8]
CsCl	918	60.2	3.84	11.34	0.100	4.84	18.13	17.34 [8]; 18.0 [9]
NaBr	1020	44.1	3.50	10.08	0.224	6.24	16.06	16.26 [10,11]
KBr	1007	55.9	3.91	11.97	0.166	6.10	16.54	11.0 [11]
RbBr	995	61.2	3.95	12.22	0.135	5.57	17.39	—
CsBr	909	68.0	3.89	10.13 *	0.268	5.64	18.61	—
NaI	933	54.6	3.48	11.67	0.186	5.64	15.67	16.04 [10]
KI	954	68.0	3.89	14.76 *	0.159	5.74	16.31	—
RbI	920	73.5	3.96	14.27	0.127 **	5.27	17.23	—
CsI	899	81.8	3.74	13.72	0.285	5.64	17.76	17.2 [9]

* ref.[14]

** interpolated value

[5] "J.A.N.A.F." Thermochemical Tables", (ed. D. R. Stull) Dow Chemical Company, Midland, 1965.

[6] T. B. DOUGLAS, Declass. Rep. U.S. At. En. Com. BNL 2426, 13 (1955).

[7] W. T. THOMPSON and S. N. FLENGAS, *Canad. J. Chem.*, **49**, 1550 (1971).

[8] B. F. MARKOV, T. A. TISURA and A. N. BUDARINA, *Ukrain. Khim. Zhur.*, **38**, 826 (1972); **39**, 757 (1973).

[9] C. E. KAYLOR, G. E. WALDEN and D. F. SMITH, *J. Phys. Chem.*, **60**, 1125 (1960).

[10] T. E. GARDNER and A. R. TAYLOR jr., *Rep. Bureau of Mines*, 7040 (1967).

[11] A. BIBAS and J. LEONARDI, *Compt. rend.*, **268C**, 877 (1969).

DISCUSSION

The information regarding the reciprocal disposal of ions in the melt are obtained from the $g(r)$ radial distribution curve calculated from X ray and neutrons diffraction measurements.[16] At small distances compared to the atomic dimensions, $g(r)$ presents damped oscillations which is in agreement with the recognized fact that the long-distance order is destroyed in liquids. On the other hand, the persistence of a certain ordering is indicated by the shape and the size of the first and the second peak in $g(r)$. The long-distance nature of coulombian forces determines an alternating arrangement of cations and of anions. Compared to the solid, the anion-cation distance decreases (by 0.1—0.2 Å) and the anion-anion distance increases; the coordination number decreases from 6 to 4—5 in the first sphere and from 12 to 7—8 in the second neighbouring sphere. Consequently, the melting process in not due to the increase of interionic distances but rather to the appearance of some gaps, which destroy the crystalline ordering.

For alkaline halides, the defects are of a Schottky type, the electroneutrality of the melt imposing the simultaneous creation of an anionic vacancy and of a cationic vacancy. It must be underlined that a defect in the melt cannot be defined by a geometrical structure, but rather by its energy and volume. The equilibrium value of the number of defects is obtained by minimizing their free energy of formation:

$$\Delta G = ng - kT \ln\left[\frac{N!}{n!(N-n)!}\,\frac{N!}{n!(N-n)!}\right]$$

If the volume variation on melting is due to the occurrence of holes,

$$\frac{n}{N} = \frac{\Delta V}{V_s} = \exp\left(-\frac{g_0}{2kT}\right) \tag{3}$$

In the holes theory developed by Furth[17] the energy of formation of a singular hole at the melting temperature is:

$$\varepsilon_0 = \frac{7}{2} kT \tag{4}$$

The cooperative effect in the formation of holes determines a drop in the energy of formation with the increasing concentration of holes, i.e.:

$$g = g_0 z \frac{V_s}{V} \quad (5) \qquad\qquad \varepsilon = \varepsilon_0 z \frac{V_s}{V} \quad (6)$$

---

[16] K. Furukawa, *Discuss. Faraday Soc.*, **32**, 53 (1961).

[17] R. Furth, *Proc. Cambridge Phil. Soc.*, **37**, 28, 252 (1941).

where $z(V_s/V)$ is the coordination number in the melt and $z = 6$, corresponds to a cubic structure with centered sides.

Finally if the heat of melting is due to the formation of $N(\Delta V/V_s)$ holes then the energy of formation of a hole is :

$$h = h_0 z \frac{V_s}{V} = \frac{\Delta H}{N(\Delta V/V_s)} \tag{7}$$

Table 3 gives comparative results obtained from eqns (5), (6), (7) with the values calculated from the cellular model with vacancies.[18] ε_T is the energy of formation of vacancies extrapolated to the melting point and θ the theoretically calculated occupation ratio. The agreement obtained seems promising and supports the idea that most holes will form by the melting of ionic crystals.

Table 3

Energy of holes formation

Salt	$g \cdot 10^{20}$ J	$\varepsilon \cdot 10^{20}$ J	$h \cdot 10^{20}$ J	$\varepsilon_T \cdot \theta 10^{20}$ J
NaCl	19.71	24.86	18.58	22.55
KCl	25.83	25.76	25.45	27.52
RbCl	28.02	25.22	27.53	27.15
CsCl	31.83	24.22	33.61	—
NaBr	20.63	24.14	19.34	21.31
KBr	25.66	25.04	25.51	25.40
RbBr	28.20	25.43	28.64	25.06
CsBr	15.62	20.76	14.61	—
NaI	21.89	22.78	21.05	—
KI	25.08	23.87	25.07	—
RbI	27.90	23.68	28.81	—
CsI	14.56	20.28	10.57	—

In the melt, the particles perform harmonic vibration motions in the cell formed from the neighbouring particles, so that :

$$c_v = 6\ R = 11.92 \text{ cal/mole} \tag{8}$$

The inharmonic effects are probably insignificant considering the rapid relaxation possibilities in the liquid disordered structure.

The contribution of holes to the heat capacity may be obtained from eq. (5) :

$$c^g = \mathrm{N} \times g_0 \frac{\mathrm{d}x}{\mathrm{d}T} \tag{9}$$

---

[18] I. G. Murgulescu and Gh. Vasu, *Rev. Roumaine Chim.*, **11**, 681 (1966).

where $x = (\Delta V/V_s)$. A similar relation is obtained from the assumption that the necessary energy for a ΔV volume increase is equal to the ΔH melting heat:

$$c^g = \alpha \frac{\Delta H}{\Delta V} \tag{10}$$

From the theory of holes,[17] we see that:

$$c^g = \frac{3}{2} R(1 - \theta) = \frac{3}{2} R \frac{\Delta V}{V} \tag{11}$$

where θ represents the liquid part with "solid-like" properties and may be replaced by V_s/V. As seen from table 4, the values obtained from the three equations (9), (10), (11) are fairly close.

Table 4

Contributions to the heat capacity

Salt	c^g			c^p	c_v calc. eq. 13			exp.
	eq. 9 (I)	eq. 10 (II)	eq. 11 (III)	eq. 12	(I)	(II)	(III)	c_v
NaCl	0.48	0.31	0.60	0.01	12.41	12.24	12.53	12.31
KCl	0.36	0.34	0.44	0.03	12.31	12.29	12.39	12.46
RbCl	0.31	0.33	0.38	0.09	12.32	12.34	12.39	12.31
CsCl	0.21	0.34	0.27	0.15	12.28	12.41	12.34	12.99
NaBr	0.45	0.27	0.55	0.02	12.39	12.21	12.49	11.99
KBr	0.35	0.30	0.43	0.05	12.27	12.27	12.40	11.53
RbBr	0.29	0.10	0.36	0.12	12.33	12.14	12.40	12.13
CsBr	0.50	0.15	0.63	0.21	12.63	12.28	12.76	12.44
NaI	0.39	0.23	0.47	0.03	12.34	12.18	12.42	11.72
KI	0.34	0.24	0.41	0.07	12.33	12.23	12.40	10.79
RbI	0.27	0.24	0.34	0.16	12.35	12.32	12.42	12.04
CsI	0.51	0.12	0.66	0.27	12.69	12.31	12.85	13.40

An additional contribution to the heat capacity results from the ion polarization in the electric field of neighbouring ions. The polarization of the electronic cloud of a ion due to the electric field of the neighbouring ions can be written under the form[19]:

$$E_p = -\frac{A}{2r^4} \qquad A = e^2(Z_+^2\, \alpha_- + Z_-^2 \alpha_+)$$

where r is the distance between ions, $\alpha_\mp$ the polarizability and Z, the atomic number. With the temperature increase:

$$\frac{dE_p}{dT} = \frac{2}{3} \frac{A}{2r^4} \alpha$$

---

[19] F. H. Stillinger in "Molten Salts", ed. M. Blander, London, 1964, p. 1.

where α is the linear dilatation coefficient. To consider the effect of the more remote ions, the given expression is multiplied by $(4/e^2)$[20]:

$$c^p = \frac{8}{2r^4}(Z_+^2\,\alpha_- + Z_-^2\,\alpha_+) \tag{12}$$

Summing up the calculated contributions we obtain:

$$c_v = 6R + c^g + c^p \tag{13}$$

The heat capacities calculated in this way (Table 4) agree well enough with experimental values.

The model that could be advanced for a kind of "ideal liquid" is the following. The particles perform harmonic vibration motions around some centres which, in turn, are being displaced by translation motions throughout the volume occupied by the liquid. The particle degrees of freedom may be separated into harmonic vibrations and translation degrees of freedom in the volume determined by holes in which particles behave as an ideal gas. The transition from a motion state to another occurs with an expense of energy depending on the surface separating the two phases. The quasitotality of holes is formed on melting. The number of holes increases with the temperature rise. At the same time singular holes will group into complex holes which determine the liquid conversion into vapour state when reaching a certain value.

CONCLUSIONS

A Calvet calorimeter in a dynamic regime was used to measure the heat capacities in molten alkaline halides. Within the limit of experimental errors (1—2%) c_p are constant over limited temperature intervals (approx. 100° above the melting temperature). The c_v constant volume heat capacities are close to 6R. Admitting that melting means the occurrence of holes in an equal concentration with the volume variation on melting, the values calculated for c_v agree satisfactorily with the experimental c_v.

---

[20] J. Lumsden, *Discuss, Faraday Soc.*, **32**, 138 (1961).

Revue Roumaine de Chimie, 22, 5, 691–695 (1977)

Dedicated to the 70th anniversary
of Professor Coriolan Drăgulescu

CONTRIBUTIONS TO THE BISMUTH HYDROLYSIS STUDY. IV[1–3]

EQUILIBRIUM AND RATE CONSTANTS OF BISMUTH PERCHLORATE HYDROLYSIS STUDIED BY POLAROGRAPHY

ANA NIMARĂ and I. JULEAN
Chemical Research Centre, Bd. Mihai Viteazul 24, Timişoara, Romania

Received September 6, 1976

By means of direct current polarography the product between the hydrolysis constant and the rate constant in light and heavy water was determined at the bismuth perchlorate hydrolysis. The hydrolysis constant value in D_2O was also calculated. The ratio of these constants K_h/K_D is equal to 2.4. By means of these values the rate constants were computed. The kinetic isotope effects are :

$k_{H_2O}/k_{D_2O} = 1.1$ and $k_H^+/k_D^+ = 2.3$.

In the case of electrode processes, where the charge transfer reaction is coupled with a chemical reaction, it is possible to determine from polarographic data the product between the equilibrium and rate constants, corresponding to the respective chemical reactions.[4]

In our previous research [5] concerning the elucidation of the hydrolysis process of Bi(III) it was shown that in the 1–2 pH range, the electrode process is accompanied by two chemical reactions, one consisting in the formation of the hydrolysis products $BiOH^{2+}$ and $Bi(OH)_2^+$ and the other in the decomposition of the $Bi(OH)_2^+$ species into $BiOH^{2+}$.

In the present paper the product $K_h k$ was determined polarographically, at the hydrolysis of bismuth perchlorate in light and heavy water, as well as the hydrolysis constant in D_2O and kinetic isotope effects were also computed.

---

[1] Part III : C. Drăgulescu, A. Nimară and I. Julean, *Rev. Roumaine Chim.*, **19**, 1455 (1974).

[2] Part II : C. Drăgulescu, A. Nimară and I. Julean, *Rev. Roumaine Chim.*, **17**, 1181 (1972).

[3] Part I : C. Drăgulescu, A. Nimară and I. Julean, *Chem. Analit.*, **17**, 631 (1972).

[4] A. Căluşaru, I. Crişan and J. Kuta, *J. Electroanalyt. Chem.*, **46**, 51 (1973).

EXPERIMENTAL

Solutions in light water. The aqueous $BiOClO_4 \cdot H_2O$ solutions were prepared following the already described procedure.[5] $HClO_4$ and $NaClO_4$ were p.a. Merck products.

Solutions in heavy water. The heavy water used for the preparation of the solutions was 99.5% $D_2O \cdot DClO_4$, $NaClO_4$, NaOD were prepared by dissolving the crystals, respectively the $HClO_4$ 70% in D_2O. The solutions of $BiOClO_4 \cdot D_2O$ were obtained by dissolving the bismuthyl perchlorate crystals in D_2O.

Apparatus. The polarographic curves were recorded using a PO4 Radiometer polarograph. The characteristics of the capillary are : $h = 58$ cm, $t = 3$ sec., $m = 2.09$ mg/s, open circuit. The pH measurements were accomplished on a Radiometer pH-meter, with a glass electrode G–202 C, and with an accuracy of 0.005 pH-units.

RESULTS AND DISCUSSION

The study of the polarographic reduction of Bi^{3+} as a function of pH(D), in 1 M $NaClO_4$ solutions, showed the splitting of the initial wave characteristic to Bi^{3+} into 2 waves, proportional to the pH(D) increase (figure 1).

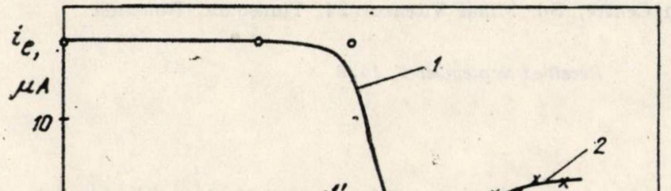

Fig. 1. — Dependence of the limiting current, corresponding of two waves on the pH (D) : 1, 2 — H_2O ; 1', 2', — D_2O.

The chemical equilibria, which accompany the electrode process and which are responsible for this splitting in the pH range 1–2, may be shown as follows :

$$\begin{tikzcd} Bi^{3+} \arrow[r, shift left, "k_1"] & BiOH^{2+} \arrow[l, shift left, "k_1'"] \arrow[r, shift left, "k_2'"] \arrow[d, "+e"] & Bi(OH)_2^+ \arrow[l, shift left, "k_2"] \\ & Bi(Hg) & \end{tikzcd} \qquad (1)$$

---

[5] C. Drăgulescu, A. Nimară, I. Julean and D. Marandiuc, *Rev. Roumaine Chim.*, 18, 583(1973).

while the chemical reactions are:

$$Bi^{3+} + H_2O \underset{k_1'}{\overset{k_1}{\rightleftharpoons}} BiOH^{2+} + H^+ \qquad (2)$$

$$BiOH^{2+} + H_2O \underset{k_2}{\overset{k_2'}{\rightleftharpoons}} Bi(OH)_2^+ + H^+ \qquad (3)$$

$$K_h = \frac{[Bi(OH)_2^+]\,[H^+]^2}{[Bi^{3+}]\,[H_2O]}$$

It follows that the $BiOH^{2+}$ species which is reducing is generated by both the hydrolysis reaction (2) and the regressing reaction (3) of the hydrolysis process. The kinetic current corresponding to the sum of the two waves may be expressed as follows:

$$i_k = \{k_1[Bi^{3+}] - k_2'[BiOH^{2+}]\}\,H_2O + \{k_2[Bi(OH)_2^+] - - k_1'[BiOH^+]\}\,[H^+] \qquad (4)$$

Supposing that both previous chemical reactions take place at a rather high rate so that in the reaction layer the constant state is prevailing, the product between the hydrolysis constant and the total rate constant may be calculated by means of the Weber and Koutecky relation [6]:

$$i_k/i_d = 0.886\ (K_h k t_1)^{1/2}/[1 + 0.886\ K_h k t_1)^{1/2}] \qquad (5)$$

In formula (5) t_1 is the dropping time at the limiting current and i_d is the hypothetical diffusion controlled current, which corresponds to the analytical concentration of Bi^{3+} ($pH = 0$).

The total rate constant k is given by the formula [7]:

$$k = k_{X_2O} + k_{X^+}[X^+] \qquad X = [H];\ [D] \qquad (6)$$

which shows that the total rate constant represents a contribution of the water and of the hydrogen, of the deuterium ions respectively.

According to equation (6) representing $K_h k$ as a function of $[X^+]$, a straight line is obtained with the slope $K_h k_X$ and the intercept $K_h k_{X_2O}$ (figure 2).

The obtained values are presented in table 1.

---

[6] J. Weber and J. Koutecky, *Coll. Czech. Chem. Comm.*, **20**, 980 (1955).

[7] R. Brdicka, *Z. Elektrochem.*, **59**, 787 (1955).

In both solvents at pH < 1.2, that is in strong acidic environment, the product between the hydrolysis constant and the rate constant, which is depending on the solvent, $K_h k_{X_2O}$ has a negative value. This means that the hydrolysis does not occur but instead the reverse process of the Bi^{3+} species formation is taking place. This result is in agreement with the experimental data as it was observed that the current value does not vary.

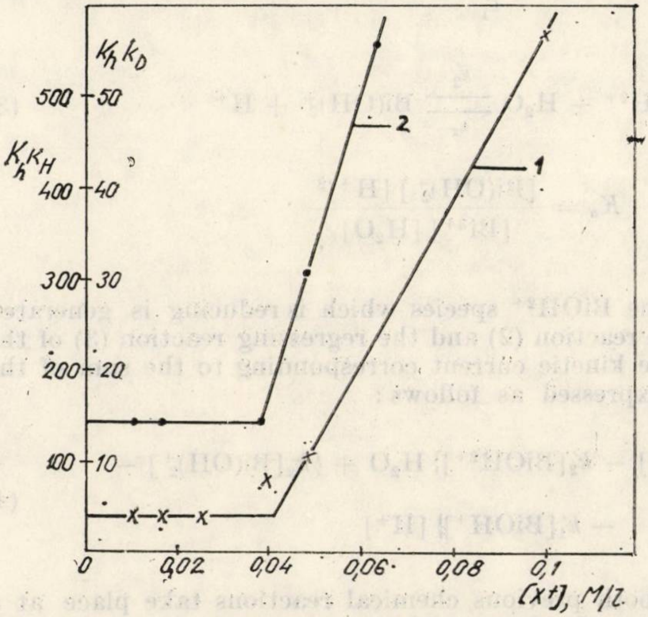

Fig. 2. — Variation of the value $K_h k$ as a function of $[X^+]$ mol/l : 1 — H_2O ; 2 — D_2O.

Table 1

Values of the product of the equilibrium and rate constants at 25°

Solvent	pH (D)	$K_h k_X + /1\ mol^{-1}\ s^{-1}$	$K_h k_{X_2O}/s^{-1}$
H_2O	0 —1.3	$9.37 \cdot 10^3$	neg.
H_2O	1.3—2.0	0	40
D_2O	0—1.3	$1.66 \cdot 10^3$	neg.
D_2O	1.3—2.0	0	14.5

At a pH > 1.2, the hydrolysis process expressed by the $K_h k$ product is independent of the hydrogen ions concentration, depending entirely on the solvent.

From the pD value corresponding to equal concentrations of the $BiOH^{2+}$ and $Bi(OH)_2^+$ species, the hydrolysis constant in D_2O has been calculated, obtaining $K_{h,D_2O} = 0.63 \cdot 10^{-3}$. The hydrolysis constant in light water, previously determined,[3] has the value $K_{h,H_2O} = 1.53 \cdot 10^{-3}$. The ratio of these constants is :

$$K_{h,H_2O}/K_{h,D_2O} = 2.4$$

The 2.4 value shows a direct isotope effect resulted from the differences that exist between pK_{H_2O} and pK_{D_2O}[4].

Using the experimental values of the $K_h k$ product and the hydrolysis constants K_h, the rate constants values and the kinetic isotope effects were computed and presented in table 2.

Table 2

Rate constants and related kinetic isotope effects at 25°

System	k_{X_2O}/s^{-1}	$k_{X^+}/1\ mol^{-1}s^{-1}$
H	$2.61 \cdot 10^4$	$6.1 \cdot 10^6$
D	$2.3 \cdot 10^4$	$2.6 \cdot 10^6$
k_H/k_D	1.1	2.3

It follows therefrom that both in light water as well as in heavy water the rate constants have approximately the same value. The isotope effect due to the solvent has therefore a relatively small value. This fact may be explained considering that in hydrolysis reactions water has the role of a reactant. The water molecules being in great excess and in the rate determining step no bond breaking is taking place, and no great change is occurring in the system.

The isotope effect of the K_{X^+} constant is determined by the acid dissociation, which is smaller in D_2O than in H_2O.[8]

As a conclusion, the kinetic and thermodynamic analysis of the Bi^{3+} hydrolysis process in light and in heavy water has revealed that in both solvents the hydrolysis process takes place similarly, with the formation of the same species. If the hydrolysis rate is the same, $(k_{H^+}/k_{D^+} = 1)$ the stability of the species will be greater in H_2O than in D_2O.

---

[8] P. KRUMMBIEGEL, "Isotopieeffekte", Akademie Verlag, Berlin, 1970.

Revue Roumaine de Chimie, 22, *5*, 697 – 704 (1977)

Dedicated to the 70th anniversary
***of Professor* Coriolan Drăgulescu**

ON THE PHOTOLYSIS OF $[Mn(C_2O_4)_2\,(H_2O)_2]K$ IN DIMETHYL-FORMAMIDE. II[1]

CONCENTRATION AND OXYGEN EFFECTS

TATIANA ONCESCU, S. G. IONESCU and C. ANDREESCU
Physical Chemistry Department, Institute of Chemistry, Bd. Republicii 13, Bucharest, Romania.

Received June 7, 1976

The photolysis of $[Mn(C_2O_4)_2(H_2O)_2]K$ in N, N-dimethylformamide (DMF), on irradiation at $\lambda = 313$ nm, in the LMCT band, within the concentration range, $1\times 10^{-4} - 2.5 \times 10^{-3}$ M was studied. A marked dependence of quantum yields on the O_2 and complex concentrations was observed. The photolysis quantum yield on irradiation at $\lambda = 405$ nm was also determined. These data complete and support the photolysis mechanism proposed in the previous part. [1]

1. INTRODUCTION

We studied earlier [1] the photolysis of $[Mn(C_2O_4)_2(H_2O)_2]K$ in DMF aerated solutions, on irradiation in the LMCT band (λ=313nm, λ=366nm) and in (*d*–*d*) band ($\lambda = 436$ nm) within the concentration range, $2\times10^{-3} - 3\times10^{-3}$ M. The quantum yield values obtained were : $1.94 \pm \pm\, 0.06$ at $\lambda = 313$, $\lambda = 366$ nm and 0.74 ± 0.05 at $\lambda = 436$ nm.

The quantum yield of about 2 as well as the similar nature of the photolysis products with those of the thermolysis suggested a reaction mechanism which involves two intermediates : $[Mn(C_2O_4)(C_2O_4^{\cdot -})(H_2O)_2]^-$ and $C_2O_4^{\cdot -}$. These transients have been detected by ESR spectrometry on irradiation at 77 K.

The aim of the present work was to provide supplementary data concerning this photolysis mechanism in order to explain the oxygen effect on the quantum yield and the large quantum yield value obtained for $\lambda = 405$ nm, corresponding to a minimum in the electronic absorption spectrum of the complex.

---

[1] Part. I, I. G. Murgulescu, T. Oncescu and S. G. Ionescu, *Rev. Roumaine Chim.*, **17**, 423 (1972).

2. EXPERIMENTAL

a) *Reagents*: $[Mn(C_2O_4)_2(H_2O)_2]K \cdot 3H_2O$, the yellow complex, presumed to be the *trans*-isomer,[2] was prepared according to the literature,[3] from $KMnO_4$ and $H_2C_2O_4 \cdot 2H_2O$, Merck, p.a.

DMF, Carlo Erba, for chromatography, was used as solvent. Its water content of 0.1 percent was determined by biamperometric titration with Karl-Fischer reagent. The content of dimethylamine of about 5×10^{-5} M was determined spectrophotometrically[4] by using 3-phenyl-2 benzofuranone as indicator.[5]

The solutions were deoxygenated by bubbling nitrogen gas for more than half an hour before each experiment.

Hydrogen peroxide (H_2O_2) traces appeared during photolysis were detected spectrophotometrically by using $Ti(SO_4)_2$ as developing reagent.

b) *The photochemical set-up* is shown in Figure 1.

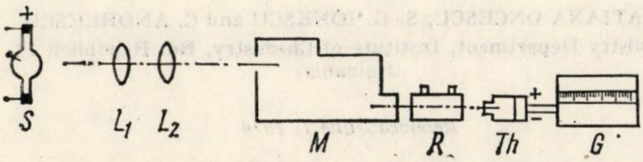

Fig. 1. — The schematic diagram of the photochemical set-up. *S* Mercury lamp HBO—500; L_1, L_2 Collimating and focusing quarz lenses; *M* Bausch-Lomb monochromator; *R* Thermostated reaction cell; *Th* Compensated thermophile VTh—1; *G* Multiflex galvanometer ($R_i = 15\Omega$, $S = 10^{-8}$ A/mm).

VTh-1 thermopile-Multiflex galvanometer system was calibrated by chemical actinometry with $[Fe(C_2O_4)_3]K_3$[6-8] directly in M. min^{-1}. mm^{-1} reaching the reaction system. The calibration was repeated weekly and ordinary values of 1.44×10^{-7} M.min.$^{-1}$ mm^{-1} were determined. Radiant flux energy was constant within 0.5—1 percent.

c) *Irradiation procedure*: Aerated, oxygen saturated, or deoxygenated samples of complex solutions were irradiated in 12 ml stoppered quartz cells of 3 cm optical depth, thermostated at 25° ± 0.1. The samples were shaken manually after every 5 minutes, corresponding to a small reaction extent. The electronic spectra of the samples were recorded by using even the irradiation cells, at a SP—800 Pye Unicam spectrophotometer. As the thermal decomposition of the complex is significantly slowed down in DMF solutions,[1] there was no need to carry out such a correction in the overall chemical change value.

d) *Quantum yield calculation*: was done by using peculiar forms of Kling, Nikolaïski and Schläfer[9] equation, established for simple photochemical systems under inner filtering condition:

$$\varphi = \frac{1}{\varepsilon_A \cdot Q_0\, t}\left[(\varepsilon_A - \varepsilon_B)(C_0 - C) + 2.303\, \varepsilon_B\, C_0 \lg \frac{C_0}{C} + \frac{1}{l} \lg\left(\frac{1 - T_0}{1 - T}\right) + \varepsilon_B\, C_0 \bar{R}_1\right] \tag{1}$$

φ is the quantum yield value.

---

[2] T. Oncescu and V. Sahini, *Rev. Chim. Acad. R.P.R.*, **1**, 73 (1963).

[3] G. H. Cartledge and W. P. Eriks, *J. Amer. Chem. Soc.*, **58**, 2061 (1936).

[4] H. E. Zaugg and A. D. Schaeffer, *Analyt. Chem.*, **36**, 2121 (1964).

[5] A. Bistrzycki and J. Flatau, a) *Ber. dtsch. chem. Ges.*, **28**, 989 (1895); b) *ibidem* **30**, 124 (1897).

[6] C. A. Parker, *Proc. Roy. Soc. A.*, **220**, 104 (1953).

[7] C. A. Parker and C. G. Hatchard, *Proc. Roy. Soc.* A, **235**, 518 (1956).

[8] J. Lee and H. H. Seliger, *J. Chem. Phys.*, **40**, 519 (1964).

[9] O. Kling, E. Nikolaïski and H. L. Schläfer, *Ber. Bunsengesellschaft Phys. Chem.*, **67**, 883 (1963).

$\bar{Q}_0$ is the number of Einstein per volume unit(liter) per time unit (minute) (M. min^{-1}).
ϵ_A, ϵ_B are decimal molar absorptivities of the complex A and the photoproduct B, ($M^{-1}.cm^{-1}$) respectively.
l is the optical depth of the reaction system (cm).
T_0, T are the reaction system trasmittancy values at zero time and t time of irradiation, respectively.
C_0, C are the concentration values of the complex A at zero time and t time of irradiation, respectively (M).
t is the irradiation time (min)
R_1 is the average of the errors which affect the value by neglecting an infinite expansion series in the exact formula given by Kling, Nikolaïski and Schläfer.
Relationship (1) was used in the case of incomplete absorption of diluted complex solutions of high inner filtering effect ($\epsilon_A \neq \epsilon_B \neq 0$).

This relationship changes in the case of complete absorption ($T = T_0$) as follows :

$$\varphi = \frac{1}{\epsilon_A \bar{Q}_0 \cdot t}\left[(\epsilon_A - \epsilon_B)(C_0 - C) + 2.303\, \epsilon_B\, C_0 \lg \frac{C_0}{C}\right] \tag{2}$$

The quantum yield values for $\lambda = 405$ nm irradiation were estimated considering relationship (1) in the case of incomplete absorption ($T \neq T_0 \neq 0$) and no inner filtering effect ($\epsilon_B = 0$) :

$$\varphi = \frac{1}{\bar{Q}_0 \cdot t}\left[(C_0 - C) + \frac{1}{\epsilon_A\, l} \lg\left(\frac{1 - T_0}{1 - T}\right)\right]. \tag{3}$$

The quantum yield values calculated with relationship (2) did not differ significantly from those obtained with relationship (4) :

$$\varphi = \frac{C_0 - C}{\bar{Q}_0 \cdot t}. \tag{4}$$

established in the case of concentrated complex solutions, $2 \times 10^{-3} - 3 \times 10^{-3}$ M and moderated reaction extent, 10–20 percent, when $\epsilon_B = 0$. We have checked previously the Beer-Lambert law, because the derivation of formulae (1)–(4) assumes its validity.
The decimal molar absorptivities of the complex A and of the final product B at the wavelengths used are :

$$\epsilon_A^{313} = 2.92 \times 10^3\, M^{-1} cm^{-1};\ \epsilon_A^{405} = 74;\ \ \epsilon_B^{313} = 5.75 \times 10^2\, M^{-1}.\, cm^{-1}.$$

3. RESULTS AND DISCUSSION

The spectra of diluted solutions of $[Mn(C_2O_4)_2(H_2O)_2]K$ in DMF at various irradiation intervals are shown in Figure 2.

The quantum yield values determined for low concentrations of complex in the presence of atmospheric or bubbled oxygen approach unity. In deoxygenated solutions the quantum yield is about twice of its value in aerated solution at low concentrations of the complex. In tables 1 and 2 typical quantum yield data are given.

Another remark on the present experimental determination is that the quantum yield value approaching unity for diluted solutions in the presence of atmospheric or bubbled oxygen is about a half from the corresponding value in concentrated aerated [1] or deoxygenated solutions of the complex.

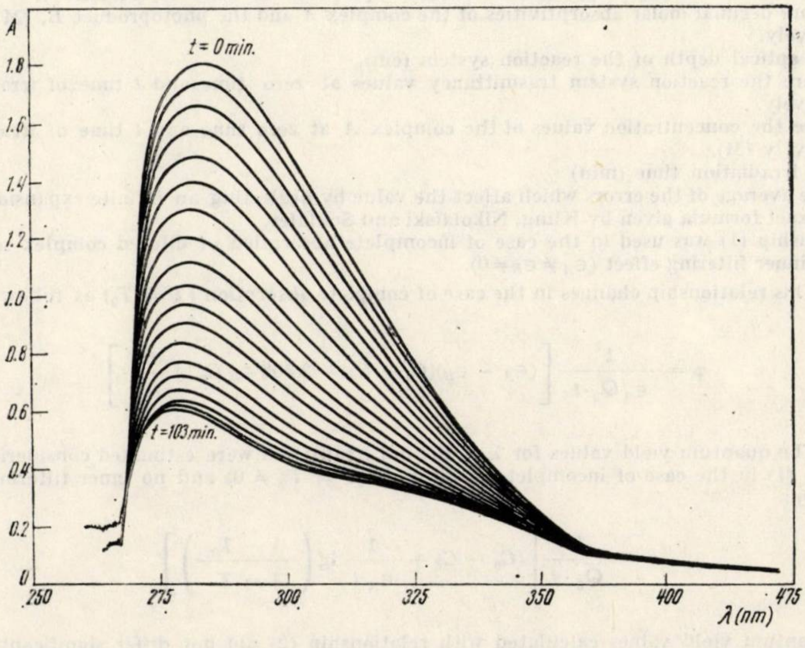

Fig. 2. — $[Mn(C_2O_4)_2(H_2O)_2]K$ spectra in DMF at various moments of photolysis. $\lambda = 313$ nm ; $C_0 = 1.28 \times 10^{-4}$M ; $\overline{Q}_0 = 4.66 \times 10^{-6}$ M · min^{-1} ; $T = 25°$.

Such a change in the quantum yield value required its determination at various concentrations within the range, $1\times10^{-4} - 2.5\times10^{-3}$ M. Our results confirmed that there is a marked dependence of the quantum yield value upon the complex concentration, as can be seen in Figure 3.

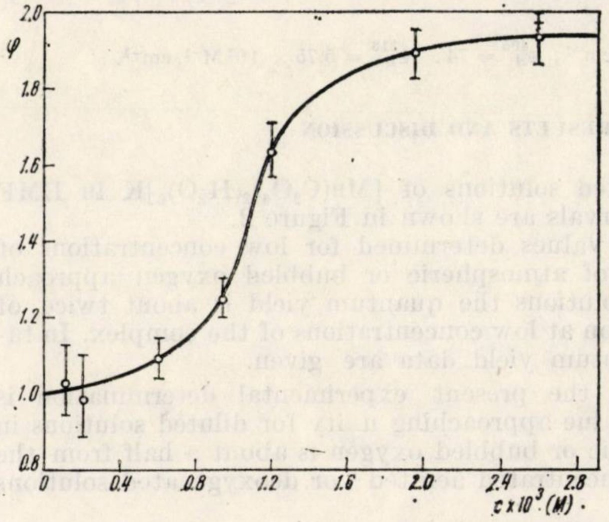

Fig. 3. — Quantum yield dependence on the average concentration of $[Mn(C_2O_4)_2(H_2O)_2]K$ in aerated solutions. $\lambda = 313$ nm ; $T = 25°$.

Table 1

Quantum yields of $[Mn(C_2O_4)_2(H_2O)_2]$ K photolysis in DMF oxygen saturated solution. λ = 313 nm; $C_0 = 1.04 \times 10^{-4}$ M; $Q_0 = 2.09 \times 10^{-6}$ M.min^{-1}; T = 25°

t (min)	$\left(\frac{1}{l}\ \lg\frac{1-T_0}{1-T}\right)\times 10^3$ (cm^{-1})	$(\epsilon_A - \epsilon_B)(C_0 - C)\times 10^3$ (cm^{-1})	$\left(2.303\ \epsilon_B C_0 \lg\frac{C_0}{C}\right)\times 10^3$ (cm^{-1})	$\epsilon_B C_0 R_1 \times 10^3$ (cm^{-1})	$\epsilon_A Q_0 \cdot t \times 10^3$ (cm^{-1})	α (%)	φ
0	0.00	0.00	0.00	0.00	0.00	0.00	—
5	3.00	21.10	5.40	0.83	30.50	8.70	0.99
10	6.70	39.90	10.60	1.80	61.00	16.40	0.97
20	14.00	75.00	22.10	4.70	122.10	30.80	0.95
30	25.40	110.20	36.00	10.70	183.10	45.20	0.99
40	37.70	140.70	51.60	22.00	244.10	57.70	1.03
55	56.70	197.00	74.50	53.80	355.70	71.20	1.01
							0.99±0.04

Table 2

Quantum yields of $[Mn(C_2O_4)_2(H_2O)_2]$ K photolysis in DMF deoxygenated (N_2) solution. λ = 313 nm; $C_0 = 1.56 \times 10^{-4}$ M; $Q_0 = 2.45 \times 10^{-6}$ M.min^{-1}; T = 25°

t (min)	$\left(\frac{1}{l}\ \lg\frac{1-T_0}{1-T}\right)\times 10^3$ (cm^{-1})	$(\epsilon_A - \epsilon_B)(C_0 - C)\times 10^3$ (cm^{-1})	$\left(2.303\ \epsilon_B C_0 \lg\frac{C_0}{C}\right)\times 10^3$ (cm^{-1})	$\epsilon_B C_0 R \times 10^3$ (cm^{-1})	$\epsilon_A Q_0 \cdot t \times 10^3$ (cm^{-1})	α (%)	φ
0	0.00	0.00	0.00	0.00	0.00	0.00	—
4	2.33	37.52	9.67	0.60	28.06	11.00	1.79
9	6.00	82.10	23.02	1.57	64.60	24.00	1.75
14	11.00	124.30	37.90	2.99	100.20	36.30	1.75
19	17.34	161.80	53.80	4.86	135.90	47.30	1.75
24	26.00	201.70	74.70	7.90	171.70	58.90	1.81
29	36.35	234.50	97.10	11.90	207.50	68.50	1.83
34	52.00	272.00	132.90	19.00	243.20	79.50	1.96
							1.81±0.08

These data led us to consider three other simple reactions, (3), (4), (5), in the previously proposed mechanism of photolysis [1] in order to explain the influence of O_2 and complex concentration upon the quantum yield values :

$$[Mn(C_2O_4)_2(H_2O)_2]^- \xrightarrow[Q_a]{h\nu} [Mn(C_2O_4)(C_2O_4^{\cdot -})(H_2O)_2]^{-\star} \qquad (0)$$

$$[Mn(C_2O_4)(C_2O_4^{\cdot -})(H_2O)_2]^{-\star} \xrightarrow{k_1} MnC_2O_4 + 2\ H_2O + C_2O_4^{\cdot -} \qquad (1)$$

$$[Mn(C_2O_4)_2(H_2O)_2]^- + C_2O_4^{\cdot -} \xrightarrow{k_2} MnC_2O_4 + 2\ H_2O + C_2O_4^{2-} + 2CO_2 \qquad (2)$$

$$[Mn(C_2O_4)(C_2O_4^{\cdot -})(H_2O)_2]^{-\star} + O_2 \xrightarrow{k_3} MnC_2O_4 + 2\ H_2O + 2\ CO_2 + O_2^- \qquad (3)$$

$$C_2O_4^{\cdot -} + O_2 \xrightarrow{k_4} 2\ CO_2 + O_2^- \qquad (4)$$

$$O_2^- + H_3O^+ \xrightarrow[(C_2O_4^{2-})]{k_5} H_2O_2 + OH^- \qquad (5)$$

The three secondary reactions are in good agreement with the similar behaviour of Mn(III) oxalato-complexes thermolysis in aqueous solutions.[10]

In order to obtain some experimental proofs on these last three processes we detected the presence of H_2O_2 with $Ti(SO_4)_2$, when the characteristic yellow product appeared. Figure 4 illustrates the generation of H_2O_2, namely in aerated but non-irradiated solutions, at complex concentrations of 1×10^{-3} M, we detected H_2O_2 traces due to the slow thermal decomposition of the complex. In aerated irradiated solutions we detected important amounts of H_2O_2 whereas in deoxygenated irradiated solutions the H_2O_2 content was lower than in the previous case.

In addition, according to the process (5), we observed an increase in the pH of aerated irradiated samples of 2 units. It is evident that the

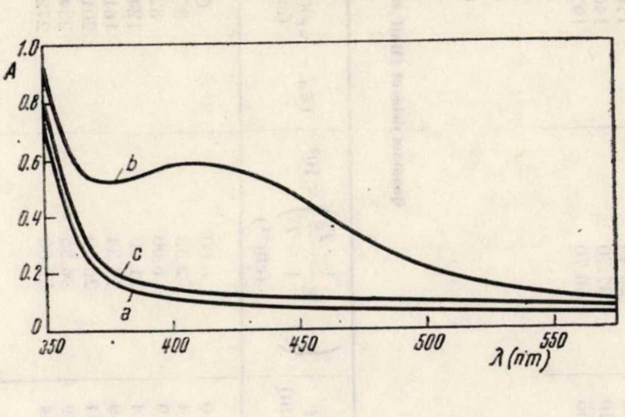

Fig. 4. — Hydrogen peroxide generation in :
(a) aerated non-irradiated, (b) aerated irradiated, (c) deoxygenated irradiated $[Mn(C_2O_4)_2(H_2O)_2]K$ solutions in DMF. $\lambda = 313$ nm ; $T = 25°$ $C_0 = 1 \times 10^{-3}$ M ; conversion = 100 percent.

---

[10] N. S. Rowan, R. M. Milburn and M. Z. Hoffman, *Inorg. Chem.*, **11**, 2272 (1972).

water content of the solvent (0.1 percent) is high enough to produce reaction (5).

In the above proposed mechanism we did not consider the $[Mn(C_2O_4)(C_2O_4^{\cdot -})(H_2O)_2]^{-*}$ decay by internal conversion or other kind of photophysic process to the ground state because of the quantum yield value of about 2 obtained in diluted deoxygenated or in aerated concentrated solutions.

By using the steady state approximation this photolysis mechanism leads to the following relationship:

$$\varphi = 1 + \frac{k_1}{k_1 + k_3 CO_2}\left[1 - \frac{k_1\, CO_2}{k_2 C + k_4 CO_2}\right] \qquad (5)$$

where C is the complex concentration and CO_2 is the O_2 concentration. This relationship permits some discussion about the influence of O_2 and complex concentration upon the quantum yield values. Thus in deoxygenated solutions, $CO_2 \cong 0$, over the entire complex concentration range, φ approaches 2.

In diluted, $\sim 10^{-4}$ M, aerated or oxygen-saturated solutions $\varphi = 1$, that is $k_2 C \ll k_4 CO_2$ because the oxygen concentration is high enough to ensure the same effect in processes (3) and (4).

In aerated but more concentrated complex solutions, $\sim 10^{-3}$ M, the quantum yield value approaches 2 that is $k_2 C \gg k_4 CO_2$ and $k_3 CO_2 \ll k_1$. Thus a simplified relationship can be derived from equation (5):

$$\varphi = 2 - \frac{k_4 CO_2}{k_2 C + k_4 CO_2} \qquad (6)$$

If k_2 and k_4 are close enough, then CO_2/C ratio will decide the extent of process (4) in competition with process (2). In concentrated aerated solutions $C > CO_2$ and φ approaches 2, supposing CO_2 as high as in diluted aerated solutions. Alternatively, the oxygen solubility decreases as the complex concentration increases and the effect can be the same as in deoxygenated solutions. Equation (6) leads to:

$$\frac{\varphi - 1}{2 - \varphi} = \frac{k_2\, C_0}{k_4 CO_2} \qquad (7)$$

The plot of equation (7) was not linear and this can be explained in two ways:

a. It is difficult to assign the right value for C.

b. There is an overlapping of the two situations discussed above regarding equation (7).

Finally we performed quantum yield measurements at $\lambda = 405$ nm and obtained $\varphi = 1.22 \pm 0.12$ in aerated concentrated solutions of the complex, that is under the same conditions of our previous investigation.[1] This value exceeds $\varphi = 0.74 \pm 0.05$ at $\lambda = 436$ nm, though $\lambda = 405$ nm corresponds to a minimum and $\lambda = 436$ nm to a maximum in the $(d-d)$ band of the complex absorption spectrum. This behaviour is similar to other oxalato-complexes.[11] It can be explained by an increasing CT character of $(d-d)$ band at this wavelength.

---

[11] G. B. Porter, J. G. W. Doering and S. Karanka, *J. Amer. Chem. Soc.*, **84**, 4027 (1962).

Revue Roumaine de Chimie, **22**, *5*, 705–712 (1977)

Dedicated to the 70th anniversary
of Professor Coriolan Drăgulescu

STUDIES IN THE FIELD OF BIURET REACTION. X[1]

INFRARED ABSORPTION SPECTRA FOR SOME COPPER(II) COMPLEXES OF THE CYANURIC ACID

G. OSTROGOVICH, MARIA NUŢIU and R. NUŢIU *
The "Traian Vuia" Polytechnic Institute, Department of Organic Chemistry, Str. Bocşa 6,
Timişoara, Romania

Received June 9, 1976

The infrared spectra of the following copper(II) complexes of cyanuric acid ($C_3H_3N_3O_3$) are studied : (Cu Cyur^{II})$_n$ **(1)**, Li[Cu Cyur^{III}] · $2H_2O$ **(2)**, Li[Cu Cyur^{III}] **(3)**, Li[Cu Cyur^{I} Cyur^{II}(H_2O)$_2$] (4), Li[Cu Cyur^{I}Cyur^{II}] **(5)**, Na_2[Cu Cyur$^{I}_{4}$] · $6H_2O$ **(6)**, α-Na_2[Cu Cyur$^{I}_{4}$] **(7)**, β-Na_2[Cu Cyur$^{I}_{4}$] **(8)**, K_2[Cu Cyur$^{I}_{4}$(H_2O)$_2$] · $4H_2O$ **(9)** and K_2[Cu Cyur$^{I}_{4}$] **(10)** where Cyur^{I}, Cyur^{II}, and Cyur^{III} are mono-, di-, and tri-anions of the cyanuric acid. It has been established that cyanuric acid presents different structures in these complexes, namely : monolactamic structure in **(1)**, dilactamic in **(2)** and **(3)**, and trilactamic in the others. In all cases the ligand donor atoms are nitrogen atoms, except the polynuclear complex **(1)**, in which Cu–O bonds are formed. The force constant of the Cu–N bond was calculated. Its value, 2.27×10^5 dyn/cm is in good agreement with the covalence degree previously evaluated for this bond.

In order to determine the structures of some cyanuratocopper(II) complexes obtained and characterized by us in previous works,[1–4] we performed an infrared spectral study on these compounds. The following compounds were studied: (Cu Cyur^{II})$_n$ **(1)**, Li[Cu Cyur^{III}] 2 H_2O **(2)**, Li Cu Cyur^{III} **(3)**, Li[Cu Cyur^{I} Cyur^{II} (H_2O)$_2$] **(4)**, Li[Cu Cyur^{I} Cyur^{II}] **(5)**, Na_2[Cu Cyur$^{I}_{4}$]·$6H_2O$ **(6)**, α–Na_2[Cu Cyur$^{I}_{4}$] **(7)**, β–Na_2[Cu Cyur$^{I}_{4}$] **(8)**, K_2[Cu Cyur$^{I}_{4}$(H_2O)$_2$]·$4H_2O$ **(9)**, and K_2[Cu Cyur$^{I}_{4}$] **(10)**, where Cyur^{I}, Cyur^{II} and Cyur^{III} are mono-, di-, and trianions of the cyanuric acid.

---

* University of Timişoara, Department of Organic Chemistry.

[1] Part IX : M. Nuţiu, F. Marx, and G. Ostrogovich, *Bul. St. Tehnic Inst., Politehnic "Traian Vuia" Timişoara, seria Chimie*, **18**, 155 (1973).

[2] G. Ostrogovich and M. Nuţiu, *Rev. Roumaine Chim.*, **16**, 1473 (1971).

[3] Z. Simon, M. Nuţiu and G. Ostrogovich, *Rev. Roumaine Chim.*, **17**, 573 (1972).

[4] M. Nuţiu, F. Marx, V. Cristea and G. Ostrogovich, *Bul. St. Tehnic Inst., Politehnic "Traian Vuia" Timişoara, seria Chimie*, **18**, 131 (1973).

Considering the great number of possible structures of the cyanuric anions in its salts[5–7] (formulae **11**–**13**) we followed both the characteristic bands of the ligand and those of the bonds formed with the copper(II) ion. These bonds can be either O–Cu or N–Cu bonds.

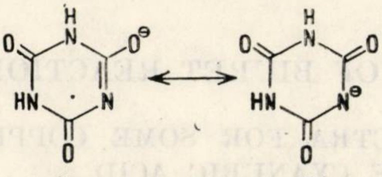

11a **11b**

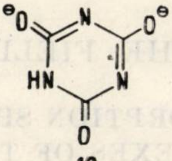

12

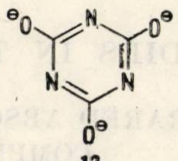

13

We also studied the characteristic bands for water molecules which in some cases are ligands corresponding to the formation of cyanurato aquo-complexes.

EXPERIMENTAL PART

The compounds were prepared according to indications given in literature data.[2,8,9] The infrared absorption spectra were recorded on an UR–10 Carl Zeiss Jena double beam spectrophotometer. The samples were studied as pellet in KBr as well as suspensions in nujol and in hexachlorobutadiene. The experimental technique was the usual one.[10]

RESULTS AND DISCUSSIONS

The infrared absorption bands of the monosodic cyanurate, Na Cyur^{I}·H_2O, and the cupric cyanurate, Cu Cyur^{II}, recorded as comparison terms in order to elucidate the yet unknown structure of Cu Cyur^{II}, together with those of our coordinated compounds are presented in Table 1.

In the case of the monosodic salt, only the mesomeric forms of a dilactamic structure **(11a)** can be taken into account. The spectrum of this compound presents a broad band at 1640–1670 cm^{-1} which can be attributed[11] to a superposition of the C=N valence vibration with a carbonyl group stretching vibration. Also the characteristic carbonyl

---

[5] E. M. Smolin and L. Rapoport, "s-Triazines and Derivatives", Interscience Publishers Inc., New York, 1959, p. 34–43.

[6] E. Agallidis, H. Fromberg and A. Hartzmann, *Dtsch. chem. Ber.*, **71 B**, 1391 (1938).

[7] M. Ito, *Bull. Chem. Soc. Japan*, **26**, 339 (1953).

[8] A. Ostrogovich and G. Ostrogovich, "Atti del II Congresso Nazzionale di Chimica Pura ed Applicata", Sardegna, Maggio e Giugno, 1935; *Chem. Zentr.*, **1937**, I, 2146.

[9] G. Ostrogovich and M. Nuţiu, *Bul. St. Tehnic Inst. Politehnic Timişoara, seria Chimie*, **15**, 151 (1970).

[10] L. J. Bellamy, "The Infrared Spectra of Complex Molecules", Translated in Russian, Izd. Inostr. Lit., Moskva, 1957.

[11] M. Avram and Gh. D. Mateescu, "Infrared Spectroscopy. Applications in Organic Chemistry", Wiley, New York, 1972, p. 333, 335, 441–449.

group bands ($\nu C{=}O$) at 1700–1800 cm^{-1} as well as the absorption at 1050 cm^{-1} which is almost surely due to the stretching vibration of the C–O bond, are arguments in favour of structure **(11a)**.

For the cupric cyanurate **(1)**, based on the molecular formula $Cu(C_3HO_3N_3)$ and taking into account its building up by the thermolysis[9] of two neutral complexes, Cu $Cyur^{II}$ $Py_2 \cdot H_2O$ and Cu $Cyur^{I}_2$ $(NH_3)_2$, we must admit a polymeric structure. The strong band at 1710 cm^{-1} and the broad one in the 1620–60 cm^{-1} range are encountered as common vibrations with the monosodium salt. It is also remarkable that the 1470 cm^{-1} band is intensified, as compared to the cyanuric acid[12] and its monosodium salt, while the strong band at 1400 cm^{-1}, encountered also for the free acid and the sodium salt are recorded here as a triplet of a lower intensity. (The splitting may be due to the crystalline field). If the absorptions at 1020 cm^{-1} (s), 1055 cm^{-1} (sh) and 1170 cm^{-1} (w) are attributed[12] to stretching vibrations of the C–O bond, the 1470 cm^{-1} to the plane degenerated vibration of the cycle, and the 1400 cm^{-1} band to the $\delta N{-}H$ deformation vibration, the cupric cyanurate may correspond to a monolactamic polynuclear structure **(14)**:

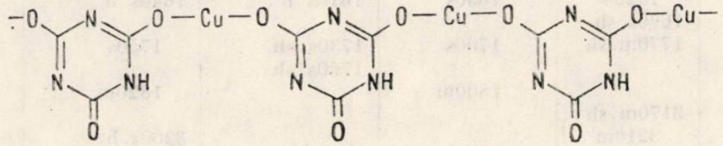

14

For monosodic and cupric cyanurates as for the complexes of cyanuric acid studied by us, the characteristic bands for the secondary amidic, and lactamic groups,[10,13–17] respectively, are found at higher values than in the cyanuric acid, these indicating the existence of some simple associations,[11] probably

$-NH\ldots O=C-$
$\qquad\qquad\qquad\quad \mid$
trans$(\cdots O = C - \qquad - NH\ldots)$. In the cyanuric acid
cis $(- C = O\ldots H - N -)$ associations were demonstrated.[18]
$\qquad \mid \qquad\qquad\qquad \mid$
$-N - H\ldots O = C-$

The doublet at 535 cm^{-1} is attributed[18] to the deformation vibration of the carbonyl group ($\delta C = O$).

---

[12] R. Newmann and R. M. Badger, *J. Amer. Chem. Soc.*, **74**, 3545 (1952).

[13] A. W. McLellan and G. A. Melson, *J. Chem. Soc. (A)*, **1967**, 137.

[14] G. Ostrogovich, R. Bacaloglu, A. Nemes, E. Catalina and M. Nuţiu, *Studii şi Cercetări Sti. Chim., Baza Cercetări Sti., Timişoara*, **10**, 71 (1963).

[15] K. Aida, *J. Inorg. Nuclear Chem.*, **23**, 155 (1961).

[16] K. Aida, *J. Inorg. Nuclear Chem.*, **25**, 165 (1963).

[17] R. Ch. Paul, B. R. Sreenathan and S. L. Chadita, *J. Inorg. Nuclear Chem.*, **28**, 1225 (1966).

[18] E. H. Wiebenga, *J. Amer. Chem. Soc.*, **74**, 6156 (1952).

Table 1

IR spectra of the copper(II) complexes

$\mathrm{NaCyur^{I}\cdot H_2O}$	$\mathrm{CuCyur^{II}}$ **(1)**	$\mathrm{Li[CuCyur^{III}]\ 2H_2O}$ **(2)**	$\mathrm{Li[CuCyur^{III}]}$ **(3)**	$\mathrm{Li[CuCyur^{I}\ Cyur^{II}\ (H_2O)_2]}$ **(4)**	$\mathrm{Li[CuCyur^{I}\ Cyur^{II}]}$ **(5)**
550m	535m	560m	550m	560s	530s, 550s
	545m	580w.sh	570w.sh	590s	595m
			585w		
705w	670w, 690w				
760w	735w, 745w	740w, 755w		720w	740m sh
775m	775w	765w	760w		760m sh
790m	785w, 800m	785s,820w	790m, 800m.sh	790s	790s
				845m	
1050m	1020s,	1015m	1020m	1020m, 1100m	1020m
	1055m.sh	1080w,			
	1170w	1100w			
	1300w.sh	1240w,	1250w	1260m	1250m.sh
		1260w			
1400s	1430 s	1405s.b	1430s.sh	1440s	1450s.b
1475m.b	1470s.b	1470s.b	1470s.b	1490s	
1640—	1620—	1650s	1610s.b	1640s.b	1620s.b
1670m.sh	1660s.sh				
1760m	1770m.sh	1760s	1730s.sh,	1750s	1780s.sh
			1760s.sh		
1790m		1800m		1820m	
3200s.b	3170m.sh				
	3210m			3200s.b	3220s.b
3460s.b				3400m.b	
3560s.b		3570s·b			

In the recent studies [19,20] of bis (isocyanurato) diammine copper(II), $\mathrm{Cu(C_3H_2O_3N_3)_2(NH_3)_2}$, which has been known for a long time,[21] the 450 cm^{-1} and 431 cm^{-1} vibrations are attributed to the Cu—N bond. We consider that the 450 cm^{-1} and 460 cm^{-1} bands in the infrared spectrum of the copper cyanurate cannot be attributed to a Cu—N bond, because these bands appear in the spectrum of trimethylcyanurate as well. The splitting in the copper cyanurate spectrum can be explained by the influence of the crystalline field.

In the spectra of the cyanuric acid complexes studied by us, besides the bands observed for the monosodic and copper cyanurates, one can also remark the characteristic band for the Cu—N bond at 580 cm^{-1}. The attribution of this band is confirmed by the fact that its position is not sensibly modified by ligand changes.[22,23]

---

[19] P. G. SLADE, M. RAUPACH and E. W. RADOSLOVICH, *Acta Crist.*, **B 29(2)**, 279 (1973).

[20] R. M. TAYLOR, *Z. anorg. Chem.*, **390**, 85 (1972).

[21] A. CLAUS and O. PUTENSEN, *J. prakt. Chem.*, **38**, 208 (1888); A. BENRATH, *Z. anorg. Chem.*, **151**, 35 (1926); G. OSTROGOVICH and A. NEMES, *Studii și Cercetări Sti. Chim., Baza Cercetări Sti. Timișoara*, **7**, 285 (1960).

[22] K. NAKAMOTO, "Infrared Spectra of Inorganic and Coordination Compounds", J. Wiley Inc., New York, 1963, p. 146.

[23] K. NAKAMOTO, "Instrument News", The Perkin-Elmer Coorporation, Norwalk Connecticut, vol. 20, 1970, p. 1.

of the cyanuric acid (in KBr pellet)

$Na_2[CuCyur^I_4]$ $6H_2O$ **(6)**	α— $Na_2[CuCyur^I_4]$ **(7)**	β— $Na_2[CuCyur^I_4]$ **(8)**	$K_2[CuCyur^I_4$ $(H_2O)_2] \cdot 4H_2O$ **(9)**	$K_2[CuCyur^I_4]$ **(10)**
		530w.sh		535w·sn
560s	565	560m	560s	560s
		590w.sh		
610m			650w.b	615m
675w	685w			685w
705w	730w		710m	705w
760m ; 780s	790s	790s	780s ; 800m.sh	780s ; 805w·sh
850—880m			840—850m	
990w				
1020w	1020w	1020w	1010w	1015w
1090w	1075w	1060w	1080w	1080w
1130w	1105w	1105w		1100w
1260w	1260w·sh	1260w.sh	1230w	1250w
1420s	1460s	1450s	1430s.sh	1410s.sh
1480m.sh	1490m	1490m	1470m.sh	1450s ; 1490s
1500s			1490s	
1650s	1690s	1650s.sh	1650s	1670s.sh
1720m·sh	1730m.sh	1720s	1720s	1705s
1755s			1750s	1735s
			1790m.sh	1800m.sh
3180m·sh	3210m	3210m.b	3100s.sh	3200m
			3180m.sh	
3480s			3430m	
3570s			3585m.sh	

There are several mentioned works [17,24,25] concerning the attribution of characteristic bands for the coordinatively bounded water in aquo complexes. These absorptions are usually found between 650 and 900 cm^{-1}, and they can be observed rather easily by comparing the spectrum of the hydrated compound with that of the anhydrous one. In our complexes these absorptions appear very clearly between 840 and 880 cm^{-1} as bands of mean or weak intensity.

For the characteristic absorption bands of the "nonbiuretie" blue lithium cyanurato-copper(II) **(2)** and of its anhydride **(3)** (Table 1), one observes their similarity with the spectrum of the sodium cyanurate for the bands at higher frequencies than 1000 cm^{-1}. This confirms a dilactamic structure for the cyanuric ligand in these compounds.

In these spectra a weak and broad absorption between 570—590 cm^{-1}, which can be attributed to the Cu—N bond, is observed.

Taking into account these considerations as well as the molecular formulae of these compounds, their structure can be conceived only as polynuclear. The infrared spectrum of compound **(2)** indicates, by the absorption at 3570 cm^{-1}, the existence of net water which does not influence the structure of the complex anion. This anion, common to the dihy-

---

[24] P. X. Armendarez and K. Nakamoto, *Inorg. Chem.*, **5**, 796 (1966).
[25] J. Nakagawa and S. Mizushima, *Bull. Chem. Soc. Japan*, **28**, 589 (1955).

drated (2) and anhydrous (3) compounds, can be illustrated by structure (15):

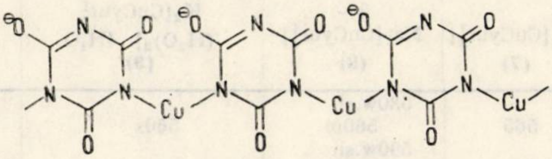

15

In the spectrum of compound (4), two very characteristic bands are recorded with certainty: the 590 cm^{-1} band characteristic for the Cu—N bond and the 845 cm^{-1} one which indicates the presence of coordinated water. Thus, the two lithium cyanurato-copper(II), of blue colour (2), and of violet colour (4) differ not only concerning the cyanuric acid : copper composition quotient (which is 1 :1 in (2) and 2 :1 in (4)), but also concerning the environment of the copper(II) ion, compound (4) being an aquo-complex.

The spectra of compounds (4) and (5) contain also the characteristic absorptions for the C—O bond at 1050 cm^{-1}, as well as the characteristic bands for the stretching vibration of the carbonyl groups; therefore we suppose that one of the cyanuric ligands in the complex has the same dicarbonylic structure as in the previously discussed lythium-cyanurato-copper(II) (2). As concerns the second cyanuric ligand of the complex anion of compound (4), we cannot decide if its structure is a di- or a tricarbonylic one. The violet colour of the compound would indicate an imidic structure for the coordinated nitrogen atoms in both cyanuric residues. Thus, the structure of these complexes can be represented as (16) (with the observation that the second cyanuric ligand may also be dicarbonylic):

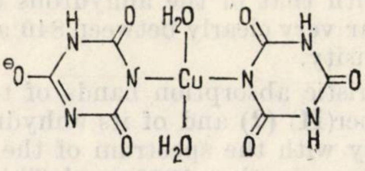

16

The presence of water molecules bound in three different ways results in the spectrum of disodium-tetracyanurato-copper(II) hexahydrate (6); at 3480 cm^{-1} one records the characteristic bands[22] for water molecules which participate in molecular associations by hydrogen bonds with the cyanuric ligand; the band at 3570 cm^{-1} corresponds to crystalline net water, while the coordinatively bounded water is responsible for the broad absorption, of medium intensity, at 850—80 cm^{-1}. The characteristic band for the Cu—N bond appears in this compound at higher wavenumbers, namely at 610 cm^{-1}, probably due to the higher coordination number of the copper(II) ion in this compound. Nevertheless one must observe that the thermogravimetric analysis of this compound [2] did not demonstrate distinct steps for the elimination of water molecules, steps corresponding to different modes of binding. The temperature interval in which dehydration takes place [2] does not conflict however with these aspects suggested by the infrared spectral analysis and the high value of the activation energy calculated for the dehydration reaction considered as one step may indicate that water could be also bound coordinatively. Nothing can be said, with the available data, concerning the number, whole or fractional, of each type of water molecules.

A band characteristic to the metal-nitrogen bond appears also in the spectra of the two anhydrous forms of the disodium tetracyanuratocopper(II), but at a lower frequency than in the hydrate, namely at 565 cm^{-1}.

No characteristic bands for the C–O bond are registered in the spectra of these three complexes and therefore we consider the cyanuric acid to have a trilactamic structure in their anions. As mentioned before we cannot evaluate how many from the six water molecules coordinate to the copper cation. The structure of the anion of the two anhydrous compounds is given in **(17)**.

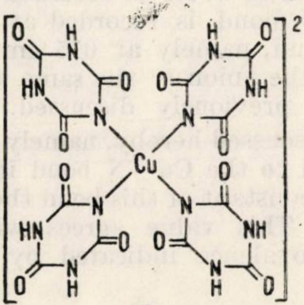

17

In the spectrum of the complex potassium salt **(9)** an important shift of the characteristic band to the metal-copper bond is observed. This band is recorded at 650 cm^{-1}, probably due to the increased coordination number of the copper(II) ion in this complex. The characteristic absorption of water bonded in three different ways is observed in this compound too: the valence vibration frequency of the OH group in association water — at 3430 cm^{-1}, crystalline net water — at 3585 cm^{-1}, and a medium intense absorption at 840–850 cm^{-1}, indicating the existence of coordination water. The thermogravimetric analysis of this compound [2] clearly demonstrated that the water molecules are not equally bonded. The activation energies [2] seem to indicate that the two pairs of water molecules are differently bonded: the first two eliminated molecules are considered by us as crystalline net water, the following two retained by protonic bonds to the cyanuric ligand, while the last two, whose elimination produces a radical colour change (from sky-blue to pink-violet), are probably molecules of coordinated water. The copper in this complex must thus be hexacoordinated. As no characteristic bands for the C—O bond are recorded, a tricarbonylic structure must be attributed to the cyanuric acid and the anion of this complex may be represented as a tetraiso cyanuratodiaquo complex (18):

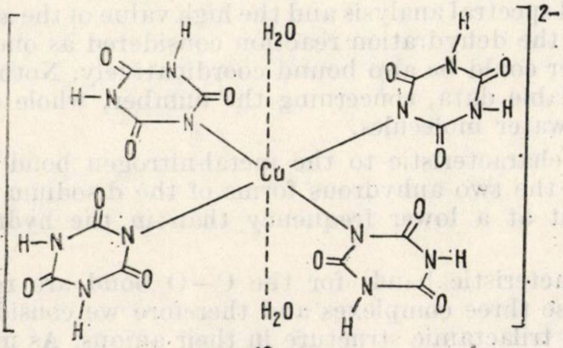

18

In the spectrum of the anhydrous compound, as expected, neither characteristic absorption band of water is recorded, while the characteristic absorption of the Cu—N bond is recorded at a lower frequency than for the hydrated compound, namely at 615 cm^{-1}. The spectrum of this compound suggests that the anion is the same as for the two anhydrous sodium salts, α and β, previously discussed.

The spectral data discussed hereby, namely the value for the absorption frequency attributed to the Cu—N bond in these complexes, allow to calculate for the force constant of this bond the value 2.77×10^5 dyn/cm (for $\nu_{Cu-N} = 580$ cm^{-1}). This value agrees with the conclusions concerning the degree of covalençe indicated by electron spin resonance studies.[23]

Revue Roumaine de Chimie, **22**, *5*, 713–717 (1977)

Herrn Professor Dr. Coriolan Drăgulescu
zum 70. Geburtstag gewidmet

ZUR KOMPLEXBILDUNG BEI DER HF-EXTRAKTION AUS CHLORIDHALTIGEN LÖSUNGEN UNTER VERWENDUNG VON HEXYLDIANTIPYRILMETHAN

B. I. PETROV,* V. V. STRELKOV,* A. I. BUSEV* und P. NENNING **
* Gorki-Universität Perm, Lomonossov-Universität Moskau,
** Karl-Marx-Universität Leipzig

Eingegangen am 11. September 1976

Im ternären System $\{A \cdot HfCl_4\}$ – $A \cdot HCl$ – nichtwäßriges Medium, in dem A für Hexyldiantipyrilmethan steht, bildet sich ein Adduckt $\{(A \cdot HfCl_4)\ (A \cdot HCl)\}$, wenn als nichtwäßriges Medium Chloroform verwendet wird. Bei einem $\geqslant$10-fachen Überschuß von Hexyldiantipyrilmethan läßt sich Hf so aus stark salzsaurer Lösung quantitativ extrahieren.

Hexyldiantipyrilmethan (HDAPM) ist als wirksames Extraktionsmittel bekannt. Ein ca 10-facher stöchiometrischer Überschuß reicht für die quantitative Extraktion einer Vielzahl von Elementen in Chloroform, Dichloräthan oder Nitrobenzol aus.[1] Wenn die HDAPM-Konzentration jedoch in der Größenordnung der Elementkonzentration liegt oder stöchiometrisch ist, scheidet sich – besonders bei Verwendung von Chloroform als Extraktionsmittel – der extrahierte Komplex als Niederschlag ab. Diese Erscheinung wird auch bei Verwendung anderer Diantipyrilmethanderivate beobachtet, z.B. bei der Chloroformextraktion von Th aus Nitrat-,[2] Ti, Zr, Hf-extraktion aus Chlorid-,[3,4] Cd-extraktion aus Jodid-,[5] Sc, Ti, Zr, Hf, Th-extraktion aus Rhodanidlösungen.[5–7] Den Einfluß des Reagenzüberschusses auf die Löslichkeit der extrahierten Verbindung stellen wir im folgenden am Beispiel des Hf dar.

---

[1] „Diantipyrilmethan und seine Homologen als analytische Reagenzien" (ruß.), Sammelband unter Redaktion von S. I. Gusev, Perm, Universitätsverlag, 1974.

[2] V. P. Zhivopistsev und L. P. Pjatosin, *Zhur. analit. Khim.*, **22**, 70 (1967).

[3] B. I. Petrov, Dissertation, Universität Perm, 1968.

[4] B. I. Petrov, V. P. Zhivopistsev und Ju. A. Makhnev, *Zhur. analit. Khim.*, **28**, 505 (1973).

[5] V. P. Zhivopistsev, Habilitationsschrift, Universität Perm, 1965.

[6] V. P. Zhivopistsev, B. I. Petrov und N. F. Sibirjakov, *Wiss. Ber. der Univ. Perm (ruß.)*, **207**, 144 (1970).

[7] V. P. Zhivopistsev und I. S. Kalmykova, *Wiss. Ber. der Univ. Perm (ruß.)*, **207**, 192 (1970).

Die Untersuchung der Verteilung von 0,01–0,02 g-Ion/l Hf(IV) zwischen HCl und Lösungen von Homologen und Derivaten des Diantipyrilmethans in verschiedenen Lösungsmitteln zeigt, daß eine HDAPM-Lösung in Chloroform bzw. Dichloräthan oder Nitrobenzol das beste Extraktionsmittel ist.[1,3] Ist die Acidität der Lösung $\geqslant$ 7 M HCl, wird Hf zu mehr als 95% extrahiert. Wird Chloroform als Extraktionsmittel verwendet, bildet sich bei vergleichbaren Konzentrationen an Hf und HDAPM ein Niederschlag, der das gesamte Hf enthält. Steigende HDAPM-Konzentration führt zu einer teilweisen Hf-extraktion, bis bei einem 10–15-fachem HDAPM-Überschuß das Hf quantitativ extrahiert wird. Bei Verwendung von Dichloräthan und Nitrobenzol als Extraktionsmittel bildet sich kein Niederschlag, zur quantitativen Extraktion reicht hier ein 2–3-facher molarer HDAPM-Überschuß. Im Gleichgewicht liegt Hf in Dichloräthan und in Nitrobenzol als $\{A \cdot HfCl_4\}$ vor, wobei A für HDAPM steht. Bei hoher HCl-konzentration ($\geqslant$ 7 M) bildet sich in der organischen Phase das Chlorid des HDAPM. Deshalb ist es notwendig, den Einfluß des Reagenzüberschusses auf die Hf-extraktion am ternären System Lösungsmittel–Hf-komplex–HDAPM-chlorid zu studieren.

Reagenzien und Arbeitsmethode. HDAPM wird aus Antipyrin hergestellt.[3] F.: 111°. — HDAPM-chlorid scheidet sich als farbloser kristalliner Niederschlag aus einer HDAPM-Lösung in wasserfreiem Äther nach Durchleiten eines trockenen HCl-stromes ab. F.: 210° (Z.) $\{A \cdot HfCl_4\}$ entsteht beim Zusammenfügen äquimolarer Mengen von HDAPM und $HfCl_4$ in wasserfreiem Äther als farbloser, feinkristalliner Niederschlag, F.: 252° (Z.).

Im Komplex und im HDAPM-chlorid sind alle Komponenten analytisch bestimmt worden (Reagenz, Hf, Zahl der Protonen, Chlorid). Hf wird komplexometrisch titriert, HDAPM durch Zweiphasentitration nach Überführen in $A \cdot HJ$[3] bestimmt. Mit 0,1 N NaOH wird der Tetrachloro-HDAPM-Hf-komplex gegen Phenolphthalein ohne und mit NaF-zusatz titriert. Die NaF-zugabe führt zur Bildung des stabilen HfF_4[8] und NaOH würde nur zur Neutralisation der H^+ verbraucht, während in Abwesenheit von NaF NaOH auch zur Bildung von Hafniumhydroxid verbraucht werden würde. Die erhaltenen Titrationswerte beweisen aber das Fehlen von H^+ im Tetrachloro-HDAPM-Hf-komplex und die Richtigkeit der Formel $\{A \cdot HfCl_4\}$. Chlorid wird potentiometrisch bestimmt.

Chloroform, Dichloräthan und Nitrobenzol werden zur Reinigung wie üblich behandelt.[9] Im ternären System bestimmen wir die Grenzen der Kristallisationszonen nach der von R. Merzlin beschriebenen Methodik[10] und nach F. Schreinemakers.[11] Meßgröße ist der Brechungsindex der flüssigen Phase.

Tabelle 1

Analysenwerte für $\{A \cdot HfCl_4\}$ und $A \cdot HCl$

Verbindung	berechnet	gefunden
$\{A \cdot HfCl_4\}$	A = 59,61%	A = 58,52%
	Hf = 22,51%	Hf = 22,37%
	Cl = 17,88%	Cl = 17,63%
$A \cdot HCl$	A = 92,84%	A = 91,70%
	Cl = 6,96%	Cl = 6,57%

---

[8] I. V. Tananaev und E. N. Deitkhan, *Nachr. Akad. Wiss. UdSSR, Abt. Chem. Wiss. (ruß.)*, **6** 593 (1947).

[9] E. A. Masurenko, „Handbuch der Extraktion" (ruß.), Kiev, Verlag Tekhnika, 1972.

[10] R. V. Merzlin, *Nachr. biol. wiss. Forsch.-Institut der Univ. Perm (ruß.)*, **11**, 1 (1937).

[11] F. Schreinemakers, *Z. phys. Chem.*, **11**, 76 (1893).

Das System $\{A \cdot HfCl_4\} - A \cdot HCl - CHCl_3$. Die Löslichkeitsisotherme dieses Systems (Abb. 1 a) besteht aus 3 Ästen, die der Abscheidung von 3 festen Phasen entsprechen. Der Ast $\overline{ab}$ entspricht gesättigten Lösungen, aus denen die Komplexverbindung auskristallisiert. Der Ast $\overline{bc}$ entspricht der Kristallisation einer Verbindung mit dem Verhältnis $\{A \cdot HfCl_4\} : A \cdot HCl = 1:1$. Der Ast $\overline{cd}$ entspricht dem Übergang von A HCl in die feste Phase.

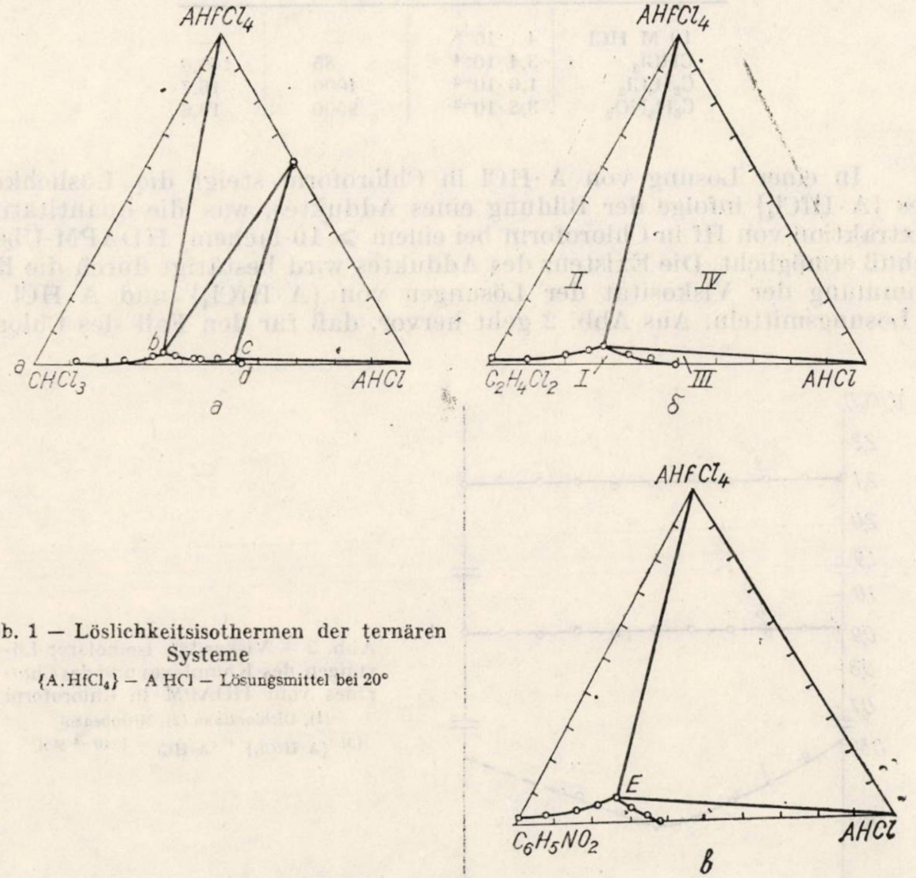

Abb. 1 — Löslichkeitsisothermen der ternären Systeme
$\{A.HfCl_4\} - A\,HCl -$ Lösungsmittel bei 20°

Das System $\{A \cdot HfCl_4\} - A \cdot HCl - C_2H_4Cl_2$ Dieses System ist vom einfachen ternären Typ (Abb. 1b). In der Dreiecksfläche existieren 4 Felder : I — homogene, ungesättigte Lösung; II — Kristallisation von $\{A \cdot HfCl_4\}$; III — Kristallisation von $A \cdot HCl$; IV — Dreiphasengleichgewicht (Kristalle von $\{A \cdot HfCl_4\}$, von $A \cdot HCl$ und Flüssigkeit der ——— Zusammensetzung E). Das Gebiet des Dreiphasengleichgewichts wird begrenzt durch die Linien E — $\{A \cdot HfCl_4\}$ und E — $A \cdot HCl$.

Das System mit Nitrobenzol stellt ebenfalls ein System von einfachem ternären Typ dar (Abb. 1c)

Erörterung der Meßergebnisse. Die untersuchten ternären Systeme gehören zu 2 unterschiedlichen Typen. Die Löslichkeit des Komplexes $\{A \cdot HfCl_4\}$ in HCl ($\geqslant 7$ M) und in $CHCl_3$ ist hinreichend gering, daß der Verteilungskoeffizient des Hf bei einem stöchiometrischen Verhältnis $A : Hf = 1 : 1$ durch Ermitteln der Löslichkeiten des Komplexes in der wäßrigen und der organischen Phase bestimmt werden kann.

Tabelle 2

Löslichkeit von $\{A \cdot HfCl_4\}$ in wäßriger und nichtwäßriger Phase

Lösungsmittel	Löslichkeit Mol/l	S_o/S_w	D
10 M HCl	$4 \cdot 10^{-6}$	—	—
$CHCl_3$	$3{,}4 \cdot 10^{-4}$	85	100,0
$C_2H_4Cl_2$	$1{,}6 \cdot 10^{-2}$	4000	16,7
$C_6H_5NO_2$	$3{,}8 \cdot 10^{-2}$	9500	13,6

In einer Lösung von $A \cdot HCl$ in Chloroform steigt die Löslichkeit des $\{A \cdot HfCl_4\}$ infolge der Bildung eines Adduktes, was die quantitative Extraktion von Hf in Chloroform bei einem ⩾ 10-fachem HDAPM-Überschuß ermöglicht. Die Existenz des Adduktes wird bestätigt durch die Bestimmung der Viskosität der Lösungen von $\{A \cdot HfCl_4\}$ und $A \cdot HCl$ in 3 Lösungsmitteln. Aus Abb. 2 geht hervor, daß für den Fall des Chloroforms in der Kurve Viskosität/Zusammensetzung ein Minimum für das Verhältnis $\{A \cdot HfCl_4\} : A \cdot HCl = 1 : 1$ existiert. Die Viskositäten der isomolaren Lösungen in Dichloräthan und Nitrobenzol sind additiv.

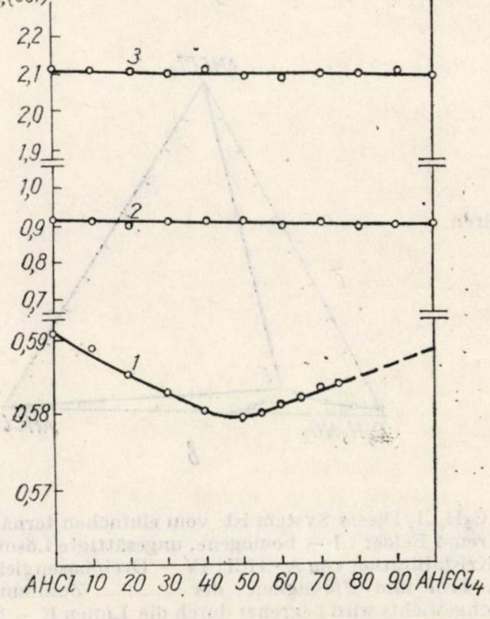

Abb. 2 — Viskosität isomolarer Lösungen des Komplexes und des Chlorides vom HDAPM in Chloroform (1), Dichloräthan (2), Nitrobenzol (3) $c_{\{A \cdot HfCl_4\}} + c_{A \cdot HCl} = 1 \cdot 10^{-2}$ Mol

Aus der Zunahme der Löslichkeit des $\{A \cdot HfCl_4\}$ in A HCl-haltigem Chloroform errechnet sich die Adduktbildungskonstante gemäß der Gleichung

$$\{A \cdot HfCl_4\} + A \cdot HCl \rightleftarrows \{(A \cdot HfCl_4)(A \cdot HCl)\}$$

zu $K = 0{,}140 \pm 0{,}016$ bei $\alpha = 0{,}95$, was auf die geringe Stabilität des Adduktes hinweist (Tabelle 3).

Tabelle 3

Bildungskonstante des Adduktes $\{(A \cdot HfCl_4)(A \cdot HCl)\}$ in $CHCl_3$

$A \cdot HCl$ Ausgangsmenge in Mol/l	$A \cdot HCl$ im Gleichgewicht Mol/l	Hf(IV) im Gleichgewicht g-Ion/l	Addukt im Gleichgewicht Mol/l	K
0,005	0,00441	0,00093	0,00059	0,134
0,01	0,00894	0,0014	0,00106	0,119
0,05	0,0435	0,0068	0,00646	0,148
0,10	0,0867	0,0136	0,0133	0,153
0,15	0,131	0,0196	0,0193	0,147
				$\overline{K} = 00{,}140$

Daraus folgt, daß bei der Extraktion des Hf aus salzsauren Lösungen unter Gleichgewichtsbedingungen das Element in Dichloräthan und in Nitrobenzol als $\{A \cdot HfCl_4\}$ vorliegt, in Chloroform als wenig stabiles Addukt der Zusammensetzung $\{(A \cdot HfCl_4)(A \cdot HCl)\}$.

Revue Roumaine de Chimie, 22, 5, 719–724 (1977)

Hommage au Professeur CORIOLAN DRĂGULESCU
à l'occasion de son 70ᵉ anniversaire

HEXACHLOROANTIMONATES(V) MÉTALLIQUES COMPLEXES AYANT COMME LIGAND LA PYRIDINE

E. PETROVICI * et IULIANA LUPU **

* Institut Polytechnique « Traian Vuia », Faculté d'ingénieurs chimistes, str. Bocşa, Timişoara, Roumanie.
** Université de Braşov, Faculté des Sciences, Str. Gh. Gheorghiu-Dej, 21, Braşov, Roumanie

Reçu le 30 juin 1976

On présente quelques complexes de la classe des hexachloroantimonates obtenus dans un milieu de tétrachlorure de carbone ayant la pyridine comme ligand. Ces complexes résultent du transfert de l'ion de chlorure entre deux chlorures aux degrés d'oxydation différents : $SbCl_5$ comme accepteur de l'ion de chlorure, et MCl_n comme donneur. Au cation M^{n+} le ligand, la pyridine est coordinée. On a isolé en état solide les complexes du type : $MPy_m(SbCl_6)_n$ ou $M = K$, Ca, Mn, Ni, Cd, Al, Fe ($m = 2$; 4 ou 6 et $n = 1$; 2 ou 3). On présente la synthèse, les données analytiques, les déterminations thermogravimétriques et les données rœntgénographiques.

Nos études sur la synthèse de quelques complexes coordinatifs de la classe des hexachloroantimonates dans un milieu de tétrachlorure de carbone aux ligands de petite donnicité (DN = 2,7 ; 4,4) [1-3] s'étendent aussi aux complexes avec la pyridine comme ligand de grande donnicité ($DN_{Py} = 33$). Ces complexes s'obtiennent par le transfert de l'ion de chlorure entre deux chlorures aux degrés d'oxydation différents [4] ; $SbCl_5$ avec fonction APE (accepteur de paires d'électrons) et MCl_n (ou $M = K$, Ca, Mn, Cd, Al, Fe et $n = 1$; 2 ou 3) avec fonction DPE (donneurs de paires d'électrons).[5] On obtient l'anion $SbCl_6^-$ et le cation M^{n+} qui coordinnent la pyridine, étant donné que $SbCl_5$ préfère coordiner Cl^- d'autres ligands.

Pendant que les hexachloroantimonates métalliques avec des nitrodérivés comme ligands de petite donnicité qui sont très instables se décom-

---

[1] C. DRĂGULESCU, E. PETROVICI et I. LUPU, *Monatsh.*, **105**, 1170 (1974).
[2] C. DRĂGULESCU, E. PETROVICI et I. LUPU, *Monatsh.*, **105**, 1176 (1974).
[3] C. DRĂGULESCU, E. PETROVICI et I. LUPU, *Monatsh.*, **105**, 1184 (1974).
[4] A. P. ZUUR et W. L. GROENEVELD, *Rec. Trav. chim.*, **86**, 1089 (1967).
[5] V. GUTMANN, « Chemische Funktionslehre », Springer-Verlag, Wien, 1971, p. 4 ; 6.

posent presque instantanément en contact avec l'humidité de l'air, les hexachloroantimonates métalliques complexes ayant la pyridine comme ligand sont stables à l'humidité et même difficilement solubles dans l'eau, fait prévisible théoriquement.[6]

PARTIE EXPÉRIMENTALE

LA SYNTHÈSE DES COMPLEXES

La préparation des réactants pour la synthèse s'est réalisée de la manière suivante : la pyridine a été séchée de façon supplémentaire étant maintenue sur KOH, le tétrachlorure de carbone a été séché étant maintenu sur un treillis moléculaire de kaolin de 4Å. On a utilisé $SbCl_5$ d'une pureté poussée (Merck — Darmastadt). La déshydratation des chlorures métalliques s'est réalisée soit par la méthode de la déshydratation thermique soit par le chauffage et la refluxation du chlorure respectif avec le chlorure de thyonile.

La synthèse de ces complexes s'est réalisée dans un milieu de tétrachlorure de carbone, où les chlorures des métaux mono- et bivalents sont insolubles, et le trichlorure d'aluminium et de fer tout comme la pyridine sont solubles dans les mêmes conditions. Par le traitement de ces systèmes avec du pentachlorure d'antimoine a lieu une réaction énergique, exothermique avec la formation de quelques précipités abondants qui se déposent facilement. Pour diminuer l'effet thermique de la réaction on a employé du pentachlorure d'antimoine diluée avec du tétrachlorure de carbone ayant un rapport de dilution de 1 : 10.

La synthèse de ces complexes s'est réalisée dans un espace fermé, qui manque le plus possible d'humidité, conditions qui ont été présentées dans une note antérieure,[1] ces conditions anhydres étant imposées par l'utilisation des chlorures métalliques anhydres. L'analyse des complexes obtenus s'est réalisée de la manière suivante : le chlore a été dosé par la méthode de Mohr, l'antimoine[7] et le potassium[8] par celle gravimétrique et les cations métalliques bivalents et trivalents par la voie complexométrique[9] et gravimétrique.

RÉSULTATS ET DISCUSSIONS

1. DONNÉES ANALYTIQUES

On a obtenu par cette voie les types suivants de complexes :

$KPy_2(SbCl_6)$

$M^{II}Py_4(SbCl_6)_2$; M^{II} = Ca, Mn, Ni, Cd

$M^{III}Py_6(SbCl_6)_3$ M^{III} = Al, Fe

Complexes avec potassium

On les a obtenus en utilisant pour la synthèse le rapport molaire de 1 : 1 entre le chlorure de potassium et le pentachlorure d'antimoine, avec des quantités variables de ligand et notamment dans une variante avec le rapport molaire de 1 : 2 entre le chlorure métallique et le ligand et aussi dans une autre variante avec le rapport molaire de 1 : 4 entre le chlorure métallique et le ligand. Dans les deux cas on a obtenu le même composé, à savoir celui qui a la formule KPy_2SbCl_6. Le produit se présente sous forme de poudre unitaire de couleur blanche-crème.

---

[6] V. Gutmann, E. Wychera, *Inorg. Nucl. Chem. Letters*, 2, 257 (1966).

[7] P. Spacu et A. Pop, *Z. analyt. Chem.*, 3, 254 (1937).

[8] J. M. Kolthoff, « Treatise on Analytical Chemistry », IIe partie, Ier vol., Interscience, New York, 1961, p. 359.

[9] R. Pribil, « Complexoni în chimia analitică », Ed. tehnică, Bucaresti, 1961, p. 255.

Complexes avec des métaux bivalents (Ca, Mn, Ni, Cd)

Les hexachloroantimonates des métaux bivalents ayant comme ligand la pyridine, correspondent à la formule : $MPy_4(SbCl_6)_2$. Les complexes obtenus ont la couleur blanche-crème pour le calcium, crème-rose pour le manganèse, crème-jaune pour le nickel et crème pour le cadmium, avec un aspect pulvérulent et unitaire.

Complexes avec des métaux trivalents (Al, Fe)

Les complexes de cette série correspondent à la formule $MPy_6(SbCl_6)_3$; M = Al, Fe mais ils sont partiellement impurifiés par des produits intermédiaires qui ne se transforment pas intégralement pendant la double complexation. La couleur des complexes à l'aluminium est crème, et celle des complexes au fer, moutarde. Les données analytiques sont présentées dans le premier tableau.

Tableau 1

Données analytiques pour hexachloroantimonates métalliques ayant la pyridine comme ligand

Complexes	%Cl		%Sb		%Metal	
	théorique	expérimental	théorique	expérimental	théorique	expérimental
$KPy_2(SbCl_6)$	40,02	40,86	22,90	22,03	7,35	7,08
$CaPy_4(SbCl_6)_2$	41,50	42,38	23,76	22,93	3,90	3,07
$MnPy_4(SbCl_6)_2$	40,91	40,05	23,42	22,85	5,28	5,02
$NiPy_4(SbCl_6)_2$	40,76	41,51	23,34	23,49	5,62	5,43
$CdPy_4(SbCl_6)_2$	38,50	38,65	22,01	21,77	10,98	10,54
$AlPy_6(SbCl_6)_3$	42,41	41,24	24,30	24,47	1,78	1,69
$FePy_6(SbCl_6)_3$	41,62	41,38	23,82	22,26	3,64	3,82

2. DONNÉES THERMOGRAVIMÉTRIQUES

Pour l'enregistrement simultané des courbes thermogravimétriques TG, des courbes thermogravimétriques dérivées DTG, et thermodifférentielles DTA, ainsi que pour celle de la température *T*, on a utilisé un dérivatographe MOM — Budapest type Pauling, Pauling-Erdey.

Conditions d'enregistrement : la quantité pesée a été de 90—100 mg, la sensibilité de la courbe TG, 100 mg, DTA, DTG, 1/15, la durée de l'enregistrement 50 minutes, l'échelle de la température 600°, la vitesse 5°/min.

Dans la figure 1 est présenté le dérivatogramme de l'essai $KPy_2(SbCl_6)$.

Le seul processus significatif qui peut être remarqué sur les courbes de thermolyse consiste dans la décomposition du complexe qui a lieu dans une seule étape quand on perd le ligand, Cl_2 et $SbCl_3$. La décomposition commence à 108° et on la considère finie à 490°, et quand la vitesse de la diminution du poids de la substance est très petite. La vitesse de décomposition maximale est enregistrée à 340°. La diminution totale du poids est de 85,43 % et le résidu de 14,57 % représente KCl, par rapport au pourcentage calculé de 14,03 %.

Les effets thermiques marqués sur la courbe DTA dont l'un est faiblement endothermique pendant la décomposition, montre une dépense d'énergie pour éliminer les produits volatils, suivi d'un faible effet exothermique après la décomposition, ce qui prouve la formation du réseau cristallin de KCl.

La décomposition du complexe $CaPy_4(SbCl_6)_2$ a lieu dans une seule étape. Le commencement de la décomposition a lieu à 110°, la vitesse de décomposition baisse beaucoup à 480°. La vitesse maximale de décomposition a lieu à 300° par une réaction endothermique, succédant une réaction facilement exothermique à 525°.

La perte totale en poids est de 85,2%, le résidu représente 14,8% par rapport à 10,8% $CaCl_2$ (calculé théoriquement). La différence est attribuée à de petites quantités de $SbCl_3$ encore non décomposées, probablement partiellement complexées comme $Ca(SbCl_4)_2$.

La décomposition du complexe $FePy_6(SbCl_6)_3$ a lieu en deux étapes comme l'on peut lire sur le diagramme DTC. Le début du commencement de la décomposition a lieu à 200°, la fin, à 480°, avec une vitesse maximale de décomposition à 348°. La diminution totale du poids est de 83,25%, le résidu, 16,73% d'où 11% $FeCl_3$ (calculé théoriquement), le reste étant probablement $SbCl_3$, complexé et indécomposable.

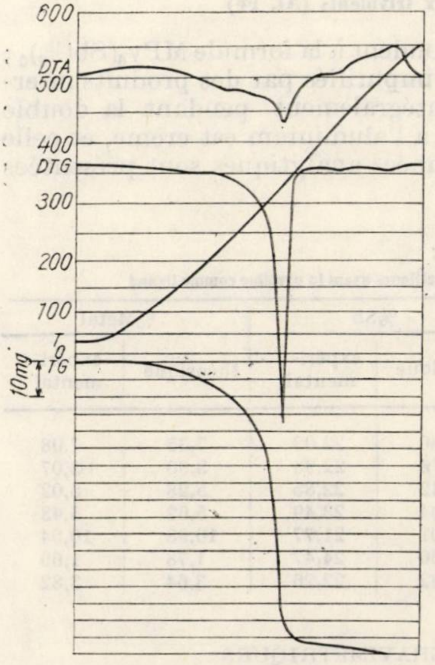

Fig. 1. — Dérivatogramme du complexe $KPy_2(SbCl_6)$.

3. DONNÉES RŒNTGÉNOGRAPHIQUES

Pour obtenir des informations concernant le réseau spatial et la cellule élémentaire des complexes synthétisés, on a effectué des déterminations rœntgénographiques.

On a travaillé avec un diffractomètre TÜR—M—61, RDG à l'anticathode de cuivre, U = 35 Kw, I = 15 mA. La vitesse du goniomètre 30'/mn, la vitesse du papier à enregistrer 600 mm/h, le compteur G M à 1500 V, la sensibilité 18.10^3 impulsions/mn.

Pour savoir si le composé est libre d'adducts, nous avons enregistré aussi le rœntgénogramme de l'adduct pure $SbCl_5Py$ qui est présenté dans le tableau 2.

Le troisième tableau présente les rœntgénogrammes du complexe KPy_2SbCl_6 exécutées dans des conditions différentes : avec le rapport de 2 : 1 pyridine/KCl, et avec le rapport 4 : 1 pyridine/KCl.

Tableau 2

Rœntgénogrammes de l'adduct $SbCl_5 \cdot Py$

I/I_0	d(Å)	I/I_0	d(Å)
88	8,34	13	3,04
45	7,06	9	2,90
12	6,32	72	2,82
12	6,04	26	2,62
100	5,76	21	2,56
19	5,40	28	2,39
58	5,02	4	2,36
39	4,59	43	2,31
64	4,21	4	2,27
64	3,99	12	2,20
29	3,74	26	2,05

Les diagrammes étant très semblables on a vérifié aussi par voie de diffraction des rayons X et on a obtenu les mêmes substances, quand on travaille avec un rapport molaire de 1 : 2 ou 1 : 4 chlorure de potassium/pyridine.

Tableau 3

Rœntgénogrammes du complexe KPy_2SbCl_6

KPy_2SbCl_6 (synthétisé avec le rapport 2 : 1 pyridine KCl)		KPy_2SbCl_6 (synthétisé avec le rapport 4 : 1 pyridine KCl)	
I/I_0	d(Å)	I/I_0	d(Å)
26	7,84	24	7,81
31	6,58	40	6,58
23	6,39	25	6,37
55	5,03	45	5,04
15	4,96	35	4,96
12	3,92	9	3,92
12	3,88	9	3,88
14	3,73	15	3,73
7	3,40	6	3,39
62	3,31	5	3,32
100	3,11	100	3,12
7	2,74	5	2,73
10	2,62	9	2,63
5	2,59	5	2,54
12	2,46	12	2,45
21	2,20	20	2,21

Dans le quatrième tableau on présente les données rœntgénographiques des complexes avec quelques métaux bivalents de type $MPy_4(SbCl_6)_2$ ou M = Ca, Mn, Ni, Cd.

Basés sur les données rœntgénographiques des hexachloroantimonates métalliques ayant la pyridine comme ligand on peut conclure :

— Les complexes ont des structures cristallines parce qu'il y a des maximums nets de diffraction des rayons X.

— Ils ont une symétrie basse et des cellules élémentaires grandes, caractérisées par des diagrammes avec beaucoup de lignes, dont la longueur de demi-onde est comparable à 1/3 de degré.

Tableau 4

Rœntgénogrammes des complexes $MPy_4(SbCl_6)_2$

$CaPy_4(SbCl_6)_2$		$MnPy_4(SbCl_6)_2$		$NiPy_4(SbCl_6)_2$		$CdPy_4(SbCl_6)_2$	
I/I_0	d(Å)	I/I_0	d(Å)	$^0I/I$	d(Å)	I/I_0	d(Å)
37	7,72	35	7,72	50	7,67	39	7,72
52	7,69						
35	6,95	85	6,58	89	6,54	90	6,58
54	6,46						
37	5,64	10	5,62	11	5,45	19	5,79
100	4,92	100	5,03	100	5,03	100	5,03
	4,23						
40	3,90	29	3,89	34	3,90	19	3,90
42	3,80	35	3,81	47	3,83	26	3,80
15	3,33	12	3,36	15	3,35	19	3,33
		12	3,36	5	3,29	14	2,98

— Hexachloroantimonates de calcium, manganèse, nickel et cadmium ayant la pyridine comme ligand ont les cellules élémentaires analogues des systèmes cristallins. Ce fait concorde avec les données analytiques sur la base desquelles on a établi la même formule $MPy_4(SbCl_6)_2$, où M = Ca, Mn, Ni et Cd.

— Grâce à la différence des rayons ioniques, le complexe de calcium a la tendance de passer dans une symétrie plus basse, fait observé par la scission des lignes.

— On remarque des groupes spatiaux différents dans le cas des complexes $KPy_2(SbCl_6)$ et $MPy_4(SbCl_6)_2$, où M = Ca, Mn, Ni, et Cd, ce qui indique des structures différentes.

CONCLUSIONS

Les hexacloroantimonates métalliques avec la pyridine ont été synthétisés, dans le but de poursuivre la voie dans laquelle la donnicité du ligand modifie les propriétés des complexes de cette classe.

Les hexachloroantimonates métalliques avec les ligands de petite donnicité : nitrométhane ($DN_{NM} = 2{,}7$), nitrobenzène ($DN_{NB} = 4{,}4$) et α-nitronaphtaline ($DN_{\alpha\text{-}NN}$ avec donnicité comparable à celui du nitrobenzène) sont très sensibles à l'humidité de l'air, se décomposant presque instantanément, les composés similaires ayant la pyridine comme ligand ($DN_{Py} = 33{,}1$) sont difficilement solubles dans l'eau.

Les complexes à ligands de petite donnicité ont un aspect cristallin macroscopique, ceux avec la pyridine, précipitent avec une grande vitesse, de sorte que leur aspect cristallin est mis en évidence seulement à l'aide des diagrammes des rayons X.

Revue Roumaine de Chimie, **22**, *5*, 725–732 (1977)

Hommage au Professeur Coriolan Drăgulescu
à l'occasion de son 70ᵉ anniversaire

SÉPARATION ET CONCENTRATION DU MAGNÉSIUM DES FONTES AU GRAPHITE SPHÉROÏDAL AU MOYEN DES RÉSINES ÉCHANGEUSES D'IONS

GRIGORE POPA et LUMINIŢA VLĂDESCU
Institut de Chimie, Faculté de Chimie; Laboratoire de Chimie Analytique,
79, Splaiul Independenţei, Bucarest

Reçu le 30 août 1976

On propose la séparation du magnésium trouvé dans les fontes au graphite sphéroïdal, au moyen des résines échangeuses d'ions en utilisant l'acide sulfosalicylique et le sulfocyanure de potassium comme agents de complexation pour le fer.

Le problème de la détermination quantitative du magnésium des fontes au graphite sphéroïdal est particulièrement important, vu que la présence de cet élément en petites quantités détermine d'importantes modifications dans la structure et les propriétés de la fonte. Du point de vue analytique, des difficultés apparaissent étant donné qu'on doit déterminer de très faibles quantités de magnésium en présence de fortes quantités de fer.

La littérature recommande pour le dosage du magnésium la méthode au phosphate,[1] le titrage spectrophotométrique en utilisant comme indicateur l'Eriochrom noir T[2,3] ou un mélange d'Erio T et de rouge de méthyle,[4] ou la détermination spectrophotométrique en présence de différents réactifs organiques, parmi lesquels le plus utilisé est le jaune de titanium.[5,6]

Quelle que soit la méthode de détermination choisie, il faut tenir compte que, dans le cas de l'application aux fontes au graphite sphéroïdal, le rapport Fe : Mg étant plus grand que 1000 : 1, il est absolument nécessaire le masquage du fer ou la séparation des deux éléments.[7] Dans ce but, la littérature recommande l'utilisation des cyanures,[8] de la triéthanolamine,[9] ou leur mélange, [10] l'acétylacétone, [11] la pyridine, [12] la diéthyldithiocarbamate de sodium.[3,14]

---

[1] N. V. Tikhonov, «Analiticheskaya khimia elementov : Magnii», Ed. Nauka, Moscou, 1973, p. 25.

[2] L. L. Lewis et L. M. Melnick, *Analyt. Chem.*, **32**, 38 (1960).

[3] T. A. Niss et T. M. Suranyi, *Mikrochim. Acta*, **5**, 1102 (1960).

[4] M. J. Miles, W. J. Mesimer et M. Atkin, *Analyt. Chem.*, **30**, 361 (1958).

[5] M. Drossdoff et D. C. Nearpass, *Analyt. Chem.*, **20**, 673 (1948).

[6] A. K. Babko et N. B. Lutohina, *Zhur. analit. Khim.*, **17**, 416 (1962).

Dans le présent travail, on propose la séparation du magnésium de fer, au moyen des résines échangeuses d'ions, en utilisant l'acide sulfosalicylique et le sulfocyanure de potassium comme agents de complexation pour le fer.

La séparation peut être effectuée aussi bien avec des résines échangeuses de cations, quand les ions Mg^{2+} sont fixés dans la résine, pendant que le fer, transformé dans des combinaisons complexes, reste dans la solution, qu'avec des résines échangeuses d'anions, quand les anions complexes du fer sont retenus et les cations Mg^{2+} passent dans l'effluent.

MATÉRIAUX ET APPAREILS

— résines échangeuses de cations fortement acides Merck I et Vionit CS–3,
— résines échangeuses d'anions fortement basiques Amberlite IRA–400 et Vionit AT–1 ;
— acide sulfosalicylique (Reanal), KSCN (Merk) ;
— solutions à titre connu d'azotate de magnésium et de fer (Merck) ;
— solutions 10^{-2}M et 10^{-3}M de Complexon III (Serva) ;
— solutions de HCl, NH_3, NH_4Cl (Reactivul) ;
— spectrophotomètres SPEKORD VV–VIS et SPEKOL ;
— pH-mètre MV–11S.

Les ions ont été déterminés quantitativement par titrage complexonométrique à l'EDTA pour le Mg^{2+}[12] et spectrophotométriquement pour le Fe^{3+}.[2]

RÉSULTATS ET DISCUSSIONS

Pour établir les conditions optimales de travail, on a étudié l'influence de la concentration des agents de complexation, du PH, et de la forme ionique de la résine, sur la fixation des ions du magnésium et du fer. Dans ce but, on a travaillé avec des cationites en formes H^+, K^+ et NH_4^+ et avec des anionites en formes Cl^- et SCN^-. On a fait passer par la résine des quantités connues d'ions Fe^{3+} et Mg^{2+}, et respectivement, en présence des anions complexants sulfosalicylate et sulfocyanure. Ensuite, on a déterminé la quantité d'ion métallique trouvée dans les solutions effluent : du passage de l'échantillon, après le lavage de la résine au réactif complexant et après l'élution des ions éventuellement fixés dans la résine, à l'HCl. Les résultats obtenus sont présentés dans le tableau 1.

---

[7] I. Nachev et D. Filipov, *Doklady Bolg. Akad. Nauk*, **22**, 767 (1969).

[8] A. Bussman, *Z. analyt. Chem.*, **148**, 413 (1956).

[9] E. G. Bradfield, *Analyst*, **85**, 666 (1960).

[10] A. J. Sterges et W. H. McIntire, *Analyt. Chem.*, **22**, 51 (1950).

[11] G. P. Patil et V. M. Schinde, *Z. analyt. Chem.*, **265**, 349 (1973).

[12] M. Zimmermann, « Photometric Metal and Water Analysis », W.V.C., M.B.H., Stuttgart, 1962, Section B-b 6/1(61) et 6/2(61)

[13] V. N. Tikhonov, N. A. Gordeeva et G. B. Karnaerkov, *Zavodskaya Lab.*, **40**, 940 (1974).

[14] T. L. Barbash, V. A. Goldireva et E. Ya. Khatkevich, *Issled. Inst. Stand. Obraztsov Spectral. Etalonov*, **4**, 80 (1968) ; *Ref. Zhur. Khim.*, Abstr. Nº 11G116 (1969) ; *Chem. Abstr.*, **72**, 139326 (1970).

Des données du tableau 1 il résulte que la présence des anions complexants, comme prévu, n'affecte pas la rétention du magnésium dans des résines échangeuses de cations et ne détermine pas sa fixation dans des anionites. En ce qui concerne le fer, son comportement à l'échange ionique est beaucoup influencé par les conditions de travail. Ainsi, en présence de KSCN (0,5—2M), il est partiellement fixé dans des cationites et totalement retenu dans des anionites. On peut expliquer ce fait par l'existence, en équilibre dans la solution, de tous les complexes de cet élément avec le SCN^-.[15] Cet équilibre est déplacé vers la formation des complexes électropositifs en contact avec une résine échangeuse de cations qui retient ces ions et vers la formation des complexes électronégatifs en contact avec un anionite. Ce comportement fait possible la séparation Mg—Fe en présence de KSCN en utilisant des résines échangeuses d'anions mais ne permet pas l'obtention des résultats quantitatifs à l'emploi d'un cationite.

A partir des conditions optimales de travail pour la détermination spectrophotométrique du fer en présence de KSCN, quand on recommande l'utilisation des solutions acides, on a étudié l'influence de l'acidité sur la rétention des ions dans les résines échangeuses de cations. On a observé que dans les milieux acides, le fer passe totalement dans l'effluent, mais une acidité trop grande détermine également l'élution de magnésium (tableau 1).

L'utilisation de l'acide sulfosalicylique n'est efficace que dans le domaine du pH de 4,5 à 9, quand le fer forme des complexes électronégatifs, mais seulement si l'on travaille avec des cationites qui excluent ces anions et fixent seulement les cations Mg^{2+}. Dans le cas des anionites, les mêmes anions complexes ne sont pas retenus, comme c'était à prévoir, probablement à cause de la différence entre la composition des solutions à l'intérieur et à l'extérieur de la résine, la dernière étant favorable à l'existence des complexes négatifs ($pH \geqslant 4{,}5$).

Donc, il y a la possibilité de séparer le magnésium de fer, au moyen des résines échangeuses d'ions, en présence de l'acide sulfosalicylique au pH 4,5—9, ou également, avec des résines échangeuses d'anions en présence de KSCN.

Prenant comme base les résultats obtenus, on a appliqué les méthodes de séparation sur des mélanges synthétiques contenant des quantités connues de Mg(II) et de Fe(III) en différentes proportions, à partir des quantités équimolaires, jusqu'aux compositions similaires à celles trouvées dans les fontes au graphite sphéroïdal.

Les résultats sont présentés dans le tableau 2 et montrent une bonne concordance entre les quantités prises dans l'échantillon et les quantités trouvées après la séparation. Mais, il y a l'inconvénient de l'utilisation d'un volume très grand d'éluant si l'on emploit le KSCN.

---

[15] V. I. Vasiliev et I. S. Muhina, *Zhur. neorg. Khim.*, **9**, 1134(1964).

Tableau 1

Influence de l'agent de complexation et de la forme ionique de la résine sur la fixation du fer et du magnésium dans des résines échangeuses d'ions

Résine Type	Forme ionique	Agent de complexation		pH	Fe(III)			Mg(II)		
			Conc.		Pris dans l'échantillon (g)	Trouvé dans la		Pris dans l'échantillon (g)	Résine (g)	Trouvé dans la solution (g)
						Résine (g)	Solution (g)			
Merck I	K+	KSCN	0,5M		0,0056	0,0042	0,0014			
			1M		0,0056	0,0028	0,0028			
			2M		0,0056	0,0014	0,0042	0,0046	0,0046	—
Amberlite IRA 400	SCN⁻	KSCN	2M		0,0056	0,0056	—	0,0023	—	0,0025
			0,1M		0,0056	0,0056	—			
			0,01M		0,0056	0,0056	—			
Vionit AT — 1	SCN⁻	KSCN	0,06M		0,0056	0,0056	—			
			0,06M		0,0056	0,0056	—			
Merck I	H+	KSCN HCl	0,5M 1M		0,0056	—	0,0056	0,0023	—	0,0023
		KSCN HCl	0,5M 0,1M		0,0112	0,0012	0,0100	0,0046	0,0046	—
		KSCN HCl	1M 0,1M		0,0056	—	0,0054	0,0023	0,0023	—
Merck I	H+	Acide sulfosalicylique	20%	1,5	0,0056	0,0054	—	0,0046	0,0048	—
	NH_4^+		20%	1,5	0,0056	0,0054	—			
			10%	8—9	0,0056	—	0,0056	0,0046	0,0044	—
			5%	8—9	0,0056	—	0,0056	0,0046	0,0044	—
			5%	4—5	0,0056	—	0,0056	0,0046	0,0044	—
Vionit CS — 3	NH_4^+	Acide sulfosalicylique	5%	8—9	0,0056	—	0,0054	0,0046	0,0046	—
Amberlite IRA 400	Cl⁻	Acide sulfosalicylique	30%	8—9	0,0056	—	0,0056	0,0046	—	0,0046

Tableau 2

Résultats de la séparation du Mg(II) – Fe(III) des mélanges synthétiques (solutions aqueuses)

Résine		Agent de complexation		pH	Fe(III)			Mg(II)		
Type	Forme ionique		Conc.		Pris dans l'échantillon (g)	Trouvé (g)	Volume d'effluent (cm³)	Pris dans l'échantillon g × 10^{-5}	Trouvé g × 10^{-5}	Volume d'effluent (cm³)
Merck I	H^+	KSCN HCl	1M 10^{-1}M		0,0090	0,0089	325	0,5	0,8	20
Amberlite IRA – 400	SCN^-	KSCN	2M		0,00056	0,00050	500	24	25	50
Merck I	NH_4^+	Acide sulfosalicylique $+NH_3$	10 %	8 – 9	0,0090	0,0093	75	0,5	0,7	20
				4 – 5	0,0011	0,0013	75	48	50	20

Tableau 3

Influence de l'acétone sur la fixation du fer dans des résines échangeuses d'ions, en présence de KSCN

Résine	KSCN conc. M	Acétone conc. %	Fe(III)			Observation
			pris dans l'échantillon (mg)	trouvé dans la résine (mg)	trouvé dans la solution (mg)	
Merck I	0,1	90	0,28	—	0,28	$V_{effluent} = 100$ cm³
	2	75	0,56	—	0,58	
Amberlite IRA – 400	0,53	57	0,28	0,20	—	le fer n'est pas apparu dans l'effluent
	2	75	0,28	0,24	—	le fer a été fixé dans la résine, mais il est apparu dans l'effluent au lavage à la solution de travail
	0,06	90	0,28	0,30		
	0,06	90	0,56	0,60	—	

Dans le but d'amender les méthodes proposées on a étudié l'influence de l'acétone sur la fixation du fer dans les résines échangeuses d'ions en présence de KSCN.

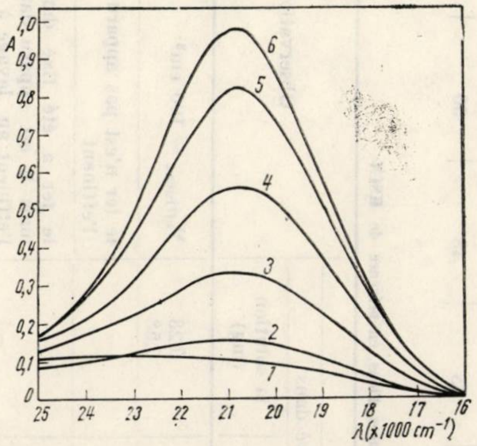

Fig. 1. — Influence de la proportion de l'acétone sur l'absorption optique des complexes $Fe^{3+} - SCN^{-}$.
1, sans acétone ; *2*, 50% acétone ; *3*, 60% acétone ; *4*, 75% acétone ; *5*, 90% acétone ; *6*, 94% acétone.

La figure 1 montre qu'un remplacement partiel de l'eau par de l'acétome, même en présence d'une petite quantité de réactif, détermine le déplacement des équilibres vers la formation de complexes supérieurs : plus la proportion du solvant organique s'accroît, plus l'absorption optique augmente.

Les données du tableau 3 montrent que, si l'on travaille avec des solvants mixtes eau-acétone, le fer est complètement exclu d'une résine échangeuse de cations en présence de KSCN et on peut le retrouver dans un petit volume d'effluent. Le fer est totalement fixé dans les résines échangeuses d'anions au cas où on n'utilise pas une concentration trop grande d'acétone. Si l'on travaille avec des solutions plus concentrées d'acétone et avec des résines gonflées dans l'eau, les complexes y sont retenus, mais au lavage à la solution de travail ils commencent à passer dans l'effluent, parce qu'on y trouve de meilleures conditions pour leur stabilité. Si on travaille avec une résine gonflée dans le mélange des solvants utilisés, les complexes se fixent et ils n'apparaissent pas dans l'effluent.

En ce qui concerne le magnésium, les données de la littérature montrent l'augmentation de ses coefficients de partage entre la résine échangeuses de cations et la solution, en présence de l'acétone.[16,17]

Prenant comme base ces résultats on a effectué les séparations présentées dans le tableau 4.

On observe la possibilité d'obtenir de bons résultats et la diminution du volume d'effluent, dans le processus du travail avec des cationites en solvants mixtes eau-acétone.

---

[16] J. Korkisch et S. S. Ahluwalia, *Talanta*, **14**, 155 (1967).

[17] J. M. Peters et G. Del Fiore, *Radiochem. Radioanal. Lett.*, **21**, 11 (1975).

Tableau 4

Résultats de la séparation du Mg(II) – Fe(III) des mélanges synthétiques (solvants eau-acétone)

Résine		Agent de complexation		Fe(III)			Mg(II)		
Type	Forme ionique		Conc.	Pris dans l'échantillon (mg)	Trouvé (mg)	Volume d'effluent (cm³)	Pris dans l'échantillon (mg)	Trouvé (mg)	Volume d'effluent (cm³)
Merck I	K⁺	KSCN acétone	2M 75%	0,56	0,48	100	0,24	0,20	20
		KSCN acétone	2M 90%	0,28	0,20	50	0,12	0,10	20
		KSCN acétone	2M 75%	9,00	9,20	100	0,005	0,009	20

Tableau 5

Résultats de la séparation Mg(II) – Fe(III) des fontes au graphite sphéroïdal

Résine		Agent de complexation		pH	Echantillon de fonte (g)	Fe(III) Mét. d'échange ionique		Autres méthodes	Mg(II) Mét. d'échange ionique		Autres méthodes
Type	Forme ionique		Conc.			(g)	%	%	(g)	%	%
Merck I	NH_4^+	Acide sulfosalicylique	10%	8–9	0,9721	0,9419	97		0,0003691	0,039	
			10%	8–9	0,9930	0,9600	96,67	98%	0,000516	0,052	0,04–0,06
Vionit CS–3	NH_4^+		10%	4–5	0,9930	0,9721	97,8		0,00054	0,054	
Merck I	K⁺	KSCN Acétone	2M 75%		0,9960	0,9711	97,5	98%	0,000468	0,047	0,04–0,06

On a choisi parmi ces possibilités, les méthodes de séparation les plus efficaces pour les appliquer sur des solutions obtenues par la désagrégation des échantillons des fontes au graphite sphéroïdal. Les résultats sont présentés dans le tableau 5.

On observe une bonne concordance avec les résultats obtenus en appliquant d'autres méthodes, bien que les quantités de magnésium soient extrêmement petites.

CONCLUSIONS

Par l'utilisation des résines échangeuses d'ions, en présence de l'acide sulfosalicylique ou de KSCN, on peut donc séparer, en bonnes conditions, le magnésium de fer. On peut fixer les cations Mg^{2+} dans des résines échangeuses de cations, pendant que les anions complexes du fer passent dans l'effluent, ou bien, on peut fixer ces anions complexes dans des résines échangeuses d'anions, pendant que les cations Mg^{2+} passent dans l'effluent.

Ce comportement différent est favorisé par l'utilisation des solvants mixtes eau-acétone.

L'emploi des cationites présente l'avantage de permettre en même temps la séparation et la concentration du magnésium dans la résine, pendant que la solution d'effluent, qui contient les ions complexes du fer, peut servir à sa détermination quantitative spectrophotométrique. En même temps, la quantité de résine est moindre parce que c'est l'ion trouvé dans la plus faible quantité qui est fixé dans la résine.

Revue Roumaine de Chimie, 22, 5, 733–737 (1977)

Dedicated to the 70th anniversary
of Professor CORIOLAN DRĂGULESCU

EQUILIBRIA OF REDISTRIBUTION REACTIONS OF ORGANOMETALLIC COMPOUNDS

O. A. REUTOV and K. P. BUTIN
Physical Organic Laboratory, Chemical Department, University of Moscow,
Moscow, U.S.S.R.

Received August 25, 1976

An approach is discussed that allows to rationalize the structural effects on positions of redistribution equilibria of organometallic compounds. The approach is based on the comparison of relative stabilities of anions corresponding to exchanging groups and complexochemical properties of organometallic cations in which the exchange occurs.

Reactions in which a redistribution of organic (or inorganic) groups takes place have a common use in organometallic chemistry; they are one of the most important methods for preparing various organometallic compounds. The general principle, which is commonly used in synthetic practice, involves the action of a salt of one metal on an inorganic compound of another, more electropositive, metal. Reactions (1) and (2) may be written as illustration:

$$RHgY + SnX_4 \longrightarrow HgXY + RSnX_3 \qquad (1)$$

$$R'_2BR' + HgX_2 \longrightarrow R'_2BX + R'HgX \qquad (2)$$

However, such ligand exchange may also take place between metals that are similar or between two compounds of the same metal. Furthermore, examples exist which show that depending on the nature of exchanging groups, R (organic) and X (inorganic), the redistribution reactions may occur by means of R group transfer both from a more electropositive to a more electronegative and from a more electronegative to a relatively electropositive element:

$$RSnR'_3 + HgX_2 \rightarrow R'_3SnX + RHgX \qquad (3)$$

$$R_2Hg + BX_3 \rightarrow RHgX + RBX_2 \qquad (4)$$

The transfer of organic groups from one organometallic compound to another has been originally observed by Frankland, Friedel, Crafts and Ladenburg as early as more than 100 years ago (see refs. [1–3] for example). Ladenburg was the first who supposed, in 1866, that it is organic radical transfers that are responsible for the formation of complex mixtures of products on heating organometallic compounds with (or without) $AlCl_3$. [3]

Many experimental data on redistribution of organic and inorganic groups have been accumulated for 100 years but our knowledge of the direction of redistribution processes is strictly empirical nowadays. (Some empirical rules have been formulated, e.g., "lighter halogen transfers from tin to silicon while heavier halogen from silicon to tin", etc.)

We want to discuss now structure effects on the position of redistribution equilibria, not concerning the specific reaction mechanisms. Although the mechanism of carbon-metal bond fission and formation might be variable (homolytic, heterolytic in variant of S_{E^2}, S_{E^1} S_{Ei}, with ion pair participation, etc.), the position of redistribution equilibrium does not depend on the specific reaction mechanism.

Let us consider the following scheme :

$$\begin{array}{ll}
m - T \to m\cdot + T\cdot & D\,(m - T) \\
m' - Z \to m'\cdot + Z\cdot & D\,(m' - Z) \\
m\cdot + Z\cdot \to m - Z & -D\,(m - Z) \\
m'\cdot + T\cdot \to m' - T & -D\,(m' - T) \\
\hline
m - T + m' - Z \rightleftharpoons m - Z + m' - T\,; & \Delta H = \sum D(\cdot/.)
\end{array}$$

$$\begin{array}{ll}
m - T \to m^+ + T^- & D(m^+ - T^-) \\
m' - Z \to m'^+ + Z^- & D(m'^+ - Z^-) \\
m^+ + Z^- \to m - Z & -D(m^+ - Z^-) \\
m'^+ + T^- \to m' - T & -D(m'^+ - T^-) \\
\hline
m - T + m' - Z = m - Z + m' - T\,; & \Delta H = \sum D(^+/_-)
\end{array}$$

$$\sum D(\cdot/.) = \sum D(^+/_-)$$

In this scheme two thermodynamical cycles are given for the redistribution process in gas phase from which one may, in principle, calculate the gas phase reaction enthalpy. The exchanging groups are denoted by symbols *T* and *Z*, while the organometallic groups by symbols *m* and *m'*. The first cycle involves homolysis and colligation, the second cycle heterolysis and coordination. Obviously, the sum of the energies of homolysis and colligation is equal to the sum of the energies of heterolysis and coordination.

[1] C. Friedel and J.-M. Crafts, *Ann. Chim. Phys.*, **9**, 5 (1866).

[2] C. Friedel and A. Ladenburg, *Liebigs Ann. Chem.*, **143**, 124 (1867).

[3] A. Ladenburg, *Ber. dtsch. chem. Ges.*, **7**, 387 (1874).

Let us consider organometallic compounds as complexes of anions, T^- and Z^-, with organometallic cations, m^+ and m'^+. Thus the equilibrium constant, K, for the reaction

$$m - T + m' - Z \rightleftharpoons m - Z + m' - T$$

may be written as follows [4-6]:

$$K = \frac{[mZ]\,[m'T]}{[mT]\,[m'Z]} = \frac{\dfrac{[mZ]}{[m^+]\,[Z^-]} \times \dfrac{[m'T]}{[m'^+]\,[T^-]}}{\dfrac{[mT]}{[m^+]\,[T^-]} \times \dfrac{[m'Z]}{[m'^+]\,[Z^-]}} = \frac{K(m^+, Z^-) \times K(m'^+, T^-)}{K(m^+, T^-) \times K(m'^+, Z^-]}$$

where $K(m^+, Z^-)$, $K(m'^+, T^-)$, $K(m^+, T^-)$ and $K(m'^+, Z^-)$ are the equilibrium constants for the formation of complexes of the anions, T^- and Z^-, with the organometallic cations, m^+ and m'^+.

In the logarithmic form

$$\lg K = \Delta \lg K_{m^+}^{Z^-,T^-} - \Delta \lg K_{m'^+}^{Z^-,T^-} \qquad (5)$$

where $\Delta \lg K_{m^+}^{Z^-,T^-}$ and $\Delta \lg K_{m'^+}^{Z^-,T^-}$ are the relative affinities of the anions, Z^- and T^-, for the organometallic cations, m^+ and m'^+, respectively.

If we know the relative affinities of T^- and Z^- anions for m^+ and m'^+ cations, equation (5) would allow to calculate the equilibrium constant for a given redistribution reaction. However, one cannot operate with the complex formation constants because of a very limited number of data available on complexochemical properties of organometallic cations. Therefore, when equation (5) is used to predict a redistribution equilibrium position, one needs to choose a suitable, not mandatorily organometallic, standard cation for which the following two points are valid:

(1) The affinities of the exchanging anions for such a cation must be known or be easily determinable, and

(2) A linear dependence must exist between the anion affinities for a standard cation and for the both organometallic cations, m^+ and m'^+:

$$\Delta \lg K_{m^+}^{Z^-,T^-} = A(m^+) \cdot \Delta \lg K_{\text{stand}}^{Z^-,T^-}$$

and

$$\Delta \lg K_{m'^+}^{Z^-,T^-} = A'(m'^+) \cdot \Delta \lg K_{\text{stand}}^{Z^-,T^-}$$

where $K_{\text{stand}}^{Z^-,T^-}$ is the relative affinity of Z^- and T^- anions for a standard cation. A and A' are constants.

---

[4] K. P. Butin, V. N. Shishkin, I. P. Beletskaya and O. A. Reutov, *Doklady Acad. Nauk S.S.S.R.*, **218**, 371 (1974).

[5] K. P. Butin, V. N. Shishkin, I. P. Beletskaya and O. A. Reutov, *Vestnik MGU, Khimiya*, **1974**, 718.

[6] K. P. Butin, V. N. Shishkin, I. P. Beletskaya and O. A. Reutov, *J. Organometal. Chem.*, **93**, 139 (1975).

Then, instead of eq. (5), one may use eq. (6) in which the logarithm of the equilibrium constant is a product of two factors: $\Delta \lg K_{\mathrm{stand}}$ was called "force factor" and $\Delta A(m^+, m'^+)$ "differentiating factor".

$$\lg K = \Delta A(m^+, m'^+) \cdot \Delta \lg K_{\mathrm{stand}}^{Z^-,T^-} \tag{6}$$

Proton seems to be the most suitable standard cation. The proton affinities are known practically for all anions, and it may be supposed that, if the nature of a donor atom remains the same in a series of exchanging anions, a linear dependence will be observed between the anion affinities for proton and organometallic cations. Recently such a supposition was shown to be valid for the interaction of methylmercury cation with different O—, N—, P—, and S-bases.[7] *

Thus $\Delta \lg K_{\mathrm{stand}}^{Z^-,T^-}$ in eq. (6) may be substituted for $\Delta pK_a\,(\mathrm{ZH, TH}) = pK_a\,(\mathrm{ZH}) - pK_a\,(\mathrm{TH})$:

$$\lg K = \Delta A\,(m^+, m'^+) \cdot \Delta pK_a\,(ZH, TH) \tag{7}$$

While it is rather easy to calculate the force factor magnitude (as a difference between pK_a's of ZH and TH), an estimation of the differentiating factor is a very difficult problem. The latter factor depends on experimental conditions (solvent, temperature, etc.) to a greater extent than the former. We were successful, for instance, in estimating $\Delta A\,(\mathrm{H_3Si^+, H_3Ge^+})$ from Cradock and Ebsworth data.[8] These authors studied the equilibria that are written in the caption of Table 1. From the data of Table 1 one may calculate the ΔA magnitudes for the anion exchange between the cations $\mathrm{H_3Si^+}$ and $\mathrm{H_3Ge^+}$.[6] Since, by definition, $A(H^+) = 1$, $A(\mathrm{H_3Si^+}) = 1.7$ and $A(\mathrm{H_3Ge^+}) = -0.3$. The positive sign of A, in the first case, and negative in the second, means that $\mathrm{H_3Si^+}$ is a harder, while $\mathrm{H_3Ge}$ is a softer acid when compared with proton. Table 1 shows also that

Table 1

Experimental equilibrium constants for the reaction

$$\mathrm{H_3MT + HZ \rightleftharpoons H_3MZ + HT}$$

and magnitudes of $\triangle$A and A for silyl and germyl cations as calculated from the equation

$$\mathrm{Lg\,K} = \triangle \mathrm{A(H_3M^+, H^+)}\ \Delta \mathrm{pK}_a\mathrm{(ZH, TH)} = [\mathrm{A(H_3M^+)} - 1\ ]\Delta \mathrm{pK}_a\mathrm{(ZH, TH)}$$

$\mathrm{H_3MT}$	HZ	$\lg K$	ΔpK_a[6]	$\Delta A(\mathrm{H_3M^+, H^+})$	$A(\mathrm{H_3M^+})$
$\mathrm{H_3SiCl}$	HBr	−0.05	−1.6	0.03	
$\mathrm{H_3SiBr}$	HI	−1.22	−0.8	1.53	
$\mathrm{H_3Si\ Cl}$	HI	−1.27	−2.4	0.55	
				MEAN: 0.70	1.70
$\mathrm{H_3GeCl}$	HBr	2.86	−1.6	−1.80	
$\mathrm{H_3GeBr}$	HI	0.55	−0.8	−0.69	
$\mathrm{H_3GeCl}$	HI	3.41	−2.4	−1.41	
				MEAN: −1.30	−0.30

---

* In the series of halide ions, $\mathrm{F^-, Cl^-, Br^-, I^-}$, the affinities for proton and other "hard" cations change in an inverse order from that of the affinities for "soft" organometallic cations such as $\mathrm{CH_3Hg^+}$ or $\mathrm{R_3Sn^+}$.

[7] G. Geiger and I. W. Erni, *Chimia (Basel)*, **27**, 635 (1973).

[8] S. Cradock and E. A. V. Ebsworth, *J. Chem. Soc.*, **1967** A, 1226.

the differentiating factor is to be equal to +2.0 for the anion exchange between silyl and germyl cations that is confirmed by experimental data.[8]

Also, the ΔA values were calculated for six substituted silyl cations from Moedritzer and Van Vazer data [9,10] on the H/Cl exchange between organosilicon compounds (Table 2). In this case the difference between the A magnitudes is significantly lesser than in the H_3Si/H_3Ge system.

Table 2

Calculated Δ A magnitudes for substituted silyl cations

$CH_3SiCl_2^+$	0.045				
CH_3SiHCl^+		0.056			
	0.011		0.064	0.096	
$(CH_3)_2SiCl^+$					0.116
	0.008				
$CH_3SiH_2^+$					
$(CH_3)_2SiH^+$	0.032				
$(CH_3)_3Si^+$	0.020				

The analysis of literature and data obtained in our laboratory [11] allows to conclude that the most preferable state of a system is that in which both central metal atoms have the least difference, in chemical sense, from one another. When, for example, a system of two organomercury compounds is under consideration in which pK_a's of four groups attached to two mercury atoms increases in the order $R_1 < R_2 < R_3 < R_4$, the equilibrium mixture will contain as main components the compounds in which one mercury atom is attached to the most and the least acidic groups (R_1 and R_4) while another to the groups of intermediate acidities (R_3 and R_4):

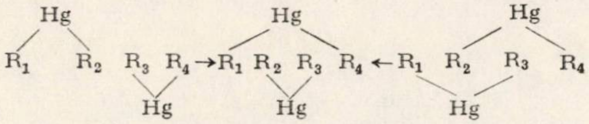

the most symmetrical

Also, in a mixture of organotin compounds, R_2SnX_2 is a preferable component:

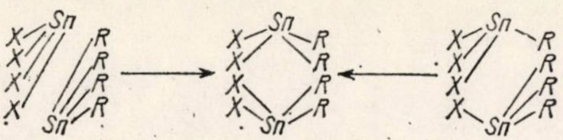

the most symmetrical

---

[9] K. Moedritzer and J. R. Van Wazer, *J. Organometal. Chem.*, **12**, 69, (1968).
[10] J. R. Van Wazer and K. Moedritzer, *J. Inorg. Nuclear Chem.*, **26**, 737 (1964).
[11] V. N. Shishkin, Dissertation, Moscow University, Moscow, 1975.

Revue Roumaine de Chimie, **22**, 5, 739–743 (1977)

Dedicated to the 70th anniversary
of Professor Coriolan Drăgulescu

CIRCULAR DICHROISM OF OPTICALLY ACTIVE SQUARE PLANAR COMPLEXES CONTAINING η^2-OLEFINS

KAZUO SAITO
Chemistry Department, Faculty of Science, Tohoku University, Sendai, 980, Japan

Received September 11, 1976

Square planar complexes of platinum(II) and rhodium(I) exhibit characteristic circular dichroism peaks in the regions 20000 to 30000 and around 40000 cm^{-1}. *R*, *R*-Configuration of η^2-olefins gives rise to marked minus CD peak in the latter region regardless of the kind of other ligands and the central metal ion. On the other hand, the sign of CD in the 20000 to 30000 cm^{-1} region seems to depend on the central metal ion.

INTRODUCTION

Optical activity of coordination compounds has drawn attention of chemists particularly in these two decades. Since the determination of absolute configuration of tris(ethylenediamine)cobalt(III) by X-ray crystallography [1], the relationship between the absolute configuration and the circular dichroism (CD) spectra has been discussed by many chemists.[2] However, most of the work concerned octahedral complexes.

Square planar complexes are not optically active by themselves. However, when some kind of olefin coordinates to a square planar complex such as platinum(II) and dihapto (η^2) ligand (Zeise-type structure), a new asymmetry is brought about as shown in Fig. 1. Not all olefins can produce such an asymmetry; *e.g.* propylene, *trans*-2-butene, 2-methyl-2-butene, and styrene are prochiral, but ethylene, *cis*-2-butene and 1,2-dimethyl-2-butene are not. Complexes containing η^2-olefins are not only interesting structurally, but also important as catalyst for various organic syntheses, *e.g.* polymerization, isomerization, and hydrogenation.

Optical activity of this kind was first demonstrated in 1964 by Paiaro and Panunzi in the preparation of a diasteroisomeric pair of *trans*-

---

[1] K. Nakatsu, M. Shiro, Y. Saito, and H. Kuroya, *Bull. Chem. Soc. Japan*, **30**, 158 (1957).

[2] *e.g.* C. J. Hawkins, "Absolute configuration of metal complexes", Wiley-Interscience, New York, 1971.

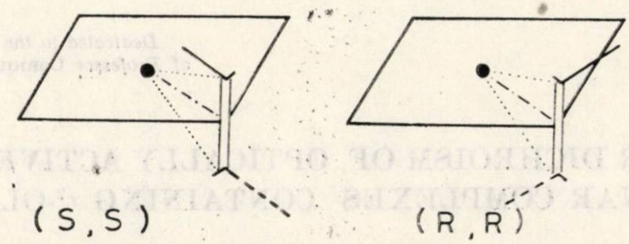

Fig. 1. — Asymmetry brought about by the coordination of prochiral olefin molecules. (*R* and *S* denote the absolute configuration of the coordinated carbon atoms; perpendicular double lines indicate the C—C double bonds.

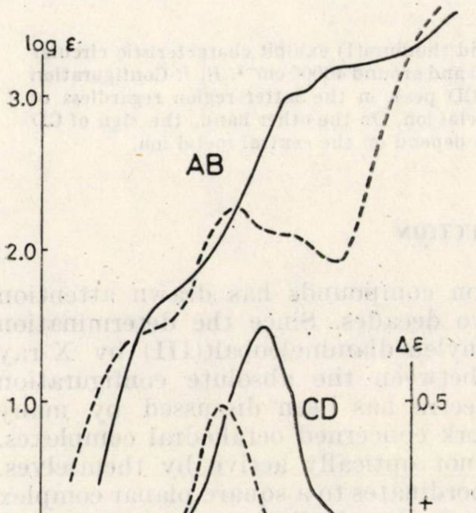

Fig. 2.— Absorption and circular dichroism spectra (AB and CD, respectively) of *trans* (*N*, [PtCl(L-prol)-(C_2H_4)] in methanol (solid line) and *K*[PtCl$_2$(L-prol)] in water (broken line).

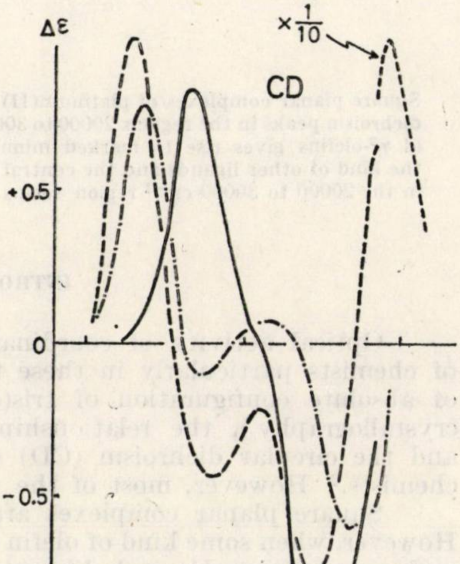

Fig. 3. — CD spectra of (+) Δε-*trans* (*N*, olefin) [PtCl(L-prol)-(*trans*-2-butene)] in ethanol (solid line) and in concentrated hydrochlorid acid (broken line with dots) and [Pt$_2$Cl$_4$(*S*, *S*- *trans*- coe)] (broken line).

-dichloro-(R, or S-α-phenethylamine) *trans*-2-buteneplatinum(II).[3] These complexes were oily products, but since then several complexes have been prepared, which exhibit this type of optical activity. The relationship between the absolute configuration and CD spectrum has been mainly discussed on the basis of experimental data with platinum(II) complexes.[4] Scott *et al.* reported that S, S-η^2 and R, R-η^2 configurations give plus and minus CD peak in the *d-d* transition region at *ca.* 27000 cm^{-1}.[5] Less information is available for complexes with other metal ions.[6] Musco *et al.* found that [$Fe(CO)_4$(R, R-η^2-fumaric acid)] gave a CD peak at 28000 cm^{-1}.

With the aim of elucidating the relationship between CD spectra and absolute configuration of η^2-olefins, we have prepared various platinum(II) and rhodium(I) complexes in crystalline state, and measured the CD spectra in visible and ultra-violet region.

Platinum(II) complexes containing η^2-olefin and various aminocarboxylates: Our group has synthesised a variety of optically active platinum(II) complexes of the type *trans*- and *cis* (n, olefin)-[PtCl(am)(η^2-olefin)] (am, aminocarboxylate; alaninate, leucinate, prolinate [prol], n-methyl-prolinate, n-benzylprolinate *etc.*; olefins, ethylene, propylene, *cis*- and *trans*-2-butene, 2-methyl-2-butene, 1,2-dimethyl-2-butene and styrene), and separated the diastereoisomers by use of the difference in solubility in mixed organic solvents, *e.g.* chloroform-hexane and acetone-hexane.[7-9] This type of complexes has geometrical isomers *cis*- and *trans* (n, olefin), and they are distinguished by infra-red spectroscopy, and also by synthetic route. All the platinum(II) complexes discussed in this paper have trans (n, olefin) structure.

These complexes have two asymmetric ligands, *i.e.* the aminocarboxylate[10] and the η^2-olefin. Platinum (II) complexes containing non-prochiral olefin (*e.g.* ethylene) give only the CD of vicinal effect coming from asymmetric aminocarboxylate.

Figure 2 shows the absorption and CD spectra of [PtCl(L-prol)(C_2H_4)] and [$PtCl_2$(L-prol)]. The CD peaks are remarkable in the region 25000 to 38000 cm^{-1}, and the difference in the peak location can be interpreted by the spectrochemical series. The corresponding *trans*-2-butene complexes separated into diasteroisomers give CD spectra as shown in Fig. 3. In ethanol a large peak plus is seen in the region 25000 to 30000 cm^{-1}, where only a small vicinal effect of L-prolinate is observed. Also there is a minus peak in the region 31000 to 38000 cm^{-1}; the strength of this peak must have been made smaller by the plus vicinal peak due to L-prolinate. These peaks are shifted to a lower wave number region in hydrochloric acid solution, owing to the replacement of L-prolinate by chloride.

---

[3] G. Paiaro and A. Panumzi, *J. Amer. Chem. Soc.*, **86**, 5148 (1964); A. Panunzi and G. Paiaro, *ibid.*, **88**, 4843 (1966).

[4] G. Paiaro, *Organometallic Chem. Rev.*, **A**, **6**, 319 (1970).

[5] A. Musco, G. Paiaro, and R. Palumbo, *Ricerca. sci.*, **39**, 417 (1969).

[6] A. I. Scott and A. D. Wrixon, *Tetrahedron*, **27**, 2339 (1970).

[7] Y. Terai, H. Kido, J. Fujita and K. Saito, *Bull. Chem. Soc. Japan*, **48**, 1233 (1975).

[8] K. Konya, J. Fujita, and K. Nakamoto, *Inorg. Chem.*, **10**, 1699 (1971).

[9] Y. Terai, K. Kashiwabara, H. Kido, J. Fujita, and K. Saito, *Bull. Chem. Soc. Japan*, **50**, in press (1977).

[10] When the methyl or benzyl group is introduced on the nitrogen in prolinate, another asymmetry is caused by the nitrogen atom. However, its contribution on CD is reckoned as a part of vicinal effect.

In organic solvents such as acetone, the CD strengths of the diastereoisomers decrease on addition of an excess of *trans*-2-butene. This phenomenon is understood as to be due to S_N2 substitution of *trans*-2-butene with inversion of configuration. Comparison of the rates of such an inversion and of the isotopic exchange with *trans*-2-butene[^{3}H] disclosed that the substitution of *trans*-2-butene with retention of configuration proceeds faster than that with inversion of configuration by one order. (For details, *cf.* Ref. [7]) *trans*-Cyclo-octene (*trans*-coe) gives an enantiomeric pair, but, because of its ring structure, it can coordinate to a metal ion only in one way. The $(-)_D$ isomer gives only *S*, *S*-configuration.[11] The absolute configuration of a binuclear complex $[Pt_2Cl_4(\textit{trans}\text{-coe})_2]$ doubly bridged by chlorides, was determined chemically by Cope and Mehta.[12] Its CD spectrum is included in Fig. 3. The pattern is very similar to our $[PtCl_3(\textit{trans}\text{-2-butene})]$ and also to $[PtCl(\text{L-prol})(\textit{trans}\text{-2-butene})]$, which exhibits $(+)$—CD peak at 26300 cm^{-1} (380 nm). Thus we can see that our two complexes have *S*, *S*-η^2-configuration, and the pattern with a plus peak at *ca.* 25000 cm^{-1} represents those of *S*, *S*-η^2-olefin. This observation agrees with the result that *cis*$[PtCl_2\text{-}(S\text{-}\alpha\text{-methylbenzylamine})(R,R\text{-}\textit{trans}\text{-coe})]$, the absolute configuration of which was determined by X-ray crystallography, has a minus peak at 26700 cm^{-1}.[13] We have thus made clear that the absolute configuration of η^2-olefins coordinated to platinum(II) can be judged from the CD sign in 23000 to 28000 cm^{-1} region; plus and minus peak to *S*, *S* and *R*, *R* configuration, respectively.

Rhodium(I) complexes containing *trans*-cyclo-octene: In order to find whether such an empirical rule is applicable to other square planar complexes with d^8 configuration, we intended to prepare optically active rhodium(I) complexes containing *trans*-2-butene and resolve them. However, the resolution has been unsuccessful so far. Alternatively we have resolved *trans*-cyclo-octene by the method of Cope *et al.*,[14] and prepared several of its complexes with rhodium(I) by use of $[Rh(acac)(C_2H_4)_2]$ (acac = enolate anion of acetylacetone) and $[Rh_2Cl_2(C_2H_4)_4]$ as starting compounds.[15] All the complexes contain two moles of *trans*-cyclo-octene per mole of rhodium(I). Details of the preparative work have been published elsewhere.[16]

Figure 4 shows the absorption and CD spectra in *n*-hexane. No discussion has ever been made on the assignment of the absorption peaks of square planar rhodium(I) complexes containing η^2-olefin. We have found that the absorption peaks in the wave number regions <30000 and>

---

[11] The absolute configuration of $(-)_D$-*trans*-cyclo-octene itself is *R*, but as an η^2-ligand of platinum(II) or rhodium(I) the absolute configuration is *S*, *S*, according to the sequence rule.

[12] A. C. Cope and A. S. Mehta, *J. Amer. Chem. Soc.*, **86**, 5626 (1964).

[13] P. Corradini, G. Paiaro, A. Panunzi, S. F. Mason, and G. H. Searle, *J. Amer. Chem. Soc.*, **88**, 2864 (1966).

[14] A. C. Cope, *J. Amer. Chem. Soc.*, **85**, 3275 (1963).

[15] R. Cramer, *J. Amer. Chem. Soc.*, **89**, 4621 (1967).

[16] I. Kinoshita, Y. Terai, K. Kashiwabara, H. Kido, and K. Saito, *J. Organomet. Chem.* (in press).

40000 cm^{-1} are related to the η^2-olefin, since the corresponding bis(carbonyl) complex $[Rh(acac)(CO)_2]$ gave no absorption peak in these two regions. The absorption peak in the former region has log ε *ca.* 3, and does not seem to be due to *d-d* transitions; there must be some mixing of charge transfer transition. On the other hand, the peak in the high wave number region must be due to $\pi-\pi^*$ transition of η^2-olefin. (The dbm complex [dbm = enolate anion of dibenzoylmethane] gives a more complicated pattern, presumably owing to the benzene ring. [curve not shown]) $(+)_D$-*trans*-Cyclooctene gives exclusively *R*,*R*-configuration on coordination to a metal ion. All the rhodium(I) complexes in Fig. 4 give plus peaks in the region $<29000\ cm^{-1}$, and large minus peaks at *ca.* 40000 cm^{-1}. Between these two regions the pattern is complicated, and must be related to other ligands than *trans*-cyclooctene (*e.g.* β-diketonate and chloride). Figure 4 includes the CD curve of [PtCl(L-prol)—(*R*, *R*-*trans*-coe)], which gives minus peaks at *ca.* 29000 and 40500cm^{-1}. The former peak must correspond to the plus CD peak of *S*, *S*-*trans*-2-butene complexes of platinum (II) in the same region, the sign being reversed by the reversed configuration. In this region, the rhodium(I) complexes have plus CD peaks, presumably because of the different nature of absorption. (*loc. cit.*)

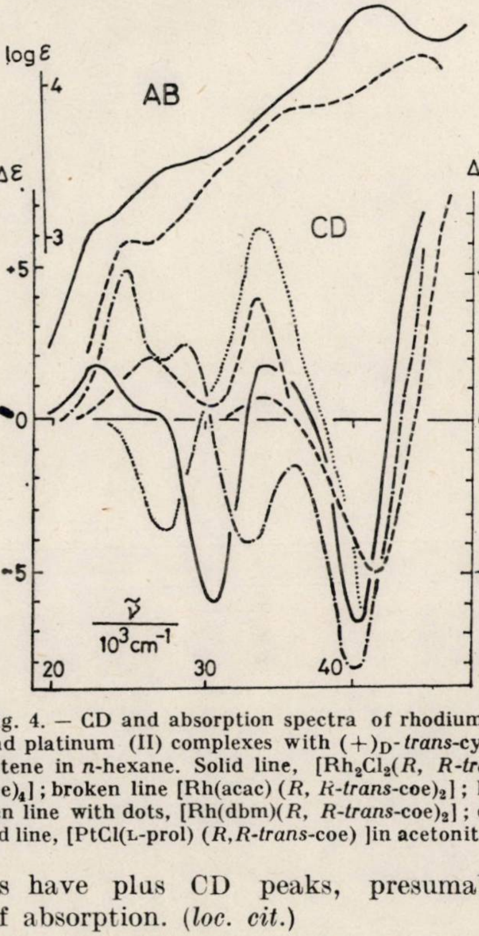

Fig. 4. — CD and absorption spectra of rhodium (I) and platinum (II) complexes with $(+)_D$-*trans*-cyclooctene in *n*-hexane. Solid line, $[Rh_2Cl_2(R, R\text{-}trans\text{-}coe)_4]$; broken line $[Rh(acac)(R, R\text{-}trans\text{-}coe)_2]$; broken line with dots, $[Rh(dbm)(R, R\text{-}trans\text{-}coe)_2]$; dotted line, [PtCl(L-prol) (*R*,*R*-*trans*-coe)]in acetonitrile.

On the other hand, in the region *ca.* 40000 cm^{-1}, the sign of CD peak is common for the rhodium(I) and platinum(II) complexes. Figure 3 shows that *S*, *S*-*trans*-cyclo-octene gives a very large plus CD peak in this region. Thus we can conclude that the CD sign in this high wave number region can be a good indicator of the absolute configuration of η^2-olefins coordinated to square planar complexes with d^8 configuration.

Acknowledgment. This work was undertaken jointly with the coworkers mentioned below on the financial support given by the Ministry of Education of the Japanese Government, to which the authors' thanks are due: Professor Junnosuke Fujita, Dr. Kazuo Kashiwabara, and Mr. Isamu Kinoshita who are now in Chemistry Department of Nagoya University, and Messrs. Hiroaki Kido and Yoshiro Terai in our Department.

Revue Roumaine de Chimie, 22, 5, 745–751 (1977)

Dedicated to the 70th anniversary
of Professor Coriolan Drăgulescu

SPECTROPHOTOMETRIC DETERMINATION OF PALLADIUM(II), CERIUM(IV), ARSENIC (III) AND NITRITE WITH FLUPHENAZINE HYDROCHLORIDE

H. SANKE GOWDA, K. N. THIMMAIAH and B. NARAYANA ACHAR
Department of Post-Graduate Studies and Research in Chemistry, University of Mysore,
Manasagangotri, Mysore, India

Received September 6, 1976

Fluphenazine hydrochloride (FPH) forms 1 : 1 complex with palladium instantaneously at pH 0.9–2.4 and red coloured radical with cerium(IV) in 3.8–6.5 M phosphoric acid. The Pd–FPH complex exhibits absorption maximum at 480 nm with molar absorptivity 3.984×10^3 litre mole^{-1} cm^{-1}. The red coloured radical has absorption maximum at 500 nm with molar absorptivity 7.283×10^3 litre mole^{-1} cm^{-1}. Beer's law is valid over the concentration range 0.5–24 ppm of Pd(II) and 0.4–16 ppm of Ce(IV). The effects of pH, time, order of addition of reagents, temperature, reagent concentration and diverse ions are reported. Arsenic (III) and nitrite are indirectly determined spectrophotometrically.

INTRODUCTION

Sanke Gowda *et al.* proposed phenothiazines as spectrophotometric reagents for the determination of palladium(II), [1–7] ruthenium(III), [8,9] osmium(VIII) [10] and gold(III). [11] In the present investigation the authors have studied the reaction of fluphenazine hydrochloride (FPH), 4-[3-(2-trifluoromethyl)-phenothiazine-10-*yl*]-propyl-1-piperazine ethanol hydro-

---

[1] H. Sanke Gowda and B. Keshavan, *Mikrochim. Acta*, **1**, 437 (1975).

[2] H. Sanke Gowda and B. Keshavan, *Z. analyt. Chem.*, **273**, 31 (1975).

[3] H. Sanke Gowda and B. Keshavan, *Indian J. Chem.*, **14**, 293 (1976).

[4] H. Sanke Gowda and P. G. Ramappa, *Indian J. Chem.*, **13**, 418 (1975).

[5] H. Sanke Gowda and P. G. Ramappa, *J. Indian Chem. Soc.*, **52**, 1123 (1975).

[6] H. Sanke Gowda, P. G. Ramappa and B. Narayana Achar, *Z. analyt. Chem.*, **275**, 127 (1975).

[7] H. Sanke Gowda and K. N. Thimmaiah, *Z. analyt. Chem.*, **208**, 279 (1976).

[8] H. Sanke Gowda and P. G. Ramappa, *Analyt. Chim. Acta*, **83**, 283 (1976).

[9] H. Sanke Gowda and P. G. Ramappa, *Current Sci.*, **45**, 218 (1976).

[10] H. Sanke Gowda and P. G. Ramappa, *Analyt. Chim. Acta*, **84**, 189 (1976).

[11] H. Sanke Gowda and P. G. Ramappa, *Z. analyt. Chem.*, **280**, 221 (1976).

chloride with palladium(II) and cerium(IV) and proposed FPH as a sensitive reagent for the spectrophotometric determination of palladium (II), cerium(IV), arsenic(III) and nitrite. The proposed methods offer the advantages of simplicity and stability without the need for extraction.

EXPERIMENTAL

REAGENTS

A stock solution of palladium(II) was prepared by dissolving 0.3402 g of palladium(II) chloride (M/s Johnson Matthey Chemicals Ltd., London) in 500 ml of 0.1 M hydrochloric acid and standardized gravimetrically by the dimethylglyoxime method.[12]

A stock solution of cerium(IV) sulphate was prepared in 0.5 M sulphuric acid and standardized with arsenic(III) solution.

A 0.2% solution of FPH was prepared in doubly distilled water and stored in an amber bottle in a refrigerator.

Walpole buffer solutions [13] (pH range 0.65—5.2) were prepared from 1M sodium acetate and 1M hydrochloric acid solutions.

Solutions of diverse ions of suitable concentrations were prepared using analytical grade reagents.

A 0.1N sodium arsenite was prepared and standardized as described by Bright.[14]

A 0.02N sodium nitrite solution was prepared in doubly distilled water and standardized by ceric sulphate method.[15]

APPARATUS

Beckman spectrophotometer model DB with matched 1 cm silica cells was used for absorbance measurements. The pH's of the solutions were measured (Vs SCE) with pH meter model L1—10 (M/s Electronic & Industrial Instruments, Hyderabad, India).

PROCEDURE FOR THE DETERMINATION OF PALLADIUM(II)

An aliquot of the stock solution containing 12.5—600 μg of palladium was transferred to a 25 ml volumetric flask. 5 ml of hydrochloric acid-sodium acetate buffer of pH 1.1 and 3 ml of 0.2% FPH solution were added and the volume was made up to the mark with doubly distilled water. The absorbance was measured at 480 nm against a corresponding reagent blank. The amount of palladium was then deduced from the standard calibration curve.

PROCEDURE FOR THE DETERMINATION OF CERIUM(IV)

An aliquot of the stock solution containing 10—400 μg of cerium(IV), 10 ml of 12M H_3PO_4 and 3 ml of 0.2% FPH solution were taken in a 25 ml volumetric flask and the solution was diluted to the mark with doubly distilled water. The absorbance was measured at 500 nm against a corresponding reagent blank prepared in the same manner. The amount of cerium was then deduced from the standard calibration curve.

PROCEDURE FOR THE DETERMINATION OF ARSENIC(III)

Aliquots of 0.5, 1.0, 1.5. . . . . 6.0 ml of arsenic(III) solution (3.75—67.50 μg), 2 ml of 2.5M sulphuric acid, 0.5 ml of osmium(VIII) solution (1.2 μg) and 2 ml of 0.001M ceric sulphate were taken in twelve 25 ml volumetric flasks and the solutions were thoroughly mixed.

---

[12] A. I. VOGEL, "A text book of quantitative inorganic analysis", The Elbs & Longmans, London, 1968, p. 512.

[13] H. T. S. BRITTON, "Hydrogen Ions", Vol. I, Chapman & Hall, London, 1955, p. 353.

[14] H. A. BRIGHT, *Ind. Eng. Chem. Analyt. Edn.*, **9**, 577 (1937).

[15] A. I. VOGEL, "A Text Book of Quantitative Inorganic Analysis", The Elbs & Longmans, London, 1968, p. 322.

10 ml of 12M phosphoric acid and 3 ml of 0.2% FPH solution were added and the volume was made up to the mark with doubly distilled water. A thirteenth 25 ml flask was used for preparation of the blank containing all the reagents except arsenic(III). All the thirteen solutions were shaken thoroughly and their absorbances were measured at 500 nm against the reagent blank containing no cerium(IV) and arsenic(III). The amount of arsenic(III) in a test solution was then deduced from the standard calibration curve constructed by plotting the concentration of arsenic(III) versus the difference in the absorbance readings between the blank (in thirteenth flask) and the sample.

PROCEDURE FOR THE DETERMINATION OF NITRITE

4 ml of 1M sulphuric acid and 2 ml of 0.001M ceric sulphate solution were taken in twelve 25 ml volumetric flasks. 4 ml of sodium nitrite solution containing 1—41 μg of nitrite was pipetted into each flask. The solutions were mixed well. After 5 min, 10 ml of 12M phosphoric acid and 3 ml of 0.2% FPH solution were added and the volume was made up to the mark with doubly distilled water. A blank containing all the reagents except nitrite was prepared in the thirteenth 25 ml flask. The absorbances of thirteen solutions were measured at 500 nm against the reagent blank containing no cerium(IV) and nitrite. The amount of nitrite in a test solution was deduced from the calibration curve of the concentration of nitrite versus the difference in the absorbance readings between the blank (in the thirteenth flask) and the sample.

RESULTS AND DISCUSSION

DETERMINATION OF Pd(II)

FPH forms a red coloured complex with palladium(II) instantaneously at room temperature in the presence of hydrochloric acid, sulphuric acid, phosphoric acid or Walpole buffer. The study of palladium(II) -FPH complex in hydrochloric, sulphuric or phosphoric acid medium is not recommended because the complex is less stable (30 min) and many foreign ions interfere even at very low concentrations. The complex is stable for 6 hours in the presence of the Walpole buffer. Maximum colouration takes place between pH 0.9 and 2.4. All studied were therefore confined to pH 1.7.

The absorption spectra of the Pd—FPH complex, palladium(II) chloride and the reagent in the buffer are shown in Fig. 1. The maximum absorbance of the complex is at 476—492 nm where the reagent and Pd(II) do not absorb.

The effect of reagent concentration was examined by measuring the absorbance at 480 nm of the solutions containing a known concentration of palladium and varying amounts of the reagent. A thirteen-fold molar excess of the reagent over palladium is required in order to obtain maximum absorbance.

The effect of varying temperature on the stability of the complex was investigated. The absorbance readings were constant in the temperature range 10—95°. The order of the addition of reagents was not critical.

CALIBRATION, RANGE AND SENSITIVITY

The Pd—FPH complex obeys Beer's law over the concentration range 0.5—24 ppm of palladium. The optimum concentration range evaluated by Ringbom's method[16] is 1.0—23.5 ppm.

---

[16] A. Ringbom, *Z. analyt. Chem.*, **115**, 332 (1938).

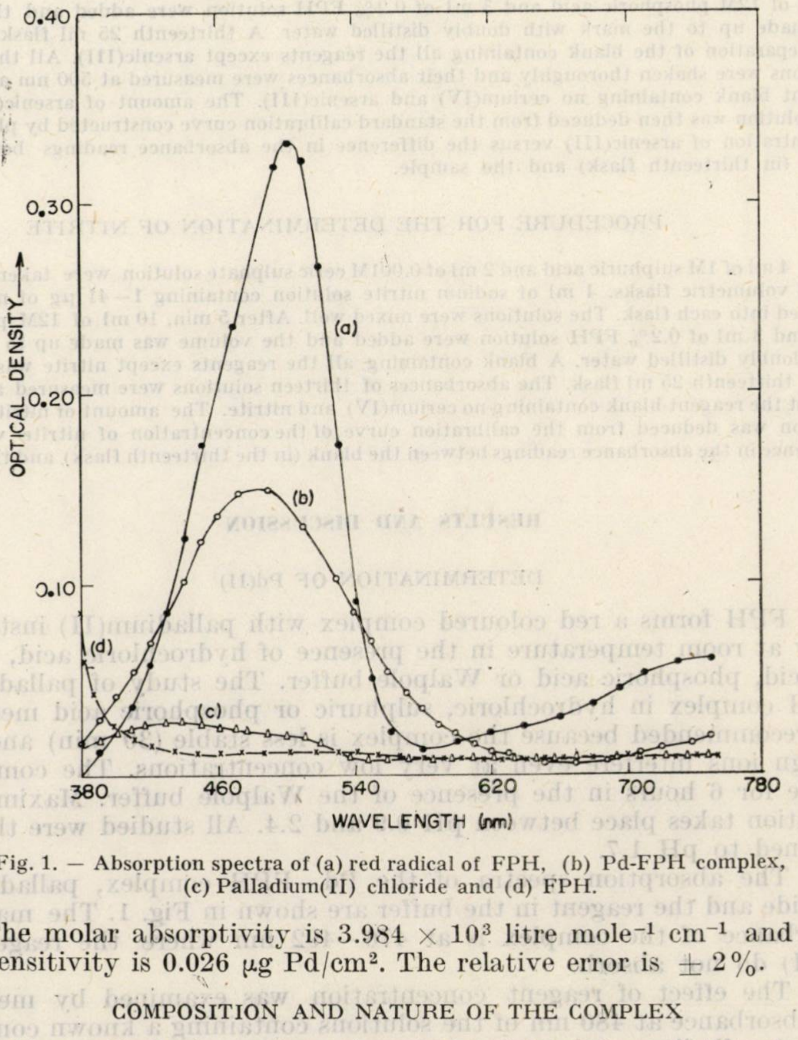

Fig. 1. — Absorption spectra of (a) red radical of FPH, (b) Pd-FPH complex, (c) Palladium(II) chloride and (d) FPH.

The molar absorptivity is 3.984 × 10^3 litre mole^{-1} cm^{-1} and Sandell's sensitivity is 0.026 μg Pd/cm^2. The relative error is ± 2 %.

COMPOSITION AND NATURE OF THE COMPLEX

Job's method of continuous variation,[17,18] mole ratio[19] and slope ratio[20] method were employed to establish the composition of the complex. The determinations were made in a medium of constant ionic strength (0.1 M sodium nitrate) at a pH value of 1.7 ± 0.1 and a temperature 26 ± 1°. The absorbance of the solutions was measured at 480 nm. The results indicated the formation of 1 : 1 complex between the metal and the reagent.

The apparent stability constant of the complex was calculated from the absorbance data by the mole ratio method. The value of log K obtai-

---

[17] P. Job, *Liebigs Ann. Chem.*, **9**, 113 (1928).

[18] H. Irving and T. B. Pierce, *J. Chem. Soc.*, 1959, 2565.

[19] J. H. Yoe and A. L. Jones, *Ind. Eng. Chem.*, **16**, 111 (1944).

[20] A. E. Harvey and D. L. Manning, *J. Amer. Chem. Soc.*, **72**, 4448 (1950).

ned for the Pd—FPH complex at 26 ± 1°, pH 1.7 ± 0.1 and ionic strength 0.1 M sodium nitrate was 6.0 ± 0.1.

The electrolytic nature of the complex was found by ion-exchange experiments. When 25 ml of 10^{-5}M solution of the complex was passed through Dowex 50W—X8 cation exchange resin column (30 × 1.4 cm) the red colour was completely adsorbed. The eluent was colourless. When Dowex 1—X8 anionic resin column was used the eluent was red coloured. This indicated that the complex was cationic.

The following amounts (μg/ml) of foreign ions were found to give less than 2% error in the determination of 10 μg of palladium per ml. Os(VIII) 10, Pt(IV) 3, Ru(III) 4.0, Rh(III) 13, Ir(III) 20, Co(II) 290, Ni(II) 600, Cu(II) 400, Fe(III) 1, Au(III) 0.10, Ce(IV) 0.2, fluoride 600, chloride 480, bromide 300, iodide 0.40, nitrate 1500, sulphate 3000, phosphate 250, acetate 1200, tartrate 44, citrate 20, oxalate 4, thiosulphate 0.09 and EDTA 1.0.

DETERMINATION OF PALLADIUM IN SYNTHETIC MIXTURES CORRESPONDING TO JEWELLERY ALLOY

A typical jewellery alloy contains 95.5% Pd and 4.5% Ru. With the increasing use of palladium for jewellery and industrial alloys a need has arisen for a simple, rapid and accurate method for determining palladium in its alloys. Synthetic mixtures containing palladium and ruthenium corresponding to jewellery alloy were prepared and palladium content was determined by the recommended procedure. The results of analysis of synthetic mixtures are given in Table 1.

Table 1

Determination of palladium in synthetic mixtures corresponding to jewellery alloy

Pd present ppm	Ru ppm	Pd found ppm
2.50	0.14	2.50
5.00	0.28	4.99
7.50	0.35	7.51
10.00	0.47	10.09

DETERMINATION OF CERIUM(IV)

FPH is oxidized to red coloured species by cerium(IV) in sulphuric or phosphoric acid medium. The red colour is less stable in 0.5—2M sulphuric acid medium (5—10 min). The maximum colour development takes place instantaneously at room temperature (27°) in 3.8—6.5 M phosphoric acid solutions as shown by the constancy of λ_{max}. The absorbance of the red coloured species remains constant for 45 min. The maximum colour intensity is not observed below 3.8 M. phosphoric acid. The reagent is slowly oxidized by phosphoric acid above 6.5 M. The red coloured species assumed to be a free radical exhibits absorption maximum at 498—504 nm (Fig. 1) with molar absorptivity 7.283×10^3 litre mole^{-1}

cm^{-1} and the Sandell's sensitivity is 0.019 $\mu g/cm^2$. There is no absorption of the reagent at this wavelength. For full development of colour intensity a nine-fold molar excess of the reagent is necessary. The absorbance values are insensitive to temperature in the range 10–60°. The order of addition of the reagents has no effect on the intensity of the red colour. Beer's law is obeyed in the concentration range 0.4–16 ppm of cerium(IV). However, the optimum range for the effective spectrophotometric determination is 1–15.6 ppm. The relative error is $\pm 2\%$.

The following mounts ($\mu g/ml$) of foreign ions are found to give less than 2% error in the determination of 8 $\mu g/ml$ of cerium(IV), La(III), 4000, Pr(III) 4000, Nd(III) 4000, Gd(III) 4000, Dy(III) 4000, Ho(III) 4000, Er(III) 4000, Yb(III) 4000, Y(III) 4000, Tb(III) 4000, Os(VIII) 2.5, Ru(III) 6, Pd(II) 0.40, Pt(IV) 8, Ir(III) 19, Rh(III) 19, Au(III) 0.5, Cu(II) 480, Ni(II) 200, Co(II) 116, Fe(III) 200, Ag(I) 20, Mg(II) 1600, Zn(II) 1620, Th(IV) 400, Mo(VI) 200, Zr(IV) 506, U(VI) 830, As(V) 4000, chloride 4800, bromide 10400, iodide 0.24, fluoride 400, sulphate 15000, acetate 1600, phosphate 5200, citrate 1200, tartrate 5720, nitrate 6490, thiosulphate 0.40 and EDTA 1.0.

It can be seen that many diverse cations especially lanthanides do not interfere in the determination of cerium(IV). The major advantage of this method is that FPH can be used as a selective reagent for the determination of cerium (IV) in presence of large quantities of other lanthanides in readily attainable oxidation states without the use of masking agents.

DETERMINATION OF CERIUM IN MISCH METAL

Commercial misch metal generally contains 50% Ce, 25% La, 15% Nd, 5% Fe and 5% of mixtures of Pr, Eu, Gd and Er. Analysed samples of misch metals were not available. Therefore solutions containing known amounts of cerium simulating the composition of the alloy were prepared and analysed by the proposed method. The results are presented in Table 2.

Table 2

Determination of cerium in synthetic mixtures corresponding to misch metal

Ce present ppm	La ppm	Nd ppm	Fe ppm	Pr ppm	Eu ppm	Gd ppm	Er ppm	Ce found ppm
4.00	2.00	1.20	0.40	0.10	0.10	0.10	0.10	4.09
5.00	2.50	1.50	0.50	0.125	0.125	0.125	0.125	5.00
8.00	4.00	2.40	0.80	0.20	0.20	0.20	0.20	8.15

DETERMINATION OF ARSENIC(III) AND NITRITE

Arsenic(III) and nitrite are indirectly determined spectrophotometrically. As(III) is quantitatively oxidized instantaneously by a known excess of ceric sulphate (20–120%) in sulphuric acid medium containing

1.2 μg of osmium(VIII) which does not interfere under the experimental conditions. Nitrite is oxidized in 0.5 M sulphuric acid in 5 min by a known excess of ceric sulphate. Cerium(IV) oxidizes FPH to red colour which is stable for 45 min in 4.8 M phosphoric acid solution containing 0.25 M sulphuric acid. The unreacted cerium(IV) is determined colorimetrically by the proposed method. In the absence of other reducing substances, the reduction in the absorbance of the red colour produced by the fixed amount of ceric sulphate is directly proportional to the amount of arsenic (III) or nitrite present. C(III), As(V) and nitrate formed in the reaction are colourless and do not interfere. 0.15—2.7 μg/ml of arsenic(III) and 0.04—1.6 μg/ml of nitrite can be determined. This method can be used for the spectrophotometric determination of micro quantities of other substances which are quantitatively oxidized by cerium(IV) in sulphuric acid to colourless, noninterfering products.

Acknowledgment. The authors thank the Council of Scientific and Industrial Research, New Delhi, for the award of Junior Research Fellowship to one of them (K.N.T.).

Dr. N. Rekhi, Essex Chemie AG, Switzerland is thanked for supplying FPH from M/s Schering Corporation, U.S.A.

Revue Roumaine de Chimie, **22**, *5*, 753–759 (1977)

Dedicated to the 70th anniversary
of Professor Coriolan Drăgulescu

FERROCENE POLYMERS AS POLYMERIZATION INITIATORS

CR. SIMIONESCU and I. MAZILU
Department of Organic Chemistry Polytechnic Institute of Jassy Str. 23 August, 11, Jassy, Romania

Received October 1, 1976

In the present paper we tested some ferrocene polymers as potential redox initiators in the polymerization of some substituted vinyl monomers. The influence of a range of initiators, their concentration and the yield of polymers is also reported. Better results are obtained at low temperatures. The obtained polymers have electrophysical properties.

INTRODUCTION

Studies on the correlation between structure, properties and catalytic activity, an interesting and very complex item for the investigators, especially in polymer field, are frequently reported.[1–3]

The catalytic activity in heterogeneous systems of certain polymers stable at high temperatures showing special physical properties such as paramagnetism and semiconductivity, has been studied for decomposition reactions of hydroperoxides, nitrogen oxide as well as for dehydration and dehydrogenation reactions of alcohols.[4,5]

The catalytic properties of the ferrocene polymers have been studied for dehydration and dehydrogenation reactions of alcohols [6] and the influence followed of the thermal treatment on the catalyst.

---

[1] K. H. Keier and I. Astofiev, *Kinetica i kataliza*, **3**, 364 (1962).

[2] J. Manassen and J. Wallach, *J. Amer. Chem. Soc.*, **87**, 2671 (1965).

[3] A. A. Slinkin, A. A. Dulov, I. M. Glavteva and L. M. Rutenstein, *Kinetica i kataliza*, **8**, 136 (1967).

[4] J. Gallard, Th. Lacaderlich, R. Salle and Ph. Fraynard, *Bull. Soc. chim. France*, **10**, 2204 (1963).

[5] J. Gallard, M. Nechtshein, M. Sontif and Ph. Fraynard, *Bull. Soc. chim. France*, **10**, 2209 (1963).

[6] M. A. Voronina, P. P. Vishnyakova, Ya. M. Paushkin, M. A. Bojilova and L. A. Aliev, *Vysokomol. Soedineniya*, **11**, 882 (1969).

Taking into account the structure and the properties of certain ferrocene polymers previously studied such as poly-*p*-ferrocenyl-phenylacetylenes [7,8] we studied in the present paper their behaviour as potential redox initiators in polymerizations of some vinyl monomers.

EXPERIMENTAL

The polymerization was carried out by bulk procedure in inert medium, using sealed glass ampoules. Products soluble in common organic solvents have been obtained and then purified by solving in benzene followed by initiator removal by filtration and precipitation with acidified methanol. The conversions were calculated based on gravimetric data.

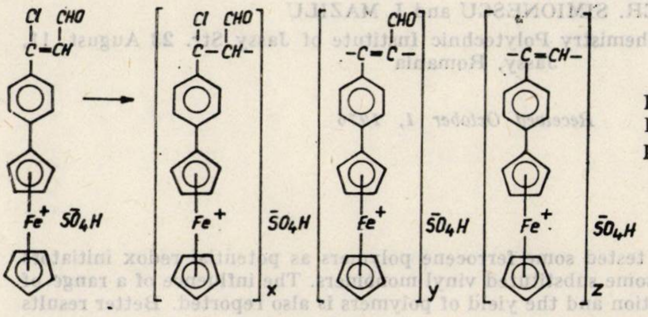

Fig. 1 — Structure of the polymers obtained by thermal polymerization of α-chloro-β-formyl-*p*-ferrocenyl-styrene.

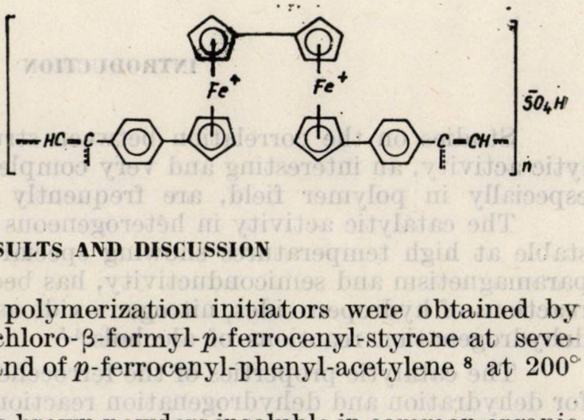

Fig. 2. — Structure of the polymers obtained by thermal polymerization of *p*-ferrocenyl-phenylacetylene at 200°.

RESULTS AND DISCUSSION

The polymers used as polymerization initiators were obtained by thermal polymerization of α-chloro-β-formyl-*p*-ferrocenyl-styrene at several temperatures [7] (Figure 1) and of *p*-ferrocenyl-phenyl-acetylene [8] at 200° (Figure 2).

These polymers are dark-brown powders insoluble in common organic solvents, infusible up to 350°.

It is worth noticing that both polymers do not show semiconducting properties although the RES spectra indicate for poly-*p*-ferrocenyl-phenylacetylene a paramagnetic particle concentration of 10^{17} spins/g order. This behaviour might be caused by the sterical hindrances of the bulky substituents which disturb the molecule planarity hindering the conjugation extension.[7,8]

---

[7] Cr. Simionescu, T. Lixandru, L. Tătaru, I. Mazilu and I. Cocîrlă, *J. Organomet. Chem.*, **102**, 219 (1975).

[8] Cr. Simionescu, T. Lixandru, I. Mazilu and L. Tătaru, *J. Organomet. Chem.*, **113**, 23 (1976).

The initiating action of these compounds in polymerizations was tested for some substituted vinyl monomers of the α-chloro-β-formyl-*p*-X-styrene type where X stands for either chlorine or bromine atoms.

The thermal polymerization of these monomers failed at 140° when the monomer was recovered entirely; at temperatures under 180° the conversions were quite insignificant. The benzoyl peroxide is not an efficient initiator since it cannot be used at high temperatures.

In the presence of ferrocene polymers the conversion was found to increase compared to that obtained by thermal polymerization under similar conditions, the yields at 140° varying between 18 and 21%. These findings might be explained by means of the ion pair in tested polymers which participates under the reaction conditions in an electronic exchange acting as redox initiators according to the following scheme:

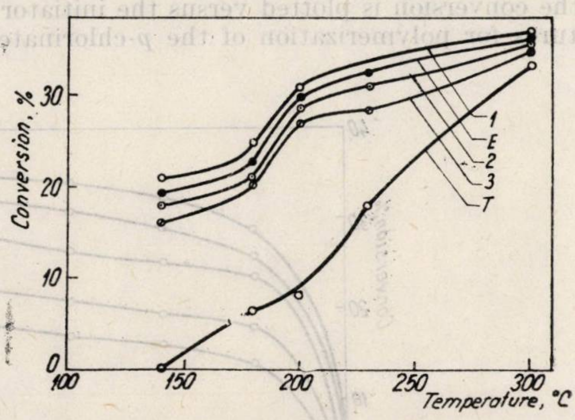

Fig. 3. — Conversion variation with temperature. Initiator 1%. *1.* Initiator synthesised from α-chloro-β-formyl-*p*-ferrocenyl-styrene at 180°; *2.* Initiator synthesised from α-chloro-β-formyl-*p*-ferrocenyl-styrene at 200°; *3.* Initiator synthesised from α-chloro-β-formyl-*p*-ferrocenyl-styrene at 300°; E. Initiator synthesised from *p*-ferrocenyl-phenyl-acetylene at 200°. Polymerization without initiator.

$$Fe^{+3} + HSO_4^- \xrightarrow{t^0} Fe^+ + \cdot SO_4H$$

The $\cdot SO_4H$ radical might be responsible for the polymerization initiation.

The fact that the $\cdot SO_4H$ radical could not be evidenced at the macromolecular chain ends as well as the failure in using the initiator with classical monomers like styrene and methylmetacrylate suggest a more complex initiation. In this connection it seems probable for the hydrogen chloride or formyl chloride appearing in the reaction medium to play an important role.[9-11] First, the influence of the initiator nature (synthesised at several temperatures) on the conversion was followed. In Figure 3 the conversion change with temperature using different initiators is shown for the *p*-chlorinated monomer.

[9] T. Lixandru, L. Tătaru, I. Mazilu and I. Cocîrlă, *Rev. Roum. Chim.*, **20**, 129 (1975).

[10] T. Lixandru, L. Tătaru, I. Mazilu and I. Cocîrlă, *Bul. Inst. Polit. Iași*, **21 (25)**, Fasc. 3–4, 69 (1975).

[11] T. Lixandru, L. Tătaru, I. Mazilu and I. Cocîrlă, *Bul. Inst. Polit. Iași*, **22 (26)**, Fasc. 1–2, 55 (1976).

The highest yields were obtained with the initiator (1) synthesised at 180°. This better activity might be attributed to the initiator structure which is less cross-linked facilitating thus the electronic exchange in the redox system. The initiators synthesised at higher temperatures are less active because of their tridimensional structure[7] in which the ferricinium cation is more screened. The fact that in the redox system the paramagnetic character of the initiator is not involved supports the above assumption. Although the polymer (E) has a high content of paramagnetic particles ($5.38\ 10^{18}$ spins/g) its activity is somewhat diminished because it was synthesised at 200°.

Using the initiator found as the most efficient, the influence of its concentration and of the temperature on the yield was followed. In Figure 4 the conversion is plotted versus the initiator amount at several temperatures for polymerization of the *p*-chlorinated monomer.

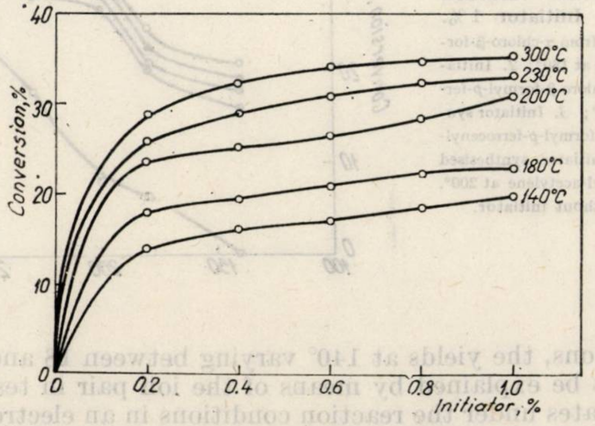

Fig. 4. — Conversion versus initiator amount.

The conversion is seen to increase with increasing temperature up to 230° remaining then within the values obtained for thermal polymerization.[9] This fact might be caused rather by the thermal destruction of the resulting product than by the modification of the initiator structure, fact which will be later discussed in connection with the polymer structure. The yield was found to increase with increasing initiator concentration up to 1%; above this value the yield varied insignificantly.

As for a reaction duration greater than 10 hours the conversion variation was rather small, all runs have been carried out varying the temperature at a constant reaction time (10 hours). In Figure 5 the conversion is plotted versus reaction time at 230° with 1% initiator concentration for the *p*-chlorinated monomer.

In table 1 some comparative data are listed on thermal polymerization and that in the initiator presence for the *p*-chlorinated and *p*-brominated monomers.

Table 1

The influence of temperature on conversion and degree of polymerization. The concentration of initiator 1%. The reaction time 10 hours

Polymer	Temperature	Conversion, %	$\sqrt{\mathrm{P}}$	M.P.
A	140	—	—	—
$\sqrt{\mathrm{A}}$*	140	21.0	6	205
A	180	6.98	6	204
$\sqrt{\mathrm{A}}$*	180	23.1	6	206
A	200	8.03	8	218
$\sqrt{\mathrm{A}}$*	200	31.0	9	218
A	230	18.00	12	195
$\sqrt{\mathrm{A}}$*	230	37.7	13	200
A	300	35.82	4	249
$\sqrt{\mathrm{A}}$*	300	37.31	3	250
B	140	—	—	—
$\sqrt{\mathrm{B}}$*	140	22.37	7	227
B	180	35.01	7	230
$\sqrt{\mathrm{B}}$*	180	36.25	7	231
B	200	43.79	6	250
$\sqrt{\mathrm{B}}$*	200	45.01	6	250
B	230	43.98	9	266
$\sqrt{\mathrm{B}}$*	230	44.80	9	270
B	300	51.72	3	294
$\sqrt{\mathrm{B}}$*	300	50.95	3	295

A = Products obtained by thermal polymerization of α-chloro-β formyl-*p*-chloro-styrene; B = Products obtained by thermal polymerization of α-chloro-β-formyl-*p*-bromo-styrene; X = Products obtained by monomer polymerizations in the initiator presence.

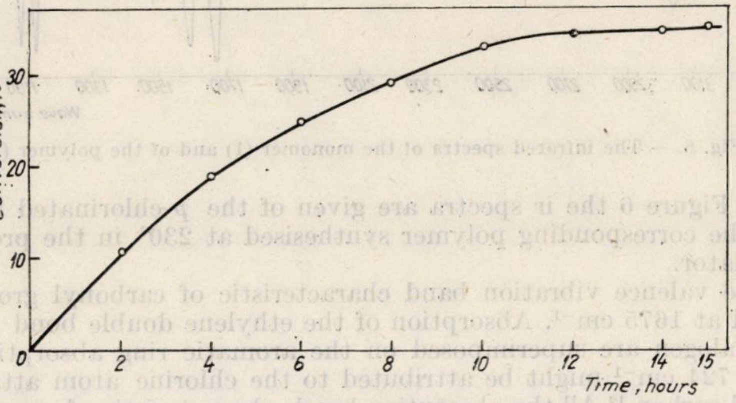

Fig. 5. — Conversion versus time at 230°.

The data listed in table 1 evidence the better efficiency of the initiator in case of the *p*-chlorinated monomer. This fact might be explained by taking into account the different reactivities of the two monomers evidenced by both MO-Hückel calculations and experimental data on thermal polymerization.[9]

The conversion increase in the initiated polymerization compared to the thermal one is much more pronounced for the less active *p*-chlorinated monomer than for the *p*-brominated derivative.

The initiators are generally noticed to be effective at low temperature when the thermal polymerization leads to poor results.

CHARACTERIZATION OF POLYMERS

Structures of the obtained products were elucidated based on ir spectral measurements, thermal differential analyses as well as on elemental analysis data.

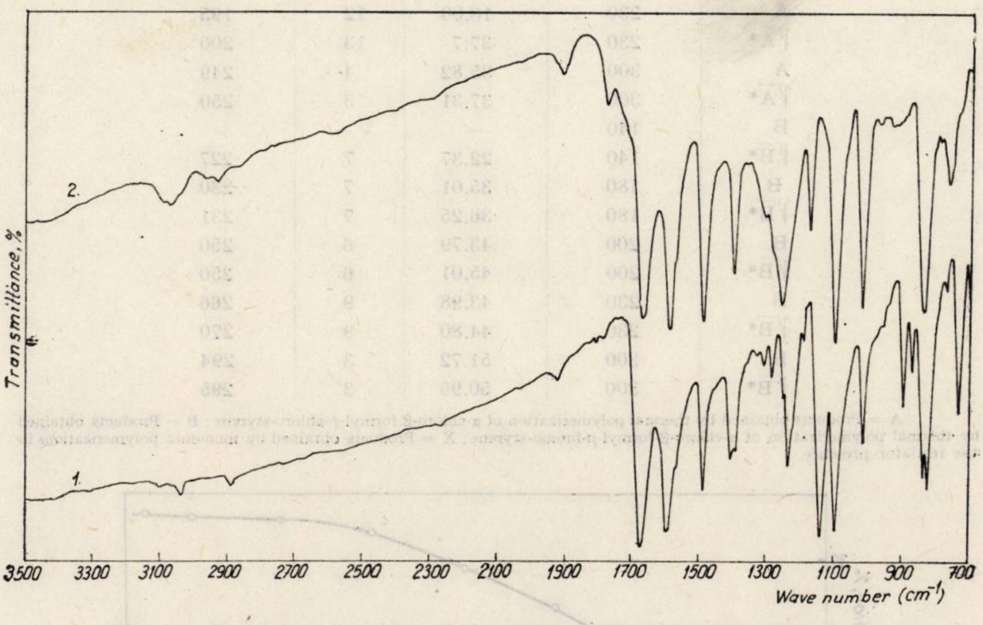

Fig. 6. — The infrared spectra of the monomer (1) and of the polymer (2).

In Figure 6 the ir spectra are given of the *p*-chlorinated monomer and of the corresponding polymer synthesised at 230° in the presence of 1% initiator.

The valence vibration band characteristic of carbonyl group is to be found at 1675 cm^{-1}. Absorption of the ethylene double bond and that of the halogen are superimposed on the aromatic ring absorption. The band at 724 cm^{-1} might be attributed to the chlorine atom attached to the vinyl carbon.[12] All the absorption bands characteristic of monomer are found in the spectrum of the polymer (2), but less intensive. The lower intensity of the band at 724 cm^{-1} in polymer spectrum might be caused by the removal as hydrogen chloride of formyl chloride of chlorine atom at the vinyl carbon.

---

[12] M. Avram and Gh. D. Mateescu, "Spectroscopia în infraroşu, aplicaţii în chimia organică", Ed. tehnică, Bucharest, 1966.

The spectra of the products obtained at different temperatures, reaction times and initiators are identical.

As can be seen in table 1 the average polymerization degrees vary between 13 and 3 the lowest value being noticed for temperatures above 230° which leads to the assumption of a concurrent depolymerization reaction till trimer at higher temperatures.

The thermal stability of the products has been investigated by means of thermal differential analyses. Figure 7 shows the weight losses as a function of temperature for the *p*-chlorinated (1) and *p*-brominated (2) derivatives obtained at 230° in the presence of 1% initiator.

The thermal destruction takes place in several stages among which only one is more important. As can be seen in figure 7 the weight losses are insignificant up to 260° and, consequently, the products may be considered stable.

The synthesized polymers show signal in RES the paramagnetic particle concentration being of $2.8 \cdot 10^{16}$ spins/g for the *p*-chlorinated derivative and $8.55\ 10^{16}$ spins/g for the *p*-brominated one.

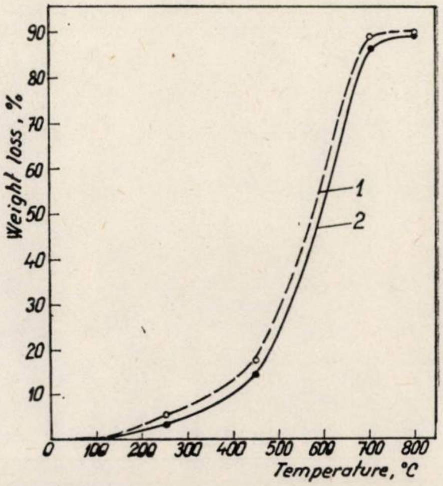

Fig. 7 — Weight losses as a function of temperature :
1. *p*-chlorinated polymer; 2. *p*-brominated polymer.

CONCLUSIONS

In the present paper some ferrocene polymers are tested as potential redox initiators in the polymerization of some substituted vinyl monomers.

1. α-Chloro-β-formyl-*p*-chloro-styrene and α-chloro-β-formyl *p*-bromo-styrene have been polymerized, the conversions being higher than those found in thermal polymerization at the same temperature. The obtained products are oligomers with average polymerization degrees between 3 and 13.

2. The initiator efficiency is better at lower temperatures and especially for the *p*-chlorinated monomer.

3. The investigated initiators have no influence on the polymerization of styrene and methylmethacrylate, the initiating action being specific for chloroformylated vinyl monomers.

4. The RES spectra evidence a paramagnetic particle concentration of the 10^{16} spin/g order.

Revue Roumaine de Chimie, 22, 5, 761–764 (1977)

Dedicated to the 70th anniversary
of Professor Coriolan Drăgulescu

ON PREFERENTIAL ORIENTATION OF THIN MAGNESIUM FILMS SUPPORTED ON GLASS

I. SITARU * and E. SEGAL **

* Center of Physical Chemistry, str. Galaţi 31, Bucharest
** I.P.B., Institute of Chemistry, Department of Physical Chemistry and Electrochemical Technology, Bd. Republicii 13, Bucharest

Received September 17, 1976

The authors present some remarks concerning the behaviour of thin magnesium films evaporated in vacuum.

INTRODUCTION

In the last two decades, a few data concerning thin metallic films preferentially oriented on various supports were reported.[1-6] In this paper, we present the results obtained with thin magnesium films evaporated in vacuum on glass.

EXPERIMENTAL

The thin magnesium films on glass were obtained in a glass backable vacuum equipment, provided with a diffusion oil pump and liquid nitrogen traps. The pressure lower limit was 10^{-7} Torr and the residual gases pressure during evaporation of magnesium was 10^{-5} Torr. Given amounts of metallic magnesium were evaporated by electrical heating of a tungsten basket. In order to obtain a uniform thickness, the glass support (20 × 20 sq. mm.) was placed at 90 mm distance from the tungsten basket. The thickness of the films was measured using an apparatus Talysurf 4. The X-ray analysis of the films was performed with a Philips PW 1140/90 diffractometer, using the Kα radiation of a copper anode.

---

[1] R. C. Newman, *Phil. Mag.*, **2**, 750 (1957).
[2] E. Grunbaum, *Proc. Phys. Soc.* (*London*), **72**, 459 (1958).
[3] D. W. Pashley, *Phil. Mag.*, **4**, 316 (1959).
[4] J. W. Matthews, *Phil. Mag.* **13**, 1207 (1966).
[5] J. W. Matthews and W. A. Jesser, *Acta Met.*, **15**, 595 (1967).
[6] R. L. Moss, H. R. Gibbens and D. H. Thomas, *J. Catalysis*, **16**, 117 (1970).

RESULTS AND DISCUSSSION

The values of the thickness for the magnesium films used in this work, as well as the results of X-ray diffraction measurements are given in table 1.

Table 1

The crystalline planes of magnesium thin films which exhibit X-ray diffraction peaks

Film N°	Thickness Å	Miller's indexes for the exhibited crystalline planes			
1	200	(002)			
2	400	(002)			
3	1500	(002)		(103)	
4	1000	(002)	(204)		
5	1000	(002)	(204)		
6		(002)	(204)	(103)	(101)
7	2000	(002)	(204)	(103)	
8		(002)	(204)		
9		(002)			

From the data presented in this table, one can see that every magnesium thin film exhibits the diffraction peak corresponding to the (002) crystalline plane. The following diffraction peaks, in order of the intensity and frequency of appearance, correspond with (204), (103) and (101) crystalline planes. The last peak appears only once.

Without a preferential orientation, according to ASTM tables for magnesium, the peaks corresponding to the crystalline planes with the highest intensities (101), (002) and (100) (with the intensities 100%, 41% and 35%, respectively) should appear. In the ASTM tables for magnesium, the intensities corresponding to (204) and (103) crystalline planes are comparatively small, namely 1% and 18%, respectively.

In table 2, the calculated surface atomic density for the magnesium crystalline planes with the densest package as well as the angles between these planes and the (002) plane are given.

Table 2

The surface atomic density in the crystalline magnesium planes with the densest package, the angles between these planes and the (002) plane calculated according to crystallographic data and the differences $2R - d_{hkl}$

(*hkl*) plane	(002)	(100)	(101)	(204)	(103)	(102)
Density at/100Å^2	11.21	5.98	5.28	4.09	3.19	2.89
φ between (*hkl*) and (002) planes	0	90°	61° 55′	43° 10′	33° 10′	75° 4′
$2R - d_{hkl}$ Å^2	0.5911	0.4171	0.7441	2.2466	1.7241	1.2961

The last row of table 2 contains the values of the difference $2R - d_{hkl}$ which enters as a factor in Yatsimirskii's formula [7] for the surface energy σ_{hkl} of the plane (hkl)

$$\sigma_{hkl} = \rho_v \left(R - \frac{1}{2} d_{hkl} \right) \tag{1}$$

In formula (1), ρ_v and R stand for the bulk cohesion energy of the crystal and rigid sphere atomic radius, respectively. According to tables [8] for magnesium, $R = 3.1971$ Å.

Taking into account the surface energy, the crystalline plane which must appear with the highest probability is (100) and from the planes given in table 2, the crystalline plane with the smallest probability of appearance is (204). If one considers the surface atomic densities given in table 2, the value of this property for the (002) plane is (twice) higher than the corresponding value for the (100) plane. On the other hand, from the same table 2, one can see that the (002) plane follows immediately after the (100) plane in the sequence of surface energy. According to our experimental results given in table 1, the thin magnesium films used in this work always exhibit a very sharp peak, corresponding to the (002) plane, but not the peak corresponding to the crystalline plane (100).

Therefore, the surface energies corresponding to these crystalline planes being approximately the same, the crystalline plane with higher surface energy appears with higher probability, due to the higher value of the surface atomic density.

According to the data given in table 1, the following plane exhibited by the magnesium thin films in the sequence of the intensities and frequencies among different samples is (204), no matter the favourable values of surface energy and surface atomic density for the (100) plane. Moreover, the intensity corresponding to the (204) plane of our magnesium films is much higher than the 1% value given in the ASTM tables.

The above mentioned inversion can be explained taking into account a geometrical factor. After the appearance of the (002) plane, due to the already mentioned reasons, it is natural to assume that the higher probabilities for the formation of different crystalline planes correspond to the lower values of the angles between these planes and the first formed one, the other factors being unchanged.

As one can see from table 2, the angles between the (100), (101), (204) planes and (002) plane are respectively 90°, 61°55′ and 43°10′. This accounts for the higher observed frequency of the (204) plane appearance in the X-ray diffractograms.

---

[7] V. K. Yatsimirskii, *Ukrain. Khim. J.*, 33, 881 (1967).

[8] "Handbook of Chemistry and Physics", 55th edition, C.R.C. Press, Cleveland, Ohio, 1974, p. F–201.

As concerns the (103) plane, according to the data given in table 2 and taking into account the geometrical factor, one can conclude that it is also favoured with respect to (100) and (101) plane. The geometrical factor does not account for the frequencies of (204) and (103) planes appearance, as given in table 1. Thus, for small differences between the angles, the other factors responsible for the appearance of crystalline planes prevail (the main factor being, in our case, the surface atomic density).

CONCLUSIONS

By means of X-ray diffraction, some preferential orientations of the crystalline planes in magnesium thin films on glass were evidenced.

Revue Roumaine de Chimie, 22, 5, 765–771 (1977)

Herrn Professor Dr. CORIOLAN DRĂGULESCU
zum 70. Geburtstag gewidmet

CHEMISCHE PARAMETER DER GEWÄSSERVERSCHMUTZUNG

HEINRICH SONTHEIMER
Universität Karlsruhe, Lehrstuhl für Wasserchemie

Eingegangen am 3. September 1976

Untersuchungen der Gewässergüte haben sich früher nahezu ausschließlich biologischer Untersuchungsmethoden bedient. Mit der Zunahme der chemischen Gewässerverunreinigung gewinnen moderne chemische Untersuchungsmethoden aber zunehmend an Bedeutung. Dabei ist von den Summenparametern die Messung der Konzentration an gelöstem organisch gebundenem Kohlenstoff am wichtigsten. Die Abhängigkeit der Fracht von der Wasserführung erlaubt dabei erste Aussagen über den Anteil an biologisch schwer abbaubaren Stoffen. Noch weitergehende Informationen liefern die erst in den letzten Jahren entwickelten Methoden zur Bestimmung von Gruppenparametern. Derartige Untersuchungen geben klare Hinweise auf die Priorität von notwendigen Abwasserreinigungsmaßnahmen.

PROBLEMSTELLUNG

Die Beurteilung der organischen Belastung eines Oberflächenwassers erfolgt seit vielen Jahren mit Hilfe von biologischen Untersuchungsmethoden. Dabei erfolgt in der Regel die Ermittlung einer Gewässergüteklasse anhand einer Einteilung der gefundenen Organismen nach dem Saprobiensystem. Als zusätzlicher chemischer Parameter wird dabei meist nur die Sauerstoffkonzentration und -zehrung für eine Beurteilung mit herangezogen.

Nachteilig an dieser Art des Vorgehens ist, wie insbesondere unsere eingehenden Untersuchungen am Rhein gezeigt haben, daß sich auf diese Weise keine oder nur sehr unvollkommene Angaben über die Wiederverwendbarkeit eines Flußwassers für die Wasserversorgung gewinnen lassen. Hier stehen in einer modernen Industriegesellschaft heute Probleme im Vordergrund des Interesses, die sich unter dem Begriff der chemischen Gewässerverunreinigung zusammenfassen lassen. Die zunehmende Bedeutung der so zu charakterisierenden Schadstoffe hängt damit zusammen, daß heute in steigendem Ausmaß organische Substanzen erzeugt und verwendet werden, die gegen biologische und chemische Angriffe sehr beständig sind. Diese schwer abbaubaren organischen Stoffe behindern zwar ähnlich wie die Schwermetallverbindungen kaum den Sauerstoffhaushalt eines Gewässers, gefährden aber unter anderem die Aufbereitung von stets einwandfreiem Trinkwasser und auch die Bereitstellung von gutem Betriebswasser.

Dieser hier nur skizzierte Sachverhalt macht es erforderlich, Untersuchungsmethoden zu entwickeln und anzuwenden, die eine laufende Kontrolle der chemischen Gewässerverunreiningungen gestatten. Die folgenden Ausführungen befassen sich mit dieser Fragestellung am Beispiel der Rheinwasseruntersuchungen, die unser Institut für die Wasserwerke im Rheineinzugsgebiet durchführt.

SUMMARISCHE PARAMETER FÜR DIE GELÖSTEN ORGANISCHEN STOFFE

Von besonderer Bedeutung für die Beurteilung eines Gewässers ist die Gesamtkonzentration an gelösten organischen Stoffen. Von den hierfür bisher vorgeschlagenen Analysenmethoden liefern jedoch nur zwei Verfahren zuverlässige und eindeutige Aussagen. Es handelt sich hierbei um :

1) Die Messung der Konzentration an gelöstem organisch gebundenen Kohlenstoff (DOC = Dissolved Organic Carbon).

2) Den chemischen Sauerstoffbedarf nach der Bichromatmethode (COD = Chemical Oxygen Demand).

Zwischen den beiden Größen besteht eine von der mittleren Zusammensetzung der organischen Stoffe abhängige Relation, die als spezifischer Sauerstoffbedarf (COD/DOC) bezeichnet wird. In vielen Gewässern liegt dieser Wert bei Angabe der Einzelwerte in g/m^3 C bzw. O_2 zwischen 2,5 und 3,5. Manche Industrieabwässer haben jedoch höhere Werte, da die organischen Inhaltsstoffe weniger weit oxidiert sind.

Für beide Meßgrößen sind verschiedene Geräte und Analysenverfahren bekannt. Führt man eine laufende Messung derartiger Werte an einem Fließgewässer durch, so beobachtet man, daß die Fracht an organischen Stoffen mit der Wasserführung deutlich zunimmt. Ein Beispiel für diese Abhängigkeit für eine Stelle am Rhein zeigt die erste Abbildung.

Man erkennt aus dieser Darstellung einmal, daß die Werte für den DOC weniger um die Ausgleichskurve streuen als die Resultate für den COD, so daß die Konzentration an gelöstem organischen Kohlenstoff für die Beschreibung der Gesamtbelastung eines Gewässers besser geeignet ist als der chemische Sauerstoffbedarf.

Eingehende Überprüfungen haben gezeigt, daß sich diese Veränderung der Fracht mit der Wasserführung recht genau mit der folgenden Beziehung beschreiben läßt.

$$F_G = F_R + F_{A,\mathrm{rep}} \cdot e^{-K/Q^n} = F_R + F_A$$

F_G = Gesamtfracht an DOC (kg/s)
F_R = Fracht an resistenten, biologisch schwer abbaubaren Stoffen als DOC (kg/s)
F_A = Fracht an biologisch abbaubaren Stoffen als DOC (kg/s)

$F_{A,\text{rep}}$ = Repräsentative Frachtzufuhr an biol. abbaubaren Stoffen als DOC (kg/s), die durch Selbstreinigung nach einer *e*-Funktion abnimmt und die Änderung der Gesamtfracht mit der Wasserführung bestimmt

n = Exponent der Wasserführung Q (m^3/s), der aussagt wie sich die Fließgeschwindigkeit mit der Wasserführung ändert. Am Rhein gilt $n = 0{,}43$. Übliche Werte für andere Flüsse liegen zwischen 0,2 und 0,8

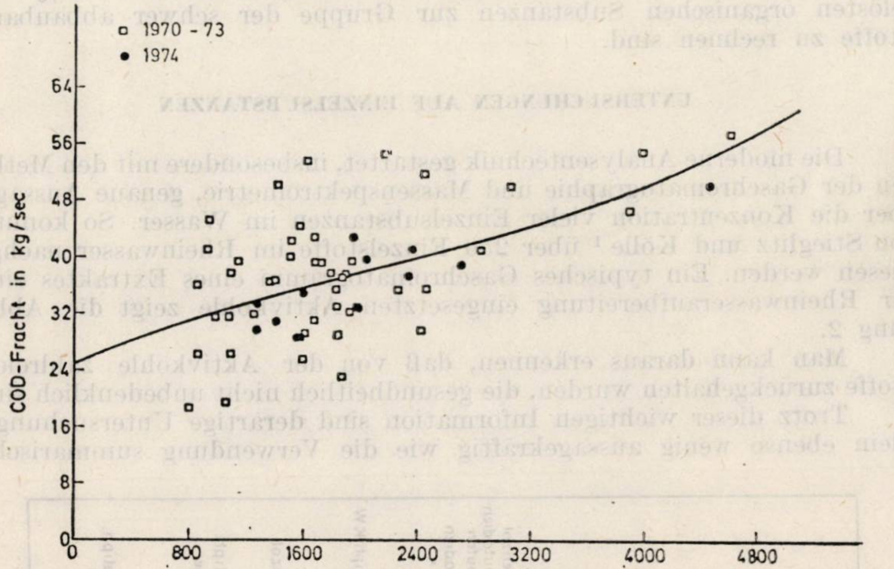

Abb. 1 — Abhängigkeit der COD- und DOC-Fracht von der Wasserführung des Rheins bei Flehe.

K = Exponent, der Aussagen über die Kinetik der Selbstreinigung macht. Am Rhein beträgt der Wert im Mittel etwa 65.

K und *n* lassen sich beim Vorliegen von ausreichendem Datenmaterial, ebenso wie die anderen Konstanten nach der Methode der kleinsten Fehlerquadratsumme über ein Rechnerprogramm ermitteln. Man erhält dann Angaben über die Fracht bzw. Konzentration der schwer bzw. nicht abbaubaren organischen Stoffe und damit bereits wichtige erste Informationen über die Art der Gewässerbelastung. Mit dieser Methode konnte am Rhein festgestellt werden, daß bei Niedrigwasser rund 75% aller gelösten organischen Substanzen zur Gruppe der schwer abbaubaren Stoffe zu rechnen sind.

UNTERSUCHUNGEN AUF EINZELSUBSTANZEN

Die moderne Analysentechnik gestattet, insbesondere mit den Methoden der Gaschromatographie und Massenspektrometrie, genaue Aussagen über die Konzentration vieler Einzelsubstanzen im Wasser. So konnten von Stieglitz und Kölle [1] über 250 Einzelstoffe im Rheinwasser nachgewiesen werden. Ein typisches Gaschromatogramm eines Extraktes einer zur Rheinwasseraufbereitung eingesetzten Aktivkohle zeigt die Abbildung 2.

Man kann daraus erkennen, daß von der Aktivkohle zahlreiche Stoffe zurückgehalten wurden, die gesundheitlich nicht unbedenklich sind.

Trotz dieser wichtigen Information sind derartige Untersuchungen allein ebenso wenig aussagekräftig wie die Verwendung summarischer

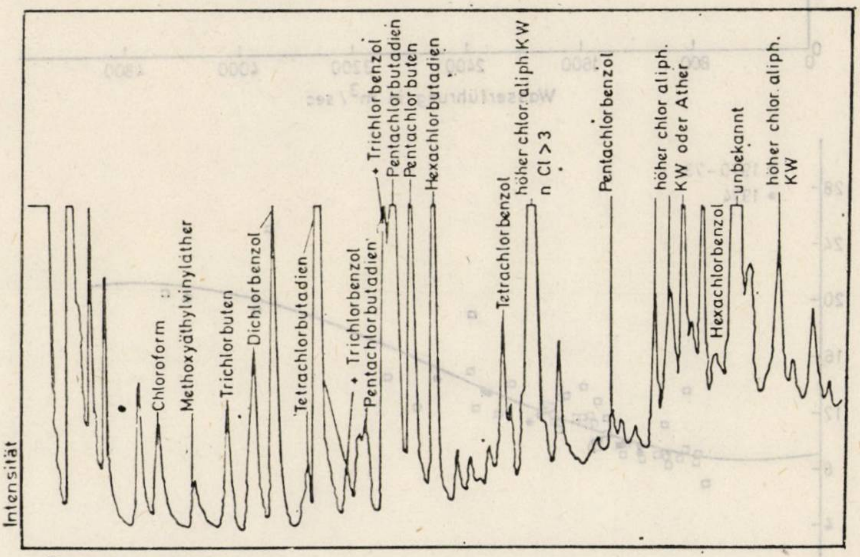

Abb. 2 — Gaschromatogramm aus dem Extrakt einer Aktivkohle in einem Wasserwerk.

---

[1] W. Kölle, K. H. Schweer, H. Gusten und L. Stieglitz, *Vom Wasser*, **39**, 109 (1972).

Parameter allein, die ja nur etwas über die Gesamtmenge an organischen Stoffen aussagen, aber nichts über deren hygienische und sonstige Bedeutung. Mit Einzelsubstanzbestimmungen ermittelt man zwar definierte organische Substanzen, kann aber auch bei sehr großem Zeit- und Materialaufwand kaum mehr als 2—5% aller organischen Stoffe erfassen. Aus diesen Gründen ist in den letzten Jahren in steigendem Maße versucht worden, einen Mittelweg zu finden, durch die Erfassung und Analyse von ganzen Gruppen von gelösten organischen Stoffen. Diese Art der Analytik ist am Rhein zum ersten Mal erfolgreich eingesetzt worden.

GRUPPENPARAMETER FÜR GELÖSTE ORGANISCHE STOFFE

Analysenmethoden mit denen eine durch bestimmte Eigenschaften charakterisierte Gruppe von organischen Stoffen erfaßt wird, werden schon seit langem angewendet, denn auch der BSB, der biochemische Sauerstoffbedarf ist hier einzuordnen. Man erfaßt damit die biologisch abbaubaren organischen Substanzen.

Auch die durch ihre Einfachheit und Schnelligkeit vorteilhafte Messung der UV-Extinktion ist hier einzuordnen. Sie hat jedoch den Vorteil, daß für viele Wässer eine nahezu konstante Relation zwischen UV und DOC besteht. Für den Rhein gilt beispielsweise für die gesamte Fließstrecke recht gut die Beziehung:

$$\mathrm{DOC} = (\mathrm{UV})^{2/3} \quad \text{(UV bei 254 nm und 1 m Schichtdicke)}$$

Insofern ist die Messung der UV-Extinktion eher eine schneller durchzuführende Ersatzmessung für den DOC, ähnlich wie der früher viel verwendete $KMnO_4$-Verbrauch.

Von ganz anderer Art sind die in den letzten Jahren vorgeschlagenen chemischen Gruppenparameter, mit denen organische Stoffe mit gleichen Strukturelementen erfaßt werden. Folgende Verfahren haben heute besondere Bedeutung erlangt:

1) Bestimmung der organischen Säuren. Dabei erfolgt nach einer von Eberle [2] vorgeschlagenen, von Wagner und Hoyer [3] und Sontheimer [4] weiterentwickelten Methode eine Extraktion der organischen Säuren aus dem zu untersuchenden Wasser mit einer Lösung von Trioctylamin in Chloroform. Durch Rückextraktion mit NaOH-Lösung und Entfernung der Na^+ Ionen über einem Kationenaustauscher erhält man die Lösungen der reinen Säuren und kann diese in Substanz isolieren.

In den Rückextrakten läßt sich über UV-Messungen bei verschiedenen Wellenlängen die Konzentration an Huminsäure und die der als Abfallprodukt der Zellstoffindustrie in den Rhein gelangenden Ligninsulfonsäure getrennt bestimmen.

2) Bestimmung des organisch gebundenen Chlors. Hier hat sich die von Kühn und Sontheimer [5] vorgeschlagene Anreicherung an Aktiv-

---

[2] S. H. Eberle und K. H. Schweer, *Vom Wasser* **41**, 27 (1973).

[3] I. Wagner und D. Hoyer, *Vom Wasser*, **45**, 207 (1975).

[4] H. Sontheimer und I. Wagner, „7. Bericht der Arbeitsgemeinschaft Wasserwerke Bodensee-Rhein“ Analysenverfahren, 120 (1975).

[5] W. Kühn und H. Sontheimer, *Vom Wasser*, **41**, 65 (1973).

kohle und die Bestimmung des Chlors auf der Kohle durch Pyrohydrolyse und Chloridmessung gut bewährt. Unpolare Chlorverbindungen können unabhängig davon durch Direktextraktion und Erfassung des Chlors in einem Mikrocoulometer bestimmt werden.

3) Ganz ähnlich wie die Chlorverbindungen lassen sich auch die Schwefelverbindungen bestimmen. Der größte Teil dieser Stoffe liegt als Sulfonsäuren vor und wird auch bei der Säurebestimmung mit erfaßt.

4) Leicht zu ermitteln aber weniger aussagekräftig sind Messungen der Konzentration an organisch gebundenem Stickstoff.

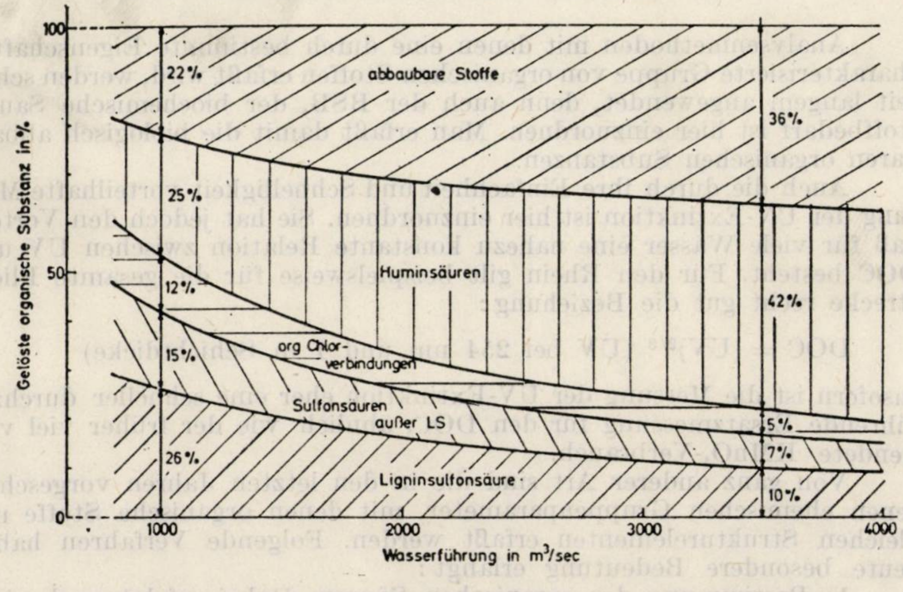

Abb. 3 — Aufteilung der gelösten organischen Stoffe auf die Hauptkomponenten bei verschidener Wasserführung am Niederrhein.

Mit den beschriebenen Methoden können wichtige Informationen über die Verschmutzung eines Gewässers erhalten werden. Dies zeigt die Abbildung 3 am Beispiel des Rheins.

Aufgetragen sind hier die Anteile der jeweiligen Gesamtmenge an gelösten organischen Stoffen, die auf die einzelnen Gruppen an organischen Stoffen entfallen. Man erkennt die große Bedeutung der Ligninsulfonsäure, der anderen Sulfonsäuren und der organischen Chlorverbindungen für die Rheinwasserqualität. Sie ist besonders ausgeprägt bei niederer Wasserführung. Hier ist außerdem auch die Gesamtkonzentration an gelösten organischen Stoffen besonders hoch.

Derartige Meßergebnisse lassen erkennen, wo die Schwerpunkte von Abwasserreinigungsmaßnahmen zu liegen haben, wenn eine wirksame Qualitätsverbesserung des Rheinwassers insbesondere bei niederer Wasserführung erreicht werden soll. Die in der Abbildung 3 dargestellten Resultate aus dem Jahre 1974 haben deshalb auch bereits zu entsprechenden Maßnahmen geführt. In der zweiten Hälfte 1975 konnte deshalb erstmals seit 30 Jahren wieder eine meßbare Qualitätsverbesserung am Rhein beobachtet werden. Dieser Hinweis zeigt besonders deutlich die große Bedeutung, die chemische Gruppenparameter für die Beurteilung der Wasserqualität haben.

MÖGLICHE WEITERENTWICKLUNGEN

Gewässeruntersuchungen sollen nicht nur irgendwelche Zahlenwerte sondern konkrete und verwendbare Aussagen für den Gewässerschutz liefern. Während die chemischen Gruppenparameter in erster Linie Angaben über die Art der Schmutzstoffe liefern, fehlen zur Zeit noch geeignete Methoden, die etwas über die Verwendbarkeit des Wassers aussagen. Hier kann man einmal, wie das von der Internationalen Arbeitsgemeinschaft der Wasserwerke im Rheineinzugsgebiet (IAWR) [6] geschehen ist, für viele einzelne Parameter Gewässergütestandards festlegen, oder aber, man kann durch dafür geeignete analytische Verfahren direkte Aussagen über die Aufbereitbarkeit erhalten. Erste Untersuchungen zur Prüfung der Adsorbierbarkeit, der Oxidierbarkeit und der Flockungswirkung haben erkennen lassen, daß es möglich sein wird, mit solchen an den verfahrenstechnischen Aufgaben bei der Wasseraufbereitung orientierten Methoden wichtige Aussagen zu erhalten. Es sind jedoch noch viele Untersuchungen erforderlich bevor die Analysenverfahren so weit standardisiert sind, daß ihre allgemeine Anwendung möglich ist.

Insgesamt gesehen zeigen jedoch diese Ausführungen, daß es zweckmäßig ist mit Hilfe von geeigneten chemischen Analysenverfahren wirklich aussagekräftige Informationen über die Gewässerverschmutzung zu erhalten und damit insbesondere auch alle die Fragestellungen zu beantworten, die sich in einer modernen Industriegesellschaft hinsichtlich der chemischen Gewässerverschmutzung ergeben. Dabei ist jedoch darauf hinzuweisen, daß die hier gemachten Ausführungen nur Teilaspekte des Gesamtproblems behandeln konnten, und daß je nach der im Einzelfall bestehenden Aufgabenstellung auch andere Untersuchungen und Analysenmethoden notwendig sein werden. Man kann jedoch gerade am Beispiel des Rheins zeigen, wie groß die Bedeutung und Aussagekraft chemischer Untersuchungen zur Gewässergüte sein kann und wie wichtig die Beschäftigung mit diesen Fragen und Problemen ist.

---

[6] W. Kölle. K. H. Schweer, H. Gusten und L. Stieglitz, *Vom Wasser*, **39**, 109 (1972).

Revue Roumaine de Chimie, 22, 5, 773–779 (1977)

Hommage au Professeur Coriolan Drăgulescu
à l'occasion de son 70ᵉ anniversaire

EFFETS DES PARTICULARITÉS CINÉTIQUES DES COMPLEXES DES ÉLÉMENTS DES TERRES RARES SUR LE MÉCANISME DU PROCESSUS DE SÉPARATION PAR ÉCHANGE IONIQUE

V. I. SPITSINE et L. I. MARTYNENKO
Institut de Chimie Physique de l'Académie des sciences de l'U.R.S.S.

Reçu le 13 octobre, 1976

La cinétique d'interaction du cationite avec des solutions des complexes des ETR a été étudiée. On a démontré que l'échange des ions ETR entre la solution du complexe et le cationite suit les lois de la cinétique d'interdiffusion dans le cas des ETR cériques et ceux de la cinétique chimique dans le cas des ETR yttriques. On a établi que la formation des complexes mixtes augmente la vitesse d'échange des ions ETR en solution.

Un des procédés technologiques dont l'efficacité d'utilisation pratique est en majeure partie déterminée par les propriétés cinétiques des complexes consiste en l'application de la chromatographie d'échange ionique des complexes. Dans la présente communication nous nous sommes proposé d'examiner un aspect cinétique du processus de la formation des complexes relatif à la séparation par échange ionique des mélanges des terres rares.

Il était admis jusqu'à présent que la vitesse de l'échange par les ions des éléments des terres rares (ETR, Ln) entre les phases constituées par une solution et un échangeur cationique (par exemple, sulfocationite KU–2) est déterminée aussi bien en présence qu'en l'absence des complexants par la vitesse de diffusion des ions ETR dans la phase de l'échangeur cationique. En particulier, on a trouvé[1] que la désorption de microquantités des ETR contenus dans le sulfocationite par les solutions de l'acide éthylènediaminotétracétique (EDTA, H_4A) et de l'acide éthylènetriaminopentacétique (ETPA, H_5A) suit les lois de la cinétique d'intradiffusion. Ce résultat a abouti aux équations proposées[2,3] pour le calcul des conditions optimales de la formation des complexes lors de la séparation par échange ionique des mélanges des ETR. Dans ce calcul seulement les paramètres statistiques du processus de la formation de complexes étaient pris en considération. Il est donc admis que le processus d'échange ionique n'est pas limité par la vitesse de l'échange entre les ions complexes des ETR et les ions hydratés $Ln^{3+}\cdot$ aq (le mécanisme de la cinétique chimique [4] n'était pas pris en considération).

---

[1] L. V. Shepetuk, Thèse. Moscou, 1970.

[2] A. M. Sorochyan et M. M. Senyavin, « Théorie de l'échange ionique et de la chromatographie », Ed. Nauka, Moscou, 1968, p. 170.

[3] N. N. Matorina, *Zhur. fiz. Khim.*, **38**, 932 (1964).

En même temps, dans certaines publications [5,6] consacrées à l'application de la chromatographie d'échange ionique des ETR on proposait que les processus de la séparation réelle des mélanges des ETR suivent les lois de la cinétique chimique.

Il est difficile de trouver une justification réaliste pour cette hypothèse, les complexes des ETR (et en particulier ceux couramment utilisés dans la chromatographie) étant labiles. Le caractère labile des complexes des ETR formés par n'importe quel ligand est dû à la formation des liaiosns sensiblement ioniques entre l'ion ETR et un ligand,[7,8] ce qui traduit le fait que les ions ETR ne possèdent pas les orbitales se prêtant facilement au recouvrement avec les orbitales du coordinant. Cependant il est à noter que les complexes des ETR avec des coordinats organiques sont souvent très stables.

Ainsi, les complexes dérivés d'acide ETPA se caractérisent par les constantes de stabilité de $10^{20}-10^{23}$, pour les dérivés d'acides EDTA les valeurs de cette constante se situent [8] entre $10^{16}-10^{19}$. La stabilité élevée de ces complexes s'explique par l'apparition de l'effet chélate. On a montré [9] que l'échange entre les ions hydratés ETR et les complexes des ETR a lieu lors de la dissociation du complexe donnant un ion central et des ligands ; l'association des ions hydrogène au ligand lié dans le complexe à l'atome central ETR précède une telle dissociation. Il s'ést avéré [9] que la croissance de la stabilité des complexes observée dans le cas des ligands polydentés provoque la diminution de la vitesse de l'échange par les ions ETR entre les complexes dissous dans l'eau et les ions hydratés.

Lors des études du processus de la formation de complexes dans le cas de la séparation chromatographique par échange d'ions des mélanges des ETR pris en macroquantité, nous avons observé un certain nombre de phénomènes difficiles à expliquer en admettant l'effet prépondérant de la cinétique d'intradiffusion. Ainsi, en mesurant le temps indispensable pour que le système $Ln^{3+}\cdot$ aq—EDTA— cationite arrive à l'équilibre, nous avons trouvé [10-12] que cet équilibre s'établissait plus vite dans le cas des

---

[4] F. Gelferich, «Ionites», Ed. I. L., Moscou, 1962, p. 237.

[5] M. M. Senyavin, «Echange ionique et ses applications», Ed. A. N., S.S.S.R., Moscou, 1959, p. 99.

[6] F. W. Cornish, G. Phillips et A. Thomas, *Canad. J. Chem.*, **34**, 1471 (1956).

[7] L. I. Martynenko, N. P. Potapova et V. I. Spitsine, *Zhur. neorg. Khim.*, **17**, 98 (1972).

[8] «Composés complexes des éléments des terres rares», sous la direction de K. B. Yatsimirski, Ed. Naukova Dumka, Kiev, 1966.

[9] P. Glenworth, B. Wiseall et C. L. Wright, *J. Inorg Chem.*, **30**, 967 (1968).

[10] L. I. Martynenko, V. I. Spitsine et G. A. Artukhina, *Zhur. neorg. Khim.*, **15**, 931 (1970).

[11] M. G. Yashkarova et L. I. Martynenko, *Zhur. neorg. Khim.*, **18**, 3136 (1973).

[12] L. I. Martynenko, M. G. Yashkarova et V. I. Spitsine, *Zhur. neorg. Khim.*, **18**, 2475 (1973).

ETR du groupe cérique que dans le cas des ETR faisant partie du groupe yttrique. Ce résultat est illustré sur la figure 1 qui montre la variation du coefficient de partage α_{exp} en fonction du temps de contact entre les phases dans le cas des mélanges de ETR du groupe cérique (néodime/praséodime) et dans celui des mélanges de ETR du groupe yttrique (erbium/holmium). Vu que le coefficient de partage théoriquement calculé est le même dans les deux cas (égal à 2 environ *), on pourrait s'attendre à la même efficacité de séparation par échange ionique de ces mélanges. Cependant, l'expérience montre que les mélanges des complexes des terres cériques avec l'acide EDTA sont beaucoup plus faciles à séparer queles mélanges des complexes des ETR yttriques. La différence observée suggère l'importance des effets cinétiques. Pour vérifier cette hypothèse nous nous sommes proposé de trouver le stade limite du processus d'échange ionique dans son ensemble.

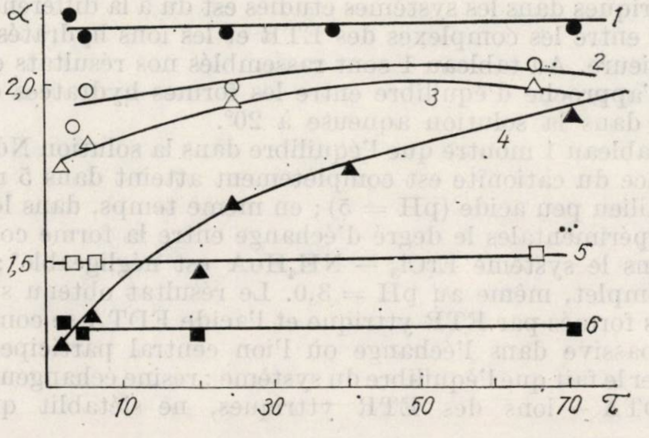

Fig. 1. — Variation du coefficient de partage α_{exp} en fonction du temps de contact entre les phases dans le cas des mélanges des ETR du groupe cérique (neodime/praséodine) et dans celui des mélanges des ETR du groupe yttrique (erbium/holmium).

La différence entre le coefficient de partage expérimental α_{exp} (α_{exp} est égal au rapport des coefficients de partage des ETR à séparer trouvé expérimentalement : voir la description donnée dans les travaux [10-12]) et celui d'équilibre, α_{eq}, a été prise comme mesure de non-équilibre du système d'échange ionique. La valeur de α_{eq} trouvée dans le cas des complexes de l'acide EDTA examinés était pratiquement la même que celle de l'$\alpha_{théor}$ calculée.[11,12]

La vitesse d'établissement d'équilibre du système : acide EDTA-cationite—mélange Nd^{3+}/Pr^{3+}, est influencée par la dimension des grains de la résine échangeuse d'ions, par la concentration de la solution exté-

---

* Dans le cas des complexes formés par l'acide EDTA $\alpha_{théor}$ est égal à $K^{n'A^-}_{stab^-}/K^{LnA^-}_{stab}$ [2,8]/.

rieure à toute vitesse d'agitation des phases et ne dépend pas du temps d'interruption du contact entre les phases.[11,12]

Les particularités observées caractérisent [4] les systèmes à cinétique d'intradiffusion. Par contre, le même système constitué par le mélange Er^{3+}/Ho^{3+} indique l'absence de la dépendance entre la vitesse d'établissement d'équilibre et la dimension des grains de la résine. L'interruption du contact entre les phases ne provoque pas toujours des changements notables de la vitesse d'échange ; on observe en même temps une variation de la vitesse d'échange avec la concentration de la solution extérieure. Un tel comportement suggère [4] la présence de la cinétique chimique.

Nous avons supposé que le comportement différent des ETR yttriques et cériques dans les systèmes étudiés est dû à la différence des vitesses d'échange entre les complexes des ETR et les ions hydratés dans la solution extérieure. Au tableau 1 sont rassemblés nos résultats concernant les vitesses d'approche d'équilibre entre les formes hydratées et complexées des ETR dans la solution aqueuse à 20°.

Le tableau 1 montre que l'équilibre dans la solution $NdCl_3-NH_4PrA$ en l'absence du cationite est complètement atteint dans 5 minutes même dans le milieu peu acide (pH = 5) ; en même temps, dans les mêmes conditions expérimentales le degré d'échange entre la forme complexe et hydratée dans le système $ErCl_3 - NH_4HoA$ est négligeable* ; cet échange reste incomplet, même au pH = 3,0. Le résultat obtenu signifie que les complexes formés par ETR yttrique et l'acide EDTA se comportent d'une manière passive dans l'échange où l'ion central participe. Ceci permet d'expliquer le fait que l'équilibre du système : résine échangeuse de cations — acide EDTA — ions des ETR yttriques, ne s'établit que lentement.

Tableau 1

Degré d'approche d'équilibre dans le système en l'absence du cationite (le temps de contact = 5 mn)

n°	Composition de la solution de départ	Concentration en ETR (totale) ion-g/l	pH de la solution en équilibre	Composition en ETR après l'échange, %				exp.	eq.
				$LnCl_3$		NH_4LnA			
				a	b	c	d		
1	$ErCl_3-NH_4HoA$	$6{,}8\cdot10^{-3}$	5,50	8,0	89,0	86,0	19,0	0,02	2,08
2	$ErCl_3-NH_4HoA$	$7{,}8\cdot10^{-3}$	3,80	57,0	42,0	48,0	52,0	1,48	2,08
3	$NdCl_3-NH_4PrA$	$7{,}5\cdot10^{-3}$	5,20	62,0	43,0	41,0	56,0	1,98	2,04

a = Nd(Er); b = (Pr(Ho); c = Nd(Er); d = Pr(Ho).

Est-ce qu'il est possible d'attribuer le caractère passif des complexes de ETR yttriques de l'acide EDTA à la plus grande stabilité de ces complexes dans la solution ou à la formation d'un autre type de liaison entre l'atome central et les EDTA dans les complexes des terres yttriques? Il est peu probable qu'une telle explication soit correcte. En effet, une étude [7,9] du type de la liaison existant entre l'ion des ETR et le ligand

---

* Les ions $Ln^{3+}\cdot$ aq et LnA^- ont été isolés sans utilisation de cationite par précipitation au pH = 6,0 de l'ion hydrate sous forme d'oxalate.

(EDTA) dans ces complexes, basée sur l'analyse des spectres IR a montré que le renforcement de la liaison covalente : $Ln^{3+}-N_{EDTA}$ et $Ln^{3+}-O_{EDTA}$ n'est pas important. Une augmentation de la stabilité des complexes observée lorsqu'on passe des ETR cériques aux ETR yttriques s'explique par le renforcement de l'interaction électrostatique à : Ln^{3+} — EDTA dû à la diminution du rayon ionique pour les ETR plus lourds.

Bien que le renforcement résultant de la stabilité soit assez important ($\lg_{stab}^{NdA^-} = 16{,}4$; $\lg_{stab}^{ErA^-} = 19{,}0$)[8], à notre avis, cet effet ne permet pas d'expliquer le caractère passif des composés des ETR yttriques dans les processus d'échange ionique. En effet, les recherches effectuées dans notre laboratoire sur les complexes beaucoup plus stables des ETR avec l'ETPA[8] n'ont pas montré l'existence d'une telle passivité.

L'indifférence entre les propriétés d'échange des complexes d'EDTA avec les ETR cériques et yttriques peut s'expliquer par les mécanismes différents de l'échange : $Ln^{3+\cdot}$ aq — LnA^- qui a lieu dans les deux cas. Nous avons montré[13] que dans les systèmes à échange ionique contenant un sulfocationite, l'EDTA et les ions des ETR la formation simultanée de plusieurs types de complexes est observée (monocomplexe protoné, HLnA ; monocomplexe neutre, M^ILnA ; complexe d'une composition Ln_4A_3 qui peut être considéré comme sel $Ln[LnA]_3$ dérivé de l'acide complexe HLnA. Nous avons établi que les complexes Ln_4A_3 se forment suivant la réaction :

$$3M^I\,LnA + LnR_3 \rightleftarrows Ln_4A_3 + 3M^IR$$

où R^- = radical du sulfocationite.

Lors de l'échange ionique le taux de complexes Ln_4A_3 dans les solutions d'équilibre est une fonction de la concentration des ETR dans le système. Dans le cas de la séparation des mélanges des ETR en macroquantité on trouve presque la moitié des groupes EDTA présents dans la solution liés dans les complexes Ln_4A_3.[13-16] Dans les systèmes contenant les ETR en microquantité ces complexes sont presque complètement dissociés ce qui empêche de mettre en évidence leur existence.

Il s'est avéré que les complexes Ln_4A_3 formés par les ETR cériques peuvent être sorbés dans le cationite en forme Ln^{3+} par le mécanisme différent de celui d'échange ionique qui n'existe pas dans le cas des complexes formés par les ETR yttriques.[13,16,17] Nous avons expliqué cette différence des propriétés des complexes des ETR yttriques et cériques en admettant que l'état de quatre ions Ln^{3+} dans le complexe Ln_4A_3 soit équilibré de telle manière qu'il se présente sous forme de polycomplexe neutre. Ce complexe est capable de pénétrer dans la phase de cationite sans trouver une barrière énergétique à franchir ; la concentration de ses solutions provoque la formation d'un précipité vitreux qui ne se transforme que très lentement à l'état cristallin.[17] Les complexes des ETR yttriques contiennent le quatrième ion Ln^{3+} dans la sphère de coordination extérieure. C'est pour cette raison que le complexe $Er[ErA]_3$ se dissocie complètement dans la solution aqueuse en Er^{3+} et 3 ErA^- ce qui rend impossible la sorption de l'Er_4A_3 par un autre mécanisme que celui d'échange ionique. La concentration des solutions aqueuses de tel complexe provoque une cristallisation assez rapide étant donné les dimensions réduites des ions qui sont donc capables de former un réseau cristallin compact. Par contre, l'organisation cristalline est compliquée dans le cas des grosses molécules Nd_4A.[8]

---

[13] L. I. Martynenko, Thèse, Moscou, 1959.

[14] Ali Khadi, Thèse, Moscou, 1973.

[15] G. L. Varlamova, Thèse, Moscou, 1971.

[16] L. I. Martynenko, *Nauchn. Dokl. Vysh. Shkoly. Khim. i Khim. Tekhnol.*, **1959**, 84.

[17] L. I. Martynenko, *Zhur. neorg. Khim.*, **1961**, 2704.

Observée spectrographiquement, la différence de la structure des complexes des ETR avec l'acide EDTA de composition Ln_4A_3 permet d'expliquer le comportement différent des ETR yttriques et cériques lors de la séparation par échange ionique des macroquantités des ETR[11,12]. En effet, les terres cériques qui forment les complexes Ln_4A_3 où l'état de quatre ions des ETR est équilibré [18] sont capables d'échanger rapidement par le mécanisme intracomplexe les ions des sphère de coordination extérieure contre ceux de sphère intérieure. Par exemple :

$$Nd^{3+} \cdot aq + 3\,PrA^- \rightleftarrows NdPr_3A_3 \rightleftarrows Pr^{3+} + NdA^- + 2PrA^-$$

Les terres yttriques participent forcément dans un autre mécanisme lié au stade lent de dissociation du complexe stable LnA^-.

Nous avons proposé [10,19] le moyen d'accélérer le processus d'échange qui intervient dans les systèmes contenant les complexes de l'acide EDTA formés par les terres yttriques. Il s'est avéré [10,20] que l'addition dans la solution de LnA^- des acides carboxyliques hydroxylés (citrique, tartrique) provoque la formation des complexes mixtes ; le tableau 2 montre que l'addition d'un acide carboxylique hydroxylé dans le système constitué par acide EDTA, le sulfocationite et les ETR provoque la suppression de la cinétique chimique dans le cas des terres yttriques : en présence de l'acide carboxylique hydroxylé la vitesse d'établissement d'équilibre dans le système est une fonction de la dimension des grains de cationite, de la concentration de solution extérieure et ne dépend pas du temps de contact entre les phases. Nous sommes donc amenés à constater qu'en présence des acides carboxyliques hydroxylés le système d'échange suit les lois de la cinétique d'interdiffusion.

L'introduction d'un ligand concurrent dans le système contenant un complexe relativement stable rend ce complexe labile.

La formation des complexes polynucléaires et ceux aux ligands mixtes, ainsi que des complexes supérieurs favorise donc l'échange entre les ions des ETR se trouvant dans les sphères extérieures et intérieures.

L'ensemble des résultats obtenus suggère la nécessité de prendre en considération les paramètres cinétiques des complexes participants dans le processus de séparation par échange ionique dans la chromatographie à formation des complexes des ETR, afin d'optimiser les régimes technologiques du processus.

---

[18] L. I. Martynenko, G. N. Kupriyanova, N. I. Pechurova, G. L. Varlamova et G. K. Tugusheva, *Zhur. neorg. Khim.*, **16**, 1286 (1971).

[19] L. I. Martynenko, M. G. Yashkarova, V. I. Spitsine et G. A. Artukhina, Rec. travaux sci. déposés VINITI, n° 5470–73 (12 février 1973).

[20] L. I. Martynenko, G. A. Artukhina et V. I. Spitsine, *Doklady Akad. Nauk. S.S.S.R.*, **185**, 600 (1969).

Tableau 2

Variation de $\alpha^{Pr/Nd}$ et de $\alpha^{Er/Ho}$ avec les conditions d'expérience en présence de l'acide citrique (H_3Cit) et tartrique (H_2tart) (la concentration des ions K^+ dans les solutions nos 12 et 13 est la même)

Composition LnR_3 4 g	Diamètre des grains, mm	Eluent	Concentration d'éluent, %		pH de la solution		Temps de contact	α_{exp}
			H_4A	H_2tart (H_3 Cit)	de départ	à l'équilibre		
(Nd, Pr)R_3	0,5	H_4A+ H_3Cit	1,5	1,5	8,10	4,00	0,5	1,84
”	0,5	”	1,5	1,5	8,10	4,60	0,5×2	1,87
”	0,5	H_4A+ H_2tart	0,25	0,25	6,90	4,20	0,5	1,62
”	0,25	”	0,25	0,25	6,90	4,20	0,5×2	1,80
”	0,5	H_4A	0,25	—	8,98	3,95	1,0	1,62
”	0,5	H_4A+ H_2tart	”	0,25	6,80	4,00	1,0	1,94
(Er, Ho)R_3	0,5	”	”	”	6,95	4,30	0,5	1,35
”	0,5	”	”	”	6,95	4,30	0,5×2	1,33
”	0,25	”	”	”	6,95	4,30	0,5	1,62
”	0,5	H_4A	”	”	8,87	4,30	1,0	0,79
(Nd, Pr)R_3	0,5	H_4A	”	—	8,95	3,45	0,5	1,45
”	0,5	H_4A+ H_2tart	”	0,25	6,05	3,60	0,5	1,72

Revue Roumaine de Chimie, 22, 5, 781–786 (1977)

Dedicated to the 70th anniversary
of Professor **CORIOLAN DRĂGULESCU**

ISOMERISM IN COPPER(II) COMPLEXES WITH N-ISOPROPYL- AND N-CYCLOHEXYL-SALICYLALDIMINATES

AKIRA TAKEUCHI and SHOICHIRO YAMADA
Institute of Chemistry, College of General Education, Osaka University, Toyonaka,
Osaka 560, Japan

Received July 12, 1976

Several pairs of planar-tetrahedral isomers and other related species have been isolated for copper(II) complexes with N-α-branched alkyl-salicylaldiminates. Their structures and interconversion have been examined and discussed on the basis of spectral, thermal and X-ray data.

INTRODUCTION

Previous extensive studies have shown that bis(N-alkyl-salicylaldiminato)nickel(II) (abbreviated as Ni(X-sal-alkyl)$_2$) in non-donor solvent exists as an equilibrium mixture consisting of the planar, tetrahedral and associated species. Possibility to isolate various isomeric forms of

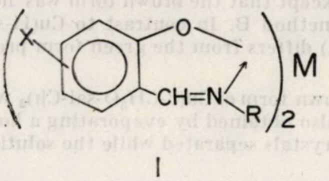

I

the same parent complex is expected to be high, when the energy difference between various configurations is small. This condition may be satisfied, if the ligand is so bulky as to cause steric hindrance to one of the possible structures that is otherwise the most stable.[1] Thus we have recently succeeded in isolating several pairs of isomeric species of Ni(X-sal-i-C_3H_7)$_2$ in crystals.[2,3]

---

[1] S. YAMADA, "Novel in Coordination Chemistry" (ed. by B. J. - Trzebiatowska and M. Rudolph), Polish Academy of Sciences (1974), p. 189.

The stereochemistry of Schiff base copper(II) complexes is similar to that of the nickel(II) complexes in many respects. However, the structural versatility is much more pronounced in the copper(II) than in the nickel(II) complexes, and the stereochemical nature of the species of these copper(II) complexes in solution, including whether any equilibrium may exist or not, has not been completely elucidated.[4-6] It was reported previously that either a planar or a tetrahedral species, and not both, could be obtained in crystals for bis(N-isopropyl-ring-substituted salicylaldiminato)copper(II), the structure of the isolated species being dependent upon X.[7] In spite of extensive studies in the past, no isomeric pairs have been isolated so far, except for some crystal modifications of the N-metyl- and the N-ethyl-analogue.[6] The present paper describes the isolation of the isomers and other related species of Cu(X-sal-α-branched-alkyl)$_2$ and examination of their structures.

EXPERIMENTAL

Materials. Green and brown forms of *Cu(3-CH$_3$O-sal-i-C$_3$H$_7$)$_2$* were obtained, as reported previously.[8]

Cu(5,6,-benzo-sal-i-C$_3$H$_7$)$_2$. The green form was prepared as described previously.[7] The brown form was newly obtained in the following way. A mixture of Cu(5,6-benzo-salal)$_2$ (0.02 mole) and isopropylamine (0.04 mole) in methanol was stirred at 50° ; in 15 min an olive-green precipitate started to separate out. To the suspension was added isopropylamine (0.04 mole), and the solution was heated with stirring for 30 min, when flaky brown crystals separated. Purification was carried out by evaporating at 30° a solution of the brown crystals in benzene or chloroform. The brown form was also obtained by heating the green form on an oil-bath at 105—110° for a few hours.

Cu(H-sal-Ch)$_2$. The brown form was obtained by recrystallizing from hot chloroform the crude product, which had been prepared from Cu(salal)$_2$ and cyclohexylamine, Ch being cyclohexyl.[9]

The green form was isolated in crystals by evaporating at room temperature a solution of the brown form in chloroform (method A). The green form was also obtained by heating the brown form on an oil-bath at 170—180° for a few hours (method B). The green form obtained by method A gave an X-ray diffraction pattern identical with that of the product by method B.

Cu(5-Br-sal-Ch)$_2$. Both the green and the brown form were isolated by methods similar to those for Cu(H-sal-Ch)$_2$, except that the brown form was heated on an oil-bath at 210—220° to yield the green form in method B. In contrast to Cu(H-sal-Ch)$_2$, the green form obtained from the solution (method A) differs from the green form prepared by method B, as discussed later in the present paper.

The green and the brown form of Cu(3-CH$_3$O-sal-Ch)$_2$ were isolated as reported previously.[10] The brown form was also obtained by evaporating a hot chloroform solution of the green form and collecting brown crystals separated while the solution was hot.

---

[2] A. Takeuchi and S. Yamada, *Bull. Chem. Soc. Japan*, **42**, 3046 (1969).

[3] A. Takeuchi and S. Yamada, *Inorg. Chim. Acta*, **8**, 225 (1974).

[4] S. Yamada, *Coord. Chem. Rev.*, **1**, 415 (1966).

[5] R. H. Holm and M. J. O'Connor, *Progr. Inorg. Chem.*, **14**, 253 (1971).

[6] H. S. Maslen and T. N. Waters, *Coord. Chem. Rev.*, **17**, 137 (1975).

[7] L. Sacconi, *Coord. Chem. Rev.*, **1**, 126 (1966) ; L. Sacconi and M. Ciampolini, *J. Chem. Soc.*, **1964**, 276.

[8] A. Takeuchi and S. Yamada, *Bull. Chem. Soc. Japan*, **43**, 3628 (1970).

[9] S. Yamada and H. Nishikawa, *Bull. Chem. Soc. Japan*, **36**, 755 (1963).

[10] A. Takeuchi and S. Yamada, *Bull. Chem. Soc. Japan*, **43**, 3629 (1970).

Adducts of $Cu(3\text{-}CH_3O\text{-sal-Ch})_2$ with CHX_3, X being Cl and Br, were obtained in red-brown crystals by recrystallizing the parent complex from haloform or by exposing the parent complex to the vapour of the haloform.

Cu(5,6-benzo-sal-Ch)$_2$. The green form was obtained in crystals by recrystallizing the crude product prepared from $Cu(5,6\text{-benzo-salal})_2$ and cyclohexylamine. The brown form was obtained by heating the green form on an oil-bath at 220–230°.

Elemental analysis for C, H and N of all the complexes agreed with theoretical values.

Measurements. All the measurements were carried out as reported previously. [3]

RESULTS AND DISCUSSION

Both the square-planar and the pseudo-tetrahedral structure may be allowed for $Cu(X\text{-sal-}\alpha\text{-branched alkyl})_2$, judging from the steric effect arising from the α-branched alkyl. In the present work, we have succeeded in isolating several isomeric pairs and related species of $Cu(X\text{-sal-}i\text{-}C_3H_7)_2$ and $Cu(X\text{-sal-Ch})_2$.

Bis(N-isopropylsalicylaldiminato)copper(II). Both the green and the brown form of $Cu(3\text{-}CH_3O\text{-sal-}i\text{-}C_3H_7)_2$ were isolated.[8] The green form I shows two endothermic peaks at 101 and 123° in the DTA curve, while the brown form II shows only one peak at 123°. With the rise of temperature, form I is transformed at 101° into the brown form II, which eventually melts at 123°.

The structures of the two forms have been determined recently by X-ray crystal analysis. Although form I was once assumed to consist of planar molecules, [8] the X-ray study has revealed that the $Cu(N)_2(O)_2$ in form I (orthorhombic) is not planar but distorted markedly from the planar structure. [11] Form II (monoclinic) is also pseudo-tetrahedral, [12] as presumed previously on the basis of the electronic spectrum.[8] The dihedral angles between the two CuNO planes in the independent complex molecules are 47.4° (I) and 57.9° (II), respectively. A remarkable difference between the two structures lies in the manner of the distortion. The two fold angles between the CuNO plane and $O-C=C-CH=N$ and between the $O-C=C-CH=N$ and the benzene nucleus are 18.2 and 5.3° (averages) for form I, while those for form II are 6.0 and 3.6° (averages), respectively. The form I may be called to be "twisted-umbrella-shaped", being more twisted than form II. The spectrum of I has a *d-d* band at 10.5 and another more intense shoulder at 14.5 kK.

Brown crystals of $Cu(5,6\text{-benzo-sal-}i\text{-}C_3H_7)_2$ have now been isolated, in addition to the olive-green form of the same complex, which was reported previously. [7] The DTA curves indicate that the green, planar form is transformed at 102° into the brown, tetrahedral form, which melts at 190° after undergoing another phase transition at 172°. The brown form shows only one peak at 190°. The spectrum of the brown form has absorption bands at 11.5, 15.3 and 20.5 kK, in agreement with the tetrahedral geometry. Judging from the low transition temperature, which is as low as that of $Cu(3\text{-}CH_3O\text{-sal-}i\text{-}C_3H_7)_2$, it is likely that the green form of $Cu\text{-}(5,6\text{-benzo-sal-}i\text{-}C_3H_7)_2$ may also have a "twisted-umbrella-shaped" structure similar to that of $Cu(3\text{-}CH_3O\text{-sal-}i\text{-}C_3H_7)_2$.

---

[11] H. Tamura, K. Ogawa, A. Takeuchi and S. Yamada, to be published.

[12] T. Ashida, private communication.

Bis(N-cyclohexylsalicylaldiminato ((copper(II). The brown form of $Cu(H\text{-}sal\text{-}Ch)_2$ was previously reported and presumed to have a pseudotetrahedral configuration in non-donor solvents.[9]

The DTA curve of the brown form has two endothermic peaks at 166 and 177°, while that of the olive-green form has only one peak at 177°. Recent X-ray studies have revealed that the $Cu(N)_2\text{-}(O)_2$ in the brown form of $Cu(H\text{-}sal\text{-}Ch)_2$ is perfectly planar.[13] It is highly probable that the olive-green form may have a pseudotetrahedral configuration, since it is the higher temperature form. It may thus be assumed that the brown, planar form is transformed at 166° into the green, tetrahedral one, which eventually melts at 177°. The brown, planar form shows a weak band at 14.1 kK, in addition to more intense shoulders at about 17 and 20 kK. Appearance of the weak band at a very low frequency (14 kK) for the planar copper(II) complex is noteworthy. The olive-green, pseudotetrahedral form shows a broad band at 17.2 kK.

The solid electronic spectrum of the brown form of $Cu(5\text{-}Br\text{-}sal\text{-}Ch)_2$ closely resembles that of the brown, planar form of $Cu(H\text{-}sal\text{-}Ch)_2$, implying that the brown form of $Cu(5\text{-}Br\text{-}sal\text{-}Ch)_2$ also consists of planar molecules similar to those of $Cu(H\text{-}sal\text{-}Ch)_2$.

The DTA curve of the brown form shows two endothermic peaks at 202 and 217°. It is considered that the brown, planar form is transformed at 202° into the green form II, which most probably has a tetrahedral structure. The green form II obtained by heating the brown form shows one peak at 217°, which corresponds to the melting process of the green, tetrahedral form. The electronic spectrum of form II is remarkably similar to that of the green form of $Cu(H\text{-}sal\text{-}Ch)_2$.

The green form I, which is obtained from the chloroform solution, shows only one peak at 185° and no peak at 217°. It is thus clear that the green form I is different from form II. The X-ray powder pattern of form I also differs distinctly from that of form II. One of the most probable structures for form I may be a binuclear structure.

Both the green and the brown form of $Cu(5,6\text{-}benzo\text{-}sal\text{-}Ch)_2$ were isolated in crystals. The green form was obtained by recrystallizing from methanol-chloroform the crude product, which had been prepared by a reaction of $Cu(5,6\text{-}benzo\text{-}salal)_2$ with cyclohexylamine in methanol. The brown form was isolated by heating the green form on an oil-bath at 210°.

The green form probably has a planar configuration, since it exhibits the main *d-d* band maximum at a comparatively high frequency (16.5 kK), in addition to a much weaker band at 8.6 kK. The spectrum of the brown form has bands at 10.5, 14.6 and 20 kK, and is consistent with the tetrahedral configuration.

The DTA curve of the green form has two endothermic peaks at 217 and 239°, while that of the brown form shows only one peak at 239°. The DTA data indicate that the green (planar) form is transformed at 217° into the brown (tetrahedral) form, which eventually melts at 239°.

---

[13] H. TAMURA, K. OGAWA, A. TAKEUCHI and S. YAMADA, Proceedings of the Ann. Meeting of Japan Chem. Soc., Tokyo, April (1975), p. 176; R. P. KASHYAP, J. M. BINDLISH, S. C. BHATIA and P. C. JAIN, *Acta Cryst.*, **15**, S 146 (1975).

Both the green and the brown form of $Cu(3\text{-}CH_3O\text{-sal-Ch})_2$ were isolated in crystals. Since the green form shows an electronic spectrum, which is almost identical with that of the green form of Cu(5,6-benzo-sal-Ch)$_2$, it probably has a planar configuration. The DTA curve of the green form has two endothermic peaks at 177 and 179°, the separation between the two peaks being enormously small. It is thus considered that the green, planar form is transformed at 177° into the brown form, which probably has a tetrahedral structure. The green form shows another endothermic peak at 300°. The brown form thus prepared again turns back into the olive-green, planar form, when allowed to stand in the atmosphere at room temperature for a few hours.

Adducts of the type $Cu(3\text{-}CH_3O\text{-sal-Ch})_2 \cdot 2CHX_3$, X being Cl and Br, have been isolated in brown crystals. The spectrum of the bromoform adduct is almost identical with that of the brown form of the parent complex, having bands at 10.5, 14.5 and 21 kK and resembles the spectrum of $Cu(3\text{-}CH_3O\text{-sal-}t\text{-}C_4H_9)_2$, which has a tetrahedral stereochemistry. The brown chloroform adduct lost chloroform molecules in the atmosphere so readily that it was not possible to measure its solid spectrum. Judging from its apparent similarity in many respects to the bromoform adduct, the chloroform adduct may also consist of tetrahedral copper(II) complexes. In the adducts of this type the CHX_3 molecules may not be involved in the bonding with copper(II) ion, but the hydrogen atom of the CHX_3 molecule is considered to form hydrogen bonding with the phenolic oxygen atom. The electron density on the oxygen atom would thereby become lower, and the ligand field weakened, the geometry other than the original planar one being more favoured. The chloroform solution is brown, and the solution spectrum shows that in chloroform the tetrahedral species does exist in an appreciable amount.

CONCLUSIONS

As summarized in table 1, two or three forms having different stereochemistries have been isolated in crystals for the same parent complexes. It has so far been believed that one form only can be isolated in the solid state. However, the present study has clearly shown that this view is no longer correct. The present work also supports the assumption that in solutions of these copper(II) complexes in non-donor solvents there may exist an equilibrium mixture of various species having different stereochemistries.[14]

Inspection of Table 1 indicates that there seem to be two types of electronic spectra for the "essentially planar" copper(II) complexes, probably suggestive of variation in the more detailed structure. The copper(II) complexes present more varieties in the manner and extent of distortion from the square-planar structure than the corresponding nickel(II) complexes.[1,4-6] Since even a slight change in the distortion may give rise to a delicate but apparent spectral change, one cannot safely

---

[14] H. P. Fritz, B. M. Golla, H. J. Keller, and K. E. Schwarzhaus, *Z. Naturforsch.*, **21b**, 725 (1966).

Table 1

Isolated species of bis(N-isopropyl- and N-cyclohexylsalicylaldiminato)copper(II), Cu(X-sal-R)$_2$[a,b]

R	X	low temp. form	high temp. form	trans. temp. °C
i-C_3H_7	3-CH_3O	ps-td(green)[c] 10.5, 14.5, 20.2	ps-td(brown) 8.7, 13.3, 18.5	101
i-C_3H_7	5,6-benzo	ps-td(green) 11.4, 14.0, 20.1	ps-td(brown) 11.5, 15.3, 20.5	102
Ch	H	pl(brown) 14.1, 17.0, 20.0	ps-td(green) 17br	166
Ch	5-Br[d]	pl(brown) 14.0, 17.0, 20.1	ps-td(green) 17br	202
Ch	5,6-benzo	pl(green) 8.6, 16.5, 20.3	ps-td(brown) 10.5, 14.5, 21.0	217
Ch	3-CH_3O	pl(green) 8.7, 16.5, 20.2	ps-td(brown) 10.5, 14.5, 21.0	177

a In the table there are also included band maxima or shoulders in kK; b ps-td: pseudo-tetrahedral, pl: planar; c twisted-umbrella-shaped; d There is the third form.

guess the approximate stereochemistry of the Schiff base copper(II) complexes from their colours alone, contrary to the current view.

The copper(II) complexes studied in the present work show very similar solution spectra, which have bands or shoulders at 9—10.5, 14—15 and 20.5—22 kK, though they are not as well-defined as the solid spectra. Inspection of the solution spectra indicates that in such non-donor solvents as chloroform and ethanol Cu(X-sal-*i*-C_3H_7)$_2$ and Cu(X-sal-Ch)$_2$ exist rather predominantly as tetrahedral species, probably in equilibrium with other species having planar (and even multinuclear) structures.

The authors are grateful to Dr. K. Ogawa and Mrs. H. Tamura for helpful discussion.

Revue Roumaine de Chimie, **22**, 5, 787–792 (1977)

Dedicated to the 70th anniversary
of Professor Coriolan Drăgulescu

RED-BROWN PIGMENTS IN THE $Cr_2O_3-TiO_2-WO_3$ SYSTEM

T. P. TĂVALĂ *, N. GR. BRÎNZAN * and V. FLOREA **
* Chemical Research Center, Bv. Mihai Viteazul 24, Timişoara, Romania
** "Emailul Roşu" Factory Mediaş, Romania

Received September 3, 1976

A method for preparing red-brown pigments in the $Cr_2O_3-TiO_2-WO_3$ system has been worked out taking into account the "heterovalent isomorphism" condition of the reaction product. The variation effect of the ratio between the chromophoric group and the other oxide reactants, as well as the effect of the mineralizers on the development of the colour have been studied. The mechanism of colour formation, the synthesis conditions, the higher pigmentation properties and the wide variety of colour shades increase the theoretical interest and the practical value of these pigments.

1. INTRODUCTION

The red-brown pigments were prepared by the pyrosynthesis method, from finely powdered mixtures of oxides of the $Cr_2O_3-TiO_2-WO_3$ system, with and without mineralizers.

The literature[1-3] describes this oxidic system as a generator of ochre-red-brown shades under certain synthesis conditions.

The Cr^{3+} ion inserted in the TiO_2 host lattice with rutile-structure, in the presence of WO_3, does not preserve its green colour but develops red-brown shades depending on the:

- ratio of the oxidic reagents;
- absence or presence of mineralizers and their nature;
- non-stoichiometry of the composition;
- thermal parameters of the synthesis.

In the present paper we investigated the influence of some of these factors upon the development of shades from the oxidic $Cr_2O_3-TiO_2-WO_3$ system.

---

[1] O. Reuman, *Glas-Email-Keramo-Technik*, **16**, 289 (1965).
[2] R. Regnier, *L'Industrie céramique*, **636**, 21 (1971).
[3] P. Eisbein, *Keramische Zeitschrift*, **23**, 214 (1971).

Table 1

The composition and the main spectral characteristics of the pigments from the Cr_2O_3 – TiO_2 – WO_3 system

Number of the pigment	Ratio of oxide components, TiO_2 : Cr_2O_3 : WO_3	Mineralizer %	Chromaticity co-ordinates			Range of spectral absorption $\Delta\lambda$, nm	Dominant wavelength λ_d, nm	Luminosity Y
			x	y	z			
1	1.00 : 0.13 : 0.22	—	0.4404	0.3828	0.1768	442–502	485.0	13.10
2	1.00 : 0.13 : 0.22	LiCl-x	0.4042	0.3713	0.2245	420–506	484.1	10.60
3	1.00 : 0.13 : 0.22	NaCl-x	0.4458	0.3855	0.1687	436–506	485.1	12.70
4	1.00 : 0.13 : 0.22	KCl-x	0.4391	0.3511	0.2098	480–564 716–742	487.4	10.90
5	1.00 : 0.13 : 0.22	H_3BO_3-x	0.4293	0.3717	0.1990	454–520	485.8	9.00
6	1.00 : 0.13 : 0.22	Borax-4x	0.3737	0.3681	0.2582	458–518	480.8	7.70
7	1.00 : 0.14 : 0.28	NaCl-x	0.4241	0.3848	0.1911	444–506	483.8	13.30
8	1.00 : 0.40 : 0.60	LiCl-x	0.3663	0.3454	0.2883	450–530	485.3	7.00
9	1.00 : 0.40 : 0.60	NaCl-x	0.4145	0.3670	0.2185	442–508	485.4	8.10
10	1.00 : 0.04 : 0.07	LiCl-x	0.3790	0.4518	0.1692	428–508	437.0	16.50
11	1.00 : 0.04 : 0.07	NaCl-x	0.4253	0.4854	0.0893	450–510	477.3	19.60
12	1.00 : 0.13 : 0,22	NaCl-10x	0.4457	0.3870	0.1673	430–502	485.0	13.50
13	1.00 : 0.13 : 0.22	KCl-10x	0.4417	0.3991	0.1592	420–508	483.4	15.90
14	— 1.00 : 1.60	—	0.3562	0.3475	0.2963	480–564 716–742	483.1	4.80
15	— 1.00 : 1.60	NaCl-x	0.3788	0.3581	0.2631	446–508 714–742	483.9	6.20
16	1.00 : 0.53 —	—	0.3690	0.3224	0.3066	458–465 598–614	602.0	10.50

2. EXPERIMENTAL

The details concerning the intimate mixture preparation of the powders of raw and auxiliary materials as well as the main technological operations have been described in a previous paper.[4]

The raw materials used were : titanium dioxide — anatase, chromic oxide and hydrated ammonium tungstate. Lithium, natrium, and sodium chlorides, as well as boric acid and borax were used as mineralizers.

All the reactants were of analytical grade; the size of powder particles was of 36 ± 5 microns.

The optimal thermal factors, temperature *(T)* and time *(t)* were established experimentally.

The proportion of oxidic components, the mineralizers and the spectral characteristics of the pigments prepared, numbered from 1 to 16, are presented in table 1.

The mechanism of colour formation and the influence of the main factors determining the red-brown shades, developed by the compositions of the prepared pigments, was studied by means of the derivatographic, roentgenographic, spectrophotometric, colorimetric and magnetic analysis.

With the purpose of determining the optimal thermal factors and the physico-chemical transformations which take place during the pyrosynthesis, derivatograms were recorded with a Paulik-Erdely derivatograph type MOM (Hungary). The heating rate was of 12°/minute.

The X-ray diffraction was accomplished with the TUR—M—61 Roentgen diffractometer, using the CuKα radiation.

The pigment shades were defined by their reflexion spectra, recorded with a UNICAM SP 800, spectrophotometer, England adapted for powders.

The colour components of each pigment were determined with the MOMCOLOR Tristimulus Colorimeter, Hungary. The zero method was used in conditions of diffused illumination, C illuminant, 45° observation angle, with a standard of achromatic colour, and a 2° visual field. In order to achieve a diffuse surface of the pigment tablets submitted to determination, the pieces of the tablet-pressing device were sanded. The dosage and pressing of powders were accomplished in similar conditions at a 2.4×10^7 N/m^2 pressure.

The x, y, z colour coordinates of the pigments 1—16 were obtained by calculation.[5] On this basis, the dominant wavelength λ_d was calculated for each pigment.

The magnetic susceptibility was measured by means of the Gouy method.

3. INTERPRETATION OF THE RESULTS

Figure 1 presents the derivatogram of pigment 3 from table 1. It shows the successive physico-chemical changes, taking place during the pyrosynthesis of the pigments in the $Cr_2O_3-TiO_2-WO_3$ system in the presence of mineralizers.

The crystalline structures and the pigments colour are formed in reactions taking place in the 750°—1080° temperature range. This range is characterized by endothermic effects due to a partial ionization of the reagents (including the mineralizer) and to a slight reduction of the composition. These are the conditions for the insertion of the Cr^{3+} colour centre and of the W^{6+} charge compensating ion, in the rutile lattice which becomes distorted.

The nonstoichiometry of the intermediate compositions is determined by the formation of vacancies in the two crystalline sublattices :[4]

---

[4] T. P. Tăvală, N. Gr. Brînzan and V. Florea, *Revista Materiale de construcţii*, **6**, 135 (1976).

[5] W. D. Wright, "The Measurement of Colour", Third Edition, Hilger & Watts LTS, London, 1964, p. 118.

in the anionic sublattice, V_a anionic vacancies caused by the substitution of Ti^{+4} ion by Cr^{3+} of the chromophore grouping, thus :

$$Ti^{4+}_{1-3x}\, Cr^{3+}_{4x}\, (V_a)_x O^{2-}_2, \qquad (1)$$

in the cationic sublattice, V_c cationic vacancies as a consequence of the substitution of Ti^{4+} ion by the W^{6+} charge compensating ion, thus :

$$Ti^{4+}_{1-3x}\, W^{6+}_{2x}\, (V_c)_x\, O^{2-}_2. \qquad (2)$$

This mechanism leaves unchanged the oxidation degree of the system, as the electronic defects, which appear in the intermediary phases at the cations, are finally compensated in the rutile-type distorted crystalline structure of the mixed oxides, thus :

$$Ti^{4+}_{1-3x}\, Cr^{3+}_{2x}\, W^{6+}_x\, O^{2-}_2, \qquad (3)$$

the condition of the "heterovalent isomorphism" being respected.

The W^{6+} cation imposes octahedral symmetry to the Cr^{3+} cation during the insertion in the rutile lattice with the same symmetry, thus making it responsible for the formation of red-brown shades.

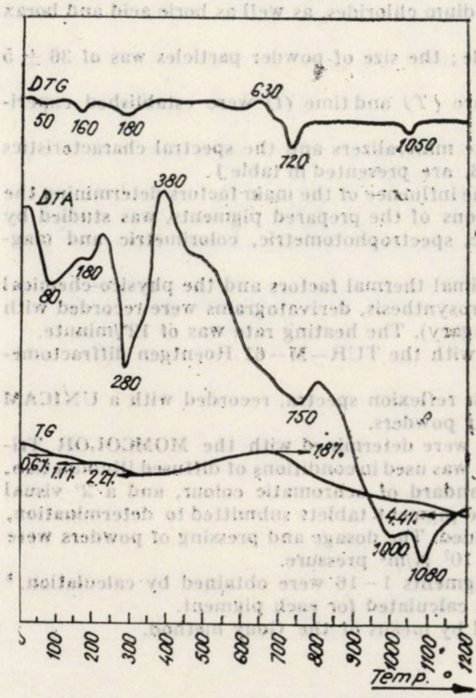

Fig. 1. — Derivatogram of pigment 3.

In the absence of the TiO_2 host lattice, the dark red-brown colour is obtained from the reaction between chromic oxide and tungsten trioxide. In our case pigments number 13 and 14 (table 1) were obtained, corresponding to the chromium tungstate composition, Cr_2WO_6, or to the mixed oxide, $Cr_2O_3 \cdot WO_3$.

The colour formation mechanism in these compositions is different. It is based on the alloying of an oxide in which the cation, W^{6+}, has a noble gas electronic configuration, with the oxide of a transition metal, Cr^{3+}, the structure of which may generate defects. [6]

The chromic oxide reacts with titanium dioxide under the same technological conditions but in the absence of a charge compensating ion, it confers to the composition, (pigment 16), the green colour specific to the Cr^{3+} ion in tetrahedral coordination.

The heating of the $TiO_2 - WO_3$ powder mixture does not lead to pigment formation.

---

[6] L. Tcheichvili and W. A. Weyl, *The Glass Industry*, **44**, 145 (1963).

The crystalline structure and the mechanism of red-brown shades formation in the oxidic $Cr_2O_3-TiO_2-WO_3$ system with and without mineralizers, described above, is confirmed by the X-ray diffractograms of pigments number 15 and 3 (table 1), presented in figures 2 and 3, respectively.

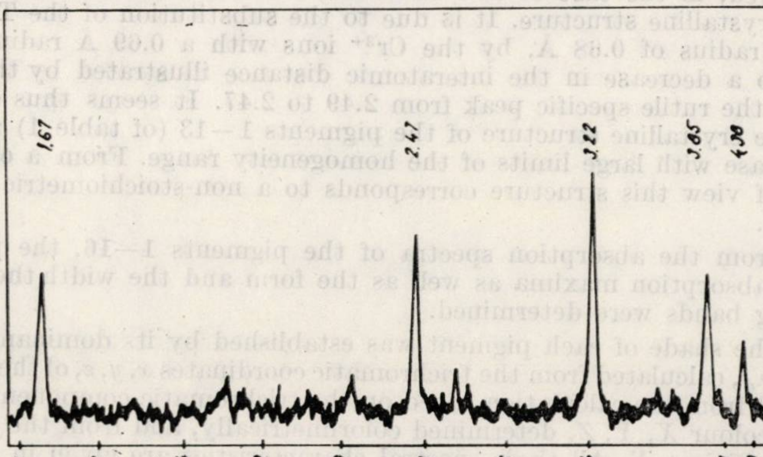

Fig. 2. — X-ray diffraction pattern of pigment 15.

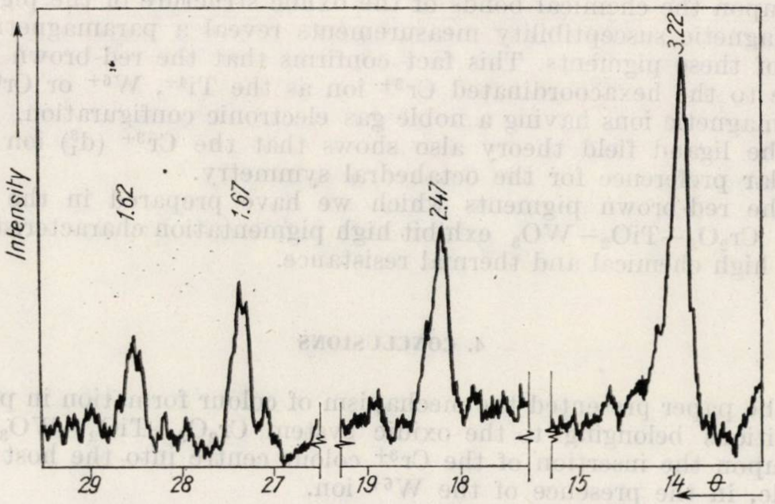

Fig. 3. — X-ray diffraction pattern of pigment 3.

Both diffractograms illustrate mixed crystal structures of the distorted rutile lattice. Thus, the peaks corresponding to the interplanar distances 4.38, 3.22, 2.47 and 1.67 from figure 2 are characteristic of the X-ray diffraction pattern of the mixed $Cr_2O_3 \cdot WO_3$ oxides, and the peak at 3.85 belongs to the unreacted WO_3. In figure 3 the peaks from 3.22, 2.47 and 1.67 are of the same relative intensities as the corresponding ones in fig. 2 ; the 1.62 peak belongs to TiO_2. The peak from 2.47 may be considered, in the case of this structure, characteristic of the distorted rutile crystalline structure. It is due to the substitution of the Ti^{4+} ion, with a radius of 0.68 Å, by the Cr^{3+} ions with a 0.69 Å radius. This leads to a decrease in the interatomic distance illustrated by the shifting of the rutile specific peak from 2.49 to 2.47. It seems thus obvious that the crystalline structure of the pigments 1—13 (of table 1) appears as a phase with large limits of the homogeneity range. From a chemical point of view this structure corresponds to a non-stoichiometric combination[7].

From the absorption spectra of the pigments 1—16, the position of the absorption maxima as well as the form and the width the corresponding bands were determined.

The shade of each pigment was established by its dominant wavelength λ_d, calculated from the trichromatic coordinates x, y, z, of the colour, resulted from the calculation based on the trichromatic component values of the colour X, Y, Z, determined colorimetrically, and from the luminosity coefficient Y. All these spectral characteristics are given in table 1.

A slight increase of the bathochromic effect in the development of the red-brown shades was observed with the increase of the Cr_2O_3 and WO_3 content, as a function of the specific polarising action of the mineralizer upon the chemical bonds of the oxidic structure of the pigments.

Magnetic susceptibility measurements reveal a paramagnetic character of these pigments. This fact confirms that the red-brown shades are due to the hexacoordinated Cr^{3+} ion as the Ti^{4+}, W^{6+} or Cr^{6+} ions are diamagnetic ions having a noble gas electronic configuration.

The ligand field theory also shows that the Cr^{3+} (d_1^3) ion has a particular preference for the octahedral symmetry.

The red-brown pigments which we have prepared in the oxidic system $Cr_2O_3—TiO_2—WO_3$ exhibit high pigmentation characteristics as well as high chemical and thermal resistance.

4. CONCLUSIONS

The paper presented the mechanism of colour formation in pigment compositions belonging to the oxidic system $Cr_2O_3—TiO_2—WO_3$. It is based upon the insertion of the Cr^{3+} colour centre into the host lattice of rutile, in the presence of the W^{6+} ion.

The latter has a charge compensating role, in accordance with the heterovalent isomorphism rule. Under these conditions, the Cr^{3+} ion assumes an octahedral symmetry and determines the development of red-brown shades, depending upon the oxidic reagent ratio, the mineralizer nature, the thermal factors and the asymmetry of the rutile crystalline lattice, of the pigments studied.

---

[7] R. Colonques, "La Non-stoechiométrie", Masson et Cie, Paris, 1971, p. 102.

Revue Roumaine de Chimie, 22, 5, 793–799 (1977)

Herrn Professor Dr. Coriolan Drăgulescu
zum 70. Geburtstag gewidmet

DIE THERMISCHE ZERSETZUNG EINIGER HEXACYANOKOMPLEXEN. I

SILBER-AMMONIUM ODER ALKYLAMMONIUM HEXACYANOFERRATE

P. TRIBUNESCU, ECATERINA MERCA und OTILIA FACSKÓ
Fakultät für Industriechemie, Str. Bocşa 6, Timişoara

Eingegangen am 3. September 1976

Es wurde die thermische Zersetzung der Mischverbindungen $Ag_2NH_4[Fe(CN)_6]$, $Ag_2[(CH_3)_4N]$ $[Fe(CN)_6]$ und $Ag_2[(C_2H_5)_4N]$ $[Fe(CN)_6]$ in Inertgasatmosphäre untersucht und mit der thermischen Zersetzung unter gleichen Bedingungen der Verbindung $Ag_3[Fe(CN)_6]$ verglichen. An Hand von T.G. und D.T.A.-Kurven sowie auf Grund von Chromatogrammen der Gasgemische die bei der Zersetzung entstanden, wurden die Etappen der Zersetzung festgelegt. Diese Etappen sind im Großen dieselben, unabhängig von den untersuchten Verbindungen. Anderseits wurden für die verschiedenen Etappen unterschiedliche Temperaturen festgestellt was der Art der äußeren Kationen zugeschrieben werden kann.

In unseren früher erschienen Mitteilungenen[1,2] wurden die Ergebnisse von Untersuchungen über Gleichgewichte bei Niederschlägen aus Lösungen mitgeteilt, wobei die Bedingungen zur Bildung von Mischverbindungen $Ag_2NH_4[Fe(CN)_6]$, $Ag_2[(CH_3)_4N]$ $[Fe(CN)_6]$ und $Ag_2[(C_2H_5)_4N]$ $[Fe(CN)_6]$ festgelegt wurden. In der vorliegenden Arbeit sind die Ergebnisse die sich auf die thermische Zersetzung der oben erwähnten Verbindungen im Vergleich mit denen die sich bei der Zersetzung der Silberverbindung $Ag_3[Fe(CN)_6]$ erhalten, gegeben.

Die Untersuchungen über thermische Zersetzungen von Hexacyanokomplexen sind in letzter Zeit recht häufig. Verschiedene Fachzeitschriften bringen über verschiedene Verbindungen umgehend Auskunft. [3-6]

---

[1] P. Tribunescu, E. Merca und O. Facskó, *Bcl. şt. tehn. Inst. Polit. „Traian Vuia" Timişoara, Seria Chimie*, **20** (34), 107 (1975).

[2] P. Tribunescu, O. Facskó und E. Merca, *Bul. şt. tehn. Inst. Polit. „Traian Vuia" Timişoara, Seria Chimie*, **21** (35) (1976) im Druck.

[3] P. K. Gallagher und B. Pescott, *Inorg. Chem.* **9**, 2510 (1970).

[4] G. B. Seifer, *Zhur. neorg. Khim.*, **5**, 68 (1960).

[5] B. Mohai, *Acta Chim. Acad. Sci. Hung.*, **62**, 217 (1969).

[6] P. Tribunescu, G. Pârlea und C. Drăgulescu, *Zhur. neorg. Khim.*, **13**, 3256 (1968).

Aus diesem Grund haben wir es für notwendig empfunden, diese Ergebnisse mit den von uns erarbeiteten, über die neu synthetisierten Verbindungen, zu vervollständigen.

EXPERIMENTELLES

Die thermische Zersetzung der untersuchten Verbindungen erfolgte im Temperaturbereich von Zimmertemperatur bis 800° mit Hilfe eines „Setaram"-Derivatographs. Diese Einrichtung ermöglichte die gleichzeitige Aufnahme sämtlicher thermischer Kurven und die gaschromatographische Analyse der erhaltenen Gase aus derselben Probe. Die thermische Zersetzung erfolgte in Helium, für einige Verbindungen auch vergleichsweise in Luft, indem die Derivatogramme mit einer Aufheizgeschwindigkeit von 5°/Min aufgenommen wurden.

Die zu untersuchenden Substanzen wurden in den unter [1,2] angeführten Bedingungen erhalten und ihre Reinheit auch durch chemische Analyse geprüft. Die bei der thermischen Zersetzung erhaltenen Diagramme sowie die bei jeder Temperatur stattfindenden Prozesse sind im weiteren für jede Verbindung dargestellt.

ERGEBNISSE UND DISKUSSIONEN

$Ag_3[Fe(CN)_6]$. Das bei der thermischen Zersetzung von $Ag_3[Fe(CN)_6]$ erhaltene Diagramm ist in Abbildung 1 dargestellt. Sowohl die Kennlinien vom typ T.G. als auch D.T.A. weisen auf drei hintereinander folgende Prozesse. Dabei ist der erste (bei 220°) und der letzte (bei 640°) exotherm, hingegen der zweite (bei 405°) endotherm.

Im ersten Prozeß wird das dreiwertige Eisen zu zweiwertigem reduziert. Dabei entsteht eine Gitteränderung gefolgt von Ausscheidung von Dicyan, entsprechend der Reaktion :

$$\text{I. } 6\, Ag_3[Fe(CN)_6] \xrightarrow[\text{exotherm}]{180-320^\circ} Ag_2Fe[Fe(CN)_6] \cdot 4\, Ag_4[Fe(CN)_6] + 3(CN)_2$$

Der zweite Prozeß erfolgt bedeutend schneller zwischen 380–410° und besteht in der Reduktion des Silbers, bedingt durch das CN^--Anion, das als Dicyan ausgeschieden wird :

$$\text{II. } Ag_2Fe[Fe(CN)_6] \cdot 4\, Ag_4[Fe(CN)_6] \xrightarrow[\text{endotherm}]{380-410^\circ} 6\, Fe(CN)_2 + 18\, Ag + 9(CN)_2$$

Aus der oben angeführten Reaktion ist neben der Silberreduktion noch eine Depolymerisation des Eisen(II)hexacyanoferrats(II) zu Eisencyanid auf Grund des Schemas :

$$Fe_2[Fe(CN)_6] \longrightarrow 3\, Fe(CN)_2$$

zu beachten.

Die Untersuchungen mit Röntgenstrahlen von Seifer [4] haben bewiesen, daß die Depolymerisation etwa bei 410° stattfindet. Da aber auch die Silberreduktion etwa bei dieser Temperatur stattfindet ist anzunehmen, daß die Depolymerisation und die Silberreduktion gleichzeitig stattfinden.

Die Wärmeaufnahmen bei 405° ist als Symptom der endothermen Depolymerisation anzusehen.

Im letzten Prozeß findet die Zersetzung von $Fe(CN)_2$ mit Bildung von Stickstoff und Dicyan als gasförmige Stoffe und festem Fe_3C statt:

$$\text{III. } 6\ Fe(CN)_2 \xrightarrow[\text{exotherm}]{560-720^\circ} 2\ Fe_3C + N_2 + 5(CN)_2$$

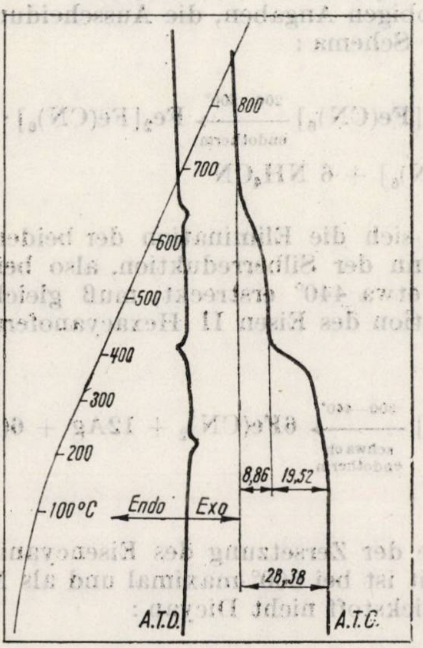

Abb. 1 — T.G. und D.T.A.-Kurven der Verbindung $Ag_3[Fe(CN)_6]$.

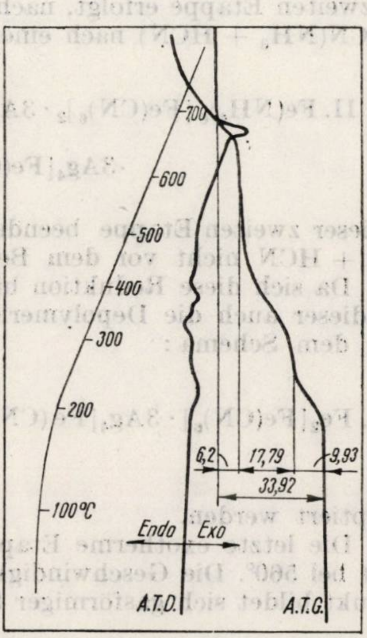

Abb. 2 — T.G. und D.T.A.-Kurven der Mischverbindung $Ag_2NH_4([Fe(CN)_6]$.

Es ist als sehr wahrscheinlich anzunehmen, daß das Verhältnis Stickstoff-Dicyan nicht dem aus dem Schema entspricht. Es muß in Betracht gezogen werden, daß das Dicyan sich teilweise in Kohlenstoff und Stickstoff zersetzt. Die gemessenen partiellen sowie totalen Gewichtschwunde entsprechen laut Kennlinie T.G., sehr gut mit den berechneten Werten. Dabei muß in Betracht gezogen werden, daß bei niederen Temperaturen die Ausscheidung von Dicyan verspätet sein kann und das Verhältnis Stickstoff-Dicyan in der letzten Etappe nicht rigurös konstant sein muß.

$Ag_2NH_4[Fe(CN)_6]$. Zum Unterschied von der vorgehenden Verbindung hat die Zersetzung von $Ag_2NH_4[Fe(CN)_6]$ vier Etappen. Von diesen sind die ersten drei nicht klar unterscheidbar sondern teilweise überlappt. Das Diagramm der Erwärmung ist in Abbildung 2 dargestellt. Die erste Etappe, leicht exotherm beginnt bei 140°, etwas niedriger als bei der einfachen Silberverbindung und entspricht der Eisenreduktion nach dem

Schema :

$$\text{I. } 6\ Ag_2NH_4[Fe(CN)_6] \xrightarrow[\text{exotherm}]{140-220^\circ} Fe(NH_4)_6[Fe(CN)_6]_2 \cdot 3Ag_4[Fe(CN)_6] + \\ + 3(CN)_2$$

Die niedrigere Temperatur am Anfang dieses Prozesses bewirkt eine Verspätung der Ausscheidung der CN-Gruppen. Somit überlappt sich teilweise die zweite Etappe der NH_4CN Elimination mit der ersten. In der zweiten Etappe erfolgt, nach obigen Angaben, die Ausscheidung von $NH_4CN(NH_3 + HCN)$ nach einem Schema :

$$\text{II. } Fe(NH_4)_6[Fe(CN)_6]_2 \cdot 3Ag_4[Fe(CN)_6] \xrightarrow[\text{endotherm}]{200-300^\circ} Fe_2[Fe(CN)_6] \cdot \\ \cdot 3Ag_4[Fe(CN)_6] + 6\ NH_4CN$$

In dieser zweiten Etappe beendet sich die Elimination der beiden Gase $NH_3 + HCN$ nicht vor dem Beginn der Silberreduktion, also bei etwa 300°. Da sich diese Reduktion bis etwa 440° erstreckt, muß gleichzeitig mit dieser auch die Depolymerisation des Eisen II -Hexacyanoferrats II nach dem Schema :

$$\text{III. } Fe_2[Fe(CN)_6] \cdot 3Ag_4[Fe(CN)_6] \xrightarrow[\substack{\text{schwach} \\ \text{endotherm}}]{300-440^\circ} 6Fe(CN)_2 + 12Ag + 6(CN)_2$$

akzeptiert werden.

Die letzte exotherme Etappe der Zersetzung des Eisencyanids beginnt bei 560°. Die Geschwindigkeit ist bei 660° maximal und als Nebenprodukt bildet sich gasförmiger Stickstoff nicht Dicyan :

$$\text{IV. } 6\ Fe(CN)_2 \xrightarrow[\text{exotherm}]{560-700^\circ} 2\ Fe_3C + 10C + 6N_2$$

In den Etappen I und II wurde eine Differenz von ± 1% zwischen berechneten und experimentellen Verlusten gefunden. Die Ursachen liegen an den oben angeführten Überlappungen. Bei den Gesamtverlusten besteht eine sehr gute Übereinstimmung (33,65% berechnet; 33,80% experimentell). Bei der Zersetzung in der Luft werden dieselben Etappen, mit Unterschied der letzteren, festgestellt.

$Ag_2[(CH_3)_4N]\ [Fe(CN)_6]$. Die vier oben erwähnten Etappen sind auch hier vorhanden, bloß daß die drei ersten bei höheren Temperaturen stattfinden. Das läßt darauf schließen, daß die Tetramethyl-ammonium-Gruppe, entgegen jeder Erwartung, der Mischverbindung mehr thermische Stabilität zuführt als die Ammonium-Gruppe. Selbst die Ausscheidung des Tetramethylammoniumcyanids beginnt erst bei 300°, also mit 100° höher als das des Ammoniumcyanids. In Abbildung 3 ist das Diagramm des thermischen Verhaltens von $Ag_2[(CH_3)_4N]\ [Fe(CN)_6]$ aufgezeichnet. Die erste Etappe erfolgt zwischen 220—250° und die D.T.A. - Kurve ist durch exotherme Effekte gekennzeichnet. Es folgt ein endothermer Effekt — wahrscheinlich eine Änderung der festen Phase. Die Reaktion ist :

$$\text{I. } 6\ Ag_2[(CH_3)_4N]\,[Fe(CN)_6] \xrightarrow[\text{exotherm}]{220-250^\circ}$$

$$\rightarrow Fe[(CH_3)_4N]_6\,[Fe(CN)_6]_2 \cdot 3\ Ag_4[Fe(CN)\,(CN_6)] + 3\ (CN)_2$$

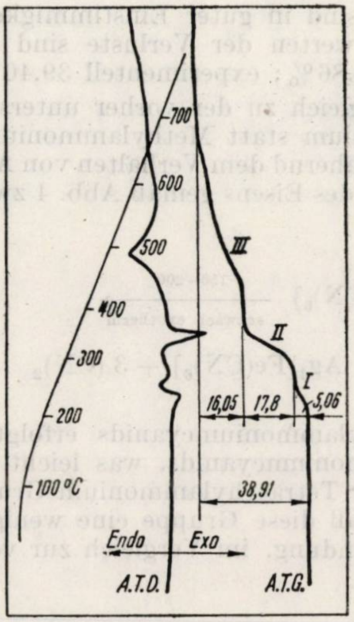

Abb. 3 — G.T. nud D.T.A.-Kurven der Mischverbindung $Ag_2[(CH_3)_4N][Fe(CN)_6]$.

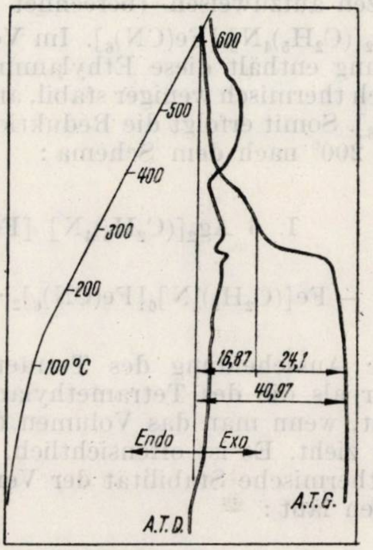

Abb. 4 — T. G. und D.T.A.-Kurven der Mischverbindung $Ag_2[(C_2H_5)_4N][Fe(CN)_6]$.

Nach der Reduktion des dreiwertigen Eisens in zweiwertiges und der Ausscheidung von sechs CN-Gruppen — die die Einsenreduktion bedingt haben — folgt der Prozeß der Ausscheidung des Methylammoniumcyanids — gekennzeichnet durch einen sehr ausgeprägten exothermen Effekt bei 330° :

$$\text{II. } Fe[(CH_3)_4N]_6\,[Fe(CN)_6] \cdot 3\ Ag_4[Fe(CN)_6] \xrightarrow[\text{exotherm}]{300-350^\circ}$$

$$\rightarrow Fe_2[Fe(CN)_6] \cdot 3\ Ag_4[Fe(CN)_6] + 6\ (CH_3)_4NCN$$

In der dritten Etappe findet die Reduktion des Silbers mit der Depolymerisation des komplexen Anions gleichzeitig statt :

$$\text{III. } Fe_2[Fe(CN)_6] \cdot 3\ Ag_4[Fe(CN)_6] \xrightarrow[\text{endotherm}]{420-520^\circ} 6\ Fe(CN)_2 + 12\ Ag + 6(CN)_2$$

Die letzte Etappe, die Zersetzung des Eisencyanids, erfolgt in demselben Temperaturbereich, und wird von Bildung gasförmigen Stickstoffs nach dem Schema :

$$\text{IV. } 6\ \mathrm{Fe(CN)_2} \xrightarrow[\text{exotherm}]{560-750^\circ} 2\ \mathrm{Fe_3C} + 10\ \mathrm{C} + 6\mathrm{N_2}$$

begleitet.

Die pro Etappe berechneten Verluste sind in guter Einstimmigkeit mit den experimentellen. Bei den Gesamtwerten der Verluste sind jedoch Differenzen aufzuweisen (berechnet 40,86 %; experimentell 39,40 %).

$Ag_2[(C_2H_5)_4N]\,[Fe(CN)_6]$. Im Vergleich zu der vorher untersuchten Verbindung enthält diese Ethylammonium statt Methylammonium und ist folglich thermisch weniger stabil, annähernd dem Verhalten von $Ag_2NH_4\,[Fe(CN)_6]$. Somit erfolgt die Reduktion des Eisens gemäß Abb. 4 zwischen 150 und 200° nach dem Schema :

$$\text{I. } 6\ \mathrm{Ag_2[(C_2H_5)_4N]\ [Fe(CN)_6]} \xrightarrow[\text{schwach exotherm}]{150-200^\circ}$$

$$\to \mathrm{Fe[(C_2H_5)_4N]_6[Fe(CN)_6]_2 \cdot 3\ Ag_4[Fe(CN)_6]} + 3\ \mathrm{(CN)_2}$$

Die Ausscheidung des Tetraethylammoniumcyanids erfolgt etwa 50° tiefer als die des Tetramethylammoniumcyanids, was leicht zu erklären ist, wenn man das Volumen der Tetraethylammonium-Gruppe in Betracht zieht. Es ist offensichtlich, daß diese Gruppe eine weniger gediegene thermische Stabilität der Verbindung, im Vergleich zur vorigen, zukommen läßt :

$$\text{II. } \mathrm{Fe[(C_2H_5)_4N]_6\ [Fe(CN)_6]_2 \cdot 3\ Ag_4[Fe(CN)_6]} \xrightarrow[\text{endotherm}]{250-280^\circ}$$

$$\to \mathrm{Fe_2[Fe(CN)_6] \cdot 3\ Ag_4[Fe(CN)_6]} + 6\ \mathrm{(C_2H_5)_4NCN}$$

Die oben angegebene Reaktion erfolgt mit großer Geschwindigkeit innerhalb eines kleinen Temperaturbereiches, wobei die Reduktion des Silbers langsamer, zwischen 330—430°, und wahrscheinlich begleitet von der Depolymerisation des Hexacyanoanions stattfindet :

$$\text{III. } \mathrm{Fe_2[Fe(CN)_6) \cdot 3Ag_4[Fe(CN)_6]} \xrightarrow[\text{endotherm}]{330-430^\circ} 6\ \mathrm{Fe(CN)_2} + 12\ \mathrm{Ag} + 6\mathrm{(CN)_2}$$

Die letzte Etappe der Zersetzung des Eisencyanids beginnt bei 580°, mit Ausscheidung von gasförmigem Stickstoff und kleinen Mengen von Dicyan statt :

$$\text{IV. } 6\ \mathrm{Fe(CN)_2} \xrightarrow[\text{exotherm}]{580-700^\circ} 2\ \mathrm{Fe_3C} + 10\ \mathrm{C} + 6\ \mathrm{N_2}$$

Es wird auch diesmal eine sehr gute Übereinstimmung der berechneten Gewichtsverluste mit den experimentellen verzeichnet (berechnet 46,93 %; experimentell 46,60 %).

ZUSAMMENFASSUNG

Aus den vorgelegten und ausgearbeiteten Ergebnissen steht fest, daß die thermische Zersetzung von Komplexverbindungen in Inertgasen in vier getrennten identischen Etappen stattfindet. Eine Ausnahme bildet das einfache Silberhexacyanoferrat(III), das sich in drei Etappen zersetzt.

Die erste Etappe ist durch die Eisenreduktion vom drei zum zweiwertigen Eisen gekennzeichnet. Mit Ausnahme der Verbindung mit Silber und Tetramethylammonium, erfolgt die Zersetzung unter 200°.

In der zweiten Etappe erfolgt die Ausscheidung der volatilen Cyanverbindungen und somit ist diese Etappe bei der einfachen Silberverbindung nicht anwesend. Die minimale Temperatur entspricht NH_4CN, die maximale $(CH_3)_4NCN$.

In der dritten Etappe, zwischen 350—400° finden gleichzeitig zwei Prozesse statt : die Reduktion des Silbers zu Metall und die Depolymerisation des Hexacyanianions mit Bildung des Eisencyanids. Dieses zersetzt sich dann in der letzten Etappe — bei etwa 600° — in Fe_3C, Stickstoff und Kohlenstoff. Bei der einfachen Silber-Verbindung wird in der letzten Etappe Dicyan und Stickstoff in Verhältnis 5 : 1 frei. Bei den anderen Verbindungen ist das dominierende Gas der Stickstoff. Dieser Stickstoff enthält am Anfang der Etappe Dicyan wie es deutlich aus der chromatographischen Analyse ersichtlich ist.

Revue Roumaine de Chimie, **22**, *5*, 801–804 (1977)

Dedicated to the 70th anniversary
of Professor Coriolan Drăgulescu

CORRELATION BETWEEN ABSOLUTE CONFIGURATIONS OF COBALT(III) COMPLEXES AND THEIR CHROMATOGRAPHIC BEHAVIOUR ON ION-EXCHANGE CELLULOSE *

KAZUO YAMASAKI and YUZO YOSHIKAWA
Department of Chemistry, Faculty of Science, Nagoya University, Nagoya, 464 Japan

Received September 6, 1976

Relationships between absolute configurations of cobalt(III) complexes, and the elution order from a column of ion-exchange cellulose were studied. For tervalent complex cations the Δ-form was eluted first by HCl from the column of *P*-cellulose, while for univalent complex cations the Λ-form first. For both univalent and tervalent complex anions the Δ-form was eluted first by HCl from the column of DEAE-cellulose.

Since Werner succeeded in resolving the $[CoCl(NH_3)(en)_2]^{2+}$ ion by the fractional crystallization of its diastereoisomers,[1] various methods were devised for resolution of metal complexes. Among them the preferential adsorption technique on quartz crystals was first used by Tsuchida [2] and co-workers in 1936 to achieve a partial resolution of non-ionic $[CoCl(dmgH)_2(NH_3)]$ (dmgH=dimethylglyoximate ion) by shaking a solution of the complex with powdered laevo- and dextro-rotatory quartz crystals. Complex ions such as $[Co(en)_3]^{3+}$, $[CoCl(NH_3)(en)_2]^{2+}$, and $[CoCl_2(en)_2]^+$, and $[Co(C_2O_4)_3]^{3-}$ were also partially resolved by this technique.[2] Several other investigators have applied this technique to numerous substances including metal complexes with various optically active adsorbents like powdered starch,[3] lactose,[4] ion-exchange resins with optically active groups,[5] ion-exchange resins loaded with optically active substances,[6] etc. In no instances, however, complete resolution of complexes was reported.

---

* A part of this paper was read at the XIIth ICCC (1969) held in Sydney, Australia.

[1] A. Werner, *Ber. dtsch. chem. oses.* **45**, 121 (1912).

[2] R. Tsuchida, M. Kobayashi and A. Nakamura, *Bull. Chem. Soc. Japan*, **11**, 38 (1936).

[3] H. Krebs and R. Rasche, *Z. anorg. Chem.*, **276**, 236 (1954).

[4] T. Moeller and E. Gulyas, *J. Inorg. Nuclear Chem.*, **5**, 245 (1958).

[5] S. Tsuboyama and M. Yanagita, *Sci. Papers Inst. Phys. Chem. Res. Tokyo*, **53**, 245 (1959).

We have used ion-exchange cellulose, P- and DEAE-cellulose as adsorbents to resolve cobalt(III) complexes, and succeeded in achieving partial resolutions of $[\mathrm{Co(en_3)}]\mathrm{Cl_3}$ and $\mathrm{K[Co(edta)]}$ with HCl as an eluent.[7] The sign of rotation and the resolution percentage found for the first eluted fraction were $(-)_{589}$ and 7% for the former complex, and $(-)_{589}$ and 51% for the latter complex. Then we have studied several other procedures[8] to increase resolution percentages. First a 0.2M sodium $(+)_{589}$-tartrate solution was used to elute $[\mathrm{Co(en)_3}]^{3+}$ ion adsorbed on a *P*-cellulose column. The $(+)_{589}$ enantiomer was eluted first with the resolution percentage of 80%. Thus the optically active eluent, sodium $(+)_{589}$-tartrate enhanced remarkably the resolution percentage. Next butyl alcohol saturated with water was used as the solvent of the same complex, and a solution of tartaric acid in a mixture of concentrated HCl and butyl alcohol as the eluent. The resolution percentage of the first fraction increased up to 92%, but still no complete resolution was achieved. Finally an ion-exchange dextran, SE-Sephadex (Pharmacia, Sweden) was used as the adsorbent for resolving the same complex with sodium $(+)_{589}$-tartrate as the eluent. The elution curve showed two completely separated peaks corresponding to the enantiomers, the Δ- and Λ-forms, and the complete chromatographic separation of $[\mathrm{Co(en)_3}]^{3+}$ ion was achieved for the first time.[8]

Since then this technique, column chromatography on SP-Sephadex[*] with an optically active eluent, has been successfully applied to complete resolution of various complexes such as $[\mathrm{Co(dien)_2}]^{3+}$,[9] $[\mathrm{Co(ibn)_3}]^{3+}$,[10] $[\mathrm{Co(penten)}]^{3+}$,[11] $[\mathrm{Co(linpen)}]^{3+}$,[12] $[\mathrm{Co(tmd)_3}]^{3+}$,[13] u-*cis*-$[\mathrm{Co(ida)(dien)}]^{+}$,[14] $[\mathrm{Rh(en)_3}]^{3+}$,[15] etc. The abbreviations used for the above complexes are dien = diethylenetriamine, ibn = 2-methyl-1,-2,-propanediamine, penten = N, N, N′, N′-tetrakis(2-aminoethyl)ethylenediamine, linpen = linear pentaethylenehexamine, tmd = tetramethylenediamine, and ida = iminodiacetate ion. This technique is effective not only to resolve complexes, but also to separate geometrical isomers and diastereoisomers which cannot be isolated by other techniques. The examples are $[\mathrm{Co(dien)_2}]^{3+}$,[9] $[\mathrm{Co\{(R)\,pn\}_3}]^{3+}$,[16] $[\mathrm{Co\{(-)cptn\}_3}]^{3+}$,[17]

---

[*] The SE-Sephadex is now replaced by the SP-Sephadex with sulfopropyl groups.

[6] Y. Yoshino, H. Sugiyama, S. Nogaito and H. Kinoshita, *Sci. Papers Coll. General Educa. Univ. Tokyo*, **16**, 57 (1966).

[7] Y. Yoshikawa and K. Yamasaki, *Inorg. Nucl. Chem. Lett.*, **4**, 697 (1968).

[8] Y. Yoshikawa and K. Yamasaki, *Inorg. Nucl. Chem. Lett.*, **6**, 523 (1970).

[9] F. R. Keene, G. H. Searle, Y. Yoshikawa, A. Imai and K. Yamasaki, *Chem. Commun.*, **1970**, 784; Y. Yoshikawa and K. Yamasaki, *Bull. Chem. Soc. Japan*, **45**, 179 (1972).

[10] M. Kojima, Y. Yoshikawa and K. Yamasaki, *Bull. Chem. Soc. Japan*, **46**, 1687 (1973).

[11] Y. Yoshikawa, E. Fujii and K. Yamasaki, *Bull. Chem. Soc. Japan*, **45**, 3451 (1972).

[12] Y. Yoshikawa and K. Yamasaki, *Bull. Chem. Soc. Japan*, **46**, 3448 (1973).

[13] J. Fujita and H. Ogino, *Chem. Lett.*, **1974**, 57.

[14] Y. Yoshikawa, A. Kondo and K. Yamasaki, *Inorg. Nucl. Chem. Lett.*, **12**, 351 (1976).

[15] Unpublished result of K. Yamasaki.

[16] M. Kojima, Y. Yoshikawa and K. Yamasaki, *Inorg. Nucl. Chem. Lett.*, **9**, 689 (1973).

[17] H. Toftlund, E. Pedersen, *Acta Chem. Scand.*, **26**, 4019 (1972).

$[Co(dabp)\{(R)pn\}_2]^{3+}$,[18] etc., where (R)pn, (−)cptn and dabp denote R-propylenediamine, $(-)_{589}$-*trans*-1,2-diaminocyclopentane, and 2,2′-diaminobiphenyl respectively.

So far commercially available adsorbents with chiral structures have been used, but, if optically active exchanging groups are introduced into Sephadex itself, a more efficient cation-exchanger will be produced. Fujita, Yoshikawa and Yamatera prepared Sephadex having $(-)_{589}$-tartrate residues as exchanging groups, and used it to resolve $[Co(en_3)]Cl_3$ with naturally occurring $(+)_{589}$-tartrate as eluent.[19] A highly efficient and complete resolution was achieved for $[Co(en_3)]Cl_3$ and $[Co(tn)_3]Cl_3$.[20]

Resolution by the column chromatographic technique is based on the interaction of chiral adsorbents with complexes having chiral structures in the presence of chiral eluents. Therefore the use of optically inactive eluents like hydrochloric acid or sodium sulfate as mentioned above is not effective, achieving only a partial resolution. Although resolution percentages are low in these cases, optically active complexes with the same sign of rotation are eluted first, that is, a correlation seems to exist between the absolute configuration of the enantiomer eluted, and the elution order. If such a correlation exists, it may be useful for determining absolute configurations. We have first studied the system, *P*-cellulose(adsorbent) — HCl(eluent).[21] The results are shown in Table 1. In Table 1 the sign of the longer wavelength CD peak in the first absorption region of the cobalt(III) complexes are given for the first eluted fraction, CD being circular dichroism. The absolute configurations determined by the X-ray method [22] are also shown. The absolute configurations assigned indirectly are shown by (Δ) and (Λ).

The results show that for the tris(diamine)complexes, the 6N-type complexes (No. 1 — No. 10), the enantiomers with the Δ-configuration are eluted first except for the $[Co(tn)_3]^{3+}$ ion which forms six-membered chelate rings. All the other complexes form five-membered chelate rings. For the univalent cations (No. 11—14) the enantiomers with the Δ-configuration are eluted first by HCl.

In Table 2 the results for the system, DEAE-cellulose (adsorbent) — HCl (eluent) are shown. As in Table 1 the sign of the CD peak, and the absolute configuration of the first eluted fraction are given.

The results show that for the tervalent and univalent complex anions (N°15 — N°19) the enantiomers with the Δ-configuration are eluted first by HCl from DEAE-cellulose.

The above results may be useful for determining the absolute configurations of the complex cations and anions, although the numbers of the cobalt(III) complexes studied are not large, and some exceptions are found.

---

[18] T. Tanimura, H. Ito, J. Fujita, K. Saito, S. Hirai and K. Yamasaki, *J. Coord. Chem.*, 3, 161 (1973).

[19] M. Fujita, Y. Yoshikawa and H. Yamatera, *Chem. Lett.*, **1974**, 1515; **1975**, 473.

[21] M. Fujita, Y. Yoshikawa and K. Yamatera, *Chem. Commun.*, **1975**, 941.

[21] K. Yamasaki and Y. Yoshikawa, *Proc. XII Intern. Conf. Coord. Chem. Sydney, Australia*, **1969**, 98.

[22] Y. Saito, *Coord. Chem. Reviews*, 13, 305 (1974). In this paper a complete list of the coordination compounds whose absolute configurations were determined by X-rays during the period of 1955—1972 is found.

Table 1

Correlation between the sign of the CD peak of the first eluted fraction and the absolute configuration, P-cellulose

N⁰	Ions	Sign of the longer wave-length CD peak in the first absorption region	Absolute configuration determined by X-rays (IUPAC Nomenclature)
1	$[Co(en)_3]^{3+}$	−(minus)	Δ ref. [22]
2	$[Co(chxn)_3]^{3+}$ ·(lel)$_3$-form	−	Δ [22]
3	$[Co\{(R)pn\}_3]^{3+}$, (lel)$_3$-form	−	Δ [22]
4	$[Co(tn)_3]^{3+}$	+(plus)	Λ [22]
5	$[Co(bpy)_3]^{3+}$	− *	(Δ) [23]
6	Cis-$[Co(NH_3)(en)_2]^{3+}$	−	(Δ) [24]
7	U-fac-$[Co(dien)_2]^{3+}$	−	ΔΛΔ [9,22]
8	$[Co(penten)]^{3+}$	−	ΔΛΔ [10,22]
9	$[Co(mepenten)]^{3+}$ **	−	ΔΛΔ [10,22]
10	$[Co(linpen)]^{3+}$ (isomer V)	− *	(ΔΛΔΔΛΔ) [12]
11	$[Co(C_2O_4)(en)_2]^{+}$	+	Λ [25]
12	Cis-$[Co(NO_2)_2(en)_2]^{+}$	+	Λ [26]
13	Cis-α-$[Co(NO_2)_2(trien)]^{+}$	+	(Λ) [27]
14	U-cis-$[Co(ida)(dien)]^{+}$	−	(ΛΔΛ) [14]

* Sign of the main CD peak, not of the longer wavelength peak.

** Mepenten denotes N,N,N′,N′-tetrakis(2-aminoethyl)-1,2-propanediamine.

Table 2

Correlation between the sign of the CD peak of the first eluted fraction and the absolute configuration. DEAE-cellulose

Ions	Sign of the longer wavelength CD peak in the first absorption region	Absolute configuration determined by X-rays
15. $[Co(C_2O_4)_3]^{3-}$	−(minus)	Δ ref. [28]
16. $[Co(rdas)_3]^{3-}$*	−	(Δ) [29]
17. $[Co(C_2O_4)_2(en)]^{-}$	−	(Δ) [30]
18. Cis-$[Co(ida)_2]^{-}$	−	(Δ Λ Δ) [31]
19. $[Co(edta)]^{-}$	−	(Δ Λ Δ) [32]

* rdas denotes rac-diaminosuccinate ion.

As for the system, ion-exchange Sephadex — optically active eluents, the situation is more complicated, and it is difficult to find a simple relationship between the elution order of a cobalt(III) complex and its absolute configuration, although a complete resolution is achieved.

---

[23] J. Ferguson, C. J. Hawkins, N. A. P. Kane-Maguire and H. Lip, *Inorg. Chem.*, **8**, 771 (1969).

[24] A. J. McCaffery, S. F. Mason and B. J. Norman, *J. Chem. Soc.*, **1965**, 5094.

[25] T. Aoki, K. Matsumoto, S. Ooi and H. Kuroya, *Bull. Chem. Soc. Japan*, **46**, 159 (1973).

[26] K. Matsumoto and H. Kuroya, *Bull. Chem. Soc. Japan*, **45**, 1755 (1972).

[27] The absolute configuration of this complex was assigned in analogy with that of the complex containing 3,8-dimethyltriethylenetetramine. See M. Ito, F. Marumo and Y. Saito, *Acta Crystallogr.*, **B28**, 457 (1972).

[28] K. R. Butler and M. R. Snow, *J. Chem. Soc. A*, **1971**, 565.

[29] M. Kojima, Y. Yoshikawa and K. Yamasaki, *Bull. Chem. Soc. Japan*, **48**, 879 (1975).

[31] F. P. Dwyer, and D. P. Mellor, Editors, "Chelating Agents and Metal Chelates", Academic Press, New York, 1964, p. 228.

[31] C. W. V. Saum and B. E. Douglas, *Inorg. Chem.*, **8**, 1145 (1969).

[32] R. D. Gillard, *Spectrochim. Acta*, **20**, 1431 (1964).

NOTE POUR LES AUTEURS

La Revue Roumaine de Chimie publie des articles en anglais, français, russe, allemand ou espagnol. Les auteurs sont priés d'envoyer des articles et comptes rendus inédits.

Les manuscrits seront dactylographiés à deux intervalles. La bibliographie, les tableaux et la légende des figures seront placés après le texte.

Si l'article fait partie d'une série numérotée, le titre de la partie précédente sera indiqué dans une note au bas de la première page.

Chaque article sera précédé d'un résumé comprenant quinze lignes au maximum.

Les références bibliographiques dans le texte seront faites par des exposants sans parenthèses, et paraîtront comme des notes au bas de chaque page.

Les publications périodiques mentionnées dans la bibliographie seront présentées suivant les prescriptions internationales : le nom de l'auteur précédé de l'initiale du prénom, le titre du périodique abbrégé conformément à « Chemical Abstracts », et souligné par une ligne, le numéro du tome indiqué par des chiffres arabes et souligné par deux lignes, suivi de la première page de l'article ; à la fin, l'année de la parution sera placée entre parenthèses. Le numéro de la revue ne sera pas indiqué si les pages du volume sont numérotées consécutivement.

Les textes des livres ou traités inclueront : les noms des auteurs, les initiales du prénom, le titre du livre entre guillemets et sans être souligné, le numéro du tome précédé par l'abbréviation « vol. » (ou « Bd. »), le numéro de l'édition, les éditions (the publisher), la localité de la parution du livre, l'année de la parution et la page de la référence précédée(s) par l'abbréviation « p » (ou « S »).

Les brevets seront indiqués comme suit : l'auteur ou la firme, le pays et le numéro du brevet, la date et la revue (Chem. Abstr.). Par ex. : M. Jones (to Union Carbide C$^{o.}$), Brit. Pat. 601 238,2 Sept. 1959, *Chem. Abstr.* 54, 12808 (1960).

Les diagrammes seront tracés à l'encre de Chine sur papier calque. Les tableaux et les figures (en nombre strictement nécessaire) seront numerotés par des chiffres arabes. Les courbes dans les figures seront numérotées par des chiffres arabes et leur explication sera donnée dans la légende des figures. Prière de ne pas inscrire les mêmes données dans les tableaux et les figures. Chaque tableau aura un titre. On indiquera dans le texte la place approximative des tableaux et des figures. Les formules chimiques seront incluses dans le texte ; en outre, elles seront transcrites sur papier calque, à l'encre de Chine.

Les auteurs sont priés d'indiquer les caractères italiques (en soulignant les lettres au croyon), ainsi que tout autre caractère spécial ; les préfixes *ortho*, *meta*, *para*, *cis*, *trans*, etc. seront soulignés pour indiquer leurs caractères italiques et ne seront jamais écrites avec des majuscules.

Aucune correction à main ne sera admise sur le manuscrit. Les corrections seront frappées à la machine. Les lettres grecques ou autres symboles spéciaux seront insérés à la main à l'encre clairement.

Le manuscrit sera signé par l'auteur.

Le colonne-titre aura 50 lettres au maximum.

L'entière responsabilité du contenu des articles appartient aux auteurs.

PRINTED IN ROMANIA

TRAVAUX PARUS AUX ÉDITIONS DE L'ACADÉMIE DE LA RÉPUBLIQUE SOCIALISTE DE ROUMANIE

I. G. MURGULESCU, **Introducere în Chimia fizică. Vol. I. Atomi, molecule, legătură chimică** (Introduction à la Chimie Physique, Ier vol. Atomes, molécules, liaison chimique), 1976, 559 p,. 36 lei .

P. BALTĂ, E. BALTĂ, **Introduction to the physical chemistry of the vitreous state**, co-édition avec Abacus Press, 1976, 400 p., 39 lei.

I. GĂLĂŢEANU, **Radiochimia aplicată. Metode şi probleme** (La radiochimie appliquée. Méthodes et problèmes), 1976, 305 p., 19 lei.

FR. A GOTHARD, **Echilibre lichid-vapori. I. Baze teoretice şi metode de calcul** (Equilibres liquide-vapeurs, I. Bases théoriques et méthodes de calcul), 1975, 262 p., 28 lei.

CONST. GH. MACAROVICI, DAN MACAROVICI, **Chimia oxizilor dubli şi utilizările lor** (La Chimie des oxydes doubles et leur utilisation), 1975, 194 p,. 13 lei.

ELENA CEAUŞESCU, **Research work on synthesis and caracterization of macromolecular compounds. Contributions**, 1974, 251 p., 20 lei.

I. ZUGRĂVESCU et MAGDA PETROVANU, **Chimia N-Ilidelor** (La chimie des N-Ylures), 1974, 347 p., 19 lei.

MARGARETA AVRAM, **Antidăunători** (Pesticides), 1974, 494 p., 41 lei.

CR. SIMIONESCU, VIORICA RUSAN et N. POPA, **Chimia algelor marine** (La Chimie des algues marines), 1974, 211 p., 18 lei.

TIBERIU NĂŞCUŢIU, **Metode radiochimice de analiză** (Méthodes radiochimiques d'analyse), 1973, 384, p. 23 lei.

MARIA FITI, **Dozimetria chimică a radiaţiilor ionizate** (La dosimétrie chimique des radiations ionisantes), 1973, 240 p., 13,50 lei.

MIHAI FLORESCU, **Eficienţa economică a cercetării ştiinţifice** (L'efficience économique de la recherche scientifique), 1972, 115 p., 15 lei.

GEORGETA LĂZĂRESCU, **Sistematizarea informaţiilor în Chimia organică** (La systématisation des informations dans la Chimie organique), 1972, 252 p., 10,50 lei.

LYDIA-MARIA VAICUM, **Biodegrabilitatea detergenţilor** (La biodégrabilité des détergents), 1971, 254 p., 16 lei.

TIBERIU NĂŞCUŢIU, **Metode radiometrice de analiză** (Méthodes radiométriques d'analyse), 1971, 346 p., p., 19,50 lei.

I. ZUGRĂVESCU et L.. STOICESCU-CRIVETZ, **Polimeri heterociclici** (Polymères hétérocycliques) 1971, 190 p., 9,50 lei.

1978 FEB 16

43426

Lei 25.—
($ 30 pour un abonnement annuel)

I. P. I. – c. 7119

F 1103

ACADÉMIE DE LA RÉPUBLIQUE SOCIALISTE DE ROUMANIE

REFERÁLVA

Vagy -

Fu

REVUE ROUMAINE DE CHIMIE

TOME 22
N° 6
Juin 1977

EDITURA ACADEMIEI REPUBLICII SOCIALISTE ROMÂNIA

Rev. Roumaine Chim.

RECHAX, 22, 6, p. 805–964 (1977), Bucarest

ACADÉMIE DE LA RÉPUBLIQUE SOCIALISTE DE ROUMANIE

COMITÉ DE RÉDACTION

Rédacteur en chef :

I. G. MURGULESCU, membre de l'Académie de la République Socialiste de Roumanie

Rédacteurs en chef adjoints :

A. T. BALABAN et V. EM. SAHINI, membres correspondants de l'Académie de la République Socialiste de Roumanie

Collège de rédaction :

EM. BRATU, ELENA CEAUŞESCU, ECATERINA CIORĂNESCU-NENITZESCU, C. DRĂGULESCU, CR. SIMIONESCU, membres de l'Académie de la République Socialiste de Roumanie; P. SPACU, membre correspondant de l'Académie de la République Socialiste de Roumanie; MARGARETA AVRAM, I. HAIDUC, D. I. MARCHIDAN, I. MOLDOVAN, G. NIAC et D. SĂNDULESCU

La Revue Roumaine de Chimie paraît 10 fois par an. Toute commande de l'étranger (fascicules ou abonnements) sera adressée à ILEXIM — Departamentul Export-Import Carte (Livres)/Departamentul Export-Import Presă (Revues), P.O.B. 136—137 télex 11226, Bucarest 12, 3, str. 13 Decembrie, Roumanie

Les manuscrits, les livres et les revues proposés en échange ains que toute correspondance seront envoyés à la rédaction :

REVUE ROUMAINE DE CHIMIE

23, str. Dumbrava Roşie, Bucarest, Roumanie, téléphone 12 41 60

EDITURA ACADEMIEI REPUBLICII SOCIALISTE ROMÂNIA

125, Calea Victoriei, Bucarest, 71021, Roumanie, téléphone : 50 76 80

ORSZÁGOS MŰSZAKI KÖNYVTÁR ÉS DOKUMENTÁCIÓS KÖZPONT 1883

REVUE ROUMAINE DE CHIMIE

Tome 22, N° 6 Juin 1977

I. G. MURGULESCU and MARILENA ŞERBAN, On the viscosity of molten metals. V. Dependence of viscosity on the mean vibration frequency . . . 807–809

V. EM. SAHINI and SIMONA BĂDILESCU, Collision-induced light absorption in liquid mixtures . . . 811–814

F. ARCE, J. L. ARMESTO, J. CASADO y M. A. RIOS, Estudio conformacional y de constantes de acoplamiento hiperfino en radicales libres. Aproximacion INDO . . . 815–825

RODICA VÎLCU, I. GĂINAR and C. LEPĂDATU, Second interaction virial coefficient. II. Ar + H_2 and CH_4 + H_2 systems . . . 827–838

CAMELIA BELDIE, Thermodynamic and transport properties of the polyelectrolyte solutions . . . 839–848

GH. MARCU, MARIANA RUSU and LIVIA OCHEŞEL, Heteropolytungstates with U(IV) as central ion. Synthesis and physico-chemical studies . . 849–855

A. DAOUD, A. THRIERR-SOREL, R. PERRET et B. CHAILLOT, Préparation et caractérisation de tétrachloromanganates (II) d'ammoniums monosubstitués linéaires . . . 857–863

ILEANA I. STĂNOIU, MARIA PARASCHIV, EUGENIA GÂRD and A. T. BALABAN, Isotope effects in electronic absorption spectra of CH_3/CD_3-substituted six-membered heteroaromatics . . . 865–867

F. CUIBAN, ALFA LUPEA, MARCELA SILAŞI and MARIANA ŞORA, Obtention of the *o*-nitrophenylsuccinic acid and of some functional derivatives . . . 869–875

R. BACALOGLU, T. KORODI, A. FLORESCU und G. OSTROGOVICH, Nucleophile Substitutionen an Kohlensäure-Derivate. IX. Kinetik und Mechanismus der Alkoholyse von Kohlensäure-Dichlorid-N-Aryl-Imiden 877–883

ILEANA BARACU, EUSTANŢA TĂRNĂUCEANU and I. NICULESCU-DUVĂZ, Potential anticancer agents. XIII. Synthesis of new aliphatic and cycloaliphatic N-nitrosoureas . . . 885–898

H. KHALIFA, Y. M. ISSA and A. T. HAJ-HUSSEIN, Spectrophotometric studies on some chromotropic acid azo dyes in aqueous buffer solutions 899–906

E. G. GEORGESCU and M. D. GHEORGHIU, The reaction of cyclobutadiene with sterically hindered dienophiles . . . 907–909

CR. I. SIMIONESCU and MIHAELA MACOVEANU, The grafting of the poly(ethylene-terephthalate) under radiofrequency electrical discharge conditions . . . 911–921

Rev. Roumaine Chim. **22**, *6*, 805–964 (1977), Bucarest

D. MUNTEANU and I. NANU, Perspectives for industrial production of poly(olefins) graft copolymers 923–930

C. LITEANU and IOANA ILEANA PANOVICI, Frequentometric determination under the detection limit of N-methyl-2-pyrrolidone in styrene by IR spectrometry 931–936

T. SIMONESCU and V. RUSU, New analytical applications of some sulphonamide compounds. VI. Sodium *m*-silversulphamoylbenzoate, a new reagent for the determination of carbon monoxide in the air 937–944

NATALIA HURDUC und I.-A. SCHNEIDER, Der thermische Abbau von Poly(methylmethacrylat) unter nicht isothermen Bedingungen 945–951

I. MANOVICIU, VIRGINIA MANOVICIU und C. DAVIDESCU, Ölmodifizierte Terephthalatglycerinalkydharze 953–961

COMPTES RENDUS 963–964

Revue Roumaine de Chimie, 22, 6, 807–809 (1977)

ON THE VISCOSITY OF MOLTEN METALS. V[1]

DEPENDENCE OF VISCOSITY ON THE MEAN VIBRATION FREQUENCY

I. G. MURGULESCU and MARILENA ŞERBAN
Institute of Chemistry, Department of Physical Chemistry and Electrochemical Technology,
Bd. Republicii 13, Bucharest, Romania

Received September 29, 1976

The aim of this paper is to evaluate the viscosity coefficient of metallic melts starting from a model involving the mean vibration frequencies. The mean vibration frequency of liquid particles is assumed to be equal to that of solid particles, at the melting point. The theoretical values of the preexponential constant agree with the experimental values.

A previous work [2] has suggested to evaluate the viscosity coefficient of metal melts, by using relation :

$$\eta = \frac{R}{\gamma M}\frac{\rho T}{\nu}\exp(E/RT) \qquad \textbf{(1)}$$

in which ν represents the vibration frequency of atoms in liquid state supposed to be independent of temperature and equal to that corresponding to the melting temperature. It represents a unique frequency which was evaluated by means of Mott's relation [3] whereby it is correlated to the vibration frequency of solid particles at the melting point. Thus equation (1) becomes :

$$\eta = \frac{R}{\gamma M}\frac{\exp(L/3RT_m)}{\nu_S}\rho T\exp(E/RT) \qquad (2)$$

The packing coefficient γ is $\sqrt{2}$. The vibration frequency of solid particles at the melting point has been evaluated by Lindemann's relation.[4]

The present paper shows that an acceptable relation can be obtained for the viscosity coefficient of the metal melt by introducing, instead of

---

[1] Part IV: M. Şerban, *Rev. Roumaine Chim.*, **22**, 35 (1977).
[2] I. G. Murgulescu and M. Şerban, *Rev. Roumaine Chim.*, **19**, 1417 (1974).
[3] N. F. Mott, *Proc. Roy. Soc.*, **146**, 465 (1934).
[4] F. A. Lindemann, *Phys. Ztschr.*, **11**, 609 (1910).

ν frequency in eqn. (1), $\bar{\nu}$ mean frequency defined by relation :

$$\bar{\nu} = \frac{\int_0^{\nu_m} \nu \, \mathrm{d}Z}{3N} \tag{3}$$

dZ represents the number of frequencies comprised between ν and $\nu + \mathrm{d}\nu$ and ν_m, the maximum vibration frequency of the system supposedly assimilable with $3N$ harmonic oscillators per mole.

Assuming that the mean frequency will not change when passing from the solid state to the liquid state, it is possible to evaluate the dZ number by using expression :

$$\mathrm{d}Z = \frac{9N}{\nu_m^3} \nu^2 \, \mathrm{d}\nu \tag{4}$$

from the Debye theory, concerning the specific heats of solids.

By introducing the dZ number from eqn. (4) into eqn. (3) and by integrating, there results :

$$\bar{\nu} = \frac{3}{4} \nu m \tag{5}$$

The ν_m frequency is correlated to the characteristic Debye temperature θ_D by the known relation :

$$\nu_m = \frac{k}{h} \theta_D \tag{6}$$

Therefore, the mean frequency assumes the value :

$$\bar{\nu} = \frac{3}{4} \frac{k}{h} \theta_D \tag{7}$$

By introducing this value into eqn. (1) we obtain the new equation of viscosity :

$$\eta = \frac{4}{3} \frac{Nh}{\gamma} \frac{\rho T}{M \theta_D} \exp{(E/RT)} \tag{8}$$

which, by introducing the numerical values of physical constants, becomes :

$$\eta = 3.76 \times 10^{-3} \frac{\rho T}{M \theta_D} \exp(E/RT) \tag{9}$$

Since values θ_D are known in metals, eqn. (9) can be verified. Table 1 lists comparatively the values of preexponential constants calculated by means of equation (9) and their experimental values in normal metals. The last but one column also contains data calculated by means of equation (8) of the work mentioned above, [2] deduced from equation (2) by simplification of $\exp(L/3RT_m)$ with γ and by evaluation of the ν_S frequency with Lindemann's relation.

Table 1

Comparison between the theoretical values of the preexponential constant given by eqn. (9) and the experimental values

Element	θ_D, K	$A \times 10^7$, $\mathrm{cm^2 s^{-1} degree^{-1}}$		
		eqn. (9)	eqn. (8)^2	experim.
Na	164	9.973	9.285	9.346 ; 8.841
K	99.4	9.674	9.267	8.976 ; 13.13
Rb	58	7.584	6.974	7.146
Cs	42	6.736	6.141	6.209
Cu	318	1.861	1.981	2.697 ; 0.779
Ag	211	1.652	1.804	1.893 ; 1.946 ; 1.975
Au	160	1.193	1.274	1.766
Al	375	3.716	4.096	4.209 ; 5.630
Pb	88	2.062	2.235	2.061 ; 2.819 ; 2.905
Fe	423	1.592	1.848	2.515 ; 0.958 ; 0.897
Co	385	1.657	1.766	1.155 ; 0.972
Ni	375	1.708	1.788	1.521 ; 1.348 ; 1.382

The agreement between the new theoretical and experimental values is as good as that obtained in the previous work. The two groups of theoretical values are very close to each other in the case of compact metals; they differ more markedly in alkaline metals.

A paper in press [5] demonstrates that the frequencies calculated from the characteristic temperatures lead to Lindemann's relation with 2.44×10^{12} coefficient in alkaline metals and 2.81×10^{12} in compact metals. Since all the data reported in the previous paper have been obtained by using Lindemann's relation with 2.8×10^{12} coefficient, the data corresponding to alkaline metals are somewhat smaller.

The θ_D values listed in the table have been selected from a larger number of data, being the values which have led to the coefficients of Lindemann's relation mentioned above.[5]

A better estimation of the new viscosity relation could be made in the case in which the values of the characteristic temperature at the melting point were known.

From the observed agreement, there results that the approximation regarding the mean vibration frequency is experimentally verified by the viscous behaviour of melts; the lowering of the mean vibration frequency on melting is hardly noticeable.

---

[5] M. ŞERBAN, *Rev. Roumaine Chim.*, in press.

Revue Roumaine de Chimie, 22, 6, 811–814 (1977)

COLLISION-INDUCED LIGHT ABSORPTION IN LIQUID MIXTURES*

V. EM. SAHINI ** and SIMONA BĂDILESCU ***

** Department of Physical Chemistry, Institute of Chemistry, B-dul Republicii 13, Bucharest

*** Central Laboratory of Petrochemical Works, Pitești, Șos. Giurgiului, 127, Pitești

Received April 15, 1976

The isolated binary collision model of light scattering in liquids has been developed to obtain an analytical expression for the spectral intensity of infrared simultaneous transition spectrum in liquid mixtures. The dependence of the spectral intensity on interaction potential energy between molecules in the collision pair and on frequency shift from the centre of the band was evidenced.

INTRODUCTION

Bucaro and Litovitz [1] introduced the idea of isolated binary collisions in studies of vibrational energy transfer in gases to explain the collision-induced Rayleigh spectra.

SHIN [2–4] derived an expression based on this model and performed a comparison with existing Rayleigh experiments.

The model of isolated binary collisions (IBC) has the advantage of conceptual and mathematical simplicity and leads to results that are in close agreement with experiment.[1]

In the present paper we shall verify the applicability of IBC model to infrared simultaneous transition (ST) spectra.

The intensity of ST vibration band depends, in the same manner as Rayleigh spectra, on induced dipole moment in the colliding pair and on the number of collisions :

$$I(\omega, T) = C_2\int_0^\infty\int_0^\infty N(b, v)\times\left|\int_{-\infty}^{+\infty}\mu^{\text{ind}}[r(t)]\exp(i\omega t)\,\mathrm{d}t\right|^2 \mathrm{d}b\,\mathrm{d}v \qquad (1)$$

---

* Paper presented at the National Conference of Pure and Applied Physical Chemistry, held in Bucharest, September 1–4, 1974.

[1] J. A. BUCARO and T. A. LITOVITZ, *J. Chem. Phys.*, **54**, 3846 (1971).

[2] H. K. SHIN, *J. Chem. Phys.*, **56**, 2617 (1972).

[3] H. K. SHIN, *J. Chem. Phys.*, **46**, 744 (1967).

[4] H. K. SHIN, *J. Phys. Chem.*, **73**, 4321 (1969).

where μ^{ind} is the induced dipole moment ($\mu^{\text{ind}} = C/r^m$), $r(t)$ is the distance r parametrized in time and $N(b, v)$ is the number of collisions per unit time for which the impact parameter is b and the magnitude of the relative velocity is v. We choose the Lennard-Jones potential for the interaction energy :

$$U(r) = 4D[(\sigma/r)^{12} - (\sigma/r)^{6}]$$

Taking into account only the repulsive part of this interaction potential (at very small separations), eq. (1) can be obtained as

$$I\,(\omega,\,T) \propto T^{4/19}\;\omega^{[2(m-7)/7]+[4/19]}\exp\left(-2.714\frac{\beta\omega^{12/19}}{kT^{7/19}} + 1.346\frac{(D\beta)^{1/2}\,\omega^{6/19}}{kT^{13/19}} - 0.838\frac{D}{kT}\right) \tag{2}$$

RESULTS AND DISCUSSIONS

The applicability of expression (2) to ST band intensity was tested for different liquid systems for which experimental data are available. [5-8] As in SHIN's work, we plot $I\omega^{-1.9248}$ *versus* $\nu^{12/19}$ assuming m to be equal with 9. Figure 1 presents the ST experimental data for a $CS_2 - CCl_4$ mixture (*a* and *a'*) comparatively with SHIN'S [2] calculated values from Rayleigh spectrum of carbon tetrachloride (*b* and *b'*). In the same manner was represented the intensity distribution in the ST bands belonging to the following systems[8] : $CS_2 + Br_2(a)$, $CS_2 + PBr_3(b)$ and $CS_2 + I_2(c)$.

The dependence of the intensity distribution on the form of assumed interaction potential was followed in figure 3, and one assumed the m value was given in the same figure ($m9 \div 13$).

Figure 1 shows a good agreement between SHIN's calculated values and our ST experimental data. The magnitude of the terms in the exponent given by eq. (2) is probably the same in Rayleigh spectrum of carbon tetrachloride and in ST spectrum of their mixture with CS_2, owing to the similar values of potential constants in both systems. The most important term in eq. (2) is the repulsive term, which increases rapidly as the frequency shift increases. The deviation from the linearity observed at small values of ν is due to the effect of the attractive interaction.

In the IBC model, m may have any physically realistic value. As in the work of BUCARO and LITOVITZ [1] we assume $m = 9$ as the minimal value because this represents the origin of the induced anisotropy by electronic overlap for monoatomic liquids. Figure 3 shows a correct picture of the simultaneous transition band at $m = 13$. The assumed m

[5] S. Bădilescu, *Rev. Roumaine Chim.*, **13**, 1297 (1968).

[6] S. Bădilescu, *Rev. Roumaine Chim.*, **19**, 1139 (1974).

[7] S. Bădilescu, *Rev. Roumaine Chim.*, **19**, 1145 (1974).

[8] F. N. Hooge, Thesis, Amsterdam, 1956.

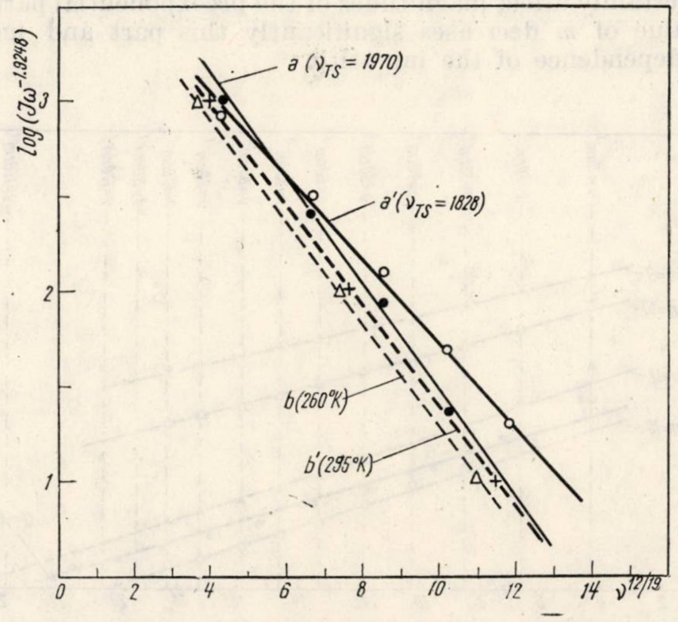

Fig. 1. — The intensity distribution in ST-band belonging to $CS_2 - CCl_4$ mixture : a — experimental data for ST = 1970 cm^{-1}; a' — experimental data for ST = 1828 cm^{-1}; b — SHIN's calculated values from Rayleigh spectra of CCl_4 (260 K) ; b' — SHIN's calculated values at 295 K.

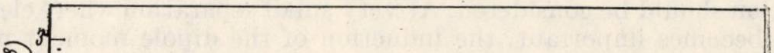

Fig. 2. — The intensity distribution in ST-bands : a — $CS_2 - Br_2$ mixture ; b — $CS_2 - PBr_3$; c — $CS_2 - I_2$.

value will certainly affect magnitudes of the preexponential part in eq. (2). A small value of *m* decreases significantly this part and modifies the frequency dependence of the intensity.

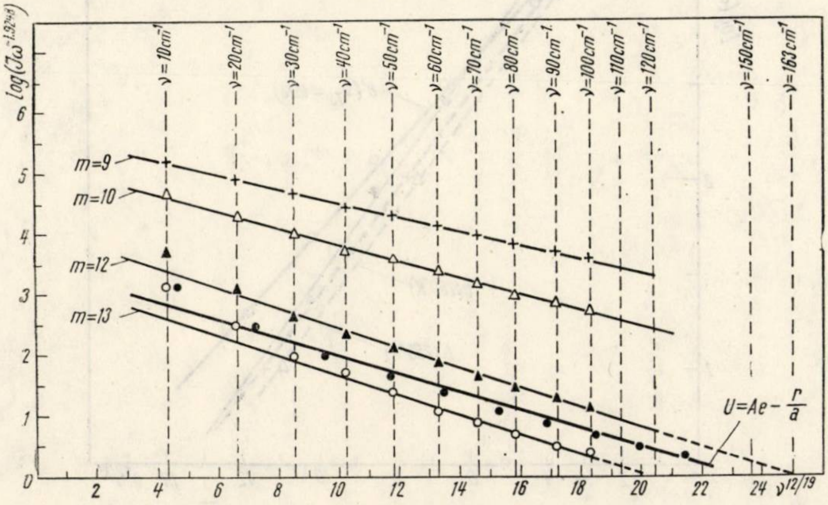

Fig. 3. — The dependence of intensity distribution on the form of interaction potential and on assumed *m* value.

The applicability of the IBC model to simultaneous transition spectra shows that in studies of this kind of induced spectra the repulsive part of interaction should be considered. At very small separation where electronic overlap becomes important, the induction of the dipole moment may be controlled more by the repulsive forces than by a "dipole-induced dipole" interaction. It is obvious that it is not sufficient to consider exclusively the electrostatic interactions to explain the existing data.

Our results suggest a resemblance between the simultaneous transition absorption spectra and Rayleigh scattering spectra and the inclusion of both kinds of spectra in the framework of the collision-induced molecular spectra.

Revue Roumaine de Chimie, **22**, *6*, 815–825 (1977)

ESTUDIO CONFORMACIONAL Y DE CONSTANTES DE ACOPLAMIENTO HIPERFINO EN RADICALES LIBRES. APROXIMACION INDO

F. ARCE, J. L. ARMESTO, J. CASADO y M. A. RIOS

Departamento de Química-Física. Facultad de Ciencias. Universidad de Santiago. España.
Centro Coordinado del C.S.I.C.

28 Apr. 1975

Se han establecido las geometrías de equilibrio de una serie de radicales que presentan una amplia gama de valores en sus constantes de acoplamiento, utilizando un criterio de minimación parcial, dentro del esquema de métodos sin restricciones de spin y haciendo uso de la aproximación INDO. Se han calculado también las densidades de spin de dichos radicales. Se ha obtenido un valor de 488,96 para la constante de proporcionalidad protónica y las constantes de acoplamiento calculadas de este modo concuerdan satisfactoriamente con los valores experimentales.

INTRODUCCION

La magnitud estructural más asequible experimentalmente para radicales libres, como sistemas de capa abierta, es la constante de acoplamiento hiperfino isótropa, que se obtiene de los espectros de RSE. Su interpretación teórica se lleva a cabo ordinariamente a través de la densidad de spin calculada mecanocuánticamente, haciendo uso de la relación lineal que debe de existir entre esta magnitud teórica y los valores experimentales de dichas constantes. Como resultado de este planteamiento se obtiene, para cada tipo de núcleos, el factor de proporcionalidad que correlaciona ambas variables.

Otro aspecto importante, sobre el que en general existe muy poca información experimental, lo constituye la geometría de los radicales, cuyo conocimiento es necesario para el cálculo de densidades de spin.

Existen en la bibliografía diversas publicaciones relativas a estudios teóricos en que se establece la geometría de radicales pequeños por minimación total y/o se calculan densidades de spin, la constante de proporcionalidad anteriormente aludida y constantes de acoplamiento hiperfino. Entre ellas merecen destacarse las de Pople [1] y Benson.[2] Sin embargo, estas investigaciones se refieren unas veces a radicales pequeños, otras veces adoptan geometrías estándar con criterios excesivamente drásticos y/o se refieren a radicales cuyas constantes de acoplamiento presentan valores relativamente próximos.

En el presente trabajo se seleccionan una serie de radicales de características diversas, con constantes de acoplamiento en un amplio margen de valores (Tabla 1); se establecen sus geometrías de equilibrio siguiendo un criterio de minimación parcial y se calculan sus densidades de spin de acuerdo con la aproximación INDO. Estos resultados se utilizan para obtener un nuevo valor del factor de proporcionalidad constante de acoplamiento protónico-densidad de spin, así como los valores teóricos para las constantes de acoplamiento.

---

[1] J. A. Pople, D. L. Beveridge y P. A. Dobosh, *J. Amer. Chem. Soc.*, **90**, 4201 (1968).

[2] H. G. Benson y A. Hudson, *Theor. Chim. Acta*, **23**, 259 (1971).

PLANTEAMIENTO DEL PROBLEMA

La constante de acoplamiento hiperfino isótropa experimental, que aparece como consecuencia de la interacción entre el spin electrónico y los spines de cualquier núcleo magnético de la molécula, está relacionada con la función de onda del sistema en la forma:

$$a_N = \frac{8\pi}{3} g \beta g_N \beta_N \rho(r_N) \qquad (1)$$

donde g, β, g_N, β_N tienen su significado habitual y $\rho(r_N)$ representa la densidad de spin en el núcleo.

Si la función de onda para el radical, ψ, se define, dentro del formalismo LCAO, como un determinante de Slater simple, el valor promedio del operador densidad de spin puede escribirse como:

$$\langle \psi | \rho^{\text{spin}}(r_N) | \psi \rangle = \sum_{\mu\nu} \rho^{\text{spin}}_{\mu\nu} \Phi_\mu(r) \Phi_\nu(r) \qquad (2)$$

donde $\rho^{\text{spin}}_{\mu\nu}$ es la densidad de electrones desapareados.

Para el cálculo de la densidad de electrón desapareado es importante retener las integrales de canje atómicas, puesto que dan cuenta de la diferente energía de repulsión de los electrones sobre un mismo átomo según sus spines y por las importantes consecuencias que tienen sobre la distribución de electrones desapareados en el sistema. La forma más simple de introducir el canje es retener el recubrimiento diferencial monoatómico en las integrales de un centro, que es la principal característica del método INDO [3] en el que dichas integrales se estiman a partir de los parámetros de Slater-Condon.[4]

De acuerdo con las aproximaciones implicadas en el método INDO, el valor promedio del operador densidad de spin se reduce a:

$$\langle \psi | \rho^{\text{spin}}(r_N) | \psi \rangle = \rho^{\text{spin}}_{s_N s_N} | \Phi s_N(r_N) |^2 \qquad (3)$$

obteniéndose para la constante de acoplamiento la expresión final:

$$a_N = \frac{8\pi}{3} g \beta g_N \beta_N | \Phi_{s_N}(r_N) |^2 \rho^{\text{spin}}_{s_N s_N} \qquad (4)$$

---

[3] J. A. Pople, D. L. Beveridge y P. A. Dobosh, *J. Chem. Phys.*, **47**, 2026 (1967).

[4] J. C. Slater, "Quantum Theory of Atomic Structure", vol. 1, McGraw-Hill Book Company, New York, 1960, p. 339–43.

según la cual se pueden calcular constantes de acoplamiento a partir de densidades de electrón desapareado evaluadas semiempíricamente, una vez establecidos los valores de la constante de proporcionalidad para cada núcleo. Dado que la base STO utilizada no permite una evaluación correcta de la densidad de orbitales s en el núcleo, $|\psi_{s_N}(r_N)|^2$, la constante de proporcionalidad se obtiene a partir de datos experimentales de a_N.

Para el establecimiento de geometrías existen, fundamentalmente, dos alternativas : adoptar valores estándar o realizar una minimación energética respecto a los parámetros geométricos de los radicales.

Dentro del primer tipo se encuentran los referidos trabajos de Pople, que toma para los ángulos y distancias de enlace valores que dependen únicamente de la naturaleza de los átomos enlazados y no del tipo de enlace. Este criterio resulta, en un elevado número de casos, demasiado drástico.

La minimación energética total presenta limitaciones prácticas en el caso de radicales grandes, como consecuencia del elevado número de parámetros geométricos que definen la hipersuperficie de energía potencial molecular.

Como consecuencia, en el presente trabajo se adopta un criterio de minimación energética parcial, que resuelve los inconvenientes de las geometrías estándar a la vez que aminora el problema de cálculo. Salvo pequeñas variaciones en el caso de algún radical de caracteristicas especiales, este criterio consiste en obtener por minimación los ángulos de enlace más directamente afectados por la formación del radical, manteniendo para los demás parámetros geométricos los valores correspondientes a las moléculas de que procede el radical. Su justificación radica en que :

i) Un análisis de los resultados, tanto teóricos como experimentales, que aparecen en la bibliografía, permite concluir que en la zona de la molécula no directamente afectada por la formación del radical, no se observan variaciones significativas ni en las distancias ni en los ángulos de enlace, como consecuencia de la formación de aquél.

ii) Dentro de la zona que se supone directamente afectada por la formación del radical, una minimación respecto a las longitudes de enlace no conduce en general a mayores diferencias (en relación a las de la molécula estable) que las atribuibles al error del propio método teórico utilizado.

RESULTADOS Y DISCUSION

En la Tabla 1 se incluyen las densidades protónicas de spin calculadas para cada uno de los radicales, así como los valores experimentales de las constantes de acoplamiento. Relacionando ambas variables se ha obtenido para el factor de proporcionalidad de los núcleos de hidrógeno el valor 488,96, con un coeficiente de correlación de 0,95. Dicho valor es del orden de los establecidos por otros autores y su coeficiente de correlación, superior al obtenido por Pople (0,88), es muy próximo al encontrado por Benson (0,96), si bien presenta la ventaja de estar referido a una amplia gama de valores de constantes de acoplamiento, pertenecientes a sistemas de características variadas. En la referida tabla se incluyen también las constantes de acoplamiento calculadas utilizando la anterior constante de proporcionalidad.

Tabla 1

Densidades de spin y constantes de acoplamiento de los radicales estudiados

Radical	atomo	ρ^{spin}	a_H(calc.)	a_H(exp.)	(Ref.)
Metilo	H	−0,04022	−19,67	(−) 23,04	5
Monofluometilo	H	−0,01321	− 6,46	(−) 21,1	6
Difluometilo	H	0,04298	21,02	(+) 22,20	6
Etinilo	H	0,06444	31,51	(+) 16,10	7
Formilo	H	0,15960	78,04	(+)137,00	8
CNH^-	H	0,26087	127,55	(+)137,00	9
BOH^-	H	0,14320	70,08	(+) 94,00	10
Metilenimino	H	0,13534	66,18	(+) 87,4	11
Piridilo	H_2	0,01470			
	H_3	0,01680			
	H_4	0,01059			
	$\bar{H}$	0,01403	6,86	(+) 4,3	12
Vinilo	$H(CH_2)$	0,15074	73,71	(+)65,0	5
	$H'(CH_2)$	0,08671	42,40	(+)37,0	5
	$H(CH)$	−0,00640	− 3,13	(−)13,4	5
Etilo	$H(CH_3)$	0,05150	25,18	(+)26,87	5
	$H(CH_2)$	−0,04138	−20,23	(−)22,38	5
Metilvinilo	$\bar{H}(CH_3)$	0,04335	21,20	(+)19,48	5
	$H(CH_2)$	0,09978	48,79	(+)32,92	5
	$H'(CH_2)$	0,14490	70,85	(+)57,89	5
Ciclopropilo	H_1	−0,00305	− 1,9	(−) 6,51	5
	H_2	0,03747			
	$H_{2'}$	0,03888			
	$\bar{H}$	0,03817			
Ciclobutilo	H_1	−0,02944	−14,40	(−)21,20	5
	H_2	0,05159			
	$H_{2'}$	0,05472			
	$\bar{H}$	0,05315	25,99	(+)36,66	5
	H_3	−0,00420			
	$H_{3'}$	−0,00254			
	$\bar{H}$	−0,00337	− 1,65		
Ciclopentilo	H_1	−0,03725	−18,21	(−)21,48	5
	H_2	0,06898	33,73	(+)35,16	5
	H_3	−0,00315	− 1,54	(−) 0,53	5
Isopropilo	$H(CH_3)$	0,00349			
	$H(CH_3)$	0,06887			
	$H(CH_3)$	0,06887			
	$\bar{H}(CH_3)$	0,04707	22,78	(+)24,68	5
	$H(CH)$	−0,03729	−18,23		
Terbutilo	$H(CH_3)$	0,06240			
	$H(CH_3)$	0,06240			
	$H(CH_3)$	0,00296			
	$\bar{H}(CH_3)$	0,04587	22,43	(+)22,72	5
Fenilo	H_2	0,03611	17,66	(+)19,50	5
	H_3	0,01143	5,59	(+) 6,50	5
	H_4	0,00757	3,70		

---

[5] R. W. FESSENDEN y R. H. SCHULER, *J. Chem. Phys.*, **39**, 2147 (1963).

[6] R. W. FESSENDEN y R. H. SCHULER, *J. Chem. Phys.*, **43**, 2704 (1965).

[7] E. L. COCHRAN, F. J. ADRIAN y V. A. BOWERS, *J. Chem. Phys.*, **40**, 213 (1964).

[8] F. J. ADRIAN, E. L. COCHRAN y V. A. BOWERS, *J. Chem. Phys.*, **36**, 1661 (1962).

[9] E. L. COCHRAN, B. C. WEATHERLEY, V. A. BOWERS y F. J. ADRIAN, *Bull. Amer. J. Physics*, **13**, 35 (1968).

[10] W. J. LAFFERTY, E. K. PLYLER y E. D. TIDWELL, *J. Chem. Phys.*, **37**, 1981 (1962).

[11] E. L. COCHRAN, F. J. ADRIAN y V. A. BOWERS, *J. Chem. Phys.*, **36**, 1938 (1962).

[12] B. BAK, L. HANSEN-HYGAARD y J. KASTRUP-ANDERSEN, *J. Mol. Spectroscopy*, **2**, 361 (1958).

Tabla 1 (Continuación)

Radical	atomo	θ^{spin}	*a* (calc.)	*a* (exp.)	(ref.)
Alilo	$H(CH_2)$	$-0,02749$	$-13,44$	$(-)13,93$	5
	$H'(CH_2)$	$-0,02790$	$-13,64$	$(-)14,83$	5
	$H(CH)$	$0,01318$	$6,44$	$(+)\ 4,06$	5
Ciclopentadienilo	H_1	$0,00075$			
	H_2	$-0,02195$			
	H_3	$0,00540$			
	H_4	$-0,01742$			
	H_5	$-0,01194$			
	$\bar{H}$	$-0,00902$	$-\ 4,41$	$(-)\ 5,60$	13
Ciclohexadienilo	H_1	$-0,01993$	$-\ 9,75$	$(-)13,04$	5
	H_2	$0,01078$	$5,27$	$(+)\ 2,65$	5
	H_3	$-0,01974$	$-\ 9,65$	$(-)\ 8,99$	5
	H_4	$0,12639$	$61,80$	$(+)47,71$	5

La numeración en los radicales cíclicos comienza en el átomo a partir del cual se ha formado el radical y continua la secuencia en el sentido de las agujas del reloj. En los radicales no cíclicos se especifica en cada caso el grupo al cual pertenece el átomo de hidrógeno. Constantes de acoplamiento expresadas en gauss.

a) RADICALES METILO, MONOFLUOMETILO Y DIFLUOMETILO

Las geometrías obtenidas para estos radicales son análogas a las calculadas por otros autores dentro del mismo esquema de trabajo. En la Tabla 2 se comparan los valores de distancias y ángulos de enlace con los obtenidos por Beveridge et al.[14] dentro del esquema INDO realizando la minimación sobre los ángulos de enlace, así como con los obtenidos por Pople [15] realizando una minimación energética total. Como es lógico, las densidades de spin son semejantes a las calculadas por estos autores, así como las constantes de acoplamiento resultantes.

Tabla 2
Geometrías de equilibrio

Radical		R(C−H) (Å)	R(C−F) (Å)	θ_{HCH}(°)	θ_{HCF}(°)	θ_{FCF}(°)
CH_3	a	1,0936[16]		119,4		
	b	1,08		119,7		
	c	1,11		119,0		
CH_2F	a	1,105[17]	1,385	121,1	113,3	
	b	1,08	1,35	121,0	114,0	
	c	1,11	1,32	119,6	114,4	
CHF_2	a	1,09[18]	1,36		116,0	108,1
	b	1,08	1,35		116,0	109,0
	c	1,12	1,33		115,9	109,5

a − presente trabajo, b − Ref.[14], c − Ref.[15]

[13] S. Ohnisi y I. Nitta, *J. Chem. Phys.*, **39**, 2848 (1963).

[14] D. L. Beveridge, P. A. Dobosh y J. A. Pople, *J. Chem. Phys.*, **48**, 4802 (1968).

[15] J. A. Pople y D. L. Beveridge, "Aproximate Molecular Orbital Theory", McGraw-Hill Book Company, New York, p. 94.

[16] G. Herzberg, "Infra-red and Raman Spectra of Polyatomic Molecules", Van Nostrand Co., New York, 1945, p. 439−56.

[17] D. R. Gilliam, H. D. Edwards y W. Gordy, *Phys. Rev.*, **75**, 1014 (1949).

[18] G. G. Thornton, University Microfilms, Ann. Arbor, Michigan Pub. No. 7746; *Diss. Abs.*, **14**, 604 (1954).

b) RADICALES FORMILO, CNH^- y BOH^-

En la Tabla 3 se comparan las geometrías establecidas en el presente trabajo con las obtenidas por una minimación total dentro del esquema INDO.

Tabla 3

Geometrías de equilibrio

XYH		R(X−Y) (Å)	R(X−H)(Å)	θ_{XYH}(°)
COH	a	1,2078[19]	1,1161	132
	b	1,22	1,11	131,2
BOH^-	a	1,365[21]	1,25[22]	129
	b	1,37	1,25	129
CNH^-	a	1,155[20]	1,063	139,5
	b	1,23	1,18	133

a — presente trabajo, b — Ref.[23]

En los tres radicales hay una importante densidad de spin en los orbitales s tanto de los hidrógenos como del oxígeno, boro y carbono, lo que los caracteriza como radicales tipo σ.

En valor excesivamente bajo de la constante de acoplamiento protónica del formilo es comparable al calculado por Pople [1] con geometrías estándar, $a_H = 74,9$ G., o por Thomson [23] para la geometría de equilibrio. En el caso del BOH^- se predice satisfactoriamente el bajo valor de la constante de acoplamiento protónico en este radical.

c) RADICAL ETINILO

Con las distancias interatómicas del etilo [24] el mínimo energético corresponde a una geometría lineal, análoga a la calculada por minimación respecto a las longitudes y ángulos de enlace dentro del esquema INDO.[15]

Las mayores densidades de spin aparecen sobre los orbitales del carbono 2s (0,3356) y 2p en la dirección del eje del enlace (0,5454) lo que lo caracteriza como un radical tipo σ, en contra de la suposición hecha por Petersson y McLachlan [25] ante los malos valores obtenidos para la constante de acoplamiento protónico (74,0 G.) dentro de un esquema Hückel extendido. Las densidades de spin sobre los dos carbonos son positivas y nó una positiva y otra negativa como encuentra Pople, quizás debido a que las geometrías estándar no constituyen una buena aproximación para este caso.

---

[19] K. Takagi y T. Oka, *J. Phys. Soc. Japan*, **18**, 1174 (1963).
[20] J. K. Tyler y J. Sheridan, *Trans. Faraday Soc.*, **59**, 2661 (1963).
[21] A. C. Zachariasen, *Acta Cryst.*, **7**, 305 (1954).
[22] P. T. Ford y R. E. Richards, *Discuss. Faraday Soc.*, **19**, 230 (1955).
[23] C. Thomson, *Theor. Chim. Acta*, **17**, 320 (1970).
[24] W. J. Lafferty, E. K. Plyler y E. D. Tidwell, *J. Chem. Phys.*, **37**, 1981 (1962).
[25] G. A. Petersson y A. D. McLachlan, *J. Chem. Phys.*, **45**, 628 (1966).

d) RADICAL METILENIMINO

La geometría establecida en el presente trabajo, adoptando las distancias interatómicas de la metilenimina [26] y un mínimo para el ángulo HCN de 123°, concuerda satisfactoriamente con la calculada por minimación energética total dentro del esquema INDO.[15]

La mayor fracción de densidad de electrón desapareado (0,86) aparece sobre el orbital 2p del nitrógeno sobre el plano de la molécula y en cantidad relativamente grande sobre los hidrógenos (0,135). Esta concentración de densidad sobre el orbital $2p_y$ del nitrógeno puede ser la causa de la gran constante de acoplamiento protónico en este radical, 87,4 G.[11]

e) RADICAL PIRIDILO

Se adopta la geometría propuesta por Bak et al.[27] para la piridina. La densidad protónica de spin utilizada es el valor medio de las calculadas para los hidrógenos en las posiciones 2, 3 y 4. La buena concordancia entre las constantes de acoplamiento hiperfino calculadas (6,86G.) y el valor experimental (4,3 G.) corroboran la sugerencia de Symons [28] de que el radical que se obtiene por radiación de la piridina es el 2-piridilo y no el catión piridina.

f) RADICALES ETILO, ISOPROPILO Y TERBUTILO

La geometría establecida para el radical etilo presenta un esqueleto $C-CH_2$ plano [29] y un grupo metilo rotando libremente con todas las posiciones isoenergéticas y, aunque no hay referencias al respecto para este radical, la geometría indicada corresponde a la que en primera aproximación se podía prever.

La geometría establecida para el isopropilo supone una hibridación sp^2 en el átomo de carbono central y una conformación más estable en la que el hidrógeno α y dos de los dos grupos metilo se encuentran en el plano del esqueleto carbonado. Para el terbutilo se encuentra una estructura plana para el esqueleto carbonado y la conformación de máximo estrellamiento de los tres metilos, adoptándose para la densidad de spin protónica el valor medio de las calculadas para cada uno de los hidrógenos.

Los valores y signos obtenidos para las densidades de spin del radical etilo indican claramente como el método INDO da cuenta tanto de los efectos de polarización de spin, ya que incluye el canje monocéntrico, como de la delocalización electrónica, por tratarse de un método de orbitales moleculares. El radical etilo, al igual que el isopropilo y terbutilo, quedan caracterizados como radicales tipo π, ya que prácticamente toda la densidad de electrón desapareado aparece sobre el orbital $2p_z$ del carbono a partir del cual se ha formado el radical.

---

[26] J. H. SCAHTSCHENEIDER y R. G. SNYDFR, *Spectrochim. Acta*, **19**, 117 (1963).

[27] B. BAK, L. HANSEN y J. RASTRUP-ANDERSEN, *J. Chem. Phys.*, **22**, 2042 (1954).

[28] J. BOWER, J. A. MCRAE y M. C. R. SYMONS, *Chem. Comm.*, **1967**, 542.

[29] A. ALMENNINGEN y O. BASTIANSEN, *Acta Chem. Soc.*, **1955**, 9815.

En la Tabla 4 se comparan las constantes de acoplamiento protónico (en posición β) calculadas en el presente trabajo con las obtenidas por vía experimental en estos tres radicales, así como con valores obtenidos por otros autores, concretamente por Dixon,[30] utilizando un modelo hiperconjugativo, y por Petersson et al.[25] dentro de un esquema Hückel extendido.

Tabla 4

Constantes de acoplamiento calculadas y experimentales

Radical	a_H^a	a_H^b	a_H^c	a_H(exp.)
Etilo	25,18	27,1	21,4	26,87
Isopropilo	22,78	22,8	18,8	24,68
Terbutilo	22,43	20,3	16,8	22,72

a — presente trabajo, b — Ref.[30], c — Ref.[25]
Constantes de acoplamiento expresadas en gauss.

Los valores obtenidos, aunque algo más bajos, concuerdan satisfactoriamente con los experimentales y son comparables a los calculados por medio de un modelo hiperconjugativo, lo que confirma la hiperconjugación como posible mecanismo de la aparición de densidades de spin en las posiciones β.

g) RADICALES VINILO Y METILVINILO

Realizando la minimación energética según el criterio establecido, se encuentra para el radical vinilo un valor del ángulo HCC de 150°. En el metilvinilo el mínimo energético aparece para un ángulo CCC de 162°. El radical vinilo, así como el metilvinilo, quedan caracterizados como radicales σ, pues prácticamente toda la densidad de electrón desapareado aparece sobre la parte σ de los mismos. La pequeña densidad de spin encontrada para el hidrógeno en la posición α, en el vinilo, resulta insuficiente para justificar la constante de acoplamiento de 13,4 G., siendo los valores calculados para las constantes hiperfinas de los otros dos hidrógenos concordantes con los valores experimentales. El valor medio obtenido para los hidrógenos del grupo CH_3, en el metilvinilo, concuerda con el valor experimental; los valores obtenidos para los hidrógenos del grupo metilénico resultan algo más elevados que los valores experimentales.

h) RADICALES CICLOPROPILO, CICLOBUTILO Y CICLOPENTILO

Para el ciclopropilo se adopta la geometría del ciclopropano,[31] variando el ángulo entre el enlace C—H radical y el plano del esqueleto carbonado; el mínimo energético aparece a $\theta = 35°$. En el ciclobutilo, con las distancias interatómicas del ciclobutano,[32] el mínimo energético aparece a 20° y para el ciclopentilo corresponde a la situación en la que el hidrógeno radical se encuentra en el plano del anillo. Los valores más bajos del referido ángulo en los dos últimos radicales eran, en parte, deducibles de los valores más elevados de las constantes de acoplamiento de los correspondientes hidrógenos α.

---

[30] W. T. Dixon, *Mol. Phys.*, **9**, 201 (1965).

[31] S. P. Sinha, *J. Chem. Phys.*, **18**, 217 (1950).

[32] J. D. Dunitz y V. Schomaker, *J. Chem. Phys.*, **20**, 555 (1952).

En la Tabla 5 se indican las densidades de spin obtenidas para los diferentes valores del ángulo α en el ciclopropilo. Los resultados teóricos indican que el hidrógeno α se encuentra fuera del plano. El hecho de que las constantes de acoplamiento de los hidrógenos en las posiciones β y β' sean iguales parece indicar que el hidrógeno α oscila entre dos posiciones equivalentes a ambos lados del anillo. De los valores de la energía total incluídos en la Tabla 5 se obtiene el valor de 0,15 eV. para la altura de la doble barrera de energía correspondiente a esta oscilación, de modo que, si se adopta para la constante de acoplamiento protónico el valor medio de todas las posiciones posibles, tenido en cuenta su peso estadístico, la constante $a_{H'}$ disiminuirá, aproximándose al valor experimental. Estas conclusiones concuerdan con las predicciones empíricas sugeridas por Fessenden y Shuler [5] al observar el espectro RSE del ciclopropilo.

Tabla 5

Variación de las densidades de spin y energía total con el ángulo α (ciclopropilo)

α	ρ_{H_α}	ρ_{H_β}	$\rho_{H_{\beta'}}$	E_T(eV.)
0°	−0,04541	0,05148	0,05148	−657,6077
10°	−0,03971	0,04996	0,04995	−657,6247
20°	−0,02588	0,04586	0,04615	−657,6974
30°	−0,01017	0,04039	0,04135	−657,7529
35°	−0,00305	0,03747	0,03888	−657,7632
40°	0,00319	0,03456	0,03646	−657,7545
50°	0,01272	0,02896	0,03190	−657,6625
60°	0,01835	0,02883	0,02778	−756,4452

En la Tabla 6 se comparan los valores obtenidos para las constantes de acoplamiento del radical ciclobutilo con los valores experimentales y los obtenidos dentro de otros sistemas de cálculo.

Tabla 6

Constantes de acoplamiento. Ciclobutilo

Posición	a_H^a	a_H^b	a_H^c	a_H^d	a_H(exp.)
H_1	−14,40	27,20		20,28	−21,20
H_2, $H_{2'}$	25,99	34,17	38,2	9,92	36,60
H_3, $H_{3'}$	− 1,65	1,07	2,9	2,10	− 1,12

a — presente trabajo, b — Ref.[33], c — Ref.[30], d — Ref.[34]
Constantes de acoplamiento expresadas en gauss.

---

[33] R. S. DRAGO y H. PETERSSEN JR., *J. Amer. Chem. Soc.*, **89**, 16 (1967).

[34] N. M. ATHERTON y A. HINCHLIFFE, *Mol. Phys.*, **12**, 349 (1967).

En el ciclopentilo las constantes de acoplamiento protónico concuerdan satisfactoriamente con los valores experimentales, como se puede observar en la Tabla 7, donde se comparan también con otros valores calculados.

Tabla 7

Constantes de acoplamiento. Ciclopentilo

Posición	a^{a}_{H}	a^{b}_{H}	a^{c}_{H}	a_{H}(exp.)
H_1	18,21	27,54		21,48
H^2, $H_{2'}$	33,73	33,42	37,2	35,16
H_3, $H_{3'}$	1,54	0,22	0,57	0,53

a — presente trabajo, b — Ref.[34], c — Ref.[30]

Constantes de acoplamiento expresadas en gauss.

i) RADICAL FENILO

La geometría establecida para el radical fenilo es la experimental del benceno.[35]

Las mayores densidades de spin se encuentran sobre los orbitales $2p_y$ (0,64) y 2s (0,18) del átomo de carbono que ha perdido el hidrógeno en la formación del radical, lo que lo caracteriza como un radical tipo σ. Las densidades de spin de los hidrógenos siguen el orden orto>meta>para, como se ve en la Tabla 8, secuencia que no puede obtenerse dentro de un esquema de electrón independiente tipo Hückel.

Tabla 8

Constantes de acoplamiento. Fenilo

Posición	a^{a}_{H}	a^{b}_{H}	a^{c}_{H}	a^{d}_{H}	a_{H}(exp,)
orto	17,66	39,98	12,5	23,3	19,5
meta	5,59	10,42	5,3	4,2	6,50
para	3,70	1,02	11,0	17,9	—

a – presente trabajo, b – Ref. [34], c – Ref. [30], d – Ref. [25]

Constantes de acoplamiento expresadas en gauss.

j) RADICALES ALILO Y CICLOPENTADIENILO

En el radical alilo la minimación se ha llevado a cabo sobre la distancia C—C y el ángulo CCC. La distancia calculada es 1,37 Å y el ángulo de 126°.

El radical queda caracterizado como tipo π. El método distingue entre los hidrógenos 1 y 2, aunque la diferencia entre sus densidades de spin es pequeña comparada con la existente entre los valores experimentales de sus respectivas constantes de acoplamiento.

En el ciclopentadienilo, puesto que experimentalmente solo muestra un valor de la constante de acoplamiento protónica, se supuso el anillo regular plano y la minimación se llevó a cabo sobre la distancia C—C. Como consecuencia de dificultades de convergencia surgidas en el estudio de este radical, las densidades de spin obtenidas para átomos equivalentes muestran pequeñas variaciones, por lo que se han utilizado valores medios para el cálculo de la constante de acoplamiento protónico, cuyo valor (—4,41 G.) concuerda satisfactoriamente con el valor experimental (—5,60 G.) y es análogo al calculado utilizando geometrías estándas.[1] Las mayores densidades de electrón desapareado aparecen en los orbitales $2p_z$ de los carbonos, como corresponde a un radical tipo π.

---

[35] J. L. Karle, *J. Chem. Phys.*, **20**, 65 (1952).

k) RADICAL CICLOHEXADIENILO

La geometría establecida está de acuerdo con la formación de un sistema conjugado en que participa el carbono que ha perdido un hidrógeno en la formación del radical. El hidrógeno permanente sobre este carbono se encuentra en el plano de dicho sistema, cuya distancia C—C, obtenida por minimación supuestos ángulos de 120°, es de 1,40 Å. Para el resto del radical se ha mantenido la geometría del ciclohexadieno, propuesta por Ermer.[36]

Las constantes de acoplamiento calculadas concuerdan relativamente bien con las experimentales, como se observa en la Tabla 9 en la que se comparan también estos valores con otros referidos en la bibliografía.

Tabla 9

Constantes de acoplamiento. Ciclohexadienilo

Posición	a_H^a	a_H^b	a_H^c	a_H^d	a_H(exp.)
H_4	61,80	97,6	42,0	54,0	47,71
H_3	−9,65	−11,1			− 8,99
H_2	5,27	5,1			2,65
H_1	−9,75	−9,8			−13,04

a — presente trabajo, b — Ref.,[1] c — Ref.,[25] d — Ref.[10]
Las posiciones estan numeradas a partir del átomo en el cual se ha formado el radical
Constantes de acoplamiento expresadas en gauss.

Como resumen se puede concluir que el método INDO es apto para dar cuenta de todo tipo de radicales dentro de un esquema simple de trabajo y sin necesidad de utilizar parametrización adicional alguna, permitiendo el cálculo directo de constantes de acoplamiento en todas las posiciones moleculares, sin recurrir a mecanismos de polarización de spin o delocalización hiperconjugativa.

Los cálculos fueron realizados con un ordenador UNIVAC 1108 del Centro del Proceso de Datos del Ministerio de Educación y Ciencia a través de la terminal DCT 2000 del Centro de Cálculo de la Universidad de Santiago. Se ha elaborado un programa original en el lenguaje FORTRAN V para el cálculo de densidades de spin dentro del esquema INDO; este programa incluye como subrutinas el cálculo de coordenadas y el de integrales electrónicas implicadas en el método.

AGRADECIMIENTO. Uno de los autores (JLA) agradece la concesión de una beca de formación de personal investigador por el Ministerio de Educación y Ciencia de España con la que sa ha podido realizar este trabajo.

---

[36] O. Ermer y S. Lifson, *J. Amer. Chem. Soc.*, **95**, 13, 4121 (1973).

Revue Roumaine de Chimie, 22, 6, 827–838 (1977)

Dedicated to the 70th anniversary
of Professor Coriolan Drăgulescu

SECOND INTERACTION VIRIAL COEFFICIENT. II[1]

$Ar + H_2$ AND $CH_4 + H_2$ SYSTEMS

RODICA VÎLCU, I. GĂINAR and C. LEPĂDATU
Department of Physical Chemistry and Electrochemical Technology, Polytechnic Institute
Bucharest, Chemistry Institute, Faculty of Chemistry

Received June 9, 1976

With the help of an original equipment described in a previous paper, the excess volumes and the second interaction virial coefficients were estimated for $Ar + H_2$ and CH_4+H_2 mixtures, at high pressures (max. 80 atm) and at standard temperature. On the other hand, the variation with pressure of second excess virial coefficient was observed. A qualitative interpretation for the pressure variations appearing as an effect of the gas mixing on the basis of the assumption of uniformly distributed positive electric charges on the sphere surrounding the molecule was proposed. The existence as well as the value of these charges were remarked by the quantum mechanical calculus of the electron population before and after the molecule formation.

RESULTS AND DISCUSSIONS. $Ar+H_2$ SYSTEM

As remarked by other authors [2] the dynamical behaviour of $Ar + H_2$ system should be very similar to that of $N_2 + H_2$ system as long as the non-sphericity of the nitrogen molecule plays only an unessential role.

The values of the excess volumes (V^E) computed for the pressure interval where the measurements were carried out (10–80 atm) wholly confirm this hypothesis; some of these values are recorded in table 1 and a few are represented graphically in figure 1.

In table 2 we presented the experimental values of the excess volumes, the pressure variations (appearing as an effect of the gas mixing) and the numbers of moles that should be removed from the system in order that the pressure would recover its initial charge value.

The comparative examination of our experimental data referring to the excess volumes and those obtained by Zandbergen and Beenakker [2] within the same interval of pressure and approximate temperature (292.16 K) points out a good agreement, if the various means of experimental technique used there are taken into account.

---

[1] R. Vîlcu and I. Găinar, *Rev. Roumaine Chim.*, **19**, 1123 (1974).

[2] P. Zandbergen and J. J. M. Beenakker, *Physica*, **33**, 343 (1967).

Table 1

Excess volumes of Ar + H_2 mixture for various pressures and compositions at standard temperature (l/mol)

	P_{atm}								
x_{H_2}	10	20	30	40	50	60	70	80	90
0.1	1.793	1.823	1.849	1.874	1.895	1.912	1.926	1.96	1.941
0.2	3.180	3.225	3.266	3.302	3.332	3.357	3.375	3.386	3.3390
0.3	3.165	4.215	4.261	4.300	4.332	4.356	4.372	4.380	4.380
0.4	4.750	4.801	4.844	4.874	4.908	4.928	4.939	4.942	4.936
0.5	4.940	4.984	4.021	5.050	5.072	5.086	5.091	5.088	5.077
0.6	4.736	4.770	4.799	4.821	4.835	4.843	4.843	4.835	4.820
0.7	4.138	4.163	4.183	4.197	3.205	4.207	4.203	4.193	4.177
0.8	3.149	3.165	3.176	3.187	3.187	3.186	3.180	3.170	3.156
0.9	1.770	1.778	1.782	1.784	1.784	1.782	1.778	1.772	1.763

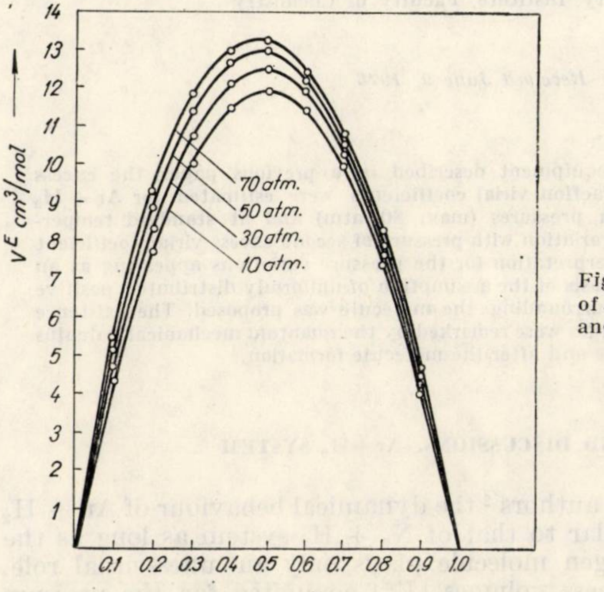

Fig. 1. — Variation of excess volume of Ar + H_2 mixture with composition and pressure at the standard temperature.

Table 2

Excess volumes of Ar + H_2 mixture from experimental data

P_{atm}	x_{H_2}	$n_{Ar} + n_{N_2}$ mol	$\Delta n.10^3$ mol	ΔP mm Hg	P^E mm Hg	$V^{M,id}$ cm³/mol	V^E cm³/mol
10	0.421	0.480	0.65	0.96	6.40	2450–56	3.30
20	0.460	0.848	2.48	34.00	24.48	1227.61	3.32
30	0.470	1.215	4.90	74.75	48.57	820.21	3.30
40	0.480	1.583	8.10	127.15	80.20	616.70	3.55
50	0.487	1.947	13.50	180.08	133.40	494.74	3.41
60	0.489	2.317	18.80	239.40	185.80	413.55	3.30
70	0.491	2.684	25.13	297.54	248.20	355.65	3.31
80	0.494	3.051	34.85	357.69	304.00	312.32	3.58

Table 3

Excess volumes of Ar+H$_2$ mixture from experimental (a) and from comparative data[2] (b)

$T = 298.10$ K$^{a)}$			$T = 292.10$ K$^{b)}$		
P_{atm}	x_{H_2}	V^E(cm^3/mol)	P_{atm}	x_{H_2}	V^E(cm^3/mol)
10	0.421	3.30	10	0.5	3.07
20	0.466	3.32	20	0.5	3.67
30	0.470	3.30	30	0.5	3.67
40	0.480	3.55	40	0.5	3.62
50	0.487	3.41	50	0.5	3.66
60	0.489	3.36	60	0.5	3.63
70	0.491	3.31	70	0.5	3.60
80	0.494	3.58	80	0.5	3.60

Figure 2 represents the variation with pressure of experimental quantities P and P^E that give explicitly the deviation of the Ar + H$_2$ system from ideality. As in the case of the N$_2$ + H$_2$ system the deviation becomes more marked starting from the value of about 30 atm.

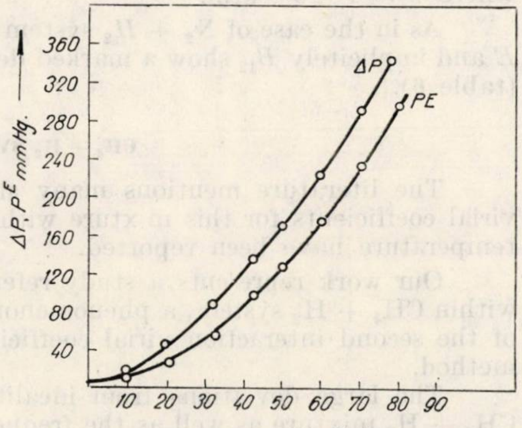

Fig. 2. — Variation of ΔP and P^E with the pressure of Ar + H$_2$ mixture.

If the excess volume is extrapolated for pressure zero the experimental value $V^E = 3.61$ cm^3/mol will result : by using this value together with the virial coefficients of the single gases (table 4) the experimental value of the second interaction virial coefficient $B_{12} = 6.38$ cm^3/mol is found.

For the theoretical estimation of the second interaction virial coefficient we made use of a Lennard-Jones potential (6, 12) and of the simple combination rules.

The examination of the results recorded in table 5 shows that the theoretical value of B$_{12}$ is particularly sensitive as concerns the choice of the intermolecular potential parameters.

Table 4

The second virial coefficients of H_2 and Ar at standard temperature

Gas	$B_{298} \cdot 10$(cm^3/mol)
H_2	13.81[3]
Ar	−15.49[4]

Table 5

The potential parameters for H_2 and Ar and the second interaction virial coefficient of the Ar+H_2 mixture

Single gas or mixture	σ(Å)	ε.10^{14} erg	B_{12} cm^3/mol
H_2	2.928[5]	0.5106	
Ar	3.820[5]	1.649	
	3.405[5]	1.67	
Ar + H_2	3.374[5]	0.917	8.98
	3.164[5]	0.923	7.23

The use of the experimental data regarding the pressure variations ΔP that result as an effect of the mixing of the two gases leads to the following relation [1] which expresses the dependence of the second excess virial coefficient (E) upon the pressure:

$$E = 0.6438 \frac{P}{n^2} - 2(216.6225 + 0.84\, E)\, 4.10^{-4}\, n$$

where $n = P \cdot 10^{-1}$ atm.

As in the case of $N_2 + H_2$ system the second excess virial coefficient E and implicitely B_{12} show a marked decrease when the pressure increases (table 6).

$CH_4 + H_2$ SYSTEM

The literature mentions many studies where [6–8] measurements of virial coefficients for this mixture within a wide interval of pressure and temperature have been reported.

Our work represents a study referring to the molecular interaction within $CH_4 + H_2$ system, a phenomenon emphasized by the measurement of the second interaction virial coefficient at high pressures by a direct method.

The large deviations from ideality to be expected in the case of $CH_4 + H_2$ mixture as well as the frequency of the appearance of the two components in the industrial practice [9] justify the importance we have granted to the study of this mixture.

As in the previous study we shall give first the computation results of the excess volumes at standard temperature and for pressures going from 10 to 80 atm.

---

[3] A. Michels and H. Wijker, *Physica's Grav.*, **15**, 627 (1949).

[4] A. Michels and M. Goudeket, *Physica's Grav.*, **8**, 347 (1941).

[5] C. W. Solbrig and R. T. Ellington, *Chem. Eng.*, **59**, 127 (1963).

[6] I. R. Kritschewsky and G. T. Lerchenko, *Acta Phys. Chim.*, URSS, **14**, 271 (1941).

[7] D. M. Mason and B. E. Eakin, *J. Chem. Eng. Data*, **6**, 499 (1961).

[8] M. H. Mueller and T. W. Leland Jr., *Amer. Inst. Chem. Engr.*, **7**, 267 (1961).

[9] C. D. Nenițescu, "Chimie Organică", vol. I, Editura Tehnică, București, 1958, p. 218–222.

From the examination of the excess volume values recorded in table 6 and graphically represented in figure 3, there results that the largest deviations determined for molar fraction 0.5 are approximately 3.5 times greater than in the case of $N_2 + H_2$ and $Ar + H_2$ systems.

Table 6

Excess volumes of CH_4+H_2 mixture for various pressures and compositions at the standard temperature (l/mol)

x_{H_2} \ P_{atm}	10	20	30	40	50	60	70	80
0.1	4.370	4.569	4.767	4.959	5.140	5.306	5.450	5.569
0.2	7.726	8.033	8.332	8.616	8.876	9.110	9.306	9.461
0.3	10.090	10.437	10.771	11.080	11.359	11.600	11.979	11.944
0.4	11.477	11.821	12.142	12.435	12.693	12.910	13.081	13.200
0.5	11.907	12.212	12.494	12.746	12.963	13.140	13.272	13.356
0.6	11.389	11.637	11.864	12.063	12.229	12.360	12.452	12.502
0.7	9.931	10.117	10.282	10.423	10.539	10.626	10.682	10.704
0.8	7.545	7.664	7.768	7.856	7.925	7.973	8.001	8.005
0.9	4.234	3.291	4.338	4.378	4.408	4.427	4.436	4.332

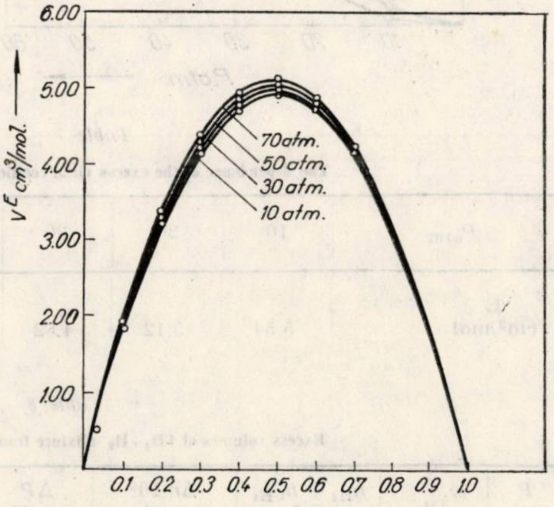

Fig. 3. — Variation of excess volume of $CH_4 + H_2$ mixture with composition and pressure at the standard temperature.

The experimental values recorded in table 7 are smaller than the computed ones, though the variation of V^E with the composition is the same.

The extrapolation value of the excess volume at pressure zero which is equal to 10.63 cm³/mol together with the values of the virial coefficients of single components (in table 9) lead to the experimental value $B_{12} = 6.42$ cm³/mol of the second interaction virial coefficient in good agreement with the theoretical values of 6.03 cm³/mol or 5.78 cm³/mol (see Table 10).

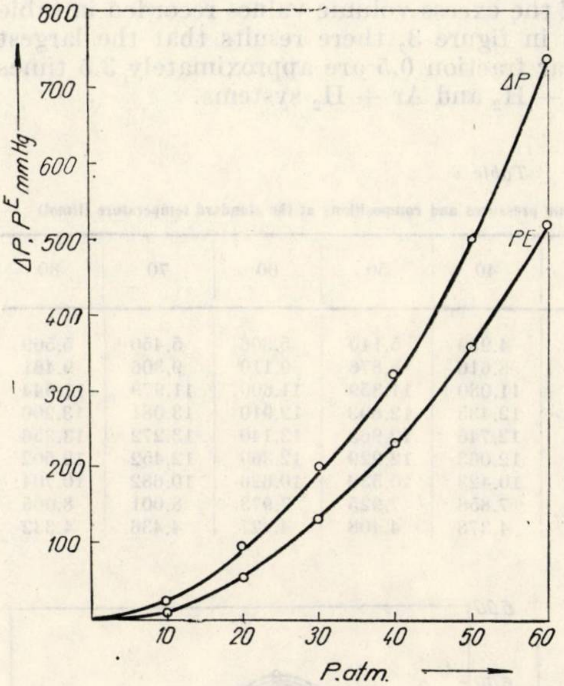

Fig. 4. – Variation of ΔP and P^E with the pressure of $CH_4 + H_2$ mixture.

Table 7

The dependence of the excess virial coefficient on pressure

P_{atm}	10	20	30	40	50	60	70	80
E cm³/mol	5.54	5.12	4.82	4.42	3.76	3.24	2.69	2.12

Table 8

Excess volumes of CH_4+H_2 mixture from experimental data

P atm	x_{H_2}	$n_{H_2} + n_{CH_4}$ mol	$\Delta n.10^3$ mol	ΔP mm Hg	P_E mm Hg	$V^{M,id}$ cm³/mol	V^E cm³/mol
10	0.370	0.547	1.4	21.77	13.91	2444.31	6.23
20	0.427	1.908	5.68	91.41	56.13	1221.50	7.54
30	0.452	1.270	13.26	200.20	130.95	831.16	6.41
40	0.466	1.632	21.85	312.09	214.98	615.92	8.09
50	0.475	1.915	38.30	497.15	356.10	494.12	9.25
60	0.481	2.356	59.76	735.72	518.37	413.09	10.25

By introducing the values of the second virial coefficients of the single components CH_4 and H_2 into the equation expressing the dependence of the second excess virial coefficient of pressure and variation of pressure

Table 9

The second virial coefficients for CH_4 and H_2 at standard temperature

Gas	$B_{298.16}$(cm^3/mol)
H_2	13.81[3]
CH_4	−43.38[10]

Table 10

The potential parameters of CH_4 and H_2 and the interaction second virial coefficient of $CH_4 + H_2$ mixture

Single gas or mixture	(Å)	ε/k(°k)	B_{12}(cm^3/mol)
H_2	2.928	37.00	
CH_4	3.796	144 from viscosity coefficients	
	3.81	148.2 from $B(T)$	
$CH_4 + H_2$	3.369	72.99	6.03
	3.369	73.00	5.78

which appears as an effect of the gas mixing,[1] we are led to the following equation :

$$E = 0.64387\,\frac{\Delta P}{n^2} - 2(220.25 + 14.84\ \mathrm{E})\,4\cdot 10^{-4}\,n$$

where $n = P.10^{-1}$ atm.

In table 11, there are to be found the results of our computations within the pressure interval where the measurements were made.

Table 11

The dependence of the excess virial coefficient on pressure

P_{atm}	10	20	30	40	50	60
E(cm^3/mol)	13.66	14.02	13.32	11.31	11.25	11.29

Let us remark the much less pronounced variation with pressure of the excess second virial coefficient (E) than in the case of $N_2 + H_2$ and $Ar + H_2$ systems.

QUALITATIVE THEORETICAL INTERPRETATION OF THE EXPERIMENTAL RESULTS

It is well known that in general the intermolecular forces are of electric nature. This is true even when there are also possibilities of magnetic interactions which are usually negligible even in the border-line case of the ferromagnetism.

If the interacting molecules are situated far from one another, their interactions are determined by the permanent electric moments (charges, dipoles, quadrupoles, etc.) of the free molecules. On the other hand, the permanent electric moments of the individual molecules polarize (distort) the electronic structure of other molecules they contact and produce an induction energy that can be expressed by the permanent moments of the individual molecules and by polarizabilities (induced electric moments).

The interaction between the electric moments resulting from the fluctuations of the charge distributions of the molecules leads to the London energy dispersion occurring even in the molecules devoid of permanent electric moments. This dispersion energy is expressed by the polarizabilities of the individual molecules in the electric fields where they oscillate at imaginary frequencies [10,11] or it can be approximated by the molecular polarizabilities and by the ionization potentials of the free molecules.[12,13]

The appearance of a positive pressure variation as an effect of the gas mixing — in the case of $N_2 + H_2$ and $CH_4 + H_2$ systems can be qualitatively explained if we admit the existence of uniformly distributed positive charges upon the surface of the sphere surrounding the molecule.

The existence of these positive charges as well as their values for each individual molecule — in spite of the fact that the molecules are electrically neutral — was taken into account and numerically computed by quantum methods, by the analysis of the electron population before and after the formation of the chemical bonds. The computation is developed in extenso in the appendix.

In case of the hydrogen molecule the net proton charge of each hydrogen atom in the molecule is

$$\delta_{\mathrm{H}} = + \frac{S}{1+S} = +0.429 \text{ proton charges}$$

while the density of the two proton charges distributed on the sphere area (A_{H_2}) of radius $r_{\mathrm{H-H}} = 0.74$ Å will be :

$$\rho_{\mathrm{H}_2} = \frac{2\,\delta_{\mathrm{H}}}{A_{\mathrm{H}_2}} = + 0.4997.10^{16} \text{ e/cm}^2$$

---

[10] Mc. Lachlan, *Proc. Roy. Soc.*, **A 271**, 387 (1963).

[11] A. Dalgarno and W. D. Davison, *Adv. At. Mol. Phys.*, **2**, 1 (1966).

[12] F. London, *Trans. Faraday Soc.*, **33**, 8 (1937).

[13] A. D. Backingham, *Adv. Chem. Phys.*, **12**, 107 (1967).

In the nitrogen case $\delta_N = +0.1625$ proton charges which means that on a hydrogen atom of a hydrogen molecule there are 2.623 times more proton charges than on a nitrogen atom of a nitrogen molecule.

The density of the two proton charges distributed on area A_{N_2} ($r_{N-N} = 1.10$ Å) will be :

$$\rho_{N_2} = \frac{2\,\delta_N}{A_{N_2}} = 0.0855.10^{16}\ \mathrm{e/cm^2}$$

which is 5.844 smaller than δ_{H_2}.

Assuming that the methane molecule is like a sphere of diameter $2r_{C-H} = 2.186$ Å, the density of the four proton charges will be

$$\rho_{CH_4} = \frac{4\,\delta_H}{A_{CH_4}} = 0.0053.10^{16}\ \mathrm{e/cm^2}$$

Therefore, the methane molecule can be considered as a double electric layer having negative electric charges on the central carbon atom and positive electric charges on the peripheral hydrogen atoms of the molecule.

The repulsive forces of electric nature appearing between the components of the two chemical species and possessing a uniformly distributed positive charge on a spherical surface are a function of the separating distance which depends in turn on the pressure within the mixture.

In the case of $H_2 + Ar$ and $N_2 + Ar$ systems owing to the lack of electric interactions between permanent electric dipolar or charges on the molecule atoms as in the case of $N_2 + H_2$ and $CH_4 + H_2$ systems, the London interactions are the most probable ones.

The dispersion interactions depend on the molecular polarizabilities. For the above-mentioned systems the experimentally determined molecular polarizabilities and refractions are :[14]

Table 12

The experimental values for the molecular polarizabilities and refractions

Gas	R_0(cm^3/mol)	$\alpha_0 = \frac{3R_0}{4\pi N_0} \cdot 10^{24}$cm^3/mol
Ar	4.143	1.6264
H_2	2.037	0.8023
N_2	4.402	1.7340
CH_4	6.855	2.6990

from which there results that the interaction forces of London type will be prevalent in $N_2 + Ar$ system which explains, moreover, the presence of attractive energies within the system (negative variations of the mixing pressure).

---

[14] E. A. Moelwyn-Hughes, "Physical Chemistry", Pergamon Press, London, 1961, chap. 9.

In the $H_2 + Ar$ system owing to the small polarizability of the hydrogen molecule, the prevailing energy will be the repulsive one because of the diffusion at high pressures of the electron cloud of the other molecule.

The quantitative estimation of the interaction energies acting between the molecules of a gas mixture under given conditions of pressure and temperature constitutes a particularly difficult problem that requires the design of a computing model the validity of which will only be confirmed by its confrontation with experiment.

APPENDIX

ELECTRON POPULATION ANALYSIS FOR MOLECULES H_2, N_2 AND CH_4

1. Molecules H_2 and N_2 are diatomic molecules, the distances between their two atoms being $r_{H-H} = 0.74$ Å and $r_{N-N} = 1.10$ Å.

The electron population analysis was made by the Mulliken method for the following fundamental molecular configurations :

$$H_2\ [(\psi)^2] \text{ where } \quad \psi = \sqrt{\frac{1}{2(1+S_{AB})}}\,(1s_A + 1s_B)$$

$$N_2\ [(\sigma_s)^2\,(\sigma_s^*)^2\,(\pi_{x(y)})^4\,(\sigma_z)^2]$$

where

$$\sigma_s = \sqrt{\frac{1}{2\,(1+S_{AB})}}\,(2s_A + 2s_B), \quad \sigma_s^* = \sqrt{\frac{1}{2\,(1-S_{AB})}}\,(2s_A - 2s_B)$$

$$\pi_{x(y)} = \sqrt{\frac{1}{2\,(1+S_\pi)}}\,\left(2p_{x(y)_A} + 2p_{x(y)_B}\right)$$

$$\sigma_z = \sqrt{\frac{1}{2\,(1+S_\sigma)}}\,\left(2p_{z_A} + 2p_{z_B}\right)$$

where S are the diatomic overlap integrals.

By making use of Slater type atomic orbitals ($\zeta_H = 1$; $\zeta_N = 1.95$) and by estimating the diatomic overlap integrals for the above mentioned interatomic distances, the electron population analysis supplies the following values for the proton charges on hydrogen and nitrogen atoms : $\delta_H = +0.429$ and $\delta_N = 0.1625$.

If molecules H_2 and N_2 are considered as spheres, the diameters of which are equal to the intermolecular distances, it is easy to see that the density of the proton charges distributed on the sphere area will be :

$$\rho_{H_2} = \frac{2\,\delta_H}{A_{H2}} = +\,0.4997.10^{16}\,e/\,cm^2$$

$$\rho_{N_2} = \frac{2\,\delta_N}{A_{N2}} = +\,0.0855.10^{16}\ e/cm$$

where A_{H_2} and A_{N_2} are the areas of the two spheres.

Since the chemical bonds of molecules H_2 and N_2 are homopolar the mixing coefficients of the molecular orbitals can be directly given by the topological properties of molecule and are independent of the nature of the various approximations used for estimating the energies of the molecular levels. Since in the methane molecule C—H bonds are heteropolar, there results that the values of these coefficients will depend on the nature of the MO approximations used for determining the energies of the molecular states. Hereafter we give the values of the net electron charges estimated by means of a few approximations of well known molecular orbitals by making use of the Slater type atomic orbitals (Table 13).

Let us remark that the net proton charges on the hydrogen and carbon atoms are very small and that in a single case (INDO) can negative electric charges be forecast, on the hydrogen atoms.

So as to be able to choose the most sensible values of the proton charges we should appeal to data about the dipole moment of the molecule. But it is known that the dipole moment of the methane molecule is equal to zero since a contingent vector sum of the dipole moment of the four C—H bonds, whatever their values, would be equal to zero owing to the symmetry of the molecule.[15]

Nevertheless, the kinetic data [16,17] permitted to estimate that the dipole moment of the $C^- - H^+$ bond would be approximately $\mu_{C^- - H^+} = 0.33.10^{-18}$ electrostatic units.

From the data supplied by the above-mentioned approximations LCAOMO, the following values result for the dipole moments of bond C—H.

Table 13

Electron charges in methane estimated by different MO methods [18]

CNDO	$C^{-0.073}$	$H^{+0.0018}$
INDO	$C^{+0.043}$	$H^{-0.011}$
RCNDO	$C^{-0.084}$	$H^{+0.021}$
SCFMO	$C^{-0.192}$	$H^{+0.048}$

Table 14

The calculated dipole moments C—H in methane [18] **in $C^- - H^+$** (10 — [18] es. u.

CNDO	+0.288
INDO	−0.168
RCNDO	+0.330
SCFMO	+0.755

---

[15] *Idem*, chap. 7.

[16] C. P. Smith, *J. Phys. Chem.*, **41**, 209 (1937).

[17] J. R. Partington, "An Anvanced Treatise on Physical Chemistry", vol. 5, Pergamon Press, New York, 1954, p. 476, 1954, p. 476.

Hereafter we shall use the value of the proton charge on the hydrogen atom $\delta_H = +0.02$ supplied by methods CNDO and RCNDO because versions CNDO supply generally good values for the dipole moments of the chemical bonds,[18] as, on the other hand, the same results were deduced from the above mentioned values.

If molecule CH_4 is considered as a sphere the diameter of which is $2r_{C-H} = +2.186$ Å, this sphere area will be equal to $4 \times 3.751.10^{-16}$ cm^2 while the density of the four proton charges, distributed on area A_{CH_4}, will be

$$\rho_{CH_4} = \frac{4\,\delta_H}{A_{CH_4}} = 0.0053.10^{16}\ \mathrm{e/cm^2}.$$

---

[18] G. Klopman and B. O'Leary, "All-Valence Electrons SCF Calculations", Springer Verlag, Berlin, 1970.

Revue Roumaine de Chimie, 22, 6, 839–848 (1977)

THERMODYNAMIC AND TRANSPORT PROPERTIES OF THE POLYELECTROLYTE SOLUTIONS

CAMELIA BELDIE

Department of Physical Chemistry,
Polytechnic Institute of Jassy

Received April 1, 1975

This paper reports the measurement data on the behaviour in an aqueous solution of a few samples of poly(acrylic)acid (PAA) and poly(methacrylic)acid (PMA) of different molecular weights. The mixture volume and viscosity measurements were studied within the temperature range of 20–50°, and the concentration of 0.0009–0.01 g/ml. The molal apparent volumes, the mixture volumes referred to monomer, the reduced viscosity and the "viscous flow activation energy" were also computed.

The properties of the polyelectrolyte solutions are of great theoretical and practical interest, taking into account that many natural substances, important from the biochemical viewpoint, behave like polyelectrolytes.

Although many investigations on polyelectrolytes have been made, particularly in the last decades, an agreement has not yet been found concerning their behaviour in different media and especially in aqueous solutions, the closest state of natural conditions.

The experimental data as regards the behaviour and conformation in aqueous solution of a few poly(acrylic)acid (PAA) and poly(methacrylic)acid (PMA) samples of different molecular weights, depending on concentration and temperature, are presented in this paper.

It must be recalled that the PAA and PMA are weak acids (weak polyelectrolytes) in an aqueous solution, while their salts are strongly dissociated (strong polyelectrolytes).

Owing to the carboxylic groups in the macromolecular chain, PAA and PMA can form intra- and intermolecular hydrogen bonds. The hydrogen bonds are influenced by concentration and temperature of the solution.

The existence of both the hydrogen bonds and the other interaction types (counter ion-macroion, counter ion-dipole, macroion-dipole), which take place in these kinds of solutions, will influence certain properties, for instance mixture volume, viscosity, conductivity, etc.

EXPERIMENTAL RESULTS

PAA and PMA were carried out by monomer polymerization in solution.[1] Samples with different molecular weights were prepared, as follows :

$$\mathrm{PAA} - \bar{M}_w = 1.5 \times 10^5 ; 3.0 \times 10^5 ; 4.5 \times 10^5.$$

$$\mathrm{PMA} - \bar{M}_w = 1.5 \times 10^5 ; 3.0 \times 10^5.$$

The mixture volumes and the viscosities of the above polyelectrolytes within 20 – 50° temperature range, were measured.

PAA and PMA solutions were used for 24 hours, in order to avoid autodegradation in time.

Solutions of 0.0009 – 0.01 g/ml concentration were used in all measurements.

1. APPARENT MOLAL VOLUMES AND MIXTURE VOLUMES

The apparent molal volumes and the mixture volumes, referred to the monomer unity, were computed from the density measurements (pyknometry).

The apparent molal volume was computed employing the equation

$$\Phi_v = \frac{M}{d} + \frac{W_{55.51}(d_0 - d)}{d d_0 m} \tag{1}$$

where M – is monomer molecular weight,
d – solution density,
m – solution concentration (moles monomer/1000 g solvent),
$W_{55.51}$ – weight of 55.51 moles of water.

The molal apparent volume and the mixture volume data are given in Table 1. One can see that these values increase with decreasing concentration.

All density measurements were made within 20–25° temperature range. Our samples show a positive mixture volume except two determinations for PAA_2 ($\bar{M}_w = 3.0 \times 10^5$), at higher concentrations.

2. VISCOSITIES

The viscosity was measured employing a Ubbelohde viscometer, within 20 – 50 ± 0.05° temperature range.

The η_{sp}/c ratio plotted against concentration and the intrinsic viscosities were obtained by extrapolating the plottings (Fig. 1 and Fig. 2).

The η_{sp}/c ratio decreases, for the range of used concentration, simultaneously with the concentration for PAA (Fig. 1 and Fig. 2) and shows a minimum for PMA, which become smooth by increasing temperature (Fig. 3).

---

[1] A. Packter, *J. Polymer Sci.*, A, 3021 (1963).

Table 1

Apparent molal and mixture volumes

Sample	Conc. (monomer moles/1000 g solvent)	$t°C$	Φ_v (ml/mol monomer)	Δv_2^m(ml/mol monomer)
PAA(1)	0.13993	21.5	73.6708	1.4432
	0.05609	20.0	119.7980	41.4166
	0.02242	21.5	142.8518	70.5249
PAA(2)	0.18950	20.8	59.9601	−12.0704
	0.16070	20.8	63.5888	− 8.5080
	0.07603	20.8	82.7709	10.5180
	0.03805	21.6	143.7820	71.3737
PAA(3)	0.15050	20.2	74.2677	2.0546
	0.07535	19.4	98.9002	26.5770
	0.03772	20.0	152.2018	79.7972
	0.01886	21.2	253.1571	180.7055
PMA(1)	0.16013	21.2	86.2849	0.0200
	0.12234	21.8	94.1978	7.9218
	0.07646	20.2	108.3501	21.9595
	0.06143	21.2	122.8195	36.3695
PMA(2)	0.14450	20.8	89.7893	3.4893
	0.10510	23.4	98.4251	12.0076
	0.06622	20.2	123.0696	36.6150
	0.03354	19.4	179.7970	93.2953

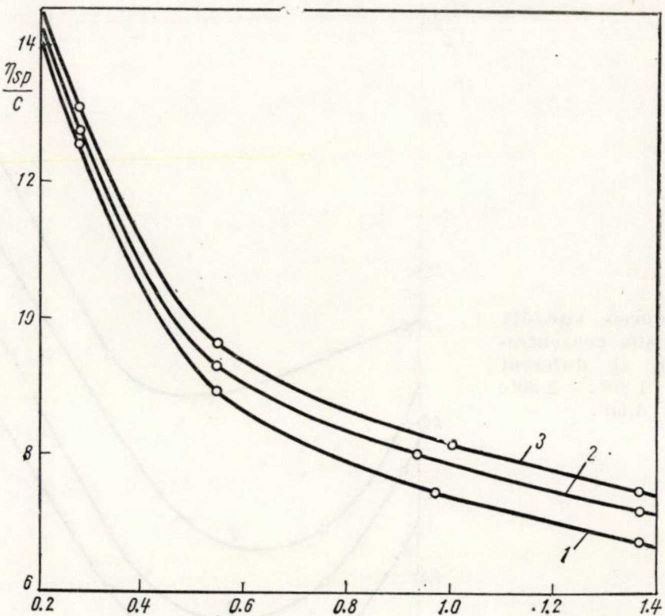

Fig. 1. — Reduced viscosity of PAA(2) versus concentration (g/100 ml), at different temperatures, 1.20° ; 2.30° ; 3.35°.

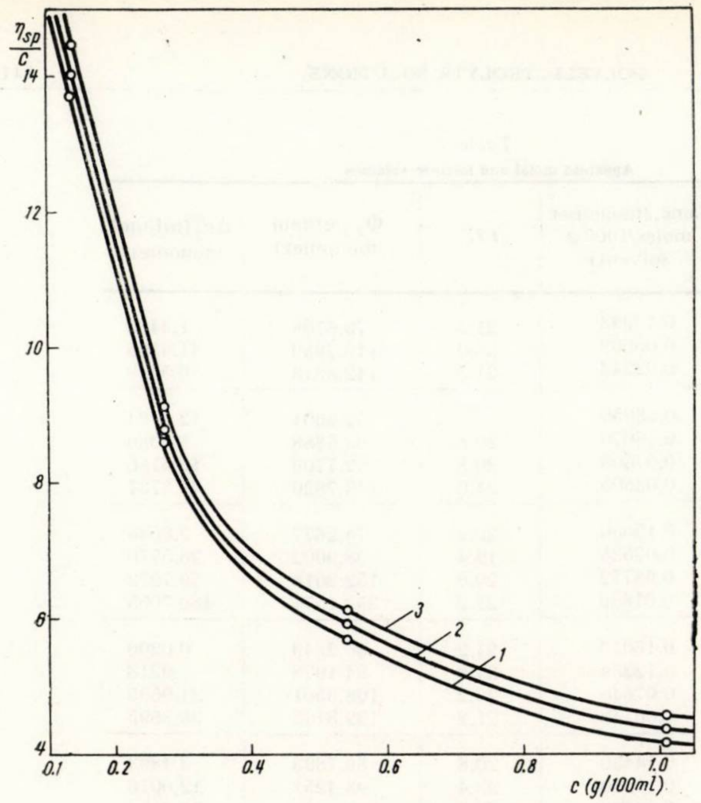

Fig. 2. — Reduced viscosity of PAA(3) versus concentration (g/100 ml), at different temperatures, 1.20° ; 2.30° ; 3.35°.

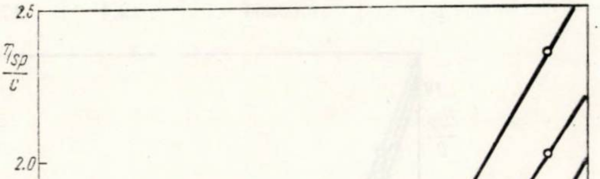

Fig. 3. — Reduced viscosity of PMA(2) versus concentration (g/100 ml), at different temperatures, 1.20° ; 2.30° ; 3.40° ; 4.50°.

DISCUSSION

It is well known that the ratio η_{sp}/c increases nonlinearly and quickly with the system dilution for polyelectrolytes in the salt-free solutions. Different equations were suggested in order to describe the reduced viscosity dependence upon concentration. Here are several examples :

The Fuoss' equation [2] is the most well-known one,

$$\eta_{sp}/c = \frac{A}{1 + B\sqrt{c}} + D \tag{2}$$

Liberti-Stivala's equation,[3]

$$\eta_{sp}/c = \frac{A}{1 + B(\sqrt{c} - k'c)} \tag{3}$$

Schaefgen-Trivisonno's equation,[4]

$$\eta_{sp}/c = \frac{A}{1 + Bc} \tag{4}$$

These equations are empirical in essence and they involve the knowledge of two or three parameters that can hardly be precisely determined.

A and B are specific to polyelectrolyte-solvent couple, D serves primarily as a linearizing device and k' is understood as interaction parameter.

The employment of equations (2) — (4) for the viscosimetrical study data of the polyelectrolyte solutions is not always satisfactory.[3] For instance Schaefgen-Trivisonno[4] and Liberti-Stivala[5] have got infinite or negative values for the intrinsic viscosity employing equation (2).

A new semiempirical equation was proposed by Yuan, Dougherty and Stivala [3] under the following form :

$$\eta_{sp}/c = [\eta]_\infty + k[\eta]_\infty/\sqrt{c} \tag{5}$$

or

$$\eta_{sp}/c = [\eta]_\infty[1 + k/\sqrt{c}]$$

This equation was verified for a number of polyelectrolytes by its authors [3] as long as the concentration is not too low and only for strong polyelectrolytes.

One could see that in our case the ratio η_{sp}/c plotted against concentration is not a linear relationship (Fig. 1 ; Fig. 2).

---

[2] R. M. Fuoss, *J. Polymer Sci.*, **3**, 602, 603 (1948).
R. M. Fuoss and U. P. Strauss, *Ann. N. Y. Acad. Sci.*, **51**, 836 (1949).

[3] L. Yuan, T. J. Dougherty and S. S. Stivala, *J. Polymer Sci.*, Part A2, **10**, 171 (1972).

[4] J. R. Schaefgen and C. F. Trivisonno, *J. Amer. Chem. Soc.*, **74**, 2715 (1952).

[5] P. A. Liberti and S. S. Stivala, *J. Polymer Sci.*, B, **4**, 137 (1966).

Attempts were made to straighten this dependence plotting η_{sp}/c versus $1/\sqrt{c}$, according to equation (5). Such a plotting might be a straight line for strong polyelectrolytes in agreement with the authors' comments.[3]

For our data the η_{sp}/c parameter depending on $1/\sqrt{c}$ can be estimated as straight lines only for the PAA samples with the smallest molecular weight (Fig. 4), except the two samples where some curves are really obtained according to our experimental data.

The curves may be extrapolated in order to get the values for infinite concentration (Fig. 5).

In the case of PMA a straight line was only obtained for a sample, at higher temperature, between 40 and 50° (Fig. 6).

At the same time, an evident variation was found for the obtained plots depending on temperature, as it can be seen from figures 5 and 6.

The intrinsic viscosity $[\eta]$ varies with the molecular weight of the polyelectrolyte samples, as one can see in Fig. 7, where the η_{sp}/c ratio was plotted versus c for the PAA samples of different molecular weights, at 25°.

The apparent molal volume data are correlated with corresponding partial molal volume v_2 by equation :

$$v_2 = \Phi_v + n_2(\partial\Phi_v/\partial n_2)_{n_1} \tag{6}$$

where n_2 are moles of solute and n_1 moles of solvent.

Φ_v and v_2 are usually obtained at infinite dilution[6] (v_2^{∞}) by extrapolating v_2 or Φ_v in terms of $c^{1/2}$; v_2^{∞} can then be interpreted in terms of solvation effects.

The apparent molal volume increases with dilution show a similar behaviour to the viscosity measurements, therefore we think that the same reason used for the explanation of the solution viscosity of the two polyelectrolytes can be also employed in order to interpret the apparent molal volumes.

In aqueous solution, the dissociation degree increases by increasing dilution and the counter ions, in bigger amount, will contribute to the increasing of the repulsion forces between macroion segments leading to the expansion of the macroion. The molecules of the two polyelectrolytes expand owing to the repulsion between the electrical groups upon macroion, that increase by increasing dilution at the same time.

If the molecules straighten, the solution viscosity will decrease at the same time. This effect is in fact typical of the salt-free polyelectrolyte solutions.

The suggested relationships, for the dependence of the η_{sp}/c on the concentration, for the soluble polyelectrolytes will be applied better to PAA than PMA samples.

In order to evidence the temperature influence upon the solution viscosity, an exponential dependence of the viscosity on temperature was taken into consideration, as it was used for the polymers in the liquid

---

[6] GH. IORDACHE, *Materiale plastice*, **9**, 191 (1972).

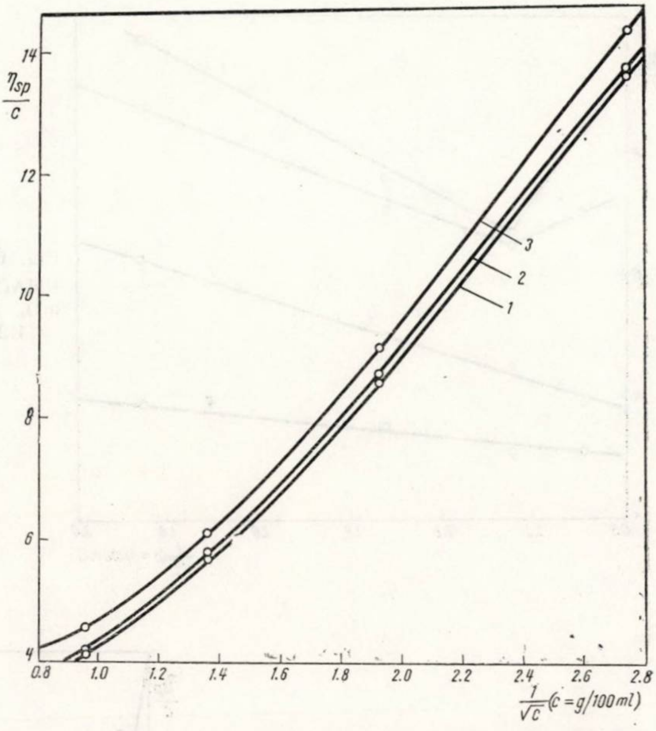

Fig. 4. — Reduced viscosity of PAA(1) versus $1/\sqrt{c}$ ($c =$ g/100 ml), at different temperatures, 1.20° ; 2.25° ; 3.35°.

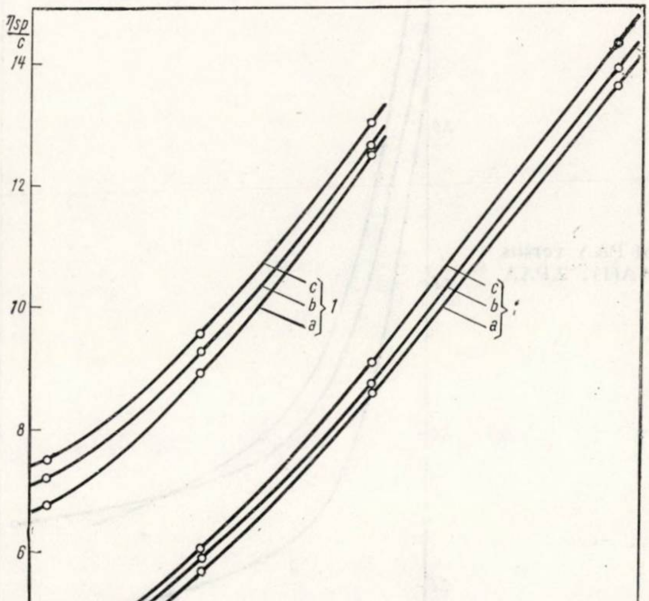

Fig. 5. — Reduced viscosity of PAA versus $1/\sqrt{c}$ ($c =$ g/100 ml), at different temperatures and molecular weights, 1. PAA(2) ; 2. PAA (3) ; a. 20° ; b. 30° ; c. 35°.

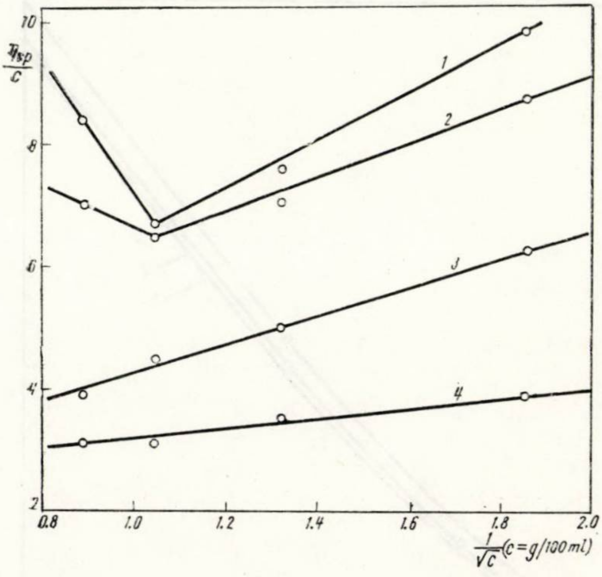

Fig. 6. — Reduced viscosity of PMA(2) versus $1/\sqrt{c}$ (c = g/100 ml), at different temperatures, 1.20° ; 2.30° ; 3.40° ; 4.50°.

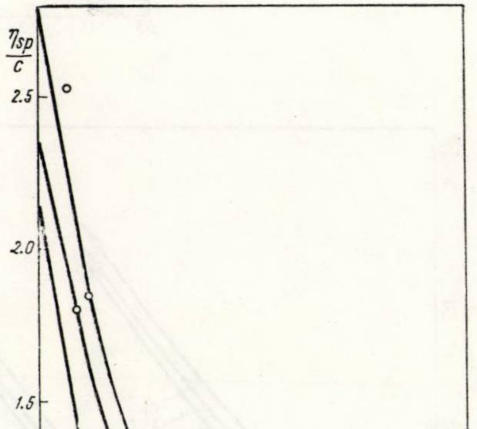

Fig. 7. — Intrinsic viscosity of PAA versus molecular weight, at 25°. 1.PAA(1) ; 2.PAA (2) ; 3.PAA(3).

state,[6–10]

$$\eta = a \exp (B/RT)$$

where B may be a "viscous flow activation energy", and a a preexponential parameter, which may depend on the couple polyelectrolyte-solvent nature.

Using such a relationship for the temperature range 20—35° for PAA and the temperature range 20—50° for PMA, one can notice as follows;

The a value varies between 3.051×10^{-2} and 6.5×10^{-3} for a concentration variation of $9.657 \times 10^{-4} - 1.366 \times 10^{-2}$ g/ml of those two polyelectrolytes.

B is equivalent to kilocalories order and it depends more on solution concentration than on molecular weight of polyelectrolyte, as one can see from Table 2.

Table 2 a

a and B values

Sample	Temp. range (°C)	Conc. (g/ml) $\times 10^3$	$a \times 10^2$	B(cal/mol)
PAA(1)	20—35	10.060	5.586	2897.8
		1.609	1.253	3346.8
		0.966	1.052	3365.0
PAA(2)	20—35	13.660	8.345	2799.6
		5.464	2.442	3191.6
		2.732	0.967	3566.3
PAA(3)	20—35	10.820	3.051	3019.0
		5.410	1.414	3297.2
		2.705	0.829	3489.6
		1.352	0.653	3539.5

Table 2 b

a and B values

Sample	Temp. range (°C)	Conc. (g/ml) $\times 10^3$	$a \times 10^5$	B (cal/mol)
PMA(1)	20—50	13.770	8.694	6326.2
		10.500	0.450	7710.3
		6.560	5.110	6028.8
		5.266	20.220	5255.8
PMA(2)	20—50	9.016	10.610	5654.1
		5.677	19.770	5201.3
		2.874	29.370	4900.4

---

[7] E. C. Bernhardt, "Pererabotka termoplastichinyh materialov", Izdatelstvo Moskva, 1965.

[8] J. R. Pearson, "Mechanical principles of polymer melt processing", Pergamon Press, London, 1966.

[9] M. McKelvey, "Polymer processing", John Wiley, New York, 1962.

[10] B. E. Conway, *J. Macromol. Sci., Revs. Macromol. Chem.*, **C6(2)**, 113 (1972).

From the experimental data of the two value categories, one can draw a conclusion, which agrees with the literature data,[10] that the studied polyelectrolytes exist under the form of coil flexible sticks. These macromolecules expand during their dilution removing each other owing to the penetration of the water molecules within chain segments. This exchange in the macroion neighbourhood leads to the osmotic effects which acquire an increasing importance and cause the ion expansion which might be a loose coil.

CONCLUSIONS

The following conclusions can be drawn from the obtained results: Poly(acrylic)acid has a behaviour characteristic of the soluble polyelectrolytes in the salt-free solution.

Yuan-Dougherty-Stivala relationship may be applied sometimes and it is more valid for smaller molecular weights. At the same time it applies better to PAA than PMA samples.

The $[\eta]$ or $[\eta]_\infty$ values are temperature-dependent, namely, they increase by increasing temperature for PAA. They decrease, at the same time, by increasing temperature for PMA.

The "viscous flow activation energy" of the two polyelectrolytes in aqueous solution is dependent on the solution concentration and it is of the order of kilocalory.

The apparent molal volumes increase by increasing dilution, and this behaviour may be explained employing the same reason as in the viscosity case.

Revue Roumaine de Chimie, **22**, *6*, 849–855 (1977)

Dedicated to the 70th anniversary
of Professor CORIOLAN DRĂGULESCU

HETEROPOLYTUNGSTATES WITH U(IV) AS CENTRAL ION

SYNTHESIS AND PHYSICO-CHEMICAL STUDIES

GHEORGHE MARCU, MARIANA RUSU and LIVIA OCHEŞEL

"Babeş-Bolyai" University, Department of Inorganic
Chemistry, str. Arany Janos, 11, Cluj-Napoca, Romania

Received August 2, 1976

The U(IV) ion reacts rapidly with unsaturated heteropolyanions, forming complexes of the UL_2 type, where $L = P_2W_{17}O_{61}{}^{10-}$, $PW_{11}O_{39}{}^{7-}$ and $SiW_{11}O_{39}{}^{8-}$. The K^+, $NH_4{}^+$, Cs^+ and Tl^+ salts of the $[U(SiW_{11}O_{39})_2]^{12-}$ heteropolyanion were isolated. The chemical individuality and the oxidation state of uranium in this heteropolycompound were analysed.

1. GENERAL CONSIDERATIONS

The unsaturated heteropolyanions of the $[U(SiW_{11}O_{39})_2]^{12-}$ type are obtained after a partial degradation of the $SiW_{12}O_{40}{}^{4-}$ anions at pH $= 6-7$ by adding the potassium hydrogencarbonate, in the presence of the U(IV) metallic ions.

Our investigations indicate that the U(IV) ion forms UL_2 heteropolycompounds, where $L = [P_2W_{17}O_{61}]^{10-}$, [1] $[PW_{11}O_{39}]^{7-}$, [2] and $[SiW_{11}O_{39}]^{8-}$ (this paper).

2. EXPERIMENTAL PART

The potassium salt of the $[U(SiW_{11}O_{39})_2]^{12-}$ heteropolyanion has been obtained by a method generally used for obtaining heteropolycompounds of this type : a solution containing 2 g U(IV) sulphate in 10 ml water was added stepwise under continuous stirring to a $K_8SiW_{11}O_{39}$[3] solution containing 25 g of solid salt in 50 ml distilled water having the pH$=4.5$ adjusted with 2N H_2SO_4 and heated at 70° (the U(IV) salt has been obtained by reducing a U(VI) salt using Jones method [4]). Finally the solution is cooled to 5° and filtered.

[1] GH. MARCU, M. RUSU and A. V. BOTAR, *Rev. Roumaine Chim.*, **19**, 827 (1974).
[2] GH. MARCU and M. RUSU, *Rev. Roumaine Chim.*, (under press).
[3] P. SOUCHAY, *Ann. Chim. (France)*, **18**, 61 (1943).
[4] J. H. KENEDY, *Analyt. Chem.*, **32**, 150 (1960).

Deep brown microcrystals were obtained after 48 hours of resting at 5° and were purified by repeated recrystallization from distilled water (70°, pH = 4.5).

The NH_4^+, Cs^+ and Tl^+ salts of $[U(SiW_{11}O_{39})_2]^{12-}$ heteropolyanion were obtained by adding calculated amounts of NH_4Cl, Cs_2SO_4 and $TlCH_3COO$ (aqueous solutions) under continuous stirring at 70° to a freshly prepared and concentrated solution of potassium salt of $[U(SiW_{11}O_{39})_2]^{12-}$ heteropolyanion.

Pure crystals of salts having a deep brown colour are obtained after threefold recrystallization from distilled water at 70° and the pH = 4.5, in each case.

2.1. ANALYTICAL ANALYSIS

The K^+, NH_4^+, Cs^+ and Tl^+ salts were chemically analysed according to the general procedure shown in reference[5]. Uranium was photocolorimetrically analysed with Arsenazo III reagent.[6]

The amount of tungsten was measured by precipitation with cinchonine followed by an ignition to WO_3 at 800°.[7] The silicon was volatilized with HF.[8] Potassium and caesium were obtained as tetraphenylborates.[9] Thallium (I) was analysed as TlI.[10] Nitrogen was measured by Kjeldhal method.[11] The water content was thermogravimetrically established. The results of the chemical analysis are given in table 1.

2.2. OTHER MEASUREMENTS

The basicity has been determined by conductometric titration of 50 ml solution of $K_{12}[U(SiW_{11}O_{39})_2].30\ H_2O$ ($T_W = 0.0275$) with a $TlCH_3COO$ solution ($T_{Tl} = 0.0199$) (see figure 1). Measurements have been carried out by a Radelkis OK–102 conductometer.

Table 1

The analytical data for K+, NH_4^+, Cs+ and Tl+ salts of $(U(SiW_{11}O_{39})_2]^{12-}$ heteropolyanion

Compound		%							
		W	U	Si	H_2O	K	N	Cs	Tl
$K_{12}[U(SiW_{11}O_{39})_2].30H_2O$	Calcd.	61.32	3.60	0.85	8.84	7.09	—	—	—
	Found.	61.30	3.58	0.83	8.82	7.08	—	—	—
$(NH_4)_{12}[U(SiW_{11}O_{39})_2].26H_2O$	Calcd.	64.49	3.79	0.89	7.46	—	2.69	—	—
	Found.	64.45	3.77	0.88	7.42	—	2.64	—	—
$Cs_{12}[U(SiW_{11}O_{39})_2].20H_2O$	Calcd.	53.63	3.15	0.74	4.76	—	—	21.14	—
	Found.	53.59	3.12	0.73	4.75	—	—	21.10	
$Tl_{12}[U(SiW_{11}O_{39})_2].16H_2O$	Calcd.	48.57	2.85	0.67	3.45	—	—	—	29.44
	Found.	48.54	2.84	0.66	3.44	—	—	—	29.43

---

[5] V. E. Simmons, Ph. D. Thesis, Boston University, 1963.

[6] B. V. Savvin, *Talanta*, **8**, 673 (1961).

[7] A. I. Vogel, "A textbook of quantitative inorganic analysis", 2nd. edn. London, 1951, p. 418.

[8] A. I. Kokorin and R.-L. Dimant, *Zhur. obshchei Khim.*, **24**, 971 (1954).

[9] M. Kohler, *Z. analyt. Chem. B.*, **138**, 9 (1953).

[10] I. M. Kolthoff and P. J. Elving, "Treatise on analytical chemistry", Part II, vol. 2, Interscience Publishers, New York, 1962, p. 92.

[11] F. P. Treadwell, "Kurzes Lehrbuch der analytichen Chemie", vol. 2, edn. 11, Franz Deutiche, Wien, 1941, p. 483.

The chemical individuality of potassium salt $K_{12}[U(SiW_{11}O_{39})_2].30\,H_2O$ (I) was controlled by recording the UV spectrum of a solution of the compound (I) having a tungsten concentration of 10^{-4}M which was recorded on a "Specord-UV-VIS" spectrophotometer and the IR spectrum of solid salt which was recorded on a "UR-10-Zeiss Jena" spectrophotometer. Both spectra were recorded at room temperature.

The oxidation state of uranium in this heteropolycompound was established using the absorption spectrum in the visible domain of a solution with a tungsten concentration of 10^{-2} M (see figure 4), the electronic reflection spectrum (see figure 5), and the measurements of magnetical susceptibility (see figure 6).

The electronic absorption spectrum in the visible domain was recorded on a "Specord-UV-VIS" spectrophotometer with automatical recording. The electronic reflectance spectrum was recorded on a "WSH-1-Zeiss" spectrophotometer on pellets made of heteropolycompound (I) diluted by MgO in a ratio 1 : 1. The measurements of the magnetical susceptibility and its temperature dependence were made by using a Forrer type balance in the temperature range 75–232° and with liquid nitrogen cooling of the sample. The experimental data are shown in figure 6.

3. RESULTS AND DISCUSSION

The newly obtained heteropolycompound has the formula: $K_{12}[U(SiW_{11}O_{39})_2].30\,H_2O$, in good agreement with the experimental data, and this compound is formed according to the following equation:

$$2\,K_8SiW_{11}O_{39} + U(SO_4)_2 = K_{12}\,[U(SiW_{11}O_{39})_2] + 2\,K_2SO_4$$

We were able to prepare the free acid by a cationic exchange method on Zerolit 225 resin in the H^+ form, but it decomposes rapidly.

The good agreement between the theoretical basicity and the experimental value obtained by conductometrical titration of the potassium salt of the $[U(SiW_{11}O_{39})_2]^{12-}$ heteropolyanion and by chemical analysis of the K^+, NH_4^+, Cs^+ and Tl^+ salts (see table 1) was proved.

The UV spectrum of a solution of the $K_{12}[U(SiW_{11}O_{39})_2].30\,H_2O$ exhibits an absorption band with a peak at 254 nm (figure 2) assigned to a charge transfer from the oxigen to the tungsten atoms i.e. to a $p_\pi - d_\pi$ [12] electron transfer respectively.

This band si also characteristic of the 1 : 12 and 2 : 11 heteropolyanions, respectively.

The IR spectrum of the $K_{12}[U(SiW_{11}O_{39})_2].30\,H_2O$ compound shows three absorption bands from 700 to 1000 cm^{-1}, which are due to stretching vibration of the W–O bonds. The absorption maxima are found at 800, 900 and 960 cm^{-1}; the absorption bands in the above-mentioned

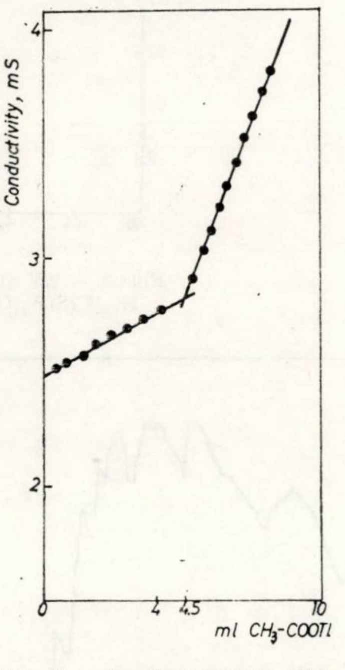

Fig. 1. – Conductometric titration curve of 50 ml solution $K_{12}[U(SiW_{11}O_{39})_2].30\,H_2O$ with $T_W = 0.0275$ with $TlCH_3COO$ with $T_{Tl} = 0.0199$.

---

[12] G. M. Varga Jr., E. Papaconstantinou and M. T. Pope, *Inorg. Chem.*, **9**, 662 (1970).

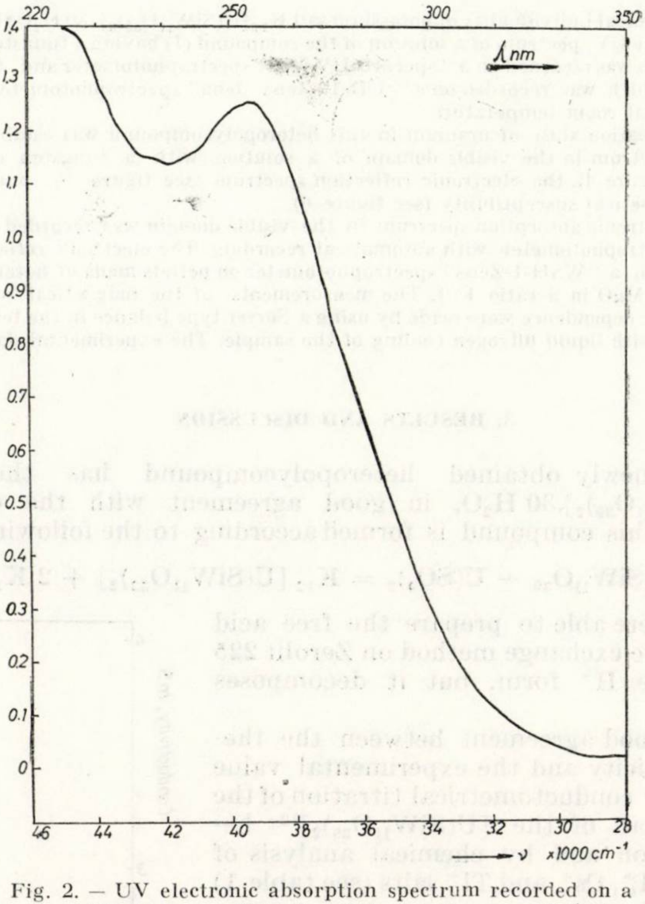

Fig. 2. — UV electronic absorption spectrum recorded on a $K_{12}[U(SiW_{11}O_{39})_2].30\ H_2O$ solution with $c_W = 10^{-4}$ M.

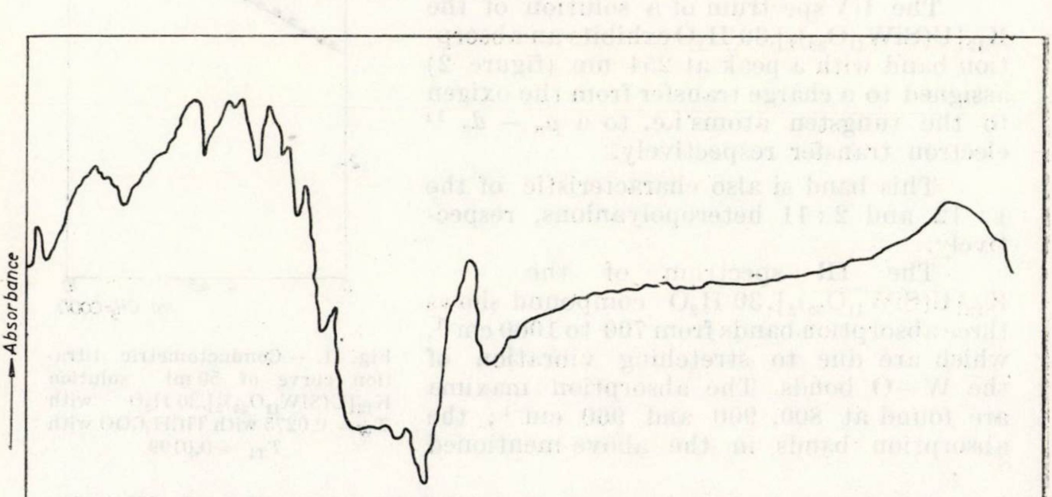

Fig. 3. — IR spectrum of $K_{12}[U(SiW_{11}O_{39})_2].30\ H_2O$, recorded on solid salt.

range are also characteristic of the heteropolytungstates, particularly of the 2 : 11 series and allow to identify this compounds based on IR spectra. [13–15]

The three absorption maxima located at 1020, 1120 and 1460 cm^{-1} seen in the IR spectrum (figure 3) are due to Si^{4+}, U^{4+} and to HOH bending vibrations, respectively.

The broad absorption bands situated between 3400 and 3600 cm^{-1} are indicative of the HOH bending vibration.

By studying the electronic absorption spectrum of the heteropolycompound (I) on a solution having a tungsten concentration $c_W = 5.10^{-2}$ M (figure 4), in the visible region, we observed that the *L* band at 14,490 cm^{-1}

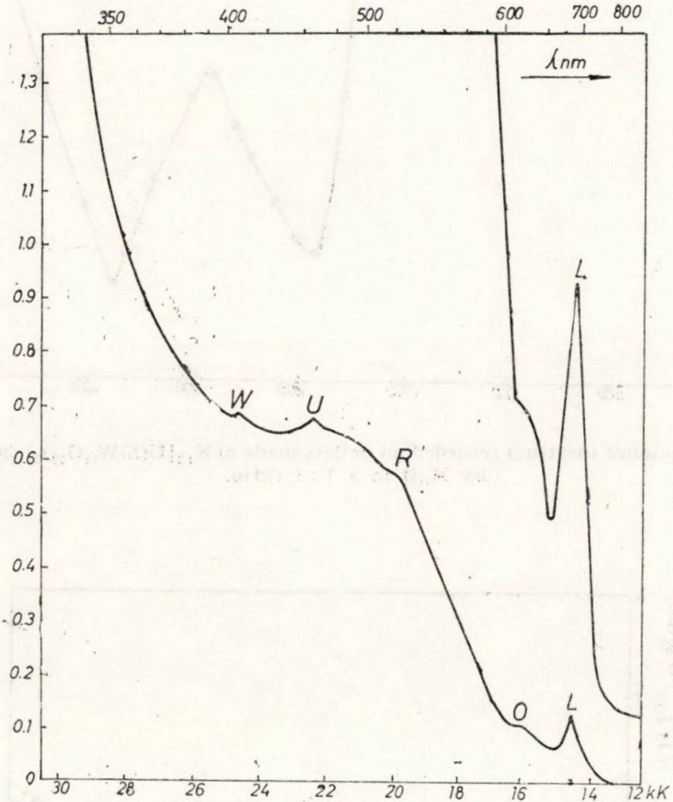

Fig. 4. — Absorption spectrum in the visible domain, recorded on a $K_{12}[U(SiW_{11}O_{39})_2].30\ H_2O$ solution with $c_W = 10^{-2}$ M and 5.10^{-2} M at room temperature.

---

[13] O. Glemser, W. Holznagel, W. Hopte and E. Schwarzmann, *Z. Naturforsch.*, **20b**, 725 (1965).

[14] G. Lange, H. Helm and K. Debrike, *Z. Naturforsch.*, **24b**, 1498 (1969).

[15] C. M. Flynn, Jr. and M. T. Pope, *Inorg. Chem.*, **10**, 2745 (1971).

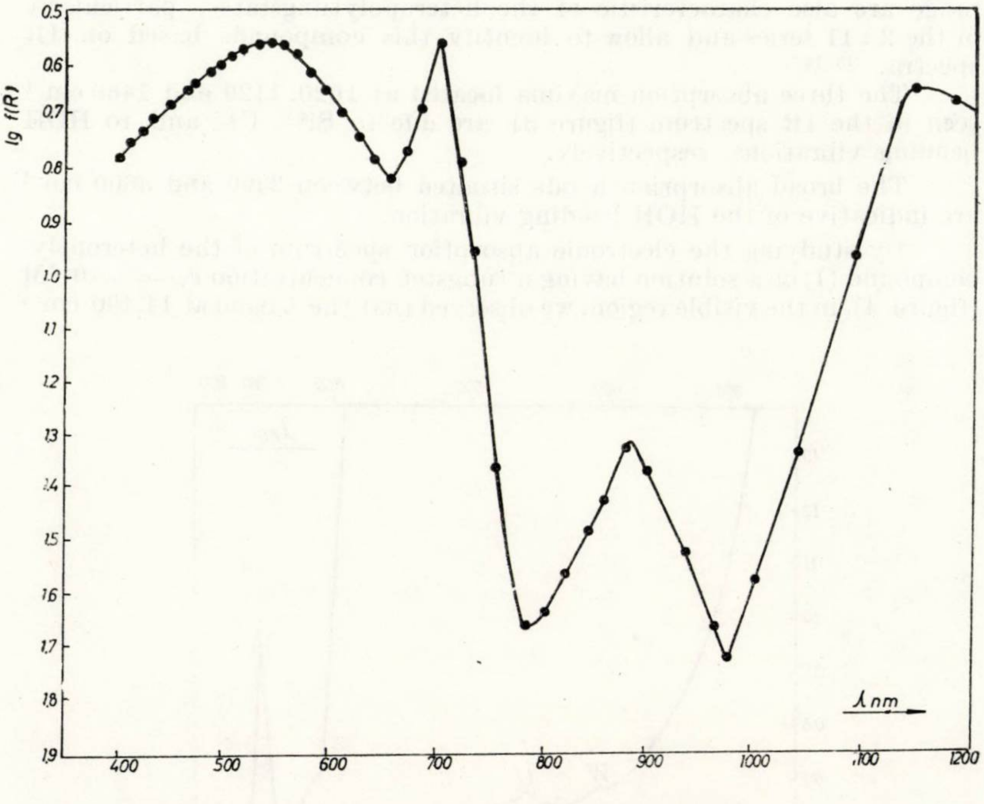

Fig. 5. — Reflectance spectrum recorded on pellets made of $K_{12}[U(SiW_{11}O_{39})_2].30\ H_2O$ diluted by MgO in a 1 : 1 ratio.

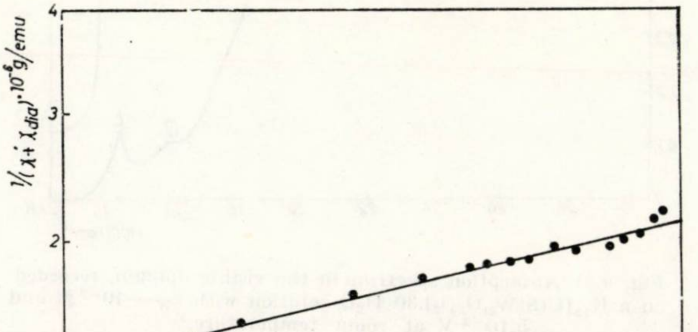

Fig. 6. — Variation of $1/\chi$ depending on temperature T for $K_{12}[U(SiW_{11}O_{39})_2].30\ H_2O$.

is well resolved and by increasing dilution ($c_W = 10^{-2}$M), it appeared that the O, R, U and W bands could be also resolved.

A value of the oscillator strength was found to be $f = 4.15.10^{-5}$, which is in good agreement with a value of $f \sim 3.10^{-5}$ obtained for L band of the Cs_2UCl_6 where U(IV) is octacoordinated.[16] The broad absorption band at 20,000 – 25,000 cm^{-1} with superimposed $f - f$ peaks is due to *a* from U(IV) to U(VI) charge transfer.

A diffuse reflectance spectrum was also recorded (see figure 5). The band at 8,700 cm^{-1} and that at 14,490 cm^{-1} are due to the electronic transitions between U(IV) and W(VI) either by using the oxygen atom as a bridge, or directly the metal-metal orbitals.

These two bands suggest an octahedral configuration of the U(IV) ion.

The heteropolycompound (I) has a reflexion spectrum of high intensity in good agreement with data given by Gans.[17]

Our investigations were completed with magnetochemical measurements. Figure 6 shows the temperature dependence of the magnetic susceptibility. The linear dependence follows the Curie law.

The effective magnetic moment was calculated from :

$$\mu_{\mathrm{eff}} = 2.839\ C^{1/2} \tag{1}$$

where C is obtained from the slope of the line in figure 6.

A value of 2.81 Bohr magnetons is found for μ_{eff}. This value of μ_{eff} obtained by the Curie-Weiss method, as well as he electronic absorption spectrum in the visible domain and the diffuse reflectance spectrum suggest that the $K_{12}[U(SiW_{11}O_{39})_2].30\,H_2O$ compound belongs to octahedrally-coordinated U(IV) compounds, and the U(IV) has an oxidation state equal to +4.

4. CONCLUSIONS

The K^+, NH_4^+, Cs^+ and Tl^+ salts of the $[U(SiW_{11}O_{39})_2]^{12-}$ heteropolyanion were synthesised.

The chemical individuality of these compounds was established by recording the UV and IR spectra, and the oxidation state of uranium in these compounds was determined by recording the electronic absorption spectrum in the visible range, the electronic reflection spectrum and the measurements of magnetical susceptibility.

The experimental results suggest an octahedral configuration of the U(IV) ion and an oxidation state equal to +4 in the studied compounds.

---

[16] R. Pappalardo and C. K. Jorgensen, *Helv. Phys. Acta*, **37**, 79 (1964).

[17] P. Gans, B. J. Hathaway and B. C. Smith, *Spectrochim. Acta*, **21**, 1589 (1965).

Revue Roumaine de Chimie, 22, 6, 857–863 (1977)

PRÉPARATION ET CARACTÉRISATION DE TÉTRACHLOROMANGANATES (II) D'AMMONIUMS MONOSUBSTITUÉS LINÉAIRES

ABDELAZIZ DAOUD,* ALINE THRIERR-SOREL,** RENÉ PERRET **
et BERNARD CHAILLOT ***

* Institut de Recherches Scientifiques et Techniques, Carthage, Tunisie

** Laboratoire de Recherches sur la Réactivité des Solides, associé au C.N.R.S., Faculté des Sciences Mirande, 21000, Dijon, France.

*** Laboratoire de Chimie Analytique, Faculté des Sciences Pharmaceutiques et Biologiques, 21000, Dijon, France

Reçu le 5 mai 1975

Les tétrachloromanganates (II) d'ammoniums monosubstitués $(RNH_3)_2MnCl_4$, dérivant d'amines aliphatiques, de la méthylamine à la pentadécylamine et de la benzylamine à la butylphénylamine, ont été préparés sous forme de fines plaquettes roses très pâles. Ces composés sont isotypes et le même arrangement cristallin se trouve conservé dans toute la série. L'environnement octaédrique de l'ion Mn^{2+} semble stabilisé par les chaînes linéaires des ions ammoniums monosubstitués.

Les tétrachloromanganates (II) d'ammoniums monosubstitués linéaires demeurent encore peu connus : seuls semblent avoir été préparés et étudiés les sels de méthylammonium [1] et de propylammonium.[2] Dans le présent travail, nous avons essayé de généraliser ces résultats en nous limitant au cas des sels d'ammoniums monosubstitués dans lesquels le groupement $-NH_3$ se trouve situé en bout d'une chaîne linéaire, pour montrer que l'allongement de cette chaîne carbonée ne paraît modifier ni l'environnement octaédrique du cation Mn^{2+}, ni les arrangements structuraux de leurs mailles.

MÉTHODES DE PRÉPARATION

Il parait en effet possible de préparer d'autres composés de même formule globale $(RNH_3)_2MnCl_4$ que ceux déjà décrits. Le mode opératoire proposé par Foster et Gill [1] et repris par Peterson et Willett [2] nous a effectivement permis de les obtenir facilement à l'état pur.

Les chlorures d'ammoniums sont facilement préparés par action du chlorure d'hydrogène sur les amines correspondantes dissoutes dans l'éther.

Le chlorure de manganèse II hydraté d'une part, le chlorure d'ammonium substitué d'autre part, pris dans les proportions stœchiométriques 1/2, sont dissous séparément dans le minimum de méthanol ou d'éthanol ; ces deux solutions sont ensuite mélangées : le sel complexe précipite rapidement. Il peut être recristallisé dans le même solvant. Un refroidissement très lent laisse cristalliser de fines plaquettes d'allure rectangulaire. Tous ces composés sont toutefois assez solubles et le rendement de la préparation reste faible.

---

[1] J. J. Foster et N. S. Gill, *J. Chem. Soc.* A, **1968**, 2625.

[2] E. R. Peterson et R. D. Willett, *J. Chem. Phys.*, **56**, 1879 (1972).

En dissolvant dans l'eau les chlorures simples dans le rapport stœchiométrique et en acidifiant la solution aqueuse par l'acide chlorhydrique jusqu'à pH 1 environ, une évaporation lente permet de recueillir des plaquettes d'allure semblable, en général plus épaisses.

Ainsi ont pu être préparés les tétrachloromanganates (II) d'ammoniums substitués dérivant d'amines aliphatiques, de la méthylamine à la pentadécylamine, de l'aniline, de la benzylamine, de l'éthyl-, la propyl- et la butylphénylamine. L'analyse chimique confirme leur formule globale $(RNH_3)_2MnCl_4$ comme nous le montrons sur quelques exemples dans le tableau 1.

Tableau 1

Exemples de résultats analytiques

	Mn %		Cl %		N %		C %	
	cal.	obs.	cal.	obs.	cal.	obs.	cal.	obs.
$(CH_3NH_3)_2MnCl_4$	21,05	21,0	54,35	54,1	10,73	10,6	9,20	9,4
$(C_2H_5NH_3)_2MnCl_4$	19,01	18,8	49,08	48,9	9,70	9,5	16,63	16,7
$(C_4H_9NH_3)_2MnCl_4$	15,92	16,0	41,09	40,9	8,11	8,0	27,82	27,9
$(C_5H_{11}NH_3)_2MnCl_4$	14,72	14,6	38,00	38,2	7,50	7,5	32,16	32,2
$(C_8H_{17}NH_3)_2MnCl_4$	12,01	12,0	31,02	31,3	6,13	6,0	42,02	41,8
$(C_{12}H_{25}NH_3)_2MnCl_4$	9,64	9,4	24,89	24,6	4,92	4,6	50,56	50,4
$(C_6H_5NH_3)_2MnCl_4$	14,27	14,4	36,83	36,6	7,28	7,3	37,43	37,5
$(C_6H_5CH_2NH_3)_2MnCl_4$	13,30	13,4	34,33	34,1	6,78	6,9	40,70	40,5

Tous ces composés sont roses très pâles, indice probable d'une coordination octaédrique de l'ion Mn^{2+}, la présence d'anions à coordination tétraédrique se manifestant habituellement par une coloration jaune ou jaune verdâtre très claire des sels complexes.[1] Ils sont assez peu hygroscopiques ; ils sont très solubles dans l'eau, assez solubles dans le méthanol et l'éthanol et presque insolubles dans l'éther. Chauffés au-dessus de 130—150°, ils fondent en se décomposant.

ÉTUDE RADIOCRISTALLOGRAPHIQUE

Ces différents composés ont été caractérisés par radiocristallographie ; leurs diffractogrammes ont été obtenus à partir d'échantillons pulvérulents avec le rayonnement K_α du cuivre. Ils ont tous une allure semblable et, dans la série $(C_nH_{2n+1}NH_3)_2MnCl_4$ comme dans la série $(C_6H_5-(CH_2)_m-NH_3)_2MnCl_4$, l'allongement de la chaîne se traduit par un déplacement global des raies de diffraction vers les petits angles.

Seul composé dont la structure soit connue, le sel $(CH_3CH_2CH_2NH_3)_2MnCl_4$, a été décrit comme orthorhombique, de groupe d'espace Cmca.[2] Par analogie nous avons essayé d'indexer les diffractogrammes dans une maille orthorhombique, les valeurs des paramètres obtenus sont rassemblées dans les tableaux 2 et 3. En particulier, nous avons trouvé que $(CH_3NH_3)_2MnCl_4$ cristallise dans ce même type structural, bien qu'il ait été précédemment décrit dans le système quadratique : $a = 7{,}20$ Å, $c = 19{,}37$ Å[1] ; $a = 7{,}235$ Å, $c = 19{,}399$ Å.[3,4] Ce résultat vient de se trouver confirmé : ce composé présente plusieurs transformations structurales liées à des modifications d'orientation des groupements

---

[3] W. D. Van Amstel et L. J. de Jongh, *Solid State Commun.*, **11**, 1423 (1972).

[4] G. Heger, E. Henrich et B. Kanellopulos, *Solid State Commun.*, **12**, 1157 (1973).

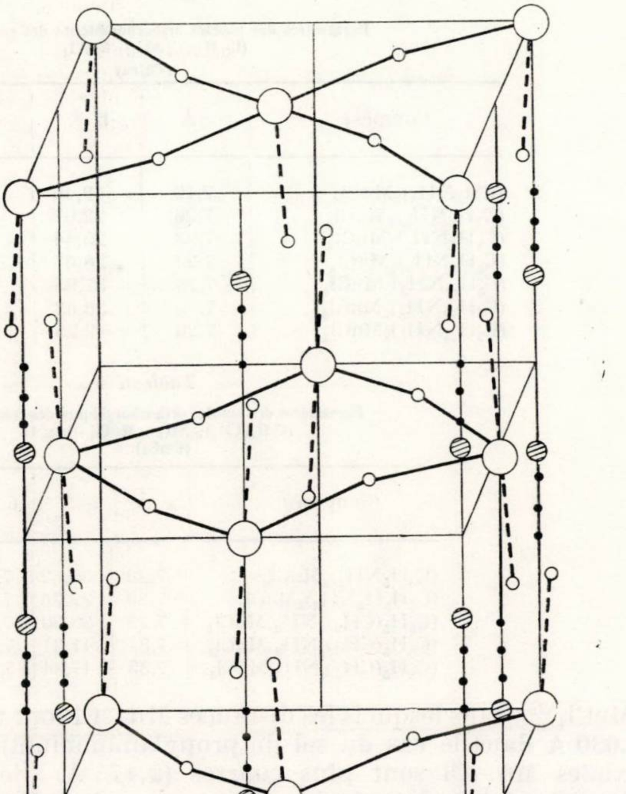

Fig. 1. — Représentation schématique de $(C_3H_7NH_3)_2MnCl_4$ d'après.[2]

$(CH_3{-}NH_3)$: la forme stable à la température ambiante est la forme orthorhombique Cmca : a = 7,215 Å, b = 19,41 Å, c = 7,276 Å.[5] D'autres composés $(RNH_3)_2MnCl_4$ semblent présenter des transitions de phase semblables.[6] Des mesures de densité confirment la présence de quatre groupements formulaires par maille.

A partir de la structure de chlorure de propylammonium, [2] il est possible de décrire schématiquement l'édifice structural présenté par ces composés. Les atomes de manganèse, situés dans des sites de symétrie 2/m, se trouvent placés aux sommets et aux centres des faces de la maille et se trouvent entourés d'octaèdres d'ions chlorures ; dans le plan (010) ces octaèdres se trouvent réunis par leurs sommets pour former des feuillets

---

[5] K. Knorr, I. R. Jahn et G. Heger, *Solid State Commun.*, **15**, 231 (1974).
[6] H. Arend, R. Hofmann et F. Waldner, *Solid State Commun.*, **13**, 1632 (1973).

Tableau 2

Paramètres des mailles orthorhombiques des composés
$(C_nH_{2n+1}NH_3)_2MnCl_4$
(Cmca)

Composés	a Å	b Å	c Å	V Å³
$(CH_3NH_3)_2MnCl_4$	7,19	19,40	7,28	1015
$(C_2H_5NH_3)_2MnCl_4$	7,26	22,07	7,36	1180
$(C_3H_7NH_3)_2MnCl_4$	7,23	25,44	7,44	1368
$(C_4H_9NH_3)_2MnCl_4$	7,24	28,61	7,40	1533
$(C_5H_{11}NH_3)_2MnCl_4$	7,28	31,95	7,36	1711
$(C_6H_{13}NH_3)_2MnCl_4$	7,30	36,63	7,32	1957
$(C_7H_{15}NH_3)_2MnCl_4$	7,26	42,25	7,37	2261

Tableau 3

Paramètres des mailles orthorhombiques des composés
$(C_6H_5(CH_2)_mNH_3)_2MnCl_4$ ($m \leqslant 4$)
(CmCa)

Composés	a Å	b Å	c Å	V Å³
$(C_6H_5NH_3)_2MnCl_4$	7,29	30,32	7,36	1627
$(C_6H_5H_2NH_3)_2MnCl_4$	7,29	32,26	7,36	1731
$(C_6H_5(CH_2)_2NH_3)MnCl_4$	7,29	38,30	7,35	2052
$(C_6H_5(CH_2)_3NH_3)MnCl_4$	7,31	41,31	7,37	2225
$(C_6H_5(CH_2)_4NH_3)MnCl_4$	7,35	47,34	7,38	2567

$(MnCl_4)_n^{2n-}$ dans lesquels les distances Mn—Cl sont toutes égales (elles valent 2,630 Å dans le cas du sel de propylammonium), tandis que les liaisons axiales Mn—Cl sont plus courtes (2,475 Å) : les octaèdres $MnCl_6$ sont légèrement déformés et admettent une symétrie D_{4h}. Les chaînes alkylammonium enfin, localisées dans des sites délimités par des ions chlorures, sont sensiblement parallèles à la direction b : elles se situent sur les arêtes et les droites passant par le milieu des arêtes.

Si ce motif structural se trouve effectivement conservé dans tous les composés envisagés, la longueur d'une diagonale de la face (010) devrait, au moins en première approximation, représenter sensiblement quatre fois la longueur d'une liaison Mn—Cl ; les valeurs déduites des données cristallographiques restent voisines de 2,60 Å, c'est-à-dire proches des valeurs couramment admises pour les liaisons Mn—Cl en environnement octaédrique, par exemple 2,57 Å pour Cs_2MnCl_4 [3] ; en fait, ces résultats ne peuvent qu'être approchés car, par suite d'un léger basculement des octaèdres, dû à des liaisons hydrogènes entre les atomes d'azote et de chlore, les quatre liaisons coplanaires équivalentes s'écartent légèrement de la face (010) et l'angle Mn—Cl—Mn est inférieur à 180°.

Ces caractères structuraux, peu différents d'ailleurs des composés de cuivre correspondants, [7-10] permettent de rendre compte de l'augmen-

---

[7] L. J. DE JONGH, A. C. BOTTERMAN, F. R. DE BOER et A. R. MIEDEMA, *J. Appl. Phys.*, **40**, 1363 (1969).

[8] J. P. STEADMAN et R. D. WILLETT, *Inorg. Chim. Acta*, **4**, 367 (1970).

[9] B. ZASLOW et G. L. FERGUSON, *Chem. Comm.*, **1967**, 822.

[10] F. BARENDREGHT et H. SCHENK, *Physica*, **49**, 465 (1970).

tation du paramètre b avec l'allongement de la chaîne, l'impossibilité de préparer des chlorures mixtes contenant des ammoniums substitués par des chaînes de longueur différente ainsi que les possibilités de clivage de ces composés selon le plan (010).

ÉTUDE SPECTROSCOPIQUE

Les méthodes spectroscopiques nous ont permis de montrer que, dans tous ces composés, l'ion Mn^{2+} conserve un environnement octaédrique.

SPECTROSCOPIE R.P.E.

Cette étude a été effectuée sur des échantillons pulvérulents, à l'aide d'un spectromètre Microspin type ESR3 bande X, avec un champ directeur modulé à 100 Kc/s. L'étalonnage est fait par rapport au DDPH ($g = 2,0036$).

Les observations faites en spectroscopie RPE viennent apparemment confirmer l'existence d'une coordination octaédrique de l'ion Mn^{2+} dans toute la série. Les signaux obtenus aussi bien à la température ambiante qu'à la température de l'azote liquide restent parfaitement symétriques (fig. 2). A la température ambiante, le facteur spectroscopique conserve la valeur constante $g = 2,02$; à la température de l'azote liquide, il diminue légèrement et vaut $g = 2,007$. Ces valeurs sont voisines de celles observées pour d'autres composés de manganèse présentant ce type d'environnement.[11]

SPECTROSCOPIE ÉLECTRONIQUE D'ABSORPTION

Les spectres de réflectance, obtenus à partir d'échantillons microcristallins, présentent tous une allure semblable, avec, en particulier, une bande caractéristique intense située à 24.000 cm^{-1} environ. La dilatation de la maille, liée à un allongement des groupements ammoniums provoque une diminution d'intensité et un aplatissement des maxima d'absorption, difficilement repérable

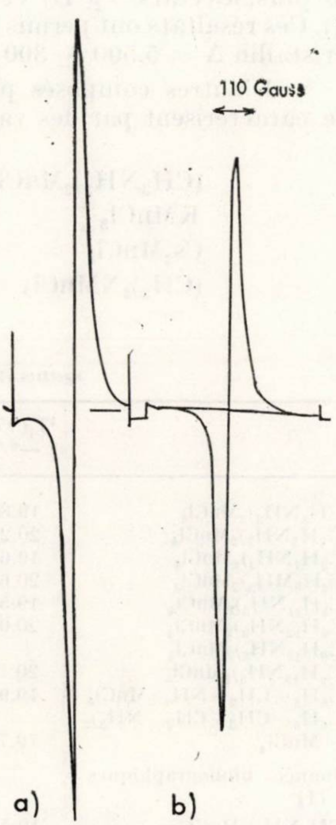

Fig. 2. — Signaux RPE de $(C_3H_7NH_3)_2MnCl_4$. a) température ambiante ; b) température de l'azote liquide.

---

[11] R. D. Dowsing, J. F. Gibson, D. M. L. Goodgame, M. Goodgame et P. J. Hayward, *Nature*, **219**, 1037 (1968).

avec précision. Des indications fournies par des études antérieures ont permis d'attribuer les transitions électroniques aux bandes observées expérimentalement. A partir de l'état fondamental $^6A_1$, les six bandes d'absorption de faible intensité repérées dans le visible et le proche ultra-violet, correspondent aux transitions interdites entre cet état $^6A_1$ et les niveaux supérieurs excités ^4G, ^4P et ^4D de l'ion libre. Le diagramme des niveaux d'énergie de l'ion Mn^{2+} montre la succession des transitions possibles :

$$^4T_1\,(^4G) \leftarrow {}^6A_1 < {}^4T_2\,(^4G) \leftarrow {}^6A_1 < {}^4E,\, {}^4A_1\,(^4G) \leftarrow {}^6A_1 <$$

$$^4T_2\,(^4D) \leftarrow {}^6A_1 < {}^4E\,(^4D) \leftarrow {}^6A_1 < {}^4T_1\,(^4P) \leftarrow {}^6A_1\,;$$

de plus, les états $^4T_2(^4D)$ et $^4E(^4D)$ sont très proches l'un de l'autre (tableau 4). Ces résultats ont permis de déterminer la valeur du paramètre du champ cristallin $\Delta = 5.500 \pm 300\ cm^{-1}$.

D'autres composés présentant le même motif $MnCl_6^{4-}$ octaédrique se caractérisent par des valeurs voisines de [1] :

$(CH_3NH_3)_2MnCl_4$	$= 5.500\ cm^{-1}$
$KMnCl_3$	$5.400\ cm^{-1}$
Cs_2MnCl_4	$5.200\ cm^{-1}$
$(CH_3)_4NMnCl_3$	$5.600\ cm^{-1}$

Tableau 4

Spectres électroniques (cm^{-1}) : attribution des bandes

	$^4T_1(^4G) \leftarrow$ $\leftarrow {}^6A_1$	$^4T_2(^4G) \leftarrow$ $\leftarrow {}^6A_1$	$^4E,\, {}^4A_1(^4G) \leftarrow {}^6A_1$	$^4T_2,\, {}^4E(^4D) \leftarrow {}^6A_1$	$^4T_1(^4P) \leftarrow$ $\leftarrow {}^6A_1$
$(CH_3NH_3)_2MnCl_4$	19.800	21.800	24.000	28.200	30.000
$(C_2H_5NH_3)_2MnCl_4$	20.200	21.800	24.000	28.100	30.000
$(C_3H_7NH_3)_2MnCl_4$	19.600		24.100, 23.600	28.200	
$(C_4H_9MH_3)_2MnCl_4$	20.600		24.100, 23.400	28.200	
$(C_5H_{11}NH_3)_2MnCl_4$	19.500	22.000	24.100, 23.800	27.800	
$(C_6H_{12}NH_3)_2MnCl_4$	20.000	21.800	24.100, 23.400	28.200	
$(C_8H_{17}NH_3)_2MnCl_4$		21.000	24.100	27.700	30.000
$(C_9H_{19}NH_3)_2MnCl_4$	20.100	22.300	24.100	27.800	
$(C_6H_5-CH_2-NH_3)_2MnCl_4$	19.900	21.600	23.900, 23.600	28.000	30.000
$(C_6H_5-CH_2-CH_2-NH_3)_2$ $MnCl_4$	19.700	21.900	24.000, 23.600	28.100	
Données bibliographiques (1)					
$(CH_3NH_3)_2MnCl_4$	19.560	22.100	23.980, 23.440	27.600, 28.120	29.980
Cs_2MnCl_4	19.920	22.640	24.180, 23.660	27.380, 28.340	29.900

Dans un environnement tétraédrique, l'ion complexe $(MnCl_4)^{2-}$ se caractérise par une valeur de $\Delta_T = 3.100\ cm^{-1}$; le rapport expérimental $\frac{\Delta_T}{\Delta_0} = 0{,}56$ est supérieur à la valeur théorique $4/9 = 0{,}44$ car, dans un environnement tétraédrique réel, les longueurs des liaisons ion central-coordinat sont légèrement inférieures à celles de l'arrangement octaédrique.

Les valeurs de Δ_0 et Δ_T sont donc suffisamment différentes pour déterminer sans ambiguïté le type de coordination de l'ion métallique.

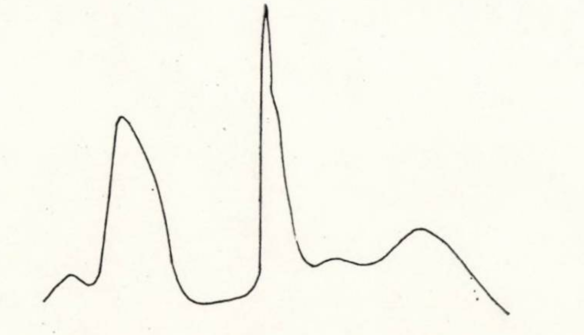

Fig. 3. — Spectre électronique de $(C_2H_5NH_3)_2MnCl_4$.

Ce travail nous a permis de préparer et de caractériser une famille de tétrachloromanganates (II) d'ammoniums monosubstitués. Ces composés sont isotypes : ils présentent le même arrangement structural dans lequel les chaînes alkylammonium sont «alignées» parallèlement à l'axe b ; les ions divalents, situés dans des plans perpendiculaires à cet axe, sont au centre d'octaèdres légèrement déformés d'ions chlorures. L'influence des ions ammoniums ne doit toutefois pas être complètement négligée : l'édifice structural avec coordination octaédrique autour du manganèse est stabilisé par un ion ammonium monosubstitué car, dans les tétrachloromanganates contenant des ions ammoniums polysubstitués, le manganèse possède un environnement tétraédrique.

Revue Roumaine de Chimie, **22**, *6*, 865–867 (1977)

ISOTOPE EFFECTS IN ELECTRONIC ABSORPTION SPECTRA OF CH_3/CD_3-SUBSTITUTED SIX-MEMBERED HETEROAROMATICS

ILEANA I. STĂNOIU, MARIA PARASCHIV, EUGENIA GÂRD and A. T. BALABAN*

Institute of Atomic Physics, P.O.B. 5206, Bucharest, Romania
* Department of Organic Chemistry, The Polytechnic Institute of Bucharest

Received October 27, 1976

The ^1L_b absorption maximum of 2,4,6-trimethylpyridine is shifted to lower wavelengths on deuterating the α-standing methyl groups, by 0.9 nm in polar solvents and 0.4 nm in non-polar ones. Deuteration of the γ-methyl group has no detectable influence.

It was recently reported[1] that deuteration of the α-methyl or methylene groups in 2,4,6-trimethylpyridine (Ia → IIIa) and in 2,6-diethyl-4-methylpyridine, respectively, caused a marked isotope effect in the lanthanide-induced chemical shift observed for the β-hydrogen in ^1H–NMR spectra; deuteration of the γ-standing methyl group had no detectable effect, i. e. IIa behaved like Ia, and IIIa like IVa. This was interpreted as indicating a steric origin of this isotope effect: the CD_3 group, with smaller volume than CH_3,[2] allows a shorter heteroatom-to-europium distance in the complex. By contrast, the pK_a values vary additively in the series Ia–IIa–IIIa–IVa, increasing with ca. 0.025 pH units per CD_3 group,[3] in agreement with the known[4] electron-releasing effect of CD_3 *versus* CH_3 groups.

We investigated the electronic absorption spectra of methyl-deuterated 2,4,6-trimethylpyridine (Ia–IVa) and 2,4,6-trimethylpyrylium perchlorate (Ib–IVb). The spectra were recorded with a CF-4 Optica (Milan) grating spectrophotometer, expanding as much as possible the wavelength

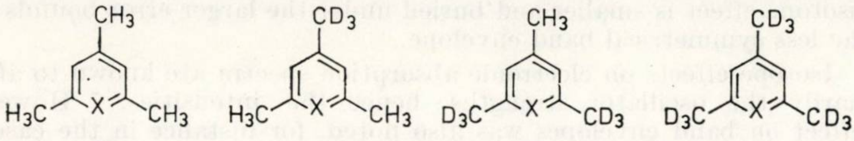

I II III IV

a, X = N ; b, X = O^+ ClO_4^-

---

[*] To whom correspondence should be addressed.

[1] A. T. Balaban, I. I. Stănoiu and F. Chiraleu, *Chem. Commun.*, **1976**, 984.

[2] K. Clusius and K. Weigand, *Z. physik. Chem.*, **B 46**, 1 (1940).

[3] A. T. Balaban, I. I. Stănoiu and E. Gârd, *Rev. Roumaine Chim.* **22**, Nr. 8 (1977).

[4] E. A. Halevi, M. Nussim and A. Ron, *J. Chem. Soc.*, **1963**, 866.

scale (7 mm for one nm). The position of the maximum absorption was determined graphically by intersecting the absorption curve with the straight line (fig. 1) determined from the condition that this line should be equidistant from the slopes of the absorption curve at all absorbances. Concentrations were equal and conditions were selected so as to lead to absorbance ca. 0.8 at the maximum, as indicated in figure 1. Determinations were carried out in cells thermostated at 25 ± 0.1°, because a separate reproducibility study had shown that, without a thermostat, variations up to 0.25 nm occurred ; at constant temperature, absorption maxima were reproducible within 0.15 nm.

Experimental results are presented in Table 1 for three solvents ; each value is the average of several determinations (at least three solutions, each recorded three times).

Table 1

UV Absorption maxima (in nm) at 25 ± 0.1° (accuracy ± 0,15 nm)

Solvent / Compound	Water	*n*-Heptane	Methanol
Ia	265.1	264.1	265.0
IIa	265.0	264.2	265.1
IIIa	264.1	263.8	264.3
IVa	264.4	263.7	264.3

It can be observed that in polar solvents (water, methanol), pyridines Ia and IIa have λ_{max} at ca. 265.1 nm, while IIIa and IVa have it at ca. 264.2 nm, i. e. one observes a hypsochromic shift of 0.9 nm due to a secondary isotope effect in electronic absorption spectra. In the non-polar *n*-heptane, the band appears at slightly lower wavelength, and the hypsochromic effect on deuterating the α-methyl groups is smaller (0.4 nm). Deuteration of the γ-methyl group has no detectable effect in any solvent (the slightly larger deviation between IIIa and IVa in water is compatible with the error bounds of ±0.15 nm).

In the UV absorption maxima of deuterated pyrylium salts Ib—IVb, in water or acetic acid as solvents, there is no detectable trend ; probably the isotope effect is smaller and buried under the larger error bounds due to the less symmetrical band envelope.

Isotope effects on electronic absorption spectra are known to affect primarily the oscillator strengths, hence the intensities.[5-7] However, an effect on band envelopes was also noted, for instance in the case of $n-\pi^*$ bands of aliphatic ketones, whose maxima move to lower wavelengths on deuteration adjacent to the carbonyl group (e. g. 400 cm^{-1}, ca. 2 nm, difference between $H_3C-CO-CH_3$ and $D_3C-CO-CD_3$).[7]

---

[5] C. N. R. Rao and A. S. N. Murthy, *Proc. Phys. Soc. (London)*, **87**, 771 (1966).

[6] C. N. R. Rao, G. C. Chaturvedi and H. S. Randhawa, *Chem. Phys. Letters*, **7**, 563 (1970).

[7] E. F. Worden Jr., *Spectrochim. Acta*, **22**, 21 (1966).

This isotope effect was assigned to a difference in the position of maximum Franck-Condon overlap for the hypersurface of the combining electronic states (rather than to zero-point energy differences, which only determine the position of the $0 - 0'$ band, and not of the absorption maximum).

In the present case of the ^1L_b band in pyridines, the $\pi - \pi^*$, HOMO–LUMO, transition is involved. As for acetone,[7] the absorption curves coincide at lower wavelengths for deuterated and non-deuterated substrates, and differ only at higher wavelengths (figure 1), leading to the observed difference in the wavelength of the maximum. In *n*-heptane, as solvent, the vibrational structure of the ^1L_b band was apparent. The reason for the exclusive effect of α-methyl deuteration and for the undetectable influence of γ-methyl deuteration is probably the following: the ^1L_b band is polarized parallel to the line connecting the α and α′ substituents; therefore, as in phenyl-substituted pyrylium salts,[8] the position of this band is markedly affected by electronic effects of α-substituents, and hardly by γ-substituents (the reverse is true for the shorter-wavelength ^1L_a band around 200 nm).

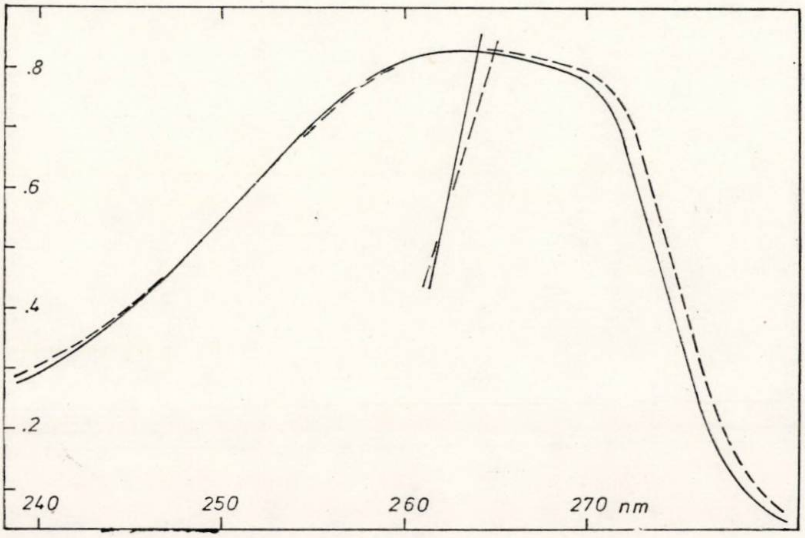

Fig. 1. — Ultraviolet absorption curves for Ia (broken line) and IVa (full line) and determination of their absorption maxima.

The preparation of deuterated pyrylium salts Ib–IVb, and therefrom of pyridines Ia–IVa, was described elsewhere.[1,3,9] Compounds II and III had isotopic purity of ca. 85–90%, while I and IV were 99–100% isotopically pure.

---

[8] A. T. Balaban, V. E. Sahini and E. Keplinger, *Tetrahedron*, **9**, 163 (1960).

[9] E. Gârd, A. Vasilescu, G. D. Mateescu and A. T. Balaban, *J. Labelled Comp.*, **3**, 196 (1967).

Revue Roumaine de Chimie, 22, *6*, 869–875 (1977)

OBTENTION OF THE *o*-NITROPHENYLSUCCINIC ACID AND OF SOME FUNCTIONAL DERIVATIVES

F. CUIBAN, ALFA LUPEA, MARCELA SILAŞI and MARIANA ŞORA
Chemical Engineering Faculty, Polytechnic Institute
"Traian Vuia" Timişoara, P.O.B. 103, Romania

Received July 16, 1976

Instrumental analysis methods (UV, IR, NMR, polarography) have been used to study both the nitration of phenylsuccinic acid and of its anhydride and the synthesis of compounds mentioned in the title by the derivatives of the malonic acid. Improved yields in *ortho* isomer (35%) have been obtained on anhydride nitration, as against only 17% obtained on nitration of phenylsuccinic acid. The secondary reactions accompanying the CN^- addition to the derivatives of the *o*-nitro-benzylidene malonic acid can be avoided by using acetone-cyanhydrine as a CN^- source. The amidation of the anhydride of *o*-nitro-phenylsuccinic acid leads to the formation of α and β isomeric amides.

In recent years, special attention has been given to internal oxidoreduction processes between the *o*-nitro group of the aromatic derivatives and the lateral chain, new working methods being developed for heterocyclic compounds with nitrogen.[1] The cyclization reactions, in which the reduction of the nitro group occurs with external reducing agents, have been less studied so far. In a previous work,[2] we have established that depending on the reaction conditions and on the substituent nature the catalytic hydrogenation of some *o*-nitrophenyl-substituted derivatives leads in particular to benzo-lactames or N-hydroxy-lactames, without being able to specify the difference between the cyclization tendency for the formation of 5 atom cycles, as against 6-atom cycles. The *o*-nitrophenylsuccinic acid and its functional derivatives have been found to be adequate molecular models for such a study since both benzo-lactame systems may form on their reduction.

NITRATION OF PHENYLSUCCINIC ACID

The *o*-nitrophenylsuccinic acid may be obtained by nitration of phenylsuccinic acid with a great excess [3] of HNO_3 or by condensation of *o*-nitrobenzaldehyde with the derivatives of malonic acid.[4–6] However,

[1] P. N. Preston and G. Tennant, *Chem. Rev.*, **72**, 627 (1972).
[2] F. Cuiban, *Tetrahedron Letters*, **1971**, 2471; *Rev. Roumaine Chim.*, **17**, 897 1(972).
[3] F. Fichter and O. Walter, *Ber. dtsch. chem. Ges.*, **42**, 4312 (1909).
[4] L. Horner, K. Klüpfel and W. Sahler, *Liebigs. Ann. Chem.*, **591**, 85 (1955).
[5] J. D. Loudon and J. Wellings, *J. Chem. Soc.*, **1960**, 3462.
[6] H. le Moal, A. Foucaud and R. Carrié, *Bull. Soc. chim. France*, **1964**, 579.

in both cases, the global yields are low. We have attempted to improve such methods in the phases which affect more markedly the yield.

Under the mentioned nitration conditions which do not rule out the possibility of some polynitrations, it has been however stated [3] that only mononitrated products are being obtained : 24% *o*-nitrophenylsuccinic acid and 65% *para*, separated on the basis of the more reduced water solubility of the *para* isomer. The inconclusive results obtained by reproducing this procedure have prompted us to investigate suitable analysis methods to determine the isomer ratio in the mixture, to evidence the formation of polynitrated products and to possibly improve the *o*-nitrophenylsuccinic acid ratio, resorting in our study to instrumental analysis techniques, such as UV, IR and RMN spectroscopy, polarography, potentiometry and thin-layer chromatographic analysis.

On nitration of phenylsuccinic acid with sulphonitric mixtures under stronger conditions one obtains the isomer mixture : 2,4- and 2,6-dinitrophenylsuccinic and the trinitrated product is not formed. The 2,4-dinitrophenylsuccinic acid can be conveniently obtained in pure state by nitration of the *p*-nitrophenylsuccinic acid. In general, the acidity constants of the nitrated products are close enough without offering a separation possibility based on the acidity difference.

On polarographing the nitroderivatives of the phenylsuccinic acid, the limit diffusion current is proportional with the concentration of the substance within $10^{-3} - 10^{-5}$ mole.l^{-1} limits, which permits the dosage of each product in pure state or in mixture, relative to the non-nitrated product (e.g. phenylsuccinic acid), yet the very close half wave potentials will not permit the dosage of an isomer in the presence of another nitrated product, although the 2,4-dinitrophenylsuccinic acid is more readily electroreduced than mononitrophenylsuccinic acids.

The UV spectra of *o*- and *p*-nitrophenylsuccinic acids in methanol solution have their absorption maxima at 258 nm ($\varepsilon = 4706$), respectively 277 nm ($\varepsilon = 10303$) and the Lambert-Beer law is obeyed within the limits of $4.10^{-5} - 1{,}2.10^{-4}$ mole.l^{-1}. A hypsochromic shift of absorption maxima is observed with the increasing concentrations. In the spectrum of an isomer mixture, the two very close maxima cannot be separately distinguished and one single maximum appears. In order to be able to dose the two isomers in the mixture, we have used relations deduced on the basis of extinction additivity within a concentration range which obeys the Lambert-Beer law. The validity of the deduced relations was verified by dosing mixtures with known concentrations. The conclusion reached was that they are possible when no other substances absorbing in the same domain are present (see experimental section). By nitration of the phenylsuccinic acid there also result oxidation products whose presence affects the UV absorption and the IR spectrometry failed to perform quantitative determinations of isomers in the mixture. The more reduced symmetry of the molecule of the *o*-nitrophenylsuccinic acid relative to the *para* isomer determines different chemical shifts of the benzyl proton signal in the NMR spectrum. The dimethyl ester of the pure *p*-nitrophenylsuccinic acid is observed in the NMR spectrum by the symmetry of aromatic protons ($\delta = 7.8$ ppm) and by the quartet of the benzyl proton at $\delta = 4.2$ ppm whereas in the *ortho* isomer, the benzyl proton signal, also split into a quartet, is shifted to the value $\delta = 4.65$ ppm. From the integration curves of benzyl protons it was possible to estimate quantitatively the isomer ratio in the mixture. The results of the nitration process can be quantitatively followed after esterification of the raw product with diazomethan and after recording NMR spectra.

A detailed verification of data obtained from the nitration of the phenylsuccinic acid, according to the indications given in the literature, has shown that in reality the isomer ratio is 17% *ortho* and 83% *para* rather than 24% and 65% respectively, as appreciated from the separations based on solubility. The nitration result, somehow surprising compared to the nitration of toluene and of phenylacetic acid, where the *ortho* isomer is preponderantly obtained, has suggested the assumption that the steric effect due to the high volume of the substituent and to the free rotations in the chain, hinders the *ortho* nitration, the isomer ratio being controlled only kinetically. To improve the ratio between isomers in favour of the *ortho* isomer, we subjected to nitration the anhydride of phenylsuccinic acid in which the relative motion of chains involving carboxyl group is hindered. The nitration of the anhydride of phenylsuccinic acid took place with acetyl nitrate in the presence of acetic anhydride with or without sulphuric acid addition. After hydrolysis to the corresponding acids, the mixture was analysed by thin-layer chromatography and by NMR spectrometry. On nitration with acetyl nitrate without sulphuric acid addition, the ratio of the two isomers is sensibly enriched in *ortho* isomer (35% as against 65% *para*). However, the presence of non-nitrated phenylsuccinic acid in proportion of 3—5%, which complicates the separation process of nitrated isomers, was revealed both by thin-layer chromatography and by NMR spectra (5 aromatic protons equivalent to $\delta = 7.3$ ppm). Considering the equilibria being formed when mixing the nitric acid with acetic anhydride[7] which have also been confirmed by our experiments (non-nitrated product when using stoichiometric quantities of nitric acid, releases of nitrogen oxides and formation of oxidized products with excess of nitric acid and particularly when raising the temperature without performing a total nitration), and the higher nitration capacity of the protonated acetyl nitrate, we used catalytic quantities of conc. H_2SO_4, when the product was integrally nitrated and the *ortho-para* isomer ratio remained enriched in *ortho* isomer by almost twice that obtained by direct nitration of the phenylsuccinic acid. The separation of the pure *o*-nitrophenylsuccinic acid by recrystallizations from aqueous solution or from various solvents implies great difficulties. In contrast to the anhydride of the *o*-nitrophenylsuccinic acid which is crystalline, sublimable with definite b.p. and m.p., the anhydride of the *para* isomer is an uncrystallizable oil distilling over a large interval, with partial decompositions, suggesting to be a mixture of oligomers. This difference of properties has allowed us to develop a separation procedure of the *o*-nitrophenylsuccinic acid from a mixture enriched in *ortho* isomer by changing it into anhydrides, crystallization and then hydrolysis of the *o*-nitrophenylsuccinic anhydride (see experimental section).

---

[7] F. G. Bordwell and E. W. Garbisch, jr., *J. Amer. Chem. Soc.*, **82**, 3588 (1960).

OBTENTION OF *o*-NITROPHENYLSUCCINIC ACID FROM *o*-NITROBENZALDEHYDE

The synthesis approach is similar to the preparation of the phenylsuccinic acid and the main difficulty is related to the CN^- addition to *o*-nitrobenzylidene derivatives of the malonic acid, particularly due to the internal oxidoreductions on account of the nitro group and of the hydrolysis reactions, amplified by the alkalinity of the cyanide used in the reaction.[1,5] The rigorous control of the pH by buffering the medium with acetic acid or monopotassium phosphate has permitted the partial elimination of side reactions; however the IR and NMR-analysis of the finite product has revealed that the CN^- addition was not complete. The comparative absorptions of the CN group at 2248 cm^{-1} and of the double bond at 1640 cm^{-1} and also the RMN analysis on account of the benzyl proton from the addition product, split into a doublet at $\delta = 5.35$ ppm, and of the vinyl proton from the ethyl *o*-nitrobenzylidene-malonate overlapped with the multiplet of the aromatic protons at 7.5 — 8.2 ppm have shown that in certain samples the impurification with raw material, diethyl *o*-nitrobenzylidene diethyl malonate, reaches 50%. The course of the reaction in a heterogeneous medium, due to the reduced solubility of diethyl-nitrobenzylidene-malonate and of the nitrile resulted by addition, in the reaction medium suggested in the literature,[5] as well as the possibility of a better control of the pH have prompted us to use acetonecyanhydrine as a CN^- source while performing a controlled alkalinization with NaOH solution. Under these conditions, the reaction takes place in a homogeneous solution and develops almost quantitatively, at pH 10. 8—11.5 (yields 90—95% of the theory), the obtained product being of a corresponding quality. The nitrile saponification to *o*-nitrophenylsuccinic acid took place by separating intermediately α-carbamoyl-α-(2-nitrobenzyl)-diethylmalonate and on its hydrolysis the reaction time was prolonged and a more efficient purification method was adopted (see experimental section).

PREPARATION OF THE AMIDES OF *o*-NITROPHENYLSUCCINIC ACID

The amides of *o*-nitrophenylsuccinic acid were readily obtained particularly from anhydride, prepared without dificulties based on the indications given in the literature.[8] Although in the amidation of the anhydrides of the substituted succinic acid one obtains a mixture of α- and β-isomer amides in variable proportions,[9,10] depending on the nature of substituents and of the amine, for the anhydride of the *o*-nitrophenylsuccinic acid, the literature[4] states that one single amide will be obtained by treating with ammonia, without specifying the position of the amide group.

We have established that on treating the *o*-nitrophenylsuccinic anhydride with ammonia there results 30% α-amide and 70% β-amide,

[8] V. Askam and R. H. L. Deeks, *J. Chem. Soc. C.*, **1968**, 1243.

[9] A. Foucaud, *Bull. Soc. Sci. Bretagne*, **35**, 88 (1960); in *Chem. Abstr.*, **55**, 35616 (1961).

[10] A. Foucaud, *Bull. Soc. chim. France*, **1963**, 873.

a composition determined by RMN analysis of the mixture from amidation after a previous transformation into methylic esters with diazomethane. The subsequent purifications result in the elimination of the α-isomer and explain the yield drops recorded in the meantime. By mild hydrolysis with acids of α-carbamoyl-α-(2-nitrobenzyl)diethyl-malonate we obtained the α-amide of the *o*-nitrophenylsuccinic acid, with physico-chemical properties clearly differing from that obtained in the amidation with ammonia of the *o*-nitrophenylsuccinic anhydride. The α-amide also results as a partial hydrolysis product in the preparation of the *o*-nitrophenylsuccinic acid. By treating the *o*-nitrophenylsuccinic anhydride with secondary amides, such as diethyl-amine or with aromatic amines such as aniline, only the corresponding β-amides will form almost exclusively.

EXPERIMENTAL SECTION

UV spectroscopy. Determinations were made on a "Specord UV-VIS" Karl Zeiss Jena spectrophotometer in 1 cm cuve, thermostated at 20°, using as a solvent methyl alcohol purified according to the standards in use. The total concentration of nitrated products was approximately 7.10^{-5} mole.l^{-1} and the molar ratio between the *o*-nitrophenylsuccinic acid and the *para*-isomer has varied from 1 : 1 to 1 : 6,5. The (c_0) concentration of the *o*-nitrophenylsuccinic acid in the isomer mixture was calculated by relation :

$$c_0 = \frac{\varepsilon''_p . E'_{0+p} - \varepsilon'_p . E_{0+p}}{\varepsilon''_p . \varepsilon'_0 - \varepsilon'_p . \varepsilon''_0} \qquad \text{in which}$$

E'_{0+p} and E''_{0+p} represent the extinctions measured at wavelengths corresponding to the absorption maxima for the two isomers $\lambda' = 258$ nm, $\lambda'' = 277$ nm and ε'_0, ε''_0, respectively, and ε'_p, ε''_p represent the molar extinction coefficients determined at the two wavelengths used for reading. The relative error in the determination of isomer concentrations varies between +3 and −1%.

IR spectroscopy. The spectra were recorded on a "Specord 71 IR" Karl Zeiss Jena spectrophotometer in a $CHCl_3$ or CCl_4 solution or in KBr pellet. The characteristic absorption frequencies are mentioned in each separate product.

NMR spectroscopy. Determinations were made on a Varian 60 A Spectrometer in $CDCl_3$ solutions and TMS as reference.

Polarography. Determinations were carried out on a Heyrovski LP 55 apparatus, the polarization domain 0−2 V, the Hg° column height of the dropping electrode being of 20 cm for 10 ml solution. The electrolyte solution was prepared from 3.725 g (50 mM) KCl dissolved in water to which are added 13.1 ml conc. HCl and 48 ml ethanol, diluting thereafter with water to 500 ml. Adequate nitroderivative concentrations are diluted with electrolyte solution, 1−2 drops of 0.5% gelatine solution are added, hydrogen is bubbled through the solution for 10 minutes and the polarograms are performed. The halfwave potential $E_{1/2}$ for *o*- and *p*-nitrophenylsuccinic acids : −0.1875 V and for 2,4-dinitrophenylsuccinic : −0.175 V.

Nitration of phenylsuccinic anhydride : *i)* Preparation of the solution of succinic anhydride. 1.94 g (10 mM) phenylsuccinic acid are heated under reflux with 3.1 g acetic anhydride for 3 hrs and are left to cool at room temperature. *ii)* Obtention of acetyl nitrate. 1.08 g HNO_3 67% (d = 1.42) are introduced under stirring, over a mixture of 7 g acetic anhydride and 0.63 g acetic acid, cooled to 15° adding shortly thereafter a drop of conc. H_2SO_4 so that the temperature should not exceed 20°. *iii)* Nitration. Over the solution of phenylsuccinic anhydride one adds in portions, maintaining the temperature below 20°, a solution of acetyl nitrate. After 24 hrs, the mixture is poured over 25 g ice when the resulting oily product is solubilized as the anhydride undergoes hydrolysis. After the solvent elimination under vacuum, washing with water and drying on P_2O_5, one obtains 2.5 g (96% of the theory) mixture of mononitrated acids : thin-layer chromatography on silicagel G plates with the ethyl methyl ketone (EMK) system : Ethanol :

NH_3 25% = 65 : 15 : 28, *o*-nitrophenylsuccinic acid $R_f = 0.16$; *p*-nitrophenylsuccinic acid $R_f = 0.24$; with the mixture phenol : *p*-xylene : formic acid 80% = 5 : 7 : 1, after two elutions for mononitrated products $R_f = 0.456$ and the result is neither phenylsuccinic acid $R_f = 0.30$ nor 2,4-dinitrophenylsuccinic acid $R_f = 0.376$, revealed with authentic samples (developing with bromophenol blue solution).

Separation of the o-nitrophenylsuccinic acid from a mixture of ortho-para isomers by means of the anhydride. The *o*-nitrophenylsuccinic acid 2.39 g (10 mM) separated from parent waters[3] left after removal of the *p*-nitrophenylsuccinic acid are treated with 8 ml acetyl chloride under reflux until total dissolution. The unreacted acetyl chloride is removed by distillation and the residue is mixed with 10 ml anhydrous benzene and it is filtered. It is recrystallized from 15 ml anhydrous benzene, obtaining 1.1 g *o*-nitrophenylsuccinic anhydride under the form of white crystals with m.p. 129°. After its hydrolysis under reflux in 15 ml water acidulated with 2 drops of conc. HCl, 1.05 g pure *o*-nitrophenylsuccinic acid separates by filtration on cooling, under the form of white crystals with m.p. 188° (decomposition) : $K_{a_1} : 2.82.10^{-4}$; $K_{a_2} : 1.22.10^{-5}$; IR(KBr) $\nu NO_{2\,sym}$: 1360, $\nu NO_{2\,asym}$: 1528 ; $\nu C = O$: 1700 cm^{-1}.

Dimethyl ester of the o-nitrophenylsuccinic acid : m.p. 70°; b.p. 115°/0.4 mmHg. NMR ($CDCl_3$) δ3(2H, for the center of CH_2 multiplet) 3.7 (6H, the center of CH_3 triplet) 4.65 (H, benzyl, middle of the quartet) 7.3 – 8.1 (4H, aromatic multiplet).

p-Nitrophenylsuccinic acid : m.p. 210° (decomposition) ; $K_{a_1} : 5.01.10^{-4}$; $K_{a_2} : 1.58.10^{-5}$; anhydride, noncrystallizable oil, b.p. 110–165° 0.2 mmHg.

Dimethyl ester of the p-nitrophenylsuccinic acid : m.p. 91–92°; b.p. 105°/0.3 mmHg; NMR ($CDCl_3$) δ 3(2H, center of the octet for CH_2) 3.7 (6H, center of CH_3 triplet) 4.2 (H, benzyl, middle of the quartet) 7.8 (4H, center of the aromatic symmetric multiplet).

2,4-Dinitrophenylsuccinic acid : To 2.39 g (10 mM) 4-nitrophenylsuccinic acid dissolved in 11 g H_2SO_4 is added a mixture of 2.17 g HNO_3 98% and 7.5 g conc. H_2SO_4 maintaining the temperature at 55–60° for 3 hr. The following day, the mixture is poured over 80 g ice, it is filtered and washed with water, obtaining after two recrystallizations from an ethanol : water (1 : 2) mixture, 2.05 g (72.3% of the theory) dinitrophenylsuccinic acid, yellow crystals with the m.p. 200° (decomposition) chromatographically unitary on silicagel G plates with phenol : *p*-xylene : HCOOH 80% = 3 : 7 : 1, $R_f = 0.376$ or with the (EMK) mixture : ethanol : ammonia 25% = 65 : 15 : 28; $R_f = 0.24$. $Ka_1 = 7.60.10^{-4}$; $Ka_2 = 2.09.10^{-5}$; IR (KBr); $\nu NO_{2\,sym}$: 1360; $\nu NO_{2\,asym}$: 1540 ; $\nu C=O$: 1720 cm^{-1}. Calculated % for $C_{10}H_8N_2O_8$, C : 42.26 ; H : 2.85 ; N : 9.85 ; Found, C : 42.40 ; H : 3.0 ; N : 9.60.

o-NITROPHENYLSUCCINIC ACID FROM *o*-NITROBENZALDEHYDE

o-Nitrobenzylidenediethylmalonate. Prepared according to the data from the literature.[5] IR(CCl_4) ; $\nu NO_{2\,sym}$: 1345 ; $\nu NO_{2\,asym}$: 1530 ; $\nu C = C$: 1640 ; $\nu C=O$: 1720–30 cm^{-1}. NMR ($CDCl_3$) δ 1.3(6H, CH_3 interpenetrated triplets); 4.18 (4H, quadruplet) 7.5 – 8.2 (5H, aromatic multiplet and vinyl H).

α-Cyano-α-o-nitrobenzyl-diethylmalonate. Over a solution of 29.3 g (10 mM) diethyl-*o*-nitrobenzylidene-malonate dissolved in 70 ml ethanol one adds at normal temperature 8.9 g (10.5 mM) acetonecyanhydrine and the pH of the solution is brought with NaOH 40% to 10.8 – 11.5 using a type 26 "Radiometer" pH-meter. The solution is stirred for 5 hr and after cooling to 10° the formed precipitate is filtered obtaining 29.5 g (92% of the theory) crystalline, light yellow with m.p. 54–55°. IR (CCl_4) $\nu NO_{2\,sym}$: 1345, $\nu NO_{2\,asym}$: 1550, $\nu C\equiv N$: 2248, $\nu C=O$: 1725–1745 (split) cm^{-1}. NMR ($CDCl_3$) δ 1.3 (6H, CH_3 interpenetrated triplets) 4.2 (5H, CH_2 multiplet and malonic proton), 5.35 (H, benzyl), 7.8 – 8.1 (4H, aromatic multiplet).

α-Carbamoyl-α-o-nitrobenzyl-diethylmalonate. It was prepared by nitrile hydrolysis with conc. H_2SO_4 according to the data from the literature.[5] IR (KBr) $\nu NO_{2\,sym}$: 1345 ; $\nu NO_{2\,asym}$: 1530 ; $\nu_{C=O}$ amide I 1605, $\nu_{C=O}$ ester 1735 cm^{-1}.

o-Nitrophenylsuccinic acid. In contrast to the indications from the literature,[6] we observed that the hydrolysis of α-carbamoyl-α-*o*-nitrobenzyl-diethylmalonate with concentrated HCl on boiling is not completed in 3 hrs and thus the duration was prolonged to 30 hr. Even in such conditions there still remain products resulted from the partial hydrolysis and the purification by more recrystallization from water is not sufficient. For a more advanced purification we proceeded as follows : 19 g *o*-nitrophenylsuccinic raw acid is suspended in 30 ml water and treated with NaOH 10% to reach a pH = 5.5 – 6, when the majority of the product is dissolved. The insoluble product is filtered, the solution discoloured with coal is precipitated with conc. HCl at pH 2.5 and after filtration and recrystallization from water one obtains the pure *o*-nitrophenylsuccinic acid with the m.p. 188° (decomposed). By recrystallization from methanol of the insoluble product at pH 5–6, one obtains variable quantities (3 – 10%) of α-amide of the *o*-nitrophenylsuccinic acid with m.p. 148–149°.

β-AMIDES OF THE *o*-NITROPHENYLSUCCINIC ACID

α-Amide of the o-nitrophenylsuccinic acid. A solution of 8 g (23.8 mM) α-carbamoyl-α-*o*-nitrobenzyl diethylmalonate in 133 ml dioxane is treated with 21 g HCl 17.5% and is heated under reflux on a water bath for 20 hr. After vacuum distillation of the solvent, the residue is triturated with 20 ml benzene and after filtration it is dried. The raw product is triturated with saturated solution of sodium bicarbonate and is washed with water, then it recrystallizes from methanol, obtaining 2.85 g (50.5% of the theory) of α-amide of the *o*-nitrophenylsuccinic acid with the m.p. 148—149°. Chromatographed on silicagel G plates in the system benzene : methanol : glacial acetic acid : 45 : 8 : 4 it has $R_f=0.7$, development with iodine vapours or with a solution of bromophenol blue. K_a 1.12.10^{-9} (alcohol-water 25%), IR (CCl_4) νNO_{2sym} : 1345, νNO_{2asym}: 1530, $\nu_{C=O}$ amide I = 1660 — 1680 (shoulder), $\nu_{C=O}$ 1710—20 (split) cm^{-1}. Calculated % for $C_{10}H_{10}O_5N_2$, C : 50.42 ; H : 4.23 ; N : 11.76 ; Found, C : 50.20 ; H : 4.00 ; N : 12.00. NMR methyl ester ($CDCl_3$) δ : 3.1 (3H, triplet), 4.5 (H, benzyl) 7.3 (aromatic multiplet).

β-Amide of the o-nitrophenylsuccinic acid. Prepared after the indications given in the literature[4] and the raw amide, separated after acidulation has m.p.158—162°. The methyl ester obtained in methanol solution with diazomethan shows in the RMN spectrum a content of about 25—30% α-amide. By recrystallization of the raw product from water, on cooling, only β-amide deposits, approximately 50% of the initial product with m.p. 182°. In the chromatography on silicagel *G* plates, with the EMK system : ethanol : NH_3 25% in the ratio 65 : 15 : 28, the pure product has $R_f = 0.32$ as against α-amide with $R_f = 0.60$ (development with iodine). NMR methyl ester ($CDCl_3$) δ 3.68 (3H, CH_3 triplet) 4.8 (H, benzyl) 7.3 (aromatic multiplet).

β-Anilide of the o-nitrophenylsuccinic acid. To a solution of 5 g (22 mM) anhydride of the *o*-nitrophenylsuccinic acid in 100 ml anh. $CHCl_3$ is added 2.1 g (120 mM) aniline and it is heated on a water bath under reflux for 2.5 hr. After filtration and recrystallization from methanol one obtains 5.2 g (73.3% of the theory) anilide, white crystals with m.p. 153—154°. The chromatography on G silicagel plates with benzene : dioxan : acetic acid = 45. : 12.5 : 2 and developed with iodine or 5% solution of bromophenol blue R_f=0.6 ; K_a 1.34.10^{-6} (methanol-water 75%). Ir (KBr) $\nu NO_{2\,sym}$: 1340 ; $\nu NO_{2\,asym}$: 1520 ; $\nu_{C=O}$ amide I 1660, $\nu C=O$: 1715 cm^{-1}. Calculated % for $C_{16}H_{14}N_2O_5$, C : 61.11 ; H : 4.48 ; N : 8.91 ; Found : C : 61.5 ; H : 4.7 ; N : 9.10.

Methyl ester of β-anilide of the o-nitrophenylsuccinic acid. It was obtained by esterification of anilide, dissolved in tetrahydrofuran with diazomethan etheric solution, under the form of white crystals with m.p. 119—120.5°, chromatographically unitary $R_f = 0.60$ on silicagel G plates in the system benzene : methanol : glacial acetic acid=45 : 8 : 4. NMR ($CDCl_3$) δ 3(CH_2) 3.67 (triplet CH_3) 4.8 (H, benzyl) 7.5 (aromatic multiplet).

β-Diethylamide of the o-nitrophenylsuccinic acid. The anhydride of the *o*-nitrophenylsuccinic acid 7.3 g (33 mM) dissolved in 70 ml tetrahydrofuran is treated with 6.33 g (86.5 mM) diethylamine at a temperature of 10°. After 24 hr, it is acidulated with a HCl etheric solution up to a pH = 2 and the diethylamine hydrochloride is filtered. The residue left after removal of the solvent under vacuum is washed with a diluted HCl solution and with water. After recrystallization from benzene one obtains 5.7 g diethylamide (59% of the theory), white crystals with m.p. 122°, chromatographically unitary, R_f : 0.6 plates of G silicagel, with the system benzene : methyl alcohol : glacial acetic acid = 45 : 8 : 4, development with 5% solution of bromophenol blue. K_a 4.5.10^{-5} (methanol-water 75%) IR (KBr)$\nu_{NO_{2\,sym}}$: 1355, $\nu_{NO_{2\,asym}}$: 1525 ; $\nu_{C=O}$ amide I 1640, $\nu_{C=O}$ 1713 cm^{-1}. Calculated % for $C_{14}H_{18}N_2O_5$, C : 57.13 ; H : 6.16 ; N : 9.52 ; Found, C : 57.4 ; H : 6.3 ; N : 9.6.

Methyl ester of β-diethylamide of the o-nitrophenylsuccinic acid. By treating diethylamide in tetrahydrofuran with a diazomethan etheric solution, it was obtained as white crystals with m.p. 95.5°, chromatographically unitary $R_f = 0.59$ on silicagel G plates in the system benzene : methanol : glacial acetic acid = 45 : 8 : 4. NMR ($CDCl_3$) δ : 1.0 (CH_3 of the amide), 3.0 (CH_2), 3.4 (CH_2 of the amide) 4.8 (H, benzyl), 7.6 (aromatic multiplet).

β-AMIDES OF THE o-NITROPHENYLSUCCINIC ACID

α-Amide of the o-nitrophenylsuccinic acid. A solution of 8 g (23.8 mM) α-carbamoyl-(o-nitrobenzyl) diethylmalonate in 132 ml dioxane is treated with 21 g HCl 17.5% and is heated under reflux on a water bath for 20 hr. After vacuum distillation of the solvent, the residue is triturated with 20 ml benzene and after filtration it is dried. The raw product is triturated with saturated solution of sodium bicarbonate and is washed with water, then it recrystallizes from methanol, obtaining 2.85 g (50.5% of the theory) of α-amide of the o-nitrophenylsuccinic acid with the m.p. 148–149°. Chromatographed on silica gel G plates in the system benzene : methanol : glacial acetic acid 45 : 8 : 4 it has R_f = 0.[illegible], development with iodine vapours or with a solution of bromophenol blue. R_E 1.23.10^{-3} (alcohol-water 25%). IR (KCl) $\nu NO_{2\,as}$ 1525, $\nu NO_{2\,sym}$ 1345; $\nu C{=}O$ amide I = 1660 – 1680 (shoulder), $\nu C{=}O$ 1710–1720 (split) cm^{-1}. Calculated % for $C_{10}H_{10}O_5N_2$: C: 50.42; H: 4.23; N: 11.76. Found, C: 50.20; H: 4.06; N: 12.06. NMR methyl ester ($CDCl_3$) δ 3.1 (2H, triplet), 4.0 (1H, benzyl) 7.5 (aromatic multiplet).

β-Amide of the o-nitrophenylsuccinic acid. Prepared after the indications given in the literature[1] and the raw amide, separated after acidulation has m.p. 155–162°. The methyl ester obtained in methanol solution with diazomethane shows in the NMR spectrum a content of about 25–30% α-amide. By recrystallization of the raw product from water, on cooling, only β-amide deposits, approximately 50% of the initial product with m.p. 182°. In the chromatography on silica gel G plates, with the BMK system (ethanol : NH_4OH 25% in the ratio 65 : 15 : 28, the pure product has R_f = 0.32 as against α-amide with R_f = 0.40 (development with iodine). NMR methyl ester ($CDCl_3$) δ 2.68 (2H, CH_2 triplet) 4.3 (1H, benzyl) 7.5 (aromatic multiplet).

β-Anilide of the o-nitrophenylsuccinic acid. To a solution of 5 g (22 mM) anhydride of the o-nitrophenylsuccinic acid in 100 ml anh. $CHCl_3$ is added 2.1 g (22.0 mM) aniline and it is heated on a water bath under reflux for 2.5 hr. After filtration and recrystallization from methanol one obtains 5.2 g (73.3% of the theory) anilide, white crystals with m.p. 153–154°. The chromatography on G silica gel plates with benzene : dioxan : acetic acid = 45 : 12.5 : 2 and developed with iodine or 5% solution of bromophenol blue R_f = 0.6. R_E 1.34.10^{-3} (methanol-water 75%). IR (KCl) $\nu NO_{2\,as}$ 1540; $\nu NO_{2\,sym}$ 1350; $\nu C{=}O$ amide I 1660, $\nu C{=}O$ 1715 cm^{-1}. Calculated % for $C_{16}H_{14}N_2O_5$: C: 61.14; H: 4.48; N: 8.91. Found: C: 61.5; H: 4.7; N: 9.10.

Methyl ester of β-anilide of the o-nitrophenylsuccinic acid. It was obtained by esterification of anilide, dissolved in tetrahydrofuran with diazomethane etheric solution, under the form of white crystals with m.p. 119–120.5°, chromatographically unitary R_f = 0.60 on silica gel G plates in the system benzene : methanol : glacial acetic acid = 45 : 8 : 4. NMR ($CDCl_3$) δ 2.82 (2H, triplet, CH_2) 4.8 (1H, benzyl) 7.5 (aromatic multiplet).

β-Diethylamide of the o-nitrophenylsuccinic acid. The anhydride of the o-nitrophenylsuccinic acid 7.5 g (33 mM) dissolved in 70 ml tetrahydrofuran is treated with 2.88 g (39.5 mM) diethylamine at a temperature of 10°. After 2 hr, it is acidulated with a HCl etheric solution up to a pH = 2 and the diethylamine hydrochloride is filtered. The residue left after removal of the solvent under vacuum is washed with a diluted HCl solution and with water. After recrystallization from benzene one obtains 5.7 g diethylamide (58% of the theory), white crystals with m.p. 122°, chromatographically unitary, R_f = [illegible] plates of G silica gel, with the system benzene : methyl alcohol : glacial acetic acid = 45 : 8 : 4, development with 5% solution of bromophenol blue. R_M 1.03.10^{-3} (methanol-water 75%). IR (KBr) $\nu NO_{2\,as}$ 1530; $\nu NO_{2\,sym}$ 1355; $\nu C{=}O$ 1725; $\nu C{=}O$ amide I 1640, $\nu C{=}O$ 1718 cm^{-1}. Calculated % for $C_{14}H_{18}N_2O_5$: C: 57.13; H: 6.16; N: 9.52; Found, C: 57.[illegible]; H: 6.3[illegible]; N: 9.6[illegible].

Methyl ester of β-diethylamide of the o-nitrophenylsuccinic acid. By treating diethylamide in tetrahydrofuran with a diazomethan etheric solution, it was obtained as white crystals, with m.p. 92.5°, chromatographically unitary R_f = 0.56 on silica gel G plates in the system benzene : methanol : glacial acetic acid = 45 : 8 : 4. NMR ($CDCl_3$) δ 1.0 (CH_3 of the amide), 3.3 (CH_2 of the amide), 4.8 (1H, benzyl), 7.6 (aromatic multiplet).

Revue Roumaine de Chimie, 22, 6, 877–883 (1977)

Herrn Professor Dr. Coriolan Drăgulescu
zum 70. Geburtstag gewidmet

NUCLEOPHILE SUBSTITUTIONEN AN KOHLENSÄURE-DERIVATE.

IX[1]. KINETIK UND MECHANISMUS DER ALKOHOLYSE VON KOHLENSÄURE-DICHLORID-N-ARYL-IMIDEN

R. BACALOGLU, T. KORODI, A. FLORESCU und G. OSTROGOVICH
Laboratorium für Organische Chemie, Technische Hochschule „Traian Vuia“
Timişoara, Str. Bocşa 6.

Eingegangen 3. Sept. 1976

Die Kinetik der Alkoholyse von Kohlensäure-dichlorid-N-aryl-imiden wurde durch Leitfähigkeitsmessungen in Gegenwart von tertiären Aminen verfolgt. Auf Grund der experimentellen Daten wurde im langsamen Schritt ein trimolekularer Additionsmechanismus festgestellt, welcher auf dem nucleophilen Angriff des tertiären Amins an das Assoziat Alkohol mit Kohlensäure-dichlorid-N-aryl-imid, beruht.

In der Literatur findet man wenige Angaben über die Reaktion der Kohlensäure-dichlorid-N-aryl-imide mit Alkoholen. Wenn man Kohlensäure-dichlorid-N-aryl-imide im Molverhältnis 1 : 1 mit Natriumäthoxyd versetzt, erhält man den N-Aryl-imino-chlorameisensäure-äthylester,[2] während bei einem Überschuß von Alkoxyd über das Verhältnis 1 : 2 N-Aryl-imino-äthylkarbonat gebildet wird.[3] Es ist weiterhin bekannt, daß in Gegenwart tertiärer Amine die Kohlensäure-dichlorid-N-acyl-imide[4,5] bzw. die Kohlensäure-dichlorid-N-dimethylphosphoryl-imide [6] mit Alkoholen Iminokarbonate bilden. Die Chlorameisensäure-imine als Zwischenprodukte konnten nicht isoliert werden. In vorliegender Arbeit werden die Reaktionsprodukte, sowie die Kinetik der Reaktion der Kohlensäure-dichlorid-N-aryl-imide mit Alkoholen in Gegenwart tertiärer Amine verfolgt.

REAKTIONSPRODUKTE

Das einzig nachweisbare Produkt bei der Reaktion des Kohlensäure-dichlorid-N-phenyl-imids mit Methanol in Gegenwart des Triäthylamins in Dioxan war das N-Phenylimino-methylkarbonat. Das Reaktionsgemisch wurde zu verschiedenen Zeiten gaschromatographisch analysiert. Es konnten nur die Peaks entsprechend den Kohlensäure-dichlorid-N-phenylimiden, N-Phenylimino-methyl-karbonaten, sowie des Triäthylamins und des Lösungsmittels identifiziert werden. Im I.R. Spektrum des Reaktionsgemisches sieht man klar, daß die charakteristischen Banden der Kohlensäure-dichlorid-N-phenylimide verschwinden und an ihrer Stelle die der N-Phenylimino-methylkarbonate erscheinen. Sowohl bei der chromatographischen, als auch bei der I.R.-spektroskopischen Überprüfung der Reaktionsprodukte wurden zum Vergleich authentische Proben von N-Phenyl-imino-methylkarbonat sowie N-Phenyliminochlorameisensäuremethylester verwendet.

---

[1] Mitteilung VIII. R. Bacaloglu und C. Dăescu, *Rev. Roumaine Chim.* im Druck.

[2] F. Langfeld und J. Stieglitz, *Amer. Chem. J.*, **16**, 70 (1894).

[3] W. R. Smith, *Amer. Chem. J.*, **16**, 372 (1894).

[4] J. M. Ivanova, N. A. Kirsanova, E. A. Stucalo und Cs. I. Dercaci, *Zhur. org. Khim.*, **3**, 480 (1966).

[5] R. Neidlein und W. Haussmann, *Arch. Pharm.*, **300**, 609 (1967).

[6] P. I. Alimov und L. I. Levcova, *Izvest. Akad. Nauk. S.S.S.R., Otdel. khim. Nauk*, **1964**, 1889.

Die Reaktionsprodukte wurden in Dioxan identifiziert, obwohl die kinetischen Messungen in Aceton durchgeführt wurden, weil Aceton in dem I.R.-Bereich 1800–1550 cm^{-1} nicht durchlässig ist.

REAKTIONSKINETIK

Die Kinetik der Reaktion der Kohlensäure-dichlorid-N-aryl-imide mit verschiedenen Alkoholen wurde in Gegenwart tertiärer Amine, in wasserfreiem Aceton durch Leitfähigkeitsmessungen verfolgt.

In Tabelle 1 sind die Geschwindigkeitskonstanten pseudoerster Ordnung aufgeführt. In allen Fällen waren diese mit der Pyridinkonzentration proportionell, wodurch die R.G. Konstanten zweiter Ordnung berechnet werden konnten. Die Reaktionsgeschwindigkeit war um so größer, je saurer der betreffende Alkohol war. Der sterische Effekt des organischen

Tabelle 1

Geschwindigkeitskonstanten erster und zweiter Ordnung der Reaktion von Kohlensäure-dichlorid-N-phenyl-imid (3×10^{-3}M/L mit verschiedenen Alkoholen, in Gegenwart von Pyridin bei 45°

Alkoholkonz. M/L	σ^{*7}	E_s^7	Py Konz. M/L	$k_1 \times 10^4$ Sek.$^{-1}$	$k_2 \times 10^4$ Sek.$^{-1}$. M^{-1}L
1 $\begin{matrix}CH_3\\CH_3\end{matrix}\!\!>\!CH-OH$			0,600	4,00	
	−0,19	−0,47	0,703	4,69	4,74
4,86			0,813	5,15	
			0,908	5,47	$r = 0{,}988$
2 C_2H_5-OH			0,130	1,28	
6,65	−0,1	−0,07	0,372	2,84	6,56
			0,614	4,45	$r = 0{,}999$
3 CH_3-OH			0,131	1,32	
9,35	0	0	0,372	3,19	7,58
			0,620	5,03	$r = 0{,}999$
4 $CH_3OCH_2CH_2-OH$			0,595	6,49	
4,80	0,07	−0,77	0,707	7,50	9,36
			0,817	8,57	$r = 0{,}999$
5 $C_6H_5-CH_2-OH$			0,700	9,41	
3,58	0,212	−0,38	0,817	11,05	11,43
			0,916	12,07	
			0,022	13,11	$r = 0{,}996$

---

[7] J. E. LEFFER und E. GRUNWALD, „Rates and Equilibria of Organic Reactions“, Wiley, New York, 1963.

Alkoholradikals konnte vernachlässigt werden, so daß eine gute Korrelation mit den σ^*-Taft Konstante möglich war.

$$\log k_2 = 0{,}804\ \sigma^* - 3{,}138 \quad r = 0{,}969$$

Bei kleinen Alkoholkonzentrationen hängen die Konstanten zweiter Ordnung, linear von derselben ab, während sie bei Konzentrationen, die den Grenzwert 3 Mol/Liter überschreiten, praktisch unabhängig von der Alkoholkonzentration sind, wie aus Tabelle 2 hervorgeht.

Tabelle 2

Geschwindigkeitskonstanten zweiter Ordnung der Reaktion von Kohlensäure-dichlorid-N-phenyl-imid (1 : 4 : 3 × 10^{-4} M/L und 5 : 9 : 3 × 10^{-3} M/L) mit Methanol in Gegenwart von Pyridin (0,84 M/L) bei 45°

	Alkoholkonzentration M/L	$k^2 \times 10^4$ Sek.$^{-1}$ M^{-1}L
1	0,183	2,57
2	0,373	2,83
3	0,733	4,43
4	1,282	6,20
5	2,340	7,84
6	4,680	8,00
7	7,600	7,94
8	8,770	7,78
9	9,350	7,86

Da das tertiäre Amin am langsamen Schritt der Reaktion teilnimmt, wurde der Einfluß seiner Basizität und sterischen Effekte auf die Geschwindigkeitskonstante zweiter Ordnung (Tabelle 3) untersucht.

Wie aus Abb. 1 ersichtlich ist, kann für die tertiären sterisch wenig behinderten Amine eine liniare Brönstedt-Korrelation in Betracht gezogen werden :

$$\log k_2 = 0{,}776 . pK_a - 7{,}137 \quad r = 0{,}993$$

Bei Aminen mit größerer sterischer Hinderung kann man feststellen, daß die Reaktionsgeschwindigkeit beträchtlich abnimmt(Tabelle 3). Der stark elektrophile Charakter des Kohlensäure-dichlorid-N-phenyl-imids bei der Reaktion mit tertiären Aminen wird durch die

Tabelle 3

Geschwindigkeitskonstanten pseudoerster und zweiter Ordnung der Reaktion von Kohlensäure-dichlorid-N-phenylimid (3 × 10^{-3}M/L) mit Methanol (9,35 M/L) bei 45°

	Tertiäres Amin Art	pK_a[8]	Konz. M/L	$k_1 \times 10^4$ Sek.$^{-1}$	$k_2 \times 10^4$ Sek.$^{-1}$ M^{-1} L	$\log \frac{k_2^*}{k_2^c}$
1	Pyridin	5,18	0,601	4,38	7,28	—
2	Isochinolin	5,38	0,573	8,85	15,45	—
3	β-Picolin	5,52	0,491	6,73	13,70	—
4	α-Picolin	5,94	0,690	0,88	1,277	−1,36
5	γ-Picolin	6,08	0,494	12,79	25,90	—
6	N-Äthyl-morpholin	7,67	0,523	5,53	10,57	−1,79
7	Diazobycyclo Octan	8,19	0,206	744,8	1805	—
8	NN-Dimethyl-ethanolamin	9,31	0,671	26,8	40	−2,48
9	Triäthylamin	10,67	0,485	1,25	2,58	−4,73

* k_2^c berechnet nach Brönsted's Korrelation

---

[8] D. D. Perrin ,,Dissociation Constants of Organic Bases in Aqueous Solution'', Butterworths, London, 1965.

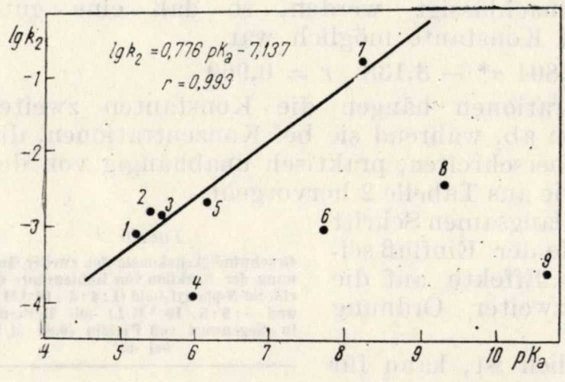

Abb. 1.—Abhängigkeit des Logarithmus der Geschwindigkeitskonstante zweiter Ordnung gegen pK_a der tertiären Amine (Tabelle 3).

Tabelle 4

Geschwindigkeitskonstanten zweiter Ordnung der Reaktion von Kohlensäure-dichlorid-N-phenyl-imid (2,5 – 3 × 10^{-3}M/L) (am Benzolkern verschieden substituiert) mit Methanol (9,35 M/L) in Gegenwart von Pyridin (0,60 M/L) bei 45°

	R	σ^7	$k_2 \times 10^{-4}$ Sek.$^{-1}$M^{-1}L
1	$p-CH_3O$	0,268	4,06
2	$p-CH_3$	−0,17	4,43
3	H	0	7,28
4	$p-Cl$	0,227	26,2
5	$p-CH_3OCO$	0,45	59,5
6	$m-NO_2$	0,71	131,4
7	$p-NO_2$	0,778	245

Tabelle 5

Aktivierungsenthalpie und -Entropie der Reaktion von Kohlensäure-dichlorid-N-Phenyl-imid (2 × 10^{-3}M/L) mit Methanol und Metoxy-äthanol in Gegenwart von Pyridin (0,1 – 0,8 M/L)

Alkohol	Temperatur °C	$k_2 \times 10^4$ Sek.$^{-1}$M^{-1}L	scheinbare Aktivierungsparameter
CH_3-OH (9,35 M/L)	45 35 25	7,58 4,35 2,71	$\Delta H^{\#} = 9{,}0$ kcal/Mol $\Delta S^{\#} = -42{,}4$ u.e.
$CH_3OCH_2CH_2-OH$ (4,80 M/L)	45 35 25	9,36 8,66 2,96	$\Delta H^{\#} = 10{,}3$ kcal/Mol $\Delta S^{\#} = -37{,}6$ u.e.

Hammet-Korrelation für die am aromatischen Kern verschieden substituierte Produkte veranschaulicht (Tabelle 4)

$$\log k_2 = 1{,}72\sigma - 3{,}022 \qquad r = 0.994$$

Die verhältnismäßig niederen Aktivierungsentropien zeigen eine höhere Ordnung im Übergangszustand als im Anfangsstadium, während die relativ kleinen Aktivierungsenergien einen guten Energieausgleich zwischen Reißen und Bilden chemischer Bindungen veranschaulichen (Tabelle 5).

DISKUSSION

Da die Reaktionsgeschwindigkeit bei ansteigender Acidität der Alkohole in Abwesenheit sterischer Effekte wächst, gelangt man zu der Schlußfolgerung, daß der Alkohol im langsamen Schritt als Protonenspender und nicht als nucleophiles Agenz anzusehen ist. Sie bilden in einem Gleichgewichtsprozeß wahrscheinlich ein Assoziat mit den Kohlensäuredichlorid-N-aryl-imiden:

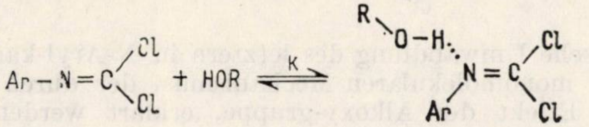

Im Falle eines großen Alkoholüberschusses kann die Konzentration des Assoziats gegen die Gesamtkonzentration des Kohlensäuredichlorids-N-aryl-imids und des Alkohols durch eine Gleichung mit folgender Form ausgedrückt werden:

$$[\mathrm{I}] = K\,\frac{[\mathrm{ArNCCl_2}]\ [\mathrm{ROH}]}{1 + K\,[\mathrm{ROH}]}$$

Dieser Ausdruck entspricht der gefundenen linearen Abhängigkeit für kleine Alkoholkonzentrationen ($K[\mathrm{ROH}] \ll 1$) und ist praktisch unabhängig für große Konzentrationen des Alkohols ($K\ [\mathrm{ROH}] \gg 1$).

Wenn man den stark elektrophilen Charakter des Kohlensäuredichlorid-N-aryl-imids und den nucleophilen Charakter des Amins in Betracht zieht, so kommt man zu dem Schluß, daß im langsamen Schritt der nucleophile Angriff des Amins an das oben genannte Assoziat, erfolgt.

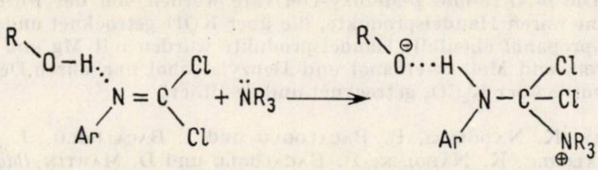

Somit können die sterischen Effekte am Niveau des tertiären Amins, sowie die niederen Enthalpien und Entropien eine Erklärung finden. Von vornherein muß der Mechanismus, der einen nucleophilen Angrif des Assoziats Alkohol mit dem tertiären Amin an das Kohlensäure-dichlorid-N-aryl-imid voraussetzt, ausgeschlossen werden, weil dieser durch die Abhängigkeit der Geschwindigkeitskonstanten von der Acidität der Alkohole sowie ihrer Konzentration nicht erklärt werden kann.

Zusammenfassend kann gesagt werden, daß es sich um eine trimolekulare Additionsreaktion analog derer die bei einer Reihe von Additionen an heterosubstituierte Nitrile[9] anzutreffen sind, handelt. Das oben angegebene Reaktionszwischenprodukt stabilisiert sich durch Chloreliminierung und nucleophile Addition des Alkohols durch Bildung von Chlorameisensäure-N-imino-alkylester.

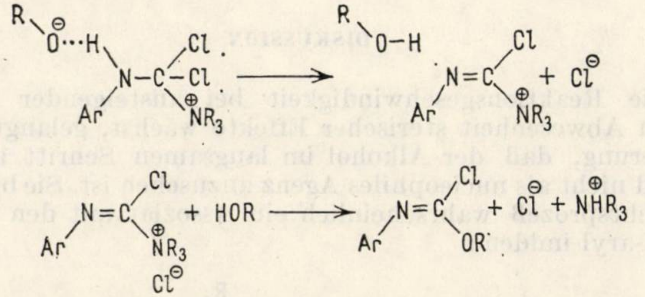

Die rasche Umwandlung des letztern in N-Aryl-karbonat kann nur durch einen monomolekularen Mechanismus, der durch den elektronenabgebenden Effekt der Alkoxy-gruppe, erklärt werden kann, möglich werden.

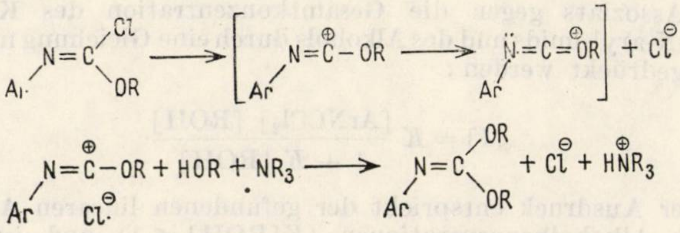

EXPERIMENTELLER TEIL

Substanzen : Die Kohlensäure-dichlorid-N-aryl-imide wurden durch Chlorieren von Isothiocyanat (3 Tab. 4), Isonitril (2 Tab. 4) oder Ameisensäure-N-aryl-imiden dargestellt (4–6 Tab. 4).[10] Die *p*-Nitro-und *p*-Metoxy-Derivate wurden von der Firma Bayer erhalten. Die tertiären Amine waren Handelsprodukte, die über KOH getrocknet und destilliert wurden. Methanol und Isopropanol ebenfalls Handelsprodukte wurden mit Mg und Jod, Athanol mit CaO behandelt, während Metoxy-ethanol und Benzylalkohol nur durch Destillieren gereinigt wurden. Aceton wurde über K_2CO_3 getrocknet und destilliert.

---

[9] D. Martin, K. Nadolski, R. Bacaloglu und I. Bacaloglu, *J. prakt. Chem.*, **313**, 58 (1971) ; I. Bacaloglu, K. Nadolski, R. Bacaloglu und D. Martin, *ibid.*, 839 ; D. Martin, A. Berger, H. I. Niclas und R. Bacaloglu, *ibid.*, **315**, 274 (1973) ; I. Bacaloglu, R. Bacaloglu, C. Viragh, H. Glatt und G. Ostrogovich, *ibid.*, **317**, 907 (1975) ; I. Bacaloglu, R. Bacaloglu, H. Glatt, C. Viragh und G. Ostrogovich, *J. Chim. Soc. Perkin Trans. II. Phys. Org. Chem.*, **1976**, 524.

[10] E. Kuhle, B. Anders und G. Zumach, *Angew. Chem.*, **79**, 663 (1967).

Die Synthese des Chlorameisensäure-N-phenyl-imin-methylesters[2] und des N-Phenyl-imino-methyl-karbonates[3] wurde nach Literaturangaben ausgeführt und ihre Struktur durch I.R.- und N.M.R. - Spektroskopie geprüft.

IDENTIFIZIERUNG DER REAKTIONSPRODUKTE

Das Gemisch, gebildet von Kohlensäure-dichlorid-N-phenyl-imid (0,0063 M), Methanol (0,025 M), Triäthylamin (0,010 M) und 1 ml Dioxan wurde auf 45° thermostatiert. Die von Zeit zu Zeit entnommenen Proben wurden I.R. - spektroskopisch (Spektrograph Specord I.R. 71 Carl-Zeiss Jena in Arsensulfid Küvetten) und gas-chromatographisch (Chromatograph Chromatron G.C.H.F. 18.3) unter folgenden Bedingungen untersucht: Säule von 3 m aus methyl-silikonhaltigem Gummi SE 30 10% auf Chromosorb P, Wasserstoffdurchflußmenge 1 ml/Sek., Eingangstemperatur 260°, in der Säule Anfang 130° 5 Minuten, Ende 170° 5 Minuten; Gradient 3°/Min.

REAKTIONSKINETIK

In eine thermostatierte Leitfähigkeitszelle versehen mit Rührer wurde ein Gemisch von Aceton, Alkohol und tertiärem Amin eingeführt. Das Kohlensäure-dichlorid-N-imid wurde in wenig Aceton gelöst und in ein dünnwandiges Reagenzglas, welches im Moment Null durchstochen wurde, eingeführt. Die Änderung der Leitfähigkeit im Verhältnis zur Zeit wurde mit einem Radiometer - Konduktometer samt Registriergerät (Radelkis Typ Oh 814 l) gemessen.

Die Berechnungen wurden nach Guggenheim's[11] Methode durchgeführt. Die scheinbaren Aktivierungsparameter wurden für 300 K berechnet.

---

[11] A. A. Frost, R. G. Pearson, „Kinetics and Mechanism", Wiley, New York, 1953.

Revue Roumaine de Chimie, **22**, *6*, 885–898 (1977)

POTENTIAL ANTICANCER AGENTS. XIII[1]

SYNTHESIS OF NEW ALIPHATIC AND CYCLOALIPHATIC N-NITROSOUREAS

ILEANA BARACU *, EUSTANŢA TĂRNĂUCEANU and I. NICULESCU-DUVĂZ
Oncological Institute Bucharest
Bul. 1 Mai 11, Romania

Received February 11, 1975

Eighteen new aromatic, aliphatic and cycloaliphatic nitrosoureas were synthetised. The synthesis of the intermediate ureas and nitrosoureas was disscused. From these derivatives *n*-hexan-1 : 6-1′-N-nitroso-3′-N-(2-chloroethyl)-urea and *n*-octan-1 : 8-bis-1′-N-nitroso-3′-N-(2-chloroethyl)-urea showed to be effective against L-1210.

The considerable interest for N-nitrosourea derivatives arises both from their significant activity against intraperitoneally and intracerebrally implanted experimental leukemia (i.c. and i.p. L-1210, P-388), and their outsanding clinical results obtained in several forms of neoplasia (i.e. Hodgkin disease, central nervous system tumors, etc.). From this group four compounds namely: 1,3 bis-(2-chloroethyl)-1-nitrosourea (**1**, B.C.N.U.),[2–4] 1-(2-chloroethyl)-3-cyclohexyl-1-nitrosourea (**2**, C.C.N.U.),[5–7] 1-(2-chloroethyl)-3-(4-methyl-cyclohexyl)-1-nitrosourea (**3**, MeCCNU),[8,9] and more recently 2-[3-(2-chloroethyl)-3-nitrosoureido]-2-

---

* This work represents a part of Ph. D. Thesis, supervised by Prof. dr. G. Ostrogovich.

[1] Part XII. I. Dragotă, D. Ionescu, E. Tărnăuceanu, V. Dobre and I. Niculescu-Duvăz, *Rev. Roumaine Chim.*, in press.

[2] V. T. De Vita, P. P. Carbone, A. B. Owens, G. L. Gold, M. J. Krant and J. Edmonson, *Cancer Res.*, **25**, 1876 (1965).

[3] T. P. Johnston, G. S. McCaleb and J. A. Montgomery, *J. Med. Chem.*, **6**, 669 (1963).

[4] S. K. Carter and J. W. Newman, *Cancer Chemother. Rep.*, **1**, 115 (1968).

[5] T. P. Johnston, G. S. McCaleb, P. S. Oplinger and J. A. Montgomery, *J. Med. Chem.*, **9**, 892 (1966).

[6] S. B. Wilson, E. B. Boldrey and K. J. Enot, *Cancer Chemother. Rep.*, **54**, 273 (1970).

[7] H. H. Hansen, O. S. Selawry, F. M. Muggia and M. D. Walker, *Cancer Res.*, **31**, 223 (1971).

[8] T. P. Johnston, G. S. McCaleb, P. S. Opliger, W. R. Laster and J. A. Montgomery, *J. Med. Chem.*, **14**, 600 (1971).

[9] C. R. Joung, D. M. Walker, P. G. Canellos, S. P. Schein, A. B. Chabner and V. T. De Vita, *Cancer Res.*, **31**, 1164 (1973).

deoxy-D-glucopyranose (**4**, chlorozotocin),[10] have had the most extensive clinical trial and have reached the point of commercial application.

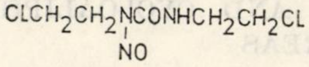

$ClCH_2CH_2N(NO)CONHCH_2CH_2Cl$

1

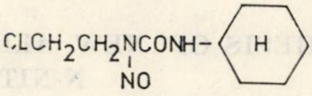

2

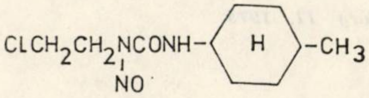

3

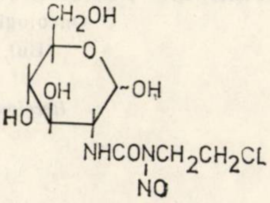

4

One of the most important properties of N-nitrosourea derivatives was their ability to cross the blood-brain barrier and to kill intracerebrally injected leukemic cells.[11] Moreover the reasonable correlation found between their biological effectiveness and their lipid solubility, expressed as log P, supported this assumption.[12-14] Recently it was stated that the range $-1.0 \leqslant \log P \leqslant 2.0$ was the most interesting area to be explored for active nitrosourea design.[15]

No one knows the molecular mechanism responsible for the antitumor activity of these cell cycle non specific agents. Observations related to the mechanism of action which included : 1) the inhibition of the DNA and RNA synthesis ;[16-18] 2) the cross resistance with alkylating agents observed with the hamster plasmocytoma (between B.C.N.U. and cyclophosphamide) and microorganisms ;[19-21] 3) the reaction with 4-(*p*-nitrobenzyl)pyridine (N.B.P.),[22,23] led to the inclusion of nitrosoureas in the class of alkylating agents. But several factors would indicate that nitrosoureas did not alkylate through their β carbon : 1) derivatives **5** with Z = F were highly active against L-1210,[4] although the 2-fluoroethyl compounds were less chemically reactive than the 2-chloroethyl ones ;[24] 2) the parent ureas seemed to be devoid of antileukemic activity ;[25] and 3) B.C.N.U. did not induce cross resistance with other alkylating agents in Hodgkin disease.[4]

---

[10] T. P. Johnston, G. S. Mc Caleb and J. A. Montgomery, *J. Med. Chem.*, **18**, 104 (1975).

[11] M. F. Schabel Jr., T. P. Johnston, G. S. McCaleb, J. A. Montgomery, W. R. Laster and H. E. Skipper, *Cancer Res.*, **23**, 725 (1963).

[12] V. A. Levin and P. Kabra, *Cancer Chemother. Rep.*, **58**, 787 (1974).

[13] C. Hansch and Y. M. Clayton, *J. Pharm. Sci.*, **62**, 1 (1973).

[14] C. Hansch, N. Smith, R. Engle and H. Wood, *Cancer Chemother. Rep.*, **56**, 443 (1972).

[15] J. A. Montgomery and J. G. Mayo, *J. Med. Chem.*, **17**, 477 (1974).

[16] T. Sugimura, Sh. Fujimura, N. Nagao, T. Yokoshima and T. Hasegawa, *Biochim. Biophys. Acta*, **170**, 44 (1968).

[17] N. P. Buu-Hoi, *Cancer Res.*, **30**, 559 (1970).

[18] D. R. McCalla and S. A. Reuver, *Can. J. Biochem. Physiol.*, **46**, 1411 (1968).

[19] G. P. Wheeler and B. J. Bowdon, *Cancer Res.*, **25**, 1770 (1965).

[20] G. Gale, *Biochem. Pharmacol.*, **14**, 1707 (1965).

[21] R. F. Pittilo, A. J. Narkates and J. Burns, *Cancer Res.*, **24**, 1222 (1964).

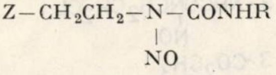

$$\underset{\displaystyle NO}{Z-CH_2CH_2-N}-CONHR$$

5 (Z = F, Cl)

These collected data and the fact that B.C.N.U. and C.C.N.U. are extremely unstable compounds suggested that the nitrosoureas function as suitable carriers of some alkylating or carbamoilating moieties.[12,26] The knowledge of the structures of these breakdown products is the critical step in the design of such effective derivatives.

The *in vitro* degradation studies of N-alkyl-N-nitrosoureas, B.C.N.U., C.C.N.U., etc., as well as the reaction with N.B.P., provided some data for the elucidation of their biological activity.[23,25] These results indicated that nitrosoureas breakdown initially into a diazohydroxide and an isocyanate (the former releasing N_2 and a carbonium ion which leads to the corresponding alcohol or aldehyde), so that they may be considered both alkylating and carbamoilating agents.[25] In agreement with this assumption, recent reports related the alkylating activity of nitrosoureas to their antitumor effectiveness and their carbamoilating activity to systemic toxicity (at least in the case of solid tumor systems).[12] From a comparative investigation on the mode of decomposition of B.C.N.U., C.C.N.U. and B.F.N.U. (1,3bis-(2-fluoroethyl)-1-nitrosourea) it appeared that the biologic activity of these compounds may also result from their carbamoylating activity.[27]

---

[22] D. Bray, V. T. Oliverio, R. Adamson and V. T. De Vita, *Proc. Amer. Ass. Cancer Res.*, **30**, 133 (1970).

[23] G. P. Wheeler and S. Chumley, *J.Med.Chem.*, **10**, 259 (1967).

[24] P. L. Levins and Z. B. Papanastassion, *J.Amer.Chem. Soc.*, **87**, 826 (1965).

[25] J. A. Montgomery, R. James, G. S. Mc Caleb and T. P. Johnston, *J. Med. Chem.*, **10**, 668 (1967).

[26] S. K. Carter, F. M. Schabel Jr., L. E. Broder and T. P. Johnston, *Adv. Cancer Res.*, **16**, 273 (1972).

[27] G. P. Wheeler, B. J. Bowdon, J. A. Grimsley and H. H. Lloyd, *Cancer Res.*, **34**, 194 (1974).

In order to provide additional data in this area the synthesis of three new types of nitrosoureas **6, 7,** and **8** was undertaken.[28]

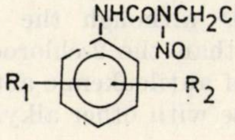

6

6a $R_1 = 3-\underset{NO}{NHCONCH_2CH_2Cl}$ $R_2 = 4-CH_3$

b $3-CO_2CH_3$ $6-CH_3$

c $2-CO_2CH_3$ $6-CH_3$

d $2-CO_2CH_3$ $4-CH_3$

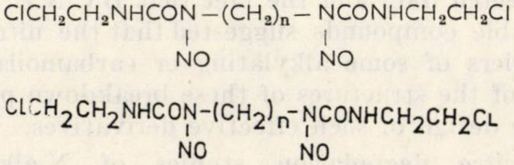

$$ClCH_2CH_2NHCO\underset{NO}{N}-(CH_2)_n-\underset{NO}{N}CONHCH_2CH_2Cl$$

$$ClCH_2CH_2NHCO\underset{NO}{N}-(CH_2)_n-\underset{NO}{N}CONHCH_2CH_2Cl$$

7 (a−f), n = 2−6,8

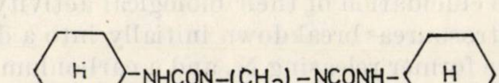

8 (a−g), n = 2−8,

1. SYNTHESIS

UREAS SYNTHESIS

Two main procedures, adapted from the known methods were used in the preparation of the ureas,[3,5,8] namely the coupling between : a) a suitable amine and 2-chloroethyl[29−32] or cyclohexyl isocyanate ; [33−36]

---

[28] I. NICULESCU-DUVĂZ, I. BARACU, V. FEYNS, G. CIUȘTEA, Communication at the 6th National Congress of Pharmacy, Bucharest, 1973.

[29] H. WENKER, *J. Amer. Chem. Soc.*, **58**, 2608 (1936).

[30] H. NAJER, P. CHABRIER and R. GIUDICELLI, *Bull. Soc. Chim. France*, **1960**, 956.

[31] W. SIEFKEN, *Liebigs Ann. Chem.*, **562**, 74 (1949).

[32] C. K. JOHNSTON, *J. Org. Chem.*, **32**, 1508 (1967).

[33] A. SKITA and M. ROLFES, *Ber. dtsch. chem. Ges.*, **53**, 1242 (1920).

[34] R. J. SLOCOMBE, E. E. HARDY, J. H. SAUNDERS and R. L. JENKIS, *J. Amer. Chem. Soc.*, **72**, 1888 (1950).

[35] A. GEMASSMER, Ger. Pat. 949227, 1956 ; *Chem. Abstr.*, **53**, 4243 (1959).

[36] R. BARDAY JR. and R. P. KURKJY, U. S. Pat. 3 054 819, 1962 ; *Chem. Abstr.*, **58**, 3332 (1962).

b) an appropriate isocyanate and 2-chloroethyl or cyclohexyl amine :

$$\text{a) } R-NH_2 + \underset{\mathbf{9}}{ClCH_2CH_2NCO} \rightarrow \underset{\mathbf{10}}{RNHCONH-CH_2CH_2Cl}$$

$$\text{b) } \underset{\mathbf{11}}{R-NCO} + H_2NCH_2CH_2Cl \rightarrow \mathbf{10}$$

The aromatic ureas **12 (a-g)** (see Table 1) were obtained by the first mentioned procedure, but the excessive toxicity of 2-chloroethyl isocyanate (9) made this route unsuitable for the preparation of large amounts.

Some synthetic methods for this intermediate **9** have previously been described,[29-32] but the reported over-all yields remain usually under 50%. In an attempt to increase the over-all yield of 2-chloroethyl isocyanate **9** the Wenker method [29] (with PCl_5) was modified. The intermediate **9** was obtained *via* 2-hydroxyethyl-urethan [37] in the following two-step procedure :

$$\underset{\mathbf{13}}{HOCH_2CH_2NH_2} + \underset{\mathbf{14}}{(C_2H_5O)_2CO} \rightarrow \underset{\mathbf{15}}{HOCH_2CH_2NHCOOC_2H_5} \xrightarrow{PCl_5} \mathbf{9}$$

The replacement of ethylchloroformate with ethylcarbonate in this reaction led to a very convenient route (yield 95—98%) for preparation of **15**.

The aromatic urea structures **12 (a—d)** were in good agreement with the i.r. spectral data (see table 1).

Table 1

Aromatic ureas

$R_1R_2C_6H_3NHCONHCH_2CH_2Cl$ (**12**)

No.	Substituent		m.p. °C	Method[a]	Analysis %				Yield %
	R_1	R_2			C	H	N	Cl	
12 a[b]	$3-NHCONH(CH_2)_2Cl$	$4\ CH_3$	204—6	A	47.10	5.25	17.05	21.31	62
12 b[c]	$3-COOCH_3$	$6\ CH_3$	154	B	52.90	5.75	10.45	13.52	97
12 c[c]	$2-COOCH_3$	$6\ CH_3$	144—6	B	53.49	5.82	10.56	13.52	52
12 d[c]	$2-COOCH_3$	$4\ CH_3$	166—8	B	52.99	5.66	10.50	13.25	70

a. Typical procedures given : A. $R_1R_2C_6H_3(NCO)_2 + H_2NCH_2CH_2Cl$; B. $R_1R_2C_6H_3NH_2 + ClCH_2CH_2NCO$; b. Formula $C_{13}H_{18}N_4O_2Cl_2$, calcd. : C = 46.85, H=5.45, N = 16.81, Cl = 21.27; c. Formula $C_{12}H_{15}N_2O_3Cl$, calcd. : C = 53.23, H = 5.59, N = 10.35, Cl = 13.09.

---

[37] N. P. A. FRANCHIMONT and A. LUBLIN, *Rec. Trav. chim.*, **21**, 48 (1902) ; *Chem. Zentr.*, **1**, 975 (1902).

The synthesis of aliphatic and cycloaliphatic bisureas was achieved according to scheme 1.

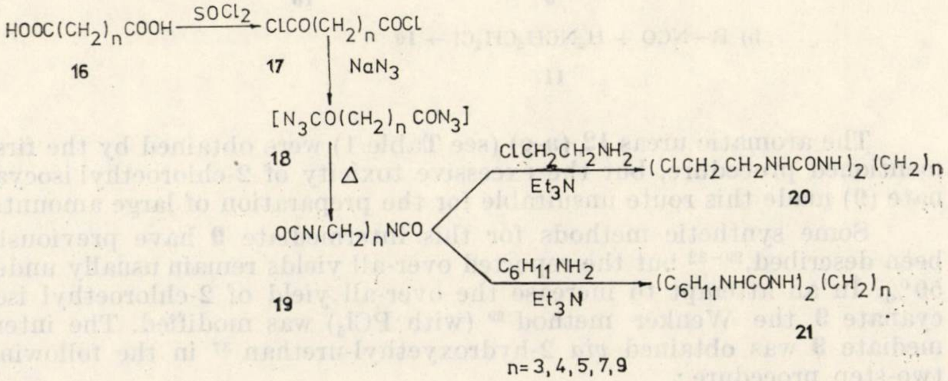
HOOC(CH2)nCOOH
SOCl2
ClCO(CH2)nCOCl
16
17
NaN3
[N3CO(CH2)nCON3]
18
Δ
OCN(CH2)nNCO
19
ClCH2CH2NH2
Et3N
(ClCH2CH2NHCONH)2(CH2)n
20
C6H11NH2
Et3N
(C6H11NHCONH)2(CH2)n
21
n=3, 4, 5, 7, 9

The reaction of the acid chlorides **17** with activated sodium azide [38] afforded the intermediate azides **18**. Their conversion to ureas was accomplished by a two-step procedure involving : a) their thermal decomposition into the corresponding isocyanates **19** and b) reaction of the isocyanates, thus obtained (without further purification) with 2-chloroethylamine or cyclohexylamine. The use of triethylamine as catalyst considerably improved the yield of this reaction. The formation of both azides and isocyanates was spectrometrically controlled (see table 2).

Table 2

Characteristic i.r. absorption maxima for 17, 18 and 19 intermediates [a]

Compound n	Acid chlorides (**17**) $\nu_{C=O}$ (cm^{-1})	Azides (**18**) $\nu_{CON_3}^{(a)}$ cm^{-1}	Isocyanates (**19**) $\nu_{NCO}^{(a)}$ cm^{-1}
3	1805^b	2135	2285
4	1805^b	2140^c	2280^c
5	1800^b	2142^c	2280^c
7	1725	2140	2285
8	1730	2138	2280

a. The i.r. spectra were run in ethylic ether solution when no otherwise noted; b. CCl_4 c. benzene.

Unexpected low yields were obtained during the preparation by this procedure of ureas **20 b** (n=3) and **20 d** (n=5).

The assigned structure of the new ureas **20** (**a**–**f**) and **21** (**a**–**g**) (summarized in table 3) was also supported by their i.r. spectra.

---

[38] P. A. S. Smith in "Organic Reactions", vol. III, 7th ed., John Wiley & Sons, Inc., New York, 1959, p. 373.

Table 3

Aliphatic and cycloaliphatic ureas

$RNHCONH(CH_2)_n NHCONHR$ **20**, $R = CH_2CH_2Cl$ **21**, $R = C_6H_{11}$

No.	n	Formula	m.p. °C	Me-thod[a]	Analysis								Yield %
					calcd.				found				
					C	H	N	Cl	C	H	N	Cl	
20 a	2	$C_8H_{16}N_4O_2Cl_2$	180–3	A_1	35.43	5.96	20.66	26.14	35.55	5.92	20.70	26.60	25
20 b	3	$C_9H_{18}N_4O_2Cl_2$	141–3	B_1	37.90	6.37	19.64	24.86	38.25	6.59	19.64	24.63	30
20 c	4	$C_{10}H_{20}N_4O_2Cl_2$	165	B_1	40.13	6.75	18.73	23.69	40.00	6.83	18.87	23.54	72
20 d	5	$C_{11}H_{22}N_4O_2Cl_2$	131–3	B_1	42.17	7.09	17.89	22.63	42.48	7.40	17.63	22.37	49
20 e	6	$C_{12}H_{24}N_4O_2Cl_2$	150–3	A_1	44.03	7.41	17.12	21.66	43.85	7.50	16.90	21.43	91
20 f	8	$C_{14}H_{28}N_4O_2Cl_2$	157	B_1	47.32	7.96	15.77	19.95	47.81	7.98	15.27	—	80
21 a	2	$C_{16}H_{30}N_4O_2$	242–3	A_2	61.88	9.76	18.05	—	61.53	10.05	18.20	—	83
21 b	3	$C_{17}H_{32}N_4O_2$	220	B_2	62.91	9.96	17.27	—	62.53	10.00	14.47	—	95
21 c	4	$C_{18}H_{34}N_4O_2$	300	B_2	63.85	10.14	16.55	—	63.44	9.68	16.46	—	89
21 d	5	$C_{19}H_{36}N_4O_2$	235–7	B_2	64.72	10.31	15.89	—	64.96	10.63	16.23	—	98
21 e	6	$C_{20}H_{38}N_4O_2$	225	A_2	65.52	10.47	15.28	—	66.09	10.56	15.39	—	75
21 f	7	$C_{21}H_{40}N_4O_2$	221–3	B_2	66.25	10.61	14.72	—	66.70	10.10	14.57	—	78
21 g	8	$C_{22}H_{42}N_4O_2$	208	B_2	66.94	10.74	14.20	—	67.42	10.60	14.43	—	67

a. Typical procedures given in the Experimental part: $A_1 \cdot H_2N(CH_2)_nNH_2 + ClCH_2CH_2NCO$; $A_2 \cdot H_2N(CH_2)_nNH_2 + C_8H_{11}NCO$; $B_1 \cdot OCN(CH_2)_nNCO + ClCH_2CH_2NH_2 \cdot HCl$; $B_2 \cdot OCN(CH_2)_nNCO + C_6H_{11}NH_2$.

In some cases the previously described procedure provided impure isocyanates, containing variable amounts of precursor acid chlorides. The condensation of this material with amines afforded a mixture of desired urea with the corresponding amide **22**, attempts to obtain pure ureas from such mixtures being unsuccessful. It appeared that the isocyanate

$$\mathrm{RNHCO{-}(CH_2)_n{-}CONHR}$$

22

purity must be carefully controlled during its preparation. Spectral distinction between ureas and amide-derivatives was made in the i.r. spectra, the medium intensity band at 3080 $\mathrm{cm^{-1}}$ being attributed to the amide N−H (ν_{N-H}).[39]

N-NITROSOUREAS SYNTHESIS

Nitrosation of previously reported ureas was achieved using the known methods.[2,4,7] In order to minimize random nitrosation undiluted formic acid (98−100%) and dry $\mathrm{NaNO_2}$ were used.[4]

The isomeric pure nitrosoureas **6** (**a**−**d**), **7** (**a**−**f**) and 8 (**a**−**g**) were obtained in good yields by dissolution of the crude material in undiluted formic acid, and after a time, reprecipitation by addition of water.

The nitrosation of ureas (**20** ; n = 3, 5, 8) and (**21** ; n = 8) with $\mathrm{HCO_2H}$/dry $\mathrm{NaNO_2}$ failed in a number of attempts. In concentrated HCl (10N) the reaction was complete and proceeded in good yields. The nitrosation of *n*-heptan 1 : 7 bis-3′-N-cyclohexylurea (**21 f** ; n=7) was performed using dry $\mathrm{NaNO_2}$ in the following media : 1) AcOH−$\mathrm{Ac_2O}$; 2) 98−100% HCOOH, 3) 80% HCOOH, 4) HCl 10N, and 5) mixture of HCl (10*N*) : HCOOH (98−100%) 1 : 1 (vol : vol). The first four methods afforded oils containing unnitrosated ureas whereas the last procedure gave a precipitate which after purification produced an analytically pure sample.

The new nitrosoureas **6** (**a**−**d**), **7** (**a**−**f**) and 8 (**a**−**g**) thus obtained were summarized in tables 4 and 5.

2. SPECTRAL DATA

The structure of N-nitrosoureas was checked using both spectroscopic data (i.r., n.m.r.) and decomposition studies (with amines, etc.). These last data will be reported in detail elsewhere.

I.R. Spectra. The i.r. spectra of precursor ureas were in good agreement with the literature data.[40,41] As expected the carbonyl absorption was definitely shifted by nitrosation of the precursor urea,[4,14] (with a $\Delta\nu = 75-90\ \mathrm{cm^{-1}}$) the $\nu_{C=O}$ frecquency in nitrosoderivatives being located in the range 1705−1715 $\mathrm{cm^{-1}}$ (see table 6). This band was very useful

---

[39] L. J. Bellamy, "The Infra-red Spectra of Complex Molecules", John Wiley & Sons Inc., New York, 1960, p. 208.

[40] Y. Mido, *Spectrochim. Acta*, **28A**, 1503 (1972).

[41] Y. Mido, *Spectrochim. Acta*, **29A**, 1 (1973).

Table 4

Aromatic nitrosoureas

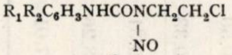

$$R_1R_2C_6H_3NHCO\underset{\displaystyle NO}{N}CH_2CH_2Cl$$

6

No.	Substituent		m.p. °C	Method[a]	Analysis %				Yield %
	R_1	R_2			C	H	N	Cl	
6 a[b]	$3-NHCO\underset{NO}{N}CH_2CH_2Cl$	$4-CH_3$	100	A	40.00	4.51	20.88	18.36	77
6 b[c]	$3-COOCH_3$	$6-CH_3$	98	B	48.10	4.85	13.97	11.79	50
6 e[c]	$2-COOCH_3$	$6-CH_3$	71–72	B	48.20	5.10	14.15	11.05	53
6 d[c]	$2-COOCH_3$	$4-CH_3$	96–8	A	47.61	5.18	13.90	12.23	89

a) method A) 98–100% $HCOOH/NaNO_2$; B) $H_2SO_4 : H_2O/NaNO_2$

b) formula: $C_{13}H_{16}N_6O_4Cl_2$, calcd.: C = 39.90, H = 4.12, N = 21.48, Cl = 18.12%; c) formula $C_{12}H_{14}N_3O_4Cl$, calcd.: C = 48.08, H = 4.72, N = 14.02, Cl = 11.83%.

to control the completeness of nitrosation. The N-nitroso absorption appeared in the 1488–1505 cm^{-1} range as a medium band.

N.M.R. Spectra. The spectra of ureas were not recorded because of their poor solubility in suitable solvents. The n.m.r. spectra were used in order to establish the isomeric purity of new compounds **6** (**a**–**d**), **7** (**a**–**f**) and **8** (**a**–**g**). The absorptions obtained for the several protons were given in table 7.

The data thus obtained for aliphatic and cycloaliphatic nitrosoureas (**7** and **8**) supported the assigned structures (i.e. the splitting of N–*H* absorption into a doublet ($J = 7.0$ cps) in **8** (**a**–**g**) compounds, the singlet and respectively the triplet obtained for H^A protons – (see table 7 – in compounds **8 a** and **8 b**, etc.).

Nitrosation of ureas **20** (**a**–**f**) gave in some cases an isomeric mixture. For example the n.m.r. spectra of the unpurified solid obtained after **20 e** nitrosation (compound **7 e**) exhibited two weak but well defined triplets at $\delta = 3.62$ (CH_2Cl) and 4.19 (CH_2–N–NO) ($J_{CD} = 7.0$ cps) corresponding to the absorption pattern of H^C and H^D protons in structure **23**, and the N–H absorption was shifted to $\delta = 7.90$ ppm.

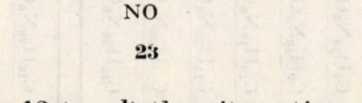

$$(ClCH_2^C\,CH_2^D\underset{\displaystyle NO}{N}-CO-NH)_2(CH_2)_n$$

23

In aromatic ureas **12** (**a**–**d**) the nitrosation afforded in all cases the isomeric structure **5**(Z=Cl) characterized by the two triplets arising at $\delta = 3.50 - 3.68$ (2H) and $4.22 - 4.28$ (2H) ($J = 6.0 - 7.0$ cps) corresponding to H^C and H^D protons. Mention should be made of the unusual low field absorption of N–*H* proton in compound **6 c** ($\delta = 10.1$).

Table 5

Aliphatic and cycloaliphatic nitrosoureas

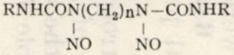

$$\mathrm{RNHCO\underset{NO}{N}(CH_2)_n\underset{NO}{N}-CONHR}$$

7 R = CH_2CH_2Cl

8 R = C_6H_{11}

No.	n	Formula	m.p. °C	Method[a]	Analysis %								Yield %
					calcd.				found				
					C	H	N	Cl	C	H	N	Cl	
7 a	2	$C_8H_{14}N_6O_4Cl_2$	145–6	A	29.19	4.30	25.54	21.54	29.65	3.96	25.42	21.67	85
7 b	3	$C_9H_{16}N_6O_4Cl_2$	68–70	B	31.49	4.71	24.49	20.66	31.73	4.88	24.19	20.50	70
7 c	4	$C_{10}H_{18}N_6O_4Cl_2$	137	A	33.64	5.09	20.54	19.86	34.00	5.50	23.64	20.33	95
7 d	5	$C_{11}H_{20}N_6O_4Cl_2$	55–7	B	35.59	5.41	22.64	19.10	35.59	5.30	22.82	19.31	75
7 e	6	$C_{12}H_{22}N_6O_4Cl_2$	92	A	37.41	5.77	21.82	18.40	36.95	5.90	21.78	18.26	90
7 f	8	$C_{14}H_{26}N_6O_4Cl_2$	82	B	40.68	6.35	20.34	17.15	41.11	6.62	20.70	17.01	92
8 a	2	$C_{16}H_{28}N_6O_4$	135	A	52.15	7.81	22.81	–	52.54	7.68	23.22	–	58
8 b	3	$C_{17}H_{30}N_6O_4$	137	A	53.33	7.92	21.98	–	52.96	7.93	21.95	–	74
8 c	4	$C_{18}H_{32}N_6O_4$	112	A	54.52	8.15	21.20	–	54.56	8.05	21.24	–	96
8 d	5	$C_{19}H_{34}N_6O_4$	100–102	A	55.58	8.36	20.47	–	55.73	8.64	20.80	–	97
8 e	6	$C_{20}H_{36}N_6O_4$	103–105	A	56.57	8.56	19.79	–	57.00	8.90	20.11	–	90
8 f	7	$C_{21}H_{38}N_6O_4$	57–60	C	57.50	8.75	19.16	–	57.25	8.90	19.40	–	87
8 g	8	$C_{22}H_{40}N_6O_4$	93–94.5	B	58.37	8.93	18.57	–	58.78	9.35	18.24	–	80

a. Typical procedures (see Experimental part) : A) HCOOH 98–100%/$NaNO_2$; B) HCl d 1.19/$NaNO_2$; C) HCl d 1.19 : HCOOH 98–100%/$NaNO_2$.

Table 6

The infra-red spectra of aliphatic and cycloaliphatic ureas and nitrosoureas

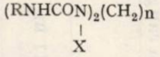

$(RNHCO\underset{X}{N})_2(CH_2)_n$

X = H, NO; n = 2–8

No.	R	X	Infra-red absorption[a, b], cm^{-1}				$\Delta\nu_{C=O}$ [c]
			$\nu_{C=O}$ amide I	$\nu_{CN} + \delta_{NH}$ amide II	ν_{NH}	ν_{N-NO}	
20	$ClCH_2CH_2$	H	1620–1635 *s*	1575–1595 *s*	3335–3355 *s* 3325–3330 *sh*	—	—
7	$ClCH_2CH_2$	NO	1710–1715 *s*	1535–1550 *s*	3325–3365 *m*	1490–1505 *m*	80–90
21	C_6H_{11}	H	1625–1640 *s*	1575–1595 *s*	3350–3360 *s* 3325–3330 *s*	—	—
8	C_6H_{11}	NO	1710–1715 s	1538–1548 s	3310–3365 m	1488–1495 *m*	75–85

a) KBr disks; b) *s* = strong; *m* = medium; *sh* = shoulder; c) $\nu_{C=O} = \nu_{C=O}(X{=}NO) - \nu_{C=O}(X{=}H)$

Table 7

N.M.R. Spectra of aliphatic and cycloaliphatic nitrosoureas

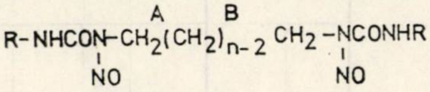
$$R\text{-}NHCO\underset{NO}{N}\text{-}\overset{A}{CH_2}(\overset{B}{CH_2})_{n-2}CH_2\text{-}\underset{NO}{N}CONHR$$

n=2−8

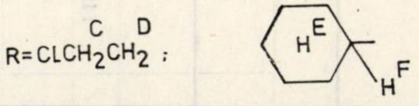

$$R = Cl\overset{C}{CH_2}\overset{D}{CH_2}\ ;$$

Chemical shift (ppm)[(a)]	Compounds	
	7 (a–f)	8 (a–g)
H^A	3.92 s[b)] (4H)	3.73–3.90 m[c)] (4H)
H^B	1.25–1.55 m (4–12 H)	overlapped on the H_E proton range[d)]
	3.74–3.78 m (8H)	– –
H^E	–	1.27–2.11 m (22H)
H^F	–	3.84 m[e)] (2H)
N–H	7.30–7.60 s (2H)	6.74–6.80 (2H ;J_{F-H}=7.0 cps)

a) internal standard TMS ; solvent $CDCl_3$; b) determined in compound **7 a**(n = 2). In the other similar derivatives (n = 3–8) the absorption arose in the range of H^C and HD protons ; c) in compound **8a** (n=2) the band appeared as a singlet ; in the compound **8 b** (n=3) as a triplet (J_{AB}=7.0 cps) and in the compounds with n>3 it appeared as a multiplet ; d) the absorption is located in the range of H^E protons probably around a $\delta = 1.27 - 1.30$ (m, 2 – 12 H) ; e) the absorption of proton H_F overlaps the H_A protons peak.

3. BIOLOGICAL DATA

A detailed discussion of antitumor (against W-256) and antileukemic (against L-1210) activity of these derivatives will be reported elsewhere.

Nitrosoureas **7 e** (n = 6) and **7 g** (n = 8) were significantly effective against L-1210 (see table 8). None of the new aromatic and bis-cyclohexyl ureas **6** and **8** showed any significant activity against L-1210. Derivative **7 a** (n = 2) was effective against both the vaccinal virus and a viral agent extracted from Hodgkin's lymphoma (in contrast with C.C.N.U. completely inactive in these tests).

Table 8

Effectiveness of some derivatives of type 7 against L-1210 Leukemia

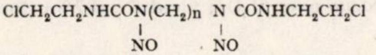

$ClCH_2CH_2NHCON(CH_2)_n\underset{NO}{N}CONHCH_2CH_2Cl$ with NO under the first N: $ClCH_2CH_2\underset{NO}{N}CON(CH_2)_n\underset{NO}{N}CONHCH_2CH_2Cl$

7

No.	n	DL$_{50}$		L.-1210 1)	
		mg/kg	mmole/kg	dosis(mg/kg)× nr. adm. 2)	I.L.S. 3) %
2	C.C.N.U.	93.5	0.40	4× 14	113
7 e	6	417	1.08	20× 10	63
7 a	2	1300	3.14	100× 10	47

1) The screening was performed on L-1210 bearing BDF$_1$ mice, according to NCI rules, by Dr. V. Dobre; 2) daily administration; 3) I.L.S. – increase in the life span.

EXPERIMENTAL PART

Melting points were determined with a Franz Küstner-Dresden apparatus and were uncorrected.

The infrared spectra were determined in pressed KBr disks (ureas, nitrosoureas) or $CHCl_3$, CCl_4 solutions (nitrosoureas) on a U.R.10 (Carl Zeiss, Jena) spectrophotometer.

The n.m.r. spectra were run on a Varian T-60 spectrophotometer in $CDCl_3$ or $(CD_3)_2SO$ solutions, using tetramethylsilane as internal standard.

T.L.C. were performed on Merck silica gel F$_{254}$ plates using the following solvent systems: $C_6H_6 : EtOH : CHCl_3/9 : 1 : 1$ and $C_6H_6 : EtOH/5 : 1$; nitrosoureas could often be detected in ultraviolet light ($\lambda = 2540$ Å) or with iodine vapors.

The starting acid chlorides **17** were synthetized according to the literature data, b.p. (°C/mmHg): 80/10, **17 b** (n=3);[42–44] 111/12, **17 c** (n=4);[42–45] 122/4, **17 d** (n=5);[44] 151/10, **17 f** (n=7)[46,47] and 170/14, **17 g** (n=8).[42,48] Their purity was spectrometrically controlled (see table 2).

n-Butan-1:4 bis- 3′-N-(2-chloroethyl)urea, **20 c** (method B$_1$, table 3).

To a stirred solution of n-butan-1 : 4-diacid chloride (2 g, 10.9 mmoles) in dry benzene (40 ml) activated NaN_3 (4.45 g, 68.7 mmoles) was gradually added. The mixture was refluxed until the evolution of N_2 ceased. The reaction was finished when acid chloride and azide bands ($\nu_{COCl} = 1805$ cm^{-1} and $\nu_{CON_3} = 2140$ cm^{-1}) dissappeared from the i.r. spectrum of the reaction mixture. The isocyanate thus obtained was used without further purification.

2-Chloroethylamine-hydrochloride (3.9 g, 33.6 mmoles) in cold water was made basic with 50% aqueous NaOH and extracted with three (20 ml) portions of benzene. To the dried (Na_2SO_4) and stirred benzene solution triethylamine (5.8 ml, 41 mmoles) was added, and after cooling, it was treated with the previously prepared *n*-butan-1,4 diisocyanate. The mixture was stirred for 0,5 hrs at 5° and at room temperature for 7 hrs. The bis-urea was collected by filtration, washed with petroleum ether (b.p. 30–60°), water, again with petroleum ether (b.p. 30–60°) and dried in vacuo over P_2O_5; afforded **20 c** 5.2 g (98%), m.p. 153–157° (for analytical data see table 3).

[42] K. V. Auwers and M. Schmidt, *Ber. dtsch. chem. Ges.*, **46**, 457 (1913).
[43] P. Ruggli, *Liebigs Ann. Chem.*, **399**, 174 (1913).
[44] H. J. Backer and J. D. H. Homan, *Rec. Trav. chim.*, **58**, 1050 (1939).
[45] D. Holde, *Ber. dtsch. chem. Ges.*, **45**, 3701 (1912).
[46] H. Erlenmeyer and W. Büchler, *Helv. Chim. Acta*, **29**, 1924 (1946).
[47] L. Ruzicka and H. A. Brekenoogen, *Helv. Chim. Acta*, **14**, 1319 (1931).
[48] V. Anger, *Ann. Chim. Physique*, **22**, 289 (1891).

n-Butan 1 : 4 bis (3'-N-cyclohexylurea), **21 e** (method B_2, table 3).

To a cooled and stirred solution of cyclohexylamine (4 g, 40 mmoles) and triethylamine 5.8 ml, 41 mmoles) a benzenic solution of previously prepared (see 1) *n*-butan 1 : 4 diisocyanate was added. After 0.5 hrs at 5° and 7 hrs at room temperature, the white precipitate formed was collected and washed with petroleum ether (30—60°) water, again with petroleum ether (30—60°) and then dried *in vacuo* over P_2O_5 ; yield 6 g (87%) (for analytical data see table 3).

Ethan 1 : 2 bis-3'-N-(2-chloroethylurea), **20 a** (method A_1, table 3).

2-Chloroethyl isocyanate (6.33 g, 61 mmoles) was added dropwise to a chilled (5°) and stirred ethereal (10 ml) solution of ethan-1.2 diamine (1.8 g, 30 mmoles) and triethylamine (4.35 ml, 30 mmoles). The mixture was gradually allowed to stand at room temperature, and after 7 hrs the white solid formed was collected by filtration, washed with water, then with petroleum ether (b.p. 30—60°), and dried *in vacuo* over P_2O_5 ; yield **20 a** (5.2 g, 62%) (for analytical data see table 3).

n-Hexan 1 : 6 bis-1'-N-nitroso-3'-N-cyclohexyl-urea, **8 e** (method A, table 5).

Dry $NaNO_2$ (2.24 g, 32.5 mmoles) was added in small increments to a 5°, stirred solution of **21 e** (1.0 g, 2.73 mmoles) in 98—100% formic acid (10 ml).

The mixture was stirred at 0—5° for 1 hr, slowly diluted with cold water (30 ml), and stirred 30 min more, at 0—5°. The light yellow precipitate was washed with water and dried *in vacuo* over P_2O_5.

The dried precipitate was dissolved in 98—100% formic acid (20 ml). The solution was stirred for 2 hrs at 5°, diluted with cold water (20 ml), and the stirring continued for 30 min at 5°. The light yellow solid was collected, washed with water and dried *in vacuo* over P_2O_5 ; yield 0.9 g (76%) (for analytical data see table 5).

n-Heptan 1 : 7 bis-1'-N-nitroso-3'-N-cyclohexyl-urea, **8 f** (method C, table 5).

21 f (0.5 g, 1.35 mmoles) was dissolved under stirring at room temperature in HCl (d.1.19,5 ml) and 98—100% HCOOH (5 ml). The mixture was chilled (5°) and $NaNO_2$ (0.5 g, 7.24 mmoles) was added in small increments. The mixture was subsequently stirred for 1 hr at 0—5°, diluted with cold water and the stirring continued for 1 more hr at 0—5°. The separated oil was extracted with three 15 ml portions of chloroform. The washed chloroformic extract was evaporated under *vacuo* to an oil which crystallized after 24—30 hrs. The light yellow solid was triturated with petroleum ether (b.p. 30—60°) and dissolved in cold 98—100% HCOOH (10 ml). The solution was cooled, stirred for 2 hrs at 0—5°, diluted with cold water (10 ml) and the stirring continued for 1 more hr at 5°. The obtained oil solidified on standing. The nitrosoureas was collected, washed with petroleum ether (b.p. 30—60°) and dried ; yield **8 f** (0.5 g, 86.7%) (for analytical data see table 5).

N-hydroxyethyl-urethan, **15**

A solution of monoethanolamine (81 g, 1 mole) and ethylcarbonate (129.8 g, 1.1 moles) was refluxed for 12 hrs and then distilled under *vacuo*. Fraction with b.p. 169—172/12 mm was redistilled under *vacuo* ; yield **15** (130 g, 98%) b.p. 177—180/12 mm.

ACKNOWLEDGMENTS. The authors are grateful to Dr. M. Elian for performing n.m.r. spectra and for his valuable cooperation in this area.

Revue Roumaine de Chimie, 22, 6, 899–906 (1977)

SPECTROPHOTOMETRIC STUDIES ON SOME CHROMOTROPIC ACID AZO DYES IN AQUEOUS BUFFER SOLUTIONS

H. KHALIFA, Y. M. ISSA and A. T. HAJ-HUSSEIN
Chemistry Department, Faculty of Science, Cairo University,
Giza, EGYPT

Received May 5, 1975

The absorption spectra of *o*-, *m*-, and *p*-methoxyphenylazo-, 1-, and 2-naphthylazo-, *m*-,nitrophenylazo-, and *p*-sulphonamide-phenylazo-chromotropic acid are studied in buffer solutions of varying pH values. The variation of spectra with pH indicates the presence of two equilibria. The *pK* values of the naphthalenic OH- groups are determined spectrophotometrically, while those of the sulphonic groups are determined potentiometrically.

INTRODUCTION

Chromotropic acid (1,8-dihydroxynaphthalene-3,6-disulphonic acid disodium salt) azo dyes find wide application as chromophoric and metallochromic indicators. Few studies were concerned with the effect of pH on the absorption spectra and calculation of the ionization constants of both the strong sulphonic and the somewhat weak hydroxyl groups.

The present investigation is a study of the absorption spectra of *o*-, *m*-, and *p*-methoxyphenylazo-, 1-, and 2-naphthylazo-, *m*-, nitrophenylazo- and *p*-sulphonamidephenylazochromotropic acid (I—VII respectively) in buffer solutions of varying pH values.

EXPERIMENTAL

The water used was always twice distilled from all glass equipment. The chemicals were all of the highest purity available. The chromotropic acid azo dyes under investigation were prepared by coupling the diazotized corresponding amines with chromotropic acid in carbonate medium.[1] The 10^{-3} M solution of each dye was prepared by dissolving the accurately weighed amount in the appropriate volume of water. Britton and Robinson [2] modified universal buffer series was used to control the pH. Solutions for spectral measurements were obtained by diluting known volumes of the stock solution of the dye with the buffer solutions. The spectra of the resulting solutions were obtained at room temperature using Beckman DK recording spectrophotometer using water as the blank in the visible region. The potentiometric titrations of the above mentioned dyes were performed as mentioned before.[3]

---

[1] N. N. Basargain, *Metody poluncheniniya Kim. Reaktivavi preparatov Gas. Sov. SSSR. Po. Khim.*, **6**, 29 (1962); *Chem. Abstr.*, **61**, 1890 (1964).

[2] H. T. S. Britton, "Hydrogen Ions", 4th Ed., Chapman and Hall, London, 1952.

RESULTS AND DISCUSSION

The absorption spectra of I, II, III, IV, V, VI, and VII in buffer solutions of pH values 2–6 are characterized by bands exhibiting maximum absorption at 524, 506, 524, 536, 518, 498, and 500 nm respectively (Figs. 1–7). The absorption of these bands decreases with increasing pH up to pH 9.0. A sharp decrease in absorbance is observed between pH values 6 and 8. These bands may be assigned to $\pi - \pi^*$ transition of the azo group influenced by intermolecular charge transfer. They are due to the absorption of the acid form and the form containing one ionized naphthalenic OH group. The ionization of the sulphonic acid groups is not considered, since it does not cause any colour or absorption changes,[4] as revealed by the overlapping absorption spectra in the acid range of pH. This is due to the fact that, unlike the hydroxyl naphthalenic groups, the ionizable strong acidic groups are not conjugated with the N=N center. As the pH is further increased the absorbance of the whole band increases gradually up to pH 11–12, where it tends to attain a limiting value. The first decrease in absorbance (pH 6–9) is due to the ionization of the first naphthalenic OH group namely that far from the azo group. This is substantiated by the fact that the ionization of the OH group not involved in a hydrogen bonding requires a lower energy.[5] Also the tautomerism favouring the participation of phenylhydrazone structure retards the deprotonation of the second naphthalenic OH group of the chromotropic acid moiety, which is confirmed by the increase in the absorbance in the pH range 9–12.

The presence of some isosbestic points is an indication of existing equilibria, only up to a certain pH value above which deviation from the isosbestic points takes place (Figs. 1–7).

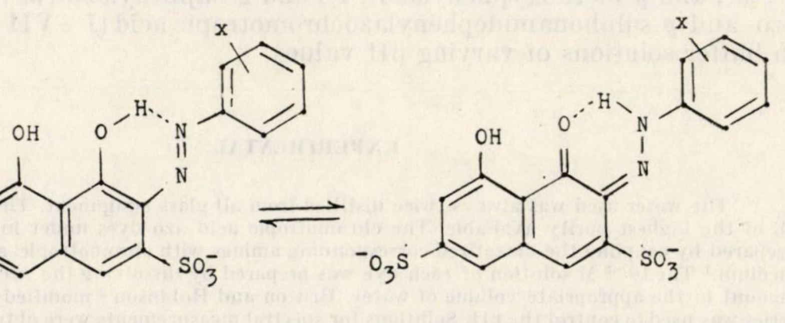

---

[3] H. Khalifa, M. M. Khater and A. A. El-Sirafy, *Z. Analyt. Chem.*, **237**, 111 (1968); H. Khalifa and Y. M. Issa, *J. Chem. Egypt.*, **18**, (1975).

[4] G. Schwarzenbach, "Complexometric Titrations", Interscience Publishers Inc., New York, 1957.

[5] R. M. Issa, M. S. El-Ezabey and A. H. Zewail, *Z. Phys. Chem.* Leipzig, **244**, 155 (1970).

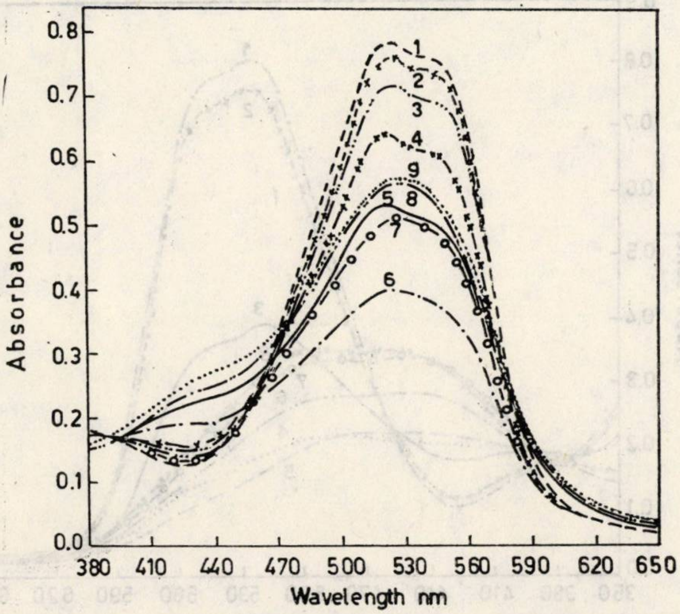

Fig. 1. — Absorption spectra of 4×10^{-5} M *o*-methoxyphenylazochromotropic acid in aqueous solutions of varying pH values. pH = 2.0 (1), 6.0 (2), 7.0 (3), 7.5 (4), 8.0 (5), 9.0 (6), 10.0 (7), 11.0 (8), 12.0 (9).

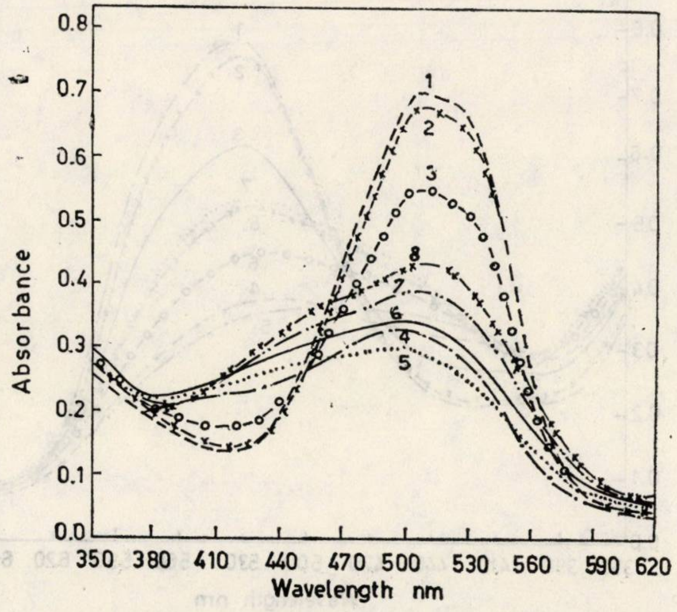

Fig. 2. — Absorption spectra of 4×10^{-5} M *m*-methoxyphenylazochromotropic acid in aqueous solutions of varying pH values. pH = 2.0 (1), 6.0 (2), 7.0 (3), 8.0 (4), 9.0 (5), 9.5 (6), 10.0 (7), 11–12 (8).

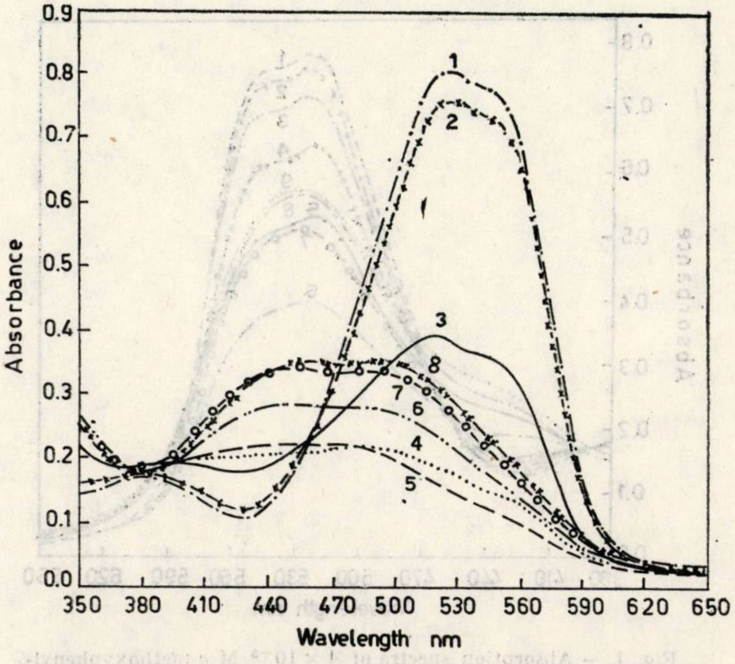

Fig. 3. — Absorption spectra of 4×10^{-5} M *p*-methoxyphenylazo-chromotropic acid in aqueous solutions of varying pH values.
pH = 2.0 (1), 6.0 (2), 7.0 (3), 8.0 (4), 9.0 (5), 10.0 (6), 11.0 (7), 12.0 (8).

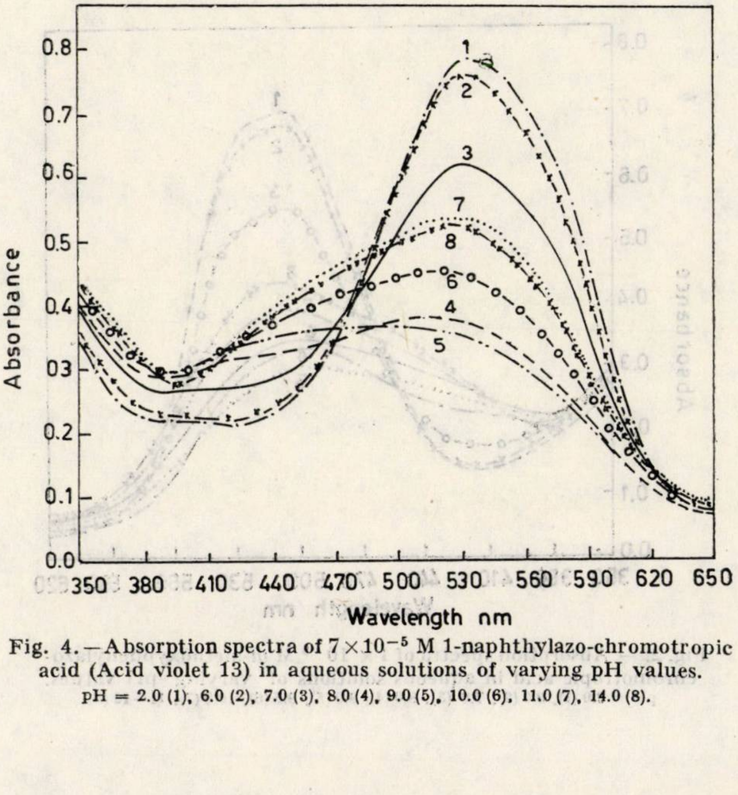

Fig. 4. — Absorption spectra of 7×10^{-5} M 1-naphthylazo-chromotropic acid (Acid violet 13) in aqueous solutions of varying pH values.
pH = 2.0 (1), 6.0 (2), 7.0 (3), 8.0 (4), 9.0 (5), 10.0 (6), 11.0 (7), 14.0 (8).

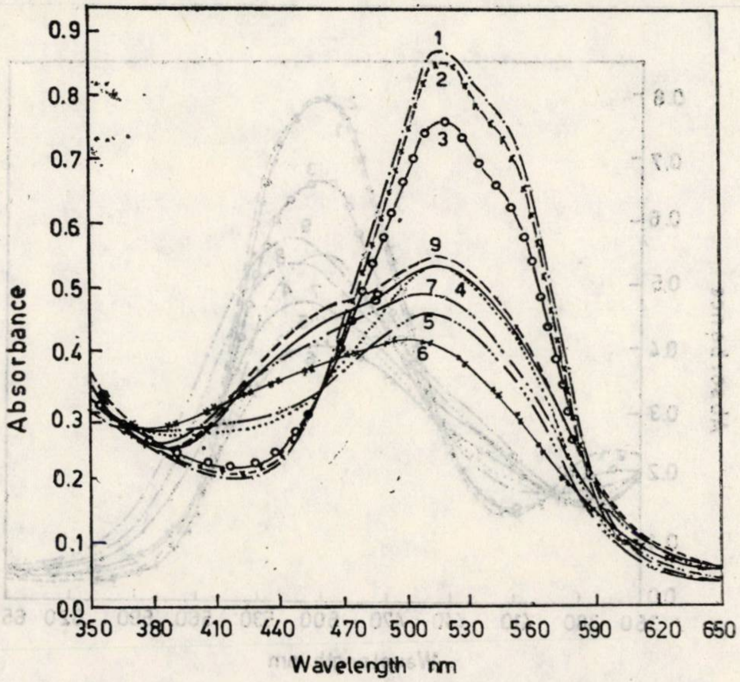

Fig. 5. — Absorption spectra of 5×10^{-5} M 2-naphthylazo-chromotropic acid in aqueous solutions of varying pH values.
pH = 2.0 (1), 6.0 (2), 7.0 (3), 7.5 (4), 8.0 (5), 9.0 (6), 10.0 (7), 11.0 (8), 12.0 (9).

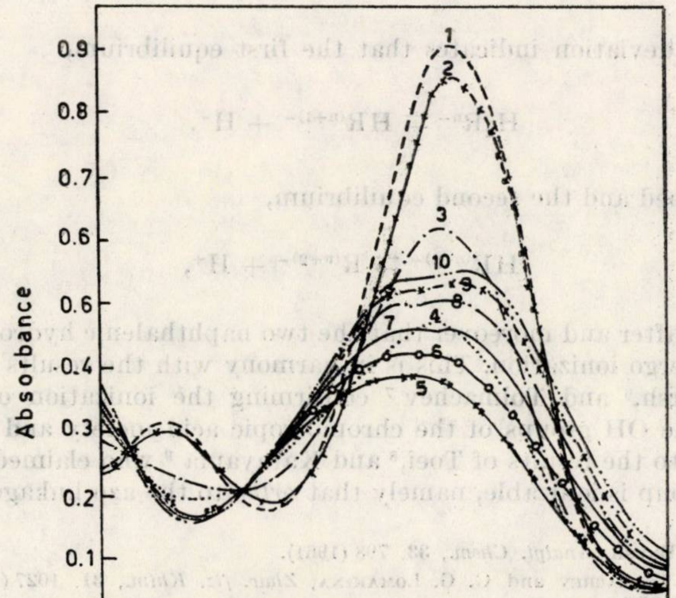

Fig. 6. — Absorption spectra of 4×10^{-5} M *m*-nitrophenylazo-chromotropic acid in aqueous solutions of varying pH values.
pH=2.0 (1), 6.0 (2), 7.0 (3), 7.5 (4), 8.5 (5), 9.0 (6), 9.5 (7), 10.0 (8), 11.0 (9), 13.0 (10).

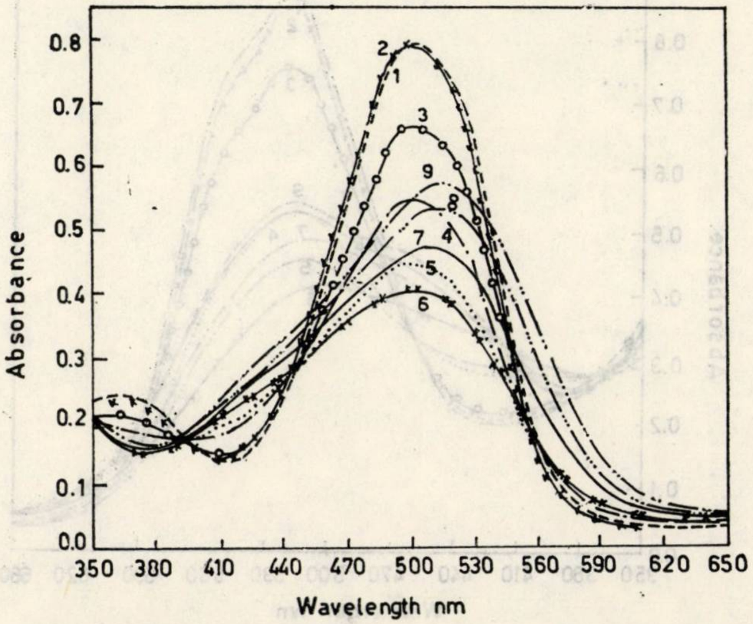

Fig. 7. — Absorption spectra of 3×10^{-5} M *p*-sulphonamidephenyl-azo-chromotropic acid in aqueous solutions of varying pH values. pH = 2.0 (1), 6.0 (2), 7.0 (3), 7.5 (4), 8.0 (5), 8.5 (6), 9.5 (7), 10.5 (8), 14.0 (9).

Such deviation indicates that the first equilibrium,

$$H_2R^{n-} \leftrightarrows HR^{(n+1)-} + H^+,$$

is overstepped and the second equilibrium,

$$HR^{(n+1)-} \leftrightarrows R^{(n+2)-} + H^+,$$

starts thereafter and moreover that the two naphthalenic hydroxyl groups should undergo ionization. This is in harmony with the results of Khalifa et al.,[3] Bursh,[6] and Tolmachev [7] confirming the ionization of the two naphthalenic OH groups of the chromotropic acid moiety and in contradistinction to the results of Toei,[8] and Katayama [9] who claimed that only one OH group is ionizable, namely that *ortho* to the azo linkage.

[6] J. S. Brush, *Analyt. Chem.*, **33**, 798 (1961).

[7] V. N. Tolmachev and G. G. Lomakina, *Zhur. fiz. Khim.*, **31**, 1027 (1957); *Chem. Abstr.*, **52**, 50 (1958).

[8] K. Toei, H. Miyata and H. Kimura, *Bull. Chem. Soc. Japan*, **40**, 1141 (1967); **40**, 1273 (1967); **38**, 1050 (1965).

[9] T. Katayama, M. Miyata and K. Toei, *Bull. Chem. Soc. Japan*, **40**, 2712 (1967)

The absorbance-pH curves obtained at some wavelengths at which a pronounced change in absorbance is observed are characterized by two branches. Representative curves are shown in Fig. 8. The first branch within the pH range 5—9 is descending, while the second within the pH range 9—12 is ascending. The corresponding values are used for calculating *pK* values of the first and the second naphthalenic hydroxyl groups. The results are collected in table (1), applying the half height method [10] and limiting the absorbance method.[10]

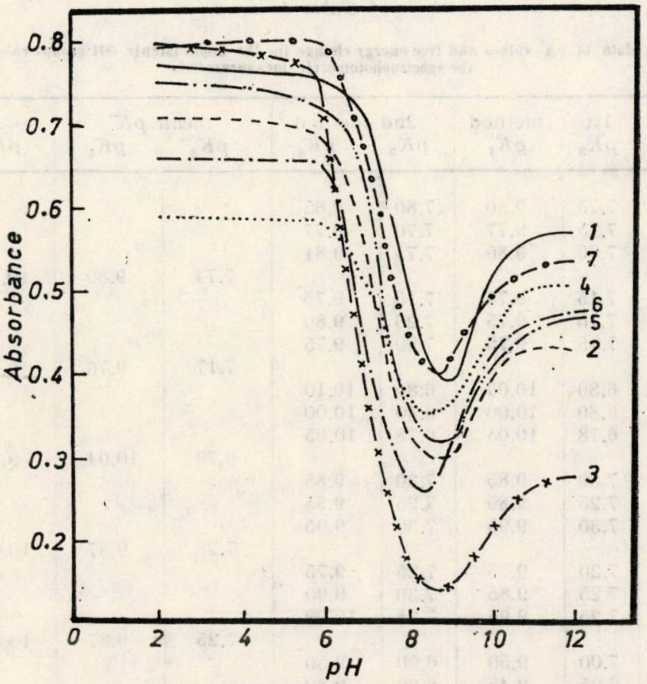

Fig. 8. — Absorbance — pH curves : 1 — *o*-OCH_3 (λ = 530 nm); 2 — *m*-OCH_3 (λ = 506 nm); 3 — *p*-OCH_3 (λ = 530 nm); 4 — 1-naphthyl (λ = 500 nm); 5 — 2-naphthyl (λ = 548 nm); 6 — *m*-NO_2 (λ = 528 nm); and 7 — *p*-SO_2NH_2 (λ = 500 nm).

The difference in free energy changes between the ionization of the two hydroxyl groups amounted to 2.85, 3.58, 4.53, 3.58, 3.62, 3.56, and 3.32 for the compounds I to VII, respectively, which are close to the energy required for the hydrogen bond formation indicating that the *ortho* hydroxyl groups are involved in a hydrogen bond with the azo linkage, while the other one is free.

Dissociation of the two sulphonic groups takes place more or less simultaneously as indicated from the titration curves of the acid form against NaOH solution, and the pK values calculated from the potentiometric method amounted to 3.63, 3.76, 3.78, 3.60, 3.70, 3.67, and 3.72 for I — VII, respectively.

---

[10] R. M. ISSA and A. H. ZEWAIL, *J. Chem. U.A.R.*, **14**, 261 (1971).

Table 1

Cumulative data of pK values and free energy change for the naphthalenic OH groups calculated from the spectrophotometric measurements

	λ_{nm}	1st method pK_3	pK_4	2nd method pK_3	pK_4	mean pK pK_3	pK_4	$-\Delta G°$ KCal/mole pK_3	pK_4
I	500	7.75	9.80	7.80	9.85	7.74	9.80	10.72	13.57
	530	7.75	9.77	7.70	9.77				
	548	7.70	9.80	7.75	9.81				
II	482	7.15	9.75	7.15	9.75	7.17	9.76	9.93	13.51
	506	7.15	9.75	7.20	9.80				
	530	7.15	9.75	7.20	9.75				
III	476	6.80	10.05	6.80	10.10	6.79	10.04	9.37	13.90
	500	6.80	10.00	6.80	10.00				
	530	6.78	10.05	6.78	10.05				
IV	500	7.30	9.85	7.30	9.85	7.28	9.87	10.08	13.66
	530	7.25	9.85	7.25	9.85				
	560	7.30	9.95	7.30	9.95				
V	488	7.20	9.75	7.25	9.75	7.25	9.87	10.04	13.66
	518	7.25	9.85	7.30	9.90				
	548	7.25	9.95	7.25	10.00				
VI	480	7.00	9.50	6.90	9.50	6.93	9.49	9.58	13.14
	510	6.95	9.45	6.90	9.50				
	528	6.95	9.50	6.90	9.50				
VII	500	7.30	9.75	7.30	9.70	7.30	9.70	10.11	13.43
	518	7.30	9.70	7.30	9.66				
	580	7.30	9.65	7.30	9.75				

Revue Roumaine de Chimie, 22, 6, 907–909 (1977)

THE REACTION OF CYCLOBUTADIENE WITH STERICALLY HINDERED DIENOPHILES

E. G. GEORGESCU and M. D. GHEORGHIU
Center of Organic Chemistry, Spl. Independenței 202 B,
76300 Bucharest 15

Received May 5, 1975

Diels-Alder reactions of cyclobutadiene with various quinones bearing bulky groups (**3**–**6**) are described.

It is well known that classical dienes or dienophiles become unreactive in the Diels-Alder reaction if they are substituted with bulky groups.[1,2] Their lack of reactivity was attributed to steric hindrance exerted by the bulky group rather than to electronic effects.

Considering the early transition state character of the normal 4 + 2 cycloaddition reactions[3] it was assumed that more reactive diene or dienophile partners could minimize the steric hindrance effect in the transition state.

The ability of the small-sized, extremely reactive cyclobutadiene (**1**) molecule to act as diene or dienophile is well-known.[4,5] Consequently the investigation of **1** with hindered dienes or dienophiles seemed appropriate.

In this paper we wish to report about the reaction of cyclobutadiene with 2,5-di-*t*-butyl-benzoquinone derivatives (**3**–**6**)[6] used as hindered dienophiles. The latter failed to undergo Diels-Alder reaction with classical dienes such as butadiene, cyclopentadiene and dimethoxytetrachlorocyclopentadiene even at elevated temperatures.

---

[1] J. Sauer, *Angew. Chem.*, **78**, 233 (1966) and literature therein cited.

[2] L. W. Butz and A. W. Rytina, in R. Adams, "Organic Reactions", vol. 5, Wiley, New York, 1957, p. 136.

[3] F. Badea, "Mecanisme de reacție în chimia organică", Ed. II, Edit. științifică, București, 1973, p. 657.

[4] G. Maier, *Angew. Chem. Intern. Edit.*, **13**, 425 (1974) ; P. M. Maitlis and K. W. Eberius, Cyclobutadiene-Metal Complexes, in J. P. Snyder, "Nonbenzoid Aromatics", Academic Press, New York, 1971, p. 359.

[5] L. Watts, J. D. Fitzpatrick and R. Pettit, *J. Amer. Chem. Soc.*, **88**, 623 (1966) ; *ibid.*, **87**, 3253 (1965).

[6] H. W. Moore and W. Weyler jr., *J. Amer. Chem. Soc.*, **93**, 2812 (1971) ; R. J. Wikholm and H. W. Moore, *ibid.*, **94**, 6152 (1972) ; H. W. Moore, D. L. Maurer, D. S. Pearce and M. S. Lee, *J. Org. Chem.*, **37**, 1984 (1972) ; M. D. Gheorghiu and M. Avram, *Org. Prep. Proced. Int.*, **6**, 231 (1974).

Cyclobutadiene **2** was generated *in situ* by the decomposition of the cyclobutadieneiron tricarbonyl complex **1** [7] with ceric ions in acetone solution at room temperature. Working in presence of an excess of the quinones **3** — **6** the adducts **7** — **10** were obtained in 50—60% yield.

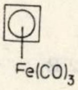

1

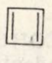

2

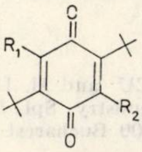

3, $R_1=R_2=H$
4, $R_1=Cl, R_2=H$
5, $R_1=R_2=Cl$
6, $R_1=R_2=N_3$

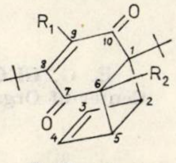

7, $R_1=R_2=H$
8, $R_1=Cl, R_2=H$
9, $R_1=R_2=Cl$
10, $R_1=R_2=N_3$

The structure of the adducts was ascribed on the basis of elemental analyses data and of NMR and IR spectral data. The *endo* configuration was tentatively attributed on theoretical grounds [8] and by analogy with the earlier described adducts,[4,5] especially that with 2,5-dibromoquinone [9] and was strongly supported by NMR spectra.

The synthesis of the adducts **7** — **10** from the hindered benzoquinones **3** — **6** demonstrates, as we expected, that the energy of small-sized dienes such as cyclobutadiene may compensate the steric hindrance effect of the bulky groups. These results suggested the possibility of using the cyclobutadiene molecule as a Diels-Alder reference substrate in testing the cycloaddition ability of sterically hindered, apparently unreactive Diels-Alder reagents (dienes or dienophiles).

Further investigations on these reactions involving bulky dienes are in progress.

EXPERIMENTAL

Microanalyses were performed by E. Şliam and V. Daniel. IR spectra were recorded with a double beam UR 20 spectrophotometer. NMR spectra were determined with Varian A-60A spectrometer.

GENERAL PROCEDURE

Into a stirred solution of 1.0 mmoles cyclobutadieneiron tricarbonyl (**1**) and 1.0 mmoles benzoquinone **3** — **6** in 10 ml dry acetone, 1.5—2.0 g cerium amonium nitrate were added in small portions, at room temperature, over a period of 5—10 min. After 5 min. additional stirring, 30 ml ether and 10 ml water were added and the organic layer was washed with 10 portions of 5 ml water and dried. The yellowish ethereal solution after evaporation of solvent afforded a crystalline residue, in which the content in desired adduct was determined by means of NMR spectra. The isolation of the compounds was achieved by column chromatography (ether or petroleum ether/Al_2O_3) and recrystallization from methanol.

---

[7] G. F. Emerson, L. Watts and R. Pettit, *J. Amer. Chem. Soc.*, **87**, 131 (1965).
[8] Reference 3, p. 666.
[9] R. Pettit, J. C. Barborak and L. Watts, *J. Amer. Chem. Soc.*, **88**, 1328 (1966)

1,8-DI-T-BUTYL-*ENDO*-TRICYCLO$[4.4.0.0^{2,5}]$DECA-3,8-DIEN-7,10-DIONE (**7**)

Working as above, from 0.19 g (1 mmole) **2** and 0.22 g (1 mmole) **3**, 0.25 g reaction mixture were obtained in which, by means of NMR a content of 45% unreacted **3** and 55% **7** was determined, corresponding to 0.14 g (51%). By chromatography, pure **7** was obtained, m.p. (from methanol).

$C_{18}H_{24}O_2$ (272.4) *Calcd.* : C, 79.37 ; H, 8.88.
Found : C, 79.30 ; H, 8.96.

NMR (CCl_4, δ, ppm) : 0.98 (s, 9H, t-Bu-1), 1.21 (s, 9H, t-Bu-8), 3.10–3.60 (m, 3H, H-2, H-5, H-6), 6.00–6.10 (m, 2 olefinic H, H-3, H-4), 6.42 (s, 1H, H-9).

9-CHLORO-1,8-DI-T-BUTYL-*ENDO*-TRICYCLO$[4.4.0.0^{2,5}]$DECA-3,8-DIEN-7,10-DIONE [8]

Working after the general procedure, from 0.19 g (1 mmole) **2** and 0.25 g (1 mmole) **4**, 0.30 g reaction mixture were obtained, which was found by NMR to contain 50% unreacted **4** and 50% **8**, corresponding to 0.15 g (49%).

By chromatography, pure **8** was obtained, m.p. 95° (from methanol).

$C_{18}H_{23}ClO_2$ (306.8) *Calcd.* : C, 70.46 ; H, 7.55 ; Cl, 11.55.
Found : C, 69.90 ; H, 7.62 ; Cl, 11.89.

NMR (CCl_4, δ, ppm) : 1.08 (s, 9H, t-Bu-1), 1.39 (s, 9H, t-Bu-8), 3.10-3.60 (m, 3H, H-2, H-5, H-6), 5.97 and 6.14 (2 broad s, 2H, H-3, H-4).

6,9-DICHLORO-1,8-DI-T-BUTYL-*ENDO*-TRICYCLO$[4.4.0.0^{2,5}]$DECA-3,8-DIEN-7,10-DIONE (**9**)

Working in the usual way, from 0.19 g (1 mmole) **2** and 0.29 g (1 mmole) **5**, 0.29 g reaction mixture were resulted, containing 40% unreacted **5** and 60% **9** ; thus 0.18 g (51%) **9** were formed. By chromatography, pure **9** was obtained, m.p. 78° (from methanol).

$C_{18}H_{22}Cl_2O_2$ (341.3) *Calcd.* : C 63.35 ; H, 6.50 ; Cl, 20.77.
Found : C 63.39 ; H, 6.70 ; Cl, 21.03.

NMR ($CDCl_3$, δ, ppm) : 1.20 (s, 9H, t-Bu-1), 1.40 (s, 9H, t-Bu-8), 3.58 (broad s, 2H, H-2, H-5), 6.05 and 6.25 (2 broad s, 2H, H-3, H-4).

6,9-DIAZIDO-1,8-DI-T-BUTYL-*ENDO*-TRICYCLO$[4.4.0.0^{2,5}]$DECA-3,8-DIEN-7,10-DIONE (**10**)

Using the general procedure, from 0.19 g (1 mmole) **2** and 0.30 g (1 mmole) **6**, 0.84 g reaction product were isolated. By NMR, this was found to be a mixture of 40% **6** and 60% **10**, which corresponds to 0.21 g (61%) **10**. By chromatography, pure **10** was isolated as colourless crystals with m.p. 112° (from methanol) ; in the presence of air and/or at light, **10** are unstable and the crystals became coloured.

NMR ($CDCl_3$, δ, ppm) : 1.13 (*s*, 9H, t-Bu-1), 1.33 (s, 9H, t-Bu-8), 3.51 (broad *s*, 2H, H-2, H-5), 6.10 (broad *s*, 2H, H-3, H-4).

$C_{18}H_{22}N_6O_2$ (326.4) *Calcd.* : C, 61.00 ; H, 6.26 ; N, 23.71.
Found : C, 61.42 ; H, 6.57 ; N, 22.09.

ACKNOWLEDGEMENTS. We are grateful to Professor Margareta Avram and Dr.-Ing. I. G. Dinulescu for several helpful discussions.

Revue Roumaine de Chimie, **22**, *6*, 911–921 (1977)

THE GRAFTING OF THE POLY(ETHYLENE-TEREPHTHALATE) UNDER RADIOFREQUENCY ELECTRICAL DISCHARGE CONDITIONS

CRISTOFOR I. SIMIONESCU and MIHAELA MACOVEANU

Institute of Macromolecular Chemistry "Petru Poni" JASSY,
Aleea Grigore Ghica-Vodă, n° 41 A, JASSY

Received April 13, 1976

The grafting *in situ* of the poly(ethylene-terephthalate) with acrylamide under radiofrequency electrical discharge conditions has been studied. The experiments were carried out according to the factorial design, followed by dispersional analysis in order to establish the optimum grafting conditions. The final products show better hydrophilic properties.

The specialized literature reports the change of poly(ethylene-terephthalate) (films) by acrylic acid[1] or nylon 6–10[2,3] in view of improving its moisture-proof features.

This paper studies the grafting of the poly(ethylene-terephthalate; fibre and thread) with acrylamide by means of a direct method under electrical discharge and the results relative to the grafted polymer concerned as a function of experimental conditions have been interpreted by statistical analysis.

1. EXPERIMENTAL

1.1 MATERIALS

— Poly(ethylene-terephthalate) PET under the form of threads (6 den) and fibres (4 den), with 25000 molecular-weight, was extracted by means of a solvent on warming (ethanol : benzene ;1 : 1 volumetric ratio) to remove the textile auxiliaries. The samples were dried and conditioned at room temperature (R.H. 65 %).

— Acrylamide (AA ; Eastman Organic Chemicals) was purified by recrystallization from methanol ; melting point = 79.5°

1.2 APPARATUS AND PROCEDURE

The grafting was carried out in the installation shown in Fig. 1. PET samples wrapped on a glass base (Fig. 1 (*3*)) were immersed in an aqueous solution of acrylamide (50 %) for 24 hours, then dried and conditioned. The glass base (*3*) was introduced into the reactor (*1*) under inert gas (nitrogen).

---

[1] A. Bradley and J. D. Fales, *Chem. Tech.*, **1**, 232 (1971).

[2] P. H. Hay, *Adv. Chem.*, **80**, 350 (1969).

[3] P. Blais, D. J. Carlsson, T. Suprunckuk and D. W. Wiles, *Textile Res. J.*, **41**, 485 (1971).

The working conditions (the generator power and the grafting time) were established according to the 2^2 factorial design of the experiments.

The grafted poly(ethylene-terephthalate) was extracted with methanol in the warm (for 48 hours) to remove the unreacted monomer and the formed homopolymer. The samples extracted and dried were subjected to physico-chemical analysis both to study the structural changes and to determine the properties acquired by grafting.

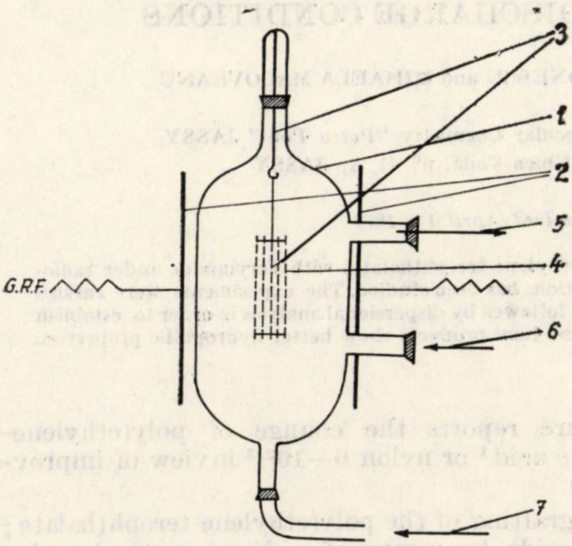

Fig. 1. — Scheme of the installation used for polymers treatment under cold radiofrequency plasma.

1 – glass reactor; 2 – copper condensator connected to the RF generator; 3 – device for polymer sustaining; 4 – polymer to be treated; 5 – to vacuum pump; 6 – gas supply; 7 – to vacuum checking apparatus.

A PAULIK PAULIK ERDELY MOM Budapesta derivatograph (rate of heating 12 grd/min, in air, substance 20 mg, temperature 20 – 600°) was used for the study of the thermal behaviour. Both the activation energy and the order of the degradation reaction were calculated according to the Freeman-Carroll method.[4]

The content of the grafted polymer was calculated from the quantity of nitrogen available in the grafted products (micro-Kjeldahl method).

2. RESULTS AND DISCUSSIONS

2.1 CHARACTERIZATION OF GRAFTED POLYMER

The action of the active species formed in nitrogen plasma upon solid compounds, both on the base-polymer and on the solid monomer, leads to the activation *in situ*, at the same time with the proper grafting. Generally speaking, while the real value of the quantities of the grafted copolymer must necessarily be established for theoretical purposes,[5] for practical reasons it is important that the content of the "apparent" grafted copolymer (represented by the sum of the quantities of base-polymer, grafted base-polymer and synthetized but unextractable homopolymer) should be determined.

This paper has studied the "apparent" quantity of the grafted polymer, trying to keep the fibre or thread integrity for practical purposes.

---

[4] E. S. Freeman and B. Carroll, *J. Phys. Chem.*, **62**, 398 (1958).

[5] I. Sakurada, T. Okada and Y. Ikada, *Cell. Chem. and Tech.*, **6**, 35 (1972).

The samples after extraction were investigated by IR spectroscopy (Fig. 2), to point out the existence of the grafted copolymers synthetized under the action of electrical discharge.

The grafted copolymers (curves *3* and *4*, fig. 2) presented the bands characteristic for poly(ethylene-terephthalate) alongside with new vibrations in 3350 cm^{-1} (ν—CO—NH—CO—), 3450 cm^{-1}, 1600 cm^{-1} (ν—NH—) and 1650 cm^{-1} (ν—CO—) bands, which are slightly shifted, compared to the polyacrylamide spectrum (synthetized under plasma conditions). The existence of these bands and the recorded shifts were a proof supporting the presence of the grafted copolymer.

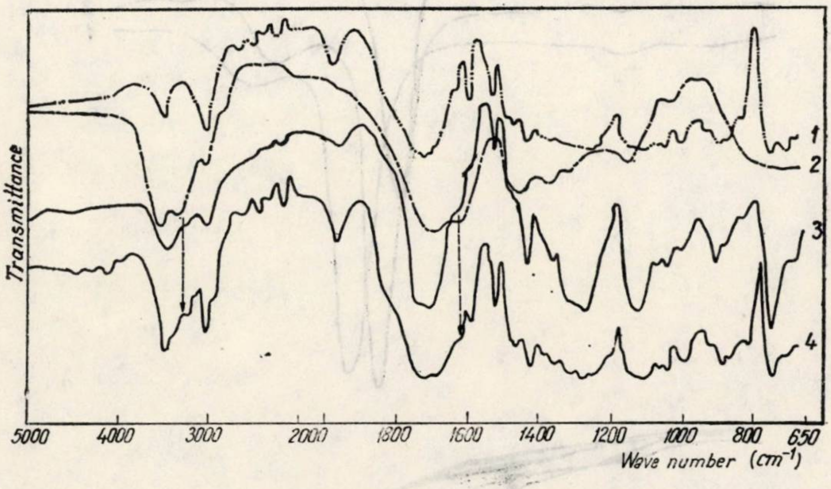

Fig. 2. — IR spectra of PET control (*1*); polyacrylamide synthetized under plasma conditions (*2*); PET-fibre-co-g-PAA (*3*); PET-thread-co-g-PAA (*4*); (UNICAM SP 200 in potassium bromide).

On the other hand, the behaviour of grafted copolymers to thermo-oxidative destruction, copolymers which have been obtained in various experimental conditions compared to that of the unchanged PET (control) and of the physical mixture (PET—PAA ; 90 :10) is shown in Figures 3 ***a***, ***b*** and 4 ***a***, ***b***.

The DTG and TG curves of grafted copolymers are placed between that of the physical mixture and of unchanged PET, and this shows that new products have been obtained. In the case of copolymers with a high-grafted polymer content (15.57 % and 16.53 % ; curve *3* and *4*, respectively, Fig. 3 ***a***) the appearance of a new destruction process ($T_i = 270°$, $T_f = 340°$, peak *I*) is observed beside the flattening of the peak III ($T_i = 480°$, $T_f = 600°$) which underlines the various behaviour to thermo-oxidative destruction compared to the analysed PET controls. The values of the activation energy and of the orders of destruction reactions (Table 1) were much higher than those of the unchanged PET.

Considering the sensitivity of the method it is normal that we should observe, in the case of the products having a low grafted polymer content

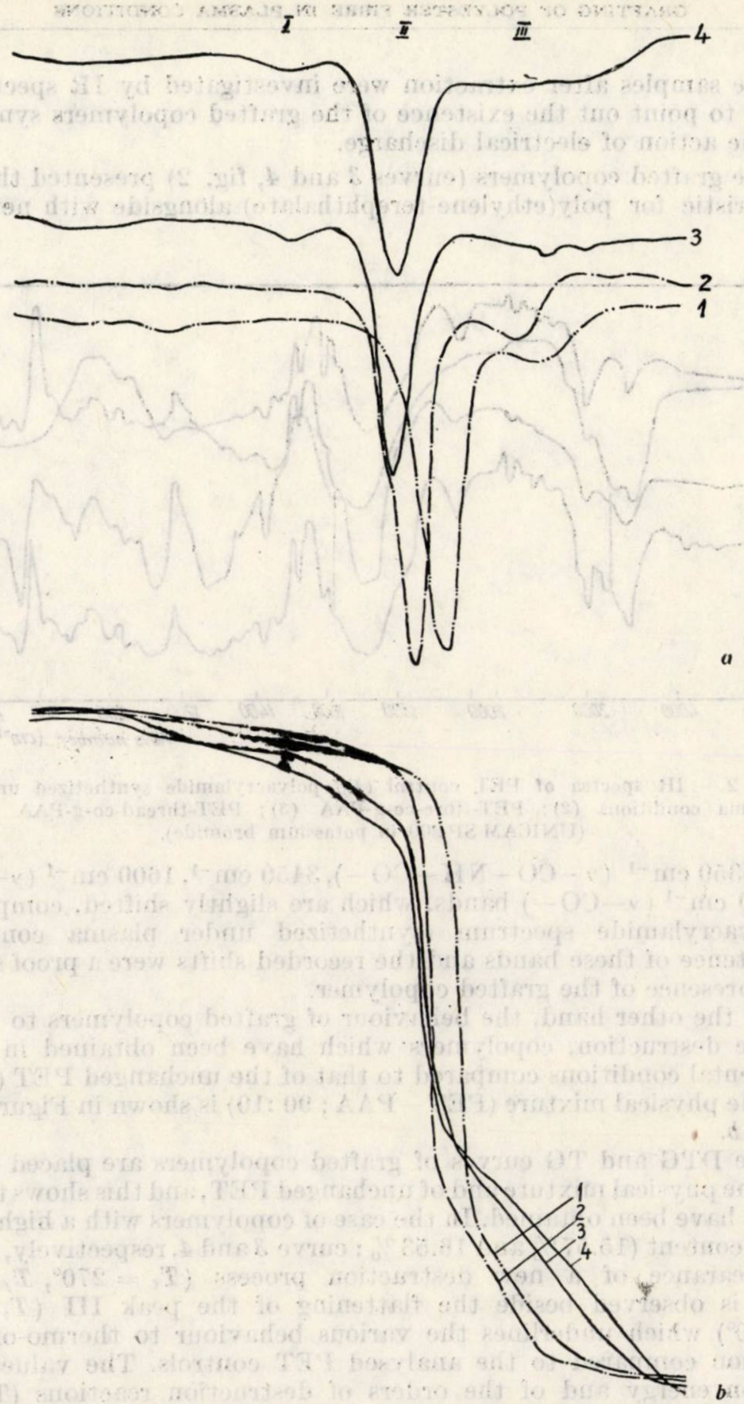

Fig. 3. — *a*) DTG curves recorded for : PET control fibre (*1*) ; physica mixture PET-PAA 90 : 10 (*2*) ; PET-co-g-PAA 15.57 % (*3*) ; PET-co-g-PAA 16.53 % (*4*).
b) TG curves recorded for the same polymers.

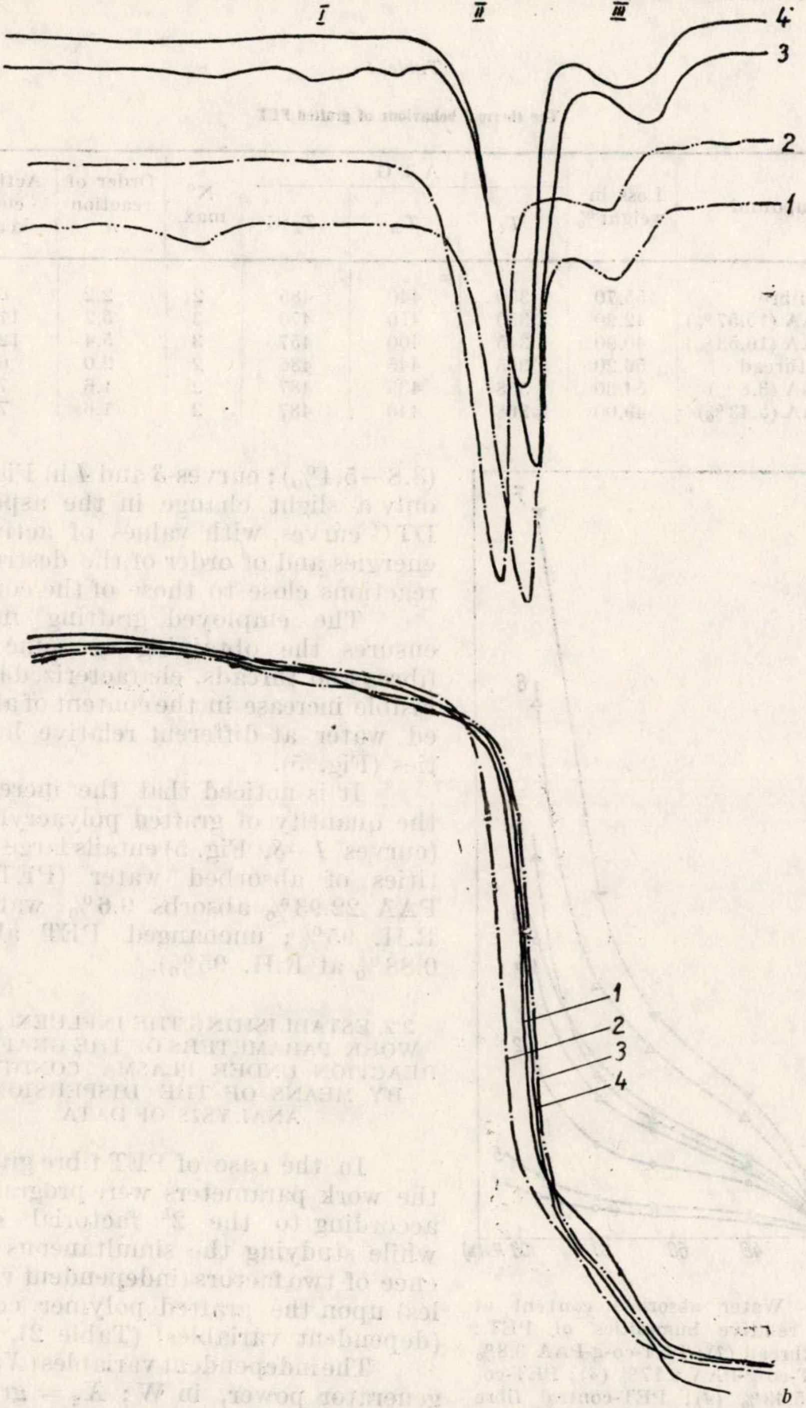

Fig. 4 — *a*) DTG curves recorded for : PET control thread (*1*) ; physical mixture PET-PAA 90 : 10 (*2*) ; PET-co-g-PAA 3.80 % (*3*) ; PET-co-g-PAA 5.43 % (*4*).

b) TG curves recorded for the same polymers.

Table 1

The thermal behaviour of grafted PET

Compound	Loss in weight %	ATG			N° max.	Order of reaction *n*	Activation energy kcal/mol
		T_i	T_m	T_f °C			
PET fibre	55.70	350	440	485	2	2.2	69.56
PET–AA (15.57%)	42.90	350	410	470	3	5,2	111.33
PET–AA (16.53%)	40.90	345	400	457	3	5.4	120.62
PET thread	56.20	355	445	485	2	2.0	68.64
PET–AA (3.8%)	54.30	358	435	487	2	1.6	70.51
PET–AA (5.43%)	49.00	368	440	487	2	1.6	71.29

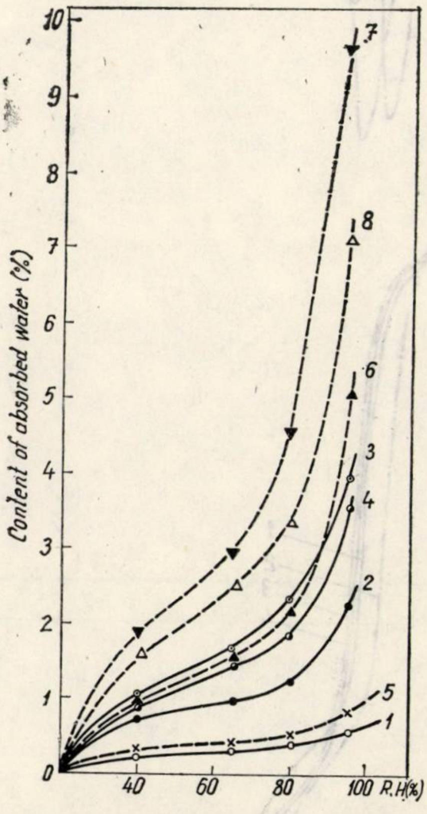

Fig. 5. – Water absorbed content at various relative humidities of PET: control thread (*1*); PET-co-g-PAA 3.8% (*2*); PET-co-g-PAA 8.17% (*3*); PET-co-g-PAA 5.43% (*4*); PET-control fibre (*5*); PET-co-g-PAA 15.57% (*6*); PET-co-g-PAA 22.93% (*7*); PET-co-g-PAA 16.53% (*8*).

(3.8–5.4%); curves *3* and *4* in Fig. 4 *a*), only a slight change in the aspect of DTG curves, with values of activation energies and of order of the destruction reactions close to those of the controls.

The employed grafting method ensures the obtaining of some PET fibres and threads, characterized by the visible increase in the content of absorbed water at different relative humidities (Fig. 5).

It is noticed that the increase in the quantity of grafted polyacrylamide (curves *1*–*8*, Fig. 5) entails large quantities of absorbed water (PET-co-g-PAA 22.93% absorbs 9.6% water at R.H. 95%; unchanged PET absorbs 0.88% at R.H. 95%).

2.2. ESTABLISHING THE INFLUENCE OF WORK PARAMETERS OF THE GRAFTING REACTION UNDER PLASMA CONDITIONS, BY MEANS OF THE DISPERSIONAL ANALYSIS OF DATA

In the case of PET fibre grafting, the work parameters were programmed according to the 2^k factorial design while studying the simultaneous influence of two factors (independent variables) upon the grafted polymer content (dependent variables) (Table 2).

The independent variables (X_1 = the generator power, in W; X_2 = grafting time in minutes) varied between two levels (I = 1300 W and II = 1920 W;

I = 5 min and II = 15 min). All the four series of experiments were accomplished according to the programme shown in Table 2, two graftings being performed for each level combination of the parameters.

Table 3 lists the results obtained from this set of experiments. In order to calculate the dispersions caused by the considered parameters the mean squares were determined (Table 4) the degrees of freedom for each partial mean square being established.

On the basis of these results Table 5 has been set up to show the dispersional bifactorial analysis in the presence of the interaction effect of variable factors.

By using the Fischer test (F) and by comparing the calculated values F with the value $F_{\alpha(1.4)}$ tabulated at $\alpha = 0.05$ corresponding to the 95% confidence level (7.71) it has been found that the effect of the interactions

Table 2

Experiments Programme

No. exp.	Coded value of independent variables	
	X_1	X_2
1	-1	-1
2	-1	$+1$
3	$+1$	-1
4	$+1$	$+1$

Table 3

Results of Determinations

X_2	X_1		X_j
	I	II	
I	22.52 23.35	17.60 15.47	78.94
II	50.58 49.25	46.85 46.00	192.68
X_i	145.70	125.92	271.62

Table 4

Determination of Mean Squares

S_i	$S_1 = \sum\limits_{ij} X_{ij}^2$	$S_2 = \dfrac{\left(\sum\limits_{i=1}^{m} X_i\right)^2}{n}$	$S_3 = \dfrac{\left(\sum\limits_{j=1}^{n} X_j\right)^2}{m}$	$S_4 = \dfrac{\left(\sum\limits_{ij} X_{ij}\right)^2}{mn}$	$S_5 = \dfrac{\sum\limits_{i}^{2} X_i^2 + \sum\limits_{j}^{2} X_j^2}{k}$
Calculated value	10 896.27	9 271.27	10 839.27	9 222.17	10 892.41

Table 5

Dispersional Analysis

No.	Dispersion source	Sum of squares	Degree of freedom	Dispersion	F calculated
1	X_1	48.90	1	48.90	50.73
2	X_2	1617.09	1	1617.09	1677.48
3	X_1X_2	4.23	1	4.23	4.39
4	Residual	3.85	4	0.96	

(X_1X_2) is negligible while the effects of independent variables are noteworthy.[6]

The same method was employed, as well, in the case of grafting the PET thread by considering two levels for X_1 and X_2 factors (I$=$1300 W and II $=$ 1920 W ; I $=$ 3 min. and II $=$ 10 min.).

The results of the experiments carried out according to the programme displayed in Table 2 are shown in Table 6.

Two parallel tests were performed for each level combination of parameters. The mean squares calculated with experimental data are those from Table 7.

These values (from Table 7) and the established degree of freedom were useful for the dispersional analysis (Table 8).

Table 6

Results of the Determinations In The Case of PET Grafted Thread

X_2	X_1		X_j
	I	II	
I	8.24 8.10	5.00 5.86	27.20
II	9.15 11.85	7.90 8.10	37.00
X_i	37.40	26.86	64.20

Table 7

Determinations of the Mean Squares in the Case of PET Thread

S_i	S_1	S_2	S_3	S_4	S_5
Calculated value	545.01	528.93	527.21	515.20	540.96

Table 8

Dispersional Analysis

No.	Dispersion source	Sum of squares	Degree of freedom	Dispersion	F calculated
1	X_1	13.73	1	13.73	13.50
2	X_2	12.01	1	12.01	10.80
3	X_1X_2	0.02	1	0.02	0.01
4	Residual	4.05	4	1.01	

By a similar methodology, if the values of the calculated F test are compared to those of the $F_{\alpha(1.4)} = 7.71$ it can be noted, in this case as well, that the content of the grafted polymer on PET thread is considerably influenced by the separate variation of the two studied parameters.

---

[6] A. GLÜCK, "Metode matematice în industria chimică", Editura Tehnică, București, 1971, p. 66.

The confidence interval enclosing the values of real effects at the meaning threshold $\alpha = 0.05$ for the transition from the inferior level of the independent variables to the superior one, was calculated by means of the relations :

$$\bar{Y}_1 - \bar{Y}_2 \pm t_{0.05(1.4)}\, S_r \sqrt{1/k_1 + 1/k_2} \tag{1}$$

where $\bar{Y}_1$ and $\bar{Y}_2$ are the mean values of the dependent variables at the two levels of independent variables, and where S_r, $t_{0.05(1.4)}$ and k_1 and k_2 are, respectively, the residual dispersion, the Student test and the number of experiments accomplished for each level. In conformity with the calculated data it has been recorded that :

— for the variation of the generator power :

in the case of the fibre, the interval is made up of values 4.94 ± 2.08, therefore $2.86 \div 7.02$

in the case of the thread 2.88 ± 2.14 ; $0.74 \div 5.02$

— for the variation of the grafting time :

in the case of the fibre : 28.84 ± 2.08 ; $26.76 \div 30.92$

in the case of the thread : 2.45 ± 2.14 ; $0.31 \div 4.59$.

2.3 ESTABLISHING THE OPTIMAL GRAFTING CONDITIONS FOR POLY(ETHYLENE-TEREPHTHALATE) UNDER ELECTRICAL DISCHARGE CONDITIONS

As a result of the facts presented above, we studied the variation in the content of the "apparent" grafted polymer on PET fibre thread as a function of a larger area of powers applied to the generator (Figures 6 and 7) and of the reaction times (Figs. 8 and 9).

From Figs 6 and 7 we can notice that, in the domain 700 – 1300 W the ratio of grafted polymer increased while a sensible decrease was recorded in the domain 1300 – 1920 W. That is why it can be assumed that the optimal power applied to the generator in order to obtain a grafted polymer having an optimal content of polyacrylamide is, both for the fibre (22.52 %) and for PET thread (8.24 %) equal to 1300 W. In Figs. 8 and 9 there can be noticed a minimum at 7 and 6 minutes, respectively, followed by an increase in the content of the grafted polymer. This peculiar behaviour in what grafting is concerned, can be explained by the specific conditions created in the plasma. At the same time with the increase in the power applied to the generator or in the duration of the grafting reaction, polyacrylamide and acrylamide are subjected to secondary reactions. These reactions imply both molecule splitting and fragments recombination, which lead to the setting of the film on the reactor wall (the depth of which increases when the power or the duration of the reaction is increased). The IR analysis of the deposited film reveals polymer reticulated with $-C{\equiv}N$ groups beside the groups characteristic to polyacrylamide. The reactions in which the acrylamide monomer and polymer are spent take place to the detriment of the grafting reaction. On the other hand, with higher durations (over 10 min) the homopolymer deposit from the samples subjected to the action of the plasma is reticulated and becomes unextractible.

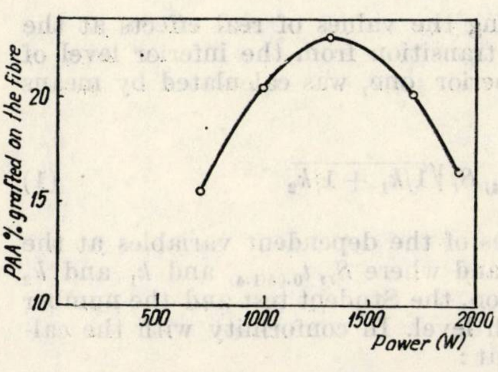

Fig. 6. — Dependence of the content of polymer grafted on PET fibre upon the generator power W ($t = 5$ minutes; $p = 0.7$ mmHg).

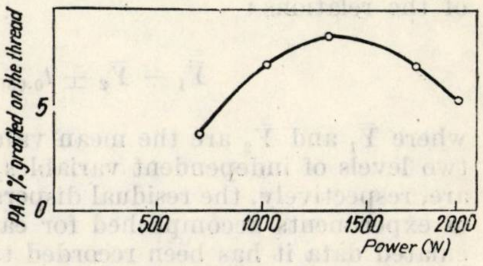

Fig. 7. — Variation of the content of polymer grafted on PET thread as a function of the generator power W ($t = 3$ min.; $p = 0.7$ mmHg).

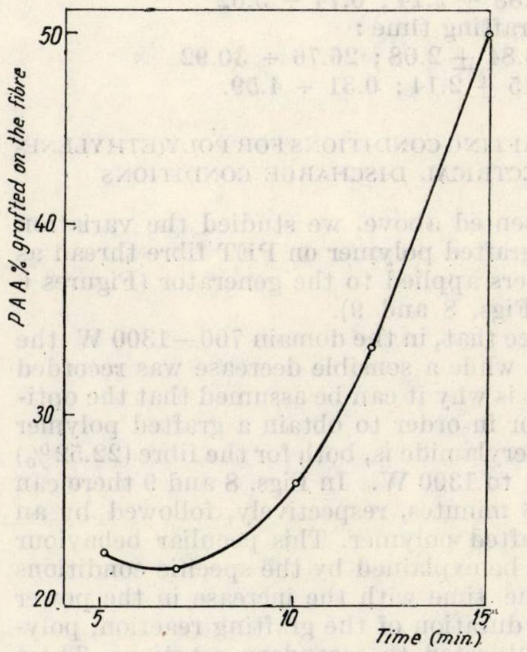

Fig. 8. — Dependence of the polymer grafted on PET fibre upon the reaction time ($W = 1300$ W; $p = 0.7$ mmHg).

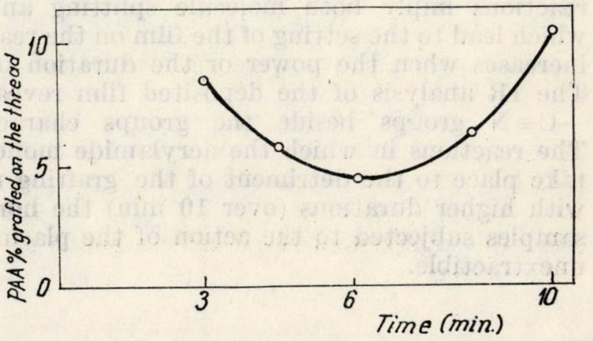

Fig. 9. — Variation in the content of polymer grafted on PET thread as a function of the grafting time ($W = 1300$ W; $p = 0.7$ mm Hg).

Relying on these notes we conclude that the achievement of a copolymer grafted on the basis of poly(ethylene-terephthalate) and polyacrylamide requires durations up to 5 minutes in the case of fibre and up to 3 minutes in the case of PET thread.

CONCLUSIONS

The PET base polymer under the action of active species in the plasma covers two distinct steps : the activation reaction and the proper grafting reaction, which virtually take place, at the same time ("*in situ* activation"). The grafted copolymer, poly(ethylene-terephthalate)-co-g-acrylamide was obtained in the presence of acrylamide.

The grafting reaction taking place on the base surface strongly modifies only the surface properties (the increase of water absorption). The thermal behaviour and the physico-mechanical properties of the synthetized products remain within the characteristic limits, for the industrial made poly(ethylene-terephthalate). Under the same experimental conditions the content of the "apparent" grafted polymer varies differently when the fibre or the thread is used. This finding is perfectly explained by the action of plasma at the polymer surface (the fibre and the thread having various specific surfaces).

By using the dispersional analysis, both in the case of the fibre and of the thread of PET grafting, it has been established that the parameters considerably and independently influencing the content of the grafted polymer are the generator power (W) and the reaction time (minutes).

The optimum grafting conditions have been established from the experimental data, i.e. the generator power 1300 W, reaction time 5 minutes and 3 minutes for PET fibre and thread, respectively.

Relying on these notes we conclude that the achievement of a copolymer grafted on the basis of poly(ethylene-terephthalate) and polyacrylamide requires durations up to 5 minutes in the case of fibre and up to 3 minutes in the case of PET thread.

CONCLUSIONS

The PET base polymer under the action of active species in the plasma covers two distinct steps : the activation reaction and the proper grafting reaction, which virtually take place, at the same time ("in situ activation"). The grafted copolymer, poly(ethylene-terephthalate)-co-g-acrylamide was obtained in the presence of acrylamide.

The grafting reaction taking place on the base surface strongly modifies only the surface properties (the increase of *water absorption*). The thermal behaviour and the physico-mechanical properties of the synthetized products remain within the characteristic limits, for the industrial made poly(ethylene-terephthalate). Under the same experimental conditions the content of the "apparent" grafted polymer varies differently when the fibre or the thread is used. This finding is perfectly explained by the action of plasma at the polymer surface (the fibre and the thread having various specific surfaces).

By using the dispersional analysis, both in the case of the fibre and of the thread of PET grafting, it has been established that the parameters considerably and independently influencing the content of the grafted polymer are the generator power (W) and the reaction time (minutes).

The optimum grafting conditions have been established from the experimental data, i.e. the generator power 1300 W, reaction time 5 minutes and 3 minutes for PET fibre and thread, respectively.

Revue Roumaine de Chimie, 22, 6, 923–930 (1977)

Dedicated to the 70th anniversary
of Professor CORIOLAN DRĂGULESCU

PERSPECTIVES FOR INDUSTRIAL PRODUCTION OF POLY(OLEFINS) GRAFT COPOLYMERS

D. MUNTEANU* and I. NANU**

* ICECHIM — Research Laboratory Piteşti, Şos. Giurgiului 127
** Polytechnic Institute, Timişoara, Chemical Engineering Faculty, Str. Karl Marx 3

Received August 25, 1976

The melt grafting in plastics processing equipments has great perspectives to become an industrial synthesizing method of the poly(olefins) graft copolymers. Therefore it was utilized for the grafting of VA onto PE. Through the injection of VA containing a dissolved peroxidic initiator, in the cylinder of a twin screw extruder, graft systems are obtained in which a part of VA is bonded as side chains onto PF chains, and the other one as homopolymer chains — PVA. The study of the main factors which determine the grafting process (reaction temperature and time, VA concentration in reaction mixture, type and concentration of the initiator) shows that it is possible to obtain, with good yields, a large scale of graft systems having up to 30% VA pol. and 15% VA g.

INTRODUCTION

In the development of macromolecular chemistry, an initial discovery, whether made systematically or to some extent accidentally, has been very rapidly exploited and finalized in industrial applications of the respective product. The main reason is that the properties of a homopolymer or random copolymer are often unique, so that its industrial applications are obvious from the very beginning. In the case of block and graft copolymers, even though their methods of synthesizing have been known for many years and considerable efforts have been made to find practical uses, only a few materials have been developed to the stage of a mass production. From these, the blockcopolymers are situated on the first place, as the proportion of the graft copolymers is much smaller. However, if in the general field of the graft copolymers a few classes have succeeded in reaching the level of an industrial production: ABS terpolymers, some anti-shock poly(styrene) types, natural rubber and cellulose graft copolymers, a single example is known so far in the peculiar field of poly(olefins) graft copolymers: the vinyl chloride grafting onto ethylene-vinyl acetate random copolymers.

The main reason for this situation is the fact that although very many synthesis methods are known, most of them utilize small amounts and the grafting techniques are clumsy, hindering thus the development of an industrial process. The large majority of the methods of synthesizing poly(olefins) graft copolymers lead to a mixture of the graft copolymers with the homopolymer corresponding to the grafting monomer. Therefore, it seems that until some economical methods are discovered, either of "pure" graft copolymers synthesis or of separation of the homopolymers formed during grafting, the commercial development of the graft copolymers will be restricted only to those systems in which the presence of homopolymers does not disturb the desired properties and utilization fields.

From the synthesizing methods, the melt grafting in plastics processing equipments can be considered as having great perspectives for industrial application. It is based on carrying out the grafting reaction in a plastics processing equipment (mixer, extruder) in contact with the molten poly(olefin) at a certain temperature, in the presence of a radicalic initiator (rarely ionic). The literature referring to this method is composed only of patents which claim the grafting of a series of monomers onto different poly(olefins).[1–15] None of the patents contain data about the influence of the grafting conditions on grafting yields and on properties of the synthesized products. Although an equipment which is suited to an industrial application has been utilized for grafting, graft copolymers obtained by this method and which should have reached the stage of a mass production have not been reported so far.

Because of the perspectives of this method we have applied it for semiindustrial or industrial obtaining of some high pressure poly(ethylene) graft copolymers which have been utilized in various fields.[16–19] Through

---

[1] R. M. Nowak and G. D. Jones, U. S. Pat., 3177269 (1965); *Chem. Abstr.*, **62**, 16462 (1965).

[2] G. D. Jones and R. M. Nowak, U.S. Pat., 3177270 (1965); *Chem. Abstr.*, **63**, 1953 (1965),

[3] G. Zeitler and T. H. Müller, Ger. Offen Pat., 2342486 (1975); *Chem. Abstr.*, **82**, 171732 (1975).

[4] Asahi Kasei Kogyo Kabushiki Kaisha, Fr. Pat., 1564548 (1969); *Chem. Abstr.*, **71**, 102598 (1969).

[5] Allied Chem. Corp., U.S. Pat., 3267173 (1966); *Chem. Abstr.*, **65**, 18721 (1966).

[6] W. R. Grace and Co., Fr. Pat., 1367558 (1963); *Chem. Abstr.*, **58**, 13728 (1963).

[7] W. R. Grace and Co., Fr. Pat., 1466197 (1967); *Chem. Abstr.*, **67**, 117722 (1967).

[8] Allied Chem. Corp., Brit. Pat., 1168959 (1969); *Chem. Abstr.*, **72**, 13423 (1970).

[9] Dow Chemical Co., Fr. Pat., 1395993 (1965); *Chem. Abstr.*, **63**, 18307 (1965).

[10] R. A. Steinham and T. Y. Grail, Fr. Pat., 2132780 (1972); *Chem. Abstr.*, **79**, 6161 (1973).

[11] C. Andrei, V. Părăuşanu, D. Mihăiţă and D. Munteanu, Pat. Rom., 52431 (1970).

[12] Y. Fujisaki, Japan Pat., 19315 (1968); *Chem. Abstr.*, **70**, 58507 (1969).

[13] I. Aijima, H. Sakurai, Y. Takatsuchi and T. Ozaki, Japan Pat., 30111 (1972); *Chem. Abstr.*, **78**, 112347 (1973).

[14] I. Iwaomi, T. Nishikage and H. Kawasaki, Japan Pat., 32829 (1972); *Chem. Abstr.*, **78**, 112117 (1973).

[15] T. Aijima, H. Sakurai and A. Kitaoha, Japan Pat., 21211 (1971); *Chem. Abstr.*, **75**, 152609 (1971).

[16] V. Aslan, D. Munteanu and C. Nică, Rom. Pat., 58137 (1974).

[17] V. Aslan, D. Munteanu and V. Irodiu, Rom. Pat., 57903 (1974).

[18] V. Aslan, D. Munteanu, C. Variu, S. Turcu, V. Badea, G. Boncea, R. Necşescu and M. Toader, Rom. Pat., 73535 (1973).

[19] V. Aslan, D. Munteanu and I. Tincul, Rom. Pat., 60243 (1975).

the grafting of zinc acrylate, graft copolymers having an ionomer character are obtained and they are utilized for extrusion coating of cellophane.[16] The grafting of N-vinyl carbazole, confers on the poly(ethylene) a higher value of the dielectric strength, which permits the use of the graft copolymers for high voltage cable insulating.[17] The grafting of a monomer containing an ultraviolet rays absorption group : 2-hydroxy-4-(2′-hydroxy-3′-acryloxy)propoxybenzophenone permits the obtaining of an UV stabilized poly(ethylene). The chemical bonds obtained through grafting remove the main disadvantages of the usual stabilization (compounding with small molecular weight UV absorbers) : the poor compatibility and the migration at the surface of films.[18] The grafting of the vinyl acetate [19] is the subject of the present paper.

EXPERIMENTAL

The object of this paper is the grafting of vinyl acetate (VA) onto high pressure poly(ethylene) (PE), with the view to achieving some products, which, due their properties, may be utilized in the same fields as the ethylene-vinyl acetate random copolymers, but would also have other specific properties supposed to open the way for other fields of utilization. To obtain them, the melt grafting in a plastics processing equipment was carried out. A detailed study of this method was undertaken, so as to use it as an industrial process.

MATERIALS

Since the goal was to develop an industrial process, only technical materials have been utilized :

Low density poly(ethylene)-commercial type 17M08 produced by the Petrochemical Works Piteşti through the autoclave high pressure process. Vinyl acetate "polymerization grade" produced by the Chemical Works Craiova and inhibited with 12—24 ppm. hydroquinone.

Initiators—Three radicalic initiators have been utilized : ditertbutyl peroxide (initiator A) lauroyl peroxyde (initiator B), tertbutylperbenzoate (initiator C).

EQUIPMENT AND WORKING TECHNIQUE

A twin screw extruder (Werner Pfleiderer, type ZSK-53L/v) and the corresponding, granulating line have been utilized, the injection of VA being achieved with a metering twin pump. The whole equipment has specially been adapted for effectuation of the grafting reaction. The twin screw extruder is fed with PE from a hopper, through the agency of a twin screw dosing feeder which allows to set the feeding output with PE (O_{PE}). PE fails in the extruder cylinder (screw barrels), composed from 5 zones, maintained by constant temperature, and is taken over by the two screws which turn in the same direction with a constant revolution (100 RPM). VA in which the initiator was dissolved at the desired concentration (c_{VA}), is taken over out of a dosing vessel by a metering twin pump and is injected with a certain volumetric output (O_{VA}), in the first zone of the extruder cylinder, where PE is already melted. The reaction mixture (PE+VA+I) taken over by the two screws, passes through the extruder cylinder at a constant temperature (*t*-reaction temperature) in a certain time (*T*-reaction time). The last zone of the cylinder is provided with an exhaust connection tied to a vacuum pump, through which the unreacted VA is removed. The screws have been composed of a lot of screw bushing and kneading blocks, which have been so assembled that in each zone they should assure the necessary conditions — zone 1 : injection of VA ; zone 2—4 : homogenizing of reaction mixture ; zone 5 : vacuum degassing of VA. At the end of the extruder cylinder, by means of a granulating line (vertical die, cooling bath, ventilator, pelletizer) the reaction products are obtained under the form of granules, which are packed up in bags, measuring the realized output (O_{GR}).

RESULTS AND DISCUSSIONS

The initiator dissolved in the VA injected in the extruder cylinder decomposes at a rate characterized by the half-time(T ½) corresponding to the working temperature. A part of the free radicals formed in this way initiates the homopolymerization reaction of VA. The other radicals are stabilized through the removing of some H atoms along the PE chains, thus forming the macroradicals on which the VA is grafted. Thus, graft systems are obtained, in which a part of VA is bonded as side chains grafted on the PE chain, and the other one as homopolymer chains : poly(vinyl acetate).

To study the grafting reaction, the influence of the main parameters (reaction temperature and time, type and concentration of the initiator, VA concentration in the reaction mixture) on the composition and forming yields of the synthesized products was pursued. The composition of the graft systems was expressed through the total polymerized VA content (%VA pol. : homopolymerized + grafted) and through the grafted VA content (%VAg.) and it was determined with the aid of two methods adapted for this purpose : saponification of the acetoxy groups [20] and infrared spectroscopy.[21] Corresponding to the composition, the polymerization yield (*Y*pol.) and the grafting yield (*Y*g.) was calculated from the VA balance of materials. The study of the influence of each parameter has been carried out by maintaining the others unchanged, the working conditions and the experimental results being comprised in Table 1. To compare the activity of the three initiators, the molar concentration expressed as 10^{-3} mol.g. initiator/100 g.PE ($c_{\text{mol.}}$) was used.

INFLUENCE OF TEMPERATURE

Table 1 (samples 1—18) shows that by increasing the temperature %VApol., %VAg., *Y*pol., *Y*g. decrease the more so as the initiator is more stable. At the same temperature the corresponding values decrease in the increasing order of the activity of the three initiators (A—C—B). This behaviour is caused by the variation of the decomposition rate of each initiator depending on temperature. At a high temperature the initiator dissolved in the VA injected in the cylinder decomposes completely into free radicals, with a high rate ($T\frac{1}{2}$ is small). The reaction mixture is only for a short time in the presence of the free radicals (from the moment of injection). In the rest of time, the reaction mixture traverses the cylinder of the extruder without disposing of new quantities of free radicals, freshly formed through the decomposition of the initiator (practically consumed entirely in the first moments of the reaction). At a low temperature, the decomposition ratio of the initiator is small, $T\frac{1}{2}$ is great, the reaction mixture disposing of ever newer quantities of free radicals which can initiate the homopolymerization and grafting of new quantities of VA.

INFLUENCE OF TYPE AND CONCENTRATION OF INITIATOR

To compare the efficiency of the three initiators (A—C—B), worked at different temperatures (240°—215°—170°) which should assure the same $T\frac{1}{2}$ (1 sec.), therefore the same decomposition rate. Table 1 (samples 19—30) shows that in all initiators, with an increasing concentration, %VApol., %VAg., *Y*pol., *Y*g. initially increase sharply until a maximum limiting value is reached. A part of the free radicals formed through the decomposition of the initiator initiates the homopolymerization of VA and the other one, through the attack on PE chains, forms macroradicals on which VA is grafted. By increasing the initiator concentration, the number of the free radicals increases, consequently increasing the number of PE radicals, so that the yields grow too. From a certain level of concentrations, the rate of initiation of the homopolymerization and grafting reaction is no more determining for the total rate of reaction, so that a limiting value is reached. At the same concentration of the initiator, the yields are the greater as the initiator is more stable (they increase in the order B—C—A), high values being obtained only with the initiators A and C. These are characteristic initiators, both of VA homopolymerization and of PE crosslinking (great capacity of H atoms removal from the saturated chain of PE) being industrially utilized for these purposes. Therefore, greater values are obtained with them than with the initiator B.

---

[20] D. MUNTEANU and N. SAVU, *Rev. Chim.*, (Bucureşti), **27**, 906 (1976).

[21] D. MUNTEANU, M. TOADER and M. LAIBER, *Materiale Plastice*, **13**, 97 (1976).

INFLUENCE OF VA CONCENTRATION IN REACTION MIXTURE

To modify the VA concentration in the reaction mixture (X), O_{PE} was maintained constant and O_{VA} was changed. From Table 1 (samples 31÷35) it is found that %VApol. and %VAg. increase continually. At the beginning *Y*pol. and *Y*g. increase, reach a maximum and then decrease, the difference between the maximum and minimum value being very small. It follows that graft systems having the most varied compositions can be obtained with good yields.

INFLUENCE OF THE REACTION TIME

To modify the reaction time, O_{PE} and O_{VA} were proportionally increased, thus maintaining constant the VA concentration in the reaction mixture. This traverses the extruder cylinder with an increasing speed, so that the reaction time decreases. Table 1 (samples 36—40) shows that in the range 60—160 sec. the reaction time has practically no influence on %VApol., %VAg., *Y*pol., *Y*g., the high ratio of the grafting process becoming thus conspicuous. The conclusion is very important because it allows the accomplishment of the grafting process at small reaction times, therefore at high extrusion outputs, without a decrease of the yields. This ensures the obtaining of a great capacity, a determining factor for an industrial process.

The synthesized products have been industrially used to obtain: "hot-melt" adhesives, hydroisolating bituminous materials, injected parts with a great environmental stress cracking resistance.

A more detailed study of the influence of the previously examined factors, of other factors which influence the grafting process (inhibitor type and concentration, PE type, introduction manner of the initiator) as well as of the structure, properties and utilization fields, will be published in subsequent papers.

Table

Experimental conditions of vinyl

Spl. No.	O_{VA} 1/h	O_{PE} kh/h	O_{GR} kg/h	Type I	c_{VA}	c_{mol}	t °C
1	3.65	12.43	12.94	C	0.49	0.65	260
2	3.65	12.43	13.43	C	0.49	0.65	240
3	3.65	12.43	14.25	C	0.49	0.65	220
4	3.65	12.43	14.53	C	0.49	0.65	200
5	3.65	12.43	15.12	C	0.49	0.65	180
6	3.65	12.43	15.42	C	0.49	0.65	160
7	3.61	12.17	12.49	A	0.37	0.65	270
8	3.61	12.17	12.52	A	0.37	0.65	250
9	3.61	12.17	13.73	A	0.37	0.65	230
10	3.61	12.17	14.75	A	0.37	0.65	210
11	3.61	12.17	14.96	A	0.37	0.65	190
12	3.61	12.21	14.41	B	1.00	0.65	130
13	3.61	12.21	13.97	B	1.00	0.65	150
14	3.61	12.21	13.78	B	1.00	0.65	170
15	3.61	12.21	13.57	B	1.00	0.65	190
16	3.61	12.21	13.11	B	1.00	0.65	210
17	3.61	12.21	12.70	B	1.00	0.65	230
18	3.61	12.21	12.51	B	1.00	0.65	260
19	4.50	13.95	14.79	A	0.50	1.00	240
20	4.50	13.95	16.80	A	1.50	1.98	240
21	4.50	13.95	17.17	A	2.00	3.91	240
22	4.50	13.95	17.12	A	3.00	7.62	240
23	4.50	13.95	15.98	C	0.50	0.75	215
24	4.50	13.95	16.52	C	1.00	1.44	215
25	4.50	13.95	16.50	C	2.00	2.97	215
26	4.50	13.95	16.59	C	4.00	5.75	215
27	4.50	13.95	15.63	B	1.00	0.70	170
28	4.50	13.95	16.05	B	2.00	1.45	170
29	4.50	13.95	16.11	B	4.00	2.84	170
30	4.50	13.95	16.17	B	8.00	5.48	170
31	1.00	13.90	14.53	C	3.00	1.00	200
32	2.00	13.90	15.41	C	1.60	1.00	200
33	4.00	13.90	16.90	C	0.75	1.00	200
34	6.00	13.90	18.05	C	0.50	1.00	200
35	8.90	13.90	19.82	C	0.33	1.00	200
36	0.78	2.60	3.32	C	0.50	0.67	200
37	1.66	5.80	7.05	C	0.50	0.67	200
38	2.53	9.00	11.26	C	0.50	0.67	200
39	3.38	12.20	14.57	C	0.50	0.67	200
40	9.25	31.40	40.32	C	0.50	0.67	200

1

acetate grafting onto poly(ethylene)

T sec.	*T* ½ sec.	*X* %VA	%VA pol.	%VA g.	$Y_{pol.}$ %	$Y_{g.}$ %
95	0.05	21.0	3.94	2.50	15.5	9.8
95	0.20	21.0	8.05	4.42	33.0	18.0
95	0.65	21.0	12.76	6.53	55.2	28.2
95	3.00	21.0	14.45	8.18	63.6	36.0
95	15.00	21.0	17.75	9.70	81.5	44.5
95	90.00	21.0	19.37	9.80	90.5	45.8
95	0.16	21.0	2.56	0.58	7.4	1.7
95	0.60	21.0	2.79	1.64	10.7	6.3
95	2.40	21.0	11.35	7.75	47.7	32.6
95	12.00	21.0	17.45	10.13	78.9	45.7
95	65.00	21.0	18.64	9.87	85.3	45.2
95	20.00	21.0	15.28	6.49	67.5	28.7
95	4.00	21.0	12.60	6.20	54.0	28.6
95	0.90	21.0	11.40	3.50	48.2	14.8
95	0.20	21.0	10.00	2.70	41.7	11.3
95	0.05	21.0	6.86	2.17	27.6	8.7
95	0.02	21.0	3.86	1.33	15.0	5.2
95	0.01	21.0	2.40	0.68	9.2	2.6
85	1.00	22.4	5.67	5.38	20.6	19,6
85	1.00	22.4	16.90	7.56	70.3	31.4
85	1.00	22.4	18.80	8.20	80.7	35.2
85	1.00	22.4	18.40	7.80	80.1	33.8
85	1.00	22.4	8.80	6.05	50.0	29.0
85	1.00	22.4	15.50	6.84	63.2	31.4
85	1.00	22.4	15.50	7.70	63.2	28.0
85	1.00	22.4	15.90	7.38	66.6	25.4
85	1.00	22.4	10.70	2.33	41.2	9.0
85	1.00	22.4	13.10	2.28	52.1	9.1
85	1.00	22.4	13.40	3.22	54.6	13.1
85	1.00	22.4	13.80	4.06	58.5	17.3
85	3.00	5.9	4.33	2.13	72.4	35.8
85	3.00	11.4	9.80	4.97	84.2	42.7
85	3.00	20.6	17.75	8.27	82.9	38.5
85	3.00	28.0	23.00	11.66	76.6	40.0
85	3.00	36.8	29.80	15.00	73.2	36.8
165	3.00	20.5	6.75	4.49	28.7	21.1
140	3.00	20.5	9.22	7.10	43.2	33.3
115	3.00	20.5	9.00	6.93	44.3	34.1
95	3.00	20.5	8.66	7.95	41.3	37.9
60	3.00	20.5	9.22	8.57	44.2	41.3

CONCLUSIONS

1. An equipment and a working technique were established, allowing to graft VA onto PE in conditions which assure the industrial development of the process.

2. The influence of the main factors which determine the grafting process was studied : reaction temperature and time, VA concentration in reaction mixture, type and concentration of the initiator.

3. Graft systems with variable composition (up to 30%VApol. and 15%VAg.) have been obtained with good yields.

Revue Roumaine de Chimie, **22**, *6*, 931–936 (1977)

FREQUENTOMETRIC DETERMINATION UNDER THE DETECTION LIMIT OF N-METHYL-2-PYRROLIDONE IN STYRENE BY IR SPECTROMETRY

CANDIN LITEANU * and IOANA ILEANA PANOVICI **

* University of Cluj-Napoca, Department of Analytical Chemistry, Str. Arany Jànos 11, Cluj-Napoca

** Technological Research and Design Institute for Refineries and Petrochemical Plants, Bd. Republicii 295, Ploieşti

Received March 21, 1975

After a short presentation of the theoretical basis for frequentometric determination under the detection limit, the results obtained for N-methyl-2-pyrrolidone solutions of known concentrations are shown (the calibration curve). The method was tested and applied to solutions of various concentrations in N-methyl-2-pyrrolidone.

As the c concentration can take practically any value in the $(0, a)$ interval, where a is the maximum possible concentration, we may consider it as a continuous type random variable, so that the expression for frequency distribution can be written as:

$$F(c) = P(0 < c < a) = \left\{ \begin{array}{l} 0 \\ \int_0^a f(c)\mathrm{d}c = \varphi(c) \\ 1 \end{array} \right\} \begin{array}{l} c = 0 \\ 0 < c < a \\ c = a \end{array} \qquad (1)$$

It results that relation $F(c) = f(c)$ can be used as a calibration function for the determination of concentrations,[1,2] even under the detection limit.[3] In practice, due to the limited number of repetitions for a certain sample, it is obvious that empirical $F_n(c)$ frequencies will be obtained which estimate, according to Glivenko's theorem,[4] the theoretical frequencies and therefore a dispersion range must be attached[5] to the calibration function $F_n(c) = f(c)$.

Considering that $p(y_0)$ is the probability distribution for the background noise and $p(y)$ for the analytical signal, as it results [6] from fig. 1

---

[1] C. Liteanu and I. Florea, *Mikrochim. Acta* [*Wien*], **1966**, 983.

[2] C. Liteanu and R. Alexandru, *Mikrochim. Acta* [*Wien*], **1968**, 639.

[3] C. Liteanu, *Mikrochim. Acta* [*Wien*], **1970**, 715.

[4] In. V. V. Nalimov, "Primenenie matematicheskoi statistik pri analize vestechestva", Gosud. izd. fiziko-matem. literatur, Moskva, 1960, p. 172.

[5] C. Liteanu and I. Rîcă, *Pure Appl. Chem.*, **44**, 535 (1975).

[6] C. Liteanu and I. Rîcă, *Mikrochim. Acta* [*Wien*]. **1973**, 745.

and especially from fig. 2 one can notice that the superposition degree of both probability fields increases with the concentration decrease. The appearance frequency of values $y > y_0$, namely of the positive samples, decreases similarly (the cross-hatched area in figure 2).

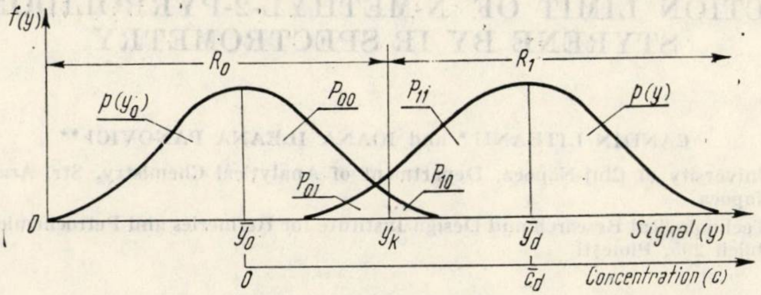
f(y)
R0
R1
p(y0')
P00
P11
p(y)
P01
P10
0
ȳ0
yK
ȳd
Signal (y)
0
c̄d
Concentration (c)

Fig. 1. — Two-step statistical model for defining the detection limit.

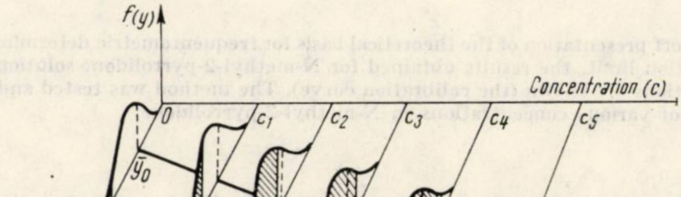
f(y)
Concentration (c)
0
c1
c2
c3
c4
c5
ȳ0
yk
ȳ = ȳ0 + bc
Signal
y
▨ – „Positive" samples (y > yK)
yk – Detection level

Fig. 2. — Graphical model of signal distribution variation for a linear dependence between concentration c and analytical signal y, in the presence of a gaussian noise.

Therefore, under the cd detection limit, the calibration curve will take the form:

$$F_n(c) = n_+/n = f(c) \tag{2}$$

where n_+ is the number of positive samples $(y > y_0)$ from the set of n samples for each value of the concentration $c < \bar{c}_d$.

With a view to discriminating the analytical signal values as compared with the background, namely $y > y_k$ "positive" or $y \leqslant y_k$ "negative" sample, to estimate the appearance frequency of the positive samples, one considers [7] as a threshold the y_k level of detection estimated by the Neyman-Pearson criterion, i.e. by attaching to the y_k value a certain value of the P_{10} false detection probability[8].

Thus, admitting a normal distribution of the background values, after normalization $z_k = (y_k - \bar{y}_0)/\sigma_{y_0}$ one obtains:

$$y_k = \bar{y}_0 + z_k\,\sigma_{y_0} \tag{3}$$

where $\bar{y}_0$ and σ_{y_0} represent the mean and the standard deviations of the background values.

The "S"-shaped calibration curve $F_n(c) = n_+/n = P(y > y_k) = f(c)$, plotted in fig. 3, can be linearized, after normalization, $z = (c - \bar{c})/\sigma$, being thus of the form:

$$z = \frac{\bar{c}}{\sigma} + \frac{1}{\sigma}\,c = a + bc \tag{4}$$

starting from the relation $F_n(c) = 0.5 \pm \Phi(z)$, respectively

$$\Phi(z) = F_n(c) - 0.5 = \frac{n_+}{n} - 0.5 \tag{5}$$

for $F_n(c) > 0.5$ and, respectively

$$\Phi(z) = 0.5 - F_n(c) = 0.5 - \frac{n_+}{n} \tag{5'}$$

for $F_n(c) < 0.5$.

The values of the normalized variable z (obtained from tables [9]) obviously act here as the assignment of the analytical signal.[7]

Obs. The discrimination operation, namely the decision $y > y_k$ or $y \leqslant y_k$ can be made very easily when the analytical signal is digitalized.

EXPERIMENTAL PART

a) *Apparatus.* A UR-10 spectrophotometer C. Zeiss with double beam was utilized, to which an integrating digital system from a Willy-Giede chromatograph cell with NaCl windows, was adapted, $d = 0.2$ cm.

b) *Recording conditions.* The measurements were carried out at 1682 cm^{-1} fixed frequency, prism NaCl, slit 2, amplification 6, with retarder, sensitivity 2, compensation-cell with CCl_4.

c) *Plotting of the calibration curve.* As a first stage, the value of detection level must be calculated, thus a blank sample (background) was recorded for $n = 20$ times and the mean $\bar{y}_0 = 282$ and the standard deviation $\sigma_{y_0} = 6.3$ were found from the obtained values. A false detection probability $P_{10} = 0.025$ ($z_k = 1.96$) was fixed, so that equation 3 will yield : $y_k = 282 + 6.3 \times 1.96 = 294$. A series of standards were further prepared from N-methyl-2-pyrrolidone in styrene. From each standard, the same quantity was measured for $n = 20$ times. Each sample was treated with 10 cm³ CCl_4, homogenized and recorded in the above mentioned conditions. For each set of $n = 20$ samples, a number of positive samples $n_+(y > y_k)$ will be obtained as a function of the $y_k = 294$ detection level value obtaining therefore pairs of the concentration appearance frequency values of the positive samples $P(y > y_k) = n_+/n = F_n(c)$.

---

[7] C. Liteanu and I. Rîcă, *Mikrochim. Acta* [*Wien*], **1975**, 311.

[8] In C. W. Helstrom, "Statistical Theory of Signal Detection", Pergamon Press, Oxford, 1960, p. 59.

[9] P. D. Lark, B. R. Craven and R. C. L. Bosworth, "The Handling of Chemical Data", Pergamon Press, Oxford, 1969, p. 335.

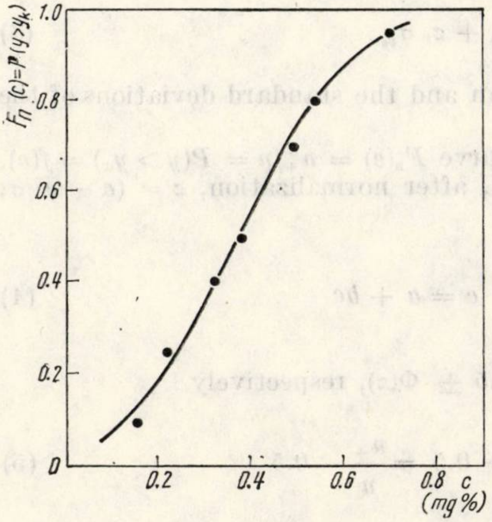

Fig. 3.— Calibration curve$F_n(c) = f(c)$.

The results thus obtained are listed in table 1, and fig. 3 reproduces the calibration curve $P(y > y_k) = f(c)$.

Table 1

The frequencies of appearance for positive tests for N-methyl-2-pyrrolidone solutions of different concentrations and the linearization of $F_n(c) = f(c)$ function

No.	Conc. mg % (x)	n	n_+	$n_+/n = P(y > y_k)$	$\Phi(z)$	z (y)
1	0.701	20	19	0.95	0.45	1.650
2	0.535	20	16	0.80	0.30	0.842
3	0.490	20	14	0.70	0.20	0.525
4	0.377	20	10	0.50	0.00	0.000
5	0.320	20	8	0.40	0.10	−0.255
6	0.231	20	5	0.25	0.25	−0.675
7	0.150	20	2	0.10	0.40	−1.285

The data in table 2 were obtained after linearization of the curve $P(y > y_k) = f(c)$, and the calibration function $z = a + bc$ (eq. 4) was represented in fig. 4.

The calibration straight-line equation was calculated from the pairs of values $z - c$, using the least squares method, obtaining :

$$z = -1.96 + 5.18\,c \tag{6}$$

According to Glivenko's theorem, experimental frequencies thus obtained estimate the theoretical frequencies. It is obvious that z values are also estimative, therefore a dispersion range must be attached [5] to the $z=f(c)$ function, which is limited by two hyperbola arcs, [10] described by the following equations :

$$z = z_i \pm 0.14\sqrt{0.215 + 7\,(0.4006 - c_i\,)^2} \qquad (7)$$

d) *Procedure.* The sample to be analyzed is measured so that the concentration in N-methyl-2-pyrrolidone be within the appearance limits of both the positive and the negative samples. This quantity is repeated in 20 identical samples, 10 cm^3 CCl$_4$ are added to each sample. After homogenization, the whole set is recorded in the conditions already shown. In this way, the number of positive samples $n_+(y > y_k)$ is determined, then $P(y > y_k) = n_+/n$. The value of the Laplace function is determined and the suitable value of z variable is found in the tables, finally the c concentration is calculated by introducing the z value in the calibration straight-line equation (6). The value thus obtained is referred to 100 g sample.

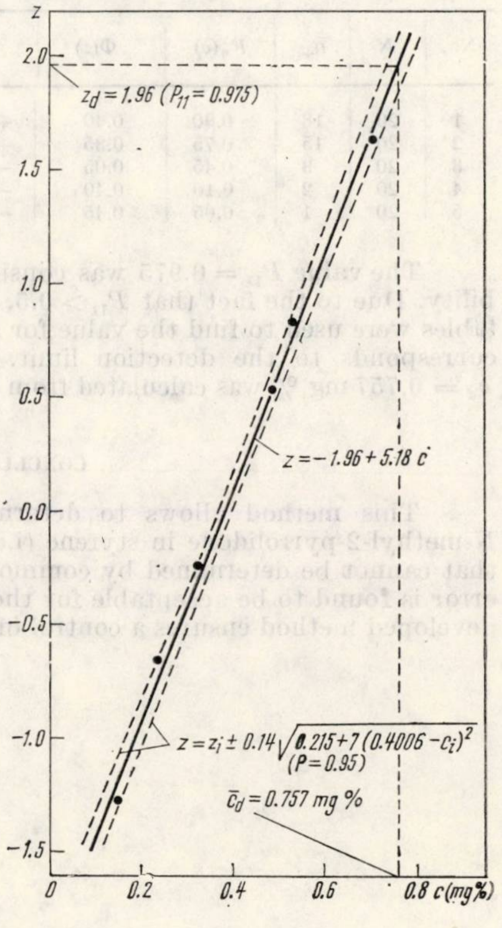

Fig. 4. — Calibration equation $z = f(c)$, respectively $z = a + bc$.

---

[10] F. S. Acton, "Analysis of Straight Line Data", J. Wiley, New York, 1959, p. 34.

RESULTS AND DISCUSSION

To verify the developed method, a number of synthetical mixtures were prepared and analyzed according to the recording conditions. The results obtained are exhibited in table 2.

Table 2

The results of frequentometric determination for N-methyl-2-pyrolidone in solutions of various concentrations based on the calibration equation (6)

No.	N	n_+	$F_n(c)$	$\Phi(z)$	z	Taken mg %	Given mg %	Error %
1	20	18	0.90	0.40	+1.285	0.645	0.626	− 2.9
2	20	15	0.75	0.35	+1.040	0.600	0.579	− 3.5
3	20	9	0.45	0.05	−0.130	0.325	0.353	+ 8.6
4	20	2	0.10	0.40	−1.285	0.115	0.130	+13.0
5	20	1	0.05	0.45	−1.650	0.072	0.060	+16.6

The value $P_{11} = 0.975$ was considered for the true detection probability. Due to the fact that $P_{11} > 0.5$, $\Phi(z) = 0.475$, the Laplace function tables were used to find the value for $z_d = 1.96$, namely the z value which corresponds to the detection limit. The value of the detection limit $\bar{c}_d = 0.757$ mg % was calculated from the calibration straight line (eqn. 6).

CONCLUSIONS

This method allows to determine very small concentrations of N-methyl-2-pyrrolidone in styrene (i.e. 0.072 ... 0.757 mg %), quantities that cannot be determined by common working procedures. The relative error is found to be acceptable for the concentration range involved. The developed method ensures a control of styrene purity.

Revue Roumaine de Chimie, **22**, *6*, 937–944 (1977)

NEW ANALYTICAL APPLICATIONS OF SOME SULPHONAMIDE COMPOUNDS. VI*

SODIUM *m*-SILVERSULPHAMOYLBENZOATE, A NEW REAGENT FOR THE DETERMINATION OF CARBON MONOXIDE IN THE AIR

TULIU SIMONESCU and VASILE RUSU
University of Timişoara, The Laboratory for Analytical
Chemistry, Strada Pestalozzi 16

Received March 26, 1975

The silver compound of *m*-sulphamoylbenzoic acid in alkaline solution is proposed as a reagent for the determination of carbon monoxide in the air. Lambert-Beer's law is obeyed in a concentration range of 5 to 500 ppm, and the determination errors do not exceed 3%.

There are rather few reagents proposed for determining micro-amounts of carbon monoxide in air.[1–10]

From equimolecular amounts of sodium *p*-sulphamoylbenzoate and silver nitrate, an alkali-soluble silver compound of this acid is obtained. The carbon monoxide reduces the alkaline solution of sodium *p*-silversulphamoylbenzoate, resulting a silver sol (Ciuhandu's reaction),[11] which is intensively coloured, finely powdered, very stable, and follows Lambert-Beer's law in a large concentration range. The high sensitivity of the re-

---

[*] Part V. T. Simonescu and V. Rusu, *Rev. Roumaine Chim.*, **22**, 435 (1977).

[1] P. Bourbon, *Chimie et Industrie*, **92**, 17 (1964).

[2] B. Smaller and J. F. Hall, *Ind. Eng. Chem.*, **16**, 64 (1944).

[3] W. Manchot and H. Gall, *Ber. dtsch. chem. Ges.*, **58**, 2175 (1925).

[4] C. H. Gray and M. Sandiford., *Analyst.*, **71**, 107 (1946).

[5] M. Shepherd, *Analyt. Chem.*, **17**, 77 (1947).

[6] M. Shepherd, S. Schuhmann and M. V. Kilday, *Analyt. Chem.*, **27**, 380 (1955).

[7] A. O. Beckman, J. D. McCullough and R. A. Crane, *Analyt. Chem.*, **20**, 674 (1948).

[8] W. Manchot and G. Lehman, *Ber. dtsch. chem. Ges.*, **64**, 1261 (1931).

[9] Z. Burianec and J. Burianova, *Coll. Czech. Chem. Comm.*, **28**, 2895 (1963).

[10] J. L. Lambert and P. A. Hamlin, *Analyt. Letters*, **4**, 745 (1971).

[11] G. Ciuhandu, *Studii şi Cercetări Chim. Acad. R.P.R.*, **3–4**, 243 (1955).

agent led to more researches in this field, the method being subsequently improved by the author of this work[12-16] as well as by other researchers.[17-22]

Taking into account that the oxidizing character of the alkaline solution of sodium *p*-silversulphamoylbenzoate towards the carbon monoxide is due to the complexing possibilities of silver ions, we undertook to study if there are other silversulphonamidic compounds which behave similarly. We have found the silver compound of the *m*-sulphamoylbenzoic acid which is recommended as a new reagent for the determination of carbon monoxide microamounts in air.

EXPERIMENTAL PART

APPARATUS

The absorption of light by the silver sol was measured with a spectrophotometer "Spekol" Carl Zeiss Jena.

The thermal control of samples was done by means of an ultrathermostat U-10 VEB Prüfgeräte Werk Medingen Dresden.

Mechanical stirring of samples was done with a stirrer Typ Thys II VEB Labortechnik Ilmenau.

The conductometric determinations were carried out with a conductometer Radelkis Typ OK-102.

pH-meter MV-11 Clamann-Grahnert.

Electrophoresis apparatus made at "Electrotehnica" Bucharest.

REAGENTS

10^{-1} M silver nitrate *p.a.*

10^{-1}M sodium *m*-sulphamoylbenzoate *p.a.* The solution is prepared by solving 20.1204 g of *m*-sulphamoylbenzoic acid[23] (standard substance for the determination of the titer for NaOH) in 100 ml of NaOH 1 M, and by adding distilled water to a final volume of 1000 ml.

1 M NaOH solution *p.a.*

10^{-1} M NaOH solution *p.a.*

Sodium *m*-silversulphamoylbenzoate (the reagent solution). It is prepared by mixing two volumes of silver nitrate 10^{-1} M solution with two volumes of sodium *m*-sulphamoylbenzoate 10^{-1} M solution. To this mixture, after homogenization, a volume of NaOH 1 M solution is added. The resultant solution should be clear and colourless.

Carbon monoxide prepared from formic acid and stored in a gas collector.

METHODS AND RESULTS

Although the *m*-sulphamoylbenzoic acid is well-known it has only a few analytical applications. As there are three hydrogen atoms in its composition which could dissociate, the stability of the combination

[12] G. Ciuhandu, *Studii și Cercetări Chim. Acad. R.P.R.*, **3–4**, 189 (1956).

[13] G. Ciuhandu, *Z. analyt. Chem.*, **155**, 321 (1957).

[14] G. Ciuhandu, *Z. analyt. Chem.*, **161**, 345 (1958).

[15] G. Ciuhandu and V. Rusu, *Rev. Chim. (București)*, **25**, 601 (1965).

[16] G. Ciuhandu and V. Bockel, *Chem. analyt.*, **52**, 525 (1970).

[17] D. A. Levaggi and M. Feldstein, *Amer. Ind. Hyg. Assoc. J.*, **25**, 64 (1964).

[18] E. Stamm, *VDI-Zeitung*, **18**, 796 (1967).

[19] E. Stamm, *Z. f. die gesamte Hygiene*, **3**, 160 (1967).

[20] V. Rusu, "The IIIrd National Conference on Analytical Chemistry Brașov – România" 22nd – 26th September, Vol. III, 1971, pp. 243.

[21] R. Bock and B. Bockholt, *Z. analyt. Chem.*, **260**, 274 (1972).

[22] T. Simonescu, V. Rusu and L. Kiss, *Rev. Chim. (București).*, **26**, 75 (1975).

[23] V. Rusu "The Vth National Conference on Physical Chemistry", Bucharest, September 1–4, 1976, p. 280.

resulting from the interaction of equimolecular amounts of silver nitrate and *m*-sulphamoylbenzoic acid should be largely influenced by pH. If we follow potentiometrically the variation of the concentration of free silver ions in solution (silver indicator electrode) for an equimolecular mixture of silver nitrate and *m*-sulphamoylbenzoic acid, we can see that it is considerably influenced by pH. It is well-known that in a strong alkaline medium the concentration of the free silver ions is very low. In a strong alkaline medium the resulting silver compound has a maximum stability, which can be explained by subsequent deprotonation steps of the *m*-sulphamoylbenzoic acid.

In figure 1 the pH-metric titration curve of *m*-sulphamoylbenzoic acid with sodium hydroxide is plotted. It emphasizes the presence of two protons which can dissociate. The extremely small value of the second pH jump indicates that in this stage the acid is much weaker than in the first one.

The elimination of the second proton must be favoured by the presence of silver ions in case they take part in an equilibrium. Figure 2 shows the variation of hydrogen ions concentration of the pH-metric titration of an equimolecular mixture of silver nitrate and *m*-sulphamoylbenzoic acid with sodium hydroxide. If we study the plotted curve we can see that there is a larger pH-jump for the second stage of deprotonation.

The elimination of the third proton could not be evidenced by means of a pH-meter. The equilibria of the first two stages can be formulated as follows:

$$Ag^+ + H_2N - SO_2 - C_6H_4 - COOH + OH^- \rightleftharpoons H_2N - SO_2 - \\ - C_6H_4 - COOAg + H_2O \qquad (1)$$

and

$$H_2N - SO_2 - C_6H_4 - COOAg + OH^- \rightleftharpoons AgHN - SO_2 - C_6H_4 - \\ - COO^- + H_2O \qquad (2)$$

The existence of these two equilibria formulated so far is supported by the titration curve from fig. 2, and by the fact that the two silver compounds which result from (1) and (2) could be separated and characterized by analysis. The existence of the second equilibrium is supported by the fact that we could also separate the disodium salt of *m*-sulphamoylbenzoic acid, used as a standard reagent [24] for hydrochloric acid solutions.

In order to evidence the elimination of the third proton we used the conductometric method. The $^-HN-SO_2-C_6H_4-COO^-$ ion (whose existence is confirmed by the presence of the disodium salt of *m*-sulphamoylbenzoic acid [24]) which can be considered a weak acid will deprotonate itself easier in the presence of silver ions. This is explained by the equilibrium shift to the right:

$$AgHN - SO_2 - C_6H_4 - COO^- + OH^- \rightleftharpoons [Ag - N - SO_2 - \\ - C_6H_4 - COO]^{2-} + H_2O \qquad (3)$$

---

[24] V. Rusu, (*unpublished work*).

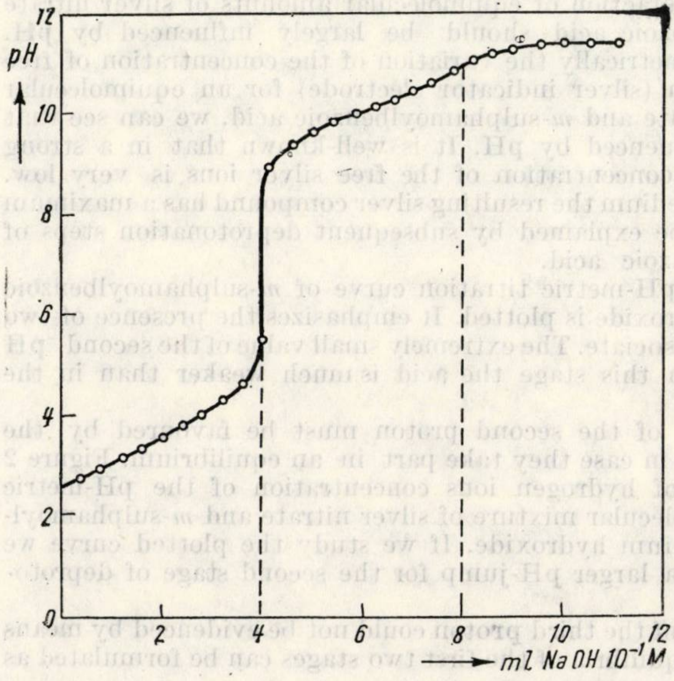

Fig. 1. — pH-metric titration of 0.0804 g *m*-sulphamoylbenzoic acid dissolved in 20 ml water with sodium hydroxide 10^{-1} M.

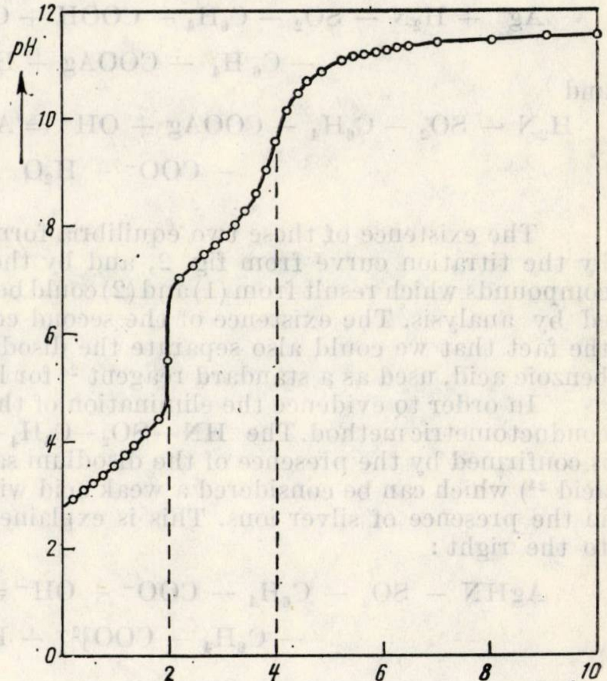

Fig. 2. — pH-metric titration of 20 ml 1 : 1 mixture of 2×10^{-2} M silver nitrate and 2×10^{-2} M *m*-sulphamoylbenzoic acid with 10^{-1} M sodium hydroxide.

The presence of the third slope change on the conductometric titration curve, plotted in fig. 3, when an equimolecular mixture of silver nitrate and *m*-sulphamoylbenzoic acid is added to sodium hydroxide, can be thus interpreted.

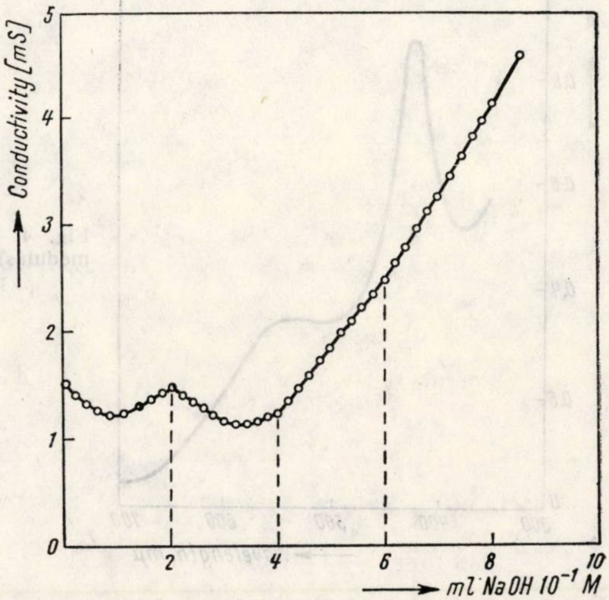

Fig. 3. — Conductivity (mS) at the titration of 20 ml 1 : 1 mixture of 2×10^{-2} M silver nitrate and 2×10^{-2} M *m*-sulphamoylbenzoic acid with 10^{-1} M sodium hydroxide.

The concentration of the free silver ions is maintained at a practically constant value by means of the equilibrium:

$$[Ag-N-SO_2-C_6H_4-COO]^{2-} + H_2O \rightleftharpoons Ag^+ + OH^- + + {}^-HN - SO_2 - C_6H_4 - COO^- \qquad (4)$$

It is very likely that the free silver ions are reduced to metal in accordance with the formulation for the silver compound of *p*-sulphamoylbenzoic acid adopted by Ciuhandu.[11]

$$2\,Ag^+ + CO + 4\,OH^- \rightarrow 2Ag^\circ + CO_3^{2-} + 2\,H_2O \qquad (5)$$

The reaction speed between carbon monoxide and the reagent is controlled by the distribution of CO between the liquid and the gaseous phases. Solute CO reduces rapidly the silver ions to metallic silver, while the *m*-sulphamoylbenzoate ion is involved in the mechanism supplying free silver ions and, probably contributing to the outstanding stability of the colloidal particle. The reduced silver looks like a very stable colloidal solution with an intense absorption of light.

The variation of the silver sol light absorption versus the wavelength is plotted in fig. 4. The peak at 425 nm allows measurements at this wavelength.

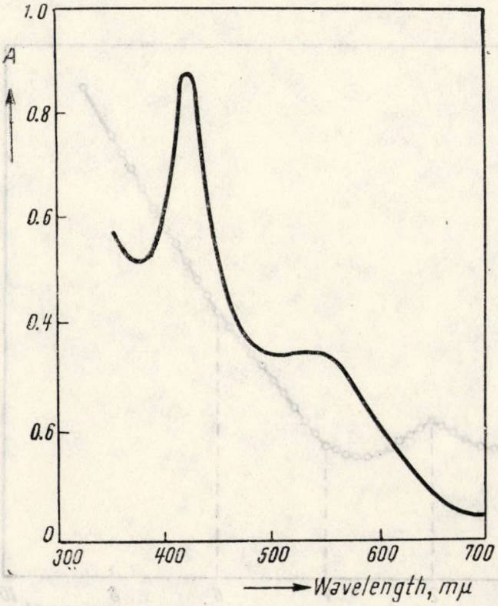

Fig. 4. — Light absorption (*A*-absorbance modulus) of the silver colloidal solution plotted versus wavelength.

The negative charge found by electrophoresis, the conditions in which the silver colloidal solution is formed as well as the analogous formulation with the silver compound of *p*-sulphamoylbenzoic acid [25] led us to the following possible structure of the particle :

$$[m\,\mathrm{Ag}^{\circ}.n\,\mathrm{Ag}^{+}.p\,\mathrm{OH}^{-}.r^{-}\mathrm{HN} - \mathrm{SO}_2 - \mathrm{C}_6\mathrm{H}_4 - \mathrm{COO}^{-}]^{x-} \qquad (6)$$

$$\text{where } n < p + 2r \qquad (7)$$

The known CO and air concentrations are obtained by diluting CO with clean air.[26] The experimental device is made up to 100 ml Erlenmeyer flasks, where the contact of the gas and the reagent takes place.[13,26]

The gasous mixture to be analysed is introduced in the Erlenmeyer flask by displacing the distilled water from it. The sampling of gas from atmosphere is done analogously by emptying the distilled water from the flasks. In the gas samples, 10 ml of alkaline sodium *m*-silversulphamoylbenzoate is introduced and consequently the same amount of gas is evacuated.

There are two possibilities of carrying out a determination. The first is based on maintaining the samples in a thermostatic bath for 20 hours, and on measuring the absorption of light at 425 nm wavelength. The other one requires mechanical stirring of the samples for 2 hours in order to increase the reaction speed of CO with the reagent, by increasing the contact surface. In both cases the reagent solution is taken as blank test.

---

[25] G. Ciuhandu and V. Giuran, *Z. analyt. Chem.*, **159**, 250 (1958).

[26] G. Ciuhandu, V. Rusu and M. Diaconovici, *Z. analyt. Chem.*, **208**, 81 (1965).

The variation of the absorbance modulus versus the CO content of the samples, at 25°, is plotted in fig. 5.

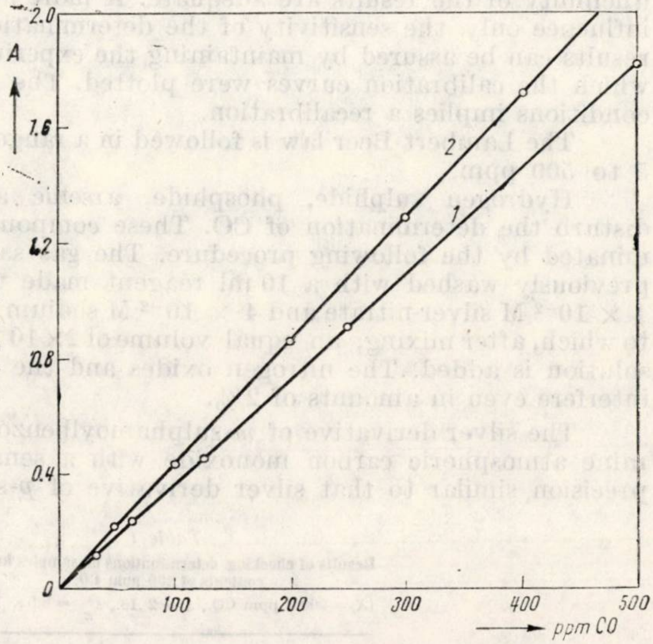

Fig. 5. — Standard curves for the determination of CO in the air. (A — absorbance modulus) Curve *1*. A 20 hours contact between the gas and the reagent at 25°. Curve *2*. Samples stirred for 2 hours at 25°.

The variation of absorbance (A) with time, for samples with a given concentration of CO, can be expressed by the following law :

$$A = K \times f(t) \tag{8}$$

where t is the time, and K a constant [20,22] depending on the gas concentration C, on the gas-reagent interface S, on the diffusion coefficient D, on temperature $t°$.

$$K = f(C, S, D, t°) \tag{9}$$

By maintaining constant all these parameters and by determining the absorption of light at a certain time, the value of $f(t)$ is the same because, under these conditions, A undergoes modifications due exclusively to the variation of concentration C. If we consider for a certain time

$$K \times f(t) = K', \tag{10}$$

K' having a well-defined value resulting from the experimental conditions, the law which gives the modification of light absorption of the samples as a function of their carbon monoxide content will become :

$$A = K' \times C \tag{11}$$

Relation (11) is a linear equation whose variables are A and C, and K' represents the slope of the calibration curves which has a constant value under the given conditions.

The calibration curves will serve later on to find out the carbon monoxide content in the unknown samples. Although the carbon monoxide absorption in the reagent is not quantitative, the accuracy and reproducibility of the results are adequate. A more advanced absorption will influence only the sensitivity of the determination. The accuracy of the results can be assured by maintaining the experimental conditions under which the calibration curves were plotted. The change of experimental conditions implies a recalibration.

The Lambert-Beer law is followed in a range of concentrations from 5 to 500 ppm.

Hydrogen sulphide, phosphide, arsenic and antimony hydride disturb the determination of CO. These compounds are completely eliminated by the following procedure. The gas sample to be analysed is previously washed with a 10 ml reagent made up to equal volumes of 4×10^{-2} M silver nitrate and 4×10^{-2} M sodium *m*-sulphamoylbenzoate to which, after mixing, an equal volume of 2×10^{-1} M aqueous piperazine solution is added. The nitrogen oxides and the sulphur dioxide do not interfere even in amounts of 2%.

The silver derivative of *m*-sulphamoylbenzoic acid allows to determine atmospheric carbon monoxide with a sensibility, specificity, and precision similar to that silver derivative of *p*-sulphamoylbenzoic acid.

Table 1

Results of checking determinations on samples known contents of 200 ppm CO

($\bar{X}$ = 200.3 ppm CO., s = 2 .16., $s_{\bar{x}}$ = 6.8×10^{-1})

ppm CO found	Deviation in ppm	Error %
196	−4	−2
202	+2	+1
202	+2	+1
198	−2	−1
195	−5	−2.5
198	−2	−1
201	+1	+0.5
198	−2	−1
202	+2	+1
201	+1	+0.5

The proposed method has a good reproducibility as it results from table 1.

The simplicity of execution and specificity of this method recommends it for immediate practical application.

Revue Roumaine de Chimie, **22**, 6, 945–951 (1977)

Herrn Professor Dr. C. Drăgulescu
zum 70. Geburtstag gewidmet

DER THERMISCHE ABBAU VON POLY(METHYLMETHACRYLAT) UNTER NICHT ISOTHERMEN BEDINGUNGEN

NATALIA HURDUC und IOAN-ADAM SCHNEIDER
Lehrstuhl für phys. Chemie, Polytechnisches Institut,
R-6600 Iassy, Splaiul Bahlui Stîng, 61

Eingegangen am 31. August 1976

Dynamisch thermische Abbauuntersuchungen an radikalischem und ionischem PMMA haben gezeigt, daß das unterschiedliche Verhalten sowohl beim Abbau in Luft, als auch in Stickstoff vor allem an das Vorhandensein oder nicht von endständigen Doppelbindungen gebunden ist, wobei die Thermostabilität umso geringer ist, je größer die Anzahl dieser endständigen Doppelbindungen ist.

Obwohl in der Literatur zahlreiche Arbeiten über den thermischen Abbau von Poly(methylmethacrylat) — abgekürzt PMMA — anzutreffen sind, gibt es wenige Studien über den Abbau unter nicht isothermen Bedingungen. So fanden Sazanov und Mitarb.[2] auf Grund von vergleichenden derivatographischen Untersuchungen, daß unter thermogravimetrischen Bedingungen bei einer Aufheizgeschwindigkeit von 6°/Min., anionisches PMMA molekulargewichtsbedingt, bis zu 70° thermostabiler als radikalisches PMMA ist. Zu ähnlichen Schlüssen gelangte auch McNeill[2] während seiner TVA-Untersuchungen.

Schon isotherme Untersuchungen haben gezeigt, daß bei radikalischem PMMA, infolge der beim Polymerisationsabbruch durch Disproportionieren gebildeten endständigen Doppelbindungen, der Start bei tieferen Temperaturen vom Kettenende her erfolgt, wogegen er bei höheren Temperaturen und bei ionischem PMMA statistisch stattfindet, wobei der Mechanismus zusätzlich auch vom mittleren Polymerisationsgrad bedingt ist.[3]

[1] Yu. N. Sazanov, E. P. Skvortsevich und E. B. Milovskaia, *J. Therm. Anal.*, **6**, 53 (1974).

[2] J. C. McNeill, *European Polymer J.*, **4**, 21 (1968).

[3] H. H. G. Jellinek und Ming Dean Luh, *Makromol. Chem.*, **115**, 89 (1968); N. Grassie und H. W. Melville, *Proc. Roy. Soc.*, **A190**, 1 (1949); S. Straus und S. L. Madorsky, *J. Res. Nat. Bur. Stand.*, **50**, 165 (1953); J. R. Mac Callum, *Makromol. Chem.*, **83**, 137 (1965) und A. Barlow, R. S. Lehrle, J. C. Robb und D. Sunderland, *Polymer*, **8**, 557 (1967).

In vorliegender Arbeit wird nun versucht unsere Kenntnisse über das thermogravimetrische Verhalten von PMMA unter nicht isothermen Bedingungen zu erweitern, wozu radikalisches (PMMA$-$R$_1$) und ionisches (PMMA$-$I$_1$) Polymeres verwendet wurden.

Da in nicht isothermen Bedingungen sowohl der Abbauprozeß, als auch seine kinetischen Parameter zusätzlich von den Arbeitsbedingungen abhängen, wurde der Abbau von PMMA nicht nur in Luft, sondern auch in inerter Atmosphäre bei verschiedenen Aufheizgeschwindigkeiten untersucht.

EXPERIMENTELLER TEIL UND DISKUSSIONEN

Die charakteristischen Merkmale der in dieser Arbeit verwendeten Polymerproben sind in Tabelle 1 wiedergegeben. Die Molekulargewichtsmittel sind nach viskosimetrischen Messungen in Acetonlösung bei 25° aus $[\eta] = 0{,}96.10^{-2}\,\bar{M}_{\text{visk}}^{0{,}69}$ abgeleitet worden.[4]

Tabelle 1

Charakteristische Merkmale der untersuchten Polymerproben

	PMMA$-$R$_1$	PMMA$-$I$_1$
viskosimetrisches Molekulargewichtsmittel $\bar{M}_{\text{visk}}$	84500	93800
Monomergehalt Mol %	0,77	0,54
Bromzahl	16,77	8,49
Doppelbindungen/Makromolekül	0,26	0,029
scheinbare Aktivierungsenergie kcal/Mol für : 4,6°C/Min	39,9*	54,6
12,4 ,,	34,2	31,0
19,4 ,,	34,2	26,8

* Die Werte sind nur für Reaktionsbeginn gültig und weitgehend unsicher.

Die Polydispersität der untersuchten Proben ist an einem Gelpermeationchromatographen WATERS gemessen worden. Die erhaltenen Dispersionskurven sind in Abb. 1 dargestellt.

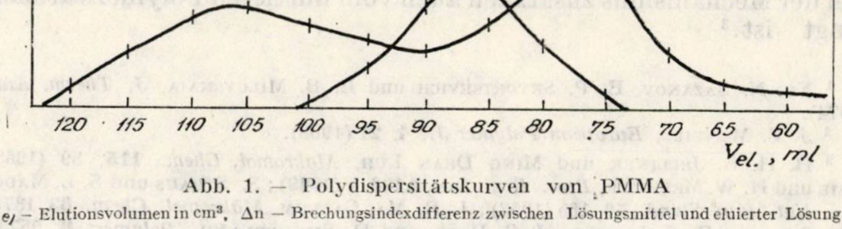

Abb. 1. — Polydispersitätskurven von PMMA

v_{el} – Elutionsvolumen in cm³, Δn – Brechungsindexdifferenz zwischen Lösungsmittel und eluierter Lösung.

---

[4] J. Mureșan, ,,Chimia macromoleculelor'', Ed. Didactică și Pedagogică, București, 1967, S. 279.

Aus obigen Ergebnissen geht klar hervor, daß das anionische PMMA$-I_1$ weitaus einheitlicher ist und weniger endständige Doppelbindungen als das radikalische PMMA$-R_1$ enthält. Die ausgewählten Proben besaßen zusätzlich vergleichbare Molekulargewichte, da sowohl isotherme, als auch nicht isotherme Untersuchungen gezeit haben, daß das thermische Verhalten des PMMA auch vom mittleren Polymerisationsgrad bedingt ist.

Der thermogravimetrische Abbau wurde sowohl in einem Derivatographen MOM-Budapest (für den Abbau in Luft), als auch in einer Mettler'schen Thermowaage (für den Abbau in Luft und in inerter Atmosphäre) untersucht. Dabei wurden pulverförmige Proben von bzw. 20 mg und 2,5 mg und Aufheizgeschwindigkeiten von 2 bis 20°/Min benützt.

Charakteristische Thermogramme für den Abbau in Stickstoff von 2,5 mg Polymerproben bei einer Aufheizgeschwindigkeit von 10°/Min sind in Abb. 2 wiedergegeben.

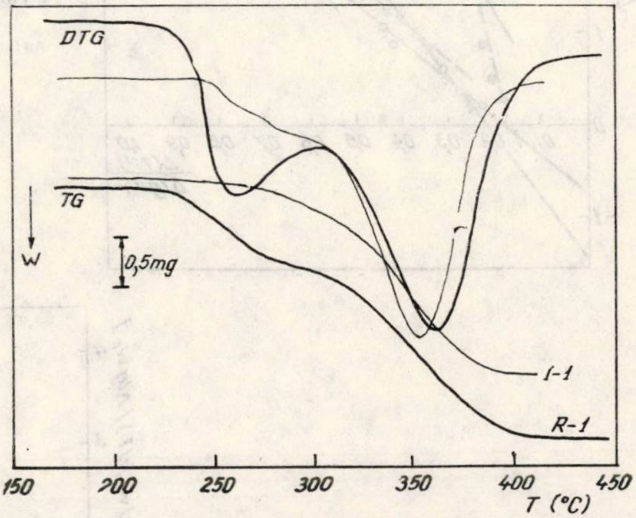

Abb. 2. — Thermogramme von PMMA für den Abbau in Stickstoff.
Aufheizgeschw.: 10°C/Min, Probenmenge: 2,5 mg, w — Gewichtsverlust.

Aus dieser Abbildung geht hervor, daß das PMMA$-I_1$ nicht nur thermostabiler ist, sondern sich auch thermogravimetrisch einheitlicher verhält, da es praktisch in einer Stufe abbaut, wogegen PMMA$-R_1$ sich in deutlich zwei Abbaustufen zersetzt. Damit wird noch einmal bestätigt, daß die Polymermoleküle mit endständiger Doppelbindung bei tieferen Temperaturen als die gesättigten Makromoleküle angegriffen werden.

Dieses unterschiedliche Verhalten zeichnet sich auch bei einem Versuch, die thermogravimetrischen Daten kinetisch auszuwerten ab.

So sind in den Abb. 3 und 4 die Freeman-Carroll'schen [5] Kurven für den derivatographischen Abbau in Luft der beiden Polymerproben dargestellt. Während diese Kurven für PMMA$-R_1$ uneinheitlich erscheinen, was auf Überlagerung komplexer Abbauprozesse hindeutet, sind die entsprechenden Kurven für PMMA$-I_1$ einheitlich linear. Doch auch im letzteren Falle besteht ein deutlicher Einfluß der Aufheizgeschwindigkeit, was sich auch in den abgeleiteten scheinbaren Aktivierungsenergien in Tabelle 1 widerspiegelt.

Der Einfluß des Umsatzgrades auf die kinetischen Parameter, der für den Ablauf komplexer Prozesse unter nicht isothermen Bedingungen

---

[5] E. S. Freeman und B. Carroll, *J. Phys. Chem.*, **62**, 394 (1958).

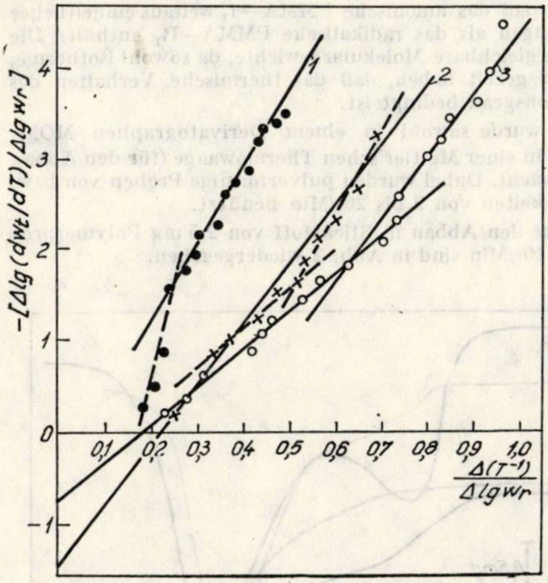

Abb. 3. — Kinetische Auswertung der Umsatzkurven von PMMA−R$_1$ nach Freeman-Carroll. Abbau von 20 mg Proben in Luft.

Aufheizgeschw.: ● − 4,6; × − 12,4 und ○ − 19,4°C/Min.

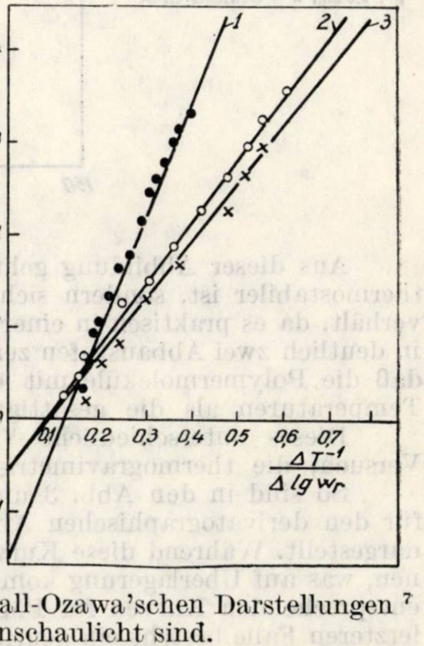

Abb. 4. — Kinetische Auswertung der Umsatzkurven von PMMA−I$_1$ nach Freeman-Carroll. Abbau von 20 mg Proben in Luft.

Aufheizgeschw.: ● − 4,6; ○ − 12,4 und × − 19,4°C/Min.

charakteristisch ist,[6] wird in den Flynn-Wall-Ozawa'schen Darstellungen [7] verdeutlicht, die in den Abb. 5 und 6 veranschaulicht sind.

Der kurvenartige Verlauf in Abb. 5 zeigt eine Änderung des Abbaumechanismuses von PMMA−R$_1$, sowohl während des Prozesses, als auch mit der Aufheizgeschwindigkeit an. Dagegen deutet der Neigungsabfall der Graden mit Anstieg des Umsatzes (Abb. 6) auf einen entsprechenden Abfall der scheinbaren Aktivierungsenergie des Abbauprozesses von PMMA – I_1 hin, was für einen Kettenablauf der thermischen Abbaureaktion charakteristisch ist.[6]

---

[6] I. A. Schneider, *Rev. Roumaine Chim.*, **17**, 291 (1972).

[7] J. H. Flynn und L. A. Wall, *J. Polymer Sci., Part B*, **4**, 323 (1966); T. Ozawa, *Bull. Chem. Soc. Japan*, **38**, 1881 (1965).

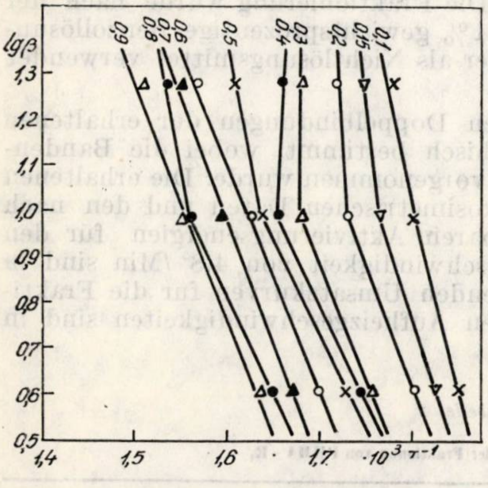

Abb. 5. – Auswertung der Umsatzkurven von PMMA – R_1 nach Flynn-Wall-Ozawa. Abbau von 20 mg Proben in Luft.

β – Aufheizgeschw. in °C/Min., T – Temperatur in °K. Die angeführten Zahlen bedeuten den Umsatz.

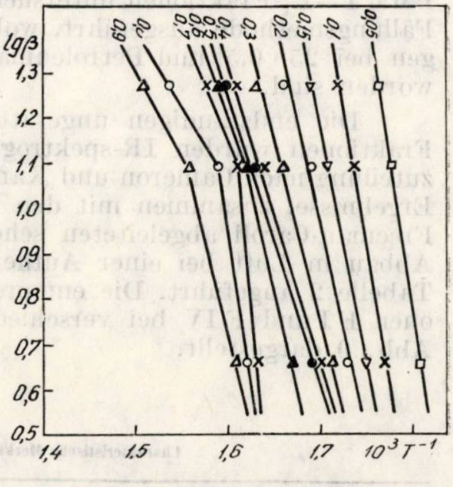

Abb. 6. – Auswertung der Umsatzkurven von PMMA – I_1 nach Flynn-Wall-Ozawa. Bedingungen wie in Abb. 5.

Die mit Hilfe einer Mettler'schen Thermowaage erhaltenen Ergebnisse für den Abbau der Polymerproben in inerter Atmosphäre bestätigen weitgehend oben angeführte Unterschiede. Zur Veranschaulichung sind in den Abb. 7 und 8 die entsprechenden Flynn-Wall-Ozawa'schen Diagramme dargestellt.

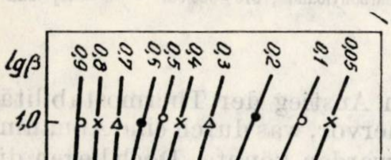

Abb. 7. – Auswertung der Umsatzkurven von PMMA – R_1 nach F-W-O. Abbau von 2,5 mg Proben in Stickstoff.

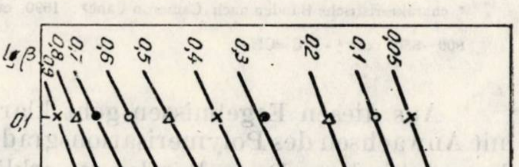

Abb. 8. – Auswertung der Umsatzkurven von PMMA – I_1 nach F-W-O. Bedingungen wie in Abb. 7.

Ausgehend von dem Gedanken, daß die Fraktionen kleineren Polymerisationsgrades von PMMA$-$R$_1$ einen größeren Anteil endständiger Doppelbindungen, als die Fraktionen höheren Polymerisationsgrade enthalten müßten, wurde auch das thermogravimetrische Verhalten von PMMA$-$R$_1$-Fraktionen untersucht. Die Fraktionierung wurde nach der Fällungsmethode ausgeführt, wobei 1% gewichtsprozentige Benzollösungen bei 25± 0,5° und Petroleumaether als Nichtlösungsmittel verwendet worden sind.

Die endständigen ungesättigten Doppelbindungen der erhaltenen Fraktionen wurden IR-spektrographisch bestimmt, wobei die Bandenzuteilung nach Cameron und Kane [8] vorgenommen wurde. Die erhaltenen Ergebnisse, zusammen mit den viskosimetrischen Daten und den nach Freeman-Caroll abgeleiteten scheinbaren Aktivierungsenergien für den Abbau in Luft bei einer Aufheizgeschwindigkeit von 4,8° /Min sind in Tabelle 2 angeführt. Die entsprechenden Umsatzkurven für die Fraktionen F I und F IV bei verschiedenen Aufheizgeschwindigkeiten sind in Abb. 9 dargestellt.

Tabelle 2

Charakteristische Merkmale der Fraktionen von PMMA$-$R$_1$

Fraktion	$[\eta]$ ml/g	$\overline{M}_{\text{visk}}$	Verhältnis der ungesättigten Banden		scheinbare E, kcal/Mol für 12,4°C /Min
			845/1690 cm^{-1}	990/1690 cm^{-1}	
I	31,7	126000	0,127*	0,24	77
II	20,0	64000	0,13	0,31	62
III	13,2	35000	0,20	0,42	52
IV	10,0	23000	0,29	0,55	46

* charakteristische Banden nach Cameron-Cane[8]: 1690 cm^{-1}-Carbonylbande; 870–920 cm^{-1}- $>$C=CH$_2$ und 800–850 cm^{-1}- $>$C=CH–

Aus diesen Ergebnissen geht klar ein Anstieg der Thermostabilität mit Anwachsen des Polymerisationsgrades hervor, was durch eine Abnahme der endständigen Doppelbindungen erklärt werden könnte. Doch liegen die Verhältnisse nicht so einfach, da die entsprechenden Freeman-Carroll'schen (Abb. 10) und Flynn-Wall-Ozawa'schen Darstellungen (Abb. 11) eindeutig anzeigen, daß der komplexe Charakter der Abbauprozesse bei allen Fraktionen anzutreffen ist.

Da der Abbau in Luft erfolgt, könnte dieses, neben den endständigen Doppelbindungen zusätzliche Komplikationen bringen, obwohl gewöhnlich in thermisch dynamischen Bedingungen, infolge des hohen Austrittspotentials der flüchtigen Abbauprodukte, der Abbau in deren Atmosphäre stattfindet.

---

[8] G. C. CAMERON und D. R. CANE, *Chem. listy*, **109**, 194 (1967) und **113**, 75 (1968).

Abb. 9. — Umsatzkurven für den Abbau in Luft von 20 mg PMMA–R_1-Fraktionen.

Aufheizgeschw.: F IV, ● – 4,8; △ – 12 und ■ – 20°C/Min. F I, ○ – 4,8; △ – 12 und □ – 20°C/Min.

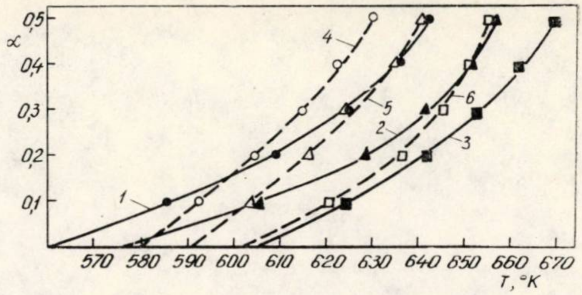

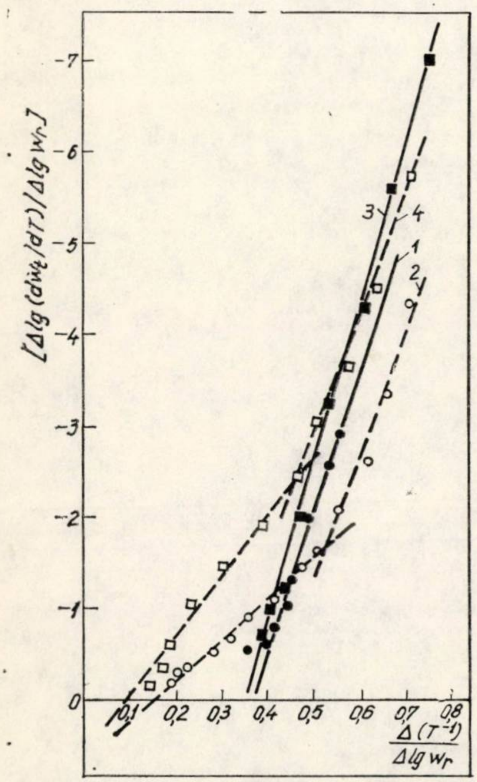

Abb. 10. — Kinetische Auswertung der Umsatzkurven von PMMA-Fraktionen nach F-C. Abbau von 20 mg Proben in Luft.

Aufheizgeschwin.: F III, ● – 4,8 und ○ – 20°C/Min. F ■ – 4,8 und □ – 20°C/Min.

Abb. 11. — Auswertung der Umsatzkurven von PMMA-Fraktionen nach F-W-O. Bedingungen wie in Abb. 10.

● bzw. ○-F IV und bzw. △-F I.

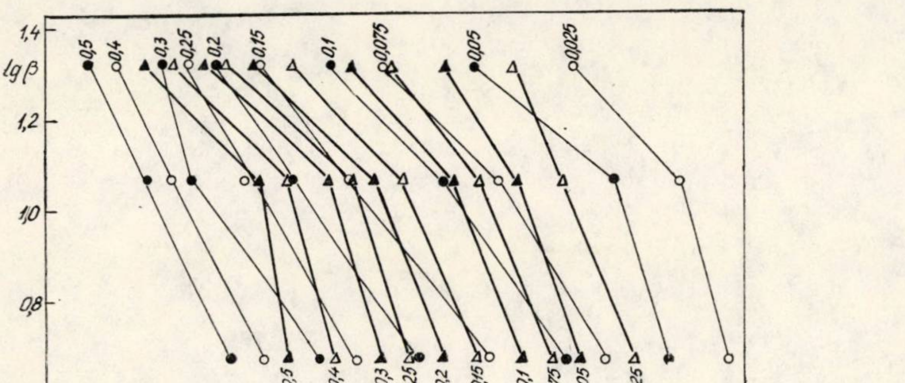

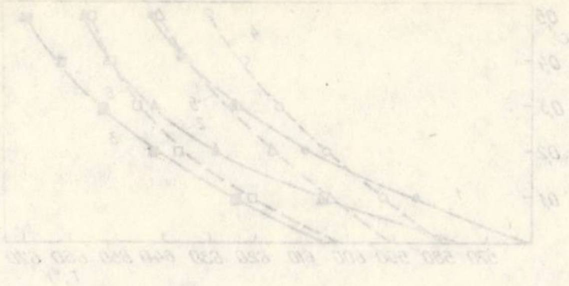

Abb. 9 — Umsatzkurven für den Abbau in Luft von 20 mg PMMA-U_1-Fraktionen.

[illegible] I IV; ● – 4; Δ – 12 und ▩ – 20°C/Min. F I; □ – 4,8; Δ – 12 und [illegible] 20°C/Min.

Abb. 10. — Kinetische Auswertung der Umsatzkurven von PMMA-Fraktionen nach [illegible] Abbau von 20 mg Proben in Luft.

[illegible] F IV, ● – 4,8 und □ – 20°C/Min. F [illegible] ▩ – 4,8 und [illegible] 20°C/Min.

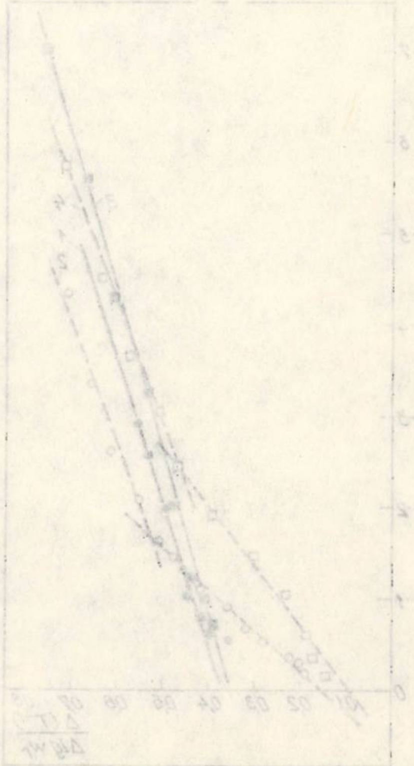

Abb. 11 — Auswertung der Umsatzkurven von PMMA-Fraktionen nach F-W-O. Bedingungen wie in Abb. 10.

● bzw. □ F IV und ▩ bzw. □ F I.

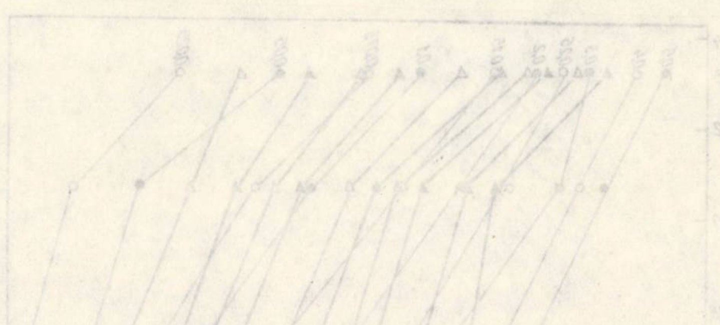

Revue Roumaine de Chimie, **22**, *6*, 953–961 (1977)

Herrn Professor Dr. Coriolan Drăgulescu
zum 70. Geburtstag gewidmet

ÖLMODIFIZIERTE TEREPHTHALATGLYCERINALKYDHARZE

I. MANOVICIU, VIRGINIA MANOVICIU und C. DAVIDESCU
Polytechnisches Institut „Traian Vuia", Fakultät für chemische Inginieurie,
Timişoara Bd. 30 Decembrie Nr. 2

Eingegangen am 26. Juli 1976

In der vorliegenden Arbeit werden die ölmodifizierten Terephthalatglycerinharze, die als Säurekomponente Dimethylterephtalat verwenden, behandelt. Die mit einem Ölgehalt von 46,5-und 61,5 % synthetisierten Harze, zeigten entsprechende filmbildende Eigenschaften. Einige davon haben sehr gute Trocknungsfähigkeit, sowie verbesserte physikalische und mechanische Eigenschaften im Vergleich zu den entsprechenden Phthalatharzen.

Die Erfindung der Terephthalatalkydharze im Jahre 1950 bei General Electric Co [1] entsprang der Notwendigkeit elektroisolierende Lacke mit verbesserten Eigenschaften, wie Dehnbarkeit, Wärmebeständigkeit und mechanische Festigkeit [2,3] zu erzeugen, Eigenschaften die auf diesem Gebiet nur von den Silikonharzen oder silikonmodifizierten Alkydharzen erreicht werden können.[2,4] Die Literatur über die bisherigen Forschungen auf diesem Gebiet erwähnt eine Reihe von Darstellungsmöglichkeiten,[2,5–12] die von Ölen (die gebräuchlichste Methode) oder entsprechenden Fettsäuren, Glycerin, Terephthalsäure (TS) oder TS und Dimethylterephthalat (DMT) (im Verhältnis von 10–30 % zur gesamten Säuremenge [2]) ausgehen.

---

[1] * * * „Encyclopedia of Polymer Science", Bd. I, Interscience Publishers, New-York, 1964, S. 663.

[2] R. H. Thielking, U. S. Pat. 3.080.331, 5. März 1963; *Chem. Abstr.*, **58**, 14.308 (1963).

[3] * * * Brit. Pat. 991.020,5. Mai 1965; *Chem. Abstr.*, **63**, 5902 (1965).

[4] A. L. Smith, L. H. Brown, L. Y. Tyler und M. Y. Hunter, *Ind. Eng. Chem.*, **49**, 1903 (1957).

[5] M. Dubrova und N. V. Burenkova, *Lakokras. mater. ikh. primen.*, **1960**, 20.

[6] J. Smoczynski und A. Lausch, Pol. Pat. 43.451. 31. August 1960; *Chem. Abstr.*, **58**, 3609 (1963).

[7] I. Eikichi, Japan Pat. 2976, 30. Mai 1962; *Chem. Abstr.*, **59**, 14.200 (1963).

[8] A. O. Focşăneanu, *Farbe u. Lack*, **1965**, 643.

[9] I. R. Klare und G. O. Sedgwick, U.S. Pat. 3.423.341, 21. Januar 1969; *Chem. Abstr.*, **70**, 58.998 (1969).

[10] F. I. Tonner, Fr. Pat. 1.522.793, 26. April 1968; *Chem. Abstr.*, **70**, 116.328 (1969).

[11] K. Reiser, E. Sydney, I. Fry und M. Jonason, Brit. Pat. 968.322, 2. September 1964; *Chem. Abstr.*, **61**, 12.159 (1964).

[12] * * * „Encyclopedia of Polymer Science", Bd. I, Interscience Publishers, New York, 1964, S. 687.

Die Alkoholyse der Öle ist schon lange bekannt.[13–19] Hinsichtlich dieser Reaktion, die in heterogener basischer Katalyse [13–20] verläuft, wurden kinetische,[13] thermodynamische [21] Untersuchungen durchgeführt, ein Reaktionsmechanismus sowie die Bedingungen für die Verschiebung des Gleichgewichtes zugunsten einer Höchstausbeute in Monogliycerid [13–18,22] vorgeschlagen.

In der weniger untersuchten zweiten Phase der Reaktion d.h. der Polykondensation erfolgt durch Abspalten von Wasser die Verlagerung des Gleichgewichtes nach rechts. Die Reaktion wird in der Schmelze unter Bedingungen die eine Vernetzung und Vergilbung des Produkte vermeiden, durchgeführt.[22]

Vom Standpunkt des Einflusses verschiedener Komponenten des Alkydsystems auf die filmbildenden Eigenschaften der erhaltenen Produkte wurden in vorhergehenden Arbeiten [23,24] der Einfluß der Isophthalsäure und des Pentaerythrits, sowie die Möglichkeit einer Kompensation der schwächeren Fähigkeit zur oxydativen Vernetzung der halbtrocknenden Öle durch entsprechenden Formulierung des Polyesters untersucht.

Die vorliegende Arbeit untersucht die Möglichkeit DMT für die Synthese der fetten und halbfetten ölmodifizierten Terephthalatalkyde zu verwenden und den Einfluß der Art und Menge des Öls auf die filmbildenden Eigenschaften der so erhaltenen Harze zu erforschen.

EXPERIMENTELLER TEIL

Für die Synthese wurden folgende Rohstoffe verwendet:

- Glycerin: 99,64 %, $\rho = 1{,}27$ g/cm³, $n_D^{20} = 1{,}4748$; Säuregehalt = 0,0035 %, Feuchtigkeit = 0,3 %;
- DMT: 99,9 %, Säurezahl = 0,07 mgKOH/g; Asche = 0,08 %, flüchtige Bestandteile = 0,01 %;
- Bleiglätte (PbO): 99,5 %, Alkoholysekatalysator;
- Leinöl, Sojaöl und Sonnenblumenöl, deren Eigenschaften in Tabelle 1. angeführt sind.

---

[13] N. A. Ghanem und F. F. Abd El-Mohsen, *J. Paint. Technol.*, **38**, 381 (1966).

[14] N. A. Ghanem und F. F. Abd El-Mohsen, *Paint Technol.*, **30**, 14 (1966).

[15] N. A. Ghanem und F. F. Abd El-Mohsen, *J. Oil Colour Chemists' Assoc.*, **49**, 490 (1966).

[16] N. A. Ghanem und F. F. Abd El-Mohsen, *J. Oil Colour Chemists' Assoc.*, **50**, 441 (1967).

[17] N. A. Ghanem, M. A. El-Azmirly und Z. H. Abd El-Latif, *J. Oil Colour Chemists' Assoc.*, **55**, 114 (1972).

[18] J. Peredi, *Elelmezesi ipar*, **1952**, 244.

[19] T. Pintilie, *Bul. Tehn. Inform. Lab. Centr. Cercet. Lacuri şi Cerneluri, Buc.*, **1**, 39 (1970).

[20] R. H. Runk, *Ind. Eng. Chem.*, **44**, 1124 (1952).

[21] Z. Hippe und W. Mauberg, *Przem. chem.*, **42**, 309 (1963).

[22] D. Feldman, ,,Tehnologia compuşilor macromoleculari'', Ed. Tehn. Buc., 1974, S. 397.

[23] I. Nanu, I. Manoviciu und V. Manoviciu, *Mat. Plast.*, **8**, 305 (1971).

[24] I. Manoviciu, E. Schuster und I. Nanu, *Mat. Plast.*, **11**, 231 (1974).

Tabelle 1

Eigenschaften der verwendeten Öle

Öl	Spez. Gewicht	Brechungs- ind.	Säurezahl	OH-zahl	Jodfarbe	Feuchtigkeit
	g/cm³	n_D^{20}	mgKOH/g		mg I/100 g	%
Lein	0,934	1,4800	0,79	198,44	7,64	0,25
Soja	0,928	1,4725	0,68	196,20	7,73	0,20
Sonnenblumen	0,926	1,4722	0,48	194,32	6,66	0,18

Für die Synthese wurde das Schmelzverfahren verwendet. Die hiefür verwendete entsprechende Apparatur für Polyesterifizierungen wurde mit einer thermostatierten Kolonne (70°) und einem Kratzgerät für die Rücknahme des DMT, welches durch Methanol mitgenommen oder durch Sublimierung sich an der Kolonne absetzt, versehen. Der Abschluß der Glycerolyse wurde durch Löslichkeitsproben des Produktes in Ethanol im Verhältnis 1 : 10[25−28] geprüft.

Der Abschluß der Polykondensationsreaktion wurde durch die gebildete Methanolmenge, sowie Aussehen und Eigenschaften des Harzes bestimmt. Die theoretisch gebildete Menge Methanol wurde berechnet, indem die in allen Fällen möglichen Grenzwerte in Betracht gezogen wurden. Die Ausbeute unter diesen Bedingungen kann mit genügender Genauigkeit im Verhältnis zur gebildeten Methanolmenge berechnet werden. Das so erhaltene Methanol wurde durch Brechungsindex und chromatographische Analyse auf Reinheit geprüft.

Die für die alkydsynthesenverwendeten Rezepte wurden nach der Methode von Patton[29] berechnet. Die diesen Synthesen zu Grunde liegende Idee ist, Produkte mit entsprechenden filmbildenden Eigenschaften zu erzeugen. Um die Vernetzung des Harzes zu verhindern, sowie Lösungen mit viel Festkörper und entsprechender Zähigkeit zu erhalten, mußte die Begrenzung der Molekulargewichte in Betracht gezogen werden. Zu diesem Zweck wurden Rezepte mit einem Überschuß von Polyol verwendet, der die Kette durch OH-Gruppen blockiert und somit gute Bedingungen für die Polykondensation schafft.

Nach Pattons Methode,[29] werden die Werte von R, A_1, A_2 und B_x wie vorher beschrieben,[24] berechnet und dann die Rezepte nach den Angaben der Tabelle 2 ausgearbeitet. Wenn mit Ölen gearbeitet wird, werden die Rezepte nach Daten der Tabelle 3 berechnet. Auf Grund dieser Angaben wurden die Rezepte für 8 Typen fett- und halbfett-ölmodifizierte Terephthalatalkyde mit verschiedenem OH-Überschuß, ausgearbeitet. Für die Synthese wurden diejenigen Rezepte verwendet, die den größten OH-Gruppenüberschuß garantieren, welcher notwendig ist um das Molekulargewicht zu begrenzen und so die Vernetzung der Reaktionsmasse zu verhindern (Tabelle 4).

Tabelle 2

Rezeptberechnung auf Grund von Fettsäuren

	Total Äquivalente zu Beginn der Reaktion	Äquivalentgewicht	Gewicht	Prozentgewicht
	e_0	E	W	$W.\%$
Fettsäure	A_1	E_1	$A_1.E_1$	$A_1.E_1.100/\Sigma X$
DMT	A_2	E_2	$A_2.E_2$	$A_2.E_2.100/\Sigma X$
Polyol	B_x	E_x	$B_x.E_x$	$B_x.E_x.100/\Sigma X$
	1,00		ΣX	100 %

---

[25] W. MÜLLER und K. BERGER, *Plaste u. Kautschuk,* **10**, 632 (1964).

[26] K. M. GOLDBERG, N. M. GELDFANDBENI, M. N. FALKOVICI und N. V. PRILUTSKAJA, *Lakokras. mater. ikh. primen.*, **1960**, 75.

[27] R. S. MCKEE und A. W. E. STADDON, *J. Oil Colour Chemists' Assoc.*, **44**, 77 (1961).

[28] I. MLEZIVA und V. HANZLIK, *Chem. průmysl.*, **4**, 442 (1954) ; **5**, 422 (1955).

[29] T. C. PATTON, ,,Alkyd Resin Technology'', Interscience Publishers, New York, 1962.

Tabelle 3

Rezepteberechnung auf Grund von Ölen

	Total Äquivalente zu Beginn der Reaktion	Äquivalentgewicht	Gewicht	Prozentgewicht
	e_0	E	W	$W.\%$
Öl	A_1	E_u	$A_1.E_u$	$A_1.E_u.100/\Sigma Y$
DMT	A_2	E_2	$A_2.E_2$	$A_2.E_2.100/\Sigma Y$
Polyol	B_x-A_1	E_x	$(B_x-A_1).E_x$	$(B_x-A_1).E_x.100/\Sigma Y$
			ΣY	100 %

Tabelle 4

Synthetisierte Harztypen

Harz Nr.	Öl	Ölgehalt %	OH-Überschuß %	Alkydkonstante K
1	Lein	46,5	26	1,0470
2	Lein	61,5	13	1,0785
3	Soja	46,5	26	1,0470
4	Soja	61,5	13	1,0785
5	Sonnenblumen	46,5	26	1,0470
6	Sonnenblumen	61,5	13	1,0785
7	Soja	46,5	26	1,0470

ERGEBNISSE UND DISKUSSIONEN

In Abbildung 1 und 2 werden die kinetischen Kurven als Umsatz zur Zeit dargestellt. Diese haben das Aussehen typischer Polykondensationskurven. Nach Abschluß der Polykondensationsreaktion wurden die erhaltenen Harze im Vakuum behandelt, um die Reste des nicht reaktionierten DMT zu entfernen, welches eine Trübung der Harze hervorufen würde.

Aus den erhaltenen experimentellen Daten geht hervor:

a) Der Katalysator bestehend aus Bleiglätte (bei der Glycerolyse) und Cd-Acetat (bei der Polytransestherifizierung) wurde aus einer Reihe von vorangegangenen Versuchen mit verschiedenen Katalysationssystemen gewählt. Das oben gewählte Katalysationssystem ermöglicht größere Reaktionsgeschwindigkeiten dank des sich ergebenden größeren synergetischen Effektes. Die gebrauchten optimalen Katalysatormengen sind im Einklang mit denen der Literatur;[13–17.22]

b) Die Reaktionsdauer der Glycerolyse bzw. der Polytransestherifizierung ist größer bei den fetten als bei den halbfetten Alkyden;

c) Die anhand des Methanols berechneten Umsätze sind größer als 90%;

d) Die Glycerolysegeschwindigkeit der Öle ist verschieden, wie aus weiter unten angegebener Reihenfolge zu ersehen ist: Sonnenblumenöl > > Leinöl > Sojaöl. Die erhaltenen Resultate sind im Einklang mit den Literaturangaben,[13,15,30] die dies Phänomen als Kombination zweier Effekte erklären und zwar das der Säurezahl und das der Jodzahl der Öle.

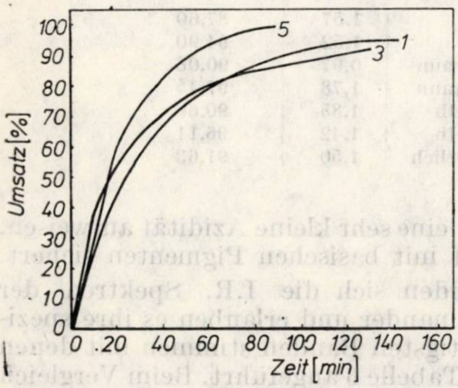

Abb. 1. — Umsatz im Verhältnis zur Zeit für die halbfetten Terephthalatalkydharze (46,5 % Ölgehalt). Die Kurven 1, 3, 5 beziehen sich auf die in Tab. 4 erwähnten Proben.

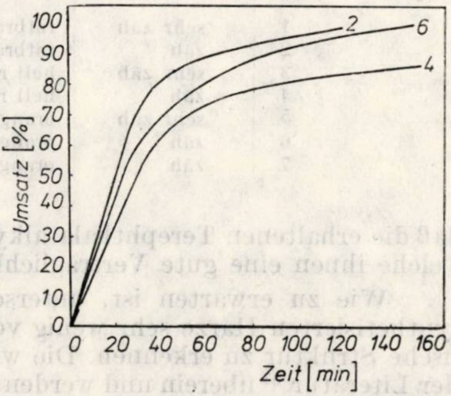

Abb. 2. — Umsatz im Verhältnis zur Zeit für die fetten Terephthalatalkydharze (61,5 % Ölgehalt). Die Kurven 2, 4, 6 beziehen sich auf die in Tab. 4 erwähnten Proben.

Der Effekt der Säurezahl ist größer als der der Jodzahl. Somit verläuft die Glycerolyse des Sonnenblumenöls (halbtrocknendes Öl aber mit kleinerer S.Z.) schneller als die des Leinöls (trocknendes Öl aber mit größerer S.Z.);

e) Die Art des Öls ausgedrückt durch S.Z. und J.Z. beeinflußt auch den Umsatz, so daß die trocknenden Öle größere Ausbeuten in Monoglyzeriden und größere Konversionen gegenüber Methanol geben;

f) Die Behandlung des Harzes im Vakuum beeinflußt auch die Farbe der Produkte, welche eine Nachdunkelung als Resultat der Oxydationsprozesse erleiden. Dieser Effekt kann durch Thermostabilisatoren wie Triphenylphosphit vermindert werden. Letzteres beeinflußt auch die Trockeneigenschaften der aus den synthetisierten Harzen erzeugten Lacke (vergleiche die Lacke 7 und 4 aus Tabelle 7);

g) Um eine entsprechende Farbe des Produktes zu erhalten ist es notwendig auch inertes Gas, sowohl bei der Synthese als auch beim Auflösen des Harzes zu verwenden, sowie die Qualität der benützten Öle zu berücksichtigen.

Einige Eigenschaften der synthetisierten Harze sind in Tabelle 5 angeführt. Die Löslichkeit der erhaltenen Alkyde ist vom aromatischen bzw. aliphatischen Anteil abhängig. Alkyde mit 46,5 % Ölgehalt sind in aromatischen Lösungsmitteln (Toluol, Xylol, Kresole) und solche mit 61,5 % Ölgehalt in Whitespirit löslich. Die halbfetten Alkyde sind sehr zäh, während die fetten flüssigzähen Zustand haben. Es ist zu bemerken,

---

[30] P. K. Kochhar, S. K. Dey und R. K. Bhatnagar, *Indian Oilseeds J.*, **7**, 46 (1963).

Tabelle 5

Einige Eigenschaften der Alkydharze

Harz Nr.	Konsistenz	Farbe	Säurezahl mgKOH/g	OH-Zahl mgKOH/g
1	sehr zäh	rotbraun	1,57	87,60
2	zäh	rotbraun	1,52	94,90
3	sehr zäh	hell rotbraun	0,97	90,08
4	zäh	hell rotbraun	1,78	97,45
5	sehr zäh	orange-gelb	1,85	90,66
6	zäh	orange-gelb	1,42	96,11
7	zäh	orange-rötlich	1,50	91,63

daß die erhaltenen Terephthalatalkyde eine sehr kleine Azidität aufweisen, welche ihnen eine gute Verträglichkeit mit basischen Pigmenten sichert.

Wie zu erwarten ist, unterscheiden sich die I.R. Spektren der synthetisierten Harze sehr wenig voneinander und erlauben es ihre spezifische Struktur zu erkennen. Die wichtigsten Banden stimmen mit denen der Literatur [31] überein und werden in Tabelle 6 angeführt. Beim Vergleich der Spektren geht hervor, daß die Valenzschwingungsbanden $-CH_3$, $-CH_2-$, $-\underset{|}{C}H-$ im Bereich 2800–3000 cm^{-1} der fetten Alkyde an Intensität gegenüber den halbfetten zunehmen (es steigt der Ölgehalt im Alkyd), während die breite OH-Bande bei 3300-3500 cm^{-1} ihre Intensität im Verhältnis zum bleibenden OH-Gehalt im Alkyd, ändert.

Tabelle 6

Charakteristische I.R.-Absorbtionsbanden der Alkyde

Bereich (μm)	Gruppe
2,8–2,95	Hydroxil
3,3–3,4	Kohlenwasserstoff
5,7–5,9	Ester und Säure
6,0–6,75	Aromatischer Kern
6,75–7,5	Aliphatischer Kohlenwasserstoff
7,5–10	Ester
10,0–10,5	trans-Ungesättigte
10,5–14,5	Aromatischer Kern

Um die erhaltenen Harze als Anstrichstoffe zu verwenden, wurden sie bis zu einer standardisierten Zähigkeit verdünnt und mit Pb, Mn und Co sikkativiert.

Aus den so erhaltenen Lacken wurden Filme gebildet, welche auf Trockeneigenschaften (Tabelle 7), physikalisch-mechanische und chemische Eigenschaften hingeprüft wurden. Die physikalisch-mechanischen Bestimmungen sind in den Tabellen 8 und 9 aufgeführt.

---

[31] * * * *Pure Appl. Chem.*, **33**, 411 (1973).

Aus den experimentellen Daten geht hervor:

— Die synthetisierten halbfetten Terephthalatalkyde (1, 3, 5) zeigen sehr gute Staub- und Durchtrocknungsfähigkeit. Außergewöhnlich gut ist das Verhalten des halbfetten Alkyds 1 auf Grund von Leinöl. Der Thermostabilisator (Triphenylphosphit) wirkt sich sehr günstig auf die Trockendauer aus (vergleiche Tab. 7, Versuch 7 thermostabilisiert und 4 unstabilisiert);

— Die synthetisierten Alkyde zeigen sehr gute Dehnungseigenschaften. Dies entspricht einigen Erwartungen betreffend die Verbes-

Tabelle 7

Trocknungsgrad (STAS 2875–51)

Alkydlack	Staubtrocken (Stunden)	Durchtrocknung (Tage)	Bemerkung
1	2	4	—
2	24	8	—
3	4	7	—
4	27	14	—
5	4	7	—
6	36	—	Ofentrocknung
7	24	8	-

Tabelle 8

Einige physikalisch-mechanische Eigenschaften der Filme

Alkydlack	Dornbiegeprüfung (mm) (STAS 2312–51)	Elastizität nach Erichsen (mm) (STAS 3046–52)
1	1	5,5
2	1	4,1
3	1	7,1
4	1	3,6
5	1	4,1
6	1	4,5
7	1	5,4

Tabelle 9

Pendelhärte der Filme

Alkydlack	Härte, in Sek. nach				
	48 h	96 h	120 h	144	336 h
1	100	128	152	170	190
2	26	28	34	34	34
3	30	33	36	36	36
4	29	31	32	34	34
5	38	40	41	42	47
6	29	30	31	31	31
7	24	25	29	29	29

serung der Dehnungseigenschaften durch Einfügen des Terephthalatrestes in die Struktur der Alkyde[5];

— Die Elastizität der so erhaltenen Filme ist gut. Hierbei bemerkt man wieder, daß bei Alkyd 7 diese Eigenschaft besser ist als bei Alkyd 4;

— Die halbfetten Alkyde auf Grund von Soja- und Leinöl (3 undl) zeigen sehr gute mechanische Eigenschaften. Die oben genannten Alkyde haben, wie erwartet, eine größere Härte im Vergleich zu den fetten. Die Härte vom leinölhaltigen Alkyd 1 ist 5—6 mal besser als die der anderen Filme.

Die chemische Beständigkeit der Filme (STAS 2113—70) wurde gegenüber distilliertem Wasser, 3%-iger HCl—, 3%-iger NaOH-Lösung sowie 3,5%-ige Salzlösung bestimmt. Das Verhalten der Filme ist, wie erwartet, im Einklang mit der Struktur der Terephthalatalkyde. Die Filme wurden nur von der alkalischen Lösung angegriffen.

Um die Verwendungseigenschaften der Produkte festzustellen, wurden aus den erhaltenen Lacken, weiße Emaille nach folgender Rezeptur dargestellt: Lack 340 Tl., TiO_2 107 Tl., ZnO 60 Tl., Co-Naphthenat 2,5 Tl. (33%-ige Lösung in Xylol), Pb-Naphthenat 5 Tl. (33%-ige Lösung in Xylol). Für den Vergleich wurde der industriell hergestellte Phthalatemail E 105—1 (60% Leinölgehalt) verwendet. Die dargestellten Emaille wurden hinsichtlich ihrer physikalisch-mechanischen und chemischen Eigenschaften geprüft. In Tabelle 10 sind die physikalisch-mechanischen Eigenschaften angeführt.

Tabelle 10

Physikalisch-mechanische Haupteigenschaften der Filme

Alkydemail / Charakteristik	1	2	3	4	5	6	7	E 105—1
Staubfrei (Std.)	1,45	4,5	3,5	48	3,5	48	3,5	72
Durchtrocknung (Tage)	6	7	6	—	6	—	7	6
Elastizität nach Erichsen (mm)	6,6	6,2	7,0	6,7	7,4	7,8	5,7	6,0
Dornbiegeprüfung (mm)	1	1	1	1	1	1	1	1
Pendelhärte nach 7 Tagen (Sek.)	145	62	58	21	48	45	50	70

Die experimentellen Daten besagen folgendes:

— Im Verhältnis zur Vergleichsprobe besitzen die Terephthalat-Emaille eine bessere Staubtrocknungsfähigkeit und eine vergleichbare Durchtrocknungsfähigkeit. Nur die fetten Terephthalatemaille auf Grund von halbtroknenden Ölen (4-Soja und 6-Sonnenblumen) benötigen Ofentrocknung.

— Die dargestellten Emaille haben bessere Dehnungs- und Elastizitätseigenschaften im Verhältnis zur Vergleichsprobe. Besonders hervorzuheben sind die Emaille 3 und 5 auf Grund von Soja- bzw. Sonnenblumenöl.

— Die Härte der Emailfilme 3—7 ist kleiner als die der Vergleichsprobe. Dies ist auf das jeweils verwendete Öl zurückzuführen. Die Emailfilme auf Grund halbtrocknender Öle (3—7) haben eine kleinere Härte als diejenigen mit trocknenden Ölen (1, 2, E 105—1). Die besten Eigenschaften besitzt der Email der aus halbfettem leinölmodifiziertem Alkyd hergestellt wurde, welches zweimal härter als der industriell hergestellte Email ist.

— Vergleicht man die Härte der auf Grund von Leinöl erzeugten Emaille 1, 2 und E 105—1 so bewahrheitet sich die Abhängigkeit der Härte vom Ölgehalt des betreffenden Harzes. Die Härte steigt in folgender Reihenfolge : 2 < E 105—1 < 1, und in derselben sinkt auch der Ölgehalt, welcher 61,5%, 60% bzw. 46,5% beträgt. Somit gelangt man zu derselben Schlußfolgerung wie auch bei den anderen synthetisierten Harzen (3—7), daß die Härte der Filme mit abnehmendem Ölgehalt steigt.

Die chemische Beständigkeit der Emaille wurde unter denselben Bedingungen wie bei den Lacken getestet und führte zu denselben Schlußfolgerungen.

Bei den Emailfilmen, die durch Spritzen erhalten wurden, bestimmte man auch die Durchschlagfestigkeit. Die Ergebnisse sind in Tabelle 11 angeführt. Aus den gegebenen Daten geht hervor, daß der Terephthalatrest in der Alkydstruktur einen günstigen Einfluß ausübt.

Tabelle 11

Durchschlagfestigkeit der Emailfilme

Alkydemail	1	2	3	4	5	6	E 105—1
Durchschlagfestigkeit kV/mm	22	30	14	20	10	10	11

SCHLUSSFOLGERUNGEN

a) Es wurden 6 verschiedene halbfette- (46,5% Ölgehalt) und fette (61,5% Ölgehalt) Alkyde auf Grund von DMT, Glycerin, Lein-, Soja- und Sonnenblumenöl dargestellt.

b) Die experimentellen Ergebnisse haben gezeigt, daß es möglich ist, die Terephthalsäure für die Synthese der Terephthalatalkyde gänzlich mit DMT zu ersetzen, wodurch mehrere Vorteile erzielt werden.

c) Es wurden eine Reihe von Rezepten für die Synthese der halbfetten und fetten Alkydharze ausgearbeitet, die ausschließlich DMT als Säurekomponente verwenden.

d) Es wurden Terephthalatalkyde bei kurzer Reaktionsdauer mit einem praktisch Null-Säuregehalt erhalten.

e) Die Filmprüfungen der Lacke und Emaille hoben die außergewöhnlichen Eigenschaften des leinölmodifizierten halbfetten Alkyds (1) hervor.

Revue Roumaine de Chimie, 22, 6, 963–964 (1977)

COMPTES RENDUS

G. LIPTAY, "Atlas of thermoanalytical curves", vol. V, Akadémiai Kiadó, Budapest, 1976, 169 p.

The fifth volume of the "Atlas of thermoanalytical curves" includes 92 diagrams for substances, taken under different experimental conditions. The readers will certainly find useful the much more complete information provided for the same material, in many cases, by combining the simultaneous technique with parallel recordings on instruments of other type (Metler, Sartorius, Du Pont). The widespread use of thermoanalytical methods and differences in the instruments required the preparation of standards. The National Bureau of Standards, in co-operation with the Standardization Committee of the International Confederation for Thermal Analysis has recently made standards available ($KClO_4$, K_2SO_4, KNO_3, K_2CrO_4, $SrCO_3$, $BaCO_3$, SiO_2, Ag_2SO_4). It was of course evident to include them into this volume. The standards were tested by complex thermoanalysis completed with micro DTA and DSC or TG, DTG measurements. For these standards the temperature values of peaks are always given, unlike the rest of the materials, in order to help the readers in comparing these results with the data obtained on their own instruments.

D. I. Marchidan

"STRUCTURE AND BONDING", Volume 27, Springer-Verlag, Berlin, Heidelberg, New York, 1976, 220 p.

The volume 27 of Structure and Bonding contains three different article reviews.

The first article review, "Extended Hückel Investigation of Reaction Mechanisms" by M. Simonetta and A. Gavezotti summarizes in 43 pages the recent papers (between 1968–1975) regarding the application of the EHT to various research fields, such as i) different chemical reactions in organic chemistry; ii) the reactions of PH_5 — a covalent compound which does not contain carbon; iii) coordination compounds of the transition metal ions, and iv) the applications to the surface chemistry. Ii is worth mentioning the attention paid by the authors in discussing the last results reported by R. Hoffmann (in organic chemistry, reactions of PH_5, transition metal complexes). The results published by other authors are also discussed. The review is very concise and interesting, clearly exposed and therefore accessible to the readers who want a general view about the recent applications of the EHT. This article review has 50 up-to-data bibliographic quotations.

The second review entitled: "Ligand Field Theory of Metal Sandwich Complexes" is written by K. Warren. It presents in 114 pages, with 180 bibliographic, quotations the present theoretical treatment of the sandwich complexes from the viewpoint of the Ligand Field Theory (L.F.T.). The numerous theoretical and experimental studies devoted to this kind of complexes, known for about 25 years, must be mentioned. These studies have allowed the progress of our knowledge concerning the structure and the chemical bonding in what the coordination compounds is concerned. The history of the theoretical interpretations of the sandwich complexes has known many stages. After a period of pioneering works, it was concluded by 1965 that only the Molecular Orbital Theory should be able to explain in details the structure of these complexes. Then the papers of D.R. Scott and R. S. Becker published after 1965 have revealed that the traditional method of the L.F.T. may be successfully used to interpret the main physico-chemical properties (electronic spectra and magnetic susceptibilities) of the sandwich complexes. Moreover, the adapted L.F.T. was able to predict, in good agreement with the experimental data, the molecular properties of numerous newly-synthesized sandwich compounds. The aim of Warren's article review is to present in the frame of L.F.T. the explanation and especially the interpretation of the electronic spectra and of the "classical" measurements of magnetic susceptibility obtained with these kinds of complexes. An excellent ligand field treatment of the d^x ions in a pseudo-axial symmetry is described. The author's contributions must be mentioned with regard to the $d-d$ transitions in the electronic spectra of the sandwich complexes. The $d-d$ spectra of the $3d^x$, (x= 3 — 8), metallocenes, as well as of the cationic species $Cr(Cp)_2^+$, $Fe(Cp)_2^+$, $Co(Cp)_2^+$ and $Ni(Cp)_2^+$, ($Cp = C_6H_6$), are exhaustively analyzed. The ferrocene, as a classical example, is, of course, studied in all details. The data regarding the bis-arrene complexes, such as $Cr(Bz)_2^+$ and $Cr(Bz)_2$, ($Bz = C_6H_6$), are also presented. The next chapter deals in detail with the magnetic susceptibility of the sandwich complexes. Here are also presented many of the recent works (1974) of the author. After a detailed description of the ESR data a chapter follows devoted to the charge transfer spectra and MO calculations. The reader is familiarized with the most recent results regarding the interpretation of the structure of the sandwich complexes by means of the L.F.T. and MO theory. A new chapter deals with the photoelectron spectroscopy of the sandwich complexes. Only three domains are not treated, namely the vibration spectroscopy, the nuclear resonance spectroscopy and the magnetic circular dichroism. However the review represents a very valuable contribution to the understanding and explanation of one of the newest domains of the coordination chemistry.

The third article review is "Calculation of Molecular Properties Using Force Fields. Applications in Organic Chemistry" by O. Ermer. It contains 50 pages and 113 bibliographic quotations and is divided into two distinct parts. The first one represents a concise theoretical treatment, on 20 pages, of the types of force fields, of the energy minimization techniques as well as of the procedures to fit the force field parameters. The second part presents the various applications, especially those regarding the organic chemistry, with which the author himself is acquainted. These applications are numerous, various and extremely interesting (for instance the calculations of the conformational interconversions). The review represents a useful guide for the physico-chemists who want to apply such calculations to different domains of organic chemistry.

A. C. Banciu

"Topics in Current Chemistry", vol. 61, Physical and Chemical Applications of Dyestuffs. Editors: F. P. Schäfer, H. Gerischer, F. Willig, H. Meier, H. Jahnke, M. Schönborn, G. Zimmermann, 187 p.

Since the first volume of the series was published in 1973, we come now to the 61st of "Topics in Current Chemistry", edited by Springer Verlag. The purpose the editors proposed themselves is to give an outlook of the present position and future trends in modern chemical research to all industrial and research chemists.

Applications of dyes in different fields are presented, four articles making the content of the present volume.

The first to open the series, "Organic Dyes in Laser Technology" by F. P. Schäfer, comes to discuss applications of organic dyes in laser field which have been reported up to present. The term "dye" is used in the context in its broadest meaning, and it is meant to include all organic compounds with conjugated double bonds since the mechanism of their interaction with light always involves the excitation or deactivation of π electrons. Nonlinear absorption of dyes is treated first, followed by the applications making use of this property. Dye lasers are examined next, and finally frequency tripling in dyes is considered.

"Reaction of Excited Dye Molecules at Electrodes" by H. Genscher and F. Willig is discussing redox reactions of excited molecules in electrodes in comparison with reactions in the ground state. Examples for the best studied types of reactions are presented, concerning two cases: semiconductor and insulator electrodes, respectively.

The next paper, "Application of the Semiconductor Properties of Dyes Possibilities and Problems" by H. Meier deals with industrial application of the dark- and photo-conductor properties of organic dyes in connection with their electronic properties. The significance of the semiconductivity of organic dyes and other classes of organic solids is analysed and possible industrial applications of organic semiconductors are proposed.

The final paper of this volume is "Organic Dyestuffs as Catalysts for Fuel Cells" by H. Jahnke, M. Schönborn and G. Zimmermann. Dyestuffs with electrocatalytic properties are discussed and their applications in fuel cells are presented. First, electrochemical aspects of fuel cells are shown and different dyestuffs with electrocatalytic properties are introduced. It is pointed out that from the various classes of dyestuffs only metal chelates are to present electrocatalytic properties. Some experimental results are given, making the basis for a final theoretical discussion of the electrochemical mechanisms in which these dyestuffs are involved.

An author index gives the literature references for the above mentioned papers.

Florian Urseanu

NOTE POUR LES AUTEURS

La Revue Roumaine de Chimie publie des articles en anglais, français, russe, allemand ou espagnol. Les auteurs sont priés d'envoyer des articles et comptes rendus inédits.

Les manuscrits seront dactylographiés à deux intervalles. La bibliographie, les tableaux et la légende des figures seront placés après le texte.

Si l'article fait partie d'une série numérotée, le titre de la partie précédente sera indiqué dans une note au bas de la première page.

Chaque article sera précédé d'un résumé comprenant quinze lignes au maximum.

Les références bibliographiques dans le texte seront faites par des exposants sans parenthèse et paraîtront comme des notes au bas de chaque page.

Les publications périodiques mentionnées dans la bibliographie seront présentées suivant les prescriptions internationales : le nom de l'auteur précédé de l'initiale du prénom, le titre du périodique abrégé conformément à « Chemical Abstracts » et souligné par une ligne, le numéro du tome, indiqué par des chiffres arabes et souligné par deux lignes, suivi de la première page de l'article ; à la fin, l'année de la parution sera placée entre parenthèses. Le numéro de la revue ne sera pas indiqué si les pages du volume sont numérotées consécutivement. Pour les revues dont les tomes ne sont pas numérotés (par ex. Bull. Soc. Chim. France, etc.), l'année de la parution soulignée par deux lignes précèdera l'indication de la page.

Les textes des livres ou traités inclueront : les noms des auteurs, les initiales du prénom, le titre du livre entre guillemets et sans être souligné, le numéro du tome précédé par l'abréviation «vol». (ou «Bd»), le numéro de l'édition, les éditions (the publisher), la localité de la parution du livre, l'année de la parution et la page de la référence précédée (s) par l'abréviation « p » (ou « S »).

Les brevets seront indiqués comme il suit : L'auteur ou la firme, le pays et le numéro du brevet, la date et la revue (Chem. Abstr.). Par ex. : M. Jones (to Union Carbide C^{o}), Brit. Pat. 601 238, 2 Sept. 1959, *Chem. Abstr.*, **54**, 12808 (1960).

Si la référence n'a pas été lue en original, on indiquera aussi la revue de références consultée.

Les diagrammes seront tracés à l'encre de Chine sur papier calque. Les tableaux et les figures (en nombre strictement nécessaire) seront numérotés par des chiffres arabes et leur explication sera donnée dans la légende des figures. Prière de ne pas inscrire les mêmes données dans les tableaux et les figures. Chaque tableau aura un titre. On indiquera dans le texte la place approximative des tableaux et des figures. Les formules chimiques seront incluses dans le texte ; en outre, elles seront transcrites sur papier calque, à l'encre de Chine.

Les auteurs sont priés d'indiquer les caractères italiques (en soulignant les lettres au crayon), ainsi que tout autre caractère spécial ; les préfixes *ortho*, *meta*, *para*, *cis*, *trans*, etc. seront soulignés pour indiquer leurs caractères italiques et ne seront jamais écrits avec des majuscules.

Aucune correction à la main ne sera admise sur le manuscrit. Les corrections seront frappées à la machine. Les lettres grecques ou d'autres symboles spéciaux seront insérés à la main à l'encre clairement.

Le manuscrit sera signé par l'auteur. Le colonne-titre aura 50 lettres au maximum. L'entière responsabilité du contenu des articles appartient aux auteurs.

PRINTED IN ROMANIA

TRAVAUX PARUS AUX ÉDITIONS DE L'ACADÉMIE DE LA RÉPUBLIQUE SOCIALISTE DE ROUMANIE

C. DRĂGULESCU, E. PETROVICI, **Chimie structurală modernă. Chimia coordinanței** (La chimie structurale moderne. La chimie de la coordinence), 1977, 947 p., 70 lei.

I. G. MURGULESCU, **Introducere în Chimia fizică. Vol. I. 1. Atomi, molecule, legătură fizică** (Introduction à la Chimie Physique, Ier vol. 1. Atomes, molécules, liaison chimique), 1976, 560 p., 36 lei.

E. P. BALTĂ, E. BALTĂ, **Introduction to the physical chemistry of the vitreous state**, coédition avec Abacus Press, 1976, 287 p., 31 lei.

H. I. GĂLĂȚEANU, **Radiochimia aplicată. Metode și probleme** (La radiochimie appliquée. Méthodes et problèmes), 1976, 307 p., 19 lei.

CONST. V. UGLEA, **Cromatografia pe gel permeabil. Noi domenii de aplicare** (La chromatographie sur gel perméable. Nouveaux domaines d'application), 1976, 123 p., 6,75 lei.

FRANCISC A. GOTHARD, **Echilibre lichid-vapori. I. Baze teoretice și metode de calcul** (Equilibres liquide-vapeurs. I. Bases théoriques et méthodes de calcul), 1975, 263 p., 2 pl., 28 lei.

CONST. GH. MACAROVICI, D. MACAROVICI, **Chimia oxizilor dubli și utilizările lor** (La chimie des oxydes doubles et leur utilisation), 1975, 195 p., 13 lei.

M. AVRAM, **Antidăunători** (Pesticides), 1974, 496 p., 41 lei.

ELENA CEAUȘESCU, **Research work on synthesis and characterization of macromolecular compounds. Contributions**, 1974, 251 p., 20 lei.

DUMITRU COSTACHE, **Analiza chimică prin metoda cinetică** (L'Analyse chimique par la méthode cinétique), 1974, 251 p., 20 lei.

G. A. RĂDULESCU, **Proprietățile țițeiurilor românești** (Les propriétés des pétroles roumains), 1974, 267 p., 2 pl., 18 lei.

CR. SIMIONESCU, VIORICA RUSAN, V. POPA, **Chimia algelor marine** (La chimie des algues marines), 1974, 212 p., 1 pl., 18 lei. ,

I. ZUGRĂVESCU, MAGDA PETROVANU **Chimia n-ilidelor** (La chimie des n-Ilures), 1974, 348 p., 19 lei.

MARIA FITI, **Dozimetria chimică a radiațiilor ionizante** (La dosimétrie chimique des radiations ionisantes), 1973, 240 p., 13,50 lei.

TIBERIU NĂȘCUȚIU, **Metode radiochimice de analiză** (Méthodes radiochimiques d'analyse), 1973, 384 p., 23 lei.

CRISTOFOR SIMIONESCU, MARGARETA GRIGORAȘ, AGATA CERNĂTESCU-SANDEI, GHEORGHE ROZMARIN, **Chimia lemnului în România. Plopul și salcia** (La Chimie du bois en Roumanie. Le peuplier et le saule), 1973, 299 p., 13 pl., 26 lei.

MIHAI FLORESCU, **Eficiența economică a cercetării științifice** (L'efficience économique de la recherche scientifique), 1972, 115 p., 15 lei.

GEORGETA LĂZĂRESCU, **Sistematizarea informațiilor în chimia organică** (Systématisation des informations en Chimie organique), 1972, 243 p., 1 pl., 10,50 lei.

I. P. I. c. 7107

43426

1978 FEB 16

Lei 25.—

F 1103

REFERÁLVA

ACADÉMIE DE LA RÉPUBLIQUE SOCIALISTE DE ROUMANIE

REVUE ROUMAINE DE CHIMIE

TOME 22
N° 7
Juillet 1977

EDITURA ACADEMIEI REPUBLICII SOCIALISTE ROMÂNIA

Rev. Roumaine Chim.   RECHAX, 22, 7, p. 965–1114 (1977), Bucarest

ACADÉMIE DE LA RÉPUBLIQUE SOCIALISTE DE ROUMANIE

COMITÉ DE RÉDACTION

Rédacteur en chef:

I. G. MURGULESCU, membre de l'Académie de la République Socialiste de Roumanie

Rédacteurs en chef adjoints:

A. T. BALABAN et V. EM. SAHINI, membres correspondants de l'Académie de la République Socialiste de Roumanie

Collège de rédaction:

EM. BRATU, ELENA CEAUȘESCU, ECATERINA CIORĂNESCU-NENITZESCU, C. DRĂGULESCU, CR. I. SIMIONESCU, membres de l'Académie de la République Socialiste de Roumanie; P. SPACU, membre correspondant de l'Académie de la République Socialiste de Roumanie; MARGARETA AVRAM, I. HAIDUC, D. I. MARCHIDAN, I. MOLDOVAN, G. NIAC et D. SĂNDULESCU

La Revue Roumaine de Chimie parait 10 fois par an. Toute commande de l'étranger (fascicules ou abonnements) sera adressée à ILEXIM Departamentul Export-Import Carte/Departamentul Export-Import Presă (Revues), P.O.B. 136–137, Télex 11226, Bucarest, 3, str. 13 Decembrie, Roumanie

Les manuscrits, les livres et les revues proposés en échange, ainsi que toute correspondance seront envoyés à la rédaction
REVUE ROUMAINE DE CHIMIE
23, str. Dumbrava Roșie, Bucarest, Roumanie, téléphone 12 41 60

EDITURA ACADEMIEI REPUBLICII SOCIALISTE ROMÂNIA
125, Calea Victoriei, Bucarest, Roumanie, téléphone: 50 76 80

ORSZÁGOS MŰSZAKI KÖNYVTÁR ÉS DOKUMENTÁCIÓS KÖZPONT 1883

REVUE ROUMAINE DE CHIMIE

Tome 22, N° 7 Juillet 1977

The 75th Anniversary of Professor **C. D. Nenitzescu** 967–968

N. ANGHELIDE, ELVIRA ŞLIAM and D. RĂILEANU, Electron transfer *vs* proton capture in the formation of dienamino esters 969–976

R. BACALOGLU und C. DĂESCU, Nucleophile Substitutionen an Kohlensäurederivaten. X Kinetik und Mechanismus der Hydrolyse von N,N-disubstituierten Thiocarbamidsäure-chloriden 977–985

ALEXANDRU T. BALABAN, Chemical graphs. XXXI. Benzo-homovalenes 987–1001

A. T. BALABAN, ANISIA BOTA, F. CHIRALEU, ELVIRA ŞLIAM, ANA HANEŞ and C. DRĂGHICI, Pyrylium salts formed by diacylation of olefins. XXIII. Isomeric ethyltrimethylpyridines and dimethyl-n-propylpyridines from the diacetylation of hexenes and methylpentenes 1003–1015

M. BANCIU, RODICA VLAD, C. DRĂGHICI and ECATERINA CIORĂNESCU, Carbenium ion reactions. XIV. Solvolysis of "Dibenzobullvalene bromide" 1017–1025

VICTORIA CIURDARU and F. HODOŞAN, Reactions with sodium hydridoborate on silica gel 1027–1035

I. G. DINULESCU, M. S. POP and MARGARETE AVRAM, Investigations in the cyclobutane series. XLV. Dibenzotricyclo[4.3.1.0 ^{2,5}]decadiene system. Behaviour and retrorearrangement into dibenzo-$(CH)_{10}$ Nenitzescu's hydrocarbon derivatives 1037–1043

V. DRĂGUŢAN, LIGIA STĂNESCU and ALICE MARIE GLATZ, Aluminium chloride catalyzed reactions of unsaturated acids with benzene. X. Reaction of cyclohexylidene- and 1-cyclohexenylacetic acids 1045–1052

IOSIF DRIMUŞ and M. TRIFAN, Oxidation of n-dodecanitrile in liquid state with molecular oxygen, in the presence of pseudo-homogeneous catalysts. I. Peroxides, acids and esters concentration 1053–1059

L. ENESCU and MARGARETA AVRAM, Investigations in the cyclobutane series. XLIV. Ring contraction of 8-diazo-*exo*-benzo[*c*]tricyclo[4.2.1.0 ^{2,5}] non-3-en-7-one on photolysis 1061–1067

M. D. GHEORGHIU, A model of the transition state in the cycloaddition of ketene to acetylene 1069–1074

S. MAGER and I. HOPÂRTEAN, Infrared, ^1H-NMR and mass spectra of some triphenylmethane derivatives 1075–1083

Rev. Roumaine Chim. **22**, 7, p. 965–1114 (1977), Bucarest

DOINA OȘIANU, ELENA NICOARĂ and C. BODEA, Inchain-Epoxides of carotenoids. V. Canthaxanthin-11,12-epoxide and 9,12-furanoid oxide . 1085–1088

LUMINIȚA PÂRVULESCU and M. D. GHEORGHIU, Synthesis of bicyclo [3.2.1]octane derivatives *via* Makosza reaction 1089–1095

I. I. SCHIKETANZ, ANA HANEȘ and ILEANA NECȘOIU, Étard reaction. XI. Oxidation of dibenzo[*c*, *g*]bicyclo[4.2.0]octa-3,7-diene with chromyl chloride 1097–1103

CR. I. SIMIONESCU, SVETLANA DUMITRESCU, V. PERCEC and M. GRIGORAȘ On the polymerization of acetylenic derivatives. XXXII. Heats of *cis-trans* isomerization of polyacetylene isomers 1105–1109

M. VLASSA and F. HODOȘAN, Amidation with bis-(α-aryliminobenzyl)-disulphides 1111–1114

SEVENTY-FIVE YEARS SINCE THE BIRTHDAY OF *COSTIN D. NENITZESCU*

This issue of *Revue Roumaine de Chimie* contains papers dedicated to the seventy-fifth anniversary of C. D. Nenitzescu's birthday.

The activity of C. D. Nenitzescu (born July 2/15, 1902; deceased July 28, 1970), the best-known Romanian organic chemist, included scientific achievements (e.g. the Nenitzescu indole syntheses, the Nenitzescu $(CH)_{10}$ hydrocarbon), technological advances (catalysts for low-pressure polyethylene, new processes for organic chemicals), teaching duties (his treatises of Organic Chemistry and General Chemistry are still used by students in Romania and abroad), and organizational duties (creation of the first chemical research institutes, directing the chemistry section of the Romanian Academy, editor of this journal).

The reader may find extensive information about the biography and scientific activity,[1–18] as well as about the chemical impact[19–56] of C. D. Nenitzescu's scientific output in the following selected bibliography.

[1] * * * *Rev. Chim. Acad. R.P. Roumaine*, **7**, 651 (1962).

[2] * * * *Angew. Chem. Nachr. Chem. Tech.*, **10**, 200 (1962).

[3] * * * *Scinteia*, **39**, N° 8500 of 29 July 1970.

[4] G. Bogza, *Contemporanul*, N° 1238 of 31 July 1970; "Paznic de far", Editura Minerva, București, 1974, p. 328; *Tribuna*, 10 February 1977.

[5] G. Rădoi, *România Literară*, **32**, 6 August 1970.

[6] * * * *Rev. Roumaine Chim.*, **15**, N^{o} *8*, I (1970); *Studii și Cercetări Chim. Acad. R.S. România*, **18**, N^{o} *8*, I (1970).

[7] * * * *Revista de Chimie* (*Bucharest*), **21**, 383 (1970).

[8] * * * *Contemporanul*, N° 1249 of 16 October 1970.

[9] * * * *Revista "Ing." (Inst. Politehnic Bucharest)*, N° 11–12, 8 (1970).

[10] B. Timm, *Angew. Chem.*, **82**, 381 (1970).

[11] F. Runge, *Jahrber, Sächs. Akad. Wiss. Leipzig.*, 1969/70 (1972) 281.

[12] M. Avram, *Studii și Cercetări Chim. Acad. R.S. România*, **19**, 583 (1971); *Rev. Roumaine Chim.*, **16**, 959 (1971); *Chem. Ber.*, **104**, XVII (1971).

[13] S. Ifrim, *Comun. Şt. Inst. Pedag. Univ. A. I Cuza (Iași)*, 515 (1971).

[14] R. Huisgen, *Jahrbuch* **1971** *der Bayerischen Akad. Wiss.*, 221 (1971).

[15] P. F. G. Praill, *Chem. Brit.*, **7**, 252 (1971).

[16] A. T. Balaban, *Scinteia*, **46**, Nr. 9196 of 2 July 1972.

[17] A. T. Balaban, *Analele Academiei R. S. România*, Ser. IV, **104** (XX), 226 (1976).

[18] * * * J. C. Poggendorff-Redaktion , "Biographisch-Literarisches Handwörterbuch der exakten Naturwissenschaften", Band VIIb.

[19] P. Karrer, "Kurzes Lehrbuch der organischen Chemie", 3. Aufl., Leipzig, 1933, S. 738.

[20] G. Kränzlein, "Aluminiumchlorid in der organischen Chemie", 3. Aufl., Verlag Chemie, Berlin, 1939.

[21] C. A. Thomas, "Anhydrous Aluminium Chloride in Organic Chemistry", Reinhold Publ. Corp., New York, 1941.

[22] S. L. Friess and R. Pinson, *J. Amer. Chem. Soc.*, **73**, 3512 (1951).

[23] H. H. Inhoffen und E. Prinz, *Chem. Ber.*, **87**, 684 (1954).

[24] W. C. Sumpter and F. M. Miller, in "The Chemistry of Heterocyclic Compounds" (A. Weissberger, Ed.), Vol. 8, Wiley-Interscience, New York, 1954.

[25] H. L. Lochte and E. R. Littmann, "The Petroleum Acids and Bases", Constable, London, 1955.

[26] J. E. Gowan and T. S. Wheeler, "Name Index of Organic Reactions", Longmans Green and Co., London, 1960, p. 179, 180.

[27] G. W. Griffin and D. V. Veber, *Chem. and Ind.*, 1162 (1961).

[28] Y. Yukawa and T. Hanafusa, *J. Chem. Soc. Japan*, **82**, 1563 (1961).

[29] R. Criegee, *Ref. Chim. Acad. R. P. Roumanie*, **7**, 771 (1962).

[30] H. Krauch und W. Kunz, "Namenreaktionen der organischen Chemie", 2. Aufl., A. Hüthig Verlag, Heidelberg, 1962, S. 327, 328.

[31] R. Criegee, *Bull. Soc. chim. France*, **1965**, 1.

[32] G. Domschke, *Z. Chem.*, **6**, 41 (1966) ; *Studii şi Cercetări Chim. Acad. R.S. România* **14**, 673 (1966).

[33] W. von E. Doering and J. W. Rosenthal, *J. Amer. Chem. Soc.*, **88**, 2078 (1966).

[34] J. Hanuise et R. R. Smolders, *Bull. Soc. chim. France*, 2139 (1967).

[35] J. Yanez, *Dissert. Abstr.*, **28**, 854–B (1967).

[36] M. P. Cava and M. J. Mitchell, "Cyclobutadiene and Related Compounds", Academic Press, New York, 1967.

[37] W. von E. Doering and J. W. Rosenthal, *Tetrahedron Letters*, 349 (1967).

[38] * * * "The Merck Index", Merck and Co., Rahway, N. J., 8th Ed., 1968, p. 1195.

[39] A. Albert, "Heterocyclic Chemistry", 2nd Ed., The Athlone Press, London, 1968, p. 240.

[40] G. R. Allen Jr. and M. J. Weiss, *J. Org. Chem.*, **33**, 198 (1968).

[41] R. Littell, G. O. Morton and G. R. Allen Jr., *Chem. Commun.*, 1144 (1969).

[42] G. Maier, *Chem. Ber.*, **102**, 3310 (1969).

[43] R. J. Sundberg, "The Chemistry of Indoles", Academic Press, New York, 1970, p. 171.

[44] J. F. Poletto and M. J. Weiss, *J. Org. Chem.*, **35**, 1190 (1970).

[45] U. Kuckländer, *Tetrahedron Letters*, 157, 2093 (1971).

[46] U. Kuckländer, *Arch. Pharm.*, **304**, 602 (1971).

[47] F. Eiden und U. Kuckländer, *Arch. Pharm.*, **304**, 57 (1971).

[48] G. A. Olah, Preface to "Carbonium Ions", Vol. 3, Interscience, New York, 1971.

[49] U. Kuckländer, *Tetrahedron*, **28**, 5251 (1972).

[50] G. A. Olah, *J. Amer. Chem. Soc.*, **94**, 808 (1972).

[51] R. M. Roberts, *Intra-Science Chem. Reports*, **6**, 89 (1972).

[52] G. R. Allen Jr., "The Synthesis of 5-Hydroxyindoles by the Nenitzescu Reaction" *Org. Reactions*, **20**, 337 (1973).

[53] U. Kuckländer, *Tetrahedron*, **29**, 921 (1973).

[54] G. Maier, *Angew. Chem.*, **86**, 491 (1974).

[55] E. Vedejs and E.S.C. Wu, *J. Amer. Chem. Soc.*, **97**, 4706 (1975).

[56] T. W. Wickersham, J. P. Li and E. J. Warawa, *Synthesis*, **1975**, 399.

Revue Roumaine de Chimie, **22**, 7, 969–976 (1977)

Dedicated to the 75th anniversary of
Prof. C.D.NENITZESCU'*s birthady (1902–1970)*

ELECTRON TRANSFER *vs* PROTON CAPTURE IN THE FORMATION OF DIENAMINO ESTERS

N. ANGHELIDE, ELVIRA ŞLIAM and D. RĂILEANU *
Organic Chemistry Center, Bucharest 15, C.P. 2322

Received February 5, 1977

The reaction of the dimedone monoenamine **13** with acetylenedicarboxylic ester (**3a**) was carried out at room temperature in DMSO as a solvent. Competition occurred between nucleophilic addition and a ionic (2 + 2) cycloaddition with intermediate formation of a cyclobutene adduct **16**. The first mechanism gave the *s-cis*-dienamino este *Z*–**15** while the condensed "push-pull cyclobutene" **16** underwent ring-expansion with formation of a cyclooctadienone (**17**). The electron transfer inside the zwitterion **14** was possible owing to the fact that proton capture was made difficult by the existence of strong hydrogen-bonding with the negative end of the DMSO molecules. Evidence is presented which eliminates the possibility of a concerted $(2\pi_s + 2\pi_a)$ cycloaddition in which the acetylenic ester would play the antarafacial role.

In the first paper of this series [1] the mechanism of the addition of enamino esters **1** and **2** to acetylenic esters **3** with formation of dienamino esters (**6**–**10**) was described as occurring through the intermediate of the zwitterion **4** formed by a head-to-tail attachment. In the case of nontertiary enamino esters a 1,5-proton transfer occurred as an intermediate stage. The tertiary enamino esters, where such transfer was not possible, cyclized to a cyclobutene intermediate **5** which further stabilized itself by conrotatory ring opening or possibly by a push-pull heterolytic cleavage. In the latter case ($\mathbf{R'} \neq \mathbf{H}$) an aprotic zwitterion intermediate could be trapped by a 1,4-dipolar cycloaddition [2] to an electrophilic dipolarophile **3a** and formation of a benzene nucleus (**12**). In fact as it turned out from NMR analysis and comparison with model compounds the trapped dipole was **11**, resulted from the ring-opening of the intermediate cyclobutene adduct **5** rather than the primary zwitterion **4**. Cisoid conformations **7** and **8** are the characteristic feature of the acetylenedicarboxylic ester adducts.

---

* To whom correspondence should be addressed.

[1] N. ANGHELIDE, C. DRĂGHICI and D. RĂILEANU, *Tetrahedron*, **30**, 623, (1974).

[2] R. HUISGEN, *Z. Chem*, **8**, 290, (1968).

More recently an analogous reaction pattern has been described by Schug and Huisgen.[3] The zwitterionic intermediate of the (2+2) cycloaddition of TCNE to vinyl ether was cyclized to a four-membered ring adduct, trapped by 1,4-dipolar cycloaddition or stabilized by alcohol addition.

CHART I*

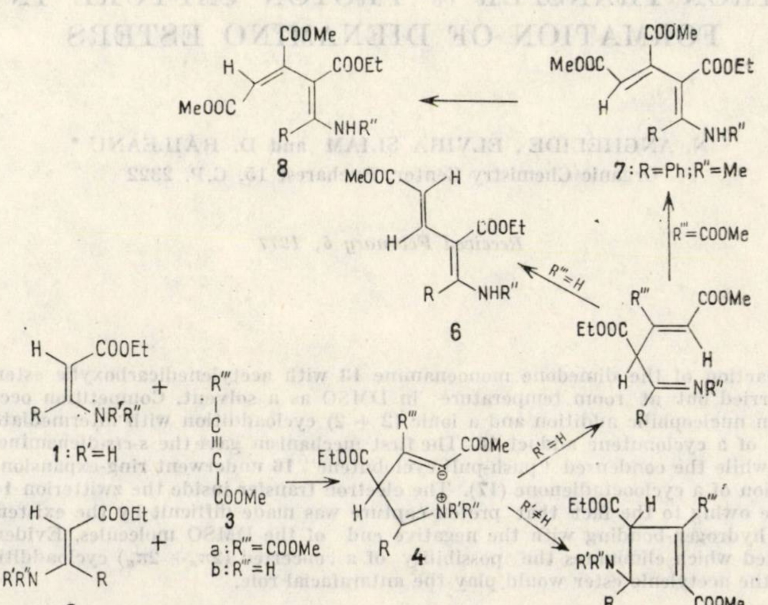
COOMe
H
COOEt
MeOOC
R
NHR″
8
COOMe
MeOOC
COOEt
H
R
NHR″
7 : R=Ph; R″=Me
MeOOC
H
COOEt
H
R
NHR″
6
R‴=COOMe
R‴=H
R‴
COOMe
EtOOC
H
H
NR″
R
H
COOEt
R
NR′R″
1 : R′=H
R‴
C
C
COOMe
3
a : R‴=COOMe
b : R‴=H
H
COOEt
R′R″N
R
2
a : R=Ph; R′R″=−(CH₂)₄−
b : R=Ph; R′R″=−(CH₂)₂−
R‴
EtOOC
COOMe
H
NR′R″
R
4
R′=H
R′≠H
EtOOC
H
R‴
R′R″N
R
COOMe
5
R‴=H
R‴=COOMe
H
COOEt
R
COOMe
NR′R″
11
COOEt
H
H
R
COOMe
NR′R″
H
COOMe
EtOOC
R′R″N
COOMe
R
10 : R=Ph
R′R″=−(CH₂)₄−
−HNR′R″
3a
COOEt
MeOOC
COOMe
R
12
EtOOC
H
COOMe
H
R
NR′R″
9

* The R symbols are not explicated in this general scheme except for the compounds which are directly implied in the present work. R may be generally considered as being alkyl or aryl. For details see ref. [1] Benzene was the solvent throughout.

[3] R. Schug and R. Huisgen, *Chem. Comm.*, **1975**, 60.

In the present paper we wish to describe an interesting case of electron transfer *vs.* proton capture, [4] namely the competition between the 1,5-proton transfer earlier described [1] and the formation of a cyclobutene as second step of the ionic (2+2) cycloaddition. That was made obvious by using the cyclic primary monoenamine of dimedone **13** whose unstable cyclobutene adduct **16** expands itself into a cyclic eight-membered enamino ketone (**17**)[5,6] which provides unambiguous proof for the path followed, being easily distinguishable from the head-to-tail attachment product. The reaction between **13** and **3a** was carried out at room temperature in DMSO which appears to be a better hydrogen-bond acceptor than most solvents. The reaction product was formed by fairly equal amounts of the head-to-tail adduct **15** and the cyclooctadienone **17.** Although it has been generally found that proton transfers take place at diffusion controlled rates, when the destruction of electric charge involves hydrogen-bond breaking, this takes place not without an important amount of energy, required to reorganize solvent molecules. This might be of the order of 10 kcal/mole or more, [7] therefore an appreciable contribution to the free energy of activation. The fact that (2+2) cycloaddition competes very effectively with proton transfer suggests strong hydrogen-bonding between DMSO and the immonium hydrogens of **14**.

CHART II

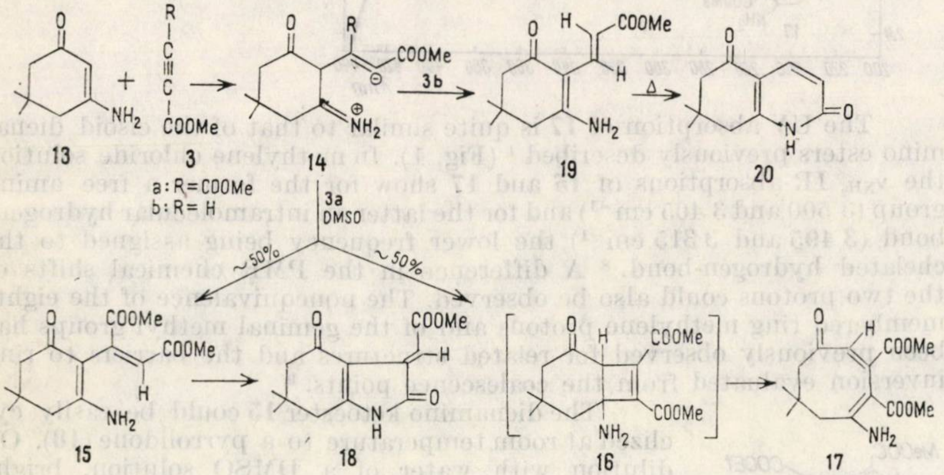

To our knowledge this is the first case of an intramolecular 1,5-prototropic shift competed by electron transfer with formation of a new bond and completion of a cyclobutene ring.

---

[4] R. D. GUTHRIE, *Intra-Sci-Chem. Rep.*, **7**, 27 (1973).

[5] K. BRANNOCK, R. BURPITT, V. GOODLETT and J. THWEATT, J. Org. Chem. **28**, 1464 (1963).

[6] C. HUEBNER, L. DORFMAN, M. ROBINSON, E. DONOGHUE, W. PIERSON and P. STRACHAN, *ibid.*, **28**, 3134 (1963).

[7] E. F. CALDIN, *J. Chem. Soc.*. **1959**, 3345.

The electrocyclic opening of ring-condensed cyclobutenes would be extremely difficult because the constraint imposed by the four-carbon bridge does not permit a thermal and conrotatory ring-opening. The readiness with whom the reaction takes place can be explained by the "push-pull cyclobutene" structure involved whose substituents at the 3- and 4-positions are electron-donating and-withdrawing respectively. Heterolytic cleavage thus becomes possible.

The structures of **15** and **17** are based on spectral data and chemical behaviour.

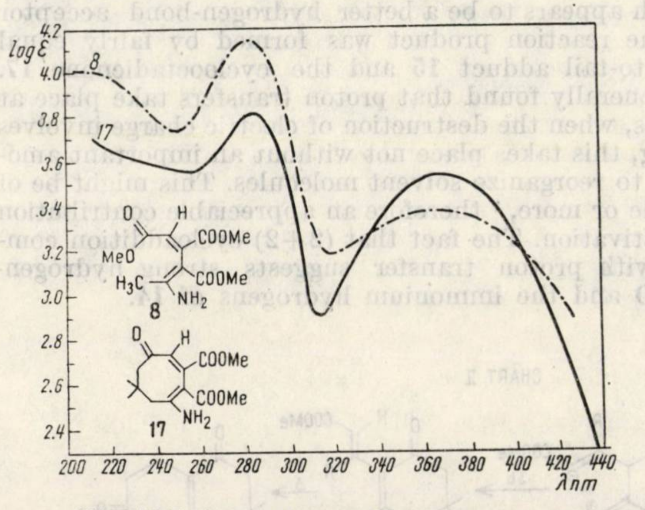

Fig. 1. — UV spectra of cyclooctadienone **17** and of *s-cis*-dienamino ester *Z,E*—**8** (R = Me ; R″ = H).

The UV absorption of **17** is quite similar to that of the cisoid dienamino esters previously described [1] (Fig. 1). In methylene chloride solution the ν_{NH_2} IR-absorptions of **15** and **17** show for the former a free amino group (3 500 and 3 405 cm^{-1}) and for the latter an intramolecular hydrogen-bond (3 495 and 3 315 cm^{-1}) the lower frequency being assigned to the chelated hydrogen-bond. [8] A difference in the PMR chemical shifts of the two protons could also be observed. The nonequivalence of the eight-membered ring methylene protons and of the geminal methyl groups has been previously observed for related structures and the barriers to ring inversion evaluated from the coalescence points. [9]

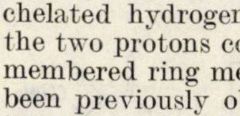

21

a: R=Me; R′=H
b: R=Ph; R′=H
c: R=Ph; R′=Me

The dienamino ketoester **15** could be easily cyclized at room temperature to a pyrrolidone (**18**). On dilution with water of a DMSO solution, bright yellow crystals separated of the tetrahydrooxindole derivative **18**. Huebner *et al.* [6] were able to perform this cyclization only in the case of one enamino ketone adduct. Attempts with adducts of anilinocrotonic ester were unsuccessful. In order to determine the scope of the reaction several cisoid dienamino esters : **7** and **8** (R=Me and Ph ; R″=H) were cyclized in the same conditions as for **18** and the corresponding pyrrolidones **21** were obtained. [§] Spectral data are given in table 2.

---

[8] A. Gomez-Sanchez, A. M. Valle and J. Bellanato, *J. Chem. Soc., Perkin Trans. 2*, **1973**, 15.

[9] E. J. Cone, R. H. Garner and A. Wallace Hayes, *Tetrahedron Letters*, **1972**, 57.

The reaction of the dimedone monoenamine **13** with propiolic ester, as expected, took place less readily because of the lower electrophilicity of **3b**. Heating on a steam bath for several hours was necessary and as a result the enamino ketoester **19** was obtained as sole reaction product. The energy furnished by the increase in temperature seems to compensate solvent reorganization imposed by breaking of the hydrogen-bonds. The structure of **19** is the result of 1,5-proton transfer inside **14** ($R'''=H$). It could be cyclized by a moderate thermal reaction to the tetrahydroquinolone **20**. It is worth mentioning that for the dienamino esters of type **6** with an internal hydrogen-bond, previously described,[1] in order to achieve cyclization to the corresponding pyridones, heating under reflux in DMFA or even heating at 180—190° in a Carius tube was necessary, while **19** underwent rapid cyclization by simple heating to its melting point. This fact reconfirms the importance of hydrogen-bonding which has to be taken into account in **6** but not in **19**.

Concerning the formation of the cyclobutene intermediates **5** and **16** one should also take into consideration the possibility of a $(2\pi_s + 2\pi_a)$ concerted cycloaddition where the acetylenic ester would play the antarafacial role in the same way as ketenes in their cycloaddition to olefins. This concerted cycloaddition is supposed to occur with nonsynchronous bond formation[10] and regioselectivity is expected in a head-to-tail manner as predicted by the perturbation theory [11].

In order to furnish more evidence for the described mechanism of cycloaddition *via* dipolar ions the dependence of the reaction upon solvents and substituent effects were taken into consideration. The stereoselectivity, which is observed in the formation of dienamino esters, does not necessarily imply a concerted mechanism. [12] On the other hand, isomerization to the more stable isomer *via* imino-enaminic tautomerism or immonium type resonance reduces at a minimum the possibility of a retention of configuration.

Solvent dependence was emphasized by NMR controlled experiments. In chloroform solution after 24 hours at room temperature no reaction occurred between **13** and **3a** while in benzene solution at reflux only proton capture took place with the cyclization of the intermediate cisoid dienamino ester **15** to the corresponding pyrrolidone derivative **18** which was isolated from the reaction mixture.

Substituent effect dependence was observed by the cycloaddition of the N-methyl derivative of **13** [13] which has one single hydrogen atom bonded to DMSO, therefore, a smaller probability of proton capture. The evolution of the reaction was followed by NMR and an almost exclusive formation of the corresponding cyclooctadienone was observed, i.e. a strongly reduced proton transfer owing to the hydrogen-bonding by the solvent. Similar results were obtained with HMPT.

[§] Very probably the addition of water, which forms strong hydrogen-bonds, liberates the NH_2 group which becomes able to lactamize the neighbouring ester group.

[10] R. W. Holder, *J. Chem. Educ.* **53**, 81, (1976).

[11] N. D. Epiotis *J. Amer. Chem. Soc.*, **95**, 5624 (1973).

[12] P. D. Bartlett, *Quart. Rev.*, **24**, 473 (1970).

[13] J. Goerdeler and V. Keuser, *Chem. Ber.*, **97**, 2209, (1964).

To substantiate our rationale further evidence was provided by the study of reactivity of enamino esters with various degrees of charge separation as reflected in the PMR chemical shifts of the vinylic proton. That may be considered as a measure of the nucleophilic reactivity of the α-carbon though a correlation cannot be expressed, but only a general tendency.

The 3-pyrrolidinocinnamic ester (**2a**) reacted at room temperature with **3a** according to the scheme shown in Chart I. That was in accordance with its good charge-separation and nucleophilic reactivity for which the chemical shift of the α-H is indicative ($\delta = 4.55$). The structure of the resulted product corresponds to *s-cis*-(*E*, *E*) — **10**. Its configuration can be deduced from the NMR spectrum which exhibits a strong shielding effect exerted by a noncoplanary phenyl group on the vicinal carbomethoxy group in the *cis* position. The chemical shift of the vinylic hydrogen indicates a *trans* configuration of the ester groups.

Both isomers of the aziridinocinnamic ester **2b** did not react with **3a** although the reaction conditions were varied as regards both solvent and temperature. That was in accordance with the reduced nucleophilicity of the α-position as expressed by the chemical shifts of the α-H in the two isomers : $\delta_E = 5.26$ and $\delta_Z = 5.46$ ppm.

To end with, we should point out that only the lack of solubility of the dimedone monoenamine in benzene which was the usual solvent, has brought to our attention the above described solvent effect of DMSO.

EXPERIMENTAL PART

NMR spectra were recorded on a Varian A60-A spectrometer with TMS as internal standard. UV spectra were measured with a Specord Carl Zeiss-Jena instrument and IR spectra with a UR-20 Carl-Zeiss-Jena spectrometer.

Characterization, purification, yields and analyses of all new compounds are given in table 1.

Table 1

Characterization of new compounds

	Yield %	Recrystallization solvent	m.p.°C	Calcd. %			Found %		
				C	H	N	C	H	N
15	35	C_6H_6	137	59.77	6.81	5.04	60.01	6.90	5.50
17	27	C_6H_6	223	59.77	6.81	5.04	59.92	6.99	5.04
18	100 (from **17**)	C_6H_6	180	62.70	6.10	5.57	62.64	6.07	5.61
19	86	CH_3CN	202	64.55	7.67	6.27	64.20	7.50	6.15
20	100	CH_3CN	289	69.10	6.85	7.32	69.34	7.02	7.53
7	88	*n*-heptane	73	62.24	6.09	4.21	62.30	6.27	4.21
21a	80	CCl_4	142	55.22	5.48	5.85	55.26	5.63	5.91
21b	60	CCl_4	136	63.78	5.02	4.65	63.94	5.21	4.62
21c	75	$C_6H_6-C_6H_{12}$	129	64.43	5.43	4.44	64.50	5.45	4.37
2a	67	C_6H_{12}	54	73.44	7.80	5.71	73.18	7.74	5.85
10	80	*n*-heptane	115	65.10	6.50	3.63	65.28	6.69	3.58

3-Amino-5,5-dimethyl-2-cyclohexen-1-one (**13**) was prepared as described in literature.[14]

Dimethyl 3-amino-5,5-dimethyl-7-oxo-2,8-cyclooctadiene-1,2-dicarboxylate (**17**). Equivalent amounts of the enamino ketone **13** (2.8 g) and **3a** (2 ml) in DMSO (40 ml) were kept at room temperature for 24 hr. After removal of the solvent *in vacuo* (2 mm Hg) at a temperature below 60°, the residue was triturated with ethyl alcohol, when compound **17** crystallized (m.p. 220°, 1.5 g). UV $\lambda_{\max}^{\mathrm{EtOH}}$ mμ (log ε): 367.6 (3.52), 284 (3.80); IR cm^{-1} (CH_2Cl_2): 3495 and 3315 (chelated NH_2), 1730 (unchelated ester-CO), 1685 (chelated ester-CO); NMR δ(Py-d_5): 1.0 and 1.15 (singlets, 6, gem-CH_3), 2.2 and 2.65 (AB system, J = 13 cps, 2, 4−CH_2), 2.2 and 3.06 (AB system, J = 11.5 cps, 2, 6−CH_2), 3.76 and 3.81 (singlets, 6, COOMe), 6.83 (t, J = 1.5 cps, 8-CH), 8.40 and 9.80 (broadened singlets, 2, unchelated and chelated NH_2-protons).

Dimethyl (3-amino-5,5-dimethyl-1-oxo-2-cyclohexen-2-yl)-maleate (**15**). The mother liquors of **17** on dilution with water gave 2 g of **15**, m.p. 133−135°. UV $\lambda_{\max}^{\mathrm{EtOH}}$ mμ(logε); 353 (3.63), 272 (3.88); IR cm^{-1} (CH_2Cl_2): 3500 and 3405 (unchelated NH_2), 1730 (unchelated ester-CO); NMR δ ($CDCl_3$): 1.08 (s, 6, gem−CH_3), 2.23 and 2.40 (singlets, 4, CH_2), 3.74 and 3.82 (singlets, 6, COOMe), 5.26 (broadened singlet, 2, NH_2), 6.10 (s, 1, ω−H).

Methyl 4,5,6,7-tetrahydro-6,6-dimethyl-2,4-dioxo-$\Delta^{3,\alpha}$-indolineacetate (**18**) Dienamine **15** (1.4 g) was dissolved in the minimum amount of DMSO (about 10 ml) and the solution was diluted dropwise with water. Compound **18** separated quantitatively as beautiful bright yellow crystals with m.p. 178−180°. UV $\lambda_{\max}^{\mathrm{EtOH}}$ mμ (log ε): 347 (3.74), 274(3.84); IR cm^{-1}(CH_2Cl_2): 3430 (NH), 1740, 1670, 1655, (CO); NMR δ ($CDCl_3$−DMSO-d_6): 1.15 (s, 6, gem-CH_3), 2.28 and 2.55 (singlets, 4, CH_2), 3.81 (s, 3,COOMe), 7.10 (s, 1, vinyl-H), 9.90 (broadened singlet, 1, NH).

18 *and* **17** *from* **13**. Equivalent amounts of **13** (1.4 g) and **3a** (1.5 ml) were dissolved in DMSO (15 ml) and the solution was kept at room temperature for 24 hr. The reaction mixture was diluted with water and a mixture of about equal amounts of **17** and **18** (about 2 g) separated. By recrystallization from EtOH, **17** was obtained (0.7 g) and by dilution with water of the filtrate **18** separated (0.8 g, crude).

Methyl Z,Z-4-carbethoxy-3-carbomethoxy-5-methylamino-5-phenyl-2,4-pentadienoate (**7**) was obtained according to the previously described method[1]. UV $\lambda_{\max}^{\mathrm{EtOH}}$ mμ (log ε): 389 (3.44), 264 (3.90); IR cm^{-1} (CCl_4): 3250 (chelated NH), 1730 (ester-CO), 1665 (chelated ester-CO); NMR δ ($CDCl_3$): 1.23 (t, 3, $COOCH_2CH_3$), 2.70 (d, J = 5.5 cps, 3, N−CH_3), 3.53 and 3.70 (singlets, 6, COOMe), 4.16 (q, 2, $COOCH_2CH_3$), 5.30 (s, 1, vinyl-H), 7.30 (s, 5, Ph), 9.90 (broadened singlet, 1, NH).

Ethyl 4-carbomethoxymethylene-4,5-dihydro-2-methyl-5-oxo-1H-pyrrole-3-carboxylate (**21a**), *Ethyl 4-carbomethoxymethylene-4,5-dihydro-5-oxo-2-phenyl-1H-pyrrole-3-carboxylate* (**21b**), *Ethyl 4-carbomethoxymethylene-4,5-dihydro-1-methyl-5-oxo-2-phenyl-1H-pyrrole-3-carboxylate* (**21c**). The same cyclization method was used as for obtaining **18** from **15**. The starting materials were the corresponding cisoid dienamino esters from which only **7** had not been described before.[1] The spectral data are given in table 2.

Table 2

Spectral Data of Compounds 21

	UV $\lambda_{\max}^{\mathrm{EtOH}}$ mμ (log ε)	IR cm^{-1}		NMR (δ)					
		CO	NH_2	vinyl-H	COOEt q	COOEt t	COOMe s	R	R′
21a	370 (3.52), 246 (3.91)	1740 1710	3430	7.15	4.30	1.35	3.86	2.50 (s, 3)	9.20 (s, 1)
21b	390 (3.74), 273 (4.07)	1740 1710	3430	7.30	4.21	1.17	3.80	7.55 (m, 5)	9.30 (s, 1)
21c	388 (3.52), 266 (3.96)	1735 1715	—	7.34	4.03	0.98	3.93	7.48 (m, 5)	2.90 (s, 3)

---

[14] a) F. Zymalkowski and H. Rimek, *Arch. Pharm.*, **294**, 759 (1961); b) D. L. Ostercamp, *J. Org. Chem.*, **35**, 1632 (1970).

Methyl E-3-(3-amino-5,5-dimethyl-1-oxo-2-cyclohexen-2-yl)-δ-acrylate (**19**). Almost stoichiometric amounts of **13** (4 g) and **3b** (2.5 ml) were heated in DMFA (50 ml) on a steam bath for 5–6 hr. After removal of the solvent at reduced pressure (30 mm Hg), distilled water (about 100 ml) was added to the residue when crude **19** separated (5 g) with m.p. 195–197°. IR cm^{-1} (CH_2Cl_2) : 3505 and 3410 (unchelated NH_2), 1710 (unchelated ester-CO), 1645 (CO); NMR δ (DMSO-d_6) : 1.0 (s, 6, gem-CH_3), 2,13 and 2.40 (singlets, 4, CH_2), 3.66 (s, 3, COOMe), 6.8 (d, 1, ω-H), 7.63 (d, 1, α–H), $J\alpha,\omega$ = 16cps, 7.65 (broadened singlet, 2, NH_2).

*7,8-Dihydro-7,7-dimethyl-2,5(1*H, *6*H)*-quinolinedione* (**20**). The crude dienamine **19** was heated up to its melting point when resolidification occurred and the quinolinedione **20** was quantitatively formed (m.p. 286–288°) IR cm^{-1} (CH_2Cl_2) : 3370 (NH), 1680 and 1660 (CO); NMR δ (DMSO-d_6) : 1.09 (s, 6, gem-CH_3), 2.33 and 2.70 (singlets, 4, CH_2), 6.2 (d, 1, 3–H), 7.8 (d, 1, 4–H), $J_{3,4}$ = 9.5 cps, 12.0 (broadened singlet, 1, NH).

Ethyl E-3-pyrrolidino-cinnamate (**2a**). Ethyl benzoylacetate (19 g, 0.10 moles) and pyrrolidine (8.5 g, 0.12 moles) in benzene (250 ml) were refluxed in the presence of a small amount of *p*-toluenesulfonic acid with azeotropic removal of the water until 2 ml were collected. The cooled reaction mixture was washed with aqueous $NaHCO_3$ and water and subsequently dried over Na_2SO_4. After removal of the solvent the product was distilled *in vacuo* (b.p. $_{0.2}$ =165–167°). On cooling the product crystallized (16 g). UV λ_{max}^{EtOH} mμ (log ε) : 291 (4.33); IR cm^{-1} (CCl_4) : 1698 (ester-CO); NMR δ (CCl_4) : 1.05 (t, 3, $COOCH_2CH_3$), 3.80 (q, 2, $COOCH_2CH_3$), 1.82 and 3.05 (multiplets, 8, pyrrolidine protons), 4.55 (s, 1, α–H), 7.20 (m, 5, Ph).

Ethyl E,E-*3,4-dicarbomethoxy-5-phenyl-5-pyrrolidino-2,4-pentadienoate* (**10**). In 50 ml of benzene 6 g of **2a** and 3.5 ml of **3a** were added and the solution was kept over night at room temperature. The solvent was removed *in vacuo* and the residue was triturated with petroleum ether when an orange solid crystallized (7.75 g) with m.p. 110–112°. UV λ_{max}^{EtOH} mμ (logε) : 401 (3.70), 314 (3.95); NMR δ ($CDCl_3$) : 1.10 (t, 3, $COOCH_2CH_3$), 1.90 and 3.20 (multiplets, 8, pyrrolidine protons), 3.45 and 3.80 (singlets, 6, COOMe), 4.13 (q, 2, $COOCH_2CH_3$), 6,46 (s, 1, 2–H), 7.40 (m, 5, Ph).

Ethyl 3-aziridino-cinnamate (**2b**). To 16 g (0.1 moles) of methyl phenylpropiolate in 50 ml of dry ether, 5 g (0.11 moles) of aziridine were added and the reaction mixture left to stay for 24 hr at room temperature. After removal of the ether the reaction product was a mixture of the two isomers (*E* : 2p and *Z* : 1p). After a fractionation attempt on a Vigreux column the proportion between isomers remained unchanged (b.p.$_{3-4}$: 143–145°). *Found* : C, 70.97; H, 6.72; N, 6.60. *Calcd.* for $C_{12}H_{13}NO_2$: C, 70. 93; H, 6.70; N, 6.84 %. UV λ_{max}^{EtOH} mμ (logε) : 274 (4.12). IR cm^{-1} (CCl_4) : 1718. NMR δ (CCl_4) : 1.90 and 2.15 (singlets, 4 + 4, CH_2), 3.47 and 3.62 (singlets, 3 + 3, COOMe), 5.26 and 5.46 (singlets, 1 + 1, α–H) for the *E*-and *Z*-isomers respectively, 7.3 (m, 5, Ph).

Revue Roumaine de Chimie, 22, 7, 977–985 (1977)

Dedicated to the 75th anniversary o
Prof. C. D. NENITZESCU'*s birthday (1902–1970)*

NUCLEOPHILE SUBSTITUTIONEN AN KOHLENSÄURE-DERIVATEN. X[1]

KINETIK UND MECHANISMUS DER HYDROLYSE VON N,N-DISUBSTITUIERTEN THIOCARBAMIDSÄURE-CHLORIDEN

R. BACALOGLU und C. DĂESCU
Laboratorium für organische Chemie der Technischen Hochschule ,,Traian Vuia"
Str. Bocşa 6 Timişoara

Eingegangen am 19. Mai 1976

Die Kinetik der Hydrolyse von N, N-disubstituierten Thiocarbamidsäure-chloriden in wäßrigem Aceton wurde durch potentiometrische und Leitfähigkeitsmessungen bestimmt. Im langsamen Schritt der Reaktion findet eine monomolekulare Dissoziation statt. Die gebildeten N, N-disubstituierten Thiocarbamidsäuren zersetzen sich zu COS, das langsam durch eine Kinetik zweiter Ordnung zu H_2S hydrolysiert.

Die nucleophilen Substitutionsreaktionen an Carbamid- und Thiocarbamidsäure-chloride wurden relativ wenig studiert, obzwar der elektronenabstoßende Effekt des an die Carbonylgruppe gebundenen Stickstoffatoms voraussichtlich interessante Auswirkungen auf die Reaktivität haben kann.

Im Falle der Hydrolyse des N,N-Dimethyl-carbamidsäure-chlorids in Wasser, Aceton-Wasser und Dioxan-Wasser, wurde ein monomolekularer Mechanismus gefunden.[2–5] Dieser Reaktionsmechanismus erwies sich als allgemein für die Substitution durch schwache Nucleophile (z.B. die sauerstoffhaltigen) und wurde von uns durch das Studium der Hydrolyse und Alkoholyse einer großen Anzahl von N,N-disubstituierten Carbamidsäure-chloriden bestätigt.[6]

Im Falle der stärkeren Nucleophile (z. B. aliphatische Amine) wurde durch Hall für das N,N-Dimethyl-carbamidsäure-chlorid ein bimolekularer Mechanismus ermittelt.[7]

---

[1] R. BACALOGLU, T. KORODI, A. FLORESCU und G. OSTROGOVICH, *Rev. Roum. Chem.*, unter Druck.

[2] H. K. HALL, *J. Amer. Chem. Soc.*, **77**, 5993 (1955).

[3] H. K. HALL und C. H. LUECK, *J. Org. Chem*, **28**, 2818 (1963).

[4] I. UGI und F. BECK, *Chem. Ber.*, **94**, 1829 (1963).

[5] A. QUEEN, *Canad J. Chem.*, **45**, 1619 (1967).

[6] R. BACALOGLU, C. DĂESCU und G. OSTROGOVICH, *J. Chem. Soc. Perkin II. Trans.*, **1972**, 1011.

[7] H. K. HALL, *J. Org. Chem.*, **29**, 3539 (1964).

Das schwächer nucleophile Pyridin reagiert hingegen in polaren nichtprotischen Lösungmitteln mit dem N,N-Dimethyl-carbamidsäurechlorid über einen monomolekularen Mechanismus. [8]

Für die N-monosubstituierten- im Vergleich zu den N,N-disubstituierten Carbamidsäure-chloriden wurde eine wesentliche Mechanismusänderung bei der Reaktion mit Nucleophilen festgestellt. So reagieren die N-Aryl-carbamidsäure-chloride mit den aromatischen Aminen über einen E_2-Mechanismus. Im langsamen Schritt der Reaktion bildet sich das entsprechende Isocyanat durch Abspalten von HCl. [9]

Die Einführung des Schwefelatoms anstatt des Carbonyl-Sauerstoffatoms in die Aryl-chloroformiate führt nicht zur Änderung des bimolekularen Mechanismus der Hydrolyse und Alkoholyse. Die Reaktionsgeschwindigkeit verkleinert sich wesentlich, das sowohl einem enthalpischen (wahrscheinlich durch die kleinere Polarität der $C=S$ Bindung als die der $C=O$ Bindung) als auch einem entropischen Effekt (durch das etwas größere Volumen des S-Atoms als das des O-Atoms) zuzuschreiben ist.[10-12]

Die Alkyl-thiolchloroformiate hydrolysieren in Wasser über einen monomolekularen Mechanismus, [13] der auch im Falle der Alkyl-dithiochloroformiate beibehalten wird.[14]

In der vorliegenden Arbeit wurde die Hydrolyse der N,N-disubstituierten Thiocarbamidsäure-chloride zur Erläuterung ihres Reaktionsmechanismus studiert.

ERGEBNISSE

Durch die Hydrolyse der N,N-disubstituierten Thiocarbamidsäurechloride in wäßrigem Aceton konnten als einzige Reaktionsprodukte die entsprechenden Aminchlorhydrate und H_2S isoliert werden. Die Chlorhydrate wurden durch Vergleichen ihrer IR-Spektren mit denen autentischer Proben indentifiziert. Die Bildung des Chloridions und des H_2S während der Reaktion, wurde mit Hilfe selektiver Cl^- und S^{2-} Elektroden verfolgt.

Die Kinetik der Hydrolyse der N,N-disubstituierten Thiocarbamidsäure-chloride wurde durch Leitfähigkeitsmessungen bestimmt. Die Reaktionsgeschwindigkeitskonstanten erster Ordnung sowie die scheinbaren Aktivierungsparameter sind in Tab. 1 eingetragen.

Die durch kontinuierliche potentiometrische Messungen der Cl^--Konzentration im Falle der Hydrolyse des N,N-Dimethyl-carbamidsäurechlorids erhaltenen Reaktionsgeschwindigkeitskonstanten und scheinbaren Aktivierungsparameter sind aus Tab. 2 ersichtlich.

---

[8] S. L. Johnson und K. A. Runeon *J. Phys. Chem.*, **68**, 3149 (1964).

[9] R. Bacaloglu und C. A. Bunton, *Tetrahedron*, **29**, 2725 (1973).

[10] G. Ostrogovich, C. Csunderlik und R. Bacaloglu, *J. prakt. Chem.*, **317**, 62 (1975).

[11] C. Csunderlik, R. Bacaloglu und G. Ostrogovich, *J. prakt. Chem.*, **317**, 73, 81 (1975).

[12] C. Csunderlik, R. Bacaloglu und G. Ostrogovich, *Bull. șt. și tehn. al I.P.T. Seria Chimie*, **19**, 27 (1974).

[13] A. Queen, T. A. Nour, M. N. Paddon-Row und K. Preston, *Canad. J. Chem.*, **48**, 522 (1970).

[14] D. M. Mc Kinnon und A. Queen, *Canad. J. Chem.*, **50**, 1401 (1972).

Tabelle 1

Geschwindigkeitskonstanten und scheinbare Aktivierungsparameter der durch Leitfähigkeitsmessungen verfolgten Hydrolyse der N,N-disubstituierten Thio-carbamidsäure-chloride in Aceton-Wasser (70:40=V/V)

Nr.	Verbindung	t °C	$k \cdot 10^3$ sec^{-1}	$\Delta H^{\neq}$ kcal/M	$\Delta S^{\neq}$ cal/M·grd	σ^{*15}	$E_s{}^{15}$	pK_a R_2NH
1	Me_2NCSCl	5	1,03					
		10	2,02					
		15	3,45	17,1	−10,4	0,00	0,00	10,73[16]
		20	4,58					
		25	10,97					
		30	13,90					
2	Et_2NCSCl	0	1,79					
		5	3,69					
		10	6,44	19,7	−1,0	−0,10	−0,07	11,04[17]
			7,14					
		15	11,25					
		20	21,30					
3	Pr_2NCSCl	5	1,95					
		10	4,35	23,2	12,7	−0,115	−0,36	11,00[18]
		15	8,72					
		20	11,90					
4	iBu_2NCSCl	−5	1,82					
		0	2,37	12,8	−23,1	−0,125	−0,93	10,91[19]
		10	5,76					
		15	10,42					
5	$(CH_2)_5NCSCl$	0	2,89					
		5	5,94	15,6	−12,7	—	—	11,123[20]
		10	7,52					
		15	14,70					
			17,30					
		20	22,06					
6	$O(C_2H_4)_2NCSCl$	5	0,96					
		10	1,57					
		15	3,63	23,0	10,1	—	—	8,39[21]
			4,03					
		20	6,16					
7	PhMeNCSCl	15	0,36					
		20	0,55	16,5	−17,1	0,60	−2,55	4,85[22]
		25	0,97			0,00	0,00	
8	PhEtNCSCl	15	0,56					
		20	1,04	22,5	4,8	0,60	−2,55	5,12[19]
		25	2,20			−0,10	−0,07	
		30	4,04					

---

[15] N. B. CHAPMAN und J. SHORTER, „Advances in Linear Free Energy Relationships" Plenum Press, London, 1972, S. 76.

[16] H. S. HARVED und B. B. OWEN, *J. Amer. Chem. Soc.*, **52**, 5079 (1930).

[17] W. C. SOMMERVILLE, *J. Phys. Chem.*, **35**, 2412 (1931).

[18] G. GIRAULT-VEXLEARSKI, *Bull. Soc. Chem. France*, **1956**, 589.

[19] N. F. HALL und M. R. SPRINKLE, *J. Amer. Chem. Soc.*, **54**, 3469 (1932).

[20] R. G. BATES und V. E. BOWER, *J. Res. Nat. Bur. Stand.*, **57**, 153 (1956).

[21] A. R. INGRAM und W. F. LUDER, *J. Amer. Chem. Soc.*, **64**, 3043 (1942).

[22] A. L. BACARELLA, E. GRUNWALD, H. P. MARSHALL und E. L. PURLEE, *J. org. Chem.*, **20**, 747 (1955).

Tabelle 2

Durch potentiometrische Methoden bestimmte Geschwindigkeitskonstanten erster Ordnung und scheinbare Aktivierungsparameter der Hydrolyse des N,N-Dimethyl-thiocarbamidsäure-chlorids in Aceton-Wasser (70:30=V/V)

t °C	$k \cdot 10^3$ sec^{-1}	$\Delta H^{\ddagger}$ kcal/M	$\Delta S^{\ddagger}$ cal/M.grd K
5	1,13	18,9	−3,80
10	2,17		
15	3,63		
20	5,79		
25	13,42		

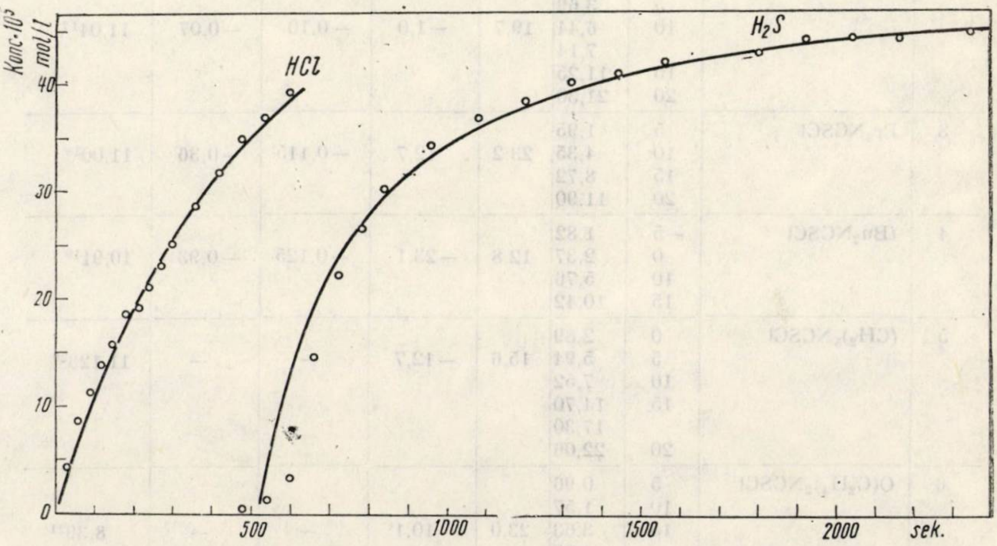

Abb. 1. —Die Veränderung der Konzentration der HCl und H_2S mit der Zeit für die Hydrolyse der N, N-Dimethyl-thiocarbamidsäure-chloride (10°, Aceton : Wasser = 70 : 30 V/V).

Sowie es leicht bemerkbar ist, sind die durch Leitfähigkeits- und durch potentiometrische Messungen erhaltenen Konstanten innerhalb der Fehlergrenze der Bestimmungen gleich. Dies beweist eindeutig, daß durch die Leitfähigkeitsmessungen die Cl^--Bildung verfolgt wurde. Durch den Vergleich der durch die beiden Methoden erhaltenen scheinbaren Aktivierungsparameter kann man auf die Größenordnung des Fehlers dieser Parameter-Bestimmungen schließen.

Das Abspalten des H_2S ist eine der Cl^--Eliminierung folgende Etappe. In Abb. 1 wurde die Zeitabhängigkeit der Konzentration der sich durch die Hydrolyse des N,N-Dimethyl-thiocarbamidsäure-chlorids in wäßrigem Aceton (30 : 70 = V/V) bei 10° gebildeten Cl^- und S^{2-} Ionen dargestellt

Die im Falle der Hydrolyse des N,N-Dimethyl-thiocarbamidsäurechlorids in Aceton-Wasser vorgenommenen quantitativen Interpretierungsversuche der S^{-2}-Konzentrationsänderung in der Zeit, führten zu den besten Ergebnissen wenn man eine Induktionszeit und die Reaktionsordnung 2 annimmt. Die so erhaltenen Reaktionsgeschwindigkeitskonstanten sind aus Tab. 3 ersichtlich.

Tabelle 3

Durch potentiometrische Messungen bestimmte Geschwindigkeitskonstante zweiter Ordnung und scheinbare Aktivierungsparameter der S^2-Bildung durch die Hydrolyse des N,N-Dimethyl-thiocarbamidsäure-chlorids in Aceton-Wasser (70:30=V/V)

t °C	Induktionszeit sec.	*k* l. $sec^{-1}M^{-1}$	$\Delta H^{\ddagger}$ kcal/M	$\Delta S^{\ddagger}$ cal/M grd K
5	900	0,44	13,0	−9,18
10	522	0,87		
20	378	1,62		

Sowie aus Tab. 4 folgt, wird die Geschwindigkeit der Cl^--Bildung im Falle der Hydrolyse des N,N-Dimethyl-thiocarbamidsäure-chlorids beträchtlich von der Polarität des Lösungsmittels beeinflußt.

Tabelle 4

Durch Leitfähigkeitsmessungen bei 10° bestimmte Reaktionsgeschwindigkeitskonstanten erster Ordung der Hydrolyse des N,N-Dimethyl-thiocarbamidsäurechlorids in wäßrigem Aceton von verschiedenen Konzentrationen

Wasserkonzentration		E_T^*	$k \cdot 10^3$ sec^{-1}
% Vol.	M/l		
5	3,520	48,3	0,043
10	7,020	50.3	0,223
20	13,940	52,2	1,75
30	20,740	53,3	13,89

*aus l.c. [23]

DISKUSSIONEN

Die für die Hydrolyse der N,N-disubstituierten Thicarbamidsäurechloride gefundenen Aktivierungsentropien sind im allgemeinen größer als die im Falle der entsprechenden Carbamidsäure-chloride. Dies weist ebenfalls auf einen monomolekularen Reaktionsmechanismus hin. Im langsamen Schritt der Reaktion bilden sich Cl^--Ionen.

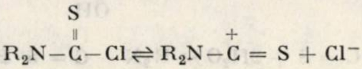

$$R_2N-\overset{\overset{S}{\|}}{C}-Cl \rightleftharpoons R_2N-\overset{+}{C}=S+Cl^-$$

Das Studium der induktiven, mesomeren und sterischen Effekte der Reste (R) bestätigt diesen Mechanismus.

Eine Taft-Korrelation (15° Nr. 1—4, 7, 8 aus Tab. 1) führt zur folgenden Gleichung :

$$\log k = 2{,}401 - 1{,}730 \sum\sigma^* + 0{,}002 \sum E_s \; (r = 0{,}996)$$

Sowie es leicht bemerkbar ist, wird die Reaktionsgeschwindigkeit von den elektronenabstoßenden Substituenten (*R*) beschleunigt, während der Einfluß der sterischen Hinderung praktisch unbedeutend ist. Der Vergleich der im Falle des Pyperidin- und des Morpholinderivates erhaltenen Reaktionsgeschwindigkeitskonstanten (Nr. 5 und 6 aus Tab. 1) führt zum selben Schluß.

---

[23] Ch. Reinhard und K. Dimroth, *Fortschr. Chem. Forsch.*, **11**, 1 (1968).

Die aromatischen elektronenanziehenden Reste (R) verkleinern durch ihren mesomeren Effekt die Elektronendichte am Stickstoffatom und so die Stabilität des sich bildenden Kations. Dies führt zur Verminderung der Reaktionsgeschwindigkeit (Nr. 7, 8 aus Tab. 1).

Es erscheint nun wahrscheinlich, eine gute Korrelation der Logarithmen der Reaktionsgeschwindigkeitskonstanten und der pK_a-Werte der den N,N-disubstitutierten Thiocarbamidsäure-chloriden entsprechenden sekundären Amine zu finden. Diese Korrelation führt zur unteren Gleichung:

$$\log k = 0{,}219\, pK_a - 4{,}384 \quad (r = 0{,}967)$$

Wie es zu erwarten war, wird die Geschwindigkeit der Ionisierung von der steigenden Polarität des Lösungsmittels stark vergrößert. Die in Tab. 4 dargelegten Ergebnisse erlauben gute Korrelationen der Geschwindigkeitskonstanten mit dem E_T-Parameter und dem Logarithmus der Wasserkonzentration:

$$\log k = 0{,}488\, E_T - 28{,}05 \qquad (r = 0{,}986)$$

$$\log k = 3{,}160 \log [H_2O] - 6{,}211 \qquad (r = 0{,}987)$$

Ebenfalls gut korrelierbar sind die in vergleichbaren Reaktionsbedingungen erhaltenen Geschwindigkeitskonstanten der Hydrolyse der N,N-disubstituierten Carbamidsäure-chloride $(k^{\circ})^6$ und der entsprechenden N,N-disubstituierten Thiocarbamidsäure-chloride (k^S):

$$\log k^S = 0{,}724 \log k^{\circ} + 0{,}673 \qquad (r = 0{,}993)$$

Dies entspricht der Annahme eines gemeinsamen monomolekularen Reaktionsmechanismus. [6]

Als nächste Etappe folgt eine schnelle Reaktion des Kations mit dem Wasser:

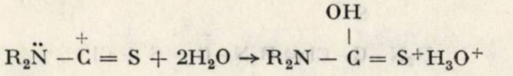

$$R_2\ddot{N} - \overset{+}{C} = S + 2H_2O \rightarrow R_2N - \overset{\overset{\displaystyle OH}{|}}{C} = S + H_3O^+$$

Die so gebildeten Thiocarbamidsäuren sind unbeständig.

Die Zersetzung der N,N-disubstituierten Carbamidsäuren [24] sowie der N,N-disubstituierten Dithiocarbamidsäuren [25] führt zu CO_2 und H_2S und ist in der Literatur beschrieben. Diese Reaktionen sind allgemein säurekatalysiert.

---

[24] D. De Filippo und F. Devillanova, E. F. Trogu und G. Verani, *Gazz. chim. Ital.*, **104**, 1227 (1974).

[25] D. De Fillipo, P. Deplano, F. Devillanova, E. F. Trogu und G. Verani, *J. Org. Chem.*, **38**, 560 (1973).

Aus den in der Literatur angegebenen Daten kann man die Geschwindigkeitskonstanten zweiter Ordnung der Zersetzung des $(CH_2)_5NCSSH$ als $2{,}5 \cdot 10^2$ l/M sec. [25] und des $(CH_2)_5$ NCOOH als $7 \cdot 10^8$ l/M sec. [25]. annehmen, obzwar das Lösungsmittel (Wasser-Methanol verschiedener Konzentration) nicht das gleiche mit dem von uns verwendeten ist. Selbst bei großer Fehlergenze legt diese Annäherung den Schluß nahe, daß die Geschwindigkeitskonstante der Zersetzungsreaktion der disubstituierten Thiocarbamidsäuren viel größer als die von uns ermittelte sein muß (Tab. 3). Es folgt, daß die schnelle nächste Etappe, deren Geschwindigkeit nicht bestimmt wurde, die unten angegebene ist :

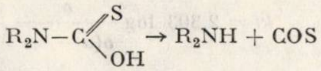

$$R_2N{-}C(=S)OH \rightarrow R_2NH + COS$$

Durch Messen der Bildungsgeschwindigkeit des H_2S, wurde eigentlich die Kinetik der Hydrolyse des COS studiert.

$$COS + H_2O \xrightarrow{R_2N_2HCl} CO_2 + H_2S$$

Diese Etappe ist wahrscheinlich die langsamste des ganzen Reaktionssystems. Sie scheint durch das Aminchlorhydrat katalysiert zu werden und hat dadurch eine Kinetik zweiter Ordnung. Eingehendere Studien dieser Reaktion wurden nicht unternommen.

BESCHREIBUNG DER VERSUCHE

SUBSTANZEN

Die N, N-disubstituierten Thiocarbamidsäure-chloride wurden nach bekannten Verfahren (Chlorierung der N, N-Tetraalkyl-thiuram-disulfide [26] oder Thiophosgenierung der entsprechenden Amine [27]) hergestellt sowie in einer vorhergehenden Arbeit gezeigt wurde.[28] Die erhaltenen Produkte wurden i. Vak. destilliert und IR-spektroskopisch auf Reinheit geprüft.[28]

Aceton (pa) wurde über K_2CO_3 getrocknet und destilliert.

KINETISCHE MESSUNGEN

Die Leitfähigkeitsmessungen wurden in einer mit Rührer und Thermometer vorgesehenen und an einen Leitfähigkeitsmesser (Radelkis Typ OK 102/1) angeschlossenen, thermostatierten Zelle durchgeführt. Im Falle der potentiometrischen Bestimmungen haben wir uns einer, der oberen ähnlichen Meßtechnik bedient, nur war die Zelle mit einer Kalomel-Elektrode und einer spezifischen Cl^-- bzw.S^{2-}- Elektrode ausgestattet und an ein Präzisionspotentiometer (Radelkis OP-205) angeschlossen. Die spezifische Cl^- -Elektrode (Radelkis OP—Cl—7111c) wurde mit einer Me_2NH_2Cl-Lösung in Aceton-Wasser (70 :30 = V/V) geeicht, wobei eine relativ gute lineare Abhängigkeit des gemessenen Potentials von dem Logarithmus der Cl^--Konzentration (im Bereich $0-6.10^{-3}$M/l) gefunden wurde. Um die Diffusion der Cl^-- Ionen aus der Kalomel-Elektrode zu vermeiden wurde zwischen ihr und dem Meßsystem eine Agar-agar Brücke mit KNO_3 als Elektrolyt gelegt.

Die spezifische S^{2-}- Elektrode (Radelkis OP—S—7112 D) wurde ebenfalls in Aceton-Wasser (70 : 30 = V/V) bei den Bestimmungstemperaturen mit einem Na_2S und H_2SO_4 Gemisch (M/M) geeicht. Da für den gesuchten Konzentrationsbereich ($0-6{,}10^{-3}$ M/l) die Abhängigkeit des Potentials von dem Logarithmus der S^{2-}-Konzentration nicht linear war, wurde eine Etalonierungskurve verwendet.

---

[26] G. H. Gashovn, W. Lewis, E. Jaul und. E. J. Ritter, *Org. Synth.*, **35**, 55 (1955).

[27] O. Bitter, *Ber. dtsch. chem. Ges.*, **20**, 1629, 1893 (1887), **26**, 1686 (1893).

[28] C. Dăescu und R. Bacaloglu, *Bull. şt. şi tehn. al I.P.T. Seria Chimie* 1976 (unter Druck).

Um die kinetischen Bestimmungen durchzuführen, wurde das Lösungsmittel in die Zelle und das in Aceton gelöste Thicarbamidsäurechlorid in ein dünnwandiges Reagenzglas eingeführt. Zum Zeitpunkt Null wurde dieses Reagenzglas durchstochen, und die Reaktion durch zeitweiliges Messen der Leitfähigkeit bzw. des Potentials verfolgt. Die Geschwindigkeitskon tanten wurden aus Daten der Leitfähigkeitsmessugen durch graphische Darstellung errechnet,

$$kt = 2{,}303 \log \frac{\Lambda_\infty - \Lambda_0}{\Lambda_\infty - \Lambda_t}$$

Die Reaktion blieb erster Ordnung bis zu Konversionen von 85 bis 95%.

Im Falle der potentiometrischen Messungen, wurden zuerst die Cl^- -Konzentrationen zu verschiedenen Zeitpunkten errechnet und die Geschwindigkeitskonstanten durch die graphische Methode bestimmt.

$$kt = 2{,}303 \log \frac{a}{a(a - c_t)}$$

Die Reaktionsordnung blieb bis zu Konversionen von 85–95% erhalten. Zur Berechnung der Reaktionsgeschwindigkeitskonstanten zweiter Ordnung im Falle der S^{2-} -Bildung fand ebenfalls die graphische Methode Verwendung.

$$k(t - t_i) = \frac{c_t}{a(a - c_t)}$$

wobei a und c_t die Konzentration des Thiocarbamidsäure-chlorids zum Zeitpunkt Null und die Konzentration des H_2S zum Zeitpunkt t darstellen.

In den Tabellen 5–7 sind die berechneten Daten für die Reaktionen des N, N-Dimethylthiocarbamidsäure-chlorids in wäßrigem Aceton (30 : 70 = V/V) bei 10° angegeben.

Tabelle 5

Rechenbeispiel der Geschwindigkeitskonstante erster Ordnung der durch Leitfähigkeitsmessungen verfolgten Hydrolyse des N,N-Dimethyl-thiocarbamidsäure-chlorids in Aceton-Wasser (70:30=V/V) bei 10°
$ClSCNMe_2 = 3{,}24 . 10^{-3}$ M/l
$\Lambda_\infty = 480$; $\Lambda_\circ = 10$

Zeit sec.	$\Lambda_t . 10^6$ Ω^{-1}	$\log \frac{\Lambda_\infty - \Lambda_\circ}{\Lambda_\infty - \Lambda_t}$
90	105	0,098
120	135	0,134
150	160	0,167
180	183	0,202
210	205	0,234
240	220	0,249
270	235	0,283
300	250	0,310
330	270	0,350
360	280	0,371
420	300	0,416
480	325	0,482
540	340	0,526
600	355	0,575
660	370	0,630
720	385	0,694
780	395	0,743
840	405	0,797
900	413	0,846
1 120	427	0,948
1 200	444	1,116

$k = (2{,}017 \pm 0.023) . 10^{-3}\ \mathrm{sec}^{-1}$.
$(r = 0{,}997)$

Tabelle 6

Rechenbeispiel der Geschwindigkeitskonstante erster Ordnung der durch potentiometrische Messungen verfolgten Hydrolyse des N,N-Dimethyl-thiocarbamidsäure-chlorids in Aceton-Wasser (70:30=V/V) bei 10° $ClCSNMe_2 = 5{,}340 . 10^{-3}$ M/l

Zeit sec.	V mV	$c_{HCl} . 10^4$ M/l	$\log \frac{a}{a - c_{HCl}}$
0	131,2	0,0	0,000
30	87,0	4,3	0,037
60	72,7	8,6	0,076
90	65,0	11,3	0,103
120	59,5	13,7	0,130
150	55,7	15,7	0,150
180	52,7	18,5	0,180
210	50,2	19,2	0,196
240	48,2	21,1	0,220
270	46,4	23,3	0,250
300	44,8	25,2	0,267
360	42,0	28,8	0,338
420	40,0	31,9	0,395
480	38,2	35,0	0,462
540	37,0	37,0	0,515
600	35,8	39,3	0,598
	28,7	53,4	—

$k = 2{,}171 + 0{,}025) . 10^{-3}\ \mathrm{sec}^{-2}$ $(r = 0{,}997)$

Tabelle 7

Rechenbeispiel der Geschwindigkeitskonstante zweiter Ordnung der Bildung des H_2S durch die Hydrolyse des N,N-Dimethyl-thiocarbamidsäure-chlorids in Aceton-Wasser (70:30 = V/V) bei 10°
$[ClCSNMe_2] = 5{,}125.10^{-3}$ M/l

Zeit sec.	V mV	$c_{H_2S} \cdot 10^4$ M/l	$\frac{c_{H_2S}}{a(a - c_{H_2S})}$
360	−224,0	0,00	0,000
420	−248,0	0,00	0,000
480	−270,0	0,34	1,305
540	−288,5	1,41	5,52
600	−308,0	3,37	13,75
660	−322,0	14,75	78,69
720	−332,0	22,4	151,7
780	−338,5	26,8	213,4
840	−343,0	30,4	283,5
960	−349,5	34,5	400,4
1 080	−354,0	37,1	507,7
1 200	−357,4	38,7	600,9
1 320	−361,0	40,5	733,6
1 440	−363,5	41,3	805,0
1 560	−366,0	42,5	935,4
1 780	−367,3	42,9	1004,9
1 800	−369,0	43,5	1083,9
1 920	−371,0	44,5	1276,7
2 040	−372,5	44,8	1334,3
2 160	−373,6	45,0	1396,8
2 340	−375,0	45,5	1538,3

$k = 0{,}8657 \pm 0{,}0100$ l/M.sec. $(r = 0.997)$

Revue Roumaine de Chimie , **22**, 7, 987 – 1001 (1977)

Dedicated to the 75 th anniversary of
Prof. C. D. NENITZESCU'*s birthday (1902–1970)*

CHEMICAL GRAPHS. XXXI.[1]

BENZO-HOMOVALENES

ALEXANDRU T. BALABAN

Department of Organic Chemistry, The Polytechnic Institute, Bucharest, Romania

Received January 7, 1977

All possible mono- to tetrabenzo-homovalenes (benzoderivatives of valence isomers $C_{n+1}H_{n+2}$, i.e. CH_2-homologues of [n]valenes $(CH)_n$) are enumerated for n=2 to 8, i.e. for benzo-C_3H_4 to benzo-C_9H_{10} systems. Known representatives are reviewed.

INTRODUCTION

In the first part of this series, the valence isomers of annulenes $(CH)_n$, named for short [n]valenes,* were defined and enumerated on a graph-theoretical basis.[2] The algorithm was expanded later, to include general cubic graphs.[3]

Homo[n]valenes are defined as homologues of valenes, $C_{n+1}H_{n+2}$; they differ from valenes by the presence of a methylene group. They may be enumerated by using general cubic graphs with one loop ; the vertex to which the loop is attached corresponds to the methylene group.[4]

Benzovalenes, i.e. benzoderivatives of valence of isomers of annulenes, such as benzocyclobutadiene,* naphthalene, Dewar-naphthalene, or benzocyclooctateraene,** are no longer cubic graphs, since their formulas (without hydrogens ***) contain vertices of degree four, not only three (namely, for each benzo ring, two points of degree four). Procedures for the systematic enumeration of benzovalenes were presented in a preceding paper.[7]

---

* According to a well-known theorem in graph theory, in [n]valenes which correspond to cubic multigraphs with n points or vertices, the number n must be even. Therefore as will be seen in the following, all homovalenes will have an odd number of vertices, one of which is of degree two, and the remaining vertices of degree three.

** These names are at variance with the new Chemical Abstracts nomenclature system [5] which calls these two compounds benzocyclobutene and benzocyclooctene, respectively.

*** Such formulas are called reduced structural graphs[6].

[1] Preceding part, A. T. BALABAN, *Rev. Roumaine Chim.*, **22**, 243 (1977).

[2] A. T. BALABAN, *Rev. Roumaine Chim.*, **11**, 1096 (1966) ; erratum, *ibid.*, **12**, N° 1, 103 (1967).

[3] A. T. BALABAN, *Rev. Roumaine Chim.*, **17**, 865 (1972).

[4] A. T. BALABAN, *Rev. Roumaine Chim.*, **19**, 1611 (1974).

[5] *Chemical Abstracts*, Index Guide Introduction, **76**, 151 (1972).

[6] A. T. BALABAN, *Rev. Roumaine Chim.*, **19**, 1323 (1974).

Continuing these enumerations, the present paper concentrates on [b]benzo-homo[n]valenes. Such a molecule contains b benzo-annelations of a homo[n]valene $C_{n+1}H_{n+2}$: the molecular formula of a [b]benzo-homo[n]valene is $C_{n+4b+1}H_{n+2b+2}$.

ENUMERATION OF BENZO-HOMOVALENES

The notations of preceding papers will be followed :[4,7] since a homo[n]-valene is derived from a general cubic graph with $p = n + 2$ points with one loop by deleting the loop-point, a homo [n] valene has $p - 1 = n + 1$ carbon atoms or vertices in the reduced structural graph. We shall classify [b]benzo-homo[n]valenes according to the number b of benzo-annelations, and according to the number $p = n + 2$ of vertices in the general cubic graph ; the former number b, followed by the letter B is the first index of the [b]benzo-homo[n]valene, the latter number is the second index. The third, fourth, fifth and sixth indices are the numbers of loops, double bonds, cyclopropane and cyclobutane rings in the general cubic graph corresponding to the homo[n] valene ; the last, seventh index is a serial number, starting with 1, which orders the graphs (when all indices from the first to the sixth were identical for two or more non-isomorphic graphs) according to the increasing number of circuits with 5, 6, etc. vertices. In all cases to be discussed in the present paper, the number of loops is 1, so that for convenience the third index (which is 1 in all present cases) will be omitted leaving only six indices. As a bonus of the classification, in the tables, the benzoderivatives are ordered according to the increasing number of double bonds.

It should be mentioned that this is only one of the possible ways to devise an ordering of graphs ; an alternative procedure, based on expressing adjacency matrices as binary numbers, was developed by Randić.[8]

When one and the same homo[n]valene gives rise by annelation to several [b]benzoderivatives with the same b, these are distinguished by an index i following the letter B : $bB_i - p - \ldots$

The order in which indices i are assigned is the same as outlined in the previous paper :[7] the hierarchy of previous [7] precedence criteria is supplemented by the criterion (v) below :

(i) Normal structures have precedence over *ortho*-quinonoid ones (see below the definitions) :

(ii) Acyclic bonds to be annelated have precedence over bonds involved in rings :

(iii) Bonds to be annelated, involved in smaller rings, have precedence over those in larger rings ;

(iv) Bonds closer to smaller rings have precedence ;

(v) Bonds closer to the black dot have precedence ;

(vi) In polybenzoderivatives, bonds further apart have precedence over bonds closer to one another.

---

[7] A. T. Balaban, *Rev. Roumaine Chim.*, **19**, 1185 (1974) ; erratum : in table 5A, the single bond between the two three-membered rings of $1B_3 - 10 - 3 - 2 - 1 - 3$ must be replaced by a $-CH{=}CH-$ unit.

[8] M. Randić, *J. Chem. Phys.*, **60**, 3920 (1974) ; **62**, 309 (1975).

These criteria are applied in sequence until factors are no longer equal. A few examples of how these precedence rules are applied appear from figure 1, where the order of indices i for monobenzo-annelation is obtained by applying in sequence the rules indicated under each formula. For polybenzo-derivatives the same rules apply.

Only planar graphs are considered and they will be drawn so as to emphasize their graph theoretical planarity by avoiding crossing lines.

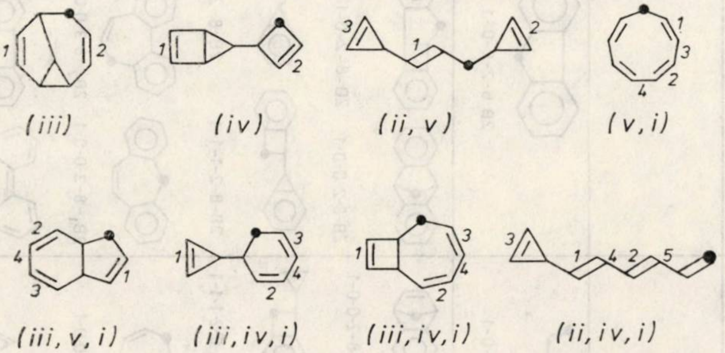

Fig. 1. — Indices *i* giving the order in which the corresponding bonds of homovalenes are to be annelated in order to afford monobenzo-homovalenes; under each formula, the relevant precedence criteria are indicated.

Stereoisomerism is disregarded, only constitutional isomers are treated as distinct.

Two kinds of benzoderivatives can exist: when, in an [n]valene or a homo[n]valene which possesses isolated or conjugated double bonds, b of these double bonds become benzo-annelated, a normal [b]benzoderivative results; this is symbolized by inscribed circles in the benzenoid rings. When, in an [n]valene or a homo[n]valene with conjugated double bonds, at least one benzo-annelation takes place at a formal single bond in the conjugated system, an *ortho*-quinonoid or *ortho*-xylylenoid benzoderivative results; this is symbolized by an asterisk following the index B, and by the absence of inscribed circles. *ortho*-Quinonoid benzoderivatives follow normal ones derived from the same homo[n]valene.

Table 1 presents all possible constitutional isomers of mono- and dibenzo-homo[n]valenes with $p-1 = n+1 = 3$, 5 and 7; table 2 presents monobenzo-homo[8]valenes, table 3 the dibenzo-homo[8]valenes, and table 4 the tri- and tetra-benzo-derivatives with $n+1 = p-1 = 7$, and 9. The numbers of all these [b]benzo-homo[n]valenes are presented in table 5.

In order to find these [b]benzo-homo[n]valenes, two procedures are available, starting either from the table of homo[n]valenes, or from the table of benzovalenes. In the former case, double bonds become benzo-annelated (for conjugated double bonds, the annelation may also take place at single bonds within the conjugated system, leading to *ortho*-

Table 1

Mono- and dibenzo- homo[n]valenes with $p-1=n+1=3,5$ and 7 vertices.

p-1 \ b	1	2
3	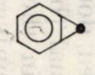 1B-4-1-1-0-1	
5	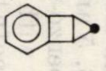 1B-6-1-1-1-1 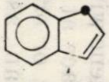 1B$_1$-6-2-0-0-1 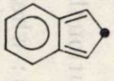 1B$_2^*$-6-2-0-0-1 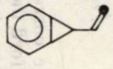 1B-6-2-1-0-1	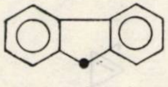 2B-6-2-0-0-1
7	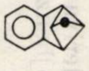 1B-8-1-0-3-1 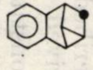 1B-8-1-1-1-1 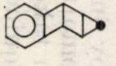 1B-8-1-1-2-1 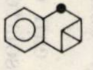 1B-8-1-2-1-1 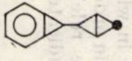 1B-8-1-3-1-1 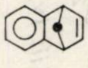 1B-8-2-0-0-1 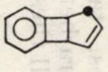 1B$_1$-8-2-0-1-1 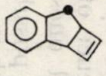 1B$_2$-8-2-0-1-1 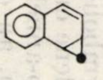 1B$_1$-8-2-1-0-1 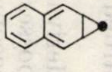 1B$_2^*$-8-2-1-0-1 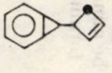 1B$_1$-8-2-1-1-1 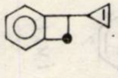 1B$_2$-8-2-1-1-1 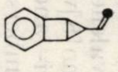 1B-8-2-1-1-2 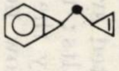 1B-8-2-2-0-1 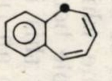 1B$_1$-8-3-0-0-1 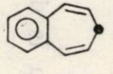 1B$_2$-8-3-0-0-1 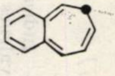 1B$_3^*$-8-3-0-0-1 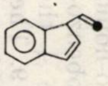 1B$_1$-8-3-0-0-2 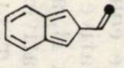 1B$_2^*$-8-3-0-0-2 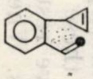 1B$_1$-8-3-1-0-1 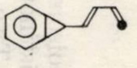 1B$_2$-8-3-1-0-1 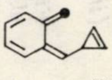 1B$_3^*$-8-3-1-0-1	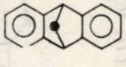 2B-8-2-0-0-1 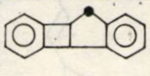 2B-8-2-0-1-1 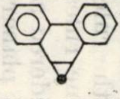 2B-8-2-1-0-1 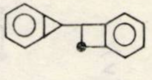 2B-8-2-1-1-1 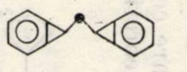 2B-8-2-2-0-1 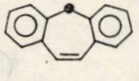 2B$_1$-8-3-0-0-1 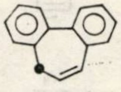 2B$_2$-8-3-0-0-1 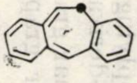 2B$_3^*$-8-3-0-0-1 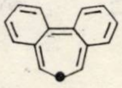 2B$_4^*$-8-3-0-0-1 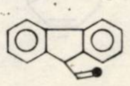 2B-8-3-0-0-2 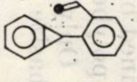 2B-8-3-1-0-1

Table 2

Monobenzo-homo[8]valenes, with $p-1 = n+1 = 9$ vertices.

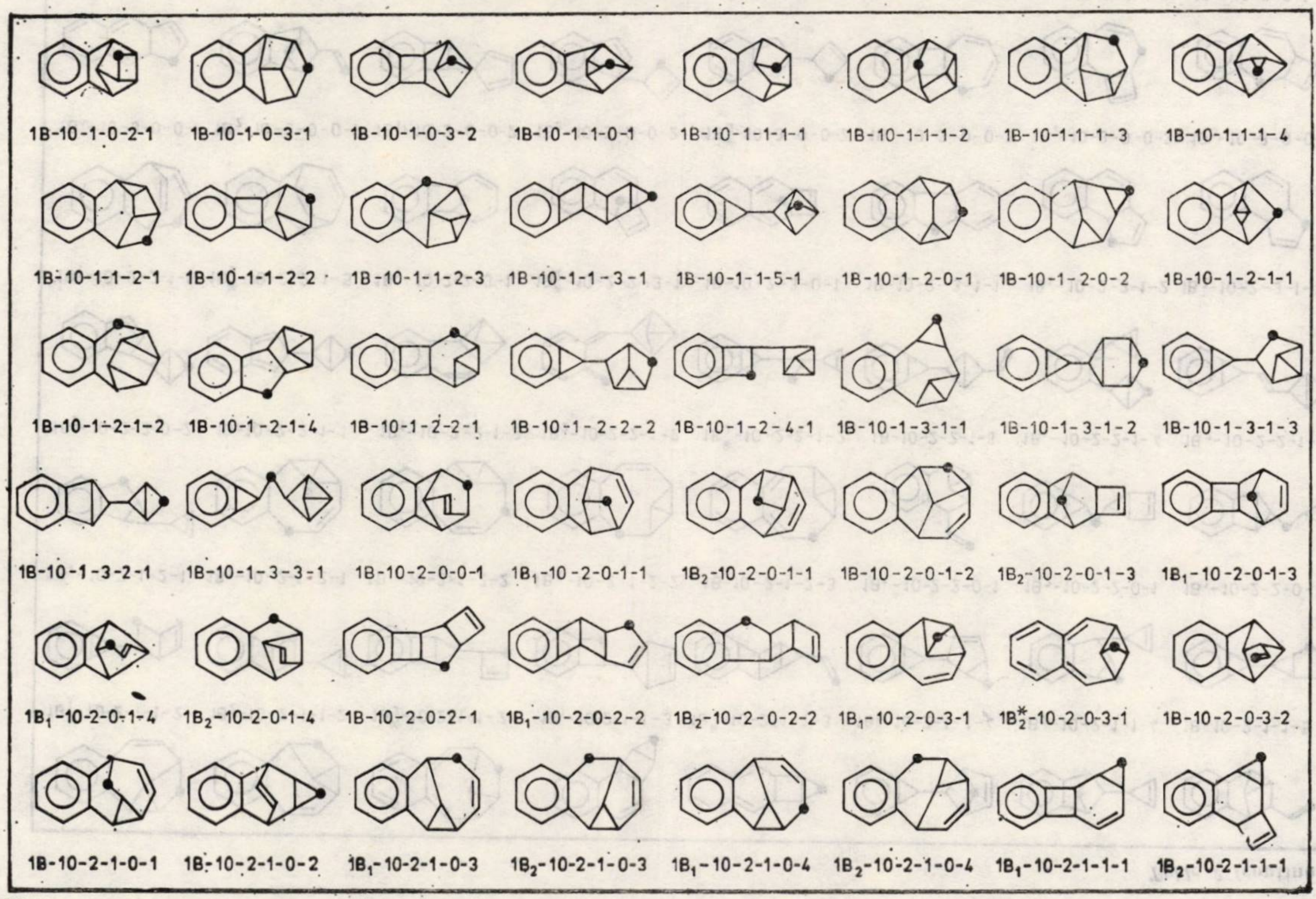

1B-10-1-0-2-1	1B-10-1-0-3-1	1B-10-1-0-3-2	1B-10-1-1-0-1	1B-10-1-1-1-1	1B-10-1-1-1-2	1B-10-1-1-1-3	1B-10-1-1-1-4
1B-10-1-1-2-1	1B-10-1-1-2-2	1B-10-1-1-2-3	1B-10-1-1-3-1	1B-10-1-1-5-1	1B-10-1-2-0-1	1B-10-1-2-0-2	1B-10-1-2-1-1
1B-10-1-2-1-2	1B-10-1-2-1-4	1B-10-1-2-2-1	1B-10-1-2-2-2	1B-10-1-2-4-1	1B-10-1-3-1-1	1B-10-1-3-1-2	1B-10-1-3-1-3
1B-10-1-3-2-1	1B-10-1-3-3-1	1B-10-2-0-0-1	$1B_1$-10-2-0-1-1	$1B_2$-10-2-0-1-1	1B-10-2-0-1-2	$1B_2$-10-2-0-1-3	$1B_1$-10-2-0-1-3
$1B_1$-10-2-0-1-4	$1B_2$-10-2-0-1-4	1B-10-2-0-2-1	$1B_1$-10-2-0-2-2	$1B_2$-10-2-0-2-2	$1B_1$-10-2-0-3-1	$1B_2^*$-10-2-0-3-1	1B-10-2-0-3-2
1B-10-2-1-0-1	1B-10-2-1-0-2	$1B_1$-10-2-1-0-3	$1B_2$-10-2-1-0-3	$1B_1$-10-2-1-0-4	$1B_2$-10-2-1-0-4	$1B_1$-10-2-1-1-1	$1B_2$-10-2-1-1-1

Table 2 (continued)

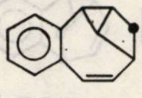	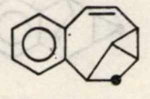	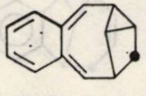	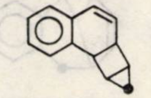	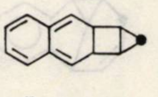	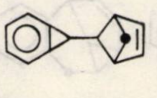	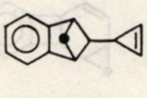	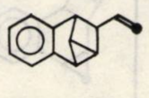
$1B_1$-10-2-1-1-2	$1B_2$-10-2-1-1-2	$1B_3^*$-10-2-1-1-2	$1B_1$-10-2-1-1-3	$1B_2^*$-10-2-1-1-3	$1B_1$-10-2-1-1-4	$1B_2$-10-2-1-1-4	1B-10-2-1-1-5
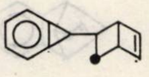	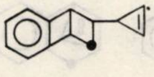	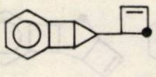	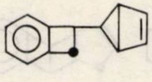	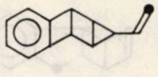	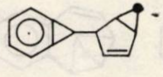	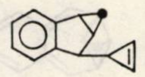	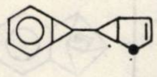
$1B_1$-10-2-1-2-1	$1B_2$-10-2-1-2-1	$1B_1$-10-2-1-2-2	$1B_2$-10-2-1-2-2	1B-10-2-1-2-3	$1B_1$-10-2-2-0-1	$1B_2$-10-2-2-0-1	$1B_1$-10-2-2-0-2
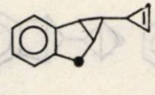	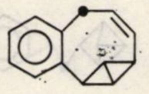	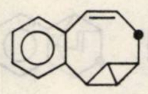	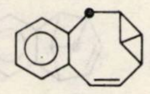	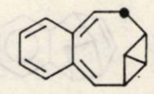	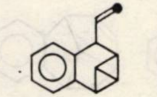	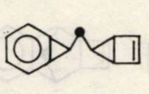	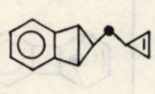
$1B_2$-10-2-2-0-2	1B-10-2-2-1-1	$1B_1$-10-2-2-1-2	$1B_2$-10-2-2-1-2	$1B_3^*$-10-2-2-1-2	1B-10-2-2-1-3	$1B_1$-10-2-2-1-4	$1B_2$-10-2-2-1-4
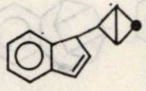	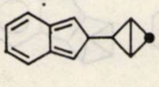	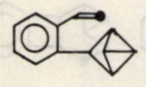	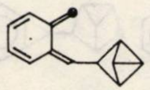	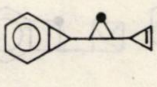	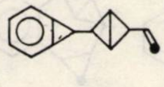	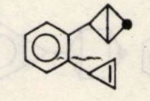	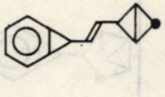
$1B_1$-10-2-2-1-5	$1B_2^*$-10-2-2-1-5	$1B_1$-10-2-2-3-1	$1B_2^*$-10-2-2-3-1	1B-10-2-3-0-1	1B-10-2-3-1-1	$1B_1$-10-2-3-1-2	$1B_2$-10-2-3-1-2
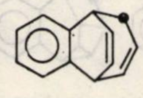	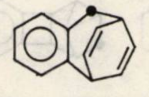	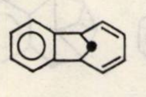	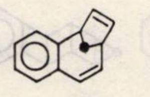	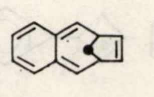	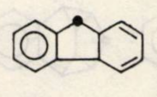	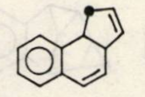	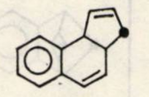
$1B_1$-10-3-0-0-1	$1B_2$-10-3-0-0-1	$1B_1$-10-3-0-0-2	$1B_2$-10-3-0-0-2	$1B_3^*$-10-3-0-0-2	$1B_1$-10-3-0-0-3	$1B_2$-10-3-0-0-3	$1B_3$-10-3-0-0-3
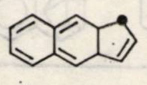	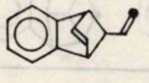	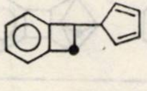	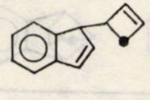	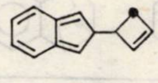	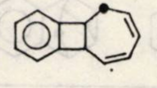	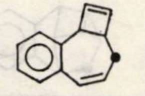	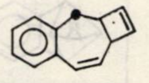
$1B_4^*$-10-3-0-0-3	1B-10-3-0-0-4	$1B_1$-10-3-0-1-1	$1B_2$-10-3-0-1-1	$1B_3^*$-10-3-0-1-1	$1B_1$-10-3-0-1-3	$1B_2$-10-3-0-1-3	$1B_3$-10-3-0-1-3

Table 2 (continued)

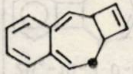

$1B^*_4$-10-3-0-1-3

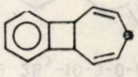

$1B_1$-10-3-0-1-4

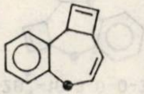

$1B_2$-10-3-0-1-4

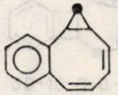

$1B_1$-10-3-1-0-1

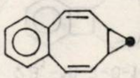

$1B_2$-10-3-1-0-1

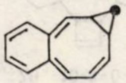

$1B^*_3$-10-3-1-0-1

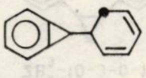

$1B_1$-10-3-1-0-2

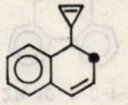

$1B_2$-10-3-1-0-2

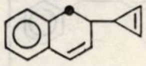

$1B_3$-10-3-1-0-2

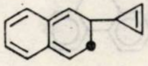

$1B^*_4$-10-3-1-0-2

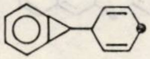

$1B_1$-10-3-1-0-3

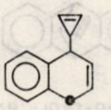

$1B_2$-10-3-1-0-3

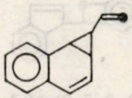

$1B_1$-10-3-1-0-4

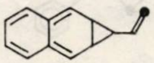

$1B^*_2$-10-3-1-0-4

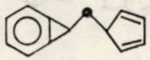

$1B_1$-10-3-1-0-5

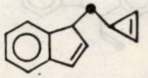

$1B_2$-10-3-1-0-5

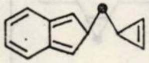

$1B^*_3$-10-3-1-0-5

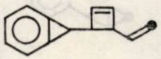

$1B_1$-10-3-1-1-1

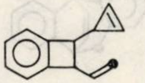

$1B_2$-10-3-1-1-1

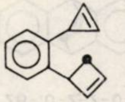

$1B_1$-10-3-1-1-2

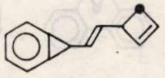

$1B_2$-10-3-1-1-2

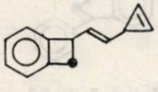

$1B_3$-10-3-1-1-2

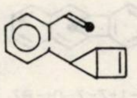

$1B_1$-10-3-1-1-3

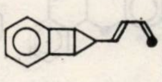

$1B_2$-10-3-1-1-3

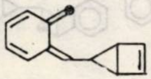

$1B^*_3$-10-3-1-1-3

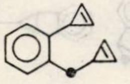

$1B_1$-10-3-2-0-1

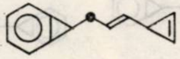

$1B_2$-10-3-2-0-1

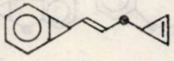

$1B_3$-10-3-2-0-1

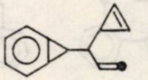

1B-10-3-2-0-2

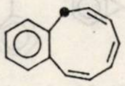

$1B_1$-10-4-0-0-1

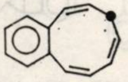

$1B_2$-10-4-0-0-1

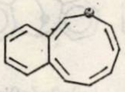

$1B^*_3$-10-4-0-0-

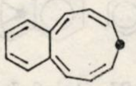

$1B^*_4$-10-4-0-0-1

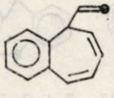

$1B_1$-10-4-0-0-2

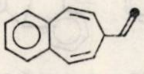

$1B_2$-10-4-0-0-2

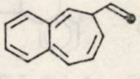

$1B^*_3$-10-4-0-0-2

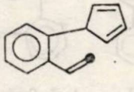

$1B_1$-10-4-0-0-3

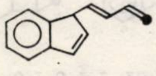

$1B_2$-10-4-0-0-3

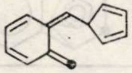

$1B^*_3$-10-4-0-0-3

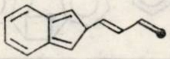

$1B^*_4$-10-4-0-0-3

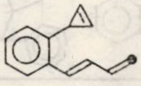

$1B_1$-10-4-1-0-1

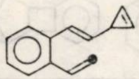

$1B_2$-10-4-1-0-1

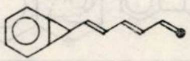

$1B_3$-10-4-1-0-1

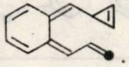

$1B^*_4$-10-4-1-0-1

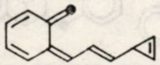

$1B^*_5$-10-4-1-0-1

Table 3

Dibenzo-homo [8] valenes, with $p-1=n+1=9$ vertices.

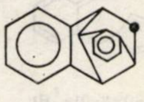
2B-10-2-0-0-1

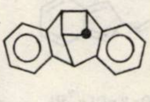
2B-10-2-0-1-1

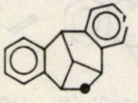
2B-10-2-0-1-2

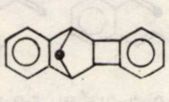
2B-10-2-0-1-3

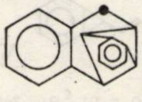
2B-10-2-0-1-4

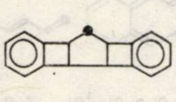
2B-10-2-0-2-1

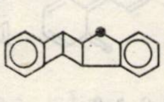
2B-10-2-0-2-2

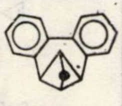
2B-10-2-0-3-1

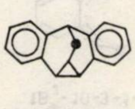
2B-10-2-1-0-1

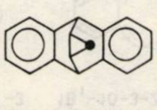
2B-10-2-1-0-2

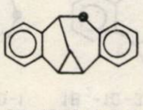
2B-10-2-1-0-3

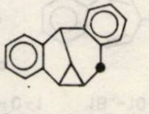
2B-10-2-1-0-4

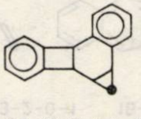
2B-10-2-1-1-1

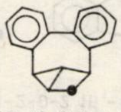
2B-10-2-1-1-2

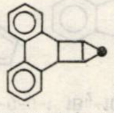
2B-10-2-1-1-3

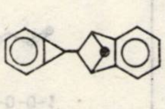
2B-10-2-1-1-4

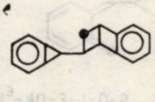
2B-10-2-1-2-1

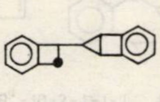
2B-10-2-1-2-2

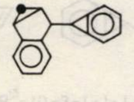
2B-10-2-2-0-1

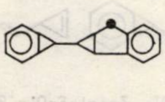
2B-10-2-2-0-2

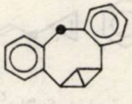
2B-10-2-2-1-1

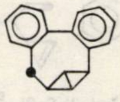
2B-10-2-2-1-2

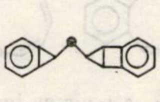
2B-10-2-2-1-4

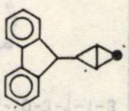
2B-10-2-2-1-5

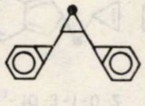
2B-10-2-3-0-1

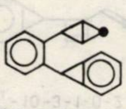
2B-10-2-3-1-2

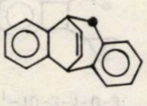
$2B_2$-10-3-0-0-1

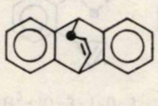
$2B_1$-10-3-0-0-1

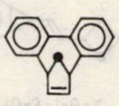
$2B_2$-10-3-0-0-2

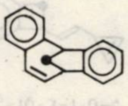
$2B_1$-10-3-0-0-2

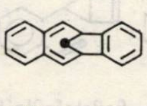
$2B_3^*$-10-3-0-0-2

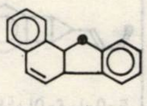
$2B_1$-10-3-0-0-3

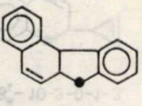
$2B_2$-10-3-0-0-3

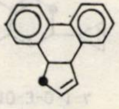
$2B_3$-10-3-0-0-3

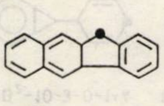
$2B_4^*$-10-3-0-0-3

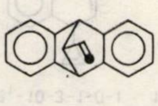
2B-10-3-0-0-4.

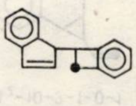
$2B_1$-10-3-0-1-1

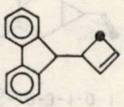
$2B_2$-10-3-0-1-1

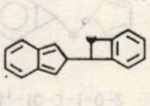
$2B_3^*$-10-3-0-1-1

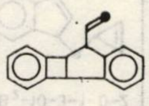
2B-10-3-0-1-2

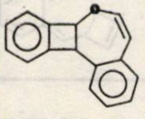
$2B_1$-10-3-0-1-3

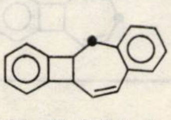
$2B_2$-10-3-0-1-3

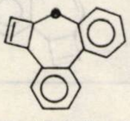
$2B_3$-10-3-0-1-3

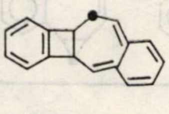
$2B_4^*$-10-3-0-1-3

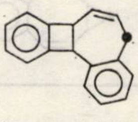
$2B_1$-10-3-0-1-4

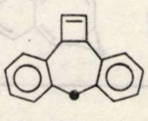
$2B_2$-10-3-0-1-4

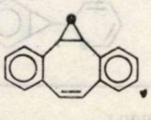
$2B_1$-10-3-1-0-1

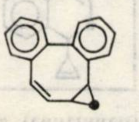
$2B_2$-10-3-1-0-1

Table 3 (continued)

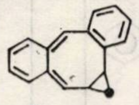	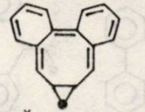	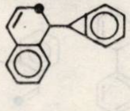	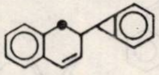	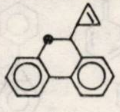	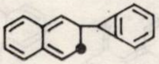	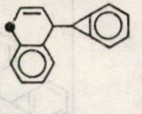	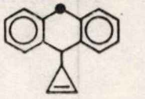
$2B_3^*$-10-3-1-0-1	$2B_4^*$-10-3-1-0-1	$2B_1$-10-3-1-0-2	$2B_2$-10-3-1-0-2	$2B_3$-10-3-1-0-2	$2B_4^*$-10-3-1-0-2	$2B_1$-10-3-1-0-3	$2B_2$-10-3-1-0-3
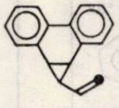	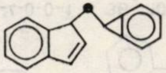	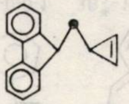	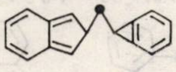	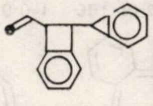	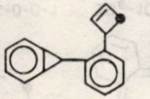	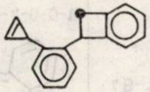	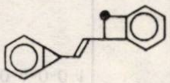
2B -10-3-1-0-4	$2B_1$-10-3-1-0-5	$2B_2$-10-3-1-0-5	$2B_3^*$-10-3-1-0-5	2B-10-3-1-1-1	$2B_1$-10-3-1-1-2	$2B_2$-10-3-1-1-2	$2B_3$-10-3-1-1-2
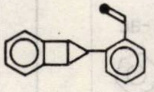	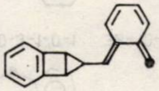	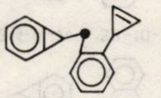	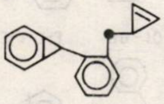	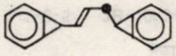	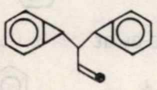	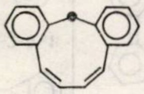	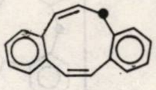
$2B_1$-10-3-1-1-3	$2B_2$-10-3-1-1-3	$2B_1$-10-3-2-0-1	$2B_2$-10-3-2-0-1	$2B_3$-10-3-2-0-1	2B-10-3-2-0-2	$2B_1$-10-4-0-0-1	$2B_2$-10-4-0-0-1
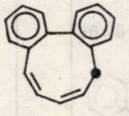	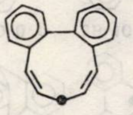	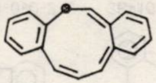	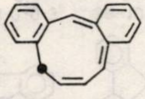	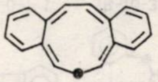	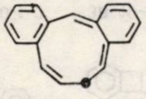	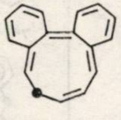	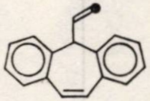
$2B_3$-10-4-0-0-1	$2B_4$-10-4-0-0-1	$2B_5^*$-10-4-0-0-1	$2B_6^*$-10-4-0-0-1	$2B_7^*$-10-4-0-0-1	$2B_8^*$-10-4-0-0-1	$2B_9^*$-10-4-0-0-1	$2B_1$-10-4-0-0-2
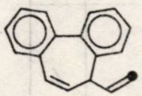	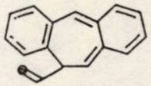	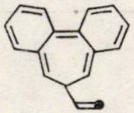	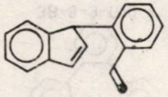	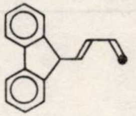	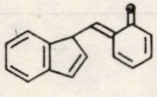	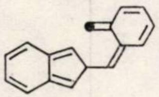	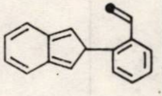
$2B_2$-10-4-0-0-2	$2B_3^*$-10-4-0-0-2	$2B_4^*$-10-4-0-0-2	$2B_1$-10-4-0-0-3	$2B_2$-10-4-0-0-3	$2B_3^*$-10-4-0-0-3	$2B_4^*$-10-4-0-0-3	$2B_5^*$-10-4-0-0-3
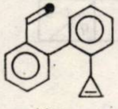	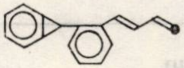	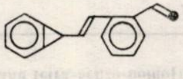	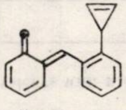	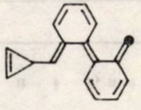	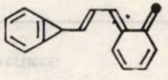	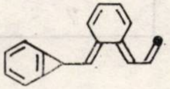	
$2B_1$-10-4-1-0-1	$2B_2$-10-4-1-0-1	$2B_3$-10-4-1-0-1	$2B_4^*$-10-4-1-0-1	$2B_5^*$-10-4-1-0-1	$2B_6^*$-10-4-1-0-1	$2B_7^*$-10-4-1-0-1	

Table 4

Tri- and tetra-benzo-homo[n]valenes with p − 1 = n + 1 = 7, and 9, vertices.

p-1 \ b	3	4
7	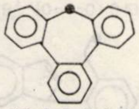 3B-8-3-0-0-1	
9	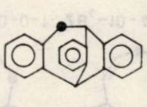 3B-10-3-0-0-1 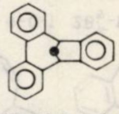 3B-10-3-0-0-2 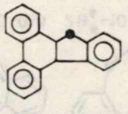 3B-10-3-0-0-3 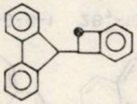 3B-10-3-0-1-1 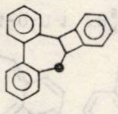 3B-10-3-0-1-3 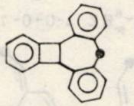 3B-10-3-0-1-4 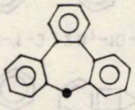 3B-10-3-1-0-1 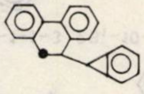 3B-10-3-1-0-2 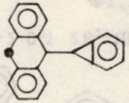 3B-10-3-1-0-3 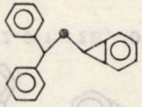 3B-10-3-1-0-5 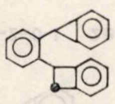 3B-10-3-1-1-2 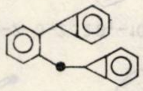 3B-10-3-2-0-1 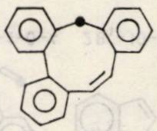 3B$_1$-10-4-0-0-1 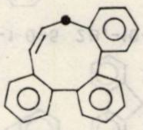 3B$_2$-10-4-0-0-1 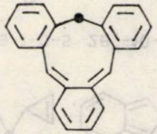 3B$_3^*$-10-4-0-0-1 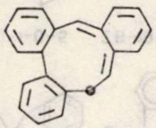 3B$_4^*$-10-4-0-0-1 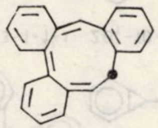 3B$_5^*$-10-4-0-0-1 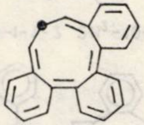 3B$_6^*$-10-4-0-0-1 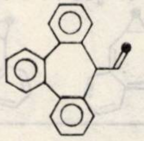 3B-10-4-0-0-2 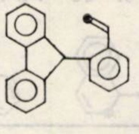 3B$_1$-10-4-0-0-3 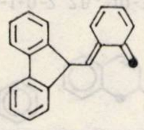 3B$_2^*$-10-4-0-0-3 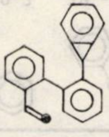 3B$_1$-10-4-1-0-1 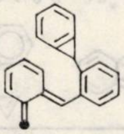 3B$_2^*$-10-4-1-0-1 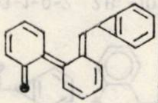 3B$_3^*$-10-4-1-0-1	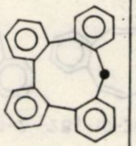 4B-10-4-0-0-1

Table 5

Numbers of planar [b]benzo-homo[n]valenes as functions of b and p − 1 = n + 1

b p − 1	1	2	3	4
3	1	—	—	—
5	4	1	—	—
7	22	11	1	—
9	141	95	24	1

quinonoid structures). In the latter procedure, two adjacent points joined by a double bond are replaced by a point of degree two, symbolizing the CH_2 group. In all formulas from tables 1—4, this point is marked by a black dot. However, the latter procedure does not generate all *ortho*-quinonoid systems, and therefore it was only used as a check-up for normal benzo-homovalenes.

All double bonds in a homo[n]valene may be benzo-annelated, with the exception of double bonds ending in a black dot; therefore, not all homo[n]valenes have corresponding benzo-derivatives, e.g. the last example in figure 1 cannot have the terminal double bond annelated.

A warning is necessary : it may appear artificial to include 1-vinylindene $1B_1$ —8—3—0—0—2 or *ortho*-cyclopropenyl-styrene $1B_1$ —8—3 — —1—0—1 among benzo-homovalenes; however, it was considered better to adhere to a strict definition than to make room to subjective criteria of classification. Since homovalenes were defined as hydrocarbons, whose structural graphs depicting only carbon atoms have all points but one, of degree three and one point of degree two, everything else follows from this definition.

Unlike benzovalenes, where the known, stable anthracene is an *ortho*-quinonoid benzoderivative, in the case of benzohomovalenes, *ortho*-quinonoid systems are too unstable to be isolated; they tautomerize to non-*ortho*-quinonoid structures.

SURVEY OF SOME KNOWN SYSTEMS

On the basis of tables 1—4, one can have a reliable and systematic approach to all possible benzo-homovalenes where the black dot symbolizes a $-CH_2-$ group as in barbaralane, or cognate systems where the black dot symbolizes a heteroatom (—O—, —S—, —NR—), or a carbonyl group —CO— as in barbaralone. On the other hand, in cases when the black dot symbolizes a charged carbon atom or carbon atom with unpaired spin, tables 1—4 indicate limiting structures for carbocations or free radicals.

A brief non-exhaustive survey of a few benzo-homovalenes follows.

The simplest benzo-homovalene is benzocyclopropene (norcaratriene) $1B-4-1-0-0-1$. Despite its steric strain, it was obtained in 1965 by Vogel and coworkers.[9] The structure and the strain were confirmed by NMR measurements.[10]

From the benzo-C_5H_6 systems, indene $1B_1-6-2-0-0-1$ and fluorene $2B-6-2-0-0-1$ are too well-known to warrant more than a cursory mention.

The mono,- di-, and tri-benzo-C_7H_8 systems include the benzotropylidenes $1B_1-8-3-0-0-1$ (unable to valence-isomerize, but able to afford the benzotropyl radical on pyrolysis[11]), $1B_2-8-3-0-0-1$ and $1B_3-8-3-0-0-1$, whose valence isomerization to benzo-norcaradienes $1B_1-8-2-1-0-1$ and $1B_2-8-2-1-0-1$ is no longer a mobile equilibrium as for tropylidene, but is completely displaced to one side, in both cases favouring the non-*ortho*-quinonoid valence isomer: $1B_2-8-3-0-0 \rightleftarrows 1B_2^*-2-1-0-1$ and $1B_3^*-8-3-0-0-1 \rightleftarrows 1B_1-8-2-1-0-1$.[12,13] Benzonorbornadiene or 1,4-methano-1,4-dihydronaphthalene $1B-8-2-0-0-1$ was first obtained by Wittig and coworkers from benzyne and cyclopentadiene,[14] though some derivatives had been prepared from *p*-benzoquinone and cyclopentadiene.[15] Pyrolysis of benzonorbornadiene affords 1,2-benzotropylidene $1B_1-8-3-0-0-1$ which at higher temperature rearranges to 1- and 2-methylnaphthalenes; as intermediates in this rearrangement, $1B_2-8-2-0-1-1$, $1B_1-8-2-1-0-1$ and $1B_2-8-3-0-0-1$ were discussed.[16] 3,4-Benzotricyclo[4.1.0.0^{2,7}]heptene $1B-8-1-2-1-1$ was obtained;[17] its thermal isomerization afforded $1B_2-8-2-0-1-1$, while transition-metal-catalyzed isomerizations gave different products, among which was benzotropylidene $1B_1-8-3-0-0-1$.[17]

Thermal, photochemical and transition-metal-catalyzed rearrangements between 3H-benzo[*a*]cycloheptatriene ($1B_1-8-3-0-0-1$) and its valence isomers $1B-8-1-2-1-1$ and $1B_2-8-2-0-1-1$ were studied by Japanese authors.[13]

Along with studies of benzo-C_7H_8 hydrocarbons, $1B_1-8-3-0-0-1$, $1B_2-8-2-0-1-1$ and $1B-8-1-2-1-1$, mention should be made of heteroanalogues, with the black dot symbolizing a divalent heteroatom or group (O, S, NR), i.e. valence isomers of benzoxepin,[18] benzothiepin,[19] benzazepin.

---

[9] E. Vogel, W. Grimme and S. Korte, *Tetrahedron Letters*, **1965**, 3625.

[10] H. Guenther and J. B. Pawliczek, *J. Amer. Chem. Soc.*, **93**, 2050 (1971); E. Hedaya and M. E. Kent, *ibid.*, **92**, 2149 (1970); M. A. Cooper and S. L. Manatt, *ibid.*, **92**, 1605 (1970).

[11] M. Pomerantz and A. S. Ross, *J. Amer. Chem. Soc.*, **97**, 5850 (1975).

[12] G. Maier, "Valenzisomerisierungen", Verlag Chemie, Weinheim, 1972, p. 107 and further references therein.

[13] G. Wittig, H. Eggers and P. Duffner, *Liebigs, Ann. Chem.*, **619**, 10 (1958).

[14] G. Wittig and E. Krauss, *Chem. Ber.*, **91**, 895 (1958); G. Wittig, H. Härle, E. Krauss and K. Niethammer, *ibid.*, **93**, 951 (1960); cf. also P. D. Bartlett and W. P. Giddings, *J. Amer. Chem. Soc.*, **82**, 1240 (1960).

[15] J. Meinwald and G. A. Wiley, *J. Amer. Chem. Soc.*, **80**, 3667 (1958).

[16] S. J. Cristol and R. Caple, *J. Org. Chem.*, **31**, 585 (1966).

[17] J. Murata, T. Nakazawa, M. Kato, T. Tatsuoka and J. Sugihara, *Tetrahedron Letters*, **1975**, 1647.

[18] M. Uyegachi, S. Ito, J. Sugihara and I. Murata, *Tetrahedron Letters*, **1976**, 4473.

[19] I. Murata, T. Tatsuoka and J. Sugihara, *Tetrahedron Letters*, **1973**, 4261; **1974**, 199.

3H-Dibenzo[*a*,*d*]cycloheptatriene ($2B_1-8-3-0-0-1$) and its heteroanalogues, dibenzo[*b*, *f*]oxepine or -azepine were intensely studied for two reasons: some of these derivatives possess psychotropic activity;[20,21] the conformational inversion of the seven-membered ring gives rise[22] to temperature-dependent NMR spectra and in certain cases to stable conformational isomers[23] which can be separated; these possess different chemical reactivities and NMR spectra, and their energy barriers for inversion can be conveniently measured.[24,25] Conformational studies were also effected on 5H-dibenzo[*a*,*c*]-cycloheptatriene ($2B_2-8-3-0-0-1$)[26] and on 9H-tribenzo[*a*,*c*,*e*]cycloheptatriene ($3B-8-3-0-0-1$).[22,24] On homologation of anthracene with diazomethane in the presence of copper(I) bromide, dibenzo-norbornadiene ($2B-8-2-0-0-1$) was obtained, along with $2B_1-8-3-0-0-1$.[27]

The numerous class of benzo-C_9H_{10} systems is fairly well represented, and new such compounds are prepared each year. To facilitate the review, compounds will be discussed in the order of increasing last three indices, and decreasing number of double bonds. Benzocyclononatetraenes $1B_1-10-4-0-0-1$ and $1B_2-10-4-0-0-1$ were prepared by Anastassiou and coworkers: the latter from α-pyrone and homocyclooctatetraene (bicyclo[6.1.0]nonatriene);[28] conversion into the anion and treatment with ethanol affords both isomers.[29] While $1B_2-10-4-0-0-1$ is stable,[28,29] $1B_1-10-4-0-0-1$ undergoes rapidly ($\Delta G = 22.3$ kcal/mol) the thermally allowed electrocyclization to $1B_1-10-3-0-0-3$, which can be dehydrogenated by chloranil to fluorene.[29]

The reaction of benzyne with tropone affords a derivative with structure $1B_1-10-3-0-0-2$ (the black dot corresponding to a carbonyl group).[30] By analogy, benzyne and cycloheptatriene were supposed to react in an analogous fashion;[31] this assumption was proved later to be in error, the product has structure $1B_1-10-3-0-1-3$ instead;[32,33] thermolysis of this hydrocarbon yields $1B_1-10-3-1-0-1$,[34-36] which was synthesized independently from benzocyclooctatetraene

---

[20] S. O. Winthrop, M. A. Davis, G. S. Myers, J. G. Gavin, R. Thomas and R. Barber *J. Org. Chem.*, **27**, 230 (1962).

[21] J. O. Jilek, V. Seidlova, E. Svatek, M. Protiva, J. Promylacek and Z. Sedivy, *Monatsh. Chem.*, **96**, 182 (1965).

[22] W. Tochtermann, *Fortschr. Chem. Forsch.*, **15**, 378 (1971).

[23] W. Tochtermann, G. Schnabel and A. Mannschreck, *Liebigs Ann. Chem.*, **705**, 169 (1967).

[24] M. Nogradi, W. D. Ollis and I. O. Sutherland, *Chem. Commun.*, **1970**, 158.

[25] H. J. Bestmann, A. Armsen and H. Wagner, *Chem. Ber.*, **102**, 2259 (1969).

[26] I. O. Sutherland and M. V. J. Ramsay, *Tetrahedron*, **21**, 3401 (1965).

[27] E. Müller and H. Kessler, *Liebigs Ann. Chem.*, **692**, 58 (1966).

[28] A. G. Anastassiou, S. S. Libsch and R. C. Griffith, *Tetrahedron Letters*, **1973**, 3101.

[29] A. G. Anastassiou and R. C. Griffith, *J. Amer. Chem. Soc.*, **96**, 611 (1974).

[30] T. Miwa, M. Kato and T. Tamano, *Tetrahedron Letters*, **1969**, 1761; H. Tanida and T. Irie, *J. Org. Chem.*, **36**, 2777 (1971).

[31] I. Tabushi, H. Yamada, Z. Yoshida and H. Kuroda, *Tetrahedron Letters*, **1971**, 1093.

[32] L. Lombardo and D. Wege, *Tetrahedron Letters*, **1971**, 3981.

[33] P. Crews, M. Loffgren and D. J. Bertelli, *Tetrahedron Letters*, **1971**, 4697.

[34] M. Kato, T. Sawa and T. Miwa, *Chem. Commun.*, **1971**, 1635.

and methylene dichloride;[35] this reaction also afforded $1B_2-10-3-1-0-1$ which was also formed by decarbonylation of a polycyclic ketone. In turn, thermolysis of the structurally similar systems gave specifically (without leakage) structurally related hydrocarbons, namely: $1B_1-10-3-1-0-1 \xrightarrow{\Delta} 1B_2-10-3-0-0-3$;[35,36] $1B_2-10-3-1-0-1 \xrightarrow{\Delta} 1B_3-10-3-0-0-3$.[35] In the same paper, isomeric systems $1B_1-10-3-0-1-4$ and $1B_1-10-3-0-0-1$ were discussed theoretically.[35] The latter hydrocarbon was tested under pyrolytic conditions; it was found to afford benzobarbaralane $1B-10-2-1-0-1$, *cis*-$1B_3-10-3-0-0-3$ and an unidentified product.[37] The first two systems are also formed pyrolytically from $1B_1-10-2-0-1-3$ *via* $1B-10-1-2-0-1$, which at higher temperatures rearranges (by homolysis and 1,2-alkyl migration) to $1B-10-2-1-0-1$ which then gives $1B_3-10-3-0-0-3$.[37,38]

On the other hand, photochemical rearrangement of $1B_1-10-3-0-1-3$ affords [36] two hydrocarbons: $1B-10-2-0-2-1$, and $1B-10-1-1-1-2$; the intermediacy of all possible isomeric benzocyclononatetraenes was discussed; the most plausible is $1B_3^*-10-4-0-0-1$.[36] Photochemical rearrangement of $1B_1-10-3-1-0-1$ yields $1B-10-2-1-1-1$.[36] In order to make structural assignments, a computer program[39] giving all possible isomeric systems was used;[36] along with the above structures, which were finally proved, plausible candidates from the computer output had been $1B-10-1-3-1-1$ and $1B-10-1-1-2-1$, but these were disproved.[36] It would have been simpler to employ the present approach.

An entry into the 7,8-benzobicyclo[4.2.1]nona-2,4,7-triene system ($1B_1-10-3-0-0-2$) was found in the addition of (di)chlorocarbene to 6,7-benzo[3.2.1]octa-2,6-diene followed by dehydrochlorination;[40] the photochemical rearrangement, with or without sensitisers, converts substituted $1B_1-10-3-0-0-3$ hydrocarbons into stereoisomeric benzobarbaralane derivatives ($1B-10-2-1-0-1$) and/or $1B_2-10-2-0-1-3$; the former process, sensitized, involves a di-π-methane rearrangement, the latter, direct, rearrangement is a ring closure of a butadiene to a cyclobutene; thus $1B_1-10-3-0-0-2$ is a "four-way threat",[41] offering alternative structural and stereochemical pathways. Hydrocarbon $1B_1-10-3-0-0-2$ is stable at elevated temperature.[40]

---

[35] L. Lombardo and D. Wege, *Tetrahedron*, **30**, 3945 (1974).

[36] R. C. Hahn and R. P. Johnson, *J. Amer. Chem. Soc.*, **98**, 2600 (1976).

[37] D. R. Miller and D. L. Dolce, *Tetrahedron Letters*, **1976**, 1059.

[38] H. D. Martin, S. Kagabu and H.-J. Schiwek, *Tetrahedron Letters*, **1975**, 3311.

[39] R. E. Carhart, D. H. Smith, H. Brown and C. Djerassi, *J. Amer. Chem. Soc.*, **97**, 5755 (1975).

[40] R. C. Hahn and R. P. Johnson, *Tetrahedron Letters*, **1973**, 2149.

[41] R. C. Hahn and R. P. Johnson, *J. Amer. Chem. Soc.*, **97**, 212 (1975).

To conclude the present discussion, mention should be made of haloderivatives (from tetrachloro- or tetrafluorobenzyne) with structure $1B-10-1-1-0-1$ and $1B_1-10-2-0-1-3$,[42] of structures $1B-10-2-1-0-1$ and $1B_3-10-3-0-0-3$ mentioned by Tanida and coworkers,[43] and a study by Gheorghiu and Pârvulescu of the addition of dichlorocarbene to hydrocarbons and oxygen-bridged hetereoanalogues with structures $1B-8-2-0-0-1$ and $1B_1-10-2-0-1-3$.[44]

Dibenzo-heterocyclic systems $2B_4-10-4-0-0-1$ with the black dot symbolizing an oxygen or sulphur heteroatom were prepared by Anastassiou.[45,46]

---

[42] H. Heany and J. M. Jablonski, *Tetrahedron Letters*, **1967**, 2733.

[43] T. Tsuji, H. Ishitobi and H. Tanida, *Bull. Chem. Soc. Japan*, **44**, 2447 (1971).

[44] M. D. Gheorghiu and L. Pârvulescu, *Rev. Roumaine Chim.*, **22**, 1089 (1977).

[45] A. G. Anastassiou, *Acc. Chem. Res.*, **8**, 281 (1972).

[46] A. G. Anastassiou and B. Chao, *Chem. Commun.*, **1972**, 277.

Revue Roumaine de Chimie, **22**, 7, 1003–1015. (1977)

Dedicated to the 75th anniversary of
prof. C. D. NENITZESCU'*s birthday (1902–1970)*

PYRYLIUM SALTS FORMED BY DIACYLATION OF OLEFINS. XXIII[1]

ISOMERIC ETHYLTRIMETHYLPYRIDINES AND DIMETHYL-n-PROPYLPYRIDINES FROM THE DIACETYLATION OF HEXENES AND METHYLPENTENES

A. T. BALABAN,[a] ANISIA BOTA,[a] F. CHIRALEU,[b] ELVIRA ŞLIAM,[b]
ANA HANEŞ[b] and C. DRĂGHICI[b]
[a] Department of Organic Chemistry, The Polytechnic Institute, Bucharest
[b] Research Centre for Organic Chemistry, Bucharest

(*Received January 11, 1977*)

Of the ten possible ethyltrimethylpyridines, four were prepared *via* pyrylium salts. Diacetylation of 3-methyl-2-pentene **4** and reaction of the resulting mixture of pyrylium-salts with ammonia afforded pentamethylpyridine **7** and 4-ethyl-2,3,6-trimethylpyridine **9**. 2-Butanone **1** yielded, on treatment with acetic anhydride and perchloric acid, and then with ammonia, 6-ethyl-2,3,4-trimethylpyridine **17** in addition to the above two pyridines **7** and **9**. This pyridine **17** is believed to be the unidentified product in an earlier heterogeneously-catalyzed reaction of 2-butanone with ammonia. Similarly, 2-methyl-2-pentene **22** yielded 2,6-dimethyl-4-*n*-propylpyridine **27** and 3-ethyl-2,4,6-trimethyl pyridine **25**. 1-Hexene **29** yielded analogously 2,6-dimethyl-3-*n*-propylpyridine **33**, while 2-hexene **28** afforded the known 3-ethyl-2,5,6-trimethylpyridine **31**. 2,6-Dimethyl-4-*n*-propylpyrylium perchlorate **26** was isolated in crystalline state, and then converted to the corresponding pyridine **27**. The structures of the pyridines were demonstrated by NMR spectroscopy, using also lanthanide-induced shifts (LIS) and partial deuteration of pyrylium salts.

INTRODUCTION

In previous papers [2,3] and reviews [4,5] it was shown that diacylation of substituted propenes to pyrylium salts afforded different products according to the reaction conditions: in the case of 2-methyl-2-butene, diacetylation with acetyl chloride and strong Lewis acids, such as aluminium or antimony(V) chlorides, yielded 2,6-dimethyl-4-ethylpyrylium, whereas weak Lewis acids, such as beryllium chloride,[6] or acetic anhydride with Lewis or Brönsted acids, afforded mostyl 2,3,4,6-tetramethylpyrylium. This was interpreted as being due to the ease of olefin isomerization : stronger Lewis acids make this isomerization fast and reversible so that the pyrylium salt is derived from the more reactive olefin with marginal double bond (2-methyl-1-butene), present in small amount in the equilibrium mixture ; with weak Lewis acids the isomerization is not fast enough so that the olefin reacts in its form with "internal" double bond, 2-methyl-2-butene. This interpretation rests on tracer experiments which evidenced the reversibility of the aliphatic monoacylation.[7,8] However, not only the catalyst but also the nature of the acyl reagent influence the outcome of the reaction, since dipropionylation [2] or dibenzoylation of 2-methyl-2-butene only afforded the tetrasubstituted pyrylium salt, even with aluminium chloride as catalyst.[9]

---

[1] Preceding part, A. T. BALABAN and I. I. BĂDILESCU, *Rev. Roumaine Chim.*, **21**, 1339 (1976).

[2] A. T. BALABAN and C. D. NENITZESCU, *J. Chem. Soc.*, **1961**, 3553.

[3] P. F. G. PRAILL and A. L. WHITEAR, *J. Chem. Soc.*, **1961**, 3573.

[4] A. T. BALABAN and C. D. NENITZESCU, *Rev. Chim. Acad. R. P. Roumaine*, **6**, 269 (1961); *Studii şi Cercetări Chim. Acad. R. P. România*, **9**, 251 (1961).

[5] A. T. BALABAN, W. SCHROTH and G. FISCHER, *Adv. Heterocyclic Chem.* **10**, 241 (1969).

[6] A. T. BALABAN, E. BARABAS and M. FĂRCAŞIU, *Chem. and Ind.* **1962**, 781.

In the present paper we report further results where the olefin may isomerize ; whereas the two olefins discussed above, 2-methyl-2-butene and 2-methyl-1-butene, are both derived from the dimethylethylcarbenium ion, we started by investigating an olefin derived from the diethylmethylcarbenium ion, 3-methyl-2-hexene **4**. This afforded a mixture of pyrylium salts which was converted into the difficulty accessible pentamethylpyridine **7** and an unreported ethyltrimethylpyridine, **9**, in different amounts with different acylating agents. We obtained this same ethyltrimethylpyridine **9** starting from ethyl methyl ketone, acetic anhydride and perchloric acid, along with an isomeric ethyltrimethylpyridine **17** and with pentamethylpyridine **7**. We then investigated other olefins which could lead to isomers of ethyltrimethylpyridines, namely 2-methyl-2-pentene **22**, 1- and 2-hexene, **28** and **29**.

Theoretically, there are ten possible ethyltrimethyl-pyridines, as shown by applying Polya's enumeration theorem [10] to $(CH)_6$; substituting

$$C_i = (r + s + t + u)^i$$

into the cycle index of benzene

$$\frac{1}{12}\,(C_1^6 + 3C_1^2\,C_2^2 + 4C_2^3 + 2C^2 + 2C_6)$$

one finds [11] for r^3stu or rs^3tu, etc. the coefficient 10, indicating the number of isomers in a benzene with four different substituents (ethyltrimethylpyridine may be considered as such, the three different substituents being

---

[7] M. Frangopol, A. Genunche, P. T. Frangopol and A. T. Balaban, *Tetrahedron*, **20**, 1881 (1964) ; D. Fărcașiu, A. T. Balaban and M. Gutman, *Rev. Roumaine Chim.*, **9**, 727 (1964).

[8] M. Frangopol, A. Genunche, N. Negoiță, P. T. Frangopol and A. T. Balaban, *Tetrahedron*, **23**, 841 (1967) ; A. T. Balaban, in "Omagiu pentru Prof. Raluca Ripan", Editura Academiei, Bucharest, 1966, p. 103.

[9] A. T. Balaban, *Tetrahedron Letters*, **1963**, 91 ; A. Bota, A. T. Balaban and F. Chiraleu, *Rev. Roumaine Chim.*, **21**, 101 (1976).

[10] F. Harary, E. M. Palmer, R. W. Robinson and R. C. Read, in "Chemical Applications of Graph Theory" (editor A. T. Balaban), Academic Press, London, 1976, p. 11.

[11] A. T. Balaban, D. Fărcașiu and F. Harary, *J. Labelled Comp.* **6**, 211 (1970).

the ethyl group, the aromatic proton and the nitrogen heteroatom). Only one of these isomers, **31**, had been reported.[12]

Pentamethylpyridine **7** had been prepared [13–15] by a complicated procedure starting from 3,5-dicarbethoxy-2,4,6-trimethylpyridine, and was isolated also from other sources.[16,17]

DIACETYLATION OF 3-METHYL-2-PENTENE OR OF DIETHYLMETHYLCARBINOL

Diethylmethylcarbinol (3-methyl-3-pentanol) **3** was prepared from ethylmagnesium bromide with either 2-butanone (ethyl methyl ketone) **1**,[18] or ethyl acetate, **2**.[19] Its iodine-catalysed or oxalic acid promoted dehydration followed by fractionation afforded the diastereomeric 3-methyl-2-pentenes **4** and 2-ethyl-1-butene **5**.[20] Diacetylation of either the olefins or of the carbinol (which dehydrates *in situ*) was performed at 80–100° with excess acetic anhydride by adding 70% perchloric acid; alternatively, the olefin was added to the acetyl chloride-aluminium chloride complex at room temperature. The crude mixture of pyrylium salts was converted by aqueous ammonia into pyridines which were analyzed and separated by gas-liquid chromatography (GLC). Two products were identified as shown below: 4-ethyl-2,3,6-trimethylpyridine **9** and pentamethylpyridine **7** (in the order of increasing retention times); the relative amounts are 60 : 40 for $AlCl_3$ + AcCl and 33 : 67 for Ac_2O + $HClO_4$, in agreement with the above theoretical interpretation; the ethyltrimethylpyridine must originate from the isomeric olefin **5** with the terminal double bond, and this is favoured by AcCl + $AlCl_3$; in the present case, however, the selectivity is lower than with 2-methyl-2-butene.

Pentamethylpyridine **7** is easily identified by the fact that it forms a less volatile crystalline hemihydrate [15] so that the pyridine mixture exposed to the atmosphere on a dish overnight becomes almost pure pentamethylpyridine hemihydrate.

---

[12] G. N. Dorofeenko, V. I. Dulenko and N. V. Kovalenko, *Zh. Obshchei Khim.*, **34**, 332 (1964).

[13] P. Karrer and S. Mainoni, *Helv. Chim. Acta*, **34**, 2151 (1951).

[14] V. Galik and S. Landa, *Coll. Czech. Chem. Comm.*, **29**, 2562 (1964).

[15] H. G. Biedermann, K. Oefele, N. Schubauer and J. Tajtelbaum, *Angew. Chem.* **87**, 634 (1975); *Angew. Chem. Internat. Edit.* **14**, 639 (1975).

[16] E. D. Vasilieva, I. L. Kotlyarevsky and Y. M. Faiershtein, *Izv. Akad. Nauk. Ser. Khim.*, **1965**, 322.

[17] G. R. Clemo, *Tetrahedron*, **29**, 3987 (1973).

[18] A. E. Favorskii and I. Zalesskaya-Kibardina, *Bull. Soc. Chim. France*, [4] **37**, 1227 (1925); *Zh. Russ. Fiz-Khim. Obshchestva*, **57**, 287 (1925); H. Gilman and F. Schulze, *J. Amer. Chem. Soc.*, **49**, 2328 (1927).

[19] L. Henry, *Compt. rend.*, **144**, 552 (1907); *Rec. Trav. chim.*, **26**, 94 (1904); M. Willcox and R. F. Brunel, *J. Amer. Chem. Soc.*, **38**, 1821 (1916).

[20] H. Van Risseghem, *Bull. Soc. chim. belges*, **30**, 8 (1921); **31**, 213 (1922); **32**, 144 (1923); **33**, 115 (1924).

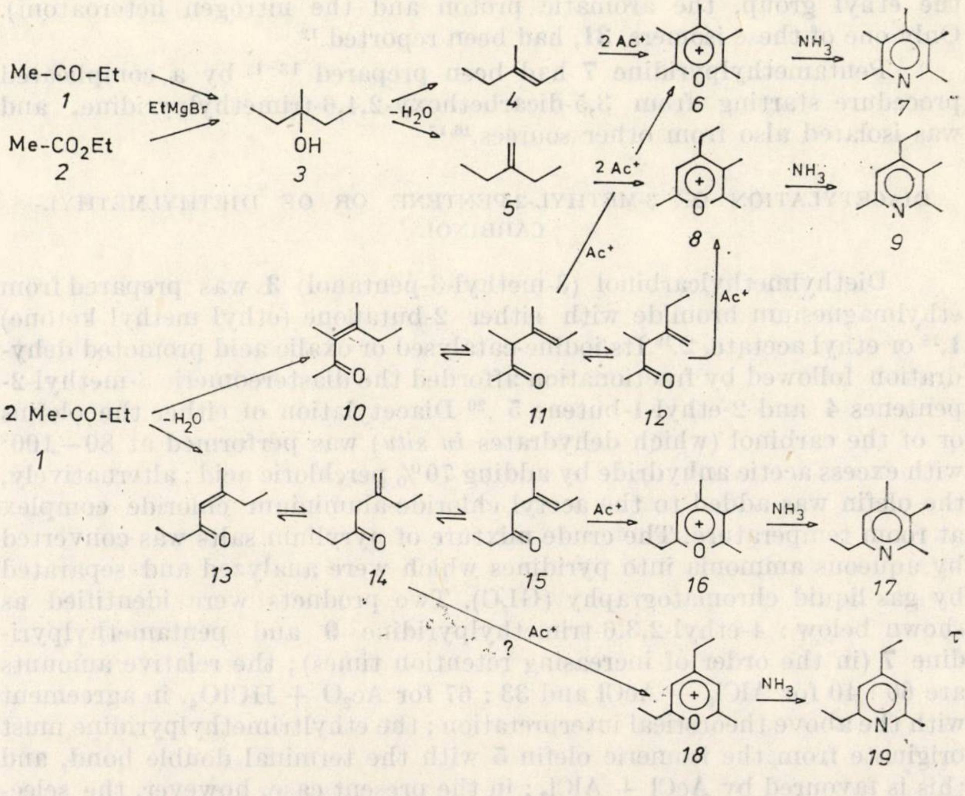

The NMR spectrum of **7** (table 1) presents, unlike all other pyridines to be discussed in the present paper, no peak in the aromatic proton region; the accidental degeneracy of the β and γ methyl groups in CS_2, $CDCl_3$ or CCl_4 is resolved in C_6H_6 or C_6D_6 (α-CH_3, τ 7.51; β-CH_3, τ 8.10; γ-CH_3, τ 8.13) which cause [21] marked downfield shifts for the α-methyl and upfield shifts for the β- and γ-methyl groups; the degeneracy is also resolved by lanthanide shift reagents (table 1) or by protonation to the conjugate acid; this protonation may be achieved either by using trifluoroacetic acid (TFA) as solvent (table 2) or by preparing the crystalline perchlorate and recording its NMR spectrum in deuterochloroform (the solubility is satisfactory), when in addition to the α, β, and γ-methyl peaks at τ 7.28, 7.64 and 7.54 ppm, respectively, the NH proton at τ 2.67 may be seen, since it does not exchange with the solvent as it happens in TFA.

4-Ethyl-2,3,6-trimethylpyridine **9** presents in CS_2 an NMR spectrum (table 1) with two closely spaced α-methyl peaks and another methyl peak at higher field. The LIS data (table 1) are in agreement with the struc-

[21] P. Laszlo, *Progress NMR Spectroscopy*, **3**, 231 (1967).

ture and so are also the NMR spectra in TFA (table 2): the α-methyl groups become degenerate in the latter solvent. One may generalize the data in tables 1 and 2 to the conclusions presented in table 3 : this table is to be applied with caution, however, and not used for compounds with widely different structure from those few ethyl- and/or methyl-pyridines for, and from which, it was devised.

A chemical proof of the structure of **7** and **9** was provided by studying the deuteration of the pyrylium salt mixture in CH_3-COOD for a time insufficient for complete deuteration ; conversion into pyridine, followed by preparative GLC separation and NMR spectral study revealed that the pentamethylpyridine (in TFA) had extensive γ-methyl deuteration, no β-methyl deuteration and slight α-methyl deuteration in agreement with the kinetics of pyrylium methyl deuteration ; [22–24] the 4-ethyl-2,3,6-trimethylpyridine **9** had extensive deuteration of the ethyl methylene group, evident both in the depression of the methylene quadruplet integral, and in the changed pattern of the coupled methyl signal : in CS_2, between the components of the 1 : 2 : 1 triplet, a doublet of closely-spaced 1 : 1 : 1 triplets appears due to the methyl group bonded to a CHD group, since the proton causes the doublet splitting, and the deuteron the small 1 : 1 : 1 triplet splitting ; the two α-methyl groups had slight deuteration and the β-methyl no deuteration.

ACETYLATING CONDENSATION OF 2-BUTANONE

In addition to the above pyridines, **7** and **9**, in some runs a third isomeric pyridine **17** was present. By its NMR spectrum it was a different ethyltrimethylpyridine. Finally, it could be traced to those runs which were based on the diethylmethylcarbinol prepared from 2-butanone (ethyl methyl ketone) **1**, which contained unreacted 2-butanone **1** as an impurity. As a confirmation, when pure 2-butanone **1** was introduced into a mixture of AcCl + $AlCl_3$ and worked up as above, the same three pyridines were obtained : 27% **17**, 21% **9** and 52% **7** (in the order of increasing retention times).

The structure of the new isomer is 6-ethyl-2,3,4-trimethylpyridine, **17**, as it was proved by the NMR spectrum with one α-methyl peak, at lower field, two methyl peaks at higher field and one β-hydrogen. The chemical shifts of the ethyl group are not characteristic, as seen from table 1, therefore they do not discriminate among isomeric ethyltrimethylpyridines. The assignment of the three methyl groups is nicely confirmed by partial deuteration of the pyrylium salt mixture followed by conversion

---

[22] A. T. Balaban, E. Gârd, A. Vasilescu and A. Barabas, *J. Labelled Comp.*, **1**, 266 (1965).

[23] E. Gârd, A. Vasilescu, G. D. Mateescu and A. T. Balaban, *J. Labelled Comp.*, **3**, 196 (1967).

[24] E. Gârd, I. I. Stănoiu, F. Chiraleu and A. T. Balaban, *Rev. Roumaine Chim.*, **18**, 257 (1973).

Table

¹H-NMR Spectra of alkyl-substituted pyridines in CS_2 (τ-values),

Compound / Position	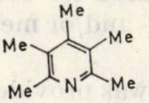 7	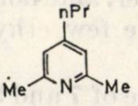 *27*	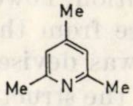 *35*	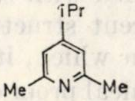 *39*	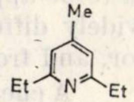 *41*
2	7.67 (13.0)	7.62	7.63 (15.0)	7.62	7.34 (6.5) 8.78 (1.8)
3	7.89 (3.6)	3.35	3.33 (6.0)	3.32	3.33 (2.5)
4	7.89 (3.3)	7.58 8.42	7.78 (3.8)	7.27 8.80	7.75 (1.6)
5	7.89 (3.6)	3.35	3.33 (6.0)	3.32	3.33 (2.5)
6	7.67 (13.0)	7.62	7.63 (15.0)	7.62	7.34 (6.5) 8.78 (1.8)

into pyridines, GLC separation and NMR study in CS_2; only the γ-methyl peak is appreciably decreased relatively to the NMR spectrum of non-deuterated **17**.

Russian investigators [16] had obtained from 2-butanone and ammonia an unidentified pyridine $C_{10}H_{15}N$ (picrate m.p. 120—121°, chloroplatinate m.p. 211° dec.). Since the melting points of the same derivatives of **17** are 113—114° and 205°, respectively, we believe that the unidentified [16] pyridine is identical to **17**.

The formation of three pyrylium salts and pyridines in the acetylation of 2-butanone may be rationalized by the condensation leading to unsaturated ketones **10**—**15**; then, the β,γ-unsaturated isomers **11**, **12** and **15** afford pyrylium salts **6**, **8**, and **16**, and pyridines **7**, **9** and **17**, respectively, by monoacetylation. The only other such isomeric β, γ-enone, which could exist in equilibrium with those mentioned above, is **14**: its further acetylation would afford 2,4-diethyl-6-methylpyrylium **18** and this would be converted into the corresponding pyridine **19**. Since GLC separation evidenced a few minor components of the pyridine mixture, one cannot exclude the presence of **19**; however, this amounts to at most 5%.

1

and MIS data (in brackets) in the presence of Eu (dpm)$_3$

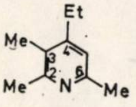 9	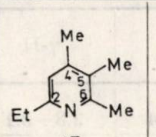 17	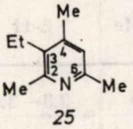 25	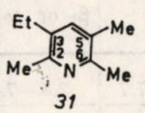 31	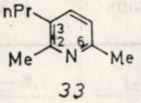 33	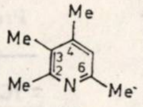 37	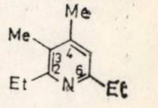 43
7.63 (15.2)	7.41 (11.3) 8.82 (3.0)	7.61 (14.1)	7.64 (11.0)	7.62 (13.8)	7.64 (13.0)	7.29 (4.2) 8.80 (1.5)
7.88 (4.4)	3.35 (4.1)	7.43 (3.9) 8.92 (2.5)	7.50 (3.2) 8.85 (2.0)	7.50 (3.7) 8.50 (2.8) 9.04 (1.7)	7.98 (3.7)	7.87 (1.2)
7.45 (3.7) 8.64 (2.6)	7.80 (2.6)	7.80 (3.6)	3.02 (3.5)	2.86 (4.5)	7.88 (3.7)	7.82 (1.0)
3.34 (6.4)	7.87 (2.7)	3.38 (6.2)	7.85 (2.8)	3.24 (5.3)	3.36 (7.9)	3.40 (1.6)
7.68 (15.7)	7.61 (9.41)	7.70 (14.6)	7.68 (10.4)	7.64 (14.5)	7.70 (14.7)	7.43 (4.5) 8.80 (1.8)

Table 2

^{1}H-NMR Spectra of alkyl-substituted pyridines in F$_3$C – COOH (τ-values)

Compound / Position	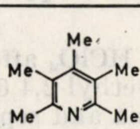 7	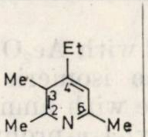 9	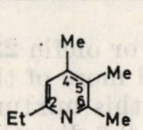 17	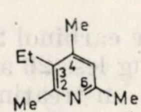 25	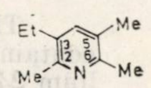 31
2	7.25	7.22	6.97 8.55	7.25	7.23
3	7.53	7.54	2.48	7.13 8.67	7.15 8.65
4	7.41	7.04 8.61	7.37	7.38	1.87
5	7.53	2.50	7.57	2.60	7.48
6	7.25	7.22	7.22	7.32	7.23

Table 3

Ranges of chemical shifts (τ-values), and of MIS values with Eu $(dpm)_3$ (in ppm), for methyl and aromatic proton peaks of pyridines with two α-methyl substituents (solvents in brackets)

Protons	α-Me	β- or γ-Me	β-H	γ-H
τ (CS_2)	7.6– 7.7	7.8–7.9	3.3–3.4	2.8–3.1
τ (TFA)	7.2– 7.3	7.4–7.6	2.4–2.6	1.8–1.9
MIS (CS_2)	10.0–15.0	3.5–6.0	6.0–8.0	3.0–4.0

DIACETYLATION OF DIMETHYL-n-PROPYLCARBINOL

Dimethyl-n-propylcarbinol (2-methyl-2-pentanol) **21** was prepared from ethyl butyrate **20** and methylmagnesium iodide [19,25] or from acetone and n-propylmagnesium bromide.[26] Its dehydration [20] affords 2-methyl-2-pentene **22**. This olefin with acetyl chloride and aluminium chloride afforded a mixture of two pyrylium salts, with 2,6-dimethyl-4-n-propylpyrylium prevailing, so that the perchlorate **26** could be isolated crystalline.

Conversion of the pyrylium salt mixture into pyridines and preparative GLC separation yielded 78% **27**, 2% an unidentified compound and 20% **25** (in the order of increasing retention times).

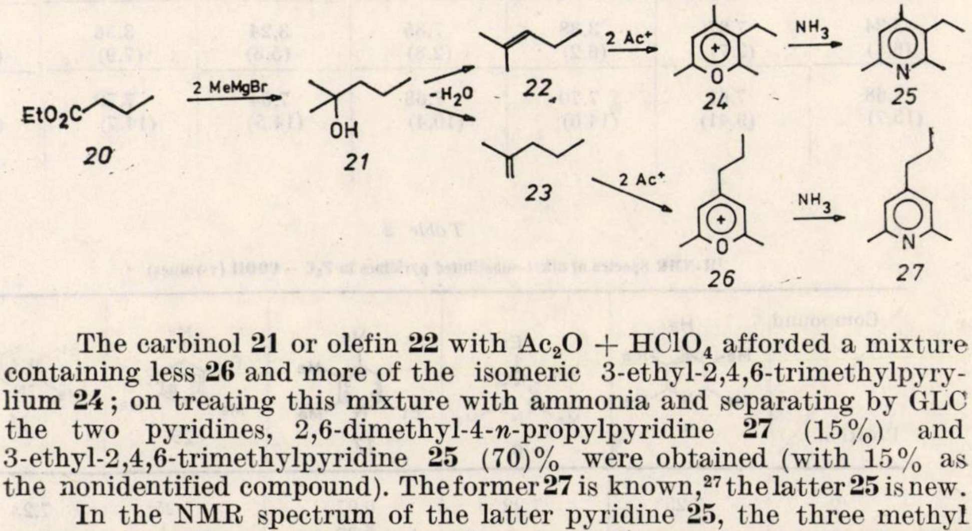

The carbinol **21** or olefin **22** with $Ac_2O + HClO_4$ afforded a mixture containing less **26** and more of the isomeric 3-ethyl-2,4,6-trimethylpyrylium **24**; on treating this mixture with ammonia and separating by GLC the two pyridines, 2,6-dimethyl-4-*n*-propylpyridine **27** (15%) and 3-ethyl-2,4,6-trimethylpyridine **25** (70)% were obtained (with 15% as the nonidentified compound). The former **27** is known,[27] the latter **25** is new.

In the NMR spectrum of the latter pyridine **25**, the three methyl peaks are equally spaced, both in CS_2 and in TFA as solvents (in all other cases, the difference in chemical shifts between α-standing methyl groups is so small in CS_2, that in TFA they become degenerate, cf. tables 1 and 2).

---

[25] H. Masson, *Compt. rend.*, **132**, 483 (1901); L. Jawein, *Liebigs Ann. Chem.*, **195**, 258 (1879).

[26] J. P. Wibaut, H. Hoog, S. L. Langedijk, J. Overhoff and. J. Smittenberg, *Rec. trav. chim.*, **58**, 329 (1939).

[27] A. Jaeckle, *Liebigs Ann. Chem.*, **246**, 32 (1888).

The formation mechanism of the two pyrylium salts **24** and **26**, and of the two corresponding pyridines **25** and **27**, is simple, involving the two possible olefins **22** and **23**; in the presence of $AlCl_3$, the product **26** formed from the marginal olefin **23** prevails, in agreement with the accepted mechanism.

DIACETYLATION OF 1- AND 2-HEXENE

To complete the picture, the diacetylation of a mixture of 1- (**29**) and 2-hexenes (**28**) was reinvestigated. The 3-ethyl-2,5,6-trimethylpyridine, **31**, resulted from 2-hexene, which had been obtained similarly by Dorofeenko *et al.*[12] on diacetylating 2-acetoxy-*n*-hexane, has a normal NMR spectrum as seen from tables 1 and 2 : the chemical shifts of methyl and ethyl protons in **31** are quite similar to those of 4-ethyl-2,3,6 trimethylypyridine **9** but the aromatic proton presents a significant difference : in agreement with table 3, a γ-standing proton in pyridines appears at lower field than a β-standing proton.

The new 2,6-dimethyl-3-*n*-propylpyridine **33**, formed *via* the corresponding pyrylium salt **32** from 1-hexene, also has a normal ^{1}H-NMR spectrum (table 1) which may be compared with that of the isomeric 2,6-dimethyl-4-n-propylpyridine **27** ; the main difference is in the position of the aromatic protons : γ-proton at τ 2.86, β-proton at τ 3.35.

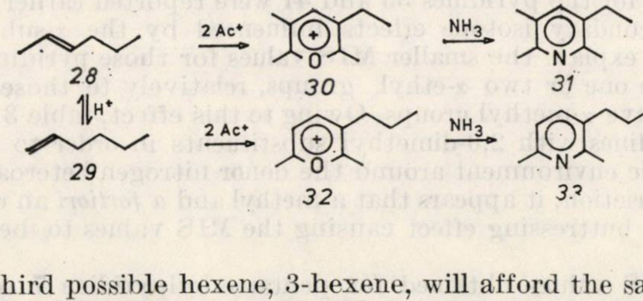

The third possible hexene, 3-hexene, will afford the same pyrylium salt **30** and pyridine **31** as 2-hexene ; therefore it was not investigated. It is obvious that geometrical (*cis-trans*) isomerism is expected to exert little or no influence on the outcome of a reaction performed under strong acid catalysis.

NMR SPECTRA OF PYRIDINES IN THE PRESENCE OF LANTHANIDE SHIFT REAGENTS

In order to better differentiate between α, β, and γ-standing hydrogens or alkyl groups in pyridines for structure assignments, we investi-

---

[28] A. F. Cockerill, G. L. O. Davies, R. C. Harden and D. M. Rackham, *Chem. Rev.* **73**, 553 (1973) ; R. von Ammon and R. D. Fischer, *Angew. Chem.*, **84**, 737 (1972) ; I. Ya. Slonim and A. Kh. Bulai, *Uspekhi Khim.*, **42**, 1976 (1973) ; English transl., p. 904 ; M. R. Petterson and G. H. Wahl, *J. Chem. Educ.*, **49**, 790 (1972) ; J. K. M. Sanders and D. H. Williams, *Nature*, **240**, 385 (1972) ; B. C. Mayo, *Chem. Soc. Revs.*, **2**, 49 (1973).

gated the lanthanide-induced shifts (LIS) (cf. reviews [28, 29], previous data in CS_2,[30] relevant papers on pyridines [31–35]) in the presence of tris (dipivaloylmethanato)europium (III), $Eu(dpm)_3$, in the ^1H-NMR spectra, in carbon disulphide solution. The results are presented in tables 1 and 3; the data presented are molar induced shifts (MIS) determined by extrapolation from the linear dependence obtained with molar ratios $Eu(dpm)_3$/pyridine in the range 0–0.5. The absolute MIS values have an accuracy of 10–15%.

Table 1 also includes for comparison 2,4,6-tri- (**35**) and 2,3,4,6-tetramethylpyridine (**37**), 2,6-dimethyl-4-isopropylpyridine (**39**), 2,6-diethyl-4-methylpyridine (**41**) and 2,6-diethyl-3,4-dimethylpyridine (**43**), all obtained *via* pyrylium salts **34, 36, 38, 40** and **42**, and described earlier; [2,36*]

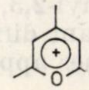
34

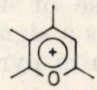
36

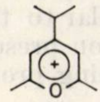
38

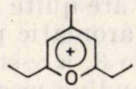
40

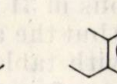
42

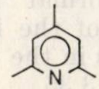
35

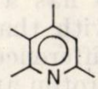
37

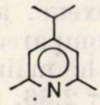
39

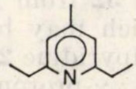
41

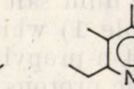
43

the LIS data for the pyridines **35** and **41** were reported earlier in connection with secondary isotope effects influenced by the α-substituents.[37] These effects explain the smaller MIS values for those pyridines in table 1 which have one or two α-ethyl groups, relatively to those pyridines which only have α-methyl groups. Owing to this effect, table 3 refers only to such pyridines with 2,6-dimethyl substituents in order to maintain a constant steric environment around the donor nitrogen heteroatom. Even with this restriction, it appears that a methyl and *a fortiori* an ethyl group in β exerts a buttressing effect causing the MIS values to be somewhat smaller.

The MIS values obtained for pentamethylpyridine **7** refer to the liquid hygroscopic anhydrous pyridine; the crystalline hemihydrate of

---

[*] It will be observed that with the exception of compounds **1–5, 10–15, 20–23, 28** and **29**, an even number indicates a pyrylium cation, while the next odd number indicates the corresponding pyridine.

[29] R. E. Sievers (editor), "Nuclear Magnetic Resonance Shift Reagents", Academic Press, New York, 1973.

[30] D. B. Walters, *Analyt. Chim. Acta*, **60**, 421 (1972).

[31] M. Hirayama, E. Edagawa and Y. Hanyu, *Chem. Comm.*, **1972**, 1343; R. K. Mackie and T. M. Shepherd, *Org. Magn. Resonance*, **4**, 557 (1972).

[32] K. Tori, Y. Yoshimura, M. Kainosho and K. Ajisaka, *Tetrahedron Letters*, **1973**, 3127.

[33] W. L. F. Armarego, T. J. Batterham and J. R. Kershaw, *Org. Magn. Resonance*, **3**, 575 (1971).

[34] H. Huber and J. Seelig, *Helv. Chim. Acta*, **55**, 135 (1972).

[35] J. Reuben and J. S. Leigh, *J. Amer. Chem. Soc.*, **94**, 2879 (1972).

[36] A. T. Balaban and C. D. Nenitzescu, *Liebigs Ann. Chem.*, **625**, 74 (1959).

[37] A. T. Balaban, F. Chiraleu, I. I. Stănoiu and E. Gârd, *Chem. Comm.* **1976**, 984.

7 yields appreciably lower MIS values, with partial decomposition of $Eu(dpm)_3$, namely 6.4 for α-, 1.5 for β-, and 1.3 ppm for γ-methyl groups. These values are all a little smaller than half the MIS values of the anhydrous base.

The data from table 1 indicate that the MIS values are approximately equal for methyl or methylene groups (the latter belonging to ethyl groups) when they are situated in the same positions. On the other hand, there are significant differences between the MIS values of an aromatic proton and a methyl, or between two aromatic protons, when these are in β or γ, but not between two methyl groups when these are in β and γ. This is most readily apparent in the LIS of 2,3,4,6-tetramethylpyridine, **37**, where the distinct β and γ-methyl peaks have the same MIS value. This effect is probably due to the inductive effect of the methyl group : the dipole moment in such asymmetrically substituted pyridines lies no longer along the axis passing through the nitrogen heteroatom, hence the europium atom in the complex is also no longer on this axis ; thus, introduction of an extra β-methyl group in 2,4,6-collidine causes the β and γ-methyl groups to be equally deshielded by the europium atom. It appears, therefore, that the β-methyl causes the europium atom to coordinate the nitrogen in a non-axial position opposite the β-methyl (fig. 1). As a consequence, the α-methyl groups have significantly different MIS values (13. and 14.7 ppm). It will be observed from table 1 that this is a general phenomenon in unsymmetrical pyridines, where α-methyl groups have different chemical shifts and MIS values. Since the differences between the 2- and 6-methyl values for the latter (MIS) are more significant than the former (τ), this may assist in the assignment of chemical shifts. Table 1 evidences that for all 2,3,4,6-tetrasubstitutes pyridines with two α-methyl groups, namely **9**, **25** and **37**, the higher α-methyl chemical shift is always associated with the higher MIS value. The latter, as shown in figure 1, is due to the europium being closer to the less crowded (or, at least, less buttressed) 6-methyl group ; therefore, this methyl has the higher chemical shift, probably due to the fact that only this methyl has an electron-releasing alkyl in a *para* position. The only 2,3,5,6-tetrasubstituted pyridine in table 1, namely **31**, presents the reversed phenomenon : the α-methyl with the higher chemical shift has the lower MIS value ; it appears therefore in this case, as indicated in figure 1, that if europium is again closer to the less crowded 6-methyl, this methyl is the one with the lower chemical shift ; this fact can be rationalized on the basis of the hyperconjugative donor ability of the 5-methyl *para* to the 2-methyl prevailing over the 3-ethyl *para* to the 6-methyl.

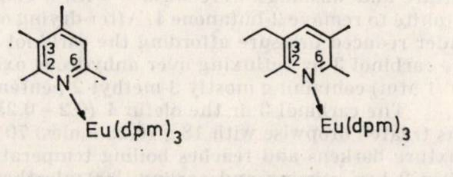

Fig. 1. — Non-axial complexes of pyridines **37** (left) and **31** (right) accounting for the chemical shifts induced by $Eu(dpm)_3$.

Detailed calculations and computer simulations of lanthanide-induced shifts in alkylpyridines will be published separately.

Since LIS data for symmetrically substituted pyridines are less interesting than for unsymmetrical ones, we did not investigate LIS for two such symmetrical pyridines, namely **27** and **39** from table 1.

An interesting conclusion is that coordination to Eu(dpm)$_3$ is strongly influenced by steric factors : a comparison between (i) MIS values for pyridines with two α-methyl groups (tables 1 and 3), (ii) those of **17** with one α-methyl and one α-ethyl, and (iii) those of **41** and **43** with two α-ethyl groups shows how these MIS values drop with increasing size of α-substituents. This is dramatically evidenced by the fact that 2,6-diisopropyl-4-methylpyridine no longer presents any LIS, either with Eu (dpm)$_3$ or with Eu(fod)$_3$ in CS$_2$.[37] Also, literature data [31b] show that LIS values are much larger in 4-picoline than in 2,4,6-trimethylpyridine, owing to steric effects. We reported separately on the steric origin of secondary isotope effects in lanthanide-induced shifts.[37]

EXPERIMENTAL PART

PREPARATION OF PYRIDINES 7 AND 9

Diethylmethylcarbinol **3** was prepared from ethylmagnesium bromide (2.5 moles) and ethyl acetate (1 mole) or from ethylmagnesium bromide and 2-butanone **1** in equimolar amounts. After decomposing the reaction mixture with a saturated aqueous ammonium chloride solution,[38] the magnesium-ammonium complex was filtered off and the combined ethereal filtrate and washings were washed with a concentrated aqueous solution of sodium hydrogen sulphite to remove 2-butanone **1**. After drying on magnesium sulphate, the product was distilled under reduced pressure affording the carbinol **3** (b.p. 122°/1 atm) (90% yield). Dehydration of the carbinol **3** by refluxing over anhydrous oxalic acid yielded a mixture of olefins (b.p.55—69°/1 atm) containing mostly 3-methyl-2-pentene **4**.

The carbinol **3** or the olefin **4** (0.2—0.25 moles) with 145 g (1.4 moles) acetic anhydride was treated dropwise with 18 g (0.23 moles) 70% perchloric acid with stirring under reflux. The mixture darkens and reaches boiling temperature owing to the exothermicity of the reaction. After 2 hrs' stirring and cooling, 300 ml ether were added, the black lower layer containing pyrylium salts was separated and introduced into an excess of aqueous ammonia affording pyridines. These were extracted with ether and separated from non-basic side-products by extraction into 10% hydrochloric acid, extraction with ether, alkalinization of the aqueous layer, extraction with ether, drying over sodium hydroxide and distillation under reduced pressure. The distillate was analyzed and separated by GLC. On standing overnight in an open vessel, pentamethylpyridine **7** affords the less volatile crystalline hemihydrate, while **9** volatilizes so that the residue is almost pure hemihydrate.

The black lower layer of pyrylium salts can be deuterated by heating in an excess of CH_3-COOD (obtained by refluxing equimolar amounts of D_2O and acetic anhydride for two hours) : partial γ-deuteration takes place in 30 minutes at 100° (total γ- and α-deuteration would require refluxation for a few hours). Then ether was added, and the lower layer was converted as above into pyridines, taking care to effect the first step of the reaction with aqueous ammonia at 0° (once formed, the pyridines do not exchange the methyl hydrogens in these conditions).

The olefin **4** (20 g) was introduced dropwise into a mixture, prepared at 0°, of 40 g acetyl chloride and 30 g freshly sublimed aluminium chloride with mechanical stirring. After standing overnight, the mixture was decomposed by pouring it over cracked ice and hydrochloric acid, extracted with ether, and the aqueous layer was introduced into an excess of aqueous ammonia. To dissolve the aluminium hydroxide, a concentrated solution of sodium hydroxide was then added, the pyridine mixture was extracted with ether, and worked up as described above.

Pentamethylpyridine, **7** : Hemihydrate, m.p. 50° :[15] *Found*, C, 75.71 ; H, 10.26 ; N, 7.99. *Calcd.* for $C_{10}H_{15}N.\frac{1}{2}H_2O$, C, 75.95 ; H, 10.15 ; N, 8.86%. On dehydration with $LiAlH_4$

---

[38] L. F. Fieser and M. Fieser, "Reagents for Organic Synthesis", Wiley, New York, 1967, p. 419.

in ether and subsequent distillation in vacuum, the anhydrous hygroscopic pentamethylpyridine was obtained.[15] *Picrolonate*, m.p. 265—7°,*Found*: C, 58.30; H, 5.76; N, 16.78.$C_{20}H_{23}N_5O_5$ requires C, 58.10; H, 5.61; N, 16,94%. *Picrate*, m.p. 135—7°; *Found*, C, 50.85; H, 4.94; N, 15.02. $C_{16}H_{18}N_4O_7$ requires C, 50.79; H, 4.79; N, 14.81%.

4-Ethyl-2,3,6-trimethylpyridine, **9**: *Picrolonate*, m.p. 210° (from ethanol); *Found*, C, 58.45; H. 5.79; N, 16.89. $C_{20}H_{23}N_5O_5$ requires C, 58.10; H, 5.61; N, 16,94%. *Picrate*, m.p. 110—112° (from ethanol): *Found*: C, 50.77; H, 4.87; N, 14.55. $C_{16}H_{18}N_4O_7$ requires C, 50.79; H, 4.79; N, 14.81%.

REACTION OF 2-BUTANONE WITH ACETIC ANHYDRIDE AND $HClO_4$

Ethyl methyl ketone **1** (2-butanone, 19 g, 0.26 moles) was mixed with 160 g (1.46 moles acetic anhydride and treated dropwise under stirring with 32 g (0.26 moles) 70% perchloric acid. The temperature raises above 100°, and after 3 hrs' stirring ether was added, and the black lower pyrylium salt layer was worked up as above. Preparative GLC separation of the pyridines afforded, in addition to **7** and **9**, an isomeric pyridine **17** with lower retention time.

6-Ethyl-2,3,4-trimethylpyridine, **17**: *Picrolonate*, m.p. 185—186° (From ethanol); *Found*, C, 58.06; H, 5.69; N, 16.68. $C_{20}H_{23}N_5O_5$ requires C, 58.10; H, 5.61; N, 16.94%. *Picrate*, m.p. 113—114° (from ethanol); lit.[16] 120—121°. *Hexachloroplatinate*, m.p. (dec.) 205° (from 1% HCl); lit.[16] 211°.

PREPARATION OF PYRYLIUM SALT 26 AND OF PYRIDINES 25 AND 27

Ethyl *n*-butyrate (58 g, 0.5 moles) was added dropwise into methyl magnesium bromide prepared from 34.3 g magnesium and 141 g methyl iodide (one mole) in ether. Dimethyl-*n*-propylcarbinol **21**, b.p. 120°, was obtained in a similar manner as described above for diethylmethylcarbinol **3**, in 70% yield. On dehydration over anhydrous oxalic acid, the carbinol **21** afforded an olefin mixture containing mostly 2-methyl-2-pentene **22**, b.p. 67°.

This olefin **22** (11 g, 0.13 moles) was added under stirring to a mixture of acetyl chloride (51 g, 0.65 moles) and 14 g (0.13 moles) freshly sublimed aluminium chloride. After 3 hrs' stirring and standing overnight at room temperature, the mixture was poured on ice and hydrochloric acid. The aqueous layer, after extraction with ether, was concentrated to 50 ml in vacuum, and then either worked up to a pyridine mixture, or treated with perchloric acid; the crystalline precipitate was filtered off and recrystallized from ethanol-ether.

2,6-Dimethyl-4-n-propylpyrylium perchlorate, **26**, m.p. 93°; *Found*: C, 47.61; H, 6.20; Cl, 13.99. $C_{10}H_{15}ClO_5$ requires: C, 47.91; H, 6.03; Cl, 14.14%. On treatment with ammonia, this perchlorate affords **27** (see below). The ^1H-NMR spectrum of **26** in trifluoroacetic acid: the β-hydrogens at τ 2.28, the α-methyls at τ 7.03, and the $-CH_2-CH_2-CH_3$ hydrogens at τ.6.97, 8.10 and 8.90, respectively ($J = 7$ Hz). Its IR spectrum (KBr pellet) has strong bands at 1030, 1535 and 1640 cm^{-1} in addition to the ClO_4 bands at 625 and 1100 cm^{-1}.

The carbinol (20 g, 0.2 moles) in 120 g acetic anhydride was treated with 30 g 70% perchloric acid and worked up as above. The lower layer of pyrylium salts which separated after addition of ether was converted into a mixture of pyridines by reaction with ammonia, which were freed from non-basic products and distilled under reduced pressure. Preparative GLC separation afforded 2,6-dimethyl-4-*n*-propyl-pyridine, **27**, and 3-ethyl-2,4- 6, trimethylpyridine, **25**.

PREPARATION OF PYRIDINES 31 AND 33

1-Hexanol (214 g) was dehydrated with 150 ml conc. sulphuric acid affording a mixture of 1- (**29**) and 2-hexene (**29**) which was washed neutral and fractionated collecting the fraction b.p. 63—69°. This mixture (18 g, 0.21 moles) was diacetylated with 133 g acetic anhydride and 30 g 70% perchloric acid, then worked up to a mixture of pyridines as above, which by GLC revealed two major components: 70% *3-ethyl-2,5,6-trimethylpyridine*, **31**: picrolonate m.p.230° (from ethanol); chloroplatinate m.p. 200° dec.; picrate m.p. 142° in agreement with literature data; and 21% *2,6-dimethyl-3-n-propylpyridine*, **33**, whose structure is evident from the ^1H-NMR spectra; picrolonate m.p. 169° (from ethanol); *Found*: C, 58.00; H, 5.50; N, 16.79.$C_{20}H_{23}N_5O_5$ requires C, 58.10; H, 5.61; N, 16.94%.

IR Spectra were recorded with a Jena UR-10 instrument, and *NMR spectra* with a Varian A-60A instrument. Preparative gas-liquid chromatographic separations were run at 120° on a Carlo Erba Model GV instrument with a 2m/10 mm inox column packed with acid-washed chromosorb W (30—60 mesh), coated with 10% polyethylene glycol 20 M.

Revue Roumaine de Chimie, 22, 7, 1017–1025 (1977)

Dedicated to the 75th anniversary of
Prof. C. D. NENITZESCU's *birthday (1902–1970)*

CARBENIUM ION REACTIONS. XIV[**]

SOLVOLYSIS OF "DIBENZOBULLVALENE BROMIDE"

M. BANCIU, RODICA VLAD, C. DRĂGHICI and ECATERINA CIORĂNESCU
Laboratory of Organic Chemistry, Polytechnic Institute,
Str. Polizu 1, Bucharest 12, Romania

Received February 1, 1977

The buffered acetolysis of bromide **2** affords (after $LiAlH_4$ reduction) the alcohol *endo*-**6** as major product beside the alkenes **4** and **5** and the alcohols **7** and **8**. In the unbuffered acetolysis of **2** the allylic alcohols **7** and **8** become the main products. The structures and interconversions of alcohols **6**, **7** and **8** as well as the solvolysis mechanism of **2** are discussed.

The various cationic rearrangements observed[1,2] in the series of dibenzobicyclic compounds of type **1** (n=1, 2) determined us to continue these studies by extending them to the series of higher homologues (**1**, n=3). The bromide **2**, a precursor in the synthesis of dibenzobullvalene, described in a previous paper,[3] is a convenient starting material.

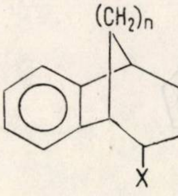

1

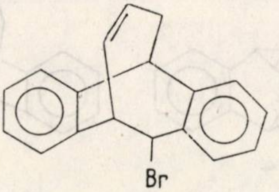

2

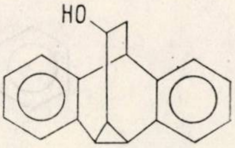

3

One would expect the solvolytic rearrangements of "dibenzobullvalene bromide"[**] (**2**) to proceed in a way similar to those of the known

---

[*] Part XIII. E. DRAGU, M. BANCIU, C. DRĂGHICI, M. ELIAN and E. CIORĂNESCU, *Rev. Roumaine Chim.*, **21**, 1497 (1976).

[**] Name employed by analogy with the parent bullvalene bromide[4] in spite of the fact that the tricyclic skeleton of bullvalene is lost.

[1] S. J. CRISTOL, F. P. PARUNGO, D. E. PLORDE and K. SCHWARZENBACH. *J. Amer. Chem. Soc.*, **87**, 2879 (1965); S. J. CRISTOL, R. M. SEQUEIRA and G. O. MAYO, *ibid.*, **90**, 5564 (1968)

[2] E. CIORĂNESCU, A. MIHAI, G. MIHAI, M. ELIAN and C. D. NENITZESCU, *Rev. Roumaine Chim.*, **10**, 175 (1965); E. CIORĂNESCU, M. BANCIU, R. JELESCU, M. RENTZEA, M. ELIAN and C. D. NENITZESCU, *Rev. Roumaine Chim.*, **14**, 911 (1969); *Tetrahedron Letters*, **1969**, 1871.

[3] M. BANCIU, M. ELIAN, E. CIORĂNESCU and C. D. NENITZESCU, *Tetrahedron Letters*, **1972**, 2573; M. ELIAN, M. BANCIU, L. STĂNESCU and E. CIORĂNESCU, *Rev. Roumaine Chim.*, **21**, 89 (1976).

[4] a) G. SCHRÖDER and J. THIO, unpublished; see references 4b and 4c; b) H. P. LÖFFLER, *Tetrahedron Letters*, **1971**, 4893; c) *ibid.*, **1974**, 2121.

system (**1**, $n=1, 2$). However, the solvolysis (accompanied by elimination) of this 10-carbon bicyclic system may lead to dibenzo $(CH)_{10}$ hydrocarbons, the thermal and photochemical rearrangements of which have been investigated previously.[3] On the other hand, a comparison with the parent "bullvalene bromide" (**2** with no benzene rings, obtained by Schröder[4] from bullvalene and HBr), the solvolysis of which has been recently studied by Löffler,[4] seemed attractive.

RESULTS AND DISCUSSION

The bromide **2**, synthesized previously [3] from alcohol **3** and PBr_3, was also obtained by addition of HBr to dibenzobullvalene (**4**). In both cases, only the *endo* epimer resulted. The assignment of the stereochemistry was made on the basis of NMR analysis (*vide infra*).

The NaOAc-buffered acetolysis of the bromide **2** (1.5 equivalents NaOAc, ten half-lives at 55°) gave a product which after $LiAlH_4$ reduction, was v.p.c. analyzed (93% yield calculated on **2**).

Two hydrocarbons, **4** and **5**, and three alcohols, *endo*-**6**, **7** and **8**, were identified (table 1, entry 1), the main component being the alcohol *endo*-**6**. When the acetolysis was carried out with 6 equivalents of NaOAc, the product distribution was found to be unaltered. On the other hand, when the bromide **2** was acetolyzed in the absence of buffer (NaOAc), the major component was the alcohol **8** (50%) (table 1, entry 6).

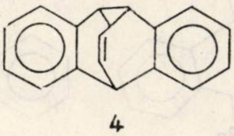
4

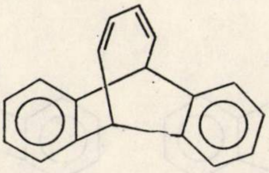
5

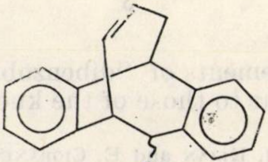

6

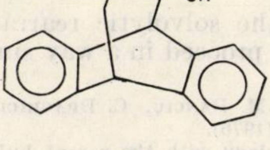

7

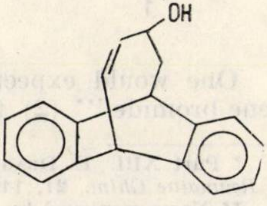

8

Separation of the acetolysis products was accomplished by column chromatography on neutral alumina.

The two hydrocarbons (obtained as a mixture in the first chromatography fraction) were identified as dibenzobullvalene (**4**) and butadienodihydroanthracene (**5**) by v.p.c. comparison with authentic samples.[3]

The structure of alcohols **6**, **7** and **8** and the configuration of alcohols **6** were ascribed by means of NMR spectroscopy analysis. In order to gain more information, the three alcohols were converted to the corresponding ketones **9**, **10** and **11** using Sarett's[5] procedure.

Table 1

Acetolysis products of 2 at 55°

(v.p.c. analysis after $LiAlH_4$ reduction)

	Conditions \ Products[a] (%)	4	5	*endo*-6	7	8	*exo*-6
1	6.5 hrs [b]	6	2	67.5	11.5	5.5	2.5
2	24 hrs [b]	6	1.5	68	13	2.5	3
3	48 hrs [b]	7	2	63	16	2.5	3.5
4	96 hrs [b]	7.5	2	56	23	3	3.5
5	6.5 hrs [b;c]	13.5	5	4	65	10	—
6	6.5 hrs [d]	2	3	7	22	50	—

[a] the differences up 100% are due to many minor unidentified components;

[b] 1.5 moles NaOAc/mole **2**; [c] at 118°; [d] without added NaOAc.

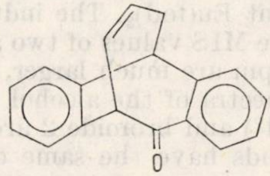

9

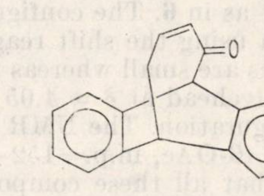

10

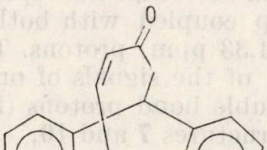

11

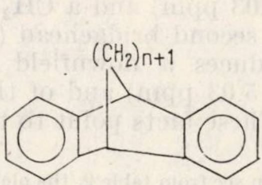

12

Some spectral data concerning the alcohols **6**—**8** and the related ketones are presented in table 2.

All the NMR spectra of the ketones show signals corresponding to two olefinic protons, two CH groups (bridgeheads), one CH_2 group and eight aromatic protons. The spectra of the alcohols present two more signals due to the $CH-OH$ group and to the hydroxylic proton.

The structure of the alcohol **6** and ketone **9** resulted from the following spectral data. The IR and NMR spectra ($\nu_{CO} = 1679$ cm^{-1}; one of the aromatic protons at $\delta = 8.15$ ppm) of **9** point to a bezylic ketone.

---

[5] G. I. Poos, G. E. Arth, R. E. Beyler and L. H. Sarett, *J. Amer. Chem. Soc.*, **75**, 422 (1953).

Table 2

Spectral data for alcohols *endo*-6, 7, 8 and ketones 9, 10 and 11

	IR (cm^{-1})		NMR * (δ, ppm)				
	ν_{OH}	$\nu_{C=O}$	CH	CH=CH	CH_2	*C*H–OH	Aromatic
endo-**6**	3584	—	3.68(dd)+4.05(t)	5.5(m)+5.9(m)	2.4–2.9(m)	4.88(d)	7.1–7.5(m)
9	—	1679	4.47(d)+4.22(t)	5.5–6.2(m)	2.5–3.0(m)	—	7.0–7.5(m ; 7H) +8.15(m ; 1H)
7	3585	—	4.14(t)+4.28(d)	4.8–5.3(m)	2.7–3.1(m)	4.55(m)	7.15–7.60(m)
10	—	1663	4.33(t)+5.03(s)	5.3–5.8(m)	3.05(m)	—	7.15–7.5(m)
8	3626	—	4.26(m)+4.40(d)	5.25(m)+6.02(m)	1.94(m)+2.50(m)	3.85(m)	7.0–7.4(m)
11	—	1678	5.63(d)+6.85(dd)	4.36(t)+4.67(d)	3.28(d)	—	7.11–7.5(m)

* s = singlet ; d = doublet ; t = triplet ; m = multiplet

One of the bridgeheads ($\delta = 4.47$) and the CH_2 unit are both coupled with the double bond protons, whereas the second bridgehead ($\delta = 4.22$) is coupled only with the CH_2 protons, which hints to a proton sequence as in structure **9**. When the alcohol **6** is oxidized to **9**, two protons, in the NMR spectra, are strongly deshielded : one bridgehead (from 3.68 in **6** to 4.47 ppm in **9**) and an aromatic proton. These facts show the position of the OH group as in **6**. The configuration of this alcohol resulted from the NMR spectra using the shift reagent $Eu(fod)_3$. The induced shifts of the bridge protons are small whereas the MIS values of two aromatic protons and the bridgehead at $\delta = 4.05$ ppm are much larger, which points to the *endo* configuration. The NMR spectra of the alcohol **6**, the corresponding acetate (**6**-OAc, m.p.=152–4°) and bromide **2** are much alike, which suggests that all these compounds have the same configuration.

The ketone **10** is, according to the IR spectrum ($\nu_{CO} = 1663$ cm^{-1}), a conjugated ketone. The NMR spectrum shows an uncoupled bridgehead proton ($\delta = 5.03$ ppm) and a CH_2-group coupled with both the double bond and the second bridgehead ($\delta = 4.33$ ppm) protons. The oxidation of **7** to **10** induces a downfield shift of the signals of one bridgehead (from 4.28 to 5.03 ppm) and of the double bond protons (from about 5 to 5.5 ppm). These facts point to the structures **7** and **10**.

As one can see from table 2, the olefinic proton β- with respect to CO is not deshielded with regard to the α-proton, as usual in α, β-unsaturated ketones. The Dreiding stereomodels show a nonplanar bridge with orthogonal CO and double bond π-orbitals. If one assumes that, in order to gain some conjugation, the double bond is slightly twisted, then the β-proton enters the shielding region of the neighbour aromatic ring, so that the peculiar position of the NMR signal of this particular proton is understandable.

The IR spectrum of ketone **11** shows also a conjugated system ($\nu_{CO} = 1678$ cm^{-1}). The couplings in the NMR spectrum (one bridgehead proton coupled with the olefinic protons and the other one with the methylenic protons), as well as the deshielding of the double bond and methylenic protons when the alcohol is oxidized to the corresponding ketone, strongly support the structures **8** and **11**.

These data point to two types of compounds : with dibenzobicyclo [3.3.2] decatriene skeleton, like alcohol *endo*-**6** and ketone **9**, and with dibenzobicyclo[4.2.2]decatriene (or -tetraene) skeleton, like alcohols **7**, **8** and ketones **10**, **11** (and hydrocarbon **5**).

Since the solvolysis of bromide **2** afforded only the *endo*-**6** isomer, we tried to convert the latter (at least partially) into the *exo* isomer, by oxidation to ketone **9**, followed by hydride reduction. The crude reaction mixture contained two alcohols in the ratio 2 : 1, as shown by v.p.c. analysis. The main component was found to be the *endo*-**6** alcohol. The second component, which is very likely *exo*-**6**, has the same v.p.c. retention time as the product which results, in small amounts, in the solvolysis of **2** (table 1, last column). All attempts to isolate pure *exo*-**6** (from the mixture obtained on reduction of ketone **9**) either by elution or by preparative gas-chromatography were unsuccessful.

In order to establish whether the small amounts of *exo*-**6** isomer (2.5–3.5%) are formed primarily or result by an equilibration subsequent to the solvolysis, the mixture of alcohols (obtained by reduction of ketone **9**) was heated with a NaOAc solution in acetic acid (55°, 6.5 hrs). The ratio between the two alcohols was found to remain unchanged.

The interconversions between the alcohols *endo*-**6**, **7** and **8** (the corresponding acetates, respectively) are reflected in the data shown in table 1.

Under buffered conditions, the main solvolysis product (67.5%) is the alcohol *endo*-**6** with bicyclo [3.3.2] skeleton. With longer reaction times the amount of *endo*-**6** decreases slightly, in favour of alcohol **7** (table 1, entries 2–4). The alcohol **7** with bicyclo [4.2.2] skeleton becomes the main product (65%) even under buffered conditions, by carrying out the acetolysis at 118° (instead of 55°); only minor amounts of *endo*-**6** are found under these conditions (table 1, entry 5). It appears, therefore, that even in the buffered acetolysis the raise of temperature or prolongation of the reaction time may favour the conversion of bicyclo [3.3.2] compounds of type **1** ($n = 3$) into bicyclo [4.2.2] compounds of type **12** ($n = 3$).

In the unbuffered solvolysis, the allyl alcohols **7** and **8** (1 : 2 ratio) represent 72% of the reaction products (table 1, entry 6).

The bromide **2** displayed good first-order behaviour in acetolysis ($k_{50^\circ} = 2.85 \times 10^{-4} s^{-1}$). The structures **13**, **14** and **15** are considered for the cationic intermediates involved in this reaction. The possibility of obtaining further support for them is currently investigated in our laboratory.

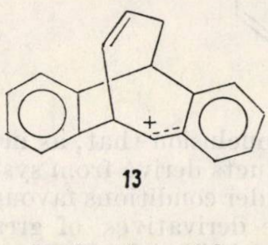

13

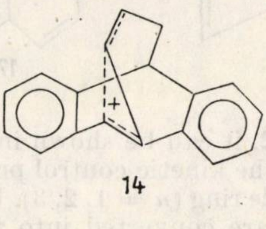

14

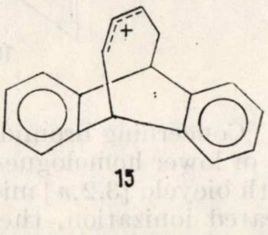

15

Ionization of bromide **2** would produce the stable benzyl cation **13**. However, the steric course of the reaction, namely the almost exclusive formation of the *endo*-**6** isomer (*endo*/*exo*=27/1; no interconversion under the conditions used) is not consistent with the intervention of this intermediate.

The examination of the model of the *endo*-**2** bromide shows that the double bond is particularly well oriented for *exo*-attack, through its π-electron pair, upon the carbon bearing the leaving group, which leads to the relatively stable cyclopropylcarbinyl ion **14**. It would be, therefore, seen that the double bond may compete favourably with the benzene ring in assisting the ionization. Solvent collapse at any of the two benzyl positions of ion **14** can occur only *endo*, holding the stereochemistry of the initial bromide **2**. Cyclopropylcarbinyl to homoallyl isomerizations have been found to be highly stereoselective in several systems, as Winstein and his collab.[6] have shown in a series of papers. Dibenzobullvalene (**4**), which is found among the solvolysis products of bromide **2**, supports the intervention of cyclopropylcarbinyl ion.

The absence of the tricyclic compound **3-OAc**, which could result by attack at the other end of the cyclopropylcarbinyl system **14**, may be due to the ease of its reionization which may lead to further transformations.

The formation of small amounts of *exo*-**6**, in addition to the *endo*-**6** epimer, may indicate the intervention, at least to a small extent, of the benzyl ion **13**. On the other hand, a phenyl shift in this intermediate could lead to an allyl ion **15**. This rearrangement, favoured by the higher stability of the system **12**, related to dihydroanthracene, determines the main reaction course under conditions facilitating the ionization.

The products generated by the ion **15**, the alcohols **7**, **8** and the hydrocarbon **5**, may thus accumulate, amounting to 75% of the acetolysis products (table 1, entry 6).

The solvolysis [4] of the bromide analogous to **2** ("bullvalene bromide") in which the two benzene rings are replaced by two double bonds, affords products similar to **6**, **7** and **8** (about 50% of the total). In addition to these, other compounds like **16** and **17** are formed, by double bond participation, involving ionic intermediates which are not possible in the case of annelation with the two benzene rings.

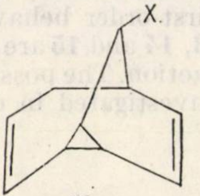

16

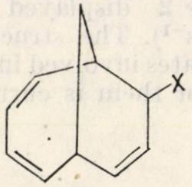

17

Concerning bromide **2**, it can be shown in conclusion that, as in the case of lower homologues, the kinetic control products derive from system **1** with bicyclo [3.2.*n*] middle ring ($n = 1, 2, 3$). Under conditions favouring repeated ionization, they are converted into the derivatives of greater thermodynamic stability related to system **12** with bicyclo [$2.2.n + 1$] skeleton.

---

[6] C. DALE and S. WINSTEIN, *J. Amer. Chem. Soc.*, **92**, 4282 (1970) and the literature cited therein.

EXPERIMENTAL

Melting points are uncorrected. IR spectra were recorded with a double-beam C. Zeiss Jena UR-20 spectrophotometer. NMR spectra were obtained on a Varian A-60A spectrometer using TMS as internal standard. The v.p.c. analyses were performed on a Carlo Erba model D gas-chromatograph using neopentylglycolsuccinate columns (5% on 60—80 mesh silanized Chromosorb W) 1 m long, 2 mm diameter, at 190°, with a nitrogen rate-flow of 30 ml/min.

11-BROMO-10,11-DIHYDRO-10,5-PROPENO-5H-DIBENZO[a,d]CYCLOHEPTENE ("DIBENZOBULLVALENE BROMIDE") (2)

a) *From alcohol* **3** *and* PBr_3. The synthesis of bromoderivative **2** from tricyclic alcohol **3** on treatment with PBr_3 was described previously.[3]

b) *From dibenzobullvalene and HBr.* Dried gaseous HBr (from tetraline and Br_2) was bubbled into a cooled (—25°) stirred solution of dibenzobullvalene (**4**) (50 mg ; 0.21 mmoles) in 50 ml anhydrous methylene chloride. When HBr was no more absorbed in the reaction (about 10 minutes), the bubbling was stopped and the reaction mixture was stirred for 0.5 hr at —25°. The clear colourless solution was washed with water, Na_2CO_3 solution and again with water until neutral pH. After drying and evaporation of the solvent the crude bromide **2** m.p.106—118°, was obtained (64.8 mg; 96%). Recrystallization from *n*-hexane afforded the bromide **2** with a m.p. 120—122°.

IR spectrum (CS_2 ; CCl_4 ; cm^{-1}) : 715 m, 729 m, 735 m, 1129 s, 1147 s, 1416 m, 1452 m, 1480 m, 1488 m, 2816 w, 2894 m, 3028 s and 3071 m.

NMR spectrum ($CDCl_3$; δ, ppm) : 6.9—7.6 (m ; 8H ; H_{arom}) ; 5.3—6.1 (m ; 3H ; $H_{1'}, _{2'}, _{11}$; d ; J = 4.5 Hz at 5.81) ; 4.08 (t ; J = 4 Hz ; 1H ; H_5) ; 3.87 (dd ; J = 4.5 ; 8Hz ; 1H ; H_{10}) and 2.1—3.1 (m ; 2H ; $H_{3'}$).

NaOAc-buffered acetolysis of bromide 2. A solution of bromide **2** (2 g ; 6.4 mmoles) and freshly fused NaOAc (0.79 g ; 11.3 mmoles) in 150 ml anhydrous acetic acid was heated in a thermostat at 55° for 6.5 hrs. The reaction mixture was poured into water (200 ml), neutralized with solid Na_2CO_3, then ether-extracted. The combined organic layers were washed with water, dried and evaporated *in vacuo*, affording a solid residue. This crude mixture of acetates was subsequently reduced with 0.3 g (7.9 mmoles) $LiAlH_4$ in 100 ml anhydrous ether. After the usual work-up a partially crystallized oil (1.5 g; 93%) was obtained. The v.p.c. analysis of the reaction mixture is indicated in table 1. The preparative separation of the acetolysis mixture was performed on a neutral alumina column. On elution with petroleum ether (b.p. 30—40°) a mixture of alkenes **4** and **5** was obtained (0.2 g; 12%). The elution was then continued with progressively enriched mixtures of diethyl ether in petroleum ether. With mixtures of more than 7 : 3 petroleum ether : diethyl ether only small quantities (0.13 g; 8%) of thick oil (which later crystallized) were obtained. The spectral analysis (IR and NMR) of this product indicated a mixture of alcohols **7** and **8**. By continuing the elution with a 1 : 1 mixture of petroleum ether and diethyl ether, a white solid was obtained (0.85 g ; 57%). After two recrystallizations from cyclohexane the pure *endo-10, 11-dihydro-10,5-propeno-5H-dibenzo*[a, d]*cyclohepten-11-ol* (**6**), m.p. 138—140° was obtained. *Found* : C, 86.92 ; H, 6.69 ; $C_{18}H_{16}O$ requires : C, 87.05 ; H, 6.5%.

IR spectrum (CS_2 ; CCl_4 ; cm^{-1}) : 734 vs, 754 s, 763 vs, 1004 s, 1027 m, 1379 m, 2822 w, 2913 m, 3024 m, 3065 m, 3300—3500 m and 3584 m.

NMR spectrum ($CDCl_3$, δ, ppm) : 7.1—7.5 (m, 8H, H_{arom}) ; 5.3—6.15 (m ; 2H ; $H_{1'}, _{2'}$) ; 4.88 (d ; J = 5 Hz ; 1H ; H_{11}) ; 4.05 (t ; J = 4.5 Hz ; 1H ; H_5) ; 3.68 (dd ; J = 5 ; 8Hz ; 1H ; H_{10}) ; 2.4—2.9 (m ; 2H ; $H_{3'}$) and 1.6 (s ; 1H ; OH).

NMR spectrum with chemical shift reagent $Eu(fod)_3$; molar induced shift data : 24.7 (H_{11}) ; 15.7 (H_{10}) ; 13.2 (H_1) ; 7.0 (H_9) ; 6.6 (H_5) ; 4.5 ($H_{3'}$) and 4.0 ppm ($H_{1'}$; $H_{2'}$).

Acetate **6-OAc**, from the alcohol **6** and acetic anhydride in the presence of pyridine, m.p. 152—154°.

IR spectrum (CCl_4 ; CS_2 ; cm^{-1}) : 748 s, 754 s, 762 s, 1237 vs, 1729 vs, 2822 vw, 2895 w, 2918 w, 3024 w and 3067 w.

NMR spectrum ($CDCl_3$; δ, ppm) : 6.9—7.4 (m ; 8H ; H_{arom}) ; 6.24 (*d* ; J = 5.0 Hz ; 1H ; H_{11}) ; 5.4—6.2 (m ; 2H ; $H_{1'}, _{2'}$) ; 4.15 (*t* ; J = 4 Hz ; 1H ; H_5) ; 3.91 (dd ; J = 8.0 ; 5.0 Hz ; 1H ; H_{10}) ; 2.2—3.2 (m ; 2H ; $H_{3'}$) and 1.88 (s ; 3H ; $-COCH_3$).

By continuing the elution with solvent mixtures enriched in diethyl ether small quantities (0.08 g; 5 %) of an oily solid were obtained. The IR spectrum of this product indicated the presence of the impure alcohol **6**.

Unbuffered acetolysis of bromide 2. A solution of bromide **2** (2.5 g; 8.36 mmoles) in 200 ml anhydrous acetic acid was heated in a thermostat at 55° for 6.5 hrs. The reaction mixture was worked up and $LiAlH_4$ reduced (yield 1.9 g; 95 %) in the manner described for the buffered acetolysis of **2** (see above). The v.p.c. analysis of this mixture is indicated in table 1. The preparative separation of the acetolysis mixture was performed on a column filled with neutral alumina. The elution with petroleum ether (b.p. 30–40°) afforded a crystalline residue (0.14 g; 7 %). The IR and NMR spectra indicated the presence of the alkenes **4** and **5**. Further elution with mixtures of petroleum ether and diethyl ether (7 : 3) afforded a new fraction of white crystals (0.40 g; 21 %). After two recrystallizations from methanol, the pure *9,10-dihydro-9,10[1'-hydroxy-2'-buteno]anthracene* (**7**), m.p. 146–7° was obtained. *Found* : C, 87.0 ; H, 6.42 ; $C_{18}H_{16}O$ requires : C, 87.05 ; H, 6.5 %.

IR spectrum (CS_2 ; CCl_4 ; cm^{-1}) : 704 s, 732 s, 778 m, 1009 s, 1415 m, 1452 m, 1482 m, 2812 w, 2885 w, 3008 w, 3031 w, 3071 w and 3585 m.

NMR spectrum ($CDCl_3$; δ, ppm): 7.15–7.60 (m ; 8H ; H_{arom}) ; 4.8–5.3 (m ; 2H ; $H_{2',3'}$) ; 4.55 (m ; 1H ; $H_{1'}$) ; 4.28 (d ; J = 4.5 Hz ; 1H ; H_9) ; 4.14 (t ; J = 4.5 Hz ; 1H ; H_{10}) ; 2.7–3.1 (m ; 2H ; $H_{4'}$) and 2.08 (s ; 1H ; OH).

By continuing the elution with a mixture of petroleum ether and diethyl ether (6.5: 3.5) a new crystalline compound was obtained (0.93g ; 49 %). After two recrystallizations from methanol the pure *9,10-dihydro-9,10[2'-hydroxy-3'-buteno]anthracene* (**8**), m.p. 180–2°, was obtained. *Found* : C, 86.83 ; H, 6.75 ; $C_{18}H_{16}O$ requires : C, 87.05 ; H, 6.5 %.

IR spectrum (CS_2 ; CCl_4 ; cm^{-1}) ; 706 w, 745 m, 773 w, 1045 m, 1454 w, 1481 w, 2851 w, 2909 w, 3024 w, 3045 w and 3626 w.

NMR spectrum ($CDCl_3$; δ, ppm) ; 7.0–7.4 (m ; 8H ; H_{arom}) ; 6.02 (m ; J_{cis} = 12 ; J_{vic} = = 8.5 ; J_{allyl} = 2.5 Hz ; 1H ; $H_{4'}$) ; 5.25 (m ; J_{cis} = 12 ; J_{vic} = 3 ; J_{allyl} = 1 – 1.5 Hz ; 1H ; $H_{3'}$) ; 4.40 (d ; J = 8.5 Hz ; 1H ; H_{10}) ; 4.26 (m ; 1H ; H_9) ; 3.85 (m ; 1H ; $H_{2'}$) ; 2.21 – 2.80 (m ; 1H ; $H_{1'}$) ; 1.94 (m ; 1H ; $H_{1'}$) and 1.48 (s ; 1H ; OH).

The final elution with pure diethyl ether afforded 0.05 g (2.6 %) of an yellow oily solid which was not further investigated.

The CrO_3 oxidation of alcohols 6, 7 and 8. The alcohols **6, 7** and **8** were oxidized after the same procedure (illustrated below for **6**) giving rise to ketones **9, 10** and respectively **11.**

A solution of alcohol **6** (0.85 g ; 3.4 mmoles) in 20 ml anhydrous pyridine was poured with vigorous stirring and cooling during 1 hr over a preformed complex of CrO_3 (0.7 g ; 7 mmoles) with 10 ml anhydrous pyridine. The temperature was allowed to rise to the room temperature, continuing the stirring for about 8 hrs. The reaction mixture was then left overnight. After decomposition with cold water (30 ml) the reaction mixture was ether-extracted (4 × 40 ml). The organic layers were washed successively with water, diluted HCl, again with water, then dried and evaporated *in vacuo*. The crystalline residue (0.75 g ; 88 %) was then recrystallized from ethanol, affording *10,11-dihydro-10,5-propeno-5H-dibenzo* [a, d] *cyclohepten-11-one* (**9**), m.p. 133–134°. *Found* : C, 87.68 ; H, 5.94 ; $C_{18}H_{14}O$ requires : C, 87.77 ; H, 5.73 %.

IR spectrum (CS_2 ; CCl_4 ; cm^{-1}) : 720 s, 741 s, 755 vs, 1281 s, 1679 vs, 2821 w, 2893 m, 2914 m, 3029 m and 3069 m.

NMR spectrum ($CDCl_3$; δ, ppm) : 8.1–8.3 (m ; 1H ; H^{ortho}_{arom}) ; 7.0–7.5 (m ; 7H ; H_{arom}) ; 5.5–6.2 (m ; 2H ; $H_{1',2'}$) ; 4.47 (d ; J = 8 Hz ; 1H ; H_{10}) ; 4.22 (t ; J = 4 Hz ; 1H ; H_5) and 2.5–3.0 (m ; 2H ; $H_{3'}$).

The ketone **10** was similarly obtained from alcohol **7** in a 40 % yield. After three recrystallizations from methanol *9,10-dihydro-9,10[1'keto-2'-buteno]anthracene* (**10**) showed a m.p. of 155–157°. *Found* : C, 87.44 ; H, 6.09 ; $C_{18}H_{14}O$ requires : C, 87.77 ; H, 5.73 %.

IR spectrum (CS_2 ; CCl_4 ; cm^{-1}) : 716 s, 751 m, 786 m, 1663 vs, 2884 shoulder, 2899 w, 3027 m and 3070 m.

NMR spectrum ($CDCl_3$; δ, ppm) : 7.15—7.5 (m ; 8H ; H_{arom} ; 5.30—5.80 (m ; 2H ; $H_{2',3'}$) ; 5.03 (s ; 1H ; H_9) ; 4.33 (t ; J = 4 Hz ; 1H ; H_{10}) ; 3.05 (m ; 2H ; $H_{4'}$).

9,10-dihydro-9,10-[2'-keto-3'-buteno]anthracene (**11**) was obtained similarly from **8** in a 30% yield. $\nu_{C=O} = 1678$ cm^{-1}.

NMR spectrum ($CDCl_3$; δ, ppm ; 7.1—7.5 (m ; 8H ; H_{arom}) ; 6.85 (dd ; J = 12.5 ; 9.5 Hz ; 1H ; $H_{4'}$) ; 5.63 (d ; J = 12.5 Hz ; 1H ; $H_{3'}$) ; 4.67 (d ; J = 9.5 Hz ; 1H ; H_{10}) ; 4.36 (t ; J = 5 Hz ; 1H ; H_9) and 3.28 (d ; J = 5 Hz ; 2H ; $H_{1'}$).

Kinetic procedure. For kinetic determinations the ampoule technique was used. The hydrobromic acid formed in the reaction was completely neutralized by the excess of NaOAc present in every sample and the remaining NaOAc was titrated with a solution of 0.05 M perchloric acid in acetic acid in the presence of crystal-violet. The concentrations used were 10^{-2} mol/l for bromide **2** and 3×10^{-2} mol/l for NaOAc.

Acknowledgements. We wish to thank Dr. M. Elian for helpful discussions, Miss Ligia Stănescu and Miss Doina Georgescu for v.p.c. analyses and Miss Elvira Sliam for elemental analyses.

Revue Roumaine de Chimie, 22, 7, 1027–1035 (1977)

Dedicated to the 75th anniversary of
Prof. C.D.NENITZESCU'*s birthday (1902–1970)*

REACTIONS WITH SODIUM HYDRIDOBORATE ON SILICA GEL[1]

Received June 15, 1973

VICTORIA CIURDARU and F. HODOŞAN
Laboratory of Natural Products, Institute of Chemistry, Cluj-Napoca, Romania

The title reagent transfers to suitable acceptors a H^-/H^+ pair and/or a BH_3 group. Thus oximes are converted into hydroxylamine(N–B)boranes and tert. amines into amine-boranes.

We already reported the ability of sodium hydridoborate adsorbed on aluminium oxide ($NaBH_4/Al_2O_3$)[2] or on silica gel ($NaBH_4$ /SG)[3] to reduce readily ketones in non-polar solvents to the corresponding alcohols. In order to check the reducing power of these reagents we examined their action on compounds containing functional groups non reducible under usual conditions.

It is known that sodium hydridoborate does not react with oximes ;[4,5] only systems such as $NaBH_4$/LiBr [6] or $NaBH_4/AlCl_3$[7] are able to reduce these to primary amines. Our preliminary investigations with $NaBH_4/Al_2O_3$ and $NaBH_4$/SG respectively, showed that both convert oximes into rather complex mixtures. Since $NaBH_4$/SG gave fewer reaction products we decided to perform our subsequent experiments exclusively with this reagent. Oxosteroid oximes and cyclohexanone oxime were used as substrates.

RESULTS

REDUCTION OF 5α-CHOLESTAN-3-ONE OXIME (1)

When treated with $NaBH_4$/SG in benzene at room temperature compound **1** gave a mixture of two less and three more polar reaction products than the starting substance. Their separation was performed by preparative t.l.c. on silica gel *G*. From the more polar fractions a very small amount of 5α-cholestan-3β-ol was isolated. The ability of silica gel to slowly cleave oxime **1** to the starting ketone accounts for the formation of this alcohol.

[1] F. HODOŞAN and V. CIURDARU, *Tetrahedron Letters*, **1971**, 1997.
[2] F. HODOŞAN and N. SERBAN, *Rev. Roumaine Chim.*, **14**, 121 (1969).
[3] V. CIURDARU, Dissertation, 1972, Cluj (Romania).
[4] S. G. BROOKS, R. M. EVANS, G. F. H. GREEN, J. S. HUNT, A. G. LONG, B. MOONEY and L. J. WYMAN, *J. Chem. Soc.*, **1958**, 4614.
[5] C. W. SHOPPEE, D. E. EVANS, H. C. RICHARDS and G. H. R. SUMMERS, *J. Chem. Soc.*, **1956**, 1649.
[6] J. H. BOYER and S. E. ELLZEY, *J. Amer. Chem. Soc.*, **82**, 2525 (1960).
[7] C. S. FRANKLIN and A. C. WHITE, *J. Chem. Soc.*, **1963**, 1335.

The other two more polar products were found to be very unstable; purification attempts or even storage in non-polar solvents resulted in their rapid and complete decomposition. On the contrary, the less polar fractions were stable enough to permit careful purifications leading to two pure compounds of spectral and chemical properties consistent with the epimeric hydroxylamine(N—B)borane structures **2a** and **2b**.

The IR spectrum of the main product **2a** (Y : 60%) (Fig. 1) displays *inter alia* a rather complex and strong band between 2275—2410 cm^{-1} consisting of five peaks and resembling the absorption pattern in the same region of the co-ordinated BH_3 group in trialkylamine-boranes.[8,9] The sharp bands at 3250 and 3500 cm^{-1} are associated with N—H and O—H stretching respectively. The ability of the $=NH-BH_3$ group to form associated species in CCl_4 solutions[9,10] may account for the occurrence of the broad and concentration dependent band at 3180 cm^{-1}. For the other prominent bands the literature[11] data suggest the following assignments: 1140 C—N stretching, 1175 B—H bending, and 1410 cm^{-1} N—B stretching.

Compound **2a** reduces 5α-cholestan-3-one to the epimeric cholestanols.* This is certainly due to the co-ordinated BH_3 group and supports its structural similarity with the amine-boranes which are also reducing agents.[12]

Compound **2a** was found to be sensitive to acids. Treatment with hydrochloric acid resulted in the loss of the BH_3 group (disappearance of B—H bands) and conversion into the hydroxylamine hydrochloride **3a** from which sodium hydroxide liberated the rather unstable free hydroxylamine **4a**. When tested with silver nitrate — ammonium hydroxide solution, compounds **3a** and **4a** exhibited reducing properties. The IR spectrum of compound **4a** is consistent with the hydroxylamine structure. The sharp band at 3590 cm^{-1} is certainly due to the O—H stretching vibration. The N—H stretching band appears splitted at 3220 and 3240 cm^{-1} suggesting the existence of two rotamers. The rather sharp and concentration independent band at 3170 cm^{-1} may be tentatively attributed to a rather stable dimeric species.**

Schotten-Baumann benzoylation of compound **3a** gave the very stable O,N-dibenzoyl-hydroxylamine derivative **5a** of spectral and analytical data in agreement with the assigned formula.

A finding which is consistent with the dative character of the N—B bond was the reconversion of the free hydroxylamine **4a** into the hydroxylamine-borane **2a** under the action of $NaBH_4$/SG.

---

[8] R. Köster, G. Bruno and P. Binger, *Liebigs Ann. Chem.*, **644**, 1 (1961).

[9] M. P. Brown, R. W. Heseltine, P. A. Smith and P. J. Walker, *J. Chem. Soc.*, **1970**, 410.

[10] M. P. Brown and R. W. Heseltine, *Chem. Comm.*, **1968**, 1551.

[11] D. W. Aubrey, M. F. Lappert and H. Pyszora, *J. Chem. Soc.*, **1960**, 5239; J. N. G. Faulks, N. N. Greenwood and J. H. Morris, *J. Inorg. Nuclear Chem.*, **29**, 329 (1967).

[12] H. Nöth and H. Beyer, *Chem. Ber.*, **93**, 1078 (1960).

* Only qualitative information was obtained by t.l.c.; no preparative experiments were carried out.

** The reliability of these assignments is altered to some extent by the unstability of compound **4a** in solution.

Consequently, when no suitable hydrogen acceptor is present, the reagent acts on basic species only as a borane donor. This was also confirmed by contacting $NaBH_4$/SG with triethylamine in benzene solution when triethylamine-borane [8] was obtained.

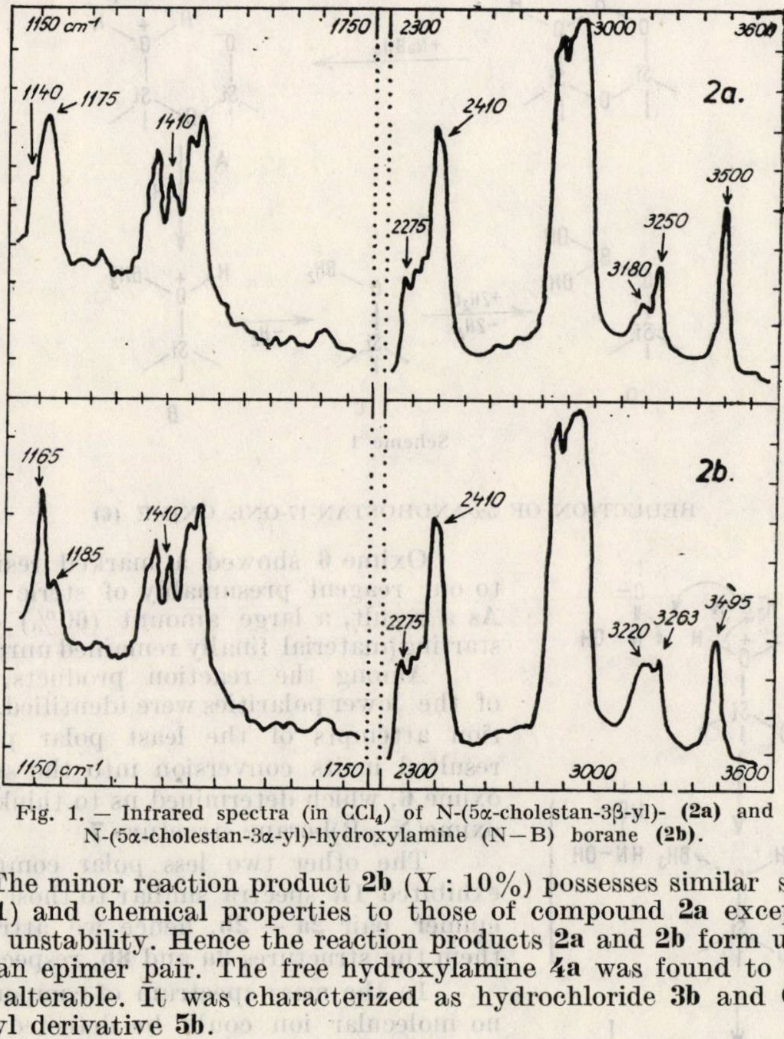

Fig. 1. — Infrared spectra (in CCl_4) of N-(5α-cholestan-3β-yl)- (**2a**) and N-(5α-cholestan-3α-yl)-hydroxylamine (N—B) borane (**2b**).

The minor reaction product **2b** (Y : 10%) possesses similar spectral (Fig. 1) and chemical properties to those of compound **2a** excepting a higher unstability. Hence the reaction products **2a** and **2b** form undoubtedly an epimer pair. The free hydroxylamine **4a** was found to be also easily alterable. It was characterized as hydrochloride **3b** and O,N-dibenzoyl derivative **5b**.

The stereochemistry of the reaction products could not be ascertained by conversion of hydroxylamine **4a** into the corresponding amine of known orientation. [5,13] Treatment with reducing agents such as lithium hydridoaluminate, sodium in isopropyl-alcohol, stannous chloride, titanium trichloride, and zinc in hydrochloric acid, resulted in the recovering of the starting material. Similar difficulties were encountered with the other hydroxylamines mentioned further on. Consequently, the configurations reported in this paper are only tentative ones. These were derived from

---

[13] L. Labler, V. Cerny and F. Sorm, *Coll. Czech. Chem. Comm.*, **19**, 1249 (1954).

the known rule concerning the relative stability of conformer (epimer) pairs and the assumption that similar steric factors are operative as in the case of the reduction of oxosteroids with $NaBH_4/SG$.[3]

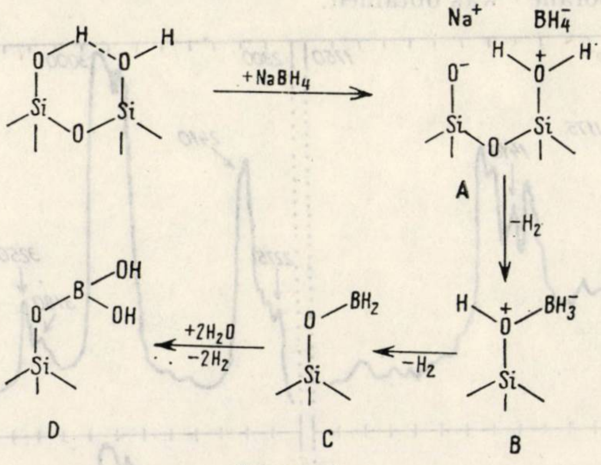

Scheme 1

REDUCTION OF 5α-ANDROSTAN-17-ONE OXIME (6)

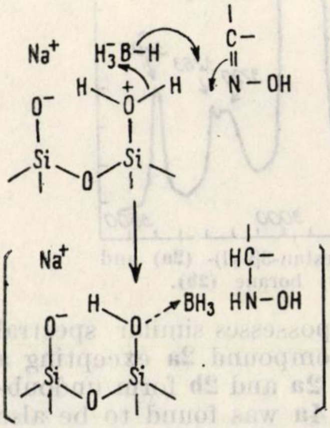

Scheme 2

Oxime **6** showed a marked resistance to our reagent presumably of steric origin. As a result, a large amount (60%) of the starting material finally remained unreacted.

Among the reaction products, three of the lower polarities were identified. Isolation attempts of the least polar product resulted in its conversion into the starting oxime **6**, which determined us to think of an oxime(N—B)borane structure **7**.

The other two less polar compounds exhibited IR spectra similar to those of the epimer pair **2a** — **2b**, hence we attributed them the structures **8a** and **8b**, respectively.

In the mass spectrum of compound **8a** no molecular ion could be detected; very small peaks at masses 303 (M^+-2) and 302 ($\overline{M}^+-3$) were observable instead. Conclusive from the structural point of view is the base peak *m/e* 291 which corresponds to the hydroxylamine radical-ion and derives from the molecular ion by loss of 14 mass units

---

[14] J. J. BARIEUX and J. GORE, *Tetrahedron*, **28**, 1537 (1972).

$(^{11}BH_3)$.* Subsequent fragmentation generated a prominent peak *m/e* 274 by loss of a hydroxyl radical. The fragments *m/e* 259, 258 and 217 characterize the 17-monosubstituted androstanes [15] ** (Fig. 2).

Chemical evidences supporting structure **8a** were brought about by conversion into the hydrochloride **9a** and subsequently into the O,N-dibenzoyl derivative **10a**.

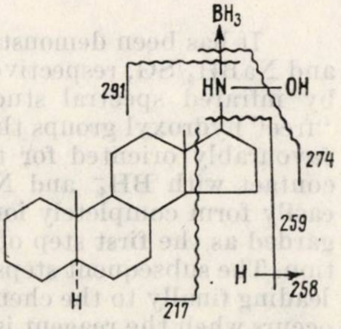

Fig. 2. — Fragmentation pattern of N-(5α-androstan-17β-yl)-hydroxylamine (N—B)borane (**8a**).

REDUCTION OF 3β-ACETOXY-5α,$25\alpha_F$-SPIROSTAN-12-ONE OXIME (**11**)

Compound **11** reacted also sluggishly with our reagent. Besides unreacted starting substance (17%), two hydroxylamine-boranes **12a** (25%) and **12b** (8%) were isolated by preparative t.l.c., and examined spectrometrically. No chemical proofs concerning their structures could be produced, since it was not possible to convert them into stable hydroxylamine derivatives. As to the relative stability of the reaction products, **12b** was found to be much more labile than **12a**.

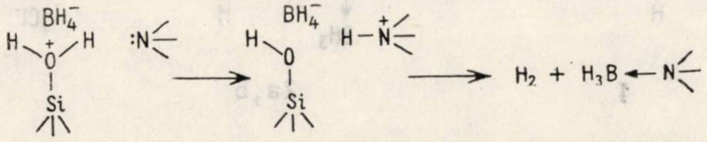

REDUCTION OF CYCLOHEXANONE OXIME

In spite of its rapid and complete disappearance from the reaction mixture (t.l.c.), cyclohexanone oxime was identified among the reaction products. As with oxime **6**, formation of cyclohexanone oxime-borane, $C_6H_{10} = \underset{\underset{BH_3}{\downarrow}}{N}OH$, which decomposes during the processing of the reaction mixture, accounts presumably for this fact. The existence of a fraction of low polarity, which liberated the starting oxime during the isolation, supported this assumption.

---

[15] M. Spiteller-Friedmann and G. Spiteller, "Massenspktren von Steroiden. Fortschritte der chemischen Forschung", Vol. 12, Springer-Verlag, Berlin, 1969, p. 440.

* Fragments M^{+}—14 were detected recently also in the mass spectra of certain steroidal amine-boranes[14].

** Thanks are due to Dr. I. Oprean (Institute of Chemistry, Cluj-Napoca) for his advice in the interpretation of the mass spectral data.

Cyclohexyl hydroxylamine-borane, the main reaction product, was converted into the known cyclohexyl-hydroxylamine[16] and subsequently into the corresponding O,N-dibenzoyl derivative.

DISCUSSION

It has been demonstrated that reductions by means of $NaBH_4/Al_2O_3$ and $NaBH_4$/SG, respectively, are surface processes.[2,3] It has been shown by infrared spectral studies on silica gel that besides non-interacting "free" hydroxyl groups the surface carries closely situated hydroxyl groups favourably oriented for the formation of mutual hydrogen bonds.[17] In contact with BH_4^- and Na^+ ions such interacting hydroxyl groups can easily form completely ionized systems (Scheme 1, A), which may be regarded as the first step of the sodium hydridoborate — silica gel interaction. The subsequent steps involve very likely the surface species *B* and *C*, leading finally to the chemisorbed boric acid *D*.* This deactivation process occurs when the reagent is stored at room temperature and is accompanied by a slow evolution of hydrogen.[3]

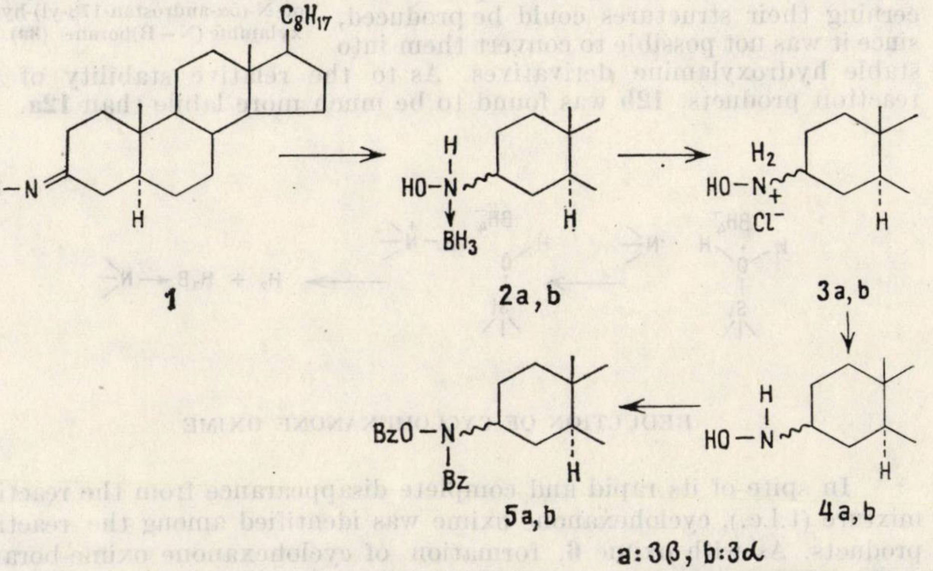

One can see that *A*, *B*, and *C* are all reducing entities. Infrared measurements performed on fresh and partially deactivated reagent showed, in the B—H stretching region, an absorption pattern similar with that of crystalline $NaBH_4$; no bands associated with the $O-BH-O$, $-BH_2$ and BH_3 surface groups* were observed. Hence one may admit that the only species involved in these reductions is the ion pair $=Si-OH_2^+ . BH_4^-$ (A). Because of their high lability [19], the species *B* and *C* should be present in very small amounts and therefore cannot be identified by IR spectrometry; presumably they do not play a significant role in the reactions.

---

[16] H. Feuer, B. F. Vincent jr. and R. S. Bartlett, *J. Org. Chem.*, **30**, 2877 (1965); S. L. Yoffe, V. A. Tartakovski, A. A. Medvedeva and S. S. Novikov, *Isvest. Akad. Nauk. S.S.S.R.*, **1964**, 1537; J. M. Lalancette and J. R. Bridle, *Canad. J. Chem.*, **48**, 735 (1970).

[17] L. H. Little, "Infrared Spectra of Adsorbed Species", Academic Press, New York, 1966, p. 276; L. R. Snyder and J. W. Ward, *J. Chem. Phys.*, **70**, 3941 (1966).

[18] A. Hajós, "Komplexe Hydride und ihre Anwendung in der organischen Chemie", VEB Deutscher Verlag der Wissenschaften, Berlin, 1966, p. 45.

* Similar sequences have been postulated for the acidic hydrolysis of the hydridoborate anion.[18]

The reducing property of the species $=Si-OH_2^+ . BH_4^-$ is obviously due to its ability to transfer a H^-/H^+ pair to a suitable acceptor. The resulted Lewis acid BH_3 is first accepted by a surface hydroxyl and transfered immediately to the more basic nitrogen atom of the hydroxylamine group (Scheme 2).

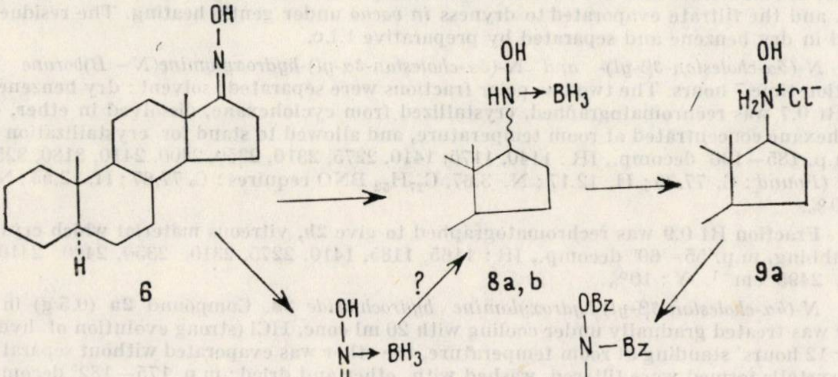

With non-reducible basic compounds (amines, hydroxylamines) the reaction proceeds as shown in Scheme 3: (below)

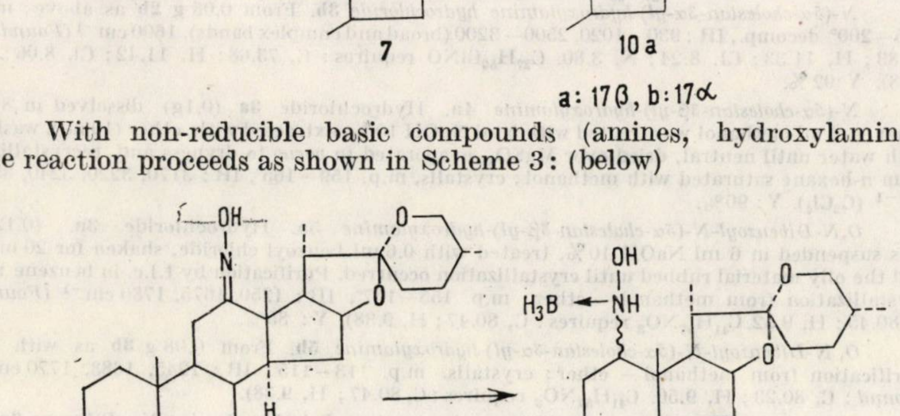

---

* These were identified when diborane interacted with dry silica gel; traces of water entailed immediate disappearance of these bands.[19]

[19] J. J. Fripiat and Van Tongelen, *J. Catalysis*, **1966**, 158.

EXPERIMENTAL

Infrared spectra were recorded in CCl_4, unless otherwise stated, with an Unicam SP 200 *G* instrument. The mass spectrum was taken with a Varian MAT SN-1 spectrometer at 70 eV and source temperature 210° using a direct insertion system. All melting points were determined in capillaries and are uncorrected. T.l.c. were carried out on silica gel *G* using phosphomolybdenic acid as indicator.

Reagent. $NaBH_4$ (1g) in 2 ml dist. water is added to 2.5 g silica gel (Merck, 70—325 mesh ASTM, extra pure, for column chromatography) previously dried for 3 hours at 120°. After vigorous shaking, the homogenized material is heated at 40—45° and 5—10 mm, in a recipient containing P_2O_5, until water evolution appears to be complete.

General reduction procedure. In a stirred solution of 0.2 g oxime in 20 ml dry benzene 10 g reagent is added in two portions in 20 minutes time. The stirring is continued at room temperature for several hours and the reaction followed by t.l.c. The reagent is filtered, washed with ether, and the filtrate evaporated to dryness *in vacuo* under gentle heating. The residue is dissolved in dry benzene and separated by preparative t.l.c.

N-(5α-cholestan-3β-yl)- and N-(5α-cholestan-3α-yl)-hydroxylamine(N—B)borane **2a, b**. Reaction time 7 hours. The two less polar fractions were separated; solvent: dry benzene. Fraction Rf 0.7 was rechromatographed, crystallized from cyclohexane, dissolved in ether, diluted with hexane concentrated at room temperature, and allowed to stand for crystallization to give **2a**, m.p. 185—190° decomp., IR : 1140, 1175, 1410, 2275, 2310, 2350, 2400, 2410, 3180, 3250,3500 cm^{-1} (*Found* : C, 77.36 ; H, 12.17 ; N, 3.67. $C_{27}H_{52}$ BNO requires : C, 77.67 ; H, 12.55 ; N, 3.35). Y : 60%.

Fraction Rf 0.9 was rechromatographed to give **2b**, vitreous material which crystallized by rubbing, m.p. 55—60° decomp., IR : 1165, 1185, 1410, 2275, 2310, 2350, 2400, 2410, 3220, 3263, 2495 cm^{-1}. Y : 10%.

N-(5α-cholestan-3β-yl)-hydroxylamine hydrochloride **3a**. Compound **2a** (0.5 g) in 20 ml ether was treated gradually under cooling with 20 ml conc. HCl (strong evolution of hydrogen). After 12 hours' standing at room temperature, the ether was evaporated without separation and the crystalls formed were filtered, washed with ether and dried; m.p. 175—182° decomp., IR : 950—1040, 2450—3500 (broad and complex bands), 1585 cm^{-1} (KBr) (*Found* : C, 73.92 ; H, 11.42 ; N, 3.44 ; Cl, 8.03. $C_{27}H_{50}ClNO$ requires : C, 73.68 ; H, 11.44 ; N, 3.18 ; Cl, 8.06). Y : 90%.

N-(5α-cholestan-3α-yl)-hydroxylamine hydrochloride **3b**. From 0.08 g **2b** as above; m.p. 185—200° decomp., IR : 930—1020, 2500—3200 (broad and complex bands), 1600 cm^{-1} (*Found* : C 73.83 ; H, 11.33 ; Cl, 8.24 ; N, 3.80. $C_{27}H_{50}ClNO$ requires : C, 73.68 ; H, 11.42 ; Cl, 8.06 ; N, 3.18). Y :92%.

N-(5α-cholestan-3β-yl)-hydroxylamine **4a**. Hydrochloride **3a** (0.1g) dissolved in 8 ml ether + 4 ml methanol was treated with 5 ml NaOH 10%, extracted with ether (10 ml), washed with water until neutral, dried over $MgSO_4$, evaporated *in vacuo* to dryness and recrystallized from *n*-hexane saturated with methanol; crystalls, m.p. 159—165°, IR : 3170, 3220, 3240, 3590 cm^{-1} (C_2Cl_4). Y : 90%.

O,N-Dibenzoyl-N-(5α-cholestan-3β-yl)-hydroxylamine **5a**. Hydrochloride **3a**. (0.12 g) was suspended in 6 ml NaOH 10%, treated with 0.6 ml benzoyl chloride, shaken for 20 min., and the oily material rubbed until crystallization occurred. Purification by t.l.c. in benzene and crystallization from methanol — ether; m.p. 155—157°, IR : 1250, 1675, 1780 cm^{-1} (*Found* : C, 80.45 ; H, 9.52. $C_{41}H_{57}NO_3$ requires : C, 80.47 ; H, 9.38). Y : 85%.

O, N-Dibenzoyl-N-(5α-cholestan-3α-yl)-hydroxylamine **5b**. From 0.08 g **3b** as with **5a**. Purification from methanol — ether; crystalls. m.p. 113—115°, IR : 1245, 1683, 1770 cm^{-1} (*Found* : C, 80.23 ; H, 9.50. $C_{41}H_{57}NO_3$ requires : C, 80.47 ; H, 9.38).

N-(5α-androstan-17β-yl)- and N-(5α-androstan-17α-yl)-hydroxylamine(N—B)borane **8a, b**. From **6**; reaction time 10 hours. An additional portion of reagent and 14 ml benzene were added 6 hours after the start. Developing agent : benzene — ether 19 : 1. Fraction Rf 0.1 : unreacted oxime **6**. Fraction Rf 0.8 liberated during isolation oxime **6**. Fraction Rf 0.7 was recrystallized from hexane — ether to give **8a**; needles, m.p. 192—194° decomp., IR : 1165, 1175sh, 1180, 1415, 2260, 2300, 2320, 2340sh, 2370, 2400, 3180, 3240, 3478 cm^{-1} (CCl_4), mass m/e 303 (1), 302 (2), 291 (100), 287 (5), 286 (10), 275 (85), 274 (98), 260 (7), 259 (20), 258 (17), 257 (19), 243 (8), 231 (7), 219 (4), 218 (4), 217 (17) (*Found* : C, 74.80 ; H, 11.70 ; N, 4.73. $C_{19}H_{35}$ BNO requires : C, 75.02 ; H, 11.59 ; N, 4.60). Y : 15%.

Fraction Rf 0.65 was rechromatographed to give **8b**; crystalls, m.p. 165—167° decomp., IR : 1160, 1170, 1185, 1410, 2270, 2310, 2340, 2380, 2410, 3190, 3250, 3480 cm^{-1}. Y : 2%.

N-(5α-androstan-17β-yl)-hydroxylamine hydrochloride **9a**. From 0.04 g **8a** as with **3a**. Crystals, m.p. 200—215° decomp., IR : 940—1060, 2400—3500 (broad and complex bands), 1580 cm^{-1} (KBr). Y : 73%.

O,N-Dibenzoyl-N-(5α-androstan-17β-yl)-hydroxylamine **10a**. From 0.02 g **9a** as with **5a**. Purification by t.l.c. in benzene and crystallization from aqueous methanol; plates, m.p. 132—134°. IR : 1240, 1255sh, 1670, 1770 cm^{-1} (CCl_4). (*Found* : C, 79.58; H, 8.06. $C_{33}H_{41}NO_3$ requires : C, 79.32; H, 8.27).

N-(3β-acetoxy-5α,$25\alpha_F$ *-spirostan-12β-yl)- and N-(3β-acetoxy-5α,* $25\alpha_F$ *-spirostan-12α-yl)-hydroxylamine (N—B)borane* **12a**, **b**. From **11**; reaction time 11 hours, with two portions of reagent in 50 ml benzene. T.l.c. with benzene — ether 9 : 1. Fraction Rf 0.5 : starting oxime **11**. Fraction Rf 0.8 was rechromatographed to give **12a**; m.p. 220—226° decomp., IR : 1735, 2270, 2310, 2350 sh, 2380, 3250, 3480 cm^{-1} (CCl_4). Y : 25%.

Fraction Rf 0.65 was rechromatographed to give **12b**, m.p. 205—220° decomp., IR : 2270, 2320, 2350, 2380, 2420, 3220, 3460 cm^{-1} (CCl_4). Y : 18%.

N-Cyclohexyl-hydroxylamine(N—B) borane. Viscous, colourless liquid, IR : 1165, 1185, 1410, 2280, 2315, 2350sh, 2390, 2410sh, 3180, 3250, 3490 cm^{-1} (CCl_4). (*Found* : C, 55.50; H, 11.97; N, 10.90. $C_6H_{16}BNO$ requires : C, 55.86; H, 12.50; N, 10.85). Y : 46%.

N-Cyclohexyl-hydroxylamine hydrochloride. From the preceding compound as with **3a**. Sparkling plates, m.p. 130—136° decomp., IR : 1580, 2500—3500 (broad and complex band) (KBr). Y : 90%.

N-Cyclohexyl-hydroxylamine. The preceding compound was treated in aqueous solution with NaOH 10%, the precipitate filtered, washed, and dried; crystalls, m.p. 140—142° [16], IR : 3160, 3260 cm^{-1} (KBr) (*Found* : N. 11.94. $C_6H_{13}NO$ requires : N, 12.16). Y : 40%.

O,N-Dibenzoyl-N-cyclohexyl-hydroxylamine. Prisms from aqueous methanol; m.p. 110—111°, IR : 1145, 1670, 1770 cm^{-1} (CCl_4). (*Found* : C, 74.50; H, 6.33; N, 4.48. $C_{20}H_{21}NO_3$ requires : C, 74.27; H. 6.55; N, 4.33). Y : 75%.

Revue. Roumaine de Chimie, **22**, 7, 1037 – 1043 (1977)

Dedicated to the 75th anniversary of
Prof. C. D. NENITZESCU'S *birthday (1902–1970)*

INVESTIGATIONS IN THE CYCLOBUTANE SERIES. XLV.[1]

DIBENZOTRICYCLO[4.3.1.$0^{2,5}$]DECADIENE SYSTEM. BEHAVIOUR AND RETROREARRANGEMENT INTO DIBENZO-$(CH)_{10}$ NENITZESCU'S HYDROCARBON DERIVATIVES

I. G. DINULESCU, M. S. POP and MARGARETA AVRAM
Center of Organic Chemistry, Spl. Independenţei 202 B, 76.300 Bucharest 15, POB 2354

Received February 1, 1977

The retrorearrangement of the dibenzotricyclo[4.3.1.$0^{2,5}$]decadiene system into a [4.2.2.$0^{2,5}$] system is described. The stereochemistry and some mechanistic aspects of the rearrangements occurring in this series are discussed.

The interest in the general area of $(CH)_{10}$ hydrocarbon chemistry was dramatically awakened by the first skeletal rearrangement of Nenitzescu's hydrocarbon **(1)** with tricyclo[4.2.2.$0^{2,5}$]deca-3.7.9-triene skeleton.[2,3,4] Similar interest was manifested towards dibenzo-$(CH)_{10}$ derivatives.[5]

From the three possible dibenzo-$(CH)_{10}$ Nenitzescu's hydrocarbons (**2**–**4**), two isomers, **1**[6] and **2**[7], were obtained by Nenitzescu himself. The third one has not been obtained so far.

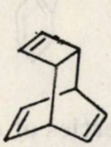
1

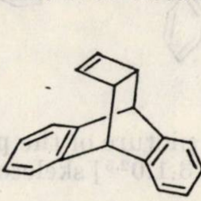
2

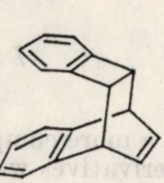
3

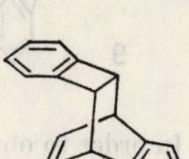
4

---

[1] Part XLIV : L. ENESCU and M. AVRAM, *Rev. Roumaine Chim.*, **22**, 1061 (1977).

[2] L. T. SCOTT and M. JONES, jr., *Chem. Rev.*, **1972**, 181.

[3] C. D. NENITZESCU, M. AVRAM and E. MARICA, *Chem. Ber.*, **90**, 2541 (1957).

[4] C. D. NENITZESCU, M. AVRAM, I. POGANY, G. D. MATEESCU and M. FĂRCAŞIU, *Studii şi Cercetări Chim. Acad. R.P.R.*, **11**, 7 (1963).

[5] M. ELIAN, M. BANCIU, L. STĂNESCU and E. CIORĂNESCU, *Rev. Roumaine Chim.*, **21**, 89 (1976), and literature therein cited.

[6] M. AVRAM, I. G. DINULESCU and C.D. NENITZESCU, *Liebigs Ann. Chem.*, **691**, 9 (1966).

[7] I. G. DINULESCU, M. S. POP, F. CHIRALEU, M. AVRAM and C. D. NENITZESCU, *Rev. Roumaine Chim.*, **19**, 1197 (1974).

While thermal and photochemical interconversions have been intensively investigated,[2,5] less data are available about the ionic reactions.

In a previous paper [8] we have reported on the behaviour of the dibenzo-$(CH)_{10}$ hydrocarbon **3** with $[4.2.2.0^{2,5}]$ skeleton. It was shown that, in electrophilic additions under kinetically controlled conditions, rearrangement of dibenzotricyclo$[4.2.2.0^{2,5}]$decadiene system into two new polycyclic systems, dibenzo[*c,h*]tricyclo$[5.2.1.0^{2,5}]$- and $[4.3.1.0^{2,5}]$deca -3.7-diene, occurs.

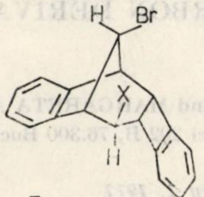

5 X = OAc

7 X = Br

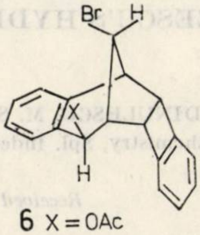

6 X = OAc

8 X = Br

Further investigations showed that the derivatives with $[5.2.1.0^{2,5}]$ skeleton and with one ionizable group in α position of the cyclobutene ring, for instance **7**, undergoes a reversible rearrangement into the $[4.2.2.0^{2,5}]$ system, [8] by a thermodynamically controlled SN reaction. Thus, **7** is converted into **9** in presence of silver bromide in carbon tetrachloride, and into **10** on treatment with hydrobromic acid in acetic acid.

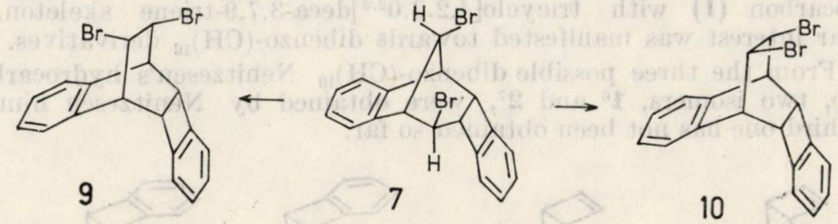

9 **7** **10**

In order to obtain a more complete picture of the properties of these systems, the study of derivatives with $[4.3.1.0^{2,5}]$ skeleton appeared necessary.

In this paper we report on the synthesis of the parent compound of the dibenzotricyclo$[4.3.1.0^{2,5}]$decadiene series and on the behaviour of its derivatives with ionisable groups in the benzylic position, in different SN reactions.

By heating the dibromide **8** with sodium acetate in acetic acid, the bromoacetoxy-derivative **6** resulted, identical with that obtained by the solvolytic addition of bromine to **3**. [8] The base-catalyzed hydrolysis of **6** yielded the bromohydroxyderivative **11**. The *exo* orientation of the hydroxy group, and respectively *endo* for H-7 proton, results from the small value of the $J_{6,7}$ coupling, [9,10] as well as from the intramolecular association of the hydroxy group with the *anti* oriented 10-bromine (ν OH 3570 cm^{-1}).

---

[8] I. G. Dinulescu, M. S. Pop, F. Chiraleu and M. Avram, *Chem. Ber.*, **108**, 283 (1975).

The oxidation of **11** with chromic anhydride-pyridine afforded the bromoketone **12**. In the IR spectrum of **12** the ν CO absorption at 1692 cm^{-1} is characteristic for the benzylic carbonyl group.[11] When **12** is reduced with $LiAlH_4$ in ethereal solution, the *endo*-hydroxy-derivative **13** is obtained. Its epimer, the *exo*-hydroxy-derivative **14**, was obtained by reduction with $LiAlH_4$ of the bromoacetoxy-derivative **6**. The epimerism of the two alcohols was evidenced chemically and by spectral means.

Both hydroxy-derivatives **13** and **14**, by oxidation were converted in the same ketone **15**. This chemical evidence was substantiated by proton magnetic resonance studies, based on the $J_{6,7}$ coupling constant values. Thus, in the NMR spectrum of **13** the benzylic proton H-7 at δ 4.96 ppm presents a large singlet due to the coupling of the latter with H-6 and OH group proton. On deuteration, the broad signal becomes doublet, with $J_{6,7} = 5.0$ Hz, corresponding to the proposed stereochemistry. In

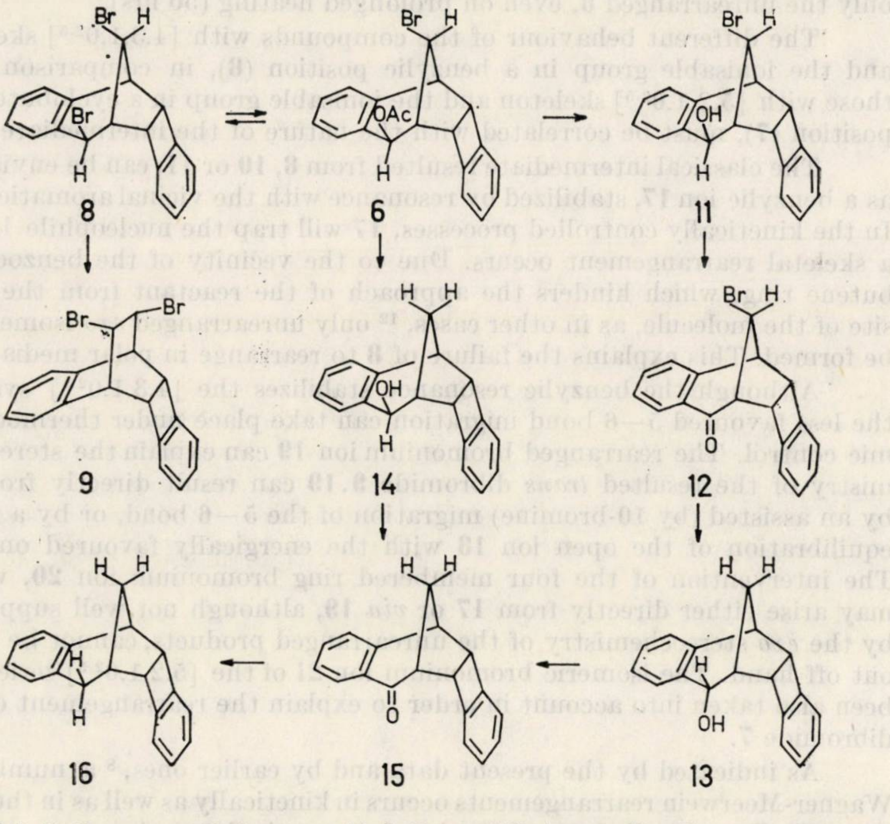

---

[9] I. G. Dinulescu, F. Chiraleu, M. S. Pop and M. Avram, *Rev. Roumaine Chim.*, **20**, 85 (1975).

[10] A. R. Katritzky and B. Wallis, *Chem. and Ind.*, **1964**, 2025.

[11] M. Avram and G. D. Mateescu, "Infrared Spectroscopy. Applications in Organic Chemistry", Wiley-Interscience, New York, 1972.

the IR spectrum, the ν OH frequencies at 3580 cm^{-1} is in agreement with an intramolecular association bond with the benzene ring.

The *exo* alcohol **14** can be characterized by the H-7 proton resonance at δ 4.33 ppm, doublet by coupling with H-6, with $J_{6,7} = 2.0$ Hz, corresponding to a dihedral angle of 75°. In the IR spectrum of **14**, two absorptions for the hydroxy group are visible : at 3005 cm^{-1}, for the free OH group, and a large one at 3490 cm^{-1}, corresponding to a intermolecular association.

By reduction of the ketone **15** with aluminium hydride, the parent hydrocarbon of the series, **16**, was obtained.

By prolonged heating of **8**, in carbon tetrachloride solution, in presence of silver bromide as catalyst, the rearrangement of the dibromide **8** into the *trans* dibromide **9** (with [$4.2.2.0^{2,5}$] skeleton) was achieved.

The treatment of the bromoacetoxy-derivative **6**, as well as of the bromohydroxy-derivative **11**, with hydrobromic acid, in acetic acid solution, or with anhydrous hydrogen bromide in dichloromethane, afforded only the unrearranged **8**, even on prolonged heating (50 hrs).

The different behaviour of the compounds with [$4.3.1.0^{2,5}$] skeleton and the ionisable group in a benzylic position (**8**), in comparison with those with [$5.2.1.0^{2,5}$] skeleton and the ionisable group in a cyclobutenylic position (**7**), must be correlated with the nature of the intermediate ions.

The classical intermediate resulted from **8**, **10** or **11**, can be envisaged as a benzylic ion **17**, stabilized by resonance with the vicinal aromatic ring. In the kinetically controlled processes, **17** will trap the nucleophile before a skeletal rearrangement occurs. Due to the vecinity of the benzocyclobutene ring, which hinders the approach of the reactant from the *endo* site of the molecule, as in other cases, [12] only unrearranged *exo* isomer will be formed. This explains the failure of **8** to rearrange in polar media.

Although the benzylic resonance stabilizes the [$4.3.1.0^{2,5}$] system, the less favoured 5—6 bond migration can take place under thermodynamic control. The rearranged bromonium ion **19** can explain the stereochemistry of the resulted *trans* dibromide **9**. **19** can result directly from **17** by an assisted (by 10-bromine) migration of the 5—6 bond, or by a rapid equilibration of the open ion **18** with the energically favoured one **19**. The intervention of the four membered ring bromonium ion **20**, which may arise either directly from **17** or *via* **19**, although not well supported by the *exo* stereochemistry of the unrearranged products, cannot be ruled out off hand. The isomeric bromonium ion **21** of the [$5.2.1.0^{2,5}$] series has been also taken into account in order to explain the rearrangement of the dibromide **7**.

As indicated by the present data and by earlier ones, [8] a number of Wagner-Meerwein rearrangements occurs in kinetically as well as in thermodynamically controlled reactions, involving cationic species.

---

[12] N. ŞTEFAN, I. G. DINULESCU, F. CHIRALEU and M. AVRAM, *Rev. Roumaine Chim.*, **20**, 1473 (1975).

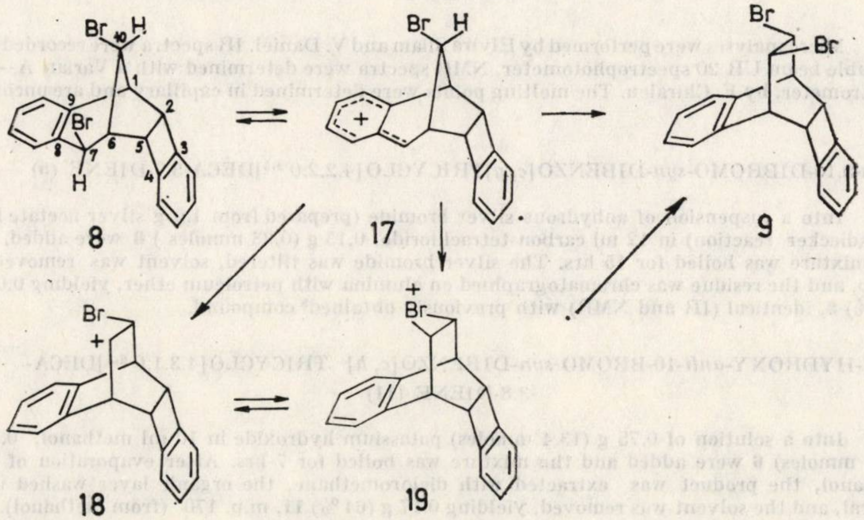

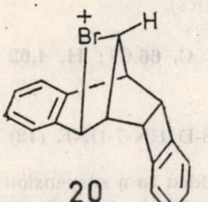

20

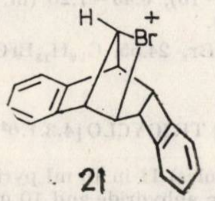

21

By electrophilic addition to dibenzo-$(CH)_{10}$ Nenitzescu's hydrocarbon **3**, the $[4.2.2.0^{2,5}]$ system was converted into $[5.2.1.0^{2,5}]$ and $[4.3.1.0^{2,5}]$ systems. The ionisation of the cyclobutenylic bromine in $[5.2.1.0^{2,5}]$ system or of the benzylic one in $[4.3.1.0^{2,5}]$ system leads to the retrorearrangement of these two systems into those with $[4.2.2.0^{2,5}]$ skeleton.

Experimental data show that between the three systems under discussion, the order of stability in thermodynamically controlled conditions follow the sequence : $[4.2.2.0^{2,5}] > [4.3.1.0^{2,5}] > [5.2.1.0^{2,5}]$.

The comparison of the behaviour of studied systems with those of the extensively studied[13,14] dibenzobicyclo[2.2.2]- and [3.2.1]octadiene, may show some similarities. However, by the replacement of a benzene ring with a benzocyclobutene ring, the molecule losses its symmetry, and consequently new aspects appear in the possibilities of rearrangement.

---

[13] S. J. Cristol, F. P. Parungo, D. E. Plorde and K. Schwarzenbach, *J. Amer. Chem. Soc.*, **87**, 2879 (1965), and literature therein cited.

[14] I. G. Dinulescu, M. Avram, G. D. Mateescu and C. D. Nenitzescu, *Chem. and. Ind.*, **1964**, 2023; *Rev. Roumaine Chim.*, **9**, 351 (1964).

EXPERIMENTAL

Microanalyses were performed by Elvira Şliam and V. Daniel. IR spectra were recorded with a double beam UR 20 spectrophotometer. NMR spectra were determined with a Varian A—60A spectrometer, by F. Chiraleu. The melting points were determined in capillary and are uncorrected.

trans-9,10-DIBROMO-*syn*-DIBENZO[*c*, *g*]TRICYCLO[4.2.2.0 ^{2,5}]DECA-3.7-DIENE (**9**)

Into a suspension of anhydrous silver bromide (prepared from 1.0 g silver acetate by a Hunsdiecker reaction) in 12 ml carbon tetrachloride, 0,15 g (0,38 mmoles) **8** were added, and the mixture was boiled for 15 hrs. The silver bromide was filtered, solvent was removed *in vacuo*, and the residue was chromatographied on alumina with petroleum ether, yielding 0,050 g (33 %) **9**, identical (IR and NMR) with previously obtained[8] compound.

exo-7-HYDROXY-*anti*-10-BROMO-*syn*-DIBENZO[*c*, *h*] TRICYCLO[4.3.1.0 ^{2,5}]DECA--3.8-DIENE (**11**)

Into a solution of 0.75 g (13.4 mmoles) potassium hydroxide in 10 ml methanol, 0.30 g (0.81 mmoles) **6** were added and the mixture was boiled for 7 hrs. After evaporation of the methanol, the product was extracted with dicloromethane, the organic layer washed until neutral, and the solvent was removed, yielding 0.17 g (64 %) **11**, m.p. 170° (from methanol).

NMR ($CDCl_3$, δ, ppm): 3.01 (d, 1H, OH, $J_{7,OH} = 12.0$ Hz), 3.15 (m, 1H, H—6, $J_{6,10} = 4.5$ Hz), 3.65 (m, 1H, H—1, $J_{1,10} = 4.5$ Hz), 3.95—4.20 (m, 2H, H—2 and H—5), 4.38 (d, 1H, H—7), 4.53 (t, 1H, H—10), 6.45—7.20 (m, 8H aromatics).

IR (CCl_4, cm^{-1}) : ν OH 3570.

Found : C, 65.27 ; H, 4.91 ; Br, 24.55. $C_{18}H_{15}BrO$ requires : C, 66.07 ; H, 4.62 ; Br, 24.42.

anti-10-BROMO-*syn*-DIBENZO[*c*, *h*] TRICYCLO[4.3.1.0^{2,5}]DECA-3,8-DIEN-7-ONE (**12**)

A solution of 0.45 g (1.38 mmoles) **11** in 10 ml pyridine was added to a suspension of a complex prepared from 1.0 g chromic anhydride and 10 ml pyridine, and the mixture was left for 24 hrs at room temperature. Water was added and the product was extracted with ether. After washing with water, with 2% hydrochloric acid, with water until neutral, and drying, the ether was removed, yielding 0.42 g (94 %) **12**, m.p. 145° (from methanol).

NMR ($CDCl_3$, δ, ppm) : 3.53 (m, 1H, H—6, $J_{6,10} = 4.5$ Hz), 3.83 (m, 1H, H—1, $J_{1,10} = 4.5$ Hz), 4.15—4.55 (m, 2H, H—2 and H—5), 4.61 (t, 1H, H—10), 6.70—7.40 (m, 7H aromatics). 7.53 (d, 1H, aromatic, $J_{ortho} = 7.0$ Hz).

IR (CCl_4, cm^{-1}) : ν CO 1692.

Found : C, 66.23 ; H, 4.20 ; Br. 24.81. $C_{18}H_{13}BrO$ requires : C, 66.48 ; H, 4.03 ; Br, 24.57.

endo-7-HYDROXY-*syn*-DIBENZO[*c*, *h*]TRICYCLO[4.3.1.0^{2,5}]DECA-3.8-DIENE (**13**)

A solution of 0.25 g (0.75 mmoles) **12** in 25 ml anhydrous ether was added dropwise into a suspension of 0.50 g (13.2 mmoles) lithium aluminium hydride U.C.B., and the mixture was stirred at room temperature for 2 hrs. After working up, 0.18 g (94%) **13** were obtained; m.p. 92° (from methanol).

NMR ($CDCl_3$, δ, ppm) : 2.00—2.50 (m, 3H, 2H—10 and OH), 2.88 (m, 1H, H—6, $J_{6,7} = 5.0$ Hz), 3.40 (m, 1H, H—1), 3.90—4.35 (m, 2H, H—2 and H—5), 4.96 (broad s, 1H, H—7), 6.45—7.25 (m, 8H aromatics).

IR (CH_2Cl_2, cm^{-1}) : ν OH 3580

Found : C, 87.44 ; H, 6.80. $C_{18}H_{16}O$ requires : C, 87.06 ; H, 6.50.

exo-7-HYDROXY-*syn*-DIBENZO[*c*, *h*]TRICYCLO[4.3.1.0^{2,5}]DECA-3.8-DIENE (**14**)

Bromoacetoxy-derivative **6** (0.25 g, 0.68 mmoles) was reduced as above with lithium aluminium hydride U.C.B., yielding 0.21 g (95 %) **14**, colourless oil.

NMR ($CDCl_3$, δ, ppm): 1.96 (dt, 1H, *syn*-H—10, $J_{1,10} = J_{7,10}$ = 4.0 Hz), 2.33 (d, 1H, *anti*-H—10, J_{10gem} = 11.0 Hz), 2.66 and 3.30 (broad s, 3H, H—1, H—6 and OH), 3.85—4.20 (m, 2H, H—2 and H—5), 4.33 (d, 1H, H—7, $J_{6,7}$ = 2.0 Hz), 6.30—7.20 (m, 8H aromatics).

IR (CH_2Cl_2, cm^{-1}) : ν OH 3490, 3605.

syn-DIBENZO[*c*, *h*] TRICYCLO[4.3.1.$0^{2,5}$]DECA-3.8-DIEN-7-ONE (**15**)

To a suspension of complex prepared from 0.50 g chromic anhydride in 5 ml pyridine, a solution of 0.080 g (0.32 mmoles) **13** in 5 ml pyridine was added. After working up as above, 0.050 g (63 %) **15** were obtained. RMN and IR spectra were identical with those of the previously obtained [8] (by oxidation of **14**) compound.

syn-DIBENZO[*c*, *h*]TRICYCLO[4.3.1.$0^{2,5}$]DECA-3.8-DIENE (**16**)

A solution of 0.10 g (0.4 mmoles) **15** in 25 ml ether was added dropwise into a stirred solution of aluminium hydride (prepared from 1.40 g (10.6 mmoles) anhydrous aluminium chloride, 0.20 g (5.2 mmoles) lithium aluminium hydride and 20 ml ether). After 15 min. at room temperature, the mixture was boiled for 5 hrs. After working up, the crude product was chromatographed on Al_2O_3 with petroleum ether, yielding 0.070 g (75 %) **16**, m.p. 71°.

NMR (CCl_4, δ, ppm) : 2.10—2.27 (m, 2H, 2H—10), 2.40—3.60 (m, 3H, H—1, H—6 and H—7), 3.85—4.25 (m, 2H, H—2 and H—5), 6.30—6.90 (m, 8H aromatics).

exo-7-*anti*-10-DIBROMO-*syn*-DIBENZO[*c*,*h*]TRICYCLO[4.3.1.$0^{2,5}$]DECA-3,8-DIENE (**8**)

a). From bromoacetoxy-derivative **6** : A solution of 0.20 g (0.54 mmoles) **6** in 10 ml dichloromethane was saturated with anhydrous hydrogen bromide, and the mixture was left at room temperature for 24 hrs. After washing with water, the solvent was evaporated yielding 0.19 g (90 %) **8**, identical with the previously[8] obtained compound.

b). From bromohydroxy-derivative **11** : A solution of 70 mg (0.21 mmoles) **11** and 0.50 ml 63 % hydrobromic acid in 5 ml acetic acid was boiled for 50 hrs. After working up, 70 mg (84 %) **8** were obtained.

Revue Roumaine de Chimie, **22**, 7, 1045–1052 (1977)

Dedicated to the 75th anniversary o
Prof. C. D. NENITZESCU*'s birthday (1902–1970*

ALUMINIUM CHLORIDE CATALYZED REACTIONS OF UNSATURATED ACIDS WITH BENZENE. X[1]

REACTION OF CYCLOHEXYLIDENE- AND 1-CYCLOHEXENYLACETIC ACIDS

V. DRĂGUŢAN, LIGIA STĂNESCU and ALICE MARIE GLATZ
Center of Organic Chemistry, Spl. Independenţei 202–B, Bucharest 15

Received February 5, 1977

The reaction between cyclohexylidene- or 1-cyclohexenylacetic acids and benzene in the presence of aluminium chloride at 40–45° is described. Equilibrium mixtures of phenylated acids were obtained in which the phenyl group enters the 2,3 or 4 position (*trans, cis,* and *trans,* respectively). The reaction was also carried out at 80° and beside the above phenylated acids three bicyclic ketones were obtained by the cycliacylation of the corresponding phenylcyclohexaneacetic acids. The mechanisms of the involved reactions are also discussed.

In 1937, Nenitzescu and Gavăt [2] and simultaneously Cook and Goulden [3,4] described the reaction of cyclohexylidene- and 1-cyclohexenylacetic acids with benzene in the presence of aluminium chloride and indicated 4-phenylcyclohexaneacetic acid as main reaction product.

This was the first report [1] of a migration of a phenyl group in the most remote position of the alicyclic ring during the Friedel-Crafts arylation of an alicyclic derivative.

In the same year, Gosh[5] carried out the reaction of 1-cyclohexenylacetic acid and reported 2-phenylcyclohexaneacetic acid as reaction product.

In a more recent work, Nenitzescu and coworkers studied in detail the reactions of unsaturated aliphatic [6–8] and alicyclic acids [9–13] with benzene in the presence of aluminium chloride. It was found that three main competitive phemomena occur in these types of reactions : the rearrangement of the alkylating agent, the alkylation of the aromatic substrate and the isomerisation of the reaction products. These results have been confirmed by the work of other investigators as well.[1,14,15]

---

[1] A. M. GLATZ, *Rev. Roumaine Chim.*, **19**, 455 (1974) considered as part IX.

[2] C. D. NENITZESCU and I. GAVĂT, *Ber. dtsch. chem. Ges.*, **70**, 1883 (1937).

[3] J. W. COOK, *Chem. and. Ind.*, **56**, 290 (1937).

[4] J. W. COOK and F. GOULDEN, *J. Chem. Soc.*, **1937**, 1559.

[5] R. GHOSH, *Sci. Cult.* (*Calcutta*), 3, 55 (1937).

[6] C. D. NENITZESCU and A. M. GLATZ, *Bull. Soc. chim. France*, **1961**, 218.

[7] A. M. GLATZ, A. C. RĂZUŞ and C. D. NENITZESCU, *Rev. Roumaine Chim.*, **11**, 555 (1966).

[8] A. M. GLATZ, F. BADEA, ZS. ARVAY, V. DRĂGUŢAN, F. CHIRALEU and A. C. RĂZUŞ, *Rev. Roumaine Chim.*, **18**, 2087, (1973).

[9] A. M. GLATZ, A. C. RĂZUŞ, M. ELIAN and C. D. NENITZESCU, *Rev. Roumaine Chim.*, **16**, 1579 (1971).

[10] A. M. GLATZ, A. C. RĂZUŞ, F. BADEA and C. D. NENITZESCU, *Rev. Roumaine Chim.*, **16**, 1567 (1971).

[11] A. C. RĂZUŞ, F. CHIRALEU and A. M. GLATZ, *Rev. Roumaine Chim.*, **20**, 781 (1975).

[12] A. M. GLATZ, V. WERTHEIMER and F. BADEA, *Rev. Roumaine Chim.*, **19**, 87 (1974).

[13] A. C. RĂZUŞ, ZS. ARVAY, A. HANEŞ and A. M. GLATZ, *Rev. Roumaine Chim.*, **21**, 727 (1976).

In the series of alicyclic compounds the behaviour of the following acids in the presence of aluminium chloride has been studied : cyclobutylidene-[9], cyclopentylidene- and cyclopentenyl-,[10,13] 1-indenylidene- and 3-indenylacetic[11] acids and cyclopentylacrylic[12] acid. From the data obtained so far it became interesting to reinvestigate the pionneering work on cyclohexylidene- and 1-cyclohexenylacetic acids mentioned above using modern analytical tools.

In the present work we undertook the study of the reaction of cyclohexylideneacetic (**1**) and 1-cyclohexenylacetic (**2**) acids with benzene using the same conditions as those reported by Nenitzescu and Gavăt.[2] A mixture of the following three positional isomers was obtained (scheme 1, table 1) : *trans*-2- (**3**), *cis*-3- (**4**) and *trans*-4-phenylcyclohexaneacetic (**5**) acids. The reaction at a higher temperature was also examined. Besides the acids, a mixture of bicyclic ketones was obtained : benzo [*b*] bicyclo-[4.4.0] decen-4-one (**6**), benzo [*b*] bicyclo [4.3.1] decen-4-one (**7**) and benzo [*b*] bicyclo [4.2.2] decen-4-one (**8**). These ketones resulted by the cycliacylation of the corresponding acids.

REACTION OF CYCLOHEXYLIDENEACETIC (1) AND 1-CYCLOHEXENYLACETIC (2) ACIDS WITH BENZENE AT 40—45°

The acids **1** and **2** were phenylated at 45° using a molar ratio acid : $AlCl_3$: benzene of 1 : 1.5 : 20. The composition of the reaction product was determined by v.p.c. at various reaction times. Both acid **1** and **2** gave the same reaction products, the *trans*-2- (**3**), *cis*-3- (**4**) and *trans*-4-phenylcyclohexaneacetic (**5**) acids in an equilibrium ratio of 2.6 : 60 : 35 after 1 hr. (see table 1).

Table 1

The reaction of cyclohexylidene-(1) and 1-cyclohexenylacetic (2) acids with benzene at 40–45°

Starting material	Reaction time min	Phenylcyclohexylacetic acids, %		
		trans-2 (3)	*cis*-3 (4)	*trans*-4 (5)
Acid **1**	1	1.1	55	43
	5	1.2	56	42
	15	1.6	59	38
	60	2.6	60	35
	240	2.7	60	35
Acid **2**	1	1.3	52	46
	5	1.4	54	44
	15	1.8	58	38
	60	2.7	59	35
	240	2.8	60	35

[14] M. F. ANSELL and G. F. WHITFIELD, *Tetrahedron Letters*, **1968**, 3075.

[15] P. FOUR and D. LEFORT, *Compt. rend. C*,. **264**, 786 (1967)

Table 1 shows that only slight differences exist between the composition of the product mixtures starting either from acid 1 or acid 2. The absence of some isomers among the reaction products, the great amount of 3- and 4- in respect with 2-phenylated acids and the high quantity of the 1,4-disubstituted isomer, at short reaction times require an explanation.

Thus, as previously mentioned,[1] ions 9 and 10 are initially formed (scheme 1).

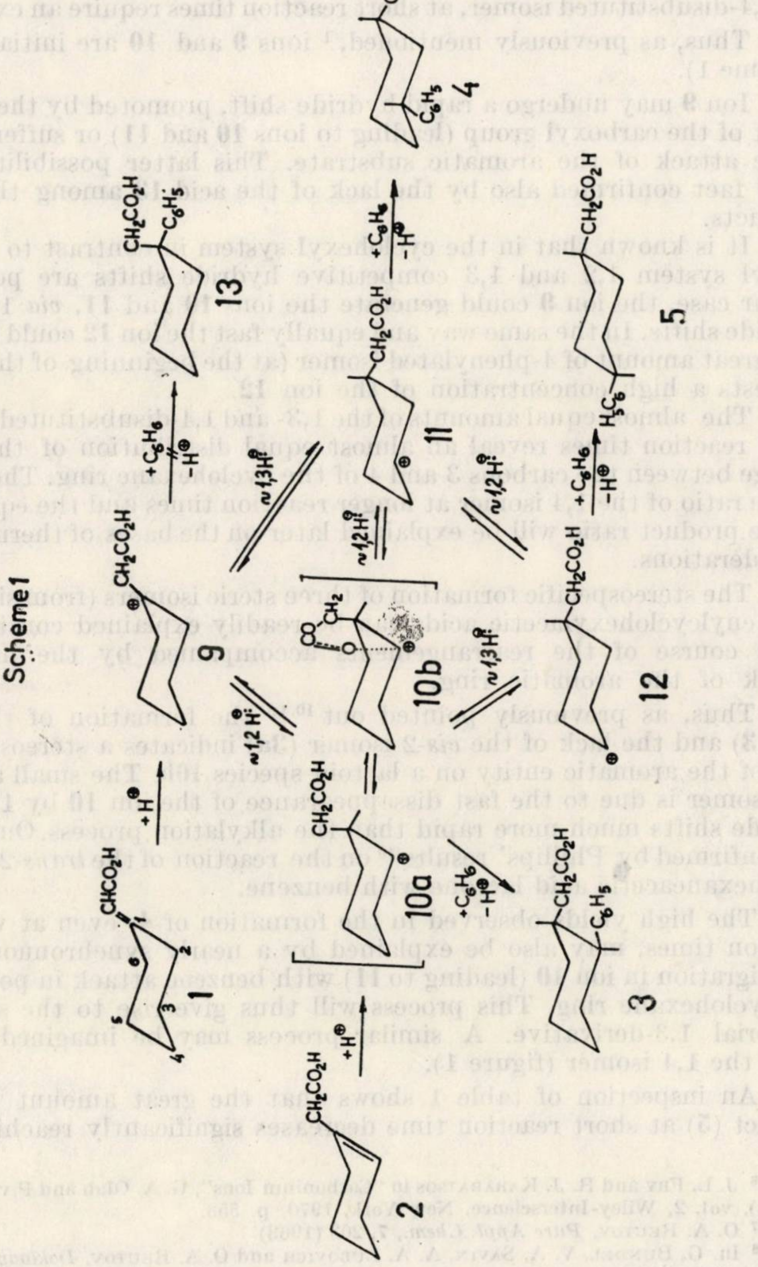
Scheme 1

Ion 9 may undergo a rapid hydride shift, promoted by the inductive effect of the carboxyl group (leading to ions 10 and 11) or suffer a nucleophilic attack of the aromatic substrate. This latter possibility is ruled out,[1] fact confirmed also by the lack of the acid 13 among the reaction products.

It is known that in the cyclohexyl system in contrast to the cyclopentyl system 1,2 and 1,3 consecutive hydride shifts are possible.[16-18] In our case, the ion 9 could generate the ions 10 and 11, *via* 1,2 and 1,3 hydride shifts. In the same way and equally fast the ion 12 could be formed. The great amount of 4-phenylated isomer (at the beginning of the reaction) suggests a high concentration of the ion 12.

The almost equal amounts of the 1,3- and 1,4-disubstituted isomers at short reaction times reveal an almost equal distribution of the positive charge between the carbons 3 and 4 of the cyclohexane ring. The decrease of the ratio of the 1,4 isomer at longer reaction times and the equilibration of the product ratio will be explained later on the basis of thermodynamic considerations.

The stereospecific formation of three steric isomers (from six possible) of phenylcyclohexaneacetic acids is readily explained considering the steric course of the rearrangements accompanied by the nucleophilic attack of the aromatic ring.

Thus, as previously pointed out[10,19] the formation of the *trans*-2 acid (3) and the lack of the *cis*-2 isomer (3a) indicates a stereospecific attack of the aromatic entity on a bridged species 10b. The small amount of this isomer is due to the fast disappearance of the ion 10 by 1,2 and 1,3 hydride shifts much more rapid than the alkylation process. Our findings are confirmed by Phillips' results[19] on the reaction of the *trans*-2-hydroxycyclohexaneacetic acid lactone with benzene.

The high yields observed in the formation of 4 even at very short reaction times, may also be explained by a nearly synchronous hydride ion migration in ion 10 (leading to 11) with benzene attack in position 3 of the cyclohexane ring. This process will thus give rise to the stable diequatorial 1,3-derivative. A similar process may be imagined from ion 11 to the 1,4 isomer (figure 1).

An inspection of table 1 shows that the great amount of *trans*-4 product (5) at short reaction time decreases significantly reaching a cor-

---

[16] J. L. Fry and E. J. Karabatsos in "Carbonium Ions", G. A. Olah and P. v. R. Schleyer (editors), vol. 2, Wiley-Interscience, New York, 1970, p. 555.

[17] O. A. Reutov, *Pure Appl. Chem.*, 7, 203 (1963).

[18] In. G. Bundel, V. A. Savin, A. A. Lebovitch and O. A. Reutov, *Doklady Akad. Nauk S.S.S.R.*, 165, 1078 (1965).

[19] D. D. Phillips and D. N. Chatterjee, *J. Amer. Chem. Soc.*, 80, 1360 (1958).

Table 1 shows that only slight differences exist between the composition of the product mixtures starting either from acid **1** or acid **2**. The absence of some isomers among the reaction products, the great amount of 3- and 4- in respect with 2-phenylated acids and the high quantity of the 1,4-disubstituted isomer, at short reaction times require an explanation.

Thus, as previously mentioned, [1] ions **9** and **10** are initially formed (scheme 1).

Ion **9** may undergo a rapid hydride shift, promoted by the inductive effect of the carboxyl group (leading to ions **10** and **11**) or suffer a nucleophilic attack of the aromatic substrate. This latter possibility is ruled out, [1] fact confirmed also by the lack of the acid **13** among the reaction products.

It is known that in the cyclohexyl system in contrast to the cyclopentyl system 1,2 and 1,3 competitive hydride shifts are possible. [16,18] In our case, the ion **9** could generate the ions **10** and **11**, *via* 1,2 and 1,3 hydride shifts. In the same way and equally fast the ion **12** could be formed. The great amount of 4-phenylated isomer (at the beginning of the reaction) suggests a high concentration of the ion **12**.

The almost equal amounts of the 1,3- and 1,4-disubstituted isomers at short reaction times reveal an almost equal distribution of the positive charge between the carbons 3 and 4 of the cyclohexane ring. The decrease of the ratio of the 1,4 isomer at longer reaction times and the equilibration of the product ratio will be explained later on the bases of thermodynamic considerations.

The stereospecific formation of three steric isomers (from six possible) of phenylcyclohexylacetic acids can be readily explained considering the steric course of the rearrangements accompanied by the nucleophilic attack of the aromatic ring.

Thus, as previously pointed out [10,13] the formation of the *trans*-2 acid (**3**) and the lack of the *cis*-2 isomer (**3a**) indicates a stereospecific attack of the aromatic entity on a lactoid species **10b**. The small amount of this isomer is due to the fast dissappearance of the ion **10** by 1,2 and 1,3 hydride shifts much more rapid than the alkylation process. Our findings are confirmed by Phillips' results [19] on the reaction of the *trans*-2-hydroxycyclohexaneacetic acid lactone with benzene.

The high yields observed in the formation of **4**, even at very short reaction times, may also be explained by a nearly synchronuous hydride ion migration in ion **10** (leading to **11**) with benzene attack in position 3 of the cyclohexane ring. This process will thus give rise to the stable diequatorial 1,3-derivative. A similar process may be imagined from ion **11** to the 1,4 isomer (figure 1).

An inspection of table 1 shows that the great amount of *trans*-4 product (**5**) at short reaction time decreases significantly reaching a con-

---

[16] J. L. Fry and R. J. Karabatsos in "Carbonium Ions", G. A. Olah and P v R. Schleyer (editors), vol. 2, Wiley-Interscience, New York, 1970, p. 553.

[17] O. A. Reutov, *Pure Appl. Chem.*, **7**, 203 (1963).

[18] Iu. G. Bundel, V. A. Savin, A. A. Lubovich and O. A. Reutov, *Doklady Acad. Nauk S.S.S.R.*, **165**, 1078 (1965).

[19] D. D. Phillips and D. N. Chatterjee, *J. Amer. Chem. Soc.*, **80**, 1360 (1958).

stant value after 1 hour. While the reaction is progressing the other two positional isomers change gradually towards equilibrium values. These results indicate that the reaction is under kinetic control at short reaction

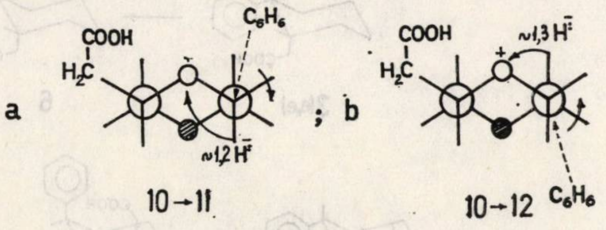

Fig. 1. — Synchronous attack of benzene with hydride ion migration; *a* leading to **4**, *b* leading to **5**.

times being then thermodynamically controlled. The thermodynamic equilibration of reaction products occurs as a result of the isomerization of phenylcyclohexaneacetic acids. [12]

These data demonstrate that the constant amount of *trans*-2 (**3**) isomer during the reaction course is due to the low tendency of *cis*-3 (**4**) and *trans*-4 (**5**) isomers to isomerize to acid **3** because of the strong inductive effect of the carboxyl group.

The mechanism of these isomerizations involving phenonium ions as transition states has been previously discussed. [12] It is probable that phenyl migration would be assisted by 1,2-hydride shift from the adjacent carbon atom.

To prove the above intramolecular mechanism we undertook the isomerization reaction of phenylcyclohexaneacetic acids in the presence of an excess of toluene. The reaction mixture analysis indicated as only isomerization products phenylcyclohexaneacetic acids and no methylphenylcyclohexaneacetic acids that could be formed in an intermolecular pathway.

REACTION OF CYCLOHEXYLIDENEACETIC (1) AND 1-CYCLOHEXENYLACETIC (2) ACIDS WITH BENZENE AT 80°

The reaction of the acids **1** and **2** with benzene was carried out in refluxing benzene in a molar ratio acid : $AlCl_3$: benzene of 1 : 1.5 : 20. The reaction products were analyzed by v.p.c. As expected [7,10,20] benzo [*b*] bicyclo [4.4.0] decen-4-one (**6**), benzo [*b*] bicyclo [4.3.1] decen-4-one (**7**) and benzo [*b*] bicyclo [4.2.2] decen-4-one (**8**) were formed by cycliacylation of the phenylated cyclohexaneacetic acids (scheme 2).

---

[20] A. M. Glatz and C. Răzuş, *Rev. Roumaine Chim.*, **11**, 551 (1966).

Scheme 2

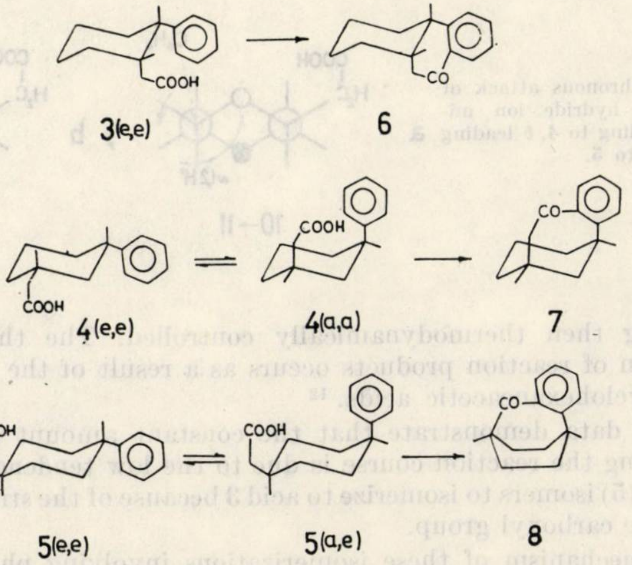

These ketones were identified by comparison with authentic samples.

Table 2

The reaction of cyclohexylidene- (1) and 1-cyclohexenylacetic acids with benzene at 80°

Starting material	Reaction time hr	Reaction products, %						
		3	**4**	**5**	**6**	**7**	**8**	Unidentified products
Acid **1**	1/2	1.2	47	51	traces	traces	traces	2.5
	1	1.3	58	36	0.1	0.2	traces	3.5
	10	2.0	46.6	26	3.4	4.2	1.0	15.5
Acid **2**	1	1.5	56	37	0.2	0.2	traces	3.4
	10	2.0	46	26	3.2	4.0	1.1	15.0

The maximum overall yield in benzobicyclic ketones obtained in the reaction at 80° was 9% in contrast to five-membered ring.[10] At longer reaction times this yield decreased due to the formation of unidentified polymeric products. It is noteworthy that the equilibrium ratio of the phenylated cyclohexaneacetic acids **3**, **4** and **5** is maintained at 80° too.

Obviously, only the favourable conformations of the acids **3**, **4** and **5** (**4**e,e, **5**a,a and **6**a,e, respectively) can cyclize to the corresponding ketones (scheme 2). Ketone **8** results from the boat conformation of the acid **5** a,e.

EXPERIMENTAL

All melting points are uncorrected. IR spectra were recorded on UR—20 Carl Zeiss-Jena spectrophotometer. NMR spectra were recorded on a Varian A 60—A spectrometer, using TMS as internal standard. The v.p.c. analyses were carried out on a Willy Giede model 18—3 gas-chromatograph using a 3m × 4 mm column packed with 10% ethylene-gycol succinate on Chromosorb W (60—80 mesh); column temperature 190°.

A. SYNTHESES OF THE STARTING MATERIALS AND AUTHENTIC SAMPLES

The structure and purity of the starting materials and authentic samples were checked by g.p.c., NMR and elemental analysis.

Cyclohexylideneacetic acid (**1**). The acid **1** was prepared by Wittig reaction starting from cyclohexanone and triethylphosphonoacetate using the procedure of Wiberg and Hiatt. [21].

To a stirred suspension of 2.4 g NaH (100 mmol) in 100 ml dimethoxyethane 22.4 g triethylphosphonoacetate (100 mmol) were added dropwise at 32°. The reaction mixture was stirred for the further 30 min, then a solution of 9.8 g cyclohexanone (100 mmol) in 10 ml dimethoxyethane was added dropwise at 35°. After 1 hr stirring at room temperature the reaction mixture was quenched with 250 ml water and extracted with ether. The extracts were dried over $MgSO_4$, the solvent removed and the residue distilled in vaccuum yielding 14 g of ethyl-cyclohexylideneacetate. Alkaline hydrolysis and recrystallization from aqueous ethanol gave 6.5 g (56%) cyclohexylideneacetic acid, m.p. 91—92°. (*Found* : C, 68.39 ; H, 8.73 ; *Calcd.* for $C_8H_{12}O_2$: C, 68.54 ; H, 8.63) NMR spectrum (CCl_4, δ, ppm) : 11.6 (1 carboxylic proton) ; 5.63 (1 vinylic proton, singlet) ; 2.88 (2 protons, multiplet) ; 2.27 (2 protons, multiplet) ; 1.65 (6. protons).

1-Cyclohexenylacetic acid (**2**). The acid **2** was obtained in 60% yield by alkaline hydrolysis of its ethyl ester prepared by Reformatsky reaction and subsequent dehydration,[22] b.p. $_1$ 98°. (*Found* : C, 67.98 ; H, 8.93 ; *Calcd.* for $C_8H_{12}O_2$: C, 68.54 ; H, 8.63).

NMR spectrum (CCl_4, δ, ppm) : 10.7 (1 carboxylic proton) ; 5.55 (1 vinylic proton) ; 2.92 (2 exocyclic protons, singlet) ; 2.2—1.4 (8 protons).

trans-2-(**3**), *cis-3-* (**4**)*-Phenylcyclohexaneacetic* (**5**) *acids* were prepared in the same way as previously described. [12] Their esters, used as authentic samples in v.p.c. identifications were obtained by esterification with diazomethane.

cis-2-Phenylcyclohexaneacetic acid (**3a**) was obtained according to Gutsche [23] starting from 2-phenylcycohexanone. Reformatsky reaction followed by dehydration and reduction gave acid **3a**, m.p. 162—164° (aqueous ethanol), in 40% yield. (*Found* : C, 76,98 ; H. 8.39 ; *Calcd.* for $C_{14}H_{18}O_2$: C, 77.03 ; H, 8.31).

NMR spectrum (CCl_4, δ,ppm) : 10.5 (1 carboxylic proton), 7.17 (5 aromatic protons, singlet) ; 2.9 (1 benzylic proton, multiplet) ; 2.5 (exo-cyclic-CH_2-, 2 protons, broadened singlet) ; 2.2—1.1 (9 protons).

Benzo [b] bicyclo [4.4.0] decen-4-one (**6**) was prepared by PPA cyclization of the acid **3** in 78% yield, m.p. 95—96° (96—97° reported by Buchta and Ziener.) [24]

Benzo [b] bicyclo [4.3.1] decen-4-one (**7**) was obtained in the same way starting from acid **4**.

To a mixture of 30 g P_2O_5 and 21 ml of 89% H_3PO_4 stirred for 1 hr at 100°, 2 g (9.2 mmol) of *cis*-3-phenylcyclohexaneacetic acid (4) were added. The temperature was raised at 130° and stirring continued for the further 3 hrs. The reaction mixture was then poured into 50 ml ice-water and allowed to stand overnight. After extraction with ether, washing with 5% KOH and water, drying over $MgSO_4$ and removal of the solvent the residue was purified by column chromatography (neutral alumina, eluent a mixture of 95% petroleum ether and ethyl ether) affording 1.2 g of an oil, b.p.$_1$ 130—132°, yield 66%, (*Found* : C, 83.80 ; H, 8.21 ; *Calcd.* for $C_{14}H_{16}O$: C, 83.96 ; H, 8.05).

IR (CCl_4, cm^{-1}) : 1285 s, 1457 s, 1608 m, 1680 v.s., 2860 s, 2875 s, 2940 v.s., 3030 w, 3070 w.

NMR spectrum (CCl_4, δ, ppm) : 7.5—6.7 (4 aromatic protons, multiplet), 3.17 (1 benzylic proton, multiplet) ; 2.74 (2 protons, doublet) ; 2.25—1.25 (9 protons).

---

[21] K. B. Wiberg and H. Hiatt, *J. Amer. Chem. Soc.*, **90**, 6495 (1968).

[22] R. L. Shriner, "Organic Reactions", vol. 1, J. Wiley, New -York, 1942, p. 1.

[23] C. D. Gutsche, *J. Amer. Chem. Soc.*, **70**, 4152 (1948).

[24] E. Buchta and H. Ziener, *Liebigs Ann. Chem.*, **601**, 155 (1956).

Oxime, white crystals, m.p. 138–139° (ethanol) (*Found* : N, 6.35 ; *Calcd.* for $C_{14}H_{17}NO$: N, 6.51).

Benzo [b] bicyclo [4.2.2] decen-4-one (**8**) was obtained by cyclization of the acid **5** in 32% yield, b.p. 126–128°.

NMR spectrum (CCl_4, δ, ppm) : 7.5–6.9 (4 aromatic protons, multiplet) ; 3.25 (1 benzylic proton, multiplet) ; 2.8 (2 protons, doublet) ; 2.3–1.2 (9 protons).

B. REACTION OF CYCLOHEXYLIDENE-(1) AND 1-CYCLOHEXENYLACETIC (2) ACID WITH BENZENE AT 40–45°

A solution of 4 g (28.6 mmol) cyclohexylideneacetic acid (**1**) in 20 ml anhydrous benzene was added dropwise to a stirred suspension of 5.7 g (43 mmol) of aluminium chloride in 30 ml anhydrous benzene, at 40–45°. The mixture was stirred at this temperature for 4 hrs. After quenching in ice-water, extraction with ether, drying over magnesium sulfate and removal of the solvent 5.6 g (89%) of a crystalline product, m.p. 68–70° were obtained. (*Found:* C, 76.14 ; H, 8.75 ; *Calcd.* for $C_{14}H_{18}O_2$: C, 77.03 ; H, 8.31.) The v.p.c. analysis of this product after esterification with diazomethane indicated the following composition : 2.6% of acid **3**, 62% of acid **4** and 35% of acid **5**.

A similar experiment was carried out at a 10 hrs reaction time. At various intervals samples were withdrawn and after being worked-up as above the product compositions were determined by v.p.c. (Table 1).

C. REACTION OF CYCLOHEXYLIDENEACETIC (1) AND 1-CYCLOHEXENYLACETIC (2) ACIDS WITH BENZENE AT 80°

A solution of 6 g (42.9 mmol) cyclohexylideneacetic (**1**) acid in 30 ml anhydrous benzene was added dropwise to a stirred suspension of 8.7 g (64.5 mmol) of aluminium chloride in 45 ml anhydrous benzene at 80°. The mixture was stirred at this temperature for 10 hrs. Samples were withdrawn at the intervals mentioned in Table 2 and after the usual work-up the product-compositions were determined by v.p.c. (Table 2).

After 10 hrs the reaction mixture was quenched with ice-water, extracted with ether. The ethereal solution was extracted with 5% potassium hydroxide, the alkaline solution acidified and the separated material gave 7.1 g (75%) of a solid m.p. 66–68°. The v.p.c. after esterification with diazomethane gave the following composition : 2.6% of acid **3**, 62.5% of acid **4** and 35.0% of acid **5**.

The neutral portion yielded after removal of the solvent and purification by column chromatography 0.8 g, yield 9% of a pale yelow oil, b.p.$_2$ 162–166°. (*Found* : C, 83.75 ; H, 8.25 ; *Calcd.* for $C_{14}H_{16}O$: C, 83.96 ; H, 8.25). V.p.c. showed the composition : 37% ketone **6**, 11% ketone **7** and 51% ketone **12**.

The reaction carried out with 1-cyclohexenylacetic (**2**) acid gave a similar product composition (Table 2).

D. ISOMERIZATION REACTIONS

Isomerization reactions of the phenylcyclohexaneacetic acids were carried out for 8 hrs under the same reaction conditions except that a mixture of 2 :3 benzene : toluene was used as solvent. The product composition during the reaction and after 8 hrs corresponded to that of a mixture of phenylated cyclohexaneacetic acids.

Acknowledgements. We thank Elvira Sliam and Violeta Daniel for elemental analyses and C. Drăghici for NMR spectra. We are also deeply indebted to Professor Florin Badea for helpful discussions.

Revue Roumaine de Chimie, 22, 7, 1053–1059 (1977)

Dedicated to the 75th anniversary of
Prof. C. D. NENITZESCU*'c birthday*

OXIDATION OF *n*-DODECANITRILE IN LIQUID STATE WITH MOLECULAR OXYGEN, IN THE PRESENCE OF PSEUDO-HOMOGENEOUS CATALYSTS. I

PEROXIDES, ACIDS AND ESTERS CONCENTRATION

IOSIF DRIMUŞ and MARIAN TRIFAN

Polytechnic Institute Bucharest, The Laboratory of Organic Technology

Received: June 23, 1976

The oxidation of *n*-dodecanitrile in liquid state with molecular oxygen, the thermal process of oxidation and the oxidation in the presence of pseudo-homogeneous catalysts on the basis of metallic naphthenates were studied. The development of the oxidation process was appreciated by determining peroxide, carboxylic and estereal oxygen within the reaction mass. The formation of peroxide type oxygen was positively influenced by the presence of metal salts in the following order: Fe> Cr> Ni> Cu> Co> Pb> Mn. For the final concentration with regard to the final amount of carboxylic oxygen the order was: Cr> Co> Fe> Ni> Cu> thermal process > Mn> Pb, meanwhile for the final concentration of esters the order of activity was: Cr> Co> Fe> Cu> Ni thermal process> Pb> Mn.

INTRODUCTION

One common feature of the oxidation of liquid hydrocarbons with molecular oxygen, in the absence of catalysts is the appearence of an induction stage; in the presence of catalyts, this period diminishes and the reaction takes place faster; the oxidation process may develop under less severe conditions, thus determining a reduction of the amount of the secondary degradation products, which are typical for a very advanced oxidation.

Literature shows that by means of the oxidation of saturated nitriles, which include 3–5 carbon atoms in their chain, in the presence of metallic catalysts (Ag, Au, Pt, Pd, Ru and Ir) at temperatures of 300–800°, unsaturated nitriles with a smaller number of carbon atoms can be obtained.[1]

The oxidation of the mono-olefinic fatty acids nitriles (i.e. oleonitrile) by using a Cr_2O_3 and concentrate sulphuric acid catalysts or by using $KMnO_4$ at 80—90°, takes place by breaking the double bond; the nitrile group is preserved. Nitriles, saturated cyanoacides (i.e. $NC-(CH_2)_8-COOH$) and other acid products are formed alongside with unreacted products. [2]

---

[1] H. J. HAGMEYER, JR., (Eastman Kodak Co.), U.S. 2.701.260, 1 Feb., 1955; *Chem. Abstr.*, **50**, 1893 (1956).

In the oxidation of propionitrile and acrylonitrile[3] in the presence of bismuth and molybdenum, at 460°, the products obtained out of the reaction were:

a. in the oxidation of propionitrile: acrylonitrile 2.4%, acetonitrile 7.8%, cyanhidric acid 3%, acetic aldehyde 0.7%, carbon monooxide and carbon dioxide 70%;

b. in the oxidation of acrylonitrile: cyanhidric acid 3%, acetylene 12.5%, carbon monooxide and carbon dioxide 70%.

For the oxidation of acrylonitrile, the molar ratio air : acrylonitrile 20 : 1 was used.

The oxidation of cyanoalkanes with molecular oxygen in the presence of metallic catalysts (Cu, Ag, Pt, Pb) lead to the cyanoalkene.[4]

The biological oxidation,[5] the oxidation with O_3, H_2O_2 and peracids[6] of the residual waters containing organic and anorganic cyanides has been carried out for their purification in order to change the nitrile group into a carboxylic group. Literature also describes the oxidation reaction of liquid hydrocarbones, taking place in the presence of pseudo-homogeneous catalysts. These catalysts have an intermediate position between the homogeneous and heterogenous catalysts; accordingly they are either pseudo-homogeneous or pseudo-heterogeneous.[7] Studies on the oxidation of hydrocarbons, particulary that of *n*-dodecane [8,9] by means of pseudo-homogeneous catalysts are well known. It was generally accepted that in the presence of pseudo-homogeneous catalysts, which have in their composition metals of variable valency, the initiation of the reaction chain takes place by modifying the valency of metals; in the presence of bivalent metals, it may be noticed a change in colour during the process of oxidation. For instance a solution of bivalent cobalt stearate or naphthenate and a hydrocarbon has a slighly violet colour before the oxidation starts and it gets dark green [10,11,12] after oxidation; this phenomenon is also confirmed by the spectral analysis.[12,13]

---

[2] J. D. Fitzpatrick and L. D. Myers (Emery Industries, Inc.), U. S. 2.468.436, 26 Apr., 1949; *Chem. Abstr.*, **43**, 7502 (1949).

[3] C. Michel, E. Jean, *Bull. Soc. chim. France*, **1971**, 2990; *Chem. Abstr.*, **75**, 117763 (1971).

[4] R. E. Gee, Jr., and H. J. Hagmeyer, Jr., (Eastman Kodak Co.), U.S. 2.734.909, 14 Feb., 1956; *Chem. Abstr.*, **50**, 16826 (1956).

[5] F. J. Ludzack, R. B. Schaffer, R. N. Bloomhuff and M. B. Ettinger, *Sewage and Ind. Wastes*, **31**, 33 (1959).

[6] H. Claude, Boeglin and Jean C., (Inst. Rech. Hydrol., Nancy, Fr.), Trib. CEBEDEAU (Centr. Belge Etude Doc. Eaux), **24**, 282—294, 331—332 (1971); *Chem. Abstr.*, **75**, 121105 (1971).

[7] E. T. Denisov and N. M. Emanuel, *Uspekhi Khim.*, **29**, 1409 (1960).

[8] I. Drimuş and L. Papahagi, *Rev. Roumaine Chim.*, **20**, 973 (1975).

[9] I. Drimuş and A. Lupu, *Rev. Romaine Chim.*, **17**, 8 (1972).

[10] E. T. Denisov and N. M. Emanuel, *Zhur. fiz. Khim.*, **30**, 2327 (1956).

[11] G. A. Knorre, Z. K. Maizis and N. M. Emanuel, *Zhur. fiz. Khim.*, **29**, 710 (1955).

[12] B. G. Freidin, *Zhur. priklad. Khim.*, **30**, 768 (1957).

[13] R. Lombard and L. Rommert, *Bull. Soc. chim. France*, **1956**, 36.

Denisov and Emanuel[7] show that cobalt does not entirely change from a bivalent into a trivalent state during the oxidation of cyclohexane in the presence of pseudo-homogeneous cobalt catalyst.

As far as we know, literature does not describe either uncatalytic or catalytic oxidation of *n*-dodecanitrile nor the fatty *n*-alkylnitriles, with molecular oxygen, in liquid state.

In the present work, we have studied the influence of the following metals: Cu, Mn, Co, Fe, Cr, Ni, Pb (in the form of naphthenates) on the oxidation process of the *n*-dodecanitrile in liquid state, with molecular oxygen.

The rate of the oxidation process has been established by measuring the variation of the acidity and peroxid indexes, respectively.

EXPERIMENTAL

Preparing of catalysts. For the preparing of the Co, Cr, Mn, Fe, etc. naphthenates, naphthenic acids of Romanian provenience with the following characteristics, have been used :

— average molecular weight 217
— unsaponificabile = 3 %
— acidity index = 260 mgKOH/g
— $d_4^{20} = 0.970$ g/cm³

The naphthenate which was used as a catalyst was obtained through a double exchange reaction starting from a water soluble naphthenate (sodium naphthenate) and a salt of the metal. For instance in the case of a bivalent metal the reaction may be written as :

$$2\,RCOONa + MeSO_4 \longrightarrow (RCOO)_2Me + Na_2SO_4$$

$RCOONa, MeSO_4$ = soluble in water, (Me = Co, Fe, Ni, Mn, Cu, Pb, Cr).

The naphthenates obtained $(RCOO)_2Me$ to be used as catalysts, are insoluble in water but they are soluble in *n*-dodecanitrile.

PROCEDURE FOR OXIDATION

The catalytic or uncatalytic oxidation of the *n*-dodecanitrile with molecular oxygen has been achieved in a vertical tubular glass reactor. 50 g of *n*-dodecanitrile have been oxidised at a flow rate of 30 l/h of oxygen at a temperature of 120° for a period of 300 minutes. The temperature was kept with an accurancy of ±2°.

The volatile fraction has been condensed and collected.

The uncondensed gas is set free into air after being previously washed up succesively with H_2SO_4, NaOH and H_2O.

A weight ratio metal : *n*-dodecanitrile 1 :1000 has been used in the reaction.

Analysis. A determination of the acidity and peroxide indices of the reaction mass has taken place every 15 minutes. The saponification indices have been established at various stages of the reaction and finally at the end of it.

RESULTS AND DISCUSSION

A. THE VARIATION OF PEROXID CONCENTRATION

Figure 1 reveals that for the oxidation of *n*-dodecanitrile, in the absence of catalysts there is a period (about 30 minutes) of delay in the forming of the peroxides. After this period of induction was surpassed, the concentration of peroxides grows gradually, reaching a maximum after a period of 200 minutes; further the existing peroxides start gradually disappearing, down to 1 mgO/g.

In the case when the oxidation of the n-dodecanitrile with molecular oxygen was carried out in the presence of Fe, Cr, Cu, Ni, Co, Mn, Pb naphthenates, the concentration of peroxides runs as follows : in the presence of Fe naphthenate a rapid accumulation of peroxides takes place during the first 20 minutes of the reaction, reaching a value that maintains itself for about 50 minutes ; further the peroxides gradually disappear from the reaction medium ; in the case of a Cr naphthenate, the concentration of peroxides grows slowlier than in the case of a Fe naphthenate, reaching a higher value within 60 – 70 minutes ; after this period the thus-formed peroxides are rather rapidly degraded, resulting in a very low value within a relatively short period of time ; in the presence of Ni, Cu and Co naphthenates, a more pronounced increase of concentration of peroxides appears after 40 – 50 minutes starting from the moment in which the regimen conditions have been reached ; the concentration of peroxides maintains their high value up to a period of time of about 60 minutes and afterwards starts to disappear gradually, reaching at the end reaction period levels under 0.5 mgO/g.

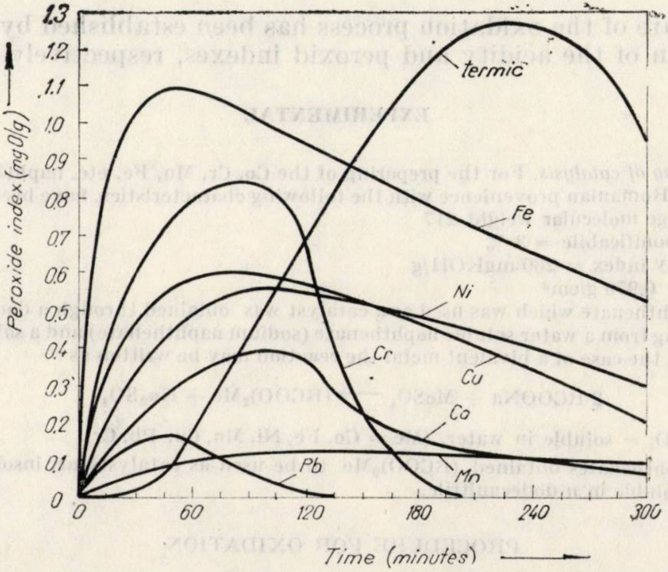

Fig. 1. – The concentration of peroxides for the oxidation of n-dodecanitrile, in liquid state, with molecular oxygen.

The oxidation of n-dodecanitrile in the presence of the Mn and Pb naphthenates shows that the concentration of peroxides is lower than in the previous cases ; in the case of Mn, higher values are being preserved even after 120 minutes, without marked decreases as for the other catalysts.

B. ACID AND ESTER CONCENTRATIONS

The concentration of acids expressed by means of the acidity index (I_a, mgKOH/g) in the case of the oxidation of n-dodecanitrile in the absence of catalysts begins to get a measurable value after 15 minutes of reaction (figure 2). The curve of acid concentration versus time is in this case slightly ascending until the end of the reaction. The use of metallic catalysts (in the form of naphthenates) for the oxidation of *n*-dodecanitrile accelerates the forming up of acids as soon as the reaction has rached its established work conditions.

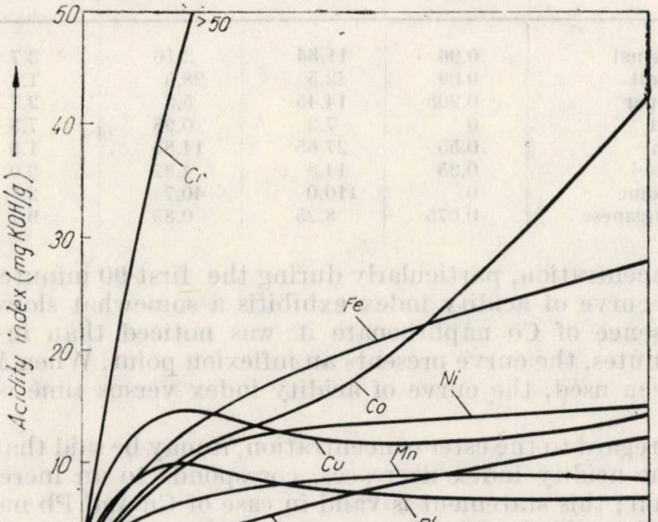

Fig. 2. — The concentration of acids for the oxidation of *n*-dodecanitrile, in liquid state, with molecular oxygen.

In the presence of Cr naphthenate, the acid concentration rapidly increases, reaching, after 30 minutes an acidity index higher than 33 and finally having the value given in Table 1.

In the presence of Cu naphthenate, after 30 minutes of reaction the acidity index gets to a value that is kept constant for a period of about 20 minutes and then falls slowly for the next 60 minutes by approximately 2.4 mgKOH/g; afterwards it is once again slowly increasing towards the final part of the reaction.

The same phenomenom, namely the decrease of the acidity index after reaching a maximum, was also noticed when lead naphthenate was used; in this case, the decrease of the acidity index is smaller than in the presence of copper (see figure 2).

The use of nickel naphthenate leads to a marked increase of the acid concentration, as soon as the reaction begins; in this case, the curve of acidity index is slightly increasing. For the Fe and Co naphthenates, the acid concentration begins to increase from the first moments of the reaction. The presence of iron naphthenate determines the augmentation of

Table 1

Concentration of peroxides, acids and esters after 300 minutes, in the process of the oxidation of *n*.dodecanitrile, in liquid state, with molecular oxigen

Catalyst (naphthenate)	Peroxide index mg0/g	Acidity index mgKOH/g	Ester index mgKOH/g	Acidity index / ester index
thermal	0.96	11.84	3.16	3.7
cobalt	0.09	42.5	28.5	1.4
copper	0.205	14.45	5.3	2.7
lead	0	7.2	0.98	7.3
iron	0.55	27.65	14.85	1.8
nickel	0.35	14.8	4.92	3.0
chrome	0	110.0	40.7	2.7
manganese	0.075	8.25	0.85	9.7

the acid concentration, particularly during the first 90 minutes ; after this period, the curve of acidity index exhibitis a somewhat slower increase. In the presence of Co naphthenate it was noticed than in the period 60—120 minutes, the curve presents an inflexion point. When Mn naphthenate has been used, the curve of acidity index versus time is practically linear.

With regard to the ester concentration, it may be said that the period, in which the acidity index decreases, coresponds to an increase of ester concentration ; this statement is valid in case of Cu and Pb naphthenates. The ester index, obtained in the presence of Mn naphthenate, has resulted in small and unsignificant values. The ester concentration, resulted after 50—60 minutes in the presence of Cu, Ni, Pb naphthenates (or just thermal oxidation), tends to remain approximately constant till the end of the reaction. In the cases in which, Fe, Co or Cr naphthenates were used, the ester indexes increase in time ; their final values are given in Table 1.

We suppose that in case of lead and copper naphthenates, the ester formation is not accompanied by the formation of new acid products ; the ester production takes place on the basis of the acids formed in the first stage of the reaction, resulting in the decrease of acidity indexes (figure 2).

The final ratios between acidity and ester indexes are presented in Table 1.

CONCLUSIONS

1. In the oxidation of *n*-dodecanitrile, the peroxides and acids are generated as soon as the work conditions are fulfilled ; induction period present at the formation of peroxides and acids in the case of the uncatalytic oxidation is to a great extent diminished in the presence of the Co, Pb, Fe, Cr, Cu, Bi and Mn naphthenates.

2. In the oxidation of *n*-dodecane [8] and that of *n*-dodecanitrile in the presence of metals (in the form of naphthenates), the maximum peroxid concentration presents various series of order, namely :

a. for the oxidation of *n*-dodecane [8] Al > Ni > Zn > Cr > Co > Mn > Fe > Cu > Pb.

b. for the oxidation of *n*-dodecanitrile Fe> Cr> Ni> Cu> Co> Pb> Mn.

3. In the presence of the same catalysts, in the case of the oxidation of *n*-dodecanitrile, the peroxides are more rapidly generated, i.e. 30 minutes earlier than in the case of *n*-dodecane.

4. In the presence of catalysts studied, the disappearance of peroxides formed, after reaching a maximum, takes place at different rates; the order is: Cr> Fe> Co> Pb> Cu> Ni> Mn.

5. By catalytic oxidation of *n*-dodecanitrile not only acids are formed, but also esters.

6. Catalysts present the following order of activity (expressed as final acid concentration):

a. for the oxidation of *n*-dodecane [8] Zn> Cd> Co> Fe> Cr> Al> Ni> Mn> Pb> Ag> Hg> Cu> Sn.

b. for the oxidation of *n*-dodecanitrile Cr> Co> Fe> Ni> Cu> Mn> Pb.

Revue Roumaine de Chimie, **22**, 7, 1061–1067 (1977)

Dedicated to the 75th anniversary o
Prof. C.D. Nenitzescu's *birthday (1902–1970)*

INVESTIGATIONS IN THE CYCLOBUTANE SERIES. XLIV[1]

RING CONTRACTION OF 8-DIAZO-*exo*-BENZO[*c*]TRICYCLO [4.2.1.0 ^{2,5}]NON-3-EN-7-ONE ON PHOTOLYSIS

L. ENESCU and MARGARETA AVRAM
Laboratory of Organic Chemistry, Polytechnic Institute, str. Polizu 1, 7000 Bucharest 12, Romania

Received January 22, 1977

The synthesis of diazoketone 9 from the formylketone 8 and that of *exo*-benzo[*c*] tricyclo[4.1.1.0^{2,5}]oct-3-en-7-carboxylic acid (3) by photolysis of 9 are presented.

As part of our studies aiming at the synthesis and behaviour of polycyclic systems with cyclobutane ring, we reported previously on the synthesis of *endo*-benzo[*c*]tricyclo[4.1.1.0 ^{2,5}]oct-3-en-7-carboxylic acid **(1)** and *exo*-8-bromo-*exo*-benzo[*c*]tricyclo[4.1.1.0 ^{2,5}]oct-3-en-7-carboxylic acid (**2**).[2, 3]

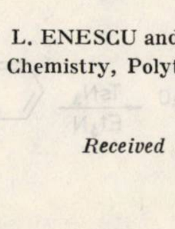

1a R = H
b R = CH_3

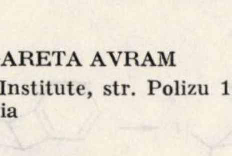

2 R = H X = Br
3 R = H X = H
4 R = CH_3 X = H

In the present paper we report on the synthesis of the corresponding compound in the *exo* series, namely *exo*-benzo[*c*]tricyclo[4.1.1.0 ^{2,5}] oct-3-en-7-carboxylic acid **(3)** by photolysis of 8-diazo-*exo*-benzo[*c*]tricyclo[4.2.1.0 ^{2,5}]non-3-en-7-one (**9**).

---

[1] Part XLIII: I. G. Dinulescu, E. G. Georgescu and M. Avram, *J. Organometal. Chem.*, **127**, 193 (1977).

[2] M. Avram, L. Enescu, I. G. Dinulescu, F. Chiraleu and C. D. Nenitzescu, *Rev. Roumaine Chim.*, **16**, 1783 (1971).

[3] L. Enescu, F. Chiraleu and M. Avram, *Rev. Roumaine Chim.*, **20**, 957 (1975).

The diazoketone **9** was prepared through a five-step sequence starting with *exo*-benzo[*c*]tricyclo$[4.2.1.0^{2,5}]$nona-3.7-diene (*exo*-benzocyclobuteno-norbornene) (**5**).

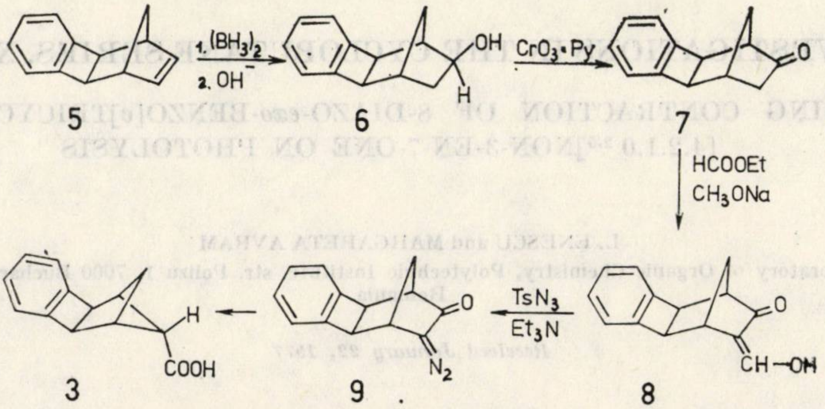

The *exo*-benzocyclobuteno-norbornene (**5**), available from the reaction of benzyne with norbornadiene,[4] was more conveniently prepared using benzyne generated *in situ*, after the procedure described by Logullo.[5] By heating a suspension of diazo-anthranilic acid hydrochloride[6] in dichloroethane with norbornadiene in the presence of propylene oxide, an oily fraction was obtained (b.p. 82—90°/2 mm) which was found to be a mixture of **5** and benzo[*f*]tetracyclo$[3.2.1.1^{3,8}.0^{2,4}]$non-6-ene (**10**)

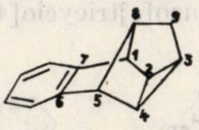

10

in 3 : 1 ratio.[5,7] This mixture could be used as such in hydroboration, yielding the *exo*-hydroxy derivative **6**[8] and the unreacted **10**. Oxidation of **6** with CrO_3-pyridine afforded ketone **7**.[8] The attempt to oxidize **7** with selenium dioxide was unsuccessful, and the synthesis of the diazoketone **9** was achieved using the general procedure of Rosenberger and Yates involving as intermediate formylketones.[9]

---

[4] H. E. Simmons, *J. Amer. Chem. Soc.*, **83**, 1657 (1961).

[5] L. Friedman, R. L. Rice, quoted by F. M. Logullo, Ph. D. Thesis, Case Institute of Technology, Cleveland, 1965.

[6] G. R. Ziegler, *J. Amer. Chem. Soc.*, **91**, 446 (1969).

[7] a) I. Tabushi, H. Yamada, Z. Yoshida and H. Kuroda, *Tetrahedron Letters*, **1971**, 1093. b) The compound **10** was characterized by comparing his NMR spectra with those of the tetrahalogeno compounds obtained by H. Heaney (H. Heaney, J. M. Jablonski, K. G. Mason and J. M. Sketchley, *J. Chem. Soc.* (*C*), **1971**, 3129).

[8] R. Baker and J. Hudec, *Chem. Comm.*, **1967**, 929.

[9] M. Rossenberger, P. Yates, J. B. Hendrickson and W. Wolf, *Tetrahedron Letters*, **1964**, 2285.

The treatment of **7** with ethyl formate in the presence of sodium methoxide afforded **8**, an unstable oily product, in 80% yield. Treatment of the latter with toluenesulfonyl azide[10] and triethylamine, at room temperature, yielded the diazoketone **9**, yellow crystals, m.p. 170 – 173°, in 50% yield.

The mechanism proposed for the formation of the diazoketone **9** is presented in the following scheme:

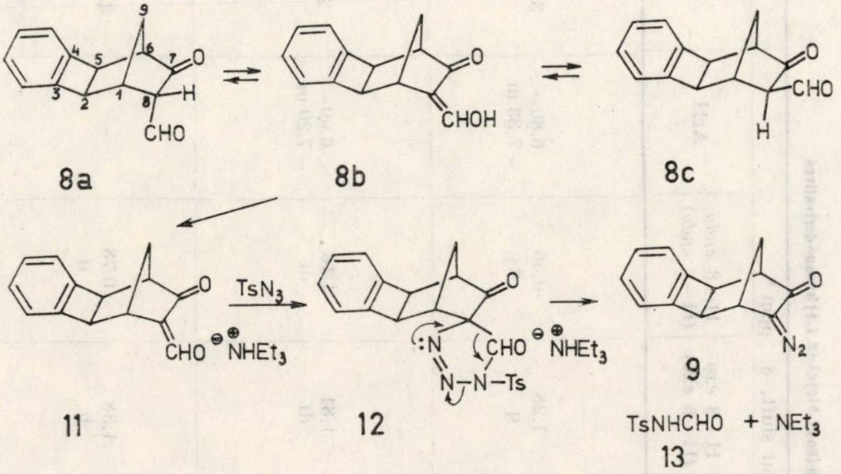

The addition of the tosylazide to the triethylamine salt of the enol **8b** (**11**) led to a strained spiro-cyclic intermediate **12**; cleavage of the N–N bond gave the stabilized diazo-group together with the formylsulfonamide **13**.

The existence of the enol **8b** in equilibrium with the carbonyl forms **8a** and **8c** has been evidenced in the IR and NMR spectra of **8**.

In the IR spectrum (CCl_4) the aldehydes **8a** and **8c** present characteristic carbonyl absorptions ν_{CO} at 1702 and 1735 cm^{-1}; for the aldehyde hydrogen the ν_{CH} stretching appears at 2865–2895 cm^{-1}.[11] The enol **8b** presents the $\nu_{C=C}$ at 1605 cm^{-1} and the associated ν_{OH} at 3400–3600 cm^{-1}.

In the NMR spectrum in CCl_4 the ratio between **8a** : **8b** : **8c** was evaluated at 16 : 51 : 33. **8b** was characterized by the singlet at $\delta = 3.50$ (H–2, H–5) and by the OH signal at $\delta = 8.58$ ppm. For **8a**, the *endo*-aldehyde group induces a non equivalence of the H–2 and H–5 protons; the splitted signal at 3.80 (d, H–5) and the singlet at $\delta = 9.69$ ppm (*endo*–CHO proton) were thus ascribed to **8a**. **8c** displays a singlet at $\delta = 9.56$ due to the *exo*-CHO and H–2, H–5 proton signals at 3.50, as a singlet, superposed on the similar signals of **8b**.

The photolysis of the diazoketone **9** was carried out in a mixture of dioxane : water (1 : 1) by irradiation with a high-pressure lamp (Hanovia,

---

[10] W. von E. Doering and C. De Puy, *J. Amer. Chem. Soc.*, **75**, 5955 (1953).

[11] M. Avram and G. D. Mateescu, "Infrared Spectroscopy. Applications in Organic Chemistry", Wiley-Interscience, New York, 1972.

Table 1

NMR spectral data of some endo-carbomethoxy-bicyclo[2.1.1]hexane derivatives

Compound	Chemical shift, δ, ppm *							Coupling constant J, Hz
	H−2 H−5 (H−2) (H−3)	H−1 H−6 (H−1) (H−4)	H−7 *exo* (H−5 *exo*)	H−8 *exo* (H−6 *exo*)	H−8 *endo* (H−6 *endo*)	ArH	CH_3	
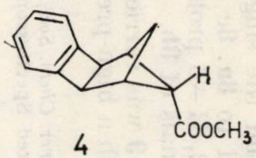 4	3.85 m	2.83 m	3.00 t	1.28 q	0.56 d	6.80− −7.33 m	3.63 s	$J_{7,1}$ 2.5 $J_{8,8}$ 7.5
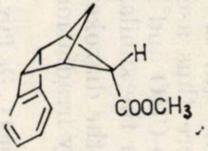 1b	3.78 m	3.11 m	2.43 t	1.81 dt	1.16 dt	6.90− −7.20 m	2.99 s	$J_{7,1}$ 3.0 $J_{8,8}$ 6.8 $J_{8,1}$ 2.5 $J_{8,7}$ 1.5
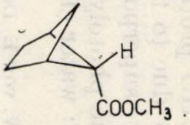 14	1.63 m	2.70 t	2.74 b	1.38 b	0.78 d	—	3.54 s	$J_{7,1}$ 2.9 $J_{8,8}$ 6.3

* The protons in parenthesis correspond to *endo*-5-carbomethoxy-bicyclo[2.1.1]hexane (**14**).[13]

75W), for 72 hrs, until the evolution of gas ceased. The crude acid **3**, white crystals, m.p. 143—145°, was converted by treatment with diazomethane into its methyl ester **4**.

The structure of *exo*-benzo[*c*]tricyclo[4.1.1.0 ^{2,5}]oct-3-en-7-*endo*-carbomethoxylate (**4**) was ascribed on the basis of spectral data and by comparison with the previously described *endo*-isomer **1b** [3,12] and methylbicyclo[2.1.1]hexan-carboxylate **14** [13] (table 1).

In **4**, where the benzocyclobutene ring is *exo*-oriented, more shielded signals are observed for the bridgehead protons (H—1, H—6) and for the bridge protons H—8, and less shielded than in **1b** for H—7-*exo* and H—2, H—5 protons. The coupling constant $J_{8,8}$ in **4** is greater than that for **1b**, while both are greater than those of **14**. [13]

It should be mentioned that neither the *exo* carboxylate [2] nor the acid-catalysed ring opening product [3] were observed in this reaction, in detectable amounts.

EXPERIMENTAL

Microanalyses were performed by Mrs. V. Mateescu. The IR spectra were run on a double beam UR 20 spectrophotometer. NMR spectra were recorded on a Varian A-60A spectrometer using TMS as internal standard, by F. Chiraleu.

Gas-chromatography analyses were carried out on a Cromatron gas-chromatograph, using a 2.0 m× 4 mm diameter column filled with 20% methylsilicone SE 30 on Chromosorb W 30—60 mesh, at 180° and with 30 ml /min hydrogen as carrier gas.

REACTION OF BENZYNE WITH BICYCLO[2.2.1]HEPTA-2.5-DIENE. *exo*-BENZO-[*c*]TRICYCLO[4.2.1.0^{2,5}]NONA-3.7-DIENE (5)

In a three-necked flask fitted with an overhead stirrer, dropping funnel and condenser were placed 23.0 g (217 mmoles) bicyclo[2.2.1]hepta-2.5-diene, 5 ml propylene oxide dissolved in 1500 ml dichloroethane and 9.2 g (46.5 mmoles) diazo-anthranilic acid hydrochloride.[6] The well stirred suspension was gently boiled for 5 hrs until evolution of carbon dioxide ceased. The solvent was evaporated *in vacuo* and the residue was extracted with petroleum ether (500 ml). After filtration from the polymeric material, the solution was washed with water, with saturated sodium bicarbonate solution (five runs of 50 ml) and then dried. The solvent was removed *in vacuo*. The distillation of the residue using a Vigreux column (200 mm× 15 mm diameter) afforded 7.0 g (89.9%) colourless oily product, b.p. 82—90°/2.0 mm.

The gas-chromatography analysis of this fraction indicated a content of two hydrocarbons, **5**[4] (73.1%) and **10**[7] (26.9%) (isolated after hydroboration, see later).

The NMR spectrum of this mixture evidences *exo*-benzo[*c*]tricyclo[4.2.1.0^{2,5}]non-3.7-diene (**5**) by the signals at 3.07 (2H), 2.71 (2H), 6.12 (2H), 1.28 (1H) and 0.86 (1H) in agreement with literature data [4] and with the spectrum of an authentic sample.

exo-7-HYDROXY-*exo*-BENZO[*c*]TRICYCLO[4.2.1.0^{2,5}]NON-3-ENE (6)[8] AND BENZO[*f*] TETRACYCLO[3.2.1.1^{3,8}.0^{2,4}]NON-6-ENE (10)

The hydroxy-derivative **6** described by Baker [8] without experimental details was obtained by hydroboration of the mixture of **5** and **10**. Thus, 26.6 g mixture (containing 19.5 g **5** and 7.2 g **10**, respectively, as indicated by gas-chromatography analysis) afforded 25.0 g crude product. The chromatography on neutral alumina with petroleum ether as eluent yielded 7.0 g oily fraction of **10**[7] with b.p. 93—95°/2.5 mm.

---

[12] M. p. 78° (petroleum ether). IR (CCl$_4$, cm^{-1}): ν_{CO} 1740, ν_{COR} 1224.

[13] K. B. Wiberg, B. R. Lowry and B. J. Nist, *J. Amer. Chem. Soc.*, **84**, 1594 (1962).

$C_{13}H_{12}$ (168.2) *Calcd.* : C, 92.80 ; H, 7.19. *Found* : C, 92.61 ; H, 7.04

IR (CCl_4, cm^{-1}) : ν_{arom} 1140, 1250, ν_{CH,CH_2} 1450, 2850, 2940. 3040.

NMR (CCl_4, δ, ppm) : 3.05 (m, 2H, H−1, H−5), 2.25 (m, 1H, H−8), 1.66 (m, 2H, H−9), 0.83−1.50 (m, 3H, H−2, H−4, H−3).

Further elution with ethyl ether gave 17.0 g (78.7 %) *exo*-alcohol **6** (m.p. 71°) with spectral data in agreement with literature data. [8]

exo-BENZO[*c*]TRICYCLO[4.2.1.0^{2,5}]NON-3-EN-7-ONE (7) [8]

The ketone **7** (m.p. 53°) was obtained in 82 % yield by oxidation of the alcohol **6** with CrO_3-pyridine complex, using a usual procedure. The product was identified by comparison of the IR and NMR spectra with those of the compound obtained by Baker. [8]

8-FORMYL-*exo*-BENZO[*c*]TRICYCLO[4.2.1.0^{2,5}]NON-3-EN-7-ONE (8)

In a 100 ml three-necked flask, sodium methoxide was prepared from 10 ml methanol and 0.6 g (0.026 at.g) sodium and after removal of the methanol in excess, 20 ml anhydrous benzene was added. The mixture was cooled at 0° and under stirring a solution of 2.73 g (0.037 mmoles) ethyl formate, 3.25 g (0.017 mmoles) ketone **7** and 5 ml benzene, was introduced dropwise, during 1 hr. After additional 12 hrs stirring at room temperature, the suspension was extracted with 100 ml aqueous 1N-sodium hydroxide solution. The alkaline extract was filtered, acidified with hydrochloric acid, under cooling and extracted with ether. The organic layer was dried and evaporated to yield 3.0 g (80.2 %) formyl-derivative **8**, an unstable, colourless, oily product, which was characterized by its IR and NMR spectra.

IR (CCl_4, cm^{-1}) : ν_{CO} 1702, 1735, $\nu_{CO-chel.}$ 1680, $\nu_{C=C}$ 1605, ν_{CHO} 2865−2895, ν_{OH} 3400−3600.

NMR ($CDCl_3$, δ, ppm) : 9.69 (s, 1H, CHO-*endo*), 9.56 (s, 1H, CHO-*exo*), 8.58 (bs, 1H, OH-enolic), 6.83−7.45 (m, 5H, aromatic and CH-enolic), 3.80 (m, 1H, H−5 of **8a**), 3.51 (s) 2H, H−2, H−5 of **8b**, m, 2H, H−2, H−5 of **8c**), 2.58−3.16 (m, unresolved, H−1, H−6 and H−8 of **8a−c**, H−2, of **8a**), 1.28 and 1.55 (2d, H−9*endo*, H−9*exo* of **8a−c**, $J_{9,9}$ = 11.0 Hz).

Acetyl-derivative of **8b** : m.p. 95−97°.

IR (CCl_4, cm^{-1}) : ν_{CO} 1740, 1780, $\nu_{C=C}$ 1675.

NMR (CCl_4, δ, ppm) : 7.96 (s, 1H, CH-enolic), 6.88−7.40 (m, 4H, aromatic), 3.55 (s, 2H, H−2, H−5), 2.25 (s, 3H, CH_3), 2.00−2.40 (m, 2H, H−1, H−6), 1.33 and 1.51 (2d, 2H, H−9*endo*, H−9*exo*, $J_{9,9}$ = 11.O Hz).

8-DIAZO-*exo*-BENZO[*c*]TRICYCLO[4.2.1.0^{2,5}]NON-3-EN-7-ONE (9)

Into a well-stirred solution of 3.0 g (14.0 mmoles) formyl derivative **8** in 36 ml ether cooled at 0°, 2.78 g (14.1 mmoles) tosylazide [10] was added and then, during 4 hrs, 2.85 g (28.0 mmoles triethylamine were dropped. After stirring for additional 6 hrs, 35 ml water were added slowly until two layers separated. The aqueous layer was extracted with ether (five portions of 15 ml) and the combined organic layers were washed with water, then dried on magnesium sulfate. The ethereal solution was chromatographed on basic alumina with ether and methylene chloride as eluents. After solvent removal *in vacuo*, 1.5 g (50.6 %) diazoketone **9**, yellow crystals, m.p. 170−173°, were obtained.

$C_{13}H_{10}ON_2$ (210.2) *Calcd.* : N, 13.32. *Found* : N, 13.60.

IR (CCl_4, cm^{-1}): ν_{CO} 1715, 1615, $\nu_{N\equiv N}$ 2085, 1370.

endo-7-CARBOMETHOXY-*exo*-BENZO[*c*]TRICYCLO[4.1.1.$0^{2,5}$]OCT-3-ENE (**4**)

A solution of 1.0 g (4.75 mmoles) diazoketone **9** in a mixture of 20 ml dioxane and 6 ml water was irradiated for 72 hrs with a high-pressure mercury lamp (Hanau 75W) until the evolution of nitrogen ceased and the $\nu_{N\equiv N}$ band disappeared. After removal of the solvent *in vacuo*, the oily residue was dissolved in ether and the ethereal layer was extracted with a saturated sodium bicarbonate solution (four portions of 15 ml). The collected alkaline aqueous layer was acidified with diluted hydrochloric acid and the organic acid was extracted with ether. Evaporation of the dried organic layer provided 0.14 g (14.7%) crude acid **3**, m.p. 143—145° (methanol).

0.14 g crude acid **3** were esterified by treatment with an ethereal solution of diazomethane. After the usual working up the crude ester was purified by chromatography on neutral alumina using a mixture of petroleum ether : ethyl ether (1 :1) as eluent. Removal of the solvent afforded 0.13 g (86.6%) methylester **4**, a colourless oil.

$C_{14}H_{14}O_2$ (214.3) *Calcd.* : C, 78.48 ; H, 6.58. *Found* : C, 78.18 ; H, 6.22.

IR (CCl_4, cm^{-1}) : ν_{CO} 1760.

NMR ($CDCl_3$, δ, ppm) : 6.80—7.33 (m, 4H, aromatics), 3.85 (m, 2H, H—2, H—5), 3.00 (t, 1H, H—7, $J_{1,7} = J_{6,7} = 2.5$ Hz), 2.83 (m, 2H, H—1, H—6), 1.28 (q, 1H, H—8 *exo*), 0.56 (d, 1H, H-8*endo*, $J_{8,8} = 7.5$ Hz), 3.63 (s, 3H, carbomethoxy group).

Revue Roumaine de Chimie, **22**, 7, 1069–1074 (1977)

Dedicated to the 75th anniversary of
Prof. C. D. Nenitzescu*'s birthday (1902–1970)*

A MODEL OF THE TRANSITION STATE IN THE CYCLOADDITION OF KETENE TO ACETYLENE[1]

M. D. GHEORGHIU
Laboratory of Organic Chemistry, Polytechnic Institute, Str. Polizu 1, Bucharest 12, Romania

Received January 17, 1977

Cycloaddition of acetylene to ketene, according to Extended Hückel Calculations, occurs through an asymmetric orthogonal transition state.

The cycloaddition of a ketene to an acetylene represents an attractive synthesis of cyclobutenone derivatives. However, this reaction has received only sporadic attention since only few examples are known so far. Thus, the only reactions reported to give cyclobutenones are illustrated by bis (trifluoromethyl)-ketene,[2] dichloroketene[3] and *t*-butylcyanoketene[4] with various substituted acetylenes.

Rational aspects of the cycloaddition of ketene to acetylenes are obscure. There are no systematic kinetic studies, no discussions of reaction mechanisms and no theoretical studies regarding electronic aspects of this cycloaddition. This status contrasts with the related area of the cycloaddition of ketenes to olefins, where there is satisfactory evidence for both experimental[5–8] and theoretical[9] aspects of this reaction. Thus, it is generally accepted that, if concerted, the addition of ketene to an olefin occurs through a ${}_\pi 2_s + {}_\pi 2_a$ transition state,[5] the suprafacial component is the olefinic double bond, while the ketene is the antarafacial component. This reaction image is substantiated by kinetic studies [6,7] and by the stereochemistry of the resulting cyclobutanones.[8]

---

[1] Presented in part at the 5th National Conference of Physical Chemistry, Bucharest 1–4 Sept. 1976, Abstract N° I – 9.

[2] D. C. England and C. G. Krespan, *J. Org. Chem.*, **35**, 3308 (1970); D. C. England and C. G. Krespan, *J. Amer. Chem. Soc.*, **87**, 4019 (1965).

[3] H. Knoche, *Ann.*, **722**, 232 (1969); A. Krebs and H. Kimling, *Ann.*, **1974**, 2074; H.N.C. Wong, F. Sondheimer, R. Gwodin and R. Breslow, *Tetrahedron Letters*, **1976**, 2715.

[4] M. D. Gheorghiu, C. Drăghici, L. Stănescu and M. Avram, *Tetrahedron Letters*, **1973**, 9.

[5] R. B. Woodward and R. Hoffmann, "The Conservation of Orbital Symmetry", Verlag Chemie, Weinheim, 1970, p. 163; for a recent review see: R. W. Holder, *J. Chem. Educ.*, **53**, 81 (1976).

[6] R. Huisgen, L. Feiler and G. Binsch, *Angew. Chem.*, **76**, 892 (1964); W. T. Brady and H. R. O'Neal, *J. Org. Chem.*, **32**, 612, 2705 (1967); R. Huisgen, L. A. Feiler and P. Otto, *Tetrahedron Letters*, **1968**, 4485; R. Huisgen and L. A. Feiler, *Chem. Ber.*, **102**, 3444 (1969); T. DoMinh and O. P. Strausz, *J. Amer. Chem. Soc.*, **92**, 1766 (1970); F. Effenberger, G. Prossel and P. Fischer, *Chem. Ber.*, **104**, 2002 (1971).

[7] N. S. Isaacs and P. Stanbury, *J. C.S. Perkin II*, **1973**, 166.

[8] M. Rey, S. Roberts, A. Dieffenbacher and A. S. Dreiding, *Helv. Chim. Acta.* **53**, 417 (1970); W. T. Brady and R. Roe, Jr., *J. Amer. Chem. Soc.*, **92**, 4618 (1970); P. R. Brook, A. J. Duke and J. R. Duke, *Chem. Comm.*, **1970**, 574; W. T. Brady and R. Roe, Jr., *J. Amer. Chem. Soc.*, **93**, 1662 (1971); W. Weyler, Jr., L. R. Byrd, M. C. Caserio and H. W. Moore,

We would like to present here a few theoretical results concerning the cycloaddition of ketene to acetylene. However, the exploration of the reaction hypersurface of this cycloaddition would be an extraordinarily difficult task which is beyond our computational facilities. Therefore, we could not undertake a systematic study and we attempted an exploratory investigation of the cycloaddition of ketene to acetylene, in fact a first step which could trigger more advanced and sophisticated studies.

Information about the features of a transition state for the ketene + acetylene reaction were obtained, in the present paper, considering only a section in the reaction hypersurface. This section was defined by the following geometrical parameters : the acetylene and the ketene approach each other in parallel planes. The distance between the planes, measured along the y axis which intersects both C—C bonds in their central points, is denoted by r (fig. 1). The acetylene molecule was allowed to rotate in the plane around this y axis with an angle represented in the figure by α, measured from the x' axis. The intermolecular distance, r, was varied between 2 and 3 Å, with an increment of 0.5 A, while for each distance the relative rotation angle was considered as being 0°, 30°, 45°, 60° and 90°.

All the calculations were carried out using standard Extended Hückel [10] formalism.

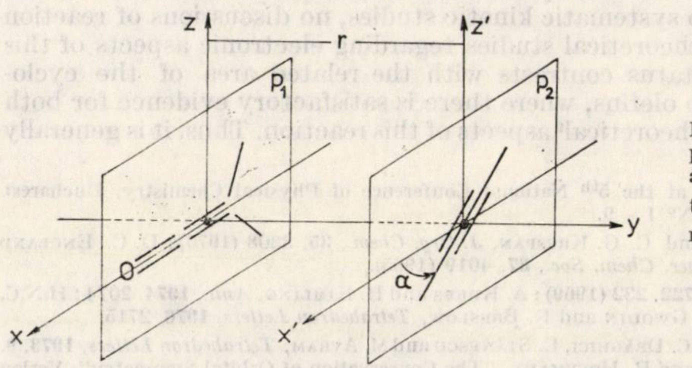

Fig. 1. — The geometrical parameters of the ketene-acetylene approach ; r — intermolecular distance ; α — relative rotational angle.

J. Amer. Chem. Soc., **94**, 1027 (1973) ; M. D. GHEORGHIU, F. KEREK and M. AVRAM, *Rev. Roumaine Chim.*, **20**, 75 (1975) ; M. D. GHEORGHIU, P. FILIP, C. DRĂGHICI and L. PÂRVULESCU, *J. C. S. Chem. Comm.*, **1975**, 635 ; M. D. GHEORGHIU and L. PÂRVULESCU, unpublished results regarding the stereochemistry of cycloaddition of *t*-butylcyanoketene to bicyclo [2.2.1] heptene derivatives.

[9] For theoretical studies regarding the cycloaddition of ketene to olefin see : S. INAGAKI and K. FUKUI, *J. Amer. Chem. Soc.*, **97**, 7480 (1975) ; N. E. EPIOTIS, *J. Amer. Chem. Soc.*, **94**, 1924 (1972) ; R. SUSTMAN, A. AUSMANN and F. VAHRENHOLT, *J. Amer. Chem. Soc.*, **94**, 8099 (1972) ; for other 2+2 thermal cycloadditions see : S. INAGAKI, T. MINATO, S. YAMABE, H. FUJIMOTO and K. FUKUI, *Tetrahedron*, **30**, 2165 (1974).

[10] R. HOFFMAN, *J. Chem. Phys.*, **39**, 1397 (1963).

DISCUSSION OF THE RESULTS

We are concerned with two aspects regarding the cycloaddition of an acetylene to a ketene. The first problem refers to the energetics of the reaction, i.e. information regarding the general features of the geometry of the transition state. The second part of the present discussion is devoted to a comparative reactivity between acetylene and ethylene as ketenophiles, a discussion which is based entirely on electronic arguments.

A. FEATURES OF THE TRANSITION STATE

1. The transition state involves orthogonal approach ;

The total energies for various geometrical approaches of ketene to acetylene are presented in table 1.

Table 1

The total electronic energy of the cycloaddition of ketene to acetylene (in eV) ; r-distance between reactants ; α-the relative rotational angle between the reactants

r (Å)	0°	30°	45°	60°	90°
2	−476.42	−476.85	−477.10	−477.27	−477.38
2.5	−481.38	−481.43	−481.47	−481.51	−481.55
3	−482.49	−482.49	−482.50	−482.51	−482.51

It may be noted from table 1 that the lowest energy for all distances results at orthogonal approaches of the reagents, representing in fact the geometry corresponding to a ${}_{\pi}2_{a}+{}_{\pi}2_{s}$ reaction mode, according to Woodward and Hoffmann's terminology.[5] Therefore, we believe that in this sense the Woodward-Hoffmann rules for concerted cycloaddition of ketene to nonpolar olefins, can be extended to the reactions of ketene to nonpolar acetylenes.

In order to gain more confidence in our results regarding the cycloaddition of ketene to acetylene we have repeated the same kind of calculations for the cycloaddition of ethylene to ketene : the reagents approach each other in a similar geometry as before, along the line connecting the middle of the two C=C bonds. The six atoms of ethylene molecule are all contained in the plane, leaving the π lobes directed parallel to the y axis. The ethylene is allowed to make a rotation from a parallel ($\alpha = 0°$) to an orthogonal ($\alpha = 90°$) position (fig. 2). The results of these calculations are presented in table 2.

Indeed, Extended Hückel Theory calculations provide the accepted reaction mode, ketene and ethylene added through an orthogonal approach, e.g. the reaction mode is ${}_{\pi}2_{s}+{}_{\pi}2_{a}$.

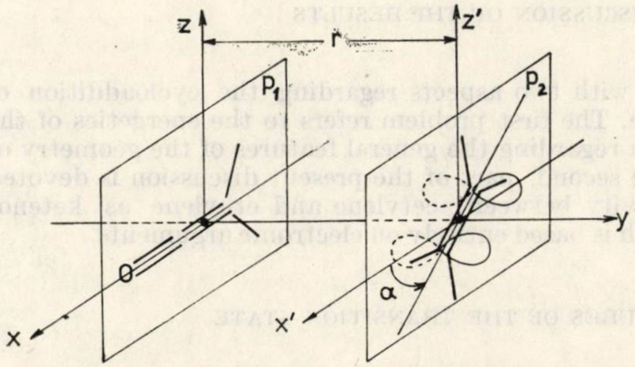

Fig. 2. — The geometric approach of ketene to ethylene ; r — intermolecular distance ; α — relative rotational angle.

Table 2

The total energy of the cycloaddition of ketene to ethylene (in eV) ; r-distance between reactants, α-the relative rotational angle

r (Å)	0°	30°	45°	60°	90°
2	−511.00	−511.14	−511.29	−511.41	−511.44
2.5	−515.53	−515.56	−515.59	−515.63	−515.67
3	−516.62	−516.62	−516.63	−516.63	−516.64

2. The transition state is asymmetric

The Extended Hückel Theory (EHT) gives poor results for the geometry of molecules. However, we believe that EHT can be used to give qualitative results, obtained from the analysis of Mulliken populations.[11] Generally, it is observed that although one assumes for example a symmetrical geometry for certain molecules, the Mulliken overlap populations appear as distributed non-symmetrically, suggesting in fact the tendency for molecular distortions.

Thus, although the ketene and acetylene are made to approach one another symmetrically by geometrical constraint, the overlap populations of the newly formed bonds r_1 and r_2, resulted unequal, $r_1 < r_2$.

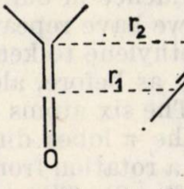

The arrowhead of the reaction is the electrophilic attack of the carbonyl-carbon from the ketene. Therefore, the transition state of ketene addition to acetylene is asymmetric.

---

[11] R. S. Mulliken, *J. Chem. Phys.*, **23**, 1833, 1841, 2338, 2343 (1955).

The fact that, on testing the same method (EHT) for the cycloaddition of ketene to ethylene, Mulliken overlap populations for the two newly formed bonds also appear asymmetrically distributed, strengthens the confidence in these conclusions.

B. COMPARATIVE KETENOPHILE REACTIVITY OF ACETYLENE AND ETHYLENE

It is quite interesting to answer the question whether the cycloaddition of acetylene to ketene occurs more easily than that of ethylene to ketene. Unfortunately, experimental evidence is rare. Thus, dimethylketene reacts with the triple bond of compound ,[12] *although the same molecule contains also a nucleophilic double bond.*

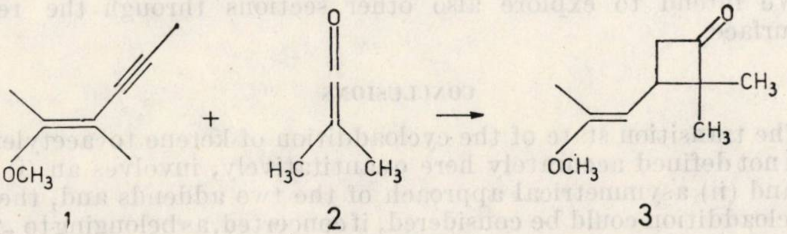

This observation is supported also by kinetic data, although the only competition study existing so far to our best knowledge is in the case of addition of dimethylketene to ethoxyacetylene and butyl vinyl ether.[7] The acetylene reacts *ca.* 2.5 times faster than the olefin.

A higher reactivity of an acetylene as ketenophile than that of an ethylene resulted also from EHT calculations. If one considers that the energy required to obtain the transition state, ΔE, is proportional to the difference between the total energy of the activated complex E_{R-S}, and the total energy of the isolated fragments E_R (acetylene or ethylene) and E_S (the ketene), the values presented in table 3 ore obtained.

The values were obtained only for othogonal approach of the reagents. As a general trend it is observed that the lowest energy required

Table 3

The total energy difference (in eV) between the activated complex and the sum of total energy of the isolated fragments*

r(Å)	2	2.5	3
ketene + acetylene	5.349	1.179	0.219
ketene + ethylene	5.416	1.186	0.216

* see the text for some cautionary comments.

---

[12] H. HASEK, P. G. GOTT and J. C. MARTIN, *J. Org. Chem.*, **29**, 2510 (1964).

to attain the transition state is that of the cycloaddition of ketene to acetylene rather than the cycloaddition of ketene to ethylene.

Some caution must be exercised here. The figures presented in table 3 should be taken only with a semiquantitative meaning, i.e. with an unknown proportionality coefficient. The unacceptable value of *ca.* 5 eV for the energy of transition state in both cycloadditions, probably represents either a deficiency of the computational method or is the energy of a configuration which already passed beyond the transition state. We think that the transition state should be located at about 2.5 Å distance between the reacting molecules. In fact many cycloadditions of ketenes are exothermic and, according to Hammond's principle,[14] the transition state should be located closer to a geometrical configuration resembling the reactants rather than the product.[13]

We intend to explore also other sections through the reaction hypersurface.

CONCLUSIONS

The transition state of the cycloaddition of ketene to acetylene, although not defined accurately here quantitatively, involves an (i) orthogonal and (ii) asymmetrical approach of the two addends and, therefore, this cycloaddition could be considered, if concerted, as belonging to ${}_{\pi}2_s + {}_{\pi}2_a$ reaction mode. It seems that, electronically, acetylene is a better ketenophile than ethylene.

Acknowledgements. The author is indebted to Prof. Roald Hoffmann (Cornell University, Ithaca, New York) for a generous gift of computational time, to Dr. Mihai Elian for carrying out the calculations and some helpful observations and to Prof. A. T. Balaban for many helpful comments.

APPENDIX

The diagonal term, $H_{ii} = I_p$, represents the ionization potential of the corresponding valence state considered $1s_H = -13.6$ eV, $2s_C = -$ -21.40 eV, $2s_O = -32.3$ eV, $2p_C = -11.40$; $2p_O = 14.8$ eV. The off-diagonal term, H_{ij}, was calculated according to Wolfsberg-Helmholtz relationship $H_{ij} = (K/2)\, S_{ij}(H_{ii} + H_{ij})$, where $K = 1.75$ and S_{ij} is the overlap integral between orbitals "*i*" and "*j*". Population analysis was carried out according to Mulliken formulas [11].

The geometry: of ketene [15] was considered as having $r_{C=O} = 1.16$, $r_{C=C} = 1.135$, $r_{C-H} = 1.079$ and HCH bond angle as equal with 122°; of acetylene [16] $r_{C\equiv C} = 1.2$ and $r_{C-H} = 1.057$; of ethylene $r_{C=C} = 1.34$, $r_{C-H} = 1.1$ and the HCH bond angle as equal with 120°.

---

[13] R. Huisgen and H. Mayer, *Tetrahedron Letters*, **1975**, 2965.

[14] G. D. Hammond, *J. Amer. Chem. Soc.*, **77**, 334 (1955); for a critical discussion see: D. Fărcaşiu, *J. Chem. Educ.*, **52**, 76 (1975).

[15] G. Herzberg, "Electronic Spectra and Electronic Structure of Polyatomic Molecules", D. van Nostrand, Toronto, 1966 p. 622.

[16] G. W. King and S. P. So, *J. Mol. Spectroscopy*, **36**, 468 (1970).

Revue Roumaine de Chimie, **22**, 7, 1075–1083 (1977)

Dedicated to the 75th anniversary of
Prof. C. D. NENITZESCU*'s birthday (1902–1970)*

INFRARED, ^{1}H-NMR AND MASS SPECTRA OF SOME TRIPHENYLMETHANE DERIVATIVES

SORIN MAGER and IONEL HOPÂRTEAN
Department of Organic Chemistry, Babeş-Bolyai University, Str. Arany Janos 11,
Cluj-Napoca, Romania

Received July 20, 1976

An IR, ^{1}H–NMR and mass spectral study of the 2′, 2″, 4′, 4″-tetramethoxy-2,4-dinitro-triphenylmethane (I) and of its derivatives II and III was performed. Characteristic vibrations of the benzenic ring and of the alkoxy group are given. The influences of the nitro and methoxy groups on the chemical shifts of aromatic protons are discussed. The formation of the base peak (m/e 165, the fluorenyl ion) and of all major fragments in the mass spectrum of I is explained.

The study of the condensation reaction of nitrobenzaldehydes with phenolic ethers (in order to obtain anthranils, respectively acridones) leads to the observation that in the reaction between 2,4-dinitrobenzaldehyde and dimethylether of the resorcinol a triphenylmethane derivative was obtained.[1]

Changing the condensation agent (conc. sulphuric acid) with phosphoric acid ($d = 1.70$) or polyphosphoric acid we succeeded to improve the yield of the reaction from 53–54 % to 65 % and to shorten the reaction time from 24 to 8 hours (warming at 80°).

The structures of 2′, 2″, 4′, 4″-tetramethoxy-2,4-dinitrotriphenylmethane (I) and of its derivatives II and III, obtained by reduction of I and benzoylation of II, were confirmed and an infrared ^{1}H–NMR and mass spectral study was performed.

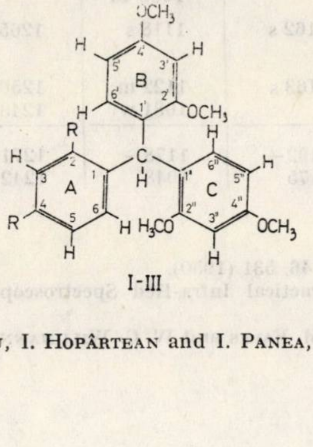

I-III

I R = NO_2
II R = NH_2
III R = $HNCOC_6H_5$

---

[1] M. IONESCU, I. HOPÂRTEAN and I. PANEA, *Stud. Univ. Babeş-Bolyai, Chem.*, **19** (1), 53 (1974).

INFRARED SPECTRA

As a result of the reduction of compound I, using Raney Nickel and hydrazine hydrate, the formation of the corresponding amino derivative II was proved by the replacement of the ν_{NO_2} asymm. and symm. vibrations (at 1544 respectively 1352 cm^{-1} in compound I) by the characteristic ν_{NH_2} asym. and symm. vibration at 3450 respectively 3372 cm^{-1}.

In compound III the absorption bands of the aromatic $-NH_2$ groups are replaced by the ν_{NH} vibration of the secondary amines at 3440 cm^{-1} and the ν_{NH} bending vibration ("Amide II" band) at 1537 cm^{-1}; the ν_{CO} stretching vibration ("Amide I" band) appears at 1692 cm^{-1}.

The ν_{CC} vibrations of the triphenylmethanes I—III (table 1) are in agreement with those known for the benzenic ring.[2]

Table 1

The $\nu_{C-C_6H_5}$ and ν_{C-C} vibration bands (cm^{-1})

Compound	$\nu_{C-C_6H_5}$ vibrations		ν_{CC} vibrations			
TPM*	1184 m*	1290 w*	1603 s*	1567 m	1502 s	1455 s
I	1186 s	1283 s	1616 s	1592 s	1511 s	1468 s
II	1183 m	1296 m	1618 s	1589 s	1510 s	1460 m
III	1182 m	1295 m	1611 s	1592 s	1511 s	1475 s
Vibration ranges [2,3]	1190—1179	1290—1270	1600±20	1580±20	1500±20	1450±20

* TPM = Triphenylmethane; s = strong, m = medium, w = weak.

The further analysis of the spectra of compounds I—III also shows the presence of the (γ_r) rocking vibrations at about 1163—1068 cm^{-1} as well as the symmetrical and antisymmetrical stretching vibrations of the CH (from CH—O—Ar) group in the 2978—2845 cm^{-1} range and of the $C_{aliphatic}$—O—$C_{aromatic}$ group in the 1269—1038 range (table 2).

Table 2

The characteristic alkoxy group vibrations (cm^{-1})

Compound	CH (from CH—O—Ar) vibrations				C—O—C vibrations	
	ν_{as}	ν_s	γ_r		ν_{as}	ν_s
I	2978 m 2949 m	2851 m	1163 s	1124 s 1112 s 1068 m	1269 s 1245 s	1043 s 1038 s
II	2970 m 2948 m	2845 m	1162 s	1118 s	1265 s	1043 s
III	2958 m	2845 m	1163 s	1122 m 1081 w	1250 m 1248 m	1045 s 1038 s
Vibration ranges [4]	2976—2941	2857—2833	1192—1175	1178—1048	1271—1242	1042—1000

s = strong; m = medium; w = weak

---

[2] N. Sheppard, *Trans. Faraday Soc.*, **46**, 531 (1950).

[3] R. D. Cross, "Introduction to Practical Infra-Red Spectroscopy", Butterworths, London, 1960, p. 59.

[4] L. H. Briggs, L. D. Colebook, H. M. Fales and W. C. Wildmann, *Analyt. Chem.*, **29**, 940 (1957).

The aromatic ν_{CH} stretching vibrations, occurring in the 3115 — 3012 cm^{-1} range, are presented in table 3.

Table 3

γ_{CH} **and** ν_{CH} **vibrations (cm^{-1})**

Compound	γ_{CH} vibrations of the substituted benzenic ring (1, 2, 4)		aromatic ν_{CH} vibrations		
TPM	—	—	3094 s	3076 s	3036 s
I	811 m	868 m 879 w	3110 m	3090 m	3012 m
II	805 m	885 w	3115 w	3070 w	3050 w
III	821 w 803 w	880 w 865	3112 w	3070 w	3017 w
Vibration ranges [5]	825—805	885—870	3100—3000		

s = strong ; m = medium ; w = weak

^{1}H-NMR SPECTRA

The ^1H-NMR spectra of compounds I and II have been studied in comparison with those of the triphenylmethane, on the one hand, and with those of the starting materials, *m*-dimethoxybenzene (IV) and 2,4-dinitrobenzaldehyde (VII), on the other hand.

The substitution of the aromatic ring of the triphenylmethane in *ortho* and *para* positions with methoxy and nitro groups (compound I) brings about a strong low field shift ($\Delta\delta = 0.99$ ppm) of the tertiary proton from the triphenylmethane (from $\delta = 5.42$ ppm to $\delta = 6.41$ ppm).

In the part of the spectrum corresponding to the benzenic ring which contains the two nitro groups (ring A), it is easy to recognize an ABX-coupling pattern in which the chemical shifts of the three protons are $\delta_{H^3} = 8.65$ ppm, $\delta_{H^5} = 8.21$ ppm, $\delta_{H^6} = 7.29$ ppm (table 4) and the coupling constants are $J_{H^5H^6} = 8.6$ Hz and $J_{H^3H^5} = 2.4$ Hz ($J_{H^3H^6} = 0$).

Table 4 also shows, for comparison, the chemical shifts of the corresponding protons of the *m*-dinitrobenzene (V), 2,4-dinitrotoluene (VI) and 2,4-dinitrobenzaldehyde (VII). (The spectra of these compounds were also run). While protons H^3 and H^5 have practically the same chemical shifts in 2,4-dinitrotoluene and in compound I, the position of proton H^6 differs with $\Delta\delta = 0.26$ ppm as a result of its location in the influence area of the neighbouring benzenic rings.

---

[5] M. AVRAM and G. D. MATEESCU "Spectroscopia în Infraroşu. Aplicaţii în Chimia Organică", Ed. tehnică, Bucharest, 1966, p. 269, 277.

Table 4

Chemical shifts for I, II and related compounds (IV – VII) in $CDCl_3$

Reference compound for table 4.

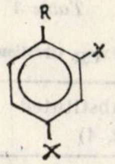

Compound	R	X	Chemical shifts δ (ppm) H³	H⁵	H⁶	OCH_3
I	HC<cycle B*, cycle C	NO_2	8.65	8.21	7.29	3.68 (*p*) 3.78 (*o*)
II	HC<cycle B*, cycle C	NH_2	6	—	6.75	3.77 (*p*) 3.76 (*o*)
IV	H	OCH_3	6.16	6.24	6.85	3.42
V	H	NO_2	8.90	8.49	7.77	—
VI	CH_3	NO_2	8.65	8.26	7.55	—
VII	CHO	NO_2	8.87	8.57	8.05	—

* See formula 1.

The protons located between the two methoxy groups are situated in spectrum at the highest field in concordance with the additivity rule[6] of the increments brought by different substituents (table 5 gives the values of these increments for $-NO_2$, $-OCH_3$ and $-NH_2$ groups) which give for the $H^{3'}$ ($H^{3''}$) proton the value $\delta = 6.20$ ppm ($7.06 - 2 \times 0.43$) in comparison with the experimental value $\delta = 6.22$ ppm. The signal of the proton situated in the 6′(6″) position ($\delta = 6.64$ ppm) is shifted by $\Delta\delta = 0.21$ ppm in comparison with the similar proton from *m*-dimethoxybenzene ($\delta = 6.85$ ppm) as a result of the influence through space caused by the neighbouring benzenic ring.

---

[6] L. M. Jackman and S. S. Sternhell "Applications of NMR Spectroscopy in Organic Chemistry", 2nd edition, Pergamon Press, London, 1969, p. 202.

The chemical shifts of the protons 3′ and 3″, 5′ and 5″, 6′ and 6″ are not identical; as a result, instead of the simple ABX pattern (easy to identify in the case of protons H^3, H^5 and H^6), one observes an agglomeration and partial superposition of the two different ABX coupling patterns in which it is possible to identify the coupling constants $J_{H^{5'}(5'')H^{6'}(6'')} = 9Hz$ and $J_{H^{5'}(5'')H^{3'}(3'')} = 2.2$ Hz ($J_{H^3H^6} = 0$) but it is not possible to ascertain without doubt the chemical shifts of each of the three protons. The differentiation of the protons belonging to the two benzenic rings must be the result of a hindrance of the free rotation of the benzenic rings caused by the existence of the bulky methoxy and nitro groups in the *ortho* positions. On the other hand, while in the case of the ring A the increments brought by the NO_2 groups situated in *ortho*, *meta* and *para* positions are different enough (table 5), the two OCH_3 groups situated in *ortho* positions bring about the same shift (0.86 ppm) for proton 3′ as do the two OCH_3 groups situated in *ortho* and *para* ($0.43 + 0.37 = 0.8$ ppm) for proton 5′. As a result, all chemical shifts for protons situated on rings B and C are concentrated in a narrow range (between 6.64 and 6.22 ppm).

Table 5

The increments brought by different substituents for aromatic protons[6]

Substituent	δ (ppm)		
	ortho	*meta*	*para*
NO_2	0.95	0.17	0.33
OCH_3	−0.45	−0.09	−0.37
NH_2	−0.75	−0.24	−0.63

The spectrum of compound II shows the contrary effect of the $-NH_2$ groups (in comparison with $-NO_2$) on the protons of the ring A.

The chemical shifts of these protons are strongly shifted towards higher fields, the signals being partially superposed over those of the protons belonging to B and C benzenic rings. From the spectrum it is possible to establish with strong probability the unsplitted signal from $\delta = 5.80$ ppm (shifted upfield as compared to that one of the compound I) as belonging to the tertiary proton of the triphenylmethane.

The signal at $\delta = 6$ ppm belongs to the proton H^3 and is strongly shifted towards higher field due to the influence of the two NH_2 groups situated in *ortho* position. The signal at $\delta = 6.75$ ppm splitted as a doublet ($J = 8.5$ Hz) belongs to the proton H^6, its position being in agreement with the calculated one by means of the aditivity rule of the increments brought by the NH_2 groups.

MASS SPECTRUM

The mass spectrum of compound I (Fig. 1) brings the confirmation of its established structure, showing, not only a molecular weight of 454, in agreement with the molecular formula $C_{23}H_{22}N_2O_8$, but also the corresponding number of rings plus double bonds calculated by means ofthe

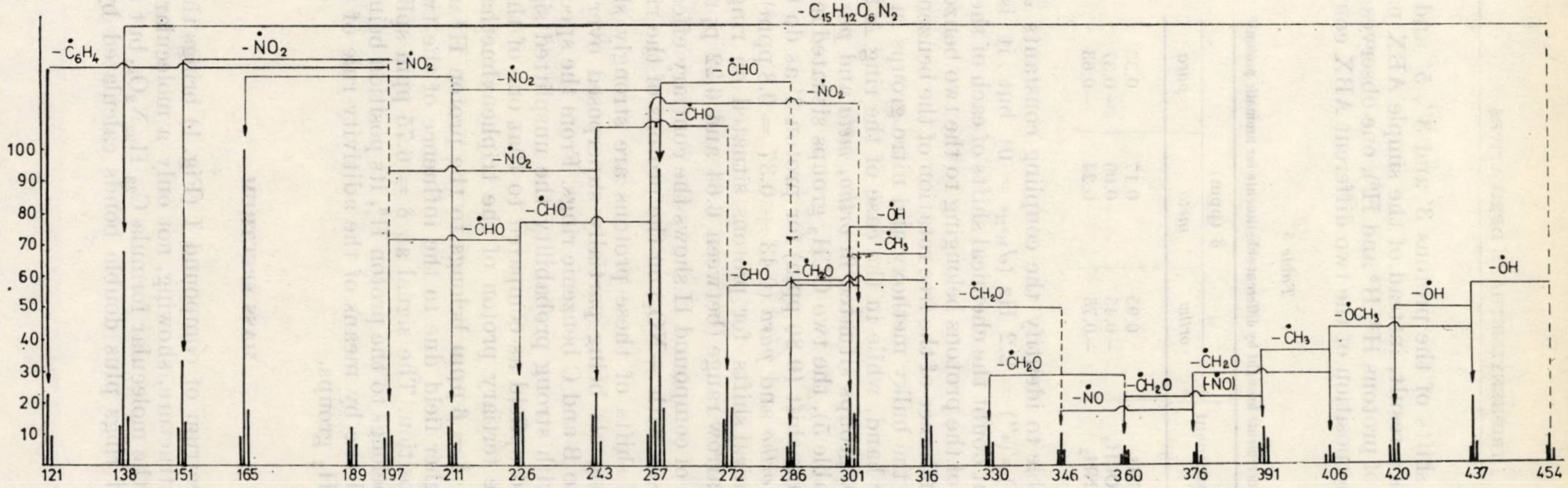

Fig. 1 — The mass spectrum of compound I.

well-known equation (1)

$$N = x - {}^1/_2 y + {}^1/_2 z + 1 = 14 \tag{1}$$

in which $x = 23$, $y = 22$, and $z = 2$.

The fragmentation pattern may be explained taking into account two significant fragmentation ways of the molecular ion (m/e 454), shown in the scheme I.

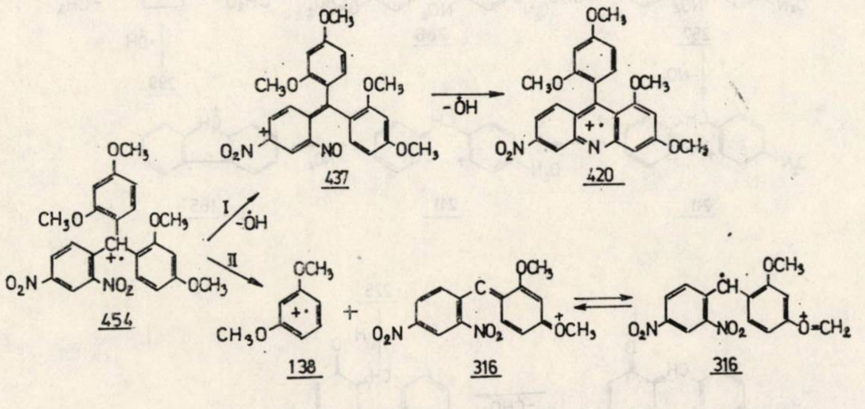

SCHEME I

The loss of an OH fragment (scheme I) typical for the "*ortho* effect" in the *ortho*-nitrotoluene derivatives leads to the fragment m/e 437 which subsequently may undergo two different fragmentations:

$$\begin{tikzcd}
\text{a)} & 420 \arrow[r, "-CH_2O\ (-NO)"'] & 390 \arrow[r, "-CH_2O"'] & 360 \arrow[r, "-CH_2O"'] & 330 \arrow[r, "-CH_2O"'] & 300 \\
437 \arrow[ur, "-OH"'] \arrow[dr, "-OCH_3"'] & 391 \arrow[r, "-CH_2O\ (-NO)"'] & 361 \arrow[dr, "-CH_3"] & & & \\
\text{b)} & 406 \arrow[u, "-CH_3"] \arrow[r, "-CH_2O"'] & 376 \arrow[u] \arrow[r, "-NO"'] & 346 \arrow[r, "-CH_2O"'] & 316 \arrow[r, "-CH_3"'] & 301
\end{tikzcd}$$

a) A new OH elimination followed by a cyclisation has as a result the formation of the fragment m/e 420 representing a phenylacridinic derivative (Scheme I) which subsequently undergoes the typical fragmentation of polymethoxyderivatives losing CH_2O fragments. The result is the symmetric and regular disposition of the groups of peaks (fig. 1) at m/e values 390, 360, 330, 300.

b) The loss of an OCH_3 group leads to the fragment m/e 406 which may be further considered the starting point of typical losses of CH_2O

and NO groups, whose result is another group of regular spaced peaks (m/e 376, 346, 316).

The most important and significant fragmentation pattern is that one presented in scheme II, which contains all the major peaks of the spectrum (316, 301, 272, 257, 255, 243, 226, 197, 151, 138) including the base peak, m/e 165. The central fragment, which gives account of all subsequent transformations, is the fragment ion m/e 316 (abundance 35%), obtained by the breaking of the dimethoxy-benzene ion (m/e 138) from the parent ion m/e 454 (Scheme I). The further elimination of a methyl group leads to the high abundance (50%) ion m/e 301 which losing twice CHO groups and once a NO_2 group (in different order, as shown in scheme II) gives, after a rearrangement accompanied by a cyclisation, the aromatic tricyclic nitroderivative m/e 197. The final loss of the nitro group leads to the aromatic abundant (33%) fragment ion m/e 151.

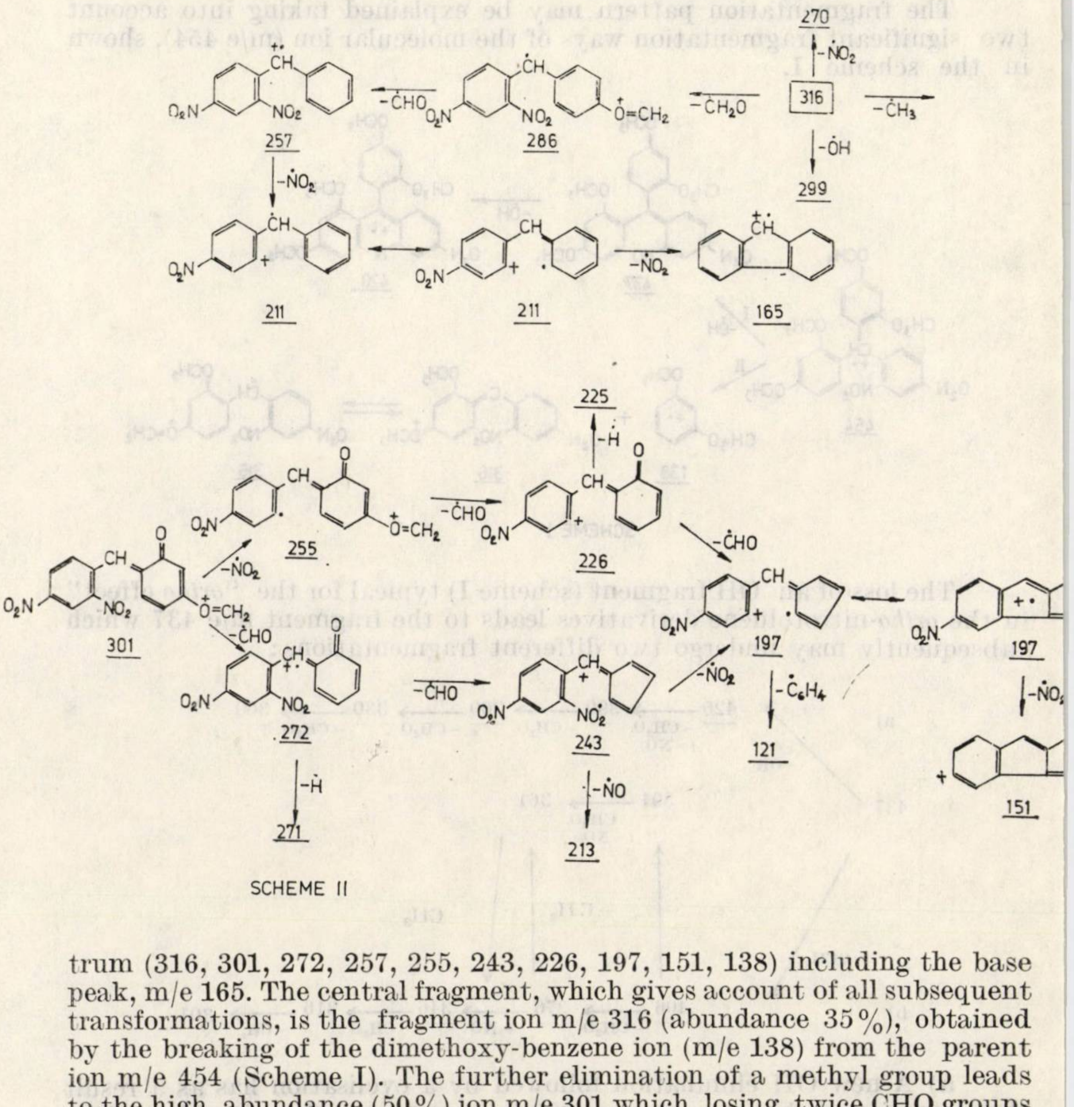
270
-ṄO₂
257
-ĊHO
286
-ĊH₂O
316
-ĊH₃
-ȮH
299
-ṄO₂
211
211
-ṄO₂
165
225
-Ḣ
255
-ĊHO
226
-ĊHO
301
-ṄO₂
-ĊHO
197
197
272
-ĊHO
243
-ṄO₂
-Ċ₆H₄
121
-ṄO₂
151
-Ḣ
271
-ṄO
213

SCHEME II

Another important fragmentation pathway, having as starting point the same m/e 316 ion, is that one represented by the successive losses of the CH_2O and CHO fragments, which leads to the very abundant (93%) dinitrodiphenylmethane ion (m/e 257). By means of the subsequent eliminations of the two nitro groups accompanied by a cyclisation one arrives at the most stable fluorenyl ion, m/e 165, representing the base peak of the mass spectrum.

EXPERIMENTAL PART

IR spectra were recorded in KBr pellets using a Carl-Zeiss Jena UR 20 spectrophotometer.

^1H—NMR spectra were recorded by means of a TESLA BS 487 C spectrometer operating at 80 MHz, using $CDCl_3$, as solvent and TMS as internal standard.

Mass spectrum was recorded using a Perkin-Elmer RMU 6L mass spectrometer operating at 70 eV with the source and all-glass inlet system maintained at 180—200°; a pressure of 2×10^{-7} Torr was used.

Compounds I—III were prepared according to the literature.[1]

Revue Roumaine de Chimie, 22, 7, 1085–1088 (1977)

Dedicated to the 75th anniversary of
Prof. C. D. NENITZESCU'*s birthday (1902—1970o*

INCHAIN-EPOXIDES OF CAROTENOIDS. V[1]

CANTHAXANTHIN-11,12-EPOXIDE AND 9,12-FURANOID OXIDE

DOINA OŞIANU, ELENA NICOARĂ and C. BODEA
Institute of Agronomy "Dr. Petru Groza"
Department of Chemistry and Biochemistry
Str. Mănăştur 3, Cluj-Napoca, Romania

Received December 16, 1975

Buffered epoxidation of canthaxanthin with perbenzoic acid affords as main reaction products canthaxanthin-11,12-epoxide and 9,12-furanoid oxide. Hydrogenolytic ring opening and reduction reactions of these new inchain-epoxides are described.

In previous papers we have described the preparation and some properties of 9,10- and 13,14-monoepoxy- and of 9,10—9′,10′-diepoxy-canthaxanthin.[1–4] It is to be noticed that in all these cases addition of the oxygen atom took place to a methylated double bond.

Considering the sensibility of the canthaxanthin inchain-epoxides known so far towards acids, as shown in the previous papers, we have examined the action of perbenzoic acid upon canthaxanthin, I, in the presence of anhydrous sodium acetate. In these conditions the epoxidation reaction follows a different way. The main reaction products are two new compounds showing the characteristics of inchain-epoxides. They are accompanied by small quantities of the already known 9,10- and 13,14-epoxides and of other non identified reaction products.

One of the new inchain-epoxides gives the characteristic colour reaction with HCl in ether and metal chlorides, it undergoes deepoxidation reverting to canthaxanthin and shows the main absorption maximum at 414 nm (benzene) corresponding to a polyene system of seven conjugated double bonds, showing position 11,12- of the epoxidic ring (II, Scheme 1). This means that the addition of the peroxidic oxygen took place to a nonmethylated double bond.

As in the case of the above mentioned 9,10- and 13,14-epoxides, hydrogenolytical ring opening of the 11,12-epoxide, II, resulted in the formation of 11-hydroxy-11,12-dihydro-isozeaxanthin, III, and 12-hydroxy-11,12-dihydro-isozeaxanthin, IV, while on treatment with $NaBH_4$ only the two carbonyl-groups were reduced to give 11,12-epoxy-isozeaxanthin, V.

---

[1] D. Oşianu, E. Nicoară and C. Bodea, *Rev. Roumaine Chim.*, **19**, 1203 (1974).
[2] E. Nicoară, D. Oşianu and C. Bodea, *Rev. Roumaine Chim.*, **15**, 1965 (1970).
[3] D. Oşianu, E. Nicoară and C. Bodea, *Rev. Roumaine Chim.*, **16**, 765 (1971).
[4] D. Oşianu, E. Nicoară and C. Bodea, *Rev. Roumaine Chim.*, **16**, 925 (1971).

The other inchain-epoxide formed on buffered epoxidation of canthaxanthin gives a blue colour reaction with HCl in ether and shows absorption maximum at 386 nm. Reduction with $LiAlH_4$ yields a triol identical

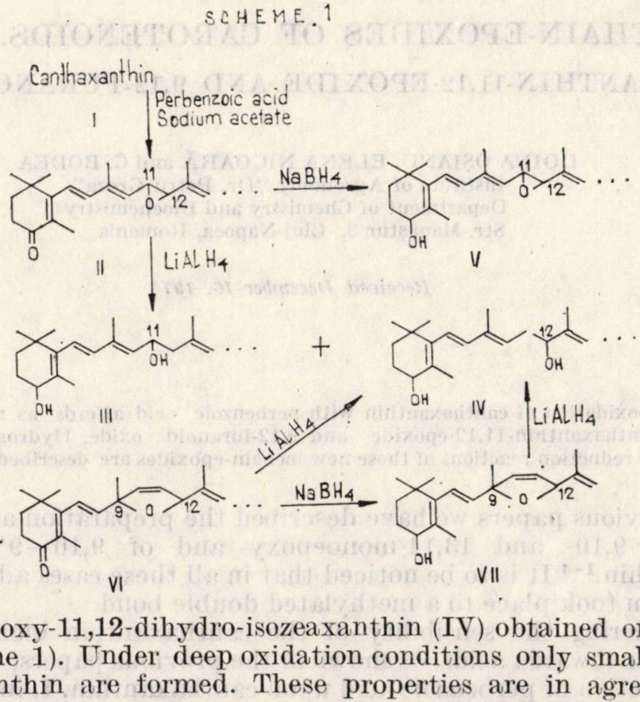
SCHEME 1
Canthaxanthin
I
Perbenzoic acid
Sodium acetate
11
O
12
II
NaBH4
OH
V
LiAlH4
11
OH
III
+
12
OH
OH
IV
LiAlH4
LiAlH4
9
O
12
VI
NaBH4
9
O
12
OH
VII

with 12-hydroxy-11,12-dihydro-isozeaxanthin (IV) obtained on reduction of II (Scheme 1). Under deep oxidation conditions only small quantities of canthaxanthin are formed. These properties are in agreement with structure 9,12-furanoid oxide, VI, which is formed by ring expansion of 11,12-epoxy-canthaxanthin (II). The IR spectrum supports structure VI. Reduction of VI with $NaBH_4$ gives isozeaxanthin-9,12-furanoid oxide, VII.

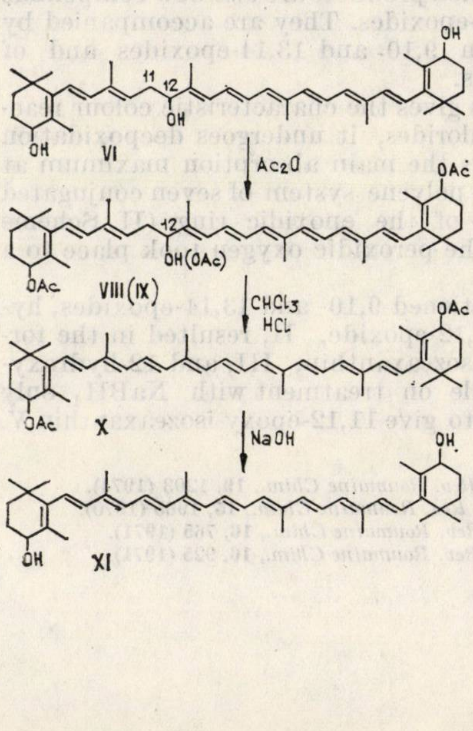
SCHEME 2
11
12
OH
OH
OH
VI
Ac2O
OAc
12
OH(OAc)
OAc
VIII (IX)
CHCl3
HCL
OAc
OAc
X
NaOH
OH
OH
XI

The triol IV obtained by reduction with $LiAlH_4$ of 11, 12-epoxide (II) as well as of 9,12-furanoid oxide (VI), was acetylated with acetic anhydride and the dynamics of the reaction was followed up. The 4,4′-diacetate, VIII, is first formed and the triacetate IX (Scheme 2) appears after a longer period.

The diacetate VIII undergoes easily dehydration on treatment with acidified chloroform to give the isozeaxanthin-acetate X, which on hydrolysis affords isozeaxanthin, XI.

EXPERIMENTAL

BUFFERED EPOXIDATION OF CANTHAXANTHIN

To a chloroformic solution of $0{,}2.10^{-3}$ moles canthaxanthin an ethereal solution of perbenzoic acid [2] was added in a quantity to achieve a molar ratio of 1 : 2 and the mixture was treated with 2 g powdered anhydrous NaOAc. The reaction mixture was kept for 20 h in the dark at 0°C. After dilution with petroleum ether in a double volume, the solution was submitted to chromatographic separation on MgO-celite (1 :4) column (6× 40 cm). The chromatogram developed with petroleum ether containing increased amounts of acetone up to 6% is shown in Table 1.

Table 1

Chromatogram of buffered epoxidation of canthaxanthin

Zone	Colour	λ_{max}(nm) in benzene	Pigment
6	yellow	386	9,12-furanoidoxid of canthaxanthin (VI)
5	yellow	414	11,12-epoxy-canthaxanthin (II)
4	red-violet	480	canthaxanthin (I)
3	deep yellow	432	9,10-epoxy-canthaxanthin
2	yelow	426	non identified
1	pale yellow	376	13,14-epoxy-canthaxanthin

ISOLATION AND CHARACTERISATION OF CANTHAXANTHIN-11,12-EPOXIDE (II)

The pigment (II) of zone 5 was purified by chromatography on a MgO-celite (1 :4) column using petroleum ether — acetone (6%) as developing solvent. λ_{max}=414 nm in benzene and 400 nm in methanol. Relative polarity value = 2.00 units. The IR spectrum (in CCl_4) of II had ν_{max}·3020—2820 (C—H), 1660(conj. C=O), 1370 (gem. CH_3), 1220, 880 ring vibration C—O—C, 970 (all trans) cm^{-1}. The metal-chloride complex of II obtained with $FeCl_3$ in benzene [1] showed in the electronic spectrum λ_{max} at 700 nm.

The reduction of II with $NaBH_4$ gives 11, 12-epoxy-isozeaxanthin (V) (λ_{max}=386 nm in benzene, 378 nm in methanol, relative polarity = 2,6 units, blue colour reaction with HCl).

Upon treatment with $LiAlH_4$ the epoxide is converted into the isomeric triols, 11-hydroxy- and 12-hydroxy-11,12-dihydro-isozeaxanthin, III and IV. The triol III has λ_{max} in benzene at 384 nm, in methanol at 374 nm and relative polarity value of 3.15 units. The triol IV has λ_{max} in benzene at 384 nm, in methanol at 372 nm, relative polarity 3.10 units. The two triols III and IV were easily dehydrated in acidic chloroform medium with formation of dehydrocarotenoids.

ISOLATION AND CHARACTERISATION OF CANTHAXANTHIN-9,12-FURANOID OXIDE (VI)

The pigment (VI) of zone 6 was purified by chromatography on MgO-celite (1 :4) column using petroleum ether — acetone (10 %) as developing solvent. The compound VI gives a blue colour reaction with HCl.λ_{max}= 384 nm in benzene and 376 nm in methanol. Relative polarity value = 2.00 units. The IR spectrum (in CCl_4) of VI had ν_{max}= 3000—2820 (C—H), 1675 (conj. C = O), 1645 (isolated C = C), 1380—1320 (gem. CH_3), 1100—1070 (cyclic C—O—C), 970 (all trans) cm^{-1}. Yield 10—12 %.

Upon treatment with $NaBH_4$ pigment VI is converted into isozeaxanthin-9,12-furanoid oxide (VII). λ_{max}= 366 nm in benzene, relative polarity = 2.5 units.

The reduction of VI with $LiAlH_4$ gives compound IV, characterized above.

Reduction with $NaBH_4$, $LiAlH_4$, elimination reaction of the allylic hydroxyl groups, as well as deepoxidation reaction, were performed as shown in a previous paper.[2]

The relative polarity was determined according to Krinsky,[5] using both systems of solvents, depending on the polarity of the tested compound.

ACETYLATION OF 12-HYDROXY-11,12-DIHYDRO-ISOZEAXANTHIN (IV)

10 mg IV in 2 cm^3 anhydrous pyridine were treated with 0.4 cm^3 acetic anhydride and kept for 24 h at room temperature in the dark. The reaction was then interrupted by adding a double volume of petroleum ether. After washing the pyridine off with water, the reaction products were separated on a MgO-celite column (1 :4). Development was performed with petroleum ether containing up to 3% acetone. The two separated zones contain the diacetate VIII (λ_{max}=380 nm in benzene) and the triacetate IX (λ_{max}= 382 nm in benzene).

Elimination reaction of the allylic hydroxy-group from 12-position of the diacetate VIII with acidic chloroform[2] gives isozeaxanthin diacetate (X), chromatographically identical with the authentic isozeaxanthin-diacetate, obtained by acetylation of isozeaxanthin.

Hydrolysis of the isozeaxanthin-diacetate X resulted in the formation of isozeaxanthin, XI.

This work is part of a joint research program between our Department and the Department of Food and Resource Chemistry , University of Rhode Island, Kingston, Rhode Island, U.S.A.

---

[5] N. I. Krinsky, *Analyt Biochem.*, **6**, 293 (1963).

Revue Roumaine de Chimie, 22, 7, 1089–1095 (1977)

Dedicated to the 75th anniversary of
Prof. C. D. NENITZESCU*'s birthday (1902–1970)*

SYNTHESIS OF BICYCLO[3.2.1]OCTANE DERIVATIVES *via* MAKOSZA REACTION

LUMINIŢA PÂRVULESCU and M. D. GHEORGHIU
Laboratory of Organic Chemistry, Polytechnic Institute,
Str. Polizu 1, Bucharest 12, Romania

Received December 2, 1976

The cycloaddition of dichlorocarbene, generated by the Makosza technique (phase-transfer catalysis) to polycyclic hydrocarbons having bicyclo[2.2.1]heptene skeleton gave with 50%–62% yield *exo*-2,3-dichlorobicyclo[3.2.1]oct-3-ene-derivatives.

The discovery in 1969 that chloroform is readily converted into dichlorocarbene by a concentrated aqueous solution of sodium hydroxide and catalytic amounts of triethylbenzylammonium chloride (TEBA)[1,2] developed into a very useful synthetic technique for the preparation of dichlorocyclopropane derivatives. The synthetical advantages are remarkable : (i) the reaction can be carried out in aqueous medium, (ii) yields are generally higher than in the case of conventional nonaqueous methods, (iii) in some cases the reaction course was more selective,[3] (iv) it represents the only entry method for the synthesis of certain compounds.[4]

Among the olefinic substrates, bicyclo[2.2.1]heptene derivatives present an intriguing behaviour in the reaction with dichlorocarbene.[5,6] It seems that the dichlorocyclopropane derivatives **1a** and **1b** are unstable[6c] under the reaction conditions and rearrange to skeleton of structural type **2**. Although details regarding the rearrangement process are obscure, three facets presumably will be incorporated in a rationale of this reaction. There is evidence that the first stage of the reaction involves cyclopropane derivatives of type **1a** and/or **1b**, which rearrange thermally into *exo*-2,3-dichlorobicyclo [3.2.1] oct-3-ene derivatives.[6b] Second, the magnitude of the host cycle, a five-membered ring [6c] should also be responsible for the rearrangement of the dichlorocyclopropane derivatives. Third, the rear-

---

[1] M. MAKOSZA and M. WAWZYWIEWICZ, *Tetrahedron Letters*, **1969**, 4459.

[2] M. MAKOSZA, *Pure and Applied Chemistry*, **43**, 439 (1975) ; E. V. DEHMLOW, *Angew. Chem.*, **86**, 187 (1974) ; J. DOCKS, *Synthesis*, **1973**, 441.

[3] See for example : T. HIYAMA, H. SAWADA, M. TSUKANADA and H. NOZAKI, *Tetrahedron Letters*, **1975**, 3013.

[4] See for example : T. SASAKI, K. KANEMATSU and N. OKAMURA, *J. Org. Chem.*, **40**, 3322 (1975).

[5] For reviews see : (a) D. WENDISH, "Carbocyclische Dreiring-Verbindungen", Houben-Weyl "Methoden der Organischen Chemie", E. Müller, Ed., Band IV/3, Georg Thieme Verlag, Stuttgart, 1971, pag. 193 ; (b) C.W. JEFFORD, *Chimia*, **24**, 357 (1970).

[6] (a) W. R. MOORE, W. R. MOSER and J. E. LA PRADE, *J. Org. Chem.*, **28**, 2201 (1963) ;
(b) R. C. DE SELMS and C. M. COMBS, *J. Org. Chem.*, **28** , 2206 (1963) ;
(c) E. BERGMAN, *J. Org. Chem.*, **28**, 2210 (1963) ;
(d) C. W. JEFFORD, S. MAHAJAN, J. WASLYN and B. WAEGELL, *J. Amer. Chem. Soc.*, **87**, 2183 (1965).

rangement occurs only if the halogen stereochemistry is *syn.*[7] as required from the geometrical constraint imposed by the bicyclic system **1a** to the electrocyclic transformation of **1a** into **2**.

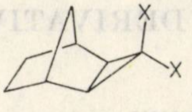

1a

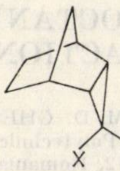

1b

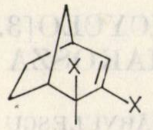

2

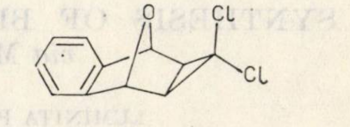

3

X = F, Cl, Br

The isolation of the dichlorocyclopropane **3** (from the reaction of dichlorocarbene, generated by phase-transfer catalysis) to 1,4-epoxynaphthalene [8] suggested us that the same reaction might proceed in the same manner to benzonorbornadiene * (**4**), *exo* ** and *endo*-benzocyclobutenonorbornenes ***, **5**, and **6** respectively. Unfortunately, the conclusion of the present work is that phase-transfer catalysis does not change the pattern of the dichlorocarbene cycloaddition reactions to the olefins **4**, **5** and **6**, as was expected by analogy with 1,4-epoxynaphthalene; rather the thermodynamically more stable exo-2,3-dichlorobicyclo[3.2.1]oct-3-ene derivatives were isolated, in analogy to reactions of dichlorocarbene with related bicyclo[2.2.1]heptene derivatives.

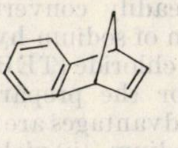

4

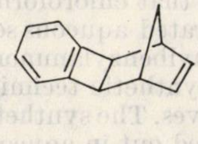

5

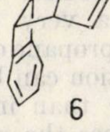

6

RESULTS AND DISCUSSIONS

REACTION OF BENZONORBORNENE (4) WITH CCl_2

Benzonorbornene was reported to react with dichlorocarbene generated from chloroform and t-BuOK, forming in 5.2% yield[9a] the dichloroderivative 7, while on using chloroform with a 50% aqueous solution of sodium hydroxide and triethylbenzylammonium chloride (TEBA) as phase-transfer catalyst, the yield of dichloroderivative **7** was improved up to 65%.[9b] Independently of Goldschmidt and Gutman,[9b] we performed the cycloaddition of dichlorocarbene to benzonorbornene with phase-transfer catalyst but in a standard fashion, which involves benzene as solvent. In our procedure the yield however, never exceeded 50%.

---

* 1,4-dihydro-1,4-methanonaphthalene

** 1,4,4a,8b-tetrahydro-1,4-methanobiphenylene (1α, 4α, 4aα, 8bα)

*** 1,4,4a,8b-tetrahydro-1,4-methanobiphenylene (1α, 4α, 4aβ, 8bβ)

[7] L. Ghosez, P. Laroche, G. Slinckx, *Tetrahedron Letters*, **1967**, 2767.

[8] M. D. Gheorghiu and L. Pârvulescu, (manuscript in preparation).

[9] (a) H. Tanida, K. Tori and K. Kitahonoki, *J. Amer. Chem. Soc.*, **89**, 3212 (1967); (b) L. Goldschmidt and U. Gutman, *Tetrahedron*, **30**, 3327 (1974); C. Bernard and M. Bernard, *Compte rendu*, Ser.C, 1975, 1003; *Chem. Abstr.*, **83**, 113735 (1975).

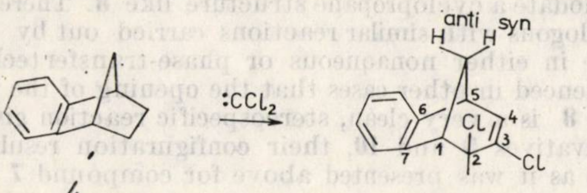

4

7

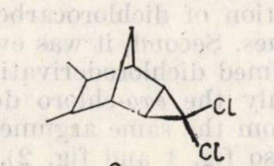

8

The structure of the *exo*-2,3-dichlorobenzobicyclo[3.2.1]-octene-3 is supported by the NMR and IR spectra which parallel the patterns of similar structures.[6] The *exo*-configuration of the chlorine at C—2, results from the magnitude of the $H_1—H_2$ coupling constant. There are firm evidences both directly [10] and indirectly [6b] the $H_1—H_2$ *endo* coupling constant is ca 2 Hz, while the $H_1—H_2$ *exo* coupling constant is ca 5 Hz. Since in the NMR spectrum of **7** there is a 2 Hz coupling constant between the $H_2—H_1$ protons one could assign the *exo* configuration to the chlorine at position 2 in **7**.

The addition of dichlorocarbene, generated from $CHCl_3$ and 50% aqueous NaOH in the presence of catalytic amounts of TEBA to *exo*- and *endo*-benzocyclobutenonorbornene, **5** and **6**, respectively, gave the rearranged products **9** and **10**. The reaction yields for dichloroderivatives **9** and **10** are 60% and 50% respectively, but one should note that the unreacted olefins are easily recoverable by chromatography on silicagel.

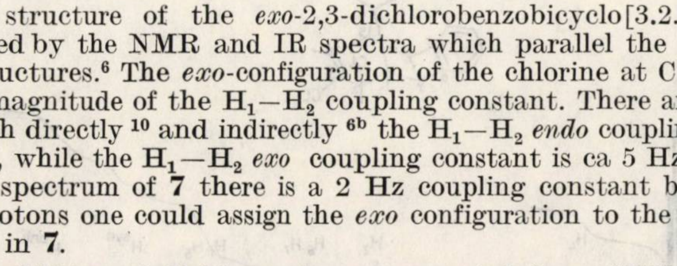

5

9

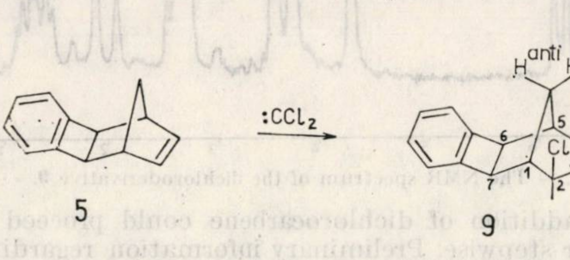

6

10

---

[10] C. W. Jefford, J. Mareda, J.-C. E. Gehret, n Tanda Kabengele, W. D. Graha n and U. Burger, *J. Amer. Chem. Soc.*, **98**, 2585 (1976).

We believe that three aspects regarding the reactions **5** → **9** and **6** → **10** are worthwhile to be noted.

First, the bicyclo[2.2.1]heptene skeleton, of olefins **5** and **6** are inappropriate to accommodate a cyclopropane structure like **8**. Therefore the reaction course is analogous with similar reactions carried out by addition of dichlorocarbene in either nonaqueous or phase-transfer techniques. Second, it was evidenced in other cases that the opening of the presumed dichloroderivative **8** is a very clean, stereospecific reaction giving only the *exo*-chloro derivatives **9** and **10**, their configuration resulting from the same argument as it was presented above for compound **7** (see also fig. 1 and fig. 2).

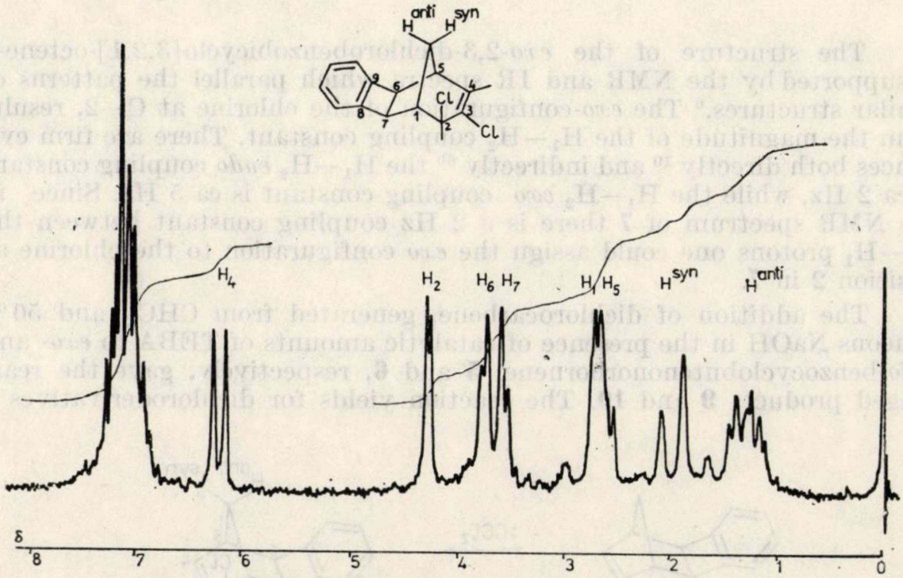

Fig. 1. — The NMR spectrum of the dichloroderivative **9**.

Third, the addition of dichlorocarbene could proceed either in a concerted mode or stepwise. Preliminary information regarding the reaction course could be tested using olefins prone to easy rearrangements, if the reaction would occur in an unconcerted manner.

The addition of bromine [11] to endo-benzocyclobutenonorbornene and solvolysis of 2-tosylderivatives [12] gave only rearranged products. In both cases a bicyclo[2.2.1]hept-2-enyl cation was invoked, a very unstable species which rearranges rapidly.

In our case, should the cycloaddition of dichlorocarbene proceed *via* an unconcerted mode, then one would expect among the reaction products compounds of structural types **11, 12, 13** and **14,** to mention only a part of all possibilities.

---

[11] M. Avram, I. Pogany, I. G. Dinulescu, F. Chiraleu and C. D. Nenitzescu, *Rev. Roumaine Chim.*, **15**, 1207 (1970); M. Avram, I. Pogani, F. Badea, I. G. Dinulescu and C. D. Nenitzescu, *Tetrahedron Letters*, **1969**, 3857.

[12] R. Baker and T. Mason, *J. C. S. Perkin II*, 1972, 18 and references cited therein.

The examination of crude reaction mixture for both cycloaddition **5** → **9** and **6** → **10** did not reveal any of the rearranged compounds **12** and **14**, nor compounds **11** and **13**.

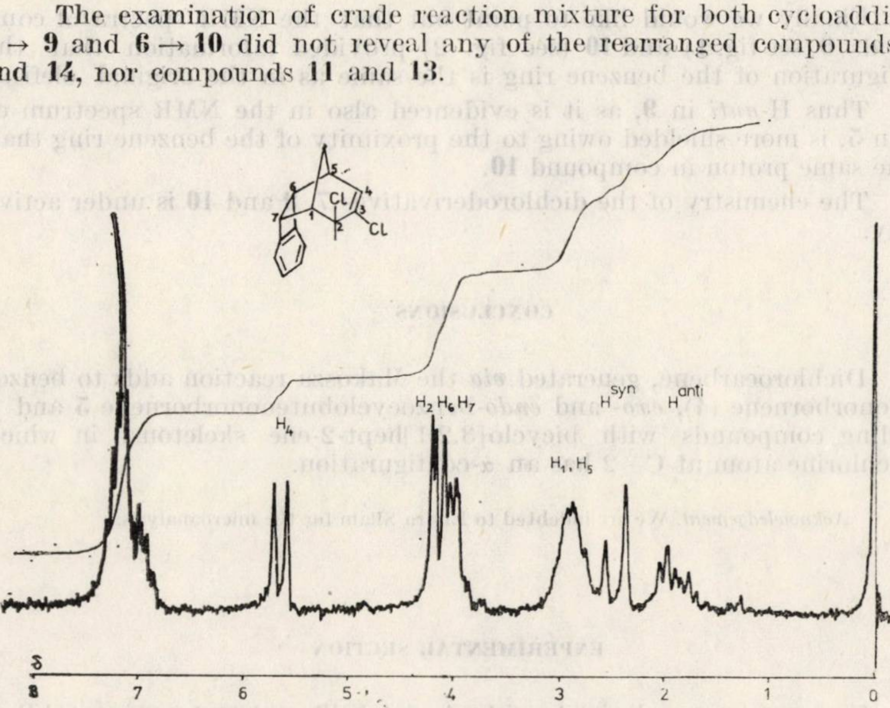

Fig. 2. — The NMR spectrum of the dichloroderivative **10**.

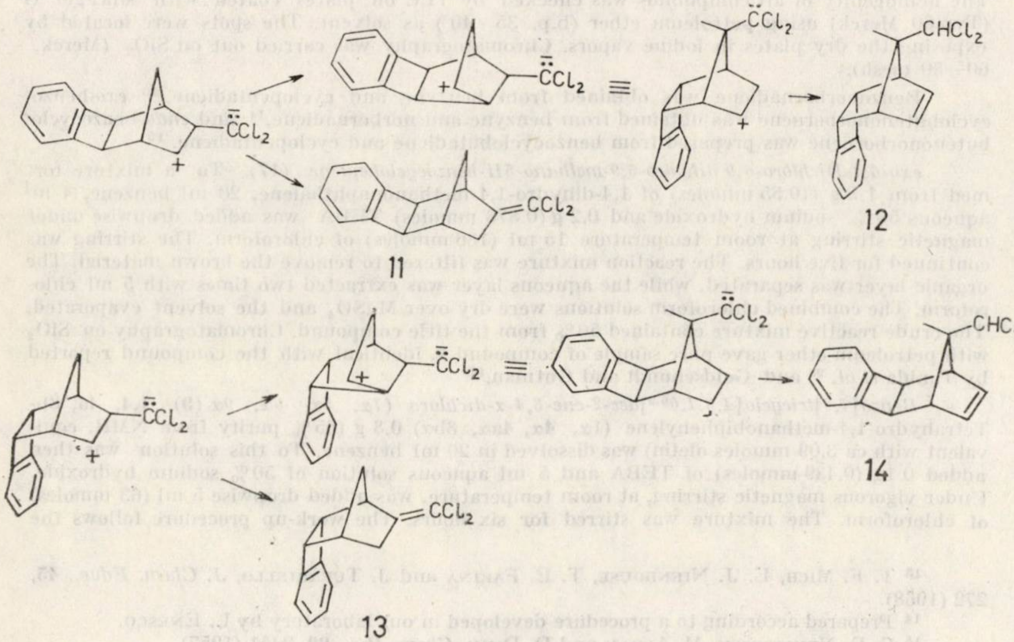
CCl2
+
CCl2
CCl2
CHCl2
11
12
CCl2
CCl2
CCl2
CHCl2
14
13

Finally we would like to point out that the NMR spectra of compounds **9** (see fig. 1) and **10** (see fig. 2) provided information that the configuration of the benzene ring is the same as in the original olefins.

Thus H-*anti* in **9**, as it is evidenced also in the NMR spectrum of olefin **5**, is more shielded owing to the proximity of the benzene ring than is the same proton in compound **10**.

The chemistry of the dichloroderivatives **7**, **9** and **10** is under active study.

CONCLUSIONS

Dichlorocarbene, generated *via* the Makosza reaction adds to benzocyclonorbornene (**4**), *exo*- and *endo*-benzocyclobutenonorbornene **5** and **6** yielding compounds with bicyclo[3.2.1]hept-2-ene skeletons, in which the chlorine atom at C—2 has an α-configuration.

Acknowledgement. We are indebted to Elvira Sliam for the microanalysis.

EXPERIMENTAL SECTION

Spectra were run on Varian Associates A—60A NMR spectrometer and on a UR—20 Carl Zeiss Jena ir spectrometer. The NMR spectra were taken in carbontetrachloride; chemical shifts (δ) are reported as parts per million from tetramethylsilane as internal standard. The homogenity of all compounds was checked by TLC on plates coated with silicagel G (Typ 60 Merck) using petroleum ether (b.p. 35—40°) as solvent. The spots were located by exposing the dry plates in iodine vapors. Chromatography was carried out on SiO_2 (Merck, 60—80 mesh).

Benzonorbornadiene was obtained from benzyne and cyclopentadiene,[13] *exo*-benzocyclobutenonorbornene was obtained from benzyne and norbornadiene,[14] and *endo*-benzocyclobutenonorbornene was prepared from benzocyclobutadiene and cyclopentadiene.[15]

exo-6,7-Dichloro-6,9 dihydro-5,9-methano-5H-benzocycloheptene (**17**). To a mixture formed from 1.5 g (10.55 mmoles) of 1,4-dihydro-1,4-methanonaphthalene, 20 ml benzene, 4 ml aqueous 50% sodium hydroxide and 0.2 g (0.878 mmoles) TEBA was added dropwise under magnetic stirring at room temperature 15 ml (186 mmoles) of chloroform. The stirring was continued for five hours. The reaction mixture was filtered to remove the brown material. The organic layer was separated, while the aqueous layer was extracted two times with 5 ml chloroform. The combined chloroform solutions were dry over $MgSO_4$ and the solvent evaporated. The crude reactive mixture contained 50% from the title compound. Chromatography on SiO_2 with petroleum ether gave pure sample of compound **7**, identical with the compound reported by Tanida *et al.*[9a] and Goldschmidt and Gutman.[9b]

Benzo[7,8]tricyclo[4.3.1.0^{6,9}]dec-2-ene-3,4-α-dichloro (1α, 5α, 6α, 9α (**9**). 1,4, 4a, 8b-Tetrahydro-1,4-methanobiphenylene (1α, 4α, 4aα, 8bα) 0.8 g (65% purity from NMR, equivalent with ca 3.09 mmoles olefin) was dissolved in 20 ml benzene. To this solution was then added 0.1g (0.439 mmoles) of TEBA and 5 ml aqueous solution of 50% sodium hydroxide. Under vigorous magnetic stirring, at room temperature, was added dropwise 5 ml (63 mmoles) of chloroform. The mixture was stirred for six hours. The work-up procedure follows the same line as above. From the NMR spectrum of the crude product one could estimate a 62 % yield of the title compound. Pure sample, colorless oil was obtained by chromatography on SiO_2 with petroleum ether (b.p. 35 – 40°).

---

[13] T. F. Mich, E. J. Nienhouse, T. E. Farina and J. Tufariello, *J. Chem. Educ.*, **45**, 272 (1968).

[14] Prepared according to a procedure developed in our laboratory by L. Enescu.

[15] C. D. Nenitzescu, M. Avram and D. Dinu, *Chem. Ber.*, **90**, 2451 (1957).

Found : C, 66.86 ; H. 5.15 ; Cl, 27.90. $C_{14}H_{12}Cl_2$ requires : C, 66.94 ; H, 4,81 ; Cl, 28.23 %.

IR : 700 m, 750 s, 875 m, 962 m, 1042 w, 1210 w, 1169 m, 1460 w, 1535 m, 2950 s, 3072 w.

NMR : 1.125 – 1.433 m (1p) ; 1.99 d (1p, J = 12.5 Hz) ; 2.5 – 2.95 m (2p), 3.54 d (1p, J = 3 Hz) ; 3.74 d (1p, J = 3 Hz) ; 4.25 d (1p, J = 2.5 Hz) ; 6.20 d (1p, J = 7 Hz) ; 6.82 – 7.15 m (4p).

Benzo[a-, 7,8]tricyclo[4.3.1.0 ^{6,9}*]dec-2-ene-3,4*α*-dichloro-(1*α*, 5*α*, 6*β*, 9*β*).* The reaction was carried out as above, using the following quantities 1,4, 4a, 8b-tetrahydro-1,4-methanobiphenylene (1α, 4α, 4aβ, 8bβ), 0,4 g (2.83 mmoles), benzene 20 ml TEBA 0.1 g (0.439 mmoles), 5 ml aqueous sodium hydroxide 56 % and 5 ml (63 mmoles) of chloroform. The estimated yield based on the NMR of the crude mixture is 50 %. Pure sample, colorless oil, was isolated by chromatography on SiO_2 using petroleum ether.

Found : C, 66.67 ; H, 5.02 ; Cl, 27.91 ; $C_{14}H_{12}Cl_2$ requires : C, 66.94 ; H, 4.81 ; Cl, 28.23 %.

IR (CS_2, CCl_4) : 695 m, 755 s, 778 s, 790 s, 1062 m, 1365 m, 1461 m, 1640 w, 2879 w, 2960 m, 3082 w.

NMR : 1.68 – 2.02 m (1p) ; 2.43 d (1p, J = 12 Hz) ; 2.66 – 3.16 m (2p) ; 3.9 – 4.05 m (2p) ; 4.13 d (1p, J = 2.5 Hz) ; 5.06 d (1p, J = 7.5 Hz) ; 6.73 – 7.33 m (4p).

Revue Roumaine de Chimie, 22, 7, 1097–1103 (1977)

Dedicated to the 75th anniversary of
Prof. C. D. NENITZESCU*'s birthday (1902–1970)*

ÉTARD REACTION. XI*

OXIDATION OF DIBENZO[*c,g*]BICYCLO[4.2.0]OCTA-3,7-DIENE WITH CHROMYL CHLORIDE

I. I. SCHIKETANZ, ANA HANEŞ[a] and ILEANA NECŞOIU
Laboratory of Organic Chemistry, Polytechnic Institute
Bucharest, Romania
[a]Center of Organic Chemistry, Splaiul Independenţei 202B, Bucharest.

Received November 23, 1976

Étard oxidation of dibenzo[*c,g*]bicyclo[4.2.0]octa-3,7-diene (**1**) yields ketones (**5**) and (**6**), chlorohydrine (**7**) and chloroketone (**8**). The filtrate of the Étard complex contains *syn*-8-chloro-dibenzo[*b,f*]bicyclo[3.2.1]octa-2,6-diene (**4**). Compounds (**7**) and (**8**) can be obtained by oxidizing the chloroderivative (**4**) with chromyl chloride. The ionic mechanism of this reaction is discussed.

The Diels-Alder reaction between *ortho*-quinodimethane and benzocyclobutadiene, both in nascent state,[1,2] yielded dibenzo[*c,g*]bicyclo[4.2.0]octa-3,7-diene which formed on bromination with *N*-bromosuccinimide the dibromoderivative (**2**).

Solvolysis of 2,5-dibromo-dibenzo[*c,g*]bicyclo[4.2.0]octa-3,7-diene (**2**) leads to rearranged products, derivatives of *syn*-8-bromo-dibenzo[*b, f*]bicyclo[3.2.1]octa-2,6-diene (**3**).[3]

These results prompted us to investigate the behaviour of hydrocarbon **1** in other reactions involving carbonium ions, for instance the Étard reaction.[4–9]

---

* Part X is reference 8.

[1] M. AVRAM, I. G. DINULESCU, D. DINU, G. D. MATEESCU and C. D. NENITZESCU, *Tetrahedron*, **19**, 309 (1963).

[2] M. AVRAM, I. G. DINULESCU, D. DINU and C. D. NENITZESCU, *Chem. and. Ind.*, **1962**, 555.

[3] I. G. DINULESCU, M. AVRAM, G. D. MATEESCU and C. D. NENITZESCU, *Rev. Roumaine Chim.*, **8**, 351 (1964).

[4] C. N. RENTZEA, I. NECŞOIU, M. RENTZEA, A. GHENCIULESCU and C. D. NENITZESCU, *Tetrahedron*, **22**, 3501 (1966).

[5] C. N. RENTZEA, M. RENTZEA, I. NECŞOIU and C. D. NENITZESCU, *Rev. Roumaine Chim.*, **12**, 1495 (1967).

[6] C. N. RENTZEA, M. RENTZEA, I. NECŞOIU and C. D. NENITZESCU, *Tetrahedrom*, **24**, 4667 (1968).

[7] I. I. SCHIKETANZ, I. NECŞOIU, M. RENTZEA and C. D. NENITZESCU, *Rev. Roumaine Chim.*, **13**, 1385 (1968).

[8] V. PRZEMETCHI, I. NECŞOIU, M. RENTZEA and C. D. NENITZESCU, *Rev. Roumaine Chim.*, **14**, 1567 (1969).

[9] A. GHENCIULESCU, I. NECŞOIU, M. RENTZEA and C. D. NENITZESCU, *Rev. Roumaine Chim.*, **14**, 1543 (1969).

The Étard complex of dibenzo[*c*,*g*]bicyclo[4.2.0]octa-3,7-diene was obtained at 0°C, using carbon tetrachloride as solvent, the molar ratio hydrocarbon **1** : chromyl chloride being 1 : 2.[10] The reaction is complete in 2 hours.

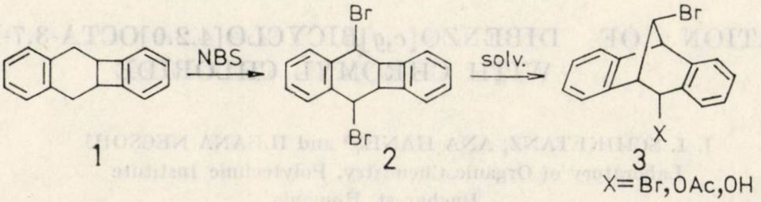

The decomposition of the Étard complex with water and ice led to a mixture of products, from which we identified : *syn*-8-chloro-dibenzo [*b*,*f*]bicyclo[3.2.1]octa-2,6-diene (**4**), dibenzo[*b*,*f*]bicyclo[3.2.1]octa-2,6-dien-4-one (**5**), dibenzo[*b*,*e*]bicyclo[2.2.2]octa-2,5-dien-7-one (**6**), *exo*-4-hydroxy-*syn*-8-chloro-dibenzo[*b*,*f*]bicyclo[3.2.1]octa-2,6-diene (**7**) and *syn*-8-chloro-dibenzo[*b*,*f*]bicyclo[3.2.1]octa-2,6-dien-4-one (**8**) (Table 1), representing 76.4 % of the total products.

Table 1

Products of the Étard reaction of dibenzo [*c*, *g*] bicyclo [4.2.0] octa-3,7-diene resulted by decomposition of the solid complex

Oxidation products [a]	[b] 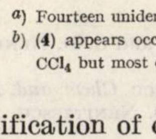 4	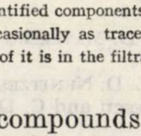 5	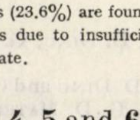 6	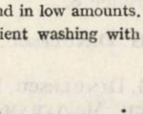 7	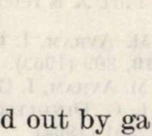 8
mole %	1.2	0.5	3.8	25.6	45.3

[a] Fourteen unidentified components (23.6%) are found in low amounts.

[b] (**4**) appears occasionally as traces due to insufficient washing with CCl_4 but most of it is in the filtrate.

Identification of compounds **4**, **5** and **6** was carried out by gas-chromatography comparing the retention times with those of autentic samples ; compounds **7** and **8** were isolated by preparative gas-chromatography. The elemental analyses, the IR and n.m.r. spectra are in accordance with the proposed structures.

The filtrate of the Étard complex of hydrocarbon **1** contains only one product, that is *syn*-8-chloro-dibenzo[*b*,*f*]bicyclo[3.2.1]octa-2,6-diene (**4**).

---

[10] I. Necşoiu, A. T. Balaban, I. Pascaru, E. Sliam, M. Elian and C. D. Nenitzescu, *Tetrahedron*, **19**, 1135 (1963).

DISCUSSION

The formation of Étard complexes during the reaction of the hydrocarbons with chromyl chloride involves an electrophilic attack of the chromyl chloride at a C—H bond of a saturated carbon atom in a concerted cyclic mechanism :[10]

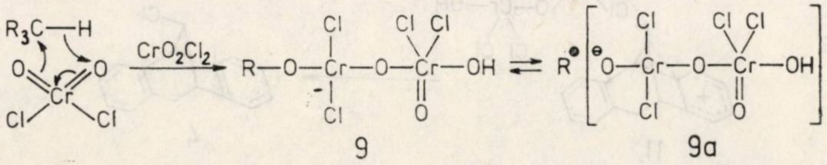

9 9a

In non-polar solvents (carbon tetrachloride), the Étard complex **9** is partly ionized to ion pairs **9a**, the process being facilitated by the formation of a stable carbonium ion.

The intervention of carbonium ions was proved by trapping with azide ions, by hydride ion exchange with ethers, cycloheptatriene and xantene,[11] by hydrolysis[12] of the complexes with $H_2{}^{18}O$, and by the formation of Friedel-Crafts-type products during the oxidation of toluene and ethylbenzene with chromyl chloride.[13] The alcohols resulted by the hydrolysis of the Étard complexes, are further oxidized, partly or totally, to carbonyl compounds by the chromic acid formed.

In the reaction of dibenzo[*c*,*g*]bicyclo[4.2.0]octa-3,7-diene (**1**), chromyl chloride attacks a benzylic C—H bond, forming a chromium ester (**10**). The ionization of the latter, assisted by the $C_8—C_1$ bond, leads to the ion pair (**11**):

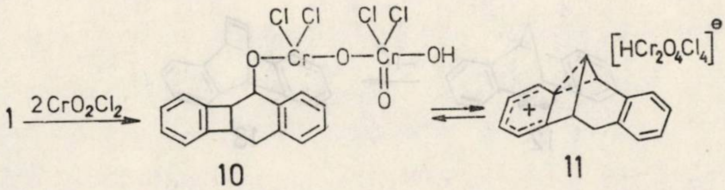

10 11

The trapping of the carbonium ion by the chloride ion yields the chloroderivative (**4**).

At the same time, the carbonium ion can stabilize itself by a hydride ion transfer from the 4-*exo* position which is close to the *p* orbital at C_8; the process affords thus the benzyl ion (**12**).

---

[11] C. D. Nenitzescu, *Bull. Soc. chim. France*, **1968**, 1349; I. Necşoiu and C. D. Nenitzescu, *Chem. and Ind.*, **1960**, 377.

[12] L. V. Sulima and I. P. Gragerov, *Zhur. obshchei Khim.*, **29**, 3825 (1959).

[13] I. Necşoiu, A. Ghenciulescu, M. Rentzea, C. N. Rentzea and C. D. Nenitzescu, *Rev. Roumaine Chim.*, **12**, 1503 (1967).

The rather uncommon 1,3-hydride ion migration has been proved in some cases: the solvolysis of norbornane derivatives,[14] which involves a similarly rigid system, the solvolysis of deuterated cyclohexyl tosylate,[15] the deamination of ^{14}C labelled propylamine.[16]

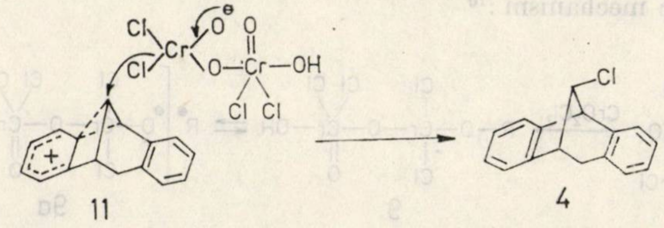

Carbonium ion (**12**) appears as an intermediate during the reversible transformations of dibenzo[*b,e*]bicyclo[2.2.2]octa-2,5-diene and dibenzo [*b,f*]bicyclo[3.2.1]octa-2,6-diene systems.[17]

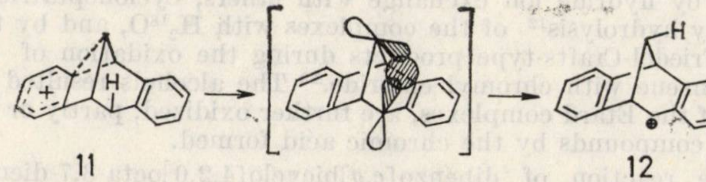

Elimination of one proton from C_8 and migration of the C_5-C_6 bond in the carbonium ion (**12**) yields alchene (**13**).

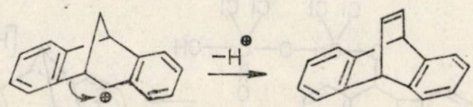

The intervention of alkenes as intermediates during the reaction of saturated hydrocarbons with chromyl chloride has already been proved previously.[4–9] The reaction of alkene **13** with chromyl chloride leads to an oxonium ion **14**. In most cases such compounds are the accepted intermediates of the oxidation of alkenes.[4–9, 12,18] The opening of the oxirane

[14] J. D. Roberts and C. C. Lee, *J. Amer. Chem. Soc.*, **73**, 5009 (1951); J. D. Roberts, C. C. Lee and W. H. Saunders, *J. Amer. Chem. Soc.*, **76**, 4501 (1954).

[15] Y. G. Bundel, V. A. Savin, A. A. Lubovich and O. A. Reutov, *Proc. Acad. Sci. USSR Chem. Sect.*, **165**, 1180 (1965).

[16] A. A. Aboderin and R. L. Baird, *J. Amer. Chem. Soc.*, **86**, 2300 (1964).

[17] S. J. Cristol, R. J. Bopp and E. Johnson, *J. Org. Chem.*, **34**, 3574 (1969); S. J. Cristol, F. P. Parungo, D. E. Plorde and K. Schwarzenbach, *J. Amer. Chem. Soc.*, **87**, 2879 (1965).

[18] F. Freeman, P. J. Cameron and R. H. Du Bois, *J. Org. Chem.*, **33**, 3970 (1968).

ring, assisted by the C_2-C_1 bond, leads to the zwitter-ion (**15**). The frontal attack of chloride ion and the migration of the inorganic part yields chloroester (**16**):

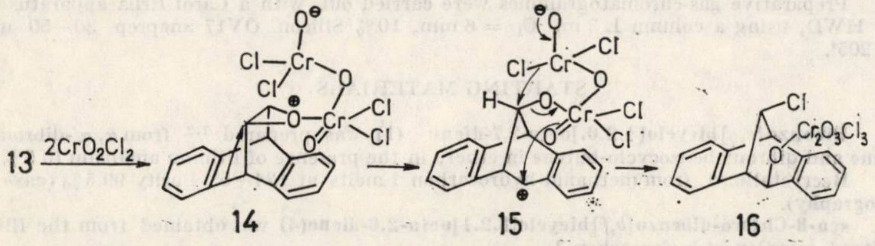

The hydrolysis and the oxidation of (**16**) afforded chlorohydrine (**7**) and chloroketone (**8**). These two products may also result by the attack of chromyl chloride at the bezylic position of chloroderivative (**4**), followed by hydrolysis and oxidation.

The Étard reaction performed with the chloroderivative (**4**) leads to a complex which gives by hydrolysis the compounds (**7**) and (**8**). These compounds are unlikely to result by the oxidation of chloroderivative (**4**) because of the very low rate of formation of the corresponding complex (see the Experimental part).

Carbonium ion (**12**) may also undergo a nucleophilic attack of water during the hydrolysis of the Étard complex. The attack can take place at C_4 (a) or at C_5 (b) with migration of the C_6-C_5 bond (c). The oxidation of the alcohols formed yielded ketones (**5**) and (**6**).

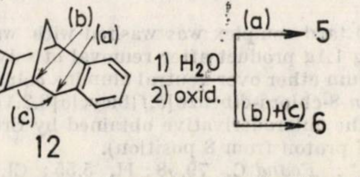

The formation of rearranged products during the Étard reaction of hydrocarbon (**1**) confirms the ionic mechanism proposed previously,[11] according to which the chromyl chloride acts as an electrophilic reagent.

The study of the reaction of hydrocarbon (**1**) with aluminium chloride activated by water,[19] showed the presence of dibenzo[*b,e*]bicyclo[2.2.2]octa-2,5-diene (**17**), dibenzo[*b,f*]bicyclo[3.2.1.]octa-2,6-diene (**18**) and untransformed hydrocarbon (**1**) among the reaction products (see Experimental part). These bicyclic systems appear also as the result of the Étard reaction, which indicates the similarity of the intermediates involved in the two cases.

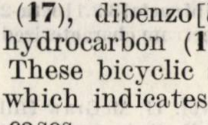
17

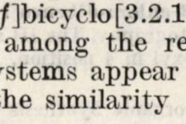
18

---

[19] C. D. Nenitzescu in G. A. Olah, P. von R. Schleyer, (editor) "Carbonium Ions", vol. 2, Wiley, New York, 1970.

EXPERIMENTAL

Analytical gas-chromatogrammes were carried out with a Carol Erba apparatus, type D, FID, using a column L 2m $Ø_i = 2$ mm, 3% NPGS chromosorb W silanized 60—80 mesh, t=190°.

Preparative gas-chromatogrammes were carried out with a Carol Erba apparatus type GV, HWD, using a column L 3 m, $Ø_i = 6$ mm, 10% Silicon OV17 anaprep. 30—50 mesh, t = 205°.

STARTING MATERIALS

Dibenzo[*c,g*]bicyclo[4.2.0.]octa-3,7-diene (1) was prepared [1,2] from α, α′-dibromo-o-xylene and dibromobenzocyclo-butene in ether, in the presence of lithium amalgam (0.5% Li).

Recrystallized from methanol hydrocarbon **1** melts at 124—5°. Purity 99.5% (gas-chromatography).

syn-8-Chloro-dibenzo[*b,f*]bicyclo[3.2.1]octa-2,6-diene(4) was obtained from the filtrate of Etard complex of hydrocarbon **1**.

Chromyl chloride was prepared according to Sisler[20] and used immediately after distillation.

The Étard complex of dibenzo[*c,g*]bycyclo[4.2.0.]octa-3,7-diene (1). In a 250 ml 3-necked round-bottomed flask provided with a dropping funnel, a reflux condenser (with $CaCl_2$ tube), a thermometer and inert gas (nitrogen) inlet tube, placed in an ice-water bath, a solution of 2.06 g (10 mmoles) hydrocarbon (**1**) in 40 ml dry CCl_4 was introduced. To this solution, stirred with a magnetic stirrer, a solution of 3.1 g (20 mmoles) chromyl chloride in 30 ml dyr CCl_4 was added dropwise in the course of 1 hr, in an inert gas atmosphere (nitrogen) at 0—5°C. The reaction mixture was stirred at room temperature for 1hr, so that the chromyl chloride was completely consumed.

The complex was then filtered off under inert gas and thoroughly washed with dry CCl_4. The dry complex (2.8 g) was thus obtained as a brown, insoluble, hydroscopic powder. The complex was decomposed in ice-water in the presence of CH_2Cl_2. The organic layer was separated and the aqueous layer was extracted four times with 50 ml portions CH_2Cl_2.

The combined organic layers were washed with water until neutral, dried over anhydrous $MgSO_4$, yielding 0.5 g liquid residue after removal of solvent.

The qualitative and quantitative results are given in Table 1 (gas-chromatography identifications).

The filtrate of the Étard complex was washed with water, then with 5% $NaHCO_3$ aq, dried over $MgSO_4$, yielding 1.1g product after removal of solvent.

Elution with petroleum ether over neutral alumina column afforded 1 g (41.7%) product, m.p. 143°, identified as *syn*-8-chloro-dibenzo[*b,f*]bicyclo[3.2.1]octa-2,6-diene (4) n.m.r. spectrum identical to that of the chloroderivative obtained by Cristol[21,22] (characteristic triplet at $\delta = 4.76$ ppm for the *anti* proton from 8 position).

Elemental analysis*: *Found* C, 79.58; H, 5.55; Cl, 14.85; *Calculated* for $C_{16}H_{13}Cl$: C, 79.85; H, 5.44; Cl, 14.73.

The results of the experiments are given in Table 1 so that in the following only the identification of the reaction products will be described.

Dibenzo[*b,f*]bicyclo[3.2.1]octa-2,6-dien-4-one (5) and dibenzo[*b,c*]bicyclo [2.2.2] octa-2,5-dien-7-one (6). Gas chromatography retention times identical to those of authentic samples[23–27].

exo-4-Hydroxy-syn-8-chloro-dibenzo[*b,f*]bicyclo[3.2.1]octa-2,6-diene (7) was isolated by preparative gas-chromatography. The IR spectrum characterized by $\nu = 3574\ cm^{-1}$, a band corresponding to *exo*-hydroxyl in 4 position.

---

[20] H. E. SISLER, "Inorganic Synthesis", vol. II, McGraw-Hill, New York, 1946 p. 205.

[21] S. J. CRISTOL, R. P. ARGANBRIGHT and D. D. TANNER, *J. Org. Chem.*, **28**, 1374 (1963).

[22] S. J. CRISTOL, J. R. MOHRIG and D. E. PLORDE, *J. Org. Chem.*, **30**, 1956 (1965).

[23] K. ALDER and H. F. RICKERT, *Liebigs Ann. Chem.*, **543**, 1 (1939).

[24] S. WAWZONEK and J. V. HALLUM, *J. Org. Chem.*, **18**, 288 (1953).

[25] E. CIORĂNESCU, A. MIHAI, G. MIHAI, M. ELIAN and C. D. NENITZESCU, *Rev. Roumaine Chim.*, **10**, 175 (1965).

[26] S. J. CRISTOL, J. R. MOHRIG and G. T. TIEDEMAN, *J. Org. Chem.*, **37**, 3239 (1972).

[27] S. J. CRISTOL, F. P. PARUNGO and D. E. PLORDE, *J. Amer. Chem. Soc.*, **87**, 2870 (1965).

* The elementary analyses were performed by Elvira Sliam and Violeta Daniel.

The n.m.r. spectrum displayed the following signals : $\delta = 4.96$ ppm (triplet *anti*-H_8), $\delta = 4.60$ ppm (H_4), $\delta = 4.12$ ppm (doublet H_1), $\delta = 3.75$ ppm (doublet H_5) and $\delta = 2.80$ pm (hydroxyl).

Elemental analysis of chlorohydrine **(7)** : *Found* C, 74.54 ; H, 5.19 ; Cl, 13.15 ; *Calculated for* $C_{16}H_{13}ClO$: C, 74.85 ; H, 5.10 ; Cl, 13.81.

8-syn-Chloro-dibenzo[*b*, *f*]bicyclo[3.2.1.]octa-2,6-dien-4-one (8) was isolated by preparative gas-chromatography.

The IR spectrum : $\nu = 1705$ cm^{-1}, a carbonyl band ; the n.m.r. spectrum identical to that reported in literature.[22]

Elemental analysis : *Found* C, 75.56 ; H, 4.52 ; Cl, 13.58 ; *Calculated for* $C_{16}H_{11}ClO$: C, 75.46 ; H, 4.35 ; Cl, 13.92.

The Étard complex of syn-8-chloro-dibenzo[*b*, *f*]bicyclo[3.2.1]octa-2,6-diene (4) was prepared by the same method as for the previous compound, the ratio halogenate derivative : chromyl chloride being 1 : 2 and the temperature 0°C. The reaction time was 20 hrs. The residue of the decomposition of the complex was filtered and worked up. Identification by gas-chromatography showed the presence of chlorohydrine **(7)** (20.4 %) and chloroketone **(8)** (76.1 %).

Izomerization of dibenzo[*c*, *g*]bicyclo[4.2.0.]octa-3,7-diene (1) with aluminium chloride. 0.62g (3 mmoles) hydrocarbon **1** and 0.14 g wet aluminium chloride (obtained[28] from anhydrous aluminium chloride and $AlCl_3 \cdot 6\,H_2O$ so that the final molar ratio $AlCl_3 : H_2O$ was 2 : 1) dissolved in 40 ml CS_2, were introduced in a 100 ml round-bottomed flask. The reaction mixture was refluxed for 3 hours and after cooling was decomposed with water. The organic layer was separated and washed with 5 % $NaHCO_3$, then with water, dried on anhydrous $MgSO_4$ and evaporated *in vacuo*. The residue was analyzed by gas-chromatography ; the main components were found to be : dibenzo[*b*, *e*]bicyclo[2.2.2]octa-2,5-diene **(17)** (3 %), dibenzo[*b*,*f*] bicyclo[3.2.1]octa-2,6-diene **(18)** (31.1 %) and untransformed hydrocarbon 1 (1.9 %). The gas-chromatography retention times were identical to those of authentic samples.[27,29]

---

[28] I. Necşoiu and C. D. Nenitzescu, *Studii şi cercetări Chimie. Acad. R.S. România*, **2**, 241 (1961).

[29] S. J. Cristol and N. L. Hause, *J. Amer. Chem. Soc.*, **74**, 2193 (1952).

Revue Roumaine de Chimie, **22**, 7, 1105–1109 (1977)

Dedicated to the 75th anniversary of
Prof. C. D. Nenitzescu*'s birthday (1902–1970)*

ON THE POLYMERIZATION OF ACETYLENIC DERIVATIVES. XXXII[1]

HEATS OF *cis-trans* ISOMERIZATION OF POLYACETYLENE ISOMERS

CR. I. SIMIONESCU, SVETLANA DUMITRESCU, V. PERCEC and M. GRIGORAŞ
Institute of Macromolecular Chemistry "P. Poni",
Aleea Gr. Ghica Vodă n° 41 A, Iaşi-6600, Romania

Received October 14, 1976

The enthalpy changes associated with *cis-trans* thermal isomerization phenomena of polyarylacetylenes have been calculated.

The literature data present the heat of *cis-trans* thermal isomerization in the polyacetylene case only.[2,3] Ito *et al.*[3] studied the thermal behaviour of *cis* polyacetylene and showed that the thermal *cis-trans* isomerization takes place at 145°.

The enthalpy change, associated with the exothermic phenomenon at around 145°, was found to be 1.85 kcal/mole (calibrated to 100% *cis* polyacetylene), and includes : *cis-trans* isomerization (exothermic phenomenon), in-plane disorder of moleclar chains (endothermic phenomenon) and rearrangement (exothermic phenomenon).

In some of our previous papers, the synthesis and properties of *cis* and *trans* isomers of polyphenylacetylene (PPA),[1,4,5] poly (α-ethynylnaphthalene) (Pα — EN)[1,6,7], poly (β-ethynylnaphthalene) (Pβ — EN), [8,9] poly (N-ethynylcarbazole) (PEK), [10,11] poly-(9-ethynylanthracene) (P-9-EA) [4,12] and poly (3-ethynylphenanthrene) (P-3-EPh)[13] were reported. Three fractions were separated from the polymers obtained with Ziegler catalysts. Polymer structures according to these fractions are presented in table 1.

---

[1] Part. XXXI : Sv. Dumitrescu, V. Percec and C. I. Simionescu, Rev. Roumaine Chim, **22**, 000 (1977)

[2] F. D. Kleist and N. R. Byrd, *J. Polym. Sci., Part A–1*, **7**, 3419 (1969).

[3] T. Ito, H. Shirakawa and S. Ikeda, *J. Polym. Sci., Polym. Chem. Ed.*, **13**, 1943 (1975).

[4] I. Simionescu, Sv. Dumitrescu, I. Negulescu, V. Percec, M. Grigoraş, I. Diaconu M. Leancă and L. Goraş, *Visokomol. Soedineniya*, A, **16**, 791 (1974).

[5] C. I. Simionescu, V. Percec and Sv. Dumitrescu, *J. Polym. Sci., Polym. Chem. Ed.*, in press.

[6] C. I. Simionescu, Sv. Dumitrescu, V. Percec, I. Negulescu and I. Diaconu, *J. Polym. Sci., Polym. Symposium Ed.*, **42**, 201 (1973).

[7] C. I. Simionescu, Sv. Dumitrescu and V. Percec, *Polymer J.*, **4**, 313 (1976).

[8] C. I. Simionescu, Sv. Dumitrescu and V. Percec, "IVth Polymer Symposium", Varna October 4–6 (1973), Preprint Vol. I, p. 466.

[9] C. I. Simionescu, Sv. Dumitrescu and V. Percec, *Polymer J.*, **8**, 139 (1976).

Table 1

Structure of Polyarylacetylenes obtained with Ziegler catalysts

MONOMER	STRUCTURE[a]			Literature
	fraction I[b]	fraction II	fraction III	
PA	c—c	c—t	—	1, 4, 5
α-EN	c—c	c—c	t—c	1, 6, 7
β-EN	c—c	t—c	t—c	8, 9
NEK	c—c/c—t	c—c/c—t	—	10, 11
9-EA	c—c	c—c	—	4, 12
3-EPh	c—c	t—c	—	13

[a] c—c = *cis-cisoidal* structure, c—t = *cis-transoidal* structure, t—c = = *trans-cisoidal* structure, c—c/c—t = *cis-cisoidal* and *cis-transoidal* stereoblocks structure; [b] fraction I = benzene-insoluble polymer fraction, fraction II = methanol-insoluble polymer fraction, fraction III = 3/1 methanol-water insoluble polymer fraction.

By thermal polymerization of the corresponding monomers, *trans-cisoidal* structures were obtained only.

The present paper presents the experimental values of enthalpy changes which accompany the *cis-trans* thermal isomerization of PPA, Pα-EN, Pβ-EN, PEK, P-9-EA and P-3-EPh.

EXPERIMENTAL

cis Polymers were prepared by the polymerization of acetylenic monomers with $AlEt_3/Fe\ (dmg)_2 \cdot 2Py$ catalyst, using the following experimental conditions: Al/Fe = 10 (molar ratio), catalyst = 5% (molar concentration), solvent/monomer = 10/1 (volumetric ratio), polymerization temperature = 20°. *Trans* polymers were synthesized by thermal polymerization at 140°. The polymerizations and purifications of the corresponding polymers were carried out as previously reported.[9] The *cis* content was determined in the case of PPA only using a previously reported method.[5]

The enthalpy changes were calculated from DTA curves recorded on a Mettler thermobalance (nitrogen, heating rate = 10°/minute). Tin was used as internal standard, its melting point (232)° being in the field of *cis-trans* thermal isomerization temperatures. The caloric effect which accompanies the melting of tin is 14.4 cal/g.[14]

---

[10] C. I. Simionescu, Sv. Dumitrescu and V. Percec, "XXIII IUPAC International Symposium on Macromolecules", Madrid (1974), Preprint I. 5—13.

[11] Sv. Dumitrescu, V. Percec and C. I. Simionescu, J. *Polym. Sci., Polym. Chem. Ed.*, in press.

[12] C. I. Simionescu, Sv. Dumitrescu, M. Grigoraş and I. Negulescu, "IVth Polymer Symposium "Varna, October 4—6, 1973, Preprint Vol. I, p. 479.

[13] C. I. Simionescu, Sv. Dumitrescu, M. Grigoraş and I. Diaconu, "XXIII IUPAC International Symposium on Macromolecules", Madrid (1974), Preprint I. 5—14.

[14] "Handbook of Physics and Chemistry", RCA, New York, 1973.

RESULTS AND DISCUSSIONS

The thermograms of various polyacetylenes are presented in fig. 1. All *cis* polymers present an exothermic peak in a temperature range depending on the polymer nature. No peaks have been observed in the cases of the *trans* polymers.[15] The extohermic effects are not accompanied by weight losses, except for the cases of *cis* PEK and *cis* P-9-EA. The weight losses represent 1—10 % of the sample weight. It has to be mentioned that in the cases of *trans* PEK and P-9-EA, this first step of thermal degradation is not accompanied by caloric effects. IR, UV, NMR and XRD spectroscopy data [5,9,11] showed that these exothermic peaks are connected to a *cis-trans* isomerization, which changes the *cis* insoluble or soluble, crystalline or amorphous polymer into a *trans-cisoidal* amorphous and soluble

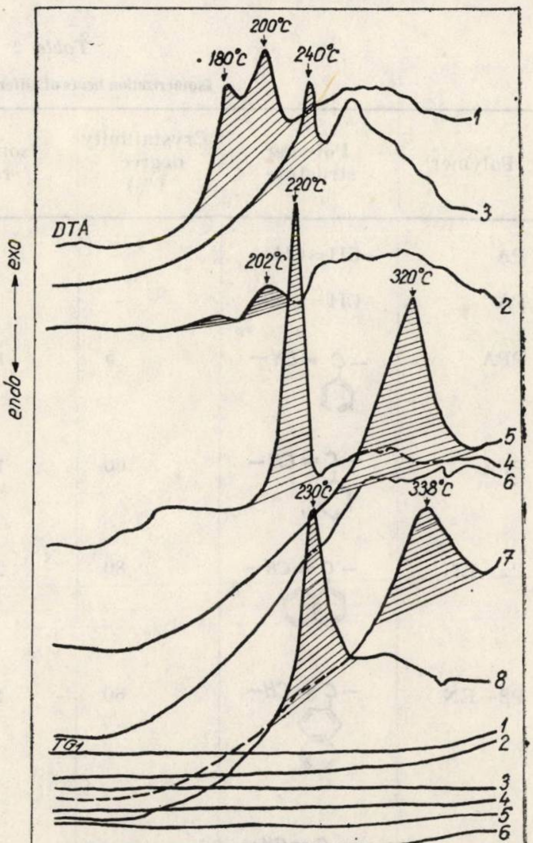

Fig. 1. — DTA and TG curves of : PPA with *cis-transoidal* structure (1), PPA with *cis-cisoidal* structure (2), Pα-EN with *cis-cisoidal* structure (3), Pβ-EN with *cis-cisoidal* structure (4), PEK with *cis-cisoidal/cis-transoidal* stereoblocks structure (5), PEK with *trans-cisoidal* structure (6), P—9—EA with *cis-cisoidal* structure (7), and P—3—EPh with *cis-cisoidal* structure (8).

---

[15] C. I. Simionescu, Sv. Dumitrescu, S. Vasiliu and V. Percec, *J. Thermal. Anal.*, **6**, 389 (1974).

polymer. In the case of PEK only, the exothermic peak appears at a temperature range of 200 and 330°. The temperature value is a function of the *cis-transoidal* vs. *cis-cisoidal* stereoblocks ratio.[10,11]

The enthalpy changes associated with the exothermic phenomena are presented in table 2.

Table 2

Isomerization heats of different polyacetylenes

Polymer	Polymer structure	Crystallinity degree (%)	Isomerization range (°)	Temp. of exothermic phenomenon (°)	Isomerization heat (kcal/mole)
PA	—CH=CH—	—	47–227	47–227	1.6–1.7[a]
PA	—CH=CH—	—	145	145	1.85[b]
PPA	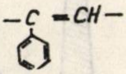	5	130–210	180–200	6.35[c]
PPA	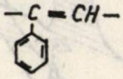	60	135–225	135–225	1.45[d]
Pα–EN	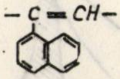	80	220–250	240	2.30
Pβ–EN	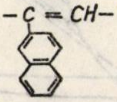	60	190–240	220	5.08
PEK	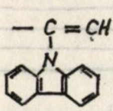	60	275–360	320	19.80
P–9–EA	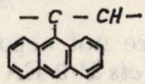	amorph	266–370	338	12.40
P–3–EPh	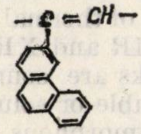	amorph	190–265	230	12.56

[a] after Kleist and Byrd (1969), (60–70% *cis* content, corrected to 100% *cis* content); [b] after Ito *et. al.*, (1975), (88% *cis* content, corrected to 100% *cis* content); [c] *cis-transoidal* structure, (94.45% *cis* content, corrected to 100% *cis* content); [d] *cis-cisoidal* structure, (90.10% *cis* content, corrected to 100% *cis* content).

Almost in all cases, the exothermic peaks include the exothermic phenomenon of *cis-trans* isomerization and the endothermic phenomenon of in-plane disorder of molecular chains.

The *cis-trans* isomerization of *cis* P-9-EA and P-3-EPh with amorphous structures is not accompanied by the disordering of molecular chains of a crystalline structure into an amorphous one, but by a conformational change from a *cis-cisoidal* conformation into a *trans-cisoidal* conformation.

At present it is impossible to determine independently the heat of isomerization from the apparent enthalpy change. This is the reason for which the enthalpy changes obtained for *cis-transoidal* PPA (5% crystallinity degree), P-9-EA and P-3-EPh both having an amorphous *cis-cisoidal* structure, are close to *cis-trans* heat of isomerization.

The difference between enthalpy changes of the transformation of *cis-cisoidal* and *cis-transoidal* PPA structures into *trans-cisoidal* structures, and that between *cis-cisoidal* structures of Pα-EN and Pβ-EN can be explained by the crystallinity degree differences of the corresponding polymers (table 2).

The enthalpy changes at *cis-trans* isomerization temperature are increasing with the size of acetylene substituent. The highest caloric effect found in the case of PEK can be explained by the rigidity of the polymeric chains.[11]

Revue Roumaine de Chimie, **22**, 7, 1111–1114 (1977)

Dedicated to the 75th anniversary of
Prof. C. D. NENITZESCU*'s birthday (1902–1970)*

AMIDATION WITH BIS-(α-ARYLIMINOBENZYL)-DISULPHIDES

M. VLASSA and F. HODOŞAN
Laboratory of Natural Products, Institute of Chemistry,
Str. Donath 65–103, Cluj-Napoca, Romania

Received June 21, 1976

The title reagents react with organic acids in the presence of triphenylphosphine to give, depending on the isolation conditions, N-aryl-amides or their N-benzoyl derivatives.

It has been reported [1] that disulphide **1** (Ar = Ph), when melted with benzoic acid, gives a mixture of thiobenzanilide (**2**, Ar = Ph), N,N-dibenzoylaniline (**3**, Ar = R = Ph), and sulphur. Under milder conditions (room temperature, benzene solution) dichloroacetic acid entails similar transformations leading to N-dichloroacetyl-N-benzoylaniline (**3**, Ar = Ph, R = Cl_2CH) as main product.[2] Our recent investigations showed that weaker acids, such as N-protected amino acids, do not react under these conditions.

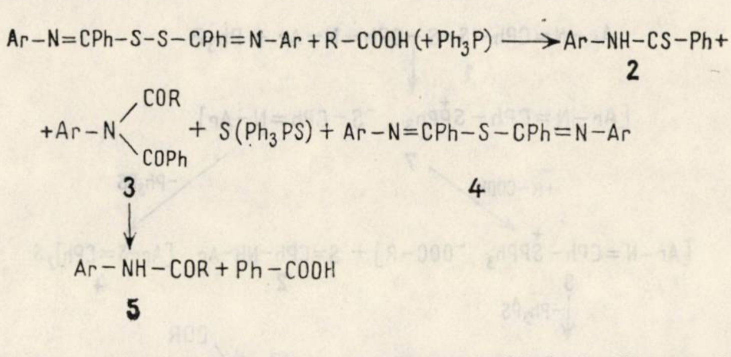

$$\mathrm{Ar{-}N{=}CPh{-}S{-}S{-}CPh{=}N{-}Ar + R{-}COOH\,(+Ph_3P) \longrightarrow \underset{\mathbf{2}}{Ar{-}NH{-}CS{-}Ph} +}$$

$$\mathrm{+\underset{\mathbf{3}}{Ar{-}N\begin{matrix}COR\\COPh\end{matrix}} + S\,(Ph_3PS) + \underset{\mathbf{4}}{Ar{-}N{=}CPh{-}S{-}CPh{=}N{-}Ar}}$$

$$\mathbf{3}\ \downarrow\ \mathrm{\underset{\mathbf{5}}{Ar{-}NH{-}COR} + Ph{-}COOH}$$

Starting with the idea that a reagent which facilitates disulphide bond cleavage [3] will promote the reaction with an acidic component, we treated disulphide **1** (Ar = Ph) with Z-Val in the presence of triphenylphosphine, in benzene solution, at room temperature. Column chromatography enables us to isolate a very small amount of sulphide **4**(Ar = Ph), thiobenzanilide (**2**, Ar = Ph), triphenylphosphine sulphide, and compounds containing the amino acid moiety whose structure varied depending on the nature of the adsorbent used and/or its activity grade. Thus, working on silica gel the unsymmetrical N,N-diacylaniline **3** (Ar = Ph, RCO = = Z—Val) was isolated. Neutral alumina activity grade I entailed loss of benzoyl radical from compound **3** affording aniline **5** (Ar = Ph, RCO = = Z—Val)(Y : 48 %) ; the latter appeared along with the hydantoin derivative **6** when less active alumina (activity grade IV) was used. Compound **6** resulted from the diacyl derivative **3** (Ar = Ph, RCO = *Z*—Val) by loss of a benzoyl and a benzyloxy radical.

---

[1] F. HODOŞAN and N. ŞERBAN, *Bull. Soc. chim. France*, **1959**, 507.
[2] F. HODOŞAN, *Bull. Soc. chim. France*, **1957**, 633.
[3] T. ENDO, S. IKENAGA, and T. MUKAIYAMA, *Bull. Chem. Soc. Japan*, **43**, 2632 (1970).

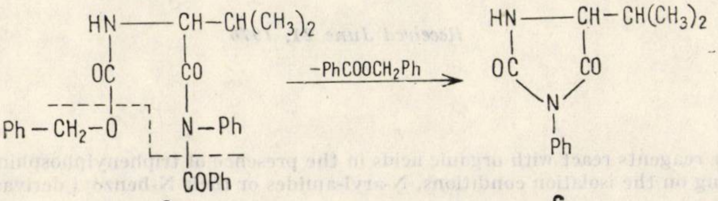
HN—CH—CH(CH3)2
OC
CO
Ph—CH2—O
N—Ph
COPh
−PhCOOCH2Ph
HN—CH—CH(CH3)2
OC
CO
N
Ph

3 **6**

Z—Ala, disulphide **1** (Ar = Ph) and Ph_3P gave under the above mentioned conditions anilide **5** (Ar = Ph, RCO = Z—Ala) (Y : 58 %).

Experiments were carried out also with another disulphide **1** (Ar = = *p* — C_6H_4 COOEt), prepared by benzoylperoxide oxidation of the corresponding thioamide.[1] With Z—Val and Ph_3P the anilide **5** (Ar = *p*— — C_6H_4COOEt, RCO = Z—Val) was obtained after isolation on alumina with activity grade I.

The transformations reported here can be rationalized as follows :

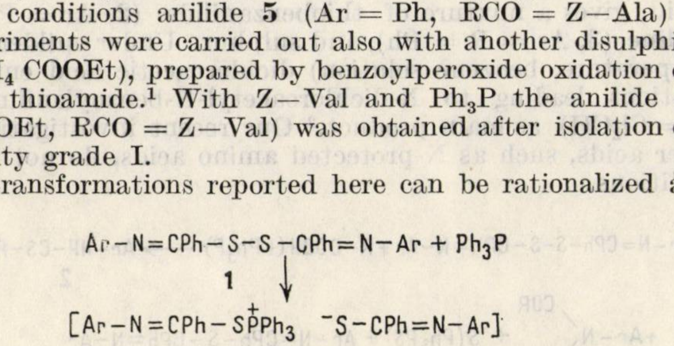
Ar—N=CPh—S—S—CPh=N—Ar + Ph3P
1
[Ar—N=CPh—S+PPh3 −S—CPh=N—Ar]
7
+R—COOH
−Ph3PS
[Ar—N=CPh—S+PPh3 −OOC—R] + S=CPh—NH—Ar [Ar—S=CPh]2S
8
2
4
−Ph3PS
[Ar—N=CPh—O—CO—R] ⟶ Ar—N(COR)(COPh)
9
3

When no organic acid was present, the transformations proceeded following exclusively the route **1**→**7**→**4**, as was shown by the reaction of disulphide **1** (Ar = Ph) with triphenylphosphine (molar ratio 1 : 1) in benzene solution, at room temperature, leading quantitatively to a mixture of sulphide **4** (Ar = Ph) and triphenylphosphine sulphide.

A rapid displacement of the anion in the intermediary compound **7**, preceding the Ph_3PS elimination from the phosphonium cation, and formation of a new intermediary compound **8**, took place when worked in the presence of an organic acid. The O-acyl derivative **9**, formed from **8**, gave instantly the rearranged, stable final compound **3**.

EXPERIMENTAL

All melting points are uncorrected. The NMR spectra were determined at 60 Mc with a Bruker WP—60 FT spectrometer and TMS as an internal standard. The IR spectra were taken on a Unicam SP 200G recording spectrophotometer.

N-Benzoyl-N-(N′-carbobenzoxyvalinyl)-aniline (**3**, Ar = Ph, RCO = Z—Val). A solution of Z—Val (1.25 g, 5 mmols), disulphide **1** (Ar = Ph) (2.13 g, 5 mmols), and Ph_3P (1.3 g, 5 mmols), in benzene (25 ml) was kept overnight at room temperature. The solution was washed with $NaHCO_3$ solution, then with water, dried on $MgSO_4$ and chromatographed on a silica gel column (200 g). A yellow fraction containing Ph_3PS, **2** (Ar = Ph), and **4** (Ar = Ph) was firstly removed by elution with hexane-benzene 1 : 1 and then with benzene. Compound **3** was subsequently eluted with ethyl acetate. M.p. 143—45° (hexane-ethyl acetate). Yield : 1.24 g IR(KBr) : $\nu_{max}=3250, 1705, 1680, 1530\ cm^{-1}$. $^1H-NMR\ (CDCl_3)$: $\delta = 1.00$ (q, 6H, $(CH_3)_2CH-$, $J = 2.0$, 7.0 Hz), 2.27 (m, 1H, $(CH_3)_2CH-$), 4.48 (m, 1H, $-NH-CH-CO-$), 5.10 (s, 2H, $Ph-CH_2-$ $-O-CO-$), 6.09 (d, 1H, $-O-CO-NH-CH-$, $J = 8.5$ Hz), 7.18 (s, 15 H_{arom}). *Found* : C, 72.58 ; H, 6.30 ; N, 6.43. *Calcd.* for $C_{26}H_{26}N_2O_4$: C, 72.53 ; H, 6.08 ; N, 6.50.

N-(N′-carbobenzoxyvalinyl)-aniline (**5**, Ar, = Ph, RCO = Z—Val). The compound was prepared following the procedure described above for **3**. The crude reaction products were separated on neutral alumina (Whoelm 200, activity grade Super I) (50 g). After removal of Ph_3PS, **2** (Ar = Ph), and **4** (Ar = Ph) with benzene and benzene-ethyl acetate 4 : 1, the compound was eluted with ethyl acetate. M.p. 184—186° (hexane-ethyl acetate). Yield : 0.78 g. IR(KBr) : $\nu_{max}=3280, 1690, 1660, 1540\ cm^{-1}$. $^1H-NMR(CDCl_3)$: $\delta=1.025$ (q, 6H, $(CH_3)_2CH-$, $J = 1.5$, 7.0 Hz), 2.10 (m, 1H, $(CH_3)_2CH-$, $J = 7.0$ Hz), 4.26 (q, 1H, $-NH-CH-CO-$, $J = 7.0$, 9.0 Hz), 5.25 (s, 2H, $Ph-CH_2-O-CO-$), 5.75 (d, 1H, $-O-CO-NH-$, $J =$ $= 9.0$ Hz), 7.47 (s, 10 H_{arom}), 8.50 (s, 1H, $-CO-NH-Ph$). *Found* : C, 69.75 ; H, 7.00 ; N, 8.50. *Calcd.* for $C_{19}H_{22}N_2O_3$: C, 69.91 ; H, 6.79 ; N, 8.58.

1-Phenyl-4-isopropyl-hydantoin (**6**). The mixture containing the crude reaction products prepared as described above for **3** was chromatographed on neutral alumina activity grade IV. The compound **6** was eluted with ethyl acetate immediately after **5** (Ar = Ph, RCO = Z—Val). M.p. 130—132°, $/\alpha/_D^{23} + 99°$ (ethanol) (lit.[4] m.p. 131—133°, $/\alpha/_D^{22} + 97.2°$). Yield : 0.3 g.

N-(N′-carbobenzoxyalanyl)-aniline (**5**, Ar = Ph, RCO = Z—Ala). The compound was prepared from Z—Ala (1.11 g, 5 mmols), disulphide **1** (Ar = Ph) (2.13 g, 5 mmols), and Ph_3P (1.3 g, 5 mmols) in dichloromethylene solution (25 ml), following the procedure described above for **5** (Ar = Ph, RCO = Z—Val). M.p. 163—165° (hexane-ethyl acetate). Yield : 0.75 g. IR (KBr) : $\nu_{max} = 3260, 1680, 1650, 1530\ cm^{-1}$. $^1H-NMR\ (CDCl_3)$: $\delta = 1.54$ (d, 3H, CH_3-CH-, $J=3.75$ Hz), 4.76 (q, 1H, CH_3-CH- $J=3.75$ Hz, 5.12 (s, 2H, $Ph-CH_2-O-CO-$), 6.48 (d, 1H, $-NH-CH-$, $J = 9.0$ Hz), 7.32 (s, 10 H_{arom}), 8.05 (s, 1H, $-CO-NH-Ph$). *Found* : C, 68.65 ; H, 6.04 ; N, 9.30. *Calcd.* for $C_{17}H_{18}N_2O_3$: C, 68.44 ; H, 6.09 ; N, 9.39.

Ethyl N-thiobenzoyl-p-aminobenzoate. N-thiobenzoyl-*p*-aminobenzoic acid (m.p. 200—207° ; hexane-ethyl acetate) prepared from *p*-aminobenzoic acid (1.37 g) and thiobenzoylthioacetic acid (2.12 g),[5] was esterified with anh. ethanol and thionyl chloride (2 hours at 40°). The dried crude reaction product was dissolved in benzene-ethyl acetate 4 : 1 and filtered through a small column of neutral alumina. M.p. 156—158°. Yield : 2g. *Found* : C, 67.34 ; H, 5.36 ; N, 5.00 ; S, 10.82. *Calcd.* for $C_{16}H_{15}NO_2S$: C, 67.33 ; H, 5.29 ; N, 4.90 ; S, 11.82.

---

[4] E. FISCHER, *Ber. dtsch, chem. Ges.*, **39**, 2327 (1904).

[5] K. ADAMS, *Acta Chim. Scand.*, **4**, 1347 (1950).

Bis-[α-(p-carbetoxyphenylimino)-benzyl]-disulphide (**1**, Ar = *p*-C_6H_4COOEt). The compound was prepared from ethyl N-thiobenzoyl-*p*-aminobenzoate and benzoylperoxide following the procedure reported earlier[1]. M.p. 105—107° (ethanol). Yield : 70%. *Found*: C, 67.43 ; H, 4.86 ; N, 4.80 ; S, 11.10. *Calcd.* for $C_{32}H_{28}N_2O_4S_2$: C, 67.57 ; H, 4 96 ; N, 4.92 ; S, 11.27.

Ethyl N-(N′-carbobenzoxyvalinyl)-p-aminobenzoate (**5**, Ar = *p*-C_6H_4COOEt, RCO = =Z—Val). The compound was prepared from Z—Val (1.25 g, 5 mmols), disulphide **1** (Ar= = *p*-C_6H_4COOEt) (2.85 g, 5 mmols), and Ph_3P (1.3 g, 5 mmols), following the procedure described above for **5** (Ar=Ph, RCO = Z—Val). M.p. 179—181° (hexane-ethyl acetate). Yield : 0.8 g. IR(KBr) : ν_{max}= 3250, 1700, 1680, 1655, 1520 cm^{-1}. ^1H-NMR ($CDCl_3$) : δ= 1.00(q, 6H, $(CH_3)_2CH-$, J = 2.0, 7.0 Hz), 1.33 (t, 3H, $CH_3-CH_2-O-CO-$, J = 6.0 Hz), 2.15 (m, 1H, $(CH_3)_2CH-$, J = 7.0 Hz), 4.09 (m, 1H, $-NH-CH-CO-$), 4.30 (q, 2H, $CH_3-CH_2-O-CO-$, J = 6.0 Hz), 5.07 (s, 2H, $Ph-CH_2-O-$), 5.36 (d, 1H, $-O-CO-NH-CH-$, J = 8.0 Hz), 7.24 (s, 5H, $C_6H_5-CH_2-O-CO-$), 7.36 (q, 4H, $-O-CO-C_6H_4-NH-$, J= = 9.0 Hz), 8.24 (s, 1H, $-CO-NH-C_6H_4-$). *Found*: C, 66.72 ; H, 6.30 ; N, 7.25. *Calcd.* for $C_{22}H_{26}N_2O_5$: C, 66.32 ; H, 6.57 ; N, 7.03.

NOTE POUR LES AUTEURS

La *Revue Roumaine de Chimie* publie des articles en anglais, français, russe, allemand ou espagnol. Les auteurs sont priés d'envoyer des articles et des comptes rendus inédits.

Les manuscrits seront dactylographiés à deux intervalles. La bibliographie, les tableaux et la légende des figures seront placés après le texte.

Si l'article fait partie d'une série numérotée, le titre de la partie précédente sera indiqué dans une note au bas de la première page.

Chaque article sera précédé d'un résumé comprenant quinze lignes au maximum. Les références bibliographiques dans le texte seront faites par des exposants sans parenthèses, et paraîtront comme des notes au bas de chaque page.

Les publications périodiques mentionnées dans la bibliographie seront présentées suivant les prescriptions internationales : le nom de l'auteur précédé de l'initiale du prénom, le titre du périodique abbrégé conformément à « Chemical Abstracts », et souligné par une ligne, le numéro du tome indiqué par des chiffres arabes et souligné par deux lignes, suivi de la première page de l'article ; à la fin, l'année de la parution sera placée entre parenthèses. Le numéro de la revue ne sera pas indiqué si les pages du volume sont numérotées consécutivement.

Les textes des livres ou traités inclueront : les noms des auteurs, les initiales du prénom, le titre du livre entre guillemets et sans être souligné, le numéro du tome précédé par l'abbréviation « vol. » (ou « Bd »), le numéro de l'édition, les éditions (the publisher), la localité de la parution du livre, l'année de la parution et la page de la référence précédée(s) par l'abbréviation « p » (ou « S »).

Les brevets seront indiqués comme suit : l'auteur ou la firme, le pays et le numéro du brevet, la date et la revue (Chem. Abstr.), Par ex. : M. Jones (to Union Carbide Co.), Brit. Pat. 601 238, 2 Sept. 1959, Chem. Abstr., 54, 12808 1960.

Les diagrammes seront tracés à l'encre de Chine sur papier calque. Les tableaux et les figures (en nombre strictement nécessaire) seront numérotés par des chiffres arabes. Les courbes dans les figures seront numérotées par des chiffres arabes et leur explication sera donnée dans la légende des figures. Prière de ne pas inscrire les même données dans les tableaux et les figures. Chaque tableau aura un titre. On indiquera dans le texte la place approximative des tableaux et des figures. Les formules chimiques seront incluses dans le texte ; en outre, elles seront transcrites sur papier calque, à l'encre de Chine.

Les auteurs sont priés d'indiquer les caractères italiques (en soulignant les lettres au crayon), ainsi que tout autre caractère spécial ; les préfixes *ortho, meta, para, cis, trans,* etc. seront soulignés pour indiquer leurs caractères italiques et ne seront jamais écrites avec des majuscules.

Aucune correction à la main ne sera admise sur le manuscrit. Les corrections seront frappées à la machine. Les lettres grecques ou autres symboles spéciaux seront insérés à la main à l'encre clairement.

Le manuscrit sera signé par l'auteur.

Le colonne-titre aura 50 lettres au maximum.

L'entière responsabilité du contenu des articles appartient aux auteurs.

PRINTED IN ROMANIA

TRAVAUX PARUS AUX ÉDITIONS DE L'ACADÉMIE DE LA RÉPUBLIQUE SOCIALISTE DE ROUMANIE

- I. G. MURGULESCU, **Introducere în chimia fizică. Vol. I. 1. Atomi. Molecule. Legătură chimică** (Introduction à la chimie physique. Ier vol. 1re Partie, Atomes. Molécules. Liaison chimique), 1976, 560 p., 2 pl., 36 lei.
- GR. POPA, ŞERBAN MOLDOVEANU, **Reactivii organici în chimia analitică** (Les réactifs organiques dans la chimie analytique), 1976, 255 p., 18 lei.
- I. ZUGRĂVESCU, MAGDA PETROVEANU, **N-Ylid Chemistry**, 1976, coédition avec McGraw-Hill International Book Company, SUA, 396 p., 33 lei.
- C. V. UGLEA, **Cromatografia pe gel permeabil. Noi domenii de aplicare** (La Chromatografie sur gel perméable. Nouveaux domaines d'application), 1976, 123 p., 6,75 lei.
- I. GĂLĂŢEANU, **Radiochimia aplicată. Metode şi probleme** (La radiochimie appliquée. Méthodes et problèmes), 1976, 305 p., 19 lei.
- FRANCISC A. GOTHARD, **Echilibre lichid-vapori. I. Baze teoretice şi metode de calcul** (Equilibres liquide-vapeurs. I. Bases théoriques et méthodes de calcul), 1975, 263 p., 2 pl., 28 lei.
- CONST. GH. MACAROVICI, D. MACAROVICI, **Chimia oxizilor dubli şi utilizările lor** (La chimie des oxydes doubles et leur utilisation), 1975, 195 p,. 13 lei.
- ELENA CEAUŞESCU, **Research work on synthesis and characterization of macromolecular compounds. Contributions**, 1974, 251 p., 20 lei.
- M. AVRAM, **Antidăunători** (Pesticides), 1974, 496 p., 41 lei.
- DUMITRU COSTACHE, **Analiza chimică prin metoda cinetică** (L'Analyse chimique par la méthode cinétique), 1974, 276 p., 15,50 lei.
- G. A. RĂDULESCU, **Proprietăţile ţiţeiurilor româneşti** (Les propriétés des pétroles roumains), 1974, 267 p., 2 pl., 18 lei.
- CR. SIMIONESCU, VIORICA RUSAN, V. POPA, **Chimia algelor marine** (La chimie des algues marines), 1974, 212, p., 1 pl., 18 lei ;

1977 SEP 1 6

I. P. INFORMAŢIA c. 7288

43 426

Lei 25.—

F 1103

ACADÉMIE DE LA RÉPUBLIQUE SOCIALISTE DE ROUMANIE

REVUE ROUMAINE DE CHIMIE

TOME 22
N° 8
Août 1977

EDITURA ACADEMIEI REPUBLICII SOCIALISTE ROMÂNIA

Rev. Roumaine Chim.

RECHAX, 22, 8, p. 1115 – 1276 (1977), Bucarest

ACADÉMIE DE LA RÉPUBLIQUE SOCIALISTE DE ROUMANIE

COMITÉ DE RÉDACTION

Rédacteur en chef :

I. G. MURGULESCU, membre de l'Académie de la République Socialiste de Roumanie

Rédacteurs en chef adjoints :

A. T. BALABAN et V. EM. SAHINI, membres correspondants de l'Académie de la République Socialiste de Roumanie

Collège de rédaction :

EM. BRATU, ELENA CEAUŞESCU, ECATERINA CIORĂNESCU-NENITZESCU, C. DRĂGULESCU, CR. SIMIONESCU, membres de l'Académie de la République Socialiste de Roumanie ; P. SPACU, membre correspondant de l'Académie de la République Socialiste de Roumanie ; MARGARETA AVRAM, I. HAIDUC, D. I. MARCHIDAN, I. MOLDOVAN, G. NIAC et D. SĂNDULESCU

La Revue Roumaine de Chimie paraît 10 fois par an. Toute commande de l'étranger pour les travaux parus aux Editions de l'Académie de la République Socialiste de Roumanie (fascicules ou abonnements) sera adressée à ILEXIM, Departamentul Export-Import Carte (Livres)/Departamentul Export-Import Presă (Revues), P.O.B. 136—137, télex 11226, Bucarest, 3, str. 13 Decembrie, Roumanie

Les manuscrits, les livres et les revues proposés en échange, ainsi que toute correspondance seront envoyés à la rédaction :

REVUE ROUMAINE DE CHIMIE

23, str. Dumbrava Roşie, Bucarest, Roumanie, téléphone 12 41 60

EDITURA ACADEMIEI REPUBLICII SOCIALISTE ROMÂNIA

125, Calea Victoriei, 71021, Bucarest, Roumanie, téléphone : 50 76 80

ORSZÁGOS MŰSZAKI KÖNYVTÁR ÉS DOKUMENTÁCIÓS KÖZPONT 1883

REVUE ROUMAINE DE CHIMIE

Tome 22, N° 8 Août 1977

MINODORA LECA and J. R. H. PÉREZ, Relation between hydrophilic-lipophilic balance and polarity determined by reverse gas-liquid chromatography for nonionic surfactants 1117–1123

LUCIA CIOHODARU, Electronic structure of some stilbene derivatives. V. The influence of the substituents on the HMO π-energy levels 1125–1133

V. BĂRBOIU, Some NMDR experiments improved by means of a computer 1135–1143

L. R. SINGH, P. BAHADUR and S. N. SRIVASTAVA, Studies on conductivities of some ionic surfactants in aqueous methanol 1145–1150

SULTANA CIOLAC, Irreversibility of the pitting process 1151–1164

E. UHLIG, W. HEPP, LE MY NGU und K. SCHMIEDEKNECHT, Zum Einfluß der Ringgröße auf die Struktur von Metallchelaten dreizähliger Liganden. III. Kupfer(II)-, Nickel(II)- und Eisen (II)-Chelate pyridylsubstituierter Dialkylsulfide 1165–1174

R MARIA BREZEANU and MAGDALENA DINCULESCU, Polynuclear complex compounds of iron, cobalt and nickel. II. Mercury-containing complex compounds 1175–1180

A. C. BANCIU, A tetrahedral Ni(II) complex compound derived from 1-methyl-2-carbethoxy-glyoxalanil-(1)-*m*-nitro-phenylhydrazone-(2) 1181–1186

NELLY DEMIAN, CARMEN AMBRUS and D. CAMBOLI, Complex compounds of Pd(II) with monosubstituted derivatives of thiourea 1187–1189

A. T. BALABAN, ILEANA I. STĂNOIU and EUGENIA GÂRD, Deuterium isotope effect on the basicity of 2,4,6-trimethylpyridine 1191–1193

R D. C. ŞUSTER, G. CIUŞTEA, ANA DUMITRESCU, L. V. FEYNS, EUTANŢA TĂRNĂUCEANU, GEORGETA BOTEZ, S. ANGELESCU, V. DOBRE and I. NICULESCU-DUVĂZ, Potential anticancer agents. XIV. Synthesis and biological evaluation of N[4′-{[(2,4-diamino-6(7-)-pteridinyl)-methyl]-N^{10}-methylamino}-benzoyl]-L,D and DL-glutamic(aspartic) acids 1195–1207

M. IOVU und E. VOINA, Gemischte aromatische Ester der Phosphorigen-und der Phosphorsäure 1209–1215

M. ANWAR and S. H. ETAIW, Infrared absorption spectra of some 4H-3,1-benzoxazin-4-ones and 2,3-disubstituted-4(3H)-quinazolinones 1217–1223

F. URSEANU and E. TESZLER, New disperse dyes for polyester fibres . . . 1225–1231

R D. S. MAHADEVAPPA and RANGASWAMY, Physico-chemical properties of chloramine-T. II. Conductometric study of the interaction of chloramine-T with Cr(III), Al(III) and Fe(III) solutions 1233–1241

Rev. Roumaine Chim. **22**, *8*, p. 1115–1276, (1977), Bucarest

R ELENA HOPÎRTEAN, ELISABETA VERESS and VALERIA MUREŞAN, Liquid-membrane electrodes. VII. Perchlorate-selective membrane-electrode. Construction and characterization 1243–1250

A. A. KHALAF, S. H. ETAIW, R. M. ISSA and A. K. EL-SHAFEI, Spectrophotometric study of some 1,5-diphenyl-1,5-pentadiene-3-ones . . . 1251–1259

R I. GAVĂT, OLGA BUTUFEI and MARIANA MUNTEANU, Adducts of tetrachlorohydroquinone with quinoline and piperazine 1261–1265

MARGARETA TOMESCU, I. DEMETRESCU and D. OANCEA, Structural characterization of multicomponent acrylic polymers 1267–1270

COMPTES RENDUS 1271–1275

Revue Roumaine de Chimie, **22**, *8*, 1117–1123, (1977)

RELATION BETWEEN HYDROPHILIC-LIPOPHILIC BALANCE AND POLARITY DETERMINED BY REVERSE GAS-LIQUID CHROMATOGRAPHY FOR NONIONIC SURFACTANTS

MINODORA LECA and JOSÉ RAFAEL HIDALGO PÉREZ *
Polytechnic Institute of Bucharest, Chemistry Department,
Macromolecular Chemistry Laboratory, Bd. Republicii 13, Romania

Received May 20, 1975

The polarity of nonionic surfactants was characterized by gas-liquid chromatography, using surfactants as stationary phases. MeOH have been selected as specific sensors for hydrogen bonds. The carbon atom number corresponding to the retention volume of MeOH on n-alkanes scale — the apparent carbon of MeOH on surfactant, C_{MeOH} — was taken as a relative measure of the polarity. The difference between C_{MeOH} on surfactant and C_{MeOH} on squalane — taken as nonpolar reference — C'_{MeOH} was suggested as an absolute measure of the polarity. The analytical dependence of C_{MeOH} on *HLB* for spans, tweens, mirjs and pluronics was given. C_{MeOH} or C'_{MeOH} properly describe the polarity of nonionic surfactants and polarity index, *PI*, the polarity of their binary mixtures.

The applicability of surfactants being connected with the polarity of the molecules,[1] numerical systems were searched to characterize their polarity. Three such systems were known for nonionic surfactants:

— hydrophilic-lipophilic balance, *HLB*, introduced by Griffin,[2,3] useful for surfactants as well as for their binary mixtures;

— hydrophilic/lipophilic number, *H/L*, belonging to Moore and Bell,[4] used for surfactants;

— polarity index, *PI*, by Huebner,[5] useful for binary mixtures of surfactants.

The most useful is the *HLB* system, offering the advantage of the additivity for mixtures.

The *HLB* values were assigned by determining the proportions of different emulsifier combinations needed to make the best oil in water emulsions.[2] As these were time-consuming, faster methods had to be found. With that end in view, the *HLB* values thus obtained were correlated to some specific properties of the surfactants, such as:

---

* Present address: Apartado 1827, IVIC, Caracas, Venezuela.

[1] P. Becher, "Nonionic Surfactants", Edward Arnold Publisher LTD, London, 1967.

[2] W. C. Griffin, *J. Soc. Cosmetic Chemists*, **1**, 311 (1949).

[3] W. C. Griffin, *J. Soc. Cosmetic Chemists*, **5**, 249 (1954).

[4] C. D. Moore and M. Bell, *Soap, Parfumery & Cosmetics*, **29**, 893 (1956).

[5] V. R. Huebner, *Anal. Chem.*, **34**, 488 (1962).

solubility, including water titration method[6] and liquid-liquid distribution coefficients of surfactants in water and isooctane,[7] solubilization of benzene in water and solubilization of dyes in nonaqueous solvents,[8] R_f values in paper[9] and thin-layer chromatography,[10] behaviour as a stationary phase in the gas-liquid chromatography,[5,11–14] heat of hydration,[15] phase inversion temperature,[16–18] dielectric constant,[14,19] partial molal volume.[20]

Griffin[3] developed formulas to calculate the *HLB* values of certain simple esters and ethylene oxide derivatives and Davies[21] assigned each functional group in a molecule an *HLB* contributing number. These methods are restricted to surfactants having known structure.

Pointing out that the *HLB* value means the balance of surfactant at an oil-water interface, Shinoda[18] has shown that it will change with the types of oils and with the additives to water or oil phase and it is also a function of temperature.

The above experimental methods, excepting phase inversion temperature, do not take into account the influence of medium, so that the HLB values so obtained — named ideal — will differ from the real ones.

However they are useful, allowing the surfactants selection for some specific applications.

The dependence of retention volume of a polar solute on the polarity of stationary phases is the base for the determination of the polarity of surfactants.

The *HLB* values were correlated on one side with partition coefficients[11] and a good correlation was obtained for partition coefficients of di-isobutylene, and on the other side with retention volumes[5,13,14] or time[12] and some quantities which reflect the selective retention of a polar solute in relation to nonpolar ones (hydrocarbons) on surfactants and, therefore, their polarity were determined. The ratio, ρ, of the retention times of ethanol and *n*-hexane[12] and the apparent carbon number, C,[5] were used for that purpose. The last one represents the number of carbon atoms on the *n*-hydrocarbon scale, corresponding to the peak of the selected polar solute.[5]

[6] H. L. Greenwald, G. L. Brown and M. N. Fineman, *Anal. Chem.*, **28**, 1693 (1956).

[7] H. L. Greenwald, E. B. Kice, M. Kenly and J. Kelly, *Anal. Chem.*, **33**, 465 (1961).

[8] R. C. Little, Ph. D. Thesis, Rensselaer Polytechnic Inst., Mic., 1960, cf. ref. 5.

[9] T. Nakagawa and M. Nakata, *J. Chem. Soc. Japan, Ind. Chem. Sect.*, **59**, 1154 (1956).

[10] S. Hayano and T. Asahara, "Proc. 5th Int. Congr. of Surface Activity", Barcelona, 1968.

[11] O. Harva, P. Kivalo and A. Keltakallio, *Suomen Kem.*, **B 32**, 52 (1959).

[12] P. Becher and R. L. Birkmeier, *J. Amer. Oil Chem. Soc.*, **41**, 169 (1964).

[13] J. Broniarz, M. Wisniewski and J. Szymanowski, *Tenside, Detergents*, **10**, 75 (1973).

[14] J. Broniarz, M. Wisniewski and J. Szymanowski, *Tenside, Detergents*, **11**, 27 (1974).

[15] I. Racz and E. Orban, *J. Colloid Sci.*, **20**, 99 (1965).

[16] K. Shinoda and H. Arai, *J. Phys. Chem.*, **68**, 3486 (1964).

[17] K. Shinora, *J. Colloid Interface Sci.*, **24**, 4 (1967).

[18] K. Shinoda, "Proc. 5th Int. Congr. of Surface Activity", Barcelona, 1968.

[19] W. G. Gorman and G. D. Hall, *J. Pharm. Sci.*, **52**, 442 (1963).

[20] L. Marszall, *J. Pharm. Pharmac.*, **25**, 254 (1973).

[21] J. T. Davies, "Proc. 2nd Int. Congr. of Surface Activity", Butterworths, London, 1957.

C numbers obtained from various surfactant combinations were not additive and they were converted by Huebner[5] to an empirically derived polarity index, *PI*, by the following equation:

$$PI = \lg(C - 4.7) + 60 \tag{1}$$

EXPERIMENTAL PART

Column preparation. The surfactants were dissolved in chloroform and added to the adequate quantity of 100—120 mesh chromosorb *P* (Carlo Erba). The solvent was removed by evaporation under mixing. A 6 mm o.d. copper column, 2 m in length, was packed with such materials. The column was conditioned about 2 hours in carrier gas flow (flow rate 5—20 ml/min) at temperatures ranging between 60 and 95°.

Operating conditions. The concentration of stationary phase was 10% for very polar surfactants, 15% for those having medium polarity and 20% for surfactants of small polarity and squalane.

The column temperature ranged from 60 to 95°, depending on the melting point of the surfactant, so that the surfactant be in liquid phase. The detector temperature was 150—175° and the injection temperature, 150—175°.

The thermal conductivity detector was used, with hydrogen as carrier gas. A flow rate from 30 to 40 ml/min was used, so that the analysis was completed in 15 to 20 minutes and the best resolution was obtained. A mixture of *n*-pentane, *n*-hexane, *n*-heptane, *n*-octane, methyl alcohol, and air was injected into the column and peak retention times were measured relative to the air.

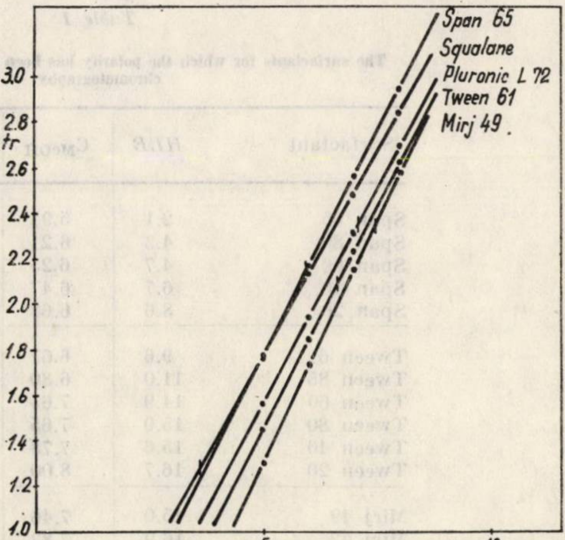

Fig. 1.— Determination of C_{MeOH} numbers by Huebner method: /depicts the C_{MeOH} numbers on surfactants.

Carbon number determination. The apparent carbon numbers of methyl alcohol, C_{MeOH}, on surfactants of the types: span, tween, mirj and pluronic were determined by Huebner method.[5] Thus, the logarithms of the hydrocarbons retention times measured after the air peak (in the same conditions) were plotted against the length of their carbon chain on semi-logarithmic scale to obtain a straight line relationship. The logarithm of the retention time of methyl alcohol is extrapolated from this plot to find its C_{MeOH}. The method is exemplified in figure 1 for one surfactant belonging to any studied type.

All the values reported in this paper are the average of three, and sometimes of four determinations.

RESULTS AND DISCUSSION

In our opinion, the problem of surfactant polarity determination using reverse gas-liquid chromatography contains two aspects : the surfactants and their binary mixtures.

The present work deals with relations between the polarity as determined by reverse gas-liquid chromatography and the *HLB* values for four types of surfactants and their binary mixtures.

C numbers were not affected by column temperature — as long as the surfactants are in liquid phase, by carrier gas flow rates, the type of support, the concentration of the stationary phase, and by the column length, so that they are expected to give the right succession of the polarity of the surfactants. With this idea in view, we decided in favour of methyl alcohol as specific sensor for hydrogen bonds, taking account of the nature of the interactions between nonionic surfactants and the aqueous phase. The carbon atom number corresponding to the retention time of methyl alcohol on the n-alkanes scale, C_{MeOH}, on surfactants was taken as a relative measure of the polarity. C_{MeOH} were determined on surfactants listed in table 1.

Table 1

The surfactants for which the polarity has been determined by gas-liquid chromatography

Surfactant	*HLB*	C_{MeOH}	C'_{MeOH}	PI_{MeOH}
Span 65	2.1	5.98	2.33	70.7
Span 80	4.3	6.21	2.56	77.9
Span 60	4.7	6.25	2.60	79.0
Span 40	6.7	6.47	2.82	84.8
Span 20	8.6	6.68	3.03	89.6
Tween 61	9.6	6.67	3.02	89.4
Tween 85	11.0	6.80	3.15	92.2
Tween 60	14.9	7.65	4.00	107.0
Tween 80	15.0	7.65	4.00	107.0
Tween 40	15.6	7.78	4.13	108.5
Tween 20	16.7	8.00	4.35	111.8
Mirj 49	15.0	7.46	3.81	104.1
Mirj 52	16.9	7.83	4.18	109.5
Mirj 59	18.8	8.17	4.52	114.0
Pluronic L 72	6.5	7.10	3.45	98.0
Pluronic F 68	29.0	7.90	4.25	110.5

Plotting C_{MeOH} of the four types of nonionic surfactants : span, tween, mirj, and pluronic in terms of HLB values, linear functions were obtained for any type, as shown in figure 2.

The analytical dependence of C_{MeOH} on *HLB* for any type was calculated using the equation of the straight lines as well as the least square method and the results are the same, as shown in table 2.

C_{MeOH} on nonpolar stationary phases are not zero, so that these numbers are not an absolute measure of the surfactant polarity. The polarity should be properly represented by the difference between C_{MeOH} on surfactant and C_{MeOH} on the lipophilic part. Since the determination of the last quantity is impossible, we have taken squalane as nonpolar reference, it being entirely non-selective for hydrocarbons.[22] C_{MeOH} on squalane had the value 3.65 and the differences are given in table 1. These are the corrected apparent carbon numbers of methyl alcohol on surfactants, C'_{MeOH}, and they are an absolute measure of the surfactant polarity. There is no difficulty to pass from $C_{MeOH} = f(HLB)$ to $C'_{MeOH} = f(HLB)$.

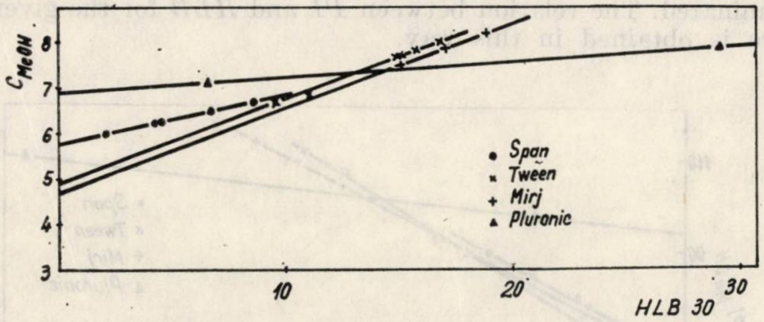

Fig. 2. – Dependence of C_{MeOH} on *HLB* for surfactants of the types: span, tween, mirj, and pluronic.

Table 2

The dependence of C_{MeOH} on *HLB*

Type of surfactant	Equation
Span	$C_{MeOH} = 5.75 + 0.110\ HLB$
Tween	$C_{MeOH} = 4.90 + 0.185\ HLB$
Mirj	$C_{MeOH} = 4.70 + 0.185\ HLB$
Pluronic	$C_{MeOH} = 6.85 + 0.035\ HLB$

PI were introduced by the necessity to preserve the linearity between the polarities determined by gas-liquid chromatography and the composition of binary surfactant mixtures. The *PI* values, according to Huebner,[5] were calculated using C_{MeOH} to verify if this system properly describes the polarity of surfactants. The values are given in table 1.

The *PI* values were plotted in terms of *HLB* (figure 3) and, as we expected, there were deviations from linearity for any type.

The deviations from linearity being small, approximate relations can be established between *PI* and *HLB* (table 3). This fact determined Broniarz et al.[13,14] to consider *PI* as a measure of surfactant polarity.

---

[22] H. M. Tenney, *Anal Chem.*, **30**, 2 (1958).

The C_{MeOH} numbers of surfactants once known, the *HLB* values of binary mixtures should be determined as follows : C_{MeOH} numbers are converted into *PI* values and then, taking into account the fact that both *HLB* and *PI* are linear function of composition, the concentration *c* is eliminated. The relation between *PI* and *HLB* for the given binary mixture is obtained in this way.

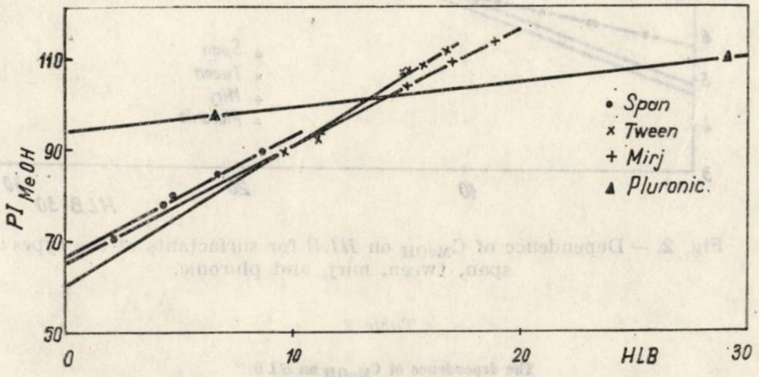

Fig. 3. – PI_{MeOH} values in terms of *HLB* for surfactants of the type : span, tween, mirj, and pluronic.

Table 3

The dependence of PI_{MeOH} on *HLB*

Type of surfactant	Equation
Span	$PI_{MeOH} = 66.2 + 2.66\ HLB$
Tween	$PI_{MeOH} = 60.0 + 3.08\ HLB$
Mirj	$PI_{MeOH} = 65.0 + 2.60\ HLB$
Pluronic	$PI_{MeOH} = 94.3 + 1.25\ HLB$

HLB and *PI*, respectively, in terms of percent concentration of the two surfactants are readily obtained, by using the corresponding values of the original surfactants. Using the subscript 1 for the less polar surfactant and the subscript 2 for the most polar one, we obtain :

$$HLB = (HLB)_1 + \frac{(HLB)_2 - (HLB)_1}{100}\,c\,; \tag{2}$$

$$PI = (PI)_1 + \frac{(PI)_2 - (PI)_1}{100}\,c. \tag{3}$$

The elimination of *c* between equation (2) and (3) gives the relation between *HLB* and *PI*.

CONCLUSIONS

We suggest to use C_{MeOH} or C'_{MeOH} to characterize the polarity of nonionic surfactants and *PI* to describe the polarity of their binary mixtures.

We gave the analytical dependence of C_{MeOH} on *HLB* for spans, tweens, mirjs and pluronics.

The way to obtain the relations between *HLB* and *PI* for binary mixtures was also emphasized.

This method is able to reduce the time to determine a *HLB* value of a surfactant to about four hours, if the calibration curve has been previously plotted for the given type of surfactant.

Revue Roumaine de Chimie, **22**, *8*, 1125–1133 (1977)

ELECTRONIC STRUCTURE OF SOME STILBENE DERIVATIVES. V[1]

THE INFLUENCE OF THE SUBSTITUENTS ON THE HMO π-ENERGY LEVELS

LUCIA CIOHODARU

Department of Physical Chemistry, Polytechnic Institute,
St. Polizu 1, Bucharest, Romania

Received January 21, 1976

Modifications of energy differences between the ground and first electronically excited states, as well as of the π-energy levels because of the substituents, for 27 stilbenes, are discussed in terms of the Hückel Molecular Orbital method. The calculations correlate well with the A band maximum in the ultraviolet spectra of the corresponding stilbene derivatives.

The Hückel Molecular Orbital (HMO) method leads to the overrating of the π-electron delocalization; however it yields satisfactory results for series of closely related compounds. Especially when these derivatives have large molecules and SCF–MO calculations are difficult, the HMO method is of good use.

There are no available literature data referring to the HMO calculations of the stilbene derivatives dealt with in this paper. Some data in connection with similar compounds were reported.[2–8]

In order to obtain the HMO π-energy levels and to evidence the substituent effects in stilbenes, LCAO–HMO calculations have been performed for a series of 27 nitro-containing stilbene derivatives.

---

[1] Part IV: L. Ciohodaru, V. E. Sahini and E. Volanschi, *Rev. Roumaine Chim.* **22**, 171 (1977).

[2] C. A. Coulson and J. Jacobs, *J. Chem. Soc.*, **1949**, 1983.

[3] H. Suzuki, *Bull. Chem. Soc. Japan*, **25**, 145 (1952).

[4] H. H. Jaffé and M. Orchin, *J. Chem. Soc.*, **1960**, 1078.

[5] R. W. Schmid, *Helv. Chim. Acta*, **45**, 1982 (1962).

[6] G. Favini, S. Trovato and A. Gamba, *Theor. Chim. Acta*, **7**, 305 (1967).

[7] H. Güsten and L. Klasinc, *Tetrahedron Letters*, **1967**, 2923.

[8] Iu. P. Egorov, V. A. Hranovschi and M. Iagupolschi, *Teor. eksper. khimiia*, **3**, 90 (1970).

RESULTS AND DISCUSSION

The studied stilbene derivatives can be described by the following general formula :

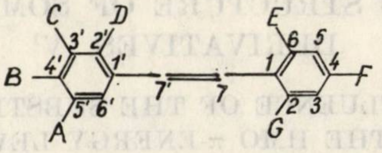

Table 1 contains the A—G substituents of the 27 stilbene derivatives, synthesized as in a previous paper.[9]

Table 1

The substituents of the stilbene derivatives studied

N⁰	A	B	C	D	E	F	G	Comments
1	H	H	H	H	H	NO_2	CN	2-cyano-4-nitro-stilbene derivatives
2	H	H	H	H	H	NO_2	$CONH_2$	
3	H	H	H	H	H	NO_2	COOH	
4	H	OH	H	H	H	NO_2	CN	
5	H	OCH_3	H	H	H	NO_2	CN	
6	H	NMe_2	H	H	H	NO_2	CN	
7	H	NMe_2	H	H	H	NO_2	COOH	
8	H	H	H	H	H	CN	NO_2	2-nitro-4-cyano-stilbene derivatives
9	H	H	H	H	H	$CONH_2$	NO_2	
10	H	H	H	H	H	COOH	NO_2	
11	H	OH	H	H	H	CN	NO_2	
12	H	OCH_3	H	H	H	CN	NO_2	
13	H	NMe_2	H	H	H	CN	NO_2	
14	H	NMe_2	H	H	H	$CONH_2$	NO_2	
15	H	NMe_2	H	H	H	COOH	NO_2	
16	H	$NHCOCH_3$	H	H	H	CN	NO_2	
17	OCH_3	OH	H	H	H	CN	NO_2	
18	OCH_3	$OCOCH_3$	H	H	H	CN	NO_2	
19	H	H	H	H	H	NO_2	NO_2	2,4-dinitrostilbene derivatives
20	H	H	H	NO_2	H	NO_2	NO_2	
21	H	H	NO_2	H	H	NO_2	NO_2	
22	H	NO_2	H	H	H	NO_2	NO_2	
23	H	NMe_2	H	H	H	NO_2	NO_2	
24	H	H	H	H	NO_2	NO_2	NO_2	2,4,6-trinitrostilbene derivatives
25	H	OCH_3	H	H	NO_2	NO_2	NO_2	
26	H	Cl	H	H	NO_2	NO_2	NO_2	
27	H	NO_2	H	H	NO_2	NO_2	NO_2	

The HMO calculations were carried out with an IBM 370/135 computer.

The parameter values used in the HMO calculations together with the corresponding references are contained in Table 2.

---

[9] L. Ciohodaru and A. Meghea, *Rev. Roumaine Chim.*, **8**, 1127 (1976).

Table 2

The parameter values of the heteroatoms used in HMO calculations

	h_X	k_{CX}	References
$>C'-CH=CH-C'<$	$h_C = 0$ $h_{C'} = 0$	$k_{C'-C} = 0.9$ $k_{C=C} = 1.1$	10
$>C=O$	$h_{\dot{O}} = 1$	$k_{C=O} = 1$	10
$>C-NH_2$	$h_{NH_2} = 1.5$	$k_{C-NH_2} = 0.8$	7
$>C-NMe_2$	$h_{NMe_2} = 1$	$k_{C-NMe_2} = 0.8$	7
$>C-OH$	$h_{OH} = 2.0$	$k_{C-OH} = 0.8$	7
$>C'-OCH_3$	$h_{OCH_3} = 1.9$	$k_{C'-OCH_3} = 0.8$	7
$>C-N<^{O}_{O}$	$h_C = 0.25$ $h_N = 1.8$ $h_O = 1.5$	$k_{C-N} = 0.9$ $k_{N-O} = 1.8$	7
$>C'-CN$	$h_{CN} = 0.5$	$k_{C'-CN} = 1$	7
$>C-Cl$	$h_{Cl} = 2.0$	$k_{C-Cl} = 0.4$	7
$>C-\ddot{C}H_3$	$h_{\ddot{C}H_3} = 2$	$k_{C-\ddot{C}H_3} = 0.7$	10

MODIFICATIONS OF THE HMO π-ENERGY LEVELS PICTURE DUE TO SUBSTITUTION

The HMO π-energy levels for the studied stilbenes are collected in Table 3.

In order to make a comparison, the HMO π-energy levels for the unsubstituted stilbene and for the other nitro-containing stilbene derivatives (namely, 4-nitro- and 4,4′-dinitro-stilbene) were calculated again, using the parameter values from Table 2. They are also given in Table 3.

Examining the values of the HMO π-energy levels of the investigated stilbene derivatives, the following can be observed :

— The energy of the lowest occupied MO in unsubstituted stilbene is $\alpha + 2.1830\,\beta$; for all derivatives studied this energy lowers at about $\alpha + 4.1872\,\beta$. At about the same value, there are a number of one to four energy levels, depending on the presence of one to four nitro groups in every molecule.

---

[10] A. Streitwieser, "Molecular Orbital Theory for Organic Chemists", John Wiley, New York, 1961, p. 135.

Table 3

The m_j values from the eigenvalues ($\varepsilon_j = \alpha + m_j\beta$) of the Hamiltonian operator, corresponding to the π-system in every molecule

N⁰ π-energy level (j)	Unsubst. stilbene	**1**	**2**	**3**	**4**	**5**	**6**	**7**	**8**	**9**
1	2.1830	4.1873	4.1873	4.1873	4.1873	4.1873	4.1873	4.1873	4.1878	4.1878
2	2.0487	2.2665	2.3968	2.5439	2.4712	2.4172	2.2736	2.5439	2.2438	2.3719
3	1.5062	2.0963	2.1279	2.1677	2.2572	2.2550	2.1688	2.2125	2.1008	2.1484
4	1.1224	1.5411	1.9571	2.0546	1.9677	1.9473	1.6936	2.0913	1.6631	1.9919
5	1.0000	1.4999	1.5411	1.5411	1.4999	1.4999	1.4999	1.6909	1.5000	1.5057
6	1.0000	1.3884	1.4999	1.4999	1.4783	1.4734	1.4197	1.4999	1.2943	1.4999
7	0.5819	1.1428	1.3018	1.4846	1.3680	1.3655	1.2994	1.4871	1.0766	1.2886
8	−0.5819	1.0000	1.1628	1.1641	1.0517	1.0437	1.0000	1.3482	1.0000	1.1130
9	−1.0000	0.6938	1.0000	1.0000	1.0000	1.0000	1.8999	1.0000	0.7489	1.0712
10	−1.0000	0.2389	1.0000	1.0000	0.6420	0.6378	0.5374	1.0000	0.2368	1.0000
11	−1.1224	−0.4538	0.6333	0.6342	0.2307	0.2302	0.2189	0.8844	−0.4705	0.6284
12	−1.5062	−0.7859	−0.3601	−0.3519	−0.4625	−0.4629	−0.4676	0.4790	−0.7330	−0.3589
13	−2.0487	−1.0000	−0.5774	−0.5663	−0.8079	−0.8086	−0.8187	−0.3689	−1.0000	−0.5818
14	−2.1830	−1.1302	−0.7981	−0.7972	−1.0000	−1.0000	−1.0000	−0.5671	−1.1447	−0.8123
15		−1.2744	−1.0000	−1.0000	−1.1396	−1.1399	−1.1432	−0.8291	−1.2747	−1.0000
16		−1.5514	−1.1797	−1.1787	−1.2968	−1.2975	−1.3067	−1.0000	−1.5834	−1.1610
17		−2.0830	−1.4355	−1.4276	−1.5703	−1.5709	−1.5788	−1.2158	−2.0836	−1.3335
18		−2.2264	−1.5517	−1.5517	−2.0981	−2.0985	−2.1035	−1.4370	−2.2124	−1.6774
19			−2.0946	−2.0991	−2.2992	−2.2292	−2.3202	−1.5788		−2.0997
20			−2.2607	−2.2595				−2.1166		−2.2356
21								−2.2614		

Table 3 (continued)

N°π-energy level (*j*)	**10**	**11**	**12**	**13**	**14**	**15**	**16**	**17**	**18**	**19**
1	4.1878	4.1878	4.1878	4.1878	4.1878	4.1878	4.1878	4.1878	4.1878	4.1968
2	2.5328	2.4711	2.4168	2.2540	2.3722	2.5328	2.5511	2.5756	2.7810	4.1781
3	2.1816	2.2339	2.2319	2.1675	2.2058	2.2196	2.2482	2.2344	2.3916	2.2027
4	2.0573	1.9793	1.9601	1.7475	2.0215	2.1014	2.1729	2.1899	2.2303	2.0724
5	1.6110	1.6180	1.6128	1.5000	1.6653	1.7042	1.8910	1.9205	2.1063	1.5411
6	1.4999	1.4999	1.5000	1.4983	1.4999	1.5139	1.6179	1.5938	1.9233	1.5000
7	1.3889	1.1826	1.1736	1.0914	1.3666	1.4999	1.4999	1.4999	1.6042	1.4999
8	1.1156	1.0678	1.0665	1.0000	1.2058	1.2331	1.3838	1.1548	1.4999	1.1890
9	1.0713	1.0000	1.0000	0.9768	1.0851	1.0851	1.1181	1.0651	1.3886	1.0748
10	1.0000	0.6824	0.6770	0.5560	1.0000	1.0000	1.0505	0.8538	1.1460	1.0000
11	0.6298	0.2284	0.2279	0.2165	0.8667	0.8672	1.0000	0.6540	1.0644	0.6407
12	−0.3503	−0.4786	−0.4789	−0.4831	−0.4773	0.4783	0.6604	0.2275	0.8538	−0.3756
13	−0.5741	−0.7528	−0.7535	−0.7629	−0.3762	−0.3671	0.2277	−0.4786	0.6538	−0.5904
14	−0.8062	−1.0000	−1.0000	−1.0000	−0.5818	−0.5742	−0.4763	−0.7538	0.2292	−0.7958
15	−1.0000	−1.1596	−1.1600	−1.1650	−0.8489	−0.8428	−0.7347	−1.0515	−0.4758	−1.0000
16	−1.1604	−1.2964	−1.2972	−1.3068	−1.0000	−1.0000	−0.9353	−1.1636	−0.7367	−1.1495
17	−1.3310	−1.6006	−1.6012	−1.6082	−1.1720	−1.1717	−1.0000	−1.3052	−0.9114	−1.2750
18	−1.6704	−2.0978	−2.0982	−2.1028	−1.3777	−1.3750	−1.1710	−1.6115	−1.0530	−1.5513
19	−2.0992	−2.2157	−2.2158	−2.2170	−1.6895	−1.6859	−1.3135	−2.1130	−1.1688	−2.0650
20	−2.2347				−2.1200	−2.1195	−1.6092	−2.2111	−1.3129	−2.1932
21					−2.2382	−2.2373	−2.1020		−1.6152	
22							−2.2168		−2.1145	
23									−2.2217	

Table 3 (continued)

N° π-energy level (j)	**20**	**21**	**22**	**23**	**24**	**25**	**26**	**27**	4-nitro	4,4′-dinitro-
1	4.1968	4.1968	4.1968	4.1968	4.2065	4.2065	4.2065	4.2065	4.1872	4.1875
2	4.1877	4.1872	4.1872	4.1781	4.1781	4.1781	4.1781	4.1872	2.1895	4.1872
3	4.1781	4.1781	4.1781	2.2296	4.1779	4.1779	4.1779	4.1781	2.0612	2.1950
4	2.2110	2.2076	2.2068	2.1271	2.2166	2.4167	2.2498	4.1789	1.5411	2.0743
5	2.0901	2.0876	2.0868	1.6898	2.0806	2.1960	2.1739	2.2196	1.4999	1.5705
6	1.5421	1.5589	1.5706	1.5000	1.5411	1.9399	1.9729	2.0960	1.1702	1.4999
7	1.5000	1.5000	1.5000	1.4999	1.5000	1.5000	1.5123	1.5706	1.0000	1.4999
8	1.5000	1.5000	1.4999	1.3621	1.5000	1.5000	1.5000	1.5000	1.0000	1.2203
9	1.4999	1.4999	1.4999	1.0871	1.4999	1.4999	1.5000	1.4999	0.6184	1.0000
10	1.1958	1.2124	1.2338	1.0000	1.1919	1.4673	1.4999	1.4999	−0.4290	1.0000
11	1.0874	1.0825	1.0790	0.8908	1.1608	1.1608	1.6111	1.5000	−0.7753	0.6577
12	1.0690	1.0621	1.0000	0.4813	1.0000	1.0810	1.1608	1.2382	−1.0000	−0.3627
13	0.6632	0.6443	0.6802	−0.3935	0.6703	1.0000	1.0000	1.1607	−1.0000	−0.5941
14	−0.3248	−0.3729	−0.3202	−0.5905	−0.3522	0.6055	0.6557	1.0000	−1.2188	−0.8958
15	−0.5733	−0.5387	−0.5817	−0.8274	−0.4883	−0.3652	−0.3554	0.7116	−1.5512	−1.0000
16	−0.5928	−0.5926	−0.5970	−1.0000	−0.6613	−0.4883	−0.4883	−0.2959	−2.0569	−1.0000
17	−0.8275	−0.8064	−0.9087	−1.1688	−0.8815	−0.6628	−0.6617	−0.4883	−2.1868	−1.3012
18	−1.1393	−1.1181	−1.0000	−1.3033	−1.0000	−0.9077	−0.8881	−0.5932		−1.5838
19	−1.2078	−1.1903	−1.1815	−1.5788	−1.2674	−1.0000	−1.0000	−0.6796		−2.0652
20	−1.2796	−1.3082	−1.3272	−2.0820	−1.3004	−1.2937	−1.2737	−0.9921		−2.1895
21	−1.5527	−1.5715	−1.5838	−2.2036	−1.5513	−1.3004	−1.3004	−1.0000		
22	−2.0755	−2.0741	−2.0736		−2.0715	−1.5709	−1.5507	−1.3004		
23	−2.1984	−2.1963	−2.1958		−2.2001	−2.0852	−2.1747	−1.3304		
24						−2.2048	−2.2011	−1.5838		
25								−2.0805		
26								−2.2023		

— The increasing of the π-electron number (from 14 for unsubstituted stilbene to 20—30 for its derivatives) leads to the crowding of the π-energy levels and to the diminishing of the energy difference between two successive levels.

— The energy of the highest occupied MO in unsubstituted stilbene is $\alpha + 0.5819\ \beta$. This value is raised if :

— NO_2 and CN groups are introduced in one benzene ring and OH, OCH_3, $NHCOCH_3$ or NMe_2 groups in the second benzene ring;

— NO_2 and $CONH_2$ (or COOH) groups are introduced in one benzene ring and NMe_2 group in the second benzene ring;
and it is lowered if $CONH_2$ (or COOH) group and one or more nitro groups (or only nitro groups) are introduced in molecules.

Furthermore, on the basis of the values of the highest occupied MO energies, the approximate order of the HMO ionization potentials for our stilbene derivatives can be predicted as : **27, 22, 24, 20, 26, 21, 19, 3, 2, 10, 9, 25**, stilbene, **23, 7, 15, 14, 1, 8, 4, 5, 18, 11, 12, 16, 17, 6, 13.**

— The energy of the lowest unoccupied MO in unsubstituted stilbene is $\alpha - 0.5819\ \beta$. The introduction of any substituent in the molecule lowers this energy. If we take into account the above discussed raising of the highest occupied MO, the effect of the substitution, the diminishing of the corresponding energy difference associated with the $\pi - \pi^*$ transition, is evident.

2,4,6,4′-tetranitro-stilbene indicates the greatest diminution, whereas 2-cyano-4-nitro-4′-methoxy-stilbene the smallest one.

On the basis of the values of the lowest unoccupied MO energies, the following approximative order of the HMO electron affinities can be predicted as : **27, 22, 20, 10, 3, 24, 26, 9, 2, 25, 15, 7, 21, 19, 14, 23, 1, 4, 6, 8, 18, 16, 17, 11, 12, 13, 5**, stilbene.

THE ENERGY DIFFERENCE BETWEEN THE GROUND STATE AND THE FIRST ELECTRONICALLY EXCITED STATE

In comparison with unsubstituted stilbene, a diminishing of the energy difference between the ground and the first electronically excited states is observed for all studied stilbene derivatives, regardless of the number, nature or position of the substituents.

The energy difference for unsubstituted stilbene is 1.1638 β. This difference decreases for 2-cyano-4-nitro-4′-dimethylamino-stilbene at a value of 0.6865 β, which is the lowest value found in the present study and agrees with the increasing wavelength associated with the $S - S(\pi - \pi^*)$ monoelectronic transition from the highest occupied to the lowest unoccupied MO. In fact, this derivative has the greatest bathochromic shift of both A and B absorption bands in the ultraviolet spectrum, due to the presence of the two substituents with the strongest opposite electronic effects (NMe_2 and NO_2), at the extremities of the conjugated system, in the direction of the long axis of the molecule.[9]

In comparison with this derivative, the energy difference between the two states increases, remaining below the value corresponding to the unsubstituted stilbene when :

— one or both substituents (NMe_2, NO_2) at the p, p'-positions are replaced by the substituents having a weaker electronic effect;

— bulky substituents at o,o'-positions are introduced, regardless of their electronic effect;

— identical or different substituents, having the same kind of electronic effects, are introduced.

The smallest diminishing of the energy difference, in comparison with unsubstituted stilbene, appears at the derivatives having only nitro groups; regardless of the number and position of the nitro groups, the energy difference is about the same (1.00—1.04 β). As a matter of fact, their electronic absorption spectra show about the same bathochromic shift of the *A* band.

The wave-number of the absorption maximum corresponding to the A band can be correlated with the HMO energy difference between the ground and first electronically excited states (Table 4).

Table 4

The $\nu_{\max_A}$* (in cm^{-1}) and Δm (in β -units) values**

N°	$\nu_{\max_A}$	Δm	N°	$\nu_{\max_A}$	Δm
1	29410	0.6927	**17**	26670	0.7061
2	29760	0.9934	**18**	27320	0.7061
4	25320	0.6932	**19**	28090	1.0163
5	25640	0.6931	**20**	29410	0.9877
6	21550	0.6865	**21**	29410	1.0172
7	22520	0.8479	**22**	28410	1.0004
8	31850	0.7073	**23**	21010	0.8748
9	32260	0.9873	**24**	28570	1.0225
11	28990	0.7070	**25**	25000	0.9707
12	29410	0.7068	**26**	28570	1.0091
13	23260	0.6996	**27**	32260	1.0075
14	25000	0.8535	unsubstituted stilbene	34010	1.1638
16	27030	0.7040	4-nitro-stilbene	28570	1.0474
			4,4'-dinitro-stilbene	27170	1.0204

* $\nu_{\max_A}$ values were reported in a previous paper,[9] excepting the last two stilbenes taken from literature;[11]

** Δm values are calculated here for the derivatives No 1—28 of Table 1 and calculated again for unsubstituted stilbene, 4-nitro-and 4,4'-dinitro-stilbene, using the parameter values from Table 2.

The equations of the regression lines have the following general form: $\nu_{\max_A} = a + b\,\Delta m$. Accordingly:

— for the 2,4-dinitro-stilbene derivatives:

$$\nu_{\max_A} \times 10^{-4} = -2.54 + 5.37\ \Delta m;\quad r = 0.936;^{12}\quad n = 5;$$

— for the 2,4-dinitro- and 2,4,6-trinitro-stilbene derivatives:

$$\nu_{\max_A} \times 10^{-4} = 2.18 + 0.61\ \Delta m;\ r = 0.848;\ n = 9;$$

[11] H. Veschambre and A. Kergomard, *Bull. Soc. chim. France*, **1966**, 336.

[12] D. Ceaușescu, "Tratarea statistică a datelor chimico-analitice", Ed. tehnică, Bucharest, 1973, p. 225.

— for the 2-cyano-4-nitro-,2,4-dinitro- and 2,4,6-trinitro-stilbene derivatives, adding to these the unsubstituted stilbene, 4-nitro- and 4,4′-dinitro-stilbene :

$$\nu_{\max_A} 10^{-4} = 1.42 + 1.42\ \Delta m;\ r = 0.611;\ n = 19.$$

A linear dependence has not been obtained for 2-nitro-4-cyano-stilbene derivatives, a fact explainable if we take into account the degree of steric hindrance to coplanarity, already reported for these compounds.[9]

To conclude, the HMO π-energy levels picture of the studied stilbene derivatives undergo changes because of substituents, regardless of their number, nature or position. The substituents bring about a diminution of the difference energy between the ground state and the first electronically excited state, in comparison with the unsubstituted stilbene. This corresponds and correlates well with the bathochromic shifts of the *A* band in the electronic absorption spectra of these stilbene derivatives.

Revue Roumaine de Chimie, **22**, *8*, 1135–1143 (1977)

SOME NMDR EXPERIMENTS IMPROVED BY MEANS OF A COMPUTER

V. BĂRBOIU
The "P. Poni" Institute of Macromolecular Chemistry, Aleea Ghica Voda, 41A,
Iași, Romania

Received May 31, 1975

Some interesting Double Resonance experiments were carried out by means of a rapid electronic computer on-line connected to a c.w. NMR spectrometer. In this way, (1) the determinations of ^{14}N–NMR parameters from ^{1}H–{^{14}N} Indor curves were much improved. Results obtained for several amides dissolved in different solvents are given and discussed. There are also described several DR experiments using periodically pulsed r.f. fields. They referred to (2) the total decoupling in systems of strong coupled nuclear spins, (3) the removal of undesirable signals in spectra, and (4) the observation of DR effects in complex spectra.

It is well known that the computers have tremendously improved the sensitivity of NMR spectrometers by the slow and fast accumulation techniques (CAT and PFT respectively). The extraction of δ and J in complex spectra is also possible only by using trial and errors computer methods.

This paper is referred to several computer applications in Double Resonance (DR) experiments. A JNM–C–60HL (60 MHz) spectrometer and a JEC–6 spectrum computer were used, but any other spectrometer-computer system can be used if the computer is able to read and generate analogous signals. In fact, most of experiments described below are periodically pulsed NMDR experiments. The idea to carry out such experiments is rather old,[1,2] and a theoretical treatment has been made on the appearance of the observed signals.[3] As it will be shown further on, such experiments can be much improved if an electronic computer is used for the modulation control of r.f. fields and for the processing of spectrometer output.

CONNECTIONS BETWEEN SPECTROMETER AND COMPUTER

Several connecting modes between the JEC–6 computer and some of the components of JNM–C–60HL NMR spectrometer are schematically drawn on figure 1. A. The standard connections to achieve the

---

[1] S. L. Gordon and J. D. Baldeschwieler, *J. Chem. Phys.*, **41**, 571 (1964).
[2] R. S. Milner and D. W. Turner, *Chem. Comm.*, **1965**, 31.
[3] S. L. Gordon, *J. Chem. Phys.*, **48**, 2129 (1968).

CAT technique are noted by c.l.. The pulsed voltage P_1, the ON and OFF periods which are adjustable by programming, command the Ox motion of the recorder pen, and of course the sweeps of the static magnetic field (H_0), the observing frequency (ν_1) or the irradiating frequency (ν_2). By means of P_1, the computer can successively accumulate spectra swept by field or observing frequency and spectra with ν_2 swept (Indor spectra).

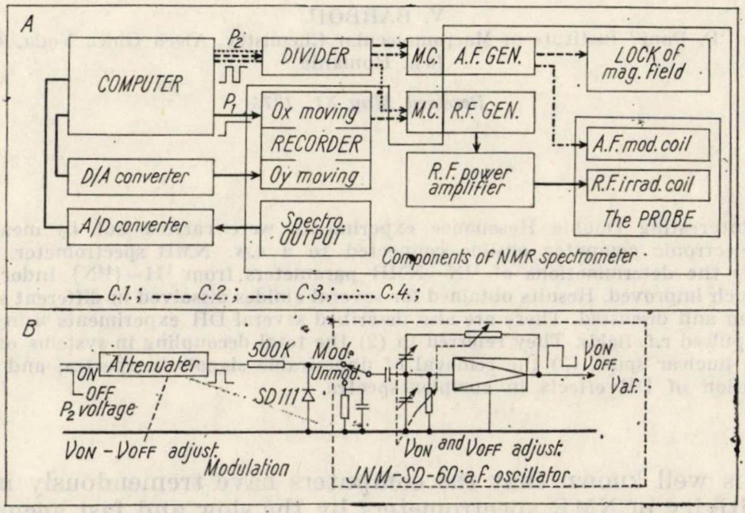
A
COMPUTER
P_2
P_1
DIVIDER
M.C.
A.F. GEN.
LOCK of mag. field
Ox moving
M.C.
R.F. GEN.
RECORDER
A.F. mod. coil
D/A converter
Oy moving
R.F. power amplifier
R.F. irrad. coil
A/D converter
Spectro. OUTPUT
The PROBE
Components of NMR spectrometer
C.1.; C.2.; C.3.; C.4.;
B
ON
OFF
P_2 voltage
Attenuater
500K
Mod.
Unmod.
SD111
V_{ON}
V_{OFF}
$V_{a.f.}$
V_{ON} - V_{OFF} adjust.
Modulation
V_{ON} and V_{OFF} adjust.
JNM-SD-60 a.f. oscillator

Fig. 1.— Connections between the NMR spectrometer and the computer to perform various types of pulsed DR experiments (*A*) and the pulse frequency modulation of an a.f. oscillator (*B*). Used notations:

c1 – standard connections, c2 – connections for heteronuclear Indor experiments, c3 – connections for homonuclear ON – OFF irradiations, c4 – connections for heteronuclear ON – OFF irradiations, M.C. modulation circuits.

Another pulsed voltage, noted by P_2, was used to modulate the frequency of various a.f. or r.f. generators. Actually, P_2 is one of the voltages energizing the relays which permit to the JEC–6 computer to successively control different apparata. To get rectangular pulses, the exciting coil of the relay was replaced by a pure resistor. Some of the P_2 characteristics are the following: the increasing and decreasing times are shorter than 1msec, the level ON is of about +5 V and the level OFF of few mV, and the periods ON and OFF can be adjusted by programming.

Figure 1.B. shows schematically how the frequency of an a.f. RC generator (which was of JNM–SD–60 type for our experiments) is modulated by P_2. The attenuator, which is a common resistor divider, is necessary to adjust the difference $|\nu_{ON} - \nu_{OFF}|$. The maximum value obtained for this difference was of about 70–80 Hz for frequencies around 4 KHz. (The frequency of side bands for JNM–C–60HL spectrometer is of 4000 Hz or near.)

Some experiments required a slow modulation of the r.f. irradiating frequencies. The standard JEOL r.f. generators JNM–RH–N–60A (4MHz) and JNM–RH–C–60A (15 MHz) were used in these experiments. The frequency modulation was performed by inserting a varicap diode into the pilot crystal circuits, and supplying the diode with the voltage P_2 suitably attenuated. The maximum modulation for the entire amplitude of P_2 is of several hundreds Hz for 4 MHz frequencies and of several KHz for 15 MHz frequencies.

THE ACCUMULATION AND COMPUTER PROCESSING OF HETERONUCLEAR INDOR SPECTRA : $^1H-\{^{14}N\}$ IRRADIATIONS TO DETERMINE THE SPECTRAL PARAMETERS OF ^{14}N NUCLEUS

It is known that the nucleus ^{14}N is a hardly observable nucleus because of its relatively small magnetic moment and the exaggerated broadening of its resonances due to the electric relaxation, which is very fast in most of the molecules. (The nucleus ^{14}N has got a quadrupole electric moment, its spin being equal to 1). However, it is possible to indirectly observe the NMR spectra of this nucleus by using DR effects in which ^1H or ^{19}F signals are observed and the nucleus ^{14}N is irradiated.[4-7] Of course, it is absolutely necessary that the observed and irradiated nuclei should be in interaction, and theseinteractions must affect the observed spectra.[6]

Such determinations are already reported for the ^{14}N resonance frequency by using the total decoupling $^1H - \{^{14}N\}$[4-7].

A more recent paper [8] shows how the selective decoupling $^1H - \{^{14}N\}$ carried out at moderate and low irradiation levels can be used to obtain all spectral parameters (resonance frequency, magnitudes and signs of coupling constants) for the nitrogen nucleus of formamide. It was also established there that the most convenient method to observe such selective decoupling effects is the Indor technique. The main disadvantage is that the precision of determination for the maxima positions, and thus for the parameters of irradiated nuclei, is quite low because these Indor spectra show broad maxima and the S/N ratio is usually too low. (The molecule of formamide particularly shows relatively sharp $^1H - \{^{14}N\}$ Indor maxima, and for this reason the ^{14}N NMR study on this molecule is experimentally easier than for other molecules containing the nitrogen atom in asymmetrical groups.)

A computer procedure will be shown below which improves this precision and eliminates some possible subjective errors. To make a short presentation, the illustration will be made for the Indor curves of A_3 and A_4 proton lines of formamide (see fig. 2). The interpretation of the $^1H - \{^{14}N\}$ selective decoupling spectra of this molecule is already made

---

[4] Hirotake Kamei, *Japan J. Appl. Phys.*, **4**, 212 (1965); Hirotake Kamei, *Bull. Chem. Soc. Japan*, **38**, 1212 (1965); Hirotake Kamei, *Bull. Chem. Soc. Japan*, **41**, 1030 (1968).

[5] R. J. Chuck, D. G. Gillies and E. W. Randall, *Mol. Phys.*, **16**, 121 (1969).

[6] P. Hampson and A. Mathias, *Mol. Phys.*, **11**, 541 (1966).

[7] P. Hampson and A. Mathias, *Mol. Phys.*, **13**, 361 (1967).

[8] V. Barboiu, *Mol. Phys.*, **28**, 707 (1974).

in the reference 8, where it is also concluded that (1) the distance between the main maxima of these two curves is just equal to J_{KX}, and (2) the distance between the secondary and main maxima of the same curve is equal to $J_{MX} - J_{AX}/2$.

EXPERIMENTAL

The $^1H-\{^{14}N\}$ Indor spectra were obtained by keeping the resonance condition fixed on each proton line and recording the intensity dependence upon the irradiating frequency. This frequency was obtained from a standard JEOL 4 MHz generator of JNM—RH—N—60A type, the local oscillator of which was modified to achieve a frequency sweep simultaneous with the motion of recorder pen (see ref. 8 for more details).

The voltage P_1 (fig. 1 a) assures the computer control for the pen motion, and, in this way, the computer is able to read and successively accumulate the Indor curves. One curve can be evidently stored into the computer memory by a CAT technique, a number of scans being necessary to get a good S/N ratio. After the accumulation job is executed, the computer can be programmed to do an additional smoothing of the read curve and to determine its maxima positions.

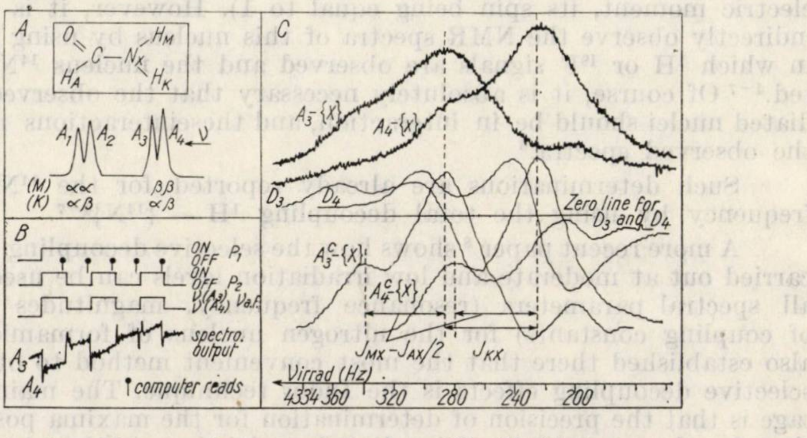

Fig. 2. — The computer processings of two $^1H-\{^{14}N\}$ Indor curves of formamide to find the NMR parameters of ^{14}N nucleus:

A, the spin state assignment for the formyl proton lines, *B*, sequences of P_1, P_2 and audio frequency for magnetic field lock, and the corresponding spectrometer output, and *C*, original $A_3, A_4 - \{X\}$ Indor curves, their derivatives and the curves with the resolution enhanced by computer.

It was however observed that these processings cause a systematic error in the determination of maxima positions, and, for this reason, it was concluded it was indicated to simultaneously read two or more Indor curves. If the same processings are made for all these curves, the above error is eliminated from the distances between their maxima, and thus from the coupling constants values. The procedure is explained on figure 2 for the two Indor curves of formamide: $A_3-\{X\}$ and $A_4-\{X\}$. Figure 2 b illustrates how the two curves are in the same time deposited in the computer memory. The voltage P_2, which is only generated when the irratiating frequency is swept at a suitable rate (and this happens when P_1 is ON), modulates the frequency of a SD—60 a.f. oscillator according to figure 1.B. This audio frequency is used to get the lock signal for the static magnetic field. The frequencies ν_{ON} and ν_{OFF} are adjusted so as to correspond to the resonance conditions for A_3 and A_4 lines respectively. In other words, the voltage P_2 permits to the computer to read alternatively the curves $A_3-\{X\}$ and $A_4-\{X\}$, the reading being made at the end of each ON and OFF periods of P_2.

These periods, evidently equal to each other, must be long enough for the recovery of observed signals to be complete. Therefore, their length of time depends on the relaxation rate of the observed spins. It was found that periods of 2 seconds are long enough for the analysed sample of 15 mol per cent aqueous solution of formamide.

The curves $A_3-\{X\}$ and $A_4-\{X\}$ on figure 2c are the single scan ones. A sensitivity improvement of $\sqrt{n}$ times can be obtained if the number of scans is taken equal to n. Additional smoothings were achieved by means of the computer, using the simple local artihmetical average.

After the smoothing job was executed, the computer was instructed to calculate the differentials of curves. The distance between the main maxima, which is equal to J_{KX}, was determined as the distance between the zero points of differential curves with a precision of about ±1 Hz. Note that this precision is about ±5 Hz if the original Indor curves are used.[8] Additionally, the possible subjective errors, which appear when the original curves are used, are excluded. The differentiation program is based on the formula :

$$F' = h^{-1}(D^{(1)} - D^{(2)}/2 + D^{(3)}/3 - \ldots.),$$

where $D^{(i)}$ is the difference at right of "i" order, and "h" is the elemental interval.

Another computer processing was the resolution enhancement of the analysed curves. It was achieved by means of a standard JEOL program based on the formula $F - k \cdot F''$, k being an optional subunit. The curves $A^{c}_{3,4} - \{X\}$ on figure 2c were obtained with $k = 0.5$. One observes that the secondary maxima become enough resolved to measure their distances from the main maxima. The value of 55 ± 5 Hz, found for both distances, corresponds to the value of $J_{MX} - J_{AX}/2$, and therefore supports the explanation of the secondary maxima origin advanced in reference 8.

The computer method described before for the determination of one of the $J(^{14}N, {}^{1}H)$ couplings in formamide is generally utilizable for ^{14}N NMR studies on many other molecules showing non-zero hydrogen-nitrogen coupling constants. The method is evidently of interest when the proton spectra do not show hydrogen-nitrogen splittings due to a very rapid relaxation of ^{14}N nucleus. To make complete determinations of ^{14}N parameters (resonance frequency and coupling constants), the investigated nitrogen nucleus must be coupled with two or more non-equivalent protons (or ^{19}F nuclei). Otherwise, the resonance frequency is only determinable.

SOME PRELIMINARY RESULTS

The table below contains the nitrogen chemical shifts values obtained by the method described before for several amides dissolved in different solvents. There is a good agreement between these values and the previous observations and suppositions,[6,7,9] and, additionally, the measurement precision was good enough to observe some solvent and concentration dependences. For example, it was found that the shielding of ^{14}N nucleus in amides decreases when the solvent is changed in the following series : acetic anhydride — acetone — water. The explanation for this is that the percentage of the charge-separated structure 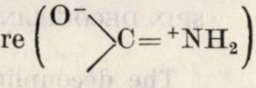 $\left({}^{O^-}_{\ }\!\!>C={}^{+}NH_2\right)$ relative to the non-charged form 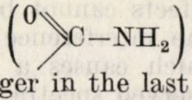 $\left({}^{O}_{\ }\!\!>C-NH_2\right)$ increases in the same mode, and the ^{14}N shielding is larger in the last form.[6] The equilibrium between the two forms depends on the solvent-solute interactions, the charge-separated form being favoured in water solutions where HO—H... ORC—NH_2 hydrogen bonds are possible, and the other form being favoured by the existenec of ORC—NH_2... $O{=}C\langle$ hydrogen bonds.

[9] D. Herbison-Evans and R. E. Richards, *Mol. Phys.*, **8**, 19 (1964).

The table with ^{14}N NMR parameters

Compound	Solvent	* Conc. mol %	** Shifts ppm	$^1J(^{14}N, ^1H)$ in Hz J_{KX}	$^1J(^{14}N, ^1H)$ in Hz J_{MX}
Formamide	Pure liquid		0.0	$+66\pm2$	$+63\pm2$
Formamide	Acetone	13.5	$+4.5\pm0.5$	idem	
Formamide	Water	14.5	-2.0 ± 0.5	idem	
Acetamide	Water	7	$+0.5\pm1$	idem	
Acetamide	Acetone	8	$+6.5\pm1$	idem	
Acetamide	Acet. anh.	8	$+9.5\pm1$	idem	
Acrylamide	Water	4	$+11.5\pm2$	idem	
Thioacetamide	Water	4	-48.5 ± 1	$+63\pm1$	$+63\pm1$
Thioacetamide	Acetone	5	-39.5 ± 0.5	idem	
Thioacetamide	Acet. anh.	5	-32.5 ± 1	$+74\pm3$	$+68\pm3$

* NMR determinated. ** Related to the pure formamide, the ^{14}N resonance frequency of which being equal to 4334582 Hz when the TMS proton resonance frequency is exactly equal to 60 MHz. The sign "−" implies a downfield shift.

This fact also explains why the nucleus ^{14}N is more shielded in oxyamides than in thioamides, the charge separated structure being more probable in thioamides because the electronegativity of sulphur atom is lower than that of oxygen atom.[7]

The coupling constants $^1J_{^{14}N, ^1H}$ were found to have the same values for all amides, excepting the thioacetamide in acetic anhydride solutions, where the values are visibly larger.

It is to mention that the method described before can be also applied for indirect observations of ^{13}C nucleus, but the tickling effects of ^1H (or ^{19}F) $-\{^{13}C\}$ type are more advantageous in this case because the nucleus ^{13}C has the spin number equal to 1/2, and therefore the lines are not affected by broadening quadrupolar effects.[10]

ALTERNATIVE ON-OFF RESONANCE IRRADIATIONS

In many cases, especially in complex spectra, the double resonance effects are hardly observable and thus interpretable. It will be shown below how a digital computer can be used to improve the observation of such effects.

SPIN DECOUPLING EXPERIMENTS IN STRONG COUPLED SPIN SYSTEMS

The decoupling effects cannot be well observed in strong coupled spin systems due to the interference between the observing and irradiating frequencies, which causes a lot of noise and seriously affects the base line in the observed spectra. These difficulties can be removed if the irradiation is alternatively ON−OFF resonance switched and the receiver is only open in the periods OFF. The OFF irradiating frequency must be taken sufficiently far from the observing frequency to avoid their interference.

---

[10] W. McFarlane, *Ann. Rev. NMR Spectroscopy*, **1**, 15 (1966); V. I. Kowalewski, *Progr. NMR Spectroscopy*, **5**, 1 (1969).

Experimental. The modulation of irradiating frequency was made by means of the pulsed voltage P_2, the two audio-frequencies ν_{ON} and ν_{OFF}, obtained at the output of JNM—SD—60 oscillator (fig. 1.B), being then used to modulate the 60 MHz field to create the two r.f. fields for ON and OFF resonance irradiations. The voltage P_2 was in the same time used to switch OFF—ON the input of receiver. This commutation was simply achieved by a gate transistor inserted between the r.f. detector and the a.f. receiver amplifier and fed with the voltage P_2.

The programming was made so that both ON and OFF periods of P_2 may be adjustable, and the computer may do one reading at the end of each OFF period. Of course, the persistency of the decoupling effects, after the irradiation is switched OFF, depends on the relaxation rate of irradiated nuclear spins, and for this reason the OFF periods were taken 5—10 times shorter than the ON periods. The length of time for ON periods has not a critical value, but, to avoid the satellites on P_2 repetitive frequency in the observed spectra, the total period of P_2 must be longer than $1/(\Delta\nu)$, $(\Delta\nu)$ being the width of the observed lines. On the other hand, this total period (which is the sum of ON and OFF periods) must not be too long because the recording time becomes too long.

Figure 3C shows, for example, the signal of methylene protons in polyacrylonitril (PAN) decoupled from the methine protons ($\Delta\delta/J \sim 7$-5) by using this ON—OFF irradiation technique. One observes that the decoupled signal is not a single line, but a doublet. A splitting like this can be interpreted as arising from the iso- and syndiotactic diads, and therefore it is possible to estimate the relative numbers of these diads for PAN. Such estimations cannot be made by any other method using 60 MHz proton spectra. It is true that the problem of PAN tacticity has already been resolved yet using ^{13}C spectra.[11]

ON—OFF decoupling experiments can be carried out evan in systems where $\Delta\delta/J = 2-3$. Such an experiment was carried out for the AA′BB′ system of benzimidazole ($\Delta\delta/J \sim 3$). The decoupled signal is a single line in both AA′—{BB′} and BB′ — {AA′} experiments. This fact demonstrates that *the magnetical non-equivalence of (say) A and A′ spins exists as long as their scalar interactions with the spins B and B′ are not annihilated.*

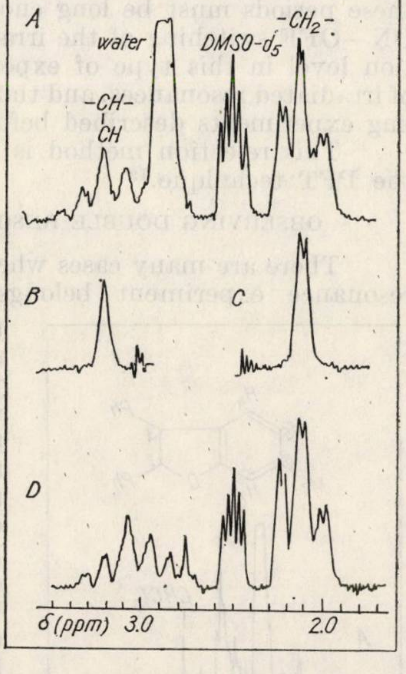

Fig. 3. — An illustration of DM experiments with ON—OFF irradiation: *A*, the normal spectrum of PAN dissolved in DMSO-d_6, *B*, the methine signal decoupled from the methylene protons, *C*, the methylene signal decoupled from the methine protons, and *D*, the spectrum in A but with the water signal ON—OFF saturated. (The length of time for the ON periods was taken equal to 2 seconds in all experiments with ON—OFF irradiation.)

THE REMOVAL OF UNDESIRABLE SIGNALS IN SPECTRA

Figure 3a shows the normal proton spectrum of PAN dissolved in DMSO—d_6. It is known that the DMSO easily hydrates, the signal on the high field side of methine multiplet arising from the water protons. It is possible to diminish or just eliminate this signal if it is alternatively ON—OFF saturated and the PAN proton spectrum is read at the end of each OFF period (fig. 3 D). This cleaning method can be evidently applied when the relaxation of irradiated nuclei is much slower than that of observed nuclei, and it is especially useful in the study of biological macromolecular compounds which either contain much water or the water is used as a solvent.

---

[11] V. D. Machel, *J. Macromol. Sci.-Revs. Macromol. Chem.*, **C8**, 289 (1972).

The rejection of undesirable signals being based on the saturation effects of these signals, the periods OFF must be short enough so that the saturation may remain complete at their ends. On the other hand, these periods must be long enough to avoid the transient effects at the ON–OFF switching of the irradiating frequency. Of course, the irradiation level in this type of experiments must only assure the saturation of irradiated resonances, and thus it is much lower than that in the decoupling experiments described before.

This rejection method is especially practicable in connection with the PFT technique.[12]

OBSERVING DOUBLE RESONANCE EFFECTS IN COMPLEX SPECTRA

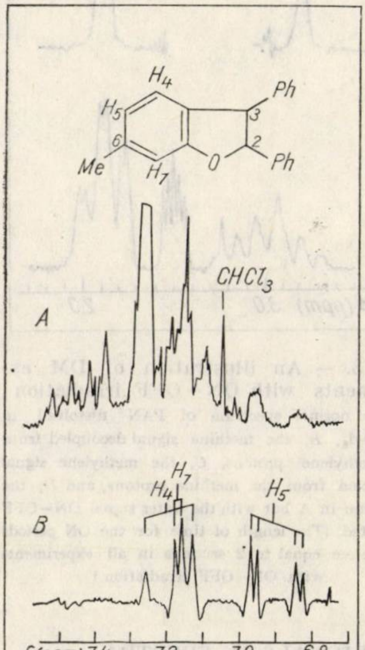

Fig. 4.—An illustration of the DR observation in very complex spectra : *A*—the normal spectrum of aromatic protons, and *B*—the spectrum in A when the methyl signal is strongly irradiated by the ON—OFF technique. (The length of time for both ON and OFF periods was taken equal to 2 seconds.)

There are many cases where the signal(s) to be observed in a double resonance experiment belongs to a complex spectrum part, and thus the effects of irradiation on different signals connected to it are difficult or just impossible to be observed and clearly interpreted. An improvement can be obtained if an ON–OFF irradiation technique, in which the computer reads the spectrometer output in both ON and OFF periods, is used. The difference between the readings ON and OFF, which can be easily made by a computer, will be different from zero only for the spectral lines connected with the irradiated line(s). A difference spectrum like this can be easily interpreted although its pattern is generally complicated.

It is evident that the periods ON and OFF in such experiments must be of the same length of time. This length of time depends on the relaxation rates of irradiated and observed nuclear spins. It must be long enough so that the spin system states to be "completely disturbed" and "completely undisturbed" at the ends of ON and OFF periods respectively, when the computer reads the spectrometer output.

Figure 4 B shows, for example, the difference between the aromatic proton spectra obtained for 2,3-diphenyl-6-methylbenzofuran (a NMR study of this

compound has already been made [13]) when the methyl resonance is ON and OFF irradiated. Taking into account the chemical structure of this compound, it results that the signals of "fused ring" protons (H_4, H_5 and H_7) will be only affected by the irradition on methyl-6 signal. The spectrum of these three protons is evidently expected to be an ABK, and the ON–OFF methyl decoupled spectrum (fig. 4.B) indicates clearly this supposition. It is very easy to do the assignment of lines for the spectrum 4.B because it is known that $J^{ortho} > J^{metha} > J^{para}$ in an aromatic system.

---

[12] *JEOL News*, **10**, 13 (1973).

The methyl irradiation effects for the H_4 lines are weaker than those for H_5 and H_7 lines because $J_{H_4,Me}$ is smaller than both $J_{H_5,Md}$ and $J_{H_7,Me}$. This explains why the lines of H_4 in 4.B spectrum are relatively weaker than the lines H_5 and H_7.

This technique is especially useful to detect the nuclear Overhauser effects when the observed signals are masked by other complex signals. In such experiments, the irradiation level is evidently lower than in decoupling experiments, and therefore the difference spectrum is quite simple.

Another utilization of this ON–OFF irradiation technique is for heteronuclear systems, for example to facilitate the observation of proton lines due to the $^2J_{^{13}C,^1H}$ geminal couplings. These lines are usually masked by the very strong signals arising from the molecules containing the isotope ^{12}C. The procedure, where the ^{13}C signals are ON–OFF irradiated and the ^1H signals observed, was initially used by Freeman.[14] The difference proton spectrum in these experiments contains only the lines arising from the ^{13}C molecules, and therefore the coupling constants $J_{^{13}C,^1H}$ and the ^{13}C resonance frequencies are easily determinable.

It is to mention that the CAT technique can be used to improve the signal-to-noise ratio in all the double resonance experiments using alternative ON–OFF irradiating techniques. This can be simply achieved by using a suitable number of P_1 periods (see fig. 1 a). To succeed in such experiments, the internal lock of magnetic field is absolutely necessary to assure a sufficiently high stability for the field/frequency ratio.

---

[13] V. BARBOIU, H. WEXLER and B. ARVENTIEV, *Org. Mag. Res.*, **6**, 327 (1974).
[14] R. FREEMAN, *J. Chem. Phys.*, **43**, 3087 (1965).

Revue Roumaine de Chimie, **22**, *8*, 1145–1150 (1977)

STUDIES ON CONDUCTIVITIES OF SOME IONIC SURFACTANTS IN AQUEOUS METHANOL

L. R. SINGH,* P. BAHADUR ** and S. N. SRIVASTAVA,**
* Chemistry Department, B.S.A. College, Mathura, (U.P.), India
** Chemistry Department, Agra college, Agra, (U.P.), India

Received May 5, 1975

Conductivities of solutions of some surfactants (both anionic and cationic) in water-methanol mixtures of various composition have been measured at 30° and critical micelle concentration (CMC) determined. The equation :

$$\log \mu = A + B \log C$$

holds good for all surfactants.

1. INTRODUCTION

Conductivities of metallic soaps and anionic surfactants have been measured by several workers.[1-3] However, the data on cationic surfactants are rather scarce. In the present report, the conductivity behaviour of some cationic surfactants with varying chain length and head group sizes has been studied over a wide range of water-alcohol mixture and surfactants themselves. Sodium lauryl sulphate, an anionic surfactant, has also been used in conductivity measurements for comparison.

EXPERIMENTAL

The Surfactants Cetyl pyridinium bromide (CPB), Cetyl trimethyl ammonium bromide (CTAB), Lauryl pyridinium chloride (LPC) and Sodium lauryl sulphate (SLS) were all BDH chemicals. Methanol was E. Merck GR grade Chemical. Water used was always doubly distilled.

Conductivities of various water-methanol mixtures in presence of varying amount of surfactants were measured by the use of simple conductivity bridge (PHILIPS PR 9500) and dipping (TYPE : PV 9055) conductivity cell with platinized electrodes. All the data were recorded at a constant temperature 30°.

[1] R. P. Verma and P. Bahadur, *Indian J. Chem.*, **10**, 1189 (1972).
[2] K. N. Mehrotra and S. C. Bhargava, *Z. phys. Chem. (Leipzig)*, **239**, 17 (1968).
[3] S. S. Bhatnagar and M. Prasad, *Kolloid-Z.*, **34**, 193 (1924).

RESULTS AND DISCUSSION

The specific conductance, K, of surfactant solutions in aqueous methanol of different composition has been measured at 30° and is plotted as a function of surfactant concentration in Figs. 1—4. All the figures are characterized by an intersection of two straight lines at CMC of the surfactant, which are 1.6×10^{-2}, $6{,}5 \times 10^{-4}$, 10.2×10^{-4} and 8.4×10^{-3}M for lauryl pyridinium chloride, cetyl pyridinium bromide, cetyl trimethyl ammonium bromide and sodium lauryl sulphate respectively. These values are very close to those reported earlier.[4] It is seen from the graphs that the CMC's of surfactants are independent of the composition of water-methanol mixture. CMC values may also be obtained by plotting the graph between molecular conductivity, μ, and surfactant concentration, C (Fig. 5). The decrease in molecular conductivity of the surfactant solution with increase in concentration might be due to the tendency of the surfactants to form aggregates at higher concentration.

In Fig. 6 the values of molecular conductivity, μ, are plotted against volume per cent of methanol and μ values are found to decrease almost linearly as volume of methanol increases to 50%. Above 60% of methanol concentration, the μ values again increase with further increase in methanol concentration. It appears that the change in nature of solvent takes place above 50%.

From the nature of the plots of log C versus log μ (Fig. 7) it is observed that the conductivity can be related to the surfactant concentration by the equation:

$$\log \mu = A + B \log C$$

where A and B are constants. The values of log μ for zero values of log C (i.e., for $C = 1$M) have been found by extrapolation for all the surfactants and the values of $\mu_{c=1}$ and the constant B have been reported in Table 1. It was however not possible to prepare the molar solution of surfactants in water, methanol or even water-methanol mixture.

Table 1

Extrapolated values of $\mu_{c=1}$ and constant B

Volume % of Methanol	LPC		CTAB		CPB		SLS	
	$\mu_{c=1}$	B	$\mu_{c=1}$	B	$\mu_{c=1}$	B	$\mu_{c=1}$	B
10	38.64	0.1339	30.20	0.1219	28.51	0.1472	31.26	0.0814
20	35.65	0.0972	27.23	0.1192	23.99	0.1443	29.17	0.0705
30	33.11	0.0953	24.27	0.1166	21.38	0.1443	26.61	0.0669
40	—	—	22.13	0.1166	18.84	0.1386	24.83	0.0633
50	27.23	0.0927	21.63	0.1113	17.38	0.1357	23.99	0.0598
60	27.23	0.0927	21.13	0.1061	16.79	0.1328	23.71	0.0598

---

[4] P. Mukerjee and K. J. Mysels, "Critical Micelle Concentrations of Aqueous Surfactant Systems" NSRDS-NBS-36 (1971).

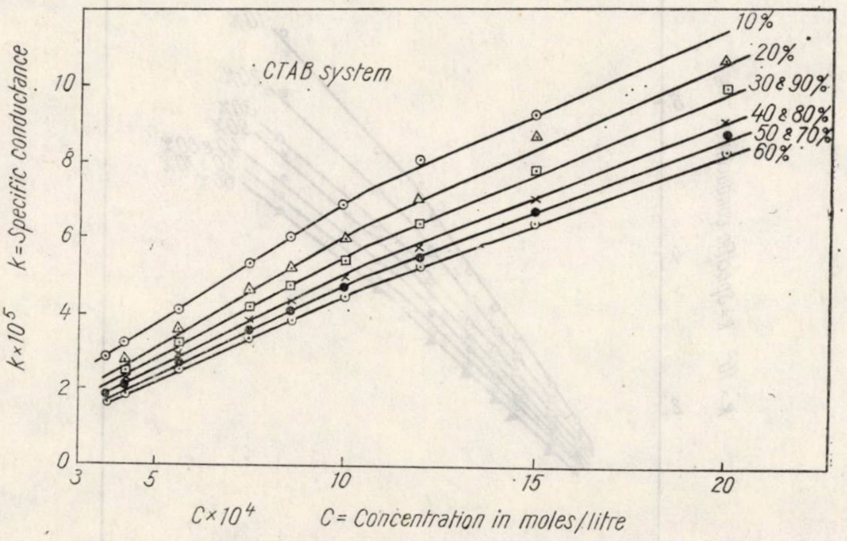

Fig. 1. — Specific conductance vs. molar concentration of CTAB.

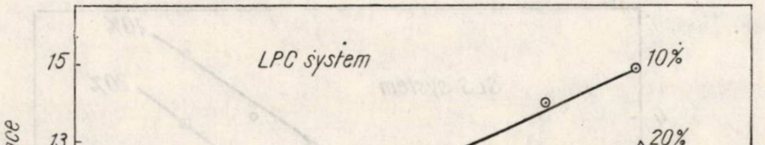

Fig. 2. — Specific conductance vs. molar concentration of LPC.

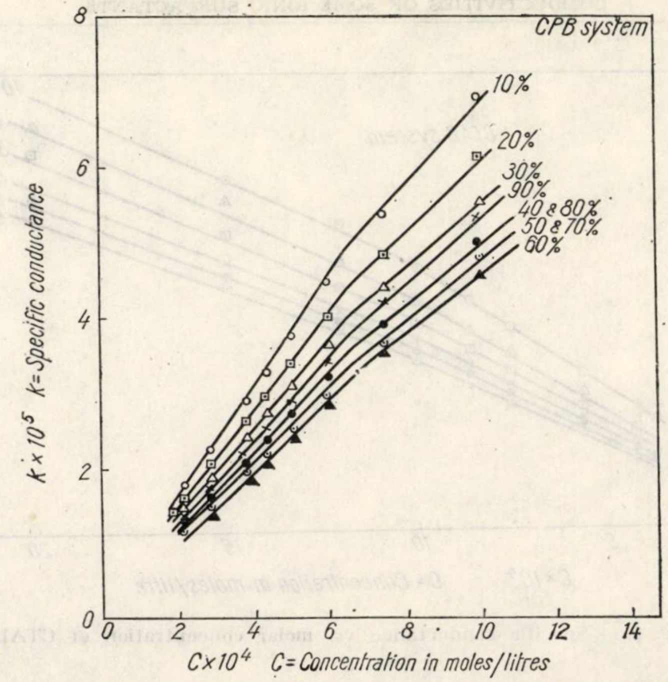

Fig. 3. — Specific conductance vs. molar concentration of CPB.

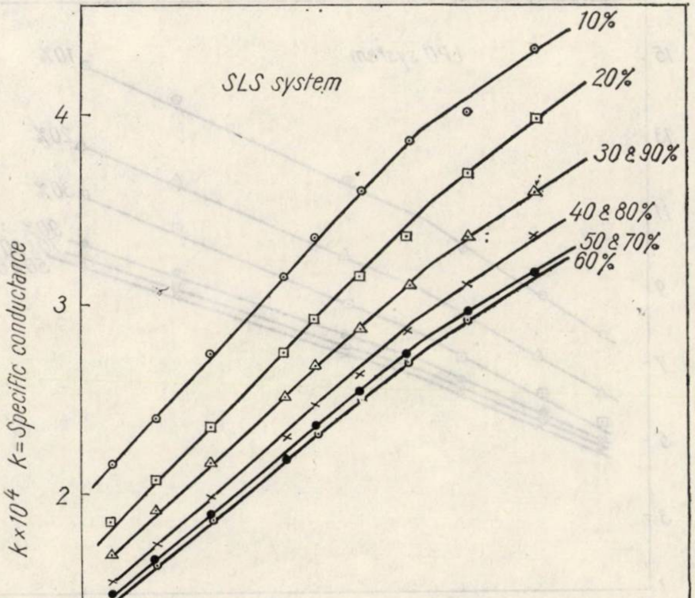

Fig. 4. — Specific conductance vs. molar concentration of SLS.

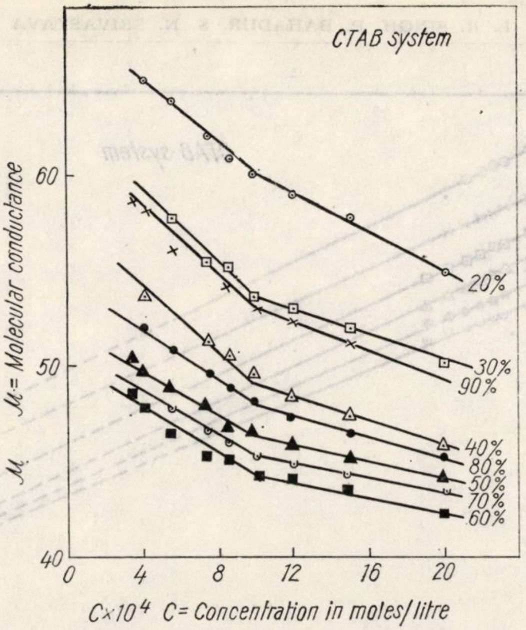

Fig. 5. — Molecular conductance vs. molar concentration of CTAB.

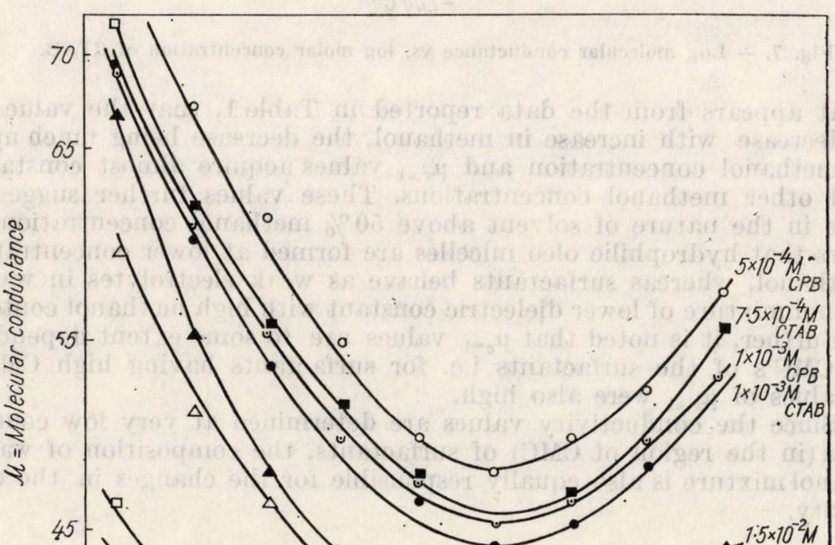

Fig. 6. — Molecular conductance vs. solvent composition as a function of surfactants concentration.

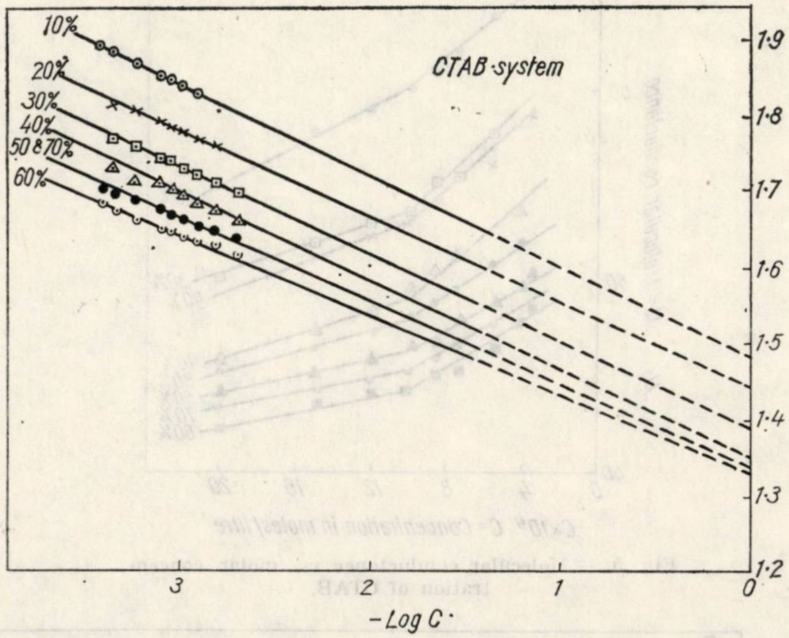

Fig. 7. — Log molecular conductance vs. log molar concentration of CTAB.

It appears from the data reported in Table 1, that the values of $\mu_{c=1}$ decrease with increase in methanol, the decrease being much up to 50 % methanol concentration and $\mu_{c=1}$ values acquire almost constancy for all other methanol concentrations. These values further suggest a change in the nature of solvent above 50 % methanol concentration. It appears that hydrophilic oleo micelles are formed at lower concentration of methanol, whereas surfactants behave as weak electrolytes in water-methanol mixture of lower dielectric constant with high methanol content.

Further, it is noted that $\mu_{c=1}$ values are to some extent dependent upon CMC's of the surfactants i.e. for surfactants having high CMC's, the values of $\mu_{c=1}$ were also high.

Since the conductivity values are determined at very low concentration (in the region of CMC) of surfactants, the composition of water-methanol mixture is also equally responsible for the changes in the conductivity.

Revue Roumaine de Chimie, **22**, *8*, 1151–1164 (1977)

IRREVERSIBILITY OF THE PITTING PROCESS

SULTANA CIOLAC
Institute of Physical Chemistry,
Str. Galați 31, Bucharest, Romania

Received April 23, 1975

The existence of two potentials characterizing the initiation (critical pitting potential, E_{cp}) and growth of pits (potential of pits repassivation, E_{rp}) is considered as a proof of the irreversibility of the pitting process. The extent of the pitting irreversibility (ΔE) is defined by the difference $E_{cp}-E_{rp}$. Our own results and the available data from the literature are used to assess the effect of the environment and metallic composition on ΔE. It is shown that the role of alloying constituents changes through the different stages of pitting development. It is suggested that the methods of protection against pitting should be directed to cutting to a minimum the extent of pitting irreversibility. The use of ΔE as a criterion of metals classification in respect with their behaviour is proposed.

Throughout a few decades the critical pitting potential has been considered as the most proper parameter to give information concerning the pitting behaviour of passivable metals.

Although explained in different ways from electrochemical and thermodynamical points of view,[1] the critical pitting potential has been extensively used as an index to pitting resistance. The protection against pitting was considered to be assured by the capacity of metals to maintain their passive state below the critical pitting potential.

The reserves shown in the acceptance of "the protection potential against pitting" defined in 1970 by Pourbaix,[2] come from the implications brought along with the new parameter into the pitting corrosion studies and the lack of experimental data in its support.

The earlier results obtained from the examination of some stainless steels (compositions shown in table 1) that are centralized in table 2, as well as some recent data concerning the inhibition of pitting corrosion produced on the same metals prove that there exist two potentials characterizing the process of pitting.

Parameters like critical pitting potential (E_{cp}), induction time (t_i) and potential of pits repassivation (E_{rp}) were established by using potentiostatic and galvanostatic techniques as elsewhere described.[3-5]

[1] S. Szklarska-Smialowska, *Corrosion*, **27**, 223 (1971).

[2] M. Pourbaix, *Corrosion*, **26**, 431 (1970).

[3] S. Ciolac and E. Vasilescu, *Rev. Roumaine Chim.*, **20**, 739 (1975).

[4] S. Ciolac and E. Vasilescu, *Rev. Roumaine Chim.*, **20**, 749 (1975).

[5] S. Ciolac, *Rev. Roumaine Chim.*, **20**, 1057 (1975).

Table 1

The chemical compositions of stainless steels (w/o)

Type of steel	C	S	P	Si	Mn	Cr	Ni	Ti	Mo	Fe
FeCr	0.04	0.016	N.D.	N.D.	0.71	13.95	—	—	—	balance
CrNi	0.04	0.012	0.01	0.64	0.71	19.43	8.09	—	0.016	,,
CrNiTi	0.05	0.007	0.03	0.4	1.34	17.76	8.79	0.52	0.07	,,
CrNiTiMo	0.08	0.01	0.02	0.09	1.82	16.90	11.90	0.7	2.36	,,

N.D. not determined

Table 2

Comparative examination of pitting electrochemical characteristics as function of the electrolyte composition

Variable	Type of dependence		
	E_{cp}	t_i	E_{rp}
Cl^- ions concentration	$E_{cp} = a - b \log a_{Cl^-}$	$1/t_i = ct. C_{Cl^-}^{-8}$	independent
°T	exponential (t_i more sensitive than E_{cp})		exponential
acidic pH $+ H_2SO_4$	exponential (t_i more sensitive than E_{cp})		independent
alkaline + KOH	maximum value at pH ~ 9.5		independent
content in nonaggressive additions	$E_{cp} = a + \log a_{Inh^-}$	—	$E_{rp} = E_T$ for total inhibition $E_{rp} \leqslant E_{st}$ for insufficient additions

E_{st} – rest potential; E_T – transpassive potential.

The similitudes and differences rising from the dependences of E_{cp}, t_i, $E_{rp} = f(a_{Cl^-}, °T, \text{pH})$ allow their separation into two groups of parameters.

E_{cp}, t_i dependences being in agreement with the observations of other investigators [6-8] do not call for additional discussion but understanding of E_{rp} behaviour requires a review of available knowledges.

The potential of pits repassivation may be assimilated with the potential settled down at the bottom of the pits as a result of localized attack that promotes high electrochemical and chemical differences between the individual areas of the surface.

---

[6] H. P. Leckie and H. H. Uhlig, *J. Electrochem. Soc.*, **113**, 1262 (1966).

[7] J. Horwath and H. H. Uhlig, *J. Electrochem. Soc.*, **115**, 792 (1968).

[8] N. D. Stolica, *Corrosion Sci.*, **9**, 205 (1959).

The active dissolution in the narrow anodic areas (pits) taking place in very aggressive conditions (high activator concentration,[9-11] low pH, deposits of salts completely or partially dissociated,[11,12] restrains of diffusion due to the corrosion products diaphragm [13-18]) follows in the establishment of inside potentials more active than those existing outside the pits.

Once started, the pitting process continues on the basès of pits aggressivity so that the composition of the more gentle outside environment cannot affect very much its development and hence the inside potential. Instead, it would be expected that the depth of the attack, the amount of anodic reaction [19] and the extent of cathodic/anodic differences are decisive for the inside potential value.

In this respect pits growth compares with crevices and cracks growth.

The data presented in table 2 show that such an independence of the electrolytic environment is found only for E_{rp}.

The determination of the potential of pits repassivation from hysteresis potentiostatic curves was based on the possibility to realize the stifling of pits activity by the electrochemical equalization of individual areas of the pitted surface through reverse polarization.

E_{rp} values were determined for the amount of pits propagation corresponding to an average current density of 500 μA/cm².

Going into a review of the previous results and some of the literature data, cyclic $E-I$ potentiostatic curves can be separated into three representative diagrams as those presented in figures 1 a, b and c, corresponding to three possible cases.

Case 1 $a \cdot E_{cp} \gg E_{rp}$; $E_{rp} \leqslant E_{st}$ (rest potential); $\Delta E \geqslant 0$ mV — was found in the investigation of FeCr,[3,4] Al and Al alloys [20] as well as in pitting inhibition attempts for insufficient inhibitor additions.

In the latter case, the tests carried out on CrNiTi s.s. in 0.1 mol. KCl + Na_2SO_4 (figure 2) have shown that insufficient SO_4^{2-} additions lead to more noble E_{cp} but more active E_{rp} potentials.

While in pure electrolyte $E_{cp} = 350$ mV and $E_{rp} = 50$ mV, the addition of 0.1 mol. Na_2SO_4 moves the critical pitting potential to +1000 mV and the potential of pits repassivation to −50 mV. Since the value of E_{rp} is actually unaffected by the content of the inhibitor (below C_{critic} for complete inhibition) it results that the more noble E_{cp}, the higher is the degree of hysteresis.

---

[9] C. Weil and D. Menzel, *Z. Elektrochem.*, **63**, 669 (1959).

[10] Y. Kitamura and T. Suzuki, "Proceedings to the 4th International Congress on Metallic Corrosion", Amsterdam, 1969, p. 716.

[11] T. Suzuki, M. Yamabe and Y. Kitamura, *Corrosion*, **29**, 18 (1973).

[12] B. E. Wilde and E. Williams, *Electrochim. Acta*, **16**, 1971 (1971).

[13] M. Pourbaix, *Corrosion*, **25**, 267 (1969).

[14] Y. M. Kolotirkin, *Corrosion*, **19**, 261t (1963).

[15] I. L. Rosenfeld and I. S. Danilov, *Z. phys. Chem. (Leipzig)*, **226**, 257 (1964).

[16] B. F. Brown, *Corrosion*, **26**, 431 (1970).

[17] F. G. Hodge and B. E. Wilde, *Corrosion*, **26**, 146 (1970).

[18] I. L. Rosenfeld, "4th Congress of European Coal and Steel Community", 1968, p. 3.

[19] B. E. Wilde, *Corrosion*, **28**, 283 (1972).

[20] O. Radovici, S. Ciolac and E. Vasilescu, Unpublished data.

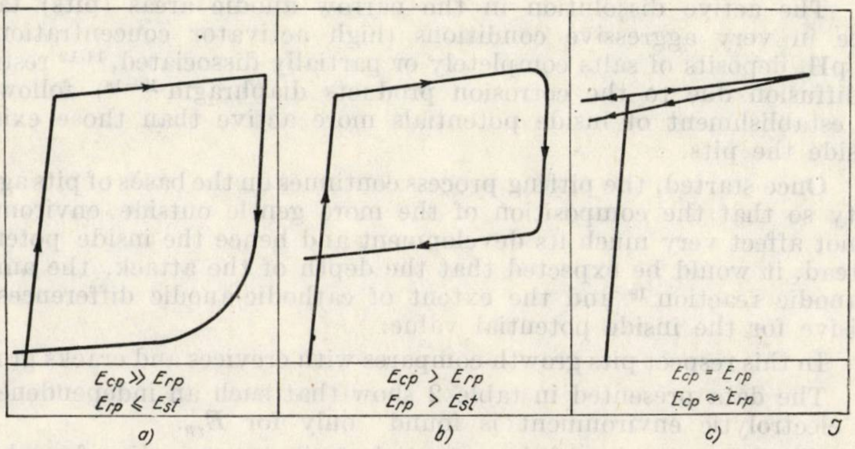

Fig. 1. a, b and c. Schematic $E-I$ hysteresis diagrams.

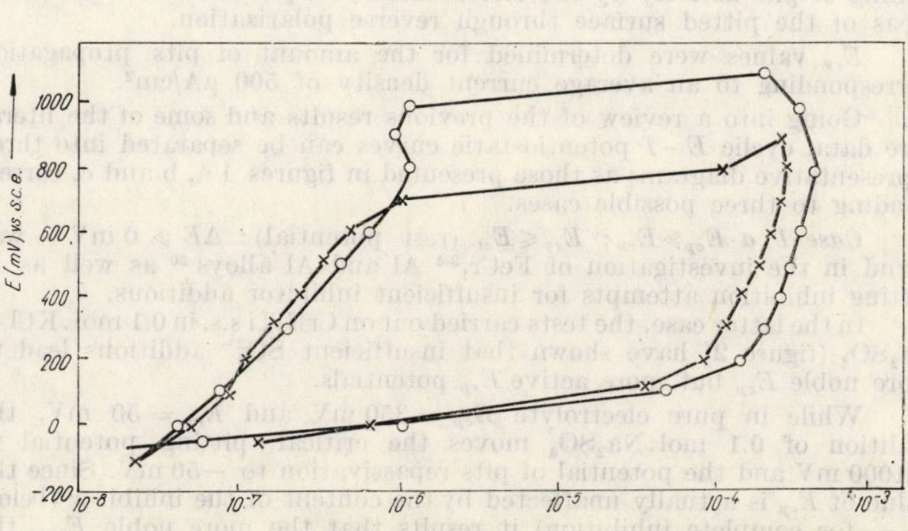

Fig. 2. — Cyclic anodic curves for CrNiTi s.s. in 0.1 mol. KCl + :
× — 0.01 mol. Na_2SO_4 ; ○ — 0.1 mol. Na_2SO_4. Aerated electrolyte, at 25°.

In all cases showing large hysteresis loops the presence of pits on the surface was always observed by microscopical examination, even $E_{cp} > 1000$ mV.

Case 1b · $E_{cp} > E_{rp}$; $E_{rp} > E_{st}$; $\Delta E > 0$ mV — was found most frequently. It has been established for austenitic stainless steels investigated in variable C_{Cl^-} (figure 3), °T and pH-s electrolyte.

Case 1 c · $E_{cp} = E_{rp}$ or $E_{cp} \approx E_{rp}$; $\Delta E = 0$ mV or $\Delta E \approx 0$ mV was supplied by some specific electrolytes and particular metallic compositions.[12]

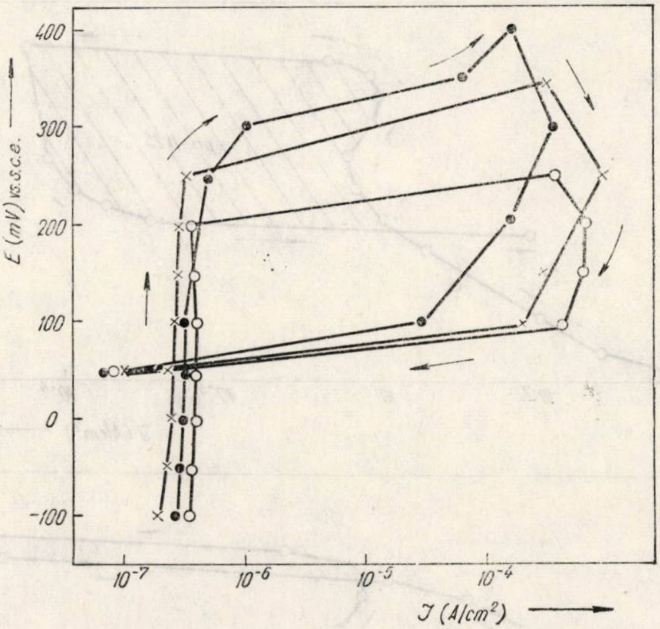

Fig. 3. — Hysteresis curves for CrNiTiMo s.s. in variable KCl concentrations at 25°.
Deaerated ● — 0.5 mol. KCl; × — 1 mol. KCl; ○ — 2 mol. KCl.

In the first case the results obtained for CrNiTi s.s. in 0.1 mol. KCl of pH = 11.25 and for 0.05 mol. KOH additions (figures 4a and b) have to be considered.

The values of E_{cp}, E_{rp} established from figure 4a were previously presented on E_{cp}, $E_{rp} = f(\mathrm{pH})$ diagrams.[4] It has then been shown that the critical pitting potentials increase (become more noble) with increasing alkaline pH, reaching maximum values at 9—10 units (as function of the metallic composition). Every increase in the pH beyond the maximum was accompanied by an activation of the critical pitting potentials. Unlike E_{cp}, the potential of pits repassivation was not affected by the pH of the electrolyte.

In the particular case of CrNiTi s.s., E_{cp} had a maximum value at pH = 9, while E_{rp} was constant and equal with + 100 mV until pH = 11.25. Depending on the E_{cp} value the hysteresis curves showed quite large loops and the surface was always pitted. For 0.05 mol. KOH additions the degree of hysteresis decreases from +500 mV (pH = 11.25) to +50 mV and the surface was free of pits.

It follows therefore that there is a strong correlation between the degree of hysteresis and pitting. The complete inhibition of the process results only for a certain $C_{\mathrm{activator}}/C_{\mathrm{Inh}}$ ratio able to reduce or render nill the difference $E_{cp}-E_{rp}$.

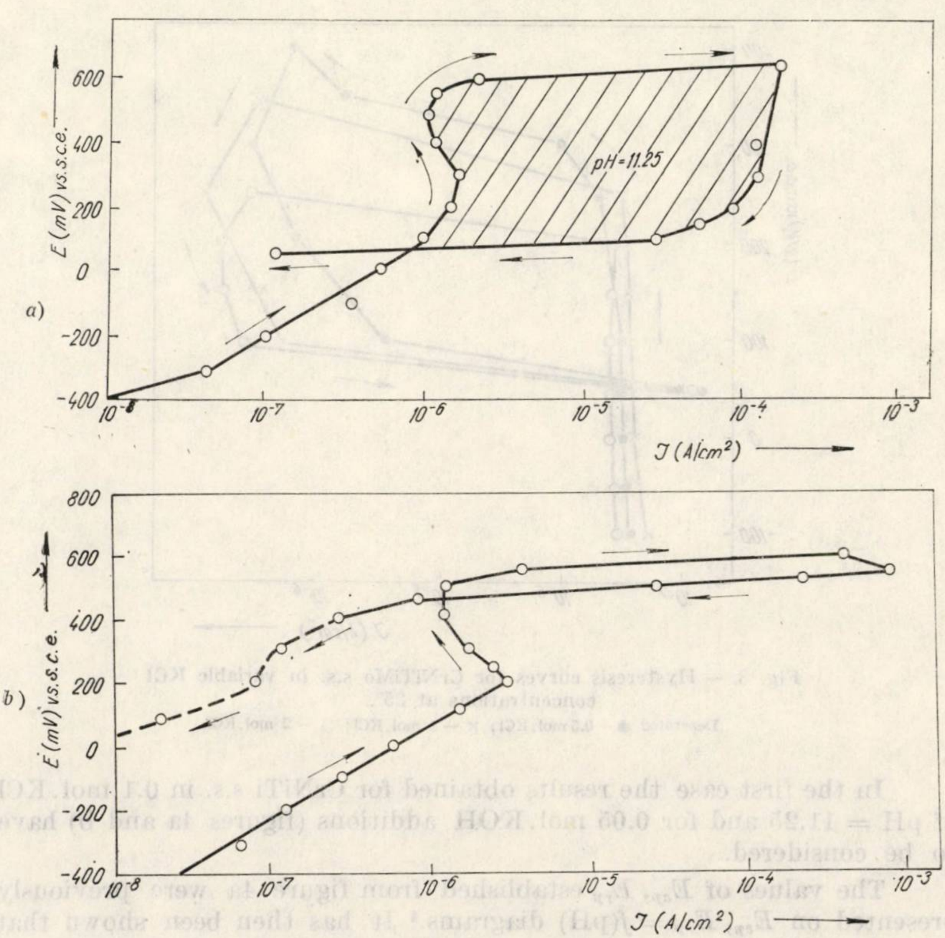

Fig. 4. — Hysteresis curves for CrNiTi s.s. in deaerated 0.1 mol. KCl + :
(a) — KOH to pH = 11.25 and (b) 0.05 mol. KOH.

Similar results were obtained when $NaHCO_3$ was added. Figure 5 illustrates E_{cp} and E_{rp} variations as a function of $NaHCO_3$ content of 0.1 mol. KCl electrolyte.

It can be seen from this figure that C_{critic} $NaHCO_3$ required for complete inhibition of pitting produced on CrNiTi s.s. is 0.4 mol. Only at this concentration the difference $E_{cp}-E_{rp}$ is minimum and the surface is not pitted. Below this concentration the potentials of pits repassivation are more active ($E_{rp} = -200$ mV) than for uninhibited electrolyte ($E_{rp} = +50$ mV) and the formed pits are larger, deeper and covered with greater amounts of corrosion products.

A content of only 0.01 mol. KNO_3 was sufficient to protect CrNiTi s.s. against pitting, $E_{cp} - E_{rp}$ being zero as shown in figure 6.

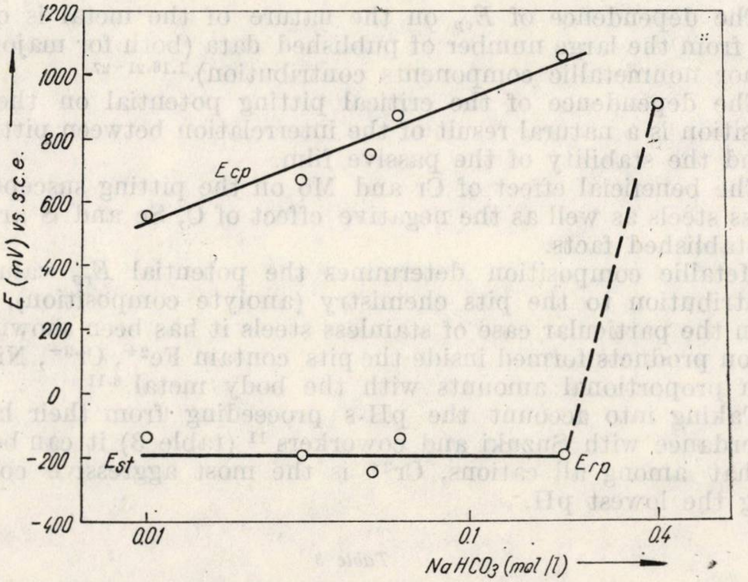

Fig. 5. — The variation of E_{cp} and E_{rp} with $NaHCO_3$ content added to aerated 0.1 mol. KCl at 25° for CrNiTi s.s.

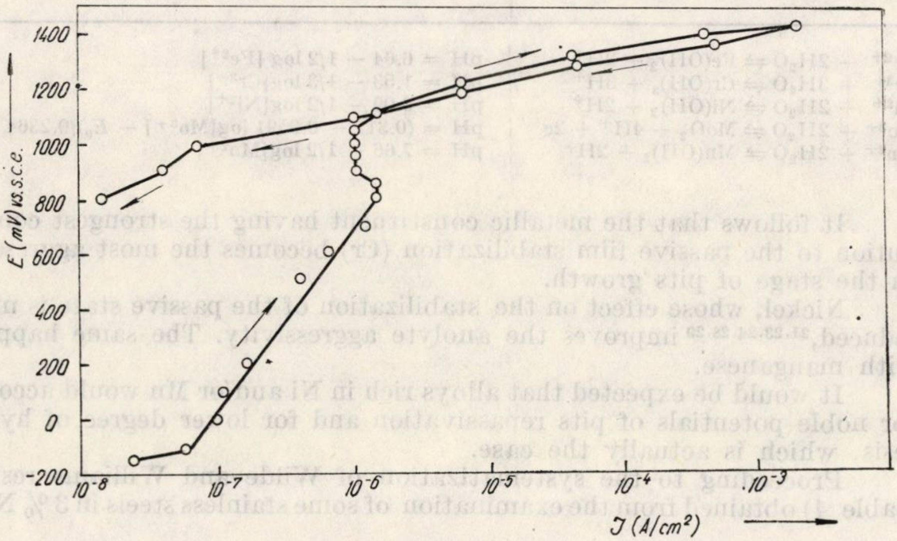

Fig. 6. — Hysteresis curves for CrNiTi s.s. in deaerated 0.1 mol. KCl + 0.01 mol. KNO_3 at 25°.

The above data prove the utility and necessity to consider the cyclic anodic curves in the aim of C_{critic} Inh^- estimation required by the complete inhibition of the process.

In the second case, as has been anticipated, the degree of hysteresis is strongly influenced by the metallic composition.

The dependence of E_{cp} on the nature of the metal is quite well known from the large number of published data (both for major metallic or minor nonmetallic components contribution).[1,16,21–27]

The dependence of the critical pitting potential on the metallic composition is a natural result of the interrelation between pitting initiation and the stability of the passive film.

The beneficial effect of Cr and Mo on the pitting susceptibility of stainless steels as well as the negative effect of C, Se and S are already well established facts.

Metallic composition determines the potential E_{rp} value due to its contribution to the pits chemistry (anolyte composition).

In the particular case of stainless steels it has been shown that the corrosion products formed inside the pits contain Fe^{2+}, Cr^{3+}, Ni^{2+}, Mo^{3+}, etc., in proportional amounts with the body metal.[8,11]

Taking into account the pH-s proceeding from their hydrolysis, in accordance with Suzuki and coworkers [11] (table 3) it can be emphasized that among all cations, Cr^{3+} is the most aggressive constituent, leaving the lowest pH.

Table 3

Hydrolysis reactions and equilibrium pH for metal ions involved in anclyte of pit of stainless steels

Hydrolysis reaction	Equilibrium pH
$Fe^{2+} + 2H_2O \rightleftharpoons Fe(OH)_2 + 2H^+$	$pH = 6.64 - 1/2 \log [Fe^{2+}]$
$Cr^{3+} + 3H_2O \rightleftharpoons Cr(OH)_3 + 3H^+$	$pH = 1.53 - 1/3 \log [Cr^{3+}]$
$Ni^{2+} + 2H_2O \rightleftharpoons Ni(OH)_2 + 2H^+$	$pH = 6.09 - 1/2 \log [Ni^{2+}]$
$Mo^{3+} + 2H_2O \rightleftharpoons MoO_2 + 4H^+ + 2e$	$pH = (0.311 - 0.0591 \log [Mo^{3+}] - E_0)/0.2364$
$Mn^{2+} + 2H_2O \rightleftharpoons Mn(OH)_2 + 2H^+$	$pH = 7.66 - 1/2 \log [Mn^{2+}]$

It follows that the metallic constituent having the strongest contribution to the passive film stabilization (Cr) becomes the most aggressive in the stage of pits growth.

Nickel, whose effect on the stabilization of the passive state is more reduced,[21,23,24,28,29] improves the anolyte aggressivity. The same happens with manganese.

It would be expected that alloys rich in Ni and/or Mn would account for noble potentials of pits repassivation and for lower degree of hysteresis, which is actually the case.

Proceeding to the systematization of Wilde and Williams results (table 4) obtained from the examination of some stainless steels in 3 % NaCl

---

[21] N. D. Tomashov, G. P. Cernova and O. N. Marcova, *Corrosion*, **20**, 166t (1964).

[22] I. L. Rosenfeld and W. P. Maximtsuch, *Z. phys. Chem., (Leipzig)*, **215**, 25 (1960).

[23] E. A. Lizlovs and A. P. Bond, *J. Electrochem. Soc.*, **116**, 574 (1969).

[24] A. P. Bond and E. A. Lizlovs, *J. Electrochem. Soc.*, **115**, 1130 (1968).

[25] M. A. Streicher, *Corrosion*, **30**, 115 (1974).

[26] R. F. Steigerwald, *Materials Performance*, **13**, 9 (1974).

[27] G. Vranglén, *Corrosion Sci.*, **9**, 585 (1969).

[28] E. Vasilescu, *Rev. Roumaine Chim.*, **20**, 491 (1975).

[29] E. A. Lizlovs and A. P. Bond, *J. Electrochem. Soc.* **118**, 22 (1971).

and sea water,[12] it appears that $E_{cp} - E_{rp}$ difference decreases or becomes zero as Ni content in alloyed composition increases.

The same regularities are followed from own experiments (even studied steels are less adequate for such discussion) as seen from table 5.

Table 4

The dependence of the extent of pitting irreversibility on the metallic composition. Electrolyte: 3% NaCl and sea water[12]

Type of steel	Main alloying components (w/o)			E_{cp}	E_{rp} (mV)	ΔE
	Cr	Ni	Mo			
Hasteloy	15.44	56.27	13.6	+970	+970	0
AISI 316	17.2	11.6	2.2	+100	− 20	120
AISI 304	18.1	8.22	0.36	0	−110	110
AISI 430	16.37	0.17	0.02	−100	−260	160
USS 100	11.6	0.19	0.05	−150	−340	190
AISI 410	12	0.34	0.08	−200	−420	220

Table 5

The extent of pitting irreversibility of austenitic stainless steels studied

Type of steel	Main alloying components (w/o)				E_{cp}	E_{rp} (mV)	ΔE
	Cr	Ni	Mo	Mn			
CrNiTiMo	16.90	11.90	2.36	1.82	+350	+150	200
CrNiTi	17.76	8.79	0.07	1.34	+350	+100	250
CrNi	19.43	8.09	0.016	0.71	+200	−100	300

IRREVERSIBILITY OF THE PITTING PROCESS

The existence of two potentials characterizing the initiation and development of the pitting process (being separated most frequently by hundreds of millivolts) that result from the uncoincidence of forward and reverse anodic curves may be considered as a proof of the pitting irreversibility.

The difference between the critical pitting potential (E_{cp}) and the potential of pits repassivation (E_{rp}) is in consequence defined as the extent of pitting irreversibility (ΔE).

Among the three types of $E-I$ variations presented in figures 1 a, b and c, the 1 c case might be considered as being generated by a reversible process. The reversibility in this case should not be looked as proceeding from an adsorption-desorption equilibrium process of activators[14,30] but as a result of a less deep attack or a less aggressive anolyte containing pits.

The repassivation of the pitted surface is caused by the cancel of pits activity and not by a desorption process.[22]

---

[30] Y. M. Kolotirkin, *J. Electrochem. Soc.*, **108**, 203 (1961).

Cases represented in figures 2, 4b and 5 showing $\Delta E \approx 0$ mV were found for inhibitor additions equal or higher than C_{critic} Inh^- required for complete inhibition. The increase in current recorded on these curves does not come from a pitting attack but from the transpassive dissolution of the metal. The reversibility of the process in these conditions is justified by the total absence of the local corrosion.

The dependence of the extent of pitting irreversibility on the depth of the pits is determined by the effect of the amount of pits propagation on E_{rp} value.[12]

For a certain metallic composition, as E_{rp} is less affected by the electrolyte composition, the extent of pitting irreversibility being estimated from the difference $E_{cp}-E_{rp}$ should increase with increasing E_{cp}.

A stabilization of the passive state able to move the critical pitting potential to more noble values but unable to realize a simultaneously E_{rp} raise will cause an increase in the extent of irreversibility. Such an effect was related for insufficient additions of inhibitors.

The above reasoning is helpful in understanding the superiority of austenitic stainless steels in comparison with ferritic steels.

The ferritic s.s. would not show high resistance to pitting but for sufficient high contents in Cr (and Mo) able to avoid the initiation of pitting even in the transpassive region. Otherwise if for some unknown reasons the attack started on the surface, it would cause deeper pits.

The beneficial effect of Ni cannot be substantial in semiaustenitic steels, but it is very strong in high nickel containing alloys. [12,23,26]

The data presented in table 4, as well as those reported by Steigerwald [26] (from chemical tests) can be used to understand the better resistance shown by Incolloy 825, Incolloy 625, Hastelloy G, J.S. 700 and Alloy 6X.

Manganese like nickel increases the resistance toward pitting justifying the good behaviour of Allegheny L type 216 and Armco 22—13—5 stainless steels.[26]

In a recent publication Streicher [25] pointed out that Cr alone (even as high as 40 %) is unable to ensure the resistance to pitting in very aggressive agents and that Mo has a great contribution to passive film stabilization. He also showed that a certain Cr/Mo ratio should be respected to get high pitting resistant compositions.

In accordance with the above considerations the avoidance of pitting or an attack leading to shallow pits is always related to noble repassivation potentials and small or zero $E_{cp} - E_{rp}$ differences.

It follows then that the potential of pits repassivation is a measure of pitting resistance while the critical pitting potential refers only to pitting susceptibility.

A reduced susceptibility toward pitting cannot be considered sufficient to avoid pitting attack and this fact can account for the disagreement between the electrochemical, chemical and immersion tests reported frequently by different investigators.

Chemical tests taken in $FeCl_3$, $KMnO_4 + Cl^-$, etc., like immersion tests in natural environments supply data on the whole process (not only on its particular stages) and thus relate the pitting resistance.

Electrochemical tests considering only the value of the critical pitting potentials relate the susceptibility of metals toward pitting, thus the chances for the process to initiate, but not the pitting resistance.

It is thus clear that the most complete and rapid information about the pitting behaviour of a metal can be supplied by the electrochemical tests that take into account E_{cp} and E_{rp} potentials.

The methods of protection against pitting corrosion should be directed toward reducing the $E_{cp} - E_{rp}$ difference, thus decreasing the extent of pitting irreversibility.

The protection seems difficult to be realized both because of the change in alloying components function throughout the different stages of the pitting process development and because of the necessity that a rigorous ratio $C_{\mathrm{activator}}/C_{\mathrm{Inh}^-}$ should be maintained.

The improvement of pitting behaviour by alloying with passivity stabilizing constituents seems to be as critical as the inhibitor addition. In this case certain ratios between the alloyed metals should be respected.

The decrease in the pitting susceptibility by alloying or inhibition (below C_{critic} Inh^-) can result in an opposite effect than that expected for a more stable passive state, if these ratios are not respected.

A low pitting susceptibility means an attack occurring on a few active centers. The development of the process on such a surface can result in much stronger electrochemical and chemical differences between cathodic and anodic areas and thus in a deeper attack than that occurring on a surface having many active but less aggressive centers of attack.

From the tested inhibitors OH^- anions seem to be more convenient because they do not move E_{cp} to very noble values (like NO_3^-, HCO_3^- or SO_4^{2-}) but are able to ennoble E_{rp} at quite low concentrations.

The same reasoning applies with regard to metallic compositions.

The austenitic stainless steels having higher susceptibilities than ferritic stainless steels follow in shallow and less dangerous attack.

The above considerations point out the necessity of a systematic study of E_{rp} as a measure of pitting resistance. Such diagrams as $\log(a_{\mathrm{activator}}) = f(\log a_{\mathrm{Inh}^-})$ reported by Uhlig and coworkers [6,31] should be build up only from the hysteresis curves.

The foregoing results and comments lead to the conclusion that the extent of pitting irreversibility is a proper informative criterion for pitting behaviour classification both in respect with metallic composition and environmental conditions.

THE DELIMITATION OF THE PITTING DEVELOPMENT STAGES

On the base of the potential-pH diagram (figure 7) [2,32] and some earlier publications [3,4] the possibility arises to make some completions of $E - I$ and $E - t$ variations (figures 8 a and b) in the view of delimiting the individual stages of pitting development.

---

[31] H. Böhni and H. H. Uhlig, *J. Electrochem. Soc.*, **116**, 906 (1969).

[32] E. Vernik Jr. and M. Pourbaix, *Corrosion*, **27**, 449 (1971).

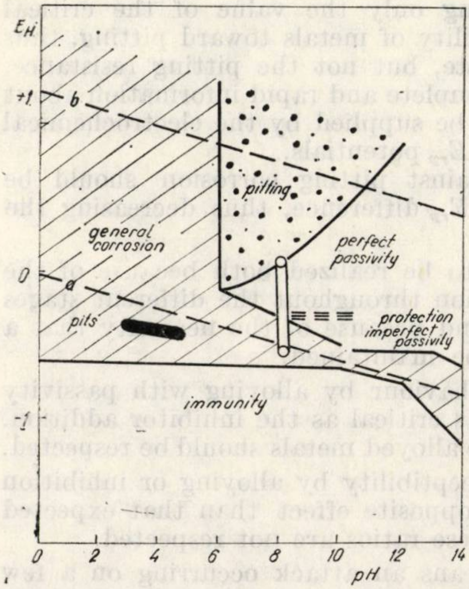

E_H
+1
b
0
a
-1
general corrosion
pitting
perfect passivity
pits
protection
imperfect passivity
immunity
0
2
4
6
8
10
12
14
pH

Fig. 7. — Thermodynamic conditions for corrosion, pitting and passivity. Fe in the presence of Cl^- ions.

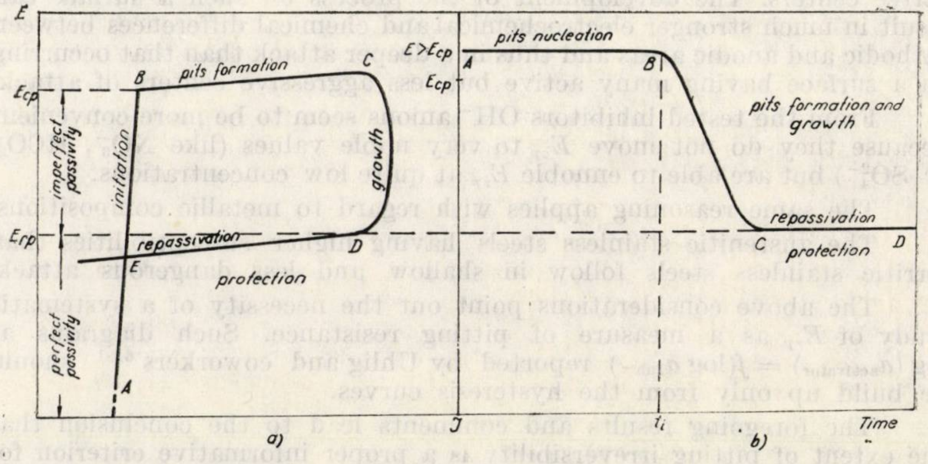

E
E_{cp}
B
pits formation
C
imperfect passivity
initiation
growth
E_{rp}
repassivation
D
E
protection
perfect passivity
A
a)
$E>E_{cp}$
A
pits nucleation
B
E_{cp}
pits formation and growth
repassivation
C
D
protection
J
t_i
Time
b)

Fig. 8. — Delimitation of the pitting process development stages on:
(a) potentiostatic curves and (b) galvanostatic curves.

In accordance with Pourbaix the potential of pits repassivation separates the conditions of perfect and imperfect passivity.

If transferred on the $E-I$ curve, this separation will make possible the division of AB range into AE and EB corresponding to the two kinds of passivity.

The occurrence of imperfect passivity cannot result other than from the interference of activator in the formation and growth of passive film. It follows then that the initiation of pitting begins at much more active potentials than E_{cp} or in other words the critical pitting potential marks the highest degree of imperfection of the passive film.

At the critical pitting potential the imperfection of the passive film should be provided by the adsorption of a certain number of An^- around a metallic cation able to break down the Me—O binding.[1]

This assertion comes from the independence of E_{cp} on a_{Cl} — reported above.

Logically E_{rp} should depend on the content of the activator in the electrolyte since its amount determines the quantity of corrosion products and consequently the inside pH-s. An E_{rp} independent of the activator content supposes an equal chemical activity inside the pits, thus the participation of the same quantities of reactants $(An^- + Me^+)$ in the process development.

In this respect pitting differentiates from the other kinds of the local attack (crevice, stress corrosion cracking).

The above proposition, namely the adsorption of a certain number of An^- around a metallic cation explains the dependence of the critical pitting potential on the activator content.

As the content of the activator in the electrolyte is smaller, it would be more difficult to realize the critical concentration of anions in the passive film and higher potentials will be required. On the contrary, for greater amounts of activator the critical concentration will be easier to achieve and the start of the attack will be possible at lower potentials.

As Me—O binding depends on the metal and environment (i.e. nature and concentration of nonaggressive anions) it results that the number of adsorbed anions varies from case to case.

This explains the results reported above for inhibited electrolytes.

The participation of a higher number of Cl^- ions in the break of Me—O binding accounts for $E_{cp} = f(C_{\mathrm{Inh}^-})$ presented in figure 5 and for the activation of E_{rp}.

The independence of the potential of pits repassivation of the content of the inhibitor (below C_{critic} Inh^-) suggests in turn that the nonaggressive anions affect only the initiation stage of the pitting process. Their contribution to the further development of the attack should be of electrochemical and not of chemical nature (the amount of the potential difference between cathodic and anodic areas).

For $E_{apl} > E_{cp}$ the break of Me—O binding will require the consumption of "an induction time". Through the induction period the premises for local cells action are settled as a result of pits nucleation (*AB* branch in figure 8b).

The above statements can explain the dependence of E_{cp} and t_i on the metallic and electrolyte compositions and the higher sensitivity of t_i on the degree of passive film stability.

While the formation and growth of pits are related by *BC* and *DE* branches of figure 8a they cannot be separated on *BC* branch of $E - t$ curve from figure 8b.

The potential settled after the decay was earlier checked to relate E_{rp} values.[5] Separating the condition of reaction from stable protection, E_{rp} can again be considered as a measure of pitting resistance of metals.

Any procedure able to enlarge the region of stable protection by moving E_{rp} to a noble direction will result in higher pitting resistance.

CONCLUSIONS

– The nature of the pitting process changes throughout its development. In the initiation stage (below critical pitting potential and until the induction time is consumed) the process has a reversible nature but as long as the attack develops, it becomes irreversible.

– The initiation of the pitting process begins as far back as the formation and growth of passive film.

The critical pitting potential assesses the maximum imperfection conditions in the passive film, being a measure of pitting susceptibility of passivable metals (or in other words a measure of passive film resistance to the breakdown by aggressive anions).

– The start of the pitting process requires a certain number of anions to be adsorbed around a metallic cation, able to break down the Me–O bond during induction period.

Both critical pitting potential and induction time should be closely related by the number of the pits on the metallic surface.

– The inhibitor anions interfere only in the initiation stage of the pitting process, their contribution to its development being of an electrochemical nature.

– The potential of pits repassivation assesses the reaction potential inside the pits. Its value is a measure of the metal resistance to the higher aggressive conditions created throughout the growth stage.

– The difference between pitting susceptibility and pitting resistance ($E_{cp} - E_{rp}$) measures the extent of pitting irreversibility.

– The function of alloying constituents changes throughout the successive stages of pitting development. The most effective constituent in passive state stabilization of stainless steels like chromium becomes the most aggressive in the reaction stage.

– The superiority of austenitic to ferritic steels is brought about by nickel which ameliorates the aggressivity of the anolyte.

– The methods of protection against pitting should be directed towards cutting to a minimum the extent of pitting irreversibility ennobeling both E_{cp} and E_{rp}.

– The extent of pitting irreversibility, ΔE, should be used as an index for pitting behaviour both in respect with metallic composition and environmental conditions (for very well established systems).

Revue Roumaine de Chimie, **22**, *8*, 1165–1174 (1977)

Herrn Professor Dr. Coriolan Drăgulescu
zum 70. Geburtstag gewidmet

ZUM EINFLUSS DER RINGGRÖSSE AUF DIE STRUKTUR VON METALLCHELATEN DREIZÄHLIGER LIGANDEN. III[1]

KUPFER(II)-, NICKEL (II)- UND EISEN(II)-CHELATE PYRIDYLSUBSTITUIERTER DIALKYLSULFIDE

E. UHLIG, W. HEPP, LE MY NGU und K. SCHMIEDEKNECHT
Jena, Sektion Chemie der Friedrich-Schiller-Universität

Eingegangen am 9. Juli 1976

Inhaltsübersicht : Bis(pyridyl-2-methyl)-sulfid ($2,2-py_2Stri$) bildet mit Nickel (II)-Salzen oktaedrische 1,2-Komplexe $[Ni(2,2-py_2Stri)_2]X_2$, in Gegenwart von Anionen, die gegenüber Nickel (II) als stärkere Donatoren wirken, auch 1,1-Komplexe $Ni(2,2-py_2Stri)\,Y_2$. (Pyridyl-2-methyl)-(β-pyridyl-2-äthyl)-sulfid($2,3-py_2Stri$) fungiert im $[Ni(2,3-py_2Stri)_2]\,(ClO_4)_2$ als dreizähliger, im $Ni(2,3-py_2Stri)_2Cl_2$ nur als zweizähliger Ligand.
Vom Kupfer (II) konnten nur 1,1-Komplexe, wie $Cu(2,2-py_2Stri)\,X_2$ ($X = Cl, Br$), $Cu(2,2-py_2Stri)\,(H_2O)\,(ClO_4)_2$ und $Cu(2,3-py_2Stri)\,Cl_2$ dargestellt werden. Bei der Reaktion von Kupfer (II)-chlorid bzw. -perchlorat mit einem Überschuß an $2,2-py_2Stri$ entstehen diamagnetische Verbindungen mit einem Verhältnis von Metall : Anion gleich 1 : 1. Bildung und Struktur dieser Verbindungen werden diskutiert. $2,2-py_2Stri$ besetzt in Koordinationsverbindungen, vorzugsweise aus sterischen Gründen, faciale Positionen und begünstigt in Verbindungen der Koordinationszahl 5 trigonalbipyramidale Strukturen.

1. EINLEITUNG

Die Liganden $2,2-py_2Stri$; $2,3-py_2Stri$ und $3,3-py_2Stri$ sind potentiell dreizählige Liganden mit dem gleichen Donatoratomsatz NSN. Sie bilden aber Chelatringe unterschiedlicher Größe. Aus diesen Gründen ist in wäßriger Lösung eine Verwandtschaft im koordinativen Verhalten von $2,3-py_2Stri$ (5,6-Ringbildner) und $3,3-py_2Stri$ (6,6-Ringbildner) gegenüber den Ionen der 3d-Elemente nicht zu verkennen.[1] Auf der anderen Seite werden aber auch Unterschiede sichtbar. So bilden zwar beide Liganden bei dreizähliger Funktion stabile 1,1-Komplexe mit Nickel (II) und Kupfer (II), und beim Kupfer (II) konnten in beiden

---

[1] E. Uhlig u. W. Hepp, *Z. anorg. Chem.*, **421**, 161 (1976).

Fällen auch 1,2-Komplexe nachgewiesen werden. Ein 1,2-Chelat des Nickel (II) wurde dagegen nur im Falle des 2,3—py$_2$Stri erfaßt. Es ist jedoch, wie die Stabilitätskonstante[1] erkennen läßt, selbst gegenüber dem Angriff schwacher Donatoren recht instabil.

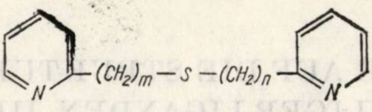

	m	n
2,2—py$_2$ Stri	1	1
2,3—py$_2$ Stri	1	2
3,3—py$_2$ Stri	2	2

Für den Liganden 2,2 — py$_2$Stri liegen keine Lösungsdaten vor. Ein Vergleich mit anderen 5,5-Ringbildnern[2] läßt jedoch eine hohe Tendenz zur Bildung von 1,2-Komplexen erwarten.

Kristalline Verbindungen wurden bisher nur vom 3,3—py$_2$Stri beschrieben.[3,4] Es handelt sich ausschließlich um 1,1-Chelate. Das ist insofern bemerkenswert, als im Falle des Kupfer(II) in Lösung auch 1,2-Komplexe nachgewiesen wurden. Wir berichten im Folgenden über Synthesen von Kupfer(II)-, Nickel(II)- und Eisen(II)-Komplexen der Liganden 2,2 — py$_2$Stri und 2,3—py$_2$Stri.

2. NICKEL(II)-KOMPLEXE

Aus äthanolischer Lösung kristallisieren die 1,1-Komplexe Ni(2,2—py$_2$Stri) Cl$_2$ und Ni(2,2—py$_2$Stri) (NCS)$_2$ (Tab. 1). Ni(2,2—py$_2$Stri) Cl$_2$ ist in Nitrobenzol ein Nichtelektrolyt. Sein VIS-Spektrum ist mit denen von Ni(3,3—py$_2$Stri) Cl$_2$[4] und Dibromo-[6,6'-dimethyldi(2-pyridylmethyl)-amin]-nickel (II)[5] vergleichbar. Da für die letztgenannte Verbindung eine Strukturanalyse vorliegt,[6] kann für Ni(2,2—py$_2$Stri) Cl$_2$ eine trigonal-bipyramidale Struktur postuliert werden. Ni(2,2—py$_2$Stri) (NCS)$_2$ entspricht im VIS-Spektrum und in bezug auf die charakteristischen Banden im IR-Bereich (Tab. 1) nicht dem Ni(3,3—py$_2$Stri) (NCS)$_2$ sondern dem Ni(3,3—py$_2$tri) (NCS)$_2$. Damit wird eine oktaedrische Struktur (Brückenfunktion der Hälfte der Thiocyanatoliganden) angezeigt.[4]

Bei der Umsetzung von 2,2—py$_2$Stri mit Nickel (II)-Salzen, deren Anionen gegenüber Nickel (II) schwächere Donatoren als Chlorid und Thiocyanat sind,[7] kristallisieren aus Äthanol die 1,2-Komplexe [Ni(2,2—py$_2$Stri)$_2$]X$_2$ (X = Br, NO$_3$, J, ClO$_4$). Diese Verbindungen sind in Methanol 1,2-Elektrolyte. Die hypsochrome Verschiebung der Valenzschwingung ν_{8a}(Valenzschwingung des Pyridinringes) um $\sim$10 cm^{-1} beim komplexgebundenen im Vergleich zum freien 2,2—py$_2$Stri,[5] sowie das Auftreten der für freie Nitrat- bzw. Perchlorationen charakteristischen Schwingungen (Tab. 1) weisen auf eine dreizählige Funktion des 2,2—py$_2$Stri bei koordinanativer Inaktivität der Anionen hin. Unter Berücksichtigung der magnetischen Momente (Tab. 1) kann daher auf eine oktaedrische

[2] R. Barbucci, L. Fabrizzi u. P. Paoletti, *Inorg. Chim. Acta*, **7**, 157 (1973).
[3] E. Uhlig u. G. Heinrich, *Z. anorg. Chem.*, **330**, 40 (1964).
[4] S. Nelson u. J Rodgers, *Inorg. Chem.*, **6**, 1390 (1967).
[5] M. da Mota, J. Rodgers u. S. Nelson, *J. Chem. Soc. (A)*, **1969**, 2036.
[6] J. Rodgers u. R. Jacobson, *J. Chem. Soc. A*, **1970**, 1826.
[7] Vgl. dazu D. Goodgame u. L. Venanzi, *J. Chem. Soc.*, **1963**, 5909.

Tabelle 1

Übergangsmetallkomplexe der Liganden 2,2-py$_2$Stri und 2,3-py$_2$Stri

	ν_{8a} a,b) (cm^{-1})	Anionenbanden (cm^{-1})	Ligandenfeld maxima (kK) d)	Λ_c (Ω^{-1}cm^2 mol^{-1}) h)	μeff (20°) (B.M.)
Ni(2,2−py$_2$Stri) Cl$_2$	1610	—	10,0 ; 11,0S ; 15,6 ; 20,8 S ; 25,2	9,3 i)	3,18
Ni(2,2−py$_2$Stri) (NCS)$_2$	1608	2070, 2090, 2115(S) 2130	10,1 ; 16,5 ; 22,0S	28 k)	3,14
[Ni(2,2−py$_2$Stri)$_2$] Br$_2$	1610	—	11,3 ; 15,4 ; 19,0	184 l)	3,16
[Ni(2,2−py$_2$Stri)$_2$] J$_2$	1610	—	11,2 ; 15,4 ; 18,5	185 l)	3,18
[Ni(2,2−py$_2$Stri)$_2$] (NO$_3$)$_2$	1610	1370 br.	11,5 ; 15,7 ; 18,7	178 e)	3,16
[Ni(2,2−py$_2$Stri)$_2$] (ClO$_4$)$_2$	1610	625, 1100 br.	11,5 ; 15,5 ; 19,0	185 e)	3,16
[Ni(2,3−py$_2$Stri)$_2$] (ClO$_4$)$_2$	1610	625, 1095 br.	11,4 ; 18,3 ;	52(1,2·10^{-3}) m)	2,92
Ni(2,3−py$_2$Stri)$_2$Cl$_2$	1604, 1592S	—	9,0 ; 13,55 ; 15,7 ; 25,0	10,6(9,1·10^{-4}) m)	3,09
Cu(2,2−py$_2$Stri) Cl$_2$	1610	—	9,5 ; 11,0S	15(1·10^{-2}) k)	1,85
Cu(2,2−py$_2$Stri) Br$_2$	1610	—	10,0 ; 12,0S	17(1·10^{-2}) k)	1,84
Cu(2,2−py$_2$Stri) (H$_2$O) (ClO$_4$)$_2$ c)	1620	630, 1100 br.	15,4	n)	1,72
Cu(2,3−py$_2$Stri) Cl$_2$	1612	—	e)	1(1,4·10^{-3}) m)	1,85
Cu(2,3−py$_2$Stri) Cl(ClO$_4$)	1613, 1608S	625, 1100, 1060		16(1,2·10^{-3}) m)	1,89
„Cu(2,2−py$_2$Stri) Cl“ (IV)	1603	—	f)	5,6(1·10^{-2}) k)	diam.
„Cu(2,2−py$_2$Stri) ClO$_4$“ (VI)	1610	625, 1100	11,3 ; 15,5 ; 25,0S	20(1·10^{-2}) k)	diam.
F(2,2−py$_2$Stri) Cl$_2$	1610	—	10,2(0,85), 15,7 (0,0) S, 16,7 (0,04) g)	91 l)	5,51

a) Lage in den freien Aminen: 2,2-py$_2$Stri 1600 cm^{-1}; 2,3-py$_2$Stri 1595 cm^{-1}. b) Zur Nomenklatur vgl. C. Klein u. J. Turkevich, J. Chem. Physics **12**, 300 (1944). c) ν_{OH} 3390−3460 cm^{-1} d) Reflexionsspektren. e) nicht gemessen. f) Intensive Absorption im gesamten sichtbaren Bereich, über die sich ein flaches Maximum im nahen IR (11,0 − 13,0 kK) erhebt. g) Spektrum einer 10^{-2} m Lösung in Methanol, Werte in Klammern: log ε. h) wenn nicht anders angegeben: $c = 10^{-3}$ m, $t = 25$°C. i) in Nitrobenzol. k) in Acetonitril. l) in Methanol. m) in Nitrobenzol bei 18°, Werte in Klammern: c (mol·l^{-1}). n) wegen möglicher Zerstezung nicht bestimmt.

Struktur der Verbindungen $[Ni(2,2-py_2Stri)_2]\ X_2$ geschlossen werden. Ein analoger Strukturvorschlag erscheint auf Grund der physikalischen Daten (Tab. 1) auch für $[Ni(2,3-py_2Stri)_2](ClO_4)_2$ gerechtfertigt.

Bei oktaedrischen Nickel (II)-Komplexen dreizähliger Liganden mit dem Donatoratomsatz NSN sind drei Isomere möglich (Abb. 1). Bei den beiden *trans*-Formen I und II ist eine starke, bei der *cis*-Form III nur eine schwache Aufspaltung der längstwelligen Ligandenfeldbande (ν_1) zu erwarten.[8,9] Wir diskutieren daher für $[Ni(2,2-py_2Stri)_2]\ X_2$ (drei Banden im sichtbaren Bereich) eine *trans*- (I oder II), für $[Ni(2,3-py_2Stri)_2](ClO_4)_2$ (zwei Banden im sichtbaren Bereich, Abb. 2) eine *cis*-Struktur.

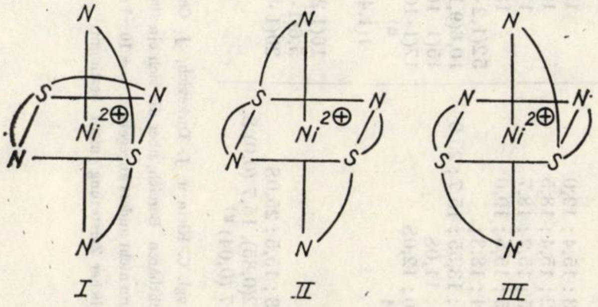

Abb. 1. — Isomere der oktaedrischen Nickel(II)-Komplexe dreizähliger Liganden mit dem Donatoratomsatz NSN.

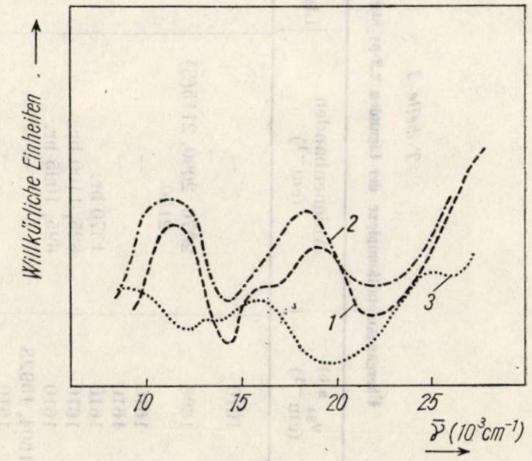

Abb. 2.— Reflexionsspektren.
1, $[Ni(2,2-py_2Stri)_2]ClO_4)_2$;
2, $[Ni(2,3-py_2Stri)_2](ClO_4)_1$;
3, $Ni(2,3-py_3Stri)_2Cl_2$.

Eine genauere Aussage darüber, ob in den Komplexen $[Ni(2,2-py_2Stri)_2]\ X_2$ die meridionale (I) oder die faciale *trans*-Form (II) realisiert ist, kann nicht getroffen werden; es sei aber auf Folgendes hingewiesen:

$3,3-py_2Stri$ ist in den planaren Komplexen $[Pd(3,3-py_2Stri)\ X]\ X$ dreizählig, $2,2-py_2Stri$ dagegen nur zweizählig (ein Pyridinhaftatom

---

[8] C. Hare u. C. Ballhausen, *J. Chem. Phys.*, **40**, 792 (1964).

[9] N. Curtis u. Y. Curtis, *Inorg. Chem.*, **4**, 804 (1965).

koordiniert nicht).[10] Offenbar kann 2,2$-$py$_2$Stri *trans*-Positionen nicht überspannen. Eine notwendige Voraussetzung für die Ausbildung des Isomeren I ist daher nicht erfüllt, und damit wird die Struktur II für die kristallin dargestellten Verbindungen [Ni(2,2$-$py$_2$Stri)$_2$] X$_2$ wahrscheinlich gemacht.

Ni(2,3$-$py$_2$Stri)$_2$Cl$_2$ hat in Nitrobenzol eine molare Leitfähigkeit, die zwischen den Erwartungswerten für Nicht- und 1,1-Elektrolyten liegt (Tab. 1). Die Valenzschwingung ν_{8a} des koordinierten 2,3$-$py$_2$Stri weist neben dem Maximum bei 1604 cm^{-1} eine Schulter bei 1592 cm^{-1} auf. Damit ist gezeigt, daß 2,3$-$py$_2$Stri weniger als drei Koordinationsstellen besetzt. Auf Grund der starken Ähnlichkeit des VIS-Spektrums mit dem des Bis[methyl-(pyridyl-2-methyl)-sulfid]-dichloronickel (II) [11] kann eine oktaedrische Struktur mit der zentralen Koordinationseinheit NiN$_2$S$_2$Cl$_2$ diskutiert werden. Da zwar mit Methyl-(pyridyl-2-methyl)-sulfid, nicht aber mit Methyl-(pyridyl-2-äthyl)-sulfid [12] Nickel (II)-Komplexe darstellbar sind, schließt das 2,3$-$py$_2$Stri im Ni(2,3$-$py$_2$Stri)$_2$Cl$_2$ wahrscheinlich den Chelatfünf- nicht aber den -sechsring. Der aus den Lösungsuntersuchungen [1] gezogene Schluß, daß der 1,2-Komplex [Ni(2,3$-$py$_2$Stri)$_2$]$^{2+}$ selbst gegenüber dem Angriff relativ schwacher Donatoren (zu denen die Chloridionen gehören) labil sei, wird damit bestätigt. Es sei darauf hingewiesen, daß nur bei der angenommnen *cis*-Struktur des [Ni(2,3$-$py$_2$Stri)$_2$]$^{2+}$ der *trans*-Effekt der Schwefelhaftatome auf Pyridinhaftgruppen wirken und deren Substitution durch Chloroliganden erleichtern kann.

3. KUPFER (II)-KOMPLEXE

2,2$-$py$_2$Stri reagiert mit Kupfer(II)-Salzen in Äthanol in ungewöhnlicher Weise. So bilden sich zwar bei Raumtemperatur normale grüne 1,1-Komplexe Cu(2,2$-$py$_2$Stri)X$_2$ (X = Cl, Br). Wird jedoch Kupfer(II)-chlorid bei 60° in Gegenwart eines Ligandenüberschusses umgesetzt, so schlägt die Farbe des ausfallenden Festkörpers von Grün nach Schwarz um. Bei der Reaktion äquimolarer Mengen von Kupfer(II)-perchlorat und 2,2$-$py$_2$Stri in der Kälte scheiden sich grüne Kristalle ab. Aus der Mutterlauge kristallisiert im Eisschrank noch eine blaue Substanz. Die grünen Kristalle sind das einzige Reaktionsprodukt, wenn im Molverhältnis 1 : 2 gearbeitet wird.

Die Analysendaten des Reaktionsproduktes von Kupfer (II)-chlorid mit 2,2$-$py$_2$Stri bei 60° (im Folgenden als „Komplex IV" bezeichnet) entsprechen denen einer Kupfer(I)-Verbindung „Cu(2,2$-$py$_2$Stri) Cl". Der Diamagnetismus und der Nichtelektrolytcharakter (Tab. 1) sind damit in völliger Übereinstimmung, nicht jedoch die schwarze Farbe. So ist das Bis[2-(2-pyridyl) äthyl]-disulfid-kupfer(I)-perchlorat, eines Koordinationspolymeres mit der zentralen Koordinationseinheit Cu^{I}(Npy)$_2$S$_2$,[13] die der einer echten Kupfer(I)-Verbindung Cu(2,2 $-$ py$_2$Stri) Cl sehr ähnlich wäre, gelbt gefärbt.

---

[10] Le My Ngu, Dissertation, Jena, 1971.

[11] P. Chia, S. Livingstone u. T. Lockyer, *Austral. J. Chem.*, **20**, 239 (1967).

[12] P. Chia, S. Livingstone u. T. Lockyer, *Austral. J. Chem.*, **19**, 1835 (1966).

[13] L. Warner, T. Ottersen u. K. Seff, *Inorg. Chem.*, **13**, 2819 (1974).

Hemmerich[14] beschreibt tiefviolette binukleare Kupfer(II)-Verbindungen des Typs V, die bei tiefer Temperatur wegen starker Spin-Spin-Kopplung über die Mercaptid-Brücken diamagnetisch sind. Wir halten es für möglich, daß der schwarze Komplex IV ein mit V vergleichbares Kupfer(II)-Chelat des Liganden $\alpha-C_5H_4N-CH_2-S^{\ominus}$ ist. Das zweite Bruchstück des 2,2−py$_2$Stri sollte dann als α-Picolin im Komplex gebunden sein. Der Übergang von Thioäther- in Mercaptidkomplexe ist aus der Chemie des Nickel(II), Platin(II) und Palladium(II) bekannt (Reaktion *a*).[15] Dabei ist der nukleophile Angriff des Halogenoliganden auf die koordinierte Thioätherfunktion der entscheidende Schritt. Die Bildung eines Komplexes mit einer zu V vergleichbaren Struktur und koordiniertem α-Picolin würde einen radikalischen Mechanismus voraussetzen. Der leichte Übergang von Kupfer(II) in Kupfer(I) und umgekehrt könnte dafür eine wichtige Voraussetzung sein.

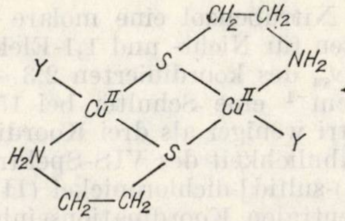

V (Y= einwertiges Anion)

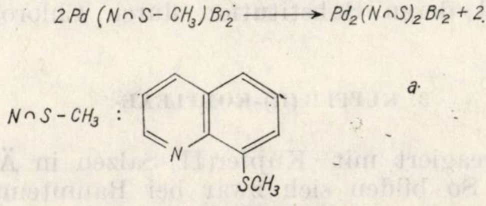

a

Während es sich bei den blauen Kristallen, die aus Kupfer(II)-perchlorat und 2,2−py$_2$Stri entstehen, um Cu(2,2−py$_2$Stri) $(H_2O)(ClO_4)_2$ handelt, kann das zweite, grüne Produkt (im Folgenden als „Komplex VI“ bezeichnet) auf Grund der Analysendaten wieder als Kupfer(I)-Verbindung „Cu(2,2−py$_2$Stri) (ClO_4)“ angesprochen werden. Es ist diamagnetisch und weist nur eine geringe elektrische Leitfähigkeit in Acetonitril auf. Im VIS-Spektrum wird ein schwaches Maximum bei 15500 cm^{-1} beobachtet, etwa an der gleichen Stelle wie bei Cu(2,2−py$_2$Stri) (H_2O) $(ClO_4)_2$. Die Vermutung liegt nahe, daß die grüne Farbe durch einen Einschluß der letzteren Verbindung bedingt ist. Komplex VI im reinen Zustand könnte also im Unterschied zu Komplex IV eine im sichtbaren Spektralgebiet nicht absorbierende Kupfer(I)-Verbindung sein.

---

[14] P. Kroneck, C. Naumann u. P. Hemmerich, *Inorg. Nucl. Chem. Letters*, **7**, 639 (1971).

[15] L. Lindoy, *Coord. Chem. Rev.*, **4**, 41 (1969).

Auf folgende Befunde sei noch verwiesen:

— Dichloro-(*o*-Methylmercapto-anilin)-kupfer(II) kann nur bei 0° dargestellt werden, sonst entsteht eine dunkel gefärbte Lösung, aus der keine Kristalle erhalten werden. Mit Kupfer(II)-perchlorat verläuft die Reaktion des *o*-Methylmercapto-anilins so schnell, daß kein reiner Komplex isoliert werden kann.[16] *o*-Methylmercapto-anilin ist strukturell dem 2,2—py_2Stri verwandt (N und S in einer für die Fünfringbildung geeigneten Position, Thioätherfunktion) und bildet Komplexe des Typs V.[17] Die von uns zwischen Kupfer(II)-Salzen und 2,2—py_2Stri beobachtete Reaktion hat also Parallelen.

— Komplexe des Typs V sind nur mit Fünfringbildnern darstellbar, das Stickstoffatom kann aber durch Sauerstoffunktionen ersetzt werden.[14] Die erfolglosen Versuche zur Darstellung Kupfer(II)-Komplexe mit 2-(Pyridyl-2)-äthylmercaptan, einem Chelatsechsringbildner, und das Ausbleiben einer Weiterreaktion von Cu(3,3—py_2Stri) Cl_2 in Äthanol [3] sprechen daher nicht gegen die oben angestellten Überlegungen zur Struktur der Verbindungen IV und VI.

Wenn auch die Untersuchungen zur Bildung und Struktur der Komplexe IV und VI nicht als abgeschlossen zu betrachten sind, so kann doch Folgendes festgestellt werden: Kupfer(II)-Salze reagieren vor allem bei höherer Temperatur mit 2,2—py_2Stri im Sinne einer Redoxreaktion. Diese wird in ihrem Verlauf in starkem Maße von den Anionen beeinflußt, und sie wird auch mit Liganden beobachtet, die dem 2,2—py_2Stri strukturell verwandt sind.

In den 1,1-Komplexen des Kupfer(II) mit den Liganden 2,2—py_2Stri und 2,3—py_2Stri sind die letzteren dreifach koordiniert (vgl. das IR-Spektrum, Tab. 1). Die Reflexionsspektren von Cu(2,2—py_2Stri) Cl_2 und Cu(2,2—py_2Stri)Br_2 sind vor der Form her denen des [Cu(Me_6tren) Br] Br[18] und des [Cu(tren) (NCS)] (NCS)[19] nahe verwandt. Letzteres hat eine trigonalbipyramidale Struktur.[20] Zwischen den Halogenokomplexen Cu(2,2—py_2Stri) X_2 und dem Perchlorat Cu(2,2—py_2Stri) (H_2O) $(ClO_4)_2$ besteht eine deutliche strukturelle Differenz. Ein Maximum bei 15,4 kK mit einer an der langwelligen Flanke angedeuteten Schulter ist am ehesten mit einer tetragonal-pyramidalen Struktur des Perchlorates in Übereinstimmung zu bringen,[21] wobei die Frage nach der speziellen Lage des 2,2—py_2Stri offen bleibt.

4. EIN EISEN(II)-KOMPLEX

Aus alkoholischen Lösungen von Eisen(II)-chlorid und 2,2—py_2Stri kristallisiert der gelbe 1,1-Komplex Fe(2,2—py_2Stri) Cl_2. Nach dem IR-Spektrum und dem magnetischen Moment (Tab. 1) kommt dem Zentralatom die Koordinationszahl 5 zu. Das VIS-Spektrum (Bande im nahen

---

[16] L. Lindoy, S. Livingstone u. T. Lockyer, *Austral. J. Chem.*, **20**, 471 (1967).

[17] T. Ottersen, L. Warner u. K. Seff, *Inorg. Chem.*, **13**, 1904 (1974).

[18] M. Ciampolini u. N. Nardi, *Inorg. Chem.*, **5**, 41 (1966).

[19] R. Barbucci, G. Cialdi, G. Ponticelli u. P. Paoletti, *J. Chem. Soc. A*, **1969**, 1775.

[20] P. Jain u. E. Lingafelter, *J. Amer. Chem. Soc.*, **89**, 6131 (1967).

[21] M. Bew, B. Hathaway u. R. Fereday, *J. Chem. Soc.*, **A 1972**, 1229.

IR mit $\varepsilon \sim 10$, schwache Maxima im sichtbaren Bereich, die auf spinverbotene Übergänge zurückgehen) entspricht dem des [Fe(Me$_2$tren) Br] Br, dem nach Ciampolini [22] eine trigonal-bipyramidale Struktur zukommt. Mit 3,3—py$_2$Stri konnte unter vergleichbaren Bedingungen kein Eisen(II)-Komplex erhalten werden.

5. DISKUSSION DER ERGEBNISSE

Ein Vergleich der isolierbaren Nickel(II)-Komplexe der Liganden 3,3—py$_2$Stri,[3,4] 2,3—py$_2$Stri und 2,2—py$_2$Stri zeigt ein deutliches Ansteigen der Tendenz zur Bildung von 1,2-Komplexen beim Übergang vom 6,6- über den 5,6- zum 5,5-Ringbildner. Eine ähnliche Tendenz wird auch bei den amin-analogen Liganden 3,3—py$_2$tri[3,4] und 2,2—py$_2$tri [23] beobachtet. Während aber 1,1-Komplexe von 2,2—py$_2$tri mit Nickel(II)-Salzen nicht dargestellt werden konnten, ist das im Falle des 2,2—py$_2$Stri dann möglich, wenn stärkere anionische Donatoren, wie Chlorid oder Thiocyanat, als Zweitliganden angeboten werden.

Beim Kupfer(II) konnten mit 3,3—py$_2$Stri, 2,3—py$_2$Stri und 2,2—py$_2$Stri [24] nur 1,1-Komplexe isoliert werden, obwohl in wäßriger Lösung der Nachweis von 1,2-Komplexen gelang.[1] Allerdings muß einschränkend bemerkt werden, daß unter Bedingungen, die im Falle des amin-analogen Liganden 2,3—py$_2$tri die Darstellung eines 1,2-Komplexes ermöglichten (Verwendung von Kupferperchlorat bei Anwendung eines Ligandenüberschusses),[2] der Ligand 2,2—py$_2$Stri die in Abschnitt 3 beschriebene Redoxreaktion eingeht.

2,2—py$_2$Stri bildet mit Kupfer(II) und Nickel(II) Komplexe gleicher Zusammensetzung wie sein aliphatisches Analogon Bis(2-aminoäthyl)-sulfid(2,2-Stri).[25] In den VIS-Spektren dieser Verbindungen zeichnen sich jedoch deutliche strukturelle Unterschiede ab. So stehen den trigonal-bipyramidalen Chelaten Cu(2,2—py$_2$Stri) X$_2$ (Abschnitt 3) die Verbindungen Cu(2,2—Stri)X$_2$ (X = Cl, Br) gegenüber, denen auf Grund des Absorptionsmaximums bei etwa 16,0 kK eine tetragonal-pyramidale oder verzerrt oktaedrische Struktur mit Halogenobrücken zugeschrieben werden kann,[21] und im Spektrum von [Ni(2,2—Stri)$_2$](NO$_3$)$_2$ (Banden bei 11,66; 18,26 und 28,77 kK) fehlt das für [Ni(2,2—py$_2$Stri)$_2$] (NO$_3$)$_2$ gefundene Maximum bei 15,7 kK. Interessanterweise sind aber die Spektren von [Ni(2,2—Stri)$_2$] (NO$_3$)$_2$ und [Ni(2,3—py$_2$Stri)$_2$] (ClO$_4$)$_2$ sehr ähnlich, so daß wir für beide die oktaedrische *cis*-Struktur III diskutieren (Abschnitt 3). Aus der längstwelligen Absorptionsbande beider Komplexe können die mittleren Ligandenfeldparameter D$_q$ für 2,2-Stri zu 1166 und für 2,3—py$_2$Stri zu 1140 cm^{-1} entnommen werden. Sie entsprechen etwa dem D_q-Wert des diens.[23]

2,3—py$_2$Stri ist infolge der zusätzlich eingeschobenen Methylengruppe weniger starr als 2,2—py$_2$Stri. Es kann daher in der Beweglichkeit des Haftatomsystems, die für den „Biß“ eines mehrzähligen Chelatliganden und seine Anpassungsfähigkeit an die sterischen Erfordernisse eines Zentralatoms von großer Bedeutung ist,[26] etwa mit dem 2,2-Stri verglichen werden. Die strukturelle Verwandtschaft der Nickel (II)-Komplexe beider Liganden findet darin eine plausible Erklärung.

---

[22] M. Ciampolini u. N. Nardi, *Inorg. Chem.*, 5, 1150 (1966).

[23] S. Nelson u. J. Rodgers, *J. Chem. Soc. A*, **1968**, 272.

[24] E. Uhlig U. B. Borek, *Z. anorg. Chem.*, **425**, 217 (1976).

[25] L. Taylor u. E. Barefield, *J. Inorg. Nucl. Chem.*, **31**, 3831 (1969).

Obwohl Strukturanalysen fehlen, so zeichnet sich aus unseren Ergebnissen doch ab, daß der Ligand 2,2$-py_2$Stri bevorzugt faciale Positionen besetzt. In Komplexen mit der Koordinationszahl 5 werden außerdem trigonal-bipyramidale Strukturen begünstigt, d.h. ein Haftatom von 2,2$-py_2$Stri besetzt eine axiale Position. Ungeklärt bleibt die Frage, ob es sich dabei um das Schwefelatom oder eines der Stickstoffatome handelt. Die Bevorzugung facialer Positionen durch 2,2$-py_2$Stri hat primär sterische Gründe, die vor allem in der Starrheit des Liganden und in seiner Unfähigkeit Transpositionen zu überspannen zu suchen sind.

7. BESCHREIBUNG DER VERSUCHE

Bis(pyridyl-2-methyl)-sulfid (2,2$-py_2$Stri) : 26 g (0,2 Mol) 2-Chlormethylpyridin[27] werden mit 36 g (0,15 Mol) $Na_2S \cdot 9H_2O$ in 30 ml Wasser und 100 ml Äthanol 5 Stunden unter Rühren auf 60° erhitzt. Dann wird das Äthanol in Vakuum abgezogen, der Rückstand mit Natronlauge alkalisch gemacht und anschließend mit Chloroform extrahiert. Der Chloroformextrakt wird nach Waschen mit Wasser und Trocknen mit Natriumsulfat destilliert. 2,2$-py_2$Stri geht bei 146–148° (1 Torr) über. 19 g (88%)
$C_{12}H_{12}N_2S$ (216,2)
Ber. C 66,60 (gef. 66,55); H 5,56 (5,71); N 12,94 (12,90%)

Darstellung der Komplexe: Cu(2,2$-py_2$Stri)Cl_2, Cu (2,2$-py_2$Stri)Br_2 und Cu(2,3$-py_2$Stri)Cl_2 entstehen bei der Umsetzung der Kupfer (II)-halogenide mit 2,2$-py_2$Stri bzw. 2,3$-py_2$Stri in Äthanol (Molverhältnis 1 : 1, Zimmertemperatur). Läßt man $CuCl_2 . 2H_2O$ oder $Cu(ClO_4)_2 \cdot 6H_2O$ mit 2,2$-py_2$Stri (Molverhältnis 1 : 2) in siedendem Äthanol reagieren, so erhält man die Komplexe IV „Cu(2,2$-py_2$Stri) Cl“ bzw. VI „Cu(2,2$-py_2$Stri) ClO_4“. Die Umsetzung von $Cu(ClO_4)_2 \cdot 6H_2O$ mit 2,2$-py_2$Stri (Molverhältnis 1 : 1) in Äthanol in der Kälte ergibt zunächst grüne Kristalle des Komplexes VI. Aus der blauen Mutterlauge kristallisiert im Eisschrank Cu(2,2$-py_2$Stri) (H_2O) $ClO_4)_2$. Die Komplexe [Ni(2,2$-py_2$Stri$)_2$] X_2 und [Ni(2,3$-py_2$Stri$)_2$] $(ClO_4)_2$ werden aus den Komponenten im Molverhältnis 1 : 2 in Äthanol hergestellt (Siedehitze).

Cu(2,3$-py_2$Stri) $Cl(ClO_4)$: Man löst Cu(2,3$-py_2$Stri) Cl_2 in 15 ml Wasser und fügt in der Hitze 1 g $NaClO_4$ (gelöst in 5 ml Wasser) hinzu. Beim langsamen Abkühlen scheiden sich blaue Kristalle ab, die aus Äthanol umkristallisiert werden. Ni(2,2$-py_2$Stri) Cl_2 : 2,0 $NiCl_2 \cdot . 6H_2O$ werden in 30 ml abs. Äthanol gelöst und dazu bei Zimmertemperatur 2,7 g 2,2$-py_2$Stri in 10 ml abs. Äthanol gegeben. Die Reaktionsmischung wird bis zur beginnenden Trübung mit Diisopropyläther versetzt. Nach mehrtägigem Stehen bei –15° scheiden sich feine Kristalle ab, die aus abs. Äthanol umkristallisiert werden.

Analog werden Ni(2,2$-py_2$Stri) $(NCS)_2$ aus $Ni(SCN)_2$ und 2,2$-py_2$Stri und Ni(2,3$-py_2$Stri$)_2Cl_2$ aus $NiCl_2 . 6H_2O$ und 2,3$-py_2$Stri dargestellt.

Fe(2,2$-py_2$Stri) Cl_2 : 1,26 g Eisen(II)-chlorid in 30 ml abs. Äthanol werden unter Rühren in eine Mischung von 2,37 g 2,2$-py_2$Stri und 10 ml abs. Äthanol gegeben. Die Farbe wechselt beim anschließenden 15 minütigen Erhitzen auf 60° von Hellblau nach Gelb. Beim Stehen im Kühlschrank scheiden sich gelbe Kristalle ab.

Analysendaten und Eigenschaften der neu dargestellten Komplexe sind der Tabelle 2 zu entnehmen.

Wegen weiteren experimentellen Einzelheiten sei auf die Dissertation von Le My Ngu, Jena, 1971, verwiesen.

---

[26] E. Uhlig, in „Neuere Enwicklungen der anorganischen Chemie“, VEB Deutscher Verlag der Wissenschaften, Berlin, 1974, S. 321.

[27] W. Mathes u. H. Schuly, *Angew. Chem.*, **75**, 235 (1963).

Tabelle 2

Eigenschaften und Analysendaten von Komplexen des 2,2-py$_2$Stri und des 2,3-py$_2$Stri

	Molmasse	Farbe	Schmelzpunkt	Metall		N		Anion	
				gef %	ber %	gef %	ber %	ber %	gef %
Ni(2,2–py$_2$Stri) Cl$_2$ $C_{12}H_{12}Cl_2N_2NiS$	345,8	taubenblau	282°	16,95	17,05	8,37	8,12	20,33	20,53
Ni(2,2–py$_2$Stri) (NCS)$_2$ $C_{14}H_{12}N_4NiS_3$	390,9	grünblau	270°	14,90	15,03	14,42	14,34	29,50	29,70
[Ni(2,2–py$_2$Stri)$_2$] Br$_2$ $C_{24}H_{24}Br_2N_4NiS_2$	651,0	violett	259°	9,02	9,03	8,57	8,51	24,20	24,00
[Ni(2,2–py$_2$Stri)$_2$] J$_2$ $C_{24}H_{24}J_2N_4NiS_2$	744,9	violett	247°	7,87	7,88	7,65	7,52	33,98	34,04
[Ni(2,2–py$_2$Stri)$_2$] (NO$_3$)$_2$ $C_{24}H_{24}N_6NiO_6S_2$	614,7	violett	245°	9,75	9,76	13,73	13,67	—	—
[Ni(2,2–py$_2$Stri)]$_2$(ClO$_4$)$_2$ $C_{24}H_{24}Cl_2N_4NiO_8S_2$	689,6	violett	—	8,44	8,52	8,22	8,12	28,65	28,85
[Ni(2,3–py$_2$Stri)$_2$] (ClO$_4$)$_2$ $C_{26}H_{28}Cl_2N_4NiO_8S_2$	718,3	rotviolett	203°	8,28	8,17	7,49	7,80	28,13	27,70
Ni(2,3–py$_2$Stri)$_2$Cl$_2$ $C_{26}H_{28}Cl_2N_4NiS_2$	590,3	hellgrün	186°	9,69	9,89	9,39	9,45	11,38	11,95
Cu(2,2–py$_2$Stri) Cl$_2$ $C_{12}H_{12}Cl_2CuN_2S$	350,5	hellgrün	127°	18,22	18,10	7,74	7,99	20,28	20,20
Cu(2,2–py$_2$Stri) Br$_2$ $C_{12}H_{12}Br_2CuN_2S$	439,6	hellgrün	132°	14,48	14,46	6,55	6,37	—	—
Cu(2,3–py$_2$Stri) Cl$_2$ $C_{13}H_{14}Cl_2CuN_2S$	364,8	türkis	141°	17,53	17,40	7,36	7,68	19,60	19,45
Cu(2,3–py$_2$Stri) Cl(ClO$_4$) $C_{13}H_{14}Cl_2CuN_2O_4S$	428,8	blau	149°	15,01	14,81	6,97	6,53	8,13[a] 22,80[b]	8,26
„Cu(2,2–py$_2$Stri) Cl“ (IV)[c] $C_{12}H_{12}ClCuN_2S$	315,1	schwarz	150°	20,33	20,17	8,59	8,86	11,21	11,26
„Cu(2,2–py$_2$Stri) (ClO$_4$)“ (VI)[d] $C_{12}H_{12}ClCu_2NO_4S$	379,2	grün	224°	18,22	18,10	7,74	7,99	20,28	20,20
Fe(2,2–py$_2$Stri) Cl$_2$ $C_{12}H_{12}Cl_2FeN_2S$	343,0	gelb	187°	16,30	16,30	8,26	8,18	20,58	20,68

[a] Chlorid, [b] Perchlorat, [c] Ber. C 45,75 (gef. 44,95); H 3,80 (3,51%), [d] Ber. C 38,00 (gef. 38,50); H 3,25(3,97%).

Revue Roumaine de Chimie, **22**, *8*, 1175–1180 (1977)

POLYNUCLEAR COMPLEX COMPOUNDS OF IRON, COBALT AND NICKEL. II[1]

MERCURY-CONTAINING COMPLEX COMPOUNDS

MARIA BREZEANU and MAGDALENA DINCULESCU
Chemistry Institute of Bucharest, Laboratory of Inorganic Chemistry,
Splaiul Independenţei, 89

Received August 31, 1976

A series of polynuclear complex compounds containing mercury and respectively iron, cobalt, nickel were synthesized. They correspond to the following general formulas : $Fe(HgCl_2en)_n(OH)_3$ where $n = 1, 2, 4$; $M(HgCl_2 en)_n(OH)_2$ where $n = 2,4$ for cobalt and $n = 2$ for nickel and $M(HgCl_4en_2)$ in which M = Co, Ni. These compounds were characterized by elemental chemical analysis, electronic and vibrational spectra and molecular electric conductivity determinations.

A previous paper[1] has reported on the results obtained from the synthesis and characterization of compounds formed in the systems : $FeCl_3-HgCl_2-B$ and MCl_2-HgCl_2-B where M = Co, Ni ; $B = NH_3$.

In view of establishing the influence of the base used on the type of compounds which may be formed in such systems, the study of the same systems was extended using ethylenediamine as a base.

A series of polynuclear complex compounds were thus obtained, which may be represented by the following general formulas : $Fe(HgCl_2\ en)_n(OH)_3$ $n = 1, 2, 4$; $M(HgCl_2\ en)_n(OH)_2$, $n = 2,4$ for Co and $n = 2$ for Ni ; $M(HgCl_4\ en_2)$ where M = Co, Ni.

These compounds were characterized by elemental chemical analysis, electronic and ir spectra and conductivity determinations.

RESULTS AND DISCUSSION

The synthesis of compounds that may form in the systems MCl_n-HgCl_2-en, M = Fe(III), Co (II), Ni(II) was conducted under various conditions relative to the MCl_n ratio (from 1 : 1 to 1 : 8 and from 1 : 1 to 8 : 1, respectively).

We shall present below the results obtained from the first series of determinations in which iron, cobalt and nickel chloride, respectively, was kept constant whereas the amount of mercury chloride was progressively varied from a ratio of 1 : 1 to 1 : 8. Three complex compounds were obtained for each of the systems under study; they are represented by the above-mentioned general formulas. It results thereof that for each of the systems studied, the maximum amount of mercury chloride corresponds to a $1:4\ MCl_n:HgCl_2$ ratio, even if using an excess of mercury chloride in the synthesis ($1MCl_n:8HgCl_2$).

---

[1] Part I : M. Brezeanu and M. Dinculescu, *Rev. Roumaine Chim.*, **22**, 539 (1977).

All these compounds exist under the form of one single modifica, tion. Unlike the compounds containing ammonia as a neuter ligand, the compounds of the form $Fe(HgCl_2\ en)\ (OH)_3$; $M(HgCl_2\ en)_n\ (OH)_2$, M = Co-$n = 2,4$ and M = Ni, $n = 2$ and $M(HgCl_4\ en_2)$ in which M = Co, Ni, are characterized by a relatively high thermal stability. When heating them to 110° they will not modify their value and their weight will remain practically constant. This difference in the behaviour of the two series of compounds may be attributed to the ethylenediamine chelating effect.

Based on the spectral data (electronic and vibration) correllated with the molecular electric conductivity determinations, it was possible to assign to the compounds $Fe(HgCl_2en)_n\ (OH)_3\ n = 1,\ 2,\ 4$ a tetrahedral structure having very likely the form :

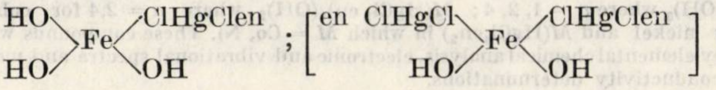

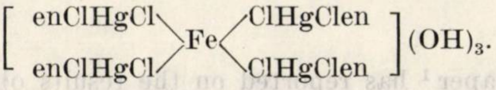

The same data were used to assign to compounds $M(HgCl_4\ en_2)$ the structure :

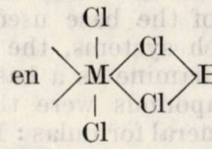

and the compounds of the form : $M(HgCl_2\ en)_n\ (OH)_2$ where $n = 2$ and M = Co, Ni, were assigned the octahedral structure :

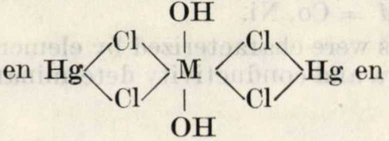

ELECTRONIC SPECTRA

The structure of the complex compounds obtained in the systems under consideration was elucidated by recording their electronic spectra. A study of these spectra (Fig. 1) shows that the most likely structure for the compounds $Fe(HgCl_2\ en)_n(OH)_3$, $n = 1, 2, 4$ is tetrahedral, the band at approx. 800 nm being attributed to the $^6A_1 \rightarrow {}^4E$ spin-forbidden transition.

The electronic spectra of compounds $Co(HgCl_2\,en)_n\,(OH)_2$, $n = 2{,}4$ and $CoHgCl_4en_2$ (Fig. 2) may be satisfactorily interpreted in terms of an octahedral structure. The band at approx. 1150 nm is assumed to be due to the ${}^4T_{1g} \rightarrow 4T_{2g}$ transition, while that situated at approx. 500 nm, to the ${}^4T_{1g} \rightarrow 4T_{1g}(P)$ transition.

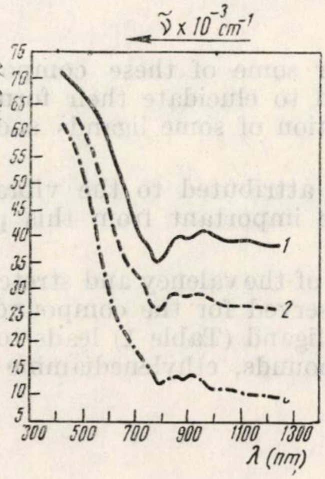

Fig. 1. — Electronic spectra of compounds :
1, $Fe(HgCl_2en)\ (OH)_3$;
2, $Fe(HgCl_2en)_2\ (OH)_3$;
3, $Fe(HgCl_2en)_4(OH)_3$.

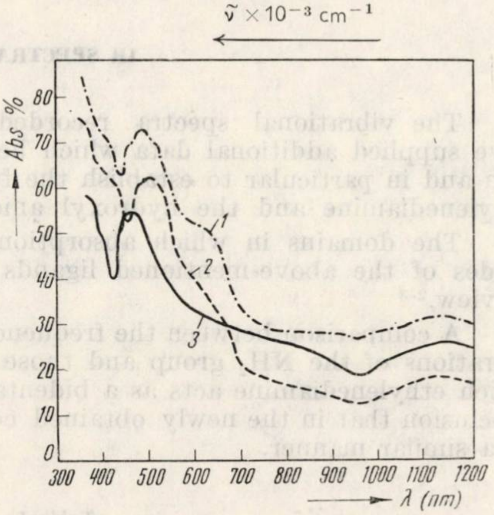

Fig. 2. — Electronic spectra of compounds :
1, $Co(HgCl_4en_2)$; *2*, $Co(HgCl_2)_2en_2(OH)_2$; *3*, $Co(HgCl_2)_4en_4(OH)_2$.

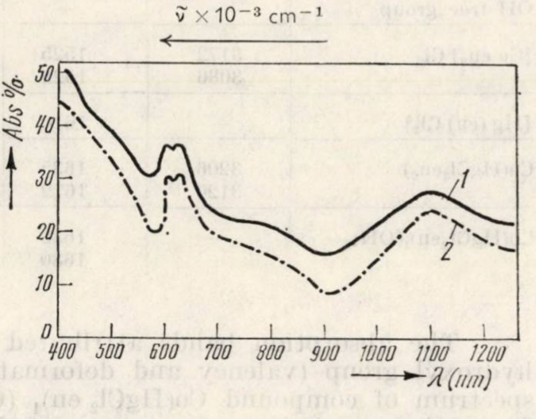

Fig. 3. — Electronic spectra of compounds :
1, $Ni(HgCl_4en_2)$; *2*, $Ni(HgCl_2)_2en_2(OH)_2$.

For the corresponding nickel compounds, the recorded electronic spectra indicate also an octahedral structure (Fig. 3). Thus, the band appearing at approx. 650 nm is attributed to the ${}^3A_{2g} \rightarrow {}^3T_{1g}(F)$ transition, the splitting being due to the spin-orbit coupling which determines the mixing of ${}^3T_{1g}(F)$ and ${}^1E_g$ states, and the band appearing at approx. 1100 nm is attributed to the ${}^3A_{2g} \rightarrow {}^3T_{2g}$ transition.

IR SPECTRA

The vibrational spectra recorded for some of these compounds have supplied additional data which helped to elucidate their formulation and in particular to establish the function of some ligands such as ethylenediamine and the hydroxyl anion.

The domains in which absorption is attributed to the vibration modes of the above-mentioned ligands are important from this point of view.[2,3]

A comparison between the frequencies of the valency and stretching vibrations of the NH_2 group and those observed for the compounds in which ethylenediamine acts as a bidentate ligand (Table 1) leads to the conclusion that in the newly obtained compounds, ethylenediamine acts in a similar manner.

Table 1

Characteristic-IR frequencies for some of the obtained compounds

Compounds	νNH_2(str.)	νNH_2(def.) asym.	$\nu M-N$	νOH(str)	νOH(def.)
Etylenediamine	3510	1595	—	—	—
OH free group	—	—	—	3590 – 3650	1260 – 1350
$[Co\ en_3]\ Cl_3$	3172 3086	1525 1529	$\nu Co-N$: 585	—	—
$[Hg\ (en)\ Cl_2]$	—	1610	—	—	—
$Co(HgCl_4en_2)$	3206 3120	1635 1672	$\nu Hg-N$: 473 $\nu Co-N$: 586	—	—
$Co(HgCl_2en)_4(OH)_2$	—	1638 1680	$\nu Hg-N$: 467	3210	1324

The absorption bands attributed to the vibration modes of the hydroxyl group (valency and deformation vibration) observed in the spectrum of compound $Co(HgCl_2\ en)_4\ (OH)_2$ indicate its coordination. The shift towards lower frequencies of the bands in question agrees with the data from the literature.

---

[2] G. Gordon and R. K. Birdwhistell, *J. Amer. Chem. Soc.*, **81**, 3567 (1959).

[3] L. J. Bellamy, "The Infrared Spectra of Complex Molecules" John Wiley Sons, Inc., New York, 1958, p. 102.

A third important domain for solving such problems is that in which absorption is attributed to the metal-ligand valency vibration (metal-nitrogen).[4,5]

Based on the data from the literature (Table 1), the two bands appearing in the spectrum of compound $Co(HgCl_4\,en_2)$ in this domain have been attributed to the valency frequencies

$$\nu_{Hg-N}(473\ cm^{-1})\ \text{and}\ \nu_{Co-N}(568\ cm^{-1}).$$

This thing indicates the ethylenediamine coordination both in mercury and in cobalt.

The presence in the spectrum of compound $Co(HgCl_2en)_4(OH)_2$ of one single absorption band attributed to the vibration mode ν_{M-N} at 467 cm^{-1} indicates the ethylenediamine coordination only in mercury.

MOLECULAR CONDUCTIVITY DETERMINATIONS

Molecular conductivity studies were also performed in order to provide additional evidence to support the formulation of these compounds.

Table 2 indicates the results obtained, and they agree with the formulations attributed on the basis of the data reported in the literature relative to the limits comprising the various electrolyte types.[6]

EXPERIMENTAL DATA

SYNTHESIS AND ANALYSIS OF COMPOUNDS

1. $Fe(HgCl_2)_n\ (en)_n\ (OH)_3$ ($n=1, 2, 4$). To a solution obtained by dissolving 0.25 g $FeCl_3 \cdot 6H_2O$ in 3 ml water one adds 0.25 g, 0.5 g and 1 g $HgCl_2$, respectively, corresponding to a

Table 2

Molecular electric conductivities of the obtained compounds in DMF solutions

Compounds	$\lambda(\Omega^{-1}\ cm^2/mol)$	Electrolyte type
$Fe(HgCl_2)\ en\ (OH_3)$	12.5	non-electrolyte
$Fe(HgCl_2)_2en_2(OH_3)$	72.9	1 : 1
$Fe(HgCl_2)_4en_4(OH_3)$	203.5	1 : 3
$Co(HgCl_4en_2)$	10.4	non-electrolyte
$Co(HgCl_2)_2en_2(OH)_2$	13.5	non-electrolyte
$Co(HgCl_2)_4en_4(OH)_2$	17.0	non-electrolyte
$Ni(HgCl_4en_2)$	16.1	non-electrolyte
$Ni(HgCl_2)_2en_2(OH)_2$	18.2	non-electrolyte

---

[4] D. B. Powell and N. Sheppard, *J. Chem. Soc.*, **1961**, 1112.

[5] K. Nakamoto, "The Infrared Spectra of Inorganic Compounds" John Wiley Sons, Inc., New York, 1963, p. 143

[6] D. J. Phillips and S.. Y. Tyree, *J. Amer. Chem. Soc.*, **83**, 1806 (1961).

1 : 1, 1 : 2 and 1 : 4 $FeCl_3 : HgCl_2$ ratio. About 25 ml ethyl alcohol is added to assure the total dissolution of salts, the compounds being then precipitated with ethylendiamine at pH = 8. The separated substance is filtered after 24 hr and thoroughly washed with alcohol.

Calcd. : Hg, 45.78; Fe, 12.75; Cl, 16.13; N, 6.38 $n = 1$
Found : 45.82; 12.69; 16.40; 6.45%

Calcd. : Hg, 52.14; Fe, 7.26; Cl, 18.41; N 7.26 $n = 2$
Found : 52.26; 7.35; 18.62; 7.43%

Calcd. : Hg 56; Fe, 3.90; Cl, 19.80; N 7.81 $n = 4$
Found : 56.12; 3.85; 19.96; 7.93%

The compound $Fe(HgCl_2)_4en_4(OH)_3$ is also obtained at $FeCl_3 : HgCl_2 > 1 : 4$ ratios, i.e. 1 : 6 and 1 : 8.

2. $CoHgCl_4en_2$; $Co(HgCl_2)_n(en)_n(OH)_2$ ($n = 2,4$). To a solution obtained by dissolving 0.2 g $CoCl_2 . 6H_2O$ in 3 ml water one adds a variable $HgCl_2$ quantity corresponding to the $CoCl_2 : HgCl_2$ ratio, i.e. : 0.25 g, 0.5 g and 1 g. About 25 ml alcohol is added with vigorously stirring until total dissolution of salts. Ethylenediamine is added to the final solution up to a pH = 8. The separated substance is filtered after 24 hr and it is thoroughly washed with alcohol to totally remove the excess of ethylenediamine. The compound $Co(HgCl_2)_4en_4(OH)_2$ is also obtained for the $CoCl_2 : HgCl_2 > 4$ ratio, i.e. for 1 : 6 and 1 : 8. In the other two compounds the existing $HgCl_2$ quantity corresponds to the quantity used in the synthesis.

Calcd. : Hg, 38.50; Co, 11.32; Cl, 27.20 N, 10.72 $n = 1$
Found : 38.75; 11.53; 26.90; 10.56%

Calcd. : Hg, 53.10; Co, 7.92; Cl, 18.75; N, 7.39 $n = 2$
Found : 53.23; 7.99; 19.01; 7.65%

Calcd. : Hg, 56.54; Co, 4.15; Cl, 20.01; N, 7.88 $n = 4$
Found : 56.72; 4.23; 20.22; 8.02%

3. $Ni(HgCl_2)_2en_2(OH)_2$; $Ni(HgCl_4\ en_2)$. To a solution obtained by dissolving 0.2 g $NiCl_2 . 6H_2O$ in 3 ml water and 2 ml alcohol one adds 0.25 g, respectively 0.5 g of $HgCl_2$. After total dissolution of salts, compound $Ni(HgCl_2)_2\ en_2(OH)_2$ precipitates with ethylenediamine at pH = 8. The separated substance is filtered after 24 hr and thoroughly washed with alcohol.

The compound $NiHgCl_4\ en_2$ is obtained under similar conditions only at a 1 : 2 $HgCl_2 : NiCl_2$ ratio.

Calcd. : Hg, 53.10; Ni, 7.79; Cl, 18.79; N, 7.39
Found : 53.32; 7.83; 18.35; 7.52%
Calcd. : Hg, 38.50; Ni, 11.30; Cl, 27.20; N 10,73
Found : 38.35; 11.15 26.95; 10.92%

Reflexion spectra were recorded at room temperature using a VSU_1 spectrophotometer and magnesium oxide as reference.

IR spectra were recorded by means of a UR 20 spectrophotometer using potassium bromide pelleting technique.

Molecular conductivity determinations were performed using a UK—120/1 conductometer.

Revue Roumaine de Chimie, 22, 8, 1181–1186, (1977)

A TETRAHEDRAL Ni(II) COMPLEX COMPOUND DERIVED FROM 1-METHYL-2-CARBETHOXY-GLYOXALANIL-(1)-*m*-NITRO-PHENYLHYDRAZONE-(2)

A. C. BANCIU

Center of Physical Chemistry Bucharest, str. Dumbrava Roşie, 23, Romania

Received June 7, 1975

Both the electronic spectrum and the magnetic moment ($\mu_{exp} = 3.2 \pm 0.1$ B.M.) of the Ni(II) complex compound derived from 1-methyl-2-carbethoxy-glyoxalanil-(1)-*m*-NO_2-phenylhydrazone-(2) indicate for the solid complex an approximately tetrahedral structure. This presents, however, a considerable distortion from the regular tetrahedral one. In solutions the complex is square-planar.

INTRODUCTION

In our previous investigations [1-3] we have prepared and studied new Ni(II) chelate complexes derived from 1-methyl-2-carbethoxy-glyoxalanil-(1)-phenylhydrazones-(2), differently substituted (*p*- and *m*-CH_3; *p*- and *m*-OCH_3) at the benzene ring of the hydrazone group. Extending these studies, in a recent paper [4] we have also synthesized the new complexes of this type, Ia and Ib, which are *para*- and respectively *meta*-NO_2-substituted at the benzene ring of the hydrazone group. In the same paper [4] we have interpreted the electronic absorption spectra of all the new Ni(II) complexes of this class, in the framework of the ligand field theory.

The present paper reports the electronic reflectance spectrum and the magnetic moment of the complex Ib in the solid state. These properties show that in solid state the structure of the complex is fundamentally different from the square-planar structure of the complex found in acetone solutions.

---

[1] P. Spacu, A. C. Banciu and C. I. Lepădatu, *Rev. Roumaine Chim.*, **18**, 7, 1143 (1973).

[2] A. C. Banciu and P. Spacu, *Rev. Roumaine Chim.*, **19**, 5, 817 (1974).

[3] A. C. Banciu and P. Spacu, *Rev. Roumaine Chim.*, **19**, 8, 1307 (1974).

[4] A. C. Banciu and C. I. Lepădatu, *Z. phys. Chem. (Frankfurt)*, **97**, 197 (1975).

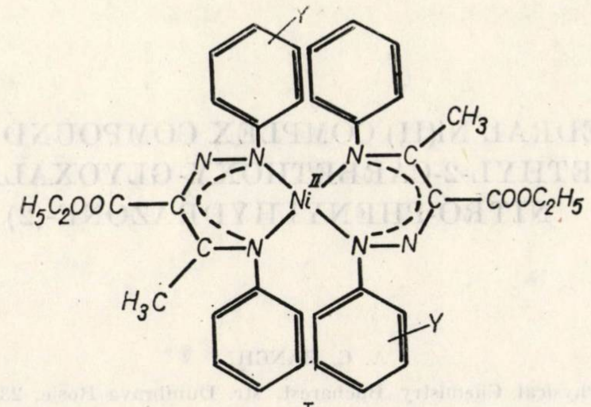

I

a : Y = p – NO_2 ; b : Y = m – NO_2

EXPERIMENTAL

The synthesis of the Ia and Ib complexes, their *analytical* data and their *electronic absorption spectra* (recorded on acetone solutions) were described in.[4]

The magnetic susceptibility measurements were performed [4] on solid complexes, at room temperature, by using the Faraday method. The magnetic moments of the complexes were calculated using the formula $\mu = 2.828\ [\chi'_M \cdot T]^{1/2}$B.M., where T is the absolute temperature and $\chi'_M = \chi_M - \chi_{\text{dia}}$ is the molar susceptibility corrected for diamagnetism. In the case of both isomeric chelates, Ia and Ib, the correction $\chi_{\text{dia}} = -361 \times 10^{-6}$ c.g.s.u. was applied for the diamagnetism. For the calculation of χ_M and χ_{dia} the complexes were formulated as monomers, according to the formulas Ia–b.

The electronic reflectance spectra of the solid complexes Ia and Ib were recorded within the 350–1200 nm range on a VSU–1 Carl Zeiss (Jena) spectrophotometer, using MgO as standard.

RESULTS AND DISCUSSION

Almost all the new Ni(II) complexes under study [1–4] are diamagnetic and therefore square-planar in the solid state. Their electronic absorption spectra (measured on acetone solutions) agree very well with the reflectance spectra measured on the solid complexes. This shows that the complexes maintain in solutions the square-planar structure for the Ni(II)–N_4 chromophore.

In contrast to all these, the complex Ib is paramagnetic in the solid state. It presents at room temperature an experimental magnetic moment of 3.2 ± 0.1 B.M., which rules out a square-planar structure for the complex. However, in solutions the complex reveals an electronic absorption spectrum practically identical to that of the other investigated Ni(II) complexes[1–4], which are square-planar both in the solid state and in solutions.

The value of the magnetic moment mentioned above suggests, with regard to the structure of the solid complex Ib, the two distinct possibilities given below.

1. The complex is ***pentacoordinated***, of high-spin type. It is known that the pentacoordinated Ni(II) high-spin complexes are formed with

ligands with N or O donor atoms and they present experimental magnetic moments of 3.2—3.4 B.M.[5] The change from the actually tetracoordinated structure of the new Ni(II) complexes[1-4] to the pentacoordinated one would take place in the case of this complex through the participation of the NO_2 group from the benzene ring of the hydrazone group in the formation of the fifth chemical bond of the central Ni(II) ion. In the series of the similar complexes formed by the Co(II) ion, which are almost without exception tetrahedral, we have recently found [6] also a pentacoordinated complex, which, similar to the complex Ib under discussion, is NO_2-substituted at the benzene ring of the hydrazone group.

2. The complex is *approximately tetrahedral*, presenting, however, a considerable distortion from the regular tetrahedral geometrical structure. It is known[7-12] that te regular tetrahedral Ni(II) complexes present strongly temperature-dependent experimental magnetic moments, measuring beyond 3.8 B.M. at room temperature. Nevertheless, the complexes whose structure presents a considerable distortion from the regular tetrahedral one, exhibit a different magnetic behaviour too. In this case, due to the quenching of the orbital contribution to the magnetic moment the experimental magnetic moments are less temperature-dependent and always smaller than in the first case. The moments measure sometimes only 3.2 B.M.[13] at room temperature, exactly as in the case of the present complex.

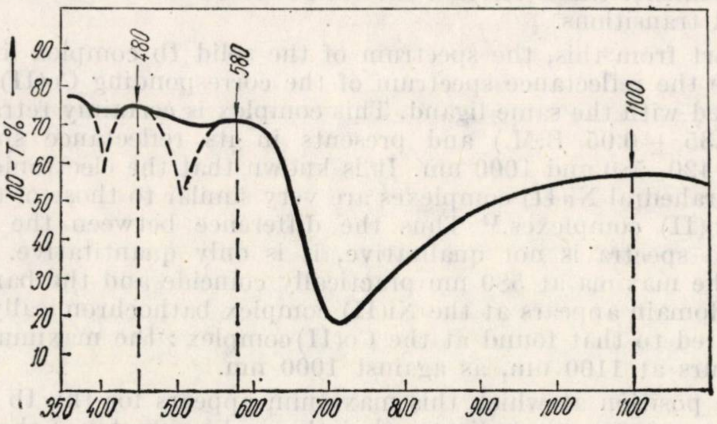

Fig. 1. — Reflectance spectrum of the complex Ib.

---

[5] P. L. Orioli, *Coord. Chem. Rev.*, **6**, 285 (1971).

[6] A. C. Banciu, *Rev. Roumaine Chim.*, under press.

[7] M. Goodgame, D. M. L. Goodgame and F. A. Cotton, *J. Amer. Chem. Soc.*, **83**, 4161 (1961).

[8] D. M. L. Goodgame and F. A. Cotton, *J. Amer. Chem. Soc.*, **82**, 5774 (1960).

[9] J. T. Donoghue and R. S. Drago, *Inorg. Chem.*, **1**, 866 (1962).

[10] C. Furlani and G. Morpurgo, *Z. phys. Chem. (Frankfurt)*, **28**, 93, (1961).

[11] K. Issleib and B. Mitscherling, *Z. anorg. Chem.*, **304**, 73 (1960).

[12] R. S. Drago, J. T. Donoghue and D. W. Herlocker, *Inorg. Chem.*, **4**, 836 (1965).

[13] L. Sacconi, "Electronic Structure and Stereochemistry of Ni(II)" in "Transition Metal Chemistry", vol. 4, Edward Arnold, London, 1968, p. 199.

The electronic reflectance spectrum of the complex Ib, as shown in figure 1, must be, obviously, interpreted in agreement with the above magnetic considerations which rule out a square-planar structure for the solid complex.

Indeed, the discussed spectrum is largely different from the reflectance spectrum of the isomeric complex, Ia, which is certainly square-planar (diamagnetic) not only in solution but also in the solid state. The last mentioned reflectance spectrum exhibits bands at ~ 430 nm (shoulder), 535 nm, 620 nm (shoulder), 740 nm (shoulder) and ~1060 nm and agrees very well with the electronic absorption spectrum[4] recorded on (acetone) solutions of the complex Ia, which shows bands at 410 nm, 520 nm (shoulder), 625 nm (shoulder) and 1150 nm.

The reflectance spectrum of the Ib complex also clearly differs from the electronic spectra of pentacoordinated Ni(II) complexes. The spectra of these complexes, regardless of the geometrical structure adopted in the frame of pentacoordination (a square pyramid or a trigonal bipyramid), will always present bands within the 600—1000 nm range as well.[13] The solid Ib complex fails however to reveal bands within this range.

Conversely, the reflectance spectrum of the complex Ib may be very reasonably assigned to an (approximately) tetrahedral Ni(II) complex. According to such an assignment, the band at 450 nm represents a charge transfer transition and the bands at 580 nm and 1100 nm represent d—d transitions.

Apart from this, the spectrum of the solid Ib complex looks very much like the reflectance spectrum of the corresponding Co(II) complex synthesized with the same ligand. This complex is certainly tetrahedral[14] ($\mu_{exp} = 4.35 \pm 0.05$ B.M.) and presents in its reflectance spectrum[14] bands at 420, 580 and 1000 nm. It is known that the electronic spectra of the tetrahedral Ni(II) complexes are very similar to those of the tetrahedral Co(II) complexes.[14] Thus the difference between the last two mentioned spectra is not qualitative, it is only quantitative. In these spectra the maxima at 580 nm practically coincide and the band in the near IR domain appears at the Ni(II) complex bathochromically shifted, as compared to that found at the Co(II) complex : the maximum of the band occurs at 1100 nm, as against 1000 nm.

The position at which this maximum appears for the Ib complex, 1100 nm (~9000 cm^{-1}), indicates that the real symmetry of the complex is lower than that of a regular tetrahedron.[13] In the case of approaching the regular tetrahedral geometry the maximum of this band appears at sensibly lower wavenumbers, such as for instance at approx. 7500 cm^{-1} for the $NiCl_4^{2-}$ tetrahedral ion.[13]

Thus, the magnetic data and the electronic reflectance spectrum of the complex Ib are in very good agreement, both indicating for the solid complex an approximately tetrahedral structure, which actually presents an appreciable distortion from the idealized tetrahedral one.

The two bands in the reflectance spectrum of the Ib complex, situated at longer wavelengths were assigned to the following *d—d* transitions, proper to the d^8 electronic configurations of the Ni(II) central ion, found in a tetrahedral surrounding.[13]

---

[14] A. C. Banciu, Ph. D. Thesis, Polytehnic Institute Bucharest, 1974.

$$\nu_2(^3T_1(F) \rightarrow {}^3A_2) = 9000 \ \text{cm}^{-1}$$

$$\nu_3(^3T_1(F) \rightarrow {}^3T_1(P)) = 17400 \ \text{cm}^{-1}$$

By neglecting the spin-orbit coupling, the energy expressions of the spin triplet levels involved in these transitions are the following [15]:

$$^3T_1(F) : 7.5\,B - 3Dq - \frac{1}{2}[225\,B^2 + 100\,Dq^2 + 180\,Dq \cdot B]^{1/2}$$

$$^3A_2 : +12\,Dq$$

$$^3T_1\,(P) : 7.5\,B - 3\,Dq + \frac{1}{2}[225\,B^2 + 100\,Dq^2 + 180\,Dq.B]^{1/2}$$

In these formulas B is the Racah parameter for the interelectronic repulsion radial integrals and $10\,Dq = \Delta$ = the orbital splitting parameter (the energetic difference between the t_2 and $\dot{e}$ subshells).

By solving the energetic expressions of the transitions ν_2 and ν_3 based on the above values one obtains the values $10\,Dq = \Delta = 4870\ \text{cm}^{-1}$ and $B = 940\ \text{cm}^{-1}$. Since for the free Ni(II) ion $B_0 = 1040\ \text{cm}^{-1}$ (according to [15]; according to [16] $B_0 = 1080\ \text{cm}^{-1}$), with the above calculated B value one obtains the β_{35} value of the nephelauxetic ratio

$$\beta_{35} = \frac{B(\text{spin allowed})}{B_0} = \frac{940}{1040} = 0.90$$

This value, unusually high, indicates a low covalency degree for the Ni(II)—N bonds of the solid Ib complex.

It is of interest to mention that for the new Co(II) complexes [1,17–19] similar to the tetrahedral Ni(II) complex in question (Ib in the solid state) the values determined [19] from electronic absorption spectra were lower for the parameter β, ranging between 0.71 and 0.82. They indicate a higher covalency degree for the Co(II)—N bonds of these complexes. This fact is not surprising since a characteristic of the tetrahedral Ni(II) complexes is the fact that they are always more ionic (less covalent) than their Co(II) analogues.

---

[15] A. B. P. Lever, "Inorganic Electronic Spectroscopy", Elsevier, Amsterdam, 1968, Chap. 8–9.

[16] J. S. Griffith, "The Theory of Transition-Metal Ions", Univ. Press, Cambridge, 1964.

[17] A. C. Banciu and P. Spacu, *Rev. Roumaine Chim.*, **19**, 6, 1019 (1974).

[18] A. C. Banciu and P. Spacu, *Rev. Roumaine Chim.*, **19**, 7, 1169 (1974).

[19] A. C. Banciu, *Rev. Roumaine Chim.*, under press.

In conclusion, it would be worth mentioning that the Ib complex is interesting not only by its unusual structural character. It is also interesting and useful for explaining the electronic spectra of the other Ni(II) complexes of this class, [1-4] i.e. derived from substituted glyoxalanil-(1)-arylhydrazones-(2). The structure of the Ib complex in question, tetrahedral in the solid state but square-planar in solution, shows that in all the other Ni(II) complexes of this class — which are square-planar both in the solid state and in solutions — a spin triplet spectral term must exist which is energetically very close to the ground state of the complexes, $^1A_{1g}$. If this was not so, it would be impossible to explain the mentioned structural conversion which is caused by a minor energetic variation (dissolution of the complex). In a recent paper [4] we have shown that the spin triplet term in question is the term $^3B_{1g}$. This has supported the assignments made in the paper [4] for the bands found in the electronic absorption spectra of the Ni(II) square-planar complexes.

ACKNOWLEDGMENT. I thank V. Mincu, lecturer at the Polytechnic Institute of Bucharest, for the magnetic susceptibility measurements.

Revue Roumaine de Chimie, **22**, *8*, 1187–1189 (1977)

COMPLEX COMPOUNDS OF Pd(II) WITH MONOSUBSTITUTED DERIVATIVES OF THIOUREA

NELLY DEMIAN, CARMEN AMBRUS and D. CAMBOLI
Department of Physical Chemistry, Polytechnic
Institute, Bucharest, Str. Polizu 1, Romania

Received April 2, 1976

The paper presents three new, stable complex compounds of Pd(II) with some monosubstituted derivatives of thiourea. The complexes were characterized by chemical analysis as well as IR spectra. They were also studied by spectrophotometry. Based on the obtained data it was established that the formula of the complex compounds is of the type $[PdA_2(SCN)_2]$, where A represents the monosubstituted thiourea derivative.

This paper is a continuation of authors concern in the field of thiocyanic complex compounds of Pd(II) with certain amines.[1,2]

There are some data in the literature concerning the complex compounds of Pd(II) with unsubstituted thiourea.[3] The purpose of this paper is the synthesis and characterization of some new complex compounds of Pd(II) with certain monosubstituted derivatives of thiourea. The amides used in the synthesis were arylated compounds of thiourea, having the following formula:

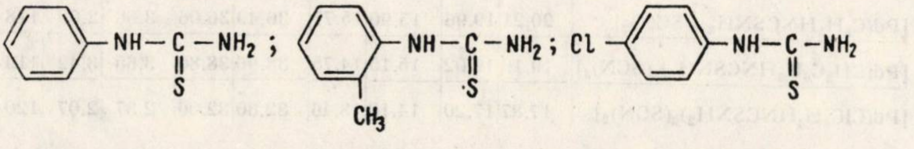

Being a weak Lewis acid, $PdCl_2$ has a good affinity for ligands with sulphur which are weak Lewis bases, as was established by Pearson.[4] Therefore, the resulted complex compounds are expected to have a good stability.

The complex compounds of Pd(II) with monosubstituted derivatives of thiourea were studied by chemical and physicochemical methods. The results permit the characterization of the new complexes regarding their structure and properties.

---

[1] D. Camboli, N. Demian and C. Ambruş, *Anal. Univ. Buc.*, **21**, 103 (1972).
[2] D. Camboli, C. Ambruş and N. Demian, *Bul. I.P.B.*, **00**, 000 (1977).
[3] P. Spacu and D. Camboli, *Anal. Univ. Buc.*, **2**, 117 (1964).
[4] R. G. Pearson, *J. Amer. Chem. Soc.*, **85**, 3533 (1963).

EXPERIMENTAL

The three amides, used as ligands, were synthetised and purified according to the data in literature.[5,6]

The complex compounds were obtained by the following method : in the aqueous solution of $PdCl_2 10^{-2}$ M, acidified with HCl, un aqueous solution of amide and crystals of KSCN was added in excess, under continuous stirring. The obtained yellow-orange precipitates were filtered on G3 crucibles, washed several times with water, ethanol and ether and dried in vacuum. The precipitates are stable in time.

For the spectrophotometric study, to the solution of $PdCl_2 10^{-3}$M was added the amine solution, also 10^{-3}M and allowed to stand for 30 minutes. The samples were then diluted with acetone and to them KSCN solution in excess was added. The total volume of the samples was maintained constant. The λ max. determined previously was 388 nm for all cases.

RESULTS AND DISCUSSION

The method by which the three new complex compounds were synthetized was in principle the same in all three cases : to an aqueous solution of $PdCl_2$ was added in excess an aqueous solution of amide and crystals of KSCN. The precipitates which were formed are abundant, mycrocrystalline, stable, easily filtered and their colour is yellow-orange. The complexes are soluble in acetone but insoluble in water, ethanol, ether, benzene. For their characterization the elementary chemical analysis was performed and their melting points were established. The results are given in table 1.

Table 1

Elementary analysis and melting points of the complexes

Complex	Pd %		N %		C %		H%		Melting points, °C
	Theor.	Exp.	Theor.	Exp.	Theor.	Exp.	Theor.	Exp.	
$[Pd(C_6H_5HNCSNH_2)_2(SCN)_2]$	20.21	19.96	15.90	15.77	36.49	36.06	3.06	2.99	118–120
$[Pd(CH_3C_6H_4HNCSNH_2)_2(SCN)_2]$	19.19	19.02	15.15	14.75	38.96	38.80	3.65	3.42	119–120
$[Pd(ClC_6H_4HNCSNH_2)_2(SCN)_2]$	17.87	17.20	14.10	13.46	32.30	32.00	2.37	2.07	120–122

The data of the elementary analysis show that all the three new synthetised complexes may be included in the class of diammines. Their general formula is of the type $[PdA_2(SCN)_2]$, where A stands for the monosubstituted derivative of thiourea.

The IR spectra of the complexes were carried out on a UR-20 Karl Zeiss-Jena spectrophotometer in the range 400–4000 cm^{-1}. The spectra reflected the maxima of the ligands, slightly displaced as a result of complexation. In the range 2000–2200 cm^{-1} all complexes exhibit maxima, which is a proof for the bonding of the thiocyano groups. The fact that the maxima correspond to values of wave numbers higher than 2100 cm^{-1}

---

[5] F. Kurzer, *Org. Synth.*, **31**, 8 (1951).

[6] F. Kurzer, Org. Synth., **31**, 21 (1951).

demonstrates that the chemical bond is achieved through the sulphur atom and therefore all obtained complexes are thiocyanic and not isothiocyanic (figure 1).

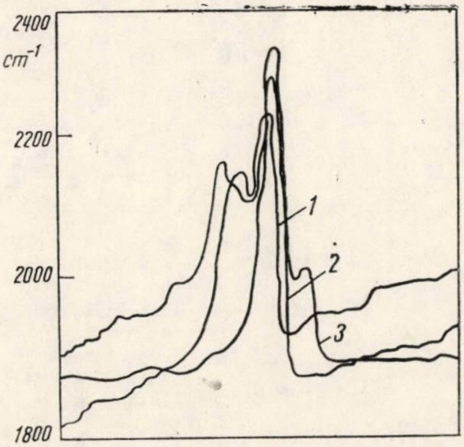

Fig. 1. — 1800—2200 cm^{-1} range of the IR spectra of the complex:

1, with phenyl-thiourea; *2*, with *o*-methyl-phenyl-thiourea; *3*, with *p*-chlorophenyl-thiourea.

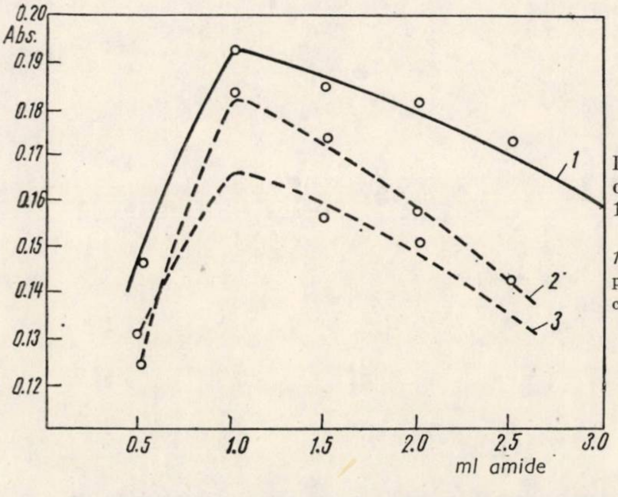

Fig. 2. — Absorbance versus ml of amide solution. Total volume: 10 ml; the samples contain 0.5 ml $PdCl_2$ 10^{-3} M.

1, complex with phenyl-thiourea; *2*, complex with *o*-methyl-phenyl-thiourea; *3*, complex with *p*-chlorophenyl-thiourea.

In order to complete the characterization of the discussed complexes, they were also subjected to a spectrophotometrical study, using a VSU-2G Karl Zeiss-Jena apparatus. The diagrams which allow to establish the combining ratio Pd : A, according to Job's method, were determined. This ratio being in all cases 1 : 2 is a confirmation of the previously assumed general formula $[PdA_2(SCN)_2]$ (figure 2).

CONCLUSIONS

The reactions which led to the obtaining of the three studied complex compounds being quantitative and the precipitates very stable in time, they may be used for gravimetric or photocolorimetric dosage of palladium.

Revue Roumaine de Chimie, 22, 8, 000–000 (1977)

DEUTERIUM ISOTOPE EFFECT ON THE BASICITY OF 2,4,6-TRIMETHYLPYRIDINE

ALEXANDRU T. BALABAN,[a,b] ILEANA I. STĂNOIU,[a]
and EUGENIA GÂRD[a]
[a] Institute of Atomic Physics, P.O.B. 5206, Bucharest
[b] The Polytechnic, Organic Chemistry Department, Bucharest, Romania

(*Received Oct. 29, 1976*)

Relative pK_a measurements for 2,4,6-trimethylpyridine and its congeners deuterated at the α, or γ, or all, methyl groups show that the basicity increment on deuteration is approximately additive and equal to 0.025 pH units.

During a recent investigation of secondary isotope effects in lanthanide-induced shifts (LIS) of ^1H–NMR peaks, we observed that on complexing the 2,4,6-trimethylpyridines **1**–**4** with $Eu(dpm)_3$ in CS_2, α-methyl deuteration (i.e. **3** and **4**) caused an appreciable isotope effect, whereas γ-methyl deuteration (i.e. **2**) gave no observable isotope effect relatively to **1**. A similar situation was encountered with 2,6-diethyl-4-methylpyridine.[1]

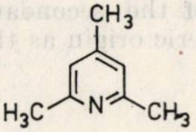
1

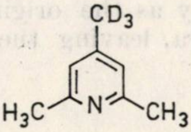
2

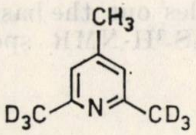
3

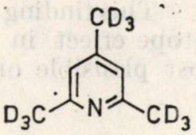
4

This observation was interpreted as indicating a steric origin of the isotope effect, rather than an electronic one as had been initially suggested by Hinckley, who discovered this type of isotope effect:[2] the larger LIS of **3** and **4** than of **1** might be due either to increased basicity on deuteration as supposed by Hinckley, or to the smaller volume of CD_3 or CD_2Me groups.[3] However, since only α-deuteration was operative, the steric origin seemed more plausible.

---

[1] A. T. Balaban, I. I. Stănoiu and F. Chiraleu, *Chem. Commun.* **1976**, 984.

[2] C. C. Hinckley, W. A. Boyd and G. V. Smith, *Tetrahadron Letters*, **1972**, 879; G. V. Smith, W. A. Boyd and C. C. Hinckley, *J. Amer. Chem. Soc.* **93**, 6319 (1971).

[3] K. Clusius and K. Weigand, *Z. physik. Chem.* **B46**, 1 (1940).

H. C. Brown [4a] presented a convincing case for steric factors determining secondary deuterium isotope effects in the kinetics of quaternization of methylpyridines, or in the thermodynamics of adduct formation with BF_3. He also found [4b] abnormal pK_a values for 2,6-di-t-butylpyridine denoting steric effects involving the proton. Surprisingly, however, the pK_a values of deuterated alkylpyridines have not yet been reported. Since this is relevant to the origin of secondary isotope effects in LIS-^{1}H—NMR spectra, we undertook this investigation.

The reported [5] pK_a value of *sym*-collidine **1** at 25° was accepted as such, and we performed comparative pK_a measurements by pH-metric titration with 0.1 N HCl in water at 25° ± 0.1°. The experimentally obtained data are reproducible within 0.01 pH units, and they are as follows: **1**, 7.45 (taken as such in all measurements); **2**, 7.47; **3**, 7.49; **4**, 7.53 (all these data have an error of ±0.01 and are relative values based on the figure for **1**).

The isotopic purity of **1** and **4** was above 97%, but owing to the method of preparation (see below), **2** was only ca. 85% pure and **3** only 80% pure, the remainder being species with different isotopic composition (as indicated by ^{1}H—NMR spectra).

These pK_a values indicate that the basicity of 2,4,6-trimethylpyridine increases on deuterating either the γ-methyl group, or the α-methyl group, with approximately the same increment; however, the pK_a values of **2** and **3** are affected by a larger error than that of **4**, owing to the lower isotopic purity of the former samples. One may conclude, therefore, that the basicity of alkylpyridines increases approximately additively on deuterating α- or γ-standing methyl groups, the increment being 0.025 ± 0.01 pH units per one d_3-methyl group.

The "electron-releasing inductive effect" of deuterium was noted previously; [6] the quotation marks are necessary because actually the effect is *on*, not *of*, the deuterium.[7]

This finding rules out the basicity as the origin of the secondary isotope effect in LIS-^{1}H-NMR spectra, leaving the steric origin as the most plausible one.

EXPERIMENTAL

2,4,6-Trimethylpyrylium perchlorate [8] heated at 80° for 10 minutes in D_2O affords mostly the γ-deuterated salt. On refluxing in D_2O all methyl groups are deuterated in 2—3 hrs; this perchlorate on dedeuteration at 80° in H_2O for 20 minutes affords mostly the α-deute-

---

[4] H. C. Brown, "Boranes in Organic Chemistry", Cornell Univ. Press, Ithaca, 1972: a, p. 71; b, p. 109 and further references therein.

[5] A. Gero and J. J. Markham, *J. Org. Chem.* **16**, 1835 (1951), also accepted by M. Tamres, S. Searles, E. M. Leighly and D. W. Mohrman, *J. Amer. Chem. Soc.* **76**, 3983 (1954), A pK_a value of 7.63 at 15° was reported by N. Ikekawa, Y. Sato and I. Maeda, *Pharm. Bull.* (*Japan*), **2**, 205 (1954).

[6] E. A. Halevi, M. Nussim and A. Ron, *J. Chem. Soc.* **1963**, 866.

[7] E. K. Thornton and E. R. Thornton, in "Isotope Effects in Chemical Reactions" (ed. C. J. Collins and N. P. Bowman), Van Nostrand, New York, 1970, p. 217.

[8] A. T. Balaban and C. D. Nenitzescu, "Org. Synth". Coll., Vol. 5, p. 1106.

rated salt. The rate ratio for $\gamma : \alpha$ deuteration is ca. 10 : 1,[9] and the kinetic isotope effect in these conditions (including the solvent isotope effect) is $k_H/k_D \cong 2$.[10]

By reaction with aqueous ammonia and ether, the four pyrylium salts are converted into the four *sym*-collidines **1**–**4**, which are purified by hydrochloric acid extraction, realkalinization, and distillation.

Titrations were performed in a thermostated cell (25° ± 0.1) under nitrogen using an automatic Potentiograph E436 and a UX glass electrode (both manufactured by Metrohm, Herisau). In all cases, 70 μl of pyridine **1**–**4** were dissolved in 20 ml distilled water using magnetic stirring. The whole pH scale was one pH unit, so that 0.01 units could be easily read; the titration curves were recorded by varying the compensation potential and towards the end of the titration the recorder was changed from pH-metric titration to d*E*/d*t* in order to determine precisely the end of the pH interval as the peak of the d*E*/d*t* curve. The pK_a value was found on the titration curve at the mid-point of the interval. The glass electrode and the set-up were checked with two buffers for pH 4.03 and 6.02, but since the latter value was too far from the pK_a, no attempt was made to obtain absolute pH values, relying only on measurements relative to 2,4,6-trimethylpyridine.

ACKNOWLEDGEMENT. The apparatus was made available by Dr. Cireşica Huch and Dr. Iuliu Pogany, to whom we express our thanks.

---

[9] E. Gârd, I. I. Stănoiu, F. Chiraleu and A. T. Balaban, *Rev. Roumaine Chim.*, **18**, 257 (1973); E. Gârd, A. Vasilescu, G. D. Mateescu and A. T. Balaban, *J. Labelled Comp.*, **3**, 196 (1967).

[10] I. I. Stănoiu, F. Chiraleu, E. Gârd and A. T. Balaban, *Rev. Roumaine Chim.*, **22**,000 (1977)

Revue Roumaine de Chimie, 22, 8, 1195–1207 (1977)

POTENTIAL ANTICANCER AGENTS. XIV[1]

SYNTHESIS AND BIOLOGICAL EVALUATION OF N[4′-{[(2,4-DIAMINO-6(7-)-PTERIDINYL)-METHYL]-N^{10}-METHYLAMINO}-BENZOYL]-L,D AND DL-GLUTAMIC (ASPARTIC) ACIDS

D. C. ȘUSTER*, G. CIUȘTEA, ANA DUMITRESCU, L. V. FEYNS,
EUTANȚA TĂRNĂUCEANU, GEORGETA BOTEZ, S. ANGELESCU, V. DOBRE
and I. NICULESCU-DUVĂZ

Oncological Institute, Bucharest, Bd. 1 Mai 11

Received February 11, 1975

The synthesis of L, D and DL enantiomeres of N[4′-{[(2,4-diamino-6-(or 7-)pteridynyl)methyl]-N^{10}-methylamino} benzoyl] glutamic (aspartic) acids was carried out by condensation of 2,4-diamino-6-(or 7-)chloromethyl pteridine with the corresponding peptides. New synthetic procedures for the preparation of these intermdiates were described. Among these the DL enantiomer of N[4′-{[(2,4-diamino-6-pteridinyl) methyl] N^{10}-methylamino}-benzoyl] glutamic acid exhibited the best chemotherapeutic index against L 1210.

The discovery of N[4′-{[(2,4-diamino-6-pteridinyl)-methyl-]-N^{10}-methylamino}-benzoyl] -L-glutamic acid, **1a** (6-L-MTX, Methotrexate),[2] highly specific in the treatment of chorioepitelioma [3] represents one of the most important successes of cancer chemotherapy.

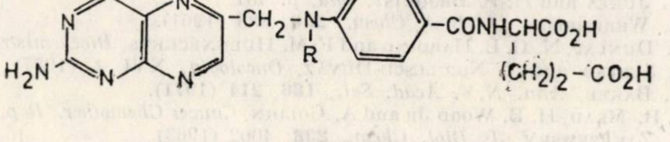

1a R=CH$_3$ (L, D, DL)

b R=H

*** This work is a part of Ph. D. Thesis, supervised by Prof. Dr. G. Ostrogovich**

---

[1] Part XIII. I. Baracu, E. Tărnăuceanu and I. Niculescu-Duvăz, *Rev. Roumaine Chim.* – in press.

[2] D. R. Seeger, D. B. Cosulich, J. M. Smith Jr and M. E. Hultquist, *J. Amer. Chem. Soc.*, **71**, 1753 (1949).

[3] M. C. Li, R. Hertz and D. B. Spencer, *Proc. Soc. Exptl. Biol. Med.*, **93**, 361 (1956).

The anticancer activity of **1a** (L) has been associated with its ability to act as antagonist of folic acid,[4–8] inhibiting the dihydrofolate reductase (DHFR) [6] and thymidilate synthetase (TS).[7] However, recent studies [9] raised the question if these mechanisms would be the only responsible for the anticancer activity of these compounds.

The examination of the structure-activity data available on this class pointed out the following important structural features :

— 4-amino moiety [10]

— N^{10}-centre, which seems to be equally important both for antitumor and antifolic activity of **1a** (L). Although some observations (i.e. the fact that the therapeutic index of **1a** (L) is superior to that of aminopterin, **1b**) [10] suggested a relationship between its basicity and biological behaviour,[11] both the marked inhibitory activity of compound **2** against DHFR [12] and the improved therapeutic index of 3′,5′-dihalo-MTX [10] did not support this point of view.

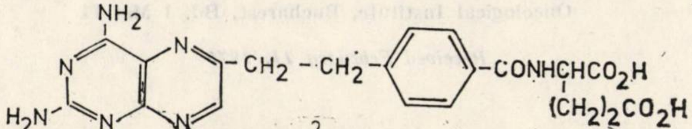

2

— structure and position of peptidic side chain :

a) drastic changes in the glutamic (or aspartic) acid residues did not improve the antitumor activity against L 1210.[13–18]

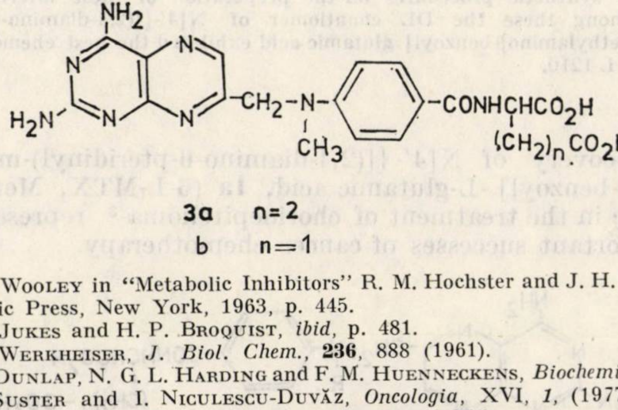

3a n=2

b n=1

[4] D. W. Wooley in "Metabolic Inhibitors" R. M. Hochster and J. H. Quastel—editors, vol. I, Academic Press, New York, 1963, p. 445.

[5] T. H. Jukes and H. P. Broquist, *ibid*, p. 481.

[6] W. C. Werkheiser, *J. Biol. Chem.*, **236**, 888 (1961).

[7] R. B. Dunlap, N. G. L. Harding and F. M. Huenneckens, *Biochemistry*, **10**, 88 (1971).

[8] D. C. Şuster and I. Niculescu-Duvăz, *Oncologia*, XVI, *1*, (1977).

[9] B. R. Baker, *Ann. N.Y. Acad. Sci.*, **186**, 214 (1971).

[10] J. A. R. Mead, H. B. Wood Jr and A. Goldin, *Cancer Chemother. Rep.*, **1**, 273 (1968).

[11] S. F. Zakrzewsky, *J. Biol. Chem.*, **238**, 4002 (1963).

[12] J. I. De Graw, R. L. Kisliuk, Y. Gaumont, C. M. Baugh and M. G. Nair, *J. Med. Chem.*, **17**, 552 (1974).

[13] A. Rosowsky, *J. Med. Chem.*, **16**, 1190 (1973).

[14] B. L. Hutchings, J. H. Mowat, J. J. Oleson, E. L. R. Stokstad, C. W. Waller, R. B. Angier, J. Semb and Y. Subbarow, *J. Biol. Chem.*, **170**, 323 (1947).

[15] W. B. Wright Jr, D. B. Cosulich, M. J. Fahrenbach, C. W. Waller, J. M. Smith Jr. and M. E. Hultquist, *J. Amer. Chem. Soc.*, **71**, 3014 (1949).

[16] M. Chaykovsky, A. Rosowsky, M. Papathanasopoulos, K. K. N. Chen and E. J. Modest, *J. Med. Chem.*, **17**, 1212 (1974).

[17] V. Dobre, M. Sbenghe, D. C. Şuster, G. Ciuştea, C. Russo-Goţ and G. Maltezeanu, Annual Session of Oncological Institute, Bucharest, 1975.

[18] W. W. Lee, A. P. Martinez and L. Goodman, *J. Med. Chem.*, **17**, 326 (1974).

b) convenient benzenic nucleus substitution (i.e. 3′,5′-dichloro-MTX, 2′-methoxy- and 3′-methoxy-aminopterin[17]) led to highly effective compounds against L 1210.

c) finally the 6-position of peptidic chain (on the pteridinic nucleus) was required, the 7-MTX (**3a**) being inactive.[19]

— the contribution of N^1, N^3, N^5 and N^8 to the biological properties of **1a** was not so easy to be established.[20,21] The excellent anticancer activity of 2,4-diaminoquinazoline derivatives [22,23] raised some questions concerning the importance of one of these centres.

Very little is known about the influence of the peptidic chain optical centre upon the general biological properties of such molecules. With the exception of a recent paper reporting the preparation of **1a** (D),[18] no literature data regarding this aspect could be found.

The present report describes the synthesis and biological evaluation of optical isomers (L, D and DL) of 6-MTX (**1a**) as well as 7-MTX (**3a**, **b**).

1. *Synthesis*. Three main approaches to the synthesis of **1a** (L) and its analogs were known starting with:

a) pyrazine derivatives. An unequivocal synthesis of **1a** (L) and structural analogs was recently reported [16,24–29];

b) 4-amino-4-deoxy-N^{10}-methyl pteroic acid. The mixed anhydrides were used as key intermediates [30–32];

c) pyrimidine derivatives. This procedure was carried out in two ways, namely:

---

[19] D. C. Șuster, L. V. Feyns, G. Ciuștea, G. Botez, V. Dobre, R. Bick and I. Niculescu-Duvăz, *J. Med. Chem.*, **17**, 758 (1974).

[20] J. A. Montgomery and N. F. Wood, *J. Org. Chem.*, **29**, 734 (1964).

[21] J. A. Montgomery, R. D. Elliott, S. S. Straigh and C. Temple Jr, *Ann. N.Y. Acad. Sci.*, **186**, 227 (1971).

[22] D. J. Hutchison, *Ann. N.Y. Acad. Sci.*, **186**, 496 (1971).

[23] J. B. Hynes, W. T. Ashton, D. Bryansmith and J. H. Freisheim, *J. Med. Chem.*, **17**, 1023 (1974).

[24] E. C. Taylor, K. L. Perlman, Y. Ho Kim, I. P. Sword and P. A. Jacobi, *J. Amer. Chem. Soc.*, **95**, 6413 (1973).

[25] E. C. Taylor, E. C. Portnoy, D. C. Hochstetler and T. Kobayaski, *J. Org. Chem.*, **40**, 2347 (1975).

[26] E. C. Taylor and T. Kobayaski, *J. Org. Chem.*, **38**, 2817 (1973).

[27] E. C. Taylor, K. L. Perlman, I. P. Sword, M. Séquin-Frey and P. A. Jacobi, *J. Amer. Chem. Soc.*, **95**, 6407 (1973).

[28] A. Rosowsky and K. K. N. Chen, *J. Med. Chem.*, **17**, 1308 (1974).

[29] A. Albert and K. Ohta, *J. Chem. Soc. D*, **1969**, 1168.

[30] M. G. Nair and C. M. Baugh, *Biochemistry*, **13**, 3923 (1973).

[31] C. L. Krumdieck and C. M. Baugh, *Biochemistry*, **8**, 1568 (1969).

[32] R. D. Elliott, C. Temple Jr. and J. A. Montgomery, *J. Org. Chem.*, **35**, 1676 (1970).

— Without isolation of pteridine intermediates.[2,33–41] It consisted in the reaction between 2,4,5,6-tetraaminopyrimidine, a (at least) difunctional carbonylic compound (i.e. dibromopropionaldehyde,[2,33–41] 1,1,3-tribromo-[42] or 1,1,3-trichloro-acetone[43,44]) and a peptide containing 4-N-methylaminobenzoic acid residue. Appropriate treatments of crude resulting material afforded **1a** with desired purity.[2,44–48]

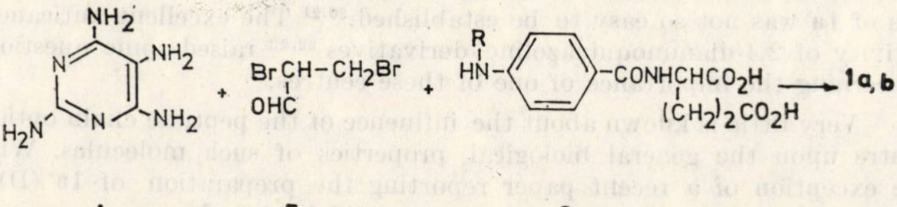

4 **5** **6**

By an alternate procedure, the treatment of 2,4-diamino-5-nitro-6-chloropyrimidine with methyl *p*-[(3-aminoacetonyl) methylamino] benzoate oxime gave 4′{[(2,4-diamino-6-pteridinyl) methyl] amino} benzoic acid.[32,49]

— With isolation of pteridine intermediate. In order to improve the previous described procedures and to obtain an isomeric pure **1a**, several attempts were made to prepare the 2,4-diamino-6-halomethyl pteri-

---

[33] J. H. Mowat, J. H. Boothe, B. L. Hutchings, E. L. R. Stokstad, C. W. Waller, R. B. Angier, J. Semb, D. B. Cosulich and Y. Subbarow, *J. Amer. Chem. Soc.*, **70**, 14 (1948).

[34] C. W. Waller, B. L. Hutchings, J. H. Mowat, E. L. R. Stokstad, J. H. Boothe, R. B. Angier, J. Semb, Y. Subbarow, D. B. Cosulich, M. J. Fahrenbach, M. E. Hultquist, E. Kuh, E. H. Northey, D. R. Seeger, J. P. Sickels and J. M. Smith Jr, *J. Amer. Chem. Soc.*, **70**, 19 (1948).

[35] M. E. Hultquist, E. Kuh, D. B. Cosulich, F. M. Fahrenbach, E. H. Northey, D. R. Seeger, J. M. Smith, J. P. Sickels, R. B. Angier, J. H. Boothe, B. L. Hutchings, J. H. Mowat, J. Semb, E. L. R. Stokstad, Y. Subbarow and C. W. Waller, *J. Amer. Chem. Soc.*, **70**, 23 (1948).

[36] R. B. Angier, E. L. R. Stokstad, J. H. Mowat, B. L. Hutchings, J. H. Boothe, C. W. Waller, J. Semb, Y. Subbarow, D. B. Cosulich, M. J. Fahrenbach, M. E. Hultquist, E. Kuh, E. H. Northey, D. R. Seeger, J. P. Sickels, and J. M. Smith Jr, *J. Amer. Chem. Soc.*, **70**, 25 (1948).

[37] J. H. Boothe, C. W. Waller, E. L. R. Stokstad, B. L. Hutchings, J. H. Mowat, R. B. Angier, J. Semb, Y. Subbarow, D. B. Cosulich, M. J. Fahrenbach, M. E. Hultquist, E. Kuh, E. H. Northey, D. R. Seeger, J. P. Sickels and J. M. Smith Jr, *J. Amer. Chem. Soc.*, **70**, 27 (1948).

[38] D. B. Cosulich and J. M. Smith Jr, *J. Amer. Chem. Soc.*, **70**, 1922 (1948).

[39] B. E. Hultquist, J. M. Smith Jr, D. R. Seeger, D. B. Cosulich and E. Kuh, *J. Amer. Chem. Soc.*, **71**, 619 (1949).

[40] A. S. Tomcufcik and D. R. Seeger, *J. Org. Chem.*, **26**, 3351 (1961).

[41] L. V. Alexeeva, H. L. Burde and B. N. Lundin, *Khim. Farm. Zhur.*, **2**, 30 (1968).

[42] M. E. Hultquist and P. F. Dreisbach, US Patent 2, 443, 165 (1948), *Chem. Abstr.*, **42**, 7944 (1948).

[43] S. Uyeo, S. Mizukami, T. Kubota and T. Takagi, *J. Amer. Chem. Soc.*, **72**, 5339 (1950).

[44] V. M. Berezovski, G. D. Glebova, E. M. Birinberg and L. V. Kazanskaya, *Khim. Farm. Zhur.*, **2**, 15 (1968).

[45] T. L. Loo, *J. Med. Chem.*, **8**, 139 (1965).

[46] V. T. Oliverio, *Analyt. Chem.*, **33**, 263 (1961).

[47] M. R. Heinrich, V. C. Dewey and G. W. Kidder, *J. Chromatogr.*, **2**, 296 (1959).

[48] E. P. Noble, *Biochem. Prep.*, **8**, 20 (1961).

[49] R. D. Elliott, C. Temple Jr, J. L. Frye and J. A. Montgomery, *J. Org. Chem.*, **36**, 2818 (1971).

dine, a key intermediate in this route. The preparation of 2,4-diamino-6-bromomethyl pteridine was achieved in two ways: a) by bromination of 2,4-diamino-6-methyl pteridine [2,24,50] using bromine-hydrobromic acid [51] or N-bromo-succinimide [52]; b) by treatment of 2,4-diamino-6-hydroxymethyl pteridine with Ph_3PBr_2.[53] The isolation of 2,4-diamino-6-bromomethyl pteridine hydrobromide and its conversion in good yields to **1a** was reported.[53]

An analogous intermediate was claimed also to be obtained by selective reduction of 2,4-diamino-6,7-dibromomethyl pteridine,[54] but the structure of resulted derivatives was questionable.[28]

In our laboratory, Seeger's method [2] gave a low yield of pure 6-L-MTX. Using 1,1,3-trichloro-acetone [44] we obtained an improvement of the overall yield, but the product, chromatographically identical with an authentic sample of **1a**, exhibited only 60% of its biological activity, together with a higher molar extinction coefficient (at 306 nm in 0.1 N HCl). Oxidation and hydrolysis of the reaction product (with alkaline $KMnO_4$) [2,19,55] gave 2-amino-4-hydroxy-pteridine carboxylic acids **(8a, b)** and provided evidence for the presence of both 6- and 7-MTX isomers. For the analytical differences between **1a** and **3a** see Table 1.

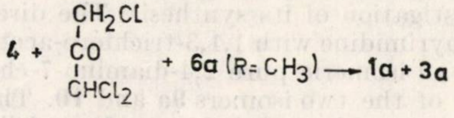

$$4 + \underset{CHCl_2}{\overset{CH_2Cl}{CO}} + 6a\,(R = CH_3) \longrightarrow 1a + 3a$$

7

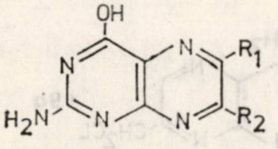

	R_1	R_2
8a	CO_2H	H
b	H	CO_2H

Table 1

Comparative analytical data of 6-MTX and 7-MTX (1a, 3a)

	6-MTX (L) **1a**(L)	7-MTX (L) **3a**(L)
I.R. Spectra [a]	Non significant	
U.V. Spectra, λnm(log ε) [b]	306(4.34)	311(4.38)
N.M.R. [c]	9.01(1H, s)	8.51(1H, s)
Mass-spectra	Non significant	

[a] in KBr disk; [b] in 0.1 N HCl; [c] in d_6-DMSO, recorded by prof. R. Bick (University Hobarth, Tasmania).

---

[50] F. E. King and P. C. Spensley, *J. Chem. Soc.*, **1952**, 2144.

[51] D. J. Brown, *J. Chem. Soc.*, **1953**, 1644.

[52] Z. V. Pushareva and L. V. Alexeeva, *Zhur. obshchei Khim.*, **2**, 1058 (1962).

[53] J. R. Piper and J. A. Montgomery, *J. Heterocycle Chem.*, **11**, 279 (1974).

[54] D. Farquhar, T. L. Loo and S. Vadlamundi, *J. Med. Chem.*, **15**, 567 (1972).

[55] R. L. Dion and T. L. Loo, *J. Org. Chem.*, **26**, 1857 (1961).

As no suitable methods for their separation could be found, other approaches for the selective synthesis of the two isomers were undertaken (A new method for the synthesis of 7-L-MTX, **3a** devoid of 6-MTX, **1a**, was reported elsewhere.[19,56])

A procedure which allowed the synthesis of isomeric pure 6-MTX (L, D and DL) via 2,4-diamino-6-chloromethyl pteridine (**9a**) was independently developed in our laboratory since 1972.[57] Thus **9a** was synthetized and its condensation with 4-N-methylaminobenzoyl-glutamic acid (**6**, $R = CH_3$) at pH 3.5—4.0 in aqueous medium afforded a crude product containing 60—70 % of **1a** (L).

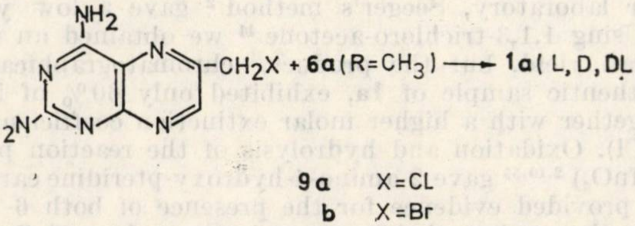

The availability of an isomeric pure 2,4-diamino-6-chloromethyl pteridine prompted an investigation of its synthesis. The direct condensation of 2,4,5,6-tetraaminopyrimidine with 1,1,3-trichloro-acetone afforded (depending on pH) either an isomeric pure 2,4-diamino-7-chloromethyl pteridine (**10**) or a mixture of the two isomers **9a** and **10**. The synthesis of isomeric pure 2,4-diamino-6-chloromethyl pteridine failed by this procedure.

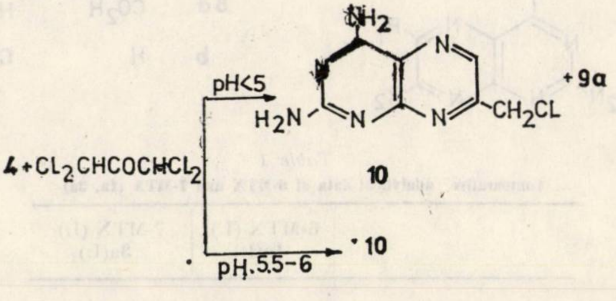

However, isomeric pure **9a** could be obtained by direct chlorination of 2,4-diamino-6-hydroxymethyl pteridine.

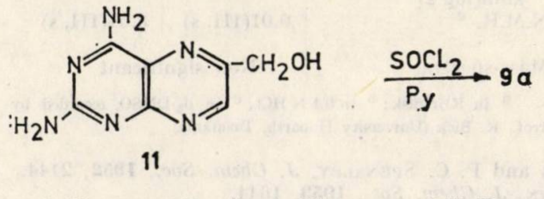

---

[56] D. C. Şuster, I. Niculescu-Duvăz, A. Pănescu and V. Dobre, Rom. Patent 56210 (1972).

[57] I. Niculescu-Duvăz, L. V. Feyns, D. C. Şuster and G. Ciuştea, Rom. Patent 55885 (1972).

The route used for the preparation of 2,4-diamino-6-hydroxymethyl pteridine, free of 7-hydroxymethyl pteridine, with an overall yield of 50–60 % was reported earlier.[58,59] In this paper we described the experimental details and some improvements of the original synthesis which allow us to obtain an overall yield of 80 %.[57,60]

$$4 + (HOCH_2)_2CO \rightarrow 11$$

The synthesis of 2,4,5,6-tetraaminopyrimidine [61–71] was accomplished according to scheme:

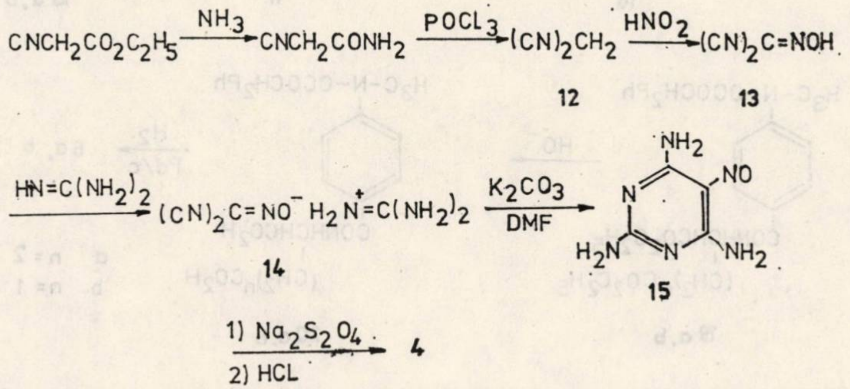

The following improvements, which led to a reproducible procedure were worth mentioning:

a) the diminution of the NaCl amount added during the preparation of malonic dinitrile (**12**), which allowed a confortable handling of reaction products;

b) the use of guanidine salts (i.e. hydrochloride, nitrate, etc.) as well as guanidine carbonate in the amidine (**14**) preparation.

c) reduction in mild conditions of 2,4,6-triamino-5-nitrosopyrimidine (**15**) was achieved with an yield of 60 % by a slight modification of the original method.

[58] C. M. Baugh and E. Shaw, *J. Org. Chem.*, **29**, 3610 (1964).

[59] H. S. Forrest and J. Walker, *J. Chem. Soc.*, **1949**, 2077.

[60] D. C. Şuster, G. Botez and V. Neagu, Rom. Patent 59968 (1972).

[61] W. Traube, *Ber. dtsch. chem. Ges.*, **37**, 4544 (1904).

[62] M. F. Mallette, E. C. Taylor and C. K. Cain, *J. Amer. Chem. Soc.*, **69**, 1814 (1947).

[63] A. Schrage and G. H. Hitchings, *J. Org. Chem.*, **16**, 207 (1951).

[64] O. Vogl and E. C. Taylor, *J. Amer. Chem. Soc.*, **79**, 1518 (1957).

[65] E. C. Taylor, O. Vogl and C. C. Cheng, *J. Amer. Chem. Soc.*, **81**, 2442 (1959).

[66] Laboratoires Lumière and Institute Merieux, Fr. Patent 1 364 734 (1964); *Chem. Abstr.*, **62**, 572 (1965).

[67] G. Longo, *Gazz. chim. Ital.*, **61**, 575 (1931).

[68] A. Surrey, *J. Amer. Chem. Soc.*, **65**, 2471 (1943).

[69] A. Surrey, *Org. Synth.*, **25**, 63 (1945).

[70] Lonza Ltd., Fr. Patent 1 365 202 (1965); *Chem. Abstr.*, **61**, 13202 (1964).

[71] Org. Synth. Coll., vol. I, H. Gilman, editor, II$_{nd}$ Ed., Wiley, 1958, p. 179.

The 4-N-methylamino-benzoyl-glutamic or aspartic acid [38,72–76] were prepared by two routes,[77] the usually one being summarized in the following scheme :

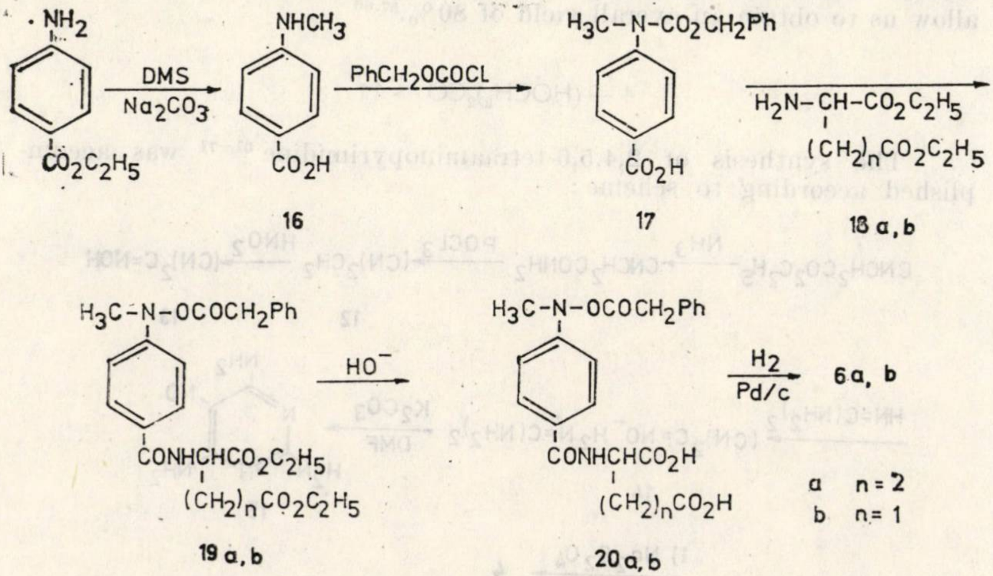
NH2
CO2C2H5
DMS
Na2CO3
NHCH3
CO2H
16
PhCH2OCOCL
H3C–N–CO2CH2Ph
CO2H
17
H2N–CH–CO2C2H5
(CH2)nCO2C2H5
18 a, b
H3C–N–OCOCH2Ph
CONHCHCO2C2H5
(CH2)nCO2C2H5
19 a, b
HO⁻
H3C–N–OCOCH2Ph
CONHCHCO2H
(CH2)nCO2H
20 a, b
H2
Pd/c
6 a, b
a n = 2
b n = 1

The following improvements which allowed these compounds to be prepared in large amounts were described :

a) the preparation of 4-N-methylaminobenzoic acid (**16**) [38,73] with an overall yield of 45 % by methylation (with DMS) of ethyl 4-aminobenzoate ;

b) the synthesis of 4-N (carbobenzoxy) methylaminobenzoic acid (**17**) using an acetic acid-sodium acetate medium. This procedure proved to be reproducible in contrast with Schotten-Baumann method ;

c) the azeotropic esterification of glutamic or aspartic acid with an yield of 85–90 % ; [78]

d) the final hydrogenolysis of carbobenzoxy compounds (**20a, b**) which avoided (in contrast with previous reported procedures [72]) the formation of hygroscopic hydrobromides.

The relevant analytical data pertaining to the new synthetized analogs of **1a** and **3a, b** and some new intermediates were listed in Tables 2 and 3.

---

[72] S. C. J. Fu, M. Reiner and T. L. Loo, *J. Org. Chem.*, **30**, 1277 (1965).

[73] M. Sekyia and K. Ito, *Chem. Pharm. Bull.* (*Tokyo*), **14**, 1007 (1966).

[74] A. Surrey and H. F. Hammer, *J. Amer. Chem. Soc.*, **66**, 2127 (1944).

[75] H. M. Chiles and W. A. Noyes, *J. Amer. Chem. Soc.*, **44**, 1798 (1922).

[76] J. H. Mowat, A. L. Gazzola, B. L. Hutchings, H. J. Boothe, C. W. Waller, R. B. Angier, J. Semb, Y. Subbarow, *J. Amer. Chem. Soc.*, **71**, 2308 (1949).

[77] G. Ciuştea, D. C. Suster, A. Dumitrescu and M. Ionescu, Rom. Patent 58475 (1971).

[78] D. C. Şuster and S. Angelescu, Rom. Patent 60252 (1973).

Table 2

Analytical data of new MTX derivatives

Compound	Formula	m.p. °C	Analytical data %						uv spectral data	NMR δ
			Calc.			Found			λ(nm) (log ε) [a]	
			C	H	N	C	H	N		
1a (D)	$C_{20}H_{22}N_8O_5 . H_2O$	208	50.90	5.10	23.70	50.53	5.65	23.86	244(4.36), 306(4.38)	
1a (DL)	$C_{20}H_{22}N_8O_5 . H_2O$	205	50.90	5.10	23.70	51.38	5.77	23.64	244(4.35), 306(4.46)	
3a (L)	$C_{20}H_{22}N_8O_5 . {}_2H_2O$	203	48.89	5.30	22.90	48.59	5.30	23.19	243.6(4.26) (sh), 311.6(4.38)	C_6-H^b 8.51(1H, s)
3a (D)	$C_{20}H_{22}N_8O_5 . {}_2H_2O$	200	48.89	5.30	22.90	49.70	5.61	22.14	238(4.30) (sh), 306(4.50)	
3a (DL)	$C_{20}H_{22}N_8O_5 . {}_2H_2O$	208−12	48.89	5.30	22.90	49.05	5.45	22.45	238(4.28) (sh), 306(4.41)	
3b (DL)	$C_{19}H_{20}N_8O_5 . H_2O$	305	49.80	4.80	24.50	50.03	5.12	24.85	240(4.28) (sh), 310(4.10)	C_6-H^c 8.21(1H, s)

[a] in 0.1 N HCl; [b] in d_6-DMSO; **1a** (L) (6−L−MTX) : C_7-H 9.01 (1H, s); [c] in DMSO.

Table 3

Analytical data of the peptidic intermediates

Compound	Formula	m.p. °C	Analytical data %						uv spectral data λ(nm) (log ε) [b]
			Calc.			Found			
			C	H	N	C	H	N	
6a (L)	$C_{13}H_{16}N_2O_5$	87−90 [a]	55.80	5.70	10.0	56.40	5.84	9.78	283(4.025)
6a (D)	$C_{13}H_{16}N_2O_5$	90−93 [a]	55.80	5.70	10.0	56.28	6.00	9.85	298(4.03) [c]
6a (DL)	$C_{13}H_{16}N_2O_5 . H_2O$	110−115 [a]	52.30	6.03	9.40	52.70	6.57	9.21	300(3.60)
6b (DL)	$C_{12}H_{14}N_2O_5 . H_2O$	114−119 [a]	50.80	6.32	9.85	50.30	6.18	9.86	300(3.69)
18a (L)	$C_9H_{17}NO_4 . HCl$	107−109	45.10	7.46	5.83	45.61	7.71	5.67	
18a (D)	$C_9H_{17}NO_4 . HCl$	110.5−111.5	45.10	7.46	5.83	44.66	7.32	5.86	
18a (DL)	$C_9H_{17}NO_4 . HCl$	73.5−75	45.10	7.46	5.83	44.65	7.46	5.94	
18b (DL)	$C_8H_{15}NO_4 . HCl$	87.5−89.5	42.60	7.09	6.21	42.46	7.57	6.31	
19a (D)	$C_{25}H_{30}N_2O_7$	66−67	63.83	6.40	5.96	64.21	6.73	5.95	260(4.21) [c]
19a (DL)	$C_{24}H_{30}N_2O_7$	86−87	63.83	6.40	5.96	64.33	6.75	5.93	260(4.11)
19b (DL)	$C_{24}H_{28}N_2O_7$	78−79	63.10	6.12	6.12	63.71	6.53	5.96	262(4.22) [c]
20a (D)	$C_{21}H_{22}N_2O_7 . H_2O$	138.5−139.5	58.30	5.53	6.50	58.73	5.60	6.50	260(4.28) [c]
20a (DL)	$C_{21}H_{22}N_2O_7 . H_2O$	93−95	58.30	5.53	6.50	58.76	5.52	6.29	260(4.11)
20b (DL)	$C_{20}H_{20}N_2O_7 . H_2O$	106−107	55.04	5.50	6.42	54.71	5.47	6.32	260(4.11)

[a] no definite melting point; [b] in MeOH when no otherwise noted; [c] in EtOH.

2. *Spectral data.* Differences in the infrared spectra of the newly obtained compounds (especially between **1a** and **3a** derivatives) were difficult to assign.

The u.v. spectral data of the new **1a** and **3a, b** derivatives and those of the main intermediates were summarized in Table 3. The u.v. spectra of 6-MTX (**1a**) and 7-MTX (**3a**) were slightly different and the molar extinction coefficient is higher for 7-MTX (Table 2).

Due to their extremely low volatility, the mass spectra of the new analogs of MTX were difficult to perform (when increasing the temperature, they decomposed so that no molecular ion appeared) and the few minor differences which appeared at $m/e < 160$ could not be used for structural analysis.

NMR spectra of compounds allowed an unequivocal structural attribution between 6- and 7-isomers. The chemical shifts of 7-H protones (in 6-MTX) and 6-H (in 7-MTX) were in agreement with literature data.[79,80] Owing to their low solubility, the NMR spectra of 2,4-diamino-6- and 7-chloromethyl pteridine could not be obtained.

3. *Biological evaluation.* The antitumor activity of the new compounds against L 1210 and Walker carcinosarcoma (W 256) were evaluated according to standard methods.[81,82] The results were given in Table 4.

Table 4

Biological evaluation of new MTX derivatives[a]

Compound	LD_{50} mg/kg b.W.	Antitumor activity			
		W 256[b]		L 1210[c]	
		Dose (mg/kg) × nr. admn.	TWI %	Dose (mg/kg)× nr. admn.	ILS %
6-MTX (**1a**, L)[d]	18.0	5×1	80	0.5×10	134
6-MTX (**1a**, D)	17.0	7×1	56	0.5×10	87
6-MTX (**1a**, DL)	34.6	7×1	95	0.5×10	150
7-MTX (**3a**, L)[e]	691	50×13	33	200×8	30
7-MTX (**3a**, D)	500			70×5	0
7-MTX (**3a**, DL)	490	45×12	35	45×10	38
7-MTX (**3b**, DL)	200	40×14	29	40×8	0

[a] The screening was achieved according to N.C.I. protocol by D_r V. Dobre and G. Meltezeanu; [b] The treatment began 7 days after tumor transplantation; [c] The treatment began 24 hrs after i.p. transplantation of 10^6 leukemic cells; [d] An authentic sample of 6-MTX gave the following comparative data: $LD_{50} = 18.7$ mg/kg; antitumor activity: W 256 (TWI%) 80% (5 mg/kg × 1); L 1210 (ILS%) 130% (0.5 mg/kg × 10); [e] See[19].

Collectively, the data presented in Table 4 suggested :

a) the modification of the peptidic chain position on the pteridine nucleus (from the 6- into 7-position) led to a drastic decrease of the antitumor activity;

b) there were significant differences between the antitumor activity against L 1210 of the L and D enantiomeres.

---

[79] A. Dieffenbacher and W. V. Philipsborn, *Helv. Chim. Acta*, **52**, 743 (1969).

[80] E. J. Pastore, *Ann. N.Y. Acad. Sci.*, **186**, 43 (1971).

[81] H. R. Adamson, S. T. Yancev, M. Ben, T. L. Loo and D. P. Rall, *Arch. Int. Pharmacodyn.*, **153**, 87 (1965).

[82] J. Cornfield and N. Mantel, *J. Amer. Statist. Assoc.*, **45**, 181 (1950).

Both the enantiomeres of 6- and 7-MTX were active against the adenovirus, the 6-MTX being more active.[83] All the new synthetized compounds inhibited the growth of Streptococcus faecalis ATCC 8043,[84,85] the most active being the 6-MTX enantiomeres.[17]

EXPERIMENTAL

The m.p. were taken on a Boetius apparatus and are uncorrected. The u.v. spectra were determined with a CF_4 Optica Milano spectrophotometer. The i.r. spectra were run on an UR_{10} Carl Zeiss Jena spectrophotometer. The n.m.r. spectra were run on a JEOL 100—Mz and on a Varian T 60 spectrophotometers. Paper chromatograms were run on a Whatman No 1 paper and the spots were detected under u.v. light. TLC were run on Merck plates (Kieselgel 60 F_{254}).

2,4-DIAMINO-6-HYDROXYMETHYL PTERIDINE (11)

10.5 g (0.05 moles) of tetraaminopyrimidine dihydrochloride (**4**) (solved in 150 ml H_2O) and 8.5 g (0.077 moles) selenium dioxide (in 150 ml H_2O) were added to a stirred solution of 330 g (4 moles) CH_3CO_2Na and 9 g (0.1 moles) dihydroxyacetone in 550 ml H_2O. The mixture was heated at 35° for 1.5 hrs with air bubbling (the end of the reaction being spectrophotometrically controlled), then rapidly cooled at 5°, stirred at this temperature for 3—4 hrs and the resulted product filtered off and washed with cold water. The obtained solid was suspended in 250 ml boiling water, treated with charcoal and filtered hot. 25 g NaCl were added to the filtrate and it was stored at 0° over night. The solid was collected by filtration, washed with H_2O, EtOH, EtOH-ether (1 : 1), ether and dried at 60°. A yield of 7.5—8.0 g (80—85%) **11** (paper chromatography on Whatman No 1, ascendent system BuOH—EtOH—H_2O 100 : 35 : 72, $R_f = 0.38$) was obtained.

N[4'{[(2,4-DIAMINO-6-PTERIDINYL)-METHYL-] N^{10}-METHYLAMINO-}-BENZOYL]-GLUTAMIC ACID (1a)

10 g (0.052 moles) of finely powdered **11** was suspended under stirring in 200 ml anhydrous $CHCl_3$, 5 ml anhydrous pyridine and 30 ml (0.41 moles) $SOCl_2$ and refluxed for 8 hrs. The mixture was cooled at room temperature, the solid was filtered, washed with $CHCl_3$ and dried to afford 2,4-diamino-6-chloromethyl pteridine **9a** (for chromatography see compound **11**, $R_f = 0.64$). The isolated **9a** was impurified with some starting materials. It was used without further purifications.

In a solution of 100 g (1.22 moles) CH_3CO_2Na in 750 ml H_2O adjusted at pH 4.0 (with 12 N HCl) and heated at 45°, 14 g (0.05 moles) peptide **6a** was dissolved. To this mixture, a solution of 10 g (0.045 moles) **9a** in 75 ml HCO_2H 98% was dropped slowly (2 hrs), the pH being maintained at 3.5—4.0 with solid Na_2CO_3. The process was carried out during 40 hrs at 45°, then the mixture was cooled at 4° for 48 hrs. The resulted precipitate was filtered, washed with H_2O, EtOH, ether and dried at 60°. It was suspended in 500 ml H_2O, the pH adjusted at 10—11 (with 1 N NaOH) and heated at 60°, maintaining the pH in the above mentioned range. After filtration, the solution was cooled, adjusted to pH 7 (with 1 N HCl), stored overnight in the refrigerator, treated with charcoal and filtered. The filtrate was adjusted to the pH 3.5—4.0 and the solid filtered, washed with H_2O, EtOH, ether and dried. It resulted cca 8 g of a partially purified product (with 60—70% **1a** content, as determined spectrophotometrically). The purification of this crude material was achieved in two steps: a) on a cellulose column by elution with 0.1 M Na_2HPO_4 buffer adjusted at pH 7.0 (with 12 N HCl) to give a 88—90% pure material; b) the previous obtained material was subjected to a second column chromatography on a cellulose-charcoal column eluted with H_2O. The overall yield was 10–15% **1a** of 95–98% purity (determined spectrophotometrically). Compounds **1a** (D) and **1a** (DL) were synthetized by the same procedure.

---

[83] C. Barbu, personal commun.

[84] L. J. Teply and C. A. Elvehjem, *J. Biol. Chem.*, **157**, 303 (1945).

[85] C. A. Nichol, S. F. Zakrzewsky and C. A. Welch, *Proc. Soc. Exptl. Biol. Med.*, **83**, 272 (1953).

N[4′-{[(2,4-DIAMINO-7-PTERIDINYL)-METHYL-] N^{10}-METHYLAMINO}-BENZOYL-] (D AND DL) GLUTAMIC (3a) AND DL-ASPARTIC ACIDS (3b)

The previous described procedure was employed using 4-methylamino-benzoyl-(D and DL)-glutamic and DL-aspartic acids. and 2,4-diamino-7-chloromethyl pteridine[19,56] (see Table 3).

2,4,5,6-TETRAAMINOPYRIMIDINE DIHYDROCHLORIDE (4)

500 g (3.25 moles) 2,4,6-triamino-5-nitrosopyrimidine[66] were suspended under stirring in 10 l H_2O and heated at 35°. At this temperature sodium dithionite (2100 g, 14.8 moles) was slowly added, when the suspension colour turned from red into yellow pink and the temperature raised to cca 55°. The solution was then heated at 75°, filtered hot, the filtrate cooled at 0–5° overnight and the solid collected, washed with H_2O and dried. 520 g of tetraaminopyrimidine bisulphite were obtained.

The product (520 g) was suspended under stirring in 5900 ml H_2O, heated under reflux and 900 ml 12 N HCl were slowly added. The solution was then treated with charcoal and filtered hot. To the filtrate 700 ml 12 N HCl were added, then it was cooled to 0–5° overnight and the solid filtered to give 410 g (60%) **4**.

4-N-METHYLAMINOBENZOIC ACID (16)

A mixture of 540 g (5.1 moles) Na_2CO_3, 825 g (5 moles) ethyl 4-aminobenzoate and 2500 ml H_2O was heated under stirring at 90–95°. 480 ml (5 moles) dimethyl sulphate (DMS) were dropped during 5 minutes when a vigourous reflux resulted. Then the reflux was continued for 6 minutes and the organic layer immediately separated and submitted to hydrolysis.

The organic layer was added to a stirred solution of 400 g (10 moles) NaOH in 10 l H_2O and heated at 95–100° for 0.5–1 hr. After cooling at room temperature, the solution was filtered, adjusted to pH 4 with 12 N HCl and stored for 24 hrs at room temperature. The solid was collected by filtration and washed with H_2O.

To a stirred solution of the previous obtained solid in 2 l 12 N HCl and 8 l H_2O a solution of 350 g/l $NaNO_2$ was added dropwise at 0–5° (to a persistent colour of iodine-starch paper) and after stirring for another 0.5 hrs in the cold, the resulted 4-N,N′-nitroso-methylamino-benzoic acid was collected by filtration and washed with 0.5 N HCl and water.

To a stirred solution of the above filtered 4-N,N′-nitroso-methylamino-benzoic acid and 1400 g (35 moles) NaOH in 5100 ml H_2O heated at 90–95°, 760 g Zn powder were added. The mixture was maintained at 90–95° for additional 30 hrs, then it was cooled at room temperature, adjusted to pH 8–9 (with 12 N HCl). The $Zn(OH)_2$ was removed by filtration and the cake washed with hot water. The combined filtrates were adjusted to pH 4 (with 12 N HCl) and stored overnight at room temperature. The deposited solid was filtered and after washing (with water) and drying yielded 400–420 g (45%) **16** (m.p. 162°, lit.[38] 158–161.5°).

4-N(CARBOBENZOXY)METHYLAMINOBENZOIC ACID (17)

To a stirred solution of 151 g (1 mol) **16**, 135 g (1.65 moles) anhydrous CH_3CO_2Na and 2250 ml CH_3CO_2H (heated at 60° for 1 hr and then cooled at 40°), 190 g (1.1 moles) carbobenzoxy chloride were added. After 40 hrs (at 40°) the reaction mixture was poured into 8–10 l H_2O, stirred for 1–2 hrs, filtered and dried. Purification of the crude material was achieved by: a) stirring with 0.5 N HCl for 16 hrs; b) dissolution in CH_3CO_2H and precipitation with cold water; c) dissolution in $CHCl_3$, washing with 0.5 N HCl and H_2O and precipitation (after drying with Na_2SO_4) with toluene. After purification, 188 g (65%) **17** were obtained (m.p. 149–150°, lit.[72] 149–151.5°).

4-N-METHYLAMINOBENZOYL-(L, D AND DL)-GLUTAMIC AND DL-ASPARTIC ACIDS (**6a, b**)

41.4 g (0.1 moles) 4-N(carbobenzoxy) methylaminobenzoyl-(L, D and DL)-glutamic acid in 415 ml MeOH were submitted to catalytical reduction (4.1 g 5% Pd/C) at atmospheric pressure and room temperature. The reaction mixture was filtered and concentrated under vacuo (at 60°) to give white platelets (22–26 g, 80–95%). By the same method, 4-N-methylaminobenzoyl-DL-aspartic acid (synthetized by S.C.J.Fu's method[72]; for analytical data see Table 3) was prepared.

DIETHYL GLUTAMATE (ASPARTATE) HYDROCHLORIDE (**18a, b**)

In the bottom of a rectification column (Ø 2.5 cm, 20 plates) 3 moles of glutamic (aspartic) acid hydrochloride, 3300 ml EtOH, 800 ml benzene and 20 g ***p*-TsOH** were introduced.

The reaction mixture was heated under reflux when at the column top two layers separated. The aqueous layer was continously discarded and the organic one was reintroduced in the column. Completion of the esterification was monitored by TLC (BuOH–AcOH–AcOEt–H_2O 1 : 1 : 1 : 1).

The reaction mixture was concentrated under vacuo and the oily residue crystallized when triturated with ether. The procedure gave a constant yield of 85–90% (For analytical data see Table 3).

Revue Roumaine de Chimie, **22**, *8*, 1209–1215, (1977)

GEMISCHTE AROMATISCHE ESTER DER PHOSPHORIGEN- UND DER PHOSPHORSÄURE

M. IOVU und E. VOINA

Fakultät für Pharmazie, Str. Traian Vuia 6, Bukarest, Rumänien

Eingegangen am 22. Oktober 1975

In den vorhergehenden Mitteilungen haben wir die Synthese des Tris(4-cyclohexylphenyl)phosphits als Antioxydant und der Tris(4-benzylphenyl)phosphite als Stabilisatoren für makromolekulare Produkte beschrieben. In der vorliegenden Arbeit sind wir zur Synthese einiger gemischten Phosphite mit der allgemeinen Formel $(Ph\text{-}CH_2\text{-}Ar\text{-}O\text{-})_2P\text{-}O\text{-}C_6H_4\text{-}Ph$ übergegangen, wo Ar einen Benzolring darstellt, der nebst einem Benzyl- auch mit Methyl-Radikalen substituiert werden kann. Die Produkte gehören zur Gruppe der Stabilisatoren für Polyvinylchlorid und für synthetischen Kautschuk. Es wurden auch die den Phosphiten entsprechenden Phosphate sowie Phosphate vom Typ $(Ph\text{-}C_6H_4\text{-}O\text{-})_2PO\text{-}O\text{-}Ar\text{-}CH_2\text{-}Ph$ synthetisiert, in welchem das Verhältnis zwischen den Radikalen umgekehrt dem der Phosphite ist.

EINLEITUNG

Um einige Antioxydationsmittel mit besonderen Eigenschaften zu erhalten, haben wir das Tris(*p*-cyclohexylphenyl)phosphit synthetisiert.[1] Ebenso haben wir auch Tris(*p*-benzylphenyl)phosphite dargestellt, die sich durch das Vorhandensein oder die Abwesenheit von Methyl-Radikalen im Phenylring unterscheiden, welche die Polymere stabilisieren und vor allen Dingen den Kautschuk vor dem Einfluß des Sauerstoffs und des Ozons schützen.[2]

Dank des Interesses für die gemischten Phosphite der allgemeinen Formel $(RC_6H_4O)_m P(OR')_n$ in der R′ ein Alkyl ist, während R ein Alkyl oder Allyl darstellt, für die Stabilisierung synthetischer Kautschuke [3] des Phenyl bis [2,4,6-tris(α-methylbenzyl)phenyl]phosphits für die Stabilisierung von Polyvinylchlorid,[4] sind wir zur Synthese einiger gemischten Phosphate vom Typ

$$Ph-C_6H_4-O-P(-O-Ar-CH_2-Ph)_2$$

---

[1] M. Iovu, E. Voina und N. Miclovici, *Analele Univ. Buc. Chimie*, **19**, 102 (1970).

[2] M. Iovu, E. Voina, *Rev. Chim. (București)*, **26**, 10 (1975).

[3] W. P. Bayer, R. Mangham und M. Melton, U.S. 3.027,348 Mar. 27, 1962, Appl. Aug. 14, 1958; *Chem. Abstr.*, **57**, 4813 (1962).

[4] J. S. Sconce, J. Haldan und L. Schall, U.S. 3, 415, 907,10 dec. 1968; *Chem. Abstr.*, **70**, 38687 (1969).

übergegangen, wo Ar ein mit einem oder zwei Methylradikalen substituierter oder nicht substituierter Benzolring ist, oder

$$\mathrm{Ph-C_6H_4-O-P(-O-C_6H_4-C_6H_{11})_2}$$

ist und zur Synthese der entsprechenden Phosphate vom Typ

$$\mathrm{Ph-C_6H_4-O-PO(-O-Ar-CH_2-Ph)_2} \text{ oder}$$

$$\mathrm{Ph-C_6H_4-O-PO(-O-C_6H_4-C_6H_{11})_2}.$$

Ebenso wurden Phosphate mit denselben Radikalen, aber im umgekehrten Verhältnis, vom Typ

$$\mathrm{(Ph-C_6H_4-O-)_2PO-O-Ar-CH_2-Ph}$$

$$\text{und } \mathrm{(Ph-C_6H_4-O-)_2PO-O-C_6H_4-C_6H_{11}}$$

synthetisiert.

Für die Synthese der gemischten Ester von den oben genannten Typen, benutzten wir als Ausgangsstoffe feste, leicht zu reinigende Benzyl-Phenole, die man durch Einwirkung des Benzylchlorids auf Phenole, Kresole oder Xylole in Gegenwart von Aluminiumchlorid [2] oder 4-Cyclohexylphenol[1] und 4-Hydroxydiphenyl erhält.

Für die Synthese der Ester der phosphorigen Säure wurde zuerst das 4-Diphenyl-Dichloranhydrid der phosphorigen Säure durch die Reaktion von 4-Hydroxybiphenyl mit Phosphortrichlorid dargestellt :

$$\mathrm{Ph-C_6H_4-OH + PCl_3 \rightarrow Ph-C_6H_4-O-PCl_2 + HCl}$$

Das 4-Diphenyl-Dichloranhydrid der phosphorigen Säure wurde mit Benzyl-Phenol kondensiert :

$$\mathrm{Ph-C_6H_4-O-PCl_2 + 2\,Ph-CH_2-C_6H_4-OH \rightarrow}$$

$$\mathrm{\rightarrow Ph-C_6H_4-O-P(-O-C_6H_4-CH_2-Ph)_2 + 2HCl}$$

Für die Synthese der gemischten Ester der Phosphorsäure mit der allgemeinen Formel :

$$\mathrm{Ph-C_6H_4-O-PO(-O-C_6H_4-CH_2-Ph)_2}$$

haben wir zwei Wege

1. Die Oxydation der entsprechenden Triphosphite :

$$\mathrm{Ph-C_6H_4-O-P(-O-C_6H_4-CH_2-Ph)_2 + 1/2\ O_2 \rightarrow}$$

$$\mathrm{\rightarrow Ph-C_6H_4-O-PO(-O-C_6H_4-CH_2-Ph)_2}$$

2. Die Erzielung des Dichloranhydrids der Phosphorsäure durch die Reaktion des 4-Hydroxydiphenyls mit Phosphoroxychlorid:

$$Ph-C_6H_4-OH + POCl_3 \rightarrow Ph-C_6H_4-O-POCl_2 + HCl$$

und Kondensation des Dichloranhydrids mit Benzyl-Phenolen:

$$Ph-C_6H_4-O-POCl_2 + 2\,Ph-CH_2-C_6H_4-OH \rightarrow$$

$$\rightarrow Ph-C_6H_4-O-PO(-O-C_6H_4-CH_2-Ph)_2 + 2HCl$$

Die auf diesen zwei Wegen erhaltenen gemischten Ester sind identisch.

Die gemischten Phosphate vom Typ

$$(Ph-C_6H_4-O-)_2PO-O-C_6H_4-CH_2-Ph$$

wurden durch Kondensierung des Monobenzylphenyl-Dichloranhydrids der Phosphorsäure in entsprechenden stöchiometrischen Verhältnissen mit dem Phosphoroxychlorid in Gegenwart von Natriumchlorid als Katalysator[5] erhalten.

BESCHREIBUNG DER VERSUCHE

Das als Ausgangsstoff verwendete Phosphoroxychlorid, Phosphortrichlorid und 4-Hydroxydiphenyl stammten aus dem Handel. Das *p*-Cyclohexylphenol wurde durch Cyclohexylierung des Phenols mit Cyclohexen erhalten, wobei als Katalysator wasserfreies $ZnCl_2$ und trockener HCl verwendet wurden.

Das *para*-Isomere wurde von dem *ortho*-Isomere durch fraktioniertes Umkristallisieren aus Petroläther abgetrennt (Schmp. 130, 5°).

Das *p*-Benzylphenol, *p*-Benzyl-2-methylphenol- *p*-Benzyl-2,5-dimethylphenol und *p*-Benzyl-3,5-dimethylphenol stammten ebenfalls aus dem Handel.

Die Bestimmung des Phosphors fand durch Oxydation zu Phosphorsäure mit einem Schwefelsäure-Salpetersäure-Gemisch statt, die dann in Ammoniumphosphomolibdat umgewandelt wurde[6].

Die UV-Spektren wurden mit Hilfe eines Spekord UV-VIS, Carl Zeiss Jena, erhalten. Die IR-Spektren wurden mit einem UR-20 Gerät, Carl Zeiss, Jena, erhalten. Die NMR-Spektren wurden mit einem Gerät vom Typ Varian A-60 A erhalten, wobei als innerer Standard Tetramethylsilan und als Lösungsmittel Tetrachlorkohlenstoff zur Anwendung gelangte.

Wir führen weiter unten Beispiele der durchgeführten Synthesen an.

1. SYNTHESE DES BIPHELYL DI(*p*-CYCLOHEXYLPHENYL)PHOSPHITS

In einem 50-ml Glaskolben mit Rückflußkühler und Kalziumchlorid-Rohr werden 2 g Biphenyldichloranhydrit der phosphorigen Säure 2,58 g *p*-Cyclohexylphenol, 1,49 g Triäthylamin und 10 ml Benzol als Lösungsmittel eingetragen. Das dabei angewandte molare Verhältnis betrug 1 : 2 : 2. Nach sechsstündigem Erhitzen wurde das Reaktionsprodukt nach Abkühlen auf einer Glasnutsche G_4 abgesaugt. Es wurden 4 g eines gelben, zähflüssigen Produktes erhalten (Ausbeute 87,33%). Die entsprechenden physikalischen Konstanten sind in Tabelle 1. enthalten.

---

[5] M. Iovu, E. Voina, *Rev. Roumaine Chim.*, **21**, 447 (1976).

[6] T. H. Kasterina und L. S. Kalinina, „Khimicheskie metody isledovania sinteticheskikh smol i plastichesskikh mass", Goshimizdat, Moskva, 1963, S. 37—38.

Tabelle 1

Gemischte aromatische Ester der Phosphorigen- und der Phosphorsäure

Strukturformel	Summenformel	P %		d_{25}	n_D^{25}	Schmp. C°	λ_{max} mμ	ε_{max}	Ausbeute %
		Ber.	Gef.						
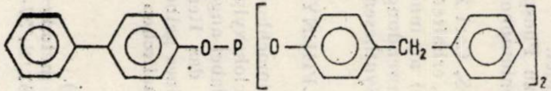	$C_{38}H_{31}O_3P$	5,46	5,48	1,2056	1,6005		261	17260	87
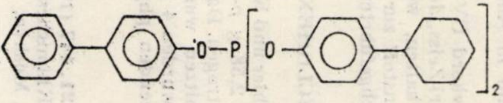	$C_{36}H_{37}O_3P$	5,65	5,55 5,58	1,1938	1,5912		260	19360	87
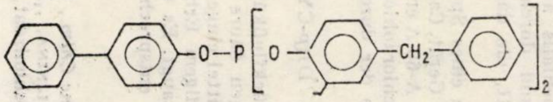	$C_{40}H_{35}O_3P$	5,29	5,30 5,34	1,2526	1,6134		259	17150	85
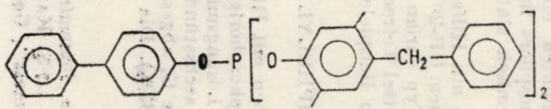	$C_{42}H_{39}O_3P$	4,98	5,04 4,96	1,2072	1,6094		259	19110	85
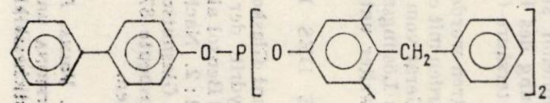	$C_{42}H_{39}O_3P$	4,98	4,88 4,92	1,2028	1,6012		256	19110	70
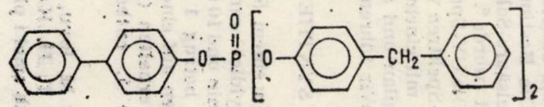	$C_{38}H_{31}O_4P$	5,40	5,38 5,44			86—87	250,5	47500	80

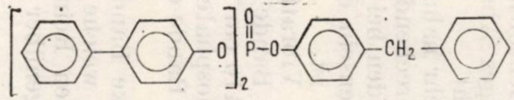	$C_{37}H_{29}O_4P$	5,45	5,59 5,54			110—111	254	47000	86
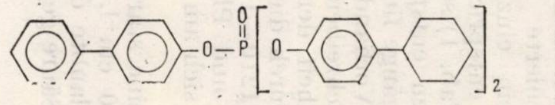	$C_{36}H_{37}O_4P$	5,49	5,53 5,56			105—106	251,5	43000	80
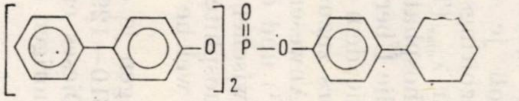	$C_{36}H_{32}O_4P$	5,54	5,63 5,67			87	251,4	42500	81
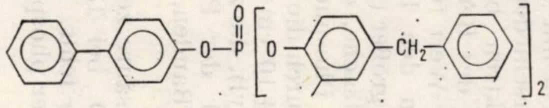	$C_{40}H_{35}O_4P$	5,07	5,10 5,13	1,2404	1,6108		252	16560	90
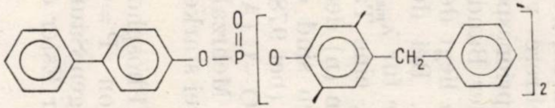	$C_{42}H_{39}O_4P$	4,92	4,87 4,80	1,2156	1,6055		251	19600	87
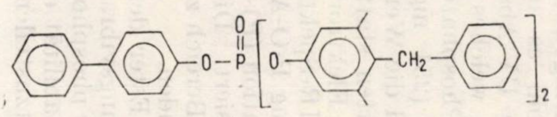	$C_{42}H_{39}O_4P$	4,92	5,00 5,08	1,2060	1,6068		251	18400	81

2, SYNTHESE DES BIPHENYL DI(*p*-CYCLOHEXYLPHENYL)PHOSPHATS

In die gleiche Vorrichtung, wie bei Punkt 1 beschrieben, werden 2 g Diphenyldichloranhydrid der Phosphorsäure, 2,45g *p*-Cyclohexylphenol, 1,41 g Triäthylamin und 10 ml Benzol als Lösungsmittel eingeführt, wobei das molare Verhältnis 1 : 2 : 2 betrug. Nach 8 Stunden bei 80° Erhitzen wurde wie bei Punkt 1 verfahren. Es wurden 3,56 g (Ausbeute 80,36%) eines festen, aus einem Benzol-Benzin-Gemisch (1 : 3) umkristallisierten Produktes erhalten, dessen physikalische Konstanten in Tabelle 1 angegeben sind.

3. OXYDATION DES DI(*p*-CYCLOHEXYLPHENYL)DIPHENYLPHOSPHITS ZU DI(*p*-CYCLOHEXYLPHENYL)DIPHENYLPHOSPHAT

In ein dickwandiges Probierglas von 50 ml Inhalt, das am oberen Teil ein Seitenrohr und außerdem auch ein Belüftungsrohr enthält, wird 0,5 g Di(*p*-cyclohexylphenyl) diphenylphosphit zusammen mit 15 ml Benzol eingeführt.

Das Probierglas wird sodann an die Wasserstrahlpumpe angeschlossen und während drei Stunden Luft eingeblasen. Wird darauf Leichtbenzin hinzugefügt, so scheidet sich ein fester Stoff aus, der aus einem Benzol-Benzin-Gemisch (1 : 3) umkristallisiert wird. Man erhält 0,48 g eines Produktes (Ausbeute 96%) mit den gleichen physikalischen Konstanten, wie das durch Kondensierung des Diphenyldichloranhydrids mit *p*-Cyclohexylphenol erhaltene Di(*p*-cyclohexylphenyl) diphenylphosphat, dessen Eigenschaften in Tabelle 1 enthalten sind.

Andere Ester der Phosphorsäure oder der phosphorigen Säure, die in Tabelle 1 angegeben sind, wurden unter ähnlichen Bedingungen erhalten.

ERGEBNISSE UND DISKUSSION

In Tabelle 1 sind die Strukturformeln der gemischten aromatischen Ester der phosphorigen und Phosphorsäure enthalten, sowie die Ergebnisse der Elementaranalyse des Phosphors, physikalische Konstanten, wie Dichte, Brechungsindex und Schmelzpunkt. Es wurden auch die durch UV-Spektroskopie erhaltenen Werte für λ_{max} und auch die entsprechenden Werte für ε_{max} eingetragen.

Alle synthetisierten Phosphite sind flüssig. Die Oxydation der Phosphite in die entsprechenden Phosphate wird durch die Schmelztemperatur angezeigt. Von den Phosphaten sind nur diejenigen feste Stoffe, die Benzolringe enthalten, welche mit Methyl-Radikalen substituiert sind.

Obwohl es mehrere verschieden substituierte Benzolringe gibt, haben die UV-Absoprionsspektren bloß je ein einziges Absorptionsmaximum, welches der Bande des Benzolrings entspricht.

Bei Phosphaten liegt der Wert für λ_{max} (Tab. 1) sehr nahe dem des Diphenyls (251 mμ). Bei den den Phosphaten entsprechenden Phosphiten sind die Werte für λ_{max} größer (die Übergänge finden bei kleineren Energiewerten statt), eine Tatsache, die dem Vorhandensein der nichtbindenden Elektronen (n) des Phosphors zuzuschreiben ist.

Die IR-Spektren sind durch die Anwesenheit der Vibrationsbande der Bindung P-O-Ar (bei 978 ± 10 cm^{-1}) und durch die Bande der Dehnungsvibration (P)—O—C (Aryl), die zwischen 1210—1110 cm^{-1}) liegen, charakterisiert. Die Mehrzahl der Phosphite und Phosphate besitzen in diesem Bereich zwei starke Banden, welche sich am Rande des Intervalls befinden.

Alle Ester der Phosphorsäure zeigen je eine starke Bande infolge der Dehnungsvibration P=O bei 1310—1290 cm^{-1}, welche bei den Estern der phosphorigen Säure fehlt. Dieses erlaubte den Reinheitsgrad und die Stabilität der Ester der phosphorigen Säure gegenüber der Oxydation festzustellen.

Die NMR-Spektrometrie zeigte mehrere Signale für δ der aromatischen Protonen, das zwischen 6,9 und 7,6 ppm lag. In Abb. 1 und 2 sind zwei Beispiele von NMR-Spektren dargestellt. Abb. 1 zeigt das NMR-Spektrum des Biphenyl di(4-cyclohexylphenyl)phosphits, indem CCl_4 als Lösungsmittel und TMS als innerer Standard verwendet wurden. Man unterscheidet 17 aromatische Protone im Bereich für δ = 7–7,6 ppm und 22 Protone im Bereich eines breiten Signals von δ = 1,0–2,5 ppm.

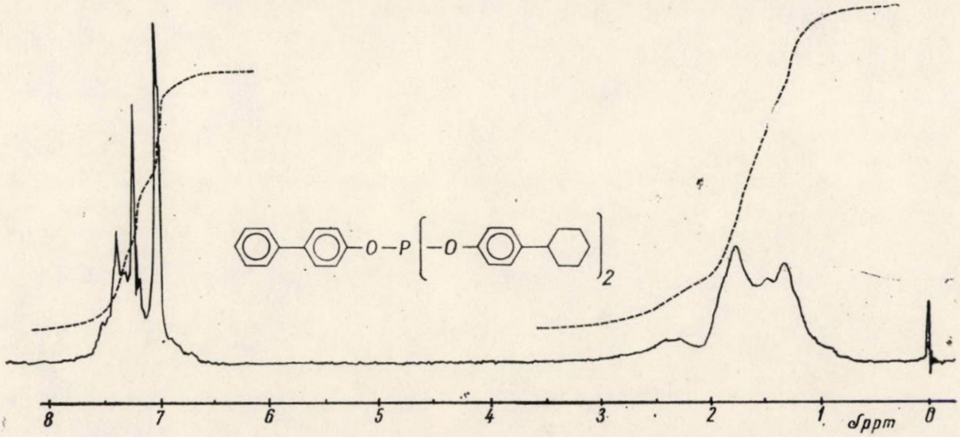

Abb. 1. – NMR-Spektrum des Biphenyl di(4-cyclohexylphenyl)phosphits.

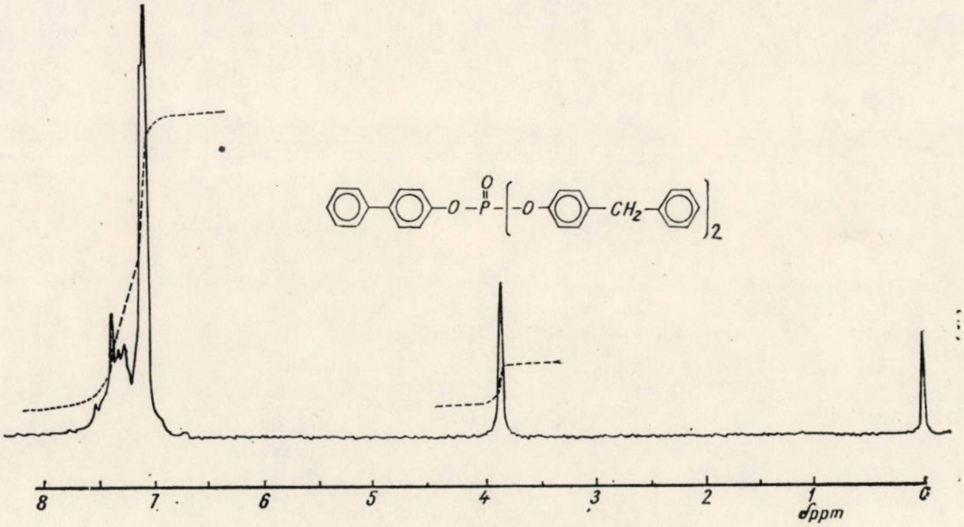

Abb. 2. – NMR-Spektrum der Biphenyl (di (4-benzylphenyl)phosphats.

In Abb. 2 ist das NMR-Spektrum des Biphenyl di(4-benzylphenyl) phosphats wiedergegeben, welches unter denselben Bedingungen, wie oben erhalten wurde. Man beobachtet die Anwesenheit der 27 aromatischen Protone, in einem vielfachen Signal im Bereich für δ = 6,9–7,6 und der 4 Protone aus den Methylen-Gruppen für δ = 3,86 ppm.

Die NMR-Spektrometrie zeigte mehrere Signale für δ der aromatischen Protonen, das zwischen 6,9 und 7,6 ppm lag. In Abb. 1 und 2 sind zwei Beispiele von NMR-Spektren dargestellt. Abb. 1 zeigt das NMR-Spektrum des Biphenyl di(4-cyclohexylphenyl)phosphits, indem CCl_4 als Lösungsmittel und TMS als innerer Standard verwendet wurden. Man unterscheidet 17 aromatische Protone im Bereich für δ = 7—7,6 ppm und 22 Protone im Bereich eines breiten Signals von δ = 1,0—2,5 ppm.

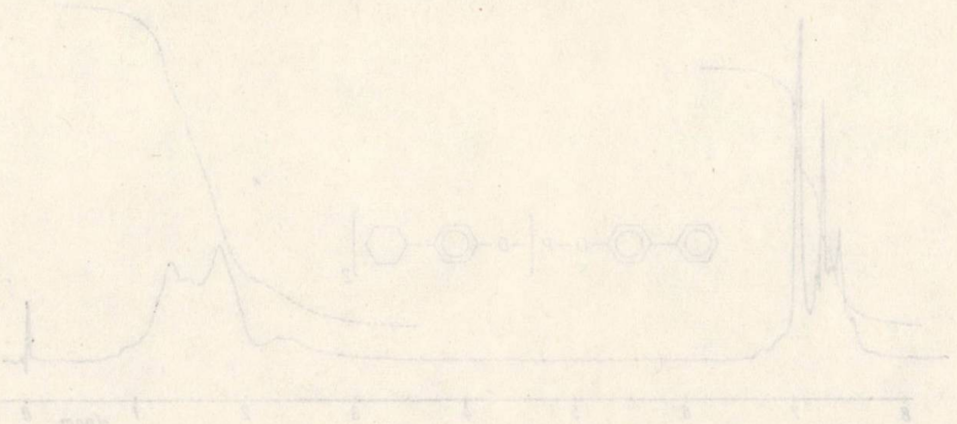

Abb. 1. — NMR-Spektrum des Biphenyl di(4-cyclohexylphenyl)phosphits.

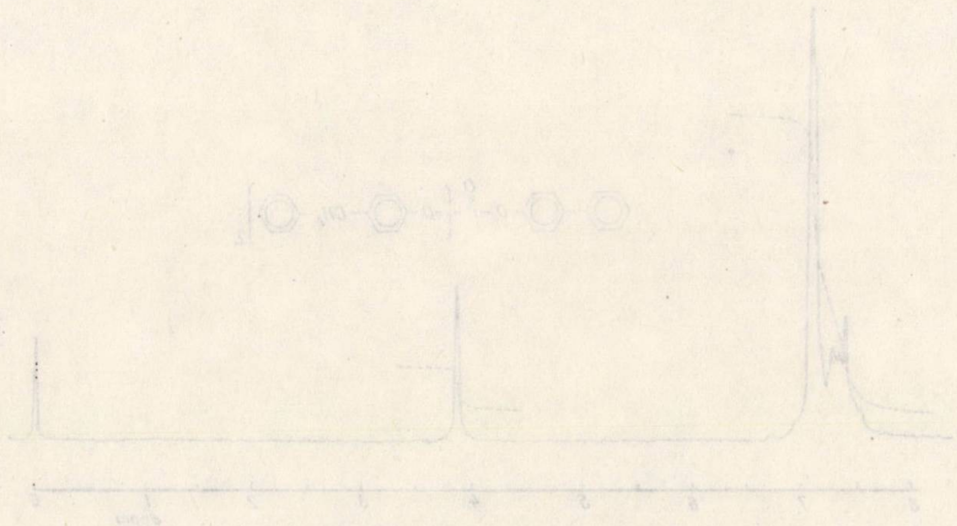

Abb. 2. — NMR-Spektrum des Biphenyl di(4-benzylphenyl)phosphats.

In Abb. 2 ist das NMR-Spektrum des Biphenyl di(4-benzylphenyl)phosphats wiedergegeben, welches unter denselben Bedingungen, wie oben erhalten wurde. Man beobachtet die Anwesenheit der 27 aromatischen Protone, in einem vielfachen Signal im Bereich für δ = 6,9—7,6 und der 4 Protone aus den Methylen-Gruppen für δ = 3,86 ppm.

Revue Roumaine de Chimie, **22**, *8*, 1217–1223, (1977)

INFRARED ABSORPTION SPECTRA OF SOME 4H-3,1-BENZOXAZIN-4-ONES AND 2,3-DISUBSTITUTED-4(3H)-QUINAZOLINONES

M. ANWAR and S. H. ETAIW

Chemistry Department, Faculty of Science, Tanta University, Tanta, A. R. Egypt

Received May 5, 1975

The ir spectra of some 4H-3,1-benzoxazin-4-ones and 4(3H) quinazolinones are studied as KBr discs. The frequency shifts of the $C=O$ and $C=N$ groups are interpreted in terms of molecular structure correlations. The ir-spectra are analysed to the extent that appears possible.

INTRODUCTION

The 4H-3,1-benzoxazin-4-ones and 4(3H) quinazolinones have become of increasing importance in recent years owing to their adequate use as pharmacological agents.[1-3] In the benzoxazonoid and quinazonoid area some investigations were already reported. The most extensive, perhaps, have been the studies of Mayer and Wagner,[4] Somasekhera[5] and Sammour.[6-8] They assigned the 1700 cm^{-1} band to $\nu C = O$ and the 1625 cm^{-1} band to $\nu C = N$. Also, the three bands at 1628–1618, 1581–1566 and 1517–1478 cm^{-1} are termed quinazoline I, II and III band, respectively.

In the present paper, we report spectral characteristics for the fundamental ring systems of some new 2-substituted 4H-3,1-benzoxazin-4-ones and their corresponding 2,3-disubstituted 4(3H)quinazolinones. Also, complete solid state spectra are reported and interpreted to the extent that appears possible.

---

[1] A. J. Tomisck and B. E. Christensen, *J. Amer. Chem. Soc.*, **67**, 2112 (1945).

[2] P. R. Dua, R. P. Kohli, R. Kumar and K. P. Bhargava, *Indian J. Physiol. Pharmacol.*, **11**, 107 (1967).

[3] G. Bonala, P. Dare, M. J. Magistretti, E. Massarans and I. Setniker, *J. Medicin. Chem.*, **11**, 1136 (1968).

[4] J. F. Meyer and E. C. Wagner, *J. Org. Chem.*, **8**, 239 (1943).

[5] S. Somasekhera, V. S. Dighe and S. L. Mukherjee, *Current Sci.*, **35**, 294 (1966).

[6] A. Sammour, M. I. B. Selim and M. Anwar, *U.A.R.J. Chem.*, **14**, *2*, 197 (1971).

[7] A. Sammour, M. I. Selim, M. Elkasaby and M. Abdalla, *Acta Chim. Acad. Sci. Hung.*, **78**, 293 (1973).

[8] A. Sammour, T. Zimaity and M. Anwar, *Egypt. J. Chem.*, **16**, 215 (1973).

EXPERIMENTAL

A number of 2-substituted 4H-3,1-benzoxazin-4-ones were prepared by the reaction of anthranilic acid and acid chlorides [9] or the condensation of 2-methyl-4H-3,1-benzoxazin-4-one with aldehydes and ketones. [6,7]

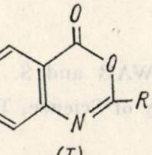

(I)

Ia, $R= CH=CH-CH=CH-C_6H_5$; Ib, $R= CH=C(CH_3)_2$; Ic, $R= CH=C(CH_3)(C_6H_5)$

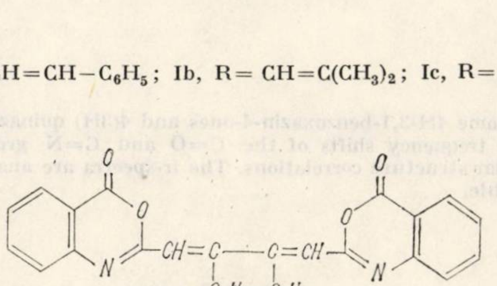

(Id)

The condensation of (I) with aromatic amines and hydrazines gives the 2,3-disubstituted 4(3H) quinazolinones (II).[6]

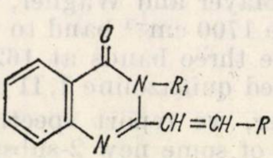

(II)

	R	R_1		R	R_1
IIa,	C_6H_5	NH_2 ;	f,	$C_6H_4OCH_3-p$	$C_{10}H_7-1$
b,	C_6H_5	$NHC_6H_4NO_2-p$;	g,	$C_6H_3O_2CH_2-3,4.$	$C_6H_4CH_3-p$
c,	C_6H_5	$C_6H_4OCH_3-p$;	h,	$C_6H_3O_2CH_2-3,4.$	C_6H_4Cl-p
d,	C_6H_5	$C_6H_4NO_2-p$;	i,	$CH=CH-CH_3$	$C_6H_4OCH_3-p$
e,	$C_6H_4OCH_3-p$	$C_6H_4OCH_3-p$			

---

[9] D. T. Bain and R. K. Smalley, *J. Chem. Soc.* (*C*), **1968**, 1593.

Compounds IIIa, b were obtained by adding thiophenol to II according to the method described in the literature.[7]

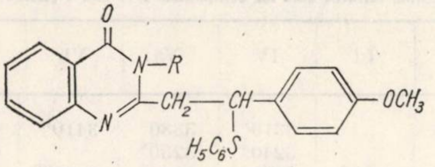

(III)

IIIa, R=OCH_3; b, R=CH_3

N-Ethyl-N′-cinnamoyl anthranilamide was obtained from the reaction of 2-styryl-4H-3,1-benzoxazin-4-one with ethylamine.[10]

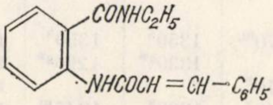

(IV)

Reaction of ethylmagnesium iodide with (I) gives the expected 2-benzamido-aryl-diethyl carbinols (Va, b).[7,11]

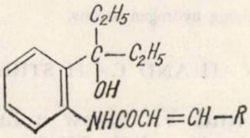

(V)

Va, R=C_6H_5; b, R=$CH{=}CH{-}C_6H_5$

The products were crystallized several times from appropriate solvents. The ir-spectra were obtained by a UNICAM S.P.200 infrared spectrophotometer using the KBr-disc technique.

RESULTS AND DISCUSSION

Infrared spectra have been determined in the 4000—650 cm^{-1} region. The solid state spectra determined in potassium bromide discs are subject to the problem that certain bands may originate from some type of crystal interaction, rather than to a vibration of the molecule itself. Absorption bands for 2-substituted 4H-3,1-benzoxazin-4-ones (I), (IV), (Va, b) in the 4000—650 cm^{-1} region are presented in Table 1. Spectral characteristics for the 2,3-disubstituted-4(3H) quinazolinones (II) in 3300—650 cm^{-1} region are outlined in Tables 2 and 3. In all ir-spectra, there is no significant absorption in the 2200—1720 cm^{-1} region.

---

[10] A. M. El-Abbady, M. Anwar, F. I. Abdel-Hay and M. F. Abdel-Megeed, *J. Chem., A.R.*, 3 (1976) (in press).

[11] T. Zimaity, M. Anwar, F. I. Abdel-Hay and M. F. Abdel-Megeed, *Acta, Chim., Sci., Hung.* (1975) (in press).

Table 1

Solid state infrared data for compounds I, IV and V (KBr; cm⁻¹)

Ia	Ib	Ic	Id	IV	Va	Vb	Band Assignment
				3310^{s}	3380^{s}	3410^{b}	νOH
				3240^{s}	3230^{s}		νNH
1690^{s}	1700^{s}	1700^{s}	1700^{s}	1680^{s}	1680^{s}	1680^{sh}	νC=O
1645^{s}	1655^{s}	1650^{s}	1650^{s}	1640^{s}	1640^{sh}	1650^{sh}	νC=N
				$1615^{v.s}$			νC=C ethylenic
1600^{s}	1600^{s}	1610^{s}	1600^{s}	$1600^{v.s}$	1610^{s}	1600^{s}	νC=C skeletal vibr.
1565^{s}	1570^{s}	1575^{s}	1580^{s}	1575^{s}	1575^{s}	1560^{sh}	νC=C skeletal vibr.
1500^{b}	1510^{b}	1500^{b}	1520^{b}	$1510^{v.s}$	$1500^{v.s}$		νC=C skeletal vibr.
1450^{s}	1450^{s}	1460^{s}	1460^{s}	1450^{s}	1445^{s}	1450^{s}	δ aromatic C−H overlapped with δ asym. aliph. C−H
1370^{m}	1375^{s}	1375^{m}	1370^{m}	1350^{s}	1350^{s}	1355^{m}	δ sym. aliph. C−H
				1330^{s*}	1290^{s*}	1315^{m}	νC−N
1295^{s}	1300^{s}	1300^{s}	1310^{s}			1300^{m}	δ arom. C−H
1225^{s}	1235^{b}	1235^{s}	1240^{s}	1280^{s}	1245^{m}	1239^{s}	γ C−O
775^{s}	785^{s}	780^{s}	785^{s}		780^{s}		γ $C-H^{(4)}$
760^{s}		760^{m}	765^{m}	$760^{v.s*}$	$775^{v.s*}$	740^{m}	γ $C-H^{(5)}$
700^{s}		705^{s}	710^{m}	720^{m}	695^{s}	$700^{v.s}$	γ $C-H^{(5)}$

Intensity of bands is given as: v.s = very strong, s = strong, m = medium, b = broad, w = weak, sh = shoulder.

* overlapped with other bands.

(4 or 5) are the number of adjacent ring hydrogen atoms.

(a) O−H, N−H AND C−H STRETCHING BANDS

The ir-curves for IV and Va show a fairly sharp strong band at 3310 and 3380 cm⁻¹, respectively, while Vb has a broad band at 3410 cm⁻¹. The band can be assigned to O−H stretching. The keto-enol shift in IV is responsible for the appearance of the band at 3310 cm⁻¹ while in Va, b the enolic O−H and hydroxylic O−H stretching bands are merged and appear as a broad one. The low frequency values of OH in Va, b can be attributed to the intramolecular hydrogen bond formed between the hydroxyl proton and the nitrogen atom. The hydrogen bond is probably quite strong, so it favours the enolic shift, phenomenon which raises the enolic OH frequency.

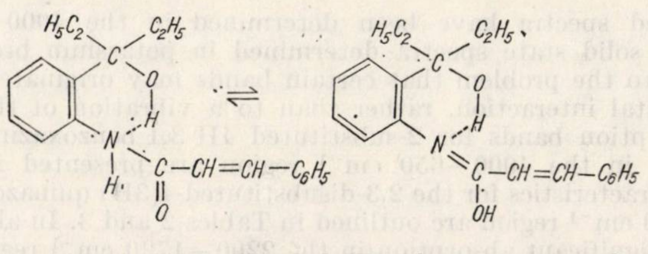

The ir- spectra of IV, Va and IIb show a strong band at 3240, 3230 and 3280 cm⁻¹, respectively, assigned to N−H stretching. The lower frequency of νNH in IV and Va relative to that in IIb arise from the keto-enol tautomerism in these compounds. However, the low frequency of νNH in IIb is due to the intramolecular hydrogen bond formed

Table 2

Solid state infrared data for compounds II and III (KBr; cm^{-1})

IIa	IIb	IIc	IId	IIe	IIf	IIg	IIh	IIi	IIIa	IIIb	Band Assignment
3070	3040	3080	3090	3050	3060	3045	3045	3090	3100	3100	δ asym. arom. C−H
3040	3015	3030	3015	3010	3010	3025	3020	3000	3020	2990	δ sym. arom. C−H
2995	2910	2955	2955	2975	2930	2930	2960	2910	2920	2910	δ asym. aliph. C−H
2890	2840	2850	2860	2865	2860	2890	2920	2830	2830	—	δ sym. aliph. C−H
1665^{s}	1668^{s}	1670^{s}	1680^{s}	1674^{s}	1670^{w}	1672^{s}	1675^{s}	1675^{s}	1670^{m}	1670^{sh}	νC=O
—	—	1655^{sh}	1650^{sh}	1650^{m}	1630^{sh}	—	1650^{sh}	1645^{w}	1630^{s}	1630^{b}	νC=N
$1625^{v.s}$	—	—	—	—	—	1620^{sh}	—	1615^{w}	—	—	νC=C ethylenic
1600^{s}	$1600^{v.s}$	1605^{s}	1610^{m}	1605^{s}	$1600^{v.s}$	—	1600^{m}	—	—	1585^{sh}	Quinazolone I
1575^{s}	1575^{s}	1580^{sh}	1580^{s}	1560^{s}	1575^{sh}	$1575^{v.s}$	1540^{s}	1580^{s}		1550^{w}	Quinazolone II
1510^{s}	—	1515^{s}	1500^{s}	$1520^{v.s}$	1510^{s}	$1515^{v.s}$	$1480^{v.s}$	$1520^{v.s}$	$1570^{v.s}$	1500^{s}	Quinazolone III
1325^{m}	1300^{s}	1320^{m}	1305^{s}	1315^{s}	1315^{m}	1315^{s}	1330^{w}	1320^{s}	1320^{w}	1315^{s}	νC−N
1195^{s}	1180^{sh}	1170^{m}	1175^{m}	1185^{s}	1170^{s}	1192^{s}	—	1195^{s}	1200^{s}	1180^{s}	δ arom. C−H
			1120^{s}	1125^{m}	—	1080^{sh}	1100^{m}	$1105^{v.s}$	1110^{w}	—	νC−C
875^{m}	—	—	$865^{m(2)}$	$840^{s(2)}$	$850^{m(2)}$	$920^{w(1)}$	$830^{m(2)}$	840_{s_2}	$870^{s(2)}$	$830^{b(2)}$	γC−H
$755^{s(4)}$	—	$830^{m(2)}$	$865^{s(2)}$	$775^{s(4)}$	$815^{m(3)}$	845_{s_2}	—	$755^{s(4)}$	—	—	γC−H
$730^{s(5)}$	—	$780^{s(4)}$	$730^{m(5)}$	—	$750^{s(4)}$	815_{s_2}	$780^{s(5)}$	—	$770^{w(4)}$	$740^{w(5)}$	γC−H
$680^{s(5)}$	—	$710^{s(5)}$	$700^{s(5)}$	—	—	$750^{m(4)}$	$700^{m(5)}$	—	$730^{(5)}$	$700^{m(5)}$	γC−H

1, 2, 3, 4 or 5 are the number of adjacent ring hydrogen atoms.

Table 3

IR – Spectral data for functional groups of II and III

IIa	IIb	IIc	IId	IIe	IIf	IIg	IIh	IIi	IIIa	IIIb	Band Assignment.
$3300^{v.s}$											ν asym. NH_2
3195^{s}											ν sym. NH_2
	$3280^{v.s}$										ν N−H
	1550^{sh}										ν asym. NO_2
1450^{s}	1445^{w}	1460^{sh}	1445^{s}	1455^{m}	1460^{m}	1460^{b}	1465^{m}	1460^{w}	1460^{w}	1460^{w}	δ asym. aliph. C−H
1350^{s}	1360^{sh}	1370^{w}	1350^{sh}	1365^{w}	1360^{m}	—	1370^{w}	1350^{w}	1355^{sh}	—	δ sym. aliph. C−H
	1340^{s}		$1340^{v.s}$								ν sym. NO_2
		$1250^{v.s}$		$1265^{v.s}$	$1250^{v.s}$	1220^{m}	—	$1255^{v.s}$	$1250^{v.s}$	$1260^{v.s}$	ν asym. = C−O−C
		1040^{m}		$1045^{v.s}$	1025^{s}	$1060^{v.s}$	—	1040^{s}	1040^{s}	1030^{s}	ν sym. = C−O−C
							675^{w}				νC−Cl
										670^{w}	νC−S

between the hydrogen atom and the carbonyl oxygen atom. On the other hand, the spectrum of IIa shows strong bands at 3300 and 3195 cm^{-1} assigned to the asymmetric and symmetric stretching vibration of the amino group, respectively. The low frequency values are usually a sufficient indication that a hydrogen bond is involved.

The fundamental benzoxazonic and quinazolonic ring systems contain C—H stretching bands near 3100 and 3030 cm^{-1}. Also, the aliphatic C—H asymmetric and symmetric stretching bands are observed near 2960 and 2860 cm^{-1}, respectively.

(b) C=O, C=N AND C=C STRETCHING BANDS

All ir- spectra of the present compounds show a strong band within 1700—1665 cm^{-1} region assigned to the C=O stretching. The carbonyl groups in IV, Va, b can be considered as α, β-unsaturated carbonyl which already absorbs at 1680 cm^{-1}. The spectra of the benzoxazone derivatives show the carbonyl stretching band near 1700 cm^{-1}. On the other hand, the carbonyl in quinazolones absorbs near 1670 cm^{-1}. The shifts toward lower frequencies on going from 4H-3,1-benzoxazin-4-ones, 2-benzamido aryl-diethyl carbinol to 4H-4(3H) quinazolinones are expected due to increased polarizability of the carbonyl group. The relatively large frequency shifts of II relative to I and V arise mainly from charge transfer interaction between the substituents at positions 2 and 3, and the carbonyl group.

Also, the ir- spectra show a shoulder or a strong band near 1650 cm^{-1}, assigned to C=N stretching. The band is directly influenced by the nature of substituent at position 2. The donor groups as well as increased conjugation cause a red shift while the saturated systems (IIIa, b) cause a blue shift. The appearance of this band near 1640 cm^{-1} in the spectra of IV, Va, b is a further support for the presence of the keto-enol tautomerism. In the spectra of IIa, b and g the νC=N is masked by the strong band due to carbonyl stretching.

The ir- spectra of IIa, h, j and IV are characterized by a strong or medium band, within the 1625—1615 cm^{-1} region, which can be assigned to ethylenic C=C stretching. The band in the remaining compounds is strongly overlapped with the band near 1600 cm^{-1} arising from skeletal vibrations.

(c) ABSORPTION DUE TO SKELETAL VIBRATIONS

In Tables 1 and 2 are listed bands possibly associated with skeletal vibrations. Other workers [12] have noted as many as three bands associated with skeletal vibrations in the spectra of 3-methyl-4(3H) quinazolinone and 2,3-dimethyl-4(3H) quinazolinones. Both the quinazolone and benzoxazone nuclei absorb at 1610—1585, 1580—1550 and 1520—1480 cm^{-1}.

(d) ABSORPTION IN 1500—1000 cm^{-1} REGION

The region is of interest, since bands due to O—H, N—H and C—H in plane deformation modes may occur here. Other bands possible in the appropriate derivatives are C—O stretching bands of the lactone link and the methoxyl group, NO_2, C—N and various C—C stretching modes, which data are listed in Tables 2 and 3.

---

[12] L. J. BELLAMY, "Infrared Spectra of Complex Molecules", Methuen, London, 1966, p. 284.

In Table 3 are listed bands possibly characteristic of the functional groups found in compounds IIa—c. The other bands observed in this region can be assigned to in-plane bending vibrations of aromatic C—H and to various C—C stretching modes.

(e) ABSORPTION IN 1000—650 cm^{-1} REGION

The out-of-plane deformation frequencies for aromatic C—H bonds are the most expected in this region. The spectra of compounds I and V exhibit a strong band at 780 cm^{-1} corresponding to out-of-plane deformation of four adjacent ring hydrogen atoms. On the other hand, five adjacent hydrogen atoms absorb near 760 and 700 cm^{-1}. Compounds II have different types of ring hydrogen atoms, however the quinazolone ring involves four adjacent ring-hydrogen atoms which absorb within 780—750 cm^{-1} region.

In addition to these out-of-plane deformation bands, there are some other peaks in the 1000—650 cm^{-1} region. These bands could be associated with various C—C and C—O stretching modes.

Revue Roumaine de Chimie, 22, 8, 1225–1231 (1977)

NEW DISPERSE DYES FOR POLYESTER FIBRES

F. URSEANU and E. TESZLER
Laboratory of Chemistry and Technology of Aromatic
Intermediates and Dyes, Polytechnic Institute, Bucharest,
Calea Victoriei 149, Romania

Received February 17, 1976

Syntheses for the preparation of disperse dyes with new heterocyclic dibenz [f,ij] isoquinoline [2,3–b] quinazoline [5,6–cd] pyrazol-6(2H)-one and dibenz [f,ij] isoquinoline [2,3–b] quinazoline [5,6–de] pyrimidin-7-one structure are described.

1. INTRODUCTION

Our study for the preparation of new disperse dyes for polyester fibres has the object to obtain some products with various structures, which have a good affinity and better fastness, when applied on the textile material.

The present work describes the results obtained concerning the synthesis of dyes with new mixed condensed: dibenz [f,ij] isoquinoline [2,3-b] quinazoline [5,6-cd] pyrazol-6(2H)-one (I) and dibenz [f,ij] isoquinoline [2,3-b] quinazoline [5,6-de] pyrimidin-7-one (II) structures:

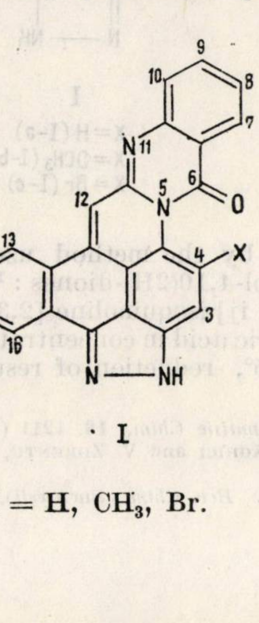

I

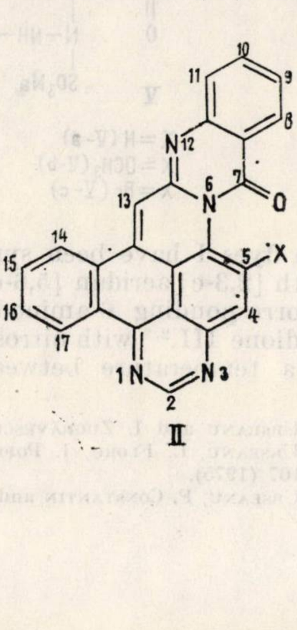

II

in which X = H, CH_3, Br.

2. SYNTHESIS OF DYES

2.1. SYNTHESIS OF DIBENZ [f, ij] ISOQUINOLINE [2,3-b] QUINAZOLINE [5,6-cd] PYRAZOL-6(S_2H)-ONE DERIVATIVES

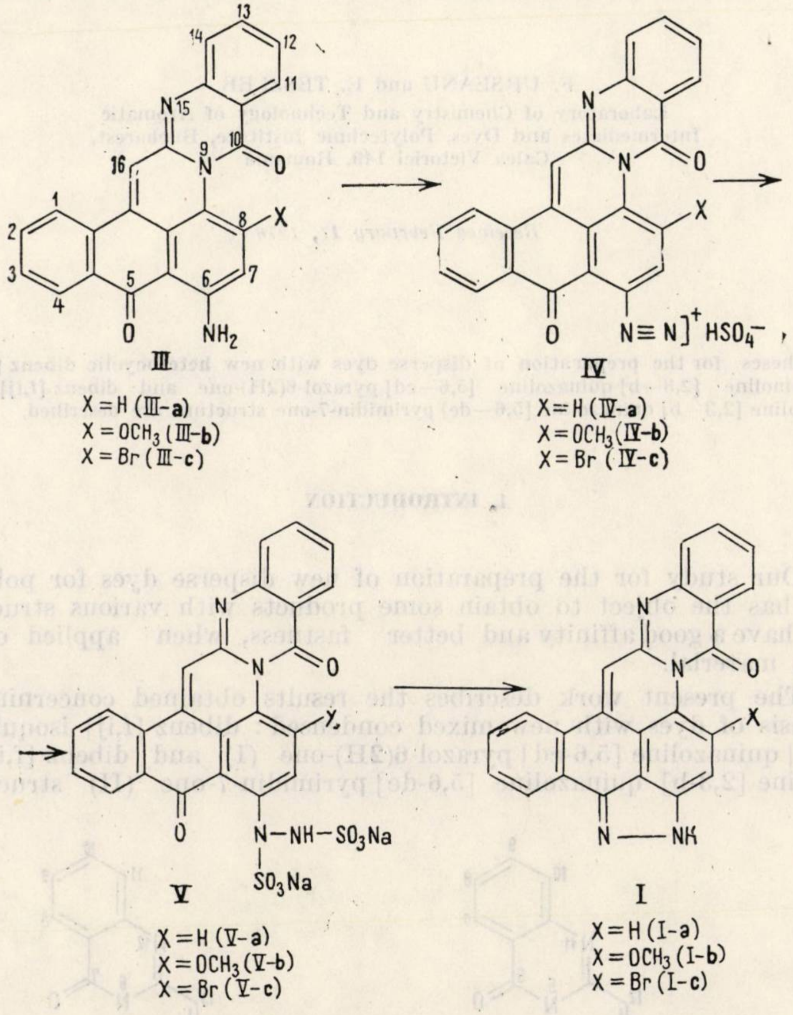
13
14
12
11
N15
10
9
16
N
O
1
8
X
2
3
5
6
7
4
O
NH2
N
N
O
X
O
N≡N]+ HSO4−
N
N
O
X
O
N—NH—SO3Na
SO3Na
N
N
O
X
N
N——NH

III
X = H (III-a)
X = OCH$_3$ (III-b)
X = Br (III-c)

IV
X = H (IV-a)
X = OCH$_3$ (IV-b)
X = Br (IV-c)

V
X = H (V-a)
X = OCH$_3$ (V-b)
X = Br (V-c)

I
X = H (I-a)
X = OCH$_3$ (I-b)
X = Br (I-c)

The dyes I have been synthesized by the method used to obtain the naphth [2,3-c] acridan [5,6-cd] pyrazol-4,10(2H)-diones :[1] diazotation of the corresponding 6-aminodibenzo [f, ij] isoquinoline [2,3-b] quinazoline-5,10-dione III,[2,3] with nitrosylsulphuric acid in concentrated sulphuric acid at a temperature between 30—35°, reduction of resulting diazonium salt IV with sodium sulphite and sodium disulphite in sodium hydrazinedisulphonic salt V and its cycling by heating in concentrated sulphuric acid at moderate temperature (50°).

---

[1] F. Urseanu and I. Zugrăvescu, *Rev. Roumaine Chim.*, **18**, 1211 (1973).

[2] F. Urseanu, L. Floru, I. Popescu, C. Drăghici and V. Zdrenţu, *Rev. Roumaine Chim.*, **20**, 107 (1975).

[3] F. Urseanu, P. Constantin and V. Zdrenţu, *Rev. Chim. (Bucureşti)*, **27**, 565 (1976).

2.2. SYNTHESIS OF DIBENZ [f,ij] ISOQUINOLINE [2,3-b] QUINAZOLINE [5,6-de] PYRIMIDIN-7-ONE DERIVATIVES

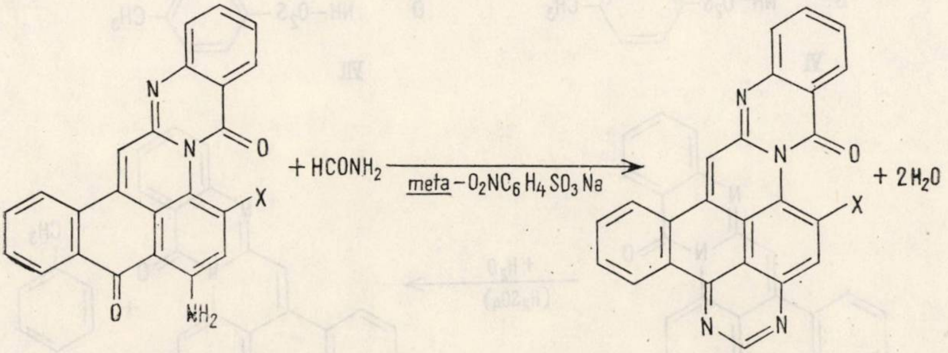

III
X = H (III-a)
X = OCH3 (III-b)
X = Br (III-c)

II
X = H (II-a)
X = OCH3 (II-b)
X = Br (II-c)

The dyes II have been synthesized according to a literature procedure,[3,4] namely by treating the corresponding 6-aminodibenzo [f,ij] isoquinoline [2,3-b] quinazoline-5,10-dione III with formamide in the presence of sodium *meta*-nitrobenzenesulphonate ; the reaction was carried out by refluxing in excess of formamide as solvent.

2.3. SYNTHESIS OF STARTING MATERIALS (III)

The synthesis of compounds III-*b* and III-*c* is described in a previous work.[3]

The compounds III-*a* have been synthesized according to the reactions given below :

The compound VI[5,6] has been refluxed in aqueous solution with glucose and sodium hydroxide in order to eliminate the sulphonic acid group, according to a literature procedure.[7] The product VII was treated with anthranilic acid by heating at 110–115° in a mixture of acetic anhydride and anhydrous zinc chloride ; the hydrolysis of the *para*-tolylsulphonamidic rest from the resulting compound IX was performed by heat-

---

[4] F. Urseanu, C. Tărăbășanu-Mihăilă, L. Floru and V. Zdrențu, *Rev. Roumaine Chim.*, **21**, 255 (1976).

[5] FIAT Final Rep., nr. 1313, vol. 2, p. 202.

[6] H. Sanielevici and L. Floru, "Tehnologia intermediarilor aromatici și a coloranților", Ed. didactică si pedagogică, Bucharest, 1971, p. 310.

[7] F. Urseanu, C. Tărăbășanu-Mihăilă, L. Floru and V. Zdrențu, *Rev. Chim.* (*București*), **25**, 873 (1974).

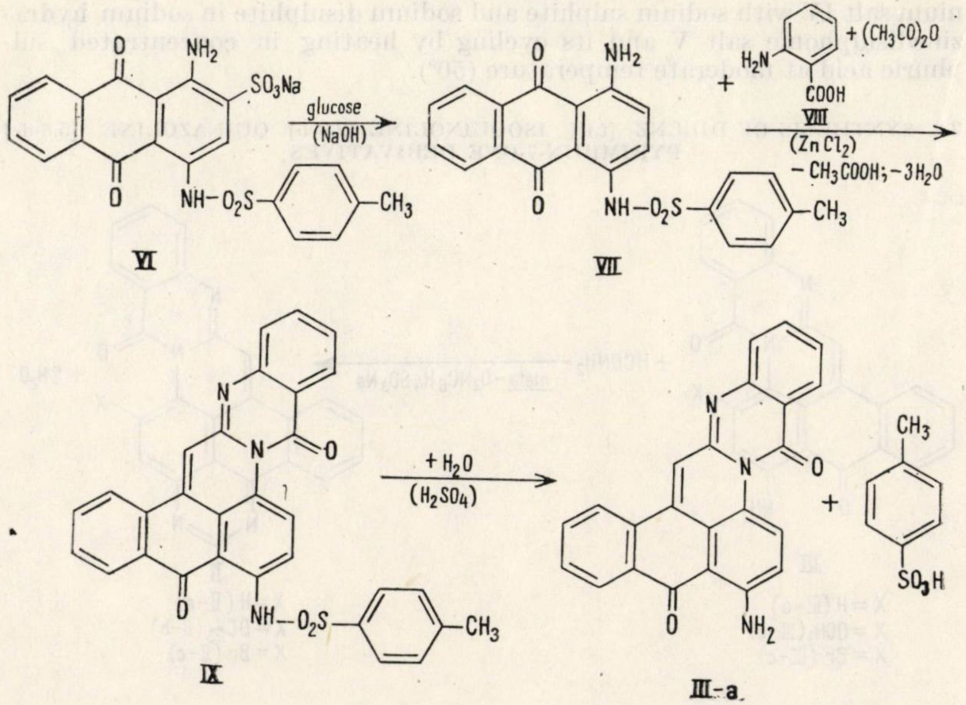

ing it at 50—60° in concentrated sulphuric acid, followed by the decomposition of the reaction mass on ice, according to a literature procedure described.[6,2]

Using analogous conditions the compound III-*b* will be synthesized if the sulphonic acid group of compound VI is replaced with the methoxy group.[6]

3. EXPERIMENTAL

3.1. 24.7 g (0.05 mol) compound VI is dissolved in a solution of 7.8 g NaOH in 250 ml water at 90—95°, then a warm solution of 16.5 g glucose in 35 ml water is added dropwise, for 10 minutes, to the solution resulted; the reaction is completed by heating at 95° for 15 minutes. The mixture is then cooled to 15—20°, neutralized with concentrated HCl to pH = 6—6.5 and filtered; the precipitate is washed with 400 ml water and dried at 75—80°, yielding 18.6 g product VII (95% yield).

3.2. A solution of 15.7 g (0.04 mol) compound VII in 60 ml acetic anhydride is heated at 100° for 20 minutes with removal of the acetic acid formed under a light vacuum; then 6 g anthranilic acid and 10 g anhydrous zinc chloride are added and the mixture is heated at 110—115° for 2 hours, with continuous distillation of the acetic acid formed. Note: During the reaction the colour of the mass turns from red to orange.

Finally, when the reaction ends, the mass is cooled to 30—40°, 500 ml water are added and the mixture is gradually heated to 100° in order to hydrolyze the excess of acetic anhydride and to precipitate the resulted compound IX and then filter it. The precipitate is washed with 500 ml lukewarm water (40—50°) and dried at 75—80° yielding 17.6 g product IX (90% yield).

3.3. 18.1 g (0.035 mol) compound IX is dissolved in 150 ml 96% H_2SO_4 and the resulted solution is heated for 2 hours at 60—70°, then the mixture is cooled at 5—10°, poured over 2000 g ice and water and filtered; the precipitate is washed with water until the filtrate is neutral, dried at 75—80°, yielding 12.2 g product III-a (96% yield).

3.4. 5.44 g (0.015 mol) compound III-*a* is added for 30 minutes, at 25—30°, to a solution of nitrosylsulphuric acid obtained from 1.7 g dry $NaNO_2$ and 50 ml 96% H_2SO_4. The diazotation reaction is completed by heating at 30—35° for 3 hours. The solution is then poured over 250 g crushed ice, mixed for 20 minutes and filtered; the precipitate is washed with 25% NaCl solution until the filtrate is neutral.

The diazonium salt IV-*a* thus obtained is added to a solution of 12 g Na_2SO_3 in 120 ml water and stirred for 2 hours at 20—25°, then 2 g $NaHSO_3$ are added and heated for 3 hours at 70—75° (a sample is completely soluble in water). The formed product V-*a* is precipitated by adding NaCl, filtered, washed with 50 ml 25% NaCl solution (when the filtrate is colourless) and dried at 40—50°.

The dried compound V-*a* is dissolved in 50 ml 96% H_2SO_4 and the solution is heated for 1.5 hours at 50—70°, then it is cooled at 15—20° and poured over 500 g ice and water; the precipitate is filtered, washed with water until the filtrate is neutral and dried at 75—80°. 4.6 g product I-*a* are obtained (85% yield).

3.5. Using analogous conditions to those of synthesis 3.4, from 5.9 g (0.015 mol) compound III-b, 4.7 g product I-*b* are obtained (80% yield).

3.6. If 6.63 g (0.015 mol) compound III-*c* are used, and work is done in the conditions described in synthesis 3.4., finally 5.4 g product I-*c* are obtained (82% yield).

3.7. A mixture of 5.44 g (0.015 mol) compound III-*a* and 3 g sodium *meta*-nitrobenzenesulphonate in 40 ml formamide is refluxed (198°) for 3 hours, then it is cooled at 25° and 100 ml water are added; the formed precipitate is filtered, washed with lukewarm water (40—50°) until the filtrate is colourless (about 150 ml) and dried at 75—80° yielding 4.6 g product II-*a* (82.5% yield).

3.8. Working in the conditions described in synthesis 3.7., from 5.9 g (0.015 mol) compound III-*b*, 4.88 g product II-*b* are obtained (81% yield).

3.9. Similarly from 6.63 g (0.015 mol) compound III—*c*, 5.5 g product II-*c* are obtained (81.5% yield).

4. ANALYSES

The analysed compounds were previously purified from an appropriate solvent: N,N-dimethylformamide, nitrobenzene glacial acetic acid (see Table 1). All the synthesized compounds have the melting point over 300°, with their decomposition.

The purified compounds were subjected to chromatographic, elementary spectral and tinctorial analyses.

The % N of synthesized compounds are determined by microcombustions and the results are presented in Table 1.

Chromatographic analyses were carried out on Whatman paper no 3 (impregnated with a 10% solution of 1-bromonaphthalene in ethanol), in ascendent system, using N,N-dimethylformamide as solvent and 80% CH_3COOH as eluent, in order to follow the reactions and to check the purity of analysed compounds.

Ultraviolet and visible spectra of the products were recorded with a "Pye Unicam SP-1800" apparatus. The determinations were carried out in N,N-dimethylformamide and the extinction coefficients ε_{max} were calculated; the characteristic absorption maxima λ_{max} and lg ε_{max} are presented in Table 1.

Table 1

Characteristics of the newly prepared compounds

Compound	Empirical formula	Solvent for recrystallization	% N Calculated Found	$\lambda_{\max}^{\mathrm{DMF}}$ [nm]	$\lg \varepsilon_{\max}^{\mathrm{DMF}}$
I-*a*	$C_{23}H_{12}ON_4$	DMF	15.55 15.62	434 458 484	4.00 4.06 3.99
I-*b*	$C_{24}H_{14}O_2N_4$	DMF	14.36 14.45	366 486 580	4.17 3.85 3.63
I-*c*	$C_{23}H_{11}ON_4Br$	DMF	12.75 12.61	358 374 470	4.25 4.22 3.88
II-*a*	$C_{24}H_{12}ON_4$	nitrobenzene	15.02 15.12	378 422 504	3.72 3.73 3.18
II-*b*	$C_{25}H_{14}O_2N_4$	nitrobenzene	13.92 13.78	340 434	4.41 3.98
II-*c*	$C_{24}H_{11}ON_4Br$	glacial acetic acid	12.41 12.32	340 422	4.20 3.89

DMF = N.N-dimethylformamide.

Table 2

Determinations with dyed fibres

Compound	Colour	Fastness					
		Light	Cold water	Washing 40°	Perspiration		Rubbing
					acid pH = 5.5	alkaline pH = 8.4	
I-*a*	olive 20	5	5/5/5	5/4–5/5	5/5/5	5/5/5	5
I-*b*	brown 24	5–6	5/4–5/5	5/4–5/5	5/4–5/5	5/4–5/4–5	5
I-*c*	yellowish brown 22	6	5/5/5	5/5/5	5/5/5	5/5/5	5
II-*a*	yellowish orange 4	5–6	5/5/5	5/5/5	5/5/5	5/5/5	5
II-*b*	brownish olive 21	5–6	5/4–5/4–5	5/4–5/4	5/4–5/4–5	5/4–5/4–5	5
II-*c*	reddish yellow (dull) 3	5–6	5/5/5	5/5/5	5/5/5	5/5/5	5

The synthesized compounds I and II were used as disperse dyes for "Terom" polyester fibres. The results of determinations with dyed fibres are presented in Table 2. The colours were defined according to C. I. Hue Chart.[8]

The dyeings obtained are distinguished by good affinity of dyes for textile material, very good fastness and brilliance of shade.

A good agreement is observed between the colours seen on the dyed samples and the value of the absorption maxima.

---

[8] C. I. HUE, "Indication Chart, American Association of Textile Chemists and Colourists", Lowell Institute, Lowell Massachusetts, U.S.A.

Revue Roumaine de Chimie, **22**, *8*, 1233–1241 (1977)

PHYSICO-CHEMICAL PROPERTIES OF CHLORAMINE-T. II

CONDUCTOMETRIC STUDY OF THE INTERACTION OF CHLORAMINE-T WITH Cr(III), Al(III) AND Fe(III) SOLUTIONS

D. S. MAHADEVAPPA and RANGASWAMY

Department of Post-graduate Studies and Research in Chemistry,
University of Mysore, Manasa Gangotri, Mysore 570 006
India

Received May 5, 1975

Chloramine-T, the sodium salt of N-chloro-*p*-toluenesulphonamide produces a white turbidity with $Cr_2(SO_4)_3$, $CrCl_3$, $Al_2(SO_4)_3$, $AlCl_3$ and $FeCl_3$ in aqueous solution. Conductometric and potentiometric titrations have been carried out, and by elemental analysis, ultraviolet and infrared spectral data, the precipitate has been identified as dichloramine-T. The breaks in the conductance graphs also substantiate the formation of the free acid, N-chloro-*p*-toluenesulphonamide, for which no experimental proof has been presented until now.

Chaloramine-T (CAT), $CH_3-C_6H_4SO_2NClNa$ is the sodium salt of N-chloro-*p*-toluenesulphonamide and it has been extensively used as an analytical reagent for oxidising many inorganic and organic compounds.[1–9] The compound behaves like a strong electrolyte in aqueous solution.[10] However, very little work has been done on the salts of N-chloro-*p*-toluenesulphonamide. The authors [11] have reported on the silver and mercuric salts of this acid. During our attempts to prepare the corresponding chromium, aluminium and ferric salts, we noticed that addition of CAT solution to aqueous solutions of these ions or the respective alums produced a white turbidity. It was found to be of interest to

---

[1] I. M. Kolthoff and R. Belcher, "Volumetric Analysis", Vol. III, Interscience Publishers, New York, 1957, p. 639.

[2] G. Aravamudan and D. Venkappayya, *Talanta*, **15**, 704 (1968).

[3] C. G. R. Nair and A. R. V. Murthy, *Monatsh*, **94**, 134 (1963).

[4] V. R. S. Rao and A. R. V. Murthy, *Talanta*, **4**, 206 (1960).

[5] D. S. Mahadevappa, *Current Sci.*, **33**, 710 (1964), **34**, 530 (1965).

[6] D. S. Mahadevappa and A. S. A. Murthy, *Talanta*, **17**, 431 (1970).

[7] D. S. Mahadevappa and A. S. A. Murthy, *Current Sci.*, **41**, 100 (1972).

[8] D. S. Mahadevappa and H. M. K. Naidu, *Talanta*, **20**, 349 (1973).

[9] N. M. Made Gowda, A. S. A. Murthy and D. S. Mahadevappa, *Current Sci.*, **44**, 5 (1975).

[10] E. Bishop and V. J. Jennings, *Talanta*, **1**, 197 (1958).

[11] D. S. Mahadevappa and Rangaswamy, *Indian J. Chem.*, **11**, 811 (1973).

establish the composition of the precipitate by performing conductometric titrations supported by potentiometric titrations of CAT with these solutions and by elemental analysis, UV and I.R. spectral studies. It was also found necessary to carry out a similar type of titrations of CAT with HCl and H_2SO_4 solutions in support of our conclusions.

MATERIALS AND METHODS

All the solutions were prepared in triply distilled water (Sp. cond. $< 1.0 \times 10^{-6}$ ohm^{-1} cm^{-1}). BDH reagent grade chromic sulphate, chromic chloride, chrome alum, aluminium sulphate, aluminium chloride, potash alum and ferric chloride were used. Chromic sulphate and ferric chloride solutions were standardized by dichrometry. Chromic chloride solution was standardized by iodometry. Aluminium solutions were filtered to remove the traces of $Al(OH)_3$ and were standardized using E.D.T.A. Chloramine-T (E Merck) was purified by the method of Morris et al.[12] and aqueous solutions of the compound were standardized by the iodometric method. Reagent grade chemicals were used in the preparation of other solutions. UV spectra were recorded on a Beckman DB Spectrophotometer. IR spectra (KBr) were obtained on a Carl-Zeiss UR-10 spectrophotometer. Equal weights of the compounds were taken for recording the spectra, to make a visual comparison of band intensities.

Conductance measurements were made at room temperature (25°) using a Philips PR 9500 conductivity bridge and a dip type conductivity cell having a cell constant 0.66 cm^{-1}.

Potentiometric titrations were carried out on an Elico model L1—10 pH meter.

PROCEDURE

The initial conductance of a known volume of the metal ion solution of known concentration was measured. To this solution a solution of CAT (5—10 times stronger) from a microburette was added in small amounts. In the initial stages, a white turbidity was formed which dissolved on stirring the solution. The resistance of the solution was recorded after the disappearance of the turbidity. The precipitate formed on further addition of CAT was allowed to settle wherever possible, before the resistance of the solution was measured. Conductance of the solution with each addition of CAT solution was calculated after applying the volume correction.[13] The end point was obtained graphically by plotting the conductance of the solution against the volume of CAT added. Reverse titrations were carried out in the same manner.

A similar procedure was adopted with HCl and H_2SO_4 solutions.

RESULTS AND DISCUSSION

Some typical conductance plots are shown in Figures 1, 2 and 3. Figure 1(1) indicates the conductance profile when CAT solution is added to chromic sulphate or HCl. The break observed corresponds to 1 : 1 molar ratio with respect to CAT and Cr^{3+} or HCl. Figure 1(2) gives the conductance plot with $CrCl_3$ solution, showing a faint break approximately at 1 : 2 molar ratio, while Figure 1(3) shows a plot for the titration of H_2SO_4 with CAT, showing a break at 1 : 2 with respect to the acid and CAT. The reverse titrations for all these reagents with CAT are similar and the conductance profile is shown by Figure 1(4). The break corresponds to 1 : 1 molar ratio while it is 2 : 1 with respect to CAT and H_2SO_4 or $CrCl_3$.

---

[12] J. C. Morris, J. A. Salazar and M. A. Wineman, *J. Amer. Chem. Soc.*, **70**, 2036 (1948).

[13] L. Meites and H. C. Thomas, "Advanced Analytical Chemistry", McGraw Hill, New York, 1958, p. 114.

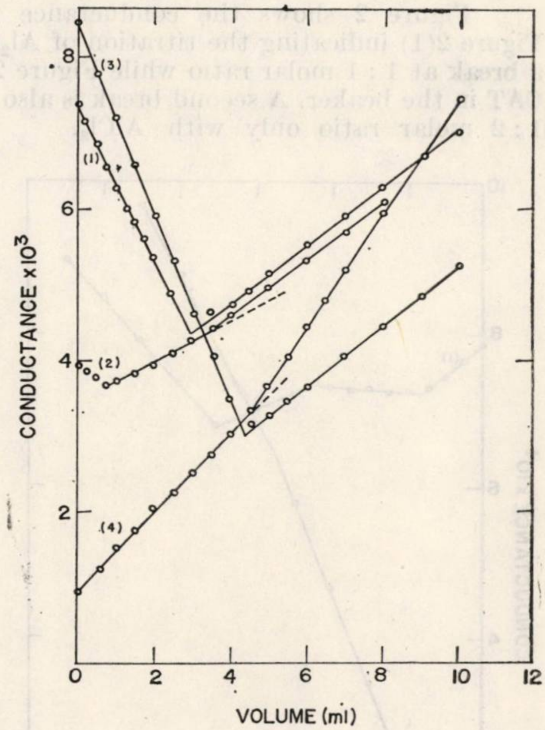

Fig. 1. — (1) $Cr_2(SO_4)_3$ (0.01133 M) VS CAT (0.1100 M); (2) $CrCl_3$ (0.01013M) VS CAT (0.09670 M); (3) H_2SO_4 (0.01109 M) VS CAT (0.09770 M); (4) CAT (0.03672 M) VS $Cr_2(SO_4)_3$ (0.03976 M).

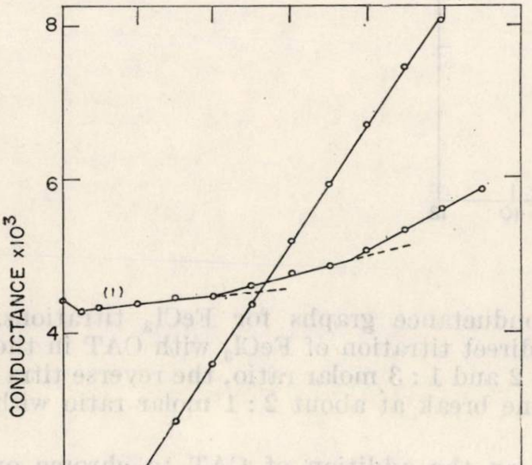

Fig. 2. — (1) $AlCl_3$ (0.01072 M) VS CAT (0.09670 M); (2) CAT (0.009985 M) VS $AlCl_3$ (0.1022 M).

Figure 2 shows the conductance plots for Al^{3+} ion solutions. Figure 2(1) indicating the titration of $Al_2(SO_4)_3$ or $AlCl_3$ with CAT shows a break at 1 : 1 molar ratio while Figure 2(2) is the reverse titration with CAT in the beaker. A second break is also observed in figure 2(1) at about 1 : 2 molar ratio only with $AlCl_3$.

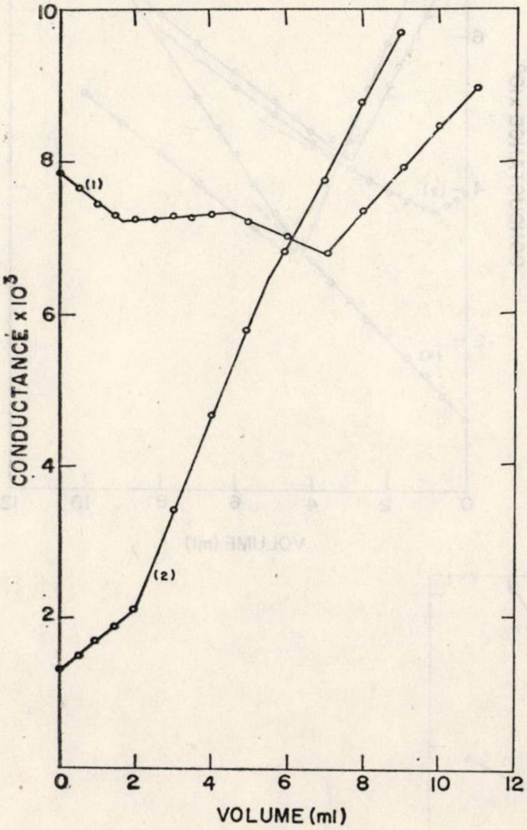

Fig. 3. — (1) $FeCl_3$ (0.01784 M) VS CAT (0.1740 M); (2) CAT (0.01392 M) VS $FeCl_3$(0.1250 M).

Figure 3 indicates the conductance graphs for $FeCl_3$ titrations. While figure 3(1) involving the direct titration of $FeCl_3$ with CAT in the burette shows breaks at 1 : 1, 1 : 2 and 1 : 3 molar ratio, the reverse titration [Figure 3(2)] shows only one break at about 2 : 1 molar ratio with respect to CAT and $FeCl_3$.

In titrations with alums, on the addition of CAT to chrome or potash alum solutions, precipitation is observed but the conductance increases regularly with only a very faint break at 1 : 1 molar ratio. A similar behaviour was observed in the reverse titrations when CAT is taken in the beaker.

pH titration curves of CAT with Cr^{3+}, Al^{3+} and Fe^{3+} ions and H_2SO_4 in the burette are similar and identical with those obtained by Morris et al.[12] in the potentiometric titration of CAT with HCl [Figure 4(1)].

The reverse potentiometric titration curves with CAT in the burette are also identical and resemble the normal acid-base titration curves [Figure 4(2)]. From the pH titration data obtained, it was found that the conductance breaks generally occurred between pH 3 and 4 and the precipitation generally continued [12] until a pH of 5.2, in both direct and reverse titrations.

It was also found that the breaks noted in the conductance graphs can be used for approximate quantitative estimation of any of the compounds if the molarity of the titrant is known or vice versa.

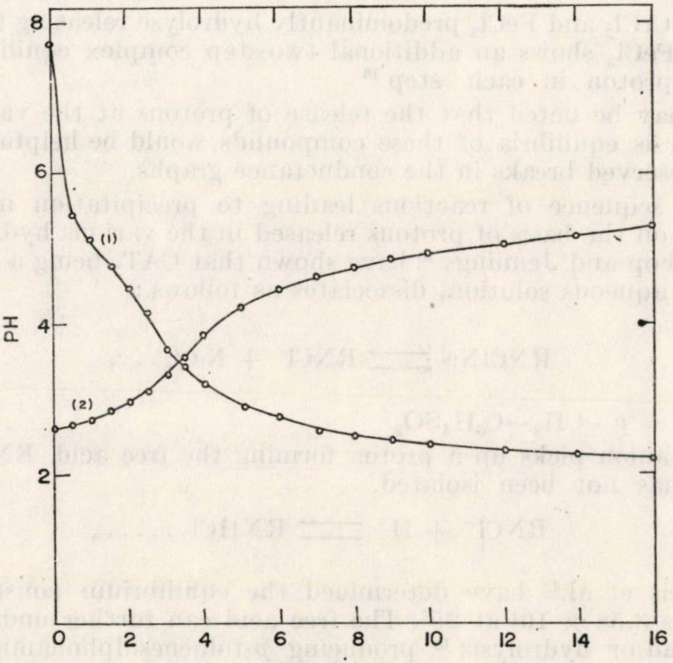

Fig. 4. — Potentiometric titration curves of: (1) CAT VS Cr^{3+}, Al^{3+}, Fe^{3+}, ion solutions and H_2SO_4; (2) Cr^{3+}, Al^{3+}, Fe^{3+}, ion solutions and H_2SO_4VS CAT.

The white precipitate formed on the addition of CAT to chromic sulphate solution turns green with the addition of excess CAT after the break. However, when the precipitate is filtered, shaken with diluted H_2SO_4, it again becomes white and Cr^{3+} can be detected in the acid solution. This indicates that $Cr(OH)_3$ gets adsorbed on the precipitate during the later stages of titration. A similar observation was made with Al^{3+} and Fe^{3+} ion solutions, with $Al(OH)_3$ and $Fe(OH)_3$ depositing on the white precipitate initially formed. However the precipitation of $Cr(OH)_3$ was not observed with $CrCl_3$ solutions. Further, when carefully neutralized solutions of Cr^{3+}, Al^{3+} and Fe^{3+} ions with NaOH were titrated against CAT, no precipitation was observed and the conductance increased continuously without a break. These results and their similarity to the conductance data obtained for HCl and H_2SO_4 indicate that the H^+ ion seems to play a prominent role in these precipitation reactions.

Chromic sulphate and aluminium sulphate and chlorides behave like monobasic acids in aqueous solution due to the release of a proton in the hydrolysis equilibria. But aluminium chloride is also found to undergo a hydrolysis reaction releasing two protons as shown below :[14,15]

$$2Al^{3+} + 2H_2O \rightleftharpoons [Al_2(OH)_2]^{4+} + 2H^+ ;$$

However, $CrCl_3$ and $FeCl_3$ predominantly hydrolyse releasing two protons, although $FeCl_3$ shows an additional two-step complex equilibrium, liberating a proton in each step.[16]

It may be noted that the release of protons at the various stages of hydrolysis equilibria of these compounds would be helpful in explaining the observed breaks in the conductance graphs.

The sequence of reactions leading to precipitation may now be envisaged on the basis of protons released in the various hydrolysis equilibria. Bishop and Jennings [10] have shown that CAT, being a strong electrolyte in aqueous solution, dissociates as follows :

$$RNClNa \rightleftharpoons RNCl^- + Na^+ \ldots, \qquad (1)$$

where $R = p{-}CH_3{-}C_6H_4SO_2$

The anion picks up a proton forming the free acid RNHCl, which however has not been isolated.

$$RNCl^+ + H^+ \rightleftharpoons RNHCl \ldots\ldots \qquad (2)$$

Morris et al.[12] have determined the equilibrium constant of this reaction as 3.58×10^4 at 25°. The free acid can further undergo disproportion and/or hydrolysis [10] producing *p*-toluenesulphonamide $(RNH)_2$, dichloramine-T $(RNCl_2)$ and HOCl.

$$2\ RNHCl \rightleftharpoons RNH_2 + RNCl_2 \ldots\ldots\ldots(3) ;\ K_d = 6.1 \times 10^{-2}$$

$$RNHCl + H_2O \rightleftharpoons RNH_2 + HOCl \ldots\ (4) ;\ K_h = 4.88 \times 10^{-8}.$$

It is likely that the precipitate obtained in the conductometric titrations is $RNCl_2$(DCT) wich is only slightly soluble in water $(0.310 \times 10^{-3}$ equivalents per litre) and the break at 1 : 1 molar ratio probably indicates the formation of RNHCl. The break found at 2 : 1 with respect to CAT and H_2SO_4 and other salt solutions could be due to the availability

---

[14] J. Aveston, *J. Chem. Soc.*, 4438 (1965).

[15] E. Grunwald and D. W. Fong., *J. Phys. Chem.*, **73**, 650 (1969).

[16] F. A. Cotton and G. Wilkinson, "Advanced Inorganic Chemistry", II Edition, Wiley Eastern, New Delhi, 1966, p. 858.

of both protons in the acid for reaction with CAT.

$$2\,\mathrm{RNCl}^- + 2\,\mathrm{H}^+ \rightleftharpoons 2\,\mathrm{RNHCl} \ldots\ldots\ldots\ldots \quad (5)$$

The initial decrease in conductance of salt solutions when CAT is taken in the burette could be attributed to the removal of H^+ from the solution, and solubility of the precipitate in the metal salt solution, while the increase noted after the breaks is due to the addition of excess titrant.

In the reverse titrations, with CAT in the beaker, the initial increase in conductance of the solution is due to the addition of metal ions sulphate ions or both or chloride ions although $RNCl^-$ ions are removed from the solution by the added H^+ ions according to equation (2). The steep increase observed after the breaks is due to the addition of excess titrant.

The absence of a sharp break in the titration curves of alums with CAT could be attributed to the decrease in hydrolysis of the double salts in solution and also to the presence of higly conducting K^+ and $SO_4^=$ ions in the solution.

IDENTIFICATION OF THE TURBIDITY

The turbidity obtained in the above titrations was suspected to be dichloramine-T (DCT). A check for mass balance was carried out in the case of chromic sulphate — CAT titrations and these results are shown in Table 1. This shows a reaction between H^+ and CAT approximately in 1 : 1 molar ratio. The precipitate was filtered, washed with water and was estimated by iodometry in glacial acetic acid medium.[17] The unreacted CAT in the filtrate was determined by iodometric titration. The amount of H^+ ions reacted was calculated by titrating against standard NaOH. It is seen that CAT and H^+ ions have reacted in the molar ratio of 1 : 1 and the amount of DCT formed is nearly half the amount of CAT reacted. Further investigations towards the identification of the precipitate were done by elemental analysis, UV and IR spectral studies.

Table 1

Mass balance in chromic sulphate – CAT reaction

CAT added mM	CAT unreacted mM	DCT obtained mM	No. of H^+ ions reacted mM	CAT reacted mM
0.3724	0.1260	0.1117	0.2484	0.2464
0.5586	0.1801	0.1802	0.4090	0.3785
0.2450	0.0864	0.0656	0.1761	0.1586
0.2450	0.0963	0.0605	0.1305	0.1487
0.2450	0.1061	0.0536	0.1069	0.1389

[17] T. J. Jacob and C. G. R. Nair, *Talanta*, **19**, 347 (1972).

ELEMENTAL ANALYSIS

Calculated for $p-CH_3-C_6H_4SO_2NCl_2$: S = 13.33 %, N = 5.84 %, Cl = 29.6 %. Found for precipitate for chromic sulphate titrations, S = 13.74 %, N = 5.11 %, Cl = 29.1 %. The precipitates obtained with the other compounds had the same elemental composition within experimental error.

UV AND IR SPECTRAL DATA

UV spectra of the compound in aqueous solution (~0.1 mM) were identical and showed a broad absorption band around 43100 cm^{-1} ($\log \varepsilon_M = 4.1$). A sample of DCT prepared by the method of Jacob and Nair[17] showed an identical band in aqueous solution.

IR spectra of the compounds were identical and the data are given in Table 2. I.R. spectral data of pure DCT have been included for comparison. Band assignments have been made[18-21] which show that they are similar compounds.

Table 2

IR Data of Dichloramine-T and the precipitate

Dichloramine-T (Jacob and Nair)	Precipitate	Assignment
542^{VS} D	542^{VS} D	Out of plane ring deformation
560^{VS}	560^{VS}	$\nu N-Cl$
660^{S}	657^{S}	In plane ring deformation
767^{S}	767^{S}	Out of plane CH bending of 2 adjacent aromatic H atoms
817^{S}	817^{S}	Out of plane CH bending of 2 adjacent aromatic H atoms
950w	950w	$\nu S-N$
1027^{m}	1027^{m}	In plane δCH
1085^{VS}	1085^{VS}	In plane δCH
1169^{VS}	1169^{VS}	$\nu s\ SO_2$
$1220^{V}w$	1220^{W}	In plane δCH
1303^{m}	1303^{m}	$\nu\ SO_2$
1387^{W}	1387 w	δCH_3
$1454^{V}w$	1454 w	$\nu C = C$
$1500^{V}w$	$1500^{V}w$	$\nu C = C$
1605^{m}	1605^{m}	$\nu C = C$
1647^{W}	1647^{W}	$\nu C = C$
2847^{VVW}	2848^{VVW}	$\nu\ CH_3$
2923^{VVW}	2923^{VVW}	$\nu\ CH_3$

VS = very strong, S = strong, m = medium, W = weak, D = doublet; VW = very weak, VVW = very very weak, ν = stretch; ν_s = symmetric stretch, ν_{as} = asymmetric stretch; δ = bending.

[18] N. B. Colthup, L. H. Daly and S. E. Wiberley, "Introduction to Infrared and Raman Spectroscopy", Academic Press, New York, 1964, p. 220, 308.

[19] K. Nakanishi, "Infrared Absorption Spectroscopy" – practical, Holden-Day, San Fancisco, 1962, p. 126, 216.

[20] L. J. Bellamy, "The Infrared Spectra of Complex Molecules", Methuen, London, 1954, p. 54.

[21] F. F. Bentley, L. D. Smithson and A. L. Rozek, "Infrared Spectra and Characteristic Frequencies: 700 – 300 cm 1" Interscience Publishers, New York, 1968, p. 66.

The above results show that the turbidity produced by the addition of CAT to Cr^{3+}, Al^{3+} or Fe^{3+} ion solution and vice versa is dichloramine-T formed by reactions (2) and (3).

In conclusion, it may be pointed out that no chromic or aluminium or ferric salt to the free acid RNHCl, similar to AgCAT and $Hg(CAT)_2$ reported by the authors,[11] can be prepared even by the addition of excess of reagents. Bishop and Jennings during their investigations on the analytical applications of CAT have stated that although the reagent is considered to be the sodium salt of RNHCl, the free acid has not been isolated. In this context, the results of our present investigations are theoretically quite significant, for the conductance breaks can be taken as conclusive evidence for the formation and existence of the free acid RNHCl, for which no other experimental proof has been presented until now. This conclusion is further supported by the mass balance given in Table 1, which shows that H^+ ions are removed by reaction (2) where the equilibrium is mainly to the right and DCT is formed by reaction (3). Higuchi et al.[22] have studied the dismutation reaction and they have shown that at $pH = 2.3$ and initial concentration of 1 mM, the half way point in he approach of equilibrium is of the order of 1 minute. It is seen that eaction (3) is fastest at $pH = 4$ and thereafter the rate decreases. This ould as well account for the decrease in the amount of precipitation ter $pH = 4$. It is probable that RNHCl formed around $pH = 3$ disapears above this pH by reaction (3), giving rise to DCT and RNH_2.

ACKNOWLEDGMENT. The authors are grateful to Prof. A. K. N. Reddy, Indian Institute of Science, Bangalore, for the IR spectra. One of us (D.S.M.) acknowledges financial assistance from the University Grants Commission, New Delhi.

---

[22] T. Higuchi, K. Ikeda and A. Hussain, *J. Chem. Soc.* (*B*), **1967**, 546.

Revue Roumaine de Chimie, **22**, *8*, 1243–1250 (1977)

LIQUID-MEMBRANE ELECTRODES. VII[*]

PERCHLORATE-SELECTIVE MEMBRANE-ELECTRODE. CONSTRUCTION AND CHARACTERIZATION

ELENA HOPÎRTEAN, ELISABETA VERESS and VALERIA MUREŞAN
Department of Analytical Chemistry, University "Babeş-Bolyai" Cluj-Napoca,
str. Arany Janos 11, Cluj-Napoca, Romania

Received May 31, 1975

The paper reports the results obtained in the construction and characterization of the perchlorate-selective membrane-electrode having as an active electrodic component [Fe(*o*-phen)$_3$]$^{2+}$, respectively [Ni(*o*-phen$_3$]$^{2+}$(perchlorate salts), in nitrobenzene solvent. The linear response of the electrodes towards perchlorate ($J = 0.15$ M, achieved with Na_2SO_4) is characterized by a 56 mV slope within $10^{-1}-5.10^{-5}$M concentration range. The selectivity series of the constructed electrodes as well as the selectivity constants relative to various anions were also established.

INTRODUCTION

Iron complexes with *o*-phenantroline or with bathophenantroline were used as active electrodic components in the construction of anion-selective liquid membrane-electrodes, namely for : iodide,[1] perchlorate,[2] maleic acid [3] and phthalic acid.[3] A close dependence was found to exist between the selectivity series of these electrodes relative to various anions and the hydration energies series of the respective anions. The perchlorate-selective liquid membrane-electrode was equally achieved based on quaternary ammonium salts [4,5] or by embedding a commercialized liquid ion exchanger into polyvinylchloride.[6] This paper deals with the construction and the study of a liquid membrane-electrode with an active electrodic compound [Ni(*o*-phen)$_3$](ClO$_4$)$_2$ in parallel with the one achieved by using [Fe(*o*-phen)$_3$] (ClO$_4$)$_2$ as an active electrodic component.

---

[*] Part. VI : E. Hopîrtean and E. Ştefănigă, *Stud. Univ. Babeş-Bolyai*, *Chem.*, **19**, 92, (1974).

[1] N. Ishibashi, H. Kohara and N. Uemura, *Bunseki Kagaku*, **21**, 1072 (1972) ; *Chem. Abstr.*, **77**, 171847 (1972).

[2] N. Ishibashi and H. Kohara, *Analyt. Lett.*, **4**, 785 (1971).

[3] A. Jyo, M. Yonemitsu and N. Ishibashi, *Bull. Chem. Soc. Jap.*, **46**, 3734 (1973).

[4] R. E. Reinsfelder and F. A. Schultz, *Analyt. Chim. Acta*, **65**, 425 (1973).

[5] T. Stworzewicz, *Pr. Nauch. Inst. Technol. Org. Tworzyw Sztucznych Politech. Wroclav*, **13**, 211 (1973) ; *Chem. Abstr.* **80**, 152382 (1974).

[6] T. J. Rohm and G. G. Guilbault, *Analyt. Chem.*, **46**, 590 (1974).

EXPERIMENTAL

The perchlorate-selective liquid electrode was obtained by soaking the pores of a G_4 glass frit rendered hydrophobic (Ø = 12 mm) fixed at the end of a glass tube ($l = 12$ cm) with the salt solution of the complex $[Fe(o\text{-phen})_3]^{2+}$, respectively of $[Ni(o\text{-phen})_3]^{2+}$ in a nitrobenzene solvent. The organic solution also serves as internal solution, introducing therein the calomel saturated electrode (SCE) to process the potential.

Potential measurements were performed on a MV-85 pH-meter (±1 mV accuracy), by e.m.f. determination of the electrochemical cell:

SCE ‖ internal organic solution | liquid membrane in the frit | test solution ‖ SCE

Determinations were made at room temperature without stirring.

Reagents and standard solutions. Reagents used were of p.a. purity. The $NaClO_4$, NaSCN, NaI and $NaNO_3$ standard solutions were prepared at a constant ionic strength ($J = 0.15$ M) by successive dilutions from the stock solution 1 M and using the necessary amounts of the solution of the non-interfering electrolyte Na_2SO_4 5×10^{-2}M.

The $NaClO_4$ standard solutions used for the determination of the electrode selectivity constants were prepared using as background the 10^{-1}M concentrated solution of the sodium salt of the respective anion.

RESULTS AND DISCUSSION

Electrode construction. At the beginning it was necessary to establish the optimum concentration of the active electrodic component in nitrobenzene. To this end, the electrodic functions of the liquid membranes obtained with different concentrations of the complexes $[Ni(o\text{-phen})_3](ClO_4)_2$ and, respectively, $[Fe(o\text{-phen})_3](ClO_4)_2$ in nitrobenzene, towards perchlorate, were established. Results are listed in table 1. The optimum concentration is 0.01 % in the case of the nickel complex and 0.005 %, respectively, in the case of the iron complex. These concentrations yield a high sensitivity within the largest perchlorate concentration range.

Table 1

Influence of the concentration of electrodic active component on the electrode function for perchlorate

Electrodic active component	Concentration (%)	Concentration range of ClO_4	Slope (mV)
$[Ni(o\text{-phen})_3](ClO_4)_2$	0.001	$10^{-1}-4\times10^{-4}$M	52
	0.01	$10^{-1}-5\times10^{-5}$M	56
	0.1	$10^{-1}-6.5\times10^{-4}$M	57
$Fe[(o\text{-phen})_3](ClO_4)_2$	0.001	$10^{-1}-10^{-4}$M	42
	0.005	$10^{-1}-8\times10^{-5}$M	55.5
	0.01	$10^{-1}-1.5\times10^{-4}$M	55.5
	0.1	$10^{-1}-5\times10^{-4}$M	56
	1.0	$10^{-1}-8\times10^{-4}$M	54.5

Studies were further made to see whether or not the electrode response towards perchlorate is influenced by the nature of the salt anion used as an active electrodic component. Results obtained are given in fig. 1.

It has been found that the use of the two complexes under the form of perchlorate or of iodide leads to similar results with regard to the sensitivity and the concentration range of the linear response. Only the standard potential of electrodes is modified.

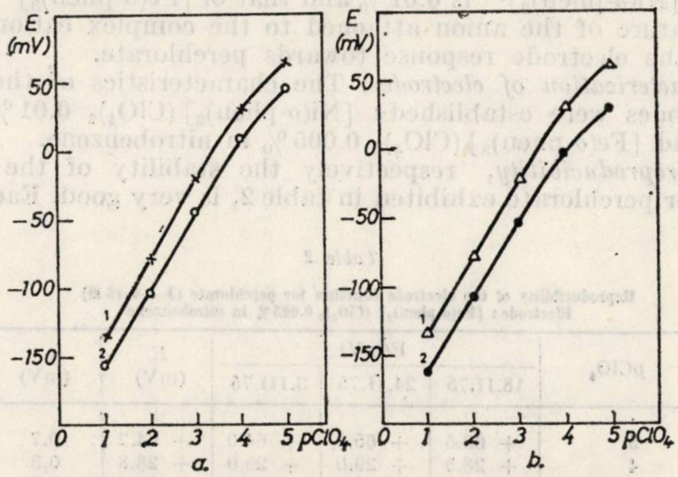

Fig. 1. — Influence of the nature of salt anion used as an active electrodic component on the perchlorate electrode function.

a) electrodic active component, nickel complex, c = 0.01% in nitrobenzene: *1* — $[Ni(o\text{-phen})_3](ClO_4)_2$; *2* — $[Ni(o\text{-phen})_3]I_2$.

b) electrodic active component, iron complex, c = 0.005% in nitrobenzene: *1* — $[Fe(o\text{-phen})_3](ClO_4)_2$; *2* — $[Fe(o\text{-phen})_3]I_2$.

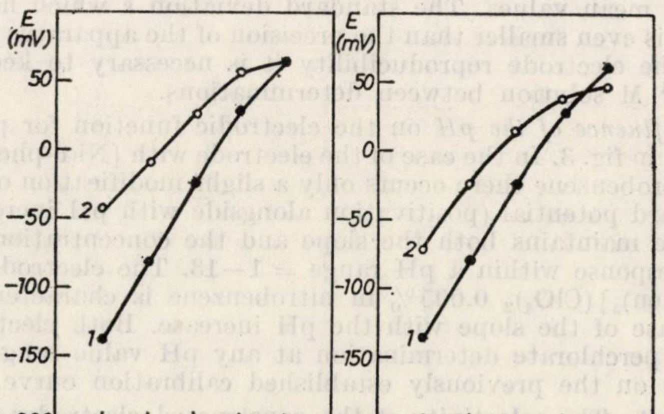

Fig. 2. — Influence of the solvent on the electrode function for perchlorate.

a) electrodic active component $[Ni(o\text{-phen})_3](ClO_4)_2$, c = 0.01% ; *1* — nitrobenzene; *2* — benzyl alcohol.

b) electrodic active component $[Fe(o\text{-pehn})_3](ClO_4)_2$, c = 0.005% : *1* — nitrobenzene; *2* — chloroform.

The influence of the solvent nature on the electrodic function for perchlorate results from figure 2. Both benzyl alcohol and chloroform prove to be sensibly inferior to nitrobenzene.

Thus it can be concluded that the adequate solvent is nitrobenzene, the optimum concentration of the active electrodic component formed of $[Ni(o\text{-phen})_3]^{2+}$ is 0.01% and that of $[Fe(o\text{-phen})_3]^{2+}$ is 0.005% and the nature of the anion attached to the complex cation does not influence the electrode response towards perchlorate.

Characterization of electrodes. The characteristics of the following two electrodes were established: $[Ni(o\text{-phen})_3](ClO_4)_2$ 0.01% in nitrobenzene and $[Fe(o\text{-phen})_3](ClO_4)_2$ 0.005% in nitrobenzene.

The reproducibility, respectively the stability of the electrodic function for perchlorate exhibited in table 2, is very good. Each separate value entered in columns 2—4 represents the mean of three successive determinations performed, and the data in column 5 represent the average of the three mean values. The standard deviation *s* which has a value below 1 mV is even smaller than the precision of the apparatus (± 1 mV). To assure the electrode reproducibility it is necessary to keep it in a $NaClO_4$ 10^{-1} M solution between determinations.

Table 2

Reproducibility of the electrode function for perchlorate (J = 0.15 M)
Electrode: $[Fe(o\text{-phen})_3](ClO_4)_2$ 0.005% in nitrobenzene

$pClO_4$	E(mV)			*E* (mV)	*s* (mV)
	18.II.75	24.II.75	3.III.75		
5	+ 63.5	+ 65.0	+ 64.0	+ 64.2	0.7
4	+ 28.5	+ 29.0	+ 29.0	+ 28.8	0.3
3	− 24.0	− 23.0	− 23.5	− 23.5	0.5
2	− 80.0	− 79.0	− 80.0	− 79.7	0.5
1	−135.0	−135.0	−135.0	−135.0	0.0

The influence of the pH on the electrodic function for perchlorate is illustrated in fig. 3. In the case of the electrode with $[Ni(o\text{-phen})_3](ClO_4)_2$ 0.01% in nitrobenzene there occurs only a slight modification of the electrode standard potential (positivation alongside with pH increase) while the electrode maintains both the slope and the concentration range of the linear response within a pH range = 1—13. The electrode response for $[Fe(o\text{-phen})_3](ClO_4)_2$ 0.005% in nitrobenzene is characterized by a slight decrease of the slope with the pH increase. Both electrodes may be used for perchlorate determination at any pH value ranging within 1—13 based on the previously established calibration curve.

Selectivity. The selectivity of the constructed electrodes was established by using the electrodic functions for perchlorate in standard solutions containing a constant concentration (0.1 M) of the salt of the interfering anion. Some of the electrodic functions obtained in this manner are presented in figure 4 and the results referring to the whole group of anions involved in the selectivity study are listed in table 3.

It has been found that the anions significantly affecting the electrodic function relative to perchlorate are: SCN^-, I^-, ClO_3^- and NO_3^-. The remaining anions have a practically insignificant influence on the electrode response. The only total interfering agent is the ion MnO_4^- in a 10^{-1} M concentration.

The electrodic functions established in this way were used to calculate the selectivity constants by formula $K = a_{\mathrm{ClO_4^-}} / a_{\mathrm{interf.}}$; evidently, taking into account the practically constant ionic strength applied, activities were replaced by concentrations. The concentration assumed for perchlorate was that which causes in the electrodic function the deviation from the linear response in the presence of the respective anion and

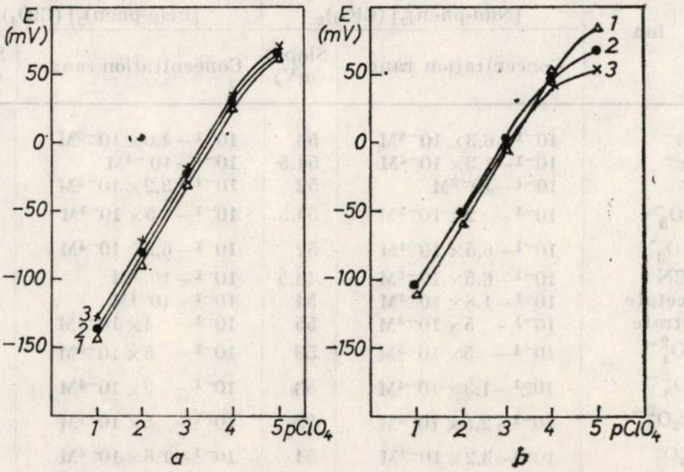

Fig. 3. — Influence of the pH on the electrodic function for perchlorate.

a) electrode: $[\mathrm{Ni}(o\text{-phen})_3](\mathrm{ClO_4})_2$ 0.01% in nitrobenzene.

b) electrode: $[\mathrm{Fe}(o\text{-phen})_3](\mathrm{ClO_4})_2$ 0.005% in nitrobenzene.

1 — pH = 1 (HCl); 2 — pH = 6 ($\mathrm{Na_2SO_4}$); 3 — pH = 13(NaOH).

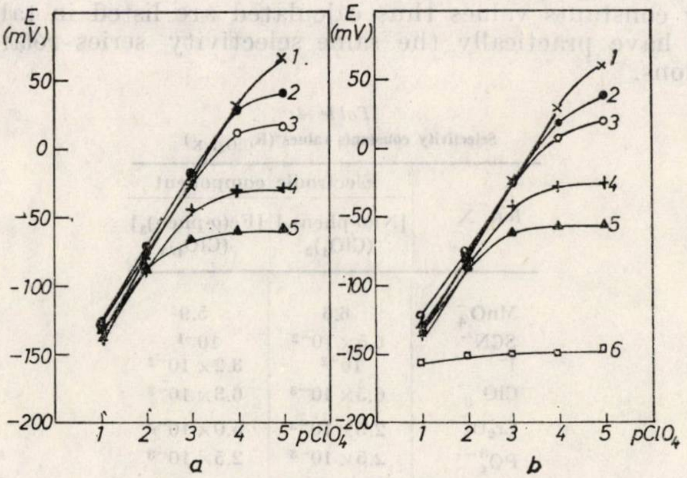

Fig. 4. — Electrodic functions for perchlorate obtained in the presence of different anions (natrium salts, c = 10^{-1}M).

a) electrode: $[\mathrm{Ni}(o\text{-phen})_3](\mathrm{ClO_4})_2$ 0.01% in nitrobenzene;

b) electrode: $[\mathrm{Fe}(o\text{-phen})_3](\mathrm{ClO_4})_2$ 0.005% in nitrobenzene.

1 — $\mathrm{SO_4^{2-}}$; 2 — $\mathrm{NO_3^-}$ 3 — $\mathrm{ClO_3^-}$; 4 — $\mathrm{I^-}$; 5 — $\mathrm{SCN^-}$; 6 — $\mathrm{MnO_3^-}$.

Table 3

Electrodic function for perchlorate obtained in the presence of different anions in a 10^{-1}M concentration

Ion	Electrode			
	$[Ni(o\text{-phen})_3](ClO_4)_2$		$[Fe(o\text{-phen})_3](ClO_4)_2$	
	Concentration range	Slope) (mV)	Concentration range	Slope (mV)
Cl^-	$10^{-1}-6.3\times10^{-5}$M	56	$10^{-1}-4.0\times10^{-5}$M	55
Br^-	$10^{-1}-1.3\times10^{-4}$M	54.5	$10^{-1}-10^{-4}$M	51.5
I^-	$10^{-1}-10^{-3}$M	52	$10^{-1}-3.2\times10^{-3}$M	51
NO_3^-	$10^{-1}-2\times10^{-4}$M	54.5	$10^{-1}-5\times10^{-4}$M	53.5
ClO_3^-	$10^{-1}-6.5\times10^{-4}$M	52	$10^{-1}-6.3\times10^{-4}$M	48.5
SCN^-	$10^{-1}-6.5\times10^{-3}$M	43.5	$10^{-1}-10^{-2}$M	42
Acetate	$10^{-1}-1.8\times10^{-4}$M	54	$10^{-1}-10^{-4}$M	53.5
Citrate	$10^{-1}-5\times10^{-5}$M	55	$10^{-1}-4\times10^{-5}$M	54
SO_4^{2-}	$10^{-1}-5\times10^{-5}$M	56	$10^{-1}-5\times10^{-5}$M	55.5
CO_3^{2-}	$10^{-1}-1.3\times10^{-4}$M	53	$10^{-1}-2\times10^{-4}$M	51
$Cr_2O_7^{2-}$	$10^{-1}-2.5\times10^{-4}$M	53	$10^{-1}-5\times10^{-4}$M	53
$B_4O_7^{2-}$	$10^{-1}-3.2\times10^{-4}$M	54	$10^{-1}-1.6\times10^{-4}$M	53.5
PO_4^{3-}	$10^{-1}-2.5\times10^{-4}$M	54	$10^{-1}-2.5\times10^{-4}$M	51.5
HSO_4^-	$10^{-1}-3\times10^{-5}$M	56	$10^{-1}-3.2\times10^{-5}$M	55
$H_2PO_4^-$	$10^{-1}-5\times10^{-5}$M	56	$10^{-1}-5\times10^{-5}$	55

for the interfering agent, the concentration was in each case 0.1 M. The selectivity constants values thus calculated are listed in table 4. Both electrodes have practically the same selectivity series relative to the tested anions.

Table 4

Selectivity constants values ($K_{ClO_4, X}$)

Ion X	Electrodic component	
	$[Ni(o\text{-phen})_3](ClO_4)_2$	$[Fe(o\text{-phen})_3](ClO_4)_2$
MnO_4^-	6.6	5.9
SCN^-	6.5×10^{-2}	10^{-1}
I^-	10^{-2}	3.2×10^{-2}
ClO_3^-	6.5×10^{-3}	6.3×10^{-3}
$Cr_2O_7^{2-}$	2.5×10^{-3}	5.0×10^{-3}
PO_4^{3-}	2.5×10^{-3}	2.5×10^{-3}
NO_3^-	2.0×10^{-3}	5.0×10^{-3}
$B_4O_7^{2-}$	3.2×10^{-3}	1.6×10^{-3}
Br^-	1.3×10^{-3}	10^{-3}
Acetate	1.8×10^{-3}	10^{-3}
Citrate	5.0×10^{-4}	4.0×10^{-4}
Cl^-	6.3×10^{-4}	4.0×10^{-4}
HSO_4^-	3.0×10^{-4}	3.2×10^{-4}
$H_2PO_4^-$	5.0×10^{-4}	5.0×10^{-4}

The response of electrodes towards SCN^-, I^- and NO_3^- was also tested (fig. 5).

The electrical resistance was measured in continuous current with a RLC bridge at a temperature of 25° using platinum counter electrodes. Depending on the concentration of the active component, the electrical resistance of the liquid membranes ranges within 1—2 MΩ.

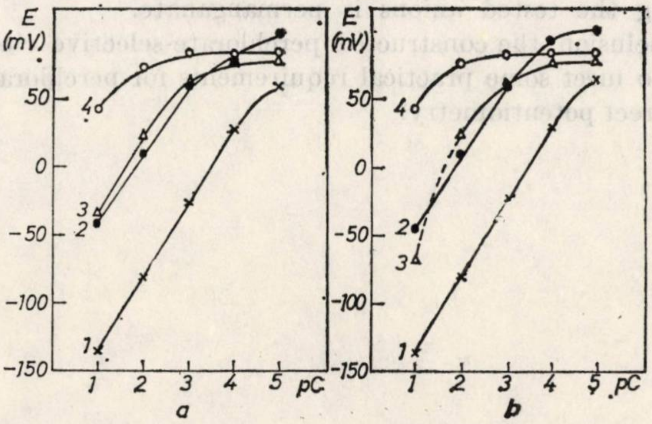

Fig. 5. — Electrodic functions for different anions ($J = 0.15$ M, achieved with Na_2SO_4).

a) electrode : $[Ni(o\text{-phen})_3]\ (ClO_4)_2$ 0.01% in nitrobenzene ; b) electrode : $[Fe(o\text{-phen})_3]\ (ClO_4)_2$ 0.005% in nitrobenzene. *1* — ClO_4^- ; *2* — SCN^- ; *3* — I^- ; *4* — NO_3^-.

The response time. At concentrations beyond 10^{-3} M, the response time of the electrode is less than 1 minute; at a 10^{-4} M concentration it is 2—3 min. and at 10^{-5} M the equilibrium is attained only after 14—15 min. Likewise, in a strongly basic medium (pH = 13) the response time is somewhat longer throughout the perchlorate concentration range (10^{-1}—10^{-5} M).

CONCLUSIONS

Perchlorate-selective liquid membrane-electrodes based on $[Ni(o\text{-phen})_3]\ (ClO_4)_2$ and, respectively, $[Fe(o\text{-phen})_3]\ (ClO_4)_2$ in nitrobenzene solvent were obtained and studied in parallel. The electrodes manifest a linear response towards perchlorate, with a 56 mV slope within the range 10^{-1}—5×10^{-5} M (standard solutions with a constant ionic strength $J = 0.15$ M, achieved with Na_2SO_4). The reproducibility of electrodes is very good being within the precision limits of the apparatus (± 1 mV). The sensitivity and the concentration range of the linear response towards perchlorate remain the same within a pH range = 1—13 in the case of the electrode with nickel complex as an active electrodic component whereas a slight modification of these factors occurs in the case of the electrode with iron complex. Both electrodes have a good selectivity towards nitrate ($K_{ClO_4,NO_3} \simeq 5 \times 10^{-3}$) and enable the perchlorate determination by direct potentiometry, in the presence of 200 times nitrate concentrations. The electrode may be used for perchlorate determination in the presence of any of the following anions : SCN^-, I^-, ClO_3^-, $Cr_2O_7^{2-}$, PO_4^{3-}, NO_3^-, $B_4O_7^{2-}$, Br^-, AcO^-, citrate, Cl^-, HSO_4^-, $H_2PO_4^-$, SO_4^{2-}, obviously having the concentration limits resulting from the selectivity constant value towards the ion in question. The only total interfering agent among the tested anions is permanganate.

In conclusion, the constructed perchlorate-selective electrodes are considered to meet some practical requirements for perchlorate determination by direct potentiometry.

Revue Roumaine de Chimie, 22, 8, 1251–1259, (1977)

SPECTROPHOTOMETRIC STUDY OF SOME 1,5-DIPHENYL 1,5-PENTADIENE-3-ONES

A. A. KHALAF, S. H. ETAIW*, R. M. ISSA* and A. K. EL-SHAFEI
Chemistry Department, Faculty of Science, Assuit University,
Assuit, A. R. Egypt

Received May 15, 1975

The electronic absorption spectra of some 1,5-diphenyl-1,5-pentadiene-3-ones are studied in organic solvents of different polarities. The spectra are discussed in terms of medium effects and molecular structure. Band assignment is also attempted. The acid dissociation constants of OH-containing compounds are determined from spectral measurements in buffer solutions. The important bands in the ir-spectra are also discussed in relation to molecular structure.

INTRODUCTION

The electronic absorption spectra of diarylidene ketones was the subject of some investigations.[1–6] These studies considered mainly the spectral—structural correlations as well as the assignment of the longer wavelength band to electronic transitions within certain parts of the molecule. In a previous investigation,[7] we studied the solvent effect on the electronic absorption spectra of some diarylidene-cyclohexanones and cyclopentanone. In continuation of our studies on diarylidene derivatives, the spectral behaviour of some substituted 1,5-diphenyl-1,5-pentadiene-3-one derivatives is investigated in organic solvents of different polarities and buffer solutions of varying pH. The study includes band assignment, determination of the acid dissociation constant of the compounds containing OH group. Also the important ir-bands are assigned to the extent that appears possible. The results are discussed in terms of molecular structure.

[1] H. S. French and M. G. T. Holden, *J. Amer. Chem. Soc.*, **67**, 1239 (1945).
[2] A. Maccioni and E. Marargu, *Ann. Chim. (Ital.)*, **49**, 1283 (1959).
[3] A. C. Hurtric and W. D. Kumelar *J. Amer. Chem. Soc.*, **78**, 614 (1956).
[4] P. G. Furrell, *Canad. J. Chem.*, **46**, 3684 (1968).
[5] N. L. Leonard and G. C. Robenson, *J. Amer. Chem. Soc.*, **75**, 2714 (1953).
[6] B. K. Razani and J. K. Sugden, *Chem. Ind. (London)*, **21**, 685 (1970).
[7] R. M. Issa, I. M. Issa, S. H. Etaiw and A. K. El-Shafie, *Acta Chim. Acad. Sci. Hung.*, in press.

* Dr. S. H. Etaiw, Prof. Dr. R. M. Issa, Chemistry Department, Faculty of Science, Tanta University, A. R. Egypt.

EXPERIMENTAL

MATERIALS AND SOLUTIONS

The diphenylpentadiene-3-one derivatives were prepared by the condensation of acetone with aromatic aldehydes under the proper experimental conditions.[2,7] The products were crystallized from the appropriate solvents and the purity was checked by m.p. determination and ir-spectra.

10^{-3} M stock solutions were prepared by dissolving the accurately weighed quantity of the compound in the requisite volume of the solvent. Lower concentrations used for spectral measurements were obtained by accurate dilution. Whenever the compound has limited solubility in a given solvent, a saturated solution was used for recording the spectra.

The solvents used were of laboratory grade and purified according to recommended procedures.[8] The universal buffer series of Britton and Robenson [9] was used for pH control.

WORKING PROCEDURE AND APPARATUS

The working procedure is the same as described previously.[10] The absorption spectra were recorded on a UNICAM S.P. 8000 self recording quartz spectrophotometer using 1 cm matched silica celis. The pH measurements were carried out by the aid of a RADIOMETER pH-meter model 28. The ir-spectra were recorded on a Beckman 37 infrared spectrophotometer using the KBr disc technique.

RESULTS AND DISCUSSION

The compounds under investigation have the general formula

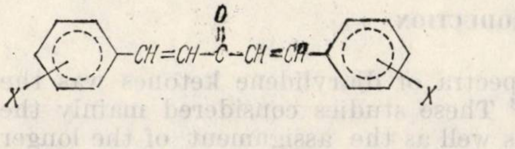

1; x = H
2; x = p-N$(CH_3)_2$
3; x = p-OCH_3
4; x = p-OH
5; x = p-Cl
6; x = o-OH
7; x = o-OH; m, m'-di-Br.

1. SPECTRA IN ORGANIC SOLVENTS

1. Band assignment and solvent shifts

The spectra of the compounds under investigation show in general two bands (Table 1 and Fig. 1). The high ε_{max} values indicate that the bands are due to $\pi-\pi^*$ transitions. The band corresponding to $n-\pi^*$ transition which should be observed in the 270–300 nm region, being of low intensity, would be masked by the intense $\pi-\pi^*$ bands. Also the dilute solutions used would not enable to record such bands of low intensity.

The short wavelength band is slightly broadened and has mostly an asymmetric appearance. This band can be assigned to the $\pi-\pi^*$ transition of the benzenoid system $({}^1L_a \leftarrow {}^1A)$ overlapping with the $\pi-\pi^*$ transition of the conjugate system $O = \overset{|}{C}-\overset{|}{C}H =$. This band shows small solvent shifts since it corresponds to locally excited transitions. However, the band is in general slightly shifted to red with increasing

---

[8] A. I. Vogel, "Practical Organic Chemistry", Longmans, London, 1964, p. 175.

[9] H. T. S. Britton, "Hydrogen Ions", Vol. I, Chapman and Hall, London, 1952, p. 365.

[10] I. M. Issa, R. M. Issa, H. R. Mahmoud and Y. M. Temerek, *Z. phys. Chem.* (*Leipzig*), **253**, 289, (1973).

Table 1

Electronic spectra of compounds 1–7 in pure organic solvents, (λ_{max}[nm]; ε_{max} = [cm^2.mole^{-1} × 10^{-4}]

N°	CCl$_4$		Ether		CHCl$_3$		Ethanol		Assignment
	λ_{max}	ε_{max}	λ_{max}	ε_{max}	λ_{max}	ε_{max}	λ_{max}	ε_{max}	
1			230	1.88	—	—	230	1.25	$\pi-\pi^*$(a)
	320	3.21	318	3.38	325	3.12	330	3.09	C.T.
2	270	0.75	—	—	271	1.11	270	1.11	$\pi-\pi^*$(a)
	420	2.53	—	—	445	3.60	456	4.60	C.T.
3	—	—	237	3.10	—	—	240	2.47	$\pi-\pi^*$(a)
	356	4.85	353	3.91	350	0.76	368	3.86	C.T.
4	—	—	240	1.40	—	—	245	1.96	$\pi-\pi^*$(a)
	—	—	355	2.94	363	S	378	3.46	C.T.
5	—	—	234	1.932	—	—	235	1.80	$\pi-\pi^*$(a)
	332	3.35	323	3.78	335	3.82	334	3.91	C.T.
6	—	—	250	0.85	—	—	255	0.90	$\pi-\pi^*$(a)
	310	S	303	0.80	313	1.17	315	1.04	C.T.
	350	S	305	0.86	355	1.65	370	1.57	C.T.
7	—	—	255	S	—	—	255	8.67	$\pi-\pi^*$(a)
	308	S	305	S	310	0.63	310	3.15	C.T.
	350	S	355	S	365	0.65	370	1.59	C.T.

(a) $^1(L_a - {}^1A)$, S – Saturated solution used; C.T. – Charge transfer band.

solvent polarity which is in accordance with the $\pi-\pi^*$ nature of the transition leading to this band.

The second band at longer wavelength corresponds probably to an intramolecular charge transfer. The charge transfer involves the location of π-electrons from highest occupied π-orbitals on the phenyl ring as donor to the lower vacant π-orbital on the C = O groups acting as acceptor.[7] The mesomeric shift representing such a charge transfer can be considered as follows :

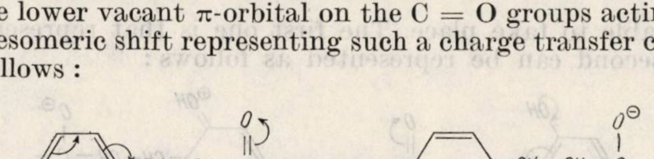

This band shows an apparent red shift with increasing solvent polarity which is in accordance with charge transfer nature of the transition leading to this band. The apparent red shift with ethanol is essentially due to its high polarity and the probable hydrogen bond formation with the C = O group. This lowers the energy levels of the acceptor center hence decreases the energy gap between the ground and excited states.

For compounds 6 and 7, a broad band is observed within the 300–315 nm region. This band can be ascribed to a second type of intramolecular charge transfer, caused by the presence of the OH-group in *o*-position. Thus for 6 and 7 two types of intramolecular charge transfer interac-

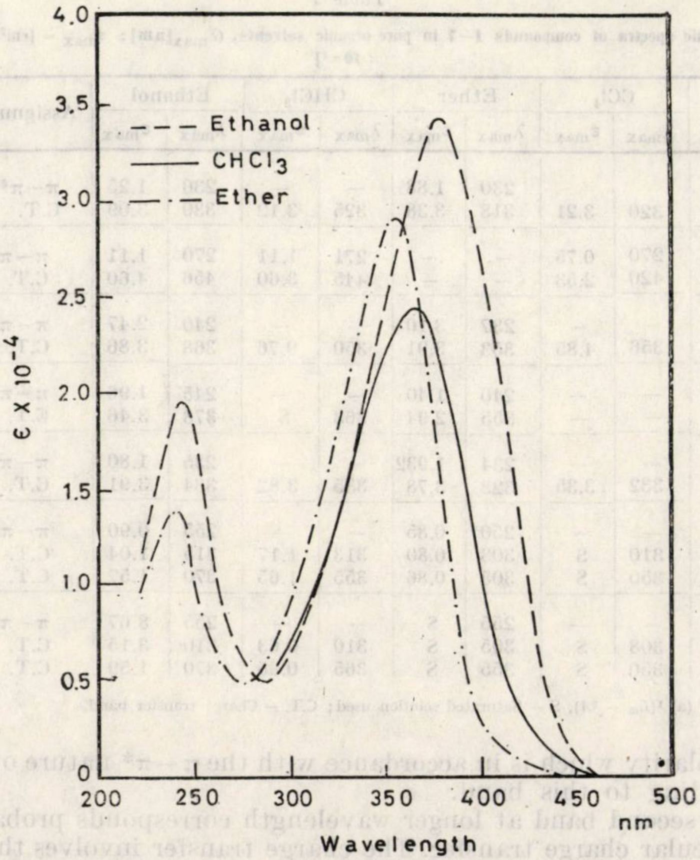

Fig. 1. — Electronic spectra of 4.

tions are liable to take place. The first one is that represented above, while the second can be represented as follows:

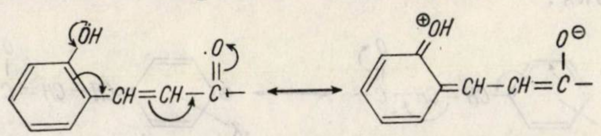

The charge transfer nature of the band is visualized from its broadening, solvent shift and high molar absorptivity.

The origin of the long wavelength band as charge transfer (C.T.) band can be supported by calculating the energy of the intramolecular charge transfer ($E_{\text{C.T.}}$). For this purpose the following relation may be applied[11]

$$E_{\text{C.T.}} = \mathrm{I} - (E_A - E_c) \qquad (1)$$

where I = Ionization potential of donor center

E_A = Electron affinity of the acceptor center

---

[11] R. ABU-EITTAH and M. M. HAMED, *Bull. Chem. Soc. Japan* (in press), c.f. M. M. HAMED, M. Sc. Thesis, Faculty of Science, Cairo University, 1972, p. 50.

E_c = Coulombic interaction between the migrating charge and the positive bole left behind on the aromatic nucleus.

For unsubstituted compound 1, the donor center is the styryl system with $I = 8.47$ eV[12] while the acceptor center is the $C = O$ group with $E_A = -1.4$ eV.[13] The value of $E_{C.T.}$ was calculated as 5.26 eV[13] for the benzene nucleus. Substituting these data in equation (1), the value of $E_{C.T.} = 4.61$ eV is obtained.

However, the experimental value determined from λ_{max}:

$$E_{C.T.} = \frac{10^7}{320} \times \frac{1.2398}{10^4} = 3.87 \text{ eV} \tag{2}$$

deviates from the calculated one to some extent. This deviation is due to approximation in the considered system, essentially for the Coulombic factor.

For charge transfer complexes of diphenyl polyenes, Brigleb, Czekalla and Hauser[14] gave the following relation for the energy of the charge transfer band:

$$E_{C.T.} = (I - 5.0) + \left(\frac{0.7}{I - 5.0}\right) \tag{3}$$

The value calculated from this equation amounts to 3.67 eV which is not much different from the experimental value. This result supports the C.T. origin of the long wavelength band.

Further support is obtained by considering the effect of substitution on the band. The values of λ_{max} in table 1 indicate that the band is progressively shifted to red as the donor character of the substituents on the phenyl ring increases. The plot of λ_{max} as a function of the σ-(Hammett) constant is a linear relation as shown in Fig. 2a.

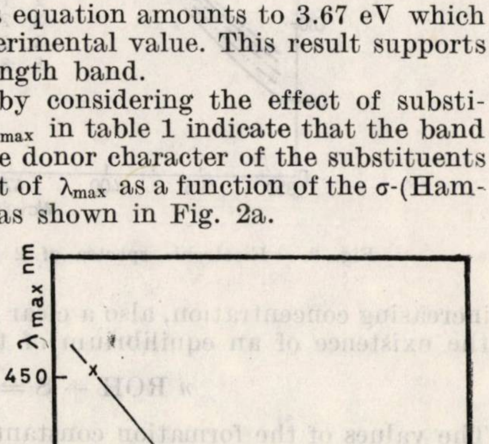

Fig. 2.—Variation of λ_{max}(a) and $\nu_{C=O}$(b) with σ (Hammett constant).

---

[12] R. C. WEAT, "Handbook of Chemistry and Physics", The Chemical Rubber Company, 50*th* Edit., Ohio, U.S.A. 1969, p. 86.

[13] K. WATANABE, *J. Chem. Phys.*, **26**, 542 (1957).

[14] G. BRIGLEB, J. CZEKALLA and A. HAUSER, *Z. phys. Chem.* (*Frankfurt*), **21**, 99 (1959).

1. SPECTRA IN MIXED ORGANIC SOLVENTS

The formation of intermolecular hydrogen bond between solute and ethanol molecules is substantiated by studiying the spectral behaviour of 2 in ether solvent containing successively increased quantities of ethanol (Fig. 3). The C.T. band acquires an apparent red shift with increasing concentration, also a clear isosbestic point is observed denoting the existence of an equilibrium of the type:

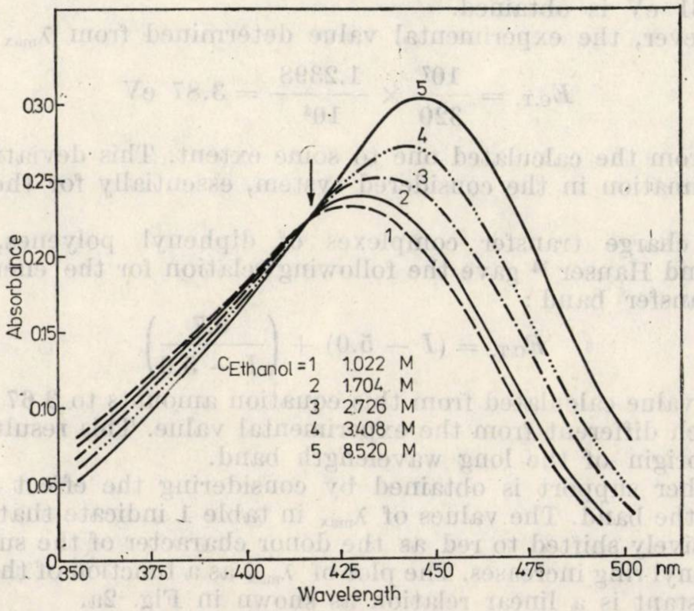

Fig. 3. — Electronic spectra of 2 in ether-ethanol mixed solvents.

$$n\ \mathrm{ROH} + \mathrm{S} \rightleftharpoons \mathrm{S} \ldots (\mathrm{ROH})_n$$

The values of the formation constant K_f of the molecular complex $\mathrm{S} \ldots (\mathrm{ROH})_n$ was determined applying the previously given [15] relation :

$$n \log C_{\mathrm{ROH}} = \log K_f + \log \left(\frac{A - A_0}{A_1 - A} \right)$$

Where : A_0 = absorbance in low polarity solvent.
A_1 = absorbance in ethanol.
A = absorbance in mixed solvent.

The values obtained from such investigation on 2 are $n \simeq 1.0$, $\log K_f = 0.47$, $\Delta G^* = -0.63$ Kcal/mol and $\Delta E = 2.84$ Kcal/mol.

These results reveal that the molecular complex dominating in solution has a stoechiometric ratio of 1 : 1 and is formed through a weak intermolecular hydrogen bond.

---

[15] F. M. Abdel-Halim, R. M., Issa, I. E. El-Kholey, and A. E. El-Kholey, *Egypt J. Chem.* (in press).

2. SPECTRA IN BUFFER SOLUTIONS

The spectra of 2, 4, 6 and 7, i.e. compounds containing $N(CH_3)_2$ or OH group, were studied in buffer solutions containing 30% by volume ethanol. The presence of ethanol was found to increase the solubility of the non-ionic forms hence enabling the recording of their spectra. The spectra represented in Fig. 4 show a band at longer wavelength in alkaline solutions. The lowering of pH causes a decrease of absorbance ; meanwhile a new band is developed at shorter wavelength. The observed isosbestic points (Fig. 4) indicate the existence of an acid-base equilibrium due to the dissociation of a proton from the OH- or $-\overset{\otimes}{N}H\ (CH_3)_2$ groups.

The absorbance-pH curves (Fig. 5) are typical dissociation curves with an ill-defined inflection on the resting part of the curve. The pH titration of the OH-containing compounds showed that two equivalents of alkali are consumed for each solute molecule. The titration curve displays two small inflections. Thus both OH-groups dissociate in a stepwise manner in spite of their symmetrical position in the molecule and absence of conjugation between the two groups in the ground state. However, when one of the electron releasing groups is ionized, its donor character will increase hence opposing the intramolecular charge transfer from the non-ionized group. This causes a firmer bonding of the proton, hence a higher pK_a value.

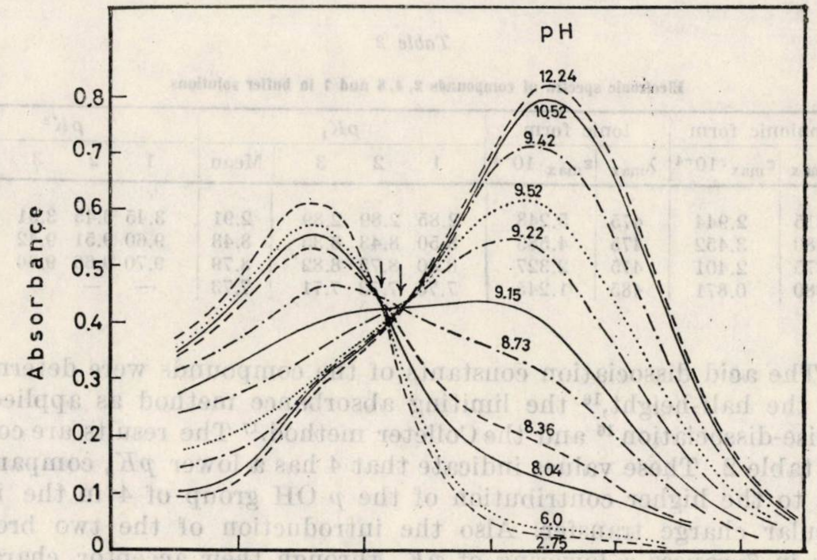

Fig. 4. — Electronic spectra of 4 in buffer solutions.

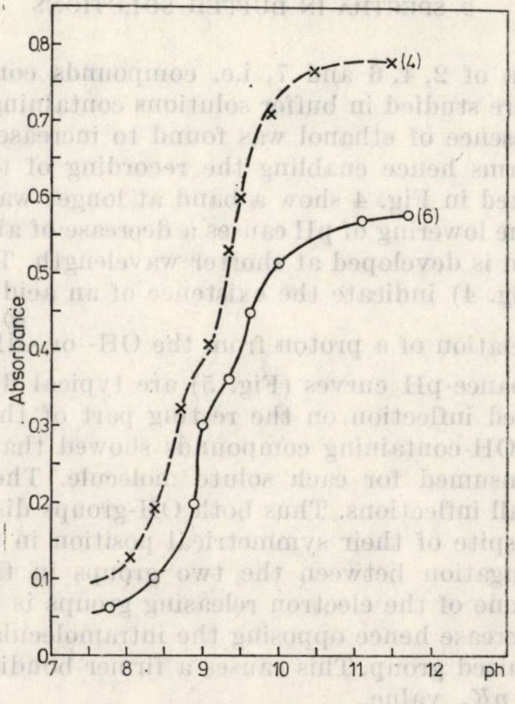

Fig. 5. — The absorbance-pH curves of 4 and 6.

Table 2

Electronic spectra of compounds 2, 4, 6 and 7 in buffer solutions

N⁰	Nonionic form		Ionic form		pK_1				pK^2			
	λ_{max}	$\varepsilon_{max} \cdot 10^{-4}$	λ_{max}	$\varepsilon_{max} \cdot 10^{-4}$	1	2	3	Mean	1	2	3	Mean
2	315	2.944	475	5.248	2.85	2.89	2.89	2.91	3.45	3.45	3.51	3.47
4	380	3.452	475	4.583	8.50	8.43	8.35	8.43	9.60	9.51	9.42	9.51
6	375	2.401	475	2.327	8.80	8.75	8.82	8.79	9.70	9.66	9.66	9.67
7	380	0.871	485	1.245	7.75	7.73	7.71	7.73	—	—	—	—

The acid dissociation constants of the compounds were determined using the half-height,[16] the limiting absorbance method as applied for stepwise-dissociation[16] and the Colleter method.[17] The results are collected in table 2. These values indicate that 4 has a lower pK_a compared to 6 due to the higher contribution of the p-OH group of 4 in the intramolecular charge transfer. Also the introduction of the two bromine atoms in 7 causes a lowering of pK_a through their acceptor character.

[16] R. M. Issa, *Z. phys. Chem. (Frankfurt)*; **74**, 17 (1971); *Egypt J. Chem.*, **14**, 113 (1971).

[17] J. C. Colleter; *Ann. Chim. (France)*, **5**, 415 (1960).

3. INFRARED ABSORPTION SPECTRA

The ir-spectra for the compounds under investigation obtained as KBr discs are reported in Table 3, and interpreted to the extent that appears possible.

Table 3

Solid state (a, b, c), infrared spectral data for 1,5-diphenyl-1,5-pentadiene-3-one derivatives

1	3	4	5	6	7	Vibrational assignment
—	—	3325 b	—	3220 b	3400 b	ν_{O-H} (associated)
1655 s	1655 s	1655 sh	1660 m	1640 sh	1670 m	$\nu_{C=O}$
1630 m	1630 s	1630 sh	1630 s	1610 vs	1615 vs	$\nu_{C=C}$ conjugated with C=0
1600 s	1600 s	1600 s	1595 s	—	1595 s	$\nu_{C=C}$skeletal vib
1580sh	1580 sh	1540 sh	1580 s	1550 s	1580 s	$\nu_{C=C}$,, ,,
1450 s	1445 w	1440 s	1450 s	1470 s	1450 s	$\nu_{C\ C}$skeletal. vib.
1350 s	1335 m	1360 s	1340 s	1350 s	1340 s	δ aromatic C−H
—	—	1290 s	—	1300 m	1290 m	ν_{C-O} (phenolic)
1195 s	1180 m	1180 s	1200 s	1160 s	—	δ aromatic C−H
1100 m	1150 m	1130 s	1100 s	1100 m	1100 s	δ aromatic C−H
760^5vs	835^2s	840^2s	830^2vs	—	860^1m	γ_{C-H}
695^5vs	820 s	760^4s	—	—	—	

(a) As KBr disc.

(b) Intensity of bands is given by: b = broad, vs = very strong, s = strong, m = medium, w = weak and sh = shoulder.

(c) Absorption band frequencies are expressed in cm^{-1}.

1, 2, 4 and 5 denote the number of adjacent ring-hydrogen atoms.

The band due to the stretching frequency of the C = O group appears in 1670—1640 cm^{-1} region. In comparison to the unsubstituted compound (1), this band is shifted to lower frequencies with electron donating group and to higher ones when the substituent is an electron acceptor. Obviously, the donor groups favour the polarization of the carbonyl group through their enhancement of the C.T. from the phenyl ring, while the electron acceptors oppose to this polarization.

The spectrum of compound 7 exhibits the carbonyl band at 1670 cm^{-1}. Thus the band is blue shifted by 30^{-1} cm compared to the corresponding compound without the bromine substituents. This indicates the diminishing of the polar character of the carbonyl link by the existence of the bromine atoms. The plot of $\nu_{C=O}$ versus the Hammett constant of the substituents results in a more or less linear relationship (Fig. 2b).

Revue Roumaine de Chimie, *22*, *8*, 1261–1265 (1977)

ADDUCTS OF TETRACHLOROHYDROQUINONE WITH QUINOLINE AND PIPERAZINE

I. GAVĂT, OLGA BUTUFEI and MARIANA MUNTEANU
Institute of Macromolecular Chemistry "P. Poni", Section Polymerization Processes,
Bucharest, str. Dumbrava Roşie, 18, Romania

Received March 3, 1976

Studies on the polycondensation reaction of chloranil with substances containing the amino group such as : hydrazine, diphenylhydrazine or piperazine in the presence of an acceptor for hydrochloric acid such as quinoline, pyridine, sodium acetate, have evidenced the formation of compounds of low molecular weight which impede the polycondensation owing to their stability. Among these compounds of low molecular weight we mention the adducts of tetrachlorohydroquinone with quinoline, hydrazine and piperazine. The adducts of tetrachlorohydroquinone with quinoline or piperazine were studied by UV and infrared spectra. In the reaction of tetrachlorohydroquinone with the above mentioned amines, the first to form is the monoanion of tetrachlorohydroquinone which becomes stable in the corresponding dianion with the formation of adducts of structure V and VI, respectively.

INTRODUCTION

Tetrachlorohydroquinone behaves in different ways towards amine depending on the reaction conditions and the amine nature.[1]

The literature reports the interaction possibilities of hydroquinone with aromatic amines,[2] with the formation of some double compounds, which can be formulated as monoammonium aryl derivatives of hydroquinone (structure I) and diammonium hydroquinone (structure II).

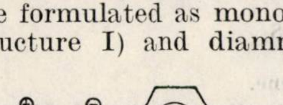

I

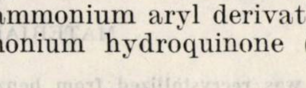

II

The aliphatic amines[3] also form a series of compounds with hydroquinone, which can be bound in various molecular proportions :

a) one molecule of hydroquinone with one molecule of amine
b) one molecule of hydroquinone with two molecules of amine
c) two molecules of hydroquinone with one molecule of amine

---

[1] I. Gavăt and O. Butufei, *Materiale Plastice* in press (1978).
[2] H. D. Gibbs, *J. Amer. Chem. Soc.*, **28**, 1395 (1906).
[3] H. D. Gibbs, *J. Amer. Chem. Soc.*, **46**, 2536 (1924).

Hydroquinone also forms double compounds with pyridine and quinoline.[4] An analogous reaction was observed by Bell[5] when the formation of a crystalline substance occurred, in the reaction of benzoquinone with quinaldine, in xylene as solvent.

Subsequently, Bother[6] explained the possible formation of stable adducts of hydroquinone with the amines which have in *ortho* pozition towards the nitrogen atom groups such as CH_3, so that the formation of the adduct takes place according to reaction 1, with the formation of the intermediate product of structure III.

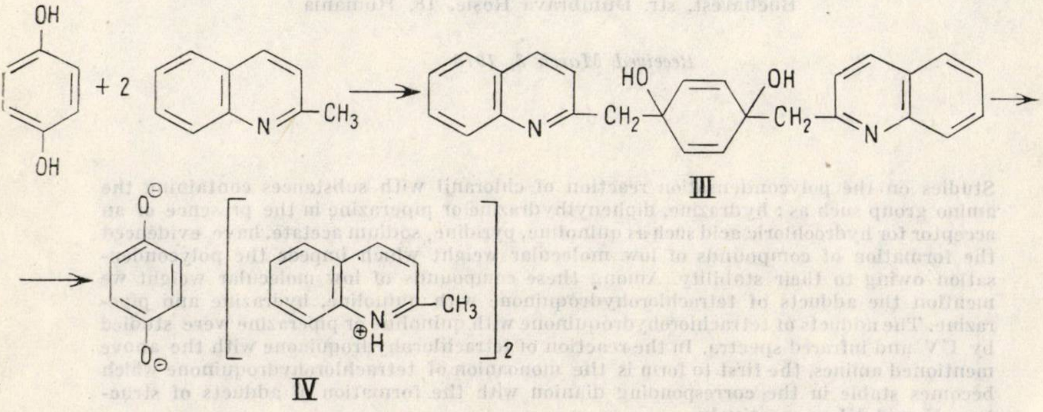

which changes into the final product of structure IV.

This paper studies the reaction of tetrachlorohydroquinone with quinoline or piperazine in ethanol solution and emphasizes the formation of the corresponding adducts by UV and infrared spectra.

EXPERIMENTAL PART

MATERIALS

— Chloranil was recrystallized from benzene.

— Tetrachlorohydroquinone was prepared by the reduction of chloranil with hydrazine[7] and was purified by recrystallization from alcohol.

— Quinoline and piperazine were freshly distilled in vacuum.

— Ethanol, *p.a.* product of "Reactivul — Bucureşti".

APPARATUS

Spectrometer UR-10 Carl Zeiss Jena for infrared spectra.
Spectrometer UV VIS—SPECORD for UV spectra.

---

[4] A. Bayer and V. Villiger, *Chem. Ber.*, **35**, 1208 (1902).
[5] F. Bell, *J. Chem. Soc.*, **1953**, 348 (1953).
[6] B. Bother, *J. Amer. Chem. Soc.*, **77**, 749 (1955).
[7] S. Sur, *J. Indian Chem. Soc.*, **49**, 4 (1972).

a) Reaction of tetrachlorohydroquinone with quinoline

0.0393 g of tetrachlorohydroquinone ($0.15.10^{-3}$M) and 0.0387 g of quinoline ($0.30.10^{-3}$M) are dissolved in 200 ml of ethanol. The mixture is heated for half an hour under reflux. The solution is concentrated to half of its volume by the distillation of ethanol and then it is cooled on an ice bath. A yellow product crystallizes.

The analysis of chlorine and nitrogen of the yellow product : *Found* : N, 5.33 ; Cl, 28.00 % ; *Calculated* : N, 5.53 ; Cl, 28.00 %.

The corresponding empirical formula of the yellow product is : $C_{24}Cl_4H_{16}O_2N_2$.

This product has the melting point 114°, and is decomposed by the diluted alkali solution into tetrachlorohydroquinone, identified by its melting point at 232° and into an oily product, identified as being quinoline, by its transformation into chlorohydrate.

b) Reaction of tetrachlorohydroquinone with piperazine

0.2568 g of tetrachlorohydroquinone ($1.02.10^{-3}$M) is dissolved in 30 ml of ethanol. 0.044 g of piperazine ($0.51.10^{-3}$M) dissolved in 10 ml of ethanol is added over 15 ml of this solution, which contains $0.51.10^{-3}$ M tetrachlorohydroquinone and 0.088 g of piperazine ($1.02.10^{-3}$ M) dissolved in 10 ml of ethanol is added to the second portion of tetrachlorohydroquinone ($0.51.10^{-3}$ M). A white-brown product precipitates from the mixture of these solutions. After filtration, the pH of the filtrate from the first portion is neutral and that from the second portion is basic.

The basic filtrate in the latter case was titrated with 0.1 N aqueous HCl and the result of the titration demonstrates the consumption of one mole of piperazine for one mole of tetrachlorohydroquinone.

The white-brown product has the melting point 185° and the elemental analysis is : *Found* : N, 8.33 ; Cl, 41.83 ; $C_{10}Cl_4H_{10}N_2O_2$ requires : N, 8.40 % ; Cl, 42.20 %.

RESULTS AND DISCUSSION

Tetrachlorohydroquinone can form with amines, complexes with charge transfer [7] and also adducts.[5,6]

At the condensation of chloranil with hydrazine [1] in the presence of quinoline as acceptor for HCl, two products were found at the interface : a black-brown product which is the polymer and another one, the yellow product. When treated with hydrochloric acid the latter decomposes into tetrachlorohydroquinone and quinoline. In this case, tetrachlorohydroquinone was formed by the reduction of chloranil with hydrazine. In turn, tetrachlorohydroquinone reacts with quinoline, to produce the above mentioned yellow product.

The same yellow product was directly synthesized from tetrachlorohydroquinone and quinoline in ethanol solution (experience a). The chlorine and nitrogen analysis of the yellow product shows that the reaction of tetrachlorohydroquinone with quinoline results in this product with an 1 : 2 of the components.

Studying the kinetics of the formation of the product from tetrachlorohydroquinone and quinoline in ethanol solution by UV spectra, the appearance of some characteristic bands of the tetrachlorohydroquinone monoion (426 and 452 mμ) [8,9] was observed in the first moments of the mixture, which disappear within a few minutes. At 300 mμ where quinoline absorbs and at 310 mμ where tetrachlorohydroquinone absorbs

---

[8] Y. Iida, *Bull. Chem. Soc. Japan*, **43**, 2772 (1970).

[9] E. Foster, *Rec. Trav. chim.*, **83**, 711 (1964).

a diminution of the absorptions in time was observed, which cannot be followed because of the superposition of these absorption bands over that of 300 mμ, characteristic of the yellow product, which is formed in this range.

Fig. 1 (curve 1) exhibits the absorption spectra if the yellow product resulted from experience (a), having a concentration of 5.10^{-4} M in ethanol solution.

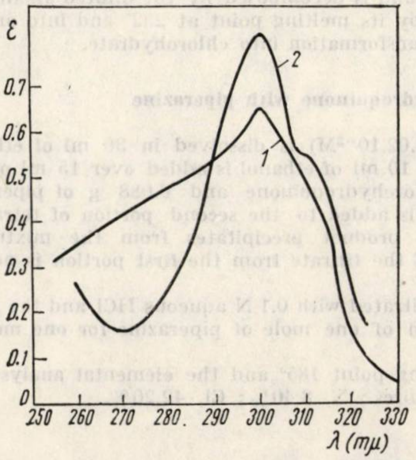

Fig. 1. — The UV spectra of : 1) The yellow product, resulted from the reaction of tetrachlorohydroquinone with quinoline, in ethanol alcohol, of concentration 5.10^{-4}M ; 2) The white-brown product, resulted from the reaction of tetrachlorohydroquinone with piperazine, in ethyl alcohol of concentration $5\ 10^{-4}$M.

The yellow product was also studied by infrared spectra. At 2500 cm^{-1} one observers the appearance of a large absorption band, which is characteristic of $-NH^{+}$ group [10]; the absorption band at 3400 cm^{-1} characteristic of the $-OH$ group is diminished, compared to the absorption band of the $-OH$ group in tetrachlorohydroquinone.

From the above mentioned facts, it results that the yellow product formed in the interaction of one mole of tetrachlorohydroquinone with two moles of quinoline is the corresponding adduct with the structure V.

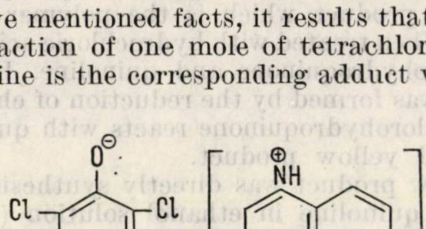

V

Tetrachlorohydroquinone behaves similarly towards aliphatic cyclic amines. Thus, in reaction (b), a white-brown product was obtained from the interaction of tetrachlorohydroquinone with piperazine.

---

[10] L. J. Bellamy, "Infra-red spectra of complex molecules", London, New York, p. 259, 1966.

From the elemental analysis and the consumption of piperazine, determined by the titration of unreacted piperazine with 0.1 N HCl, it results that the components interact in an 1 : 1 molar ratio.

The product was also examined by UV and infrared spectra.

The UV spectra of the yellow product, in ethyl alcohol, of concentration 5.10^{-4}M is presented in fig. 1, curve 2.

A maximum absorption band at 300 mμ is observed.

Thus, tetrachlorohydroquinone with quinoline and piperazine in the ethanol dilute solution form adducts with structures V and VI.

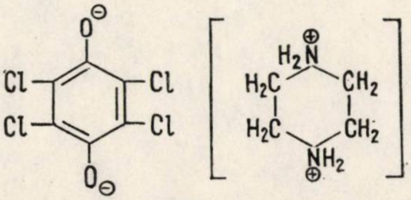

VI

Regardless of the method of preparation, these adducts contain the same proportions of the reactant components and are stable in solid state. In freshly prepared ethanol solutions the adducts obey the Lamber-Beer law of absorption in UV. The solutions of adducts prepared and stored for over an hour display the characteristic absorption bands of the decomposed products being formed.

This phenomenon is accelerated by the presence of water in ethanol alcohol. It was also observed that the aqueous solutions of the adducts are not stable in time.

Revue Roumaine de Chimie, 22, 8, 1267–1270 (1977)

STRUCTURAL CHARACTERIZATION OF MULTICOMPONENT ACRYLIC POLYMERS

MARGARETA TOMESCU, I. DEMETRESCU and D. OANCEA

Faculty of Industrial Chemistry, Polytechnic Institute, Bucharest,
Str. Polizu Nº 1 – Romania

Received April 8, 1975

This paper makes a structural characterization of some acrylic copolymers carried out by average molecular weight, intrinsic viscosity and IR spectrum.

Recent studies concerning plastics, elastomers, fibers, adhesives coating materials are particularly connected with multicomponent polymers. The special interest in copolymers results from a large variety of synthetic possibilities which allow to obtain macromolecular compounds with properties required by the field of applications.

Several previous papers have examined the copolymers synthesis, compositional distribution and some potential industrial applications for the following polymers : acrylonitrile (AN)-metacrylic acid (AM)-styrene (S)-vinylidene chloride (CV),[1] AN-*n* butyl acrylate (BA)–S–CV[2] and AN–BA–CV.[3]

A structural characterization of the same multicomponent polymers is attempted on the basis of average molecular weight, intrinsic viscosity and IR spectrum.

EXPERIMENTAL

The polymers were prepared by radical polymerization in solution at 60° in the presence of 0.5% azoisobutyronitrile, as indicated previously.[1–3] In order to reduce the induction period found when oxygen was present, the synthesis was carried out in an inert atmosphere (prepurified grade argon). The products were separated from the reaction medium by precipitation in methanol. They were subsequently purified by reprecipitation and repeated washing with methanol and finally dried in vacuum until constant weight was reached.

Taking into account the compositional heterogeneity of the copolymers studied in the papers,[2,4] we chose restrictive synthesis conditions to get only quaternary or ternary copolymers rather than physical mixtures of copolymers and homopolymers.

In order to obtain only quaternary copolymer in system AN–AM–S–CV and AN–BA–S–CV we carried out copolymerization at conversions not exceeding 55 percent in weight. Below such conversions no monomer is entirely consumed.

---

[1] M. Tomescu, V. Părăuşanu, M. Georgescu, S. Creţu, I. Hogea, D. Mihăiţă, E. Rizescu and V. Tomescu, RSR Patent 59.667, June, 1976.

[2] M. Tomescu and Cr. Simionescu, *Makromol. Chem.*, **00**, 000 (1977).

[3] M. Tomescu, M. Georgescu, S. Creţu, I. Hogea, D. Mihăiţă, E. Rizescu and V. Tomescu, RSR Patent, 59.668, June, 1976.

[4] M. Tomescu and Cr. Simionescu, unpublished data.

The AN—BA—CV copolymer studied in this note has an azeotropic composition.

The copolymers composition was established by both elemental and functional analyses. Acrylonitrile, vinylidene chloride and metacrylic acid content in polymers was found from nitrogen analysis using the micro Kjeldahl method, chlorine analysis using the Schöniger method and carboxyl groups analysis using a potentiometric titration with 0.1 N. NaOH nonaqueous medium,[5] respectively.

The viscosities of polymer solutions in DMF-were measured at 30° using a Ubbelhode viscometer. The number-average molecular weights Mn were determined from osmotic pressure measurements of 0.2% (by weight) solutions of polymers in DMF at 30° using an automatic Hallikainen osmometer.

The samples for IR study were obtained as films by evaporating the polymer solution in acetone as solvent on a mercury surface or directly on the KBr window. Spectra for copolymers insoluble in acetone were recorded in DMSO solution or in KBr pellets, when grinding was possible. The spectra were recorded using a UR-10 Karl-Zeiss Jena spectrophotometer within the range 400—4000 cm^{-1}.

RESULTS AND DISCUSSION

The experimental results on the composition, intrinsic viscosity and average molecular weight of multicomponent polymers are given in table 1. The characteristic absorption bands are given in table 2.

The assessment of IR bands was done in agreement with the IR data on the monomers and homopolymers.[6,7]

Since all multicomponent polymers examined in this paper contain AN and CV, the characteristic C ≡ N and C—Cl bands are present in spectra.

Table 1

Compositions, intrinsic viscosities and average molecular weights of copolymers

Copolymer composition % (by weight)	(DMF, 30°)	Number-average molecular weight of copolymer
AN 53.80 AM 13.56 CV 10.50 S 22.14	0.92	52,600
AN 18.39 BA 43.31 CV 25.00 S 13.30	1.67	54,000
AN 70.29 BA 26.91 CV 2.80	1.92	70,000

---

[5] A. F. Deneş, N. Asandei and Cr. Simionescu, *Analyt. Chem.*, **40**, 629 (1968).

[6] H. Volkmann, "Handbuch der Infrarot Spektroskopie", Verlag Chemie, New York, 1972.

[7] H. W. Thompson and D. A. Jameson, *Spectrochim. Acta*, **13**, 236 (1958).

Table 2

Characteristic IR bands of acrylic multicomponent polymers

Copolymers	Band (cm^{-1})	Assessment
AN—AM—CV—S	3640	$\nu_{OH\ free}$
	3030	ν_{CH} (C_6H_5 group)
	2980	ν_{as-CH_3}
	2940	ν_{as-CH_2}
	2840	ν_{sym-CH_2} and ν_{sym-CH_3}
	2240	ν_{-CN}
	1710; 1720	ν_{-CO}(COOH group)
	1605	ring stretching C_6H_5
	1500	ring stretching C_6H_5
	1460	δ_{as-CH_3}
	1370	δ_{sym-CH_3}
	1228	ν_{C-O} and δ_{O-H}
	770; 708	C—H out of plane in phase deformation (C_6H_5 group)
	655; 660	ν_{C-Cl}
	530	ν_{C-Cl}
AN—BA—CV—S	3030	ν_{CH} (C_6H_5 group)
	2960	ν_{as-CH_3}
	2920	ν_{as-CH_2}
	2880	ν_{sym-CH_2} and ν_{sym-CH_3}
	2238	ν_{CN}
	1735	ν_{CO} (butyl ester)
	1600; 1495	ring stretching C_6H_5
	1455	δ_{as-CH_3}
	1375	δ_{sym-CH_3}
	1180; 1065	ν_{C-O-R} (butyl ester)
	765; 710	C—H out of plane in phase deformation (C_6H_5-group)
	645	ν_{C-Cl}
	550	ν_{C-Cl}
AN—BA—CV	2955	ν_{as-CH_3}
	2922	ν_{as-CH_2}
	2860	ν_{sym-CH_3} and ν_{sym-CH_2}
	2238	ν_{CN}
	1716	ν_{CO} (butyl ester)
	1446	δ_{as-CH_3}
	1380	δ_{sym-CH_3}
	1168; 1060	ν_{C-O-R} (butyl ester)
	650; 525	ν_{C-Cl}

The stretching vibration of CN group in acrylonitrile (ν_{CN}) is always present at 2238 cm^{-1} as for the monomer and homopolymer. The relative intensity of this band changes from one polymer to another depending on the AN content.

A comparative IR study of polyvinylidene chloride and multicomponent polymers 1 to 3 indicates the presence of the C—Cl vibration; in the IR spectrum of the monomer the C—Cl bands appear at 715 and 585 cm^{-1}, while for the homopolymer there are three bands situated at 656, 599 and 528 cm^{-1}. In the examined multicomponent polymers the C—Cl characteristic bands are situated within the range 660—645 and

525–540 cm^{-1}. There is a shift of C–Cl peaks in the multicomponent polymers relative to homopolymers, which can be explained as an environmental effect.[8]

The spectra of multicomponent polymers 1 and 2 having styrene as a component, show two strong characteristic bands at 708–710 and 765–770 cm^{-1} assigned to the C–H deformation in phase of phenyl group. These two bands have the same intensities in the spectrum of styrene. The intensities are different for the multicomponent polymers (708–710, 770–765 cm^{-1}). The same is true for atactic polystyrene.[6]

The presence of carboxylic and CH_3 groups in the spectrum of the copolymer 1 which contains metacrylic acid was established through the following characteristic bands: ν_{OH} free — 3640 cm^{-1}, $\nu_{C=O}$ 1710 and 1720 cm^{-1}, δ_{sym, CH_3} —1370 cm^{-1} and δ_{asym, CH_3} —1460 cm^{-1}.

The spectra of the polymers 2 and 3 which contain *n* butyl acrylate exhibited the characteristic bands of ester and CH_3 group: $\nu_{C=O}$ at 1735 cm^{-1} and 1716 cm^{-1} respectively, ν_{C-O-R} at 1180–1065 cm^{-1} and 1060–1168 cm^{-1} respectively, δ_{as, CH_3} at 1455 cm^{-1} and δ_{sym, CH_3} at 1375 cm^{-1}.

---

[8] M. Avram and Gh. H. Mateescu, "Spectroscopia in IR. Aplicaţii în chimia organică", Ed. Tehnică, Bucureşti, 1966.

Revue Roumaine de Chimie, **22**, *8*, 1271–1275 (1977)

COMPTES RENDUS

"Lectures in Heterocyclic Chemistry" (R.N. Castle et al., editors), Heterocorporation, Orem, Utah, USA: vol. I, 1972; vol. II, 1974; vol. III, 1976 (12 $ per volume or 30 $ for all three volumes)

As supplements to the *Journal of Heterocyclic Chemistry* published by the Heterocorporation, the plenary invited lectures delivered at the last three International Congresses of Heterocyclic Chemistry held every two years were gathered in three volumes.

Vol. I includes seven lectures presented at the Third Congress held at Tohoku University, Sendai, Japan (23–27 August, 1971) and three abstracts of lectures which were not available (by A. N. Kost, E. E. Van Tamelen, and G. Büchi); A. Eschenmoser's lecture was printed elsewhere. The seven lectures presented in full are by J. P. Kutney (Studies of indole alkaloid biosynthesis), E. Klingsberg (On the trail of no-bond resonance), W. Nagata (Bridged azacycles), A. R. Katritzy (The aromaticity of heterocycles and tautomeric equilibria), M. Hamana (Some advances in the reaction of aromatic N-oxides), G. Märkl (Aromatic phosphorus heterocycles — synthesis, structure, and reactivity), and R. Jacquier (The chemistry of cyclic azaenamines, enehydrazines, and amidrazones). Dr. Klingsberg's fascinating account of thiothiophthene and related systems obtained by progressive replacement of sulphur atoms with first-row elements makes exciting reading; in the reviewer's opinion, one could argue that the central sulphur is tetravalent and has hypervalent character (cf. J. I. Musher, *Angew. Chem.*, 1969, **81**, 68; *Angew. Chem. Internat. Edit.* 1969, **8**, 54). Prof. Katritzky's lecture is a thorough discussion of tautomeric equilibria, methods used for determining equilibrium constants and resonance energies, and application to 2-pyridone and analogs such as uracil, 2-quinolone, etc. Both last lecturers quote Romanian contributions. Prof. Märkl's lecture describes the chemistry of phosphabenzene and related systems such as 2,4,6-triphenylphosphorine and 1,1,2,4,6-pentaphenylphosphabenzene, first obtained by him from pyrylium salts and tris(hydroxymethyl)phosphine. Prof. Jacquier's lecture deals with indoles and pyrazolines obtained from the acyclic starting materials mentioned in the title.

Vol. II comprises eight lectures and an abstract (by H. Wynberg) delivered at the Fourth Congress held at the University of Utah, Salt Lake City (8–13 July, 1973), by J. J. Fox (Pyrimidine nucleoside transformations), J. Streith et al. (Photochemical synthesis and reactivity of 1,2-diazepines), B. Stanovnik (Transformations of azolopyridazines, azinopyridazines and related systems), A. J. Boulton (Concerted rearrangements in 1,2-oxazoles and related compounds), T. Kametani (The total synthesis of natural products by the intramolecular coupling reaction), C. W. Rees and R. C. Storr (Interconversion of some nitrogen heterocyclic systems), H. C. van der Plas (Ring transformations of azines. A mechanistic study of the ring transformation of ^{14}C- and ^{15}N-labeled azines) and E. F. Elsager et al. (Synthesis of fused pyrimidines as folate antagonists). Prof. Streith's lecture deals with the photochemical ring expansion of 1-iminopyridinium ylides (formed from pyrylium salts and arylhydrazines) affording 1,2-diazepines which, like Diazepam, may possess pharmacological activity; valence isomerizations between these systems, 1,7-diazanorcaradienes and 2,3-diazabicyclo [3.2.0]-hepta-3,6-dienes are discussed, as well as various cycloadditions. Dr. Boulton's lecture describes a generalized rearrangement which is reminiscent of the "no-bond resonance" in thiothiophthenes. Prof. van der Plas's lecture describes the powerful mechanistic tool of isotopic labelling, applied to ring conversions of six-membered aza-heterocycles, most of which involve ring opening to unstable intermediates. Natural product heterocyclic chemistry is very well represented by the first, fifth and last lecture.

Vol. III includes the ten invited lectures held at the Fifth Congress (Ljubljana, 13–18 July, 1975): N. Cromwell (Some comparative and contrasting aspects of the chemistry of aziridines and azetidines), S. Gronowitz (Recent work on aromatic boron-containing heterocycles), K. Hafner (New heterocyclic conjugated π-electron systems. Syntheses and properties), A. K. Bose and M. S. Manhas (Cephalosporins, penicillins and beta-lactams), Y. Ban and T. Oishi (Synthetic studies on polyheterocyclic ring systems), J. Clark (Ring cleavage of some pyridine and pyrimidine derivatives), A. Lattes (Mechanisms of chemical and photochemical rearrangements of unsaturated amines and related heterocycles), M. L. Mihailović (The formation of cyclic ethers from alcohols by intramolecular substitution and addition processes), R. B. Moffett (New benzodiazepine analogs, synthesis and CNS activity), A. Marxer (Reactions of organometallic compounds in the heterocyclic field).

Prof. Gronowitz's lecture discusses six-membered boron-containing aromatic heterocycles possessing, in addition, nitrogen heteroatoms, as well as dithienoborepins, highly interesting through their structural similarity to dithienotropylium. Prof. Hafner's lecture describes new azaazulenes and azapentalenes.

The general presentation of lectures is in the same format and style as is usual for normal papers published in the *Journal of Heterocyclic Chemistry*. Owing to the high scientific level of the lecturers, the three volumes should be present in every organic chemical laboratory where heterocyclic chemistry is a research topic.

A. T. Balaban

"TOPICS IN CURRENT CHEMISTRY", Vol. 63, Springer Verlag, Berlin, Heidelberg, New York, 1976

The volume 63 of "Topics in Current Chemistry" contains, in 202 pages, three article reviews different in topics and extension.

The first article is "Discriminating Interactions Between Chiral Molecules" by D. P. Craig and D. P. Mellor. It is known that the differences between the "chiral" (optic active) molecules have been evidenced so far by means of optical measurements only. The paper of 48 pages and 65 bibliographic quotations is interesting by the treatment of the less studied topics and namely, of the difference between the chiral molecules which may be made obvious by studying their specific interactions. It is difficult to study chirodiastaltically ("diastaltic" = "serving to distinguish") the isolated chiral molecules. Considering that a chiral molecule is the source of an external field, which is inherently chiral, the molecule may be coupled to another chiral molecule. The possibility of chirodiastaltic investigation will be enlarged if one takes into account such pairs of molecules. In this paper, the field of a chiral molecule is imagined in general terms as the electrostatic field of the permanent molecular charge distribution, the field of the dispersion interactions and the field of the short-distance interactions. The first part of the article describes the phenomena due to chirality. The second one presents a detailed theoretical treatment of the origins and of the nature of the discriminating interactions between chiral molecules. It must be mentioned the theoretical treatment "in advance" with regard to the chiral discrimination by means of the resonance methods, not yet experimentally achieved.

The second article review of smaller extent is the "No-Bond-Resonance Compounds, Structure, Bonding and Properties", by R. Gleiter and R. Gygax. This article, of 40 pages and 147 bibliographic quotations, is devoted to the chemistry of trithiapentalenes. These compounds have aroused since 1958 the attention of the researchers, in what the chemical bonding is concerned. It has been thus established that these compounds have an unusually long-bond distance between the sulphur atoms, greater than the sum of their covalent radii but shorter than the sum of their Van der Waals radii. This unusual structure has been explained by a new bonding type, of "no-bond-resonance". In the last years the chemistry of these compounds has been rapidly developed. The introduction of various substituents as well as the replacing of the sulphur atoms with other heteroatoms in the trithiapentalene molecules have been experimentally accomplished. New spectroscopic methods have been also used in order to elucidate the structure. The theoretical investigation of the chemical bonding in these compounds has known a spectacular progress. The article review presents exhaustively these investigations and interpretations in the chemistry of the trithiapentalenes.

The third article is "The Molecular Zeeman Effect" by D. H. Sutter and W. H. Flygare. It treats on 108 pages with almost 80 bibliographic quotations a very interesting and modern research field. It is known that the microwave spectroscopy has achieved a new and considerable development especially regarding the aplication of the Zeeman effect to establish the correct values for the diagonal elements of the molecular g tensor, for the anisotropics in the diagonal elements of the magnetic susceptibility tensor, as well as for the tensor of the electric molecular quadrupole moment. The results obtained allow to predict in the future the obtaining of new significant information regarding the electronic structure of the molecules using the molecular Zeeman effect. The first part oi the paper describes the basic principles of the rotational Zeeman spectroscopy. The next part gives the latest results regarding the molecular quadrupole moments and the anisotropy of the magnetic susceptibility. The third part deals with the scientific equipment and the detailed analysis of the obtained spectra. The measurement limits are also discussed herewith. The fourth part contains the theoretical basis of the rotational Zeeman spectroscopy. The theoretical treatment starts with the most general notions, such as the Lagrangian of the molecular system, and it is gradually developed in a rigorous and interesting form. The Appendix summarizes the most recent experimental data published between 1972–1975.

A. C. Banciu

"Topics in Current Chemistry" Vol. 65, Theoretical Inorganic Chemistry II, Springer Verlag, Berlin, Heidelberg, New York, 1976, 153 p.

Under the title "Theoretical inorganic chemistry" the 65th volume from the series contains three large chapters.

The object of the first is a study of the "Diastereoisomerism and Diastereoselectivity in Metal Complexes" by K. Bernauer. The aim of this work is to dicuss, based on known examples, the factors which may lead to a structure model which should be able to transmit chiral information in a reaction chain. The stereochemical model of coordination compounds is determined by the nature of ligand molecules, the number and size of chelate rings and the nature of the central metal atom, factors which determine the topography of the complex. For the construction of a matrix-like model of definite structure, the diastereoselectivity of a single ligand molecule is of great importance. The stereoselective coordination of the different classes of ligands is discussed, based on the framework of the ligand and their characteristics.

The most investigated bidentate ligands are the 1,2-diamines, the 1,3-diamines and much less the five-membered chelate rings of amino acids.

For tridentate ligands, two different types are distinguished : linear and branched ligands. Linear ligands may be coordinated in peripheric as well as in a facial manner; for branched ligands only a facial coordination is possible. With tetradentate ligands, four basic structural types of coordination compounds can be distinguished for linear, branched and macrocyclic ligands. No optically active ligand reacts as pentadentate only, but, according to the nature of the central metal atom and the reaction conditions, these compounds may react as penta- or hexadentate ligands.

Many examples are presented for each type of ligands, but the characteristics which were taken into account give only an approach to the geometry of the most stable form of the complex. In this context, the problem of stereoselectivity is often related to the stereochemical specificity of biological systems. The limited number of optically active ligands, which can be easily synthesized was certainly a real obstacle for systematic study of diastereoselectivity in metal complexes.

In the second chapter of the volume, concerning "The photochemical reactions of coordination compounds", prof. Mark S. Wrighton acquaints us with the results of the last few years in the photochemistry of transition metal complexes of various d^n electronic configurations. A correlation of the available excited states and the nature of the possible chemical reactions, their potential application in energy conversion and optical device in general, is shown. This paper is organized according to the following reaction types : photosubstitution, intraligand photoreactions, metal-metal bond, cleavage and photoredox reactions. A large part is devoted to the photosubstitution chemistry of Cr(III) complexes, which serves nicely to introduce the important theories and some interesting experimental results applicable to other cases. Several chemical and physical applications of the light-induced ligand substitution are also presented.

Cleavage of the metal-metal bond by photolysis may be a successful way to reactive intermediates of a radical nature, such as metal carbonyls, which are remarkable with respect to their photodeclusterification. Several interesting examples of intraligand photoreaction, involving styrylpyridine complexes of Ru, Rh, Re, Ir, Mo, W, receive considerable attention, as well as the net oxidation or reduction photoreactions.

Among the coordination compounds yielding photoelectron production in solution, the Ru(2,2′-bipyridine)$^{2+}$ ion is considered as an excited state reducing agent and is studied in great details at in the same time with a series of transition metal complexes which induce a large number of photoredox reactions in inorganic systems.

Finally, inorganic based photoredox processes on semiconductor electrodes which have recently aroused considerable interest, for their connection with the important redox chemistry, are mentioned.

The third chapter — "Complexation and activation of diazenes and diazo compounds by transition metals" by Dr. A. Albini and Dr. H. Kirsch — is concerned with the coordinating properties of diazene and diazo compounds and their interaction with metal carbonyls.

Based on the results obtained from cyclic diazenes and iron carbonyls, the modes of coordination of the $-N = N-$ bond are discussed. Due to the electronic structure of these ligands, σ-coordination, via n_1 orbital is usually favoured over π-coordination. But stable π-complexes will be formed only if the metal is a very good π-donor and the diazene a good π-acceptor. The coordinating properties of diazenes receive a great part of interest because diazene complexes are probable intermediate in biological nitrogen fixation, and, on the other hand, the diazeno group activated by iron carbonyl towards unsaturated molecules, like alkines offers a convenient synthesis for novel organic heterocycles.

The material included in this volume is presented in a clear and concise manner with tables and diagrams wherever necessary. Each of the three chapters ends with an up-to-date bibliography, so that the whole work is extremely useful to all those concerned with research or development in this field.

Cristineta Mărculescu

L. B. SOKOLOV, V. D. GERASIMOV, V. M. SAVINOV and V. K. BELYAKOV, "Heat-Resistant Polyamides", Khimiya, Moscow, 1975, 254 p.

This book offers a wealth of information on aromatic polyamides including especially the authors' results (from the Institute of Synthetic Resins, Vladimir, USSR).

For a number of years the authors have published many original papers on the subject of this book.

The book starts with a short introduction concerning the classification of aromatic polyamides and contains four chapters.

The first chapter gives a general survey on the methods of synthesis. Extensive treatment is given to three of the methods : solution, emulsion and interfacial polycondensation. The properties of the most used solvents in the polyamide synthesis are shown in a table.

Structure and properties of aromatic polyamides are discussed in chapter II. Tables, graphs and equations are very clear and show details about physical, chemical and thermal properties.

In the third chapter a large amount of information is presented on the processing of aromatic polyamides. There is also a large collection of data on equipment for briquetting polyamides and polymer post-treatment.

The last chapter deals with thermal and mechanical properties of polyamides and their applications such as compositions, filled and unfilled polymers, fibers, paper-like membranes, and so on.

This book can be highly recommended, being useful to engineers and scientific researchers involved in the study and the development of heat resistant polymers.

Gh. Mandric

M. MEHRING "High Resolution NMR Spectroscopy in Solids" (vol. 11 from the series "NMR-Basic Principles and Progress", ed. : P. Diehl, E. Fluck and R. Kosfeld); Springer-Verlag, Berlin, Heidelberg, New York, 1976, 246 p, 104 fig.

In contrast with NMR spectra of liquid samples where the free motions of molecules annihilate the anisotropic interactions (chemical shift anisotropy, dipolar and quadrupolar interactions), in solid samples the anisotropic interactions becoming active lead to the broad form of the signals (possessing the well-known "bell-shaped" form). Lately, different techniques have been employed in order to surpass this disadvantage and to obtain high resolution NMR spectra of solids from which useful information could be drawn.

It is the purpose of this book (the 11th volume in the series : "NMR-Basic Principles and Progress") to present, mainly theoretically, but including also representative experimental results, these methods of line narrowing in NMR spectroscopy of solids.

After a short introduction (Chapter 1) the author gives, in Chapter 2, a review of the important mathematical notions concerning the tensorial character of spin interactions, exemplified mainly by second-rank tensors in solids.

Included in the general method of "manipulation" in spin space, capable to reduce dipolar and quadrupolar interactions, are the multiple-pulse experiments, described in Chapter 3. In the present days the most efficient multiple-pulse sequence is the four-pulse one, developed by *W*augh, *H*uber and *H*aeberlen starting from 1968 (named WAHUHA-technique or WHH-4). In this technique the repression of dipolar interactions (with retention of shift interactions) is achieved by application to the spins of rf 90° pulses in different directions (x, y, z) of the rotating frame using a sequence which can be symbolised as $(P_{\bar{y}}-2\tau-P_y-\tau-\mathrm{P}_x-2\tau-P_{\bar{x}}-\tau)_n$ (where τ is time ; $P_{x(y)}$ is the rotation operator about the x(or y) direction of rotating frame and $\bar{x}$ is $-x$) ; the magnetization is sampled once every cycle during one of the 2τ period ("window"). After the mathematical development of the theory, some illustrative spectra ($F_3C-COOAg$; fluoranil; malonic acid, etc.) obtained by this technique are presented.

Another general method for obtaining high resolution NMR spectra of solids is the "dilution" of the spins (the favourable effect of dilution could be easily understood taking into account that dipolar interactions are proportional to r^{-3}, where r is the distance of the spins).

The technique named "Proton Enhanced Induction Spectroscopy" developed by Pines, Gibby and Waugh (from 1972), based on the "dilution" method, utilizes naturally diluted spin systems, e.g. ^{13}C, ^{15}N, occurring along side with abundant spins like ^{1}H, ^{19}F. The rare spins (which possess a very weak homonuclear dipolar coupling, due to their low natural abundance) are first polarized by the abundant spins, then observed during the decoupling of abundant spins, operation which realizes the repression of heteronuclear dipolar broadening. In Chapter 4, entitled "Double Resonance Experiments", beside a basic mathematical account on double resonance, the above mentioned techniques (generally named "Cross Polarization of Dilute Spins") are detailed.

Chapter 5 of the book, "Magnetic Shielding Tensor", groups the data obtained through multiple-pulse and cross-polarization experiments, concerning the magnetic shielding tensors. The importance of such data is revealed from a very interesting point of view by the author : *"the interest in the magnetic shielding tensor can be traced back to the early days of NMR and generations of chemists have utilized the isotropic part of this quantity which is observed in a liquid, as a fingerprint of the chemical bond. In fact, the measurement of chemical shift has been developed into a tool for the investigation of molecular structure. Since now the full symmetric second rank shift tensor becomes available with the advent of the techniques described in this book and it is hoped that a better understanding of the underlying electronic structure will result".*

The data for proton shielding tensor ("the most difficult domain of high resolution NMR in solids") are given for different categories of protons — methylenic, olefinic and aromatic ones — then data for ^{19}F, ^{13}C, ^{15}N, ^{31}P are also given. Tables containing σ_{11}, σ_{22}, σ_{33} (1, 2 and 3 being the axes) and the average value σ for all the above mentioned shielding tensors are included.

In Chapter 6, the "Spin-Lattice Relaxation" is discussed in connection with line-narrowing experiments and the importance of multiple-pulse experiments in such investigation is underlined.

An appendix, in which some mathematical useful aspects of the problems referred to in the text are summarized, is also given in Chapter 7.

A total of 283 references end this interesting book which presents some very modern developments in the field of NMR spectroscopy. The book is a useful tool for physical and organic chemists. A special note for the good printing could also be made.

M. Banciu

NOTE POUR LES AUTEURS

La Revue Roumaine de Chimie publie des articles en anglais, français, russe, allemand ou espagnol. Les auteurs sont priés d'envoyer des articles et des comptes rendus inédits.

Les manuscrits seront dactylographiés à deux intervalles. La bibliographie, les tableaux et la légende des figures seront placés après le texte.

Si l'article fait partie d'une série numérotée, le titre de la partie précédente sera indiqué dans une note au bas de la première page.

Chaque article sera précédé d'un résumé comprenant quinze lignes au maximum.

Les références bibliographiques dans le texte seront faites par des exposants sans parenthèses et paraîtront comme des notes au bas de chaque page.

Les publications périodiques mentionnées dans la bibliographie seront présentées suivant les prescriptions internationales : le nom de l'auteur précédé de l'initiale du prénom, le titre du périodique abbrégé conformément à « Chemical Abstracts », et souligné par une ligne, le numéro du tome, indiqué par des chiffres arabes et souligné par deux lignes, suivi de la première page de l'article ; à la fin, l'année de la parution sera placée entre parenthèses. Le numéro de la revue ne sera pas indiqué si les pages du volume sont numérotées consécutivement. Pour les revues dont les tomes ne sont pas numérotés (par ex. Bull. Soc. Chim. France, etc.), l'année de la parution soulignée par deux lignes précèdera l'indication de la page.

Les textes des livres ou traités inclueront : les noms des auteurs, les initiales du prénom, le titre du livre entre guillemets et sans être souligné, le numéro du tome précédé par l'abréviation « vol. » (ou « Bd. »), le numéro de l'édition, les éditions (the publisher), la localité de la parution du livre, l'année de la parution et la page de la référence précédée par l'abbréviation « p » (ou « S »).

Les brevets seront indiqués comme suit : l'auteur ou la firme, le pays et le numéro du brevet, la date et la revue (Chem. Abstr.). Par ex. : M. Jones (to Union Carbide Co), Brit. Pat. 601 238, 2 septembre 1959, *Chem. Abstr.*, **54**, 12808 (1960).

Si la référence n'a pas été lue en original, on indiquera aussi la revue de référence consultée.

Les diagrammes seront tracés à l'encre de Chine sur papier calque. Les tableaux et les figures (en nombre strictement nécessaire) seront numérotés par des chiffres arabes et leur explication sera donnée dans la légende des figures. Prière de ne pas inscrire les mêmes données dans les tableaux et les figures. Chaque tableau aura un titre. On indiquera dans le texte la place approximative des tableaux et des figures. Les formules chimiques seront incluses dans le texte ; en outre, elles seront transcrites sur papier calque, à l'encre de Chine.

Les auteurs sont priés d'indiquer les caractères italiques (en soulignant les lettres au crayon), ainsi que tout autre caractère spécial ; les préfixes *ortho*, *meta*, *para*, *cis*, *trans*, etc. seront soulignés pour indiquer leurs caractères italiques et ne seront jamais écrits avec des majuscules.

Aucune correction à la main ne sera admise sur le manuscrit. Les corrections seront frappées à la machine. Les lettres grecques ou d'autres symboles spéciaux seront insérés à la main à l'encre clairement.

Le manuscrit sera signé par l'auteur.

La colonne-titre aura 50 lettres au maximum.

L'entière responsabilité du contenu des articles appartient aux auteurs.

PRINTED IN ROMANIA

TRAVAUX PARUS AUX ÉDITIONS DE L'ACADÉMIE DE LA RÉPUBLIQUE SOCIALISTE DE ROUMANIE

C. DRĂGULESCU, E. PETROVICI, **Chimia structurală modernă. Chimia coordinanței** (La Chimie structurale moderne. La Chimie de la coordinence), 1977, 947 p., 70 lei.

I. G. MURGULESCU, **Introducere în Chimia fizică. Vol. I. Atomi, molecule, legătură fizică** (Introduction à la Chimie Physique. Ier vol. Atomes, molécules, liaison chimique), 1976, 560 p., 36 lei.

E. P. BALTĂ, E. BALTĂ, **Introduction to the physical chemistry of the vitreous state**, coédition avec Abacus Press, 1976, 287 p., 31 lei.

H. I. GĂLĂȚEANU, **Radiochimia aplicată. Metode și probleme** (La radiochimie appliquée. Méthodes et problèmes), 1976, 307 p., 19 lei.

C. V. UGLEA, **Cromatografia pe gel permeabil. Noi domenii de aplicare** (La chromatographie sur gel perméable. Nouveaux domaines d'application), 1976, 120 p., 6,75 lei.

FR. A. GOTHARD, **Echilibre lichid-vapori. I. Baze teoretice și metode de calcul** (Equilibres liquide-vapeurs. I. Bases théoriques et méthodes de calcul), 1975, 262 p., 28 lei.

CONST. GH. MACAROVICI, DAN MACAROVICI, **Chimia oxizilor dubli și utilizările lor** (La Chimie des oxydes doubles et leur utilisation), 1975, 194 p., 13 lei.

ELENA CEAUȘESCU, **Research work on synthesis and caracterization of macromolecular compounds. Contributions**, 1974, 251 p., 20 lei.

I. ZUGRĂVESCU et MAGDA PETROVANU, **Chimia N-Ilidelor** (La chimie des N-Ilures, 1974, 347 p., 19 lei.

MARGARETA AVRAM, **Antidăunători** (Pesticides), 1974, 494 p., 41 lei.

CR. SIMIONESCU, VIORICA RUSAN et N. POPA, **Chimia algelor marine** (La Chimie des algues marines), 1974, 211 p., 18 lei.

TIBERIU NĂȘCUȚIU, **Metode radiochimice de analiză** (Méthodes radiochimiques d'analyse), 1973, 384 p., 23 lei.

MARIA FITI, **Dozimetria chimică a radiațiilor ionizante** (Le dosimétrie chimique des radiations ionisantes), 1973, 240 p., 13,50 lei.

MIHAI FLORESCU, **Eficiența economică a cercetării științifice** (L'efficience économique de la recherche scientifique), 1972, 115 p., 15 lei.

GEORGETA LĂZĂRESCU, **Sistematizarea informațiilor în Chimia organică** (La systématisation des informations dans la Chimie organique), 1972, 252 p., 10,50 lei.

1978 FEB 16

I. P. INFORMAȚIA c. 7206

| 43426 |

Lei 25.—

F 1103

ACADÉMIE DE LA RÉPUBLIQUE SOCIALISTE DE ROUMANIE

REFERÁLVA

REVUE ROUMAINE DE CHIMIE

TOME 22
Nos 9—10
Septembre—Octobre

EDITURA ACADEMIEI REPUBLICII SOCIALISTE ROMÂNIA

Rev. Roumaine Chim.

RECHAX, 22, 9—10, p. 1277—1430 (1977), Bucarest

ACADÉMIE DE LA RÉPUBLIQUE SOCIALISTE DE ROUMANIE

COMITÉ DE RÉDACTION

Rédacteur en chef:

I. G. MURGULESCU, membre de l'Académie de la République Socialiste de Roumanie

Rédacteurs en chef adjoints:

A. T. BALABAN et V. EM. SAHINI, membres correspondants de l'Académie de la République Socialiste de Roumanie

Collège de rédaction:

EM. BRATU, ELENA CEAUŞESCU, ECATERINA CIORĂNESCU-NENITZESCU, C. DRĂGULESCU CR. SIMIONESCU, membres de l'Académie de la République Socialiste de Roumanie; P. SPACU, membre correspondant de l'Académie de la République Socialiste de Roumanie; MARGARETA AVRAM, I. HAIDUC, D. I. MARCHIDAN, I. MOLDOVAN, G. NIAC et D. SĂNDULESCU

La Revue Roumaine de Chimie parait 10 fois par an. Toute commande de l'étranger (fascicules ou abonnements) pour les travaux parus aux Editions de l'Académie de la République Socialiste de Roumanie sera adressée à ILEXIM Departamentul Export-Import Carte (Livres)/Departamentul Export-Import Presă (Revues), P.O.B. 136—137, télex 11226, Bucarest 3, str. 13 Decembrie, Roumanie

Les manuscrits, les livres et les revues proposés en échange, ainsi que toute correspondance seront envoyés à la rédaction :

REVUE ROUMAINE DE CHIMIE

23, str. Dumbrava Roşie, Bucarest, Roumanie, téléphone 12 41 60

EDITURA ACADEMIEI REPUBLICII SOCIALISTE ROMÂNIA

125, Calea Victoriei, 71021, Bucarest, Roumanie, téléphone 50 76 80

ORSZÁGOS MŰSZAKI KÖNYVTÁR ÉS DOKUMENTÁCIÓS KÖZPONT 1883

REVUE ROUMAINE DE CHIMIE

Tome 22, Nos 9—10 Septembre—Octobre 1977

I. G. MURGULESCU and A. LEIBOVICI, Internal pressure in liquid metals 1279—1281

S. KIRSCHNER, R. MORASKI, C. MUNIR and R. POLLOCK, Application of the Pfeiffer effect, outer-sphere complexation, and photoresolution techniques to the determination of absolute configuration of dissymmetric coordination compounds . . . . 1283—1288

A. P. KRESHKOV, Proton-electron-hydride concept of the theory of acids and bases in non-aqueous solutions . . . . 1289—1295

П. Г. РОМАНКОВ, Современные проблемы инженерной химии . . . . 1297—1304

I. TSUJIKAWA and M. HARADA, Effect of uniaxial stress on absorption spectra of tetragonal crystals Cs_3CoCl_5 and Cs_3CoBr_5. . . . . 1305—1313

LUCIA CIOHODARU, The electronic structure of some stilbene derivatives. VI. The molecular diagrams of some mono-nitro-stilbene derivatives . . . 1315—1328

Z. KODEJŠ and I. SLÁMA, Viscosity of melts of hydrated lanthanum nitrate 1329—1333

R BOJANA D. ALEKSIĆ and ANA TERLECKI-BARIČEVIĆ, Investigation of the effects of chemical nature of some structural promotors on electric conductivity changes in precipitated ammonia synthesis catalysts in reductive atmosphere . . . . 1335—1342

D. SĂNDULESCU, CONSTANȚA PÂRLOG and C. I. LEPĂDATU, The electronic spectrum of $[Os(II)(NH_3)_5(N_2)]^{2+}$ and the chemical bonding of the dinitrogen molecule . . . . 1343—1346

D. NEGOIU and LIDIA PARUTA, Complex compounds of Cu(I) with triarylstibines. . . . . 1347—1351

A. C. BANCIU, A pentacoordinated Co(II) complex compound derived from 1-methyl-2-carbethoxy-glyoxalanil-(1)-*p*-nitrophenylhydrazone-(2) . . . . 1353—1358

ILEANA I. STĂNOIU, EUGENIA GÂRD, CORNELIA UNCUȚA, F. CHIRALEU and A. T. BALABAN, Isotopic exchange of active methyl hydrogens. IX. Intramolecular kinetic comparison between α-methyl and α-isopropyl groups in pyrylium salts. . . . . 1359—1361

A. TURCU, Reaction of 1,3,7,9-tetranitrophenothiazine-5-oxide with organic bases . . . . 1363—1368

R I. CIOCĂZANU, VIORICA DOGARU et D. ZĂVOIANU, La structure et la réactivité des nitriles. Sur la chaleur de combustion de quelques nitriles alpha, bêta non saturés. . . . . 1369—1373

F. POTMISCHIL und D. RÖMER, Heterocyclen mit perinaphthinden-Gerüst. I. Quartäre Ammoniumsalze des 2,3-Dihydro-benz[d.e]isochinolins . . 1375—1378

Rev. Roumaine Chim. **22**, *9—10*, p. 1277—1430 (1977), Bucarest

N. VLAHOVICI and P. T. FRANGOPOL, A simple semiempirical MO-calculations of electronic spectra and charge distribution in 2,4,6-trimethyl pyrylium cation 1379–1384

R ELENA HOPÎRTEAN, Liquid-membrane electrodes. X. Liquid-membrane electrode for iron(III) determination 1385–1389

R G. BOURCEANU, V. ABABI, GH. POPA, M. SANDULOVICIU, Phenol obtainment from benzene in oxygen plasma generated by a high frequency discharge. III. Kinetics of the process in pulse and steady-state regime . . 1391–1399

R GEORGETA POPESCU and MIRCEA MARINESCU, ^{1}H-N.M.R. characterization of anionic surfactants-polyvinylpyrrolidone interaction 1401–1412

PIERRE LAURENT, Quelques réactions inattendues dans le domaine des hétérocycles saturés 1413–1422

COMPTES RENDUS 1423–1430

Revue Roumaine de Chimie, **22**, *9–10*, 1279–1281 (1977)

INTERNAL PRESSURE IN LIQUID METALS

I. G. MURGULESCU and A. LEIBOVICI
Center of Physical Chemistry str. Galaţi 31, Bucharest, Romania

Received January 22, 1977

Two methods of calculating the internal pressure of liquid metals were developed : one based on the equation of state, the other on the heat of vaporization. The results yielded by the two methods are in good agreement.

In a previous paper [1] we have shown that if the cell model is assumed for liquid metals and the lattice energy is evaluated on the basis of Haber-Thomson [2] theory, the following equation of state is obtained :

$$PV\left(1 - \frac{\sigma}{a}\right) = RT \tag{1}$$

This is the Buehler-Hirschfelder-Curtis [3] equation, whose validity in liquid metals was verified in the work quoted above. From among the quantities in eq. (1), σ is the molecular diameter and a is a distance defined as :

$$a = \gamma^{1/3}\left(\frac{V}{N}\right)^{1/3} \tag{2}$$

The structure factor, γ, is equal to $\sqrt{2}$ as comes out of the X-ray analysis of liquid metals. Eqs. (1) and(2) yield :

$$PV\left(1 - \frac{2N^{1/3}}{\gamma^{1/3}\,V^{1/3}}\,r\right) = RT \tag{3}$$

where r is the radius of liquid particles, the other symbols having the well known meanings.

---

[1] I. G. MURGULESCU and A. LEIBOVICI, *Rev. Roumaine Chim.*, **19**, 739 (1974).

[2] F. HABER, *Berl. Akad. Ber.*, **506**, 990 (1919) ; J. J. THOMSON, *Phyl. Mag.*, **43**, 721 (1922).

[3] J. O. HIRSCHFELDER, C. F. CURTIS and R. B. BIRD, "Molecular Theory of Gases and Liquids", Wiley, New York, 1954, p. 286.

The pressure P in the equations above may be regarded as the sum of two terms

$$P = P_i + p \tag{4}$$

where P_i is the internal pressure and p the outside one. In normal conditions the outside pressure is very small as compared to the internal one, so that it can be neglected. Eq. (3) could then be employed in the evaluation of internal pressure:

$$P_i = \frac{RT}{\left(1 - \frac{2N^{1/3}}{\gamma^{1/3}V^{1/3}}\, r\right) V} \tag{5}$$

On the other hand the internal pressure is defined as:

$$P_i = \left(\frac{\partial E}{\partial V}\right)_T \tag{6}$$

which can be replaced by:

$$P_i = \frac{\lambda}{V} \tag{7}$$

where λ is the heat of vaporization and V the molar volume of the liquid

We have then available two equations for the calculation of the internal pressure of liquid metals (as it was for ionic liquids [4]), so that a comparison of the results obtained with eqs. (5) and (7) is useful; a good agreement would be a proof for the validity of assumptions on which their deduction was founded.

Table 1

Internal pressures in liquid metals

	T_m, K	V_m, cm³	r, A	cal/mol	P_i, atm	
					eq. (5)	eq. (7)
Li	453.15	13.56	1.519	32 300	101 600	68 300
Na	370.95	24.73	1.858	23 400	40 400	31 500
K	336.75	47.12	2.272	19 000	17 200	11 300
Rb	311.95	58.08	2.470	18 100	13 300	11 300
Cs	311.65	72.29	2.654	15 900	9 400	8 800
Cu	1356.15	7.95	1.278	72 800	390 600	396 500
Ag	1239.95	11.82	1.444	60 000	216 500	192 700
Au	1336.15	11.40	1.442	81 800	306 000	276 700
Al	933.15	11.39	1.432	69 600	260 600	164 200
Pb	600.55	19.02	1.750	42 000	94 200	198 200
Fe	1810.15	7.93	1.241	81 300	437 300	304 300
Co	1765.15	7.67	1.253	—	—	443 800
Ni	1726.15	7.56	1.246	89 400	504 400	432 900

---

[4] I. G. Murgulescu and E. Sălăgeanu, *Rev. Roumaine Chim.*, **17**, 603 (1972).

Table 1 is thought to facilitate such a comparison. The melting point was chosen as reference and it is listed in the first column of Table 1. The molecular volume V_m and atomic radii r have been taken from reference,[1] while the heats of vaporization from.[5]

The calculations have been restricted to true metals. The elements with complex lattices which do not behave like metals (Bi, Sn, Sb, etc.) have been left away.

Examination of Table 1 shows that the agreement between the values of internal pressure calculated by eqs. (5) and (7) is acceptable, though not excellent. Large inexplicable deviations between the two sets of values have been obtained with aluminium and lead.

The values of internal pressure of liquid metals are, for heavy metals, close to those of ionic liquids (some ten thousand atmospheres). In fused light metals the internal pressures are much lower, ranging between 1000 and 10000 atm.

---

[5] C. J. SMITHELLS, "Metals References Book", vol. 2, 2nd ed., Butterworth, London, 1955, p. 575.

Table I is thought to facilitate such comparison. The melting point was chosen as reference, and it is listed in the first column of Table I. The molecular volume V_a and atomic radii r have been taken from reference [1], while the heats of vaporization from[8].

The calculations have been restricted to true metals. The elements with complex lattices which do not behave like metals (Bi, Sn, Sb, etc.) have been left away.

Examination of Table I shows that the agreement between the values of internal pressure calculated by eqs. (6) and (7) is acceptable, though not excellent. Large inexplicable deviations between the two sets of values have been obtained with aluminium and lead.

The values of internal pressure of liquid metals are, for heavy metals, close to those of ionic liquids (some ten thousand atmospheres). In light metals the internal pressures are much lower, ranging between 1000 and 10000 atm.

---

[1] [illegible] Smithells, "Metals Reference Book", vol. 1, 2nd ed., Butterworths, London.

Revue Roumaine de Chimie, **22**, *9 – 10*, 1283–1288 (**1977**)

Dedicated to the 70th anniversary
of Professor CORIOLAN DRĂGULESCU

APPLICATION OF THE PFEIFFER EFFECT, OUTER-SPHERE COMPLEXATION, AND PHOTORESOLUTION TECHNIQUES TO THE DETERMINATION OF ABSOLUTE CONFIGURATION OF DISSYMMETRIC COORDINATION COMPOUNDS

STANLEY KIRSCHNER, RICHARD MORASKI, CHRISTY MUNIR, and RONALD POLLOCK
Department of Chemistry, Wayne State University, Detroit, Michigan, U.S.A.

Received September 6, 1976

It is possible to predict the absolute configuration of optically labile complexes utilizing the Pfeiffer Effect. The Pfeiffer Effect occurs as an equilibrium displacement of the enantiomers of a racemic mixture, which are in equilibrium in solution. The displacement is induced *via* hydrogen bonding of the optically active environment substance with the *pi* electron cloud systems of the complex. It is possible to predict the absolute configuration of optically stable complexes by utilizing outer-sphere complexation with optically active external groups. It is proposed that these interact preferentially with one enantiomer of the complex via hydrogen bonding between a donor atom on a ligand of the complex and one on the external group. Photoresolution techniques may be employed by irradiation of frozen solutions of racemic complexes with circularly polarized light of one chirality to effect preferential decomposition of one enantiomer of a racemic, photodecomposable complex.

INTRODUCTION

The Pfeiffer Effect[1] is the change in the optical rotation of a solution of an optically active compound (the "environment substance") when a racemic mixture of certain dissymmetric coordination compounds is added to it. Such a change is observed with optically labile complexes (e.g., D, L-[Ni(o-phen)$_3$]Cl$_2$), but not with optically stable complexes (e.g., D, L-[Co(en)$_3$]Cl$_3$). The Effect is known in polar solvents such as water, [2] dimethylformamide, [3] and glacial acetic acid and not in non-polar solvents such as benzene. Further, the magnitude of the Effect is proportional to the concentrations of both the complex and the environment substance, making it possible to develop a series of equations for observed Pfeiffer rotation, specific Pfeiffer rotation, and molar Pfeiffer rotation which are analogous to those for observed optical rotation, specific rotation, and molar rotation, respectively. [2] They are:

---

[1] P. PFEIFFER and K. QUEHL, *Ber., dtsch. chem. Ges.*, **64**, 2667 (1931); **65**, 560 (1932).

[2] S. KIRSCHNER, N. AHMAD, and K. MAGNELL, *Coord. Chem. Revs.*, **3**, 201 (1968).

[3] S. KIRSCHNER and K. R. MAGNELL, *Adv. Chem. Ser.* (*Am. Chem. Soc.*), **62**, 366 (1966).

Observed Pfeiffer Rotation: $\mathrm{P_{obs}} = \alpha_{e+c} - \alpha_e$

Specific Pfeiffer Rotation: $[P]^t_\lambda = P_{\mathrm{obs}}/(c)\,(e)\,(d)$

Molar Pfeiffer Rotation: $[P_M]^t_\lambda = [P]\,(\mathrm{MW})/100 = P_{\mathrm{obs}}/[c]\;[e]\,(d_m)$

where α_{e+c} is the observed rotation of the solution containing both the environment substance and the complex, α_e is the observed rotation of the solution containing only the environment substance, (c) is the complex concentration in g./ml., (e) is the environment substance concentration in g./ml., d is the path length in dm., $[c]$ is the molar concentration of the complex, $[e]$ is the molar concentration of the environment substance, and (d_m) is the path length in meters.

DISCUSSION

NATURE OF THE PFEIFFER EFFECT

It has been proposed by Dwyer and his co-workers, [4] and later by Kirschner and his co-workers, [5] that there is an equilibrium between the enantiomers of a racemic mixture of a dissymmetric complex in solution, and that this equilibrium is displaced in the presence of an optically active environment substance, in favor of one or the other of the complex enantiomers. For the $[\mathrm{Ni}(o\text{-phen})_3]\mathrm{Cl}_2$ complex, this displacement of equilibrium may be represented by the following equation, where *levo*-malic acid produces a displacement in favor of the levorotatory enantiomer (*D*-line) of the complex:

$$\Lambda_{c3}(+)_D[\mathrm{Ni}(o\text{-phen})_3]^{2+} \rightleftarrows \Delta_{c3}\,(-)_D\text{-}[\mathrm{Ni}(o\text{-phen})_3]^{2+}$$

Confirmation of this proposal can be found in the ORD and CD spectra of the $[\mathrm{Cr}(\mathrm{C_2O_4})_3]^{3-}$ and $[\mathrm{Co}(\mathrm{C_2O_4})_3]^{3-}$ anions, which are the same for the pure enantiomers, resolved by conventional means, as for the enantiomers resolved *via* the Pfeiffer Effect. [5]

pH DEPENDENCE OF THE PFEIFFER EFFECT

It was noted[6] that, for the system described above, the magnitude of the Pfeiffer Effect decreased and the rate of appearance of the Effect increased markedly with increasing pH of the solution. This was unexpected, since conversion of malic acid to monohydrogen malate (or malate) anion (negative ions) was expected to increase the interaction between the complex (positive ions) and the environment substance, which was in turn, expected to enhance the Pfeiffer Effect magnitude.[6,7] However, it is now possible to explain this observation (***vide infra***) on the basis of the nature of the interaction between the two species.

---

[4] F. P. Dwyer, E. C. Gyarfas, and M. F. O'Dwyer, *Nature*, **167**, 1036 (1951).

[5] S. Kirschner, *Rec. Chem. Prog.*, **32**, 33 (1971).

[6] N. Ahmad, Ph. D. Dissertation, Wayne State University, Detroit, Michigan, U.S.A., 1969.

THE ABSOLUTE CONFIGURATION OF DISSYMMETRIC COORDINATION COMPOUNDS

The absolute configurations of more than fifty coordination compounds have been determined by x-ray crystallographic techniques, using the anomalous scattering method. On the basis of the currently accepted IUPAC nomenclature for such complexes, the absolute configuration of the $(+)_D[\mathrm{Co(en)_3}]^{3+}$ cation is referred to as Λ_{c_3}, since this complex takes the form of a left-handed propeller when viewed along the c_3 symmetry axis. The absolute configurations of organic compounds are referred to as "R" or "S" depending upon the atomic masses of the atoms bound to the asymmetric carbon, according to a series of rules developed by Cahn, Prelog, and Ingold.[8] Absolute configurations of many organic compounds have been determined by physical and chemical techniques.

THE PFEIFFER EFFECT AND ABSOLUTE CONFIGURATION

It was observed by the present authors that the same enantiomer of $[\mathrm{Co}(o\text{-phen})_3]^{2+}$ is enriched during Pfeiffer Effect experiments, whether the environment substance is $(+)_D$ cinchonine hydrochloride, $(-)_D$ tartaric acid, or $(-)_D$ malic acid, which suggests that these three substances have the same absolute configuration. Later experiments in the authors' laboratories with a series of optically active organic environment substances confirmed the proposal that environment substances of the same absolute configuration produce an enrichment of the same complex enantiomer, regardless of the sign of rotation of the environment substance. For example, the following table shows the enantiomers which are enriched when the complex *D*, *L*-$[\mathrm{Co}(o\text{-phen})_3]^{2+}$ undergoes the Pfeiffer Effect.

Determination of the absolute configuration of organic environment Substances *via* the Pfeiffer Effect on $[\mathrm{Co}(o\text{-phen})_3]^{2+}$

Environment Compound	*Enriched Complex Enantiomer (D-line)*
$S(-)_D$ tartaric acid	levo enantiomer
$S(-)_D$ malic acid	levo enantiomer
$S(+)_D$ aspartic acid	levo enantiomer
$S(+)_D$ alanine	levo enantiomer
$R(+)_D$ tartaric acid	dextro enantiomer
$R(+)_D$ malic acid	dextro enantiomer
$R(-)_D$ mandelic acid	dextro enantiomer

The previous experiments suggested to the authors that the same environment compound (e.g., $S(-)_D$ malic acid) should enrich complex enantiomers of the same absolute configuration, regardless of the sign of

---

[7] S. Kirschner, *Coordin. Chem. Rev.*, **2**, 461 (1967).

[8] R. S. Cahn and C. K. Ingold, *J. Chem. Soc.*, **1951**, 612; R. S. Cahn, C. K. Ingold, and V. Prelog, *Experientia*, **12**, 81 (1956).

rotation of these enantiomers, and that this should permit prediction of the absolute configurations of these complexes, if the absolute configuration of the environment substance and the signs of rotation of the enriched complex enantiomers are known. This was found to be the case, as is shown in the following table :

Determination of the Absolute Configuration of Dissymmetric Coordination Compounds via the Pfeiffer Effect with $S(-)_D$ Malic Acid

Complex Enantiomer	*Absolute Configurations of the Enriched Enantiomer and Sigh of Rotation* (*D-line*)
$[\mathrm{Ni}(o\text{-phen})_3]^{2+}$	Δ_{c3} Levo
$[\mathrm{Fe}(o\text{-phen})_3]^{2+}$	Δ_{c3} Dextro
$[\mathrm{Co}(o\text{-phen})_3]^{2+}$	(Δ_{c3} predicted) Levo

Notice that $S(-)$ malic acid as an environment substance results in an enrichment of the Δ_{c_3} isomer of a complex, regardless of the sign of rotation of the complex.

NATURE OF THE INTERACTIONS OCCURRING DURING THE PFEIFFER EFFECT

In order for the Pfeiffer Effect to occur *via* the mechanism proposed for it, the environment compound and the complex must (a) attain close enough approach to each other to exert a steric influence on the equilibrium, and (b) interact with each other sufficiently to inhibit the conversion of one enantiomer into the other. It is proposed that this close approach and interaction occur during the Pfeiffer Effect. For example, for the system $[\mathrm{Ni}(o\text{-phen})_3]^{2+}$ and $S(-)_D$ malic acid, this interaction is proposed to be hydrogen bonding between the OH groups on the malic acid and the *pi* electron cloud systems [9–12] of the *ortho*-phenanthroline ligands. This proposal accounts for two important phenomena : (a) the preferential inhibition of the conversion of the $(-)_D$ enantiomer of the complex to the $(+)_D$ isomer, permitting enrichment of the $(-)_D$ enantiomer, and (b) the diminution of the magnitude of the Pfeiffer Effect with increasing pH of the system. The preferential inhibition occurs because of the more facile hydrogen bond formation of the "S" enantiomer of malic acid to the Δ_{c3} form of the complex than to the Λ_{c3} form. The diminution in the magnitude of the Pfeiffer Effect with increasing pH occurs because loss of the carboxyl hydrogens with a pH rise removes the protons necessary for hydrogen bond formation between the carboxyl oxygens and the *pi* electron clouds of the *ortho*-phenanthroline rings.

OUTER-SPHERE COMPLEXATION

It is proposed that optically stable complexes (e.g., $D, L[\mathrm{Co(en)}_3]^{3+}$) do not undergo the Pfeiffer Effect in the sense of displacement of an equilibrium between the *dextro* and *levo* enantiomers of the complex. However,

---

[9] H. Iwamura, *Tetrahedron Letters*, **26**, 2227 (1970).

[10] Zen-Ichi Yoshida, and E. Osawa, *J. Amer. Chem. Soc.*, **88**, 4019 (1966).

[11] P. J. Krueger and H. D. Mettee, *Tetrahedron Letters*, **15**, 1587 (1966).

[12] M. Oki ans H. Iwamura, *J. Amer. Chem. Soc.*, **89**, 576 (1967).

it is possible for optically stable complexes to undergo outer-sphere association with groups external to the coordination sphere. Such outer-sphere complexation may affect significantly the optical rotation and circular dichroism of such complexes, whether or not the external groups are optically active. For example, external halide ions[13] significantly alter the optical rotation of the ethylenediamine complex mentioned above, and the same halide ion in different concentrations will affect the optical rotation and circular dichroism of the complex differently.

OUTER-SPHERE COMPLEXATION AND THE ABSOLUTE CONFIGURATION OF COMPLEXES

Mason and Norman[14] noted that when a solution of optically inactive $[Co(NH_3)_6]^{3+}$ is added to a solution which contains a 400-fold excess of diethyl-*d*-tartrate, a negative Cotton Effect is induced in the circular dichroism spectrum of the complex, near the absorption peak of the optically inactive complex. The present authors have noted the inducement of a positive Cotton Effect when D, L-$[Co(en)_3]^{3+}$ is placed in contact with a 400-fold excess of $S(-)_D$ malic acid, near the absorption peak of the complex (Cotton Effect peak at 460 nm). In addition, they have found that a negative Cotton Effect is induced in the $[Cr(NH_3)_6]^{3+}$ complex upon addition of a 400-fold excess of $R(+)_D$ tartaric acid.

In order to explain these results, the authors studied the circular dichroism spectrum of each enantiomer of the $[Co(en)_3]^{3+}$ complex in the presence of a 400-fold excess of $S(-)_D$ malic acid. They noted a stronger interaction of the malic acid with the $\Delta_{c3}(-)$ enantiomer of the complex than with the opposite isomer. The increase in ellipticity in the former case is significantly greater than the decrease in the ellipticity in the latter, resulting in a net positive Cotton Effect, with an observed peak at 460 nm. Therefore, it is predicted that the enantiomer of a stable complex which shows greater interaction with $R(+)_D$ tartaric acid will be the Λ_{c_3} enantiomer. This was confirmed with the $[Co(en)_3]^{3+}$ complex, which gives a negative Cotton Effect (for the racemic complex with a 400-fold excess of $(+)_D$ tartaric acid). That is, it is the $\Lambda_{c_3}(+)_D$ enantiomer of the complex which interacts more strongly with $R(+)_D$ tartaric acid than with the opposite enantiomer, giving rise to a negative Cotton Effect when the racemic complex is treated with excess $(+)_D$ tartaric acid.

NATURE OF THE INTERACTIONS OCCURRING DURING OUTER-SPHERE COMPLEXATION

In order for the external group and the complex to interact, there must be close approach between them. The approach is not so close as to affect the visible absorption spectrum significantly. It is therefore proposed that the interaction which occurs is hydrogen bonding between the nitrogens of the ethylenediamine ligand and the oxygens of the tartrate or malate groups. Such hydrogen bonding would not be expected to occur between the complex and malate or tartrate if the ligand were N, N, N', N'-tetraethylethylenediamine, and experiments are underway to test this prediction. In such cases, outer-sphere interactions of the type described would not be expected to occur.

---

[13] M. J. Albinack, D. C. Bhatnager, S. Kirschner and A. J. Sonnessa, *Canad. J. Chem.*, **39**, 2360 (1961).

[14] S. F. Mason and B. J. Norman, *Chem. Commun.*, **1965**, 335.

PHOTORESOLUTION AND ABSOLUTE CONFIGURATION

There are conflicting reports in the literature about the ability of circularly polarized light of one chirality to decompose preferentially one enantiomer of a racemic mixture of a dissymmetric complex in solution. Jaeger[15] reports that his efforts to achieve this with *D*, *L*-$[Co(C_2O_4)_3]^{3-}$ were unsuccessful, while Tsuchida[16] reports success with this complex. The authors of this report have successfully irradiated a frozen solution of this complex with circularly polarized light of one hand, and obtained optical activity in accord with that predicted. That is, when left-handed circularly polarized light is used, the $(-)_D$ λ_{c3} enantiomer of the complex absorbs this light to a greater extent than the opposite enantiomer. Thus, the $(-)_D$ enantiomer is decomposed preferentially by the radiation ($\lambda = 420$ nm), leaving the $(+)_D$ enantiomer in excess in the solution. It is possible to identify this enantiomer by its optical rotatory dispersion curve.

ACKNOWLEDGEMENT. The authors wish to express their appreciation to the U. S. National Science Foundation for a grant which contributed significantly to the progress of this investigation, as well as to the Romanian Council for Science and Technology. The authors also wish to acknowledge the significant assistance and contributions to this work of Professor Coriolan Dragulescu (Timisoara) and Petru Spacu (Bucharest).

---

[15] F. M. Jaeger and G. Berger, *Rec. Trav. chim.*, **40**, 153 (1921).

[16] R. Tsuchida, A. Nakamura, and M. Kobayashi, *J. Chem. Soc. Japan*, **56**, 1335 (1935).

Revue Roumaine de Chimie, **22**, *9–10*, 1289–1295 (1977)

Dedicated to the 70th anniversary
of Professor CORIOLAN DRĂGULESCU

PROTON-ELECTRON-HYDRIDE CONCEPT OF THE THEORY OF ACIDS AND BASES IN NON-AQUEOUS SOLUTIONS

A. P. KRESHKOV
Mendeleev Chemical Technological Institute, Moscow, U.S.S.R.

Received September 11, 1976

Acid-base properties of compounds of different elements in non-aqueous solutions have been examined. It has been established that it is possible to predict the acid-base properties of substance in given medium and to explain acid-base properties from the position of the Proton-Electron-Hydride concept of the theory of acids and bases, based on the two reactions of protons with electrons and with the electron carriers — hydride ions — hydrogen ions antipodes.

The existing theories of acids and bases were criticized by many scientists since many new facts were discovered that did not agree with the former theories:

1) It was established that water is not the only solvent allowing for electrolytic dissociation.

2) Many substances considered non-electrolytes by Arrhenius, in certain conditions are electroconductive.

3) Acid-base interaction takes place not only in aqueous but in non-aqueous solutions as well. The latter contain acids and bases that have nothing in common with the former concepts of acids and bases.

4) Scientists have proved the existence of acids that contain no hydrogen whereas Brönsted's theory does not provide for a substance containing no hydrogen to display acidic properties.

5) In spite of Lewis and Pearson's viewpoint which does not take into account the influence of medium on the behaviour of solutes scientists have established the influence of nature and physico-chemical properties of solvent on physico-chemical properties of solutes.

Investigations in the field of analytical chemistry of non-aqueous solutions have given us new ideas about "acid" and "base", based on the two major reactions of protons (including solvated hydrogen ions) with electrons generated on the electrode and with the electron carriers — hydride ions — which are hydrogen ions antipodes.

This may be illustrated by the following scheme :

$$\text{a)}\quad p + e \rightarrow \frac{1}{2} H_2$$

$$\text{b)}\quad H^+_{sol} + H^- \rightarrow \underset{(H_2)}{H:H} + \underset{(\text{solvent})}{n\,HS}$$

Protons display acidic properties regardless of the fact whether they are capable of dissociation. Acidic properties may also be displayed by substances that contain no hydrogen.

1) From the point of view of Proton-Electron-Hydride concept the acidic properties are displayed not only by free and solvated protons but also by bound protons (proton carriers), namely :
H_2S^+, $C_2H_5OH_2^+$, $CH_3COOH_2^+$, $C_5H_5NH^+$, NH_4^+, RNH_3^+, $R_2NH_2^+$, R_3NH^+, Mg^{2+}, Ca^{2+}, Ba^{2+}, Zn^{2+}, Cd^{2+}, Hg^{2+}, Al^{3+}, Fe^{3+}, Ga^{3+}, In^{3+}, Tl^{3+}, SO_3H^+, NO^+, $SeOCl^+$, $H_2NO_3^+$, BiO^+, UO_2^{2+}, SbO^+, SbO_2^+, VO^{3+}, VO_2^+, $Fe(OH)^{2+}$, $Fe(OH)_2^+$ etc.

2) The substances listed below may also be referred to as acids : all generally known proton inorganic acids and organic acids O—H, C—H, COOH, sulphoxylic, phosphonic, etc. ;

3) positively charged compounds, complex and solvated ions in a state that corresponds to the given medium, which may form in aqueous and non-aqueous solutions, as well as in absence of a solvent under influence of various factors : electrolytic and thermal dissociation, tautomerization, polarization disproportionation, electrical charge, collision with bases attacking them etc. ;

4) negatively charged compounds, complex and solvated ions with relatively higher acidity constants than basicity constants : HSO_4^-, $H_2PO_4^-$, $HOOC-COO^-$ etc. ;

5) a number of coordinatively unsaturated compounds having no free electron pairs for the formation of stable electron attachment of one of its atoms, but capable of attracting foreign free electron pairs ; BCl_3, $AlCl_3$, PCl_3, $(C_6H_5)_3C^+$;

6) protolytic (mainly protogenic) solvents.

The strongest basic properties are displayed by free or solvated electrons neutralising not only generally known inorganic and organic acids, proton carriers, hydrogen ions etc., but also the hydrogen ions of well-known strong bases :

$$\text{a)}\quad H_3O^+ + e \rightarrow \frac{1}{2} H_2 + H_2O$$

$$\text{b)}\quad H_2O \quad + e \rightarrow \frac{1}{2} H_2 + OH^-$$

c) $OH^- + e \rightarrow \frac{1}{2}H_2 + O^{2-}$

d) $NH_4^+ + e \rightarrow \frac{1}{2}H_2 + NH_3$

e) $NH_3 + e \rightarrow \frac{1}{2}H_2 + NH_2^-$

f) $NH_2^- + e \rightarrow \frac{1}{2}H_2 + NH^{2-}$

These reactions and similar ones are essentially different from oxidation — reduction reactions when electrons transfer from a reducer to an oxidizer.

Basic properties in corresponding media under certain conditions may be displayed by :

1) all the electron carriers negatively charged simple compounds, complex and solvated ions in a state corresponding to a given medium, which may form in aqueous and non-aqueous solutions, as well as in the absence of a solvent under the influence of various factors, namely : OH^-, SH^-, O^{2-}, S^{2-}; HCO_3^-, CO_3^{2-}, PO_4^{3-} — (in H_2O); HF_2^- — (in H_2F_2); NH_2^- — (in NH_3); CH_3COO^- — (in CH_3COOH); $C_2H_5O^-$ — (in C_2H_5OH); $SeOCl_3^-$ — (in $SeOCl_2$); HSO_4^- — (in H_2SO_4); $SO_2Cl_3^-$ — (in SO_2Cl_2) etc.

The interaction of such bases with acids is accompanied by formation of weak electrolytes, stable complexes, little soluble substances and neutral molecules.

2) Positively charged compounds, complex and solvated ions characterized by relatively higher basicity constants than their acidity constants :

3) Compounds which (like hydride ions) have free electron pairs capable to unite with coordinatively unsaturated atoms of other compounds : MeO, MeOH, $MeNH_2$, NH_3, $(CH_3)_3N$ etc. ;

4) Protophilic solvents;

5) All generally known inorganic and organic bases.

A strongly marked affinity to proton (see Table I) is one of the major indications of bases. Water is the weakest of all the bases listed in table I. The bearers of electrons : NH_2^-, CO_3^{2-}, S^{2-}, O^{2-}, H^- have more affinity to proton compared with hydroxyl ions. Hydride ions which have the highest affinity to proton among other well-known ions are the strongest base of all the electron bearers.

Thus, the terms "acid" and "base" cover a greater variety of chemical compounds. These include not only mobile hydrogen and hydroxyl ions, but also compounds that under certain conditions (primarily depending on the medium and attacking agent) demonstrate acidic or basic properties.

Table 1

Proton affinity

Electron carriers	Proton carriers	kJ/Mol
H_2O	H_3O^+	773
NH_3	NH_4^+	890
ClO_4^-	$HClO_4$	1193
HSO_4^-	H_2SO_4	1239
I^-	HI	1285
Br^-	HBr	1319
NO_3^-	HNO_3	1340
Cl^-	HCl	1361
HS^-	H_2S	1436
CH_3COO^-	CH_3COOH	1436
$C_6H_5COO^-$	C_6H_5COOH	1444
$HCOO^-$	HCOOH	1453
CN^-	HCN	1457
F^-	HF	1520
OH^-	H_2O	1604
NH_2^-	NH_3	1754
SO_4^{2-}	HSO_4^-	1803
CO_3^{2-}	HCO_3^-	2085
S^{2-}	HS^-	2265
O^{2-}	OH^-	2575
H^-	H^+_{sol}	>2575

Unlike other theories of acids and bases, based on the indispensable condition that acids contain hydrogen, the above concept is not founded on the "cult of hydrogen".

According to this concept, the acid-base interaction may occur not only between reacting substances containing hydrogen, but also between aprotonic (containing no hydrogen) acids and bearers of protons and electrons. Moreover, one and the same substance may display acidic properties in some cases and basic ones in other cases depending upon various conditions.

Not only electrolytes behave in a different way in various solvents, but ions that form them display different acidic and basic properties. For example,

$$\text{a) } \underset{A}{HCl} + \underset{B}{NH_3} \xrightarrow{NH_3} NH_4^+ + Cl^-$$

$$\text{b) } \underset{B}{HCl} + \underset{A}{H_2F_2} \xrightarrow{H_2F_2} H_2Cl^+ + HF_2^-$$

$$\text{c) } \underset{B}{H_2F_2} + \underset{A}{HClO_4} \xrightarrow{H_2F_2} H_3F_2^+ + ClO_4^-$$

When dissolving HCl in amphoteric solvent (H_2O) the acidic properties are displayed by hydrogen ions, basic Cl^- ions. HCl has stronger acidic properties in protophilic (NH_3) solvent than in water, while Cl^- ions practically show no sign of basic properties in such a strong protophilic solvent as NH_3. HCl shows no acidic properties in protogenic (H_2F_2) solvent and is a base, while Cl^- ions behave like a strong base. Finally, H_2F_2 is a base in the presence of $HClO_4$.

This means that not all cations and anions (including OH^-) under all circumstances regardless of the medium display equal acidic or basic properties.

Acid-base interactions. The reactions between acids and bases may occur not only in aqueous and non-aqueous solutions, but also in vacuum (between protons and electrons) in air and gas medium, in liquified gases, in liquid solvents, melts etc.

The fundamental processes of acid-base interaction may be presented in the form of the following equations of reactions:

Acids: Bases:

1) $2\,HOH + CaH_2 \rightarrow Ca(OH)_2 + 2\,H_2$

2) $8\,HCl + Mg_3N_2 \xrightarrow{H_2O} 3\,Mg^{2+} + 2\,NH_4^+ + 8\,Cl^-$

3) $2\,HAn + KNH_2 \xrightarrow{NH_3} NH_4^+ + K^+ + 2An^-$

4) $HCl + NH_3 \xrightarrow[\text{solvent}]{\text{without}} NH_4Cl$

5) $Hg(NO_3)_2 + H_2S \xrightarrow{SO_2Cl_2} HgS + 2\,H^+ + 2\,NO_3^-$

6) $SiO_2 + Na_2CO_3 \xrightarrow{t^\circ} Na_2SiO_3 + CO_2$

7) $2\,H_2F_2 + SiO_2 \xrightarrow{H_2F_2} SiF_4 + 2\,H_2O$

8) $3\,SiF_4 + 2\,H_2O \rightarrow SiO_2 + H_2SiF_6$

9) $SiF_4 + 8\,NH_3 \xrightarrow{NH_3} 4\,NH_4^+ + Si(NH_2)_4 + 4F^-$

10) $(NH_4)_2SO_4 + K_2CO_3 \xrightarrow{NH_3} NH_4^+ + CO_2 + 2\,K^+ + SO_4^{2-} +$
$+ NH_3 + OH^-$

11) $CH{\equiv}CH + NaH \rightarrow CH{\equiv}CNa + H_2$

12) $ArCH_3 + LiH \rightarrow ArCH_2Li + H_2$

13) $4\,NH_4Cl + LiAlH_4 \xrightarrow{NH_3} AlCl_3 + 4\,NH_3 + 4\,H_2$

14) $NH_4Cl + KNH_2 \xrightarrow{NH_3} 2\,NH_3 + K^+ + Cl^-$

15) $MgCl_2 + 2\,C_2H_5ONa \xrightarrow{C_2H_5OH + RCOR} (C_2H_5O)_2Mg + 2\,NaCl$

16) $2\,HClO_4 + MgCl_2 \xrightarrow{(CH_3CO)_2O + CH_3COOH + CHCl_3} Mg(ClO_4)_2 + 2\,HCl$

As illustrated above, the acid-base interaction is not necessarily accompanied by the formation of salt and solvent molecules. In some cases the neutralization process is stipulated by the formation of covalent bond between atoms of bases and acids.

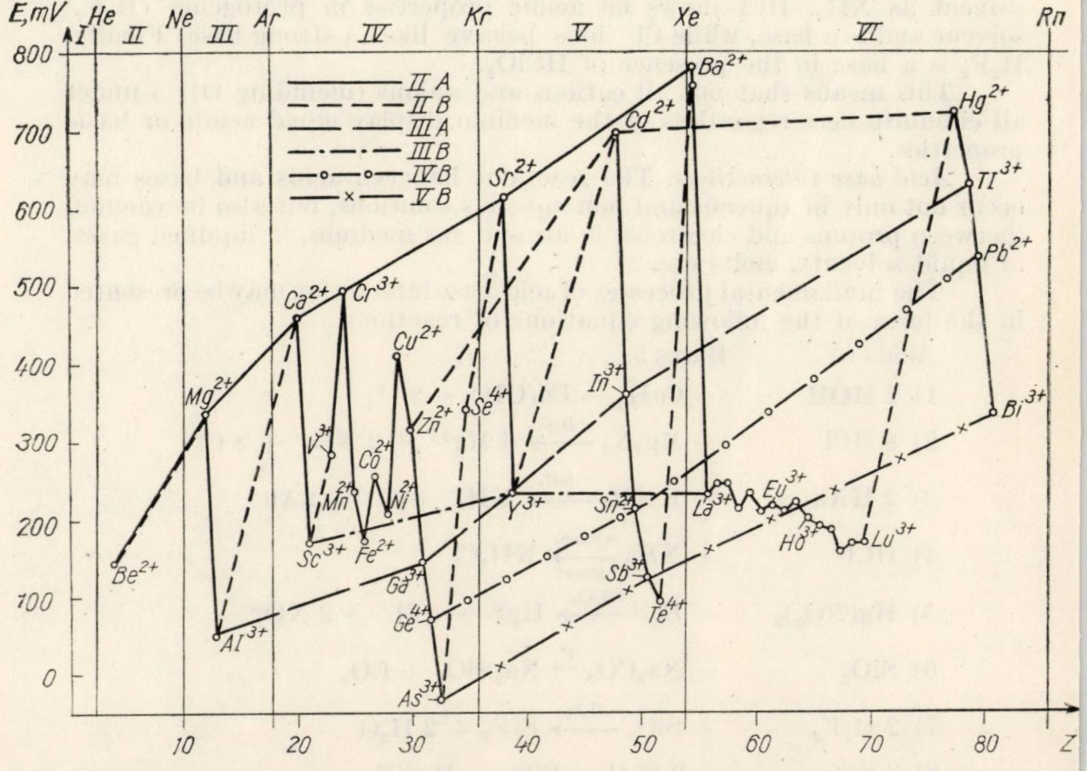

Fig. 1. — The dependence of E, mV value of iodides of some elements on ionic radius of cation in meth ethyl ketone medium (within the limits of Periodic groups).

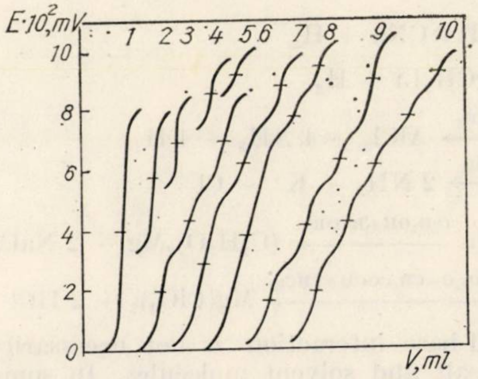

Fig. 2. — The curves of automatic titration for Mg^{2+}, Ca^{2+}, Sr^{2+}, Ba^{2+} perchlorates and their two, three and four component mixtures with perchloric acid by 0.1 N standard solution of potassium hydroxide in butanol—acetone medium: 51 — $HClO_4$; 2 — $Mg(ClO_4)_2$; 3 — $Ca(ClO_4)_2$; 4 — $Sr(ClO_4)_2$; — $Ba(ClO_4)_2$; 6 — $HClO_4 + Mg(ClO_4)_2 + Ca(ClO_4)_2$; 7 — $HClO_4 + Ca(ClO_4)_2 + Sr(ClO_4)_2$; 8 — $HClO_4 + Sr(ClO_4)_2 + Ba(ClO_4)_2$; 9 — $HClO_4 + Mg(ClO_4)_2 + Ca(ClO_4)_2 + Sr(ClO_4)_2$; 10 — $HClO_4 + Mg(ClO_4)_2 + Ca(ClO_4)_2 + Sr(ClO_4)_2 + Ba(ClO_4)_2$.

Furthermore, Proton-Electron-Hydride concept differs considerably from other fundamental concepts of acid and bases theories. At the same time it does not contradict some deeply-rooted concepts of other authors. The present theory supplements them, further developing our notion of acids and bases which was founded by Russian school headed by D. I. Mendeleev and continued by Soviet scientists.[1,2]

The above concept has definite importance for the solution of some practical problems. For example, the study of non-aqueous solutions enabled us to establish certain dependence of acid-base properties of elements in accordance with their position in the Periodical System of elements, with the degree of oxidation of elements, with ionic radius and physico-chemical properties of solvents (See Fig. 1).

It has been proved for instance, that nitrates, chlorides, iodides and perchlorates of barium, magnesium, calcium, strontium and some other compounds, which have nothing in common with acids and bases in the usual sense, display different strength of acid-base properties in the non-aqueous solutions. This enabled us to develop new methods of differentiated titration of multicomponent mixtures of the above mentioned salts, etc. (See Figs. 2, 3).[3-5]

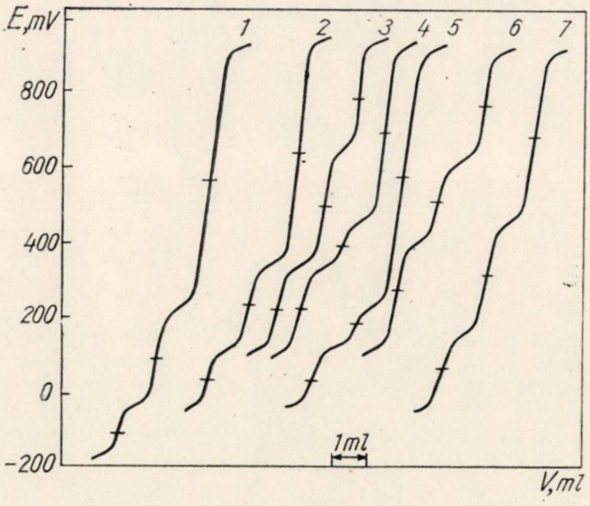

Fig. 3. — The curves of automatic titration of three component mixtures of arsenic (III), antimony (III), and bismuth (III) with iodides of other elements by 0.1 N isopropanol solution of potassium hydroxide in methyl ethyl ketone medium :

1 — $HI + AsI_3 + MnI_2$; 2 — $AsI_3 + SbI_3 + BiI_3$; 3 — $SbI_3 + BiI_3 + TlI_3$; 4 — $SbI_3 + MgI_2 + SbI_2$; 5 — $AsI_3 + GaI_3 + MnI_2$; 6 — $SbI_3 + CaI_2 + SrI_2$; 7 — $AsI_3 + FeI_2 + CaI_2$.

---

[1] A. P. Kreshkov, L. N. Bikova and N. A. Kazarian, "Titrarea în mediu neapos", Editura tehnică, București, 1969, p. 211.

[2] A. P. Kreshkov, "Osnovi analyticheskoi khimii", Moscow, Khimia, 1976, vol. 2, p. 480; vol. 3, p. 481.

[3] A. P. Kreshkov, S. M. Milaev and G. A. Chanturgaev, *Zavodskaya Lab.*, **39**, 922 (1973).

[4] S. M. Milaev, K. A. Komarova, A. P. Kreshkov and M. M. Baldanov, *Zhur. analit. Khim.*, **28**, 2157 (1973).

[5] A. P. Kreshkov, S. M. Milaev, G. A. Chanturgaev and G. I. Chanturgaeva, *Zhur. analit. Khim.*, **29**, 98 (1974).

Furthermore, [illegible] Electron-Hydrogen concept differs considerably from other fundamental concepts of acid and base theories. At the same time it does not contradict some useful selected concepts of other authors. The present theory supplements them, further developing the tradition of acids and bases which was founded in Russia and was headed by D. I. Mendeleev and continued by current scientists.

The above concept has definite importance for the solution of some practical problems. For example, the study of non-aqueous solutions enabled us to establish certain dependence of acid-base properties of elements in accordance with their position in the Periodical System of elements, with the degree of oxidation of elements, with donor factors and physico-chemical properties of solvents (see Fig. 1).

It has been proved, for instance, that nitrates, chlorides, iodides and perchlorates of bismuth, magnesium, cadmium, zirconium and some other compounds, which have nothing in common with acids and bases in the usual sense, display different strength of acid-base properties in the non-aqueous solutions. This enabled us to develop new methods of differentiated titration of multicomponent mixtures of the above mentioned salts (see Figs. 2, [illegible]).

Fig. 1. The curves of titration of [illegible] [illegible] [illegible] [illegible] [illegible]

[illegible]

Revue Roumaine de Chimie, 22, 9—10, 1297—1304 (1977)

Посвящается проф. КОРИОЛАНУ ДРЭГУЛЕСКУ
по случаю его 70-летия

СОВРЕМЕННЫЕ ПРОБЛЕМЫ ИНЖЕНЕРНОЙ ХИМИИ

П. Г. РОМАНКОВ
Ленинградский технологический институт им. Ленсовета
Московский пр. 26, Ленинград, 198013, СССР

Получена 4 августа 1976 г.

В статье изложены основные направления развития науки о процессах и аппаратах химической технологии, включая вопросы интенсификации, масштабного перехода, увеличения мощности единичных агрегатов, разработки новых методов и процессов.

Химическая технология, возникшая и развивающаяся под влиянием потребностей производства, будучи наукой о наиболее экономичных методах и процессах переработки сырых природных материалов в предметы потребления и стредства производства, представляет собой ныне своеобразный сплав химии, химической техники, кибернетики и экономики. Как показывает опыт, научно-технический прогресс химической и смежных с ней отраслей промышленности (нефтеперерабатывающей и нефтехимической, металлургической и углехимической, целлюлознобумажной, промышленности строительных материалов, многих производств пищевой промышленности, химико-фармацевтической и микробиологической, а также ряда других) во многом зависит от уровня химической техники. Успешное решение проблем химической техники позволяет осуществить достижения химии в промышленном масштабе.

В связи с громадным прогрессом во многих странах современной химической индустрии, часто при опережающих темпах ее развития по сравнению с развитием промышленности в целом, роль химической технологии как науки и ее важнейшего раздела — инженерной химии — резко возрастает. Следует также подчеркнуть, что прогресс химической промышленности во многом зависит от возможностей химического машиностроения.

Непосредственно к химической промышленности примыкает по своей технологии промышленность нефтеперерабатывющая и нефтехимическая, к которой относится весьма важное для народного хозяйства производство синтетических каучуков. И здесь проблемы инженерной химии имеют первостепенное значение.

Каковы же основные тенденции в развитии инженерной химии, призванной обеспечить ускоренное развитие химической промышленности и смежных с ней отраслей? Анализ этих тенденций очень важен для определения научных задач и нашей технической политики в этой области знаний.

Рассмотрим, вкратце, тенденции развития важнейших проблем инженерной химии.

ТЕОРЕТИЧЕСКИЕ ОСНОВЫ ХИМИЧЕСКОЙ ТЕХНОЛОГИИ

Химическая технология как наука на первом этапе своего развития основывалась на чисто эмпирических знаниях и имела описательный характер.

По мнению Н. М. Жаворонкова: «Одной из побудительных причин возникновения и развития теоретических основ химической технологии был колоссальный рост числа химических производств, когда последовательное описание каждого химического производтва при всем их многообразии стало чрезвычайно трудной и малополезной задачей. Другой причиной явилось бурное развитие таких отраслей знания, как физика, химия, математика, служащих фундаментов химической технологии. В качестве примера можно указать на исключительно возросшую за последние десятилетия благодаря развитию идей Л. Прандтля о пограничном слое и идей В. Нернста, И. Лангмюра о диффузионном слое роль гидродинамики, которая утвердилась в химической технологии, начиная примерно с 30-х годов»[1].

Идея единых кинетических закономерностей, положенная в основу современной классификации химико-технологических процессов, базируется на сходстве линейных дифференциальных уравнений, описывающих простейшие (линейные) процессы переноса.

Общеизвестными примерами линейных законов переноса являются: закон диффузии Фика, закон вязкости Ньютона, закон теплопроводности Фурье, закон Ома.

В результате сопоставления этих законов оказалось возможным разделить все химико-технологические процессы на группы, кинетические закономерности которых подчиняются общему закону: скорость процесса прямо пропорциональна движущей силе процесса и обратно пропорциональна сопротивлению. Таким образом, учение о процессах и аппаратах химической технологии оформилось в строгую научную дисциплину. Характерной особенностью этой области инженерной химии является использование объединенного метода исследования — теоретического и экспериментального позволяющего наиболее полно вскрыть кинетические закономерности процессов химической технологии и сделать наиболее широкие обобщения.[2]

Возможность использования линейных соотношений для построения точных моделей процессов химической технологии определяется степенью отклонения процесса от равновесного. Во всяком случае, для систем, близких к равновесию, линейные соотношения хорошо подтверждаются опытом.

---

[1] Н. М. Жаворонков, *Теор. основы хим. технологии*, **VI**, 659 (1972).

[2] П. Г. Романков, «Современные проблемы химической технологии», сб. трудов ЛТИ им. Ленсовета, 1975.

Поскольку большинство процессов химической технологии характеризуется значительной интенсивностью массообмена и сложной гидродинамической обстановкой (высокими относительными скоростями, движения фаз, турбулентными течениями, влиянием массообмена на характер движения фаз и т.д.), построение строгих моделей этих процессов должно базироваться на использовании нелинейных законов переноса, которые более точно описывают физико-химический механизм явлений переноса.

Вместе с тем нужно отметить, что не для всех физико-химических ситуаций известна нелинейная форма законов переноса. Получение этой информации, необходимой химикам-технологам для построения точных методов расчета технологических процессов, является неотложной задачей, стоящей перед специалистами в области теории переноса.

Одним из простейших примеров нелинейных заковов переноса является турбулентное течение жидкости или газа. При таком течении справедливы нелинейные законы переноса. Действительно, с учетом известной гипотезы Прандтля о пути смешения закона переноса импульса, выражающий связь между эффективным касательным напряжением и компонентами градиента скорости, можно записать в виде: [3]

$$\tau = -\rho l^2 \frac{\partial u}{\partial y} \left| \frac{\partial u}{\partial y} \right|$$

где τ — эффективное касательное напряжение, ρ — плотность среды, l — путь смешения, y — расстояние до поверхности тела, u — массовая скорость среды.

Данный закон записан для двумерного турбулентного погарничного слоя.

В настоящее время при исследовании законов переноса необходимо уделить особое внимание изучению кинетики *нестационарных* процессов, парамерты которых меняются во времени. Примером таких процессов являются массообменные процессы в системах с твердой фазой [4] — сушка влажных материалов (в периоде падающей скорости), адсорбция, десорбция, экстрагирование, ионообмен и др., а также тепловые процессы — охлаждение, нагревание тел и многие другие.

Существует настоятельная необходимость значительного расширения фронта научных исследований по изучению механизма массообменных процессов химической технологии и определению кинетических коэффициентов внутреннего переноса в условиях нестационарности процесса.

В связи с непрерывным ростом требований к качеству технической организации химико-технологических процессов при разработке новых процессов, а также при модернизации действующих производств все большее применение находят управляющие вычислительные машины, которые решают задачи оптимизации технологических режимов (как установившихся, так и переходных). Так как задачи динамической оптимизации решаются на основе математических моделей, описывающих переходные режимы (то есть реакции химико-технологических систем на эксплуатационные возмущения входных параметров) исследование переходных режимов химико-технологических процессов становится в последнее время обязательным элементом программы разработки любой технологической установки.[5]

---

[3] R. B. Bird, W. E. Stewart and E. N. Lightfoot, ,,Transport phenomena'', J. Wiley, New York, 1965.

[4] П. Г. Романков, Н. Б. Рашковская и В. Ф. Фролов, «Массообменные процессы химической технологии», Ленинград, изд. «Химия», 1975.

Методы и результаты исследования переходных технологических режимов объединяются научным направлением, которое получало название динамики процессов химической технологии.

ПРОБЛЕМА МАСШТАБНОГО ПЕРЕХОДА

Одной из важнейших проблем инженерной химии является проблема увеличения размеров аппаратуры. Как известно, во многих случаях увеличение размеров аппарата производит к снижению эффективности единицы рабочего объема по сравнению с лабораторной моделью. Одной из причин такого снижения эффективности можно считать изменение гидродинамической обстановки в промышленном аппарате, вызываемое нарушением равномерности распределения потоков.

А. М. Розен, В. С. Крылов и другие исследователи[6] развили положения так называемой гидравлической теории масштабного перехода.

В сложных случаях, когда в моделируемом технологическом процессе возможны отклонения от принятого технологического режима, нарушения теплообмена и других условий, допустимая величина масштабного перехода определяется на основе приближенного моделирования.

Успешно решаются задачи масштабного перехода путем создания таких аппаратурных конструкций, в которых многократно повторяются отдельные, хорошо отработанные элементы. Такой многоэлементный или многосекционный метод масштабирования нашел широкое применение в химической технике — в трубчатых выпарных, газлифтных, контактных аппаратах; близок к единице коэффициент масштабного перехода в пульсационных колонных аппаратах (рис. 1, 3).

ПРОБЛЕМА ИНТЕНСИФИКАЦИИ

Увеличение производительности единичных агрегатов может быть достигнуто не только увеличением их размеров. Не менее важной проблемой инженерной химии является интенсификация процессов химической технологии, то есть повышение производительности единицы аппаратурного объема — будь то химический реактор или ректификационная колонна. Основное внимание здесь направлено на резкое повышение скоростей жидких и газовых потоков, а это требует новых конструктивных решений для контактирующих устройств.

---

[5] D. Himmelblau and K. Bischoff, „Process analysis and simulation deterministic systems", J. Wiley, New York, 1968.

[6] А. М. Розен и В. С. Крылов, *Теор. основы хим. технологии*, 1, 297 (1967).

На примере процесса псевдоожижения можно убедиться в том, каким мощным средством увеличения интенсивности взаимодействия между фазами является *организация потоков* в химической аппаратуре (рис. 2, 4).

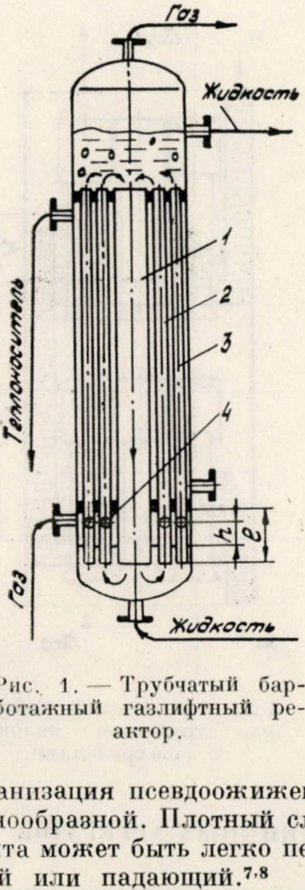

Рис. 1. — Трубчатый барботажный газлифтный реактор.

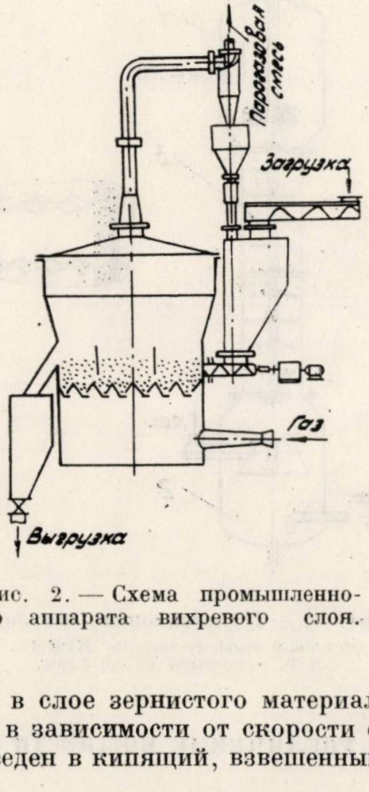

Рис. 2. — Схема промышленного аппарата вихревого слоя.

Организация псевдоожижения в слое зернистого материала может быть разнообразной. Плотный слой в зависимости от скорости ожижающего агента может быть легко переведен в кипящий, взвешенный, фонтанирующий или падающий.[7,8]

Широкое применение нашел в химической технологии также и метод организации *закрученных* (вихревых) потоков. Он хорошо известен и применяется при увеличении интенсивности взаимодействия газо-жидкостных потоков. Однако этот метод может быть применен и при псевдоожижении. В частности, можно проводить обеспыливание в фонтанирующем закрученном слое дисперсной насадки.

---

[7] J. F. Davidson and D. Harrison (edit.), „Fluidization", Acad. Press, London and New York, 1971.

[8] П. Г. Романков и М. И. Курочкина, «Гидромеханические процессы химической технологии», Ленинград, изд. «Химия», 1974.

Вибрирующие устройства также могут быть использованы для эффективной организации потоков. В промышленной практике применяется так называемый виброкипящий слой.

Внимание исследователей продолжают привлекать колонны с подвижной (плавающей) насадкой, уже вошедшие в промышленную практику в качестве абсорберов. Интенсивные гидродинамические режимы находят широкое применение и в других областях химической техники.

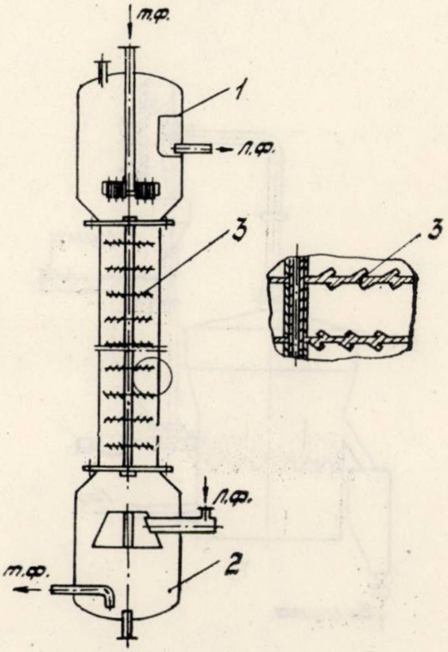

Рис. 3. — Пульсационная колонна.
1,2 – отстойные зоны, 3 – насадка КРИМЗ. Т.Ф., Л.Ф. – тяжелая легкая фазы.

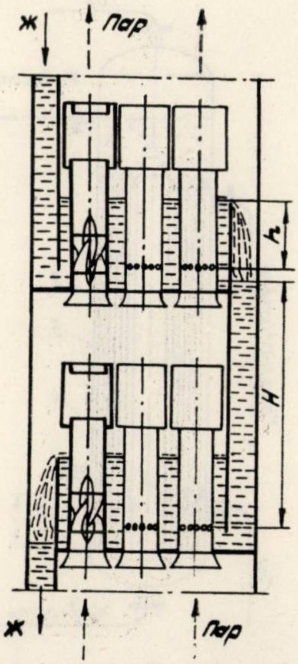

Рис. 4. — Ректификационная трубчатая колонна с завихрителями.

УВЕЛИЧЕНИЕ МОЩНОСТИ ЕДИНИЧНЫХ АГРЕГАТОВ

В связи с резким возрастанием масштаба многих химических производств становится невозможным наращивание их мощностей путем увеличения числа агрегатов пусть даже самых больших размеров, изготовляемых в настоящее время химическим машиностроением. Речь идет о создании новых единичных агрегатов громадной производительности, доведенных, однако, до оптимальных размеров при непременном соблюдении надежности их работы. Последнее требование является основным, так так внезапная остановка одного из агрегатов выводит из строя всю технологическую линию и приводит к значительному снижению производства со всеми вытекающими отсюда последствиями (невыполнение плана, снижение производительности труда и пр.).

Рассмотрим на некоторых примерах тенденцию увеличения мощности единичных агрегатов. Так, в нефтеперерабатывающей и нефтехимической промышленности СССР[9] увеличение мощности установок первичной перегонки нефти с 3 до 8 млн. т нефти в год позволило снизить удельные капиталовложения на 31%, расход металла на 47%, повысить производительность труда в 2,4 раза. Ведется подготовка к строительству аналогичных установок : мощностью до 12 млн. т нефти в год. Обсуждается возможность создания установок прямой перегонки до 24 млн. т нефти в год для заводов третьего поколения. Характерной чертой современного развития этой отрасли промышленности является комбинирование в составе одной установки процесса первичной переработки нефти с процессами термического и каталитического крекинга и стабилизации бензина. Такие крупномасштабные технологические установки потребовали жесткой связи во всей системе и автоматического управления при помощи электронно-вычислительных машин. Степень надежности всей этой техники, включая основное оборудование, должна соответствовать удлиненному сроку межремонтного пробега установок до 18—24 месяцев (особенно для процессов каталитического реформинга, гидрокрекинга, производства полиэтилена, полипропилена и др.).

Укрупнение единичных агрегатов имеет, несомненно, свой разумный предел, то есть оптимум, определяемый на данном этапе техническими возможностями и экономикой.[10]

НОВЫЕ МЕТОДЫ И НОВЫЕ ПРОЦЕССЫ

Несмотря на большие успехи, достигнутые по линии интенсификации основных процессов химической технологии, дальнейший прогресс химических производств во многом будет зависеть от разработки новых инженерных идей, новых методов и процессов химической технологии. Примером этого может служить появившаяся недавно плазмо-химическая технология.

Например, в плазме можно получить окислы азота из воздуха, ацетилен из углеводородного сырья, цианистый водород из метана и азота, тетрафторэтилен из элементов, пигментную двуокись титана из тетрахлорида титана и др. Наибольший эффект ожидается от использования неравновесной плазмы. Здесь можно ожидать получение окислов азота с концентрацией выше 12—15% при существенном снижении удельного расхода электроэнергии.

Немаловажное значение для прогресса химической технологии имеет сокращение числа стадий многостадийного химического производства вплоть до замены его одностадийным. Примером может служить оригинальный метод получения этилового спирта прямой гидратацией этилена.

Тенденция к существенному упрощению технологических схем производства проявляется и при получении ряда других промышленно важных продуктов.

---

[9] В. С. Федоров, «Нефтеперерабатывающая и нефтехимическая промышленность СССР в девятой пятилетке», Москва, изд. «Химия», 1976.

[10] Л. А. Костандов, «Химическая промышленность СССР к XXV съезду КПСС», Москва, изд. «Химия», 1976.

Ярким примером новой технологии может служить также получение белковых продуктов, аминокислот и ферментов из парафинов нефти при помощи микроогранизмов, что позволяет поставить на индустриальную основу откорм скота и повысить продуктивность животноводческих хозяйств.

Приближается полный переход в производстве синтетических каучуков от этилового спирта к бутановым и бутиленовым фракциям с применением новых эффективных катализаторов.[1,2]

Почти в каждой технологии химических продуктов иемются новые прогрессивные предложения.

Кроме перечисленных актуальных задач инженерной химии к их числу следует отнести также проблемы развития методов кибернетики (процесс — аппарат — управление), вопросы экологической технологии, а также специальную подготовку инженеров химиков-технологов и научных работников.

В заключение хотелось бы сказать, что от развития химической науки, от успехов химической технологии и ее важнейшего раздела — инженерной химии во многом зависит развитие химической и смежных с ней отраслей промышленности.

В решении этой задачи важная роль принадлежит ученым и инженерам наших социалистических стран.

Revue Roumaine de Chimie, 22, *9–10*, 1305–1313 (1977)

Dedicated to the 70th anniversary
of Professor CORIOLAN DRĂGULESCU

EFFECT OF UNIAXIAL STRESS ON ABSORPTION SPECTRA OF TETRAGONAL CRYSTALS Cs_3CoCl_5 AND Cs_3CoBr_5

IKUJI TSUJIKAWA and MASAFUMI HARADA
Department of Chemistry, Faculty of Science, Kyoto University, Kyoto, Japan

Received August 20, 1976

The effect of uniaxial stress on the absorption spectra $^4A_2 \rightarrow {}^2T_2(^2D)$ and $^4A_2 \rightarrow {}^2E\ (^2D)$ of the tetrahedral $[CoX_4]^{2-}$ complex ions (X = Cl and Br) in tetragonal crystals Cs_3CoX_5 was measured with stress up to 2.4 kbar. The dependence of the Racah parameter B on coordination-bond length and the behaviours of the ground state $^4A_2$ and the excited state ^2E with respect to the Jahn-Teller effect were investigated.

1. INTRODUCTION

Crystals of complex salts are fairly brittle. Nevertheless, if crystal plates are carefully prepared so that both surfaces are well polished and just parallel with each other, on which the uniaxial stress is applied, they are capable to be pressed without break under stress up to the order of kbar. Therefore, the measurement of the effect of uniaxial stress will be a powerful tool to investigate spectroscopic, magnetic, electrical and other properties of complex salts, as has been used for hard crystals such as oxides and fluorides.

Under the uniaxial stress, each complex ion within a crystal sustains distortions in size and shape, that is, the contraction of coordination-bond lengths and the change of coordination-bond angles. The former provides the increase of the cubic crystal field or Dq and the increase of covalency or the reduction of the Racah parameter, while, the latter does the increase or decrease of low symmetry crystal fields.

The nephelauxetic series [1] has been well known as the rule for the dependence of covalency or d-electron-cloud expansion on kinds of ligands, while the effect of contraction of bond lengths now interested will relate to a nephelauxetic effect *without replacing ligands.*

---

[1] C. K. JØRGENSEN, *Discuss, Faraday Soc.*, **26**, 110 (1958).

A distortion in shape of complex ions in crystals, namely, the presence of low symmetry field has many times hitherto been discussed in view of the Jahn-Teller effect or the crystal packing effect. Either in the effect of uniaxial stress or in the Jahn-Teller effect, the nuclear system distorts, and as was already pointed out by Ham,[2] the effect of uniaxial stress is useful for investigating the Jahn-Teller effect.

The purpose of this paper is to investigate the dependence of the Racah parameter B on the coordination-bond length [3] and the Jahn-Teller effect or, strictly speaking, the pseudo Jahn-Teller effect because of near degeneracy of the ground state $^4A_2$ [4] and the excited state $^2E(^2D)$ [5] in Cs_3CoX_5 (X=Cl and Br) by the effect of uniaxial stress on optical absorption spectra.

2. EXPERIMENTAL

Measurements of absorption spectra under uniaxial compressive stress up to 2.4 kbar at 4.2 K were made with an apparatus described elsewhere [4], using an Eagle mounting spectrograph with 0.65 Å/mm dispersion in the fourth order. Measurements of the Zeeman effect were also done with magnetic field up to 78 kOe. The crystal structure of Cs_3CoX_5 is tetragonal of which the space group is *I4/mcm* (D_{4h}^{18}) and the site symmetry at a Co^{2+} ion is D_{2d}.[6,7] A complex ion is slightly distorted along the crystallographic *c*-axis as shown in Fig. 1 where the notations of all quantities necessary for the following discussions are set down.

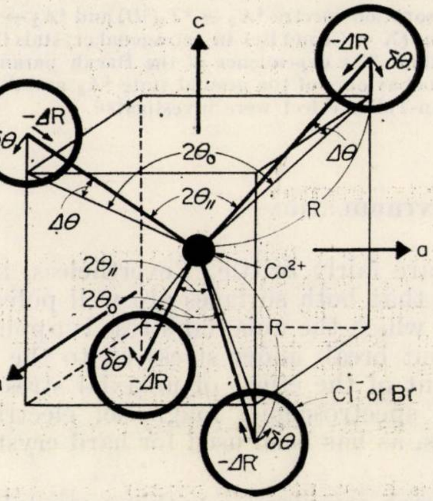

Fig. 1. — Tetragonally distorted $[CoX_4]^{2-}$ complex ion. $2\theta_0 = 109°28'$ corresponds to $2\theta_{//}$ for the regular tetrahedron and *a* and *c* denote the crystallographic *a*- and *c*-axes. ΔR and $\delta\theta$ show the two components of distortions induced by **P**//*c*.

3. EXPERIMENTAL RESULTS

The absorption spectra $^4A_2 \rightarrow {}^2T_2\,(^2D)$ for Cs_3CoBr_5 under the uniaxial compressive stress **P**//*c* (**P** < 0 as defined) are shown in Fig. 2. There are many absorption lines which can be, however, immediately classified into three groups from their different values of shift induced by **P**, $\Delta E/\Delta P$, that is, (V_1^*, V_1, V_{1-1}^* and V_{1-1}), (V_3^*, V_3 and V_{3-1}^*) and (V_4, V_{4-1} and V_{4-2}), where V_i and V_i^* ($i = 1, 3, 4$) denote transitions from the lower component $|S = 3/2, S_z = \pm 3/2>$ and the upper one $|3/2, \pm 1/2>$ of the ground state $^4A_2$, respectively, and V_{i-j} and

---

[2] F. S. Ham, *Phys. Rev.*, **166**, 307 (1968).
[3] M. Harada and I. Tsujikawa, *J. Phys. Soc. Japan*, **37**, 1367 (1974).
[4] M. Harada and I. Tsujikawa, *J. Phys. Soc. Japan*, **37**, 1353, 1359 (1974).
[5] M. Harada and I. Tsujikawa, *J. Phys. Soc. Japan*, **40**, 513 (1976).
[6] H. M. Powell and A. F. Wells, *J. Chem. Soc.*, **1935**, 359 (1935).
[7] B. N. Figgis, M. Gerloch and R. Mason, *Acta Cryst.*, **17**, 506 (1964).

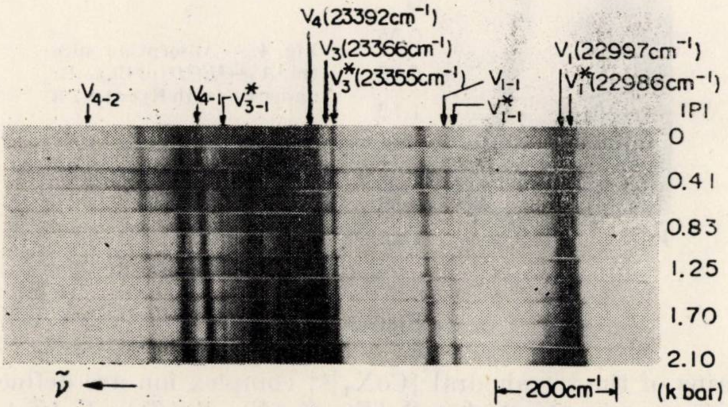

Fig. 2. — Absorption spectra $^4A_2 \rightarrow {}^2T_2\,(^2D)$ of Cs_3CoBr_5 under $\mathbf{P}//c$ with the electric vector of the incident light $\mathbf{E}\perp c$ at 4.2 K.

V_{i-j}^* are vibrational side lines of V_i and V_i^* associated with the excitation of j quanta of the totally symmetric Q_1 mode. The three final states for the V_1, V_3 and V_4 lines are the three split components of the excited state $^2T_2$. As seen above, the measurement of the effect of uniaxial stress gives direct information for the assignment of absorption lines.

The absorption spectra $^4A_2 \rightarrow {}^2E\,(^2D)$ for both salts under $\mathbf{P}//c$ are shown in Figs. 3 and 4. The energy difference between U_1 and U_1^* (U_2 and U_1) corresponds to the splitting $2D$

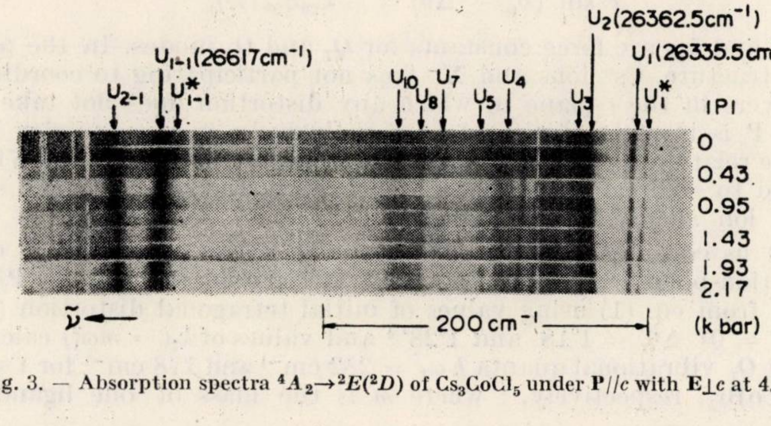

Fig. 3. — Absorption spectra $^4A_2 \rightarrow {}^2E(^2D)$ of Cs_3CoCl_5 under $\mathbf{P}//c$ with $\mathbf{E}\perp c$ at 4.2 K.

(2Δ) of the ground state $^4A_2$ (the excited state ^2E) which are 9 cm^{-1} (27 cm^{-1}) and 11 cm^{-1} (33 cm^{-1}) in the absence of **P** for Cs_3CoCl_5 and Cs_3CoBr_5, respectively. $2D$ decreases with increasing $|\mathbf{P}|$ for both salts and then critical values of $|\mathbf{P}|$ at which the splittings become zero, namely, distorted tetrahedrons become regular ones, are obtained by extrapolation to higher $|\mathbf{P}|$ side as 7.57 kbar for Cs_3CoCl_5 and 8.78 kbar for Cs_3CoBr_5. On the other hand, 2Δ increases unexpectedly with increasing $|\mathbf{P}|$ for Cs_3CoBr_5, while 2Δ decreases with increasing $|\mathbf{P}|$ for Cs_3CoCl_5. These different dependences on **P** for both salts will be explained in the next section.

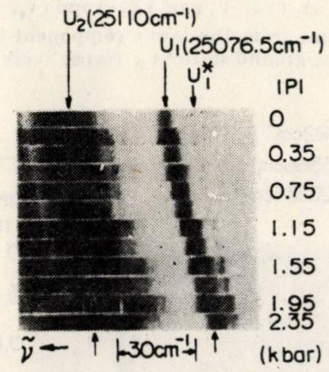

Fig. 4. — Absorption spectra $^4A_2 \rightarrow {}^2E(^2D)$ of Cs_3CoBr_5 under **P**//*c* with **E**⊥*c* at 4.2 K.

4. DISCUSSION

Strains of the tetrahedral $[CoX_4]^{2-}$ complex ion are defined by the nine strain components $S_1(A_1)$, $S_{2\theta}(E)$, $S_{2\varepsilon}(E)$, $S_{4\xi}(T_2)$, $S_{4\eta}(T_2)$, $S_{4\zeta}(T_2)$, $S_{5\zeta}(T_2)$, $S_{5\eta}(T_2)$ and $S_{5\zeta}(T_2)$ corresponding to the normal vibrational modes Q_1, Q_3, Q_2, Q_4 Q_5, Q_6, Q_8, Q_7, and Q_9,[8] respectively. In the case of **P**//*c*, strain components necessary to be taken into account are only $S_1(A_1) \equiv 2\Delta R$ and $S_{2\theta}(E) \equiv 2R \tan \delta\theta$ which are related to the force components parallel and perpendicular to a coordination — bond as follows :

$$F \cos (\theta_0 - \Delta\theta) = -k_1 S_1(A_1) \tag{1}$$

and

$$F \sin (\theta_0 - \Delta\theta) = -k_{2\theta} S_{2\theta}(E), \tag{2}$$

where k_1 and $k_{2\theta}$ are force constants for Q_1 and Q_3 modes. In the present crystal structure, Cs^+ ions and X^- ions not participating to coordination make layers in the *c*-plane in which any distortion does not take place by **P**//*c*, **P** is thought thereby to act exclusively on the complex ion to result the relation $F = 1/2\, a^2 |\mathbf{P}|$, where a is the lattice constant. When **P** is applied to a direction other than the *c*-axis, the *effective* force on the complex ion should be examined.

Let us consider the dependence of the Racah parameter B on the coordination-bond length R. Values of $\Delta R/\Delta P$ in the case of **P**//*c* are obtained from eq. (1) using values of initial tetragonal distortion (initial means $\mathbf{P} = 0$) $\Delta\theta_i = 1°18'$ and $1°28'$[4] and values of $k_1 (= m\omega_1^2)$ calculated from the Q_1 vibrational quanta $\hbar\,\omega_1 = 282\ \mathrm{cm}^{-1}$ and $178\ \mathrm{cm}^{-1}$ for Cs_3CoCl_5 and Cs_3CoBr_5, respectively,[3] where m is the mass of one ligand ion;

$$\begin{aligned} \Delta R/\Delta P &= -7.39 \times 10^{-4}\,\text{Å/kbar for } Cs_3CoCl_5, \\ &= -8.95 \times 10^{-4}\,\text{Å/kbar for } Cs_3CoBr_5. \end{aligned} \tag{3}$$

---

[8] M. D. Sturge, "Solid State Physics", ed. F. Seitz, D. D. Turnbull and H. Ehrenreich, Academic Press, New York—London, vol. 20, 1967, p. 91.

Values of $\Delta E_{av}^{exp}/\Delta P$ are shown in Table 1, where the experimentally obtained average transition energies E_{av}^{exp} denote the average energy of the V_1, V_3 and V_4 lines in the spectra ${}^4A_2 \rightarrow {}^2T_2$ and that of the U_1 and U_2 lines in the spectra ${}^4A_2 \rightarrow {}^2E$. $\Delta E_{av}^{exp}/\Delta P$ is expected to consist of $\Delta E_{av}(Dq)/\Delta P \equiv (\Delta E_{av}/\Delta Dq)(\Delta Dq/\Delta P)$ and $\Delta E_{av}(B)/\Delta P \equiv (\Delta E_{av}/\Delta B) \cdot (\Delta B/\Delta P)$. It is, however, difficult to discriminate experimentally between those two parts. Then, by assuming the point charge model, $\Delta Dq/\Delta P$ is calculated as

$$\Delta Dq/\Delta P = -0.464 \text{ cm}^{-1}/\text{kbar for } Cs_3CoCl_5, \tag{4}$$

$$= -0.518 \text{ cm}^{-1}/\text{kbar for } Cs_3CoBr_5,$$

while $\Delta E_{av}/\Delta Dq$ and $\Delta E_{av}/\Delta B$ are easily evaluated on the basis of the crystal field theory. Using these values, values of $\Delta E_{av}(Dq)/\Delta P$ and those of $\Delta E_{av}(B)/\Delta P$ are obtained, where the latters are taken as the difference between $\Delta E_{av}^{exp}/\Delta P$ and $\Delta E(Dq)/\Delta P$. The latters provide values of $\Delta B/\Delta P$. Those values are shown in Table 1, together with values of $(\Delta B/B_0)/(\Delta R/R_0)$ where B_0 is the free ion value of B for Co^{2+}, $B_0 = 997 \text{cm}^{-1}$[9] and R_0 the coordination— bond length R in the absence of **P**, $R_0 = 2.252$ Å[7] and 2391 Å[10] for Cs_3CoCl_5 and Cs_3CoBr_5, respectively. The small blue shift of the spectra ${}^4A_2 \rightarrow {}^2E$ for Cs_3CoCl_5 and the large red shift of the same spectra for Cs_3CoBr_5 come from very different values of $\Delta E_{av}(B)/\Delta P$ for both salts. $(\Delta B/B_0)/(\Delta R/R_0)$ depends linearly on the polarizability α of the ligand ions as shown in Fig. 5, which closely relates to the covalency character of the coordination bond. The nephelauxetic effect has been discussed in terms of α[9].

Table 1

Shifts of the average transition energy E_{av} of the spectra and changes of B induced by P//c and reduced gradients of B with respect to R, $(\Delta B/B_0)$ / $(\Delta R/R_0)$

Compound	Spectra	Shifts of E_{av} (cm^{-1}/kbar)			$\Delta B/\lvert\Delta P\rvert$ (cm^{-1}/kbar)	$(\Delta B/B_0)/$ $/(\Delta R/R_0)$
		$\Delta E_{av}^{exp}/\lvert\Delta P\rvert$	$\Delta E_{av}(Dq)/\lvert\Delta P\rvert$	$\Delta E(B)/\lvert\Delta P\rvert$		
Cs_3CoCl_5	${}^4A_2 \rightarrow {}^2E({}^2D)$	$+0.74 \pm 0.2$	$+11.50$	-10.76	-0.472	$+1.48$
	${}^4A_2 \rightarrow {}^2T_2({}^2D)$	-1.60 ± 0.4	$+7.87$	-9.47	-0.399	$+1.25$
Cs_3CoBr_5	${}^4A_2 \rightarrow {}^2E({}^2D)$	-6.64 ± 0.3	$+12.76$	-19.40	-0.851	$+2.34$
	${}^4A_2 \rightarrow {}^2T_2({}^2D)$	-9.12 ± 0.2	$+8.70$	-17.84	-0.750	$+2.06$

Now let us investigate the static Jahn-Teller effect of the ground state ${}^4A_2$. In order to analyse the observed changes of the splitting $2D$ of ${}^4A_2$ induced by **P**//c and to relate those with the Jahn-Teller effect, are introduced the effective Hamiltonians of the strain-induced effect and of the Jahn-Teller coupling with the doubly degenerate $\varepsilon(Q_3)$ and Q_2) mode as follows:

---

[9] H. A. Weakliem, *J. Chem. Phys.*, **36**, 2117 (1962).

[10] B. Morosin and E. C. Lingafelter, *Acta Cryst.*, **12**, 197 (1957).

$$\mathscr{H}^{\mathrm{st}} = \{D_0 + V^{\mathrm{st}}_{2\theta}\, S_{2\theta}(E)\}\, U_\theta, \tag{5}$$

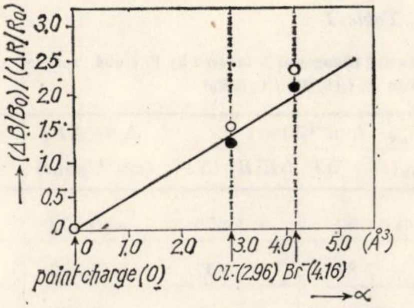

Fi.
$(\Delta B/B_0)/(\Delta R/R_0)$ and α. Values of α are t ... rom ref.

and

$$\mathscr{H}^{\mathrm{JT}} = V^{\mathrm{JT}}_{\theta}\, Q_3 U_\theta + V^{\mathrm{JT}}_{\varepsilon} Q_2 U_\varepsilon \tag{6}$$

where D_0 is D in the absence of **P**, $V^{\mathrm{st}}_{2\theta}$ the strain coefficient, V^{JT}_{θ} and $V^{\mathrm{JT}}_{\varepsilon}$ the Jahn-Teller coupling constants and U_θ and U_ε matrices defined as

$$U_\theta = \begin{pmatrix} -1 & & & 0 \\ & +1 & & \\ & & +1 & \\ 0 & & & -1 \end{pmatrix}, \quad U_\varepsilon = \begin{pmatrix} 0 & & +1 & 0 \\ & & 0 & +1 \\ +1 & 0 & & \\ 0 & +1 & & 0 \end{pmatrix}. \tag{7}$$

Thus these Hamiltonians are expressed in matrix forms with the bases $|3/2, 3/2>$, $|3/2, 1/2>$, $|3/2, -1/2>$ and $|3/2\ -3/2>$. According to Ham's theoretical treatment,[2] V^{JT}_{θ}, $V^{\mathrm{JT}}_{\varepsilon}$ and $V^{\mathrm{ST}}_{2\theta}$ are related with each other as

$$V^{\mathrm{JT}}_{\theta} = V^{\mathrm{JT}}_{\varepsilon} = V^{\mathrm{ST}}_{2\theta}. \tag{8}$$

Using eqs. (2), (5) and (8), the decrease of $2D$ induced by **P** is expressed as,

$$2D - 2D_0 = 2V^{\mathrm{st}}_{2\theta}\, S_{2\theta}(E) = 4V^{\mathrm{JT}}_{\theta}\, R_0 \tan \delta\theta, \tag{9}$$

from which V^{JT}_{θ} can be estimated. In the static Jahn-Teller effect,[8] the tetragonal distortion $\Delta\theta^{\mathrm{JT}}$ due to the Jahn-Teller coupling and the Jahn-Teller stabilization energy E_{JT} are given by

$$2R_0 \tan \Delta\theta^{\mathrm{JT}} = 2V^{\mathrm{JT}}_{\theta}/k_{2\theta}, \tag{10}$$

---

[11] J. R. Tessman, A. H. Kahn and W. Shocley, *Phys. Rev.*, **92**, 890 (1953).

and

$$E_{\mathrm{JT}} = (V_{\theta}^{\mathrm{JT}})^2/2k_{2\theta}. \tag{11}$$

k_2 $(= m\omega_2^2)$ is calculated from $\hbar\omega_2 = 110$ cm^{-1} and 75 cm^{-1} for Cs_3CoCl_5 and Cs_3CoBr_5, respectively.[4] The obtained results are listed in Table 2. It becomes clear that the contribution of the Jahn-Teller coupling to the tetragonal distortion is as small as 2–4 %, as has been expected because of the orbital singlet state.

Table 2

Estimation of the contribution of the Jahn-Teller coupling to the initial tetragonal distortion $\Delta\theta_i$

Compound	$2(D-D_0)/\lvert\mathbf{P}\rvert$ (cm^{-1}/kbar)	$V_{2\theta}^{\mathrm{st}}$ $(= V_{\theta}^{\mathrm{JT}})$ (cm^{-1} Å)	E_{JT} (cm^{-1})	$\Delta\theta^{\mathrm{JT}}$ (minutes)	$\Delta\theta^{\mathrm{JT}}/\Delta\theta_i$ (%)
Cs_3CoCl_5	1.15±0.10	38.6±2.5	0.070±0.01	2.77±0.5	3.3±1.5
Cs_3CoBr_5	1.22±0.10	39.7±2.5	0.068±0.01	2.46±0.5	2.6±1.5

Finally, let us discuss the Jahn-Teller effect of the excited state ^2E. Experimental results about the absorption spectra $^4A_2 \rightarrow {}^2E$ cannot be interpreted on the basis of the crystal field theory in the following points. 1) The splitting 2Δ of ^2E is proportional to the distortion angle $\Delta\theta$, so that 2Δ should decrease with decreasing $\Delta\theta$ by the increase of $|\mathbf{P}|$. The case of Cs_3CoBr_5 is in contradiction to the above. 2) As seen in Fig. 3, the U_5 line for instance gains its intensity with increasing $|\mathbf{P}|$, while the U_8 line loses its intensity. As far as these lines are considered as vibrational side lines of the U_1 or U_2 line, the dependence of their intensities on $\mathbf{P}$ cannot be explained. 3) The $g_{//}$-value (g-value for the case of magnetic field $\mathbf{H}//c$) of the upper component of ^2E which is the final state for the U_2 line obtained from measurements of the Zeeman effect is unexplained, as shown in Table 3.

Table 3

The $g_{//}$-values of excited states which are final states of the U_1 and U_2 lines. Calculated values *A* are on the basis of the crystal field theory and calculated values *B* are by taking into account the Jahn-Teller coupling by use of vibronic wave functions

		Exp. values	Calc. values **A**	Calc. values **B**
Cs_3CoCl_5	U_1	+0.54±0.04	+0.54	+0.54
	U_2	+0.54±0.20	+1.73	+0.74
Cs_3CoBr_5	U_1	+0.73±0.20	+0.73	+0.73
	U_2	+0.73±0.30	+1.72	+0.81

Since these experimental facts will also be beyond the scope of the adiabatic approximation, the Hamiltonian which describes the Jahn-Teller system of the electronic ^2E state with the vibrational ε mode is taken as,

$$\mathscr{H} = E_0\mathfrak{J} - \frac{1}{2}\frac{\hbar}{M}\left(\frac{\partial^2}{\partial Q_3^2} + \frac{\partial^2}{\partial Q_3^2}\right)\mathfrak{J} + \frac{1}{2}(M\,\omega_{2\theta}\,Q_3^2 + M\,\omega_{2\varepsilon}\,Q_2^2)\,\mathfrak{J} + \\ + (V_\varepsilon^{\mathrm{JT}}\,Q_3 U_\theta + V_\varepsilon^{\mathrm{JT}}\,Q_2 U_\varepsilon) + \Delta U_\theta \tag{12}$$

where E_0 is the electronic energy of the cubic term ^2E, $\mathfrak{J}$ 4×4 unit matrix, M the reduced mass for the ε mode. The second and third terms are kinetic and potential energies of the nuclear system, the fourth term the Jahn-Teller coupling energy and the last term the low symmetry crystal field that gives rise to the splitting of ^2E. The so-called vibronic wave functions for the above Hamiltonian are expressed as,

$$\Phi\left(j\Gamma_i \pm \frac{1}{2}\right) = \sum_{m,n} C_{j6i}^{mn}\left|\Gamma_6 \pm \frac{1}{2} >\right| m, n > + \sum_{m',n'} C_{j7i}^{m'n'}\left|\Gamma_7 \pm \frac{1}{2} >\right| m', n' >, \tag{13}$$

where $\Gamma_i = \Gamma_6$ and Γ_7 are the irreducible representations of the dual group D_{2d}^*, j the discriminating number of vibronic Γ_i states, $\left|\Gamma_6 \pm \frac{1}{2} >\right.$ and $\left|\Gamma_7 \pm \frac{1}{2} >\right.$ electronic wave functions, $|m, n>$ vibrational wave function with the quantum number m and n for Q_3 and Q_2 modes and C_{j6i}^{mn} and $C_{j7i}^{m'n'}$ coefficients. Using eqs. (12) and (13) and taking $E_{\mathrm{JT}} = (V_\theta^{\mathrm{JT}} + V_\varepsilon^{\mathrm{JT}})^2/8M\omega_2^2$ as equal to $\hbar\omega_2$, energies of vibronic states are calculated as function of 2Δ, which are shown in Fig. 6. An attention should be paid that 2Δ means a *virtual* splitting with $E_{\mathrm{JT}} = 0$. Then the *actual* splitting between the U_2 and U_1 lines is now replaced by ΔE which corresponds to $E(1\Gamma_6) - E(1\Gamma_7)$ in the figure. Furthermore, taking into account the splitting 2δ of the ε mode due to $\Delta\theta$, ΔE is calculated as in Fig. 7 with $2\delta = 0.16\ (2\Delta)$ and various values of E_{JT}.

The $g_{//}$-value of the $j\Gamma_i$ state is given by the expected value of $(2S_z + L_z)$ using the vibronic wave function in eq. (13) which is shown in Table 3. Thus, the $g_{//}$-value of the final state for the U_2 line agrees fairly well with the experimentally obtained $g_{//}$-value. In the process of calculation, parameters are obtained for the best fit as $E_{\mathrm{JT}}/\hbar\omega_2 = 1.4$ and $2\Delta_0/\hbar\omega_2 = 2.5$ for Cs_3CoCl_5 and $E_{\mathrm{JT}}/\hbar\omega_2 = 0.7$ and $2\Delta_0/\hbar\omega_2 = 2.5$ for Cs_3CoBr_5, where Δ_0 is Δ in the absence of $\mathbf{P}$ and their corresponding positions in Fig. 7 are indicated by open and closed circles, respectively. For Cs_3CoBr_5, Δ decreases with increasing $|\mathbf{P}|$ to result in the increase of ΔE in contrast with the case for Cs_3CoCl_5. The dependence of ΔE on $\mathbf{P}$ for both salts can be thereby understood.

The dependence of absorption intensities of the U lines for Cs_3CoCl_5 is now considered. The absorption intensity of the lines corresponding to the transition to the vibronic $j\Gamma_6(j\Gamma_7)$ state is proportional to the square of $C_{j66}^{00}(C_{j77}^{00})$. As seen in Fig. 6, the electronic $\left|\Gamma_6 \pm \frac{1}{2} >\right| 0.0 >$ state crosses

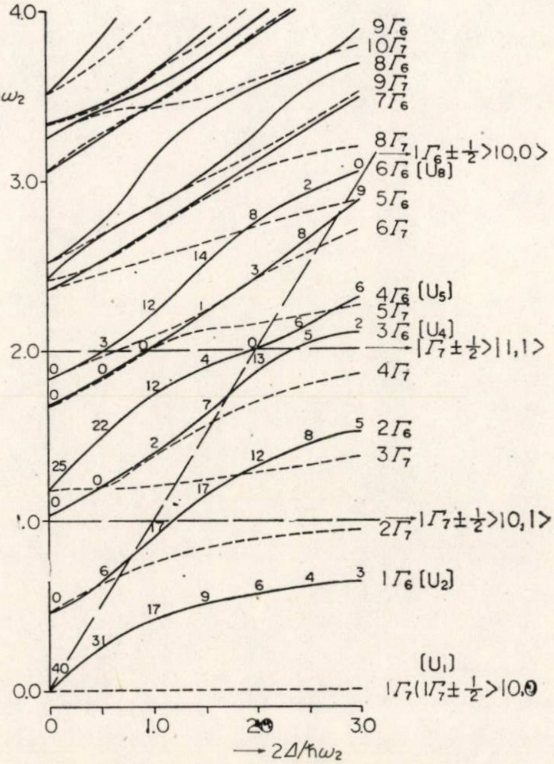

Fig. 6. — Vibronic energy levels calculated as a function of $2\Delta/\hbar\omega_2$ with $E_{JT}/\hbar\omega_2 = 1.0$. Solid and dashed lines indicate $j\Gamma_6$ and $j\Gamma_7$ vibronic states, respectively. Three broken straight lines indicate energies of $\left|\Gamma_6 \pm \frac{1}{2} > \right| 0.0>$, $\left|\Gamma_7 \pm \frac{1}{2} > \right| 0.1>$ and $\left|\Gamma_7 \pm \frac{1}{2} > \right| 1.1>$ in $E_{JT} = 0$. Some of vibronic states correspond to final states of observed absorption lines indicated in squared brackets.

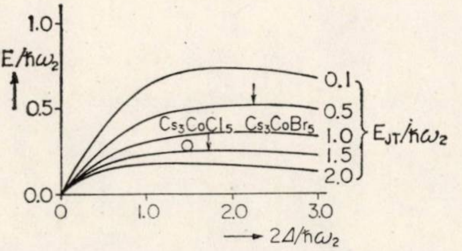

Fig. 7. — Calculated curves of $\Delta E/\hbar\omega_2$ versus $2\Delta/\hbar\omega_2$ for various values of $E_{JT}/\hbar\omega_2$ with $2\delta = 0.16$ (2Δ). Arrows show positions of maxima of curves.

with $\left|\Gamma_7 \pm \frac{1}{2} > \right| 0,1 >$, $\left|\Gamma_7 \pm \frac{1}{2} > \right| 1,1 >$ etc. so as to be the most effective intermediate state for the transition to the $j\Gamma_6$ state by mixing with the $j\Gamma_6$ state through the even parity part of vibration. Therefore the value of C^{00}_{j66} changes with $2\Delta/\hbar\omega_2$ followed by the remarkable change of intensity for vibronic lines having $j\Gamma_6$ states as the final state. In Fig. 6, the relative values of intensity are shown along each curve for these lines. It can be explained that the U_5 line for instance intensifies rapidly with increasing $|\mathbf{P}|$, while the U_8 line weakens slowly. As mentioned above, the behaviours of the excited state ^2E are well explained with the Jahn-Teller coupling by taking account of vibronic wave functions.

Revue Roumaine de Chimie, **22**, *9–10*, 1315–1328 (1977)

THE ELECTRONIC STRUCTURE OF SOME STILBENE DERIVATIVES. VI[1]

THE MOLECULAR DIAGRAMS OF SOME MONO-NITRO-STILBENE DERIVATIVES

LUCIA CIOHODARU
Department of Physical Chemistry, Polytechnic Institute, St. Polizu 1, Bucharest, Romania

Received March 4, 1976

Calculations are reported, using the method of molecular orbitals, within the framework of Hückel approximation, of the charge distribution, bond orders and free valence indices in 18 stilbene molecules. Calculations refer to the ground and first excited states of the molecules. The transmission of the substituents effects through the ethylenic bridge, as well as the alternating character of the π-charge migration and π-bond orders are discussed.

Due to the very important functions of stilbene derivatives in carcinogenesis, which may depend on the π-charge distribution, we have attempted an interpretation of their electronic structure on the basis of molecular diagrams, computed from molecular wave functions obtained by the HMO method.

Calculations are concerned both with the ground and with the first electronically excited states of 18 stilbenes molecules.

The idea of such calculations is by no means new, but there are no available literature data referring to the HMO molecular diagrams of stilbene derivatives dealt with in this paper. Some data for similar compounds were described.[2–4]

RESULTS AND DISCUSSION

The investigated stilbene derivatives have the following general formula :

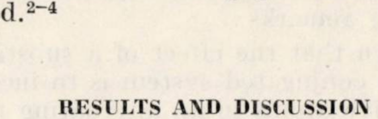

---

[1] Part V: L. Ciohodaru, *Rev. Roumaine Chim.*, **22**, 975 (1977).

[2] C. A. Coulson and J. Jacobs, *J. Chem. Soc.*, **1949**, 1983.

[3] H. H. Jaffé and M. Orchin, *J. Chem. Soc.*, **1960**, 1078.

[4] H. Güsten and L. Klasinc, *Tetrahedron Letters*, **1967**, 2923.

The significance of letters ($A-D$) is given in Table 1.

The syntheses of these compounds, according to the literature data, have been already reported, [5,6] as well as the parameter values used in HMO calculations. [1]

Table 1

The substituents of the studied stilbene derivatives

Deriv. no	A	B	C	D	Comments
1	H	H	NO_2	CN	2-cyano-4-nitro-stilbene derivatives
2	H	H	NO_2	$CONH_2$	
3	H	H	NO_2	COOH	
4	H	OH	NO_2	CN	
5	H	OCH_3	NO_2	CN	
6	H	NMe_2	NO_2	CN	
7	H	NMe_2	NO_2	COOH	
8	H	H	CN	NO_2	2-nitro-4-cyano-stilbene derivatives
9	H	H	$CONH_2$	NO_2	
10	H	H	COOH	NO_2	
11	H	OH	CN	NO_2	
12	H	OCH_3	CN	NO_2	
13	H	NMe_2	CN	NO_2	
14	H	NMe_2	$CONH_2$	NO_2	
15	H	NMe_2	COOH	NO_2	
16	H	$NHCOCH_3$	CN	NO_2	
17	OCH_3	OH	CN	NO_2	
18	OCH_3	$OCOCH_3$	CN	NO_2	

The calculated values of the static parameters of reactivity (π-electron charge density, π-bond order and free valence index), referring both to the ground state and the first excited state of every stilbene derivative, are collected in Tables 2–7.

Examining the *data in connection with the ground state of molecules* we make the following remarks :

1. It is well known that the effect of a substituent on the ground state of an aromatic or conjugated system is to increase or decrease the net charge on consecutive atoms in an alternating manner. [7] In addition, we can mention that the alternating picture of the π-charge distribution appears, also, if the conjugated system has many substituents of different electronic nature, placed in certain positions with each other depending on their nature. This effect is illustrated by all substituted stilbenes which we refer to in this paper ; they show, generally, an alternating character of the π-charge migrations, due to the perturbations introduced by substituents. Also, the value of perturbation depends on the position and electronic nature of substituents.

---

[5] L. Ciohodaru and A. Meghea, *Rev. Roumaine Chim.*, **21**, 1127 (1976).

[6] M. Bán, G. Gáspár, J. Szabó and M. Török, *Magyar Fiz. Folyoirat*, **11**, 89 (1963).

[7] C. A. Coulson and H. C. Longuet-Higgins, *Proc. Roy. Soc.*, *A* **192,** 16 (1947).

2. When one (NO_2) or two (NO_2 and CN ; NO_2 and $CONH_2$; NO_2 and COOH) electron withdrawing substituents are introduced in one benzene ring at 2- and 4-positions, the π-charge density distribution in that benzene ring has an alternating character ; this character is attenuated as we move away from the point of substitution and appears, generally, to the second carbon atom of the ethylenic bridge ; the π-charge density distribution in the unsubstituted ring resembles that in the unsubstituted stilbene. Therefore, the transmission of the substituents effects is hardly noticeable in the unsubstituted ring. This is the same conclusion resulted from IR [8] and ESR spectra [9] of some of these stilbene derivatives.

3. When one (OH, OCH_3, $NHCOCH_3$, NMe_2) electron-repelling substituent is introduced in the second benzene ring, at 4′-position, preserving the substituents in the first benzene ring, the alternating character of the π-charge distribution appears over the whole molecule ; the distribution in the first benzene ring remains like in the derivative unsubstituted in the second benzene ring. Thus the general picture of the charge migration in the derivative substituted in both benzene rings seems to be very little different from a superposition of the migrations in the derivative substituted in the first benzene ring and the derivative substituted in the second benzene ring, separately.

Considering the different electronic nature of the two substituents at 4- and 4′-positions, as well as the alternating and attenuated transmission of the substituents effects from every ring through the ethylenic bridge to its second carbon atom, we may state that these facts lead to *the addition of the electronic effects (of the substituents) just in the ethylenic region*. As a result, the highest modification of the π-charge density appears at the ethylenic bridge.

As it was to be expected, the dimethylamino substituent at 4′-position brings about the highest modification of the π-charge density distribution. In fact, the 4′-dimethylamino-stilbene derivatives containing substituents in another benzene ring are of greatest biological interest.

4. If two electron-repelling substituents (OH and OCH_3, $OCOCH_3$ and OCH_3) are introduced in the second benzene ring at 4′-and 5′-positions, respectively, preserving, also, the electron-withdrawing substituents in the first benzene ring, the alternating character of the π-charge distribution does not appear any more.

5. In comparison with the unsubstituted stilbene, the presence of the substituents in every benzene ring reduces to a great extent the π-bond orders of the adjacent bonds ; the molecular diagrams exhibit the decreasing modification of the other π-bond orders as we move away from the point of substitution. In addition to that, the π-bond order of the $7-7'$ bond decreases and those of the $1-7$ and $1'-7'$ bonds increase ; p_{1-7} increases to a greater extent ; this bond is by the side of the benzene ring substituted by two electron-withdrawing substituents ; the highest increase appears when a nitro group is placed at 2-position.

---

[8] L. Ciohodaru, *Rev. Roumaine Chim.*, **22**, 163 (1977).

[9] L. Ciohodaru, V. E. Sahini and E. Volanschi, *Rev. Roumaine Chim.*, **22**, 171 (1977).

Table 2

π-electron charge densities $(q_r)^a$ for 2-cyano-4-nitro-stilbene derivatives

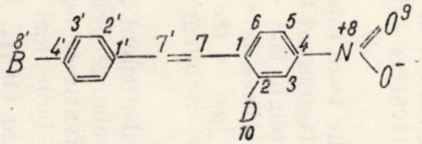

Deriv. no r^b	1	2	3	4	5	6	7	Unsubstit^c. stilbene	4-nitro^c stilbene
1	1.0568 1.0176	0.9147 1.0336	0.9123 1.0324	1.0550 1.0237	1.0559 1.0251	1.0550 1.0339	0.9128 1.0622	1.0001 1.0001	0.9572 1.0267
2	0.9503 0.9371	1.0350 1.0367	1.0360 1.0383	0.9512 0.9358	0.9517 0.9362	0.9530 0.9361	1.0398 1.0628	0.9999 0.9999	1.0051 0.9684
3	1.0396 1.0322	0.8770 0.8712	0.8736 0.8689	1.0416 1.0396	1.0423 1.0406	1.0430 1.0493	0.8726 0.8735	1.0000 1.0000	0.9391 1.0005
4	1.0922 1.1674	1.1010 1.0741	1.1011 1.0703	1.0932 1.1669	1.0941 1.1677	1.0956 1.1671	1.1047 1.1118	0.9999 0.9999	1.0995 1.1026
5	1.0336 0.9527	0.8998 1.0208	0.8987 1.0229	1.0326 0.9604	1.0333 0.9615	1.0331 0.9725	0.8999 1.0306	1.0000 1.0000	0.9391 1.0005
6	1.0044 1.0464	1.0056 0.9336	1.0056 0.9313	1.0060 1.0452	1.0069 1.0460	1.0087 1.0455	1.0096 0.9719	0.9999 0.9999	1.0051 0.9684
7	0.9964 1.0305	1.0072 0.8478	1.0073 0.8452	1.0074 1.0362	1.0086 1.0367	1.0172 1.0335	1.0287 0.9107	1.0000 1.0000	1.0035 0.8594
8	1.0715 1.2057	1.0718 1.1148	1.0718 1.1093	1.0714 1.2139	1.0717 1.2145	1.0721 1.2187	1.0723 1.1119	—	1.0721 1.1838
9	1.5045 1.6054	1.5057 1.5354	1.5056 1.5311	1.5040 1.6100	1.5050 1.6112	1.5054 1.6138	1.5065 1.5363	—	1.5060 1.5861

10	1.6955 1.2790	4.1411 4.2904	4.1497 4.3337	1.6976 1.2914	1.6984 1.2930	1.7000 1.3198	4.1536 4.3510	—	—
1′	0.9989 1.0010	1.0010 0.9377	1.0010 0.9368	1.0236 1.0263	1.0253 1.0275	1.0409 1.0335	1.0424 0.9201	1.0001 1.0001	1.0006 0.9443
2′	1.0059 1.0154	0.9917 0.9580	0.9915 0.9570	1.0010 1.0079	1.0016 1.0084	1.0004 1.0057	0.9866 0.9851	0.9999 0.9999	0.9959 0.9600
3′	0.9998 1.0014	0.9999 0.9902	0.9999 0.9902	1.0383 1.0365	1.0396 1.0376	1.0574 1.0501	1.0568 0.9863	1.0000 1.0000	0.9999 0.9913
4′	1.0059 1.0213	0.9923 0.9242	0.9920 0.9226	0.9957 0.9622	0.9552 0.9614	0.9548 0.9548	0.9416 0.8748	0.9999 0.9999	0.9961 0.9297
7′	1.0317 1.0440	1.0276 1.0407	0.9540 0.9415	1.0276 1.0407	1.0281 1.0412	1.0263 1.0422	0.9508 1.0460	1.0000 1.0000	0.9775 0.9393
8′	—	—	—	1.9384 1.9368	1.9340 1.9319	1.8719 1.8517	1.8659 1.6485	—	—

a – the charges on the atoms are shown in units of e; positions not labelled may be found by symmetry;
b – for each *r*, the first line contains the data for the ground state, and the second line the data for the first excited state;
c – in order to make a comparison, the data for the unsubstituted stilbene are calculated again in this work, although there are available literature data for it;[8] also, the data for 4-nitro-stilbene, although it does not take part in our series of stilbenes.

Table 3

π-bond orders (p_{rs}) for 2-cyano-4-nitro-stilbene derivatives[a]

Deriv. no / $r-s$[b]	1	2	3	4	5	6	7	Unsubstit.[c] stilbene	4-nitro-[c] stilbene
1−2	0.5203 0.4268	0.5527 0.4262	0.5504 0.4248	0.5200 0.4268	0.5205 0.4273	0.5205 0.4292	0.5478 0.4476	0.6173 0.4876	0.6092 0.4992
2−3	0.5763 0.5591	0.6231 0.6363	0.6206 0.6286	0.5780 0.5592	0.5781 0.5593	0.5793 0.5608	0.6204 0.6157	0.6774 0.7262	0.6818 0.7419
2−10	0.5446 0.6408	0.4184 0.4799	0.4263 0.4932	0.5424 0.6405	0.5422 0.6403	0.5411 0.6374	0.4289 0.5009	—	—
3−4	0.6488 0.5790	0.6364 0.6191	0.6366 0.6233	0.6471 0.5786	0.6490 0.5790	0.6456 0.5790	0.6366 0.6394	0.6593 0.6007	0.6184 0.5380
4−8	0.2911 0.3945	0.2939 0.3287	0.2937 0.3238	0.2918 0.3978	0.2917 0.3979	0.2925 0.3992	0.2949 0.3296	—	0.3062 0.3900
8−9	0.6692 0.5527	0.6683 0.6312	0.6683 0.6361	0.6687 0.5457	0.6688 0.5455	0.6668 0.5405	0.6677 0.6329	—	0.6676 0.5716
4−5	0.6002 0.5190	0.6067 0.5327	0.6060 0.5350	0.6008 0.5153	0.6008 0.5152	0.6012 0.5133	0.6037 0.5344	0.6593 0.6007	0.6184 0.5380
5−6	0.6806 0.7196	0.6846 0.7149	0.6844 0.7115	0.6801 0.7235	0.6800 0.7237	0.6797 0.7279	0.6870 0.7066	0.6774 0.7262	0.6888 0.7419
6−1	0.6209 0.5628	0.6154 0.5301	0.6159 0.5338	0.6215 0.5597	0.6215 0.5595	0.6215 0.5554	0.6131 0.5708	0.6173 0.4876	0.6092 0.4992
1−7	0.4107 0.5106	0.3988 0.5556	0.3999 0.5536	0.4098 0.5124	0.4097 0.5125	0.4099 0.5169	0.4069 0.5001	0.3767 0.5868	0.3828 0.5506
7−7′	0.8428 0.7365	0.8497 0.5890	0.8492 0.5924	0.8418 0.7355	0.8425 0.7361	0.8409 0.7318	0.8413 0.6901	0.8617 0.4968	0.8621 0.5864
7′−1′	0.3795 0.4337	0.3812 0.5301	0.3814 0.5283	0.3852 0.4393	0.3853 0.4394	0.3886 0.4480	0.3938 0.4938	0.3767 0.5868	0.3778 0.5349
1′−2′	0.6143 0.5863	0.6155 0.5529	0.6154 0.5238	0.6118 0.5848	0.6116 0.5844	0.6073 0.5776	0.6051 0.5295	0.6173 0.4876	0.6164 0.5199
2′−3′	0.6783 0.6882	0.6778 0.7127	0.6778 0.7124	0.6829 0.6925	0.6833 0.6929	0.6895 0.7023	0.6922 0.7395	0.6744 0.7262	0.6776 0.7138
3′−4′	0.6584 0.6476	0.6587 0.6164	0.6587 0.6164	0.6368 0.6262	0.6354 0.6251	0.6152 0.6009	0.6150 0.6007	0.6593 0.6007	0.6584 0.6149
4′−8′	—	—	—	0.2504 0.2514	0.2582 0.2595	0.3567 0.3696	0.3655 0.4955	—	—

[a] the labelling of positions is shown in Table 2; positions not labelled may be found by symmetry;

Table 4

Free valence indices (F_r) for 2-cyano-4-nitro-stilbene derivatives[a]

Deriv. no / r^b	1	2	3	4	5	6	7	Unsubstit. stilbene[c]	4-nitro-stilbene[c]
1	0.1800 0.2318	0.1651 0.2201	0.1657 0.2197	0.1807 0.2331	0.1801 0.2326	0.1800 0.2305	0.1641 0.2134	0.1206 0.1700	0.1308 0.1830
2	0.0907 0.1052	0.1377 0.1896	0.1347 0.1853	0.0928 0.1067	0.0910 0.1051	0.0909 0.1045	0.1348 0.1677	0.4373 0.5183	0.4340 0.4909
3	0.5068 0.5939	0.4725 0.4766	0.4748 0.4798	0.5068 0.6076	0.5049 0.5932	0.5070 0.5921	0.4742 0.4761	0.3953 0.4052	0.4248 0.4521
4	0.1968 0.2395	0.1950 0.2514	0.1954 0.2494	0.1923 0.2402	0.1904 0.2393	0.1927 0.2403	0.1960 0.2278	0.4134 0.5307	0.2002 0.2772
5	0.4512 0.4934	0.4406 0.4844	0.4415 0.4855	0.4511 0.4931	0.4511 0.4931	0.4511 0.4907	0.4413 0.4909	0.3953 0.4052	0.4248 0.4521
6	0.4305 0.4496	0.4320 0.4870	0.4316 0.4866	0.4304 0.4487	0.4304 0.4487	0.4308 0.4486	0.4318 0.4545	0.4373 0.5183	0.4340 0.4909
7	0.4785 0.4849	0.4840 0.5878	0.4828 0.5860	0.4804 0.4842	0.4797 0.4833	0.4812 0.4835	0.4838 0.5417	0.4935 0.6484	0.4871 0.5950
1′	0.1237 0.1256	0.1197 0.1560	0.1197 0.1559	0.1230 0.1231	0.1235 0.1236	0.1287 0.1287	0.1280 0.1791	0.1206 0.1700	0.1214 0.1573
2′	0.4393 0.4575	0.4386 0.4964	0.4387 0.4957	0.4372 0.4547	0.4371 0.4546	0.4351 0.4521	0.4343 0.4626	0.4373 0.5183	0.4380 0.4983
3′	0.3952 0.3961	0.3954 0.4029	0.3954 0.4028	0.4129 0.4133	0.4133 0.4139	0.4272 0.4288	0.4272 0.4610	0.3953 0.4052	0.3960 0.4033
4′	0.4151 0.4367	0.4145 0.4992	0.4145 0.4985	0.2079 0.2734	0.2029 0.2222	0.1448 0.1606	0.1423 0.1743	0.4134 0.5307	0.4152 0.5022
7′	0.5096 0.5617	0.5010 0.6128	0.5013 0.6113	0.4941 0.5464	0.5041 0.5564	0.5025 0.5524	0.4969 0.5481	0.4935 0.6484	0.4921 0.6107

a–c – the same significances shown in Table 3.

Table 5

π-electron charge densities (q_r)^a for 2-nitro-4-cyano-stilbene derivatives

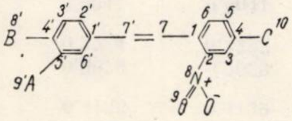

Deriv. no r^b	8	9	10	11	12	13	14	15	16	17	18
1	1.0358 0.9806	0.9094 1.0268	0.9074 1.0264	1.0348 0.9869	1.0346 0.9872	1.0341 0.9963	0.9098 1.0590	0.9077 1.0575	1.0347 0.9864	1.0347 0.9879	1.0338 0.9848
2	1.0953 1.1744	1.1042 1.1050	1.1042 1.1016	1.0972 1.1747	1.0973 1.1747	1.0988 1.1742	1.1081 1.1233	1.1080 1.1193	1.0970 1.1739	1.0970 1.1745	1.0958 1.1732
3	1.0317 0.9970	0.8761 0.8662	0.8727 0.8669	1.0335 1.0053	1.0335 1.0057	1.0346 1.0151	0.8759 0.8781	0.8727 0.8790	1.0332 1.0038	1.0333 1.0061	1.0324 1.0028
4	0.9525 0.9439	1.0335 1.0075	1.0343 1.0082	0.9539 0.9426	0.9540 0.9426	0.9553 0.9423	1.0369 1.0542	1.0379 1.0546	0.9538 0.9429	0.9540 0.9427	0.9526 0.9421
5	1.0618 1.0142	0.9074 1.0242	0.9050 1.0232	1.0621 1.0250	1.0618 1.0252	1.0617 1.0364	0.9086 1.0324	0.9063 1.0309	1.0616 1.0230	1.0717 1.0256	1.0608 1.0213
6	0.9952 0.9872	1.0048 0.9302	1.0050 0.9305	0.9972 0.9871	0.9972 0.9871	0.9984 0.9863	1.0089 0.9747	1.0089 0.9750	0.9970 0.9870	0.9971 0.9870	0.9956 0.9859
7	0.9998 1.0412	1.0080 0.8567	1.0080 0.8534	1.0115 1.0389	1.0121 1.0385	1.0206 1.0351	1.0236 0.9116	1.0288 0.9113	1.0110 1.0400	1.0111 1.0376	1.0078 1.0384
8	1.0718 1.2298	1.0720 1.1111	1.0720 1.1060	1.0720 1.2393	1.0721 1.2397	1.0724 1.2441	1.0726 1.1139	1.0726 1.1079	1.0720 1.2352	1.0720 1.2395	1.0712 1.2345
9	1.5065 1.6611	1.5067 1.5358	1.5064 1.5317	1.5059 1.6286	1.5060 1.6289	1.6063 1.7315	1.5074 1.5390	1.5074 1.5344	1.5059 1.6259	1.5059 1.5865	1.5048 1.6249

10	1.7012 1.3007	4.1668 4.3096	4.1453 4.3075	1.7044 1.3141	1.7044 1.3150	1.7062 1.3415	4.1403 4.3174	4.1493 4.3490	1.7039 1.3168	1.7041 1.3170	1.7018 1.3130
1′	0.9996 1.0118	1.0010 0.9414	1.0010 0.9402	1.0246 1.0272	1.0258 1.0280	1.0416 1.0341	1.0428 0.9229	1.0427 0.9220	1.0233 1.0270	1.0238 1.0259	1.0166 1.0215
2′	1.0052 1.0122	0.9917 0.9602	0.9912 0.9589	1.0008 1.0047	1.0010 1.0048	0.9998 1.0021	0.9869 0.9867	0.9866 0.9858	1.0015 1.0059	1.0293 1.0293	1.0292 1.0298
3′	0.9996 1.0015	1.0000 0.9909	1.0000 0.9907	1.0383 1.0366	1.0397 1.0378	1.0575 1.0503	1.0571 1.9875	1.0570 0.9872	1.0356 1.0339	1.0378 1.0360	1.0292 1.0283
4′	1.0052 1.0182	0.9926 0.9284	1.0090 0.9437	0.9553 0.9589	0.9548 0.9579	0.9545 0.9516	0.9428 0.8793	0.9425 0.8780	0.9624 0.9676	0.9906 0.9900	0.9968 0.9989
5′	0.9996 1.0015	1.0000 0.9909	1.0000 0.9907	1.0383 1.0366	1.0397 1.0378	1.0575 1.0503	1.0571 0.9875	1.0570 0.9872	1.0356 1.0339	0.9889 0.9866	0.9810 0.9800
6′	1.0052 1.0122	0.9917 0.9602	0.9912 0.9589	1.0008 1.0047	1.0010 1.0048	0.9998 1.0021	0.9869 0.9867	0.9866 0.9858	1.0015 1.0059	1.0468 1.0545	1.0458 1.0546
7′	1.0267 1.0265	0.9548 0.9462	0.9536 0.9435	1.0232 1.0223	1.0232 1.0223	1.0214 1.0230	0.9518 1.0488	0.9503 1.0453	1.0235 1.0229	1.0236 1.0232	1.0238 1.0234
8′	—	—	—	1.9384 1.9363	1.9343 1.9318	1.8720 1.8509	1.8661 1.6519	1.8661 1.6509	5.9373 5.9387	1.9413 1.9385	5.9328 5.9549
9′	—	—	—	—	—	—	—	—	—	1.9394 1.9389	1.9378 1.9374

a,*b* – the same significances shown in Table 2.

Table 6

π – bond orders (p_{rs}) for 2-nitro-4-cyano-stilbene derivatives [a]

Deriv. no $r-s^b$	**8**	**9**	**10**	**11**	**12**	**13**	**14**	**15**	**16**	**17**	**18**
1 – 2	0.5620 0.4590	0.5681 0.4508	0.5674 0.4538	0.5622 0.4561	0.5624 0.4561	0.5625 0.4545	0.5656 0.4730	0.5648 0.4765	0.5622 0.4570	0.5618 0.4556	0.5740 0.4690
2 – 3	0.6627 0.6004	0.6484 0.6900	0.6515 0.6960	0.6604 0.5986	0.6610 0.5992	0.6597 0.5994	0.6507 0.6768	0.6517 0.6810	0.6611 0.6005	0.6602 0.5984	0.6608 0.5995
2 – 8	0.2949 0.4097	0.2978 0.3330	0.2976 0.3285	0.2954 0.4130	0.2958 0.4134	0.2965 0.4147	0.2993 0.3362	0.2991 0.3311	0.2957 0.4114	0.2954 0.4130	0.2956 0.4114
8 – 9	0.6679 0.5318	0.6671 0.6327	0.6672 0.6372	0.6672 0.5239	0.6524 0.5088	0.6672 0.5204	0.6665 0.6300	0.6665 0.6352	0.6675 0.5274	0.6674 0.5239	0.6678 0.5276
3 – 4	0.5657 0.5484	0.6100 0.5567	0.6074 0.5505	0.5668 0.5479	0.5673 0.5484	0.5684 0.5497	0.6099 0.5797	0.6073 0.5727	0.5671 0.5484	0.5670 0.5484	0.5670 0.5487
4 – 10	0.5362 0.6261	0.4126 0.4710	0.4203 0.4827	0.5334 0.6254	0.5343 0.6263	0.5327 0.6232	0.4148 0.4827	0.4228 0.4953	0.5342 0.6253	0.5334 0.6241	0.5340 0.6248
4 – 5	0.5554 0.4662	0.5900 0.5126	0.5875 0.5111	0.5552 0.4662	0.5559 0.4668	0.5562 0.4692	0.5877 0.5108	0.5852 0.5091	0.5558 0.4673	0.5554 0.4666	0.5552 0.4666
5 – 6	0.7058 0.7439	0.6908 0.7262	0.6925 0.7272	0.7048 0.7414	0.7052 0.7418	0.7050 0.7407	0.6942 0.7237	0.6952 0.7244	0.7052 0.7428	0.7042 0.7408	0.7046 0.7420
6 – 1	0.5995 0.5587	0.6100 0.5146	0.6094 0.5148	0.5994 0.5603	0.5998 0.5607	0.5997 0.5613	0.6072 0.5523	0.6063 0.5519	0.5997 0.5595	0.5994 0.5603	0.5990 0.5590
1 – 7	0.4051 0.5003	0.3971 0.5543	0.3978 0.5513	0.4044 0.5013	0.4042 0.5014	0.4044 0.5052	0.4024 0.4996	0.4045 0.4980	0.4046 0.5029	0.4046 0.5020	0.4042 0.5017

7–7′	0.8452	0.8505	0.8500	0.8440	0.8448	0.8431	0.8428	0.8422	0.8442	0.8444	0.8438
	0.7422	0.5956	0.5989	0.7423	0.7431	0.7400	0.6880	0.6915	0.7405	0.7422	0.7406
1′–7′	0.3833	0.3810	0.3811	0.3846	0.3845	0.3878	0.3931	0.3935	0.3855	0.3840	0.3844
	0.4362	0.5259	0.5242	0.4370	0.4371	0.4457	0.4947	0.4931	0.4409	0.4371	0.4389
1′–2′	0.6146	0.6155	0.6154	0.6114	0.6119	0.6076	0.6052	0.6050	0.6108	0.6126	0.6116
	0.5870	0.5261	0.5269	0.5850	0.5854	0.5786	0.5292	0.5299	0.5826	0.5853	0.5837
2′–3′	0.6781	0.6779	0.6779	0.6828	0.6833	0.6896	0.6296	0.6926	0.6847	0.6762	0.6764
	0.6879	0.7115	0.7112	0.6923	0.6930	0.7026	0.7397	0.7395	0.6958	0.6864	0.6872
3′–4′	0.6585	0.6588	0.6587	0.6362	0.6355	0.6152	0.6123	0.6122	0.6306	0.6450	0.6442
	0.6478	0.6182	0.6184	0.6261	0.6251	0.6007	0.5320	0.5319	0.6186	0.6341	0.6326
4′–5′	0.6585	0.6588	0.6587	0.6362	0.6355	0.6152	0.6123	0.6122	0.6306	0.6160	0.6160
	0.6478	0.6182	0.6184	0.6261	0.6251	0.6007	0.5320	0.5319	0.6186	0.6048	0.6042
4′–8′	—	—	—	0.2508	0.2583	0.3570	0.3652	0.3655	0.2831	0.2406	0.2394
				0.2528	0.2608	0.3715	0.4933	0.4944	0.2885	0.2443	0.2438
5′–6′	0.6781	0.6779	0.6779	0.6828	0.6833	0.6896	0.6926	0.6926	0.6847	0.6644	0.6631
	0.6879	0.7115	0.7112	0.6923	0.6930	0.7026	0.7397	0.7395	0.6958	0.6740	0.6734
5′–9′	—	—	—	—	—	—	—	—	—	0.2340	0.2475
										0.2352	0.2483
6′–1′	0.6146	0.6155	0.6154	0.6114	0.6119	0.6076	0.6052	0.6050	0.6108	0.6112	0.6122
	0.5870	0.5271	0.5269	0.5850	0.5854	0.5786	0.5292	0.5299	0.5826	0.5851	0.5847

a – the labelling of position is shown in Table 5;
b – the same significance shown in Table 2.

Table 7

Free valence indices (F_r) for 2-nitro-4-cyano-stilbene derivatives[a]

Deriv. no r^b	8	9	10	11	12	13	14	15	16	17	18
1	0.1653 0.2139	0.1566 0.2123	0.1573 0.2120	0.1622 0.2143	0.1655 0.2137	0.1653 0.2109	0.1566 0.2077	0.1562 0.2056	0.1654 0.2125	0.1622 0.2141	0.1548 0.2023
2	0.2123 0.2627	0.2177 0.2582	0.2153 0.2536	0.2140 0.2643	0.2127 0.2632	0.2133 0.2634	0.2164 0.2459	0.2162 0.2433	0.2128 0.2630	0.2146 0.2650	0.2016 0.2521
3	0.5035 0.5831	0.4736 0.4853	0.4730 0.4854	0.5048 0.5855	0.5037 0.5844	0.5038 0.5829	0.4713 0.4754	0.4730 0.4782	0.5037 0.5830	0.5048 0.5852	0.5042 0.5831
4	0.0745 0.0912	0.1192 0.1917	0.1167 0.1875	0.0766 0.0925	0.0744 0.0904	0.0746 0.0899	0.1194 0.1587	0.1167 0.1547	0.0748 0.0909	0.0762 0.0921	0.0758 0.0919
5	0.4708 0.5219	0.4512 0.4932	0.4519 0.4936	0.4720 0.5244	0.4709 0.5233	0.4708 0.5220	0.4500 0.4975	0.4515 0.4983	0.4709 0.5218	0.4724 0.5246	0.4722 0.5234
6	0.4267 0.4294	0.4312 0.4912	0.4300 0.4899	0.4278 0.4304	0.4269 0.4294	0.4273 0.4299	0.4305 0.4559	0.4304 0.4556	0.4270 0.4296	0.4284 0.4309	0.4284 0.4310
7	0.4816 0.4894	0.4843 0.5821	0.4841 0.5817	0.4836 0.4884	0.4829 0.4874	0.4844 0.4875	0.4866 0.5443	0.4852 0.5424	0.4831 0.4885	0.4832 0.4880	0.4840 0.4897
1′	0.1193 0.1216	0.1199 0.1538	0.1199 0.1539	0.1246 0.1250	0.1237 0.1241	0.1289 0.1290	0.1284 0.1787	0.1283 0.1789	0.1248 0.1257	0.1242 0.1245	0.1238 0.1247
2′	0.4392 0.4570	0.4385 0.4943	0.4386 0.4938	0.4378 0.4547	0.4368 0.4536	0.4348 0.4508	0.4342 0.4630	0.4343 0.4625	0.4365 0.4535	0.4432 0.4675	0.4440 0.4611
3′	0.3953 0.3962	0.3952 0.4022	0.3953 0.4023	0.4130 0.4136	0.4131 0.4138	0.4271 0.4287	0.3953 0.4023	0.4271 0.4605	0.4167 0.4175	0.4108 0.4115	0.4114 0.4122
4′	0.4149 0.4364	0.4143 0.4955	0.4144 0.4951	0.2088 0.2270	0.2125 0.2209	0.1445 0.1591	0.1420 0.1746	0.1420 0.1738	0.1696 0.2062	0.2304 0.2488	0.2324 0.2514
5′	0.3953 0.3962	0.3952 0.4022	0.3953 0.4123	0.4130 0.4136	0.4131 0.4138	0.4271 0.4287	0.3953 0.4023	0.4271 0.4605	0.4167 0.4175	0.2176 0.2180	0.2154 0.2061
6′	0.4392 0.4570	0.4385 0.4943	0.4386 0.4938	0.4378 0.4547	0.4368 0.4536	0.4348 0.4508	0.4342 0.4630	0.4343 0.4635	0.4365 0.4535	0.4564 0.4729	0.4567 0.4739
7′	0.5034 0.5536	0.5005 0.6105	0.5018 0.6088	0.5034 0.5527	0.5030 0.5517	0.5010 0.5470	0.4960 0.5491	0.4961 0.5473	0.5022 0.5505	0.5038 0.5527	0.5038 0.5525

[a] – the labelling of positions is shown in Table 5;

[b] – the same significance shown in Table 2.

At the same time, we can mention that the dimetylamino substituent has the highest value of π-bond order $\left(\gt C-NMe_2\right)$ among the other substituents.

6. All the above mentioned results, referring to the π-bond orders, lead to the conclusion that even in the ground state of the molecule, besides the Kekulé unexcited structures, such as (I), there are some high-polar quinoid structures such as (II), having of course a small weight :

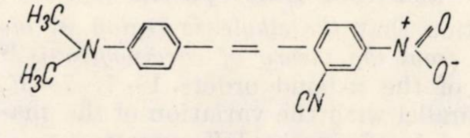

(I)

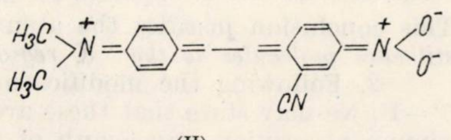

(II)

Therefore, not only the π-charge distribution has an alternating character due to the presence of certain substituents in corresponding positions ; also, the π-bond orders increase and decrease along the molecule in an alternating manner due to the presence of the same substituents.

7. Further on, the substituents bring about the modification of free valence indices ; thus, the free valence indices for carbon atoms by the side of the point of substitution increase. Simultaneously, the highest modification belongs to the ethylenic carbon atoms, depending on the nature, number and position of substituents in the two benzene rings.

In connection with *the first excited state* of the same molecules, the following conclusions may be drawn :

1. In the first excited state of the molecules it may be presumed that the weight of quinoid structure, such as (II), increases to a greater extent, due to the alternating modifications of the π-charge densities distribution and π-bond orders. (The same assumption was made, based on the UV spectra. [5]) But, the weight of such structures could not be estimated in a quantitative manner.

There are alternating modifications of the π-bond lengths along the whole conjugated system, including the substituents from the two benzene rings, namely that interaction between substituents and conjugated system of stilbene molecule is quantitatively much greater in the excited state than in the ground state. The central ethylenic bridge exhibits the highest modification of π-bond orders and of free valence indices.

2. Generally, the electronic excitation brings about an attenuation of the alternating character of the π-charge distribution corresponding to the ground state ; at the same time, the average charge migration increases.

3. In comparison with the ground state, on the whole, there is a π-charge migration in the first excited state to the electron-withdrawing substituents and from the electron-repelling substituents.

4. All free valence indices increase.

5. Therefore, in comparison with the ground state, for all investigated stilbene derivatives, the modifications of the π-bond orders, free valence indices, as well as the π-charge migrations, prove a greater reactivity in the first excited state.

In connection with *the molecular diagrams and the electronic absorption spectra of same studied stilbenes*, we may state the followings :

1. The modification, to the greatest extent, of all static parameters of reactivity for the ethylenic carbon atoms is due to the transmission of the substituents effects through the ethylenic bridge, to the second carbon atom as against every ring. Therefore, the ethylenic bridge has the greatest reactivity in stilbenes molecules. It is the same conclusion resulted from the UV spectra ($\Delta\lambda_{A_{\max}}$) [5] and from ESR spectra (a_7^{H}, $a_{7'}^{H}$).[9] This conclusion justifies the assumption that *the ethylenic region in the stilbenes molecules is the "K region" from the theory of carcinogenesis.*[10]

2. Following the modifications of the π-bond orders $1-7$, $7-7'$, $7'-1'$, we may state that these are parallel with the variation of the maximum absorption wavelength of the *A* band in the UV spectra.[5]

3. Certain stilbene derivatives show similar molecular diagrams. Thus : -no **2** and **3**, **9** and **10**, **14** and **15** ; this means that influence of the amido group at 2- or 4-positions is almost identical with that exerted by the carboxy group at the same positions ;
-no **4** and **5**, **11** and **12** ; in this case, the hydroxy or methoxy groups at 4′-positions bring about similar modifications of the studied parameters ; their UV spectra are, also, similar ;[5]
-no **17** and **18** ; the influence of the hydroxy group at 4′-position and of the methoxy one at 5′-position is almost identical with the influence of the acetoxy group at 4′-position and methoxy group at 5′-position.

4. The molecular diagrams of the couples of positional isomers (no **1** and **8**, **2** and **9**, **3** and **10**, **4** and **11**, **5** and **12**, **6** and **13**, **7** and **15**) exhibit differences concerning the π-charge distributions and π-bond orders. Their values give a theoretical evidence to our assumption, based on the UV spectra analysis, [5] that the conjugative effect of the nitro group at 2-position is stronger than its steric effect. This leads, generally, to a planar conformation of molecules. In addition to that, our HMO calculations account for the differences between the UV spectra of same positional isomers. [5]

5. For the series of compounds no **1**, **4**, **5**, **6** and **9**, **11**, **12**, **13**, the molecular diagrams exhibit differences, which show the increasing influence of the substituents at 4′-position (preserving the substituents at 2- and 4-positions), just in the expected order : H, OH, OCH_3, NMe_2. The same influence was evidenced, earlier, by their UV absorption spectra.[5]

To conclude, the molecular diagrams in both ground and first excited states, obtained by HMO calculations, of 18 stilbenes molecules, are thought to be considered as a theoretical basis for the understanding of the transmission of the substituents effects through the ethylenic bridge ; the same substituents effects have been evidenced by their UV, IR and ESR spectra.

---

[10] A. Pullman and B. Pullman, *Adv. Cancer Res.*, **3**, 117 (1955).

Revue Roumaine de Chimie, 22, *9–10*, 1329–1333 (1977)

VISCOSITY OF MELTS OF HYDRATED LANTHANUM NITRATE

Z. KODEJŠ and I. SLÁMA
Czechoslovak Academy of Sciences,
Institute of Inorganic Chemistry,
Řež near Prague, Czechoslovakia

Received June 5, 1975

The temperature and concentration dependence of the viscosity of $La(NO_3)_3$ solutions has been investigated over the temperature range 278 – 328 K and the concentration range 4 – 10 mol % $La(NO_3)_3$. An empirical equation has been applied to the mathematical description of the dependences obtained.

INTRODUCTION

An understanding of highly concentrated aqueous solutions which may be held for hydrated melts is essential to the development of complete interpretation of electrolyte solution behaviour from molten salt to dilute solution. Current interest in these melts led to the discovery of glass-forming ability of some compounds. For a number of these solutions the glass-forming concentration ranges have been determined and the corresponding glass transition temperatures at which the solution viscosity approaches values of the order of 10^{13} P have been reported. [1] Some of those solutions can persist in supercooled state and their physicochemical properties, therefore, can be investigated in the range between the thermodynamic liquidus temperature and the glass transition temperature.

The lanthanum nitrate solution has been chosen regarding the possibility of preparing supercooled solutions. [1] Spedding et al [2,3] investigated the conductance and viscosity of unsaturated solutions of lanthanum nitrate at the temperature of 298.15 K. The aim of our work is to determine the viscosity of this solution even in the supercooled state and to verify at the same time the validity of some empirical equations for the description of the temperature and concentration dependence of fluidity in this region.

[1] C. A. Angell and J. E. Sare, *J. Chem. Phys.*, **52**, 1058 (1970).
[2] J. A. Rard and F. H. Spedding, *J. Phys. Chem.*, **79**, 257 (1975).
[3] F. H. Spedding, L. E. Shiers and J. A. Rard, *J. Chem. Eng. Data*, **20**, 88 (1975).

EXPERIMENTAL

The lanthanum nitrate solution was prepared from lanthanum nitrate hexahydrate $La(NO_3)_3.6H_2O$ reagent grade. To remove any insoluble matter capable of acting as nucleation centers for crystallization, the solution was filtered through a sintered glass.

The concentration of the solution was indicated by EDTA method using methylthymol blue as indicator.

The viscosity of the solution was determined using a Höppler viscosimeter BH 2 with an inherent accuracy of $\pm 0.5\%$. The viscosimeter jacket was kept at a constant temperature by an ultra-thermostat, the temperature being measured with an accuracy of $\pm 0.1K$. The experimentally obtained viscosity values have been expressed in poise (P) units defined as $1P = 10^{-1}\,kg\,m^{-1}\,s^{-1}$.

The density of the investigated solutions used to calculate the viscosity has been determined by the method of Ewing and Mikovsky [4] and will be reported later.

RESULTS AND DISCUSSIONS

The viscosity of the solutions was determined over the temperature range 278—328 K and the concentration range 4—10 mol % $La(NO_3)_3$. To describe mathematically the temperature dependence of fluidity (φ) or viscosity (η), three types of equations have been used: an Arrhenius type equation

$$\varphi = A \exp(-E/RT) \tag{1}$$

an empirical equation of the form

$$\ln \eta = k_1 + k_2/T + k_3/T^2 \tag{2}$$

and the Vogel equation frequently applied to the correlation of temperature dependence of viscous solutions [5,6]

$$\ln \varphi = C + B/(T - T_0) \tag{3}$$

where T is the temperature, R is the gas constant, and E, A, B, C, k_1, k_2, and k_3 are the parameters.

The temperature dependence of the fluidity of variously concentrated solutions has been investigated and the parameters of equations (1), (2), and (3) have been calculated. Fig. 1 illustrates the agreement of the experimental values with the course of the temperature dependence of fluidity calculated according to equation (1). Table 1 lists the parameter values of this equation for solutions of different concentrations; the last column gives average relative percent difference between the fluidity calculated and experimentally determined according to the following relation:

$$\Delta = \frac{\sum\limits_{i=1}^{n} \frac{|\varphi_i^{\exp} - \varphi_i^{\text{calc}}|}{\varphi_i^{\exp}}}{n}\, 100 \tag{4}$$

---

[4] W. W. Ewing and R. J. Mikovsky, *J. Amer. Chem. Soc.*, **72**, 1390 (1950).

[5] J. H. Ambrus, C. T. Moynihan and P. B. Macedo, *J. Electrochem. Soc.*, **119**, 192 (1972).

[6] C. A. Angell and R. D. Bressel, *J. Phys. Chem.*, **76**, 3244 (1972).

The presented data reveal an obvious increasing disagreement between the mathematical correlation (1) and the experimental results with increasing concentration of the solutions.

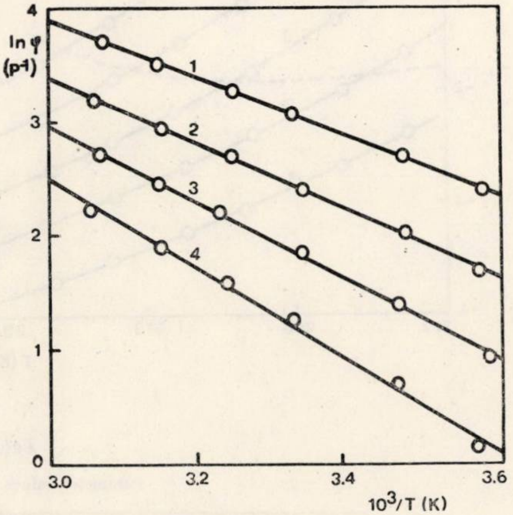

Fig. 1. — Comparison of experimentally obtained temperature dependence of fluidity with that calculated according to equation (1); mol % $La(NO_3)_3$: 1 — 4.92 ; 2 — 6.46 ; 3 — 7.61 ; 4 — 8.72 ; full line denotes calculated data.

Table 1

Parameter values of equation (1) for lanthanum nitrate solutions

concentration mol %	$A.10^{-4}$	E kcal/mol	Δ %
4.92	8.4179	4.9371	0.99
6.46	14.138	5.6158	1.44
7.61	39.457	6.5734	2.16
8.72	144.97	7.7396	3.39

Three-parameter equation (2) proved to be more appropriate for the mathematical description of the temperature dependence of viscosity. Fig. 2 shows the agreement of the experimental and calculated values. Table 2 lists the values of the found parameters k_1, k_2 and k_3 of equation (2) together with the average differences calculated according to relation (4). The maximum value of the relative difference does not exceed 1.5%, which is in accordance with the accuracy of experimentally obtained data.

Using the values listed in Table 1, the viscosity of the investigated solutions at the temperature of 298.15 K has been calculated and compared with the precise data published by Spedding et al.[3] The comparison is made in Fig. 3 and may be taken for satisfactory.

The application of equation (3) to the correlation of the temperature dependence of fluidity resulted in somewhat smaller differences between the calculated and experimental results; however, the values

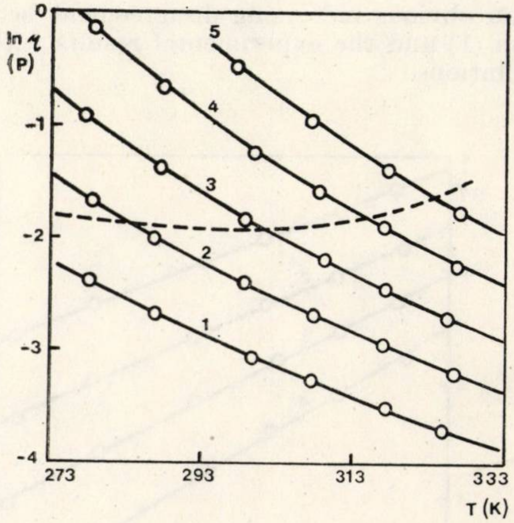

Fig. 2. — Comparison of experimentally obtained temperature dependence of viscosity with that calculated according to equation (2); mol % $La(NO_3)_3$: 1 — 4.92 ; 2 — 6.46 ; 3 — 7.61 ; 4 — 8.72 ; 5 — 9.60 ; full line denotes calculated data, broken line separates the region of saturated and unsaturated solutions.

Table 2

Parameter values of equation (2)

concentration mol %	k_1	$k_2.10^{-2}$	$k_3.10^{-5}$	Δ %
4.92	−8.4820	7.6531	2.5770	0.68
6.46	−6.5414	− 3.7881	4.8139	0.76
7.61	−4.2574	−18.787	7.7701	0.58
8.72	−0.2230	−45.272	12.660	0.92
9.60	−2.1214	−36.084	12.185	0.53

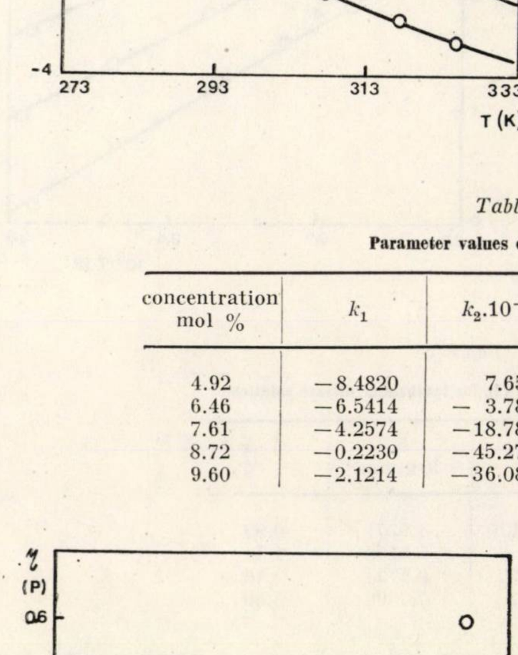

Fig. 3. — Comparison of viscosity data calculated according to equation (2) with those published by Spedding *et al;* temperature : 298.15 K ; O calculated results ; + published results.

of the parameter T_0 which is considered to be a limiting value of the glass transition temperature were considerably scattered. The correlation of the parameter T_0 and the concentration of the solution was not reliable. This was due to relatively low values of the viscosity of investigated solutions, since the preparation of sufficiently supersaturated solutions able to persist in the whole temperature range investigated had not been successful.

To describe the dependence of viscosity on the temperature and concentration, the values of the parameters of equation (2) listed in Table 2 have been expressed as a function of the concentration

$$k_i = a_i + b_i x + c_i x^2 \text{ for } i = 1, 2, \text{ and } 3 \tag{5}$$

where x is the mole fraction of $La(NO_3)_3$ and i is the index of the parameter k. The calculated values of parameters of the equation

$$\ln \eta = a_1 + b_1 x + c_1 x^2 + (a_2 + b_2 x + c_2 x^2)/T + (a_3 + b_3 x + c_3 x^2)/T^2 \tag{6}$$

describing the dependence of viscosity of lanthanum nitrate solutions on the temperature and concentration in the temperature range 278—328 K and the concentration range 4—9 mol % La $(NO_3)_3$ are summarized in Table 3. The comparison of the experimentally obtained viscosity data with those calculated according to equation (6) showed the average relative difference determined from equation (4) and the maximum value to be 0.7 % and 1.6%, respectively.

Table 3

Parameter values of equation (5)

i	a_i	b_i	c_i
1	$6.55423 \cdot 10^{-1}$	$-4.09807 \cdot 10^{2}$	$4.47392 \cdot 10^{3}$
2	$-6.18875 \cdot 10^{3}$	$2.97705 \cdot 10^{5}$	$-3.18957 \cdot 10^{6}$
3	$1.44828 \cdot 10^{6}$	$-5.25373 \cdot 10^{7}$	$5.77648 \cdot 10^{8}$

The authors wish to thank J. Štorková for technical assistance.

of the parameter T_0 which is considered to be a limiting value of the vitrification temperature were considerably scattered. The correlation of the parameter T_0 and the concentration of the solution was not possible. This was due to relatively low values of the viscosity of investigated solutions, since the preparation of sufficiently supersaturated solutions able to persist in the whole temperature range investigated had not been successful.

To describe the dependence of viscosity on the temperature and concentration, the values of the parameters of equation (2) listed in Table 2 have been expressed as a function of the concentration

$$k_i = a_i + b_i x + c_i x^2 \text{ for } i = 1, 2, \text{ and } 3 \qquad (3)$$

where x is the mole fraction of $La(NO_3)_3$ and i is the index of the parameter k. The calculated values of parameters of the equation

$$\ln \eta = a_1 + b_1 x + c_1 x^2 + (a_2 + b_2 x + c_2 x^2)\, T^{-1} + (a_3 + b_3 x + c_3 x^2)\, T^{-2}$$
(4)

describing the dependence of viscosity of lanthanum nitrate solutions on the temperature and concentration in the temperature range 278–328 K and the concentration range [illegible] and [illegible] % $La(NO_3)_3$ are summarized in Table 3. The comparison of the experimentally obtained viscosity data

Table 3

Parameter values of equation (4)

i	a_i	b_i	c_i
1	[illegible]	[illegible]	[illegible]
2	[illegible]	[illegible]	[illegible]
3	[illegible]	[illegible]	[illegible]

with those calculated according to equation (4) showed the average relative difference determined from equation (1) and the maximum value of 0.7% and 2.0%, respectively.

The authors [illegible] technical assistance.

Revue Roumaine de Chimie **22**, *9–10*, 1335–1342 (1977)

INVESTIGATION OF THE EFFECTS OF CHEMICAL NATURE OF SOME STRUCTURAL PROMOTORS ON ELECTRIC CONDUCTIVITY CHANGES IN PRECIPITATED AMMONIA SYNTHESIS CATALYSTS IN REDUCTIVE ATMOSPHERE

BOJANA D. ALEKSIĆ and ANA TERLECKI-BARIČEVIĆ
Institute for Chemistry Technology and Metallurgy, Beograd, Njegoseva, 12

Received February 12, 1975

Changes of electrical conductivity *vs* temperature in hydrogen have been measured to investigate effects of the nature of structural promotors on various properties of precipitated catalysts for ammonia synthesis. Results obtained may contribute to the knowledge of processes taking place in ammonia synthesis catalyst during its reduction.

Previous investigations of electric conductivity changes of precipitated oxide forms of catalysts for ammonia synthesis have shown that the chemical nature of structural promotors has more important effect on the course of electric conductivity changes as a function of temperature, than some other parameters varying during catalyst synthesis.[1] For this reasons, some samples of catalysts with different structural promotors — oxide of aluminium, silicium, calcium, magnesium or samarium have been selected for investigations in reductive atmosphere.

EXPERIMENTAL

Samples have been synthetized by the precipitation method, according to the previously described procedure for samples with corresponding symbols.[1]

In order to determine the attained degree of reduction, concentration of total and bivalent iron has been measured in samples, before and after the complete electric conductivity measurement cycle. The permanganometric method adjusted to the investigated systems was used. Potassium oxide content, existing in all samples as chemical promotor, has been determined by means of the flame-photomeric mehod.

Electric conductivity of the pressed tablets of catalysts was calculated on the basis of resistivity values, obtained by means of compensation method. Resistivity of sample tablets set between two nickel plates as electrodes, was measured in direct current of 4V. The cycle of electric conductivity measurement has included the following steps :

— a tablet of unreduced catalyst was evacuated in vacuum of 10^{-5} mmHg, by gradual heating up to 450°, at which temperature the sample was stabilized up to the constant resistivity, and the conductivity change was followed by resistivity measurements during cooling ;

---

[1] B. D. Aleksić and A. Terlecki-Baričević, *Bull. Soc. Chim., Beograd*, **38**, 447 (1973).

— a slow stream of purified hydrogen was introduced into the measurement cell at room temperature and resistivity was measured during gradual heating of tablet up to 450° ; tablet has been kept for three hours at 150°,250° and 450° ;

— after being cooled in hydrogen stream, the tablet was continuously heated again in hydrogen up to 550° and was kept at this temperature until constant resistivity was attained ; resistivity measurements were made during cooling in hydrogen ;

— measurement cycle terminated by heating in vacuum up to 550° and resistivity measurements were made analogously to the ones in the first step of the cycle.

RESULTS AND DISCUSSION

A survey of promotors present in the investigated samples is given in table 1. Besides the cited promotors all samples contain also (1±02) %K_2O. The sample F—II-a was synthetized analogously to the previously investigated sample F—II-b with addition of silicium oxide as a powder.

Table 1

Survey of promotors present in the investigated catalyst samples

Sample	Al_2O_3 (3±0.5%)	SiO (2±0.5%)	CaO (2.5±0.5%)	MgO (2.5±0.5%)	Sm_2O_3 (1—3%)
F—I-a	+	—	+	—	—
F—VII-a	—	—	—	—	+
F—I-d	+	+	+	—	—
F—II-a	+	+	—	+	—
F—VIII-b	+	+	—	—	+

Chemical composition of samples was chosen so as to enable the comparison of the effects of aluminium oxide substitution by samarium oxide (sample F—I-a and F—VIII-a) as well as of calcium oxide substitution by magnesium oxide (samples F—I-d and F—II-a) or by samarium oxide (samples F—I-d and F—VIII-b).

Results of chemical analysis of the total and bivalent iron contents, in weight percent, are given in table 2. The reduction degree was estimated by comparison of maximum possible and experimentally determined concentration of bivalent iron in the reduced samples. During electric conductivity measurements in vacuum, evaporation of potassium from some samples was observed after the reduction and a metal film was formed on the interior of the measuring cell outlet tube ; therefore, the content of potassium oxide in samples before and after the electric measurement cycles was analysed. These results are also given in table 2.

Based on the obtained values shown in table 2, it can be concluded that the reduction of trivalent iron was carried out, to a large extent, in all samples during their exposure to the reductive atmosphere. Higher reduction degree was observed in samples F—VIII-a and F-VIII-b with samarium oxide. Lower reducibility may result partly from the mode in which promotors were introduced ; aluminium and magnesium added by coprecipitation with hydrated oxide, as well as calcium oxide introduced by wet procedure as milk of lime, build either the mixed gels which

Table 2

Content of total and bivalent iron and potassium oxide in sample before and after reduction

Sample	Fe, total		Fe^{2+}		Fe^{3+}		K_2O			Reduction degree
	before	after	before	after	before	after	before	after		
								I*	II	
F—I-a	67.24	83.92	0.34	83.26	66.90	0.66	0.90	—	—	93.89
F—VIII-a	64.05	83.72	0.34	83.48	63.71	0.24	1.03	1.34	0.87	99.80
F—I-d	64.26	72.20	0.35	71.34	63.91	0.86	0.96	1.08	0.94	85.36
F—II-a	62.89	80.40	0.46	79.99	62.43	0.41	0.77	0.98	0.81	97.78
F—VII-b	61.85	79.21	0.23	78.81	61.62	0.40	0.81	1.03	0.97	98.99

* Values under I were calculated as the increase of promotor concentration due to the elimination of oxygen from the catalyst, and values under II were experimentally determined; the difference corresponds to the eliminated potassium oxide by evaporation.

pass into hardly reducible mixed oxides[2,3] or are distributed in the sample more homogeneously than in the case with samarium oxide. Due to this fact the approach of reductive gas to iron oxide is much easier in samples with samarium oxide.

Electric conductivity changes during the reduction of samples in hydrogen at a temperature up to 450° are shown in figures 1 and 2. Diagrams are grouped so that catalysts with the same basic composition, but with different structural promotors, can be compared.

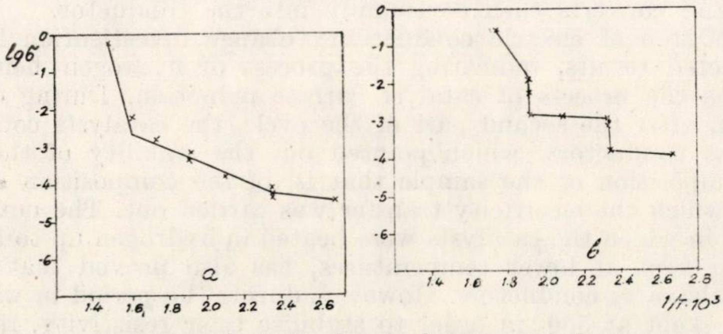

Fig. 1. — Electric conductivity changes during sample heating in hydrogen: *a*. F—I-a; *b*. F—VIII-a.

All investigated catalysts are converted, during this step of treatment in hydrogen, into conductors. Although conductivity changes are within the same interval, the course of conductivity changes indicate remarkable differences in interaction processes between catalysts and hydrogen. The catalyst F—VIII-a is reduced more easily with a higher increase of conductivity during heating at lower temperatures and even at 300° it becomes a conductor. This is the consequence of aluminium

---

[2] S. S. Latchinov, A. M. Rubinstein, V. M. Akimov, A. L. Kliachko-Gurvich, I. N. Koniuhova, L. D. Kuznetsov, T. T. Levitskaya, N. A. Prybytkova, A. A. Slinkin and R. V. Chesnokova, *Kinetika i Kataliz*, **5**, 478 (1964).

[3] M. Dimitrov and P. Banov, *Khim. i Ind.*, **39**, 16 (1967).

absence, which in the sample F—I-a is precipitated together with iron oxide.

Conductivity changes, shown in diagrams in Fig. 2, make possible the comparison of samples with calcium, magnesium or samarium oxides. Mutual differences in the way of conductivity changes are smaller in samples with magnesium and samarium oxide (F—I-a and F—VIII-b) than between these two samples and the catalyst with calcium oxide (F—I-d) which changes its conductivity more slowly at a temperature up to 250° and converts then continually into the conductor.

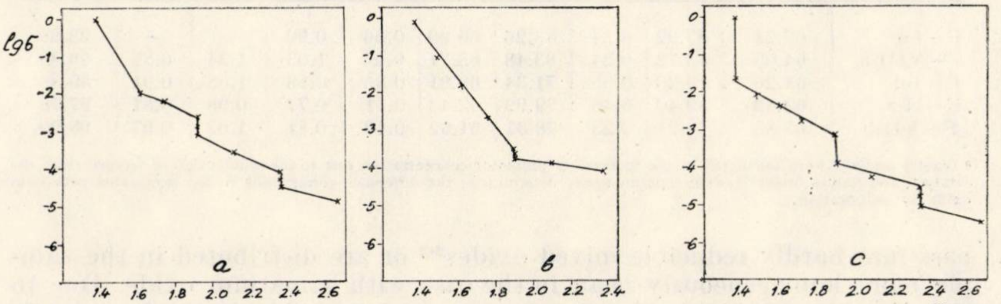

Fig. 2. — Electric conductivity change during sample heating in hydrogen: *a*. F—II-a; *b*. F—I-d; *c*. F—VIII-b.

This step of electric conductivity change investigation has given the expected results, indicating the process of hydrogen hemisorption as well as the process of catalyst surface reduction. During cooling in hydrogen, after the second part of the cycle, the catalysts continued to behave as conductors, which pointed out the stability of the reached phase composition of the sample that is, of the composition of surface through which the electricity transfer was carried out. The next step of the cycle in which the catalysts were heated in hydrogen up to 550° without being kept at lower temperatures, has also proved that catalysts tablets behave as conductors. However, during the period in which samples were kept at 550° in order to stabilize their resistivity, remarkable increase of resistivity occurred in all catalysts, except in F—VIII-a, only one hour later. Resistivity was stabilized after 8—10 hours on values corresponding to semiconductors, while the catalyst F—VIII-a retained all the time its high conductivity.

Kinetics conductivity changes at 550° are shown in diagrams in Fig. 3.

Unlike the other samples shown in Fig. 3, the sample F—I-d was not previously treated by hydrogen at 450°, its surface being only cleaned in vacuum by heating at 550° up to resistivity stabilization, after which hydrogen was introduced. The experiment was made in order to enable the comparison catalysts conductivity behaviour after different previous reduction procedures. Direct introduction of hydrogen on the sample F—I-d at 550° resulted in the first 15 min., into conductivity increase from 2.7 10^3 Ohm^{-1} cm^{-1} up to the order of magnitude of several Ohms, which correspond to the conductors and which can be ascribed to the reduction of tablet catalyst surface. [4] The results, however, have shown that resistivity during staying period at 550°, changes in the same interval with no regard to the history of the reduction at 450°. The course of experimentally obtained curves points out very complex diffusion processes taking place in promoted iron oxides during reduction by hydrogen, influencing directly the electronic state of the catalyst surface. From this group of samples too, the sample with samarium oxide (F—VIII-b) differs by the smaller decrease of conductivity. As all samples contain the same quantity of potassium oxide, differences in the magnitudes of conductivity can be ascribed to the presence of different structural promotors.

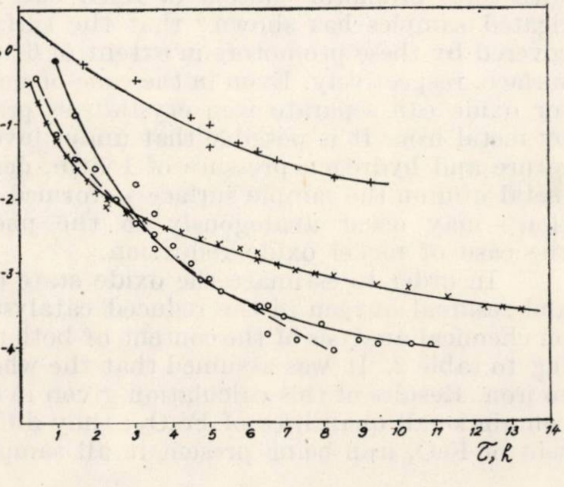

Fig. 3. — Conductivity changes of catalysts in dependence on time, at 550°

× F I d ● F II a
○ F I a + F VIII b

Coefficients of log σ change with time, calculated after linear approximation of curves from Fig. 3, as a measure of the rate of catalyst conductivity changes at 550°, are shown in table 3.

Table 3

Coefficients of log σ changes with time

Interval	log σ /Ohm^{-1} cm^{-1} min.$^{-1}$/			
	F—I-a	F—I-d	F—II-a	F—VIII-b
I	−0.0129	−0.0133	−0.0101	−0.0043
II	−0.0055	−0.0027	−0.0030	—

One of the causes of the change of the investigated catalyst behaviour in hydrogen may be due, to the fact, that by the applied method, conductivity of grain surface was measured. During thermal treatment in hydrogen, promotors migrated from the grain bulk on the surface causing thus its semiconductor character. Simultaneously with the process

[4] I. V. Nicolescu, M. Spinzi and A. Suceveanu, *Omagiu Raluca Ripan*, **1966**, 397.

of promotor diffusion, oxygen diffusion from the grain bulk to the surface takes place too, which doubtless changes the concentration of the carriers in catalyst surface.

According to Nielsen [5] in the reduced catalyst, the surface of metal iron may be covered from 88 to 93% by potassium, aluminium and calcium oxides. Surface investigation of a commercial reduced catalyst with total promotor content of K_2O, CaO and Al_2O_3 close to the investigated samples has shown [6] that the surface of the reduced grain was covered by these promotors in extent of 64.9, 25.4 and 17.8% of the total surface, respectively. Even in the case of smaller surface covering, promotor oxide can separate iron crystallites preventing electric transfer only by metal iron. It is possible that under investigated conditions of temperature and hydrogen pressure of 1 atm, destruction of the thin layer of metal iron on the sample surface — formed during the first step of reduction — may occur analogously to the phenomenon cited by Hauffe[7] in the case of nickel oxide reduction.

In order to estimate the oxide state of iron, quantities of removed and residual oxygen in the reduced catalysts have been calculated based on chemical analysis of the content of both total and bivalent iron, according to table 2. It was assumed that the whole residual oxygen was bound to iron. Results of this calculation given in table 4 show that samples can contain small quantities of Fe_2O_3; they differ mutually by potential content of FeO, iron being present in all samples mostly in free metal form.

Table 4

Quantity of the removed and residual oxygen in catalysts

Sample	Total stoichiometric content of O_2 in iron oxides, weight %		Oxide content after reduction, weight %	
	Before reduction	After reduction	Fe_2O_3	FeO
F—I-a	24.18	5.38	0.90	23.07
F—VIII-a	23.03	—	—	—
F—I-d	23.11	12.11	1.17	52.98
F—II-a	22.60	1.05	0.56	4.09
F—VIII-b	22.25	0.43	0.54	1.30

The established reduction degree (table 2.) and a relatively small content of promotor oxides in the investigated catalysts could be an indication of conductive behaviour of sample mass as a whole, but the observed changes indicate clearly the existence of differences between the surface and bulk chemical composition of catalyst grain, during reduction in hydrogen.

---

[5] A. Nielsen, "An Investigation of Promoted Iron Catalysts for the Synthesis of Ammonia", Jull. Gjellerups Forlag, 3rd ed., p. 264, Copenhagen, 1968.

[6] Hong-Chin-Chen and R. B. Anderson, *J. Catalysis*, **28**, 161 (1973).

[7] K. Hauffe, "Reakchii v tverdykh telatkh i na ikh poverkhnosti", vol. II, Izd. Inostr. Lit., Moskva, 1963, p. 243.

Conductivity changes of catalysts during cooling in hydrogen, after resistivity stabilization at 550°, are shown in diagrams in Fig. 4. Activation energies of conductivity are marked on the corresponding parts of conductivity curves.

Although the differences in conductivity value do exist, all samples show similar behaviour regarding the course of electric conductivity changes as function of temperature, and have similar activation energies.

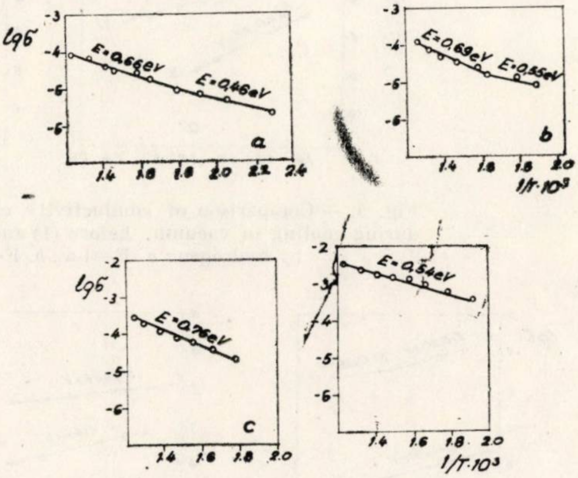

Fig. 4. —Conductivity changes of catalysts during cooling in hydrogen : *a*. F—I-a ; *b*.F—II-a : *c*. F—I-d ; *d*. F—VIII-b.

In the last step of the cycle, samples have been heated again *in vacuo* up to 550° for the purpose of hydrogen removal and resistivity stabilization at this temperature. Conductivity changes during further cooling *in vacuo* are shown in diagrams in Fig. 5 and 6. In order to make the comparison, electric conductivity changes during cooling *in vacuo* of the unreduced catalyst in the first step of measurement cycle, are also shown.

The samples do not show uniform behaviour with regard to conductivity changes before and after reduction. Catalysts F—I-a and F—II-a have lower conductivity after reduction, while F—I-d and F—VIII-b catalysts show higher conductivity, which may be the result of different promotors distribution, causing thus different concentrations of electricity carriers, their nature being not substantially changed in both cases. This can be proved also by the fact that activation energies, shown by the catalysts after reduction, are similar to the ones in unreduced form.

Potassium elimination in this step of cycle is a phenomenon which has been noticed during reduction of potassium ferrite [8] under similar conditions. Larger volatility of K_2O was noticed in F—VIII-a sample in which aluminium oxide did not exist and this is in accordance with the presumption that acid oxides connect potassium oxide on its way in the diffusion process through iron oxide during its reduction.

---

[8] S. H. Egeubaev, S. A. Rogozhina, D. A. Kuznetsov and I. E. Zubova, *Kinetika i Kataliz*, **6**, 754 (1965).

Investigation results prove the influence of structural promotor nature on electric conductivity of catalysts for ammonia synthesis. Complexity of structural changes during reduction of oxide forms of iron in precipitated catalysts as well as superposition of diffusion of separate oxide on manifold phase boundaries occurring during the reduction and promotor difusion, make difficult the differentiation of some influences of promotors on changes of both nature and concentration of electricity carriers.

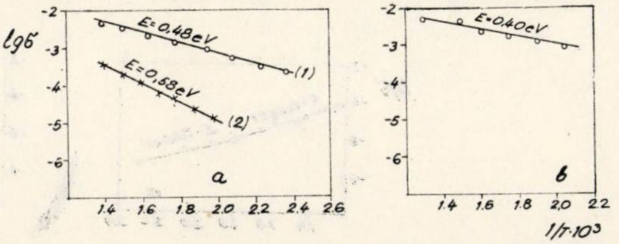

Fig. 5. — Comparison of conductivity changes of catalysts during cooling in vacuum, before (1) and after (2) reduction by hydrogen : *a*. F—I-a ; *b*. F—VIII-a.

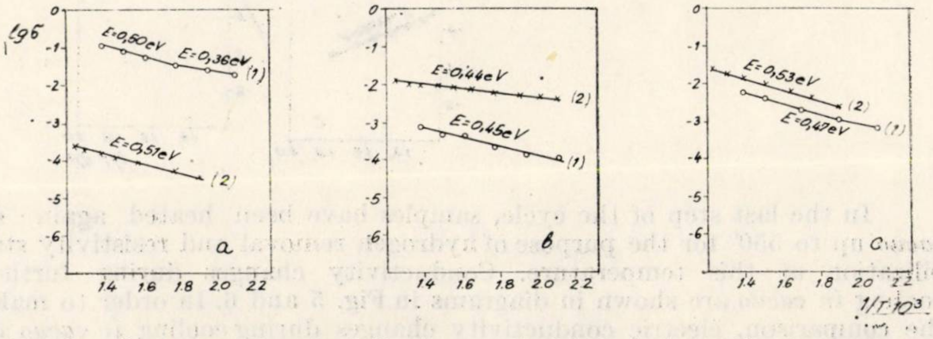

Fig. 6. — Comparison of conductivity changes of catalysts during cooling in vacuum, before (1) and after (2) reduction by hydrogen : *a*. F—II-a ; *b*. F—I-d ; *c*. F—VIII-b.

The obtained results point out, at the same time, the necessity of complementary analysis of phase composition as well as of the catalyst surface state during and after reduction, so that more complete conclusions regarding the nature of conductivity carriers in catalysts for ammonia synthesis, can be drawn.

Revue Roumaine de Chimie, **22**, *9–10*, 1343–1346 (1977)

THE ELECTRONIC SPECTRUM OF $[Os(II)(NH_3)_5(N_2)]^{2+}$ AND THE CHEMICAL BONDING OF THE DINITROGEN MOLECULE

D. SĂNDULESCU*, CONSTANŢA PÂRLOG and C. I. LEPĂDATU**

* Institute of Petroleum and Gases – Ploieşti, Romania
** Centre of Chemical Physics, 23 Dumbrava Roşie, Bucharest, Romania

Received May 28, 1974
Completed: February 21, 1977

It has been shown that the absorption maxima occurring in the electronic spectrum of $[Os(II)(NH_3)_5(N_2)]^{2+}$ may be assigned to spin-allowed transitions proper to a low-spin d^6 configuration in a C_{4v} coordination geometry. From the MO analysis of these transitions, it has been shown that the dinitrogen molecule exerts a π-bonding effect on the metal orbitals and forms σ bonds three times weaker than those with ammonia, in agreement with the chemical behaviour of the complex.

INTRODUCTION

Recently, many authors have devoted their attention to coordination compounds containing the small diatomic ligands [1] dinitrogen, dihydrogen, dioxygen, etc. There are presently no reports in the literature concerning the study of these ligand molecules approached through the interpretation of the spectral behaviour of their coordination complexes. The aim of the present report is to present a study on the already known complex $[Os(II)(NH_3)_5(N_2)]^{2+}$. This complex is of interest, because its electronic spectrum shows a splitting of an absorption band which may be used to evaluate separately the σ/π bonding contributions of the ligands.

EXPERIMENTAL

The complex has been prepared according to a previously reported method.[2] The electronic spectrum of the complex $[Os(II)(NH_3)_5(N_2)]^{2+}$ has been recorded on a VSU 1 Carl Zeiss (Jena) in aqueous solutions.

---

[1] A. D. Allen and J. R. Stevens, *Chem. Comm.*, **1967**, 1147.

[2] A. D. Allen, R. D. Harris, B. R. Loescher, J. R. Stevens and R. N. Whiteley, *Chem. Rev.*, **73**, 11 (1973).

RESULTS AND DISCUSSION

The electronic spectrum of the complex $[Os(II)(NH_3)_5(N_2)]^{2+}$ is presented in Figure 1.

There are two main absorption regions within the range of 700—200 nm. The absorption band at lower wavenumbers is asymmetric and can arise from two gaussian curves one at 22,720 cm^{-1} and another at 25,640 cm^{-1}. The absorption band at higher wavenumbers occurs at 32,260 cm^{-1}. The electronic spectrum of $[Os(II)(NH_3)_5(N_2)]^{2+}$ is quite similar [3] to that of $[Ru(II)(NH_3)_6]^{2+}$, except the $d-d$ transition $^1A_{1g} \rightarrow {}^1T_{1g}$ which is split in the case of the first complex.

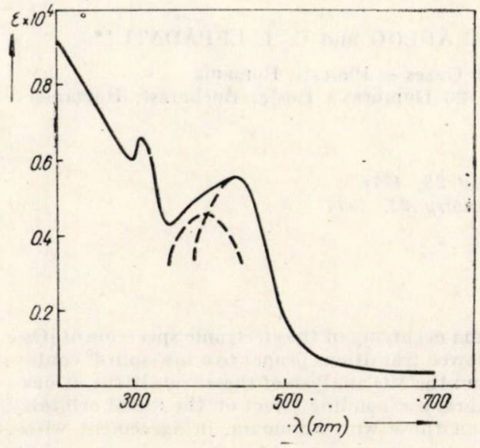

Fig. 1. — The electronic spectrum of $[Os(NH_3)_5N_2]^{2+}$.

We shall discuss the observed transitions of $[Os(II)(NH_3)_5(N_2)]^{2+}$, in order to get information concerning the metal-ligand chemical bonding with special emphasis on the coordination bond of the dinitrogen molecule. The above complex is of the MA_5B type which belongs to the C_{4v} point group. Figure 2 represents the orbital pattern obtained using the Angular Overlap Model [4]

The antibonding orbital energies $e_{\sigma(\pi)}$ belong to the $\sigma(\pi)$ bonds of the ligands A and B. Figure 2 illustrates the orbital pattern which is valid when $e_\sigma^A > e_\sigma^B$ and $e_\pi^A < e_\pi^B$.

In the strong- field coupling scheme for a low spin electron distribution, the spectral terms arising from a d^6 electron configuration in an octahedral environment and their subsequent splitting in a C_{4v} environment are as follows

$$O_h(MA_6) \qquad\qquad C_{4v}(MA_5B)$$

$$E[^1A_{1g}(t_{2g}^6)] = E_0 \qquad\qquad E[^1A_1(b_2^2e^4)] = E_0'$$

$$E[^1T_{1g}(t_{2g}^5e_g^1)] = E_0 + \Delta^A - C \qquad\qquad \begin{cases} E[^1A_2(b_2^1e^4a_1^1)] = E_0' + \Delta^A - C \\ E[^1E^a(b_2^2e^3a_1^1)] = E_0' + 3/4\Delta^A - C \end{cases}$$

---

[3] H.-H. Schmidtke and D. Garthoff, *Helv. Chim. Acta*, **49**, 2039 (1966).

[4] C. E. Schäffer and C. K. Jørgensen, *Mol. Phys.*, **9**, 401 (1965).

$$E[{}^1T_{2g}(t_{2g}^5e_g^1)] = E_0 + \Delta^A + 16B - C \begin{cases} E[{}^1B_2(b_2^1e^4b_1^1)] = E_0' + 2/3\Delta^A + \\ + 1/3\Delta^B - 4/3(e_\pi^A - e_\pi^B) + 16B - C \\ E[{}^1E^b(b_2^2e^3b_1^1)] = E_0' + 11/12\Delta^A + \\ + 1/12\Delta^B + 2/3(e_\pi^A - e_\pi^B) + 16B - C \end{cases}$$

The energy for the ground terms is represented by $E_0(E_0')$, the Racah parameters B and C for the interelectronic repulsion energies, and $\Delta^{A(B)}$ for the orbital splitting parameters in the octahedral environment. The above energy expressions have been obtained using the formulas for the orbital energies expressed in $e_{\sigma(\pi)}$parameters of the Angular Overlap Model[5] taking into account that $\Delta = 3e_\sigma - 4e_\pi$ (see Figure 2).

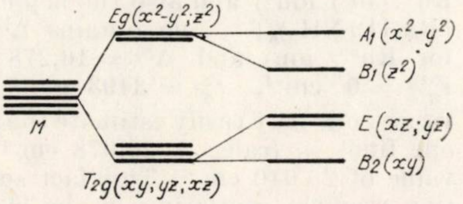

Fig. 2. — The orbital pattern obtained using the Angular Overlap Model.

If we materialize the formulas of the spectral term energies for $A = NH_3$ and $B = N_2$ considering $e_\sigma^{N_2} < e_\sigma^{NH_3}$ and $e_\pi^{NH_3} = 0$ (the nitrogen atom in ammonia has a sp^3 hybridization and therefore is unable to form π-bonds with the central metal ion), the following energy expressions of the first $d - d$ spin-allowed transitions, and the energy difference between the spectral terms are obtained

$$\nu_1({}^1A_2 \leftarrow {}^1A_1) = \Delta^{NH_3} - C$$

$$\nu_2({}^1E^a \leftarrow {}^1A_1) = 3/4\Delta^{NH_3} + 1/4\Delta^{N_2} - C$$

$$\nu_3({}^1B_2 \leftarrow {}^1A_1) = 2/3\Delta^{NH_3} + 1/3\Delta^{N_2} + 3/4e_\pi^{N_2} + 16B - C$$

$$\nu_4({}^1E^b \leftarrow {}^1A_1) = 11/12\Delta^{NH_3} + 1/12\Delta^{N_2} + 2/3e_\pi^{N_2} + 16B - C$$

The ν_1, ν_2 arise from the transition ${}^1T_{1g} \leftarrow {}^1A_{1g}$ which is split by $\delta_{\nu_1-\nu_2} = 1/4(\Delta^{NH_3} - \Delta^{N_2})$ and ν_3, ν_4 arise from the ${}^1T_{2g} \leftarrow {}^1A_{1g}$ transition which is split by $\delta_{\nu_3-\nu_4} = -1/4(\Delta^{NH_3} - \Delta^{N_2}) + 2e_\pi^{N_2}$. Since $e_\pi^{N_2} > 0$, it results that $\delta_{\nu_1-\nu_2} > \delta_{\nu_3-\nu_4}$ which is in agreement with the observed splitting, previously mentioned.

Assuming that $\Delta^{NH_3} > \Delta^{N_2}$, the experimental transitions have been assigned as follows

$$\nu_1({}^1A_2 \leftarrow {}^1A_1) = 25{,}640 \text{ cm}^{-1}$$

$$\nu_2({}^1E^a \leftarrow {}^1A_1) = 22{,}720 \text{ cm}^{-1}$$

$$\nu_3({}^1B_2 \leftarrow {}^1A_1)\,;\ \nu_4({}^1E^b \leftarrow {}^1A_1) = 32{,}260 \text{ cm}^{-1}.$$

---

[5] C. I. LEPĂDATU, *Rev. Roum. Chim.*, **11**, 1175 (1966).

We have assigned the absorption maximum at 22,720 cm^{-1} to be a double degenerate single electron transition ν_2, because this maximum is more intense than that at lower wavenumbers assigned as a transition to the singlet state ${}^1A_2$.

From the values of $\delta_{\nu_1-\nu_2}$ and $\delta_{\nu_3-\nu_4}$, it follows that $\Delta^{NH_3} - \Delta^{N_2} =$ 11,600 cm^{-1} and $e_\pi^{N_2} = 1450$ cm^{-1}. The Δ^{NH_3} and Δ^{N_2} have been estimated from ν_3, ν_4 which are according to the rule of average environment[5,6]

$$(\nu_3 + \nu_4)_{av} = 5/6\Delta^{NH_3} + 1/6\Delta^{N_2} + 25/36e_\pi^{N_2} + 16B - C$$

Using[7] $B = 620$ cm^{-1} and the well-known relationship $C \approx 4B$ (for the $Ru^{2+}(4d^6)$ ion[3]) and also the nephelauxetic ratio $\beta = 0.7$ of the complex[3] $[Ru(II)(NH_3)_6]^{2+}$, one obtains $\Delta^{NH_3} = 27,878$ cm^{-1} ($\Delta^{NH_3} = 27,100$ cm^{-1} for Ru^{2+} ion) and $\Delta^{N_2} = 16,278$ cm^{-1}, and therefore $e_\sigma^{NH_3} = 9293$ cm^{-1}, $e_\pi^{NH_3} = 0$ cm^{-1}, $e_\sigma^{N_2} = 3493$ cm^{-1} and $e_\pi^{N_2} = 1450$ cm^{-1}. With these values, one may easily estimate the absolute value of ν_1 or ν_2. For instance, one finds ν_1 (calc.) $= 26,078$ cm^{-1}, in agreement with the experimental value of 25,640 cm^{-1}. This fact supports the assignment of the absorption maxima appearing in the electronic spectrum to be spin-allowed $d-d$ transitions, in spite of their unusually high intensities. The very high intensity of the electric dipole $d-d$ transitions can be explained by the fact that the MA_5B complex belongs to the C_{4v} symmetry group, and therefore the transition probability (oscillator strength) does not depend on the vibronic coupling, as in an octahedral environment. As may be seen from the obtained values assumed by the antibonding $\sigma(\pi)$ orbital energies, the σ metal – ammonia bond must be stronger that the σ metal – dinitrogen bond, but the dinitrogen ligand exerts a noticeable π bonding effect on the central metal orbitals. The considerable difference between the σ – bonds between Os(II) – NH_3 and Os(II) – N_2 produces an obvious departure from the octahedral coordination geometry. This is reflected in the electronic spectrum by the splitting of the first spin-allowed ${}^1T_{1g} \leftarrow {}^1A_{1g}$ band.

According to the LCAOMO stabilization theory,[8,9] the d-Molecular Orbital Stabilization Energy should be equal to $5 \times (-2e_\sigma^{NH_3}) + 1 \times (-2e_\sigma^{N_2})$. This means that each coordination point does not contribute to the total stabilization energy via the π-bonding with the d-metal orbitals. Since $e_\sigma^{NH_3} > e_\sigma^{N_2}$, the stabilization energy of the Os(II) – N_2 bond is much lower than that of the Os(II) – NH_3 bond, which explains the lability of the dinitrogen which is therefore easily substituted by other ligands and removed from the inner coordination sphere of the complex.

---

[6] C. I. LEPĂDATU, *Z. phys. Chem. (Frankfurt)*, **60**, 202 (1968).

[7] J. S. GRIFFITH, "The Theory of Transition – Metal Ions", Cambridge Univ. Press, 1964.

[8] C. I. LEPĂDATU, *J. Cryst. Mol. Structure (London)*, **1**, 397 (1971).

[9] C. I. LEPĂDATU, *Rev. Roumaine Chim.*, **17**, 863 (1972).

Revue Roumaine de Chimie, **22**, *9–10*, 1347–1351 (1977)

COMPLEX COMPOUNDS OF Cu(I) WITH TRIARYLSTIBINES

D. NEGOIU* and LIDIA PARUTA**

* Faculty of Chemistry, Polytechnic Institute of Bucharest, Splaiul Independenţei, 89, Bucharest, Romania

** Center of Physical Chemistry, str. Dumbrava Roşie, 23 Bucharest-9, Romania

Received June 5, 1975

Cu(I) complex compounds containing tritolyl- and trixylylstibines of the type MXL and MXL_2, where M = Cu(I); L = *o*-tolyl$_3$Sb, *m*-tolyl$_3$Sb, *p*-tolyl$_3$Sb, *o*-xylyl$_3$ Sb and *p*-xylyl$_3$Sb ; $X=Cl^-, Br^-$, have been obtained. The compounds were prepared by prolonged heating of $CuCl_2.2H_2O$ and $CuBr_2$ with tertiary stibine under reflux. The reduction or formation of the complex depends on the solvent used as a reaction medium. The compounds are colourless or slightly yellow powders. Physical and chemical determinations prove that they are tetramers, nonelectrolytes and diamagnetic. Electronic and IR spectra of the complexes are also discussed.

RESULTS AND DISCUSSIONS

Scholder and Pattock[1] were the first who studied Cu(I) complex compounds with tertiary phosphines and arsines. The reducing action of tertiary phosphines,arsines and stibines on the halides of the first group of metals has been long known [2] and yet it has been only lately applied [3] to the preparation of the complex compounds of monovalent copper halides with these ligands. Thus, subsequent studies pointed out that compounds may be obtained having the metal : ligand combination ratio : 1 :1, 1 : 2, 1 : 3 and sometimes also 1 : 4. When using tertiary stibines as a ligand only compounds of the type 1 : 1 and 1 : 2 are obtained.

In the preparation of these complexes the solvent used as a reaction medium is of great importance as well as the stoichiometric ratio of copper (II) salt and ligand. Treating copper (II) salts with the respective ligand in ethanol, acetone, benzene or chloroform, under prolonged refluxing 13 compounds of the type $[CuX.SbR_3]$ and$[CuX.(SbR_3)_2]$, where $X = Cl^-$, Br^- ; R_3 = *ortho-*, *meta-*, *para-*tolyl$_3$Sb or *ortho-*, *meta-*, *para-*xylyl$_3$Sb were obtained.

---

[1] R. Sholder and K. Pattock, *Z. anorg. Chem.*, **220**, 250 (1934).
[2] A. Cahours and H. Gall, *Compt. rend.*, **70**, 1380 (1870).
[3] F. H. Jardine, L. Rule aud A. G. Vohra, *J. Chem. Soc., A*, **1970**, 238.

The reduction of Cu(II) salts to Cu(I) and the formation of the respective complex compound takes place over a long time interval which varies from several hours to several days. The complex compounds thus obtained as well as some of their characteristics are presented in Tables 1 and 2.

Table 1

Complex compounds of Cu(I) with tritolylstibine and trixylylstibine

Compound	Colour	Melting point °	Elemental analysis					
			C%		H%		Halogen %	
			Calc.	*Found*	*Calc.*	*Found*	*Calc.*	*Found*
CuCl $SbpT_3$	white	142−144	51.0	49.8	4.2	4.4	7.1	7.0
CuBr $SbpT_3$	white	143−145	40.7	40.5	3.3	3.6	26.0	25.8
CuCl $SboT_3$	white	181	51.0	49.7	4.2	4.5	7.1	7.0
CuBr $SboT_3$	white	161−163	40.7	40.6	3.3	3.2	26.0	25.8
CuBr $(SbpT_3)_2$	white	133−135	49.7	49.5	4.1	3.9	15.8	15.7
CuCl $(SbotT_3)_2$	white	165−167	56.7	56.4	4.7	4.9	4.5	4.4
CuCl $SbpX_3$	white	172−175	53.6	53.3	3.9	4.0	6.6	6.3
CuBr $SbpX_3$	white	157−162	43.6	43.4	4.0	4.2	24.2	23.6
CuCl $SbmX_3$	white	117−120	53.6	53.5	3.9	4.1	6.6	6.5
CuBr $SbmX_3$	white	124−128	43.6	43.5	4.0	3.9	24.2	24.0
CuCl $SboX_3$	white	80−82	53.6	53.4	3.9	4.0	6.6	6.5
CuBr $SboX_3$	white	88−91	43.6	43.3	4.0	4.1	24.2	24.1
CuCl $(SbmX_3)_2$	white	125−130	59.2	59.0	4.3	4.5	3.6	3.5

The stability of these complex compounds with phosphines, arsines and stibines decrease in the same order as the above mentioned enumeration. The yields are also lower. All the compounds are colourless or slightly yellow. This is explained by the fact that the electronic configuration of Cu(I) is $3d^{10}$, the absorption in visible being less probable, according to the crystal field theory.

Table 2

Properties of (CuXL) compounds

Compound	Molar weight		Observations	Electr. conductivity $\Lambda(\Omega^{-1}cm^2\ mol^{-1})$
	Theor.	Exper.		
CuCl $SbpT_3$	1975	1896	tetramer	1.15
CuBr $SbpT_3$	2472	2380	tetramer	1.47
CuCl $SbotT_3$	1975	1889	tetramer	0.93
CuBr $SboT_3$	2472	2365	tetramer	1.10
CuCl $SbpX_3$	2143	2069	tetramer	1.46
CuBr $SbpX_3$	2640	2550	tetramer	1.53
CuCl $SbmX_3$	2143	2056	tetramer	1.20
CuBr $SbmX_3$	2640	2532	tetramer	1.37
CuCl $SboX_3$	2143	2039	tetramer	1.43
CuBr $SboX_3$	2640	2520	tetramer	1.39
CuBr $(SbpT_3)_2$	1012	1198	monomer	1.72
CuCl $(SboT_3)_2$	888	1021	monomer	1.93
CuCl $(SbmX_3)_2$	972	1139	monomer	2.10

The molecular weights determined by the Rast method point out that compounds of the type $[CuX.SbR_3]$ are tetramers both in solid state and in benzenic solution (in chloroform a partial dissociation occurs [4], whereas those of the type $[CuX\,(SbR_3)_2]$ are monomers in benzene and nitrobenzene, thus suggesting the presence of tricoordinated copper.

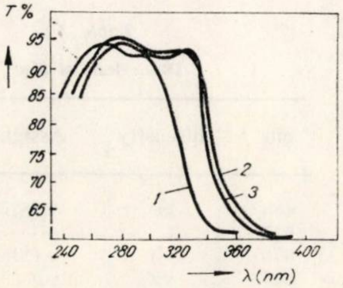

Fig. 1. — The ultraviolet absorption spectra of: 1. (Sb-p-tolyl$_3$); 2. (CuCl.Sb-p-tolyl$_3$); 3. (CuBr.Sb-p-tolyl$_3$).

Electric conductivity measurements carried out in nitrobenzene confirm the nonelectrolytic character of these compounds. Solubility tests point out that they are sparingly soluble in benzene, nitrobenzene and practically insoluble in alcohols, ethers and water.

Electronic and infrared spectra have been studied in order to obtain some data about the structure and the chemical bonding in these compounds.

The electronic spectra of stibine copper complexes show no absorption bands in visible, this proving the occurrence of copper in +1 oxidation state, for which the crystal field theory does not predict absorption bands in visible. For illustration, Fig. 1 presents the absorption spectra in ultraviolet of one of the free ligands and of Cu (I) halide complexes with the same ligand.

Similar to Cullen and Hochstrasser [5] we attribute the two ligand absorption to some $n \rightarrow \pi^*$ transitions (the intense band in 230—270 nm region) from the electronic nonbonding sp^3 orbital of the metal central ion to the tolyl group antibonding molecular orbitals, and to some $\pi \rightarrow \pi^*$ transitions (the slighter band placed in 290 nm region) between tolyl group molecular energetic levels. One notices that metal coordination affects these bands as follows:

1) the $n \rightarrow \pi^*$ transition by antimony sp^3 orbital participation in the σ coordination band with copper (I),

2) the $\pi \rightarrow \pi^*$ transition by less delocalization of tolyl group π orbitals on antimony d orbitals, as a result of their participation in coordinative bonds Cu $(3d^{10}) \rightarrow$ Sb (6d).

The study of IR absorption spectra gives interesting data, especially in the low frequencies region where bands, determined by metal-halogen and metal-ligand IR active vibrations occur.

The range of 250—800 cm^{-1} investigated by us is yet unsatisfactory, because Cu-Sb characteristic vibration frequencies which occur below this lower limit could not be determined.

---

[4] A. P. Lane and D. S. Payne, *J. Chem. Soc.*, **1963**, 4004.

[5] W. R. Cullen and R. M. Hochstrasser, *J. Mol. Spectroscopy*, **5**, 118 (1960).

The vibration spectra of free ligands, as well as those of several CuX complexes of these ligands, are discussed comparatively with the spectra of benzene substituted compounds.

Therefore, Tables 3, 4 and 5 present the IR absorption bands of one of the ligands together with the complexes obtained.

Table 3

IR spectrum of SbpT$_3$

cm^{-1}	Intensity	Assignment
488	m	γ_2(Sb-*p*-tolyl)
617	i	σR
670	v.i.	ν_2(Sb-*p*-tolyl)
695	v.i.	γR
742	i	γ(C−H)

Table 4

IR spectrum of CuCl SbpT

cm^{-1}	Intensity	Assignment
325	i	ν(Cu−Cl)
470	m	γ_2(Sb-*p*-tolyl)
615	i	σR
690	i	γR
745	i	γ(C−H)

Table 5

IR sprectrum of CuBr SbpT$_3$

cm^{-1}	Intensity	Assignment
295	i	ν(Cu−Br)
475	m	γ_2(Sb-*p*-tolyl)
620	m	σR
668	m	ν_2(Sb-*p*-tolyl)
685	m	γR
742	m	γ(C−H)

In the second column the intensities of the respective bands are marked using m = medium, i = intense, v.i. = very-intense, ; in column three the respective assignment is given.

The literature data [7] point that in copper halide complexes the vibration frequencies characteristic of the terminal M − Cl and M − Br bonds occur in the 220 − 370 cm^{-1} region and they are, generally, characterized by relative strong intensities. The frequencies of the bridging M−X bonds assume lower values.

The values found by us are identical with those existing in literature. Very close positions for the main absorption bands confirm the same strength of the Sb−C bonds.

EXPERIMENTAL

Triarylstibines were obtained in several steps. The starting material was toluidine or the respective xylyne and passing through the phase of diazonium salt the halide derivatives were obtained. Subsequently, using Würtz or Grignard reactions they were converted into the respective triarylstibines : *ortho-*, *meta-*, *para-*tolyl$_3$Sb and *meta-*, *para-*xylyl$_3$Sb. Using the same method but in different conditions we obtained the *ortho-xylyl*$_3$Sb which has not been previously reported in the literature.

---

[6] D. Wiffen, *J. Chem. Soc.*, **1956**, 1350.

[7] D. M. Adams and P. J. Lock, *J. Chem. Soc.*, **1967**, 620 ; *Nature*, **199**, 278 (1963).

($CuCl.SbR_3$) : These complexes are obtained by prolonged heating of alcoholic solutions containing stoichiometric quantities of $CuCl_2.2H_2O$ and tolylstibine, with the metal : ligand ratio 1 :1. For xylylstibines, the solvent used was a mixture of ethanol and acetone in equal volumes. The complex precipitates as almost colourless powders. They are rapidly filtered and dried *in vacuo.*

($CuBr.SbR_3$) : These compounds were obtained only in three cases, using the same method with the difference that the metal : ligand ratio was 1 :2. It must be mentioned that the chloride complexes were obtained by refluxing only under nitrogen atmosphere. In each case the solution of the obtained complexes was cooled on ice for two hours before the product was collected.

The chemical composition of these compounds was verified through chemical analysis of C, H and halogen.

The Volhard method was used to determine the halogen.

The determination of the reflectance spectra in ultraviolet was performed with a VSU_1 spectrophotometer, within 230—360 nm, magnesium oxide being taken as standard.

The determination of IR spectra was carried out in KBr pellets in the 250—800 cm^{-1} range with a UR_{10} spectrophotometer.

[illegible] These compounds are obtained by [illegible] solutions containing [illegible] and [illegible] with the [illegible] solvent [illegible] acetone [illegible]. The compound [illegible]. They are rapidly filtered and dried in vacuo.

[illegible] These components were obtained only [illegible] with the difference that the [illegible] liquid [illegible] must be [illegible] the compounds [illegible] atmosphere. In each case the [illegible] of the obtained complexes was [illegible] for two hours before the product was [illegible].

[illegible] was [illegible] through [illegible] and [illegible].

The Volhard method was used to [illegible] the halogen.

The determination of [illegible] was performed with a [illegible] spectrophotometer [illegible] 300 [illegible] taken as standard.

The determination of [illegible] with a [illegible] in the [illegible] with a [illegible] spectrophotometer.

Revue Roumaine de Chimie, **22**, *9–10*, 1353–1358 (1977)

A PENTACOORDINATED Co(II) COMPLEX COMPOUND DERIVED FROM 1-METHYL-2-CARBETHOXY-GLYOXAL-ANIL-(1)-*p*-NITROPHENYLHYDRAZONE-(2)

A. C. BANCIU
Center of Physical Chemistry, Bucharest,
Str. Dumbrava Roşie 23, Romania

Received June 7, 1975

Almost all the Co(II) chelate complexes of 1-methyl-2-carbethoxy-glyoxalanil-(1)-phenylhydrazones-(2), differently substituted at the benzene ring of the phenylhydrazone group, exhibit, both in the solid state and in solution, a tetrahedral structure for the Co(II)$-N_4$ chromophore. In contrast to these, the *p*-NO_2-substituted complex is actually tetrahedral in solution but in solid state it is pentacoordinated with a high-spin electron distribution ($\mu = 4.41 \pm 0.05$ B.M.).

In our previous works[1-3] we have studied Co(II) complexes derived from 1-methyl-2-carbethoxy-glyoxalanil-(1)-phenylhydrazones-(2) differently substituted at the benzene ring of the hydrazone group. Extending these investigations, in a recent paper [4] we have studied the absorption electronic spectra and the magnetic moments of two new Co(II) complexes derived from the chelate ligands Ia and Ib of this class.

The complexes, CoL_2 and CoL'_2, are formed by Co(II) ion with the conjugated anions L and L′, respectively (formula II).

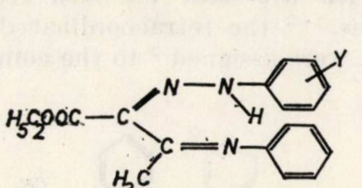

I

$a: Y = p-NO_2$; $b: Y = m-NO_2$

These result from the organic compounds Ia and Ib, by proton dissociation from the imino group, -NH-.

---

[1] P. Spacu, A. C. Banciu and C. I. Lepădatu, *Rev. Roumaine Chim.*, **18**, *7*, 1143 (1973).
[2] A. C. Banciu and P. Spacu, *Rev. Roumaine Chim.*, **19**, *6*, 1019 (1974).
[3] A. C. Banciu and P. Spacu, *Rev. Roumaine Chim.*, **19**, *7*, 1169 (1974).
[4] A. C. Banciu, *Rev. Roumaine Chim.* (to be published).

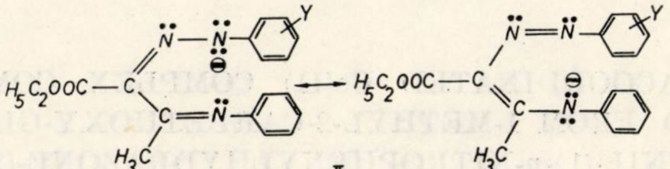

II

$L: Y = p-NO_2$; $L': Y = m-NO_2$

The present paper studies the electronic spectrum and the magnetic moment of the CoL_2 complex in the solid state. These properties indicate that in this case (solid state) the complex structure is fundamentally different from the tetrahedral structure of the complex in solution.

EXPERIMENTAL

The synthesis of the CoL_2 and CoL'_2 complexes and their *electronic absorption spectra* were described in.[4]

The magnetic susceptibility measurements were performed for the solid complexes, at room temperature, by using the Faraday method. The magnetic moments of the complexes were calculated by formula $\mu = 2.828\ [\chi'_M \cdot T]^{1/2}$ B. M., where T is the absolute temperature and $\chi'_M = \chi_M - \chi_{dia}$ is the for diamagnetism corrected molar susceptibility. In the case of both isomeric CoL_2 and CoL'_2 chelates the correction $\chi_{dia} = -361 \times 10^{-6}$ c.g.s.u. was applied. The calculation of χ_M and χ_{dia} referred to the molar weight of the complexes formulated as monomers.

The electronic reflectance spectra of the solid compounds were recorded in the 350–1200 nm range on a VSU–1 Carl Zeiss (Jena) spectrophotometer using MgO as standard substance.

RESULTS AND DISCUSSIONS

In agreement with the data obtained from chemical analysis [4] and based on analogies, [1–3] the tetracoordinated chelate formulas IIIa and IIIb, respectively, were assigned [4] to the complexes CoL_2 and CoL'_2.

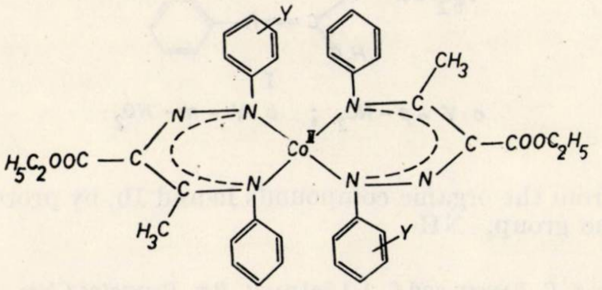

III

(a) $CoL_2 : Y = p-NO_2$; (b) $CoL'_2 : Y = m-NO_2$

The tetrahedral structure of the Co(II)$-N_4$ chromophore in CoL_2 and CoL'_2 chelates found in acetone solutions was suggested [4] by their electronic absorption spectra. Thus, in the absorption spectrum of the CoL_2 chelate – as well as in the spectra of all other analogous Co(II) chelates [1-4] – the bands situated at 550 and 1060 nm were assigned, very plausibly, – both as position and as intensity – to the transitions $\nu_3({}^4A_2\rightarrow{}^4T_1^b)$ and $\nu_2({}^4A_2\rightarrow{}^4T_1^a)$, respectively. These $d-d$ transitions are proper to the electronic configuration d^7, of the Co(II) central ion found in a tetrahedral surrounding. [5-7]

The same paper [4] has also shown that *in the solid complexes* the values of the experimentally determined magnetic moments agree very well with the values anticipated by calculations, with the formula [8-9]

$$\mu = (\mu_s - 15.59\lambda/\Delta)\text{B.M.}$$

which holds for the Co(II) tetrahedral complexes (Table 1).

Table 1

The magnetic moments of the CoL_2 and CoL'_2 complexes

Complex	Δ * [cm^{-1}]	μ calculated** [B.M.]	μ experimental [B.M.]
CoL_2	5260	4.42	4.41 ± 0.05
CoL'_2	5370	4.40	4.35 ± 0.05

* values calculated based on the absorption spectra of the complexes.
** values calculated by formula $\mu = \mu_S - 15.59\ \lambda/\Delta$, which holds for tetrahedral Co(II) complexes.

In this formula $\mu_s = 3.89$ B.M. = the spin-only magnetic moment, $\lambda = -178\ cm^{-1}$=the spin-orbit coupling constant for the free Co(II) ion and Δ = the orbital splitting parameter (the energy difference between the t_2 and e subshells). The Δ parameter was calculated [4] from electronic absorption spectral data recorded for *acetone solutions of the complexes.*

Therefore, there is a very good agreement between the magnetic susceptibility data, performed on the solid complexes, and the electronic absorption spectra, recorded on complex solutions. However, this agreement is not incidental but it is well substantiated only when both in the solid state and in solution there are predominantly the same molecular species.[10] In this case the reflectance spectra measured on the solid complexes must agree well with the absorption spectra measured on complex solutions. This is precisely the case of the CoL'_2 complex (m-NO_2-substituted at the benzene ring of the hydrazone group). In spite of some detectable band shifts, in the case of this complex the electronic reflect-

---

[5] A. B. P. Lever, "Inorganic Electronic Spectroscopy", Elsevier, Amsterdam, 1968, chap. 8–9.

[6] Y. Tanabe and S. Sugano, *J. Phys. Soc. Japan*, **9**, 753 (1954).

[7] E. König, *Struct. and Bonding*, **9**, 175 (1971).

[8] R. Stahl-Broda and W. Low, *Phys. Rev.*, **113**, 775 (1959).

[9] F. A. Cotton and M. Goodgame, *J. Amer. Chem. Soc.*, **83**, 1777 (1961).

[10] A. C. Banciu, Ph. D. Thesis, Polytechnical Institute, Bucharest, 1974.

ance spectrum, measured on the solid compound (bands at 580 and 1000 nm), presents, however, a very good agreement with the electronic absorption spectrum, measured on solutions of the complex (bands at 550 and 1040 nm). This fact shows that both in the solid state and in solutions the CoL_2' complex exhibits a type IIIb tetrahedral structure for the $Co(II)-N_4$ chromophore.

In contrast, in the case of the CoL_2 complex (p-NO_2-substituted at the benzene ring of the hydrazone group) the electronic reflectance spectrum, measured on the solid compound and plotted in Fig. 1, is essentially different from the absorption spectrum of the same compound measured in solution and discussed in detail in. [4]

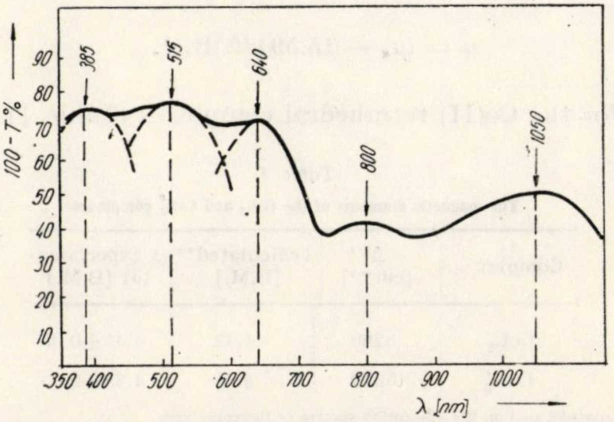

Fig. 1. — The electronic reflectance spectrum of the CoL_2 complex.

In the 350—1200 nm range the reflectance spectrum exhibits an unusually large number of bands. Their maxima occur at 385 nm (26000 cm^{-1}), 515 nm (19400 cm^{-1}), 640 nm (15600 cm^{-1}), 800 nm (12500 cm^{-1}) and 1050 nm (9500 cm^{-1}). Such a spectrum is certainly typical of a Co(II) pentacoordinated complex compound.

Thus, it is interesting to compare this spectrum with the spectra of two Co(II) pentacoordinated complexes which are positively known, from detailed X-ray determinations, to have structures close to the two geometrical limits of pentacoordination. It is known [5] that the real structures of the Co(II) pentacoordinated complexes virtually never coincide with one of the two possible ideal geometrical structures (square pyramidal and trigonal bipyramidal). The real structures exhibit always significant distortions from the ideal structures. The reference complexes are $Co(Me_6\ tren)Cl^+$, (Me_6 tren = tris(2-dimethylaminoethyl)amine), whose structure is close to that of a trigonal bipyramid, [5,11] and β-$Co(paphy)Cl_2$, (paphy = pyridine-2-aldehyde-2-pyridylhydrazone), with a structure close to that of a square pyramid. [12,13]

---

[11] P. L. ORIOLI, *Coord. Chem. Rev.*, **6**, 285 (1971).

[12] I. G. DANCE, M. GERLOCH, J. LEWIS, F. S. STEPHENS and F. LIONS, *Nature*, **210**, 298 (1966).

[13] M. GERLOCH, *J. Chem. Soc.*, **A 1966**, 1317.

Table 2 summarizes the positions of the maxima in the electronic spectra of these two complexes, compared to those found in the spectrum of the CoL_2 complex.

Table 2

Position of the bands maxima [cm^{-1}] in the electronic reflectance spectra of some Co(II) pentacoordinated complexes

$Co(Me_6\,tren)Cl^+$	CoL_2	$Co\,(paphy)Cl_2$
	26000	
		21000 (shoulder)
19600	19400	
		17500 (shoulder)
15800	15600	15500
12300	12500	12300
	9500	
5500		

It can be seen that the spectrum of the CoL_2 complex resembles more that of the trigonal bipyramidal complex $Co(Me_6tren)Cl^+$. Their spectra reveal three bands which practically coincid (at 19400, 15600 and 12500 cm^{-1}). Such a marked similarity is not found when comparing the spectrum of the CoL_2 complex to that of the β-$Co(paphy)Cl_2$ complex, with a square pyramidal structure. However, it would be risky to consider that this spectral similarity proves a structure close to the trigonal bipyramidal one for the Co(II)-donor atom chromophore of the CoL_2 complex. In fact, whatever the real structure adopted by complexes within the limits of pentacoordination (close to the square pyramid or to the trigonal bipyramid) the electronic spectra of all Co(II) pentacoordinated complexes markedly resemble each other.[5] Thus, there is also a sufficiently great similarity even between the spectra of the two reference complexes from Table 2, whose real geometrical structures differ so much (being close either to the square pyramid or to the trigonal bipyramid). Therefore, neither in general, nor in this case can certain distinctions be made between the two possible geometric structures in the case of pentacoordination, based on electronic spectra only. Conversely, the electronic spectra of the Co(II) pentacoordinated complexes, so characteristic, similar to each other and rich in bands situated in the visible and near IR domain, permit a clear distinction of these complexes — unfrequent in the case of the Co(II) ion — from the Co(II) tetrahedral or octahedral complexes, which are extremely numerous.

It remains to explain the experimental magnetic moment of the complex which, if undiscriminately applied, would have erroneously indicated a tetrahedral structure of the solid complex, in disagreement with the data from the electronic reflectance spectrum. The pentacoordinated structure of the CoL_2 complex revealed by the reflectance spectrum permits, however, a correct explanation of the experimental value of the magnetic moment.

It is known [5,11] that the Co(II) pentacoordinated complexes can be of two magnetic types : low-spin, corresponding to an unpaired electron, or high-spin, corresponding to three unpaired electrons. Low-spin complexes present experimental magnetic moments of 2.2 B.M.[14] These are generally formed with ligands having as donors, low electronegativity atoms, such as C, S, P and As, and which are often involved in the formation of strong π bonds.[11] In turn, high-spin complexes exhibit experimental magnetic moments ranging within 4.4 and 5.5 B.M.,[12,15–19] exactly as in the present case. These are formed with ligands with strongly electronegative donor atoms, such as N and O, exactly as in the present case, of the CoL_2 complex. These atoms form strong σ bonds with the central metallic ion. For this reason, the experimental value of the magnetic moment of the complex under discussion, CoL_2, of 4.5 B.M., is very well explained, and this is in perfect agreement with the data from the reflectance spectrum, on the base of a pentacoordinated, high-spin type structure of the complex.

Although pentacoordinated high-spin complexes are generally known[11] to exhibit a trigonal bipyramidal structure (D_{3h} symmetry) while low-spin complexes have a square pyramidal structure (C_{4v} symmetry) for the Co(II)-donor atom chromophore, there are, however, some exceptions. Therefore, neither the electronic spectra, nor the magnetic criterion do permit a distinction between the two possible geometric structures of pentacoordinate Co(II) ion.[11]

Regardless of the geometrical structure adopted by the CoL_2 complex, it is certain that the NO_2 group situated in the *para* position in the benzene ring of the hydrazone group also contributes to achieving the pentacoordination of the Co(II) ion. (In the isomer CoL_2' complex, with the NO_2 group situated in the *meta* position in the benzene ring of the hydrazone group, the Co(II) ion remains tetracoordinated).

All the possible assumptions on the *intra-* or *inter*molecular manner in which the NO_2 group contributes to achieving the pentacoordination of the Co(II) ion in the CoL_2 complex would be risky. This could only be shown by a detailed X-ray structural study, which would also indicate the exact geometrical structure adopted by the complex within the limits of pentacoordination.

This study has shown that in the solid CoL_2 complex the Co(II) ion is pentacoordinated and has explained the agreement between the data from the electronic reflectance spectrum and the magnetic data of the complex. It has also shown that its dissolution (in acetone) is accompanied by a major structural change : the adoption of a tetracoordinated, tetrahedral structure.

---

[14] G. Dyer and D. W. Meek, *Inorg. Chem.*, **4**, 1389 (1965).

[15] L. Sacconi, *Coord. Chem. Rev.*, **1**, 192 (1966).

[16] S. Yamada and H. Nishikawa, *Bull. Chem. Soc. Japan*, **38**, 683 (1965).

[17] M. Ciampolini and N. Nardi, *Inorg. Chem.*, **5**, 41 (1966).

[18] H. B. Gray, *Trans. Metal Chem.*, **1**, 239 (1965).

[19] J. Lewis, R. S. Nyholm and G. A. Rodley, *Nature*, **207**, 72 (1965).

Revue Roumaine de Chimie, 22, 9–10, 1359–1361 (1977)

ISOTOPIC EXCHANGE OF ACTIVE METHYL HYDROGENS. IX[1]

INTRAMOLECULAR KINETIC COMPARISON BETWEEN α-METHYL AND α-ISOPROPYL GROUPS IN PYRYLIUM SALTS

ILEANA I. STĂNOIU,[a] EUGENIA GÂRD,[a] CORNELIA UNCUȚA,[a] F. CHIRALEU[b] and A. T. BALABAN[a,c,d]

[a] Institute of Atomic Physics, P.O.B. 5206, Bucharest, Romania
[b] Organic Chemistry Research Centre, Bucharest
[c] Organic Chemistry Department, Polytechnic Institute, Bucharest
[d] To whom correspondence should be addressed[a]

Received January 11, 1977

The kinetics of the deuteration of 2,4-dimethyl-6-isopropylpyrylium (by ^{1}H—NMR, in D_2O buffer) showed that α-isopropyl and α-methyl groups are deuterated with almost equal rates, so that per one hydrogen the exchange takes place 2.6 times faster for an isopropyl group than for a methyl group.

Most of our earlier studies on the isotopic exchange in alkylpyrylium salts involved α- or γ-methyl groups.[2] However, isopropyl groups are better in that they have the simplest kinetics, because they have only one exchangeable hydrogen.

In the preceding part,[1] the kinetics of the deuteration of isopropyl groups bonded to α- or γ-positions of pyrylium cations was studied by an indirect ^{1}H—NMR technique: since the CH isopropyl signal has low intensity and is split into a septet, this signal is difficult to integrate precisely. One can, however, follow indirectly the course of the exchange from the ^{1}H—NMR methyl peaks of the isopropyl group: while the coupling with the proton splits the methyl signal into a widely spaced doublet ($J = 7$ Hz),* the coupling with the deuteron ($J = 1$ Hz) gives a central closely spaced triplet.* Integrals are reliable and precise enough, despite the isotope effect of 0.3 Hz between the centres of the $CHMe_2$ and $CDMe_2$ methyl signals. Figure 1 presents the methyl multiplet of an isopropyl group atom at an intermediate deuteration degree.

---

* The integrated intensities of the two components of the doublet are denoted by h_1 and h_2, and the integrated intensity of the triplet by d.

[1] Part VIII, I. I. Stănoiu, F. Chiraleu, E. Gârd and A. T. Balaban, *Rev. Roumaine Chim.*, **22**, 117 (1977).

[2] E. Gârd, I. I. Stănoiu, F. Chiraleu and A. T. Balaban, *Rev. Roumaine Chim.*, **18**, 257 (1973).

It was observed [1] that the overall rate of deuteration did not differ appreciably between CH_3 and $CHMe_2$ groups. However, all comparisons involved these groups in different molecules. In the present paper we report the result of an intramolecular comparison. We selected 2,4-dimethyl-6-isopropylpyrylium (**1**) [3] because the α-standing methyl and isopropyl groups do not interfere in the ^1H-NMR spectrum; thus the kinetics of the deuteration can be followed at 85° by NMR directly for the α-methyl group (by monitoring the decrease of its integrated intensity) and indirectly as described above for the isopropyl group. The γ-standing methyl group is deuterated about ten times faster than α-standing group, like all γ-alkyl groups; [2] γ-deuteration would proceed at a kinetically convenient rate around 55°.

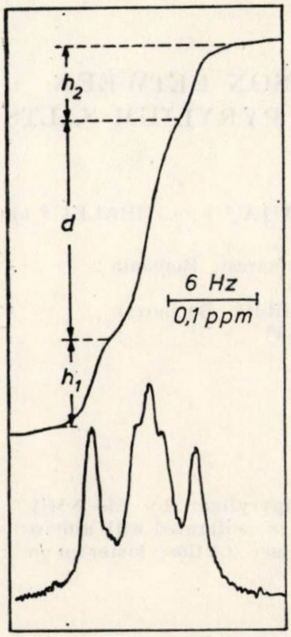

Fig. 1. —^1H-NMR spectrum (isopropyl methyl multiplet, partly deuterated) and the notations of the integral curve used in kinetic determinations.

Results for the kinetics of the deuteration in D_2O buffer at 85° are presented in table 1. They indicate that, within the limits of experimental error, the α-methyl and α-isopropyl groups in the same molecule **1** exchange with almost the same overall rate: 0.378 h^{-1} for methyl, 0.331 h^{-1} for isopropyl.

Taking into account that all hydrogens of the methyl exchange, while the isopropyl has only one exchangeable hydrogen, the statistical factor 3 must be included. Therefore an α-hydrogen in isopropyl exchanges 2.6 times faster than an α-hydrogen in methyl.

Table 1

Kinetics of the deuteration of 2,4-dimethyl -6-isopropylpyrylium perchlorate in D_2O buffer (pH=4) at 85°

Time hrs	Integrated intensities, mm					α-Methyl		α-Isopropyl	
	α-Methyl	α-Isopropyl				$-\lg Mf/M_0$		$-\lg(h_1 + h_2)f/\Sigma$	
	M	h_1	*d*	h_2	Σ	*Exp.*	*Calc.*	*Exp.*	*Calc.*
0	68	64.5	5.5	61	131	0	0.0033	0.0186	0.0306
0.083	59	56.8	10	56	122.8	0.0336	0.0347	0.0370	0.0581
0.167	56.5	53	22	49.5	124.5	0.0584	0.0664	0.0844	0.0859
0.333	48	47.2	43	36.2	126.5	0.1361	0.1291	0.1809	0.1410
0.667	35	40.8	57.5	27.7	126	0.2715	0.2551	0.2647	0.2517
1.083	26	30.2	72.5	23.5	126.2	0.4013	0.4122	0.371	0.3895

For the α-methyl group, $-\lg Mf/M_0 = 0.00336 + 0.378\ t$.
For the α-isopropyl group, $-\lg (h_1 + h_2)f/\Sigma = 0.0306 + 0.331\ t$.

All the three possible anhydrobases (methylenepyrans) **2** — **4** are constitutionally (structurally) different: the lower energy (confirmed by

---

[3] C. Uncuța and A. T. Balaban, *Rev. Roumaine Chim.*, **21**, 251 (1976).

HMO calculations) of the γ-methylenepyran **2** explains the faster γ-deuteration. The α-methylenepyrans **3** and **4** differ in that **3** has a tetrasubstituted ethylenic bond, while **4** has a 1,1-disubstituted bond. The present kinetical analysis indicates that **3** is formed ca. three times faster than **4**.

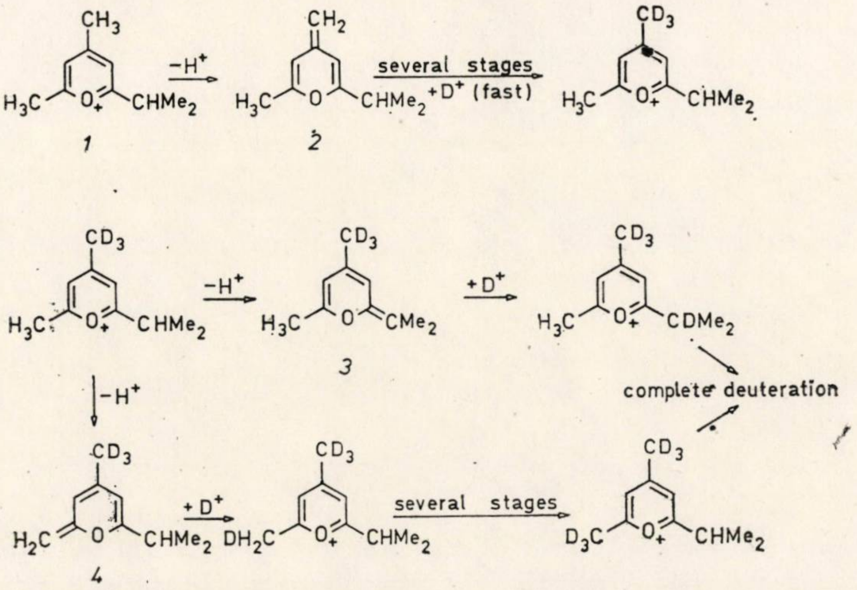

Earlier studies of the kinetic isotope effect revealed a fairly small value for $k_H/k_D = 1.6$ in acetonitrile-d_3 with a slight excess of H_2O or D_2O, respectively;[1] this finding is in agreement with the intermediacy of methylenepyrans and with the idea that their formation by C-deprotonation is the rate-determining step.

EXPERIMENTAL PART

The preparation of **1** and its ^{1}H−NMR spectrum were described earlier.[3] Solutions of **1** in D_2O buffer (prepared as described earlier[1] and checked pH-metrically with a glass electrode) were introduced into NMR vials. The ^{1}H−NMR spectra were recorded at 38°, after keeping the vial immersed for a prescribed time in a water thermostat at 85°. Four integrals for each spectrum were recorded for the α-methyl peak and the α-isopropyl methyl multiplet (at a sweep width of 100 Hz). The vial was then placed again in the thermostat until the next time elapsed, and a new spectrum was recorded. The integrated intensities were averaged and the kinetic results were obtained as indicated in table 1 by the method of least squares.

In order to take into account the slight variations of the integrator sensitivity, a correction factor $f = \Sigma_0/\Sigma$ was introduced (tab. 1), where Σ_0 is the integrated intensity of the isopropyl methyl multiplet at the initial time $t = 0$. At all times, this intensity Σ ought to remain constant, but as shown in the respective column of table 1, minor variations did occur. A slight deuteration had already taken place during the preparation of the solution, so that there is a non-zero intercept of both regression lines for the α-methyl and the α-isopropyl groups at $t = 0$, as seen from their expressions at the bottom of table 1.

An A−60A Varian instrument was used for the ^{1}H−NMR spectra, and 99.8% deuterium oxide for the solutions.

Revue Roumaine de Chimie, 22, *9–10*, 1363–1368 (1977)

REACTION OF 1,3,7,9-TETRANITROPHENOTHIAZINE-5-OXIDE WITH ORGANIC BASES

AUREL TURCU
Faculty of Biology, University of Bucharest,
Splaiul Independenţei 91–95

Received May 24, 1976

15 molecular complexes were prepared through the reaction of 1, 3, 7, 9-tetranitrophenothiazine-5-oxide with inferior aliphatic amines and quaternary ammonium bases. Two categories of compounds are evidenced through IR spectroscopy ; these are molecular complexes or salts. The thermal stability and donor-acceptor combination ratio of the complexes by an elemental and thermogravimetric analysis are determined. Hypotheses regarding their chemical structure are given.

INTRODUCTION

In previous papers [1,2] the molecular complexes formed by the reaction of 1, 3, 7, 9-tetranitrophenothiazine-5-oxide considered as acceptor with different donors were studied. The paper presents the results of research on compounds made up by this 1, 3, 7, 9-tetranitrophenothiazine-5-oxide (I) with some aliphatic amines and quaternary ammonium bases.

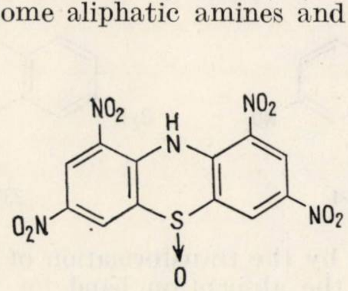

I

The nature of the issuing compounds can be explained through the structure of the nitroderivative (I), as well as through its basic component.

The hydrogen atom bound to the nitrogen atom of the nitroderivative (I) presents an acidic character owing to the presence in the molecule of the four nitro groups as well as of the sulphoxidic group.

---

[1] A. Turcu and M. Răileanu, *Rev. Roumaine Chim.*, **14**, 1579 (1969).

[2] M. Răileanu, M. Olteanu, I. Radulian, G. Volanschi, A. Turcu and H. Căldăraru, *Rev. Roumaine Chim.*, **16**, 1269 (1971).

The absorption band corresponding to the valency vibration of the N-H bond is strongly displaced from 3350 cm^{-1} to 3205 cm^{-1} regarding its situation in phenothiazine.

The reason leading to this displacement is due to the formation of an intramolecular hydrogen bond between the hydrogen atom bound to nitrogen atom and nitro group in 1 or 9 position.

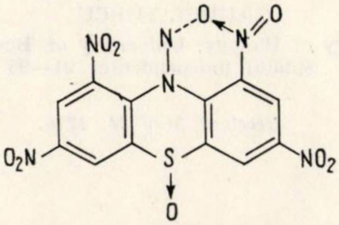

II

This conclusion was reached following the IR spectra made up by tabletation with KBr to the following compounds :

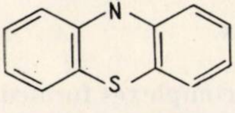

YN–H 3350 cm^{-1}

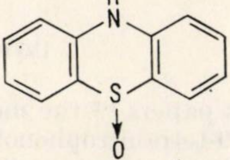

3250 cm^{-1}

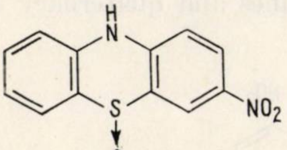

3260 cm^{-1}

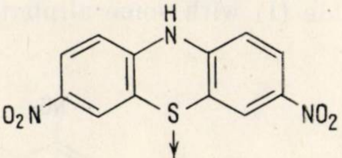

3300 cm^{-1}

One can see that by the transformation of the phenothiazine into phenothiazine-5-oxide, the absorption band for N-H valency vibration is displaced from 3350 cm^{-1} to 3250 cm^{-1}. This displacement can be explained by the formation of an intramolecular hydrogen bond, as : $>S\rightarrow O\ldots H-N<$.[3]

Through the nitration of phenothiazine-5-oxide in special conditions in order to obtain 3-nitrophenothiazine-5-oxide,[4] the absorption band for N-H of the latter is placed at 3260 cm^{-1} and for 3, 7-dinitrophenothiazine-5-oxide at 3300 cm^{-1}.

---

[3] N. A. Kudryavtseva, Z. V. Pushkareva, V. F. Gryasev. *Chim. Gheterofikl. Soedin., Akad. Nauk. Letv. S.S.R.*, **1965**, 523.

[4] M. Răileanu and A. Turcu, *Rev. Roumaine Chim.*, **11**, 1423 (1966).

Taking into account these data, we believe that by the maximum nitration of phenothiazine-5-oxide, the intermolecular hydrogen bond is transformed into an intramolecular hydrogen bond.

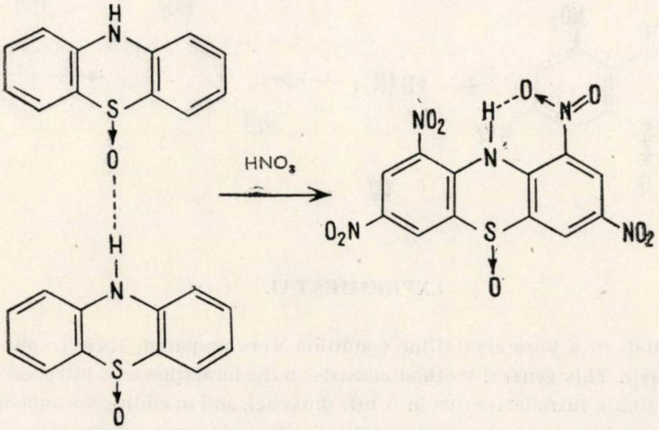
H
N
S
O
H
N
S
O
HNO₃
NO₂
H
O
N
O
N
O₂N
S
NO₂
O

In the IR spectra of 1, 3, 7, 9-tetranitrophenothiazine-5-oxide solved in dioxane and deuterated dioxane, the position of the absorption band corresponding to N—H does not show considerable displacements towards its position in IR spectrum of the solid substance.

The acidic properties of the hydrogen atom bound to the nitrogen atom of the heterocycle and the formation of the six atoms chelate are the principal factors in establishing the manner of reaction of the 1, 3, 7, 9-tetranitrophenothiazone-5-oxide with basic substances.

The quaternary ammonium bases give with this tetranitroderivate salts :

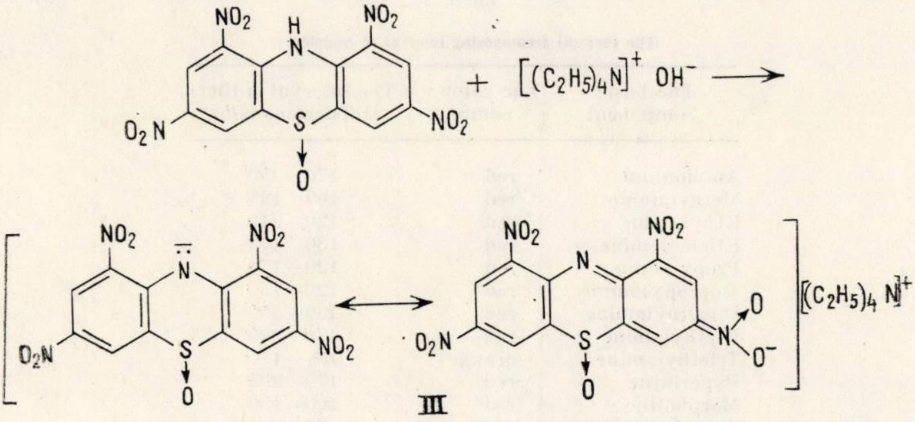
NO₂
H
N
NO₂
O₂N
S
NO₂
O
+
[(C₂H₅)₄N]⁺ OH⁻
NO₂
N
NO₂
O₂N
S
NO₂
O
NO₂
N
NO₂
O₂N
S
N
O
O⁻
O
[(C₂H₅)₄ N]⁺

III

The inferior aliphatic amines being weaker bases, we believe they react in a different way with 1, 3, 7, 9-tetranitrophenothiazine-5-oxide, leading to charge transfer complexes, in the same way as ammonium : [1]

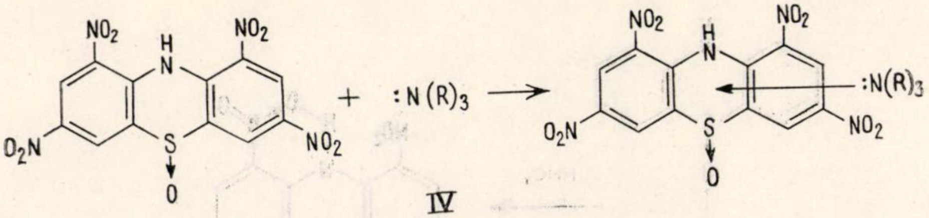

IV

EXPERIMENTAL

15 compunds in a pure crystalline condition were prepared, their colour varying from orange to dark red. This general method consists in the formation of a nitroderivative suspension in dioxane (0.2 g nitroderivative in 5 ml. dioxane), and in adding an aqueous 30% amine solution. This suspension has to be continuously shaken, till the nitroderivative dissolved and [a] clear solution of a dark red colour is obtained; distilled water is added drop by drop, shaking continuously till the first coloured crystals appear in the testtube. After leaving the solution for several hours, it is filtered and dried at 60—70°. The yield is 75—80%. The complexes are pure enough in order to determine the structure.

Through the thermogravimetric analysis it has been pointed out that the complexes of nitroderivative-ammonium and inferior aliphatic amines decompose into the two components at the temperature between 100 and 250° (table 1). These complexes have no melting point. The complexes with quaternary ammonium bases by heating to a certain temperature (table 2) get melted and by continuing the heating over the melting point, they decompose explosively.

The IR spectra have been obtained by using tabletation technique with KBr and the suspension in nuyol using a UR-10 apparatus.

Table 1

The thermal decomposing interval of complexes

The basic component	The colour of complex	The interval of thermal decomposing°
Ammonium	red	170—250
Methylamine	red	160—195
Ethylamine	red	120—210
Ethanolamine	red	130—175
Propylamine	red	120—170
Isopropylamine	red	120—150
Dimethylamine	red	130—190
Diethylamine	red	130—200
Triethylamine	orange	130—170
Pyperidine	red	170—205
Morpholine	red	100—150
Cyclohexylamine	green	20—25

Table 2

The melting points of complexes

The basic component	The colour of complex	The melting point °
Tetraethylammonium hydroxide	orange	240
Triethylbenzylammonium hydroxide	orange	180
Trimethylbenzyl-ammonium hydroxide	orange	178

DISCUSSION

The interpretation of the IR spectra of the complexes in comparison to IR spectra of the two components can lead to some hypothesis regarding their structure. The most affected divisions of the tetranitroderivative spectrum are those corresponding to the vibration of the N-H bond (3205 cm^{-1}) and the nitro groups. In the complexes with quaternary ammonium bases, the absorption band at 3205 cm^{-1} disappears and the absorption band of the nitro groups presents also some modifications.

While in the pure nitroderivative for the symmetric vibration of the nitro groups (1300—1355 cm^{-1}) there are four bands of absorption (1312, 1328, 1340 and 1355 cm^{-1}) the complexes in this divison show only two absorption bands at 1313 and 1340 cm^{-1}. For the asymmetric vibration of the nitro groups belonging to the pure nitroderivative, there are the following bands : 1495, 1515, 1525, 1542 cm^{-1} ; the complexes in this division have only two absorption bands : at 1515 and 1545 cm^{-1}.

These modifications in the IR spectrum can be interpreted as a result that in the pure nitroderivative not all the nitro groups are equivalent : one of them which is to be found in 1 or 9 position is implied in an intramolecular hydrogen bond, while the other is free ; the nitro groups of 3, 7, positions can be considered equivalent. For the complexes with quaternary ammonium bases, the IR spectra are simpler, because the above mentioned hydrogen bond disappears while the quaternary ammonium ion has characteristic frequencies in IR.

Considering these moditications in IR nitroderivative spectra, combined with quaternary ammonium bases, as compared to the pure nitroderivative, we believe that the reaction between the two substances takes place as it was shown in scheme III.

To this conclusion leads also the fact that the quaternary bases of ammonium being strong, it can take away the hydrogen atom from the nitrogen atom, even in the condition in which it belongs to a stable chelate of six atoms.

We can give the structure IV to the complexes formed by weaker bases such as the amines. In order to determine this structure, the IR spectra of the tertiary amines complexes are more relevant, because the tertiary amines do not have absorption bands in the absorption division of N – H valency vibration in the tetranitroderivative. In the triethylamine complex, the absorption band of 3205 cm^{-1} does not show significant modifications as regards its position in the pure tetranitroderivative.

The IR spectra of primary and secondary amines complexes present in the 3180 – 3380 cm^{-1} division 2 – 3 absorption bands. In this way the methylamine complex has in this division a wide band of absorption with two peaks : 3190 cm^{-1}, 3235 cm^{-1} and a shoulder at 3280 cm^{-1} ; the ethylamine complex : a band between 3200 cm^{-1} and 3245 cm^{-1} and another one at 3260 cm^{-1} ; the complex with ethanolamine has a wide band between 3200 cm^{-1} and 3300 cm^{-1} with the peak at 3250 and a wide band between 3400 and 3550 cm^{-1}, characteristic of the hydroxyl group ; the diethylamine complex has only one band between 3180 – 3205 cm^{-1}. In the case of the primary and secondary amines complexes it is more difficult to know which of these bands is due to the N-H bond vibration in the heterocycle and which one is due to the N – N vibration in the amine.

The structure of these complexes is to be studied by crystallographic analysis, with X rays, ESR and electric conductivity, because some of the complexes with charge transfer have semiconductive properties. [5]

---

[5] F. Gutmann and L. E. Lyons, "Organic Semiconductors", Wiley, London, 1967.

Revue Roumaine de Chimie, 22, *9–10*, 1369–1373 (1977)

LA STRUCTURE ET LA RÉACTIVITÉ DES NITRILES

SUR LA CHALEUR DE COMBUSTION DE QUELQUES NITRILES ALPHA, BÊTA NON SATURÉS

ION CIOCĂZANU*, VIORICA DOGARU* et DINU ZĂVOIANU**
* Laboratoire de Thermodynamique chimique
** Laboratoire de Chimie organique Faculté de Chimie, 89, Splaiul Independenţei, Bucarest

Reçu le 8 novembre 1974
Révisé le 30 septembre 1976

Pour pouvoir établir des relations entre la structure et la réactivité des nitriles on détermine les chaleurs de combustion et de formation de quelques nitriles *alpha*, *bêta* non saturés dérivés du benzylidène *o*-tolylacétonitrile et du benzylidène 2,5-diméthylphénylacétonitrile. On constate que les valeurs des chaleurs de combustion et de formation sont influencées par les effets électroniques qui se manifestent dans les molécules des nitriles.

Dans une série de notes[1–3] on a étudié le comportement dans la réaction d'hydrolyse alcaline de quelques nitriles *alpha*, *bêta* non saturés aromatiques et on a constaté que la présence des électrons π détermine la croissance des constantes de vitesse et l'abaissement des valeurs des énergies d'activation.

De même on a observé que la présence des substituants qui repoussent les électrons ou qui attirent les électrons dans la molécule des nitriles *alpha*, *bêta* non saturés déterminent la modification des valeurs des paramètres d'activation, l'enthalpie d'activation $\Delta H\neq$ et l'entropie d'activation $\Delta S\neq$.

Afin d'apporter une contribution à la connaissance des relations entre la structure et la réactivité des nitriles nous présentons les résultats obtenus en ce qui concerne les chaleurs de combustion $-\ \Delta H_c^\circ$.

La chaleur de combustion $-\ \Delta H_c^\circ$ constitue un paramètre thermodynamique très important et qui peut caractériser une certaine substance. La chaleur de combustion $-\ \Delta H_c^\circ$ se trouve en étroite liaison avec la chaleur de formation ΔH_f°, l'énergie de conjugaison des électrons π, l'énergie de résonance et de la force de liaison chimique.

Dans cette note on présente les résultats obtenus pour les nitriles suivants : *o*-chlorbenzylidène-*o*-tolylacétonitrile (1) ; *m*-chlorbenzylidène

---

[1] D. ZĂVOIANU, *Chemistry Oil and Gas in Romania*, **4**, 16 (1969).

[2] D. ZĂVOIANU et E. CAVADIA, *Rev. Chim.* (*Bucureşti*), **22**, 129 (1971).

[3] D. ZĂVOIANU, *Anal. St. Univ. Bucureşti*, **2**, 183 (1971).

o-tolylacétonitrile (2) ; *o*-nitrobenzylidène-*o*-tolylacétonitrile (3) ; *p*-nitrobenzylidène-*o*-tolylacétonitrile (4) ; *m*-nitrobenzylidène-2, 5-diméthylphénylacétonitrile (5) et *p*-nitrobenzylidène-2, 5-diméthylphénylacétonitrile (6).

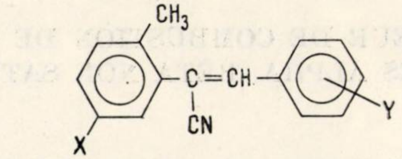

1 : $X = H ; Y = o - Cl$
2 : $X = H ; Y = m - Cl$
3 : $X = H ; Y = o - NO_2$
4 : $X = H ; Y = p - NO_2$
5 : $X = CH_3 ; Y = m - NO_2$
6 : $X = CH_3 ; Y = p - NO_2$

PARTIE EXPÉRIMENTALE

Pour la détermination des chaleurs de combustion on a utilisé une bombe calorimétrique adiabatique du type Gallenkamp, qui présente un système de thermistor en série, ce qui permet à maintenir durant la combustion une différence nulle de température entre l'enceinte intérieure et l'enceinte extérieure.

La bombe calorimétrique est munie d'un thermomètre Beckmann qui permet de lire 0,01° et même 0,001°.

Pour les déterminations effectuées on a employé des fils de Cr—Ni avec une chaleur de combustion de 335 cal/g et de cotton avec une chaleur de combustion de 4180 cal/g.

Afin d'obtenir la chaleur de combustion standard on a effectué les déterminations à 25°.

Au début on a déterminé l'équivalent calorique du système avec l'acide benzoïque (auquel on connaît la chaleur de combustion de 6317,83 cal/g[4-8] obtennant à la suite d'un grand nombre de déterminations une valeur moyenne de 510,67 cal/degré.

Pour la détermination de la chaleur de combustion on applique la relation suivante :

$$\Delta U_c = C\Delta T - Q_1 - Q_2$$

où $C = C_{\text{bombe}} + C_{\text{eau}} + C_{\text{épreuve}}$

Q_1 = la chaleur dégagée à la suite du brûlage du fil de cotton

Q_2 = la chaleur dégagée à la suite du brûlage du fil de Cr—Ni

ΔT = la différence de température entre la période finale et celle initiale.

A l'aide du thermomètre Beckmann on a déterminé la croissance de la température due aux processus de combustion dans la bombe en lisant la température à des intervalles égaux à une minute. On fait la remarque qu'il n'y a pas de corrections de température, les déterminations étant faites au moment initial et au moment final à une température constante.

Pour obtenir les valeurs plus précises des chaleurs de combustion des substances contenant dans la molécule de l'azote on fait les corrections pour la formation de l'acide azotique. Ainsi, 10% d'azote au maximum contenu dans la molécule se retrouve[9] comme acide azotique

---

[4] R. S. Jessup, *J. Res. Nat. Bur. Stand.*, **29**, 247 (1942).

[5] J. Coops et N. Adriannse, *Rec. Trav. chim.*, **75**, 237 (1956).

[6] E. J. Prosen et F. D. Rossini, *J. Res. Nat. Bur. Stand.*, **33**, 439 (1941).

[7] K. L. Churney et G. T. Armstrong, *J. Res. Nat. Bur. Stand.*, **72**, 453 (1958).

[8] H. A. Gundry, D. Harrop, A. J. Head et G. B. Lewis, *J. Chem. Thermodynamics*, **1**, 321 (1969).

[9] F. D. Rossini, "Experimental Thermochemistry". Chap. 3. Interscience Publishers Inc., New York, 1956.

(ΔH_f°=13,8 k.cal/mole). L'acide azotique est titré pour pouvoir faire les corrections respectives. De même, on tient compte[10] que 15—20 % du chlore contenu dans la molécule se retrouve comme chlore libre, et le reste sous forme d'acide chlorhydrique. Pour pouvoir transformer toute la quantité de chlore contenu dans la molécule comme ions de chlore on traite la substance à une solution d'oxyde arsénieux 0,35 N d'après la réaction suivante :

$$2Cl_2(g) + As_2O_3(aq) + 2H_2O(1) \rightarrow As_2O_5(aq) + 4HCl(aq)$$

La solution d'oxyde arsénieux qui n'a pas réagi est titrée par une solution 0,1 N $KMnO_4$. Ainsi on peut déterminer la quantité d'acide chlorhydrique et connaissant sa chaleur de formation dans les conditions de la réaction[11] on fait la correction correspondant à la chaleur de formation pour la substance étudiée. Si dans la molécule se trouve aussi de l'azote et du chlore on emploit le même procédé et on effectue la détermination colorimétrique pour l'acide azotique en présence de diphénylamine.

La chaleur de formation pour une substance ($C_mH_nN_pO_qX_r$) est déterminée à l'aide de la chaleur de combustion, H_c° d'après la loi de Hess, la relation étant :

$$\Delta H_f^\circ = -\Delta H_c^\circ - m_\Delta H_{f,CO_2} - \frac{(n-r)}{2}\Delta H_{f,H_2O(1)} - \frac{r}{2}\Delta H_{f,HX}$$

où $\Delta H_{f,CO_2}$, $\Delta H_{f,H_2O}$ et $\Delta H_{f,HX}$ sont les chaleurs de formation connues[11] pour le CO_2, H_2O et pour la solution d'acide halogéné obtenue.

Dans le tableau 1 on représente les données concernant les valeurs de la chaleur de combustion à volume constant (ΔU_c°) et à pression constante (ΔH_c°) et en même temps les valeurs pour la chaleur de formation (ΔH_f°).

Les chaleurs de combustion et de formation standard des substances étudiées sont consignées dans le tableau 2.

Pour chaque terme on a effectué 3 expériences au minimum, l'erreur étant de ±1,5 %. Les valeurs obtenues coïncident avec les valeurs calculées d'après la méthode d'Handrick[12] basée sur une relation linéaire entre la balance d'oxygène nécessaire à la combustion et la chaleur molaire de combustion.

Les substances étudiées ont été obtenues et purifiées au laboratoire de Chimie organique de la Faculté de Chimie.[1-3]

Tableau 1

Résultats pour une expérience de combustion du *para*-nitrobenzylidène *ortho*-tolylacétonitrile à 25°

m (*para* nitrobenzylidène *ortho*-tolylacétonitrile (4)/g	0,3589
m (fil de cotton)/g	0,0063
m (fil de Cr—Ni)/g	0,0077
m (H_2O)/g	1,00
q (pour allumer)/cal	28,9
q(HNO_3)/cal	3,8
$-U_c^\circ$ (298,15 K)/kcal.mole^{-1}	7397,90
$-U_c^\circ$ (298,15 K)/kcal.mole^{-1}	1955,06
$-H_c^\circ$ (298,15 K)/kcal.mole^{-1}	1955,65
$-H_f^\circ$ ($C_{16}H_{12}N_2O_2$, s, 298,15 K)/kcal.mole^{-1}	41,05

---

[10] L. Smith, L. Bjellerup, S. Krook et H. Westermark, *Acta Chem. Scand.*, **7**, 65 (1953).

[11] F. D. Rossini, D. D. Waymar, W. H. Evans, S. Levine et I. Jaffe, "Selected Values of Chemical Thermodynamic Properties", part I, National Bureau of Standards, circular 500. 1961.

[12] G. R. Handrick, *Ind. Eng. Chem.*, **48**, 1366 (1956).

Tableau 2

Chaleurs de combustion et de formation de quelques nitriles *alpha*, *bêta* non saturés dérivés du benzylidène *ortho*-tolylacétonitrile et du 2,5-diméthylphénylacétonitrile

Nitrile	ΔH_c° kcal. mole^{-1}	ΔH_f° kcal,mole^{-1}
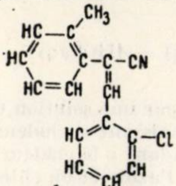 1	−1965,28	73,53
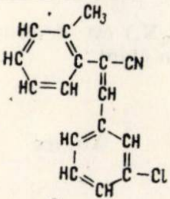 2	−1966,25	74,50
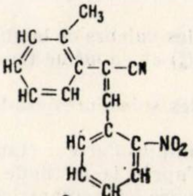 3	−1954,08	39,48
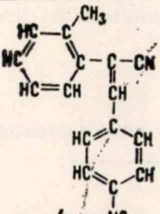 4	−1955,65	41,05
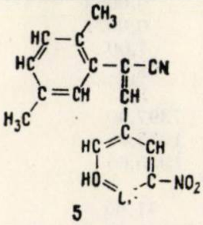 5	−2109,57	32,62
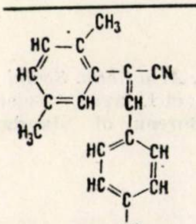 6	−2113,45	36,50

DISCUSSION DES RÉSULTATS

Des données consignées dans le tableau 2 on constate que la structure moléculaire des nitriles étudiés exerce une influence sur les valeurs de chaleurs de combustion et de formation ; ainsi une chaleur de formation petite correspond au fait que la substance donnée présente des liaisons fortes, c'est-à-dire une plus grande stabilité.

Ainsi, pour l'*ortho*-chlorbenzylidène-*ortho*-tolylacétonitrile on observe une chaleur de formation plus petite en comparaison de la chaleur de formation correspondant au dérivé *méta*-chlorbenzylidène-*ortho*-tolylacétonitrile, fait dû probablement à l'effet électromère $+E$ qui se manifeste seulement pour la position *ortho*, tandis que dans la position *méta* se manifeste seulement l'effet inductif — I. Cette influence due à l'effet $+E$ détermine une plus grande stabilité de la molécule.

Dans le cas des substituants nitro on remarque que la superposition des effets — I et — E est plus accentuée pour la position *para*, ce qui détermine une diminution de la stabilité de la molécule, la chaleur de formation présentant une valeur plus grande que pour le dérivé *ortho*.

Si on étudie les valeurs des chaleurs de formation obtenues pour les nitriles *méta*-nitrobenzylidène-2,5-diméthylphénylacétonitrile et *para* nitrobenzylidène 2,5-diméthylphénylacétonitrile on constate, de même que dans les cas précédents, que la superposition des effets électroniques $-I$ et $-E$ (seulement dans la position *para*) détermine une diminution de la stabilité moléculaire, en comparaison de la position *méta* où agit seulement l'effet inductif $-I$.

Une constatation intéressante peut être mentionnée au cas du *para*-nitrobenzylidène-2,5-diméthylphénylacétonitrile qui présente une stabilité plus grande que celle du *para*-nitrobenzylidène-*ortho*-tolylacétonitrile fait dû probablement au groupement méthyle fixé dans la position 5 qui exerce un effet inductif $+I$.

En conclusion, la stabilité moléculaire est déterminée par les effets électroniques qui repoussent les électrons ($+I$ et $+E$) et peut être diminuée par les effets qui attirent les électrons ($-I$ et $-E$).

DISCUSSION DES RÉSULTATS

Des données consignées dans le tableau 2 on constate que la structure moléculaire des nitriles étudiés exerce une influence sur les valeurs de chaleurs de combustion et de formation ; ainsi une chaleur de formation petite correspond au fait que la substance donnée présente des liaisons fortes, c'est-à-dire une plus grande stabilité.

Ainsi, pour l'*ortho*-chlorbenzylidène-*ortho*-tolylacétonitrile on observe une chaleur de formation plus petite en comparaison de la chaleur de formation correspondant au dérivé *méta*-chlorbenzylidène-*ortho*-tolylacétonitrile, fait dû probablement à l'effet électromère $+E$ qui se manifeste seulement pour la position *ortho*, tandis que dans la position *méta* se manifeste seulement l'effet inductif $-I$. Cette influence due à l'effet $+E$ détermine une plus grande stabilité de la molécule.

Dans le cas des substituants nitro on remarque que la superposition des effets $-I$ et $-E$ est plus accentuée pour la position *para*, ce qui détermine une diminution de la stabilité de la molécule, la chaleur de formation présentant une valeur plus grande que pour le dérivé *ortho*.

Si on étudie les valeurs des chaleurs de formation obtenues pour les nitriles *méta*-nitrobenzylidène-2,5-diméthylphénylacétonitrile et *para*-nitrobenzylidène-2,5-diméthylphénylacétonitrile on constate, de même que dans les cas précédents, que la superposition des effets électroniques $-I$ et $-E$ (seulement dans la position *para*) détermine une diminution de la stabilité moléculaire, en comparaison de la position *méta* où agit seulement l'effet inductif $-I$.

Une constatation intéressante peut être mentionnée au cas de *para*-nitrobenzylidène-2,5-diméthylphénylacétonitrile qui présente une stabilité plus grande que celle du *para*-nitrobenzylidène-*ortho*-tolylacétonitrile fait dû probablement au groupement méthyle fixé dans la position 5 qui exerce un effet inductif $+I$.

En conclusion, la stabilité moléculaire est déterminée par les effets électroniques qui repoussent les électrons ($+I$ et $+E$) et peut être diminuée par les effets qui attirent les électrons ($-I$ et $-E$).

Revue Roumaine de Chimie, 22, *9–10*, 1375–1378 (1977)

HETEROCYCLEN MIT PERINAPHTHINDEN-GERÜST. I

QUARTÄRE AMMONIUMSALZE DES 2,3-DIHYDRO-BENZ[d.e] ISOCHINOLINS

F. POTMISCHIL und D. RÖMER
Organisch-Chemisches Laboratorium der Universität Bukarest,
Spl. Independenței 89

Eingegangen am 28. Oktober 1974
Ergänzt: 10. Februar 1977

Eine größere Zahl quartärer Ammoniumsalze (IIIa-r) des 2,3-Dihydro-benz[d.e]isochinolins (2-Aza-perinaphthindans) wurden dargestellt und charakterisiert.

Salze tertiärer heterocyclischer Amine aus den Reihen des Dihydroisoindols, 1,3-Dihydro-benzo[f]isoindols, 2,7-Dihydro-dibenzo[c.e]azepins und 2,3-Dihydro-benz[d.e]isochinolins sind für die Pharmakologie interessante Verbindungen, als mögliche Antagonisten von Adrenalin und Serotonin. [1] In der vorliegenden Mitteilung berichten wir über die Synthese einer größeren Zahl quartärer Ammoniumsalze (**IIIa-r**) der zuletzt erwähnten Reihe, aus welcher bisher sehr wenige Vertreter beschrieben sind.

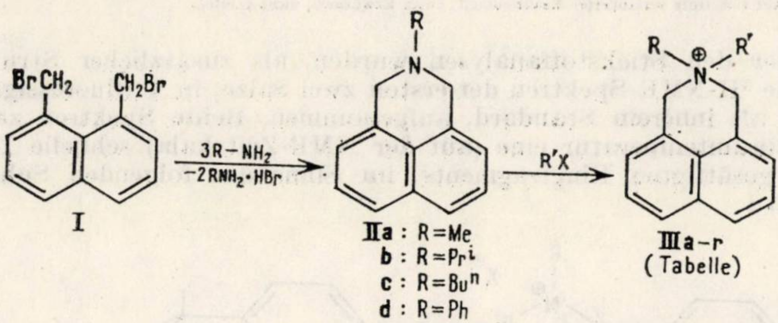

I

IIa : R=Me
b : R=Prⁱ
c : R=Buⁿ
d : R=Ph
e : R=CH₂Ph

IIIa–r
(Tabelle)

Ried und Grabosch [1] gewannen drei tertiäre Amine **II** von 1,8-Bisbrommethyl-naphthalin (**I**) und den entsprechenden primären Aminen ausgehend, wobei sich beide Reaktionspartner in Benzol gelöst befanden.

---

[1] W. Ried und J. Grabosch, *Chem. Ber.*, **91**, 2485 (1958).

Wir folgten denselben Weg und fanden, daß die sehr flüchtigen Amine (z.B. Methyl- und Äthylamin), zur Vereinfachung der Arbeitsweise, ohne weiteres auch in der Form ihrer im Handel befindlichen wäßrigen Lösungen eingesetzt werden können. Die Amine **II**, die uns nicht besonders interessierten, wurden schon in rohem Zustand der Quaternierung unterworfen, und ergaben (mit einer Ausnahme — s. Tabelle) die Salze **III** mit Ausbeuten von 26 bis 90%, auf **I** bezogen. Die fünfzehn neuen (und zwei bereits bekannte) Ammoniumsalze, mit ihren Schmelzpunkten und den Analysenwerten, sind in der Tabelle angegeben.

Tabelle

Schmelzpunkte und Analysenwerte der quartären Ammoniumsalze IIIa-r

Salz III	R	R′	X	Schmelzpunkt (°C)	Mol. — Formel	Mol. — Gew.	Analyse (%N)	
							Ber.	Gef.
a	Me	Me	I	233—235[a]	$C_{14}H_{16}NI$	325,19	4,30	4,27
b	Me	Et	I	188—190	$C_{15}H_{18}NI$	339,21	4,12	3,77
c	Me	CH_2Ph	Cl	131—132,5	$C_{20}H_{20}NCl$	309,82	4,52	4,50
d	*i*-Pr	Me	I	235—237 (Zers.)	$C_{16}H_{20}NI$	353,24	3,96	3,69
e	*i*-Pr	Et	I	211 (Zers.)	$C_{17}H_{22}NI$	367,27	3,81	[b]
f	*i*-Pr	*n*-Bu	Br	200—203 (Zers.)	$C_{19}H_{26}NBr$	348,31	4,02	3,75
g	*i*-Pr	CH_2Ph	Cl	207—208 (Zers.)	$C_{22}H_{24}NCl$	337,87	4,14	4,21
h	*n*-Bu	Me	I	192—194[c]	$C_{17}H_{22}NI$	367,27	3,81	3,65
i	*n*-Bu	Et	I	190—192 (Zers.)	$C_{18}H_{24}NI$	381,29	3,67	3,85
j	*n*-Bu	*n*-Bu	Br	121—123 (Zers.)	$C_{20}H_{28}NBr$	362,34	3,86	3,60
k	*n*-Bu	CH_2Ph	Cl	140—142 (Zers.)	$C_{23}H_{26}NCl$	351,90	3,98	4,03
l	Ph	Me	I	178	$C_{19}H_{18}NI$	387,25	3,61	3,78
m	Ph	Et	I	183 (Zers.)	$C_{20}H_{20}NI$	401,28	3,49	3,79
n	Ph	*n*-Bu	Br	183—184 (Zers.)	$C_{22}H_{24}NBr$	382,33	3,66	3.94
o	Ph	CH_2Ph	Cl	[d]				
p	CH_2Ph	Me	I	220—224	$C_{20}H_{20}NI$	401,28	3,49	3,61
q	CH_2Ph	Et	I	191	$C_{21}H_{22}NI$	415,31	3,37	3,22
r	CH_2Ph	CH_2Ph	Cl	180—181	$C_{26}H_{24}NCl$	385,91	3,62	3,82

[a] Wittig und Ludwig[2] gaben 230—231° an.

[b] Die Menge des gereinigten Salzes war für die Analyse unausreichend.

[c] Ried und Grabosch gaben 196—198° an.

[d] Dieses Salz hat sich trotz verlängerter Reaktionszeit, unter Erwärmen, nicht gebildet.

Außer den Stickstoffanalysen wurden, als zusätzlicher Strukturbeweis, die ^1H-NMR-Spektren der ersten zwei Salze, in Trifluoressigsäure mit TMS als innerem Standard, aufgenommen. Beide Spektren zeigen, daß bei Raumtemperatur eine (auf der NMR-Zeitskala) schnelle Inversion des gesättigten Ringfragments, im Sinne des folgenden Schemas stattfindet:

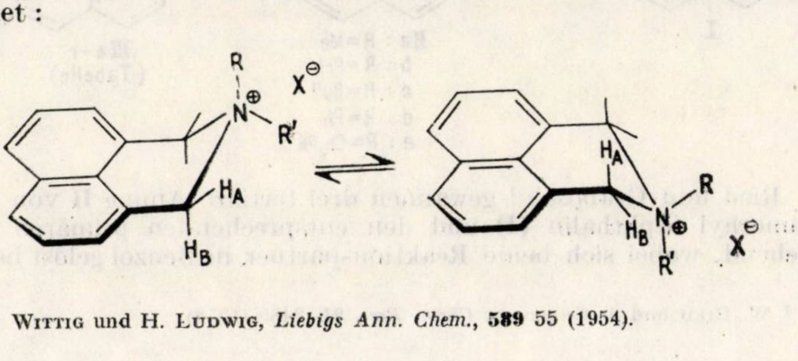

---

[2] G. Wittig und H. Ludwig, *Liebigs Ann. Chem.*, **589** 55 (1954).

Die beiden unäquivalenten Methylgruppen von 2,2-Dimethyl-2,3-dihydro-benz[d.e]isochinoliniumjodid (**IIIa**, $R = R' = CH_3$, $X = I$) geben nur ein einziges, zeitgemitteltes scharfes Singlett bei δ3,46 ppm (6 Protonen), die Protonen H_A und H_B in den benzylischen Stellungen ebenfalls ein zeitgemitteltes Singlett, bei δ5,06 ppm (4 Protonen), und die aromatischen Protonen, ein zwischen δ7,50—8,25 ppm ausgebreitetes Multiplett (6 Protonen).

Das Spektrum von 2-Äthyl-2-methyl-2,3-dihydro-benz[d.e]isochinoliniumjodid (**IIIb**, $R = CH_3$, $R' = C_2H_5$, $X = I$) wird im experimentellen Teil beschrieben.

Die Kenntnis der quantitativen Parameter der Inversion dieses *peri*-kondensierten gesättigten Ringfragments und der konformationellen Gleichgewichte einiger der quartären Salze **III** könnte für die Konformationstheorie von Nutzen sein. So ist, zum Beispiel, unter Inbetrachtnahme der geringen Deformationsfähigkeit der vom Naphthalinkern ausgehenden Bindungen, im Augenblick des Inversionsvorganges dieses Ringfragments eine Spannung von einer Größe zu vermuten, wie sie bei völlig gesättigten sechsgliederigen Ringen höchstwahrscheinlich nicht begegnet wird. Es wäre also wissenswert inwiefern die Aktivierungsenergie der Ringinversion von dieser Spannung beeinflußt wird? (Ein Vergleich zwischen **IIIa** und 1,1-Dimethyl-piperidiniumjodid). Eine andere Problemstellung, über welche die Konformationsgleichgewichte der Salze **III** gewissen Aufschluß geben könnten, wäre ob der voluminösere Substituent auch in der Abwesenheit 1,3-diaxialer Wechselwirkungen die äquatoriale Lage bevorzugt oder nicht? (Ein Vergleich zwischen **IIIb**, **IIIc**, usw. und den zutreffenden quartären Piperidiniumsalzen).

Eine quantitative Schätzung der Aktivierungsenergie der Inversion des gesättigten Ringteiles im Amin **IIa** wurde von Anderson und Oehlschlager unternommen, [3] doch es gelang den Autoren nicht ganz eindeutig zwischen Ringinversion und Inversion des Stickstoffatoms zu unterscheiden. Da die Salze **III**, bei welchen die Inversion des Stickstoffatoms nicht mehr in Frage kommt, bestens geeignet sind diese Ungewißheit zu beheben, beabsichtigen wir bei erster Möglichkeit ein Tieftemperatur-NMR-Studium einiger dieser Salze vorzunehmen.

Die Verfasser danken Professor Dr. *A. T. Balaban* für nützliche Diskussionen, und Dipl.-Phys. *F. Chiraleu* für die Aufnahme der NMR-Spektren.

BESCHREIBUNG DER VERSUCHE

Die Schmelzpunkte wurden im Röhrchen bestimmt und sind unkorrigiert. Die NMR-Spektren wurden mit einem „Varian A60—A“ -Gerät aufgenommen.

2-Methyl-2,3-dihydro-benz[d.e]isochinolin (**IIa**)* *und 2-Äthyl-2-methyl-2,3-dihydro-benz-[d.e]isochinoliniumjodid* (**IIIb**). In einer Glasröhre aus der die Luft durch einen CO_2-Strom verdrängt wurde, wurden 7,85 g (25 mMol) **I**,[4] 35 ml Benzol und 10 ml 33%-ige wäßrige Methylamin-Lösung eingeschmolzen und, unter gelegentlichem Schütteln, 20 Stdn. auf 70° erwärmt. Nach Öffnen wurde eine gewisse Menge Kristalle abfiltriert, die Benzolschicht getrennt und das

---

[3] J. E. Anderson und A. C. Oehlschlager, *Chem. Commun.*, **1968**, 284.

[4] L. A. Carpino, *J. Amer. Chem. Soc.*, **85**, 2144 (1963).

* Von Wittig und Ludwig [2] bereits durch $LiAlH_4$-Reduktion des N-Methyl-naphthalimids dargestellt.

Lösungsmittel völlig entfernt. Der Rückstand wurde in Äther aufgenommen, abermals eine kleine Menge Kristalle abfiltriert und der Äther entfernt. Der Rückstand (rohes **IIa**), der bei Kühlen sofort kristallisierte, wurde ohne weiteres in 10 ml Aceton aufgenommen, zusammen mit 6 ml Äthyljodid in einer Glasröhre eingeschmolzen, und die Röhre dann 48 Stdn. bei Raumtemperatur sich selbst überlassen. Es wurden 5,19 g Äthojodid **IIIb** (61% d. Th.) mit dem Schmp. 188—190° (aus Äthanol + Aceton) erhalten.

NMR : δ 1,61 ppm, Triplett 1 :2 :1, J = 7,5 Hz, 3 Protonen, ($N^+-CH_2-\mathbf{CH_3}$);
δ 3,34 ppm, Singlett, 3 Protonen ($N^+-\mathbf{CH_3}$);
δ 3,72 ppm, Quartett 1 :3 :3 :1, J = 7,5 Hz, 2 Protonen ($N^+-\mathbf{CH_2}-CH_3$);
δ 5,06 ppm, Singlett, 4 Protonen ($-\mathbf{CH_2}-$ in benzylischer Stellung);
δ 7,50—8,25 ppm, Multiplett, 6 Protonen (aromatische).

Die Amine **IIb-e** wurden ohne Abweichung von den Vorschriften von Ried und Grabosch[1] dargestellt, und wie weiter oben beschrieben, nötigenfalls unter Erwärmen, quaterniert.

Revue Roumaine de Chimie, **22**, *9–10*, 1379–1384 (1977)

A SIMPLE SEMIEMPIRICAL MO-CALCULATIONS OF ELECTRONIC SPECTRA AND CHARGE DISTRIBUTION IN 2,4,6-TRIMETHYL PYRYLIUM CATION

N. VLAHOVICI* and P. T. FRANGOPOL**

Institute of Physics* P.O. Box 5207 and Institute of Atomic Physics** P.O.Box 5206 ;
R-76900 Măgurele-Bucharest, Romania

Received June 3, 1975

Energetical levels, wave functions, atom net charges, transition energies and oscillator strength for the 2,4,6-trimethyl-pyrylium cation (TPC) have been calculated by a simple all valence electrons method. The results were compared with the experimental data and a good agreement was found.

In a previous paper [1] electronic spectra of 2,4,6-trimethylpyrylium cation (TPC) have been calculated taking into account only the π electrons of the molecule.

The electronic absorption spectra of TPC and most of its derivatives have been studied both theoretically and experimentally by several workers. [2–6]

The theoretical works reported so far are, however limited to their attempts, by different approximate methods,[6] to obtain a good correlation between the lowest calculated electronic transition energy and the lowest energy absorption band of TPC experimentally observed.

In view of the above, we extended in this paper the investigation of the electronic absorption spectra of TPC, all the electrons of the molecules being considered. Consequently, different values for orbital energies and wave functions resulted. Though, for the transitions, were found the same values as in our previous paper. [1] The calculated values were close to those experimentally measured without making a selection of variable parameters. Such studies of TPC would be of significant importance for a clear understanding of the absorption and emission spectral behaviour of the other pyrylium salts, which are in progress in our laboratories.

---

[1] S. K. Chakrabarti, P. T. Frangopol and M. Frangopol, *Rev. Roumaine Phys.*, **17**, 1053 (1972).

[2] G. V. Boyd and N. Singer, *Tetrahedron*, **21**, 1263 (1965) ; N. Singer, P. R. Whittington and G. V. Boyd, *Tetrahedron*, **26**, 3731 (1970) ; G. V. Boyd, *Rev. Roumaine Chim.*, **12**, 1133 (1967).

[3] H. Khediya, H. Strzelecka and M. Simalty, *Bull. Soc. chim. France*, **1972**, 3173 ; M. Simalty, H. Strzelecka and H. Khedija, *Tetrahedron*, **27**, 3503 (1971).

[4] J. Fabian, A. Melhron, and R. Zahradnik, *Theor. Chim. Acta*, **12**, 247 (1968).

[5] G. Karlsson and O. Martensen, *Theor. Chim. Acta*, **13**, 195 (1969).

[6] C. Decoret, J. Royer and B. Tinland, *Bull. Soc. chim. France*, **1972**, 2235 and references cited therein ;

The calculations were carried out by a method similar to that used by Bertus and McGlynn for the energetical states in pyridine.[7]

In order to estimate the diagonal and nondiagonal elements of the secular equation, Cusach's approximation was used.[8]

$$H_{ii} = -VSIP$$

$$H_{ij} = (2 - S_{ij})(H_{ii} + H_{jj})S_{ij}/2$$

where $VSIP$ are the ionization potentials of the orbitals involved in the chemical bond for the valence state of the molecular atoms and S_{ij} are the overlap integrals between the symmetry orbitals i and j.

Ionization potentials $VSIP$ were evaluated by the expression:

$$VSIP_{(eV)} = A + Bq$$

where, A and B are the given parameters for each type of atom and q is the net charge of the atom.[9]

The iterations were made after the net charges up to the obtaining of selfconsistent values of the ionization potentials. The method has the advantage that it is considering the $\sigma - \pi$ interaction by dependence of ionization potentials on the charges of the molecular atoms.

The method was elaborated in order to study the electronic spectra of certain molecules with similar structure. These results will be reported later.

The structure of TPC was assumed to be planar, the TPC molecule with the chosen symmetry axes and the convention for numbering the atoms, are shown in Fig. 1. In the Table 1 are tabulated the symmetry

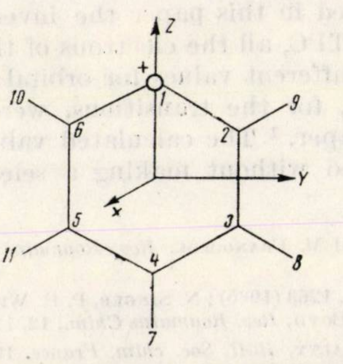

Fig. 1. — Coordinate orientation for 2,4,6-trimethyl pyrylium cation, x, y, z, represent out of plane, short and long axes of the molecule respectvely.

---

[7] B. J. **Bertus** and S. P. **McGlynn** in O. **Sinanoglu** and K. B. **Wiberg** (ed), "Sigma Molecular Orbital Theory", New Haven, Yale University Press, 1970, p. 293—300.

[8] L. C. **Cusachs**, *J. Phys. Chem.*, **71**, 1060 (1967).

[9] L. C. **Cusachs** and J. W. **Reynolds**, *J. Chem. Phys.*, **43**, S160 (1965).

atom orbitals, adapted for the symmetry class of group C_{2v}, where the molecule belongs. Trigonal hybridization orbitals were noted with t, tetragonal hybridization orbitals with T, and π orbitals with p.

Table 1

Symmetry orbitals of 2,4,6-trimethyl pyrilium cation

Simmetry orbitals	Class of symmetry			
	ΓA_1	ΓA_2	ΓB_1	ΓB_2
1	$\frac{1}{\sqrt{2}}(t_{1.2} + t_{1.6})$	$\frac{1}{\sqrt{2}}(p_2 - p_6)$	$\frac{1}{\sqrt{2}}(p_2 + p_6)$	$\frac{1}{\sqrt{2}}(t_{1.2} - t_{1.6})$
2	$\frac{1}{\sqrt{2}}(t_{2.1} + t_{6.1})$	$\frac{1}{\sqrt{2}}(p_3 - p_5)$	$\frac{1}{\sqrt{2}}(p_3 + p_6)$	$\frac{1}{\sqrt{2}}(t_{2.1} - t_{6.1})$
3	$\frac{1}{\sqrt{2}}(t_{6.5} + t_{2.3})$		p_1	$\frac{1}{\sqrt{2}}(t_{6.5} - t_{2.3})$
4	$\frac{1}{\sqrt{2}}(t_{5.6} + t_{3.2})$		p_4	$\frac{1}{\sqrt{2}}(t_{5.6} - t_{3.2})$
5	$\frac{1}{\sqrt{2}}(t_{5.4} + t_{3.4})$			$\frac{1}{\sqrt{2}}(t_{5.4} - t_{3.4})$
6	$\frac{1}{\sqrt{2}}(t_{4.5} + t_{4.3})$			$\frac{1}{\sqrt{2}}(t_{4.5} - t_{4.3})$
7	$\frac{1}{\sqrt{2}}(t_{6.10} + t_{2.9})$			$\frac{1}{\sqrt{2}}(t_{6.10} - t_{2.9})$
8	$\frac{1}{\sqrt{2}}(T_{10.6} + T_{9.2})$			$\frac{1}{\sqrt{2}}(T_{10.6} - T_{9.2})$
9	$\frac{1}{\sqrt{2}}(t_{5.11} + t_{3.8})$			$\frac{1}{\sqrt{2}}(t_{5.11} - t_{3.8})$
10	$\frac{1}{\sqrt{2}}(s_{11.5} + s_{8.3})$			$\frac{1}{\sqrt{2}}(s_{11.5} - s_{8.3})$
11	$t_{4.7}$			
12	$T_{7.4}$			
13	sp^2			

The symmetry classes being orthogonal, the secular equation:

$$\|H_{ij} - S_{ij}\| = 0$$

is factorised as following:

$$A_1(12 \times 12),\ A_2(2 \times 2),\ B_1(10 \times 10),\ B_2(4 \times 4)$$

The group overlap integrals between the symmetry orbitals have been reduced to the simplest case of the biatomic overlap integrals. For this reason the following relationships were used :

$$< t_i | t_j > = < \frac{1}{\sqrt{3}}(s_i + \sqrt{2}p_i) \Big| \frac{1}{\sqrt{3}}(s_j + \sqrt{2}p_j) > = \frac{1}{3} < s_i | s_j > +$$

$$+ \frac{\sqrt{2}}{3} < s_i | p_j > + \frac{\sqrt{2}}{3} < s_j | p_i > + \frac{2}{3} < p_i | p_j >$$

$$< t_i | T_j > = < \frac{1}{\sqrt{3}}(s_i + \sqrt{2}p_i) \Big| \frac{1}{2}(s_j + \sqrt{3}p_j) > = \frac{1}{2\sqrt{3}} < s_i | s_j > +$$

$$+ \frac{1}{2} < s_i | p_j > + \frac{1}{\sqrt{6}} < s_j | p_i > + \frac{1}{\sqrt{2}} < p_i | p_j >$$

etc.

Biatomic overlap integrals were evaluated for the following interatomic distances obtained for substances with similar structure[10]

$$R_{C-C} = 1.397 \text{ Å}; \quad R_{C-C_{methyl}} = 1.52 \text{ Å}; \quad R_{C-O} = 1.371 \text{ Å};$$

$$R_{C-H} = 1.084 \text{ Å}$$

The used orbitals were of Slater type (STO), and the Slater exponents in atomic units are :

$$C : \zeta_{2s,\ 2p} = 1.625$$

$$O : \zeta_{2s;\ 2p} = 2.45$$

$$H : \zeta_{1s} = 1$$

With these data, the overlap integrals were taken from tables[11] after calculating the parameter values :

$$p = \frac{\zeta A + \zeta B}{2} R_{AB} \qquad \text{and} \qquad t = \frac{\zeta A - \zeta B}{\zeta A + \zeta B}$$

The values of overlap integrals are the following :

$$S_{\sigma CO} = 0.623 \qquad S_{\sigma CC} = 0.747 \qquad S_{\sigma CH} = 0.709$$

$$S_{\pi CC_{methyl}} = 0.516 \qquad S_{\pi CC} = 0.243 \qquad S_{\pi CO} = 0.140$$

---

[10] "Tables of Interatomic Distances and Configuration in Molecules and Ions", Special Publication No. 18, London, The Chemical Society, Burlington House, 1965.

[11] R. S. Mullikan, C. A. Rieke and D. Orloff, *J. Chem. Phys.*, **47**, 1248 (1949).

Parameters A and B from the expression for ionization potentials $VSIP$ were the following :[9,12]

	A	B
C_{2s}	21.20	11.90
C_{2p}	11.40	11.90
O_{2s}	30.74	15.95
O_{2p}	15.84	15.95
H_{1s}	13.60	14.00

The atom net charge q was evaluated from the analysis of electronic population using Mullikan approximation[13] and the iterative procedure was carried out calculating after each iteration the atom net charge and ionization potential ($VSIP$). Interatomic distances and overlap integrals were maintained for all the iterations.

In order to increase the convergence rate, the following procedure[7] to iteration was used :

$$VSIP_{n+1} = 0.9\ VSIP_{n-1} + VSIP_n$$

n being the iteration order.

Selfconsistence was obtained after ten iterations. The distribution of net charges on the atoms of TPC molecule is shown in Fig. 2. As could be seen from Fig. 2, the charge on the oxygen atom tends to be reduced from $+1$ to -0.08 as a consequence of chemical bonds formation. The carbon atoms, neighbouring the oxygen atom present a deficit of electronic density, becoming more electropositive (net charges $+0.15$ to $+0.13$), while the distant carbon atoms are less affected by the inductive effect produced by the oxygen ion (net charges $+0.09$ to $+0.07$).

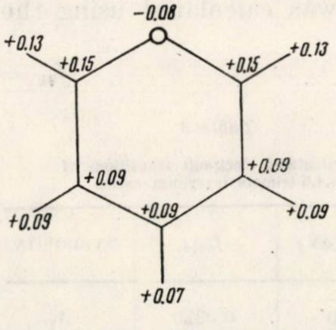

Fig. 2. — Distribution of net charges on the molecular atoms of 2,4,6-trimethyl pyrylium cation.

The molecular energetic levels and wave functions interesting the transitions which can appear in electronic spectra of molecule of TPC type, were summarized in Table 2. Since the hamiltonian operator was approximated to an operator of monoelectronic type, it is not possible to distinguish between the singlet and triplet electronic state. This distinction was done on the basis of experimental data. A more elaborated method

---

[12] R. REIN, N. FUKUDA, H. WIN, G. A. CLARKE and F. E. HARRIS, *J. Chem. Phys.*, **45**, 4743 (1966).

[13] R. S. MULLIKEN, *J. Chem. Phys.*, **46**, 675 (1949).

Table 2

The molecular energetic levels and wavefunctions for the 2, 4, 6 trimethyl pyrylium cation

Orbital energy	Wavefunction	Orbital type
− 7.67	$0.6945(t_{6.10} \pm t_{2.9}) - 0.7407(T_{10.6} \pm T_{9.2})$	$A^*_{1(\sigma)}$, $B^*_{2(\sigma)}$
− 9.68	$0.5408(p_2 - p_6) - 0.6057(p_3 - p_5)$	$A^*_2(\pi)$
−11.56	$-0.5783p_1 + 0.4628(p_2 + p_6) + 0.1255(p_3 + p_5) - 0.6106p_4$	$B^*_1(\pi)$
−14.56	$0.4982p_1 + 0.0002(p_2 + p_6) + 0.3746(p_3 + p_5) - 0.5292p_4$	$B_1(\pi)$
−14.75	$0.4889(p_2 - p_6) + 0.4087(p_3 - p_5)$	$A_2(\pi)$
−16.07	$0.6213p_1 + 0.3777(p_2 + p_6) + 0.2033(p_3 + p_5) + 0.1257p_4$	$B_1(\pi)$
−17.34	$0.4394(t_{5.11} \pm t_{3.8}) + 0.3241(s_{11.5} \pm s_{8.3})$	$A_1(\sigma)$, $B_2(\sigma)$
−17.72	$0.3783(t_{5.4} \pm t_{3.4}) + 0.3783(t_{4.5} \pm t_{4.3})$	$A_1(\sigma)$, $B_2(\sigma)$
−17.92	$0.6466t_{4.7} + 0.4989T_{7.4}$	$A_1(\sigma)$
−17.98	$0.4029(t_{0.5} \pm t_{2.3}) + 0.3534(t_{5.6} \pm t_{3.2})$	$A_1(\sigma)$, $B_2(\sigma)$
−18.58	$0.4463(t_{6.10} \pm t_{2.9}) + 3646(T_{10.6} \pm T_{9.2})$	$A_1(\sigma)$, $B_2(\sigma)$
−19.51	sp_0^2	$A_1(\eta)$
−20.85	$0.5009(t_{1.2} \pm t_{1.6}) + 0.2766(t_{2.1} \pm t_{6.1})$	$A_1(\sigma)$, $B_2(\sigma)$

performed on the ground closed-shell configuration and excited open-shell configuration of 2,4,6-trimethylpyrylium cation,[7] presents little or no relevance when discussing $\pi^* \leftarrow \pi$ transition. As result, a new more elaborated method is now under consideration and the data will be reported. However, the presently discussed method, despite its limitations, by its simplicity could be useful in computations of large molecules.

Electronic transition which could take place in the accesible range of the spectrum are shown in Table 3. Also the strength of dipole oscillator was calculated using the expression:

$$f_{ik} = \left| \int \psi_i^* \, r \psi_k \mathrm{d}\tau \right|^2$$

where r is the direction of electric dipole momentum, ψ_i and ψ_k are the wave functions for the initial and respectively the final state between the transitions.

Table 3

Calculated electronic transitions of 2,4,6-trimethylpyrylium cation

E_{calc} (eV)	f_{calc}	Symmetry
3.00	0.0220	A_1
3.19	0.0000	B_2
4.51	0.0309	A_1
4.88	0.0000	B_2
5.07	0.0022	A_1
6.39	0.0000	B_2

Table 4

Comparison between calculated and observed transition energy

E_{calc}(eV)	E^*_{obs}	f_{calc}	$\varepsilon^{\text{abs}}_{\text{max}}$
3.00	3.06	0.0220	—
4.51	4.34	0.0309	11.800*
5.07	5.39	0.0022	3.600*

* The observed data are from Ref.[1]

The comparison of the calculated data with those experimentally determined are summarized in Table 4 and a good agreement is evident. The concordance was obtained without fitting the variable parameters as in Parizer — Parr's method. Though, as well as Bertus and McGlynn,[7] we do also emphasize the absolute need of obtaining selfconsistence.

The authors express their thanks to Dr. C. Ghiță for his continuous support during this work.

Revue Roumaine de Chimie, 22, 9–10, 1385–1389 (1977)

LIQUID-MEMBRANE ELECTRODES. X*

LIQUID-MEMBRANE ELECTRODE FOR IRON (III) DETERMINATION

ELENA HOPÎRTEAN
Department of Analytical Chemistry, University of Cluj-Napoca
Str. Arany Janos 11, Cluj-Napoca, Romania

Received June 14, 1975

The results regarding the use of the triphenylpyrylium tetrachloroferrate (III) in tetrachloroethane for $FeCl_4^-$-selective liquid membrane electrode obtention are presented. The electrode response is nernstian towards $FeCl_4^-$ in $10^{-1}-10^{-4}$ M concentration range (slope 58.5 mV) and highly selective in the presence of Zn^{2+}, Cu^{2+}, Cl^-, SO_4^{2-}, BF_4^- and NO_3^- ions.

The obtention of membrane-electrodes for polyvalent cations has been lately extended by applying new approaches. Liquid membrane-electrodes based on quaternary ammonium salts for Zn^{2+} or Pd^{2+} in the chlorocomplex form have been obtained. [1] The coated metallic wire electrode for Fe^{3+} determination as $FeCl_4^-$ was recently obtained.[2] The active electrode component was in this case trimethylammonium tetrachloroferrate (III) obtained from trimethylcaprylammonium chloride (Aliquat 336 S.)

The present paper reports results with regard to the obtention and behaviour of the $FeCl_4^-$-selective liquid membrane-electrode with electrode active compound triphenylpyrylium tetrachloroferrate ($TPh\pi.\ FeCl_4$) in the solvent tetrachloroethane.

EXPERIMENTAL

Electrode active component, $TPh\pi.FeCl_4$, has been synthetized[3] in the Laboratory of Organic Chemistry of the Babeş-Bolyai University of Cluj-Napoca.

The liquid membrane-electrode has been obtained by soaking the pores of a glass frit G_4 made hydrophobic, attached to the extremity of a glass tube with $TPh\pi.FeCl_4$ solution in tetrachloroethane. The organic solution was used as internal solution, too. A saturated calomel electrode (SCE) was used as inner reference electrode. The outer reference electrode was also SCE. To stabilize the standard potential of the liquid membrane-electrode, this was maintained in a 10^{-1} M $FeCl_4^-$ solution.

---

* Part IX: E. Hopîrtean, M. Preda and V. Liteanu, *Chem. Analit.*, **22** (1977).

[1] G. Scibona, L. Mantella and P. R. Danesi, *Analyt. Chem.*, **42**, 845 (1970).

[2] R. W. Cattrall and P. Chin-Poh, *Analyt. Chem.*, **47**, 93 (1975).

[3] W. Dilthey and E. Last, *J. prakt. Chem.*, **94**, 65 (1916).

Potential measurements have been performed with a MV–85 pH-meter, at room temperature, no stirring being used. The measurements precision was ± 1 mV.

Reagents and solutions. Analytical grade reagents were used.

Standard Fe^{3+} solutions were prepared[2] starting from ferriammonium sulphate, in a 6M chloride medium (5M LiCl+1M HCl), by successive dilutions from a 2×10^{-1} M Fe^{3+} stock solution down to 2×10^{-5} M concentration. The following standard solutions have also been prepared :

Fe^{3+} standard solutions containing Zn^{2+}, in the following conditions : *a*) with constant ratio between concentrations of the two cations, namely $[Fe^{3+}]/[Zn^{2+}]=1:25$, in the $2\times10^{-1} - 2\times10^{-5}$ M Fe^{3+} concentration range, and *b*) maintaining Zn^{2+} concentration constant in all Fe^{3+} standard solutions. Two series of *b* standard solutions have been prepared, namely with Zn^{2+} concentration 10^{-1} M and 1M, respectively.

Fe^{3+} standard solutions containing Cu^{2+}. The iron concentration interval was $2\times10^{-1} - 2\times10^{-5}$ M and Cu^{2+} concentration was maintained 10^{-1}M in all standard solutions. All the standard solutions containing Zn^{2+} or Cu^{2+} were prepared in 6M chloride medium (5M LiCl + 1M HCl).

Standard ClO_4^-, SCN^-, BF_4^-, NO_3^- solutions were prepared by successive dilutions from the 1M stock solution of the natrium salt of the respective anion and by adjusting the ionic strength with Na_2SO_4 ($J = 0.15$ M).

RESULTS AND DISCUSSIONS

The concentration influence of the pyrylium salt in tetrachloroethane on the electrode function towards $FeCl_4^-$ is given in Fig. 1. While for a 0.05% concentration the linear response range is between $10^{-1} - 10^{-4}$M $FeCl_4^-$, in the case of 0.1% concentration it is restricted to $8\times10^{-2} - 4\times\times10^{-4}$M $FeCl_4^-$, and at the same time a slight sensitivity decrease from 58.5 to 57 mV occurs.

The interference of zinc and copper is given in figures 2, 3, 4 and table 1.

The electrode functions from fig. 2 illustrate the absence of Zn^{2+} interference on the electrode response towards $FeCl_4^-$ in the case of a constant concentration ratio ($[Fe^{3+}]/[Zn^{2+}] = 1:25$) between the two cations at each iron concentration level. From the data shown in fig. 3, the selectivity constant for $FeCl_4^-$ in the presence of Zn^{2+} has been found to be independent of the zinc concentration level (10^{-1}M and 1M respectively) in standard iron solutions. Consequently, the electrode is highly selective for $FeCl_4^-$ in the presence of Zn^{2+} ($K_{FeCl_4^- \, ZnCl_4^{2-}} = 4\times10^{-3}$). With regard to the copper interference, a 6×10^{-3} selectivity constant has been obtained denoting a high selectivity even in the presence of this ion. The low interference of zinc and copper ions also results from the electrode functions obtained for these ions (fig. 4). The electrode shows a sensitivity towards $ZnCl_4^{2-}$ and $CuCl_4^{2-}$ only between $10^{-1} - 1$ M concentration. The selectivity constants given in table 1 were calculated by the ratio between minimum $FeCl_4^-$ concentration for which the linear response in the presence of a given ion is maintained and the concentration of this ion, considering the constant ionic strength of standard solutions.

In order to better outline the possibility for practical application of the electrode, its sensitivity towards the main anions supposed to interfere, namely ClO_4^-, SCN^-, BF_4^- and NO_3^-, has been tested. The obtained results are shown in fig. 5 and table 2.

From the obtained electrode functions it results that the presence of BF_4^- and of NO_3^- respectively, even in a 10^{-1} M concentration, will not

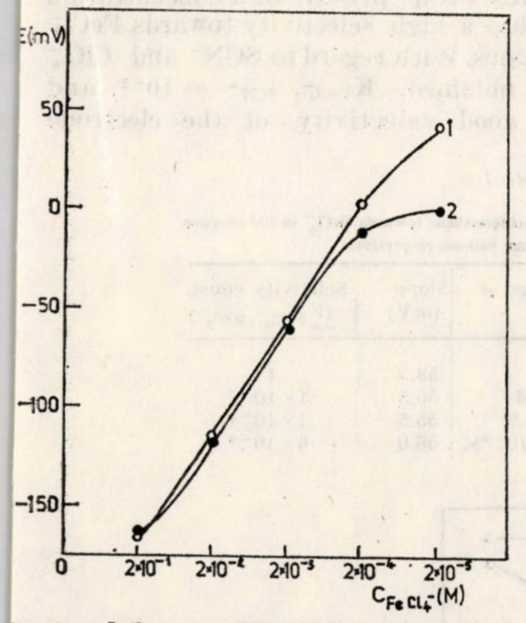

ig. 1. — Influence of TPhπ. $FeCl_4$ concentration in etrachloroethane on the electrode function for $FeCl_4^-$ ·1 — c = 0.05 %; 2—c = 0.1 %.

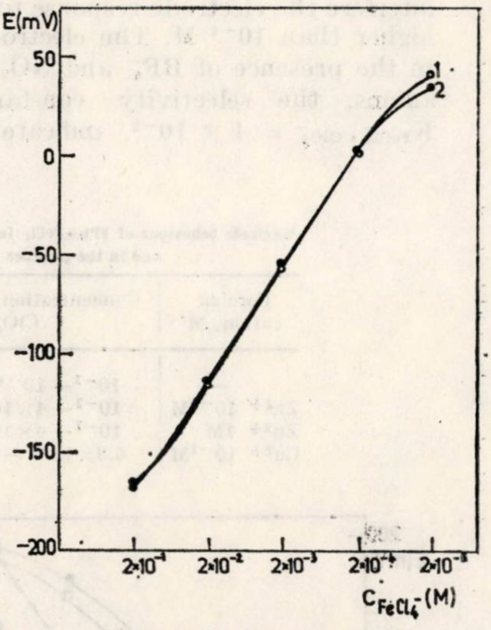

Fig. 2. — Electrode functions for $FeCl^-$ ·1 — in the absence of Zn^{2+}; 2 — in standard solutions with $[Fe^{3+}]/[Zn^{2+}] = 1:25$.

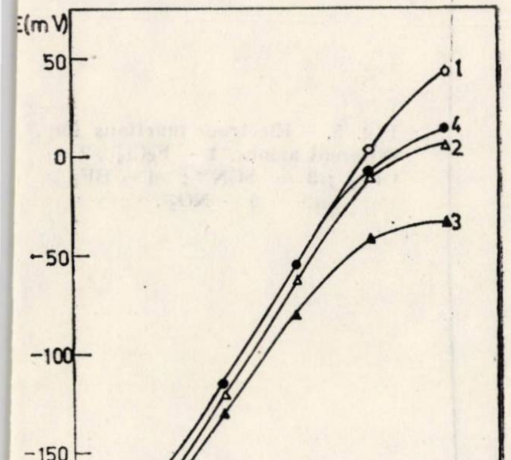

Fig. 3. — Electrode functions for $FeCl_4^-$ ·1 — pure $FeCl_4^-$ solutions; 2 — standard Fe^{3+} — solutions with 10^{-1} M Zn^{2+}; 3 — standard Fe^{3+} — solutions with 1M Zn^{2+}; 4 — standard Fe^{3+} — solutions with 10^{-1} M Cu^{2+}.

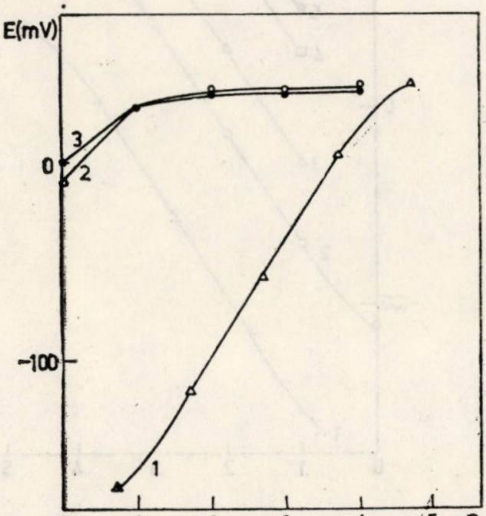

Fig. 4. — Electrode functions. 1 — for $FeCl_4^-$; 2 — for $ZnCl_4^{2-}$; 3 — for $CuCl_4^{2-}$.

interfere the electrode response towards $FeCl_4^-$ present in a concentration higher than 10^{-4} M. The electrode has a high selectivity towards $FeCl_4^-$ in the presence of BF_4^- and NO_3^- anions. With regard to SCN^- and ClO_4^- anions, the selectivity constants obtained, $K_{FeCl_4^-, SCN^-} = 10^{-2}$ and $K_{FeCl_4^-, ClO_4^-} = 4 \times 10^{-2}$, indicate a good selectivity of the electrode

Table 1

Electrode behaviour of $TPh\pi.FeCl_4$ in tetrachloroethane towards $FeCl_4^-$ in the absence and in the presence of some cations, respectively

Foreign cation, M^{2+}	Concentration range of ClO_4^-	Slope (mV)	Selctivity const. ($K_{FeCl_4^-, MCl_4^-}$)
—	10^{-1} – 10^{-4}M	58.5	1
Zn^{2+} 10^{-1}M	10^{-1} – 4×10^{-4}M	55.5	4×10^{-3}
Zn^{2+} 1M	10^{-1} – 4×10^{-3} M	55.5	4×10^{-3}
Cu^{2+} 10^{-1}M	6.3×10^{-2} – 6×10^{-4}M	56.0	6×10^{-3}

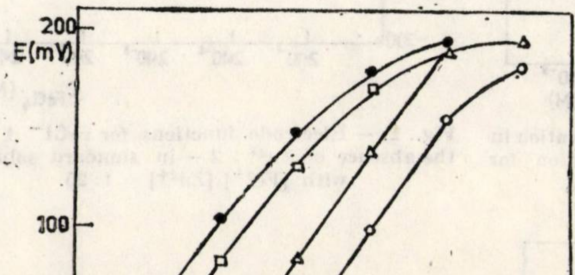

Fig. 5. — Electrode functions for different anions. 1 — $FeCl_4^-$; 2 — ClO_4^- ; 3 — SCN^- ; 4 — BF_4^- ; 5 — NO_3^-.

for $FeCl_4^-$ in the presence of these ions. The selectivity constants were calculated for these ions by using the potential values of the electrode in solutions of the two anions of 10^{-1} M concentration.

As a matter of fact, in the absence of $FeCl_4^-$ the electrode may serve as ClO_4^--selective electrode, or in the absence of $FeCl_4^-$ and ClO_4^- as SCN^- — selective electrode. The electrode response towards ClO_4^- and SCN^- respectively is nearly nernstian within a very large concentration range (table 2).

Table 2

Electrode behaviour of $TPh\pi.FeCl_4$ in tetrachloroethane towards different anions

Anion	Concentration range of linear response	Slope (mV)
$FeCl_4^-$	$10^{-1} - 10^{-4}M$	58.5
ClO_4^-	$3\times10^{-1} - 8\times10^{-6}M$	57.0
SCN^-	$10^{-1} - 10^{-5}M$	55.5
BF_4^-	$10^{-1} - 3.2\times10^{-3}M$	54.0
NO_3^-	$10^{-1} - 5\times10^{-3}M$	54.0
$CuCl_4^{2-}$	$10^{-1} - 10^{-2}M$	30.0
$ZnCl_4^{2-}$	$10^{-1} - 10^{-2}M$	36.0

The electrode response time is 4—5 min in a 2×10^{-5} M $FeCl_4^-$ solution, 1—2 min in a 2×10^{-4} M $FeCl_4^-$ solution and attains 20—30 sec in solutions more concentrated than 2×10^{-3} M.

CONCLUSIONS

$TPh\ \pi.FeCl_4$ was found to be a very good electrode active compound for $FeCl_4^-$, ClO_4^- and SCN^- ions. Tetrachloroethane is a suitable solvent for obtaining $FeCl_4^-$-selective liquid membrane-electrode based on $TPh\pi.FeCl_4$. The electrode response is nernstian towards $FeCl_4^-$ in a $10^{-1} - 10^{-4}$ M, concentration range (slope 58.5 mV) and highly selective in the presence of Zn^{2+}, Cu^{2+}, BF_4^- and NO_3^-. The high selectivity towards chloride, supported at a 6M concentration in standard iron solutions, or towards sulphate, used in order to adjust the ionic strength for ClO_4^-, SCN^-, BF_4^- and NO_3^- standard solutions, must be outlined. The absence of electrode sensitivity towards zinc and copper chlorocomplex will allow the iron determination without separation in the iron ore mining by using the above electrode. Further, the use of pyrylium salts as $TPh\pi.BF_4$, $TPh\pi.SCN$, etc, for the obtention of anion-selective liquid membrane-electrodes, will be examined.

The author gratefully acknowledges the assistance of Sorin Mager, Mihai Horn and Ionel Hopîrtean for providing the compound $TPh\pi.FeCl_4$.

Revue Roumaine de Chimie, 22, 9–10, 1391–1399 (1977)

PHENOL OBTAINMENT FROM BENZENE IN OXYGEN PLASMA GENERATED BY A HIGH FREQUENCY DISCHARGE. III[1]

KINETICS OF THE PROCESS IN PULSE AND STEADY-STATE REGIME

G. BOURCEANU *, V. ABABI *, GH. POPA ** and M. SANDULOVICIU **

* Faculty of Chemistry and Chemical Engineering, Polytechnic Institute of Jassy, Splai Bahlui 71;

** Faculty of Physics, "Al. I. Cuza" University, Jassy, Calea 23 August 11, Romania

Received April 2, 1975

The kinetics of benzene transformation and phenol formation in oxygen plasma has been studied. On the basis of the experimental data, the benzene disappearance process in oxygen plasma follows a kinetics that varies between the first and the second order. A comparison of phenol rate formation in high frequency electrical discharges, in pulse and steady-state regime, has also been made.

A detailed treatment of kinetics of the elementary reactions which take place in plasma is very difficult to be made especially when the molecules involved are more complex. However, theoretically, the kinetics of the chemical reactions in plasma can be treated as follows:

— In the case of the monomolecular reactions, particularly the decomposition reactions, according to R.R.K.M.'s theory, the whole rate constant is given by the sum of contributions of all vibration levels, formulating for each vibration level one rate equation. In order to formulate the coupled set of reaction rates one starts from Pauli's equation applied to the case of monomolecular reactions which take place in a thermostat of inert gas. For monomolecular reactions, too, particularly for the dissociative capture, when only the molecule which dissociates has vibration freedom degrees, the rate constant can be computed starting from Boltzmann's kinetical equation[2–6].

— In the case of bimolecular reactions, when two species of molecules with distribution functions of different rates are involved, the rate constant expression can be obtained starting from Boltzmann's kinetical equation too.[6]

---

[1] Part II: G. Bourceanu, V. Ababi, Gh. Popa and M. Sanduloviciu, *Rev. Roumaine Chim.*, **21**, (1976).

[2] G. Bourceanu, V. Ababi, Gh. Popa and M. Sanduloviciu, *Rev. Roumaine Chim.*, under print.

[3] G. Bourceanu, *Studii și Cercetări Chim., Acad. R. S. Romania*, **21**, 1399 (1973).

[4] R. A. Marcus, *J. Chem. Phys.*, **43**, 2658 (1965).

[5] W. S. Valence and E. W. Schlag, *J. Chem. Phys.*, **45**, 216 (1966).

[6] L. S. Polak, A. N. Temcin and A. V. Hocioian, *Kinetica i kataliz*, **11**, 831 (1970).

In both cases, the problem of the rate constant finding is difficult enough except the rate constant calculation for the dissociative capture.

According to R.R.K.M's theory,[3,4] the transition probabilities of molecules in different energetical states must be known, which is very difficult in the case of complex molecules.

To find the rate constant of the bimolecular reactions starting from Boltzmann's kinetical equation, the efficacious sections of collision among the reacting molecules and the rate distribution functions must be known. For these objective reasons a detailed treatment is made of simple systems [7] while with the complex ones only macroscopic parameters are investigated such as the generator power that creates plasma, concentration of the reactants and residence time in the discharge zone.

1. KINETICS OF THE BENZENE TRANSFORMATION AND PHENOL YIELDING IN OXYGEN PLASMA, IN PULSE REGIME

To discuss the kinetics of the phenol formation it is first necessary to analyze the kinetics of the benzene disappearance. The graphical representation of the $1/[C_6H_6]_t$ ratio against the residence time in the discharge zone, at constant power and benzene flow rate, has given the curves plotted on Fig. 1. However, it can be seen that the points which correspond to the larger residence times, for the three conditions, are situated in a first approximation, on a straight line. To the shorter residence times, the points are scatterd, finally resulting in a curve. From this plotting, it results that with larger residence times in the discharge zone the benzene disappearance follows a kinetics close to the second order, while with shorter residence times the kinetics of benzene transformation approaches the first order.

Indeed, it was shown that when the residence time in the discharge zone is larger, namely when the oxygen flow rate is low, the preponderent reactions are $(11-13)^2$ due to the high atomic oxygen concentration in the discharge zone. As the oxygen flow rate increases, the atomic oxygen concentration and mean energy of the electrons in plasma decrease, therefore the benzene transformation could be due to the electron-molecular collisions, a process that follows a first order kinetics as shown in the toluene decomposition kinetics.[8]

The result is that the order of benzene transformation reaction has its value between one and two. As it results from Fig. 1, at larger residence times, namely at low oxygen flow rate, $1/[C_6H_6]$ is larger and it decreases as the residence time decreases, or, in other words, benzene conversion increases as the residence time increases. This is due both to large electrons energy (Tab. 1) and to high atomic oxygen concentration which promotes the reactions (11—13).

For a better evidence of the oxygen flow rate effect on benzene transformation in plasma, the graph $1/[C_6H_6]$ against oxygen flow rate was plotted (Fig. 2). It can be seen that the larger the oxygen flow rate,

[7] A. M. Gubanov, E. K. Ereşenkov, O. A. Malkin and L. S. Polak, *Kinetica i kataliz*, **13**, 33 (1972).

[8] G. Bourceanu, V. Ababi, Gh. Popa and M. Sanduloviciu, *Rev. Roumaine Chim.*, **20**, 627 (1975).

the less is $1/[C_6H_6]_t$, namely the unreacted benzene concentration increases with the increase of the oxygen flow rate. It seems that these results are contradictory to the data obtained regarding the phenol yield increase as the oxygen flow rate increases.[1]

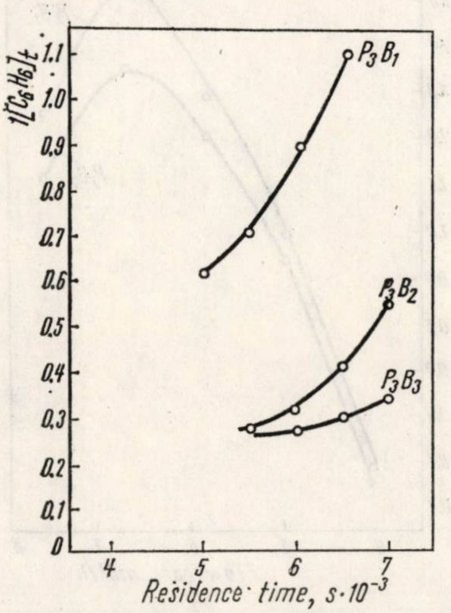

Fig. 1. — Dependence of $1/[C_6H_6]_t$ on the residence time.

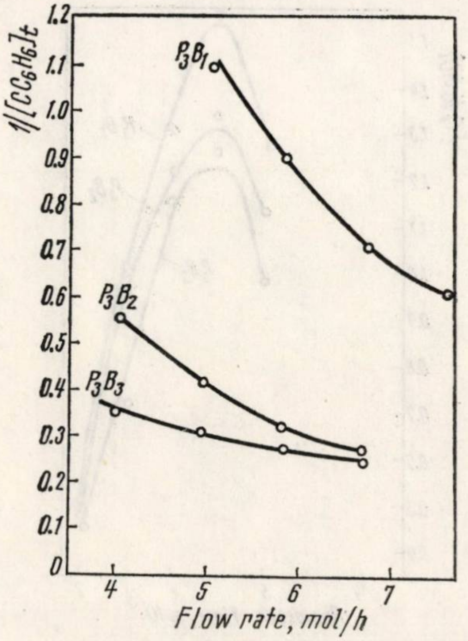

Fig. 2. — Dependence of $1/[C_6H_6]_t$ on the oxygen flow rate.

If the phenol concentrations are plotted against the residence time, a series of curves will be obtained (Fig. 3). From these curves it can be seen that the larger the residence time, the less is the phenol concentration in the discharge zone and it increases to a certain value after which it decreases as the residence time decreases. On the contrary, if the phenol concentration is plotted against the oxygen flow rate, it can be seen that as the oxygen flow rate increases, the phenol concentration increases to a certain value after which it decreases, (Fig. 4).

These experimental findings as regard the kinetics of benzene decomposition and phenol formation can be explained as follows:

Fig. 3. shows that the larger the residence time, the less is the phenol concentration. But a small oxygen flow rate corresponds to larger residence time, or it was shown that in this case the atomic oxygen concentration is large (Tab. 1), so that the reactions (31) and (32)[2] of phenol generation are not favoured.

On the contrary, Fig. 1 shows that the unreacted benzene concentration decreases as the residence time increases, namely as the oxygen flow rate decreases (Fig. 2). As oxygen flow rate increases, the atomic oxygen concentration decreases, while that of molecular oxygen increases, so that reactions (31) and (32) are favoured and reactions (11—13)[2] are not.

The concentration of unreacted benzene increases as the residence time decreases, namely with the increase of oxygen flow rate, because in this case the electron mean energy and atomic oxygen concentration, respectively (Tab. 1), decreases. It results that the C_6H_5-H bonds with their bond energy of 4.4 eV[9] will break in the largest amount portion and the C $\underline{\cdots}$ C bonds in benzene nucleus with their bond energy of 5.1 eV[10,11] will break in a smaller amount. This fact is proved by the

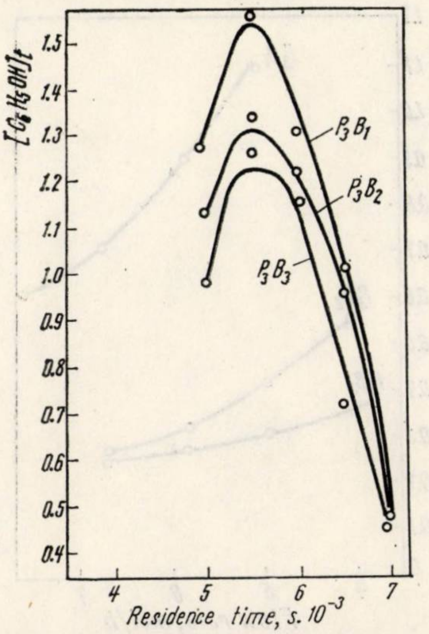

Fig. 3. — Variation of the phenol concentration *versus* the residence time.

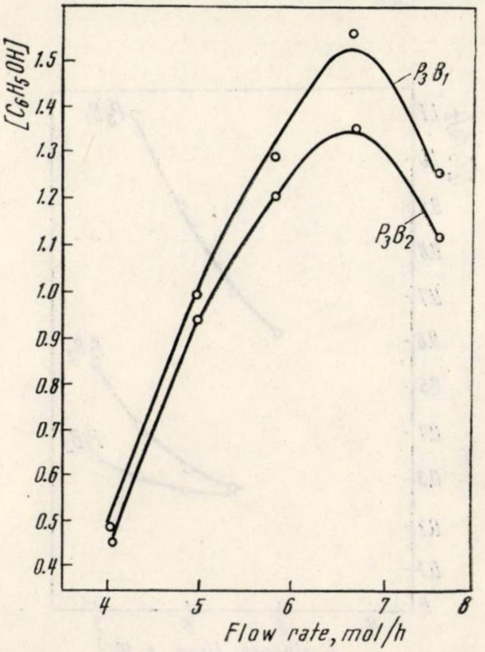

Fig. 4. — Variation of the phenol concentration *versus* the oxygen flow rate.

Table 1

The atomic oxygen concentration versus the electron energy and molecular oxygen flow rate at power of 305.5 W

The O_2 flow rate (mol/h)	Mean energy of the electr. (eV)	Concentration of the atomic oxygen, %	The molar ratio oxygen to benzene
4.01	6.0—6.3	26.43	80
4.95	5.6	22.41	99
5.80	5.0	17.60	116
6.65	4.2—5.0	11.70	134
7.58	3.1	6.25	151

---

[9] M. Szwarc, *Chem. Rev.*, **47**, 75 (1950).

[10] Lo H. Donald and M. A. Whitehead, *Canad. J. Chem.*, **16**, 2027 (1968).

[11] V. I. Vedenyev, L. V. Gurvich, V. N. Kondratiev, V. A. Medvedev and Ye. L. Frankevich, "Bond Energies Ionisation Potentials and Electron Affinities", Eduard Arnold Ltd., London, 1966, p. 56.

smaller quantity of gaseous mixture and polymer. Finally, we must say that the kinetical data agree with the proposed mechanism for the phenol formation from benzene in oxygen plasma.

Taking into account the fact that the benzene transformation increases as the residence time decreases, while the phenol concentration increases up to a certain value after which it decreases as the residence time decreases, another explanation of the experimental observations could be that the phenol formation takes place according to some successive reactions :

$$C_6H_6 \xrightarrow{\vec{e}^-} \dot{C}_6H_5 \xrightarrow{O_2} C_6H_5-O-O^{\cdot} \xrightarrow{H_2O}$$

$$\longrightarrow C_6H_5-OH \longrightarrow CO_2 + H_2O \qquad (1)$$

Indeed, if we plot on the same graph the benzene concentration and phenol concentration against the residence time, at a generator power of 305.5 W and benzene flow rate of 0.05 mol/h,[1] some curves characteristic of the successive reactionsare obtained, (Fig. 5).

In accordance with this interpretation, it results that in fact phenol is an intermediate product and its concentration diminishing with the residence time should be due to its transformation in final products such as CO_2 and H_2O according to the reaction (1). Which of these explanations is true remains to be studied in the future.

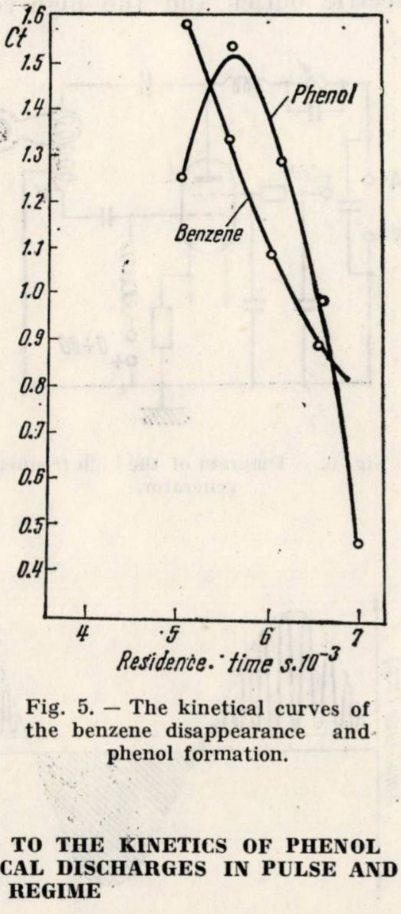

Fig. 5. — The kinetical curves of the benzene disappearance and phenol formation.

2. COMPARATIVE RESULTS WITH REGARD TO THE KINETICS OF PHENOL FORMATION IN HIGH FREQUENCY ELECTRICAL DISCHARGES IN PULSE AND STEADY-STATE REGIME

As we have already reported,[1] plasma was obtained by means of a high frequency electromagnetical field in a cylindrical tube (T) placed between the armatures of condenser (C_1) of an oscillating circuit. This circuit was coupled inductively with the oscillating circuit (C_2) of an oscillator equipped with a tetrode (L), (Fig. 6).

The generator frequency was 30 MHz. The inductive couple between the two oscillating circuits (C_1 and C_2) was adjusted by the help of the intermediary mobile contact M on the coil C_2.

The power supply of the oscillator was realized between A and B in two regimes :

1. To A and B was connected a supplying source of 3 KW. The power source is made up of a high-voltage transformer, a high-vacuum rectifier valve and a filter cell which assures a modulation factor less than 1% of the rectified voltage.

The voltage between A and B was adjusted uniformly from 0.0 to 3000 V by means of a self-transformer connected between the 220 V electric outlet and the high-voltage transformer of the power source.

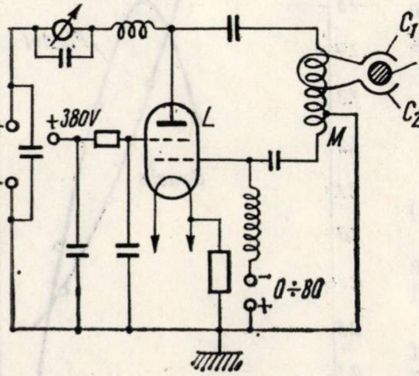

Fig. 6. — Diagram of the high frequency generator.

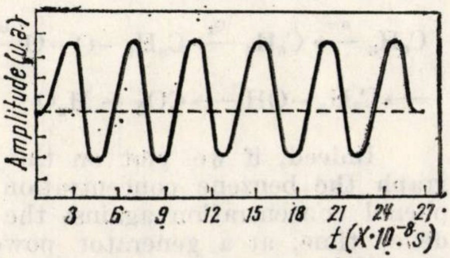

Fig. 7. — The oscillation amplitude of the high frequency field in steady-state regime in the presence of a rectifying bridge.

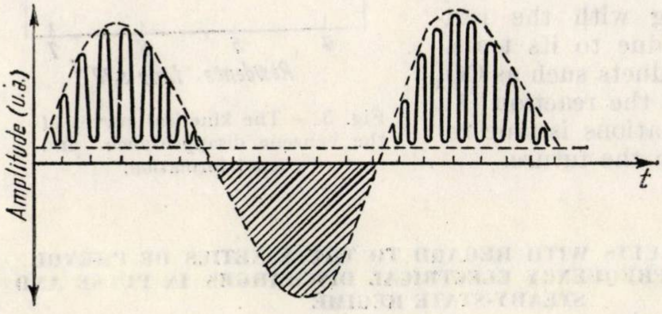

Fig. 8. — The oscillation amplitude of the high frequency field in impulse regime in the absence of a rectifying bridge.

In this case, the amplitude of high frequency oscillations can be modified by changing the oscillator voltage. If the voltage between A and B is maintained constant, then the oscillations will have the same amplitude, (Fig. 7).

2. To A and B was connected directly an a.c. voltage of 50 Hz supplied by the power transformer of the supplying source presented in the former case. In the latter case tetrode (L) of the oscillator is also a rectifier. In this case the oscillator will work with its own frequency also of 30 MHz only on positive alternance of the a.c. voltage applied between A and B (A_1 and A_2, Fig. 8). Here, the amplitude of high frequency field oscillations will be modified as presented in Fig. 8.

The high frequency discharge takes place in 50 Hz pulses namely the frequency of the supplying alternating field.

The difference between the two regimes of high frequency discharge does not consist only in the fact that in pulse regime the oscillations amplitude varies continuously (Fig. 8) but also from the fact that in steady-state regime plasma takes continuous energy from the electromagnetic field, while in the pulse regime plasma takes energy only from the positive alternance (Fig. 8).

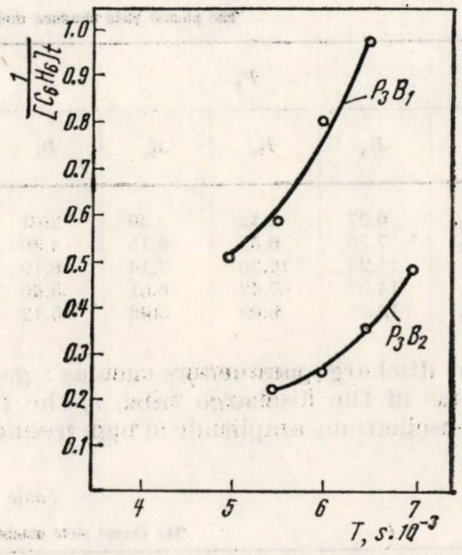

Fig. 9. — Dependence of $1/[C_6H_6]_t$ on the residence time under steady-state regime.

Starting from these considerations and from the remark made at the kinetical study of toluene decomposition, where it was shown that the toluene transformation rate increases with the electron concentration increase, we considered that a larger phenol yield will be obtained by working in steady-state regime, namely in the presence of the rectifying bridge, where the electron concentration is larger than in the pulse regime.

But, contrary to expectations, both the unreacted benzene concentration and phenol yield decreased. Of course in both cases the generator power and the oxygen to benzene ratio was the same.

In Fig. 9, $1/[C_6H_6]_t$ is plotted against time. As shown in this figure, the unreacted benzene concentration in the steady-state regime is larger than in pulse regime under the same conditions.

The phenol yield obtained under the conditions of steady-state regime only for the levels P_2 and P_3 and the other level combinations of the parameters B and O is given in Table 2.

The phenol yield obtained under conditions of pulse regime for the same generator powers P_2 and P_3 and the other level combinations of parameters B and O is presented in Table 3.

A qualitative explanation of these experimental remarks will be attempted below. First of all we will make clear that in both studied cases the frequency of the electromagnetic field was the same i.e. 30 MHz; but the oscillations amplitude was variable.

It is known that plasma occurring in a high frequency discharge with either interior or exterior electrodes is controlled by the characteristic discharge parameters such as: gas pressure, p, in the discharge tube, radius of the discharge tube, r, the free mean path of the electrons, λ_e, the oscillations amplitude of high frequency electromagnetic field and so on.

Table 2

The phenol yield obtained under steady-state regime

	P_2				P_3			
	B_1	B_2	B_3	B_4	B_1	B_2	B_3	B_4
O_1	6.27	5.12	3.59	2.01	6.45	6.51	6.39	4.76
O_2	7.70	6.52	6.15	4.30	11.79	11.14	8.33	6.63
O_3	11.29	10.26	7.14	6.19	15.32	14.22	13.96	8.29
O_4	14.31	7.42	6.51	5.93	16.41	15.03	14.87	8.58
O_5	12.23	6.98	5.68	5.12	12.13	11.74	9.96	6.91

Table 3

The phenol yield obtained under pulse regime

	P_2				P_3			
	B_1	B_2	B_3	B_4	B_1	B_2	B_3	B_4
O_1	7.92	6.32	4.28	2.88	7.76	7.56	7.52	5.71
O_2	9.62	8.54	8.62	6.02	16.54	15.82	11.76	8.66
O_3	18.90	17.34	9.70	8.40	22.72	20.02	21.30	12.56
O_4	21.42	11.44	12.62	8.40	26.28	22.04	22.04	15.52
O_5	16.48	9.04	8.34	7.50	20.90	18.54	16.20	13.52

In the two cases studied, the pressure variation could not be evidenced, because this was measured using a differential manometer with a precision of 7.10^{-2} torr, but it is known that even to a smaller variation of the 10^{-3} torr order the electrons mean energy is largely modified due to the free mean path of these. The radius of the discharging tube was constant. We know very well that the oscillations amplitude varies in the case of the discharges in pulse regime, while it is constant in the steady-state regime.

Under a pressure of about 1 torr (the way it was in our operating conditions),[2] the frequency of collisions among electrons and oxygen molecules calculated by us was $\nu_c = 4.10^9$, and the free mean path of electrons corresponding to this frequency, $\lambda_e \cong 4.1.10^{-2}$ cm. Under these conditions (when $\lambda_e < r$ and $\nu_c > \nu$, where ν is the frequency of electromagnetic field) the electrons carry out many collisions for each oscillation of the field, so that they get a training velocity in phase with the field, i.e. they can follow the phase change of the field.[12] If the oscillation's amplitude is low, in comparison with the radius of the discharge tube, the gas ionization in the tube is kept up by the electron collisions, and the electron losses take place especially by diffusion towards the tube wall. Or, if the oscillation amplitude becomes larger than the tube radius, some electrons in the discharge zone are lost after their collisions with the discharge tube. It results that the oscillation's amplitude is efficacious only when this is a little less than the discharge tube radius.

Since a larger phenol yield was obtained in the pulse regime, we think that from the multitude of oscillations with different amplitude (Fig. 8) some of them have a little less amplitude than the discharge tube radius and, during a cycle, the electron in its motion carries out a high number of collisions with the molecules in the discharge zone. Without any demonstration, the greater the energy received by the electron during a cycle, the greater is the number of its collisions with molecules, which is the effect of the ordered oscillating motion transformation into disordered motion. Since in the ordered motion the electron velocity is diphased by $\pi/2$, from the field phase, the energy won by the electron on a half cycle is lost on a next half cycle.[12]

In the steady-state regime, when the phenol yield becomes less it is possible that the constant oscillations amplitude may be either much smaller in comparison with the discharge tube radius, and consequently the electrons carry out a smaller number of collisions with the molecules in the discharge zone, or that it may be much higher than the discharge tube radius, and consequently the electron concentration becomes lower due to their collision with the tube wall. The latter possibility cannot be considered because in the steady-state regime the electron concentration was approximately twice that in the pulse regime.

It must be admitted that the oscillations amplitude is much smaller than the tube radius and the number of collisions carried out by the electrons with molecules is smaller, and consequently, their transformation degree is also small.

CONCLUSIONS

From this kinetical study the following two significant conclusions can be detached :

1. It is difficult to determine precisely the reaction order of benzene disappearance and the phenol formation due to the reaction mechanism complexity.

2. The phenol yield increases when discharge takes place in pulse regime.

---

[12] E. Bădărău and I. Popescu, "Gaze ionizate, descărcări electrice în gaze", Editura tehnică, București, 1965, p. 80.

Revue Roumaine de Chimie, **22**, *9–10*, 1401–1412 (1977)

^{1}H-N.M.R. CHARACTERIZATION OF ANIONIC SURFACTANTS-POLYVINYLPYRROLIDONE INTERACTION

GEORGETA POPESCU and MIRCEA MARINESCU
Institute of Macromolecular Chemistry "P. Poni"
Department of Colloids Bucharest, Splaiul Independenței 89

Received 14 July, 1975

The nature of nonionic polymer polyvinylpyrrolidone (PVP) interaction with anionic surfactants sodium dodecyl sulphate (SDS) and sodium laurate (SL) is described with the aid of high resolution N.M.R. technique. The chemical shift difference between $-CH_2-$ and $-CH_3$ peaks and the chemical shifts of these signals relative to water peak, are surfactant concentration-dependent. The chemical shift difference between $-CH_2-$ and $-CH_3$ peaks could be taken as a measure of surfactant aqueous solution hydrophobicity both in the presence and in the absence of polymer. The obtained information was discussed in the light of some existing models of micellization and water structure of aqueous solutions and on this basis some suggestions for an improved model of micellization at concentrations higher than the critical micellar concentration (CMC) were given.

INTRODUCTION

Recent works in the field of physical characterization of aqueous solutions of surfactants revealed an increased interest in the use of magnetic resonance techniques such as nuclear magnetic resonance N.M.R. (on ^{1}H, ^{19}P, ^{13}C nuclei),[1–6] electronic spin resonance E.S.R. [7–10] or nuclear quadrupole resonance N.Q.R. (on ^{81}Br, ^{35}Cl nuclei).[11–13]

The information obtained by these techniques completes the already existing information on the physical and chemical properties of association colloids, giving new insight into a series of problems like polyphase dynamic equilibria [14] or the type of interaction between components of such systems.

---

[1] J. Clifford and B. A. Pethica, *Trans. Faraday Soc.*, **60**, 1483 (1964).

[2] J. Clifford, *Trans. Faraday Soc.*, **61**, 1276 (1965).

[3] T. Walker, *J. Colloid. Interf. Sci.*, **45**, 372 (1973).

[4] U. Henriksson and L. Ödberg, *J. Colloid. Interf. Sci.*, **46**, 212 (1974).

[5] R. E. Atkinson, G. E. Clint and T. Walker, *J. Colloid. Interf. Sci.*, **46**, 32 (1974).

[6] T. Björn, D. Berg and B. Lindman, *J. Colloid. Interf. Sci.*, **44**, 784 (1973).

[7] A. S. Waggoner, D. H. Griffith and C. R. Christensen, *Proc. Nat. Acad. Sci. U.S.A*, **57**, 1198 (1967).

[8] A. S. Waggoner, A. D. Keith and O. H. Griffith, *J. Phys. Chem.*, **72**, 4129 (1968).

[9] J. Chavolin and P. Rioxy, *Compt. rend.*, **224**, Serie B, 269 (1969).

[10] H. Sillescu and R. Brüssen, *Chem. Physics Letters*, **5**, 525 (1972).

[11] G. Lindblom, B. Lindman and L. Mandell, *J. Colloid. Interf. Sci.*, **34**, 262 (1970).

[12] B. Lindman and B. Bernard, *J. Colloid. Interf. Sci.*, **42**, 298 (1973).

[13] G. Lindblom, B. Lindman and L. Mandell, *J. Colloid. Interf. Sci.*, **42**, 400 (1973).

[14] N. Müller in "Reaction Kinetics in Micelles", Edited by E. Codes, Plenum Publishing Corp., New York, 1973.

The present work presents the results obtained by a high resolution N.M.R. study of aqueous solutions (in D_2O) of sodium dodecyl sulphate (SDS) and sodium laurate (SL) at various concentrations, containing or not polyvinylpyrrolidone (PVP). The relative chemical shifts of surfactant solution peaks from the high resolution N.M.R. spectra and the halfheight width of the $-CH_2-$ peak were followed at various surfactant concentration, in the presence and in the absence of PVP.

The results were discussed in light of some existing models of micellization and water structure of aqueous solutions and on this basis some suggestions for an improved model of the micellization at concentrations higher than the critical micellar concentration (CMC) were given.

EXPERIMENTAL

Reagent grade chemicals were used as follows: Sodium dodecyl sulphate (SDS) from Merck, of purity higher than 99%; sodium laurate (SL) from Chemische Fabrik E. Mickel; polyvinylpyrrolidone (PVP) from B.A.S.F., with N = 250 and a mean molecular weight M_w 30000; D_2O of 98% purity from the Institute of Atomic Physics, Bucharest.

The measurements were carried out on a "JEOL" JNM-C-60HL N.M.R. spectrometer with opperating frequency of 60 MHz (c/s). The magnetic field was internally locked on the residual H_2O peak of deuterated water. This peak was also used as a reference for $-CH_2-$ and $-CH_3$ peaks. The peak positions were determined with a precision of ±0.1 Hz by means of a digital frequency counter. The halfheight width of $-CH_2-$ peak of surfactants was measured with a precision better than 0.3 Hz. All measurements were carried out at room temperature (22°).

The solutions were prepared in D_2O and their concentrations have been expressed in grammes at 100 ml D_2O in the case of pure surfactant solutions, or at 100 ml grwt. % D_2O polymer solution, when the polymer was added.

RESULTS AND DISCUSSIONS

The experimental data were represented in Figs. 1 – 6. For every surfactant in both presence and absence of the polymer, the reference measurement was the surfactant solution of the smallest concentration. Thus from chemical shifts difference between $-CH_2-$ peak and $-CH_3$ peak, respectively, and the H_2O peak for the SDS 0.1% and SL 0.2% solutions, the chemical shifts of all other solutions were subtracted, for both surfactants apart. These differences of chemical shifts were plotted versus surfactant concentration.

The halfheight width of $-CH_2-$ peak of surfactants was represented as function of surfactant concentration, respectively for SDS (Fig. 7, curve 1) and SL (Fig. 8, curve 1). Curves 2 and 3 (Fig. 7 and 8) represent the halfheight width of surfactant peak at addition of polymer in various concentrations.

A rise on the curves plotted in Fig. 1 – 6 represents a close-in of the peaks $-CH_2-$ and $-CH_3$ relative to H_2O peak on curves 1 and 2 and a setting apart of the $-CH_2-$ and $-CH_3$ peaks on curves 3. On curves 3 the chemical shifts between $-CH_2-$ and $-CH_3$ peaks were represented as they are, function of concentration.

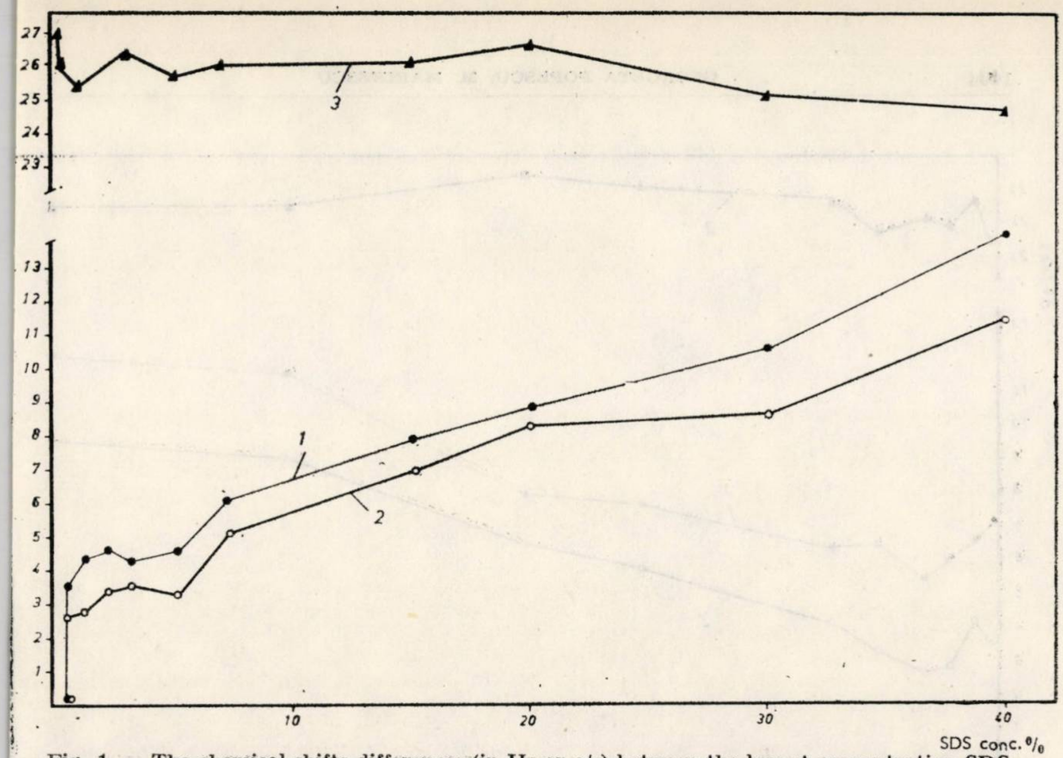

Fig. 1. — The chemical shifts differences (in Hz or c/s) between the lowest concentration SDS solution (0.1 % grams per 100 ml) and higher concentration SDS solutions. Chemical shifts differences between : $-CH_3$ peak and residual H_2O peak — curve 1 (●) ; $-CH_2-$ peak and residual H_2O peak — curve 2 (○) ; $-CH_2-$ and $-CH_3$ peaks — curve 3 (▲).

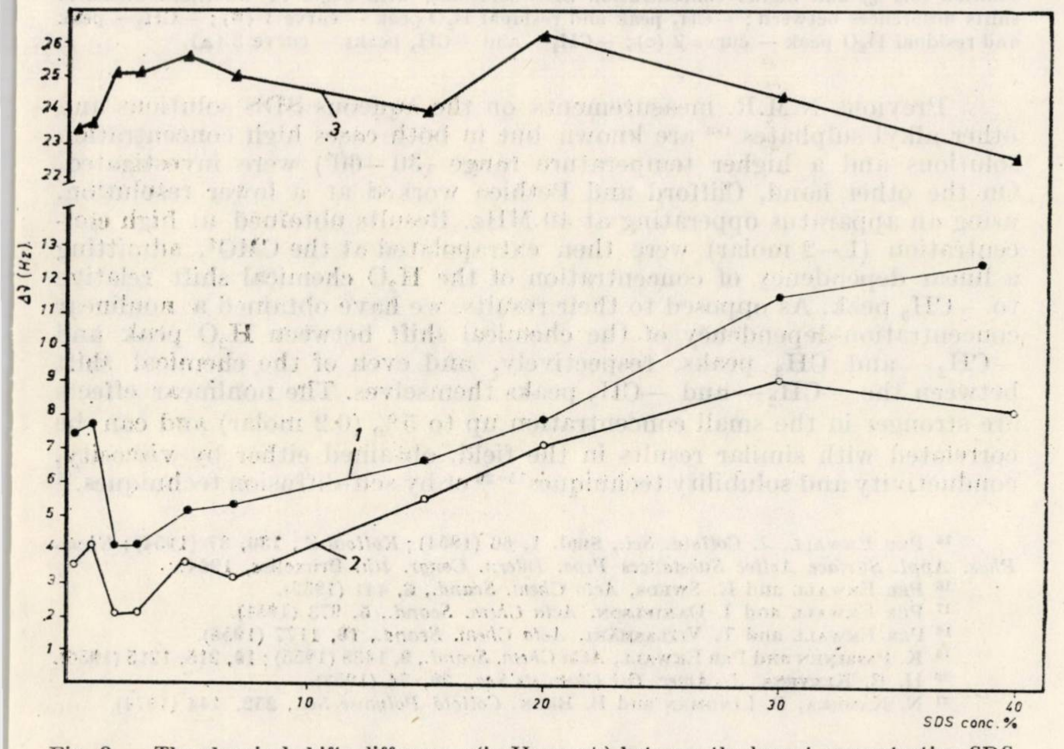

Fig. 2. — The chemical shifts differences (in Hz or c/s) between the lowest concentration SDS solution (0.1 %) and higher concentration SDS solutions, with 1 % PVP addition. Chemical shifts differences between ; $-CH_3$ peak and residual H_2O peak — curve 1 (●) ; $-CH_2-$ peak and residual H_2O peak — curve 2 (○) ; $-CH_2-$ and $-CH_3$ peaks — curve 3 (▲).

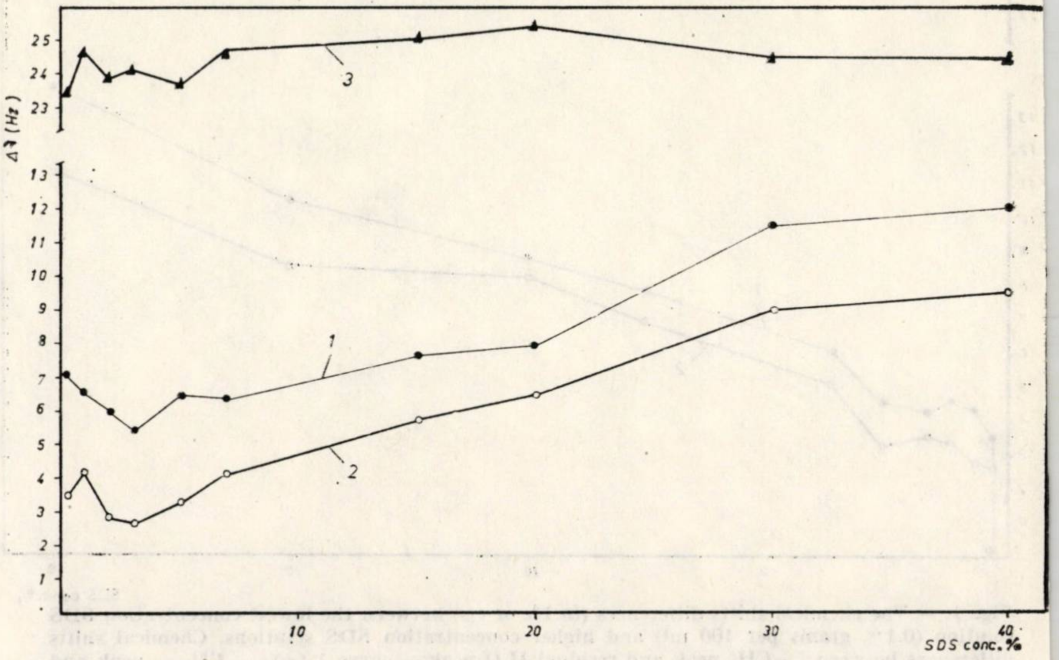

Fig. 3. — The chemical shifts differences (in Hz or c/s) between the lowest concentration SDS solution (0.1%) and higher concentration SDS solutions, with 3% PVP addition. Chemical shifts differences between : $-CH_3$ peak and residual H_2O peak — curve 1 (●) ; $-CH_2-$ peak and residual H_2O peak — curve 2 (○) ; $-CH_2-$ and $-CH_3$ peaks — curve 3 (▲).

Previous N.M.R. measurements on the aqueous SDS solutions and other alkyl sulphates [1,3] are known but in both cases high concentration solutions and a higher temperature range (30—60°) were investigated. On the other hand, Clifford and Pethica worked at a lower resolution, using an apparatus opperating at 40 MHz. Results obtained at high concentration (1—2 molar) were then extrapolated at the CMC[3], admitting a linear dependency of concentration of the H_2O chemical shift relative to $-CH_3$ peak. As opposed to their results, we have obtained a nonlinear concentration-dependency of the chemical shift between H_2O peak and $-CH_2-$ and CH_3 peaks, respectively, and even of the chemical shift between the $-CH_2-$ and $-CH_3$ peaks themselves. The nonlinear effects are stronger in the small concentration up to 5% (0.2 molar) and can be correlated with similar results in the field, obtained either by viscosity, conductivity and solubility techniques[15–20] or by self-diffusion techniques.[21]

---

[15] Per Ekwall, *J. Colloid. Sci.*, **Supl. 1**, 66 (1954) ; *Kolloid-Z.*, **136**, 37 (1954) ; *Chem. Phys. Appl. Surface Active Substances Proc. Intern. Congr. 4th*, Bruxelles, 1964.

[16] Per Ekwall and K. Sweds, *Acta Chem. Scand.*, **6**, 441 (1952).

[17] Per Ekwall and I. Danielson, *Acta Chem. Scand.*, **5**, 973 (1951).

[18] Per Ekwall and T. Vitlasmäki, *Acta Chem. Scand.*, **10**, 1177 (1956).

[19] K. Passinen and Per Ekwall, *Acta Chem. Scand.*, **9**, 1438 (1955) ; **10**, 215, 1215 (1956).

[20] H. B. Klevens, *J. Amer. Oil Chemists'Soc.*, **30**, 74 (1953).

[21] N. Kameka, B. Lindman and B. Brun, *Colloid Polymer Sci.*, **252**, 144 (1974).

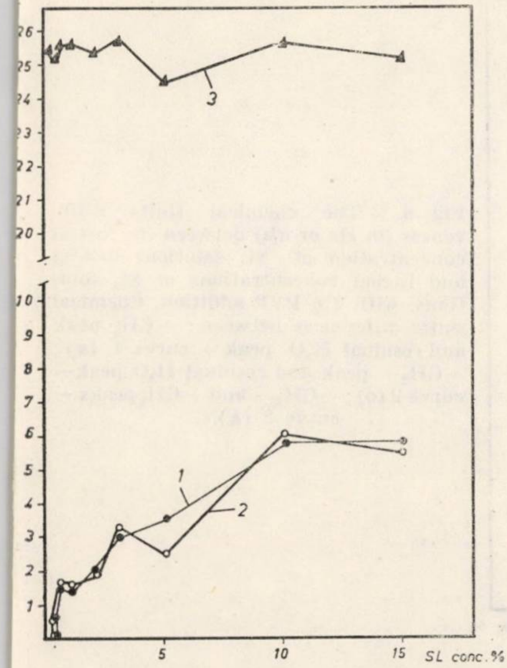

g. 4. — The chemical shifts differences (in Hz c/s) between the lowest concentration SL solun (0.2%) and higher concentration SL solutions. emical shifts differences between: — CH_3 ak and residual H_2O peak — curve 1 (●); $-CH_2-$ ak and residual H_2O peak — curve 2 (○); $-CH_2-$ d $-CH_3$ peaks — curve 3 (▲).

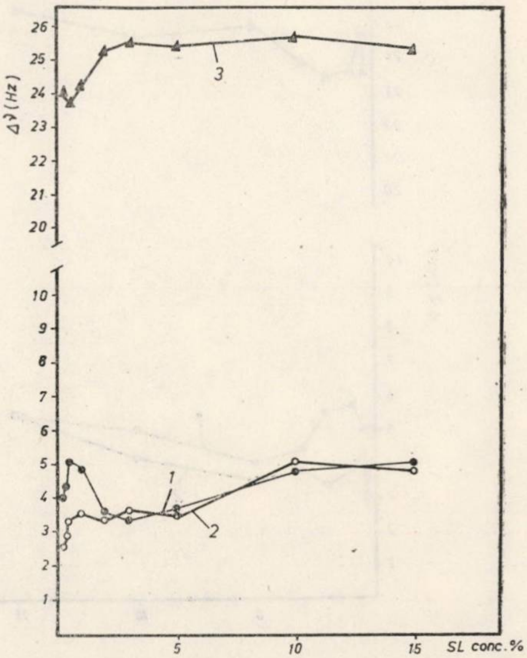

Fig. 5. — The chemical shifts differences (in Hz or c/s) between the lowest concentration SL solutions (0.2%) and higher concentrations SL solutions, with 1% PVP addition. Chemical shifts differences between: — CH_3 peak and residual H_2O peak — curve 1 (●); $-CH_2-$ peak and residual H_2O peak — curve 2 (○); $-CH_2-$ and $-CH_3$ peaks — curve 3 (▲).

Both the SDS and SL surfactants exhibit nonlinearities in the region just over CMC (0.2% SDS and 0.4% SL) and up to approximately 5%, after which the chemical shifts are nearly proportional with the concentration in the respective domains which were up to 40% for SDS and up to 15% for SL.

For both surfactants the CMC is exhibited as a sudden increase on the curves 1 and 2, and as a decrease on curves 3 (Fig. 1 and 4). For the SDS (Fig. 1) at higher concentration a maximum at 1–2% — curve 1, and 3% — curve 2 is observed followed by a minimum at 3% — curve 1 and 5% — curve 2. Accordingly, on curve 3 a minimum at 1% is observed, followed by a maximum at 3%. For the SL (Fig. 4) curves 1 and 2 represent a growth between 0.2–0.5%, followed by a maximum at 3% and a minimum at 5% on curve 2. On curves 3 a slight minimum at 0.4% is observed followed by a flat between 0.5–2% and a minimum at 5%.

In order to find a coherent explanation of the shape of the curves, we can correlate the variation of the curves to the known behaviour of the solutions at the CMC. Thus the CMC is known to be the concentra-

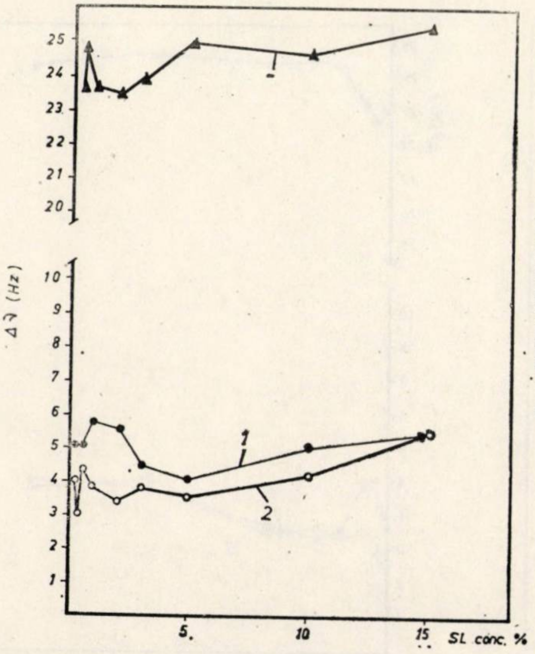

Fig. 6. — The chemical shifts differences (in Hz or c/s) between the lowest concentration of SL solutions (0.4%) and higher concentrations of SL solutions, with 2% PVP addition. Chemical shifts differences between : $-CH_3$ peak and residual H_2O peak — curve 1 (●); $-CH_2-$ peak and residual H_2O peak— curve 2 (o); $-CH_2-$ and $-CH_3$ peaks — curve 3 (▲).

tion range at which the specific contact surface of the surfactant with water is abruptly diminished by the association of simple molecules in aggregates called micelles. The micellar core can be considered as a different hydrocarbonate phase from the aqueous phase, since water is not considered as part of the micelles.

It can be considered that a close-in of the peaks representative for $-CH_2-$ and $-CH_3$, or a simultaneous close in of the specific signal of water to the peaks of $-CH_2-$ and $-CH_3$, indicates a growth of the nonpolar character of the hydrocarbonate phase, meaning that over the CMC the aggregation number of micelles is growing. Consequently, the growing separation between the peaks representative for water and $-CH_2-$ and $-CH_3$, respectively between the characteristic signals of the $-CH_2-$ and $-CH_3$ can be regarded as an increased degree of polar behaviour against the nonpolar phase, which could be interpreted as a growth in the number of micelles, hence a growth of the specific contact surface with the aqueous solvent, supposing that the aggregation number is constant.

It is observed that besides the nonlinearities at the CMC, there are other concentration ranges in which the hydrocarbonate phase is growing. These nonlinearities appear for the SDS about 5% (Fig. 1, curves 1, 2) and at the same concentration for SL (Fig. 4, curves 1, 2). Because in this region the chemical shift between the $-CH_2-$ and $-CH_3$ signals is decreasing it follows that the differences in chemical vicinity are diminshed in the very regions of the hydrocarbonate phase growth, whereas the number of contacts with the polar type vicinities is decreased.

In fact the nonlinearities at concentrations over CMC are also exhibited by the curves of the halfheight width of the $-CH_2-$ signal versus concentration, which are shown in Figs 7 and 8, curves 1.

For the SDS (Fig. 7, curve 1) the CMC is appearing as an increase of the halfheight width band. This is approximately equal to $1/T_2$-where T_2 is the spin-spin relaxation time-, i.e. the spin-spin relaxation velocity. After a maximum at 2%, the curve shows a minimum at 3% only to grow again to 5%. For the SL curve 1 (Fig. 8) is similar except that, apart from the first small amplitude maximum at 0.4%, there are two other maxima at 1% and 3% separated by a minimum at 2%. Over 5% the transversal relaxation velocity is growing as for the SDS at similar concentration.

It comes out that the second nonlinearity of the curve would appear, by comparison with the first, between 3 –5% for the SDS, and 2 –5% for the SL.

The spin-spin relaxation velocity growth may be due to the increase of the number of contacts between the $-CH_2-$ chains as compared to the number of contacts of these same chains with water, considering that the spin-spin relaxation velocity of the $-CH_2-$ protons are greater in the hydrocarbonate phase than in aqueous phase.

The nonlinearity showing between 3 –5% for both surfactants may be correlated with the second CMC which information can be found in the literature.[15,20,22,23] Figure 1 shows that at a concentration between 5% and 20% SDS curves 1 and 2 are linear. At 20% SDS on curve 3 a maximum appears that can be interpreted as the beginning of a slower growth rate of the hydrocarbonate phase up to 40% SDS.

The nonlinear effects manifest themselves after a region of constant growth of the spin-spin relaxation velocity (Fig. 7, curve 1) and also of the chemical shift of the $-CH_2-$, $-CH_3$ peaks (Fig. 1 and 4, curves 3) and, as it has been shown before, they can be associated to the number of micelles that grow for a relatively constant aggregation number. As concentration grows further, the tendency to the diminution of the specific contact surface grows at a concentration of about 20%, thus explaining the peak of curve 3 (Fig. 1) for the SDS, which can be considered as a growth of the aggregation number. This growth can be regarded as a passage from the Debye-type large micelles (rods form) to a bilamellar structure, in which the structure of the solution resembles microscopically to that of a sandwich (water bilamellar surfactant-water.

Figure 7, curve 1 shows that the SDS exhibits a strong growth of the spin-spin relaxation velocity at 20 –30% which means that the existent hydrocarbonate phase is tending to compact. To conclude, taking account of the chemical shifts (Fig. 1 and 4) and the variation of the relaxation velocity (Fig. 7), there is another nonlinear region in the domain of 20%, this being the third CMC domain, when the whole solution contains the bilamellar micelles.

Adding PVP at a concentration of 1% (Fig. 2 and 5), the shape of the curves of the chemical shifts versus concentration is modified. At,

---

[22] P. A. Demchenko and A. V. Dumanski, *Doklady Akad. Nauk S.S.S.R.*, **131**, 120 (1960).

[23] Z. N. Markina, N. N. Tsikurina, N. Z. Kostora and P. A. Rebinder, *Kolloid-Zhur.*, **26**, 76 (1964).

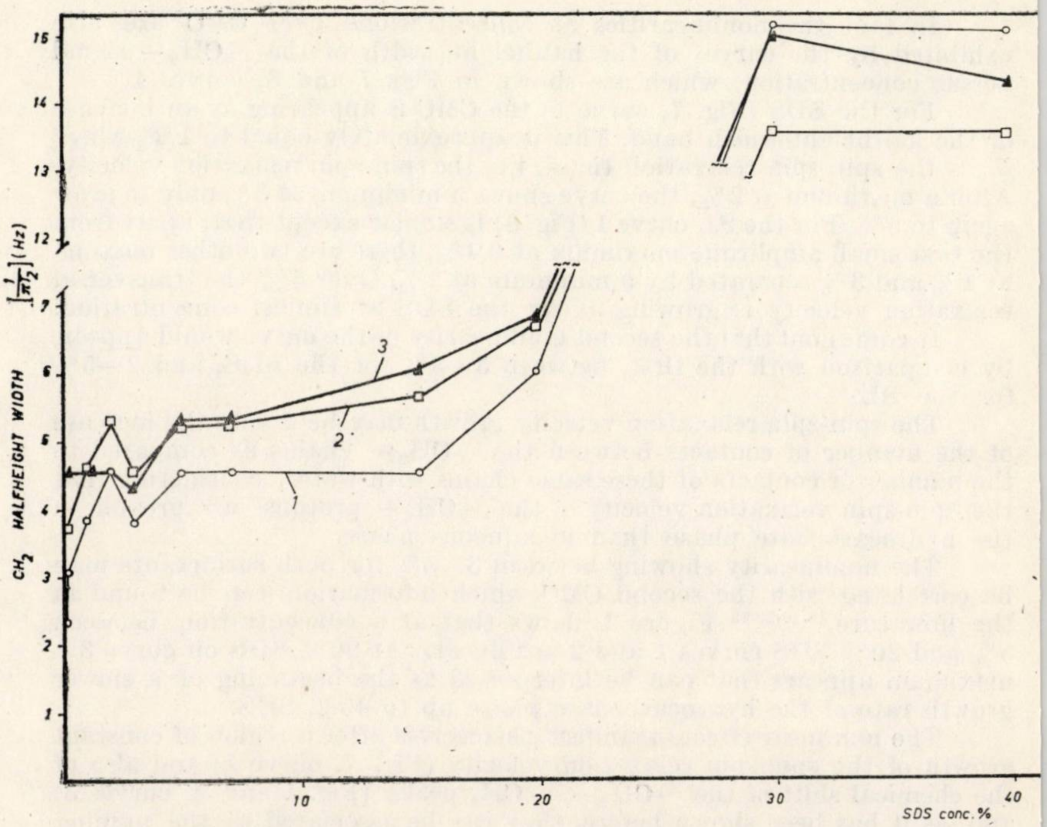

Fig. 7. — The halfheight width (in Hz or c/s) of $-CH_2-$ peak plotted against SDS concentration : pure SDS — curve 1 (○) ; SDS with 1 % PVP addition — curve 2 (□) ; SDS with 3 % PVP addition — curve 3 (▲).

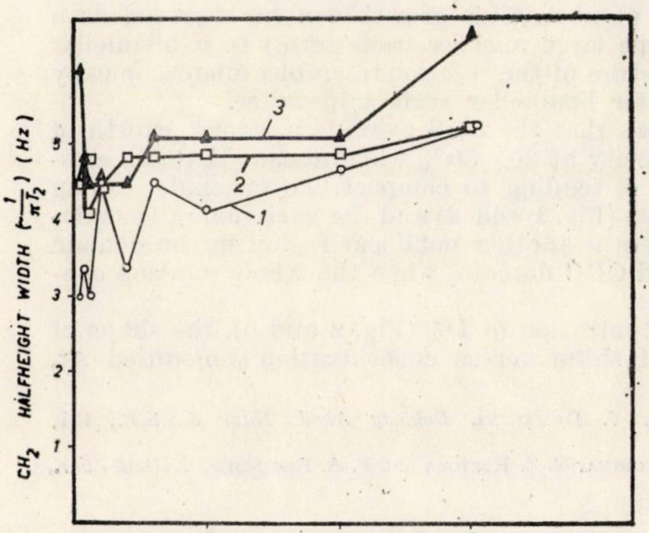

Fig. 8.—The halfheight width (in H
c/s) of $-CH_2-$ peak plotted agains
concentration : pure SL — curve 1
SL with 1 % PVP addition—curve 2
SL with 2 % PVP addition — curve 3

small concentration the hydrocarbonate phase appears to be already formed around the CMC, hence the CMC must have a much smaller value (at such concentrations the surfactant signal was smaller than the noise signal of the N.M.R. apparatus).

An explanation could be that the surfactant molecules are adsorbed on the polymer, and the total number of contacts with water molecules appears to be very reduced as compared to the pure surfactant for which, at the same concentrations, all monomers are contacted by water molecules. As the surfactant adsorption on the polymer saturates, the number of micelles grows at a constant aggregation number.

Curves 1 and 2 (Fig. 2 and 5) decrease and curve 3 increases for both surfactants between 1 –3 %. The two tendencies reequilibrate at 5 –15 % for the SDS and at 4 –15 % for the SL (Fig. 2 and 5, curves 3) indicating a growth in hydrophobicity, hence a compacting of the surfactant polymer complex. The same is true for the micelles organized in bigger units and could be even transformed to bilamellar structure of the surfactant in which the polymer is embedded, a phenomenon accentuated for the SDS (Fig. 2, curve 3) between 20 –40 %. Then, three zones of hydrophobicity (Figs 2 and 5, curves 3) can be distinguished : the first, at concentrations between 0.2 –2 % SDS and 0.4 –2 % SL, the first CMC being lowered by the presence of polymer ; the second between 5 –15 % SDS corresponding to the second CMC, extended on a whole domain of concentrations for the SDS ; the third between 20 –40 %, where the hydrophobicity zone is the same as for the surfactant (Fig. 1, curve 3).

The spin-spin relaxation velocity for 1 % PVP (Figs 7 and 8, curves 2) presents no severe modifications from the relaxation velocity of the surfactant in the absence of the polymer, exhibiting however a decrease and an increase between 4 –5 % SDS and 1 –3 % SL, respectively, which could be related to the second CMC which lowered at smaller concentrations in the presence of the polymer.

At higher polymer concentrations, 3 % PVP added to SDS and 2 % PVP added to SL, the compaction zone of the polymer-micelles complexes seems to appear at smaller concentrations, 1 –5 % SDS and 1 –3 % SL (Figs 3 and 6, curves 1, 2, 3) due to the polymer-dominated concentration. At higher surfactant concentrations both for the SDS and SL the differences are not so accentuated, nonlinearities appearing at 20 % SDS and at 10 % SL. For the SL, figure 6 shows a growth of the polar contact surface at a constant aggregation number between 2 –5 %.

The information obtained from the relaxation velocity curves leads to some supplementary conclusions. Figure 8, curve 3, shows that the spin-spin relaxation velocity for the SL considerably increases in the presence of the polymer, at small surfactant concentrations (0.2 %). The same velocity decreases with the increase of the polar contact with the solvent, by the growth of the micelles number. Then it increases again between 3 –4 %, growth associated with a second CMC, the first being at much smaller concentrations. The next increase will take place at 10 – 15 %. The formation of the bilamellar structure (third CMC) is produced similar to the pure surfactant even in the presence of the PVP 3 % between 20 –30 %, when the spin-spin relaxation velocity exhibits a fast growth.

It is obvious that the relaxation velocity values increase with the increase of the polymer concentration (Figs 7 and 8). The explanation resides in the facility of the movement of hydrocarbonate chains in the vicinity of the nonpolar polymers, compared to the same movement in the presence of the polar water molecules. The same conclusions can be reached if we compare curves 3 or 1, 2 of Figs 1, 2, 3 for SDS or of Figs 4, 5, 6 for SL. The closing- in of the signals $-CH_3$, $-CH_2-$ to the water signal and of the signals $-CH_3$ and $-CH_2-$ between themselves is more marked with the increase of the polymer concentration. Hence we may conclude that the presence of the polymer biases the solution to a hydrocarbonate phase with respect to the aqueous phase and that the formation of the adsorption complex realised by hydrophobic forces is the most evident explanation.

From the material above, we may draw the following conclusions :

1. The curve of the chemical shifts between the N.M.R. peaks of $-CH_2-$ and $-CH_3$ of the SDS and SL surfactants can be taken as a relative measure of the hydrophobicity or the polar character of the aqueous solutions of these substances. Thus the closing- in of these signals means a growth of the aggregation number of the micelles produced and their setting apart as an increase of the solution polar character, hence a growth of the number of micelles at a constant aggregation number.

2. The surfactant molecular association is not a continuous process. Apart from the known nonlinearities at CMC there are other, less accentuated nonlinearities, at a higher concentration (5–7 % i.e. 0.2–0.25 M), called the second CMC.

At still higher concentrations, 20 % or 0.7 M (a larger domain studied for the SDS) there is another nonlinear zone, less accentuated in the chemical shifts curve, but evident on the spin relaxation velocity curve, which could be called the third CMC and would represent a passage to the sandwich structure of the solution of surfactants.

3. These results lead to a model in which the micellization could be determined by two interdependent factors : specific contact surface and micellar aggregation number stability.

The specific contact surface between the nonpolar ends of the unassociated surfactant molecules and the water molecules, as well as between the polar ends of the associated or unassociated surfactant molecules and water molecules, is steadily decreasing. On the other hand, there is a tendency of stability of the micellar aggregation number. This does not vary rapidly and can be considered statistically constant at constant concentrations, temperatures and chemical potentials.[24] It varies only when the hydrophobic forces of association between surfactant chains enforces a restructure of the micelles. Except for certain ranges of high stability, determined by the equilibrium between the hydrophobic forces of surfactant chains with the polar forces established between the water and polar heads of surfactants, there is a restructuring of the aggregates with a decrease in the polar contact surface. This restructuring of micelles, produced with concentration growth, is equivalent with an increase of the micellar aggregation number, i.e. a new chemical and physical equilibrium or a new macroscopic state of the surfactant solution.

---

[24] T. NAKAGAWA, *Colloid Polymer Sci.*, **252**, 56 (1974).

The continuous equilibrium between the hydrophobic nonpolar forces and the polar ones leads to a step variation of the physicochemical properties of the surfactant solutions, with respect to the concentration and by no means to a linear behaviour above the first CMC.

We can mention as a further argument the results obtained by Per Ekwall[15] who has pointed out that there must be another "limit of the association concentration", under the CMC, which he named LAC (limiting association concentration). This LAC is also due to the decrease tendency of the contact surface of surfactant molecules in the vicinity of water, being linked to small aggregation numbers.

4. Addition of polymer to the surfactant solution drastically modifies their properties in the domain of small concentration (CMC up to 5%), a fact proven also by other techniques. [25,26] An important role is played by the equilibrium between the solution components already discussed. [27]

5. The type of interaction taking place between the surfactant molecules and between the polymer and the surfactant is not qualitatively different. These are electrostatic type of interactions (dipole-dipole and induced dipole) exhibiting a strong statistical character (London van der Waals mode) and they take place because of the tendency of these molecules to have as small a contact with the water molecules as possible.

The most important energy distribution modifications do not take place in the surfactant molecules, nor at the level of the polymer (where the electric gradient of the whole molecule does not change too much), but at the level of the solvent, i.e. the water. This has been shown [1,3] by the fact that the peak signal of water is largely displaced from internal or external standards compared to the $-CH_2-$ and $-CH_3$ signals, namely toward larger field values.

In the present study even though the water signal was the one which shifted, we preferred to use this signal for an internal lock for the control of both $-CH_2-$ and $-CH_3$ chemical shifts. Actually the measured chemical shifts were belonging to the water signal which is much more sensitive to the concentration growth of the surfactant.

Generally the sensitivity of the water signal to the dissolved substances and in particular for surfactant agents is associated either with the breaking of the hydrogen bonds [28] or with the growth of the covalent character of the existent hydrogen bonds. [1] We tend to support the second of these hypotheses.

The thermodynamic data as interpreted by Nemethy Scheraga[29,30] plead in this respect, and moreover, for an increase of the hydrogen bonds in water, as stated previously by Frank and Wenn. [31] In fact, the dependency of the N.M.R. properties of the polymer surfactant solutions in water on the surfactant concentration or, according to our hypotheses, on the specific contact surface of undissociated surfactant, micelle, polymer

[25] S SAITO, *Kolloid-Z.*, **154**, 19 (1957); **158**, (120 (1958).

[26] S. SAITO, *Kolloid-Z.u.Z. Polymere*, **215**, 316 (1967) ; **226**, 10 (1968).

[27] G. POPESCU, M. MARINESCU and I. BRAD, *Kolloid-Z.u.z. Polymere*, **254**, 55 (1976).

[28] A. POPLE, *Proc. Roy. Soc.*, **205**, 155 (1951).

[29] G. NEMETHY and A. SHERAGA, *J. Chem. Phys.*, **36**, 3401 (1962).

[30] A. T. HAGLER and A. SCHERAGA, *Ann. New York Acad. Sci.*, **204**, 51 (1973).

[31] A. S. FRANK and W. Y. WENN, *Discuss. Faraday Soc.*, **24**, 133 (1957).

(when it applies) and water may be explaned using the model of the statistical distribution of the energy levels belonging to the water molecule, as Scheraga postulates.

This may also be supported by another experimental argument, drawn from the transversal (spin-lattice) relaxation T_1 (Fig. 9); we have represented the spin-lattice relaxation velocity $(1/T_1)$ of the protons

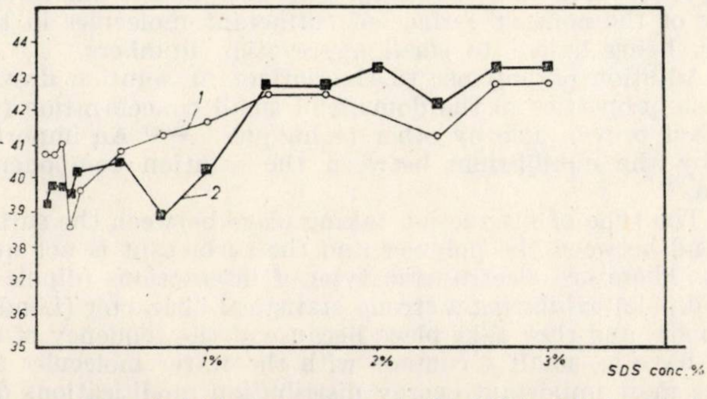

Fig. 9. — The spin-lattice relaxation velocity $(1/T_1)$ plotted against water solutions SDS concentration: pure SDS — curve 1 (ŏ); SDS with 0.5% PVP addition — curve 2 (□).

from SDS aqueous solutions for concentrations of 0.075—3% and in the presence of PVP 0.5%. It can be seen that this velocity decreases at the CMC and at a concentration of 2.35%, while at the formation of the micelles, the spin-spin relaxation velocity of $-CH_2-$ proton chains grows and the corresponding spin-lattice relaxation velocity decreases. Hence, water molecules are more inhibited from contacting by the formation of micelles, by the growth of their individual energy.

This study will be continued in order to give a better insight into these questions yet too obscure to be taken for definite answers.

The authors would like to express their gratitude to Dr. V. Bărboiu and Miss A. Natansohn for their help and kind assistance in the realization of N.M.R. spectra, presented in this work.

Revue Roumaine de Chimie, 22, *9–10*, 1413–1422 (1977)

Dédié au Professeur Coriolan Drăgulescu *à*
l'occasion de son 70e anniversaire

QUELQUES RÉACTIONS INATTENDUES DANS LE DOMAINE DES HÉTÉROCYCLES SATURÉS

PIERRE A. LAURENT
Laboratoire de Chimie Organique — Pau Université, France

Reçu le 26 juillet 1976

Quelques réactions inattendues de certains hétérocycles sont rapportées. L'oxazolidine se trimérise selon une réaction autocatalytique. Une expression numérique précise a été trouvée. Elle ne s'applique cependant pas à la trimérisation de la tétrahydroxazine. L'hydrolyse des trioxocanne- 1, 3, 6, dioxathiocanne- 1, 3, 6 et de l'oxadithiocanne-1, 3,6 suivent des lois normales. Par contre, l'hydrolyse de l'oxadithiocanne-1, 4, 6 suit une loi autocatalytique difficile à interpréter. Une expression semi-empirique satisfaisante a été trouvée. L'hydrolyse de quelques trioxocannes alkylés en 2 donne des constantes de vitesse à peu près égales. Elles sont cependant 10^4 fois plus grandes que celles du trioxocanne non substitué.

1. INTRODUCTION

Nous donnons ci-dessous un certain nombre de résultats qui ont été trouvés et confirmés du point de vue expérimental, mais dont l'interprétation théorique reste très hasardeuse.

Appartenant encore à la vieille chimie nous serions très heureux de trouver une collaboration chez de jeunes chimistes théoriciens pour l'interprétation de ces phénomènes.

La chimie des hétérocycles saturés paraît à première vue comme étant sans intérêt.

En effet, il n'y a pas de possibilité de mésomérie comme dans les hétérocycles non saturés et par suite on s'attend à ce que ces composés aient les propriétés classiques des chaînes saturées.

L'expérience montre qu'il n'en est rien, et nous avons trouvé de nombreux cas intéressants dont nous rapportons quelques exemples ci-dessous mais que nous avons beaucoup de peine à interpréter.

2. OXAZOLIDINE (avec M. RIEHL)

La thiazolidine est un composé parfaitement stable qui manifeste des propriétés qu'on attend de sa formule. Il devrait en être de même pour l'oxazolidine.

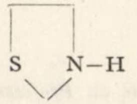

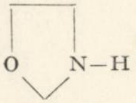

Or, on constate que ce composé n'est pas stable, et qu'il se transforme spontanément en un trimère.

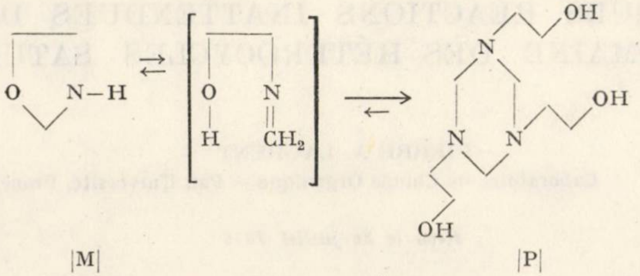

Le mécanisme exact n'est pas élucidé mais on peut supposer que cela passe par l'intermédiaire d'un imino-alcool.

Nous n'avons cependant jamais pu mettre en évidence la double liaison $>C{=}N-$

La réaction est réversible mais l'équilibre est pratiquement à 100 % de trimère dans le domaine de températures étudié.

L'allure cinétique de la polymérisation est reportée sur la figure 1. Elle fait penser à une réaction autocatalytique et on peut imaginer une oi cinétique du type :

$$v = f(|M|^{\alpha},\ |P|^{\beta})$$

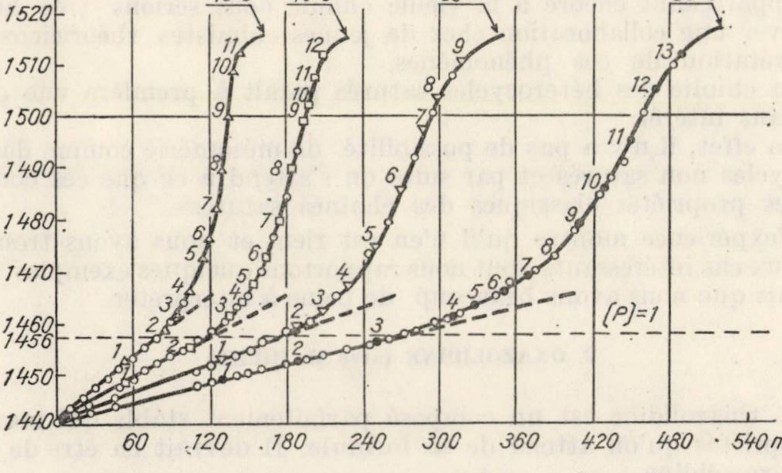

Fig. 1. — Polymérisation de l'oxazolidine $n = f$ (temps).

où $|M|$ et $|P|$ sont les concentrations en monomère et en polymère. La loi la plus simple, puisqu'il s'agit d'une trimérisation serait :

$$v = k|M|^3|P|$$

Elle n'est pas vérifiée.

On peut aussi imaginer la superposition de deux réactions. L'une normale et l'autre catalysée par le polymère. Ce qui donne :

$$v = k_1\,|M| + k_2\,|M|\,|P|$$

$$\text{soit}\ \frac{v}{|M|} = k_1 + k_2|P|$$

Elle n'est pas vérifiée non plus (fig. 2).

Par contre, la loi

$$v = k_1\,|M| + k_2|M|\,|P|^3$$

$$\text{soit}\ \frac{v}{|M|} = k_1 + k_2|P|^3$$

est remarquablement bien vérifiée comme on peut le constater sur la figure 3, avec les valeurs suivantes pour k_1 et k_2

Température °C	30°	35°	40°	45°
$k_1 \times 10^5$ s^{-1}	0,4	0,8	1,3	1,9
$k_2 \times 10^6$ mole^{-3}, s^{-1} . .	2,3	3,3	4,9	8,6

Il reste le problème non résolu de l'interprétation théorique de cette loi empirique.

3. TÉTRAHYDRO OXAZINE (avec W. WU KOR HSIEN)

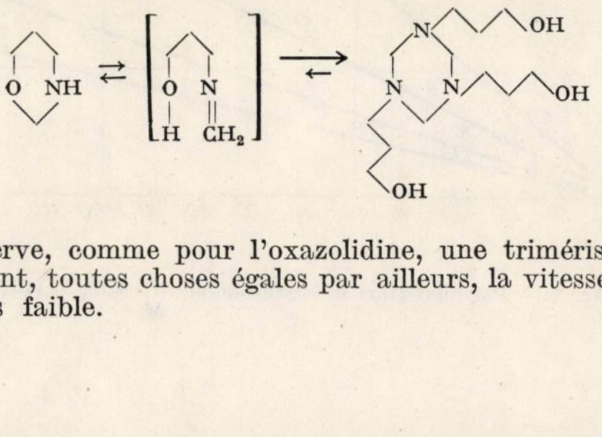

On observe, comme pour l'oxazolidine, une trimérisation.

Cependant, toutes choses égales par ailleurs, la vitesse est environ 100 fois plus faible.

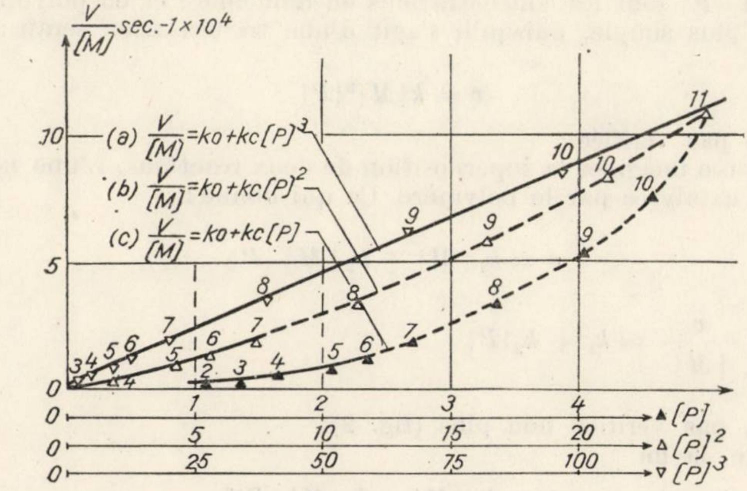

Fig. 2. — Polymérisation de l'oxazolidine $\frac{v}{|M|} = k_1 + k_2 |P|^n$.

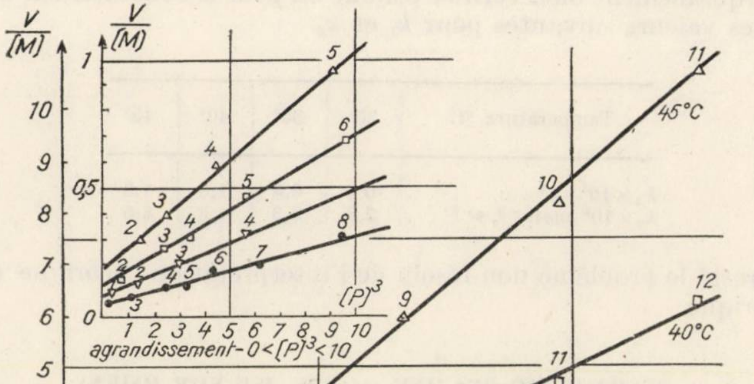

Fig. 3. — Polymérisation de l'oxazolidine $\frac{v}{M} = k_1 + k_2 |P|^3$.

Mais surtout le mécanisme est certainement beaucoup plus complexe que pour l'oxazolidine et la loi empirique trouvée pour l'oxazolidine ne s'applique pas.

4. HYDROLYSE DE QUELQUES OCANNES (avec F. CLARIGET)

Ces hydrolyses ont été faites à différentes températures et différentes concentrations en acide. Le milieu réactionnel est en général un mélange eau (60 %) dioxanne (40 %).

4 – 1) TRIOXOCANNE-1, 3, 6

Le trioxocanne-1, 3, 6 est un acétal cyclique. Son hydrolyse a été étudiée

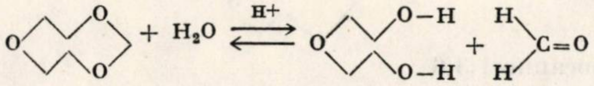

$t = 0$	a_0	$\vert H_2O \vert$	b_0	c_0
$t = \theta$	$a_0 - x$		$b_0 + x$	$c_0 + x$
$t = \infty$				ρ

La cinétique de la réaction ci-dessus donne avec les notations habituelles l'expression suivante :

$$\frac{\mathrm{d}x}{\mathrm{d}t}\overrightarrow{\mathbf{k}} = (a_0 - x) - \overleftarrow{\mathbf{k}}(b_0 - x)(c_0 - x) \qquad (1)$$

en admettant que $\vert H_2O \vert$ est constant.
Si au départ on a $b_0 = c_0 = 0$, la relation ci-dessus devient :

$$\frac{\mathrm{d}x}{\mathrm{d}t} = \overrightarrow{\mathbf{k}}(a_0 - x) - \overleftarrow{\mathbf{k}}x_2 \qquad (2)$$

$$\text{avec } \frac{\overrightarrow{\mathbf{k}}}{\overleftarrow{\mathbf{k}}} = \frac{\rho^2}{a_0 - \rho} = K_c \qquad (3)$$

où ρ est la concentration de formol en fin d'expérience. La combinaison de (2) et de (3) donne, tous calculs faits :

$$\frac{\mathrm{d}x}{\mathrm{d}t} = \overrightarrow{\mathbf{k}}(a_0 - x) - \frac{\overleftarrow{\mathbf{k}}}{K_c}\, x^2$$

soit après intégration :

$$\vec{\mathbf{k}}t = \frac{2{,}3\,\rho}{2a_0 - \rho}\left|\log\frac{\rho}{\rho - x} - \log\frac{\rho}{(a_0 - \rho)x + \rho a_0}\right|$$

ou

$$\vec{\mathbf{k}}t = \frac{\rho}{2a_0 - \rho}\,|\log A - \log B|$$

en posant :

$$\frac{\rho}{\rho - x} = A \quad \text{et} \quad \frac{\rho}{|(a_0 - \rho)x + \rho a_0|} = B$$

ρ étant accessible à l'expérience on doit avoir une droite en portant l'expression ($\log A - \log B$) en fonction du temps.

La loi est effectivement vérifiée pour le trioxocanne (fig. 4, 4′, 4″) Pour l'oxadithiocanne-1,3,6

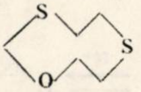

et le dioxathiocanne-1,3,6

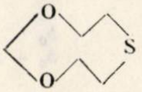

les résultats sont analogues et le tableau ci-dessous rassemble les constantes de vitesse et les constantes d'équilibre trouvées.

Tableau 1

Constantes de vitesse et d'hydrolyse dans l'équilibre des trioxocanne-1,3,6,dioxathiocanne-1,3,6 oxadithiocanne-1,3,6

		40°C	45,5°C	52,5°C	60°C	80°C
$\vert H^+\vert = 0{,}1$ N 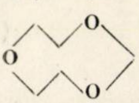	$\vec{\mathbf{k}}(s^{-1})$	$1{,}2 \cdot 10^{-4}$	$2{,}6 \cdot 10^{-4}$	$5{,}6 \cdot 10^{-4}$	$12{,}2 \cdot 10^{-4}$	—
	k_c	$1{,}1 \cdot 10^{-2}$	$1{,}0 \cdot 10^{-2}$	$1{,}0 \cdot 10^{-2}$	$1{,}0 \cdot 10^{-2}$	—
$\vert H^+\vert = 0{,}2$ N 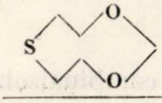	$\vec{\mathbf{k}}(s^{-1})$	$0{,}45 \cdot 10^{-4}$	$0{,}9 \cdot 10^{-4}$	$2{,}3 \cdot 10^{-4}$	$5{,}6 \cdot 10^{-4}$	$2{,}7 \cdot 10^{-2}$
	k_c	$0{,}8 \cdot 10^{-2}$	$0{,}9 \cdot 10^{-2}$	$1{,}05 \cdot 10^{-2}$	$1{,}4 \cdot 10^{-2}$	—
$\vert H^+\vert = 1$ N 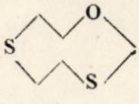	$\vec{\mathbf{k}}(s^{-1})$	—	—	—	—	$7{,}5 \cdot 10^{-6}$
	k_c	—	—	—	—	$8{,}3 \cdot 10^{-4}$

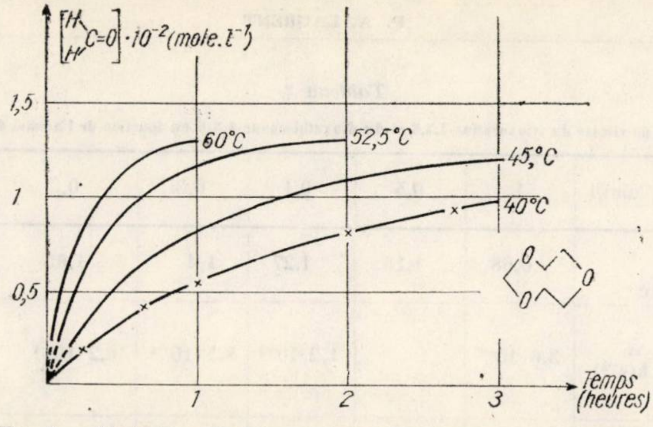

Fig. 4. — Hydrolyse du trioxocanne-1, 3, 6 à différentes températures. Variation de la concentration en formaldéhyde en fonction du temps.

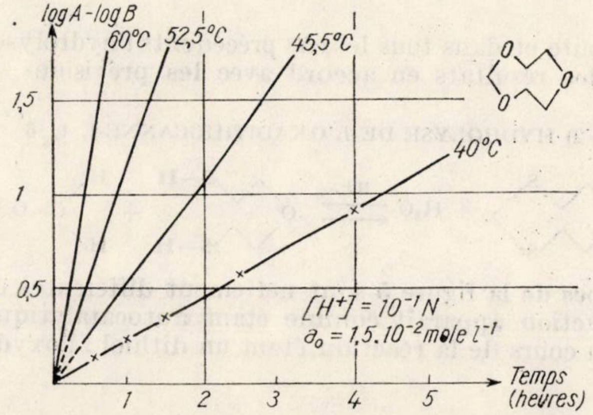

Fig. 4′. — Hydrolyse du trioxocanne-1, 3, 6 à différentes températures. Variation de log A — log B en fonction du temps.

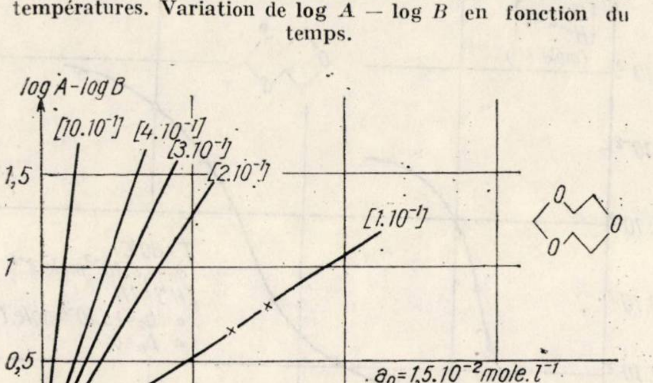

Fig. 4″. — Hydrolyse du trioxocanne-1, 3, 6 à 45°5 à différentes concentrations en acide. Variation de log A — log B en fonction du temps.

Tableau 2

Constantes de vitesse du trioxocanne-1,3,6 et du dioxathiocanne-1,3,6 en fonction de l'acidité du milieu

$t = 45{,}5°C$ $\vert H^+ \vert$ mol/l	1	0,5	0,4	0,3	0,2	0,1
H_0 fonction d'acidité	0,68	1,15	1,27	1,4	1,65	2,14
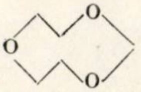 $\vec{k}(s^{-1})$	$3{,}6 \cdot 10^{-3}$	—	$1{,}2 \cdot 10^{-3}$	$8{,}5 \cdot 10^{-4}$	$6{,}2 \cdot 10^{-4}$	$2{,}6 \cdot 10^{-2}$
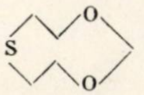 $\vec{k}(s^{-1})$	$4 \cdot 10^{-4}$	$2{,}5 \cdot 10^{-4}$	—	$1{,}3 \cdot 10^{-4}$	$0{,}9 \cdot 10^{-4}$	—

Somme toute et dans tous les cas précédents l'hydrolyse est classique et on trouve des résultats en accord avec les prévisions.

4–2) HYDROLYSE DE L'OXADITHIOCANNE-1, 4, 6

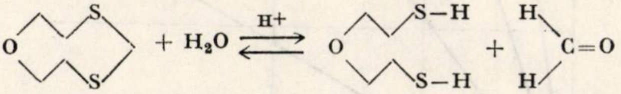

Les courbes de la figure 5 sont nettement différentes des cas précédents et la réaction apparaît comme étant autocatalytique, le produit qui se forme au cours de la réaction étant un dithiol : l'oxyde de bis(mercapto-éthyle).

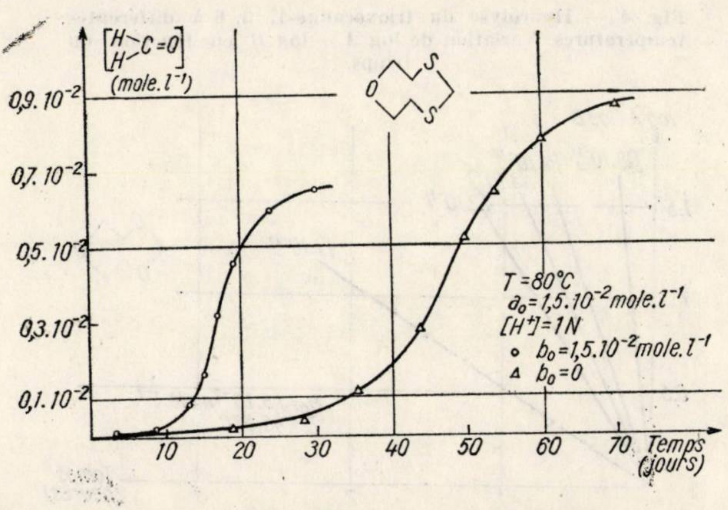

Fig. 5. — Hydrolyse de l'oxadithiocanne-1, 4, 6. Variation de la concentration en formaldéhyde en fonction du temps.

Nous avons vérifié que l'addition de ce produit en cours de réaction augmentait effectivement la vitesse de l'hydrolyse et que les résultats étaient en excellent accord avec une relation empirique dont nous donnons ci-dessous quelques éléments de calculs avec des notations analogues à celles du trioxocanne.

Nous admettons la superposition de deux réactions :

— l'une catalysée par les ions H^+, sa vitesse pouvant être représentée par :

$$v_1 = \overrightarrow{\mathbf{k}}_1(a_0 - x) - \overleftarrow{\mathbf{k}}_1 x^2$$

— l'autre catalysée par le dithiol avec pour vitesse :

$$v_2 = \overrightarrow{\mathbf{k}}_2 x^n(a_0 - x) - \overleftarrow{\mathbf{k}}_2 x^{n+2}$$

La vitesse totale V est donnée par :

$$V = \frac{\mathrm{d}x}{\mathrm{d}t} = v_1 + v_2 = \overrightarrow{\mathbf{k}}_1(a_0 - x) - k_1 x^2 + \overrightarrow{\mathbf{k}}_2 x^n(a_0 - x) - \overleftarrow{\mathbf{k}}_2 x^{n+2}$$

à l'équilibre $V = 0$

$v_1 = 0$

$v_2 = 0$

donc

$$\frac{\overrightarrow{\mathbf{k}}_1}{\overleftarrow{\mathbf{k}}_2} = \frac{\overrightarrow{\mathbf{k}}_2}{\overleftarrow{\mathbf{k}}_2} = \frac{\rho^2}{a_0 - \rho} = K_c$$

avec K_c = constante d'équilibre
et $x = \rho$ quand $t \to \infty$
ce qui donne :

$$V = v_1 + v_2 = \vec{k}_1 \left| a_0 - x - \frac{x^2}{K_c} \right| + \overrightarrow{\mathbf{k}}_2 x^n \left| a_0 - x - \frac{x^2}{K_c} \right|$$

un ensemble de mesures et de calculs nous a conduits à admettre que $n = 1$ ce qui conduit à l'expression :

$$\frac{\mathrm{d}x}{\mathrm{d}t} = \overrightarrow{\mathbf{k}}_1 \left| a_0 - x - \frac{x^2}{K_c} \right| + \overrightarrow{\mathbf{k}}_2 x \left| a_0 - x - \frac{x^2}{K_c} \right|$$

avec $\overrightarrow{\mathbf{k}}_1 = 1{,}2 \times 10^{-8}\ s^{-1}$

$\overrightarrow{\mathbf{k}}_2 = 3 \times 10^{-4}\ \mathrm{mol}^{-1} \times \mathrm{e} \times s^{-1}$ et $t = 80°\mathrm{C}$

$K_c = 1{,}37 \times 10^{-2}\ \mathrm{mol} \times \mathrm{e}^{-1}$

L'excellent accord de la formule précédente avec les résultats expérimentaux ne donne cependant aucune indication sur le mécanisme de cette autocatalyse.

En effet, l'acidité du dithiol est bien trop faible pour provoquer une protolyse. Et nous n'avons pas non plus pû mettre en évidence un complexe correspondant à un acide fort.

4 – 3) HYDROLYSE DES TRIOXOCANNES SUBSTITUÉS EN 2

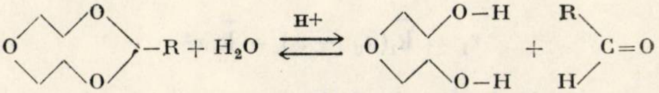

Elles ont été faites à 10°C dans un mélange eau (60%) dioxanne (40%) à une concentration en $H^+ = 10^{-3}N$ et une force ionique égale à 1 mole/l par addition de KCl

Voici les résultats

R	$-H$	$-CH_3$	$-C_2H_5$	$-C_3H_2$	$-CH(CH_3)_2$
k en s^{-1}	$1{,}3 \times 10^{-8}$	$1{,}1 \times 10^{-4}$	$0{,}95 \times 10^{-4}$	$0{,}4 \times 10^{-4}$	$0{,}55 \times 10^{-4}$

Quand R varie du méthyle à l'isopropyle les variations de k sont faibles et pratiquement de l'ordre de 10^{-4}.

Par contre, quand $R = H$ c'est-à-dire le trioxocanne non substitué k est de l'ordre de 10^{-8}.

L'effet inducteur ou l'hyperconjugaison peuvent être invoqués. Mais les influences sont bien trop faibles pour expliquer une différence de l'ordre de 10^4.

Revue Roumaine de Chimie **22**, *9–10*, 1413–1416 (1977)

COMPTES RENDUS

M. TUBIS and W. WOLF (editors), "Radiopharmacy", Wiley-Interscience, New York, 1976, 911 p., $ 51,90

To indicate the contents of this valuable book, the six parts are listed, followed by the titles of the chapters ; then the authors are indicated in brackets, and lastly the number of pages in each chapter.

Part 1, History: History of Radiopharmacy (G. A. Andrews) 24.

Part 2, Physics and Instrumentation: Physics of Radioactivity (R. K. Cole) 36 ; Interaction of Radiation with Matter (W. Wolf) 14 ; Basis of Measurement (L. S. Graham and L. Akers) 18 ; Instruments for *In Vivo* Counting and Imaging (R. Adams) 28.

Part 3, Biology: Radiation Biology (C. S. Marcus) 28 ; Principles of Radiation Safety (S. Kinsman) 28 ; Elements of Dosimetry (M. A. Greenfield and R. G. Lane) 24.

Part 4, Chemistry: Radiochemistry (W. Wolf) 22 ; Production and Purification of Radionuclides (H. B. Hupf) 30 ; Radioisotope Generators (G. Subramanian and J. G. McAfee) 24 ; Cyclotron-Produced Radiopharmaceuticals (W. Wolf and M. Tubis) 24 ; Synthesis of Labeled Compounds (R. J. Bayly, E. A. Evans, J. S. Glover and J. L. Rabinowitz) 76 ; Purity and Stability of Labeled Compounds (Y. Cohen) 26.

Part 5, Radiopharmaceutics: Radiopharmaceutics (M. Tubis) 82 ; Hospital Preparation and Dispensing of Radiopharmaceuticals (M. Tubis) 14 ; Industrial Production of Radiopharmaceuticals (R. S. Mani and N. G. S. Gopal) 54 ; Quality Control of Radiopharmaceuticals (M. Tubis) 24 ; The Design of New Radiopharmaceuticals (M. Tubis) 12 ; The Radiopharmacy (C. H. Wang and T. K. Kawada) 8 ; Radionuclides and Radiation in the Pharmaceutical Industry (G. S. Banker) 22 ; Radionuclides in Pharmacology (Y. Cohen and L. J. Roth) 64 ; Regulations and Legal Aspects of Radiopharmaceuticals (E. L. Meyers and R. E. Cunningham) 28.

Part 6, Nuclear Medicine: Stable Nuclides in Clinical Pharmacology (W. Sadee and C. Finn) 8 ; Nuclear Medicine (J. K. Siemsen and N. Talfer) 112 ; Principles of Competitive Binding Assays (W. D. Odell) 28 ; Radionuclides in Space Biology and Space Medicine (H. S. Winchell and S. A. Landaw) 10.

As it may be seen from the above detailed table of contents, this is the first book in the world's literature aiming to treat comprehensively the whole field of radiopharmacy. Each chapter is written by one or several international leading experts in the field, but is part of a general plan, in order to ensure complete coverage. It should be stated from the outset that the ambitious goal was fulfilled, despite the considerable difficulties of such a venture.

Slight overlap between a few chapters was unavoidable (e.g. legal aspects are discussed at pages 551 and 685–710) but it is minimal, and as there are no conflicting views, consistency is achieved. Actually, it is better to have some overlap than to leave gaps.

Each chapter is provided with a bibliography through 1973/4 and in several cases also with later quotations (1975/6), which provides the reader with supplementary reading ; an advantage is that titles of papers are included. As expected, the four larger chapters (those above 60 pages) have more than 100 references each (at most 435 references for the chapter 'Radiopharmaceutics'), the remainder have between 12 and 99 references per chapter. In the reviewer's opinion, a good balance of literature quotations is very important, and this balance was well achieved in the present volume.

Especially commendable is the fact that, in spite of inherent problems connected with commercial aspects, the essential problems of the user are not eluded. Indeed, in Drs. Mani and Gopal's chapter 'Industrial Production of Radiopharmaceuticals', detailed tables are included, indicating the main large-scale manufacturers and their principal products, the optimum specifications of important radiopharmaceuticals, and the main nuclear reactors and cyclotrons used for the production of radioisotopes for medical applications. These tables were not easy to prepare, because they raise the problem to define "main", "principal" and "optimum" ; these tables are quite valuable and informative. In table 17.4, the maximum thermal neutron flux of nuclear reactors would have been easier to compare, if it would have been given as multiples of 10^{13} n. $cm^{-2}.s^{-1}$.

The monograph contains several chapters with problems specific to the United States of America, notably the last one on space biology and medicine, and the chapter concerning legal aspects. However, most chapters are of interest to readers throughout the world ; as an example in this respect, in Dr. Tubis's chapter 'Radiopharmaceutics', not only the monographs contained in the 18th edition of the United States Pharmacopeia are listed, but also those from the International Pharmacopoeia published by the World Health Organization.

The whole book is permeated by the philosophy that the radiopharmaceuticals have come to stay and to grow, and that a new profession, the radiopharmacist, must emerge. Indeed, both editors of this volume, who authored together or separately several chapters, have been personally involved in obtaining recognition for this profession, and initiated the Radiopharmacy Program at the University of Southern California in Los Angeles. Because of that, the whole book and especially the fifth part "Radiopharmaceutics", provide the reader with a host of useful informations which are difficult to locate elsewhere in the specialist literature.

The outlay of the book, the detailed subject index, and the remarkable absence of errors (a minor one is an arrow instead of a plus sign in equation 2—22 on page 47) make the reading attractive and easy. The equilibration of theoretical and practical aspects of the topics discussed in all chapters is very commendable.

Besides the rapid progress in this field, one of the most dynamically developing areas of the seventies, the extensive coverage of the book ensures that this monograph will be a valuable guide and reference work for many years to come, for all those who are interested in radiopharmaceuticals and in nuclear medicine.

Alexandru T. Balaban

G. O. ASPINALL, (ed.) "CARBOHYDRATES", International Review of Science, Organic Chemistry, Series Two, vol. 7, Butterworth, London, 1976, 323 p.

By means of International Review of Science, the publishers have assumed the difficult task to present periodically, by means of the most reputed specialists, the advances made in various fields of chemistry and parachemical schiences. The present volume completes the first series of organic chemistry devoted to carbohydrates, aiming at covering the literature of the years 1972—1973, However some of the most important breakthroughs of the years 1974 and even 1975 have been captured therein.

As it was expected, the second series dealing with carbohydrates does not totally treat the topics discussed in the first volume. The subjects chosen here cover more extended domains both from the sphere of monosaccharides and of polysaccharides. Account was taken of the fact that the biochemical aspects of carbohydrates would be treated in the corresponding biochemistry series.

1. *^{13}C-NMR Spectroscopy of Carbohydrates* (A. S. Perlin, McGill Univ., Montreal). The characteristics of ^{13}C spectra are described discussing the demonstrated or potential applications which may provide data that cannot be obtained by other techniques. In this context, the book presents the chemical shifts, the analysis of the equilibrium mixture of ketoses, the spectra of polysaccharides, the spin-spin ^{13}C—^{1}H coupling and the applications of such couplings to problems of stereochemistry (34 pages and 89 ref.).

2. *Displacement, Elimination and Rearrangement Reactions* (R. J. Ferrier, Victoria Univ. Wellington). The first volume of the series is completed by extending the aspects concerning the elimination and transposition reactions which are in fact interrelated with nucleophilic shift reactions. Many data of the years 1974 and even 1973 are presented by the additional notes introduced on the proof-galleys (54 pages, 215 ref.).

3. *General Carbohydrate Synthesis* (W. A. Szarek and D. M. Vyas Queen's Univ., Kingston). The chapters presented in the first volume: oxidation in the chemistry of carbohydrates, reactions of chain extension and branching, addition reactions to unsaturated saccharides, deoxyhalogenated saccharides and total synthesis of carbohydrates were completed by a new subject dedicated to the problems of photochemistry of saccharides derivatives (30 pages, 313 ref.).

4. *The Nitro Sugars* (A. C. Richardson, Univ. London). Compared to the corresponding chapter in the first series, treating "Amino and Nitro Sugars", the present volume treats only the recent advances in the synthesis of nitro sugars and of nitro alditols as well as the reactions and properties of nitro sugars (15 pages, 53 ref.).

5. *Sugar — containing Antibiotics.* (S. Umezawa, Keio Univ., Yokohama). Referring also to older data on sugar-containing antibiotics, the author presents the progress recorded in recent years in aminoglycosidic antibiotics, nucleosidic and macrolidic antibiotics, antibiotics with aromatic groups and others. (40 pages, 268 ref.).

6. *Polysaccharide Methodology* (G. O. Aspinall, York Univ., Toronto). As in the previous edition, the article is particularly concerned with analytical methods, including gas- liquid

chromatography, mass spectrometry and NMR, besides the chemical procedures for glucides, fragmentation and transformation in view of structure determination (16 pages, 148 ref.).

7. *Glycolipids of Animal Cell Membranes* (S. Hakomori, University of Washington). After pointing out the main historical stages in the study of glycolipids, the author reports the more important aspects in the structure of glycosphyngolipids and the present trends in the study of glycolipids (22 pages, 183 ref.).

8. *Glycoproteins with Blood Group Activity* (K. O. Lloyd, Columbia Univ.). The problematics related to glycoproteins in secretions of the ovary and of gastric mucous, in submaxillary glands is presented as well as problems concerning sulphated glycoproteins and glycoproteins in erithrocytes (24 pages, 111 ref.).

9. *Structure and Biosynthesis of Iduronic Acid containing Glycosaminoglycans.* (U. Lindale, Royal Veterinary College of Sweden). The author deals mainly with the structure and biosynthesis of glycosaminoglycans in animal tissues (23 pages, 135 ref.).

Undoubtedly, a critical appraisal of advances made in recent years in the field of the carbohydrates chemistry is of a real use to teaching staff, to undergraduate students, to those preparing for their doctoral thesis and to researchers working with such aspects or having contingencies with them. To read all the articles in the field directly from journals is almost impossible for a person today. Therefore the various monographs, journals and comprehensive articles are irreplaceable for keeping researchers up-to-date. However, in general, there is the problem of the proliferation of this type of information disseminated by publishers in various compendia where many subjects (sometimes even of the same authors) are overlapping to a variable extent. This leads to an appreciable time-consuming activity to read them and to additional expenses to procure the volumes in question. An agreement between publishers concerning these types of publications would have a beneficial effect, thus restricting the proliferation of data having a similar coverage.

F. Cuiban

E. PRETSCH, TH. CLERC, J. SEIBL and W. SIMAN: "TABELLEN ZUR STRUKTURAUFKLÄRUNG ORGANISCHER VERBINDUNGEN MIT SPEKTROSKOPISCHEN METHODES" (Tabele pentru lămurirea (elucidarea) structurii compuşilor organici cu metode spectroscopice), Springer-Verlag, Berlin, 1976, 300 p.

The book contains a collection of tables and of spectroscopic data ^{13}C$-$NMR, ^{1}H$-$NMR, IR, MS and UV/VIS separately ordered for each method and with supporting tables to compare the data referring to various classes of chemical compounds. The combined use of spectroscopic methods to elucidate the structure of organic compounds has become for a long time a current practice of organic analysts. The younger chemists have learnt this method in colleges while the older ones have become familiar with the basic knowledge, considering it is of interest or of need; thus it may be considered that everybody can choose the most adequate spectroscopic methods to solve these problems and to transpose the data obtained into structural information. For those who are not concerned with the daily analysis of such spectra, the consultation of some multilateral, well-ordered and revised reference data is extremely useful. The specialists themselves are sometimes forced to resort to additional information for some less familiar types of compounds consulting the literature but this implies a special effort.

The collection of data in this book supports such requirements, being an auxiliary means for the interpretation of various types of spectra and it represents an useful additional source of information for the books and monographs having such spectroscopic methods as an object. The use of the book supposes a knowledge of basic notions related to the interpretation of spectra. It is conceived so that even a beginner can consult it and also the representative literature for the domain in question while the specialists may use it for consulting purposes. According to the statement of the authors who have had a long teaching experience, *an important member of tabulated data are given from their own measurements*, yet correlated with a large volume of indications given by the literature. For certain problems, references are made to the original sources. The fact that spectra were recorded under the most usual routine conditions is extremely important. Thus the $CDCl_3$ or CCl_4 solvents were used for NMR chemical shift the reference substance being tetramethyl silane. IR frequencies were given for less polar solvents such as $CHCl_3$ or CS_2. Mass spectroscopic data were obtained at a ionization energy of 70 eV.

In general, all the data listed in tables were collected from the recent literature, in particular monographs published in the period 1960–1975, which attributes them an important reference value.

The general conception of the book is also of interest, including the page numbering every 5 pages and their grouping by methods to enable the completion of the collection with new data without modifying the general paging. For an easier orientation on the more relevant data, indications regarding the content are circled on the pages, as follows:

KOMB — a comprehensive view according to structural elements on characteristic spectroscopic data, on pages $B_5 - B_{245}$;

^{13}C–NMR — spectral resonance data ^{13}C ordered according to classes of substances, pages $H_5 - H_{370}$;

IR — IR absorption frequencies ordered by functional groups, respectively classes of substances, pages $I_5 - I_{280}$;

MS — tables and indications for the interpretation of mass spectra, pages $M_5 - M_{170}$;

UV/VIS — tables, indications and reference spectra for electronic spectra rationalization, pages $U_5 - U_{155}$.

The consultation of tables may provide the first structural indications, particularly where no preliminary or adjacent information is available from the examination of the general data on pages $B_5 - B_{70}$. In the second stage, based on the mentioned structural elements, it is easy to study the spectroscopic data for the most important classes of substances, in tables $B_{75} - B_{245}$ which exhibit the chemical shifts $\delta - {}^{13}C$ and $\delta - {}^{1}H$ and the coupling constants, the strong IR, UV and VIS absorption bands as well as the characteristic mass fragments. For instance, spectroscopic data characteristic of alkanes and alycyclic compunds are given (^{13}C, ^{1}H, IR, MS, UV) as well as references to more detailed tables of data for each spectroscopic method. Further, similar data are given for unsaturated aliphatic compounds, aromatic and heteroaromatic hydrocarbons, halogenated derivatives, alcohols, phenols, ethers, amines, aldehydes, carbonyl acids, etc.

The other tables are generally used to foresee the spectroscopic behaviour of a certain compound. They are supportive for the correlation of the structure of organic compounds with spectroscopic data and are presented according to methods and to classes of substances. In ^{13}C–NMR for alkanes, the chemical shifts are given together with indications for the calculus of chemical shifts ^{13}C in aliphatic compounds, steric and conformation correction factors and examples of additive calculation of chemical shifts, of coupling constants in various classes of compounds, as well as characteristic data for solvents more frequently used in ^{13}C–NMR. Tables and data devoted to ^{1}H–NMR have a similar structure. For the IR spectroscopy, in addition to the characteristic frequencies and their assignment in the normal domain of absorption, the more frequent exceptions are presented, grouped as observations: the influence of adjacent groups, the shape of bands for special cases and the overlapping with other functional groups.

The tables for mass-correlations contain indications on the mass of the most frequent ions or radical-ions, the generator ion, the class to which it could belong, the natural isotopic abundance and the isotopic distribution calculation, the mass fragments typical of certain classes of compounds, the contribution of heteroatoms to the aspect of mass spectra and also the mass spectra of the principal solvents.

Tables UV–VIS give the transitions, the characteristic absorptions and their intensity for various types of compounds, the calculation possibilities for the characteristic absorptions in the unsaturated carbonyl compounds, in dienes and polyenes and a series of schematic reference spectra. A subject index facilitates the study of the problems of interest.

The authors' experience in vehiculating and using spectroscopic data permitted an excellent rational and functional ordering for the examination of reference elements. The content of the book is characterized by concision, clarity and rigorous systematization of the multitude of data used at present in various spectroscopic methods. It is of a real use to students and the teaching staff in the chemical higher education, to researchers and specialists in industry, helping them to solve the numerous problems raised by the modern chemical industry. The preoccupations of builders of apparatus to improve the performances of spectrometers, to simplify their handling and to reduce their price recorded remarkable success so that spectroscopic methods became routine methods. Due to the great advantages they offer, they are largely used in current practice: in research, in industry and in the qualitative and quantitative analysis of products.

This book is a valuable auxiliary for the combined use of such methods without which the progress recorded in chemistry at present would be inconceivable.

F. Cuiban

"Topics in Current Chemistry" (Fortschritte der chemischen Forschung), **68**, Theory, Springer-Verlag, Berlin, Heidelberg, New York, 1976

X. CHAPUISAT and Y. JEAN, "Theoretical Chemical Dynamics : A Tool in Organic Chemistry", p. 1–57.

This paper refers to one of the most interesting domain of modern theoretical chemistry in which the authors are responsable for original contributions — chemical dynamics.

After an introductory chapter about the purpose of chemical dynamics and the present status of trajectory studies in chemical dynamics, the authors develop a general method for the dynamical study of chemical reactions. The expressions for the potential energy functions are deduced on the bases of spline theory. Further, a formulation of classical mechanics for constrained molecular systems within Lagrangian and Hamiltonian formalisms is given. A special attention is paid to the mode of selection of initial conditions in such calculations.

The final part of the paper contains an application of this method to the optical and geometrical isomerization of cyclopropane.

It is relevant that the dynamical study presented furnishes more complete information about the mechanistic details of organic reactions than those obtained from static considerations alone.

The paper is of valuable help for all chemists interested in theoretical chemistry.

D. PAPOUSEK and V. SPIRKO, "A New Theoretical Look at the Inversion Problem in Molecules", p. 59–102.

This paper describes the molecular inversion in ammonia based on a new model of the vibration-inversion-rotation Hamiltonian lately developed by the authors.

In this model the inversion motion is removed from the vibrational problem and considered with the rotational problem by allowing the molecular reference configuration to be a function of the large amplitude motion coordinate.

Characteristic is that the form of the Hamiltonian obtained is very close to the standard Hamiltonian used in the study of rigid molecules and allows for a treatment of the inversion motion in a way which is very similar to that for the study of molecules with internal rotation.

The approach is largely developed for the ammonia molecule and for the isotope substituted molecules.

The limitations and advantages of this new approach are outlined.

The paper is of particular interest for chemists working in theoretical chemistry and spectroscopy.

H. SCHNEIDER, "Ion Solvation in Mixed Solvents", p. 103–144.

Schneider's paper approaches the ion-solvent interaction or ion solvation based on studies on electrolytes in mixed solvents.

After a short introduction the free energy of transfer of individual ions between two solvent media is discussed. The experimental methods which are frequently used to determine the free energy transfer of electrolytes and neutral combinations of ions are at first presented and then various models used for estimating single ions' free energy of transfer.

The next chapter refers to the complex formation of solvent molecules with ions. A treatment to derive a formula for the free energy of ions transfer in terms of the contribution of solvated ions and of solvent composition is developed. The experimental techniques for the evaluation of coordination numbers and of formation constants of ion-solvent complexes are also shown with emphasis on potentiometric and spectroscopic methods.

The last chapter deals with the transport of a solvated component in a mixed solvent electrolyte solution. The transference numbers for a binary electrolyte in a single solvent and an electrolyte in a binary solvent mixture are discussed. Finally two experimental methods for the determination of solvent transport in mixed solvent electrolyte solutions are exposed : the Hittorf transference method and the electromotive force method.

Schneider's work on ion solvation in mixed solvents is a well-documented treatment of the subject. It is of valuable help for all chemists interested in solvation phenomena.

Valerian Drăguţan

"Topics in Current Chemistry" (Fortschritte der chemischen Forschung), **67**, Preparative Organic Chemistry, Springer-Verlag, Berlin, Heidelberg, New York, 1976

G. WITTIG, "Old and New in the Field of Directed Aldol Condensations", p. 1—14.

Wittig's paper discusses a new method for extending the chain of an aldehyde or ketone to an α, β-unsaturated ketone or aldehyde by means of organometallic directed aldol condensation.

Preceeded by a short introduction, the general procedure for directed aldol condensation is exposed. This procedure consists of converting the aldehyde carbonyl group to an azomethine group, metalling the Schiff base with an appropriate lithium compound and reacting the product with a carbonyl compound to give an aldimine adduct. The protective group is subsequently removed by treatment with acid.

The optimal conditions under which the various steps in the directed aldol condensations should proceed were determined. Cyclohexylamine and lithium diisopropylamide are recommended as the most appropriate amine component of the Schiff base and metallating agent, respectively. The Schiff bases of ketones can also be used in the condensation step.

Some examples of the application of the method to the synthesis of natural products are also included.

In the third chapter the author makes a comparison between directed aldol condensation and the modified carbonyl-olefination. Both methods make possible a desired extension of the chain of carbonyl compounds but the first gives good results with ketones, whereas the latter with aldehydes as substrate.

The final chapter is a preliminary report on Wittig's still unfinished work regarding syntheses which combine the directed aldol condensation and the carbonyl-olefination with phosphorous ylides.

Wittig's paper is of particular interest for all organic chemists. By his new method it is now possible to control the aldol condensation of aromatic ketones with α-CH groups of aldehydes.

C. GANTER, "Dihetero-tricyclodecanes", p. 15—106. Ganter's paper is a comprehensive review of the published data about the synthesis of dihetero-tricyclodecanes including the classes of adamantanes, isotwistanes, twistanes, homotwistbrendanes and tricyclo $[3.2.2.0^{3,7}]$ decanes. These substances are widely used today in organic synthesis.

After a short introduction three chapters deal with the syntheses of the above compounds. Special attention is paid to the synthesis of compounds from suitable 9-hetero[3.3.1]- and 9-heterobicyclo[4.2.1]nonanes as well as by molecular rearrangements of dihetero-tricyclodecanes involving neighbouring group participation. Further transformations and derivatives of dihetero-tricyclodecanes are also included.

In this part of the paper the author largely illustrates the many possible for the synthesis of dihetero-tricyclodecanes and numberous examples of such syntheses are mentioned.

In the last chapter some structural assignments of various dihetero-tricyclodecanes, namely constitutions and conformations of substituents, are discussed. These structural assignments are based on chemical conversions to already-known compounds an d on spectrosopical measurements including IR, UV and NMR spectroscopy.

The material is very concise and clearly organized. The paper is well-written and the reader will find in Ganter's review an useful guide for the synthesis of these types of compounds or of their derivatives.

G. HENRICI-OLIVE and S. OLIVE, "Olefin Insertion in Transition Metal Catalysis", p. 107—127. This review deals with one of the most interesting problem of transition metal chemistry, olefin insertion in transition metal complexes.

After an introductory chapter the authors focuses on the electronic structure of reaction partners in olefin insertion and the regioselectivity of this type of reaction. The polarity of metal-carbon and metal-hydrogen bonds in transition metal complexes and of olefinic double bonds are considered.

A relevant point of the paper is the interpretation given for the insertion step of the coordinated olefin into metal-carbon or metal-hydrogen bond. The olefin insertion is assumed to take place by a concerted reaction path through a more or less polar, cyclic transition state, with simultaneous bond breaking and bond making.

Some considerations are given as whether the insertion takes place at the coordination site of the σ-bonded ligand or this ligand migrates to the site of the coordinated substrate olefin. *cis*-Migration mechanism of the ligand to the site of the coordinated substrate is presented as a very attractive model for olefin insertion, at least in octahedral complexes. On the other hand, in square-planar complexes, olefin insertion is thought to take place at the site of the σ-bonded ligand in order to maintain the square-planar symmetry.

A special attention is paid to the regioselectivity in olefin insertion. The discussion of regioselectivity is based on the definitions of the Markownikoff and anti-Markownikoff modes of insertion and on the electronic structure of metal-carbon and metal-hydrogen bonds as well as of olefinic bonds. To explain the anti-Markownikoff mode a mechanism is suggested in which the metal centers that possess a high *d*-electron population in the presence of electron donor ligands might provoke the inversion of the polarization of the weakly polar double bonds of substrate olefin. This hypothesis is rationalized according to the Dewar-Chatt-Ducanson model of the metal-olefin bond and taking into account the unsymmetric habitus of the π-orbital of the olefinic substrate.

The paper has a real significance for our theoretical knowledge about homogenous catalysis by transition metal complexes.

Valerian Drăguţan

NOTE POUR LES AUTEURS

La Revue Roumaine de Chimie publie des articles en anglais, français, russe, allemand ou espagnol. Les auteurs sont priés d'envoyer des articles et des comptes rendus inédits.

Les manuscrits seront dactylographiés à deux intervalles. La bibliographie, les tableaux et la légende des figures seront placés après le texte.

Si l'article fait partie d'une série numérotée, le titre de la partie précédente sera indiqué dans une note au bas de la première page.

Chaque article sera précédé d'un résumé comprenant quinze lignes au maximum.

Les références bibliographiques dans le texte seront faites par des exposants sans parenthèse et paraîtront comme des notes au bas de chaque page.

Les publications périodiques mentionnées dans la bibliographie seront présentées suivant les prescriptions internationales : le nom de l'auteur précédé de l'initiale du prénom, le titre du périodique abrégé conformément à «Chemical Abstracts» et souligné par une ligne, le numéro du tome, indiqué par des chiffres arabes et souligné par deux lignes, suivi de la première page de l'article ; à la fin, l'année de la parution sera placée entre parenthèses. Le numéro de la revue ne sera pas indiqué si les pages du volume sont numérotées consécutivement. Pour les revues dont les tomes ne sont pas numérotés (par ex. Bull. Soc. Chim. France, etc.), l'année de la parution soulignée par deux lignes précèdera l'indication de la page.

Les textes des livres ou traités incluront : les noms des auteurs, les initiales du prénom, le titre du livre entre guillemets et sans être souligné, le numéro du tome précédé par l'abbréviation «vol.» (ou «Bd.»), le numéro de l'édition, les éditions (the publisher), la localité de la parution de livre, l'année de la parution et la page de la référence précédée par l'abréviation «p.» (ou «S.»).

Les brevets seront indiqués comme suit : L'auteur ou la firme, le pays et le numéro du brevet, la date et la revue (Chem. Abstr.). Par ex. : M. Jones (to Union Carbide Co.), Brit. Pat. 601 238, 2 septembre 1959, *Chem. Abstr.*, 54, 12808 (1960).

Si la référence n'a pas été lue en original, on indiquera aussi la revue de références consultée.

Les diagrammes seront tracés à l'encre de Chine sur papier calque. Les tableaux et les figures (en nombre strictement nécessaire) seront numérotés par des chiffres arabes et leur explication sera donnée dans la légende des figures. Prière de ne pas inscrire les mêmes données dans les tableaux et les figures. Chaque tableau aura un titre. On indiquera dans le texte la place approximative des tableaux et des figures. Les formules chimiques seront incluses dans le texte ; en outre, elles seront transcrites sur papier calque, à l'encre de Chine.

Les auteurs sont priés d'indiquer les caractères italiques (en soulignant les lettres au crayon), ainsi que tout autre caractère spécial ; les préfixes *ortho*, *meta*, *para*, *cis*, *trans*, etc. seront soulignés pour indiquer leurs caractères italiques et ne seront jamais écrits avec des majuscules.

Aucune correction à main ne sera admise sur le manuscrit. Les corrections seront frappées à la machine. Les lettres grecques ou autres symboles spéciaux seront insérés à la main à l'encre clairement.

Le manuscrit sera signé par l'auteur.

Le colonne-titre aura 50 lettres au maximum.

L'entière responsabilité du contenu des articles appartient aux auteurs.

PRINTED IN ROMANIA

NOTE POUR LES AUTEURS

La Revue Roumaine de Chimie publie des articles en anglais, allemand, russe, ou exceptionnellement en français. Les auteurs sont priés d'envoyer des articles et des comptes rendus inédits.

Les manuscrits seront dactylographiés à deux interlignes. La bibliographie, les tableaux et la légende des figures seront placés après le texte.

Si l'article fait partie d'une série numérotée, le titre de la partie précédente sera indiqué dans une note au bas de la première page.

Chaque article sera précédé d'un résumé comprenant quinze lignes au maximum.

Les références bibliographiques dans le texte seront faites par des exposants sans parenthèse et paraîtront comme des notes au bas de chaque page.

Les publications périodiques mentionnées dans la bibliographie seront présentées suivant les prescriptions internationales : le nom de l'auteur précédé de l'initiale du prénom, le titre du périodique abrégé conformément à «Chemical Abstracts» et souligné par une ligne, le numéro du tome, indiqué par des chiffres arabes et souligné par deux lignes, suivi de la première page de l'article ; à la fin, l'année de la parution sera placée entre parenthèses. Le numéro de la revue ne sera pas indiqué si les pages du volume sont numérotées consécutivement. Pour les revues dont les tomes ne sont pas numérotés (par ex. Bull. Soc. Chim. France, etc.), l'année de la parution soulignée par deux lignes précédera l'indication de la page.

Les textes des livres ou traités mentionnés : les noms des auteurs, les initiales du prénom, le titre du livre entre guillemets et sans être souligné, le numéro du tome précédé par l'abréviation vol. (ou Bd.), le numéro de l'édition, les éditeurs (the publisher), la localité de la parution du livre, l'année de la parution et la page de la référence précédée par l'abréviation p. (ou S.).

Les brevets seront indiqués comme suit : l'auteur ou la firme, le pays et le numéro du brevet, la date et la revue (Chem. Abstr.) (par ex. : W. Jones (to Union Carbide Co.), Brit. Pat. 801 339, 2 septembre 1959; Chem. Abstr., 54, 22635 (1960).

Si la référence n'a pas été lue à l'original, on indiquera aussi la revue de références consultée.

Les diagrammes seront tracés à l'encre de Chine sur papier calque. Les tableaux et les figures (en nombre strictement nécessaire) seront numérotés par des chiffres arabes et leur explication sera donnée dans la légende des figures. Éviter de ne pas inscrire les mêmes données dans les tableaux et les figures. Chaque tableau aura un titre. On indiquera dans le texte la place approximative des tableaux et des figures. Les formules chimiques seront incluses dans le texte ou, en outre, elles seront transcrites sur papier calque, à l'encre de Chine.

Les auteurs sont priés d'indiquer les caractères italiques (en soulignant les lettres en crayon ainsi que tout autre caractère spécial) ; les préfixes cis, trans, méta, para, o, m, p, etc. seront soulignés pour indiquer leurs caractères italiques et ne seront pas écrits avec des majuscules.

Aucune correction à main ne sera admise sur le manuscrit. Les corrections seront tapées à la machine. Les lettres grecques ou autres symboles spéciaux seront inscrits à la main à l'encre distinctement.

Le manuscrit sera signé par l'auteur.

Le colonne titre aura [illegible] lettres au maximum.

L'entière responsabilité du contenu des articles appartient aux auteurs.

PRINTED IN ROMANIA

1978 APR 6

TRAVAUX PARUS AUX ÉDITIONS DE L'ACADÉMIE DE LA RÉPUBLIQUE SOCIALISTE DE ROUMANIE

C. DRĂGULESCU, E. PETROVICI, **Chimia structurală modernă. Chimia coordinanței** (La Chimie structurale moderne. La Chimie de la coordinance), 1977, 947 p., 70 lei.

I. G. MURGULESCU, **Introducere în Chimia fizică, vol. I. 1. Atomi, molecule, legătură chimică** (Introduction à la Chimie physique, Ier vol., 1. Atomes, molécules, liaison chimique), 1976, 560 p., 36 lei.

E. P. BALTĂ, E. BALTĂ, **Introduction to the physical chemistry of the vitreous state**, coédition avec Abacus Press, 1976, 287 p., 31 lei.

H. I. GĂLĂȚEANU, **Radiochimia aplicată. Metode și probleme** (La radiochimie appliquée. Méthodes et problèmes), 1976, 307 p., 19 lei.

CONST. V. UGLEA **Cromatografia pe gel permeabil. Noi domenii de aplicare** (La chromatographie sur gel perméable. Nouveaux domaines d'application), 1976, 122 p., 6,75 lei.

GR. POPA, ȘERBAN MOLDOVEANU, **Reactivii organici în chimia analitică** (Les réactifs organiques dans la chimie analytique), 1976, 255 p., 18 lei.

FRANCISC A. GOTHARD, **Echilibre lichid-vapori. I. Baze teoretice și metode de calcul** (Equilibres liquide-vapeurs. I. Bases théoriques et méthodes de calcul), 1975, 263 p., 2 pl., 28 lei.

CONST. GH. MACAROVICI, D. MACAROVICI, **Chimia oxizilor dubli și utilizările lor** (La chimie des oxydes doubles et leur utilisation), 1975, 195 p., 13 lei.

M. AVRAM, **Antidăunători** (Pesticides), 1974, 496 p., 41 lei.

ELENA CEAUȘESCU, **Research work on synthesis and characterization of macromolecular compounds. Contributions**, 1974, 251 p., 20 lei.

DUMITRU COSTACHE, **Analiza chimică prin metoda cinetică** (L'Analyse chimique par la méthode cinétique), 1974, 276, p., 15,50 lei.

G. A. RĂDULESCU, **Proprietățile țițeiurilor românești** (Les propriétés des pétroles roumains), 1974, 267 p., 2 pl., 18 lei.

CR. SIMIONESCU, VIORICA RUSAN, V. POPA, **Chimia algelor marine** (La chimie des algues marines), 1974, 212 p., 1 pl., 18 lei.

I. ZUGRĂVESCU, MAGDA PETROVANU, **Chimia n-ilidelor** (La chimie des n-Ilures), 1974, 348 p., 19 lei.

MARIA FITI, **Dozimetria chimică a radiațiilor ionizante** (La dosimétrie chimique des radiations ionisantes), 1973, 240 p., 13,50 lei.

TIBERIU NĂȘCUȚIU, **Metode radiochimice de analiză** (Méthodes radiochimiques d'analyse), 1973, 384 p., 23 lei.

CRISTOFOR SIMIONESCU, MARGARETA GRIGORAȘ, AGATA CERNĂTESCU-ASANDEI, GHEORGHE ROZMARIN, **Chimia lemnului în România. Plopul și salcia** (La Chimie du bois en Roumanie. Le peuplier et le saule), 1973, 299 p., 13 pl., 26 lei.

MIHAI FLORESCU, **Eficiența economică a cercetării științifice** (L'efficience économique de la recherche scientifique), 1972, 115 p., 15 lei.

GEORGETA LĂZĂRESCU, **Sistematizarea informațiilor în chimia organică** (Systématisation des informations en Chimie organique), 1972, 243 p., 1 pl., 10,50 lei.

I. P. I. — c. 7356

43426

Lei 25.—

F1103

ACADÉMIE DE LA RÉPUBLIQUE SOCIALISTE DE ROUMANIE

REFERÁLVA

REVUE ROUMAINE DE CHIMIE

TOME 22

Nos 11—12

Novembre — Décembre 1977

EDITURA ACADEMIEI REPUBLICII SOCIALISTE ROMÂNIA

Rev. Roumaine Chim. RECHAX, 22, *11—12*, p. 1431—1571 (1977), Bucarest

ACADÉMIE DE LA RÉPUBLIQUE SOCIALISTE DE ROUMANIE

COMITÉ DE RÉDACTION

Rédacteur en chef:

I. G. MURGULESCU, membre de l'Académie de la République Socialiste de Roumanie

Rédacteurs en chef adjoints:

A. T. BALABAN et V. EM. SAHINI, membres correspondants de l'Académie de la République Socialiste de Roumanie

Collège de rédaction:

EM. BRATU, ELENA CEAUŞESCU, ECATERINA CIORĂNESCU-NENITZESCU, C. DRĂGULESCU, CR. SIMIONESCU, membres de l'Académie de la République Socialiste de Roumanie; P. SPACU, membre correspondant de l'Académie de la République Socialiste de Roumanie; MARGARETA AVRAM, I. HAIDUC, D. I. MARCHIDAN, I. MOLDOVAN, G. NIAC et D. SĂNDULESCU

La Revue Roumaine de Chimie paraît 10 fois par an. Toute commande de l'étranger pour les travaux parus aux Editions de l'Académie de la République Socialiste de Roumanie sera adressée à ILEXIM, Departamentul Export-Import Carte (Livres)/Departamentul Export-Import Presă (Revues), P. O. B. 136—137, télex 11226, 3, str, 13 Decembrie, Bucarest, Roumanie

Les manuscrits, les livres et les revues proposés en échange, ainsi que toute correspondance seront envoyés à la rédaction :
REVUE ROUMAINE DE CHIMIE
125, Calea Victoriei, Bucarest, Roumanie, téléphone 50 76 80

EDITURA ACADEMIEI REPUBLICII SOCIALISTE ROMÂNIA
125, 71021, Calea Victoriei, Bucarest, Roumanie, téléphone 50 76 80

ORSZÁGOS MŰSZAKI KÖNYVTÁR ÉS DOKUMENTÁCIÓS KÖZPONT 1883

REVUE ROUMAINE DE CHIMIE

Tome 22, N°s 11—12 Novembre—Décembre 1977

I. G. MURGULESCU and C. MISDOLEA, A relation for the viscosity of ionic liquids . . . . 1433—1439

MARIANA CIUREANU and V. E. SAHINI, A spectroscopic study of iodine complexes with some heterocycles in the azoles series . . . . 1441—1446

RODICA VÎLCU and SANDA SAMSON, Thermodynamic characterization of some binary solutions of non-electrolytes, by a cellular model with holes 1447—1456

R O. RADOVICI and VIORICA LĂZĂRESCU, Some results concerning nickel electrodeposition on thin films . . . . 1457—1461

P. PACÁK and I. SLÁMA, Diffusion of cadmium and silver ions in concentrated aqueous solutions of calcium nitrate . . . . 1463—1469

TATIANA ONCESCU and ECATERINA JURCONI, Thermal decomposition of tris(oxalato) manganese(III) complex in aqueous solutions. . . . . 1471—1477

N. S. BIRADAR, B. R. PATIL and V. H. KULKARNI, A spectroscopic study of tin(IV) complexes with 2,2′-dihydroxychalkones . . . . 1479—1486

D. NEGOIU and LIDIA PARUTA, Preparation and investigation of Hg(II) complex compounds with triarylstibines . . . . 1487—1492

R P. V. SIVAPULLAIAH and S. SOUNDARARAJAN, Pyridine-N-oxide complexes of rare-earth bromides. . . . . 1493—1497

ILEANA I. STĂNOIU, A. T. BALABAN and F. CHIRALEU, Isotopic exchange of active methyl groups. X. Activation parameters for deuteriation and de-deuteriation of isopropylpyrylium salts . . . . 1499—1504

V. WERTHEIMER, A. M. GLATZ and A. C. RĂZUȘ, Solvolytic behaviour of strained systems: The 1-, 4- and 5-methylbenzo[*b*]bicyclo[3.1.0]hex-2-en-4-yl cations . . . . 1505—1511

A. O. FULEA and CORNELIA FULEA, Relations between the electronic structure and reactivity of some thioamides. II. UV and IR spectra . . . 1513—1520

В. В. КОРШАК, А. И. ПАВЛОВ, Г. МАНДРИК, И. ЗУГРЭВЕСКУ, Полибензимидазолимиды . . . . 1521—1532

V. ARMEANU and ELENA DRĂGUȘIN, Spectrophotometric study of cadmium complex with 6-(6-methoxy-benzothiazol-2-ylazo)-2,4-dichlorophenol . . 1533—1538

Rev. Roumaine Chim. **22**, *11—12*, p. 1431—1571 1977. Bucarest

R **T. HODIŞAN and C. LITEANU, Optimization of the separation process in temperature gradient chromatography. I. Determination of the optimum temperature gradient necessary for the separation of certain component mixtures 1539–1542**

COMPTES RENDUS **. 1543–1550**

INDEX DES AUTEURS **. 1551–1563**

INDEX DES SUJETS **. 1564–1571**

Revue Roumaine de Chimie, **22**, *11—12*, 1433—1439 (1977)

A RELATION FOR THE VISCOSITY OF IONIC LIQUIDS

I. G. MURGULESCU and C. MISDOLEA
Centre of Physical Chemistry,
Str. Galaţi, 31, Bucharest, Romania

Received December 10, 1976

A relation is suggested for the calculation of viscosity in the particular case of ionic liquids, starting from one of the primary equations of viscosity, established by Eyring. Supposing that the vibration motion of molecules is similar to that of a harmonic oscillator and using Debye's approximation for the crystalline solid, a viscosity equation is established including magnitudes accessible to experiment (θ_D, ρ, etc.) and an adjustable parameter — the activation energy. The values deduced with this relation are compared for some ionic liquids with the experimental values of viscosity.

INTRODUCTION

In addition to properties which differentiate them from non-polar liquids (higher electric conductibility and superficial tension, lower molar volumes), for a series of properties — among which viscosity — the ionic liquids have values comparable in magnitude with those found in molecular liquids. For this reason, in the theoretical study of the liquid state, models initially worked out for molecular liquids — e. g. cellular model, free volume theory — could be successfully extended to ionic liquids.

Starting from theoretical considerations on the structure of the liquid and on the mechanism of viscous flow and applying the theory of the transition state, Eyring[1] established as a primary equation of viscosity the relation :

$$\eta = h \frac{\lambda_1}{\lambda_2 \lambda_3 \lambda^2} \frac{E}{F^*} e^{E/RT} \tag{1}$$

where λ_1 λ_2, λ_3 are lattice parameters, λ is the equilibrium distance, F and F^* are partition functions of particles on the volume unit, in normal and activated state, respectively and E is the activation energy of the viscous flow.

---

[1] S. Glasstone, K. J. Laidler and H. Eyring, "The Theory of Rate Processes", McGraw-Hill, London, 1941, p. 483.

If we admit that the flow occurs through ion pairs, then[2]

$$\lambda_2 \lambda_3 = \frac{\sqrt{3}}{2} a^2, \quad \lambda_1 = \frac{\sqrt{3}}{2} a, \tag{2}$$

$$\lambda = a$$

such that:

$$\frac{\lambda_1}{\lambda_2 \lambda_3 \lambda^2} = \frac{1}{a^3} \tag{3}$$

where a is the distance between the nearest neighbours. Liquids, as compared to solids, maintain a short-distance order. This makes it possible to write:

$$\frac{1}{a^3} = \frac{\mathfrak{N}}{\gamma V} \tag{4}$$

where V is the molar volume of the liquid, $\mathfrak{N}$ is Avogadro's number and γ is a factor which depends on the liquid structure. Account being taken of the above relations, we can write for viscosity:

$$\eta = \frac{\mathfrak{N} h}{\gamma V} \frac{F}{F^*} \mathrm{e}^{E/RT} \tag{5}$$

In the following, starting from eq. (5), we shall try to deduce a relation for the viscosity of ionic liquids. Supposing that the liquid, similarly to the solid, maintains the prevalence of vibration movements of the particles in relation to the other movements (translation and rotation) and if we suppose that the partition function of the transition state F^* has one freedom degree less than the partition function in the normal state, F, then the F/F^* relation becomes equal to the partition function of a harmonic oscillator:

$$\frac{F}{F^*} = (1 - \mathrm{e}^{-h\bar{\nu}/kT})^{-1} \tag{6}$$

where an average vibration frequency occurs, whose amplitude is to be determined. In the case of ionic liquids where the temperatures of existence in the liquid phase are high, one can obtain a good approximation if only the first two terms are kept in the series development of the exponential from the above relation. We may write then:

$$\frac{F}{F^*} \simeq \frac{kT}{h\bar{\nu}} \tag{7}$$

---

[2] H. Eyring and T. Ree, *Proc. Nat. Acad. Sci. U. S. A.*, **47**, 526 (1961).

Magnitude $\overline{\nu}$ is calculated as a weighted mean of frequencies, after the number of dZ oscillators with a frequency ν. The values of these frequencies range between zero and a maximum value, ν_m, according to Debye's approximation:

$$\overline{\nu} = \frac{1}{3\mathfrak{N}} \int_0^{\nu_m} \nu \, \mathrm{d}Z \tag{8}$$

In Debye's theory of specific heats it is shown[3,4] that there exists the relation:

$$\mathrm{d}Z = \frac{9\mathfrak{N}}{\nu m^3} \nu^2 \mathrm{d}\nu \tag{9}$$

such that for the mean frequency we get:

$$\overline{\nu} = \frac{3}{4} \nu_m \tag{10}$$

Considering equation (10), the ratio of the partition functions F/F^* shown in eq. (7) becomes:

$$\frac{F}{F^*} = \frac{4kT}{3h\nu_m} \tag{11}$$

The maximum vibration frequency can be replaced by the characteristic Debye temperature θ_D if we use the relation which defines this temperature

$$\frac{h\nu_m}{k} = \theta_D \tag{12}$$

Then relation (11) becomes:

$$\frac{F}{F^*} = \frac{4}{3} \frac{T}{\theta_D} \tag{13}$$

We thus have obtained an expression of the ratio of normal and activated partition functions where there occur magnitude accessible to experimental measurements (θ_D determined by specific heats, elastic constants, etc.).

Relation (5) of viscosity, using eq. (13), becomes:

$$\eta = \frac{4\mathfrak{N}h}{3\gamma V} \frac{T}{\theta_D} e^{E/RT} \tag{14}$$

---

[3] A. H. Wilson, "Thermodynamics and Statistical Mechanics", University Press, Cambridge, 1960, p. 153.

[4] A. J. Dekker, "Solid State Physics", McMillan, London, 1962, pp. 41–42.

Diffraction studies with X-radiations have shown that in the case of ionic liquids the $\sqrt{2}$ value for γ is in good agreement with experimental structure data. Moreover $V = M/\rho$, so that we get the final relation of viscosity:

$$\eta = \frac{2\sqrt{2}}{3}\,\frac{\mathcal{N}h}{M}\,\frac{\rho T}{\theta_D}\,e^{E/RT} \tag{15}$$

CALCULATIONS AND RESULTS

To check up relation (15), in addition to the knowledge of density and of the Debye temperature, it is also necessary to know the activation energy E. If experimental data of viscosity satisfy a relation of type (15), i. e. a relation where $\log \eta/\rho T$ is a linear function of $1/T$, then the activation energy can be obtained from the slope of the straight line. Indeed, using experimental data of viscosity and density depending on temperature, we determined (Figs. 1 and 2) the activation energy for ionic liquids for which we also had characteristic Debye temperatures, θ_D.[5,6] According to the way in which activation energy is determined, relation (15) is an equation of viscosity with an adjustable parameter.

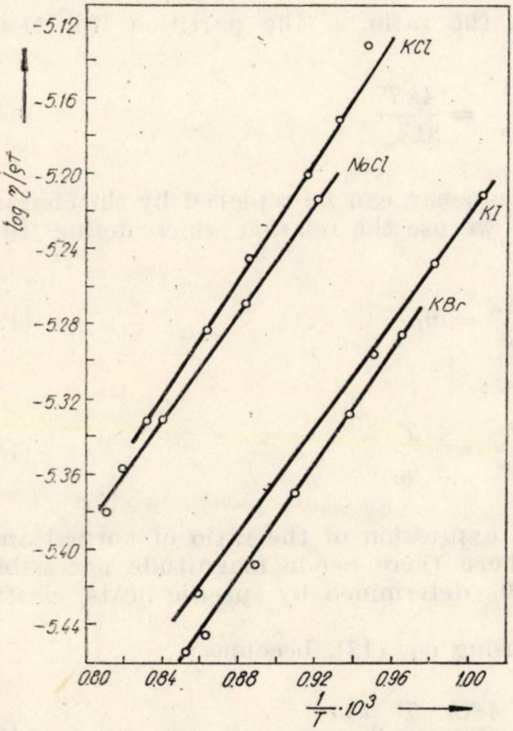

Fig. 1. — Dependence of $\log \eta/\rho\, T$ on $1/T$ for NaCl, KCl, KBr and KI.

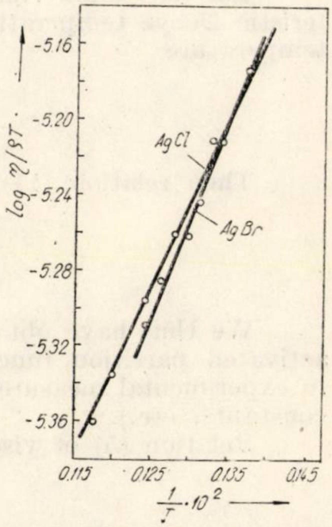

Fig. 2. — Dependence of $\log \eta/\rho T$ on $1/T$ for AgCl and AgBr.

---

[5] A. J. DEKKER, "Solid State Physics", McMillan, London, 1962, p. 44.
[6] K. S. SHOLOBOV and V. A. GRISHUKOV, *Izv. Vyssh, Ucheb. Zaved. Fiz.*, **14,** 58 (1971).

Except for KCl and KI, new data[7,8] were used as experimental values of viscosity, for the determination of which experimental techniques were much improved.

All necessary data are now available to calculate the viscosity with relation (15). The results of calculations, compared with experimental values, are recorded in tables 1–5.

Table 1

Viscosity of NaCl

$E = 6995$ cal/mol $\theta_D = 281$ K

T (K)	ρ (g/cm^3)	$\eta.10^2$ (Poise) exp.[7]	$\eta.10^2$ (Poise) calc.	Δ %
1085.5	1.5481[a]	1.031	0.987	4.3
1133	1.5222	0.931	0.884	5.0
1190.5	1.4909	0.828	0.783	5.4
1220	1.4749	0.792	0.739	6.7
1235	1.4667	0.757	0.718	5.2

[a] Reference [9]

Table 2

Viscosity of KCl

$E = 7380$ cal/mol $\theta_D = 230$ K

T (K)	ρ (g/cm^3)	$\eta.10^2$ (Poise) exp.[10]	$\eta.10^2$ (Poise) calc.	%
1056.4	1.5201[a]	1.172	1.187	1.3
1073	1.5083	1.080	1.107	2.5
1093.6	1.4983	1.030	1.074	4.3
1129	1.4833	0.960	0.987	2.8
1158	1.4606	0.881	0.918	4.2
1201.9	1.4353	0.804	0.836	4

[a] Reference [10]

Table 3

Viscosity of KBr

$E = 7063$ cal/mol $\theta_D = 177$ K

T (K)	ρ (g/cm^3)	$\eta.10^2$ (Poise) exp.[7]	$\eta.10^2$ (Poise) calc.	Δ (%)
1037.2	2.1026[a]	1.132	1.201	6.1
1067.4	2.0778	1.043	1.108	6.2
1100.6	2.0505	0.965	1.020	5.7
1127.7	2.0282	0.895	0.956	6.8
1161	2.0008	0.832	0.887	6.6
1172.9	1.9910	0.816	0.864	5.9

[a] Reference [9]

---

[7] ST. ZUCA and R. BORCAN, to be published.

[8] ST. ZUCA and R. COSTIN, to be published.

[9] ST. ZUCA and L. IONESCU-VASU, *Rev. Roumaine Chim.*, **12,** 1285 (1967).

[10] I. G. MURGULESCU and ŞT. ZUCA, *Rev. Roumaine Chim.*, **10,** 129 (1965).

Table 4

Viscosity of KI

$E = 6788$ cal/mol $\theta_D = 133$ K

T (K)	ρ (g/cm^3)	$\eta.10^2$ (Poise) exp.[11]	calc.	Δ (%)
993	2.4111[a]	1.471	1.274	13.4
1019.7	2.3863	1.380	1.183	14.3
1052.2	2.3561	1.255	1.087	13.4
1117.2	2.2957	1.100	0.931	15.4
1165.2	2.2511	0.990	0.839	15.3

[a] Reference. [9]

Table 5

Viscosity of AgBr

$E = 5384$ cal/mol $\theta_D = 144$ K

T (K)	ρ (g/cm^3)	$\eta.10^2$ (Poise) exp.[8]	calc.	Δ (%)
727	5.5546[a]	2.707	2.338	13.6
744	5.5370	2.537	2.190	13.7
760	5.5204	2.397	2.066	13.8
771	5.5090	2.326	1.988	14.5
789	5.4904	2.248	1.871	16.8
803	5.4759	2.162	1.789	17.3

[a] Reference.[12]

A general observation is the fact that, for all liquids where calculations were made (AgCl included), viscosity decreases with the rise in temperature, in agreement with the variation shown by experimental data. For KCl, the agreement of calculated and experimental values is very good, as illustrated by percentage deviations. For NaCl and KBr, the agreement of theoretical and experimental values is good and for KI and AgBr it is only acceptable. For AgCl, calculated values differ more from the experimental ones (for $T = 850$ K, $\eta_{exp}/\eta_{calc} = 2.08$). Among the liquids where calculations were made, KCl is the most stable and experimental data can be more reliable while KI is a more instable substance, which might affect experimental measurements. For this substance, experimental data ought to be recalculated with new techniques, considerably improved as against the 1965 ones.

---

[11] I. G. Murgulescu and Şt. Zuca, *Rev. Roumaine Chim.*, **10**, 123 (1965).

[12] G. J. Janz, F. W. Dampier, G. R. Lakshminarayanan, P. K. Lorent and R. P. T. Tomkins, "Molten Salts", Vol. 1, NSRDS-NBS 15, U. S. Government Printing Office, Washington, 1968, p. 70.

As shown in a previous work,[13] molten salts can be real ionic liquids formed exclusively of free ions (Na, K, Rb, Cs halides and nitrates) or liquids with a mixed character, where, in addition to ionic bond there also exists a covalent bond (Ag, Cu halides, etc). The values of viscosity calculated with relation (15) seem to confirm this fact, since it is for AgCl that no agreement with experimental data could be obtained. This might be due to the presence of covalent bonds in a proportion that might be considerable.

The presence of these bonds to a lower extent in the case of AgBr might account for the satisfactory agreement of calculated and experimental values. For the substantiation of a positive opinion in this connection, theoretical calculations for a higher number of substances of the two discussed categories as well as new experimental data determined with improved calculations might be necessary.

Acknowledgement. Thanks are expressed to Dr. Stefania Zuca for making available unpublished data.

---

[13] I. G. Murgulescu, *Rev. Roumaine Chim.*, **14**, 965 (1969).

Revue Roumaine de Chimie, **22**, *11-12*, 1441—1446 (1977)

A SPECTROSCOPIC STUDY OF IODINE COMPLEXES WITH SOME HETEROCYCLES IN THE AZOLES SERIES

MARIANA CIUREANU and V. E. SAHINI
Physical Chemistry Department, Polytechnical Institute of Bucharest, Bucharest,
Bd. Republicii 13, Romania

Received October 8, 1976

Spectroscopic studies are reported for iodine complexes with several heterocycles in the azoles series : imidazole, benzimidazole, 2-methylbenzimidazole, 1-[H]-benzotriazole and benzoxazole. The shift of the iodine visible band has been investigated in several solvents and the effect of the polarity of the solvent has been discussed. From the position of the charge transfer band it was concluded that these complexes are of an $n-\sigma$ type. The measured absorbance of the iodine visible band in the complexes has been analysed by the Liptay procedure to give K_f and ε ; measurements at different temperatures gave ΔH_f^0 and ΔS_f^0. The experimental data were compared with the theoretical data calculated by an original method.

1. INTRODUCTION

Heterocycles of the azoles series have well-known donor properties, [1-3]; however, there are not reports on complexes formed with typical acceptors such as iodine. Therefore, the purpose of the present paper is to investigate the spectral, thermodynamic and structural properties of the molecular complexes formed by iodine with some of these heterocycles : imidazole, benzimidazole, 2-methylbenzimidazole, 1-[H]-benzotriazole and benzoxazole. Besides, we were concerned with the problem of establishing the extent to which the electronic structure of the donor molecule influences the properties of the complex.

---

[1] M. Ciureanu and V. E. Sahini, *Rev. Roumaine Chim.*, **20**, 1205 (1975).

[2] [a] K. M. Iunusov, N. L. Fursova, A. D. Garnovskii, I. B. Kolodiajnîi and O. A. Osipov, *Zhur. obshchei Khim.*, **41**, 1128 (1971).

[b] K. M. Iunusov, A. D. Garnovskii, O. A. Osipov and N. D. Vitkevitschi, *Zhur. neorg. Khim.*, **15**, 1802 (1970),

[c] A. D. Garnovskii, O. A. Osipov, V. T. Paniuskii and A. F. Potarskii, *Zhur. obshchei Khim.*, **36**, 1063 (1966),

[d] V. T. Paniuskii, A. D. Garnovskii, O. A. Osipov, A. L. Siniavin and A. F. Pojarskii, *Zhur. obshchei Khim.*, **37**, 312 (1967).

[3] a) P. Linda, *Tetrahedron*, **25**, 3297 (1969),
b) W. C. Aten and K. Buechel, *Z. Naturforsch B*, **25**, 961 (1970),
c) H. Walba and V. R. Ruiz, *J. Org. Chem.*, **34**, 3315 (1969).

2. EXPERIMENTAL SECTION

The donors were synthetized and purified according to literature data.[4] The solvents were purified according to standard procedures; iodine was resublimed and stored in a dark bottle until use. The solutions were freshly prepared before use.

The spectra were recorded in the region 600—220 nm with an Unicam SP 800 spectrophotometer. The quartz cells (0.1, 1 and 2 cm) were used in the temperature regulated cell holder; the temperature in the cells could be controlled to ± 0.2° over a range from 16° to 50°.

3. RESULTS AND DISCUSSION

3.1. SPECTRA

The visible and ultraviolet spectra of the complexes were investigated in the region 600—220 nm. In the 600—260 nm region, the spectra were recorded in a series of solvents of increasing polarity: chloroform, methylene chloride, ethylene dichloride, acetonitrile. Below 260 nm, owing to the solvent absorbance, the spectra could be recorded in methyelene chloride only. Our results are presented in tables 1 and 2.

Table 1

The blue shifted visible band of iodine in the complex (in nm)

Complex	Solvent			
	$CHCl_3$ $\varepsilon=4.81$	CH_2Cl_2 $\varepsilon=9.08$	$C_2H_4Cl_2$ $\varepsilon=10.66$	CH_3CN^a $\varepsilon=36.01$
Imidazole — I_2	370	368	365	361
2-Methylbenzimidazole — I_2	386	382	380	362
Benzimidazole — I_2	394	385	378	362
1-[H]-Benzotriazole — I_2	414	408	372	365
Benzoxazole — I_2	425	423	410	362

[a] The absorbance of the sample solutions in CH_3CN was measured relative to a reference cell containing a matching solution of iodine.

Table 2

Experimental and calculated CT spectra (in nm)

Complex	$\lambda_{exp}(nm)$	$\lambda_{calc}(nm)$
Imidazole — I_2	236	241
2-Methylbenzimidazole — I_2	237	242
Benzimidazole — I_2	234	242
Benzotriazole — I_2	239	230
Benzoxazole — I_2	238	227

As seen from these tables, there are several important spectral changes occurring on complex formation:

i) a large blue shift of the iodine visible band (situated at 520 nm in inert solvents). A typical spectrum in this region is presented in figure 1 : the 2-methyl benzimidazole-I_2 complex in chloroform ; the absorption at 510 nm decreases as the donor concentration increases and a new band develops at lower wavelengths, with the appearance of a sharp isosbestic point.

---

[4] E. Wundt, *Ber. dtsch. chem., Ges.*, **11**, 826 (1878),
O. Ladenburg, *Ber dtsch. chem. Ges.*, **10**, 1123 (1877).

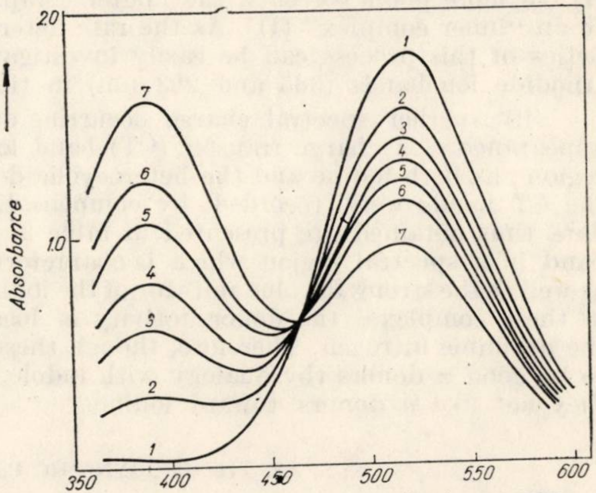

Fig. 1. — The blue shifted band iodine ($CI_2 = 1.9 \cdot 10^{-3}$ mole/l) with various concentrations of 2-methyl-benzimidazole :
2) $1.43.10^{-3}$ mole/l ;
3) $2.85.10^{-3}$ mole/l ;
4) $3.58.10^{-3}$ mole/l ;
5) $4.66.10^{-3}$ mole/l ;
6) $5.37.10^{-3}$ mole/l ;
7) $7.16.10^{-3}$ mole/l.

As seen from table 1, the magnitude of the blue shift increases with the solvent polarity.

The data presented in table 1 are given for large excess of the donor component. If the concentration of the donor is lowered, the band will exhibit a further blue shift. This shift is hardly noticeable in chloroform ; in more polar media, like methylene chloride, ethylene dichloride, acetonitrile, the limiting value of this shift is at about 360—365 nm, which is the characteristic absorption of the I_3^- ions in solution. [5] The existence of triiodide ions in solution is also confirmed by the appearance of a second characteristic ultraviolet absorption at about 293 nm. Therefore, we conclude that the polarization of the iodine molecule in the complex increases to the extent where a clear-cut separation of charges occurs with the resulting formation of triiodide ion. By analogy with other $n-\sigma$ complexes, [6] we conclude that the following reactions occur between the heterocyclic donors (B) and iodine in solution :

$$\underset{}{B + I_2} \rightleftharpoons \underset{\text{I}}{B \cdot I_2} \qquad \text{fast (1)}$$

$$B \cdot I_2 \rightarrow \underset{\text{II}}{(B - I)^+ I^-} \qquad \text{slow (2)}$$

$$(B-I)^+I^- + I_2 \rightleftharpoons \underset{\text{III}}{(B-I)^+} + \underset{\text{IV}}{I_3^-} \qquad \text{fast (3)}$$

---

[5] A. I. Popov and R. F. Swensen, *J. Amer. Chem. Soc.*, **77**, 3724, (1955).

[6] a) R. S. Mulliken and C. Reid, *J. Amer. Chem. Soc.*, **76**, 3869 (1954),
b) S. N. Bhat and C. N. Rao, *J. Amer. Chem. Soc.*, **88**, 3216 (1965),
c) P. Klaboe, *Acta Chem. Scand*, **18**, 27 (1964),
d) B. Muslin, W. J. Jones and M. J. Bleen, *J. Inorg. Nuclear Chem.*, **26**, 239 (1964).

In chloroform, except for imidazole — I_2, the only stage of the reaction is (1), leading instantaneously to the formation of an "outer complex" (I). In more polar solvents, the "outer complex" is partly transformed to an "inner complex" (II). As the rate determining stage is (2), the kinetics of this process can be easily investigated by the increase of the triiodide ion bands (365 and 293 nm) in time.[7]

ii) Another spectral charge occurring on complex formation is the appearance of a charge transfer (CT) band located in the 230–240 nm region; as both iodine and the heterocyclic donors absorb in this region, the CT bands were recorded by compensating for both of them. The data thus obtained are presented in table 2. The appearance of the CT band in a spectral region which is characteristic for $(n-\sigma)$ complexes,[8] as well as the strong for blue shift for of the iodine visible band, show that in these complexes the donor activity is located at the lone pair of the pyridinic nitrogen. Therefore, though these heterocycles are expected to be good π donors (by analogy with indole, pyrrole and benzofurane), they act like n donors toward iodine.

3.2. THERMODYNAMIC PARAMETERS

The thermodynamic constants were evaluated from the shifted visible iodine band for benzimidazole I_2, 2-methylbenzimidazole-I_2, 1-[H]-benzotriazole–I_2 and benzoxazole–I_2 in chloroform.

The formation constants K_f and the molar absorptivities were obtained at several temperatures between 16° and 43° following the Liptay procedure[9]; the values of K_f were computed using a program for the Liptay procedure (in Fortran IV for the IMB 360 computer).

The ΔH_f^0 and ΔS_f^0 for these complexes were evaluated from a Van't Hoff plot of the values of K_f at different temperatures *vs.* $1/T$. The data thus obtained are shown in table 3. As seen from the data presented in tables 1 and 3 the stability of the complex is the greater when the blue shift of the visible iodine band is larger.

Table 3

Thermodynamic parameters

Complex	$K_{298°}$ (l/mole)	ε	$-\Delta G_f^0$ (kcal/mole)	$-\Delta H_{f_f}^0$ (kcal/mole)	$-\Delta S_f^0$ e. u.
2-Methylbenzimidazole$-I_2$	314	2100	3.48	7.72	14,44
Benzimidazole$-I_2$	27.2	3530	2.09	7.26	17.37
Benzotriazole$-I_2$	2.59	920	0.56	2.85	7,69
Benzoxazole$-I_2$	0,995	2000	-0.002	2.63	8.84

---

[7] M. Ciureanu, unpublished results.

[3] E. N. Gurianova, I. P. Goldstein and I. P. Room, "Donorno actzeptornaia Sviazi", Izd. Khimia, Moskva, 1973.

[9] G. Briegleb "Elektronen Donator Acceptor Complexe" Springer Verlag, Berlin, 1961.

A comparison of the stabilization energies in the series under consideration shows that a CH_3 introduced in the position 2 of benzimidazole produces an increase in the donor ability of the molecule, whereas on azasubstitution in the same position the donor ability is lowered. If the pyrrolic nitrogen is replaced by oxygen, a marked decrease of the donor capacity of the molecule is observed. The same features were noted in the series of pK_a values of these molecules, as well as for the calculated n ionization potentials I_n calc.[10]

4. THEORETICAL PART

An original method proposed in a preceding paper[1] was used to investigate the electronic structure of the following complexes: imidazole—I_2, benzimidazole—I_2, 1-[H]-benzotriazole—I_2, benzoxazole—I_2. The n ionization potentials of the donors were calculated as shown in ref.[10]; we made use of the π electronic charges calculated by the PPP SCF MO method.

The σ atomic charges were calculated by Del Re's procedure.[11] The N—I distance was considered to be 2.31A in all cases, the same as for other iodine complexes with azaheteroaromatic donors. The intermolecular resonance integral β_{NI} was calculated by the formula:

$$\beta_{NI} = \frac{1}{2} K (W_N + W_I)\ S_{NI}$$

where W_N and W_I are the ionization potentials of nitrogen and iodine and S_{NI} is the ovelap integral calculated after Mulliken.[12]

The theoretical charge transfer spectra are presented in table 2, together with the experimental data. As seen from this table, the agreement between the calculated and experimental values is very good in all cases. The calculated stabilization energies are much higher than the experimental ΔH_f^0 values; fortunately, they seem to predict very well the experimental order of variation in the series under consideration

ΔH^0-imidazole $> \Delta H$-^{0}benzimidazole $> \Delta H^0$-benzotriazole $> \Delta\ H^0$-benzoxazole

The same trend is shown by the calculated n ionization potentials which are presented in table 4. We must note that for benzotriazole there were two isomeric complexes taken into account, with iodine located either at N(2) or at N(3) in the five-membered ring; our results plead in favour of the first possibility, which led to a higher stabilization energy for the complex.

---

[10] M. Ciureanu and V. E. Sahini, *Rev. Roumaine Chim.*, **20**, 1037 (1975).

[11] G. Del Re and B. Pullman, *J. Chim. phys.*, **62**, 942 (1965).

[12] R. S. Mulliken, C. A. Rieke, D. Orloff and H. Orloff, *J. Chem. Phys.*, **17**, 1248 (1949).

Table 4

Charge displacements on complex formation and calculated *n* ionization potentials for the donor molecules

Complex	Δq_N	Δq_{I_1}	Δq_{I_2}	$\Delta\lambda_{I_2}$ (nm) (in $CHCl_3$)	calc I_n (eV)
Imidazole $-I_2$	-0.1430	-0.0941	$+0.2371$	140	9.33
Benzimidazole $-I_2$	-0.1363	-0.0680	$+0.2043$	106	9.67
Benzotriazole $-I_2$	-0.1158	-0.0628	$+0.1786$	96	9.96
Benzoxazole $-I_2$	-0.1077	-0.0535	$+0.1612$	85	10.41

The calculated charge displacements occurring on complex formation are presented in table 4. As seen from this table, the polarization of the iodine molecule, as well as the total amount of charge transferred by the donor, increase in the same order as the experimental blue shift of the iodine band, that is:

Δq_N-imidazole $>$ Δq_N-benzimidazole $>$ Δq_N-benzotriazole $\geq$ Δq_N-benzoxazole

This observation supports previous theories considering this blue shift to be a consequence of a strong polarization of the iodine molecule in the complex.

Revue Roumaine de Chimie, **22**, *11—12*, 1447—1456 (1977)

THERMODYNAMIC CHARACTERIZATION OF SOME BINARY SOLUTIONS OF NON-ELECTROLYTES, BY A CELLULAR MODEL WITH HOLES

RODICA VÎLCU and SANDA SAMSON
Institute of Chemistry, Department of Physical
Chemistry, Bd. Republicii 13, Bucharest, Romania

Received April 17, 1976

Taking as a working basis a cellular model with holes, used by Hlavaty to characterize the solutions constituted of simple molecules, several modifications have been suggested for a more accurate estimation of the distances between molecules, of the number of holes and of the free volumes with a view to extending this model to more complicated non-polar molecules. An improved formulation of the partition function led to results consistent with the experiment of certain thermodynamic quantities. Tests were achieved by computation of Helmholtz's free energy, of the excess internal energy and of the compressibility in the case of systems : $CCl_4+C_6H_6$, $CCl_4+C_6H_{12}$, and $C_6H_6+C_6H_{12}$ for various values of molar fractions. By so doing, the premises were created for the formulation and verification of state equations of the solutions under study.

INTRODUCTION

This paper presents the ways of improving the peculiarities of a cellular model with holes, applied with satisfactory results to the thermodynamic characterization of some binary solutions consisting of molecules of liquids with similar dimensional and energetic characteristics.

The theory of cells with holes [1] offers a working model for liquids, much closer to the physical reality than the Lennard-Jones and Devonshire (L. J. D)[2] cellular model, by diminishing the absoluteness of the characteristic features of solids in the theories of lattices and introducing elements specific to the liquid phase.

Even if the statistical valorization of mixing and excess functions according to the L. J. D. model offers advantage of partial compensation ot the errors occurring at statistical characterization of individual liquids, the strict estimation of such functions however requires the introduction of a more advanced model of liquids.

EXTENSION OF THE CELLULAR MODEL WITH HOLES OF THE INDIVIDUAL LIQUIDS TO THE TREATMENT OF SOLUTIONS

The correct treatment of solutions according to models requires precise knowldege of the interaction forces between the molecules of the systems, capable of reflecting the peculiarities occurring at their constitution. We however remark the approximate character of the estimation of certain quantities specific to the solution, generally obtained by conventional rules which do not entirely correspond to their behaviour.

---

[1] J. S. Rowlinson and C. F. Curtiss, *J. Chem. Phys.*, **19**, 1519 (1951).

[2] J. E. Lennard Jones and A. F. Devonshire, *Proc. Roy. Soc.* (*A*), **163**, 53 (1937).

The cellular model with holes for individual liquids was extended to the solutions given by Hlavaty, [3] by using Henderson's assumption concerning the linear dependence of the free volume on the number of neighbouring holes. Two models were developed, according to one of the following hypotheses :

a) The cells of the model are equal to those of the binary mixture components and

b) the cells of the model have sizes specific to each component of the binary mixture.

These versions of the theory supply similar results if the systems consist of molecules of nearly equal sizes.

PECULIARITIES OF THE CELLULAR MODEL WITH HOLES IN THE SOLUTIONS

The analysis of the cellular model with holes of the solutions consisting of molecules with similar properites, suggested by Hlavaty, reveals some deficiencies. With a view to present some ways of improving this model, as well as their consequences upon the computed quantities, we shall synthetically expound the peculiarities of Hlavaty's model, by assuming that Henderson's version of the cellular model with holes for a singular liquid with a configurational partition function, Q, is known and equal to :

$$Q(N, V, T) = \frac{L\,!}{N\,!(L-N)\,!}\exp\left[-\frac{N\psi(0)}{2kT}\right]^{N} v_f(y, q, T) \tag{1}$$

where L is the number of cells into which volume V of the liquid is divided, N is the number of molecules ($L > N$), T the absolute temperature, k the Boltzmann constant, $\psi(0)$ is the potential energy of a molecule and v_f, the free volume accessible to the latter.

In order to determine the potential energy of a molecule in the field of its immediate neighbours, the Lennard-Jones 6–12 potential of interaction was used :

$$\psi(0) = 4\,zy\varepsilon\left[\left(\frac{\sigma}{a}\right)^{12} - \left(\frac{\sigma}{a}\right)^{6}\right] \tag{2}$$

where z is the coordination number, a the distance between two neighbouring molecules, y the molecule fraction in the liquid and ε and σ the potential parameters.

---

[3] K. Hlavaty, *Coll. Czech. Chem. Comm.*, **35,** 3666 (1970).

For the free volume, Henderson[4] assumes its linear dependence on the hole fraction, the knowledge of the free volume in the absence of the holes $v_f(1, q, T)$ and the cell size, q:

$$v_f\,(y, q, T) = yv_f\,(1, q, T) + (1-y)q \tag{3}$$

To the free volume in the absence of the holes, an approximate expression is substituted, that is valid for the systems of rigid spheres

$$v_f\,(1, q, T) = \frac{4\pi}{3}\,(a-\sigma)^3 \tag{4}$$

The extension to the solutions of the cellular model with holes was based in the first version (Hlavaty) on the fact that volume V is fulfilled by two different types of molecules, N_1 and N_2 and is divided into L cells with $L > N_1 + N_2$. Consequently, a lattice of cells was conceived, the cells being empty or containing one molecule each of them, the cell volume being $q = \frac{V}{L}$, for which, on the assumption of a random mixing of molecules and holes, in Bragg-Williams approximation, the following configurational partition function was deduced:

$$Q = \frac{\mathrm{L}\,!}{N_1\,!N_2\,!(\mathrm{L}-N)\,!}\exp\left[-\frac{N_1\psi_1(0) + N_2\psi_2(0)}{2kT}\right]^{N_1} v_{f_1}(y, q, T)^{N_2}\, v_{f^2}(y, q, T) \tag{5}$$

where:

$$V = Nv = Lq \tag{6}$$

$$y = \frac{N}{L} = \frac{q}{v} \tag{7}$$

$$q = a^3\sqrt{2} \tag{8}$$

$$\psi_i(0) = 4zy\,\varepsilon_{x_i}\left[\left(\frac{\sigma_{x_i}}{a}\right)^{12} - \left(\frac{\sigma_{x_i}}{a}\right)^{6}\right] \tag{9}$$

$$\varepsilon_{x_i} = \frac{\sum\limits_{j=1}^{2} x_j\,\varepsilon_{ij}\,\sigma_{ij}^6}{\sum\limits_{j=1}^{2} x_j\,\varepsilon_{ij}\,\sigma_{ij}^{12}}\,; \qquad \sigma_{x_i}^6 = \frac{\sum\limits_{j=1}^{2} x_j\,\varepsilon_{ij}\,\sigma_{ij}^{12}}{\sum\limits_{j=1}^{2} x_j\,\varepsilon_{ij}\,\sigma_{ij}^{6}} \tag{10}$$

$$\varepsilon_{12} = (\varepsilon_{11}\,\varepsilon_{22})^{1/2}\,; \qquad \sigma_{12} = \frac{\sigma_{11} + \sigma_{22}}{2} \tag{11}$$

$$v_{f_i} = \frac{4\pi}{3}\,y(a-\sigma_{x_i})^3 + (1-y)q \tag{12}$$

---

[4] D. Henderson, *J. Chem. Phys.*, **37**, 631 (1962).

The cellular volume, q, and the volume per molecule, v, were deduced from the minimizing condition of the free energy with regard to q, respectively to v:

$$\left(\frac{\partial E}{\partial q}\right)_{v,T,x_i} = 0; \quad \left(\frac{\partial E}{\partial v}\right)_{T,x_i} = 0 \tag{13}$$

The second version of the cellular model with holes considers, the differences between the molecules of the two components, by considering that the mixture volume is divided into L_1 cells of volume q_1 and L_2 cells of volume q_2, according to relation:

$$V = L_1 q_1 + L_2 q_2 = N_1 v_{x_1} + N_2 v_{x_2} \tag{14}$$

The computation method is followed, as described in the first version of the model, but assuming moreover that:

$$\frac{q_1}{q_2} = \frac{v_{x_1}}{v_{x_2}} = \frac{\sigma_{x_1}^3}{\sigma_{x_2}^3} \tag{15}$$

The two versions of the cellular model with holes, described by Hlavaty, lead to similar values of the excess functions of the binary mixtures consisting of molecules of the same size. The models do not supply satisfactory values for mixtures consisting of molecules of various sizes; this shortcoming is largely due to the computation method applied to the determination of the potential parameters of the solution components.

However the computations emphasized that the percentage of empty cells in the neighbourhood of an occupied cell is equal to 10–20%, which brings a significant contribution to the thermodynamic properties of the solutions, their contribution to the free volume of a molecule is not accurately conveyed by relation (12).

This constitutes an additional element of error in the estimation of the mixture quantities that depend on the volume.

The rectifying and extension of the cellular model with holes to the solutions consisting of non-polar complicated molecules.

The cell theory with holes of the binary mixtures formed by equal cells was corrected by us, by a more accurate estimation of the distances between molecules and of the number of holes and free volumes, with a view to extending the model to more complex non-polar molecules. As a consequence, the partition function was improved by taking a few surmises into account. Thus, from the theory of significant structures [5], we took over the approximation of the fraction of molecules and holes by means of the molar volume of the solid at the melting point, i. e. the molar volume of the liquid:

$$y = \frac{V_s}{V}\ ; \quad 1 - y = \frac{V - V_s}{V} \tag{16}$$

---

[5] H. Eyring, T. Ree and N. Hirai, *Proc. Nat. Acad. Sci. U. S. A.*, **44**, 683 (1958).

This approximation is justified by the possibility of the occurrence in the lattice of a hole number, proportional to the volume increase associated with the transformation of the solid into liquid, but neglecting the contribution of the cellular volume increase to t is change.

The second hypothesis supposes a sufficiently compact organization of the molecules for determining a minimum value of the potential energy of the system. As a result, distance *a* between any two molecules in the lattice can be estimated with the help of the minimization condition of the potential energy of the system.

$$\frac{\partial}{\partial a}(x_1\psi_1 + x_2\psi_2) = 0. \tag{17}$$

The hypothesis is correclty adopted, the more so as the kinetic energy of the molecules which could make translation motions into the neighbouring holes is independent of distance *a*.

Lastly, a third consideration consists in improving the technique of the correlation between the free volume and the fraction holes especially concerning the systems formed by molecules with more complex structure. An expression of the type of equation (3) that reproduces the linear dependence of the free volume on the fraction of holes has an arbitrary character and a validity limited to quite simple systems. Its application emphasizes too great a dependence of the computed thermodynamic properties upon the number of holes, in disagreement with the experiments. As a result, we suggested a more suitable dependence of the free volume of the molecules upon the fraction of the empty molecules, in the form:

$$V_{fi}(y, q, T) = \left[\frac{4\pi}{3}\, y(a - \sigma_{xi})^3 + (1 - y)q\right]^{1/2} \tag{18}$$

We specify that relation (18), although preserving the empriric feature presented by former formulations, describes better the real behaviour ot the molecules in solutions; the fact was estabilished by comparing the calculated properties with the experimental ones.

RESULTS AND DISCUSSIONS

In agreement with the modifications suggested by us the cellular model with holes was applied in the new form to binaries $CCl_4 + C_6H_6$, $CCl_4+C_6H_{12}$ and $C_6H_6+C_6H_{12}$ and a few thermodynamic excess functions as well as the compressibilities of the systems were calculated with satisfactory results. At the same time, the premises were created for the formulation and verification of state equations of these systems. Taking into account the partition function established by these models and the general equations of certain thermodynamic quantities, some relations were deduced for certain quantities of the mixture, such as Helmholtz's free energy, the internal energy and the compressibility:

$$F = RT(x_1 \ln x_1 + x_2 \ln x_2) + RT\frac{V}{V_s}\left[\frac{V_s}{V}\ln\frac{V_s}{V} + \left(1-\frac{V_s}{V}\right)\ln\left(1-\frac{V_s}{V}\right)\right] + $$

$$+\frac{N}{2}\left[x_1\psi_1(0) + x_2\psi_2(0)\right] - RT(x_1 \ln V_{f_1} + x_2 \ln V_{f_2}) \qquad (19)$$

$$E = RT^2\left(\frac{(\partial \ln Q}{\partial T}\right)_v = \frac{N}{2}\left[x_1\psi_1(0) + v_2\psi_2(0)\right] \qquad (20)$$

$$C_p = -\frac{1}{v}\frac{1}{\left(\frac{\partial P}{\partial V}\right)_T} \qquad (21)$$

$$\left(\frac{\partial P}{\partial V}\right)_T = -\frac{RT}{V_s}\frac{1}{V-V_s} - \frac{2N}{V^2}\left[X_1\psi_1(0) + X_2\psi_2(0)\right] -$$

$$-\frac{RT}{N^2}\sum_{i=1}^{2}\frac{X_i}{\left[\frac{4\pi}{3}(a-\sigma_{x_i})^3 + \frac{V-V_s}{N}\right]^2 + \frac{RT}{V^2}} \qquad (22)$$

The excess quantities, Y^E, were computed by means of their equations of definition:[6]

$$Y^E = Y - Y^{id} \qquad (23)$$

where Y is a generalized function.

In the particular case of Helmholtz's free energy

$$F^E = F + RT(x_1 \ln x_1 + x_2 \ln x_2) - (x_1F_1 + x_2F_2), \qquad (24)$$

where the values corresponding to the pure components are deduced from the boundary values of the functions for $x_1=0$ and $x_1=1$. We mention that Lennard-Jones parameters, ε and σ, of the mixture components were computed by relations (10) and (11), while the molar volumes of the liquids as well as the molecule fractions, y, in the solution at various compositions were estimated by relatios:

$$V = x_1V_1 + x_2V_2 + V^M \qquad (25)$$

$$y = x_1y_1 + x_2y_2 \qquad (26)$$

---

[6] R. Vîlcu, "Termodinamică chimică", Ed. Tehnică, Bucureşti 1975.

The quantities corresponding to the pure components entering the present computations, are recorded in table 1.

Table 1

Parameters of the pure components necessary for estimating some thermodynamic quantities

Component	σ(A)	ε/k (K)	V_s (cm^3)
C_6H_6	5.628	335	77
CCl_4	5.881	327	88.66
C_6H_{12}	6.093	324	99.81

The excess functions and the compressibilities of the three mixtures, estimated for various compositions, were compared with the values supplied by Hildebrand and Scatchard[7] and by Wood[8] as well as by the theory of significant structures[9], in tables 2–4.

Table 2

Computed and observed excess energies at V = constant (T = 298.16 K) for the system $CCl_4 + C_6H_6$

x_{CCl_4}	F^E cal/mol			E^E cal mol				
	Calc.[9]	Calc.*	Exp.[10]	Calc.[7]	Calc.[8]	Calc.[9]	Calc.*	Exp.[10]
0.1	6.3	9.1	7.1	2.9	2.5	8.9	11.7	10.5
0.2	11.7	15.9	12.6	5.1	5.1	20.1	21.0	18.6
0.3	15.9	18.7	16.5	6.7	7.0	24.7	25.6	24.4
0.4	19.0	20.5	18.8	7.5	8.1	28.6	28.6	27.9
0.5	20.6	20.5	19.5	7.8	8.8	29.1	29.1	29.0
0.6	20.6	18.8	18.7	7.5	8.6	28.6	27.2	27.8
0.7	18.8	16.4	16.3	6.4	7.6	24.9	23.2	24.3
0.8	14.9	11.8	12.4	4.4	5.7	19.0	17.3	18.5
0.9	8.8	5.8	7.0	2.7	2.9	10.7	9.6	10.4

* This work

Let us remark that excess energies, E^E, estimated by means of this model, approximate very well the experimental values corresponding to the solutions of molecules the constants of which, ε and σ, have nearly the same values. These results are fairly higher than those deduced by Hildebrand and Scatchard and by Wood and can be compared with those supplied by the theory of significant structures, which is a praiseworthy model from the standpoint of the numerical results given for the thermodynamic properties while introducing several adjustable parameters.

---

[7] G. B. CARPENTER and R. S. HALFORD, *J. Chem. Phys.*, **15,** 99 (1947).

[8] I. PRIGOGINE, "The Molecular Theory of Solutions", North Holland Publ., Amsterdam, 1957.

[9] KAY LIANG, H. EYRING and R. P. MARCHI, *Proc. Nat. Acad. Sci.*, **52,** 1107 (1964).

[10] S. E. WOOD and J. A. GRAY, *J. Chem. Phys.*, **74,** 3729 (1952).

Table 3

Computed and observed excess energies at V = constant (T = 298.16 K) for the system $CCl_4 + C_6H_{12}$

x_{CCl_4}	F^E cal/mol			E^E cal/mol				
	Calc.[9]	Calc. *	Exp.[10]	Calc.[7]	Calc.[8]	Calc.[9]	Calc. *	Exp.[10]
0.1	5.9	5.3	6.0	1.0	10.0	9.8	6.3	9.0
0.2	10.6	10.5	10.0	2.0	19.0	17.4	11.9	15.0
0.3	13.9	14.0	14.0	3.0	26.0	22.8	16	21.0
0.4	15.9	16.5	16.0	4.0	30.0	26.1	18.7	24.0
0.5	16.5	17.7	17.0	4.0	32.0	27.3	20	25.0
0.6	15.9	17.4	16.0	4.0	32.0	26.2	19.6	25.0
0.7	13.9	16.2	14.0	3.0	29.0	23.0	17.6	22.0
0.8	10.6	12.2	11.0	3.0	23.0	17.6	13.8	17.0
0.9	6.0	6.9	6.0	2.0	14.0	9.9	8	10.0

* This work

Table 4

Computed and observed excess energies at V = constant (T = 298.16 K) for the system $C_6H_6 + C_6H_{12}$

$x_{C_6H_6}$	F^E cal/mol			E^E cal/mol				
	Calc.[9]	Calc.*	Exp.[10]	Calc.[7]	Calc.[8]	Calc.[9]	Calc.*	Exp.[10]
0.1	27	19.6	29	8	29	56	51.1	53
0.2	47	38.5	51	14	52	89	93.1	93
0.3	62	56.8	66	19	69	114	125.4	123
0.4	72	71.5	75	22	82	128	147.6	142
0.5	76	81.4	77	23	86	131	158.9	150
0.6	74	85.0	73	23	85	126	159.0	146
0.7	66	81.0	63	20	78	90	144.0	130
0.8	51	66.5	48	16	63	83	114.0	101
0.9	31	40.9	27	19	38	47	68.0	58

* This work

Computations emphasized the uncommon influence of a suitable choice of the interaction parameters and of the most accurate estimation of the hole percentage in the liquid. We find that an increase of the values of σ, according to sequence C_6H_6, CCl_4, C_6H_{12}, is accompanied by an increase of both molar volumes, V and V_s and the fraction of the molecules in the liquid. It seams therefore that the smaller the molecules, the greater the number of holes appearing in the liquid lattice, although their volume is smaller.

At the time of the solution formation, the ratio between the number of molecules and the number of holes as well as the compact arrangement of the latter in the lattice corresponding to the solution depend both on the sizes of the molecules and cells corresponding to them in pure liquids and on their fractions of holes as well as on the structural resemblances with one another of the molecules characterized by parameters ε and σ. Since with pure components CCl_4 and C_6H_6, respectively CCl_4 and C_6H_{12}, the values of parameters ε, σ and y are close to one another, their correspondents in the solution can be computed according to the additivity rules already described.

In the case of solutions C_6H_6 and C_6H_{12} with great differences between the values of ε, σ and y of the pure components, the y values for various compositions could not be simply computed by the rule of additivity and so a corrective term was introduced in the fundamental relation, proportional to the size difference between molecules, to molar fractions x_1 and x_2 and to the molecular fraction of pure components, y_1 and y_2.

$$y = x_1y_1 + x_2y_2 - \delta x_1x_2\sqrt{y_1y_2}\ ; \quad \delta = \frac{4\pi}{3}\frac{N}{V}(r^3_{x_i} - r^3_{x_2}) \tag{27}$$

$$r_{x_i} = \frac{\sigma_{x_i}}{2}$$

The accuracy of these considerations is revealed by the satisfactory values of excess energy which represent both qualitatively and quantitatively the actual behaviour of the solutions.

As to values F^E of the free energies for various compositions, they correctly approximate the variation with the given composition supplied by experiment of systems $CCl_4+C_6H_6$ and $CCl_4+C_6H_{12}$ and less satisfactorily that for the system $C_6H_6+C_6H_{12}$. On values F^E, a particular influence is exerted by the choice of a rigorous expression of the free volume. For the studied mixtures, equation (18) for the free volume leads to satisfactory results for the values of the excess free energies, but less acceptable for compressibilities. (tables 5—7).

Table 5

Computed and observed compressibilities of the mixture $CCl_4+C_6H_6$

x_{CCl_4}	$\beta\ 10^5$ 1/atm		
	Calc.[9]	Calc.*	Exp.[10]
0.1	8.99	17.55	9.55
0.2	9.1	16.10	9.77
0.3	9.21	14.00	10.03
0.4	9.32	13.50	10.28
0.5	9.41	12.37	10.52
0.6	9.50	11.27	10.77
0.7	9.56	10.19	11.01
0.8	9.61	9.26	11.25
0.9	9.63	8.39	11.50

* This work

Computations have emphasized that a correct relation of dependence of the free volume on the number of holes in the solution cannot ascribe an absolute role to the number of holes even though these bring

Table 6

Computed and observed compressibilities of the mixture $CCl_4 + C_6H_{12}$

x_{CCl_4}	$\beta.10^5$ l/atm		
	Calc.[9]	Calc.*	Exp.[10]
0.1	11.0	7.25	11.0
0.2	10.8	7.29	11.0
0.3	10.7	7.35	11.0
0.4	10.6	7.38	11.0
0.5	10.4	7.41	11.0
0.6	10.3	7.45	11.0
0.7	10.1	7.48	11.0
0.8	10.0	7.50	11.0
0.9	9.8	7.52	11.0

* This work

Table 7

Computed and observed compressibilities of the mixture $C_6H_6 + C_6H_{12}$

x_{CCl_4}	$\beta.10^5$ l/atm		
	Calc.[9]	Calc.*	Exp.[10]
0.1	9.17	9.29	10.03
0.2	9.47	11.42	10.16
0.3	9.77	13.55	10.28
0.4	10.04	15.68	10.39
0.5	10.30	17.26	10.50
0.6	10.54	18.65	10.61
0.7	10.75	19.59	10.71
0.8	10.93	20.02	10.81
0.9	11.08	19.93	10.91

* This work

a significant contribution to the properties of liquids, so that the contributions of their volume should also be taken into account in a more accurate form.

CONCLUSIONS

It can be stated that the version of the cellular model with holes improved by us can be satisfactorily applied to the solutions the components of which are formed by molecules resembling with one another from the standpoint of both their dimensional and energetic characteristics and of the ratio of molecules to holes in individual lattices. For the solutions formed by dissimilar molecules, the version could be applied of a cellular model with holes which takes into consideration the lattice of a solution consisting of two kinds of cells. On the other hand, some additional improvements can be brought by optimizing the computation relation of both the free volume and the number of holes.

Revue Roumaine de Chimie, **22,** *11–12*, 1457–1461 (1977)

SOME RESULTS CONCERNING NICKEL ELECTRODEPOSITION ON THIN FILMS

O. RADOVICI and VIORICA LĂZĂRESCU
Institute of Physical Chemistry, str. Galaţi 31,
Bucharest, Romania

Received July 5, 1975

The cathodic polarization curves for nickel electrodeposition on copper thin films were obtained by means of the single pulse galvanostatic method. The results show that the curve slope and the exchange current density are dependent on the copper thin film thickness.

Thin films are widely used to study the solid/gas interface phenomena appearing in catalyses processes. Up to now thin films are only occasionally used in electrochemistry [1-6].

This paper deals with the influence of copper film thickness, obtained with vacuum evaporation technique, on the electrochemical parameters of the nickel electrodeposition.

EXPERIMENTAL

The experimental goal was to obtain the cathodic polarization curves $i=f(E)$, using the single pulse galvanostatic method.

One has worked with acid solution, pH=3.5, at constant temperature = 60°, because nickel ions do not precipitate too much nickel hydroxide at a pH value smaller than 6, and the deposition and dissolution reactions between metal and its ions can occur without any solid compound interference. To eliminate any traces of impurities the solution has been submitted to a pre-electrolysis for 12 hours at 3 mA/cm^2 current density. The composition of the solution was: $NiSO_4.7H_2O$ ... 240, $NiCl_2.6H_2O$ ... 40, H_3BO_3 ... 30 g/l.

For experiments, a special electrode with eight separate minielectrodes was made (fig. 2) with pure copper (99.99%) evaporation in vacuum and deposition on a steel surface embedded in teflon. Different minielectrodes are chosen for measurements with an electric switch. The Luggin capillary is set up in such a way to permit the whole electrode surface exploration. The thin film thickness was calculated from the total copper amount deposited on a Jena glass rectangular piece, optically polished and placed in vacuum, near the work-

---

[1] G. Trümpler and H. E. Hintermann, *Helv. Chim. Acta*, **11,** 205 (1947).

[2] T. Hagyard, W. B. Earl, J. K. Kirkpatrik and I. G. Watson, *J. Electrochem. Soc.*, **113,** 926 (1966).

[3] R. Piontelli, B. Rivolta and L. Giuliani, *Electrochim. Metal.*, **1,** 3 (1968).

[4] I. Vartires, Studii şi *Cercetări Chim. Acad. R. S. R.*, **18,** 683 (1970).

[5] O. Radovici and M. E. Macovschi, *Rev. Roumanie Chim.*, **16,** 1819 (1971).

[6] M. E. Macovschi, *Studii şi Cercetări Chim. Acad. R. S. R.*, **20,** 849 (1972).

ing electrode. The copper amount was measured spectrophotometrically.[7] A nickel strap was used as auxiliary electrode and a calomel electrode as reference electrode.

The working cell, made from Jena glass, is shown in figure 3, and the general electrical diagram in figure 4. Current pulses were obtained from a rectangular pulse generator type Tacussel and the potential transients have been recorded with an Orion EMG syncroscope equipped with a photographic device.

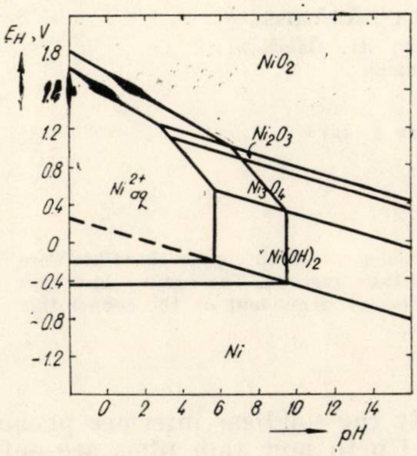

Fig. 1. — Potential/pH diagram for the $Ni-H_2O$ system (after Pourbaix).

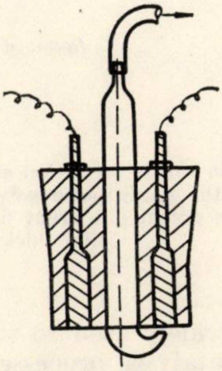

Fig. 2. — Working electrode.

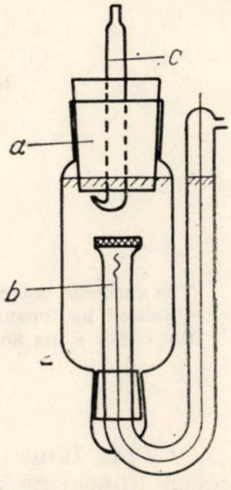

Fig. 3. — Electrolytic cell : *a*, working electrode ; *b*, counter electrode ; *c*, Luggin capillary.

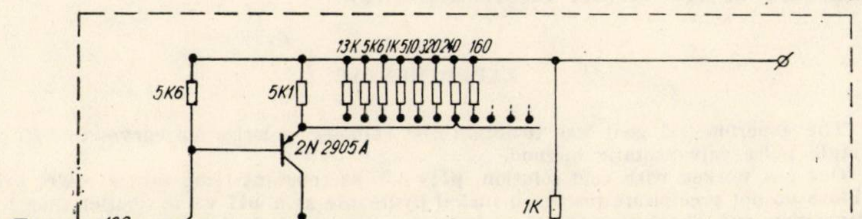
13K 5K6 1K 510 320 240 160
5K6
5K1
2N 2905A
100
2N 2222
Generator
1K
10K
BZ 488
120K
2N 5245
b
c
a
100K
3K9
330
2K7
10K
500µF
mA
Oscilloscope
Oscilloscope

Fig. 4. — Electrical arrangement : *a*, working electrode ; *b*, counter electrode ; *c*, reference electrode.

---

[7] M. E. Macovschi and V. Nițu, *Rev. Roumanie Chim.*, **15,** 605 (1970).

RESULTS AND DISCUSSION

The current density range for the measurements was chosen so as to have a great cathodic deposition efficiency for nickel. This range is from 3 to 14 A/dm², as can be seen from figure 5.

For the cathodic overpotential curves, a Tafel type equation has been used :

$$i = i_0 \exp\left(\eta_a\, z\, F/RT\right) - \exp\left(-\, \eta_c\, z\, F/RT\right)$$

where all symbols have their usual meaning.

In this paper, the kinetic constants **b** and i_0 for the nickel electrodeposition are measured. At the same time, their dependence on the copper film thickness is studied. The experimental data obtained with the galvanostatic method are presented in table 1.

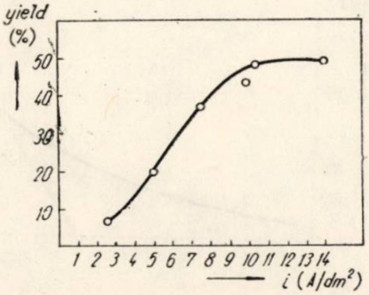

Fig. 5. — The dependence of cathodic deposition efficiency for nickel on current density.

Table 1

Kinetic parameters for the electrodeposition of nickel on thin copper films

Copper film thickness nm	i_0 mA/cm²	log i_0	Polarization curve slope
0	1.55	0.19	120
4.7	3.9	0.60	170
32.3	4.5	0.65	185
52.4	5	0.69	200
79.7	7.6	0.88	315
85.1	17.4	1.24	380
	4.9	0.69	175
96	2.18	0.34	150
	1.58	0.2	125
122	1.4	0.15	115
181	1.90	0.28	125
	0.7	−0.15	85
massive copper	0.025	−1.6	180

The experimental current-potential curves and the b and i_0 values are shown in figure 6. The copper film thickness was 85 nm and the maximum overpotential 200 mV.

Figures 7a and 7b give the results of kinetic constants b and i_0 for different film thickness.

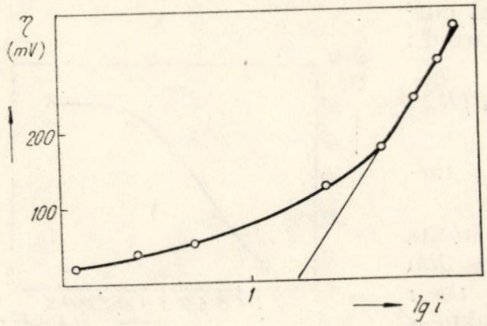

Fig. 6. — The dependence of activation overpotential η(mV) on the logarithm of current density, log i(copper film thickness = 85 nm).

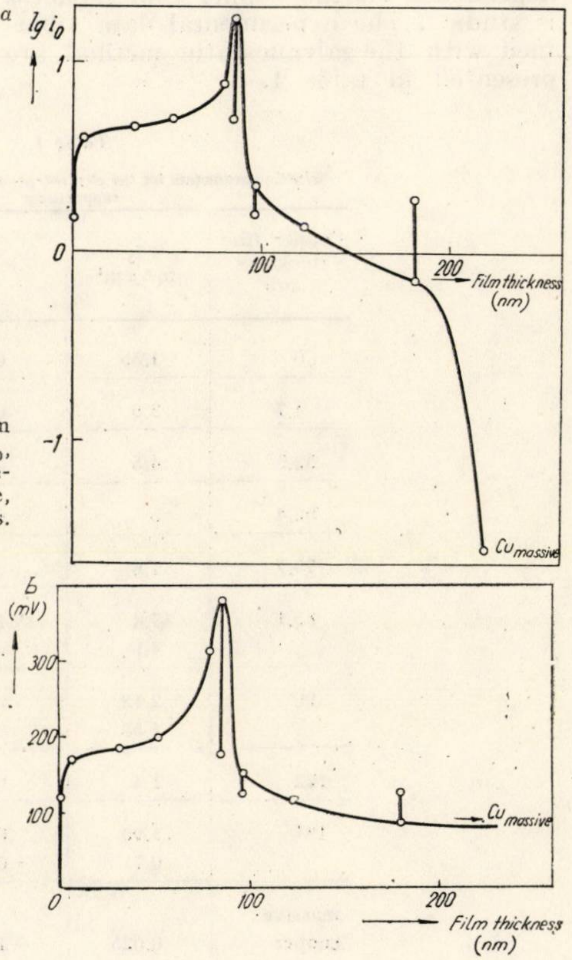

Fig. 7 *a*. — The dependence of logarithm of the exchange current density, log i_0, on copper film thickness; *b*. — The dependence of the polarization curve slope, b(mV), on the copper film thickness.

As can be seen from the experimental results, the exchange current density for nickel electrodeposition is very near the corresponding values for pure steel, if the film thickness is in the range 1—70 nm.

For the film thickness between 80 and 100 nm the exchange current density increases sharply and decreases again for greater copper film thickness, with a tendency towards the value corresponding to the massive copper electrode.

The exchange current density variation with the copper film thickness for values smaller than 70 nm shows that nickel electrodeposition is very weakly influenced by the film thickness. This is why the results are about the same as in the case of a steel electrode. If film thickness is in the range 80—100 nm, the thin film has a clear influence on the nickel electrodeposition. For a film thickness greater than 100 nm this influence is no more present.

The polarization curve slope variation with the copper film thickness was obtained in figure 7b. This is similar with the exchange current density variation.

CONCLUSIONS

Because the exchange current density is correlated with the standard speed of the reaction, the speed of the nickel electrodeposition depends on the copper support thickness. This means, in the case of nickel on steel electrodeposition, that the nickel deposition is faster and the adherence is better, if the copper thickness initially deposited is greater than 70 nm.

Usually, nickel electrodeposition is associated with hydrogen release, because their standard potentials are about the same. This is evident from the great values, sometimes near 380 mV, of the polarization curves slope.

As can be seen from the experimental results, the exchange current density for nickel electrodeposition [illegible] very near the same [illegible] values [illegible] of the film thickness in the range [illegible]—75 nm. [illegible] film thickness between 85 and 100 nm the exchange current density increases sharply and decreases again for greater copper film thickness, which tend to reach the value corresponding to the massive copper electrode.

The exchange current density variation with the copper film thickness [illegible] smaller than 70 nm shows that nickel electrodeposition is not essentially influenced by the film thickness. This is why the results are about the same as in the case of a massive copper electrode. If the film thickness is in the range 80—100 nm, the copper film has a great influence on the nickel electrodeposition. For a film thickness greater than 100 nm this influence [illegible] gradually.

The [illegible] curves show variation with the copper film thickness as outlined in Figure 7b. This is similar with the exchange current density variation.

CONCLUSIONS

[illegible] exchange current density is correlated with the [illegible] of the reaction, the speed of the nickel electrodeposition depends on the copper film thickness. This means, in the case of copper [illegible] electrodes, that the nickel deposition is faster and the adherence is better, if the copper thickness generally deposited is greater than 75 nm.

Usually, nickel electrodeposition is associated with hydrogen release, because their standard potentials are about the same. This is evident from the given values, as high as 700 mV, of the polarization curves slope.

Revue Roumaine de Chimie, 22, 11–12, 1463–1469 (1977)

DIFFUSION OF CADMIUM AND SILVER IONS IN CONCENTRATED AQUEOUS SOLUTIONS OF CALCIUM NITRATE

P. PACÁK and I. SLÁMA
Czechoslovak Academy of Sciences,
Institute of Inorganic Chemistry
Řež near Prague

Received June 5, 1975

Diffusion coefficients of Cd^{2+} and Ag^{+} ions in the system $Ca(NO_3)_2-H_2O$ of various composition were measured within the temperature range 15–60° using chronopotentiometric method. To evaluate the results, the Vogel-Tamann-Fulcher equation describing the temperature dependence of transport phenomena in supercooled liquids has been applied. The results have been compared with those obtained by conductance and viscosity measurements.

A characteristic feature of some concentrated aqueous solutions of electrolytes is their ability to form glasses. For a number of such solutions Angell and Sare [1] have published the concentration ranges of the glass formation in which the viscosity of solutions reaches values of the order of 10^{13} P. In some cases these solutions can remain supercooled for a very long time so that physico-chemical measurements may be performed over a wide range between the thermodynamic melting temperature and the transition temperature of the glass formation.

The fact that most aqueous solutions of a concetration higher than 7 mol % have high viscosity and may be supercooled into the vitreous state motivated the application of the theory and equations of relaxation processes in other liquids forming glasses to these solutions. Angell[2] interpreted the temperature dependence of the conductance of calcium and magnesium nitrate solutions in terms of the empirical Vogel-Tamann-Fulcher equation [3–5] describing the transport property, $W(T)$, of the glass-forming liquids as a function of temperature:

$$W(T)=A.T^{-1/2} \ .\exp\left(-B/(T-T_0)\right) \qquad (1)$$

---

[1] C. A. ANGELL, and E. J. SARE, *J. Chem. Phys.*, **52**, 1058 (1970).
[2] C. A. ANGELL, *J. Phys. Chem.*, **70**, 3988 (1966).
[3] H. VOGEL, *Z. Physyk*, **22**, 645 (1921).
[4] V. G. TAMMANN, and W. HOSSE, *Z. anorg. Chem.*, **156**, 245 (1926).
[5] G. S. FULCHER, *J. Amer. Ceram. Soc.*, **8**, 339 (1925).

where A, B, and T_0 are constants, W is the equivalent conductance (λ), the reciprocal of the viscosity ($1/\eta$), or the ratio of the diffusion coefficient and temperature (D/T), respectively, and T_0 is the temperature at which the ionic mobility equals zero. Equation (1) has also been transformed into an isothermal form[2] by taking into consideration the changes of the three constants in dependence on the composition. However, the real validity of this approach to the interpretation of the properties of concentrated electrolyte solutions has not been completely verified because of the lack of experimental data covering a sufficiently wide range of temperature and composition.

In recent years, therefore, attention has been paid to the study of the temperature dependence of transport properties, especially of viscosity and conductance, in supercooled systems of $Ca(NO_3)_2.H_2O$,[2,6-8] $Mg(NO_3)_2.H_2O$[2] and $Na_2S_2O_3.5H_2O$.[6] The diffusion coefficients of cadmium ions in calcium nitrate tetrahydrate and in its mixture with potassium nitrate were measured polarographically[9] and those of cadmium, thallium, and silver ions also in calcium nitrate tetrahydrate were measured chronopotentiometrically.[10] Lovering[11] studied polarographically the diffusion coefficients of zinc, cadmium, silver, and nickel ions in aqueous melts of $Ca(NO_3)_2.4H_2O$, $CaCl_2.6H_2O$, and $LiNO_3.3H_2O$.

The dependence of the diffusion coefficients on composition of the solvent has not been hitherto examined and is the subject of the present work. We have investigated the temperature dependence of the diffusion coefficients of cadmium and silver ions in the system calcium nitrate—water over the concentration range 2—22 mol % $Ca(NO_3)_2$.

EXPERIMENTAL

Chronopotentiometric method was used to measure the diffusion coefficients of cadmium and silver ions in the system $Ca(NO_3)_2$—water. The diffusion coefficient of the electrochemically active ion i is given by Sand equation

$$D_i = \frac{4I^2\tau}{\pi\mathfrak{F}^2 n_i^2 A^2 c_i^2} \tag{2}$$

where I is the current in amperes, σ the transition time in sec, F the Faraday constant, n_i the number of electrons required for electrolysis, A the electrode area in cm^2, and c_i the concentration of ions in mol/cm^3.

Equation (2) was derived on the asumption that all the current is consumed in the electrolysis. In fact, a part of the current is required to charge the electric double-layer. Some authors[12-14] have paid attention to this problem and found the effect of the double-layer charging to be compensated when measuring the transition time in a proper fashion.

---

[6] C. T. Moynihan, *J. Phys. Chem.*, **70,** 3399 (1966).

[7] J. H. Ambrus, C. T. Moynihan, and P. B. Macedo, *J. Electrochem. Soc.*, **119,** 192 (1972).

[8] C. A. Angell, and R. D. Bressel, *J. Phys. Chem.*, **76,** 3244 (1972).

[9] J. Braunstein, L. Orr, A. R. Alvarez-Funes, and H. Braunstein, *J. Electroanalyt. Chem.*, **15,** 337 (1967).

[10] C. T. Moynihan, and C. A. Angell, *J. Phys. Chem.*, **74,** 736 (1970).

[11] D. G. Lovering, *Coll. Czech. Chem. Comm.*, **37,** 3697 (1972).

[12] M. L. Olmstead, and R. S. Nicholson, *J. Phys. Chem.*, **72,** 1650 (1968).

[13] P. Delahay, and T. Berzins, *J. Amer. Chem. Soc.*, **75,** 2486 (1953).

[14] R. S. Rodgers, and L. Meites, *J. Electroanalyt. Chem.*, **16,** 1 (1968).

Our equipement for the chronopotentiometric measurement of the diffusion coefficients consisted of a 15 cm long test-tube of 3 cm in diameter placed in water thermostate where the required temperature was maintained by means of proportional temperature controller employing a platinum resistance sensor with an accuracy of ± 0.05°. Into the test-tube we weighed approximately 20 g $Ca(NO_3)_2$ with the corresponding water content and approximately 30 mg $Cd(NO_3)_2 . 4H_2$ Oor $AgNO_3$ which, according to the density of the basic electrolyte, corresponded to the concentration of aproximately $7-8.10^{-6}$ mol Cd^{2+} /cm³ or $0.9-1.1.10^{-5}$ mol Ag^+/cm³, respectively. Into the solution in the test-tube there were inserted indicator, counter and reference electrodes, a stirrer made of Teflon and a platinum resistance thermometer. The test-tubes for silver ions experiments were painted black on the outside to prevent the decomposition of Ag^+ ions. For the measurement of the diffusion of cadmium ions we used as cathode a mercury cup electrode, the surface of which was determined by measuring the diameter of the cup and the height of the mercury meniscus. Calculation was made assuming that the mercury surface is spherical-shaped and the electrode area was found to be 1.11 ± 0.04 cm². The counter electrode was a platinum wire of 0.5 mm in diameter placed in a glass tube serving to separate the anodic space. The reference saturated calomel electrode was situated in such a way that its lower end was 1—2 mm over the surface of the mercury cathode in order to obtain the ohmic resistance between the two electrodes as low as possible. When measuring the diffusion coefficients of silver ions, we used as indicator electrode a platinum foil of the surface of 2.53 ± 0.02 cm² and as reference electrode a silver wire 1 mm in diameter.

As constant current source we used a stabilized power supply (200 V) connected in series with two potentiometers of 0.15 MΩ and 33 kΩ serving as adjustable resistors to regulate the current. The magnitude of the current was measured by a digital voltamperemeter NR 50 (Metra Blansko) and the potential-time curves were recorded by a Philips $x-y$ recorder. As time base we used an integrator made of operational amplifier AS 101 (ZPA Trutnov). The pen speed used in recording the chronopotentiograms was 1.4 cm/sec. To eliminate the possibility of influencing the transition time either by the presence of impurities or by dissolved oxygen, we performed repeatedly blank runs both with mercury and silver cathodes on the samples of calcium nitrate to which no reducible cation had been added. Using the same current densities as in the following runs, no transition times were indicated.

PROCEDURE

The solution of cadmium or silver ions in calcium nitrate with the corresponding water content was allowed to temper in a tube dipped in the thermostate to the temperature of about 60°. After measuring the transition time, tempeature was lowered by 8—10° and the measurement was repeated. Temperature was gradually lowered until crystallization of the solution. At each temperature 3—4 runs were performed resulting in transition times not differing from one another by more than 2%. Other runs were made such that after tempering the solution to the temperature of about 60°, we turned off the heating and recorded the chronopotentiograms at continuous cooling of the solution in five-minute intervals, the temperature of the solution being measured simultaneously (see curves 3, 4, and 5 in Fig. 1 and curves 3, 4, and 6 in Fig. 2). Between individual measurements the solution was intensively stirred. The obtained temperature dependences of the diffusion coefficients were the same as in the runs with gradual cooling. Current densities were chosen such that the transition times were not longer than 8 sec.

The used calcium nitrate tetrahydrate from Lachema had to be repeatedly purified by filtration at 60°. Samples with various water content were made up by diluting the original tetrahydrate and the calcium content was determined complexometrically using Kalkon indicator. The silver and cadmium nitrates were used without further purification.

RESULTS AND DISCUSSION

The transition times were evaluated following the method of Delahay and Berzin[13] and the diffusion coefficients were calculated according to equation (2). The concentrations of cadmium and silver ions were calculated from the weight of the components present using the density data of the calcium nitrate-water systems from the paper of Ewing and Mikovsky.[15]

The relative error of the determination of cadmium ion diffusion coefficients, depending primarily on the accuracy of determination of the mercury electrode area and the water content in the solution, was estimated to be approximately 8%. For silver ions where the platinum electrode area can be determined more precisely, the estimated relative error amounts approximately to 5%.

The diffusion coefficients of cadmium and silver ions in calcium nitrate with 4.09 mole H_2O/mole Ca^{2+} at 50° were measured to be 4.10^{-7} cm²/sec and $8.2.10^{-7}$ cm²/sec, respectively. Under the same conditions, Moynihan and Angell[10] obtained the values $3.5.10^{-7}$ and $7.15.10^{-7}$ cm²/sec, respectively. From polarographic measurements, Braunstein and coworkers[9] found the value $3.12.10^{-7}$ cm²/sec for cadmium ions in $Ca(NO_3)_2.4H_2O$ which corresponds to the value $3.4.10^{-7}$ in $Ca(NO_3)_2.4{,}09\ H_2O$. Lovering[11], on the other hand, found the polarographically-measured diffusion coefficient of cadmium and silver ions in calcium nitrate tetrahydrate to be somewhat lower ($2.45.10^{-7}$ and $2.15.10^{-7}$ cm²/sec at 50° respectively).

From experimental data we evaluated the parameters A and B of equation (1) for variously concentrated solutions of calcium nitrate by inserting into the equation the T_0 values determined by conductance measurements given in paper[16]. After linearizing the equation, parameters were calculated by the least squares treatment. Figs 1 and 2 show the diffusion coefficient versus temperature dependences (full line) for Cd^{2+} and Ag^+ ions, respectively, calculated from equation (1) together with experimental coefficient measurement of cadmium ions is not greater than 6% and that of silver ions does not exceed 3%. As it has been

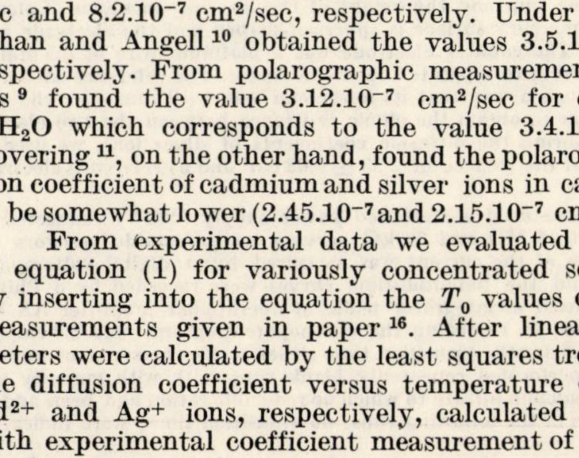

Fig. 1. — Temperature dependence of diffusion coefficients of cadmium ions, $D_{Cd^{2+}}$ (cm² sec^{-1}), in $Ca(NO_3)_2-H_2O$ system (curves 1 to 7 correspond to 20.75, 19.05, 17.64, 13.40, 12.14, 6.15, and 2.00 mol% $Ca(NO_3)_2$, respectively).

---

[15] W. W. Ewing, and R. J. Mikovsky, *J. Amer. Chem. Soc.*, **72**, 1390 (1950).
[16] R. Bressel, Ph. D. Thesis, Purdue University, 1972.

noted above, the magnitude of the error is connected primarily with the accuracy in determining the area of the electrode. Fig. 3 shows the dependence of the diffusion coefficients on the composition of calcium nitrate solution. The dependences of parameters *A* and *B* on the composition are displayed in Fig. 4. It can be seen from this figure that the

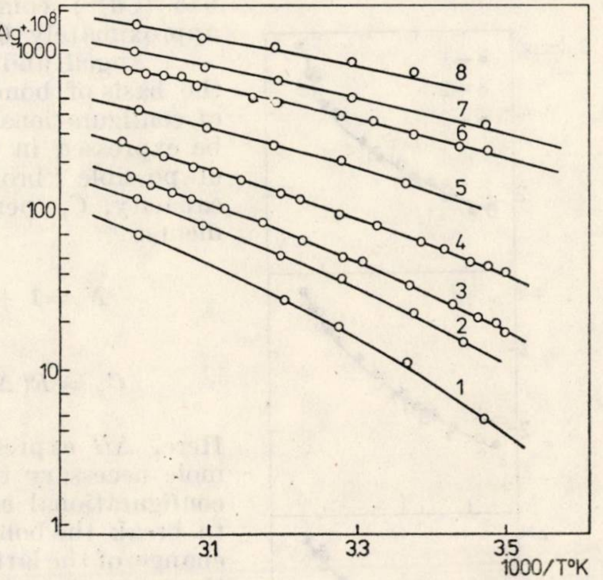

Fig. 2. — Temperature dependence of diffusion coefficients of silver ions, D_{Ag^+} (cm^2sec^{-1}), in $Ca(NO_3)_2-H_2O$ system (curves 1 to 8 correspond to 21.16, 19.53, 18.00, 15.87, 14.05, 10.02, 8.39, and 6.47 mol% $Ca(NO_3)_2$, respectively).

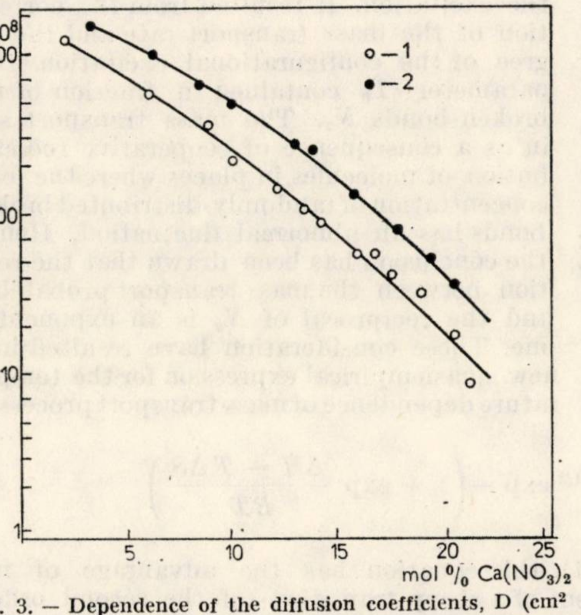

Fig. 3. — Dependence of the diffusion coefficients, D ($cm^2 sec^{-1}$), of cadmium and silver ions on the composition of calcium nitrate solution : *1*, (Cd^{2+}) ; *2*, Ag^+.

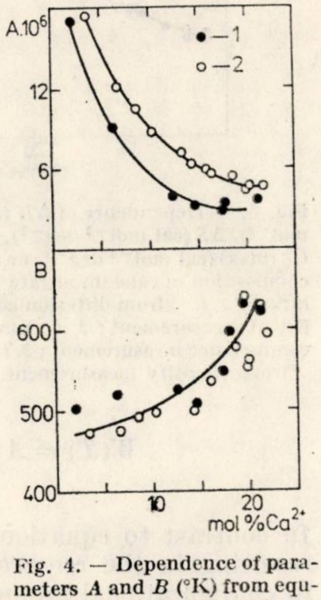

Fig. 4. — Dependence of parameters *A* and *B* (°K) from equation (1) on the composition of calcium nitrate solution : *1*,( ) Cd^{2+}; ( )*2*, Ag^+.

values of A are lower for Cd^{2+} ions. This is in accordance with the data given in [10] where the values of the coefficient A for $Ca(NO_3)_2.4,09\ H_2O$ amount on an average to $5.5.10^{-6}$ for Ag^+ and $4.2.10^{-6}$ for Cd^{2+} . Our mean values corresponding to the same composition are 5.10^{-6} and 3.10^{-6}, respectively. The values of parameter B given in [10] are 587 (Ag^+) and 645 (Cd^{2+}) compared with our values of approximately 600 for both cations.

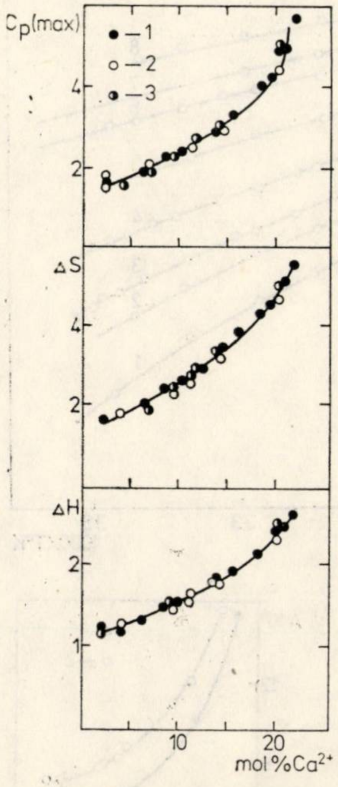

Fig. 5. — Dependence of ΔH (kcal mol^{-1}), ΔS (cal mol^{-1} deg^{-1}), and C_p (max) (cal mol^{-1} deg^{-1}) on the composition of calcium nitrate solution : *1*, ( ) from diffusion coefficient measurement ; *2*, ( ) from conductance measurement ; *3*, ( ) from viscosity measurement.

Angell and Rao [17] have shown that on the basis of bond lattice model [18] the degree of configurational excitation of a liquid may be expressed in terms of the fraction, N_w, of possible "broken bonds" and the heat capacity, C_p, per mole of bond lattice elements.

$$N_x = 1 + \exp \frac{\Delta H - T\,\Delta S}{RT} \tag{3}$$

$$C_p = R(\Delta H/RT)^2 N_x (1 - N_x) \tag{4}$$

Here, ΔH expresses the average energy per mole necessary to produce the elementary configurational excitation of the lattice (i. e., to break the bond), ΔS is the average molar change of the lattice entropy associated with the excitation. It resulted from the correlation of the mass transport rate and the degree of the configurational excitation that parameter T_0 contained a fraction of the broken bonds N_x. The mass transport sets in as a consequence of cooperative redistribution of molecules in places where the local concentration of randomly-distributed broken bonds has an abnormal fluctuation. Hence, the conclusion has been drawn that the relation between the mass transport probability and the reciprocal of N_x is an exponential one. These consideration have resulted in a new quasiempirical expression for the temperature dependence of mass transport processes:

$$W(T) = A\,T^{-1/2} \exp -\left(1 + \exp \frac{\Delta H - T\,\Delta S}{RT}\right) \tag{5}$$

In contrast to equation (1), this equation has the advantage of not resulting in the requirement of a sharp transition (of the second order) to configurational ground state at a finite temperature T_0. From theoretical considerations it follows that, in fact, there is no actual temperature, T_0, of the ideal glass transition. This parameter should be understood as a quantity in relation to the simple temperature dependence of important thermodynamic excess quantities. On the curve of the temperature dependence of heat capacity, T_0 lies approximately at the half of the steeply falling part of the curve.[17]

By iterative least squares treatment we received the values of ΔH and ΔS optimally fitting equation (5). These values were found to be the same through diffusion coefficient measurements both of cadmium and silver ions. The dependences of ΔH and ΔS on the composition of calcium nitrate solution are shown in Fig. 5. Here, the points calculated from the viscosity and conductance measurements performed by Bressel[16] are also included for comparison.

Parameters ΔH and ΔS contain the information which enables us to determine approximately the maximum configurational heat capacity, C_p (max), per mole of bonds according to equations (3) and (4). By comparison of this value with the results of calorimetric measurements of the heat capacity per mole of liquid, the number of excited bonds per mole of liquid can be calculated which may be of value for clarification of transport processes in these solutions. The dependence of theoretical values of the maximum configurational heat capacity of the calcium nitrate-water system on the composition is shown in Fig. 5 a. Again the comparison with the results calculated on the basis of Bressel's data[16] on conductance and viscosity of these systems has been performed. Up to now, the data on experimentally measured heat capacities of these systems are lacking. Only for calcium nitrate tetrahydrate there are calorimetric data, the comparison of which with the results calculated from transport data has been made in the paper of Angell and Bressel.[8] As far as this system is concerned, we obtained the same results.

Finally, it should be noted that the results of the diffusion coefficient measurement are generally less precise than that of conductance and viscosity measurements. Nevertheless, a good agreement between them should be stated as well as the fact that the obtained results satisfy the theoretical conclusions following from the bond lattice model.

---

[17] C. A. Angell, and K. J. Rao, *J. Chem. Phys.*, **57**, 470 (1972).

[18] C. A. Angell, *J. Phys. Chem.*, **75**, 3698 (1971).

Revue Roumaine de Chimie, 22, *11–12*, 1471–1477 (1977)

THERMAL DECOMPOSITION OF TRIS(OXALATO) MANGANESE(III)

COMPLEX IN AQUEOUS SOLUTIONS

TATIANA ONCESCU and ECATERINA JURCONI
Physical Chemistry Department,
Bucharest Institute of Chemistry,
Bd. Republicii 13, Romania

Received June 26, 1975

The kinetics and mechanism of the thermal decomposition of $[Mn(C_2O_4)_3]^{3-}$ in aqueous solutions which give Mn(II) and CO_2 were investigated at different pH values and various temperatures. The activation parameters were reported. Similar studies were carried out in the presence of a large excess of $C_2O_4^{--}$. In both cases the rate constant values were influenced by the pH values of the solutions used and slightly affected by the ionic strength. The kinetic results are consistent with a free radical mechanism.

1. INTRODUCTION

The thermal decomposition of the oxalate complexes of some transitional metals in aqueous solution has been investigated by several groups of workers; most of them admitted the aquation mechanism. While the Cr(III)[1,2] and Rh(III)[3,4] tris (oxalato) complexes are very stable and their aquation leads only to the corresponding dioxalato complexes, the tris (oxalato) complexes of Co[5–7] and Mn[8,9] undergo redox thermal decomposition to give Me(II) and CO_2. Regarding the thermal decomposition of $[Mn(C_2O_4)_3]^{3-}$ at various concentrations of oxalate and hydrogen ions, Wronska and Ernst [9] pointed out the existence of three kinds of complexes in equilibrium, undergoing decomposition with various velocities, but they did not present a detailed reaction mechanism.

The purpose of this study is to establish the kinetics and mechanism of the thermal decomposition of $[Mn(C_2O_4)_3]^{3-}$ in aqueous solution in

[1] F. D. Graziano and G. M. Harris, *J. Phys. Chem.*, **63**, 330 (1959).
[2] K. V. Krishnamurty and G. M. Harris, *J. Phys. Chem.*, **64**, 346 (1960).
[3] D. Barton and G. M. Harris, *Inorg. Chem.*, **1**, 251 (1962).
[4] K. V. Krishnamurty, *Inorg. Chem.*, **1**, 422 (1962).
[5] I. G. Murgulescu and T. Oncescu, *Z. phys. Chem.*, (*Leipzig*), **214**, 238 (1960).
[6] Lee Hin-Fat and W. C. E. Higginson, *J. Chem. Soc.*, (*A*), **1970**, 2836.
[7] N. S. Rowan, R. M. Mulburn and M. Z. Hoffman, *Inorg. Chem.*, **11**, 2272 (1972).
[8] I. G. Murgulescu and T. Oncescu, *Rev. Roumaine Chim.*, **10**, 3 (1965).
[9] M. Wronska and T. Ernst, *Roczniki Chem.*, **46**, 643 (1972).

the presence and absence of oxalate. At the same time we investigate the medium effect on the reaction rate as : pH of solution, ionic strength, Mn(II) and O_2 influences, which are explained in terms of the mechanism proposed.

2. EXPERIMENTAL

Tris(oxalato) Mn(III) complex was prepared as a crystalline substance by using the Cartledge and Ericks method.[10] The pH influence and the salt effects studies were made as in the previous paper[11] for the bis (oxalato) complex and the remarks concerning the substances and the experimental spectrophotometrical technique used are consistent with those made before.

In this paper two series of experiments were carried out : some of them were made in aqueous solutions of complex at different pH values in the presence of fifty time exces of $K_2C_2O_4$ and others in the absence of oxalate. In the first case, kinetic experiments were made at $\lambda = 520$ nm, in the absorption band of the red tris(oxalato) complex (fig. 1.*1*.) In the second case the kinetics runs were effected at $\lambda = 450$ nm in the absorption band of the yellow bis (oxalato) complex (fig. 1.*2*) because by dissolving the red tris(oxalato) complex, in solutions the red color of the solutions turns instantaneously yellow as also observed by other authors.[9,10]

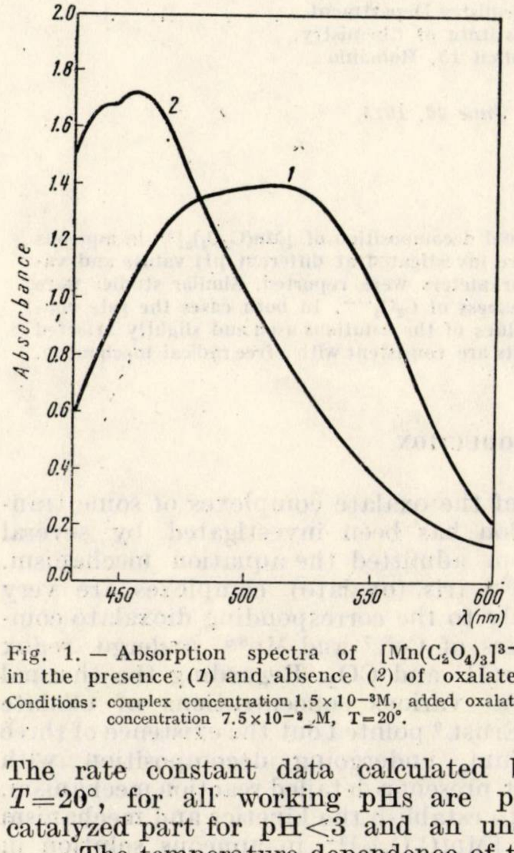

Fig. 1. — Absorption spectra of $[Mn(C_2O_4)_3]^{3-}$ in the presence (*1*) and absence (*2*) of oxalate. Conditions: complex concentration 1.5×10^{-3}M, added oxalate concentration 7.5×10^{-2} M, T=20°.

3. RESULTS

a. DECOMPOSITION STUDIES IN THE PRESENCE OF OXALATE

Series of runs confirmed the first order of reaction in respect to Mn(III) complex concentration. We present as example the data obtained for one of the pH values used (fig. 2). The rate constant data calculated by the least square method at $T = 20°$, for all working pHs are plotted in Fig 3.*1* which shows a catalyzed part for pH<3 and an uncatalyzed behaviour for pH >3.*2*.

The temperature dependence of the rate constant is shown in table 1 which presents the corresponding kinetic and thermodynamic parameters at two different pH values (2.34 and 4.5) from the two distinct regions of the above plot.

Investigation of the salt effect on the reaction rate were not made because the added inert salt does not dissolve in the presence of the large excess of oxalate.

[10] G. H. Cartledge and W. P. Ericks, *J. Amer. Chem. Soc.*, **58,** 2061 (1936).

[11] T. Oncescu and E. Jurconi, *Rev. Roumaine Chim.*, **21,** 805 (1976).

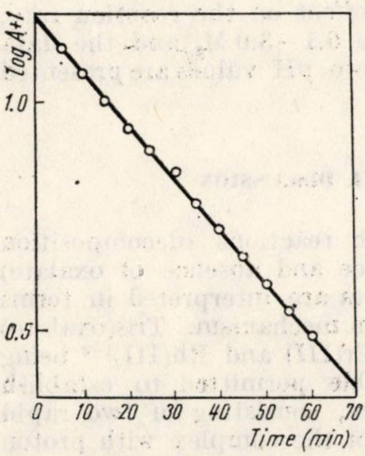

Fig. 2. — Typical first order dependence; pH = 2.6 in excess of oxalate at $T = 20°$.

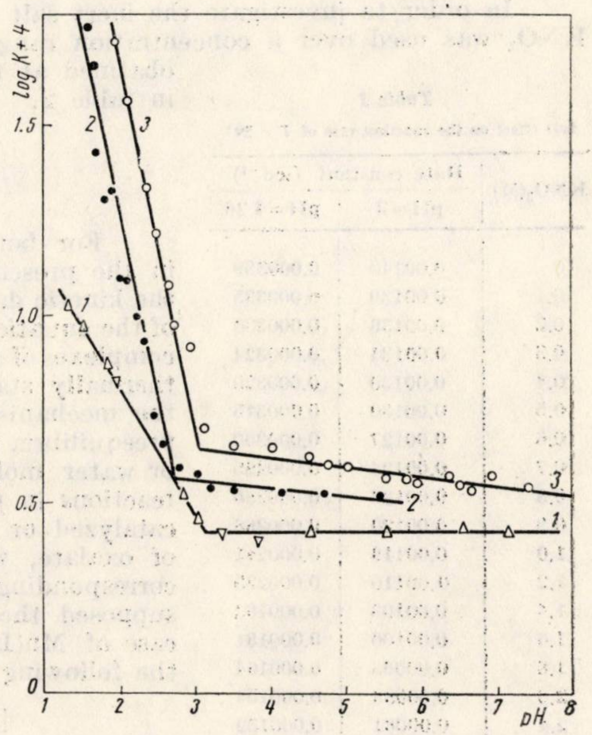

Fig. 3. — Variation of rate constant with pH at $T=20°$: for $[Mn(C_2O_4)_3]^{3-}$, in the presence (*1*) and absence (*2*) of oxalate, and for $[Mn(C_2O_4)_2(H_2O)_2]^{-}$ (*3*).

Table 1

Temperature dependence of the rate constants and activation parameters for the decomposition of $[Mn(C_2O_4)_3]^{3-}$

pH / T°	Rate constant 15.5°	20°	25°	E_{Arrh} kcal mole^{-1}	log A	$\Delta H^{\neq}$ kcal mole^{-1}	$S\Delta^{\neq}$ u. e.
1.65	0.00157	0.00266	0.00447	19.2	11.76	18.6	−2.94
2.34	0.000277	0.000482	0.000878	20.6	12.07	20.0	−2.30
4.26	0.000189	0.000339	0.000631	21.7	12.73	12.73	−2.20
4.50	0.000152	0.000270	0.000502	21.9	12.79	21.3	−0.87

b. DECOMPOSITION STUDIES IN THE ABSENCE OF OXALATE

In this case, the reaction is also of the first order in respect to Mn(III) concentration and the rate constant data are plotted in Fig. 3 b. One observes also the two different behaviours the first being typical of specific acid-catalyzed reactions.

From the temperature variation of the rate constant at two pH values (1.65 and 4.26), the activation parameters given in table 1 were calculated.

In order to investigate the inert salt effect on the reaction rate, KNO_3 was used over a concentration range 0.1–3.0 M, and the data obatined at two pH values are presented in table 2.

Table 2

Salt effect on the reaction rate of $T = 20°$

KNO_3(M)	Rate constant (sec^{-1})	
	pH=2	pH=4.26
0	0.00140	0.000339
0.1	0.00139	0.000335
0.2	0.00136	0.000330
0.3	0.00134	0.000324
0.4	0.00130	0.000320
0.5	0.00130	0.000315
0.6	0.00127	0.000300
0.7	0.00124	0.000295
0.8	0.00123	0.000280
0.9	0.00120	0.000266
1.0	0.00119	0.000241
1.2	0.00110	0.000235
1.4	0.00103	0.000182
1.6	0.00100	0.000181
1.8	0.00093	0.000164
2.0	0.00088	0.000154
2.4	0.00081	0.000132
2.6	0.00082	0.000110
2.8	0.00080	0.000095
3.0	0.00079	0.000101

4. DISCUSSION

For both reactions (decomposition in the presence and absence of oxalate) the kinetic data are interpreted in terms of the aquation mechanism. Tris(oxalato) complexes of Cr(III) and Rh(III)[1–4] being thermally stable permitted to establish the mechanism, consisting of two rapid preequilibria of the complex with proton or water molecule, followed by opposite reactions in parallel involving either non-catalyzed or acid catalyzed substitution of oxalate, with the formation of the corresponding bis(oxalato) complex. We supposed the same mechanism[11] in the case of Mn(III) complex, illustrated by the following sequences:

$$[Mn(C_2O_4)_3]^{3-} + H_3O^+ \underset{k_7'}{\overset{k_7}{\rightleftharpoons}} [Mn(C_2O_4)_2OC_2O_3H_3O]^{2-} \quad \text{(very fast)} \qquad (7)$$

$$[Mn(C_2O_4)_3]^{3-} + H_2O \underset{k_8'}{\overset{k_8}{\rightleftharpoons}} [Mn(C_2O_4)_2OC_2O_3H_2O]^{3-} \quad \text{(very fast)} \qquad (8)$$

$$[Mn(C_2O_4)_2OC_2O_3H_3O]^{2-} + H_2O \underset{k_9'}{\overset{k_9}{\rightleftharpoons}} [Mn(C_2O_4)_2(H_2O)_2]^- + HC_2O_4^- \quad \text{(fast)} \qquad (9)$$

$$[Mn(C_2O_4)_2OC_2O_3H_2O]^{3-} + H_2O \underset{k_{10}'}{\overset{k_{10}}{\rightleftharpoons}} [Mn(C_2O_4)_2(H_2O)_2]^- + C_2O_4^{--} \quad \text{(fast)} \qquad (10)$$

a. DECOMPOSITION IN THE PRESENCE OF OXALATE

In the first series of experiments, the concentration of added oxalate is very large so that the reactions (9) and (10) are shifted practically to the left. Under these conditions the equilibria (7) and (8) are also displaced to the left and $[Mn(C_2O_4)_3]^{3-}$ is preponderantly present in solution, the fraction as dioxalato complex being smaller than 0.10.[12]

---

[12] G. H Cartledge and W. P. Ericks, *J. Amer. Chem. Soc.*, **58**, 2065 (1936)

Because MnC_2O_4 and CO_2 are the final products, we must admit the presence in the system of the competitive paths for the protonated and aquated intermediates, leading to the formation of the free radical $C_2O_4^{\cdot -}$, followed by the $C_2O_4^{\cdot -}$ attack on the initial complex:

$$[Mn(C_2O_4)_2OC_2O_3H_3O]^{2-} + H_2O \rightarrow MnC_2O_4 + HC_2O_4^{-} + C_2O_4^{\cdot -} + 2H_2O \quad \text{(slow)} \tag{11}$$

$$[Mn(C_2O_4)_2OC_2O_3H_2O]^{3-} + H_2O \rightarrow MnC_2O_4 + C_2O_4^{--} + C_2O_4^{\cdot -} + 2H_2O \quad \text{(slow)} \tag{12}$$

$$[Mn(C_2O_4)_3]^{3-} + C_2O_4^{\cdot -} \rightarrow MnC_2O_4 + 2C_2O_4^{--} + 2CO_2 \quad \text{(fast)} \tag{13}$$

Consequently, kinetics followed spectrophotometrically at $\lambda = 520$ nm is preponderantly the recomposition of the tris(oxalato) complex.

On the basis of the proposed mechanism and taking into account the reaction stoichiometry, the differential kinetic equation for the decomposition reaction is:

$$\frac{dC_T}{dt} = k_7 C_T^2 C_{H_3O^+} - k_7 C_c^2 + k_8 C_T^2 C_{H_2O^+} - k_8 C_D^2 + k_{13} C_T^2 C_{ox}^2 \tag{14}$$

where: C_T = concentration of the tris (oxalato) complex

C_c = concentration of the protonated complex

C_D = concentration of the aquated complex

C_{ox} = concentration of the oxalyl radical-ion

By applying the stationary-state approximation to *c*, *D* and *ox*, we obtained the rate equation:

$$\frac{dCT}{dt} = (k_{11}\sqrt{k_7} C_{H_2O} C_{H_3O} + k_{12}\sqrt{k_8} C_{H_2O}^2) C_T - (k_9 C_{HC_2O_4} + k_{10} C_{C_2O_4}) C_{DA} \tag{15}$$

where C_{DA} is the concentration of the bis(oxalato) complex which appeared in the system. The equation (15) can be written as:

$$\frac{dC_T}{dt} = (k'_H + k''_H) C_T - k''' C_{DA} \tag{16}$$

where: k'_H = rate constant of the hydrogen ion catalyzed reaction

k' = rate constant of the uncatalyzed reaction

k''' = total rate constant of the disappearance of bis (oxalato) complex processes.

Our experimental data verify this equation: the first order in respect to Mn(III) concentration, (fig. 2) and the distinct behaviour of the rate constant as a function of pH (fig. 3). The slope of the catalytic region is however smaller than unity (about 0.4). It is to expect such a result because the second term of equation (16) diminishes at any moment the decomposition rate, by the re-formation of the substrate.

b. DECOMPOSITION IN THE ABSENCE OF OXALATE

According to the mechanism proposed, in this case, the sequences (9) and (10) are the most probable and this diminishes the contribution of the sequences (11) and (12). Under these conditions, as Cartledge and Ereks showed,[12] the tris(oxalato) complex solution is converted into bis (oxalato) complex in proportion of about 80 %. Therefore, the reaction mechanism involves the steps (7)—(13) followed by the steps (1), (3) and (5) discussed in the previous paper.[11] As seen in Fig. 1.*2*, by dissolving the red complex in water takes place a rapid conversion into yellow di(oxalato) complex, so that the kinetics followed spectrophotometrically is preponderantly the thermal decomposition of $[Mn(C_2O_4)_2(H_2O)_2]^-$.

The kinetic equation of the bis(oxalato) decomposition is:

$$\frac{dC_{DA}}{dt} = -k_9 C_c C_{H_2O} + k'_9 C_{DA} C_{HC_2O_4} - k_{10} C_D C_{H_2O} + k'_{10} C_{DA} C_{C_2O_4} + \\ + k_1 C_{DA} C_{H_3O} - k'_1 C_A + k_5 C_{DA} C_{ox} \qquad (17)$$

By applying the stationary-state approximation to A, c, D and ox we obtain:

$$\frac{dC_{DA}}{dt} = 2k_3 C_A C_{H_2O} - (k_7 C_T^2 C_{H_3O}^2 - k'_7 C_c^2 + k_8 C_T^2 C_{H_2O} - k'_8 C_D^2 + k_{13} C_T^2 C_{ox}^2) \qquad (18)$$

Taking into account the relationship (14), the equation (18) becomes

$$\frac{dC_{DA}}{dt} = 2K_1 k_3 C_{H_2O} C_{H_3O} C_{DA}^{-} \left(-\frac{dC_T}{dt} \right) \qquad (19)$$

One observes that the first term in the last equation represents the decomposition rate of the bis(oxalato) complex in acidic media, and the second is the rate of the tris(oxalato) in the presence of oxalate. Our experimental data plotted in Fig. 3.*2*. illustrate this equation. One notices that for the catalyzed part the slope is about unity, as in the case of the bis(oxalato) complex (Fig. 3.*3*) but, at the same time, all the rate constants are smaller than in the case of pure $[Mn(C_2O_4)_2(H_2O)_2]^-$. Equation (19) explains such a behaviour, because of the decrease of the bis (oxalato) rate with the corresponding rate of the tris(oxalato) complex present in solution in proportion of about 20 %.

In order to obtain evidence for the reaction mechanism, series of experiments were done in KNO_3 media. The results presented in Table 2 show that the rate constants are slightly affected by ionic strengths. Also, the decrease of the rate with ionic strength is larger for pH=4.26 than for pH=2, corresponding respectively to the uncalalyzed and catalyzed region. As in the case of bis(oxalato) complex[11] the explanation of this behaviour refers to the charge involved in the rate determining step: the aquated and protonated complex in the first and second case, respectively.

c. GENERAL REMARKS CONCERNING THE DECOMPOSITION OF $[Mn(C_2O_4)_3]^{3-}$

The kinetic data of acid catalyzed redox decomposition of $[Mn(C_2O_4)_3]^{3-}$ presented above confirm the aquation mechanism involving free radicals as intermediates. The evidences for the formation of $C_2O_4^{\cdot -}$ were offered in our previous paper.[11] But we point out that the rate constants in deoxygenated solution by bubbling argon are larger than in the presence of air. For example : at pH=2.34 (in the presence of oxalate), $k_{Ar} = 0.000530\ sec^{-1}$ and $k_{air} = 0.000482\ sec^{-1}$.

In connection with the presence of $C_2O_4^{\cdot -}$ we mention the appearance of H_2O_2 in solution and the catalytic action of Mn(II) upon H_2O_2 formation and the thermal decomposition of $[Mn(C_2O_4)_3]^{3-}$. These effects were interpreted before[11] in terms of the mechanism proposed and the assumption made there can be also applied in this case. As seen in Fig. 4, H_2O_2 quantity increases with the increase of hydrogen ion concentration (curves *1* and *3*) and added Mn(II) concentration (curve *4*) as well as in the presence of an oxalate excess (curve *2*).

Regarding the catalyzed action of Mn(II), as shown in table 3, the rate constant changes markedly with the increase of the added Mn(II) concentration, as in the case of $[Mn(C_2O_4)_2(H_2O)_2]^-$.

Another interesting observation, resulting from table 1, is the difference obtanied between the activation parameters corresponding to the catalyzed and uncatalyzed region. In all cases, as was to be expected, these parameters are smaller for the catalyzed part than for the uncatalyzed one.

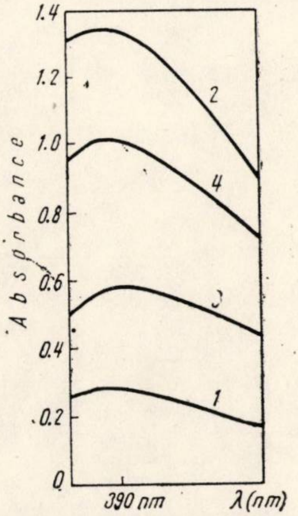

Fig. 4. —The increase of final absorption of solution by adding $Ti(SO_4)_2$ at pH=1.85 in the absence (curve *1*) and presence of oxalate (curve *2*), pH=6.75 (curve *3*) and pH=1.85 in the presence of $Mn(NO_3)_2$ 1.74×10^{-3} (curve *4*).

Table 3

Rate constants at different concentrations of added $Mn(NO_3)_2$ (pH = 1.85, T = 20°C) in the absence of oxalate

$Mn(NO_3)_2$ M	0	0.87×10^{-3}	1.7×10^{-3}	3.48×10^{-3}
Rate constant	0.00210	0.0112	0.0165	0.0192

In conclusion, the present study, as well as the previous one, permitted a unitary treatment of the Mn(III) oxalate complexes confirming, at the same time, the reaction mechanism proposed.

Revue Roumaine de Chimie, **22** *11–12*, 1479–1486 (1977)

A SPECTROSCOPIC STUDY OF TIN(IV) COMPLEXES WITH 2,2′-DIHYDROXYCHALKONES

N. S. BIRADAR
Department of Chemistry, Karnatak University, Dharwar-580003, India

B. R. PATIL and V. H. KULKARNI
Department of Chemistry, Karnatak University Post-graduate Centre,
Gulbarga-585105, India

Received July 14, 1975

A few complexes of tin (IV) have been prepared by reacting *2,2′*-dihydroxychalkones with tin (IV) chloride in benzene medium. The complexes are characterized by the elemental analysis and molar conductance in DMF. The infrared spectra have been studied in the 4 000–200 cm^{-1} region. The tin(IV) complexes formed with *2,2′*-dihydroxychalkones are shown to have hexacoordinated halogen-bridged structures.

INTRODUCTION

The examples of tin(IV) complexes with bases containing —O— and —N— donor atoms are numerous and well documented in the literature. [1] In most of the cases tin(IV) is shown to have an octahedral stereochemistry. The complexes of tin(IV) with ligands containing —O— and —N— donor atoms are, however, known to a limited extent. [2,3]

Though the work on tin(IV) complexes with bifunctional tridentate ligands containing —O, N, O— sequences seeems to be limited[4], no work on the bifunctional tridentate ligands containing —O, O, O— sequences is recorded in the literature.

---

[1] *a*. N. S. Biradar and V. H. Kulkarni, *J. Inorg. Nuclear Chem.*, **33**, 245 ; 3781 (1971), and references therein ; *Rev. Roumaine Chim.*, **18**, 63 (1973) ; *b*. N. S. Biradar, V. B. Mahale and V. H. Kulkarni, *Indian J. Chem.*, **9**, 1410 (1971) and *J. Karnatak Univ.* (*Science*), **17**, 7 (1972) ; *c*. K. Kawakani, M. Miya-Uchi and T. Tanaka, *J. Inorg. Nuclear Chem.*, **33**, 3773 (1971) ; *d*. F. Maggio, R. Bosco, R. Cefalu and R. Barbieri, *Inorg. Nucl. Chem. Lett.*, **4**, 389 (1968) ; *e*. G. Faraglia, F. Maggio, R. Bosco, R. Cefalu and R. Barbieri, *Inorg. Nucl. Chem. Lett.*, **5**, 117 (1969) ; *f*. F.D. Bianca, E. Rivarola, G. C. Stocco and R. Barbieri, *Z. anorg. Chem.*, **387**, 126 (1972) ; *g*. R. Cefalu, F. Maggio, L. Pellerito and V. Romano, *Inorg. Nucl. Chem. Lett.*, **10**, 529 (1974).

[2] J. W. Faller and A. Davison, *Inorg. Chem.*, **6**, 182 (1967).

[3] R. W. Jones and R. C. Fay, *Inorg. Chem.*, **12**, 2599 (1973).

[4] *a*. F. Maggio, R. Cefalu, R. Rosco and R. Flavio, *Atti. Acad. Sci. Lett., Arti Paleramo. Parte I*, **28**, 5 (1969) ; *Chem. Abstr*,. **73**, 31154 (1970) ; *b*. R. Barbieri, *Inorg. Nucl. Chem. Lett.*, **8**, 481 (1972) ; *c*. H. Preut, F. Huber, H. J. Hauft, R. Cefalu and R. Barbieri, *Z. anorg. Chem.*, **410**, 88 (1974) ; *d*. G. C. Srocco, G. Alonzo, A. Silvestri, N. Bertazzi, L. Pellerito and R. Barbieri, *Z. anorg. Chem.*, **409**, 248 (1974).

It has, therefore, been thought to synthesize tin(IV) complexes with a few tridentate ligands containing —O, O, O— sequences and study their stereochemistry.

In this paper, we report the synthesis and spectral study of a few tin(IV) complexes with the following *2,2'*-dihydroxychalkones

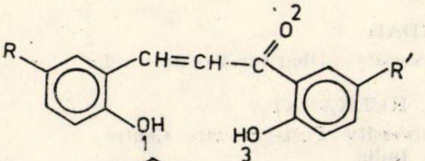

	R	R'
I.	H	CH_3
II.	CH_3	CH_3
III.	Cl	CH_3
IV.	CH_3	Cl
V.	Cl	Cl

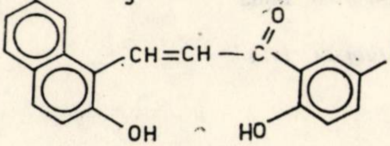

VI

EXPERIMENTAL

MATERIALS

All the chemicals used for preparing substituted aldehydes and acetophenones we. of reagent grade.

Substituted *o*-hydroxyacetophenones were prepared starting with *p*-cresol and *p*-chlorophenol subjecting them to acetylation followed by Fries-migration.

5-methyl and *5*-chloro salicylaldehydes and *2*-hydroxy, *1*-naphthaldehyde were prepared according to the known method.[5]

Salicylaldehyde was of Bush make and was used as such without further purification.

METHODS

Preparation of chalkones

Chalkones I—VI were prepared according to the method of Dhar,[6] and crystallized from benzene.

Preparation of the complexes

Anhydrous tin(IV) chloride was of Riedel make and used as such for complexation Commercial grade benzene was purified by repeated distillation and stored over sodium metal.

Tin(IV) chloride (0.01 mole) was treated with 0.012 mole of chalkone in benzene medium with vigorous shaking. The reaction mixture was kept under reflux on an oil bath until the evolution of HCl gas ceased. The complex separated out was filtered, washed with little benzene then with *n*-hexane and dried in vacuum.

The dry complex was powdered and extracted in a Soxhlet thimble with *n*-hexane to remove excess of the reagent. The complex was then dried in vacuum.

---

[5] J. C. Duff, *J. Chem. Soc.*, **1941**, 547.

[6] *a.* D. N. Dhar and J. B. Lal, *J. Org. Chem.*, **23**, 1159 (1958); *b.* D. N. Dhar, *J. Org. Chem.*, **25**, 1247 (1960); *c.* D. N. Dhar, *J. Indian Chem. Soc.*, **37**, 363 (1960).

ANALYSIS

Tin in the complexes was estimated gravimetrically as SnO_2 and chloride as AgCl.

PHYSICAL MEASUREMENTS

Molar conductivities of the complexes in DMF were measured at concentration of 10^{-3}M, on an ELICO conductivity bridge CM–82 having a cellconstant 0.829 cm^{-1} manufactured by Electrical Industrial Instrument Co. Hyderabad.

The infrared spectra of the complexes in Nujol mull were recorded on a Perkin Elmer-220 in the 4000–200 cm^{-1} region.

RESULTS AND DISCUSSION

The complexes are orange red to brownish yellow in colour, insoluble in common organic solvents and soluble to a limited extent in DMF. This insoluble nature of the complexes did not permit the determination of molecular weight. The elemental analyses summarized in Table 1 agree well with the 1:1 stoichiometry.

Table 1

Elemental analyses of tin (IV) chalkonates

Lig. No.	Comp. No.	Empirical Formula	% Sn		% Cl	
			Cald.	Found	Cald.	Found
I	VII	$(C_{16}H_{12}O_3)\ SnCl_2$	26.93	26.56	16.11	16.05
II	VIII	$(C_{17}H_{14}O_3)\ SnCl_2$	26.05	25.90	15.58	15.58
III	IX	$(C_{16}H_{11}ClO_3)\ SnCl_2$	24.93	24.88	14.91	15.01
IV	X	$(C_{16}H_{11}ClO_3)\ SnCl_2$	24.93	24.65	14.65	15.40
V	XI	$(C_{16}H_{10}Cl_2O_3)\ Sn\ Cl_2$	23.91	23.49	14.30	14.67
VI	XII	$(C_{19}H_{11}ClO_3)\ SnCl_2$	24.91	24.40	14.89	14.55

MOLAR CONDUCTIVITY

The molar conductance values determined at the concentration $\sim 10^{-3}$M fall in the range of 5–10 $ohm^{-1}\ cm^2\ mole^{-1}$ for the complexes VII–XII suggesting that all these complexes in DMF exhibit non-electrolytic behaviour.

INFRARED SPECTRA

The important infrared frequences of ligands I–VI and their tin (IV) complexes VII–XII are listed in Table 2 along with their assignments.

The infrared spectra of ligands I–V and VI exhibit two bands in the region 3300–2600 cm^{-1}. The medium intensity band in the region 3300–3200 cm^{-1} (Table 2) and broad weak band with fine structure in the region 2675–2650 cm^{-1} are, respectively, ascribed to the inter-

Table

Infrared frequencies (in cm^{-1}) of 2,2′-dihydroxy

S. No.	Assignments	I	VII	II	VIII
1	Aromatic CH and =CH stretching vibrations	2950	2960 2940 2850 2850	2900	2960 2940 2870
2	Intermolecular H-bonded OH stretching vibration	3200 m	—	3300 m	—
3	Intramolecular H-bonded OH–stretching vibration	2650 br, w	—	2675 br, w	—
4	C=O stretching vibration	1640 s	1620 s	1646 s	1635 s
5	HC=CH stretching vibration	1595 m	1520 s	1600 m	1620 m
6	Aromatic C=C stretching vibration	1570 s 1495 m 1480 s	1600 m 1590 m 1580 m 1545 s	1575 s 1500 m 1470 m	1590 w 1580 w 1560 s 1550 sh
7	Phenolic C–O stretching vibration	1265 s	1315 s	1275 s	1292 s
8	Sn–O stretching vibration	—	460 m 445 sh 425 m	—	470 m 450 m —
9	Sn–Cl stretching vibration	—	350 w,sh 310 s, br 230 s 220 sh	—	370 w 340 sh 320 s,br 230 m

Note: w = weak; m = medium; s = strong; br = broad and sh = shoulder.

molecular and intramolecular hydrogen bonded OH groups. These assignments closely agree with the previous assignments.[7]

The high intensity band observed in the region 1650–1640 cm^{-1} for these ligands is assigned to the C=O stretching vibration. The shift of the C=O from its normal value to the lower frequency may be due to the conjugation and hydrogen bondings in the molecule. Analogous assignments have also been made by previous authors.[8] A high intensity band observed in the region 1600–1580 cm^{-1} for all these ligands is atributed to the stretching vibration due to the ethylenic double-bond

[7] N. S. Biradar and V. B. Mahale, *J. Less. Common Metals,* **31,** 159 (1973); *b.* K. K. Ramaswamy, C. I. Jose and D. N. Sen, *Indian J. Chem.,* **5,** 156 (1967); *c.* H. I. Hegert and E. F. Kurth, *J. Amer. Chem. Soc.,* **75,** 1622 (1953).

[8] *a.* C. N. R. Rao, "Chemical Applications of Infrared Spectroscopy" Academic Press, London, 1958; *b.* H. W. Thomson and P. J. Torkington, *J. Chem. Soc.,* **1945,** 640; *c.* N. L. Silver and D. W. Bovkin (Jr.), *J. Org. Chem.,* **35,** 759 (1970).

2

chalkones, their tin (IV) complexes and assignments

III	IX	IV	X	V	XI	VI	XII
2900	2960	2950	2940	2900	2960	2900	2940
	2920		2900		2920		2930
	2860		2840		2850		2920
							2850
3200 br,m	—	3250 m	—	3280 m	—	3250 br,m	—
2650 br,w	—	2675 br,w	—	2650 br,w	—	2650 br,w	—
1648 s	1630 s	1648 s	1630 s	1646 s	1630 s	1650 s	1610 s
1600 s	1590 m	1590 s	1580 s	1580 s	1600 m	1600 m	1595 s
							1565 s
1558 s	1580 m	1575 s	—	1560 m	1578 s	1525 m	1540 s
—	1555 s	1525 w	1555 s	—	1555 s	1470 s	1500 s
1470	1505 w	1470 s	1500 s	1470 s	1480 w		
	1490 w						
1280 as	1320 m	1280 s	1320 s	1286 s	1360 br,s	1290 m	1310 s
—	470 m	—	470 m	—	460 w	—	490 s
	460 w		460 w		450 s		460 s
	450 m		450 m		430 w		415 w
							400
—	330 s	—	360 m	—	350br.m	—	360 m
	310 m		330br,m		335 sh		330 s
			260 w		310 sh		320 s
							290 m

conjugated to the aromatic ring system in view of the previous assignments.[9,10] The medium to high-intensity bands appearing in the region 1600—1470 cm^{-1} are assigned to the aromatic C=C stretching vibrations. The high intensity band in the region 1280—1265 cm^{-1} of the ligands (I—VI) is due to the phenolic C—O stretch. This band is found to be absent in benzalacetophenone.

We observe quite discernible changes in these characteristic frequencies in the tin(IV) complexes.

The bands due to the intramolecular and intermolecular hydrogen bonded —OH disappear in the complexes and the phenolic C—O vibration shifts to higher frequency and appears in the region 1360—1290 cm^{-1}. These observations suggest that the hydroxy groups of the ligands I—VI are utilized in the formation of Sn—O bonds.

---

[9] N. K. Freeman, *J. Amer. Chem. Soc.*, **75,** 1859 (1953).

[10] D. N. Dhar and V. P. Gupta, *Indian J. Chem.*, **9,** 818 (1971).

The C=O stretch is displaced to the lower frequency in complexes and appears in the region 1635–1610 cm^{-1}. This low frequency shift of about 10–40 cm^{-1} in complexes may be interpreted as due to the coordination of the C=O group to the metal moiety through oxygen. This results in lowering the bond order of carbon-to-oxygen link.

All these observations suggest that the two hydroxy groups (1 and 3), and coordinating group (2) in I–VI are involved in the complex formation. Hence, one can predict the following structure for these complexes.

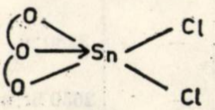

(A)

The construction of models for complexes indicates that the formation of monomeric structure (*A*) involves much strain because of the steric demands, whereas the dimeric structure (B) can be formed without much strain.

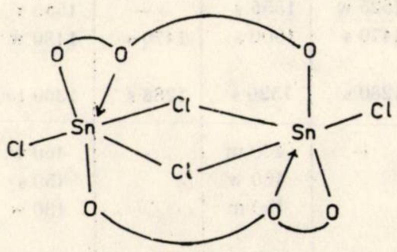

(B)

The molecular weights cannot be determined because of their insolubility in common organic solvents. This also suggests the formation of dimeric rather than monomeric complex.

The study of the low region spectra (600–250 cm^{-1}) throws some light on the structural probabilities.

$\nu(Sn-O)$

The assignments made in the region 600–200 cm^{-1} are tentative and based on the previous assignments.

Nakamoto and coworkers [10–14] have demonstrated that pure $\nu(M-O)$ occurs in the 500–400 cm^{-1} region of the infrared spectra of acetyl-

---

[11] K. Nakamoto and A. E. Martell, *J. Chem. Phys.*, **32**, 583 (1960).

[12] K. Nakamoto, P. J. McCarthy, A. Ruby and A. E. Martell, *J. Amer. Chem. Soc.*, **83**, 1066 (1961).

[13] K. Nakamoto, P. J. McCarthy and A. E. Martell, *J. Amer. Chem. Soc.*, **83**, 1272 (1961).

[14] G. T. Behnke and K. Nakamoto, *Inorg. Chem.*, **6**, 433 (1967).

acetone complexes of transition metals. A few authors[15-17] have reported metal sensitive bands in the same region. In glycino complexes of Pt(II), the Pt—O band is reported to occur in the 400 cm^{-1} region.[18] Fay and Pinnavaia[19] have assigned a medium intensity band in the region 422—398 cm^{-1}. Biradar and coworkers[20-23] report almost the same region for the ν(M—O) vibrations of Schiff base complexes of quadrivalent metal ions. On the basis of these reported data, we assign the bands of strong to medium intensity in the region 495—410 cm^{-1} to the ν(Sn—O) vibrations. These assignments closely agree with those of Kawasaki *et al.*,[24] Jain and Rivest.[25]

ν(Sn—Cl)

The previous studies on metal halogen stretching frequencies have shown that ν(M—X) vibrations are sensitive to the oxidation state, coordination number of the central metal ion,[26] and useful in predicting the stereochemistry of the complexes.[27-30] In the complexes of the type $[M(en)_2X_2]^+$ only one ν(M—X) band is expected for the *trans* arrangement and two bands for the *cis* arrangement.[18] Fay and Pinnavaia[19] have assigned the ν(Zr—Cl) and ν(Hf—Cl) bands in the region 361—273 cm^{-1} for the Zr(IV) and Hf(IV) acetylacetonates. Douek *et al.*[31] and Cox *et al.*[32] claim that ν(Sn—Cl) occurs in the region 338—264 cm^{-1} for Sn(IV) acetylacetonates. Recently Jones and Fay[3], Ohkaku and Nakamoto[33] have assigned a strong band in the vicinity of 340 cm^{-1} to the ν(Sn—Cl) in Sn(IV) acetylacetonates and adducts, respectively. Considering all these evidences, we have assigned a strong-to-medium

---

[15] C. Djordjevic, *Spectrochim. Acta*, **17**, 448 (1961).

[16] *a*. C. P. Prabhakaran, and C. C. Patel, *J. Inorg. Nuclear Chem.*, **31**, 3316 (1969); *b*. B. C. Sharma and C. C. Patel, *Indian J. Chem.*, **8**, 747 (1970).

[17] J. A. Faniran, and K. S. Patel, *J. Inorg. Nuclear Chem.*, **36**, 2261 (1974).

[18] K. Nakamoto, "Spectroscopy and Structure of Metal Chelate Compounds", Edited by K. Nakamoto and P. J. McCarthy, Wiley, New York, 1968, p. 216.

[19] R. C. Fay and T. J. Pinnavaia, *Inorg. Chem.*, **7**, 508 (1968).

[20] N. S. Biradar and V. H. Kulkarni, *J. Inorg. Nuclear Chem.*, **33**, 3847 (1971); *Z. anorg. Chem.*, **387**, 275 (1972).

[21] N. S. Biradar, V. H. Kulkarni and N. N. Sirmokadam, *J. Inorg. Nuclear Chem.*, **34**, 3651 (1972).

[22] N. S. Biradar, V. B. Mahale and V. H. Kulkarni, *Inorg. Chim. Acta*, **7**, 267 (1973).

[23] N. S. Biradar and A. L. Locker, *J. Inorg. Nuclear Chem.*, **36**, 1915 (1974).

[24] V. Kawasaki, T. Tanaka and R. Okawara, *Spectrochim. Acta*, **22A**, 157 (1966).

[25] S. C. Jain and R. Rivest, *J. Inorg. Nuclear Chem.*, **31**, 399 (1969).

[26] *a*. D. M. Adams and H. A. Gebbie, *Spectrochim. Acta*, **19**, 925 (1963); *b*. D. M. Adams, J. Chatt, J. M. Davidson and J. Gerratt, *J. Chem. Soc.*, **1963**, 2189.

[27] D. M. Adams, J. Chatt, J. Gerrat and A. D. Westland, *J. Chem. Soc.*, **1964**, 734.

[28] A. Sabatini and L. Sacconi, *J. Amer. Chem. Soc.*, **86**, 17 (1964).

[29] R. J. H. Clark and C. S. Williams, *Inorg. Chem.*, **4**, 350 (1965).

[30] *a*. I. R. Beattie, G. B. McQuillan, L. Rule and M. Webster, *J. Chem. Soc.*, **1963**, 1514; *b*. I. R. Beattie and L. Rule, *J. Chem. Soc.*, **1964**, 3267.

[31] I. Douek, M. J. Frazer, Z. Goffer, M. Goldstein, B. Rimmer and H. A. Willis, *Spectrochim. Acta*, **23A**, 373 (1967).

[32] M. Cox, R. J. H. Clark and H. J. Milledge, *Nature*, **212**, 2357 (1966).

[33] N. Ohkaku and K. Nakamoto, *Inorg. Chem.*, **12**, 2440, 2446 (1973).

intensity bands in the region 360–330 cm^{-1} for the ν(Sn–Cl) vibration in these complexes.

Adams and Chandler[34] have used ν(M–Cl) vibrations to decide the stereochemistry of halogen-bridged complexes of platinum (II) and palladium (II) and have distinguished between bridging and terminal metal halogen bonds. They have fixed the region 370–340 cm^{-1} for the terminal and 335–300 cm^{-1}, 290–250 cm^{-1} regions for bridging ν(M–Cl) vibrations. Jain and Rivest[25] have assigned a band in the vicinity of 397 cm^{-1} to the ν(Ti–Cl) in the hexacoordinated Ti(IV) complexes, and the band at 262 cm^{-1} to the $Ti-Cl\rightarrow Ti$ type bonding.

The choice between structures *A* and *B* of the tin (IV) complexes under present investigation is made on the observed ν(Sn–Cl) vibrations in the region 360–330 cm^{-1}. This is the characteristic band for the hexacoordinated tin(IV) complexes. The bands in the region 310–230 cm^{-1} suggest that the $Sn-Cl\rightarrow Sn$ type bondings may be present in the complexes VII–XII.

All these evidences suggest that complexes VII—XII favour structure *B*.

ACKNOWLEDGEMENT. Authors wish to thank Prof. D. W. A. Sharp, Departement of Chemistry, University of Glasgow, Scotland, for the infrared spectra. One of the authors (B. R. P.) is thankful to Dr. S. P. Hiremath, Head, Department of Chemistry, P. G. Centre, Gulbarga, for his encouragement.

[34] D. M. Adams and P. J. Chandler, *Chem. Comm.*, 3, 69 (1966).

Revue Roumaine de Chimie, **22**, *11—12*, 1487 – 1492 (1977)

PREPARATION AND INVESTIGATION OF Hg(II) COMPLEX COMPOUNDS WITH TRIARYLSTIBINES

D. NEGOIU [*] and LIDIA PARUTA [**]

[*] Faculty of Chemistry, Polytechnic Institute of Bucharest, Splaiul Independenţei 89,
Bucharest, Romania
[**] Center of Physical Chemistry, Str. Dumbrava Roşie 23, Bucharest — 9, Romania

Received June 5, 1975

The present paper reports the preparation of two series of Hg(II) complex compounds with triarylstibines of the type: $[(HgX_2)_2L_2]$ and $[(HgX_2)_3L_2]$, where $X = Cl^-$, Br^-, I^- and $L = (o\text{-}, m\text{-}, p\text{-tolyl})_3Sb$; $(o\text{-}, m\text{-}, p\text{-xylyl})_3Sb$. The compounds are characterized by elemental analysis, melting points, molecular weight, conductivity measurements, UV and infrared spectra.

The first preparation of complex compounds of trialkylstibines with mercuric iodide has been described by Partheil and Mannheim.[1] These syntheses are connected with some difficulties, related to air sensitivity of alkylstibines, the slight affinity of stibium for organic groups (especially the alkyl ones), and also to their easy reduction to metal, when stibines are added even to cold mercuric chloride solution. [2] Another influencing factor may be the poor crystallizability of the stibium salts.

Subsequent investigations of similar Hg(II) and Cd(II) compounds with several types of phosphines and arsines were also carried out since 1940 by Evans, Mann and Puedie. [3] They point out that basically Hg(II) halides can form five classes of such nonionic compounds, namely: $[HgX_2L_2]$, $[(HgX_2)_2L_2]$, $[(HgX_2)_3L_2]$, $[(HgX_2)_4L_2]$ and $[(HgX_2)_2L_3]$, where L = phosphine, arsine and $X = Cl^-$, Br^-, I^-.

Our investigations pointed out that under the same conditions tertiary arylstibines form only compounds of the type: $[(HgX_2)_2L_2]$ and $[(HgX_2)_3L_2]$. Compounds with another metal : ligand combination ratio are unstable; they dissociate in solution and each time the above mentioned compounds are obtained.

In the present work 24 compounds have been prepared: $[(HgX_2)_2L_2]$ class has been obtained by refluxing alcoholic solutions of Hg(II) halides with tolyl or xylylstibines, whereas the $[(HgX_2)_3L_2]$ class has been synthetized by the interaction of $[(HgX_2)_2L_2]$ compounds with an excess of Hg(II) halide in alcohol or hot acetone. The compounds thus obtained are crystalline colourless of slightly yellow, with well defined melting points (table 1).

---

[1] R. Partheil and E. Mannheim, *Arch. Pharm.*, **238**, 166 (1900).

[2] W. Dyke and W. Jones, *J. Chem., Soc.*, **1930**, 1921.

[3] R. C. Evans, F. G. Mann, A. Preiser and D. Puedie, *J. Chem. Soc.*, **1940**, 1209.

Some characteristics of the compounds are presented in table 2.

Table 1

Complex compounds of Hg(II) with tritolylstibines and trixylylstibines of the type $[(HgX_2)_2L_2]$ and $[(HgX_2)_3L_2]$

Compound	Colour	Melting point °C	Elemntal analysis					
			C %		H %		Halogen %	
			Calcd.	*Found*	*Calcd.*	*Found*	*Calcd.*	*Found*
$(HgCl_2)_2(SboT_3)_2$	white	163–165	37.8	37.5	3.1	2.8	10.6	9.9
$(HgBr_2)_2(SboT_3)_2$	white	183–185	33.3	33.0	2.6	2.0	21.1	20.6
$(HgI_2)_2(SboT_3)_2$	yellow	175–176	29.6	29.2	2.4	1.8	29.8	29.6
$(HgBr_2)_3(SboT_3)_2$	white	178–180	26.9	30.0	2.2	1.6	25.6	25.0
$(HgCl_2)_3(SbmT_3)_2$	white	300	31.4	29.9	2.6	2.0	13.2	13.0
$(HgBr_2)_3(SbmT_3)_2$	white	300	26.9	26.6	2.2	1.7	25.6	25.3
$(HgI_2)_3(SbmT_3)_2$	yellow	300	23.4	23.3	1.9	1.4	35.3	34.8
$(HgCl_2)_2(SbpT_3)_2$	white	195–198	37.8	37.5	3.1	2.6	10.6	10.1
$(HgBr_2)_2(SbpT_3)_2$	white	178–180	33.3	33.0	2.6	2.2	21.1	19.6
$(HgCl_2)_3(SbpT_3)_2$	white	235–240	31.4	31.1	2.6	2.4	13.2	12.7
$(HgBr_2)_3(SbpT_3)_2$	white	220–225	26.9	26.5	2.2	2.0	25.6	25.2
$(HgI_2)_3(SbpT_3)_2$	yellow	147–149	23.4	23.2	1.9	1.5	35.3	34.7
$(HgCl_2)_2(SbpX_3)_2$	white	172–173	40.6	40.5	3.7	3.0	11.1	10.6
$(HgBr_2)_2(SbpX_3)_2$	white	166–170	36.1	35.8	3.3	2.8	20.0	19.3
$(HgI_2)_2(SbpX_3)_2$	yellow	160	32.3	31.9	3.0	2.4	28.0	27.5
$(HgI_2)_3(SbpX_3)_2$	yellow	168–171	25.7	25.4	2.4	1.9	34.0	33.4
$(HgCl_2)_2(SbmX_3)_2$	white	163–165	40.6	40.2	3.7	3.1	11.1	10.8
$(HgBr_2)_2(SbmX_3)_2$	white	213–215	36.1	36.0	3.3	2.8	20.0	19.6
$(HgI_2)_2(SbmX_3)_2$	yellow	196–200	32.3	32.1	3.0	2.6	28.0	27.5
$(HgI_2)_3(SbmX_3)_2$	yellow	210–215	25.7	25.5	2.4	2.0	34.0	33.6
$(HgCl_2)_2(SboX_3)_2$	white	90– 92	46.0	39.0	3.7	3.1	11.1	10.7
$(HgBr_2)_2(SboX_3)_2$	white	85– 88	36.1	35.6	3.3	2.9	20.0	19.7
$(HgI_2)_2(SboX_3)_2$	yellow	76– 77	25.7	25.6	2.4	1.8	28.0	27.5
$(HgI_2)_3(SboX_3)_2$	yellow	138–140	25.7	25.4	2.4	1.9	34.0	33.4

Lindqvist[4] was the first to describe some similar compounds with various phosphines or arsines formulated as simple compounds of the type $(R_3P.HgX_2)$, but Evans and Mann[3] assigned to such compounds a dimeric formula. This conclusion was also fully confirmed by the results of our investigations on compounds of the type: (HgX_2L) (see table 2).

Electric conductivity measurements carried out in nitrobenzene, and the determinations of magnetic susceptibility point out that all these compounds are not electrolytes and are diamagnetic. This is explained by the electronic configuration of Hg(II) with the electrons coupled.

---

[4] I. Lindqvist, *Acta Chim. Scand.*, **13**, 1353 (1959).

Table 2

Some properties of Hg(II) complexes

Compound	Molecular weight		Molecular state	Electrical conductivity $\Lambda(\Omega^{-1}\,cm^2\,mol^{-1})$
	Calcd.	*Found*		
$(\mathrm{HgCl_2})_2(\mathrm{Sb}o\mathrm{T_3})_2$	1 332	1 095	dimeric	0.97
$(\mathrm{HgBr_2})_2(\mathrm{Sb}o\mathrm{T_3})_2$	1 510	1 181	dimeric	1.15
$(\mathrm{HgI_2})_2(\mathrm{Sb}o\mathrm{T_3})_2$	1 698	1 339	dimeric	0.75
$(\mathrm{HgBr_2})_3(\mathrm{Sb}o\mathrm{T_3})_2$	1 870	1 595	monomeric	1.68
$(\mathrm{HgCl_2})_2(\mathrm{Sb}p\mathrm{T_3})_2$	1 332	1 154	dimeric	0.83
$(\mathrm{HgBr_2})_2(\mathrm{Sb}p\mathrm{T_3})_2$	1 510	1 269	dimeric	0.69
$(\mathrm{HgCl_2})_3(\mathrm{Sb}p\mathrm{T_3})_2$	1 604	1 320	monomeric	1.10
$(\mathrm{HgCl_2})_2(\mathrm{Sb}p\mathrm{X_3})_2$	2 290	1 963	dimeric	0.90
$(\mathrm{HgBr_2})_2(\mathrm{Sb}p\mathrm{X_3})_2$	2 467	2 130	dimeric	0.75
$(\mathrm{HgI_2})_2(\mathrm{Sb}p\mathrm{X_3})_2$	2 655	2 467	dimeric	0.55
$(\mathrm{HgCl_2})_2(\mathrm{Sb}m\mathrm{X_3})_2$	2 290	1 890	dimeric	0.65
$(\mathrm{HgBr_2})_2(\mathrm{Sb}m\mathrm{X_3})_2$	2 467	2 149	dimeric	1.05
$(\mathrm{HgI_2})_2(\mathrm{Sb}m\mathrm{X_3})_2$	2 655	2 315	dimeric	0.85
$(\mathrm{HgI_2})_3(\mathrm{Sb}m\mathrm{X_3})_2$	2 236	2 098	monomeric	1.89

According to the crystal field theory, which does not allow absorption bands in visible for d^{10} configuration, the Hg(II) compounds will have bands placed in the ultraviolet range. These are due to transitions in coordinated tritolyl and trixylylstibine.

Pointing out that the electronic spectrum of the substituted arylstibines can be satisfactorily interpreted in terms of a charge transfer model, Cullen and Hochstrassen[5] reported two systems of bands within the 210—360 nm range. Our data also point to the presence of two bands : the first band is atributed to the transition of one electron from the lone pair of antimony atom to a π antibonding orbital of the benzene ring ($n \rightarrow \pi^*$). According to LACO — MO[6] description, such a transition consists in the excitation of one electron in nonbonding orbital (n orbital), localized mainly on a certain atom into an antibonding orbital (π^* orbital), extended over more atoms in the molecule. This band is affected both by the nature, the position and number of substituents.

In arylstibines with methyl substituents on the aromatic nucleus the $n \rightarrow \pi^*$ transition exhibits a red shift, suggesting a greater conjugation interaction between the antimony free electron pair and the aromatic ring. The electron pair is thus less available for coordinative bond formation than in triphenylstibine. This shift takes place gradually, depending on the nature, position and number of the substituents, as can be seen from figures 1, 2, 3.

Therefore, in the arylstibines series, triphenylstibine presents more characteristic donor properties. This is confirmed by the experimental findings, namely : the stability of the prepared complexes diminishes with the increase of methyl groups on the aromatic ring and with the increasing distance to the donor atom.

---

[5] W. R. Cullen and R. M. Hochstrasser, *J. Mol. Spectroscopy,* **5,** 118 (1960).

[6] J. W. Sidman, *Chem. Rev.*, **58,** 689 (1958).

The second band recorded in the electronic spectrum is marked with $\pi \rightarrow \pi^*$ and it is attributed to an aromatic ring transition. In contrast to the first one, the latter band is not affected by any factor.

As it has been mentioned above the compounds of the type: $(HgX_2)_2L_2]$ are presented in dimeric form, i. e. as dihalogeno-bis(tristibino)-μ-dihalogeno-dimercury compounds.

It is obvious that a correct structural formula must indicate halogen bridges. Theoretically three isomeric forms can exist: asymmetrical (I), *cis*-symmetrical (II) and *trans*-symmetrical (III),

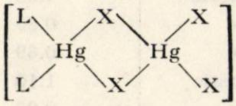

(I)

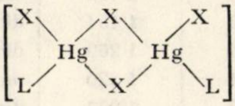

(II)

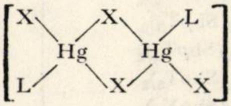

(III)

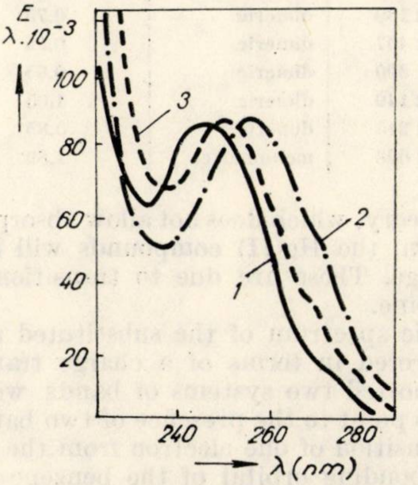

Fig. 1. — Ultraviolet absorption spectra of: *1.* $[Sb(C_6H_5)_3]$; *2.* $[Sb\text{-}o\text{-}tolyl_3]$; *3.* $[Sb\text{-}m\text{-}tolyl_3]$;

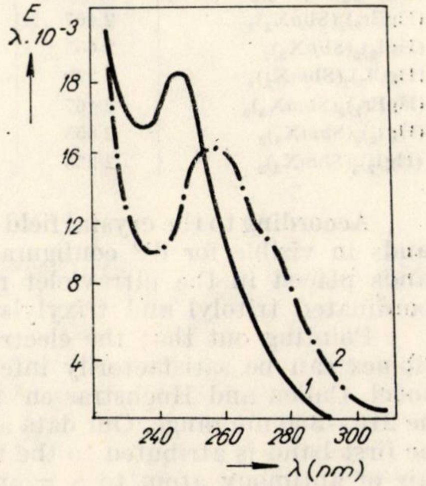

Fig. 2. — Ultraviolet absorption spectra of: *1.* $[Sb\text{-}m\text{-}tolyl_3]$; *2.* $[Sb\text{-}m\text{-}xylyl_3]$;

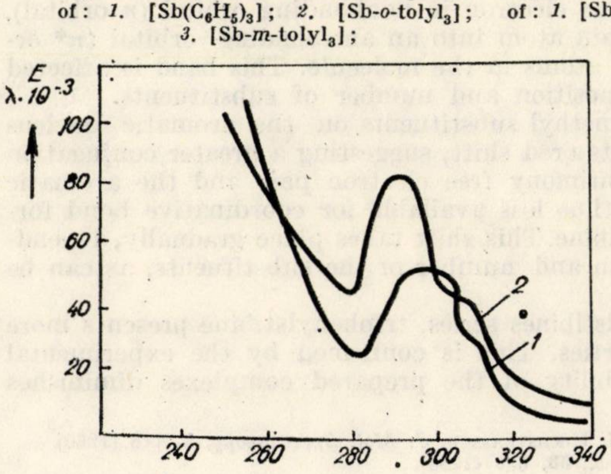

Fig. 3. — The electronic spectra of: *1.* $[HgCl_2.Sb\text{-}p\text{-}tolyl_3]$; *2.* $[HgCl_2.Sb\text{-}p\text{-}xylyl_3]$;

Numerous crystallographical studies performed for analogous compounds with dipalladium, dicadmium and dimercury bridges suggest a single structure, namely the *trans*-symmetrical (III) form, with a tetrahedral arrangement of the four groups, around each mercury atom. In the case of the type $[(HgX_2)_3L_2]$ compounds, a bicyclic doubly bridged structure, without a symmetry center can be considered :

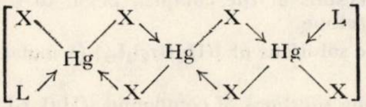

But in some cases compounds with completely different structures were obtained, which this time have a symmetry center and contain bridges between the molecular compounds $[(HgX_2)_2L_2]$ and simple molecules HgX_2. Such a bridged molecule could be of the type :

$$(Tolyl_3Sb)XHgX_2HgX(Tolyl_3Sb) \quad X{=}halogen$$

where each bridged mercury atom is linked to four groups, with a considerable distortion of the normal tetrahedral arrangement. On both sides of this molecular bridge there are molecules of HgX_2.

Because of the continuous alternation of bridges and HgX_2 molecules, a symmetry center may exist in the crystal at each mercury atom, and also at the center of each bridge in the ring at point X. Therefore, the different structure of this class of compounds is not completely known.

The vibration spectra within the 250—800 cm^{-1} range were of litlle use for establishing the structure of the compounds, because both terminal and bridge Hg—X vibration frequencies occur below the lower limit of the instrument used. Thus, only the bands assigned to the respective ligands were identified.

EXPERIMENTAL

The preparation of tritolyl- and trixylylstibines was described in a previous paper[7].

THE PREPARATION OF $[(HgX_2)_2L_2]$ compounds, where L = *o*-, *m*-, *p*-tolyl$_3$Sb, *o*-, *m*-*p*-xylyl$_3$Sb

$[(HgCl_2)_2L_2\ ]$ are obtained by treating an alcoholic solution of stibine (2 moles) with a solution of mercuric chloride (2 moles) in water, under reflux and continuous stirring. After some time a bulky precipitate is separated; after storrage on ice for several hours it is filtered and washed with alcohol and acetone.

$[(HgBr_2)_2L_2]$ are obtained by the same method, with the difference that only alcoholic solutions are used.

$[(HgI_2)_2L_2]$ The alcohol solution of stibine (2 moles) is added in small quantities, under stirring, to an alcoholic solution of mercuric iodide (2 moles) to which a 12% KI solution

---

[7] D. Negoiu and L. Paruta, *Rev. Roumaine Chim.*, **18**, 2059 (1973).

has been added. A viscous yellow oil is immediately separated and this solidifies. It is purified by recrystallization from acetone. One must work carefully as the compound is unstable in the presence of solvent excess and is quickly converted into $[(HgI_2)_3L_2]$.

THE PREPARATION OF $[(HgX_2)_3L_2]$ COMPOUND

$[(HgCl_2)_3L_2]$; these are obtained by treating an alcoholic solution of stibine (1 mole) with an excess of mercuric chloride (3 moles) in water solution, for a longer time under refluxing. After *ca* 5 hours crystals of the complex begin to separate. They are filtered and washed with alcohol and acetone.

$[(HgBr_2)_3L_2]$; alcoholic solutions of $[(HgBr_2)_2L_2]$ (1 mole) are treated under reflux with $HgBr_2$ (2 moles).

$[(HgI_2)_3L_2]$; hot acetone solutions of compound $|(HgI_2)_2L_2|$ (1 mole) and HgI_2 (1 mole) are mixed. The precipitate thus obtained is purified by dilution with a hot solution of alcohol and acetone (in equal amounts).

Revue Roumaine de Chimie, **22**, *11–12*, 1493–1497 (1977)

PYRIDINE-N-OXIDE COMPLEXES OF RARE-EARTH BROMIDES

P. V. SIVAPULLAIAH and S. SOUNDARARAJAN

Department of Inorganic and Physical Chemistry
Indian Institute of Science, Bangalore-560012, India

Received July 2, 1975

Pyridine-N-oxide (PyO) complexes of eight rare-earth bromides of the composition $MBr_3(PyO)_6.2H_2O$ where M=La, Pr, Nd, Sm, Gd, Dy, Yb and Y have been prepared and characterized by analysis, molecular weight, conductance and infrared data. Infrared studies reveal the coordination of PyO through the oxygen of the N–O group and also the coordination of water to the metal. Conductivity data in acetonitrile indicate a coordination number of ten for all rare-earths.

INTRODUCTION

While many complexes of rare-earth chlorides, nitrates, perchlorates and thiocyanates are known, those of bromides are very few.[1–4] As is known, the anion plays an important role in the coordination of ligands to the rare-earth ions. So far, only little work has been done to study the role of bromide ion in the rare-earth complexes. Our recent studies on dimethylsulphoxide (DMSO) complexes of rare-earth bromides reveal that two bromide ions are coordinated to the rare-earth ions as well as eight DMSO molecules so as to make a coordination number of ten for all rare-earths.[5] In order to study further the effect of the bromide ion on the coordination number of rare-earth ions, we started the work on PyO complexes of rare-earth bromides.

PyO complexes of transition and non-transition metal salts have been studied.[6–8] PyO complexes of rare-earth perchlorates[9] and nitrates[10] are known as well as the complexes[11] with the anion $[Cr(SCN)_6]^{3-}$.

---

[1] T. Moeller and G. Giffin, PB Report 136 162; *Chem. Abstr.*, **54.** 10623 (1960).

[2] K. Rossmanith, *Monatsh. Chem.*, **97**, 1357 (1966).

[3] G. Vicentini and C. Airoldi, *J. Inorg. Nuclear Chem.*, **17**, 1733 (1971).

[4] M. I. Labanov, *Russ. J. Inorg. Chem.*, **17**, 1490 (1972).

[5] P. V. Sivapullaiah and S. Soundararajan, *Current Science*, **44** (11), 374 (1975).

[6] N. M. Karayannis, L. L. Pytlewski and C. M. Mikulski, *Coord. Chem. Rev.*, **11**, 93 (1973).

[7] R. G. Garvey, J. H. Nelson and R. O. Ragsdale, *Coord. Chem. Rev.*, **3**, 375 (1968).

[8] M. Orchin and P. J. Schmidt, *Coord. Chem. Rev.*, **3**, 345 (1968).

[9] V. N. Krishnamurthy and S. Soundararajan, *Canad. J. Chem.*, **45,** 189 (1967).

[10] G. A. Pneumaticakis, *Chem. and Ind.*, *(London)*, **1968,** 770.

[11] E. S. Pavlenko, V. N. Kumok, Z. A. Grankina and V.V. Serebrennikov, *Tr. Tomsk. Univ.*, 1971, No. 204, 327; *Chem. Abstr.*, **78,** 131517 (1973).

Very recently PyO complexes of rare-earth iodides have been prepared and characterized in this laboratory.[12] PyO complexes of europium bromide and other salts of europium have been prepared and their fluorescence spectra studied.[13] The present paper described the preparation and characterization of eight complexes of rare-earth bromides with PyO. The preparative method employed for the present complexes is simple and different from that reported for the europium complex.[13]

EXPERIMENTAL

Materials used (1) Pyridine-N-oxide: This was prepared according to the method of Ochiai[14] and purified by vacuum distillation (129°/2 mm).

(2) Rare-earth bromides: Hydrated rare-earth bromides were prepared by dissolving the corresponding oxide (obtained from American Potash and Chemicals Corporation, U. S. A.) in dilute hydrobromic acid and evaporating the solution on a water bath to near dryness. The product was dried in a desiccator over calcium chloride. The crystals were then washed with dry benzene to remove any excess of free acid and maintained in a desiccator over calcium chloride.

All the solvents used were purified by standard methods.

Preparation of the complexes. All the complexes were prepared by the same method. To 0.5 gm of the hydrated rare-earth bromide was added 1 gm of PyO and the mixture was triturated. Then about 20 ml of acetone was added and the contents were stirred well. The fine crystalline product obtained was filtered off through a sintered crucible and washed well with cold acetone to remove any free PyO present. The complexes were dried over phosphorus (V) oxide in a vacuum desiccator.

Analyses. The complexes were analysed for the metal, bromide and Py O parts. The metal content was estimated by EDTA titrations using xylenol orange as indicator.[15] Bromide content was estimated by Volhard's method.[16] PyO was estimated spectrophotomerically at 257 nm using the calibration curve method.[17] The analytical results are presented in table 1.

Table 1

Analytical data

Complex	% Metal		% Bromide		% PyO	
	Found	Calcd.	Found	Calcd.	Found	Calcd.
$LaBr_3(PyO)_6.2H_2O$	14.13	14.10	24.21	24.35	58.24	57.92
$PrBr_3(PyO)_6.2H_2O$	14.26	14.27	24.18	24.31	57.98	57.80
$NdBr_3(Py)O)_6.2H_2O$	14.43	14.56	24.10	24.22	57.22	57.59
$SmBr_3(PyO)_6.2H_2O$	15.05	15.09	23.97	24.07	56.92	57.24
$GdBr_3(PyO)_6.2H_2O$	15.58	15.67	23.92	23.91	56.54	56.84
$DyBr_3(PyO)_6.2H_2O$	16.08	16.11	23.85	23.80	56.39	56.58
$YbBr_3(PyO)_6.2H_2O$	17.23	17.10	23.60	23.72	56.32	56.40
$YBr_3(PyO)_6.2H_2O$	9.34	9.50	25.42	25.65	61.73	61.01

---

[12] L. Ramakrishnan and S. Soundararajan, *Monatsh. Chem.*, (in press).

[13] E. Butter and W. Seifert, *Z. anorg. chem.*, **368,** 133 (1969).

[14] E. Ochiai, *J. Org. Chem.*, **18,** 534 (1953).

[15] I. M. Kolthoff and P. J. Elwing, "Treatise on Analytical Chemistry", Part II, Vol. 8, Interscience, New York, 1963, p. 57.

[16] A. I. Vogel, "A Text-book of Quantitative Inorganic Analysis", Third edition, Longmans, London, 1962, p. 287.

[17] H. H. Willard, L. L. Merrit and J. A. Dean, "Instrumental Methods of Analysis", 4th edition, Affiliated East-West Press Pvt., Ltd., New Delhi, 1965, p. 89.

Infrared studies. The infrared spectra of the complexes were recorded in nujol mulls in a Carl-Zeiss UR-10 spectrophotometer. The important absorbtion bands and their assignments are given in table 2.

Table 2

IR spectral data

PyO in solution cm^{-1}	$GdBr_3(PyO)_6 .2H_2O$** in mull.cm^{-1}	Assignment
	3 320 w	
	3 280 w	O—H stretching
	3 230 w	
3 070 w*	3 116 w	C—H stretching
	3 056 w	
	1 640 m	H—O—H bending and ring
1 610 m*		stretching ring deformation
1 463 s*	1 472 vs	ring deformation C—H in-plane
	1 258 m	deformation
		N—O stretching
1 265 vs	1 230 vs	
1 188 w	1 185 m	
1 166 s	1 172 m	
	1 152 w	C—H in-plane deformation
	1 095 w	
1 068 w	1 076 w	
1 014 s	1 028 s	ring breathing
887 m	930 w	C—H out-of-plane vibration
840 s	840 s	N—O bending
758 vs	785 vs	C—H out-of-plane deformation
	678 s	rocking mode of coordinated H_2O

Abbreviations: vs = very strong; s = strong; m = medium; w = weak;
* = CCl_4 solution spectrum, others in CS_2
** = The spectra of other complexes are very similar (within ± 2 cm^{-1})

Conductivity measurements. Molar conductance data were obtained in a Siemens conductivity bridge using an immersion cell (type LTA) previously calibrated with standard KCl solutions. The concentrations of the solutions used were of the order of 0.001M. The molar conductances of the complexes in water, dimethylformamide (DMF) and acetonitrile were determined.

Molecular weight measurements. Molecular weights of a few representative complexes were determined in water using the Beckmann's freezing point method. However, molecular weight determinations in organic solvents by collegative methods were not possible because of the low solubility of the complexes in suitable solvents.

The molecular weight and conductance data are given in table 3.

RESULTS AND DISCUSSION

Analytical results conform to the formula $MBr_3(PyO)_6.2H_2O$ where M=La, Pr, Nd, Sm, Gd, Dy, Yb or Y. The composition of the present complexes is different from the one reported[13] for the PyO complex

Table 3

Conductance and molecular weight data

Complex	Molar conductance, $ohm^{-1} cm^2 mole^{-1}$			Molecular weight in water	
	in water*	in DMF **	in acetonitrile ***	Observed	Calculated for complete dissociation
$LaBr_3(PyO).2H_2O$	380.3	175.2	110.1	99.1	98.5
$PrBr_3(PyO).2H_2O$	370.9	170.7	112.3	..	..
$NdBr_3(PyO).2H_2O$	377.9	166.0	110.9	..	..
$SmBr_3(PyO).2H_2O$	387.4	160.4	112.7	99.8	99.7
$GdBr_3(PyO).2H_2O$	368.4	176.7	111.3	..	..
$DyBr_3(PyO).2H_2O$	371.4	174.0	111.8	..	..
$YbBr_3(PyO).2H_2O$	369.7	162.3	109.5	102.2	101.9
$YBr_3(PyO).2H_2O$	375.0	162.1	118.2	..	..

* In water, 1 : 3 electrolytes have a molar conductance 360 $ohm^{-1} cm^2 mole^{-1}$ (ref.[23]),

** In DMF, 1 : 2 electrolytes have a molar conductance in the range 140 – 170 $ohm^{-1} cm^2 mole^{-1}$ (ref[24]).

*** In acetonitrile, 1 : 1 electrolytes have a molar conductance in the range 120 – 160 $ohm^{-1} cm^2 mole^{-1}$).

of europium bromide. By varying the method of preparation, such changes in the composition are known to occur.[18]

The complexes are very hygroscopic and soluble in water, methanol, DMF, dimethylsulphoxide, acetonitrile and are insoluble in nonpolar solvents and acetone. In their colour, the complexes closely resemble their parent salts.

The infrared spectra of the complexes are almost similar irrespective of the central metal ion. The N–O stretching vibration occurring at 1265 cm^{-1} in the free ligand[19] (in CS_2 solution) is shifted to about 1230 cm^{-1} in the complexes indicating the coordination of the PyO through oxygen of the N–O group. The shift observed (*ca.* 35 cm^{-1}) in this series is less than that observed in the corresponding perchlorate complexes[9] which indicates the weaker metal-ligand bond in the lanthanide bromide complexes compared to that in the lanthanide perchlorate complexes. This shift is slightly more (*ca.* 3 cm^{-1}) than that observed in the iodide complexes.[12]

The N–O bending vibration of PyO, tentatively assigned[19] to a strong band at about 840 cm^{-1}, undergoes no appreciable change upon coordination as in other PyO complexes indicating that the two opposing influences, (1) the effect of the bonded metal atom on the N–O group which would cause a vibrational shift to higher frequencies and (2) the decrease in the double bond character of the N–O bond arising from the coordination which would tend to lower the frequency, are very nearly equal.

The C–H out-of-plane vibration appearing at 758 cm^{-1} in the free ligand[19] (in CS_2 solution) is shifted to higher frequencies by about 25 cm^{-1} in the complexes. But the C–H out-of-plane vibration of PyO occurring at 887 cm^{-1} (in CS_2 solution) is shifted to about 930 cm^{-1} in the complexes. Such shifts are also known in other PyO complexes. Both these shifts are attributed to a decrease in the electron density in the ring consequent upon the formation of the metal to ligand bond.[20]

---

[18] C. H. Harrison and W. H. Watson, *J. Inorg. Nuclear Chem.*, **32**, 2255 (1970).

[19] S. Kida, J. V. Quagliano, J. A. Walmsley and S. Y. Tyre, *Spectrochim. Acta*, **19**, 189 (1963).

The strong band at 1014 cm^{-1} in the spectrum of PyO (in CS_2 solution) due to ring breathing vibration[19] undergoes a shift of about 14 cm^{-1} to higher frequencies in the complexes. The 1610 cm^{-1} band of the PyO ascribed to the in-plane vibration of the pyridine ring is overlapped by the H_2O bending vibration.

New bands appearing in the region 3360—3250 cm^{-1} in the complexes can be assigned to O—H stretching vibrations of water.[21] The band at 1640 cm^{-1} in the complexes is assigned to H—O—H bending vibration of water. The occurrence of stretching frequencies at a relatively lower frequencies and bending frequency at a slightly higher frequency, coupled with the fact that a new band is appearing at 678 cm^{-1} (which can be assigned to rocking mode of the coordinated water) lead us to the conclusion that the water in the present complexes is coordinated to the metal.[22]

Conductance data in water, DMF and acetonitrile are in good agreement with those reported for 1: 3, 1: 2, and 1: 1 electrolytes respectively.[23,24] This suggests that two of the bromide ions are coordinated to the metal in acetonitrile, a solvent of poor donor properties. Thus, a coordination number of ten can be postulated for all rare-earths.

It is of interest to note that the coordination number of the rare-earths in the corresponding perchlorates[9] and iodides[12] is eight and the number of PyO entering the coordination sphere is also eight. But in the present bromides, though the number of PyO entering the coordination sphere is only six, a coordination number of ten has been observed.

Molecular weight data in water show that the complexes dissociate completely in water.

ACKNOWLEDGEMENT. One of the authors (P. V. S.) thanks the C. S. I. R., India for a fellowship. The authors thank Mr. D. K. Koppikar and Mr. L. Ramakrishnan for helpful discussions.

---

[20] Y. Kakiuti, S. Kida and J. V. Quagliano, *Spectrochim. Acta*, **19**, 201 (1963).

[21] K. Nakamoto, "Infrared Spectra of Inorganic and Coordination Compounds", 2nd edition, Wiley Interscience, New York, 1970, p. 166.

[22] G. Sartori, C. Furlani and A. Damiani, *J. Inorg. Nuclear Chem.* **8**, 119 (1958).

[23] A. Weissberger and B. W. Rossiter, "Physical Methods in Chemistry", "Techniques of Chemistry", Vol. I, Part II-A, Wiley Interscience, New York, 1971, p. 199.

[24] W. J. Geary, *Coord. Chem. Rev.*, **7**, 81 (1971).

at [illegible] cm⁻¹ (in CS_2 solution) is shifted to about [illegible] cm⁻¹ in the complexes. Such shifts are also known in other PyO complexes. Such shifts are attributed to a decrease in the electron density in the ring consequent upon the formation of the metal to ligand bond.[4]

The strong band at 1011 cm⁻¹ in the spectrum of PyO (in CS_2 solution) due to ring breathing vibration[5] undergoes a shift of about [illegible] cm⁻¹ to higher frequencies in the complexes. The 1610 cm⁻¹ band of the PyO ascribed to the in-plane vibration of the pyridine ring is overlapped by the H_2O bending vibration.

New bands appearing in the region 3380–3200 cm⁻¹ in the complexes can be assigned to O–H stretching vibrations of water.[6] The band at 1640 cm⁻¹ in the complexes is assigned to H–O–H bending vibration of water. The occurrence of stretching frequencies at relatively lower frequencies and bending frequency at a slightly higher frequency, coupled with the fact that a new band is appearing at [illegible] cm⁻¹ (which can be assigned to rocking mode of the coordinated water) lead us to the conclusion that the water in the present complexes is coordinated to the metal.[6]

Conductance data in water, DMF and acetonitrile are in good agreement with those reported for 1:3, 1:2, and 1:1 electrolytes respectively.[7,8] This suggests that two of the [illegible] ions are coordinated to the metal in acetonitrile, a solvent of poor donor properties. Hence a coordination number of [illegible] can be postulated for all these complexes.

It is of interest to note that the coordination number of the rare earths in the corresponding perchlorates and iodides[9] is eight and the number of PyO entering the coordination sphere is also eight. But in the present complexes, though the number of PyO entering the coordination sphere is only six a coordination number of eight is [illegible].

Molecular weight data in water show that the complexes dissociate completely in water.

ACKNOWLEDGEMENT. One of the authors ([illegible]) is [illegible] to the [illegible] for a fellowship. The authors thank Mr. [illegible] for helpful discussions.

---

[4] [illegible] Kakiuti, [illegible] and [illegible], Spectrochim. Acta, 19, 201 (1963).

[5] K. Nakamoto, "Infrared Spectra of Inorganic and Coordination Compounds", 2nd edition, Wiley Interscience, New York 1970, p. [illegible].

[6] [illegible] and [illegible], J. Inorg. Nucl. Chem. 8, [illegible] (1958).

[7,8] [illegible] and [illegible], "Physical Methods in [illegible] Chemistry", Vol. 1, [illegible] Wiley Interscience, New York, 19[illegible], p. [illegible].

[9] [illegible], Coord. Chem. Rev. [illegible] (1971).

Revue Roumaine de Chimie, 22, 11–12, 1499–1504 (1977

ISOTOPIC EXCHANGE OF ACTIVE METHYL GROUPS. X[1]

ACTIVATION PARAMETERS FOR DEUTERIATION AND DE-DEUTERIATION OF ISOPROPYLPYRYLIUM SALTS

ILEANA I. STĂNOIU,[a] ALEXANDRU T. BALABAN,[a,b,c] and FILIP CHIRALEU [d]

[a] Institute of Atomic Physics, P. O. B. 5206, Bucharest, Romania
[b] To whom correspondence should be addressed
[c] Department of Organic Chemistry, The Polytechnic, Bucharest
[d] Research Centre of Organic Chemistry, Bucharest

Received April 7, 1977

The activation parameters were determined for the deuteriation (in buffered deuterium oxide) and de-deuteriation (in buffered aqueous solution) for the isotopic exchange of the isopropyl benzylic proton in 2,6-dimethyl-4-isopropyrylium perchlorate ($I \rightleftharpoons I-d_1$).

In previous parts of this series, [2,3] the kinetics of deuteriation and de-deuteriation of isopropyl groups bonded to α- or γ-positions of pyrylium salts I–III was studied; in these cases the kinetic expressions are quite simple because only one hydrogen atom undergoes isotopic exchange in an isopropyl group. The kinetic isotope effect was determined for I and II, [2] and rates of exchange for α-standing methyl and isopropyl groups were compared intramolecularly for III. [3]

The present study completes the kinetic investigation of isotopic exchange for isopropyl groups by determining activation parameters for the γ-isopropyl group in 2,6-dimethyl-4-isopropylpyrylium perchlorate (I): deuteriations were effected in buffered deuterium oxide solutions, de-deuteriations in buffered aqueous solutions of approximately the same pH and ionic strengths.

---

[1] Previous part is ref. 3.

[2] I. I. Stănoiu, F. Chiraleu, E. Gârd and A. T. Balaban, *Rev. Roumaine Chim.*, **22**, 117 (1977).

[3] I. I. Stănoiu, E. Gârd, C. Uncuţa, F. Chiraleu and A. T. Balaban, *Rev. Roumaine Chim.*, **22**, 1359 (1977).

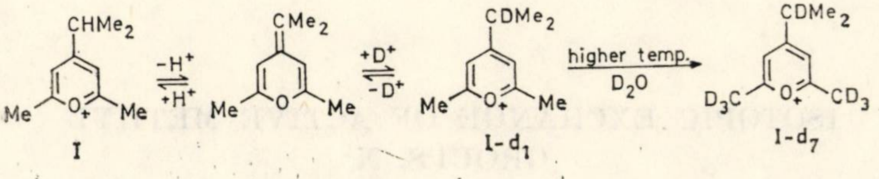

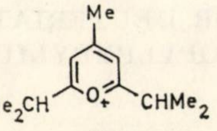

II

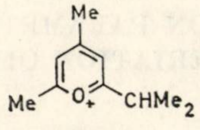

III

EXPERIMENTAL PART

2,6-Dimethyl-4-isopropylpyrylium perchlorate (I) was obtained by diacetylation of 2,3-dimethyl-2-butene with acetyl chloride and aluminium chloride, followed by hydrolysis and treatment with perchloric acid.[4] It was recrystallized from 1% perchloric acid in the presence of decolourizing carbon.

The kinetic conditions were similar to those described previously:[2,3] solutions of the pyrylium salt in buffered H_2O or D_2O, respectively, were introduced into the NMR vials; concentrations were low, as in the previous parts,[2,3] so that reactions were pseudounimolecular. The ^1H-NMR spectra were recorded after prescribed times of standing in a thermostated bath; chilling of the samples to the temperature of the NMR spectrometer (ca. 35°) was rapid, so that it may be safely assumed that, during the recording of the NMR spectra, the isotopic exchange is practically stopped.

The preparation of deuteriated and non-deuteriated buffers was described previously.[2,3] The pH values (determined electrochemically under the same conditions) were 1.94 in D_2O, and 1.87 in H_2O. It must be remembered[5] that pD=pH reading + 0.40.

Deuteriated $I-d_7$ was obtained by refluxation of I in excess D_2O for three hours; the six α-methyl hydrogens and the single γ-isopropyl hydrogen undergo complete isotopic exchange, as evidenced by the NMR spectrum.

At the reaction temperatures employed in the present kinetic study, little or no isotopic exchange is observed for the α-methyl hydrogens. The α-alkyl isotopic exchange requires higher temperatures than the γ-alkyl exchange.[2,3,6]

The evaluation of the kinetic results involved the integral NMR curves for the methyl part of the isopropyl resonance peaks: the methyl signal of $CHMe_2$ in I is a widely spaced (J=6.9 Hz) doublet, while $CDMe_2$ in $I-d_1$ is a closely spaced (J=0.7 Hz) triplet, appearing between the components of the doublet.[2,3] In order to ensure a good separation of these peaks, the NMR spectra were recorded with sweep width 100 Hz. Four integral curves were recorded after each reaction time, and at each temperature at least six reaction times were observed (tables 1 and 2). The integrated intensities were measured and averaged. The least-squares fitting of straight lines for $\ln [(h_1+h_2)f/\Sigma]$ in deuteriations, and for $\ln (fd/\Sigma)$ on dedeuteriations *versus* time yielded the reaction rates presented in tables 1–3. The significance of all terms in the above expressions is the same as in the previous papers:[2,3] h_1 and h_2 are the two integrated components of the $CHMe_2$ doublet, d is the integrated $CDMe_2$ triplet, Σ is the integrated total methyl hydrogen content ($\Sigma = h_1 + h_2 + d$), and f is a correction factor representing the ratio Σ_0/Σ, where Σ_0 is the initial Σ value; this correction was necessary because the sensitivity of the NMR integrator varied slightly in time, resulting in small variations of the Σ value which ought to remain constant.

[4] A. T. BALABAN and C. D. NENITZESCU, *Liebigs Ann. Chem.*, **625**, 74 (1959).

[5] P. K. GLASOE and F. A. LONG, *J. Phys. Chem.*, **64**, 188 (1960); cf. also V. GOLD and M. A. KESSICK, *Discuss. Faraday Soc.*, **39**, 84 (1965).

[6] E. GÂRD, F. CHIRALEU, I. I. STĂNOIU and A. T. BALABAN, *Rev. Roumaine Chim.*, **18**, 257 (1973).

Table 1

Deuteriation of I in buffered D_2O

Temp. (°C)	Time t (hrs.)	Integral averaged intensities (mm) Measured h_1	h_2	d	Σ	Corrected $(h_1+h_2)f/\Sigma$	$-\ln\ [(h_1+h_2)f/\Sigma]$ Exper.	Calc.	Expression
58	0	71.5	58.8	19.5	149.8	0.870	0.139	0.165	$0.165+1.907\ t$
	0.067	60.5	51.8	34.0	146.3	0.786	0.241	0.293	
	0.133	53.0	38.5	56.5	148.0	0.626	0.469	0.419	
	0.250	41.0	30.0	72.5	143.5	0.516	0.661	0.642	
	0.417	28.5	20.2	93.2	142.0	0.362	1.017	0.960	
	0.667	18.5	13.0	106.0	137.5	0.250	1.388	1.435	
62	0	90.2	85.0	8.5	183.7	0.954	0.047	0.063	$0.063+2.985\ t$
	0.050	75.8	68.2	34.5	178.5	0.830	0.186	0.212	
	0.100	65.5	55.8	59.2	180.5	0.684	0.380	0.361	
	0.167	51.2	42.0	81.5	174.7	0.561	0.578	0.561	
	0.267	40.2	33.0	108.5	181.7	0.407	0.898	0.860	
	0.417	26.5	20.5	128.8	175.8	0.279	1.275	1.308	
66	0	67.0	57.0	11.0	135.0	0.919	0.085	0.128	$0.128+4.061\ t$
	0.050	52.0	41.0	39.0	132.0	0.721	0.328	0.331	
	0.100	41.8	33.2	58.0	133.0	0.572	0.558	0.534	
	0.167	29.5	25.5	75.5	130.5	0.436	0.830	0.806	
	0.250	22.8	15.5	93.2	131.5	0.299	1.207	1.143	
	0.333	17.0	13.0	99.0	129.0	0.243	1.413	1.480	
70	0	88.5	80.5	14.0	183.0	0.923	0.080	0.133	$0.133+5.056\ t$
	0.033	72.0	61.5	47.0	180.5	0.750	0.288	0.300	
	0.067	60.5	52.5	69.5	182.5	0.621	0.477	0.472	
	0.117	48.0	32.8	102.0	182.8	0.442	0.815	0.725	
	0.167	37.2	25.5	116.5	179.2	0.357	1.029	0.977	
	0.233	27.8	21.8	127.5	176.1	0.293	1.229	1.311	
74	0	66.8	53.8	19.2	139.8	0.863	0.148	0.160	$0.160+7.798\ t$
	0.017	55.2	47.2	31.2	133.6	0.802	0.221	0.293	
	0.033	47.0	31.5	56.2	134.7	0.605	0.503	0.417	
	0.067	35.5	25.0	70.2	130.7	0.495	0.703	0.683	
	0.100	27.2	17.2	87.5	131.9	0.357	1.031	0.940	
	0.150	21.5	12.5	98.5	132.5	0.271	1.307	1.330	
	0.200	15.5	9.2	108.0	132.7	0.196	1.629	1.720	

Table 2

De-deuteriation of I − d_7 in buffered H_2O

Temp. (°C)	Time t (hrs.)	Integral averaged intensities (mm)					− ln (fd/Σ)		
		Measured				Corrected			
		h_1	h_2	d	Σ	fd/Σ	Exper.	Calc.	Expression
58	0	16.2	10.4	122.6	149.2	0.822	0.196	0.239	$0.239+0.663\,t$
	0.067	21.8	13.5	119.2	154.5	0.745	0.294	0.283	
	0.133	27.0	17.0	109.0	153.0	0.695	0.364	0.327	
	0.250	30.0	19.5	102.0	151.5	0.663	0.411	0.405	
	0.417	35.2	24.0	90.2	149.5	0.602	0.507	0.532	
	0.667	42.2	31.5	75.8	150.0	0.503	0.688	0.681	
	0.883	48.0	35.0	65.0	148.0	0.443	0.815	0.824	
62	0	14.2	8.0	107.5	129.7	0.829	0.188	0.242	$0.242+1.024\,t$
	0.050	18.5	11.8	104.0	134.3	0.748	0.291	0.293	
	0.100	22.0	14.0	95.5	131.5	0.716	0.334	0.344	
	0.167	27.5	17.8	91.0	136.3	0.635	0.454	0.413	
	0.267	31.2	21.5	81.0	133.7	0.588	0.532	0.515	
	0.417	37.0	29.2	67.2	133.4	0.490	0.714	0.669	
	0.583	42.2	31.8	57.8	131.8	0.432	0.840	0.839	
	0.783	46.5	36.0	48.0	130.5	0.366	1.006	1.044	
66	0	17.2	13.3	127.0	157.2	0.806	0.215	0.198	$0.198+1.762\,t$
	0.050	22.8	18.0	115.8	156.5	0.745	0.295	0.286	
	0.100	28.5	20.0	108.0	156.5	0.695	0.365	0.375	
	0.167	34.2	27.0	96.8	158.0	0.611	0.493	0.493	
	0.250	40.5	31.0	84.0	155.5	0.547	0.603	0.639	
	0.333	46.5	39.0	69.5	155.0	0.456	0.786	0.785	
	0.483	55.2	48.0	53.8	157.0	0.344	1.068	1.049	
70	0	11.8	7.8	84.0	103.6	0.811	0.210	0.180	$0.180+2.481\,t$
	0.033	14.8	11.8	71.0	97.6	0.772	0.259	0.262	
	0.067	17.2	14.2	64.2	95.6	0.728	0.318	0.346	
	0.117	22.5	17.8	58.8	99.1	0.620	0.478	0.470	
	0.167	24.2	22.0	48.0	94.2	0.560	0.579	0.594	
	0.233	28.0	25.5	41.5	95.0	0.476	0.742	0.758	
	0.333	34.0	31.2	33.0	98.2	0.355	1.037	1.006	
	0.417	36.0	34.5	28.0	98.5	0.299	1.207	1.214	
74	0	18.0	10.0	106.5	134.5	0.792	0.233	0.225	$0.225+3.178\,t$
	0.017	22.2	12.0	97.2	131.4	0.757	0.278	0.279	
	0.033	24.8	14.5	90.2	129.5	0.723	0.324	0.330	
	0.067	30.8	19.5	82.0	132.3	0.630	0.462	0.438	
	0.100	32.8	21.8	73.0	127.6	0.603	0.506	0.543	
	0.150	40.0	28.2	60.2	128.4	0.491	0.711	0.702	
	0.200	43.0	32.8	50.0	125.8	0.425	0.856	0.861	
	0.267	48.5	37.2	40.0	125.7	0.340	1.077	1.070	

RESULTS AND DISCUSSION

Tables 1 and 2 present the experimental kinetic data for deuteriations of I and de-deuteriations of I$-$d$_7$, respectively, at the γ-isopropyl benzylic hydrogen. The rate constants, k_H and k_D, respectively, obtained by a least-squares straight line fitting, together with the intercept (due to incipient isotopic exchange during the preparation of the sample) are indicated in the last column of tables 1 and 2 for each temperature.

Table 3 groups together the rate constants k_H for deuteriation and k_D for de-deuteriation; the calculated values for k_H and k_D from table 3 were obtained by means of the activation parameters indicated at the bottom of table 3; these activation parameters were also obtained by a least-squares fitting of straight lines. As seen from figure 1, the Arrhenius correlations are satisfactory both for deuteriation and for the de-deuteriation.

Table 3

Rate constants and activation parameters

Temp. °C	Deuteriation of I			De-deuteriation of I$-$d$_7$		
	Experimental		Calcd.	Experimental		Calcd.
	k_H	ln k_H	ln k_H	k_D	ln k_D	ln k_D
58	1.907	0.646	0.709	0.663	−0.411	−0.342
62	2.985	1.094	1.055	1.024	0.024	0.076
66	4.061	1.401	1.393	1.762	0.566	0.483
70	5.056	1.621	1.723	2.481	0.909	0.881
74	7.798	2.054	2.046	3.178	1.156	1.270

Deuteriation : $\ln k_H = 29.7 - 19020/(RT)$; De-deuteriation : $\ln k_D = 34.6 - 22900/(RT)$.

The larger activation energy found for the de-deuteriation (22.9 kcal/mol) than for the deuteriation (19.0 kcal/mol) agrees with the known fact that the isotopic effects, k_H/k_D, decrease with increasing temperatures. The values of the activation energies and of the pre-exponential factors agree with those found earlier for the isotopic exchange of 2,4,6-trimethylpyrylium perchlorate.[6]

It must be borne in mind that the rate constants determined in different solvents (buffered D_2O for deuteriations, buffered H_2O for de-deuteriations) also include a factor due to solvent effects: indeed, isotopic effects at one and the same temperature were found in such conditions to be higher ($k_H/k_D=2.2\pm0.3$) than in one and the same main solvent, acetonitrile-d$_3$ with small additions of D_2O and H_2O, respectively, at the same temperature as for the above data (in D_3C-CN, $k_H/k_D=1.6\pm0.3$).[2]

In previous papers [2,3] the pseudounimolecular reaction rates for the isotope exchange which were presented resulted from plots of decimal logarithms $-$ lg $[(h_1+h_2)f/\Sigma]$, and $-$ lg(fd/Σ), respectively, *versus* time, since only the ratios of these rates were interesting, e. g. for isotope effects [2] or for the intramolecular comparison of the ease of exchange at α-methyl and α-isopropyl groups. [3] In the present paper, however, where true individual absolute rate constants k_H and k_D are employed, we use natural, not decimal logarithms.

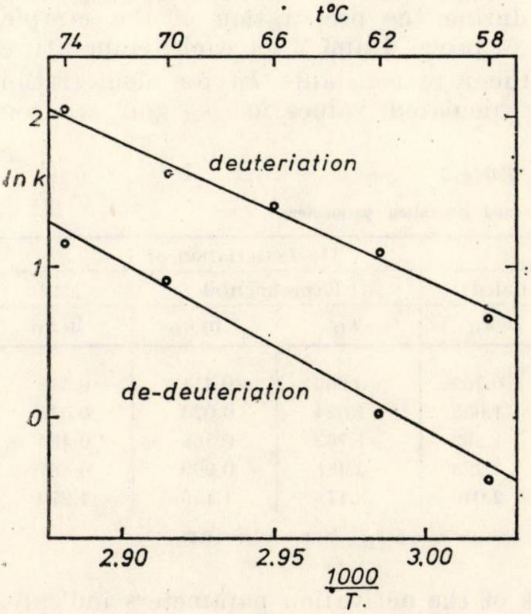

Fig. 1. — Arrhenius plots for the deuteration of 2,6-dimethyl-4-isopropylpyrylium perchlorate (I) in buffered D_2O (upper line), and for the de-deuteriation of 2,6-di-d_3-methyl-4-(isopropyl-d_1)-pyrylium perchlorate ($I-d_7$) in buffered H_2O (lower line).

Revue Roumaine de Chimie, **22**, *11–12*, 1505–1511 (1977)

Dedicated to the 75th anniversary of
Prof. C. D. NENITZESCU'*s birthday (1902–1970)*

SOLVOLYTIC BEHAVIOUR OF STRAINED SYSTEMS : THE 1-, 4- AND 5-METHYLBENZO[*b*] BICYCLO[3.1.0]HEX-2-EN-4-YL CATIONS

V. WERTHEIMER, A. M. GLATZ and A. C. RĂZUŞ
Centre of Organic Chemistry, Spl. Independenţei 202B,
Bucharest 15, Romania

Received March 15, 1976

Pathways for the cyclopropane ring opening in the solvolytically generated 1- and 4-methylbenzo[*b*]bicyclo[3.1.0]hex-2-en-4-yl cations are described. The 4-methyl cation behaves similarly to the "parent" system. The methyl substitution in position 1 changes dramatically the behaviour of the system, the opening of the 1–5 bond occurring also in the ground state. The methyl-substituted alcohol in position 5 exhibits a very low reactivity. The mechanism of the opening is discussed.

In our preceding paper [1] we have discussed the cyclopropane ring opening in the solvolytically generated benzo[*b*]bicyclo[3.1.0]hex-2-en-4-yl cation. It has been shown that the concerted opening of the ring fused linkage 1–5 occurs (as in Winstein's cation [2,3]) only photochemically and the opening of the 5–6 linkage occurs by homoallylic delocalization leading to indenylmethyl derivatives.

The present paper reports our results on the reactions of the 4- and 1-methylbenzo[*b*]bicyclo[3.1.0]hex-2-en-4-yl cations **5**[4] and **6** generated from the corresponding alcohols **1** and **2** (*endo*–OH) in aqueous dioxane with perchloric acid as well as the behaviour of the 5-methyl [*b*]bicyclo[3.1.0] hex-2-en-4-ol in the same conditions.

As seen from the results (table 1), the tertiary alcohol **1** behaves in a highly similar way to the parent compound reported previously. Thus, in nonirradiated acid catalysis a mixture of epimeric **1** and methylene derivative **3** is formed, whereas in the UV-irradiated solvolysis a significant amount of 1-methylnaphthalene **4** accompanies the same products.

---

[1] A. C. RĂZUŞ, V. WERTHEIMER, F. BADEA and A. M. GLATZ, *Tetrahedron Letters*, **1975** 1799.

[2] R. F. CHILDS, M. SAKAI, B. D. PARRINGTON and S. WINSTEIN, *J. Amer. Chem. Soc.*, **96**, 6403 (1974).

[3] R. F. CHILDS and S. WINSTEIN, *J. Amer. Chem. Soc.*, **96**, 6409 (1974).

[4] The obtention and the ^{1}H and ^{13}C NMR spectra of cation **5** were recently reported by G. A. OLAH, G. LIANG and S. P. JINDAL, *J. Org. Chem.*, **40**, 3259 (1975).

The 1-methylderivative **2** exhibits a quite different behaviour. Although the irradiated solvolysis of **2** leads to epimeric **2** and **4**, the same products are also formed without irradiation. Naphthalene is formed fast in the ground state reaction of **2** (overall catalytic rate constant $=1.38\times10^{-4}\ \mathrm{s}^{-1}$ at 65.7°)[5] and the reaction can be monitored up to the quantitative conversion into **4**.

As seen from the data herein reported, alcohol **1** strongly resembles the parent compound, the only cyclopropane ring opening in ion **5** being the concerted cleavage of the 1−5 linkage. This process is accomplished photochemically leading to the naphthalene precursor **7**. Irradiation of **1** in nonionizing condition (*n*-hexane) affords the conclusion that at least 75% of **4** formed in run 2 arises by a cationic pathway.

Table 1

Product distributions in the rearrangements of 1 and 2

Run	Substrate	Conditions[a]	Products, % moles (g. l. c.)			
			1(*endo*−OH)	**1**(*exo*−OH)	**3**	**4**
1	**1** (*endo*−OH)	42°, 4.5h	39.9	56.1	4	0
2		42°, 3.5h, hν	30.9	42.3	2.7	24.1
			2(*endo*−OH)	**2**(*exo*−OH)		**4**
3	**2** (*endo*−OH)	49.6°, 5.5h	28.8	48.8		22.4
4		80°, 3h	0	0		100
5[b]		14°, 1.5h, hν	35.5	46.1		18.4

[a] Runs 1, 3, 4 in dioxane-water (1 : 1), runs 2, 5 in dioxane-water (1 : 3). All acid-catalysed isomerizations have been performed with 0.3 M $HClO_4$. Irradiations have been performed under argon with a medium pressure 125 W-mercury lamp.

[b] Extrapolated kinetic data showed that the nonirradiated solvolysis yields maximum 6% **4** under these conditions.

No opening of the 5−6 bond in **5** has been observed under the employed conditions. Undesired secondary reactions operate when more energetic conditions are used, conditions under which 5−6 cleavage occurred in the parent compound.[1,6]

1-Methylnaphthalene **4** can arise from **2** *via* **6** by two distinct pathways: either a stepwise breakage of the ring fused linkage in the ground state, or by a photochemically concerted one. In the former case the formation of the delocalized cation **8** can be a satisfactory explanation of the results. This cyclopropylcarbinyl type delocalization should be favoured by the methyl group adjacent to the participating bond. A

[5] A new report is in preparation containing the kinetic and thermodynamic data obtained in the case of the parent system and the substituted derivatives; some results are already reported in the present paper.

[6] We found the overall catalytic rate constant for the parent alcohol in 1-indenyl methanol equal to $3.14\times10^{-6}\ \mathrm{s}^{-1}$ at 69.5°.

nonconcerted thermal pathway is further proved by the high positive value of the entropy of activation found in this reaction ($\Delta S^{\neq}=16.1$ eu at 65.7°). 1-Methylnaphthalene **4** can arise either directly from **8**, or *via* **7**. In the irradiate solvolysis of **2** at least 65 % of the 1-methylnaphthalene **4** should be formed directly from **6**, the remainder arising by the stepwise path discussed above (see table 1).

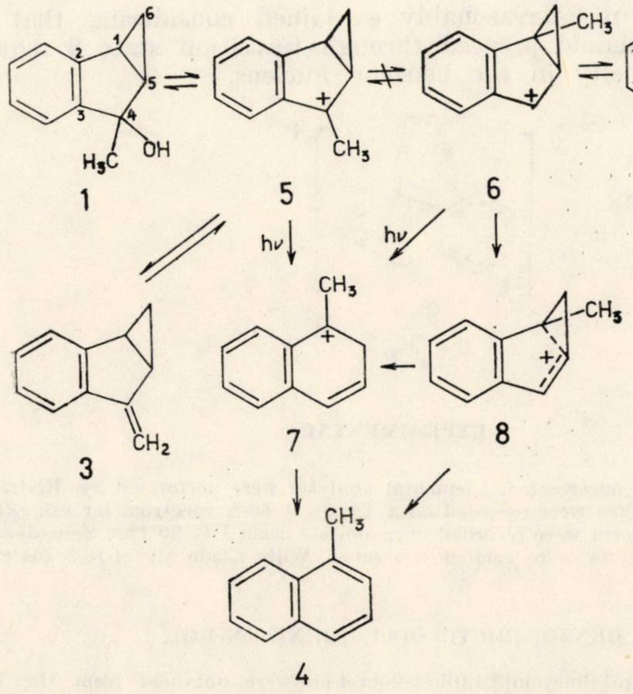

With a view to corroborate the supposition concerning the activation of the 1—5 bond opening by a contiguous methyl group, we attempted the solvolysis of 5-methylbenzo[*b*]bicyclo[3.1.0]hex-2-en-4-ol (*endo*—OH). Working in the conditions of run 3 (see table 1), the conversion of the alcohol was smaller than 4 %. The absence of an internal return with epimerisation or any other transformation proceeding from an ionic intermediate which can be formed, pleads for the unusual stability of the alcohol in the conditions of an SN1 reaction. This stability results also from the comparison between irradiating a solution of the 5-methylbenzo[*b*]bicyclo[3.1.0]hex-2-en-4-ol in aqueous dioxane, in the presence or absence of perchloric acid at 49.6°, for 3.5 hrs. In both cases the conversion was 22—25 %, 2-methylnaphthalene representing over 95 % of the product transformed. Therefore, in irradiated acid medium, no processes involving ionic intermediates occur, as they do in the above systems.

Excepting the photochemically formed 1-methylnaphthalene, there is no further cross-over between the products of **1** and **2**, either in the irradiated, or in the nonirradiated solvolysis. This clearly shows that cations **5** and **6** are not interconverting, though these two ions could exhibit a suprafacial 1,4 sigmatropic shift.[3,7] The fact that no deuterium scrambling between C4 and C1 could be detected in both irradiated and nonirradiated solvolysis of 4-deutero-benzo[*b*]bicyclo[3.1.0]hex-2-en-4-ol, also points to the absence of such sigmatropic shifts within these benzobicyclic systems.

These facts can be reasonably explained considering that such sigmatropic shifts should proceed through transition state **9** requiring the loss of aromaticity in the benzene nucleus.

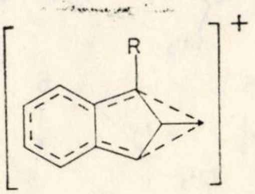

9

R = CH_3, D

EXPERIMENTAL

Melting points are uncorrected. Elemental analyses were performed by Elvira Şliam and V. Daniel. NMR spectra were recorded on a Varian A 60-A spectrometer using TMS as internal standard. IR spectra were recorded on a double beam UR 20 Carl Zeiss-Jena spectrometer. The g.l.c. analyses were carried out on a Willy Giede Model 18.3 gas chromatograph.

BENZO[*b*]BICYCLO[3.1.0]HEX-2-EN-4-OL

exo- and *endo*-Benzo[*b*]bicyclo[3.1.0]hex-2-en-4-ols were obtained from the ketone[8] by reduction with sodium borohydride in methanol (isopropanol). After the usual working up, a mixture of epimeric alcohols (crystals and viscous liquid) was obtained; yield over 98%; the ratio *endo* : *exo*=26.5 : 73.5 in both solvents. The trituration with petroleum ether of the mixture followed by filtration led to the separation of a crystalline residue, which after recrystallization yielded the *endo*-epimer gas-chromatographically pure, m. p. 83.5° (alcohol/water). (*Found*: C, 82.36; H, 7.08; *Calcd.* for $C_{10}H_{10}O$: C, 82.16; H, 6.90).

NMR spectrum ($CDCl_3$, δ ppm, J = Hz): 0.48 (multiplet, 1H, 6H-*endo*; J=4.4; 4.2; 3.4); 0.92 (multiplet, 1H, 6H-*exo*; J=8.2; 7.5; 4.4); 2.01 (multiplet, 1H, H-5, J is deduced from the signals of the other protons), 2.06 (singlet, 1H, OH), 2.40 (multiplet, 1H, 1−*H*, J = 7.5; 6.0; 3.4); 5.56 (doublet, 1H, 4−H *exo*; J=6.4); 7.00−7.50 (multiplet, 4 aromatic protons).

The *exo*-epimer, pale yellow oil, was separated by preparative gas-chromatography (the same conditions as for the analytical g. l. c. of *endo*-epimer). (*Found*: C, 82.00; H, 7.10; *Calcd.* for $C_{10}H_{10}O$: C, 82.16; H, 6.90).

NMR spectrum ($CDCl_3$, δ ppm, J=Hz): 0.01 (multiplet, 1H, 6−H *endo*: J=4.5; 4.5; 3.4); 1.10 (multiplet, 1H, 6−H *exo*; J=8.6; 7.6; 4.5); 1.96 (multiplet, 1H, 1−H; J=8.6; 5.8; 4.5); 2.31 (singlet, 1H, OH); 2.43 (multiplet, 1H, 5−H; J deduced from the other sig-

---

[7] J. A. Berson and N. M. Hasty, Jr., *J. Amer. Chem. Soc.*, **93**, 1549 (1971); P. Vogel, M. Saunders, N. M. Hasty, Jr. and J. A. Berson, *ibid.*, **93**, 1551 (1971).

[8] G. R. Elling, R. C. Hahn and G. Schwab, *J. Amer. Chem. Soc.*, **95**, 5659 (1973).

nals); 4.83 (broad singlet, 1H, 4—H *endo*); 7.15—7.65 (multiplet, 4 aromatic protons). The NMR spectrum can be used to establish the *endo* or *exo* position of the OH group at C4. The first indication is the coupling between the protons 4 and 5. When these protons are in opposition a big coupling (6.4—6.2) appears between them, that means the group OH has an *endo* orientation. When the dihedral angle between the two hydrogens is near 90°, the coupling constant becomes small or zero and the OH group has an *exo* position.

The chemical shift of the 6-*endo*-H is another indication which can be used also in the case when there is no proton in position 4. For a series of products δ corresponding to 6—H *endo* varies from 0.40 to 0.50 ppm while for another series a stronger shielding of the δ of 6—H *endo* occurs varying between 0.00 and 0.10 ppm. We consider that the deshielding of 6—H *endo* can be due to the approach of this proton from the OH group.

exo- and *endo-4-Deutero-benzo[b]bicyclo[3.1.0]hex-2-en-4-ols* were obtained by the reduction with $LiAlD_4$ of the respective ketone. A complete isotopic labelling of the position 4 was found from the NMR spectrum.

4-METHYL-*exo*- and -*endo*-BENZO[*b*]BICYCLO[3.1.0]HEX-2-EN-4-OLS (**1**)

The alcohols **1** (*endo*- and *exo*-OH) were obtained by treating benzo[*b*]bicyclo[3.1.0]hex-2-en-4-one (4 mmol) with methylmagnesium iodide (6 mmol methyliodide and 6.5 mmol magnesium); yield 70.0%. The gas-chromatographic analysis was very tedious, the results were denaturated by the partial thermal decomposition on the column of tertiary alcohols. (For a correct appreciation of the ratios, the analyses were performed in two different conditions: a 3 m× 4 mm column packed with 0.25% silicon OV7 on glass beads, column temperature 155°, carrying gas: argon, 80 ml/min and a 3 m× 4 mm column packed with 10% Carbowax 20 M on Chromosorb W (30—60 M), column temperature 170°, carrying gas: hydrogen 66 ml/min).

The separation by preparative g. l. c. of the *endo*-isomer was performed on a 2 m× 6 mm silicon OV7 10% on Chromosorb W (45—60 M) column; column temperature 150°; carrier-gas: argon 250 ml/min. The crystalline *endo*-isomer was recrystallized from petroleum ether; m. p. 57.5° (*Found*: C, 82.20; H, 7.57; *Calcd.* for $C_{11}H_{12}O$: C, 82.46; H, 7.55).

NMR spectrum ($CDCl_3$, δ ppm, J=Hz): 0.41 (multiplet, 1H, 6—H *endo*, J=4.2; 3,4); 0.98 (multiplet, 1H, 6—H *exo*, J=8.2; 7.5; 4.2); 1.60 (singlet, 3H, CH_3); 1.85 (multiplet, 1H, 5—H; J=8.2; 6.0; 4.2); 1.91 (singlet, 1H, OH); 2.41 (multiplet, 1H, 1—H, J=7.5; 6.0; 3.4); 7.00—7.30 (broad singlet, 4 aromatic protons).

In the above separation also a small quantity of *exo*-isomer was obtained.

NMR spectrum (CCl_4, δ ppm, J=Hz): 0.10 (multiplet, 1H, 6—H *endo*, J=4.5; 3.2); 1.08 (multiplet, 1H, 6—H *exo*, J=8.5; 7.5; 4.5); 1.53 (singlet, 3H, CH_3); 1.60 (singlet, 1H, OH); 1.93 (multiplet, 1H, 1—H; J=7.5; 5.8; 4.5); 2.35 (multiplet, 1H, 1—H; 5—H; J=8.5; 5.8; 3.2); 7.00—7.30 (multiplet, 4 aromatic protons).

1-METHYLBENZO[*b*]BICYCLO[3.1.0]HEX-2-EN-4-ONE

Diethyl phthalate was converted into 3,3-dimethylphthalide[9] and by alkaline melting[10] the 2-isopropenylbenzoic acid was obtained. The acyl chloride was prepared at room temperature by adding dropwise 24 mmol thionyl chloride into a solution of 22 mmol acid and 44 mmol pyridine dissolved in 20 ml dry ether. After 4 hrs, benzene was added and the solution was concentrated *in vacuo* when the thionyl chloride in excess is carried away by benzene. The remaining benzenic solution was washed with water and ice, dried with magnesium sulphate and concentrated *in vacuo*. (The usual methods to obtain acyl chlorides, without pyridine, give again 3,3-dimethylphthalide).

The NMR spectrum of the acyl chloride shows the absence of dimethylphthalide. The crude acyl chloride treated with diazomethane gave the corresponding diazoketone, pale yellow oil; yield 68% (relating to the acid).

IR spectrum (CCl_4, cm^{-1}): 2210 vi; 1640 vi; 1360 vi.

The diazoketone was cyclized after a method described by Nenitzescu and coworkers.[11] After distillation, the 1-methylbenzo[*b*]bicyclo[3.1.0]hex-2-en-4-one (96.2% pure) was obtained. The purification on a chromatographic column, packed with silicagel, carbon tetrachloride: ethyl ether (5:1) eluent gave a purity of 98.0%.

[9] B. B. Elsner, H. E. Strauss and E. J. Forbes, *J. Chem. Soc.*, **1957,** 578.

[10] G. Berti, G. Kabas and A. Marsili, *Ann. Chim.* (*Ital.*), **49,** 1994 (1959).

[11] M. Popovici, V. Ioan, M. Elian and C. D. Nenitzescu, *Rev. Roumaine Chim.*, **12,** 583 (1967).

1-METHYL-*exo*- and -*endo*-BENZO[*b*]BICYCLO[3.1.0]HEX-2-EN-4-OLS **(2)**

These alcohols were obtained in nearly quantitative yield by the reduction of the respective ketone on treatment with $NaBH_4$. In the crude mixture of products the ratio *exo* : *endo* was 30 :70. The isomers were separated in pure form by prep. g. l. c.

The *endo*-isomer was recrystallized from petroleum ether: m. p. 76°. (*Found* : C, 81.83 ; H, 7.63 ; *Calcd.* for $C_{11}H_{22}O$: C, 82.46 ; H, 7.55).

NMR spectrum (CCl_4, δ ppm, J=Hz) : 0.50–0.83 (multiplet, 2H, 6–H *endo* and 6–H *exo*) ; 1.50 (singlet, 3H, CH_3) ; 1.70 (multiplet, 1H, 5–H, J=7.8 ; 6.5 ; 4.7) ; 2.43 (singlet, 1H, OH) ; 5.42 (doublet, 1H, 4–H, J=6.2) ; 6.85–7.20 (multiplet, 4 aromatic protons).

The *exo*-isomer was separated in very small quantity. (*Found* : C, 81.83 ; H, 7.63 ; *Calcd.* for $C_{11}H_{12}O$: C, 82.46 ; H, 7.55).

NMR spectrum (CCl_4, δ ppm, J=Hz) : 0.09 (triplet, 1H, 6–H *endo*, J=4.2) ; 0.91 (multiplet, 1H, 6–H *anti*, J=8.5 ; 4.2) ; 1.54 (singlet, 3H, CH_3) ; 1.68 (multiplet, 1H, 5–H ; J= =8.5 ; 4.2) ; 2.76 (singlet, 1H, 4–H) ; 7.00–7.50 (multiplet, 4 aromatic protons).

5-METHYL-*endo*- and -*exo*-BENZO[*b*]BICYCLO[3.1.0] HEX-2-EN-4-OL

2-Methylinden-1-one was prepared by the method employed by Floyd and Allen[12] for obtaining 2-alkylindenones. By a Reformatsky reaction between benzaldehyde and ethyl α-bromopropionate, the ethyl ester of the 3-hydroxy-3-phenyl-2-methylpropionic acid was obtained ; yield 70%. The ester after saponification gave the respective acid ; yield 98%. (The NMR spectrum confirms the presence of two stable conformers at room temperature). From the acid treated with thionyl chloride, the acyl chloride of the chloroacid was obtained (Cl instead of OH). The above acyl chloride was cyclized to chloroindanone, and by means of pyridine the dehydrochlorination was performed ; yield 40% based on the acid.

IR spectrum (CH_2Cl_2, cm^{-1}) : 1728 vi.

NMR spectrum (CCl_4, δ ppm, J=Hz) : 1.83 (doublet, 3H, CH_3, J=1.7) : 6.75–7.40 (multiplet, 4 aromatic protons and 1 alkene proton).

2-Methylinden-1-ol was obtained by the reduction of the respectively ketone with $NaBH_4$ in a mixture of ethanol : water (5 :1) at room temperature, b.p.$_1$ 100–105°. The alcohol has a 96% purity (g. l. c. analysis) ; yield 90%.

NMR spectrum ($CDCl_3$, δ ppm, J=Hz) : 2.00 (doublet, 3H, CH_3, J=1.5) ; 2.23 (singlet, 1H, OH) ; 4.70 (singlet, 1H, 3–H) ; 6.26 (broad singlet, 1H, 1–H) ; 6.90–7.50 (multiplet, 4 aromatic protons).

5-Methyl-endo- and -exo-benzo[b]bicyclo[3.1.0] hex-2-en-4-ols were obtained by the cyclopropanation of 2-methylinden-1-ol according to known methods described in the literature for the cyclopropanation of cyclopentenol[13] and indene[14]. A solution of 2-methylindene-1-ol (11.5 mmol) in ether was added to an organo-metallic derivative obtained from methylene iodide (20 mmol) and the Zn–Cu couple[15] (from 2 g Zn). The mixture was stirred and heated under reflux for 24 hrs. The resulting precipitate was filtered after cooling on cellite, the filtrate was washed with a hydrochloride acid solution, a sodium hydrogen carbonate solution and then with a saturated solution of sodium chloride. The solvent was evaporated *in vacuo* and 1.6 g of crude product was obtained which contains 60% of the cyclopropanated product and 30% of the starting material. The separation of the two alcohols (the cyclopropanated and the starting alcohol) was performed on a column packed with neutral alumina and chloroform : petroleum ether (4 :1) as eluent. The other impurities were separated by preparative g. l. c. (column packed with silicon OV7 10% on Carbowax W silanized (60–80 M), column temperature 160°, carrier gas : argon, 300 ml/min). This yielded a pale yellow oil, which contains 94% *endo*-alcohol (configuration assigned by the NMR spectrum) and 6% other unidentified components.

NMR spectrum (CCl_4, δ ppm, J=Hz) : 0.48 (multiplet, 1H, 6–H *endo*, J=7.5 ; 4.2) ; 1.42 (singlet, 3H, CH_3) ; 1.70 (singlet, 1H, OH) ; 2.09 (multiplet, 1H, 1–H, J=7.5 ; 3.2) ; 5.09 (singlet, 1H, 4–H *exo*) ; 6.90–7.30 (multiplet, 4 aromatic protons).

---

[12] M. B. Floyd and G. R. Allen, Jr., *J. Org. Chem.*, **35**, 2647 (1970).

[13] E. Corey and R. R. Dawson, *J. Amer. Chem. Soc.*, **85**, 1782 (1963).

[14] A. L. Goodman and R. H. Eastman, *J. Amer. Chem. Soc.*, **86**, 908 (1964).

[15] E. LeGoff, *J. Org. Chem.*, **29**, 2048 (1964).

4-METHYLENEBENZO[*b*]BICYCLO[3.1.0]HEX-2-EN (**3**)

The mixture of the *endo*- and *exo*-4-methylbenzo [*b*] bicyclo[3.1.0]hex-2-en-4-ols (**1**) was dehydrated by means of phosphorus oxychloride in the presence of pyridine;[16] yield 70.0%; pale yellow oil.

IR spectrum (CCl_4, cm^{-1}): 880 i, 1650 i.

UV spectrum (ethanol): λ_{max} (log ε) 257.4 (4.023), 266.5 (3.908), 295.1 (3.368), 306.8 (3.287).

SOLVOLYSIS REACTIONS

The solvolysis reactions of the alcohols were carried out in a solution of 0.3 M perchloric acid in dioxane-water (1 : 1), the concentration of the alcohol being 0.1 M. The samples after solvolysis were neutralized with 2% sodium hydrogen carbonate solution extracted three times with ether. The organic layer was dried with magnesium sulphate and distilled at normal pressure on a fractionation column. The etheral fraction had no traces of products (g. l. c. analysis).

The irradiated solvolysis was carried out in a mixture of dioxane : water (1 : 3). After neutralization with a two percent sodium hydrogen carbonate solution, the product was extracted with ether in a continuous extractor. The ether was removed as above.

The reaction product, after irradiation in *n*-hexane, was directly analysed without removing the solvent, in order to retain all the reaction products.

---

[16] W. L. Dilling and J. A. Alford, *J. Amer. Chem. Soc.*, **96**, 3615 (1974).

Revue Roumaine de Chimie, 22, *11–12*, 1513–1520 (1977)

RELATIONS BETWEEN THE ELECTRONIC STRUCTURE AND REACTIVITY OF SOME THIOAMIDES. II[1]

UV AND IR SPECTRA

A. O. FULEA* and CORNELIA FULEA**

* Department of Physical Chemistry, Institute of Chemistry, Polytechnic Institute of Bucharest, Bd. Republicii n°. 13

** Department of Organic Chemistry, Institute of Chemistry, Polytechnic Institute of Bucharest, Splaiul Independenţei, n° 89, Bucharest, Romania

Received July 14, 1975

The studies carried out previously on some thioamides were extended, to establish some correlations between the calculated data and the UV and IR data of these thioamides. A complete set of parametres for the sulphur and the nitrogen atoms was used, taking into account all the possible structures for the thioamide group, unprotonated as well as protonated.

In a previous paper [1] we have applied HMO and ω techniques on some thioamides to study reactivity. A complete set of parameters has been used for both sulphur and nitrogen atoms * for structures A, B, C and D, between which the chemical equilibria from Scheme I can be put down:

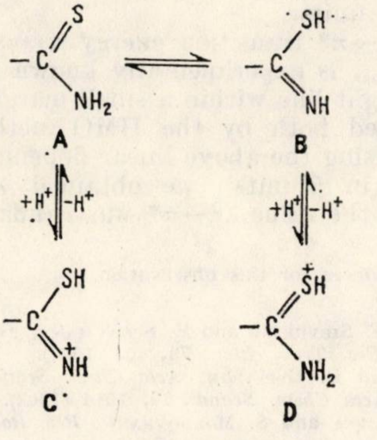

---

* Table 1, reference.[1]

[1] F. Cornea, C. Fulea and A. O. Fulea, *Rev. Roumaine Chim.*, 18, 111 (1973).

Recent studies by Walter *et al* [2] have experimentally shown that the protonation site in primary thioamides is the sulphur atom. Whereas the structure C can pass to the structure D by a process of deprotonation, one of tautomery and one of protonation, the two structures are also mesomers** :

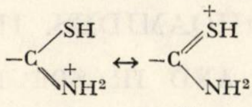

C D

i. e. the same chemical species is obtained by both processes of protonation in Scheme I.

The study was done on nine thioamides : thioformamide (I), thioacetamide (II), phenylthioacetamide (III), thiobenzamide (IV), thioacrylamide (V), cinnamthioamide (VI), thiourea (VII), dithiobiuret (VIII) and dithiomalonamide (IX). The obtained results [1] allowed a good correlation of the chemical behaviour with the electronic structure.

In this paper we have tried to obtain some correlations between the electronic structure and the UV and IR spectra for the above compounds.

UV SPECTRA

The spectral studies on thioamides have shown that the thioamide group absorbs in UV at two wavelengths : a band around 360 nm and the other, more intense, at 260−270 nm, [2] the former being atributed to a $n\rightarrow\pi^*$ transition and the latter to a $\pi\rightarrow\pi^*$ transition. [3−5] For the thioamides studied here, the UV spectra are given only for thioacetamide, thiobenzamide, [5] phenylthioacetamide, [6] cinnamthioamide [7] and thiourea. [8] For the other thioamides we have calculated $\lambda_{\max}$ for the $\pi\rightarrow\pi^*$ transition using the relation $E\lambda=hc$. Table 1 gives the values of the transition energies in β units.

Plotting the $\pi\rightarrow\pi^*$ transition energy *versus* the value $1/\lambda_{\max}$ for the thioamides whose $\lambda_{\max}$ is experimentally known we have found that the points are on a straight line within a small margin. In figure 1 are given these results obtained both by the HMO method (line *1*) and the ω technique (line *2*). Using the above linear dependence and the calculated transition energies (in β units), we obtained $\lambda_{\pi\rightarrow\pi^*}$ and denoted this by λ'. Furthermore, the value $\lambda\pi\rightarrow\pi^*$ was calulated from $E\lambda=hc$ using

** We thank the referee for this observation.

[2] W. Walter, M. F. Sieveking and E. Schaumann, *Tetrahedron Letters*, **1974**, 839.
[3] M. J. Janssen, *Rec. Trav. chim.*, **79**, 464 (1960).
[4] J. Sandström and B. Uppström, *Acta Chem. Scand.*, **19**, 2432 (1965).
[5] J. Sandström, *Acta Chem. Scand.*, **16**, 1616 (1962).
[6] F. Cornea, C. Fulea and S. Moldoveanu, *Rev. Roumaine Chim.*, **19**, 429 (1974).
[7] G. Pappalardo, B. Tornetta and P. Condorelli, *Il Farmaco, Ed. Sci.* **22**, 808 (1967).
[8] R. K. Ritchie and H. Spedding, *Spectrochim. Acta*, **26A**, 9 (1970).

Table 1

$\pi \to \pi^*$ transition energies in β units

		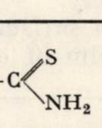		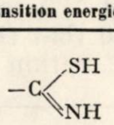		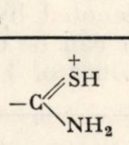		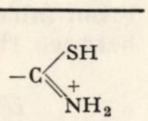	
		H	ω	H	ω	H	ω	H	ω
I		−0.622	−1.125	−0.902	−1.172	−0.500	−0.721	−0.607	−0.641
		0.730	0.974	0.834	0.764	1.500	1.335	1.154	1.298
	$\pi \to \pi^*$	−1.352	−2.099	−1.736	−1.936	−2.000	−2.056	−1.761	−1.939
II		−0.750	−1.236	−1.006	−1.279	−0.650	−0.867	−0.748	−0.793
		0.693	0.816	0.815	0.663	1.500	1.197	1.127	1.224
	$\pi \to \pi^*$	−1.443	−2.052	−1.821	−1.942	−2.150	−2.064	−1.875	−2.017
III		−0.729	−1.021	−0.951	−1.021	−0.632	−0.827	−0.726	−0.760
		0.679	0.736	0.788	0.642	0.880	0.841	0.872	0.854
	$\pi \to \pi^*$	−1.408	−1.757	−1.739	−1.663	−1.512	−1.668	−1.598	−1.614
IV		−0.395	−0.724	−0.556	−0.746	−0.304	−0.495	−0.369	−0.440
		0.659	0.770	0.771	0.675	1.000	0.970	1.000	1.017
	$\pi \to \pi^*$	−1.054	−1.494	−1.336	−1.421	−1.304	−1.465	−1.369	−1.457
V		−0.357	−0.769	−0.517	−0.797	−0.271	−0.497	−0.330	−0.436
		0.644	0.813	0.753	0.691	1.137	1.110	1.000	1.202
	$\pi \to \pi^*$	−1.001	−1.582	−1.270	−1.488	−1.408	−1.607	−1.330	−1.638
VI		−0.270	−0.584	−0.386	−0.600	−0.201	−0.396	−0.244	−0.348
		0.572	0.650	0.614	0.606	0.822	0.775	0.776	0.802
	$\pi \to \pi^*$	−0.842	−1.234	−1.000	−1.206	−1.023	−1.171	−1.020	−1.150
VII		−0.823	−1.264	−1.064	−1.305	−0.728	−0.936	−0.826	−0.839
		0.664	0.744	0.792	0.618	1.500	1.666	1.095	1.194
	$\pi \to \pi^*$	−1.487	−2.008	−1.856	−1.923	−2.228	−2.602	−1.921	−2.033
VIII		−0.622	−1.135	−0.585	−0.899	−0.558	−0.851	−0.583	−0.719
		0.627	0.670	0.590	0.471	0.679	0.785	0.677	0.734
	$\pi \to \pi^*$	−1.249	−1.805	−1.175	−1.370	−1.237	−1.636	−1.260	−1.453
IX		−0.622	−1.131	−0.706	−1.152	−0.553	−0.830	−0.615	−0.759
		0.666	0.749	0.690	0.651	0.699	0.835	0.697	0.844
	$\pi \to \pi^*$	−1.288	−1.880	−1.396	−1.803	−1.252	−1.665	−1.312	−1.603

the value $\beta = 2.62$ eV,[9] for both thioamide and isothioamide forms, the results being denoted by λ'' and λ''', respectively.

From table 2 it can be concluded that there is a satisfactory agreement between the values of λ' and λ'' within the realm of ω technique, but

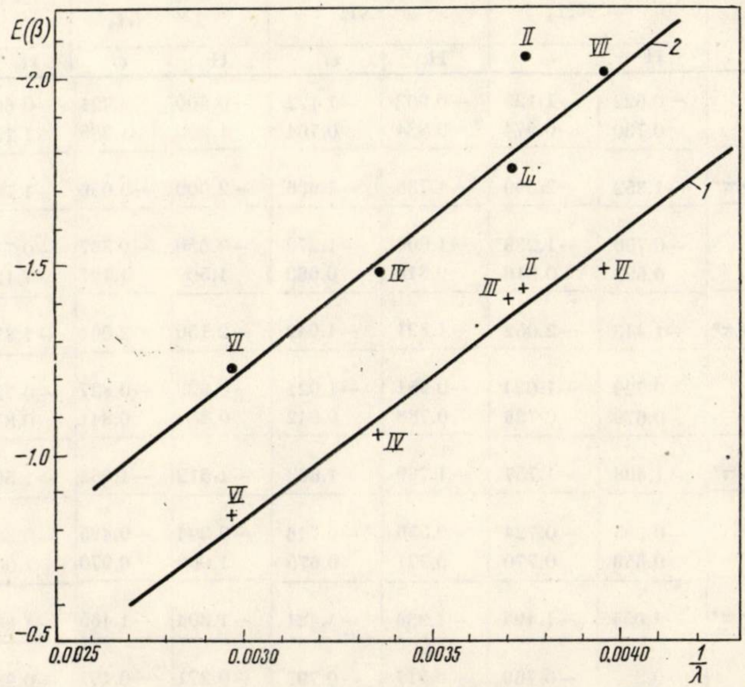

Fig. 1. — The dependence of $E = hc/\lambda$ obtained by the HMO method (*1*) and by ω technique (*2*).

Table 2

The calculated values

	λ exp (nm)	$-C(=S)NH_2$ $E_{\pi\to\pi^*}$ (β)		λ′(nm)		λ″(nm)		$-C(SH)=NH$ $E_{\pi\to\pi^*}$(β)		λ‴ (nm)	
		H	ω	H	ω	H	ω	H	ω	H	ω
I		−1.352	−2.099	277	240	365	277	−1.736	−1.936	273	243
II	267	−1.443	−2.052			325	231	−1.821	−1.942	260	240
III	270	−1.408	−1.757			337	269	−1.739	−1.663	272	285
IV	298	−1.054	−1.494			451	318	−1.336	−1.421	353	334
V		−1.001	−1.582	312	294	474	300	−1.270	−1.488	373	326
VI	338	−0.842	−1.234			564	385	−1.000	−1.206	474	391
VII	253	−1.487	−2.008			318	235	−1.856	−1.923	255	246
VIII		−1.249	−1.805	285	270	380	263	−1.175	−1.370	403	346
IX		−1.288	−1.880	277	263	367	251	−1.396	−1.803	339	261

---

[9] A. Streitwieser, "Molecular Orbital Theory for Organic Chemists", Wiley Inc., New York, 1961, chap. 8.

not for the HMO method. Also for II, III, IV, VI and VII λ_{max} observed experimentally agrees with λ'' obtained by ω technique but not with that obtained by the HMO method.

The values λ''' obtained by the ω technique for the isothioamide form are close to λ' and λ''. Therefore, on the basis of these results we can not eliminate the isothioamide form.

As far as the $n \rightarrow \pi^*$ transition is concerned we gave in table 3 the energy of the lowest unoccupied π^* orbital as well as the wavelength of this band.

Table 3

$\lambda_{n} \rightarrow \pi^*$ and the energy of the first unoccupied orbital

	$\lambda_{(nm)}$	π^*	
		H	ω
II	367	−0.750	−1.236
III	374	−0.729	−1.021
IV	412	−0.395	−0.724
VI	445	−0.270	−0.584
VII	357	−0.823	−1.264

It can be seen that for a lower absolute value of the energy of the π^* orbital a higher value of $\lambda_{n \rightarrow \pi^*}$ is found experimentally. This can be rationalized taking into account the fact that the non-participant electrons of the sulphur atom are much less influenced by the substituent of the thioamide group than the π electrons.

THE BOND ORDERS AND A TENTATIVE CORRELATION WITH IR FREQUENCIES

The bond orders are given in table 4 for all the thioamides studied here. As it is known these bond orders may be correlated with the IR frequencies.

In the present work, we have tried to correlate the bond order of CN bond of the unprotonated thioamide form with the frequency of the *B* vibration [10] of thioamides. For the stretching frequencies of the carbonyl group a linear dependence upon the bond order of C=O bond has been found. [11] The thioamide group is a complex vibrational group, each of its frequencies being group frequencies in which more vibrations are coupled. [12]

From table 5 it can be seen that the frequency *B* has the highest value for I. This can be explained by the fact that in I the cross conjugation is absent and, therefore, the bond order of CN bond has the

---

[10] K. A. Jensen and P. H. Nielsen, *Acta Chem. Scand.*, **20**, 597 (1966).

[11] G. Berthier, B. Pullman and J. Pontis, *J. Chim. phys.*, **49**, 367 (1952).

[12] L. J. Bellamy, "Advances in Infrared Group Frequencies", Methuen, Bungay, 1969, p. 214, 287.

Table 4

The bond orders

	Thioamide	Bond	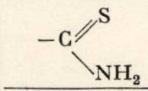		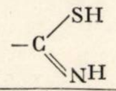		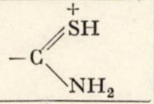		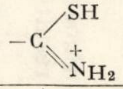	
			H	ω	H	ω	H	ω	H	ω
I	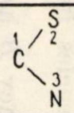	1−2	0.745	0.941	0.392	0.389	0.480	0.855	0.580	0.611
		1−3	0.528	0.325	0.887	0.918	0.640	0.452	0.596	0.735
II	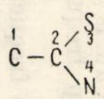	1−2	0.358	0.261	0.293	0.255	0.411	0.345	0.387	0.367
		2−3	0.675	0.908	0.377	0.375	0.434	0.800	0.522	0.565
		2−4	0.500	0.312	0.838	0.887	0.578	0.422	0.553	0.682
III	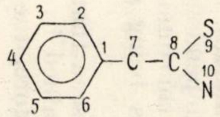	1−2 (6−1)	0.650	0.648	0.650	0.647	0.650	0.648	0.650	0.648
		2−3 (5−6)	0.670	0.672	0.670	0.672	0.670	0.671	0.670	0.671
		3−4 (4−5)	0.665	0.664	0.665	0.664	0.665	0.664	0.665	0.664
		1−7	0.261	0.228	0.216	0.228	0.216	0.225	0.215	0.224
		7−8	0.357	0.257	0.293	0.252	0.409	0.339	0.385	0.360
		8−9	0.674	0.907	0.377	0.373	0.432	0.799	0.521	0.564
		8−10	0.498	0.312	0.837	0.887	0.576	0.421	0.552	0.680
IV	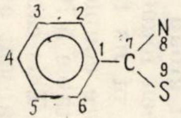	1−2 (6−1)	0.595	0.632	0.612	0.633	0.585	0.623	0.593	0.621
		2−3 (5−6)	0.683	0.676	0.678	0.676	0.686	0.679	0.684	0.680
		3−4 (4−5)	0.655	0.661	0.639	0.661	0.652	0.659	0.654	0.658
		1−7	0.447	0.312	0.396	0.307	0.474	0.342	0.449	0.351
		7−8	0.659	0.892	0.355	0.371	0.407	0.794	0.503	0.561
		7−9	0.461	0.309	0.808	0.871	0.542	0.418	0.518	0.677
V	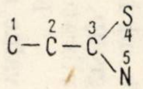	1−2	0.861	0.947	0.896	0.948	0.838	0.937	0.855	0.933
		2−3	0.498	0.319	0.437	0.317	0.530	0.342	0.502	0.349
		3−4	0.640	0.891	0.348	0.370	0.392	0.796	0.486	0.564
		3−5	0.448	0.309	0.793	0.870	0.522	0.419	0.502	0.680

VI	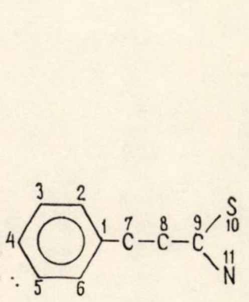 1 2 3 4 5 6 7 8 9 10 11 C C C S N	1−2 (6−1)	0.593	0.622	0.599	0.623	0.588	0.619	0.591	0.617
		2−3 (5−6)	0.684	0.679	0.682	0.670	0.685	0.680	0.684	0.681
		3−4 (4−5)	0.654	0.659	0.656	0.659	0.653	0.658	0.654	0.657
		1−7	0.452	0.351	0.437	0.350	0.463	0.362	0.455	0.366
		7−8	0.762	0.881	0.802	0.884	0.732	0.865	0.752	0.859
		8−9	0.542	0.347	0.469	0.340	0.585	0.382	0.551	0.393
		9−10	0.612	0.879	0.341	0.367	0.370	0.778	0.462	0.548
		9−11	0.432	0.306	0.775	0.860	0.493	0.409	0.481	0.662
VII	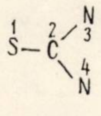	1−2	0.629	0.896	0.365	0.368	0.427	0.837	0.486	0.547
		2−3	0.477	0.307	0.392	0.300	0.564	0.370	0.509	0.437
		2−4	0.477	0.307	0.804	0.876	0.563	0.370	0.524	0.660
VIII	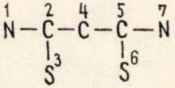 1 2 3 4 5 6 7 N C C C N S S	1−2	0.482	0.309	0.432	0.296	0.519	0.449	0.551	0.412
		2−3	0.646	0.898	0.572	0.861	0.501	0.564	0.413	0.783
		2−4	0.436	0.293	0.587	0.395	0.477	0.604	0.490	0.388
		4−5	0.436	0.293	0.641	0.787	0.439	0.331	0.424	0.283
		5−6	0.646	0.898	0.433	0.415	0.640	0.887	0.654	0.901
		5−7	0.482	0.309	0.452	0.335	0.480	0.306	0.485	0.301
IX	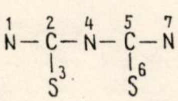 1 2 3 4 5 6 7 N C N C N S S	1−2	0.501	0.313	0.841	0.888	0.556	0.683	0.582	0.423
		2−3	0.681	0.909	0.378	0.374	0.526	0.566	0.437	0.802
		2−4	0.342	0.254	0.284	0.249	0.368	0.354	0.390	0.333
		4−5	0.342	0.254	0.348	0.255	0.338	0.248	0.336	0.249
		5−6	0.681	0.909	0.679	0.908	0.684	0.910	0.685	0.910
		5−7	0.501	0.313	0.500	0.313	0.502	0.314	0.502	0.314

highest values. On the other hand, this shows that indeed a significant part of the energy of the *B* vibration is used to stretch the CN bond.

From table 5 it can be also seen that there is no linear relation between the CN bond order and the frequency of the *B* vibration, as expected on the basis of the coupled character of this vibration.

Table 5

Bond orders and the IR frequencies of *B* vibration in cm^{-1} (KBr)

	Thioamide	Bond order C—N		νC—N (cm^{-1})
		H	ω	
I	$HCSNH_2$	0.5288	0.3247	1 433
IV	$C_6H_5-CSNH_2$	0.4610	0.3092	1 400
V	$CH_2=CH-CSNH_2$	0.4482	0.3088	—
VI	$C_6H_5-CH=CH-CSNH_2$	0.4317	0.3062	1 410

While the molecular orbital calculations make sense for all A, B, C and D structures from Scheme I, finally it should be pointed out the different electronic structures for the protonated form, which were obtained starting from C and D. *

If an electronic structure should be picked up, the one calculated from the C structure would be probably closer to the real structure of the protonated form, taking into account the n.m.r. studies of Walter *et al.* **

---

* See table 2, reference[1] and tables 1, 4 in the present paper.

** See δ_{CH_3}, δ_{H_A}, δ_{H_B}, $'\tau_{^{15}N-H_A}$, $'\tau_{^{15}N-H_B}$, $\Delta G^{\neq}$ values for unprotonated and protonated thioamides in reference[2].

Revue Roumaine de Chimie, **22**, *11–12*, 1521–1532 (1977)

ПОЛИБЕНЗИМИДАЗОЛИМИДЫ

В. В. КОРШАК *, А. И. ПАВЛОВ *, Г. МАНДРИК **, И. ЗУГРАВЕСКУ **
* Московский химико-технологический институт им. Д. И. Менделеева.
** Ясский институт макромолекулярной химии им. П. Пони.

Получена 2 мая 1974 года

Синтезированы диамины, содержащие гетероциклы: 2,2′-бис-п-(м)-аминофенил-5,5′-бис-бензимидазолоксиды (I). I получали низкотемпературной конденсацией 3,3′, 4,4′-тетрааминодифенилового эфира с хлорангидридами п-(м-)-нитробензойных кислот, высокотемпературной циклизацией полученных продуктов в ПФК и последующим восстановлением гидразингидратом на никеле Ренея. Низкотемпературной поликонденсацией I и пирромеллитового диангидрида в ДМАА получены полибензимидазоламидокислоты, термической циклодегидратацией которых синтезированы полибензимидазолимиды (ПБИИ). ПБИИ начинают разлагаться на воздухе при 400—420° и имеют 100%-ную потерю веса при 1000—1100° ($\Delta T = 12°$/мин).

В настоящее время большое внимание исследователей уделяется синтезу смешанных гетероциклических полимеров на основе мономеров большого молекулярного веса, содержащих готовые гетероциклы. Такой вариант синтеза позволяет повысить термостойкость полимеров за счет уменьшения общего количества «дефектных» звеньев в полимерной цепи.[1–10]

С целью получения полибензимидазолимидов на основе мономеров, содержащих бензимидазольные группировки, нами синтезирован ряд бис-амифенилбензимидазолов общей формулы:

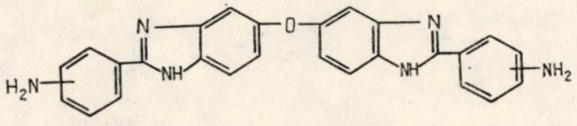

1

Iа (Iб) а: п-изомер; б: м-изомер

---

[1] J. Preston and W. B. Black, *J. Polymer Sci.*, **B 3,** 845 (1965).

[2] J. Preston and W. B. Black, *J. Polymer Sci.*, **B 4,** 267 (1966).

[3] J. Preston, W. DeWinter and W. L. Hofferbert, *J. Heterocyclic Chem.*, **5,** 269 (1968).

[4] J. Preston, W. DeWinter and W. L. Hofferbert, *J. Heterocyclic Chem.*, **6,** 119 (1969).

[5] J. Preston and W. B. Black, *J. Polymer Sci.*, **C 23,** 441 (1968).

[6] J. Preston, W. B. Black and W. Bruce, *J. Polymer Sci.*, **A1,** 7, 283 (1969).

[7] J. Preston, W. DeWinter, W. B. Black, W. Bruce and W. L. Hofferbert, *J. Polymer Sci.*, **A 1,** 7, 3027 (1969).

[8] W. DeWinter, R. Stein and H. Uwents, *J. Polymer Sci.*, **A 1,** 8, 1955 (1970).

[9] J. Iwakura, K. Uno, Y. Imai and M. Fukui, *Macromol. Chem.*, **77,** 41 (1965).

[10] Н. Н. Кузнецов, М. И. Бессонов, Т. М. Килселева и М. М. Котон, — *Высокомол. соединения*, **А 14,** 2034 (1972).

Эти мономеры были получены как по одностадийной схеме, описанной в литературе [9], путем прямой конденсации тетрагидрохлоридов тетрааминозойными кислотами

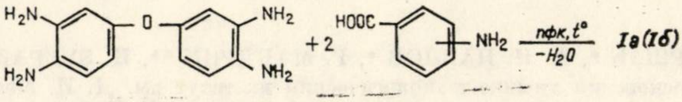

2

так и по трехстадийной схеме

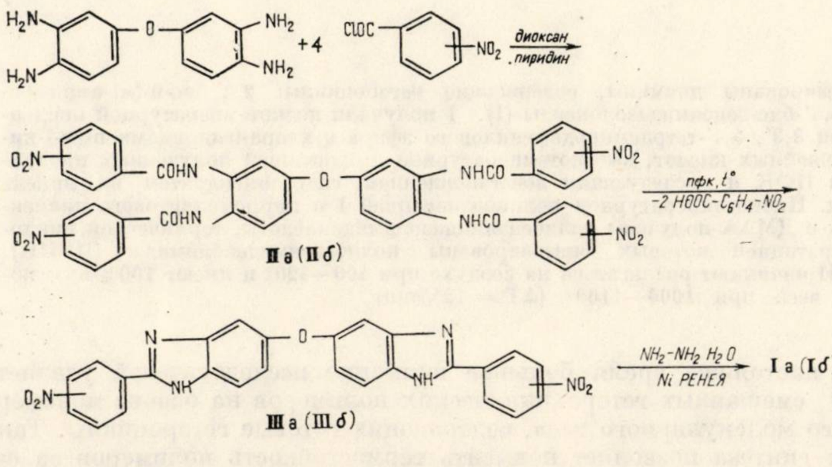

3

Для идентификации целевых продуктов и облегчения расшировки ИК-спектров промежуточных веществ, получаемых по трехстадийной схеме, нами был синтезирован ряд модельных соединений :

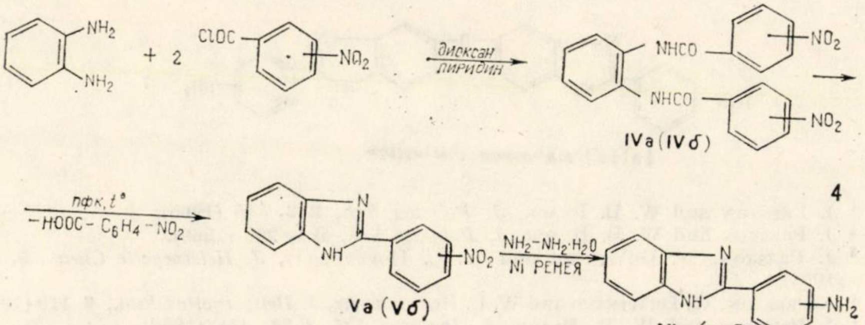

4

При рассмотрении ИК-спектров модельных соединений и их промежуточных продуктов (Рис 1 и 2) видно, что при переходе от N,N′-биснитропроизводных о-фенилендиамина (IV) к нитрофенилбензимидазолам (V) исчезает полоса поглощения 1660—1665 см$^{-1}$ (амид-1) и появляются полосы 1620, 1400, 965 см$^{-1}$, характерные для бензимидазольного цикла.[11] При переходе от нитрофенилбензимидазолов (V) к аминофенилбензимидазолам (VI) исчезают полосы поглощения 1540 (ν_{as} C—NO$_2$) и 1350 см$^{-1}$ (ν_s C—NO$_2$ и появляется полоса 1620 см$^{-1}$ (δ N—H).

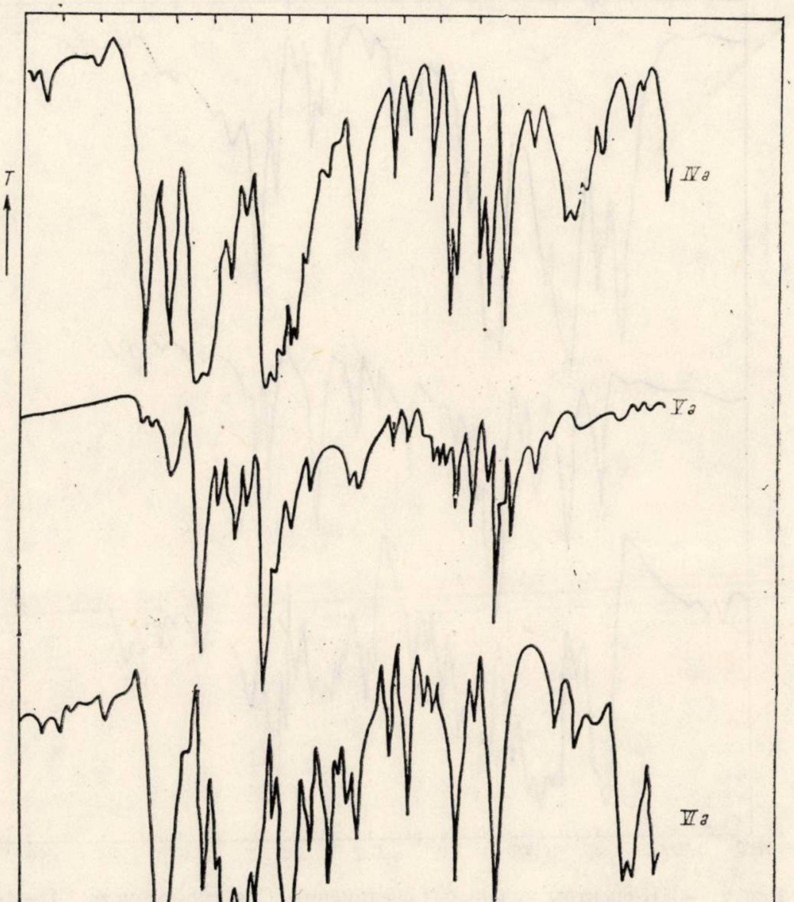

Рис. 1 — ИК-спектры модельных соединений. Спектрофотометр UR-10. Таблетки в KBr.

В ИК-спектрах бис-аминофенилбензимидазолов и их промежуточных продуктов (Рис 3 и 4) наблюдаются те же изменения, что и в спектрах модельных соединений.

---

[11] K. J. Morgan, *J. Chem. Soc.*, **1961**, 2343.

Из ИК-спектров (Рис 3 и 4) также видно, что бис-аминофенилбензимидазолы, получаемые как по одностадийной, так и по трехстадийной схеме идентичны (спектры 1 и 2). Следует отметить, что мономеры, полученные трехстадийным методом, несколько чище, о чем свидетельствует более высокая приведенная вязкость растворов полимеров на их основе (Табл № 1). Однако, общий выход мономеров трехстадийного синтеза (46—58%) ниже по сравнению с выходом мономеров прямой конденсации (62—68%).

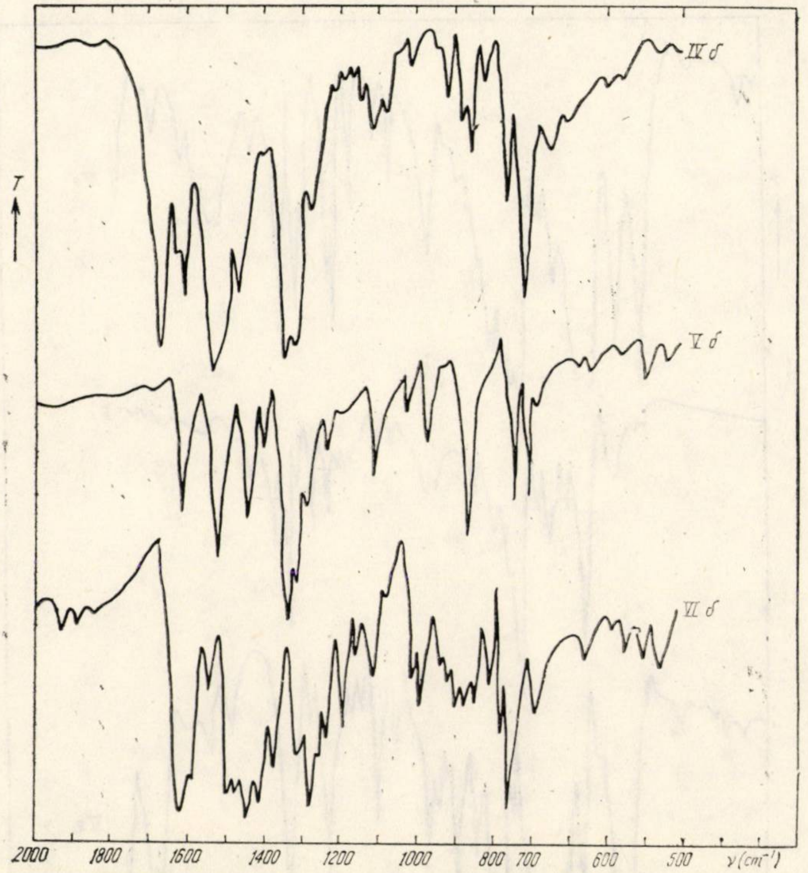

Рис. 2.— ИК-спектры модельных соединений. Спектрофотометр UR—10. Таблетки в KBr.

Исследование термического разложения модельных аминофенилбензимидазолов и бис-аминофенилбензимидазолов* при 300° в приборе Бурдона [12, 13] показало, что модельные соединения не образуют кристаллогидратов, в то время как бис-функциональные соединения образуют криcлаллогидраты с 1,5 H_2O. Для более полного удаления кристаллизационной воды после обычной сушки необходима термообработка под вакуумом при высоких температурах (~250°), о чем отмечали ранее и другие авторы.[9]

---

* Вещества переосаждались из метанола в воду и подвергались термическому разложению после сушки под вакуумом над NaOH при комнатной температуре в течение 3-х суток.

[12] К. К. Андреев, « Термическое разложение и горение взрывчатых веществ », Изд. « Наука » , М. 1966, стр. 15.

[13] А. И. Гольбиндер, « Лабораторные работы по курсу теории взрывчатых веществ », Розвузиздат, 1963, стр. 9.

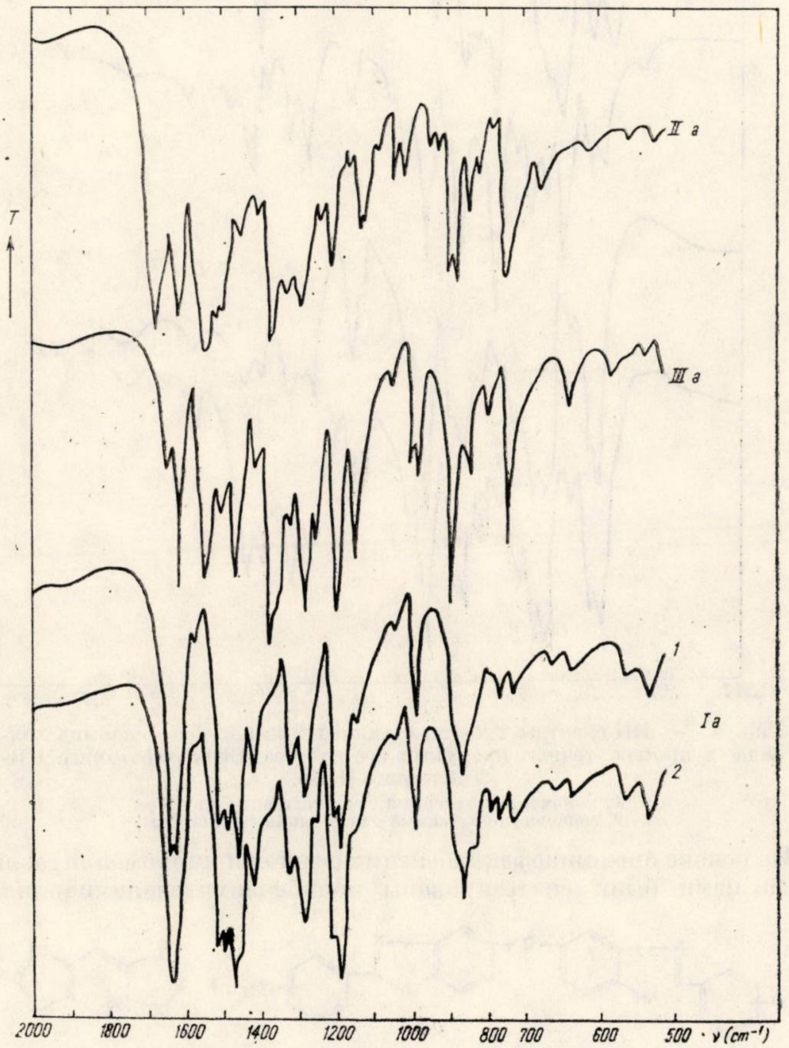

Рис. 3. — ИК-спектры 2,2′-бис-п-аминофенил-5,5′-бис-бензимидазолоксида и промежуточных продуктов его синтеза. Спектрофотометр UR-10. Таблетки в КВ.

1, мономер, полученный трехстадийным способом;
2, мономер, полученный одностадийным способом .

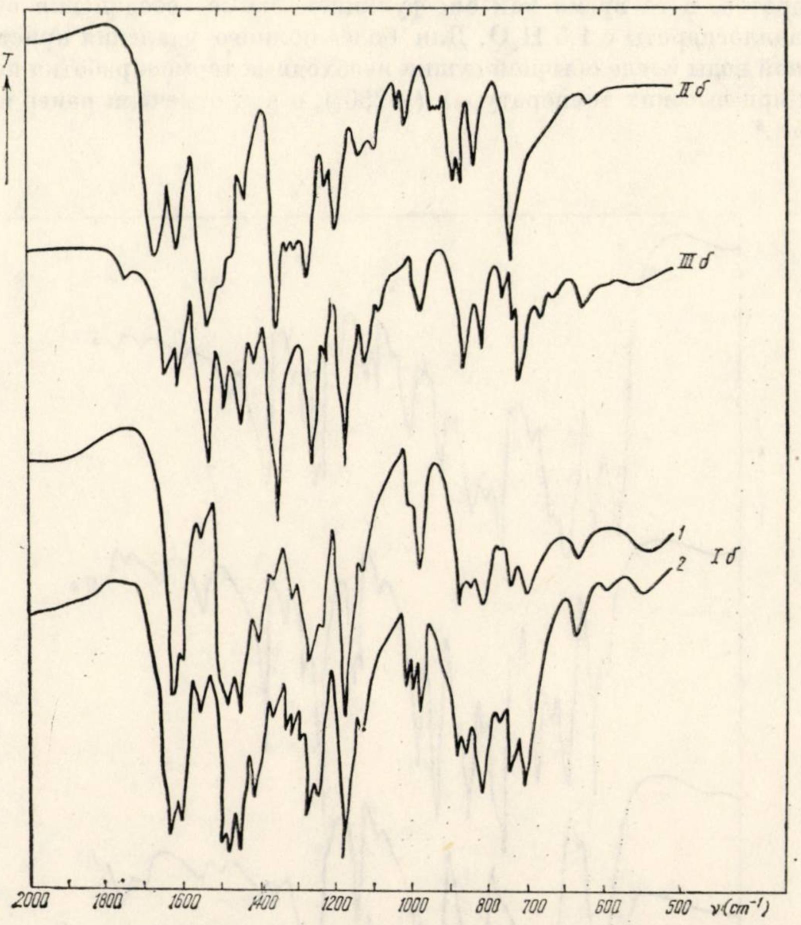

Рис. 4. — ИК-спектры 2,2′-бис-м-аминофенил-5,5′-бис-бензимидазол-оксида и промежуточных продуктов его синтеза. Спектрофотометр UR-10. Таблетки в KBr.

1, мономер, полученный трехстадийным способом,
2, мономер, полученный одностадийным способом.

На основе бис-аминофенилбензимидазолов и пиромеллитового диангидрида нами были синтезированы полибензимидазоламидокислоты

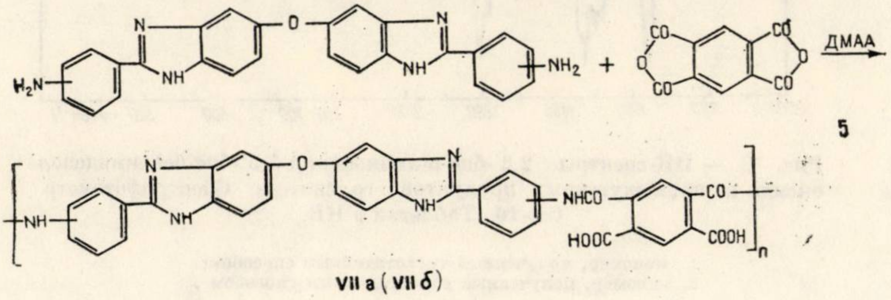

5

VII а (VII б)

путем термической циклодегидратации которых получены полибензимидазолимиды

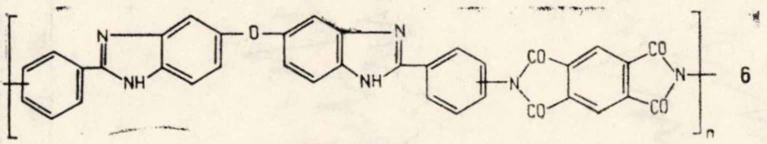

6

VIII а (VIII б)

Для идентификации полимеров были синтезированы модельные соединения:

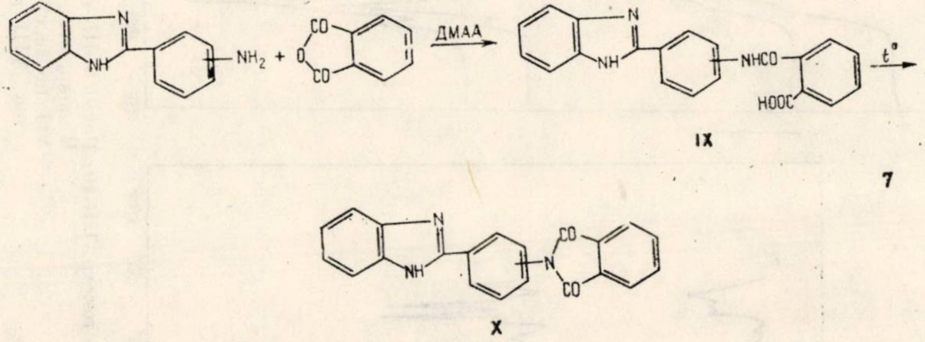

7

IX

X

Из ИК-спектров этих соединений (Рис 5) видно, что при переходе от амидокислотной модели (IX) к имидной (*X*) исчезает полоса поглощения 1660 см^{-1} (амид-1) и появляются полосы 1780, 1710 (νCO) и 1380 см^{-1} (νCH), характерные для имидного цикла. [14]

В ИК-спектрах полимеров (Рис. 6) при переходе от VII к VIII наблюдаются аналогичные изменения.

Свойства полибензимидазоламидокислот и полибензимидазолимидов приведены в таблице № 1.

Как следует из данных динамического термогравиметрического анализа на воздухе (Рис. 7), синтезированные полибензимидазолимиды начинают разлагаться при температурах 400—420°, при температуре 700° сохраняют 50% исходного веса и разлагаются нацело лишь при 1000—1100°.

---

[14] S. Nishizaki and A. Fukami, *J. Chem. Soc. Jap. Ind. Chem. Soc.*, **66**, 382 (1963); **67**, 474 (1964).

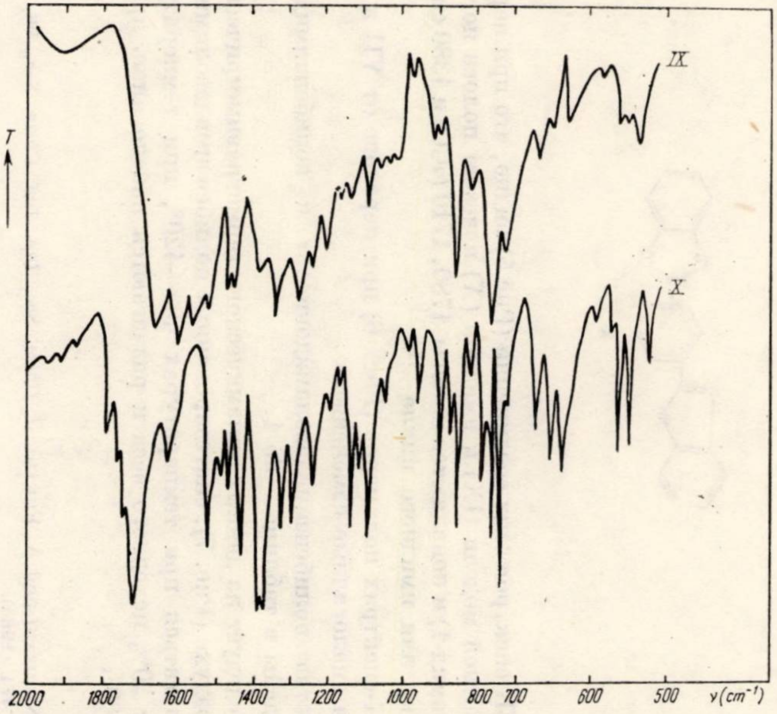

Рис. 5. — ИК-спектры моделей полимеров. Спектрофотометр UR-10. Таблетки в KBr.

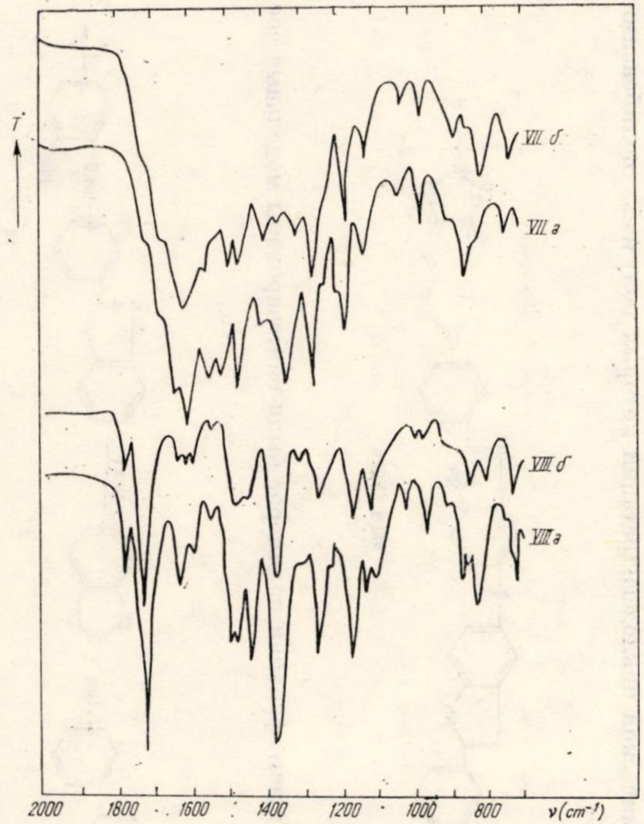

Рис. 6.—ИК-спектры полимеров. Спектрофотометр UR-10. Пленки, отлитые из раствора в ДМАА на пластины NaCl. VII после сушки под вакуумом при 50° в течение 3-х суток, VIII после термообработки при 100—280° (280°—3 часа).

Таблица 1

Свойства полимеров

Полимер	Формула брутто	η пр в ДМАА, дл/г	Растворимость при комнатной температуре	Содержание азота %	
				Вычислено	найдено
VII а	$(C_{36}H_{22}N_6O_7)_n$	0,55*; 1,05**	ДМАА, N-МП, ГМФТА, ДМСО, HCOOH, H_2SO_4	12,90	12,25 12,16
VII σ	,,	1,2* 1,4**	ДМАА, ДМФА, ГМФТА, ДМСО, N-МП, HCOOH, H_2SO_4	,,	12,36 12,48
VIII а	$(C_{36}H_{18}N_6O_5)_n$	—	Растворяется при нагревании в конц H_2SO_4	13,68	13,47 13,25
VIII σ	,,	—	—	,,	13,28 13,42

ДМАА — диметилацетамид; ДМФА — диметилформамид; N — МП — N-метилпирролидон; ГМФТА — гексаметилфосфортиамид; ДМСО — диметилсульфоксид; * — на основе одностадийного диамина; ** — на основе трехстадийного диамина.

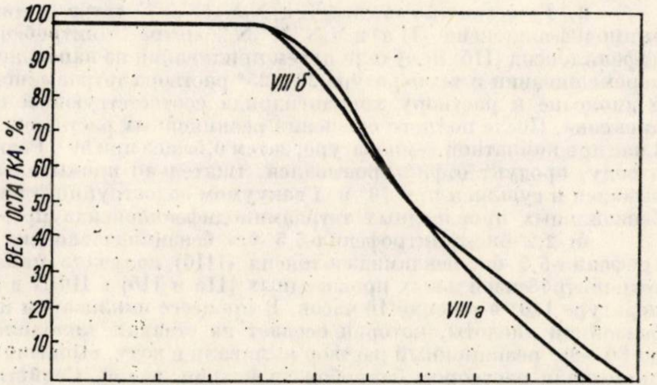

Рис. 7. — Термогравиметрические кривые полибензимидазолимидов. Дериватограф системы Ж. Паулик. Навеска образца 100 мг, атмосфера — воздух, $\Delta T = 12°$/мин.

ЭКСПЕРИМЕНТАЛЬНАЯ ЧАСТЬ

А. МОНОМЕРЫ

1. *Одностадийный способ*. Синтез бис-аминофенилбензимидазолов осуществлялся путем конденсации тетрагидрохлорида 3,3′, 4,4′-тетрааминодифенилоксида с аминобензойными кислотами в полифосфорной кислоте (ПФК) по известной методике.[9] Целевые продукты выделялись из раствора в ПФК путем осаждения в воду. Выпавшие вещества отфильтровывали, промывали раствором бикарбоната натрия, водой, растворяли в смеси (1:1) метанола и воды. Растворы при кипении дважды обрабатывали активированным углем, затем небольшим количеством гидросульфита натрия. После охлаждения до 30—40° растворы при тщательном перемешивании выливали в большой объем воды, подсоленной поваренной солью. После фильтрации и сушки под вакуумом при 80° вещества подвергали термообработке при температуре 250° и вакууме 1 мм тр. ст. в течение 2-х часов. Свойства бис-аминофенилбензимидазолов приведены в таблице № 2.

Таблица 2

Данные по одностадийному синтезу и свойствам бис-аминофенилбензимидазолов

Мономер	Формула брутто	Исходные компоненты	Выход		Т.пл., °С	Содержание азота, %	
			г	%		Вычислено	Найдено
I а 2,2′-бис-п-аминофенил-5,5′-бис-бензимидазолоксид	$C_{26}H_{20}N_6O$	ТГХ ТАДФО — 18,5 г п-АБК — 13,2 ПФК — 300 г	14,5	68	211—220 209—211*	19,42	19,08 19,22
I б 2,2′-бис-м-аминофенил-5,5′-бис-бензимидазолоксид	,,	ТГХ ТАДФО — 18,8 г м-АБК— 13,7 г ПФК — 300 г	13,4	62	198—204	,,	19,11 19,24

ТГХ ТАДФО — тетрагидрохлорид 3,3′, 4,4′-тетрааминодифенилоксида; м-АБК — м-аминобензойная кислота; п-АБК — п-аминобензойная кислота; * — по литературным данным.[10]

2. *Трехстадийный способ.* а) N,N′,N″,N‴ -тетра-(п-нитробензоил)-3,3′4, 4′-тетрааминодифенилоксид (II а) и N,N′,N″,N‴ -тетра-(м-нитробензоил)-3,3′, 4,4′-тетрааминодифенилоксид (IIб) получали путем приливания из капельной воронки при тщательном перемешивании и температуре 20—25° раствора тетрааминодифенилоксида и пиридина в диоксане к раствору хлорангидрида соответствующей нитробензойной кислоты в диоксане. После полного смешения реакционных растворов масса перемешивалась еще 1 час при комнатной температуре, затем 0,5 часа при 50°. Реакционная масса выливалась в воду, продукт отфильтровывался, тщательно промывался водой, перекристаллизовывался и сушился при 70° под вакуумом водоструйного насоса. Свойства тетранитробензоильных производных тетрааминодифенилоксида представлены в таблице № 3.

б) 2,2′-бис-п-нитрофенил-5,5′-бис-бензимидазолоксид (III а) и 2,2′-бис-м-нитрофенил-5,5′-бис-бензимидазолоксид (IIIб) получали циклизацией соответствующих тетранитробензоильных производных (IIа и IIб) в ПФК в атмосфере аргона при температуре 170° в течение 10 часов. В процессе циклизации происходит возгонка нитробензойной кислоты, которая оседает на стенках холодильника. После охлаждения до 80—90° реакционный раствор выливали в воду, выпавший осадок отфильтровывали, промывали раствором бикарбоната натрия, водой. Свойства продуктов III а и III б приведены в таблице № 3.

в) 2,2′-бис-п-аминофенил-5,5′-бис-бензимидазолоксид (I а) и 2,2′-бис-м-аминофенил-5,5′-бис-бензимидазолоксид (Iб) получали восстановлением соответствующих бис-нитрофенилбензимидазолов (III а и III б) при комнатной температуре гидразингидратом на никеле Ренея.[15] После восстановления в течение 3-х часов катализатор отфильтровывали, раствор упаривали досуха под вакуумом водоструйного насоса. Продукт растворяли в смеси метанола и воды (1: 1), кипятили дважды с активированным углем и после фильтрации осаждали в воду. Свойства мономеров приведены в таблице № 3.

Б. МОДЕЛЬНЫЕ СОЕДИНЕНИЯ

1. *Модельные соединения мономеров.* Модельные соединения IV—VI получали аналогично соответствующим веществам I—III. Свойства полученных продуктов представлены в таблице № 4.

2. *Модельные соединения полимеров.* IX получали прибавлением эквимолекулярного количества твердого фталевого ангидрида к раствору 2-(п-аминофенил)-бензимидазола (VI а) в ДМАА. После перемешивания при комнатной температуре в те-

---

[15] R. Mozingo, *Org. Syntheses*, **21**, 15 (1941).

Таблица 3

Данные по трехстадийному синтезу и свойствам бис-аминофенилбензимидазолов

Вещество, формула	Исходные компоненты	Выход			Т. пл, °С	Содержание азота	
		г	%	% от первой стадии		Вычислено	Найдено
II а $C_{40}H_{26}N_8O_{13}$	В капельной воронке: ТАДФО — 5,1 г, пиридин — 6,5 мл, диоксан — 125 мл.	17,0	92		не плавится до 320 (из ДМФА)	13,57	13,52 13,60
II б $C_{40}H_{26}N_8O_{13}$	В колбе: ХА п-НБК — 18 г, диоксан — 125 мл. В капельной воронке: ТАДФО — 21,8 г, пиридин — 28 мл, диоксан — 400 мл.	66,0	84		242—245 (из диоксана с водой)	,,	13,38 13,47
III а $C_{26}H_{16}N_6O_5$	В колбе: ХА м-НБК — 75 г, диоксан — 350 мл. IIа — 13,6 г, ПФК — 90 г	6,5	80	73,5	296—300 (переосаждение из изопропилового спирта в гексан)	17,07	16,84 17,01
III σ $C_{26}H_{16}N_6O_5$	II б—40,7 г, ПФК—250 г	18,2	75	63	207—210 (переосаждение из диоксана в воду)	17,07	16,96 16,82
I а $C_{26}H_{20}N_6O$	IIIа — 2,6 г, MeOH— 50 мл, гидразингидрат — 4 мл, никель Ренея ~ —0,2 см³	1,8	79	58	209—214 209—211*	19,42	19,43 19,31
I σ $C_{26}H_{20}N_6O$	IIIб — 5,0 г, MeOH — 150 мл, гидразингидрат — 10 мл, никель Ренея ~ 0,5 см³	3,2	73	46	224—229	19,42	19,29 19,35

ТАДФО — 3,3′, 4,4′-тетрааминодифенилоксид; ХА п-НБК — хлорангидрид п-нитробензойной кислоты; ХА м-НБК — хлорангидрид м-нитробензойной кислоты; ; * — по литературным данным.[10]

чение 2-х часов раствор вылили в воду, выпавший продукт отфильтровали и промыли горячим метанолом. Вещество не плавится до 320°. Вычислено для $C_{21}H_{15}N_3O_3$ N 11,76%. Найдено N 11,58; 11,65%.

Термообработкой IX при 200—280° под вакуумом 1 мм рт. ст. в течение 5 часов получен продукт X, не плавящийся до 320°. Вычислено для $C_{21}H_{13}N_3O_2$ N12,38%. Найдено N 12,18; 12,22%.

В. Полимеры. VII а (VII б) получали путем прибавления при тщательном перемешивании в атмосфере аргона эквимолекулярного количества твердого пирромеллитового диангидрида к 7%-ному раствору соответствующего диаминодибензимидазола в ДМАА. Температура реакции 20°; продолжительность 1—3 часа (до момента, когда раствор полимера начинал наматываться на мешалку). Раствор осаждали в хлороформ, декантировали, заливали свежей порцией хлороформа, выдерживали в течение ночи и сушили под вакуумом при 50°. VIII а (VIII б) получали термической обработкой VII а (VIIб) под вакуумом 1 мм рт. ст. при подъеме температуре от 100 до 280° в течение 2-х часов и выдержке при 280° продолжительностью 3 часа.

Таблица 4

Данные по синтезу и свойствам модельных соединений

Продукт, наименование, формула	Исходные компоненты	Выход		Т. пл., °C	Т. пл. по лит. данным		Содержание азота, %	
		г	%		°C	лит. ссылка	Вычислено	Найдено
IV а, N, N′-бис-(п-нитробензоил)-о-фенилендиамин, $C_{20}H_{11}N_4O_6$	Капельная воронка о-фенилендиамин 3 г, пиридин — 4 мл, диоксан — 50 мл, Колба: ХА п-НБК-10,8 г, диоксан-5 ил.	10,2	90	259—261 из ДМФА с водой	267	16	13,79	13,68 13,64
IV, б N,N′-бис-(м-нитробензоил)-о-фенилендиамин, $C_{20}H_{14}N_4O_6$	Капельная воронка: о-фенилендиамин 11 г, пиридин — 15 мл, диоксан — 150 мл, Колба: ХА м-НБК—3,8 г, диоксан—150 мл.	35,5	86	213—215 из диоксана с водой	240	17	13,79	13,75 13,67
V а, 2-(п-нитрофенил)-бензимидазол, $C_{13}H_9N_3O_2$	IV а — 6,6 г, ПФК — 50 г.	3,3	85	307—309 из диоксана	210 не пл. 310 322	16 17 18	17,58	17,48 17,53
V б, 2-(м-нитрофенил)-бензимидазол, $C_{13}H_9N_3O_2$	IV б — 34,6 г, ПФК — 190 г.	16,7	82	203—205 из изопропил. спирта и воды	204—205 204	19 17	17,58	—
VI а, 2-(п-аминофенил)-бензимидазол, $C_{13}H_{11}N_3$	V а — 3,0 г, MeOH — 60 мл, диоксан — 50 мл, гидразингидрат — 7 мл, никель Ренея ~ 0,2 см³	2,5	95	249—250 возгонка при 260° (1 мм)	240 235—236	20 21	20,09	20,18 20,14
VI б, 2-(м-аминофенил)-бензимидазол, $C_{13}H_{11}N_3$	V б — 5,0 г, MeOH — 125 мл, гидразингидрат—12 мл, никель Ренея ~ 0,2 см³	4,0	91	257—258 возгонка	251—252	20	20,09	20,18 20,14

---

[16] O. Fischer and F. Limmer, *J. prakt. Chem.*, **74**, 72 (1906).

[17] R. Walter and Th. von Pulawski, *J. prakt. Chem.*, **59**, 259 (1899).

[18] O. Hinsberg and F. Funcke, *Ber. dtsch. chem. Ges.*, **27**, 2191 (1894).

[19] J. Pinnow and F. Wiskott, *Ber. dtsch. chem. Ges.*, **32**, 905 (1899).

[20] B. Miklaszewski and St. von Niementowski, *Berd. dtsch. chem. Ges.*, **34**, 2958 (1901).

[21] O. Kym, *Ber. dtsch. chem. Ges.*, **33**, 2848 (1900).

Revue Roumaine de Chimie, **22**, *11–12*, 1533–1538 (1977)

SPECTROPHOTOMETRIC STUDY OF CADMIUM COMPLEX WITH 6-(6-METHOXY-BENZOTHIAZOL-2-YLAZO)-2,4-DICHLOROPHENOL

V. ARMEANU * and ELENA DRĂGUȘIN **

* Academy of Economic Studies, Department of Chemistry and Physics, Piața Română 6, Bucharest, Romania

** Petrochemical Works, Pitești, ICECHIM Laboratory, Sos. Giurgiului 127, Pitești, Romania

Received July 21, 1975

The paper deals with the qualitative and quantitative spectrophotometric study of the cadmium-6-(6-methoxy-benzothiazol-2-ylazo)-2,4-dichlorophenol system. The structure and stability of the complex combination formed, and also the optimum working condiditions are determined.

In a previous paper[1] we have presented a spectrophotometric study of complexes formed by Cd^{2+} with the 6-(6-benzothiazol-2-ylazo)-2,4-dichlorophenol reagent. In that case, it was shown that two complexes may be obtained, depending on the working conditions.

In the present study, it was found that 6-(6-methoxy-benzothiazol-2-ylazo)-2,4-dichlorophenol (I), Cd^{2+} affords only one type of complex, in an acetone-water solution, at pH $= 7-8$. The combination ratio was found to be R : Me$=1:1$, and the complex exhibits an absorption maximum at $\lambda=530$ nm.

The chemical formula of the reagent is the following:

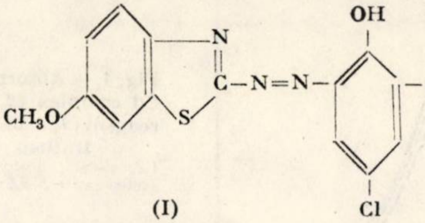

$C_{14}H_9N_3O_2SCl_2$

(I)

The reagent is a brown-reddish powder, but the colour of its acetone-water solution (at pH$=8$) is reddish-purple, while that of the cadmium complex is yellow.

---

[1] V. Armeanu and E. Drăgușin, *Rev. Roumaine Chim.*, **18**, 1475 (1973).

EXPERIMENTAL

The starting material for the synthesis of I was 2-amino-6-methoxy-benzothiazole, which was prepared according to the literature data [2], and then diazotized with nitrosyl-sulphuric acid and subsequently coupled with 2,4-dichlorophenol to give I, m. p. 248−249°.

By the elemental analysis method we obtained:

Calculated for $C_{14}H_9N_3O_2SCl_2$: C, 43.75 ; H, 2.34 ; N, 10.93 %. Found : C, 44.02 ; H, 2.32 ; N, 10,82 %.

The infrared spectrum of this compound shows absorption bands in agreement with the structure I :1,115 (ν C−O, OCH_3) ; 1,375 and 1,480 (δ C−H, OCH_3) ; 1, 600 ; 1,595 and 1,550 (ring vibrations) ; 940 and 1,440 (−N=N−) and 750 (νC−Cl) cm^{-1}.

Buffer solutions for pH adjustment were prepared by mixing 0.1 M citric acid and 0.2 M disodium hydrogenophosphate solutions.

The spectrophotometric study was carried out by means of a spectrophotocolorimeter SPEKOL, using 10 mm cells.

The study was carried out in water-acetone solutions, pH values being obtained by adding the corresponding buffer solution. The pH-values were read on a pH-Meter 28.

The concentration of the reagent and of the cadmium chloride solutions used was 1×10^{-3}M.

To establish optimum working conditions we have first carried out a qualitative study of the Cd-reagent system. We have observed by spectrophotometry the variation of the absorption of the reagent as compared to that of the complex, versus the wavelength and the pH.

The quantitative study of the system was performed in order to establish the combination ratio, the degree of dissociation, and the dissociation constant, as well as the acidity constant (pK_a) of the reagent.

1. ABSORPTION SPECTRA

Figure 1 presents the absorption spectra of the reagent and of the Cd complex in acetone at various concentrations (in the visible range $\lambda=420-660$ nm at pH=8). The colours of the complex and of the reagent solution are yellow and red, respectively.

An analytical wavelength of 530 nm was selected and the solvent concentration chosen was 84 per cent.

The complex was found to be stable, as indicated by the constant absorption value and by the fact that no discolouration of the complex solution was observed over 24 hours.

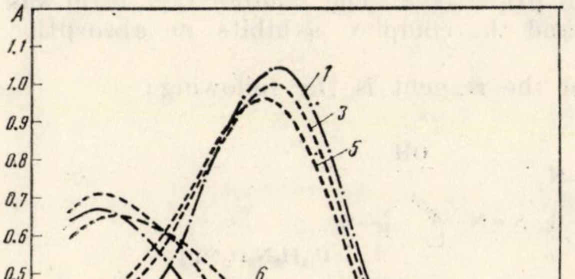

Fig. 1.— Absorption spectra of the Cd complex (*2*, *4*, *6*) and of the reagent (*1*, *3*; *5*) at various concentrations of solutions.

1,2: $c=84\%$ acetone-water ; *3,4:* $c=70\%$ acetone-water ; *5,6:* $c=50\%$ acetone-water

---

[2] J. METZER and H. PLANK, *Bull. Soc. Chim. France*, **1956**, 1697.

2. OPTIMUM WORKING CONDITIONS

The absorption spectra of the complex in the range of pH 2–10 are ilustrated in fig. 2. The working pH was chosen 8.

3. STRUCTURE OF THE CADMIUM COMPLEX

The quantitative study of the system carried out by means of the continuous variations method [3] by using equimolecular solutions of reagents, indicated a R :Cd combination ratio of 1 :1.

The general aspect of the diagram $A=f(C_{Cd}/C_R + C_{Cd})$ in the case of the complex 6-(6-methoxy-benzothiazol-2-ylazo)-2,4-dichlorophenol with Cd is given in figure 3.

The molar ratio method [4,5] gives the same results, respectively a Me :R= =1 :1 ratio (Fig. 4).

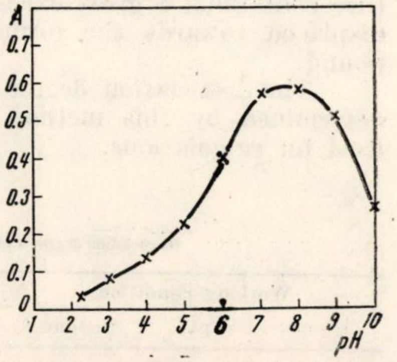

Fig. 2. – Variation of the absorbance of the complex versus pH in water-acetone 84% solution ; $\lambda = 530$ nm ; $A = A_R - A_{CX}$.

The quantitative study of the system was carried out under optimum conditions, established by the study of complex formation, i. e. a water-acetone (84 %) solution, at pH=8 (buffer : citric acid and disodium hydrogenophosphate).

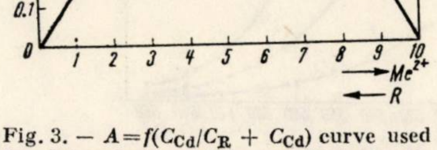

Fig. 3. – $A=f(C_{Cd}/C_R + C_{Cd})$ curve used for determination of the combininig ratio according to Job ; 84% acetone in water solution ; pH=8 ; λ=530 nm.

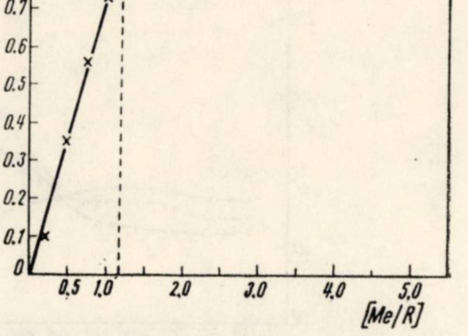

Fig. 4. – Determination of the combining ratio by molar ratio method. Reagent concentration : 4×10^{-5} M ; 84% acetone in water solution ; pH=8 ; λ=530 nm.

---

[3] P. Job, *Ann. Chim.* (*France*), **9**, 113 (1928).

[4] Y. A. Yoe and L. A. Jones, *Ing. Eng. Chem.*, *Analyt. Ed.*, **16**, 111 (1944).

[5] Y. A. Yoe and A. E. Harvey, *J. Amer. Chem. Soc.*, **70**, 648 (1943).

4. STABILITY OF THE COMPLEX

The dissociation degree and dissociation constant of the complex were determined by the Harvey-Manning method [6,7] by measuring the absorbance of the stoichiometric mixture of reactants (A_s) and of a mixture containing a great excess of Cd^{2+} (A_m) so that the equilibrium be displaced towards the formation of a practically undissociated compound.

The dissociation degree and the instability constant of the complex determined by this method are given in table 1 together with the data used for calçulations.

Table 1

Dissociation degree and dissociation constant of the complex

Working conditions			C Mol/l	A_m	A_s	α	K
λ(nm)	pH	Acetone %					
530	8.0	84	4×10^{-5}	0.845	0.369	0.563	2.9×10^{-5}

5. ACIDITY CONSTANT OF THE 6-(6-METHOXY-BENZOTHIAZOL-2-YLAZO)-2,4-DICHLOROPHENOL

Fig. 5 shows the absorption curves of the reagent at various pH-values. As it may be observed, an isosbestic point was obtained at 440 nm wavelength. The solutions of acid forms are yellow and the solution of alkaline forms are red (maximum at 520 nm).

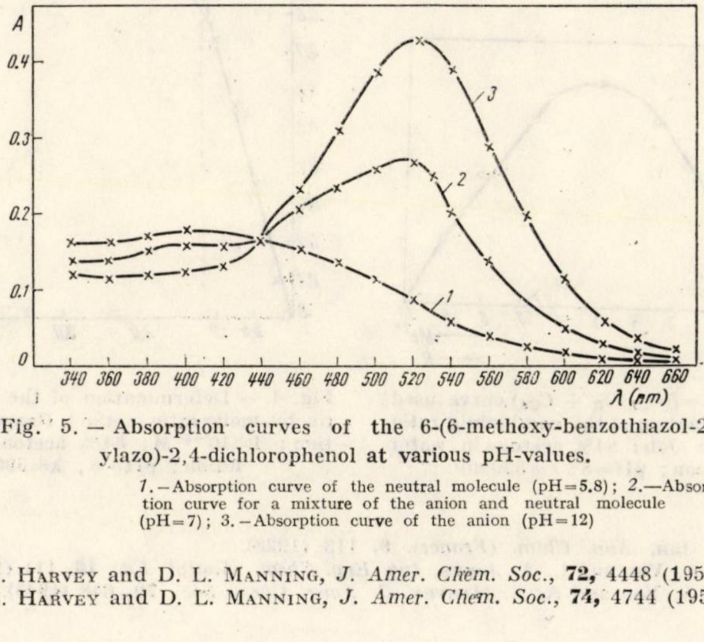

Fig. 5. — Absorption curves of the 6-(6-methoxy-benzothiazol-2-ylazo)-2,4-dichlorophenol at various pH-values.

1. — Absorption curve of the neutral molecule (pH = 5.8); 2. — Absorption curve for a mixture of the anion and neutral molecule (pH = 7); 3. — Absorption curve of the anion (pH = 12)

---

[6] A. E. Harvey and D. L. Manning, *J. Amer. Chem. Soc.*, **72**, 4448 (1950).

[7] A. E. Harvey and D. L. Manning, *J. Amer. Chem. Soc.*, **74**, 4744 (1952).

The acidity constant value of the reagent established by spectrophotometric method [8] was calculated from the following expression:

$$pK_a = \text{pH} - \log \frac{a_{M_1} - a_{M_2}}{a_{M_3} - a_{M_1}}$$

in which:

a_{M_1} = molar absorption index corresponding to the changing of colour;

a_{M_2} = molar absorption index in acid medium;

a_{M_3} = molar absorption index in alkaline medium.

The value obtained for pK_a is 6.80, the function-determining group being the OH(phenol)group.

6. SPECTROPHOTOMETRIC DETERMINATION OF Cd^{2+}

The Bouguer-Lambert-Beer law is obeyed by the reagent studied for amounts up to 104 μg Cd for 25 ml solution.

Fig. 6 represents the dependence of the absorption versus the Cd^{2+} content of the solution, according to this law.

The molar absorbance value of the complex calculated according to the diagram in figure 6 is 20,000 ± 500.

7. SELECTIVITY OF REAGENT

The 6-(6-methoxy-benzothiazol-2-ylazo)-2,4-dichlorophenol reagent shows no particular selectivity for the Cd ion, giving colour reactions with other ions as well.

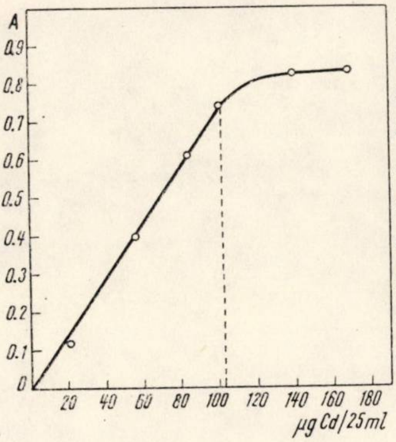

Fig. 6. — Checking of the Bouguer-Lambert-Breer law in an 84 % acetone-water solution.

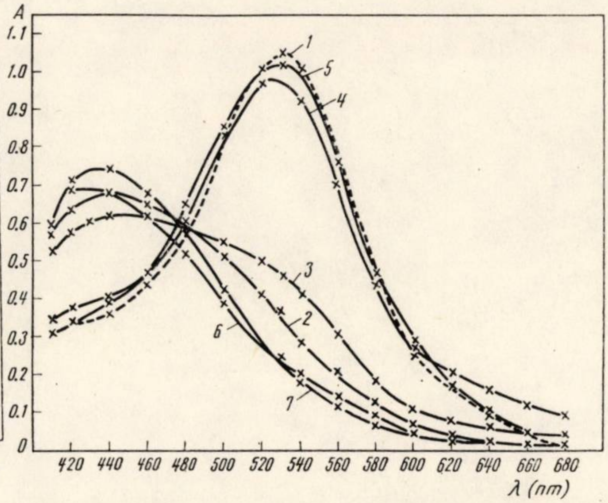

Fig. 7.—Absorption curves of the reagent (*1*) and of Cd^{2+} (*2*), Zn^{2+} (*3*), Hg^{2+} (*4*), Ba^{2+} (5), Fe^{3+} (*6*) Al^{3+} (7) ions in an 84 % acetone-water solution at pH = 8 (buffer: citric acid and disodium hydrogeno-phosphate).

---

[8] A. Albert and E. Sergent, "Konstanty ionizatsii Kislot i osnovanii", Izd. Akad. S. S. S. R., Moskva, 1964, p. 64.

Under the working conditions studied, an interference with Zn^{2+}, Fe^{3+}, Al^{3+} was observed while the Fe^{2+}, Cu^{2+} Co^{2+} and Ni^{2+} interference is negligible. No interference is found for Hg^{2+}, alkaline and earth-alkaline metals.

CONCLUSIONS

A new benzothiazolylazoic reagent was synthetized and the spectrophotometric study of its complex with Cd was carried out in water-acetone solution.

The study was carried out in buffered solutions prepared with citric acid and disodium hydrogenophosphate, the optimum value of pH being 7–8.

The quantitative study established the combination ratio of the complex (Me : R = 1 : 1) as well as the value of the dissociation constant.

The value of the acidity constant was also established using the spectrophotometric method.

The Bouguer-Lambert-Beer law is obeyed for amounts up to 104 μg Cd^{2+} for 25 ml solution.

Revue Roumaine de Chimie, 22, *11–12*, 1539–1542, (1977)

OPTIMIZATION OF THE SEPARATION PROCESS IN TEMPERATURE GRADIENT CHROMATOGRAPHY. I

DETERMINATION OF THE OPTIMUM TEMPERATURE GRADIENT NECESSARY FOR THE SEPARATION OF CERTAIN COMPONENT MIXTURES

T. HODIȘAN and C. LITEANU
Department of Analytical Chemistry, University of Cluj-Napoca,
Str. Arany János n⁰ 11, Cluj-Napoca

Received July 18, 1975

The possible utilizations of the ascending or the descending branch of the curve illustrating the variation of the resolution with the temperature gradient are shown. Each case is exemplified with actual mixtures to be separated. The modality for determining that particular value of the temperature gradient, for which an optimum resolution is obtained, is shown.

One of the most important problems to be considered by a chromatographic analysis is the optimization of the separation process. In the case of chromatography with a temperature gradient, the problem of optimization may be considered under various aspects. The first aspect which will be discussed in the present paper is related to the determination of the optimum temperature gradient necessary for obtaining quantitative separations.

As it was shown[1], the following relation exists between the resolution of two components and the temperature gradient:

$$(1/R_s)_{\text{grad.}t} = (1/R_s)_{\text{izo}(ti)}| + b.\text{grad.}t \qquad (1)$$

This equation permits, on the one hand, the determination by extrapolation of very low resolutions which cannot be determined from the aspect of the densitogram since no "rupture" appears between zones; on the other hand, equation (1) permits the determination of a temperature gradient corresponding to a certain resolution.

Considering two components whose R_f values vary with the temperature gradient as shown by the curve plotted in figure 1a[2] and whose resolution varies according to curve in fig. 1b, one finds that, on the one hand, a certain value of the resolution may be attained for two values of the gradient and, on the other hand, in order to obtain a maximum resolution, the chromatographic process will have to be conducted at a gradient value equal to the limit temperature gradient of the first component $(\text{grad}\,_l t)_1$ (the limit temperature gradient is that gradient value for which the considered component assumes a $R_f = 1.0$ value). The dotted curve in figure 1b illustrates the theoretical decrease of the resolution with the temperature gradient. However, practically, resolutions become higher than theoretical values as the value of the gradient increases, due to the zone narrowing in its migration direction. Evidently, the differences are gradually reduced as the applied temperature gradient gets closer to the value of the limit gradient of the second component.

---

[1] C. Liteanu and T. Hodișan, *Rev. Roumaine Chim.*, **17**, 1985 (1972)
[2] C. Liteanuu and T. Hodișan, *St. și cerc. chim. Acad. R.S.R.*, **21**, 875 (1973).

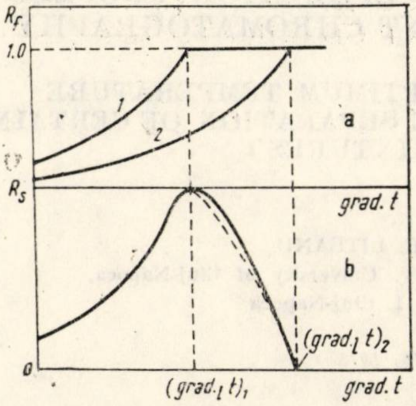

Fig. 1. — Determination of the maximum resolution of two components from the variation of their R_f values.

In the case of a binary mixture, in order to obtain a certain resolution it makes obviously no sense to work a higher temperature gradient than the limit temperature gradient of the component with the higher R_f, i. e. on the descending branch of curve $R_s = f(\text{grad}.t)$, since this would uselessly lengthen the separation time, because the migration speed of the eluent and of the zone decreases with the rise of the temperature gradient.

In the case of a complex mixture formed of n components one may plot for each component the variation of R_f values with the temperature gradient, as seen in fig. 2 a, for $n=5$ components, for instance. For each component pair, a similar curve to that seen in fig. 1 b may be plotted (fig. 2 b). Since the maximum resolution between two components is obtained when the first component reaches the eluent front ($R_f = 1.0$), the use of the descending branch of curves $R_s = f(\text{grad}.t)$ is meaningless, as it actually corresponds to $R_s = 0$, at least for two other components. Therefore, in the case of complex mixtures, only the following two situations may arise from a practical point of view: 1) to use the ascending branch of curve $R_s = f(\text{grad}.\ t)$ for all components, or 2) to use the ascending branch for $n-2$ components and the descending branch for the other two components.

Figure 2 also reveals that it is pointless to construct curves $R_s = f(\text{grad}.\ t)$ for all components and that they should be plotted only for those having the neighbouring R_f values in an increasing succession (e. g. components 1 and 2, 2 and 3, 3 and 4, 4 and 5, etc.). Therefore, $n-1$ $R_s = f(\text{grad}.\ t)$ curves will be plotted determining thereby that value of the temperature gradient for which condition $R_s > 1.0$ is satisfied for all components, as seen in fig. 2 b.

The use of the ascending branch of the curves $R_s = f(\text{grad}.\ t)$ in the optimization process is illustrated in the separation of an amino-

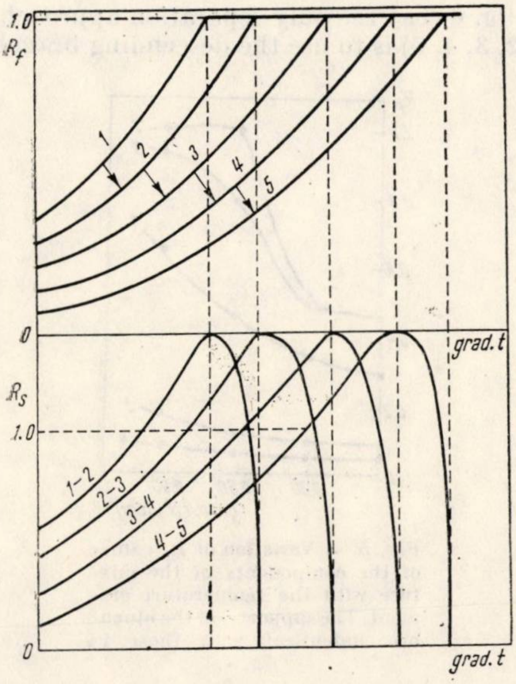

Fig. 2. — Variation of R_f values and of the resolution with the temperature gradient for a mixture formed of five components.

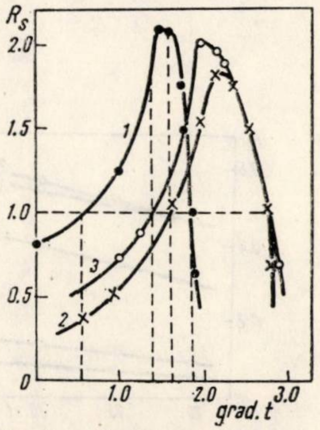

Fig. 3. — Variation of the resolution with the temperature gradient for mixtures of leucine-phenylalanine (*1*) alanine-glutamic acid (*2*) and alanine, glutamine (*3*). Support, microcrystalline cellulose; eluent, the organic phase of the mixture *n*-butanol-acetic-acid-water (40:10:50,v/v).

acid mixture (see fig. 3). It results from this figure that by working with a gradient for which the mixture that separates with difficulty (alanine-glutamic acid) has $R_s = 1.0$, one obtains supraunitary values for the resolutions of the other two mixtures. The same conclusion also holds in the case in which one works at a value of the temperature gradient for which $R_s = 1.0$ for the leucine-phenylalanine mixture (which separates very easily) but on the descending branch of the curve $R_s = f(\text{grad}.t)$. In conclusion, it results clearly that from the standpoint of the optimization of the separation process, the optimum gradient value to work with is that for which the resolution of the poorly separating mixture (alanine-glutamic acid) equals unity on the ascending branch of the curve.

The other possibility (the use of the descending branch) supposes an increase of the temperature gradient by a certain value, which implicitly leads to the extension of the analysis time. Such a case is materialized in the separation of the following mixture of steroidic compounds: 5α-androstane-3 β-ol (1), 5α-androstane-3α-ol (2), 5α-androstane-17β-ol (3), 5β-androstane-3α-17β-diol (4) and 5α-androstane-3β-17β-diol (5).

Figures 4 and 5 show the variation of R_f values under isothermal conditions and in a temperature gradient, respectively.

An inspection of the two figures shows that from the four possible combinations, the problem of separation arises particularly in the case of pairs 2+3 and 4+5. Therefore, figure 6 exhibits the variation of the resolutions of these two mixtures with the temperature gradient.

It results from the study of fig. 6 that the only separation approach, the case of the four components (2, 3, 4, 5) is to use the descending branch

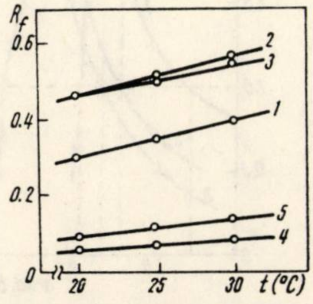

Fig. 4. — Variation of R_f values of the five individual steroidic compounds with temperature. Support, silicagel G; eluent, benzene-ethyl ether (60 :10, v/v).

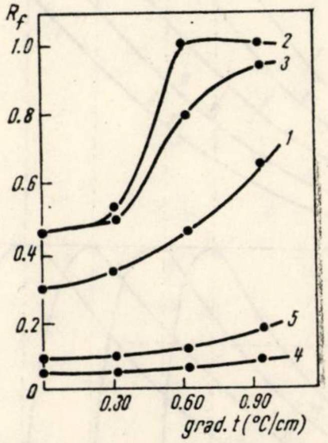

Fig. 5. — Variation of R_f values of the components of the mixture with the temperature gradient. The support and the eluent are indentical with those in fig. 4.

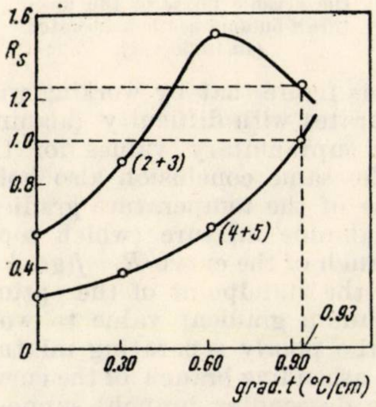

Fig. 6. — Variation of the resolution of mixtures formed of components 2,3 and 4,5 with the temperature gradient.

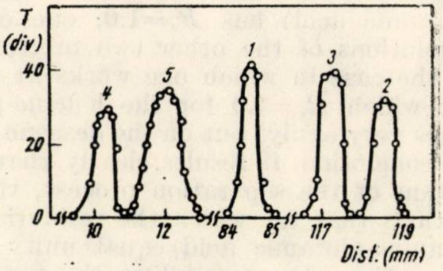

Fig. 7. — Densitograms of the five components of the mixture, obtained at a grad. t=0.93°C/cm.

for components 2+3 and the ascending branch for components 4+5, at a 0.93° C/cm gradient value.

The densitograms of the five components in the mixture, obtained at this gradient in fig. 7, are presented.

As the separations are definitely quantitative, it results that the method suits perfectly to the quantitative determination of these components.

Revue Roumaine de Chimie, 22, *11–12*, 1543–1550 (1977)

COMPTES RENDUS

GR. POPA and S. MOLDOVEANU, „Reactivii organici în Chimia analitică" ("Organic reagents in analytical chemistry"), Ed. Academiei, Bucharest, 1976, 254 p.

The book "Organic reagents in analytical chemistry" by Grigore Popa and Serban Moldoveanu, published at Editura Academiei, Bucharest 1976, presents an important and topical subject of analytical chemistry as well as of chemical analysis.

Although organic reagents were introduced in analytical laboratories since the beginning of this century, their use is very important also at present, the oldest gravimetric and volumetric techniques being completed by new physical methods, especially optical and electrometric.

In this field, many books have been issued by Romanian and foreign authors, such as the book published by the same authors in 1969, at Editura Tehnică, Bucharest. Their main drawback lies in the fact that they describe especially the use of organic reagents in chemical analysis and make only few considerations concerning the operational parameters and characteristics of these reagents and their compounds with inorganic ions.

The present book presents in few pages the theoretical and practical characteristics of the use of organic reagents in analytical chemistry. We consider that the present book is the best monograph published by now in this field (in my opinion as a specialist in organic reagents and as an old coworker of the authors).

The first two chapters of the book deal from a theoretical point of view with the formation and the properties of the compounds formed of inorganic ions and organic reagents. The third chapter presents the main types of organic reagents. The classification is made on the basis of different active groups present in organic reagents, this being the most efficient and rational point of view. Tables include the main groups of organic reagents as well as their characteristics. The data provided by these tables enable us to understand the importance of the use of this kind of reagents in analytical laboratories.

Chapter 4 presents the use of organic reagents for the concentration and separation of inorganic ions. This is only an informative chapter since many books have been published in this field.

The last chapter presents in many tables the use of organic reagents for the determination of inorganic ions. The importance of this chapter lies in the fact that it supplies the analytical chemist with a lot of significant data also referring to up-to-date literature.

We consider the publication of the book as necessary due to the large number of chemists, biologists, physicists and students from the chemical faculties interested in this modern field of analytical chemistry.

We suggest the translation of the book into English and Russian.

George-Emil Baiulescu

"Renormalization theory", G. Velo and A. S. Wightman Ed. D. Reidel Publishing Company, Dordrecht, Holland, Boston, U.S.A., 1976, 482 + VII

The lecture notes from the session of the International School of Mathematical Physics "Ettore Majorana" that took place in Erice (Sicily) in August 17 – 31, 1975, are collected in this book. The principal efforts in the last period of 30 years for the development of the quantum field theory in 4-dimensional space (space-time) are reviewed in this so-called renormalization theory. The starting point is the formula of Gell-Mann and Low (1951) for the Lagrangian form of quantum field theory. The mathematical improvement of this formula has an object to solve certain theoretical problems as : ultraviolet renormalization, infrared power counting, the construction of the scattering matrix, composite fields, etc. The basic notions are systematically introduced and in-depth treated in the development of this theory, namely : analytical and dimensional renormalization, the normal product technique, the Bogoliubov-Shirkov-Epstein-Glaser method, etc. all these for the perturbative renormalization theory. On the other hand, the advances of the methods of constructive field theory in models in space-time of two and three dimensions in the non-perturbative renormalization theory are reviewed. On this occasion some limitations and errors of the renormalization theory, and in general quantum field theory, were revealed. A series of open problems are expressed ("Achievements, limitations and open problems in renormalized perturbation theory", lectures given by B. Schroer) as the non-perturbative expression of solution in terms of functional integrals. The lucidity of the introductory presentation on the historical development of the renormalization theory (lectures given by professor A. S. Wightman) must be remarked.

Since formalism uses Feynman integrals, it is ununderstandable that their topological properties already studied ten years ago were not reviewed (Fotiadi, Froissart, Lascoux, Pham, 1965, and taken again in detail in the book of R. C. Hwa and V. I. Teplitz, 1966).

This book is of didactc interest, to familiarize the future specialists with the present mathematic difficulties in the iquantum field and particles theory. At the same time this book is a good guide for algebrists who are expected to give their point of view in the general theory of interactions. However, professor J. Fröhlich also remarks that this theory which becomes more and more sophisticated owing to a heavy and not always efficient mathematical gauge has to be more relevant especially for physicists.

The strong linkage between Lagrangian quantum field theory and statistical mechanics is briefly mentioned by Kadanoff parametrization of the Gell-Mann and Low formula. This expression leads to the differential version of the Kadanoff's scaling law introduced in the statistical-mechanics treatment of the critical phenomena. We can complete this picture by reminding that the renormalization group approach (1973) has been recently constructed for the particular case of the critical behaviour of the magnetic systems. Taking into account the fact that recent studies upon non-equilibrium thermodynamics have introduced new working principles, their extension to the case of the electromagnetic, weak and strong interactions would establish a unitary formalism.

Gh. Drăgan

"Hydrogen energy" T. N. Veziroğlu Ed. Plenum Press, (in two volumes), 1975, 1369 pages

Published after the Hydrogen Economy Miami Energy (THEME) Conference held in Miami Beach on 18 — 20 March 1974 this excellent edition of the Proceedings will serve as the platform from which the new Conference will commence. Indeed, the Conference has attempted to provide the best information available today on the obtaining of the most viable solution to the energy crisis and has devoted much time to considering the use of hydrogen as an energy-carrier and long-range benefit of energy supply. For the most part, the papers of this issue are future-oriented. There is a strong emphasis on the relationship between findings and views in the hydrogen production from solar, nuclear, thermochemical and other sources and the economic, technical and operational aspects of feasibility. The consensus of the authors is that there are problems regarding the question of feasibility but, at least, in principle, they can be solved.

This two-volumes work does not follow the division of the scientific programme and the papers have been organized under two parts and five major headings : 1) Primary energy sources, 2) Hydrogen production, 3) Hydrogen storage and trasmissions, 4) Hydrogen utilization and 5) General considerations.

Chapter 1 contains five well-informed papers on the problem of conversion of solar and geothermal energy to electricity and a study on the effect of atmospheric turbulence on windmill performance.

The long Chapter 2 (418 pages) contains 29 papers on hydrogen production by electrolysis of water (including the developments of high temperature electrolysis and static feed water electrolysis), thermochemical water splitting cycles, sea thermal power and photolysis of water.

Chapter 3 devotes 126 pages to the subject of metal-hydride storage systems (five papers) and pipeline transportation of hydrogen (two papers).

Chapter 4 presents a number of the most interesting aspects of hydrogen utilization : experimental investigations of the performance of internal combustion engine on hydrogen, ammonia as a hydrogen carrier and its applications as a fuel, hydrogen-oxygen fuel cells and liquid hydrogen as a fuel for aircraft.

Chapter 5 is concerned with the various aspects of hydrogen technology (hydrogen in metals, hydrogen-environment embrittlement of metals and hydrogen distribution) and discusses some of the problems that have to be solved before we can develop a commercial hydrogen economy (social and environmental context of the hydrogen economy, technical problems facing the hydrogen economy, the hydrogen economy and the law, mechanisms and strategies of market penetration, etc.).

As a whole, the book is well put together and presents an authoritative view of the subject. It will certainly be of great utility to all workers engaged in hydrogen technology research.

Cezar Ungurenașu

HEINZ ENGELHARDT : "Hohdruckflussigkeits-Chromatographie", Springer Verlag, Berlin, 1975, 213 p.

The book provides a valuable material for all those who want to learn about the theoretical and practical bases of liquid chromatography. It deals with theoretical problems and also presents the appparatus required in high-pressure liquid-chromatography (HPLC). The book has 12 chapters. The first chapter discusses the chromatographic procedures. Chapter II presents the bases of liquid chromatography : retention values, problems relating to the flow through porous media, the reasons for the zone enlargement, the resolution, the optimization of the separation process and the column selectivity. Chapter III and IV deal with problems regarding the apparatus and various detector types used in liquid-chromatography. Chapter V handles the problem of the stationary phases in liquid-chromatography (adsorption, distribution, ion exchange and steric exclusion). Chemically bound stationary phases are also discussed. The next four chapters VI — IX handle, at a high scientific level and with much clarity, the most important basic problems of the four separation elementary processes : adsorption, distribution, ion exchange and steric exclusion.

The last three chapters (X — XII) summarize some problems related to the choice of the separation system, preparatory chromatography, quantitative analysis and the solvent purification. As the author is a famous and well-known research worker in the field of liquid chromatography, he has succeeded in making a clear presentation of the basic problems of liquid chromatography in a reduced number of pages. The book is adequately illustrated with the most representative examples which significantly complete its content. This work has a rich scientific content and it is intended both for research workers and for students who wish to specialize in the field of liquid chromatography.

S. Gocan

"Radioaktive Isotope in Klinik und Forschung", vol. 10 (Gasteiner Internationales Symposium 1972), edited by K. Fellinger and R. Höfer, Urban & Schwarzenberg Verlag München—Berlin—Vienna, 1973 ; 516 pp., 353 illustrations, 83 tables, cloth-bound, DM 150.

As special volume 72 of *Strahlentherapie*, the Proceedings of the biennial Bad Gastein International Symposium 1972 make a useful addition to the existing records of these well-known symposia in nuclear medicine, which started twenty years ago.

The 68 papers presented in this volume belong to one of the following nine sections :

1. Organizational problems in nuclear medicine (7 papers)
2. Data processing instruments in nuclear medicine (8 papers)
3. Renal circulation and renal function (7 papers)
4. Liver scintigraphy (4 papers)
5. Spinal circulation (7 papers)
6. Isotope therapy (5 papers)
7. Radiocardiography (4 papers)
8. Regional lung function (6 papers)
9. Free lectures (20 papers).

The papers are presented in German, English or French in full, or in one case only, as an extended summary. All papers have summaries (but not titles) in all of the above three languages. Most papers are followed by a reproduction of the discussions.

The papers in the first section make an interesting reading for radioisotope producers, radiopharmacists and clinical nuclear physicians alike. Until now, organizational problems have seldom been solved favourably for all factors involved : good and inexpensive medical assistance, quick and regular delivery of the radiopharmaceutical, efficient stimulation of research and development. Therefore, the various approaches are very instructive, since they differ not only by magnitude and social outlook of the country, but also by the viewpoint of different professions : physicists, chemists, biophysicists and physicians.

Some problems raised in this section are connected with those examined in the second section ; indeed, the paper by Hundeshagen discussing the planification, construction and facilities of an institute of nuclear medicine within a large hospital, intended to perform 50,000—80,000 examinations yearly (for 15,000—20,000 patients), evidences the necessity of computerized data processing.

Several papers presented in the third section discuss radioisotopic methods for the functional evaluation of isolated kidneys, preserved in view of transplanation. This is a rapidly developing area during the last years, and these papers are therefore valuable.

In the sixth section, McDougall, Greig and Gillespie discuss ^{125}I therapy for thyrotoxicosis after trials with 148 patients, comparing the effects and doses with ^{125}I and ^{131}I ; since the range of ^{131}I β-rays is 400—2 000 μm, and those of ^{125} I have a range of only 30 μm being lower-energy positrons, theoretically the latter radioisotope should give better results for localized cell destruction ; the practical conclusions, however, require testing over longer periods.

In the eighth section, three papers discuss the use of ^{133}Xe for lung scintigraphy. These papers retain their usefulness and interest ; especially important is the problem of discerning operable from non-operable lung carcinomas using this technique.

The last section discusses various topics, from which we will point out the last papers on oncotropic radiopharmaceuticals, using ^{67}Ga, ^{111}In, ^{75}Se, as well as the first report on ^{57}Co-labelled Bleomycin ; despite the fact that today, ^{111}In-labelled Bleomycin has reached a competing level, this last paper still retains its high interest.

The volume contains an alphabetical list of participants, and a subject index. However, this latter index includes topics in their original language without translation or cross-referencing, as it may be ascertained by looking under the three separate headings *kidney*, *rein*, and *Niere*.

This book must be present in all units of nuclear medicine, and is useful to all those interested in the production and use of radiopharmaceuticals, in the medical applications of radionuclides.

Alexandru T. Balaban

„Atlas of Thermoanalytical Curves", ed. by G. Liptay (Cumulative Index for volumes 1—5), Akademiai Kiado, Budapest, 1977.

With the publication of volume 5, the editor introduced the cumulative index, comprising cumulative subject and formula indexes, plus a list of the contributions, their affiliations and the names of the materials examined by them. A special feature of this ring-clamped loose-leaf system is that it allows the user to arrange the curves in a manner best suited to his particular needs. The serial number given by the user during this procedure can be written in a frame reserved for this purpose on the data side of each page.

The materials investigated include inorganic and organic compounds, coordination compounds, minerals, amino acids, drugs, pesticides and coal samples.

The compounds in the index have been classified into three main categories :

— compound index

— chemical formula index (inorganic and organic)

— class index (ICTA Standards, Minerals, Rocks, Coals, Amino Acids, Pharmaceutical Products, Pesticides).

D. I. Marchidan

HENRY T. KERNER, *Foam Control Agents*, Ed. Noyes Data Corp. Park Ridge, New Jersey, U. S. A. 1976, 372 p.

In many industrial processes the foaming is an indesirable phenomenon interfering with the process efficiency and sometimes affecting the quality of the products. To avoid these inconveniences there are used small amounts of substances that prevent or damp the foam without any undesirable side effect, known as antifoaming agents, defoamers, foam control agents, foam-preventing agents or foam-dampening agents.

The problem being extremely important for many technical processes, substances were looked for, having antifoaming properties and resisting a long time under heavy acidic or basic conditions. The most of the data obtained constitute the subject of many patents.

The volume "Foam Control Agents" includes descriptive information upon the types of antifoaming agents, their application areas, the methods of preventing and decreasing the foaming. In the form it is drawn up the book can supply technical information and at the same time it is a guide to the U. S. patents issued since 1960s in the field of the foam control agents.

There are presented the main fields of utilisation, such as : detergents and cleansers, pulp and paper, lubricants, fuels and organic liquids, textiles, phosphoric acid processes, latex, coating and photographic applications, fermentation, pharmaceuticals and foodstuffs, polymerisation and distillation, antifreeze, drilling fluids, acid gas separation from liquid mixtures. Finally, a chapter deals with the general processes of the foam control.

Among the classes of antifoaming agents, the most useful are the silicones as polydimethylsiloxanes treated or not with SiO_2, substituted organopolysiloxanes, siloxane copolymers with hydrosylated polyalkylenes, organofunctional silicones, amides, polyoxyalkyleneamines, polyalkyleneimines, polyoxyalkylated fatty acids and their alkaline salts, ethoxylated fatty alcohols, etc.

The author presents also some equipments meant to be used in the processes where the liquids tend to foam upon agitation or aeration, electrical control signals for the increase or the decrease of the foam amount and some methods of reducing the degree of foaming of the aqueous liquids by passing them through a porous mass, wettable and permeable to aqueous liquids.

Due to the great number of data comprised in the 210 patents described, the book represents a very precious documentary guide for the specialists meeting with foaming problems both in aqueous or nonaqueous systems.

Besides the table of contents, the volume provides a company index, an index of the inventors and an U. S. patents number index, to facilitate the going over the material and the finding of the information desired.

Aglaia Ciobanu

CRISTOFOR SIMIONESCU und Mitarbeiter : ,,Handbuch der Makromolekularchemie", 3 Bände. Ed. didactică şi pedagogică, Bukarest 1973-76

Das Handbuch des Akademikers Cristofor Simionescu, Professor am Polytechnischen Institut Iaşi, stellt eine weitläufige, vier Bände umfassende Arbeit dar, wovon zur Zeit drei erschienen sind.

Der erste Band — Autoren Cristofor Simionescu und Cleopatra Vasiliu-Oprea, 1973, 693 Seiten — behandelt die allgemeine Problematik dieses Gebietes und beschäftigt sich mit den anorganischen und den elementorganischen Polymeren sowie mit der Synthese von hochmolekularen Verbindungen durch Radikalkettenpolymerisation.

Der sich auf allgemeine Aspekte beziehende einführende Teil bringt einen kurzen geschichtlichen Überblick, behandelt Grundbegriffe, die Klassifizierung der Polymere sowie Nomenklaturfragen. Der übrige Teil des Bandes ist in drei Teilen gegliedert.

Der erste Teil bezieht sich auf die Herstellung von anorganischen Polymeren. In diesem Sinne wird die Fähigkeit der verschiedenen Elemente solche Polymere zu bilden, untersucht und deren allgemeine Darstellungsverfahren gebracht. Es folgt eine Systematisierung dieser Polymere, welche acht Klassen umfaßt.

Mit den elementorganischen hochmolekularen Verbindungen beschäftigt sich der zweite Teil. Gemäß dem im ersten Teil angewandten Behandlungsprinzip, wird die Fähigkeit verschiedener Elemente elementorganische Polymere zu bilden analysiert und deren allgemeine Syntheseverfahren dargestellt. Anschließend geht der Autor auf die verschiedenen Klassen von elementorganischen Polymeren ein : — die eigentlichen Polymere (solche die Bor, Aluminium, Silizium, Germanium, Zinn, Blei, Arsen, Phosphor, Antimon, Schwefel, Selen, Tellur enthalten, sowie Metalle die Alkoxyde und Carboxylate bilden) — und die Koordinationspolymere.

Im dritten Teil des ersten Bandes — Syntheseverfahren für hochmolekulare organische Verbindungen — gehen die Autoren von einer Klassifizierung dieser Verfahren nach drei Richtlinien aus: Polymerisation, Polykondensation und Polyaddition. Dem erstgenannten Verfahren — der Polymerisation — ist der gesamte restliche Teil des ersten Bandes gewidmet. Es werden allgemeine Überlegungen, die Polymerisationsverfahren, der Kettencharakter des chemischen Prozesses und die gegenseitige Wechselwirkung Monomer-Reaktionsmedium betreffend, gebracht und in einer logischen Reihenfolge Probleme wie: die freien Radikale, die Fähigkeit der Monomere eine Radikalhomopolymerisation einzugehen, die einzelnen Phasen des chemischen Prozesses (Kettenstart, Kettenwachstum und Kettenabbruch), die Polymerisationskinetik in homogenem System, die Polymerisation in heterogenem System, die radikale Kopolymerisation, die Polymerisation nichtkonjugierter Diene und die Polymerisation in festem Zustand, untersucht.

Der zweite Band — Autoren Cristofor Simionescu und Dorel Feldman, 1974, 256 Seiten — ist ausschließlich der ionischen Polymerisation gewidmet. Zunächst gehen die Autoren auf einige spezielle Probleme bezüglich des Reaktionsmechanismus und der Kinetik der Polymerisation, Telomerisation und der anionischen Kopolymerisation ein. Es werden ausführlich die anionische koordinative Polymerisation behandelt sowie Eigenarten der stereoregulären Polymere. Desgleichen beziehen sich die Autoren auf die Problematik der kationischen Homo- und Kopolymerisation. Im abschließenden Teil werden die Blockkopolymerisation und die Herstellung von Pfropfpolymeren nach dem Ionenmechanismus bahandelt.

Der dritte Band — Autoren Cristofor Simionescu und Victor Bulacovschi, 1976, 325 Seiten — behandelt die Synthese von hochmolekularen Verbindungen nach dem Polykondensationsverfahren. Im Verlauf von elf Kapiteln beziehen sich die Autoren auf folgende Aspekte: die Grundprinzipien dieses Verfahrens, das Verhalten der Monomere im Polykondensationsprozeß, die Thermodynamik und Kinetik der Polykondensation, die Molekulargewichtsverteilung der Polykondensate, die Grenzflächenpolykondensation, die Lösungspolykondensation, die elektrochemische und mechanoschemische Polykondensation, die linearen Polykondensate (Polyester, Polyäther, Polyacetale, Polyamide, heterozyklische Polymere), die Polykondensate mit räumlich vernetzter Struktur und die Kopolykondensation.

Der vierte Band wird auf die Polyaddition, die polymer-analogen Umsetzungen, die Polymere mit speziellen Eigenschaften und die makromolekularen Naturstoffe eingehen.

Das Handbuch der Makromolekularchemie ist nach modernen Gesichtspunkten verfaßt und stützt sich auf umfassende bibliographische Studien. Allein die ersten drei Bände enthalten 2757 Literaturhinweise, welche die veröffentlichte Literatur bis 1975 berücksichtigen. 290 Tabellen und 242 Abbildungen tragen zu einer übersichtlichen Veranschaulichung der behandelten Problematik bei.

Das Handbuch des Akademikers Cristofor Simionescu und Mitarbeiter stellt einen bedeutenden Literaturbeitrag von hohem theoretischen und praktischen Wert dar und zeichnet sich durch ein hohes wissenschaftliches Niveau, eine zusammenfassende und übersichtliche Darstellung der auf diesem Gebiete veröffentlichten Arbeiten aus.

Die einheitliche und kritische Darstellungsweise der theoretischen Grundlagen verleiht der Arbeit einen erhabenen und praxisbezogenen Charakter.

Das Handbuch der Makromolekularchemie ist die erste rumänische Arbeit dieses Inhaltes, welche in einheitlicher Form die physikalischen und chemischen Grundlagen der Polymere, deren Herstellungsverfahren und ihre strukturbedingten Eigenschaften darlegt. Demzufolge ist dieses Buch eine wertvolle Ergänzung der zahlenmäßig geringen Arbeiten solchen Ausmaßes, die zur Zeit auf Weltebene veröffentlicht sind.

Durch die Vielzahl der übermittelten Sachkenntnisse stellt dieses Handbuch ein besonders nützliches Hilfsmittel für Studenten, Kandidaten der Wissenschaften und alle Fachleute der Makromolekularchemie dar.

I. Manoviciu

PETER HEDVIG "Dielectric Spectroscopy of Polymers", Akademiai Kiado, Budapest, 1977, 431 p.

This book presents the dielectric spectra of polymers. This new method of polymer characterization is compared with others such as thermomechanical measurements and dilatometry, mechanical relaxation spectroscopy, differential scanning calorimetry, nuclear magnetic resonance.

The first part discusses the theoretical principles of dielectric spectroscopy : the origin of dipole moments of low and high molecular weights materials, statistical, thermodynamical and phenomenological models used in this field.

With regard to the polymers the sttuctural transitions and molecular mobilities are presented. Comparatively with other methods the book reviews the kind of transitions that can be detected by dielectric spectroscopy.

The esperimental part presents the methods and instruments used to obtain the dielectric spectra of polymers. The other techniques such as thermomechanical measurements and dilatometry, mechanical relaxation spectroscopy, differential scanning calorimetry, nuclear magnetic resonance are also discussed.

Dielectric spectra of pure polymers are reviewed function of the chemical structure of their main chains and side groups. These polymers are : nonpolar polymers (polyethylene, polytetrafluoroethylene), polymers with flexible polar side groups (polyvinyl acrylates and methacrylates, polyvinyl esters, polyvinyl alkylethers), polymers with polar side groups rigidly attached to their apolar main chain (polyvinyl chloride and related halogen polymers, polyvinyl acetals) polymers with polar main chain (oxide polymers, polyesters and polycarbonates, polyethylene terephthalate), polymers with hydrogen bond (polyamides, polyurethanes, cellulose derivatives).

The author also presents the efficiency of dielectric spectroscopy in the study of polymer compounds. Polymer compounds are divided in three main groups. The first group is that which forms a homogeneous phase : plasticized compounds and polymer solutions. The second group consists in inhomogeneous phases : compounds of polymers with fillers, dyes, stabilizers and impurities. The third group is that of polymer blends and copolymers.

The last two chapters discuss the possibilities of the dielectric spectroscopy in following the crosslinking processes and ageing process of polymers.

The temperature dependences of relaxation times associated with the main transitions in various polymers are plotted in the appendix.

The references are given at the end of the book.

In the polymer field this book is a vey important contribution regarding polymer characterization.

Dan Donescu

M. HARGITTAI and I. HARGITTAI, "The Molecular Geometries of Coordination Compounds in the Vapour Phase", Akadémiai Kiadó, Budapest, 1977, 276 p.

The book entitled "The molecular geometries of coordination compounds in the vapour phase" by M. Hargittai and I. Hargittai is the English version of the Volume 23 in the series A Kémia Ujabb Eredményei (Advances in Chemistry), edited by Béla Csakvári, Akadémiai Kiadó, Budapest, 1974. The book is intended to be a review of the data published on molecular geometry determination of coordination compounds in vapour phase up to the end of 1973. Some references from the beginning of 1974 are also included.

The first part of this monograph describes the general concepts related to coordination compounds and makes an introduction regarding the structural measurements of this kind of compounds.

When comparing the vapour phase and the liquid- or crystal-phase data the changes in molecular geometry might be significant. The molecules with a low barrier to internal rotation, intramolecular hydrogen bridges or coordination-type linkages show the largest deviations. The origins of the differences in bond lengths and bond angles of various compounds derived from vapour phase and condensed phases measurements are discussed.

In this introductory part the authors give also a short review of the current physical methods used in molecular geometry determination. The special merits of the electron diffraction and microwave spectroscopy are emphasized.

The second part of the book largely illustrates the structural data of seven classes of compounds obtained in vapour phase by electron diffraction and microwave spectroscopic studies. Some comments about their significance are also given. The material is organized in seven chapters.

The first chapter, "Addition compounds", focuses on the results of vapour phase structural determinations of some charge transfer complexes of the type Lewis acid — Lewis base. The boron-nitrogen, boron-phosphorus and aluminium-nitrogen compounds are included. In addition to reviewing the determinations of the molecular geometries of individual compounds, the variations of the geometrical parameters and possible correlations between geometry and bonding are also considered.

The electron-deficient molecules are the subject of the second chapter. The vapour phase determinations on boron hydrides, carboranes, metal borohydrides and some metal-alkyl bridge compounds are gathered and the structures of these compounds are successfully interpreted by the concept of multi-centre bonds.

Very interesting studies on halogen bridging compounds are treated in the next chapter. The dimeric, trimeric and tetrameric halides as well as structural information on monomeric species are included. Mixed halides with the formula $M^nMe^m X_{n+m}$ (where M and Me are n- and m-valent metals, X is a halogen) are also surveyed and the importance of these data for chemical bonding is outlined.

Inorganic salts of some oxyacids as metaborates, nitrates, sulfates, chromates, molybdates and perrhenates are next described. The structural data compiled for these low-volatility compounds are based especially on electron diffraction determinations at high temperatures. The authors emphasize the importance of various techniques such as "matrix isolation technique" used for structural determinations in this class. The data including details which are obtained by tedious studies and delicate techniques have a particular significance for the knowledge of the structure of a wide class of inorganic compounds. This chapter gives some information on structural peculiarities of compounds of the formula $MeXO_4$ (where Me=monovalent metal and X=S, Cr, Mo or W) demonstrating the coordination character of these structures while the metaborates and nitrates are considered to be borderline cases.

The electron diffraction method constitutes the main technique for the structure determination of polymeric oxides as shown in the fifth chapter. Starting with structural data on nitrogen and sulfur oxides attention is then granted to the oxides of the formula A_4O_6 (where A=P, PO, As and Sb), the oxides of the chromium group, the selenium tetroxide tetramer and dimethylaluminium methoxide trimer.

The sixth chapter on complexes with hydrogen bonds is a short one but it has a theoretical value. The authors firstly discuss the influence of intermolecular hydrogen bonds on internal structure of dimeric compounds (dimeric organic acids) or of bimolecules (trifluoroacetic acid — formic acid) and then that of isotopic substitution on the hydrogen bonds. The data given on hydrogen fluoride, dimeric or polymeric, have an increased value in supplementing the recent theoretical calculations in this field. In the study of monomeric amonium chloride a structure with one hydrogen bond has been revealed based on the comparison of the electron diffraction data with those obtained by infrared measurements or *ab initio* calculations.

The final chapter on transition metal complexes represents a valuable information source for all the chemists interested in this large area of coordination chemistry. Although the molecular geometries of relatively few transition metal complexes have been determined up to now in the vapour phase the data compiled have a real significance for the nature of the coordination bonds of these compounds. Structural determinations by electron diffraction on complexes of the π-acceptor ligands of carbonyls, olefin and allyl complexes of metal carbonyls and cyclopentadienyl metal complexes are described and their geometries are commented. In the last part of this chapter a comparison for various types of metalocenes is made. Based on these data the authors give some correlations between molecular geometries and the nature of coordination bonds. In some cases (e. g. for ferocene) the contribution of the d orbitals in the π bond formation is outlined.

The most original feature of this monograph is that the molecular geometry of the coordination compounds is determined from vapour phase measurements. These measurements refer to free, isolated molecules, uninfluenced by intermolecular forces which is particular important when weaker interactions can play a significant role in shaping the molecular geometries. The compiled data are the most appropriate for comparison with the theoretical calculations on the bonding in coordination compounds.

The book is the first to provide a comprehensive survey of structural determinations of coordination compounds in the vapour phase. As the number of such determinations is not yet too large for the above classes of coordination compounds all the published data were included.

Valerian Drăguţan

REVUE ROUMAINE DE CHIMIE

INDEX DU TOME 22, 1977

INDEX DES AUTEURS

A

Page

ABABI V., voir BOURCEANU G. 459, 1391
ABBE J. CH., voir CONSTANTIN E. 327
AGASIAN P. K. i E. P. NIKOLAEVA, R. D. CHIAVDAROVA, Kulonometricheskie metody opredelenyia renyia 491
ALEKSIC B. D. and A. TERLECKI-BARICEVIC, Investigation of the effects of chemical nature of some structural promotors on electric conductivity changes in precipitated ammonia synthesis catalysts in reductive atmosphere 1335
ALIMARIN I. P. i A.P. GOLOVINA, A. K. RUNOV, Ionnye assosiaty rodaminovykh krasitelei s anionnymi kelatami i ikh khimikoanaliticheskoe ispolzovanye 503
AMBRUS C., voir DEMIAN N. 1187
ANDREESCU C., voir ONCESCU T. 697
ANDREI R., voir TOTIR N. 137
ANGELESCU S., voir ŞUSTER D. C. 1195
ANGHELIDE N. and E. ŞLIAM, D. RĂILEANU, Electron transfer *vs* proton capture in the formation of dienamino esters 969
ANTONESCU L., voir SPACU P. 61
ANWAR M. and S. H. ETAIW, Infrared absorption spectra of some 4H-3,1-benzoxazin-4-ones and 2,3-disubstituted-4(3H)-quinazolinones 1217
ARCE F. y J. L. ARMESTO, J. CASADO, M. A. RIOS, Estudio conformacional y de constantes de acoplamiento hiperfino en radicales libres. Aproximacion INDO 815
— y J. CASADO, M. A. RIOS, V. TATO, Estudio teorico de la naturaleza de constantes de fuerza. I. Moleculas diatomicas 335
— y J. CASADO, M. A. RIOS, V. TATO, Estudio teorico de la naturaleza de constantes de fuerza. II. Moleculas triatomicas 345
ARMEANU V. and E. DRĂGUŞIN, Spectrophotometric study of cadmium complex with 6-(6-methoxy-bezothiazol-2-ylazo)-2,4-dichlorophenol 1533
ARMESTO J. L., voir ARCE F. 815
ASANDEI N., voir SIMIONESCU CR. I. 283
ASHKENAZI P., voir CAIS M. 545
AURIAN-BLĂJENI B., voir IONESCU N.I. 353
AVRAM M., voir ENESCU L. 1061
— , voir DINULESCU I. G. 1037

B

BACALOGLU I.-I. und R. BACALOGIU, D. MARTIN, A. PRÜFER, Struktur-Reaktivitätsuntersuchungen mit heterosubstituierten Nitrilen. XVII. Kinetik und Mechanismus der Trimerisation der Arylcyanate in Gegenwart von $AlCl_3$ 511
BACALOGLU R., voir BACALOGLU I.-I. 511
— und C. DĂESCU, Nucleophile Substitutionen an Kohlensäurederivaten. VIII. Kinetik und Mechanismus der Hydrolyse von N,N-disubstituierten Thiocarbamidsäurechloriden 977

Rev. Roumaine Chim. 22, *11–12*, p. 1551–1571 (1977), Bucarest

Page

BACALOGLU R. and T. KORODI, A. FLORESCU, G. OSTROGOVICH, Nucleophile Substitutionen an Kohlensäure-Derivate. IX. Kinetik und Mechanismus der Alkoholyse von Kohlensäure-Dichlorid-N-Aryl-Imiden 877
BĂDILESCU S., voir SAHINI V. EM. 811
BAHADUR P., voir SINGH L. R. 1145
BALABAN A. T., Chemical graphs. XXVIII. A new topological index for catafusenes : L-transform of their three-digit codes 45
— , Chemical graphs. XXX. Reaction graphs for degenerate rearrangements of homovalenium cations 243
— , Chemical graphs. XXXI. Benzo-homovalenes 987
— and A. BOTA, F. CHIRALEU, E. ŞLIAM, A. HANEŞ, C. DRĂGHICI, Pyrylium salts formed by diacylation of olefins. XXIII. Isomeric ethyltrimethylpyridines and dimethyl-n-propylpyridines from the diacetylation of hexenes and methylpentenes. 1003
— and E. M. PALMER, F. HARARY, Chemical graphs. XXIX. Numbers of isomers with naphthalene and adamantane skeletons 517
— , voir STĂNOIU I.I. 117, 865, 1359, 1499
— and I.I. STĂNOIU, E. GÂRD, Deuterium isotope effect on the basicity of 2,4,6-trimethylpyridine. 1191
BALABAN C., voir BRATU EM. A. 271
BALÁZS I. and V. FĂRCĂŞAN, I. HAIDUC, Synthesis of di- and triphenyllead polychloroacetates 379
BALTĂ P. and D. RADU, Some information about the geometry of the molecules in molten and solid glasses 525
BANCIU A. C., A pentacoordinated Co(II) complex compound derived from 1-methyl-2-carbethoxy-glyoxalanil-(1)-*p*-nitrophenylhydrazone-(2). 1353
— , A tetrahedral Ni(II) complex compound derived from 1-methyl-2-carbethoxy-glyoxalanil-(1)-*m*-nitro-phenylhydrazone-(2) 1181
BANCIU M. and R. VLAD, C. DRĂGHICI E. CIORĂNESCU, Carbenium ion reactions. XIV. Solvolysis of "Dibenzobullvalene bromide" 1017
BARACU I. and E. TĂRNĂUCEANU, I. NICULESCU-DUVĂZ, Potential anticancer agents. XIII. Synthesis of new aliphatic and cycloaliphatic N-nitrosoureas . . . 885
BĂRBOIU V., Some NMDR experiments improved by means of a computer 1135
BÉCZY O., voir CIUHANDU GH. 583
BEICU S., voir HAIDUC I. 427
BEJAN L., voir STERNBERG S. 21
BELCHER R. and H. PUZANOWSKA-TARASIEWICZ, W. I. STEPHEN, An examination of various phenothiazine derivatives as indicators in vanadometry . . . 531
BELDIE C., Thermodynamic and transport properties of the polyelectrolyte solutions 839
— and O. MIHĂILESCU, Dielectric constants and refractive indices in polyelectrolyte solutions 201
BIELAŃSKI A. and J. M. ŁAGAN, An EPR study of oxygen and nitrous oxide chemisorption on manganese substituted X-type zeolites 191
BIRADAR N. S. and B. R. PATIL, V. H. KULKARNI, A spectroscopic study of tin(IV) complexes with 2,2′-dihydroxychalkones 1479
BODEA C., voir OŞIANU D. 1085
— , voir SZEKELY Z. 421
BOLDEA A., voir MRACEC M.. 401
BOTA A., voir BALABAN A. T. 1003
BOTEZ G., voir ŞUSTER D.C. 257, 1195
BOURCEANU G. and V. ABABI, GH. POPA, M. SANDULOVICIU, Phenol obtainment from benzene in oxygen plasma generated by a high frequency discharge. II. The phenol formation mechanism 459
— and V. ABABI, GH. POPA, M. SANDULOVICIU, Phenol obtainment from benzene in oxygen plasma generated by a high frequency discharge. III. Kinetics of the process in pulse and steady-state regime 1391
BRANDT-PETRIK E., voir LIPTAY G 647

Page

BRATU EM. A. and C. BALABAN, G. I. JINESCU, Mass transfer from dispersed particles to continuous fluid media. II. Oscillating fluid media, particularly due to ultrasonic energy 271
BREZEANU M. and M. DINCULESCU, Polynuclear complex compounds of iron, cobalt and nickel. I. Mercury containing complex compounds 539
— and M. DINCULESCU, Polynuclear complex compounds of iron, cobalt and nickel. II. Mercury-containing complex compounds 1175
— and I. JITARU, Cr(III) coordination compounds with 3-amino-1-propanol . . 371
— , voir TEODORESCU M. 221
BRÎNZAN N. GR., voir TĂVALĂ T. P. 787
BUCHWALD P. and F. DOMNARIU, Cyanoethylation of ketoximes. III. Preparation of *para*-substituted-(benzylidene-aminoxy)-propionic acids 263
BUSEV A.I., voir PETROV B. I. 713
BUTIN K. P., voir REUTOV O. A. 733
BUTUFEI O., voir GAVĂT I. 1261

C

CACHAZA J. M. y J. CASADO, A. VARELA, Estudio de reacciones de Arbuzov. I. Mecanismo de reacciones de trialquil(-aril) fosfitos con yoduros de alquilo . . 213
CAIS M. and P. ASHKENAZI, J. GOTTLIEB, Spin-trapping experiments with pentadienyl- and cycloheptadienyl-iron tricarbonyl cations 545
CALU N. and N. FOCA, M. LUCHIAN, The UV, VIS and IR spectra of the $Pd(p\text{-}NO.C_6H_4N(CH_3)_2)_2Cl_2.H_2O$ 551
CĂLUŞARU A., Hydroxide precipitation and metal dendrite formation at the limiting current on DME 557
CAMBOLI D., voir DEMIAN N. 1187
— , voir FĂTU D. 133
CASADO J., voir ARCE F. 335, 345, 815
— , voir CACHAZA J. M. 213
CEAUŞESCU D. and V. ELIU-CEAUŞESCU, The equivalence point and the confidence interval of linear titration curves in the outlook of normal bidimensional distribution of branches 563
ĆELAP M. B., and M. J. MALINAR, Synthesis and absolute configuration of the nitro-bis(aminoacidato)amminecobalt(III) complexes 569
CHAILLOT B., voir DAOUD A. 857
CHALMERS R. A. and A. F. J. JACKSON, Critical evaluation of fluorimetric assay methods for morphine 575
CHIRALEU F., voir BALABAN A.T. 1003
— , voir STĂNOIU I. I. 117, 1359, 1499
CHIŞ E., voir MACAROVICI CONST. GH. 657
CIAVDAROVA, R. D., voir AGASIAN P.K. 491
CIMPOERU N., voir TOTIR N. 137
CIMPU V., voir FĂTU D. 133
CIOCĂZANU I. et V. DOGARIU, D. ZĂVOIANU, La structure et la réactivité des nitriles. Sur la chaleur de combustion de quelques nitriles *alpha*, *bêta* non saturés 1369
CIOHODARU L., The electronic structure of some stilbene derivatives. III. The infrared spectra of some nitro-containing *trans*-stilbene derivatives 163
— , Electronic structure of some stilbene derivatives. V. The influence of the substituents on the HMO π-energy levels 1125
— , The electronic structure of some stilbene derivatives. VI. The molecular diagrams of some mono-nitro-stilbene derivatives 1315
— and V. EM. SAHINI, E. VOLANSCHI, The electronic structure of some stilbene derivatives. IV. ESR spectra of some nitro-containing stilbene anion-radicals 171
CIOLAC S., Irreversibility of the pitting process 1151
CIORĂNESCU E., voir BANCIU M. 1017
— , voir DRĂGUŢAN I. 607

Page

CIUHANDU GH. und O. BÉCZY, GH. OANCEA, Photometrische Bestimmung einiger aromatischer Amine durch Kupplung mit dem *p*-Nitrobenzoldiazonium-Ion 583
CIURDARU V. and F. HODOȘAN, Reactions with sodium hydridoborate on silica gel 1027
CIUREANU M. and V. E. SAHINI, A spectroscopic study of iodine complexes with some heterocycles in the azoles series 1441
CIUȘTEA G., voir ȘUSTER D.C. 1195
CLARAMUNT R. M., voir FAYET J. P. 471
COMPTES RENDUS, 153, 153, 154, 155, 156, 158, 313, 313, 314, 316, 317, 475, 476, 477, 478, 963, 963, 964, 1271, 1272, 1273, 1274, 1274, 1413, 1414, 1415, 1543, 1543, 1544, 1545, 1544, 1546, 1546, 1548, 1548, 1549 . . . .
CONSTANTIN E. et J. CH. ABBE, Étude des réactions entre D_2^+ et CH_nD_{4-n} à l'aide d'un spectromètre de masse à deux étages 327
CONSTANTINESCU M., voir GHEORGHIU C. 385
CONSTANTINESCU O., voir GHEORGHIU C. 385
CUIBAN F. and A. LUPEA, M. SILAȘI, M. ȘORA, Obtention of the *o*-nitrophenylsuccinic acid and of some functional derivatives 869
CURTUI M., voir HAIDUC I 625

D

DĂESCU C., voir BACALOGLU C. 977
DAMINESCU C., voir FACSKÓ GH.. 611
DANCE J. M. et A. TRESSAUD, J. PORTIER, P. HAGENMULLER, Sur quelques nouvelles séries de fluorures ferrimagnétiques 587
DAOUD A. et A. THRIERR-SOREL, R. PERRET, B. CHAILLOT, Préparation et caractérisation de tétrachloromanganates (II) d'ammoniums monosubstitués linéaires. 857
DAVIDECU C., voir MANOVICIU V. 953
DEMETRESCU I., voir TOMESCU M. 1267
DEMIAN N. and C. AMBRUȘ, D. CAMBOLI, Complex compounds of Pd(II) with monosubstituted derivatives of thiourea 1187
DENIELOU L. et. J. P. PETITET, C. TEQUI, Étude dilatométrique et volumétrique de sels fondus—application au sulfate d'argent, aux sulfates, chromates, molybdates et tungstates alcalins 27
DINCULESCU M., voir BREZEANU M. 539, 1175
DINULESCU I. G. and M. S. POP, M. AVRAM. Investigations in the cyclobutane series. XLV. Dibenzotricyclo [4.3.1.$0^{2,5}$] decadiene system. Behaviour and retrorearrangement into dibenzo-$(CH)_{10}$ Nenițescu's hydrocarbon derivatives . . 1037
DJORDJEVIC C., Heteroligand peroxo complexes of some d° transition metal ions 601
DOBRE V., voir ȘUSTER D.C. 257, 1195
DOGARIU V., voir CIOCĂZANU I. 1369
DOMNARIU F., voir BUCHWALD P. 263
DRĂGHICI C., voir BALABAN A. T. 1003
— , voir BANCIU M.. 1017
DRĂGULESCU C. and S. POLICEC, T. SIMONESCU, Complexes of anthranil-N, N-diacetic acid with trivalent metals. IV. Stability interpretation 55
DRĂGUȘIN E., voir ARMEANU V. 1533
DRĂGUȚAN I. and M. ELIAN, E. CIORĂNESCU, Rearrangements of the benzobicyclo [3.2.2.] nonene to the bezobicyclo [3.2.1] nonene system 607
DRĂGUȚAN V. and L. STĂNESCU, A. M. GLATZ, Aluminium chloride catalyzed reactions of unsaturated acids with benzene. X. Reaction of cyclohexyldene- and 1-cyclohexenylacetic acid 1045
DRASKOVITZ-SCHUCH E., voir SIMON Z. 87
DRIMUȘ I. and M. TRIFAN, Oxidation of *n*-dodecanitrile in liquid state with molecular oxygen, in the presence of pseudo-homogeneous catalysts. I. Peroxides, acids and esters concentrations 1053
DRUGĂRIN C., voir MRACEC M. 401
DUMITRESCU A., voir ȘUSTER D.C. 1195
DUMITRESCU S., voir SIMIONESCU CR. I. 1105

Page

E

EL-KASHEF H. S., voir ISSA I. M. 411

EL-SAMAHY A. A., voir ISSA I. M. 411

EL-SHAFEI A. K. 1251

ELGUERO J., voir FAYET J. P. 471

ELIAN M., voir DRĂGUŢAN I. 607

ELIU-CEAUŞESCU V., voir CEAUŞESCU D. 563

ENESCU L. and M. AVRAM, Investigations in the cyclobutane series. XLIV. Ring contraction of 8-diazo-*exo*-benzo [*c*] tricyclo [4.2.$10^{2,5}$] non-3-en-7-one on photolysis 1061

ETAIW S. H., voir ANWAR M. 1217

— , voir ISSA I. M. 411

— , voir KHALAF A. A 1251

F

FACSKÓ GH. und C. RADOVAN, C. DAMINESCU, Eine Deutung des Einflusses der Arbeitsbedingungen auf die Stromausbeute bei der elektrolytischen Abscheidung von metallischen Pulvern 611

FACSKÓ O., voir TRIBUNESCU P. 793

FĂRCĂŞAN V., voir BALÁZS I. 379

FĂTU D. et V. CIMPU, D. CAMBOLI, La décomposition thermique des combinaisons complexes thiocyaniques du Pd(II) avec la thio-urée 133

FAYET J. P. et M. C. VERTUT, P. MAURET, R. M. CLARAMUNT, J. ELGUERO, Azolides. IX. Étude de la conformation des azolides par dipôlemétrie 471

FEYNS L. V., voir ŞUSTER D. C. 257, 1195

FIŞEL S. et C. SIMION, Concentration et séparation d'éléments à l'aide de chélateurs par la méthode de la zone fondue. I. Systèmes Cu(II)—Co(II) ou Cu(II)—Ni(II) et mercaptoacétanilide 305

FLOREA V., voir TĂVALĂ T. P. 787

FLORESCU A., voir BACALOGLU R. 877

FOCA N., voir CALU N. 551

FRANGOPOL T., voir VLAHOVICI N. 1379

FULEA C., voir FULEA A. O. 1513

FULEA A. O. and C. FULEA, Relations between the electronic structure and the reactivity of some thioamides. II. UV and IR spectra 1513

FÜLÖP J., voir POLINSZKY K. 181

FUNDUC I., voir TOTIR N. 137

G

GĂINAR I., voir VÎLCU R. 827

GÅRD E., voir BALABAN A. T. 1191, 117, 865, 1359

GAVĂT I. and O. BUTUFEI, M. MUNTEANU, Adducts of tetrachlorohydroquinone with quinoline and piperazine 1267

GEORGESCU E. G. and M. D. GHEORGHIU, The reaction of cyclobutadiene with sterically hindered dienophiles 907

GHEORGHIU C. and. C. MĂRCULESCU, M. CONSTANTINESCU, O. CONSTANTINESCU, Contributions to the coordination chemistry of s-triazines. III. The condensation reaction of phenylbiguanide with phenylsothiocyanate in the presence of Cu ions 385

GHEORGHIU M. D., A model of the transition state in the cycloaddition of ketene to acetylene 1069

— , voir GEORGESCU E. G. 907

— , voir PÂRVULESCU L. 1089

GLATZ A. M., voir DRĂGUŢAN V. 1045

— , voir WERTHEIMER V. 1505

GOLOVINA A. P., voir ALIMARIN I. P. 503

Page

GOTTLIEB J., voir CAIS M. 545
GRIGORAŞ M., voir SIMIONESCU CR. I. 1105
GUTMANN V., Ladungsdichteveränderungen durch Donator-Acceptor-Wechselwirkungen 619

H

HAGENMULLER P., voir DANCE J. M. 587
HAIDUC I., voir BALÁZS I. 379
— and S. BEICU, C. LITEANU, Determination of xanthates from flotation pulps with an Ag_2S membrane electrode 427
— and GH. MARCU, M. CURTUI, Solvent extraction of uranium (VI) with dialkylphosphorodithioic acids. V. Synergistic effect of tributylphosphate 625
HAJ-HUSSEIN A. T., voir KHALIFA H. 899
HĂLĂLĂU M., voir POPESCU I. C. 443
HANEŞ A. voir BALABAN A. T. 1003
— , voir SCHIKETANZ I. I. 1097
HARADA M., voir TSUJIKAWA I. 1305
HARARY F., voir BALABAN A. T. 517
HEPP W., voir UHLIG E. 1165
HODIŞAN T. and. C. LITEANU, Optimization of the separation process in temperature gradient chromatography. I. Determination of the optimum temperature gradient necessary for the separation of certain component mixtures 1539
HODOŞAN F., voir CIURDARU V. 1027
— , voir VLASSA M. 1111
HOPÎRTEANU E., Liquid-membrane electrodes. X. Liquid-membrane electrode for iron (III) determination 1385
— , voir LITEANU C. 653
— and E. VERESS, V. MUREŞAN, Liquid-membrane electrodes. VII. Perchlorate-selective membrane-electrode. Construction and characterization 1243
HOPÂRTEAN I., voir MAGER S. 1075
HURDUC N. und I. A. SCHNEIDER, Der termische Abbau von Poly (methyl-methacrylat) unter nicht isothermen Bedingungen 945

I

IONESCU N. I. et B. AURIAN-BLĂJENI, Considérations sur le modèle de Landsberg relatif à l'équation logarithmique 353
IONESCU S. G., voir ONCESCU T. 697
IOVU M. und E. VOINA, Gemischte aromatische Ester der Phosphorigen- und der Phosphorsäure 1209
ISSA I. M. and A. A. EL-SAMAHY, R. M. ISSA, H. S. EL-KASHEF, S. H. ETAIW, The electronic and vibrational spectra of some N-substituted carbazoloquinones 411
ISSA R. M., voir ISSA I. M. 411
— , voir KHALAF A. A. 1251
ISSA Y. M., voir KHALIFA H. 899

J

JACKSON A. F. J., voir CHALMERS R. A. 575
JINESCU G. I., voir BRATU EM. A. 271
JITARU I., voir BREZEANU M. 371
JULEAN I., voir NIMARA A. 691
JURCONI E., voir ONCESCU T. 69
— , voir ONCESCU T. 1471

K

KÉKEDY L. and M. ŞERBAN, Zero-current bipotentiometric endpoint indication with pretreated electrodes. IV. Use of pretreated silver electrodes 633
KHALAF A. A. and S. H. ETAIW, R. M. ISSA, A. K. EL-SHAFEI, Spectrophotometric study of some 1,5-diphenyl-1,5-pentadiene-3-ones 1251
KHALIFA H. and Y. M. ISSA, A. T. HAJ-HUSSEIN, Spectrophotometric studies on some chromotropic acid azo dyes in aqueous buffer solutions 899

Page

KIRSCHNER S. and R. MORASKI, C. MUNIR, R. POLLOCK, Application of the Pfeiffer effect, outer-sphere complexation, and photoresolution techniques to the determination of absolute configuration of dissymetric coordination compounds 1283
KLEMM W., Some considerations on the nomenclature of inorganic chemistry 639
KODEJS Z. and I. SLAMA, Viscosity of melts of hydrated lanthanum nitrate 1329
KORȘAK V. V. i A. I. PAVLOV, G. MANDRIC, I. ZUGRĂVESCU, Polibezimidazolimidy 1521
KORODI T., voir BACALOGLU R. 877
KRESHKOV A. P., Proton-electron-hydride concept of the theory of acids and bases in non-aqueous solutions 1289
KULKARNI V. H., voir BIRADAR N. S. 1479

L

LAGAN J. M., voir BIELÁNSKI A. 191
LAURENT P. A., Quelques réactions inattendues dans le domaine des hétérocycles saturés 1297
LĂZĂRESCU V., voir RADOVICI O. 1457
LE MY NGU, voir UHLIG E. 1165
LECA M. and J. R. H. PÉREZ, Relation between hydrophilic-lipophilic balance and polarity determined by reverse gas-liquid chromatography for nonionic surfactants 1117
LEIBOVICI A., voir MURGULESCU I. G. 1279
LEPĂDATU C., voir SĂNDULESCU D. 1343
— , voir VÎLCU R. 827
LIGA A., voir SIMIONESCU CR. I. 49, 283
LIGETHY L., voir LIPTAY G. 647
LIPTAY G. und L. LIGETHY, E. BRANDT-PETRIK, Thermoanalytische Untersuchungen von Polyäthylen 647
LITEANU C., voir HAIDUC I. 427
— , voir HODIȘAN T. 1539
— and E. HOPÎRTEAN, E. ȘTEFĂNIGĂ, Liquid-membrane electrodes. XI. Tetrafluoroborate-selective liquid membrane-electrode 653
— and I. I. PANOVICI, Frequentometric determination under the detection limit of N-methyl-2-pyrrolidone in styrene by IR spectrometry 931
— and GH. RĂDULESCU, GY. STEINBRECHER, A. MASCAȘ, M. PREDA, Study of the rectification properties of heterogeneous membranes. V. Behaviour of the celluloid membrane systems. Cationite-Ag + Anionite-S, Cationite-Ag + Anionite-Cl, Cationite-Hg + Anionite-Br 293
LUCHIAN M., voir CALU N. 551
LUPEA A., voir CUIBAN F. 869
LUPU I., voir PETROVICI E. 719

M

MACAROVICI CONST. GH. und E. CHIȘ, Ein neues Reagenz vom EDTA Typus. II. Komplexsalze der 4,4′-Diaminodiphenylmethan-N,N′-diessigsäure mit verschiedenen Metallionen 657
MACOVEANU M., voir SIMIONESCU CR. I. 911
MAGER S. and I. HOPÂRTEAN, Infrared ^{1}H-NMR and mass spectra of some triphenylmethane derivatives 1075
MAHADEVAPPA D. S. and RANGASWAMY, Physico-chemical properties of chloramine-T. II. Conductometric study of the interaction of chloramine-T with Cr(III), Al(III) and Fe(III) solutions 1233
MALINAR M. J., voir ĆELAP M. B. 569
MANDRIC G., voir KORȘAK V. V. 1521
MANOVICIU I. und V. MANOVICIU, C. DAVIDESCU, Ölmodifizierte Terephthalatglycerinalkidharze 953
MANOVICIU V., voir MANOVICIU I. 953
MARCHIDAN D. I. and L. PANDELE, Thermal properties of the mixture $BaCl_2$-KCl 7
MARCHIDAN S., Polarographic reduction of some s-triazine herbicides 127
— , voir TOTIR N. 137
MARCU GH., voir HAIDUC I. 625
— and M. RUSU, Heteropolytungstates with U(IV) as central atom. Synthesis and physico-chemical study of the $K_{10}\,U(PW_{11}O_{39})_2\cdot 22H_2O$ complex 227

Page

— and M. RUSU, L. OCHEŞEL, Heteropolytungstates with U(IV) as central ion. Synthesis and physico-chemical studies 849

MĂRCULESCU C., voir GHEORGHIU C. 385

MARINESCU M., voir POPESCU G. 1401

MARKOV B. F., Thermodynamic information on the structure of molten salt systems with chemical interaction between the components 13

MARTIN D., voir BACALOGLU I. I. 511

MARTYNENKO L. I., voir SPITSINE V. I. 773

MASCAŞ A., voir LITEANU C. 293

MATHIS F., Quelques aspects de la recherche en chimie organique du phosphore : résultats et perspectives 665

MAURER A., voir MRACEC M. 675

MAURET P., voir FAYET J. P. 471

MAVRODIN-TĂRĂBÎC M., voir RADOVICI O. 145

MAZILU I., voir SIMIONESCU CR. 753

MERCA E., voir TRIBUNESCU P. 793

MIHAILESCU O., voir BELDIE R. 201

MISDOLEA C., voir MURGULESCU I. G. 1433

MOLDOVEANU S., voir POPA GR. 301

MORASKI R., voir KIRSCHNER S. 1283

MRACEC M. und A. MAURER, S. POLICEC, Z. SIMON, Bildung und Stabilität von Metallchelaten mit Liganden die Donoratome aus der 6. Gruppe enthalten. I. HMO-Berechnungen an den Liganden (*o*-Carboxyphenoxy)-essigsäure und (*o*-Carboxyphenylthio)-essigsäure 675

— and S. RADULY, Z. SIMON, A. BOLDEA, C. DRUGĂRIN, New urea and thiourea derivatives. II. HMO and Del Ré molecular orbital calculations . . . 401

MUNIR C., voir KIRSCHNER S. 1283

MUNTEANU D. and I. NANU, Perspectives for industrial production of poly(olefins) graft copolymers 923

MUNTEANU M., voir GAVĂT I. 1261

MUREŞAN V., voir HOPÎRTEAN E. 1243

MURGULESCU I. G. and A. LEIBOVICI, Internal pressure in liquid metals 1279

— and C. MISDOLEA, A relation for the viscosity of ionic liquids 1433

— and M. ŞERBAN, On the viscosity of molten metals. V. Dependence of viscosity on the mean vibration frequency 807

— and CR. TELEA, Heat capacities in molten alkaline halides 683

N

NANU I., voir MUNTEANU D. 923

NARAYANA ACHAR B., voir SANKE GOWDA H. 745

NAŞCU C., voir RIPAN R. 361

NECŞOIU I., voir SCHIKETANZ I. I. 1097

NEGOIU D. and L. PARUTA, Complex compounds of Cu(I) with triarylstibines . . 1347

— and L. PARUTA, Preparation and investigation of Hg(II) complex compounds with triarylstibines 1487

NENNING P., voir PETROV B. I. 713

NICOARĂ E., voir OŞIANU D. 1085

NICOLESCU I. V. and O. ŞERBAN, I. SĂNDULESCU, L. STOICESCU, The origin and the type of active centers in solid acid catalysts. II. Transalkylation of toluene on $Al_2O_3-SiO_2$ catalyst 97

NICULESCU-DUVĂZ I., voir BARACU I. 885

— , voir ŞUSTER D. C. 257, 1195

NIKOLAEVA E. P., voir AGASIAN P. K. 491

NIMARĂ A. and I. JULEAN, Contributions to the bismuth hydrolysis study. IV. Equilibrium and rate constants of bismuth perchlorate hydrolysis studied by polarography 691

NUŢIU M., voir OSTROGOVICH G. 705

NUŢIU R., voir OSTROGOVICH G. 705

Page

O

OANCEA D., voir TOMESCU M. 1267
OANCEA GH., voir CIUHANDU GH. 583
OCHEȘEL L., voir MARCU GH. 849
ONACĂ I., voir RADOVICI O. 145
ONCESCU T. and S. G. IONESCU, C. ANDREESCU, On the photolysis of $Mn(C_2O_4)_2(H_2O)_2K$ in dimethyl-formamide. II. Concentration and oxygen effects 697
— and E. JURCONI, Thermal decomposition of bis(oxalate) diaquomanganese (III). Complex in acidic aqueous solution 69
— and E. JURCONI, Thermal decomposition of tris(oxalate) manganese(III) complex in aqueous solutions 1471
OȘIANU D. and E. NICOARĂ, C. BODEA, Inchain-epoxides of carotenoids. V. Canthaxanthin—11,12-epoxide and 9,12-furanoid oxide 1085
OSTROGOVICH G., voir BACALOGLU R. 877
— and M. NUȚIU, R. NUȚIU, Studies in the field of biuret reaction. X. Infrared absorption spectra for some copper(II) complexes of the cyanuric acid 705

P

PACÁK P. and I. SLÁMA, Diffusion of cadmium and silver ions in concentrated aqueous solutions of calcium nitrate 1463
PALMER E. M., voir BALABAN A. T. 517
PANDELE L., voir D. I. MARCHIDAN 7
PANEA T., voir SZEKELY Z. 421
PANOVICI I. I., voir LITEANU C. 931
PARASCHIV M., voir STĂNOIU I. I. 865
PÂRLOG C., voir SĂNDULESCU D. 1343
PARUTA L., voir NEGOIU D. 1347, 1487
PÂRVULESCU L. and M. D. GHEORGHIU, Synthesis of bicyclo [3.2.1] octane derivatives *via* Makosza reaction 1089
PATIL B. R., voir BIRADAR N. S. 1479
PAVLOV A. I., voir KORSAK V. V. 1521
PERCEC V., voir SIMIONESCU CR. I. 1105
PERÉZ J. R. H., voir LECA M. 1117
PERRET R., voir DAOUD A. 857
PETITET J. P., voir DENIELOU L. 27
PETROV B. I. und V. V. STRELKOV, A. I. BUSEV, P. NENNING, Zur Komplexbildung bei der Hf-Extraktion aus Hexyldiantipyrilmethan 713
PETROVICI E. et I. LUPU, Hexachloroantimonates (V) metalliques complexes ayant comme ligand la pyridine 719
POLICEC S., voir DRĂGULESCU C. 55
— , voir MRACEC M. 675
POLINSZKY K. and E. VASANITS, J. FÜLÖP, Approximate analytic determination of the average values of potential functions occuring in chemical transport phenomena 181
POLLOCK R., voir KIRSCHNER S. 1283
POP GH., voir RIPAN R. 361
POP I., voir RIPAN R 361
POP M. S., voir DINULESCU I. G. 1037
POPA GH., voir BOURCEANU G. 459, 1391
POPA GR. and Ș. MOLDOVEANU, Theoretical study of the acidity of some organic reagents 301
— et L. VLĂDESCU, Séparation et concentration du magnésium des fontes au graphite sphéroïdal au moyen des résines échangeuses d'ions . . . .
POPESCU G. and M. MARINESCU, ^{1}H-NMR characterization of anionic surfactants-polyvinylpyrrolidone interaction 1401

Page

POPESCU I. C. and M. HĂLĂLĂU, Studies on the electroanalytical behaviour of membrane-electrodes under current. VI. Potentiometry at continuous and constant current using a $Hg/AgI\text{-}Ag_2S$ membrane-electrode 443
PORTIER J., voir DANCE J. M. 587
POTMISCHIL F. und D. RÖMER, Heterocyclen mit perinaphtinden-Gerüst. I. Quartäre Ammoniumsalze des 2,3-dihydro-benz[d, e]Isochinolins 1375
PREDA M., voir LITEANU C. 293
PRÜFER A., voir BACALOGLU I. I. 511
PUZANOWSKA-TARASIEWICZ H., voir BELCHER R. 531

R

RADOVAN C., voir FACSKÓ GH. 611
RADOVICI O. and V. LĂZĂRESCU, Some results concerning the nickel electrodeposition on thin films 1457
— and M. MAVRODIN-TĂRĂBÎC, I. ONACA, I. SOLACOLU, Oxygen reduction on silver gas electrodes. V. The effect of compression and sintering conditions on electrode performances 145
RADU D., voir BALTĂ P. 525
RĂDULESCU GH., voir LITEANU C. 293
RADULY S., voir MRACEC M. 401
RĂILEANU D., voir ANGHELIDE N. 969
RAMAKRISHNAN L. and SOUNDARARAJAN S., Quinoline-1-oxide complexes of lanthanide iodides 395
RANGASWAMY, voir MAHADEVAPPA 1233
RĂZUȘ A. C., voir WERTHEIMER V. 1505
REUTOV O. A. and K. P. BUTIN, Equilibria of redistribution reactions of organometallic compounds 733
RIOS M. A., voir ARCE F. 335, 345, 815
RIPAN R. et GH. POP, I. POP, C. NAȘCU, Acide ascorbique comme agent réducteur. V. Cinétique de la réduction des ions Au(III) par acide ascorbique 361
ROMANKOV P. G., Sovremenyie problemy insenernoi khimii 1297
RÖMER D., voir POTMISCHIL 1375
RUNOV V. K., voir ALIMARIN I. P. 503
RUSU M., voir MARCU GH. 227, 849
RUSU V., voir SIMONESCU T. 435, 937

S

SAHINI V. EM. and S. BĂDILESCU, Collision-induced light absorption in liquid mixtures 811
— , voir CIOHODARU L. 171
— , voir CIUREANU M. 1441
— and A. SAVIN, On the stability of aromatic hydrocarbons. IV. On the linearity of the delocalization energy relationships 39
SAITO K., Circular dichroism of optically active square planar complexes containing η^2-olefins 739
SAMSON S., voir VÎLCU R. 1447
SĂNDULESCU D. and C. PÂRLOG, C. I. LEPĂDATU, The electronic spectrum of $[Os(II)(NH_3)_5(N_2)]^{2+}$ and the chemical bonding of the dinitrogen molecule . . 1343
SĂNDULESCU I., voir NICOLESCU I. V. 97
SANDULOVICIU M., voir BOURCEANU G. 459, 1391
SANKE GOWDA H. and K. N. THIMMAIAH, B. NARAYANA ACHAR, Spectrophotometric determination of palladium (II), cerium (IV), arsenic (III) and nitrite with fluphenazine hydrochloride 745
SAVIN A., voir SAHINI V. E. 39
SCHIKETANZ I. I. and A. HANEȘ, I. NECȘOIU, Étard reaction. XI. Oxidation of dibenzo[c, g]bicyclo[4.2.0]octa-3,7-diene with chromyl chloride 1097

Page

SCHMIEDEKNECHT K., voir UHLIG E. 1165
SCHNEIDER I. A., voir HURDUC N. 945
— , voir SCHUSTER R. H. 103
SCHUSTER R. H. und I. A. SCHNEIDER, Mediummeinflüsse bei der Solvolyse von Alkylhalogeniden. II. Solvolyse von *t*-Butylchlorid in Aceton-Wasser-Gemischen mittlerer Konzentration 103
SEGAL E., voir SITARU I. 761
— , voir VLAD M.. 77
ŞERBAN M., On the viscosity of molten metals. IV. A comparison between gas and liquid viscosities. 35
— , voir KÉKEDY L. 633
— , voir MURGULESCU I. G.. 807
ŞERBAN O., voir NICOLESCU I. V. 97
SILAŞI M., voir CUIBAN F. 869
SIMION C., voir FIŞEL S. 305
SIMIONESCU CR. I. and S. DUMITRESCU, V. PERCEC, M. GRIGORAŞ, On the polymerization of polyacetylene derives. XXXII. Heats of *cis-trans* isomerization of polyacetylene isomers 1105
— and A, LIGA, Researches in the terpolymerization field. VIII. Theoretical structural study of the high conversion acrylonitrile-methacrylic acid-methyl methacrylate terpolymer 49
— and A. LIGA, N. ASANDEI, Researches in the terpolymerization field. IX. Chemical structure-properties correlation 283
— and M. MACOVEANU, The grafting of the poly(ethylene-terephtalate) under radiofrequency electrical discharge conditions 911
— and I. MAZILU, Ferrocene polymers as polymerization initiators 753
SIMON Z. and E. DRASKOVITZ-SCHUCH, Partition coefficients and intermolecular force parameters 87
— , voir MRACEC M. 401, 675
SIMONESCU T., voir DRĂGULESCU C. 55
— and V. RUSU, New analytical applications of some sulphonamide compounds. V. Arsenic traces determined with silver sulphanilamide 435
— and V. RUSU, New analytical applications of some sulphonamide compounds. VI. Sodium m-silver-sulphamoylbenzoate a new reagent for the determination of carbon monoxide in the air. 937
SINGH L. R. and P. BAHADUR, S. N. SRIVASTAVA, Studies on conductivies of some ionic surfactants in aqueous methanol 1145
SITARU I. and E. SEGAL, On preferential orientation of thin magnesium films supported on glass 761
SIVAPULLAIAH P. V. and S. SOUNDARARAJAN, Pyridine-N-oxide complexes of rare-earth bromides. 1493
SLÁMA I., voir KODEJS Z. 1329
— , voir PACÁK P. 1463
ŞLIAM E., voir BALABAN A. T. 1003
— , voir ANGHELIDE N. 963
SOLACOLU I., voir RADOVICI O. 145
SONTHEIMER H., Chemische Parameter der Gewässerverschmutzung 765
ŞORA M., voir CUIBAN F. 869
SOUNDARARAJAN S., voir RAMAKRISHNAN L. 395
— , voir SIVAPULLAIAH P. V. 1493
SPACU P. and L. ANTONESCU, Contribution to the coordination chemistry of molybdenum. IV. Biguanidonium aquo-tetrachloro-oxomolybdates (V) 61
SPITINE V. I. et L. I. MARTYNENKO, Effets des particularites cinétiques des complexes des éléments des terres rares sur le mécanisme du processus de séparation par échange ionique 773
SRIVASTAVA S. N. 1145
STĂNESCU L., voir DRĂGUŢAN V. 1045
STĂNOIU I. I., voir BALABAN A. T. 1191

Page

— and A. T. BALABAN, F. CHIRALEU, Isotopic exhange of active methyl groups. X. Activation parameters for deuteriation and de-deuteriation of isopropyl-pyrylium salts 1499
— and, F. CHIRALEU, E. GÂRD, A. T. BALABAN, Isotopic exchange of active methyl hydrogens. VIII. Deuterium kinetic isotope effects for α- and γ-isopropyl-substituted pyrylium salts 117
— and E. GÂRD, C. UNCUȚA, F. CHIRALEU, A. T. BALABAN, Isotopic exchange of active methy hydrogens. IX. Intramolecular kinetic comparison between α-methyl and γ-isopropyl groups in pyrylium salts 1359
— and M. PARASCHIV, E. GÂRD, A. T. BALABAN, Isotope effects in electronic absorption spectra of CH_3/CD_3-substituted six-membered heteroaromatics 865
ȘTEFĂNIGĂ E., voir LITEANU C. 653
STEINBRECHER GY., voir LITEANU C. 293
STEPHEN W. I., voir BELCHER R. 531
STERNBERG S. and L. BEJAN, Thermodynamic properties fused salt ternary system $AgI + NaI + CsI$ by formation cell method 21
— and T. VIȘAN, A chronopotentiometric study of the strontium (II) ion in molten potassium nitrate 321
STOICESCU L., voir NICOLESCU I. V. 97
STRELKOV V. V., voir PETROV B. I. 713
ȘUSTER D. C. and G. BOTEZ, L. V. FEYNS, V. DOBRE, I. NICULESCU-DUVĂZ, Potential anticancer agents. XI. Derivatives prepared from diazotized pyrimidines 257
— and G. CIUȘTEA, A. DUMITRESCU, L. V. FEYNS, E. TĂRNĂUCEANU, G. BOTEZ, S. ANGELESCU, V. DOBRE, I. NICULESCU-DUVĂZ, Potential anticancer agents. XIV. Synthesis and biological evaluation of N [4′-{[2,4-diamino-6(7)-pteridinyl)-methyl]-N^{10}-methylamino}-benzoyl]-L,D and DL-glutamic (aspartic) acids 1195
SZEKELY Z. and T. PANEA, C. BODEA, Hydroxyphenothiazine-5,5-dioxides (Hydroxyphenothiazine-sulphones). II. Determination of disociation constants of some 3-hydroxyphenothiazine-sulphone 421

T

TAKEUCHI A. and S. YAMADA, Isomerism in copper(II) complexes with N-Isopropyl- and N-cyclohexyl-salicyl-aldiminates 781
TĂRNĂUCEANU E., voir BARACU I. 885
— , voir ȘUSTER D. C. 1195
TATO V., voir ARCE F. 345
— , voir CASADO J. 335
TĂVALĂ T. P. and N. GR. BRÎNZAN, V. FLOREA, Red-brown pigments in the $Cr_2O_3-TiO_2-WO_3$ system 787
TELEA CR., voir MURGULESCU I. G. 683
TEODORESCU M. and M. BREZEANU, Steric effects in a series of tetracoordinates complexes of Co(II) containing phenanthroline derivatives 221
TEQUI C., voir DENIELOU L. 27
TERLECKI-BARIČEVIĆ A., voir ALEKSIĆ B. D. 1335
TESZLER E., voir URSEANU F. 1225
THIMMAIAH K. N., voir SANKE GOWDA H. 745
THRIERR-SOREL A.. voir DAOUD A. 857
TOMESCU M. and I. DEMETRESCU, D. OANCEA, Structural characterization of multicomponent acrylic polymers 1267
TOTIR N. and S. MARCHIDAN, C. VOLANSCHI, N. CIMPOERU, R. ANDREI, I. FUNDUC, Quantitative determination of trace amounts of s-triazine herbicides in waste waters by physico-chemical methods 137
TRESSAUD A., voir DANCE J. M. 587
TRIBUNESCU P. und E. MERCA, O. FACSKÓ, Die thermische Zersetzung einiger Hexacyanokomplexen. I. Silber Ammonium oder Alkylammonium Hexacyanoferrate 793
TRIFAN M., voir DRIMUȘ I. 1053
TSUJIKAWA I. and M. HARADA, Effect of uniaxial stress on absorption spectra of tetragonal crystals Cs_3CoCl_5 and Cs_3CoBr_5 1305
TURCU A., Reaction of 1,3,7,9-tetranitrophenothiazine-5-oxide with organic bases 1363

Page

U

UHLIG. E., und W. HEPP, LE MY NGU, K. SCHMIEDEKNECHT, Zum Einfluß der Ringgröße auf die Struktur von Metallchelaten dreizähliger Liganden. III. Kupfer (II)-Nichel(II)- und Eisen (II)-Chelate pyridylsubstituierter Dialkylsulfide . . 1165
UNCUŢA C., voir STĂNOIU I. I. 1359
URSEANU F. and E. TESZLER, New disperse dyes for polyester fibres 1225

V

VARELA A., voir CACHAZA J. M. 213
VASANITS E., voir POLINSZKY K. 181
VERESS E., voir HOPÎRTEAN E. 1243
VERTUT M. C., voir FAYET J. P. 471
VÎLCU R. and I. GĂINAR, C. LEPĂDATU, Second interaction virial coefficient. II. $Ar + H_2$ and $CH_4 + H_2$ systems 827
— and S. SAMSON, Thermodynamic characterization of some binary solution of non-electrolytes, by a cellular model with holes 1447
VIŞAN T., voir STERNBERG S. 321
VLAD M. and E. SEGAL, A kinetic analysis of addition polymerization reaction . . 77
VLAD R., voir BANCIU M. 1017
VLĂDESCU L., voir POPA GR. 725
VLAHOVICI N. and P. T. FRANGOPOL, A simple semiempirical MO-calculations of electronic spectra and charge distribution in 2,4,6-trimethyl pyrylium cation 1379
VLASSA M. and F. HODOŞAN, Amidation with bis-(α-arylminobenzyl)-disulphides 1111
VOICULESCU N., Reactions of coordinated ligands. IX. Chloroaluminium-organic derivatives of coordinated dimethyl-and diphenylglyoxime 237
— , Reactions of coordinated ligands. X. Aluminium-organic compounds of salicylaldoxime with Ni(II), Pd(II) and Cu(II) ions and their adducts with nitrogen Lewis bases 451
VOINA E., voir IOVU M. 1209
VOLANSCHI C., voir TOTIR N. 137
VOLANSCHI E., voir CIOHODARU L. 171

Z

ZUGRĂVESCU I., voir KORŞAK V. V. 1521

W

WERTHEIMER V. and A. M. GLATZ, A. C. RĂZUŞ, Solvolytic behaviour of strained systems: The 1-, 4- and 5-methylbenzo [*b*] bicyclo [3.1.0] hex-2-en-4-yl cations 1505
ZĂVOIANU D., voir CIOCĂZANU I. 1369

Y

YAMADA S., voir TAKEUCHI W. 781
YAMASAKI K. and Y. YOSHIKAWA, Correlation between absolute configurations of cobalt(III) complexes and their chromatographic behaviour on ion-exchange cellulose 801
YOSHIKAWA Y., voir YAMASAKI K. 801

INDEX DES SUJETS

Page

A

Absorption spectra of tetragonal crystals Cs_3CoCl_5 and $CsCoBr_5$. Effect of uniaxial stress on —, I. TSUJIKAWA and M. HARADA 1305

Acetylenic derivatives. XXXII. Heats of *cis-trans* isomerization of polyacetylene isomers, On the polymerization of —, Cr. I. SIMIONESCU, S. DUMITRESCU, V. PERCEC and M. GRIGORAŞ 1105

Acide ascorbique comme agent réducteur. V. Cinétique de la réduction des ions Au(III) par acide ascorbique, R. RIPAN, GH. POP, I. POP et C. NAŞCU 361

Acrylic polymers, Structural characterization of multicomponent —, M. TOMESCU, I. DEMETRESCU and D. OANCEA 1267

Addition polymerization reaction, A kinetic analysis of —, M. VLAD and E. SEGAL . . 77

Alkylhalogeniden. II. Solvolyse von t-Butylchlorid in Aceton-Wasser-Gemischen mittlerer Konzentration, Mediumeinflüsse bei der Solvolyse von —, R. H. SCHUSTER and I. A. SCHNEIDER 103

Aluminium chloride catalyzed reactions of unsaturated acids with benzene. X. Reaction of cyclohexylidene- and 1-cyclohexenylacetic acids, V. DRĂGUŢAN, L. STĂNESCU and A. M. GLATZ 1045

Ammidation with bis-(α-arylimino-bezyl)-disulphides, M. VLASSA and F. HODOŞAN 1111

Ammonia synthesis catalysts in reductive atmosphere, Investigation of the effects of chemical nature of some structural promotors on electric conductivity changes in precipitated —, B. D. ALEKSIĆ and A. TERLECKI-BARIČEVIĆ 1335

Aromatic hydrocarbons. IV. On the linearity of the delocalization energy relationships, On the stability of —, V. E. SAHINI and A. SAVIN 39

Azo dyes in aqueous buffer solutions, Spectrophotometric studies on some chromotropic acid —, H. KHALIFA, Y. M. ISSA and A. T. HAJ-HUSSEIN 899

Azolides. IX. Étude de la conformation des azolides par dipôlemétrie, J. P. FAYET, M. C. VERTUT, P. MAURET, R. M. CLARAMUNT et J. ELGUERO 471

B

Benzobicyclo [3.3.1] nonene system, Rearrangements of the benzobicyclo[3.2.2.] nonene to the —, I. DRĂGUŢAN, M. ELIAN and E. CIORĂNESCU . . . 607

Bicyclo [3.2.1] octane derivatives via Makosza reaction, Synthesis of —, L. PÂRVULESCU and M. D. GHEORGHIU 1089

Bis(oxalato)diaquomanganese(III). Complex in acidic aqueous solution, Thermal decomposition of-, T. ONCESCU and E. JURCONI 69

Bismuth hydrolysis study. IV. Equilibrium and rate constants of bismuth perchlorate hydrolysis studied by polarography, Contributions to the —, A. NIMARA and I. JULEAN. 691

Biuret reaction. X. Infrared absorption spectra for some copper(II) complexes of the cyanuric acid. Studies in the field of —, G. OSTROGOVICH, M. NUŢIU and R. NUŢIU 705

C

Cadmium complex with 6-(6-methoxy-benzothiazol-2-ylazo)-2,4-dichlorophenol, Spectrophotometric study of —, V. ARMEANU and E. DRĂGUŞIN 1533

Carbazoloquinones, The electronic and vibrational spectra of some N-substituted —, I. M. ISSA, A. A. EL-SAMAHY, R. M. ISSA, M. S. EL-KASHEF and S. H. ETAIW. 411

Carbenium ion reactions. XIV. Solvolysis of "Dibenzobullvalene bromide", M. BANCIU, R. VLAD, C. DRĂGHICI and E. CIORĂNESCU 1017

Carotenoids. V. Canthaxanthin-11,12-epoxide and 9,12-furanoid oxide, Inchain-epoxides of —, D. OSIANU, E. NICOARĂ and C. BODEA 1085

Page

Chemical graphs. XXVIII. A new topological index for catafusenes: L-transform of their three-digit codes, A. T. BALABAN 45

Chemical graphs. XXIX. Numbers of isomers with naphtalene and adamantane skeletone, A. T. BALABAN, E. M. PALMER und F. HARARY. 517

Chemical graphs. XXX. Reaction graphs for degenerate rearrangements of homovalenium cations, A. T. BALABAN 243

Chemical graphs. XXXI. Benzo-homovalenes, A. T. BALABAN 987

Chemisorption on manganese substituted X-type zoelites, An EPR study of oxygen and nitrous oxide—, A. BIELANSKI and J. M. LAGAN 191

Chloramine-T. II. Conductometric study of the interaction of chloramine-T with Cr(III), Al(III) anf Fe(III) solutions, Physico-chemical properties of—, D. S. MAHADEVAPPA and RANGASWAMY 1233

Chromatography. I. Determination of the optimum temperature gradient necessary for the separation of certain component mixtures, Optimization of the separation process, in temperature gradient —, T. HODIȘAN and C. LITEANU 1539

Circular dichroism of optically active square planar complexes containing η^2-olefins, K. SAITO. 739

Cobalt(III) complexes and their chromatographic behaviour on ion-exchange cellulose, Correlation between absolute configurations of—, K. YAMASAKI and Y. YOSHIKAWA 801

Complex compound derived from 1-methyl-2-carbethoxy-glyoxal-anil-(1)-*p*-nitro-phenylhydrazone-(2), A pentacoordinated Co(II)—, A. C. BANCIU 1353

Complex compounds of Cu(I) with triarylstibines, D. NEGOIU and L. PARUTA . . . 1347

Complexes des éléments des terres rares sur le mécanisme du processus de séparation par échange ionique. Effets des particularités cinétiques des—, V. I. SPITSINE et L. I. MARTYNENKO 773

Complexes of anthranil-N,N-diacetic acid with trivalent metals. IV. Stability interpretation, C. DRĂGULESCU, S. POLICEC and T. SIMONESCU 55

Complexes of Co(II) containing phenanthroline derivatives, Steric effects on a series of tetracoordinated—, M. TEODORESCU and M. BREZEANU 221

Complexes of rare-earth bromides, Pyridine-N-oxide—, P. V. SIVAPULLAIAH and S. SOUNDARARAJAN 1493

Complexes thiocyaniques du Pd(II) avec la thio-urée, La décomposition thermique des combinaisons—, D. FĂTU, V. CIMPU et D. CAMBOLI 133

Complexes with some heterocycles in the azoles series, A spectroscopic study of iodine—, M. CIUREANU and V. E. SAHINI 1441

COMPTES RENDUS, 153, 153, 154, 155, 156, 158, 313, 313, 314, 316, 317, 475, 476, 477, 478, 963, 963, 964, 1271, 1272, 1273, 1274, 1274, 1413, 1414, 1415, 1543, 1543, 1544, 1545, 1545, 1546, 1546, 1548, 1548, 1549

Conductivities of some ionic surfactants in aqueous methanol, Studies on—, L. R. SINGH, P. BAHADUR and S. N. SRIVASTAVA 1145

Constantes de fuerza. I. Moleculas diatomicas, Estudio teorico de la naturaleza de—, F. ARCE, J. CASADO, M. A. RIOS y V. TATO 335

Constantes de fuerza. II. Moleculas triatomicas, Estudio teorico de la naturaleza de-, F. ARCE, J. CASADO, M. A. RIOS y V. TATO 345

Coordonated ligands. IX. Chloraluminium-organic derivatives of coordinated dimethyl- and diphenylglyoxime, Reactions of —, N. VOICULESCU 237

Coordinated ligans. X. Aluminumorganic compounds of salicylaldoxime, witb Ni(II), Pd(II) and Cu(II) ions and their adducts with nitrogen Lewis bases, Reactions of—, N. VOICULESCU 451

Coordination compunds, Application of the Pfeiffer effect, outer-sphere complexation and photoresolution techniques to the determination of absolute configuration of dissymetric —, S. KIRSCHNER, R. MORASKI, C. MUNIR and R. POLLOCK 1283

Copper(II) complexes with N-isopropyl- and N-cyclohexyl-salicylaldiminates, Isomerism in —, A. TAKEUCHI and S. YAMADA 781

Cr(III) coordination compounds with 3-amino-1-propanol, M. BREZEANU and I. JITARU 371

Cycloaddition of ketene to acetylene, A model of the transition state in the —, M. D. GHEORGHIU. 1069

Page

Cyclobutadiene with sterically hindered dienophiles, The reaction of —, E. G. GEORGESCU and M. D. GHEORGHIU 907

Cyclobutane series. XLIV. Ring contraction of 8-diazo-exo-benzo[c]tricyclo$[4.2.1.0^{2,5}]$non-3-en-7-one on photolysis, Investigations in the —, L. ENESCU and M. AVRAM 1061

Cyclobutane series. XLV. Dibenzotricyclo$[4.3.1.0^{2,5}]$decadiene system. Behaviour and retrorearrangement into dibenzo-$(CH)_{10}$ Nenitzescu's hydrocarbon derivatives, Investigations in the —, I. G. DINULESCU, M. S. POP and M. AVRAM . . 1037

D

Deuterium isotope effect on the basicity of 2,4,6-trimethyl-pyridine, A. T. BALABAN, I. I. STĂNOIU and E. GÂRD 1191

Dienamino esters, Electron transfer *vs* proton capture in the formation of —, N. ANGHELIDE, E. ŞLIAM and D. RĂILEANU 969

Diffusion of cadmium and silver ions in concentrated aqueous solutions of calcium nitrate, P. PACAK and I. SLAMA 1463

n-Dodecanitrile in liquid state with molecular oxygen, in the presence of pseudo-homogeneous catalysts. I. Peroxides, acids and esters concentration, Oxidation of —, I. DRIMUŞ, and M. TRIFAN 1053

Dyes for polyester fibres, New disperse —, F. URSEANU and E. TESZLER 1225

E

Equivalence point and the confidence interval of linear titration curves in the outlook of normal bidimensional distribution of branches, The —, D. CEAUŞESCU and V. ELIU-CEAUŞESCU. 563

Electrodeposition on thin films, Some results concerning the nickel —, O. RADOVICI and V. LĂZĂRESCU 1457

Electrodes. IV. Use of pretreated silver electrodes, Zero-current bipotentiometric endpoint indication with pretreated —, L. KEKEDY and M. ŞERBAN 633

Electronic spectrum of $Os(II)(NH_3)_5(N_2)^{2+}$ and the chemical bonding of the dinitrogen molecule, The —, D. SĂNDULESCU, C. PÂRLOG and C. I. LEPĂDATU . . . 1343

Etard reaction. XI. Oxidation of dibenzo c, g bicyclo 4.2.0 octa-3,7-diene with chromyl chloride, I. I. SCHIKETANZ, A. HANEŞ and I. NECŞOIU 1097

F

Ferrocene polymers as polymerization initiators, CR. SIMIONESCU and I. MAZILU 753

Fluorures ferrimagnetiques, Sur quelques nouvelles séries de—, J. M. DANCE, A. TRESSAUD, J. PORTIER et P. HAGENMULLER 587

Frequentometric determination under the detection limit of N-methyl-2-pyrrolidone in styrene by IR spectrometry, C. LITEANU and I. I. PANOVICI 931

Fused salt ternary system AgI + NaI + CsI by formation cell method, Thermodynamic information on the structure of —, S. STERNBERG and L. BEJAN 21

G

Gas-liquid chromatography for nonionic surfactants, Relation between hydrophilic-lipophilic balance and polarity determined by reverse—, M. LECA and J. R. H. PEREZ 1117

Gewässerverschmutzung, Chemische Parameter der —, H. SONTHEIMER 765

H

Herbicides in waste waters by physico-chemical methods, Quantitative determination of trace amounts of s-triazine, —, N. TOTIR, S. MARCHIDAN, C. VOLANSCHI, N. CIMPOERU, R. ANDREI and I. FUNDUC 137

Herbicides, Polarografic reduction of some s-triazine —, S. MARCHIDAN 127

Heteroaromatics, Isotope effects in electronic absorption spectra of CH_3/CD_3 — substituted six-membered —, I. I. STĂNOIU, M. PARASCHIV, E. GÂRD and A. T. BALABAN 865

Heterocyclen mit perinaphtinden -Gerüst. I. Quartäre Ammoniumsalze des 2,3-Dihydrobenz[d,e]Isochinolins, F. POTMISCHIL und D. RÖMER 1375

Hétérocycles saturés, Quelques réactions inattendues dans le domaine des —, P. A. LAURENT 1297

Page

Heterogeneous membranes. V. Behaviour of the celluloid membrane systems : cationite-Ag + anionite-S, cationite-Ag + anionite-Cl, cationite-Hg + anionite-Br, Study of the rectification properties of —, C. LITEANU, GH. RĂDULESCU, GY. STEINBRECHER, A. MASCAS and M. PREDA 293

Heteroligand peroxo complexes of some d° transition metal ions, C. DJORJEVIĆ . . 601

Heteropolytungstates with U(IV) as central atom. Synthesis and physico-chemical study of the K_{10} $U(PW_{11}O_{39})_2 \cdot 22H_2O$ complex, GH. MARCU and M. RUSU . 227

Heteropolytungstates with U(IV) as central ion. Synthesis and physico-chemical studies, GH. MARCU, M. RUSU and L. OCHEȘEL 849

Hexachloroantimonates (V) metalliques complexes ayant comme ligand la pyridine, E. PETROVICI et I. LUPU 719

Hexacyanokomplexen. I. Silber Ammonium oder Alkylammonium Hexacyanoferrate, Die thermische Zersetzung einiger —, P. TRIBUNESCU, E. MERCA und O. FACSKÓ 793

Hf-Extraktion aus chloridhaltigen Lösungen unter Verwendung von Hexyldiantipyrilmethan, Zur Komplex-bildung bei der —, B. I. PETROV, V. V. STRELKOV, A. I. BUSEV und P. NENNING 713

Hg(II) complex compounds with triarylstibines, Preparation and investigation of —, D. NEGOIU and L. PARUTA 1487

Hydroxide precipitation and metal dendrite formation at the limiting current on DME, A. CĂLUȘARU 557

Hydroxyphenothiazine-5,5-dioxides(Hydroxyphenothiazine-sulphones). II. Determination of dissociation constants of some 3-hydroxyphenothiazine-sulphones, Z. SZEKELY, T. PANEA and C. BODEA 421

I

Infrared absorption spectra of some 4H-3,1-benzoxazin-4-ones and 2,3-disubstituted-4(3H)-quinazolinones, M. ANWAR and S. H. ETAIW 1217

Insenernoi khimii, Sovremenyiie problemy —, ROMANKOV P. G. 1297

Ionnye assotsiaty rodaminovykh krasitelei S anionnymi khelatami i ikh khimiko-analiticheskoe ispolzovanye, I. P. ALIMARIN, A. P. GOLOVINA i V. K. RUNOV 503

Isotopic exchange of active methyl hydrogens. VIII. Deuterium kinetic isotope effects for α and γ isopropyl-substituted pyrylium salts, I. I. STĂNOIU, F. CHIRALEU, E. GÂRD and A. T. BALABAN 117

K

Ketoximes. III. Preparation of *para*-substituted-(bezylidene-aminoxy)-propionic acids, Cyanoethylation of —, F. BUCHWALD and F. DOMNARIU 263

Kohlensäure-Derivate. IX. Kinetik und Mechanismus der Alkoholyse von Kohlensäure-Dichlorid-N-Aryl-Imiden, Nucleophile Substitutionen an —, R. BACALOGLU, T. KORODI, A. FLORESCU and G. OSTROGOVICH 877

Kohlensäurederivaten. X. Kinetik und Mechanismus der Hydrolyse von N,N-disubstituierten Thiocarbamidsäurechloriden, Nucleophile Substitutionen an —, R. BACALOGLU und C. DĂESCU 977

Kulonometricheskye metody opredelenyia renyia, P. K. AGASIAN, E. P. NIKOLAEVA i R. D. DJAVDAROVA 491

L

Ladungsdichteveränderungen durch Donator-Acceptor-Wechselwirkungen, V. GUTMANN 619

Liquid-membrane electrodes. VII. Perchlorate-selective membrane-electrode. Construction and characterization, E. HOPÎRTEAN, E. VERESS and V. MUREȘAN 1243

Liquid-membrane electrodes. XI. Tetrafluoroborate-selective liquid membrane-electrode. C. LITEANU, E. HOPÎRTEAN and E. ȘTEFĂNIGĂ 653

Liquid-membrane electrodes. X. Liquid-membrane electrode for iron(III) determination, E. HOPÎRTEAN 1385

Liquid metals, Internal pressure in —, I. G. MURGULESCU and A. LEIBOVICI . . 1279

Liquid mixtures, Collision-induced light absorption in —, V. EM. SAHINI and S. BĂDILESCU 811

Page

M

Magnésium des fontes au graphite sphéroïdal au moyen des résines-échangeuses d'ions, Séparation et concentration du —, GR. POPA et L. VLĂDESCU 725
Magnesium films supported on glass, On preferential orientation of thin —, I. SITARU and E. SEGAL 761
Mass transfer from dispersed particles to continuous fluid media. II. Oscillating fluid media, particularly due to ultrasonic energy, EM. A. BRATU, C. BALABAN G. I. JINESCU 271
Membrane-electrodes under current. VI. Potentiometry at continuous and constant current using a $Hg/AgI\text{-}Ag_2S$ membrane-electrode, Studies on the electroanalytical behaviour of —, I. C. POPESCU and M. HĂLĂLĂU 443
Metallchelaten dreizähliger Liganden. III. Kupfer(II)-Nickel(II)- und Eisen(II)-Chelate pyridylsubstituierter Dialkylsulfide, Zum Einfluss der Ringgrösse auf die Struktur von —, E. UHLIG, W. HEPP, LE MY NGU und K. SCHMIEDEKNECHT 1165
Metallchelaten mit Liganden die Donoratome aus der 6. Gruppe enthalten. I. HMO-Berechnungen an den Liganden (*o*-Carboxyphenoxy)-essigsäure und (*o*-Carboxyphenylthio)-essigsäure, Bildung und Stabilität von —, M. MRACEC, A. MAURER, S. POLICEC und Z. SIMON 675
Metallischen Pulvern, Eine Deutung des Einflusses der Arbeitsbedingungen auf die Stromausbeute bei der elektrolytischen Abscheidung von —, GH. FACSKÓ, C. RADOVAN und C. DAMINESCU 611
Modele de Landsberg relatif à l'équation logaritmique, Considération sur le —, N. I. IONESCU et B. AURIAN-BLĂJENI 353
Molten alkaline halides, Heat capacities in —, I. G. MURGULESCU and CR. TELEA 683
Molten and solid glasses, Some information about the geometry of the molecules in —, P. BALTĂ and D. RADU 525
Molten metals. IV. A comparison between gas and liquid viscosities, On the viscosity of —, M. ȘERBAN 35
Molten metals. V. Dependence of viscosity on the mean vibration frequency, On the viscosity of —, I. G. MURGULESCU and M. ȘERBAN 807
Molten salt systems with chemical interaction between the components, Thermodynamic information on the structure of —, B. F. MARKOV 13
Molybdenum. IV. Biguanidonium aquo-tetrachloro-oxomolybdates (V), Contribution to the coordination chemistry of —, P. SPACU and L. ANTONESCU 61
Morphine, Critical evaluation of fluorimetric assay methods for —, R. A. CHALMERS and A. F. JACKSON 575

N

Ni(II) complex compound derived from 1-methyl-2-carbethoxy-glyoxalanil-(1)-m-nitrophenylhydrazone-(2), A tetrahedral —, A. C. BANCIU 1181
Nitrilen. XVII. Kinetik und Mechanismus der Trimerisation der Arylcyanate in Gegewart von $AlCl_3$, Struktur-Reaktivitätsuntersuchungen mit heterosubstituierten —, I. I. BACALOGLU, R. BACALOGLU, D. MARTIN und A. PRÜFER . . . 511
Nitriles. Sur la chaleur de combustion de quelques nitriles *alpha, bêta* non saturés, La structure et la réactivité des —, I. CIOCĂZANU, V. DOGARU et D. ZĂVOIANU 1369
Nitrobis(aminoacidato) amminecobalt(III) complexes, Synthesis and absolute configuration of the, Synthesis and absolute configuration of the —, M. B. CELAP and M. J. MALINAR 569
o-Nitrophenylsuccinic acid and of some functional derivatives, Obtention of the —, F. CUIBAN, A. LUPEA, M. SILAȘI and M. SORA 869
NMDR experiments improved by means of a computer, Some —, V. BĂRBOIU . . 1135
Nomenclature of inorganic chemistry, Some considerations on the —, W. KLEMM . . 639
Non-electrolytes, by a cellular model with holes, Thermodynamic characterization of some binary solution of —, R. VÎLCU and S. SAMSON 1447

O

Organometallic compounds, Equilibria of redistribution reactions of —, O. A. REUTOV and K. P. BUTIN 733

Page

P

Palladium(II), cerium(IV), arsenic (III) and nitrite with fluphenazine hydrochloride, Spectrophotometric determination of —, H. SANKE GOWDA, K. N. THIMMAIAN and B. NARAYANA ACHAR 745

Partition coefficients and intermolecular force parameters, Z. SIMON and E. DRASKOVITS-SCHUCH 87

Pd(II) with monosubstituted derivatives of thiourea, Complex compounds of —, N. DEMIAN, C. AMBRUS and D. CAMBOLI 1187

Phenol obtainment from benzene in oxygen plasma generated by a high frequency discharge. II. The phenol formation mechanism, G. BOURCEANU and V. ABABI, GH. POPA, M. SANDULOVICIU 459

Phenol obtainment from benzene in oxygen plasma generated by a high frequency discharge. III. Kinetics of the process in pulse and steady-state regime, G. BOURCEANU, V. ABABI, GH. POPA and M. SANDULOVICIU 1391

Phenothiazine derivatives as indicators in vanadometry, An examination of various —, R. BELCHER, H. PUZANOWSKA-TARASIEWICZ and W. I. STEPHEN 531

Phosphore : résultats et perspectives, Quelques aspects de la recherches en chimie organique du —, F. MATHIS 665

Phosphorsäure, Gemischte aromatische Ester der Phosphorigen und der —, M. IOVU und E. VOINA 1209

Photolysis of $Mn(C_2O_4)_2(H_2O)_2K$ in dimethyl-formamide. II. Concentration and oxygen effects, On the —, T. ONCESCU, S. G. IONESCU and C. ANDREESCU 697

Photometrische Bestimmung einiger aromatischer Amine durch Kupplung mit dem p-Nitrobenzoldiazonium-Ion, GH. CIUHANDU, O. BECZY und GH. OANCEA 583

Pigments in the $Cr_2O_3-TiO_2-WO_3$ system, Red-brown-, T. P. TĂVALĂ, N. GR. BRÎNZAN and V. FLOREA 787

Pitting process, Irreversibility of the —, S. CIOLAC 1151

Polibenzimidazolimidy, V. V. KORSHAK, A. I. PAVLOV, G. MANDRIC i I. ZUGRĂVESCU 1521

Polyäthylen, Thermoanalytische Untersuchungen von —, G. LIPTAY, L. LIGETHY und E. BRANDT-PETRIK 647

Polychloroacetates, Synthesis of di- and triphenyllead —, I. BALAZS, V. FĂRCĂŞAN and I. HAIDUC 379

Polyelectrolyte solutions, Dielectric constants and refractive indices in —, C. BELDIE and O. MIHĂILESCU 201

Polyelectrolyte solutions, Thermodynamic and transport properties of the —, C. BELDIE 839

Poly(ethylene-terephtalate) under radiofrequency electrical discharge conditions, The grafting of the —, CR. I. SIMIONESCU and M. MACOVEANU 911

Poly(methylmethacrylat) unter nicht isothermen Bedingungen, Der thermische Abbau von —, N. HURDUC and I. A. SCHNEIDER 945

Polynuclear complex compounds of iron, cobalt and nickel. I. Mercury containing complex compounds, M. BREZEANU and M. DINCULESCU 539

Polynuclear complex compounds of iron, cobalt and nickel. II. Mercury-containing complex compounds, M. BREZEANU and M. DINCULESCU 1175

Poly(olefins) graft copolymers, Perspectives for industrial production of —, D. MUNTEANU and I. NANU 923

Potential anticancer agents. XIII. Synthesis of new aliphatic and cycloaliphatic N-nitrosoureas, I. BARACU, E. TĂRNĂUCEANU and I. NICULESCU-DUVĂZ 885

Potential anticancer agents. XIV. Synthesis and biological evaluation of N [4′-{[(2,4-diamino-6(7)-pteridinyl)-methyl]-N^{10} -methylamino}-benzoyl]-L,D and DL-glutamic (aspartic) acids, D. C. ŞUSTER, G. CIUŞTEA, A. DUMITRESCU, L. V. FEYNS, E. TĂRNĂUCEANU, G. BOTEZ, S. ANGELESCU, V. DOBRE and I. NICULESCU-DUVĂZ 1195

Proton-electron-hydride concept of the theory of acids and bases in non-aqueous solutions, A. P. KRESHKOV 1289

Pyrimidines, Potential anticancer agents. XI. Derivatives prepared from diazotized —, D. C. ŞUSTER, G. BOTEZ, L. V. FEYNS, V. DOBRE and I. NICULESCU-DUVĂZ 257

Page

Pyrylium cation, A simple semiempirical MO-calculations of electronic spectra and charge distribution in 2,4,6-trimethyl —, N. VLAHOVICI and P. T. FRANGOPOL . 1379

Pyrylium salts formed by diacylation of olefins. XXIII. Isomeric ethyltrimethylpyridines and dimethyl-n-propyl-pyridines from the diacetylation of hexenes and methylpentenes, A. T. BALABAN, A. BOTA, F. CHIRALEU, E. ŞLIAM, A. HANEŞ and C. DRĂGHICI 1003

Pyrylium salts, Isotopic exchange of active methyl hydrogens. IX. Intramolecular kinetic comparison between α-methyl and α-isopropyl groups in —, I. I. STĂNOIU, E. GÂRD, C. UNCUŢA, F. CHIRALEU and A. T. BALABAN 1359

Pyrylium salts, Isotopic exchange of active methyl groups. X. Activation parameters for deuteriation and de-deuteriation of isopropyl- —, I. I. STĂNOIU, A. T. BALABAN and F. CHIRALEU 1499

Q

Quinoline-1-oxide complexes of lanthanide iodides, I. RAMAKRISHNAN and S. SOUNDARARAJAN 395

R

Radicales libres. Approximation INDO, Estudio conformacional y de constantes de acoplamiento hiperfino en —, F. ARCE, J. L. ARMESTO, J. CASADO y M. A. RIOS 815

Reacciones de Arbuzov. I. Mecanismo de reacciones de trialquil (-aril) fosfitos con yoduros de alquilo, Estudio de —, J. M. CACHAZA, J. CASADO y A. VARELA 213

Reagents, Theoretical study of the acidity of some organic —, GR. POPA and S. MOLDOVEANU 301

Reagenz von EDTA Typus. II. Komplexsalze der 4,4'-Diaminodiphenyl-methan-N,N'-diessigsäure mit verschiedenen Metallionen, Ein neues —, CONST. GH. MACAROVICI und E. CHIŞ 657

S

Sels fondus-application au sulfate d'argent, aux sulfates, chromates, molybdates et tungstates alcalins. Étude dilatométrique et volumétrique de —, L. DENIELOU, J. P. PETITET et C. TEQUI 27

Silica gel, Reactions with sodium hydridoborate on —, V. CIURDARU and F. HODOŞAN. 1027

Silver gas electrodes. V. The effect of compression and sintering conditions on electrode performances, Oxygen reduction on —, O. RADOVICI, M. MAVRODIN-TĂRĂBÎC, I. ONACA and I. SOLACOLU 145

Solid acid catalysts. II. Transalkylation of toluene on $Al_2O_3-SiO_2$ catalyst, The origin and the type of active centers in —, I. V. NICOLESCU, O. ŞERBAN, I. SĂNDULESCU and L. STOICESCU 97

Solvolytic behaviour of strained systems. The 1-, 4- and 5-methylbenzo[b]cicyclo[3.1.0]hex-2-en-4-yl cations, V. WERTHEIMER, A. M. GLATZ and A. C. RĂZUŞ 1505

Spectromètre de masse à deux étages, Étude des réactions entre D_2^+ et CH_nD_{4-n} à l'aide d'un —, E. CONSTANTIN et J. CH. ABBE 327

Spectrophotometric study of some 1,5-diphenyl-1,5-pentadiene-3-ones, A. A. KHALAF, S. H. ETAIW, R. M. ISSA and A. K. EL-SHAFEI 1251

Spin-trapping experiments with pentadienyl- and cycloheptadienyl-iron tricarbonyl cations, M. CAIS, P. ASHKENAZI and J. GOTTLIEB 545

Stilbene derivatives. III. The infrared spectra of some nitro-containing *trans*-stilbene derivatives, The electronic structure of some —, L. CIOHODARU 163

Stilbene derivatives. IV. ESR spectra of some nitro-containing stilbene anion-radicals, The electronic structure of some —, L. CIOHODARU, V. EM. SAHINI and E. VOLANSCHI. 171

Stilbene derivatives. V. The influence of the substituents on the HMO π-energy levels, Electronic structure of some —, L. CIOHODARU 1125

Stilbene derivatives. VI. The molecular diagrams of some mono-nitro-stilbene derivatives, The electronic structure of some —, L. CIOHODARU 1315

Strontium(II) ion in molten potassium nitrate, A chronopotentiometric study of the —, S. STERNBERG and T. VIŞAN 321

Sulphonamide compounds. V. Arsenic traces determined with silver sulphanilamide, New analytical applications of some —, T. SIMONESCU and V. RUSU . . . 435

Page

Sulphonamide compounds. VI. Sodium *m*-silver-sulphamoyl-benzoate, a new reagent for the determination of carbon monoxide in the air, New analytical applications of some —, T. SIMONESCU and V. RUSU 937

Surfactants-polyvinlypyrrolidone interaction, ^{1}H-NMR characterization of anionic —, G. POPESCU and M. MARINESCU 1401

T

Terephtalatglycerinalkydharze, Ölmodifizierte —, I. MANOVICIU, V. MANOVICIU und C. DAVIDESCU 953

Terpolymerization tield. VIII. Theoretical structural study of the high conversion acrylonitrile-methacrylic acid- methyl methacrylate terpolymer, CR. I. SIMIONESCU and A. LIGA 49

Terpolymerization field. IX. Chemical structure-properties correlation, Researches in the —, CR. I SIMIONESCU, A. LIGA and A. ASANDEI 283

Tetrachlorohydroquinone with quinoline and piperazine, Adducts of —, I. GAVĂT, O BUTUFEI and M. MUNTEANU 1261

Tétrachloromanganates(II) d'ammoniums monosubstitués linéaires, Préparation et caractérisation de —, A. DAOUD, A. THRIERR-SOREL, R. PERRET et B. CHAILLOT 857

1,3,7,9-Tetranitrophenothiazine-5-oxide with organic bases, Reaction of —, A. TURCU 1363

Thermal decomposition of tris(oxalato) manganese(III) complex in aqueous solutions, T. ONCESCU and E. JURCONI 1471

Thermal properties of the mixture $BaCl_2-KCl$, D. I. MARCHIDAN and L. PANDELE 7

Thioamides. II. UV and IR spectra, Relations between the electronic structure and the reactivity of some —, A. O. FULEA and C. FULEA 1513

Tin(IV) complexes with 2,2'-dihydroxychalkones, A spectroscopic study of —, N. S. BIRADAR, B. R. PATIL and V. H. KULKARNI 1479

Transport phenomena, Approximate analytic determination of the average values of potential functions occuring in chemical —, K. POLINSZKY, E. VASANITS and J. FÜLOP 181

s-Triazines. III. The condensation reaction of phenylbiguanide with phenylisothiocyanate in the presence of Cu ions, Contributions to the coordination chemistry of —, C. GHEORGHIU, C. MĂRCULESCU, M. CONSTANTINESCU and O. CONSTANTINESCU 385

Triphenylmethane derivatives, Infrared, ^{1}H-NMR and mass spectra of some —, S. MAGER and I. HOPÂRTEAN 1075

U

Uranium(VI) with dialkylphosphorodithioic acids. V. Synergistic effect of tributyl-phosphate, Solvent extraction of —, I. HAIDUC, GH. MARCU and M. CURTUI . . 625

Urea and thiourea derivatives. II. HMO and DEL RÉ molecular orbital calculations, New—, M. MRACEC, S. RADULY, Z. SIMON, A. BOLDEA and C. DRUGARIN 401

UV, VIS and IR spectra of the $Pd(p-NO.C_6H_4N(CH_3)_2)_2.Cl_2H_2O$, The —, N. CALU, N. FOCA and M. LUCHIAN 551

V

Virial coefficient. III. $Ar + H_2$ and $CH_4 + H_2$ systems, Second interaction —, R. VÎLCU, I. GĂINAR and C. LEPĂDATU 827

Viscosity of ionic liquids, A relation for the —, I. G. MURGULESCU and C. MISDOLEA 1433

Viscosity of melts of hydrated lanthanum nitrate, Z. KODEJS and I. SLAMA 1329

Z

Zone fondue. I. Systèmes Cu(II)—Co(II) ou Cu(II)-Ni(II) et mercaptoacétanilide. Concentration et séparation d'éléments à l'aide de chélateurs par la méthode de la —, S. FIȘEL et C. SIMION 305

X

Xanthates from flotation pulps with an Ag_2S membrane electrode, Determination of —, I. HAIDUC, S. BEICU and C. LITEANU 427

Surfactants [illegible] and [illegible]
[illegible] and [illegible]

T

[illegible] and [illegible]
[illegible] and [illegible]
Tension [illegible] properties [illegible]
[illegible] and [illegible]
[illegible]
[illegible] and M. [illegible]
[illegible] and [illegible]
[illegible] and [illegible]
[illegible] and [illegible]
[illegible] and [illegible]
[illegible] and [illegible]
[illegible]

U

[illegible] and [illegible]
[illegible] and [illegible]

V

[illegible] and [illegible]
[illegible]

Z

[illegible] and [illegible]
[illegible] and [illegible]

NOTE POUR LES AUTEURS

La Revue Roumaine de Chimie publie des articles en anglais, français, russe, allemand ou espagnol. Les auteurs sont priés d'envoyer des articles et des comptes rendus inédits.

Les manuscrits seront dactylographiés à deux intervalles. La bibliographie, les tableaux et la légende des figures seront placés après le texte.

Si l'article fait partie d'une série numérotée, le titre de la partie précédente sera indiqué dans une note au bas de la première page.

Chaque article sera précédé d'un résumé comprenant quinze lignes au maximum. Les références bibliographiques dans le texte seront faites par des exposants sans parenthèses et paraîtront comme des notes au bas de chaque page.

Les publications périodiques mentionnées dans la bibliographie seront présentées suivant les prescriptions internationales : le nom de l'auteur précédé de l'initiale du prénom, le titre du périodique abbrégé conformément à « Chemical Abstracts », et souligné par une ligne, le numéro du tome indiqué par des chiffres arabes et souligné par deux lignes, suivi de la première page de l'article ; à la fin, l'année de la parution sera placée entre parenthèses. Le numéro de la revue ne sera pas indiqué si les pages du volume sont numérotées consécutivement.

Les textes des livres ou traités inclueront : les noms des auteurs, les initiales du prénom le titre du livre entre guillemets et sans être souligné, le numéro du tome précédé par l'abréviation « vol. » (ou (« Bd »), le numéro de l'édition, les éditions (the publisher), la localité de la parution du livre, l'année de la parution et la page de la référence précédée(s) par l'abréviation « p » (ou « S »).

Les brevets seront indiqués comme suit : l'auteur ou la firme, le pays et le numéro du brevet, la date et la revue (Chem. Abstr.). Par ex. : M. Jones (to Union Carbide C^{o}), Brit. Pat. 601 238, 2 Sept. 1959, Chem. Abstr., **54**, 12808 (1960).

Les diagrammes seront tracés à l'encre de Chine sur papier calque. Les tableaux et les figures (en nombre strictement nécessaire) seront numérotés par des chiffres arabes. Les courbes dans les figures seront numérotées par des chiffres arabes et leur explication sera donnée dans la légende des figures. Prière de ne pas inscrire les mêmes données dans les tableaux et les figures. Chaque tableau aura un titre. On indiquera dans le texte la place approximative des tableaux et des figures. Les formules chimiques seront incluses dans le texte ; en outre, elles seront transcrites sur papier calque, à l'encre de Chine.

Les auteurs sont priés d'indiquer les caractères italiques (en soulignant les lettres au crayon), ainsi que tout autre caractère spécial ; les préfixes *ortho*, *meta*, *para*, *cis*, *trans*, etc. seront soulignés pour indiquer leurs caractères italiques et ne seront jamais écrits avec des majuscules.

Aucune correction à la main ne sera admise sur le manuscrit. Les corrections seront frappées à la machine. Les letters grecques ou autres symboles spéciaux seront insérés à la main à l'encre clairement.

Le manuscrit sera signé par l'auteur.

Le colonne-titre aura 50 lettres au maximum.

L'entière responsabilité du contenu des articles appartient aux auteurs.

[illegible] POUR LES AUTEURS

La Revue [illegible] publie des articles en anglais, français, allemand, espagnol [illegible] des articles et des [illegible]

[illegible] les figures seront placées dans le texte.

[illegible]

Chaque article sera [illegible] cinq [illegible] bibliographie [illegible] le texte [illegible] bas de chaque page.

[illegible] dans la [illegible]

[illegible] la date [illegible] 1868 [illegible]

[illegible] figures [illegible] chiffres arabes [illegible]

Les auteurs sont priés d'[illegible]

Aucune correction à la [illegible]

Le nombre de pages [illegible]

[illegible] 50 tirés à part [illegible]

[illegible] responsabilité du contenu des articles [illegible] aux auteurs.

1978 APR 8

TRAVAUX PARUS AUX ÉDITIONS DE L'ACADÉMIE DE LA RÉPUBLIQUE SOCIALISTE DE ROUMANIE

C. DRĂGULESCU, E. PETROVICI, **Chimie structurală modernă. Chimia coordinanţei** (Chimie structurale moderne. La Chimie de la coordinence), 1977, 947 p., 70 lei.

P. BALTĂ, E. BALTĂ, **Introduction to the physical chemistry of the vitreous state**, coédition avec Abacus Press, Kent, 1976, 287 p., 31 lei.

I. G. MURGULESCU, **Introducere în chimia fizică. Vol. I. 1. Atomi. Molecule. Legătură chimică** (Introduction à la Chimie physique. Ier vol. 1re Partie. Atomes. Molécules. Liaison chimique), 1976, 560 p., 2 pl., 36 lei.

GR. POPA, ŞERBAN MOLDOVEANU, **Reactivii organici în chimia analitică** (Les réactifs organiques dans la Chimie analytique), 1976, 255 p., 18 lei.

I. ZUGRĂVESCU, MAGDA PETROVEANU, **N-ylid Chemistry**, 1976, coédition avec McGraw-Hill International Book Company, SUA, 396 p., 33 lei.

C. V. UGLEA, **Cromatografia pe gel permeabil. Noi domenii de aplicare** (La Chromatographie sur gel perméable. Nouveaux domaines d'application), 1976, 123 p., 6, 75 lei.

I. GĂLĂŢEANU, **Radiochimia aplicată. Metode şi probleme** (La radiochimie appliquée. Méthodes et problèmes), 1976, 307 p., 19 lei.

FRANCISC A. GOTHARD, **Echilibre lichid-vapori. I. Baze teoretice şi metode de calcul** (Equilibres liquide-vapeurs. I. Bases théoriques et méthodes de calcul), 1975, 263 p, 2 pl., 28 lei.

CONST. GH. MACAROVICI, D. MACAROVICI, **Chimia oxizilor dubli şi utilizările lor** (La chimie des oxydes doubles et leur utilisation), 1975, 195 p., 13 lei.

ELENA CEAUŞESCU, **Research work on synthesis and characterization of macromolecular compounds. Contributions**, 1974, 251 p., 20 lei.

M. AVRAM, **Antidăunători (Pesticides)**, 1974, 496 p., 41 lei.

DUMITRU COSTACHE, **Analiza chimică prin metoda cinetică** (L'Analyse chimique par la méthode cinétique), 1974, 276 p., 15,50 lei.

G. A. RĂDULESCU, **Proprietăţile ţiţeiurilor româneşti** (Les propriétés des pétroles roumains), 1974, 267 p., 2 pl., 18 lei.

CR. SIMIONESCU, VIORICA RUSAN, V. POPA, **Chimia algelor marine** (La chimie des algues marines), 1974, 212 p., 1 pl., 18 lei.

MARIA FITI, **Dozimetria chimică a radiaţiilor ionizante** (La dosimétrie chimique des radiations ionisantes), 1973, 240 p., 13,50 lei.

TIBERIU NĂŞCUŢIU, **Metode radiochimice de analiză** (Méthodes radiochimiques d'analyse), 1973, 384 p., 23 lei.

CRISTOFOR SIMIONESCU, MARGARETA GRIGORAŞ, AGATA CERNĂTESCU-ASANDEI, GHEORGHE ROZMARIN, **Chimia lemnului în România. Plopul şi salcia** (La Chimie du bois en Roumanie. Le peuplier et le saule), 1973, 299 p., 13 pl., 26 lei.

MIHAI FLORESCU, **Eficienţa economică a cercetării ştiinţifice** (L'Efficience economique de la recherches scientifique), 1972, 115 p., 15 lei.

GEORGETA LĂZĂRESCU, **Sistematizarea informaţiilor în chimia organică** (La systématisation des informations en Chimie organique), 1972, 243 p., 1 pl., 10.50 lei.

I. P. INFORMAŢIA c. 7437

43426

Lei 25.—